UNIVERSAL
LIBRARY
OU_166627
UNIVERSAL
LIBRARY

OSMANIA UNIVERSITY LIBRARY

Call No. 539.76/Int61P Accession No. 36095

Author International Conference Atomic Energy

Title Proceedings v 9 1956

This book should be returned on or before the date last marked below.

PROCEEDINGS
OF THE
INTERNATIONAL CONFERENCE ON THE
PEACEFUL USES OF ATOMIC ENERGY

Volume 9
REACTOR TECHNOLOGY
AND CHEMICAL PROCESSING

Proceedings of the International Conference on the Peaceful Uses of Atomic Energy

Held in Geneva
8 August - 20 August 1955

Volume 9

Reactor Technology and Chemical Processing



UNITED NATIONS
New York
1956

UNITED NATIONS PUBLICATIONS

Sales No 1956 IX 1 Vol 9

A/CONF 8/9

Price U S $10 00, 72/-stg , 42 00 Sw frs
(or equivalent in other currencies)

PREFACE

The Proceedings of the International Conference on the Peaceful Uses of Atomic Energy are published in a series of 16 volumes, as follows

Volume Number	Title	Sessions Included
1	The World's Requirements for Energy, The Role of Nuclear Power	2, 3.2, 4.1, 4.2, 5, 24.2.
2	Physics; Research Reactors	6A, 7A, 8A, 9A, 10A.1.
3	Power Reactors	10A.2, 3.1, 11A, 12A, 13A, 14A.
4	Cross Sections Important to Reactor Design	15A, 16A, 17A, 18A.
5	Physics of Reactor Design	19A, 20A, 21A, 22A, 23A.
6	Geology of Uranium and Thorium	6B, 7B.
7	Nuclear Chemistry and the Effects of Irradiation	8B, 9B, 10B, 11B, 12B, 13B.
8	Production Technology of the Materials Used for Nuclear Energy	14B, 15B, 16B, 17B.
9	Reactor Technology and Chemical Processing	7 3, 18B, 19B, 20B, 21B, 22B, 23B.
10	Radioactive Isotopes and Nuclear Radiations in Medicine	7 2 (Med), 8C, 9C, 10C.
11	Biological Effects of Radiation	6 1, 11C, 12C, 13C.1.
12	Radioactive Isotopes and Ionizing Radiations in Agriculture, Physiology and Biochemistry	7.2 (Agric.), 13C.2, 14C, 15C, 16C.
13	Legal, Administrative, Health and Safety Aspects of Large-Scale Use of Nuclear Energy	4.3, 6.2, 17C, 18C.
14	General Aspects of the Use of Radioactive Isotopes, Dosimetry	7 1, 19C, 20C
15	Applications of Radioactive Isotopes and Fission Products in Research and Industry	21C, 22C, 23C.
16	Record of the Conference	1, 24 1, 24.3.

These volumes include all the papers submitted to the Geneva Conference, as edited by the Scientific Secretaries The efforts of the Scientific Secretaries have been directed primarily towards scientific accuracy Editing for style has been minimal in the interests of early publication This may be noted especially in the English translations of certain papers submitted in French, Russian and Spanish In a few instances, the titles of papers have been edited to reflect more accurately the content of those papers.

The editors principally responsible for the preparation of these volumes were Robert A Charpie, Donald J Dewar, André Finkelstein, John Gaunt, Jacob A Goedkoop, Elwyn O. Hughes, Leonard F. Lamerton, Aleksandar Milojević, Clifford Mosbacher, César A. Sastre, and Brian E. Urquhart.

The verbatim records of the Conference are included in the pertinent volumes These verbatim records contain the author's corrections and, where necessary for scientific accuracy, the editing changes of the Scientific Secretaries, who have also been responsible for inserting slides, diagrams and sketches at appropriate points In the record of each session, slides are numbered in numerical order through all presentations Where the slide duplicates an illustration in the submitted paper, appropriate reference is made and the illustration does not appear in the record of the session

Volume 16, "The Record of the Conference," includes the complete programme of the Conference, a numerical index of papers and an author's index, the list of delegates, the records of the opening and closing sessions and the complete texts of the evening lectures

TABLE OF CONTENTS

Session 7 3 Waste Disposal Problems			*Page*
P/398	Glueckauf	Long Term Aspect of Disposal	3
P/310	Wolman, Gorman	Management and Disposal of Wastes	9
P/848	Claus	Considerations in the Release of Wastes	17
P/312	Geyer *et al*	Low-Level Radioactive Waste Disposal	19
P/311	Straub *et al*	Decontamination of Liquid Wastes	24
Record of Session			28

Session 18B 1 Metallurgy of Thorium, Uranium and their Alloys			
P/555	Foote	Physical Metallurgy of Uranium	33
P/786	Kiessling	Reaction between U and Al	69
P/556	Carlson *et al*	Metallurgy of Thorium	74
P/558	Saller, Rough	Alloys of Uranium	107
P/416	Pfeil	Alloys of U and Th	117
P/352	Cabane *et al*	Uranium-Aluminum Alloys	120
P/826	Coffinberry, Ellinger	Intermetallic Compounds of Pu	138
P/557	Chiswik, Kelman	Thermal Cycling in Uranium	147
P/351	Stohr, Chevigny	Uranium Extrusion	159
P/559	Johnson, Curtis	Technology of UO_2 and ThO_2	169
Record of Session			174

Session 18B 2 Fabrication of Fuel Elements			
P/825	Howe	Reactor Fuel Metallurgy	179
P/561	Weber, Hirsch	Dispersion-Type Elements	196
P/953	Cunningham, Boyle	MTR-Type Elements	203
P/947	Boeschoten	Heat Transfer between U and Al	208
P/827	Kaufmann	Fabrication of Uranium Alloys	210
P/562	Saller	Aluminum-Uranium Alloys	214
P/828	Gurinsky *et al*	BNL Fuel Elements	221
P/961	Ristić	Thermal Strains in Fuel Rods	231
Record of Session			234

Session 19B.1 Handling Liquid Metals *Page*

P/123 Trocki *et al* — Na and NaK for Reactor Cooling — 241
P/866 Bauer ... ... — Liquid Metal Handling — 252
P/121 Barnes ..... — Pumping Liquid Metals — 259
P/637 Sajin, Dulkina . . . — High-Purity Bismuth — 265
P/812 Jackson, Werner — Manufacture of NaK Alloy — 270
P/766 Smales . . . . . — Impurities in Liquid Metals — 273
Record of Session — 280

Session 19B 2· Liquid Metal Heat Transfer

P/639 Mikheyev *et al* — Heat Transfer of Molten Metals — 285
P/120 Lyon . . — Heat Transfer Predictions — 290
P/417 Hall — Liquid Metal Heat Transfer — 295
P/1103 Hoyaux — Comparison of Coolant Efficiency — 302
Record of Session . — 305

Session 19B 3 Corrosion in Liquid Metal Systems

P/119 Epstein — Corrosion by Liquid Metals — 311
P/787 Mogard — Corrosion of U in Liquid Na — 318
P/829 Siegel *et al* — Sodium Graphite Reactor — 321
P/122 Bonilla — Molten Metal Systems — 331
P/118 Weeks *et al* — Bismuth-Uranium Fuel — 341
P/124 Baus *et al* — Solubility of Materials in Na — 356
P/638 Tsuprun, Tarytina — Behaviour of Stainless Steel — 364
Record of Session — 368

Session 20B Chemical Aspects of Nuclear Reactors

P/900 Hurst, Wright — Chemical Problems of Power Reactors — 373
P/821 Secoy — Homogeneous Reactor Chemistry . — 377
P/348 Chenouard *et al* — Heavy Water in C E A Piles — 384
P/535 Draley, Ruther — Corrosion of Aluminium Alloys — 391
P/880 Carlsen — High Temperature Corrosion of Al Alloys — 397
P/411 Huddle — Fundamental Aspects of Al Corrosion — 403
P/537 Thomas — Corrosion of Zirconium Alloys . . — 407
P/811 Kitzes, Lyon — Aqueous Slurries of U and Th — 414
P/536 Rockwell, Cohen . — Water Chemistry of PWR . . — 423
P/412 Ferrett, Milner — Square-Wave Polarograph in Analysis — 436
Record of Session . . . . . — 441

Session 21B: Chemical Processing of Irradiated Fuel Elements *Page*

P/414	Nicholls	Selection of Separation Processes	453
P/413	Fletcher	Chemical Principles in Separation	459
P/822	Culler	Reprocessing of Reactor Fuel	464
P/541	Culler, Bruce	Processing of U-Al Fuel Elements	484
P/349	Goldschmidt *et al*	Solvent Extraction of Plutonium	492
P/785	Haeffner *et al*	The Extraction of Uranium and Plutonium	498
P/540	Gresky	Extraction of U^{233} and Th by TBP	505
P/824	Tomlinson	Limitations of Solvent Extraction	511
P/551	Ferguson	Processing of Homogeneous Reactor Fuel	514
P/765	Pratt	Liquid-Liquid Extraction Equipment	520
P/539	Flanary	Solvent Extraction of U and Pu by TBP	528
P/543	Lemon, Reid	Direct Maintenance Processing Plant	532
P/547	Foster *et al*	Nuclear Reactor Fuel Dissolution	546
P/548	Campbell	Removal of Fission Products from Steel	551
P/549	Landry	High-Level Sampling Devices	555
Record of Session			559

Session 22B.1 Chemical Processing of Irradiated Fuel Elements (*concluded*)

P/823	Lawroski	Separations Processes	575
P/350	Chesne, Regnaut	Extraction of Irradiated U^{233} and Th	583
P/544	Feder	Pyrometallurgical Processing	586
P/545	Voigt	Liquid-Metal Extraction	591
P/542	Motta	High Temperature Processing	596
P/550	Dwyer *et al*	Processing Liquid-Metal Fuels	604
P/546	Hyman *et al*	Fractional Distillation Processes	613
Record of Session			627

Session 22B.2 Separation and Storage of Fission Products

P/415	Glueckauf, Healy	Processing of Fission Products	635
P/552	Anderson, Rohrmann	High-Level Waste Storage	640
P/553	Hatch *et al*	Radioactive Waste Disposal	648
Record of Session			659

Session 23B.1: Disposal in the Ground

P/565	Brown *et al*	Disposal of Liquid Wastes to Ground	669
P/12	Mawson	Waste Disposal into the Ground	676
P/564	Theis	Ground Disposal of Nuclear Wastes	679
P/554	Struxness *et al.*	Liquid Wastes in Terrestrial Pits	684
Record of Session			692

Session 23B 2. Disposal in the Sea *Page*

P/418	Seligman	Discharge of Waste Products at Sea I	701
P/419	Dunster	Discharge of Waste Products at Sea II	712
P/420	Fair, McLean	Discharge of Waste Products at Sea III	716
P/569	Renn	Disposal of Radioactive Wastes at Sea	718
Record of Session			722

Session 23B 3 Airborne Problems

P/571	Silverman	Air and Gas Cleaning	727
P/567	Smith	Concentrations from a Point Source	736
P/1051	Central Meteorological Observatory, Tokyo	Air and Rain Water Radioactivity	745
P/1056	Ishii	Measurement of Radioactive Dusts	747
P/353	Labeyrie, Weill	Atmospheric Radioactivity Measurement	752
P/975	Barreira, Laranjeira	Determination of Radioactivity	756
P/995	Facchini, Malvicini	Fast Ionization Chamber	761
P/788	Bergstedt	Electrostatic Precipitators	764
Record of Session			767

Session 7.3

WASTE DISPOSAL PROBLEMS

LIST OF PAPERS

			Page
P/398	Long-term aspect of fission product disposal	E Glueckauf	3
P/310	The management and disposal of radioactive wastes	A Wolman and A E Gorman	9
P/848	Fundamental considerations in the release of large quantities of radioactive wastes to land and sea	W D Claus	17
P/312	Low-level radioactive waste disposal	J C Geyer *et al*	19
P/311	Methods for decontamination of low-level radioactive liquid wastes	C P Straub *et al*	24

Long-Term Aspect of Fission Product Disposal

By E. Glueckauf,* UK

THE LEVEL OF NUCLEAR ENERGY PRODUCTION

In order to appreciate fully the fission product problem it is necessary to estimate the possible expansion of nuclear energy production

The British atomic energy program envisages in the foreseeable future a substitution of nuclear energy for approximately 60 million tons of coal which would otherwise annually be burnt for production of electricity towards the end of this century In order to do this, it would be necessary to burn up approximately 20 tons of nuclear fuel annually

From the British requirements one can estimate that world consumption of nuclear fuel may eventually reach figures of not less than 200 tons annually On the other hand, it is unlikely that a world consumption of 1000 tons will be exceeded in the foreseeable future, as this would imply an electricity consumption per head of the world population equal to the present USA level and derived essentially from nuclear energy From the point of view of the fission product nuisance, a world level of 1000 tons annually in the distant future is thus the most pessimistic outlook we can reasonably accept today Similar figures have been estimated by Hatch[1] and by Rodger[2] This level of nuclear energy would be equivalent to twice the present world coal production estimated at 1500 million tons of coal If, therefore, we can decide on ways and means to dispose, economically and without danger to ourselves and future generations, of a quantity of fission products of this order, we shall have no need to restrict later on the expansion of nuclear industries on account of the fission product nuisance

THE QUANTITY OF RADIATION FROM FISSION PRODUCTS

With present-day type of reactors, using solid fuel elements, by far the largest proportion of the energy of the fission products is spent while they are in the reactors and in various stages of the recycling process, and it is only those with half-lives longer than months with which the disposal process is seriously concerned

By the time the fission products are about one year old, 99 9% of the β and γ radiation emitted is due to eight elements only—from an original number of 35

A useful picture, and one which gives a pointer to the actions to be taken, can be obtained if we imagine that the fission products of over 1 year of age would all be accumulated in one place where they would continue to decay while every year the waste from 1000 tons of burned up material would be added The activity, under these conditions, would then increase, until for every element there is annually as much decay as there is addition, so that for a steady level of production a steady level of fission product activity would eventually be reached The equilibrium level of energy dissipation measured in Mev curies (1 Mev-curie = 0 0059 watt) for individual fission products is shown in Fig 1 (highest line) This level will not be exceeded, unless an annual production of 1000 tons is exceeded The quantities are enormous by all previously known standards, but these figures are put into their proper perspective, if we compare them with the amount of radiation produced by the small percentage of potassium (K^{40}) in the oceans of the world This almost unnoticeable activity adds up to $2\,8 \times 10^{11}$ Mev-curies which is just about the amount of activity to which this hypothetical nuclear energy program could ever lead It is interesting to see how this diagram would change if the fission products would be stored not for 1 year but for 20 years before being discharged into the common pool Under these conditions the nuclides of 1 year or less half-life have decayed to an insignificant level, and an equilibrium activity distribution would result which is indicated by the shaded portions of Fig 1 (For very high burn-up rates in enriched reactors, Sm^{151} disappears but another rare earth, Eu^{154} with a 16 year half-life is produced, with a similar energy dissipation) The scene is now completely dominated by the activity from Sr^{90} and Cs^{137} If these two species could be quantitatively removed and stored separately, the activity level of the remaining bulk solutions would fall by a factor of 1000 Indeed, as the toxicity of Sr^{90} is about 25 times greater than that of other β-emitting fission products, the reduction in toxicity caused by a quantitative removal of Sr and Cs would be by a factor of about 25,000 Figure 2 shows the decay of biologically weighted activity for a solution batch, first without and then after removal of Sr and Cs It shows clearly that in the former case the solution remains at a high level of toxicity for a very long time, while in the latter case there is a rapid and continuing decrease of activity This feature is of considerable importance in the subsequent discussions on fission product disposal

* Atomic Energy Research Establishment, Harwell, Berks

It may be worthwhile to comment here on the level of activity which is introduced into the atmosphere by Kr^{85} which, being a rare gas, is in the normal course of events, released into the atmosphere. A permanent level of the order of 10^9 Mev-curies (see Fig. 1) may appear to be very large. But, by comparing it with the amount of energy released in air at sea level by cosmic radiation, we find that, when completely dissipated in the atmosphere, the equilibrium Kr activity, even from such a huge nuclear energy program, would still be less than that constantly dissipated by cosmic radiation. Its influence on living matter would be less still than that of cosmic radiation, as the latter is a body absorption while the Kr activity affects mostly the skin only. We therefore can consider the gradual release of Kr^{85} into the air as innocuous for some time to come, though at the highest production levels its storage may become desirable.

COMPOSITION AND QUANTITIES OF FISSION PRODUCT SOLUTIONS

The composition of the fission products, resulting from 1 ton of U^{235} burnt up, depends somewhat on the rate to which the burn-up has proceeded and on the time elapsed since their removal from the reactor. A typical example is represented by Table I in which the main elements are ordered according to their position in the periodic table.

These fission products are extracted during a recycling process and, consequently, are mixed with

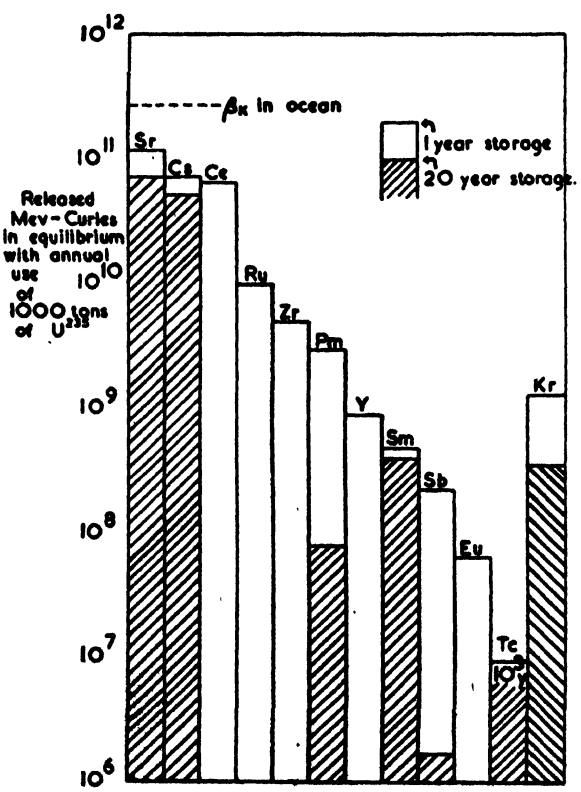

Figure 1. Equilibrium activities of individual fission products built up by the annual use of 1000 tons of fissile material; (a) after 1 year's storage before disposal; (b) after 20 years' storage before disposal. For comparison: total β-activity of K^{40} of the oceans

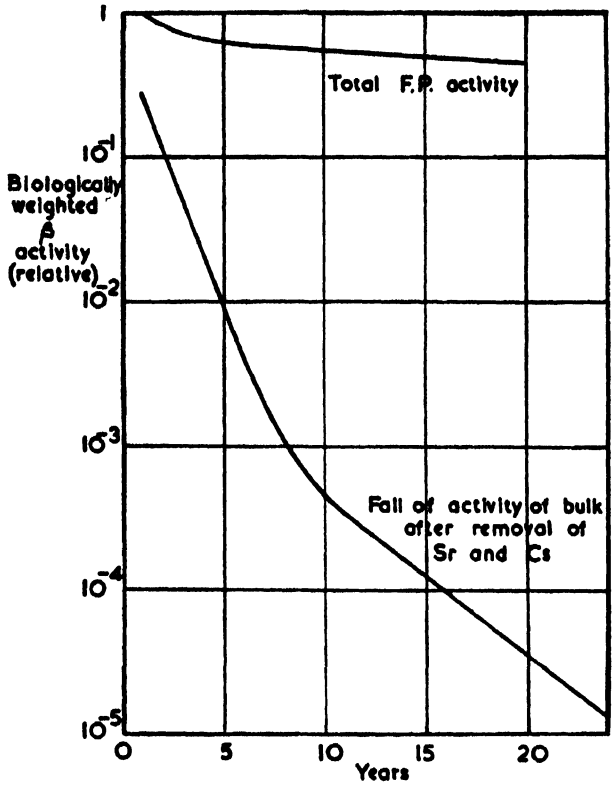

Figure 2. The decay of "biological" β-activity in a batch of mixed fission products; (a) with, (b) without prior removal of Sr and Cs

a comparatively large quantity of chemicals which are derived from (1) impurities of the reactor fuel, (2) products of the interaction of neutrons with the reactor fuel (Np, Am, Pu etc.), (3) incompletely separated reactor fuel (U or Pu), (4) incompletely removed canning or alloying material (Al, Zr etc.), (5) chemicals added during recycling separation, and (6) corrosion products from plant and storage vessels.

The quantities of these will vary greatly both according to the reactor materials (U, natural or enriched, Pu, alloys of these, etc.) and according to the recycling process employed (dissolving and extraction, re-melting with slag formation, etc.). They may be insignificant, if the fission products are extracted from the gas evolved in homogeneous reactors.

It is essential from the point of view of fission product disposal and utilisation, that the solutions arising can be concentrated to the smallest possible volume. If solid electrolytes arising from canning or alloying materials, or from salting-out agents employed during the solvent extraction process, are present in excessively large amounts, large volumes will eventually arise and the cost of storage, transport or any type of operation will go up almost proportional to the final volume. These factors should be considered when selecting reactor fuel elements and recycling processes, and have been provided for in the British fuel element and processing designs.

An example of the type of F.P. (fission product) solution arising under comparatively favourable conditions in graphite-moderated reactors using slightly

enriched uranium as fuel elements is shown in Table II. HNO_3 has been used as salting-out agent in the solvent extraction process which removes the uranium and plutonium. The bulk of original solution is very large, and it is apparent that primary concentration is an essential step before any disposal scheme becomes economical. (The only exception to this would be disposal of the original solutions into exhausted oil wells, if such are situated close to the processing plant[8].)

Table I. Quantities of Fission Products Derived from 1 Ton of U^{235} (150 days' irradiation, 30 days' cooling)

Group	*Element*	*kg*
0	Kr + Xe	128
1	Rb	15
	Cs	118
2	Sr	42
	Ba	43
3	Rare earths + Y	317
4	Zr	125
5	Nb	5
6	Mo	92
	Te	16
7	Tc	29
	I	7
8	Ru, Rh, Pd	61

Table II refers again to 1 ton of burnt-up U^{235}. There are also minor constituents such as C, Si, F', Cl', Np, Am, Pu, which are variable according to irradiation and purity of the original materials used. If future arisings should have a similar composition then, their total quantity in Great Britain, corresponding to 20 tons fissile material burnt, would be approximately $20 \times 25 = 500$ m³ of solution per annum.

There are now open various possibilities, of which the most useful ones are discussed:

(A) Indefinite storage in tanks, annual storage capacity to be added 500 m³.

(B) Immediate and complete disposal of approximately 1-year old solutions.

(C) Processing, involving the separation of the long-lived Sr and Cs. This might be followed (*a*) by immediate disposal of the bulk of solution, (*b*) by 13 years' storage, recovery of useful materials from the substantially inactive solutions, and subsequent disposal of the bulk.

Table II

Total volume of solution	*Before concentration 5–10,000 m³*	*After concentration 25 m³*
Main constituents:		
HNO_3	1300 tons	10.5 tons
$Fe(NO_3)_3$		6.8 tons
$Cr(NO_3)_3$		1.5 tons
$Al(NO_3)_3$		0.6 tons
$Ni(NO_3)_2$		0.5 tons
$UO_2(NO_3)_2$		1.3 tons
Mixed fission products (less gases) 870 kg in nitrate form		1.8 tons

(D) Separation of Sr, Cs, Ce, Zr for the economical utilisation of the radiations, followed by C, (*a*) or C, (*b*). (A discussion of this point would be premature, until there is a large industrial demand for radiation.)

It is necessary to amplify the concept of disposal. The pressure of public opinion is such that we need consider for a disposal only conditions where we have absolute safeguard (1) against F.P. entering human food or water supplies, (2) against accidental exposure of the public to radiation levels above tolerance, (3) against adversely affecting the access to the mineral wealth above or below ground, and, in addition, we require that the proposed scheme be economical. Even then a great deal of uninformed public opposition may be encountered.

POSSIBILITIES OF DISPOSAL AT SEA

We have seen already that complete and uniform dissipation of all fission products in the sea eventually would reach the activity level of K^{40}, and the high toxicity of Sr^{90} would have the result that the toxicity of the natural K^{40} in the sea would be considerably exceeded. This is therefore undesirable.

After a quantitative removal of Sr and Cs, an immediate and uniform dissipation of all the remaining fission products in the oceans could be considered as safe, but as uniform dissipation cannot be achieved in practice, this scheme would also be undesirable.

However, quantitative removal of Sr and Cs, combined with 13 years' storage, would lead to a product, the equilibrium activity of which is less than $\frac{1}{1000}$ of that of the natural K^{40} of the sea. For this type of F.P. solution safe methods can be found for disposal into the sea. One of many possible suggestions would be to drop these solutions in plastic containers into the deepest parts of the ocean, where, due to their high specific weight (>1.5), they would sink and become embedded in the mud of the sea bottom. As the activity is no longer sufficient to cause destruction of the resin, the release into the ocean by occasional leakages would be so slow that no appreciable local build-up of activity would be expected.

POSSIBILITIES OF DISPOSAL ON LAND

For disposal on land, it will require exceptional circumstances when case B is being considered. As, due to the long life of Cs and Sr, these solutions will remain highly active for a 1000 years, we shall require either completely deserted and inaccessible areas for the disposal of solutions, or else it will be necessary to turn the radioactive materials into solid products from which the fission products cannot be leached, e.g., as glasses or ignited clays.[4,5]

For disposal in solution form, places might be found in the vast and deserted arctic areas of Canada, Greenland, Northern Siberia or the Antarctic and possibly in deserts and steppes. With present-day type of fission products it is doubtful whether economic means of transport to such isolated places can be found, but this situation may disappear if fission

products later on should arise in much greater purity, e.g., from the gaseous discharge of homogeneous reactors.

Less drastic precautions would be required after the separation of Sr and Cs. The type of sandy strata which, at moderate depth, serves both domestic and industrial water supplies, becomes greatly compacted when at depths of more than 500 m. In these conditions there is practically no water flow. These sandy deposits usually have a substantial ion exchange capacity and therefore would represent an ideal burial ground. The F.P. of lowest adsorption, which diffuse fastest—such as Ru—have only a short life, and, though able to diffuse, do not get very far in their short life time. On the other hand, the tri-valent elements Pm and Sm as well as Np and Am which have a comparatively long life, are very strongly adsorbed and therefore would not move any significant distance within thousands of years.

DISPOSAL OF Sr AND Cs

It is not likely that Sr or Cs would need to be disposed of until their activities have considerably decayed. These two materials can be of great value as sources of radiation. This is almost certain to be the case for the γ-radiating Cs. Even if the industrial utilisation of the β radiation of Sr should not be practicable, the heat obtained from its decay would make it worthwhile to retain this material (which due to the absence of γ radiation requires little shielding), if only for heating purposes.

After a substantial decay, when the specific activity of these elements would become too low for economical use, disposal may be considered. As the quantities involved are quite small, one could then consider comparatively expensive treatment, such as adsorption in silica-bonded clays,[5] or in the naturally occurring montmorillonitic greensands[6] followed by baking at 1000 degrees (which leads to insoluble ceramic materials) and final disposal in safe areas. These greensands have the advantage over the clays used by Ginell, Martin and Hatch[4] that they are suitable for column packing without special treatment, though they have a smaller ion exchange capacity. For this kind of disposal, it is not necessary to have expensive heat treatment apparatus. One can visualise burying the dried clays or greensands, saturated with Sr or Cs, in water-impenetrable strata such as clays or gaults, under such conditions that the heat developed by radioactive decay raises the temperature above 1000°C. Perring[7] has calculated that the diameter of the holes required for obtaining such temperatures is only a few feet, depending on the exchange capacity of the adsorbing material and the specific activity of the final product.

Table III

Element	Fission kg/ton	Value £/kg	Total value (£) for 20-ton programme
Ru	38 kg	380	288,000
Rh	16 kg	680	220,000
Pd	7 kg	125	17,000
Xe	13 m³	£3000/m³	780,000

RECOVERY OF VALUABLE MATERIALS FROM OLD SOLUTIONS

Among the fission products which are effectively inactive after 13 years, there is a number of elements of very high specific value, such as ruthenium, rhodium, palladium and the rare gas xenon. Their approximate present-day value is shown in Table III. In addition to this the old fission product solutions contain 29 kg (per ton fission) of technetium, a long-lived element which does not occur in nature, and substantial quantities of neptunium and americium, which can be gainfully recovered. Indeed, the latter (mainly Am^{241}, half-life = 4.70 yr, α = 5.5 Mev), though at present a comparatively unimportant contribution of radiation to the fission product solutions, will become a first-order radiation hazard of old solutions when, at the later stages of the nuclear energy programme, extensive recycling of Pu takes place. At this future stage, the presence of americium in large quantities may well cause a bias against any disposal in the ground or at sea.

Xenon, which, with the present recycling processes, arises during the dissolving of the reactor elements in gaseous form, can easily be separated from the long-lived β-active krypton, by a process of gas chromatography.[8] If produced in large quantity, its price is likely to fall, but even so it would be a useful by-product.

CHOICE OF SUITABLE DISPOSAL SCHEME ON ECONOMICAL GROUNDS

Conditions may vary greatly from one country to another and, while it is not possible to consider all variations, a few possibilities will be discussed from an economical angle applicable to Great Britain.

Primary Evaporation

The cost of the primary evaporation is by far the biggest item in the whole disposal process. McCullough[9] has estimated the cost of evaporation at about 10 cents/gal processed. A somewhat smaller cost would apply in Britain. Assuming an initial volume of 5000 m³/ton fission and an evaporating cost of £6.10 per m³ of original solution, the total evaporating cost of a 20-ton programme would be £M 0.65 per annum. As such a programme is equivalent to 60 million tons of coal produced, the evaporation cost is equivalent to 2½d per ton of coal-equivalent. This represents roughly 0.4% of the present-day value of coal. We can also roughly estimate the cost of subsequent operations and shall compare "permanent storage" with "separation-disposal scheme" on the basis of a 20-ton programme.

Tank Storage

Tanks for the storage of 500 m³ per annum would involve in Britain an annual construction cost of

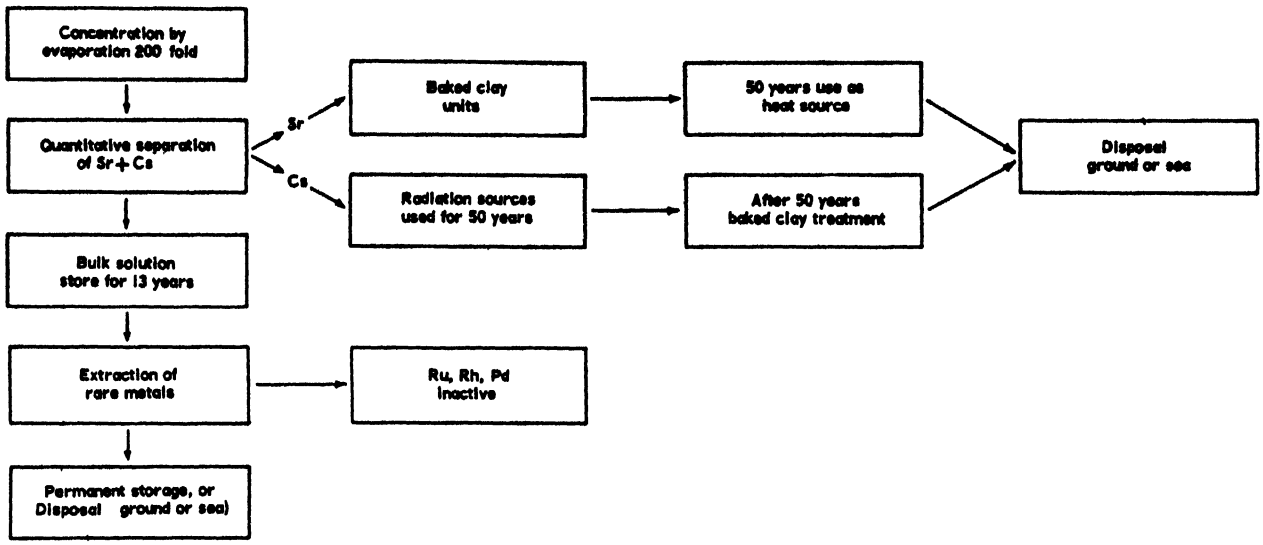

Figure 3

£50,000. Allowing another £10,000 per annum for maintenance, administration and occasional replacement, an annual expenditure of £60,000 would have to be set aside.

If a tank becomes empty again after n years, then, allowing a discount rate of 4%, the actual cost per annum is given by applying a factor of $[1-(1.04)^{-n}]$, i.e., £24,000 per annum for a storage period of 13 years.

Separation of Cs and Sr from Highly Active Solutions

It is not possible at this stage to give a cost estimate of the separation process of cesium, in view of the uncertainties as regards the composition of future fuels which may require different processing and thus give a different raw material from which the cesium is to be extracted. In view of the complexity of this operation it is safe to say, however, that the cost of separation will be very much larger than the cost of the evaporation stage.

Separation of Rare Metals from Old Solutions

A useful method for separating both the rare metals and technetium could be based on electrolytic de-acidification combined with metal deposition. No details have been worked out for such a process but in view of the fact that only a little shielding would be required, the cost would be considerably less than the value of the rare metals which latter is of the order of £250,000 per annum.

Separation of Am

This would probably require, (*a*) de-acidification, (*b*) fluoride precipitation of rare earths, and (*c*) column separation of Am from rare earths. In view of the high α-activity of Am^{241}, this is bound to be an expensive process and it is doubtful whether this would ever be economical.

In spite of the uncertainties in these assessments, it is clear that it is not possible to consider the economics of the disposal problem separately from fission product utilisation, as there are no economic advantages of any disposal scheme as compared with permanent storage for concentrated fission product solutions. The situation might be different if we had to deal with solutions, the electrolyte content of which is so high, that little or no concentration is possible, and where the volumes are increased by a factor of 25 or more. Only in such cases, separation of the long-lived Cs and Sr followed by limited storage and subsequent disposal may offer economic advantages by themselves. Otherwise, utilisation of the products has to be taken into account.

The recovery of Cs and its total utilisation could, however, pay not only for the separation but also for the concentration process. The recovery of Sr would pay only if utilisation for radiation purposes is feasible. However, its removal from the bulk solution is desirable if the remaining bulk has a low Am content as this renders the bulk fission product solutions comparatively harmless after aging.

The recovery of the rare metals Ru, Rh, Pd from old solutions is apparently a paying proposition and makes it worthwhile to retain the solutions, after the removal of Cs and Sr, sufficiently long to reach a low-activity level. It would be much more costly to recover these materials either at an earlier date or if Sr and Cs were left in solution.

It is very doubtful whether the recovery of Am and Np will ever be an economical process unless they are required for special reasons. In a future age of Pu reactors, their increasing presence in F.P. solutions might well weight the balance between disposal and permanent storage completely in favour of the latter, except for fission products arising with exceptionally small bulk.

A well balanced disposal and utilisation scheme, which is likely to be economical and self-paying and thus does not increase the cost of the power produced from nuclear energy, is outlined in Fig. 3.

No attempt has been made here to assess the value of a utilisation of the radiation energy from fission products while they are still present in the fuel elements, or the value of isolated species like Zr or Ce as source of extra-high intensity radiations. This is a field which should be treated separately under the subject of fission product utilisation. The separation of Cs and Sr comes under a different heading because their removal from the bulk facilitates the process of disposal and at the same time reduces its cost.

REFERENCES

1. Hatch, L. P., Ultimate Disposal of Radioactive Wastes, American Scientist, *41*: No. 5 (July 1953).
2. Rodger, W. A., Radioactive Wastes, Treatment, Use and Disposal, Chem. Eng. Prog. *50*: 263 (1954).
3. Herrington, A. C., Shaver, R. G. and Sorenson, C. W., Economic Evaluation of Permanent Disposal of Radioactive Wastes, Nucleonics 1953, *11*: No. 9, p 34-37.
4. Ginell, W. S., Martin, J. J. and Hatch, L. P., Ultimate Disposal of Radioactive Wastes, Nucleonics, *12*: No. 12, pp 14-18 (1954).
5. Berne, T., Grover, J. R. and Hutcheon, J. M., A.E.R.E., Harwell, Bonded Montmorillonite for the Ultimate Disposal of Long-lived Fission Products, CE/R 1658 (1955).
6. Amphlett, C. B. and Warren, D. T., A.E.R.E., Harwell, The Fixation of Fission-products on a Lower Greensand Soil, C/R 1686 (1955).
7. Perring, J. K., A.E.R.E., Harwell, The Cooling of Underground Fission Wastes, C/R 1294 (1953).
8. Glueckauf, E. and Kitt, G. P., Gas-chromatographic Separation of Kr and Xe Fission Products, Analyst, *77*: 903 (1952).
9. McCullough, G. E., Concentration of Radioactive Liquid Waste by Evaporation, Ind. Eng. Chem. *43*: 1505 (1951).

The Management and Disposal of Radioactive Wastes

By Abel Wolman* and Arthur E. Gorman,† USA

As the nuclear industry expands more and more toward centers of population far more economical methods of disposal of radioactive wastes will become necessary. The Atomic Energy Commission is preparing for this eventuality through research and development activities, broader in scope and more intensive in character than the attacks upon waste-disposal problems of any other major American industry in its early development.

In less than a decade the capital investment, including construction work in progress,[1] in the new atomic energy industry has reached nearly six billion dollars, exceeding that of any other major industry in this country. In spite of this phenomenal increase in plant and related production, hazards in the disposal of radiation wastes so far have been kept at a minimum. This is not to say that hazards do not exist nor that problems have not arisen. However, the problems are being met even though the costs are relatively high. Improvement in methods and facilities for control of radioactive wastes and reduction in cost are among the most important challenges to the industry in its progress.

As a prelude to the discussion which follows, it should be remembered that in utilization of fissionable material, in the controlled production of thermal energy power or in a sudden explosion, highly radioactive products result. These products, so aptly called radioactive ashes, represent significant hazards, whether they originate in production of fissionable materials—such as uranium or plutonium, within the reactor itself, or in subsequent chemical processing of spent fuel for recovery of valuable materials. The industry produces such wastes with great variations in quantity, level of activity, toxicity and physical form.

CHARACTERISTICS OF RADIOACTIVE WASTES

Levels of Activity

In general, high-level wastes in the atomic energy industry are those requiring extensive shielding to protect persons handling them from exposure to damaging radiation. Such waste may contain as much as 10^2 curies per liter. Fortunately they are produced in much less volume than those of intermediate and low levels. It is difficult to estimate the percentage of total waste production which is of high-level activity, because of the variety of the kinds of wastes. They might be as low as 0.5 and as high as 50 per cent depending upon the material being processed at a plant.

Intermediate-level wastes also require shielding and must be handled with much care. The low-level wastes are those which, if decontaminated by a factor of 10^2 or 10^3, would approach permissible limits[2] for human exposure. The range of their activity would be from 10^{-4} to 10^{-3} microcuries per milliliter.

Kinds of Wastes

Radioactive wastes may be in liquid, gaseous, solid states, or in some intermediate form. They may be combustible or noncombustible. The kind and intensity of radioactive wastes are not detectable by human senses. This insidious characteristic makes radioactive wastes especially dangerous because they could be released to the air, the soil, or to surface waterways without detection. With proper instrumentation and radiometric analytical techniques, however, the constituents and characteristics of radioactive wastes may be determined with accuracy.

Important from the waste-disposal point of view are the long half-lives and known damaging properties to human tissues of certain of the isotopes. Regardless of what is done to, or what use is made of a radioisotope, it will continue to give off radiation at its natural decay rate. As long as its radioactivity is in excess of permissible limits of exposure a radioisotope is a potential hazard to man.

These unique properties of radioactive wastes place more than average responsibility on those responsible for their disposal and also on officials charged with the protection of public health and natural resources.

SOURCES AND TREATMENT OF RADIOACTIVE WASTES

Radioactive waste products have numerous sources and must be evaluated carefully before wastes are treated and disposed of. This is especially true as the use of nuclear energy by competitive industry expands and reveals the true cost of waste treatment and disposal as a substantial item for consideration. Current practices, while adequate, are costly and necessarily conservative. Special emphasis is being given to environmental problems in the disposal of these wastes because, as private industry uses atomic energy, its plants must be reasonably near the popula-

* The Johns Hopkins University.
† US Atomic Energy Commission.

tions they are to serve. This is in contrast with some of the early large plants operated by the AEC which have been deliberately located remotely from large centers of population and other industries.

Raw Materials

Every industry creates some waste in progress from raw material to finished product. In the atomic energy industry the levels of activity of radioactive wastes increase progressively as industrial processes move closer to fission action.

Ores

The important raw materials for the moment are the radioactive ores of uranium. A product of radioactive decay of these ores, radon, when breathed into the lungs in sufficient concentrations can cause serious harm. With good ventilation the level of radon may be held to a minimum by methods familiar in other mining operations.

The progressive processing of the radioactive ores to the ultimate preparation of enriched feed material results in considerable volumes of long-lived alpha-emitting wastes. These processes are chemical and metallurgical and involve some machining. Chemical sludges containing uranium and giving off radon usually are held in concrete storage basins. The sludges are low in specific activity and generally represent no serious local hazard. Because of the very long periods that they will remain radioactive they will continue to present a real problem in storage. The dusts and chips from metallurgical and machining processes are usually recoverable and can be prevented from being a health hazard by good housekeeping and adequate ventilation facilities.

Fumes and Dusts

Fumes and dusts are removed as near as possible to the source of production by mechanical ventilating systems. Various air-cleaning facilities[3] are used, such as inertial separators, bag, bed and membrane filters, scrubbers and electrostatic precipitators. Experience has shown that the size, mass, and other characteristics of wastes in these feed-material operations vary widely and are often different from similar wastes of other industries. Specifications for air-cleaning equipment, therefore, must be much more rigid than in most industries.

Coolants from Nuclear Reactors

When the fuel is irradiated by neutrons in reactors, tremendous amounts of heat are produced. Reactors may be cooled by air, water, liquid chemicals, or by other media with suitable fluid and heat-exchange properties. Since, in the reactor core, these media are exposed to neutrons, they become irradiated. The radioisotopes formed depend on the composition of the cooling media. The problem of disposal of the irradiated media varies, depending on volume, radioactivity level and the suitability of local conditions for release of the coolant without creating environmental hazards.

Air

In an air-cooled reactor, such as the one at the Brookhaven National Laboratory, the coolant flows through the reactor[4] at a rate of 300,000 cubic feet per minute. The air in this system is prefiltered to remove dusts which otherwise would become radioactive when passing through the reactor. Under the neutron bombardment of the air coolant, radioactive argon, xenon and krypton are formed. The irradiated air is discharged to the atmosphere through a stack over 300 feet high. The dilution is normally such that the radioactivity is well below permissible limits in air breathed by humans. While the reactor is operating, the air in the vicinity is monitored. Should permissible limits of radioactivity for any of these isotopes be exceeded, the power level of the reactor would be reduced or the unit would be shut down entirely. The results of such control have been good.

Single-pass Water

The Hanford reactors are cooled by a single pass of water from the Columbia River. The river water is purified by chemical coagulation, settling and filtration in much the same way that water is treated for public water-supply systems. The water plants at the Hanford Works are some of the largest in the nation. The volume of cooling water used in a day is equivalent to the total water used in several large American cities. During the first few hours after leaving the reactor the rate of decay of radioactivity in the cooling water is high.

The water is held in retention basins for various periods prior to release to the river. The residual activity in the effluent water is diluted in the river after release through multiple outlets to improve dispersal. There is uptake of this activity by suspended matter and plankton in the water as well as by biologic growth and slimes in the stream-bed material. Since the spent cooling water is clear it is not objectionable from an aesthetic standpoint as are wastes from many other industries. The nearest sources of public water supply from the river are at Pasco and Kennewick, Washington, some 40 miles downstream from the nearest reactor. The activity in the river water at these intakes is within permissible levels for life-time human consumption. The river water is carefully monitored for radioactivity.

Recirculated Water

Other types of reactors, such as the Materials Testing Reactor (MTR) at the National Reactor Testing Station in Idaho, use closed cooling systems. They, too, are not free of problems of disposal of wastes. In a closed system using water it is customary to filter and to demineralize the coolant so that there will be little or no material in the water to become irradiated. Since this water must pass through pipes,

Table I. Magnitude of Low-Level Waste Output, July 1952–June 1953

Installation	Gallons liquid	Solids cubic feet: pounds		Sludge from evaporators, gallons
Argonne National Laboratory	182,400*	9600		6000
Westinghouse Atomic Power Division, Bettis Field	1,000,000*	1820		3000
Brookhaven National Laboratory	260,000*	8600		3900
California Research and Development Co.	385	1600	8000	
Iowa State College		195	4700	
Knolls Atomic Power Laboratory	2,000,000 Evap. 9300 Other	9300	168,600	11,000
Massachusetts Institute of Technology	1000			
Mound Laboratory		17,700	520,000†	
National Institutes of Health		240	1400	
National Reactor Test Station:				
Chemical Processing Plant	637,500*			
Materials Testing Reactor	42,000,000			
Oak Ridge National Laboratory (plus others)		394,000		
University of California Radiation Laboratory	330	2400	11,900	
U.S. Naval Radiological Defense Laboratory	13,200	960		

* Evaporable liquids only; may have other radioactive liquids which may or may not be treated in some other fashion such as a biological waste treatment method.

† Includes sludge from dewatering process.

pumps, and heat exchange facilities of one sort or another, it will eventually pick up some contamination, due to corrosion, dissolving properties of the water or abrasion. In order to prevent any marked increase in radioactivity in such systems, a small percentage of the total flow is bled off, filtered, passed through demineralizing media and then returned to the main stream. In other cases the bleed-off water is wasted. The waste water or the spent filter media and the demineralizing materials eventually acquire radioactivity and are disposed of usually by land burial.

Other Reactor Waste Problems

When a reactor is disassembled, or parts which have become irradiated are removed, a problem in disposal of the first order is presented. Extraordinary care is taken to shield workers, and the time and amount of their exposure is rigidly controlled. Highly active material is held in a designated fenced-off area or is buried in a burial ground with adequate cover to shield against surface exposure. An inventory of buried radioactive materials is maintained.

In case of a serious accident to a reactor, resulting in the release of enough excessive heat from nuclear reactions to volatilize fuel materials, a radioactive cloud would be formed which could spread contamination over a wide area. The extent of exposure hazard would depend on the kind and amount of radioactive material which was released and meteorological conditions at the time. The potentialities of an accident are given careful consideration. An Advisory Committee on Reactor Safeguards reviews all proposals for new reactors to be sure such matters are considered adequately and that reasonable preventive measures are taken. Additional special safety methods and devices are used to prevent serious accidents. An example of preventive measures of this kind is the 225 foot diameter steel sphere which encloses completely the submarine test reactor near West Milton, N. Y.

The general order of magnitude of low-level waste output from July 1952 to June 1953 is shown in Table I.

Chemical Processing

The high-level wastes originate principally, but not entirely, from the chemical processing of fuel from nuclear reactors in order to recover unburned portions. Associated with the irradiated fuel are many fission products with radioactive half-lives varying from seconds to millions of years. Such products have fixed rates of radioactive decay which never vary. Customarily the irradiated fuels, as removed from a reactor, are stored under water in order to permit decay of the short-lived fission products. Storage from 90 to 120 days is desirable, but processing within shorter periods may be necessary. With shorter periods of storage, problems of handling and disposing of the product are intensified.

These high-level wastes contain the entire spectrum of fission products when the uranium atoms are split. The waste solutions contain various salts and acids beside the fission products. The manner in which the uranium is utilized in the reactor, whether in solid or liquid form, determines the particular chemical separations process used. It determines likewise the physical, chemical and radiochemical properties of the waste solution ensuing. The characteristics of typical reactor fuel processing wastes to be expected are shown in Table II.

Table II. Characteristics of Typical Reactor Fuel Processing Wastes (High-Level Waste)

Gross beta activity, $1.6 \times 10^8 - 2.2 \times 10^{10}$ cpm/ml
Alpha activity, $6.0 \times 10^8 - 6.0 \times 10^9$ cpm/ml
Radioactivity, 1 to 4 $\times 10^8$ curries per gallon (neutralized)
Effective life, about 600 years
Heat generation, 1 to 3 BTU/hr/gallon
Power equivalent, 1 gm U^{235} = 24,000 kwh (100% efficiency)
Fission product wastes, 1 gm U^{235} forms 1 gm fission products
Wastes from processing, 0.5 to 5.0 gal waste solution/gm U^{235} consumed

Waste chemistry:

Ions	*Concentration in moles per liter*
Al	0.5 - 2.5
NO_3	2.0 - 8.0
H	0.5 - 3.0
Na	0.1 - 0.2
F	2.0 - 3.0
Zr	0.3 - 0.6
SO_4	0.3 - 0.6

Specific gravity, 1.1 to 1.4

Early Practice

During the earlier days of the industry emphasis was given in chemical processing to separating the weapons materials from the unburned fuel and the fission products. These by-products were held in large underground steel and concrete tanks. No attempt was made at that time to reclaim the unburned fuel or to use the fission products. Processing directed toward fuel recovery and re-use of unspent fuel is common today. The fission products are still being stored in underground tanks. Suitable uses for the energy in mixed or selected fission products are being sought. Even if found, such uses will aid in the economics of waste handling, but not in the reduction of the necessity for permanent policing of long-lived materials.

Significant Isotopes

Of special significance, because of half-life or radiotoxicity in disposal of atomic energy wastes from chemical processing are the following isotopes:

Radioisotope	*Mass number*	*Atomic number*	*Half-life*
Cesium	137	55	33.0 years
Strontium	90	38	19.9 years
Strontium	89	38	53 days
Iodine	131	53	8.1 days
Niobium	95	41	35 days
Cerium-praseodymium	144	58-59	280 days
Yttrium	91	39	61 days
Barium	140	56	12.8 days
Zirconium	95	40	65 days

Newer Methods

Improvements have been consistently made in the chemical dissolving, extraction, and stripping processes and facilities. Most important is the effort to remove these highly active wastes at the point of origin—where the volume is small—rather than to permit them to mix with and contaminate a high volume system where decontamination is very expensive. Formerly nitrogen oxide fumes and iodine vapors arising from fuel dissolving operations were released to the atmosphere through high stacks. Now these fractions of gaseous effluents are removed by scrubbers and by the use of a chemical reaction involving silver nitrate. Highly radioactive particulates, varying in size from 50 microns to fractions of a micron, are now being removed in deep-bed sand and glass-fiber filters of high efficiency. Glass-fiber filters (99.95 per cent removal efficiency for 0.3-micron particles) are manufactured commercially based on research and development work financed[5] by AEC. Presently these filters will handle gaseous effluents up to 600°F. Similar media to perform satisfactorily at 1500°F are being developed.

Prior to discharging liquid wastes to tanks and in an effort to concentrate radioactivity in as small a volume as practical, coprecipitation[6] processes in series are sometimes used. The supernatants of low activity are released to the ground usually through cribs and reverse wells. Concentrates are buried or stored in underground tanks. A disadvantage of coprecipitation is the volume of sludge which must be handled. Evaporation[7] has also been used extensively to reduce the volume of liquid wastes, both of high and intermediate levels of activity. At costs ranging from 5 to 70 cents per gallon, it is an expensive process of low- and intermediate-level wastes. Evaporation can be used to give a decontamination factor of 10^5 and even higher. High-level radioactive wastes also can be reduced in volume by ion exchange methods.[7] They are quite expensive, however, and the problem of disposal of the highly active resins remains. In all cases a balance must be arrived at between the over-all decontamination value of the process, the volume of by-product wastes resulting and the cost of the process in relation to other waste-disposal possibilities.

Storage Underground in Tanks

Storage of highly radioactive wastes in large underground steel and steel-and-concrete tanks as currently practiced presents a real problem. In the first place, it is costly, the capital cost varying from $0.35 to $2.00 per gallon of capacity. The thermal heat which results from gamma radiation is very high. In order to protect the tanks from deterioration by corrosion, excess heat must be carried away by a cooling system. To detect leakage from these tanks a system of drains is installed around them leading to a monitoring pit. The true life of these tanks is unknown. It is certainly much shorter than the length of time some of the long-lived radioactive materials will continue to be hazardous. It is not a simple task to remove entirely the high-level radioactive material after it has been stored in a tank over an extended period. Steam jetting is one method in use.

Although the costs of tank retention are high, the method has one advantage in the present stage of only limited knowledge, namely, that the wastes are under control.

Environmental Considerations

Environmental factors, such as the capacity of soils in the vicinity of these tanks to adsorb radioactive wastes should they leak and the rate of movement of such wastes through the soils, especially to underground sources of water supply, are extremely important. They are being studied under AEC sponsorship in cooperation with US Geological Survey. The possibility is under study of fixing high-level radioactivity in wastes by natural or prepared soils or by chemical compounds so that they may be disposed of safely by burial or underground storage with little likelihood of release to the environment. Removal of the more hazardous and long-lived radioisotopes such as Sr^{90}, Cs^{137} and Ce^{144} before discharge to the tanks or to the soils would reduce environmental hazards, provided these radioisotopes were adequately fixed or retained for disposal.

Ultimate Disposal

At the Brookhaven National Laboratory, Hatch[8] and his associates still seek a means of ultimate disposal of radioactive wastes. They have developed a method of adsorbing high-level fission products in specially prepared and extruded montmorillonite clay pellets. These pellets are then subjected to high temperature (800–1000°C) in a kiln to form hard ceramic beads from which the radioactive material cannot be leached. This process is in the pilot-plant stage and may have economic feasibility. Waste so treated could be placed in the ground or be stored in suitably shielded places with assurance of insignificant release to the environment. The process has some possibilities as a method of providing radioactive sources from wastes.

Ranges of costs of some of the methods discussed above are shown in Table III.

Ocean Disposal

Proposals have been made that high-level radioactive wastes be disposed of by dumping to the oceans in deeps far off shore, as is now practiced for disposal of some miscellaneous industrial wastes. The cost of shielding and transportation militates against this method for high-level wastes for many present and future plant locations. Other factors which make ocean disposal of such wastes of doubtful value are the high levels of radioactivity and heat in these wastes, the inability of recovery and uncertainties as to the effect of these wastes on other uses of the oceans in the service of mankind. The whole problem of ocean disposal is now under careful study at The Johns Hopkins University, with the collaboration of the skilled oceanographers of the United States. Until the oceanographers provide a greater assurance of ultimate safe fate of high-level wastes dumped into the ocean, the practice of withholding such materials will be continued by the Atomic Energy Commission. The uncertainty regarding the safety of sea disposal stems from the fact that the physical, chemical and biochemical behavior of the oceans cannot be satisfactorily predicted. Rates of circulation, diffusivity and turnover have not been firmly established. Even the instrumentation for so doing is not at hand.

Low- and intermediate-level radioactive wastes from the industry are being disposed of in selected dumping areas in the Atlantic and Pacific Oceans. The wastes are mixed in concrete and held in steel drums. Present studies by the staff of The Johns Hopkins University reveal that the cost of disposing of intermediate- and low-level wastes in oceans, including packaging, handling and disposal, vary from $0.30 per pound for installations within reasonable shipping distance from New York Harbor to $0.80 to $1.00 per pound for wastes from installations in the vicinity of San Francisco. On the East Coast wastes totalling from 20 to 30 tons per year are disposed of in the ocean and on the West Coast 4 to 5 tons. The difference in amounts is reflected in the costs. In The Johns Hopkins report the need was pointed out of special reinforcing of concrete in the containers to provide strength to meet the impact when the container strikes the hard ocean floor and the high hydrostatic pressures in 500 or 1000 fathoms of sea water.

Miscellaneous Wastes

In most industries significant plant wastes can be satisfactorily disposed of. The normal residual-waste products such as litter, dusts, chips, paper, wipes, clothing, obsolete material, and equipment furnishings, as well as structural material from plant renovation or wrecking, may be sold on the open market, lagooned locally, or dumped with normal waste materials of the community. In the atomic energy industry such wastes are usually segregated in special containers at the plants. They are then monitored for the kind and level of activity. Material contaminated by short-lived radioactivity may be stored for decay and then be disposed of normally. Where the half-life of the radioisotope is long the problem is complicated and still unsolved.

Incinerators

Combustible radioactive material such as paper, wipes, animal carcasses, bedding material for animals, and pieces of wood or cardboard may be disposed of

Table III. Range of Costs* of Treatment and Disposal Methods

	High-level wastes	*Low-level wastes*
Tank storage	$0.37 to $2.00/gal	
Evaporation	$0.14 to $0.71/gal	$0.14 to $2.00/ft³
Land burial	Limited practice	Approx. $10.00/ft³
Sea burial	Not practiced	
Land transport	See note†	

* All costs include interest, depreciation and overhead.

† Land transportation commonly costs about 4 cents per ton mile. However, in transporting high-level wastes under ICC regulations, about 95 to 99 per cent of the tonnage shipped is shielding which makes this item relatively costly.

by incineration. Incinerators, each different, were built to serve the AEC research and development areas—Los Alamos Scientific Laboratory (LASL), Argonne National Laboratory (ANL), and the Knolls Atomic Power Laboratory (KAPL). Each unit was provided with equipment for a high degree of clean-up of the products of combustion resulting in radioactive solutions to be disposed of, as well as the incinerator ash. The LASL unit has given considerable difficulty and is being remodeled. The ANL incinerator has performed satisfactorily at relatively high costs of $2.68 per cubic foot, including overhead and amortization charges.

The KAPL unit was a pilot plant and used oxygen to complete combustion. Its costs were also high, about $5.00 per cubic foot. Realizing the need for satisfactory and economical incinerators at its installations and also at research institutions working on problems of the industry and using radioisotopes, the AEC contracted with the Bureau of Mines, Combustion Research Laboratory, for development of a suitable unit. The staff of that Laboratory after many months of study of combustion parameters is now completing designs and specifications on two incinerators having capacities of 25 and 200 pounds per hour respectively. Each uses a tangential overfeed air-supply system in the combustion chamber[9] resulting in such a high degree of burn-up that all that is required for treatment of the gases of combustion is an inertial type separator for the larger particulates, followed by a high-temperature high-efficiency all-glass-fiber filter.

Baling

At KAPL wastes of the kind formerly incinerated are now being baled using an electric baler. The bales are stored and then shipped by rail to a storage area operated by the AEC in a part of the old Lake Ontario Works near Youngstown, N. Y. Here the bales are stored along with certain radioactive sludges and miscellaneous obsolete equipment and material which cannot be reclaimed or salvaged for scrap because of radioactivity.

Burial

Burial of radioactive wastes, particularly solids, is widely practiced at the larger AEC installations such as the Hanford Works, the Oak Ridge National Laboratory, the National Reactor Testing Station, and the Los Alamos Scientific Laboratory. The selection of burial grounds is made with the assistance of a qualified geologist, to take adequate account of (*a*) the characteristics of the soil to retain radioactivity, (*b*) the rate of release of waste from the burial area, (*c*) the elevation at and the rate of movement of ground water from the area, (*d*) the effect of release in contamination of the ground water, and (*e*) the distance to downstream users of ground water. Burial has the advantage of low cost and effective shielding. If movement of water through the soil is slow and the distance to ground water users large, a very substantial decay of radioactivity may take place before any source of water supply is affected. In the case of long-lived wastes, however, serious consideration must be given to the possible effect of any burial practice on the natural resources of the area. It is not likely that in movement through the soils there would be much lateral spread of contaminants released from a point source. Research on the selective adsorption of radioactivity in soils and movement through them under various conditions is in progress.

Deep Wells

Consideration also has been given to the possibility of disposal of radioactive waste solutions by discharge to abandoned oil and gas domes through deep wells. The economic aspects of the problem rest on the cost of shielding and delivery to the chosen well site. This method of disposal is being explored because it has obvious advantages. The feasibility of the use of abandoned mines and caves as storage places for high-level radioactive wastes also is being considered.

The use of any subterranean method of disposal of high-level wastes will require the most intensive scrutiny by the earth sciences practitioners working in collaboration with the specialists in the nuclear fission industry. This collaboration has recently been initiated by the AEC through the cooperative efforts of The Johns Hopkins University and the National Research Council. The Council has formed an Earth Sciences Committee of distinguished composition to spearhead these studies. Although in the United States several areas are underlain by geological formations possibly suitable for the disposal of high-level wastes, it is agreed by experienced geologists that the use of such formations for the purposes discussed should be deferred until these formations have been further explored and evaluated. In such explorations and studies, the baffling problems, among others, of heat dissipation and general thermal behavior will require detailed attention and diagnosis.

Laundry Wastes

In laboratories and production areas using radioactive material, protective clothing such as rubber and leather gloves, cloth coats, caps and shoe coverings are used extensively. Formerly evaporation of the wastes from laundering these materials was common practice, but usually the levels of activity were not sufficiently high to justify this expensive treatment. Such wastes may be mixed with the domestic sewage as at the National Reactor Testing Station. Here a plain settling and trickling filter plant[10] was designed with facilities for recirculation of the effluent. The laundry wastes and the domestic sewage are mixed and treated effectively. About 90 per cent of the radioactivity is found in the dried sewage sludge and the remainder in the effluent which is discharged to the ground. At Los Alamos, laundry wastes containing plutonium have been decontaminated by a co-precipitation method.[6]

Radioisotopes

The AEC manufactures and sells radioisotopes to hundreds of users in this country and throughout the world. They are used for research purposes in medicine, biology, chemistry and other professional and industrial fields. The most widely used isotopes[11] are P^{32}, I^{131}, C^{14}, Na^{24}, and Au^{198}. The Isotopes Division at Oak Ridge exercises a control over the users of these isotopes and requires purchasers to observe certain precautions[12] in the disposal of radioactive wastes. The levels of activity used are such that, in general, waste disposal is not a serious problem.[13] Current practice in many institutions is to discharge radioactive wastes to one or more holding tanks. They are monitored periodically and, if activity is at or below a prescribed level, the contents are released, usually to a public sewer system; otherwise they are held for decay to the prescribed levels for release. At places where flow in the sewers is adequate to give the desired dilution to safe levels, direct discharge without holding is practiced. Research at New York, Johns Hopkins, California, and Illinois[13] Universities has demonstrated that no adverse effect on processes of sewage treatment used by most municipalities would result from release of radioisotopes to public and institutional sewer systems.[14] Workmen should not work on or enter facilities until the level of activity have been determined and then only under the advice and supervision of a health physicist.

FUTURE PROBLEMS

Most observers are of the judgment that the next 25 years will produce major developments in the production of nuclear fuel power. Whether one shares optimistic or conservative views on these prophecies or hopes, one conclusion is clear. The disposal of reactor and fuel processing wastes will be one of the major controlling factors in determining the extent of the use of power reactors competitively with other sources of fuel for energy production. Whether we accept the calculations and assumptions as to waste production of Rodger,[15] Hatch,[8] Davis,[16] Hafstad[17] or Terrill *et al.*[18] for example, the resulting total fission products on hand to plague the operator and regulatory agency will be prodigious. To dispose of these materials will undoubtedly challenge the ingenuity and imagination of the scientist and industrialist. The economics of packaging, transporting, storing, treating and releasing these materials at some future time are still a source of great worry. The return of these wastes to nature will be undertaken with caution.

Some general indication of the magnitude of these prospective accumulations of radioactive materials with an assumed nuclear power production over the years, may be obtained from the following calculations. The amounts may be cut in half or multiplied by two, depending upon one's status as a prophet.

In 1953 the total electric-energy output of the United States was approximately 4.40×10^{11} kilowatt-hours (of this about 70 per cent was produced by fuels). The 1953 per capita consumption $= 4.40 \times 10^{11}$kwh/160×10^6 pop. $= 2.75 \times 10^3$ kilowatt hours per capita per year. Assuming that by the year 2000 the United States population will double, that the per capita consumption will triple and that 10 per cent of the increase in electrical energy produced will be generated by atomic reactors, then the nuclear power would be $(2 \times 1.60 \times 10^8 \times 3 \times 2.75 \times 10^3$ minus $4.40 \times 10^{11}) \times 10$ per cent $= 2.2 \times 10^{11}$ kilowatt hours per year.

One gram of U^{235} will furnish approximately 24,000 kwh and will produce about 1 gram of fission products. At 25 per cent heat-to-power efficiency, the nuclear reactors would, therefore, produce 2.2×10^{11} kwh $\times$ 1 gm FP/gm $U^{235}/24 \times 10^3$ kwh/gm $U^{235} \times 0.25 = 3.67 \times 10^7$ gm fission products per year. 3.67×10^7 gm $=$ 83,000 lb $=$ approximately 41 tons per year.

Under current processing techniques these fission products are dissolved or suspended in liquids. Depending on the type of reactor and the chemical separations process employed, the liquid volumes may measure as little as 0.5 gallons per gram U^{235} or as much as 5 gallons per gram U^{235} for unneutralized waste. The gallons of waste expected then would be about 1.8×10^7 to 18×10^7 gallons per year, or roughly 50,000 to 500,000 gallons per day.

One hundred days after removal from the reactor, the radioactivity of these fission products will be approximately 800 curies per gram. The half-lives of the radioactive fission products of any consequence vary from minutes or less for isotopes such as Pr^{146} and Ce^{146} to 33 years for Cs^{137} and 20 years for Sr^{90}. It would take about 600 years for the latter two isotopes to decay to the concentrations allowable in drinking water, assuming no evaporation or dilution.

Continual addition of fresh wastes to a partially decayed accumulation would build up the total activity to a rather high equilibrium level. Emerson, *et al.*,[21] have calculated such an equilibrium value for a 450 megawatt (electric power) reactor operating at 1000 megawatts total power. They assumed that an aqueous, homogeneous reactor is used and that the circulating fuel is processed every day. The total equilibrium activity of the wastes accumulated at the end of 10 years was calculated to be 625,000,000 curies.

CONCLUSION

The problems in waste disposal for the atomic energy industry are many. The control of waste is currently adequate, but expensive. As the industry expands, especially in the power field, less expensive methods will be required if atomic energy is to compete favorably in cost with other fuels. Anticipating this situation, the AEC has placed research and development contracts with universities, private industry, the national laboratories and other federal agencies to evaluate various waste-disposal methods and particularly the extent to which the ocean, the ground, surface waterways and the air may be used to store,

shield, dilute and disperse radioactive wastes. For maximum protection of the public, high-level radioactive wastes are now stored on or off site of operations under rigid supervision and management. Disposal, in its orthodox meaning as applied to familiar industrial wastes, is not yet at hand.

REFERENCES

1. *Major Activities in Atomic Energy Program—July- December 1953,* Supt. of Documents, Washington, D. C. (1954).
2. *Maximum Permissible Amounts of Radioisotopes in the Human Body and Maximum Permissible Concentrations in Air and Water,* National Bureau of Standards Handbook No. 52, Supt. of Documents, Washington, D.C. (1953 Manual).
3. Friedlander, S. K. *et al., Handbook on Air Cleaning—AEC,* Supt. of Documents, Washington, D.C. (1952).
4. Borst, L. B., *The Brookhaven Nuclear Reactor,* (AECU-1089), Physics Today, 4-6 (January 1951).
5. Little, A. D., Inc., *Development of a High Temperature-High Efficiency Air Filter,* Summary Report to AEC (August 1953).
6. Christensen, C. W. *et al., The Removal of Plutonium from Laboratory Wastes,* AECU-836.
7. *Symposium on Radioactive Wastes,* Industrial and Engineering Chemistry, *43*: 1499-1541 (July 1951).
8. Hatch, L. P., *Ultimate Disposal of Radioactive Wastes,* American Scientist, *41*: 410-421 (July 1953).
9. Corey, R. C., *Experimental Study of Effects on Tangential Orifice of Air in Incinerators,* Air Pollution Control Association, Baltimore, Md. (26 May 1952).
10. Biladeau, A. L., *Trickling Filter Sewage to Remove Radioactive Wastes,* Civil Engineering, *23*: 58 (August 1952).
11. *16th Semi-Annual Report of AEC to Congress,* Supt. of Documents, Washington, D.C. (1954).
12. *Interim Recommendations for Disposal of Radioactive Waste by Off-Commission Users,* Isotopes Division Circular B-6, Oak Ridge, Tenn.
13. Dietz, J. C., *Effect of Radioactive Wastes on Sludge Digestion,* Chemical Engineering News, *32* (24 May 1954).
14. Ruchhoft, C. C., Gorman, A. E. and Christensen, C. W., *Wastes Containing Radioactive Isotopes,* Industrial and Engineering Chemistry, *44*: 545 (March 1952).
15. Rodger, W. A., *Radioactive Wastes, Treatment, Use and Disposal,* Chemical Engineering Progress, 264-266 (May 1954).
16. Davis, W. Kenneth, *Atomic Power,* Engineering News-Record, 19 (7 April 1955).
17. Hafstad, Lawrence R., *The Industrial Application of Atomic Energy,* New York State Bankers Association (24 January 1955).
18. Terrill, J. G., Jr., Moeller, D. W. and Ingraham, S. C., II, *Fission Products from Nuclear Reactors,* Proceedings American Society of Civil Engineers, *81*: Separate No. 643 (March 1955).
19. *Proceedings AEC Sanitary Engineering Conference, Chicago, Ill.,* AEC—Washington, 129 (September 1952).
20. Wolman, Abel and Gorman, Arthur E., *Disposal of Radioactive Wastes,* Mechanical Engineering, *77*:4, 321 (April 1955).
21. Emerson, L. C., Straub, C. P. and Struxness, E. G., *Preliminary Estimates of Fission Product Quantities Associated with Radioactive Wastes from a Hypothetical Homogeneous Power Reactor,* Oak Ridge National Laboratory (15 July 1954).
22. Joseph, Arnold B., *Report of Meeting on Ocean Disposal of Reactor Wastes,* The Johns Hopkins University-AEC—No. AT-(30-1)-1477 (15 March 1955).
23. Joseph, Arnold B., *Report of Meeting on Subterranean Disposal of Reactor Wastes,* The Johns Hopkins University-AEC—No. AT-(30A)-1477 (15 March 1955).
24. Culler, F. L., Jr., *Fission Product from Proposed Power Reactors,* Oak Ridge National Laboratory (4 March 1955).

Fundamental Considerations in the Release of Large Quantities of Radioactive Wastes to Land and Sea

By Walter D. Claus,* USA

Health and safety must be given first consideration in the disposal of atomic wastes. Economy is of secondary importance. The prospective availability of plentiful power would be little blessing indeed if its unwelcome by-products were to result in illness and detrimental genetic changes for the human race—perhaps even for all life on earth. We may, however, confidently assume that engineering competence will devise economical means to meet health and safety requirements.

Fortunately, we still have a few years in which to solve the problem of what to do with dangerous radioactive by-products. The problem may offer very little sparkle and glamor to attract brilliant scientific and engineering minds to its solution. Compared to reactor engineering, it may be an unattractive endeavor, but the problem of safe and economical waste disposal may very well constitute the ceiling which will limit the production of power from nuclear fission. In the few years which we still have before the problem becomes acute, the nations of the world must pool their intelligence, their imagination and their ingenuity to determine what to do with the radioactive by-products which will result from the large-scale use of power reactors.

Sometime within the reasonably near future, we might look forward to the production of one-third of the world's present power requirements by nuclear fission. To orient our thinking, let's look at a few calculations. One-third of today's power needs is one million megawatts. To produce this amount at 25% efficiency will require the nuclear fission of four thousand kilograms of uranium per day. Let us assume further that on the average, the fission products will be ready for disposal 100 days after production. This allows for time in the reactor, for chemical processing, use, etc. After 100 days of hold-up, the daily disposal will consist of 2300 megacuries of radioactivity.

Approximate equilibrium will be reached in about ten years, when the daily radioactive decay will nearly equal the daily addition of 2300 megacuries. At this time, the world's stockpile of atomic waste will be about 6×10^5 megacuries of gamma activity. If this activity were distributed uniformly over one-tenth of the world's land surfaces (that is, over areas supporting power-consuming populations), it would produce a radiation field of 100–500 mr/hour, or several hundred times the amount which is considered to be permissible for safety. In addition, populations would be exposed to the hazardous ingestion and inhalation of large quantities of radioactive isotopes. The strontium-90 alone would build up to an equilibrium amount of 4.5×10^7 grams or 7×10^9 curies. Uniform distribution over populated areas would result in soil concentrations of strontium-90 several hundred times the calculated permissible concentration.

Of course, much of the venom of fission product wastes, such as strontium, ruthenium and cesium, can be removed during the chemical processing and put to specialized uses or be stored separately and more carefully. Valuable uses may be found for the remainder, such as for irradiation of various food and chemical products, or for its residual heat. Such uses are much to be desired, not only for their intrinsic worth, but because they will have increased the value of the by-products to the point where we can afford to dispose of them properly—for despite their use, there will still come a time when the residual specific activity (radioactivity per unit of mass of waste) will have become so small that it is useless and must be disposed of on land or in the sea. Again it should be repeated, safe and economical disposal of these wastes may very well constitute the ceiling which will limit the use of nuclear fission processes for the production of power.

Two philosophies of waste disposal prevail: "concentrate and contain" and "dilute and disperse." The figures quoted above show that dispersal of large quantities of activity over land areas is obviously unthinkable. Disposal on land must necessarily depend on concentration and containment. Some progress has been made toward permanent binding of the activity to clays[1] which can then be safely buried. Liquids might be disposed of in surface pits, possibly in desert areas of no known value, or in perma-frost areas. Engineering studies on pit-disposal methods are presently being conducted. Liquids could perhaps be consigned to abandoned mines, or to spent oil or gas wells, or to salt domes. Disposal of this nature would appear to be most economical, since the processing plants could be built near the disposal grounds,

* US Atomic Energy Commission.

resulting in a minimum of shipping and handling of bulky, dangerous radioactive liquids. The matters of primary concern, however, are those of health and safety: that excessive activity shall not be picked up as dust or spray by the winds, or seep into ground water or into other oil or gas pools.

Some people believe that significant adverse effects on the ecology of the storage areas could occur. If certain portions of the food web (particularly microorganisms in the soil) were seriously damaged, the ecology and productivity of agricultural and forest lands might be seriously impaired. Other people believe, however, that if the incidental dispersal of the activity from disposal areas is so controlled that it is harmless to human beings, it will certainly be harmless to lower organisms which in general are much more resistant than humans to radioactivity. Surface deposits certainly have the very serious disadvantage of removing their areas from all other uses, whereas the experience of man has been that sooner or later any or all areas may have some unexpected value.

Disposal at sea is now carried on only under very limited conditions[2] but it would seem to offer some advantages under both of the two philosophies of "contain" and "disperse." Just as small amounts of laboratory wastes are now deposited below 1000 fathoms of ocean in steel drums, so bulk process wastes might be deposited in some type of larger container—perhaps in a tank of steel or perhaps in one as fragile and temporary as a plastic balloon—which would carry them to selected ocean depths. Or they might be pumped in bulk below the thermocline where there is evidence of slow turn-over rates and very little sea life. Or they might be pumped into surface layers from a moving barge under conditions which are known to produce an immediate dilution[3] of a thousand to ten thousand times.

Various features bearing on the feasibility of sea disposal are under study by several American oceanographic institutes, and it is expected that much of the data which will be evolved by the oceanographic program of the International Geophysical Year in 1956–57 will have a direct bearing on the feasibility of sea disposal. The primary consideration is again health and safety: the amount of radioactivity which would be picked up in ocean spray and held in our atmosphere; and the manner in which radioactivity would affect sea life and our present and future food resources. How fast does the deep water flow from the cold latitudes toward the equator, and how fast does it turn over to mix eventually with the surface waters of economic importance? What about the waters of intermediate depth, which may be even more immobile than the bottom waters? What will be the eventual dilution of deeply deposited radioactivity if and when it finally becomes available to sea life? What will be the effect of the eventual surface concentrations on sea life, particularly since we know that certain forms of marine organisms have the property of concentrating within themselves, by hundreds or thousands of times, the radioactivity which occurs in the water? And lastly, even though such concentrated activity may not be so great as to affect the ecology of the sea at all, will that concentration in the edible forms be so great as to render the fish unsuitable for human consumption?

In all these questions, there exists wide latitude for interpretation of the facts when they are obtained. Public reaction and international relationships are involved. This makes it of greatest importance that studies on the feasibility of sea disposal be conducted on an international basis. The United States does not presently contemplate sea disposal in anything more than relatively small experimental quantities. But the possibility of world-wide power reactors will soon make radioactive waste disposal a world-wide problem in dire need of solution on an international basis. Does the sea offer the solution to this problem?

In summary, there is a real possibility that the problems posed by the accumulation of waste radioactivity from power reactors may very well place a limit on the benefits to be expected from nuclear power production. Disposal on land and in the sea both appear to offer possibilities of solution to the problems. Health and safety requirements are of primary importance, but in questions of land disposal they are largely matters of local concern. But the use of ocean depths has international implications, and the feasibility of sea disposal requires determined international study and cooperation. Fortunately we have already at hand, in the United Nations, an organization through which planning can be done, results distributed and evaluations prepared on an international plane. It is strongly urged that such studies be conducted diligently before the disposal problem reaches an acute stage.

REFERENCES

1. Ginell, W. S., Martin, J. J. and Hatch, L. P., *Ultimate Disposal of Radioactive Wastes,* Nucleonics *12*: 14-18 (1954).
2. US National Bureau of Standards Handbook 58, *Radioactive-Waste Disposal in the Ocean* (1954).
3. Redfield, A. C. and Walford, L. A., *A Study of the Disposal of Chemical Waste at Sea,* National Research Council Publication 201 (1951).

*

Low-Level Radioactive Waste Disposal

By John C. Geyer, Lloyd C. MacMurray, Albert P. Talboys and Helen W. Brown,* USA

"High"-level radioactive wastes are primarily the manufacturing residues from the chemical processing of irradiated reactor fuel elements. "Low"-level radioactive wastes are all other radioactive contaminated materials. They are the discards from all types of scientific experimentation, from medical diagnosis and therapy, and from industry. Often they are short-lived, weak energy emitters, and by comparison with reactor wastes, the total quantity of radiation in a single place is small.

The problem of disposal arises because the low-level wastes are widely distributed, originating from within such places as educational institutions, hospitals, and industrial laboratories. Flushings from laboratory equipment and glassware, bits of tissue, wipes, patients' bodily discharges, completed experimental complexes, pipes and tubing, workers' garments, and sometimes large equipment may be contaminated. If the contamination were other than radioactive, disposal could be routine by means of dilution, filtering, biological processing, burning, burying, and sludge concentration. The presence of the radiation component, however, alters the situation, and disposal of even small quantities of this kind of waste requires careful control.

University research on low-level waste disposal is primarily directed to obtaining information of practical value in actual disposal operations. This research includes: testing the ability of conventional waste-treatment processes to remove radioactive contaminants; developing special processes; studying isotope and ion exchange, adsorption, and chemical reactions which may concentrate radioisotopes; and determining the hazards which may arise in treatment and ultimate disposal. This work has been extensively sponsored by the United States Atomic Energy Commission as a part of its over-all responsibility for the nuclear radiation program.

The general purpose of this paper is to show the development of ideas and lines of experimental thinking and not to provide a comprehensive summary of all research in the field. It includes descriptions of some projects, giving information on the nature of the problem, the experimental method used, and some of the findings. Since The Johns Hopkins University research activity in the field of low-level waste disposal is representative of work being done throughout the country, several of its projects are summarized here, such as investigations of waste drain systems, institutional incinerators, and laundry methods. Also included is a report on a study conducted by the University of California on the biological treatment of radioactive wastes.

* Department of Sanitary Engineering, The Johns Hopkins University, Baltimore, Maryland.

CONCENTRATION OF RADIOACTIVITY IN WASTE DRAIN SYSTEMS[1]

A preliminary survey of the drain systems of a number of hospitals and laboratories using radioisotopes indicated that radioactivity is concentrated in traps, clean-outs, and pipe lines. Laboratory experiments were then devised to determine the mechanisms involved in the contamination of slimed and bare surfaces by radioactive wastes, and the extent of contamination under various conditions.

Uptake of P^{32} and I^{131} by bacterial slimes present in drain systems was studied first. Uniform slime films deposited on glass microscopic slides were dipped into solutions of the radioisotopes. Immersion in P^{32} solutions for short periods, which simulated rapid flushing of wastes through a drain, indicated that adsorption occurred. During immersions of several hours, which duplicated retention in traps and crevices over a long period, metabolic assimilation of the phosphate took place and isotopic exchange was found to be significant. With I^{131} solutions, only small amounts of the isotope were retained by the slimes, mainly resulting from the diffusion of active waste liquid into the matrix. There was little evidence of selective adsorption, and any I^{131} that was retained was easily washed out.

The contamination of bare metallic surfaces by I^{131} was then investigated. The metals selected were those commonly used in plumbing and in laboratory equipment, such as lead, copper, yellow brass, black iron, galvanized iron, monel, and stainless steel. Chemisorption was found to be primarily responsible for high uptake of I^{131} by some of the metals. The most important variables were type of metal, condition of surface, concentration of I^{131} in solution, pH and temperature of solution, and contact time. Lead, copper, brass, and monel were found to be most readily contaminated, forming insoluble metal iodides which were strongly bound to the metallic surfaces. Galvanized iron and stainless steel adsorbed very little of the I^{131}. Similar experiments with P^{32} and Sr^{89} demonstrated marked differences in behavior of the metals when

exposed to solutions of the different isotopes. Variations in pH also affected the extent of the contamination of the metals.

Solutions of I^{131}, P^{32}, and Sr^{89} were run through a set-up of several lengths of iron pipe and galvanized and brass fittings. GM tubes were used to monitor selected points. The pipes and fittings retained about 16% of the I^{131} and Sr^{89} and about 22% of the P^{32}, mainly as a result of selective adsorption of the isotope on the metal surfaces. In general, the more complex fittings became more highly contaminated than did the straight sections.

Counts also were made after various rinses to determine how effectively simple flushing removes activity. Water removed nearly 30% of the I^{131}, 40% of the Sr^{89}, bu only 25% of the P^{32}. With highly alkaline solutions, however, more than 90% of the P^{32} was removed. Nitric acid rinses were similarly effective in reducing Sr^{89} contamination.

USE OF INSTITUTIONAL INCINERATORS FOR RADIOACTIVE WASTES[2]

Disposal of radioactive wastes by incineration in a conventional refuse-type destructor is a convenient method if it can be accomplished without creating health hazards. Incineration reduces the volumes of waste and renders inoffensive the organic materials, but does not alter the radioactivity itself. It either passes up the flue as a gas or as particulate matter, is removed with the ash, or remains on the interior of the furnace and its stack. Ashes and dust may become a hazard to the operator, to the collector, and to the public when their ultimate disposal is on an open dump. Material remaining on the walls may present a radiation hazard to those working in the vicinity of the incinerator. Stack effluents may create a similar atmospheric hazard.

A study was made of the behavior of institutional incinerators when used to burn radioactive wastes. Its twofold purpose was: (1) to develop test methods for determining the distribution of radioactivity from contaminated material burned in an incinerator; and (2) to formulate operational standards for the safe incineration of such material. The techniques were to be such that they could be used routinely in similar examinations by local health departments. This investigation applied only to the conventional type incinerator; it was not concerned with incinerators that are being designed especially to burn radioactive materials in quantities far in excess of those anticipated by the average hospital or research institution.

The greater part of the study was with P^{32} and I^{131}, as they are used so frequently in biological experiment. Some preliminary observations were made with Sr^{89}. Radioisotopes in amounts ranging from 100 to 2000 microcuries were added to the incinerator in the form of chick embryos or cotton and sawdust wetted with the isotope solution. Determinations were made of the quantities of radioactivity discharged through the stack, dispersed in the atmosphere, distributed on the stack walls, and remaining in the ash. The atmosphere in the incineration room also was sampled during ash removal.

The method used to determine the stack-gas concentration of radioisotope varied. In the case of P^{32}, it was determined by settling and filtration, while for the I^{131} and Sr^{89}, filtration and gas scrubbing were used.

After the gas discharge was complete, several techniques were employed to measure the amount of activity on the stack walls: direct counting by a GM tube inserted through a hole bored in the metal portion of the stack about 5 feet above the roof level; or counting the activity on a disk removed from the wall, the activity in soot scraped from the wall, or in soot from the disk.

To determine the activity in the ash, the entire contents of the incinerator, some thirty-five pounds, were removed to a drum and mixed. Ten-milligram samples were removed and counted. The results varied so widely that larger samples (70 to 100 grams) were digested with a suitable liquid and the activity determined. The counts were still variable, but better agreement was obtained than with the dry method.

Test results indicate that of the P^{32} charged into the incinerator, about 12% was retained on the stack wall and 2% was recovered from the stack gas; of the Sr^{89}, 9% was retained on the wall and 1% recovered in the gas; while of the I^{131}, about 11% was deposited on the wall and 80% escaped in the gas. Since the techniques for determining stack discharge were considered to be much more accurate than those for ash determination, ash activity was assumed to be the balance of the charge not otherwise accounted for.

Atmospheric samples at breathing level were taken during ash removal, with both a high-volume air sampler and an electrostatic filter. In the P^{32} studies the atmospheric activity ranged from 4×10^{-10} to 5×10^{-8} microcuries per cubic centimeter with loadings of 100 to 2000 microcuries. This is below the maximum accepted level of 10×10^{-7} microcuries for the more hazardous and common beta-gamma emitting isotopes. With I^{131}, the low percentage remaining in the ash limits the problem of dust during ash removal, but inconclusive test results were obtained. Similar tests with Sr^{89} were not made, but the high percentage of radiostrontium remaining in the ash indicates a possible hazard during ash removal and disposal.

COTTON CLOTHING DECONTAMINATION[3]

An investigation of the decontamination of protective clothing worn by workers handling radioactive wastes was limited to cotton, since it is the most popular material for laboratory wear. One aim of the study was to evaluate the various types of decontaminating agents; a second was to determine which techniques, including dry cleaning, afford maximum decontaminating efficiency and also result in minimum volumes of waste.

The contaminants studied included Sr^{89}, Y^{91}, Ce^{141}, Fe^{59}, P^{32} and I^{131}. Effects of varying wash-bath tem-

perature, type and concentration of decontaminating agent, loading of washwheel, duration of washing, and level of contamination were investigated. Tests were conducted to determine if insoluble particulate matter could be removed more readily than could adsorbed or precipitated contaminants; and also to note the effects of previous laundering, soiling, starching, or wet-proofing.

All the tests were made on a laboratory scale. Small samples of contaminated cotton cloth were immersed in detergent solutions and agitated. Various washing and rinsing cycles were used, with the cloths removed, dried, and analyzed after each operation to determine residual radioactivity.

Results indicate that insoluble radioactive dusts mechanically occluded on the fabric can be removed satisfactorily by ordinary soap. However, where water-soluble compounds of the alkaline earths or heavy metals are deposited on the cloth as a result of evaporation of active solution, soap tends to precipitate the metallic elements. The insoluble compounds thus formed adhere to the fabric and accumulate through repeated contamination-decontamination cycles. The use of plain water to remove soluble deposits also was unsuccessful, for the radioactive metallic ions liberated upon solution of the deposited substances tended to adsorb on the cloth and to contaminate previously uncontaminated portions.

Complexing agents such as sodium hexametaphosphate and the tetrasodium salt of ethylenediaminetetraacetic acid were found to be most effective in removing metallic ions adsorbed on the fibers. Soluble metal complexes are formed of such stability that the ions are quickly lifted from the fabric and inactivated chemically.

Anionic and non-ionic detergents proved to be of considerably less value than did the complexing agents in removing metallic isotopes. Cationic exchange of the large numbers of sodium ions liberated by some types of detergent largely accounted for whatever effectiveness the detergents did exhibit. Maximum soil removal along with isotope removal was obtained when detergents and complexing agents were used in combination. Cationic sanitizing agents appeared to have very limited applicability in decontamination, and pre-treatment of cotton cloth with water-repellent finishes proved valueless. High wash-bath temperatures were generally advantageous, especially with soap, but long washing periods were not necessary.

The study indicated that only low concentrations of effective decontaminants need be used in laundering cotton clothing, thus reducing the strength of the wastes requiring treatment. By far the greatest part of the contamination present was found to be removed in the initial two or three washing and rinsing steps in the laundry procedure.

As a means of reducing to a minimum the volume of radioactive waste produced by laundering, dry cleaning techniques were tested. Organic solvents such as Stoddard solvent, carbon tetrachloride, trichlorethylene, and perchlorethylene were substituted for water as the bulk phase of the cleaning bath. Only a small, immiscible aqueous phase was retained to wet and convey the decontaminating agent to the cloth and to carry off radioactive substances removed from the cloth. Tests were made to determine extent of contamination of the solvent phase, percentage of moisture required, and decontaminating efficiency of the agents found most effective in the laundering tests.

Results indicate that modified methods of dry cleaning are just as effective as is laundering. In nearly all cases the solvents remained essentially free of contamination and were re-used a number of times. A considerable reduction in the volume of radioactive waste produced was effected, since the activity is concentrated in the easily separated aqueous phase which constitutes only a fraction of the total volume of cleaning solution used.

TREATMENT OF RADIOACTIVE LAUNDRY WASTE[4]

A study was made to determine the effects of treating radioactive laundry waste by the activated sludge process, and to find out what proportion of the radioactivity could be removed. Fresh activated sludge was obtained regularly from the municipal sewage treatment plant. Settled sewage, to which various detergents, complexing agents, and radioisotopes were added to simulate the laundry waste components, was obtained from the same source.

Isotopes studied included I^{131}, P^{32}, Sr^{89}, Fe^{59}, and S^{35}. Soap, synthetic anionic detergent, non-ionic detergent, sodium citrate and citric acid, and a complexing agent, in concentrations up to 10,000 ppm, were used individually and in combinations. Variables were time of aeration of mixed liquor, suspended solids in the mixed liquor, pH, concentration of isotope, concentration of isotopic dilutants, temperature, biochemical oxygen demand loading, and viability of the sludge. The aerating mixtures were fed during long period runs, and small samples were withdrawn periodically for centrifuging, evaporation of the supernatant, and counting. All the tests were conducted batchwise and on a laboratory scale.

In all cases isotope removals were best when the mixed liquor had a high suspended solids content. Moderate alkalinity also was generally favorable. The effect of aeration time varied with the individual isotope. For instance, Fe^{59} and Sr^{89} were removed from solution after a short aeration period, while I^{131} required a long period. With P^{32}, excessively long aeration periods resulted in the partial regeneration of the isotope. The effect of detergent concentration also showed considerable variations in accordance with the particular type used.

Removals of Sr^{89} and I^{131} seemed to be about the same with sterile as with viable sludge. In the case of P^{32}, however, there was a noticeable decrease in removal efficiency with the sterile sludge.

Extent of removal of trace amounts of I^{131} from water by adsorption on various kinds of metal particle slurries was investigated. Copper, lead, and silver, in that order, were quite effective at pH 3 to 4, in the

presence of nitric acid. Fine particles with their greater surface area gave substantially higher removals than did much greater weights of relatively large-sized material.

Further tests with copper, the best of all metals tested, demonstrated that the high uptake of I^{131} is due to adsorption of Cu_2I_2 molecules formed right at the surface of the copper particles. The Freundlich-type isotherm was not found applicable, and calculation of the theoretical number of monolayers of Cu_2I_2 gave a very high figure. It appeared that most of the adsorption occurred at isolated "active centers," and that the bonds were of such strength that no activity could be removed by rinsing with water, despite violent agitation.

BIOLOGICAL TREATMENT OF RADIOACTIVE WASTES[5]

An investigation was made to, (1) evaluate the use of biological waste treatment for concentration of radioisotopes of the fission-products group; (2) determine the relative effectiveness of various biological sewage treatments in their uptake of radioisotopes; and (3) study the significant factors in the removal of radioisotopes by biological systems. The contaminants studied were P^{32}, Sr^{89}, and Sr^{90}, and mixed fission products. Both synthetic and natural sewages were used. The activated sludge and the trickling filter processes were investigated in detail, and a preliminary inquiry made of oxidation ponds.

Factors determining the efficiency of a particular process were divided into two categories: those describing waste characteristics, such as mineral composition, presence of complexing agents, and organic nature; and those associated with the operation of the process, including organic and hydraulic loadings, duration of the treatment period, and recirculation. The procedure followed was to investigate the influence of a factor first on a batch scale and then in a laboratory-scale continuous-flow pilot plant. Here the contaminant concentration and the operating conditions were maintained constant long enough to establish dynamic equilibrium.

In these studies activated sludge flocs and trickling filter slimes were similar in the efficiency of removing radioisotopes. From 70 to 80% of the gross beta activity resulting from fission products in the organic waste was removed; this result applied to fission products ranging in age from 1.3 to 2.7 years, and a wide variety of operating conditions and waste composition. Cations had little influence on the removal of such products, Versene, a chelating agent, caused the elution of fission products from the trickling filter slimes and reduced removals to nearly zero.

In the trickling filter process the removal of P^{32} was affected by temperature in an inverse relationship: removals were low at high temperatures. The removal of P^{32} by the oxidation pond was found to be directly proportional to the rate of algal growth. Higher removals of radiophosphorus were obtained by this process than by other biological treatments.

From the public health standpoint, however, the most important fraction of the fission products is Sr^{90}. Aerobic biologic treatment probably does not remove more than 20% of the Sr^{90} from wastes having the mineral and organic compositions of natural sewages.

SORPTIVE PROPERTIES OF SILTS IN NATURAL WATERS FOR RADIOACTIVE WASTES[6]

These studies were undertaken to learn something of the nature and magnitude of the interaction of radioactive wastes and the suspended solids that are present in natural waters. Radioisotopes of phosphorus and strontium were used since they are representative of radioactive substances found under field conditions, and at the same time are conveniently studied in the laboratory. The solids used were representative of several kinds found suspended in natural waters. They included materials from cores taken in the Chesapeake Bay; a sample of sediment from the Roanoke River in Virginia; and samples of commercial Bentonite, Fullers Earth, and powdered Pyrex glass. The following environmental factors were either controlled or measured: pH, temperature, concentrations of suspended solids and reacting dissolved substance, and ionic strength.

A simple experimental method was used: measured quantities of inactive electrolytes, suspended solids, and radioactive materials were assembled in a stoppered Erlenmeyer flask which was then put on a shaking machine to keep the solids suspended. Zero time was taken as the instant the active and carrier materials were added to the system. After measured intervals of time, samples were withdrawn and centrifuged, and the solids and the supernatant solution were sampled for radioanalysis. From these analyses the amount of activity sorbed was calculated.

Phosphorus

Studies with P^{32} indicated that an adsorption reaction of some sort is responsible for the accumulation of phosphorus on the surface of solids. In one isotherm experiment a solution initially containing 11.5 microgram-atoms of phosphorus per liter and 620 milligrams per liter of solids was found to contain 10.4 microgram-atoms of phosphorus per liter after one-minute equilibration. If the number of $H_2PO_4^-$ ions in solution that initially would be in contact with the solids is compared with the number in contact after a short interval, the extent of the accumulation can be estimated. Within the limits set by the geometric model used, comparison showed that the phosphorus was over 10,000 times more concentrated on the surface of the particles than it was in the solution in contact with them.

If the adsorption process reaches equilibrium shortly after the components are mixed, further loss of phosphorus to the solids can occur only by a migration into the solids, a diffusion-like process. If the latter process is slow compared with the former, the systems should quickly come to equilibrium with respect to adsorption, and then show a gradual in-

crease of phosphorus in the solids component. This hypothesis was proved to be correct.

The rate at which phosphorus can be removed from the solids-phosphorus complex should be controlled by the amount of diffusion into the solids. If the solids have been in contact with the phosphorus solution only a short time, the greater part of the phosphorus will then be in the adsorbed layer and should be removed easily. If after longer lengths of time more diffusion has occurred, desorption processes should be less effective. This was confirmed by measurement of desorption from solids that had been in contact with phosphorus for various intervals up to seven days. The nature of the reaction following adsorption undoubtedly is complex, but the evidence indicates that the reaction rate is diffusion controlled.

Strontium

Frequently the chemical concentration of a radioactive contaminant may be many orders of magnitude below that normally encountered in usual water-treatment practices, yet be above permissible radioactivity limits. For example, the concentration of strontium produced by dispersing one gram of Sr^{90} in 100 million gallons of water is approximately 2.0 parts per trillion (2.65×10^{-6} milligrams per liter). This concentration could be neglected for most purposes, but its radioactivity would be several times above the maximum permissible level in drinking water. The practical problem here is to reduce by over a hundredfold a substance that is present initially in a concentration approximately a million times below the permissible limits of most substances normally found in water-treatment practices.

The first system studied consisted of raw and treated river water with added mixed fission products as the contaminant, treated by conventional flocculation procedures. Later studies concentrated on radiostrontium. It was found that a lime-ferrous sulphate system and trisodium phosphate treatment, both at high pH, gave removals of more than 90% of the radioactivity. The natural turbidity of the river water alone showed considerable ability to "carry" the fission products. However, with mixed fission products it is difficult to know which of the several radioisotopes have been removed and which of the several processes is responsible for removal.

The high pH suggested that precipitation of compounds formed from anions of weak acids, e.g., carbonates and phosphates, might be the mechanism by which activity is removed. The presence of suspended solids suggested adsorption or exchange mechanisms. The removal of radiostrontium, which accounts for over 17% of mixed fission products, was studied under conditions that would accentuate each process. The conclusion was reached that the adsorption-controlled process, using added solids, is more feasible and satisfactory experimentally than is the precipitation process, which requires impractically large amounts of added chemicals.

CONCLUSIONS

Low-level radioactive wastes are so ubiquitous that they may be considered as almost normal components of the solid and liquid wastes from many communities. Sometimes they need to be separated from other wastes and given special supervision. In other instances customary treatment and disposal are satisfactory. In any event, their nature, behavior, and biological effects need to be understood prior to deciding what to do with them. The background information required to make these decisions is now only partially available, although many important concepts have been established, particularly with respect to the isotopes most commonly used in medicine and biology. Investigation should continue until the radioactive component of wastes is as thoroughly known as is their pH, alkalinity, or oxygen requirement.

Contributions to this body of knowledge are being made regularly by universities, industrial laboratories, and state and local governmental agencies. The Atomic Energy Commission is supplying the stimulus and coordination for this program, as well as major financial support.

This résumé of a number of projects fixes attention on the type of study needed to give definitive, practical answers to the question of how to dispose of low-level radioactive wastes.

REFERENCES

1. Talboys, A. P., *Do Radioactive Wastes Contaminate Drain Piping?* Heating, Piping and Air Conditioning, *24*: 80-83, 87 (1952).
2. Kruse, C. W., Freese, P. V., Machis, A. and Behn, V. C,. *Behavior of Institutional Incinerators When Used to Burn Radioactive Wastes,* Final Project Report, NYO-4517, The Johns Hopkins University, Baltimore, Md. (1 November 1952) (Available from Office of Technical Services, Department of Commerce, Washington 25, D.C.).
3. Talboys, A. P. and Spratt, E. C., *An Evaluation of Laundering Agents and Techniques Used in the Decontamination of Clothing,* Progress Report JHUX-4, NYO-4590, Department of Sanitary Engineering and Water Resources, The Johns Hopkins University, Baltimore, Md. (1 August 1953).
4. Talboys, A. P., Unpublished material, Department of Sanitary Engineering, The Johns Hopkins University, Baltimore, Md.
5. Klein, G., Greenberg, A. E. and Kaufman, W. J., *Biological Treatment of Radioactive Wastes,* Institute of Engineering Research Series No. 64, Issue No. 3, Sanitary Engineering Research Laboratory, University of California, Berkeley, Calif. (30 June 1954).
6. Carritt, D. E. and Goodgal, S. H., *The Sorptive and Zeolitic Properties of Natural Water Borne Silts, with Relation to Their Capacities to Remove, Transport, Concentrate, and Regenerate Radioactive Waste Components in Natural Waters,* Final Report, NYO-4591, Department of Sanitary Engineering, The Johns Hopkins University, Baltimore, Md. (October 1953).

Methods for Decontamination of Low-Level Radioactive Liquid Wastes

By C. P. Straub,* W. J. Lacy† and R. J. Morton,‡ USA

With the availability of a great variety of radioisotopes at low cost, many applications have been found for their use in medicine, industry, and research. Naturally, this increased demand for radioactive materials has resulted in increased discharge of these materials into the environment. One of the most obvious and convenient methods of disposal is through discharge into the sewerage system as indicated by a survey of the disposal practices of 1027 users of radioisotopes.[1] Forty-one per cent of the users disposed of their spent radioactive materials by dilution and discharge to the sewer.

Following release into the sewerage system, the radioactive wastes may discharge directly into a stream or other body of water, or they may pass through a sewage treatment plant before entering the stream. Some radioactive materials will be taken out by the physical, chemical, and biological processes employed in the treatment of domestic sewage and industrial wastes. The efficiency of sewage treatment processes for the removal of radionuclides has been covered in a progress report of the Committee on the Sanitary Engineering Aspects of Nuclear Energy.[2]

Many water courses, in addition to providing for the disposal and dilution of sewage, serve as sources of public water supply, and the release of radioactive materials into such streams must be carefully controlled so as not to exceed the maximum permissible concentrations in water.[3,4]

Since the last point of control between the release of radioactive materials and the ultimate consumer of the water-treatment plant, conventional water-treatment procedures have been investigated for the removal of low level activity (10^{-1} to 10^{-7} μc/ml) from single radioisotopes and mixtures of radioelements from waste solutions.

CONVENTIONAL WATER-TREATMENT PROCESSES FOR REMOVAL OF RADIOISOTOPES

The conventional water-treatment processes investigated to determine their efficiency for the removal of radioactive materials included coagulation, sedimentation, filtration, lime-soda ash softening, and ion exchange.

* US Public Health Service.
† Corps of Engineers, US Army.
‡ Oak Ridge National Laboratory.

Coagulation

Coagulation involves the formation of chemical flocs that adsorb, entrap, or otherwise bring together suspended matter, particularly suspended matter that is colloidal. The addition of coagulating chemicals will result in the precipitation of some of the soluble constituents in the waste as metal hydroxides, generally hydroxides of aluminum or iron, since alum and iron salts are the most common coagulants.

Coagulation with settling has been studied rather extensively at the Oak Ridge National Laboratory. The results of these studies are summarized in Table I, and show that with the exception of most cations of valence 3, 4 or 5, including the rare-earths group, coagulation is not very effective for the removal of radioactive materials from water. Removals in excess of 98 per cent have been reported for phosphorus-32 as the orthophosphate. Coagulation with alum or iron is not effective for the removal of iodine-131 (as the iodide) but the addition of small amounts of copper sulfate,[5] activated carbon,[5] or silver nitrate,[5,6] will increase the removal of this anion from water to about 96 per cent.[6]

Coagulation will be helpful in the removal of radioactive material attached to or adsorbed on the natural turbidity found in surface waters. Since coagulation will remove much of the turbidity, the activity attached will also be taken out.

Sand Filtration

Except for removal by simple straining or simple sorption by biological life contained in the "Schmutzdecke," sand filters have not been effective for the removal of radioactive materials. Their major function is to remove the radioactivity previously incorporated in floc particles. As shown in Table I removals vary depending on the nature of the materials. For example, scandium, yttrium, and zirconium-niobium, probably present in the colloidal state, were removed by mechanical straining, whereas other materials such as strontium, cesium, and possibly tungsten, present in true solution, were not affected by passage through the sand filter.

Softening

Softening with lime and soda ash has been studied and under proper conditions effective removals of

Table I. Removal of Radioactive Materials by Conventional Water Treatment Processes*

Isotope	Ranges of removal in per cent					
	Chemical coagulation and settling	Sand filtration	Soda-ash softening	Ion exchange resins		
				Cation	Anion	Mixed bed
Cs^{137}-Ba^{137} (Cl)	0–37	10–70	< 50	99+	9	99+
Sr^{89} (Cl)	0–15	1–13	50–95	99+	5–7	99+
Ba^{140}-La^{140} (Cl)	1–84	39–99	50–95	96–99	36–42	99+
Cd^{115} (NO_3)		60–99	50–99	98	0	99+
Sc^{46} (Cl)	62–99+	94–99	50–95	96–97	99	99
Y^{91} (Cl)	1–99+	84–89	50–95	75–93	94–98	98–99
Zr^{95}-Nb^{95} (oxalate complex)	2–99	91–96	50–99+	58–75	96–99+	91–99+
P^{32} (phosphate)	68–99+					99+
Cr^{51} (Cl)	0–60					
Mo^{99} (MoO_4)	0–60					
W^{185} (tungstate)	1–96	3-18	< 50	9–16	97–99+	99
Re^{186} (metal)	0–29					
I^{131} (iodide)	0–96				99+	99+
Ru^{103} (Cl)	43–96					
Pr^{143} (Pr_2O_3)	83–99+					
Ce^{144}-Pr^{144} (Cl)	28–99+					99+
Pm^{147} (Cl)	4–99+					
Sm^{153} (Sm_2O_3)	44–99+					

* Variable chemical dose, coagulants, pH conditions, activity concentrations, and waters.

strontium, barium, cadmium, yttrium, scandium, and zirconium-niobium were obtained. As shown in Table I, removals of 95 to 99 per cent or better are possible. As shown in Table II, for most satisfactory removal of strontium, increased amounts of both lime and soda ash were required.[7]

If relatively high chemical dosages are employed, lime-soda ash softening is fairly effective in removing certain radioelements from waste solutions. From the standpoint of emergency water treatment, and using higher chemical dosages, the softening process could be adapted to the treatment of a waste containing radiostrontium. Other water treatment processes, with the exception of ion exchange, are relatively ineffective in removing this particular element, whereas softening, under optimum conditions, can result in greater than 99 per cent removals.

Ion Exchange

The ion exchange process is also used in softening municipal water supplies. Removal of radioactive materials by this process is feasible, and for most effective removal mixed resins in series is recommended. Results with various types of exchange materials are shown in Table I. Following ion exchange, it may be necessary to adjust the pH of the effluent water.

Although the ion exchange process offers one of the most promising methods for removing radioactive contaminants, the initial and operating costs may prohibit widespread usage unless suitable regeneration techniques are developed.

MODIFIED PROCESSES

Several other methods have been studied for the removal of radioactive constituents from water. The most promising of these, phosphate coagulation,[8] has

Table II. Results of Lime-Soda Ash Treatment for Removal of Strontium

Treatment	Per cent removal of activity
Stoichiometric amounts	75.0
20 ppm excess lime-soda ash	77.0
50 ppm excess lime-soda ash	80.1
100 ppm excess lime-soda ash	85.3
150 ppm excess lime-soda ash	97.3
200 ppm excess lime-soda ash	99.4
300 ppm excess lime-soda ash	99.7

Table III. Removal of Radioactive Materials by Modified Processes*

Isotope	Ranges of removal in per cent		
	Phosphate coagulation	Metallic dusts	Clay additions†
Cs^{137}-Ba^{137} (Cl)		9	98
Sr^{89} (Cl)	81–98		49–52
Ba^{140}-La^{140} (Cl)		66–95	85–98
Zn^{65} (Cl)	99+	98–99+	
Cd^{115} (No_3)			64
Sc^{46} (Cl)			97
Y^{91} (Cl)	99+	98	94
Zr^{95}-Nb^{95} (oxalate complex)	99+		98
P^{32} (phosphate)		84–99+	78–82
Sb^{124} (Cl)	66		
W^{185} (tungstate)	11		49
I^{131} (iodide)		23–46	9–20
Ru^{106}-Rh^{106}		93–99+	
Co^{60} (Cl)		30–92	85–99+
Ce^{144}-Pr^{144} (Cl)	99+	99+	99+

* Variable chemical quantities, levels of activity, and pH conditions.

† 5000 mg/l of clay added.

Table IV. Removal of Radioactive Materials by Distillation*

Run no.	Contaminant	Initial activity dpm/ml	Per cent removal	Concentration in distillate μc/ml	Decontamination factor
	Without anti-entrainment device				
1	MFP-1†	97,900	99.98	9.1×10^{-6}	5.0×10^{3}
2	MFP-3	22,060	99.98	2.5×10^{-6}	4.1×10^{3}
3	MFP-5	62,400	99.72	8.2×10^{-5}	3.5×10^{2}
4	MFP-7	31,150	99.97	3.6×10^{-6}	3.6×10^{3}
5	I^{131}	60,900	99.86	3.9×10^{-5}	7.0×10^{2}
	With anti-entrainment device				
6	MFP-2	38,910	99.91	1.6×10^{-5}	1.1×10^{3}
7	MFP-3	12,000	99.99+	3.2×10^{-7}	1.7×10^{4}
8	MFP-5	69,700	99.99	3.2×10^{-6}	1.0×10^{4}
9	I^{131}	45,600	99.92	1.6×10^{-5}	5.8×10^{3}

* Data obtained during operation of a 1200-gallon per day thermocompression distillation unit. Runs of 24 to 30-hour duration.

† MFP-1: Two-week-old fission products mixture; MFP-2: Synthetic bomb mixture (10 days after blast); MFP-3: Three-year-old fission products mixture; MFP-5: Mixed fission products waste containing Cs^{137}-Ba^{137} and Ru^{106}-Rh^{106}; MFP-7: Composite mixture of fission products from waste tanks.

effected removals up to 99.9 per cent as shown by the data included in Table III. Also, relatively high removals of strontium are possible by this method, but these can be secured only under carefully controlled conditions of pH and of calcium hydroxide to trisodium phosphate ratio. Phosphate coagulation is of considerable interest to the managers of water works since this method can be employed in many existing water treatment plants employing coagulation and sedimentation for treatment with little modification of plant facilities.

Studies utilizing an electrodialytic cell with permselective ion exchange membranes[9] indicated the necessity of removing all colloidal radioelements prior to concentration of the soluble radioisotopes in the cell. Passage of various radiocolloids through a millipore filter has shown that the larger colloids such as Zr^{95}-Nb^{95} were completely removed, whereas others such as Ru^{103} and Ce^{144}-Pr^{144} were removed only in part. Therefore, if the dialytic cell is to be effective for the removal of the soluble radioactive materials, the radiocolloids should be removed beforehand.

Other methods for the removal of radioactive materials include the addition of metal powders or clay materials. Laboratory jar-test studies used iron, zinc, aluminum and copper dusts[10] for the removal of specific radioactive contaminants. The results are shown in Table III. In general, the highest removals were obtained with iron dust and exceeded 90 per cent, except for iodine, cesium and a fission products mixture.

Considerable work has been reported[5,11,12,18] on the use of clay materials for the removal of specific radioisotopes from water and waste solutions. Some results are listed in Table III. Although this method is feasible, large volumes of clay must be handled both initially and finally as a mass of contaminated material for disposal. If combined with chemical coagulation, still larger volumes of contaminated sludge must be handled. Providing no health hazard will result from the release of these materials, this method has its greatest potential use where geological and hydrological conditions are such as to permit use of the ground for disposal.

Distillation

Although not a generally accepted municipal water treatment method, distillation is included in this discussion as it is the most effective process presently available for concentrating radioactive materials. Under proper conditions, it is possible to produce a condensate of very low activity. Thus, high decontamination factors are possible, but the cost is too great for normal use; however, under emergency conditions evaporation should prove feasible. Results obtained in the operation of a 1200 gallon per hour thermocompression distillation unit with and without an anti-entrainment device are summarized in Table IV.

REMOVAL OF MIXED RADIOISOTOPES

In the case of a mixture of radioisotopes, the efficiency of removal is a function of the individual radioisotopes comprising the mixture. Removal efficiencies are included in Table V.

SUMMARY AND CONCLUSIONS

Unless related to the initial concentration of the radioactive materials present, the per cent removal values cited in the various tables have little practical significance. It is only when these are considered in terms of the initial concentration of activity and the maximum permissible concentration, that one can be sure that the treated water is safe for human consumption. Generally speaking, water treatment processes will not be effective for reducing the activity in the water to acceptable safe limits, unless the initial

Table V. Removal of Mixed Fission Product Isotopes

Mixture*	Treatment process	Per cent removal
FPM-1	Coagulation and settling plus clay	61–84
FPM-2	Coagulation and settling	9–71
	Coagulation and settling plus clay	12–73
	Coagulation and settling plus clay	46
	Coagulation and settling plus filtration plus clay	70–73
FPM-3	Coagulation and settling	46
FPM-4	Coagulation and settling	89
	Mixed cation-anion exchange slurry	83–99
FPM-5	Coagulation and settling	51–59
	Mixed cation-anion exchange slurry	38
	Metallic dust slurry	8–56
FPM-6	Metallic dust slurry	77–92

* FPM-1: Iodine dissolver solution; FPM-2: Synthetic mixture; FPM-3: Three-year-old fission products mixture; FPM-4: Iodine dissolver solution aged 30 days; FPM-5: Mixed fission product waste containing Cs^{137}-Ba^{137} and Ru^{106}-Rh^{106}; FPM-6: Iodine dissolver solution aged 20 days.

levels of activity are very low, that is, in the 10^{-1} to 10^{-7} μc/ml range.

Radioactive materials should be treated and retained as close to their source of production as possible. The practice at present is predominantly storage in suitable underground tanks. In employing any of the separation or concentrating procedures described, activity is transferred from the liquid to the solid phase. This does not solve the waste disposal problem, since suitable storage or disposal facilities will have to be provided for the radioactive sludges.

REFERENCES

1. Miller, H. S., Fahnoe, F. and Peterson, W. R., *Survey of Radioactive Waste Disposal Practices,* Nucleonics, *12*: 1, 68 (January 1954).
2. Straub, Conrad P., Chairman, Sanitary Engineering Aspects of Nuclear Energy, Progress Report of the Committee of the Sanitary Engineering Division on the Sanitary Engineering Aspects of Nuclear Energy. Proceedings, Am. Soc. Civil Engrs. *81*: 11 pp. Separate No. 646 (March 1955).
3. National Bureau of Standards, US Department of Commerce, NBS Handbook 52. "Maximum Permissible Amounts of Radioisotopes in the Human Body and Maximum Permissible Concentrations in Air and Water," US Government Printing Office, Washington, D.C. (20 March 1953).
4. Recommendations of the International Commission on Radiological Protection (unpublished) (1954).
5. Straub, Conrad P., Morton, R. J. and Placak, O. R., *Studies on the Removal of Radioactive Contaminants from Water,* Jour., A.W.W.A., *43*: 773 (October 1951).
6. Eden, G. E., Downing, A. L. and Wheatland, A. B., *Observations on the Removal of Radioisotopes during Purification of Domestic Water Supplies: I. Radioiodine,* Jour. Inst. Water Engrs., *VI*: 511 (November 1952).
7. Hoyt, W. A., *The Effects of the Lima-Soda Water Softening Process on the Removal of Radioactive Strontium-90-Yttrium-90,* Master of Science Thesis submitted to the Faculty of the North Carolina State College, Raleigh, North Carolina (1952).
8. Lauderdale, Robert A., Jr., "Studies on the Removal of Radioisotopes from Liquid Wastes by Coagulation," Report ORNL-932. Oak Ridge National Laboratory, Oak Ridge, Tennessee (23 January 1951). See also: Ind. Eng. Chem., *43*: 1538 (1951).
9. Seal, M. S. and Pecsok, D. A., "Preliminary Laboratory Evaluation of an Electrolytic Method for the Treatment of Radioactive Waters," Unpublished report. Oak Ridge National Laboratory, Oak Ridge, Tennessee (July 1954).
10. Lacy, William J., *Removal of Radioactive Material from water by Slurrying with Powdered Metal,* Journal, A.W.W.A., *44*: 824 (September 1952).
11. Brockett, T. W., Jr. and Placak, O. R., "Removal of Radioisotopes from Waste Solutions by Soils—Soil Studies with Conasauga Shale," Proceedings, 8th Industrial Waste Conference, Purdue University, Lafayette, Ind. (4-6 May 1953). Extension Series No. 83, pp 393-409 (January 1954).
12. Straub, Conrad P. and Krieger, Herman L., "Removal of Radioisotopes from Waste Solutions—Soil Suspension Studies," Proceedings, 8th Industrial Waste Conference, Purdue University, Lafayette, Ind., (4-6 May 1953). Extension Series No. 83, pp 415-438 (January 1954).
13. Lacy, William J., *Decontamination of Radioactively Contaminated Water by Slurrying with Clay.* Ind. Eng. Chem., *46*: 1061 (May 1954).

Record of Proceedings of Session 7.3

THURSDAY MORNING, 11 AUGUST 1955

***Chairman:* Mr. B. C. de Mattos (Brazil)**

***Scientific Secretaries:* Messrs. L. F. Lamerton, A. Finkelstein and I. D. Rojanski**

PROGRAMME

P/398	Long-term aspect of fission product disposal	E. Glueckauf
P/310	The management and disposal of radioactive wastes	A. Wolman and A. E. Gorman
	DISCUSSION	

Mr. E. GLUECKAUF (UK) presented paper P/398.

Mr. A. WOLMAN (USA) presented paper P/310 as follows: Mr. Glueckauf has already indicated to you that one of the collateral problems of the development of nuclear power is how to handle safely the radiation that is present in the waste products of nuclear fission. This is one of the more difficult problems facing the development of nuclear power as a new source of energy. These wastes frequently are very toxic and, from the standpoint of administrative control, the radiations they give off cannot be seen, felt or tasted, but must be detected and measured by instrumentation, which has so far been developed to a very high degree. The paper which I summarize reviews current practices in the United States and the accompanying costs and makes some attempt to visualize the problems of the future.

By the year 2000, in our own country, approximately 41 tons of radioactive fission products may be produced annually by nuclear power reactors in the United States. The reason for the difference between this estimate and the one which was presented by Mr. Glueckauf rests upon the fact that, as in all of these anticipated prophecies, we differ as to the method by which we arrive at our conclusions. In our case, we have assumed a doubling of the population of the United States by the year 2000 and a three-fold increase in per capita use of electric energy. But we have likewise assumed that only 10 per cent of that increase in electric power production will be provided by nuclear fission power.

The disposal of reactor and particularly fuel processing wastes may be one of the major controlling factors in determining the extent of the use of power reactors from a comparative cost standpoint with other sources of fuel for energy production. To dispose of these materials will undoubtedly challenge, and I am sure the challenge will be met by, the ingenuity and the imagination of scientists and industrial technologists.

Of course, the problems in waste disposal, as has already been suggested, are many. Present controls of radioactive wastes are adequate but, I should say, comparatively expensive with respect to any effort at disposal. It should be pointed out in addition that disposal, as we have known it in the past with respect to its orthodox meaning and its application to familiar industrial wastes, is not yet at hand, particularly for high-level radioactive material.

These wastes are of gaseous, liquid and solid origin and are normal by-products of nuclear power production and of the essential chemical processing of fuel elements. They are of varying hazard to workers and to the public unless they are adequately collected, treated and intelligently released or stored for long periods of time.

In our particular paper, the problem is divided into the handling of low, intermediate or middle-level, and high-level wastes—a purely arbitrary classification on the part of the authors. The first category, namely, that of low-level wastes, is generally made up of those radioactive products of relatively short half-life, with activities ranging from 10^{-4} to 10^{-8} microcuries per ml. These offer no particularly difficult technical issue. They are now being returned without hazard to nature via water, air and soil. When properly applied, this system is wholly without danger to human, plant or lower animal life. The method presupposes, of course, a careful monitoring system and equally careful management with respect to each local situation.

Middle-level wastes, usually of liquid or solid nature, are held for decay long enough to permit a similar ultimately harmless discharge to nature.

The problems, however, of getting rid of high-level wastes are difficult because, as we have pointed out before, no method for real disposal in its orthodox sense is at hand or at the moment foreseeable. Such wastes in the high-level range may contain as much as 100 curies per liter and their amount may vary from 0.5 to 50 per cent of the total waste production in this field, depending, of course, upon the varieties of prior processing and handling.

For the best protection of the public, these highly radioactive wastes are now stored, in the United States, under rigid supervision and management. Recognizing the importance of the problem, the United States Atomic Energy Commission has placed research and development contracts with universities,

private industry, its own laboratories and other federal agencies, to study various methods of disposal, particularly the extent to which the ocean, ground, and surface waterways may be used to shield, dilute and disperse the material.

It is not too early in this connection to consider the international significance of the disposal of these wastes in the air and in the sea. Obviously, indiscriminate discharges may lead to objectionable environmental results of long duration if more and more countries adopt similar practices, under highly variable conditions and locations, without agreed upon standards of practice.

In the United States, federal, state and local procedures for control and regulation of the disposal of such high-level wastes are under study and will be placed in force in the near future.

Some of the characteristics of these reactor fuel processing wastes are, of course, of interest and have already been referred to. Their gross beta and alpha activities are high. Their radioactivity may range from 1 to 4 $\times$ 10^2 curies per gallon, with long effective lives. The Cs^{137} and the Sr^{90} represent the isotopes of major concern. If they are recoverable for widespread industrial and biological purposes, they would offer at least an economic return in relation to this problem. The administrative supervision of their use would then take its place in the normal administrative control which is already in force in the country.

In addition to these troublesome features, the heat production capacity of the wastes is great, of the order of 1–3 BTU per gallon. This thermal aspect alone creates problems in storage, whether in artificial structures or under the normal conditions of nature.

Much progress has been made in recent years in chemical processing so as to remove the highly active wastes at their source when their volume is at a minimum. Co-precipitation, evaporation and ion-exchange techniques are practiced. All are still relatively costly and none are without their disadvantages in creating problems of sludge disposal or holding.

Storage in underground tanks is reasonably satisfactory but, in absolute terms, remains expensive, in order to provide adequately against corrosion, to provide for heat dispersion by cooling systems, and to provide complete structural durability during the decades to come.

Much of the current practice, however, in high-level waste disposal and holding is in isolated areas. It is important to point out that, if the power industry develops as all of us hope it may, we will be pushed toward centers of highly populated areas. Then the problem of the handling and processing of fuel elements and their consequent wastes will probably not be advantageous in local areas. It may indicate the development of regional chemical fuel processing locations, where the waste products could be pooled and their disposal could be under better control, with less potential hazard to individual areas.

I might repeat that the principle of discharging these materials into nature is a long-term and sound principle. It carries with it, however, the necessity for meeting each local situation on its own terms and developing devices, processes and modifications in current understanding, all tending toward greater economy and greater safety.

DISCUSSION OF P/398 AND P/310

Mr. R. R. D. Revelle (USA): It is clear from computations similar to those made by Mr. Glueckauf that fission products, if uniformly mixed in the seas and not concentrated by organisms, would not be dangerous. The problem is to avoid dangerous concentrations in organisms of importance to man, primarily marine fishes and marine invertebrates. I do not believe that the subsidiary problem, of the effect of introduced radioactivity on the ecology of the sea, is nearly as serious. It is possible that we can take advantage of the vertical stratification in the ocean, that is, its stability due to the increase of density with depth, to age the fission products until their activity has been reduced to acceptable levels.

To find out whether this is possible, much more information must be obtained on the rate of interchange between the deep water and the surface water of the ocean. At present, oceanographers differ on their estimates of this rate by a factor of about 300, some saying that this interchange between the deep and the surface waters takes thousands of years, while others say that it takes only a few decades.

Research is now beginning, using radioactive tracer techniques in an attempt to refine this estimate.

Possibly more serious than the movement of the water is the concentration of fission products by marine organisms, which, we already know, results in a concentration by factors of at least a thousand. In the open sea far from land, the great majority of marine animals migrate vertically each day from depths of 400 to 800 meters, up to the sea surface and back again. This might well result in a significant transport of fission products into the upper few hundred meters of the sea, where the marine plants and virtually all the marine animals of importance to man spend their lives. This problem of the vertical transport by marine animals of substances present in trace amounts is being investigated, as is the whole problem of the concentrations of fission products and other trace elements by marine organisms.

I should point out that Mr. Wolman asked me to elaborate somewhat on the questions that he raised concerning the oceanic disposal of radioactive waste.

Mr. H. M. Parker (USA): Mr. Wolman spoke of high-level waste storage as being expensive. According to our calculations, the storage cost of high-level waste would be less than 1 per cent of the sales price of nuclear power. Does Mr. Wolman wish to comment on this point?

Mr. Wolman (USA): I think that the difference in point of view rests entirely on the following basis: when we state that the cost of storage is high, we are comparing the unit cost per unit volume of innocuous

liquids with which we have had to deal over the years. On that basis, the costs of long-term storage, in absolute figures, run anywhere from ten to thirty or forty times as high. From the standpoint of this cost with respect to the part which it plays in the ultimate cost of producing a kilowatt, the cost is, of course, comparatively small. I think that that accounts for the difference brought out in Mr. Parker's comment.

Mr. WILHELMSEN (Norway): I believe that Mr. Wolman more or less indirectly answered my question, but I should like to put it nevertheless.

When considering ocean disposal of reactor wastes, would you depend on the effectiveness of the container to maintain necessary shielding to prevent poisoning of the ocean bed during all the disintegration period of interest, or would you depend equally on the underwater currents to diffuse and maintain the radioactive wastes at considerable depth during the less dangerous disintegration time?

Mr. WOLMAN (USA): The question in fact answers itself to this extent: there are as many points of view about how these discharges may be controlled as there are either sources of problems or individuals. Some would advocate, for certain levels of radiation discharge, taking advantage of currents, of dilution and of dispersion. Others dealing with other levels of radiation which may have a much higher toxic potential would attempt to fix these materials initially before they are deposited either in the deep or in shallower shelves of the ocean. A great deal of work is going on in our own country on both aspects of this application of principle. Considerable work is being done, of course, with the attempt to fix materials with an assurance of permanence—no matter where the materials are deposited—either by taking advantage of natural clay, such as montmorillonite, or, as in the case of some of our studies, by direct chemical means. In the interim, the policy of the United States Atomic Energy Commission is certainly, I think, a sound one. Until all of these issues have been comparatively well resolved, the Commission has taken the position with wastes of a high-level nature that they should be manageably stored, easy to contact, easy to monitor, awaiting the day when some more successful disposal—in the air, in the soil or in the ocean—is at hand.

Mr. L. S. TAYLOR (USA): Mr. Glueckauf's paper stated that, because public opinion is so sensitive, we may consider ocean disposal only under conditions which guarantee absolute safeguards against, first, fission products entering human food or water supplies and, second, accidental exposure of the public to radiation levels above tolerance.

The words "absolute safeguards" are strong words, we all appreciate. I think that it would be very interesting if both Mr. Glueckauf and Mr. Wolman could discuss the possibility that public opinion may become less sensitive in time and that controlled release of radioactivity into the environment may become a more acceptable procedure.

Mr. GLUECKAUF (UK): At present, public opinion is no doubt the controlling factor, and it is perhaps even more restrictive than is sometimes desirable. When, however, public opinion has become more acquiescent—as is bound to happen—I feel it will be the duty of governments and scientists to evaluate the limits of release and to enforce them. If by "controlled release" Mr. Taylor means the restricted release of small quantities, this is no doubt the course that will eventually be taken. If, however, he means a release into the environment of the total activity, my answer would have to be in the negative, as may be clearly discerned from the contents of my paper.

Mr. WOLMAN (USA): Mr. Glueckauf's last sentence of course summarizes the attitude with respect to high-level materials of great concentration and, in some respects, of unknown characteristics. The answer undoubtedly is "no." I am sure that Mr. Taylor was referring, however, to the very large amounts of other radioactive materials which, as we have pointed out and as Mr. Glueckauf has pointed out, are released to nature. This is reminiscent in a way of the lessons we have learned in the disposal of other industrial wastes over the last half century. The waters of the world have a very high capacity for assimilating industrial wastes. The half century has been taken up in determining the characteristics of that capacity to assimilate—what are the parameters, how are they measured in nature, and so forth. We now have, of course, the techniques for such measurements, and similar techniques are being developed with great speed in the radioactive field. When the technologists in this field have assured themselves both that the measurement is at hand and that the controlled discharges are without hazard, my prediction is that the public, in turn, will follow a very sound principle: that nature is a good receiver of all kinds of industrial wastes, when properly managed.

Mr. S. LAWROSKI (USA): My question is directed to Mr. Glueckauf. The prospect of recovering precious metals, mentioned in your presentation, is interesting. However, would that not lead to some problems of contamination of these metals in commerce, just as would access of wastes to mineral supplies?

Mr. GLUECKAUF (UK): The contamination of these metals would be more or less entirely due to ruthenium, as chemical methods could easily be devised to remove all other contaminants from rare metals. The longer-lived ruthenium has a half-life of one year. That means that within twenty years its activity will fall to roughly one millionth of its original activity. If it should turn out that that activity level is still too high for an industrial application of these metals, one could no doubt wait another ten years before utilizing the materials. Then the value would have fallen to one thousandths of a million. I think that that more or less answers the question.

Session 18.1

METALLURGY OF THORIUM, URANIUM AND THEIR ALLOYS

LIST OF PAPERS

			Page
P/555	Physical metallurgy of uranium and its alloys	F. G. Foote	33
P/786	The solid state reaction between uranium and aluminium	R. Kiessling	69
P/556	The metallurgy of thorium and its alloys	O. N. Carlson *et al.*	74
P/558	The alloys of uranium	H. A. Saller and F. A. Rough	107
P/416	Alloys of uranium and thorium	P. C. L. Pfeil	117
P/352	Low aluminum uranium-aluminum alloys	G. Cabane *et al.*	120
P/826	The intermetallic compounds of plutonium	A. S. Coffinberry and F. H. Ellinger	138
P/557	Thermal cycling effects in uranium	H. H. Chiswik and L. R. Kelman	147
P/351	Gamma phase uranium extrusion	J. A. Stohr and R. Chevigny	159
P/559	The technology of UO_2 and ThO_2	J. R. Johnson and C. E. Curtis	169

Physical Metallurgy of Uranium and Its Alloys

By Frank G. Foote,* USA

During the last thirteen years there has been a very considerable development of uranium metallurgy including exploration for ores, their concentration and refinement, reduction of uranium compounds to metal, the melting, casting and fabrication of metal and the study of the properties and behavior of metallic uranium. This paper deals only with the latter subject, commonly described as physical metallurgy. The information on this topic is quite extensive and for the most part not yet available in the open literature. In the time available for the preparation of this manuscript it has not been possible to cover all topics in the general field of physical metallurgy nor to adequately abstract the reports of all investigators in this field. I have attempted to include a moderately detailed discussion of certain characteristics of uranium which are of importance in the development of its technology and in the understanding of its behavior during use.

I. PHYSICAL AND THERMAL PROPERTIES OF URANIUM

Certain of the properties of a metal are independent or nearly independent of the prior metallurgical history or, within limits, of the exact state of purity of the sample. Many of these properties are listed in Table I, and a few are also presented in summary form in Figs. 1 and 2. These properties will not be further discussed in this paper, although in some cases they form the basis for the discussion of other properties, such as grain size, recrystallization behavior, and tensile properties, which are markedly dependent upon prior history. The remainder of this paper is devoted to the presentation of data on these more structure-sensitive properties.

II. PLASTIC DEFORMATION MECHANISMS IN ALPHA URANIUM

Studies of the plastic deformation mechanisms in alpha uranium at room temperature have been carried out by Lloyd and Chiswik at Argonne National Laboratory (ANL). The operative deformation elements in alpha uranium have been determined as a function of the crystallographic direction of testing. Single crystals, produced by grain coarsening techniques, were tested under compression at room temperature. The location of the compression directions studied are plotted in (001) standard projection in Fig. 3.

The most frequently observed deformation mechanism was slip on the (010) plane. All crystals except *E* yielded evidence of (010) plane slip. The slip direction for the (010) system was determined to be the [100] from the following considerations: (1) it is the most densely packed direction in the slip plane; (2) the rotational asterism of Laue spots; and (3) it is in accord with the crystallography of kinking deformation discussed later. The critical shear stress value for this (010)–[100] slip system was determined to be 0.34 ± 0.02 kilogram per square millimeter.

A minor slip plane, of identity {011}, was identified by pole-locus analysis of eight slip traces observed on two crystals. The most probable slip direction for this system would be the [100]—the most densely packed direction in that plane. It must be emphasized that this system was observed in only two crystals compressed in directions unfavorable for slip on the major (010) system; hence, its role as a room temperature deformation mechanism must be viewed as minor.

Several crystals deformed principally by kinking; others showed evidences of cross-slip. Kinking was obtained in crystals which were compressed in a direction nearly parallel to the [100] slip direction and the (010) slip plane. The operative slip plane in this type of deformation was identified as the (010) by Laue spot asterism. The cross-slip appeared in crystals whose compression directions were also nearly parallel to the (010) slip plane but displaced from the [100] direction. The major slip traces were identified as (010) plane traces. The minor cross-slip traces were found to correspond to (001) planes. In

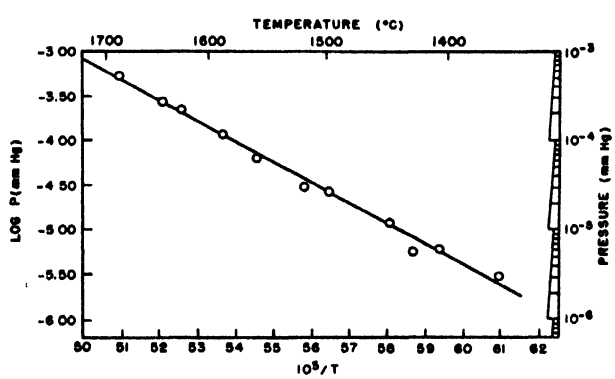

Figure 1. Vapor pressure of uranium (Rauh and Thorn). log *P* (in mm) = (2330/*T*) + 8.583

* Argonne National Laboratory.

Table I. Physical and Thermal Properties of Uranium

Density:		
High-purity uranium, directionally solidified (at 25°C)	19.05 ± 0.02 gm/cm³	(a)
Calculated from X-ray data on high purity uranium (at 25°C)	19.04 gm/cm³	(b)
Wrought material	18.7 to 19.08 gm/cm³	(c)
Transformation points:		
α - β	668°C	
β - γ	774°C	(d)
Melting point:	1132 ± 1°C	(e)
Boiling point:		
Extrapolated from vapor pressure measurements	3818°C	(f)
Vapor pressure from 1630° to 1970°K: (see also Fig. 1)		
$\log P \text{ (mm)} = \frac{2330 \pm 21}{T} + (8.583 \pm 0.011)$		(f)
Heat of fusion (estimate):	4.7 kcal/mole	(f)
Heat of vaporization:	106.7 ± 0.1 kcal/mole	(f)
Heat of sublimation at 0°k:	116.6 ± 0.1 kcal/mole	(f)
Enthalpy at 25°C:	1521.4 ± 1.6 cal/mole	(g)
Heat capacity at 25°C:	6.612 ± 0.007 cal/deg-mole	(g)
Entropy at 25°C:	11.99 ± 0.02 cal/deg-mole	(g)
Heats of transformation:		
α - β, ΔH at 668°C	0.674 kcal/mole	(h)
β - γ, ΔH at 774°C	1.131 kcal/mole	
Entropy of transformation:		
α - β, ΔS at 668°C	0.717 cal/deg-mole	(h)
β - γ, ΔS at 774°C	1.081 cal/deg-mole	
Thermal conductivity (70°C)	0.071 cal/cm-sec-°C	(i)
Temperature coefficient (100 - 225°C)	$+1.5 \times 10^{-3}$	(j)
Temperature coefficient (225 - 450°C)	$+0.4 \times 10^{-3}$	

LATTICE CONSTANTS:

I. Alpha phase, orthorhombic space group - Cmcm 4 atoms per unit cell (k)

Temperature (°C)	Lattice constants (Å)	Volume of unit cell (10^{-24} cm³)	Volume per atom (10^{-24} cm³)	Calculated density (gm/cm⁻³)
Room (25°C) (b)	$a_0 = 2.8541 \pm 0.0003$ $b_0 = 5.8692 \pm 0.0015$ $c_0 = 4.9563 \pm 0.0004$	83.02	20.75	19.04
200 (1)	$a_0 = 2.8675$ $b_0 = 5.8660$ $c_0 = 4.9775$	83.73	20.93	18.88
400 (1)	$a_0 = 2.886$ $b_0 = 5.861$ $c_0 = 5.005$	84.66	21.17	18.67
650 (1)	$a_0 = 2.920$ $b_0 = 5.834$ $c_0 = 5.064$	86.27	21.57	18.33

Thermal expansions (10^{-6} per °C) from X-ray data, parallel to:

	axis	25–125°C	25–325°C	25–650°C
(1)	a_0	21.7	26.5	36.7
	b_0	-1.5	-2.4	-9.3
	c_0	23.2	23.9	34.2

II-a. Beta phase (1.4 at % Cr) Tucker's (m) sample contained 1.4 at % Cr and the beta phase was retained to room temperature. Thewlis (n) has also reported lattice constant values for a similar alloy at 720° and 20°C

Temperature (°C)	Lattice constants (Å)	Volume of unit cell (10^{-24} cm³)	Volume per atom (10^{-24} cm³)	Calculated density (gm/cm⁻³)
720 (n)	$a_0 = 10.763 \pm 0.005$ $c_0 = 5.652 \pm 0.005$	654.7	21.82	18.11
20 (n)	$a_0 = 10.590 \pm 0.001$ $c_0 = 5.634 \pm 0.001$	631.8	21.06	18.77
20 (m)	$a_0 = 10.52$ $c_0 = 5.57$			

Linear coefficients of thermal expansion from 20 - 720°C.

(n) along $a_0 = 23 \times 10^{-6}$ per °C
along $c_0 = 4.6 \times 10^{-6}$ °C

II. Beta phase, tetragonal space group - P4/mnm 30 atoms per unit cell (m)

720 (n)	$a_0 = 10.759 \pm 0.001$ $c_0 = 5.656 \pm 0.001$	654.7	21.82	18.11

III. Gamma phase, body-centered cubic, 2 atoms per unit cell (o)

(p) 805	$a_0 = 3.525$	43.76	21.88	18.06
800	$a_0 = 3.49$			
(q) 25	$a_0 = 3.474$	41.93	20.96	18.85

Value at 25°C extrapolated from measurements on U-Mo in which gamma phase can be retained by quenching.

Approximate linear expansion coefficient = 18×10^{-6} per °C

(a) Blumenthal, B., Argonne National Laboratory.
(b) Mueller, M. H., Argonne National Laboratory.
(c) Kittel, J. H., Argonne National Laboratory.
(d) Selected values from several sources.
(e) Dahl, A. I. and Cleaves, H. E., *The Freezing Point of Uranium*, J. Research Natl. Bur. Standards, *43*: 513 (1949).
(f) Rauh, E. G. and Thorn, K. J., *Vapor Pressure of Uranium*, J. Chem. Phys. *22*: 1414 (1954).
(g) Flotow, H. E. and Lohr, H. R., Argonne National Laboratory.
(h) Ginnings, D. C. and Corruccini, R. J., *Heat Capacities at High Temperatures of Uranium, Uranium Trichloride and Uranium Tetrachloride*, J. Research Natl. Bur. Standards, *39*: 309 (1947).
(i) Weeks, J. L., *Thermal Conductivity of Uranium and Several Uranium Alloys*, J. Metals 7, AIME Trans, *203*: 192 (1955).
(j) Katz, J. J. and Rabinowitch, E., *The Chemistry of Uranium:* National Nuclear Energy Series, Division VIII, Vol. 5, McGraw-Hill Book Co., New York (1951).
(k) Jacob, C. W. and Warren, B. E., *Crystalline Structure of Uranium*, J. Am. Chem. Soc. *69*: 2588-91 (1937).
(l) Schwartz, C. M. and Vaughan, D. A., Battelle Memorial Institute.
(m) Tucker, C. W., *Acta Cryst. 4*: 425 (1951); see also Tucker, C. W. and Senio, P., *The Refined Crystal Structure of Beta Uranium*, KAPL-844 (1952).
(n) Thewlis, J., *X-ray Power Study of β-Uranium Acta Cryst. 5*: 790 (1952).
(o) Battelle Memorial Institute.
(p) Thewlis, J., *Structure of Uranium*, Nature, *168*: 198 (1951).
(q) Wilson, A. S. and Rundle, R. E., *The Structures of Uranium Metal, Acta Cryst. 2*: 126-127 (1949).

a cross-slip system the slip direction should be common to both cooperating planes, which in this case would be the [100] direction.

The second most frequently observed deformation mechanism and the most frequently observed twinning system were on the {130} composition plane. The occurrence of extensive {130} twinning was always accompanied by (010) slip. This was even true in the case of a crystal which was compressed nearly perpendicular to the (010) slip plane. The occurrence of (010) slip in such a crystal would indicate that extensive {130} twinning is always accompanied by an accommodating slip.

Two additional twin systems of irrational composition planes having indices of approximately {172} and {176} were observed. The more prevalent of these two twins were those occurring on the {172} planes. The various crystallographic elements of the three twinning systems were identified by X-ray and/or goniometric measurements; these are tabulated in Table II.

The deformation mechanisms that were identified as operative in the various crystals are summarized in Table III. In the case of twinning systems, only those unmistakably identified by a two surface analysis and/or X-ray Laue determinations are included. Similarly, the slip deformation mechanisms indicated are only those that resulted in microscopically visible traces on the polished surfaces. The major and most frequently occurring deformation mechanisms were: (010) slip, {130} twinning, and {172} twinning.

PHASE	TEMP (°C.)	NO. OF ATOMS PER UNIT CELL	VOL. PER ATOM (10^{-24} cm^3)	DENSITY (gm/cc)
α	ROOM (25°C)	4	20.75	19.04
α	200	4	20.93	18.88
α	400	4	21.17	18.67
α	650	4	21.57	18.33
β	720	30	21.82	18.11
γ	805	2	21.88	18.06

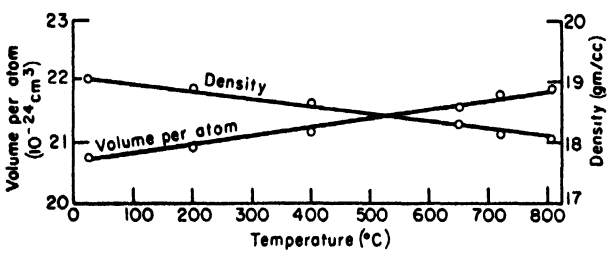

Figure 2. Some physical constants of uranium metal

Under special cases of stress application, deformation by {176} twinning, {011} slip, kinking and cross-slip were noted. The areas of crystallographic directions for which these deformation mechanisms operate are shown in Fig. 3. The depicted boundaries are not to be considered as exact, but rather as outlines which include the crystals for which the various deformation mechanisms operated. Evidence of slip on the (010) plane was observed in all crystals except E.

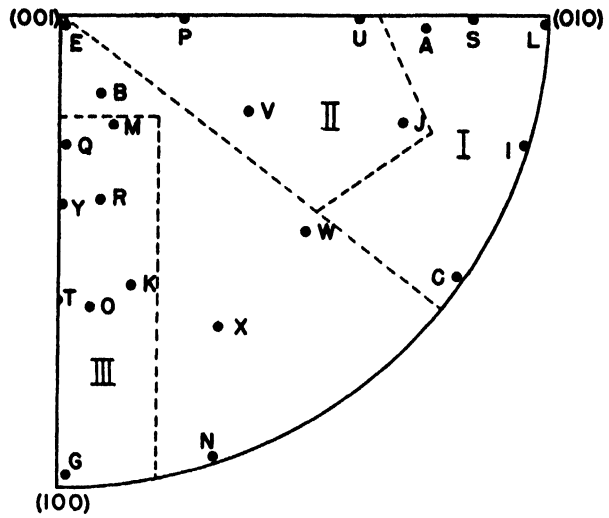

Figure 3. Compression directions studied. Dotted lines delineate areas of operation of the various deformation mechanisms. Macro 16, 615

Twinning on {130} planes was observed in the crystals within area I and II. {172} twinning occurred for crystals in area II. Twinning on {176} planes and slip on the {011} planes were confined primarily to crystals compressed in the [001] direction. Kinking and cross-slip were observed in crystals within area III.

III. PREFERRED ORIENTATION IN ALPHA URANIUM

Rod (Rolled, Swaged or Extruded)

The early investigations of the preferred orientation developed in uranium, as a result of rolling or swaging, were carried out using an X-ray photographic technique. Although this method at its best was only qualitative, it did give a good indication of some of the types of textures which were obtained. Fischer (ANL) reported that a rod swaged at 300°C and annealed two hours at 575°C showed (002) poles perpendicular to the rolling direction and (010) poles parallel to the rolling direction. In rods rolled at 300°C without an anneal, a duplex texture with the (010) and (110) poles parallel to the rod axis was reported by the Knolls Atomic Power Laboratory (KAPL) staff.

Table II. Twinning Systems*

K_1	K_2	η_1	η_2	2ϕ	S
(130)	$(1\bar{1}0)$	$[3\bar{1}0]$	[110]	81°30′	0.299
~ (172)	(112)	[312]	X^b	83°32′	0.229
~ (176)	(111)	[512]	X	83°50′	0.216

*K_1 is the first undistorted plane or twin composition plane. K_2 is the second undistorted plane. Its identity and shape is maintained both in the parent and twinned metal. η_1 is the shear direction. The plane containing the shear direction and perpendicular to the twin composition plane is the plane of shear. η_2 is the intersection of the plane of shear with the K_2 plane. 2ϕ is the angle between the K_1 and K_2 planes. S is the magnitude of shear and it is equal to 2 cot 2ϕ. X^b indicates the lack of rational direction indices.

Table III. Operative Deformation Mechanisms

Crystal*	Operative twin systems†			Slip deformation mechanisms‡			
	{130}	{172}	{176}	(010)	(010)-(001) Cross-slip	Kinking	(011)
A	2	–	–	–	–	–	–
B	–	–	–	X	–	–	–
C	1	–	–	X	–	–	–
E	–	–	4	–	–	–	X
G	–	–	–	X	–	X	–
I	2	–	–	X	–	–	–
J	1	1	–	X	–	–	–
K	–	–	–	X	–	X	–
L	2	–	–	X	–	–	–
M	–	–	–	X	X	–	–
N	–	–	–	X	–	–	–
O	–	–	–	X	–	X	–
P	2	2	–	X	–	–	–
Q	–	–	–	X	X	–	–
R	–	–	–	X	X	–	–
S	2	–	–	X	–	–	–
T	–	–	–	X	X	X	–
U	2	2	–	X	–	–	–
V	1	1	–	X	–	–	–
W	–	–	–	X	–	–	–
X	–	–	–	X	–	–	–
Y	–	–	2	X	X	–	X

*A pictorial representation of the crystal compression direction may be found in Fig. 3.

†Only twin systems identified by two-surface analysis and constituting a principal portion of the deformation observed are indicated. The number refers to the number of operative twin planes.

‡X indicates that deformation of the indicated type was observed microscopically.

As a result of this earlier work by Fischer (ANL), Burnham, Jr. and Bach, Hanford Atomic Products Operations (HAPO), and the KAPL staff, it was felt that the texture of swaged or rolled rods and rolled uranium sheet did not change after recrystallization.

Uranium rods which were either slow or fast beta treated after deformation appeared to be very nearly random, as reported by Fischer (ANL) and by Burnham, Jr. and Bach (HAPO).

Practically all of the more recent investigations of the preferred orientation in uranium have been carried out with an X-ray diffractometer using a Geiger tube as a detecting device. Several different types of sample holders have been designed and built for imparting the necessary motion or movement to the sample in order to collect the necessary intensity data from the X-ray diffractometer for the construction of pole figures, pole charts and inverse pole figures.

In a method described by Jetter and Borie, Jr.[1] spheres are machined from rods by a rather unique method to very close tolerances and have an attached stem for support. By providing two independent motions, perpendicular to each other, it is possible to obtain the necessary intensity data for the construction of one-half of a complete pole figure from one specimen.

The modified Schulz reflection technique[2] employing flat samples has been used by Holden and Seymour (KAPL), Chernock, Sylvania Electric Products, Inc. (SEP), and Mueller (ANL), for the determination of textures in uranium, with the X-ray diffractometer. The instrumental arrangement for this technique has been described by Holden[3] and by Mueller and others.[4] Each particular instrument varied somewhat in detail with respect to sample movements and recording of intensity data. In most cases, however, three samples were cut in different directions from rods and a number of small flat pieces were assembled together for the determination of sheet textures. The number of sections used for plotting a pole figure for sheet textures varied from the one large cube used by Chernock (SEP), several large cubes used by Seymour,[5] to seven different assembled sections used by Mueller and Knott.[6] In addition, Seymour and Duffey (KAPL) have made use of the Norton technique.[7]

Bach and Burnham, Jr.[8] and Morris, National Lead Company of Ohio (NLO), have made use of the X-ray diffractometer for evaluating the preferred orientation of rods on an industrial control basis. In this method the ratio or "psi" value is obtained between the intensity for a particular reflection from a sample and a randomly oriented specimen. It has been shown by Mueller and Beck (ANL) that the intensity of various reflections from the sample connot be compared directly to the (111) intensity. It was once thought that the (111) would serve as an internal standard.

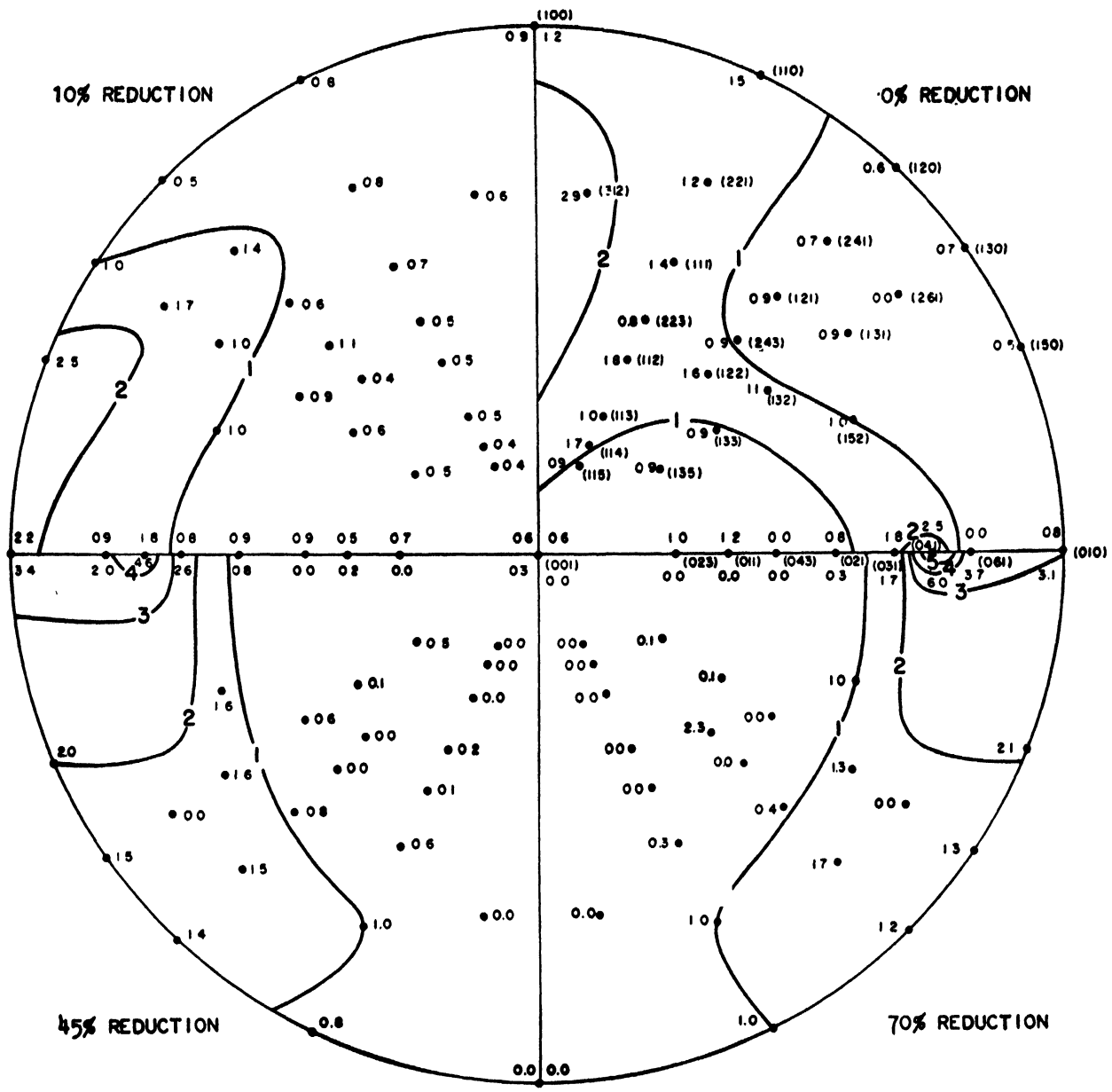

Figure 4. Inverse pole figure of uranium rods rolled at 300°C (0, 10, 45 and 70% reductions). Initial condition: water quenched from the beta phase

Rods rolled at 300°C or 600°C both contained the (010) and (110) components; however, the relative amounts of these two components varied, depending upon temperature of rolling. The (010) component seems to predominate at the lower temperature and (110) at the higher temperature, as reported by the KAPL staff, and by Chernock and Beck (ANL). A similar duplex fiber texture has also been reported by 500°C swaged rods by Jetter, Oak Ridge National Laboratory (ORNL).

Since considerable spread in intensity has been observed, some workers [Jetter (ORNL); Mueller and Beck (ANL); Seymour (KAPL)] have indicated that some of this intensity might be accounted for by minor texture components such as (451), (021), (131) in rolled rods or [031], [431], [100] directions found in 500°C swaged rods. Some evidence has been found by Sanderson (HAPO) for the development of a (100) component at high rolling temperature or after beta treatment.

It was found by Mueller, Knott and Beck (ANL) that if uranium rods are rolled at 300°C to a sufficiently high reduction (70% or greater) the preferred orientation obtained will be practically the same regardless of the prior fabrication history, that is, whether the rods were previously beta treated, 600°C rolled or 300°C rolled and annealed. The texture obtained after 70% reduction may be described by a concentration of the fiber axis between (010) and (041), with considerable scatter in the direction of the (100) including a minor maximum near (120). Below 70% reduction the type of orientation ob-

tained may vary considerably, depending upon the starting material. For example, inverse pole figures prepared according to a modified Harris method[9] indicated that the beta treated material initially was nearly random and showed a gradual increase of fiber axis concentration near the (010) and (120) poles (Fig. 4) as the reduction at 300°C increased.

Rods rolled at 600°C after beta treating varied from a nearly random condition, produced by beta treating, to a strong (110) component with considerable spread toward and including the (010) pole and some spread towards the (100) pole.

Jetter (ORNL) has prepared inverse type pole figures for 500°C swaged rods as shown in Fig. 5. A study was also made by Mueller (ANL) of the radial symmetry of the (001) planes which lie parallel to the rod axis. It was found that this symmetry was in the form of a "cloverleaf" when rods were rolled with the oval-round or oval edge-oval pass sequence (Fig. 6). Rods rolled with hand round passes showed a more nearly symmetrical intensity distribution.

The results obtained by Jetter (ORNL) and Chernock and Beck (ANL) from the X-ray diffractometer indicated that there were definite textural changes occurring upon recrystallization of rolled or swaged rods. Some of the results indicated that the (010) component remained after recrystallization, although it may have decreased in amount, and that the (110) component is replaced by an approximately (140) component with considerable spread which in some cases has been described as a (131) orientation.

Powder Compacts

An X-ray diffractometer study [Mueller (ANL); Sanderson (HAPO)] of the preferred orientation in hot-pressed uranium compacts indicated that there appeared to be very little orientation and that the samples were essentially random.

Rolled Sheet and Strip

The preferred orientations obtained in uranium sheet formed under various conditions have been investigated [Seymour,[5] Chernock (SEP); Mueller, Knott and Beck (ANL)]. The types of material investigated are summarized in Table IV. Although some preliminary texture studies were made on uranium sheet with the photographic technique [KAPL staff and Fischer (ANL)], more complete studies were made on the sheet specimens tabulated.

Since the specimens were fabricated under various conditions it would not be expected that all the pole figures would be the same. However, it was observed in general that there was a high (010) pole concentration in "as rolled" material near the rolling direction as shown in Fig. 7. In sheet rolled at the higher temperatures there was also a high (110) pole con-

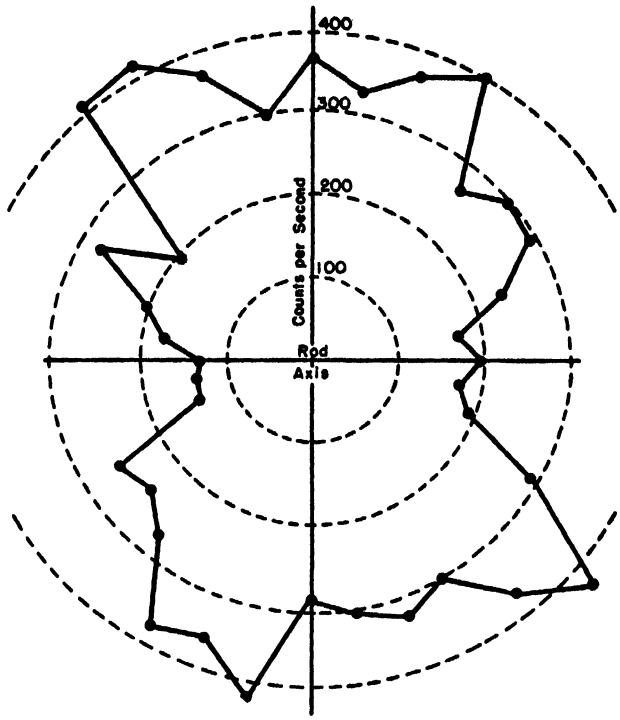

Figure 6. Radial intensity of the (002) reflection in an uranium rod rolled in an oval-edge-oval pass sequence

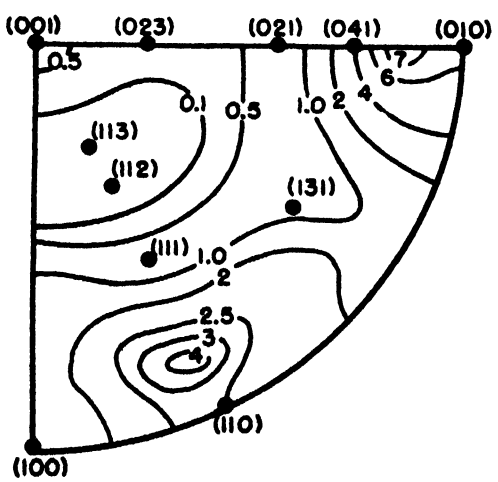

Figure 5. Preferred orientation plot for alpha-extruded uranium rod, as extruded

Table IV. Uranium Sheet Used for Preferred Orientation Studies

Investigator	*Material*	*Type of material*
Seymour (KAPL)	1	Foil formed at room temperature by a 91% reduction in area; also annealed 10 minutes, 600°C.
Seymour & Duffey (KAPL)	2	Sheet formed at 275°C by an 85% reduction in area.
Seymour & Duffey (KAPL)	3	Sheet formed at 600°C by an 85% reduction in area.
Chernock (SEP)	4	Sheet formed at 600°C by 30%, 60% and 90% reduction in area; also annealed 20 minutes at 580°C.
Mueller, Knott and Beck (ANL)	5	⅛ in. sheet formed at 300°C by an 87% reduction; also annealed 1 hour at 525°C.

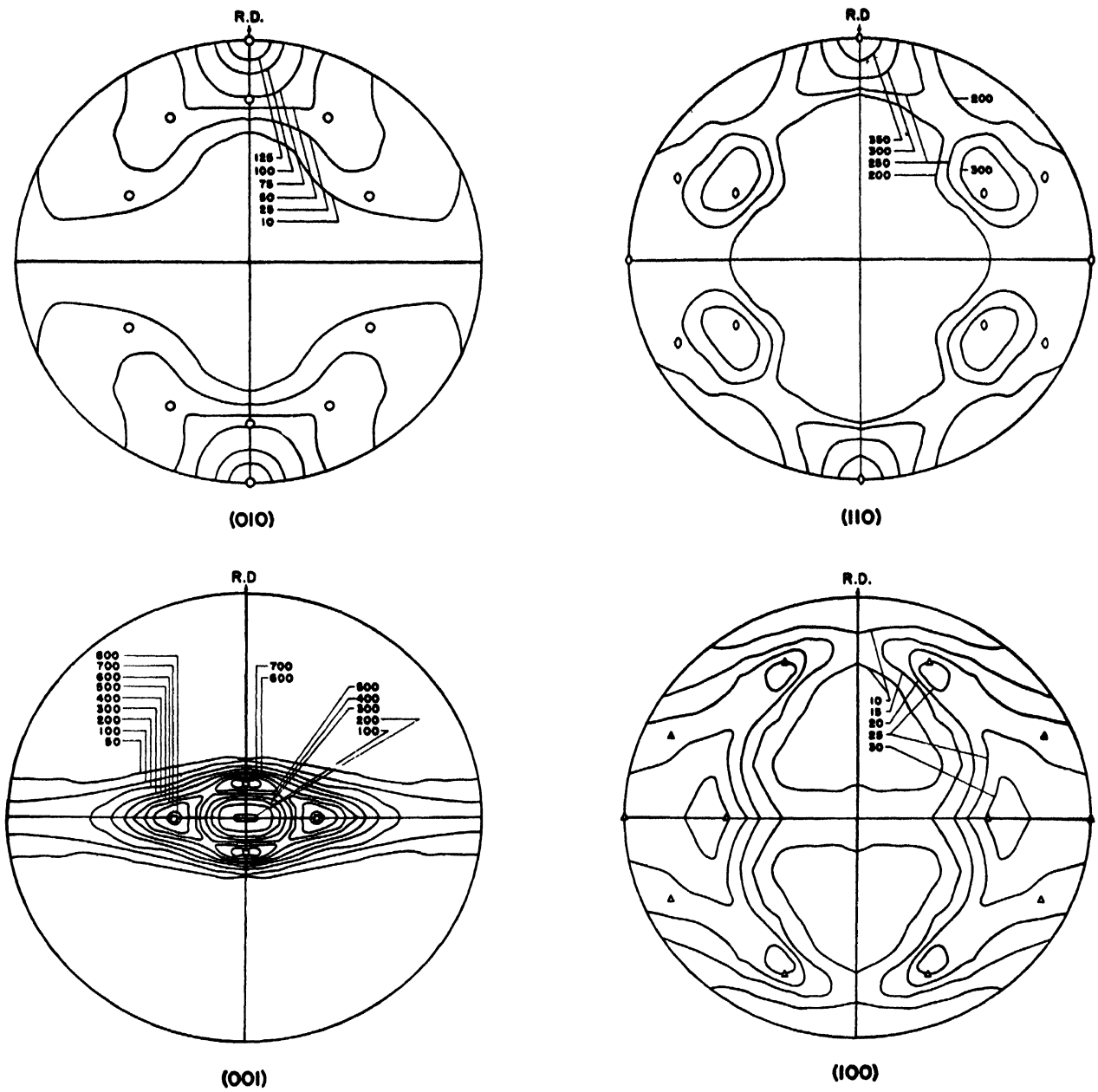

Figure 7. Pole figures for uranium sheet rolled at 300°C to an 87% reduction

centration near the rolling direction. These two observations are very reminiscent of the textures observed in rolled uranium rod. In addition, the (001) pole figures showed a high concentration near the center of the pole figure but displaced towards the transverse direction and in some cases towards the rolling direction.

The high intensity areas observed on the various pole figures shown in Fig. 7 are indicated by a separate symbol on each pole figure. These symbols, without the contour lines, have been transferred to the pole figures shown in Fig. 8 in order to show the compatibility of these high intensity areas which appear in the (010), (110), (001) and (100) pole figures. Although these quadrangles may be thought of as "ideal orientations" they may be only reasonably close to the true orientation or may only represent a spread in the orientation.

The lines which form the quadrangles shown in Fig. 8 connect one maximum or high intensity area from each of the pole figures mentioned above. The four symbols which form the corners of these quadrangles have the correct angular relationship appropriate to the corresponding poles. The "ideal orientations" represented by the various quadrangles are described under each figure in terms of (1) plane parallel to rolling plane, (2) direction parallel to rolling direction, and (3) plane perpendicular to rolling direction.

The pole figures for the 300°C rolled uranium sheet after recrystallization at 525°C are shown in Fig. 9. The (010) pole figure is very similar to that

Table V. Comparison of Results of Various Investigators

	Components in 300°C rolled sheet, Mueller, Knott and Beck (ANL)			
	Components reported under conditions as stated below by			
	Seymour (KAPL)	*Seymour and Duffey (KAPL)*	*Seymour and Duffey (KAPL)*	*Chernock (SEP)**
I.			600°C rolled to 85% reduction	600°C rolled to 60% reduction 600°C rolled to 90% reduction 600°C rolled and recrystallized
II.	Room temperature rolled to 91% reduction	275°C rolled to 85% reduction	600°C rolled to 85% reduction	600°C rolled to 60% reduction 600°C rolled to 90% reduction 600°C rolled and recrystallized
III.				
IV.	Room temperature rolled to 91% reduction	275°C rolled to 85% reduction		
	Components in sheet recrystallized at 525°C			
	Components reported under conditions as stated below by			
	Seymour (KAPL)	*Seymour and Duffey (KAPL)*	*Seymour and Duffey (KAPL)*	*Chernock (SEP)**
II.				
V.	Room temperature rolled and recrystallized 10 min at 600°C			600°C rolled to 30% reduction 600°C rolled to 60% reduction
VI.				600°C rolled to 60% reduction 600°C rolled to 90% reduction 600°C rolled and recrystallized
VII.				

* The sheet rolled at 600°C to 60% reduction also shows a minor (035) [100] component.

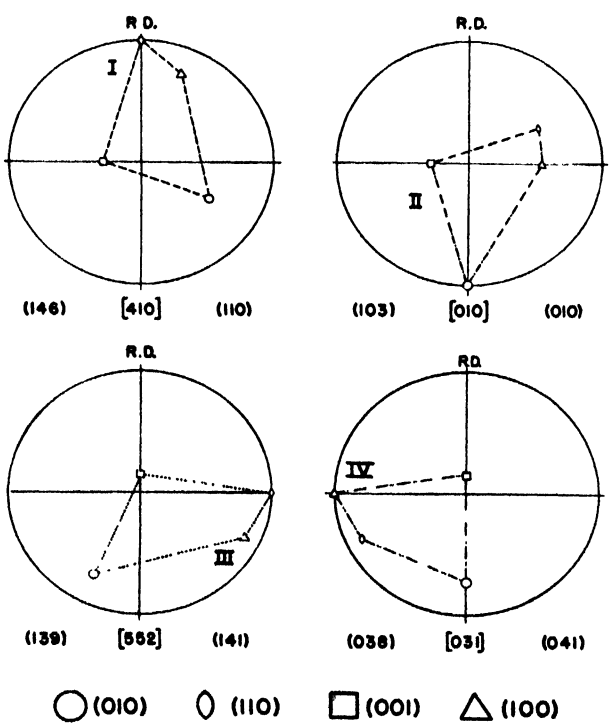

Figure 8. Pole figures showing the "ideal orientations" used to explain the relationship between the intensities found on the (010), (110), (001) and (100) pole figures of the as-rolled sheet

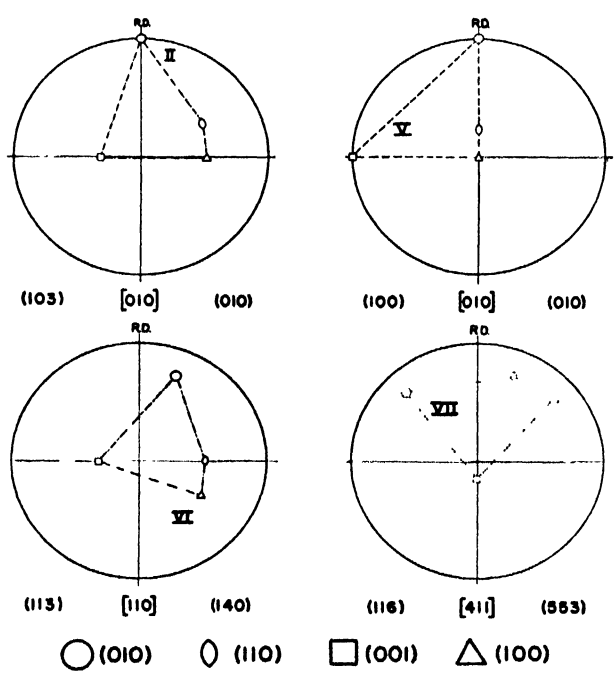

Figure 10. Pole figures showing the "ideal orientations" used to explain the relationship between the intensities found on the (010), (110), (001), and (100) pole figures of the recrystallized sheet

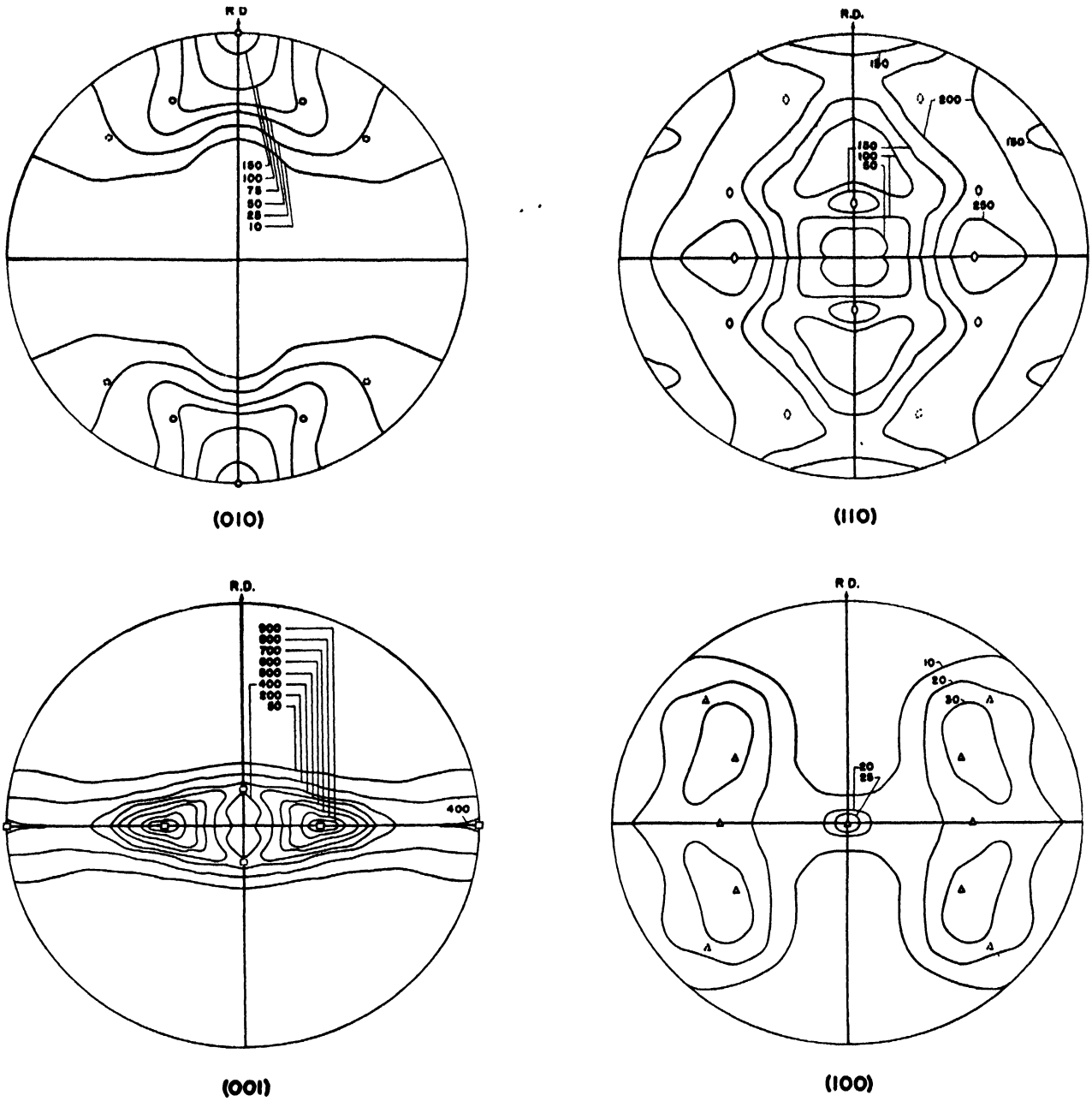

Figure 9. Pole figures for uranium sheet 300°C rolled and recrystallized

obtained for the as rolled sheet; however, the distribution of the (110) and (100) pole intensity has changed considerably.

Symbols have again been used, as in the rolled material, to mark maximum or high intensity areas on the various pole figures. These symbols have been connected together, as shown in Fig. 10, in the form of quadrangles to form "ideal orientations" and are again described under each quadrangle.

Since the 300°C rolled and the recrystallized sheet seemed to show most of the texture components reported for sheet rolled at lower and higher temperatures, these results will be compared to the "ideal orientations" reported by Mueller, Knott and Beck (ANL) for the 300°C material. Although in some cases the texture components do not agree exactly, they are in most cases reasonably close. A summary of the sheet textures as reported by the various investigators is given in Table V.

It is not surprising that other investigators do not report an intensity maximum described by III and VII in Table V since these intensity areas may only be a spread from the true texture component.

IV. RECRYSTALLIZATION AND GRAIN GROWTH IN URANIUM

A study of recrystallization and grain growth in metals involves a large number of variables. A complete study of the effects of all the factors requires considerable time as well as careful experimentation.

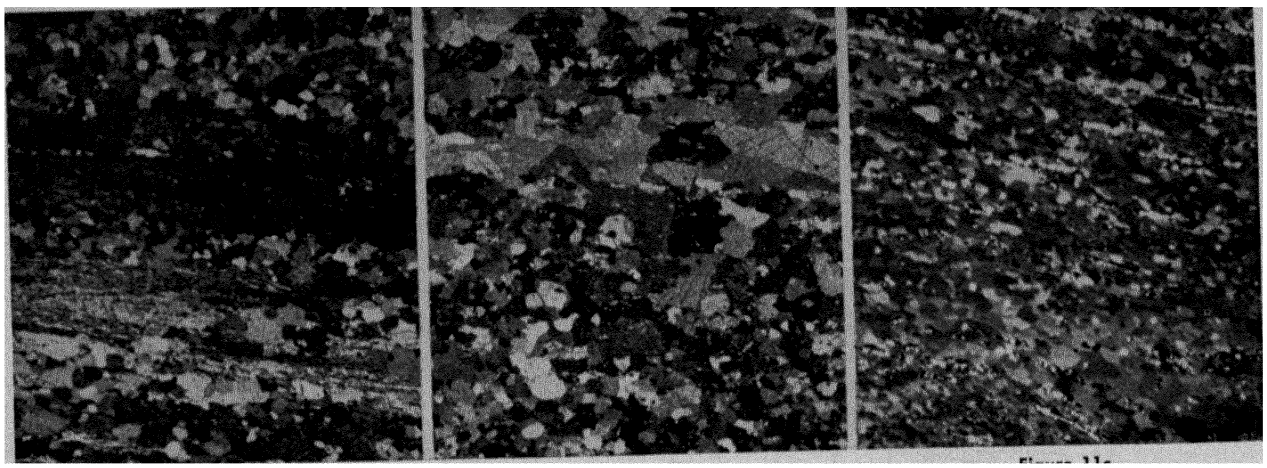

Figure 11a Figure 11b Figure 11c

A review of the literature indicates that grain growth and recrystallization in uranium has been studied to some extent at many different laboratories and production centers. Most of these studies were comparatively brief and were statistical studies of the effects of a few variables under production conditions. Systematic studies under laboratory conditions are relatively scarce. Only the laboratories at Massachusetts Institute of Technology (MIT) and Argonne have reported factors studied on a laboratory scale.

One of the reasons for the absence of more systematic data is understandable. The need for quick information on the properties of uranium appeared simultaneously with the availability of the metal. However, another reason may be the complexity of the problem, as indicated in the conclusions of the reports on statistical studies with a large number of specimens. Inconsistencies appeared to be the rule. In order to explain the inconsistencies it was first necessary to know the sources. Although most of the report writers reasoned that the impurities, the anisotropy of the crystal structure, and the allotropic transformations were the primary sources of the lack of uniformity in results, the effects of these factors were not easily studied. Some better understanding has resulted from the studies of Fisher (ANL) on high purity uranium. This work has shown that impurities have a very pronounced effect on grain growth and recrystallization and that the anisotropic properties of uranium result in nonuniform microstructures.

In this paper an attempt is made to summarize the effects of various factors on the recrystallization kinetics, grain growth after recrystallization, and the grain sizes produced by transformation of high temperature phases to alpha uranium. A brief summary of a method used to prepare single crystals and the attempts to do so by strain-anneal and phase transformation is included.

Since this report is concerned with uranium in general, rather than specific lots of uranium, the significance of any data depends on how representative it is in terms of structural uniformity and chemical composition. These two factors are discussed before describing effects of other variables.

Effect of Method of Fabrication on Uniformity of Recrystallized Structures

When uranium metal is rolled to high reductions in area in the case of rods, or in thickness in the case of plate, the recrystallized grains appear to be grouped in longitudinal bands which differ in average grain size and in orientation with respect to the longitudinal plane of examination. Figures 11a, 11b and 11c show the appearance of bands in longitudinal sections of a rod reduced 89% in area from a 0.9-inch diameter casting at a temperature between 500°C and 600°C (11a), the same rod as recrystallized at 600°C (11b), and a rod reduced 87% in area at 300°C and recrystallized at 475°C (11c). The bands appear to form as a result of differences in degree and modes of deformation of the grains existing prior to deformation. In Fig. 11a differences in degree of recrystallization during rolling are very obvious. The result of difference in degree of deformation on the uniformity of grain size after recrystallization is apparent in Fig. 11b. Even after heavy deformations below the recrystallization temperature, marked differences in grain size and orientation are evident after recrystallization.

The differences in grain size between such bands are magnified when grain growth is less inhibited, as shown in Fig. 11d. This material was reduced approximately 90% in area from an ingot of relatively high purity and annealed at 525°C for two hours. If a quantitative correlation between per cent reduction, annealing treatment, and grain size were attempted from such nonuniform structures the data would be of little significance.

The differences in grain size between bands can be reduced to a minimum if the coarse-grained billets are reduced in small steps with intermediate recrystallization between each reduction step. Figure 11e shows a longitudinal section of a high purity rod which was rolled from a 1-in. diameter ingot by a 5-step schedule with a 40% final reduction in area

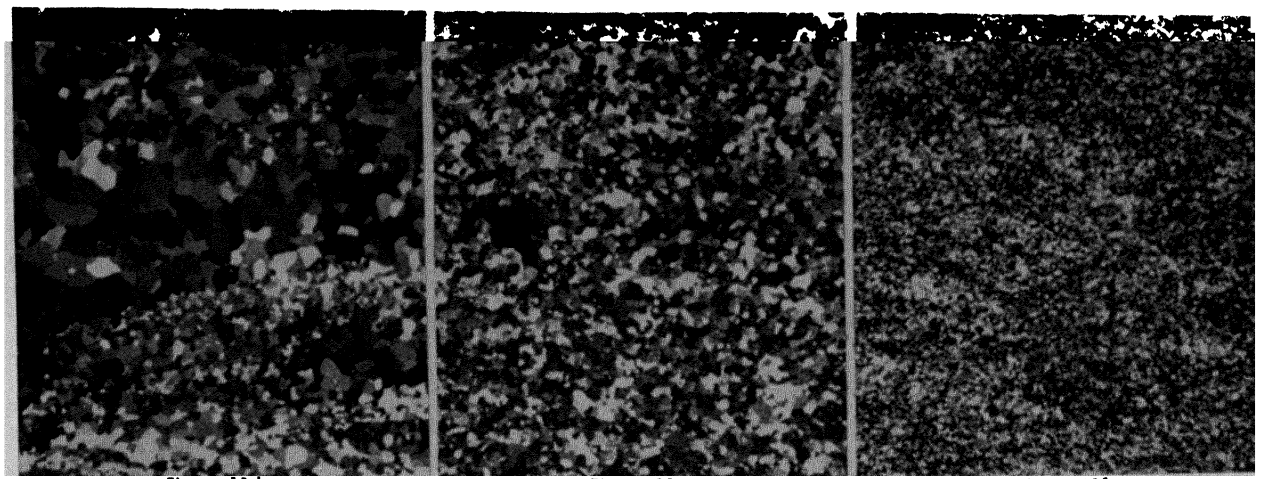

Figure 11d Figure 11e Figure 11f

Figure 11. Banding in rolled and recrystallized uranium rods

(11a) Micro 10908, 50X. 89% reduction in area at 600°C.

(11b) Micro 10940, 50X. Same as (a) recrystallized 600°C – one hour.

(11c) Micro 13094, 50X 87% reduction in area at 300°C, annealed one hour at 475°C.

(11d) Micro 10237, 100X High purity rod, 90% reduction in area at 300°C, annealed two hours at 525°C

(11e) Micro 10477, 100X. 90% total reduction in area at 300°C in five steps (15%, 30%, 30%, 48% and 48%) with intermediate recrystallization. Final anneal one hour at 475°C.

(11f) Micro 11078, 50X 73% reduction in area at 600°C, heated to 725° C for three minutes and water quenched, 47% reduction in area at 300°C and annealed one hour at 525°C.

(11g) Micro 10050 100X. Coarse grains within bands after long anneal.

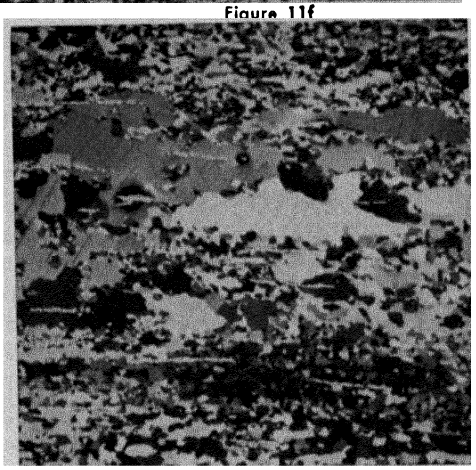

Figure 11g

and annealed one hour at 475°C. Very little variation in grain size was observed, but a careful study of the structure using polarized light revealed that traces of banding were still present.

Both differences in orientation and grain size between bands can be minimized by subjecting the rod to a fast beta treatment at some intermediate stage of rolling. Figure 11f shows the structure of an impure material which was reduced 73% in area at 550°C from a 1-in. diameter ingot, heated at 700°C for 3 minutes and water quenched, further reduced 47% in area at 300°C and recrystallized at 525°C. Instead of the longitudinal fibrous appearance, small patches of similarly oriented grains are observed.

An interesting effect of banding occurs when heavily reduced rods, even of impure material, are annealed at temperatures between 600°C and 650°C. Those bands which recrystallized to very fine grain sizes in the early stages of annealing may contain abnormally large gains after prolonged annealing (Fig. 11g)

Effect of Impurities

A. Effect of Inclusions on Grain Growth

From a lengthy study by Fisher (ANL) of grain growth in uranium containing different quantities of impurities it is concluded that most elements are nearly insoluble in alpha uranium, i.e., very small weight per cents can produce a second phase. Consequently, grain growth in uranium is extremely sensitive to differences in purity and to the heat treatments that affect the dispersion of the second phase. If the inclusions are in finely dispersed form they will have a much greater inhibiting effect on grain boundary movement than the same amount of material in relatively large inclusions. The inhibiting effect of both types will increase with their concentration.

It was also concluded that some or most impurities are much more soluble in gamma uranium than in the alpha phase, with the solubility increasing with increasing temperature in the gamma phase. If the metal is quenched to room temperature from some solution temperature in the gamma range, the solute reprecipitates during 300°C rolling and inhibits grain growth after recrystallization to a degree dependent on concentration. However, at temperatures between 600°C and 660°C the inhibiting effect of the precipitate is decreased with time because of coalescence of particles or because of slightly higher solubility in the high alpha range, so that the character of grain growth changes to a discontinuous type.

The above conclusions are based on correlations between chemical composition, microscopic observa-

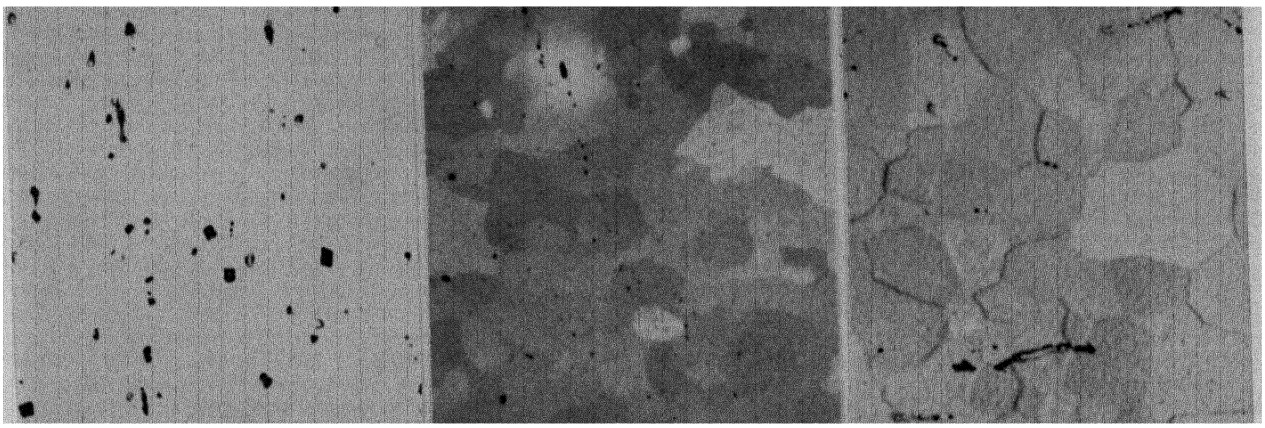

Figure 12a Figure 12b Figure 12c

Figure 12. Inclusions in different lots of uranium (electrolytic etch in 2% citric acid): (12a) Micro 13089, 500X. Large inclusions in impure uranium (230 ppm C, 40 ppm N, 30 ppm Fe, 30 ppm Si); (12b) Micro 13060, 500X. Relatively clean microstructure in impure uranium containing tantalum (230 ppm C, 10 ppm each N, Fe and Si, 220 ppm Ta); and (12c) Micro 13164, 500X. Relatively clean microstructure in high purity uranium (18 ppm C, <10 N, 10 ppm Si, 2 ppm Fe).

tions of inclusions, and grain size. Examples of this type of correlation are shown in Figs. 12 and 13. Figure 13 shows grain size versus temperature curves of five different lots of material for one-hour anneals after 300°C rolling. All the rods were reduced by a step reduction process with a 50% final reduction in area. Curve *A* is for an impure material containing 230 ppm carbon, 40 ppm nitrogen, 30 ppm silicon and 30 ppm iron. The as-etched microstructure showed numerous inclusions (Fig. 12a). The grain sizes at temperatures up to 600°C were relatively small, as might be expected from the inclusion concentration. However, a direct correlation with microstructure was not always observed, as shown by Curve *B* and Fig. 12b. This material contained 200 ppm carbon, approximately 10 ppm each of nitrogen, silicon and iron, plus 200 ppm of tantalum. The microstructure appeared free of inclusions, but grain growth was strongly inhibited as indicated by very insignificant effect of annealing temperature.

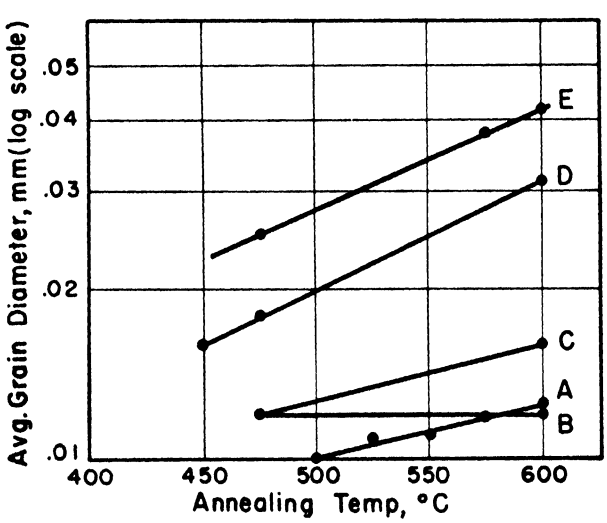

Figure 13. Average grain size after 1-hour anneals at different temperatures for different inclusion dispersions; all rods similarly fabricated. Curves *A*: impure material (Fig. 12a); *B*: impure material plus tantalum (Fig. 12b), *C*: high purity uranium, high concentration of submicroscopic inclusions; *D*: high purity uranium, low concentration of submicroscopic inclusions; *E*: high purity uranium, very low concentration of submicroscopic inclusions

The high purity metals, containing 10–40 ppm carbon and less than 15 ppm of the other impurities, all appeared relatively free of inclusions (Fig. 12c). Grain growth, however, varied considerably, with no direct correlation between grain growth and chemical composition. Curves *C*, *D* and *E* are examples of the types of grain growth curves one could obtain from some lots of material by proper choice of heat treatment prior to fabrication. In other lots of material the range of inhibition was narrower, i.e., curves such as *D* and *E* could be produced but the highly inhibited structures could not.

Discontinuous grain growth, or grain coarsening, at annealing temperatures above 600°C was a further indication of the differences in inhibition between lots. Figure 14 shows grain size versus time of annealing at 650°C for the five different lots of material. The vertical parts of the curves indicate grain coarsening and the relative heights indicate the coarse grain sizes resulting from coarsening after prolonged annealing. Note that the impure material, Curve *A*, exhibited coarsening, whereas the inclusion-free materials, Curves *B* and *C*, remained fine grained. The coarse grain size in the impure material was, however, limited by the inhibition due to the large inclusions (grain sizes up to 1 mm could be produced in such material). In the high purity material, the coarse grain size and the incubation period for coarsening varied with the concentration of fine particles and with differences in matrix grain sizes before coarsening occurred. Figure 15 is a schematic representation of the effect of fine particle concentration on grain size after prolonged anneals at 650°C. For the maximum grain size an optimum concentration exists. Figures 16a

and 16b show the start of coarsening and a completely coarsened sample in material represented by curve *D* in Fig. 14.

B. Effect of Impurities on Recrystallization

Although it seems probable that the recrystallization temperatures would be affected by inclusion dispersion as is continuous grain growth, this effect has not been extensively investigated. Figure 17 shows the relative recrystallization temperatures after one-hour anneals for the material represented by curves

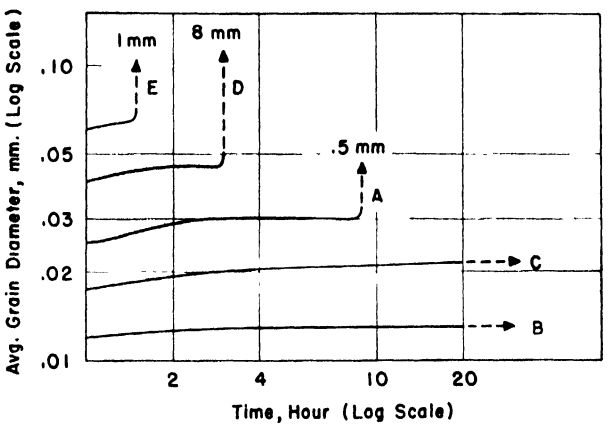

Figure 14. Average grain versus time at 650°C for the 5 different materials described in Fig. 13. Vertical arrow indicates beginning of grain coarsening; relative heights indicate relative size of coarse grains after completion of coarsening

A and *D*, respectively, in Fig. 14, as determined from Vicker's hardness measurements on metallographically polished longitudinal sections. Metallographic observations showed the high purity material to be completely recrystallized at 425°C, whereas the impure material was completely recrystallized at 475°C. In both of these materials the grain sizes were relatively uniform throughout the specimens as a result of step-reduction rolling prior to recrystallization.

From a study of critical strain in various materials it was found that, other conditions being similar, the critical strain, as determined from grain size observations, for 650°C anneals decreased with decreasing concentration of both large and submicroscopic par-

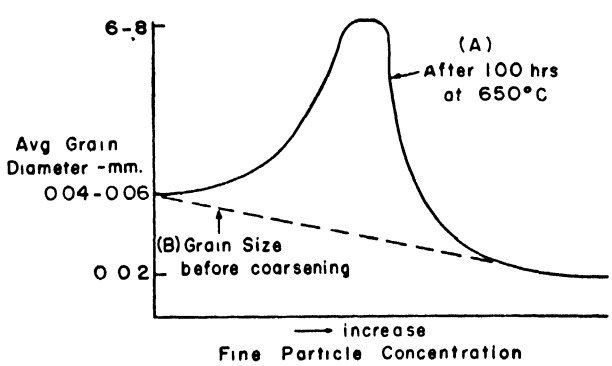

Figure 15. Postulated curves relating average grain size, after (A) 100 hours at 650°C, and (B) before coarsening, and fine particle concentration

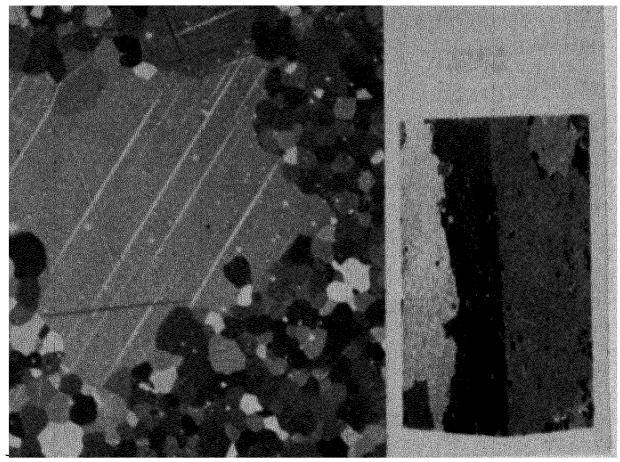

Figure 16a Figure 16b

Figure 16. Appearance of coarse grain. (a) Beginning of coarsening in material represented by curve *D* in Figure 13 (*b*) Macro 11689, 7X. Completion of coarsening in specimen of material represented by curve *D* in Figure 13

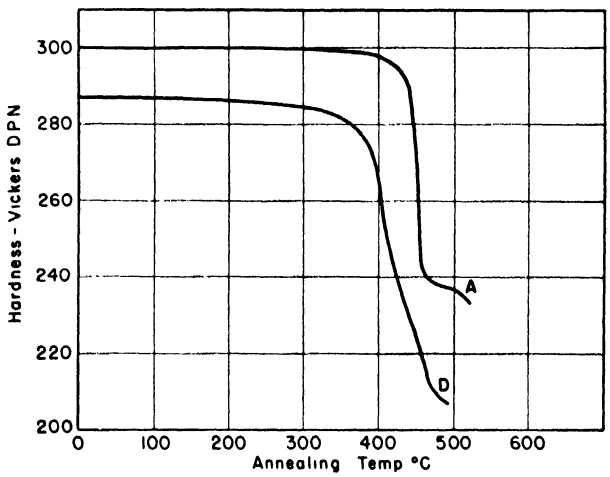

Figure 17. Effect of inclusion dispersion on recrystallization. Vickers hardness versus annealing temperature after 50% final reduction at 300°C for high purity material (*D*) and low purity material (*A*); both curves are for 1-hour anneals

ticles. Impure materials (curve *A* in Fig. 13) had a critical room-temperature tensile strain of approximately 1.2% elongation, as did the materials represented by curve *C* of Fig. 13. Critical strains of 0.5% were found in lesser inhibited specimens, decreasing to 0% for the high purity material which exhibited grain coarsening.

Effect of Degree of Work Hardening on Recrystallization

A. Recrystallization Temperature Versus Room Temperature Strain in Polycrystalline Material

Hayes (MIT) has studied recrystallization versus temperature and time for sheet specimens of impure uranium (500 ppm C, 60 ppm Fe) which were reduced 2% to 94% in thickness by room temperature rolling. To prepare the specimens, the casting was extruded at 600°C, rolled at 500°C and machined to $\frac{3}{16}$ in. thick slabs; one set was annealed at 600°C

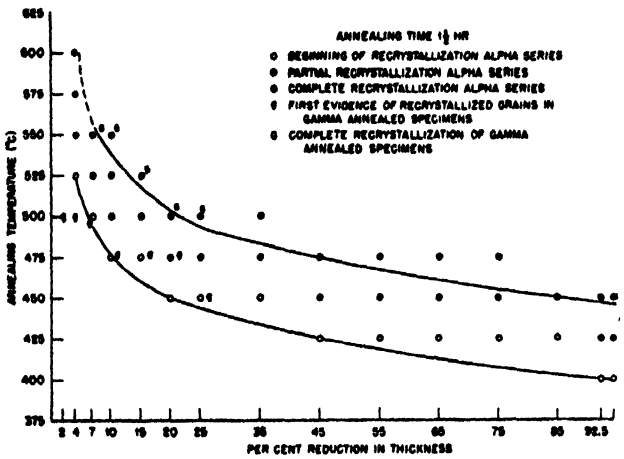

Figure 18. Recrystallization temperatures as function of per cent reduction of uranium plate at room temperature (Hayes, MIT)

(alpha series) and a second set annealed at 843°C (gamma series) prior to final rolling. The specimens were annealed for 1½ hours after room temperature rolling at temperatures up to 600°C and subsequently examined metallographically for the degree of recrystallization. The composite results appear in Fig. 18. For 94% reduction, recrystallization began at 425°C and was completed at 450°C. For 4% reduction, recrystallization started at 525°C and was not complete in the 600°C annealed sample. The results for both sets of specimens were not significantly different.

During strain-anneal studies by Fisher (ANL) the effect of per cent elongation in tension on recrystallized grain size was determined for various conditions as described in a later section. With a starting grain size of approximately 0.012 mm in impure material, a sharp drop occurred in the grain size after 45 hours at 640°C versus per cent elongation curve at approximately 1.2% (see Fig. 19). It can be concluded that recrystallization did not occur in specimens strained less than 1.2%. For the same material and starting grain size the critical strain for 625°C annealing occurred at 1.6% elongation.

Although the material strained less than the critical strains noted above did not show evidence of recrystallization, examination of the microstructures and X-ray diffraction evidence indicated that the relief of strain by gradual grain growth had occurred.

Hayes (MIT) studied the appearance of Debye-Scherrer back-reflection rings as a function of per cent reduction by rolling in sheet. After 2% reduction the reflections from the individual grains showed no effect of deformation; after 4% reductions appreciable continuous background between high intensity spots was observed, and after 10% reduction the rings were continuous.

B. Recrystallization Time Versus Strain at Room Temperature

Hayes (MIT) studied the effect of time for recrystallization at various temperatures after 85% reduction at room temperature with the same specimens described in Part A above. The data are shown in Table VI. After 24 hours at 400°C recrystallization had started. After one minute at 500°C recrystallization was complete. Using these data the activation energy for the start of recrystallization is calculated to be close to 100,000 calories per mol.

C. Recrystallization After 300°C Rolling

There is no record of a systematic study of recrystallization temperature as a function of strain at 300°C. Scattered data are available but an accurate compilation is not possible because of differences in other conditions. However, the 475°C recrystallization temperature for a final reduction of 50% in impure material, Fig. 17, corresponds to the recrystallization temperature for impure sheet reduced 50% at room temperature as reported by Hayes. The annealing times, one hour and 1½ hours, respectively, are close enough to permit comparison. Further ANL data show that for 87% reduction of impure rods at 300°C, the recrystallization temperature after two hours is also 475°C. Hayes' data for 85% cold worked sheet show a 450°C recrystallization temperature.

D. Effect of Grain Size Prior to Strain

It is quite probable that the grain size prior to deformation can have a marked effect on recrystallization after small strains. Strain-anneal studies by Fisher (ANL) show that a 1-mm grain size bar strained 1.3% in elongation did not recrystallize at 650°C, whereas 0.010-mm penultimate grain size showed a critical strain of 1.0%. It is also probable that a large grain size will lead to nonuniform recrystallization after small reductions by rolling, as discussed in Section I.

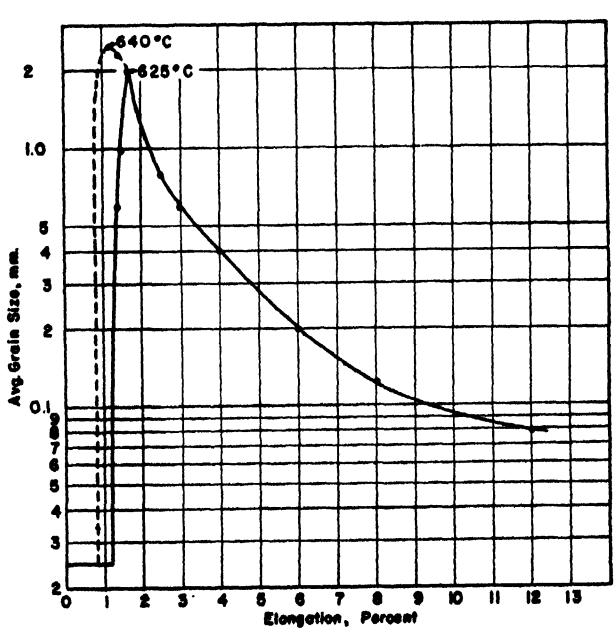

Figure 19. Grain size vs strain in impure uranium; increase of grain size with decreasing strain in elongated, tapered tensile bar annealed by heating at 5°C per hour to 625°C (solid line), and subsequently heated at 640°C for 45 hours (dotted line)

Table VI. Effect of Time on Recrystallization Range after 85% Reduction at Room Temperature of Impure Material. (Hayes, MIT)

Annealing temperature (°C)	Recrystallization time	
	Beginning	Complete
350	over 2 weeks	
375	over 1 week	
400	24 hours	
425	1½ hours	24 hours
450	5 min	1½ hours
475	1 min	5 min
500		1 min

Recrystallization after large reduction in impure material apparently is not affected significantly by grain size difference, as indicated by Hayes (MIT).

E. Effect of Rolling Temperature on Recrystallization During Rolling

The effect of rolling temperature on the as-rolled microstructure is of interest in the processing of uranium where reproducibility of structure and properties is desired. However, based on inconsistent data gathered from various sources, this temperature is not easily regulated. Although the temperature of the billet before entering the rolls can be controlled by careful operation, the change in temperature during deformation is markedly affected by the type of mill and the reduction per pass. It is also probable that the reduction per pass determines the effect of the actual temperature. A study of the problem by Mayfield (ANL) using a single stand mill indicated that rod finishing temperatures less than 600°C did not yield completely recrystallized structures. The structure shown in Fig. 11a is the result of rolling in a single stand mill at temperatures between 500°C and 550°C.

A study of a large number of rods by Rideout (duPont-ANL) which were rolled in a 6-stand commercial mill showed that the rods which finished at temperatures above 500°C were generally completely recrystallized.

F. Effect of Rolling Temperature on Recrystallization After Rolling

A comparison of the data on room temperature rolled sheet (Part A) and 300°C rolled rod (Part C), both of impure material, indicates that recrystallization temperatures after 50% final reduction are similar. After 85% reduction the room temperature rolled sheet recrystallized at 450°C after 1½ hours, whereas 300°C rolled rod was not completely recrystallized after two hours at this temperature.

Rideout (duPont-ANL) reports that rods rolled in a 6-stand mill which finished at 480°C required over 20 minutes of annealing at 500°C for complete recrystallization. This may be compared with one minute after 500°C for cold-rolled sheet reduced 85%; however, actual degree of reduction at 480°C is not known.

Grain Size After Recrystallization

A. Effect of Time at Temperature

In the section titled "Effect of Impurities," the occurrence of discontinuous grain growth at high alpha temperatures was described. The effect of time depends on the inclusion dispersion, the as-recrystallized grain size and on the type of grain growth under consideration, i.e., continuous or discontinuous grain growth. From observations in different materials there appears to be an equilibrium average grain size after reductions above 40% which increases with temperatures up to the range at which coarsening can occur. The rate of approach to equilibrium decreases with increasing inhibition and with increasing time. For example, the grain size in high purity material represented by curve *D* in Fig. 13 showed no significant increase in grain size after ½ hour at 450°C, i.e., the equilibrium grain size was rapidly approached. The impure materials (curve *A* in Fig. 13) showed a gradual increase in grain size over a 2-hour annealing period at 475°C and very little change in subsequent annealing. The heavily inhibited high purity materials showed an even less effect of time. At 650°C the grain size increased from 0.018–0.022 mm over a 115-hour period.

The effect of time on grain size in metals which tended to coarsen was, of coarse, very marked. The final grain size depended on how fast the first grains to coarsen could grow before a general release in inhibition occurred, which was primarily a function of temperature and the degree of inhibition. It was generally noted that structures attained after 20 hours were close to equilibrium, i.e., longer annealing had little effect on the grain size distribution.

B. Effect of Temperature of Annealing

The temperature of annealing determines the character of grain growth after recrystallization as described above. The effect of temperature on grain size from anneals after 50% final reduction for 5 different lots of material is shown in Fig. 13. It can be concluded from these curves that the effect of temperature on continuous grain growth decreases with increasing quantity of fine inhibitor. The grain size in rods from impure castings increase significantly with temperature whereas heavily inhibited high purity material was less affected.

Temperature has a significant effect on the coarse grain size. The maximum coarse grain size was attained at the highest annealing temperatures. At the lower coarsening temperatures the rate of coarse grain growth was not sufficient to prevent the formation of additional coarse grains or a gradual increase in matrix grain size.

C. Effect of Matrix Grain Size on Coarse Grain Growth

If a high purity specimen was annealed at a low coarsening temperature (600–625°C) and developed a matrix grain size mixture ranging from 0.04 to 1 mm, further anneals at high temperatures had little



Figure 20a



Figure 20b



Figure 20c



Figure 20d

Figure 20. Grain sizes in alpha uranium after different transformation heat treatments. (20a) Micro 17263, 100X. Heated two hours at 675°C and water quenched. (20b) Micro 17273, 100X. Heated two hours at 675°C and furnace cooled. (20c) Micro 17267, 100X. Heated two hours at 1000°C, cooled to 800°C, held one and one half hours, water quenched. (20d) Micro 17277, 100X. Same as 20c, furnace cooled

effect on the structure. Consequently, slow rates of heating to 650°C produced relatively small coarse grains.

D. Effect of Strain on Grain Size After Recrystallization

In Fig. 19 grain size after 45 hours at 640°C is plotted against per cent elongation at room temperature [Fischer (ANL)]. These data are for impure tensile specimens which were machined from rods reduced 90% in area and recrystallized to a fine grain size prior to extension. The curve shows a significant effect of strain differences below 13% elongation, the effect increasing with decreasing strain. Other data indicates that strain differences above 40% reduction in area at 300°C have very little effect on the grain size after recrystallization.

Data by Bach (HAPO) and Rideout (duPont-ANL) indicate a marked effect of rolling temperature on grain size after recrystallization. As is to be expected, the grain size increases with temperature of rolling.

Grain Size and Structure Resulting From Transformation

A. Definitions

When high purity uranium or impure uranium in which carbon is the predominant impurity is cooled to temperatures below 660°C, grains of the alpha phase form and replace the high temperature phase. Unless the transformation occurs under very special conditions, i.e., extremely slow cooling rates in high purity metal, the grains present at room temperature contain sub-boundaries separating regions of slightly differing orientation. These subgrains can be detected by polarized light examination because of the differences in orientation across boundaries as shown in Fig. 20 and by X-ray diffraction Laue patterns from single grains (Fig. 21). The grain size can be defined as the cross-sectional diameter of the volume occupied by a number of subgrains which were formed within the same grain. However, when the difference in orientation between subgrains becomes relatively large this volume will no longer approximate the behavior of a single orientation and the size of the subgrains may act as the effective grain size. In this review the effect of various factors on the grain size, as defined above, and the degree of orientation difference is summarized.

B. Factors Affecting Grain Size in Uniformly Cooled Specimens

When small specimens are uniformly heated into the beta or gamma phase and then transformed to the alpha phase by quenching all of the metal in water or

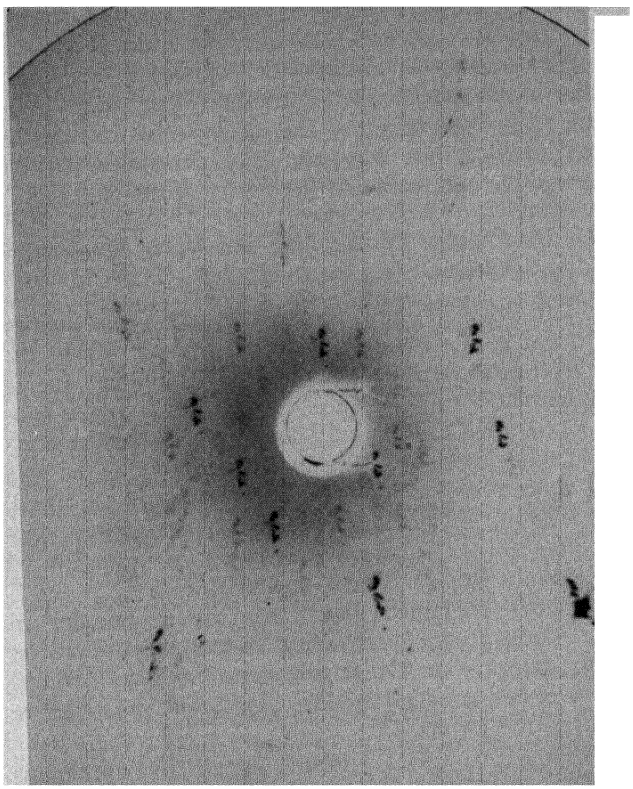

Figure 21. Orientation spread in crystals produced by phase change; reproduction of Laue pattern from large alpha grain produced by transforming; note segmentation of reflection spots. Met No. 13865

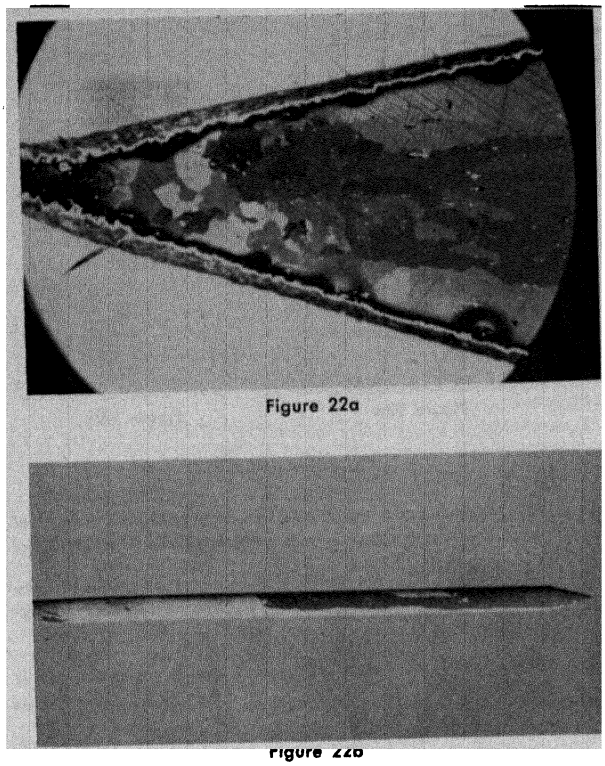

Figure 22a

Figure 22b

Figure 22. Grain size distribution resulting from transformation in temperature gradient. (22a) Micro 7664, 50X. Grain size distribution in longitudinal section at pointed end of pencil specimen after transformation in temperature gradient. (22b) Macro 4644, 1X. Macro photo of etched pencil after transformation through temperature gradient

air or by furnace cooling, all parts of the sample transform at about the same time. Data from various sources indicate that the alpha grain size produced under these conditions is primarily dependent on the rate of cooling through the transformation and, to a lesser degree, on the grain size prior to transformation. The importance of the rate of cooling is demonstrated in numerous data from actual measurements of cooling rates or from drastically different methods of cooling. Figures 20a and 20b (from experiments by Lloyd, ANL) show the alpha grain size in two specimens, both heated in the beta phase under the same conditions, but cooled by quenching in water (20a) and furnace cooling (20b), respectively. Water quenching not only produces smaller grains, but the grain boundaries are markedly jagged in comparison to the relatively straight grain boundaries in more slowly cooled specimens. The fast cooling rate apparently prevents appreciable movement of grain boundaries.

The importance of the grain size prior to transformation is indicated by the correlation with temperature and time of heating prior to transformation (Figs. 20a and 20c).

The grain size prior to heating above the transformation temperature and the rate of heating appear to have little effect on the final grain size. Annealing in the alpha phase subsequent to transformation does not affect the grain size significantly, although there is some effect on the shape of the grain boundaries and sub-structure in high purity metals, as discussed in Part D.

C. Effect of Temperature Gradient on Grain Size

Uranium specimens which are cooled through the beta to alpha transformation so that a systematic temperature gradient exists contain grains which are generally columnar in shape. These observations were made from numerous experiments by Fisher (ANL) to prepare single crystals by moving pencil-shaped specimens through a temperature gradient so that the point transformed first. It was observed that the pointed or tapered parts contained a region of equiaxed grains, as shown in Fig. 22a, but the grains above this region were longer in the general direction of the temperature gradient. The number of columnar grains at a section decreased with increasing distance above the point. With impure material a single columnar grain occupying a complete cross section could not be obtained in specimens larger than ⅛-in. diameter (Fig. 22b). A high purity specimen produced a single crystal slightly less than ¼-in. diameter. It was concluded that grains tend to grow in a preferred crystallographic direction. If the nuclei were oriented with this direction close to parallel with the

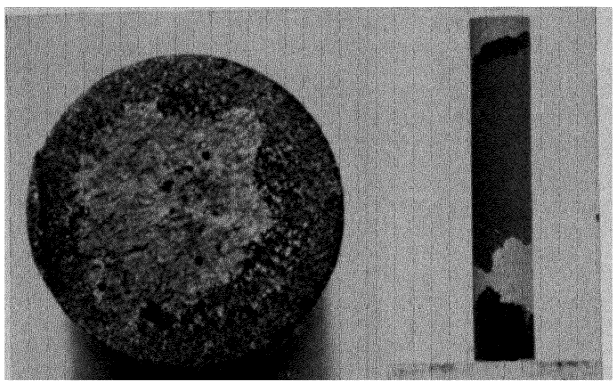

Figure 23. Characteristics of coarse grain growth and structural perfection of crystals in specimens containing gradient of inhibitor:

(23a) Macro 13359, 7X. Macrophoto of etched coarsened specimen containing gradient of inhibitor. Specimen annealed twenty-four hours at 635°C.

(23b) Macro 12482, 2X Macrophoto of etched specimen containing five single crystals.

(23c) Macro 16651, 1X. Back-reflection Laue pattern from polished face of uranium single crystal ("b" axis parallel to X-ray beam, unfiltered tungsten radiation and 0.030" collimator).

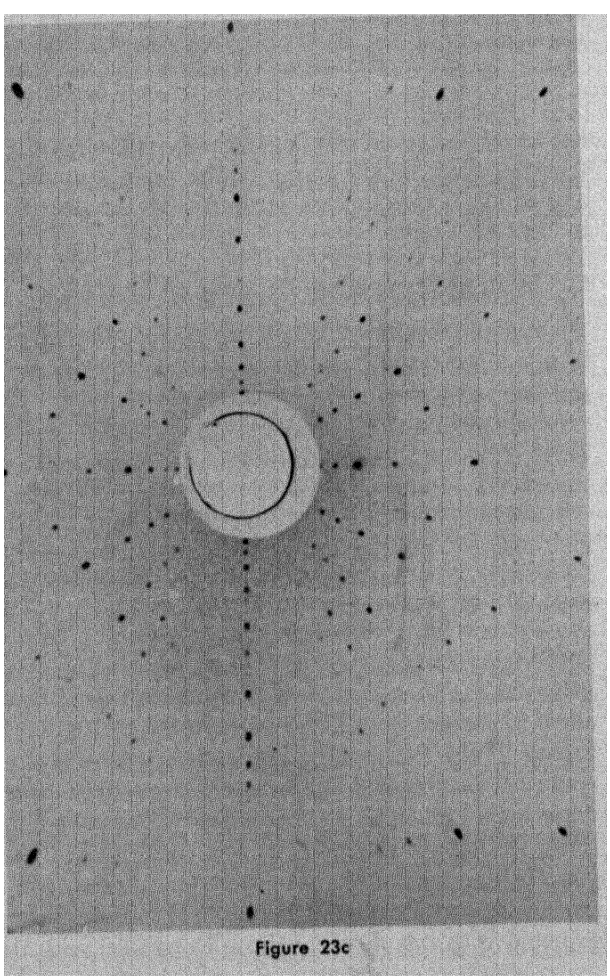

Figure 23c

specimen axis they grew to long grains; otherwise, the grains would terminate at the cylindrical surface.

The number of grains which existed in the upper part of the specimens did not depend significantly on the rate of movement of the specimen or the starting temperature, but was primarily dependent on the size of the specimen and the purity of the material.

D. The Effect of Cooling Rate and Alpha Annealing on Subgrains

The single crystals prepared by the phase change method exhibited scatters in orientation within the crystal boundaries of the order of 10 degrees due to accumulation of differences in orientation across sub-boundaries. Chiswik and Lloyd (ANL) have shown that the number of sub-boundaries formed by the beta to alpha phase change can be considerably reduced, at least in high purity uranium, by extremely slow cooling rates. Small specimens which were heated uniformly to 725°C and cooled to 625°C at ½°C per hour contained grains which were similar in perfection to those resulting from recrystallization after deformation. Other specimens which were cooled at 4°C per hour exhibited a significant substructure within the grains.

Blumenthal (ANL) heated high purity specimens which were water quenched from 1000°C to 650°C for 3½ weeks. The grain boundaries appeared relatively straight and no significant substructure was observed within the grain boundaries. It is quite probable that coalescence of subgrains and straightening of pre-existing grain boundaries accounted for this change in structure.

Preparation of Alpha Uranium Single Crystals

Because of the imperfections in single crystals formed by the phase change method it is desirable to prepare single crystals by inducing growth of alpha grains which are more perfect. Attempts to prepare such crystals by strain-anneal techniques have been carried out by a number of laboratories with no success. This lack of success can be attributed to the following causes:

(*a*) Deformation by twinning causes copious nucleation.

(*b*) Optimum conditions are difficult to attain (considering inhibition by inclusions, penultimate grain size, degree of strain and temperature of final annealing).

Fisher (ANL) has developed a second method by which single crystals can be produced from fine, recrystallized alpha grains in high purity uranium. This method makes use of the grain-coarsening phenomenon described in the section titled "Effect of Impurities." Considering rod-shaped specimens, a concentration gradient of fine inhibitor is produced by diffusion of small quantities of silicon from the cylindrical surface. The rod is then quenched from the gamma phase and fabricated by a step reduction–annealing schedule so that a fine and close to uniform

grain size exists after primary recrystallization. Referring now to Fig. 15, if a close-to-optimum concentration of fine inhibitor exists at the region about the rod axis (as determined by the temperature from which the rod was quenched prior to fabrication) a minimum number of coarse grains will form in this region during prolonged annealing at high temperatures (640–660°C) and grow radially into the fine grained matrix. Under optimum conditions only one coarse grain is produced which grows almost to the cylindrical surface (Fig. 23a). In most cases a thin layer of fine surface grains remain because of the high silicon concentrations in the outer volume. However, in some cases the grains grow to the surface as shown in Fig. 23b.

Up to the present no single crystals larger than ¼-in. diameter have been made by this method. The single crystals exhibited no substructure under polarized light examination. The X-ray diffraction spots from normal Laue techniques show no segmentation (Fig. 23c).

V. THERMAL EXPANSION CHARACTERISTICS OF URANIUM

Two of the uranium allotropic modifications are anisotropic in nature, namely, the orthorhombic alpha uranium and the tetragonal beta uranium. Because of these lattice anisotropies, their linear thermal expansion coefficients are dependent upon the specific crystallographic direction under consideration. True measurements of linear thermal expansion coefficients cannot be obtained from polycrystalline samples of these phases; they must be either calculated from X-ray determinations of lattice parameters as a function of temperature, or determined by dilatometric measurements performed on single crystals. On the other hand, true measurements of linear thermal expansion coefficients of the body-centered cubic gamma uranium can be obtained from dilatometric studies of polycrystalline materials.

Thermal Expansion Coefficients Determined From X-ray Measurements

No systematic studies have been made of the beta and gamma uranium lattice parameters as a function of temperature. Values of the alpha uranium lattice parameters over the temperature range 25°C to 625°C have been reported by Schwartz and Vaughan (BMI). These values have been used to calculate the volumetric and linear thermal expansion coefficients for alpha uranium.

Table VII. Mean Volumetric and Linear Thermal Expansion Coefficients of Alpha Uranium

Temperature °C	Mean thermal expansion coefficient per °C			
	$a \times 10^6$	$b \times 10^6$	$c \times 10^6$	$v \times 10^6$
25–100	17.74	–0.68	22.6	39.70
25–175	21.02	–0.91	22.3	42.40
25–250	24.92	–1.28	22.96	46.60
25–325	27.33	–2.10	24.01	49.20
25–400	28.79	–3.27	25.61	51.10
25–475	30.75	–4.62	28.03	54.20
25–550	33.24	–6.49	30.36	57.10
25–625	35.16	–8.49	32.62	59.30

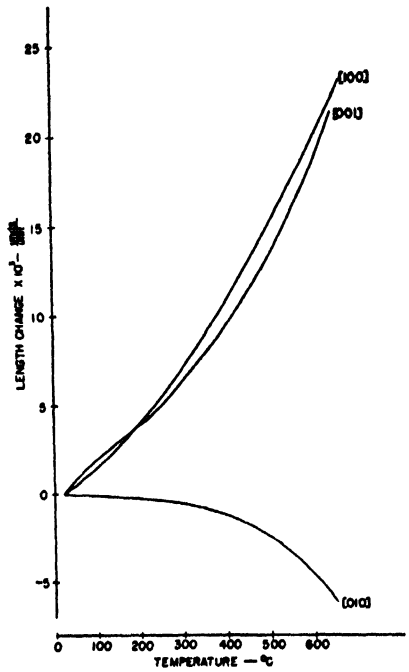

Figure 24. Length changes of the three alpha uranium principal crystallographic directions as a function of temperature; macro M-17545

Table VII records the volumetric thermal expansion coefficients and the linear thermal expansion coefficients for the three principal crystallographic directions of alpha uranium. The values were determined from the mean expansions over the temperature intervals indicated. The equations which express the volume and the three principal crystallographic directions at temperature T (°C) as a function of the original dimensions and the temperature are as follows:

$$V_T = V_{25}\,(1 + 32.03 \times 10^{-6}T + 32.87 \times 10^{-9}T^2 + 16.25 \times 10^{-12}T^3) \quad (1)$$

$$L_{[100]T} = L_{[100]25}\,(1 + 10.64 \times 10^{-6}T + 47.46 \times 10^{-9}T^2 - 16.65 \times 10^{-12}T^3) \quad (2)$$

$$L_{[010]T} = L_{[010]25}\,(1 - 1.503 \times 10^{-6}T + 9.09 \times 10^{-9}T^2 - 31.79 \times 10^{-12}T^3) \quad (3)$$

$$L_{[001]T} = L_{[001]25}\,(1 + 19.69 \times 10^{-6}T - 7.79 \times 10^{-9}T^2 + 43.26 \times 10^{-12}T^3) \quad (4)$$

Figure 24 shows the curves of the length changes for the three principal crystallographic directions as a function of temperature. The length changes for the [100] and [001] directions are similar, the former being slightly larger. The length change for the [010] direction is negative; the higher the temperature the smaller the dimension becomes.

Table VIII. Mean Thermal Expansion Coefficients of Alpha Uranium Rods for Varying Fabrication Treatments and Per Cent Reductions in Area, (Mayfield, ANL)

Treatment prior to final rolling	Nominal finish Rolling temperature, °C	Mean thermal expansion coefficients (25°–100°C) × 10^6 units/unit/°C			
		0% reduction	10% reduction	45% reduction	70% reduction
600°C rolled - 80%	300	13.42	10.16	8.62	8.94
600°C rolled - 80% and beta treated	300	15.98	12.8	10.02	9.17
600°C rolled - 80% and beta treated	600	15.86	14.9	13.39	12.71

Thermal Expansion Coefficients and Characteristics Determined From Dilatometric Measurements

Dilatometric curves of single crystal expansions have been determined for five alpha uranium samples by Lloyd (ANL). The crystallographic directions of testing for all these crystals were within a few degrees of the [010] axes. A typical expansion curve as a function of thermocouple millivoltage is shown in Fig. 25. The thermal expansion coefficient is slightly positive at low temperatures. As the temperature increases the thermal expansion coefficient decreases, passes through an inversion, and becomes negative. The temperature at which the inversion occurs is dependent upon the angular misorientation of the testing direction from the [010] direction; the greater this misorientation the higher is the temperature of inversion. These experimental determinations prove physically that the linear thermal expansion coefficient in the [010] direction is negative. No attempt has been made to analyze these data for thermal expansion coefficients in the three principal directions of the alpha uranium lattice. The errors in the coefficients for the [100] and [001] directions would be great because these are considerably displaced (nearly 90 degrees) from the direction along which the thermal expansion measurements were made.

The pronounced anisotropy of thermal expansion in alpha uranium is exemplified by the dependency of the measured values upon the previous fabrication history, thermal history, and direction of testing of polycrystalline samples. Tables VIII and IX give representative values of the mean thermal expansion

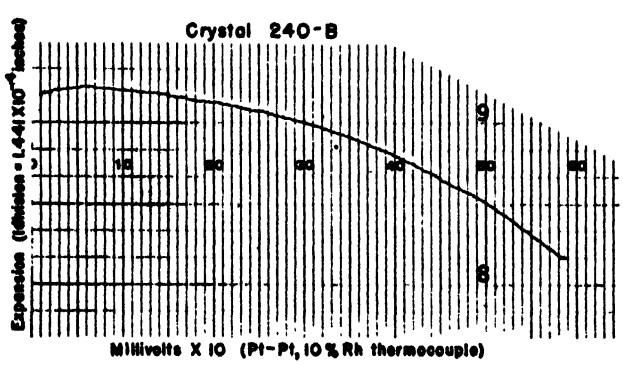

Figure 25. Typical expansion curve of an alpha uranium single crystal as a function of thermocouple millivoltage; macro M-17569; the crystallographic direction of testing was 90 degrees from the (100), 10 degrees from the (010), and 80 degrees from the (001); the initial specimen length was 0.1484 inch

coefficients of uranium rods of various histories between 25°C and 100°C. All thermal expansion coefficients were determined parallel to the axis of the rod. The mean thermal expansion coefficient of essentially randomly oriented polycrystalline material (β treated) in this temperature range is about 16 × 10^{-6} units/unit/°C. Increased per cent reduction in area at 300°C and 600°C causes the mean thermal expansion coefficient to decrease; the coefficient of the former is reduced more than the latter. For a constant per cent reduction in area, the mean thermal expansion coefficient is reduced with a decrease in rolling temperature. Recrystallization causes the mean thermal expansion coefficient to be decreased over that observed on the material in the as cold rolled condition.

These data are consistent with the preferred orientations determined for the same specimens by Mueller (ANL). Increased per cent reduction in area causes an increase in the (010) preferred orientation. The [010] direction in alpha uranium has a negative thermal expansion coefficient. An increase in the (010) preferred orientation should result in a decrease in the mean thermal expansion coefficient; the data are in agreement. At 300°C the increase in (010) preferred orientation is more pronounced than at 600°C; thus, the mean thermal expansion coefficients for material rolled at the former temperature are decreased more rapidly than those for the latter. As the temperature of rolling is increased, for a constant per cent reduction, the (010) preferred orientation is decreased; again, the mean thermal expansion coefficients are in agreement. Recrystallization causes the (110) preferred orientation component to be shifted towards the [010] direction and the (010) preferred orientation is shifted away from the [010] direction; the former component is shifted further towards the [010] than the latter is shifted away from it. Qualitatively, this indicates that the mean thermal expansion coefficient should be reduced by recrystallization. The data indicate this to be true.

The mean thermal expansion coefficient data given above do not represent the nature of the entire thermal expansion curves for these materials. This is particularly true for rods rolled at 300°C and recrystallized. A series of typical expansion curves obtained by Lloyd (ANL) in a direction parallel to the rolling direction for such a specimen is shown in Fig. 26. As the temperature increases, the specimen elongates

Table IX. Mean Thermal Expansion Coefficients of Alpha Uranium Rods for Varying Temperature of Rolling and Thermal Treatment, Uniform 75% Reduction in Area, (Mayfield, ANL)

Nominal rolling temperature, °C	*Mean thermal expansion coefficients (25°–100°C) × 10^6 units/unit/°C*	
	As rolled	*Recrystallized at approximately 625°C*
300	8.5	6.8
400	9.3	7.9
500	11.4	9.2
600	12.9	-
640	14.1	-

with a positive thermal expansion coefficient until an inversion point is reached at approximately 180°C; continued heating causes the specimen to contract. The cooling curve does not follow the heating curve because of the plastic interaction between grains. When the sample again reaches room temperature it is longer than it was prior to the thermal cycle. Additional cycling of the sample further increases its length.

Similar thermal expansion curves for 300°C rolled and alpha annealed uranium rods have been observed by Schwope (BMI). In general, an increase in length as a result of each thermal cycle occurs regardless of the temperature interval of cycling. For a particular sample, depending upon its past fabrication and thermal history, it is possible to select a temperature interval of cycling which results in a zero net length change of the specimen. Uranium rods rolled at 600°C show a similar increase in length as a result of thermal cycling, but to a lesser extent. In these cases the expansion curves do not go through an inversion, but rather the thermal expansion coefficients are positive at all temperatures.

The thermal expansion characteristics of alpha uranium developed by previous fabrication and thermal history may be changed by causing the sample to undergo phase transformation. A typical expansion versus thermocouple millivoltage curve obtained in a direction parallel to the rolling direction for a 300°C rolled and 575°C annealed sample is shown in Fig. 27 (Lloyd, ANL). The specimen shows an initial elongation at low temperatures followed by a contraction as the temperature is further increased. At the alpha to beta transformation temperature the sample increases in length abruptly. Within the beta phase expansion is at a uniform rate. At the beta to gamma transformation temperature the sample again increases in length abruptly, but to a lesser extent than at the alpha to beta transformation temperature. Expansion in the gamma phase is at a uniform rate. Upon cooling the sample contracts uniformly in the gamma phase and decreases in length as it passes through the gamma to beta transformation temperature. The contraction during this phase transformation is smaller than that observed upon heating. The specimen contracts uniformly within the beta phase, but at a different rate than that observed upon heating. This behavior would be expected because of the lattice anisotropy of the beta phase. Further cooling through the beta to alpha transformation temperature results in a sharp contraction, but of smaller amount than that observed upon heating through the alpha to beta transformation. Subsequent cooling in the alpha region results in a uniform contraction of the sample. The difference in the heating and cooling curves in the alpha region is brought about by a reorientation of the structure resulting from destruction of the preferred orientation by passage through phase transformations.

The expansion characteristics of the alpha phase, after passage through phase transformation temperatures, are not predictable. In some cases the specimen may show an expansion upon cooling after phase transformation (Fig. 28). The curve for a specific sample may and probably would be entirely different from either of the curves shown here. In general, however, there is a greater tendency for specimens to show cooling curves in the alpha region similar to that of Fig. 27, regardless of the previous fabrication and thermal history.

The thermal expansion curves for rolled uranium sheet materials differ from those obtained from rod specimens. This behavior is that which is expected as a result of the differences in preferred orientation developed in rolled uranium sheet over those developed in rolled uranium rods. Figure 29 (Lloyd, ANL) is a typical series of length change curves obtained

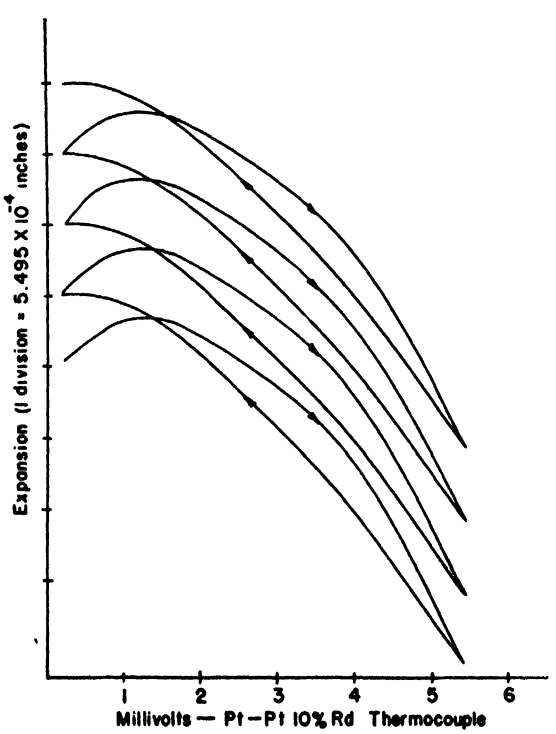

Figure 26. Thermal expansion curves for a 300°C rolled alpha uranium sample; macro M-17546; cycled in alpha range (30° to 630°C); the bottom curve represents the first thermal cycle expansion curve, the curve directly above that represents the second thermal expansion curve, etc

from uranium sheet which was given a final reduction of 75% in area at 300°C. The thermal expansion curves for three mutually perpendicular directions are shown: curve *A* is in the plane of the sheet parallel to the rolling direction, curve *B* is in the plane of the sheet perpendicular to the rolling direction, and curve *C* is perpendicular to the plane of rolling. The latter curve was obtained from the volumetric thermal expansion of alpha uranium, as calculated from X-ray lattice parameter determinations and the data of curves *A* and *B*. The thermal expansion curve in the direction parallel to the rolling direction shows a relatively low value of thermal expansion coefficient as compared to those for the other two directions. It does not, however, show a negative thermal expansion coefficient as do the curves obtained from rods reduced in area to a comparable reduction. This agrees with the preferred orientations of the two materials. Qualitatively, the (010) component in the rod orientation is stronger than that in the sheet for comparable reductions in area. The thermal expansion curves in the other two directions of the sheet material are similar despite the fact that there is a difference in the preferred orientations. These preferred orientation differences involve primarily the [100] and [001] directions. The thermal expansion curves for these crystallographic directions (Fig. 24) do not differ greatly; this accounts for the similarity of curves *B* and *C*.

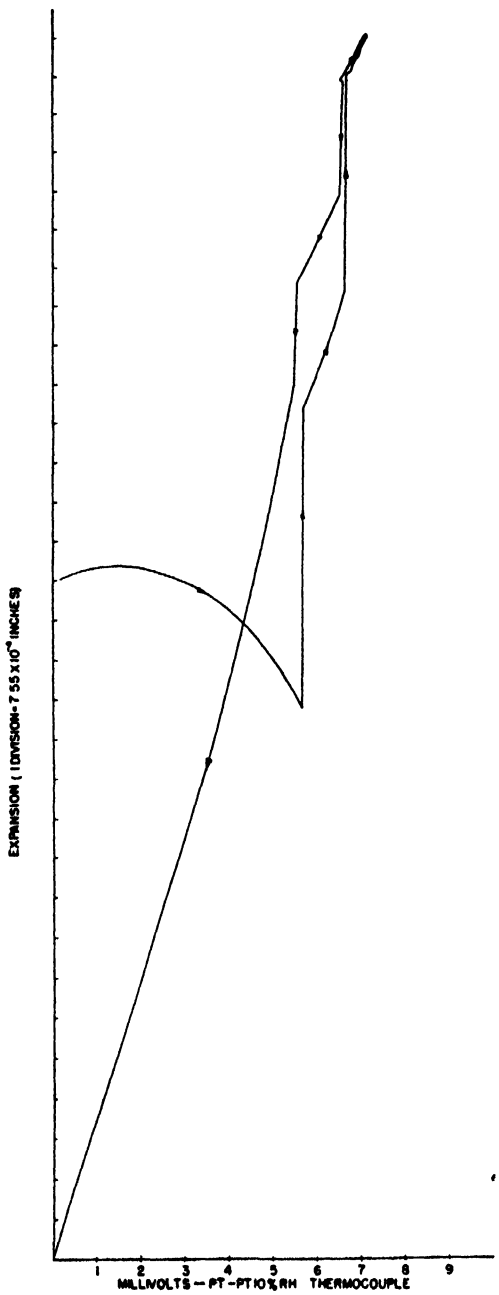

Figure 27. Typical thermal expansion curve of a 300°C rolled and 575°C annealed uranium sample; macro M-17570; the curve illustrates the changes in expansion characteristics as a result of passage through phase transformations.

It was stated above that true measurements of the thermal expansion coefficients of beta uranium cannot be obtained from polycrystalline samples because of its lattice anisotropy. No studies of the lattice parameters of pure uranium as a function of temperature are available, nor are thermal expansion curves for single crystals. Dilatometric studies of polycrystalline uranium in the beta phase indicate the mean thermal expansion coefficient over the temperature range of 675–750°C to be from 9.6 to 47.6 $\times$ 10^{-6} units/unit/°C (Lloyd, ANL). The beta uranium lattice parameters of a 1.4 weight per cent chromium-uranium alloy have been determined at 20°C and 720°C.[10] The beta phase, which is stable at 720°C in an alloy of this chromium content, can be retained in a metastable state at 20°C by quenching. From the lattice parameters determined at these two temperatures, the mean thermal expansion coefficient was calculated to be 23 $\times$ 10^{-6} units/unit/°C for the a^0 axis and 4.6 $\times$ 10^{-6} units/unit/°C for the c_0 axis. The maximum value obtained from the dilatometric studies greatly exceeds that calculated for the a_0 axis. This discrepancy can possibly be attributed to a nonlinear relationship between the a_0 lattice parameter and temperature. The slope of this curve may be greater at higher temperatures, and thereby yield a greater value of mean thermal expansion coefficient over a small temperature range at high temperatures.

The mean thermal expansion coefficient data obtained from dilatometric studies of polycrystalline gamma uranium are valid because of the isotropic nature of its crystallographic structure. The average mean thermal expansion coefficient of gamma uranium over the temperature range 775°C to 800°C, as determined from several dilatometric tests by Lloyd (ANL), is 22.6 $\pm$ 1.0 $\times$ 10^{-6} units/unit/°C. The mean thermal expansion coefficient for gamma uranium over the temperature range room temperature to 805°C can be calculated from lattice parameter data. Thewlis[11] has reported the lattice parameter for gamma uranium at 805°C. Wilson and Rundle[12] have determined the room temperature lattice parameter

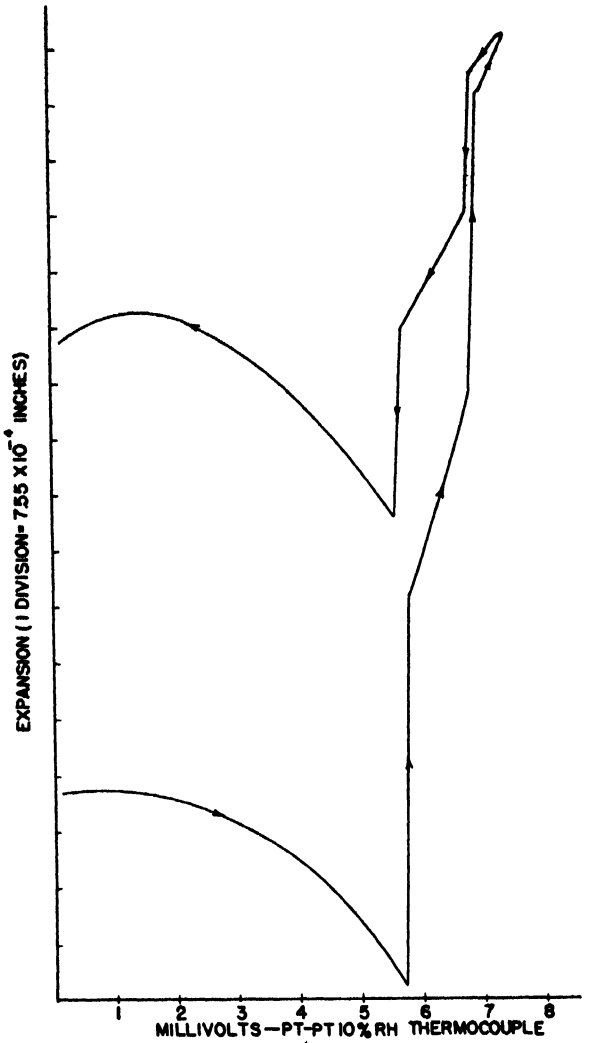

Figure 28. Thermal expansion curve for a 300°C rolled uranium sample; macro M-17571; the curve shows an anomalous expansion upon cooling in the alpha phase

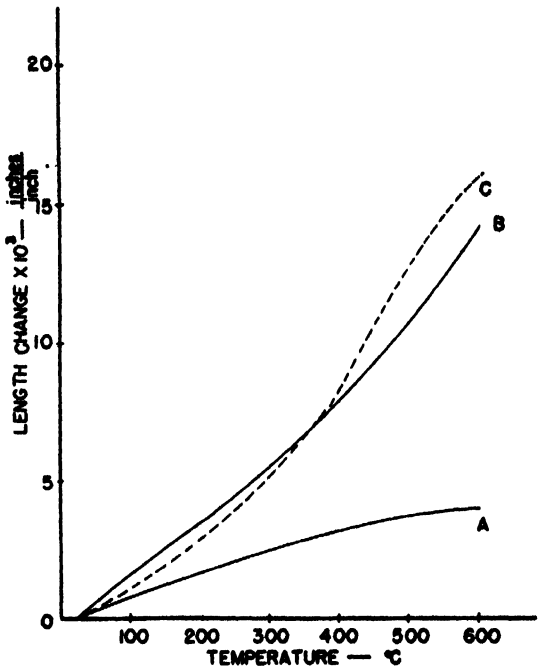

Figure 29. Thermal expansion curves for uranium sheet given a final reduction of 75% in thickness at 300°C; macro M-17547; curve A is the thermal expansion curve measured in the plane of the sheet parallel to the direction of rolling; curve B is the thermal expansion curve measured in the plane of the sheet perpendicular to the direction of rolling; curve C is the thermal expansion curve in a direction perpendicular to the plane of the sheet. The latter curve was determined from the volumetric expansion of alpha uranium as calculated from X-ray data and the experimentally measured curves A and B

of gamma uranium stabilized with molybdenum. These lattice parameters were used to extrapolate to the value at zero per cent molybdenum. The mean thermal expansion coefficient for this temperature range, as calculated from the lattice parameters, is 18×10^{-6} units/unit/°C. The difference between the value determined from dilatometric studies and that which was calculated is not excessive, taking into consideration the differences in the temperature ranges.

VI. THERMAL CYCLING EFFECTS IN URANIUM

A more detailed paper on thermal cycling effects has been prepared for Session 18B by Chiswik and Kelman.† A short abstract of their paper is included here since thermal cycling effects are a rather important feature of the physical metallurgy of uranium. It has been known since 1946 that polycrystalline uranium metal may undergo rather substantial dimensional changes when subjected to repeated heating and cooling in the alpha phase temperature range (room temperature to 660°C). In cast metal of coarse grain size, the dimensional changes manifest themselves in the form of surface roughening; in wrought metal, when fabricated in the alpha-phase temperature range, the dimensional changes take the form of substantial elongations, generally in the directions coincident with the direction of working of the metal. An example of this behavior is illustrated in Fig. 30, in which the elongation of a wrought specimen to nearly six times its original length with a corresponding decrease in diameter, has occurred.

The magnitude of the deformations is a function of the number of cycles to which the material is subjected and is affected by both structural and cycling process variables. Preferred orientation is a necessary condition for unidirectional growth to occur; the extent of the growth depends upon the sharpness of texture developed and the grain size. The highest growth rates occur in material with highly developed textures coupled with a small grain size. In conformity with these observations material rolled at 300°C elongates more than material rolled at 600°C.

Material whose prior texture has been randomized by a beta heat treatment shows the least tendency to

† P/557, Vol. 9

3695



Figure 30. Appearance of test piece after 3000 cycles between 50°C and 600°C; macro 10926, original specimen size shown

grow. Accompanying such heat treatments, however, there is usually an increase in grain size which results in an increase in surface roughening. If uranium is prepared by a process which results in both random orientation and fine grain size, such as by powder metallurgy methods, it neither grows nor surface roughens. In view of the behavior of powder metallurgical compacts one may interpret the slight growth that one observes in beta treated wrought material as being caused by remnants of texture not completely eliminated by heat treatment.

The dimensional changes are also functions of the following cycling variables: (*a*) rates of heating and cooling, (*b*) temperature level, (*c*) temperature range, and (*d*) time at temperature. The greatest growth rates per thermal cycle are obtained when slow heating and fast cooling are combined with a large temperature range of cycling. Little growth results if the upper temperature of the cycling range is below 350°C; above that temperature the higher the temperatures of cycling the greater the growth for a given temperature range. A constant growth value may be approached with increasing temperatures under certain cycling conditions. With increasing holding time above about 350°C the growth rate increases rapidly at first and then more slowly until it approaches a constant value. The higher the temperature the shorter the time required for the growth rate to level off.

Thermal cycling also results in microstructural changes, the most important of which are: polygonization or subgraining, the development of porosity with an accompanying decrease in apparent density, crystallographic slip, roughening of grain boundaries, and grain boundary migration. In material of relatively low purity thermal cycling results in extensive formation of porosity. That the formation of porosity is not inherent in the mechanism is shown by the fact that high purity uranium shows no evidence of porosity even though its rate of deformation is equivalent to that of impure metal.

The amount of internal deformation is dependent upon the relative orientations of adjoining grains; where [010] directions are almost parallel the deformation is at a minimum and increases with increasing spread between these directions. Random orientation increases the amount of internal microscopic deformation; however, these deformations do not appear as over-all dimensional changes. Preferred orientation results in less internal microscopic deformation; however, unidirectional growth along the length of the specimen does result.

The formation of a subgrain structure is most pronounced in coarse-grained material and is shown to develop near grain boundaries in coarse-grained uranium of high purity that has undergone relatively few thermal cycles. Grain boundary migration was very conspicuous in fine-grained polycrystalline specimens, but no evidence of grain boundary migration was noted in coarse-grained specimens. If any grain boundary slip had taken place it was very small and difficult to discern.

Alloying elements in low concentration do not decrease the growth of alpha-fabricated uranium; in fact, in some instances the growth is increased, presumably because of smaller grain size. Alloy additions decrease the surface roughness after a randomizing beta or gamma treatment because they promote grain refinement. To eliminate surface roughness, higher concentrations of alloying additions are often required, in some cases as high as 2 weight per cent.

Most of the mechanisms that have been proposed to explain the dimensional and structural changes that occur in uranium when thermal cycled are based on intergranular stresses developed as a result of anisotropy in the thermal expansion of alpha uranium. One proposed mechanism provides for a ratcheting condition to make the deformation nonreversible by assuming grain boundary flow to relax the stress at high temperatures and crystallographic slip to relax the oppositely directed stresses at low temperatures. Another proposed mechanism does not assume grain boundary flow but provides for continued elongation on thermal cycling as a result of creep occurring in the stronger of adjacent grains at the high temperature part of the thermal cycle and plastic deformation of the weaker grain in the low temperature part of the cycle. These mechanisms are not in complete agreement with the available experimental evidence. Objections to some of the proposed mechanisms might be minimized by resorting to the observed subgraining coupled with diffusion as a means of reorientation at grain boundaries to accommodate the necessary dimensional changes.

VII. IRRADIATION EFFECTS IN URANIUM

A more detailed paper on irradiation effects in uranium has been prepared by Paine and Kittel (ANL)‡ as a contribution to Session 11B of this

‡ P/745, Vol 7.

conference. A brief abstract of their paper is included here since irradiation effects have become an important part of the physical metallurgy of uranium.

Kittel and Paine (ANL) and Turkalo (KAPL) have shown that single crystals of alpha uranium, when irradiated in a reactor, progressively elongate in the [010], shorten in the [100], and remain relatively unaffected in the [001] lattice directions. Lineage and subgrained crystals elongate at rates appreciably greater than do single crystals, and polycrystalline rod specimens with [010] texture highly developed by cold working grow axially at more than twice the rate observed in single crystals. In the latter case, however, compensating shrinkage along the diameter occurs. The accompanying volume changes are negligible when compared with the magnitude of distortion.

A number of basic mechanisms have been proposed to explain the anisotropy of dimensional properties. Many of these models are based on thermal cycling anisotropy, and are discussed in a paper on that subject given in this Session by Chiswik and Kelman (ANL).§ The few definitive data presently available on the irridation mechanism appear to favor either the ideas of Seigle and Opinsky (SEP), based on anisotropy of diffusion of vacancies and interstitials, or the proposals of Last and McLachlan (HAPO), which are based on anisotropic flow resulting from stresses induced by fission thermal spikes within the crystalline lattice. Accentuation of irradiation growth by the presence of grain boundaries also indicates that additional mechanisms, such as the fission spike ratchet proposed by Burke, Howe and Lacy (KAPL), may operate in polycrystalline material.

The magnitude of linear distortion in irradiated uranium is quite sensitive to previous mechanical fabrication procedure and thermal treatment. The effect of these metallurgical factors may readily be understood in terms of resultant grain size and of the type and degree of preferred orientation. Rolling of rods at 300°C induces a [010] axial texture, and the resultant growth is directly dependent on the total rolling reduction. Rolling above the alpha recrystallization threshold (~400°C) brings the [110] and even the [100] components into the texture, so that for increasing rolling temperatures the positive irradiation growth rate falls off to zero and may become negative in rods rolled at 600–650°C.

Growth is most rapid in fine-grained material. Alpha recrystallization of cold rolled metal alters the preferred orientation somewhat and increases grain size and reduces the growth rates appreciably, an effect attributable mainly to grain coarsening. Beta or gamma recrystallization almost completely removes the preferred orientation resulting from alpha working, so that the growth rates are radically reduced. For example, a growth rate $G_t = 850$ microinches/inch/ppm burnup in 300°C rolled rod may be reduced to $G_t = 15$–20 microinches/inch/ppm burnup by heating into the low beta range and quenching.

Nonlinear distortions such as surface roughening and warp also occur. Grossness of surface roughening is a function of grain size; in textured material the surface bumps are elongated into ridges or striations. Warp has been shown to result from nonuniform grain size. Change in volume of irradiated uranium is about twice as great as can be accounted for by the creation of fission products.

Small additions of alloying elements to uranium affect the irradiation behavior in two possible ways: (1) by refining and stabilizing the grain size, and (2) by stabilizing the gamma phase which is isotropic under irradiation. The first effect can be achieved by the use of chromium, niobium, molybdenum or zirconium, coupled with proper heat treatment, whereas stabilization of the gamma phase can be achieved with niobium, molybdenum or zirconium in somewhat greater amounts. Carbon, a normal impurity, has no great effect on radiation growth in unalloyed uranium, but seems to accelerate radiation growth in rolled and alpha recrystallized alloys of chromium or zirconium alloys and to retard this effect in the same material after beta treatment [Kittel and Paine (ANL)].

The strength and ductility of uranium is strikingly affected by irradiation. Hueschen and Cadwell (HAPO) report that standard 0.250-inch diameter specimens which had received 0.035 (atomic) per cent burnup at 120°C suffered a loss of 27% in ultimate strength, more than doubled the yield strength and dropped from 17% to 0.36% in elongation (1-inch gage length). A 15-hour anneal in vacuo at 400°C caused a further decrease in both ultimate strength and yield, and a hot tensile test at 285°C showed no significant alteration of these values. Hardness changes are quite appreciable although erratic and dependent upon previous mechanical history. The hardness of a large number of alpha-recrystallized specimens increased from VHN 214 ± 12 before irradiation to 275 ± 10 at 0.01% burnup and to 315 ± 20 at 0.10% burnup [Kittel and Paine (ANL)].

VIII. MECHANICAL PROPERTIES OF URANIUM

Since uranium is a highly anisotropic material, the mechanical properties are affected considerably by orientation, a result of fabrication and heat treatment. So far as tensile results are concerned, uranium has a very low proportional limit, consequently there is very little straight line portion to the stress-strain curve obtained under normal practice. Grossman and Priceman[13] obtained compressive values of Young's modulus, Poisson's ratio, shear and bulk moduli, modulus of resilience, proportional limit, and yield strength using SR-4 strain gages on two specimens of hot-rolled uranium 2.5 in. long by 0.900 in. in diameter. Stress-strain curves for the low stress re-

§ P/557, Vol. 9

gions of the initial loading are illustrated in Fig. 31. A complete stress-strain curve is shown in Fig. 32. The longitudinal and transverse strains are plotted as a function of stress in Fig. 33. Elastic properties obtained are summarized in Table X. The authors conclude from their limited results that there is a very low but well-defined proportional limit (3000 psi), Poisson's ratio is not a constant but increases with increasing stress, and that any determination of Young's modulus and an offset yield strength by the standard initial tangent method is of little practical significance. Yield strength values may be obtained by an arbitrary method outlined by Chiswick, Mayfield and Mueller (ANL). Load values are chosen so that, upon removal, the resulting permanent set is near the predetermined offset value. Slight corrections may be made by passing a straight line through the required offset value and parallel to a line between the end point and zero stress point of an unloading curve.

As a result of the capricious nature of uranium, numerous attempts have been made to determine the elastic constants by dynamic means based on the measurements of sound velocities. Table XI contains the results of Laquer, McGee and Kilpatrick,[14] Reynolds,[15] and Kammer, Vigness and Cardinal of Naval Research Laboratory (NRL). The manner in which some of the elastic constants change with temperature is shown in Fig. 34. Orientation variations, differences in fabrication and treatment, as well as individual techniques, probably account for the range of values reported. Still, the most accurate elastic constant values are probably obtained in this manner in contrast with a certain amount of guesswork involved in treating ordinary tensile test data.

Mayfield and Chiswik (ANL) have determined the variation of tensile properties with rolling temperature and roll pass design in both the as-rolled and annealed conditions. Rolling temperature was measured using a radiation-type pyrometer and a fast-acting recorder. For the single stand mill used,

Table X. Elastic Properties of Uranium in Compression (Average Values)*

Modulus of elasticity, psi	25.5×10^6
Poisson's ratio (limited value at zero stress)	0.20
Shear modulus, psi	10.6×10^6
Bulk modulus, psi	14.2×10^6
Modulus of resilience in lb/in³	0.176
Proportional limit, psi	3000
Yield strength, (approx.) psi	
0.1% offset	27,000
0.2% offset	33,000

* Grossman, N. and Priceman, S., *Compressive Properties of Uranium*, Nucleonics *12*: No. 6, pp 68–69 (June 1954).

the actual finish rolling temperature was found to be considerably below the nominal preheat bath temperature for 500°, 600°, and 640°C rolling, and somewhat higher than the bath temperature for 300°C and 400°C rolling. For rods rolled at 500°C and below, the rolling direction texture was predominantly (010–120), which changes to a (140) upon annealing. [Most of the 600°C and 640°C rolled rods were recrystallized in the as-rolled condition, and the texture was predominantly (110–010).] The property test results are summarized in Figs. 35 and 36. Significant variations of tensile properties in the rolling direction with rolling temperature are apparent. The effect of roll pass design was not pronounced in most cases. Annealing at 300°C rolled uranium in an argon atmosphere was found to lower the ductility, the decrease becoming more pronounced with higher annealing temperatures for longer periods of time. Annealing in vacuum produces no such effect. Typical results are shown in Table XII. Similar observations have been reported by Hanks, Taub, and Doll (LASL), and by Waber (LASL) who attributed this behavior to a hydrogen embrittlement effect. The results of Waber indicate that hydrogen contents in the vicinity of 2 ppm will reduce the tensile elongation of uranium, and, further, that most of the dele-

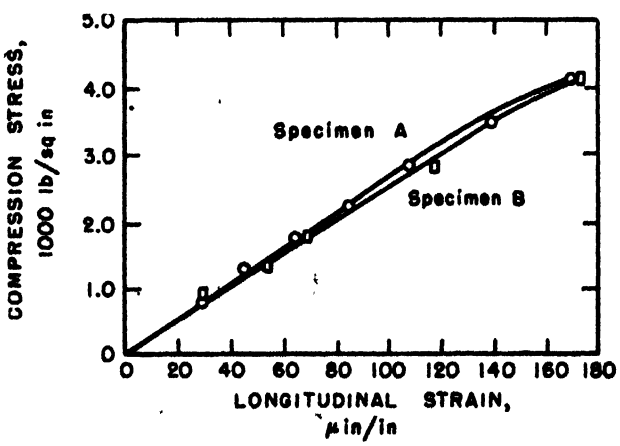

Figure 31. Compression stress-strain curves of hot-rolled uranium in low stress region (from Grossman, N., and S. Priceman, *Compressive Properties of Uranium*; Nucleonics 12: No. 6, pp 68-69, June 1954)

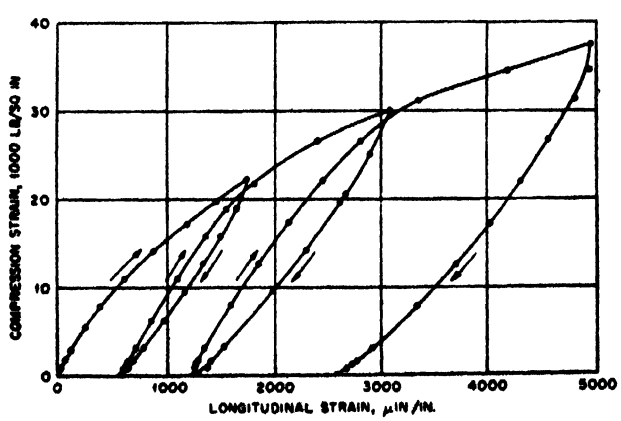

Figure 32. Complete compressive stress-strain curve for hot-rolled uranium specimen B (From Grossman, N. and S. Priceman, *Compressive Properties of Uranium*, Nucleonics 12: No. 6, pp 68-69, June 1954)

Table XI. Summary of Elastic Constant Data Obtained by Ultrasonic Techniques

Condition	*Young's modulus (psi × 10⁻⁶)*		*Shear modulus (psi × 10⁻⁶)*		*Poisson's ratio*		$\frac{1}{E}\frac{dE}{dT}$ *(10⁻⁴/°C)*
Laquer, McGee and Kilpatrick‡							
1 Swaged, annealed	29.1		11.9		0.22		5.0 avg.
3 Extruded	29.3		12.0		0.21		
4 Extruded	30.3		12.1		0.25		
7 Cast	29.5		12.1		0.22		
8 Cast	30.0		12.1		0.24		
Reynolds§ Uranium cubes, alpha-rolled and water-quenched from 740°C	25.5		10.2		0.25		
Kammer, Vigness and Cardinal (NRL)							
Group A:	25°C	300°C	25°C	300°C	25°C	300±C	
No history	27.0 25.5* 22.9†	23.3	11.5	9.61	0.18	0.22	4.9
Group B:							
Alpha-rolled and annealed	26.2	22.6	11.0	9.09	0.19	0.24	5.0
½ hour at 600°C	26.4	22.5	11.2	9.14	0.19	0.24	5.4
Alpha-rolled and Beta-treated	28.0	23.6	11.9	9.53	0.18	0.23	5.6
70 seconds at 720°C	29.1	24.1	12.3	9.76	0.19	0.24	6.3
Group C:							
Rough rolled to 1½ in. diam. at 600°C. Finish rolled to 1 in. diam. at temperature indicated:							
630°C	27.4	23.6	11.4	9.50	0.20	0.23	5.0
550°C	26.8	22.9	10.9	9.32	0.20	0.24	5.3
480°C	26.4	22.8	11.0	9.19	0.20	0.24	5.0

* Using method of Laquer, McGee and Kilpatrick.
† Static test in compression.
‡ See reference 14.
§ See reference 15.

terious effects of hydrogen can be removed by vacuum annealing. The better the vacuum the greater the improvement in elongation.

A recent study by Marsh, Muehlenkamp and Manning (BMI) on the effect of hydrogen and heat treatment on the ductile transition in alpha uranium does not completely confirm these views. A more complex phenomenon is believed to be involved. The transition from ductile to semi-brittle behavior in tension was observed in the temperature range 25°C to 65°C. Tensile data are summarized in Tables XIII and XIV. The transition was found sensitive to residual strain, strain rate, hydrogen content, and, to a smaller extent, heat treatment. The effect of hydrogen in the composition range 0.3 to 0.47 ppm is observed principally in the values for reduction of

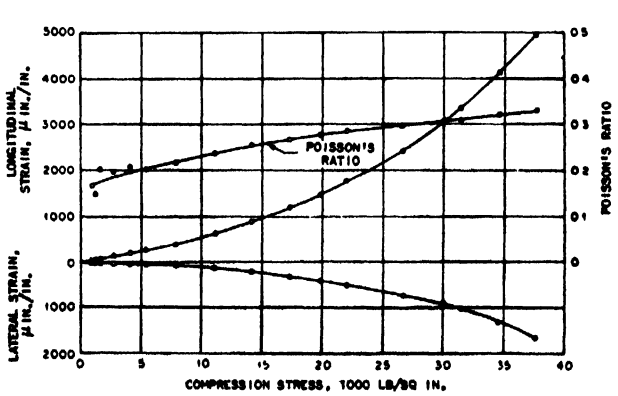

Figure 33. Longitudinal and transverse stress-strain curves and Poisson's ratio for hot-rolled uranium specimen 8 (From Grossman, N. and S. Priceman, *Compressive Properties of Uranium*, Nucleonics 12: No. 6, pp 68-69, June 1954)

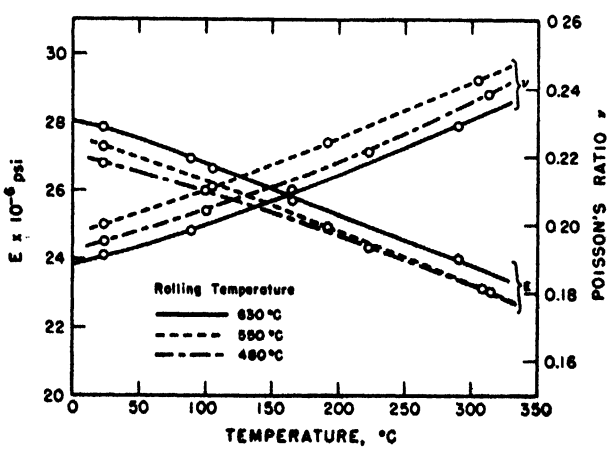

Figure 34. Young's modulus and Poisson's ratio as a function of rolling temperature (Kammer, Vigness and Cardinal (NRL))

area. At 4.7 ppm hydrogen, the reduction of area at fracture is noticeably less than for material that has been dehydrogenated. On the basis of the data available the authors conclude that the transition appears to be similar to transitions observed in other metals not of the face centered cubic type and is not the result of hydrogen embrittlement. The exact role of hydrogen on the tensile properties is not clearly resolved and further work to clarify its behavior will be required. Charpy-notched impact tests were conducted on some of this same material and the results are shown in Fig. 37. A marked transition occurs in the 100–150°C temperature range, with a further gradual decrease in energy absorbed with decreasing test temperature.

Uranium rapidly loses strength at elevated temperatures as shown by hot hardness curves (Holden, KAPL) and by tensile tests at elevated temperatures (Saller, BMI). Typical tensile properties at elevated temperatures are given in Table XV.

Other mechanical properties such as hardness, further data on impact strength, creep, etc., have received limited attention and have been reported by many investigators. In view of all the variables which affect the properties of uranium, many reported results are of little significance because the condition of the material is not clearly outlined. As an example, many previously reported creep values are questionable, since the small amount of thermal cycling which occurs during normal creep testing has been found sufficient to cause growth in uranium (Schwope, BMI).

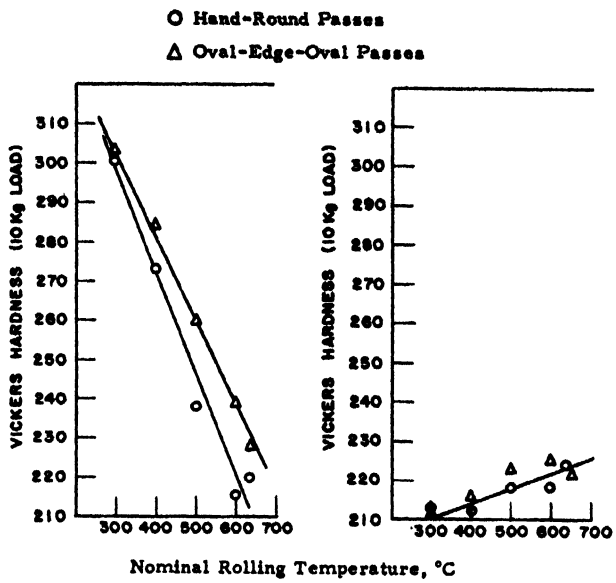

Figure 36. Hardness of uranium as rolled and annealed (Mayfield and Chiswik (ANL)

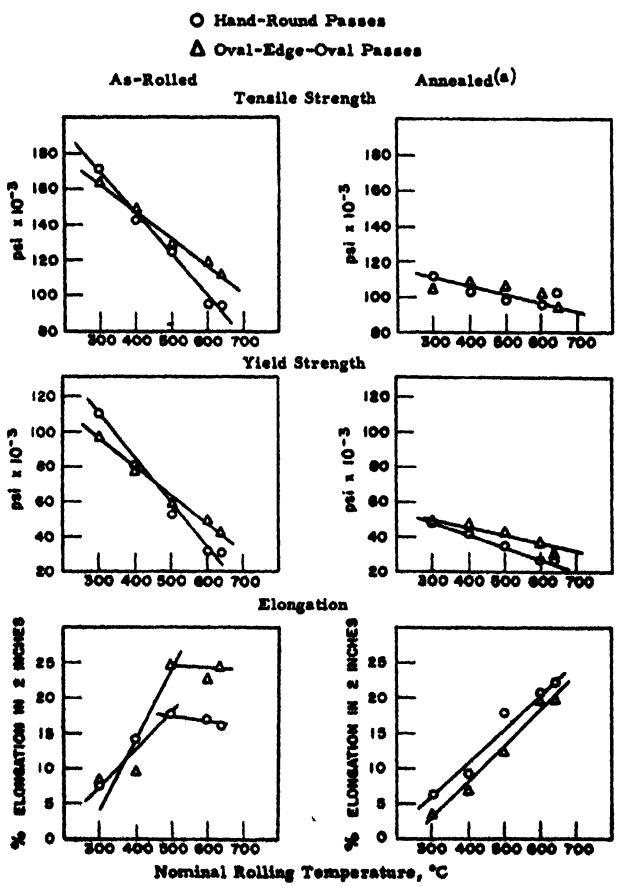

Figure 35. Tensile properties of uranium as rolled and annealed (Mayfield and Chiswik (ANL)

IX. AQUEOUS CORROSION OF URANIUM AND HIGH URANIUM ALLOYS

Uranium reacts with water to form the stable oxide UO_2 and with hydrogen to form UH_3. The reaction rate between uranium and hydrogen is at all temperatures considerably higher than that between uranium and water [Straetz and Draley of the Metallurgical Laboratory of the University of Chicago (MUC); Albrecht and Mallett (BMI)]. Two types of corrosion of uranium occur in water, depending on whether a protective film of UO_2 is formed and retained on the metal surface. In air-saturated distilled water protective films are formed, as shown

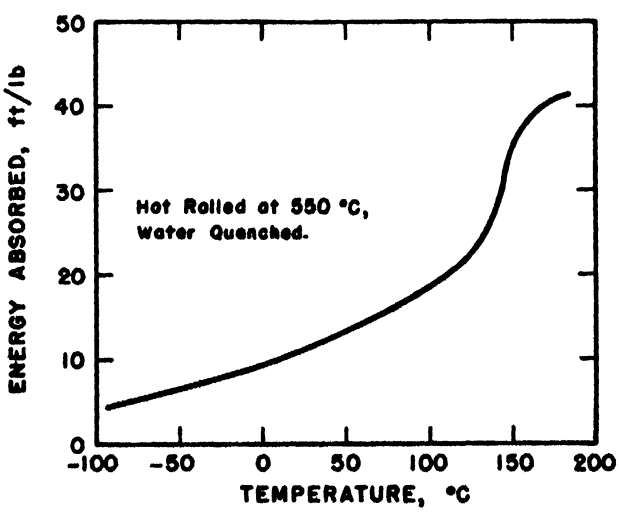

Figure 37. Impact strength of hot rolled uranium (Marsh, Muehlenkamp, and Manning (BMI))

Table XII. Variation of Properties of 300°C Round Rolled Uranium Rods with Annealing Treatment [Mayfield, Chiswik (ANL)]

Annealing treatment	Grain size average diameter (mm)	Ultimate tensile strength (psi)	Yield strength 0.2% set (psi)	Reduction of area (%)	Elongation in 2 in. (%)
575°C, 2 hours (0.54 μ vacuum)	0.012	124,000	57,000	14	12
575°C, 2 hours (argon)	0.011	120,000	52,000	13	11
635°C, 48 hours (10–20 μ vacuum)	0.03	126,000	52,000	14	11
635°C, 48 hours (argon)	0.03	125,000	57,000	6	6
630°C, 18 hours (argon)	0.035	113,000	49,000	7	7
655°C, 48 hours (argon)	0.045	107,000	51,000	2	3
As-rolled	–	171,000	109,00	14	7.5

Table XIII. Tensile Properties at Various Temperatures of Uranium Containing Different Amounts of Hydrogen and with Varying Heat Treatments [Marsh, Muehlenkamp and Manning (BMI)]

Temperature (°C)	Hydrogen content (ppm)	Tensile strength (psi)	Elongation in 2 in. (%)	Reduction of area (%)
		As hot rolled *		
−56	0.8 ± 0.1	106,000	10.5	9.2
−18	0.8 ± 0.1	118,000	10.0	9.5
+4.5	0.8 ± 0.1	119,000	11.0	9.2
+10	0.8 ± 0.1	120,000	12.5	11.2
+24	0.8 ± 0.1	126,000	32.5	28.0
+24	0.8 ± 0.1	125,500	22.0	21.2
+49	0.8 ± 0.1	111,500	32.5	34.3
+100	0.8 ± 0.1	96,500	39.0	51.0
+177	0.8 ± 0.1	63,800	35.0	53.0
		Hydrogenated †		
−18	4.7 ± 0.5	76,000	4.5	4.9
+24	4.7 ± 0.5	84,000	8.5	8.6
+24	4.7 ± 0.5	84,000	6.0	10.0
+66	4.7 ± 0.5	86,500	16.5	13.3
+66	4.7 ± 0.5	87,000	22.5	6.6
+100	4.7 ± 0.5	81,500	28.5	20.5
+149	4.7 ± 0.5	68,000	34.5	42.5
		Dehydrogenated ‡		
−18	0.3 ± 0.1	74,000	4.5	10.7
+10	0.3 ± 0.1	74,000	7.5	6.8
+24	0.3 ± 0.1	88,000	13.5	12.9
+38	0.3 ± 0.1	98,000	17.5	15.0
+66	0.3 ± 0.1	90,000	28.5	30.5
+100	0.3 ± 0.1	80,500	30.0	41.0
+149	0.3 ± 0.1	68,500	35.5	45.0

* Rolled at 550°C, water quenched to room temperature.

† Hot rolled, dehydrogenated at 600°C (vacuum), hydrogenated at 600°C (12 atm hydrogen) and water quenched, aged at 350°C for 1 hour.

‡ Hot rolled, dehydrogenated at 600°C (vacuum) and water quenched, heated at 350°C for 1 hour.

Table XIV. Tensile Properties of Uranium under Various Conditions of Heat Treament and Strain Rate [Marsh, Muehlenkamp and Manning (BMI)]

Temperature (°C)	Hydrogen content (ppm)	Tensile strength (psi)	Elongation in 2 in. (%)	Reduction of area (%)
		As rolled *		
10	0.8	122,000	16	13
24	0.8	122,000	81	16
24	0.8	127,000	20	22
93	0.8	109,000	28	39
		Alpha annealed †		
10	0.8	82,100	6.0	7.2
24	0.8	84,200	8.5	11.4
38	0.8	96,100	14.5	15.5
52	0.8	98,000	16	18.2
93	0.8	89,000	31	34.7
		Gamma phase annealed ‡		
24	–	55,200	6.2	4
52	–	74,000	16.5	24.5
66	–	60,200	11.0	37
93	–	58,500	21.3	48
149	–	49,500	23.5	48
		Beta phase impregnated §		
24	–	71,100	5	6
66	–	78,600	12	11
93	–	74,300	18	21

* Hot rolled at 550°C, water quenched; strain rate 75 in. per minute.

† Alpha annealed 10 hours at 600°C; strain rate 0.0057 in. per minute.

‡ 940°C anneal in vacuum; strain rate 0.0057 in. per minute.

§ ½ hour at 700°C (12–15 ppm hydrogen); strain rate 0.0057 in. per minute.

Table XV. Tensile Properties of Uranium at Elevated Temperatures [Saller (BMI)]

Specimen *	Test temperature (°C)	Ultimate tensile strength (psi)	Yield strength 0.2% set (psi)	Elongation (%)
300°C rolled:				
Alpha annealed †	R. T.	111,000	43,000	6.8
Beta annealed ‡	R. T.	64,000	24,500	8.5
600°C rolled:				
Alpha annealed	R. T.	88,500	26,000	13.5
Beta annealed	R. T.	62,000	25,000	6.0
300°C rolled:				
Alpha annealed	300	35,000	17,500	49.0
600°C rolled:				
Alpha annealed	300	32,000	19,000	43.0
Beta annealed	300	27,000	15,500	33.0
300°C rolled:				
Alpha annealed	500	11,100	5100	61.0
Beta annealed	500	10,500	7100	44.0
600°C rolled:				
Alpha annealed	500	10,500	5500	57.0

* All specimens were standard 0.505 in. rounds.

† Alpha anneal is 12 hours at 600°C, slow cool.

‡ Beta anneal is 12 hours at 700°C, slow cool.

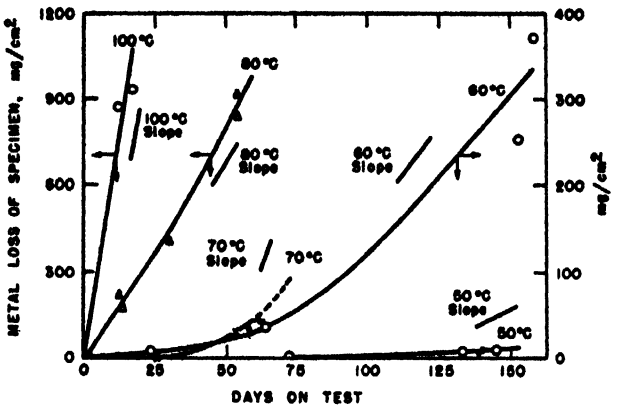

Figure 38. Corrosion of standard uranium in aerated distilled water (Mollison, English, Nelson (MUC))

in Fig. 38 [review by McWhirter and Draley (ANL)]. The curves for 50°C, 60°C and 70°C show low corrosion rates for significant periods of time, followed by increased rates of reaction. At the time when the reaction rates increased it was observed that the thin protective oxide films broke down to form areas where the corrosion product was porous and black. These areas then spread, eventually enveloping the entire sample. At the time this had occurred the corrosion rate was apparently about the same as that observed for uranium in hydrogen-saturated water, as indicated by comparison to the short lines drawn to show the slopes of the corrosion curves obtained in hydrogen-saturated water. It is observed that as the temperature is increased (and the amount of dissolved oxygen decreases) the time during which protection occurs decreases until, at 80°C and above, no apparent protection is afforded by a thin film of corrosion product.

It is believed that these experiments indicate that when thin films are formed, ionic hydrogen migrates through the oxide films and produces uranium hydride between the metal and the oxide. Such a hydride layer spoils the adherence of the oxide to the metal and its protectiveness disappears. Subsequently corrosion rates are determined by relatively rapid diffusion processes through the powdered oxide corrosion product.

In hydrogen-saturated water or degassed water corrosion is linear with respect to time, at least for significantly long periods at moderate temperatures. Corrosion rates so obtained are shown as a function of temperature in Fig. 39.

Ayres and Dillon (HAPO) have recently examined the short-time corrosion of uranium at 350°C. They report that the rate of reaction fits the extrapolated curve shown. In steam and, to a lesser extent, in water, the presence of hydride has been discovered beneath the oxide coating on samples corroded at 150°C to 180°C [Bensen, Staetz and Draley (MUC); Kelman (ANL)]. At about the time the hydride was believed to form in significant quantities the corrosion rates were observed to increase. It has generally been considered that the hydride reaction plays a significant role in increasing the total corrosion rate when the oxide corrosion product shields the metal surface from access to water. At this time the hydrogen produced in the corrosion reaction diffuses through the corrosion product (more permeable to hydrogen than to water), allowing rapid reaction of the hydrogen with uranium. When water reaches this uranium hydride, reaction occurs to form the more stable UO_2, and the hydrogen produced is free to diffuse ahead of the water again, thus providing an ample supply of the gas to react with the uranium.

The same mechanism is believed to describe the formation of uranium hydride in defectively jacketed pieces of uranium. When the jacket is not bonded to the uranium piece, water enters through the defect and reacts with the uranium to liberate hydrogen; the hydrogen is believed to diffuse along the surface of contact between jacket and uranium and may start reacting with the uranium at a considerable distance away from the jacket perforation. This distance is determined by such things as the temperature and the "induction period" which has been observed prior to initial reaction between hydrogen and uranium [Straetz and Draley (MUC); Albrecht and Mallett (BMI)]. If the reactions are allowed to proceed in unbonded jacketed pieces in water, eventually water reaches the site where uranium hydride exists and converts it to uranium oxide. Thus, if such pieces are examined when a local swelling is first observed the product is UH_3; after longer exposure the larger swellings are composed of UO_2.

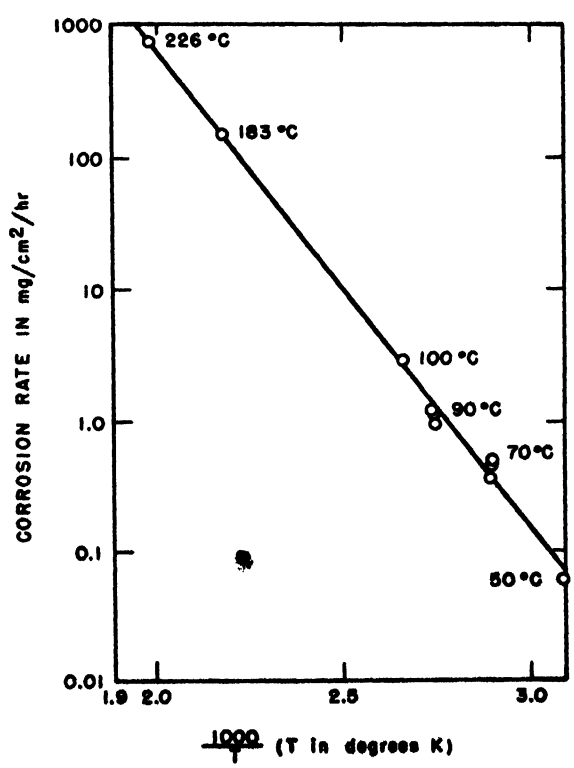

Figure 39. Corrosion rate of standard uranium in hydrogen-saturated water (McWhirter and Draley (ANL))

The corrosion behavior of uranium of usual purity is influenced by heat treatment. In boiling distilled water, where protective films do not form, corrosion rates were reduced by heating alpha-annealed material into the beta or gamma region and cooling. The lowest rates, reduced by a factor of two from the alpha-annealed metal, were obtained by furnace cooling after one hour in vacuo at 1000°C. High purity metal had essentially the same corrosion rate as the typical uranium after heat treatment, and it did not show the heat treatment effect [Draley and McWhirter (ANL)]. It was speculated that dissolution and redistribution of impurities in typical metal accounted for the changes observed in these results. Similar reduction in boiling water corrosion rate had been observed in heat-treated samples of rather miscellaneous histories [review by McWhirter and Draley (ANL)].

Alloying can be effective in stabilizing the protective oxide film on uranium metal surfaces. A U-5 weight per cent Zr alloy, for example, required a very much smaller concentration of oxygen in the water to provide the highly corrosion-resistant surface film. Thus, in actively boiling distilled water in contact with air, this alloy developed the typical thin film showing interference colors and a very low corrosion rate. Eventually these films seem to break down in much the same way as does the film formed on uranium in air-saturated water at lower temperatures. However, when oxygen-free gas is bubbled through the boiling distilled water, the corrosion rate of the U-5 weight per cent Zr alloy was nearly the same as that of unalloyed uranium and the thin protective film was not observed [Draley, McWhirter, Field and Guon (ANL)].

There are three general classes of alloys which appear to be able to form and to retain the protective oxide films, even in oxygen-free water, at temperatures as high as 350°C. These are: (1) certain metastable gamma-phase alloys; (2) certain supersaturated alpha-phase alloys; and (3) certain intermetallic compounds.

Typical of alloys of the first class are those containing more than about 7 weight per cent molybdenum or niobium. Of the corrosion-resistant alloys which have received serious study these appear to provide the lowest corrosion rates at elevated temperatures (see Fig. 40). In these alloys the alloying constituent dissolves in the uranium gamma phase which, upon moderate to rapid cooling, is retained as metastable gamma solid solution, since the transformations are sluggish. Low corrosion rates are exhibited by these materials so long as the gamma phase is retained and no transformations to other phases occur [Lustman and Thomas, Westinghouse Atomic Power Division (WAPD)].

There is a characteristic improvement in corrosion resistance of these alloys if, after their initial rapid cooling from a gamma phase, they are given a mild heat treatment. The nature of the change in the material during this treatment is not understood, but definite reductions in corrosion rates are observed.

All of these alloys are susceptible to failure induced similarly to that of uranium in air-saturated water at low temperatures. The nature of the failure is entirely different, but it apparently occurs due to the access of hydrogen to the metal. The hydrogen apparently diffuses into the alloy structure. The nature of the damage caused is not completely understood, but it is apparently true that a small amount of uranium hydride phase is formed within the structure of the metal. The lattice expansion in forming this hydride results in very high local stresses and in cracking. Such cracking results in breaking of samples into smaller pieces or in crumbling.

The supersaturated alpha-phase alloys characteristically contain small amounts of niobium. A U-3 weight per cent Nb binary alloy is a typical alloy in this series. This alloy shows moderate corrosion rates (see Fig. 40). Supersaturated alpha alloys undergo a martensitic transformation from the gamma phase, in which the alloying constituent is dissolved, to the alpha phase. If the cooling is done too slowly, a normal alpha phase is formed (not martensite) with the alloying constituents precipitated, usually as compound. These alloys are corrosion resistant only so long as the martensitic alpha phase is retained. A slight aging treatment characteristically reduces the corrosion rate of these materials in much the same way that the rate of gamma-phase alloys is reduced. Further aging causes grain boundary precipitation and reversion to the normal alpha-uranium structure. In this condition the alloy has poor corrosion resistance.

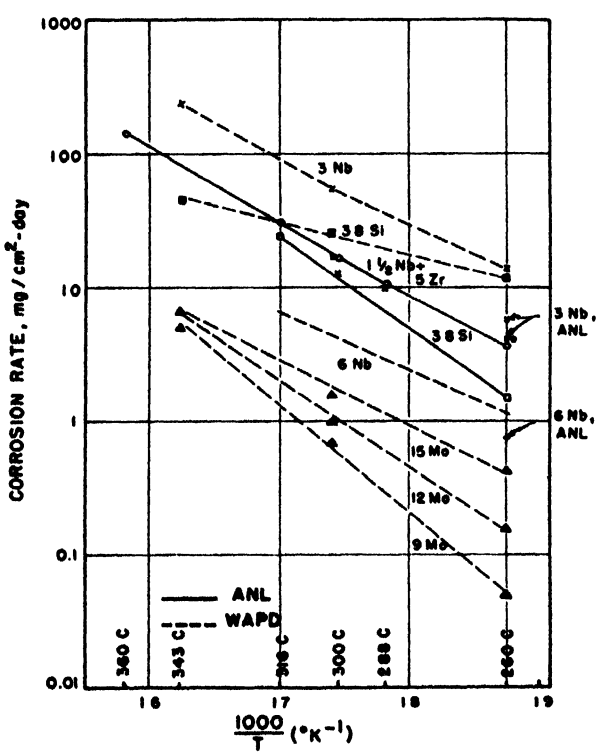

Figure 40. Corrosion of uranium base alloys in distilled water

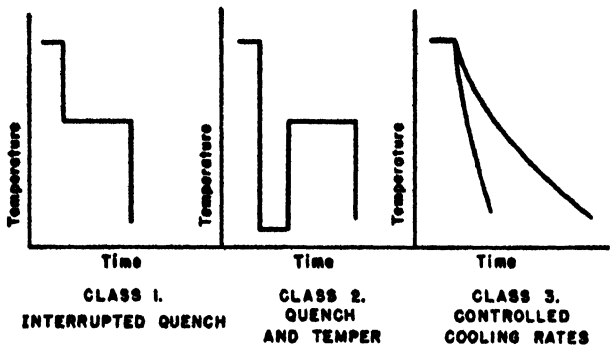

Figure 41. Heat treatments for study of time-temperature transformations

The temperature required to cause this overaging can be increased, and hence the usefulness of the alloys can be improved, by adding zirconium to the niobium alloy. A typical example of this type of alloy contain 1.5 weight per cent Nb + 5 weight per cent Zr. Its corrosion rate is approximately the same as the 3 weight per cent Nb alloy as shown in Fig 40 on page 63. Another modification contains approximately 0.7 weight per cent Sn added to the 3 weight per cent Nb alloy. This alloy is in some respects quite similar in behavior to the U-5 weight per cent Zr-1.5 weight per cent Nb alloy, but it appears to be more susceptible, during initial heat treatment, to effects such as cracking during quenching, and required the mild thermal aging treatment to avoid early corrosion cracking.

This type of alloy is susceptible to "failure" in the same fashion as the gamma-phase alloys. Failure is again by cracking or crumbling caused by the penetration of hydrogen into the metal structure. It has not been determined whether a hydride phase forms prior to the initiation of cracking.

The third type of corrosion-resistant alloy is typified by the stable epsilon phase (U_3Si) in the U-Si system. Corrosion rates are similar to those for the supersaturated alpha alloys (Fig. 40). The compound must be nearly pure to possess adequate corrosion resistance. There is only slight solubility in it of uranium and of compounds richer in silicon. Formation of the epsilon phase requires maintenance at a temperature near the maximum at which the phase is stable (850°C) for a significant period. Although formation of the epsilon phase appears to occur within the first few hours, longer times at this elevated temperature seem to provide material with a somewhat improved corrosion resistance [Kaufmann, Magel, Kneppel of Nuclear Metals, Inc. (NMI)]. This alloy has the advantage that the phase which is corrosion resistant is stable at temperatures where the metastable gamma phase and the supersaturated alpha-phase alloys are overaged and have entirely lost their corrosion-resistant characteristics.

It is not known whether this alloy is susceptible to the type of failure exhibited by the other two types of corrosion resistant alloys.

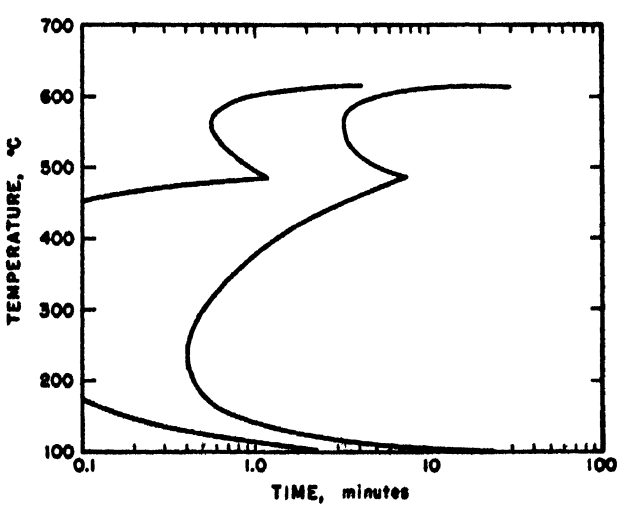

Figure 42. TTT curve for uranium-0.3 atomic per cent chromium alloy

X. URANIUM PHASE DIAGRAMS

Phase diagrams are, of course, an important part of physical metallurgy. Saller and Rough (BMI) have prepared a detailed paper¶ on the alloys of uranium for presentation at Session 18B of this conference. No attempt will be made here to summarize the extensive work on uranium phase diagrams. Such information can be best obtained from the Saller and Rough paper.

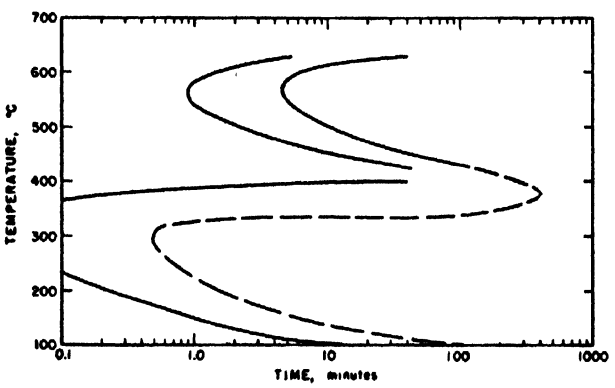

Figure 43. TTT curve for uranium-0.6 atomic per cent chromium alloy

XI. TRANSFORMATION KINETICS IN URANIUM ALLOYS

All uranium alloy systems whose transformation kinetics have thus far been studied have a common feature: the alloying component is more soluble in the gamma, body-centered cubic phase than in the tetragonal beta and orthorhombic alpha phases, and more soluble in the beta phase than in the alpha phase. In general then, when a high temperature phase is rapidly cooled to temperatures below the equilibrium temperature range, a metastable supersaturated solid

¶ P/558, Vol. 9.

solution structure results. Transformation kinetics are the time-temperature-composition relationships which describe the transformation of this metastable structure to a structure more closely approximating the equilibrium structure.

Nearly all transformation kinetic studies can be separated into three groups depending upon the type of heat treatment used. These classes are described below and shown diagrammatically in Fig. 41.

1. Interrupted quenching refers to a heat treatment wherein the specimen is held at a temperature in the gamma or beta range long enough to bring about an equilibrium structure, then is rapidly cooled to a lower temperature and held at that temperature for a measured time. The process is comparable to austempering of steel.

2. Quench and temper treatments are those wherein the specimen is heated into the gamma or beta range long enough to bring about an equilibrium structure, then drastically quenched to 100°C or below. The gamma or beta phase may be retained or may undergo a diffusionless transformation during the quench, depending on the nature and amount of the alloying elements. In either case, the structure is metastable and transforms on tempering. The study of quench and temper transformations consists of tempering the quenched specimens at various temperatures for measured times.

3. Continuous cooling treatments are those wherein the specimen is heated into the gamma or beta range long enough to bring about an equilibrium structure, then cooled to room temperature at various cooling rates, without interruption. Included are such treatments as water quenching, air cooling and furnace cooling.

The reported data on transformation kinetics can best be analysed by a breakdown into first, alloy systems, then the three classes of heat treatment.

Uranium-Chromium Alloys

White, Jr. (KAPL) has reported the transformation kinetics of the uranium-chromium system for chromium contents of 0.3, 0.6, 1.8, and 4 atomic per cent. Chromium tends to stabilize the beta-uranium phase and the study was concerned with the subcritical transformation of the beta solid solutions. The interrupted quench method was used and the transformation followed dilatometrically.

The data obtained are presented in Figs. 42 through 45. The existence of two C's in the time-temperature transformation (TTT) diagrams for the lower chromium alloys indicated that there are two transformation mechanisms, one at upper temperatures and one at lower temperatures. It is speculated that the higher temperature mechanism is controlled by rate of diffusion of chromium in beta uranium, while the lower temperature mechanism is diffusionless. The temperature of transition between the two mechanisms of transformation is depressed with increased chromium content. By qualitative extrapolation to zero per cent chromium, one would conclude that pure uranium transforms from beta to alpha entirely by the mechanism of the lower "C," and retarded transformations were observed in uranium of nominal purity. Duwez[16] has reported that the beta-alpha transformation temperature can be depressed appreciably only by extremely drastic quenching.

At higher chromium contents, the lower "C" vanished altogether and the beta phase can be retained at room temperature. This feature of the transformation was used by Tucker,[17] to obtain crystals of beta uranium for his structure studies.

Uranium-Molybdenum Alloys

The work of Jones, Hoffman, Taub and Doll (LASL) illustrates the transformation of uranium-molybdenum alloys containing 0.56, 1.12, 1.67 and 2.18 weight per cent molybdenum. The transformation was of the quench and temper type, class 2. The alloys were prepared by vacuum melting and were subsequently forged. The 1.12, 1.67, and 2.18 weight per cent molybdenum alloys, when quenched from 780°C and above (gamma solid solution phase), appear to undergo a type of transformation resulting in an acicular structure similar to martensite in appearance. These quenched alloys are entirely in the alpha condition. These supersaturated alpha solid solution alloys are relatively soft (DPN 350–380). Tempering markedly increases the hardness, as illustrated in Fig. 46. Overaging occurs rather soon at a tempering temperature of 500°C.

Saller, Rough, and Bauer (BMI) have reported on the transformation kinetics of uranium-molybdenum alloys containing 9.8, 12.6 and 14.8 weight per

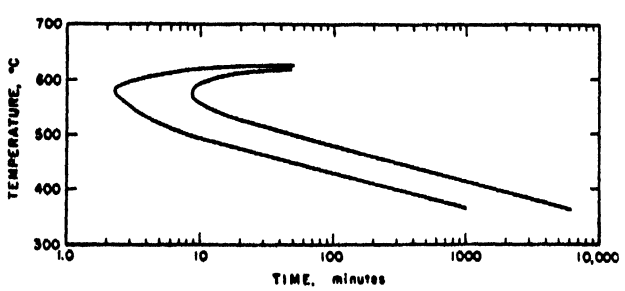

Figure 44. TTT curve for uranium-1.8 atomic per cent chromium alloy

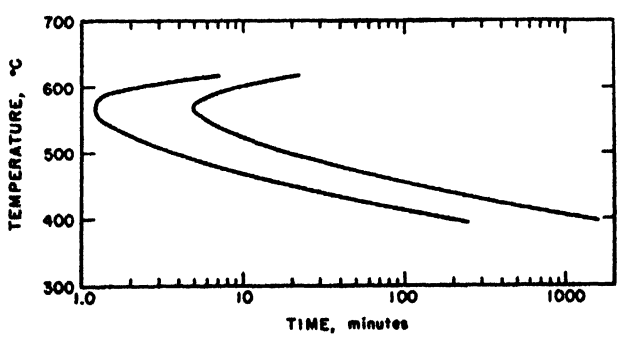

Figure 45. TTT curve for uranium-4.0 atomic per cent chromium alloy

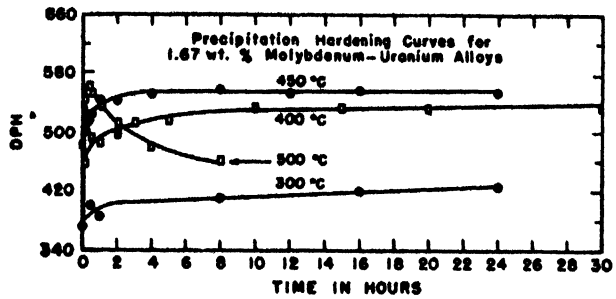

Figure 46

cent molybdenum. The class 2 heat treatment, quench and temper, are used. In this composition range, the gamma phase could be easily retained by quenching. The phases stable at room temperature are alpha uranium, solid solution, and delta (a tetragonal intermediate) phase, centered at around 16 weight per cent Mo. The transformations were quite sluggish, and the course of transformation was followed by metallographic examination and electrical resistance measurements. Transformation of the 9.8 weight per cent molybdenum alloy occurs by a nucleation and growth mechanism. The alpha and delta phases are nucleated at the gamma grain boundaries and grow inward to consume the gamma grains. The decomposition products have a lamellar distribution. The transformation curve is given in Fig. 47.

The 12.6 and 14.8 weight per cent molybdenum alloys transform by an ordering reaction which probably occurs by a nucleation and growth mechanism. Sufficient data are available to indicate that the transformation in the 14.8 weight per cent alloy has a C-curve-type behavior. During transformation of the alloys, the electrical resistance and hardness first increase and then decrease with time, the peaks in resistance and hardness almost coinciding. Transformation is not observed metallographically until after the resistance and hardness peaks are passed.

The increased hardness and resistance during aging are attributed to strain developed in the matrix as a result of the formation of coherent nuclei. Precipitation, and loss of coherency, are accompanied by a decrease in resistance and hardness. The induction period, preceding transformation, and attendant C-curve behavior originate in the temperature de-

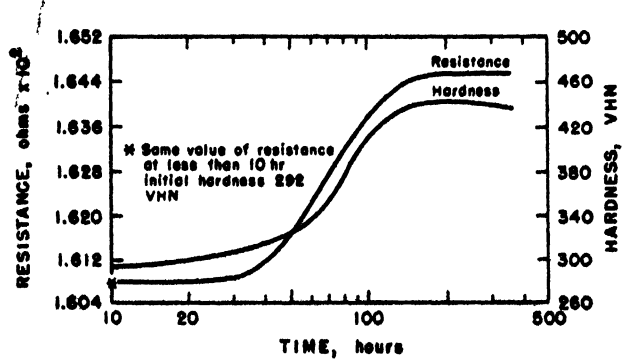

Figure 47. Resistance and hardness curves of a 9.8 weight per cent molybdenum sample during annealing at 500°C

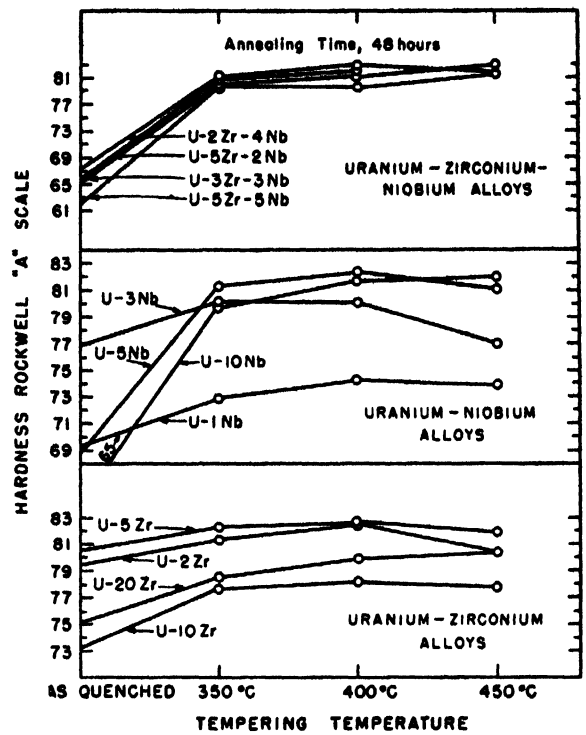

Figure 48. Effect of tempering temperatures on hardness of uranium alloys; (annealing time: 48 hours)

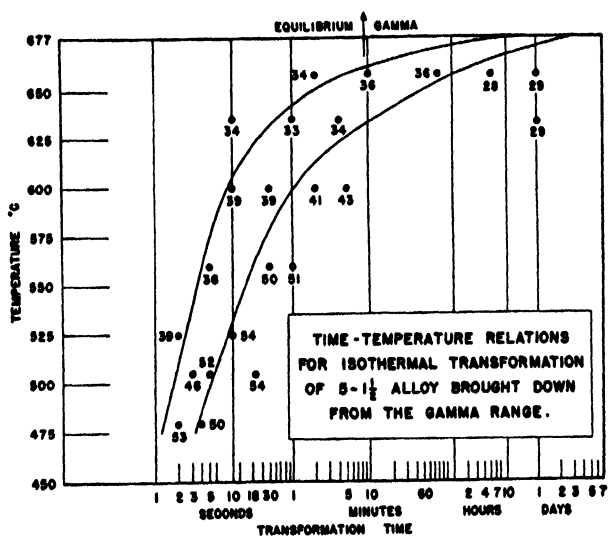

Figure 49. Time-temperature relations for isothermal transformation of uranium-5 weight per cent zirconium-1½ weight per cent niobium alloy brought down from the gamma range

pendence of the tendency of the alloy to order and of the rate of diffusion.

The transformation of gamma to delta phase is sluggish at all temperatures and the rate decreases rapidly below 440°C. The optimum temperature of transformation, or nose of the C-curve, lies close to 500°C.

Uranium-Niobium Alloys

Carlson (Iowa State College) has reported data on the transformation kinetics of the uranium-niobi-

um alloys containing 1, 3, 5, and 10 weight per cent niobium. The transformations were studied by the quench and temper method and changes followed by hardness measurements. The data are reproduced in Fig. 48. The curves show evidence of precipitation hardening followed by overaging.

Dwight (ANL) has reported a continuous cooling TTT curve for a uranium-4.9 weight per cent niobium alloy. Niobium was found to retard the decomposition of the gamma phase sufficiently so that quenching rates of 18°C per second and less will avoid touching the nose of the C curve on continuous cooling. Specimens in which the gamma phase is retained in a metastable condition by quenching have a hardness of 20 Rockwell "C."

Uranium-Zirconium Alloys

Carlson (ISC) has also studied the transformations in alloys containing 2, 5, 10, and 20 weight per cent zirconium by the quench and temper method. The data are plotted in Fig. 48 and show a moderate increase in hardness with indications that the maximum hardening occurs at 400°C in the 2, 5, and 10 weight per cent alloys.

Uranium-Zirconium-Niobium Alloys

Carlson (ISC) has studied a group of ternary alloys containing small amounts of zirconium and niobium by the same methods as those used for the U-Nb and U-Zr binary alloys. His results are included in Fig. 48 and indicate a marked hardening in all alloys at tempering temperatures up to 450°C.

Chiswik and Dwight (ANL) have studied the heat treatment of a ternary alloy containing 5 weight per cent zirconium and 1½ weight per cent niobium by several methods.

The transformation curve obtained by the interrupted quench method is shown in Fig. 49. The lines represent the beginning and end of transformation as determined by metallographic observation. The numbers represent the Rockwell "C" hardness during various stages of the transformation. The hardness after transformation is plotted as a function of transformation temperature in Fig. 50.

For a quench and temper treatment, it was found that tempering the water-quenched structure resulted in appreciable age hardening. In Fig. 51, lines of constant hardness are plotted on time-temperature coordinates, and in Fig. 52, hardness is plotted against tempering time. Both graphs exhibit behavior typical of precipitation hardening and overaging. Little change in microstructure was observed until the maximum hardness was reached and overaging had started.

XII. ACKNOWLEDGEMENTS

In a survey paper of this type which attempts to summarize the work of a great many investigators over a period of somewhat more than ten years, it is impossible to mention by name all of those whose efforts have contributed to our present knowledge of

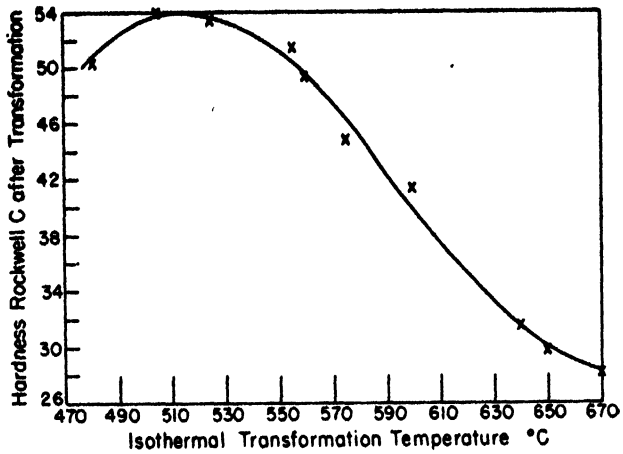

Figure 50. Hardness vs transformation temperature for conditions of isothermal transformation

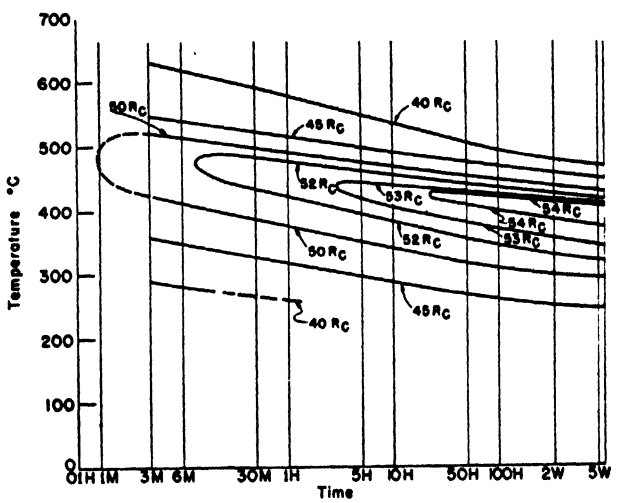

Figure 51. Effect of time and temperature of tempering on the hardness of water quenched uranium-5 weight per cent zirconium-1½ weight per cent niobium alloy

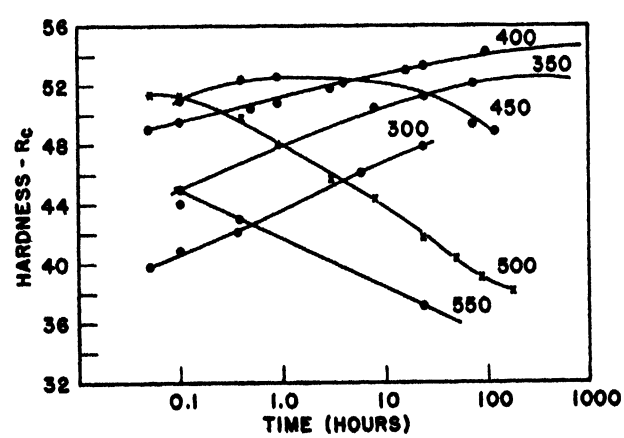

Figure 52. Age hardening of uranium-5 weight per cent zirconium-1½ weight per cent niobium

the physical metallurgy of uranium. Many authors have been mentioned throughout the text in appropriate places, but this does not infer that they are the only contributors, nor, indeed, in some cases, even the major contributors to a particular subject.

I also wish to acknowledge the very extensive assistance of many members of the Metallurgy Division of the Argonne National Laboratory in the assembling of information and for the preparation of the various sections of this paper. I wish to thank B. Blumenthal and S. S. Sidhu for the material in Section I, L. T. Lloyd for Section II, M. H. Mueller for Section III, E. S. Fisher for Section IV, L. T. Lloyd for Section V, H. H. Chiswik and L. R. Kelman for Section VI, S. H. Paine and J. H. Kittel for Section VII, R. M. Mayfield for Section VIII, J. E. Draley and S. Greenberg for Section IX, and A. E. Dwight for Section XI.

REFERENCES

1. Jetter, L. K. and Borie, B. S., Jr., *A Method for the Quantitative Determination of Preferred Orientation,* J. Appl. Phys., *24*: 532-5 (1953).
2. Schulz, L. G., *A Direct Method of Determining Preferred Orientation of a Flat Reflection Sample Using a Geiger Counter X-Ray Spectrometer,* J. Appl. Phys., *20*: 1030 (1949).
3. Holden, A. N., *Spiral Scanning X-ray Reflection Goniometer for the Rapid Determination of Preferred Orientations,* Rev. Sci. Instr., *24*: 10-12 (1953).
4. Chernock, W. P., Mueller, M. H., Fish, H. R. and Beck, P. A., *An Automatic X-Ray Reflection Specimen Holder for the Quantitative Determination of Preferred Orientation,* Rev. Sci. Instr., *24*: 925-928 (1953).
5. Seymour, W., *Preferred Orientation of Cold-Rolled Uranium Foil,* J. Metals 6, AIME Trans. *200*: 999-1003 (1954).
6. Mueller, M. H. and Knott, H. W., *Quantitative Pole Figures for Sheet Material by the Reflection Technique,* Rev. Sci. Instr., *25*: 1115-1118 (1954).
7. Norton, J. T., *A Technique for Quantitative Determination of Texture of Sheet Metals,* J. Appl. Phys., *19*: 1176 (1948).
8. Bach, J. H. and Burnham, J. B., Jr., *Determination of Preferred Orientation,* J. Metals, *4*: 1043 (1952).
9. Harris, G. B., *Quantitative Measurement of Preferred Orientation in Rolled Uranium Bars,* Phil. Mag., (7) *43*: 113 (1952).
10. Thewlis, J., *X-Ray Powder Study of β-Uranium,* Acta Cryst., *5*: 790 (1912).
11. Thewlis, J., *Structure of Uranium,* Nature, *168*: 198 (1951).
12. Wilson, A. S. and Rundle, R. E., *The Structures of Uranium Metal,* Acta Cryst., *2*: 126-127 (1949).
13. Grossman, N. and Priceman, S., *Compressive Properties of Uranium,* Nucleonics, 12, No. *6*: 68-9 (June 1954).
14. Laquer, H. L., McGee, W. E. and Kilpatrick, M. F., *The Elastic Constants of Uranium,* Trans. Am. Soc. Metals, *42*: 771 (1950).
15. Reynolds, M. B., *The Determination of the Elastic Constants of Metals by the Ultrasonic Pulse Technique,* Trans. Am. Soc. Metals, *45*: 839 (1953).
16. Duwez, P., *The Effect of the Rate of Cooling on the Allotropic Transformation Temperatures of Uranium,* J. Appl. Phys., *24*: 152 (1953).
17. Tucker, C. W., Jr., *The Crystal Structure of the β Phase of Uranium,* Acta Cryst. *4*: 425 (1951).

The Solid State Reaction Between Uranium and Aluminium

By R. Kiessling,* Sweden

If aluminium is used as a canning material for the uranium rods in a reactor, the reaction between uranium and aluminium at higher temperatures is a limiting factor for the use of this canning material. The present investigation was started in order to study the course of the solid state reaction in the boundary between uranium and aluminium at different temperatures. It is part of the Swedish contribution to the French-Swedish atomic collaboration.

The uranium-aluminium equilibrium diagram has been published by Gordon and Kaufmann,[1] who reported three intermediary phases, UAl_2, UAl_3 and UAl_5. Later Bovie[2] reported, that the ideal formula for the aluminium-rich compound "UAl_5" is UAl_4, but the compound probably has a defective uranium lattice and an extended homogeneity range between $UAl_{4.5}$ and $UAl_{4.9}$. The crystal structure of UAl_2 was given in reference,[1] and later Rundle and Wilson[3] determined the structure of UAl_3. The system is thus rather well-known and in Table I some physical constants and X-ray data for the intermediary phases have been collected. The microhardness values given have been determined during our investigation.

EXPERIMENTAL METHODS

Starting materials were cylindrical rods of natural uranium of nuclear purity with a diameter of about 8 mm and a height of about 10 mm and of aluminium† with a diameter of 3 mm and a length of about 7 mm. After degassing in vacuum at about 600°C and electrolytic polishing of the two metals the aluminium rods were pressed into drilled holes, about 5 mm deep, in the uranium plugs with a pressure of about 150 kg/cm². By pressing the aluminium into the uranium a close contact between the two metals was maintained during heating, the thermal expansion coefficient for aluminium being higher than that for uranium. The units were then heated in evacuated Pyrex tubes for different times and temperatures and the boundary zone investigated microscopically, by means of X-rays and by microhardness measurements. Microsections were prepared by polishing with diamond dust (down to 0.4 μ) and sometimes etched in a solution of 5 parts phosphoric acid, 5 parts ethylene glycol and 8 parts ethyl alcohol. The polishing technique was selected so that the boundary between uranium and aluminium and its different phases appeared as clear as possible, whereas the uranium and the aluminium phases often showed scratches because of the difference in hardness.

The most reliable identification of the different phases was by X-ray methods, and the specimens

* Dept. of Chemistry, Aktiebolaget Atomenergi, Stockholm.

† The aluminium used had a content of 0.5% magnesium ("reflectal"). This alloy is the canning material for the first Swedish reactor, and the magnesium content was considered to have no influence on the reaction.

Table I. The Properties of the Intermediary Phases in the Uranium-Aluminium System

Intermediate phase	*Density*	*Microhardness H_{50}/50 gm/15 sec*	*Melting point °C*	*Crystal structure*	*Convenient X-ray reflections for identification*				
					h	*k*	*l*	*d*	*I*
				f.c.cub. 7.745 Å	1	1	1	4.46	m
UAl_3	8.3	630	1590	C15-type, isomorphous to Cu_2Mg	2	2	0	2.722	s
					3	1	1	2.338	s
UAl_3	6.4	300	$UAl_3 \leftrightharpoons UAl_2$ + melt Peritectic at 1350°	Simple cub. 4.278Å Au Cu_3-type	1	0	0	4.25	s
					1	1	0	3.008	s
					1	1	1	2.449	s
					2	0	0	2.127	m
"UAl_4" (Ideal formula)	5.7	260	$UAl_4 \leftrightharpoons UAl_3$ + melt	Orthorhombic	0	1	1	5.64	m
				a = 4.41 Å	1	0	1	4.17	m
				b = 6.27 Å	0	1	3	3.662	m
Real formula $UAl_{4.5}$ $UAl_{4.9}$				c = 13.71 Å	0	0	4	3.414	w-m
			Peritectic at 730°	Space group I m m a	1	0	3	3.164	s

often had to be ground in different ways in order to increase the surface amount of a certain phase.

RESULTS

The specimens were heated at temperatures between 100°C and 600°C and for times from 1 hour to 1 month depending on temperature. The different heat treatments have been summarized in Table II. The course of the reaction has been illustrated by some series of microphotographs, which are referred to in the discussion and summarized in Table II.

The solid state reaction between uranium and aluminium in general proceeds in the following way. Nuclei of UAl_2 are formed at some places near the boundary uranium-aluminium *but always in the uranium phase*. These UAl_2 nuclei have a close contact with the uranium phase, giving a surface without any pores between uranium and UAl_2.

Next step seems to be a diffusion of uranium atoms through the UAl_2 phase to aluminium, and of aluminium atoms through the UAl_2 phase to uranium. The UAl_2 grains thus grow into the uranium phase and on the aluminium side the two other phases, UAl_3 and UAl_4, are formed. UAl_3 also grows on the uranium side of the initial boundary and in close contact with UAl_2. UAl_4, however, grows into the aluminium phase, forming a rather coarse and porous structure. (These steps are illustrated in Fig. 1a–d at 300°C and Fig. 2a–f at 400°C.)

The relative amount of the different phases and the rate of growing depends very much on temperature. At 250°C and usually also at 300°C only UAl_2 and UAl_4 were definitely identified (Fig. 1). UAl_3 was found only in a few specimens at 300°C forming a very narrow white border between UAl_2 and UAl_4. With increasing temperature, however, the relative amount of UAl_3 increased very rapidly, whereas the thickness of the UAl_2 zone changed very little. At these higher temperatures (for instance at 500°C Fig. 3a-b) it was often possible to see how a narrow zone of UAl_2 first was formed (etching grey). After some time the UAl_3 zone appeared (etching white) and was rapidly growing apparently through UAl_2 into the uranium phase. Also this white phase, however, had a very narrow border of grey UAl_2 on the uranium side. This rapid growth of UAl_3 will be discussed below.

At still higher temperatures UAl_3 formed by far the main part of the boundary. At 600°C after 4 hours, for instance, Fig. 4a-b) the boundary between uranium and aluminium had a thickness of about 800 μ. The following phases and phenomena were visible in this boundary zone starting from the uranium phase.

(*a*) In close contact with uranium, without any pores, a 20 μ deep layer of UAl_2 was observed. This UAl_2 phase was also found in droplets penetrating about another 20 μ into the white UAl_3 phase (Fig. 4a).

(*b*) In intimate contact with UAl_2 and without any pores the main, a 500 μ deep zone of UAl_3 appeared. This white zone seems to be rather metallic and ductile although some cracks were visible. The other side of this UAl_3 layer was situated at about the initial UAl surface, but had contact with UAl_4 or Al only on a few points. On the main part of the initial boundary and penetrating deep (200–300 μ) into the aluminium phase great pores were found.

(*c*) This porous zone, 200–300 μ thick, had nearly interrupted all contact between aluminium and the UAl_3 phase. Some small grains of a phase, probably UAl_4, were visible in some of the pores and also in some places on the aluminium side of the pores and in the aluminium phase. This porous zone was covering nearly the whole border between aluminium and UAl_3 and situated on the aluminium side of the initial boundary uranium-aluminium. The position of this zone with pores on the aluminium side shows that the diffusion rate of aluminium through the different uranium-aluminium phases into uranium is greater than for the uranium atoms through the different phases into aluminium. This higher diffusion rate for aluminium than for uranium is in accordance with the fact that the aluminium atoms are smaller than the uranium atoms ($r_{Al} = 1.35$ Å, $r_U = 1.54$ Å). It is also in accordance with the fact that aluminium is much nearer its melting point (659°C) than uranium (1133°C).

The diffusion rate of the Al atoms through UAl_3 increases much more rapidly with temperature than the diffusion rate of the U atoms through UAl_2. This is shown by the fact, that the UAl_3 layer rapidly increases in thickness with temperature, whereas the UAl_2 layer remains nearly constant in thickness.

Table II. The Reaction between Uranium and Aluminium in Vacuum

Temperature	*Time until reaction was noted (UAl_x formation)*	*Phases identified at the boundary after reaction (in decreasing amount)*	*Microphotographs*
100°C	No reaction observed	–	–
200°C	No reaction observed	–	–
250°C	~ 240 hr	UAl_2	–
300°C	24 hr	UAl_2, UAl_4, UAl_3 (trace)	Fig. 1a–d
350°C	6 hr	UAl_2, UAl_4, UAl_3	–
400°C	~1 hr	UAl_2, UAl_3, UAl_4	Fig. 2a–f
450°C	?	UAl_2, UAl_4, UAl_3	–
500°C	Immediate	UAl_2, UAl_4, UAl_3	Fig. 3a–b
600°C	Immediate	UAl_2, UAl_4, UAl_3	Fig. 4a–b

Figure 1. The reaction between aluminium (left) and uranium (right) at 300°C. Nuclei of UAl_2 are formed in the U-phase (*a*). They grow into the U-phase and UAl_4 grows into Al (*b*). UAl_4 cracks into a crystal powder (*c*), which leaves pores in the aluminium side of the contact zone (*d*). No UAl_3 is visible at this temperature

Figure 2. The reaction between aluminium (left) and uranium (right) at 400°C. A UAl_2 zone is formed in the U-phase (*a*, etching gray). It grows and a white UAl_3 zone is visible after about 20^{hr} (*c*). At the same time the porous zone, partly filled with UAl_4 appears and interrupts the contact between aluminium and uranium

→

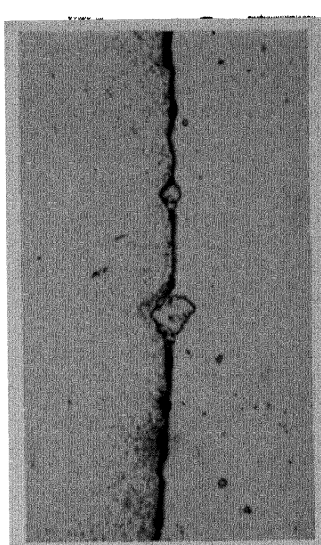

200 × Figure 1a 24 hr



200 × Figure 1b 72 hr

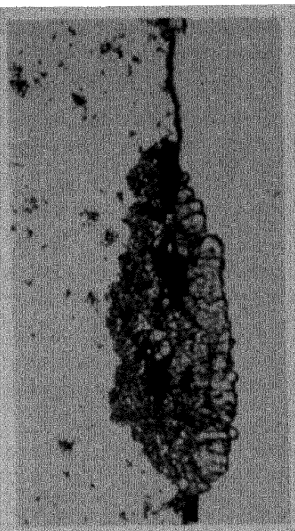

200 × Figure 1c 180 hr



200 × Figure 1d 456 hr

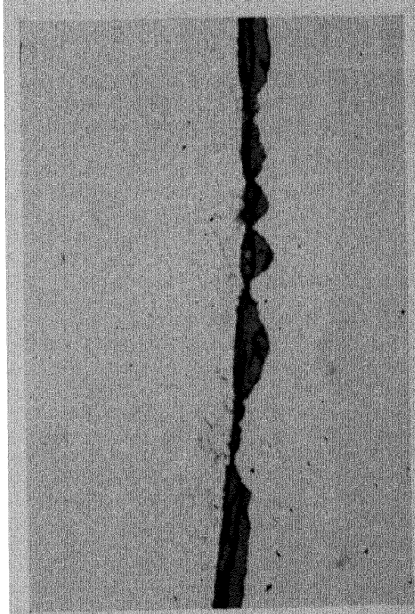

500 × Figure 2a 2 hr

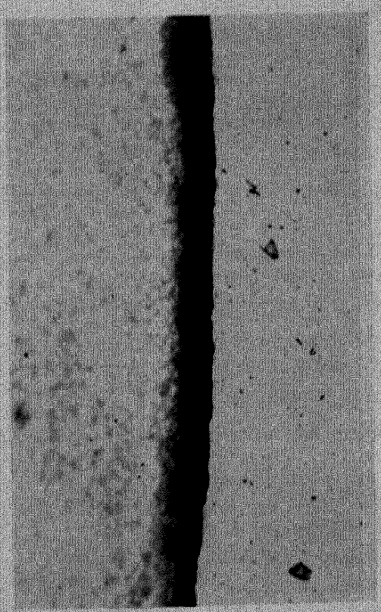

500 × Figure 2b 14 hr

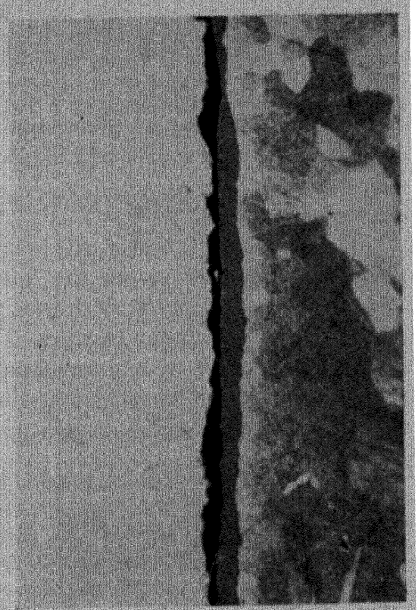

500 × Figure 2c 21 hr

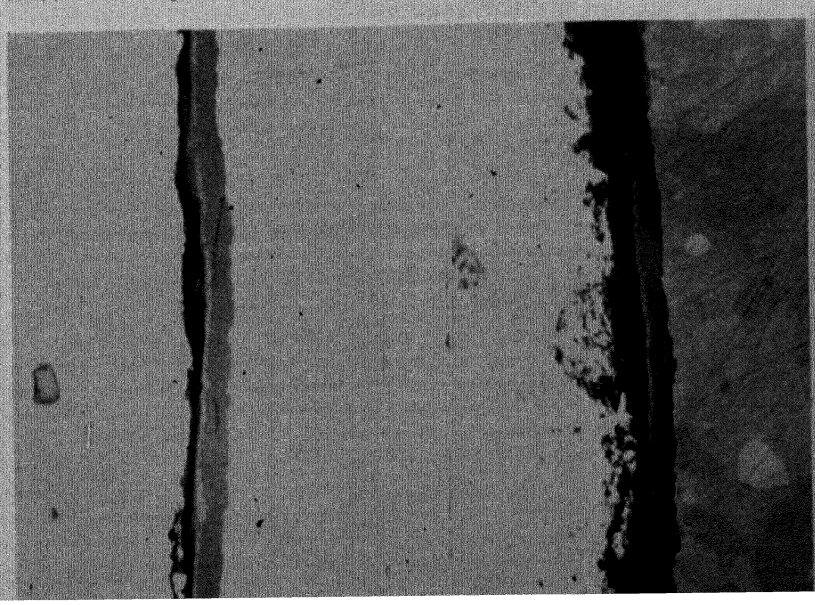

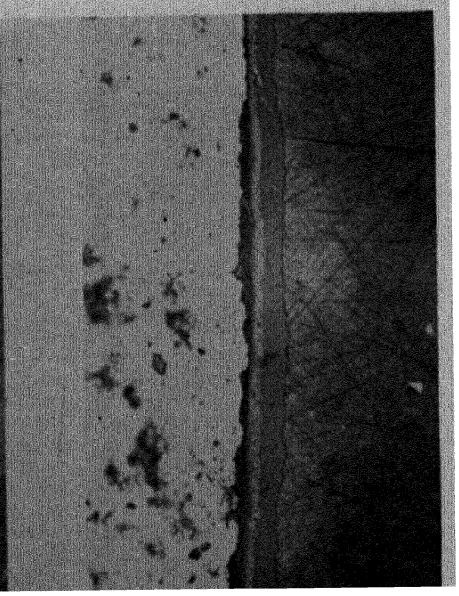

An extensive quantitative treatment of the diffusion process was not made at the present time. Such a treatment would in principle involve a careful measurement of the thickness of the different layers of the intermediary uranium-aluminium phases at different times and for some different temperatures. It was found, however, that the reaction around the cylindrical aluminium surface was not quite uniform. At certain spots there was a rapid growth of the nuclei, whereas at other places the rate of growth was slower. After each heat treatment it was also necessary to repolish the surface of the specimen and a study of exactly the same boundary was not therefore possible from time to time.

The only process, which was possible to observe with some accuracy, was the time at a certain temperature until the first visible nuclei of UAl_2 appeared in the uranium phase. These times have been given in Table II for some different temperatures and in Fig. 5 they have been plotted on a logarithmic scale against temperature. This curve thus indicates after how long a time at a certain temperature the reaction between uranium and aluminium has proceeded so far that the first nuclei of UAl_2 are visible.

INFLUENCE OF GASES (AIR)

The preceding experiments were all carried out in vacuum. In order to see the influence of air some specimens were heated in Pyrex tubes with a small hole where the air could enter. The effect was that UO_2 was formed with a comparatively high velocity on the surface of the uranium. The first traces were usually formed as UO_2 glands noted at 200°C after

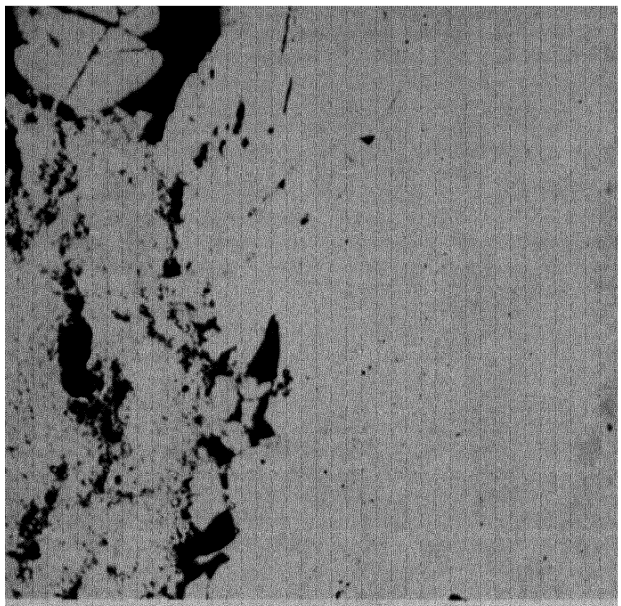

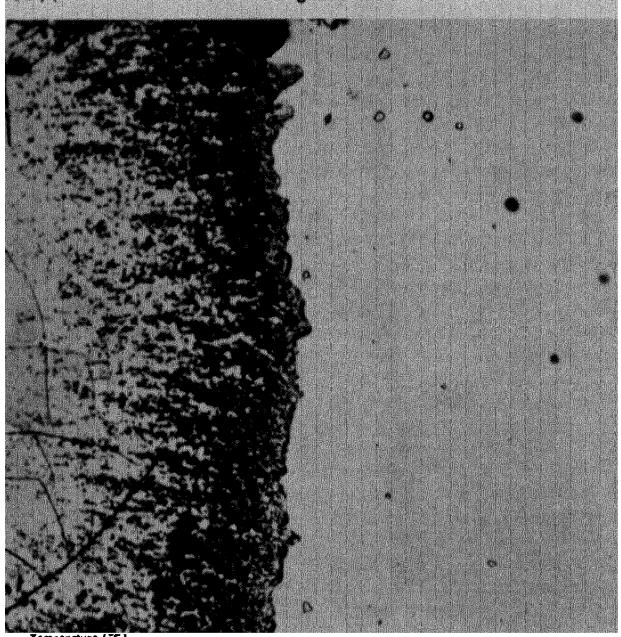

Figure 3. The reaction between aluminium (left) and uranium (right) at 500°C. UAl_2 (grey) is first formed. Later UAl_3 (white) appears, which rapidly grows through the UAl_2 zone into the U-phase. It is always preceded by a narrow grey UAl_3 zone (barely visible in *b*).

Figure 4. The reaction between uranium (right) and aluminium (left) after 600°C, 4^{hr}; a thin zone of NAl_2 (black, *b*) in close contact with both U and UAl_3; then the main part, UAl_3 (white in *a*, grey in (*b*); to the left the porous zone with UAl_4 (sharp edged grains, *a*)

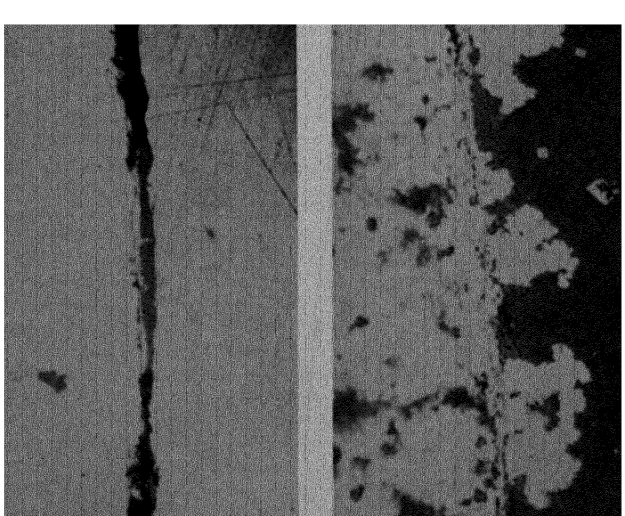

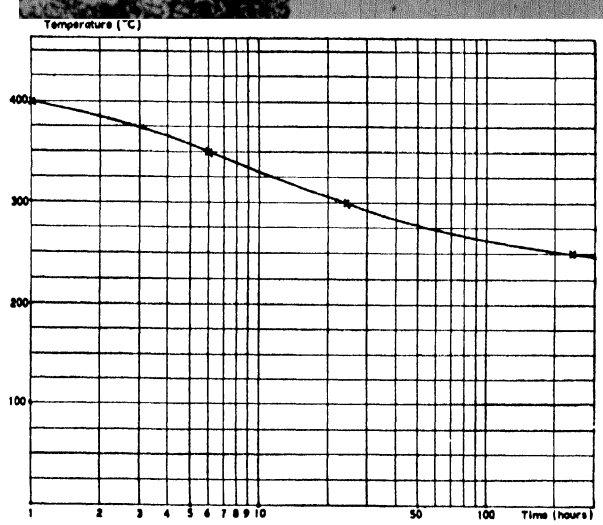

Figure 5. R. Kiessling: The solid state reaction between uranium and aluminum

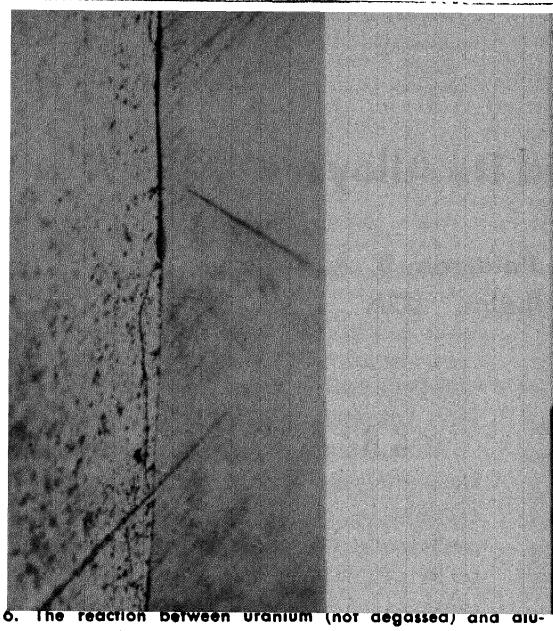

Figure 6. The reaction between uranium (not degassed) and aluminium in an atmosphere with traces of oxygen; small glands of UO_2 are formed in the contact surface; they are porous; 200°C, 13 days, 500



Figure 7. Layer of UO_2 formed at the boundary between aluminium (left) and uranium (right), if oxygen is present during the reaction; 260°C 72 hr, 1000X

13 days and at 250°C already after 1 hour (Fig. 6 above.)

A thick, porous zone of UO_2 was developed between uranium and aluminium. At 250°C (Fig. 7) it had a thickness of 30-50μ after 72 hours. This oxide layer was, of course, also developed on the other surfaces of uranium which was in contact with aluminium. On these surfaces, however, it was not adherent. The porous oxide layer interrupts the contact between uranium and aluminium and probably it has a great influence on the heat transfer.

PRACTICAL CONCLUSIONS

If the unknown radiation effects are not taken into consideration, a reaction between uranium and its aluminium can is noted at about 250°C and the reaction rate rapidly increases with the rate in temperature.

The two phases UAl_2 and UAl_3 form an adherent, metallic layer on the uranium and do not seem to have too serious an influence on the heat transfer or contact between uranium and aluminium.

UAl_4, however, does not form an adherent layer on either aluminium or UAl_3. It cracks to a powder which gives a bad contact zone.

Because of the high diffusion rate for aluminium into uranium a mass transfer from aluminium to uranium occurs and a porous zone is formed which interrupts the contact between uranium and its aluminium canning. This porous zone formation seems to be the main factor which prevents aluminium being used as a can if the temperature of uranium is about 250°C or higher.

If oxygen has access to the reaction zone, a UO_2 layer is rapidly formed which interrupts the contact between uranium and aluminium. This oxide formation starts already at about 200°C.

REFERENCES

1. Gordon, P. and Kaufmann, A. R, *The Alloy Systems Uranium-Aluminum and Uranium-Iron*, I. Metals (January 1950). Trans. AIME, *188*: 182 (1950).
2. Bovie, B. S., *Crystal Structure of UAl_4*, J. Metals (September 1951). Trans. AIME: 800.
3. Rundle, R. E. and Wilson, A. S., *The Structures of Some Metal Compounds of Uranium*, Acta Cryst. *2*: 148 (1949).

The Metallurgy of Thorium and Its Alloys

By O. N. Carlson, P. Chiotti, G. Murphy, D. Peterson, B. A. Rogers, J. F. Smith, M. Smutz, M. Voss and H. A. Wilhelm,* USA

1. INTRODUCTION

Thorium metal because of its low strength, moderately high density, poor corrosion resistance and relatively high cost is at a decided disadvantage in the field of structural materials. The use of thorium metal as an alloying constituent does have some promise of finding applications in commercial alloys. Additions of a few per cent of thorium to magnesium, for example, gives an alloy with sufficiently improved properties to warrant consideration of the use of these alloys in certain phases of commerce. Other alloying effects as well as some commercial applications of thorium metal and thorium compounds have been summarized in a general treatment of thorium by Lilliendahl.[1]

The use of thorium in the atomic energy programs has accelerated the rate of production of this element in the past few years. The nucleus of the thorium atom (Th^{232}) can undergo reaction with a neutron to form Th^{233} which is relatively short lived. Subsequent radioactive disintegrations of this isotope produce a relatively long-lived U^{233} which can be caused to fission and serve as an atomic fuel in a manner similar to U^{235} and Pu^{239}.

The transformation process from Th^{232} to U^{233} is independent of the chemical state of the thorium but for certain reactor designs the greater concentration of thorium atoms in thorium metal and other properties of the metallic state offer certain advantages. Thorium and its alloys have, therefore, received considerable study and attention in connection with atomic energy programs in recent years.

The material presented in the following pages has been selected from a large amount of data obtained by many workers and represents the present knowledge of the metallurgy of thorium and its alloys.

2. OCCURRENCE OF THORIUM AND MONAZITE PROCESSING

2.1 Occurrence of Thorium

Thorium is widely distributed in nature but rich deposits are scarce. It has been estimated that the thorium content of the earth's crust is between 0.0003 and 0.001 per cent or about two to five times that of uranium. Traces of thorium have been found in more than 100 minerals, a few of which contain more than one per cent thorium. Monazite sand, however, is the only commercially feasible source of thorium.

Monazite sand occurs as a primary mineral in granites, gneisses and pegmatites. After many years of erosion by rivers or seas, the sand is concentrated sufficiently along the courses of rivers or on beaches to be of commercial interest. The largest and richest deposits of monazite are in Brazil and India. Sizable deposits are present in the Netherlands East Indies, South Africa, and the United States.[1]

In 1893, Welsbach patented the use of a mixture containing 98 to 99 per cent thoria for gas mantles and the industry grew rapidly thereafter. In the years preceding World War I, over 300 million gas mantles were consumed annually. Brazil dominated the world market from 1895 to 1914. The wide adoption of electric lights for home lighting just prior to World War I caused a sharp decline in the demand for gas mantles and for thorium. Brazil produced less monazite from 1914 to 1941 than in the single year 1909. The advent of the atomic energy program has caused a renewed interest in thorium and thus in monazite.

Monazite sands are essentially the orthophosphates of rare earths, thorium and uranium. The chemical composition is shown in Table I. The sands are yellow to reddish-brown in color and are hard and brittle.

2.2 Processing of Monazite Sand

The first step in processing monazite is to destroy the chemical structure of the sand by a chemical reaction. Sulfuric acid digestion has been used for more than half a century to produce a water-soluble product. An alternate process starting with a caustic digestion of the sand has also been developed.[2] Both of these processes will be described briefly.

2.21 Sulfuric Acid Process

Monazite sand is added to concentrated sulfuric acid heated to about 200°C. The time of digestion depends primarily upon the particle size of the sand. If the sands are finely ground the reaction is complete in about one hour. If the sands are quite coarse, four to six hours are required. As the reaction proceeds the digested mass becomes more and more viscous. When the reaction is nearly complete, a pasty mass results. The minimum acid-to-digested sand weight ratio, based on the stoichiometry of the reaction, is

* Direct correspondence to Dr. H. A. Wilhelm, Ames Laboratory, Iowa State College, Ames, Iowa.

Table I. Chemical Composition of Monazite Sands

	Indian monazite %	*Brazilian monazite* %	*Idaho monazite* %
Total oxides	69.2	68.1	68.9
ThO_2	9.4	6.5	3.95
CeO_2	28.5	–	29.2
U_3O_8	0.37	0.18	0.15
P_2O_5	25.9	26.0	28.5

about 0.60. The actual minimum acid-to-digested sand weight ratio is limited by the solubility of the thorium phosphate in the resulting monazite sulfate solution. Shaw *et al.*[3] found the actual minimum ratio to be 1.6 for both Indian and Idaho monazite.

Dissolution of the digest mass is accomplished by adding about 10 pounds of water per pound of digested sand. Cold water is preferable because the rare earth sulfates are more soluble at lower temperatures than at higher temperatures. The resulting solution is stable and is very close to saturation with respect to rare earths and thorium. This solution is called monazite sulfate solution.

The monazite sulfate solution can be decanted immediately from the heavy undigested sand. Upon standing, the fine suspended solids will settle out of the monazite sulfate solution. These solids are primarily silica but contain a very large fraction of the radioactive daughter products of thorium and uranium. The monazite sulfate solution can be decanted from this sludge.

The separation of the desired components from the monazite sulfate solution can be accomplished in several ways. Fractional crystallization methods have been used in the past. Many attempts are being made to extract the thorium and uranium directly from the monazite sulfate solution by making use of a selective solvent.

Shaw *et al.*[3] developed a process for separating thorium, rare earths and uranium from the monazite sulfate solution. A thorium concentrate was produced by diluting the monazite sulfate solution and adjusting the pH to 1.0 by using dilute ammonium hydroxide. At this pH, about 99 per cent of the thorium and 5 per cent of the rare earths precipitated. Since the rare earths are originally present in much larger amounts than the thorium, the resulting precipitate was about half thorium phosphate and half occluded rare earth sulfates. The solids were allowed to settle, the clear solution was decanted, and the remaining mixture was filtered. The thorium concentrate was dissolved in nitric acid and fed to a multistage extractor using tributyl phosphate as a solvent. A thorium product containing only a few parts per million of rare earth contaminants was obtained as an extract product. A wide variety of inert diluents can be used to enhance phase separations.

The filtrate and decantate from the thorium precipitation was then neutralized with ammonium hydroxide to a pH of 2.3. At this pH most of the rare earths were precipitated. The precipitate was allowed to settle and the clear solution was decanted from the solids. The concentrated precipitate was then filtered. These solids were sent to a rare earth recovery unit. The individual rare earths can be separated by ion exchange[4] or solvent extraction processes.

The filtrate and decantate from the rare earth precipitation step was then neutralized to a pH of 6.0. At this pH the remainder of the rare earths and the uranium were precipitated. The filtrate and decantate were discarded, and the uranium concentrate, containing about one per cent uranium was obtained. The uranium concentrate was dissolved in nitric acid and extracted in a multistage extractor using tributyl phosphate as a solvent. A uranium product was obtained containing only a few parts per million of rare earth contaminants.

Processes starting with a sulphuric acid digestion of the monazite cause the presence of sulfate ions in the solution to be extracted. Sulfate ions decrease the distribution coefficients for thorium and uranium markedly. The addition of nitric acid helps to overcome the effect of sulfate ion. Since the phosphate and sulfate ions are not extracted into tributyl phosphate, the scrub sections of the extractors are not influenced by the presence of these ions in the feed and separations can be carried out to any desired purity.

2.22 Caustic Digestion Process

The caustic digestion process developed by Bearse *et al.*[2] at the Battelle Memorial Institute consists of the following five operations:

1. Reaction of the sand with a hot concentrated sodium hydroxide solution. This converts the metal phosphates of the sand to hydrous metal oxides and trisodium phosphate.
2. Separation of the hydrous metal oxides from the dissolved sodium phosphate and excess sodium hydroxide.
3. Dissolution of the hydrous metal oxides in hydrochloric acid.
4. Precipitation of a thorium product by partial neutralization of the acid solution.
5. Precipitation of a rare earth hydroxide product by further neutralization of the chloride solution.

The effect of the sodium hydroxide-to-sand ratio was studied and a weight ratio of 1.5 was found satisfactory. The recommended reaction time was three hours at 140°C if the sand were ground to 96.5% less than 325 mesh and the initial concentration of sodium hydroxide were about 45 per cent.

In pilot plant runs the mixture was heated to 140°C and maintained at that temperature with moderate agitation for three hours. The mixture was then diluted with a wash solution from a later step. The slurry was digested for one hour to facilitate filtration and was then filtered to remove the hydrous oxides from the trisodium phosphate and excess caustic soda. The filtration was carried out at 80°C and 60 psig. The clear filtrate was sent to an evaporator for concentration and removal of trisodium

phosphate. The cake was blown dry and sent to the acid dissolution vessel.

The hydrous oxide cake was added to 37 per cent hydrochloric acid and heated for one hour at 80°C. The solution was then diluted and partially neutralized with sodium hydroxide solution to a pH of 5.8. At this pH, all of the thorium and uranium precipitated, accompanied by about three per cent of the rare earths. The slurry was allowed to stand and then the solution was decanted and filtered from the solids. The thorium and uranium were recovered from the cake by dissolving it in nitric acid and extracting with tributyl phosphate. The thorium and uranium were selectively stripped from the solvent. The absence of phosphate and sulfate ions permitted high concentrations and high separation factors in the extraction and scrub sections of the column.

The filtrate and washings from the filtration of the hydrous oxide cake were neutralized with sodium hydroxide to precipitate the rare earths as hydroxides. The slurry was filtered giving a rare earth cake containing very small quantities of uranium and thorium.

2.23 Cost Estimates

The sulfuric acid and caustic digestion processes have been compared on a cost basis assuming the same rate of production and the same source of monazite sand. There is apparently little economic advantage of one process over the other although pilot plant work on both processes was not extensive enough to arrive at accurate costs. The actual cost of the thorium depends principally on the value credited to the by-product rare earths and on the scale of production.

3. THORIUM METAL PREPARATION

Thorium metal, because of its reactivity (especially at elevated temperatures) and its relatively high melting point, presents a number of special problems in its preparation from the readily available compounds. However, a number of methods for producing thorium metal have been described in the literature since its first preparation by Berzelius[5] who reduced thorium tetrachloride with potassium metal and obtained an impure thorium metal powder. Most of the methods described yield the metal as a powder or granular product which can be fabricated by powder metallurgical techniques to give solid metal shapes.

In general, thorium metal can be prepared from thorium halides by reduction with reactive metals such as sodium, calcium and magnesium or by electrolysis of the halide in a fused salt bath. The thermal decomposition of the iodide to give thorium metal has been used only as a means for purifying metal prepared by other processes employing more stable thorium compounds. Thorium metal can be prepared also by the reduction of thorium oxide with calcium metal and a number of processes have been developed with this reaction as their basis. The processes for virgin metal described in some detail below are selected from among those that have been demonstrated to be capable of giving good quality metal in quantity.

3.1 Thorium Oxide Reductions

The original process developed by Marden and Rentschler[6] employed calcium chloride mixed in the charge with thorium oxide and a large excess of calcium metal. The charge was heated in a closed steel bomb for one hour at 950°C. After cooling, the reacted mass was leached with dilute (1:10) nitric acid, then with water followed by a wash with alcohol and a final wash with ether. The metal powder was then dried in vacuo, compacted and then sintered at about 1300°C to give solid ductile thorium metal having a purity of at least 99.7 per cent.

Rentschler *et al.*[7] describe in detail the production of good quality thorium metal by the calcium reduction of thoria under an inert atmosphere and without additives such as calcium chloride. A variation of the process employing this reduction reaction is carried out in a refractory-lined steel crucible in an inert gas atmosphere. The liner material may be made of thin sheets of a metal such as molybdenum. The liner is to prevent reaction between the charge or products and the iron crucible at the high temperature employed in the processing.

The crucible is charged with alternate layers of calcium metal (granular) and finely divided thorium oxide with a layer of the calcium on the top. About 100 per cent excess of calcium is employed over that calculated for the reaction:

$$ThO_2 + 2\,Ca \rightarrow Th + 2\,CaO$$

The charged crucible is then placed in a larger steel vessel having a lid fitted with a pipe for admitting an inert gas. The lid is bolted on, the air is replaced with argon and the assembly is then introduced into a furnace which is capable of heating to 1200°C.

The reaction takes place as the charge heats. The charge is further heated to a temperature of 1000°C or higher in order to obtain better yields of good quality thorium powder. The crucible and its contents are then allowed to cool under the inert gas to near room temperature. The product is then leached from the crucible by dumping the crucible and its contents into just sufficient dilute (10%) acetic acid to react with all of the calcium metal and oxide.

The first leaching solution is removed leaving the product as an impure mud. This mud is further leached by agitation with more dilute acetic acid. The product is allowed to settle and the leach solution poured off. The product is similarly washed a number of times with pure water. The water is removed and the product is then washed with alcohol and then with ether. The last traces of ether are removed by vacuum drying.

The dry product is a free-flowing powder which can be formed into solid thorium metal bars by pressing and sintering. Cold pressing at about 10 tons per square inch followed by vacuum sintering at tem-

peratures up to 1450°C for 30 minutes results in a thorium metal that is almost theoretical in density.

3.2 Thorium Chloride Reductions

Calcium, magnesium or sodium can be used to produce thorium metal by the reduction of thorium tetrachloride. The tetrachloride can also be electrolyzed in a fused salt bath to give a granular deposit of thorium metal. In most cases, the processes employing the tetrachloride yield the metal in a finely divided state and powder metallurgical processes are then employed to prepare shapes. One problem that is common to a number of these methods is that ThO_2 or $ThOCl_2$ in the tetrachloride may give high oxygen values in the final metal. These oxygen-containing compounds and carbon are reduced considerably by sublimation of the tetrachloride in a vacuum.

The oxide-containing compounds are of little concern if calcium is employed as the reducing agent. A process described by Lilliendahl[8] employs a charge made up of 30 parts of granular calcium with 70 parts $ThCl_4$ and 30 parts $ThOCl_2$. The conditions for the reaction and subsequent processing are closely related to those described for thorium by the reduction of ThO_2 with calcium, and the process yields a high purity product.

The magnesium reduction of the tetrachloride offers certain advantages over the use of calcium for large scale operations since it requires less magnesium per pound of product and magnesium is obtainable usually in higher purity and at a lower cost per pound than calcium. However, experiments have shown that a high quality of thorium tetrachloride is required for good quality final metal by the magnesium reduction. Properly sublimed thorium tetrachloride meets this requirement. Since magnesium and thorium form a low melting alloy it is possible to obtain thorium sponge instead of thorium powder with magnesium reduction of the tetrachloride.

Thorium metal of reportedly good quality has been prepared in batches of several pounds each by electrolysis of thorium tetrachloride in a fused salt bath. Since the electrode products are essentially thorium metal and chlorine gas, the process has possibilities of being operated on a somewhat continuous basis by adding make-up salts. Research on this process is being conducted at Horizons, Inc., Cleveland, Ohio.

3.3 Thorium Fluoride Reductions

The successful preparation of thorium powder by the electrolysis of $ThF_4 \cdot KF$ in a fused salt bath containing sodium and potassium chlorides has been described by Driggs and Lilliendahl.[9] This process was employed in production at Westinghouse Electric Corporation but has been replaced by a process similar to that described above for the calcium reduction of thorium dioxide.

The production of thorium metal by the calcium reduction of ThF_4 has been operated on a tonnage scale by the US Atomic Energy Commission. Metal referred to later in this report as "Ames" metal was prepared by this process at Iowa State College, Ames, Iowa, USA, where the process was developed and was operated for a number of years. The ThF_4 was obtained by precipitation of thorium oxalate from a solution of purified thorium nitrate, followed by calcination of the oxalate to oxide and then hydrofluorination of the oxide to ThF_4.

In addition to the ThF_4 and the calcium metal, the charge for the Ames process for thorium contains anhydrous zinc chloride. The mixed charge which reacts spontaneously after ignition gives thorium metal, calcium fluoride, zinc metal and calcium chloride as the primary reaction products. The addition of the anhydrous zinc chloride to the charge serves three purposes in promoting the thorium separation from the slag: (1) the zinc alloys with the thorium to give a low melting metal phase, (2) the calcium chloride fluxes the calcium fluoride slag, (3) the heat of the auxiliary reaction between $ZnCl_2$ and calcium serves as a thermal booster and raises the temperature reached by the reaction mixture.

As a result of these three contributions by the addition of zinc chloride to the charge, the products of the reaction reach a temperature at which they are molten and the metal and slag phases readily separate and subsequently solidify in position on cooling. Because of the high vapor pressure of zinc metal at temperatures reached by the reaction, it is necessary to carry out the reaction in a closed pressure vessel. This vessel is lined with a refractory material such as calcium oxide or dolomitic oxide. After the charge is introduced and covered, a lid is placed on the vessel, or bomb, and the assembly then placed in a furnace.

After the products are cool the bomb is opened and the massive metal piece, referred to as a "biscuit," is cleaned of adhering slag. The biscuit is then placed in a vacuum and heated to remove the zinc, leaving thorium metal sponge. A charge containing about 275 lb of sponge and croppings is then vacuum melted by induction in a beryllia crucible and bottom-poured into a graphite mold of the proper shape for the ingot.

The Ames process has recently been turned over to the National Lead Company of Ohio and some further details of the process with some variations are presented in another paper being submitted for Session 15B.1 of this conference.†

3.4 The Iodide Process for Purifying Thorium Metal

Veigel *et al.*[10] have described the preparation of massive thorium metal of high purity, in lots of several hundred grams each, by the van Arkel-de Boer (iodide) process.

The deposition vessel used in this work was made from Pyrex glass tubing and was about 10 centimeters in diameter and 75 centimeters in length. This tube, in an upright position, was closed at the bottom while the top was sealed only after the vessel had been charged. The seal cap for the top was made

† P/817, Volume 8.

of Pyrex glass and contained a connection for the vacuum line, a side arm for about ten grams of iodine and current lead-in wires from which the starting filament for the deposition was suspended.

The vessel accommodated a perforated molybdenum cylinder, the feed retainer, of such size as to leave an annular space sufficient to hold about four kilograms of thorium chips between the cylinder and the walls of the vessel. The starting filament was made of thorium wire 0.64 mm in diameter and about 115 cm in over-all length. The two ends of this filament wire were attached to 6.35-mm diameter tungsten electrodes in the cap by means of molybdenum tie-wires. A quartz spacer ring was attached to the bottom end of the filament loop by means of tungsten wires. This ring served to hold the filament straight and keep it well-spaced from the molybdenum feed retainer.

The filament assembly was inserted in the charged deposition vessel and the top cap sealed in place. The vessel was then vacuum outgassed at 510°C for a period of 24 hours. The iodine in the side arm was kept under refrigeration during the outgassing. The vacuum system was sealed off and the vessel and its contents cooled to 260°C. The iodine was then vaporized into the vessel to form the thorium tetraiodide.

It was found that deposition of thorium on the filament took place most readily when the externally measured temperature of the unit was in the range of 455°C to 485°C. The deposition furnace was equipped with sectional heating elements and copper cooling coils to maintain the temperature in the desired range as the deposit built up and more and more heat was generated in the filament.

Since it was difficult to determine the temperature of the filament, correct operating conditions were arrived at by an indirect means. The voltage applied to the filament from a sixty-cycle ac power supply was increased in steps until onset of deposition was indicated by an increase in current while the voltage was held at a particular value. Deposition was then controlled by adjusting the voltage and current at intervals to satisfy the equation,

$$I^{1/3} E = K$$

within a range of values for K, where I is the current in amperes and E is the applied voltage. Deposition usually began when E and I were such that $K = 0.43$ per cm of filament length and burnout of the filament rarely occurred if K were equal to or less than 0.63 per cm. In building up a deposit, E and I were initially adjusted for a value of $K = 0.43$ per cm and then voltage maintained constant until a value of $K = 0.63$ was reached. Subsequently the voltage was reduced and K maintained within the operating range. Runs were terminated when the current reached values of the order of 100 amperes which produced excessive heating of the vessel.

After completion of a run the electrode cap seal was cracked and the product removed from the deposition vessel. A representative deposit was about 0.62 cm in diameter for the entire length of the filament. Approximately 200 to 250 grams of "crystal bar" thorium metal was prepared per run. A sample of this iodide process metal contained 0.02 per cent carbon and less than 0.01 per cent each of oxygen and nitrogen.

4. PHYSICAL AND THERMODYNAMIC PROPERTIES OF THORIUM

Pure, freshly cut thorium exhibits a bright silvery luster but darkens after prolonged exposure to the air. It is comparable to lead in density and is soft enough to be easily scratched with a knife. More detailed quantitative information on the properties of thorium is given in the following pages. However, for convenient reference, a summary of selected values is given in Table II.

4.1 Radioactivity

Naturally occurring thorium consists predominantly of one isotope (Th^{232}) which is radioactive. Thorium emits a 3.98 Mev alpha particle with a half-life of 1.389×10^{10} years, and is the first member of the radioactive series which decays to $_{82}Pb^{208}$. The decay scheme as summarized by Hollander, Perlman and Seaborg[11] is shown in Table III.

4.2 Crystal Form

Thorium is face-centered cubic at room temperature. The crystal structure and parameter were first reported by Bohlin[12] in 1920. An average of parameter determinations by Burgers and van Liempt,[13] Neuberger,[14] D'Eye,[15] Baenziger[16] and Borie[17] gives the 5.086 Å value selected for Table II. Borie and D'Eye used metal prepared by the iodide process while Baenziger used metal obtained by the bomb-reduction process.

Table II. Selected Values of Properties of Thorium

Atomic number	90
Atomic weight	232.12
Crystal system	
F.C.C. up to 1400°C	a_o(25°C) = 5.086±0.0005 Å
B.C.C. 1400°C to M.P.	a_o(1450°C) = 4.11±0.01 Å
Electrical resistivity	
Bomb-reduced metal	~ 18 microhm-cm
Estimated for pure thorium	13–14 microhm-cm
Density	
Theoretical (from l.p.)	11.72 gm/cm³
Bomb-reduced (as-cast)	11.5 – 11.6 gm/cm³
Arc-melted iodide	11.66 gm/cm³
Elastic constants (typical values)	
Young's modulus	10.5×10^6 psi
Shear modulus	4.0×10^6 psi
Poisson's ratio	0.27
Compressibility	16.4 cm²/dyne
Melting point	1750°C
Heat of vaporization	130–177 kcal/mol
Heat of fusion	4.6 kcal/mol
Work function	3.39 ev

Table III. Thorium Disintegration Series

Isotope	Type of emission	Energy, Mev	Half-life	Daughter
Thorium (Th^{232})	Alpha	3.98	1.389×10^{10} yr	Mesothorium I
Mesothorium I (Ra^{228})	Beta	0.053	6.7 yr	Mesothorium II
Mesothorium II (Ac^{228})	Beta	1.55	6.13 yr	Radiothorium
	Gamma	0.914		
Radiothorium (TH^{228})	Alpha	5.418	1.9 yr	Thorium X
	Gamma	0.085		
Thorium X (Ra^{224})	Alpha	5.681	3.64	Thoron
	Gamma	0.241		
Thoron (Rn^{220})	Alpha	6.282	54.5 sec	Thorium A
Thorium A (Po^{216})	Alpha	6.774	0.158 sec	Thorium B
Thorium B (Pb^{212})	Beta	0.36	10.6 hr	Thorium C
	Gamma	0.24		
Thorium C (Bi^{212})	Alpha (33.7%)	6.054		Thorium C″
	Gamma	0.04	60.5 min	
	or beta (66.3%)	2.25		Thorium C′
	Gamma	2.20		
Thorium C′ (Po^{212})	Alpha	8.776	3×10^{-7} sec	Lead (Pb^{208})
Thorium C″ (Tl^{208})	Beta	1.82	3.1 min	(Stable)
	Gamma	2.62		

Evidence for the existence of a high-temperature allotrope of thorium was obtained by Chiotti[18] while studying the temperature dependence of the electrical resistivity. His resistance-temperature plot showed a sharp increase in slope over the temperature range 1425–1525°C. Such a break in temperature-resistance curves has also been reported by Adams[19] near 1350°C. Additional evidence for the existence of this allotrope has been found by Carlson who has observed complete solid solubility at high temperature in the thorium-zirconium[20] system and, more recently, in the thorium-hafnium[21] system. McCaldin and Duwez,[22] using a Pt/Pt-Rh thermocouple, have reported a thermal arrest near 1200°C. Chiotti[23] has investigated the X-ray diffraction patterns of 99.8% thorium at high temperature. His results indicate a transition from F.C.C. to B.C.C. at 1400 ± 25°C. The observed lattice parameter of the B.C.C. phase at 1450°C was 4.11 ± 0.01 Å. The transformation temperature was found to be sensitive to impurities, particularly carbon and zirconium.

The possibility of additional polymorphic transitions in thorium is indicated by the work of Bridgman.[24] While working with Westinghouse thorium, Bridgman found a decrease in slope in the curve of shearing stress versus pressure. The mean position of the break was observed at a pressure of 12,000 kg/cm² with a shearing stress of 2500 kg/cm². Bridgman's measurements of compressibility and of electrical resistivity as functions of pressure did not show anomalies at a pressure of 12,000 kg/cm².

4.3 Density

The theoretical density of thorium, calculated on the basis of the average value of 5.086 Å given in Table II for the lattice parameter, is 11.72 gm/cm³. Typical values for cast metal lie between 11.5 and 11.6 gm/cm³. Arc-melted iodide process thorium[17] approaches theoretical density with a value of 11.66 gm/cm³, while the same metal after rolling is reported to exceed the theoretical density with a value of 11.75 gm/cm³.

4.4 Elastic Properties

The elastic constants of thorium are quite sensitive to the past history of the sample. The effects of cold working on properties will be discussed in detail later in the paper. Typical values for the cast metal are: Young's modulus, 10.5×10^6 psi; shear modulus, 4.0×10^6 psi; Poisson's ratio 0.27.

The compressibility calculated from the measurements of Reynolds[25] is 16.4×10^{-13} cm²/dyne at 25°C.

The compressibility formulae given by Bridgman[26] are:

$$\text{at } 30°\text{C} - \Delta V/V_0 = 1.818 \times 10^{-6}P - 12.78 \times 10^{-12}P^2$$

$$\text{at } 75°\text{C} - \Delta V/V_0 = 1.846 \times 10^{-6}P - 13.29 \times 10^{-12}P^2$$

with P in kg/cm².

4.5 Thermal Coefficient of Expansion

A representative value for the linear coefficient of expansion from room temperature to 1000°C is 12.5×10^{-6} per °C; from room temperature to 200°C the coefficient is about 11.0×10^{-6} per °C. No directional dependence has been noted.

4.6 Thermal Conductivity and Thermal Diffusivity

The thermal conductivity of thorium has been measured by Marsh and Keeler[27] for temperatures from 25°C to 650°C and over a less extended range by Sidles and Danielson.[28] The latter investigators used a plan of measurement that depended on a knowledge of the thermal diffusivity. The relation between conductivity and diffusivity is

$$K = kC_p d$$

in which K is the thermal conductivity, k is the thermal diffusivity, C_p is the heat capacity and d is the density. When Sidles and Danielson used their measured values of diffusivity, the heat capacity data from Spedding, Miller and Flynn[29] and a density of 11.56 gm/cm^3, they obtained values for conductivity that agreed with those of Marsh and Keeler within 5% over the range from 25°C to 200°C. As the temperature dependence of the heat capacity may be uncertain by more than 5%, this discrepancy is not unexpected.

Values of thermal conductivity as measured by Marsh and Keeler of thermal diffusivity as determined by Sidles and Danielson are given in Table IV.

4.7 Electric and Magnetic Properties

The electrical resistance of thorium is quite sensitive to impurities and to the past history of the metal. Because of this a wide range of values has been reported in the literature for the room-temperature resistivity of thorium. Typical reported values lie between 18 and 25 microhm-cm. The lowest value, 13 microhm-cm, was reported by Marden and Rentschler[6] and also by Meissner and Voigt.[30] Measurements made in recent studies on very pure thorium in this laboratory indicate the correct value is 13 to 14 microhm-cm.

Reported values for the temperature coefficient of resistance of thorium in the range 0°C to 100°C lie between 2.30×10^{-3} per °C as reported by Bender[31] and 3.96×10^{-3} per °C as reported by de Boer.[32] As the coefficient for most unalloyed metals is 4×10^{-3} or higher de Boer's value probably is more nearly correct.

The pressure dependence of electrical resistance has been determined by Bridgman[26] as

$$30°C: \Delta R/R = -2.787 \times 10^{-6} P + 1.89 \times 10^{-11} P^2$$

$$75°C: \Delta R/R = -2.966 \times 10^{-6} P + 2.18 \times 10^{-11} P^2$$

where R is the resistance in ohms at a pressure of 1 kg/cm^2.

Thorium is known to be superconducting at low temperatures. This phenomenon has been studied by Meissner,[33,34] de Haas and van Alphen,[35] Schoenberg,[36] and Daunt.[37] Based on the two most recent measurements, the transition temperature is between 1.4°K and 1.3°K. Daunt has also reported the electronic specific heat at 7.1×10^{-4} cal $\times$ mol^{-1} $\times$ deg^{-1} and the Debye temperature as 170°K.

Table IV. Thermal Conductivity and Thermal Diffusivity of Thorium

Temperature °C	Thermal conductivity (cal × sec^{-1} × cm^{-1} × deg^{-1})	Thermal diffusivity (cm^2/sec)
25	–	0.29
100	0.090	0.29
200	0.093	0.28
300	0.096	0.28
400	0.100	0.29
500	0.102	–
600	0.106	–
650	0.108	–

Table V. Reported Values for the Work Function

Authors	Reference no.	Work function, electron volts
Hamer	42	3.57
Zwikker	43	3.35
		3.38
Rentschler, Henry and Smith	44	3.38
de Boer	32	3.36
Schulze	45	3.68
Rentschler and Henry	46	3.47

The Hall coefficient of thorium has been measured[38] as -8.8×10^{-5} cm^3/coulomb. This corresponds to an electron density for the conduction electrons of 7.1×10^{22} electrons/cm^3 or 2.4 electrons/atom.

Thorium was found by Honda[39] in 1910 and Owen[40] in 1912 to be paramagnetic. In 1939, Klemm[41] measured the susceptibility by the Guoy method of a rod estimated to be 99.8% thorium. He obtained values of mass susceptibility in cgs units of 0.54×10^{-6} at 20°C and 0.64×10^{-6} at −183°C. These values indicate a negative temperature coefficient for the susceptibility whereas Honda and Owen, for probably less pure metal, had found a positive temperature coefficient.

The work function has been determined by several investigators. In Table V, the investigators and the values they obtained for the work function are given in electron volts. Zwikker obtained his values from measurements of thermionic emission. The method used by de Boer is not stated. The remainder of the values was obtained by photoelectric experiments. Values given by Hamer and by Schulze were omitted in obtaining the average value for the work function given in Table II.

4.8 Emissivity

The emissivities of both solid and liquid thorium have been measured. Smithells[47] has summarized the data and his figures were used in the preparation of Table VI.

4.9 Melting Point

Reports of the melting point of metallic thorium have given widely different values. This variation is due in part to sensitivity to kinds and amounts of impurities. Furthermore, as Chiotti and Wilhelm[48] have

pointed out, thorium tends to take up oxygen and nitrogen in such a way as to form a tenacious refractory skin that holds the molten specimen to its original form after the interior is molten. An interesting observation on the effect of crucible material on melting point has been made by Thompson,[49] who obtained melting points from 1653°C to 1782°C in beryllia crucibles and from 1569°C to 1653°C in thoria crucibles.

Illustrative of the discrepancies observed both in early reports and also in later work, which may be presumed to be on purer metal, are the figures given in Table VII. Chiotti[48] who had found values from 1695°C to 1780°C in his own investigation, in which he employed a method first used by Pirani and Alterthum,[50] has estimated that the correct value for uncontaminated thorium is near 1750°C.

4.10 Heat of Fusion

The data on the heat of fusion of thorium are meager and perhaps unreliable. Evidence of a thermal arrest associated with the solidification of thorium has not been observed at Ames, even when 100-pound masses of metal are involved. Furthermore, the rapid solidification of the liquid noted during the pouring of an ingot is indicative of an exceptionally low heat of fusion. On the other hand, Miller[57] reported an arrest at 1626°C in his time-temperature curves taken during solidification of thorium. Also, heat of fusion calculated by the Clausius-Clapeyron equation from the depression of the freezing points by addition of other elements as indicated below does indicate measurable values:

Compound involved	ΔH_f *in kcal/mol*
Th-$ThBe_{13}$	4.6
Th-Th_2Ni	3.6
Th-Th_2Cu	4.6

These data suggest 4.6 kcal/mol as the upper limit for the heat of fusion. The values calculated cannot be accurate because of uncertainty of temperatures, possibility of solid solution and possible undetected curvatures of the liquidus line, and in view of experience during production, probably are too high.

Table VI. Spectral Emissivity of Thorium

Wavelength, micron	*Temperature °C*	*Emissivity*	
		Solid	*Liquid*
0.667	1000–1700	0.380	–
0.65	below m.p.	0.36	–
0.65	above m.p.	–	0.04
0.55	below m.p.	0.36	–

Table VII. The Reported Melting Points of Thorium

Investigator	*Ref. no.*	*Year*	*M.P., °C*	*Comments*
von Bolton	51	1908	1450	
Wartenberg	52	1909	1690	
Honda	53	1910	1450	
Marden and Rentschler	6	1925	1842	
de Boer	32	1933	1827	
Thompson	54	1933	1680	Electrolytic thorium
Thompson	54	1933	1730	Calcium reduced
Alberman and Anderson	55	1949	1850	
D'Eye	15	1949	1120	
Perlman	56	1947	1690	
Miller	57	1949	1626	From thermal arrest curve
Rapperport	58	1952	1702	Iodide thorium
Rapperport	58	1952	1693	Ames thorium
Adams	19	1953	1755	Iodide thorium

Table VIII. Heat Capacity Data and Results of Some Calculations

Temperature °K	C_p	C_v	$S°$	$(H°-H_0°)/T$	$-(F°-H_0°)/T$
20	1.106	1.106	0.410	0.304	0.106
50	4.048	4.042	2.770	1.801	0.969
100	5.482	5.460	6.135	3.369	2.766
150	5.965	5.927	8.460	4.164	4.296
200	6.217	6.161	10.215	4.648	5.567
250	6.392	6.318	11.623	4.980	6.643
298.16	6.532	6.441	12.760	5.220	7.540
300	6.538	6.446	12.799	5.228	7.571

4.11 Vapor Pressure, Heat of Vaporization, and Boiling Point

There is a high degree of uncertainty in the values of these three quantities. Vapor pressure studies have been done by Andrews,[59] Swikker,[60] and de Boer.[32] The results are so divergent as to lead to boiling point values ranging from 3300°K to 4500°K and heats of vaporization from 130 to 177 kcal/mol. The data in the compilations of Brewer,[61] Dushman,[62] and Loftness[63] are based upon the earlier work of Zwikker. In view of the conflicting results, further work on the vapor pressure of thorium is desirable.

The International Critical Tables[64] lists the boiling point as greater than 3000°C. A source for the value is not given, but in view of the available data it would seem to be a safe estimate.

4.12 Heat Capacity

The heat capacity of thorium from 18°K to 300°K has been measured by Griffel and Skochdopole.[65] The measured values of the heat capacity (C_p) in cal $\times$ mol^{-1} $\times$ deg^{-1} and some calculated thermodynamic properties are shown in Table VIII. These data give a Debye temperature of 141.6°K.

Two values for C_p above room temperature have been determined by Spedding, Miller, and Flynn.[29] They are 6.59 cal $\times$ mol^{-1} $\times$ deg^{-1} at 372.42°K and 6.61 cal $\times$ mol^{-1} $\times$ deg^{-1} at 471.9°K. The values agree satisfactorily with figures obtained by extrapolation of the data of Griffel and Skochdopole. The older heat capacity figure of Jaegar and Veenstra[66] is by comparison somewhat high while the value of 6.4 cal $\times$ mol^{-1} $\times$ deg^{-1} between 0 and 100°C obtained by Nilson[67] is in fair agreement with the data in Table VIII.

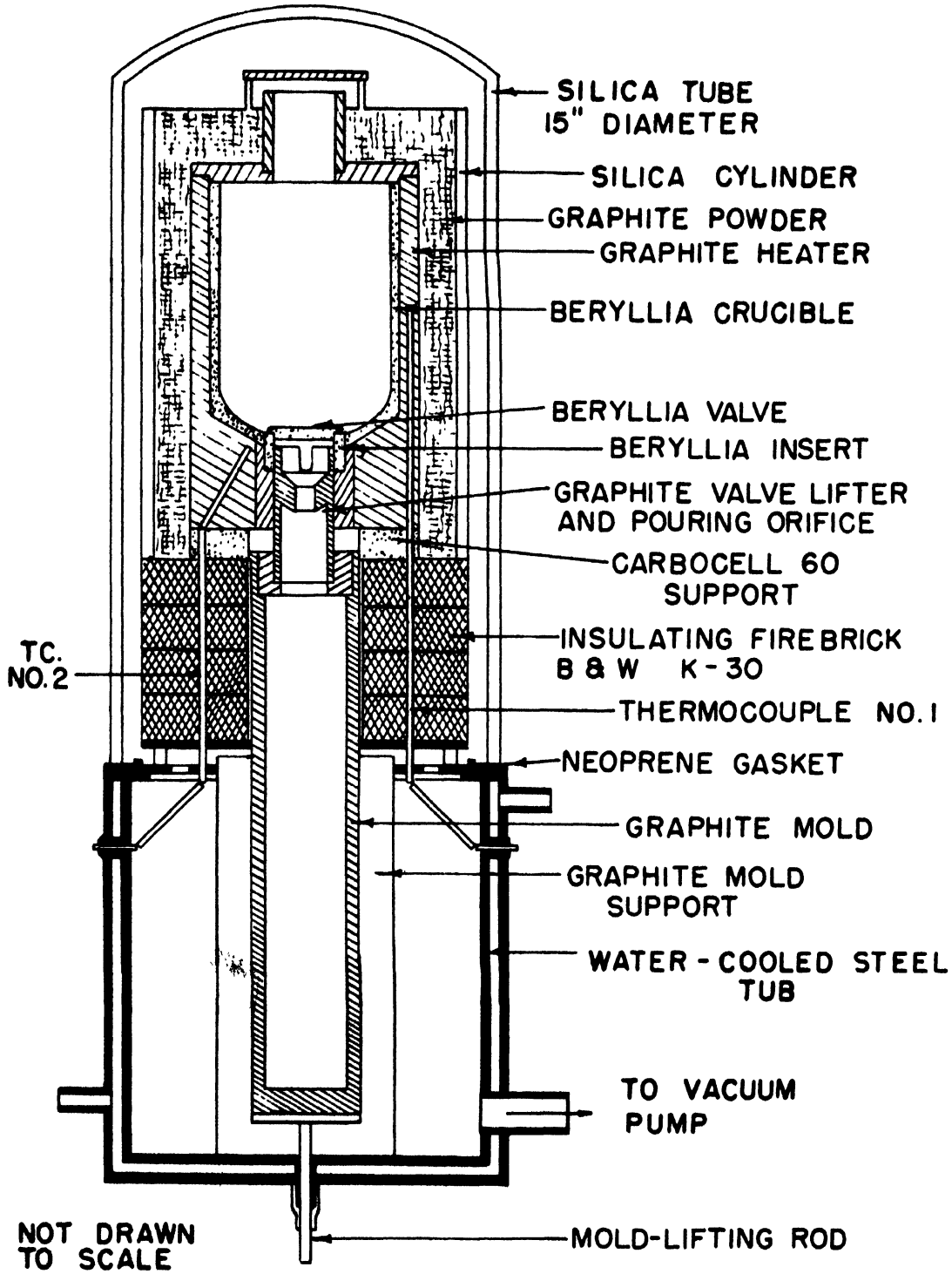

Figure 1. Equipment for melting and casting thorium in a vacuum

5. MELTING AND CASTING

The high temperature required for melting thorium and the reactivity of the metal toward crucible materials present problems in melting operations. Consequently, a variety of container materials has been investigated.

Among the oxides that have been tried, aluminum oxide, magnesium oxide and calcium oxide are attacked rapidly by molten thorium. Thorium oxide is relatively resistant but does cause contamination of the melt with oxide. Furthermore, it is undesirably susceptible to thermal shock. Stabilized zirconia has been used successfully for laboratory melts. The attack on zirconia becomes increasingly severe as the crucible temperature exceeds the melting point of thorium, consequently an induction cylinder outside the crucible should not be used. Direct inductive heat-

ing of the charge is advisable. However, the power input must be controlled carefully so that excessive temperatures do not develop. Beryllia has been the most satisfactory oxide so far tested for melting thorium. It is resistant to thermal shock and has adequate strength at high temperature. In addition, it is resistant to attack by molten thorium at 1800°C and may be used up to 1950°C.

No other container materials have been found that serve satisfactorily as melting crucibles. Graphite may be used but it contaminates the charge. For example, a melt held for 20 minutes at 1800°C picked up approximately 0.30 wt% carbon. Metallic tantalum can contain molten thorium at just above the melting point of thorium for a short time but the melt is contaminated even during the short exposure. For laboratory melting, the tungsten-arc, water-cooled copper-crucible furnace operating under helium or argon is satisfactory. With purified gas and careful handling of the arc, contamination may be held to a minimum.

At the Ames Laboratory, batches as large as 275 pounds of thorium have been vacuum melted in beryllia crucibles and the metal then poured into graphite molds. Considerable casting has been done with equipment of a size suitable for melts of 125 pounds of thorium. A drawing showing details of such equipment is presented in Fig. 1.

The apparatus consists primarily of a graphite mold mounted below a beryllia crucible designed for bottom-pouring. These items and accessory parts are enclosed in an inverted closed-end silica tube and a welded, water-cooled steel tub that is provided with a connection to a vacuum pumping system. The silica tube and the steel tub have a neoprene gasket at their junction. The tub is further designed to accommodate, with vacuum seals, two thermocouples that measure heater temperatures and a push rod for activating the pouring valve. The beryllia crucible and its charge are heated indirectly by a cylindrical graphite heater that absorbs power from an induction coil (not shown in the figure). The coil is connected to a 100 kva, 3000 cycle per second, 800 volt generator.

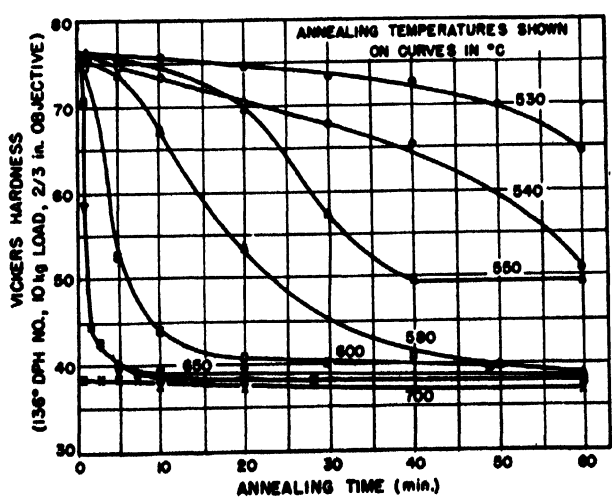

Figure 2. Isothermal recrystallization curves for iodide thorium. Reproduced from data reported by Eckert and Boyle, Oak Ridge National Laboratory, 1953

The mechanism by which the molten metal is poured from the crucible into the mold can be deduced from the figure but some description of the procedure may be helpful. An upward thrust on the mold-lifting rod raises the mold which has a cup-shaped graphite adapter with a graphite valve lifter seated in its top. The hollow valve lifter has the dual function of lifting the beryllia plug, or valve, that seals the bottom of the crucible and of providing a passageway for the molten metal released when the plug rises. Metal enters the head of the cylindrical lifter through four ports, of which one is shown, and flows downward through a central orifice. This valve lifter is machined to a large diameter in its lower portion so that the metal after it leaves the orifice makes less contact with graphite as it pours into the mold.

Thermal insulation of the heater element is provided by a layer of graphite powder, 10 to 18 mesh size, between it and the inner silica cylinder. The powder also is piled over the lid to the graphite heater. Insulation of this type and also the insulating fire brick give off some gas but the pressure can be reduced below one micron of Hg before heating is started and never rises above 50 microns of Hg on degassing. Low pressures are recovered before the metal is poured.

The time to pour a melt is determined by measurements with tungsten-niobium thermocouples that pass through vacuum tight seals and extend upward into holes drilled into the heater block. Usually, the metal is poured after the thermocouples have registered a temperature of 1800°C for 20 minutes.

With the equipment described, 125-pound charges of thorium sponge could be melted and poured in about 90 minutes. The uncropped ingot weighed about 94% to 98% of the amount of the charge. Cylindrical ingots of 3- to 7-inch diameter were the usual product but some rectangular ingots also were cast. In most instances the only apparent blow holes or shrinkage cavities were present in the top of the ingot. The surfaces were slightly rough but removal of about $\frac{1}{16}$-inch thickness of skin yielded a smooth, clean surface. A small amount of beryllium and carbon was picked up in the melting and casting. The proportions usually did not exceed 150 ppm beryllium and 300 ppm carbon.

Thorium metal has also been cast by consumable-electrode arc-melting on a rather large scale. Roberson, Beall and Caputo[88] report that the process is economical and produces good quality billets with little contamination and high casting yields. Thorium sponge metal is fabricated into electrodes by welding pieces together or by pressing smaller pieces in a die. These electrodes are arc-melted under about 250 mm Hg pressure of inert gas.

6. HEAT TREATMENT AND RECRYSTALLIZATION

As thorium is sufficiently soft to be cold worked to an extreme degree without intermediate annealing, the usual associated problem of heat treatment appears to be of minor importance. For unalloyed thorium, about the only kind of heat treatment that alters the properties of the metal is reheating to produce recovery or recrystallization. The metal has an allotropic transformation but it occurs so far above usual working and annealing temperatures as not to require consideration in unalloyed or slightly alloyed products. Effects that are possibly caused by changes in solubility of impurities, and may be related to precipitation, do sometimes make themselves evident in production metal. However, limited studies of thorium-rich alloys have not revealed significant age hardening effects.

6.1 Change in Hardness of Cold-Worked Metal with Heat Treatment

The softening of severely cold-worked, unalloyed thorium by short time annealing treatments becomes evident at a temperature of 500°C or slightly lower, according to work by Eckert and Boyle.[69] At 600°C, the softening effect is approaching completion after 20 or 30 minutes. The relationship between hardness and time at a series of temperatures is displayed graphically for iodide thorium in Fig. 2 and for Ames thorium in Fig. 3. Both kinds of thorium had been severely cold worked to about 80 per cent reduction in area. The compositions of the metals used in these tests are specified in Table IX.

As with most metals, the temperature at which softening of thorium sets in decreases as the degree of previous cold-work increases. This effect is pronounced in iodide thorium, as may be seen from Fig. 4, but is less evident in Ames thorium for which the results are presented graphically in Fig. 5. In all cases, the specimens were at temperature for 1 hour.

Eckert and Boyle also found that the addition of small amounts of carbon to iodide thorium has little effect on the temperature of recrystallization although

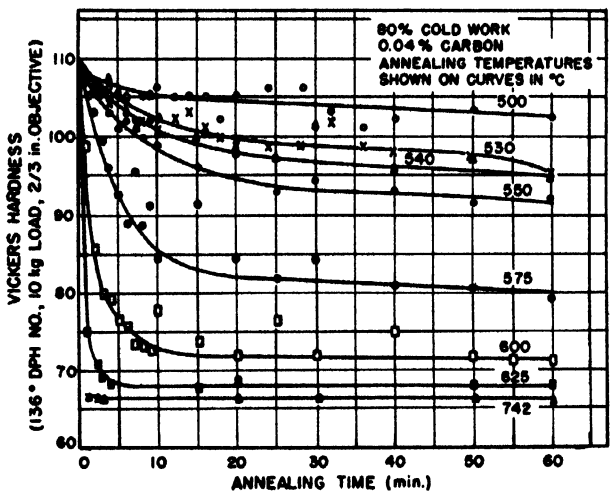

Figure 3. Recrystallization curves for Ames thorium. Reproduced from data reported by Eckert and Boyle, Oak Ridge National Laboratory, 1953

the softening curves have a different shape as may be seen in Fig. 6. A feature of these curves is the rise in hardness as the temperature of annealing increases beyond 650°C. The actual amounts of carbon in the specimens are indicated on the figure and some additional information on composition is given in Table IX.

In the preparation of these thorium-carbon alloys, Eckert and Boyle added the carbon as a master thorium-carbon alloy to iodide thorium. The melting was conducted in a tungsten-electrode arc furnace under an inert gas. Ingots were cold reduced about 35% and homogenized 12 hours at 1275°C before being subjected to reduction and the subsequent annealing treatments of Fig. 6.

As would be deduced from a study of the above figures, recrystallization begins to develop in the cold-worked material within the range 500°C to 700°C. Eckert and Boyle observed that formation of new grains begins to take place in iodide thorium as soon as the hardness decreases, whereas, no change in metallographic structure occurs in Ames thorium until the metal has decreased in hardness to about 100 on the Vickers hardness scale.

Table IX. Chemical Analyses of Thorium

	Composition (ppm)							
Material	*C*	O_2	N_2	*Al*	*Si*	*Fe*	*Be*	*Other elements*
Ames thorium billet	370	120	150	90	90	140	30	Faint traces
Iodide thorium	200	110	10		Trace	Trace		Faint traces
Thorium-carbon alloy	1350	500	600		Trace	Trace		Faint traces
Thorium-carbon alloy	1010	400	70		Trace	Trace		Faint traces
Thorium-carbon alloy	850	200	40		Trace	Trace		Faint traces
Thorium-carbon alloy	490	100	10		Trace	Trace		Faint traces

6.2 The Effect of Added Elements on the Hardness of Heat-Treated Thorium

Milko and Boyle[70] have studied the effects of larger percentages of carbon on homogenized and also on quenched specimens. Specimens homogenized 24 hours at 950°C showed a progressive rise in hardness from 22 to 66 on the Rockwell A scale as the carbon increased from 0.07% to 1.42%. At first the rise was rapid but the increase in hardness per point of carbon added decreased gradually, and an increase from 1.42% to 2.50% carbon produced little effect on hardness of these specimens. The hardness of alloys quenched from temperatures in the range of 400°C to 1600°C is summarized in Table X.

Table X shows differences in the hardness of thorium-carbon alloys quenched from different temperatures. The strengthening and hardening effect of addition of carbon in thorium has been observed by others besides Milko and Boyle. Although inspection of the thorium-carbon phase diagram indicates phase relationships that might result in extensive precipitation hardening for certain compositions, such effects are realizable to only a minor degree. The solubility of carbon in thorium probably is about 0.3 to 0.4 wt % and greater amounts cannot be held in solution by the most rapid quenching.

In general, additions of other elements to thorium have not given rise to important heat treatable alloys. Addition of low percentages of niobium, tantalum, titanium and a few other metals actually lower the hardness of Ames thorium, possible because these elements form compounds with the carbon and remove it from its role as hardener in the thorium.

Oxygen has a less pronounced effect in hardening iodide thorium than carbon does, possibly the lessened effect is due to the relatively low solubility of oxygen in thorium and the form of the oxide inclusions. An increase in oxygen content from 0.006% to 2.0% produced an increase in hardness from R_H 45 to R_H 95 in specimens that had been homogenized at 950°C for 24 hours.

6.3 Textures in Deformed and Recrystallized Thorium

Orientation has been observed in cold-rolled thorium and also in the extruded product. After being rolled,[71] the sheet is predominantly of two textures which can be described in the usual manner as (100) [001] and (011) [211]. Recrystallization removes much of the orientation effect of rolling. However, the crystals are not in a completely random arrangement, but have a slight preference for (100) [110] positions and a tendency for (111) planes to lie in the plane of the sheet.

According to Jetter, Borie and Fretague[72] speed of extrusion affects the resulting texture of the metal. If the extrusion rate is low, the texture has [111] as a major direction and [100] as a minor direction. On the other hand, high speed extrusion results in recrystallization with a single [114] texture. Metal extruded at 1 ft/min is about twice as strong as the same material extruded at 600 ft/min.

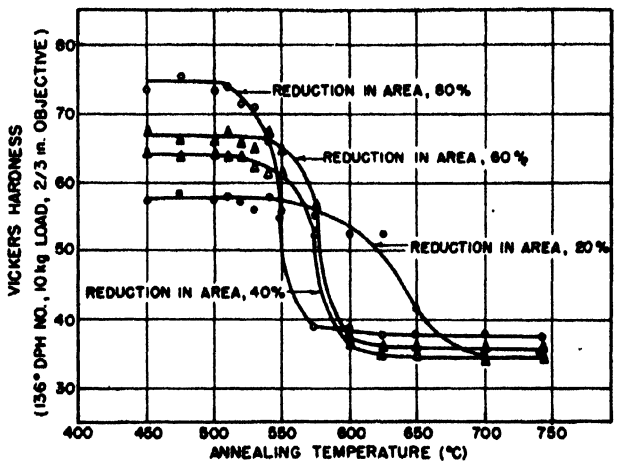

Figure 4. Effect of cold work on recrystallization of iodide thorium. (Samples annealed one hour at each temperature indicated.) Reproduced from data reported by Eckert and Boyle, Oak Ridge National Laboratory, 1953

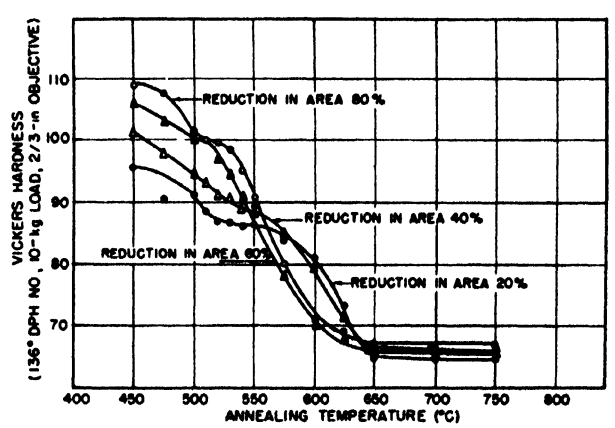

Figure 5. Effect of cold work on recrystallization of Ames thorium. (Samples annealed one hour at each temperature indicated.) Reproduced from data reported by Eckert and Boyle, Oak Ridge National Laboratory, 1953

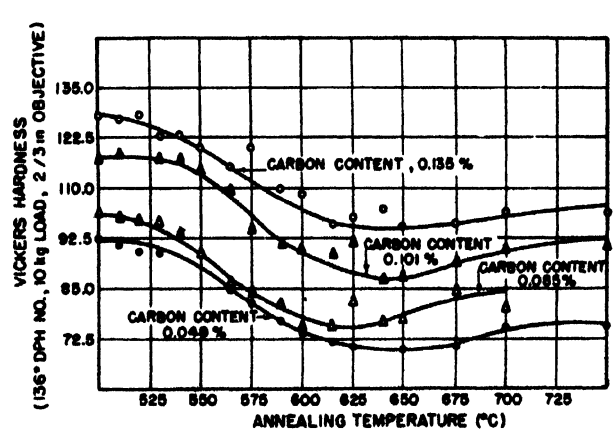

Figure 6. Effect of carbon on recrystallization of iodide thorium. (Samples annealed one hour at each temperature indicated.) Reproduced from data reported by Eckert and Boyle, Oak Ridge National Laboratory, 1953

Table X. Effects of Carbon Content on Hardness of Arc-melted Thorium-Carbon Alloys Quenched from a Series of Temperatures

Carbon (wt %)	Vickers hardness* of alloys quenched from temp. (°C)									
	1600	1500	1400	1300	1200	1100	1000	800	600	400
0.07	112	99	99	98	100	89	94	80	82	70
0.09	120	97	99	93	98	93	89	84	88	83
0.11	144	131	124	126	120	119	112	110	124	99
0.20	192	168	153	153	142	142	143	140	131	129
0.26	198	185	179	176	171	163	161	160	150	133
0.50	237	245	250	252	259	265	246	218	201	205
1.05	350	394	412	335	335	410	264	291	287	270
1.42	412	433	385	470	415	424	379	325	284	290
2.50	440	421	472	477	401	448	406	393	253	259

* Each value is the average of 5 determinations, 136-degree diamond pyramid with kg load used.

6.4 Effect of Radiation on Thorium

Brinkman and Gilbert[73] investigated the change of electrical resistance of thin sheets of thorium subjected to radiation with protons and deuterons. They observed that the resistance reached a saturation value at some value of integrated beam intensity but that the two kinds of particles produced saturation at different values of integrated intensity. Brinkman[74] studied the nature of radiation damage in thorium and other metals.

7. THE FABRICATION OF THORIUM

7.1 Forming Operations

The forming of thorium has been investigated by several contractors of the Atomic Energy Commission. Detailed descriptions of the work done by each organization appear unnecessary but the laboratories that have been most active in this work may be listed. They are: Battelle Memorial Institute, Oak Ridge National Laboratory, Massachusetts Institute of Technology and Ames Laboratory.

Although contaminating substances, particularly those that segregate in grain boundaries introduce difficulties in some instances, a good grade of thorium can be formed readily in most operations. For example, a good grade of thorium can be rolled readily either hot or cold. First grade metal can be rolled cold to reductions exceeding 99.9% without intermediate annealing. Such material is comparable to copper or silver in its amenability to fabrication. Even thorium that contains several per cent of oxygen has considerable ductility as nearly all of the element is present as small oxide inclusions and the metal simply flows around these particles.

Thorium behaves well also in forging and extrusion. Although the metal is reactive toward both oxygen and nitrogen, large pieces of thorium may be heated for such operations in ordinary fuel-fired furnaces. For smaller pieces, the proportion of metal converted to oxide becomes excessive and finely divided material is likely to be oxidized completely. Because thorium has an unusual tendency to stick in a die, drawing operations present the most trouble of any of the common processes. Tubes are particularly difficult to make.

7.2 Machining

The machining of thorium presents few problems and can be done by conventional methods either dry or under a coolant. The machining properties vary to some extent with purity. Very soft, low-carbon content thorium machines like copper but harder metal behaves more like mild steel. The softness of the metal makes the production of a fine finish difficult.

Microscopic inclusions of thorium oxide usually present throughout thorium made by the Ames process make the metal somewhat abrasive. In addition, the scale on the surface of cast or forged pieces produces rapid wear on tools. Because of this abrasive character, use of carbide tools may be advantageous in some instances.

In general, slow speeds of cutting and heavy cuts are desirable in machining operations. In lathe work, relatively high feed rates and slow spindle speeds should be used in order that the chips will be large and will not be unduly hot. The heavy chips are easy to recover efficiently and are less likely to catch fire spontaneously. For machining in turret lathes, speeds up to 300 surface feet per minute and feed rates of 0.007 inch to 0.018 inch per revolution are suitable. For sawing, a coarse high-speed steel blade in a power feed hack saw supplied with coolant works out well. Milling of thorium offers no problems but a smooth surface is difficult to obtain because of the scoring of the surface by chips that adhere to the cutter.

Hazards that are associated with the machining of thorium are described in Section 12, but the need for care cannot be over-emphasized in view of the capacity of clean thorium chips as well as chips from some types of thorium scale to ignite spontaneously. Also important is the chance of ingesting small particles of radioactive material.

7.3 Powder Metallurgy

In general, one may say that the production of thorium objects from the powder does not differ

essentially from the methods used for other metals. These methods are described in numerous journal articles and in books such as the one by Schwarzkopf.[75]

A number of the processes for producing thorium yield the metal in powder form. In other processes such as the bomb reduction of thorium fluoride, the metal in an intermediate stage may be a sponge which can be cast into massive metal. Thorium in the form of sponge, massive metal, chips or lathe turnings can be converted to metal powder by the formation and decomposition of the hydride. In the following discussion, only the preparation of thorium metal powder by the hydride process will be treated in detail, but in addition, the nature of the powders obtained by some reduction processes will be discussed here for comparison. Thorium powder and hydride, described below, offer potential explosion, fire and health hazards which are described in more detail in Section 12 of this paper.

7.31 Production of Thorium Powder by the Hydride Process

The hydride process involves, as its first stage, the treatment of metallic thorium, in pieces of any convenient size, with hydrogen. During this stage, the charged pieces disintegrate into a coarse powder as the hydrogenation progresses to completion. Decomposition of the hydrided material in a reversed process yields metallic thorium of the same particle size as was possessed by the hydrided metal.

Studies of the reaction of thorium with hydrogen have shown that two compounds are formed—one with the formula ThH_2 and one with the formula Th_4H_{15}. The dihydride has a body-centered tetragonal crystal structure with $a_0 = 4.10$ Å and $c_0 = 5.03$ Å and a density of 9.20 gm/cm^3.[76] The higher hydride is cubic with four molecules (Th_4H_{15}) per unit cell, $a_0 = 9.11$ Å, and space group $I\bar{4}3d$.[77] The density of the higher hydride is given by Nottorf[78] as 8.33 gm/cm^3. For the dissociation pressure of a system consisting of equal amounts of ThH_2 and Th, these investigators give the relation

$$\log_{10} P_{mm} = \frac{-7700}{T} + 9.54$$

where P is in mm of mercury pressure and T is in °K. The dissociation pressure for an equimolar mixture of ThH_2 and Th_4H_{15} is given by the relation

$$\log_{10} P_{mm} = \frac{-4220}{T} + 9.50$$

Mallett, Campbell *et al.*[79] also have studied the dissociation pressure of thorium-hydrogen compositions up to $ThH_{1.9}$. Their results, as well as those of Nottorf *et al.*, show that within the range investigated, the dissociation pressure is dependent upon the composition to some extent. Mallett and Campbell present equations for the dependence of the dissociation pressure on temperature for a number of specific compositions. The dissociation pressure of a composition having a hydrogen to thorium ratio of 0.05 is given as

$$\log_{10} P_{mm} = \frac{-4720}{T} + 5.7$$

This corresponds to a dissociation pressure of roughly 10 mm Hg at 1000°K. Consequently, the hydrogen content of hydride powder can be reduced to a hydrogen to thorium ratio of 0.05 at this temperature if the hydrogen pressure is reduced to 10 mm. At 700°C the decomposition pressure for a hydrogen to thorium ratio of 0.025 is of the order of 1.0 mm.

Chiotti and Rogers,[80] and Wilhelm and Chiotti[81] have described in some detail a procedure for preparing thorium powder from massive metal by means of the reaction between the metal and hydrogen. This procedure can be broken down into the following steps:

1. Formation of the dihydride, ThH_2, at 600°C to 650°C at one atmosphere hydrogen pressure. During this step the charge swells but does not break up to form a powder.
2. Formation of the higher hydride at temperatures not above 320°C. The optimum temperature for this step is about 250°C. The charge exfoliates and breaks up into a coarse powder during this operation.
3. Decomposition of the higher hydride to the lower hydride by heating to 500°C under a pressure of one atmosphere of hydrogen.
4. Decomposition of the lower hydride at 700°C at low pressure. At this temperature the dissociation pressure of $ThH_{0.025}$ is approximately 1.0 mm Hg.

For small lots of powder the preparation can be carried out in a fused silica tube. However, if ten pounds or more of powder are to be produced, a steel (preferably stainless) reaction chamber is more suitable. The remainder of the equipment consists of a mechanical vacuum pump, a diffusion pump, a suitable vacuum gauge for measuring low pressure and a manometer for measuring pressures near one atmosphere. It is possible to check the reaction rate by temporarily closing off the hydrogen supply and observing the rate of pressure drop. A purification train for the hydrogen and a liquid nitrogen trap to prevent diffusion of oil vapors from the vacuum pumps to the charge should be included.

A charge of lathe turnings or chips is preferable to massive metal since the time required to form the hydride depends on the surface to mass ratio of the charge. A ten-pound charge of shavings or chips can be converted to metal powder in eight to twelve hours. Four- to 5-pound pieces of massive metal in the form of croppings from 4-inch diameter billets have also been successfully converted to metal powder by this process but the operation required about twice as long as conversion of an equal weight of chips would require. The formation of both the dihydride and the higher hydride is exothermic. With a charge

of shavings, chips, or sponge the formation of the dihydride is sufficiently rapid and exothermic to bring the charge to a red heat and no heating of the charge is necessary once the reaction starts. The reaction becomes vigorous at 300°C to 400°C. In the case of large massive pieces of metal, the reaction is not sufficiently rapid to maintain the optimum temperature. The time required to form the higher hydride at 250°C can be reduced if some means is provided for removing the heat generated.

7.32 Properties of Thorium Powder

The thorium powder obtained by the hydride process is relatively coarse but can be broken up easily to pass a 30-mesh (0.59-mm opening) screen. If finer powder is desired, some decrease in particle size may be obtained by repeated formation and decomposition of the hydride but this method is not an effective one.[82] A more satisfactory procedure is to grind the brittle higher hydride under an inert atmosphere by some means such as ball milling and then to decompose the powdered hydride to metal at 700°C.[83] Very little sintering of the particles occurs during this stage and the metal powder can be broken up to pass through the same mesh screen as the hydride from which it was prepared.

The plasticity of the particles obtained depends to a considerable degree upon the purity of the original metal and the residual hydrogen content. If the system is pumped to a pressure below 0.5 mm Hg at 700°C, the powder produced from Ames cast metal is soft and plastic.

Chuk-Ching Ma[84] has studied some of the factors influencing the particle size of metal powders produced by fused salt electrolysis. He points out that the primary variables which affect the number of nuclei formed and their subsequent growth are the temperature, current density and bath composition. The crystal size of the deposit is decreased as the current density is increased and also as the impurity content of the bath is increased. These characteristics are believed to be due to the formation of alkali metal films on the cathode surface and to polarization effects. Polarization is more pronounced at low temperatures. He determined the particle size distribution obtained on electrolysis of a salt bath consisting of 1 part $KThF_5$, 0.5 part NaCl and 0.5 part KCl at 850°C and at 780°C. During each run the composition, temperature and current density (60 amperes per square decimeter) were held constant. It appears from Chuk-Ching Ma's curves that the thorium powder obtained at 850°C was practically all less than 250 microns, 91% less than 86 microns, and 71% less than 44 microns. At 780°C practically all the powder was less than 250 microns, 93% less than 86 microns, and 78% less than 44 microns.

In general the particle size and purity of thorium metal powder produced by electrolysis of fused salts by different investigators varied considerably.

Raynes *et al.*[71] have produced high quality metal powder by the electrolysis of fused $ThCl_4$-NaCl salt

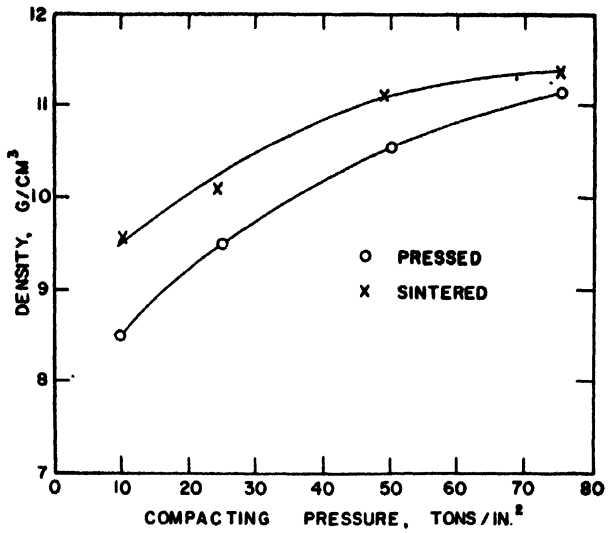

Figure 7. The density of unsintered and sintered compacts of thorium made from Ames metal by the hydride process. The specimens had been pressed at about 150,000 psi. Sintering was at 1150°C for 30 min (Wagner and Storchheim)

mixtures at 800°C to 850°C. They took special precautions to prepare pure anhydrous salts and to exclude moisture and air from the cell. The average particle size of several batches of powder tested ranged from 105 to 150 microns.

The reduction of thorium oxide with calcium and reduction of the chloride with magnesium give powders that are usually less than 150 microns, but presumably can be made coarser or finer than this depending on the final reaction temperature and other conditions.

The major impurities in the metal powder are usually oxygen, nitrogen, hydrogen, and carbon. Some recent work on the vacuum-fusion analysis of thorium powder for oxygen, nitrogen and hydrogen has been reported by Sloman *et al.*[85] Analysis of metal powder produced by the reduction of thorium halides with

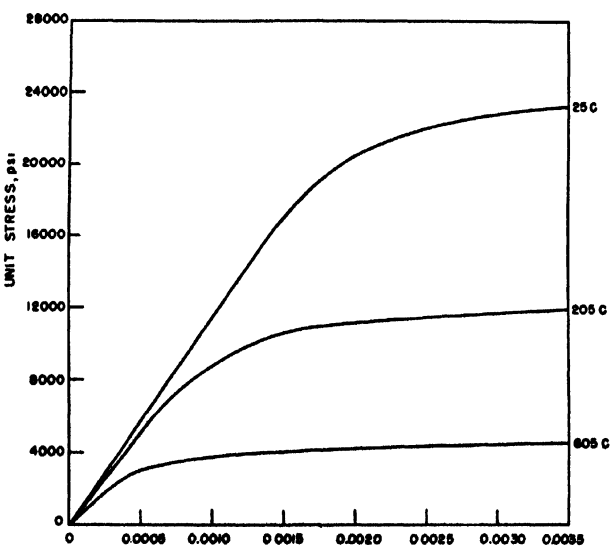

Figure 8. Typical stress-strain diagrams for cast thorium in tension

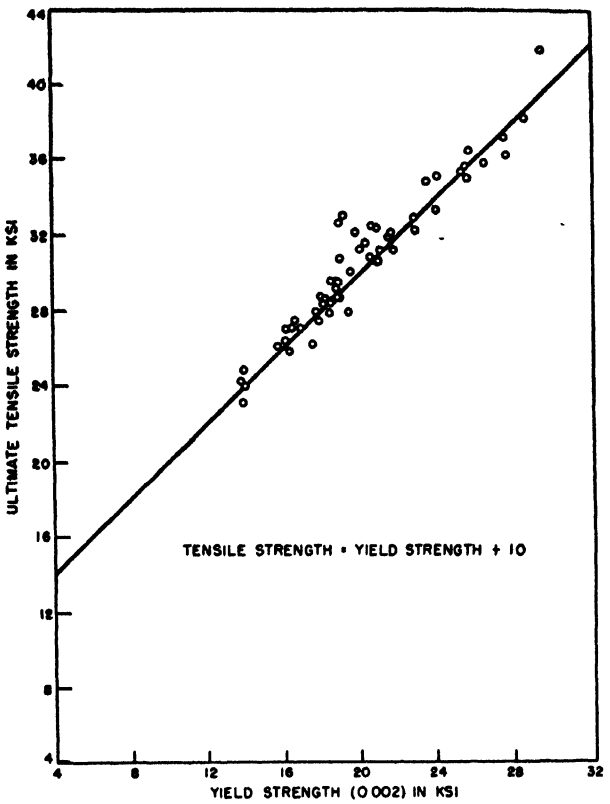

Figure 9. Variation of tensile strength with yield strength of Ames thorium

magnesium or calcium gave the following analyses: oxygen 0.2 to 1.3 wt %, nitrogen 0.1 to 0.2 wt %, and hydrogen 0.5 to 0.15 wt %. Similar powder, compacted and melted in thoria crucibles under high vacuum, analyzed: oxygen, 0.07 to 0.08 wt %; nitrogen, 0.02 to 0.03 wt %; hydrogen, 0.0010 to 0.0015 wt %. The decrease in oxygen content is believed to be due to the separation of the oxide from the melt by virtue of its lower density and its low solubility at the freezing temperature. The reduction of the hydrogen content is not surprising in view of the dissociation pressures reported for the thorium hydride compositions cited above[78,79] and the work of Wagener[86] on the reversible sorption of hydrogen by thorium. The decrease in nitrogen content might be due to separation of the nitride in a manner analogous to the separation of the oxide.

Wagener has studied the rate of sorption of oxygen by thorium at very low pressures, 10^{-3} to 10^{-7} mm Hg, over a temperature range from 27°C to 727°C. His results show that oxygen is irreversibly sorbed on the metal surface. The initial rate of sorption is very high but drops off rapidly with time. However, the surface can be reactivated by heating it to 925°C. The oxygen is not removed by this treatment and he suggests that it apparently diffuses into the metal until the gain in weight is equivalent to an oxygen content of 0.44 wt %. Since the solid solubility of oxygen in thorium is known to be much less than this proportion, a more likely explanation is that activation of the metal on heating to 925°C is principally due to a breaking up and agglomeration of the surface film and consequent exposure of new surface. Wagener also studied the sorption of hydrogen under the same conditions. The gas is sorbed reversibly by a process of solution in this case. The rate of hydrogen sorption has a maximum value between 425°C and 475°C.

7.33 The Compactability of Powder

In general particles of high purity thorium metal are quite malleable and the powder is readily fabricated by powder metallurgy techniques to give ductile shapes. Wagner and Storchheim[88] have investigated some compacting properties of metal powder produced by the hydride process. They found that the density of cold-pressed, unsintered compacts of the powder showed a continual increase with pressure up to 150,000 psi. The effect of particle size was not pronounced although the −20 to +80 screen mesh size had less satisfactory flow properties than finer powders. After being sintered under an argon atmosphere for one-half hour at 1350°C, the compacts had a density of 11.5 gm/cm^3. The change of density with pressure of both unsintered and sintered compacts is shown in Fig. 7. Klein and Wikle[88] also described fabrication of thorium by powder metallurgy.

8. MECHANICAL PROPERTIES

8.1 Tension and Compression

The tensile strength of Ames thorium has been obtained from tests on ASTM standard specimens at temperatures up to 700°C. The ultimate strength varies from 22,000 psi to 40,000 psi at room temperature depending on the method of forming and on the impurities present.

A set of typical stress-strain diagrams is given in Fig. 8. These diagrams indicate that the material very nearly exhibits a yield point, and in fact definite yield points have been observed in some tests. The yield strength (0.002 offset) at room temperature

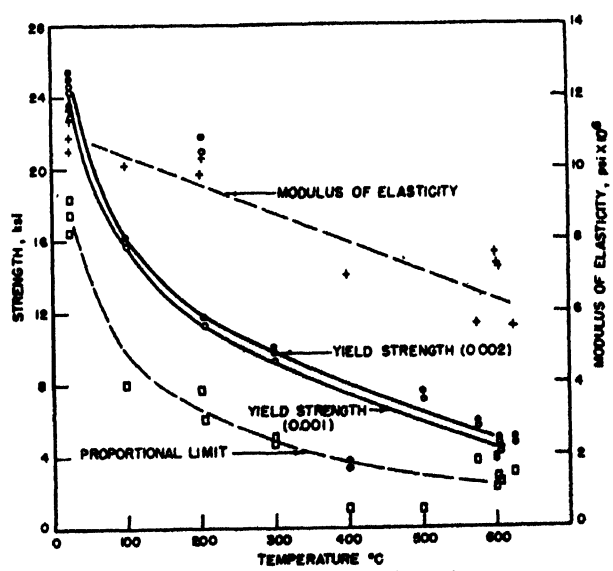

Figure 10. Tensile properties of cast thorium

is consistently 10,000 psi below the ultimate strength, as is shown in Fig. 9. The yield strength and the tensile strength at room temperature correlate well with Rockwell hardness as measured on the *E* scale.

At elevated temperatures, the yield strength is decreased, dropping to the 2000 to 8000 psi range at 700°C. Lowest values were given by the cast metal and highest by the cold-rolled material. Specimens produced by hot forging gave intermediate values, usually in the vicinity of 5000 psi. The modulus of elasticity drops from about 10.5×10^6 psi at room temperature to about 6×10^6 psi at 700°C. Typical data obtained from specimens machined from one cast billet are shown in Fig. 10.

Small amounts of impurities, particularly carbon, may have a marked effect in increasing the tensile strength and reducing the ductility of thorium. For example, the yield strength is approximately doubled when the carbon content is increased from 200 ppm to 800 ppm. Nitrogen and oxygen have similar effects, but not to as great an extent. Indium is effective in raising the yield strength. The strength properties are sensitive to the rate of straining, with an increase in the strain rate resulting in higher apparent strengths. For example, increasing the strain rate from 0.003 min^{-1} to 0.016 min^{-1} increases the yield strength approximately 32 per cent.

At room temperature Poisson's ratio is approximately 0.27.

The compressive properties are about the same as the corresponding properties in tension.

8.2 Impact

An extensive series of impact tests on standard keyhole Charpy specimens showed a marked increase in the impact strength as the temperature was increased from 200°C to 500°C. Typical data from specimens machined from two cast billets are shown in Fig. 11. In general the impact strength decreases as the carbon content of the metal increases. This is attributed to the embrittling influence of the carbon, as it has been found that increased impact strength is accompanied by an increase in the angle through which the impact specimen bends before fracturing.

8.3 Shear

Work at Battelle Memorial Institute shows the modulus of elasticity in shear, as measured by the dynamic method, to be 4.62×10^6 at room temperature. The modulus as computed from a Poisson's ratio of 0.27 and a modulus of elasticity of 10.5×10^6 psi is 4.14×10^6 psi.

8.4 Fatigue

The endurance limit of cast thorium at room temperature lies between 12,000 and 12,500 psi for rotating beam specimens. A value of approximately 15,000 psi is obtained for the endurance limit of cold-rolled material. Specimens machined from stock material formed at 600°C indicated an endurance limit of approximately 13,000 psi at room temperature. A limited number of tests reported by Battelle Memorial Institute on hot-rolled and annealed sheet specimens gave an endurance limit of 22,000 psi in repeated bending.

8.5 Creep

Relatively little work has been reported on the creep of thorium. However, it has been noted that specimens at room temperature loaded to a stress of 80 per cent of the ultimate strength may exhibit a high rate of creep initially, but the creep rate decreases with time, stabilizing at small values. At smaller stress levels the creep rate may become zero.

8.6 Work Hardening

The strength of thorium is increased by cold rolling. A reduction in area of 25 per cent increases the tensile strength by 30 to 40 per cent and increases the yield strength by 100 per cent. However, reduction in area above 25 per cent has little additional effect on the strength.

9. CORROSION OF THORIUM AND THORIUM ALLOYS

The corrosion behavior of thorium and some of its alloys in water, air, oxygen and to a lesser extent in other media, has been investigated. Most of the data presented in this section are the results of work performed at Argonne National Laboratory, Battelle Memorial Institute, Ames Laboratory at Iowa State College and Oak Ridge National Laboratory.

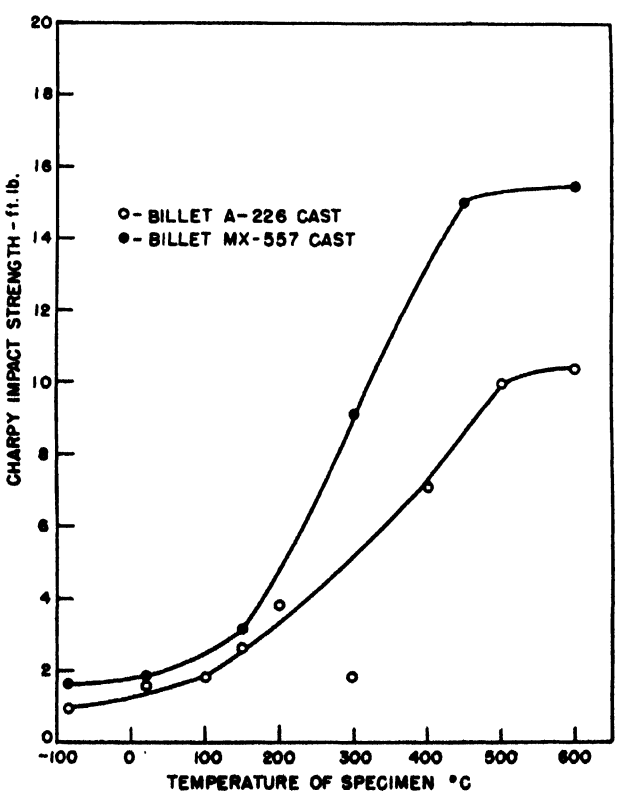

Figure 11. Effect of temperature upon Charpy impact strength of thorium

9.1 Corrosion of Thorium in Water

If exposed to boiling distilled water, thorium becomes covered with an oxide scale and usually gains weight. Considerable variation in corrosion rates has been reported for such tests; rates of gain of 0.03 mg $\times$ cm^{-2} $\times$ hr^{-1} to rates of loss of 0.02 mg $\times$ cm^{-2} $\times$ hr^{-1} have appeared in the literature.

Part of the variation can be attributed to differences in preparation and fabrication of the metal. This is shown in Table XII which gives results obtained by Olson[89] in static corrosion tests of thorium samples that had undergone different rolling and annealing treatments. The specimens were tested as received without surface preparation, and after exposure, were dried and weighed with the corrosion products adhering. From the limited data presented, the amount of corrosion seemed to be related to the degree of cold working of the metal. However, it is not impossible that the effect was due simply to the amount of operational handling, perhaps to the working of oxide into the metal. In any case the sensitivity of the metal to handling, preparation or treatment is evident.

Corrosion in 100° water as a function of time is shown by Draley's[90] results reproduced in Fig. 12 for metal prepared by different methods. The samples were cleaned by grinding before being tested and the resulting corrosion scale was removed chemically or electrochemically after completion of the test, but before weighing. Water quality was maintained by continuous replenishment. Some of the points used for the curve for Westinghouse sintered metal were for the metal as received, and some were obtained after hot rolling at the Argonne Laboratory.

For this material, hot rolling was observed to have caused relatively little change in corrosion behavior. Thorium obtained from the reduction of the oxide (Westinghouse sintered) and also the metal produced by reduction of the fluoride (Ames metal) had an initial period of rapid reaction after which the action proceeded at a slower rate. The estimated rate for Westinghouse sintered metal is about two and one-half times that for Ames metal. When Westinghouse metal was remelted, its rate of corrosion in boiling distilled water roughly approximated that of the Ames metal. Results obtained on samples tested in 178°C water showed that the corrosion rate was relatively low for a few days and then accelerated markedly, approaching a rate of 0.7 mg $\times$ cm^{-2} $\times$ hr^{-1} after 15 to 20 days. In distilled water at 315°C attack was extremely rapid.

Table XII. Corrosion of Ames Thorium in Distilled Water at 95°C after 30 Days

Sample	*Treatment*	*Rate of weight change* $mg \times cm^{-2} \times hr^{-1} \times 10^3$
1	Cold-rolled to 68% reduction, annealed at 750°C for 1 hr in vacuo	−0.40
2	Cold-rolled to 75% reduction, annealed at 750°C for 30 min	−8.3
3	Cold-rolled to 86% reduction, annealed at 750°C for 30 min	−21.0
4	Cold-rolled to 86% reduction	−6.0
5	Cold-rolled to 25% reduction	−0.27
6	Melted in ZrO_2, cold-rolled to reduction, annealed at 750°C for 1 hour	−0.12
7	Cast in ZrO_2, hot-rolled to 80% reduction, then cold-rolled to 40% and annealed at 750°C for 1 hour	−9.0

Deal and Svec[91] have made an investigation of the reaction between thorium metal and water vapor between 200°C and 600°C at water vapor pressures of 25 to 100 mm Hg. Analyses of the products indicate that ThO_2 and H_2 are the main products formed during the reaction, with formation of a thorium hydride as a possible side reaction. During these studies, the variables, time, temperature and pressure were examined. The reaction data were found to obey the logarithmic rate law

$$w = k \log (1 + 0.45t)$$

where w is the weight of water reacted per unit area of thorium surface, t is the time in hours and k is the rate constant.

The Arrhenius equation $\ln k = -E/RT + C$ in which k = rate constant, E = activation energy, T = absolute temperature and R and C are constants was used to determine the activation energy for which an average value of 6.44 $\pm$ 0.75 kcal/mol was found.

Oxide coatings of different appearance were observed in three ranges of temperature: from 200°C to 275°C, the coating was black; from 300°C to 450°C, it was gray or white; and from 450°C to 550°C, it had a metallic appearance. However, X-ray diffraction patterns of the different-appearing reaction products revealed no differences in the nature of the various colored oxide coatings.

Deal and Svec made experiments with markers in order to determine the nature of diffusion in the ThO_2 coating. They postulated that inward diffusion of water molecules or a related species is the rate-determining step of the reaction. Their experiments have shown that hydrogen produced by the reaction diffused into the metal in varying amounts depending upon temperature and water vapor pressure, thus complicating the kinetics. This hydrogen was evolved when the samples were heated under high vacuum to 1200°C.

9.2 Corrosion of Thorium in Gaseous Media

Levesque and Cubicciotti[92] have studied the reaction of thorium with oxygen in the range from 250°C to 700°C. Above 450°C, the temperature of the sample rose considerably above the temperature of the furnace. Below 450°C, the oxidation proceeded almost isothermally. From 350°C to 450°C the oxidation curves were linear with time and the energy of activation was calculated to be 22 kcal/mol. From 250°C to 350°C, the oxidation proceeded according to the parabolic law and the energy of activation for the reaction was calculated to be 31 kcal/mol.

Table XIII. The Corrosion of Thorium in Various Flowing Gases at 800°C

Atmosphere	*Time, hr*	*Weight gain, gm/cm²*
Air	1/2	6.0
Tank N_2	1/2	4.4
Purified N_2	1/2	2.0
Tank A	1/2	1.0
Purified A	1/2	0.75

Table XIV. The Effect of Temperature on Corrosion of Thorium in Air

Temperature, °C	*Time, hr*	*Weight gain, gm/cm²*
200	4	Negligible
300	4	0.12
400	4	1.72
450	4	21.4
500	4	34.75

Table XV. Behavior of Thorium in Several Media

Corroding medium	*Temp., °C*	*Time, hr*	*Results*
Bismuth	1000	4	Thorium completely dissolved
Bromine-ethyl acetate	50-60	1	50% of 5.0 gm Th sample dissolved
Gallium	600	48	Reacts extensively
Lead	1000	40	Completely dissolved
Lead–2 wt % uranium	1000	4	Substantially attacked
Lithium	600	6	Not significantly attacked
	1000	40	No attack
Sodium	500	56	No significant attack
NaK alloy	600	..	No alloying
65% HF acid	15	..	Slight weight gain, specimen covered with gray film

One-half hour scaling tests on thorium samples exposed in flowing air, nitrogen and argon at atmospheric pressure have been reported by Russell *et al.*[93] Their data, which are shown in Table XIII, indicate that air is the most corrosive of these gases at 800°C. The table does not take gas velocity into account but the investigators stated that change in rate of flow had very little effect on the rate of corrosion.

Table XIV summarizes work done by Feibig[94] on the corrosion of thorium in still air at a series of temperatures from 200°C to 500°C. The corrosion rates are averages for a 4-hour period but Feibig's results indicate that the gain in weight was approximately linear.

Hydrogen reacts with and corrodes thorium extensively at relatively low temperatures. Brugmann and Draley[95] determined the corrosion rates for thorium in hydrogen at atmospheric pressures at temperatures from 400°C to 505°C. On the assumption that the formula for the hydride was ThH_4, they calculated that the loss of thorium at 400°C was 80 mg $\times$ cm^{-2} $\times$ hr^{-1} and that it was 129 mg $\times$ cm^{-2} $\times$ hr^{-1} at 505°C. Upon continued exposure to hydrogen, the specimens turned black, started to swell and eventually disintegrated into a coarse black powder. Although the formula for the hydride has since been determined to be Th_4H_{15}, Brugmann and Draley's data may still be considered to give approximate results.

9.3 Corrosion of Thorium in Other Media

Limited tests have been made on the corrosion of thorium in several molten metals, in bromine-ethyl acetate and in hydrofluoric acid. The results obtained at several laboratories are summarized in Table XV. As indicated in the table, thorium is not significantly attacked by lithium at 600°C or at 1000°C although the specimens were decarburized to a depth of 2 mils during the test. The presence of an adherent protective film of nitride on the thorium is believed to be responsible for the lack of interaction with lithium at 600°C and 1000°C.

At 600°C, thorium reacts with any oxygen present in sodium-potassium alloys to form heavy oxide layers which spall off during the test. However, in deoxidized NaK, thorium takes on a thin oxide film but is otherwise unaffected.

The resistance to attack by hydrofluoric acid may be due to the formation of a protective fluoride film. The addition of thorium nitrate (0.3 *M*) or nitric acid (0.5 to 15.4 *M*) causes partial disintegration of pure thorium samples.

9.4 Corrosion of Thorium Alloys

The effect of alloying upon the corrosion resistance of thorium has been investigated. Most elements,

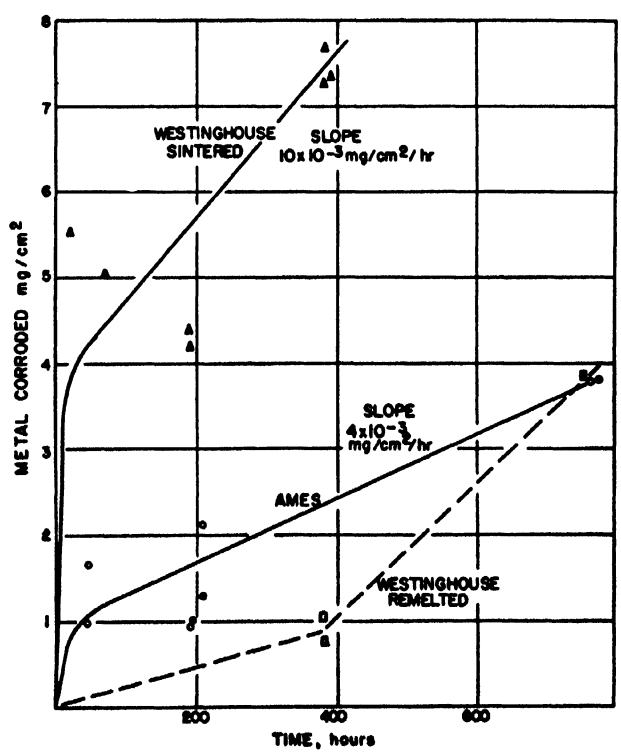

Figure 12. Graph of corrosion vs time for thorium metal in boiling water. Data supplied by J. Draley, Argonne National Laboratory, 1952

when added to thorium, exert a deleterious effect or at best impart only slight improvement to the resistance of thorium to corrosion by high temperature water. Thorium-zirconium alloys, however, exhibit good corrosion resistance to 100°C water.

Thorium-Aluminum

Thorium alloys containing 10 wt % aluminum are unstable in air, decomposing to a fine powder.

Thorium-Beryllium

The corrosion of thorium-beryllium alloys has been studied both in air and in water. Alloys containing 1 wt % and 2 wt % beryllium oxidized and scaled badly on standing in air. Corrosion rates were determined for the 2 wt % beryllium alloys at 400°C and 500°C. After 4-hours exposure, weight gains of 2.53 mg/cm^2 and 9.43 mg/cm^2 respectively were observed. Alloys containing 0.5, 1, 1.5, 2 and 2.5 wt % beryllium were tested in 100°C and 178°C distilled water for periods of 100 to 600 hours. Although the results are somewhat inconclusive, the corrosion rates are of the same order of magnitude as those for the unalloyed thorium.

Thorium-Carbon

Addition of small amounts of carbon to thorium increases its corrosion resistance to 178°C water. However, as the solid solubility limit of carbon in thorium is exceeded, the appearance of a separate carbide phase materially reduces the corrosion resistance of the metal. A 0.3 wt % carbon solid solution alloy corroded at a rate of 5.5×10^{-4} mg $\times$ cm^{-2} $\times$ hr^{-1} compared with a rate of 9.8×10^{-2} mg $\times$ cm^{-2} $\times$ hr^{-1} for a 1.24 wt % carbon alloy containing carbide as a second phase.

Thorium-Chromium

Alloys containing 1 to 10 wt % chromium failed in boiling water in less than 500 hours.

Thorium-Copper

Alloys containing 5 to 10 wt % copper decompose on standing in air.

Thorium-Iron

Addition of iron to thorium results in poor corrosion resistance in boiling water. An alloy containing 2.6 wt % iron had a corrosion rate 20 times that for unalloyed thorium and showed a similar behavior in 178°C water.

Table XVI. The Corrosion of Thorium-Silicon Alloys in Boiling Distilled Water

Silicon wt %	*Corrosion rates mg $\times$ cm^{-2} $\times$ hr^{-1}*
0	−0.0006
1.08	+0.0003
2.0	+0.0003
4.3	+0.0002

Thorium-Lanthanum

An alloy containing 5 wt % lanthanum failed in less than 500 hours in boiling distilled water.

Thorium-Lead

An alloy containing 25 wt % lead disintegrated badly after 24 hours in boiling distilled water.

Thorium-Manganese

An alloy containing 10 wt % manganese showed a weight loss of 0.30 mg/cm^2 after an 840-hour exposure to boiling water and disintegrated after 96 hours in 200°C water.

Thorium-Molybdenum

Test samples of alloys containing less than 10 wt % molybdenum failed in less than 500 hours in boiling distilled water. Additions up to 30 wt % molybdenum failed to reduce the corrosion rate appreciably.

Thorium-Niobium

The effect that niobium has upon the corrosion resistance of thorium depends somewhat upon the niobium content. Alloys containing 2, 4 and 6 wt % niobium had corrosion rates considerably higher than that of unalloyed thorium. However, alloys containing greater amounts of niobium, 25 and 30 wt %, exhibited slightly improved resistance to corrosion in 200°C water.

Thorium-Silicon

From the limited data available, silicon appears to bring about a slight improvement in corrosion resistance in both boiling and 178°C water. Grenninger's[96] results on these alloys are given in Table XVI.

Thorium-Silver

A 2 wt % silver alloy failed in boiling distilled water after 500 hours.

Thorium-Tantalum

A sample containing 10 wt % tantalum exposed to boiling distilled water exhibited a weight loss of 10 mg/cm^2 after 840 hours of testing, and disintegrated in 24 hours in 200°C distilled water.

Thorium-Tin

A test sample containing 2 wt % tin exhibited greatly accelerated corrosion in a 31-hour exposure to boiling water.

Thorium-Titanium

Several thorium-titanium alloys containing titanium in amounts varying from 2 to 30 wt % titanium were tested in boiling distilled water. All exhibited corrosion rates slightly higher than that of unalloyed thorium. In 200°C water, alloys containing 10 wt % titanium or more exhibited slightly improved corrosion resistance.

Thorium-Uranium

A 0.6 wt % of uranium alloy corrodes at about the same rate as Ames thorium in 70°C flowing water that was 0.005*N* in H_2O_2 and contained, also, 20 ppm CA^{++}, 16 ppm Mg^{++}, 85 ppm SO_4^{--} and 1 ppm Cl^-. A smooth black protective film was formed. Average rate of weight loss after 813 hours was 0.018 mg $\times$ cm^{-2} $\times$ hr^{-1}.

Thorium-Vanadium

Corrosion rates in boiling water have been determined for alloys containing 3, 20, 30 and 50 wt % vanadium. Vanadium in small quantities appears to have a slightly deleterious effect that diminishes as the vanadium content increases.

Thorium-Zirconium

Alloys containing 1 to 10 wt % zirconium were prepared by arc-melting and cold-rolling into thin sheets and were then tested in boiling distilled water. Corrosion tests showed slight but not pronounced improvement with increasing zirconium content for alloys in this composition range.

Alloys containing more than 10 wt % zirconium, however, possess good corrosion resistance in boiling water, the resistance improving as the zirconium content is increased. The results of tests in 100°C and 200°C water on a series of alloys are summarized in Table XVII. All of the alloys listed in the table were prepared by arc-melting. They were hot-rolled, vacuum-annealed at 825°C for 20 hours and cooled slowly to room temperature prior to corrosion testing. Some tests performed at higher temperatures, 315°C and 345°C, indicate that the alloys become increasingly unsatisfactory as the thorium content rises.

Thorium-Chromium-Titanium

A thorium alloy containing 2 wt % chromium and 4 wt % titanium immersed in boiling distilled water for 569 hours exhibited a corrosion rate of 2.9 mg $\times$ cm^{-2} $\times$ mo^{-1}. This rate is a little higher than that observed for thorium similarly tested.

Thorium-Titanium-Zirconium

Thorium base alloys containing small additions (1 to 2 wt %) of titanium and zirconium have been tested in 95°C water. The alloys were melted in ZrO_2, cold-rolled to 75% reduction and annealed at 750°C. In general, the corrosion resistance was not significantly better in the ternary combinations.

10. METALLOGRAPHY

The preparation of specimens of thorium for microscopic examination requires special care. As the metal is soft and ductile, its surface is easily deformed, or worked, during grinding operations. A number of procedures have been used with good results. Grinding can be done on grit papers, either dry or with kerosene or water lubricant on sizes down through 500 or 600 grit. The polishing should be done carefully to avoid leaving hard inclusions in relief. A coarse diamond paste, Linde A abrasive and silicon carbide have been used successfully. The final polishing can be done with Linde B abrasive, with fine diamond paste or with a number of other abrasive powders. A 10 per cent oxalic acid solution has been used as the suspension medium in the final polishing step.

Electropolishing techniques have been developed for thorium but they have not proven to be entirely satisfactory. Unfortunately, the electropolishing solution that probably is most nearly satisfactory for unalloyed thorium is one that contains perchloric acid and an organic compound and is therefore potentially explosive. This solution, which consists of 1 part perchloric acid and 10 parts glacial acetic acid, has been used by Roth,[97] Dickerson[98] and Pohl.[99] The bath should be maintained at a temperature of about 15°C. The electropolishing operation is conducted at 12 to 40 volts and usually lasts from 3 to 30 seconds. This electropolishing technique produces a clean surface and removes scratches left from mechanical polishing. However, it destroys the inclusions in the metal and produces serious pitting. Gray[100] has reported using a bath of 1 part perchloric acid and 15 parts ethyl alcohol. This bath is also cooled. It produces a polished sample in 15 to 45 seconds at 35 to 40 volts but leaves a thin film that can be removed if the sample is dipped in a fresh bath. The final result is a clean surface free from scratches, but again the inclusions are destroyed and the surface is pitted. Baths containing nitric acid, fluosilicic acid, sulfuric acid, phosphoric acid and combinations of these have been used with moderate success in electropolishing some samples.

No completely satisfactory chemical or electrochemical etching reagent has been found for thorium. A solution of 3*N* HNO_3 to which has been added 1% KF has been used for thorium alloys but does not give sharp outlines and has not worked out well for unalloyed thorium. Inclusions probably are more evident after mechanical polishing than after the surface has been etched. Grain boundaries of unalloyed thorium are partially revealed by electropolishing procedures. Carlson *et al.*[101] have reported good re-

Table XVII. The Corrosion of Thorium-Zirconium Alloys in 100°C and 200°C Water

Zirconium wt%	*Temp., °C*	*Time, hr*	*Weight gain, mg × cm⁻² × mo⁻¹*
10	100	662	0.07
20	100	662	0.07
25	100	662	0.08
30	100	662	0.04
40	200	100	260
50	200	100	170
60	200	100	100
70	200	100	45
80	200	100	6
90	200	100	0

sults on thorium by cathodic etching but the method has not been investigated sufficiently to establish its utility.

The identification of inclusions in thorium metal has not received sufficient study. Thorium oxide is the most common inclusion in the usual grades of thorium. The form in which the oxide occurs depends on the method of preparing the sample. Thorium which has been melted in a crucible and poured into a mold usually contains rather large globular particles of oxide randomly distributed in the metal. The oxide in arc-melted thorium usually occurs as smaller particles, often in a dendritic array. Thorium oxide is quite easily identified under the microscope by its dark gray color in as-polished samples. A typical example of thorium oxide inclusions in crucible melted thorium is shown in Fig. 13 and in arc-melted thorium in Fig. 14. Thorium monocarbide inclusions are not usually encountered in thorium metal because of solid solubility. Figure 15 shows thorium oxide as large dark particles and thorium carbide as smaller, lighter particles in a sample in the as-polished condition. Thorium nitride has not been well characterized but has been reported to appear as golden yellow-colored inclusions. A cathodically etched specimen of Ames thorium is illustrated in Fig. 16. The portion photographed includes an area of oxide inclusions; grain boundaries are well delineated.

11. THORIUM ALLOY SYSTEMS

Considerable interest has developed in the binary alloys of thorium and some of the work that has been done is summarized in this report. The material on uranium and thorium constitutional diagrams now being compiled by Saller and Rough[102] has been made available to the authors who wish to acknowledge their indebtedness for this assistance.

Thorium metal transforms from a face-centered cubic to a body-centered cubic lattice on heating at about 1400°C. Its atomic diameter for the face-centered cubic form is 3.59 Å and 3.56 Å in the high temperature form. Only a few metals have atomic diameters which differ from that of thorium by less than 14–15% and which, therefore, might be expected to form extensive solid solutions with it. These include magnesium, zirconium, hafnium, cerium, lanthanum, lead, thallium, bismuth and antimony.

The electronegativity of thorium is 1.3 on Pauling's scale and this highly electropositive value suggests the likelihood of intermetallic compound formation with many of the more noble metals. Because of these considerations only a limited degree of mutual solid solubility of thorium with other elements can be expected. However, actual knowledge of these alloys depends largely upon experimental determinations.

11.1 Thorium-Aluminum Systems

The diagram of this system shown in Fig. 17 is taken from a report by Keeler.[103] The formula of the aluminum-rich compound, $ThAl_3$, has been fairly well established from the work of Brauer,[104] who has indexed it as hexagonal with $a = 6.480$ and $c = 4.601$. The presence of other intermediate phases has been confirmed by X-ray powder data but the crystal structures and formulae of the compounds represented have not been determined.

The solid solubility of thorium in aluminum appears to have a maximum value of 0.7 to 0.8 wt % according to metallographic and thermal analyses,[102] whereas as much as 2.0 wt % thorium has been reported to be soluble in aluminum, as determined from lattice constant values.[105]

11.2 Thorium-Beryllium System

A portion of the thorium-beryllium phase diagram is shown in Fig. 18. Baenziger[106] reported the formula of the intermetallic compound to be $ThBe_{13}$. The structure is face-centered cubic with $a = 10.395$ Å. This has been confirmed by Koehler *et al.*[107] on the basis of X-ray and neutron diffraction data.

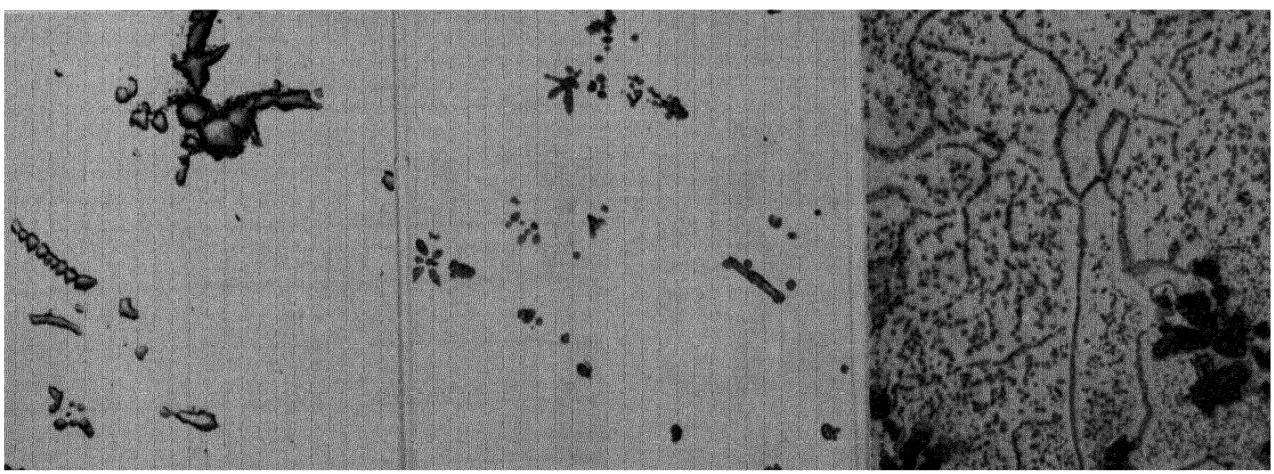

Figure 13. Thorium exide inclusions in crucible-cast thorium. As-polished. 250 ×

Figure 14. Thorium oxide inclusions in arc-melted thorium. As-polished. 250 ×

Figure 15 Thorium carbide inclusions in thorium containing 0.96% carbon. As-polished. 500 ×

11.3 Thorium-Bismuth System

The thorium-bismuth diagram shown in Fig. 19 is based upon the work of Johnson[108] and the later work of Bryner.[109] Johnson reported two compounds to which he assigned the formulae, Th_2Bi and $ThBi_3$. Recent work by Bryner has indicated that the bismuth-rich compound is actually Th_3Bi_5. He has also determined the bismuth-rich liquidus quite accurately and his results were incorporated in the proposed diagram (Fig. 19).

11.4 Thorium-Boron System

ThB_4 and ThB_6 have been reported[110] in the thorium-boron system. A eutectic, melting at 1550°C, is formed between thorium and ThB_4. The melting point of ThB_4 is probably above 2500°C. ThO_2 apparently forms extensive solid solutions with ThB_4. ThB_6 was not considered sufficiently stable to be of use as a refractory. Lafferty[111] has reported the melting point of ThB_6 as 2195°C. The crystal structure of ThB_4 has been determined by Zalkin and Templeton[112] who found it to be isomorphous with CeB_4 and UB_4. The space group is D_{4h}^5-$P4/mbm$ with lattice parameters, $a = 7.256$ Å and $c = 4.113$ Å. ThB_6 has the simple cubic CaB_6 structure[113] and is isomorphous with several other borides (BaB_6, LaB_6, CeB_6, etc.). Lafferty gives the lattice parameter of ThB_6 as 4.15 Å while Bertaut and Blum[114] give 4.1132 Å. Andersson and Kiessling[115] have reported solid solubility of boron in thorium but have not stated the limits. They also reported a phase of 50 at % boron which gave complicated powder patterns but obtained no single crystal data. The existence of a third boride at 50 at % is in conflict with the data of Brewer *et al.*[110]

11.5 Thorium-Carbon System

The diagram shown in Fig. 20 is taken from work on this system reported in 1950.[48] More recent studies have shown, however, that a small amount of carbon raises the transformation temperature and lowers the melting point. The details of these reactions are not fully understood but a proposed diagram of the low carbon region based on these later data are shown in the inset of Fig. 20. The boundaries of the alpha-beta field are based upon electrical resistivity measurements and have been confirmed by high temperature X-ray studies. The solidus has been determined from melting point observations. From an extrapolation of these data, the melting point of carbon-free thorium appears to be about 1750°C and the transformation temperature approximately 1360°C.



Figure 16. Thorium metal cathodically etched. 500 ×

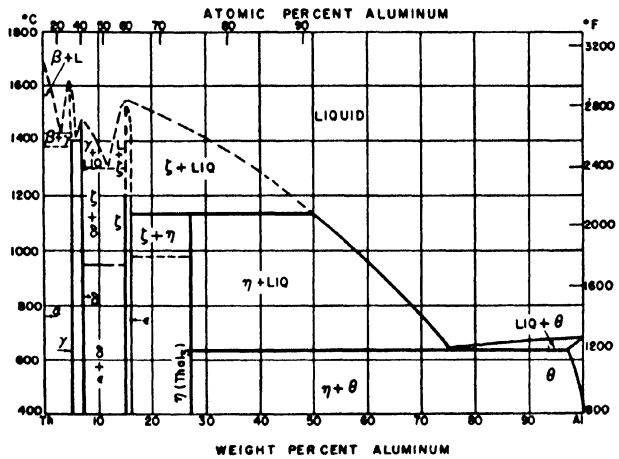

Figure 17. Thorium-aluminum system

The monocarbide phase, ThC, has considerable solid solubility for thorium. It has the sodium chloride structure with the lattice constant varying from 5.29 Å at 3.9 wt % carbon to 5.34 Å at 4.92 wt % carbon. Hunt and Rundle[116] have determined the structure of the dicarbide, ThC_2, by use of X-ray and neutron diffraction studies. They have shown the phase to be C-centered monoclinic with $a = 6.53$, $b = 4,24$, $c = 6.56$ Å and $\beta = 104$ degrees.

11.6 Thorium-Cerium and Thorium-Lanthanum Systems

Little work has been done on these systems, but early work[94,96] and very recent studies at the Ames Laboratory indicate complete solubility in the liquid state and a very wide region of solubility in the solid state. Studies of the systems have included microstructure and X-ray examinations. The cast alloys are unusually inhomogeneous.

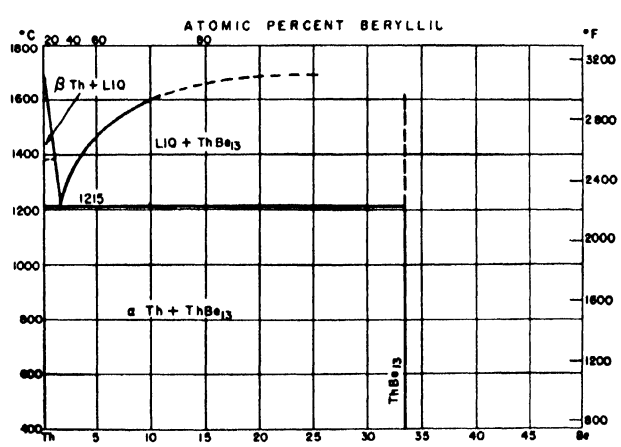

Figure 18. Thorium-beryllium system

11.7 Thorium-Chromium System

Thorium and chromium form a simple eutectic as shown in the proposed diagram of Fig. 21, which is based on work done at the Ames Laboratory. No compounds have been found in this system.

11.8 Thorium-Cobalt System

Although no phase diagram has been proposed for thorium and cobalt a considerable amount of work has been done on the crystallography of the intermetallic compounds of the system. Florio *et al.*,[116] have reported the following five intermediate phases and have determined the structure of each. Th_7CO_3 is hexagonal with $a = 9.83$ and $c = 6.17$ Å. ThCo is orthorhombic with $a = 3.74$, $b = 10.88$ and $c = 4.16$ Å. $ThCo_{2-3}$ appears to be a super lattice with such a large unit cell that it was impossible to assign an exact formula. $ThCo_5$ is hexagonal with $a = 5.01$ and $c = 3.97$ Å, and Th_2Co_{17} is monoclinic with $a = 9.62$, $b = 8.46$, $c = 6.32$ and $\beta = 99°06'$.

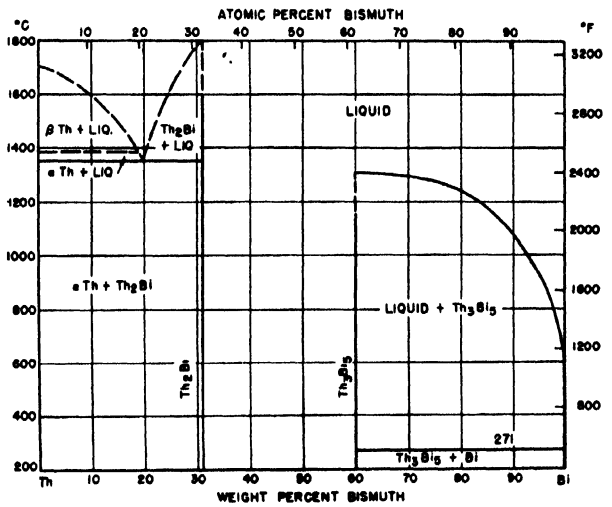

Figure 19. Thorium-bismuth system

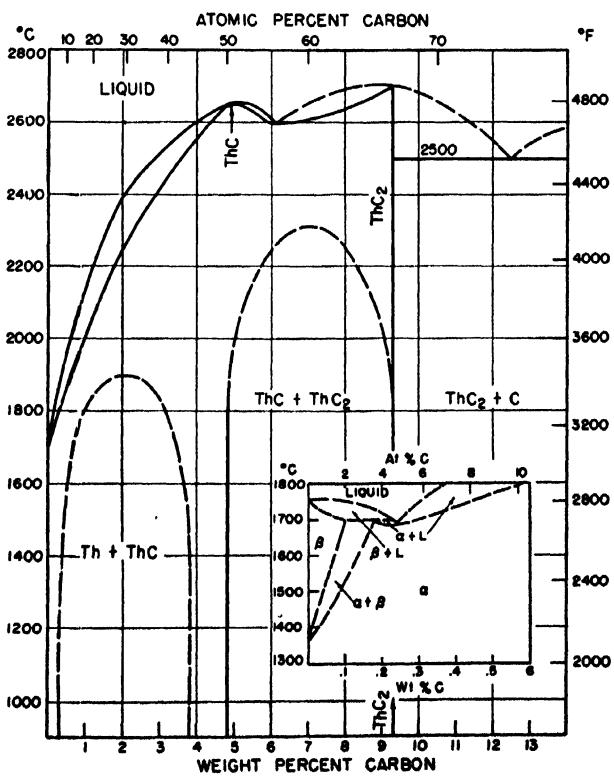

Figure 20. Thorium-carbon system

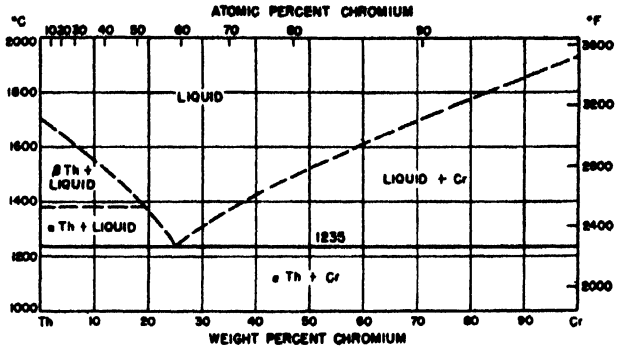

Figure 21. Thorium-chromium system

11.9 Thorium-Copper System

The diagram shown in Fig. 22 is based upon the work of Grube and Botzenhardt[105] and the crystal structure measurements of Snow and Rundle.[117] The system contains three compounds: Th_2Cu, $ThCu_2$ and $ThCu_4$: Th_2Cu is body-centered tetragonal with $a = 7.29$ and $c = 5.75$ Å. $ThCu_2$ is hexagonal with $a = 4.36$ and $c = 3.48$ Å. No information is available on the structure of $ThCu_4$. According to Raub and Engel[118] all of the compounds are brittle and pyrophoric.

11.10 Thorium-Gold System

The diagram shown in Fig. 23 (see page 98) is taken from Raub and Engel.[118] No crystallographic data have been reported for either of the compounds in this system.

11.11 Thorium-Hafnium System

An investigation of the thorium-hafnium system has been begun recently by Loomis.[119] As the solidus line is a continuous curve, complete mutual solid solubility must exist between beta thorium and beta hafnium. The solidus and liquidus curves show a minimum at 1400°C. A eutectoid horizontal occurs at 1280°C and the eutectoid composition lies near 70 wt % hafnium. There appears to be some solid solubility of each component in the other at room temperature but the limits of the alpha solubilities have not been determined.

11.12 Thorium-Hydrogen System

Two hydrides have been identified in this system. Rundle, Schull and Wollan[76] have determined the structure of ThH_2 by X-ray and neutron diffraction methods. Its structure is tetragonal with $a = 4.10$ and $c = 5.03$ Å. Zachariasen[77] has identified a second hydride, Th_4H_{15}. This phase is cubic with $a = 9.11$ Å. From studies of dissociation pressures in the interval

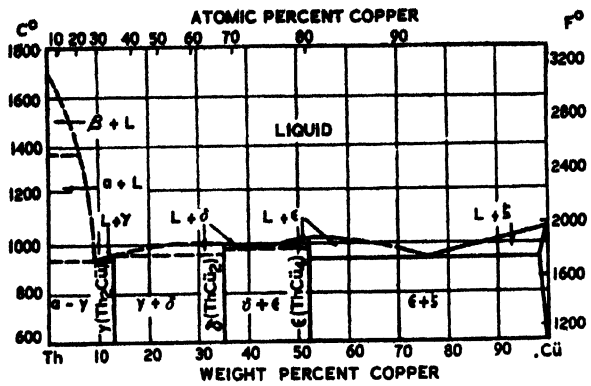

Figure 22. Thorium-copper system

between thorium and ThH_2 solubilities of 13 at % hydrogen in thorium at 650°C and 23 at % hydrogen at 900°C have been determined.[79]

11.13 Thorium-Iron System

Florio *et al.*[116] have shown that there are at least four intermetallic compounds in this system and that they are isomorphous with those of the corresponding compounds in the thorium-cobalt system. Th_7Fe_3 is hexagonal with $a = 9.85$ and $c = 6.15$ Å. It appears to form by a peritectic reaction between 850°C and 1000°C. $ThFe_3$ is hexagonal with $a = 5.22$ and $c = 24.95$ Å. $ThFe_5$ has a hexagonal lattice with $a = 5.17$ and $c = 4.02$ Å. The fourth compound, Th_2Fe_{17}, is monoclinic with $a = 9.62$, $b = 8.46$, $c = 6.32$ and $\beta = 99°06'$. A eutectic has been reported at 47.5 wt % iron which is between Th_7Fe_3 and the next compound, $ThFe_3$.[102]

11.14 Thorium-Lead System

A partial diagram proposed for this system is shown in Fig. 24. It is based upon the work of Bryner.[109] The lead-rich liquidus has been determined and an intermetallic compound has been assigned the formula $ThPb_3$. No crystallographic data are available on this phase.

The presence of small amounts of lead does not adversely affect the cold-rolling properties of thorium.

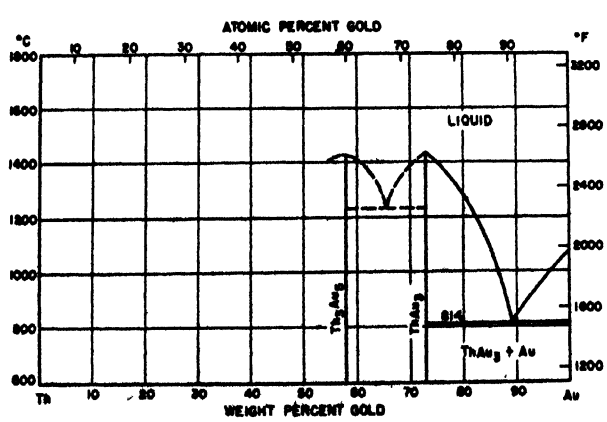

Figure 23. Thorium-gold system

11.15 Thorium-Magnesium System

Studies at the Ames Laboratory have shown that thorium and magnesium form two intermetallic compounds, $ThMg_2$ and another whose composition is yet undetermined. There is a eutectic at 63 wt % magnesium which melts at 580°C. The structure of $ThMg_2$ has been determined to be face-centered cubic with $a = 8.57$ Å. The other compound has been separated and its unit cell determined but its composition is still not fixed. It is hexagonal with $a = 6.01$ and $c = 18.98$ Å.

The solid solubility of magnesium in thorium is quite low. Leontis[120] has found that the addition of a small amount of thorium to magnesium greatly increases the high temperature creep resistance of magnesium.

11.16 Thorium-Manganese System

Florio *et al.*[121] have identified three intermetallic compounds in the thorium-manganese system; they are $ThMn_2$, Th_6Mn_{23} and $ThMn_{12}$. $ThMn_2$ is hexagonal with $a = 5.48$ and $c = 8.95$ Å. Th_6MN_{23} is face-centered cubic with $a = 12.523$ and $ThMn_{12}$ is

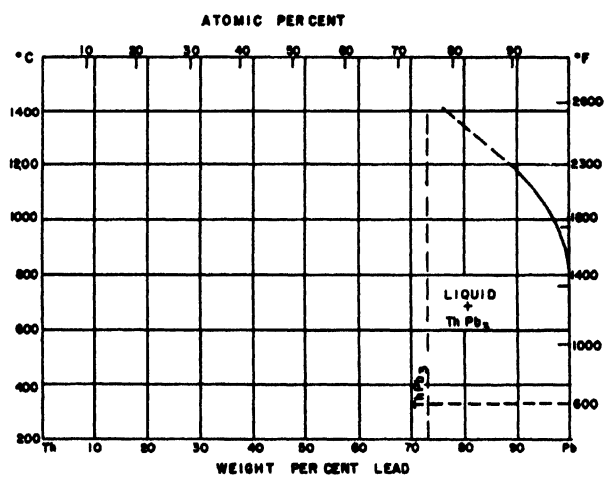

Figure 24. Thorium-lead system

tetragonal with $a = 8.74$ and $c = 4.95$ Å. Complete structures have been determined for each of these phases. There is a eutectic at 910°C at a manganese content somewhat greater than 5 wt %.

11.17 Thorium-Mercury System

Thorium and mercury react at 350°C to form an intermetallic compound[16] of the approximate composition $ThHg_3$. The structure is hexagonal with $a = 3.38$ Å and $c = 4.72$ Å. The diffraction pattern is similar to that of UHg_3. The solubility of thorium in mercury is 0.0154 wt % at 25°C according to Parks and Prime.[122]

11.18 Thorium-Nickel System

The diagram shown in Fig. 25 is based on the work of Horn and Basserman[123] but revised to agree with the crystallographic data of Florio *et al.*[116] Both in-

vestigations have shown the presence of five intermediate phases in this system all of which are compounds. These compounds are generally isomorphous with corresponding ones in thorium-cobalt and thorium-iron. Th_7Ni_3 is hexagonal with $a = 9.86$ and $c = 6.23$ Å. ThNi is orthorhombic with $a = 14.51$, $b = 4.31$ and $c = 5.73$ Å. $ThNi_2$ is hexagonal with $a = 3.95$ and $c = 3.83$ Å. $ThNi_5$ is hexagonal with $a = 4.97$ and $c = 4.01$ Å, and Th_2Ni_7 is also hexagonal

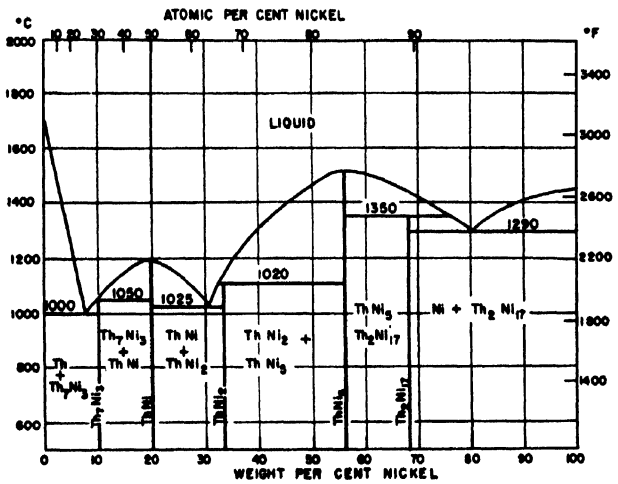

Figure 25. Thorium-nickel system

with $a = 8.37$ and $c = 8.14$ Å. Complete structures have been determined for each of these compounds.

11.19 Thorium-Niobium System

As may be seen from the diagram in Fig. 26, Carlson *et al.*[124] found that thorium and niobium form a simple eutectic system with no intermediate phases and little if any solid solubility.

11.20 Thorium-Nitrogen System

Nitrogen appears to have some solubility in solid thorium. Gerds and Mallet[125] measured the change of solubility with temperature over the range 850°C to 1500°C and found that the solubility varied almost linearly from 0.05 wt % at 850°C to 0.35 wt % at 1500°C. Chiotti[18] has observed that the presence of nitrogen raises the melting point of thorium. At least two compounds of nitrogen exist. The mononitride, ThN, has a sodium chloride structure of which the cube edge is 5.20 Å according to Rundle[126] and 5.144 Å according to Chiotti.[127] Its melting point is 2630 ± 50°C. Apparently, the compound has some solubility for thorium as it exists over a short range of composition. The compound, Th_2N_3, has the hexagonal La_2O_3 structure.[128] It is unstable at 1500°C under a vacuum.[16] A compound, Th_3N_4, has been reported but its existence is in doubt.

11.21 Thorium-Oxygen System

Thorium has one well known oxide, ThO_2, which has the CaF_2 structure. It has a very high melting point, 3050°C, and has been used as a refractory material. Evidence[18] exists that there is very little solid solubility of oxygen in thorium although particles of oxide may be present in the metal as inclusions. Attempts to prepare ThO have been made and a NaCl type of structure has been obtained, but in all cases the situation has been complicated by the presence of carbon and nitrogen as impurities. It has been suggested that oxygen, carbon and nitrogen may substitute for each other in this structure.[126]

11.22 Thorium-Phosphorus System

Two compounds have been observed to form between thorium and phosphorus. Meisel[129] has stated that the compound Th_3P_4 crystallizes in the cubic system. Zumbusch[130] has determined that ThP is an unstable compound with the NaCl structure. Both phases are isomorphous with the corresponding uranium compounds.

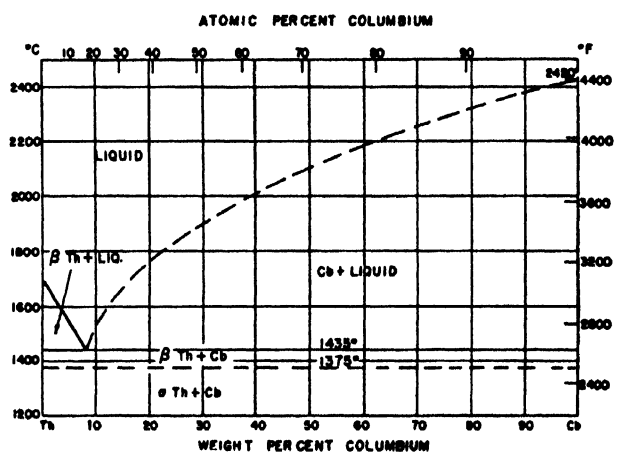

Figure 26. Thorium-niobium system

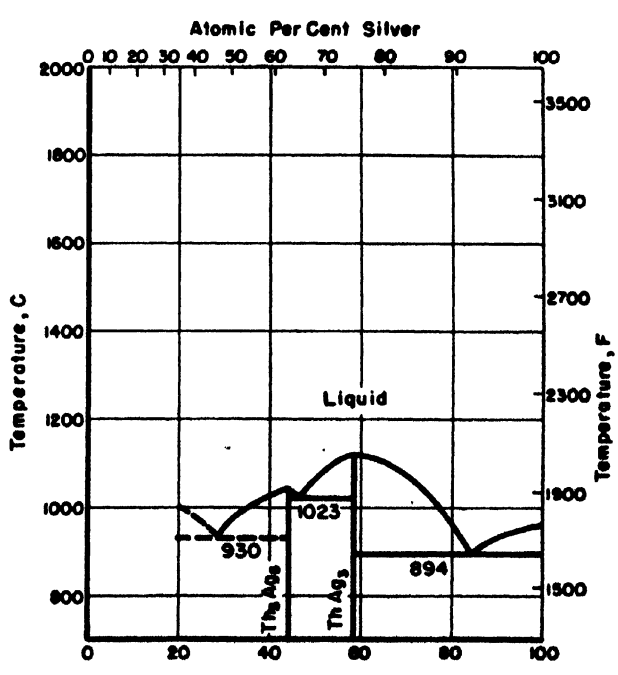

Figure 27. Thorium-silver system

11.23 Thorium-Silicon System

A compound, $ThSi_2$, has been reported in this system by Brauer and Mitius.[131] This compound has a body-centered tetragonal structure and is isomorphous with the corresponding compounds of lanthanum, cerium, and uranium. Zachariasen[132] has reported that $ThSi_2$ exists in two forms of which the alpha form is body-centered tetragonal with $a = 4.126$ Å and $c = 14.346$ Å and the beta is hexagonal with $a = 3.986$ Å and $c = 4.227$ Å. He found, also, a compound Th_3Si_2 which is tetragonal with $a = 7.841$ Å and $c = 4.166$ Å. Foote[133] has noted a eutectic with a melting point above 1300°C at about 1.3 wt % silicon.

11.24 Thorium-Silver System

The diagram shown in Fig. 27 is taken from Raub and Engel.[118] Th_3Ag_5 and $ThAg_3$ are reported to be isomorphous with similar compounds in the thorium-gold system.

11.25 Thorium-Sodium System

Early work reported by Grube and Botzenhardt[105] showed extensive solubility of thorium in liquid sodium and the presence of an intermediate phase, Na_4Th. Later work by Kelman, as reported by Saller and Rough,[102] has shown this statement to be in error and that thorium is not attached by sodium at temperatures of 650°C to 800°C.

11.26 Thorium-Sulfur and Thorium-Selenium Systems

Four compounds have been found in the thorium-sulfur system. Their structures have been studied by Strotzer and Zumbusch[134] and by Zachariasen,[135-137] and their melting points have been determined by Eastman *et al.*[138] D'Eye *et al.*[139] and D'Eye[140] have investigated the nature of the selenium compounds.

Table XVIII. The Structure and Melting Point of Some Compounds of Selenium and Sulfur with Thorium

Compound	*Lattice type*	*Cell dimensions, Å*	*Melting point °C*
ThS	F.C.C.	$a = 5.682$	2200
ThSe	F.C.C.	$a = 5.875$	1750
Th_3S_5	Orthorhombic	$a = 10.99$ $b = 10.85$ $c = 3.69$	1950 ± 50
Th_3Se_5	Orthorhombic	$a = 11.34$ $b = 11.57$ $c = 4.27$	1475 d
Th_7S_{12}	Hexagonal	$a = 11.063$ $c = 3.991$	1770 ± 30
Th_7Se_{12}	Hexagonal	$a = 11.569$ $c = 4.23$	1465
ThS_2	Orthorhombic	$a = 4.268$ $b = 7.264$ $c = 8.617$	1905 ± 30
$ThSe_2$	Orthorhombic	$a = 4.420$ $b = 7.610$ $c = 9.064$	–
Th_3Se_7	No data available	–	–

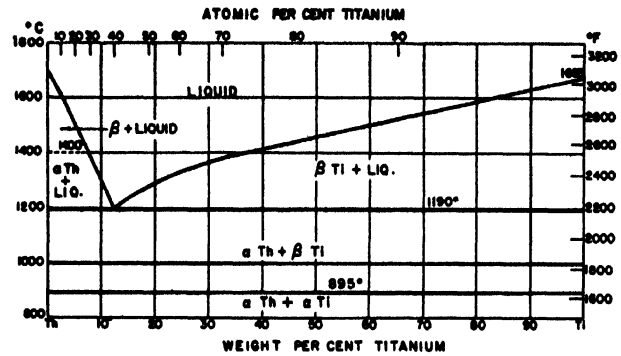

Figure 28. Thorium-titanium system

The data of these investigators are summarized in Table XVIII.

11.27 Thorium-Tantalum System

Some survey experiments at the Ames Laboratory have indicated that the solid solubility of tantalum in thorium is low and, also, that the same situation is true of the solid solubility of thorium in tantalum. The investigators at Ames did not find evidence of a compound although workers in the British Atomic Energy Establishment appear to have done so.

11.28 Thorium-Titanium System

As can be seen from Fig. 28, thorium and titanium form a eutectic at 12 wt % titanium and 1190°C. Little or no solid solubility exists in this system and no intermediate phases were found by Carlson *et al.*[124]

11.29 Thorium-Tungsten System

A survey of this system made at the Ames Laboratory indicates that this system is of the simple eutectic type. The temperature of the eutectic horizontal appears to be about 1475°C. Solid solubilities at either side probably have limits below 1 wt %. Work by the British Atomic Energy Establishment places the eutectic composition near 6 wt %.

11.30 Thorium-Uranium System

The phase diagram shown in Fig. 29 is based upon work of Carlson.[20] Recent precision X-ray data of thorium-rich alloys which have been annealed at 650°C and furnace-cooled showed very little change in the thorium lattice constant by the addition of uranium. This would indicate very little solid insolubility at this temperature. Tentative data reported by Saller and Rough[102] indicate that the solid solubility at 800°C is approximately 5 wt % uranium while at 600°C it is less than 1 wt % uranium.

11.31 Thorium-Vanadium System

The diagram shown in Fig. 30 is the result of work by Levingston and Rogers.[141] A eutectic occurs at 5 wt % vanadium and 1400°C. There are no intermetallic compounds in this system and little if any terminal solid solubility according to lattice parameter measurements.

11.32 Thorium-Zinc System

Work done at the Ames Laboratory indicates that an intermetallic compound, Th_2Zn, is formed in this system at 12 wt % zinc. This compound decomposes at 1040°C to give thorium and zinc. The compound is body-centered tetragonal with $a = 7.95$ Å and $c = 5.64$ Å. The calculated density is 10.6 gm/cm^3 which is in good agreement with observed values. The melting point of a 6 wt % zinc alloy under pressure is about 1200°C. Under vacuum, the zinc vaporizes readily at temperatures above 1040°C.

Nowotny[142] has investigated the zinc-rich end of this system from 0 to 47 wt % thorium. He noted the existence of two compounds. One was identified as $ThZn_9$ with a hexagonal structure. A compound that contained more thorium was not identified. No solubility of thorium in zinc was found.

11.33 Thorium-Zirconium System

The proposed diagram shown in Fig. 31 is based upon the early work of Carlson,[20] plus later work at the Ames Laboratory and also work reported by Saller and Rough.[102] The limits of the narrow portion of the alpha plus beta region have been established from microstructures of quenched alloys and confirmed by high temperature X-ray data. The latest estimates of the solid solubility limit of zirconium in alpha thorium at 600°C is 1.5 wt % zirconium. This value is based upon measurements of lattice constant versus composition. Because of the flattened portion of the solvus curve at 900°C a monotectoid reaction at 13 wt % zirconium has been proposed with a two-phase β_1, plus β_2 region above 900°C. However, since no evidence for such a region has been found either from microscopic or high temperature X-ray studies, this portion of the system has been constructed as shown.

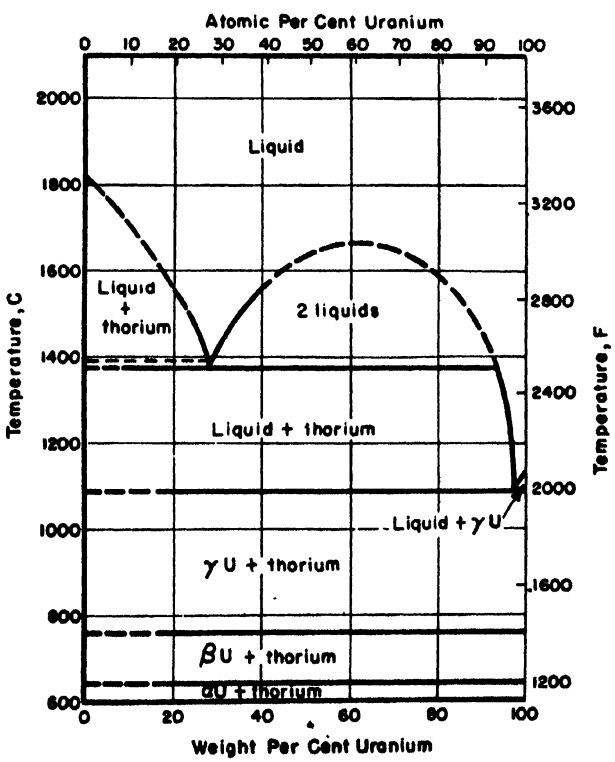

Figure 29. Thorium-uranium system

12. HAZARDS ASSOCIATED WITH THORIUM METALLURGY

Processing operations connected with the preparation, purification and treatment of thorium metal and its compounds present potential hazards due to radiological toxicity, chemical toxicity, fire and/or explosion. It is the purpose here to indicate the sources of some of these hazards in order that the novice in thorium metallurgy will be alerted to the problems bearing on health and safety.

Toxic reactions might arise from the ingress of material by inhalation, by ingestion, or by incisions. Careless handling of the metal or materials in metal preparation, especially if powdered metal is involved, can result in serious fires and explosions.

12.1 Radiological Toxicity

The radiological toxicity of thorium arises from the alpha, beta and gamma radiations that are given

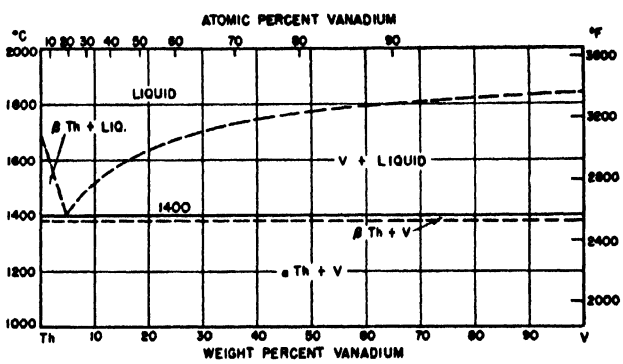

Figure 30. Thorium-vanadium system

off by the element and its decay products (see Table III, Subsection 4.1)§ In general, the greatest danger from radiation develops when the radioactive material itself enters the body, usually orally or by inhalation.

In the processing of thorium, its ores and its salts, recognition must be given to the fact that these decay products fall into several columns of the periodic table and, therefore, behave chemically in different ways. Actually, because of the short half-lives of many of the decay products, the chemical problem is essentially one of handling two elements, thorium and radium. However, these short half-lives mean, also, that after any separation into a thorium and a non-thorium fraction, the situation changes rapidly. For example, if all non-thorium decay products could be removed from thorium (Th^{232}) and its daughter

§ The growth and decay characteristics of the thorium disintegration series are complicated; the discussion in this section is an effort to present essential information in a brief, understandable manner without going into the great detail necessary for a full exposition of the subject.

isotope radiothorium (Th^{228}, which is of course truly thorium and behaves like Th^{232} chemically), only a few days would elapse before considerable concentrations of radium-type products would have formed again in the thorium fraction. The non-thorium fraction also undergoes rapid changes. It contains mesothorium I which has as one of its decay products the strongly active radiothorium (Th^{228}). As the non-thorium fraction may have considerably less physical bulk than the thorium fraction, the percentage of radiothorium in it may become relatively high—higher than it is in the thorium fraction. The thorium X in the non-thorium (i.e., the radium-type portion) fraction decays to thoron which is a short-lived radioactive gas that may build up high levels of radioactivity in working areas.

The above analysis indicates that the radiological hazards in the processing of thorium vary with the degree of separation, the concentration of the toxic members of the chain and the interval between the processing steps. In general, the non-thorium fraction poses the more serious handling, storage and disposal problems.

Illustrations of specific situations may be of value. In the sulfuric acid treatment of monazite, most of the non-thorium fraction remains in the silica sludge. The aqueous raffinate solution from the tributyl phosphate purification process will also have relatively high concentrations of the radium isotopes. In the precipitation of thorium oxalate from a thorium nitrate solution on a production scale, approximately 70% of the mesothorium I usually remained in the filtrate. Another source of radioactivity connected with treatment of ore is the thoron that is released. Thoron is not only hazardous itself but decays rapidly into radioactive products; unless it is removed by a ventilating system, dangerous levels of radioactivity may be built up in working areas. The thoron problem exists, also, in insufficiently ventilated storage spaces containing thorium or its compounds. In vacuum casting of thorium metal a good share of the residual radium isotopes escape from the metal and deposit on the interior of the furnace.

If radioactive material gains entrance to the body, the thorium-type substances tend to settle in the liver, kidneys, spleen and bone marrow whereas the radium-type substances are more likely to be in the skeleton. Hence, the body receives radiation in both bone and tissue.

As an example of the acute radiotoxicity of some of the isotopes involved, reference is made to the work on radiothorium by Finkel and Hirsch.[143] These authors report that for doses between 36 and 58 microcuries per kilogram of body weight, mice exhibited a 50% mortality in 20 to 30 days. The actual weights of materials involved are exceedingly small as one microcurie of activity is equivalent to about 10^{-9} gm of radiothorium.

Radiation from sources outside the body should also be considered. Thorium-bearing materials and wastes may have sufficient beta-gamma activity to

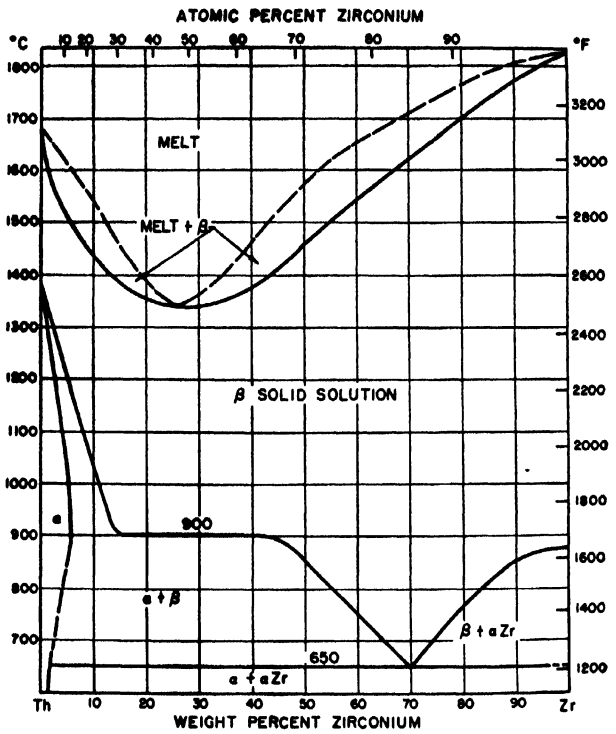

Figure 31. Thorium-zirconium system

constitute a hazard. Also deposits of radioactive material on walls and other surfaces in the areas near processing operations may have unsafe amounts of gamma radiation. Hence, frequent monitoring with radiation measuring devices is essential. This monitoring should extend to air sampling also as the amount of thoron and decay products from thoron may be present in concentrations above the safe limit.

In general, one may say that unless special precautions are taken to have adequate ventilation and to keep the areas clean, exposures in excess of accepted safe limits may occur during all processing stages including the machining of the metal.

12.2 Chemical Toxicity

Chemical toxicity of thorium and its compounds is generally low by any means of ingress. Tests made by Mattis[144] indicate that thorium nitrate, thorium chloride and thorium fluoride are relatively innocuous when administered orally. Doses of 1 to 2 grams of thorium nitrate per kilogram of body weight or 6 to 10 grams of thorium chloride per kilogram of body weight are necessary to produce severe toxic reactions in rats and mice; 10 grams of thorium fluoride per kilogram of body weight can be tolerated easily.

Subcutaneous injections of thorium nitrate solutions produced pain, necrosis and sloughing. Fifty milligrams of powdered thorium nitrate per kilogram of body weight placed in incisions was tolerated easily. On the other hand, intravenous injection of the nitrate and the chloride in the amounts of 42 mg/kg and 34 mg/kg, respectively, produced 50 per cent mortality in rats. A depression of the rate of growth of rats fed on a diet containing 1% and 4%

of thorium nitrate was shown to be due to a self-limitation of caloric intake.

Hall *et al.*[145] made studies of acute toxicity dusts of thorium nitrate—80 mg/m^3; thorium oxide—50 mg/m^3; thorium fluoride—11 mg/m^3; and thorium oxalate—26 mg/m^3. Retching, gagging and occasional vomiting but no other toxic manifestation occurred.

12.3 Fire and Explosion Hazards

The spontaneous ignition of dust layers of both thorium and thorium hydride and the relative ease of ignition of dust clouds makes it imperative that great care be taken in the handling of both powders.

Freshly prepared thorium powder, or powder which has been freed of surface adsorbed gases can ignite spontaneously when suddenly exposed to air. This tendency to ignite is less with powders made up of larger particle size. Under proper conditions the initial rate of adsorption is apparently sufficiently rapid and exothermic to raise fine particles to the ignition temperature. The tendency toward spontaneous ignition of clean thorium powder on sudden exposure to air has been observed.[6]

Metal powder suspended in air can lead to violent explosions. Hartmann *et al.*[146] have studied the explosive properties of thorium and thorium hydride (ThH_2) powders in a number of gases. The ignition temperatures were determined by propelling a weighed amount of powder by compressed air (or other gas) downward through an electrically heated cylindrical-tube furnace. The lowest temperature at which flame appeared at the open exit end of the furnace was taken as the ignition temperature. The ignition temperature of clouds of metal dust in air was found to be 270°C. Ignition temperatures for undisturbed dust layers of the metal were found to be 280°C, 450°C and 500°C in air, carbon dioxide, and nitrogen respectively. The ignition temperature of clouds of hydride dust was found to be 260°C in air, and 740°C in CO_2. No ignition was observed in nitrogen at temperatures up to 850°C. The ignition temperatures for undisturbed layers of the hydride were found to be 20°C, 340°C, and 330°C in air, carbon dioxide, and nitrogen respectively.

The limiting oxygen contents in air-inert gas mixtures for preventing spark ignition of dust clouds of these powders at room temperature were also determined by the same investigators. The limiting oxygen contents in argon, nitrogen, and helium for thorium dust were 2, 2.5, and 4.9%, respectively; the corresponding values of ThH_2 dust were 4, 5 and 5%, respectively.

In the charges employed in some thorium reduction processes there exist potential fire and explosion hazards. Charges employing halides mixed with sodium or calcium should be handled with due regard for the exothermic reaction that might be initiated prematurely.

Also in some bomb reductions excessive pressure may be built up during the bomb reaction. Moisture in materials used for the charge is one factor that could cause preignition or could cause excessive pressure by the release of hydrogen during the reduction.

In addition to structural damage, burns, and bodily injury, the radiological contamination of buildings, equipment and personnel must not be overlooked.

REFERENCES

1. Lilliendahl, W. C., *Rare Metals Handbook,* Thorium, Chapter 23, edited by Clifford A. Hampel, Reinhold Publishing Corporation, New York (1954).
2. Bearse, A. E., Calkins, G. D., Clegg, J. W. and Filbert, R. B., Jr., *Thorium and Rare Earths from Monazite,* Chem. Eng. Progr. *50*: No. 5, 235-239 (1954).
3. Smutz, M., Bridger, G. L., Shaw, K. G. and Whatley, M. E., *The Ames Process for Separation of Monazite,* Chem. Eng. Progr. Symposium Series No. 13, Nuclear Engineering - Part 3: 167-70 (1954).
4. Spedding F. H., Fulmer, E. I., Butler, T. A., Gladrow, E. M., Gobush, M., Porter, P. E., Powell, J. E. and Wright, J. M., *The Separation of Rare Earths by Ion Exchange. III. Pilot Plant Scale Separations,* J. Am. Chem. Soc. *69*: 2812-18 (1947).
5. Berzelius, J. J., *Untersuchung eines neuen Minerals und einer darin enthaltenen zuvor unbekannten Erde,* Ann. Physik *16*: (2) 385-415 (1829).
6. Marden, J. W. and Rentschler, H. C., *Metallic Thorium,* Ind. Eng. Chem. *19*: 97-103 (1927).
7. Rentschler, Harvey C., Lilliendahl, W. C. and Gray, John E., *Thorium* (to Westinghouse Electric Corporation) US Patent 2,446,062 (27 July 1948).
8. Lilliendahl, W. C., *Thorium* (to Westinghouse Electric Corporation) US Patent 2,537,067 (9 January 1951).
9. Driggs, F. H. and Lilliendahl, W. C., *Preparation of Metal Powders by Electrolysis of Fused Salts. II. Thorium.* Ind. Eng. Chem. *22*: 1302-3 (1930).
10. Veigel, N. D., Sherwood, E. M. and Campbell, I. E., *The Preparation of High Purity Thorium by the Iodide Process,* US Atomic Energy Commission Report No. AECD-3586, 16p (1953).
11. Hollander, J. M., Perlman, I. and Seaborg, G. T., *Table of Isotopes,* Rev. Mod. Phys. *25*: 469-651 (1953).
12. Bohlin, Helge, *Anordnung für röntgenkristallographische Untersuchungen von Kristallpulver,* Ann. Physik *61*: (4) 421-39 (1920).
13. Burgers, W. G. and van Liempt, J. A. M., *Zum Verhalten des Thoroxyds in Wolframglühdrähten,* Z. anorg. allgem. Chem. *193*: 144-60 (1930).
14. Neuburger, M. C., *Gitterkonstanten für das Jahr 1936,* Z. Krist. *93*: 1-36 (1936).
15. D'Eye, R. W. M., *Preparation of Pure Thorium,* US Atomic Energy Commission Report No. AERE-C/R-*425*: 6p (1949).
16. Baenziger, N. C., unpublished work, Ames Laboratory, Iowa State College (1950).
17. Borie, B. S., Jr., unpublished work, Oak Ridge National Laboratory (1951).
18. Chiotti, Premo, *The Thorium-Carbon System,* US Atomic Energy Commission Report No. AECD-3072, 52p (1950).
19. Adams, R. E., unpublished work, Oak Ridge National Laboratory (1952).
20. Carlson, O. N., *Some Studies on the Uranium-Thorium-Zirconium Ternary Alloy System,* US Atomic Energy Commission Report No. AECD-3206, 72p (1950).

21. Carlson, O. N., to be published.
22. McCaldin, James O. and Duwez, Pol, *Allotropic Transformations at High Temperature,* J. Metals *6*: 619-20 (1954).
23. Chiotti, Premo, *High Temperature Crystal Structure of Thorium,* J. Electrochem. Soc. *101*: 567-70 (1954).
24. Bridgman, P. W., *Effects of High Shearing Stress Combined with High Hydrostatic Pressure,* Phys. Rev. *48*: (2) 825-47 (1935).
25. Reynolds, Myron B., *New Elastic Constants of Some Metals,* US Atomic Energy Commission Report No. AECD-3242, 85p (1951).
26. Bridgman, P. W., *The Compressibility and Pressure Coefficient of Resistance of Ten Elements,* Proc. Am. Acad. Arts, Sciences *62*: 207-26 (1926-27).
27. Reported by Marsh, L. L. and Keeler, J. R., Battelle Memorial Institute (1951).
28. Sidles, P. H. and Danielson, G. C., unpublished work, Ames Laboratory, Iowa State College (1955).
29. Spedding, F. H., Miller, C. F. and Flynn, J. P., unpublished work, Ames Laboratory, Iowa State College (1952).
30. Meissner, W. and Voigt, B., *Messungen mit Hilfe von flüssigem Helium XI. Widerstand der reinen Metalle in tiefen Temperaturen,* Ann. Physik *7*: (5) 892-936 (1930).
31. Bender, Dietrich, *Über die elektrischen Eigenschaften des Thoriums,* Z. Metallkunde *40*: 257-60 (1949).
32. de Boer, J. H., quoted by van Arkel, A. E., in Reine Metalle, p. 217, J. Springer, Berlin (1939).
33. Meissner, W., *Supraleitfähigkeit von Thorium,* Naturwissenschaften *17*: 390-1 (1929).
34. Meissner, W., *Messungen mit Hilfe von flüssigen Helium, VII. Die Übergangskurven zur Supraleitfähigkeit für Tantal und Thorium,* Z. Physik *61*: 191-8 (1930).
35. de Haas, W. J. and van Alphen, P. M., *The change in resistance of graphite, thorium, titanium, titanium-zirconium between 20.4°K and 1.1°K.* Proc. Konink. Akad. v. Wetenschappen, Amsterdam *34*: 70-4 (1931).
36. Schoenberg, D., *Magnetic Properties of Superconductors,* Nature *142*: 874 (1938).
37. Daunt, J. G., *An Empirical Correlation Among Superconductors,* Phys. Rev. *80*: (2) 911-12 (1950).
38. Sidles, P. H. and Danielson, G. C., Quarterly Summary Research Report in Physics for April through June 1952, US Atomic Energy Commission Report ISC-283, 13p (1952).
39. Honda, K., *Magnetic Properties of Matter,* p. 129, Syokwabo and Company, Tokyo (1928).
40. Owen, M., *Magnetochemische Untersuchungen. Die thermomagnetischen Eigenschaften der Elemente. II,* Ann. Physik *37*: (4) 657-99 (1912).
41. Klemm, Li, *Magnetochemische Untersuchungen. XXXIII. Das magnetische Verhalten einiger Elemente,* Z. Elektrochem. *45*: 354-7 (1939).
42. Hamer, Richard, *Photoelectric Thresholds of Elements Under Ordinary Conditions,* J. Optical Soc. Amer. *9*: *251-7* (1924).
43. Zwikker, C., *Thermionic Emission of the Metals Tungsten, Molybdenum, Thorium, Zircon and Hafnium.* Proc. Konink, Akad. v. Wetenschappen, Amsterdam *29*: 792-802 (1926).
44. Rentschler, H. C., Henry, D. E. and Smith, K. O., *Photoelectric Emission from Different Metals,* Rev. Sci. Instr. *3*: 794-802 (1932).
45. Schulze, Rudolf, *Experimentelles über den lichtelektrischen Effect. Teil I: Reihenuntersuchung des ausseren lichtelektrischen Effektes an den Elementen des periodischen Systems,* Z. Physik *92*: 212-27 (1934).
46. Rentschler, H. C. and Henry, D. E., *Lowering of the Photoelectric Work Function of Zirconium, Titanium, Thorium, and Similar Metals by Dissolved Gases,* Trans. Electrochem. Soc. *87*: 289-97 (1945).
47. Smithells, C. J., *Metals Reference Book,* p. 469, Interscience, New York (1949).
48. Wilhelm, H. A. and Chiotti, P., *Thorium-Carbon System,* Trans. Am. Soc. Met. *42*: 1295-310 (1950).
49. Reported by Thompson, J. G., National Bureau of Standards (1945).
50. Pirani, Marcello and Alterthum, Hans, *Über eine Methode zur Schmelzpunktbestimmung an Hochschmelzenden Metallen,* Z. Elektrochem. *29*: 5-8 (1923).
51. von Bolton, Werner, *Über das Thorium,* Z. Elektrochem. *14*: 768-70 (1908).
52. von Wartenberg, H., *Über Thorium,* Z. Elektrochem. *15*: 866-72 (1909).
53. Honda, K., *Die thermomagnetischen Eigenschaften der Elemente,* Ann. Physik *32*: (4) 1027-63 (1910).
54. Thompson, J. G., *Some Physical Properties of Commercial Thorium,* Metals and Alloys *4*: 114-18 (1933).
55. Alberman, K. B. and Anderson, J. S., quoted by D'Eye in *Preparation of Pure Thorium,* US Atomic Energy Commission Report No. AERE-C/R-425, 6p (1949).
56. Reported by Perlman, I., U. of Calif. Radiation Laboratory (1947).
57. Reported by Miller, E. C., Oak Ridge National Laboratory (1949).
58. Reported by Rapperport, E. J., Mass. Institute of Technology (1952).
59. Andrews, Mary R., *The Evaporation of Thorium from Tungsten,* Phys. Rev. *33*: (2) 454-8 (1929).
60. Zwikker, C., *Samenvatting van de huidige Gegevens over Dampdrukken bij hoobe Temperaturen,* Physica *8*: 240-50 (1928).
61. Brewer, Leo, *Chemistry and Metallurgy of Miscellaneous Materials: Thermodynamics,* National Nuclear Energy Series, *IV-19B*: Paper 3, McGraw-Hill Co., New York (1950).
62. Dushman, Saul, *Scientific Foundations of Vacuum Technique,* Chapt. 11, Wiley, New York (1949).
63. Loftness, R. L., *A Vapor Pressure Chart for Metals,* US Atomic Energy Commission Report No. NAA-SR-132, 9p (1951).
64. International Critical Tables, Vol. *1*: 102 (1926).
65. Griffel, Maurice and Skochdopole, Richard E., *The Heat Capacity and Entropy of Thorium from 18 to 300°K,* J. Am. Chem. Soc. *75*: 5250-1 (1953).
66. Jaeger, F. M. and Veenstra, W. A., *The Exact Measurement of the Specific Heats of Solid Substances. XVI. The Specific Heats of Metallic Thorium and of Thoriumdioxide between 20° and 1400°C.* Proc. Konink. Akad. v. Wetenschappen, Amsterdam *37*: 327-32 (1934).
67. Nilson, L. F., *Über die Specifische Warme und die Valenz des Thoriums.* Berichte Deutsche Chem. Gesellschaft *16*: 153-63 (1883).
68. Roberson, A. H., Beall, R. A. and Caputo, F., unpublished information from US Bureau of Mines, Albany, Oregon (1955).
69. Eckert, F. H. and Boyle, E. J., unpublished work, Oak Ridge National Laboratory (1953).
70. Milko, J. A. and Boyle, E. J., unpublished work, Oak Ridge National Laboratory (1952).
71. Raynes, B. C., Bleiweiss, J. C., Sibert, M. E. and Steinberg, M. A., unpublished work, Horizons, Inc. (1954).

72. Jetter, H. K., Borie, B. S., Jr., and Fretague, W. J., unpublished work, Oak Ridge National Laboratory (1952).
73. Brinkman, J. A. and Gilbert, W. S., *Effects of Fission Fragments on Radiation Damaged Metals,* US Atomic Energy Commission Report No. NAA-SR-262, 34p (1952).
74. Brinkman, J. A., *On the Nature of Radiation Damage in Metals,* J. Applied Phys. *25*: 961-70 (1954).
75. Schwarzkopf, Paul, *Powder Metallurgy, Its Physics and Production,* Macmillan Co., New York (1947).
76. Rundle, R. E., Shull, C. G. and Wollan, E. O., *The Crystal Structure of Thorium and Zirconium Dihydrides by X-ray and Neutron Diffraction,* Acta Cryst. *5*: 22-6 (1952).
77. Zachariasen, W. H., *Crystal Chemical Studies of the 5f-Series of Elements. XIX. The Crystal Structure of the Higher Thorium Hydride, Th_4H_{15},* Acta Cryst. *6*: 393-5 (1953).
78. Nottorf, Robert William, *Some Problems in Chemistry of Uranium and Thorium of Interest to the Development of Atomic Power,* Iowa State College, J. Sci. *26*: 255-7 (1951-52).
79. Mallett, Manley W. and Campbell, Ivor E., *The Dissociation Pressures of Thorium Dihydride in the Thorium-Thorium Dihydride System,* J. Am. Chem. Soc. *73*: 4850-2 (1951).
80. Chiotti, P. and Rogers, B. A., *Production of Powdered Uranium and Thorium,* Metal Progress *60*: No. 3, 60-5 (1951).
81. Wilhelm, Harley A. and Chiotti, Premo, *Preparation of Powdered Thorium,* (To U.S.A. as represented by the Atomic Energy Commission) U.S. Patent 2,635,-956 (21 April 1953).
82. Powers, R., unpublished work, Sylvania Electric Products, Inc. (1953).
83. Wagner, R. B. and Storchheim, S., unpublished work, Sylvania Electric Products, Inc. (1954).
84. Ma, Chuk-Ching, *Crystal Size Distribution in Electrolytic Metal Powders,* Ind. Eng. Chem. *44*: 342-6 (1952).
85. Sloman, H. A., Harvey, C. A. and Kubaschewski, O., *Fundamental Reactions in the Vacuum-Fusion Method and Its Application to the Determination of O_2, N_2, and H_2 in Mo, Th, Ti, U, V, and Zr,* J. Inst. Metals, *80*: 391-407 (1952).
86. Wagener, S., *Sorption of Gases at Very Low Pressures by Thorium Powder,* Proc. Physical Soc., *66B*: 400-13 (1953).
87. Storchheim, S., unpublished work, Sylvania Electric Products, Inc. (1954).
88. Reported by Klein, J. G. and Wikle, K. G., N. Y. Operations Office of US Atomic Energy Commission (1952).
89. Olson, A. R., unpublished work, Oak Ridge National Laboratory (1951).
90. Draley, J., unpublished work, Argonne National Laboratory (1952).
91. Deal, B. E. and Svec, H. J., *Metal Water Reactions. III. Kinetics of the Reaction Between Thorium and Water Vapor,* submitted to J. Electrochem. Soc. (1955).
92. Levesque, Pascal and Cubicciotti, *The Reaction Between Oxygen and Thorium,* J. Am. Chem. Soc. *73*: 2028-31 (1951).
93. Russell, H. W., Nelson, H. R. and Grenell, L. H., unpublished work, Battelle Memorial Institute (1945).
94. Feibig, J. G., unpublished work, Ames Laboratory, Iowa State College (1945).
95. Brugmann, E. W. and Draley, J. E., unpublished work, University of Chicago Metallurgical Laboratory (1945).
96. Greninger, A. B., *et al.,* unpublished work, University of Chicago Metallurgical Laboratory (1945).
97. Roth, H. P., unpublished work, Nuclear Metals, Inc. (1952).
98. Dickerson, R. F., unpublished work, Battelle Memorial Institute (1952).
99. Pohl, Margaret S., unpublished work, Knolls Atomic Power Laboratory (1952).
100. Gray, R. J., unpublished work, Oak Ridge National Laboratory (1952).
101. Carlson, A. J., Williams, J. T., Rogers, B. A. and Manthos, E. J., *Etching Metals by Ionic Bombardment,* US Atomic Energy Commission Report No. ISC-480, 19p (1954).
102. Saller, H. A. and Rough, F. A., Editors, *Compilation of U. S. and U. K. Uranium and Thorium Constitution Diagrams,* Battelle Memorial Institute, Columbus, Ohio (1954).
103. Keeler, J. R., *Thorium Metallurgy,* Chem. Eng. Prog. Symposium Series No. 11, Nuclear Engineering–Part 1: 57-61 (1954).
104. Brauer, G., *Kristallstruktur Intermetallischer Verbindungen des Aluminiums mit Titan, Zirkon, Thorium, Niob und Tantal,* Naturwissenschaften *26*: 710 (1938).
105. Grube, G. and Botzenhardt, L., *Die Legierungen des Thorium mit Kupfer, Aluminum und Natrium,* Z. Elektrochem. *48*: 418-25 (1942).
106. Baenziger, N. C. and Rundle, R. E., *The MBe_{13} compounds,* Acta Cryst. *2*: 258 (1945).
107. Koehler, W. C., Singer, Joseph and Coffinberry, A. S., *X-Ray and neutron diffraction studies of the MBe_{13} intermetallic compounds,* Acta Cryst. *5*: 394 (1954).
108. Johnson, H. B., unpublished work, Ames Laboratory, Iowa State College (1950).
109. Bryner, J. S., unpublished work, Brookhaven National Laboratory (1955).
110. Brewer, Leo, Sawyer, Dwight L., Templeton, D. H. and Dauben, Carol H., *The Borides of Uranium and Thorium,* US Atomic Energy Commission Report No. AECD-2823, 9p (1950).
111. Lafferty, J. M., *Boride Cathodes,* J. Applied Phys. *22*: 299-309 (1951).
112. Zalkin, A. and Templeton, D. H., *The Crystal Structures of CeB_4, ThB_4, and UB_4,* US Atomic Energy Commission Report No. AECD-3080 (1950).
113. Kiessling, Roland, *Borides of Some Transition Elements,* Acta Chem. Scand. *4*: 209-27 (1950).
114. Bertaut, Felix and Blum, Pierre, *Etude des hexabornures et de la substitution alcaline,* Compt. rend. *234*: 2621-3 (1952).
115. Andersson, Lars-Henrik and Kiessling, Roland, *Investigations on the Binary Systems of Boron with Chromium, Columbium, Nickel, and Thorium, Including a Discussion of the Phase "TiB" in the Titanium-Boron System,* Acta Chem. Scand. *4*: 160-4 (1950).
116. Florio, J. V., Baenziger, N. C. and Rundle, R. E., *Compounds of Thorium with Transition Metals. II. Systems with Iron, Cobalt and Nickel,* submitted to Acta Cryst. (1955).
117. Snow, A. I. and Rundle, R. E., unpublished work, Ames Laboratory, Iowa State College (1949).
118. Raub, E. and Engel, M., *Die Legierungen des Thoriums mit Kupfer, Silber und Gold,* Z. Elektrochem. *49*: 487-92 (1943).

119. Loomis, B. A., unpublished work, Ames Laboratory, Iowa State College (1955).
120. Leontis, T. E., *Properties of Magnesium-Thorium and Magnesium-Cerium Alloys,* J. Metals *4*: 287-94 (1952).
121. Florio, John V., Rundle, R. E. and Snow, A. I., *Compounds of Thorium with Transition Metals. I. The Thorium-Manganese System,* Acta Cryst. *5*: 449-57 (1952).
122. Parks, W. George and Prime, George E., *The Solubility of Thorium in Mercury,* J. Am. Chem. Soc. *58*: 1413-14 (1936).
123. Horn, Lore and Basserman, Christl, *Das Zustandsbild Nickel-Thorium,* Z. Metallkunde *39*: 272-75 (1948).
124. Carlson, O. N., Dickinson, J. M., Lunt, H. E. and Wilhelm, H. A., *Thorium-Columbium and Thorium-Titanium Alloy Systems,* submitted to Journal of Metals (1955).
125. Gerds, A. F. and Mallett, M. W., *Reaction of Nitrogen with, and the Diffusion of Nitrogen in, Thorium,* J. Electrochem. Soc. *101*: 175-80 (1954).
126. Rundle, R. E., *A New Interpretation of Interstitial Compounds, Metallic Carbides, Nitrides and Oxides of Composition MX,* Acta Cryst. *1*: 180-7 (1948).
127. Chiotti, P., *Experimental Refractory Bodies of High-Melting Nitrides, Carbides, and Uranium Dioxide,* J. Am. Cer. Soc. *35*: 123-30 (1952).
128. Zachariasen, W. H., *The Crystal Structure of Th_3N_4,* US Atomic Energy Commission Report No. AECD-2090, 2p (1948).
129. Meisel, Karl, *Kristallstrukturen von Thoriumphosphiden,* Z. anorg. allgem, Chem. *240*: 300-12 (1938-39).
130. Zumbusch, Maria, *Über Strukturanalogie von Uran- und Thoriumphosphiden,* Z. anorg. allgem. Chem. *245*: 402-8 (1940-41).
131. Brauer, G. and Mitius, A., *Die Kristallstruktur des Thoriumsilicids $ThSi_2$,* Z. anorg. allgem. Chem. *249*: 325-39 (1952).
132. Zachariasen, W. H., unpublished work, University of Chicago (1953).
133. Foote, F., unpublished work, Argonne National Laboratory (1945).
134. Strotzer, Erich Ferdinand and Zumbusch, Maria, *Thoriumsulfide,* Z. anorg. allgem. Chem. *247*: 415-28 (1941).
135. Zachariasen, W. H., *Crystal Structure Studies of Sulfides and Oxysulfides of Uranium, Thorium and Cerium,* US Atomic Energy Commission Report No. AECD-2141.
136. Zachariasen, W. H., *Crystal Chemical Studies of the 5f-Series of Elements. IX. The Crystal Structure of Th_7S_{12},* Acta Cryst. *2*: 288-91 (1949).
137. Zachariasen, W. H., *Crystal Chemical Studies of the 5f-Series of Elements. X. Sulfides and Oxy-Sulfides,* Acta Cryst. *2*: 291-6 (1949).
138. Eastman, E. D., Brewer, Leo, Bromley, LeRoy A., Gilles, Paul W. and Lofgren, Norman L., *Preparation and Properties of the Sulfides of Thorium and Uranium,* J. Am. Chem. Soc. *72*: 4019-23 (1950).
139. D'Eye, R. W. M., Sellman, P. G. and Murray, J. R., *The Thorium-Selenium System,* J. Chem. Soc. 2555-62, (July 1952).
140. D'Eye, R. W. M., *The Crystal Structures of $ThSe_2$ and Th_7Se_{12},* J. Chem. Soc. 1670-2 (June 1953).
141. Levingston, H. L. and Rogers, B. A., *The Thorium-Vanadium System,* US Atomic Energy Commission Report No. AECD-3602, 20p (1953).
142. Nowotny, Hans, *Die Kristallstrukturen von Zn_2Th, Cd_2Ca and $(Ag,Mg)_2Ca$,* Z. Metallkunde *37*: 31-4 (1946).
143. Finkel, M. P. and Hirsch, G. M., *Preliminary Studies on the Acute Toxicity of Some Radioelements of the Mesothorium Chain,* US Atomic Energy Commission Report No. ANL-4625: 209-221 (1951).
144. Mattis, Paul A., *Toxicological Studies of Certain Thorium Salts,* US Atomic Energy Commission Report No. NYO-1607, 47p (1950).
145. Hall, Robert H., Stroud, Catherine A., Scott, James K., Root, Robert E., Steadman, Luville T. and Stokinger, Herbert E., *Acute Toxicity of Inhaled Thorium Compounds,* US Atomic Energy Commission Report No. UR-190, 27p (1951).
146. Hartmann, Irving, Nagy, John and Jacobson, Murray, *Explosive Characteristics of Titanium, Zirconium, Thorium, Uranium and Their Hydrides,* US Bureau of Mines Report of Investigation No. 4835, 16p (1951).

The Alloys of Uranium

By H. A. Saller and F. A. Rough,* USA

Fissionable isotopes of either uranium or plutonium, which is made from uranium, are used in every reactor. The metallurgy of uranium is thus important and basic to the whole atomic energy program. For this reason, there has been much interest in alloying uranium. This interest has been increased because of the relatively poor properties of the metal. It is active chemically, it is anisotropic, and its mechanical properties leave much to be desired. The study of uranium alloys has also been spurred by interest in lowering the melting point or diluting enriched uranium for power reactors.

ALLOYING OF URANIUM

Before surveying the data that are available on various uranium alloys, it is appropriate to look at the metal uranium and its alloying from a theoretical viewpoint. It has three allotropic modifications. Alpha uranium is stable up to 662°C, beta uranium is stable from 662°C to 769°C, and gamma uranium is stable from 769°C to the melting point at 1129°C.[1] The data on the crystallography of these phases are summarized in Table I.[2-7]

In alpha uranium which is orthorhombic there are two groups of interatomic distances of about 2.8 and 3.3 Å. The structure may be regarded as being composed of corrugated sheets of atoms parallel to the ac plane in which the atoms are tightly bound as indicated by the characteristic interatomic distance of 2.8 Å. The binding between the corrugated sheets is much weaker and is characterized by interatomic distances of 3.3 Å. The anisotropic nature of the atomic arrangement in alpha uranium suggests appreciable covalent bonding analogous to that occurring in arsenic, antimony and bismuth.[8]

The metal uranium has six orbital electrons outside an inert core. The electronic configuration of alpha uranium can probably be best represented by $7s^2 6d^2 5f^2$, if a single configuration can be considered to be representative, where the $7s^2$ electrons are inert, and the $6d^2$ and $5f^2$ electrons are in hybrid d-f orbitals acting with a valence of about four.[8,9] As in other transition metals, hybridized electrons do not act as a whole number of electrons, and alpha uranium may be regarded as having a valence of 3.8.

The orthorhombic crystal structure of alpha uranium is unique among metals and, since it is characterized by some degree of covalent bonding, it is to be expected that the formation of solid solutions will be restricted even though atomic sizes and valence of solute elements are favorable.

Based on the assumption that alpha uranium has a valence of about 4, or 3.8, it might be expected that the quadrivalent elements such as titanium, zirconium and hafnium would stabilize alpha relative to the beta phase. This effect has been observed experimentally in the systems uranium-titanium and uranium-zirconium, but the solid solubilities of titanium and zirconium in both alpha and beta are limited.[10] The system uranium-hafnium has not been studied. The experimental data which are available on other quadrivalent elements such as silicon and germanium where the size factors, related to the coordination number 12, are within 15 per cent, give no indication of the relative solid solubilities in the two phases.

In the gamma phase, which is body-centered cubic, uranium is in its most metallic state.[8,9] It is generally accepted that gamma uranium is characterized by a valence of 6 or perhaps 5.8. The elements which on the basis of size factor, crystal structure, and valence might be expected to form appreciable solid solutions in gamma uranium are the Group IVA elements, titanium, zirconium and halfnium; the Group VA elements, vanadium, niobium and tantalum; and the Group VIA elements, chromium, molybdenum and tungsten. Of these elements, nothing is known of the uranium-hafnium system, but titanium, zirconium, niobium and molybdenum form extensive solid solutions. Vanadium and chromium have solubilities in gamma uranium of 12 and 4 atomic per cent, respectively, while tantalum and tungsten are progressively less soluble.[10]

The complex tetragonal structure of beta and its hard nature suggest that it has some degree of nonmetallic bonding, as does alpha uranium. Its intermediate position between alpha and gamma suggests that beta may be characterized by a valence of about five. Since the structure of beta is unique among elements, only limited solid solubilities are likely.

If the assumption that beta has an effective valence of about five electrons per atom is correct, one might expect that beta would be stabilized relative to alpha and gamma, by pentavalent elements such as vanadium, niobium and tantalum. Since the crystal structures are more favorable for solid solution in the gamma, it is not surprising that these elements sta-

* Battelle Memorial Institute.

Table I. Crystallography of the Allotropes of Uranium

Phase	Unit cell Type	Unit cell Dimensions, A	Number of molecules	Density, gm/cm³ X-ray	Space group	Remarks
Alpha	Orthorhombic	$a = 2.852$ $b = 5.865$ $c = 4.945$	4	19.12	Cm cm	-
Beta	Tetragonal	$a = 10.759 \pm 0.001$ $c = 5.656 \pm 0.001$	30	18.11	P1/mnm	720°C
Gamma	Body centered-cubic	$a = 3.524$	2	18.06	-	805°C

bilize beta relative to alpha, but not relative to gamma. Many of the 6-valent gamma-stabilizing elements can also be expected to stabilize beta relative to alpha, although only limited solubilities may exist. As a result, we find that vanadium and niobium of the pentavalent elements and chromium and molybdenum of the 6-valent elements do stabilize beta relative to alpha and are capable of retaining the beta phase during quenching.

Recently, the data available from both the United States and United Kingdom on uranium-alloy systems was compiled.[10] As might be expected, the uranium alloy diagrams fall into a number of standard types. For purposes of discussion, they may be grouped as systems in which intermetallic compounds are found and those in which no true compounds are found. This latter group can be further subdivided into systems showing little solid solubility and those showing much.

Many elements form one or more intermetallic compounds when alloyed with uranium.[10] It is characteristic of these systems that limited solid solubility exists in each of the terminal phases. The uranium-aluminum system, shown in Fig. 1, may be considered typical of these compound-forming elements. Other elements in this category which have received intensive study and for which uranium-alloy diagrams have been established are beryllium, bismuth, carbon, cobalt, copper, gallium, gold, hydrogen, iron, lead, manganese, mercury, nickel, silicon and tin. Elements which form compounds with uranium but whose systems are only partially known are antimony, arsenic, boron, germanium, indium, iridium, nitrogen, oxygen, palladium, phosphorus, platinum, selenium, sulfur, tellurium, thallium and zinc. In addition, some data are available on parts of the ternary systems of uranium with aluminum and silicon, beryllium and carbon, bismuth and lead, cobalt and iron, chromium and iron, and cobalt and nickel.

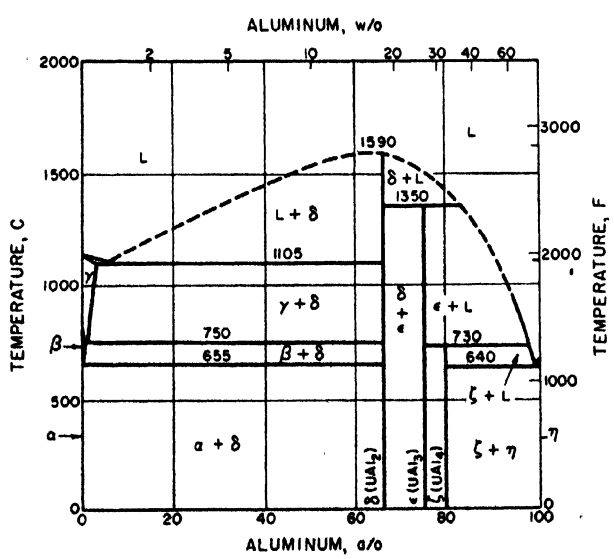

Figure 1. The system uranium-aluminum

Several elements when alloyed with uranium do not produce intermetallic compounds or show large solid solubility in the terminal phases.[10] Such systems contain either eutectic, peritectic, or monotectic reactions. Among the elements in this category for which uranium alloy diagrams are known are chromium, magnesium, silver, tantalum, thorium, tungsten and vanadium. Other elements which do not form compounds nor appreciable solid solutions, but whose uranium alloy diagrams are partially known, include calcium, cerium, lanthanum, neodymium, praseodymium and sodium.

The uranium-vanadium system, shown in Fig. 2, exemplifies the simple eutectic system. The uranium-chromium system is similar, but the eutectic reaction occurs at a somewhat lower temperature. A peritectic characterizes both the uranium-tantalum and uranium-tungsten systems. The latter is shown in Fig. 3. Because the solid solubilities are low, the details of the uranium end are not known, and the isotherms are extended to 100 per cent uranium. A typical monotectic system, that of uranium-magnesium, is shown in Fig. 4. Thorium and silver, and probably cerium, lanthanum, neodymium, and praseodymium, also form monotectic systems with uranium.[10]

Another group of elements when added to uranium produce alloys with extensive solubility at elevated temperatures, but with no true intermetallic compounds. The uranium-molybdenum system shown in Fig. 5 might be considered typical of these systems. The uranium-titanium and uranium-zirconium systems differ only in that solid solubility is complete at elevated temperatures. The uranium-niobium system has complete solid solubility at elevated temperatures, but does not have an intermediate or delta phase.[10] The intermediate phases found in the uranium-molybdenum, uranium-titanium, and uranium-zirconium systems form from a metastable gamma phase. Because they are metallic in nature, they are not considered as intermetallic compounds.

PROPERTIES OF URANIUM ALLOYS

Uranium is a relatively weak metal, and, since it is anisotropic, its mechanical properties are quite dependent on the method of fabrication. For these reasons, there has been considerable interest in alloying as a means of improving the mechanical properties.

Uranium is also very reactive chemically and alloying is also a means of developing suitably corrosion-resistant materials for various applications.

In the selection of an alloy for increased mechanical properties, or corrosion resistance, metallurgical considerations are helpful. Alloys for use as diluents in power reactors are selected primarily for nuclear reasons. This is shown by the interest in zirconium, aluminum and beryllium as diluents in thermal reactors.

A number of elements are effective in improving the high-temperature mechanical properties of uranium when added in small amounts. The tensile properties at 500°C of base uranium and some low-chromium and low-zirconium alloys are given in Table II.[11] It is apparent that a yield strength of three to five times that of uranium can be readily attained at 500°C by these additions.

A number of compound-forming elements, such as aluminum and silicon, are also effective in improving the mechanical properties of uranium when added in small amounts. In larger amounts, these elements form brittle compounds which detract from the fabricability of the alloys.

Very high strengths are possible in high-uranium alloys of the solid-solution-type systems by means

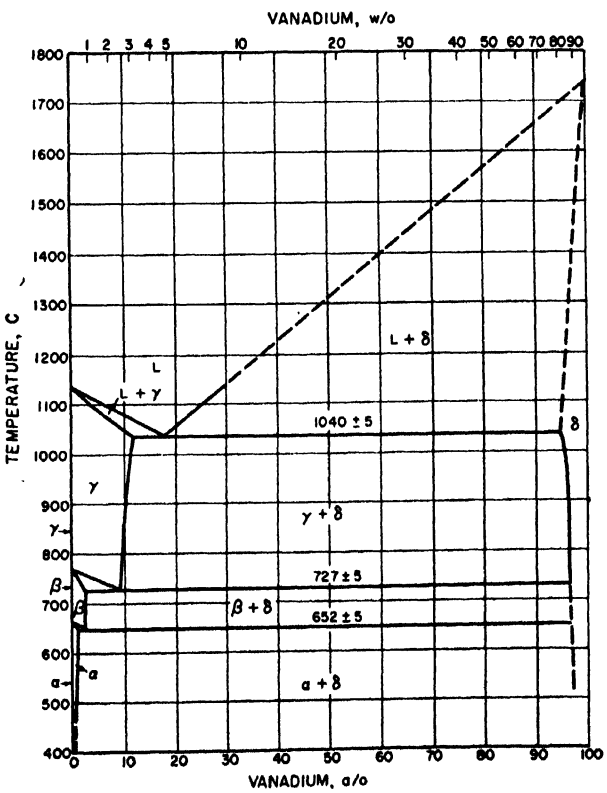

Figure 2. The system uranium-vanadium

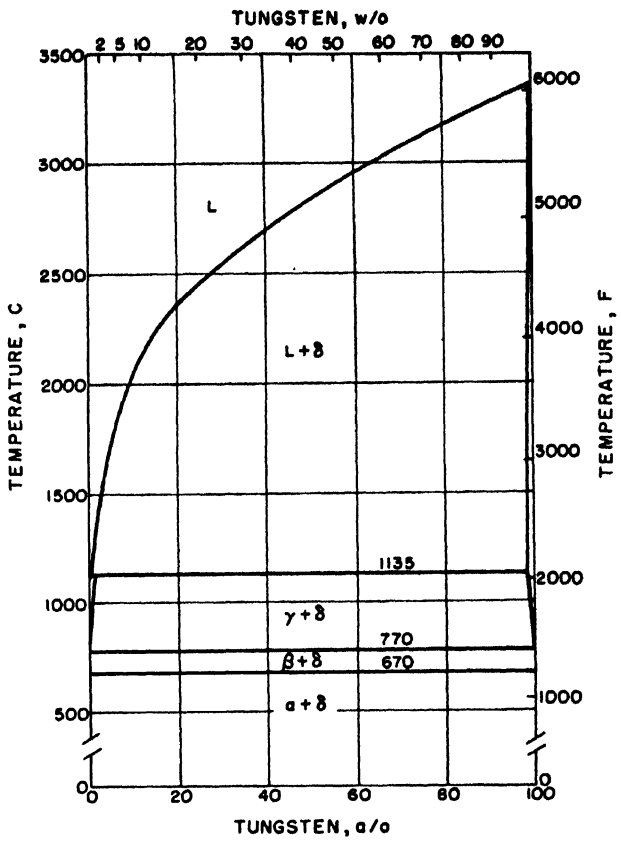

Figure 3. The system uranium-tungsten

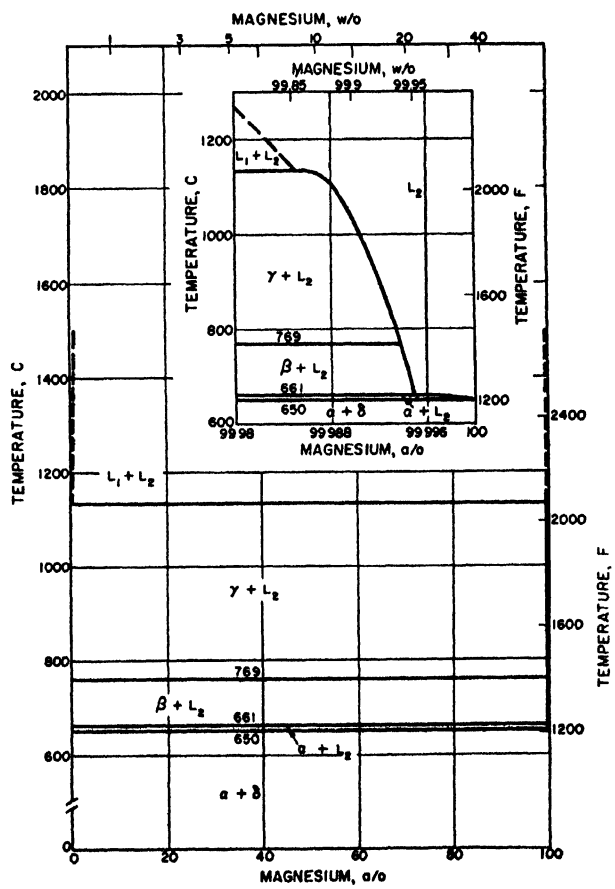

Figure 4. The system uranium-magnesium

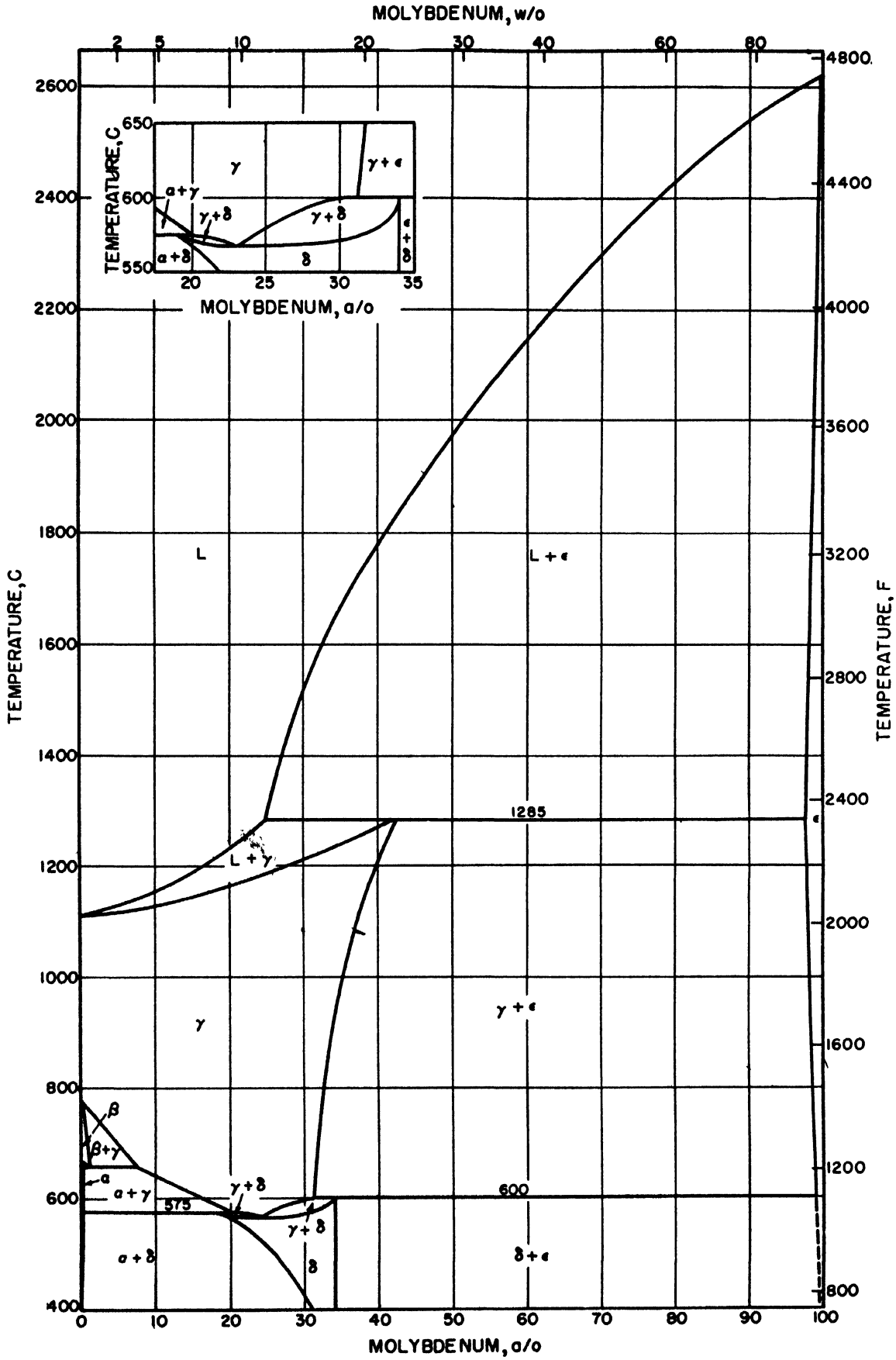

Figure 5. The system uranium-molybdenum

Table II. Tensile Properties of Uranium and Uranium Alloys at 500°C[11]

Analysis	Grain size, mm	Ultimate tensile strength, psi	0.2 per cent yield strength psi	Elongation in 2 in., %	Reduction of area, %
Base uranium,	>0.118	11,260	8330	36	~78
<0.01 carbon		12,460	7900	29	~87
0.10 chromium,	0.057	32,050	23,300	24.5	~57
<0.01 carbon		25,980	15,300	25.5	~85
0.42 chromium,	0.025	38,750	24,600	23	82
<0.01 carbon		37,100	23,800	23	82
1.11 zirconium,	0.033	43,300	31,400	11.3	61
<0.01 carbon		61,000	48,200	21	94
2.21 zirconium,	0.009	46,100	41,300	18	85
<0.01 carbon		52,400	45,000	24	94

of a martensite-type transformation. If, for example, binary alloys of 5 to 10 weight per cent zirconium are gamma quenched, a martensitic alpha-like structure (alpha prime) forms in which virtually all of the zirconium is in metastable solid solution.[12] This alpha-prime structure is very hard and strong in the quenched condition. By varying the tempering or annealing of such a structure to control the precipitation of the excess solute from solid solution, a whole range of properties can be obtained. The hardness data in Table III[12] give some indication of the vastly different properties that can be obtained by treating the uranium-5 weight per cent zirconium alloy in this manner. Similar properties can also be obtained in the other solid-solution-forming systems. In the system uranium-molybdenum, the greatest strength of the 2 weight per cent molybdenum alloy is achieved by quenching from the gamma (700°C) and aging 2 hours at 400°C. With these procedures, 0.2 per cent offset yield strengths as high as 226,000 to 248,000 psi have been obtained in the 2 weight per cent molybdenum alloy in compression at room temperature.[13] Unfortunately, the high strength of these alpha-prime materials would be lost during extended service at high temperatures by over-aging.

Perhaps the greatest improvement in high temperature mechanical properties is to be achieved in the higher alloys of the solid-solution-type systems such as uranium-molybdenum, uranium-niobium, uranium-titanium, and uranium-zirconium.

The tensile properties at 370°C of a series of uranium-zirconium alloys are shown in Table IV.[14] These samples were hot worked and heat treated 24 hours at 575°C and furnace cooled. In this case, the maximum strength was attained at about 20 weight per cent zirconium. At higher temperatures, in the gamma phase region, the maximum strength may occur at a high zirconium composition.

Table III. Vickers Hardness of Uranium-5 Weight Per Cent Zirconium Alloy[12]

Heat treatment	Hardness*
1 hr 900°C, water quenched	535
1 hr 900°C, water quenched; 2 hrs 200°C, water quenched	520
1 hr 900°C, water quenched; 2 hrs 300°C, water quenched	512
1 hr 900°C, water quenched; 2 hrs 400°C, water quenched	545
1 hr 900°C, water quenched; 2 hrs 500°C, water quenched	475
1 hr 900°C, water quenched; 2 hrs 575°C, water quenched	375
1 hr 900°C, water quenched; 2 hrs 650°C, water quenched	315

* Obtained with 30-kg load.

The tensile properties of a 12 weight per cent molybdenum alloy are shown in Table V.[15] This alloy has high strength and rather limited ductility. It is not as strong at 370°C as the strongest uranium-zirconium alloy shown in Table IV, but it may be stronger at temperatures in the gamma phase region.

Table IV. Tensile Properties of Arc-Melted Uranium-Zirconium Alloys at 370°C

Zirconium content, weight per cent	Yield strength (0.2 offset), psi	Tensile strength, psi	Elongation in 2 inches, per cent	Reduction in area, per cent
0	21,300	31,400	27.0	57.0
2.4	35,100	48,400	17.0	49.0
5.5	50,500	77,000	10.0	25.0
11.5	100,800	122,800	8.0	29.0
20.5	124,000	135,200	8.0	18.0
31.4	112,000	145,200	7.0	7.0
41.7	97,000	115,300	8.0	13.0
50.5	68,100	96,100	22.0	28.0
60.6	63,800	97,800	22.0	20.0
70.4	64,800	86,400	20.0	27.0
80.0	72,000	77,900	5.0	22.0
89.4	53,200	64,200	7.0*	11.0*
100.0	8500	17,300	42.0	-

* Specimens broke in what appeared to be rolling defects.

Table V. Tensile Properties of Uranium-12 Weight Per Cent Molybdenum Alloy[15]

Heat treatment	Test temp., °F	0.5% offset yield strength, psi	Tensile strength, psi	Per cent elongation in 1 inch		Reduction, in area, per cent
				Uniform	Total	
24 hours 900°C, water quenched	500	102,000	104,000	1.8	6.9	50
	600	107,000	108,000	2.3	3.6	23
	600	104,000	105,000	–	–	–
	700	98,000	102,000	3.0	4.3	33
24 hours 900°C, water quenched, aged 3 hours 500°C	600	103,000	104,000	15	5.8	45
24 hours 900°C, water quenched, aged 40 hours 500°C	600	114,000	118,000	2.1	5.3	32
24 hours 900°C, water quenched, aged 40 hours 500°C	500	114,000	116,000	1.4	5.2	37

Creep data for a series of uranium-zirconium and a series of uranium-titanium alloys are shown in Tables VI and VII, respectively.[16] In the zirconium system, the best results were obtained with an alloy of 47.1 weight per cent zirconium which is in the gamma solid solution near the composition of the gamma eutectoid. In the titanium alloys, near maximum results were achieved over a range of composition from 17.0 to 55.4 weight per cent titanium.[16] This range of composition is on the titanium side of the intermediate or delta phase and brackets the titanium-rich gamma eutectoid, which occurs at about 34 weight per cent titanium.

Creep data at 815°C for a series of molybdenum alloys are shown in Table VIII.[16] The best results in these alloys were obtained with a 13.3 weight per cent molybdenum alloy which is in the gamma solid solution at 815°C.

The greatest improvement in the corrosion resistance of high-uranium alloys is found in the solid-solution-type alloys. The data in Tables IX and X indicate what can be achieved in these systems.[17,18] It is apparent that a certain level of alloy addition which varies with each system is required to impart extended corrosion resistance in water at elevated temperatures, and that corrosion resistance is obtained only if the uranium alloy is heat treated in the gamma phase. Quenching produces a martensitic structure in this type of alloy which contains abnormal amounts of solute. Such a structure is metastable and will lose its enhanced corrosion resistance during aging by precipitation of a solute-rich phase; hence, these properties can be fully utilized only at limited temperatures. Moderate degrees of improvement in corrosion resistance have been achieved in high-uranium alloys in various other types of systems including the compound-forming systems. Generally, however, the corrosion resistance is produced largely by solid solution effects and in these systems, the solid solubility is too limited to give results comparable to those shown above.

Somewhat larger additions in the solid-solution-type systems produces a metastable gamma phase. In this category are the alloys of 9 to 13.3 weight

Table VI. Creep Data for Uranium-Zirconium Alloys at 815°C in Vacuum[16]

Composition, weight per cent			Condition	Stress, psi	Time for 1 per cent deformation, hour	Minimum creep rate, per cent per hour	Test time, hour†	Elongation, per cent
	Nominal analysis							
Zirconium	Zirconium*	Carbon						
5.0	7.1	0.07	Induction melted and cast in graphite, rolled at 1550°F	500	0.8	0.65	6.0	8.1
11.3	12.6	0.08	Induction melted and cast in graphite, rolled at 1550°F	1422	<0.1	43	1.0	93.8
22.4	25.8	–	Arc melted twice; jacketed, forged and rolled at 1450°F	500	0.45	1.0	11	14
46.5	47.1	–	Arc melted twice; jacketed, forged and rolled at 1450°F	500	56	0.013	169	15.1
72.3	72.6	–	Arc melted twice; jacketed, forged and rolled at 1450°F	500	40	0.021	162.7	12.3

* Zirconium by difference.

† Test discontinued before rupture.

Table VII. Creep Data for Uranium-Titanium Alloys at 815°C in Vacuum

Composition, weight per cent				Condition	Stress, psi	Time for 1 per cent deformation, hours	Minimum creep rate, per cent	Test time, hour†	Elongation, per cent
		Nominal analysis							
Alloy	Titanium	Titanium*	Carbon						
48	12.1	4.2	0.38	Induction melted and cast in graphite; rolled at 1800°F	500	0.7	0.14	30.9	6.4
Ti2-2	6.3	4.3	0.19	Induction melted and cast in copper mold‡; rolled at 1500°F	500	0.04	28	0.4	11.0
35	20.0	9.3	0.22	Induction melted and cast in graphite; rolled at 1800°F	500	3.0	0.05	78	4.6
30	20.0	12.3	0.25	Induction melted and cast in graphite; rolled at 1500°F	500	8.5	0.06	170.4	12.8
28	32.0	17.0	0.27	Induction melted and cast in graphite; rolled at 1500°F	500	35	0.0034	211	2.6
63	20.0	20.3	0.45	Induction melted and cast in graphite; rolled at 1800°F	500	23	0.008	149.5	2.9
57	25.5	25.7	1.00	Induction melted and cast in graphite; rolled at 1800°F	500	163	0.003	238.6	1.4
64	30.0	32.6	0.80	Induction melted and cast in graphite; rolled at 1800°F‡	500	40	0.0045	167.7	2.2
36	32.0	37.2	0.32	Induction melted and cast in graphite; rolled at 1800°F‡	500	44	0.0032	197	2.1
66	50.0	47.4	1.64	Induction melted and cast in graphite; rolled at 1800°F†	500	9.5	0.06	111.8	7.4
Ti54	55.0	55.4	0.19	Arc melted; remelted in BeO; forged and rolled at 1700°F	500	12.5	0.070	193	3.7
Ti62	65.0	62.2	0.95	Arc melted; remelted in BeO; forged and rolled at 1700°F	500	10.5	0.017	116	3.7
Ti75	75.0	75.6	0.49	Arc melted; remelted in BeO; forged and rolled at 1700°F	500	<0.1	12.0	1.1	12.2
Ti90	90.0	90.6	0.28	Arc melted; remelted in BeO; forged and rolled at 1700°F	500	1.7	0.4	44.7	9.4

* Ti by difference except for Ti2-2 and Ti2-4 which were analyzed directly for Ti.

† Test discontinued before rupture except for Ti2-4 which was ruptured during test.

‡ Melted twice; inverted for second melting.

Table VIII. Creep Data for Uranium-Molybdenum Alloys at 815°C in Vacuum

Composition, weight per cent			Condition	Stress, psi	Time for 1 per cent deformation, hours	Minimum creep rate, per cent	Test time, hour†	Elongation, per cent
Nominal molybdenum	Analysis: Molybdenum*	Analysis: Carbon						
Rolled								
4.3	4.8	0.50	Induction melted and cast in graphite; rolled at 1650°F	500	1	2.16	6.9	15.1
10.0	7.5	0.13	Induction melted and cast in graphite; rolled at 1650°F	500	7	0.034	160	4.5
10.0	7.8	0.13	Induction melted and cast in graphite; rolled at 1650°F	500	2	0.052	166	7.5
29.0	12.3	0.24	Induction melted and cast in graphite; canned and rolled at 2000°F	500	29	0.014	172	3.6
12.0	13.3	0.10	Induction melted and cast in graphite; canned and rolled at 2000°F	500	>330‡	0.00008‡	337‡	0.1‡
12.0	13.3	0.27	Induction melted and cast in graphite; canned and rolled at 2000°F	500	150	0.0023	191	1.1

* Molybdenum by difference except for first three alloys in which molybdenum was analyzed directly.

† All tests were discontinued before rupture.

‡ Stress subsequently raised in successive steps above 500 psi.

Table IX. Corrosion-Resistant High-Uranium Alloys (Data Obtained in Distilled Water at 100°C)

System	Composition, weight per cent: Alloy	Composition, weight per cent: Carbon	Composition, weight per cent: Nitrogen	Total weight damage, milligram/centimeter²: 24	96	336	334	after 336 hrs	Remarks
Pure Uranium*	–	0.006	0.013	-116.3	–	–	–	–	Loose oxide
Pure Uranium†				-83.9	–	–	–	–	Loose oxide
Titanium*	0.39	0.002	0.001	-12.1	–	–	–	–	Loose oxide
Titanium†				-36.6	–	–	–	–	Loose oxide
Titanium*	1.05	0.004	0.004	-3.63	–	–	–	–	Loose oxide
Titanium†				0.0	0.02	0.02	-1.52	-4.46	Tarnish film
Zirconium*	3.66	0.006	0.009	-43.4	–	–	–	–	Oxide where touched glass supports
Zirconium†				-9.72	–	–	–	–	Oxide where touched glass supports
Zirconium*	4.95	0.010	0.010	-3.52	–	–	–	–	Loose oxide
Zirconium†				-0.01	-0.01	-0.04	0.0	-0.01	Tarnish film

System	Composition, weight per cent: Alloy	Composition, weight per cent: Carbon	Composition, weight per cent: Nitrogen	Total weight damage, milligram/centimeter²: 24	96	408	1428	after 2740 hrs	Remarks
Niobium*	0.71	0.004	0.009	-48.7	–	–	–	–	Loose oxide
Niobium†				-26.2	–	–	–	–	Loose oxide
Niobium*	1.59	0.004	0.011	-57.3	–	–	–	–	Loose oxide
Niobium†				0.01	0.07	0.07	-0.03	-0.15	Tarnish film

System	Composition, weight per cent: Alloy	Composition, weight per cent: Carbon	Composition, weight per cent: Nitrogen	Total weight damage, milligram/centimeter²: 24	96	336	334	after 336 hrs	Remarks
Hafnium*	4.1	0.004	0.010	-38.8	–	–	–	–	Loose oxide
Hafnium†				-11.1	–	–	–	–	Loose-oxide
Hafnium*	9.6	0.004	0.009	-17.5	–	–	–	–	Loose oxide
Hafnium†				0.07	-0.02	-0.06	-0.65	-2.14	Yellow oxide spot and stringers at 576 hour

* 4 hour 600°C and furnace cooled.

† 1 hour 815°C and water quenched.

Table X. Corrosion of Uranium-Niobium Alloys in High-Temperature Water[18]

Composition, weight per cent	Test condition*	Hours in test	Rate of weight loss, milligram/centimeter²/hour	Remarks
		At 300°C		
3 Niobium	Degassed	64	1.3	—
3 Niobium	Air saturated	70	0.7	In contact with autoclave wall
3 Niobium	Degassed	64	0.7	Lost some water, sample above water line
3 Niobium	Air saturated	70	0.6	—
6 Niobium	Degassed	64	0.05	—
6 Niobium	Air saturated	70	0.4	Badly pitted. Porous before test
		At 260°C		
3 Niobium	Degassed	19	—0.40	
3 Niobium	Degassed	185	—0.32	
3 Niobium	Oxygen saturated	24	—1.24	
3 Niobium	Degassed	19	—0.33	
3 Niobium	Degassed	185	—0.18	
3 Niobium	Oxygen saturated	24	—0.64	
6 Per Cent Niobium	Degassed	19	+0.015	
6 Per Cent Niobium	Degassed	185	—0.064	
6 Per Cent Niobium	Oxygen saturated	24	+0.025	

* Samples heated to about 1100°C for 1 hour and water quenched.

per cent molybdenum which have been corroded in 650°F water as indicated in Table XI.[15] These alloys offer improved corrosion resistance but fail catastrophically after extended exposure, probably by the internal formation of hydride.

The effects of aging of the molybdenum alloys to form the intermediate delta phase are complex, and very long annealing times are required for complete transformation. Stable alloys of the intermediate or delta phase in the uranium zirconium system offer promise of corrosion resistance in high-temperature water. Data for alloys in this system from 50 to 100 weight per cent zirconium are included in Table XII. The delta phase is centered about the 50 weight per cent zirconium composition. It is apparent that the treatments which result in transformation to the intermediate or delta phase are the best. The eruption and cracking of the 800°C-quenched samples is attributed to the retention of the metastable gamma phase.

Another potential source of corrosion-resistant uranium alloys are the intermetallic compounds such as U_3Si, U_6Ni, U_6Fe, UAl_2, and others. The U_3Si alloy is usually tested in the as-cast and heat-treated condition. The heat treatment consists of holding for long periods of time at about 800°C to homogenize the cast structure to some degree.

Table XI. Corrosion of Uranium-Molybdenum Alloys in 650°F Water[15]

Composition, weight per cent	Heat treatment	Days to failure
9 molybdenum	24 hours 900°C, water quench	14–28
12 molybdenum	24 hours 900°C, water quench	14–28
13.5 molybdenum	24 hours 900°C, water quench	7–14

Data on the corrosion resistance of U_3Si alloys in high-temperature water are included in Tables XIII[20] and XIV.[21] Based on the results shown, it is apparent that good corrosion resistance can be attained with materials of this type. However, the application of the compounds is limited by their lack of fabricability.

Table XII. Corrosion of Arc-Melted Uranium-Zirconium Alloys in Water at 600°F

Analysis, weight per cent			Total weight gain, mg/sq cm, at hours indicated							
U	C	N	24	96	336	672	1344	2016	2688	Remarks
			1 hour at 800°C, water quenched							
49.5	0.03	0.005	0.12	–1.37	–2.89	–8.52	–	–	–	Erupted, 1175 hours
29.6	0.02	0.004	0.13	0.30	1.76	3.65	3.96	–	–	Severe cracking, 2016 hours
			1 hour at 800°C, water quenched plus 24 hours at 575°C, furnace cooled							
49.5	0.03	0.005	–0.34	–0.37	–0.56	–2.73	–13.0	–27.9	–57.7	Flaky green-yellow oxide
29.6	0.02	0.004	0.11	0.30	1.50	3.68	2.08	–18.6	–37.9	Flaky green-yellow oxide
			1 hour at 800°C, quenched to 550°C, 2 hours at 550°C, air cooled							
49.5	0.03	0.005	–0.06	0.10	–0.26	–3.47	–22.8	–49.7	–86.5	Flaky green-yellow oxide
29.6	0.02	0.004	0.17	0.25	0.96	2.99	8.04	12.1	–33.3	Flaky green-yellow oxide
20.0	0.02	0.004	0.07	0.16	0.27	0.38	0.98	2.05	3.30	Dark coating with yellow streaks
10.6	0.01	0.002	0.05	0.12	0.15	0.19	0.23	0.28	0.28	Adherent dark oxide
None	0.01	0.001	0.04	0.09	0.08	0.12	0.93	1.40	1.60	Adherent white oxide, 1008 hours

Table XIII. Corrosion of Heat-Treated U_3-Si Samples in Distilled Water at 100 and 178°C[20]

Composition weight per cent	Temperature, °C	(mg/cm²) 4 days	16 days	32 days	52.3 days	Corrosion rate, mg/cm²/hour
2.58 silicon	100	5.0		16.4		0.014
3.07 silicon	100	1.8		9.7		0.008
3.63 silicon	100	1.4		4.3		0.003
3.82 silicon	100	0.5 at 2 days		11.1		Insufficient data
2.58 silicon	178					Cracked in 1 day
3.07 silicon	178					Cracked in 2–3 days
3.63 silicon	178	2.98	10		10.9	–

The alloying of uranium has also been studied for many reasons other than to develop suitable mechanical and corrosion-resistant properties. There has been considerable study of numerous low-melting alloy systems to develop liquid metals for homogeneous reactors. Of interest are such alloys as uranium-bismuth, uranium-lead, and uranium-bismuth-lead.[22]

Table XIV. Corrosion of Heat-Treated U_3-Si Samples in Water at 260 and 316°C[21]

Composition	Heat treatment	Corrosion rate, mg/cm² month 260°C	316°C
3.70 silicon, 0.08 carbon	3 days 800°C	50	1400
3.75 silicon, 0.05 carbon	6 days 800°C	60	1400
3.82 silicon, 0.05 carbon	3 days 800°C	30	1250

Other alloys such as eutectic uranium-chromium, uranium-silicon, and uranium-vanadium are of interest in the development of power reactors, because of their lowered melting points which makes them more castable.

REFERENCES

1. Baumrucker, J. E. and Chiswik, H. H., unpublished information (March 1953).
2. Jacob, C. W. and Warren, B. E., *The Crystalline Structure of Uranium,* Journal of American Chemical Society *59*: 2588 (1937).
3. Lukesh, Joseph S., *Note on the Structure of Uranium,* Acta Cryst. *2*: 420 (1949).
4. Tucker, C. W., Jr. and Senic, Peter, *An Improved Determination of the Crystal Structure of Beta Uuranium,* Acta Cryst. *6*: 753-60 (1953).
5. Wilson, A. S. and Rundle, R. E., *The Structures of Uranium Metal,* Acta Cryst. *2*: 126-27 (1949).
6. Thewlis, J., *Structures of Uranium,* Nature *168*: 198-99 (1951).
7. Thewlis, J., *X-Ray Powder Study of Beta Uranium,* Acta Cryst. *5*: 790-94 (1952).
8. Tucker, C. W., Jr., *The Crystal Structures of Metallic Uranium,* Trans. ASM *42*: 762-70 (1950).
9. Raynor, G. V., unpublished information (1949).
10. Compilation of United States and United Kingdom Uranium and Thorium Constitutional Diagrams, compiled for the USAEC by Battelle Memorial Institute, Saller, H. A., Rough, F. A., Editors (September 1954).
11. Saller, H. A. and Rough, F. A., unpublished information (21 February 1955).
12. Saller, H. A. and Rough, F. A., unpublished information (17 May 1954).
13. Smith, C. S., unpublished information (1945).
14. Muehlenkamp, G. T., Chubb, W. and Schwope, A. D., unpublished information (20 October 1953).
15. Lustman, B., unpublished information (October 1955).
16. Saller, H. A., Stacy, J. T., Eddy, N. S. and Klebanow, H. L., unpublished information (28 May 1953).
17. Saller, H. A., Pray, H. A., Dickerson, R. F., Berry, W. E. and Foster, E. L., unpublished information (29 December 1954).
18. Draley, J. E., unpublished information (24 June 1953).
19. Pray, H. A. and Berry, W. E., unpublished information (5 October 1953).
20. Hopkins, J. M., Binger, W. W. and Nelson, F., unpublished information (14 June 1945).
21. Kaufmann, A. R. and Magel, T. T., unpublished information (February 1955).
22. Teitel, R. J., Kammerer, O. F. and Gurinsky, D. H., unpublished information (31 August 1951).

Alloys of Uranium and Thorium

By P. C. L. Pfeil,* UK

In the UK an attempt has been made to acquire an understanding of the factors affecting the constitution and properties of uranium and thorium alloys with a view to subsequent application to other cases of direct technological importance, and to serve as a guide to forecast the likely behaviour of other heavy metals, e.g., plutonium. US work has not been discussed since this is reviewed in American papers to this Conference.

CONSTITUTION OF URANIUM ALLOYS

The most noticeable constitutional features of uranium alloys that have been found are: (*a*) the formation of intermetallic compounds with a wide variety of alloying elements, see Table I, and (*b*) the lack of extensive solid solutions in α- or β-uranium, although slight solubilities can be obtained which give rise to important consequences.

Extensive solid solutions are formed by titanium,[1] zirconium,[2] niobium,[3] and molybdenum[4,5] in γ-uranium, but tantalum[6] and tungsten [7,8] which usually show marked similarities to niobium and molybdenum in their chemical and metallurgical behaviours, dissolve in uranium to a limited extent only. No element with an unfavourable size factor for solid solution formation dissolves extensively (see Fig. 1).

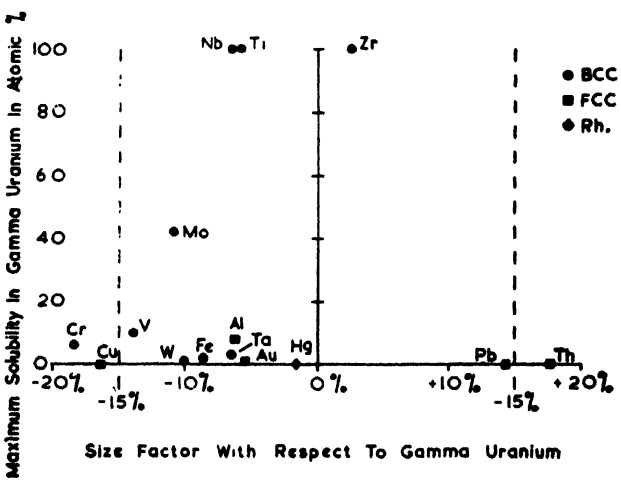

Figure 1

Titanium, zirconium and niobium form continuous solid solutions with γ-uranium at high temperatures, but at lower temperatures a compound, U_2Ti, is formed in uranium-titanium, whereas in uranium-niobium and uranium-zirconium alloys the body centred cubic solid solution splits up into two phases with the same crystal structure but of different compositions. The similar effect occurring in aluminium-zinc alloys has been attributed tentatively to electron energies.[9] An explanation on the same line has been suggested to account for the behaviour of these uranium alloys, but it does not explain all the facts and is open to considerable objection.

In uranium-molybdenum alloys the solubility range does not extend beyond 42 at %, and below 600°C the solid solution becomes tetragonal. The new phase is believed to be a superlattice, and a self-consistent, but extremely tentative electronic explanation in terms of a contribution to the lattice as a whole of four electrons from the uranium and six from the molybdenum has been advanced for the marked variation of the axial ratio of this phase with composition.

Further investigation of the behaviour of the electrons in uranium alloys is proceeding by measurements at low temperatures of the electronic specific heat and magnetic properties of selected alloys and by limited investigation of specific constitutional features of certain ternary uranium alloys. Despite the present lack of a proper understanding of the factors affecting the constitution of uranium alloys, successful predictions have been made of the effects of several further additions to uranium-molybdenum alloys to improve the age hardening characteristics.

The constitutional diagram of the uranium-zirconium system published recently[2] did not show any intermediate phases, but there is metallographic and X-ray evidence that one can form at compositions near 70 at % zirconium, although it may not be an equilibrium constituent. Powders annealed below 600°C show first an increase in the amount of this phase followed by decomposition into a mixture of α-uranium and α-zirconium.

An interesting feature of uranium-niobium alloys is the reluctance of homogeneous γ solid solution alloys to decompose into a mixture of ($\gamma_1 + \gamma_2$) at temperatures above 800°C even with prolonged annealing whereas other evidence indicates that the two phase field probably extends to above 900°C. A marked reluctance for homogeneous γ solid solution alloys to precipitate at temperatures between 620°C and 649°C is found in more dilute uranium-niobium

* Atomic Energy Research Establishment, Harwell.

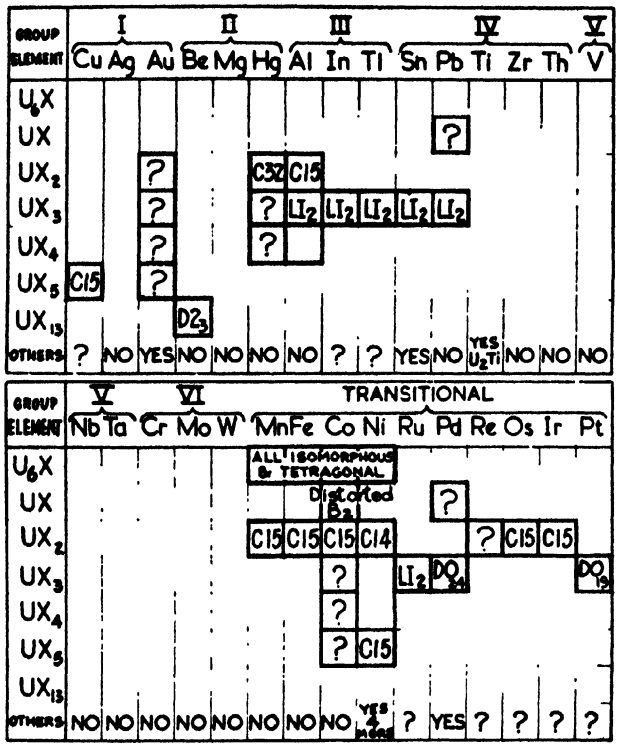

COMPOUNDS IN URANIUM ALLOY SYSTEMS

Figure 2

alloys. Reaction kinetics are extremely important to the application of alloys but in uranium alloys generally, the subject is at present insufficiently comprehended.

The first long period of the transition metals form compounds of the type U_6X and UX_2 Laves Phases (Fig. 2). UMn_2, UFe_2 and UCo_2 crystallize with the C15 structure but UNi_2 has the C14 lattice. Although manganese and iron form only the two compounds with uranium, cobalt and nickel form several more, generally with complicated structures. Pseudo-binary sections between UMn_2, UFe_2, UCo_2 on the one side and UNi_2 on the other behave systematically as regards solubility limits and the existence of a C36 ternary phase in each case[10] but no fully self-consistent explanation of the phase limits has been found in terms either of the electron concentration or of localised strains within the lattice. The second and third long periods of the transition metals do not parallel the behaviour of the first, except that in the third period the Laves Phases UOs_2 and UIr_2 are found with C15 structures, similarly to UFe_2 and UCo_2.

SOME FEATURES OF URANIUM ALLOYS OF TECHNOLOGICAL IMPORTANCE

Direct technological interest in uranium alloys arises from a variety of reasons but of especial importance are the behaviour of fission products in fuels, the improvement of fuels by deliberate alloying and possible interaction of fuels with canning and coolant materials.

Iron,[11] cobalt[12] and nickel[13] all form eutectics with uranium melting between 700°C and 750°C, and two or more intermetallic compounds in each case. Tantalum and tungsten which do not form intermetallic phases with uranium or low melting point eutectics show only limited solid solution ranges and do not react rapidly with uranium even if the uranium is molten. Zirconium, titanium, niobium and molybdenum form extensive solid solutions with uranium at a sufficiently high temperature, but although interpenetration is more rapid than in the case of tantalum and tungsten it is still fairly slow, that of uranium into niobium, for instance, being 0.1 to 0.2 mm after five weeks at 850°C. The interpenetration of uranium and aluminium is fairly rapid and is unusual in having a marked pressure dependence, especially below 570°C.[14] Uranium and magnesium show very little tendency to form alloys and seem to be almost immiscible in both solid and liquid states.

Of potential coolants, sodium and lithium have no gross alloying affinity for uranium, but it does not follow necessarily that liquid alkali metals cannot penetrate along the grain boundaries of uranium, given appropriate conditions of stress and temperature, or that they may not dissolve impurities or deliberate alloying additions. On the other hand, bismuth,[15] lead[16] and mercury[17] react fairly readily with uranium to form intermetallic compounds.

Burn-up of uranium fuels causes a complex alloy to form of a continuously varying composition, and even comparatively low concentrations of fission products may be important. The major fission products may conveniently be divided into four classes: (*a*) the inert gases krypton and xenon; (*b*) the alkali metals, the alkaline and rare earths; (*c*) the highly electronegative elements, e.g., iodine; and (*d*) metallic elements such as zirconium, niobium and molybdenum, which dissolve readily in γ-uranium and which can form supersaturated solutions in α-uranium.

The inert gases which amount to about 10% of the fission products from U^{235} are incapable of chemical combination with the uranium, while the fission products of the second group form neither solid solutions nor intermetallic compounds and in many cases show liquid immiscibility. Both classes of fission product atoms will be associated with considerable strain energy when in the uranium lattice, and if the temperature is sufficiently high to permit atomic mobility, will move elsewhere.

The highly electronegative elements will probably be chemically combined with uranium or with one of the more electropositive fission products.

Although zirconium, niobium and molybdenum all depress the γ-β transformation temperature of uranium, appreciable alloying additions are necessary for the effect to be marked. Other fission products present in the lattice, even if insoluble under equilibrium conditions, may be important, and the lattice structure may change, possibly to one not normally adopted by uranium. A further complication is that

the hard β phase is liable to be retained by sufficiently rapid cooling from high temperature.

Deliberate alloying additions may be made to uranium fuels from several motives. The paper by Pugh[18] shows that even at quite low burn-ups difficulties may arise from the wrinkling and growth of uranium slugs at temperatures below 450°C. The effect may be substantially reduced by using fine randomly oriented grains and alloying additions can help in producing such materials, either by controlled transformation of α to β by a nucleation and growth process, or by decomposition of solid solutions in the γ phase. A dispersion of the compound U_2Ti, for example, allows α-grains of average diameter, 5 to 50 microns, depending on the proportion of U_2Ti, to be stabilised sufficiently so that it takes several months at temperatures above 600°C to double the grain size. Not all second phases are effective and the requirements necessary are not yet known, although it is suspected that the misfit at the interfaces may be important.

Alloying additions can affect the behaviour of fission product atoms in various ways. First, by affecting diffusion rates in the uranium lattice, secondly by altering the mechanical properties of the fuel and thirdly by changing the number and behaviour of the grain boundary and other imperfect lattice regions of the specimen.

As an example of the kind of effects alloying can have on the mechanical properties of uranium alloys, the addition of solutes soluble in γ-uranium in insufficient quantities to allow the γ phase to be retained by quenching, can give a needle-like structure resembling martensite in steels on rapid cooling. The martensitic structure is hard, ranging from 350 to 500 Vickers depending upon the alloying element and the amount present. Unlike steels, harder alloys can often be obtained by a less rapid quench where decomposition occurs partly by precipitation and partly martensitically. In alloys containing enough solute to retain γ by quenching, subsequent decomposition to give a pearlitic type of structure has given hardnesses ranging from 300 to 600 Vickers or more.

THORIUM ALLOYS

The study of thorium alloys is less advanced. Thorium and uranium form immiscible liquids over the composition range 8–50 weight % thorium, no compounds at all and very limited solid solubilities.[19] Alteration of the extent of liquid immiscibility by ternary additions has been successfully predicted. Thorium and aluminium form at least five intermetallic compounds and show very limited solid solubilities. The crystal structures of these phases have been determined[20] and the Th-Th, Th-Al and Al-Al nearest neighbour interatomic distances related to the atomic arrangement in each particular compound. Thorium and cerium show a continuous series of solid solutions between the face-centred cubic allotropes with a large negative deviation of the lattice parameters from Vegard's law.[21] The addition of thorium may possibly affect the behaviour of the cerium atom in a way resembling that of pressure on cerium itself. Other UK constitutional work has been on the systems thorium-lead, thorium-zirconium, thorium-tungsten and the structures of compounds of thorium with copper, silver, and gold. The general conclusion to date is that the differences between the alloying behaviours of thorium and uranium arise from the larger size of the thorium atoms compared with those of uranium. This background data should be helpful in alloying thorium to improve its metallurgical characteristics as a fuel.

REFERENCES

1. Knapton, A. G., unpublished work at the Associated Electrical Industries Ltd. Research Laboratories.
2. Summers-Smith, D., *The Constitution of Uranium-Zirconium Alloys,* Journal of the Institute of Metals, *83*: 277-282 (1954-55).
3. Pfeil, P. C. L. and Browne, J. D., unpublished work at A.E.R.E., Harwell.
4. Pfeil, P. C L., *The Constitution of Uranium-Molybdenum Alloys,* Journal of the Institute of Metals, *77*: 553-570 (1950).
5. Pfeil, P. C. L. and Browne, J. D., *Superlattice Formation in Uranium-Molybdenum Alloys,* A.E.R.E. Report M/R 1333 (1954).
6. Sykes, E. C., unpublished work at A.E.R.E., Harwell.
7. Grogan, J. D., unpublished work at the National Physical Laboratory.
8. Summers-Smith, D., *The System Uranium-Tungsten,* Journal of the Institute of Metals *83*: 383-384 (1954-55).
9. Leigh, R. S., *A Theory of the γ, γ' Phases in the Al-Zn System.* Philosophical Magazine *42*: [vii]: 876-882 (1951).
10. Brook, G. B., Williams, G. I. and Smith, E. M., *Pseudo-Binary Phase Sections Between Laves Phases in Ternary Alloys of Uranium,* Journal of the Institute of Metals *83*: 271-276 (1954-55).
11. Grogan, J. D., *The Uranium-Iron System,* Journal of the Institute of Metals *77*: 571-580 (1950).
12. Waldron, M. B., unpublished work at A.E.R.E., Harwell.
13. Grogan, J. D. and Pleasance, R. J., *A Survey of the Uranium-Nickel System,* Journal of the Institute of Metals *82*: 141-147 (1953-54).
14. Le Claire, A. D. and Bear, I. J. (Miss), *The Interdiffusion Behaviour of Uranium and Aluminium,* A.E.R.E. Report M/R 878, Classified (1952).
15. Greenwood, G. W., unpublished work at A.E.R.E., Harwell.
16. Frost, B. R. T. and Maskrey, J. T., *The System Uranium-Lead,* Journal of Institute of Metals *82*: 171-180 (1953-54).
17. Frost, B. R. T., *The System Uranium-Mercury,* Journal of the Institute of Metals *82*: 456-462 (1953-54).
18. Pugh, S. F., P/443, *Damage Occurring in Uranium during Burn-up,* Volume 7, Session 11B, these Proceedings.
19. Murray, J. R. (Miss), unpublished work at A.E.R.E., Harwell.
20. Murray, J. R. (Miss), unpublished work at A.E.R.E., Harwell.
21. Freeth, W. E., unpublished work at Birmingham University.

Low Aluminum Uranium-Aluminum Alloys

By G. Cabane,* M. Englander,† Mme J. Lehmann,‡ France

Uranium, such as it is obtained following γ-phase extrusion or vacuum casting, offers a heretogeneous structure with large irregular grains. The anisotropy in the expansion of the metal leads, for rods obtained under those conditions, and subjected to thermal fatigue (200 one-hour-cycles between 20°C and 520°C), to important deformations and superficial alterations of the "orange rind" type. As regards the microstructure, there are numerous spots and groups of grains recrystallized, or in the course of evolution, showing that the anisotropy has become still sharper. Cycling being pursued beyond 200 cycles, the alterations in form and flexing increase further, which makes the use of the metal in these forms, γ cast or extruded, inacceptable according to the conditions of operation, temperature, temperature gradient, of thermal flux, such as they might be needed for certain reactors.

Various treatments have been carried out on the metal, for the purpose of looking for an isotropic structure endowed with characteristics of stability under thermal fatigue:

1. Rolling, followed by a recrystallization heat treatment, enabled us to obtain fine-grain metal rods, which were regular and equiaxial; the uranium bars so treated, subjected to thermal cycling, lead to a negligible amount of flexing, and, on the other hand, to a very good surface condition. However, an elongation reaching 7% after 1000 cycles, due to preferential orientation caused by deformation and recrystallization, makes the application of such a treatment quite difficult.

2. Hammering, followed by a recrystallization heat treatment, leads to very irregular grain structures; the heart of the rods was, in general, much less altered than the peripheral part and, moreover, the surface offered breaks due to hammering.

3. α-phase extrusion made it possible to obtain a very large grain structure, with grains 2 to 3 mm in size. Thermal cycling brought about a very small amount of flexing, but, on the other hand, the surface of the rods offered fissures which were regularly distributed along the contours of the large grains. This was sharpened during cycling, and reached the point of breaking the cohesion of the grains.

Tests were carried out for the purpose of examining the behavior of a metal much charged with impurities consisting of oxides or carbides.

One of the methods was a second melting of the metal in a graphite crucible for the purpose of adding carbides; another was to choose, for the production of the cast metal, uranium billets particularly rich in oxide.

Following cycling of the rods so obtained, there was no improvement, nor any marked increase in the deformations.

To test for refining the grain by adding an element (in a quantity acceptable from the nuclear standpoint), uranium-aluminum alloys were made. Prospection of the technological possibilities of these alloys required a fairly accurate knowledge of the equilibrium diagram in the low aluminum range.

The studies published to this date on alloys[1-4] give a complete description of the diagram from 0 to 100% aluminum, but do not show the solidus curves in the vicinity of the uranium with enough precision. Gordon and Kaufman[1] mentioned a eutectic at 1105°C at 5 at% (namely approximately 0.59% in weight) of aluminum, a low aluminum solubility in γ-uranium, and solubility of approximately zero in β and α-uranium. Kiessling[3] showed that the small proportion of the intermetallic compound UAl_2 in the eutectic substance, as well as the high speed of aluminum diffusion, account for the appearance of the 5 at % alloy, which is somewhat different from a classical eutectic.

This work was carried out within the framework of atomic cooperation between Sweden and France.

1. Solubility of Aluminum in γ-Uranium, by G. Cabane

The temperature of the eutectic alloy has been found to be somewhat less than that of uranium, so that the liquidus and solidus curves are necessarily very similar and nearly rectilinear, and the curve showing the solubility of the aluminum in γ uranium makes up the most important part of the diagram for the definition of the thermal treatment of these alloys.

Original language: French.

* Chief, Metallurgical Chemistry Department, C.E.A.
† Chief, Technology Department, C.E.A.
‡ Engineer, Technology Department, C.E.A.

PREPARATION OF THE ALLOYS

This work on the low alloys first required the production of perfectly homogeneous ingots in order to reduce the errors on the aluminum contents. They are prepared by the dilution of a hypereutectic starting alloy, in which aluminum is nearly completely combined under the form of UAl_2, an intermetallic compound which has a higher fusion point and a lower specific gravity than uranium.

Fusion in an alumina crucible, in a low frequency induction oven, makes it possible to obtain fairly homogeneous ingots. However, if graphite crucibles are used in the same oven, the risk of carbide formation limits the temperature and duration of fusion to such an extent that the grains of UAl_2 of the starting or stock alloy come to rest on the surface, and can be neither melted nor even completely dissolved in uranium.

This is why the best method of preparation of these alloys appears to be fusion in an arc oven, in which the starting alloy can be completely melted without any risk of contamination. Thus it is, in an arc oven of the laboratory type, that 10 ingots of alloys with contents of between 0.11 and 0.72% in weight were prepared.

The high temperature of the arc causes a loss of aluminum due to vaporization; but the phenomenon is perceptible only during the first fusion of the starting alloy; second fusion of the alloy, with or without uranium, takes place without any loss of aluminum, which makes it possible to obtain alloys of the desired composition.

In order to achieve perfect homogeneity, the ingots were melted again four times, and turned around between two consecutive melts. The uniformity of the aluminum content of the ingots was checked by precipitation of the UAl_2 compound in an ingot which had been quenched after being dissolved. The cross section of the ingot appeared covered with a very fine and perfectly uniform precipitate.

THERMAL TREATMENTS

In order to measure the solubility of aluminum, we noted the appearance of the UAl_2 phase as precipitated out of the solid solution in the alloys quenched at temperatures between 745°C and 1100°C. During heating, particles of UAl_2 might appear and coalesce, and might be difficult to dissolve again, if the treatment were to take place close to the solubility curve of the alloy considered. In order to avoid this drawback, we began treatment by solution for 15 hours at 1095 ± 5°C, and thereafter brought down the samples to the testing temperature by cooling off for an hour approximately. As regards the duration of treatment at that temperature, a time of four hours proved adequate to achieve equilibrium, even at the lowest temperatures tested.

Since the solubility of aluminum may be affected by a high content of impurities, great precautions were taken in order to avoid any contamination during the heat treatment; the samples were treated in a pure argon atmosphere, and rested in alumina containers. The temperatures were controlled by calibrated thermocouples placed in alumina cladding and applied against the samples.

The quenching which terminated the treatments was carried out by precipitating the samples in a 10% sodium bath; this quenching rate (200°C to 300°C per second) was not sufficient to avoid the precipitation of a UAl_2 lattice in the alloys which contained the most aluminum, at the beginning of the cooling-off period, in the two-phase range U γ + UAl_2. This did not affect the measurements, since the fine lattice was easy to distinguish from the UAl_2 particles which coalesced during the four hours the treatment lasted; but the phenomenon is a proof of the high diffusion rate of aluminum in the uranium lattice.

RESULTS

Allowing for the accuracy of the analyses (±10% of the aluminum content), the solubility curve shown (Fig. 1) is defined to ±7% in weight of aluminum.

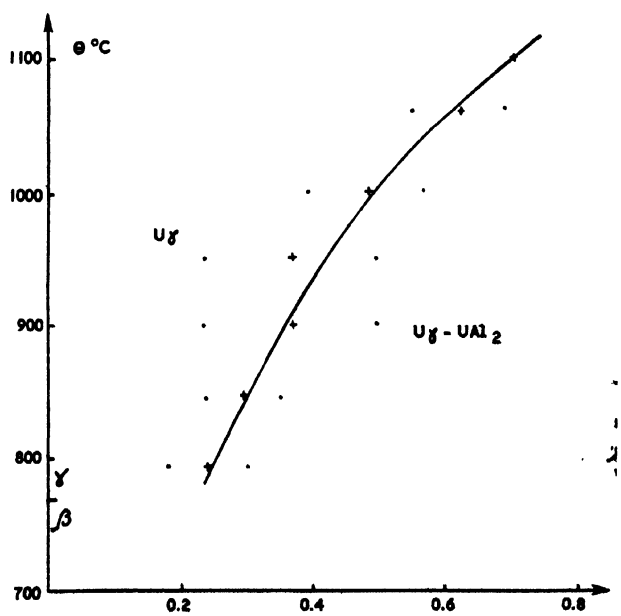

Figure 1. Solubility curve

II. Properties and Heat Treatments of Uranium-Aluminum Alloys Having Eutectoid Character, by M. Englander and Mme J. Lehmann

The uranium-aluminum equilibrium diagram (Fig. 2) reveals the presence of a eutectoid point for a content of less than 0.5% in weight. The first part of this paper shows this point to be in the vicinity of 0.2%. It was characterized by a reduction in the γ/β transformation point of 15°C. The eutectoid structure was not observed micrographically.[1]

A study of the uranium-aluminum alloys having an aluminum content in the vicinity of the eutectoid composition serves the purpose of examining the structures and behavior of the thermal fatigue of these raw cast alloys, and of searching a heat treatment which might better their physical characteristics and their resistance to thermal fatigue.

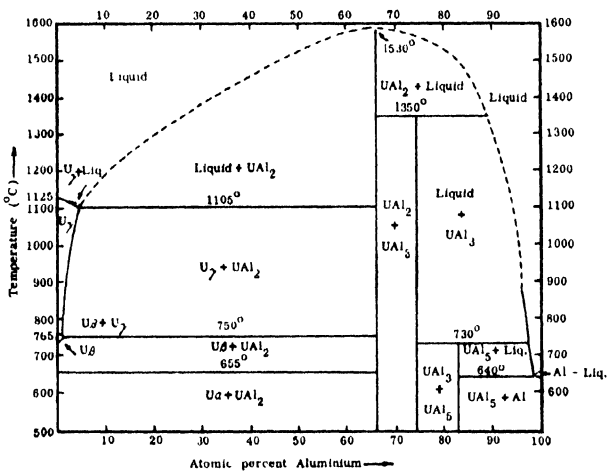

Figure 2

The eutectoid transformation made it possible to forecast that these alloys might undergo a heat treatment which would give them a fine precipitation structure with structural hardening and a greater measure of isotropy.[1]

The methods chosen were the following:

1. A homogenization treatment for the purpose of totally solubilizing aluminum in γ uranium, followed by cooling off at a controlled rate.

2. The same homogenization treatment in the γ phase, followed by quenching for the purpose of keeping solubilization in the stable phase at a low temperature, and annealing at a temperature lower than that of transformation, for the purpose of achieving fine and evenly dispersed precipitation.

CRUDE CAST ALLOYS

Alloys containing 0.15, 0.2, 0.4, and 0.5% of aluminum in weight were prepared in a graphite crucible, the inside wall of which was invested with an alumina layer. Heating was in the induction oven.

The uranium billet used was machined in the form of 2 blocks, one of which was provided with a recess so arranged as to contain the aluminum ingots, the second block formed a plug and this avoided vaporization of the aluminum when melted under vacuum. This gives rise to the formation of an intermetallic UAl_2 compound, and when a temperature of 1130°C was reached, it floated on the molten uranium. The temperature was brought up progressively to 1450–1500°C, and the UAl_2 compound was dissolved and disappeared after about 10 minutes.

Casting in the form of rods was effected by means of a device which opened in the lower part of the crucible in which the melting was carried out.

Micrographic Aspect

The crude cast alloys show a two-phase structure, one of which is uranium with irregular coarse grains, comparable to those of ordinary uranium. The other phase is the intermetallic UAl_2 compound, precipitated in different forms according to the aluminum concentration of the alloy.

For alloys containing 0.4–0.5%, UAl_2 is precipitated in the form of small rods (Fig. 3, ×650). These are arranged, particularly, according to a hex-

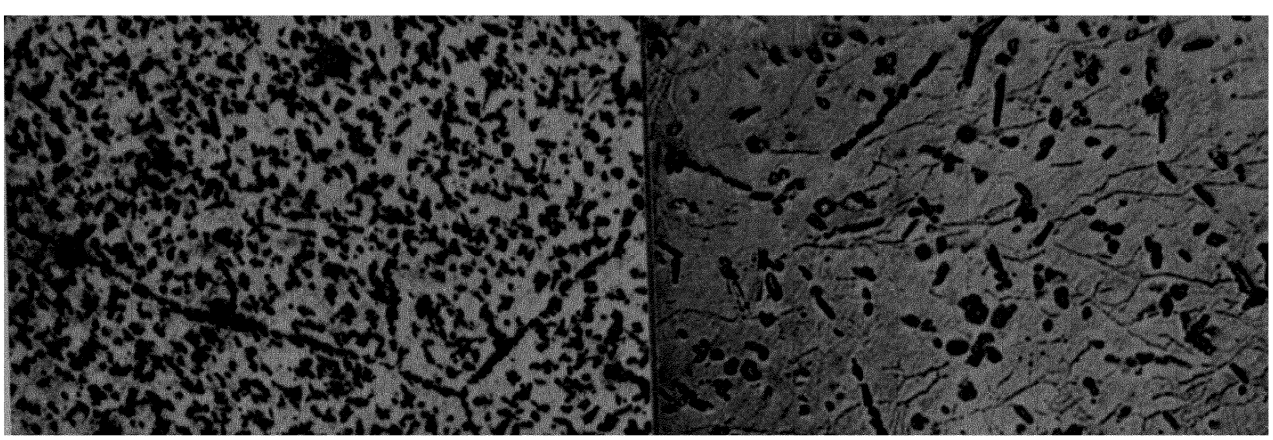

agonal type lattice inside the lattice. This probably corresponds to the contour of the former γ-grain.

For the lower content alloys (0.15 and 0.2%), UAl_2 is distributed without any great homogeneity in the matrix, in the form of spherules (Fig. 4).

Thermal Analysis

Thermal analyses were carried out by the open-circuit thermacouple method on alloys of different concentrations (0.15, 0.2 and 0.4%), as well as on the metal used for the preparation of each one of the tion in the alloy.

Comparisons were carried out on the transformation temperatures for the alloy and for the corresponding metal, and this revealed, for the alloys, a lowering of the transformation point β/γ, of approximately 15°C (when being heated up) and 20°C (when being cooled off). The α/β-phase transformation temperature was not modified. This does confirm the presence of eutectoid transformation $U_\gamma \rightarrow U_\beta + UAl_2$.

Mechanical Characteristics

The hardness of the uranium-aluminum alloy is somewhat greater than that of unalloyed uranium, but varies very little with the aluminum concentration in the alloy.

Vickers hardness, under a 40-kg load, is approximately 260 for the 0.2 and 0.4% alloys, while it is about 220 for uranium.

Impact compression[5] was carried out as a function of temperature on a 0.5% alloy, and the appearance of the "crushing as a function of temperature" curve is identical to that given for the tests on uranium. The discontinuities at the transformation points are very plain to see:

(*a*) In the α phase, and at room temperature, the alloy crushes much less than uranium. When the temperature goes up to 650°C, crushing increases from 0.03 to 0.2 mm, while for uranium, it increases from 0.12 to 0.7 mm.

(*b*) in the β phase, crushing is very small, both for the alloy and for uranium.

(*c*) In the γ phase, the behavior is the same.

The tensile tests[6] were carried out on a 0.5% alloy. They showed that the alloy had mechanical characteristics that intermediate between those of extruded γ uranium, or molded uranium, and those of hammer-hardened aluminum:

Material	*Tensile strength kg/mm²*	*Yield strength 0.2% offset*	*Elongation %*	*Reduction in area %*
U-Al alloy	63	39	2	1.8
Uranium	45 ± 9	20 ± 7	5 ± 2	9 ± 4
Hammered uranium	87	54	1	10.5

Cycling

Cycling carried out under the same conditions of temperature and time was for 30 rods (diameter = 26 mm; length = 210 mm) having concentrations of: 0.15, 0.2, 0.4, and 0.5%. This gives the following results:

Flexing	*≤0.5 mm*	*≤1 mm*
Number of bars	5	25

Buckling thus is much less than that of the non-alloyed metal, extruded in the γ phase, or crude cast. On the other hand, there was no elongation at all.

However, after 400 cycles, the formation of superficial fissures was noted, and they increased when cycling was continued up to 1000 cycles, bringing about a superficial break in the cohesion of the grains.

It would seem that this was enhanced by the hexagonal lattice. Micrography (Fig. 5) shows a break along the old γ joint, reaching a depth of 200 μ.

On the other hand, prolonged cycling tests on low content alloys (no lattice) show that it is also possible to obtain superficial fissures.

In all likelihood, the intermetallic UAl_2 compound, the hardness of which is much greater than that of α uranium (Vickers microhardening 650 kg/mm² instead of 300 kg/mm²), serves as a skeleton for the uranium and gives the metallic mass a rigidity which limits macroscopic deformation created by the anisotropy of the thermal dilatation, in a structure having coarse and irregular grains.

Summing up, it is shown experimentally that the UAl_2 alloys, crude cast, with aluminum contents of

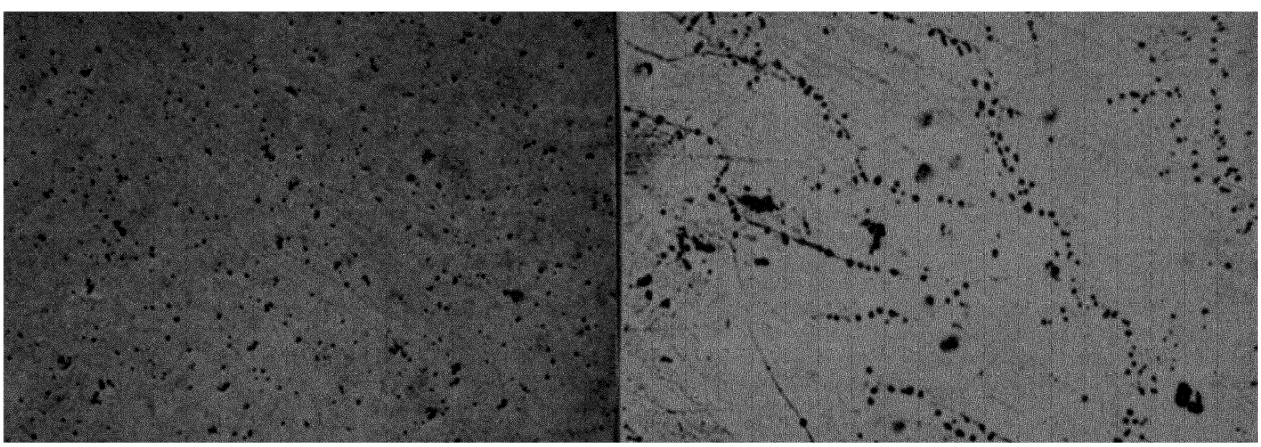

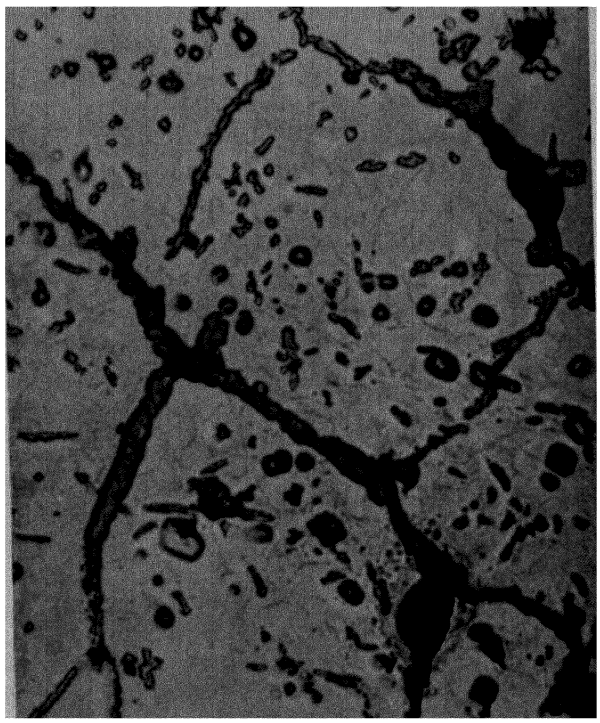

from 0.15 to 0.5%, already afford a substantial improvement, from the standpoint of resistance to thermal fatigue: buckling always under 1 mm, no superficial deformation, no elongation.

SOLUBILIZED U-Al ALLOYS

The solubilization tests were carried out for longer times, and followed by quenching in an oil or water bath, on specimens taken off crude cast alloy rods: lenses 26 mm in diameter, 5-mm thick, or rods having the same diameter and a length of 100 mm.

Tests carried out on specimens taken from bars, cold rolled to plates 4-mm thick, revealed that hardening did not promote any increase in the rate of solubilization, and the rolling process was given up.

Oil Bath Quenching

Modus Operandi

The equipment consists of an oven placed under primary vacuum, in a vertical position, the container of which is connected with the quenching bath vat, which contains oil. Heat treatment is carried out on samples suspended from tungsten wires, and quenching is begun by cutting the wires causing the specimens to drop into the quenching bath below.

Under those conditions, it was not possible to exceed a temperature of 1050°C without any risk of creeping of the alloy. In order to operate at a higher temperature, it would have been necessary to carry the samples in a crucible, and the treatment would not have been applicable to rods.

Additional treatments were carried out on samples containing 0.15, 0.2 and 0.4% of aluminum, until the major part of the intermetallic compound could no longer be seen micrographically.

The times needed in order to obtain proper solubilization near the treatment conditions mentioned above are, for a temperature of 1040°C: (*a*) 100 hours for a 0.15% alloy (AX), (*b*) 200 hours for a 0.2% alloy (BF.11), and (*c*) 300 hours for a 0.5% alloy (BF.9).

Micrographic Aspect

Following solubilization, only a few traces of the former hexagonal lattice persist for the high aluminum alloys, as well as some very fine precipitations which can be either UAl_2, reprecipitated during quenching, or insoluble impurities.

The crude solubilization alloy offers two aspects that are characteristic: either a single phase continuous structure having many structural lines, or a struc-

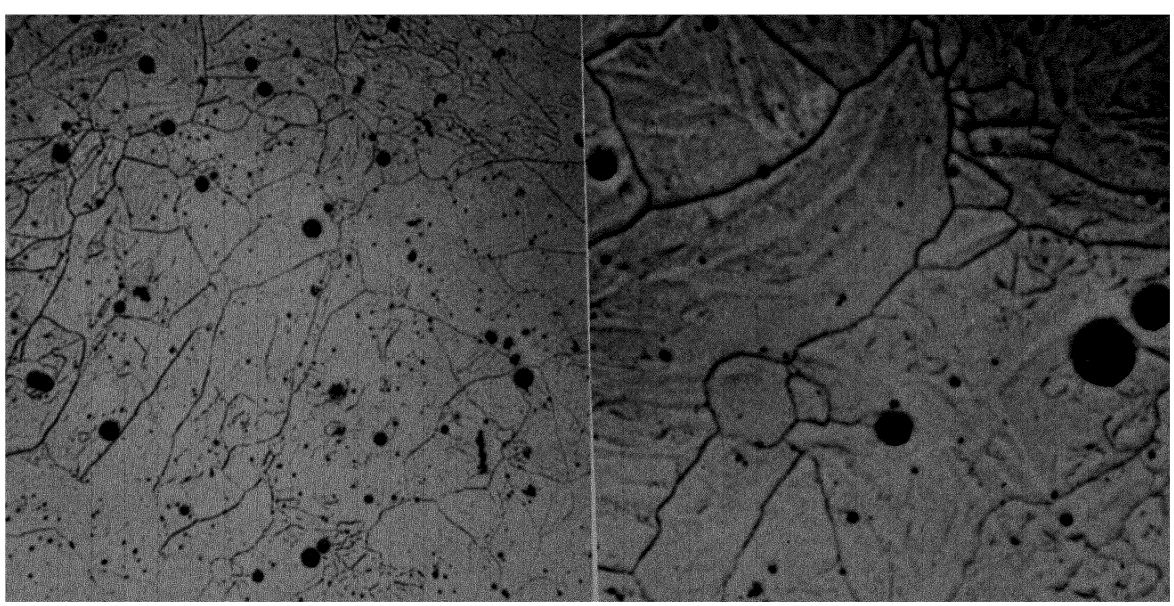

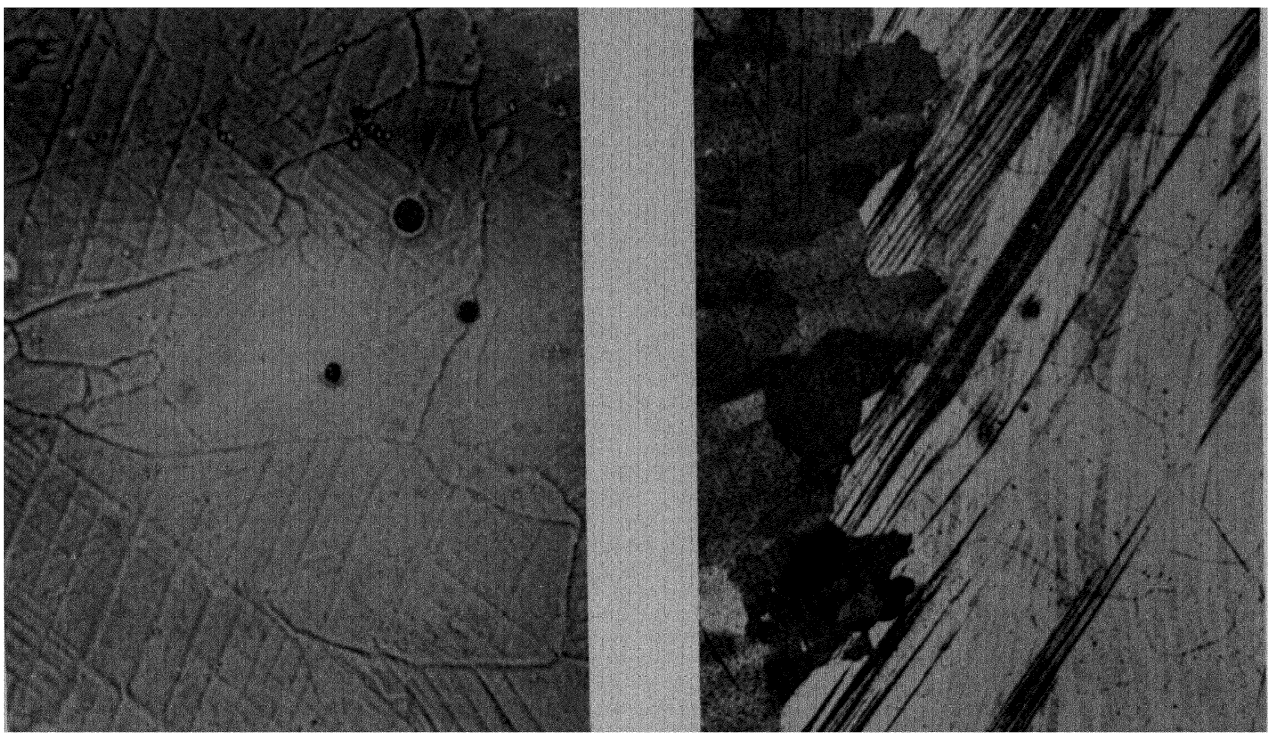

ture offering various well-marked concentration zones.

(*a*) The single-phase structure is the most frequent case. One observes a substructure which comprises domains from 30 to 100 μ, with more or less elongated forms. Inside those domains, we can see poorly resolved parallel lines (Fig. 6) and very clearly defined and rectilinear parallel lines which take the form of crossed marks or needles (Fig. 7) (This was shown only on BF.11 samples containing 0.2%.)

The substructural lines go through the junction which offers torn-up contours characteristic of the quench structure, and the areas involved show (under polarized light) no disorientation at all, one with respect to the others.

Comparisons were carried out by making identical treatments on non-alloyed uranium.

A uranium having an impurity content in the vicinity of that which was used to make the alloys was treated at 1040°C for a few hours, then quenched

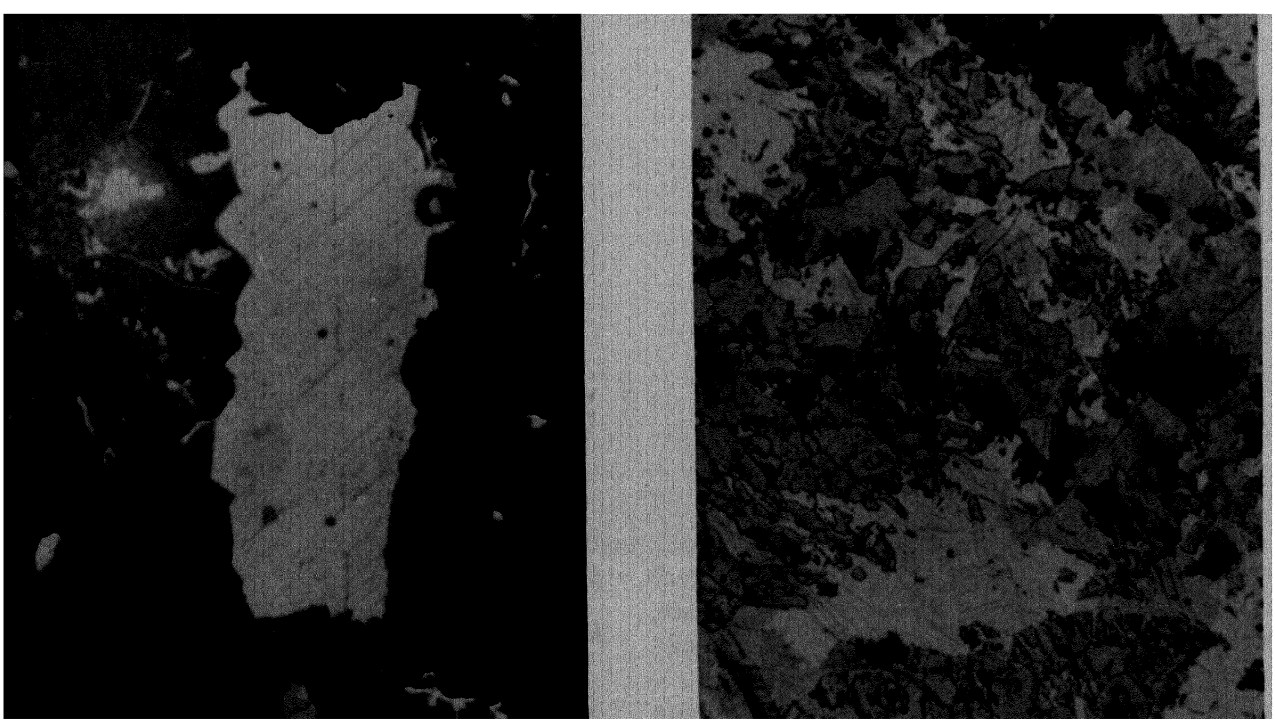

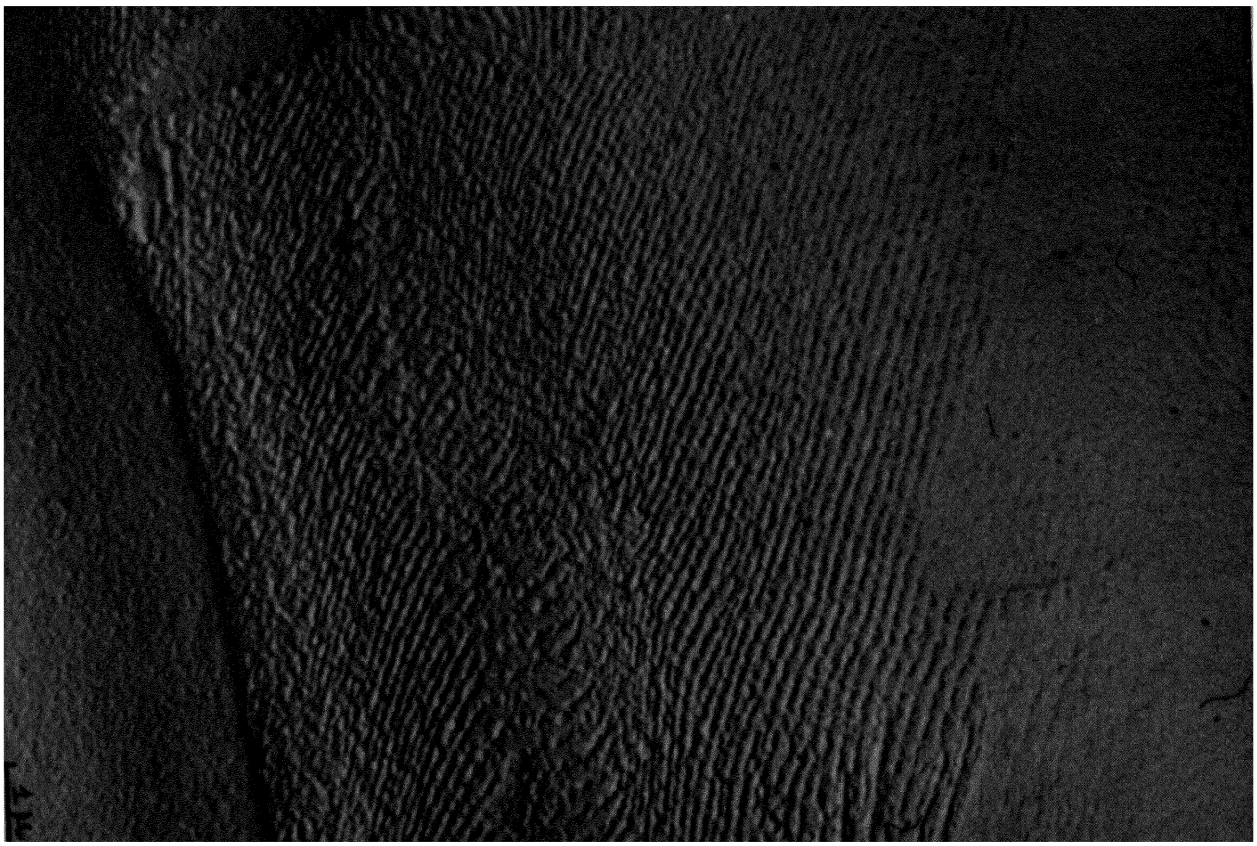

in an oil bath. It offers the same visible lattice under ordinary light, and another substructure which is visible following oxidation (Fig. 8).

Another test was carried out on the same uranium: Heating at 1040°C for a few hours, followed by slow cooling off (approximately 300°C per hour) to the top of the α phase, and at a temperature of 640°C, quenched in an oil bath.

The metal does not offer the first visible substructure under ordinary light, and, following cathodic oxidation, it is possible to reveal only the second substructure, which has all the micrographic characteristics of the polygonization of the α grain. This polygonization would take place during the quench of the α phase.

(*b*) The structure offers several zones of concentration. It is revealed on the samples which contain only 0.4%.

The zones are visible under ordinary light, and more evident after cathodic oxidation. One of them extends on either side of the former γ joint. Generally, it is recrystallized in very fine regular grains (Fig. 9). The other zone formed a series of fringes, generally perpendicular to the γ joint. It is very broken up in the vicinity of the separation surface, thereafter forms a continuous phase very rich in substructures.

The two zones are well lighted, and the α grain junction crosses them without following their contour.[9]

Electronic Microscope Examination

Examinations of aluminum-carbon replica on a 0.4% alloy in aluminum show regions which offer a perlitic structure made up of very fine lamellae, very close to one another. The perlitic zone appeared to begin at the limits of the subjoints, and to grow in a non-transformed matrix. The distance between perlite lamellae is about 2000 Å. At some points, the perlite is formed, no longer of lamellae, but rather of alignments of globe-shaped precipitates. It is possible that this structure might be undergoing evolution (Figs. 11, 12, 13).

X-ray Diffraction

The X-ray diagrams carried out on 0.4% aluminum alloys show that the spacing of the lines is comparable to that of the diagrams for the uranium-chromium alloy having an atomic chromium content of 1.4%.[25,26] In that case, the structure observed is that of a solid solution of chromium in β uranium. Adding aluminum under the same conditions would thus make it possible to retain the structure of the β phase.

Mechanical Characteristics

The solubilized alloys offer a greater hardness when compared to the crude cast alloys. This increase in hardness is greater as the aluminum content is increased.

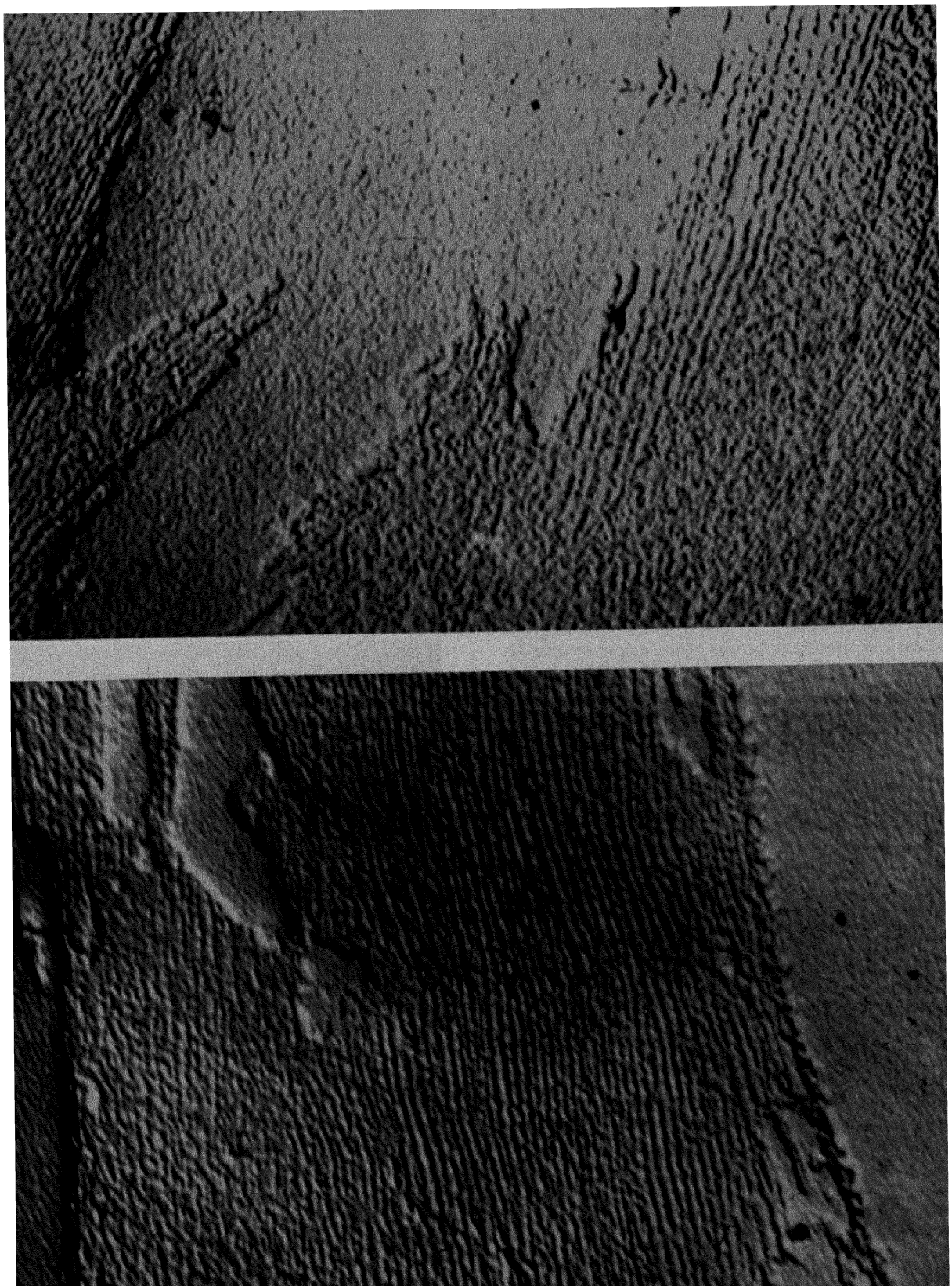

Measurements of the micro-hardness, effected under loads of 100 gm at the most, give values:

Material	*Vickers micro-hardness*
Uranium	250 kg/mm²
U-Al at 0.4%	400 at 425 kg/mm²
U-Al at 0.2%	320 at 340 kg/mm²

On the other hand, the increase in hardness due to the quenching stresses is small. Comparisons carried out between the uranium and alloys having different aluminum contents show that this increase is of the same order of magnitude.

Interpretation

According to the equilibrium diagram, there is no solubility of aluminum in α uranium. Thus, it is difficult to accept the possibility of obtaining a supersaturated solution in the orthorhombic lattice of α uranium without a distortion of the lattice.

The β structure revealed by the X-rays shows that the aluminum, in a solid solution, permits to retain, at some points, a phase which offers the same characteristics as the β phase of U-Cr at 1.4%.

The solubilized samples offer a certain degree of heterogeneity, and it is possible that the concentration zones which are revealed at times correspond to two distinct phases: α uranium and β uranium, formed according to aluminum concentrations in the specimen, which vary from one point to the next, the zones of high aluminum concentration being close to those where it is lower.

As regards the mechanical characteristics, the increase in hardness seems to be due to the stresses created by the passing of the aluminum into a solid solution and to the degree of supersaturation, rather than to the tensions brought in by the quenching.

Water Quenching

Solubilization treatments on samples containing 0.2 and 0.4% of aluminum were carried out on specimens held in vacuum-sealed quartz ampules.

Quenching was carried out by dropping and breaking the quartz ampule, brought up to a temperature of 1040°C, into a bath of iced salt water. The specimens then showed substantial cracks, thus indicating that this quenching process would not be usable for subsequent treatment of the rods.

Other tests which facilitate the modus operandi were carried out by treatment at 1040°C for 200 and 300 hours, followed by oil bath quenching, after which the samples obtained were again brought up to 1040°C in a salt bath, and then were quenched, either in ice water or in boiling water. In all the cases mentioned above, the results are identical.

Micrographic Appearance

A peculiar structure is observed in those cases. It is made up of short interlaced needles approximately 100 μ long and 5 to 10 μ broad (Figs. 14, 15).

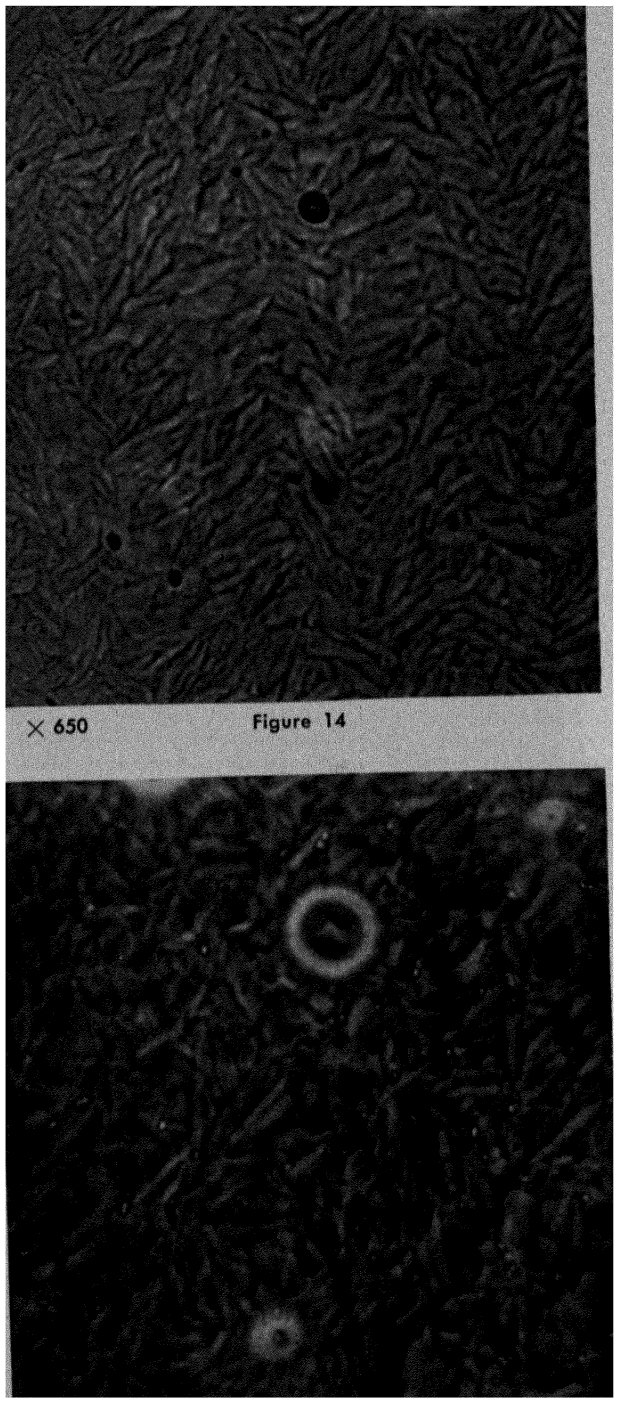

× 650 Figure 14

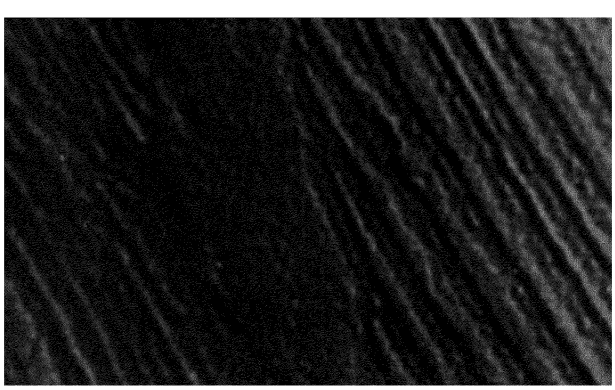

Observation under polarized light shows that each needle offers some measure of disorientation with respect to those that are around it, and that each of the domains so formed is a grain (Fig. 16). The zones located on either side of the γ junction do not show this structure, but rather a continuous phase. They also are richer in the precipitate (Figs. 17, 18).

Characteristic

The micro-hardness given by this needle structure is somewhat less than that obtained on the samples which have undergone oil quenching

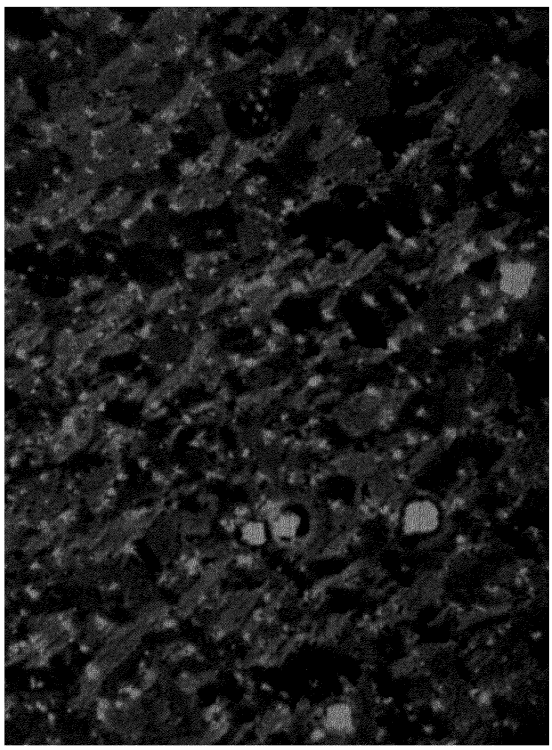

The structure is fairly stable, treatment at 580°C for 3 hours brings about no alteration.

On the other hand, the X-rays did not permit identification as yet.

It is possible that this structure is of the martensitic§ type, for the micrographic aspect of it, showing the presence of needles, is specific of water quenching, and much "dryer" than what is found in an oil bath; the measurements of the quenching speed are carried out with an oscillograph, showing that, with water, one can reach cooling off speeds of the order of 2000°C per second.

SOLUBILIZED ALLOYS, THERMALLY TREATED

Our tests served the purpose of making a study of the precipitation of the intermetallic compound, according to whether it is produced during the cooling of the solid solution, or else by an annealing treatment at temperatures lower than the eutectoid transformation point. In the last named case, the search for the optimal fine precipitation conditions will lead to establishing a "transformation-temperature-time"

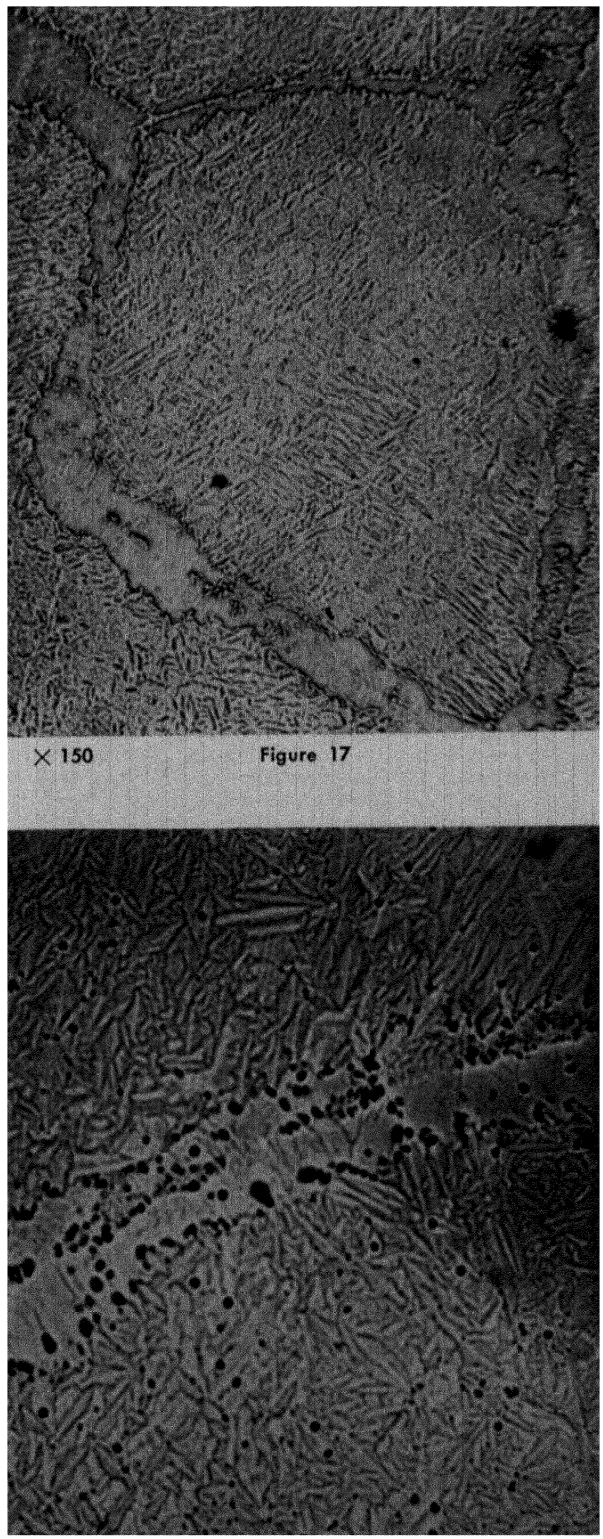

× 150 Figure 17

§ Martensitic transformation is to be found in many diagrams which have a eutectoid point; that of the Fe-C diagram is the best known. In the case of the Cu-Al diagram,[7,8] the β phase is not kept by the quench, and gives 2 martensites, γ' and β'. These Ti-Fe, Ti-Mn, Ti-Cu, Ti-Mo alloys[9-12] also show a martensitic transformation, the phase of which is stable at high temperatures, and can be kept by quenching only for concentrations which exceed a certain percentage in the second element. For the lower concentrations, the authors noted intermediary phases with martensitic characters.

These intermediate structures are not always characterized by metallography.

Their point of transformation, Ms, decreases as a function of the concentration in the second element, and may even be under 0°C in the vicinity of maximal content.

The martensitic transformation may take place, during cooling off, at speeds greater than those which will permit the elements of the eutectoid transformation to appear by diffusion. This is the case in the Fe-C diagram. Again, transformation may be isothermal: this is the case for the Fe-Ni-Mn or Fe-Cr-Ni[13,14] diagrams, and a certain induction time, which varies according to the quenching temperature, is required to have the martensitic structure appear. The formation kinetics of these isothermal martensites then gives a C type curve on the TTT diagram.

diagram, and the *C* curve "characteristic of eutectoid transformations."

Cooling of the Solid Solution of γ Uranium

Following a solubilization treatment of the 0.4% alloy, slower cooling off than that given by the quench led to precipitation of UAl_2 in different forms, according to the cooling speed.

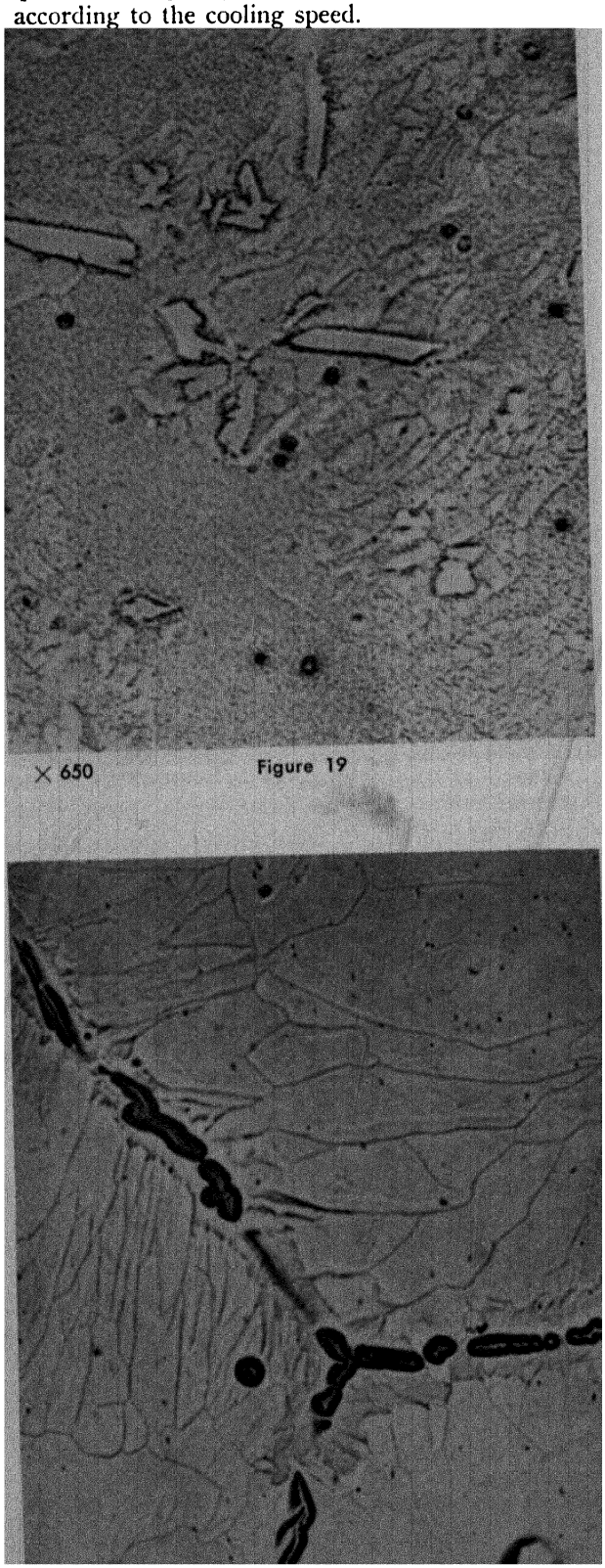

× 650 Figure 19

Very Slow Cooling

Cooling at the rate of approximately 200°C/hour, of 0.4% alloys obtained in an oven, gives large masses of UAl_2 which have a geometric contour (Fig. 19), without any preferential precipitation, whatever the aluminum concentration be.

Faster cooling of the alloy, during casting in a graphite mold, brings about, provided the aluminum contents be sufficient (and close to 0.5%), a precipitation in the form of aligned rods which form a hexagonal lattice, inside which the excess of intermetallic compound is precipitated (Fig. 3).

For the same alloy, after it has undergone solubilization at 1040°C for 200 hours cooling at the speed of 200°C/hour from 1040°C to 800°C, followed by a quench in an oil bath (initial temperature 800°C), brings about precipitation in the form of small rods, so aligned as to form an hexagonal lattice; inside the lattice, there is but little precipitation (Fig. 20).

Cooling of very short duration, between 1040°C and 980°C brings about fine precipitation in the form of platelets having a size of 2 to 4 μ, mainly at right angles to each other; their distribution in the sample is about uniform. In addition, one finds, in the matrix, a much finer precipitation, which is poorly resolved (Figs. 21, 22).

Examination under the electronic microscope shows the existence of platelets (Figs. 23, 24) which are still much smaller, approximately 0.5 μ. In addition, perlitic zones are seen, which are non-uniformly distributed, and present the same characteristics as those revealed in the solubilized and oil bath quenched alloy.¶

In the case of the U-Al alloys, γ uranium offers an extrapolated atomic diameter, at room temperature, of 2.97 Å, and aluminum gives 2.856 Å, for a difference in atomic diameter of 4.07%. Furthermore, precipitation takes place in the γ phase, and is cubical, and the UAl_2 component gives a diamond shaped structure; precipitation is favorable along certain planes of the cubic phase, to give platelets which are generally curved and oriented along a number of directions.**

Air Cooling

When the alloy BF_9 0.4% Al, solubilized at 1040°C for 300 hours, cools off freely at room temperature, gross precipitation is observed, with coalescence, and the formation of hexagonal lattice alignments.

¶ In the Al-Cu alloys, precipitation from the solid solution takes place in the form of platelets of $CuAl_2$, clearly oriented in the aluminum matrix.[16]

** Precipitation in the form of platelets is favored where the 2 components of the alloy have atomic diameters differing by more than 2%. For the very small differences in diameter, only a spherical form would be possible for the particles.

Mott and Nabarro showed that the internal energy which must be developed due to the volume difference is minimal when the form of the particles is that of very thin platelets.[17]

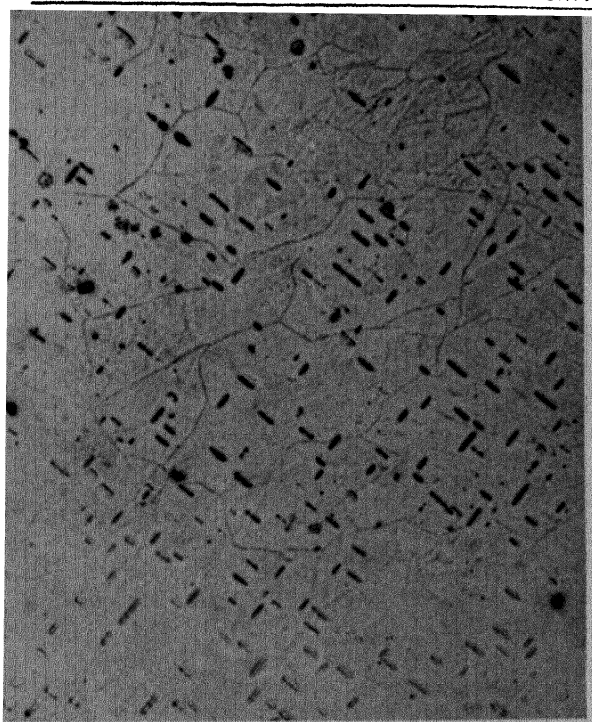

× 450 Figure 21

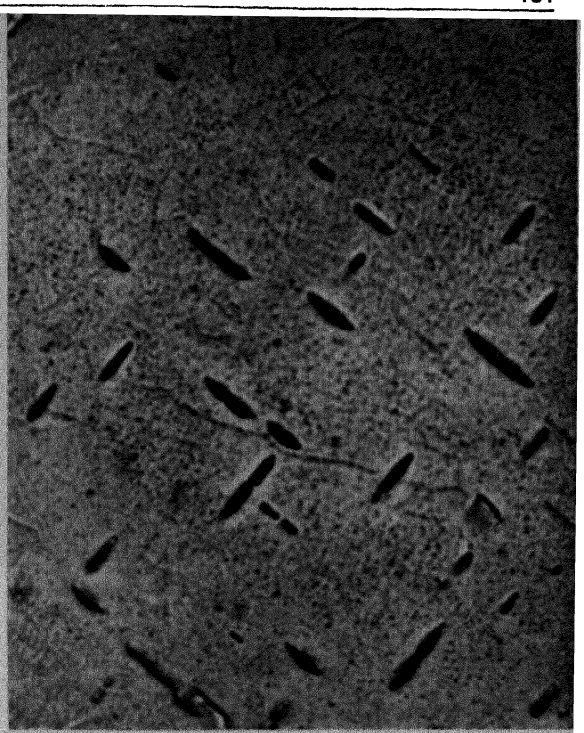

× 1400 Figure 22

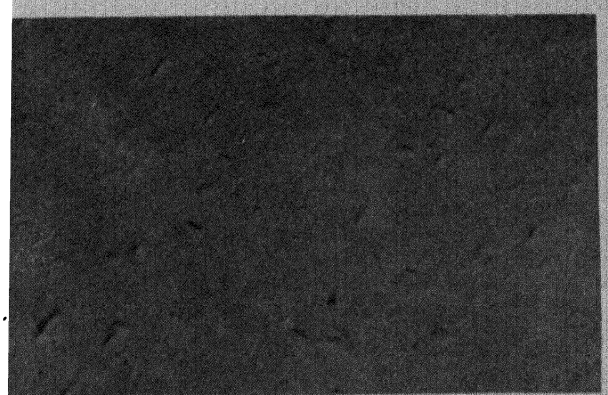

× 5000 Figure 23

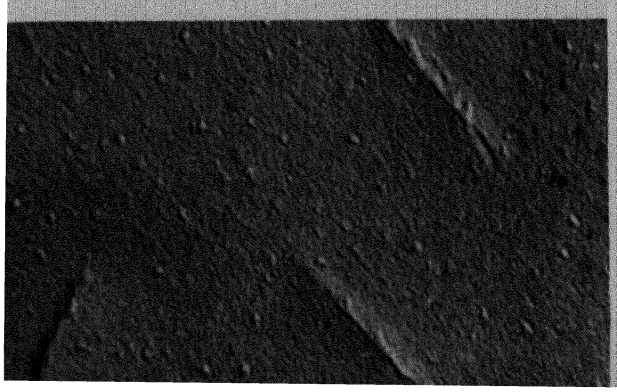

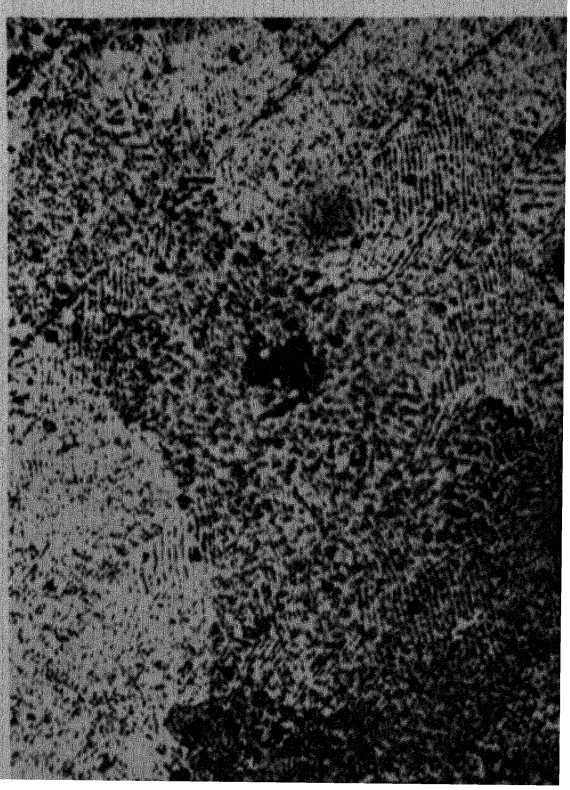

When the 0.15% AX alloy undergoes the same treatment, there is very finely dispersed precipitation, as well as a perlitic structure visible under ×1400 magnification (Fig. 25).

In this case, electronic microscope examinations show a regular perlitic structure with spacing of the lamellae 0.5 μ or 0.1 μ according to the area. In some areas, the lamellae are made up of tight alignments of thin globules (Figs. 26, 27).

Fine Precipitation by Annealing

Annealing treatments were carried out on AX, BF.11 and BF.9 samples, with respective contents of 0.15, 0.2 and 0.4%, first solubilized, and oil bath

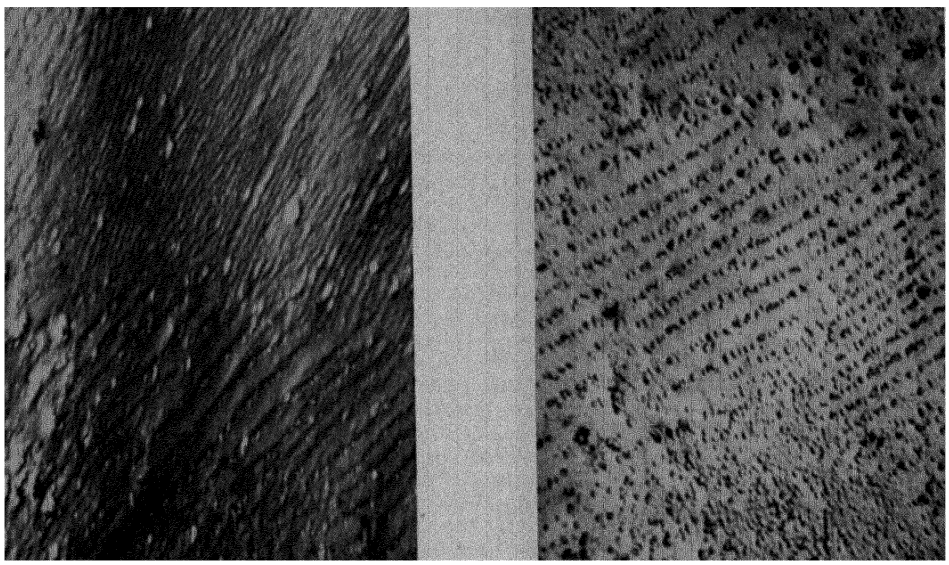

quenched. The treatments add up and are carried out under a vacuum for growing times, at temperatures of 740, 720, 700, 600, 620 and 580 C.

Physical Examinations

Micrographic Appearance

740°C: 1 hour

BF.11. Very substantial degree of coalescence
BF.9: Very substantial degree of coalescence.

720° C: 1 hour, 2 hours, 4 hours, 16 hours, 32 hours

BF.11: Ever denser fine precipitation, the grains have a torn-up outline, after 32 hours, coalescence begins.

BF.9: After 1 hour, very dense precipitation. After 2 hours, coalescence begins and the precipitates form up lines surrounding domains of about 100 μ; the precipitates are identical along the old junction. After 4 hours and 8 hours, coalescence is sharpened in the form of large occlusions, around which one can descry a depleted zone, devoid of precipitates. After 16 hours, no more large occlusions are to be found; on the other hand, the density and size of the globular precipitations have increased.

700°C: 1 hour, 2 hours, 4 hours, 8 hours, 16 hours, 32 hours

AX. Fine, ever denser, precipitation.
BF.11. Fine precipitation, which increases up to 16 hours; no more change beyond that.

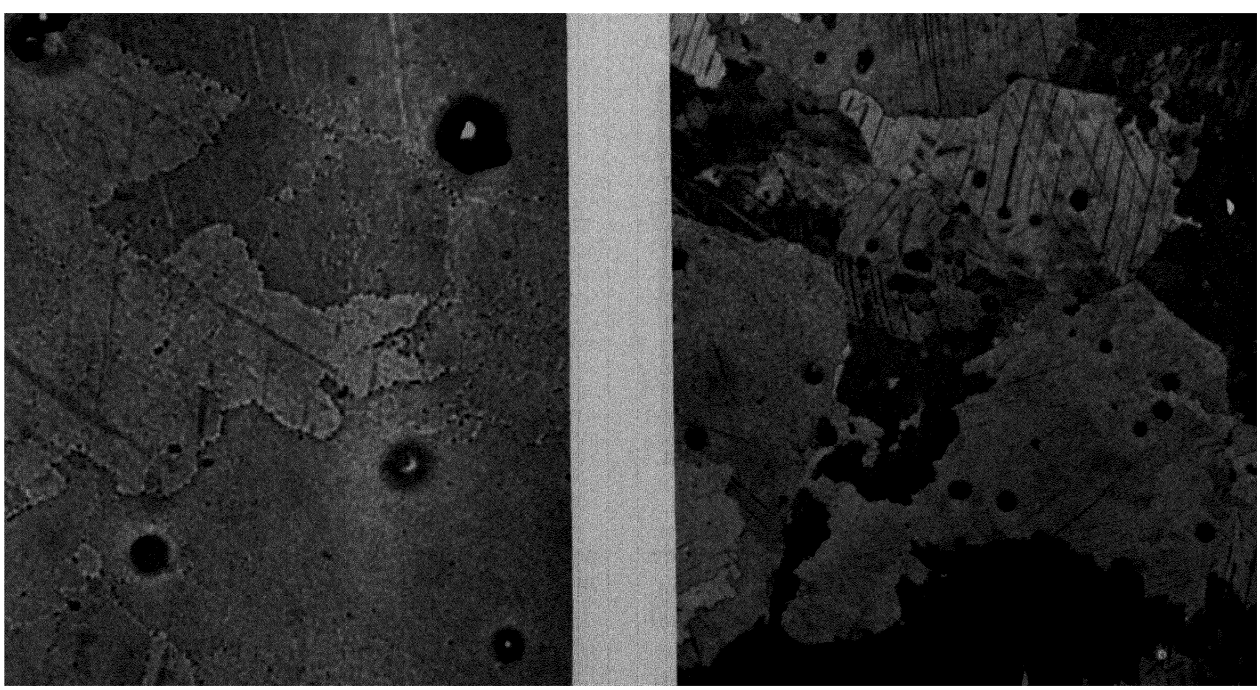

660°C: 1 hour, 2 hours, 4 hours, 8 hours, 16 hours, 32 hours

BF 11: Precipitation is regularly distributed, density increases with the duration of treatment. The outline of the grain is torn up, similar to that obtained after quenching, up to 4 hours of treatment. After 8 hours, the precipitations are aligned and form well-marked regions; these coincide with the junction points pertaining to a new structure. There is some recrystallization, with irregular grains of different sizes, rarely equiaxial (Figs. 28, 29). After 16 and 32 hours, the density of precipitation shows no marked increase; on the other hand, a considerable increase in the size of the grain is noted.

BF.9: Precipitation is denser than above. Simultaneously, recrystallization takes place, of the fine grain type, equiaxial, about 15μ. This recrystallization is very homogeneous, except for the area in the vicinity of the γ junction (Figs. 30, 31).

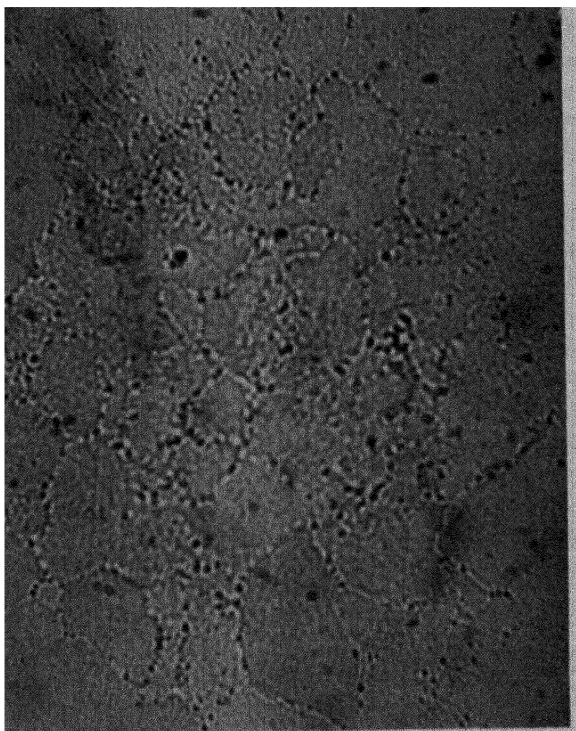

× 1400 Figure 30



× 150 Figure 31

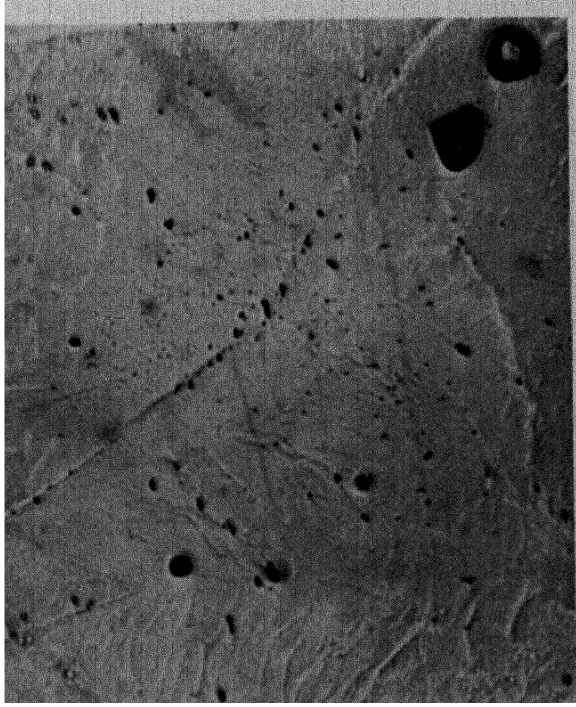

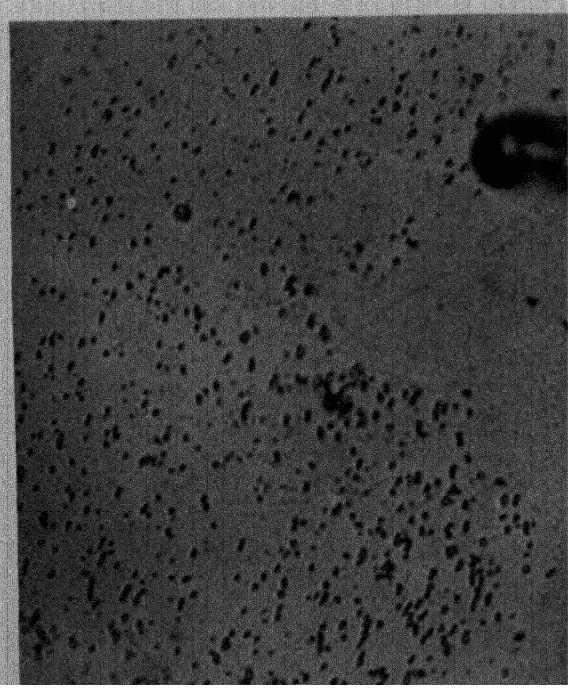

580°C: 1 minute, 3, 10, 100, 1000, 10,000 minutes

BF 11 After one minute, precipitation in the form of platelets 1 to 2 μ thick, curved, and ultra-fine very abundant precipitation, particularly along the substructural lines. The density of the last named precipitates increases up to 100 minutes, while, for the platelet-shaped precipitates, there is no evolution (Figs. 32, 33). After 100, 1000 and 10,000 minutes, there is no change.

BF.9: Two forms of precipitation as above, but much denser. After 3 min, the dimensions of the platelets have increased a bit; after 10 min, their number appears to be stationary, and ultra-fine precipitations are much more abundant; beyond that, there are no changes. Partial recrystallization at the beginning is complete after 100 min, except in the vicinity of the γ junction (Figs. 34, 35).

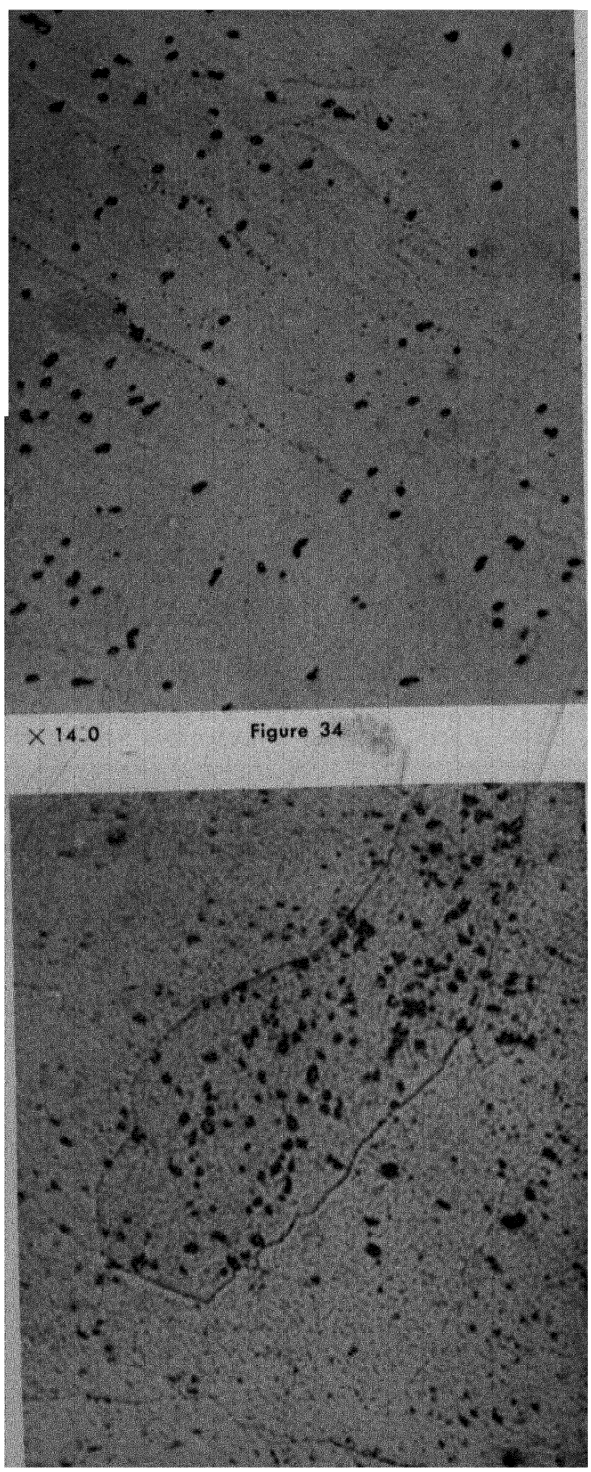

× 14.0 Figure 34

Mechanical Characteristics

Measurements of the Vickers hardness, under a 40-kg load, have been carried out on each of the BF.9 and BF.11 samples which underwent additive treatment, at temperatures of 720°C and 660°C. A reduction in the hardness is noted, which takes place rapidly, particularly at 720°C. However, the curves which represent the hardness as a function of the duration of treatment are not too accurate, and the dispersion of the measurements is much too large.

Measurements of Vickers microhardness under a maximum load of 100 gm were carried out following treatments at 580°C for 1, 3, 10, 100, 300, 1000 and 10,000 minutes. An increase in the hardness, with respect to the solubilized alloys, then is noted, after which a maximum is reached, followed by a decrease. These results correspond well to the hardness brought about by finely dispersed precipitations obtained in the alloys which have been allowed to age (Fig. 36).[18]

Electronic Microscopy

Examinations were carried out on the same sample, first examined following solubilization treatment. The sample undergoes annealing at 580°C for 3 minutes. The lamellar perlitic structure is gone, and there are fringes made up of fine globules in a matrix showing a number of lines which indicate slides (Fig. 37).

Interpretation

According to the above-mentioned results, we note that the lamellar perlitic form of the eutectoid is obtained only during the cooling of the solid solution under the conditions described. By the annealing treatment, one always obtains the precipitate in the form of platelets or globules, more or less fine according to the temperature. Electronic microscope examination confirms that this lamellar structure is none too stable, and evolves rapidly as soon as the temperature goes up.

In the alloys capable of eutectoid transformation, the perlitic form is not always observed. The eutectoid may appear under a globular form, and be considered fugitive.†† In other cases, the perlitic form is revealed only for certain conditions of temperature and duration of treatment ‡‡

The increase in hardness, with respect to the solid solution, appears during the annealing treatment, passes through a maximum, and then decreases. This is visible only following a very short annealing time; when prolonged, there is no reduction in the hard-

†† Ti-Mn,[19] Cu-Si,[20] Zr-Mo alloys.[21]

‡‡ Cu-In alloys.[22]

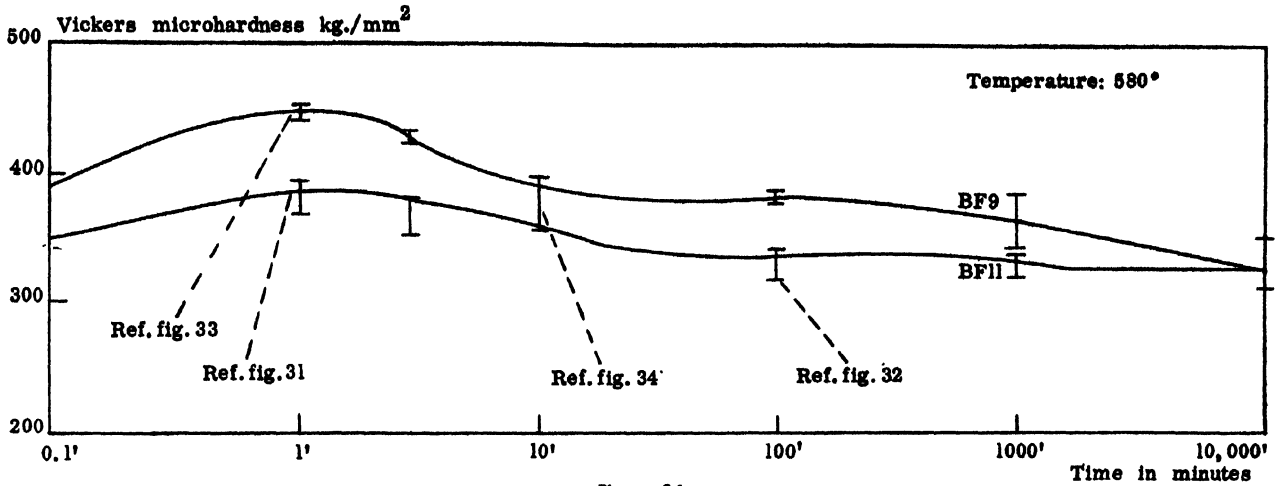

Figure 36

ness. It is likely that maximum hardness is not measured and takes place, for such a temperature, at the end of a few seconds.§§

A very important characteristic of the alloys which have undergone annealing is their recrystallization.

The alloys which contain 0.4% Al recrystallize very rapidly, giving a fine polyhedric grain structure, with dimensions of 10 to 20 μ. The lower content alloys recrystallize only after a few hours, and their structures have irregular and coarser grains.

Comparative tests carried out on uranium quenched under the same conditions show that the quenching stresses do not account for this recrystallization.

Recrystallization thus would be dependent on the degree of supersaturation and the results of the stresses created by distortions, which may be of two origins: those brought about by solubilizing the aluminum, namely the insertion of aluminum atoms in the uranium lattice; the second would be that of the distortions brought about by the formation of the precipitate which is congruent with the matrix.¶¶

In the case of uranium-aluminum alloys, it would seem that the effect of the stresses due to precipitation is larger than that due to solubilization for, in the case of the 0.2% alloy it is necessary to subject it to an 8-hour treatment at 580°C (bringing about a substantial degree of fine precipitation) to cause the recrystallization to appear.

Behavior of Finely Precipitated Alloy

Long duration and cycling treatments have been carried out in order to check on the stability of the heat treated alloy under the influence of the temperature, or of thermal fatigue.

Long-lasting Treatment

They are carried out on 0.4% alloys, following solubilization at 1040°C and 300 hours, and an annealing treatment at 550°C and 1 hour.

Following 200-hour treatments at 300°C and at 550°C, no change in structure is noted.

Cycling

This was carried out on a rod of a 0.4% alloy, 10-cm long. The rod first underwent solubilization at 1040°C for 300 hours, followed by oil bath quenching, and annealing at 580°C for 90 minutes.

The rod was subjected to cycling between 20°C and 520°C.

Following 200 cycles, there are no buckling, no surface changes, no cracking, no elongation.

The micrographs show that fine precipitation was not markedly increased. In addition, microhardness was not changed, and remained equal to 400 kg/mm² (Fig. 38).

Cycling was continued up to a total number of 800 cycles. Still no buckling, deformation, or elongation. Micrographic examinations and microhardness tests similarly failed to indicate any change.

SUMMARY AND CONCLUSIONS

This study shows that the uranium-aluminum alloys make up a material which offers important advantages as compared to pure, unalloyed uranium. The adding of aluminum as an intermetallic compound UAl_2 gives the material better resistance to thermal fatigue.

§§ From Hardy,[25] maximum hardness is associated with the formation of precipitate Θ', congruent with the matrix, and the formation of the maximum quantity of the Θ phase corresponds to a reduction in the hardness.

¶¶ From Cottrel,[24] the "stresses by coherence" are most important, and due to "short range" distortions caused by the formation of the precipitate which does not have a final crystalline structure as yet.

When precipitation is carried out at too high a temperature, the stage of coherent precipitation is very rapid, and the transition to the incoherent precipitate takes place nearly immediately so that there is no recrystallization.

According to the Orowan theory,[26] the general stress would be a consequence of interactions between the dislocations which surround the precipitate with sliding planes, and the hardness is all the greater as the distance between precipitate is smaller, since then the fields of stresses then are very close to one another, and the forces which act in a given direction at distances of only a few atoms from those which act in the opposite direction.

1. The crude cast alloys having a 0.15 to 0.5% of aluminum content already constitute an improvement with respect to the crude cast uranium, or to uranium having undergone various mechanical treatments.

These alloys behave in approximately the same manner, whether their content be in the vicinity of 0.5% and have a structure in which UAl_2 is distributed as a lattice, or this content is lower and they form a structure in which UAl_2 is dispersed in the form of nodules.

Thermal fatigue takes the form of a small amount of buckling, always less than 1 mm, without any superficial deformation: the crude cast or extruded uranium, when subjected to the same conditions of thermal fatigue, shows an average flexing of 1.5 mm and superficial deformations of the "orange rind" type.

On the other hand, thermal fatigue does not bring about any elongation; α phase rolled and recrystallized uranium, although it suffers neither distortion nor buckling following cycling, undergoes a very substantial elongation, which would make the cladding of such a material very difficult.

The main drawback of the crude cast alloys still is crack formation. This appears after only 400 cycles, and is much less than for α-phase extruded uranium, which shows a superficial decohesion of the grains after only 200 cycles

2. Thermally treated alloys make up a material which offers better resistance to thermal fatigue than the crude cast alloys.

These characteristics are due to very fine dispersion of the precipitate, leading to structural hardening and better isotropy.

To the advantage of regularly dispersed fine precipitation, let us add that of recrystallization. The fine and regular grain structure further contributes to reducing the anisotropy of the cast materials, and we have reason to believe that this structure offers no preferential orientation, so that the drawback of the elongation of the laminated rods during cycling thus can be avoided.

In this connection, the alloys which have a content in the vicinity of 0.5% would have the advantage of recrystallized structures finer than those of the low content alloys, in which the recrystallized grains are irregular.

The thermal treatments carried out on the alloys show that it is possible, in this fashion, to achieve controlled precipitation in a finely dispersed form; the treatment conditions which were conserved as likely to be applied to alloy rods having a content of approximately 0.4% are: the solubilization-homogenization treatment at 1040°C for 300 hours, followed by an oil bath quench, and annealing treatment at 580°C for about 2 hours.

The solubilization treatment offers the drawback of being very lengthy. It seems difficult to reduce its duration by increasing the temperature, without the risk of causing some creep; on the other hand, it would be possible to reduce the duration of treatment by choosing aluminum concentrations lower than 0.4–0.5%, yet sufficient to allow recrystallization in fine and regular grains.

The results of cycling a rod having a 0.4% content, and subjected to the treatments described above, show that there is but negligible flexing, no superficial deformation, no elongation.

No crack formation can be observed after 800 cycles, and on the other hand, the structure is very stable, the size and density of precipitation as well as the microhardness showing no changes.

Next to these technical conclusions, which have concrete applications, it is in order to indicate the importance which will be offered, further on in this study, by the thermal treatments of the uranium-aluminum alloys, the experimental results, which follow, were analyzed during this same study, namely:

(*a*) The lamellar perlitic structure, visible under certain conditions of cooling off, and only with the electronic microscope, by reason of its fineness (0.2 μ bands), which could be reproduced, under our experimental conditions, only by an annealing treatment. This eutectoid structure would be very unstable and would evolve rapidly

(*b*) Conservation, at room temperature, of a solid solution of aluminum in a uranium matrix offering a needle microstructure, or a crystalline structure of β uranium, according to quenching conditions.

REFERENCES

1. Gordon, Kaufman, *Uranium-Aluminium and Uranium-Iron,* J. of Metals, *188*: 182 (January 1950).
2. Borie, *Crystal Structure of UAl_4,* J. of Metals, *3*: 800 (1951).
3. Kiessling, R., Note Energie Atomique Suédoise (May 1954).
4. Beroujon, J. and Diament, A., Rapport C. E. A. Int., No. 5 (1952).
5. C. R. No. B-58, Technologie, Groupe "Essais des Matériaux" (1954).
6. C. R. No. B-85, Technologie, Groupe "Essais des Matériaux" (1955).
7. Klier and Grymko, *The transformations in β –CuAl alloys,* Transactions A.I.M.E. *185*: 611 (1949).
8. Mack, D., *The isothermal transformation of a eutectoïd aluminium bronze,* Transactions A.I.M.E. *175*: 240 (1948).
9. Polonis, Parr and Gordon, *Martensite formations in powders and lump specimens of Ti-Fe alloys,* J. of Metals, *7*: 64 (January 1955).
10. Holden, Ogden and Jaffee, *Heat Treatment structure and mechanical properties of Ti-Mn alloys,* J. of Metals *6*: 169 (February 1954).
11. Holden, *et al., Heat Treatment and mechanical properties of Ti-Cu alloys,* J. of Metals, *7*: 117 (January 1955).
12. Duwez, *Effect of rate of cooling on the γ/β transformation in Ti and Ti-Mo alloys,* J. of Metals, *3*: 765 (1951).
13. Cech and Holloman, *Rate of formation of isothermal martensitic in Fe-Ni-Mn alloy,* J. of Metals, *5*: 685 (May 1953).
14. Kulin and Speich, *Isothermal martensite formation in a Iron-Chromium Nickel,* J. of Metals, *4*: 258 (March 1952).
15. Shih, Averbach and Cohen, *Some characteristics of the isothermal martensitic transformation,* J. of Metals, *7*: 183 (January 1955).
16. Polmear and Hardy, *Some metallographic observations on aged aluminium-copper alloys,* J. of the Institute of Metals, *81*: 427 (1952-53).
17. Hardy, *Report on precipitation,* Progress in Metals Physics, 5.
18. Geisler, *Phase transformations in solids.*
19. Maykuth, Ogden and Jaffee, *Titanium-Manganese System,* J. of Metals, *5*: 225 (February 1953).
20. Kibbard and Eichelman, *The Kappa eutectoïd transformation in the Copper-Silicon system,* Transactions A.I.M.E. *180*: 92 (1949).
21. Domagala, McPherson and Hansen, *Systems Zirconium-Molybdenum and Zirconium-Wolfram,* J. of Metals, *5*: 73 (January 1953).
22. Chester, Spencer and Mack, *The Copper-Indium eutectoïd at 31, 36 wt % In.,* J. of the Institute of Metals *82*: 81 (October 1953).
23. Hardy, *The aging characteristics of binary Al-Cu alloys,* J. of the Institute of Metals, *79*: 321 (1951).
24. Cottrel, *Relation of Properties to microstructure,* Interactions of dislocations and solute atoms.
25. Holden, *Growth and crystallography of deformation of β-phase Uranium single crystals,* Acta Crystallographica, *5*: 182 (1952).
26. Holden, *The isothermal transformation of metastable β-Uranium single crystals,* Acta Metallurgica, *1, 6*: 617 (1953).

The Intermetallic Compounds of Plutonium

By A. S. Coffinberry and F. H. Ellinger,* USA

During the war years Westrum[1,2] prepared $PuSi_2$ at the Metallurgical Laboratory of the University of Chicago, and Zachariasen[3,4] determined its crystal structure. But because silicon may be regarded as a metalloid element rather than a metal, it might truthfully be stated that (so far as the authors of this paper are aware) the first preparations of compounds of plutonium with other metals were made at the Los Alamos Scientific Laboratory in the United States and at the Chalk River Project in Canada. More recently the Argonne National Laboratory has become equipped with facilities that make possible the preparation and study of plutonium intermetallic phases at that location.

The first intermetallic compounds of plutonium prepared and identified by us were the cubic phases, $PuSn_3$, $PuPb_3$ and Pu_3In. These compounds were reported in the classified literature during 1948. During 1953 the first crystal-structure determinations at Chalk River were reported by Runnalls in the classified literature. His results were for the compounds $PuAl_2$, $PuAl_3$, $PuAl_4$ and $PuBe_{13}$, and they duplicated data that had been obtained at Los Alamos during 1949–50. In a recent communication, Runnalls indicates that he has determined the crystal structures of the following: $PuAl_2$, $PuAl_3$, $PuAl_4$, $PuBe_{13}$, $PuNi_2$, $PuNi_5$, Pu_2Ni_{17}, $PuAg_3$, $PuMn_2$, $PuFe_2$ and $PuCo_2$. Although the dates of his work are not given, it seems likely that crystal structure solutions for the first six of these compounds were obtained here earlier than at Chalk River. But complete structure solutions for Pu_2Ni_{17} and $PuAg_3$ had never been obtained by us, and the solution for the isostructural series, $PuMn_2$, $PuFe_2$ and $PuCo_2$, was probably first obtained at Chalk River. Although suspected as early as 1952, we did not fully realize the isostructuralism of "$PuNi_9$" with Th_2Ni_{17} until Runnalls' recent communication directed attention to the relationship.

A summary of the compounds that are believed to have been identified by us, and crystal-structure data relating to them so far as they are now known, is given in Table I. In a number of instances, a complete investigation of the phase diagrams was not done, and therefore more compounds may exist in a particular binary system than have been reported. In order to make the table as complete as possible, Zachariasen's results for $PuSi_2$ (with revised unit-cell dimensions) are included, and account is taken of the incomplete information that has been obtained from Runnalls regarding Pu_2Ni_{17} and $PuAg_3$. Certain compounds of plutonium with nonmetallic elements and with metalloids have been included for cases in which it is believed that X-ray diffraction data that we have obtained may constitute a significant contribution to the literature. The compounds are listed in alphabetical order of chemical symbols.

With only a single exception, the crystal structures of intermetallic phases that can be reported are not new. That is, except for $PuAl_3$, all of the intermetallic compounds for which structures were determined are isostructural with compounds having previously known structures. $PuAl_3$ was found to have a structure that had not previously been reported, and this crystal structure was studied both at Los Alamos and at Chalk River. One compound of plutonium with a nonmetal, hexagonal PuH_3, appears also to have a new structure, but its determination has not yet been completed.

DISCUSSION ON TABLE I

Fifty-three phases are listed in Table I. Of this number, 8 are compounds of plutonium with nonmetals (carbon, hydrogen and oxygen), so that 45 phases consist of combinations of plutonium with either a metal or a metalloid. Among these 45, we have obtained fairly complete crystal structure data for 32—complete enough so that both the existence and the identity of each of the 32 phases may be regarded as well established, even though the compositions of two of them (Pu_2Mg and $PuMg_2$) are uncertain.

The crystal structure of one ($PuAg_3$) of the remaining 13 intermetallic phases has been determined at Chalk River, but the results are not known to us. For another ($PuBi_2$) of the 13, no recognized X-ray diffraction pattern has ever been obtained, but metallographic evidence is considered to have established its existence and its composition quite firmly. Of 11 of the tabulated intermetallic compounds it may be said, then, that the best evidence in support of their existence consists of an unsolved X-ray powder pattern. In each of these cases it cannot now be said whether eventual solution of the diffraction pattern will show the compound to be isostructural with a known structure type, or whether a new structure is represented by the pattern. Presumably both situations exist among the 11 unsolved patterns.

In most of the 11 cases the X-ray diffraction evidence is supplemented by supporting experimental

* Los Alamos Scientific Laboratory.

Table I. X-ray Diffraction and Crystal Structure Data for Some Binary Compounds of Plutonium

Compound	Structure type	Crystal lattice*	Unit cell dimensions, Å	Formula units in unit cell	Space group	Calculated density, gm/cm³
$PuAg_3$	(*see* discussion of $PuAg_3$					
Pu_2Al	Partially ordered $SrPb_3$	Tetr.	$a = 4.499 \pm 0.002$ $c = 4.538 \pm 0.002$	1		13.45
PuAl(?)	(Unsolved powder pattern;† *see* discussion of PuAl)					
$PuAl_2$	Cu_2Mg	F.C.C.	Pu-rich: $a = 7.838 \pm 0.001$ Al-rich: $a = 7.848 \pm 0.001$	8	Fd3m	8.06
$PuAl_3$	$PuAl_3$	Hex.	$a = 6.17 \pm 0.02$ $c = 14.5 \pm 0.1$	6	$P6_3/mmc$	6.67
$PuAl_4$	UAl_4	Orth.	$a = 4.41$ $b = 6.29$ $c = 13.79$	4	Imma	6.02
PuAs	NaCl	F.C.C.	$a = 5.855 \pm 0.004$	4	Fm3m	10.39
$PuBe_{13}$	$NaZn_{13}$	F.C.C.	Pu-rich: (*see* discussion) Be-rich: $a = 10.282 \pm 0.001$	8	Fm3c	4.35
PuBi	NaCl	F.C.C.	$a = 6.350 \pm 0.001$	4	Fm3m	11.62
$PuBi_3$	(Metallographic evidence only; *see* discussion of $PuBi_3$)					
PuC	NaCl	F.C.C.	$a = 4.97 \pm 0.01$ (*see* discussion of Table I)	4	Fm3m	13.6
Pu_2C_3	Pu_2C_3	B.C.C.	$a = 8.129 \pm 0.001$	8	$I\bar{4}3d$	12.70
Pu_3Co(?)	(Unsolved powder pattern; *see* discussion of Pu_3Co)					
Pu_2Co	Fe_2P (Tentative; *see* discussion of Pu_2Co)	Hex.	Pu-rich: $a = 7.902 \pm 0.004$ $c = 3.549 \pm 0.002$ Co-rich: $a = 7.762 \pm 0.003$ $c = 3.649 \pm 0.002$	3	P321	14.0
$PuCo_2$	Cu_2Mg	F.C.C.	Pu-rich: $a = 7.081 \pm 0.001$	8	Fd3m	13.35
PuCu(?)	(Unsolved powder pattern;† *see* discussion of PuCu)					
$PuCu_3$(?)	(Unsolved powder pattern;† *see* discussion of $PuCu_3$)					
$PuCu_7$(?)	(Unsolved powder pattern;† *see* discussion of $PuCu_7$)					
Pu_6Fe	U_6Mn	B.C.T.	$a = 10.41 \pm 0.01$ $c = 5.359 \pm 0.004$	4	I4/mcm	17.04
$PuFe_2$	Cu_2Mg	F.C.C.	Pu-rich: $a = 7.191 \pm 0.001$	8	Fd3m	12.53
Pu_2Ge_3	Pseudo-AlB_2		(*see* discussion of Pu_2Ge_3 and Pu_2Si_3)			
$PuGe_2$	$ThSi_2$	B.C.T.	Ge-rich: $a = 4.102 \pm 0.002$ $c = 13.81 \pm 0.01$	4	I4/amd	10.98
$PuGe_3$	Ordered $AuCu_3$	S.C.	$a = 4.223 \pm 0.001$ (*see* discussion of $PuGe_3$)	1	Pm3m	10.07
$PuH_{2.0}$-$PuH_{2.7}$	CaF_2	F.C.C.	$PuH_{2.0}$: $a = 5.359 \pm 0.001$ $PuH_{2.5}$: $a = 5.34 \pm 0.01$	4	Fm3m	10.40
PuH_3	PuH_3	Hex.	$a = 3.78 \pm 0.01$ $c = 6.76 \pm 0.01$	2	$P6_3/mmc$	9.61
$PuHg_3$	UHg_3	Hex.	(*see* discussion of $PuHg_3$)	½	$P6_3/mmc$	
$PuHg_4$	UHg_4	Pseudo-B.C.C.	(*see* discussion of $PuHg_4$)	2 in Pseudo-unit		
Pu_3In	Partially ordered $AuCu_3$	Cubic	$a = 4.703 \pm 0.002$ (*see* discussion of $PuGe_3$)	1		13.3
Pu_2Mg(?)	Probably CaF_2	F.C.C.	$a = 7.34 \pm 0.01$	4(?)		
$PuMg_3$(?)		Hex.	$a = 13.8 \pm 0.1$ $c = 9.7 \pm 0.1$			
$PuMn_2$	Cu_2Mg	F.C.C.	Pu-rich: $a = 7.292 \pm 0.001$	8	Fd3m	11.95
PuNi	(Unsolved powder pattern; *see* discussion of Table I)					
$PuNi_2$	Cu_2Mg	F.C.C.	Pu-rich: $a = 7.141 \pm 0.001$ Ni-rich: $a = 7.115 \pm 0.001$	8	Fd3m	13.1
$PuNi_3$	(Unsolved powder pattern; *see* discussion of Table I)					
$PuNi_4$	(Unsolved powder pattern;† *see* discussion of Table I)					

Table I. (cont.)

Compound	Structure type	Crystal lattice*	Unit cell dimensions, Å	Formula units in unit cell	Space group	Calculated density, gm/cm³
$PuNi_5$	$CaZn_5$	Hex.	Pu-rich: $a = 4.872 \pm 0.002$, $c = 3.980 \pm 0.001$; Ni-rich: $a = 4.861 \pm 0.002$, $c = 3.982 \pm 0.001$	1	P6/mmm	10.8
Pu_2Ni_{17}	Th_2Ni_{17}	Hex.	$a = 8.29 \pm 0.02$, $c = 8.01 \pm 0.02$	2	$P6_3/mmc$	10.3
PuO	NaCl	F.C.C.	$a = 4.96 \pm 0.01$	4	Fm3m	13.9
Pu_2O_3	La_2O_3	Hex.	$a = 3.841 \pm 0.006$, $c = 5.958 \pm 0.005$	1	$P\bar{3}ml$	11.47
Pu_2O_3 - Pu_4O_7	Mn_2O_3	B.C.C.	Pu_2O_3: $a = 11.04 \pm 0.02$	16	Ia3	10.2
PuO_2	CaF_2	F.C.C.	$a = 5.3960 \pm 0.0003$	4	Fm3m	11.46
PuP	NaCl	F.C.C.	$a = 5.664 \pm 0.004$	4	Fm3m	9.87
$PuPb_3$	Disordered $AuCu_3$	F.C.C.	$a = 4.808 \pm 0.001$ (*see* discussion of $PuGe_3$)	1	Fm3m	12.86
Pu_5Si_3(?)	(Unsolved powder pattern; *see* discussion of Table I)					
Pu_3Si_2(?)	(Unsolved powder pattern;† *see* discussion of Table I)					
PuSi	FeB	Orth.	$a = 5.727 \pm 0.005$, $b = 7.933 \pm 0.003$, $c = 3.847 \pm 0.001$	4	Pbnm	10.15
Pu_3Si_5	Pseudo-AlB_2	(*see* discussion of Pu_3Ge_5 and Pu_2Si_3)				
$PuSi_2$	$ThSi_2$	B.C.T.	Si-rich: $a = 3.967 \pm 0.001$, $c = 13.72 \pm 0.03$	4	I4/amd	9.08
$PuSn_3$	Ordered $AuCu_3$	S.C.	$a = 4.630 \pm 0.001$ (*see* discussion of $PuGe_3$)	1	Pm3m	9.96
PuTe	NaCl	F.C.C.	$a = 6.183 \pm 0.004$	4	Fm3m	10.33
Pu_3U		Apparently S.T.	$a = 10.57 \pm 0.05$, $c = 10.76 \pm 0.05$	52 atoms (*see* discussion of Pu_3U)		17.15
PuU		Apparently S.C. at room temp.	$a = 10.664 \pm 0.005$	58 atoms		18.95
Pu_xZr ($x>3$)	(Unsolved powder pattern; *see* discussion of Table 1)					

* S.C. = Simple cubic; B.C.C. = Body-centered cubic; F.C.C. = Face-centered cubic; S.T. = Simple tetragonal; B.C.T. = Body-centered tetragonal; Tetr. = Tetragonal; Hex. = Hexagonal; Orth. = Orthorhombic.

† Powder pattern not free from superimposed extraneous lines.

data obtained through metallography, thermal analysis and/or dilatometry. With very few exceptions, the combination of all types of experimental results has provided a reasonably certain indication of composition. In a number of instances the exact composition of a compound is still in doubt, however, and these cases are indicated by a question mark in parentheses following the formula of the compound in the first column of Table I. In no instance is the question mark intended to suggest uncertainty regarding the existence of the compound having approximately the indicated formula.

For 5 of the 11 powder patterns it is believed that a complete listing of valid *d*-values and observed intensities has been obtained. In 6 cases, however, the powder pattern of the phase has never been obtained free from superimposed and interfering lines of other phases, so that for these compounds there does not exist at the present time a tabulation of powder data known to be both complete and free from extraneous values. The 6 cases are indicated in Table I by a dagger following the word "pattern."

Most of the structure types listed in Table I will be found in the Strukturbericht.[5] Structure types that do not appear there are $PuAl_3$, UAl_4, Pu_2C_3, U_6Mn, $ThSi_2$, PuH_3, UHg_3, UHg_4, $CaZn_5$ and Th_2Ni_{17}. In the next section of this paper, the structures of $PuAl_3$ and PuH_3 are discussed, and references are given for the other types not found in Strukturbericht.

In establishing the isostructuralism of a plutonium compound with a known structure type, calculated interplanar spacings and calculated intensities for the plutonium compound were compared with experimental values. If possible the plutonium compound was compared with an isostructural uranium compound rather than with a structure type containing

lighter elements. Comparison with a uranium compound is especially preferable if the structure description involves variable atomic parameters. In only one instance, $PuAl_4$, was an attempt made to determine a new value of a parameter for the plutonium compound, but in all cases it was considered that atomic positions determined for the uranium compound would provide the best intensity check in confirming the isostructuralism of a plutonium phase. The following structure types listed in Table I require the evaluation of variable atomic parameters in their descriptions: $PuAl_3$, UAl_4, $NaZn_{13}$, Pu_2C_3, Fe_2P, U_6Mn, $ThSi_2$, PuH_3, UHg_4(?), Th_2Ni_{17}, La_2O_3, Mn_2O_3 and FeB.

Regarding the limits of error indicated for the unit-cell dimensions in Table I, it may be stated that in most cases the uncertainty values are not standard deviations but are indications of the quality of the diffraction patterns, and the resultant accuracy with which individual films could be measured and dimensions computed. The claims to precision should be regarded as conservative. In a few instances (those showing the lowest precision) unit-cell sizes were obtained from single-crystal patterns. But in other cases for which low precision is apparent, only powder patterns of poor quality could be obtained.

For compounds that were found to have either undetectable or negligibly small ranges of homogeneity, only one unit-cell size is given, and a small range of uncertainty is usually indicated. For phases having larger homogeneity ranges, extreme values of the unit-cell size are listed if known. For a few compounds, such as PuC and PuO, excellent powder patterns can be obtained and high precision can be ascribed to the results calculated for any one specimen. But because of variations in composition, appreciably different dimensions will be obtained for different specimens, and the composition differences are generally unknown. (PuC, PuN and PuO have appreciable mutual solid solubility, as well as homogeneity ranges for each binary phase, and differences in content of C, N and O are difficult to control or to determine.) Larger uncertainty is indicated for the unit-cell dimensions of several compounds that are subject in this way to unknown variations in composition.

DISCUSSION OF THE STRUCTURES

$PuAg_3$

The crystal structure of this compound has been determined by Runnalls at the Chalk River Project, but its description has not yet been published. We have prepared only one alloy specimen having approximately the composition $PuAg_3$. Its powder pattern appeared to indicate the presence of two phases, the predominant one being face-centered cubic with a unit-cell size larger than that of pure silver but rather small for $PuAg_3$ and $AuCu_3$ type. We suspect that our sample may contain significantly more than 75 atomic per cent silver.

Pu_3Al

This phase has a structure that was first observed for $SrPb_3$. It is a tetragonal distortion of the cubic $AuCu_3$ structure with axial ratio greater than one, and in this compound the two kinds of atoms appear to be only partially ordered. (See the discussion of $PuGe_3$, etc.)

PuAl

The powder pattern of this phase appears to be a simple one, but it has never been obtained free from the superposed patterns of other phases.

$PuAl_2$

Runnalls obtained the value, $a = 7.831 \pm 0.005$ Å, for this compound. It is perhaps worth noting that the unit-cell size is smaller when this phase contains a larger proportion of the larger plutonium atoms. To explain a similar situation for NiAl, Bradley and Taylor[6] have proposed that the increase in the proportion of larger atoms (aluminum in NiAl) is accompanied by an increase in vacant atom sites, so that the over-all result is a decrease in the size of the unit cell.

$PuAl_3$

The crystal structure of this compound was studied by Stambaugh while at Los Alamos during 1951-52. The unit-cell dimensions given in Table I are values that he obtained from a Weissenberg photograph. From rotation patterns, Runnalls obtained the values, $a = 6.08 \pm 0.01$ Å, $c = 14.40 \pm 0.03$ Å.

There is a significant reason why the structure of $PuAl_3$, but no other new structure among plutonium intermetallic phases, was investigated both at Los Alamos and at Chalk River. The rather close relationship of $PuAl_3$ to UAl_3 is immediately apparent from a comparison of the powder patterns of the two compounds, and is a relationship that made the task of finding an approximate solution for $PuAl_3$ easier than is ordinarily the case for the determination of a new structure. Disconcertingly, the investigators at Chalk River and at Los Alamos obtained different answers for this compound, but the discrepancy between the two solutions represents only a small difference in atomic positions.

UAl_3 has the simple cubic, ordered $AuCu_3$ structure. If one does not distinguish between uranium and aluminum atoms, this may be regarded as a close-packed arrangement having close packing of atoms in the (111) planes, and having (111) planes stacked in a [111] direction with equal separation (d_{111}) between any two adjacent planes. To designate the stacking sequence, or the positions occupied by atoms in successive (111) planes, as [ABC] ABCA . . . is a commonly employed and quite generally understood manner of describing the atomic configuration in cubic close packing. The approximate solution for $PuAl_3$ differs from the cubic UAl_3 structure in that the stacking sequence is [*ABCACB*]

$ABCAC\ldots$, which describes a type of hexagonal close packing having c/a three times the axial ratio that is characteristic of the ordinary $[AB]ABA\ldots$ form of hexagonal close packing. This approximate solution was the atomic arrangement first deduced at Los Alamos and is the structure that Runnalls has reported for $PuAl_3$. It is illustrated in Fig. 1 and is described† in space group $P6_3mmc$ by placing 2 Pu_I atoms in (b), 4 Pu_{II} atoms in (f) with $z_1 = 1/12$, 6 Al_I atoms in (h) with $x_1 = 1/2$, and 12 Al_{II} atoms in (k) with $x_2 = 1/6$ and $z_2 = 7/12$. (Runnalls described this structure in terms of equivalent positions in space group $P\bar{6}m2$, but the configuration is the same.)

It is apparent that for a sequence $[ABCACB]\ A\ldots$ of planes stacked in the [00·1] direction, if the configuration of atoms is the same in each plane, and if the distance between any two adjacent planes is the same, X-ray reflections will vanish for all orders to 00·1 except 00·6n (n = an integer). Runnalls must have considered that this condition was met by his rotation patterns for $PuAl_3$. But in our Weissenberg patterns it was observed that weak spots were present for 00·4, 00·8, 00·10, 00·14 and 00·16, a result indicating that the distance between planes B and C is slightly different from the distance between planes A and B and between planes A and C. Because this feature of the structure is in question, we are currently obtaining new experimental evidence. It is hoped that the new data will lead to calculations of new values of z for the 4 Pu_{II} atoms in (f) and the 12 Al_{II} atoms in (k). The new values are expected to differ only slightly from 1/12 and 7/12, respectively.

Runnalls has noted that, if in $PuAl_3$ the distances between close-packed planes were all equal, and the same as the distance between close-packed planes in UAl_3, then the value of c in $PuAl_3$ would be 14.90 Å instead of the smaller observed value (c = 14.5 Å in Table I). He attributes the contraction in the c direction of $PuAl_3$ to a mutual attraction between plutonium atoms in B planes (across BAB) and in C planes (across CAC).

Because of differences in atomic surrounding (considering both plutonium and aluminum atoms, see Fig. 1), it does seem reasonable to consider that the attraction of atoms in B planes for atoms in C planes, and vice versa, is greater than the interatomic attraction between A and B planes and between A and C planes. This condition would cause the BC distance to be less than the AB and AC distance, or in other words, it would make z_1 less than 1/12 and z_2 less than 7/12.

Figure 1. The unit cell of an approximate crystal structure solution for $PuAl_3$. The darker spheres are plutonium atoms; the lighter spheres are aluminum atoms

Stambaugh found, however, that the values, z_1 = 0.088 ± 0.002 for the 4 Pu_{II} atoms in (f), and z_2 = 0.588 ± 0.002 for the 12 Al_{II} atoms in (h), gave satisfactory agreement between calculated and observed intensities for all orders of 00·2n. But it has not been shown that this is a unique solution, and the obtaining of satisfactory intensity checks for all HK·L was not completed.

$PuAl_4$

The unit-cell dimensions given in Table I were obtained from Weissenberg patterns. From three rotation photographs Runnalls obtained the values, a = 4.42 ± 0.02 Å, b = 6.26 ± 0.02 Å, c = 13.66 ± 0.03 Å.

Singer, while working at Los Alamos during 1949–50, undertook to determine the structure of $PuAl_4$ before knowledge of Borie's[7] work on UAl_4 had reached us. From single-crystal patterns he obtained the unit-cell dimensions and space group, and he had made notable progress by Fourier methods when communication with Borie enabled him to complete the determination by taking account of the isostructuralism of UAl_4 with $PuAl_4$. Singer ultimately concluded that the value, z = 0.113 for the 4 plutonium atoms in (e) of space group Imma, gave better intensity agreement than did z = 0.111, the parameter which Borie reported for the uranium atoms in UAl_4.

† For the special values, $x_1 = 1/2$ in (h), and $x_2 = 1/6$ in (k), the atomic positions in this structure may be expressed as follows:

2 Pu_I: ± (0,0,1/4)

4 Pu_{II}: ± (1/3,2/3,z_1; 2/3,1/3,1/2+z_1) with $z_1 = 1/12$

6 Al_I: ± (1/2,0,1/4; 0,1/2,1/4; 1/2,1/2,1/4)

12 Al_{II}: ± (1/6,1/3,z_2; 2/3,5/6,z_2; 1/6,5/6,z_2; 1/6,1/3,1/2-z_2; 2/3,5/6,1/2-z_2; 1/6,5/6,1/2-z_2) with-z_2 = 7/12.

$PuBe_{13}$

It has been found at both Chalk River and Los Alamos that this phase has a measurable range of homogeneity. We have obtained a good value of the unit-cube edge for only the Be-rich limit. Runnalls found 10.284 ± 0.001 Å for the Be-rich limit and 10.278 ± 0.001Å for the Pu-rich limit. Here again, as with $PuAl_2$, the unit cell is smaller for the higher concentration of larger atoms.

Because plutonium emits alpha particles and beryllium has a strong (α,n) reaction, $PuBe_{13}$ makes a very satisfactory neutron source. Although its total yield of neutrons per second per cubic centimeter is less than that of mechanical mixtures of Po-Be or Ra-Be, it possesses a number of advantages over the stronger sources. Chief among these is its greater stability, which derives from the fact that the half-life of Pu^{239} is 24,300 years. Another important characteristic of $PuBe_{13}$ is that it is the only commonly employed neutron source ($U^{233}Be_{13}$ would also be such a substance) for which a specified weight of source material has a known and predictable neutron yield. Stewart[8] has pointed out that, Po-Be and Ra-Be being mixtures, the total yield and the neutron spectrum of these sources vary with the particle size of their constituents and with the character of mixing.

Stewart, who began her study of $PuBe_{13}$ at Los Alamos in 1950, has determined its neutron spectrum, and by integration of the energy distribution she obtained 6.1×10^4 neutrons per second per gram for the total yield. In view of the possibilities for error in her method, this result appears to be in reasonably good agreement with an average value, 6.8×10^4 n/sec/gm, obtained by comparing several specimens of $PuBe_{13}$ with Los Alamos secondary standards. The density that Stewart reports for her source, 3.7 gm/cm^3, is the bulk density of compressed powder. As indicated in Table I, the true density of $PuBe_{13}$ is appreciably higher.

PuBi and $PuBi_2$

The properties of Pu-Bi phases are such that it is extremely difficult to prepare X-ray diffraction specimens and obtain their patterns. Our securing of an unequivocal powder pattern for PuBi was largely fortuitous; and although other Pu-Bi powder patterns were also found, none of these has indicated isostructuralism of $PuBi_2$ with UBi_2. Metallographic and thermal-analysis evidence has appeared to indicate quite strongly, however, that a compound having the composition $PuBi_2$ exists.

PuC and Pu_2C_3

Both of these carbides were studied by Zachariasen[8] during the war years. The NaCl structure of PuC he determined immediately. The structure solution for Pu_2C_3 he completed later.[10] (See the last paragraph of "Discussion of Table I" for comments regarding the variable composition of PuC.)

Pu_3Co

A good powder pattern of this phase appears to have established its existence unequivocably. Although the composition has not yet been fixed, it appears to lie in the range, Pu_3Co to Pu_4Co.

Pu_2Co

The reason that the assignment of the Fe_2P structure type to Pu_2Co is now regarded as "tentative" is that an intensity check has not yet been computed. When this is done, it is believed that Pu_2Co will be shown to have the Fe_2P structure.

PuCu, $PuCu_3$ and $PuCu_7$

It is with some misgiving that these compounds have been included in Table I. Metallographic evidence has indicated that three intermediate phases exist in the Pu-Cu system, and the formulas have been assigned purely on the basis of microscopic evidence. The metallographic specimens appeared, however, to be rather badly segregated. X-ray powder patterns corroborate the conclusion that three Pu-Cu compounds exist, but from among the diffraction photographs a selection of unambiguous powder lines for each phase has not been made.

Pu_6Fe

The type structure, U_6Mn, was determined by Baenziger, *et al.*[11]

$PuGe_3$, Pu_3In, $PuPb_3$ and $PuSn_3$

These four compounds all have the face-centered cubic "phase structure" of $AuCu_3$. The true lattice of the two that appear to be fully ordered, $PuGe_3$ and $PuSn_3$, is, of course, simple cubic. The powder patterns of these two were found to contain the simple-cubic superlattice lines having intensities (relative to the intensities of the "face-centered" lines) that are characteristic of complete ordering of the Pu and group IVB atoms. Because $PuGe_3$ and $PuSn_3$ are not known to disorder at any temperature, they might best be described as simple cubic, without reference to ordering or a face-centered cubic "phase structure."

No superlattice lines could be found on the powder films of $PuPb_3$, but because of the rather small difference in scattering powers of Pu and Pb atoms, the superlattice reflections may have been too weak to be detected. It seems likely, however, that in $PuPb_3$ at room temperature the Pu and Pb atoms are fully disordered, so that only the face-centered cubic pattern is obtained.

The powder pattern of Pu_3In showed superlattice lines, but with intensities uniformly lower than would be required if this phase were fully ordered, simple cubic. The reduced intensity of the superlattice lines has been interpreted, in accordance with the theory of Bragg and Williams[12] to mean that there is partial ordering of the atoms. A similar reduced intensity of superlattice lines in the powder pattern of Pu_3Al

was also interpreted to indicate only partial ordering in this tetragonal phase.

Pu_2Ge_3 and Pu_2Si_3

During the war, Kaufmann *et al*[13] investigated the uranium-silicon phase diagram. They determined the structure of USi_3 and reported the existence of a series of additional uranium silicides that were tentatively identified as USi_2, U_2Si_3, USi, U_5Si_3 and $U_{10}Si_3$. Zachariasen[4] later obtained crystal-structure solutions for all of the compounds other than USi_3, and he revised the formulas of U_2Si_3, U_5Si_3 and $U_{10}Si_3$ to β-USi_2, U_3Si_2 and U_3Si, respectively. He then applied the designation α-USi_2 to the tetragonal form of USi_2, which he had studied earlier.[3]

According to generally accepted alloy diagram usage, to designate two different uranium-silicon phases as α-USi_2 and β-USi_2 implies that both have the same (or very close to the same) composition, and that each will transform to the other congruently at constant temperature (or within an extremely narrow range of temperature). In any case, two phases so labelled would not be expected to coexist under equilibrium conditions throughout a two-phase field having appreciable area in the phase diagram, i.e., either a wide composition range or an extensive temperature range.

In view of the tentative character of the formulas assigned by Kaufmann, *et al.*, to the uranium silicides, it was, of course, logical for Zachariasen to change the formula of the nominal U_2Si_3 to correspond to that of its structure type, AlB_2. On the other hand, it would appear that experimental evidence obtained by Kaufmann, *et al.*, must have provided some degree of justification for them to have drawn the phase diagram so as to show a two-phase field of U_2Si_3 plus USi_2 extending from 60 to 67 atomic per cent silicon, and from room temperature to over 1600°C. It is our opinion that when further work is done in this region of the uranium-silicon diagram, it will be found that a two-phase field of U_2Si_3 plus USi_2 does, in fact, exist, and that a more satisfactory designation than "β-USi_2" would be U_2Si_3, AlB_2 type, space group $P6/mmm$ with 1 U in (0,0,0,) and 1.5 Si (instead of 2 Si) in $\pm$ (1/3,2/3,1/2).

Zachariasen[4] has given 52.6 Å^3 as the volume of the unit cell in β-USi_2. Dividing this volume among three atoms gives 17.5 Å^3 per atom. He has compared this value with 18.0 Å^3 per atom in α-USi_2, with 21.1 Å^3 in USi, and with 20.6 Å^3 and 19.8 Å^3, the volume requirements of uranium and silicon atoms, respectively, in the structures of the elements. Dividing 52.6 Å^3 by 2.5 (the number of atoms in the U_2Si_3 unit cell) gives 21.0 Å^3, a value that seems to fit into the series as well as 17.5 Å^3.

The low scattering power of silicon relative to uranium would seem to make it quite unfeasible to distinguish between the effects of 2 Si or 1.5 Si in intensity calculations. Because the scattering power of germanium is greater than that of silicon, we have calculated intensities for Pu_2Ge_3 based on 1.5 Ge atoms in the AlB_2 unit cell, and we obtained satisfactory agreement with observed intensities. For this reason, and others that are stated in the next paragraph, we prefer the formulas Pu_2Si_3 and Pu_2Ge_3 to β-$PuSi_2$ and β-$PuGe_2$.

The chemical analysis (4 determinations) of a specimen that gave a powder pattern of Pu_2Si_3 quite free from PuSi or other extraneous lines showed a silicon content of only 60.5 $\pm$ 1.0 atomic per cent Si, rather than 67 atomic per cent, required to agree with $PuSi_2$. Also, we have obtained many powder patterns, representative of what we believe to be equilibrium conditions, that show Pu_2Si_3 and $PuSi_2$ coexisting throughout an appreciable temperature range and throughout the composition range of 60 to 67 atomic per cent Si.

Although we obtained acceptable intensity checks for 36 calculated lines of Pu_2Ge_3 when they were compared to the 36 corresponding lines in our observed pattern, all of our films for both Pu_2Si_3 and Pu_2Ge_3 have consistently shown several rather weak lines that are not included among these 36, and which cannot be accounted for by an AlB_2 type of unit cell. Although we have not yet found an acceptable solution, a proper multiplication of the dimensions of the AlB_2 unit appears to provide a means of explaining the weak lines. For this reason we have regarded the AlB_2 unit as a pseudo-unit, and in Table I have designated the structures of Pu_2Ge_3 and Pu_2Si_3 as pseudo-AlB_2 type. Our dimensions for the pseudo-unit are: $a = 3.975 \pm 0.002$ Å, $c = 4.198 \pm 0.002$ Å, $c/a = 1.056$, for Pu_2Ge_3; and $a = 3.876 \pm 0.002$ Å, $c = 4.090 \pm 0.002$ Å, $c/a = 1.055$, for Pu_2Si_3. Assuming formula units $PuGe_{1.5}$ and $PuSi_{1.5}$, the calculated densities are 10.06 gm/cm^3 and 8.77 gm/cm^3, respectively.

While this paper was being written, a communication was received from Runnalls and Boucher[14] on "The Crystal Structure of β-$PuSi_2$." It is interesting to note that their specimen had an "approximate composition Pu_2Si_3." They further state that "the line spacings and intensities were similar to those published for a uranium silicide, nominally of composition U_2Si_3, but described by the formula β-USi_2 as a result of Zachariasen's X-ray analysis. The Pu-Si phase has been labelled β-$PuSi_2$ to conform with the latter terminology." Powder diffraction data are reported in a table, together with calculated intensities based on the AlB_2 structure. It is concluded that "since the observed and calculated intensities are in reasonable agreement . . . β-$PuSi_2$ has the AlB_2 structure." Unit-cell dimensions are reported to be: $a = 3.884 \pm 0.003$ Å, $c = 4.082 \pm 0.003$ Å, ($c/a = 1.051$).

Their tabulated data show only observed $\sin^2\theta$ values that correspond to their calculated values for an AlB_2 type of unit cell. In other words, it appears that they observed none of the weak extra lines which we have found in all of the patterns of either Pu_2Si_3 or Pu_2Ge_3 that we have obtained so far. Their

unit-cell dimensions (and axial ratio) differ considerably from those that we have obtained for Pu_2Si_3 and Pu_2Ge_3, and thereby suggest that their specimen has a slightly different composition from any that we have studied. Although our extra lines cannot be explained by any of the patterns of neighboring phases in the Pu-Si or Pu-Ge systems, by oxides, or by any of the other familiar impurities, we realize that weak extra lines may be extraneous to the principal diffraction pattern and may therefore be misleading. It appears that only further investigation can resolve the discrepancy.

$PuGe_2$ and $PuSi_2$

The type structure is $ThSi_2$, determined by Brauer and Mitius.[15] The unit-cell dimension given in Table I are for Ge-rich and Si-rich limits of the respective homogeneity ranges. In the case of the Pu-rich solid solution in $PuSi_2$ we have observed a splitting of the high-angle lines of the powder pattern, which appears to indicate a change of structure in this composition range. The same effect may exist for Pu-rich $PuGe_2$, but we have not yet observed it.

$PuH_{2.0}$–$PuH_{2.7}$

This solid-solution phase formed by hydrogen with plutonium was the first to be discovered of a series of isostructural phases, the other members of which are formed by hydrogen with rare-earth elements. Holley *et al.*[16] have described the crystal structure of the latter, and Mulford and Sturdy[17,18] have reinvestigated the phase equilibria of plutonium and hydrogen.

The positions of the hydrogen atoms were determined for both ends of the homogeneity range, $MH_{2.0}$ to $MH_{2.7}$, by a neutron diffraction study of cerium deuteride. The composition MH_2 was found to have the CaF_2 structure. As additional hydrogen is taken into solid solution, the structure approaches that of a hypothetical face-centered cubic MH_3 having four H_{II} atoms per unit cell in the positions 1/2,0,0; 0,1/2,0; 0,0,1/2; 1/2,1/2,1/2; in addition to the eight H_I atoms in the fluorine positions and the four metal atoms in the calcium positions (0,0,0, etc.) of CaF_2. In the case of plutonium hydride the H_{II} positions are never filled, because at about $PuH_{2.75}$ the structure begins to transform to hexagonal PuH_3.

It is interesting to note that, throughout the entire solid-solution range, the unit-cell size of both plutonium hydride and the rare-earth hydrides decreases as the hydrogen content increases.

PuH_3

This compound might be regarded as the hexagonal analog of the hypothetical cubic PuH_3 described in the preceding section. In the true PuH_3 (GdH_3 and SmH_3 are isostructural with PuH_3) the metal atoms have hexagonal instead of cubic close packing, and, as in the cubic "PuH_3," the hydrogen atoms occupy positions in two different sizes of interstices among the metal atoms. For hexagonal PuH_3, Zachariasen has suggested the following probable structure in space group $P6_3/mmc$:

2 Pu in (c): $\pm$ (1/3,2/3,1/4)

2 H_I in (b): $\pm$ (0,0,1/4)

4 H_{II} in (f): $\pm$ (1/3,2/3,z; 2/3,1/3,1/2+z) with $z = 0.607$.

The correctness of this structure has not yet been proved by neutron-diffraction study of a rare-earth deuteride, but it may be noted that a similar prediction for the structure of cubic "PuH_3" was made before it was confirmed by neutron diffraction.

$PuHg_3$ and $PuHg_4$

Powder patterns have been obtained which establish the isostructuralism of these phases with UHg_3 and UHg_4, but the unit-cell dimensions have not been computed. We have not determined whether plutonium forms $PuHg_2$, isostructural with UHg_2. The structures of UHg_2, UHg_3 and UHg_4 have been studied by Rundle and Wilson.[19]

Pu_2Mg and $PuMg_2$

These phases were formed under conditions such that knowledge of their compositions could be deduced only from their X-ray diffraction patterns. The apparent fluorite structure of Pu_2Mg seems to establish its composition rather firmly, but the composition of $PuMg_2$ must be regarded as questionable.

$PuNi_5$

The type structure is $CaZn_5$, determined by Haucke.[20]

Pu_2Ni_{17}

The type structure is Th_2Ni_{17}, described by Florio and Rundle.[21]

Oxides of Plutonium

The crystal structures of PuO, PuO_2 and cubic Pu_2O_3 were determined by Zachariasen.[3,22] Only the structure of hexagonal Pu_2O_3 was established by others, by Ellinger at Los Alamos in 1949, and independently by Templeton and Dauben[23] at the University of California Radiation Laboratory in 1952. The latter investigators obtained the unit-cell dimensions, $a = 3.840 \pm 0.004$ Å and $c = 5.957 \pm 0.006$ Å.

$PuSi_2$

See discussion of $PuGe_2$ and $PuSi_2$.

Pu_3 and PuU

These phases have homogeneity ranges, and the unit-cell sizes listed in Table I were determined as closely as possible for the stoichiometric compositions indicated. The crystal lattice of Pu_3U is given in Table I as "apparently S.C." because we have not been able to obtain a good powder pattern of this phase. Presumably, because of inhomogeneity of the

specimen, the powder lines were broad and were not measurable beyond about $\sin^2\theta = 0.36$. For this reason we do not feel certain that, if the broad Debye lines could be sharpened, a somewhat different structure might not be revealed.

We have obtained much better powder patterns of PuU, and the unit cell of this phase appears to be a cube at room temperature. But it manifests the anomalous behavior of expanding anisotropically when heated. The lines of its powder pattern split in exact accordance with tetragonal symmetry. For this reason it seems likely that the crystal structure of PuU may be tetragonal with $c/a = 1.000$ at room temperature.

ACKNOWLEDGEMENTS

With very few exceptions, all of the compounds of plutonium with metallic elements were prepared by V. O. Struebing. A. E. Gorum prepared the compounds of plutonium with phosphorus, arsenic and tellurium, and determined their crystal structures. Mr. Gorum also contributed to the preparation and study of the plutonium-silicon and plutonium-germanium phases. The crystal structure by $PuAl_3$ was studied by C. K. Stambaugh, and that of $PuAl_4$ by J. Singer. The first preparations of $PuBe_{13}$ were made by C. R. Tipton and R. D. Moeller. E. M. Cramer performed and interpreted a major portion of the metallographic work that was a powerful aid in phase identification. Many other members of the plutonium physical metallurgy group at the Los Alamos Scientific Laboratory have participated in the development and use of melting, thermal-analysis, dilatometric, metallographic and X-ray diffraction techniques that have been employed in phase-diagram investigations of plutonium alloys.

REFERENCES

1. Westrum, E. F., Jr., Paper 6.5 of *The Transuranium Elements,* National Nuclear Energy Series, Division IV, Volume 14B, McGraw-Hill Book Company, Inc., New York (1949).
2. Seaborg, G. T. and Katz, J. J., *The Actinide Elements,* National Nuclear Energy Series, Division IV, Volume 14A, McGraw-Hill Book Company, Inc., New York, P 427 (1954).
3. Zachariasen, W. H., Papers 20.1, 20.2 and 20.3 of *The Transuranium Elements,* National Nuclear Energy Series, Division IV, Volume 14B, McGraw-Hill Book Company, Inc., New York (1949).
4. Zachariasen, W. H., Acta Cryst. *2*: 94-99 (1949).
5. *Strukturbericht,* Volumes I-VII, Akademische Verlagsgesellchaft, M.B.H., Leipzig (1931-43).
6. Bradley, A. J. and Taylor, A., Proc. Roy. Soc. (London), *A159*: 56-72 (1937).
7. Borie, B. S., Jr., Trans. Am. Inst. Min. Met. Eng., *191*: 800-802 (1951).
8. Stewart, L., Phys. Rev. *98*: 740-743 (1955).
9. Segré, E. and Wiegand, C., *Thick-target Excitation Functions for Alpha Particles,* US AEC Report LA-136 (MDDC-185), (1944).
10. Zachariasen, W. H., Acta Cryst. *5*: 17-19 (1952).
11. Baenziger, N. C., Rundle, R. E., Snow, A. I. and Wilson, A. S., Acta Cryst. *3*: 34.40 (1950).
12. Bragg, W. L. and Williams, E. J., Proc. Roy. Soc. (London) *A145*: 699 (1934); *A151*: 540 (1935).
13. Kaufmann, A. R., Cullity, B. D. and Bitsianes, G., unpublished information (1945). See: Saller, H. A. and Rough, F. A., *Compilation of US and UK Uranium and Thorium Constitutional Diagrams,* US AEC Report BMI-1000 (1955).
14. Runnalls, O. J. C. and Boucher, R. R., *The Crystal Structure of β-$PuSi_3$,* to be published in Acta Cryst.
15. Brauer, G. and Mitius, A., Z. anorg, Chem. *249*: 325 (1942).
16. Holley, C. E., Jr., Mulford, R. N. R., Ellinger, F. H., Koehler, W. C. and Zachariasen, W. H., *The Crystal of Some Rare Earth Hydrides,* to be published in J. Phys. Chem.
17. Mulford, R. N. R. and Sturdy, G. E., *The Plutonium-Hydrogen System, I: Plutonium Dihydride and Dideuteride,* to be published in the 20 June 1955, issue of J. Am. Chem. Soc.
18. Mulford, R. N. R. and Sturdy, G. E., *The Plutonium-Hydrogen System, II: Solid Solution of Hydrogen in Plutonium Dihydride,* to be published.
19. Rundle, R. E. and Wilson, A. S., Acta Cryst. *2*: 148-150 (1949).
20. Haucke, W., Z. anorg. allgem. Chem. *244*: 17-22 (1940).
21. Florio, J. V. and Rundle, R. E., *Compounds of Thorium with Transition Metals of the First Period,* US AEC Report ISC-273 (1952).
22. Zachariasen, W. H., Acta Cryst. *2*: 388-390 (1949).
23. Templeton, D. H. and Dauben, C. H., *The Crystal Structures of NpC and Pu_2O_3,* US AEC Report UCRL-1886 (1952).

Thermal Cycling Effects in Uranium

By H. H. Chiswik and L. R. Kelman,* USA

Polycrystalline uranium metal has been found to undergo substantial dimensional and structural changes when subjected to repeated heating and cooling in the alpha-phase temperature range (room temperature to 660°C). In cast metal the dimensional changes manifest themselves in the form of surface roughening; in wrought metal, such as rolled rod, wire, or plate fabricated in the alpha-phase temperature range, the dimensional changes take the form of substantial elongations, generally in directions coincident with the direction of working of the metal. The phenomenon may also be described as "growth." Examples of this behavior are illustrated in Fig. 1, which shows the surface roughening of a smooth cast cylindrical specimen, the growth of some plate specimens, and the growth of a 300°C-rolled specimen to nearly six times its original length when subjected to 3000 thermal cycles between 50°C and 550°C. Accompanying these macro-deformations there are also microstructural changes taking place, the chief features of which are a break-up of the grain structure and a development of porosity with a corresponding decrease in density.

The extent of these deformations and structural changes is a function of the number of cycles to which the material is subjected and is dependent upon a number of variables which may be divided into two main categories: (*a*) material variables, and (*b*) cycling variables. Among the material variables, the most important are preferred orientation, grain size, and chemical composition; the cycling variables include such considerations as the temperature limits of the cycle, the cycling range, the rate of heating and cooling, and the time of holding at each temperature limit. The effects of each of these variables on the deformation process are discussed in detail in the text and are followed at the end by a description of the mechanisms or models that have been proposed to account for this phenomenon.

MATERIAL VARIABLES

Effects of Preferred Orientation

That preferred orientation plays a significant role in the process can be demonstrated by a simple experiment as follows: if an alpha-rolled uranium rod which has a well-developed texture and grows considerably is beta-heat treated, the growth rate on thermal cycling is considerably reduced ("beta" heat treatment is defined as heating into the beta-phase temperature range followed by cooling to room temperature). By way of example, an alpha-rolled uranium rod may grow at a rate of 500 to 600 microinches/inch/cycle, whereas after beta treatment the growth rate is reduced to about 20 to 30 microinches/inch/cycle. The major effect of the beta treatment is to remove substantially the preferred grain orientations present in the rolled rods. Another example of the effect of preferred orientation on the extent of growth is the experimental observation that 300°C-rolled rods grow at higher rates than 600°C-rolled rods; as will be shown below, the reason for this is the development of different textures when rolled at different temperatures. These experimental observations indicate that preferred orientation is a necessary condition for unidirectional elongation to occur and that the extent of the growth depends upon the type of texture present. In randomly oriented material, microscopic plastic deformation of the individual grains also occurs, but it does not result in preferential growth in any given direction.

In addition to the "type" of texture present, the growth rate also depends upon the "degree of perfection" of the texture. In attempting to correlate degree of preferred orientation with growth, however, one is handicapped by the lack of a quantitative number to describe the degree of preferred orientation. In metallurgical research textures are usually described by pole figures, which, at best, are descriptive evaluations of the statistical distributions of the grain orientations. As an alternative, however, one can use the per cent reduction of area following the randomizing beta treatment as a measure of the degree of perfection of preferred orientation. This is illustrated with reference to a series of specimens that had been rolled to various reductions of area ranging from 3% to 74% following beta-treatment, as described in Fig. 2. In the preparation of such a series of specimens with varying degrees of preferred orientation, care was exercised in heat treatment to maintain the grain size constant, so as to divorce the effects of preferred orientation from those of grain size. In the case illustrated, the grain size was about 0.04 mm average diameter; this was accomplished by critical straining 5% at room temperature and recrystallizing at 575°C following the rolling at 300°C.

The specimens were in the form of cylinders, about ⅜ in. in diameter and approximately 1-in. long, and

* Argonne National Laboratory. Including works by R. M. Mayfield and S. T. Zegler.

were cycled between 50°C and 550°C under the following conditions: 5 minutes in the cold temperature zone, 10 minutes in the hot temperature zone, and 5 seconds transfer times between these temperature limits. (For the significance of these cycling conditions, see section below on cycling variables.) The growth rates are shown graphically in Fig. 2 by plotting the natural logarithm of the growth ratio L_N/L_0 as a function of N, where L_0 is the initial length of the specimen, N is the number of cycles, and L_N is the length after N cycles. This method of plotting, rather than the percentage increase in length based on the original length, permits an evaluation of the "instantaneous growth rate," thus taking into account the elongations occurring during cycling. The "instantaneous growth rate" may be expressed in terms of a growth coefficient G_t, which is the slope of the plot $\ln L_N/L_0$ versus N ($G_t = 1/L_N \times dL_N/dN$). To calculate G_t values at various cycling levels empirical equations of the form $\ln (L_N/L_0) = aN + bN^2$ were fitted to the curves by the methods of least squares. An equation of this form fitted the experimental points of most specimens rather well, indicating that the growth coefficient varies with N linearly at least up to the indicated values of N. In this connection it should be mentioned that at much higher values of N, of the order of 2000–3000 cycles, the slopes of such curves decrease, indicating a reduction in G_t value.

The effects of increasing the degree of preferred orientation by increasing the reductions in area are clearly evident in Fig. 2: the growth increased systematically with increasing reductions of area. Specimen No. 2, which had been rolled to a 3% reduction of area following beta treatment, increased in length 7.8% after 500 cycles, as compared with a growth of 22.9% for specimen No. 10, which had been rolled to a 74% reduction of area. It cannot be overemphasized that these specific growth rates are valid only for the cycling conditions given above; as will be shown below, changes in cycling variables can either increase or decrease these values.

The variation of the growth coefficient, G_t, with reduction of area and its dependence on cycling level is shown in Fig. 3, in which the G_t values at several cycling levels are plotted as a function of the per cent reduction of area. The growth rate increased sharply after only a few per cent reduction of area, and then more slowly as the reduction of area increased. A reduction of area of only 5% following beta treatment yielded a G_t value of 100 at $N = 0$, whereas an increase in the reduction of area from 46 to 74% raised the G_t value only slightly, from 302 to 331.

X-ray orientation studies of these specimens led to the following observations:

1. After slight reductions following beta treat-

Figure 1. Deformation of uranium specimens on thermal cycling; (a) cost rod, 8090, 300 cycles between 50 and 500°C; (b) rolled plate, M-4312, 700 cycles between 100 and 550°C, specimens were square before cycling; (c) 300°C-rolled rod, M-4631, 1300 cycles, 10926, 3000 cycles, before and after 1300 and 3000 cycles between 50 and 550°C

(before) Figure 1c 1 × (after) ½ ×

ment, the texture was nearly random with only a slight degree of preferredness in orientation.

2. As the amount of reduction increased the texture sharpened gradually, with an increase in the concentration of grains having (010) and (131) poles lying in the rolling direction.

3. The texture of the specimens with the highest reduction of area (74%) may be described as a fiber texture in which the majority of the grains have (131) poles, or poles close to the (131), lying in the rolling direction, with the remainder of the grains having poles between the (131) and (010) lying parallel to the rolling direction. These X-ray orientation results were in good agreement with measurements of the mean thermal expansion coefficients in the temperature range 25–100°C in the rolling direction and in two mutually perpendicular radial directions. As the reduction of area following beta treatment increased, the expansion coefficients in the rolling direction decreased, with a simultaneous increase

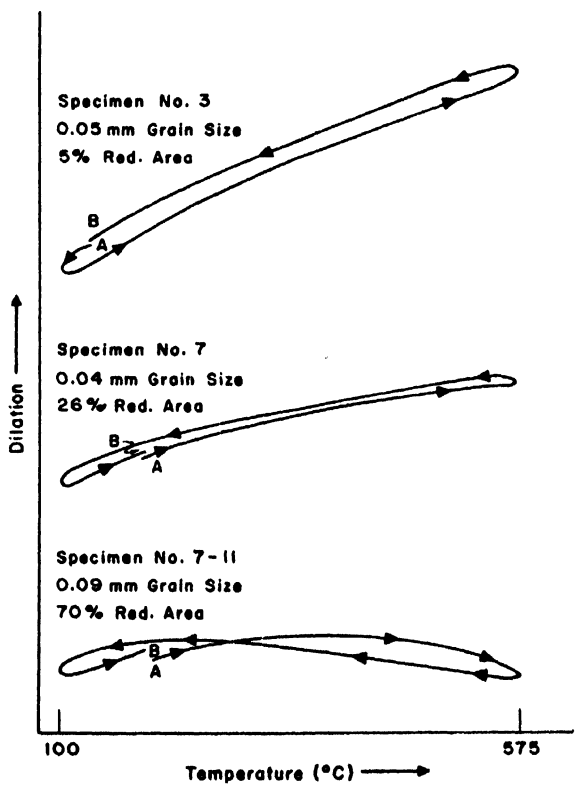

Figure 4. Typical single cycle expansion-contraction curves between 100°C and 575°C for different reductions in area

in the cross directions; this is what one would expect from a gradual alignment of the (010) poles in the rolling direction, since the [010] crystal direction has a negative expansion coefficient. It should be noted, however, that even at reductions as high as 74% the expansion coefficient in the rolling direction is still substantially positive; this is undoubtedly due to the fact that the texture centers about the (131) pole rather than the (010) pole.

Typical single cycle expansion-contraction curves between 100°C and 575°C as a function of the per

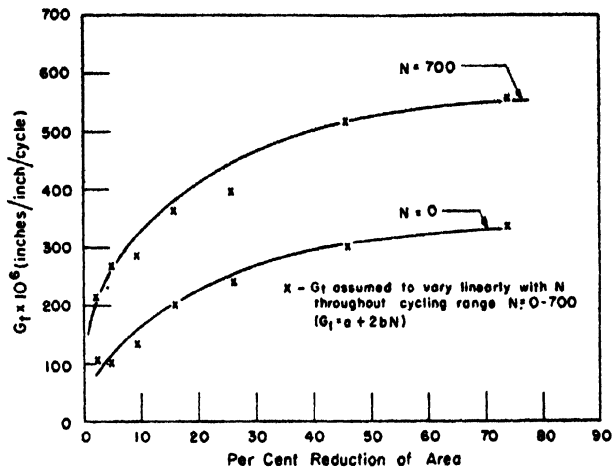

Figure 3. Effect of increasing reductions of area on growth coefficient G_t

cent reduction of area are illustrated in Fig. 4. As the reduction of area increased from 5% to 70%, the expansion coefficient became increasingly negative at the higher temperatures, and the permanent deformation per cycle increased (distance AB). It will be noted that at 70% reduction of area the length of the specimen at 575°C is actually shorter than at room temperature; this, of course, is due to the gradual alignment of the (010) poles of more and more grains in the rolling direction.

The surface appearance of such a series of specimens with constant grain size and varying preferred orientations after 500 cycles is shown in Fig. 5a. Note that the surface roughening decreased as the

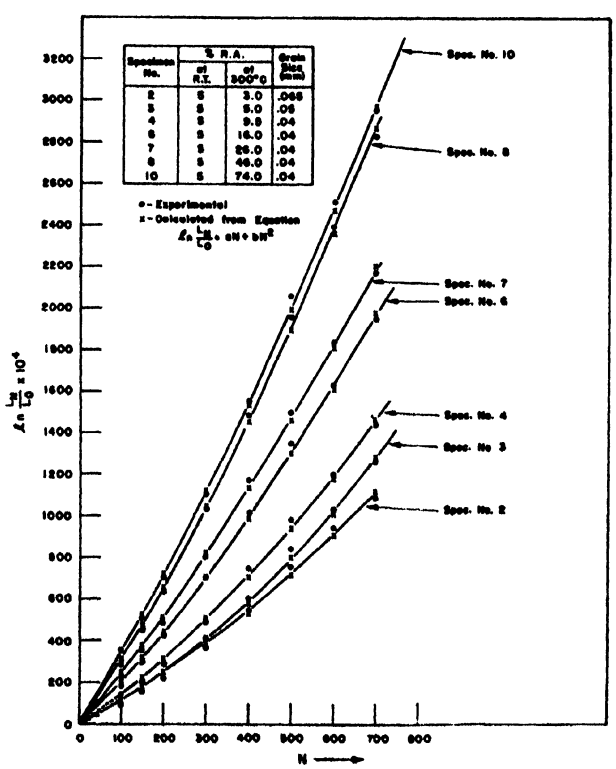

Figure 2. Plot of ln (L_n/L_0) vs N for specimens with constant grain size and variable degrees of preferred orientation

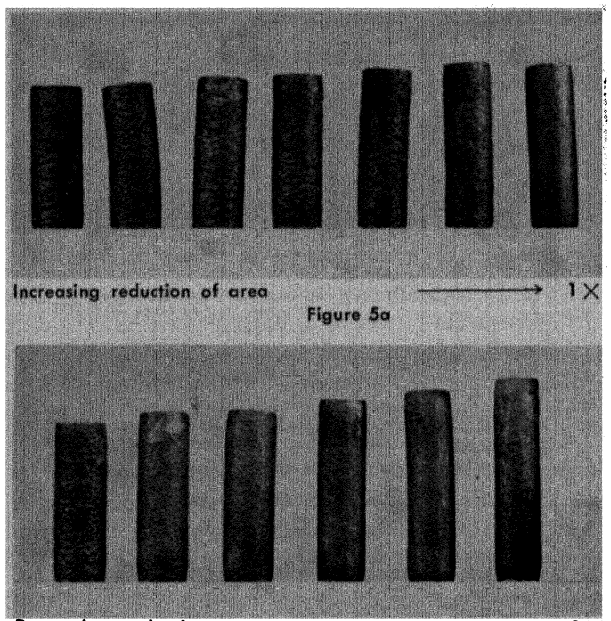

Figure 5. Macrophotographs illustrating effects of preferred orientation and grain size on growth in 500 cycles. Original lengths all 1 inch. (a) constant grain size and varying degrees of preferred orientation, M-4630; (b) constant high reductions in area and variable grain sizes, M-4629

total elongation of a specimen increased, even though the grain size was the same. It would appear, therefore, that as the tendency toward uni-directional elongation increased, the tendency for surface roughening decreased.

To exhibit the effect of a change in the "type" of texture present Fig. 6 illustrates the relative growth rates of 300°C-rolled material with a (131)-(010) texture versus a 600°C-rolled material with a (110)-(010) texture. The growth rate of material with the latter texture is considerably lower, although much of this reduction must be attributed to an increased grain size which usually results from higher temperature rolling.

Figure 6 also shows the growth rate of a specimen which has been beta treated, indicating the substantial reduction in the growth rate following such treatment. It will be noted that the growth is not eliminated entirely, even though X-ray studies indicate substantial randomization of the texture. Owing to the large grain size present after beta treatment, however, the experimental conditions for determining textures by X-ray do not permit a conclusive evaluation as to the completeness of this randomization. From a macro-property point of view, the material after beta treatment becomes essentially isotropic, as evidenced by the fact that the thermal expansion coefficients in all directions are about equal. In view of these considerations, the slight growth of beta-treated uranium may be ascribed to a remnant texture effect inherited from prior fabrication processes which is not completely eliminated in beta treatment.

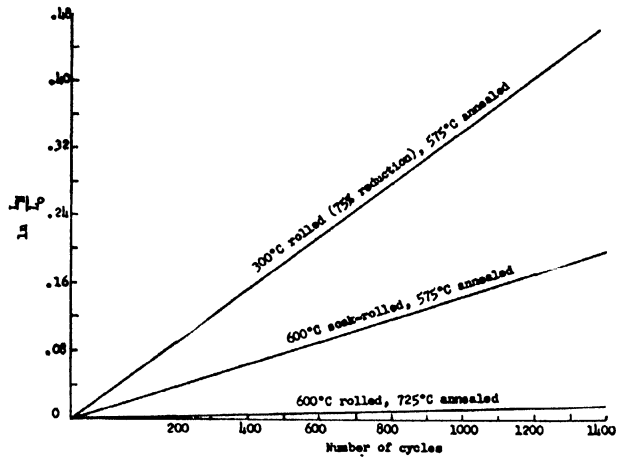

Figure 6. Elongation of 300°C-rolled, 600°C-rolled, and beta treated uranium rods due to thermal cycling between 100°C and 550°C

Effects of Grain Size

The influence of grain size on the growth rate may be illustrated with reference to a series of specimens fabricated and heat treated in such a manner as to keep the preferred orientation constant and to vary the grain size. This can be done readily by heavily cold rolling material which had been beta treated, recrystallizing it, then superimposing critical strains ranging from 1½ to 10% at room temperature, and again recrystallizing for various times in the high temperature range of the alpha phase. The growth rates of such a series of specimens of a constant preferred orientation equivalent to a 74% reduction of area and with a grain size variation from 0.01 to 0.18-

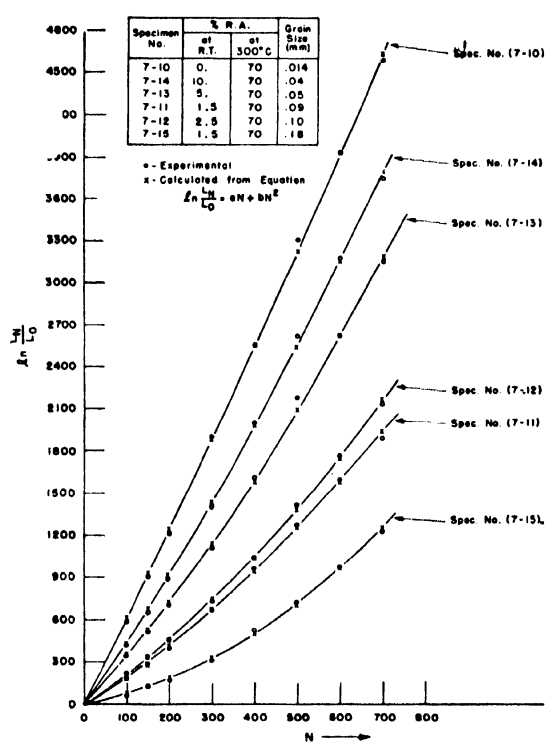

Figure 7. Plot of ln (L_n/L_o) vs N for specimens with constant high reduction of area and variable grain sizes

mm average diameter are shown in Fig. 7. The total growth in 700 cycles increased systematically with decreasing grain size; a decrease in grain size from 0.18 to 0.014 mm increased the growth in 700 cycles from 13.1% to 58.4%. The gradual increase in growth with decreasing grain size is illustrated in Fig. 5b; as in the previous set, the surface appearance improved with increase in longitudinal growth.

It is apparent from Fig. 7 that the growth coefficient increased as cycling progressed, particularly in specimens of large grain size; the variation of G_t with N is less apparent since the initial grain size is small. This dependence of the variation of G_t with N on the initial grain size may be interpreted qualitatively in terms of the marked structural changes that occur during, and as a direct result of, thermal cycling. As will be shown below, a process of subgraining akin to polygonization takes place during cycling, with each grain breaking up into a number

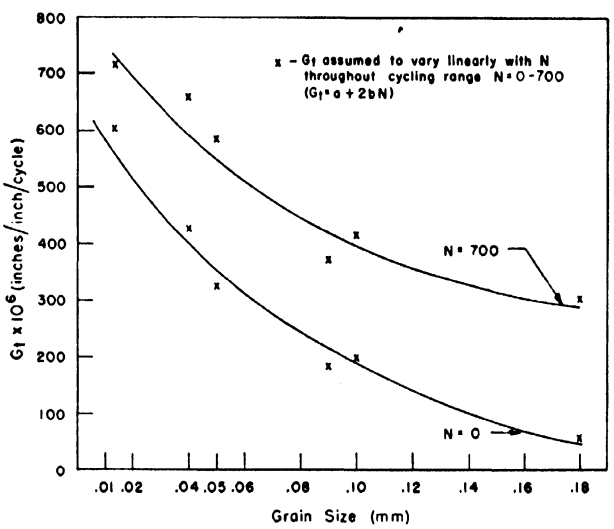

Figure 8. Effect of grain size on growth coefficient

of smaller grains differing from each other in orientation by only a few degrees. The process is most pronounced and most readily detectable microscopically in material of initially large grain size. Under conditions of a continuously changing grain size during cycling one would expect an increasing growth rate with increasing cycling level, particularly in initially large-grained material.

The variation of the growth coefficient G_t with grain size is shown at several cycling levels in Fig. 8. The pronounced effect of the initial grain size is best illustrated at $N = 0$; with an initial grain size of 0.10-mm average diameter the growth coefficient G_t was 200; decreasing the grain size to 0.014-mm average diameter raised the growth coefficient to 600.

In addition to its effect on the uni-directional growth in textured material, grain size also has an effect on the surface roughening resulting from thermal cycling; large-grained material generally shows greater surface roughening than fine-grained material. This is particularly evident in beta-treated material as illustrated in Fig. 9, which shows the greater roughening obtained in specimens which had been held for a long time in the beta-phase temperature range to allow the grains to grow as contrasted to specimens which had been held for only short periods of time in the beta phase, thereby reducing the grain size.

Effect of Chemical Composition

Additions in low concentrations of alloying elements, such as molybdenum, silicon, aluminum, titanium, zirconium, chromium and vanadium, were found ineffective in appreciably reducing the growth rate of alpha-fabricated uranium. In some cases additions of alloying elements increased the growth rate of alpha-fabricated uranium, but the increase may be interpreted as due to a smaller grain size. Carbon in concentrations up to 500–700 ppm was also found to have no effect; some experimental evidence by Seymour, Knolls Atomic Power Laboratory, however, does indicate that higher concentrations of carbon, up to 0.2 weight per cent, may reduce the growth. The alloy additions do decrease the surface roughness after a randomizing beta or gamma treatment because they promote grain refinement. To eliminate surface roughness completely, higher concentrations are often required, in some cases as high as 2 weight per cent.

As will be shown in the section on the effect of cycling on the microstructure of uranium, the porosity that develops during thermal cycling appears to be associated with the presence of inclusions. High purity uranium showed no evidence of porosity after

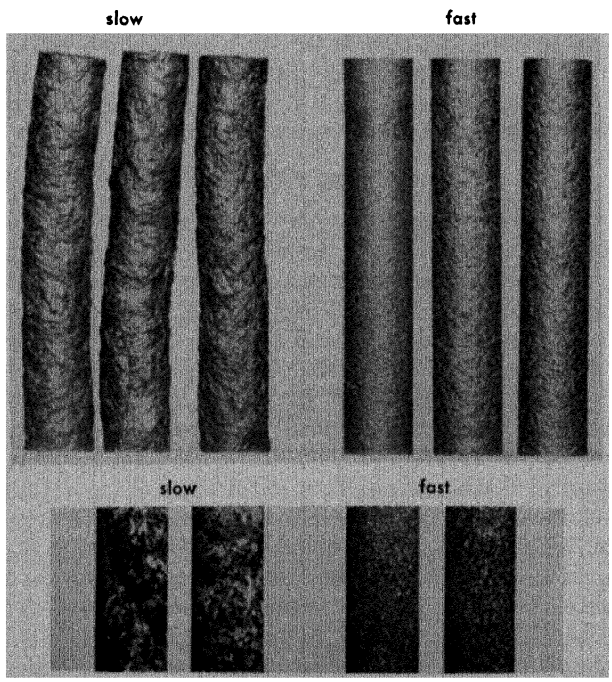

Figure 9. (a) at top, 300°C-rolled rods after 700 cycles between 100°C and 550°C (from M-4315); slow beta treatment—annealed 2 hr at 725°C; fast beta treatment—½-min dip in lead pot at 725°C and water quenched, then annealed 2 hr at 575°C. (b) at bottom, Macrostructures of the rods shown in (a) before cycling (from M-4383). Each figure 1×.

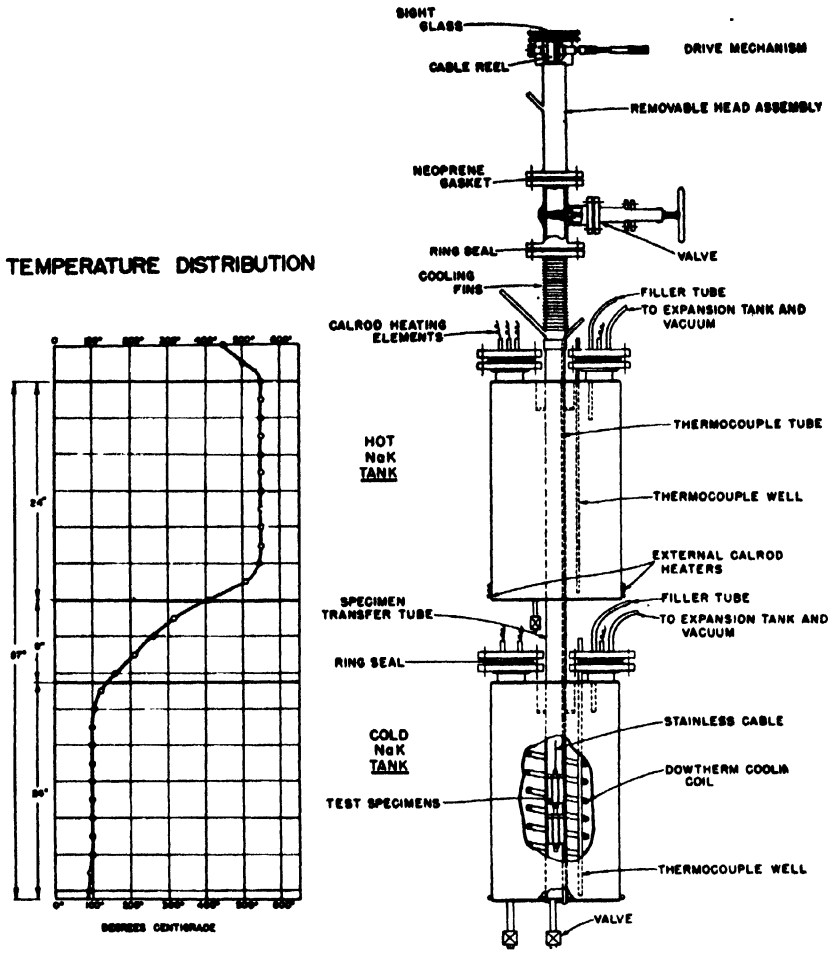

Figure 10. Schematic diagram of the vertical tube cycling unit

cycling, even though its rate of deformation under similar cycling conditions is equal to that of impure metal which developed extensive porosity.

CYCLING VARIABLES

The dimensional changes that result from thermal cycling of uranium in the alpha temperature range vary widely with the following cycling variables: (*a*) rates of heating and cooling, (*b*) temperature level, (*c*) temperature range, and (*d*) time at temperature.

Because of the importance of these cycling variables, a comparison of thermal cycling results by various investigators must take into account the method of cycling. The ensuing results on the influence of cycling variables were attained in a vertical tube cycling apparatus, shown schematically in Fig. 10, in which specimens could be cycled automatically over a wide range of conditions of temperature and time. The equipment consisted of a vertical transfer tube filled with NaK (eutectic sodium-potassium alloy) which passed through the center of two NaK-filled tanks. Thermal cycling is accomplished by automatically raising and lowering specimens between the centers of the two tanks. A typical temperature distribution plot is shown in Fig. 10. The heating and cooling rates could be varied by changing the transfer times from the center of one tank to the center of the other.

The data plotted in Figs. 11 and 12 show that the greatest growth rates per thermal cycle are obtained when slow heating and fast cooling are combined with a large temperature range of cycling. Fast heating and slow cooling result in minimum growth rates, and equal heating and cooling rates, over a wide range of values, yield intermediate growth rates.

With increasing upper cycling temperature, above about 350°C, and constant lower temperature, the growth rate increases as shown in the curves in Fig. 12. The curves verify the general relationship described above between growth rates and rates of heating and cooling. The family of curves in Fig. 13 shows conclusively that, for upper cycling temperatures above about 350°C, the greater the cycling temperature range, the greater the growth. Also, for any given temperature range the higher the temperature level, the greater the resulting growth. Although the growth rate decreases with decreasing temperature range of cycling, appreciable growths can be obtained as a result of exposing highly oriented uranium to many small thermal fluctuations in the high-alpha temperature range.

The curves in Fig. 14 indicate that the growth

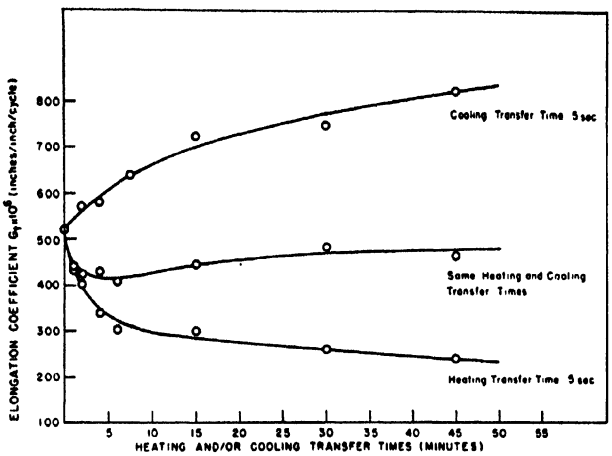

Figure 11. Effect of heating and cooling transfer times upon the elongation coefficient of 300°C rolled uranium; hot tank temp: 550°C, holding time: 5 min; cold tank temp: 50°C, holding time: 2 min

rate is also dependent upon the holding time at the upper cycling temperature. With increasing holding time above about 350°C the growth rate increases rapidly at first and then more slowly until it approaches a constant value. The higher the temperature, the shorter the time required for the growth rate to level off.

Other experiments wherein oriented uranium was given a randomizing beta treatment to minimize the degree of preferred orientation and therefore its tendency for uni-directional growth, point up the extreme importance of the cycling variables on the growth rate. In one test, using the vertical tube cycling equipment to cycle 300 times between 50°C and

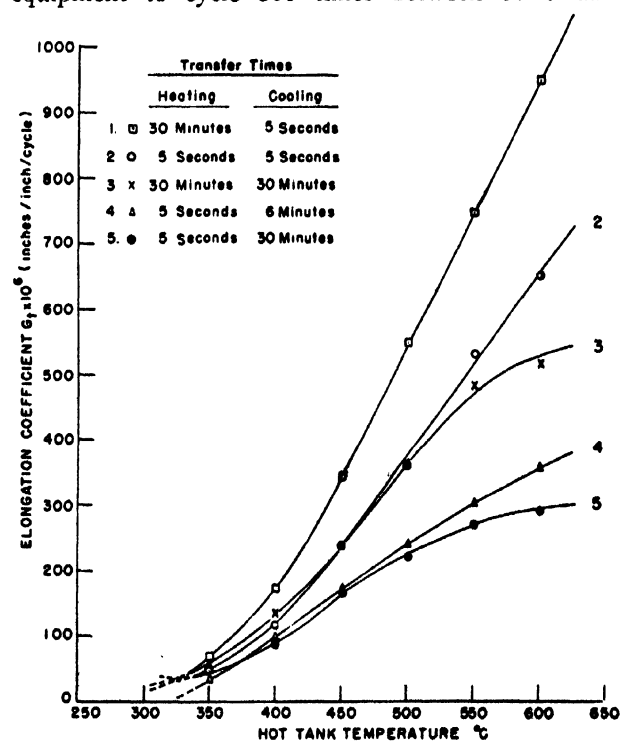

Figure 12. Variation of the elongation coefficient with hot tank temperature and transfer time; hot tank time: 5 min; cold tank time: 2 min; cold tank temperature: 50°C

550°C and with constant holding times of 5 minutes in the hot and 2 minutes in the cold zones, an elongation corresponding to $G_t = 51$ microinches/inch/cycle was obtained for 15 minutes heating and 5 seconds cooling transfer times as compared to a shrinkage equivalent to $G_t = -22$ microinches/inch/cycle for 5 seconds heating and 15 minutes cooling transfer times.

EFFECT OF CYCLING ON MICROSTRUCTURE AND PROPERTIES

Accompanying the macro-deformations discussed above, thermal cycling results in microstructural changes, the most important of which are: polygonization or subgraining; the development of porosity with an accompanying decrease in apparent density; crystallographic slip; roughening of grain boundaries; and grain boundary migration.

The formation of a subgrain structure is most pronounced and therefore easiest to follow in coarse-grained material as illustrated in Fig. 15.

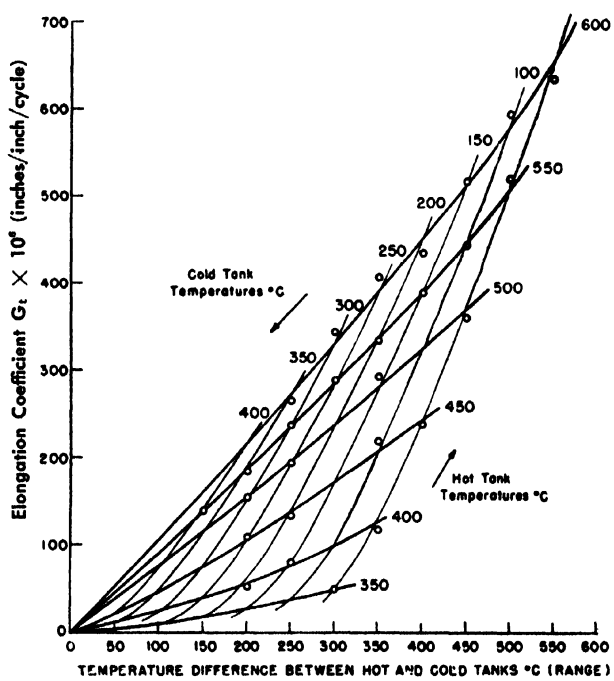

Figure 13. Composite effect of temperature range (ΔT) on the elongation coefficient; (upper and/or lower temperature variable); transfer time: 5 seconds heating and cooling; hot tank time: 5 min; cold tank time: 2 min

In Fig. 15a the starting structure is that of a highly oriented 300°C-rolled specimen wherein a coarse grain structure had been produced by a strain anneal method. As can be seen in Fig. 15b a very pronounced subgrain structure was developed in 700 cycles between 100 and 550°C.

Subgraining is shown in Fig. 16c to develop near grain boundaries in coarse-grained high purity uranium that has undergone relatively few thermal cycles.

In addition to the subgraining described above, crystallographic slip, grain boundary migration, grain boundary roughening, and surface roughening

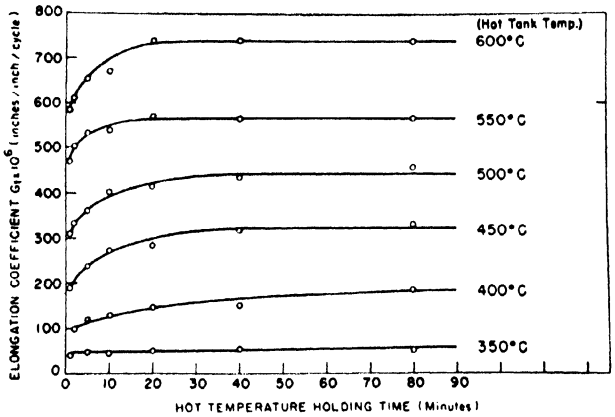

Figure 14. Influence of holding time at the upper temperature upon the elongation coefficient; transfer time: 5 seconds heating and cooling; cold tank temperature: 50°C; cold tank time: 2 minutes

have been observed on a microscopic scale as consequences of the internal stresses developed on thermal cycling. The amount of internal deformation is dependent upon the relative orientations of adjoining grains. Where [010] directions are almost parallel, the deformation is at a minimum and increases with increasing spread between these directions.

Figure 16 reveals the effect of 25 thermal cycles on a large-grained specimen. The vertical surface striations after cycling (Fig. 16b) were identified as (010) slip markings, known to be the major slip system for alpha uranium. The twin traces were identified as the (130) type. Subgraining adjacent to the grain boundary accompanied by grain boundary roughening is shown in Fig. 16c.

It was difficult from this type of experiment to determine conclusively whether or not grain boundary slip had taken place.

At any rate, if any grain boundary slip had taken place, it was very small. No evidence of grain boundary migration was noted in the coarse-grained specimens. In the relatively fine-grained polycrystalline specimens shown in Figs. 17a (300°C-rolled and annealed) and 17b (same, but beta treated) grain boundary migration was very conspicuous.

The specimens also indicate that the more random the orientation the greater the internal deformation.

It is interesting to note that single crystals of uranium undergo no dimensional changes and show no evidence of internal deformation as a result of thermal cycling in the alpha temperature range.

Another structural change that has been observed on thermal cycling is the formation of voids with a corresponding lower apparent density. The voids are not confined exclusively to grain boundaries; microstructurally, they appear to be associated more closely with inclusions than grain boundaries. This has been demonstrated clearly in a study wherein high purity uranium (10–20 ppm carbon) and uranium containing a relatively large number of inclusions (500 ppm carbon) were cycled 3000 times under similar conditions. Metallographic examinations at various

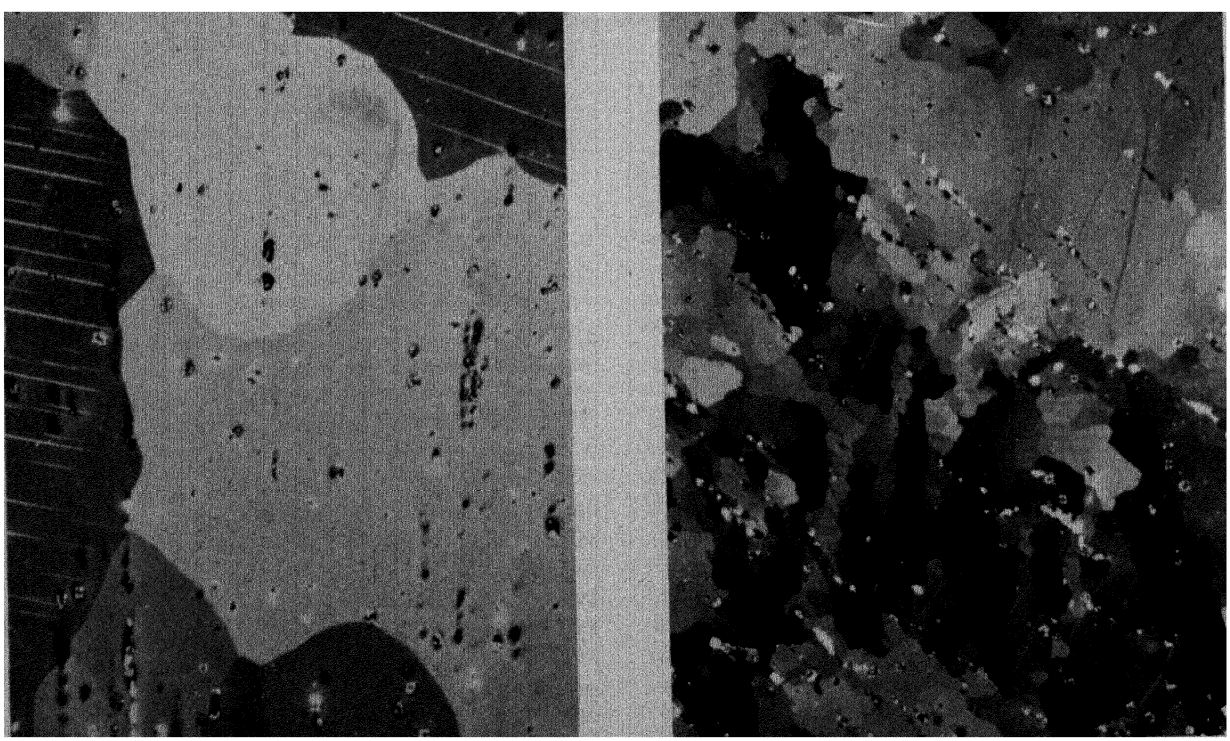

6524 Figure 15a 150× 6491 Figure 15b 150×

Figure 15. The effect of thermal cycling between 100°C and 550°C on the microstructure of a coarse-grained highly oriented uranium specimen; polarized light; (a) before cycling; (b) 700 cycles

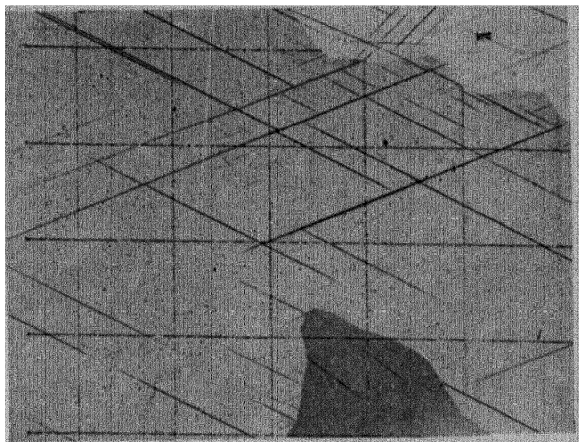

15,017 Pol. light 50×

Figure 16a. Before cycling

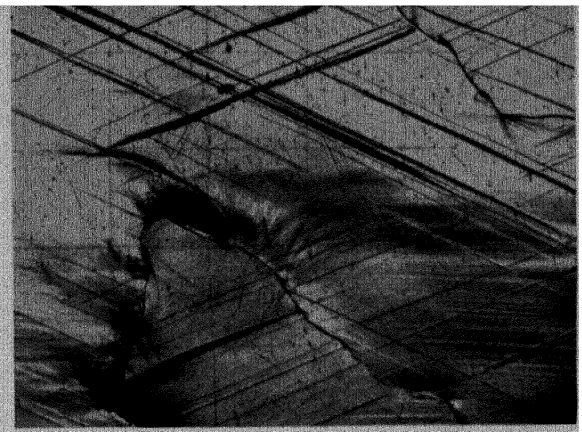

15,154 Br. field 50×

Figure 16b. After 25 cycles. Striations are (010) slip markings



15,833 Polarized light 100×

Figure 16c. Repolished after cycling

Note the subgraining and adjacent roughness boundary

Figure 16. The effect of thermal cycling on the microstructure of a polished area of a large-grained specimen

stages of cycling revealed an abundant formation of voids in the impure uranium as compared with practically no detectable voids in the pure uranium, even though both specimens grew extensively. These specimens are shown after 3000 cycles in Fig. 18 on page 157.

As regards changes in other properties on thermal cycling the following is pertinent: the thermal expansion coefficient in the range 25–100°C of 300°C-rolled and annealed rods is not altered by 500 thermal cycles between 50°C and 550°C, indicating that the degree of preferred orientation is not changed appreciably on cycling. This has been corroborated by X-ray diffraction orientation studies.

PROPOSED MECHANISMS

Several mechanisms have been proposed to account for the phenomenon of growth in uranium. Some of these are based on the fact that the coefficients of expansion of uranium are anisotropic, thus causing a stress to develop across grain boundaries of neighboring grains of different orientations. This circumstance has been proposed by Boas and Honeycombe[1] to account for the plastic deformations they noted in other anisotropic metals. In uranium, however, mechanisms proposed by Boas and Honeycombe are not sufficient, since one has to account for a continuous resulting macro-growth in one direction which was not the case in their experiments.

To account for this uni-directional continuous growth, Burke *et al.*, Knolls Atomic Power Laboratory, proposed a so-called "thermal ratcheting" mechanism which makes the deformation irreversible. These authors picture polycrystalline-textured uranium to consist of grain couples of different orientations, with stress developed across their boundary.

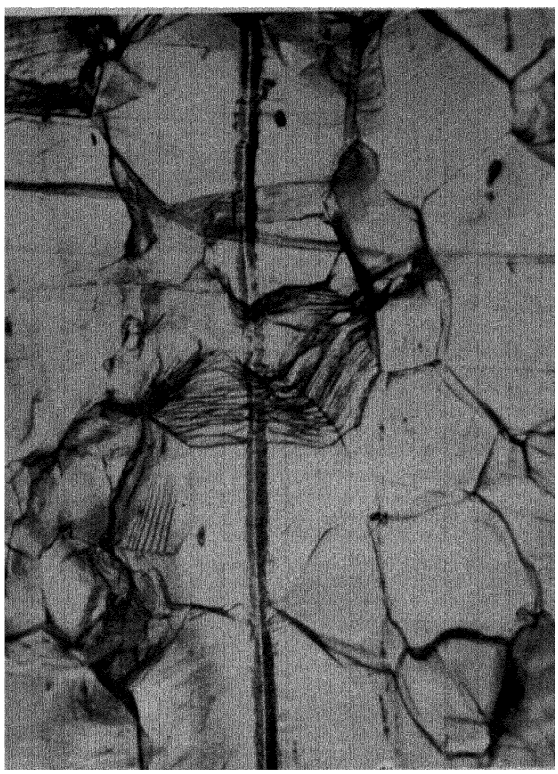

15,929 Bright Field 250 ×

Figure 17a. 300°C-rolled and annealed (oriented)
Note the grain boundary migration.
The furrow is a scribed fiducial line

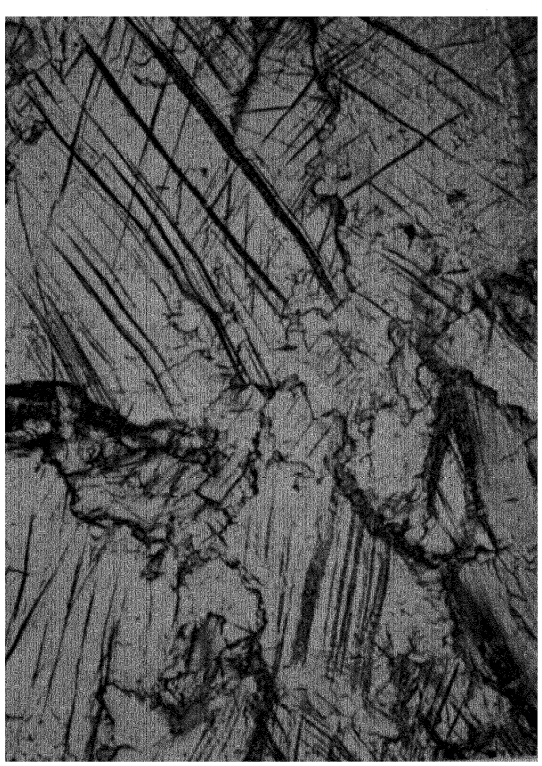

16,380 Bright Field 100 ×

Figure 17b. Beta treated (randomized)

Figure 17. The effect of thermal cycling from room temperature to 500°C on polished surfaces of oriented and randomized relatively fine-grained high purity uranium

The ratcheting or non-reversibility of the process they picture as resulting from the fact that the stress is relaxed by slip in the grain that is weaker because of its crystallographic orientation at the low temperatures, whereas at the high temperatures the stress is relaxed by grain boundary flow. In support of such a mechanism they point to the fact that experimentally one can observe grain boundary slip in thermally cycled material like zinc.[2] In essence, therefore, the mechanism pictures one of the grains to be deformed by slip or twinning at the lower temperatures and the stress to be relaxed by grain boundary flow at the higher temperatures, but no slip across the grain boundary taking place at the low temperature. Under such conditions the stronger grain of the couple never suffers plastic distortion in the direction being considered.

Bettman *et al.*, California Research and Development Co., have proposed that continued elongation on thermal cycling may occur as a result of creep in the stronger grain of a similar couple at the high temperature part of the thermal cycle, whereas the weaker grain may be deformed plastically in the low temperature part of the cycle. In this model, no flow is assumed to occur at the grain boundary. The amount of creep in the strong grain will be small because the stress in the soft grain will be equally high. Thus, the greater part of the relaxation will occur at the high temperature by creep in the softer grain. A similar mechanism has been proposed by Maringer *et al.* of the Battelle Memorial Institute.

A model has been proposed by Fisher, General Electric Research Laboratory, which attributes the growth to anisotropic diffusion of interstitial atoms and lattice vacancies under thermal cycling.

Mechanisms proposed to account for changes taking place in uranium on thermal cycling do not completely coincide with experimental observations. The anisotropic diffusion mechanism requires that single crystals of uranium show growth which is contrary to experimental fact. The stress-relaxation mechanisms must be able to account for the following: there is no evidence of preferential elongation of grains in the direction of growth as the result of even a large number of cycles; voids that develop as a consequence of thermal cycling are not confined exclusively to grain boundaries, and, in fact, appear to be associated with inclusions; cycling of high purity metal produces no voids; grain boundary slip appears to be a minor effect. Also Bettman *et al.* have criticized the Burke *et al.* mechanism as being intuitively unsatisfactory for polycrystalline metals because the proposed differential dimensional changes of adjacent grains should be prevented by the surrounding matrix of interlocking grains. The objections to some of the proposed mechanisms might be minimized by resorting to the observed subgraining as a means of reorientation at grain boundaries in order to accommodate the necessary dimensional changes. This, coupled with diffusion, could account for lack of void formation at grain boundaries.

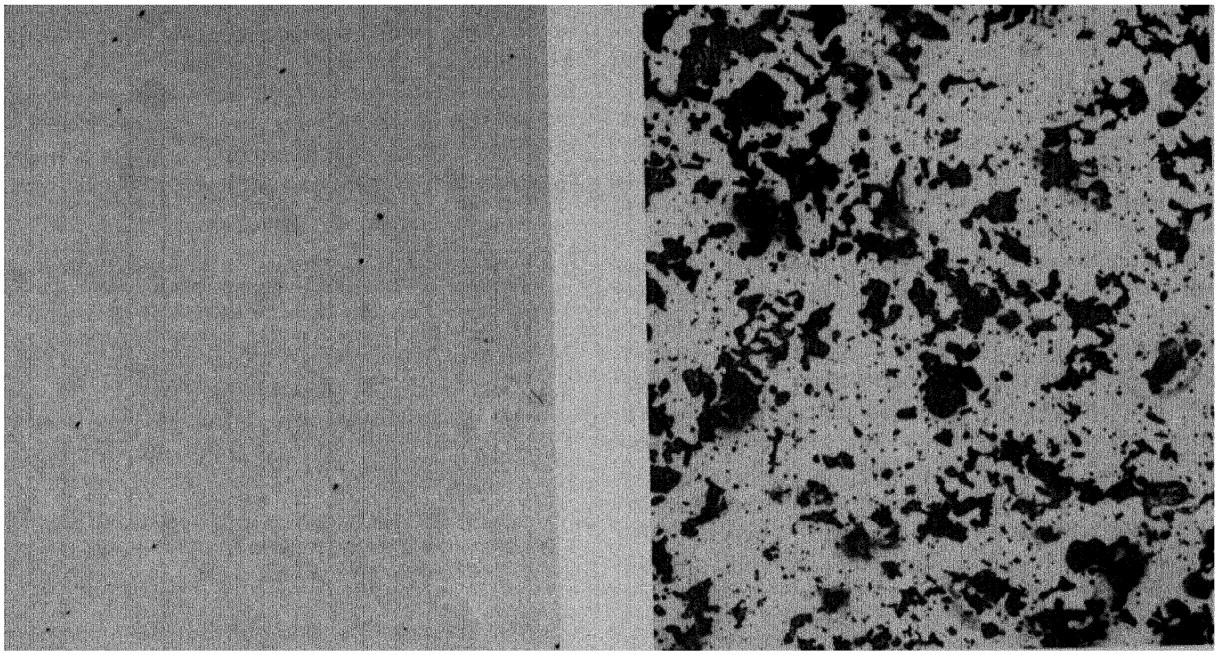

11,101 Bright Field 100×
a. High purity uranium (10-20 ppm C)

13,554 Bright Field 100×
b. Relatively impure uranium (500 ppm C)

Figure 18. Porosity formation in pure and relatively impure highly oriented uranium after 3000 cycles

SUMMARY

Polycrystalline uranium metal undergoes substantial dimensional and structural changes when subjected to repeated heating and cooling in the alpha-phase temperature range (room temperature to 660°C). In cast metal the dimensional changes manifest themselves in the form of surface roughening; in wrought metal, when fabricated in the alpha-phase temperature range, the dimensional changes take the form of substantial elongations, generally in the directions coincident with the direction of working of the metal.

The magnitude of the deformations is a function of the number of cycles to which the material is subjected and is effected by both structural and cycling process variables. Preferred orientation is a necessary condition for uni-directional growth to occur; the extent of the growth depends upon the sharpness of texture developed and the grain size. The highest growth rates occur in material with highly developed textures coupled with a small grain size. The growth rate on thermal cycling, as expressed by the growth coefficient, G_t, is not a constant; it increases with N, the number of cycles.

Material whose prior texture has been randomized by a beta heat treatment shows the least tendency to grow. Accompanying such heat treatments, however, there is usually an increase in grain size which results in an increase in surface roughening. If uranium is prepared by a process which results in both random orientation and fine grain size, such as by powder metallurgy methods, it neither grows nor is the surface roughened.

Alloying elements in low concentration do not decrease the growth of alpha-fabricated uranium; in fact, in some instances the growth is increased, presumably because of smaller grain size. Alloy additions decrease the surface roughness after a randomizing beta or gamma treatment because they promote grain refinement.

The dimensional changes are also functions of the following cycling variables: (*a*) rates of heating and cooling, (*b*) temperature level, (*c*) temperature range, and (*d*) time at temperature. The greatest growth rates per thermal cycle are obtained when slow heating and fast cooling are combined with a large temperature range of cycling.

Thermal cycling also results in microstructural changes, the most important of which are: polygonization or subgraining; the development of porosity with an accompanying decrease in apparent density; crystallographic slip; roughening of grain boundaries; and grain boundary migration. In material of relatively low purity thermal cycling also results in extensive formation of porosity. That the formation of porosity is not inherent in the mechanism is evidenced by the fact that high purity uranium develops no porosity, even though its rate of deformation is equivalent to that of impure metal.

The amount of internal deformation is dependent upon the relative orientations of adjoining grains; where [010] directions are almost parallel the deformation is at a minimum and increases with increasing spread between these directions. Random orientation increases the amount of internal microscopic deformation; however, these deformations do

not appear as over-all dimensional changes. Preferred orientation results in less internal microscopic deformation; however, uni-directional growth along the length of the specimen does result.

Most of the mechanisms that have been proposed to explain the dimensional and structural changes that occur in uranium when thermal cycled are based on intergranular stresses developed as a result of anisotropy in the thermal expansion of alpha uranium. One proposed mechanism provides for a ratcheting condition to make the deformation non-reversible by assuming grain boundary flow to relax the stress at high temperatures and crystallographic slip to relax the oppositely directed stresses at low temperatures. Another proposed mechanism does not assume grain boundary flow but provides for continued elongation on thermal cycling as a result of creep occurring in the stronger of adjacent grains at the high temperature part of the thermal cycle and plastic deformation of the weaker grain in the low temperature part of the cycle. These mechanisms are not in complete agreement with the available experimental evidence. Objections to some of the proposed mechanisms might be minimized by resorting to the observed subgraining coupled with diffusion as a means of reorientation at grain boundaries to accommodate the necessary dimensional changes.

REFERENCES

1. Boas, W. and Honeycombe, R. W. K., *The Plastic Deformation of Non-Cubic Metals by Heating and Cooling,* Proc. Roy. Soc. London, *A186*: 57-71 (1946).

   Boas, W. and Honeycombe, R. W. K., *The Deformation of Tin-Base Bearing Alloys by Heating and Cooling,* J. Inst. Metals, *73*: 433-444 (1946-47).

   Boas, W. and Honeycombe, R. W. K., *The Anisotropy of Thermal Expansion as a Cause of Deformation in Metals and Alloys,* Proc. Roy. Soc. London, *A188*: 427-439 (1947).

2. Burke, J. E. and Turkalo, A. M., *Deformation of Zinc Bicrystals by Thermal Ratcheting,* Trans, Am. Inst. Mining Met. Engrs. *194*: 651-656 (1952).

Gamma Phase Uranium Extrusion

By J. A. Stohr* and R. Chevigny,† France

STUDY OF THE FORGING PROPERTIES OF THE METAL IN THE THREE PHASES

The Bastien-Portevin method was used as a starting point. A series of tests, whereby the metal was subjected to various types of stresses, was carried out in the laboratories of the Commissariat à l'Energie Atomique. The most representative tests are summed up below.

Slow Tension Tests as a Function of Temperature (Fig. 1)

The following magnitudes were found with a 25-ton Baldwin tension machine: ultimate tensile strength: R kg/mm² (curve 1, Fig. 1), percentage elongation: $A\%$ (curve 2, Fig. 1), reduction in area: $\Sigma\%$ (curve 3, Fig. 1). The specimens used were 13.8 mm in diameter, for a length of 70 mm between ends. The ends were of the threaded type. The curves were recorded with an extensometer having an amplification factor of 1000 for a measuring base of 50 mm.

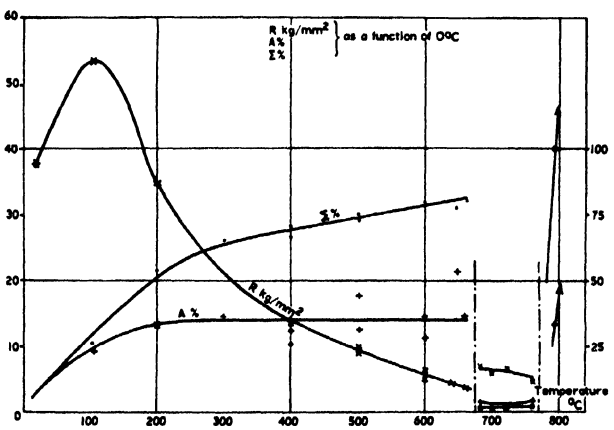

Figure 1. Tensile test on uranium at various temperatures

The samples were heated in an automatically regulated oven in an argon atmosphere.

In the α phase, the following were observed: a maximum for the value of the ultimate tensile strength at 100°C, and a slow decrease up to the α-β phase transformation point; an increase in the value of the percentage elongation up to a temperature in the vicinity of 200°C, and then a slow decrease to the point of α-β phase transformation; and a uniform increase in the magnitude of the reduction in area beyond 300°C.

In the β phase, the following were observed: a very plainly visible discontinuity in the three magnitudes as soon as phase transformation point α-β is passed, which is particularly notable for the values of the percentage elongation and reduction in area; the values of $A\%$ and of $\Sigma\%$ are comprised between 2% and 4%; they are lower than those obtained at room temperature.

In the γ phase, the following were observed: a new and no less clearly marked discontinuity in the values of the three magnitudes as soon as the β-γ phase transformation point is passed. The value of the reduction in area, for instance, goes up from 2% at 760°C to 100% at 795°C.

Slow Compression Test as a Function of Temperature

The value of the deformation in millimeters, as a function of the stress, was noted on a cylindrical specimen having a diameter of 13.8 mm and a height of 15 mm, in the temperature range 20°C to 800°C. The tests were carried out on a 25-ton Baldwin machine equipped as follows (Fig. 2):

The base of the specimen was placed in an argon circulation oven. The compression plunger (diameter of 30 mm) was made of "stubb" steel. A comparator, placed between the base plate (steel) and the part which carries the plunger, makes it possible to measure the strains. The ratio of compression used was about 1.5 kg/mm²/minute.

For the α phase, an increase in the deformation starting from a temperature in the vicinity of 550°C (Fig. 3) was observed.

For the β phase, deformation was much less marked than that noted in the upper part of the α phase.

For the γ phase, a rapid increase in the deformation as a function of the temperature was observed.

It is to be noted that the "stress-strain" curves plotted at the various temperatures (Fig. 4) reveal a new strain law, starting from a deformation comprised between 2% and 3%. The stress for which a transition point appears varies with the temperature. It goes up from 22 kg/mm², at 100°C, to 6 kg/mm² at about 600°C. The curves on Fig. 5, in double logarithmic coordinates, reveal this transition point.

Original language: French.

* Chief, Technology Department, C.E.A.

† Chief, Research Department of the Péchiney Company, Chambéry.

Tensile Impact Tests as a Function of Temperature

The tests were carried out with a pendulum-type machine specially designed for tensile impact tests. The specimens (diameter 6 mm, effective length 45 mm), were heated in an argon atmosphere oven. The tests were carried out in the oven.

The results obtained for the values of energy absorbed as the specimen is broken were too erratic to enable us to plot any curves. We are in a position to state, however, that the three phases reveal differences comparable to those revealed by the tensile tests. The differences between the phases are less marked in the tensile impact test than in the static tensile tests.

Compressive Impact Tests as a Function of the Temperature (Fig. 6)

The amount of deformation was measured on a sample having a diameter of 13.8 mm, 15-mm high, at temperatures ranging from 20°C to 900°C.

The value of the impact energy, maintained constant through the test, was chosen at 2 kg, which permits good measurements at the high tempera-

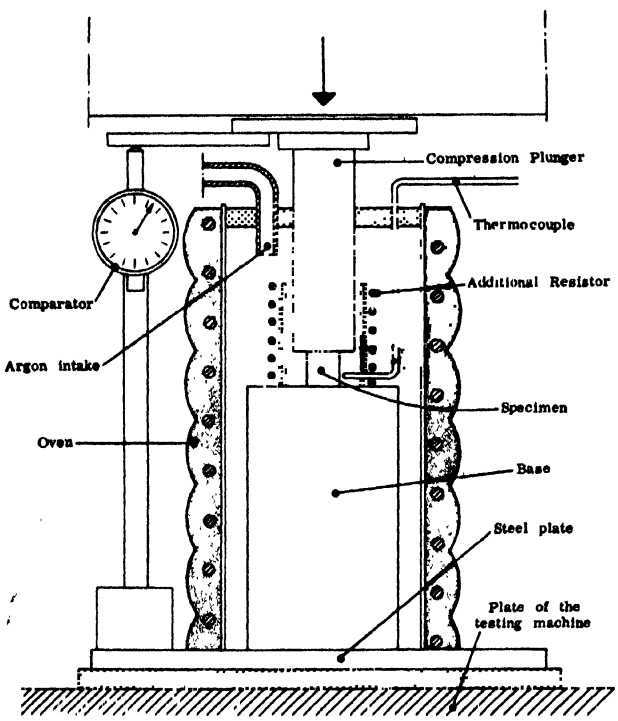

Figure 2

tures and gives a deformation that is small but readily measurable at the low temperatures. The method consists of heating the specimen in an argon atmosphere oven, of bringing it very quickly to an Amsler pendulum machine that has an 18-kg hammer (Fig. 7), and immediately carrying out the impact test.

Figure 8 shows the appearance of the specimens after impact at the various temperatures.

In the α phase, an increasing progression of the deformation as a function of the temperature was observed.

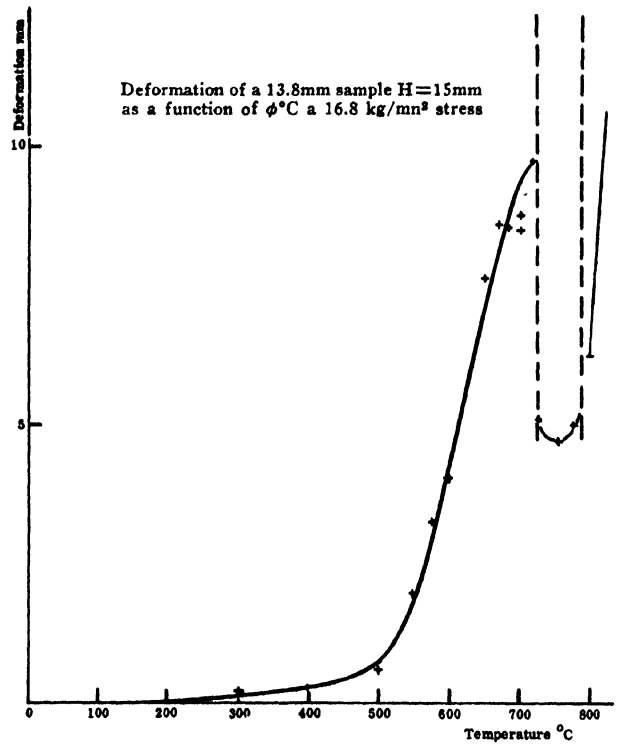

Figure 3. Uranium slow compression at high temperatures

In the β phase, a small deformation, identical to that of uranium at room temperature, and practically independent of the temperature throughout the phase was noted.

In the γ phase, a deformation which increases very rapidly with the temperature was observed.

Impact Tests as a Function of the Temperature (Figs. 9 and 10)

The amount of energy absorbed when breaking the sample at various temperatures was measured on a series of unnotched samples with dimensions of 10 × 10 × 55 mm, and on a series of notched samples, type UF, which met standard A03.106 (10 × 10 × 55 mm ; depth of notch : 5 mm). The two series of tests were conducted by using the maximum available energy of the Amsler impact hammer used, namely:

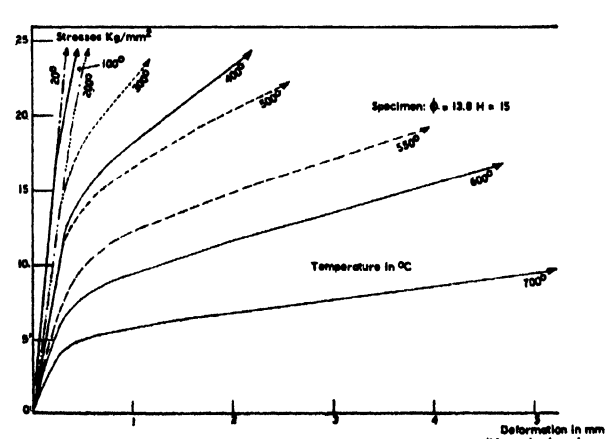

Figure 4. Uranium compression diagram at the high temperatures

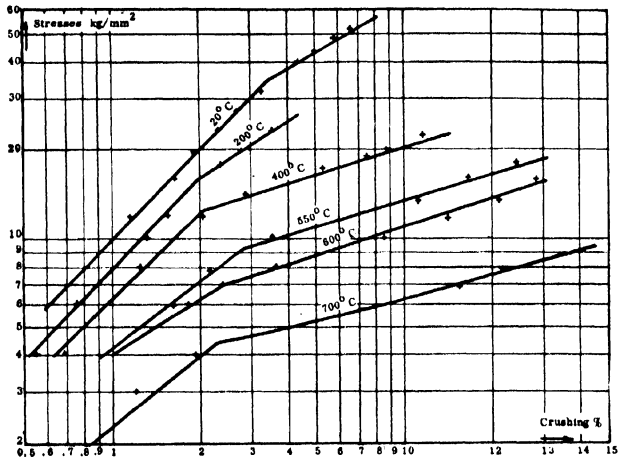

Figure 5. Uranium compression

30.5 kg-m. As was done in impact testing, the samples were heated in a circulating argon oven, and immediately placed on the rests of the impact pendulum. The handling time was about 2 seconds. Preliminary tests gave means of computing the temperature corrections due to the cooling off which takes place during the handling, in order to determine the temperature at the time of the impact. The pendulum is released as soon as the sample is set.

In the α phase, for unnotched specimens, there is an increase in the energy absorbed for temperatures of 250°C to 300°C, and a rapid decrease as soon as 300°C is exceeded. For the notched samples, the maximal energy absorbed is approximately 500°C, and then decreases. The break takes place only in the range from room temperature to 200°C; beyond this, the specimen will be distorted without breaking.

In the β phase, very great fragility was observed; all specimens were broken and there was a marked decrease in the amount of energy absorbed.

In the γ phase, no fragility, no break of specimens, and a small amount of absorbed energy, of the same

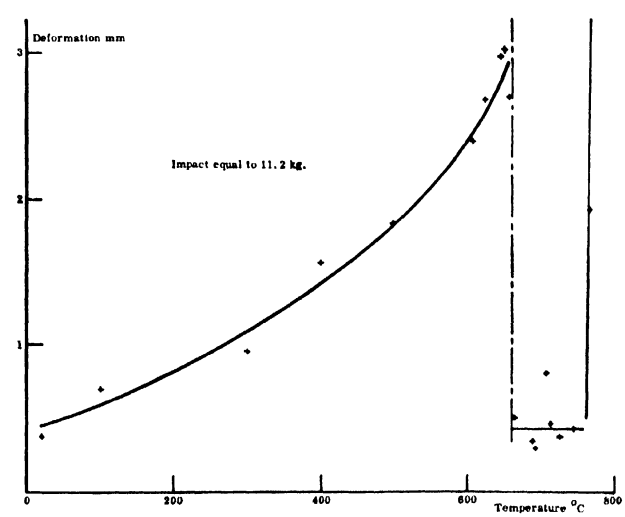

Figure 6. Uranium impact compression at the various temperatures on cylindrical samples 13.8 mm in diameter, 15 mm in height

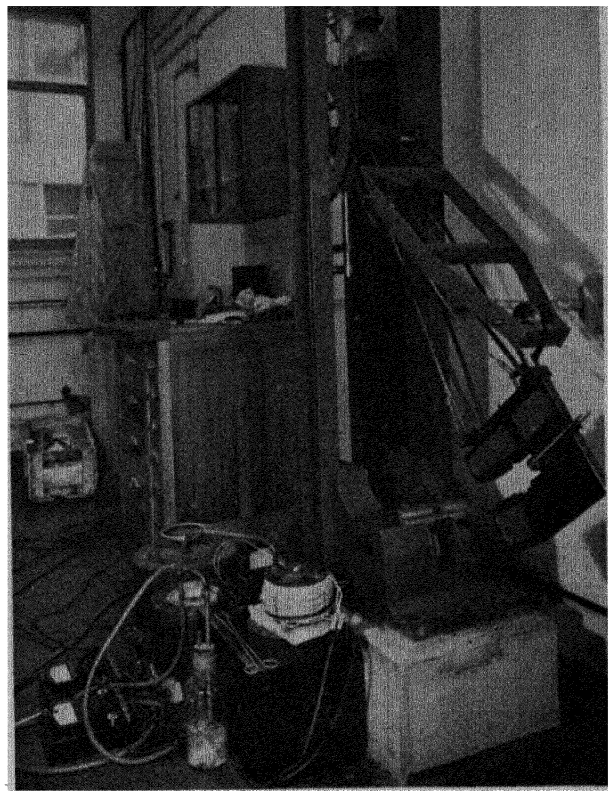

Figure 7

order of magnitude as that found in the β phase was observed. Very great plasticity was observed.

Static Flexural Tests as a Function of Temperature (Figs. 11, 12 and 13)

The flexural strength was established in several ways: (*a*) by the value of the sag, in millimeters, under the effects of a 250 kg load and of a 100-kg load respectively; and (*b*) by the definition of the yield threshold, namely the value of the stress beyond which the strain increases rapidly. The tests were carried out on parallelepiped-shaped samples having dimension of 10 × 15 × 80 mm, with a 25-ton Baldwin tension machine, equipped with special instruments, similar to that described in the section "Slow Compression Tests as a Function of the Temperature." The separation between the supports was 15 mm. The temperature range extended from 20°C to 800°C.

In the α phase, small strains which are practically reversible up to 400°C were noted. From 450°C to the α-β phase transformation point, the strain increases and the yield threshold is below the 250 kg load, corresponding to an 11.2 kg/mm² stress.

In the β phase, the plastic strain was much less than that found at the top of the α phase (550°C at the point of α-β phase transformation). An important effect due to creep was noted.

In the γ phase, a sudden drop in the flexure characteristics was noted. The metal is completely plastic

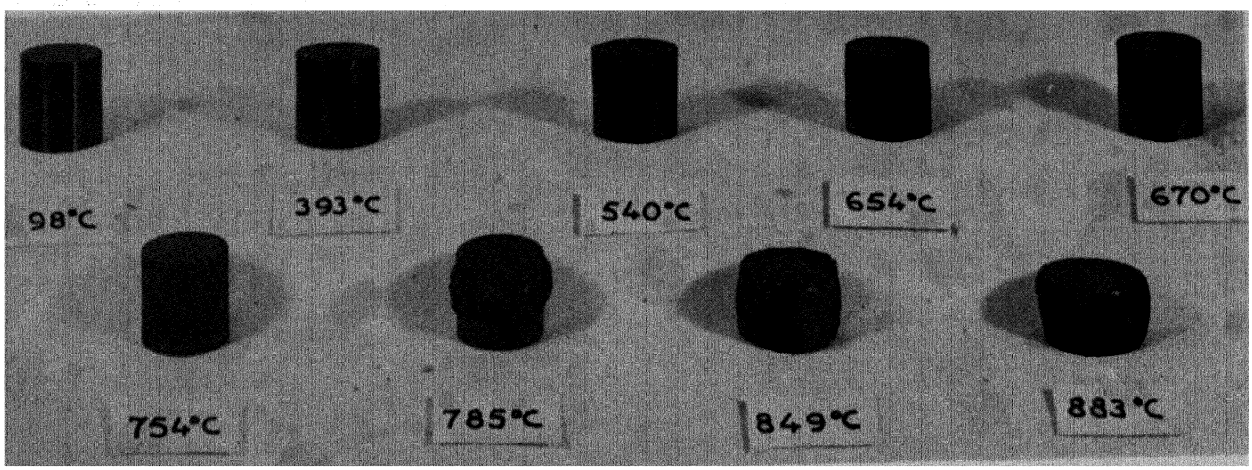

Figure 8. Impact compression at high temperature on uranium

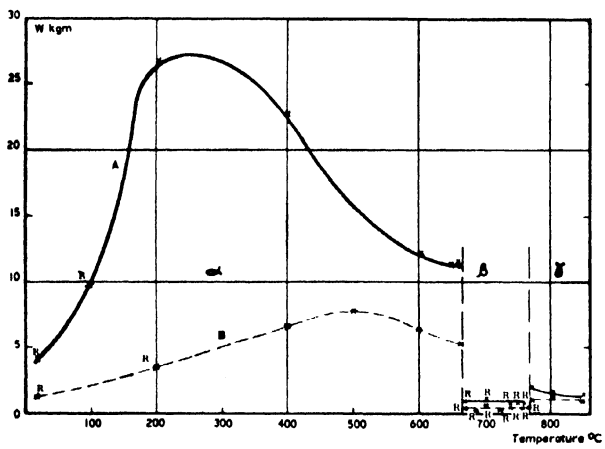

Figure 9. Resilience tests on uranium at various temperatures. See Fig. 10 for key

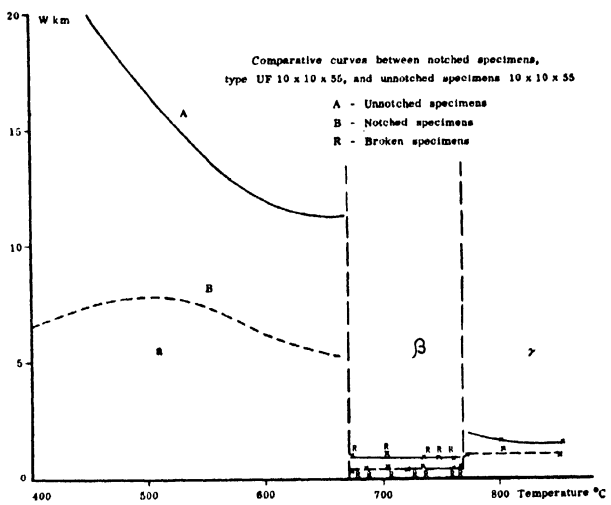

Figure 10. Resilience tests on uranium at various temperatures

in that phase; the yield threshold immediately drops to a few kilograms.

Conclusions as to the Forging Tests

The indications provided by the various tests which have just been mentioned show that uranium must be extruded under possible conditions of unit pressure at the top of phase α and in the γ phase. In the β phase, conversely, the metal seems to be of insufficient plasticity for this type of deformation.

URANIUM EXTRUSION IN THE γ PHASE‡

Since the γ phase lends itself more readily to extrusion, it was chosen for the first work.

The process used was developed at the laboratories of the Péchiney Company, at Chambéry, in cooperation with the Commissariat à l'Energie Atomique.

The characteristics of uranium at the high temperatures raised a certain number of problems due to: (*a*) the extremely high avidity of the metal for oxygen, and thus the need to avoid any contact with the air from the beginning to the end of the operation, and (*b*) the very fluid eutectic mixture which occurs at a high temperature, due to uranium-iron contact. The creation of this eutectic alloy brings about partial destruction of the equipment and makes the extruded product unusable. Accordingly, the metal must be protected against the air and any contact with steel, and in order to form the metal, use must be made of materials which can withstand large stresses at 960°C.

Principle of the Extrusion Method

The uranium billet is placed in a cylindrical stainless steel sleeve, the lower part of which is closed by the die and its mounting plate. The upper part of the sleeve is closed by a hard boss on which the extrusion pressure will be brought to bear. The boss and die are of tungsten carbide. The billet is surrounded by powdered graphite, which protects it from any metal to metal contact. The system is heated to 950°C in an argon atmosphere oven, then taken to the container of a vertical press.

Once the billet has been extruded, the rod and protecting cover, which contains the die and boss, are stored in an inert atmosphere.

‡ Brevet Péchiney No. 1 051 095.

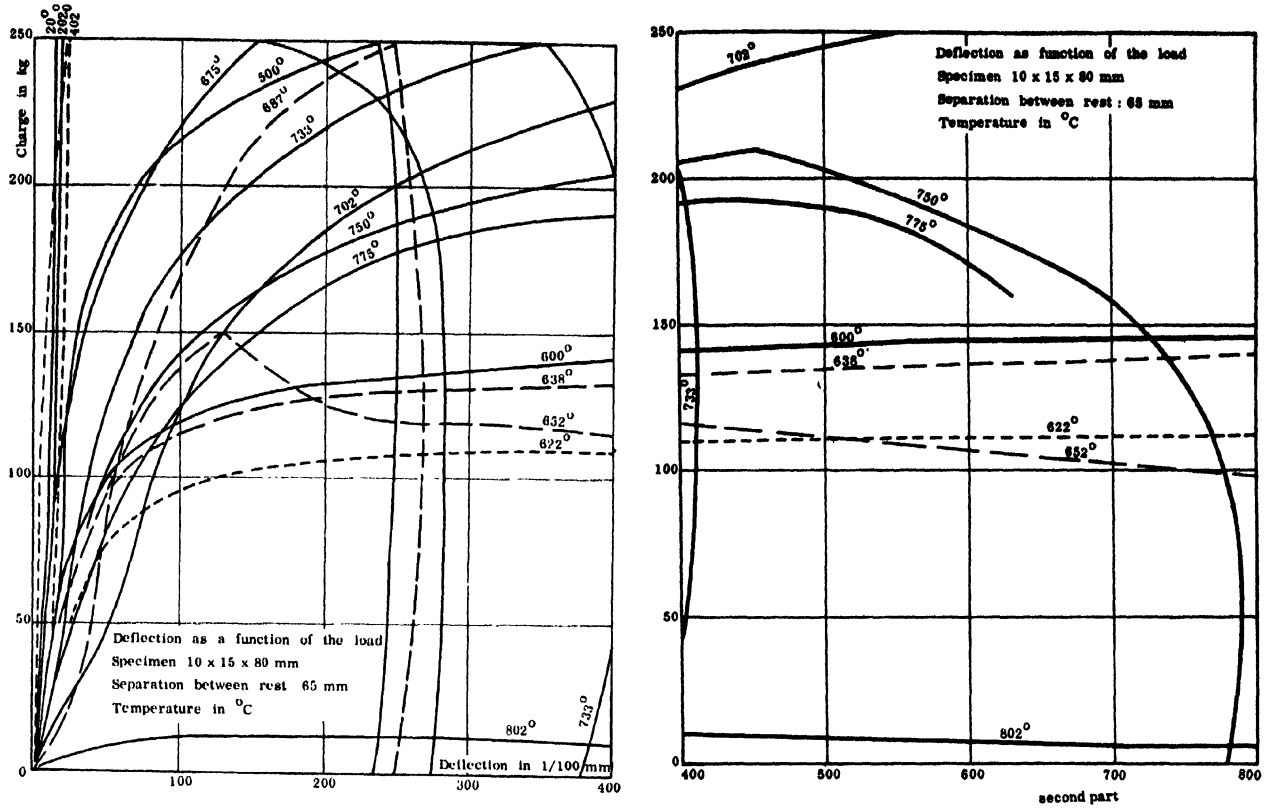

Figure 11. Uranium static flexure tests at the high temperatures

Equipment

We shall go into the equipment used in greater detail. It consists of four main units: (*a*) the extrusion unit, (*b*) the heating oven, (*c*) the extrusion press, and (*d*) the receiving tube.

Extrusion Unit

Shown on Fig. 14, this unit consists of the sleeve, the die mounting piece, the die, the billet and the boss. The stainless steel sleeve is considerably higher than the billet. Its wall thickness is such that it can stand the weight of what it contains without suffering any distortion during transfer at 970°C.

This sleeve is cylindrical in outer form. Internally, it is machined to form a series of cylinders, the diameters of which are adapted to the parts it contains.

The tungsten carbide die is of adequate thickness mechanically to resist the extrusion pressures. The cold clearance between the die and the sleeve is zero, but must be fairly substantial at 970°C, due to the differences in the expansion coefficients of stainless steel and tungsten carbide.

A stainless steel ring mounted on the die serves as a gasket between the sleeve and extrusion die. It is beveled so as to be applied against both the sleeve and die during the extrusion, thus avoiding that uranium should flow between the die and sleeve.

The billet is slightly counter-bored to make room for the gasket, and has a centering boss which fits in the opening of the die. It also has a centrally located recess, which will receive the thermocouple used to measure the metal temperature.

The space available between the billet and sleeve is filled with powdered graphite so as to avoid any and all contact between the billet and sleeve. The boss rests on the billet. The cold clearance between the boss and upper part of the sleeve is zero; it remains very small at 960°C, which reduces to a maximum the accidental air intakes during the few seconds it takes to transfer the billet from the oven to the press container. The diameter of the center part of the sleeve is such that, during the extrusion, there remains, between the boss and sleeve, a clearance which is adequate to permit the reverse extrusion

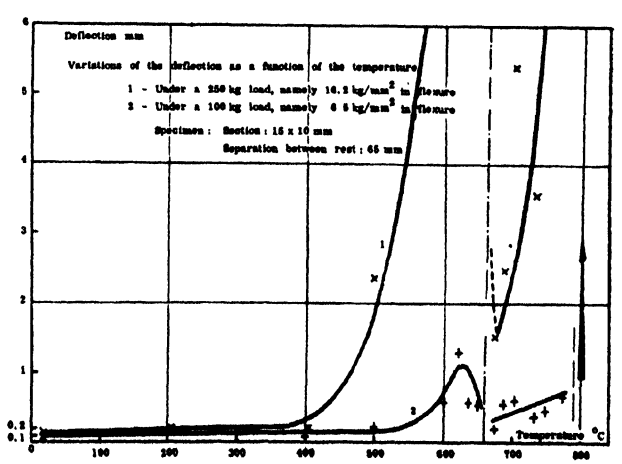

Figure 12. Static flexure, uranium

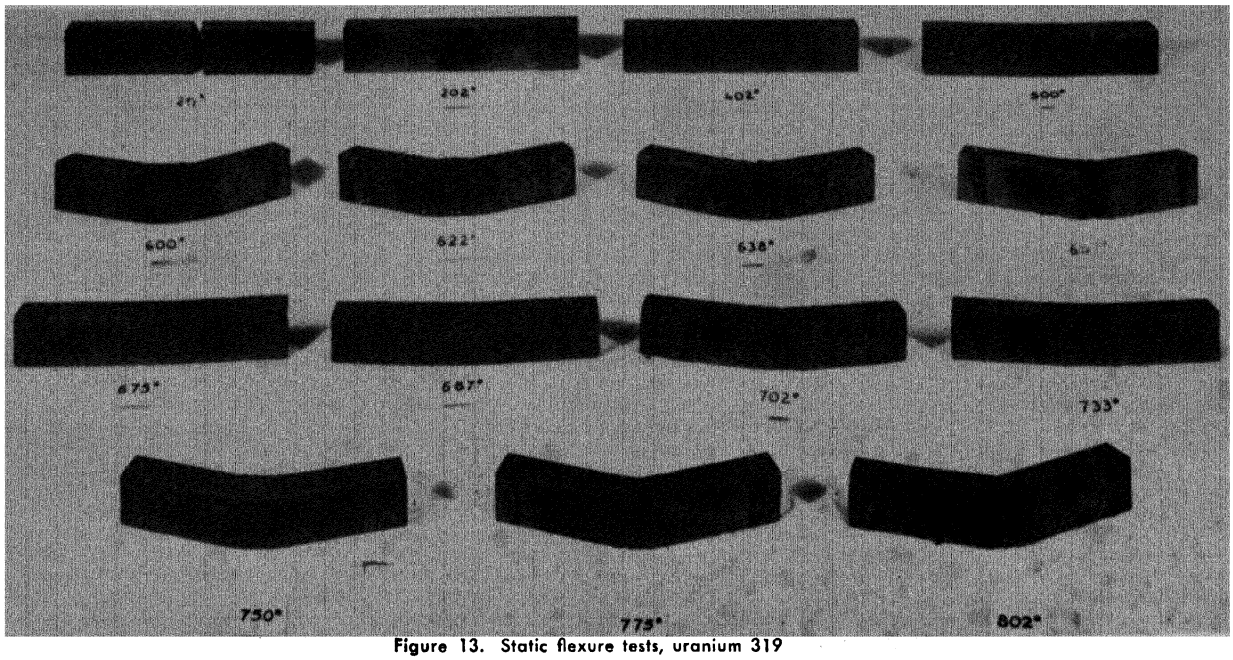

Figure 13. Static flexure tests, uranium 319

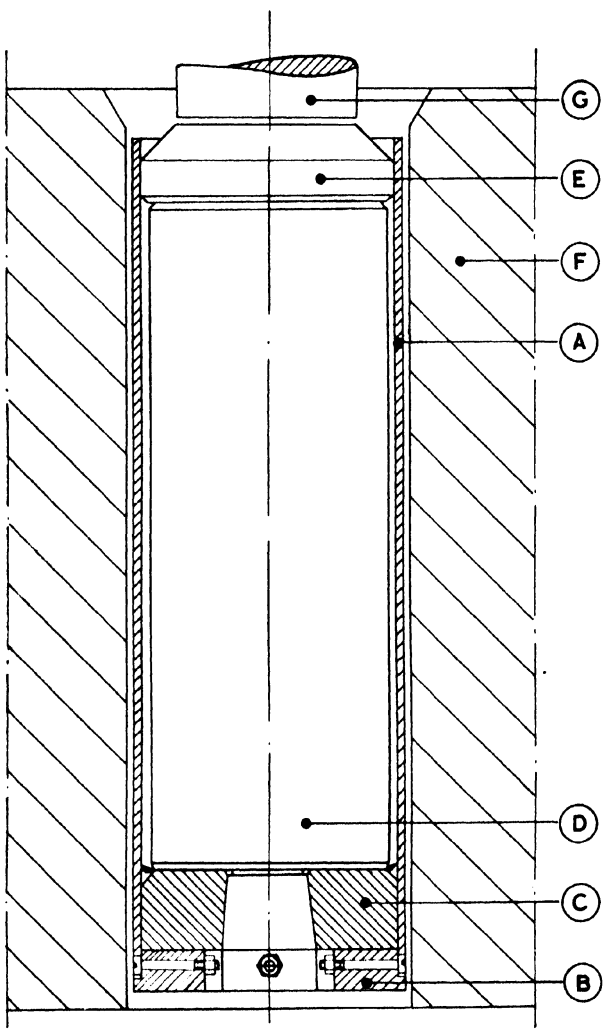

Figure 14. Extrusion unit

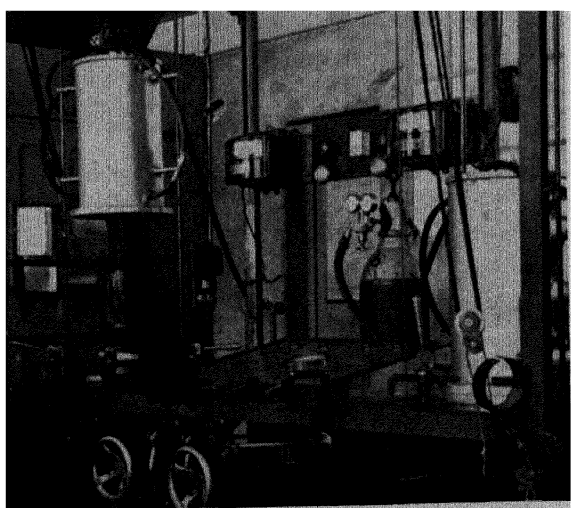

Figure 15

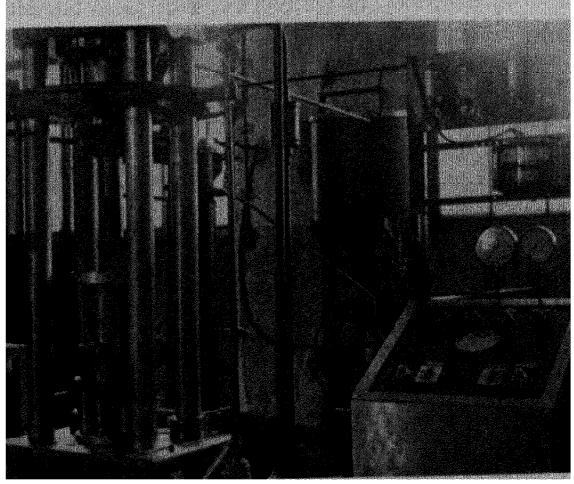

Figure 16

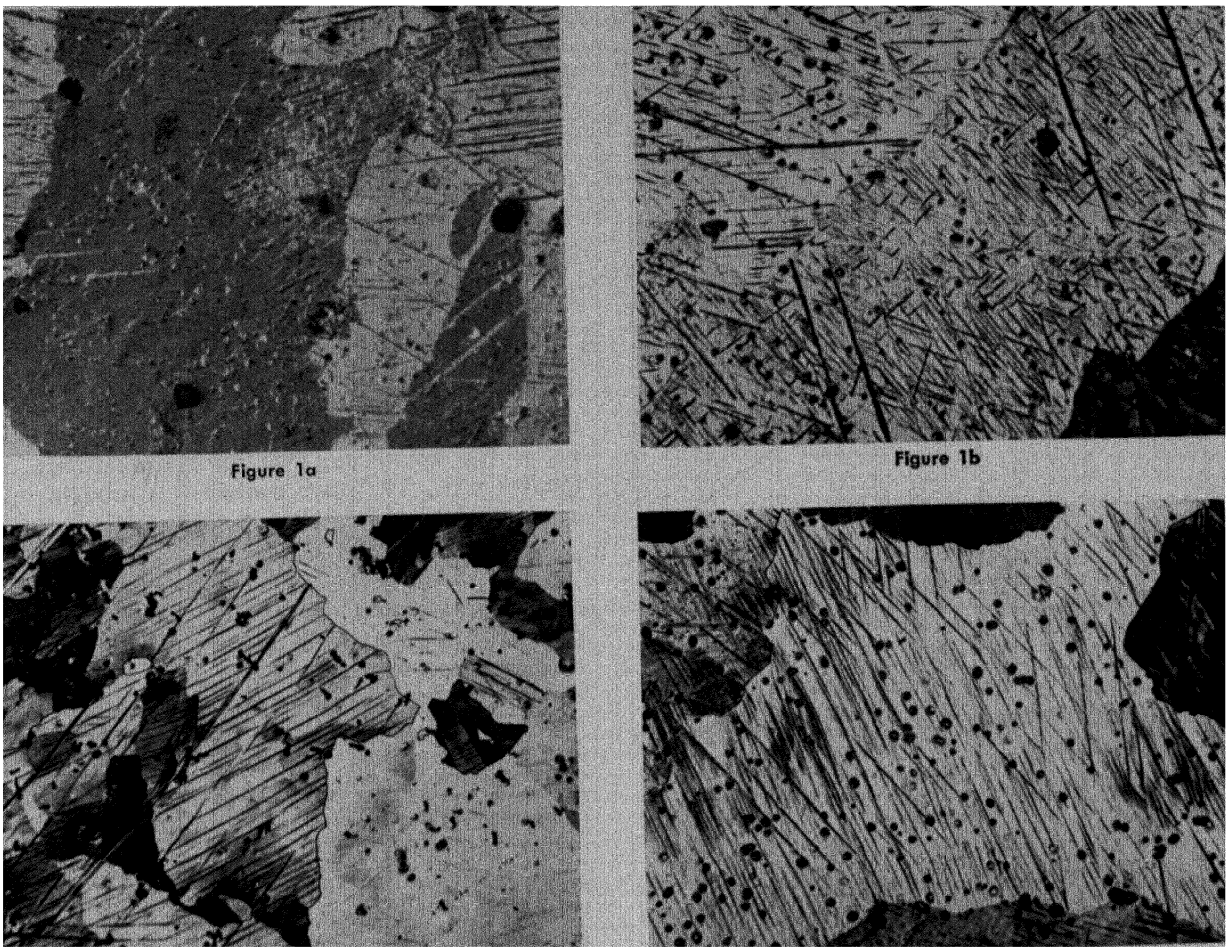

Figure 1a

Figure 1b

Figure 1c

Figure 1d

Figure 17. Uranium extruded in the γ phase without treatment, all figures 150 $\times$

motion needed to obtain a good rod. The boss is slightly counter-bored, in its lower part, in order to facilitate this reverse motion.

The carbide tungsten boss carries a stainless steel cap, which rules out thermal shock due to contact with the press punch. The die and the boss are covered with graphite to protect the tungsten carbide against direct uranium contact; under these conditions, tungsten carbide resists perfectly and these parts, which are relatively expensive, can be used for a great many operations.

The external graphite covering for the parts makes it easier to pull them out of the sleeve following extrusion. The gasket is protected by a layer of colloidal graphite. As an added precaution, it may first be covered by a metallized molybdenum layer.

Heating Oven (Fig. 15)

The heating oven imparts a uniform temperature in the vicinity of 970°C. A high vacuum and inert gas atmosphere can be established in it. It is a vertical oven with double aluminum walls cooled by a water current. A kantal ribbon resistor is wound around a refractory earth cylinder, and radiates on the extrusion unit. The base of the oven, made up of a platen provided with a torus shaped gasket, carries the extrusion unit support and is provided with the openings required for vacuum piping and argon intake, as well as with a port through which the thermocouple that makes it possible to measure the billet temperature can be passed. The heating element of the oven, which can be moved vertically, closes up the extrusion unit by applying it against the lower platen. The oven temperature is adjusted by a regulator controlled by the thermocouple.

Extrusion Press (Fig. 16)

It is an ordinary vertical press, having a maximum power of 80 tons. It has a treated steel container which can be heated by outside resistors, and an internal core. The base of the container carries the first set of keys on which the extrusion unit rests during extrusion, and which can be removed in order to allow the unit to go down into the receiver following extrusion. The second set of keys applies the receiver against the container.

The Receiving Tube (Receiver)

During extrusion the extruded rod enters the receiver in which there is argon circulation. Following

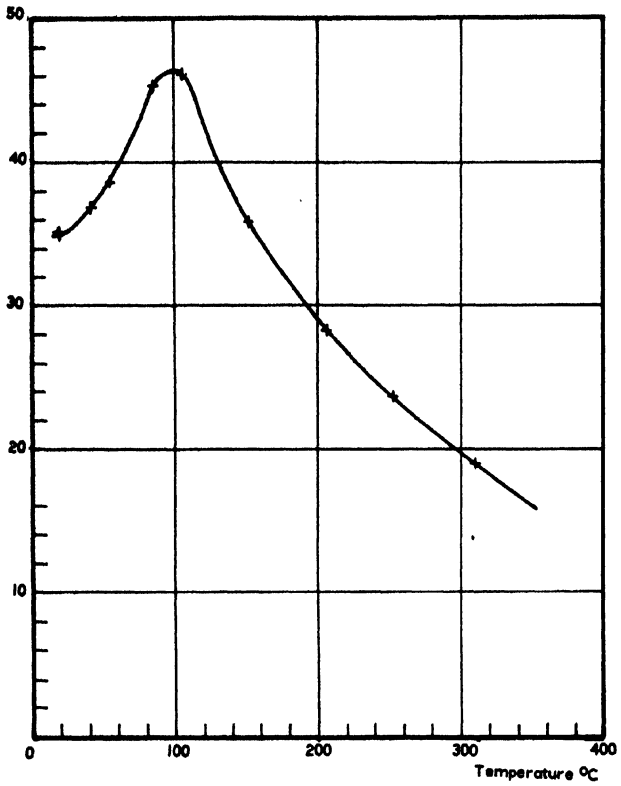

Figure 18. Uranium ultimate tensile strength, as a function of the temperature

extrusion it receives the rod, together with the extrusion unit. A spring device eliminates shock. Following removal of the keys, the receiver is closed by a tight lid. It is double walled and water cooled in order to accelerate cooling of its content.

Extrusion Process

Extrusion includes the following phases:

Preparation of the Extrusion Units

The sleeve is covered with graphite, the gasket, the extrusion unit and the boss, first heated to 200°C, after which the extrusion unit support is placed, as well as the die, gasket and the billet. The sleeve is placed on this unit, in keeping with a special set-up which makes it impossible to have the graphite layer removed by friction of the billet against the sleeve. The die carrier is screwed onto the sleeve. The annular space between the billet and the sleeve then is filled with graphite, and finally, the boss and its cap are set up.

Heating of the Metal

The extrusion unit is placed in the oven. It is placed under vacuum during the beginning of heating. At 150°C, argon is brought in, in order to obtain a slight excess pressure. The temperature is brought up in two hours and held for approximately one-quarter hour. The press container is brought up to a temperature of 500°C.

Extrusion

Extrusion proper must be carried out as fast as possible in order to avoid on the one hand, any parasitic oxidation of the metal during its passage in the atmosphere, and on the other hand, too great a temperature drop which would make it completely impossible to carry out the extrusion.

This consists of a series of operations which have to be carried out together: (*a*) removal of the inside heater core from the container; (*b*) passing the graphite grease into the container; (*c*) argon scavenging of the container through the receiving tube; (*d*) cutting off oven current; and (*e*) opening and raising the oven.

The sleeve is caught by two tongs or grips, one applied to the upper part at the level of the boss, the other being at the level of the die. The unit then is carried from the oven to the container. It slips into the container. The punch is mounted on the press. The press is operated. The whole process must not exceed one minute and can be carried out, including the extrusion, in 55 seconds.

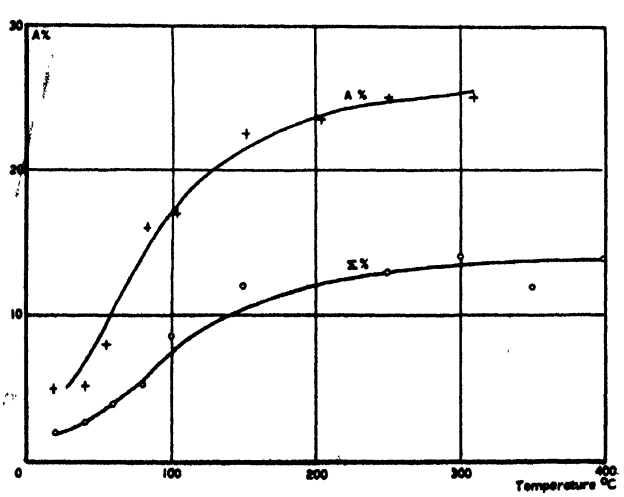

Figure 19. Uranium elongation at the breaking point, and reduction in area, as a function of the temperature

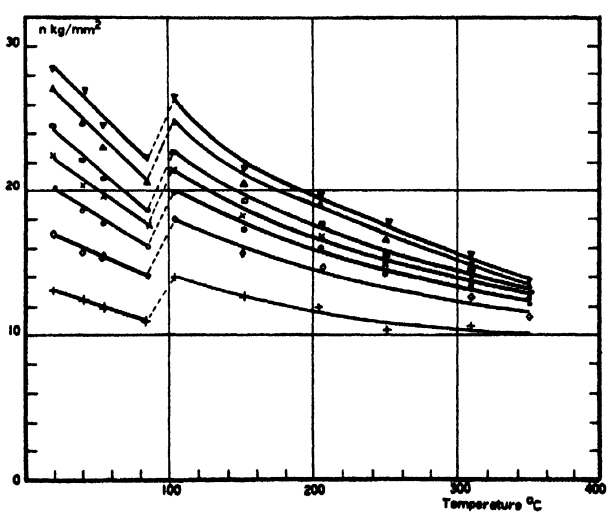

Figure 20. Uranium stresses which give a definite elongation for each temperature

Table I. Main Mechanical Characteristics of Uranium as a Function of Temperature

	Young's Modulus E kg/mm²	Ultimate tensile strength R kg/mm²	Elastic limit (kg/mm²) At 0.2%	At 0.02%	At 0.002%	Elongation at break A %	Reduction in area Σ %
Extruded uranium (tests at 20°C)	19,000 to 21,000	36 to 53	13 to 27	8 to 10	3 to 5	3 to 7	5 to 11

Temperature	Young's Modulus E kg/mm²	Ultimate tensile strength R kg/mm²	Elastic limit (kg/mm²) At 0.2%	Elongation at break A %	Reduction in area Σ %
40°C	19,300	37	14	6	14
60°C	19,200	39.5	13.2	10	20
80°C	19,100	44	12.2	12	28
100°C	18,800	46	15.2	17	38
150°C	18,100	36	14.5	21.5	53
200°C	17,700	29	13.2	24	61
250°C	17,100	24	12	25	65
300°C	16,500	20	11.2	25.5	67
350°C	15,800	16	10.6	25.5	69
400°C	15,200	15	10	26	70

The rod is then in the argon-filled receiver. The two upper keys are removed. What remains in the container (sleeve and non-extruded content) falls off, being dragged by the rod into the receiver. The keys are removed from this receiver, and it is closed by a tight lid and brought onto a rack, while water circulation is established between its walls. Following about an hour and a half of cooling, the rod is taken out of the receiver. It is separated from the remainder by sawing off. The sleeve, the extrusion die and the boss are recovered.

It is possible, with a single press, to multiply the number of ovens and receivers in order to increase the extrusion work speed.

Following extrusion, a few other operations have to be carried out:

Straightening

This is done with a conventional machine consisting of two rolls, one barrel shaped and the other hyperboloid shaped, rotating in the same direction. The rod is brought to 200°C and protected against oxidation by a silicon layer. Following 5 to 6 passes, the rod is perfectly straight.

Machining to Size

During extrusion, the sleeve expands a little in order to bear against the container. Following extrusion it is necessary, therefore, to bring down the outside diameter of the sleeve to a small value, which is done by mandrel treatment.

Conclusion

The uranium extrusion operation, conducted as just described, gives rods which are perfectly sound over their whole length. The wear on the equipment is relatively very small, so that the cost of an extrusion operation is low as regards the materials. The technique used offers complete safety and at the same time, a relatively large output if, as suggested above,

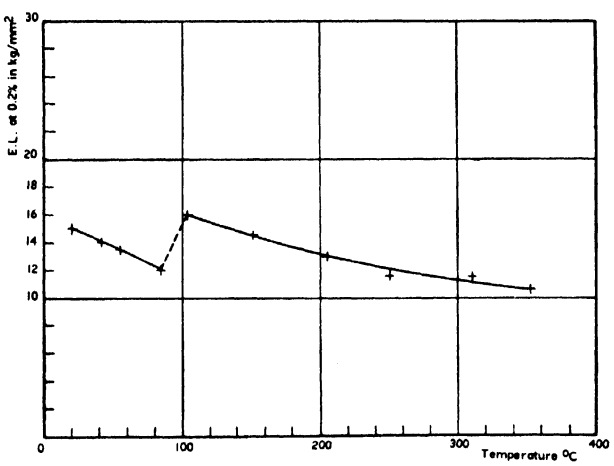

Figure 21. Uranium elastic limit at 0.2% as a function of the temperature

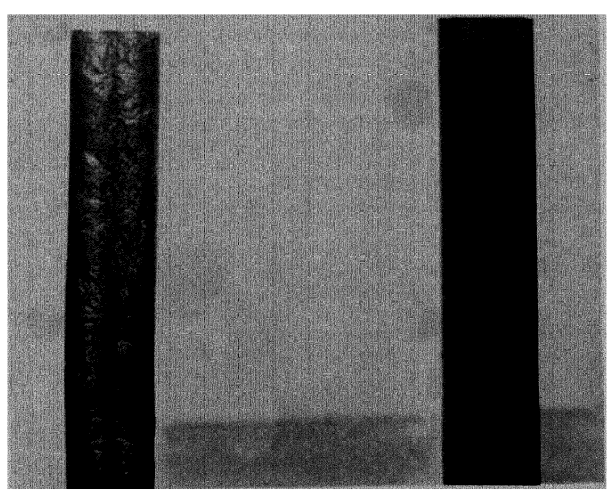

Figure 22

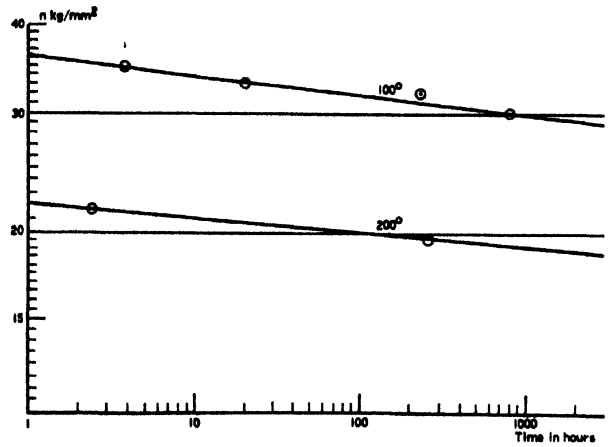

Figure 23. Uranium breaking time

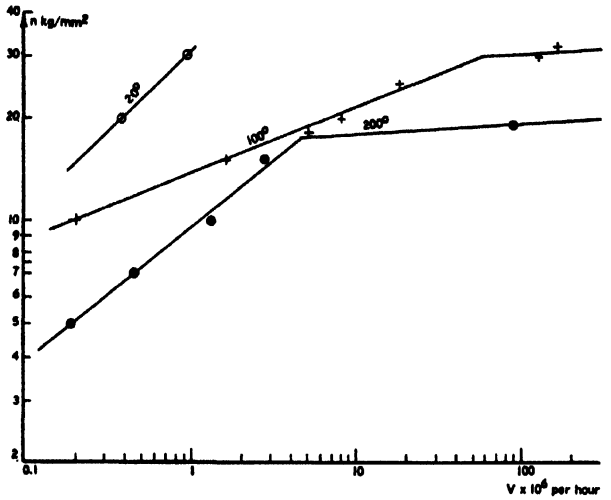

Figure 24. Uranium rates of creep

the number of heating ovens and receivers is multiplied.

CHARACTERISTICS OF THE EXTRUDED METAL

The various characteristics of the metal, noted at the C.E.A. laboratories, can be summed up as follows:

The metal extruded in the γ phase appears as a metal having very heterogeneous grains, the size of which varies from 5 to 500 μ. This metal has no characterized orientation at all (Fig. 17). The machining characteristics offer substantial variation, even on samples from the same rod. Their main values are indicated in Table I.

They are not different from the cast metal, molded under vacuum, nor from the metal which has undergone mechanical transformation and been thermally treated in the γ phase, following transformation. We may note the absence of an elastic limit, from the formal standpoint. We note a change in the ultimate tensile strength, elongation, and conventional elastic limit, in the vicinity of 100°C (Figs. 18, 19, 20 and 21). The hardness varies erratically from one point to the other, both radially and transversally. The break always is of the "fragility" type and takes place anywhere on the specimen. During thermal fatigue tests carried out by cycling between 20°C and 520°C, the metal is distorted, with local deflections which are fairly substantial and the surface looks like an orange rind (Fig. 22).

From the standpoint of creep, the following may be considered: (*a*) the breakup time, and (*b*) the rate of creep in stable regime.

Figure 23 shows the rate of creep at 100°C and 200°C, as a function of the stress. It may be noted that the stresses which bring about the break decrease very little for times between 1 hour and 1000 hours.

Figure 24 shows a few creep diagrams, plotted with different stresses, at 100°C. By eliminating the transitory creep time, one notes, from the stationary creep times, variation laws at 100°C and 200°C. We can extract the following data:

	Room	*100°C*	*200°C*
Load which gives 1% elongation in:			
100 hours	–	30.5	19
1000 hours	–	21.2	17.8
10,000 hours	31	13.5	9.6
Load which brings about a break in:			
0 hours	40	48	30
300 hours	–	30.8	19.5
1000 hours	–	29.8	19.1
10,000 hours	–	27.9	18.2

CONCLUSION

γ phase extruded uranium offers characteristics and a behavior similar to those of vacuum cast uranium. Its cost, despite the relatively low cost of extrusion, is markedly higher than that of vacuum cast aluminum and uranium particularly because of the increase in the weight of waste metal, which must be recycled.

The extrusion method makes it possible to obtain long rods more conveniently than would be possible with a continuous casting process when dealing with a small number of rods.

The Technology of UO^2 and ThO_2

By J. R. Johnson and C. E. Curtis,* USA

Consideration has been given to various forms of fissionable and fertile materials for use in atomic reactors, including the pure metals, their alloys and compounds. Of particular interest are the dioxides of uranium and thorium which are refractory and corrosion resistant in some environments. Although the atomic structures of these oxides are similar, their method of fabrication and environmental conditions of use may be quite different, primarily because of the multivalent nature of uranium.

The oxides are useful in both granular and bulk form. Small grains of uranium and thorium oxides can be mixed with other materials to form matrix-type elements where they serve either as a convenient or necessary form of fuel or fertile material. For other applications the oxides may be fabricated in bulk form such as pellets, rods, plates or blocks.

There is a need for knowledge of the properties of these oxides, particularly as it affects fabrication in the various forms required. This knowledge is also required by reactor designers and engineers. There is in addition a challenging field for basic studies of sintering rates, oxidation behavior and other phenomena.

Fabrication techniques have been developed to produce uranium and thorium oxides in various forms with consideration given to the economy of production. While thorium oxide can now be made in sintered shapes by ordinary commercial ceramic processes, uranium oxide must be given special treatment. The continued application of basic knowledge of these materials has led to simpler, more practical means of fabrication and has thus widened the scope of their use in atomic reactors.

PROPERTIES

The data in Table I show the two dioxides to be quite similar in their general physical properties.

Both oxides are also resistant to corrosion by water up to 300°C. There is a marked difference, however, in their relative stabilities in oxygen environment. While thorium dioxide is stable in oxygen to its melting point, the dioxide or uranium undergoes a number of changes. Studies of these changes have been made in many laboratories throughout the world but there exists some disagreement as to the oxides which are formed. The observations below are in substantial agreement with those of Perio[1] and of Gronvold and Haraldsen.[2]

Uranium dioxides prepared by various means were examined by differential thermal analysis and by observing weight changes on heating. Some of these data are shown in Figs. 1, 2 and 3.

In all cases a small weight loss (0.0001 to 0.001 gm/gm UO_2) was observed approximately between 50°C and 150°C with a maximum about 100°C. Approximately this amount of water was determined in the uranium. In using a weight difference method to determine the oxygen content, care must be taken to account for this water loss. On heating, the D.T.A. and weight change curves indicate two oxidation steps, $UO_2 \rightarrow (U_3O_7)$ and $(U_3O_7) \rightarrow U_3O_8$. Both steps are quite exothermic. The initial oxides vary from $UO_{2.005}$ to $UO_{2.15}$ and in general the intermediate oxides vary from $UO_{2.34}$ to $UO_{2.38}$, the lower values corresponding to those initial oxides having low values (see Table II). The oxygen ratios were calculated on the basis that the uranium oxide was U_3O_8 at its maximum weight, usually found between 500°C and 600°C.

Petrographic and X-ray diffraction studies were made on the uranium oxides as well. X-ray diffraction showed the intermediate oxides to be face-centered tetragonal with $a = 5.37$ and $c = 5.55$. The higher oxide was identified by X-ray as U_3O_8. No

Table I. Properties of UO_2 and ThO_2

Property	*UO_2*	*ThO_2*
Crystal structure	Face-centered cubic (CaF_2)	Face-centered cubic (CaF_2)
X-ray density	10.95	10.00
Melting point	2800°C	3200°C
Thermal conductivity[5] cal-cm/°C-cm²-sec (corrected to 100 per cent density)	0.02-20°C 0.008-1000°C	0.02-20°C 0.007-1000°C
Expansivity $°C^{-1}$	ca 10×10^{-6} (0-1000°C)	9.0×10^{-6} (0-1000°C)
Specific heat cal/gm-°C	0.056 (0-200°C)	0.058 (0-800°C)
Tensile strength	ca 5000 pounds per square inch	ca 5000 pounds per square inch
Modulus of elasticity		21×10^6 pounds per square inch
Metal atoms/cm³ in oxide compared with metal	51.5 per cent	78.5 per cent

* Oak Ridge National Laboratory.

Table II. UO_2-U_3O_7 Oxygen Contents from D.T.A.—Wt. Change Data

Source material	*Fused oxide*	*Ammonium diuranate precipitate oxide*	*Mallinkrodt oxide*	*Hydrogenated steam oxidized oxide*	*Oxidized U chips*	*Peroxide precipitate oxide*	*UO_3 hydrate crystal oxide*
Initial oxide calculated by wt. change UO_{2+x}	$UO_{2.005}$	$UO_{2.129}$	$UO_{2.158}$	$UO_{2.02}$	$UO_{2.028}$	$UO_{2.056}$	$UO_{2.018}$
Intermediate Oxide U_3O_{7+x}	..	$UO_{2.388}$	$UO_{2.375}$	$UO_{2.336}$	$UO_{2.351}$	$UO_{2.369}$	$UO_{2.339}$
H_2O/gm	0.0003	0.0015	0.0020	0.0003	0.0003	0.0004	0.0003
Initial oxide chemical analysis	..	$UO_{2.091}$	..	$UO_{2.021}$	$UO_{2.044}$	$UO_{2.068}$	$UO_{2.005}$

evidence was found for U_4O_9 or U_2O_5, although the methods used in this study may not be adequate for their detection.

There is evidence that the UO_2 prepared by methods yielding very small crystals reacts at lower temperatures and more readily shows the metastability range of the U_3O_7. Some extremely fine UO_2 powders are pyrophoric, reacting exothermically in air at room temperature forming U_3O_8 in a few seconds. The oxides having large crystallites or small surface areas react more slowly and at higher temperatures.

UO_2 is the stable phase above ca 1100°C so that the major difficulty in handling UO_2 arises in heating and cooling through the lower temperature stages of its processing and fabrication.

Although ThO_2 is stable in air at all processing temperatures, there is a marked physical difference in the oxide powders according to the methods of preparation. Thoria powders made by calcining oxalate or carbonate precipitates are more readily sintered if calcination takes place at a minimum temperature, ca 900°C. Calcinations made at 1200°C or higher produce a material much more crystalline that sinters with difficulty.

FABRICATION

UO_2 and ThO_2 can be fabricated into various shapes by most of the processes used for ceramics generally. Cold pressing, hot pressing, extrusion and slip casting[3] have all been used successfully. The method most often used for experimental shapes has been cold pressing followed by sintering.

Three means of obtaining high density-pressed products have been tried, all of which have produced large sintered shapes with densities ranging up to 99 per cent of theoretical. The use of large fused grains, sized and proportioned to pack densely on pressing prior to sintering has yielded products up to 92 per cent density. A second method where very fine particles were used has produced shapes having 97 per cent density while a third method using minor additions in ThO_2 has given products over 99 per cent of theoretical density when the effects of the additions are taken into account.†

† Theoretical density for ThO_2 + ½ weight per cent CaO is 9.84 gm/cm³.

The use of fused oxides of uranium and thorium in the dense packing method is limited by the poor economy of the fusion process. Another means of obtaining large crystallites of UO_2 described below overcomes this difficulty, but maximum fabrication density is more easily attained by the other methods described.

There is considerable sintering shrinkage in the products which are made with very fine powders. Control of cracking and warping is consequently difficult; however, large shapes of UO_2 are best made this way. Fine powders are also desirable for producing high density slip cast products of UO_2 and ThO_2 such as crucibles and tubes, which have relatively thin walls. The large surface area of the sub-micron powders increases the sintering rate markedly over that obtained with powders of larger crystallites.

In the case of ThO_2 a remarkable effect on sintering was found by adding less than one weight per cent CaO to the ThO_2 powders.[4] While this contaminates the thoria with a minor addition, the effect makes possible the sintering of bulk products at temperatures in the range used in some commercial tunnel kilns. Calcium has a low thermal neutron capture cross section and the addition does not alter the general properties of the ThO_2.

UO_2 FABRICATION

UO_2 has been made in bars, crucibles and rods (Fig. 4). The bars are generally made by compacting UO_2 powder in a steel die. Large rods are made by isostatically pressing the oxide in rubber forms. The most satisfactory powders for pressing are made by hydrogen reduction of ammonium diuranate precipitates or peroxide precipitates which yield very fine grains if the reduction is accomplished at temperatures less than 1000°C. There is evidence of a defect structure in the UO_2 crystals as a result of excess oxygen which the fine powders tend to pick up on exposure to air, forming UO_{2+x} to $UO_{2.15}$. The effect of this defect structure combined with the greater effect of the large surface area of the grains accelerates sintering.

Sintering of UO_2 must be accomplished in an inert or hydrogen atmosphere. The $UO_2 \rightarrow U_3O_8 \rightarrow UO_2$

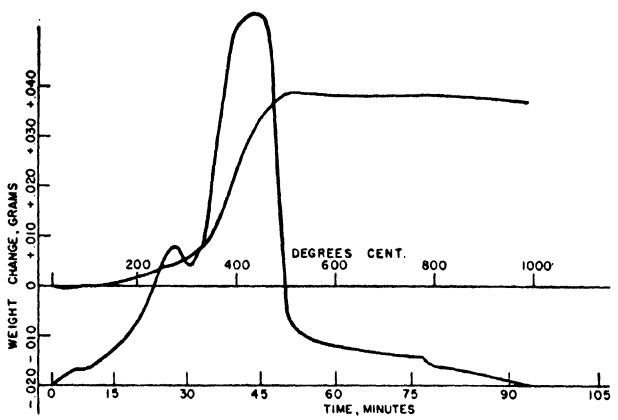

Figure 1. Fused UO_2. D.T.A. and weight change from UO_2 to U_3O_8

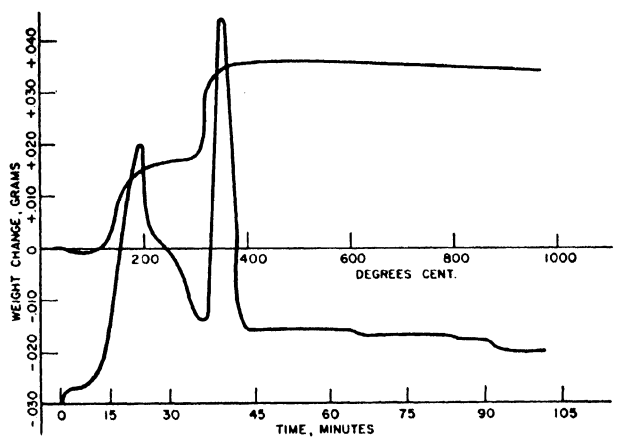

Figure 2. Peroxide Ppt. UO_2. D.T.A. and weight change from UO_2 to U_3O_8

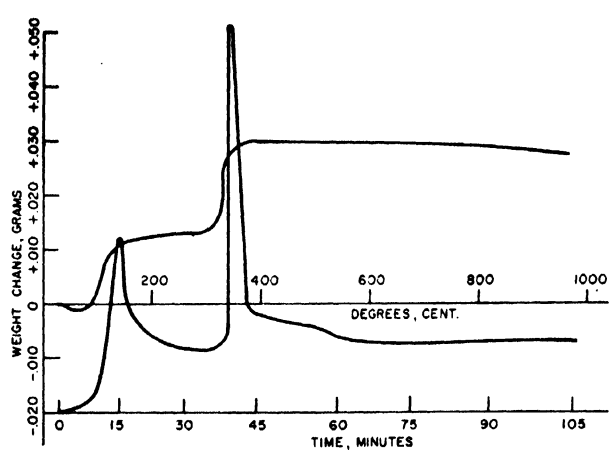

Figure 3. Ammonium diuranate Ppt. UO_2 D.T.A. and weight change from UO_2 to U_3O_8

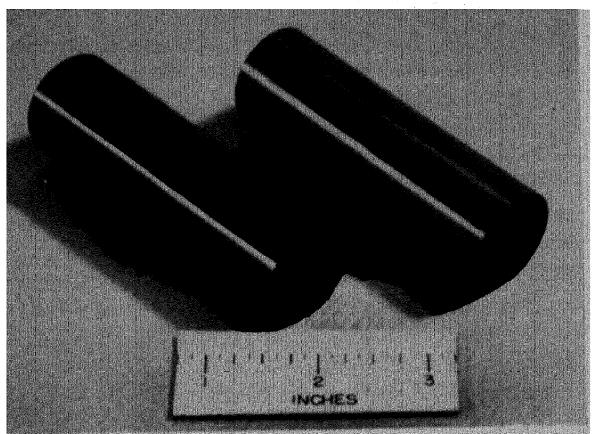

Figure 4 UO_2 rods

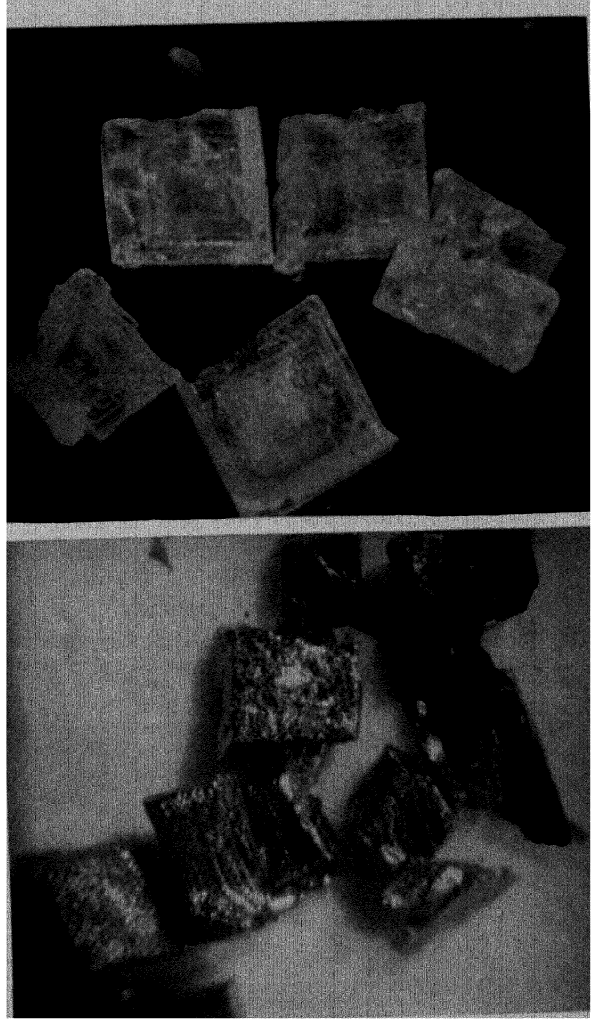

Figure 5. UO_2 particles (above) made from $UO_3 \cdot H_2O$ crystals (below)

which occurs on sintering in air is accompanied by a density change, $11 \rightarrow 8.4 \rightarrow 11$ which disrupts the product. When U_3O_8 is used as the starting product, shrinkage is excessive. A dense product can be obtained on thin shapes at 1600°C or less, but larger shapes are sintered at 1700°C to 1750°C.

UO_2 may also be hot pressed to simple shapes in graphite induction-heated dies. The general remarks about the initial powders given above also apply and very dense products can be obtained by pressing at 1500°C to 2000°C at a few thousand pounds per square inch.

UO_2 in the form of particles of specified sizes can be produced by several methods. Agglomerates of very fine UO_2 powders produced by the precipitation methods or by burning uranium metal can be screened

to the desired particle size range. These agglomerate particles are generally loosely bound and sintering is required to make a strong useful product. Depending on the size of the crystallites in the agglomerates, satisfactory particles can be made by sintering from 1700°C to 2100°C.

Very strong dense particles can be made by crushing and sieving the fused oxides to the desired particle sizes. These particles are generally red-orange and clear under transmitted light. It has been noted that the very fine particles of crushed oxide are attracted to the surfaces of the larger particles as the result of electrostatic attraction.

Still another method of obtaining large strong particles of UO_2 is by hydrogen reduction of UO_3 hydrates which have been deliberately grown hydrothermally to crystals of the desired size (see Fig. 5).

ThO_2 FABRICATION

Most ThO_2 shapes can be made readily by steel die pressing or isostatic pressing of the oxide powders. Some examples are shown in Fig. 6. Oxalate or carbonate precipitates calcined at 1200°C make satisfactory powders for fabrication provided a small amount of CaO is added to promote sintering. Calcines made at 900°C produce very fine, oxide crystallites which sinter readily at 1700°C without additions; however, a high shrinkage with tendencies for the product to warp and crack have been noted with this powder.

Sintering of ThO_2 shapes may be carried out in air, inert gases or hydrogen. Large shapes made of pure ThO_2 other than the low calcined material must be sintered at temperatures in excess of 1800°C in order to achieve 90 per cent density. Thin-walled crucibles may be sintered to 95 per cent density at 1700–1800°C using the coarser powders. The addition of about two mol per cent CaO permits sintering of bulk shapes made of coarser powders at 1700°C.

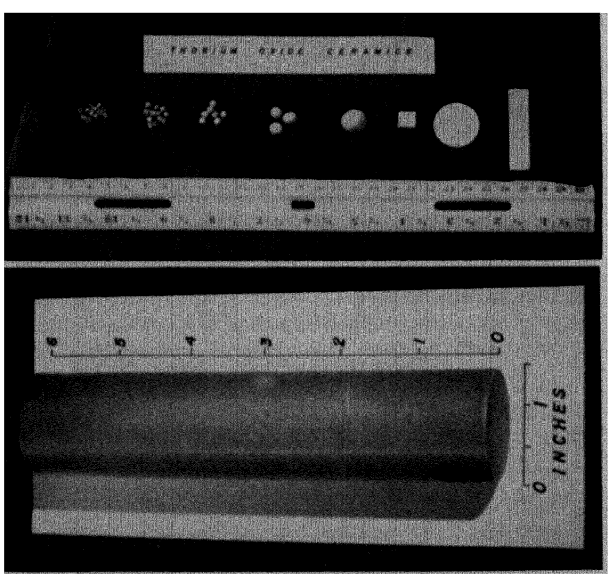

Figure 6. ThO_2 shapes

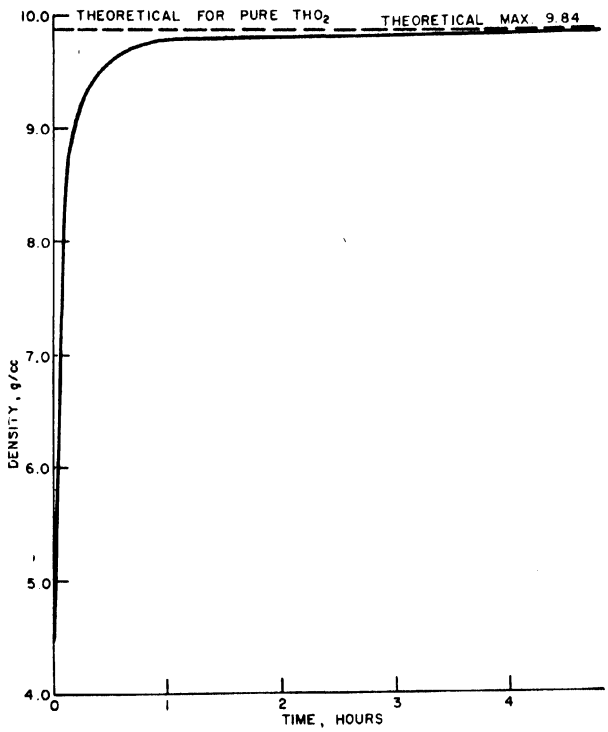

Figure 7. Sintering ThO_2 + ½ wt % CaO at 1700°C

The effect of the addition of calcium oxide on sintering is shown in Fig. 7. A study of the effect indicates that calcium is taken into solid solution in the ThO_2 lattice producing anion vacancies. The diffusion of Th^{++++}, O^{--} and Ca^{++} ions is accelerated as a result of the vacancies and more rapid sintering occurs. The Ca^{++} ion has about the same ionic radius as Th^{++++}, ca 1.0 Å so that solid solution is expected. A lowering of the index of refraction is noted as CaO is added to the ThO_2 up to 20 mol per cent. Chemical analyses show the CaO to be present after sintering, yet there is almost no measurable change in the unit cell dimensions of the ThO_2. The effect of CaO on sintering is noted beginning at 1100°C and is pronounced at 1600°C. There is no liquid phase in the ThO_2-CaO system below 2300°C so that this is a solid state reaction.

An investigation of the sintering rates indicates that surface diffusion is primarily responsible for the rapid densification of the ThO_2-CaO compacts. The mobility of Ca^{++} on the surface of ThO_2 at high temperatures is quite high and almost immediately the pores in the pressed compacts are filled to the closed pore state. Volume diffusion of the Ca^{++} and the Th^{++++} and O^{--} through the defect structure is much less rapid than migration over the surface; but is sufficiently rapid to cause much increased sintering rates in the closed pore state from ca 90 per cent to 99 per cent of theoretical density.

Grains of ThO_2 can be made by sintering agglomerates of fine particles or by crushing and sieving fused ThO_2 as in the case of UO_2.

CONCLUSIONS

The dioxides of uranium and thorium are similar in their general physical properties and atomic structure; however, because of the multivalent nature of uranium, different techniques must be applied in fabrication.

Advantage may be taken of defect structures in UO_2 as a result of oxygen excess and in ThO_2 as a result of a minor addition of CaO to accelerate their sintering. The fabrication of both bulk and granular forms of the two dioxides has been accomplished and in the case of ThO_2, using commercial ceramic practice.

A better understanding of oxidation phenomena with UO_2 and the sintering mechanisms of both oxides may make possible further improvements in fabrication techniques.

ACKNOWLEDGEMENTS

The authors would like to thank S. D. Fulkerson, who conducted the D.T.A. weight experiments with UO_2, Dr. T. N. McVay and G. D. White, who have made numerous suggestions and studied the oxides by petrography, L. M. Doney and J. A. Griffin, who fabricated the UO_2 and ThO_2 specimens, A. J. Taylor and R. L. Hamner, who have worked in developing the UO_3 to UO_2 process, Mrs. M. P. Haydon, who measured the specific heats, and Mrs. A. S. Hobbs, who assisted in editing the paper, and Dr. J. M. Warde, who encouraged this work and criticized the manuscript.

REFERENCES

1. Perio, P., *Oxidation of UO_2 at Low Temperatures,* Memoires Présentés à la Societé Chimique *39*: 256 (1953).
2. Gronvold, F. and Haraldsen, H., *Oxidation of UO_2,* Nature *69*: 162 (1948).
3. Corwin, R. E. and Everly, G. E., *Preparation of Refractories from Uranium Dioxide,* J. Amer. Ceram. Soc. *36*: 137 (1953).
4. Johnson, J. R. and Curtis, C. E., *Note on Sintering of ThO_2,* J. Amer. Ceram. Soc. *37*: 611 (1954).
5. Kingery, W. D., *Thermal Stress Resistance of Ceramic Materials,* J. Amer. Ceram. Soc. *38*: 11 (1955).
6. Katz and Rabinowitch, *The Chemistry of Uranium,* N.N.E.S. (1951).
7. Alberman, K. B. and Anderson, J. S., *The Oxides of Uranium,* J. Chem. Soc., p. 303 (1949).
8. Biltz, W. and Muller, H., Z. anorg. u. allgem. Chem. *163*: 279 (1927).
9. Jolibois, P., Compt. rend. *224*: 1935 (1947).

Record of Proceedings of Session 18B.1

WEDNESDAY AFTERNOON, 17 AUGUST 1955

Chairman: **Mr. H. M. Finniston (UK)**
Vice-Chairman: **Mr. H. J. van Eck (Union of South Africa)**
Scientific Secretaries: **Messrs. B. Prakash and J. Goedkoop**

PROGRAMME

P/555 Physical metallurgy of uranium and its alloys.....F. G. Foote
P/786 The solid state reaction between uranium and aluminium.....R. Kiessling
DISCUSSION
P/556 The metallurgy of thorium and its alloys.....O. N. Carlson *et al.*
DISCUSSION

The CHAIRMAN: This afternoon we are to concern ourselves with the metallurgy of thorium and uranium and their alloys, and the fabrication of fuel elements. With present-day reactors, no matter what the different physicists may or may not do, and no matter what the different engineers may or may not do, you have to have uranium and, if you judge by what the physicists think, thorium as well. The importance therefore of knowing the purposes of these materials cannot be overestimated, and since no reactor of the present day, with perhaps the exception of the homogeneous reactor in an aqueous solution, works without a fuel element, the methods and technique of making these elements to perform their particular tasks also cannot be overestimated.

Mr. F. G. FOOTE (USA) presented paper P/555.

Mr. R. KIESSLING (Sweden) presented paper P/786.

DISCUSSION OF P/555 AND P/786

Mr. D. H. GURINSKY (USA): The uranium-aluminum system has been studied in the United States of America from both the practical and the fundamental points of view. I would like to make a comment with respect to a practical solution of the interaction between uranium and aluminum. It has been found that if one interposes an oxide film of aluminum, such as one can obtain by anodization, one can prevent reactions between aluminum and uranium, even at elevated temperatures.

Mr. K. CARLSEN (Norway): Mr. Gurinsky says you can prevent reactions between aluminum and uranium by providing an oxide layer. Would not this layer ruin the thermal contact between the aluminum and the uranium, and what would be the temperature drop as far as the oxide layer is concerned.

Mr. GURINSKY (USA): It does of course lower the heat transferred across the interface. However, the oxide film can be kept low enough and thin enough, so that the temperature drop across the oxide film is negligible. One further comment. In any system which is air cooled, one does experience a fairly large temperature drop across the interface between the aluminum and the uranium.

Mr. S. AAS (Norway): It appears from P/555 that uranium slugs prepared by powder metallurgical methods seem to be superior in behavior in pile irradiation, in stability, and so on. If this is really so, why are not powder metallurgical methods more used to meet difficulties in reprocessing such substances? Could Mr. Foote give an indication as to that?

Mr. FOOTE (USA): I think the best reason is that we started making our fuel elements by normal fabrication methods, and I think the powder metallurgy people got started somewhat later, and they are still in the process of trying to promote the use of powder metallurgical materials in reactors. It may well be excellent material, but it requires additional testing and evaluation.

The CHAIRMAN: On one of his slides Mr. Kiessling showed that the reaction between uranium and aluminium started at very special points. Does Mr. Kiessling know why those particular points were chosen in fact?

Mr. KIESSLING (Sweden): I do not know why that is so.

Mr. A. ASCOLI (Italy): Mr. Gurinsky referred to a film of aluminum oxide at the separation surface between the uranium and the aluminum. I should like to know how this film was obtained and how its thickness was measured.

Mr. GURINSKY (USA): The best method, and the method that was finally adopted was anodization in a sulfuric acid bath, and depending on the time and the temperature of the bath as well as, of course, the control of the current, one can lay down films varying in thickness for about two-tenths of a thousandth of an inch to one thousandth of an inch. The thickness was determined metallographically.

Mr. KIESSLING (Sweden): I should like to make a statement in this connexion. We have also found

that aluminium oxide layers slow down reaction and we have started the work by comparing the anodic layers in chromic, oxalic and sulphuric acid. We have found that layers made in chromic acid are better than the aluminium oxide layers made in sulphuric acid because, owing to the thickness of the layers in sulphuric acid, they break down. Large cracks begin to appear.

Mr. GURINSKY (USA): We compared different types of layers laid down from various media; and as regards the layers laid down in a chromic acid bath, these are thinner on the average than those laid down in sulfuric acid. Further, if one tried to set this up commercially, one would find that there were skips or discontinuities in the surface. It is true that the sulfuric acid bath layer tends to crack, but this is of no importance if the thickness is sufficient to prevent the aluminum contacting the uranium. Finally, the sulfate anodic layer is more abrasion-resistant than the chromic one.

Mr. M. J. LAVIGNE (Canada): I see in Mr. Kiessling's paper that he had an electro-polished surface of both metals. It happens in some cases that oxidation takes place during the electro-polishing and this may retard the reaction between the two metals. Can you tell me what solution you have used for your electro-polishing aluminium and uranium?

Mr. KIESSLING (Sweden): Well, it was a phosphoric acid solution, which is used in the ordinary polishing of aluminium and uranium alloys.

Mr. LAVIGNE (Canada): Have you done any surface analysis?

Mr. KIESSLING (Sweden): No.

Mr. LAVIGNE (Canada): I would like to ask Mr. Foote this question: Do you think that thermal cycling is a very good method of predicting or controlling the behaviour of uranium in a reactor?

Mr. FOOTE (USA): If the fuel elements in a reactor operate at temperatures above 300°C, thermal cycling effects would be observed and the uranium core should be stabilized with respect to thermal cycling. However, the mechanisms by which dimensional changes are produced by thermal cycling and by irradiation are considerably different and while the general appearance of thermal cycled and of irradiated specimens may be similar, there does not appear to be a one-to-one correspondence between the two effects. In general, one can say that material showing dimensional changes under thermal cycling will show similar changes under irradiation, but that material which is stable under thermal cycling may or may not be stable under irradiation.

Mr. PERIO (France): I should like to know whether there is any method other than anodizing for preventing the diffusion of aluminum into the uranium.

The CHAIRMAN: I think we will give you a general answer: anything in which the diffusion rate of aluminium and uranium is low is good enough. Whether the physicists will accept it is another matter. Mr. Meierson, have you any solution to this problem?

Mr. G. A. MEIERSON (USSR): No, sir.

Mr. H. A. WILHELM (USA) presented paper P/556. There was no discussion of this paper.

Session 18B.2

METALLURGY OF THORIUM, URANIUM AND THEIR ALLOYS; FABRICATION OF FUEL ELEMENTS *(continued)*

LIST OF PAPERS

			Page
P/825	The metallurgy of reactor fuels	J. P. Howe	179
P/561	Dispersion type fuel elements	C. E. Weber and H. H. Hirsch	196
P/953	MTR-type fuel elements	J. E. Cunningham and E. J. Boyle	203
P/947	On the possibility to improve the heat transfer of uranium and aluminium surfaces in contact	F. Boeschoten	208
P/827	Fabrication of uranium alloys	A. R. Kaufmann	210
P/562	Preparation, properties and cladding of aluminum-uranium alloys	H. A. Saller	214
P/828	The fabrication of fuel elements for the BNL reactor	D. H. Gurinsky *et al.*	221
P/961	Thermal strains and deformations in the rod and canning of the heterogeneous high flux reactor	M. Ristić *et al.*	231

The Metallurgy of Reactor Fuels

By J. P. Howe,* USA

Nuclear reactors employed for research and for power production have used at least nine different fuel elements or systems. As many more systems have received detailed study and evaluation. The number of systems under study is still increasing. To make these fuel systems, materials and processes have been devised and improved. Further, a number of important physical, chemical and metallurgical phenomena, some new, have been studied in connection with the production and use of fuels. The plan of this discussion will be to view this rapidly growing field from the above three aspects and thus discuss the following: (1) the distinct types of fuel elements, their applications, the requirements on them and their limitations; (2) the essential materials and metallurgical methods used in the manufacture and processing of elements; and (3) selected studies in the field of physical and chemical metallurgy of uranium, thorium, zirconium and other materials.

The present status of the technology described in this report is the result of the efforts of a large number of workers in several laboratories. The list of persons given in the appendix represents the author's best attempt to acknowledge those who contributed ideas and leadership. It has been found convenient to abbreviate reference to individuals and organizations in the text. The appendix gives a more complete identification of persons, organizations and chronology. There are a large number of subjects on which it is impossible to touch. As a result many valuable individual contributions are not given.

The work specifically directed toward fuels started in 1942. The historical development of the field since this time can be indicated only very briefly. The time available for the preparation of this discussion has not permitted anything approaching a complete review of all pertinent reports. Illustrations of the way in which the field grew are given rather than a complete treatment since the latter is not possible in a discussion of this type. It will be seen that the subject is broader than classical metallurgy and perhaps more appropriately should be called the technology of reactor fuel materials.

FUEL TYPES, APPLICATIONS AND LIMITATIONS

The properties and performance of fuel systems are determined in large measure by the bulk material. This obvious assertion serves as the basis for a classification of fuel elements and systems from the point of view of the technology of materials. Solid and fluid systems form two distinct classes, each of which may be subdivided into several families, and so on. Perhaps the central problem in the technology of power reactor fuel systems is to maximize specific power and life, subject to a large number of conditions arising from the type reactor, the use for the power, and the methods of reprocessing.

A. Solid Fuels

Limitations

The anatomy of a solid element is illustrated in Fig. 1. The important phenomena which, in turn, establish the conditions prevailing in the element are as follows:

1. The kinetic energy of the fission recoils is dissipated to the crystal lattice producing effects generally called radiation damage in the manner described by several authors.[1]

2. The fission product atoms either take up positions close to the end of their recoil range in the material or diffuse to the most stable configuration depending on the temperature and the energy of activation for diffusion in the surroundings. Since the atomic volume of the fission product atoms is greater than that of the uranium atom, a corresponding increase in the system volume must be expected at the very minimum. If the temperature is high enough to permit movement of the inert gas fission products, nucleation and growth of gas pockets must be expected at some amount of burnup.

3. All but a very small fraction of the fission energy appears as heat in the bulk material and flows to the lower temperature coolant.

4. The steady state temperatures and gradients set up determine: (*a*) stresses and strains, (*b*) reactions between jacket and coolant, (*c*) interdiffusion between bulk material and coating, (*d*) diffusion of fission products and (*e*) generally the set of properties of the given systems.

The specific power of an element, defined as the heat rate per unit mass of fissile materials, e.g., watts per gram, may be limited by one or more of the following:

1. Limiting heat flux to coolant due to the nature of the coolant.

(*a*) Under some practical conditions of gas cooling the heat flux may be determined by surface tempera-

* North American Aviation, Inc., Nuclear Engineering & Manufacturing, Los Angeles, California.

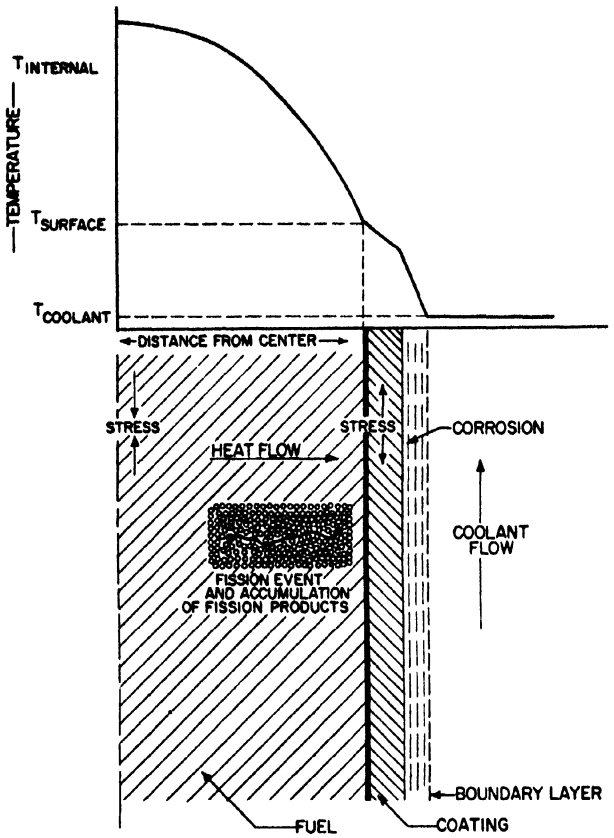

Figure 1. Diagram of fuel element heat flow, schematic

tures. The protective coating may set a limit on this temperature.

(*b*) Under practical conditions of liquid cooling, boiling of the coolant may limit the heat flux.

For this sort of limitation, the specific power of the element is given by the expression

$$P_s = \frac{2w}{r_0 \rho p} \qquad (1)$$

where P_s = specific power in watts per gram of contained fissile material, w = limiting heat flux in watts per cm^2, r_0 = radius of cylindrical element or half thickness of plate element, ρ = density of fuel bearing material, and p = weight fraction of fissile material.

2. Limiting temperature differences and flow of heat within an element.

(*a*) If the surface temperatures are fixed in a given range, for example, by a demand for power, then the maximum permissible central temperatures may limit the flow of heat. For this case

$$P_s = \frac{4\ K\ \Delta T}{r_0^2\ \rho\ p} \qquad (2)$$

where K = thermal conductivity of the fuel bearing material, e.g., watts/cm-°C, and ΔT = temperature difference center to surface.

(*b*) The stresses set up due to temperature gradients may limit the latter and hence the flow of heat for brittle, elastic materials. The following expression indicates the limiting conditions approximately

$$P_s \simeq \frac{a\ 8KS_0}{r_0^2 a E \rho p} \qquad (3)$$

where S_0 = fracture stress for fuel bearing material, a = thermal coefficient of expansion, and E = Young's modulus.

(*c*) Similarly, stresses in jacketing material may limit heat flow. For this case

$$P_s \simeq \frac{2K_j S_j}{r_{0j} a_j E_j \rho p r_0} \qquad (4)$$

where the subscript j identifies the quantities defined above with the jacket or coating material.

If comparisons of the specific power of various power systems are desired it is necessary to use as a basis all the fuel in process as well as that in the element. Also the average specific power, approximately one-half the peak, for the reactor should be used. The above maximum specific power may be corrected by multiplying by one-half the ratio of the fuel in the reactor to the total amount tied up.

Table I. Metallic Uranium–

Element	*Length*	*Length U cylinder*	*Diameter*	*Coating or jacket*		
				Metal	*Thickness*	*Nature of fuel-coating interface*
1. Unbonded Al canned natural U slug	4.06 in. (10.3 cm)	4 in. (10.2 cm)	1.1 in. (2.8 cm)	Al	0.02 in. (0.05 cm)	No bond, drawn fit
2. Ibid	4.07 in. (10.3 cm)	4 in. (10.2 cm)	1.1 in. (2.8 cm)	Al	0.035 in. (0.09 cm)	Ibid
3. Ibid	5 ft-6 in. (168 cm)	5 ft-6 in. (168 cm)	1.1 in. (2.6 cm)	Al	0.035 in. (0.09 cm)	Ibid
4. Bonded Al clad natural U slug	4.07 in. (10.3 cm)	4 in. (10.2 cm)	1.36 in. (3.45 cm)	Al	0.035 in. (0.09 cm)	Al-Si bonding material
5. NaK bonded rods	7.6 in. (19.0 cm)	1.9 in. (4.8 cm)	0.364 in. (0.92 cm)	SS	0.002 in (0.56 cm)	Slugs spaced in stainless steel tube; liquid NaK fills space between fuel and stainless steel cladding
6. NaK bonded rods	6 ft. (183 cm)	6 in. (15.3 cm)	0.75 in. (1.9 cm)	SS	0.010 in. (0.025 cm)	Ibid

The last two cases do not define limiting conditions for substances such as metals and ceramics at elevated temperature which yield plastically. If flow occurs the stresses may be relaxed to very low values. However, if the reactor is shut down, the stresses may be set up in reverse. Brittle behavior at low temperatures may then lead to fracture. Even with adequate plasticity and strength for a single cycle, a fatigue-like failure is possible after a number of cycles.

The useful life of a solid fuel element may be limited by changes in reactivity of the reactor in which it is used due to burnup of fissile material and to accumulation of fission products of appreciable cross section or physical changes in the element due to radiation damage, the accumulation of fission products or any of the conditions described above.

Specific illustrations of the above points will be given below.

Metallic Uranium Base Elements

Characteristics of uranium associated with the crystalline anisotropy of the alpha modification and with its allotropy determine the nature and behavior of several families of elements. The specific elements are listed in Table I together with their essential features. Uranium cylinders protected by aluminum cans produced the first significant amounts of nuclear heat in November, 1943, in the air-cooled graphite-moderated research reactor[2] at the X-10 site of the Plutonium Project, Oak Ridge, Tennessee. These elements, called unbonded aluminum canned slugs, may be made in any convenient size.

The second reactor to produce a reasonably large neutron flux, was the heavy water moderated and cooled CP-3[3] set in operation in June, 1944, at the Argonne Site of the Plutonium Project near Chicago, Illinois. It used long uranium rods clad in aluminum tubes fitted by drawing of the cladding on to the uranium. A cross section is pictured in Fig. 2a.

An improved version of the long element, consisting of short slugs closely spaced in a finned aluminum tube filled with slightly pressurized helium to provide for leak detection, is used in the air-cooled graphite-moderated research reactor[4] at the Brookhaven National Laboratory (BNL).

Bonded uranium cylinders enclosed in aluminum are used in the ORNL Graphite Reactor at the present time. The protective aluminum jackets are brazed to the uranium by means of an aluminum-silicon eutectic alloy. Such elements are called bonded aluminum canned slugs. A cross section is shown in Fig. 2b.

The family of aluminum-clad uranium elements may be used at surface temperatures at which aluminum gives suitable service. In air this is slightly in excess of 300°C. In water conditions of corrosion limit the temperature to near 100°C unless precautions are taken. Recently Draley[5] has found how to achieve tolerable corrosion rates at temperatures approaching 300°C. If the temperature of a clean uranium-aluminum interface exceeds 300°C interdiffusion becomes rapid compared to the life of unbonded fuel elements. In the case of the Oak Ridge unbonded aluminum canned slugs, this interaction occurred at random sites producing bumps which in some cases leaked air permitting destruction of the slug. The aluminum-silicon bonding procedure served to provide a uniform interaction layer which does not thicken significantly with time in the neighborhood of 300°C. Moreover, any leak in the aluminum can provides corroding conditions only in a very localized spot, in contrast to the case of a leak in an unbonded element. The solution of the problem of the aluminum-uranium interaction found at Brookhaven was the interposition of an anodic coating on the inside of the aluminum tube. As mentioned above, detection of leaks through the jacket is assured by a helium pressure monitoring system connected to each element. The maximum temperature of surface and center and the maximum heat flux in the respective research reactors is given in Table I.

At a given velocity of cooling air, the flux of heat depends on surface temperature of the element. Reasonable air velocities and the accompanying practical

Base Fuel Elements

Final closure	*Reactor*	*Temperature*		*Heat flux maximum*	*Specific power maximum*
		Surface	*Center*		
Seam weld, crimped end	ORNL air cooled graphite	473°F 245°C	660°F 349°C	7300 BTU/hr/ft² 2.3 watts/cm²	38,400 BTU/hr/lb U^{235} 24.8 w/gm U^{235}
Shielded arc	Ibid				
Ibid	ANL heavy water reactor (CP-3)	110°F 43°C	120°F 49°C	13,300 BTU/hr/ft² 4.2 watts/cm²	260,000 BTU/hr/lb U^{235} 168 w/gm U^{235}
Ibid	ORNL air cooled graphite (X-10)	473°F 245°C	660°F 349°C	7300 BTU/hr/ft² 2.3 watts/cm²	38,400 BTU/hr/lb U^{235} 24.8 w/gm U^{235}
Ibid	Experimental breeder reactor (EBR)	635°F 335°C	735°F 391°C	756,000 BTU/hr/ft² 240 watts/cm²	60,000 BTU/hr/lb U^{235} 38.8 w/gm U^{235}
Ibid	Sodium reactor experiment (SRE)	1000°F 538°C	1200°F 649°C	340,000 BTU/hr/ft² 107 watts/cm²	643,000 BTU/hr/lb U^{235} 415 w/gm U^{235}

Table II. Dispersion of Fissile Materials

Matrix	Dispersed Material	Shape	Thickness	Coating thickness	Width	Length	No. of plates	Method of assembly
Al	UAl_4	Curved plate	0.060 in. 0.14 cm	0.020 in. 0.046 cm	3 in. 6.9 cm	24 in. 55.5 cm	414	Sides brazed into slotted Al plates
Al	UAl_4	Flat plate	0.060 in. 0.14 cm	0.020 in. 0.046 cm	3 in. 6.9 cm	24 in. 55.5 cm		Similar
Al	UO_2							
Stainless steel (SS)	UO_2	Flat plates	0.030 in 0.069 cm	0.005 in. 0.012 cm	2.5 in. 5.8 cm	23 in. 53.0 cm	720	Brazed into SS assembly
Th	U	Cylinder	0.75 in. 1.9 cm	See SS clad NaK bonded U				

* Conditions calculated.

pumping power for research reactors, together with the limiting surface temperature, tends to limit heat flux to the range noted in Table I; depending of course, on the expense found acceptable for the cooling system. Thus the air-cooled reactor provides an example of limitation of performance by surface limitations on temperatures, case 1(*a*) above.

Liquid metal bonded uranium cylinders in steel or other material of reasonable high-temperature strength have been developed and used in a sodium-cooled reactor. The experimental fast breeder[6] reactor, built and operated at the National Reactor Testing Station in Idaho by the Argonne National Laboratory, employed 1-cm diameter highly enriched uranium slugs in stainless steel tubes filled with a sodium-potassium alloy usually called NaK. The sodium - cooled graphite - moderated experimental power reactor under construction near Los Angeles, California, uses ¾-inch slugs (1.9 cm) of slightly enriched uranium similarly contained. A schematic cross section of such an element is given in Fig. 2c.

The sodium or the sodium-potassium alloy used to cool the above-mentioned elements can provide heat transfer at least at the rate of 500 watts/cm² (1.59×10^6 BTU/ft²-hr) and with corrosion rates less than 0.0001 inch (0.00025 cm)/year at 500°C. Therefore, limitations arise from internal properties of the element.

The chief use of these elements is for power production which favors coolant temperatures near 500°C to obtain high steam plant efficiencies. If the temperatures of the alpha-beta transformation, 660°C, is taken as a limiting central temperature because of the severe distortion which can occur if uranium is repeatedly heated and cooled through the transformation, then an example of limitation under case 2(*a*) above, is provided. The use of uranium alloys may remove this limit.

With steel jackets the limiting surface temperature is lower than the iron-uranium eutectic temperature, 725°C, since near this temperature rapid interaction of jacket with slug would occur at points of contact. The use of zirconium as a jacket or as a barrier layer will obviate this difficulty.

Bonded uranium rods enclosed in zirconium would appear to offer an attractive family of elements for reactor use. The bond between these metals is strong and interdiffusion is acceptably low below 800°C. Such elements have been studied experimentally and their use contemplated in power systems, for example, the Pressurized Water Power Reactor being studied by WAPD[7] but no reactor has been built using them.

The use of uranium base elements in commercial power reactor will require as long life as can be practically obtained in order to reduce reprocessing costs. In thermal neutron power systems neutron reactivity changes limit burnup to between 1 and 2 per cent.

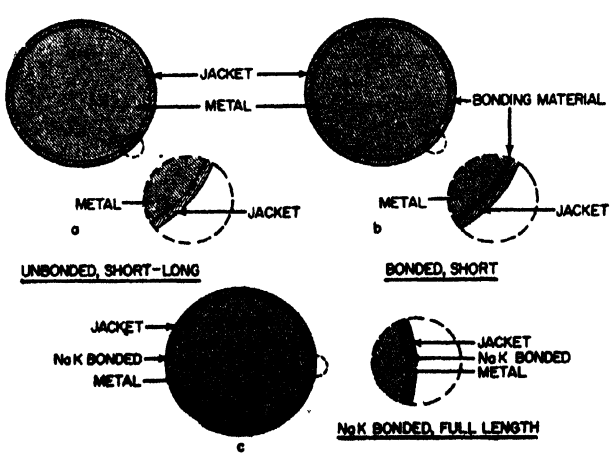

Figure 2. Schematic cross sections of bonded and unbonded cylindrical type fuel elements

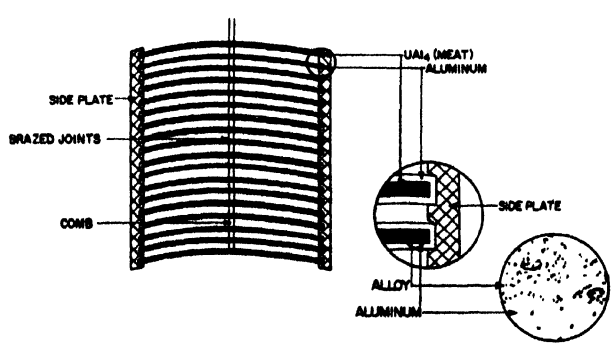

Figure 3. Schematic cross section of MTR fuel element

in Well-behaved Matrices

Reactor	Maximum temperature: Surface	Maximum temperature: Center	Maximum heat flux	Maximum specific power
Materials testing reactor	240°F 116°C	–	195 watts/cm² 6.1 × 10⁵ BTU/hr/ft²	1.5 × 10⁷ BTU/hr/lb U^{235} 9400 watts/gm U^{235}
ORNL research reactor, pool type	200°F 93°C	–	1.0 × 10⁵ BTU/hr/ft² 32 watts/cm²	3.1 × 10⁶ BTU/hr/lb U^{235} 2000 watts/gm U^{235}
Pool type reactor, Geneva, Switz.				
Pool type research*	554°F	566°F	70 watts/cm²	3.1 × 10⁶ BTU/hr/lb U^{235}
Water cooled power reactor*	290°C	297°C	2.2 × 10⁵ BTU/hr/ft²	2000 watts/gm U^{235}
Sodium graphite reactor*	960°F 516°C	1600°F 871°C	8.5 × 10⁵ BTU/hr/ft² 274 watts/cm²	1.08 × 10⁶ BTU/hr/lb U^{235} 694 watts/gm U^{235}

In the case of breeder reactors much higher burnup is permitted by this consideration. The goal of the materials technologist is therefore set to achieve fuel elements stable to 2 per cent burnup as a minimum and more if possible. It should also be clear that to increase specific power as much as possible, as small diameters as can be economically made and handled will be used.

Dispersions of Fissile Materials in Well-behaved Metallic Matrices

Aluminum-uranium alloys and the fabrication of fuel elements from them were developed by the ORNL and BMI starting in the year 1946. These elements were expressly for use in a high flux reactor for testing reactor materials. The design of this reactor[8] started at ORNL under Wigner, during the year 1946 and led, after preliminary study, to the proposed use of aluminum fuel elements containing slightly less than 2 atomic per cent U^{235} as highly enriched uranium, cooled and moderated with water. Aluminum uranium alloys of this composition after working and recrystallization have a structure in which a dispersed phase, dominantly UAl_4,[9] is in equilibrium with an aluminum phase containing a very small amount of dissolved uranium.

Details concerning these elements are listed in Table II. A schematic cross section of an MTR element is shown in Fig. 3. Besides serving very effectively in the MTR, located at NRTS, this type element is being used in the several swimming-pool research reactors now coming into use. It is also being considered for commercial power reactors by the Yankee Power Group. The specific power of such elements is limited by the permissible heat flux to the cooling water and is as indicated in Table II. Their life is beyond that permitted by reactivity changes for a reactor and may very well be equivalent to complete burnup of the fissile material. Environmental conditions permitted will be those for aluminum.

The principle of the aluminum-uranium elements may quite obviously be extended to a variety of systems in which uranium or a uranium compound is dispersed in a solid matrix, the latter chosen for its desired properties which include structural service, corrosion resistance, formability, and neutron absorption cross section. These other elements are also listed in Table II.

Aluminum-UO_2 dispersions have been developed recently by Cunningham, ORNL, and are used in the pool-type research reactor set up at Geneva, Switzerland. Other inert uranium compounds also may be dispersed in aluminum. Performance comparable to the aluminum-uranium elements may be expected.

Austenitic steel-UO_2 dispersions have similarly been developed for small water-cooled and moderated power plants. Again performance limits are probably beyond those required by practicable reactor systems. In a high power, high temperature system, thermal fatigue probably places a limit on the number of times a reactor may be started and stopped. Work at KAPL by Vandenberg and by Coffin,[10] shows that at 400°C stainless steel will fail after a few hundred cycles at bending or thermal stresses corresponding to a heat flux of 300 watts/cm² through a thickness of 0.01 inch (0.025 cm).

Thorium-uranium cylinders contained in NaK or Na filled steel tubes may serve in power reactors such as the sodium-cooled graphite[11]-moderated reactor. Details of the optimum degree and method of dispersion of the approximately 4 per cent U^{235} required are not solved but estimated performance of such elements is good. Central temperatures at least as high as 1400°C, the α-β transition temperature, should be permitted thus allowing the maximum specific power to be 720 watts/gm if the cooling sodium is at 500°C and the rod diameter is 0.75 inch (1.90 cm). By making the rod diameter 0.25 inch (0.64 cm) the specific power can be increased to 6480 watts/gm. Life corresponding to the burnup permissible in the aluminum-uranium system at corresponding temperatures relative to the melting points of the two metals should be obtainable.

Zirconium-uranium alloys clad with zirconium have been studied in some detail and have suitable properties. Here uranium may be put in solution at elevated temperatures and precipitated upon cooling

in standard metallurgical fashion. Excellent specific power and life may be obtained. However, the cost of the zirconium in such elements weighs against their use in power reactors.

Plutonium

Plutonium cylinders in steel cans served as elements in Table III in a fast reactor cooled with mercury operated for research purposes at the Los Alamos Scientific Laboratory.[12] No information exists on such elements or sources of power except that derived from the physical properties of plutonium. The specific power permitted by the low thermal conductivity and transition temperatures make this element undesirable for such purposes. It is likely that plutonium uranium alloys will be used in fast breeder power reactors. However, here the metallurgical structure will be governed largely by the uranium and hence may be considered as related to that family of elements.

Ceramic Systems

BeO-UO_2 systems were studied extensively at ANL and ORNL, and at BMI during the years 1945 to 1947. A high temperature, helium-cooled, BeO-moderated power reactor proposed by Daniels, Technical Director of the Chicago Site of the Plutonium Project at the time, was the objective of these studies. The size and shape of the elements considered are indicated in Table IV. The methods of fabrication of a variety of shapes were developed at BMI and at the Norton Company. Radiation stability was established for cylindrical shapes. Volatilization of BeO was observed during exposure to a very low partial pressure of water vapor at temperatures of 1000°C,[13] thus prescribing requirements on the dryness of any cooling gas. At operating temperatures the specific power of such elements is probably limited by the heat flux to the gas coolant. However, on shutdown, thermal stresses and brittle behavior will limit either the life or the permissible thermal strain at operating temperatures. Thus, such elements provide examples of limitations 2(*b*) and 2(*c*) above.

The reactor scheme was abandoned largely because of the expense associated with a high pressure helium cooling system and the fabrication of complicated bodies of BeO. However, these elements remain an attractive possibility.

Graphite elements, in which the UO_2 or UC_2 is dispersed in graphite (1) by impregnation of the normally porous artificial graphite or (2) by mixing and graphitizing, were developed at North American Aviation and Battelle Memorial Institute respectively. The former development was for a low power research reactor for which operating hazards were minimized. Radiation effects in such elements were studied by Hunter at ORNL and by McCarty and others at NAA. Although satisfactory under conditions customarily employed for graphite, these elements have not been used in any reactor.

Thoria and urania bodies[14] have been developed by Johnson and Curtis at ORNL. Since thoria is nearly as dense as thorium metal, its use as the fertile material in a reactor for conversion or breeding and power is indicated. Performance and life have not been investigated.

B. Fluid Fuel Systems

Fluid fuels for nuclear reactors as compared to solid fuels discussed above offer the following advantages to the materials technologist: (1) freedom from radiation damage, (2) freedom from the internal limitations on heat transfer discussed above, (3) simple preparation, and (4) less complicated and hence cheaper reprocessing. In place of the problems listed above for solid fuels there are those associated with pumping radioactive fluids, compact heat exchanger design, and corrosion of the whole reactor

Table III. Plutonium Fuel Element

Slug dimensions	*Jacket*	*Method of closure*	*Application*
5.5 in. (14.0 cm) length 0.65 in. (1.6 cm) diam	0.010 in. (0.025cm) wall; mild-steel can	Shielded arc	Fast Hg cooled research reactor

Table IV. Ceramic Fuel Elements

Matrix	*Dispersed material*	*Shape and dimensions*	*Remarks on application*
BeO	UO_2	BeO tubes impregnated with UO_2; 0.25 in. (0.63 cm) thick × 1.5 in. (3.8 cm) OD × 1 in. (2.5 cm) ID × 4.5 in. (11.5 cm) long. Suspended inside BeO moderator bricks	Proposed for high temperature power reactor by ORNL and ANL
Graphite	UO_2	Hexagonal graphite block impregnated with U_3O_8; 8.37 in. (21.3 cm) diam × 4 in. (10.2 cm) high	Low power research reactor proposed by NAA
SiC	UC_2	Ceramic blocks of SiC plus UC_2	Proposed for high temperature gas turbine power plant
ThO_2	UO_2	-	Proposed fuel for thermal breeder reactors

system. Thus one may replace a long-lived reactor assembly which contains short-lived troublesome fuel elements by a relatively short-lived reactor system. For a quantitative comparison of the two systems, more dependable data are needed on corrosion and expense of maintenance of fluid systems and fuel life and the expense of handling for solid fuel systems.

Limitations

The specific power of a fluid system may be estimated very approximately without recourse to a detailed design in the following two ways:

1. If the limiting heat flux and the surface-to-volume ratio in the exchanger are known approximately; for example, if the tube radius r_0 is known, then just as in the case of solid fuels above,

$$P_s = \frac{2w}{r_0 \rho} \qquad (1)$$

2. An alternate method may be based on the time for a round trip by the fuel through the reactor circulation system, the heat capacity, and the permissible decrease in temperature. The approximate relation

$$P_s = \frac{c_p T_{out} - T_{in}}{t\rho} \qquad (5)$$

where c_p is the specific heat (watt-sec/gm-°C), $T_{out} - T_{in}$ is the temperature rise, and t is time for round trip in seconds. With commonly feasible fluid velocities and system dimensions, the time for a round trip falls between 1 and 10 seconds.

In ways analogous to the case of solid fuels, materials may place some of the limitations on performance of the fluid system, for example:

1. Limiting upper temperature of container and heat exchanger materials due to (*a*) loss of strength, and (*b*) excessive corrosion.
2. Limiting fluid velocities due to erosion.
3. Limiting thermal stresses in heat exchanger tubes.

Several examples of fluid systems are given in Table V.

Aqueous Systems

The first nuclear reactor to use an aqueous solution was put in operation at the Los Alamos Scientific Laboratory in the year 1944. It used a solution of uranyl sulfate in light water held in a type-347 stainless steel container. Subsequent designs used uranyl nitrate solutions. Supo, now in use, dissipates up to 35 kw. Since that time five solution-type reactors have been put into operation including the Homogeneous Reactor Experiment (HRE) at ORNL.[15] Research reactors of this type avoid corrosion problems and have long life because they operate in the fractional megawatt range, using uranyl sulfate or nitrate solutions at approximately atmospheric pressure and hence below 100°C. The HRE requires higher temperatures and fluid velocities both of which promote corrosion of stainless steel and limit operating conditions and life.

Uranyl phosphate solutions investigated at Los Alamos have the interesting property that there is no discontinuity in solubility across the critical point of water, thus permitting high temperature operation. Corrosion rates of the metals gold and platinum only are sufficiently low to serve in contact with this solution. Thus corrosion of container materials is a major problem for this system.

Liquid Metal Fuels

Bismuth, primarily because of its low absorption cross section for thermal neutrons, received attention as a reactor coolant during the year 1942, particularly by Szilard. The interaction with uranium was studied

Table V. Fluid Fuel Systems

Reactor	*Fluid*	*Solute or dispersed material*	*Concentration range*	*Temperature range*	*Container material*	*Precautions*
Homogeneous Reactor Experiment	H_2O	UO_2SO_4	30–40 gm U^{235}/liter	242–250°C 467–482°F	Stainless steel	
NAA Water Boiler neutron source	H_2O	$UO_2(NO_3)_2$	45–50 gm U^{235}/liter	20–87°C 60–189°F	Stainless steel	
Los Alamos power reactor experiment	H_2O	$(UO_2)_3(PO_4)_2$	100–150 gm U^{235}/liter	20–455°C 60–851°F	Stainless steel	Gold plating on all surfaces exposed to hot solution
Intermediate scale homogeneous reactor experiment	D_2O	UO_2SO_4	4–5 gm U^{235}/liter	242–250°C 467–482°F	Stainless steel	
	Bi	U	0.05–0.66 wt % U in Bi	355–510°C 644–950°F	Low Cr, Mo-steel	Mg to getter O; Zr to inhibit mass transfer
	Bi	UBi_2(slurry)	Max. suspension of 10 wt % U	Max. temp of 950°F, 510°C	Low Cr, Mo-steel	
	Na	UO_2	Max. suspension of 30 wt % U	Max. temp of 1600°F, 870°C	Austenitic steels	

by Hoxing at Iowa State College and found to be too severe to permit direct contact. In a preliminary study of the binary system, stable intermetallic compounds were found. Exploratory studies at BMI indicated that the corrosion of iron by bismuth might be tolerable below 500°C. During the year 1943, Wigner proposed the use of a liquid bismuth-uranium alloy for a reactor but the above-mentioned work indicated an unfavorably low solubility at reasonable temperatures for systems based on natural uranium. However, more careful determinations of solubilities of uranium in liquid metals by Hayes and Gordon at MIT during the years 1945 and 1946 and by Teitel at BNL led to the careful study of the system Bi-U at BNL.[16] These studies show that a bismuth solution containing about 800 ppm U^{235} together with a few hundred ppm Mg and Zr may be contained in ferritic steel alloys or in graphite. Thus such a solution may serve as a circulating fuel in reactor systems capable of producing electric power at competitive commercial costs or better. The specific power of this fuel system should fall in the range 5000 to 10,000 watts per gram as indicated by use of the above expressions for the limits. The metallurgical problems are simply the extension of the work referred to above and include determination of the properties and nature of the liquid metal solutions and the corrosion and its limits on container materials for the solutions.

Miscellaneous Systems

A summary of other fluid fuel systems which have been suggested and studied in varying degrees but not used as yet is given in Table VI.

MATERIALS AND PROCESSES

The materials already mentioned in the foregoing section are recapitulated here for review. They either were developed or are being developed for the more important nuclear reactor fuel systems: (1) reactor grade uranium; (2) uranium alloys containing a small percentage of one or more of the following: Cr, Zr, Mo, Nb, Si; (3) aluminum-uranium alloys containing a few atom per cent uranium; (4) aluminum containing dispersed UO_2; (5) steel containing dispersed UO_2; (6) zirconium-uranium alloys; (7) thorium-uranium alloys; (8) zirconium free from hafnium for cladding; (9) BeO-UO_2 ceramics; (10) graphite impregnated with uranium; (11) SiC-UC; (12) ThO_2-UO_2; (13) liquid bismuth-uranium alloys; and (14) bismuth-thorium alloys.

Table VI. Tentative Fluid Fuel Systems (Studied only)

Fluid	*solute or dispersed solid*	*Obvious material problems*
H_2O	U oxides	Stability of suspension: (*a*) colloidal properties, (*b*) properties in water subject to ionizing radiation, (*c*) stirring, rheological properties vs settling. Erosion of system.
D_2O	UO_2	
NaK	UO_2	(1) Erosion of system, (2) settling vs stirring.
He		None, outside of possible erosion and handling.
Bi	U_2Bi_5	Similar to solution, plus erosion. Maintenance of proper particle size, preparation and make-up.
Fused fluorides	UF_4*	Corrosion due to the solubility of metals in molten salts.

* Or a complex uranium fluorine ion.

It is hoped that by discussing a sampling from this list, a picture can be drawn of the whole field of work with these materials. The procedure will be to outline most of the processes important for uranium base elements and then take up other materials to illustrate other aspects of processing.

The processes for handling these materials prior to their use in a reactor are for the most part well known to metallurgists and include: (1) extractive metallurgy; (2) melting and refining; (3) casting; (4) alloying; (5) hot and cold forming by extrusion, rolling, forging, pressing, swaging, drawing, powder methods; (6) cladding by rolling and extrusion; (7) coating by electroplating and hot dipping; (8) joining by brazing and welding; (9) machining and cutting by most of the known procedures; and (10) testing and inspection by chemical analysis, determination of physical properties, X-radiography, autoradiography, ultrasonic flaw detection, electromagnetic detection of discontinuities, and beta-ray thickness measurements.

A number of modifications of common practices and many special precautions not well known in the trade have been required and have been troublesome in some instances. Most of the precautions were related to requirements on the control of some impurities in the metals, to the need for maintaining good vacuum in melting and casting operations, and clean inert atmospheres for welding and other operations, and finally to difficult inspection and testing requirements.

The methods of handling fuel materials upon removal from the reactor are no older than reactors themselves and are unfamiliar to all except the separations chemist. The advent of commercial nuclear power will require complete economical reprocessing and recycling of fuel and fertile materials. A number of reprocessing steps for the partial elimination of fission products from fuels and the control of the complete composition of fuel systems have been found which may be said to resemble melting and refining operations.[17] If these processes are put into practice, the entire life history of metallic fuel materials may be in terms of metallurgical processes. In any event it will be advantageous to develop fuel systems with careful attention to all stages from the ore to fission product disposal or utilization and to the relations between the stages.

A. Uranium and Uranium-Base Alloys

The extractive metallurgy of uranium has been discussed by a number of authors[18] and hence will not be covered here. Highly-purified uranium oxide is produced by standardized methods. Improvements

to be expected in the future are probably in processes for working low grade ores at a reasonable cost. Traditionally, to date, the materials technologist, serving the field of nuclear reactors, has had to pay little attention to the extractive metallurgy of uranium.

Metal preparation, in contrast to ore treatment, has been correlated, with reasonable care, with reactor technology. Much of the development work toward the now standard process called the bomb reduction of UF_4 was done at the Iowa State College Laboratory of the Plutonium Project, Ames, Iowa under the direction of Spedding, *et al.* Production has been carried on at a number of industrial sites notably the Mallinckrodt Chemical Co., St. Louis, Missouri, and the Feed Materials Process Center, Fernald, Ohio.

The method mentioned above for producing uranium metal employs the steps: (1) hydrogen reduction of UO_3 to UO_2, (2) fluorination with HF to UF_4, and (3) reduction to metal with Ca or Mg in a calcium-magnesium oxide-lined steel pressure vessel. Steps for this process have also been described in the literature.[19] The metal produced directly from this process is reasonably pure except for slag inclusions and some metallic impurities usually introduced from the materials of construction of the processing equipment for the fluorination stage. Upon careful vacuum remelting in urania crucibles in the laboratory, quite pure metal results. Commercially, graphite crucibles and molds are used and the resulting castings run about 200 ppm carbon. Whereas few, if any, effects carry over from the extraction step into the fabrication procedures, the reduction step contributes effects which are primarily due to carbon, iron, nickel and chromium.

The preparation of pure uranium for laboratory work by means of electrolysis[20] was studied at the Los Alamos Scientific Laboratory by Kolodney during the years 1943 and 1944 and at ANL by Blumenthal since the year 1948. Small lots having the following composition after remelting in urania crucibles in good vacuum have been made: Fe, 1 ppm; Cu, 3 ppm; Si, 2 ppm; C, 11 ppm; K, 200 ppm; Li, 200 ppm. This material has been invaluable in the studies of the physical metallurgy of uranium and its alloys, which will be taken up later, particularly in the preparation of single crystals for studies of radiation damage and a number of crystalline properties.

Casting procedures have been used primarily for ingot and billet production. Development of these procedures started in 1942 and has been carried on at the following sites: MIT, Ames, MUC, Los Alamos, NBS, Mallinckrodt and FMPC.

Casting procedures affect the quality of uranium fuel elements directly. If inert crucibles, made for example from urania, are used and melting and casting are done under good vacuum, some refining of the material is possible. Oxides, nitrides and carbides of uranium float in the melt if it is not stirred and, therefore, may be partially removed by cropping of ingots. The graphite crucibles mentioned above contribute some carbon but the contamination may be controlled by avoiding melting temperatures above 1300°C. The nonmetallics mentioned above appear to have low solubility in the melt and do not form with great rapidity, for example, at the graphite uranium interface. If the cleanliness of the atmosphere in contact with molten uranium is not controlled either by good vacuum practice or by scrubbing of inert gases, ingots containing excessive occlusions and at times blow holes due to hydrogen may result. It is also necessary to observe principles of good ingot casting practice to avoid defects. It may be conjectured that if the melting of uranium were done in sufficiently large batches and handled so that surface-to-volume ratios were small, less exacting control of atmospheres would be required.

Direct casting of uranium fuel elements has been studied by Thompson at the US Bureau of Standards (1943–44), Wilhelm and co-workers at Ames (1943–44), and more recently by Shuck and Schumar, at ANL and by the laboratory at FMPC. Methods of standardization and of quality control appear to be the chief difficulties encountered in this work.

Uranium-base alloys have been made by co-reduction using modifications of the procedures for uranium and by additions during remelting. The structures of the alloys which result are indicated by their equilibrium diagrams most of which have been published.[9] Although the study and development of alloys were started during the year 1942, their use was not strongly indicated until enriched uranium became available. Early work was done at the laboratories mentioned above concerned with uranium. The group at MIT found (1943) that the epsilon phase in the U-Si binary system was reasonably resistant to boiling water. At MUC during the year 1943 the metastable alloys containing Mo, Cb, or Cb-Zr were also found to be somewhat resistant to boiling water. More recently, detailed investigations have been carried out at ANL, WAPD, NMI, BMI, SEP, and NAA to produce materials with resistance either to aqueous corrosion, to radiation damage, or to deformation after cyclic heating to elevated temperatures, or any combination of the three qualities. The results of the work are inconclusive as yet and discussion must be left to the future. The physical metallurgical knowledge from these studies is already of considerable value and some of it will be summarized in a later section.

The hot forming of uranium was studied initially by Creutz (1942) at MUC. After learning of the three allotropes and their transformation temperatures, he determined by hand forging tests the ductility of each modification. That of the gamma phase above 760°C appeared favorable for forming. Following this experiment, extrusion tests were arranged by Creutz and carried out at the Wolverine Tube Division of Calumet Hecla Copper Company,

Detroit, Michigan. Also at his instigation, laboratory studies were conducted by Russell, Grenel and co-workers at BMI which resulted in a large-scale production at B and T Metals Co., Columbus, Ohio, of slugs for the Oak Ridge reactor in 1943.

The laboratory studies of extrusion have been extended principally at NMI by Kaufman, Lowenstein, Arnold, and Treco. The latter two workers have summarized their work on the temperature range 199°C (390°F) to 593°C (1100°F) in Fig. 4. The studies of extrusion of uranium in the temperature range of stability of the gamma allotrope 770°C (1418°F) to 1135°C (2057°F) (the gamma range) have not been similarly systematized. Because the metal is very ductile in this range, rather more complicated extrusion operations are possible than in the lower range, providing, oxidation may be prevented.

The alloys of uranium mentioned above may be extruded in the temperature of their gamma stability. Dilute alloys, i.e., those containing up to a few atom per cent additives, may be handled in much the same manner as uranium if properly heated and annealed.

Concerted studies of the rolling of uranium started in the year 1943. However much before this time Marden of the Westinghouse Electric Corporation produced small amounts of rolled sheet. Russell and Grenel at BMI and co-workers successfully rolled approximately 1-inch diameter cylinders to ¼ inch at temperatures near 600°C. Similar studies were conducted at NBS and MIT. Larger scale studies with 4-inch ingots at temperatures near 600°C were carried out at the Joslyn Manufacturing Company, Fort Wayne, Indiana, at the instigation of metallurgists at MUC, Chipman, Greninger, Simmonds, and others. Since the year 1946 extensive studies of rolling rod, plate, and sheet at various temperatures from approximately 300°C to 660°C have been carried out at many laboratories, notably, ANL, ORNL, LASL, KAPL, and NMI. Production rolling has been done at a number of plants, notably, Joslyn, Simmons Saw and Steel, Lockport, New York, FMPC, and the Lackawanna Plant of the Bethlehem Steel Co.; however, the process is of an industrial nature that cannot readily be summarized here and is beyond the scope of this discussion. The laboratory studies established the feasibility of rolling operations in the range mentioned but are not readily summarized in terms of process variables. They, however, have yielded excellent information on the occurrence of preferred orientation in an anisotropic material. An attempt will be made to summarize the information in the later section on physical metallurgy.

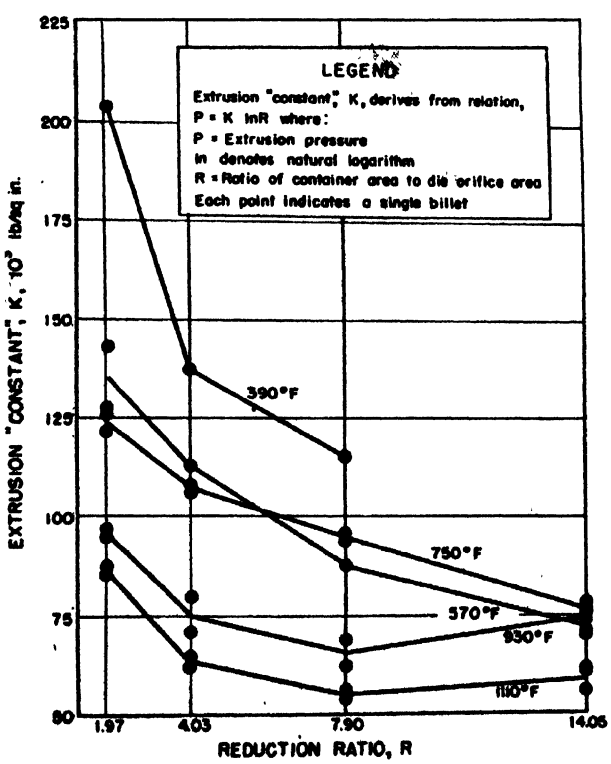

Figure 4. The extrusion constant for alpha-uranium

Swaging has proved to be a convenient laboratory method for producing various size rods down to sizes of approximately 0.050 inch (0.125 cm). Rods then may be cold drawn to approximately 0.003 inch (0.0075 cm).

Forging and pressing of uranium are straightforward operations at temperatures near 600°C (1107°F) if excessive oxidation of the billet is prevented.

Powder metallurgical methods for forming uranium and its alloys into shapes suitable for fuel elements have been studied at SEP under the direction of Kingston and Hausner.[21] The preparation of powders by [illegible] received attention earlier at Ames by Newton, and others, and at Los Alamos by Burke. The use of powders offers the familiar processing possibilities of (1) ability to mix materials which do not melt together, or which separate on solidification, (2) control of particle size, (3) elimination of preferred orientation induced in working operations, and (4) some control over the nature of the dispersed phase not always obtainable in solidification of melts. The process involves treating uranium with hydrogen to form powder, removal of oxygen, mixing of powders in the absence of air, and pressing followed by sintering, or hot pressing. Nearly any alloy may be made in this manner.

Coating, cladding, and jacketing of uranium to protect it from oxidation in hot air and corrosion by water and to retain fission products were undertaken at MUC in the year 1942 by Creutz. A successful method of coating by hot dipping in zinc was indicated. In that same year extensive studies of hot dipping and electroplating were undertaken by Boller and Gray, respectively, in the Laboratory of the Grasselli Chemical Department of the duPont Company. Objectives were successively: (1) coatings to retain fission products at 600°C in helium, (2) coatings to prevent oxidation of uranium in air at 200–250°C, and (3) coatings to prevent corrosion of uranium in water up to 100°C. Additional studies were made at BMI. Reasonably good hot-dipped coatings of zinc

containing 2 per cent aluminum and of speculum metal were developed at Grasselli and tested for oxidation resistance in air at 200–250°C. Typical of hot-dipped coatings, some porosity existed, with the result that the reactive uranium-base metal undercut the coating by oxidation. Electroplated coatings of successive layers of nickel and lead, although specifically designed to avoid porosity, suffered a somewhat similar fate. These methods, both aimed at providing coated slugs for the Oak Ridge reactor, were nearly adequate but gave way in 1943 to a canning technique invented by Marshall at MUC, developed initially by Grenel and co-workers at BMI, and further developed by Fletcher at the laboratories of the Aluminum Company of America at New Kensington, Pennsylvania. In the process tried first on a large scale, aluminum cans of 0.020-inch (0.055-cm) wall thickness were sized directly onto uranium slugs by pushing through a die. A skirted cap also held in place during this operation was joined to the extended sides of the can by seam welding. A final processing operation crimped the skirt flat onto the end face of the slug. After some use and extensive testing, seam welds were demonstrated to leak more frequently than well controlled argon-shielded arc welds. Also, after a period of operating the Oak Ridge reactor, it was felt that can walls 0.035 inch (0.088 cm) could be used. After these two modifications, unbonded slugs were used at Oak Ridge for a number of years until increased temperatures of operation favored the bonded slugs mentioned in the first section (Tables I and II).

Methods of electroplating most of the platable metals on uranium were developed by Gray at Grasselli and co-workers Wehrmann and Rebol at MUC. Alternate methods were studied at BMI by Pray and more recently by Beach and Faust.

Machining methods for uranium are adaptations of standard shop practices. By taking deep, rapid cuts with very sharp, hard tools the work hardening of uranium during cutting may be avoided. Also, advantage can be taken of less rapid hardening, and lower strength at temperatures above 150°C to 200°C. The chip, as it separates from the metal, must be completely covered with a coolant to prevent combustion.

Inspection and testing of fuel elements for power reactors at important stages of manufacture have the following major functions: (1) elimination of material possessing discontinuities which block heat flow; (2) elimination of leaks which permit the ingress of coolant to the uranium; (3) elimination of paths for the escape of fission products; and (4) assurance of proper size and amount of fissile material.

The testing procedures mentioned at the beginning of this section have all been used effectively in various ways. The rather complex subject may be summarized at best vaguely by the statement that an evaluation of the needs of a given reactor system balanced against personal local preferences has determined practice.

The reprocessing of uranium base fuel elements is at the present time accomplished by aqueous methods which return purified decontaminated metals to the fuel fabrication processes. Non-aqueous high temperature chemical studies reviewed by several authors[17] indicate the possible use of steps which might be claimed by metallurgists. They include the partition of fission product elements between (1) molten metal and solid oxide, carbide or nitride phases, the latter serving as crucible liners, and (2) molten metal and molten salt phases. Step one may be coupled with volatization of some fission products. Although most of the fission products with the largest neutron cross sections and the most damaging effects on the metal are removed, levels of radioactivity are lowered by little more than a factor of 10. If such metals are to be refabricated into fuel elements, remotely operated procedures are required. It may be speculated that for power reactors simple fuel elements, easily assembled and disassembled, using fuel shapes easily formed, may be found which may be made sufficiently inexpensively that the simplicity and low cost of the metal reprocessing steps mentioned above may be then advantageous. Such processes will reduce recycle time for fuel and thus also inventory charges.

From the very brief outline given so far, it can be seen that the processes would be analogous with the melting and refining of many metals. They also involve the oxidation reduction chemistry of fission products and heavy elements and the techniques of radiochemistry. With respect to the problem of remotely operated manufacture of fuel elements, it may be noted that the metallurgist is already compelled to handle metals remotely when they are at elevated temperatures. This area of development provides an opportunity for close cooperation of chemists and metallurgists.

B. Aluminum-Uranium Alloys

The properties and manufacture of fuel elements from aluminum alloys in which U-Al_4 is dispersed is discussed in detail by Cunningham, Weber[22] and by Saller.[23] For the discussion an outline of the unit processes is useful and is as follows: (1) melting of aluminum in graphite crucibles; (2) alloying by addition of enriched uranium (*a*) by partition from a fused salt, (*b*) as uranium metal; (3) casting into a cold graphite mold; (4) rolling of billet at 1020°F at 1110°F; (5) roll cladding with aluminum, on all sides; (6) annealing; (7) trimming; (8) inspection (9) assembly and brazing of plates into boxes; and (10) inspection.

A process for the alternate type element containing UO_2 recently developed by Cunningham and coworkers at ORNL replaces the first three steps above with (1) mixing of powder and (2) pressing. The manufacture of these two elements has its analogues in the technology of aluminum. The specifications and precautions to meet them are characteristic of atomic energy technology.

The development of the unit processes for the first manufacturing method outlined above was done at

BMI starting in the year 1946. Rolling conditions mentioned above were found satisfactory for alloys containing 20 weight per cent (2.6 atom per cent) uranium. By using an aluminum jacket, alloys containing somewhat more uranium can be handled at the same temperature. However, for elements designed to contain in the neighborhood of 10 atom per cent uranium, Cunningham has found the method using UO_2 superior. In confirmation of this, Seybolt and Hirsch at KAPL found earlier that in volume ratios up to one-third UO_2 (17.5 atom per cent U) the two powders could be compacted and formed into rods conveniently by extrusion.

The methods of producing a suitable dispersion of a fissile material in a well-behaved matrix present an interesting general problem. In the first method mentioned, chill casting, working and recrystallization produced the proper alloy structure of discrete particles of $U\text{-}Al_4$ in a matrix essentially of aluminum.

In the second method the dispersion was produced entirely by mechanical means. It may be noted that at metal working temperatures the UO_2 is wet by the aluminum, an important factor.

Thorium-uranium fuel elements will involve the same general problem mentioned above, and may yield to the same two solutions.

Investigations of the problem are not sufficiently complete, however, to permit more than the posing of the problem.

C. Ceramic Elements

The work on the ThO_2 and UO_2 systems by Johnson and Curtis[14] provides an excellent example of processes for preparing elements from high melting ceramic materials. Recent advances in this fairly old field depend on improvements in high temperature techniques and better knowledge of sintering mechanisms. Fabrication of elements containing a few per cent of UO_2 dispersed or dissolved in ThO_2 should parallel that of ThO_2 itself.

D. Liquid Metal Fuels

Laboratory methods of preparing and processing fuel bearing metals are indicated by Gurinsky[16] and co-workers and also by Bareis, *et al.*[24] In these systems the metallurgical and chemical processes are combined into one reactor system in which the steps (1) fuel makeup, (2) composition control, (3) reprocessing, and (4) reconstitution proceed continuously or almost so. Such a condensed, integrated, overall process appears to be an ideal goal.

PHYSICAL AND CHEMICAL METALLURGY OF REACTOR FUELS

Significant problems in the physics of solids, physical metallurgy, and chemistry have arisen in work with reactor fuels. Work on the general subject of the relationship between the structure and behavior of uranium is extending classical metallurgical knowledge. The observation of dimensional changes of alpha-uranium under neutron irradiation has added a new phenomenon. In this section it is hoped to illustrate these assertions with a few selected topics from these fields of knowledge.

A. Relation Between Structure and Properties of Uranium

Some progress has been made on the task of relating the properties of single crystals and polycrystalline aggregates of uranium to their structure. Models of the three known crystal structures[25] are shown in Fig. 5. These properties and structures are discussed in more detail by Foote.[26] However, the following points will serve the theme of this discussion.

Chiswick, Foote, and co-workers at ANL have prepared single crystals of uranium by using pure, cast, and wrought electrolytic material, promoting exaggerated grain growth in the center of a bar and at the same time inhibiting the growth of large grains on the surface. Crystals cut from the center of these bars have been used at ANL for determining the plastic deformation mechanisms of alpha-uranium. Cahn of the British Atomic Energy Research Establishment has also worked out the problem by means of observation on individual grains in polycrystalline specimens.[27] While agreement is not complete the dominant mechanisms given in Fig. 6 correlate in a general way with the dominant portion of the preferred orientation in rolled uranium given in Fig. 7. Work is continuing on the subject in a number of laboratories to determine in detail the origin of textures in worked uranium.

Combining the anisotropic thermal expansion of alpha-uranium crystals, the deformation mechanisms, and a partial knowledge of textures, it has been possible to account for the change in dimensions of textured alpha-uranium bars which occurs upon repeated heating and cooling, for example, from room temperature to 500°C. Burke *et al.* (1951) at KAPL and Muehlenkamp, *et al.* (1951) at BMI have shown that an active mechanism in polycrystalline uranium involves grain boundary flow to relieve stresses between differently oriented crystals at elevated temperatures followed by slip of the crystals oriented favorably to the stresses set up when cooled to a lower temperature. Other pairs of deformation mechanisms in which each mechanism depends differently on temperature may also be involved in uranium. Only slip and grain boundary flow operate in the case of zinc bicrystals, however, for which Burke and Turkalo observed a similar behavior. The relations between texture and amount of growth are given by Foote.[26]

Changes in dimensions of single crystals of uranium under neutron irradiation were observed by Turkalo at KAPL. She observed growth to be in the [010] (*b*) direction and shrinkage to be in the [100] (*a*) direction with little or no change in the [001] (*c*) direction. Textured polycrystalline wire specimens had already been observed to grow in length when irradiated. Here the single-crystal data

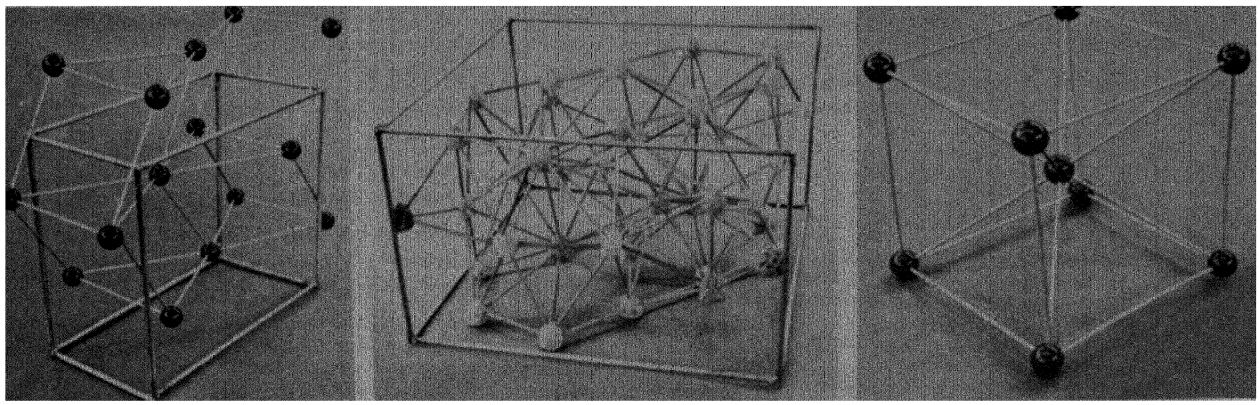

Figure 5. Models of the crystal structure of uranium allotropes; alpha, left; beta, centre; and gamma, right

correlates directly with a dominant component of the wire texture in regard to direction of growth (in this texture the (010) planes tend to be more or less perpendicular to the wire axis). The amount of growth appears to be greater in the case of the wire; however, all of the factors affecting the rate of growth are not known.

The kinetics of the beta-alpha isothermal transformation in uranium alloys containing up to 2 atom per cent chromium have been measured by White (1949) at KAPL. He found the kinetics for an alloy containing 0.3 atomic per cent Cr above 485°C (900°F) to be different from that below. Figure 8 illustrates his results which he has plotted in the familiar form of a time-temperature plot for the start and finish of the reaction. Subsequently, Holden at KAPL determined some elements of the crystallography of the transformation in the lower range, and showed it to be martensitic in nature and not controlled by diffusion.[28] The transformation occurring between 485°C and 630°C is apparently diffusion controlled. It has been suggested by members of the Metallurgy Department of the British Atomic Energy Research Establishment who have extended this work that other impurity constituents of these alloys also influence this transformation.[29] It is interesting that Holden's results supported the proof of the existence of isothermal martensite transformations in ferrous alloys[30] a point which had been debated by metallurgists.

A large number of other interesting and important problems in the physical metallurgy of uranium are under study.

B. Ductility of Thorium

Since the bulk of the physical metallurgy of thorium is that of a face-centered cubic metal only one phenomenon will be mentioned as of special interest. Thorium containing its usual impurities (e.g., 200 to 600 ppm carbon) shows a ductile brittle transition temperature in measurements of its impact strength. This is the only example of this phenomenon in face-centered cubic metals of which the author is aware. Relatively pure thorium made by the iodide process remains ductile to below the boiling point of liquid nitrogen. General discussion of the metallurgy of thorium is given elsewhere.[31]

C. Inter-diffusion of Fuels and Cladding Materials

Inter-diffusion between coating materials and uranium is important in reactor technology though not quite so much so in science at the moment. It was

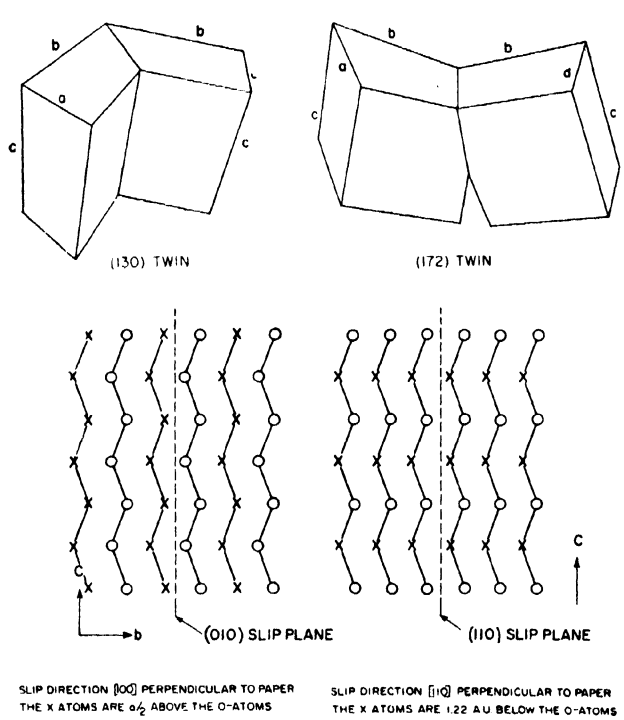

Figure 6. Deformation mechanisms for alpha-uranium

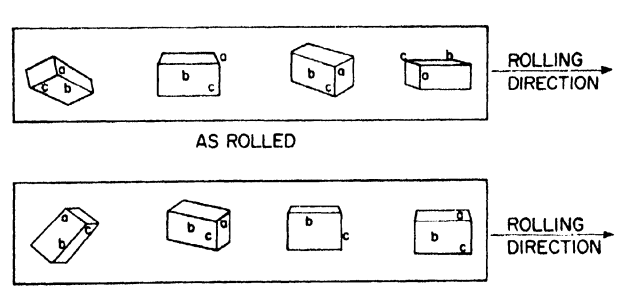

Figure 7. Orientation in rolled uranium, schematic

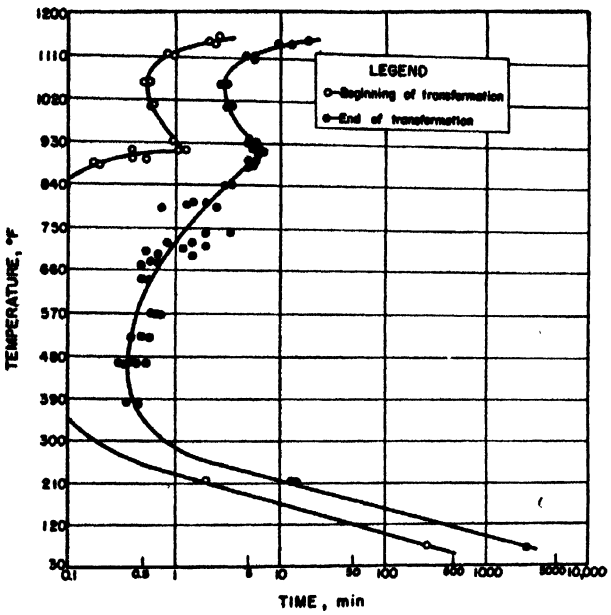

Figure 8. Rates of transformation of uranium containing 0.3 at % Cr

given earlier as the possible limitation on temperatures and hence performance of solid reactor fuels. No effect of reactor irradiation on diffusion has been detected to date. However, it has been noticed in experiments that aluminum in contact with an aluminum-uranium alloy fuel specimen in a reactor will stick to it, whereas similar conditions except for radiation would have produced no change.

In the case of iron and aluminum, the interaction is due to the growth of layers of intermetallic compound, as may be seen from their constitution diagrams. The changes in thickness may be correlated with time and temperature approximately by the following law:

$$d^n = At \qquad (6)$$

where n = an experimentally determined constant, d = thickness, t = time, $A = A_0 e^{-E/RT}$, A_0 = an experimentally determined constant, E = an activation energy in calories per mole, R = gas constant, and T = temperature in degrees Kelvin.

Table VII lists data for pertinent diffusion couples. Zirconium and uranium interdiffuse to form solid solutions which are continuous above 865°C.

So far as the author is aware, the coefficient for self-diffusion in uranium has not been measured in spite of its importance. In other metals, copper, nickel, copper-gold alloys and thorium, effects of radiation are being correlated with the production and behavior of crystal defects and with diffusion mechanisms.

D. Corrosion

The importance of corrosion by water in power reactors has led to a large number of studies which have shown a somewhat new aspect to this old problem. In the case of aluminum, Draley[5] shows that by providing sites for the catalytic combination of hydrogen atoms on the surface of aluminum, corrosion rates are tolerable in water up to approximately 300°C at a pH near 6 to 7. Under these conditions Draley believes that the corrosion rate is controlled by the rate of growth of oxide layers on the surface in standard fashion. Without catalysis, hydrogen may enter aluminum and possibly collect under the oxide causing it to spall thus greatly increasing corrosion rates.

Uranium corrosion is also affected by hydrogen. For example, between 70°C and 100°C the corrosion rate in water saturated with oxygen is 1 per cent of that in water saturated with hydrogen. Brugman (1945) at MUC showed that rates in oxygen-free water are correlated with temperature by the relation

$$\log k = \frac{3470}{T} + 9.72 \qquad (7)$$

where k = corrosion rate in mg/cm²-hr, T = temperature in degrees Kelvin.

In water containing O_2 partially protective films of UO_2 form at moderate temperatures and spall off erratically, these rates are difficult to describe. Studies of uranium corrosion have been extended and correlated by Waber at Los Alamos.

The corrosion of zirconium has been reviewed by Thomas.[32] It may be noted that effects attributable to hydrogen are mentioned in the reference.

Thus, it may be suggested that the diffusion and reaction of hydrogen atoms to form gas or hydrides may play an important role in the corrosion of the above three metals in water at elevated temperatures.

E. High Temperature Equilibria

Liquid metal fuel reactors and the new fuel processing methods mentioned above both will require extensions of our knowledge of chemical equilibria to new systems at elevated temperatures. The work

Table VII. Data on Diffusion Couples

Couple	Temp. °C	Time to penetrate 0.01 in (0.025 cm)	n	E kcal	Range applicable	A_0
Al-U	300	90 days	2.0	12.0	250–450	1.12 cm²/sec
Fe-U			2.6	20.4	600–700	–
347 Stainless steel*-U	625	1 year	2.5	17.7	500–700	–
Z4-U	740	45 days	2.0	44.3	600	0.52 cm²/sec

* A nominal 8-18 austenitic stainless steel stabilized with niobium.

at Brookhaven[16,24] makes use of solubility equilibria in liquid metals and the partition of metals between molten metals and fused salts, and has fostered their study. Several examples of phase equilibria are provided by the separations studies referred to above.[17] One study of particular interest to the author relates to the study of the partition of plutonium between molten uranium and magnesium at 1150°C studied by Barney (1955). The partition coefficient found is 0.23 expressed as the ratio of mole fraction of Pu in Mg to that in U. This ratio is constant over a wide range of concentrations and of ratios of phase volumes. By extension of equilibrium measurements of these sorts and others, the thermodynamic functions of reactor fuel systems may be determined at elevated temperatures.

ACKNOWLEDGEMENT

The author is very grateful for the help and contributions of a number of co-workers and of a large number of workers in the field of atomic energy for peaceful uses.

APPENDIX: LABORATORIES CONTRIBUTING TO REACTOR MATERIAL TECHNOLOGY

A number of laboratories are active at the present time in the technology of fuels for nuclear reactors. Some of these activities originated during the time the nuclear work was under the auspices of the Manhattan District of the United States Corps of Engineers and have had a more or less continuous existence since, in many cases under various sponsors. In order to clarify the references made in the text to these laboratories and others of more recent advent, the following listing is given.

Persons mentioned in the text are also listed with the laboratory in which they work or have worked. In addition a few names of those who contributed to the subjects taken up in the text are included. By no means has a complete allocation of credit been achieved; neither is the text a complete coverage of the important subjects in the extensive work on the metallurgy of fuel elements and fuel systems. It is to be sincerely hoped that it will be possible for some author to do justice to the work and the workers.

Alcoa	Aluminum Company of America, Research Laboratories, New Kensington, Pennsylvania	1942–1944	F. C. Frary
Ames	Chemistry Department, Plutonium Project, Iowa State College, Ames, Iowa	1942–1946	F. H. Spedding, H. A. Wilhelm, W. H. Keller, A. S. Newton, I. B. Johns, J. C. Warf, T. A. Butler.
	Atomic Engery Institute, Iowa State College, Ames, Iowa	1946–	F. H. Spedding, H. A. Wilhelm, O. N. Carlson, P. Chiotti, G. Murphy, D. Peterson, J. F. Smith, A. F. Voight, R. E. Rundle, A. S. Wilson
ANL	Argonne National Laboratory, Lemont, Illinois	1946–	W. H. Zinn, F. G. Foote, J. E. Draley, H. V. Lichtenberger, H. Chiswick, L R. Kelman, B. Blumenthal, S. Lawroski, H. M. Feder.
BMI	Battelle Memorial Institute, Columbus, Ohio	1942–	H. W. Russell, L. H. Grenel, H. A. Saller, G. T. Muehlenkamp, A. D. Schwope, L. R. Jackson, F. A. Rough
BNL	Brookhaven National Laboratory, Upton, Long Island, New York	1946–	D. Gurinsky, R. J. Teitel, D. Bareis, R. H. Wiswall, W. E. Winsche, J. S. Bryner, J. E. Atherton, O. F. Kommerer, C. Klamut, M. Silberger, B. Turovlin, J. Weeks
FMPC	Feed Material Processing Center, Fernald, Ohio	1952–	
Grasselli	Grasselli Chemicals Department, du Pont Company, Cleveland, Ohio	1942–1944	J. P. Woodhouse, A. S. Weygandt, F. R. Boller, A. G. Gray
KAPL	Knolls Atomic Power Laboratory, General Electric Company, Schenectady, New York	1946–	J. E. Burke, A. M. Turkalo, A. N. Holden, J. P. Howe, A. U. Seybolt, H. Hirsch, D. White, C. W. Tucker, C. E. Lacy, L. R. Coffin.
LASL	Los Alamos Scientific Laboratory, Los Alamos, New Mexico	1943–	E. R. Jette, M. Kolodny, C. S. Smith, J. E. Burke, J. Taube, E. T. Jurney
MIT	Massachusetts Institute of Technology, Boston, Massachusetts	1942–1952	A. R. Kaufman, R. M. Treco, S. U. Arnold, P. Lowenstein
Mallinckrodt	Mallinckrodt Chemical Works, St. Louis, Missouri	1942–	W. H. Keller

(Continued on next page)

MUC	Metallurgical Laboratory, University of Chicago, Chicago, Illinois	1942–1946	J. Chipman, F. G. Foote, A. B. Greninger, J. Simmonds, J. P. Howe, W. Brugman, E. Creutz, W. H. Zinn, F. Daniels, C. A. Hutchinson, J. G. Malm
NBS	National Bureau of Standards, Washington, D.C.	1942–	J. G. Thompson
NRTS	National Reactor Testing Station, Idaho Falls, Idaho	1948–	J. Huffman
NAA	North American Aviation, Inc., Los Angeles, California	1947–	E. E. Motta, C. Starr, S. Siegel, J. Brinkman
NMI	Nuclear Metals, Inc., Cambridge, Massachusetts	1953–	*See* Massachusetts Institute of Technology
ORNL	Oak Ridge National Laboratory, Oak Ridge, Tennessee	1947–	J. Frye, E. Boyle, J. R. Johnson, C. E. Curtis, M. E. Ramsey, C. D. Cagle, F. Seitz
SEP	Sylvania Electric Products, Inc., Bayside, Long Island, New York	1948–	W. Kingston, H. Hausner
TNX	TNX Division of Explosives Dept., duPont Company, Wilmington, Delaware	1942–1946	K. G. Jones, L. Eubank, R. C. Grills
WAPD	Westinghouse Atomic Power Division, Westinghouse Electric Corporation, Pittsburgh, Pennsylvania	1947–	W. A. Johnson, D. E. Thomas
Wolverine	Wolverine Tube Division, Calumet Hecla Copper Company, Detroit, Michigan	1942–1943	O. Klopsch, J. F. Schumar
HRE	Homogeneous Reactor Experiment		*See* Oak Ridge National Laboratory
MTR	Materials Testing Reactor		*See* National Reactor Testing Station

REFERENCES

1. Seitz, F., *Radiation Effects in Solids,* Physics Today *5(6)*: 6-9 (1952).
   Brinkman, J. A., *On The Nature of Radiation Damage in Metals,* J. App. Phy. *25(8)*: 961-970 (1954).
2. Ramsey, M. E. and Cagle, C. C., "Ten Years' Operating Experience of the ORNL Graphite-Moderator Normal-Uranium Reactor", *Nuclear Engineering—Part I, Chemical Engineering Progress Symposium Series,* Vol. 50, No. 11, pp 149-154 (1954).
3. Zinn, W. H., *The Argonne Heavy Water Reactor (CP-3 Prime),* ANL-WHZ-311 (10 August 1951).
4. Gurinsky, D. H., *et al.,* P/828, "The Fabrication of the Fuel Elements of the BNL Reactor", Vol. 9, Session 18B.2, these Proceedings.
5. Draley, J. E., P/535, "Aqueous Corrosion of Aluminum Alloys at Elevated Temperatures", Vol. 9, Session 20B, these Proceedings.
6. Lichtenberger, H. V., "The Experimental Breeder Reactor", *Nuclear Engineering—Part III, Chemical Engineering Progress Symposium Series,* Vol. 50, No. 13, pp 139-146 (1954).
7. Simpson, J. W., *et. al.,* P/815, "Description of the pressurized water reactor (PWR) power plant", Vol. 3, Session 13A, these Proceedings.
8. Huffman, J. R., *The Materials Testing Reactor,* Nucleonics *12(4)*: 20-26 (1954).
9. *Compilation of US and UK Uranium and Thorium Constitution Diagram,* BMI-1000.
10. Coffin, L. R., Jr., *The Problem of Thermal Stress Fatigue in Austenitic Steels at Elevated Temperatures,* ASTM Special Technical Publication No. 165, pp 31-50 (1954).
11. Starr, C., P/495, "A Sodium Graphite Reactor 75,000 Electrical Kilowatt Power Plant", Vol. 3, Session 11A, these Proceedings.
12. Jurney, E. T., "The Failure and disassembly of Los Alamos Fast Reactor", *Nuclear Engineering—Part III, Chemical Engineering Progress Symposium Series,* Vol. 50, No. 13, pp 191-199 (1954).
13. Hutchison, C. A., Jr. and Malm, J. G., *The Volatilization of Beryllium Oxide in the Presence of Water,* Amer. Chem. Soc. J. *71(4)*: 1338-1339 (1949).
14. Johnson, J. R. and Curtis, C. E., P/559, "The Technology of UO_2 and ThO_2", Vol. 9, Session 18B.1, these Proceedings.
15. Weinberg, A. M., *Power Reactors,* Scien. Amer. *191(6)*: 33-39 (1954).
16. Teitel, R. J., Gurinsky, D. H. and Bryner, J. S., "Liquid-Metal Fuels and Liquid-Metal Breeder Blankets", *Nuclear Engineering—Part III, Chemical Engineering Progress Symposium Series,* Vol. 50, No. 13, pp 11-13 (1954).
    Atherton, J. E., *et. al.,* "Studies in the Uranium-Bismuth Fuel System", *Nuclear Engineering—Part II, Chemical Engineering Progress Symposium Series,* Vol. 50, No. 12, pp 23-27 (1954).
17. Hawroshi, S., P/823, "Survey of Separation Processes", Vol. 9, Session 22B, these Proceedings.
    Feder, H. M., *et al.,* P/544, "Pyrometallurgical Processing of Nuclear Materials", Vol. 9, Session 22B, these Proceedings.
    Voight, A. F., P/545, "Purification of Uranium Reactor Fuels by Liquid Metal Extraction", Vol. 9., Session 22B, these Proceedings.
    Motta, E. E., P/542, "High Temperature Fuel Processing Methods", Vol. 9, Session 22B, these Proceedings.
18. For example: McDonald, R. D., "The Extractive Metallurgy of Uranium", *Nuclear Engineering—Part I, Chemical Engineering Progress Symposium Series,* Vol. 50, No. 11, pp 69-74 (1954).

19. Katz, J. J. and Rabinowitz, E., *The Chemistry of Uranium,* McGraw-Hill Co., Inc., New York (1951).

20. Meister, B., *Production of Rarer Metals,* MDDC-1673, decl. 11 February 1948; Kantan, S. K., Shreenivasan, N. and Teudolker, G. S., "Electrolytic Preparation of Uranium from a Fluoride Bath", *Nuclear Engineering—Part II, Chemical Engineering Progress Symposium Series,* Vol. 50, No. I2 (1954).

21. Hausner, H. H. and Kells, M. C., *The Role of Powder Metallurgy in the Design of Nuclear Power Reactors,* ASM Paper No. 55 (April 1955) (to be published).

22. Weber, C. E., *et al.,* P/561, "Dispersion Type Fuel Elements", Vol. 9, Session 18B, these Proceedings.

23. Saller, H. A., P/562, "Preparation, Properties, and Cladding of Al-U alloys", Vol. 9, Session 18B, these Proceedings.

24. Bareis, D. W., Wilwall, R. H., Jr. and Winsche, W. F., "Processing of Liquid Bismuth Alloys by Fused Salts", *Nuclear Engineering—Part II, Chemical Engineering Progress Symposium Series,* Vol. 50, No. 11 (1954).

25. Jacob, C. W. and Warren, B. E., *Crystal Structure of Uranium,* Amer. Chem. Soc. J. *59*: 2588-2591 (1937).
Tucker, C. W., Jr., *The Crystal Structure of the β-Phase of Uranium,* Acta Crys. *4*: 425-431 (1951).
Wilson, A. S. and Rundle, R. E., *The Structures of Uranium Metal,* Acta Crys. *2*: 126-127 (1949).

26. Foote, F. E., P/555, "The Physical Metallurgy of Uranium", Vol. 9, Session 18B, these Proceedings.

27. Cahn, R. W., *Plastic Deformation of Alpha Uranium Twinning and Slip,* Acta Met. *1*: 49-70 (1953).

28. Holden, A. N., *The Isothermal Transformation of Metastable Beta-Uranium Single Crystals,* Acta Met. *1(16)*: 617-623 (1953).

29. Private communication, 10 October 1954.

30. Kurdyumov, G. V. and Maksimova, O. P., *Kinetics of the Transformation of Austenite into Martensite at Low Temperatures,* Doklady Akad. Nauk SSSR *61*: 83-86 (1948).
Kurdyumov, G. V., *Nature of Diffusionless (Martensitic) Transformations,* Doklady Akad. Nauk SSSR *60*: 1543-1546 (1948).
Cech, R. E. and Hollomon, J. H., *Rate of Formation of Isothermal Martensite in Iron-Nickel-Maganese Alloy,* Amer. Inst. Min. and Eng. Trans. *197*: (1953) also in J. of Met. *5*: 685-689 (1953).

31. Carlson, O. N., *et al.,* P/556, Vol. 9, Session 18B, these Proceedings; Keeler, J. R., "Thorium Metallurgy", *Nuclear Engineering—Part I, Chemical Engineering Progress Symposium Series,* Vol. 50, No. 11, pp 57-61 (1954).

32. Thomas, D. E., "Corrosion of Zirconium in High-Temperature Water", *Nuclear Engineering—Part II, Chemical Engineering Progress Symposium Series,* Vol. 50, No. 12, pp 16-22 (1954).

Dispersion-Type Fuel Elements

By C. E. Weber and H. H. Hirsch,* USA

Small, compact reactors are now operating at high specific-power levels, utilizing enriched uranium as a nuclear fuel. As the specific power of such reactors is increased, the fuel element designer is asked to provide fuel elements capable of withstanding more and more damage due to generation of fission product atoms in the fuel matrix in order to keep the fuel recharging frequency low when the fuel burnup rate is high. In addition, specific reactor designs call for operation in different coolant media at different ambient temperatures, limiting the choice of fuel media.

Since, with highly enriched uranium, the U^{235} cannot be diluted with U^{238} as in natural uranium fuel elements, other diluents must be used. This article is concerned with one technique to achieve dilution; namely, through dispersion of the fuel in the diluent rather than by alloying.

Dispersion-type fuel elements are herein defined as elements in which the fuel is heterogeneous, consisting of a fissile phase dispersed in a continuous matrix of non-fissile material. For the purposes of this discussion, the non-fissile material will be limited to a pure metal or alloy. To minimize radiation damage and provide metallic properties, the diluent must predominate in volume and exist as a continuous matrix surrounding the fissile phase. The matrix metal in effect acts as the structural material in the fuel element.

DESIGN OBJECTIVES

To discuss fuel elements more effectively, the general functions of a solid fuel element for a nuclear reactor are arbitrarily defined as: (1) permanent space location of the fissile material in the reactor core; (2) retention of fission products and fissile material; (3) resistance to external and internal stresses without fracture or dimensional change; (4) minimum parasitic capture of neutrons; and (5) transfer of heat with minimum thermal gradients.

The ability of a fuel element to meet these requirements continuously during operation is a measure of its merit relative to other types. The dispersion-type fuel element offers two unique advantages over elements having a homogeneous fissile core: (1) increased operating life through localization of the fission product damage in a zone immediately adjacent to the dispersed phase, minimizing damage to the structural matrix metal; and (2) increased choice of fuel systems to permit use of normally metallurgically incompatible fuel and diluent metals and attainment of physical and mechanical properties not attainable in homogeneous fuel systems.

The specific dispersed phase and matrix metal used depends on the particular reactor design under considertion with factors such as operating temperature, type of coolant, and neutron energy spectrum limiting the materials choice. In general, however, to attain maximum endurance life, the volume fraction of the diluent metal should be large, the density of uranium in the dispersed phase should be high, and the parasitic neutron absorption cross section of the fissile phase and matrix materials should be low.

RADIATION DAMAGE IN A DISPERSION SYSTEM

Theoretical and experimental data are available in the literature on the effect of radiation and fast particle bombardment on metals and ionic or molecular compounds.[1,2] Since fissile phases may consist of metallic, intermetallic, ionic, or molecular compounds, damage may arise through either ionization or displacement of atoms through elastic collision with the fast particles. However, in both cases the major effect will be primarily due to the high energy recoiling fission products. Collision with fast neutrons will be only of secondary importance except in the fission fragment-free regions of the matrix where only the less damaging fast neutrons are available. Therefore, the major damaging effect of fast particle bombardment will be attributed primarily to the motion of fission fragments and will be ascribed to their "dynamic" properties. In fissile material, another significant metallurgical effect will be introduced by the "static" properties of fission fragments as they come to rest in the lattice atoms of the fuel. The total damage is a combination of both the "static" and "dynamic" effects, and it is clear that as higher concentrations of fission products are approached the static effect will predominate. The size and metallic (or non-metallic) properties of the fission product atoms is such that at higher concentrations considerable strain will be introduced in the lattice. The object, then, in a dispersion type element, is to concentrate the damage in the dispersed phase and in a highly localized region surrounding the dispersed fissile particle, leaving a fission product-free region of matrix metal around the zone of damage. This objective cannot

* General Electric Company, Knolls Atomic Power Laboratory, Schenectady, New York.

be achieved in a homogeneous fissile metal or in two-phase alloy systems where both phases may contain fissile atoms.

Schematic cross sections of idealized dispersant systems having a constant volume fraction of fissile dispersant (fixed at 20 volume per cent) are shown in Fig. 1. The dispersed particles are assumed to be spheres in a cubically close-packed array.

Three particle sizes are shown. A spherical zone of damaged matrix metal is shown surrounding each particle. The thickness of the zone is taken as λ, where λ, the range of the fission products in the matrix metal, determines the maximum distance that a fission fragment, leaving normal from the particle surface, can travel into the matrix metal.

For this simplified analysis, the difference in range of the light and heavy fission fragments has been neglected. For convenience, the range of fission fragments in typical materials is given in Table I.

Referring to Fig. 1, note that while the volume fraction of the dispersed particles is constant, the amount of damaged matrix metal can be varied significantly as the particle size is varied. The damage zones touch for spherical particles 37 microns in diameter and would overlap for smaller particles. For spheres 210 microns in diameter, a significant volume of undamaged matrix metal exists. The variation of the fraction of damaged matrix metal with particle size is shown in Fig. 2.

Again note that below a "critical particle size" no undamaged matrix region exists. This curve is for an idealized system containing 20 volume per cent dispersant. For other volume fractions the ordinate may be multiplied by the ratio of the actual volume fraction to the 20 per cent figure. It is obvious that as the concentration of the dispersed particles decreases, the "critical particle size" decreases.

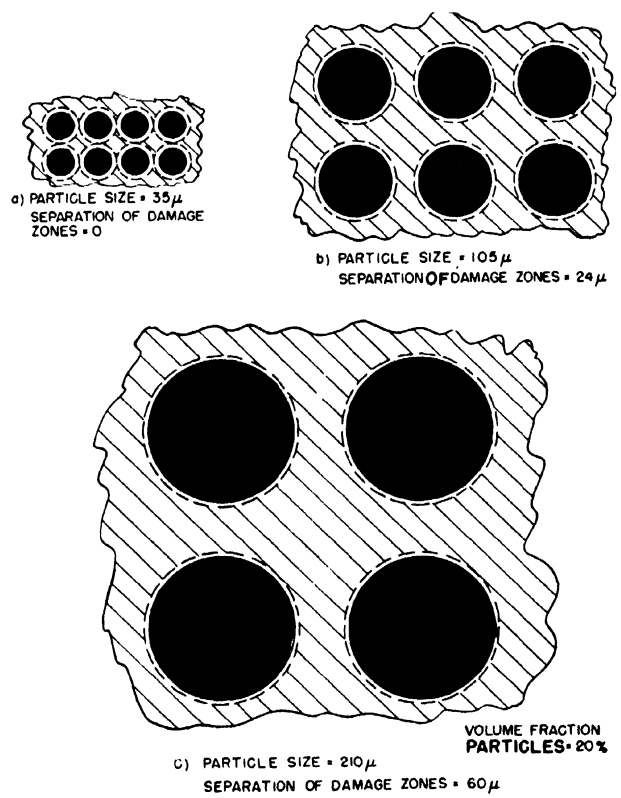

Figure 1. Damaged matrix regions for a constant volume fraction dispersant

Table I. Range of Fission Fragments in Fuel Materials

Material	*Average range mg/cm²*	*Average range microns*	*Average range inches*
U	12.6	6.8	2.7×10^{-4}
UO_2	10.0	9.4	3.7×10^{-4}
Zr	5.8	9.1	3.6×10^{-4}
Fe	5.2	6.7	2.6×10^{-4}
Al	3.7	13.7	5.4×10^{-4}

It is explicit in the previous discussion of dispersions that thermal diffusion of fission products into the undamaged matrix region does not occur during operation. Certainly at high temperatures, diffusion will occur and may change markedly the properties of both homogeneous and dispersion-type fuel media.

An additional advantage of large particles is that a significant fraction of the fission fragments will stop in the particle, whereas with small particles practically all of the fission products will recoil into the matrix metal. The fraction P_a of fission products which recoil from a sphere is given by

$$P_a = \tfrac{3}{4}\,\lambda/a - \tfrac{1}{16}\,(\lambda/a)^3 \qquad (1)$$

where a is the sphere radius and λ is the fission fragment range in the dispersed phase. This equation applies for values of λ/a equal to or less than two.

With spherical UO_2 particles, the fraction recoiling from particles of different diameters is given in Table II.

Through use of large diameter particles, the damage can be primarily retained in the dispersed particle which in itself need not contribute to the composite strength of the fuel system.

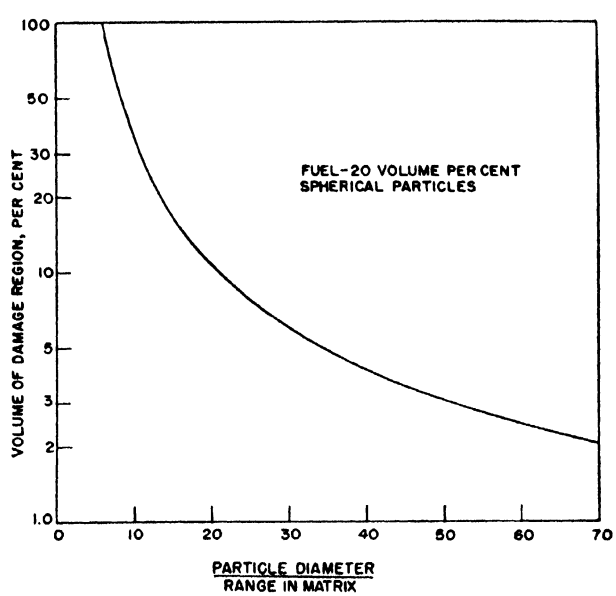

Figure 2. Per cent of matrix volume damaged by fission products

Table II. Fraction of Fission Fragments Recoiling from UO_2 Spheres

Particle diameter microns	P_e
9.4	1.0
19.0	0.69
37.0	0.37
105.0	0.068
210.0	0.034

Summarizing these analytical considerations, the design objectives to be achieved in an ideal dispersion system are: (1) dispersed particle size large compared to the fission product range; (2) uniform dispersion of particles in a metal matrix; (3) a continuous phase of matrix metal of maximum possible volume fraction; and (4) high uranium density fissile phase.

As will be discussed in the fabrication section, uniform dispersion of a particle of constant diameter cannot be attained in practice, but these idealized considerations can be approximated and serve to indicate the path for progress.

Some experimental results are available, showing that with dispersion fuels the core media is embrittled and hardened at room temperature, as is known to be the case with homogeneous fuels. Typical data on hardening of one of the systems studied, a UO_2 stainless steel system, are in Table III.

Table III. Hardening of a UO_2-Steel Media on Irradiation

Particle size	*Hardness before irradiation*	*Hardness after irradiation*
3 microns	225–250 DPH	475–500 DPH
15–44 microns	175–260 DPH	330–440 DPH

The volume fraction of dispersed UO_2 was 24 per cent. The difference in hardening is small for the two particle sizes studied, since all of the matrix metal is damaged in both cases. Annealing at high temperatures caused little change in post irradiation hardness, confirming that the "static" effect of the fission products predominated. Data on larger particle sizes are not available at the present time.

SYSTEMS FLEXIBILITY THROUGH DISPERSION TECHNIQUES

In addition to minimization of fission product damage, an equally important advantage of a dispersion system is the flexibility this technique offers in choice of fuel element materials and properties. Binary alloys of uranium and other metals vary widely in properties from those of either of the pure metals. Uranium is a reactive metal forming complicated systems with many intermetallic compounds and low melting eutectics. The thermal conductivity of alloy systems may be poor, thermal diffusion of uranium and troublesome phase changes may occur during operation, and the mechanical properties and chemical reactivity of the binary system are often poor compared to the unalloyed metals. The dispersion approach allows the fuel element designer to incorporate the fissile material in a metal matrix without metallurgical interaction and thereby retain the desirable properties of the pure matrix metal. Uranium or other fissile elements can be pre-reacted to form a stable compound, in effect metallurgically deactivated, which can be incorporated into the matrix metal without further reaction. The ideal uranium dispersion would be elemental uranium since the metal obviously offers the highest density of uranium per unit volume. However, magnesium is one of the few metals that can be mixed with uranium without reaction. Relatively high density, chemically stable compounds such as UO_2 can be employed with other metals. Intermetallic compounds may also be considered for a specific application. A number of fissile compounds of potential interest are given in Table IV. The uranium content per unit volume of dispersed phase relative to the density of uranium is given as V_r.

Table IV. Fissile Dispersants

Compound	*Density gm/cm³*	V_r	*Melting point °C* ‡
U	18.9	1.0	1120
UAl_2	8.1	0.35	1590
UAl_3	6.7	0.26	1320
UAl_4	6.0*	0.22	730
UBe_{13}	4.37	0.15	2000
UC	13.6	0.69	2270
UC_2	11.7	0.56	2400
UO_2	10.96	0.53	2500
U_6Fe	17.7	0.91	815
UFe_2	13.2	0.48	1235
UN	14.3	0.71	2630
UPb	14.5†	0.41	1280
U_3Si	15.6	0.77	930 (d)
U_3Si_2	12.2	0.59	1665
U_5Sn_4	13.0†	0.49	1500

* Calculated assuming non-ideal mixing with a deviation equal to that observed with the other U-Al compounds.

† Calculated assuming ideal mixing.

‡ The densities and melting points were taken from a paper by Katz and Rabinowitch[8] except for UBe_{13} data taken from a paper by Buzzard[4].

The melting point of the compounds has been included to provide a relative indication of chemical stability. The list is not exhaustive, but uranium dioxide stands out because it contains a relatively high density of uranium, is quite chemically stable, and its technology of manufacture and handling is well understood.

Other dispersants may be better for specific applications. Metals which may be of interest as diluents are given in Table V.

The general criterion used in choosing these metals as diluents was their thermal neutron absorption cross section. The cross section per unit volume is of interest in design and has been included. It should be pointed out that the cross section of these and other metals is quite different in non-thermal reactors.

Many of the suggested dispersants are reactive and their reaction with the diluents in Table V has not been considered. Incorporation of a specific dispersant in a particular diluent is again so direct a function of reactor design, operating temperature and fabrication temperature, that fruitful generalization is not possible.

FABRICATION

There are two general fabrication techniques available for producing dense dispersion-type fuel elements: (1) melting and casting, and (2) powder metallurgy. The material produced by either one of these methods must nearly always be mechanically reduced or worked to final size and shape. Such metal working generally improves mechanical properties and promotes bonding between the cladding and the core material. However, it can alter the structure and dispersion uniformity so that all of the potentially realizable advantages of the dispersion system are not attained. Fuel elements have, however, been prepared by both methods by applying the following principles and techniques.

Melting and Casting

Although restricted in applicability, dispersion type fuel systems can be prepared by melting and casting, and two different approaches are available. A binary alloy system can be used if the uranium rich phase can be dispersed as islands throughout the non-fissile phase. The solid solubility for uranium must be negligible in the non-fissile or matrix phase. In addition, it is important that the uranium phase be a stable compound of reasonably high melting point and contain a high percentage of uranium. It is also desirable that the compound islands be large in size for reasons previously explained, and be more or less spherical in shape.

In practice, it has been difficult to find acceptable uranium systems with which all of these specifications can be met. The desired composition must fall

Table V. Potential Matrix Metals

Matrix metal	*Melting point* °C ¶	*Microscopic absorption cross section, barns* ¶	*Macroscopic cross section,* cm^2/cm^3
Al	660	0.22	0.013
Be	1282*	0.010	0.0013
Fe	1539	2.4	0.20
Mg	651	0.059	0.0025
Mo	2625	2.4	0.15
Nb	2415	1.1	0.061
Ni	1455	4.5	0.41
Ti	1670†	5.8	0.33
V	1900‡	4.7	0.33
Zr	1852§	0.18	0.008

* See reference 4.

† See reference 6.

‡ See reference 7.

§ See reference 8.

¶ The melting points were taken from the Metals Handbook[5], except as noted. The microscopic cross sections were taken from the General Electric Chart of the Nuclides, Fourth Edition.

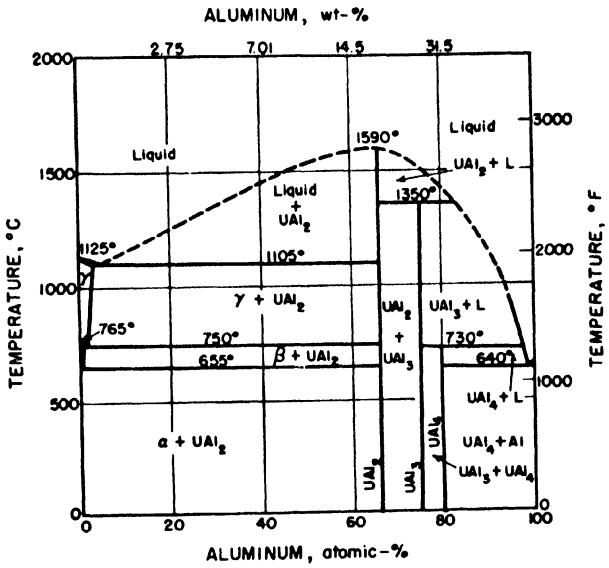

Figure 3. The constitutional diagram of the system uranium-aluminum

within a phase range bordered by a high uranium compound and the pure alloying element. If a eutectic or eutectoid is formed in this phase region, the uranium phase must be susceptible to spheroidization by heat treatment, mechanical working, or a combination of these two. Obviously only a minimum of control can be maintained over the final particle size of the uranium phase.

The application of this technique, then, to the production of acceptable dispersion-type fuel systems has been the exception rather than the rule. A notable exception is the uranium-aluminum fuel plates used in the Materials Testing Reactor. The core of the element consists of a 14 to 16 weight per cent alloy of uranium in aluminum, clad in pure aluminum. The constitution diagram for this system is shown in Fig. 3. No solubility of uranium in aluminum is indicated, the desired composition lies in a eutectoid region, and a large percentage of the aluminum is tied up in the compound UAl_4. The fine, needle-like precipitation of UAl_4 produced in the cast alloy is shown in Fig. 4. Upon hot rolling at 430°C, the matted structure of the UAl_4 shown in Fig. 5 was produced. Subsequent annealing at 375°C for one hour greatly coarsened the compound

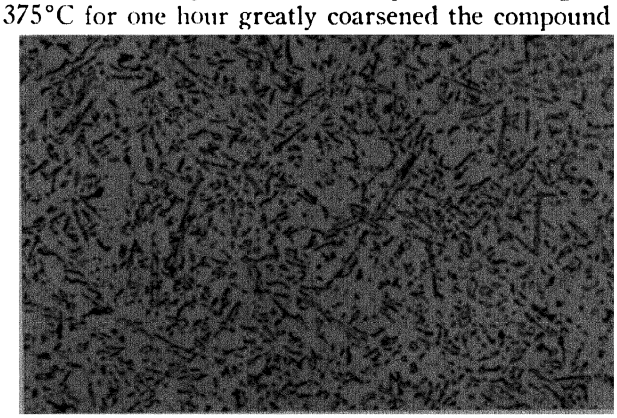

Figure 4. Cast alloy-16.8% U in Al-NaOH etch

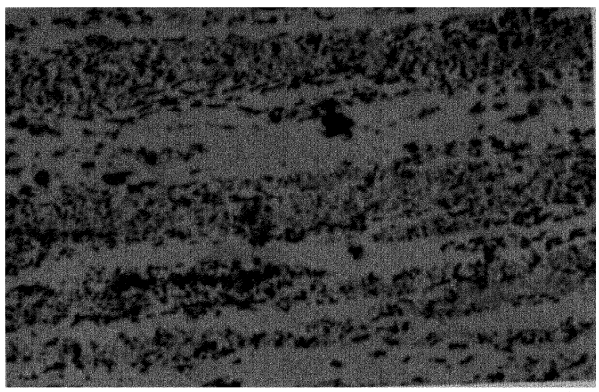

100 ×

Figure 5. Structure of rolled 11.3% U alloy Al alloy. NaOH etch

to produce the acceptable structure seen in Fig. 6. Currently, these plates are being hot rolled and annealed at 595°C, and an even better degree of dispersion is being attained. In fabrication the core is punched out and inserted into a rectangular frame of aluminum which is covered with aluminum plates. Intimate bonding between the core alloy and the cladding is achieved during a subsequent hot rolling operation. This method is generally referred to as the "picture frame technique", and is most often used for preparing clad plate-type elements.

It is also possible to prepare a fuel system by melting and casting two immiscible materials. One of these, of course, would be the fissile phase and the other the matrix phase. The matrix phase would have to be capable of being melted and cast without contamination from reaction with the crucible, mold, atmosphere, or reaction with the fissile phase. The latter would have to occupy a minor fraction of the volume. The density of the two phases would have to be matched rather closely, otherwise gravity segregation could become an important problem.

Little has been accomplished in the fuel field using this technique. Referring to Table V, Al, Fe, Ni, Mg, and possibly Zr and Ti, could be considered as matrix metals for this approach. Considering the fissile dispersants in Table IV, however, the choice is not so clear. For example, many of the fissile compounds would react with Al and Mg, and probably with Zr and Ti, and the difference in densities is great. Magnesium and uranium may be of interest since they do not interact metallurgically, but the difference in density of these two metals is about as large as possible. One system that may be feasible to fabricate by melting and casting is the iron–uranium dioxide (or nickel) system, since the oxide is chemically stable and the match in density is relatively good.

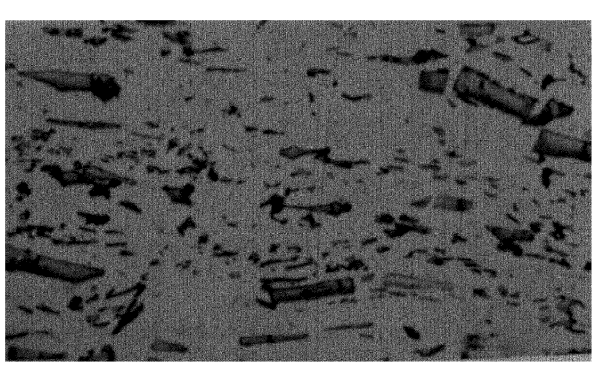

Figure 6. Structure of rolled 17.3% alloy annealed one hour at 375°C. NaOH etch

Powder Metallurgy Techniques

While melting and casting may be economically advantageous for a few specific fuel systems, the flexibility and versatility of a variety of powder metallurgy techniques offer one the possibility of producing high quality fuel elements from many combinations of materials. Because it is possible to form and work elements below the melting point of either constituent, many systems, heretofore rejected upon the basis of extensive reaction, can now be considered. Also, systems composed of two or more components possessing widely different densities can be homogeneously intermixed and subsequently alloyed if desired. Another major advantage of the method is the opportunity of incorporating the fissile phase into the matrix in its optimum shape and size.

The method does possess several disadvantages, however. Both the matrix and fissile phases have to be obtained as properly sized and shaped powders, generally of high purity. The maintenance of this high purity may require the use of special inert-atmosphere boxes for some materials which are highly reactive with the normal atmosphere. Finely divided Zr, Ti, U, UC, fall in this category. In order to produce dense bodies and develop the full strength and ductility of the matrix phase, the composite structure has to be mechanically worked. As we shall see later, this operation can destroy the shape and homogeneous distribution of the fuel phase which cannot be corrected by heat treatment as in the case of the U-Al castings.

There are several methods available for combining the components of the fuel system to produce a starting billet. The materials can be cold molded in a hardened die, sintered at a non-reacting temperature, and jacketed similar to the picture frame technique, followed by hot or cold working to final size and shape. The sintering step can be eliminated in many systems. The higher billet densities possible through the use of a hot-pressing operation often warrants the use of this more time-consuming operation. This is particularly true where subsequent working operations are to be kept to a minimum. Round elements can be prepared in a similar fashion. Pressed round slugs are loaded into metal tubes which serve the dual purpose of retaining the slugs during mechanical reduction and serving as the cladding of the final elements. The reduction to size may be carried out by groove rolling, swaging, or drawing. There are other methods of producing dense cladded elements from powder mixtures, but one in particular uses a somewhat unique approach

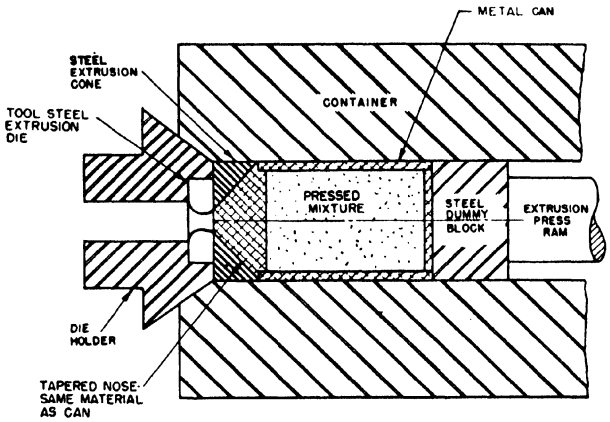

Figure 7. Arrangement for co-extruding clad rods from pressed metal powder billets

and deserves special mention here. This process is best described as a hot co-extrusion technique. Referring to Fig. 7, the powder billet is placed or pressed inside a metal can or jacket fitted with a tapered nose and flat back plate. This billet is then heated to the extrusion temperature in a separate furnace, inserted into the preheated container of the extrusion press and ejected through the die by applying pressure to the relatively cold back dummy plug. The extrusion cone fitted over the die matches that on the end of the billet and causes the walls of the can to move and be reduced concomitantly with the billet inside the can. Allowing for the porosity of the billet, both core and wall are reduced proportionate amounts. Upon establishing the proper extrusion parameters, most matrixes in Table II can be extruded into smooth concentric rods. Figure 8 shows the transverse cross section of an iron-UO_2 core clad in iron after being extruded from a 2½-inch diameter billet to ½ inch. Note the excellent uniformity of clad thickness around the whole perimeter of the core. This clad is so intimately bonded to the core that in bond strength tests the core will fail before the bond. The strength of the matrix in the core, adjusting for the volume of the fuel, is generally equal to the strength of the matrix in its solid wrought form.

Since all of the methods described for producing dispersion type elements usually call for some mechanical working to bring the elements to final size and shape, it is necessary to examine the effect of such working on the structure that has been so painstakingly created. In Fig. 9, a longitudinal cross section of an iron-clad core of iron-UO_2 is shown after approximately 50 per cent cold reduction. The UO_2 particles started out at approximately 150 microns in diameter. The fragmentation and longitudinal alignment of the UO_2 particles (most of them have been pulled out in polishing) creates a structure which could not be expected to sustain high burnups. Hot rolling this material at 1050°C produced the much more favorable structure shown in Fig. 10. These and similar results with a variety of metals and alloys clearly illustrate the need of maintaining the matrix phase in a highly plastic state during any mechanical reduction. The strength, hardness, and density of the fissile phase is also important. High firing of the UO_2 particles will, for example, greatly reduce its tendency to fragment during rolling.

In actual practice, the choice of particle size of the fissile phase is limited by the dimensions of the final element. A good rule of thumb sets the maximum particle size at one-quarter to one-third the minimum cross section of the fuel-bearing portion of the fuel element, the range reflecting the ductility of the matrix, and the relative clad and core thickness.

There is also a limitation imposed upon the maximum concentration of the fissile phase by the fabricability of the element and its ultimate mechanical properties. This limitation will vary with the size of the fissile particles and the ductility of the matrix, but for most materials there will be a sharp drop in

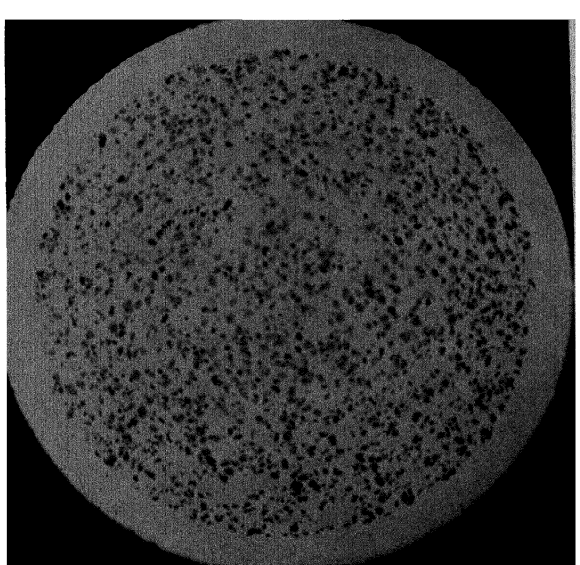

5×

Figure 8. Transverse cross section of iron clad, iron-UO_2 core co-extruded from 2½ in. diameter to ½ in. diameter

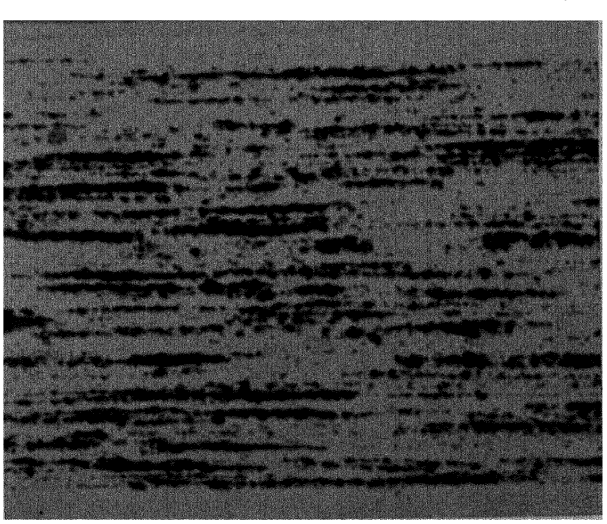

20×

Figure 9. Longitudinal cross section of cold rolled iron clad, iron-UO_2 core reduction in area—50%

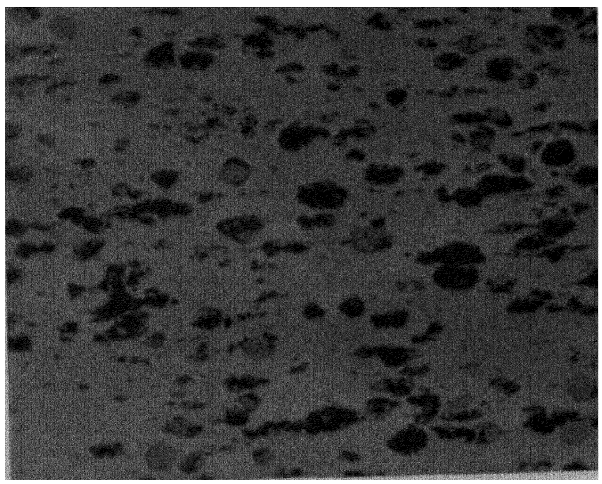

20×

Figure 10. Longitudinal cross section of iron clad, iron-UO_2 core hot rolled at 1050°C. Reduction in area 50%

mechanical properties at about 35 volume per cent of the fissile phase. If concentrations above this amount are desired, it may be necessary to select higher uranium concentration compounds. This latter concept was put to work in preparing the fuel plates for the United States reactor to be displayed at the International Conference on Peaceful Uses of Atomic Energy. The alloy core was to contain over 40 weight per cent uranium-aluminum alloy. In such an alloy an excessive amount of the aluminum would be tied up as the compound UAl_4. The resultant alloy cannot be rolled or otherwise worked into final shape. By substituting UO_2 for the uranium, the weight concentration of uranium was increased to 54 per cent, but the resultant volume concentration of the UO_2 was only 22 per cent. The powders were blended, cold pressed, and then easily hot rolled at a temperature where negligible reduction of the UO_2 by the aluminum occurred.

SUMMARY AND CONCLUSIONS

Dispersion-type fuel systems offer increased endurance life in high specific-power reactors, decreasing the refueling frequency. In addition, high uranium concentrations can be attained and fuel-diluent metal combinations used that are unattainable by conventional alloying techniques. A properly designed dispersion system calls for a fissile phase uniformly dispersed in a non-fissile matrix phase which predominates in volume so that the fissile particles are surrounded by a continuous network of matrix metal. The major damage in the fuel system is due to fission products. By proper choice of particle size, this damage can be confined to the fissile particles and a small adjacent region, leaving a continuous network of undamaged matrix metal to maintain the integrity of the element.

The fissile material should contain a high content of uranium, be relatively non-porous, and be sufficiently strong to retain its size and shape during fabrication. It should not interact with the matrix metal during fabrication or reactor operation. The matrix metal should be strong and ductile, and insensitive to neutron damage at the operating temperature. Both phases should have low parasitic neutron absorption cross sections. High thermal conductivity, low coefficient of thermal expansion, metallurgical compatibility with the cladding, and resistance to attack by the coolant are desirable features of the matrix metal used.

The features of a true dispersion system can only be achieved in a few cases using melting and casting techniques. Several different powder metallurgy techniques offer much greater flexibility, so that it is now becoming possible to design and fabricate fuel elements to a specific reactor design rather than design a reactor around the fuel element. During the fabrication by powder metallurgy methods, the problem exists of maintaining the structure and uniformity of the fissile dispersion in the process of consolidating the matrix phase and forming the element to final size and shape.

Existing data already confirm some of the advantages of the dispersion system, but much more work remains to be done. It is expected that there will be extensive effort placed on this type of system in the next few years which should supply essential data that can only be predicted today.

ACKNOWLEDGEMENTS

This paper has been written as a general survey of the dispersion-type fuel element. While based on the thoughts and experience of the authors, it includes work done by scientists at many of the laboratories of the United States Atomic Energy Commission.

Specific acknowledgement is made of work done on fabrication and heat treating at Oak Ridge National Laboratory and Battelle Memorial Institute. The work of Mr. R. J. Harrison of the Battelle Memorial Institute on the effect of particle size versus radiation damage has also been referred to in this paper. The authors are indebted to Mr. M. J. Feldman of the Oak Ridge National Laboratory for the irradiation data presented.

REFERENCES

1. Slater, J. C., *The Effects of Radiation on Materials*, Journal of Applied Physics, *22*: 237–256 (1951).
2. Dienes, G. J., *Effects of Nuclear Radiations on Mechanical Properties of Solids*, Journal of Applied Physics, *24*: 666–674 (1953).
3. Katz, J. K. and Rabinowitch, E. I., *The Chemistry of Uranium*, McGraw-Hill Book Co., Inc., New York (1951).
4. Buzzard, R. W., Journal of Research of the National Bureau of Standards, *50*: No. 2, 63–67 (1953).
5. *Metals Handbook*, 1948 Edition, The American Society of Metals, Cleveland, Ohio (1948).
6. *Metals Handbook*, 1954 Supplement, The American Society of Metals, Cleveland, Ohio (1954).
7. Adenstedt, H. K., Pequignot, J. R. and Raymer, J. M., *The Titanium-Vanadium System*, Transactions of American Society for Metals, *44*: 900–1003 (1952).
8. J. H. Keeler, Private communication, General Electric Research Laboratory, Schenectady, New York.

MTR-Type Fuel Elements

By J. E. Cunningham and E. J. Boyle,* USA

Prior to the termination of World War II, work was initiated at Oak Ridge National Laboratory to develop and produce a cheap, reliable thin-plate fuel component for service in a high neutron flux reactor. This effort culminated in the successful start-up and sustained operation of the Materials Testing Reactor at the designed 30-megawatt power level on March 31, 1952. This date was a milestone in reactor development for it not only clearly demonstrated the feasibility of constructing a high-flux research reactor, but also proved that the basic principles employed in the design and manufacture of aluminum plate-type elements were sound.

The fuel elements are made of an assembly of plates, each of which contains an enriched uranium-aluminum alloy core clad on both sides with aluminum, as shown in Fig. 1. The plates are spaced to allow water to flow between them, the water thus serving as coolant and moderator.

The fuel element lattice is surrounded by a primary beryllium reflector and the entire assembly is contained in a tank through which the water flows and which contains the control rods. No attempt will be made here to describe the reactor system in detail, since this will be covered in the session on Research Reactors.

Since the construction of the Materials Testing Reactor at the National Reactor Testing Station, Idaho Falls, Idaho, many research reactors in the United States have employed the aluminum plate fuel element. These include the Low Intensity Test Reactor, the Bulk Shielding Reactor and the Oak Ridge Research Reactor in Oak Ridge, the CP-5 Reactor at Argonne National Laboratory, the research reactors at Pennsylvania State University and the University of Michigan, and a number of others at various industrial and governmental research centers.

MATERIALS CHOICE

Aluminum was chosen for the cladding and structural material for research reactor fuel elements because of its low nuclear cross section, availability, low cost, fabricability and adequate mechanical, physical and chemical properties. The strength and thermal conductivity of aluminum are adequate for the thermal stresses and thermal gradients encountered, and its corrosion resistance is sufficient for the maximum temperatures, i.e., less than 100°C, encountered in the exit cooling water.

Fortunately, the aluminum-uranium alloy system is such that homogeneous alloys can be prepared with uranium contents up to 25 weight per cent. The aluminum-uranium phase diagram is shown in Fig. 2. It will be noted that in the composition range of interest, i.e., 14 to 25 weight per cent uranium, the structure consists of primary compounds of UAl_4 surrounded by a matrix of eutectic between aluminum and UAl_4. The techniques for preparing such alloys and insuring a homogeneous distribution of uranium will be described in a later section of this paper.

When it is necessary to prepare alloys with uranium contents greater than 25 weight per cent, difficulties with segregation and resultant non-uniform distribution of uranium are encountered. These difficulties can be obviated by the use of fuel plate cores with a powder metallurgy mixture of uranium oxide (UO_2) and aluminum powder. Fuel plates, with uranium weight percentages up to 60%, have

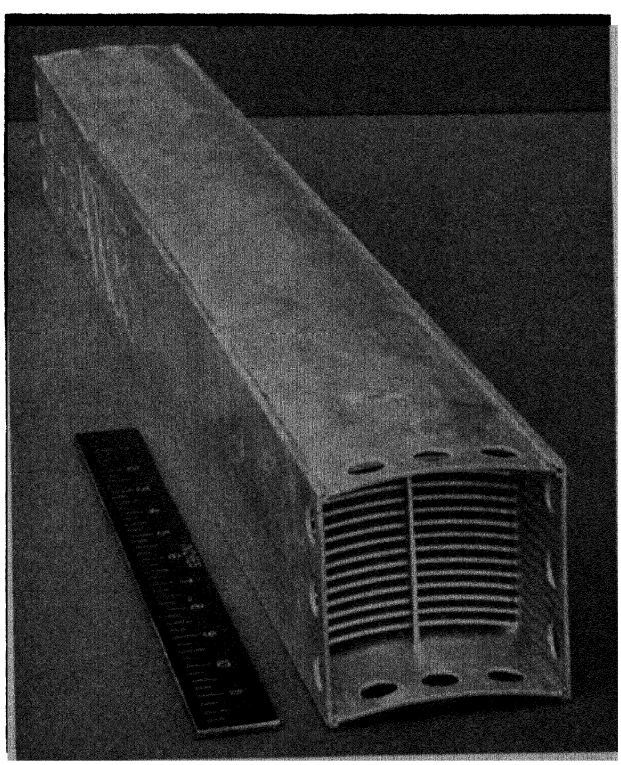

Figure 1. Brazed **MTR fuel element**

* Oak Ridge National Laboratory.

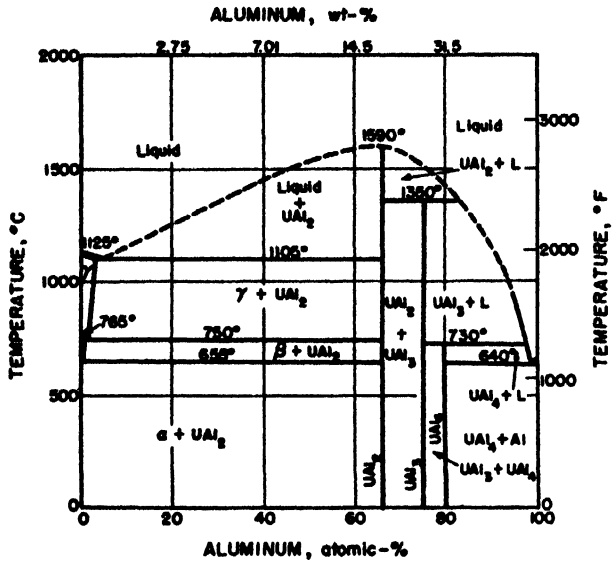

Figure 2. Aluminum-uranium phase diagram

been prepared with a uniform distribution of uranium. As will be described in detail in a later section, the fuel plates for the reactor on exhibit at this conference were prepared by this technique.

DESCRIPTION OF FUEL COMPONENT

Design and construction of aluminum plate-type elements were based on the following criteria: (1) loading the reactor with enriched uranium-235 fuel; (2) cladding to hermetically seal the fuel material from exposure to the reactor cooling water and retain the products of fission; and, (3) use of plate-type construction to give a higher surface-to-volume ratio for heat transfer purposes.

The main ingredient of the fuel element is fissionable uranium-235. The fuel is incorporated into the fuel plates of the element in the form of either aluminum-uranium alloy or as a dispersion of UO_2 in an aluminum powder matrix. The fuel plates, therefore, consist of a fuel-bearing or core section which is clad on all sides with wrought aluminum to form a three-ply composite fuel plate. The hot-rolling operation employed results in a good metallurgical bond between clad and core material.

In the case of the Materials Testing Reactor, nineteen fuel plates are assembled into a single unit which is designated as a fuel element or assembly. The fuel plates, with a nominal 0.115-inch water gap between them, are brazed into a pair of aluminum side or spacer plates.

A cross-sectional view of a Mark XI, MTR fuel element with dimensional specifications is given in Fig. 3. The spacer, or side plate, is 0.188 inches in thickness, while the 17 internal fuel-bearing plates are 0.050 inches in thickness. The external fuel plates are somewhat thicker, i.e., 0.065 inches, in order to give added cladding thickness and structural integrity to the fuel component. The center-to-center dimension in the grid for positioning the fuel component is 3.035 inches, while the over-all assembly width is 2.996 inches. This difference allows for a nominal spacing between units in this direction of 0.039 inches. The spacing in the other direction is 0.117 inches, or the same as the water gap between adjacent fuel plates in the assembly.

The water, or heat-transfer media, flows through the water passages at a velocity of 30 feet per second. The primary coolant system is not pressurized,

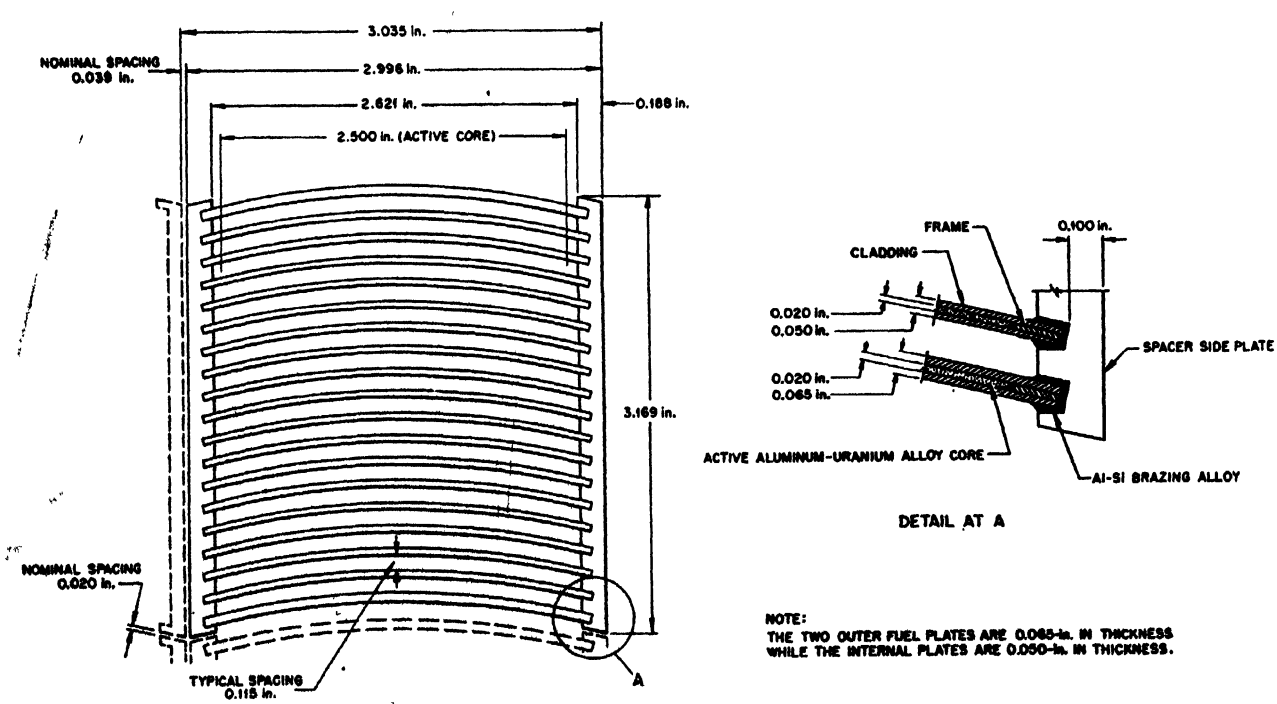

Figure 3. Dimensional drawing of MTR fuel element cross section

Table I. Design Data on Several Aluminum Fuel Components in Service

Reactor designation	*LITR and MTR*	*CP-5*	*BSR*	*GCR*
Number of fuel-bearing plates	19	10	18	18
Spacer or side plate thickness, inches	0.188	0.125	0.188	0.110
Water gap spacing, inches	0.115	0.154	0.117	0.117
Core composition, wt %	10–20 U-Al alloy	10–20 U-Al alloy	10–20 U-Al alloy	54 UO_2-46 Al powder
Metal-to-water volume ratio	0.69	0.39	0.74	0.63

since film boiling at the water-fuel plate surface interface does not occur under normal operation.

The unit is equipped with cast 356 aluminum alloy end boxes by plug welding. The purpose of the end fitting is to adapt the unit to the supporting grids which in turn firmly fix the position of the element in the reactor core. A spring is provided on the upper casting to allow for thermal expansion and tolerance limitations. These adapters also serve as transition pieces which convert the rectangular cross section of the fuel element to the smaller-sized holes in the grid. The fittings, of course, are hollow to permit free passage of the water through the fuel element. An over-all view of the finished fuel element with end adapters attached is illustrated in Fig. 4.

Additional specifications on the MTR Mark XI fuel element are given in Table I. Included for comparison, are data on similar plate-type elements employed in the operation of several other research reactors in the United States.

FABRICATION OF ALUMINUM FUEL PLATES

Aluminum-clad fuel plates containing uranium-235 are currently fabricated by two methods. These methods, referred to as the alloy and powder method, differ only in the initial preparation of the fuel-bearing core section of the composite plate. The fabrication procedure employed in the manufacture of fuel plates by both methods is described below:

In the alloy method, high purity (99.7%) aluminum and uranium metal, enriched in the U^{235} isotope, are alloyed directly to form uranium-aluminum alloy. The melt is prepared in a graphite crucible in the open atmosphere by induction heating. The melt size is confined by critical mass limitations.

After solution of the uranium and degassing of the melt are complete, the molten alloy is poured into graphite molds to produce cast-alloy slabs for rolling. Because of the large density difference in the melt constituents, careful control of casting conditions is necessary to avoid segregation. Pouring temperature varies as a function of the uranium concentration between 700–1000°C (1292–1832°F). The total uranium and U^{235} isotopic composition of the melt are verified by analyzing dip samples taken from the melt.

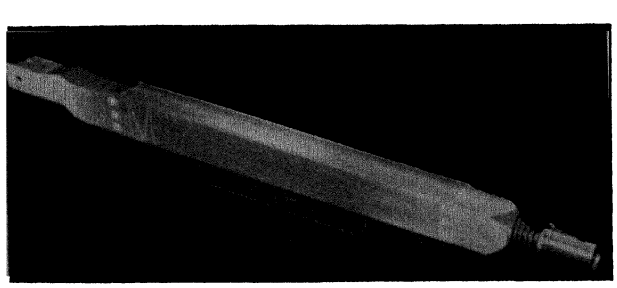

Figure 4. Over-all view of finished MTR fuel element

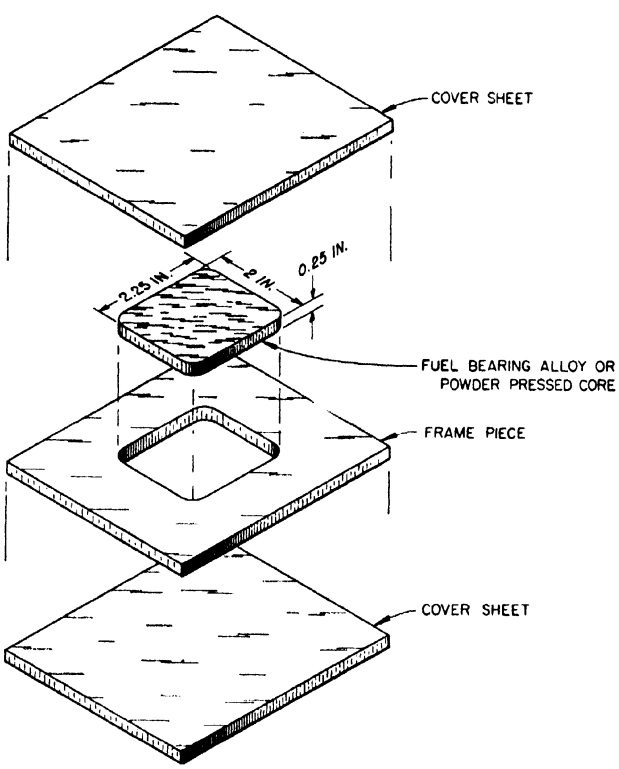

Figure 5. Exploded view showing makeup of composite fuel plate prior to rolling

The cast-alloy slab is heated for one hour at 590°C (1094°F), and hot worked by rolling to produce strip stock of 0.25 inches in thickness. Alloy blanks or fuel plate cores, 2 × 2.25 by 0.25 inches in thickness, are punched from strip stock with a conventional punch and die set.

Similar fuel-bearing cores can be prepared by powder metallurgy techniques. The starting ingredients are (—325 mesh) aluminum powder and enriched UO_2 powder in the selected 44–105 micron size. After proportioning and blending, the amount

of powder mixture required for each core compact is loaded into a die cavity and hydraulically pressed under a pressure of 33 tons per square inch.

Each alloy or pressed powder core is completely jacketed by the picture frame technique. The wrought-aluminum encasement jacket consists of a frame piece for enclosing the four lateral sides and cover sheets. An exploded view illustrating the component parts, which make up the assembled composite plate for rolling, is shown in Fig. 5.

The composite fuel plate assembly is thoroughly heated at 590°C (1094°F) and hot rolled from the starting thickness to 0.070 inches in order to achieve a sound metallurgical bond between clad and core material. The rolling schedule consists of six hot passes to yield a total reduction in thickness of 84%.

At this stage, the composite fuel plates are flux-annealed to prevent the formation of objectionable blisters which may occur on subsequent processing or during reactor service. Blisters are caused by hydrogen gas which is present in the alloy or mixture.

The flux-annealing treatment consists of coating the surface of the fuel plates with a slurry mixture of alcohol and brazing flux and annealing for one hour at 610°C (1130°F). After treatment, the water-soluble flux, which consists of a eutectic mixture of sodium, lithium, potassium fluorides and chlorides, is removed by a scrub wash. The plates are then dipped in an acid bath of 10 HNO_3-2HF-80 volume % water solution, rinsed in hot water and dried.

The composite fuel plates are reduced cold in several passes to a final thickness of 0.60 ± 0.001 inches and annealed for one hour at 590°C (1094°F). All acceptable plates are examined under a fluoroscopic X-ray screen to locate internal defects, determine straightness and delineate the fuel-bearing core section of the composite fuel plate. After rough shearing, the fuel plates are stacked and batch machined to final width and thickness.

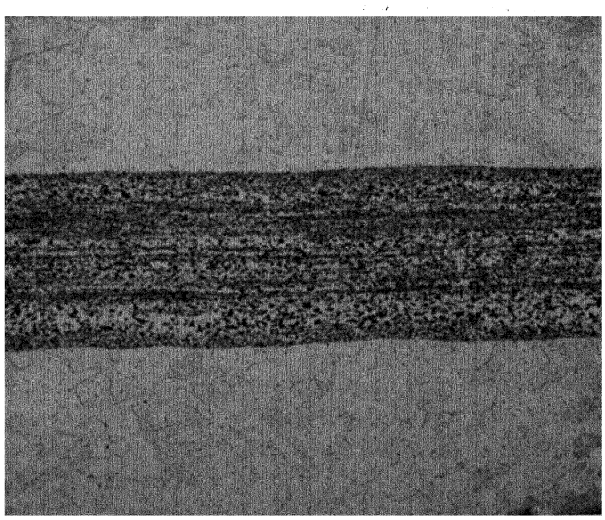

Figure 6. Micrograph of transverse section from composite fuel plate

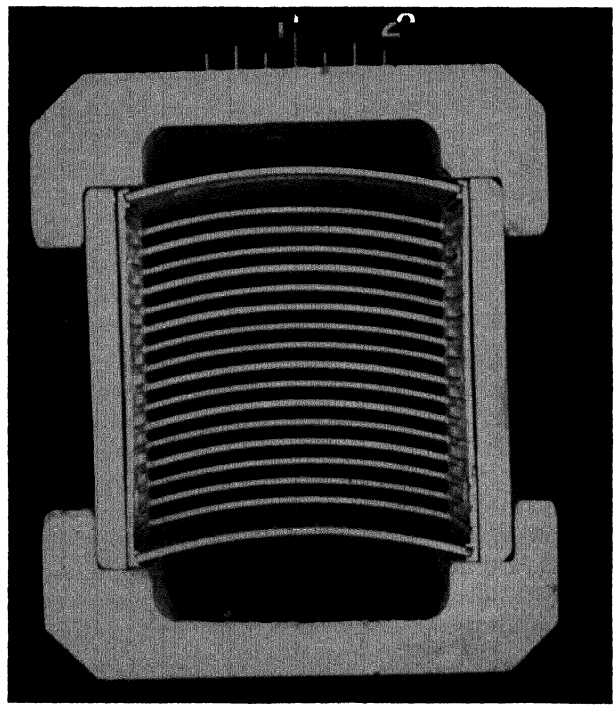

Figure 7. MTR fuel element assembled in brazing jig

The appearance of a transverse section cut from a finished fuel plate is illustrated in Fig. 6. Prior to assembly, the composite fuel plates are curved in a forming die to the desired 5.5-inch radius of curvature.

COMPONENT ASSEMBLY BY BRAZING

The curved fuel-bearing plates are joined into a single fuel assembly by brazing. In the case of the Geneva Conference Reactor, eighteen fuel-bearing plates were spaced at 117 inches apart and brazed into a pair of ⅛-inch thick side or spacer plates to form an integral fuel assembly or element.

The grooved side plates of the fuel element are prepared from braze-clad sheet stock. This material is a duplex sheet consisting of wrought aluminum sheet, clad on one side only with 12% silicon-aluminum brazing alloy. After batch machining the stock to final length and width, the grooves are cut through the braze-clad side of the plates by gang milling. The cutter is designed in a manner to permit cutting all grooves simultaneously with a minumum of chatter.

Prior to brazing, all component parts of the fuel element are thoroughly cleaned and the parts handled thereafter with white cotton gloves. The side plate grooves are coated with a slurry of brazing flux and alcohol, and positioned upright in the drying jig. The fuel plates are inserted into the proper grooves, aligned and tightened in the jig.

The assembled fuel component is taken through the following sequence of operations which constitute the brazing cycle:

1. Dry in an oven at 150°C (302°F) for three to

four hours to drive off the water and alcohol from the brazing flux.

2. Transfer from the metal drying jig to a ceramic brazing jig.

3. Preheat for one hour at 500°C (932°F) to thoroughly preheat the component and brazing jig.

4. Braze at 610°C (1130°F) in a forced-air circulation furnace for twenty-five minutes.

5. Cool to room temperature and wash to remove the water-soluble brazing flux.

6. Clean in an acid bath followed by hot water rinsing and drying.

Figure 7 illustrates an assembled aluminum fuel element in place in the self-aligning AlSiMag (aluminum, magnesium silicate) brazing jig. A cross-section slice taken from a Geneva Conference mock-up fuel element is shown in Fig. 8.

The assembly proper is equipped with a lower end box fitting to adapt the unit to the supporting grid, and firmly fix the position of the element in the reactor core. A horizontal handling bar is added to the upper end to facilitate loading and unloading the element in the reactor pool.

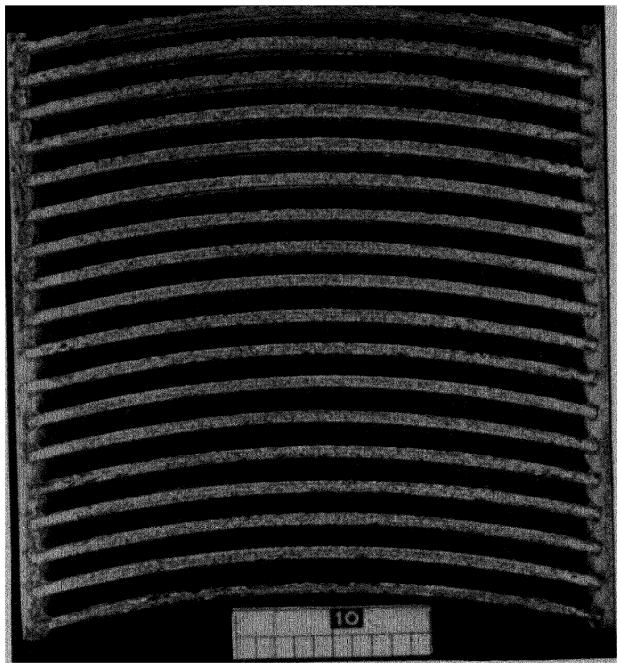

Figure 8. Cross sectional slice taken from GCR fuel assembly

REACTOR PERFORMANCE

Aluminum fuel elements, as described in the present paper, have performed satisfactorily in reactor exposure to quite high burn-ups. As described in detail in the paper, "Radiation Damage in Reactor Materials,"† there are only slight dimensional changes accompanied by slight decreases in density in such elements after long-term reactor exposure. With respect to mechanical and physical properties, it has been noted that the yield strength and hardness of an 18 weight percentage uranium-aluminum alloy was doubled after reactor exposure; and there was a marked decrease in ductility. Reductions of 20% to 30% in thermal conductivity have been recorded. However, under the operating conditions encountered in research reactors, the changes described above have not resulted in any fuel element failures or loss of operating efficiency.

† P/744, Vol. 7, Session 11B, these Proceedings.

SUMMARY

The fabrication technology has been developed to produce relatively cheap, reliable aluminum plate-type fuel elements for water-cooled research reactors. Two types of fuel elements can be produced, i.e., (1) elements with aluminum-U^{235} alloy cores, or (2) elements with aluminum-enriched UO_2 powder metallurgy cores. Many research reactors in the United States have been fueled with elements of this type, and the service performance of such reactor cores has been completely satisfactory. The development of this fuel element type has already made and will continue to make a major contribution to the peace-time applications of nuclear energy in the United States.

On the Possibility to Improve the Heat Transfer of Uranium and Aluminum Surfaces in Contact

By F. Boeschoten,* The Netherlands

A heterogeneous nuclear reactor with a high neutron flux requires necessarily a high rate of heat extraction from the fuel elements. If an aluminium canning is used, the coefficient of heat transfer for the aluminium-uranium surfaces must be as high as possible, because it soon becomes a limiting factor for the heat extraction.

The uranium and the aluminium are not in contact over the whole surface. On the contrary there is contact only on a number of small spots, depending on the roughness of the surface. In between will be a gap of varying thickness and, moreover, not the metals themselves are in contact, but their oxide layers. For these reasons the transfer between the metals is poor (about 1 watt/m²-°C).

Possibilities for improvement of the heat transfer are:

1. A closer contact between uranium and aluminium by pressure.
2. A gaseous layer between U and Al using a gas lighter than air.
3. A liquid layer between U and Al using a metal or alloy.
4. A solid layer between U and Al (powder or enamel). All lining materials should have a low neutron absorbing cross section.

An apparatus was designed[1] to measure the coefficient of heat transfer due to application of the possible improvements mentioned above. A slice of uranium (3-mm thick; 30-mm diameter) was placed between two aluminium rods, through which was sent a known heat flux. By determining the drop in temperature over the uranium slice and by dividing the heat flux by twice this amount, the coefficient of heat transfer is found for this arrangement. The temperature of the uranium was, for all tests, about 230°C, which temperature would exist at the uranium surface in a PWR type of reactor.

PRESSURE

By application of pressure, particularly in combination with a high temperature, one can expect an improvement of the contact between the metals. For our surfaces the coefficient of heat transfer increased in the following way:

1 atm	*25 atm*	*25 atm (after a week)*
0.6 watt/cm²-°C	2.0 watt/cm²-°C	3.5 watt/cm²-°C

* FOM—Researchgroup R. I, Utrecht.

Thus application of pressure gives a considerable improvement. Moreover the contact becomes better after application of the pressure over a longer time. It is necessary only that the aluminium canning be kept under pressure in the reactor (which is the case indeed for a PWR type). In considering the numbers given above, one has to be aware that they may vary easily by a factor of two, depending upon the condition of the surfaces, and that they may be appreciably different for an actual cylindrical surface.

Another possibility may be found in a pretreatment in which such a temperature and pressure are applied that the aluminium becomes plastic and joins the uranium surface. After applying a pressure of 600 atm at 150°C for 5 min an improvement by a factor of two in the heat transfer was found and better results may be expected at higher temperatures, pressures and longer time for the treatment. However, such a contact will probably be lost in the reactor unless the canning is kept under sufficient high pressure.

GASEOUS LINING

By introducing hydrogen, helium and air respectively in between the surfaces, the following coefficients of heat transfer (in watt/cm²-°C) were obtained (all gas pressures about $\frac{1}{20}$ atm):

	Hydrogen	*Helium*	*Air*
Pressure 25 atm	2.4	2.0	1.9
Pressure 50 atm	3.3	3.0	3.2

From these numbers it is obvious that most of the heat transfer takes place along the spots where the surfaces touch each other and that the transfer by the gas in the gap is relatively small.

By using these numbers and assuming an average gap width of 10 μ it is found[1] that the part of the surfaces which are really in contact is of the order of 10%, whereas presumably there is no direct contact between the metals, but only between their oxide layers.

LIQUID LINING

This must be a metal or an alloy. In our case special interest was put in metals which are liquid at about 230°C. Self-evidently it must have a low neutron absorption cross section, possible components being Bi, Pb, Al, Mg, Sn, Na.

All the low melting alloys of these metals give a big improvement; the coefficient of heat transfer for all of them is about 25 watt/cm²-°C. However, none of them except Na can be used because of their corrosive properties. In the following a short discription is given for several alloys.

To study corrosion effects a slice of uranium was put together with a slice of aluminium (both 3-mm thick; 30-mm diameter) in a glass tube under vacuum. The distance between the slices was about 1-mm and the gap between was filled with the liquid metal, similar to the rest of the tube. The whole was heated at 350°C for three days. It was expected that the corrosion under those circumstances would be comparable with the corrosion which would possibly show up after a year at 230°C. Of course, one has to be very careful with the interpretation of the results because neither threshold effects nor radiation damage is taken into account. Nevertheless, one hopes to draw some conclusions about corrosion effects in this way.

Pb(43.5)—Bi(56.5) mp 125°C

This alloy affects both the uranium and the aluminium heavily. The crystals of the intermetallic compound which is formed grow perpendicularly from the surfaces and thus ruin the aluminium canning. Moreover, because the heat transfer is very poor after the reaction occurs, no liquid metal remains.

Pb(97.5)—Mg(2.5) mp 250°C

This alloy affects the uranium and particularly the aluminium surface. Here it is clearly seen that a kind of migration takes place from the uranium to the aluminium and visa versa. The same was observed for the Pb–Bi eutectic.

Sn mp 232°C

Sn affects both the uranium and the aluminium very heavily, just like its eutectic alloys with Pb (62% Sn) and Mg (98% Sn).

Na mp 97.5°C

Only a very slight attack took place. Apparently some aluminium is transported through the sodium to the uranium surface. But the attack is so slight that application of Na may be a good solution to the problem. However, care must be taken that no moisture is present. Because the applied layer must be very thin (order of 10 μ), the effect of the sodium-water reaction in case of a breakdown of the rod will be relatively unimportant.

SOLID LINING

The application of a solid lining does not appear to give many advantages. The solid particles will tend to increase the uranium-aluminium distance so that the direct contact may be lost, without enough compensation being gained from the filling of the gap. None of the solids, except graphite, gives an improvement of the heat transfer. Most of them, particularly the oxides, give a deterioration.

The most interesting tests were:

Graphite

C as graphite increased the coefficient of heat transfer by a factor of two. The best results were obtained by smearing the graphite over the surfaces, rather than putting the crystals in between. However, blister formation on the uranium surface was observed, possibly due to formation of uranium carbides.

Mg Powder

The coefficient of heat transfer remained unaltered—about 1 watt/cm²-°C, which was lower than expected. Improvement may be obtained by applying pressure for a longer time. The uranium and particularly the aluminium were affected.

Al Powder

Al powder did not give any noticeable improvement either. As expected from the literature,[2] the uranium was affected by the aluminium.

CONCLUSION

Taking into consideration that the research so far has given only rough information rather than quantitative answers, we may conclude that the most promising improvement in the heat transfer from uranium to aluminium may be expected from pressure and/or from sodium as liquid lining. However, it is quite possible that the uranium and/or aluminium surfaces may be treated in such a way that they are not affected by compounds which otherwise would do so. Because of the numerous parameters which appear in a problem such as this it is difficult to find a solution in this direction.

REFERENCES

1. Çetinkale, T. N., Mech G. I. and Fishenden, M., Thermal Conductance of Metal Surfaces in Contact, Inst. of Mech. Eng., Gen. Disc. in Heat Transfer, page 271 (1951).
2. Gordon, P. and Kaufman, A. R., J. Metals *188*, Trans 182 (1950); Borie, S. B., J. Metals *3*, Trans 800 (1951).

Fabrication of Uranium Alloys

By A. R. Kaufmann,* USA

Uranium alloys have been extensively studied in various USA laboratories in conjunction with possible use as fuel element material in nuclear reactors. The objective has been either to get improved resistance to radiation damage or better corrosion resistance in air or water. The preparation and fabrication of these alloys present a number of problems which are often troublesome. The purpose of this paper is to discuss these difficulties in a general way in order to show that they can be solved if the investigator has a proper understanding of uranium itself and in addition has available the phase diagram of the alloy system involved. The behavior of uranium alloys during fabrication follows the same principles observed by metallurgists for other metals.

The three allotropic forms of pure uranium dominate the problem of working it. In the alpha phase (up to 660°C) uranium work-hardens when deformed at temperatures up to about 450°C. The minimum recrystallization temperature for heavily cold-worked metal is about 425°C. The minimum recrystallization temperature for heavily cold-worked metals is about 425°C. From about 450°C to 660°C true hot working can be carried out with the metal becoming softer as the temperature is raised. In the beta phase (660°C to 770°C) the forces required to hot work the metal are 2 to 3 times as great as at 650°C and the ductility is substantially less. In the gamma phase (above 770°C) uranium is so soft and plastic that difficulty is sometimes encountered in having it flow well and retain its shape. This difficulty is accentuated by certain impurities such as iron which may lead to hot shortness in the gamma phase.

The fabrication of uranium-rich alloys differs from that of the pure metal only by the extent to which the alloying element modifies the three allotropic forms of uranium. No elements having appreciable solid solubility in alpha uranium have been found. Therefore fabrication of alloys in the alpha existence range is governed by the degree of hardening caused by the second phase. If this second phase is a brittle intermetallic compound, the uranium alloy rapidly decreases in ductility with alloy addition and working in the alpha phase may become impractical. There are some cases, however, where the intermediate phase is not brittle and thus does not alter the uranium radically. Solid solubilities in the beta phase are also rather restricted and, as far as is known, there are no alloy additions which make it more feasible to fabricate in the beta phase. Presumably, alloys containing second phases are even more difficult to work in the beta phase than pure uranium. There are a number of elements such as Mo, Zr, Nb, V, and Ti which have extensive solubility in the gamma phase. In most such cases the feasibility of working above 770°C is increased since the gamma uranium is stiffened and has more high temperature ductility. In some instances the beta to gamma transformation is lowered by the alloy addition and it then becomes possible to fabricate in the body centered cubic phase below 770°C. With some alloys such as 6% to 15% Mo it is possible to retain the gamma phase in a meta stable state at room temperature and cold working of the body-centered cubic phase then can be carried out. It is possible to retain the beta phase by quenching a 1 to 2 at % Cr alloy, but this has no significance in fabrication since the beta structure apparently transforms during cold deformation.

The production and fabrication of some typical alloys is described below in order to further illustrate the problem of producing them.

URANIUM-CHROMIUM ALLOYS

In most respects the alloys with chromium constitute a simple situation since, as shown by Figure 1,† there are no intermetallic compounds. This is then a case of processing a mixture of two somewhat ductile metals.

Melting

Melting can be satisfactorily accomplished in graphite crucibles for compositions up to the eutectic at about 5.2 wt %. There is no great difficulty with regard to carbide formation or segregation.

It is interesting to note that the eutectic alloy, which melts at about 860°C, has a particularly high fluidity. When poured from about 1000°C into heated molds, it will fill very small openings. For example, plates 0.040 × 3 × 24 in. can be cast without difficulty and various intricate structures are readily produced.

* Nuclear Metals, Inc. and Massachusetts Institute of Technology, Cambridge, Mass.

† The phase diagrams given in this paper have been copied from other sources and should not be attributed to the present author.

Fabrication

Chromium alloys up to the eutectic composition can be extruded in the gamma phase at about 800°C or the alpha phase at about 600°C. Typical values for extrusion constants for several compositions are shown in Table I.‡ It is clear that chromium is stiffer than uranium and hence should make the alloys more difficult to work.

It is possible to forge the eutectic composition at about 800°C by a pressing operation using pressures of about 2000 psi. Alloys with less chromium deform still more easily at that temperature.

Rolling can be carried out readily at 600°C but cold rolling becomes increasingly difficult as the chromium content is increased. It is to be noted that chromium itself does not possess much ductility.

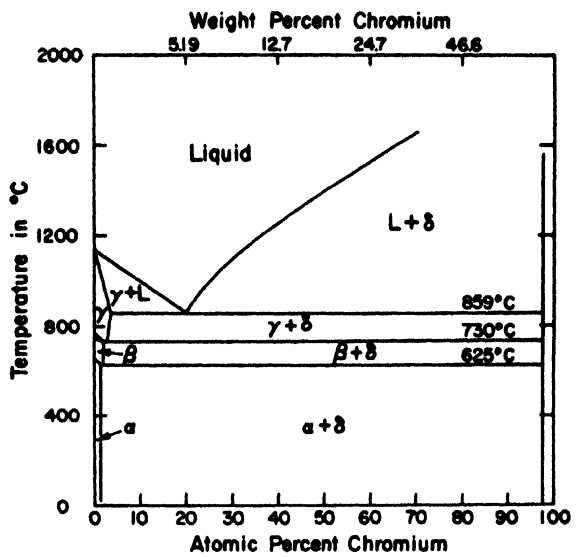

Figure 1. Uranium-chromium phase diagram

Hot swaging of alloys containing up to 2 at % Cr can be carried out at 275°C and up to 4 at % Cr at 550°C.§ Annealing at 550°C removes the effects of cold work.

URANIUM ZIRCONIUM

This system represents a case of complete solid solubility in the high temperature body-centered cubic region with no appreciable solid solubility in the low temperature phases and the occurrence of one intermetallic phase. The situation is illustrated in Fig. 2 which is a composite of the diagrams of several investigators and must be regarded as somewhat tentative. The intermetallic phase has been reported by a number of workers in the USA and recently Seymour and others of the Knolls Atomic Power Laboratory have determined the crystal structure and have concluded that it forms by an order-disorder reaction. ¶

Table I. Extrusion Constants for Some Uranium Alloys

Material wt %	Temperature °C	K psi	Remarks
Uranium	590	40,000	
	870	6500	
98U 2Zr	590	50,000	
	650	45,000	
	700	28,000	
	735	16,000	
50U 50Zr	610	50,000	
	650	42,000	
	732	32,000	
	760	29,000	
	815	28,000	
20U 80Zr	650	41,000	
	760	27,000	
	850	16,000	
	910	15,000	
8U 92Zr	760	40,000	
	815	31,000	
	870	32,000	
	927	30,000	
93.5U 5Zr 1.5 Nb	620	40,000	
	650	35,000	
	677	30,000	
	705	26,000	
	732	23,000	
	760	20,000	
	788	17,000	
99.9U 0.1Cr	635	48,000	
97.5U 2.5Cr	600	63,000	
	800	29,000	
95U 5Cr	600	68,000	
	765	44,000	
	850	31,000	
96U 4Mo	600	>94,000	Failed to extrude
	900	35,000	
92U 8Mo	600	71,000	
	900	58,000	
88U 12Mo	600	>94,000	Failed to extrude
	900	63,000	
99.9U 0.1Si	635	45,000	
97.5U 2.5Si	600	86,000	As cast
	800	34,000	
96.2U 3.8Si	850	55,000	Heat treated to form epsilon

Melting

Zirconium is even more reactive than uranium at high temperatures and therefore the choice of melting crucibles must be made carefully. Beryllium oxide and probably zirconia are satisfactory for compositions up to about 3 wt % Zr. Graphite may be used for all compositions if the molten metal is not

‡ The pressure required for extrusion may be conveniently expressed by the relation

$$P = K \ln \frac{A_1}{A_2}$$

where P is pressure on the ram in psi, K is a constant which varies with temperature, and A_1 and A_2 are the cross-sectional areas of the billet and the extruded rod respectively. K varies somewhat with the lubrication and for a given set of extrusion conditions it does not become constant until the reductions in area are greater than about 5 times. K has lower values the larger the diameter of the extrusion billet. Most of the values in Table I were determined on billets about 2 to 3 inches in diameter.

§ Personal communication from White of Knolls Atomic Power Lab.

¶ Personal communication.

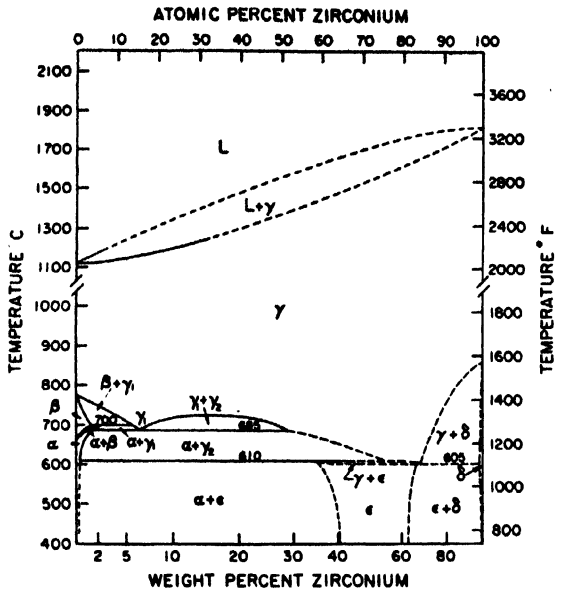

Figure 2. Uranium-zirconium constitutional diagram

overheated and is poured soon after melting. Without these precautions large amounts of zirconium carbide will form, especially in the range from 5 to 95% Zr. Arc melting in a water-cooled copper crucible must be used to produce alloys of the highest purity.

Fabrication

Zirconium is a ductile metal and its body-centered cubic phase alloys with uranium all are easy to hot work. Zirconium is much stiffer than uranium in this phase and therefore the extrusion constants at a given temperature increase with zirconium content as shown in Table I. It is interesting to note that with 2% Zr alloy it is possible to extrude in the temperature range where the uranium beta phase is normally encountered. According to Fig. 2 the alpha phase persists up to about 700°C at this composition. The relatively low K for the extrusion at 735°C is presumably due to large amounts of gamma phase mixed with beta phase. The existence range of the gamma phase may be further lowered by certain ternary alloys. As an example, an alloy containing 5 wt % Zr and 1½ wt % Nb has stable gamma phase down to about 620°C. The data in Table I show that there are no discontinuities in K for this alloy in the normal beta phase existence range. The results for the 50% Zr alloy illustrate another case of working the body-centered cubic phase at temperatures as low as 610°C.

In general it appears that the intermediate phase, epsilon, is reasonably ductile. Extrusion data below 600°C for alloys in this range have not been obtained. It may be said, however, that alloys containing epsilon may be cold rolled and cold swaged with reasonable reductions before annealing becomes necessary.

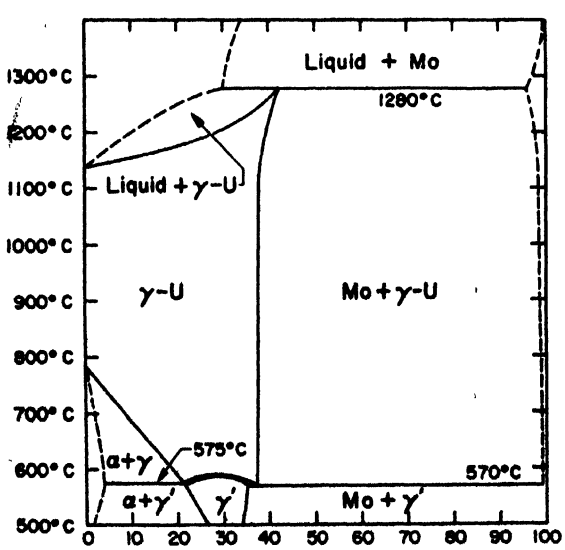

Figure 3. Uranium-molybdenum phase diagram

URANIUM-MOLYBDENUM

Molybdenum has extensive solubility in gamma uranium, as shown in Fig. 3, and forms an intermediate phase at about 15 wt % Mo. The exact location of the boundaries of this epsilon phase is somewhat uncertain but there is no doubt of its existence.** For alloys above about 5 wt % Mo the transformation of gamma to alpha becomes increasingly sluggish. Above about 10% Mo the gamma phase is retained even without quenching.

Melting

Induction melting of alloys up to 15 wt % Mo is readily carried out in crucibles suitable for melting uranium. Graphite crucibles with a zirconia wash are quite satisfactory. Arc melting is not particularly satisfactory for making these alloys since there is a possibility that the molybdenum additions may not melt completely.

Fabrication

Alloys containing up to about 3 wt % Mo may be extruded or rolled in the high alpha region. For larger amounts of molybdenum it is necessary to fabricate in the gamma phase since the alloy becomes increasingly stiff. The extrusion constants shown in Table I show that at 12% Mo the alloy is almost too stiff to extrude at 900°C†† with an appreciable reduction in area. The table shows that the 4% and 12% Mo failed to extrude at a K value of 94,000 at 600°C whereas the 8% alloy did extrude. The reasons for this are not known. One possible explanation is that the 4% alloy was in the alpha phase whereas the 8% and 12% alloys were in the gamma phase at 600°C. All the molybdenum alloys up to 12% may be cold worked to some extent by swaging. In the case of the 12% alloy, it is de-

** This diagram was obtained from British sources.

†† A unit pressure of about 200,000 psi is the practical limit for the extrusion ram.

sirable to take a heavy reduction in each pass through the machine since there is then less trouble with cracking. Cold working of the 12% alloy does not appear to transform any appreciable amount of the retained gamma phase.

URANIUM-SILICON

There are a number of intermetallic compounds in this system, as shown in Fig. 4, and all of them are quite brittle except for the epsilon phase at about 23 at % (3.6 wt %) silicon. It is not feasible to fabricate the alloys above about 30 at % Si by conventional means and the discussion will therefore be confined to the uranium-rich alloys. The epsilon phase forms rather sluggishly and hence alloys as-cast consist essentially of mixtures of uranium and U_3Si_2. A heat treatment of 4 to 24 hours duration at 800°C is required to convert most of the U_3Si_2 to epsilon although it is likely that for alloys below the eutectic composition (8 at %) the peritectoid reaction may occur more readily.

Melting

The uranium-rich alloys may be melted in any type of crucible suitable for melting uranium itself. Above about 20 at % Si it is desirable to heat to at least 1600°C in order to make sure that all the high melting compounds are in solution. It has been found that a graphite crucible which has been given a zirconia wash is suitable for this operation. An alloy of about 25 at % silicon will contain only about 0.06 wt % carbon if made in this way. It is desirable to chill-cast alloys above the eutectic composition in order that the primary U_3Si_2 particles be as small as possible. The small particle size is desirable in order that peritectoid reaction to form epsilon can go to completion readily.

Fabrication

It is possible to extrude all compositions up to about 28 at % Si in the as-cast condition where the alloy consists of uranium and U_3Si_2. At the higher silicon contents it becomes necessary to use a temperature of about 900°C. Obviously part of the U_3Si_2 will convert to epsilon during this operation. It is also possible to first convert the U_3Si_2 to epsilon and then extrude. If this composition is such that substantial amounts of free uranium remain after the heat treatment, it is necessary to use an extrusion temperature which avoids the uranium beta-phase region. Low silicon contents can be extruded at about 600°C in the uranium alpha phase. Above about 10 at % Si it is more practical to use an extrusion temperature of about 850°C which is high enough to avoid the beta phase and yet low enough to avoid decomposing the epsilon. Some typical extrusion constants are shown in Table I.

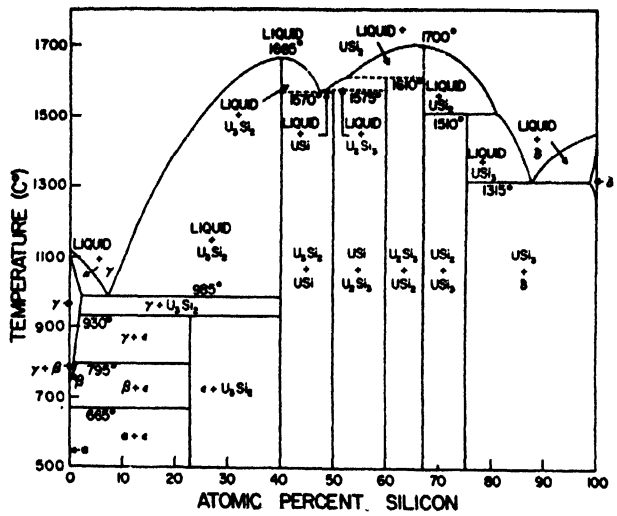

Figure 4. Uranium-silicon phase diagram

Hot rolling can be carried out at 600°C for compositions up to about 10 at % Si. It is not known whether or not rolling of higher compositions at 850°C is feasible. A limited amount of cold rolling is possible on the lower silicon compositions. An alloy consisting of essentially all epsilon has only a small amount of ductility. It can be cold swaged with 20% to 30% reduction in area but it is doubtful that rolling or drawing can be done.

CONCLUSION

Uranium-rich alloys can exist in a number of states having widely different degrees of ductility and crystal form. In alloys containing free uranium it is difficult to fabricate in the beta phase range. Alloys containing small amounts of intermetallic compound can be hot worked either in the high alpha range or in the gamma phase region. A limited amount of cold working is also possible if the amount of compound is sufficiently small. If the amount of compound is 50 to 75 volume per cent of the alloy it is necessary to work in the gamma region, preferably by extrusion. The silicon epsilon alloy is an exception to this. Elements having extensive solid solubility in the gamma phase may be fabricated conveniently in the gamma region. In some cases this can be done at lower temperatures than the beta to gamma transformation for pure uranium. With molybdenum alloys above about 10% it is possible to retain the gamma phase at room temperature and cold work does not cause the alloy to transform.

Preparation, Properties and Cladding of Aluminum-Uranium Alloys

By H. A. Saller,* USA

Aluminum-uranium alloys have long been of interest to reactor designers as a means of distributing fissionable material in a matrix of relatively low cross section. These alloys are relatively cheap, easy to fabricate, and reasonably strong. Such alloys, when clad with aluminum or one of its alloys, have excellent corrosion resistance in low-temperature water. Such elements make ideal fuel for research reactors which operate at relatively low temperatures. The usefulness of these fuel elements in power reactors is severely limited by their lack of strength and corrosion resistance at elevated temperatures.

The constitutional diagram for the system aluminum-uranium was first investigated by Kaufmann and Gordon at Massachusetts Institute of Technology.[1] As interest in low-uranium alloys increased, this portion of the system received further study at Battelle Memorial Institute[2] and Oak Ridge National Laboratory.[3] The diagram now generally accepted is shown in Fig. 1. It is plotted on a weight per cent basis to permit closer scrutiny of the aluminum-rich portion of the system. It will be noted that no significant solid solubility of uranium in aluminum is indicated. This is based primarily on early work using metallography and diffusion studies of aluminum-clad samples. The slight age hardening which has been observed in aluminum-uranium alloys does indicate a measurable solubility. Recent work by Dunnington of Savannah River Laboratory[4] confirms some solubility based on age-hardening characteristics.

The diagram shows also that eutectic between aluminum and UAl_4 occurs at 13 weight per cent uranium and 640°C. The compound UAl_4 is produced by a peritectic reaction between UAl_3 and an aluminum-rich liquid containing 18 weight per cent uranium. This occurs at 730°C. The compound UAl_3 is itself formed by peritectic reaction of UAl_2 and a uranium-aluminum alloy liquid containing 60 weight per cent uranium. This occurs at 1350°C. The compound UAl_2 melts at 1590°C.

Since alloys containing less than 35 weight per cent uranium are of greatest interest for reactor application, the major portion of the investigation is centered on the casting, fabrication, and cladding of these alloys. The second part of the study was devoted to determining the physical properties of the alloys.

* Battelle Memorial Institute, Columbus, Ohio

PREPARATION OF ALLOYS

Melting and Casting

Alloys of aluminum-uranium were prepared by open melting in graphite or clay-graphite crucibles heated either by induction or by the use of gas-air-mixtures. The uranium was added either as the pure metal, the oxide, or the fluoride. Recoveries exceeded 90 per cent.

For most applications, addition of the uranium as metal is simplest. Such melts are made by first melting the aluminum and superheating to 800°C. The uranium is added slowly with considerable stirring. Remelting is often desirable since several observers[4] have noticed that the quality of the alloys improves with remelting. Apparently considerable time is required to reach equilibrium in the liquid state and particles of UAl_2 compound persist for a considerable time.

In cases where alloys enriched in uranium-235 are desired, a great saving in cost is effected by adding the enriched uranium as the oxide or preferably the fluoride. This saves the cost of reducing the oxide or fluoride to metal and then adding it to aluminum. A number of trial melts were made using a variety of techniques for adding oxide and fluoride. Results of these tests are summarized in Table I.

The melting technique finally used consisted of melting the aluminum under a cryolite flux, then adding the cryolite-oxide or fluoride with constant stirring. The bath was stirred for one minute out

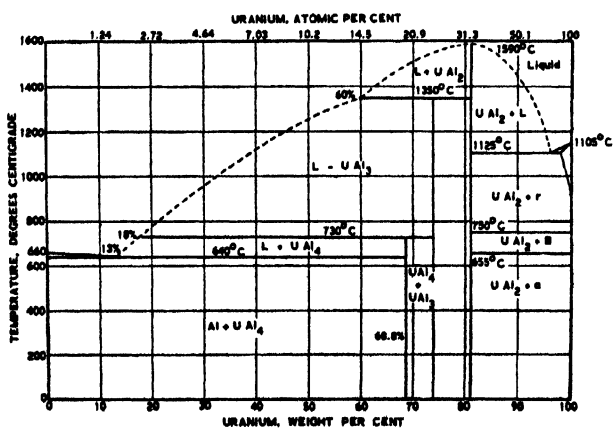

Figure 1. Aluminum-uranium equilibrium diagram

Table I. Recovery of Uranium when Added as Oxide or Fluoride to Aluminum

Treatment			Uranium, per cent		Recovery*, per cent	
Addition	Holding time, minutes	Holding temperature, °C	Charge	In alloy	Uranium	Aluminum
Exothermic mix†	60	1100/1200	8.7	2.7	20	66
Briquette, oxide and Al	5	850	8.8	0.3	3	78
Briquette, plus flux	30	1100	8.8	9.1	96	76
Oxide plus cryolite	20	1100	10.0	8.9	84	96
55% cryolite and oxide	20	1100	10.0	7.2	67	96
65% cryolite and oxide	20	1100	10.0	9.6	92	95
55% cryolite and oxide	60	1100	10.0	8.0	74	95
55% cryolite and oxide	20	1300	10.0	8.2	75	93
65% cryolite and oxide	60	1100	10.0	10.1	95	94
65% cryolite and oxide	20	1300	10.0	9.5	90	95
55% cryolite and oxide	60	1300	10.0	8.2	74	92
65% cryolite and oxide	60	1300	10.0	10.7	98	91
65% cryolite and oxide	20	1100	20.0	18.3	76	85
65% cryolite and oxide	20	1100	20.0	18.4	78	85
65% cryolite and oxide	20	1100	30.0	30.0	62‡	61
65% cryolite and fluoride	20	1100	10.0	10.5	100	94
65% cryolite and fluoride	20	1100	10.0	10.1	98	96
65% cryolite and fluoride	20	1100	10.0	10.0	96	96

* Calculated from analysis and total weight of recovered metal or product.

† Mix contained oxide, granular aluminum, $NaNO_3$, and magnesium powder.

‡ Recovery low because of poor separation of slag and metal.

of five during the holding period. The flux was then removed from the low-melting alloys by allowing it to freeze around a carbon rod. Alloys with melting points close to that of the flux were allowed to freeze in the crucible. The metal and flux were then separated mechanically, the metal remelted and cast in shape.

For the first rolling experiments, alloys were cast into ingots 6 by 8 by 1½ inches in a tilting steel mold. This casting technique facilitated rapid chilling of the ingot and duplicated commercial aluminum practice. The 35 weight per cent alloys were eventually cast into ingots 4 by 6 by ½ inches in a steel mold with 1½-inch walls. This gave the rapid chill required for these alloys. Pouring temperature ranged from 700°C to 1100°C, depending on the uranium content. The mold temperature never exceeded 150°C.

Powder Metallurgy

For some reactor applications, it is desirable to have the compound particles of a very small size. In alloys up to about 20 weight per cent uranium, this can be accomplished by careful control of casting conditions. For higher concentrations of uranium, this technique is not feasible and powder-metallurgy techniques are required.

Alloys of aluminum-42 weight per cent uranium were made up using atomized aluminum and powdered compound. Two compounds, UAl_4 and UAl_2, were used. These were prepared by melting the proper mixture of aluminum and uranium and then crushing the compound produced. Two ranges of particle sizes, minus 150 plus 20 and minus 325 mesh were used for each compound. In addition, an 8-micron UAl_2 powder was produced by grinding in an agate mortar and separating in a Haultain infrasier. Nitrogen was used in place of compressed air for agitation.

To produce alloys, the compound powder was first thoroughly mixed with minus 325-mesh aluminum. The mixture was pressed cold at pressures of 100,000 psi to produce compacts of reasonable green strength. These compacts were sintered at temperatures of 450°C and 600°C for times from 4 to 96 hours. The particle size of the compound remained unchanged during pressing and sintering. Attempts to further reduce the particle size by hot or cold rolling were not successful.

It was observed that in the compacts containing UAl_2, there was a transformation to UAl_4 upon heating. Partial conversion of UAl_2 to UAl_3 and UAl_4 occurred in 4 hours at 600°C. After 96 hours at 600°C, the UAl_2 was completely transformed to UAl_4. There was no appreciable change in compound particle size as a result of this transformation. This transformation is accelerated during hot rolling.

Fabrication

Aluminum-uranium alloys are fabricated by hot forging, hot rolling, or in some cases, cold rolling. Forging was accomplished at temperatures of 550°C to 600°C on alloys containing up to 20 weight per cent uranium. Alloys in the range 20 to 30 weight per cent uranium are forged, but with great difficulty. Alloys containing more than 30 weight per cent uranium cannot be forged.

Hot-rolling characteristics of these alloys are similar to the forging characteristics. That is, alloys up to 20 weight per cent roll very well at temperatures of 550°C to 600°C. After the cast structure is broken down, cold rolling is easily accomplished.

Higher uranium alloys, however, such as those containing 35 weight per cent uranium, required the development of special fabricating methods. From the constitutional diagram, it was observed that the 35 weight per cent uranium alloy when first cast contained a large amount of UAl_3. As solidification continued, this UAl_3 reacted with aluminum to form UAl_4. Suppression of the peritectic by rapid cooling should cause less aluminum to be combined with uranium and thus give a structure with less hard brittle compound and more soft matrix material. Such a structure should improve fabricability.

Rapid cooling alone did not insure fabrication of 35 weight per cent uranium alloys. A combination of rapid cooling and jacketing in aluminum prior to fabrication did make hot rolling possible. After an initial breakdown by hot rolling in a jacket, alloys of 35 weight per cent uranium could be stripped from the jacket and cold rolled to reductions of 50 to 60 per cent without cracking.

Cladding with Aluminum

For most reactor applications, it is essential to clad the fuel-bearing alloy on all surfaces. This is necessary both to improve corrosion resistance in water and to contain the fission fragments that are formed.

Aluminum cladding or jacketing with aluminum was accomplished by means of the "picture-frame" technique (see Fig. 2). This procedure consisted of fitting the alloy sheet into a frame of aluminum of the same thickness. A sheet of aluminum was then folded over frame and core to form a complete cover. This pack was then heated and hot rolled to produce complete cladding between the aluminum cladding and the alloy core. Bonding was insured by wire brushing all surfaces prior to assembly.

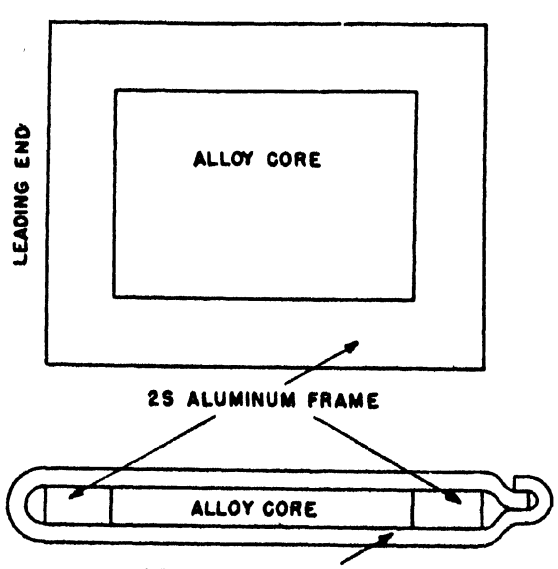

Figure 2. Details of assembly of aluminum jacket (O-7378)

Metallography

Aluminum-uranium alloys are polished quite readily using techniques normally employed for pure aluminum. Most of the alloys are etched with sodium hydroxide or other aluminum etchants. Typical cast structures are shown in Fig. 3. The 9 per cent alloy shows a typical hypoeutectoid structure. The apparently large amount of primary aluminum is caused by the high density of the compound. In the 18.1 weight per cent alloy, there are a few small crystals of UAl_3 in the UAl_4-aluminum eutectic matrix. More of the UAl_3 crystals can be seen in the 29.1 weight per cent alloy.

In order to develop casting techniques for suppressing the peritectic reaction of UAl_3 with aluminum to form UAl_4, it was desirable to develop an etchant to differentiate between UAl_3 and UAl_4. An etch consisting of chromic and acetic acids used electrolytically caused UAl_3 to be colored yellow, while UAl_4 was blue-gray. These results were confirmed by means of X-ray analysis.

Figure 4 shows the structures obtained in a 35 weight per cent alloy by chill casting and by slow cooling. In the chill-cast sample, the UAl_3 occurs as long discontinuous chains. Such a structure can be fabricated without cracking. In the slow-cooled sample, the peritectic reaction has had time to approach completion and long massive needles of the compound UAl_4 have formed. Such a structure cracks easily during fabrication. These two structures represent the extremes observed in actual castings.

The use of etchants worked very well in predicting fabricability of cast ingots. Samples containing large amounts of UAl_3 would roll while those containing only UAl_4 cracked badly.

PHYSICAL PROPERTIES

Tensile Properties

Tensile tests were run on both 0.080-inch sheet stock and 1-inch forged bars of various uranium contents. Sheet specimens containing 2.4 to 16.8 weight per cent uranium were tested in a variety of conditions including: as cold rolled (58 per cent for alloys up through 9.0 weight per cent and 45 per cent for the higher compositions), annealed 3 hours at 550°C, water quenched after 3 hours at 550°C, water quenched, and aged 6 hours at 175°C after quenching. The solution and aging temperatures were based on those used for commercial aluminum alloys. Results of these tests are shown in Table II. In the cold-rolled alloys, maximum values of ultimate tensile strength and yield strength occurred at 9 weight per cent uranium. After annealing or quenching from 550°C, all alloys showed a decrease in yield and ultimate tensile strength. In these samples, strengths increased with ultimate tensile strength. In these samples, strengths increased with increasing uranium content up to 9 weight per cent uranium. Further increases in uranium content had no appreciable effect on strength. There was

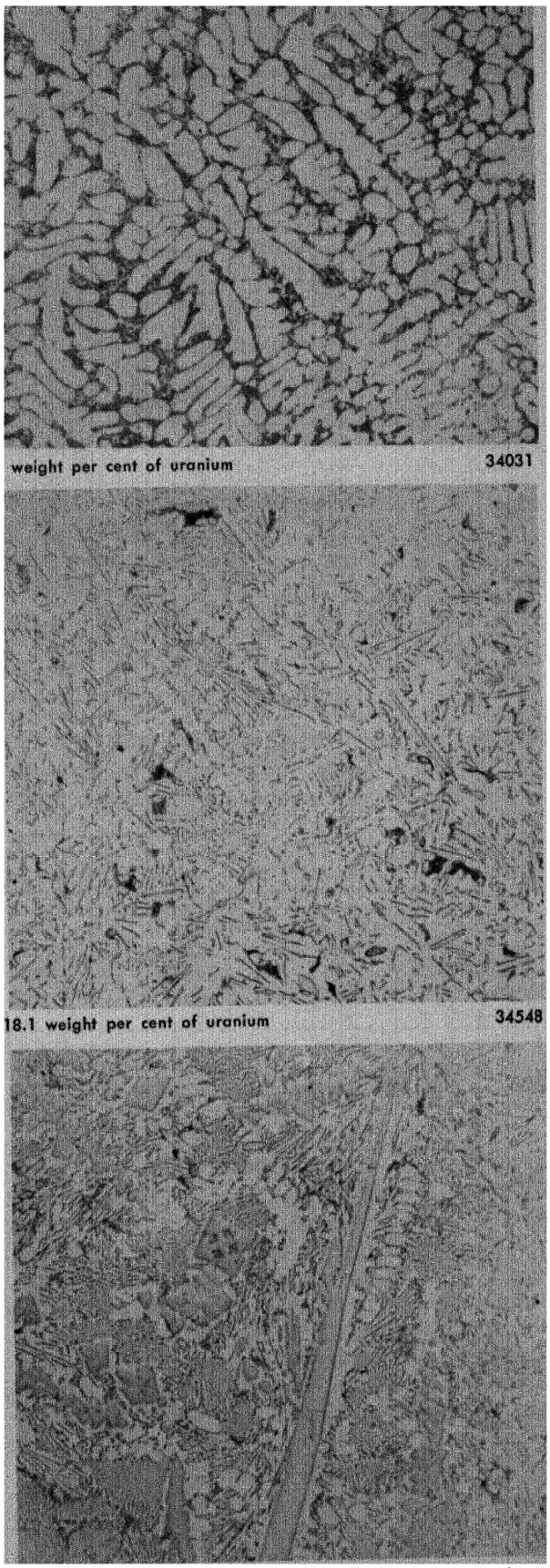

Figure 3. Structures of cast aluminum-uranium alloys, NaOH etch, 100 X

little variation in strength between alloys quenched or slow cooled from 550°C. This could indicate a lack of solid solubility of uranium in aluminum. Aging the quenched alloys gave no significant change in tensile properties.

Tensile properties of 12.5, 22.7, and 30.5 weight per cent uranium alloys are given in Table III. Samples used for these tests were standard 0.505-inch tensile specimens machined from forged bars which had been annealed ½ hour at 370°C. Modulus determinations were made by first preloading the bars, then reloading and measuring the elongations with Tuckerman strain gages.

Age Hardening and Solubility of Uranium

There now seems to be considerable doubt regarding the solid solubility of uranium in aluminum. Early work at Battelle[2] indicated little or no solid solubility of uranium in aluminum. This was based on metallographic examination of a series of alloys containing 0.16, 0.22, 0.85, 0.92, 1.65, and 3.71 weight per cent uranium. No change in structure in the alloys was effected by solution treatment. Similarly, no diffusion of uranium in aluminum in aluminum-clad samples was detected by alpha-counting techniques. There was evidence of solubility, however in a series of alloys containing 2.4 to 16.8 weight per cent uranium which were solution treated at 550°C and then aged at 175°C for various times. Results of these tests are shown in Table IV. Recent work by Dunnington[4] tends to substantiate the age-hardening effect and strongly suggests a considerable solubility of uranium in aluminum. Dunnington's tests were conducted on a 16 per cent uranium alloy which had a hardness of 52 R_H after quenching from 600°C. This value increased to 60 R_H after less than 30 days at room temperature. The same degree of increase was noted in from 1 to 5 hours at 200°C and 300°C. In view of the recent evidence, there is indication of some solubility of uranium in aluminum. Further work is in progress to clarify this point.

High-Temperature Testing

For many reactor applications, the aluminum-uranium fuel alloys operate at somewhat elevated temperatures. This makes a knowledge of elevated-temperature properties essential for the reactor designer. Tensile properties on each of two alloys were obtained at 150°C and 300°C, while creep data were obtained for one composition at 150°C.

Tensile tests were run at 150°C and 300°C on alloys containing 11.3 and 17.3 weight per cent uranium. The specimens were annealed for 1 hour at 370°C prior to testing. Results of these tests are given along with information on 2SO aluminum in Table V. Properties of the two alloys were about the same at elevated temperatures. Both were considerably stronger, but less ductile than pure uranium.

Table II. Tensile Properties of Uranium-Aluminum Alloy Sheet

Composition, weight per cent uranium	Cold reduction, per cent	Elongation, per cent	Yield strength*, psi	Tensile strength, psi	Elongation, per cent	Yield strength*, psi	Tensile strength, psi
		As rolled			Annealed 3 hours at 550°C		
2.43	58	7.5	19,300	21,800	24.8	4870	11,650
		8.5	18,500	22,200	16.5	4950	11,950
3.10	58	8.5	18,100	22,000	10.8	5250	12,200
		8.0	17,800	22,400	14.0	5120	12,300
4.95	58	7.4	17,500	23,000	34.5	5920	14,000
		7.4	17,350	22,800	35.0	5620	13,900
7.0	58	7.0	19,350	26,200	29.0	7650	16,300
		7.0	18,650	26,900	27.3	8750	16,350
9.0	58	7.5	20,040	28,200	27.5	8650	17,400
		6.0	19,800	27,600	27.5	–	17,300
11.3	45	4.5	19,250	25,600	24.5	8950	18,000
		–	–	25,700	26.5	10,400	18,200
14.3	45	4.0	18,850	25,550	22.6	8320	17,400
		6.8	18,300	26,300	26.4	9530	18,550
16.3	45	7.5	17,550	23,900	23.5	8070	17,700
		5.5	18,650	24,700	24.7	8100	17,300
16.8	45	3.5	19,500	24,200	22.7	8670	18,100
		5.0	19,500	24,600	21.3	8950	17,900
		Water quenched, 3 hours at 550°C			Aged 6 hours at 175°C after quench		
2.43	58	33.0	2600	11,600	20.0	5430	12,100
		35.0	5280	12,000	34.5	5380	11,750
3.10	58	35.5	–	12,650	35.0	5450	12,600
		38.7	5650	12,550	34.3	6000	12,600
4.95	58	34.5	5750	14,100	32.0	6230	14,350
		38.0	5420	14,100	33.0	6950	14,250
7.0	58	29.6	7250	16,300	30.5	7600	16,500
		33.0	7650	16,500	28.0	8040	16,800
9.0	58	30.0	–	16,900	27.5	–	17,000
		27.5	–	17,100	29.2	10,000	17,600
11.3	45	28.6	9760	18,850	26.5	8800	18,100
		23.5	9050	18,550	23.7	9250	18,850
14.3	45	23.5	8600	18,000	26.0	7650	17,050
		23.8	8100	17,700	22.6	7950	17,450
16.3	45	22.6	8750	17,900	21.5	8250	17,700
		26.2	8030	17,900	23.0	9050	18,500
16.8	45	27.7	8250	18,000	21.0	8450	17,800
		23.0	8350	17,700	21.5	8600	17,900

* Yield strength based on an offset of 0.2 per cent.

A sample containing 17.3 weight per cent uranium annealed 1 hour at 370°C was tested for 2000 hours at 150°C. Step loading gave the creep data tabulated below.

Load, psi	Creep rate, per cent elongation per hour	Total deformation, per cent elongation
3000	0.00004	0.134
4000	0.00035	0.420
5000	0.0027	4.21

From a log-log plot of stress versus creep rate, the stresses required to produce specified creep rates were determined and are noted below:

Creep rate, per cent per hour	Stress, psi
0.001	4480
0.0001	3410
0.00001	2620

Thermal Conductivity

Thermal-conductivity measurements were made on forged bars containing 12.5, 22.7, and 30.5 weight per cent uranium. All samples were annealed ½ hour at 370°C prior to testing. Tests were conducted using the United States Bureau of Standards method described in Research Paper RP668, April 1934. Results together with values for pure aluminum are shown in Fig. 5. The conductivity tends to decrease with increasing uranium content, as might be predicted. From the data obtained, the average values tabulated below are suggested.

Temp, °C	Conductivity in watts, $cm^{-1}\,°C^{-1}$: 12.5 weight per cent uranium	22.7 weight per cent uranium	30.5 weight per cent uranium
200	1.83	1.68	1.51
300	1.81	1.64	1.49
400	1.79	1.59	1.48

Table III. Tensile Properties of Forged Aluminum-Uranium Alloys

Composition, weight per cent uranium	Average modulus of elasticity* 10^6 psi	Tensile strength, psi	Yield strength 0.2 per cent offset psi	Elongation, per cent	Reduction of area, per cent
0	10.0	13,000	5000	45	–
12.5†	10.4	22,500	10,800	20	34
22.7	10.9	18,600	11,600	4	7
22.7	11.3	23,500	14,500	13	14
30.5	11.3	26,100	14,850	10.5	11.5

* Estimated to be correct within ± 3 per cent.
† Single specimens were used except in the 22.7 per cent uranium alloy.

Coefficient of Linear Expansion

Coefficients of thermal expansion for alloys containing 12.5, 22.7, and 30.5 weight per cent uranium were run on ½-inch-diameter specimens using standard dilatometric methods. Heating and cooling curves were made from 50°C to 500°C. Data obtained during heating and cooling were similar. Table VI shows values for the alloys as well as for pure aluminum.

CONCLUSIONS

The aluminum-uranium alloy system represents a very useful method of incorporating fuel into an alloy that is easy to fabricate, and reasonably strong.

Table IV. Hardness Data on Aluminum-Uranium Alloy Sheet

Composition, weight per cent uranium	Hardness, Rockwell H				
	As quenched*	Time aged at 175°C, hours			
		2	4	6	8
2.43	25	27–29	29–31	35–36	24
3.10	29–31	32–33	36–36	37–38	33
4.95	41–42	43–44	45–47	43	–
7.00	53–54	57	55–56	56	–
9.00	57–59	60–61	61	59–61	–
11.3	61–62	64–65	64–65	65	–
14.3	56	58	58–59	58–59	–
16.3	58–59	60–62	61–62	62–63	–
16.8	58–59	60–62	61–62	60	–

* Quenched from 550°C after holding for 3 hours.

Table V. High-Temperature Properties* of Aluminum-Uranium Alloys

Alloy	Room temperature			150°C			300°C		
	Tensile strength, psi	0.2 per cent offset yield strength, psi	Elongation, per cent	Tensile strength, psi	0.2 per cent offset yield strength, psi	Elongation, per cent	Tensile strength, psi	Elongation, per cent	Reduction in area, per cent
2SO aluminum	13,000	5000	45†	7500	3500	65	2500	90	–
11.3 weight per cent uranium	19,700	11,320	28	14,125	9200	31	8630	31	57
17.3 weight per cent uranium	20,080	11,480	28	14,700	10,000	27	8780	34	60
	19,030	8550	30	14,000	7230	34	8130	48	59.5
	–	–	–	13,650	7020	35	8210	42	58
	–	–	–	13,300	6480	35	–	–	–

* Tests on metal annealed at 370°C for 1 hour; 2SO values from "Alcoa Aluminum and Its Alloys".
† Elongation in 2 inches, others in 1 inch.

Table VI. Coefficient of Linear Expansion of Uranium-Aluminum Alloys

Temperature range, °C	Coefficient of linear expansion, 10^{-6} per degree C, for uranium content, weight per cent			
	0*	12.5	22.7	30.5
20 to 100	23.9	20.0	20.0	19.4
20 to 200	24.6	21.1	21.2	20.8
20 to 300	25.5	22.1	21.9	21.3
20 to 400	26.5	23.1	22.5	21.6
20 to 500	27.7	23.5	22.7	22.1
100 to 500	–	24.4	23.2	22.6

* Metals Handbook 1948 Edition (99.996 per cent Al).

Cladding these alloys with aluminum by the "picture-frame" technique produces a fuel element with good corrosion resistance in water. For most applications, ordinary melting and casting followed by hot fabrication are adequate. For special applications requiring controlled compound particle size, powder metallurgy works very well. The melting, casting, fabrication, and cladding of high uranium alloys are more difficult but not impossible.

In general, the alloys are stronger, but less ductile, than pure aluminum. Their properties for the most part are those to be expected in a material contain-

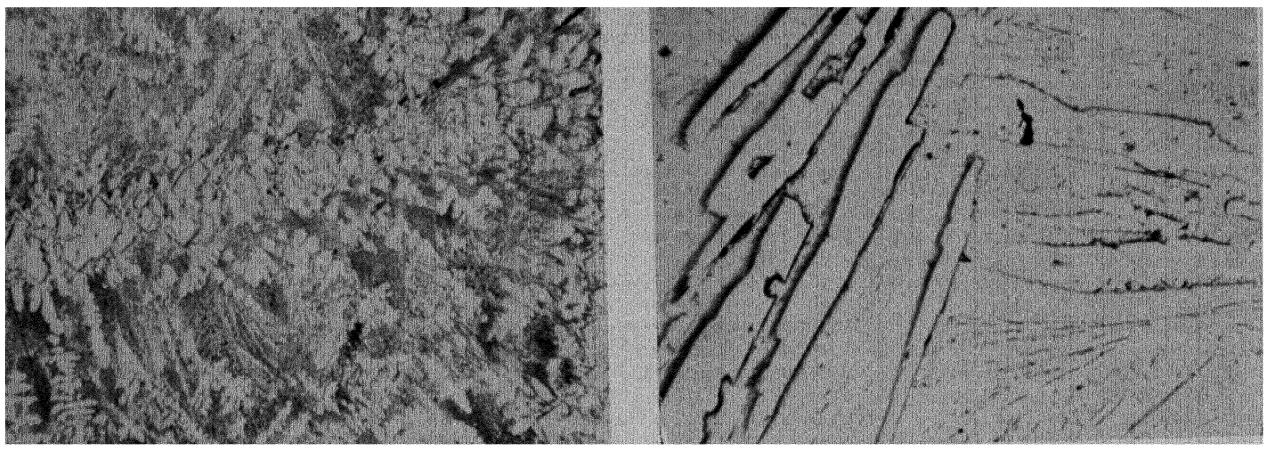

Quenched 54192 Slow cooled 54184

Figure 4. Structures obtained in a 35 weight per cent uranium alloy cooled at different rates, NaOH etch, 100×

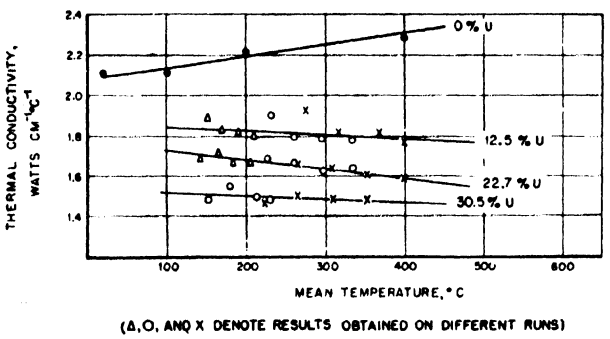

Figure 5. Thermal conductivity of uranium-aluminum alloys. (O-4547)

ing hard compound particles in a soft eutectic matrix.

The question of the extent of solid solubility of uranium in aluminum is still unresolved. Recent evidence tends to favor the idea that there is an appreciable solubility of uranium in aluminum.

REFERENCES

1. Gordon, P. and Kaufmann, A. R., *The Alloy Systems U–Al and U–Fe*, Journal of Metals, *188*: No. 1, Trans 182–94 (1950).
2. Saller, H. A., *Preparation and Properties of the Aluminum-Uranium Alloy*, Journal of Metallurgy and Ceramics *1*: No. 1, TID-65, p 9 (July 1948).
3. Borie, B. S., Jr., *Crystal Structure of UAl_4*, Journal of Metals *3*: 800–802 (September 1951).
4. Dunnington, B. W., Private communications, Savannah River Laboratory, (April 1955).

The Fabrication of Fuel Elements for the BNL Reactor

By D. H. Gurinsky, W. T. Warner, J. E. Atherton, C. Binge, H. C. Cook, L. McLean, R. J. Teitel and B. Turovlin,* USA

The Brookhaven pile is an air-cooled natural uranium graphite-moderated reactor. Design studies indicated that the rate of heat dissipation from the uranium required a heat surface area which could be obtained by using a finned aluminum casing. Since the reactor was built on a site which was relatively near populated areas, the hazards resulting from a rupture of a fuel element had to be reduced to a minimum. The decision was made that the fuel elements should consist of long finned tubes in which the slugs would be encased. In order to monitor each element for leakage, a tube (to be called the helium tube from now on) was attached to one end of each element. By monitoring the gas pressure in each element it is possible to determine the on-set of a break in the fuel element. Since a large volume of inert gas at low pressure is used to maintain the atmosphere within the element, the issuance of gas from a small leak prevents the entrance of oxygen and nitrogen which would result in the oxidation of the uranium.

For a flux of approximately 4–5 $\times$ 10^{12} neutrons cm^2/sec (design flux) calculations indicate that the interface temperature between the uranium and aluminum should be of the order of 350°C. Experiments in which 2S aluminum was held in contact with uranium showed that a reaction takes place between the uranium and aluminum at this temperature and as low as 250°C. This fact also had to be taken into account in the design of a fuel element.

One other factor which had to be considered in setting up the canning or cladding procedure involved the operation of the helium system. On raising the power level, the gas pressure in the helium system would either increase or decrease depending on the gas volume in the cartridge element. It was decided that an attempt should be made to prevent the so-called "breathing" of the element by selecting the proper gas volume at room temperature such that on attaining the expected power level the resultant change in pressure in the fuel element would be small. This requires an assumption as to the average temperature of the fuel element assembly which was taken as 350°C.

THE BASIC MATERIALS

The selection of the type of uranium, that is, its method of fabrication, was based on the following considerations: (1) uranium rods prepared by extrusion in the gamma phase do not enlongate on temperature cycling as much as rolled material; (2) the necessary tonnage of gamma extruded stock could be obtained readily from commercial sources; and (3) gamma extruded material was cheaper than the rolled material.

The operations required to convert the gamma extruded rod to slugs were performed by an outside company under the supervision of the H. K. Ferguson Company. The operations performed at this contractor's plant consisted of the following. The 1.20-inch diameter rods were first straightened in a medart straightener. They were then rough machined to rods 1.130 inches in diameter by 4-inches long. The rough-machined slugs were annealed and degassed at a temperature of 600°C for 12 hours in an atmosphere of argon gas. This step was included to decrease the hydrogen content of the metal and to relieve the machining and bending stresses. The slugs were then machined to finished dimensions indicated in Fig. 1. The finished and deburred slugs were than degreased in a vapor phase

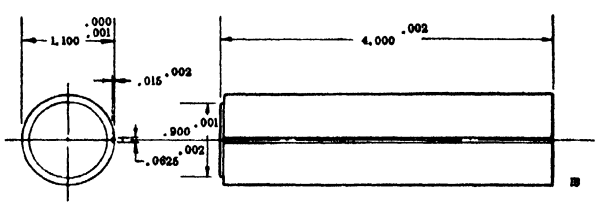

NOTES:
1. END FACES MUST BE PARALLEL WITHIN .001, IN REF. TO SLUG AXIS.
2. CYLINDRICAL SRC. TO BE GR'D. FIN.
3. TOOL MARKS NOT TO EXCEED .003" ON ENDS.
4. REMOVE ALL BURRS.

Figure 1. Uranium slug

degreaser and then degassed by heating to 400°C for 4 hours in an atmosphere of argon gas. The slugs were than examined and packed in hermetically sealed containers and shipped to BNL. Figure 2 is a photograph of the slugs in the annealing boxes after the final heat treatment. Note the use of uranium chips to prevent oxidation of the slugs in this operation.

The finned aluminum tubing was fabricated by the Aluminum Company of America. The specifications of the tubing are given in Fig. 3. Figure 4 is a photo-

* Brookhaven National Laboratory. Prepared by D. H. Gurinsky.

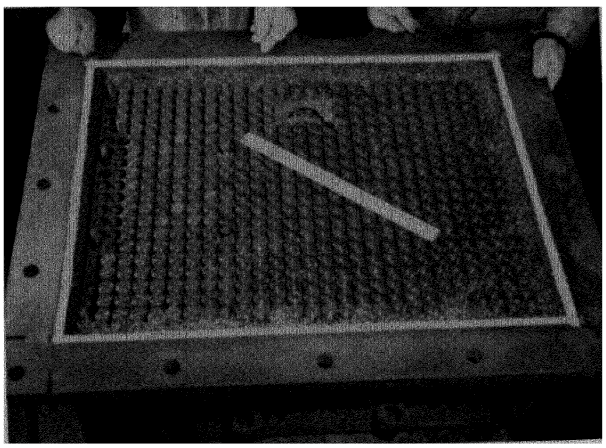

Figure 2. Uranium slugs in annealing box

graph of the as-extruded and as-drawn tubing. The tubing was formed by extruding the billets of 2S aluminum through a web type (or port hole) die. The metal is forced through 6 openings beyond which there is a mixing chamber and a stationary mandrel. After passing through the mixing chamber the metal sees a continuation of the mandrel which faces the portion of the die where the fins and walls of the tubing are formed. The extruded shape was slightly over size so as to permit a drawing operation which, as seen from the photograph resulted in a straightening of the fins and sizing of the tube. The total amount of cold work involved in this process was of the order of 15 per cent.

As pointed out in the introduction, the high temperature at the interface between the aluminum and uranium posed the problem of how to prevent the reaction of uranium with aluminum at the operating temperature. Experimentation had demonstrated that aluminum which had been anodized to give a thickness of aluminum oxide of the order of 1 mil prevented the reaction of aluminum and uranium at temperatures of the order of 550°C. The interior of the 11½ foot tubes was, therefore, anodized in a sulphuric acid medium at the proper voltage and current conditions for a sufficient length of time to yield a layer which was measured at $^{8}/_{10}$ of a mil. Further, the caps which were subsequently used to seal both ends of the fuel element were anodized on the surface which was to contact the uranium slug. Figure 5 is a drawing of the completed fuel element. Figure 6 gives the dimensions of the two caps used to close the ends of the finned tube.

The production process itself was divided into 13 operations. These are: (1) chemical stripping of the anodized film; (2) trimming of the finned tube; (3) welding of the butt closure; (4) dehydrating of the anodized film; (5) leak test No. 1; (6) loading of the welded tube; (7) trimming of the loaded tube; (8) induction brazing of the helium cap; (9) leak test No. 2; (10) hydrostatic collapsing of the finned tubing; (11) flame brazing of the anchor; (12) flame brazing of the helium tube to the fuel element; and (13) continuity and final leak test.

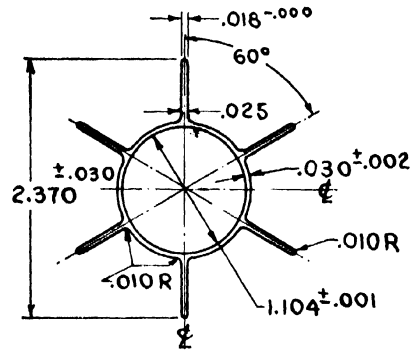

Figure 3. Finned tube specifications. Specifications: *Purity:* Standard specifications for 2S aluminum. Impurities not to exceed 1%. *Dimensions:* (1) Wall thickness 0.030 in. ± 0.002 in; (2) internal diameter 1.104 in ±0.001 in, subject to specification No. 11; (3) distance from tip of one fin to tip of opposite fin 2.370 in ± 0.030 in.; (4) fin dimensions at tip 0.018 — 0.000 +; and (5) spiral of fin 1 deg/ft. *Special specifications:* (6) Weight per foot not to exceed 0.230 lb./ft; (7) bowing of tube not greater than 0.100 in. in 10 ft; (8) plug test—the tube is acceptable if it shows no sign of rupture after a tapered steel plug has been driven into both ends so as to expand the inside diameter by ⅛ in.; (9) pressure test—a pressure of 90 psi of air shall be applied to the inside of each tube for a period of not less than five seconds. Any tube which leaks, as indicated by the formation of air bubbles in the testing fluid, shall be rejected; (10) surface inspection—the tubing and fins shall be clean, smooth, and free from seams, slivers, laminations, grooves, cracks, blisters, and other injurious defects; (11) clearance—a .500 in. × 1.101 in. od Micarta rod with chambered ends shall readily pass through each tube. This will be considered the "Go" Gage. The "No Go" Gage shall be 4.5 in. long by 1.105 in. od. and should not pass through the tube; (12) finished length 12 ft-6 in. ± 0.5 in; (13) packaging—each tube should be encased in a 3/16 in. wall mailing tube for its full length and then shipped in a substantial wooden crate, the latter to be so constructed that the material can be repacked in the same container, i.e., closure can be effected by means of screws or straps of metal

The details of these operations and the reasons for their inclusion in the procedure will be discussed below.

CHEMICAL STRIPPING OF THE ANODIZED FILM

The interior and exterior of the anodized film was stripped from an area extending ¼ inch from one end of each tube. It had been shown by experimentation that although the anodized tube could be welded, these welds are porous unless the anodized layer is removed. The solution used for removal of the

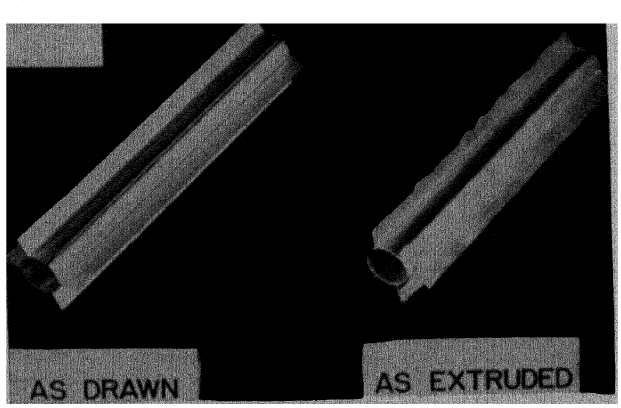

Figure 4. Finned tubing

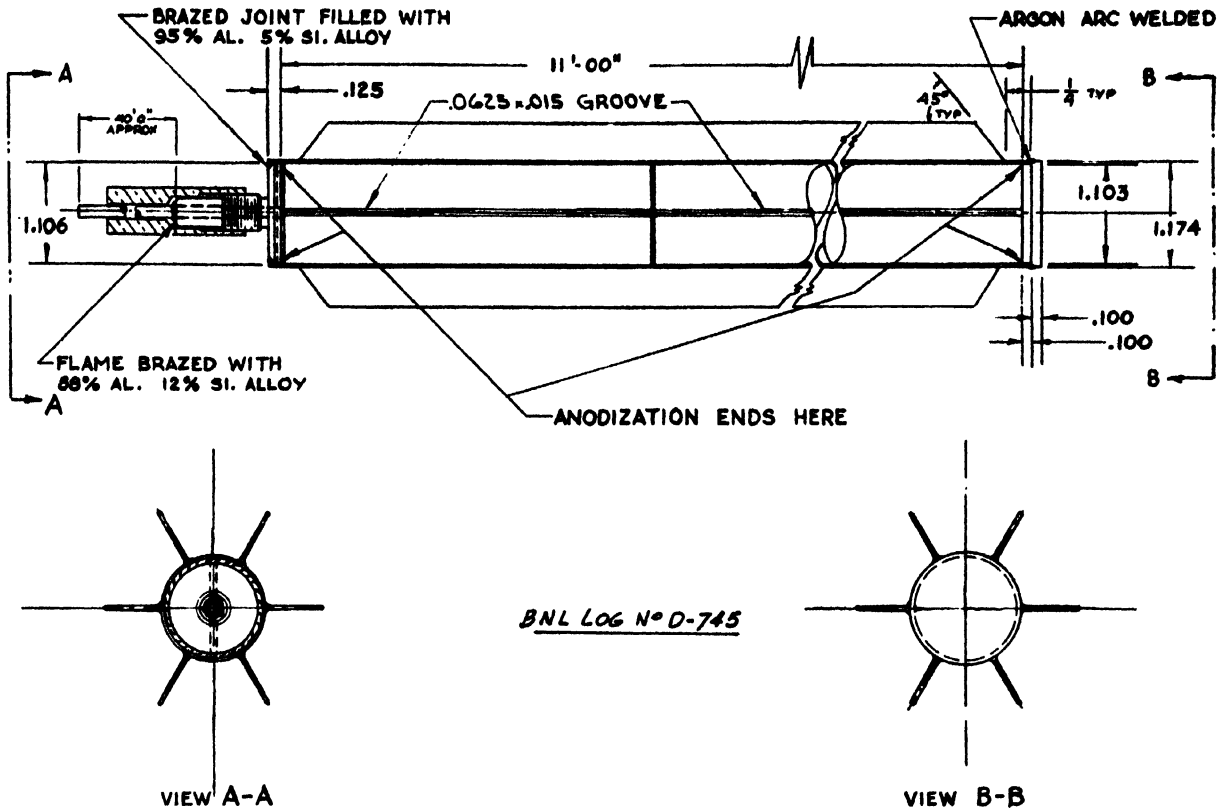

Figure 5. BNL fuel element

anodized layer from the region to be welded is a chromic and phosphoric acid solution formulated with 35 cm³ of 85 per cent phosphoric acid and 20 grams of chromium trioxide added to 1 liter of water. The solution was contained in an aluminum vessel and was maintained at 90–95°C. The liquid level was maintained by a simple constant-level device. A sieve-like platform permitted the use of a large volume of solution and prevented the submersion of the tube beyond the prescribed distance. The tubes were held in a vertical position by a device with a suspended movable plunger. The tubes were taken from the shipping boxes, bundled in units of 7, and were placed in the stripping bath for 10 minutes. A thorough rinse in hot water followed. After this, the bundle was placed, stripped-end down, into an improvised drier made from a can with a heating element in the bottom. Each tube was carefully inspected to determine whether the line of demarcation of the anodized layer was sharp. Note in Fig. 7 the line of demarcation between the anodized portion and the stripped portion.

TRIMMING OF THE FINNED TUBES

The stripped end was machined to leave a bare section of tube 1/10 of an inch long. Also in this operation the fins were cut back so that the leading edge made an angle of 45 degrees with the body of the tube. A rotary cutter was employed to trim the tube ends square and flat. A spindle mounted clipper was used to cut back the fins. The tube was cen-

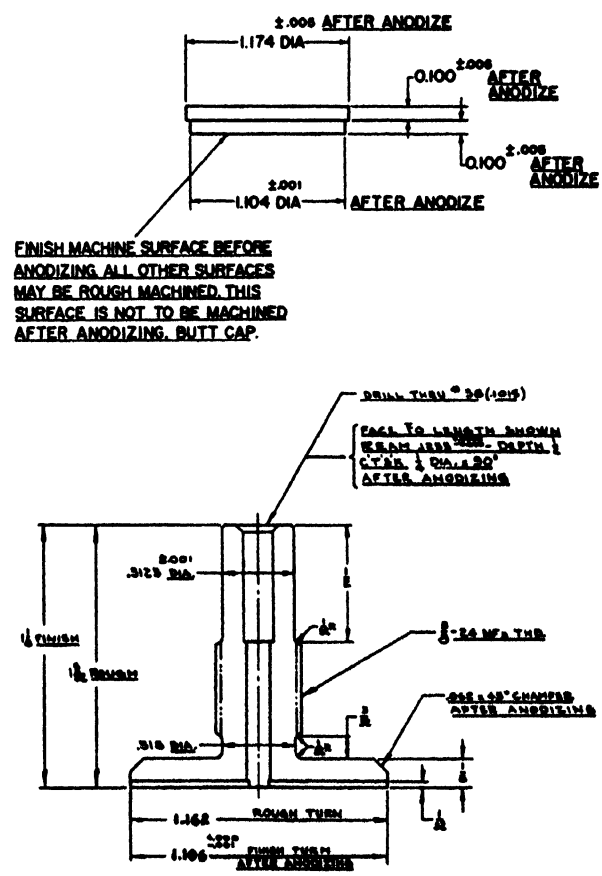

Figure 6. End caps for finned tubes: (a) above, buff cap; and (b) below, helium cap

tered by a collet which was in turn locked into position to a sliding platform. The latter was moved so that the trimming cutter engaged the tube wall to remove the excess metal. The movable platform was moved back, the finned ends clipped with tin snips and the clipper was turned on. A pre-set stop provided the correct cut back on the fins as the platform was moved into the clipper. The machine used for this operation is shown in Fig. 7.

WELDING OF THE BUTT CLOSURE

The operation consisted of insertion of the butt cap (Fig. 6A) into the de-anodized end of the tube after the tube had been inserted into a collet which, in turn, was inserted into the collet of the welding machine. The welding machine was housed in a 9-foot tower to conserve space in the fabrication area. Figure 8 shows the welding machine and housing. Figure 9 is a close up of the welding arrangement. The weld was executed using an ac inert arc bathed in argon gas. The G.E. transformer had an open circuit voltage of 100 or 150 volts and was set to deliver 95 amperes. It was found that good welds could not be made with a high degree of reproducibility unless a heat sink ("chill") was inserted in the tube. The chill used was a uranium slug. The details of the operation consisted of the following.

The trimmed tube was inserted in the collet with care to prevent torn fins, and was clamped with the end extending ¼ inch above the collet fingers. The uranium slug chill was placed in position; a cardboard tube was slipped over the tube to engage the collet; and the assembly was lifted vertically and inserted into the welding machine turntable. Two independent indexing points in the welding head assured proper line-up. The cap was dropped into place and adjusted for height by the welder (tapping with a plastic hammer) while the operator below adjusted the chill-indexing rod. When the cap was seated firmly against the slug, the torch was moved into the proper position to form an arc gap of 0.030 inches from the tip of the wolfram (tungsten) electrode to the edge of the welding cap, against which the arc is struck.

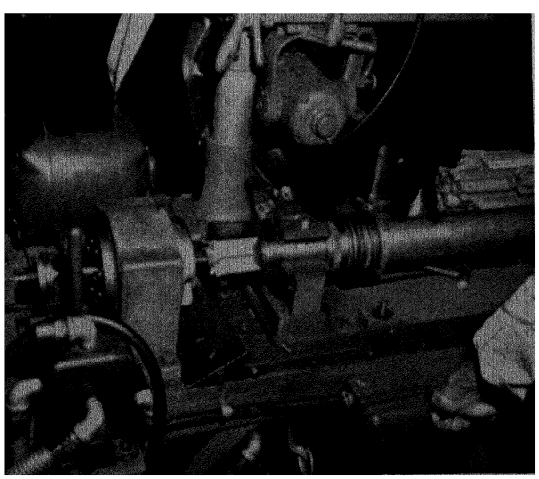

Figure 7. Machine for cutting fins and trimming tube

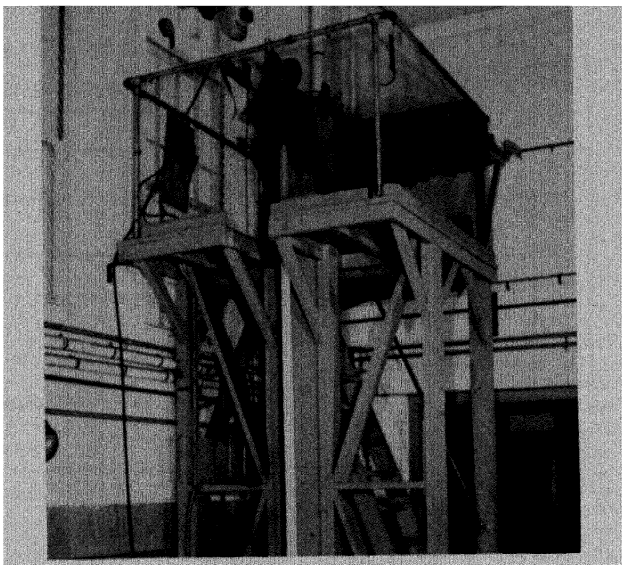

Figure 8. Welding machine and housing



Figure 9. Close up of welding arrangement

The electrode was aimed directly at the upper edge of the cap. Looking at the torch in the vertical plane, i.e., facing the welding jig with the bearing in front, the torch made an angle of 35 degrees with the horizontal. Viewing the torch in the vertical plane at 90 degrees, with the welding jig bearing to the left, the torch made an angle of approximately 55 degrees with horizontal. Looking down upon the torch, the torch was placed so that an imaginary line drawn through the axis of the electrode, through the arc point and through the center of the welding cap, would be a straight line. The cap diameter was 0.010 inches larger than the diameter of the tube to protect the thin tube wall from "burning down" when the arc was struck. The arc was initiated by depressing the start button at which time the high frequency, high voltage, ionizing pilot spark jumped the gap. The operator observed the arc and waited for a molten pool to form, at which time the rotating mechanism previously set at 4 rpm was set into motion. After the tube had rotated through

400 degrees, the start button on the control board was again depressed to begin operation of the "crater-filling". A stop switch was installed for emergency stop of the arc without "crater-filling". "Crater-filling" is an operation in which the primary of the transformer is moved away from the secondary of the transformer by actuating an air cylinder, thus the current in the arm is gradually reduced. When the primary has moved to a pre-set position the circuit is opened, turning off the power completely.

DEHYDRATING OF THE ANODIZED FILM

Preliminary heating tests had shown that when the anodized tube was heated to the neighborhood of 200°C, approximately 1 cm^3 of water was given for 11½ feet of cartridge. Since this water reacted with the uranium to form loosely held hydride and oxide, this water which was held in the aluminum oxide film was removed. Further, this operation aided greatly in the subsequent leak test procedures by decreasing the pump down time. Fifteen tubes were processed at one time with a thermocouple placed at the center of the charge and the open ends of the tube facing towards the vacuum outlet. The furnace consisted of a 10-inch diameter tube wound with heating coils and was maintained at 350°C for 1 hour under vacuum.

LEAK TEST NUMBER 1

This test was designed to determine whether the tube as a whole and the first weld were free of leaks. The finned tube was handled in a paper shipping tube. It was connected to the vacuum system shown in Fig. 10. It was first rough pumped and then, by closing and opening the proper valves, it was connected to the high vacuum system which in turn could be connected to a helium leak detector. By introducing helium gas between the shipping tube and the finned tube, the "leak tightness" of the finned tube was determined. By turning a valve which was in turn connected to a metal cup into which the welded end of the tube protruded, the weld soundness could be determined. The basic pumping system used in this test and subsequent other two tests is illustrated in the dotted portion of Fig. 11.

LOADING OF THE WELDED TUBE

This operation consisted of the loading of the uranium slugs into an aluminum tube. Since the length of the cartridge as used in the reactor is 11 feet, and the length of the slug is 4 inches, 33 slugs were inserted into the tube. The anodized layer aided in this operation in that it was a hard surface which prevented galling. All tubes were tested with respect to their abrasion resistance after they were anodized to determine whether the anodic film would be removed as a result of the rubbing which they would receive in the loading. It should also be pointed out that the high tolerance required for the uranium slugs and the finned tubing came about as a result of this operation.

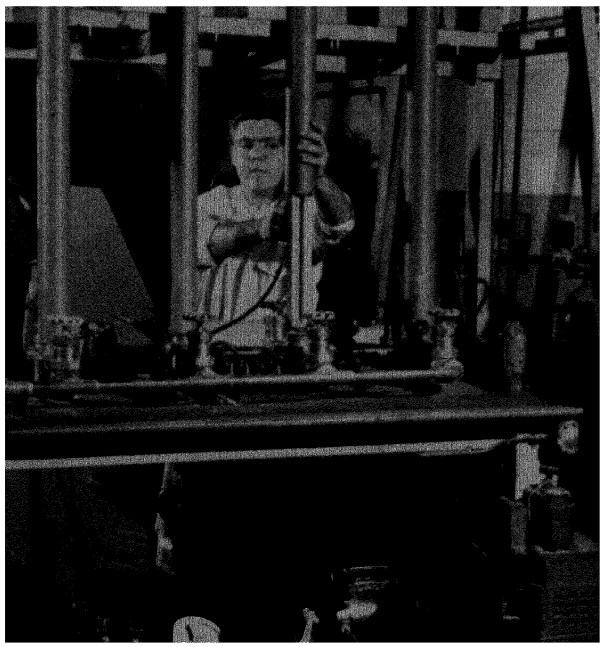

Figure 10. Equipment arrangement for leak test No. 1

Prior to the start of the loading operation, the finned tubing was inserted into a process tube so that the element could be handled in subsequent operations. The process tube consisted of an aluminum tube which had on its ends collets which held the finned tube rigidly. Each slug was seated firmly on the previous slug using a calibrated ram rod. After the slugs had been loaded, the cartridge was adjusted in the process tube so that the welded end protruded ¼ inch beyond the collet and then the collets were tightened.

TRIMMING OF THE LOADED TUBE

This operation was performed on the same machine that was used in trimming the finned tube in Step No. 2. The loaded tube was cut to size by gaging against the last slug, leaving ⅛ of an inch to receive the brazing cap.

INDUCTION BRAZING OF THE HELIUM CAP

The final closure was made by induction brazing using Alcoa No. 43S filler rod (95 per cent aluminum-5 per cent silicon) and Alcoa No. 53 flux. The decision to braze the end cap to which the helium tube was to be attached was based on the fact that it was not possible to predetermine the final position of the end slug since the cumulative error in the slugs might result in the slugs protruding a predetermined, de-anodized section, thus permitting contact between slug and aluminum. It was found that hand scraping and the use of flux permitted an effective braze to be executed. Further, leaks which were found in the brazed joint could be repaired much more readily than leaks found in a welded joint.

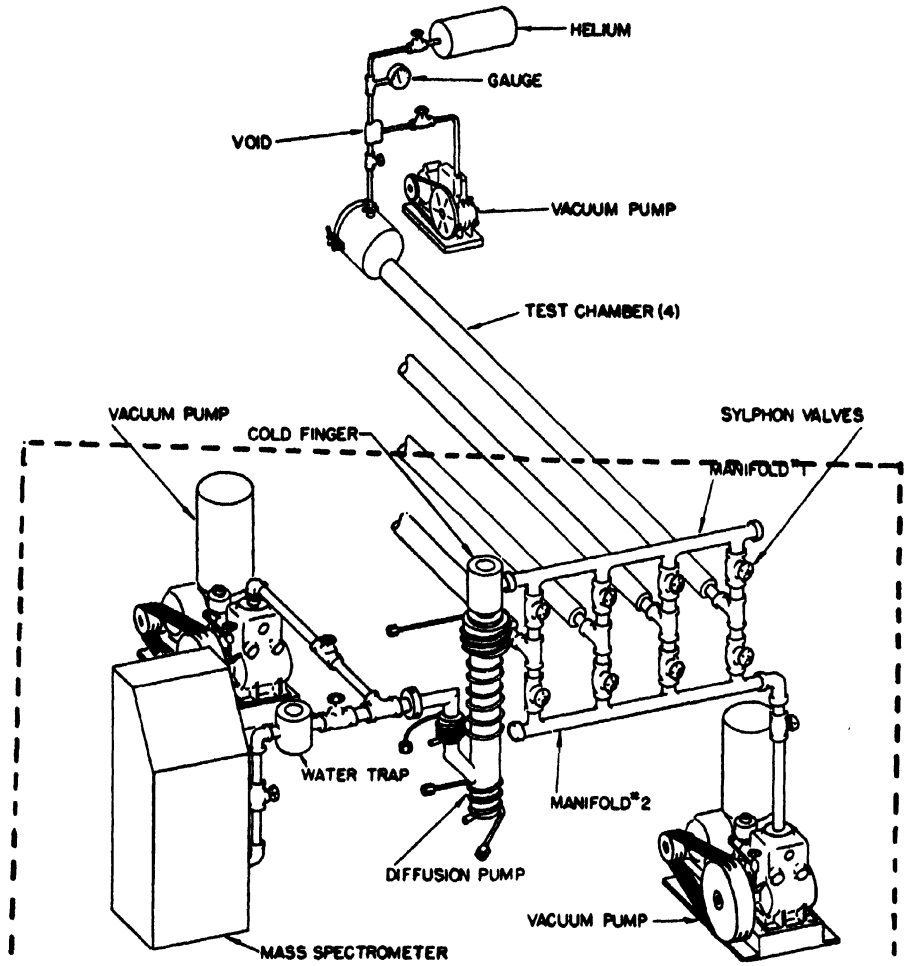

Figure 11. Equipment for final leak test

In order to achieve easier alignment, the cartridges were brazed in a vertical position. A platform 6-feet square by 9-feet high was erected to provide working space and support for the main column assembly which received the loaded process tube. The main column assembly, fixed to a semi-permanent foundation and set within a 14-inch wide by 36-inch deep recess cut into the platform, consisted of a rigid I-beam and a swinging column with a counter-balancing mechanism operated by a pneumatic cylinder. A standard 4-inch by 7.7-inch I-beam, 10 feet long, was used for the swinging column. Two ears and a transverse shaft were welded on the bottom of the column to provide a pivot within 2 bearings mounted in the frame assembly. The ears were connected to shock absorbers incorporated in the unit. The column was connected through springs and a toggle mechanism in such a way that when the column was in the downward position, i.e., about 3 feet from the floor at an inclined angle above the horizontal (supported by a swinging leg mounted on the back of the column), the springs were not under compression. The mechanism was actuated by air cylinders operated from a hand valve, which in turn, put the springs under compression and brought the toggle mechanism over center. This made it easy to swing the column plus load into the vertical. Just before the column reached the vertical, the toggle mechanism would go back over the center again, pull down the air cylinders, and release the springs. On the downward stroke, the column was restrained by the shock absorbers, as well as the friction in the air cylinders, and came down slowly to the inclined horizontal position (Fig. 12). The turntable was operated by a dc variable speed motor connected to a G.E. Thymotrol. A long rod connected the turntable to a geared wheel at the top of the platform, making it possible to either raise or lower the turntable by turning a handwheel. An annular bearing was used to index accurately the workpiece.

Because of the size and weight of the radio-frequency generator and water economizer, they were placed on the floor at one side of the platform. Copper tubing was run from the generator through stand-off insulators up the side of the platform into a step-down transformer, which was mounted on a pedestal on top of the platform. Copper leads connected the transformer to the hinged work coil. All leads and tubing up to the primary of the transformer were contained in an enclosure to prevent injury to personnel.

The loaded cartridge, contained in a process tube, was carried from the trimming table and placed on the extended pivoted column. The pneumatic valve was pressed, after which the column was raised to the vertical position to rest within latch bars built into the upper plate. The annular bearing was slipped over the collet and set into the plate recess, whereupon the operator raised the process tube so that the finned tube was above the plate.

A hand scraper was inserted into the finned tube and rotated until the anodic film was removed. The brazing cap was inserted and tapped into position against the slug button with a plastic mallet. Alcoa No. 53 flux, mixed with 4 parts of alcohol, was applied to the joint with a camel hair brush (Fig. 13). The induction coil was swung into position. After the process tube was adjusted so that the finned tube was 1/16 inches away from the coil, as shown in Fig. 14, by one operator; the other operator maintained the correct distance from coil to work. The work was rotated at 6–9 rpm. After the braze was completed, the coil was de-energized and swung back to the vertical position. The turntable was stopped to allow removal of excess flux with a bottle brush and hot water.

At this point in the production, the cartridge was removed from the process tube and handled in a carrier tube. (Preceding operations on the fuel rod required a process tube for indexing, whereas the production steps following brazing did not require that the cartridge be indexed.) After removal of the annular bearing, the process tube was lowered on the column to floor level, the collets were loosened, and the assembly was raised to a point just outside latch position. A clamp was lowered and fixed to the process tube, then it was raised up, leaving the cartridge bare. The process tube was lowered over the cartridge, after which the swinging column was lowered. The assembly was removed and placed on a rolling table for delivery to leak test number 2.

LEAK TEST NUMBER 2

The second leak test was necessary to check the brazed end and to re-check the weld and tube wall prior to compression (step No. 10), since, if a non-repairable leak were present, the cartridge could be more readily decanned before compression.

The slot on the slug was included to aid in this leak test and subsequent leak test. The apparatus used for testing was similar to that employed for the first leak test, except that the operation was done in the horizontal position. A rubber seal engaged the back (weld) end of the carrier tube, which was utilized as a helium envelope.

Each cartridge, encased in a carrier tube, was placed on the test table with the weld end engaged in the seal. A 1/4-inch id rubber vacuum tube was slipped over the brazed cap to connect the interior of the cartridge to the manifold pump.

Since the system was pumping on the equivalent of a 1/8-inch tube 11½ feet to 15 feet long, the sensitivity was inherently low, and the time interval required to observe a leak in the far (welded) end of the tube was fairly long (30 sec). It was also found that the sensitivity at the braze was quite poor. Although the sensitivity of this test was low

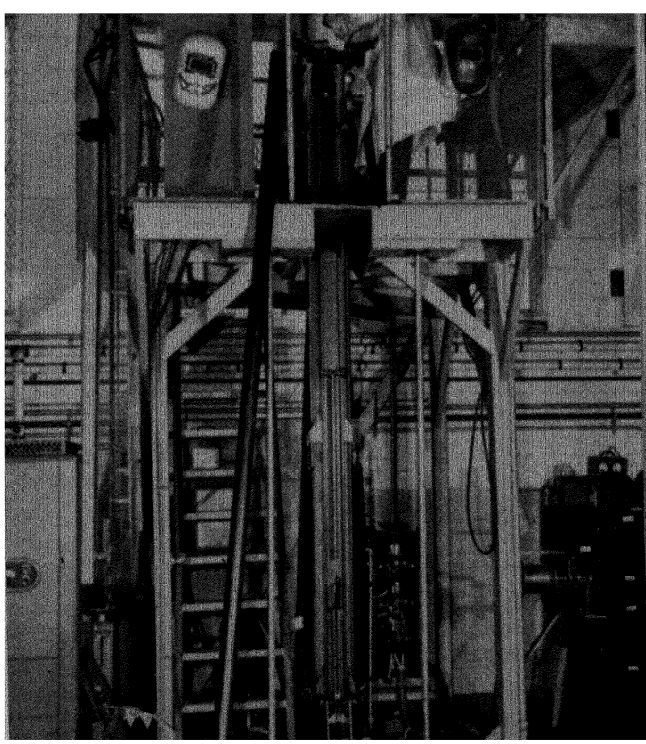

Figure 12. Induction brazing unit

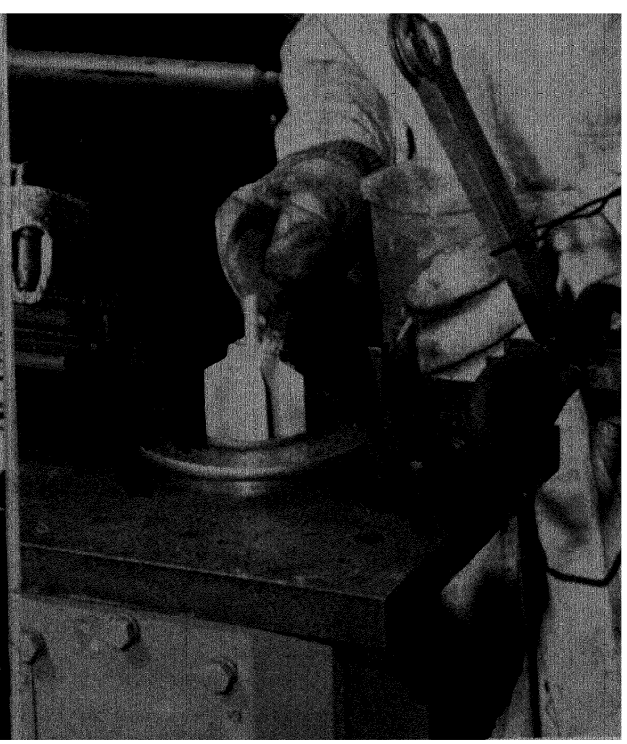

Figure 13. Fluxing of cap-tube interface

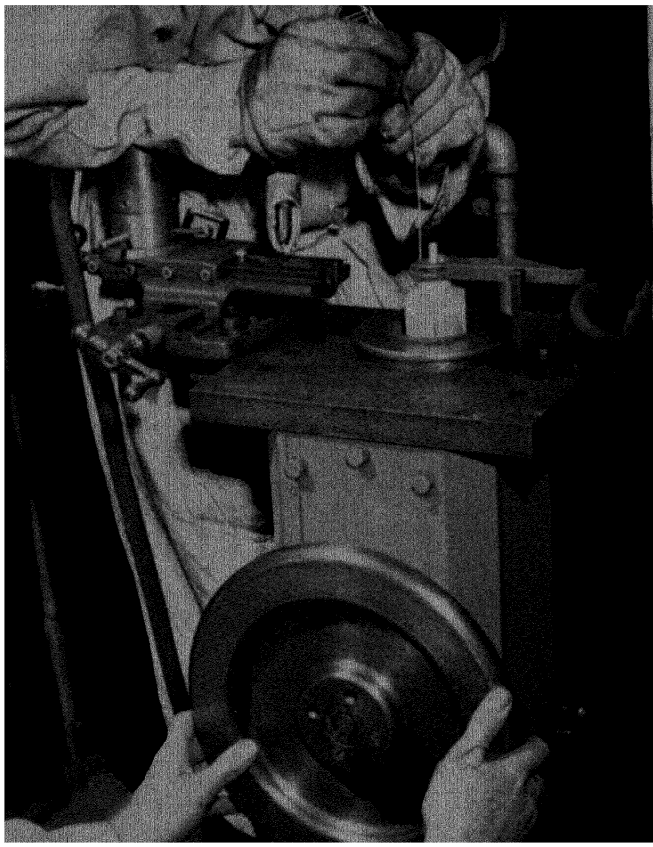

Figure 14. Feeding of brazing rod to cap-tube interface

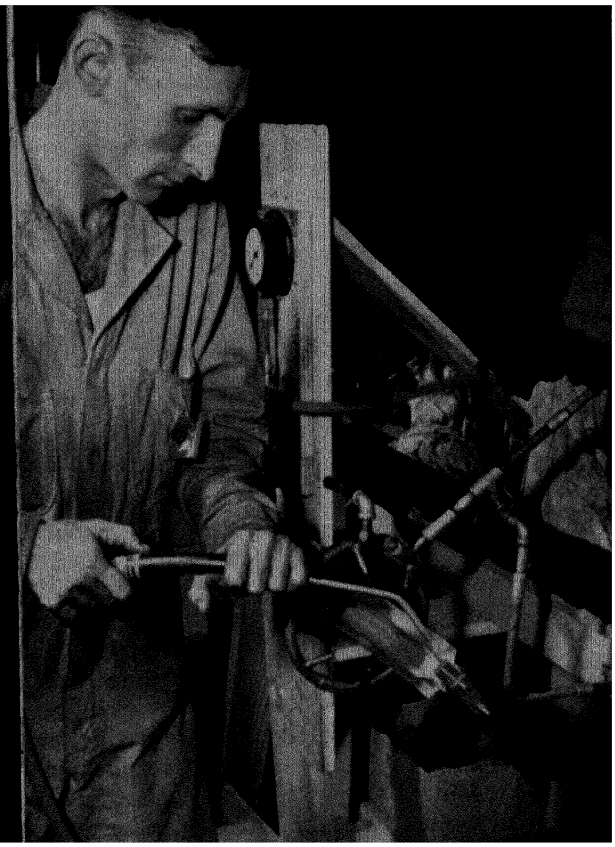

Figure 15. Air drying of finned tube after hydrostatic collapse

in comparison with later tests, it nevertheless served the purpose of sorting out tubes with leaks large enough to pass a detectable quantity of water during the next operation, hydrostatic collapse.

The finally accepted general procedure in the test was to flood the tube length and weld with helium, wait for 2 minutes to insure ample time for a leak to appear, and then probe the braze for leaks. In case of a leak other than in the braze, the tube was rejected and decanned. A leaky braze was returned to the induction-brazing operation for repair, if possible. A visual inspection of the braze was made at this leak test to insure a smooth clean braze metal deposit. If the braze was found faulty in this respect, the cartridge was immediately rejected and decanned. Tubes which showed excessive damage to the fins, braze, or weld caps due to mechanical injury were also separated here.

HYDROSTATIC COLLAPSING OF THE FINNED TUBING

The purpose of this operation was to bring the tube wall into more intimate contact with the slug to improve the heat transfer from the slug to the finned wall. The heat transfer calculations demonstrated the desirability of this operation. If it had been possible to maintain closer tolerances between slug and finned tube this step might have been eliminated. Another reason for including this step involves considerations of the helium system. As discussed previously, one of the objectives was to lock in a predetermined gas volume in the cartridge so as to minimize the breathing or surging of the detecting gas. The only way it was found possible to attain this objective was by the use of slugs of fixed dimensions in combination with the compression operation. Extensive tests were performed in which it was demonstrated that at pressures of the order of 2500 pounds per square inch, the diameter and, further, the volume of a tube could be reduced quite reproducibly.

The compression chamber was constructed using a 3½-inch stainless steel pipe, flanged and fitted to receive a plug containing O-ring seals.

A simple valving arrangement permitted rapid pressurizing with a Blackhawk Model No. 60 hydraulic pump.

Upon receipt of a cartridge from leak test number 2, a strip of absorbent paper was inserted in the brazed cap opening, and a rubber seal was screwed over the cap. The cartridge, in a carrier tube, was then loaded into the compression chamber. The plug was inserted, gate dropped into position, and the water valve and air relief valves were opened. The air relief valve was closed when water drained into an indicator that was just beyond the air relief valve, thus showing that the chamber was filled with water. The water valve was closed and the system was hand pumped to 2500 psi.

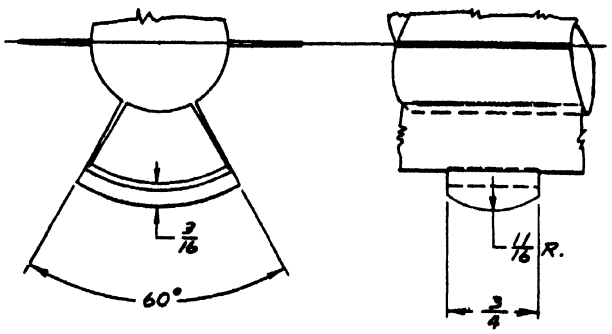

Figure 16. Anchor detail

The air relief valve was then opened permitting the pressure to drop to atmospheric and the gate was lifted. The plug was removed to aid in the drainage of water. When sufficient water was drained out of the chamber, a pair of tongs was inserted into the steel storage tube; the operator pulled the assembly out of the chamber far enough for the hands to grasp it and complete its removal. The tube and cartridge were carried to supports. The cartridge was slid, welded-end first, through an air drying ring into a dry tube. The sliding and drying action were stopped after all but a few inches of the cartridge was in the dry storage tube (Fig. 15).

The rubber stopper was removed and the brazed end inspected for leaks by examining the absorbent paper from the cap. A volume check was made after inspection of the paper. This was accomplished by connecting the cartridge to a known volume of gas at a known pressure and noting the pressure drop when the systems were joined. If the cartridge showed neither the presence of water nor volume irregularities, a rubber bumper and a spring clip were placed over the brazed cap. The cartridge was pushed completely into the carrier tube, and the assembly was placed in a storage vault.

FLAME BRAZING OF THE ANCHOR

The purpose served by the anchor was to locate the fuel element relative to the graphite structure. On going from zero power to full power the fuel element expands approximately 1 inch. On cooling down, the element can move in either direction. To prevent this, the graphite of the pile was provided with a slot 20 inches from the central gap into which the anchor would drop when the fuel element was inserted into the pile.

An "anchor" is an arc of 2S aluminum, ¾ inch wide. Its external face is convex. Each end is machined, leaving a ridge which is used to position the anchor on the fins of the cartridge (Fig. 16). A gage 20.70 inches long was designed to position the anchor accurately from the welded end of the cartridge. Alcoa No. 33 flux, mixed with two parts of alcohol, was used with filler rod composed of 88 per cent aluminum and 12 per cent silicon.

The end of each cartridge was pushed out of the storage tube onto a supporting table, exposing some 25 inches of the welded end. A small amount of flux was spread uniformly on the surfaces to be brazed. The anchor was clamped in place, using the gage to locate it, and turned a quarter turn to place the joint to be brazed in a horizontal position. An oxygen acetylene flame was used. The brazing rod, coated with flux, was applied at the proper temperature. The anchor and fins were cleaned, while still hot, with water and a fiber bristle brush to crack the flux and remove it from the surfaces. The cartridges were then dried with compressed air, pushed back into the steel storage tubes, and moved to the next operation.

FLAME BRAZING OF THE HELIUM TUBE TO THE FUEL ELEMENT

The helium tube was a ⅛-inch od, 0.032-inch wall, 40-ft long coil of 2S aluminum contained in a cardboard cylinder of approximately 2-inch id. The end of the coil was straightened for about 4 inches and the aluminum protector was slipped on. The aluminum protector tube 2-inches long was used to prevent bending of the brazed joint in subsequent handling operations. The coil of tubing was placed in a vertical holder. The end of the helium tube was cleaned and brought to size with a swaging pliers. A hydrogen gas flame and a brazing rod consisting of 88 per cent aluminum-12 per cent silicon were used to form the fillet weld about the tube. On completing this operation, water was sprayed on the hot surface to crack the flux. The joint was then cleaned and dried. Since it was felt that the cleaning operations in both brazing procedures were not stringent enough to remove the last traces of flux which might either result in corrosion of the aluminum in storage or might actually effect a temporary seal in the brazed joints, the completed assembly was given a more thorough cleaning operation in which a solution of 10 per cent nitric acid and 10 per cent sodium dichromate was dripped over both brazed joints. The total amount of solution used was 500 cm^3. The joints were then scrubbed using a monel brush to assure the removal of flux particles. This cleaning operation was followed by a rinse in hot running water. The wet areas were then dried thoroughly using compressed air. The completed assembly was then put into a storage tube and the helium coil was supported by inserting its cardboard container within the storage tube.

CONTINUITY AND FINAL LEAK TEST

Since this test was the last test to be performed to determine the soundness of the element and, therefore, its acceptance as a fuel element for insertion in the pile, this inspection was as stringent as could be devised. This test was used to determine: (1) whether the helium tube and cartridge were interconnected, and (2) whether any leaks existed in any part of the helium tubing, the joints, or the finned tubing.

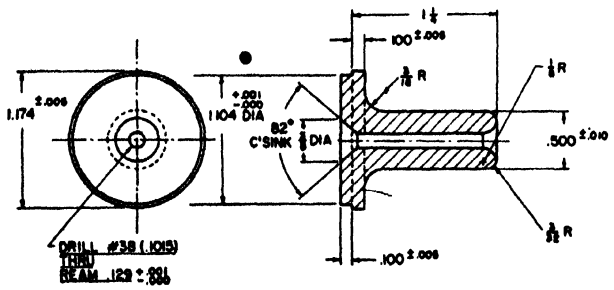

Figure 17. New helium cap

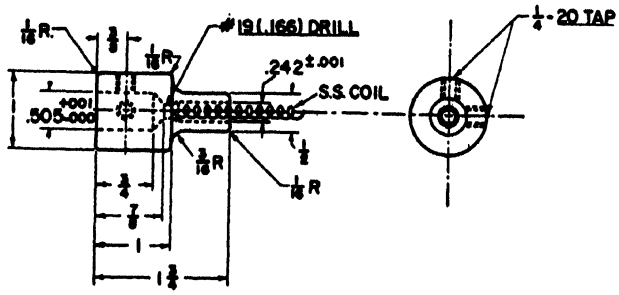

Figure 18. Helium tube cap and stainless coil

To accomplish the first of these objectives the assembly, which had been placed in the test chamber (see Fig. 11), was so oriented so that the helium tube end rested in the large cylindrical section of the test chamber. The end of the helium tube was pushed through a compression seal and connected to a reservoir gas system. The reservoir gas system was pressurized to 80 pounds. The valve connecting it to the helium tube was then opened. Since the volume of the helium tube and the fuel element were known, the reservoir volume was chosen so that it was roughly equal to that of the sum of the volume of the helium tube and fuel element. If there was continuity between the helium tube and the fuel element on opening the valve the pressure gage would drop to ½ its initial value. The "leak tightness" of the total assembly was established by a helium leak test; the vacuum door of the large cylindrical section was closed. The system was first rough pumped to 100 microns and then by closing and opening the proper valves the pressure was further reduced to about 25 microns using the diffusion pump and the other large mechanical pump. When the vacuum gage indicated that the system had been brought to 25 microns, the pressure on the interior of the assembly was raised to 80 pounds. The valve to the backing pump for the diffusion pump was turned off and the valve to the mass spectrometer was opened. A leak in the assembly could be readily noted by the characteristic change in the current in the mass spectrometer. On completion of this test the pressure within the cartridge was reduced and the unit was transferred to the storage vault ready for insertion into the reactor.

This completes the procedure used on the production of the first loading. The experience gained in operating the reactor indicated that the occasional failure that was noted in the fuel element was primarily due to the development of a leak in the helium tube, usually in the region of the brazed joint. This joint, i.e., the connection between the helium tube and the end cap was changed and also the method of joining the helium end cap to the tube was changed. Figure 17 shows the cap which is now being used in the new cartridge. In order to use this cap and an inert arc weld similar to the one that was discussed in step number 3, the end of the finned tube which is to receive this cap has to be cleaned by the same procedure as was used in step number 1. To accomplish this, the finned tube is cut longer than the summed length of 33 slugs plus the accumulated error. The two ends are chemically stripped of their anodic film. All of the operations up to number 8 are performed in the same manner as indicated in the preceding description. Step number 8 consists of the insertion of one end of the helium tube to the base of the cap shown in Fig. 17. The helium tube is flame brazed to the cap using flux and 88 per cent aluminum and 12 per cent silicon rod. This assembly, cap plus helium tube, after cleaning is seated in the cartridge. The void space, which resulted because the tube was cut too long, is filled with disks of various thicknesses of anodized aluminum so that the cap, on insertion, just makes contact with these filler disks. An inert arc weld is used to effect the closure using the same welding machine as was used in effecting step number 3. These operations are then followed by steps 10, 11, and 13 as in the previous procedure.

In preparation for insertion of the fuel element into the reactor, the helium tube is straightened and a sleeve, shown in Fig. 18, is slipped along the helium tube until it meets with the helium tube cap. It is then fastened to this cap by two set screws. Attached to this latter cap is a tight coil of stainless steel wire 22-inches long which has been swaged tight in the smaller section of the cap of Fig. 18. The purpose of the coil of wire is to prevent sharp bends from being formed in the handling operations subsequent to insertion into the pile. Discussion with Mr. Powell, who is in charge of pile operations, as to the relative advantages and disadvantages of the two helium end-cap designs resulted in the opinion that he cannot with certainty say that one was better than the other since the number of failures is low in either design and it would take a much longer time to build up statistics to show which design is superior.

Thermal Strains and Deformations in the Rod and Canning of the Heterogeneous High Flux Reactor

By M. Ristić, M. Novaković, P. Anastasijević and N. Kondić,* Yugoslavia

It is generally known that one of the factors limiting the magnitude of the thermal neutron flux in a given heterogeneous nuclear reactor is the mechanical strength of the protective canning. The main object of this paper is to examine the thermomechanical behaviour of the canning, i.e., to determine the deformation in the canning as a function of the thermal power delivered per unit volume of the uranium rod.

This paper is based on the results obtained by the examination of these effects on a model. A metal rod protected by an aluminium canning was heated by direct flow of electric current and cooled by axial circulation of water through the annulus.

I. THEORY OF THE EXPERIMENT

The power generation in a long rod with an even axial temperature distribution is given in general cases by

$$p(r) = \sum_{i=2}^{\infty} B_{i-2} r^{i-2} \tag{1}$$

The radial temperature distribution will be

$$T(r) = t_0 - t = \sum_{i=2}^{\infty} A_i r^i \tag{2}$$

and the relation between the coefficients is

$$A_i = \frac{1}{k} - \frac{B_{i-2}}{i^2} \tag{3}$$

The expressions for the mechanical stresses in the cylindrical rod are (e.g., Timoshenko: Theory of Elasticity, p. 365)

$$\sigma_r = -\sigma_{r_1} + \frac{\alpha E}{1-\nu} \sum_{i=2}^{\infty} \frac{A_i}{i+2} \cdot (r_1^i - r^i) \tag{4}$$

$$\sigma_\theta = -\sigma_{r_1} + \frac{\alpha E}{1-\nu} \sum_{i=2}^{\infty} \frac{A_i}{i+2} \cdot [r_1^i - r^i(i+1)] \tag{5}$$

$$\sigma_z = \frac{\alpha E}{1-\nu} \sum_{i=2}^{\infty} \frac{A_i}{i+2} \cdot [2r_1^i - r^i(i+2)] \tag{6}$$

where σ_{r_1} stands for the pressure on the rod by the aluminium canning. The influence of this pressure is taken into account by

$$\sigma_{r_1} = \frac{s}{r_1} \int f(\bar{\epsilon}) \approx \frac{s}{r_1} \bar{\epsilon} E_a \tag{7}$$

Due to the temperature gradient, the rod is submitted to thermal and mechanical strains. The total radial strain is given by

$$\epsilon = \epsilon_n + \epsilon_t = \frac{1}{E} [\sigma_r - \nu(\sigma_\theta + \sigma_z)] + \alpha T \tag{8}$$

and the over-all radial strain of the rod is

$$\bar{\epsilon} = \frac{1}{r_1} \int_0^{r_1} \epsilon dr = \frac{1}{r_1} \int_0^{r_1} \left\{ \frac{1}{E} [\sigma_r - \nu(\sigma_\theta + \sigma_z)] + \alpha T \right\} dr \tag{9}$$

or, after substituting Equations 4, 5, 6 and 7

$$\bar{\epsilon} = \left[\frac{1}{1 + \frac{s}{r_1} \frac{E_a}{E} (1-\nu)} \right] \alpha \sum_{i=2}^{\infty} \frac{2}{i+2} A_i r_1^i \tag{10}$$

The factor in brackets may be taken as unity since the second term in the denominator is negligible.

Substituting the coefficients A_i from Equation 3 one obtains

$$\bar{\epsilon} = \alpha \sum_{i=2}^{\infty} \frac{2}{i+2} \frac{1}{k} \frac{B_{i-2}}{i^2} r_1^i \tag{11}$$

It is seen that the over-all radial dilatation $\bar{\epsilon}$ depends on the heat generation law $p(r)$. For the uranium rod in the reactor, this function is given by

$$\frac{p(r)}{p(0)} = \frac{\phi(r)}{\phi(0)} = I_0(Kr) = 1 + \frac{1}{4}(Kr)^2 + \frac{1}{64}(Kr)^4 + \dots \tag{12}$$

and for the examined model heated by electric current, it takes the following form

$$\frac{p(r)}{p(0)} = 1 + \frac{1}{4}(Nr)^2 + \frac{5}{64}(Nr)^4 + \dots \tag{13}$$

where

$$N^2 = p(0) \frac{\theta}{k}$$

* Institute of Nuclear Sciences, "Boris Kidrich", Vinča.

It follows that the distribution of the generated heat in the model rod changes with the dissipated power, which is not the case with the fuel rod in a reactor. This might produce difficulties in the interpretation of results obtained on the model. For θ very small, the distribution of the generated heat is even and independent of the power level. In this case, Equation 11 reduces to the form

$$\bar{\epsilon} = \frac{1}{8}\left(\frac{\alpha}{k}\right) p r_1^2 = \frac{1}{8\pi}\left(\frac{\alpha}{k}\right) P \qquad (14)$$

If m and u are indices for the model and uranium rod respectively, it follows

$$\frac{\bar{\epsilon}_u}{\bar{\epsilon}_m} = \frac{(\alpha/k)_u P_u}{(\alpha/k)_m P_m} = \frac{(\alpha/k)_u P_u}{(\alpha/k)_m P_m}\left(\frac{r_{1u}}{r_{1m}}\right)^2 \qquad (15)$$

$$Ri = \frac{(\alpha/k)_m \cdot P_m \cdot t_{1m}^2}{\bar{\epsilon}_m} = \frac{(\alpha/k)_u \cdot P_u \cdot t_{1u}^2}{\bar{\epsilon}_u} \qquad (16)$$

is the similarity factor.

In such a way it is possible to determine $\bar{\epsilon}_u$ of the uranium rod submitted to a given thermal neutron flux, (i.e., to a given power generation per unit volume) by direct measurement of $\bar{\epsilon}_m$ on a model, R_i being known.

II. EXPERIMENT

A transformer of special construction, 50 kva rating 380/5 v, 50 cycles/sec was used for heating. The rod diameter was 27 mm and the effective length about 300 mm. The protective canning was made out of an aluminium (99.5% purity) tube 1.5-mm thick. Such a material was chosen in order that the effect of plastic deformation might be evident even at lower specific thermal output of the rod. The aluminium canning was drawn through a calibrated drawing pass.

To prevent the dissipation of electric power in the canning, the aluminium tube was cut into 17 sections, 15-mm long (Fig. 1). It was found that in such a way, only 5% of the total power was generated in the canning. The cooling was effected by the upward flow of water in the annulus of 36-mm outer diameter (Fig. 2).

The temperature was measured by calibrated iron-constantan thermocouples with the reference point on 0°C. The input and output water temperature was measured by mercury thermometers having the divisions at one tenth of a degree centigrade.

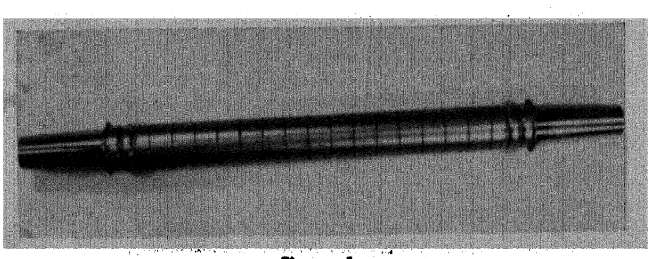

Figure 1

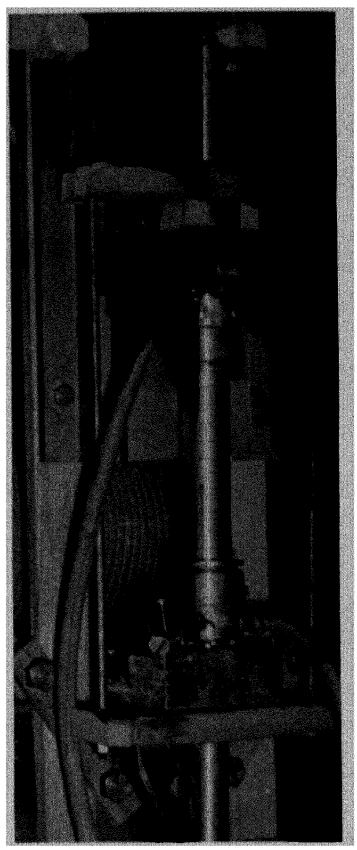

Figure 2. The experimental rod was made of material consisting of 40% of nickel, 50% of copper, while the remainder was zinc and other metals: The electrical resistivity of this alloy is nearly independent of temperature ($\theta \approx 0$) and therefore a nearly even heat generation was obtained. The power dissipated in the rod was changed and temperature measured in the centre of the rod, on the surface of the rod and in the aluminum canning, all in the middle section of the rod, in order to reduce the boundary effects

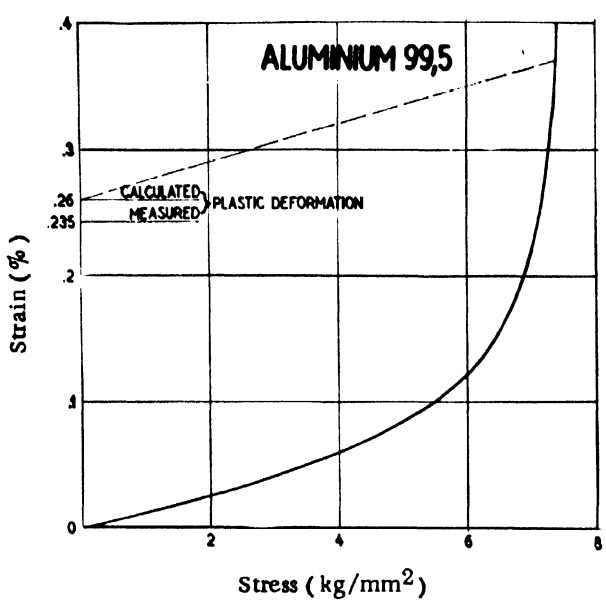

Figure 3

The generated power was determined from the relation U^2/R by measuring the potential difference between the ends of the rod and was checked calorimetrically. In order to determine the plastic deformation, the diameter of the rod and the canning were measured before and after the experiment by a precise microtester of the accuracy of one micron.

III. RESULTS

It was found that after reaching the power level of $p = 0.272$ kw/cm^3, 0.235% plastic deformation of the canning had occurred. This value was obtained by measuring outer diameters of the canning in about 70 points.

Substituting in Equation 14 the measured values for $k = 2.66 \times 10^{-4}$ (kw/cm–°C), $\alpha = 1.6 \times 10^{-5}$ (1/°C) and for the power level $p = 0.272$ kw/cm^3, the over-all deformation of the rod $\bar{\epsilon} = 0.372\%$ was obtained. From the strain-stress diagram for aluminium (Fig. 3) one can see that such a strain corresponds to the plastic deformation of 0.260%, which is in accordance with our measured value.

Applying the similarity law (Equation 16) and the relation

$$p = e \cdot \Sigma_f \cdot \bar{\phi} = 4.86 \times 10^{-15}\, \bar{\phi} \qquad (17)$$

it follows that for the heterogeneous natural uranium nuclear reactor, 25 mm rod diameter, such a plastic deformation corresponds to the flux of $\bar{\phi} = 9.3 \times 10^{13}$ (n/cm^2-sec), i.e., to a thermal power $P = 2.22$ (kw/cm), regardless of the rod diameter.

It has been proved that, during the renewed heating of the rod, the heat transfer from the rod to the canning was spoiled, evidently because of the plastic deformation which caused the worse thermal contact.

In all 20 measurements, the temperature drop from the surface of the rod to the canning per unit of the specific power has been increased by 61% on the average.

IV. NOMENCLATURE

A_i = coefficient of temperature power series
B_i = coefficient of heat generation power series
e = 2.66×10^{-14} kw-sec/fission
E = Young's modulus
E_a = Young's modulus for aluminium
I_0 = modified Bessel function of the first kind of zero order
k = heat transfer coefficient
K = reciprocal of the thermal neutron diffusion length in natural uranium
$p = B_0$ = specific power, i.e., constant power generated per unit volume of the rod
P = power generated per unit length of the rod
r = radius
r_1 = radius of the rod
R = electrical resistance of the rod
R_i = similarity factor
s = thickness of the aluminium canning
t = temperature
t_0 = temperature of the center of the rod
t_1 = temperature on the surface of the rod
t_2 = temperature of the canning
T = temperature difference
U = potential difference between the ends of the rod (electr)
α = coefficient of linear expansion (thermal)
ϵ = radial strain in the rod
$\bar{\epsilon}$ = over-all radial strain in the rod
ϵ_m = radial mechanical strain
ϵ_t = radial thermal strain
θ = temperature coefficient of electrical resistance
ν = Poisson's coefficient
π = 3.1416
σ_r = radial stress in the rod
σ_θ = tangential stress on the rod
σ_t = axial stress in the rod
σ_{r_1} = pressure by the canning to the rod
Σ_f = 0.186 cm^{-1}, macroscopic fission cross section for natural uranium
$\phi(r)$ = thermal neutron flux; $\bar{\phi}$ = average thermal neutron flux
Ψ = ratio of reactor to model rod power generation per unit length
ψ = ratio of reactor to model rod power generation per unit volume

Record of Proceedings of Session 18B.2

WEDNESDAY AFTERNOON 17 AUGUST 1955

Chairman: Mr. H. M. Finniston (UK)

Vice-Chairman: Mr. H. J. van Eck (Union of South Africa)

Scientific Secretaries: Messrs. B. Prakash and J. Goedkoop

PROGRAMME

P/825	The metallurgy of reactor fuels	J. P. Howe
P/561	Dispersion-type fuel elements	C. E. Weber and H. H. Hirsch
P/953	MTR-type fuel elements	E. J. Cunningham and J. E. Boyle
	Discussion	
P/947	On the possibility to improve the heat transfer of uranium and aluminium surfaces in contact	F. Boeschoten
	Discussion	

Mr. J. P. Howe (USA) presented paper P/825.

Mr. C. E. Weber (USA) presented paper P/561.

Mr. J. E. Cunningham (USA) presented paper P/953 and, in addition to the material already included in the paper, presented the following picture in connection with powder metallurgy techniques for the fabrication of fuel-bearing cores for fuel elements and said:

After batch proportioning and blending, the amount of powder mixture required for each core compact is loaded into a die cavity and hydraulically pressed cold under a pressure of 33 tons per square inch. The resulting dispersion of the UO_2 particles in the as-pressed core is illustrated in Slide 1.

The dark particles are UO_2, which has been magnified by about 300 diameters. Each alloy or pressed core is completely jacketed by the picture-frame technique.

DISCUSSION OF P/825, P/561 and P/953

Mr. Meyerson (USSR): One of Mr. Howe's slides showed fuel elements consisting of uranium carbide dispersed in a silicon carbide matrix. On that slide was mentioned carbide of uranium UC_2, but on the other slide mono-carbide of uranium, UC, was mentioned in the same matrix. May I ask which of those two uranium carbides it is preferable to use in this type of element, and for what reason?

Mr. Howe (USA): A carbide U_2C_3 forms at high temperature which decomposes to UC and UC_2 on cooling. If the body contains an excess of carbon, UC_2 will be present, but should the carbon content be lowered, both UC and UC_2 may be present, or at high temperature U_2C_3. It is true that the state of aggregation may depend on the thermal history. However, UC_2 should appear in both slides.

Mr. G. E. Darwin (UK): I would like to ask Mr. Howe about the solid type of uranium for the element. What is the effect of running this fuel element in such a way that the centre temperature of the rod is above the alpha-beta phase change temperature?

Mr. Howe (USA): I believe that one of the papers in the reactor session, by Mr. Siegel, gave some data on this. The effect is just about what you would expect. Since there is a large expansion when one goes from alpha to beta a portion of the center material transforms into the beta phase, and on cooling back there is too much room for the alpha material when it returns from the beta structure. As a result cracks occur, and if one does this a sufficient number of times one is very apt to have a larger element with a hole in the center, or cracks of various kinds. Generally speaking one cannot control very well when it happens.

Mr. G. N. Walton (UK): I should like to ask Mr. Weber a question on paper P/561. When fission products recoil in fissile material they are reputed to carry quite a number of other atoms as they recoil, particularly towards the end of their track. Has Mr. Weber any experimental evidence on the amount of fissile material that can be carried from a particle into the surrounding medium when a fission product recoils from it?

Mr. Weber (USA): The answer to the question is that we do not have that kind of experimental evidence. Secondly, I think this would be a fine point actually, since the main part of the range would be the fission product atom recoiling by itself and at the very end you would get this extra phenomenon you mentioned, so I do not think this would disturb the general conclusion.

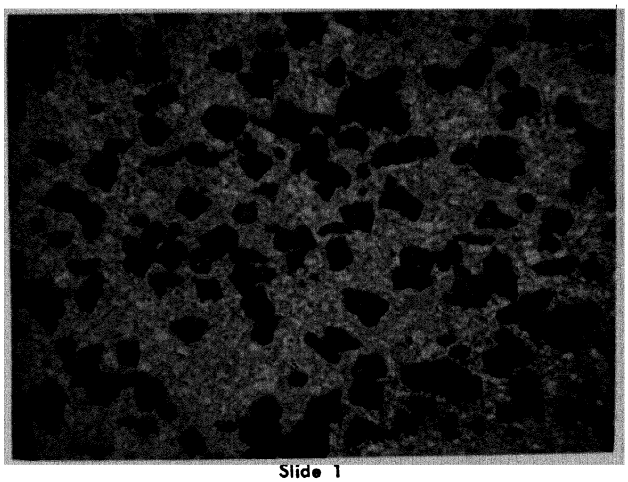

Slide 1

Mr. K. CARLSEN (Norway): In one of the papers uranium-magnesium dispersion is mentioned as a possibility. Has any work been done on this system and is it promising? It is a question for Mr. Weber.

Mr. WEBER (USA): I mentioned the uranium-magnesium as an example of two insoluble compounds. We have done some general laboratory work with various metals, but I do not know of any fuel element development.

The CHAIRMAN: A large number of fuel elements have been listed in Mr. Howe's paper and a large number of fuel elements have been mentioned by others, yet no mention is made of the amount of burn-up which has been achieved or which is possible with these fuels. Could any indication be given of this? Is it 1 per cent, 10 per cent, or $\frac{1}{10}$ per cent?

Mr. HOWE (USA): I mentioned rather hurriedly that we could expect 1 per cent burn-up at least in the dispersion type of fuel element, and this statement is backed up by data. The MTR-type elements, for instance, show—I think there are other papers on the subject—relatively small changes, at something of the order of 1 per cent burn-up. There is a small change in density. The atomic volume of the fission fragments indicates that the gases formed in these particular elements are occupying no more than their solid volume, shall we say, which is a very interesting fact, I think.

It is necessary to heat them to a very high temperature before one gets segregation of them into gas bubbles. I mention that fact because it has always fascinated me.

The CHAIRMAN: Does this mean that the element with the metallic matrix will not work at high temperature, presumably because sufficient gases can diffuse in the matrix?

Mr. HOWE (USA): That is correct. I do not know exactly what temperature one should choose. I have said 75–80 per cent of the melting point of the metal on the absolute temperature scale. That is mostly intuition, but it is corroborated by the aluminum system.

A DELEGATE (from the floor): In the dispersion type of fuel element you dilute your uranium with another metal or you disperse it. Does it pay you to disperse or to form an alloy, and under what conditions would Mr. Weber use one or the other?

Mr. WEBER (USA): The answer to the first question would be determined by the economics of the over-all fuel cycle. Whether you decide to make an alloy or disperse it would be a question of the relative manufacturing costs. Secondly you would get less damage in a dispersion element than in a very small particle size dispersion or a complete homogeneous alloy. Work is going on to get more definite data.

A DELEGATE (from the floor): I should like to ask Mr. Cunningham, in connection with aluminum-clad fuel elements, whether he would enlarge on the phenomenon of blistering, which apparently occurs at some stage during manufacture, and would he tell us what tolerance can be expected on length and width in rolling from ¼-in. thickness down to the finished size of 60 mils.

Mr. CUNNINGHAM (USA): With regard to the first question, what we have found through experience is that we do pick up hydrogen when working with the alloy type or the UO_2 aluminum powder type. We have looked at two methods for eliminating, or at least obviating, the trouble from this, and one was to vacuum cast. If you vacuum cast the metal you can get away from this hydrogen pick-up problem. This has to be followed, however, by a more expensive technique of completely encasing the core material in a jacket, welding all around, evacuating it, sealing it off and rolling it. The other method is simpler and cheaper and does not involve going through all these elaborate and expensive operations to produce the plate. You simply give it the flux annealing treatment. When these plates are flux annealed, there is some evidence to show that on heating up and annealing the hydrogen naturally goes in all directions, but it cannot normally escape through the aluminum, because of the tenacious oxide film. This flux, I believe, cuts the oxide free from the aluminum and allows a sufficient amount of hydrogen to escape, so that we no longer, in subsequent processing or in service, have the blistering problem. If we do not do this, we lose about 80 per cent of the units.

In reply to the second question, the tolerance on the fuel element width is plus or minus 10 mils. The water-gap is held to 10 per cent, or a 117-mil water-gap is held to plus or minus 12 mils.

Mr. J. E. DRALEY (USA): There is another answer to the problem of stopping blistering, and that is to alloy the aluminum to give a material which is not susceptible to blistering. For the last nine months or so we have known how to do that, but it has not gone into production so far as I know. Although the blistering phenomenon in air will not be in-

cluded, an identical process of blistering in water corrosion will be described tomorrow afternoon.

Mr. F. BOESCHOTEN (Netherlands) presented paper P/947.

DISCUSSION OF P/947

Mr. A. R. KAUFMANN (USA): I should like to point out that in the case of a solid layer between the two metals, Mr. Boeschoten did not seem to include the possibility of a metallurgical bond between the two metals and the intermediate solid layer. This can be done with an aluminum silicon brazing alloy, and you then have extremely good thermal contact and good heat transfer. Incidentally, this alloy is quite helpful in preventing reaction between aluminum and uranium at elevated temperatures.

Mr. BOESCHOTEN (Netherlands): That is quite true. I have seen it in one of the American papers, but I did not think of that solution myself.

Mr. KAUFMANN (USA): The other comment I want to make is on a point to which Mr. Boeschoten also refers. It is that even in the case of a liquid sodium layer there is the possibility of transport of metal through the sodium. This has been commonly observed in other cases, and it is considered to be a form of mass transfer.

Mr. BOESCHOTEN (Netherlands): Yes, I have observed that. I do not know whether it would give serious trouble, or what your experience in that matter is.

Mr. KAUFMANN (USA): I could not say exactly under what temperature there might begin to be trouble, but I want to point out that this is a well-known phenomenon.

Mr. BOESCHOTEN (Netherlands): I do not think it is serious at a temperature of 230° as I mentioned in my paper.

Mr. D. H. GURINSKY (USA): It seems surprising to me that uranium reacts with graphite at such low temperatures to form uranium carbide. I should like to suggest that in all probability you have formed some uranium-aluminum compound. I think that moisture may have been present, and you may have formed uranium hydride.

Mr. BOESCHOTEN (Netherlands): We evacuated very carefully, so that no moisture could be present in the tube.

A slice of uranium heated by its own in the described way did not show blister formation.

The graphite was spectroscopically pure, but perhaps it contained some moisture.

Mr. MARGEN (Sweden): I should like to have the opinion of the author, and possibly also of the meeting, on the relative merits of metal bonded elements and elements in which there is no bond and in which the contact is simply produced by pressure. It seems to me that if you have a bonded element subject to very high heat rating, and the element is fairly thick, which might be necessary from the point of view of neutron economy, particularly if you use zirconium, then, due to the greater expansion of the uranium compared with the zirconium, the zirconium will be submitted to periodic deformation under cycling. I wonder whether that could cause cracking in time, and whether a better solution might not be to rely purely on pressure and to leave a slight gap at the end for expansion purposes. Possibly the author or someone else might comment on that.

Mr. BOESCHOTEN (Netherlands): I think that by application of a gas or a liquid metal as bonding material there should be no trouble of stress, because no force is transmitted through a liquid or a gas if it can expand in a reservoir. As I mentioned, application of pressure might be a good solution, but I must say that I did not do any cycling experiments.

Mr. KAUFMANN (USA): I could undertake to say something on that question. I believe it is generally considered that if there is a good mechanical contact between two metallic surfaces the heat transfer is just about the same as if there is a metallurgical bond. The big attraction of the metallurgical bond is that it gives the assurance that the surfaces will always remain together, whereas if there is only mechanical contact that is not obvious.

With regard to a bond between zirconium and uranium, it is possible to get a metallurgical bond which is practically indestructible regardless of volume changes or anything else, so that they will not crack apart.

One other advantage of a metallurgical bond which is sometimes put forward is that if for any reason there is penetration of the coolant through the cladding it would be able to attack the underlying uranium only locally, whereas if there is no metallurgical bond the coolant can rapidly spread over the whole surface of the uranium, and the action will be a great deal faster.

Mr. HOWE (USA): The problem of differential stresses, or of stresses arising from differential expansion, is quite a general one, and arises not only because of differential metals but because of the temperature differences in the fuel elements themselves, which we tried to show as a slide. It depends on the thickness of the fuel elements, and it is true that we could have a thin heat-generating piece of metal next to a cooler one and the thermal stress might very well result in differential expansion. I think it is clear that a problem of fatigue arises in both instances at high temperature. Whereas one may have a material which is ductile and which will take the stress involved quite readily, nevertheless at moderately high temperatures, where grain-boundary flow occurs, we can run into a fatigue problem where cracks can start along grain boundaries in a matter of a few hundred cycles when the differential strains are of the order of 0.1 per cent,

whatever the cause. I am sure that does not answer the question, but it elaborates on the problem a little.

M. CABANNE (France): Mr. Kaufmann spoke of an aluminum-silicon alloy. I should like to know whether such a layer does not give rise to difficulties when the fuel elements are dissolved, in view of the fact that substances capable of hindering the diffusion of aluminum are resistant to acids.

Mr. KAUFMANN (USA): The chemists have always complained about having silicon present in dissolving up the fuel elements. I have never heard that the use of this alloy made it difficult to dissolve the elements; it is simply that when they are dissolved up there is quite a mess. The chemists, however, have apparently learned to get over that, and I do not think that it is a serious problem.

Session 19B.1

HANDLING LIQUID METALS

LIST OF PAPERS

			Page
P/123	Sodium and sodium-potassium alloy for reactor cooling and steam generation	T. Trocki *et al.*	241
P/866	Liquid metal handling	S. G. Bauer	252
P/121	Pumping of liquid metals	A. H. Barnes	259
P/637	Production of high-purity metallic bismuth	N. P. Sajin and P. Y. Dulkina	265
P/812	The use of high temperature sodium in manufacture of NaK alloy	C. B. Jackson and R. C. Werner	270
P/766	The determination of trace impurities in liquid metal coolants by radioactivation methods	A. A. Smales	273

Sodium and Sodium-Potassium Alloy for Reactor Cooling and Steam Generation

By T. Trocki,* W. H. Bruggeman† and F. E. Crever,† USA

The highly concentrated heat generation which occurs in a nuclear power reactor creates the need for cooling fluids capable of high rates of heat transfer. Liquid metals, which possess relatively high thermal conductivity, are capable of attaining high heat transfer rates at moderate velocities, and with low film temperature drop. They represent one satisfactory answer to this need. A review of the properties of the low-melting-temperature metals leads to the selection of the alkali metals, sodium and potassium, and their alloys, as the most likely to be suitable for this application. Based on this selection, extensive work with these fluids has been conducted in the United States. Their suitability for reactor cooling has been established through extensive operation of an experimental power reactor and large scale heat transfer systems and equipment. This paper is a summary of this effort.

In addition to their desirable heat transfer characteristics, the alkali metals selected are liquid over a wide range of temperature. Sodium melts at 98°C, potassium at 64°C, and one alloy of the two has a melting point as low as −11°C. The normal boiling point of these metals is between 780°C and 880°C. The low vapor pressure at reactor operating temperatures, approximately 300–500°C, is advantageous in the mechanical design of equipment using these metal coolants. Operation at temperatures permissible with these metal coolants yields power plant efficiencies not attainable today with water-cooled reactors.

The chemical reactivity of these alkali metals is well known. They burn readily in air and react vigorously with water. Although upon first consideration these characteristics would appear to limit their large-scale use, it has been established that with proper design and operating precautions the use of these metals is no less practical than many more formidable commercial chemical processes. Also, upon first consideration, these fluids appeared to be highly corrosive to structural metals. It was learned, however, that when properly purified they are practically non-corrosive to many high temperature steels. Further, since these fluids are chemical elements, they are not subject to thermal or radiation decomposition.

Sodium and potassium have sufficiently similar chemical and physical properties to permit discussion of their general applicability to reactor cooling as if they were interchangeable. For convenience, in this paper they will be referred to as liquid metals or alkali metals except where one of them is denoted specifically.

REACTOR COOLING

Liquid metals are used for power reactor cooling because they provide high rates of surface heat transfer with low film temperature drop and because their high boiling points permit high temperature operation. These characteristics become extremely desirable in reactor cores of high power density. An example of the superiority of liquid metals for heat transfer is illustrated in Table I. These data, applied to a reactor fuel element, indicate a lower fuel-operating temperature would result with liquid metal cooling for comparable operating conditions.

Table I. Temperature Drop Through Coolant Films

Coolant		*Average film temperature drop at heat flux of 200 watts/cm²*
Sodium*		30°C
Sodium-potassium alloy*		54°C
Pressurized water*	(2000 psia)	70°C
Pressurized helium	(1200 psia)	290°C

* At 15 ft/sec in tube 0.5 inches diameter.

The high boiling points of the alkali metals offer a number of advantages. Since the fluids operate with a high degree of sub-cooling, localized boiling in the reactor is avoided except under conditions of severe flow restriction. Boiling is undesirable because it may result in vapor blanketing and overheating of the fuel.

Another advantage resulting from the high boiling point is the low operating pressure possible with liquid metals. Systems and mechanisms can be designed for operation at pressures of 50–150 psig. The high boiling point also permits operation at temperatures which yield good power plant efficiency. Comparable cycle efficiencies can be obtained in gas-cooled reactors only with very high fuel tempera-

* General Electric Company, Atomic Power Equipment Department, Schenectady, N. Y.

† Knolls Atomic Power Laboratory. Operated by the General Electric Company for the United States Atomic Energy Commission. Including work by other United States government and industrial organizations.

tures and high pumping requirements. With water-cooled plants, these efficiencies are not obtainable even under conditions of high coolant pressure.

The nuclear properties of sodium and sodium-potassium alloy are acceptable over the entire range of neutron energy and particularly suitable at high energy. They possess acceptable thermal neutron absorption characteristics but they are weak moderators. Accordingly, separate moderating materials are required for thermal and low intermediate neutron energy reactors cooled with these liquid metals. Graphite and beryllium have been used for this purpose. The best application of the nuclear properties of the liquid metals is in the fast reactor in which neutron moderation is undesirable.

Another characteristic of these alkali metals is that they do not react with uranium. In event of failure of fuel cladding, corrosion of uranium by these materials is slight at reactor operating temperatures. Further, these metal coolants are essentially non-corrosive to high temperature steels and are compatible with special reactor materials such as beryllium, graphite, and zirconium. Graphite is clad to prevent the possibility of carburization of other parts of the system, and to prevent the sodium from being absorbed into the graphite. The maximum operating temperature of alkali metal cooled reactors is usually set by structural rather than by corrosion considerations.

The nuclear properties of these metals and their heat capacity dictate the need for a relatively large temperature rise of the coolant in the reactor. The percentage of liquid metal coolant volume in the reactor core is usually kept to a minimum regardless of the type of reactor. In the thermal and intermediate energy range, maximum possible core volume is devoted to the moderating material and the coolant volume reduced to improve neutron economy. In the fast reactor the moderating effect of the coolant is minimized by keeping the coolant volume to the lowest feasible percentage (25–45%). These requirements for low coolant volume result in a small coolant flow area in the core. Under these conditions a high heat capacity coolant would be desirable to permit heat removal with a moderate coolant temperature rise and low velocity. The specific heat of these metals (0.18 and 0.32 cal/gm°C) requires the use of a comparatively large temperature rise and moderate or high velocity. Of the liquid metal-cooled reactors designed or studied, most have utilized a coolant temperature rise of the order of 100 to 200°C.

A large coolant temperature difference of itself does not pose a difficult design problem. However, in a power reactor, this temperature rise may occur in a relatively short distance. In addition to this temperature gradient, there may also exist a large radial thermal gradient in a compact core. The main problem stems from the cyclic variation of these thermal gradients with varying load conditions.[1] Although such problems exist in any power reactor, they are magnified with liquid metals because of their lower heat transfer film resistance and hence, faster thermal response of the structural members.[2,3] Design to minimize thermal stresses is one of the principal problems in this type reactor.[4]

Design of vessels and sealing of control mechanisms for liquid metal-cooled reactors is simplified by the relatively low system-operating pressure. Although these metals have a low viscosity at reactor operating temperature, satisfactory bearings for control mechanisms, operating in the liquid metal, have been devised. The special problem associated with bearings in the control mechanisms is that they operate slowly and infrequently, precluding the build up of a hydrodynamic film. Extra hard materials such as tungsten carbide with a smooth surface finish have proved satisfactory. No localized corrosion similar to the crevice corrosion, experienced with high purity water, has been encountered with bearings in liquid metal.

HEAT TRANSFER AND STEAM GENERATION SYSTEM

Within the reactor, the tremendous radioactivity of the core, even after shutdown, has a predominant effect on the mechanical design of the reactor. The primary shielding around the reactor attenuates this activity to a lower level. Outside of the primary shield the radioactivity of the reactor coolant has a significant effect on the design of the heat transfer system. Both sodium and potassium become highly radioactive in passing through the reactor core and have relatively long decay half-lives (15 and 12 hours respectively). This factor, and their chemical reactivity with air and water, are primary considerations in the design of the heat transfer system. With materials as chemically active as these alkali metals, it is good practice, even when they are not radioactive, to take precautions against their leakage. The high level of radioactivity, together with their long decay half-lives after shutdown, place even greater emphasis on precaution against leakage. Of particular concern is the release of radioactivity and chemical energy which might occur if radioactive alkali metal and water mixed in the steam generator. In one design concept these hazards are separated by using a secondary non-radioactive liquid metal system for steam generation. In this arrangement the radioactive reactor coolant transfers heat to a non-radioactive secondary alkali metal coolant. In event of leakage in the steam generator, the non-radioactive reaction products can be vented to the atmosphere. Leakage of radioactive liquid metal through the heat exchanger from primary to secondary systems is prevented by operating the secondary system at a higher pressure. A schematic diagram of this arrangement is shown in Fig. 1.

This system is somewhat more complex than direct use of radioactive liquid metal in the steam generator as it requires additional heat exchangers, pumps and piping. The intermediate heat exchanger also interposes an additional temperature drop. This

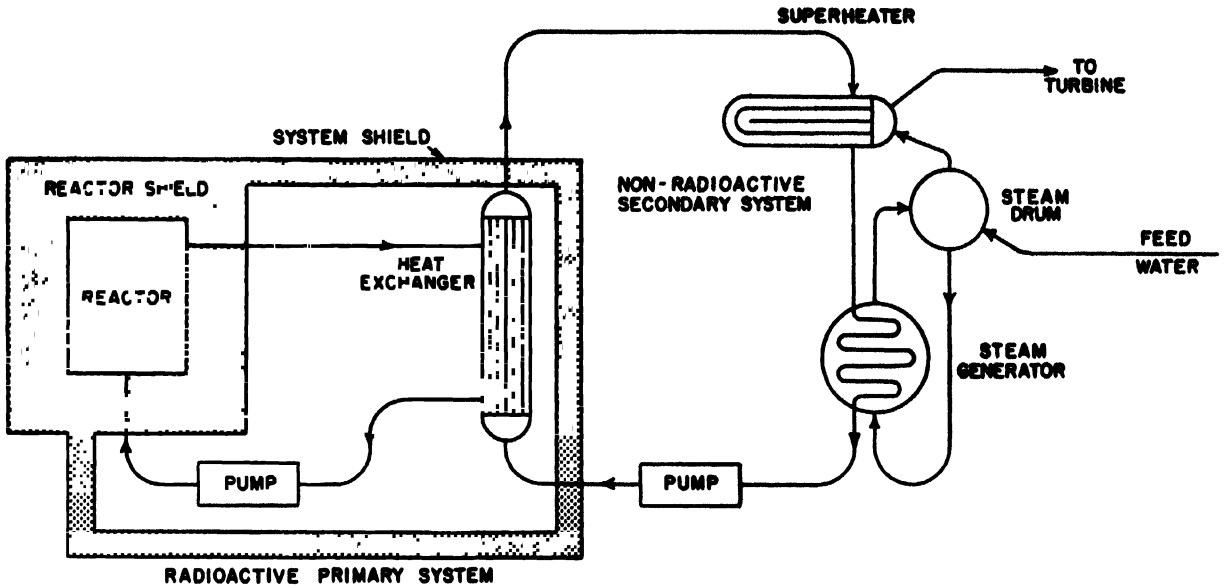

Figure 1. Flow diagram of reactor cooling and steam generation system

temperature drop, however, is minimized by the high over-all heat transfer coefficients obtainable with liquid metals on both sides of the heat exchanger wall.

Use of the radioactive reactor coolant directly in the steam generator yields a simpler system. In this configuration, the greatest possible precaution is taken to reduce the possibility of leakage through the steam generator. Units using double wall tubes with methods of detecting leakage through either wall have been developed for this service. By this technique, and by use of extreme care and inspection during fabrication, the potential hazard of a major failure is reduced to a minimum. Experience to date with steam generators of this type supports this concept. More detailed discussion is presented later.

The mechanical design and construction of the liquid metal heat-transfer system and equipment follow the basic procedures developed for high temperature power plants and processes.[5] Some of the special requirements can be inferred from the preceding discussion. In particular, the radioactivity and chemical activity require a high degree of leak tightness and soundness in fabrication. To assure leak tightness, all joints which are in continuous contact with the liquid metal are fusion welded or brazed with a nickel-manganese compound. Other somewhat special provisions are the inert gas atmosphere and preheating of all parts of the system above the melting point of the liquid metal. A blanket of inert gas, such as nitrogen or helium, is kept at a positive pressure to prevent in leakage of air. Preheating is required for sodium, which melts at 98°C, but is not required for the sodium-potassium alloy which is liquid at room temperature.

EXPERIMENTAL SYSTEMS

The most significant operating experience with these liquid metals has been accumulated in two experimental systems: a large scale heat transfer system operated at the Knolls Atomic Power Laboratory and the Experimental Breeder Reactor built by the Argonne National Laboratory and operated at the National Reactor Testing Station. The heat transfer test system utilized an oil-fired heater as the heat source. It was basically similar to the system illustrated in Fig. 1. Sodium was used in the primary circuit and sodium-potassium alloy (56 wt % K) in the secondary. The rated heat throughput of this system was 8×10^6 BTU/hr (2350 kw) with a design maximum sodium temperature of 510°C at the heater exit. The rated temperature difference in the primary system was 150°C. Design features and early operation of this system are described in previous papers.[6,7,8] This was the first successful demonstration of the use of these liquid metals on a large scale for heat transfer. In addition to being used for testing a number of model heat exchangers and steam generators, this facility was excellent for proving out large scale liquid metal handling and purification methods. It was operated for more than 8000 hours which included 500 hours at temperatures of 560–650°C. This system was later converted into a single circuit using sodium for testing of steam generator models. It is significant that such extensive changes in system piping were accomplished without excessive oxidation of the residual liquid metals in the system. After modification the system was operated satisfactorily for an additional 1450 hours before being shut down permanently.

The construction and operation of the Experimental Breeder Reactor was a milestone in the field. This was the first application of alkali metals in cooling a nuclear reactor. Although there is a separate paper given on the subject of the EBR, some aspects of the liquid metal technology involved are reviewed here. A flow diagram of the

heat transfer system is shown in Fig. 2. As in the systems previously described, two coolant circuits in series are used. Both the primary, or reactor circuit, and the secondary, or steam generator circuit use sodium-potassium alloy (78 wt % K).

A unique feature in the system is the primary coolant flow path. The alkali metal is pumped from the sump tank to a head tank as shown in Fig. 2. The alloy flows by gravity from this head tank through the reactor, then through an intermediate heat exchanger to return to the sump tank. The flow through the reactor is at 210 gpm which, at the normal 1200 kw output, raises the coolant temperature from 220°C to 320°C.

The primary circuit pump is a direct current electromagnetic type rated at 400 gpm. During operation, an excess, over that required for reactor cooling, is pumped to the head tank. The excess, approximately 100 gpm, continuously overflows, assuring a full head tank at all times during operation. When full, approximately 3000 gallons are held in this tank. This volume is more than adequate to provide cooling for reactor decay heat shortly after emergency reactor shutdown and prior to initiation of the thermal circulation standby cooling circuit. In this circuit, heat is removed from the reactor by thermal circulation of the alkali metal and is ultimately dissipated in an air cooler to a natural draft chimney.

The secondary sodium-potassium circuit also uses a sump tank, although in this case, a head tank is not employed. The secondary system pump is a mechanical centrifugal pump, which is described in some detail later. A similar centrifugal "sump type" pump is used as a spare in the primary circuit. These mechanical pumps require the use of a shallow sump tank in order to minimize variations in level.

The primary system is shielded within concrete. Heat is transferred to the non-radioactive secondary circuit through an all welded, shell and tube type heat exchanger. This unit has a double pass on both sides. The tubes are single wall, made of nickel,

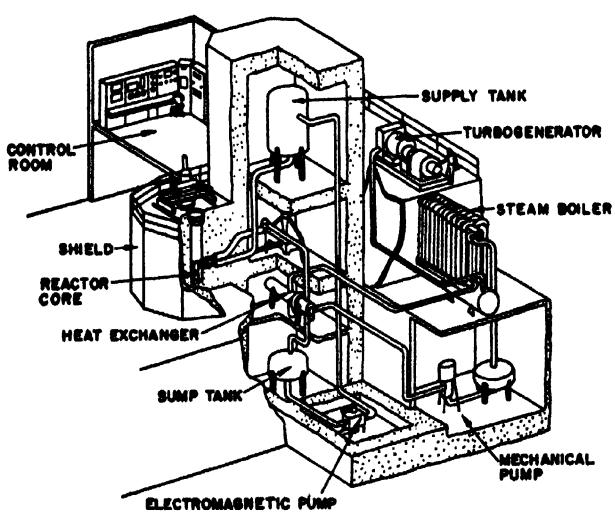

Figure 2. Experimental breeder reactor system

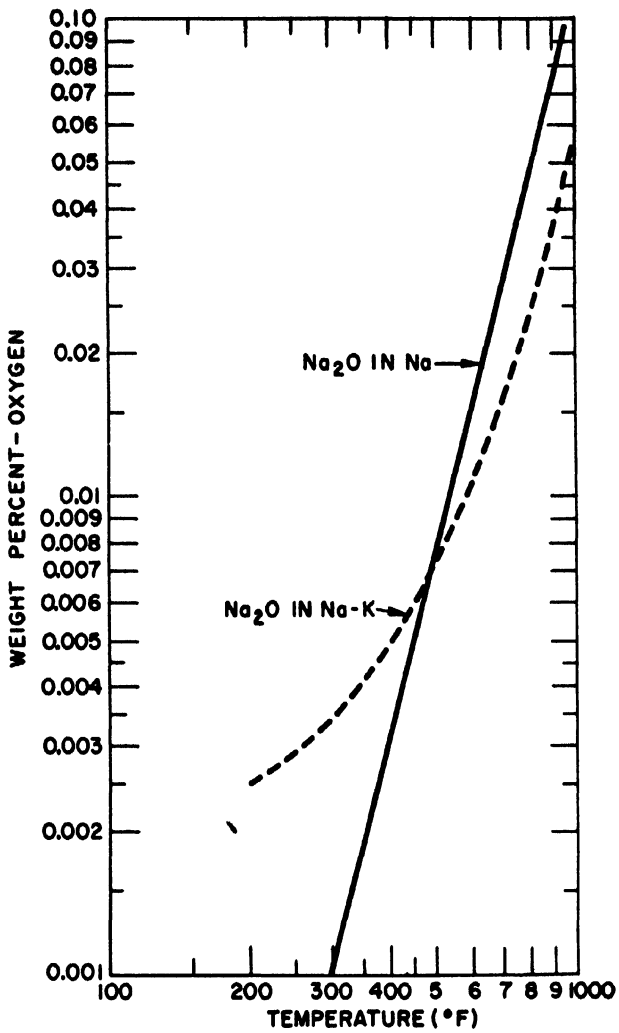

Figure 3. Solubility of sodium oxide in sodium and sodium-potassium alloy

of 0.75-inch diameter. The secondary fluid system is maintained at a higher pressure than the primary circuit in order to minimize the possibility of leakage of radioactive coolant through the heat exchanger. Heat from the secondary circuit is either dissipated to an air cooler or transferred to a steam generator. The steam generator, rated at 3630 lb/hr produces steam at 400 psig and 278°C. This unit uses the "falling film" type of flow to generate steam. This method yields high heat transfer coefficients and also provides minimum liquid water in event of leakage and reaction with the alloy. The steam drum located below the evaporator section supplies saturated water to a circulating pump. The pump lifts the water to the top of the vertical tube tank where it is sprayed on the walls of the tubes, which are externally heated by the sodium-potassium alloy. A water preheating section and superheating section are included in the steam generation equipment.

Although the EBR operates at relatively low power level, it has, during the four years of success-

ful operation, conclusively demonstrated the practicality of many aspects of alkali metal-cooled reactor systems.

CHEMICAL TECHNOLOGY

It was recognized early in laboratory investigation that oxygen accelerated the corrosion of metals by the alkali metals. The development of an analytical technique for determining oxygen in these metals was a significant advance which permitted correlation of corrosion results with oxygen content. The analytical procedure is based upon the amalgamation and solution of sodium or potassium in mercury and the separation of these elements from their oxides which are insoluble. The technique is capable of determination of the order of 0.002% oxygen in sodium.[9,10]

The amalgam analytical technique also enabled the determination of the effect of temperature on solubility of oxides in the liquid metals. Curves showing the variation are given in Fig. 3. It should be noted that over the range of power plant operating temperatures the solubility of oxides in the metals is low, less than 0.1%. At the melting temperature the oxide is the least soluble. This results in a simple method of purification by filtering the metals at a low temperature. Also of significance is the degree of variation of solubility with temperature. A system saturated with oxides at an elevated temperature will precipitate sodium oxide as the temperature is reduced. The insoluble oxides tend to form a sludge which will accumulate in small passages and form a plug. Such precipitation of oxides in colder sections has been noted in experimental systems. The relatively small passages at the cold inlet end of the reactor represent a zone for possible sludge accumulation. As this could cause flow restriction and overheating of fuel, it must be avoided. Fortunately it can be avoided by monitoring the system for oxides and repurifying as required.

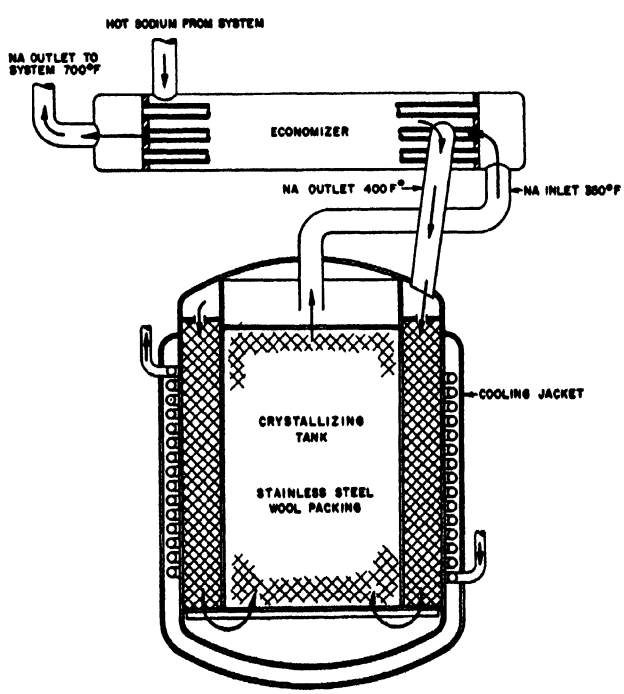

Figure 4. Cold trap and economizer

Under ordinary power operation, these liquid metal systems require no purification as they are completely sealed and covered with an inert gas. A system in which the gas is allowed to "breathe," will accumulate some contamination from the inert gas, although with purified gases, this contamination is slight. A more likely source of contamination occurs during refueling or other servicing operations which open the system to the atmosphere. After such operation is completed the liquid metal, if contaminated, must be repurified prior to returning the system to power operation.

Repurification is accomplished in a cold trap which is tied into a bypass from the main flow system. The liquid metal in the main system is held at an elevated temperature where it dissolves the maximum amount of oxide. A small portion of the flow is bypassed and cooled to precipitate the oxide. The precipitation takes place in a crystallizing tank filled with steel wool fiber to facilitate the growth of the oxide crystals. The stream is reheated before returning to the main system. A design of cold trap is shown in Fig. 4. The incoming liquid metal is cooled by the return stream in a regenerative heat exchanger to conserve heat. Additional cooling is provided in the crystallizing tank. With proper design, the leaving stream contains only that amount of oxide supported in solution at the lowest temperature of the cold trap.

A convenient method of determining the oxygen content of the liquid metal is based upon the sludging tendency of the precipitated oxide. A flow restriction, such as an orifice plate with holes of approximately 1 mm, is placed in a bypass stream in a series with a heat exchanger and flow meter. The bypass stream is cooled to reduce the temperature until a definite flow restriction is noted on the flow meter. It has been established that the flow stoppage occurs at the temperature corresponding to oxide saturation. This device, called a plugging indicator, accurately establishes the temperature at which plugging can occur in a system. The device is cleared of the restriction by permitting the bypass stream to rise to the system temperature, or by external heating if required.

With the use of the oxygen control techniques described, the level of this impurity can be kept at a low value. Large scale sodium systems operating at oxygen values of 50 ppm are not uncommon. Operation at oxide levels in this region result in extremely low corrosion rates. For example, the 18 Cr-8 Ni steels in sodium at 540°C corrode at a rate of less than 0.01 mg/cm²/month. Although corrosion of lower alloy steels is somewhat greater, their resistance is still excellent and they appear to be suitable for alkali metal systems.

Because of the success of oxygen control, little further work is being done in the United States on corrosion of conventional structural materials by alkali metals. Some of the attention in the corrosion field has shifted to study of the redistribution of radioactive stainless steel constituents in sodium.[11] Although corrosion may be negligible, the distribution of activated system structural material can present problems. Long half-life species, such as iron, cobalt and tantalum, when transferred into the heat transfer system, will cause difficulty in repair and maintenance.

This process appears to be both a net mass transfer as well as a random interchange. Order of magnitude of the transfer of 18-8 stainless steel in sodium at 450°C is 0.01 mg/cm²mo (based on reactor surface). The rate of transfer is seriously accelerated by increases in oxygen level and temperature. The radioactivity of the material transferred is, of course, a function of integrated power level and cross section of the individual species.

Impurities of lesser concern than oxygen are hydrogen and carbon. Hydrogen is of interest because it will cause moderation in reactors above thermal energy. The analytical technique for hydrogen in sodium[12] depends on thermal breakdown of the hydrogen bearing compound and subsequent diffusion of the hydrogen gas through a thin steel casing.

Carbon in alkali metals is of concern since carburization of certain steels has been observed. The determination of carbon in sodium[13] is made using a wet oxidation technique with subsequent analysis for carbon dioxide. No significant carburization difficulty has ever been encountered in a system in which oils or other carbonaceous materials have been excluded.

Other impurities in sodium and NaK are of minor interest only. Sodium, potassium and their alloys are normally quite pure, even in commercial form. A typical analysis of sodium as produced in this country is given in Table II. In general, potassium and sodium-potassium alloy have even a lower level of impurity content.

Table II. Analysis of Commercial Sodium (Analyzed at the Knolls Atomic Power Laboratory)

Element	Average parts/million	Element	Average parts/million
Ca	191.0	Hg	4*
Al	7.6	Sn	10*
Pb	1.0	Be	1*
Fe	2.4	Ti	10*
Cl	30.0	Mo	2*
S	14.0	Bi	10*
Li	17.0	Pd	5*
Cu	2.5	Ti	10*
Sr	5.0	In	2
Ni	2.0	U	5
Ce	2.0	K	100
B	4.0	Mg	5
Ba	2.0	P	10
		Cs	5

* Analyses were made for these elements, however, none was detected. The values listed are the expected sensitivity of the spectrographic detection.

HEAT EXCHANGERS AND STEAM GENERATORS

Heat exchangers for transferring heat between liquid metals can be of essentially standard configuration. One special provision is that they must be all welded to prevent leakage of the liquid metals through the heat exchanger. Another factor in design is that the tube wall thermal resistance becomes a significant proportion of the over-all resistance, because of the low film resistances of the liquid metals. This means that high conductivity tube material should be used in order to obtain minimum surface. The temperature drop across these units represents a reduction in the maximum temperature of the power cycle, and for this reason they are usually designed with a minimum temperature difference between the two fluids.

The most significant requirement of steam generators using alkali metals is to prevent leakage between the fluids. As mentioned previously, this is particularly important when radioactive liquid metal is used in the steam generator. To date, all designs have utilized concentric double wall tubes to reduce the possibility of leakage through the tube wall. Two concentric tube configurations are shown in Fig. 5. Another feature common to all designs has been some method of detecting leakage across either wall by monitoring the fluid between them. Liquid metals were used in the annulus between tubes, and gases in the grooved tube configuration of Fig. 5.

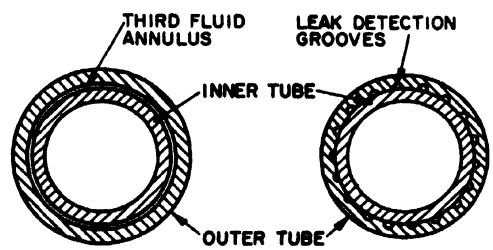

Figure 5. Concentric double wall tubes for steam generator

Each of the concentric tubes is joined to a separate tube sheet or header and the space between is filled with the monitor fluid. One type of construction is illustrated in Fig. 6, showing the outside tubes welded to a tube sheet and the inside tubes extending through to a second tube sheet.

Except for this special tube configuration, the steam generators follow conventional practice.[7] All of the units have used recirculation of water, and drums with separators to produce saturated steam which was superheated in a separate unit. Both forced and natural circulation of water has been employed. The heat transfer performance is primarily established by the water and steam conditions and the tube wall resistance. The liquid metal resistance is a minor portion of the over-all resistance (less than 35%).

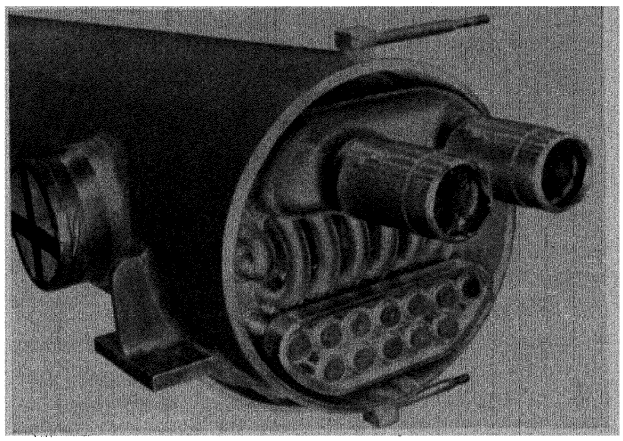

Figure 6. Construction showing concentric tubes and double tube sheets

The steam generator unit experiences approximately the same liquid metal temperature difference encountered in the reactor. This temperature difference creates a secondary effect in relation to the constant temperature of the boiling process. The temperature difference between the hot inlet liquid metal and the boiling water is of the same order as the liquid metal temperature drop in the unit. This creates thermal stress conditions at the liquid metal inlet end of the steam generator. Failure of one test unit at this location was thought to be due to thermal cycling resulting from unstable water and steam flow conditions.

The reaction mechanism of these alkali metals with water has been experimentally observed for a variety of conditions.[14,15] The principal concern is the rapid release of hydrogen which builds up in pressure. With steam this is not a problem since the reaction results in a decrease of gaseous products. The significant conclusion to be drawn from these investigations is that although the reaction with water is vigorous, it is not explosive and can be vented by conventional relief devices. The rate of reaction with water tends to be limited by the reaction contact area and also by the formation of reaction products which tend to separate the reactants. Small leaks, such as might occur through a weld crack, have been experienced in some experimental water-cooled applications. The leaks were detected by the slow steady build-up of the inert gas pressure over the liquid metal due to the release of hydrogen. In view of this experience, consideration can be given to the use of a single tube wall and single tube sheet in a steam generator using non-radioactive alkali metal.

PUMPS, VALVES, AND INSTRUMENTATION

It has been pointed out that one of the primary requirements of a heat transfer system using the alkali metals is to prevent their leakage from a system, and leakage of air and other impurities into the system. This creates a particular problem in pumps, valves, instrumentation and other mechanisms which transmit forces into or out of the liquid metal. Quite extensive investigations have been undertaken on a number of basic methods providing leak proof transmission. One of the most promising methods utilizes the relatively high electrical conductivity of the liquid metals both for pumping and instrumentation.

Electromagnetic Pumps

Pumping of these liquid metals can be accomplished by the direct application of electromagnetic forces on the liquid metal while it is carrying an electric current. This phenomenon is basically similar to a current-carrying conductor in a magnetic field. The possible configuration for electromagnetic pumping are as numerous as there are types of electric motors.[16] Many types have been investigated for various applications.[17,18] For power plant use two basic types are evolving: the direct current conduction type and the alternating current induction type.

The direct current conduction, or Faraday, pump is the simplest in concept and configuration.[19,20] It is illustrated in Fig. 7. The pumping section is a flattened rectangular duct located between the poles of an electromagnet. Direct current is passed through the liquid metal in the duct by impressing a voltage across the edges of the duct. Pumping force is produced by the interaction of magnetic fields produced by the electromagnet and the current passing through the liquid metal. This type of pump requires a high current, low voltage power supply. A 5 to 10 gpm pump of 25 psi head, requires of the order of 1000 amperes and larger capacities correspondingly larger current in the thousands of amperes at a few volts. Rectifiers or low voltage generators are used to

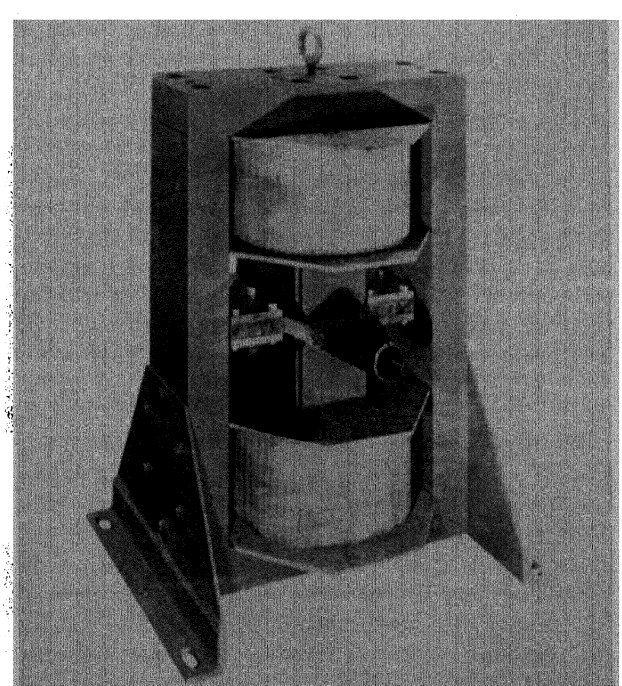

Figure 7. Direct-current electromagnetic pump

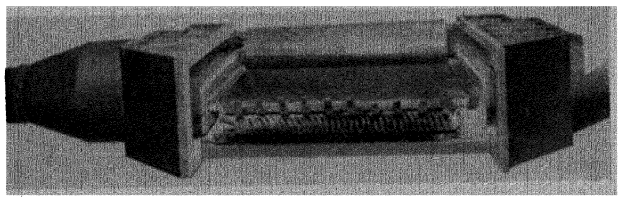

Figure 8. Alternating-current electromagnetic pump with upper half removed showing fluid duct

supply power.[21] The special power supply and large power leads are the main disadvantage of this pump. Pump efficiency with sodium is 15% to 20% in smaller sizes and 40% to 50% in larger sizes. The efficiency is reduced further by the efficiency of the power supply and input lead losses.

The advantages of this pump are its simplicity of construction and operation, and the freedom from electrical insulation problems. The windings of the electromagnet can be removed from the immediate proximity of the pumped fluid which is radioactive and hot.

The alternating current induction pump is very similar in electrical performance to the standard induction motor. Basically, a moving magnetic field, produced by a three phase field winding, induces currents in the sodium. The magnetic field due to these currents interacts with the moving field to produce a force on the liquid metal. Early models of this type of pump actually used field windings from an induction motor. Current models utilize flat field windings on both sides of a wide rectangular duct. A sodium pump of this type is illustrated in Fig. 8. The pump shown has a rating of 3300 gpm at 75 psi. It operates on 440 v 60 cycle power. The efficiency of this pump with sodium, calculated on the basis of fluid power output to electrical input, is of the order of 45% at a power factor of 42%. Its efficiency pumping NaK would be lower due to the higher electrical resistivity of NaK.

The advantages of this type of pump are mechanical simplicity and use of a standard power supply. The primary disadvantage is the location of the field windings in the immediate vicinity of the high temperature, radioactive coolant. Cooling of the windings is a problem, particularly at coolant temperatures above 400°C. Highest grades of electrical insulating materials are required to withstand the temperature and radiation in this application.

Mechanical Pumps

Mechanical pumps offer the advantage of higher efficiency and at present tend to be less costly than electromagnetic pumps. Mechanical pumps are particularly suitable for sodium-potassium alloy which has a higher electrical resistivity and consequently lower pumping efficiency in electromagnetic pumps. The primary design problems in mechanical pumps are the shaft seal and bearings. Several different methods, listed as follows, of sealing have been developed:

1. A diaphragm in the air gap of the driving motor, sealing the rotor, pumps, and bearings in the pumped fluid.
2. Gas seals in a sump-type pump with a long shaft operating in a shallow tank.
3. Frozen sodium as a shaft seal.

The diaphragm-sealed pump provides a positive welded seal and is therefore particularly suitable for pumping radioactive liquids. The welded seal makes accessibility to interior parts difficult, and the diaphragm and liquid in the motor "air gap" reduce the efficiency of this type of mechanical pump to the order of 50 to 55%. The bearings and motor assembly are insulated from the hot fluid pumped and are cooled by external means. Cooling of a pump for sodium is somewhat difficult to control because of the relatively narrow range of temperature between the sodium melting point (98°C) and the maximum allowable insulation temperature (200°C).

The gas-sealed pumps employ a configuration in which the pump shaft operates through a gas blanket over the surface of the liquid metal. A pump of this type, used in the Experimental Breeder Reactor, is illustrated in Fig. 9. This pump uses a long stiff shaft with only a guide bearing in the liquid metal at the pump casing. The driver assembly is mounted at the top of the tank and is completely enclosed. It operates in the inert gas atmosphere. A labyrinth seal is provided at the shaft to reduce transport of liquid metal vapors into the upper compartment. The upper housing is cooled by forced circulation of air.

This pump has operated satisfactorily for more than 5000 hours with only minor servicing required. It has the advantage of using conventional parts and yields efficiencies comparable to conventional pumps. It appears to be suitable for extrapolation to larger capacity. It has the disadvantage of requiring some provision to limit the range of liquid level within the length of the overhung shaft. This can be accomplished with a shallow tank in which level changes slowly with respect to volume changes.

The frozen seal pump is unique to sodium, or other higher melting point liquids. The simplest frozen seal has been devised by modifying conventional pumps to provide an annulus of sodium in the pump stuffing box. The stuffing box is cooled to keep the sodium solid. The sodium seals completely when the pump is stopped by adhering to both shaft and housing. Starting torque is of the same order experienced with ordinary tight packing and running torque is somewhat lower.

Seals of this type have been operated experimentally with varying results. Gradual extrusion of the solidified metal and shaft scoring have been encountered in some tests. The basic idea appears to be sound but the actual performance of individual applications has varied. More development work and operating experience is required to prove the utility of this type of seal. Use of the seal results in a

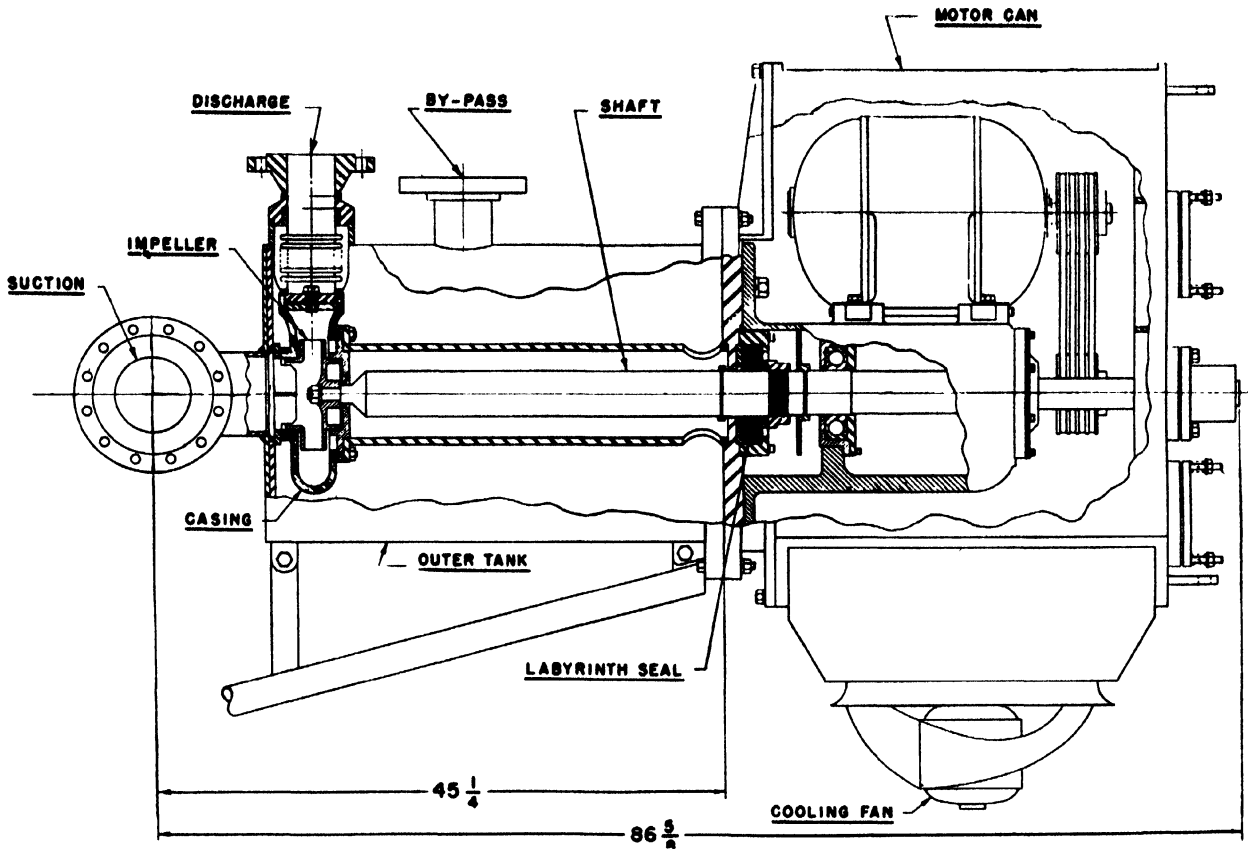

Figure 9. Gas sealed mechanical pump used in the experimental breeder reactor

relatively low cost, high efficiency pump of conventional arrangement. A pump of this type proposed for the Sodium Graphite Reactor, has performed satisfactorily on test.

Valves

As in pumps, the main problem in valves for liquid metal service is the shaft seal. No satisfactory packing materials have been developed for high temperature, hence packless, bellows-sealed valves are being used. The bellows are seal welded to both valve stem and housing. Because of the somewhat unpredictable life of bellows under these service conditions, two bellows are used in some applications. In general, globe type valves are used because of their lower stem travel which reduces the size of the bellows.

The frozen seal principle has been applied successfully to experimental valves. One of the disadvantages of this seal is that it requires a cooling system not required by the bellows-sealed valve.

Electrical and Magnetic Flow and Level Instruments

Successful flowmeters and liquid level detectors of the electromagnetic type have been developed. In the flowmeter, the voltage developed by the liquid metal flowing through the field of a permanent magnet is an accurate indication of the flow.[22,23] The voltage thus developed can be measured on commercial instruments. The permanent magnet is mounted directly on the pipe and requires no special flow section. This flowmeter is accurate over a wide range of flows and in smaller sizes is rather insensitive to approach conditions. In pipe sizes of the order of 8-inches diameter, uniform approach conditions must be insisted upon for good accuracy.

Electrical level detectors, based upon the short circuiting effect of the low resistivity liquid metal, are being used. The detector is simple, dependable in operation, and acceptably accurate for power plant use. It is inaccurate until wetted by the liquid metal, but once wetted, it does not appear to change calibration, except as affected by oxide films in a system of high oxide content.

Pressure Measurement

Many types of pressure-measuring instruments have been developed for use with these liquid metals at operating temperature. It is outside the scope of this paper to discuss the merits of all in detail. The simplest type uses a Bourdon type gage to measure inert gas pressure above a surge pot tapped into the main pipe line. This type of gage is reasonably satisfactory with the lower melting sodium-potassium alloy but has encountered freezing and plugging difficulties with sodium.

Several satisfactory pressure transmitters are available.[24] These units use either bellows or flexible diaphragms to seal the liquid metal. Pneumatic and electric transmission systems are used.

Table III. Comparison of Physical Properties

	Heat capacity cal/gm-°C, 600°C	Thermal conductivity cal/sec-cm-°C, 500°C	Thermal neutron absorption cross section at 2200 m/sec in barns
Sodium	0.2998	0.1596	0.45
Sodium-potassium			
56% Na	0.248	0.0675	1.1
Potassium	0.1825	0.0898	2.5

Temperature Measurement

Satisfactory thermocouples and resistance thermometers are available for liquid metal service. The main problems are sealing against liquid metal leakage and accuracy and reproducibility of readings at high temperature.

Special thermocouples have been developed for direct use in the liquid metal in the reactor. Chromel and alumel wires insulated with magnesium oxide are sheathed in thin stainless steel tubing of $\frac{1}{16}$ and $\frac{1}{8}$-inch diameter. Continuous lengths up to 24 feet have been made and greater lengths can be fabricated. These units can withstand both high temperature and reactor radiation.

COMPARISON OF SODIUM AND SODIUM-POTASSIUM ALLOY

Although sodium and sodium-potassium alloy are similar in many respects, they have some distinctly different characteristics. Except for the higher melting point, the physical properties of sodium are more advantageous for reactor cooling than sodium-potassium alloy. It can be seen from Table III that sodium has a higher specific heat, higher thermal and electrical conductivity, and a lower thermal neutron absorption cross section. These all favor the design of the reactor and heat transfer system. The higher melting point of sodium creates problems of preheating but has utility in providing frozen seals. Uniform preheating of sodium equipment, particularly large and complex structures with small flow passages, is not simple. Also, precaution must be taken to keep all auxiliary lines heated as they may plug due to freezing or accumulation of oxides from the main system by diffusion.

Sodium-potassium is easier to use than sodium within a piping system, primarily because of its lower melting point which eliminates the tendency of sodium to freezing and plugging. Sodium is easier to handle in air because it is less reactive and, being solid at room temperature, forms a protective coating of oxide. There have been reports of explosions in handling of highly oxidized potassium. These are attributed to the formation of potassium superoxide even at low temperatures and subsequent reaction with potassium.[5] There is no evidence of a similar reaction with sodium.

CONCLUSION

The feasibility of using sodium and sodium-potassium for reactor cooling and steam generation has been established through successful operation of liquid metal-cooled reactors and experimental heat transfer systems and equipment.

The development of successful components has been led by government sponsored laboratories, with considerable support from private industrial concerns. The active participation of industrial firms in many phases of the development work has established a commercial source for virtually all components for an alkali metal reactor cooling system. The development of this effective cooperation is one of the important advances in the technology of liquid metals. The wider application of this technology depends to a great extent upon the continued effort of these groups in reducing cost and improving performance of equipment for liquid metal-cooled reactor systems.

REFERENCES

1. Coffin, L. F., Jr., *Study of the Effects of Cyclic Thermal Stresses on a Ductile Material,* Transactions of the ASME, Vol. *76*:931 (1954).
2. Tidball, R. A., *Thermal Shocking Austenitic Stainless Steels With Molten Metals,* Transactions of the ASME, Vol. *76*:639 (1954).
3. Fritz, R. J., *Evaluation of Transient Temperatures and Stresses,* Transaction of the ASME, Vol. *76*:913 (1954).
4. Stahl, C. R., *Liquid Metal Cooled Reactors,* Mechanical Engineering, Vol. *76,* No. 12:978–80 (December 1954).
5. Lyon, R. N., *et al., Liquid-Metals Handbook,* U.S. Government Printing Office, Washington 25, D. C., 2nd Edition (June 1952).
6. Trocki, T. and Nelson, D. B., *Liquid Metal Heat Transfer System,* ASME 52 – A 140.
7. Brooks, R. D. and Rosenblatt, A. L., *Nuclear Power Plants—Design and Performance of Liquid-Metal Heat Exchangers and Steam Generators,* Mechanical Engineering, 363–68 (May 1953).
8. Clark, P. M., *Mechanical Pumps for High-Temperature Liquid Metal,* Mechanical Engineering, Vol. *75* (1953).
9. Pepkowitz, L. P. and Judd, W. C., *Determination of Sodium Monoxide in Sodium,* Analytical Chemistry *22*: 1283 (1950).
10. Bruggeman, W. H. and Billuris, G., *Sampling of High Temperature Alkali Metals,* Industrial Laboratories (January 1953).
11. Baus, R. A., Bogard, A. D., Grand, J. A. and Lockhart, L. B., Jr., *Transfer of Radioactive Components of Stainless Steel in Sodium,* Proceedings 1955 Conference on Nuclear Engineering (*27* April 1955).
12. Pepkowitz, L. P. and Proud, E. R., *Determination of Hydrogen in Sodium, Analytical Chemistry 21*:1000 (1949).
13. Pepkowitz, L. P., Knolls Atomic Power Laboratory, *Determination of Carbon in Sodium,* Private Communication.
14. King, E. C. and Wedge, C. A., Jr., *Reaction Between Sodium-Potassium and Water,* Tech. Report III, Mine Safety Appliances Company, Pittsburgh, Pennsylvania, (1 February 1950).
15. King, E. C., *Reaction Between Sodium-Potassium and Water,* Tech. Report XII, Mine Safety Appliances Company, Pittsburgh, Pennsylvania, (30 January 1952).
16. Brill, E. F., *Development of Special Pumps for Liquid Metals,* Mechanical Engineering *75,* No. 5:369 (1953).

17. Cage, J. F., *Electromagnetic Pumps for High Temperature Liquid Metals,* Mechanical Engineering *75,* No. 6: 467 (1953).

18. Cage, J. F., *Electromagnetic Pumps for High Temperature Liquid Metals,* Machine Design *25,* No. 3: 178 (1953).

19. Barnes, A. H., *Direct Current Electromagnetic Pump,* Nucleonics Vol. *11,* No. 1:16 (1953).

20. Barnes, A. H., Smith, F. A. and Witham, G. K., *Direct Current Electromagnetic Pumps,* Report ANL–4322 Argonne National Laboratory (1949).

21. Barnes, A. H., Smith, F. A. and Witham, G. K., *Large Current Homopolar Generator,* Report ANL–4361 Argonne National Laboratory (1949).

22. Gray, W. C. and Astley, E. R., *Liquid Metal Magnetic Flowmeters,* Instrument Society of American Journal (June 1954).

23. Elrod, M. G., Jr. and Fouse, R. R., *An Investigation of Electromagnetic Flowmeters,* Transactions of ASME, Vol. *74,* No. 4 (May 1952).

24. Bialous, A. J., *Pressure Transmitter for Liquid Metal Systems,* Instrument Society of America Paper No. 54–50–2.

Liquid Metal Handling

By S. G. Bauer,* UK

The stimulus of nuclear reactor development has produced many technological advances of general interest. The use of liquid or molten metals as a means of conveying heat is one of them. When the idea first came up it seemed a simple enough thing to do and the potential advantages in a large variety of industrial processes ranging from reaction kettles to reheat for steam turbines were so obvious that it was difficult to resist the temptation to tackle them all and nuclear reactors too.

Since these early days a lot of time and effort has been expended on the subject and it has become somewhat easier to see the field in perspective.

The advantages inherent in the use of liquid metals for the transport of heat are fairly obvious, the difficulties very much less so.

The greatest attraction of liquid metals is due to their high boiling points combined in favourable instances with low melting points; this enables liquid heat transfer processes to be carried out over very wide temperature ranges. Table I gives a comparison of a number of liquids.

Not all the substances mentioned are either readily available or suitable as heat transfer fluids.

Water, not mentioned in the table, is an exceptionally good heat transfer medium with relatively few limitations. These limitations are, however, of such specific importance in nuclear energy applications that they have provided the stimulus for the development of alternative coolants.

The first difficulty with water is the critical temperature of 374°C which sets a rather low limit to the upper temperature of any heat engine cycle if the heat is to be supplied by circulating water. Moreover, high temperature water requires inconveniently high pressures for its containment.

A more specific difficulty is due to the nuclear properties of hydrogen. The absorption cross section for thermal neutrons is fairly high (see Table II on the following page).

In addition water is the most effective substance for slowing down neutrons and this leads to difficulties in some designs of thermal reactors and excludes it altogether for fast reactors. Organic liquids have the same disadvantages to a greater or lesser degree in addition to limited stability under high temperatures and irradiation.

The situation might fairly be summarized by saying that in the case of the fast reactor we are forced to liquid metal coolants, while in the case of thermal power reactors there are great potential advantages to be set off against the difficulties of introducing a new technology.

The first difficulty to be met in the use of liquid metals is their chemical reactivity. The alkali metals are of course particularly reactive and will, at elevated temperatures, burn spontaneously in air. The heavy metals are less reactive in this obvious way but seriously toxic. The fire or toxicity hazard which arises with these high temperature fluids is incidental. Their reactivity makes it in any case essential that they should be most carefully confined. All the metallic oxides are very corrosive and some of the alkali metals form in contact with air nitrides, hydrides and hydroxides as well, all of which lead to serious corrosion troubles as well as the danger of plugging critical points of a flow circuit.

In all liquid metal applications it is therefore of prime importance that the whole plant should attain a very high standard of leak tightness and that any gas atmospheres present over free surfaces in the plant should be completely inert.

Table I

Substance	*Melting point °C*	*Boiling point °C*
Di-2-Napththylamine	171	471
Tetra Aryl silicate (TAS 160)	<—20	427
Triphenylamine	125	365
2-4'-Biphenyldiamine	45	363
4 Bromodiphenyl	90	310
2 Naphthyl-phenyl-methane	35.5	350
Diphenyl-diphenyloxide	182 ‡	400 ‡
Caustic soda	318.4	1390
Arsenic tri-iodide	146	403
Sulphuric acid	10.5	330
Heat transfer salt ($NaNO_2+NaNO_3+KNO_3$)	200 ‡	550 ‡
Sulphur	120	444.6
Mercury	−38.87	357
Gallium	29.92	1983
Rubidium	39.0	688
Potassium	63.7	760
Sodium	97.8	883
Lithium	179	1317
Sodium-potassium	−12	785
Lead-bismuth	125	1670

‡ Usable range.

* Rolls-Royce Ltd., Derby, England.

Table II

Substance	Thermal neutron cross section cm^2/cm^3
Water	0.0208
Sodium	0.012
Aluminium	0.013
Lead	0.0059
Mercury	15.3

Freedom from leakage is an onerous demand and can be met only with a good deal of specialised experience, particularly when the alkali metals are used, which at high temperatures are certainly the most searching crack-detectors. On the whole it is useful to model one's procedure of assembling and testing a liquid metal plant on customary high vacuum techniques. That is to say one proceeds by assembling components first and assembling them into the plant after they have been proved leak tight. It is well to remember that two separate requirements have to be met: one is to establish leak rates, if any, and the other to find the leaks.

With a vacuum test outfit the leak finding can be done either with helium mass-spectrometer or with a palladium tube ionisation gauge using hydrogen or with other more or less convenient methods which may be available. An alternative method which has been found in practice to save much time and frustration is to use a slight excess pressure in the system and use an external detector. On small components it will be found that surprisingly small leaks can be detected by pressurising the article with air and surrounding it with a glass vessel filled with methyl alcohol. It is here essential that pressure be applied before immersion, for maximum sensitivity. The reduced viscosity and surface tension makes the alcohol method very much more sensitive than a waterbath or the traditional soapsuds. On larger equipment two other detectors of high sensitivity are available. The infra-red gas analyzer using nitrous oxide as tracer and the ionisation type halogen detector using chloroform, freon or any other volatile halogen compound. Of the two, the infra-red gas analyzer is perhaps the more senitive.

In practice the joint or component to be tested, presumed to be free of gross leaks, is first wrapped in balloon fabric and then filled with the tracer-gas at a slight excess pressure. After 5 or 10 minutes the suction connection of the leak tester is inserted under the fabric so that it collects and samples all the leakage which may have taken place during the test period. In this way an exceedingly sensitive leak test can be performed without any special skill and the procedure can obviously be used to locate the actual point of leakage by successive stages.

It is most important to ensure that no potential leaks are blocked or covered during manufacture or assembly by slag, paint, oil or the like which would be attacked subsequently by the liquid metal. For this reason it is inadvisable to use, for instance, coated electrode arc-welding where a small slag inclusion might give a perfect seal under test but provide a leakage path by reaction with the liquid metal. Experience would indicate that it is best to separate functions and make seal welds by the inert arc technique and take structural loads separately. This can be done either by using edge-welding as the seal and bolts to take the structural loads or by making a butt-weld with an inert arc sealing run on the inside followed by a metallic arc structural weld over it. With care excellent results can be obtained either way provided scrupulous cleanliness is observed. It should also be remembered that all joints must be tested before they become enclosed or inaccessible in further stages of assembly. The drawing of a 1 in. sodium valve (Fig. 1) shows an assembly by edge-welding throughout, including the diaphragm stack bellows, which has proved satisfactory in high temperature service. In this instance both the weld on the gas backing line and the welds on the bellows stack are tested before final assembly. The pipe stub at the bottom shows the customary preparation for a butt-weld made as described above.

Once a leak tight plant has been assembled a supply of inert gas is required. With sodium or potassium, helium, argon or nitrogen may be used

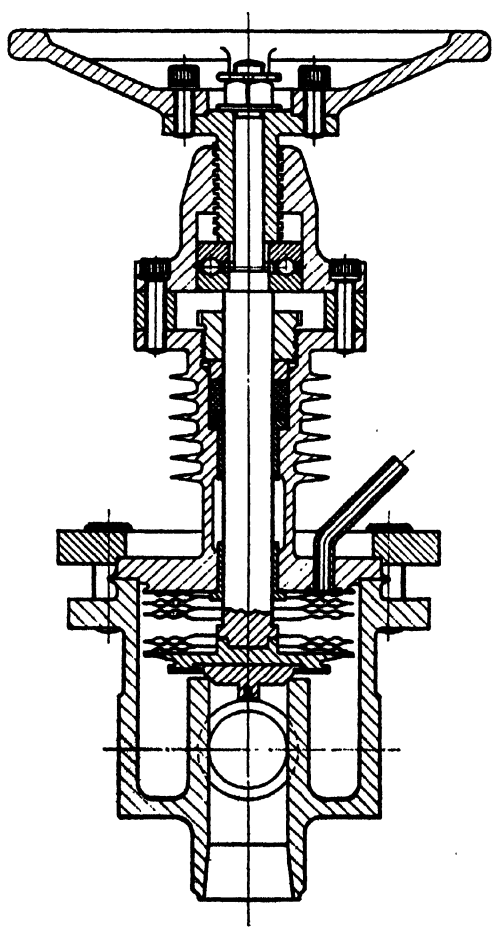

Figure 1. Frazer-Nash sodium valve

as inert atmosphere and preference must be decided on grounds of cost and convenience. With lithium a rare gas is essential while with lead a reducing atmosphere, e.g., hydrogen may be useful.

In any case a very high standard of gas purity is essential, particularly where gas pressure is used to displace liquid from one vessel to another so that large gas quantities come in contact with the liquid.

The type of gas purification train used is again largely a matter of personal preference and many types have been used successfully. In the author's experience an argon purification train consisting of a calcium packed tube at 600°C followed by a Na-K bubbler has proved satisfactory and trouble free in service. It is very difficult to determine the allowable contamination of blanket gas since the concentrations of oxygen or water involved are not measurable by any straightforward method. In practice it is relatively easy to observe an exposed area of liquid metal surface in contact with the gas and get an exceedingly sensitive indication of any objectionable impurities which may be present. If such a test is satisfactory in that no clouding of the surface appears within a minute or so, no trouble will be experienced.

However clean the assembled plant and the available gas may be, further steps are necessary to get a clean liquid circulating at high temperatures. For the original filling it is strongly advisable to evacuate the plant and remove adsorbed gas and moisture by warming if possible. The plant should then be filled with purified inert gas and carefully evacuated a second time. After that the vacuum may be used to suck in the liquid metal from a storage tank. It is usual to bring in the liquid metal through a filter of the sintered stainless steel type to keep back any suspended oxide which may be present in the tank. When the circuit is filled and brought up to temperature, remaining traces of contamination in the plant will be picked up slowly by the liquid metal, resulting as a rule in a higher oxide concentration than is advisable. If the plant is small and satisfactorily vacuum tight a final purification can be achieved by heating the liquid metal to the highest tolerable temperature in the circuit and dumping it hot back to the storage tank, letting it cool there and bringing it back again several times. With the marked increase of oxygen solubility with rising temperature, this procedure gives a satisfactory clean-up.

In a larger plant this method is not convenient and one should therefore provide a cold trap, that is a bypass line in which a small amount of the liquid metal is taken out of the circuit, cooled near to its freezing point, filtered or settled in a packed tank and then returned. If such a cold trap is the point of lowest temperature in the circuit all oxide in excess of the solubility at cold-trap temperature will eventually be deposited there.

The pumping of liquid metals can be done in a variety of ways, which have been described in the literature. The possibility of making electromagnetic pumps without moving parts is one of special interest, particularly for nuclear reactors where the presence of intense radioactivity makes pump maintenance all but impossible. The principle of all electromagnetic pumps is quite simply the interaction of force, current and magnetic field at right angles to each other. An almost unlimited number of ways of designing such pumps can be put forward and most of the more promising solutions have been investigated to a greater or lesser extent.

It has become customary to distinguish between conductive and inductive pumps, that is, pumps in which the "armature" current is supplied externally or induced internally. Both dc and ac conductive pumps have been built and operated successfully with sodium but the latter are most useful in small sizes. Conductive pumps, the dc variety in particular are apt to collect gas in solution or suspension in the liquid metal on the conductor pole pieces and this can lead to severe reduction or complete interruption of performance. This effect, if unsuspected, can lead to much trouble which is very difficult to track down. A momentary switching off of the current releases the gas so collected, but the only cure for the trouble is careful degassing of the circuit and prevention of gas entrainment at free surfaces. Inductive pumps do not show this obscure phenomenon.

Induction type electromagnetic pumps have now practically ousted all other pumps for large flow rates, at any rate of sodium. The theory and design is well understood, the manufacture is akin to normal electric machinery and their reliability is proved by many thousands of hours of operation.

The best efficiencies attained in operation are in the order of 35% for sodium and appreciably lower for sodium-potassium alloy.

Operating temperatures are limited to 300°C to 350°C depending on whether or not air cooling is applied to the windings. This applies to pole pieces wound by conventional techniques. Higher temperatures of operation are undoubtedly possible but they await the development of new and unorthodox winding and insulating methods.

It is a notable feature of liquid metal plant that all the elementary components as well as the specialized devices have to be designed and developed from scratch; no standard equipment has proved adequate. The valve shown in Fig. 1 is one example, showing how a satisfactory design for liquid metals differs from say a water or steam valve.

As illustration of the kind of design experience which has been built up it may be worth-while to quote some details of the experimental sodium-steam super heater test plant built by Messrs Foster-Wheeler at Egham. Figure 2 shows a flow diagram of the plant omitting instrumentation, safety devices and similar auxiliaries. 6400 lb/hr of steam are circulated at 1000 psi and dropped from 1025°F

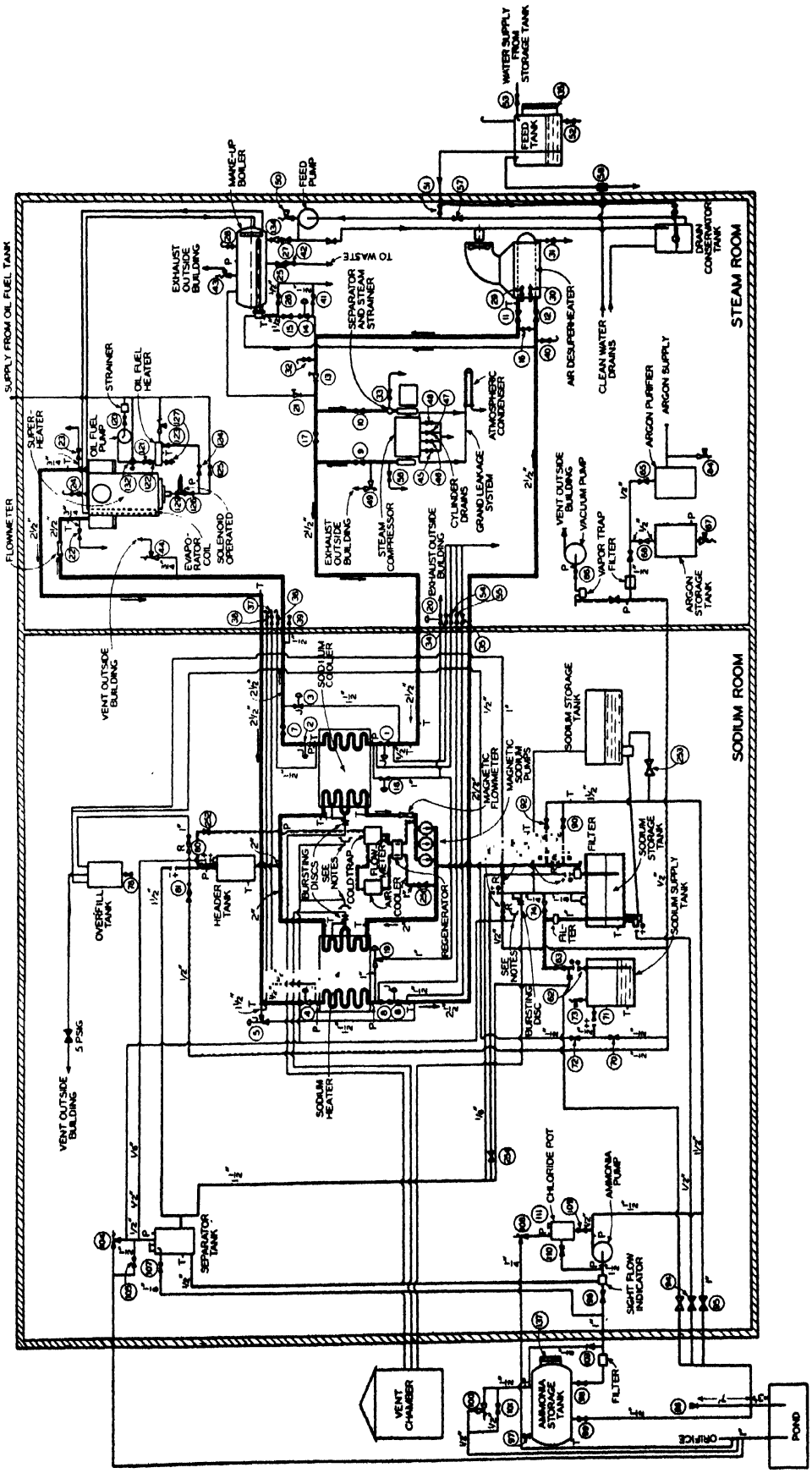

Figure 2. Foster-Wheeler sodium-steam plant

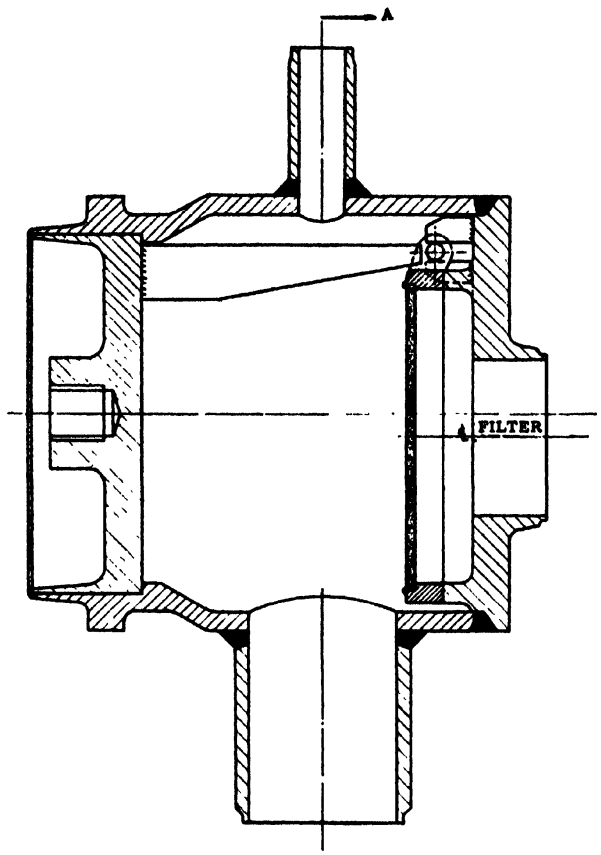

Figure 3. Flap filter for sodium

(552°C) to 735°F (390°C) in giving up heat to sodium in one heat exchanger and reheated by the circulating sodium in a second heat exchanger from 600°F (316°C) to 820°F (438°). The steam then goes on through an oil fired superheater where it is brought back to the original top temperature. The upper and lower temperatures in the sodium circuit are 900°F (482°C) and 680°F (360°C) respectively. The sodium is circulated by three small ac conduction type pumps in parallel at a rate of 15,600 lb/hr. These pumps were chosen because they happened to be available at the time as the only pumps suitable to operate at 360°C continuously.

At the time of writing, about 1500 hr of operation of the plant have been accumulated. Much useful information has been gathered and the original design has been well justified. The basic purpose of the plant was to prove whether simple, single tube heat exchangers could be operated safely with steam on one side and sodium on the other under severe practical conditions. Both heat exchangers are identical and each consists of a pair of exchangers in series. These in turn contain each bundles of 24⅜ in. tubes, 16 SWG, in U-formation, about 13 ft long and welded to their respective tube plates. The steam is on the shell-side and all parts of the plant touched by sodium are of austenitic stainless steel and welded throughout.

Several instructive mishaps have occurred. Owing to corrosion from the water-side, one tube has failed inside the tube plate, but not at the weld. Steam entered the sodium circuit and the resulting pressure broke the bursting disks and most of the sodium in the circuit was discharged through it. There was no fire nor any damage to adjacent tubes or other parts of the plant. The clearing out of the sodium hydroxide incrustation of the plant caused a lot of trouble.

One pump channel developed a fatigue crack, possibly due to incipient cavitation caused by too low a static pressure in the sodium circuit. The fault was detected by observing a slight smoke trail from the affected pump. No fire occurred, the leak being a very small one. It proved possible to go through normal shut-down procedure and wash out the sodium circuit before removing and replacing the pump. About one pound of sodium had leaked out.

A fair amount of oxide plugging was experienced in the early part of the operation. At the time there was no cold trap in circuit, the sodium being cleaned on admission through the filter shown in Fig. 3. Cold trapping cured the complaint.

The preheating of this plant is done by wrapping all pipes with Pyrotenax heater wire, placed underneath slagwool insulation. It was found necessary to cover the circuit with a very complete set of thermocouples to indicate conditions during warming up before sodium filling. Much time was wasted without them.

The whole plant is so laid out that it will drain completely and that is undoubtedly an important feature, much inconvenience being caused during cleaning even by auxiliary gas lines where the same principle had not been observed.

Many different cleaning procedures have been tried or proposed and the choice is not an easy one. Cleaning with water jets in the open air is dangerous, even with relatively open pieces of plant. Hydrogen-air explosions always occur and much damage is caused to more delicate items, even with the greatest care.

Evacuation and admission of low pressure steam with continuous evacuation of the hydrogen formed is quite a safe method and readily controllable. The disadvantages are corrosion troubles from the caustic soda formed and the likelihood of plugging smaller passages and trapping metallic sodium behind solid caustic soda. But in suitable cases and with care the method can be satisfactory.

Cleaning with alcohol is not advisable because soapy addition compounds form and block the passages and are very difficult to dislodge. Small pieces contaminated with sodium or sodium-potassium are readily and safely cleaned in a deep vessel of acetone with added dry ice. The carbon dioxide slows the reaction and keeps the liquid cool while at the same time providing a gas blanket which effectively prevents the ignition of rising hydrogen bubbles.

The sodium-steam plant described is equipped with an ammonia cleaning plant, permanently installed.

Dry liquid ammonia is the only practicable substance which will take sodium into true solution. Hence it is possible to remove residues of sodium from a plant by washing with liquid ammonia without leaving behind any residues. Thus a plant which has been operated with sodium and washed out with ammonia can be opened to the atmosphere for inspection or alteration without danger of contamination by atmospheric oxygen or moisture or hazard to the operator. Moreover, there are no deposits or corrosion during cleaning to obscure whatever changes may have taken place on surfaces during operation. In the absence of oxide in the circuit ammonia cleaning is straightforward. If there are small amounts of oxide deposits they can be cleaned out, after the removal of the metal, by a wash with a solution of ammonium chloride in ammonia, followed by a further ammonia wash. With much oxide, especially with parts of the plant plugged, the process is difficult, but it seems likely that with a good system of monitoring concentrations in the washing streams even such difficult cases could be handled satisfactorily.

Fire hazards loom rather large when a programme of liquid metal work is first embarked upon, but they diminish rapidly with experience. None the less it is essential that adequate precautions be taken. The first thing is to minimise the hazards which could arise from a sodium leak. As a rule sodium will ignite spontaneously at temperatures above 400°C (750°F) but it can ignite at much lower temperatures. Water in any form must be kept away because of the great violence of the resulting hydrogen-air explosions.

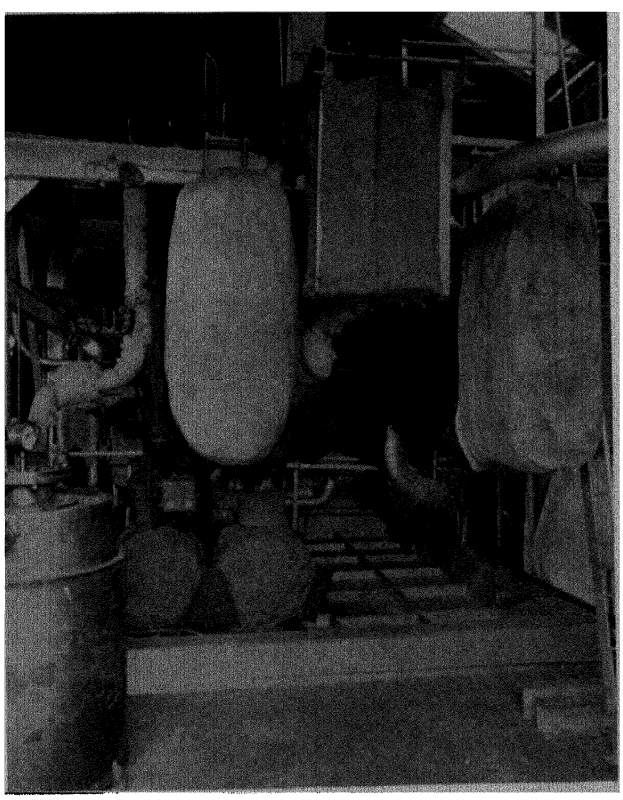

Figure 4. View of Foster-Wheeler plant showing safety trays

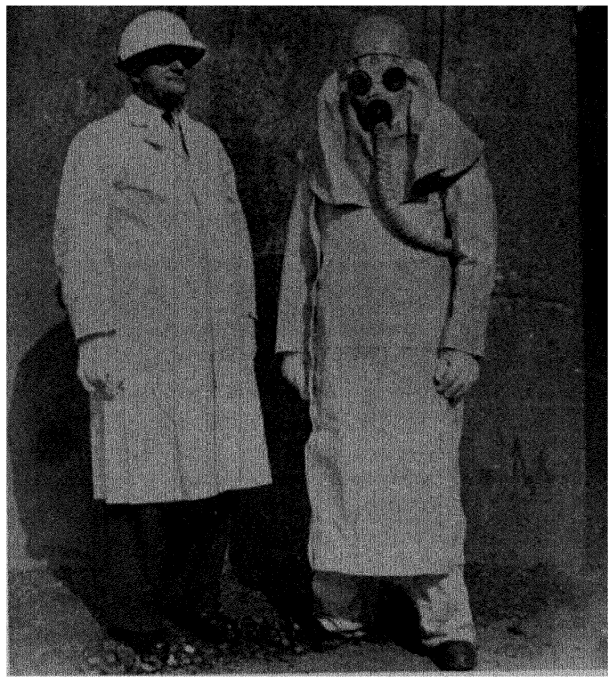

Figure 5. Protective clothing used in sodium plant

Concrete, moist sand and wood are dangerous. It is advisable to cover the floor below a sodium plant with an assembly of steel trays not more than two-feet square (see Fig. 4) to catch leaks and allow fires to be put out easily, should one occur. Insulating materials must be tested for their reaction to hot sodium, because most of them react violently. Slag wool of certain types is satisfactory.

Fire extinguishing powders are available and so are suitable applicators and even large fires can be put out in a few seconds by experienced operators, provided they occur in a place which can be covered by the powder. In a fire, thick caustic smoke is produced in great volumes and this makes fire fighting most difficult in confined places. It is advisable to have very powerful emergency ventilation to maintain some visibility, to provide easy access and to install handrails or other guides as well as low level safety lighting. It is surprisingly easy to get lost in a familiar room in thick smoke.

Two types of protective clothing are shown in Fig. 5. One is the normal working outfit of: fireproofed cotton laboratory coat, safety glasses and plastic helmet, eyes and hair being the most vulnerable points for small splashes; while the other is full protective clothing for emergency. It consists of fireproof plastic helmet with additional aluminium top, safety lenses with fine wire gauze screens in front and respirator, cape to protect neck and shoulders, a press-studded coat which can be discarded instantly, polyvinyl-chloride gumboots and moleskin gloves. The cape and coat are made of a fine chrome tanned leather with seams covered by glued joints. Any stitched joints are attacked rapidly. Seams are so arranged that no small pools or droplets can be held by them. This outfit will protect the wearer

against a shower or jet of red hot sodium. Identification marks are important, since it is impossible to tell people apart in such costume.

Fires are rare in practice and therefore it is important to have a thorough and regular fire drill practice for all concerned so that they may acquire the necessary skill and confidence to cope with any emergency which may arise.

ACKNOWLEDGEMENT

The author wishes to acknowledge his indebtedness to the Atomic Energy Research Establishment, Harwell, where most of his experience in the subject was gained, and thanks the Establishment for making available drawings, etc., of work which has been done under extra-mural contract.

Pumping of Liquid Metals

By A. H. Barnes,* USA

The increasing interest in liquid metals as reactor coolants has made necessary the development of pumps which are capable of circulating these liquids at elevated temperatures for prolonged periods. The principal design considerations arise because the liquid being pumped is not only chemically active, but, in addition, may be extremely radioactive. It is therefore necessary that the pump be free of all leakage and that it require essentially no maintenance.

In attempting to design pumps capable of satisfying these requirements, work has progressed along two lines. Mechanical pumps were redesigned and special features added in an effort to satisfy the stringent new requirements. Secondly, advantage was taken of the high electrical conductivity of liquid metals to develop pumps in which electrical forces were employed to effect pumping action.

MECHANICAL PUMPS

Centrifugal type mechanical pumps are used extensively in liquid metal systems. The significant differences in design involve the method used for containing the liquid in the pump housing. The simplest arrangement consists of mounting the impeller at the lower end of a long, vertical, overhung shaft with the shaft bearings located above the liquid level. Liquid level in the pump housing is controlled by maintaining a fixed liquid level in an overflow tank connected to the inlet side of the pump. A labyrinth is provided to restrict the diffusion of liquid metal vapor into the enclosure containing the bearings and driving motor. Figure 1 illustrates a pump of this type which has been in operation at the Experimental Breeder Reactor (EBR-I). The pumping capacity is 500 gallons per minute.

Pumps of this type are attractive because of ease of fabrication and reliable operation at moderate temperatures. Operation at high temperatures introduces problems occasioned by the loss of bearing lubricant and by the diffusion of sodium vapor into the bearing and motor enclosure. The necessity for associated equipment (liquid level control tanks, etc.) to prevent accidental flooding of the drive motor and bearing enclosure must also be considered.

The need for liquid level control may be eliminated by locating the drive motor and shaft bearings external to the pump housing and using a frozen sodium type seal at the shaft entrance to the housing. This arrangement is currently undergoing extensive study at several laboratories. The effectiveness of the seal depends upon the ability to control the temperature of a narrow annulus of sodium, surrounding the driving shaft, within rather narrow limits. This may be accomplished by flowing a coolant at a controlled temperature through channels in the shaft enclosure. Pumps of this type with capacities up to 1200 gallons/minute are at present undergoing tests.

Completely sealed mechanical pumps have been constructed by enclosing the pump impeller and driving rotor of an induction motor in a common housing. A thin annular shell is used to seal the motor armature from the field winding (Fig. 2). Enclosed rotor pumps offer the advantage of a completely sealed system, but they involve the serious problem of operating bearings in liquid metal. Although extensive effort has been applied to the solution of the bearing problem, additional development will be required before pumps of this type can be considered reliable for long time operation.

ELECTROMAGNETIC PUMPS

The high electrical conductivity of liquid metals makes them suitable for pumping by electromagnetic means. The electromagnetic pump is very attractive for circulating radioactive liquid metals because it obviates the necessity for moving parts, bearings, and seals.

The dc conduction electromagnetic pump is the most direct approach to the problem. The elements of this type of pump are illustrated in Fig. 3. A thin-walled, liquid-carrying duct, with copper conductors attached to opposite sides, is located in the magnetic field between the poles of an electromagnet. Current entering through the duct wall, traverses the liquid which fills the duct and develops in it a longitudinal thrust. The pumping rate can be shown to depend upon the current, magnetic field intensity and dimensions of the duct in accordance with the following relation:

$$Q = \frac{4(10^6)S}{B}\left[IR_b - \frac{1.75(10^6)PS}{B}(R_b + R_e)\right] \quad (1)$$

where Q = flow (gallons/minute); P = developed head (psi); B = magnetic field intensity in liquid (gauss); I = current entering pump duct (amperes); S = width of duct in magnetic field direction (inches); R_e = resistance of effective current

* Argonne National Laboratory.

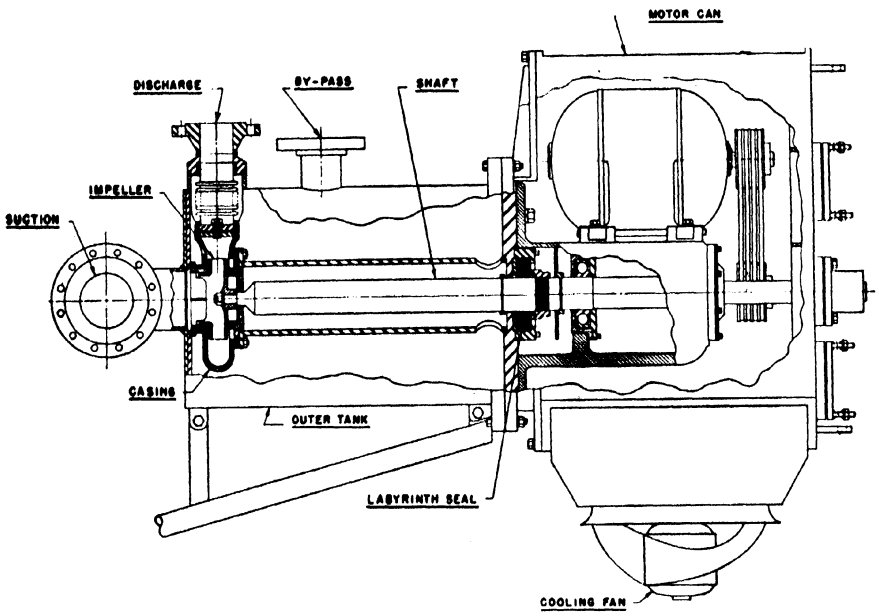

Figure 1. Mechanical liquid-metal pump. Type used to pump sodium-potassium alloy at experimental breeder reactor (EBR-1)

path through the liquid in the region between magnet poles (ohms); R_b = combined effective resistance along all bypass current paths in the duct wall and in the liquid beyond the magnet at the entrance and exit sections of the duct (ohms).

The magnitude of R_e may be calculated from the dimensions and resistivities of the liquid and duct. R_b is a complicated function of the duct geometry, fringing field distribution and liquid velocity profile. At present its magnitude is determined experimentally.

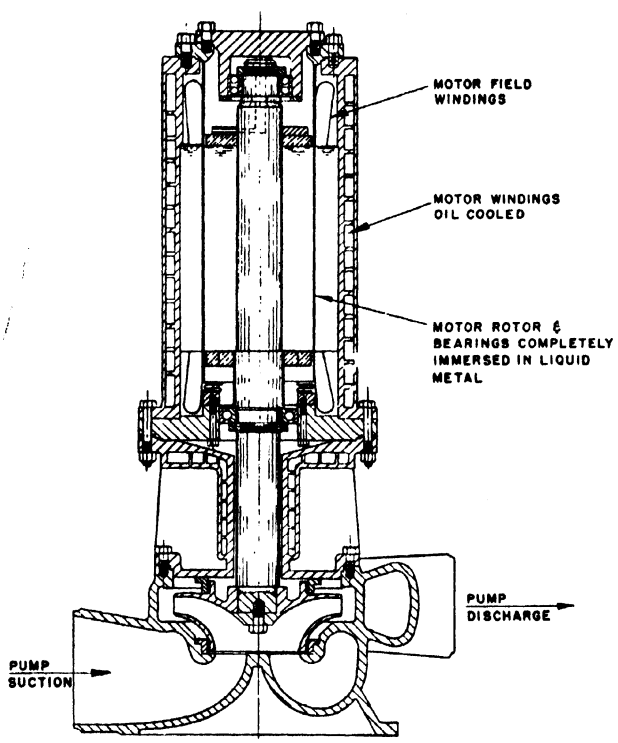

Figure 2. Enclosed-rotor pump for liquid metal use

The expression for the static (zero flow) pressure developed by the pump may be obtained from the above relation:

$$P = \frac{5.7(10^{-7})BI}{S}\left(\frac{R_b}{R_b + R_e}\right) \qquad (2)$$

The magnetic field due to the flow of current across the pump duct distorts the main field of the magnet and reduces the pump capacity and efficiency. This effect may be minimized either by properly tapering the magnet gap or by compensating for the field due to the current in the liquid by returning the current across the main field through a conductor which is adjacent to the duct in the region in which pumping occurs (Fig. 3).

The pump duct may be fabricated from sheet or formed by pressing thin-walled seamless tubing into the desired cross section. Wall thicknesses of 0.025 to 0.065 inch are normally used. Since high elec-

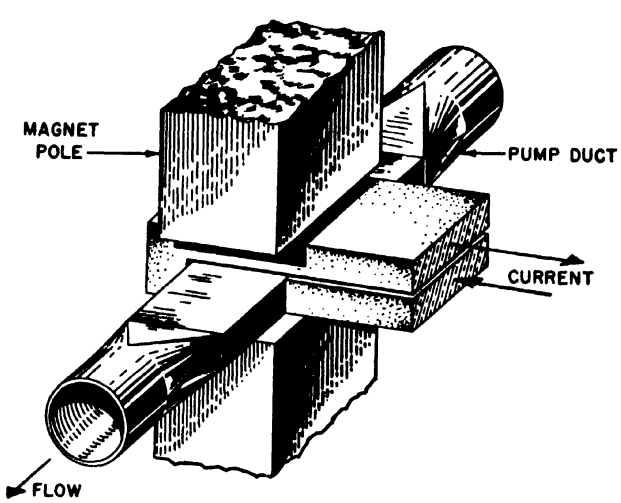

Figure 3. Direct-current electromagnetic pump

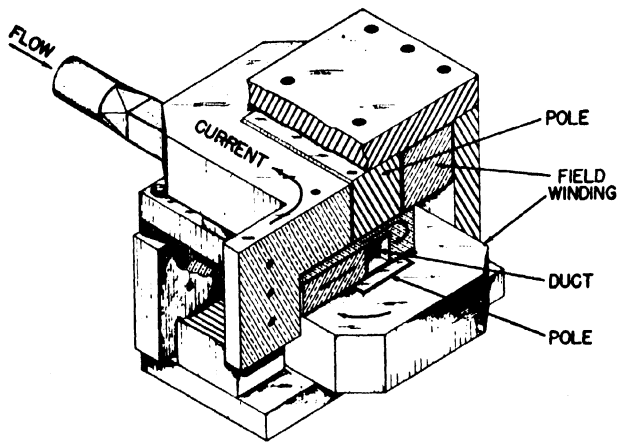

Figure 4. Direct-current pump with series field winding

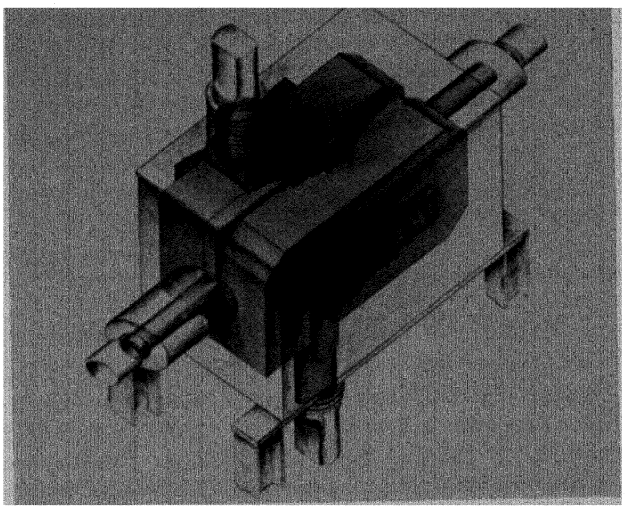

Figure 5. Electromagnetic pump used in primary coolant circuit of EBR-1

trical resistivity, as well as compatibility with sodium and sodium-potassium alloy, is necessary, the materials used are stainless steel (type 304L or 347) or 80 nickel–20 chromium alloy. The current leads are usually brazed to the duct.

The type of field winding employed is dictated by the operating requirements of the pump. For high temperature operation a series field winding consisting of one or two turns of large cross section copper is readily insulated since the voltage drop is small. Pumps with this type of field winding (Fig. 4) require no auxiliary cooling system.

The current requirements of direct current pumps range from the order of 1000 amperes for small pumps (5–10 gallons/minute) to many thousand amperes for high capacity pumps. The voltage drop across the pumps is in the vicinity of one volt. The large direct currents required may be supplied by either rectifiers or generators. Since the voltage required is low, rectifier efficiency is in the range of 20 to 40 per cent. Higher efficiency can be obtained by using a homopolar generator which uses sodium-potassium alloy as a liquid metal brush. Generators of this type have been constructed which are capable of supplying currents in the range of 20,000 to 100,000 amperes at efficiencies in excess of 80 per cent. Machines with greater capacity are at present under construction.

Pumps with capacities of several hundred gallons per minute are in use and much larger units are contemplated. The electromagnetic pump in the primary circuit of the Experimental Breeder Reactor (EBR-I) has a capacity of 500 gallons/minute against a head of 25 psi. Figure 5 shows the pump located in a stainless steel enclosure containing a helium atmosphere. This arrangement provides containment for the liquid in case of duct failure and also protects the copper against oxidation. The current-carrying copper bars are brought into the enclosure through stainless steel bellows which, by introducing a relatively high resistance path, serve as insulators as well as flexible seals. Figure 6 illustrates the operating characteristics. The efficiency of this pump (exclusive of rectifier current supply) at 300 gallons/minute against a 40 psi head is 43 per cent.

The advantages of dc electromagnetic pumps depend upon their inherent simplicity of construction and absence of insulation difficulties. Reliable operation at high temperatures for long periods has been achieved. The efficiencies obtainable vary from 15 to 20 per cent for small pumps to 40 per cent for large systems in which homopolar generators are used.

ALTERNATING CURRENT CONDUCTION PUMPS

The ac conduction pump operates on the same principle as the dc type except that the magnetic field reverses in synchronism with the current in the liquid. The field and duct currents must be properly phased in order to achieve maximum pumping efficiency. This may be accomplished most readily by connecting the field winding in series with the current path through the liquid. A step down transformer is provided to supply a large current to the

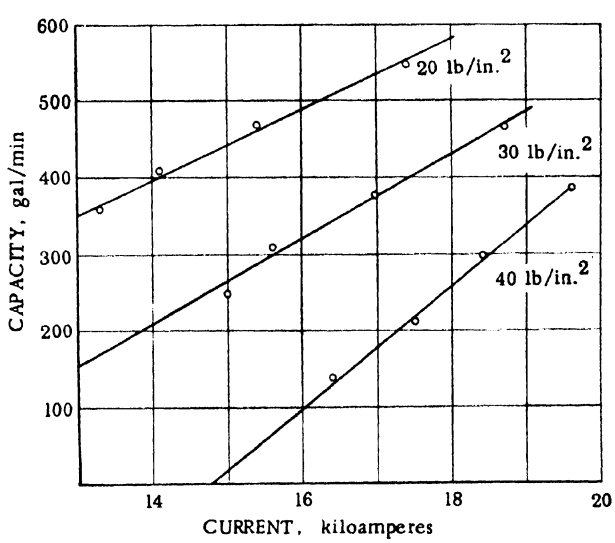

Figure 6. Operating characteristics of EBR-1 electromagnetic pump

pump duct. The magnetic circuit of the transformer may have one leg in common with the field structure of the pump (Fig. 7). The complex current and field interactions characteristic of the ac type pump have served to deter any rigorous performance analysis. While no large ac conduction pumps have been constructed, small models have been used widely since they may be operated directly from a single-phase power line. The pumping efficiencies range from 5 to 20 per cent.

ALTERNATING CURRENT INDUCTION PUMPS

Large currents may be developed directly in the flowing liquid by electromagnetic induction. The induced currents in the liquid react on the applied field so that a driving force is developed. There are numerous arrangements possible. The linear induction pump consists of a liquid duct in the form of a flattened tube which extends between two core sections containing a polyphase winding (Fig. 8). The core structure is similar to that of an induction motor stator except that it is flat so that a sliding, rather than a rotating magnetic field is produced.

Detailed analysis is similar to that followed for induction motor design except that the problem is complicated by the fact that current paths are not sharply defined. Since the magnetic gap must be relatively large, field losses are high and the power factor is low. The head developed is approximately proportional to the relative speed of the liquid and field. The core ends introduce harmonic components in the sliding field which increase losses. The use of conducting bars along the sides of the duct (equivalent to end rings on a squirrel cage rotor) have been found to provide only a slight increase in efficiency.

Mechanical vibration of the thin-walled liquid duct is a common difficulty in alternating current pumps. The vibration frequency is twice the electrical frequency and, in serious cases when resonances exist, may develop metal fatigue failure.

Pumps of this type have been constructed with capacities ranging from 100 to 3500 gallons/minute against heads up to 100 psi. Efficiencies of the large pumps have approached 40 per cent. The induction pump is extremely attractive because the large currents are developed directly in the liquid so that contact problems are avoided and auxiliary power supply equipment is obviated. Serious problems arise only when high temperature operation is required; forced cooling of the field winding and the use of associated heat removal apparatus complicates the situation.

Among the many other versions of induction pumps one which has received considerable attention is the type proposed by Einstein and Szilard. In this pump the liquid flows in an annular duct between inner and outer core sections. The outer cylindrical core contains a system of toroidal coils connected so as to produce a polyphase travelling field similar to that of the flat-type induction pump. In this case, however, the induced current paths are annular so that the edge losses of the flat type pump are avoided.

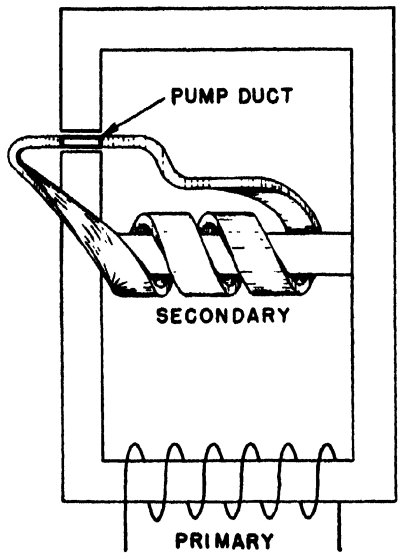

Figure 7. Typical arrangement for alternating-current conduction pumps

Although this type of pump is attractive because of its symmetry, fabrication difficulties have retarded its development and little operating experience has been acquired to date.

Another arrangement of the induction pump consists of a helical duct which is located inside a conventional type induction motor stator. A fixed, laminated core fills the interior of the helix. Several small pumps of this type have been constructed, but fabrication difficulties, together with low efficiency, have discouraged further development.

A closely related version of the helical pump is the flat rotating field type in which the liquid is driven in a spiral path by either a polyphase wound stator or by a mechanically driven rotating magnet structure (either permanent or dc electromagnets may be used). Again, fabrication problems and low efficiency have limited the use of pumps of this type.

Of the many forms of electromagnetic pump only the linear dc conduction and the linear ac induction types have as yet been used in permanent installations. The dc pump, because it operates at low voltage, avoids insulation difficulties attendant to high temperature and radiation effects. The need for a separate direct current source is a serious consideration. The alternating current pump, on the other hand, while at present limited to handling liquid

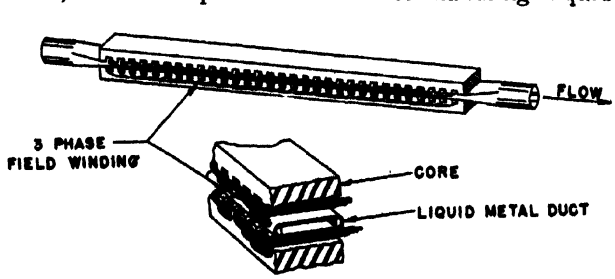

Figure 8. Alternating-current linear flow induction pump

metals at moderate temperatures, is capable of efficient operation directly from three phase power lines.

DESIGN OF LARGE DC PUMPS

The operation of large, liquid metal-cooled reactors requires the pumping of sodium or sodium-potassium alloy at rates of several thousand gallons per minute. The radioactivity of the liquid makes it mandatory that the pumps be capable of operation at elevated temperatures for prolonged periods.

In connection with the design of the Experimental Breeder Reactor II (EBR-II), a study has been made of the feasibility of using a dc conduction pump of 10,000 gallon/minute capacity. This pump would be used to circulate the primary sodium coolant through the reactor and intermediate heat exchanger. As presently envisaged, the pump would operate completely submerged in molten sodium and be supplied with current from a homopolar generator which would be located directly above it in the primary shield.

A general view of the pump is given in Fig. 9. The pump duct has a rectangular cross section of 6 inches in the magnetic field direction and 18 inches in the direction of current flow. The duct is located between magnet poles which are 42 inches long. The current is fed into the duct over a length of 24 inches. The electrical conductor system consists of stainless steel enclosures which are welded to opposite sides of the pump duct. The enclosures are packed tightly with copper bars and electrical contact with the duct wall is made by a thin layer of liquid sodium. Circulation of the liquid sodium due to stray electromotive forces is minimized by providing a tight fit on the high-pressure side of the enclosure. In this manner it is possible to fabricate an electrical connection of very low resistance which is capable of operation at high temperature. Magnetic field compensation is accomplished by returning the current, which has traversed the liquid, back across the main field through parallel paths on both sides of the duct.

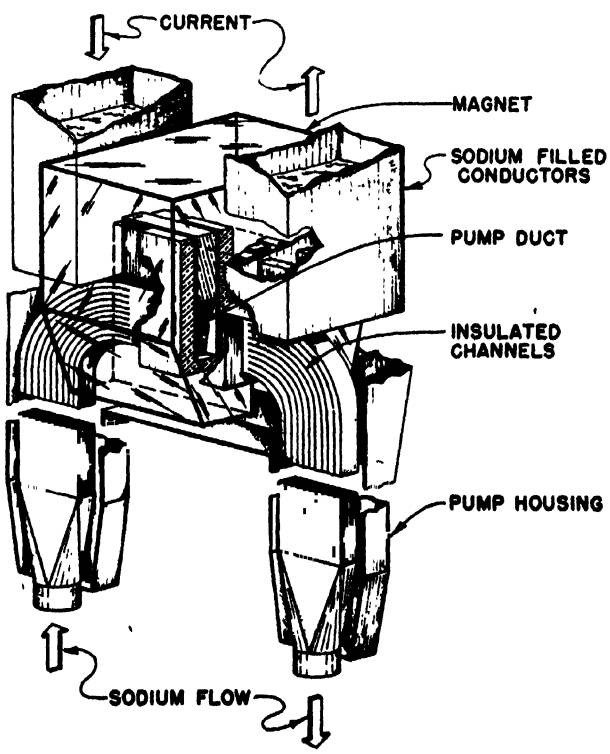

Figure 9. Proposed primary coolant pump for the experimental breeder reactor-II

Since the current traversing the duct is very large (~250,000 amperes), a single-turn field winding is sufficient to produce a magnetic field of the required intensity. The current is brought in on one side of the core structure, passed through the pump duct, and then brought out on the opposite side of the core. The pump duct in the region between the poles is fabricated from 80 nickel–20 chromium alloy sheet (0.065 inch thick). The flat sections are pressed tightly with mica insulation against the return current conductors, which, in turn, are pressed into the magnet gap. The magnet thus serves as a pressure vessel for the pump duct. In order to reduce the fringing of current in the liquid beyond the magnet poles at the entrance and exit sections, the duct has been divided into a number of separated parallel channels. Ten channels, each of 1½ inches by 6 inches cross section, extend for a distance of 6 feet on each side of the magnet. The channels are spaced externally with $\frac{1}{32}$-inch thick mica composition sheet. A reinforcing jacket encloses the channels on the exit side of the pump.

The pump duct and magnet assembly are completely enclosed in a welded stainless steel housing which will be argon pressurized. Leakage into the housing can be detected by means of probes.

The pump requires currents in the range of 200,000 to 250,000 amperes at approximately 2.5 volts. With applied currents in this range, the anticipated pumping capacity is 10,000 gallons/minute against a head of 50 to 75 psi.

The current is supplied by a homopolar generator (Fig. 10) which, in turn, is driven by a vertical-type induction motor (1250 hp, 1800 rpm). A liquid metal brush (sodium-potassium alloy) is used to establish electrical contact with the solid iron rotor (armature). The excellent wetting properties of the alloy establish a low resistance path so that large currents at low voltage can be obtained. The alloy is circulated continuously; therefore it also serves as a coolant for removing heat from the machine.

The generator is designed for a current output of 300,000 amperes at 2.5 volts. The current will be supplied to the pump through enclosures filled with sodium. A sodium conductor represents a considerable saving in fabrication, weight, and cost over a copper system of equivalent resistance.

HIGH TEMPERATURE PUMPING

It is occasionally desired to pump moderate quantities of liquid metals at relatively high temperature for prolonged periods. For this purpose a dc con-

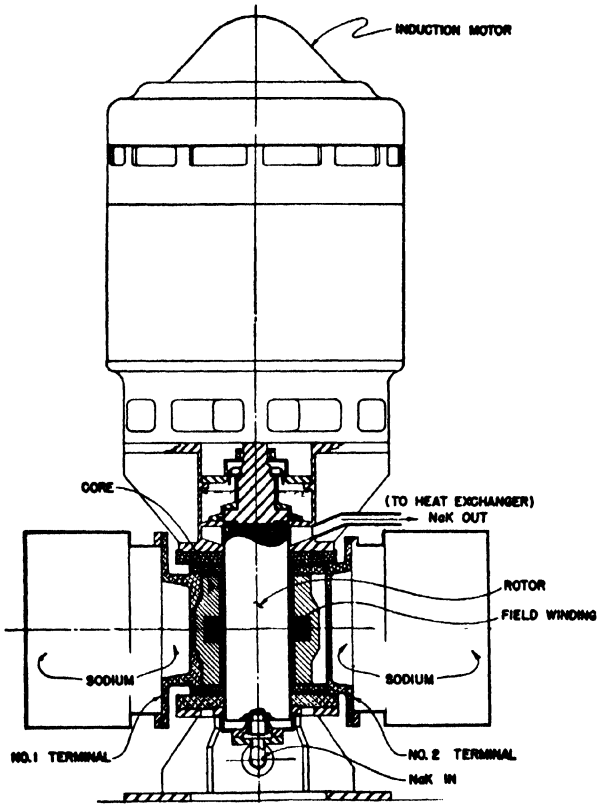

Figure 10. Homopolar generator for supplying current to dc electromagnetic pump

duction type pump (Fig. 11) of 50 gallons/minute capacity has been constructed and used for pumping sodium at 800°C.

The pump duct with a rectangular cross section, ¼ inch by 3 inches, was fabricated from 0.030-inch thick (80 nickel-20 chromium) sheet. Current is fed to the duct over a length of 5 inches and the magnetic field is applied over a length of 8 inches. Magnetic field compensation is provided by reversing the current path between the magnet poles. The copper current conductors are located inside stainless steel shells which are welded to the pump duct. The electrical bond between copper and duct wall is provided by a thin layer of sodium which is sealed in the shell. The field winding consists of two

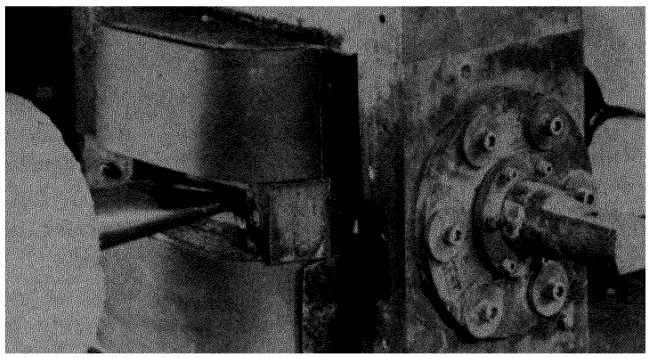

Figure 11. Fifty gallon/minute capacity dc electromagnetic pump for operation at 800°C. (Pump enclosure removed)

10-turn copper coils connected in parallel with each other and in series with the current path through the pump duct. Mica insulation is used between turns and at other points of contact. The pump is located in a helium filled enclosure to prevent oxidation and cooling is by natural convection and radiation only.

Normal operating current is 3000 amperes at approximately 2.0 volts for a flow of 50 gallons/minute. The pump forms part of a loop of 2-inch diameter, type 347 stainless steel schedule 40 pipe with an expansion bellows placed at each end of the pump duct. The flow is monitored with an electromagnetic flowmeter which is calibrated periodically against an orifice-type meter. Pressure gauges are mounted on tube extensions. The loop is brought to temperature by passing current through a system of heating coils mounted on ceramic cylinders enclosing the pipe surface. A 4-inch layer of thermal insulation covers the entire surface of the loop.

ACKNOWLEDGEMENTS

The work described in this paper represents the efforts of many individuals in several laboratories. A major share of the development of liquid metal pumps has been contributed by the following: Argonne National Laboratory, Allis-Chalmers Mfg. Co., Babcock and Wilcox Co., Knolls Atomic Power Laboratory, Oak Ridge National Laboratory, and Mine Safety Appliances Co.

Production of High-Purity Metallic Bismuth

By N. P. Sajin and P. Y. Dulkina, USSR

Power reactors working with liquid metal coolants require high-purity bismuth.

The bismuth obtained at metallurgical plants contains impurities amounting up to 1×10^{-4} to 1×10^{-2}% each.

In order to make it usable in atomic energy production it was found necessary to work out special methods of eliminating impurities such as silver.

In the present paper two methods are investigated: the hydrometallurgical method and the crystallophysical method.

HYDROMETALLURGICAL REFINING

Hydrometallurgical refining consists in dissolving the metal in acid, purification of the solution and hydrolysis of bismuth salts.

Our investigation of the possibility of utilizing hydrometallurgical methods for purifying bismuth is devoted to the problem of purifying bismuth nitrate solutions from silver.

Silver, being the more noble metal, should be isolated from the solutions during its cementation by metallic bismuth.

Despite the fact that the process of cementation is widely enough used in metallurgy, there exists no elaborated theory of this process. In practice, nearly all questions connected with cementation have to be examined experimentally.

The reference material dealing with the cementation of metals from the solutions of their salts shows that the cementation rate and the completeness of precipitation depend on a large number of factors, as, for example, on the acidity of the solution, the temperature, initial content of the principal metal, etc.[1]

There were no reference data on the conditions of silver cementation from solutions, and therefore this problem is studied in detail in the present investigation.

A study was made of the dependence of the degree of precipitation of silver from solutions of bismuth nitrate upon the following factors: (1) solution acidity, (2) coarseness of the cementing metal, (3) the concentration of Ag in the solution, and (4) the concentration of bismuth in the solution.

Optimum conditions of cementation were established as a result of the study of the influence of various factors upon the degree of precipitation of silver from solutions of bismuth nitrate by metallic bismuth. It was found that cementation should be conducted at room temperature. The acidity of the solution within the limits of from 5% to 25% does not influence precipitation degree of silver. The silver may be completely precipitated when the coarseness of the cementing metal is from −80 to +120 mesh.

In optimum conditions of precipitation, the silver may be almost entirely isolated from metallic bismuth in the case of any initial content of silver within the limits of 0.2 to 5 gm/l. The content of bismuth in the solution should not exceed 150–200 gm/l, otherwise precipitation of the basic salt is possible and the cementation process ceases.

Two series of experiments on purifying bismuth nitrate solutions of silver were conducted in two ways in optimum conditions of cementation: (1) by mixing the solution with the cementing metal, and (2) by filtering the solution through a column (Fig. 1).

The column was filled with metallic bismuth, crushed to a coarseness of −80 mesh mixed with broken glass. The height of the layer of metal in the column was 140 mm, the diameter 32 mm.

Filtration was accomplished at a rate of 1.5 liter per hour. The solution being filtered contained 1×10^{-4} gm/l of Ag. Control of the degree of purification was carried out by the radioactive tracer method. The results of the experiments are given in Tables I and II.

The metal analysis data obtained from purified solutions given in Tables I and II have been confirmed both by chemical analysis as well as by spectral analysis.

The results of investigations on purification of bismuth nitrate solutions from silver by the cementation method showed, that this method reduces the content of Ag in the metal up to 10^{-6}%.

On the basis of the investigation carried out a hydrometallurgical refining scheme consisting of the following operations has been suggested: (1) the dissolving of metal in nitric acid; (2) precipitation of the chief mass of silver by hydrochloric acid; (3) elimination of the residues of silver and other noble metals by the cementation of the nitric solution by metallic bismuth; (4) hydrolysis of the purified solution; and (5) drying, calcination, and reduction of the basic salt.

Original language: Russian.

Table I. The Cementation of Silver from Solutions of Bismuth Nitrate

No.	Quantity of solution to be purified in millilitres	Content of Ag in the solution being purified		Active silver introduced		General content of Ag in solution in gm	Quantity of metal taken for cementation in gm
		gm/l	gm	counts/minute	gm		
1	50	1.20	0.06	4,164,000	0.0009	0.0609	0.15
2	50	0.60	0.03	4,436,000	0.0009	0.0309	0.15
3	50	0.38	0.019	2,328,000	0.0009	0.0199	0.13
4	50	0.39	0.020	2,764,000	0.0009	0.0209	1.00
5	50	0.39	0.020	2,820,000	0.0009	0.0209	3.00
6	50	0.04	0.002	4,016,000	0.0009	0.0029	3.00

Activity of the precipitated cement silver in counts/minute	Activity of solution after cementation in counts/minute	Quantity of bismuth in the basic salt in gm	Content of Ag in the metal in %
4,252,000	840	6.25	2.1×10^{-4}
Not measured	785	6.25	8×10^{-5}
2,300,000	2408	13.94	1.4×10^{-4}
Not measured	412	13.94	2.1×10^{-4}
Not measured	108	13.94	5.5×10^{-6}
3,900,000	235	5.00	3.6×10^{-6}

Utilization of this scheme produces metal of the following quality (%): silver content, 3×10^{-6}; lead content, 3×10^{-3}; antimony content, 1×10^{-4}; content of iron, less than 1×10^{-3}; copper content, 1×10^{-3}; selenium + tellurium + arsenic content, 1×10^{-3}; manganese content, 5×10^{-3}; cobalt content, 5×10^{-3}; and zinc content, 1×10^{-3}.

REFINING OF BISMUTH BY CRYSTALLOPHYSICAL METHODS

Methods of obtaining pure metals by crystallization from a melt are based on the different solubility of impurities in the solid and liquid phases during the crystallisation process. In dependence on the behaviour of the impurity, the latter may concentrate in one of the phases, which results in the elimination of this impurity from the second phase.



Figure 1. Burette for filtering bismuth-nitric solutions: (1) solution, (2) metal mixed with glass, (3) glass wool

Investigations on the use of repeated crystallization of metals, in order to purify them of impurities, are extremely numerous. There are also a number of works dealing with the crystallization of bismuth from the melt; these works describe briefly, the behaviour, during the process, of certain impurities.[2-7]

In this investigation, a study has been made of the behaviour of a number of impurities during the crystallization of bismuth by pulling the metal out of the melt (the Czochralski method) and the zone-melting method. A study of the purification degree and the distribution of the impurities along the length of the samples obtained in crystallization was made.

Control of the purification degree was accomplished by the radioactive tracer method using Zn^{65}, Sb^{124}, Cu^{64}, Ag^{110}, Fe^{59}, and Sn^{113}–Sn^{123} mixture.

THE CRYSTALLIZATION OF BISMUTH BY THE CZOCHRALSKI METHOD

Experiments in pulling out bismuth crystals were carried out in a furnace (Fig. 2). The metal was melted in a graphite crucible. The pulling out was effected at a temperature of 278–280.° A study was made of the degree to which bismuth was purified of silver, zinc, antimony, iron, tin and copper.

Table II. The Filtration of Bismuth Nitrate Solutions Through a Column

Quantity of solution passed through the column (liters)	Content of silver in the metal obtained from the solutions, %	
	Column No. 1	Column No. 2
1	3.3×10^{-6}	2.9×10^{-6}
2	4.1×10^{-6}	3.8×10^{-6}
3	8×10^{-6}	7.4×10^{-6}
4	7×10^{-6}	7×10^{-6}
5	8.1×10^{-6}	7.5×10^{-6}
6	8×10^{-6}	7.8×10^{-6}
7	8×10^{-6}	7.6×10^{-6}
8	8.2×10^{-6}	8.4×10^{-6}

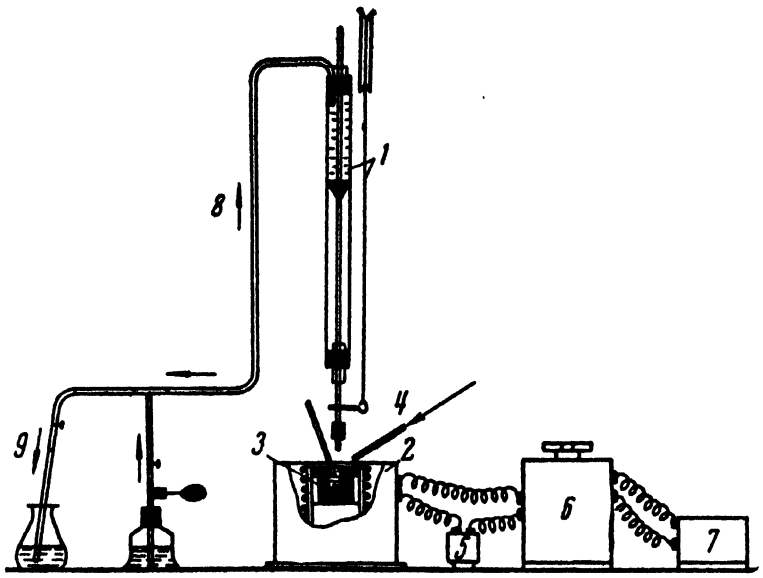

Figure 2. (1) Hoisting arrangement; (2) heating furnace; (3) graphite crucible with metal; (4) CO_2 inlet; (5) watt meter; (6) transformer; (7) potential stabilizer; (8) oil inlet; and (9) oil outlet

Results are given in Tables III, IV, V, and VI; in each experiment the metal was pulled out once.

During the experiments on bismuth purification by the pulling method, the formation of an oxide film was observed which remained in the crucible during the pulling out from the melt. In this film are concentrated, on the whole, all of the impurities.

Thus, for example, in experiment 2 on the zinc elimination the activity of the metal being purified was 4814 counts per minute, the activity of the film was 4452 counts per minute. The same was observed also in other experiments. In eliminating antimony in experiment 1, the activity of the metal was 30740 counts per minute, and the activity of the film was 22620 counts per minute.

Experiments on the elimination of tin, iron, and copper showed the same results. The remaining impurities are arranged along the length of the pulled crystal in such a way that the bottom of the crystal (~25% of the weight) is mostly contaminated. The top of the crystal, which makes up ~75% of the weight eliminates in a single crystallization the investigated impurities as follows, on an average: zinc, 8–15 times; antimony, 6–10 times; tin, 10–20 times; iron, 10–30 times; and copper, 10–30 times.

ZONE-MELTING

Zone-melting was carried out in circular tubs placed on horizontal rotating plates, the rotation speed of which permits great variation. Each tub and

Table III. Pulling of a Crystal from Bismuth Containing 5×10^{-3} % Ag

No. of experiment	Metal weight in gm	Activity of metal being pulled, recalculated to 1 gm (counts per min)	Pulling speed in cm/hr	Activity of 1 gm of pulled crystal in counts/min		Purification degree of crystal*	
				Top	Bottom	Top	Bottom
1	18	8720	4.2	20	173	436	50
2	25	7636	4.1	35	157	218	48
3	26.6	7630	3.5	39	111	195	68
4	21	7600	2.5	292	424	26	17

*The purification degree shows by what value the impurity content in the crystal was reduced.

Table IV. Pulling of a Crystal from Bismuth Containing 1×10^{-4} % Ag

No.	Metal weight in gm	Activity of metal being pulled, recalculated to 1 gm (counts per min)	Pulling speed in cm/hr	Activity of 1 gm of pulled crystal in counts/min		Purification degree	
				Top	Bottom	Top	Bottom
1	28.7	375	3.8	20	45	12	8
2	40.7	190	2.5	5	25	38	8
3	25.0	350	1.7	10	23	35	15
4	29.4	334	4.2	5	37	67	9

Table V. Pulling of Crystals from Metal Containing 1×10^{-5}% Ag

No. of experiments	Metal weight in gm	Activity of metal recalculated to 1 gm (counts per min)	Pulling speed in cm/hr	Activity of lengths of pulled crystal recalculated to 1 gm (counts per min)		Purification degree	
				Top	Bottom	Top	Bottom
1	19.2	336	3.1	174	231	1.9	1.4
2	21.6	330	3.2	163	217	2.0	1.5
3	15.6	331	2.0	92	150	3.5	2.0
4	21.0	298	3.0	121	168	2.4	1.7
5	16.6	312	4.8	157	230	2.0	1.3
6	33.0	320	10.0	300	330	not purified	

Table VI. Summary Table on Purification of Bismuth from Impurities of Zinc, Antimony, Tin, Iron, and Copper by the Method of Pulling Out from the Melt

	No. of experiments	Batch of metal in gm	Activity of initial metal in counts/min		Amount of the introduced impurity in %	Activity of lengths of crystal, recalculated to 1 gm counts per minute				Activity of the whole residue, counts per min
			Of the whole batch	1 gm		I Top	II Middle	III Middle	IV Bottom	
Elimination of zinc	1	40.5	2138	53	1.6×10^{-4}	18	15	–	16	1391
	2	17.0	4814	280	4.4×10^{-4}	11	13	–	30	4452
	3	25.0	7050	282	4.5×10^{-4}	10	16	–	7	6400
	4	16.0	602	37	5×10^{-5}	2	3	–	5	499
Elimination of antimony	1	21	30740	1450	1.8×10^{-4}	187	148	82	25	22620
	2	21.5	13669	802	8×10^{-5}	190	130	67	30	12528
	3	44.0	12136	274	3.4×10^{-5}	160	40	11	8	11105
Elimination of tin	1	29.5	1654	56	4×10^{-4}	5	–	5	20	1377
	2	27.5	4533	166	1.3×10^{-3}	9	–	10	47	3888
	3	29.0	3474	125	1×10^{-3}	6	–	4	49	2804
	4	21.0	3460	161	5×10^{-4}	22	–	48	–	2058
	5	19.0	1311	70	2×10^{-4}	17	–	19	–	919
Elimination of iron	1	26.0	950	26	5×10^{-4}	2	–	2	4	751
	2	36.0	4100	114	2×10^{-3}	6	–	6	not active	3447
	3	21.0	2010	91	1.4×10^{-3}	5	–	2	3	1322
	4	19.0	471	25	5.6×10^{-4}	3	–	2	5	350
Elimination of copper	1	21.5	18656	746	3×10^{-3}	10	19	39	692	14157
	2	21.0	2199	105	4×10^{-4}	2	10	27	65	1815

Table VII. Elimination of Impurities in Bismuth by Zone Melting. The Moving of the Melting Zone was 1.1 cm/hr

	No. of experiment	Batch of initial metal in gm	Activity of initial metal in counts per min		Quantity of introduced impurity in %	Number of crystallisations	Activity of lengths of crystal, recalculated to 1 gm counts per minute				Activity of wash waters in counts per min
			Of the whole batch	1 gm			I	II	III	IV*	
Elimination of zinc	1	24.8	161919	6529	1.3×10^{-2}	6	96	343	650	18417	11240
	2	17.6	114910	6529	1×10^{-2}	2	121	221	7655	9523	24442
	3	28.3	20000	707	3×10^{-3}	6	80	146	91	272	15753
	4	27.7	2971	107	5×10^{-4}	6	14	29	33	46	2108
Elimination of antimony	1	19.2	15093	781	1×10^{-4}	3	639	382	361	169	5002
	2	17.6	13885	781	1×10^{-4}	3	745	602	398	90	2817
	3	15.3	8659	566	1×10^{-4}	6	817	311	366	172	2390
Elimination of copper	1	20.5	716	36	4×10^{-4}	2	4	Not active	Not active	137	Without washing
	2	40	1450	36	4×10^{-4}	2	10	Not active	Not active	300	Without washing
Elimination of silver	1	23.7	4768	201	1×10^{-4}	1	30	Not active	8	509	Without washing
	2	11.8	2532	214	1×10^{-4}	2	7	Not active	8	714	Without washing
	3	17.5	3198	190	1×10^{-4}	3	Not active	Not active	6	660	Without washing

* The crystal lengths are numbered according to the direction of tub moving.

plate moves and passes together through a number of electric furnaces, which ensure the proper number of molten zones. The length of a zone is 1–2 cm.

Metallic bismuth was melted in a graphite crucible and was poured into a tub for crystallization. After cooling the metal was subjected to zone-melting with a fixed speed of zone-traveling. This operation was carried out several times in order to ensure the best purification.

Formation of an oxide film on the surface of the metal was also observed during the zone-melting experiments. Therefore at the end of the melt, the metal was washed with boiling perhydrol, hydrochloric acid and two or three times with water.* The crystal was then divided into four parts and analysed.

The results of the experiments are given in Table VII.

The experiments of Table VII showed that impurities may be eliminated from bismuth also by the method of zone-melting.

The distribution of impurities along the crystal length takes place in such a way that all impurities, with the exception of antimony concentrate at one end of the crystal, whereas antimony concentrates at the other end. Thus, the middle of the crystal is the purest. The purification degree depends upon the initial content of the impurities in the metal and the number of crystallizations.

* The hydrochloric acid and water were twice distilled.

CONCLUSION

1. A study was made of a method of purifying bismuth nitrate solutions from silver by cementation.
2. The hydrometallurgical scheme of obtaining high-purity bismuth is proposed, including the method of cementation of silver on metallic bismuth.
3. The behaviour of a number of impurities during the refining of bismuth by crystallophysical methods has been studied.
4. The possibility of obtaining high-purity bismuth by the Czochralski method and the method of zone-melting has been established.

REFERENCES

1. Plaksin, I. N. and Suvorovskaya, N. A., Non-Ferrous Metals, No. *3* (Russian) (1948).
2. Chalmers, B., Can. Journal of Phys., vol. *31,* No. 1 (1953).
3. Czohralski, Z., fur phys. chem. 92.219 (1918).
4. Pfann u. Olcen, Phys. Rev., 89, No. 1 (1953).
5. Zimmerman, W., Science, 19, N3091, 411 (1954).
6. Pfann, Journal of Met., 747–53 (1952).
7. Teal, G. K. and Little, J. B., Phys. Rev. vol. *78,* No. 5 (1950).

The Use of High Temperature Sodium in Manufacture of NaK Alloy

By C. B. Jackson and R. C. Werner,* USA

Approximately fifteen years ago a need for metallic potassium arose in the United States. The commercial process which was developed for the production of potassium and sodium-potassium alloys involved the high temperature reduction of potassium chloride with sodium—one of the earliest uses of sodium at such elevated temperatures.

It is believed that the experience obtained in these fifteen years will give assurance that sodium and fused salts can be satisfactorily handled as high temperature heat transfer media in nuclear reactor technology.[1] This paper will accordingly first describe the equipment and operating procedure used in batch and continuous processes for potassium and NaK production. Information applicable to general high temperature handling of these materials will then be pointed out.

PROCESS

Sodium is commercially prepared by the electrolysis of molten sodium chloride to which calcium chloride has been added to produce a salt mix melting lower than sodium chloride alone. The analagous process could not be used for potassium production because of attack on the graphite electrodes and the danger of explosive reaction of potassium carbonyl. Rather than work on alternate material electrodes a thermochemical process was developed, using the reduction of a potassium salt by sodium.

The comprehensive investigations of Rinck[2] described the equilibria between molten salts and alkali and alkaline earth metals. Potassium chloride was selected for the thermochemical reduction on the basis of availability and price per unit of contained potassium.

BATCH PROCESS

The initial process was a batch reaction of sodium with potassium chloride to produce a NaK mixture which was fractionally distilled to produce pure potassium. Figure 1 is a schematic diagram of the reaction vessel which was 24 inches in diameter with a vertical neck of 6-inch pipe about 3 feet long. An air-cooled condenser, 8 feet long of 2-inch pipe, connected the vertical neck with a salt trap made of a 3-foot cylinder of 12-inch pipe with a flanged top. Another length of 2-inch pipe connected the trap with the NaK collector. Reaction vessel and condenser line were of AISI Type 316 stainless steel, the remainder of the system being mild steel. The vertical neck of the reaction vessel was fitted with a charging plug.

The fractional distillation equipment (Fig. 2) was fabricated of Type 316 stainless steel. A 24-inch diameter gas-fired still pot was topped with a 14-foot column of 6-inch pipe, to which was attached a 2-inch air-cooled condensing pipe. The column was packed with ¼-inch diameter stainless steel Raschig rings contained between perforated baskets. A ½-inch NaK feed pipe was inserted to the center line of the column with another ½-inch pipe welded into the still pot for sodium removal. A ½-inch pipe was welded into the still pot for liquid level determination by nitrogen introduction.

During operation the plug was removed from the neck of the gas-fired reaction vessel and 150 pounds of 1500°F molten potassium chloride charged to the empty, hot reaction vessel. Bricks of metallic sodium were dropped into the neck. After adding 23 pounds of sodium (giving a 2/1 mole ratio of KCl/Na), the plug was replaced and nitrogen introduced by a line through the plug during heating of the reactants.

As found by Rinck the equilibrium $Na + KCl \rightleftharpoons K + NaCl$ was established rapidly. The attainment of equilibrium was aided by the mutual solubility of

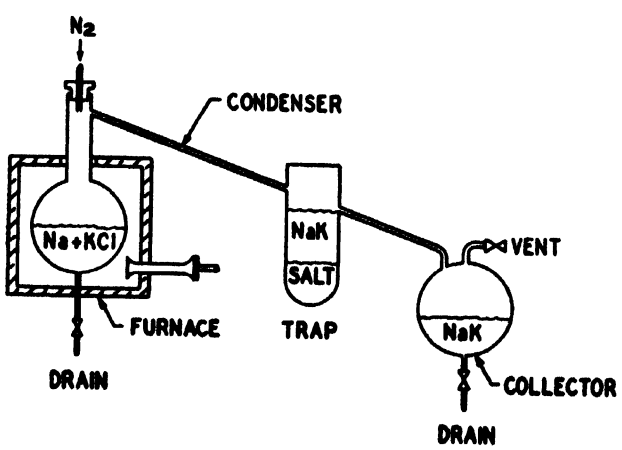

Figure 1. NaK still

* Mine Safety Appliances Company, Pittsburgh, Pennsylvania.

one phase in the other, which is appreciable at the high temperature employed.

With continued heating of the reaction vessel the more volatile metallic phase distilled from the salt phase. There was considerable vapor condensation and refluxing in the uninsulated neck, the over-all effect being a one plate distillation. Rinck had shown that the static equilibrium obtained with the initial mole ratio of reactants gives a metallic phase containing 34 atom per cent potassium. The distillate actually contained 47 atom per cent potassium, with the balance being primarily sodium. Some of the salt phase distilled off at the 1540°F distillation temperature, giving a condensate which was a mixture of NaK and sodium and potassium chlorides. This collected in the salt trap, where most of the salts dropped out of solution, the remainder running over into the collector.

The next step in producing pure potassium was to separate the NaK alloy into its components by fractional distillation at atmospheric pressure. NaK was fed into the center of the column, which was packed with Raschig rings and potassium was taken off overhead at 1400°F with sodium remaining in the 1650°F still pot. Adequate reflux was obtained simply by adjusting the heights of the insulation on the column.

Sodium was not continuously removed from the still pot, so it was necessary periodically to thaw the drain line and transfer accumulated sodium to an evacuated collector for reuse in the reaction. This operation is a striking illustration of thermal shock and thermal stress fatigue withstood by the stainless steel. The ½-inch Type 316 stainless steel drain line was heated to melt the frozen sodium plug which provided a seal during operation. When the plug melted the pipe temperature would rise from 210°F to 1600°F in a matter of seconds. There was considerable writhing and movement of the pipe; however, there were no ruptures or other serious incidents during years of operation of three of these units.

These two steps produced considerable tonnages of metallic potassium at a price far below that for which it had formerly sold. By combining the two operations into a continuous process[8] the price was lowered still further.

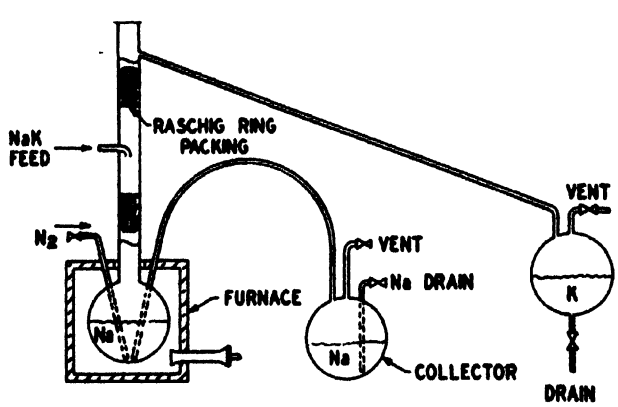

Figure 2. Fractionating column

CONTINUOUS PROCESS

Figure 3 depicts diagrammatically the equipment used in the continuous process. It consists of four basic components, all constructed of Type 316 stainless steel: (*a*) a furnace and boiler tubes for vaporizing sodium; (*b*) a column—the lower portion acting as a reaction and stripping section and the upper portion as a fractionating section; (*c*) a salt and sodium drainage system, and (*d*) a condensing system.

The energy requirements of the process are supplied from a gas-fired furnace in which boiler tubes of 3-inch pipe containing sodium are heated both by convection and radiation. The boiler tubes are of an opened hairpin type welded to the column at sufficient angles (approximately 3 degrees) to permit natural circulation of the sodium.

The column is 18 inches in diameter by 21 feet in length, fabricated from ¼-inch plates rolled and butt-welded for a total length of 720 inches of weld. The column is packed with Raschig rings contained between perforated baskets as shown. Molten potassium chloride is introduced into the column through a 2-inch pipe extending to the center line of the column, 6 feet above the bottom. An open, gas-fired pot (not shown) is fed solid potassium chloride at a variable rate. The molten potassium chloride is introduced into the column through a trap as indicated. The 6-foot length of column above the point of introduction of the potassium chloride is equipped with a 6-inch vapor take-off line, the upper portion of which serves as a condenser. Provision is made for returning condensate to the column by a ½-inch electrically heated line and a distributor head. Electromagnetic ac conduction pumps are used for condensate return and continuous sodium feed to the bottom of the column.

The bottom portion of the column is equipped with a system to drain the sodium chloride. This consists of a "T" as shown, extending from within ½ inch of the bottom of the column to a point 6 inches above the normal liquid level of the sodium. The side arm of the "T" leads through the side of the column to a trap. The molten sodium chloride is forced up the 2-inch line to the trap by the head of

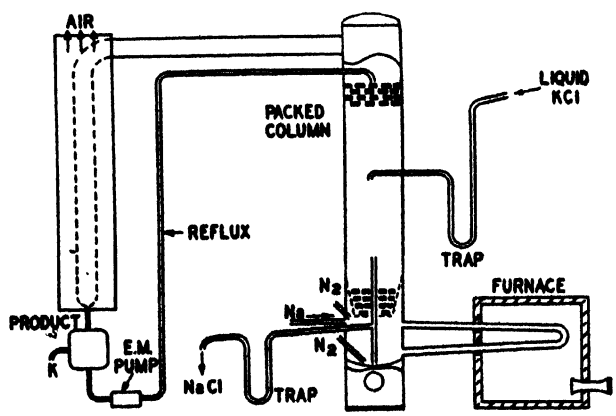

Figure 3. Continuous process for potassium

sodium overlying the denser salt phase. With proper regulation of the height of sodium the molten salt drains continuously.

During operation there is continuous introduction of molten sodium to the base of the column and molten potassium chloride to the column. The sodium is vaporized in the boiler tubes and ascends the column coming into contact with the descending potassium chloride. The equilibrium Na + KCl $\rightleftharpoons$ K + NaCl is established and the sodium-potassium vapors are separated by fractionation in the upper section of the column, condensed and collected. Sodium chloride is continuously removed as described and discarded. The column is operated slightly above atmospheric pressure by introducing nitrogen into both the sodium and molten sodium chloride phases in the bottom of the column. This arrangement serves as a liquid level device by measuring pressures required to maintain a constant flow of gas through tubes immersed in the liquids.

If suitable contact of the liquid potassium chloride and gaseous sodium is maintained all the potassium can be extracted from the potassium chloride. Proper reflux adjustment assists in maximum utilizations of the potassium chloride, and separation of potassium and sodium in the fractionating section. Reflux ratios are easily regulated by adjusting the electromagnetic pump which returns condensate to the column. Potassium of 99.5+% purity can routinely be produced at a rate of approximately 200 pounds per hour. Any desired mixture of sodium and potassium above 45 atom per cent potassium can be produced by controlling column operation.

EXPERIENCE GAINED IN THIS PROCESS

There are points encountered in overcoming difficulties in this process which are applicable to the design and operation of heat transfer systems using these media. In general, the normal design and operation criteria for high temperature high pressure water systems are translatable to liquid metal systems.

The most important consideration is the choice of fabricating materials. It was found that Type 316 stainless steel is the most satisfactory. On the basis of actual service life, stainless steels of Type 304, 310, 302, 321 and 347 were found to be less suitable. Type 310 has been used successfully in the salt melt pot, as it is more resistant to flameside oxidation.

In both processes it was found that threaded pipe and flange joints are unsatisfactory at temperatures above 500°F and that the all-welded construction of the equipment must be of good quality. Contact with sodium in the temperature range of 1400–1700°F has proven to be the best test of welding quality. Slag inclusions through a weld are invariably dissolved, resulting in a leak. Leaks experienced over the years have been small and in all cases the equipment could be cooled before serious damage was done. In every case but one the leaks have been in welds with the cause attributable to poor welding as evidenced by slag inclusions of micro-fissures in the as-welded condition. In the one exception, examination revealed gross contamination with scale, introduced into the plate when it was rolled.

Before proper techniques for welding Type 316 stainless steel were developed, leaks frequently occurred at welds within the furnace. Leak detection in the case of this operation was always visual, depending upon alkali metal oxide smoke in the exhaust gas or a small flame at the point of the leak. These leaks have always started slowly and it was found that even at 1700°F they did not rapidly increase in size. In the oxidizing atmosphere of the furnace leaking alkali metal will burn and the combustion product will accelerate corrosion around the leak. This has been evidenced by erosion around small leaks which have persisted for any length of time.

At no time has there been any indication of a reaction between sodium or NaK or potassium metal with the nitrogen cover gas, even though nitrogen is in constant contact with the alkali metals from 1700°F down to room temperature. No special precautions have been taken regarding the purity of the gas, but if large amounts of oxygen or water vapor enter the system corrosion would be increased.

With off-and-on reflux return passing through a distributor above the packing, it was found that the distributor would go to pieces within the relatively short period of a week or so. This was undoubtedly due to repetitious thermal shocks caused by rapid cooling from an initial temperature of 1400°F to a liquid potassium reflux temperature of 400°F. It is estimated that several thousand cycles of these transients resulted in almost complete failure of the Type 316 stainless steel distributor head.

Potassium chloride was melted (mp 1420°F) in 160 gallon pots, open to the atmosphere. A surface area of 35 square feet is required to melt 400 pounds per hour when the external pot surface is heated by convection and radiation from 2200°F firebrick. It is best to heat the pot on the side for highest efficiency. A deposit of corrosion products gradually builds up in the bottom and reduces the heat transfer coefficient at the bottom.

Natural convection through the boiler tubes, along with some ebullition, was sufficient to produce a heat flux of 15,000 BTU/hr-ft^2. Tube life averaged 1000 hours.

The safe operation of the processes described gave assurance that liquid metal heat transfer systems could be continuously operated at temperatures over 1000°F. This was demonstrated by the successful operation of a 1000 kw heat transfer system at a maximum temperature of 1500°F.

REFERENCES

1. The most comprehensive summary of the properties and uses of sodium and NaK as heat transfer media is the Liquid Metals Handbook (2nd Edition) published by the United States Atomic Energy Commission, Superintendent of Documents, Washington 25, D. C.
3. Jackson, C. B. and Werner, R. C., U.S.P. 2,480,655.
2. Rinck, E., Annales de Chimie *18*: 397 (1932).

The Determination of Trace Impurities in Liquid Metal Coolants by Radioactivation Methods

By A. A. Smales,* UK

The purpose of this work was to determine those impurity elements, present in a sodium-potassium alloy sample, which could contribute significantly to long-lived radioactivity after the alloy had been used as a coolant in a reactor.

Spectrographic examination of the sample was made separately for a range of elements but it was considered that in some cases this might not be sufficiently sensitive and it was therefore supplemented by radioactivation analysis. The latter work is described in this paper.

GENERAL METHOD

The samples were irradiated in the Harwell pile in five gram lots in sealed silica ampoules under reduced pressure, for a period of fourteen days. After "cooling" for a period of one week the ampoules were opened in a dry box from which all the air had been replaced by nitrogen. Approximately one gram lots were shaken out into small volumes (~30 ml) of methyl alcohol and when reaction was complete, the samples were removed from the box for individual treatment and estimation of the amount of alloy taken, by titration with acid.

An aliquot of the irradiated sample was examined on a single-channel gamma spectrometer in order to identify the major gamma emitters.

Radiochemical separations were carried out for mercury, chromium, rubidium, caesium, silver, antimony, strontium and cobalt and details are given in Appendix 1. The amounts of these elements present were determined by comparison of the beta activities with those of standards irradiated simultaneously with the sample. Where possible, radiochemical purity was checked by beta and gamma energy and half-life measurements.

A further small aliquot was, after adding carriers, taken up on an ion exchange resin and the activities separated into a number of groups depending on the differing ion exchange behaviour of the elements concerned. The radioactivity of all fractions including the residual ion exchange material was measured, thus ensuring that no significant activity in the irradiated sample was overlooked. Details of the ion exchange separations are given in Appendix 2.

* Atomic Energy Research Establishment, Harwell, Berks.

RESULTS

The gamma spectrum of the sample, 12 days after irradiation, is shown in Fig. 1 and can be compared with that from the irradiated rubidium standard in Fig. 2. It is clear that the major gamma-emitting nuclide present in the sample is the 1.1 Mev Rb^{86}. By comparison of the areas under the photopeaks the rubidium content of the sample is approximately 70 ppm. Figure 3 is the gamma spectrum of the sample 40 days after irradiation, i.e., after decay of Rb^{86} for two half-lives. Other photopeaks at 0.6 Mev and 0.8 Mev can now be seen and these energies fit Cs^{134}.

Figure 4 shows the caesium standard spectrum.

Results from the individual radiochemical separations were as follows:

	ppm
Mercury	< 0.5
Chromium	< 0.2
Rubidium	77
Caesium	0.15
Silver	< 0.02
Antimony	< 0.001
Strontium	< 0.5
Cobalt	0.02

The individual separated radionuclides from the sample were also counted on an end-window Geiger counter through a 60 mg/cm² aluminium absorber and on a sodium iodide gamma scintillation counter, and the activity of each expressed as a percentage of the total activity of an unseparated sample aliquot counted under the same conditions. The results were as follows: (*a*) beta counter (through 60 mg/cm² absorber) Rb, 100%; Cs, 0.1%; Hg, 0.015%; Sb, <0.01%; Ag, <0.01%; Cr, <0.01%; Sr, <0.01%; and (*b*) NaI gamma counter (40 days after irradiation), Rb, 90%; Cs, 10%.

The ion exchange separation results confirmed those in the preceding paragraph, i.e., that essentially the whole of the beta activity could be attributed to the alkali metals (no separation of these by ion exchange was attempted). Because of the rather small aliquots taken, the gamma activity of the fractions showed no significant increase over the background count of the gamma scintillation counter used except again in the alkali metal fraction.

DISCUSSION

Although from the above evidence of the percentage distribution of activity, it would appear that rubidium is the most significant impurity, it must be remembered that the irradiation time used here, i.e., 14 days, greatly favours rubidium, with a half-life of 19 days, at the expense of those elements giving rise to longer-lived radionuclides. From the point of view of the activity of the alloy after long use in a reactor, say for a few years, then clearly the 2.3 year Cs^{134} and, to a lesser extent, Co^{60} will also become important. The advantage of the radioactivation technique can be seen in this case over the emission spectrographic method where although rubidium was found (and said to be about 50 ppm), neither caesium nor cobalt could be detected. By the radioactivation method all three elements are readily determined and in addition, from the measurement of the gamma spectrum and distribution of activity into the several fractions, there is the assurance that other elements are unlikely to be of significance at least so far as their contribution to the long lived radioactivity of the alloy after some years irradiation, is concerned.

ACKNOWLEDGEMENTS

This work was greatly assisted by the excellent co-operation of Messrs. M. J. Cabell (ion exchange),

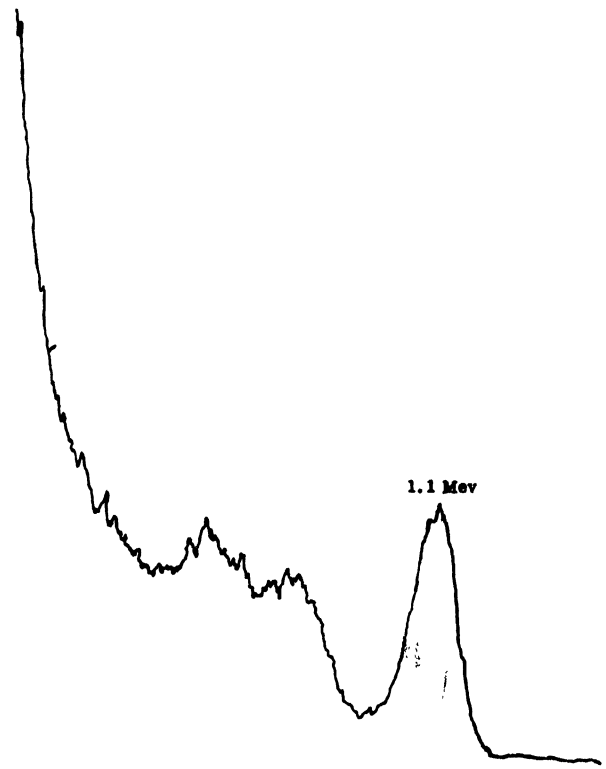

Figure 1. Gamma spectrum of NaK alloy 12 days after irradiation

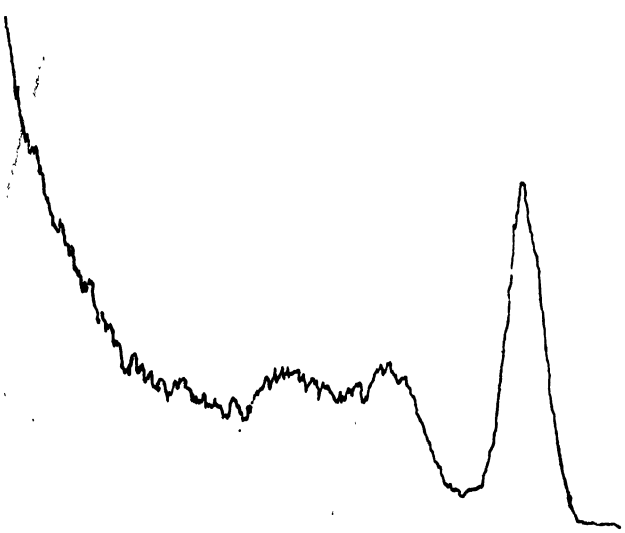

Figure 2. Gamma spectrum of irradiated rubidium standard

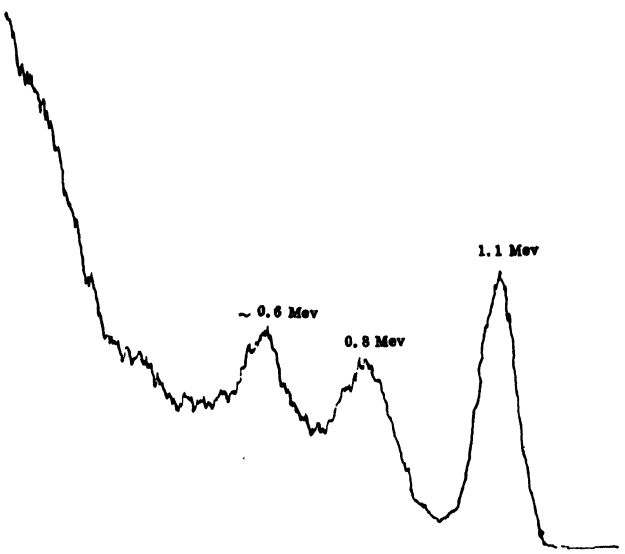

Figure 3. Gamma spectrum of NaK alloy 40 days after irradiation

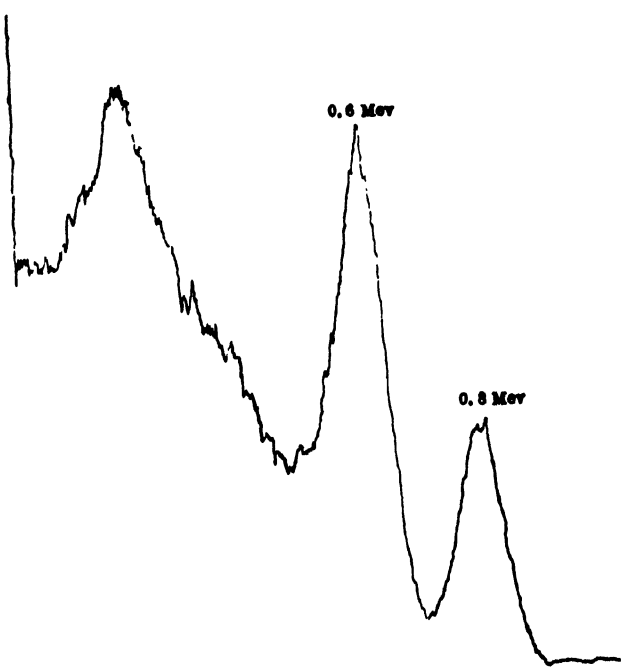

Figure. 4. Gamma spectrum of irradiated cesium standard

B. A. Loveridge (mercury and chromium), D. Mapper (silver and antimony), L. Salmon, (caesium and rubidium and gamma spectrometry), and A. J. Wood (cobalt and strontium).

APPENDIX I. RADIOCHEMICAL SEPARATION PROCEDURES

A. Mercury

Approximately 1 gram of the sample was dissolved in methanol and titrate accurately with standardised acid to a methyl red endpoint. On the basis of a 1:2 sodium-potassium ratio, the equivalent weight of the alloy samples was taken as 33.732 grams. To the titrated solution add 30 mg of Hg^{++} carrier and 3 ml of concentrated HCl, then evaporate carefully to incipient crystallisation. Dilute the sample to about 20 ml and add an excess of stannous chloride to precipitate all mercury in the metallic form. Centrifuge, discard the supernate and dissolve the metal in 3 drops of concentrated hydrochloric acid and 2 drops of concentrated nitric acid with the aid of gentle heating. Dilute again to 20 ml and carry out two silver chloride scavenges using 5 mg Ag^{+} each time and digest the precipitates for a few minutes on a boiling water bath before centrifuging. Test for complete removal of silver carrier by adding a further drop of concentrated HCl after the last centrifuging. Discard the scavenging precipitates and add 2–3 small drops of 6*N* stannous chloride reagent to the supernate. Centrifuge the mercurous chloride precipitate, wash twice with 10 ml portions of water and once with methylated spirits. Discard all supernates. Slurry the mercurous chloride with methylated spirits and transfer to the bottom of a long cold-finger condenser packet (17 × 2 cm) using a long-tipped dropping pipette for the purpose. Evaporate the alcohol with gentle heating. Cover the solid mercurous chloride with powdered iron, insert the cold finger, and adjust an asbestos shield around the jacket about one half inch above the bottom of the cold finger. Apply increasing heat from a bunsen burner until the iron is glowing red and maintain the flame for a few minutes to drive all mercury on to the tip of the cold finger. Allow to cool completely before removing the jacket and replacing it with another having 7 drops of a concentrated HCl-HNO_3 mixture in the bottom. Gently distil the acid on to the cold finger (water flow now shut off) until the grey film of mercury is dissolved. Cool again and dismantle, rinsing the cold finger thoroughly as it is withdrawn. Transfer the diluted acid washings to a 40 ml centrifuge tube, and add 2–3 small drops of stannous chloride reagent. The precipitate should be white or at worst faintly grey. If an excess of stannous reagent has made it grey, the precipitate may be centrifuged off, redissolved in a few drops of aqua regia and reprecipitated with less stannous chloride. Centrifuge, wash twice with water, once with alcohol and slurry on to a weighed counting tray and dry under an infra-red lamp. Weigh, and correct the activity for chemical yield.

B. Chromium

Approximately 1 gram of the sample was dissolved in methanol and titrated accurately with 1.206*N* HCl to a methyl red endpoint. The alloy was taken to be 2:1 potassium-sodium ratio and the equivalent weight on this basis is 33.732 grams. Chromium carrier (20 mg Cr) in the form of $K_2Cr_2O_7$ solution and 3 ml of concentrated HCl were added and the solution was evaporated down slowly to incipient crystallisation. During this evaporation the chromium was reduced to Cr^{+3} ion and the first step of the published radiochemical procedure may be omitted.

The radiochemical separations were carried out according to the method of Burgus[1] with the following modifications:

1. *Chromium carrier solution* (10 mg Cr/ml) should contain 28.28 gm $K_2Cr_2O_7$ per litre and not 56.6 gm as stated.
2. *Procedure step 12.* Considerably more H_2O_2 was required to create the blue peroxy compound for ether extraction.
3. *Procedure step 14.* A better precipitate is obtained if the ether is boiled out of the ammoniacal solution before the reprecipitation of barium chromate in Step 15. In this latter step it is preferable to wash the barium chromate with 3 × 10 ml volumes of water rather than a single 30 ml volume.
4. *Procedure step 16.* More sulphuric acid is usually required to remove all barium particularly if the washing in Step 15 has been inadequate. Using only 3 drops of 3*M* H_2SO_4 as advised can result in a heavy loss of barium chromate with the iron hydroxide scavenge of Step 17, therefore, the completeness of barium sulfate precipitation must be tested.
5. *Procedure steps 20–21.* Following the procedure often fails to produce a chromate precipitate and it appears to be necessary to establish more ammoniacal conditions and even to add further barium ion.

The final barium chromate precipitate is washed in the centrifuge tube, then washed with alcohol and slurried on to a weighed counting tray and dried under an infra-red lamp. Corrections for yield are made in the usual way.

C. Rubidium and Caesium

Take an aliquot of the neutralised sample containing about 10 mg of the alloy and add 50 mg of rubidium carrier. Add 10 mg of ferric iron as the chloride and continue from this step as described previously,[2] making allowance in the chemical yield determination for the potassium from the sample.

D. Silver

Titrate the methanol solution of sodium potassium alloy with *N* nitric acid, and then add 2 ml of silver carrier solution (*a*) plus 5 ml concentrated

nitric acid. Then add 1–2 ml of "hold-back" carrier solutions of Co, Cr, Sr, Ca, Zn, Sb, Hg, Sn, La (*b*). Boil the solution after adding an equal volume of water and allow it to cool.

Add 2–3 ml of concentrated hydrochloric acid and centrifuge off the precipitate of AgCl. Wash the precipitate twice with water and then dissolve it in a minimum amount of concentrated ammonia solution. Add a slight excess of ammonia and a few drops of ferric iron solution. Centrifuge and retain the supernatant. To this add 2–3 ml of yellow ammonium sulphide solution and centrifuge the precipitated Ag_2S. Discard the supernatant. Add 2–3 ml of concentrated nitric acid and boil strongly until no more brown fumes are evolved. Dilute to 10 ml.

To this solution (*c*) add the minimum amount of sodium hydroxide solution to precipitate the Ag_2O and then 3–4 drops in excess. Centrifuge and discard the supernatant. Add 2–3 drops of concentrated sulphuric acid to the precipitate, in the centrifuge tube, and heat gently at first, until the solution is clear, then strongly, in a bunsen flame to dryness (*d*). Allow the tube to cool.

Add 10 ml of water and boil until a clear solution is obtained, then add 1 ml of saturated potassium iodate solution and centrifuge the precipitate of $AgIO_3$. Discard the supernatant and to the precipitate, in the centrifuge tube, add 3 or 4 drops of concentrated ammonia solution to dissolve. Add 5 ml of water and 1 or 2 drops of ferric iron solution and centrifuge.[8] Pour off the supernatant into a clean centrifuge tube.

To this solution add 2 or 3 drops of sulphuric acid, to precipitate the $AgIO_3$, and centrifuge. Wash the precipitate twice with water and then transfer it to a counting tray.

Prepare the standard from 10 mg of silver foil, irradiated at the same time as the sample, by dissolving it in nitric acid, taking a suitable aliquot and adding it to the same amount of Ag carrier as used in the sample. Add 5 ml of concentrated nitric acid and heat to boiling. Precipitate Ag_2O with sodium hydroxide solution, and then proceed as from the third preceding stage above.

20 mg Ag ≡ 52.4 mg $AgIO_3$. Yields of 50% and upwards can be obtained. Calculate the yield from the weight of $AgIO_3$ on the counting tray.

Notes

(*a*) Make up a solution of $AgNO_3$ containing 10 mg/ml of silver.

(*b*) All carriers used should be non-chloride compounds and contain 10 mg/ml of the appropriate cation. 1–2 ml of each are added.

(*c*) Solution of $AgNO_3$ may be slightly turbid due to the sulphur present. This is removed at a later stage.

(*d*) It is not necessary to remove the last traces of sulphuric acid on the walls of the tube.

(*e*) The solution can be boiled at this stage, making the "iron scavenge" easier to centrifuge.

E. Antimony

Titrate the methanol solution of sodium potassium alloy with N hydrochloric acid, and then add 2 ml of antimony carrier solution (*a*) plus 5 ml of concentrated hydrochloric acid and 0.5 ml of saturated bromine water. Then add 1–2 ml of "hold-back" carrier solutions of Co, Cr, Sr, Ca, La, Zn (*b*). Boil the solution until the excess bromine is removed and allow it to cool.

Add 2 ml of silver nitrate solution (10 mg Ag/ml) and stir vigorously. Centrifuge the precipitate of AgCl and retain the supernatant. To this add some mercury hold-back carrier, as mercuric chloride solution and then add excess stannous chloride solution. Add 1–2 gm of ammonium hypophosphite and digest at 90–100°C for half an hour. Centrifuge (or filter) the precipitated mercury (*c*) and retain the supernatant.

To the hot solution add excess of pure iron powder (0.5 to 1 gm) and when evolution of hydrogen has ceased, filter off the precipitated antimony. Repeat this process twice, adding 2 or 3 ml more of concentrated hydrochloric acid, if necessary, collecting any further precipitated antimony in the filter paper. Wash the precipitate well and transfer it to a 150 ml beaker with 10 ml of water. Add 2 ml of concentrated hydrochloric acid and a few drops of 100 volume peroxide (*d*). Heat gently until the solution is clear and dilute to 50 ml.

Adjust the acidity with sodium hydroxide solution and hydrochloric acid until the solution is only just acid, adding a slight excess of dilute hydrochloric acid. Add excess yellow ammonium sulphide solution and boil gently (*e*). Filter the precipitate through a No. 40 paper and collect the filtrate. Acidify the filtrate with dilute hydrochloric acid and boil. Filter the precipitated and antimony sulphide through a No. 541 paper and wash well. Transfer the precipitate to a 150 ml beaker with 10 ml of water and add 2–3 ml of concentrated hydrochloric acid. Heat the beaker on a hot-plate and add 0.2 to 0.5 gm of solid potassium chlorate, boiling until the solution is colourless. Filter off the undissolved sulphur and retain the filtrate.

Adjust the acidity of the solution again with sodium hydroxide solution and hydrochloric acid, making certain that the solution is only just sufficiently acid to retain the antimony in solution, (*f*) and make up the volume to 150 ml.

To the hot solution add 25 ml of ammonium thiocyanate solution (*g*) and heat gently with stirring. The solution *slowly* turns yellow and a precipitate begins to form, going from yellow to deep red. This is the final precipitate of antimony trisulphide (*h*). Heat the beaker on a hot-plate for 20 min and then allow it to cool. Centrifuge the precipitate and wash it twice with water, finally transferring it to a counting tray.

Prepare the standard from Sb_2O_3, irradiated at the same time with the sample, by dissolving it in hydrochloric acid, taking a suitable aliquot and

adding it to the same amount of antimony carrier used in the sample. Add 5 ml of concentrated hydrochloric acid and 5 ml of bromine water and boil. Adjust the acidity of the solution and pass in hydrogen sulphide until precipitation of orange antimony sulphide is complete. Filter the precipitate and dissolve it in hydrochloric acid and potassium chlorate, proceeding then from the third preceding stage above.

20 mg Sb ≡ 27.9 mg Sb_2S_3. Yields of 50% and upwards can be obtained. Calculate the yield from the weight of Sb_2S_3 on the counting tray.

Notes

(*a*) The carrier solution, contains 10 mg of Sb/ml and is made by dissolving 5.66 gm of potassium antimonyl tartrate in 250 ml of water ($KSbO \cdot C_4H_4O_6$).

(*b*) Carrier solutions are made from suitable salts and contain 10 mg/ml of the appropriate ion. 1–2 ml of each are added. Copper and arsenic carriers are not added, since in this experiment, 12.8-hr Cu^{64} and 26.8-hr As^{76}, have decayed sufficiently not to affect the radiochemical purity of the final antimony precipitate. If the antimony is determined immediately after irradiation, these two carriers must be added and the procedure is still the same as given.

(*c*) If an arsenic stage has been added, arsenic is precipitated here with the mercury.

(*d*) Undissolved iron powder, carried down with the precipitated antimony, is also dissolved and is separated in the next stage.

(*e*) Fe and Cu (if added) are precipitated here.

(*f*) Excess acid must be avoided, as it interferes with the final precipitation of Sb_2S_3 in the next stage.

(*g*) The ammonium thiocyanate solution is made by dissolving 200 gm of NH_4CNS in 100 ml of water.

(*h*) If the solution has been made too acid, sulphur also precipitates. If this happens, the precipitate must be washed with carbon disulphide.

(*i*) The Sb_2O_3 is dissolved in HCl and made up to 1000 ml. 10–20 mg of Sb_2O_3 is a convenient amount to irradiate.

F. Strontium

To the acid solution of the irradiated sample add a solution containing 20 mg of strontium carrier and boil the solution gently on a hot-plate for ten minutes.

After cooling, dilute the solution to 20 ml with water, add an excess of ammonium hydroxide (specific gravity 0.88) boil gently and add 5 ml of a solution containing 1 gm of ammonium carbonate. Centrifuge and decant the supernatant.

Dissolve the precipitate in 2 ml of hydrochloric acid (specific gravity 1.18), add 1 ml of a solution containing 5 mg of ferric iron and 1 ml of a solution containing 5 mg of cobalt, 5 mg of zinc and 5 mg of manganese. Dilute the solution to 15 ml with water and add an excess of ammonium hydroxide. Boil gently and filter through a 9 cm Whatman No. 40 filter paper, washing the precipitate with 5 ml of hot water. Discard the precipitate.

Boil the filtrate and add 5 ml of a saturated solution of ammonium oxalate. Centrifuge and decant the supernatant.

Dissolve the precipitate in 2 ml of nitric acid (specific gravity 1.42) and oxidise with a solution of potassium permanganate. Add 1 ml of a solution containing 10 mg of calcium and dilute the solution to 8 ml with water. Cool the solution in an ice-bath and add 30 ml of fuming nitric acid. Digest cold for five minutes, centrifuge and decant the supernatant.

Dissolve the precipitate in 10 ml of water and add 1 ml of 6.5 *M* acetic acid and 5 ml of a solution containing 1 gm of ammonium acetate. Boil the solution and add dropwise 2 ml of a 1.5 *M* solution of sodium chromate. Digest hot for ten minutes, centrifuge and filter the supernatant through a 9 cm Whatman No. 40 filter paper. Discard the precipitate.

To the filtrate add 5 ml of ammonium hydroxide (specific gravity 0.88), boil gently and add 5 ml of a solution containing 1 gm of ammonium carbonate. Centrifuge and decant the supernatant.

Dissolve the precipitate in 2 ml of hydrochloric acid (specific gravity 1.18) and add 1 ml of a solution containing 1 mg of copper. Dilute the solution to 15 ml with water and add a slight excess of ammonium hydroxide. Add 3 *M* hydrochloric acid dropwise until the blue colouration just disappears and then add 2 ml of a solution containing 1 gm of thionalide in 100 ml of methanol. Boil the solution and filter through a 9 cm Whatman No. 541 filter paper. Discard the precipitate.

To the filtrate add 1 ml of a solution containing 5 mg of bismuth and a slight excess of carbonate-free ammonium hydroxide (specific gravity 0.88). Boil and filter through a 9 cm Whatman No. 541 filter paper. Discard the precipitate.

To the filtrate add 5 ml of a solution containing 1 gm of ammonium carbonate. Centrifuge and decant the supernatant.

Dissolve the precipitate in 2 ml of hydrochloric acid (specific gravity 1.18) and add 10 ml of absolute alcohol. Add 5 ml of 3*M* sulphuric acid and a further 10 ml of absolute alcohol. Digest for five minutes and then centrifuge. Wash the precipitate firstly with water and secondly with alcohol, centrifuging and decanting the washings.

Transfer the precipitate to a tared counting tray and evaporate to dryness under an infra-red lamp. Weigh the sample as strontium sulphate and determine the chemical yield.

Count the sample and standard under a normal end-window Geiger-Müller counter and correct for background and chemical yield.

Check the radiochemical purity by absorption measurement.

G. Cobalt

To the acid solution of the irradiated sample add a solution containing 20 mg of cobalt carrier and 1 ml of a solution containing 5 mg of ferric iron. Boil the solution gently on a hot-plate for ten minutes.

After cooling, dilute the solution to 250 ml with water and add a slight excess of a suspension of zinc oxide in water. Digest for ten minutes and then filter through a 15 cm Whatman No. 541 filter paper. Discard the precipitate.

Boil the filtrate and add dropwise 7.5 ml of a solution containing 1 gm of α-nitroso β-naphthol in 15 ml of glacial acetic acid. Boil for two minutes and filter through an 11 cm Whatman No. 31 filter paper. Wash the precipitate thoroughly with hot water and dry and ignite the filter paper and contents in a silica crucible, at 800°C. Discard the filtrate.

After cooling dissolve the ignited residue in 5 ml of hydrochloric acid (specific gravity 1.18), by warming gently on a hot-plate. Transfer the solution to a 50 ml centrifuge tube, add 1 ml of a solution containing 1 mg of ferric iron and a slight excess of ammonium hydroxide (specific gravity 0.88). Boil gently and filter through a 9 cm Whatman No. 40 filter paper into a 150 ml squat beaker. Wash the precipitate with 5 ml of hot water. Discard the precipitate.

To the filtrate add 10 ml of a solution containing 4 gm of potassium hydroxide and boil gently until all the ammonia is driven off. Wash the solution and precipitate into a centrifuge tube with water. Centrifuge and decant the washings.

To the precipitate add 5 ml of 3*M* hydrochloric acid and heat gently until a solution is obtained. Add 5 ml of glacial acetic acid and dilute to 25 ml with water. Add 5 ml of a solution containing 3 gm of potassium nitrite, digest for five minutes and then centrifuge. Wash the precipitate firstly with water and secondly with ethyl alcohol, centrifuging and decanting the washings.

Transfer the precipitate to a tared counting tray and evaporate to dryness under an infra-red lamp. Weigh the sample as potassium cobaltinitrite and determine the chemical yield.

Count the sample and standard under a normal end-window Geiger-Müller counter and correct for self-absorption, background and chemical yield.

Check the radiochemical purity by absorption measurement.

H. Method for Separation of Total Activity into Groups by Ion Exchange

10 mg each of Cs, Sr and Rb were added as chlorides to approximately 1 gm sample in 35 ml methanol. Water was also added and the solution was titrated with acid to find the amount of alloy taken, accurately. The calculated quantity of concentrated hydrochloric acid, 10 mg each of Cr^{3+}, Co^{2+}, Sb^{3+}, Sn^{2+}, Hg^{2+} and Zn^{2+} as chlorides and, with stirring, 10 mg Ag as nitrate, were added and the solution was transferred to a 250 ml flask and made up to the mark with water. The clear solution was exactly 2*M* in hydrochloric acid.

25 ml were pipetted on to a 150 mm × 7 mm diameter column of 70–100 mesh Amberlite IRA-400 which had been washed with 2*M* HCl and was allowed to feed under its own head. The column was then eluted with 37 ml 2*N* HCl, 85 ml 2*N* HNO_3 and 17 ml 7.5 *M* HN_4OH successively at an average flow-rate of 0.44 ml/min. The HCl fraction was collected for feeding to the second column, the first 25 ml of the HNO_3 fraction contained the Sn and Zn and the remainder (60 ml) contained Hg whilst the NH_4OH fraction contained Ag.

The HCl fraction from the first column was evaporated down to 10 ml and 10 ml concentrated HCl were added. The total was fed to a column of Amberlite IRA 400, identical with the first except that it had been prewashed with 8*M* HCl. After the feed had been passed it was followed by 10 ml 8*M* HCl at 0.5 ml/min and the total eluate was prepared for feeding to the third column. The second column was finally eluted with 19 ml 5*M* HCl at 0.63 ml/min to remove cobalt. Any Sb present in the original solution remained on this column.

The 8*M* HCl fraction from column two was taken to dryness under the infra-red lamp, dissolved in 5 ml 0.1*M* HCl and fed to the third column. This was approximately 4.5 cm × 1.3 cm diameter and contained < 50 μ particle size Zeokarb 225(H) which had been dried by exposure to the air; 4 gm were slurried into the column with water. After the feed had passed through elution was effected with 40 ml 0.1*M* HCl (this plus the feed contains chromium) then with 396 ml 0.5*M* HCl (alkali metals) and finally with 216 ml 1.5*M* HCl (alkaline earths), all at an average flow-rate of 1.5 ml/min.

Throughout the whole series of separations the eluate was monitored by dividing into fractions and γ-counting representative aliquots. Aliquots of the alkaline earths fraction alone were β-counted.

Each fraction was now evaporated under the infra-red lamp and transferred to successively smaller beakers until finally it could be evaporated to dryness on a platinum tray for β- and γ-counting. This was not possible with the alkali metals fraction which contained a large amount of salts and tended to creep. One-tenth of this fraction was taken for counting.

In addition the resins from the three columns were wet-ashed by boiling with 30 ml concentrated HNO_3 plus 30 ml 72% $HClO_4$ until a vigorous reaction took place. The solutions obtained were also evaporated down and finally plated out on platinum. The Zeokarb resin gave little trouble but the Amberlite resins gave a considerable amount of a salty residue which could not be completely re-

moved from the counting tray due to vigorous frothing when heat was applied.

Finally suitable aliquots of the standards and of the alloy solution were pipetted on to similar counting trays and counted together with the fractions obtained as above. In this way the distribution of the total activity in the various fractions was determined.

REFERENCES

1. Burgus, W. H., LA1566, Collected Radiochemical Procedures; 1 February 1953; Chromium pp 50–56.
2. Smales, A. A. and Salmon, L., Analyst *80*, 1955, 43.

Record of Proceedings of Session 19B.1

THURSDAY MORNING, 18 AUGUST 1955

***Chairman:* Mr. L. Rotherham (UK)**

***Vice-Chairman:* Mr. K. F. Alder (Australia)**

***Scientific Secretaries:* Messrs. B. Prakash and C. A. Sastre**

PROGRAMME

P/123 Sodium and sodium-potassium alloy for reactor cooling and steam generation ..... T. Trocki *et al.*

P/866 Liquid metal handling ..... S. G. Bauer

DISCUSSION

The CHAIRMAN: I think that everyone here will realize that there is an inevitable use for liquid metals in reactor technology. It is a use which will inevitably grow. I hope that the speakers who are presenting their papers here today will not be surprised if there are some members of the audience who do not agree exactly with everything that is said in their texts. I think that this is fortunate. It is a subject which allows of a very free exchange of views. I hope that the different opinions that exist will be fully expressed.

Mr. T. TROCKI (USA) presented paper P/123.

Mr. S. G. BAUER (UK) presented paper P/866.

DISCUSSION OF P/123 AND P/866

Mr. W. B. HALL (UK): My first question is concerned with the use of cold traps in liquid metal circuits. Can Mr. Trocki suggest approximately the quantity which he would by-pass through the cold trap as a percentage of the total flow, and can he also give a rough figure for the resident time of the liquid metal in the cold trap?

My second question concerns cavitation in liquid metal circuits. Can the author say whether any work has been done in the United States of America on cavitation, and have they tried to determine the cavitation parameters for sodium and sodium-potassium?

Mr. TROCKI (USA): The cold traps are usually sized to take about two system turnovers per hour. It is not a very large rate, and that would be only a small percentage of the normal circulating flow of a plant. With regard to the resident time, it is some time since I worked on this and I do not recall it, but it can be found in the Liquid Metal Handbook. It is of the order of a minute or more.

With regard to the work on cavitation, in the case of the large pumps of which one model was shown, the ac induction pumps, most of the models built have been tested and the cavitation parameter established for these pumps. I think that we have less trouble with cavitation than we have with included gases. It is far more important to make certain that all the gas is out of the circuit than it is to be certain about the actual cavitation parameter, although it is necessary in the circuits which we have built to use something of the order of under 1 atm of pressurization, which means 10–15 psi pressurization above atmosphere to preclude cavitation. I have heard of cavitation occurring, and it is difficult to establish the point of cavitation. It comes rather slowly. As the inlet pressure is reduced in the pump, the first evidence of cavitation is a gurgling noise at the pump inlet, and later the pump output falls off with the variation of inlet pressure.

Mr. G. W. K. FORD (UK): I want to ask Mr. Trocki whether he had found any difficulty with the type of mechanical pump which uses an inert blanket in the entrainment of the gas from the blanket into the main system, and its effect on the other functions of the circuit and whether the difficulty was greater than with other types of pump, such as interference with heat transfer, interference with filtering, and so on.

Mr. TROCKI (USA): The gas blanket pump that I have shown was the one used at the experimental reactor. I have not had very much experience with it, but I think I can answer your question. The pump is necessarily used in a rather wide and shallow tank, which provides excellent degassing facilities. Even with a small submergence of this pump there is very little danger of a vortex forming and sucking gas into that type of pump. So that, although I have never heard of any particular difficulties having been encountered at the EBR plant, I would judge, from that kind of configuration, that there should be very little difficulty with gas entrainment, once the pump has actually sucked the gas down. I think the same applies in the case of this particular pump, as with any other pump. It is desirable to detrain all the gas from the external system. I believe that this pump

and this type of system are used with a large sump tank at the bottom of the system. You will note that it will necessarily require a large tank which would limit the level of the liquid, because this pump has to operate from a condition of having the tank full of liquid up to a condition of having the system full of liquid. The sodium is transferred from the tank up into the system, and in order to do this the tank in which the pump is operating is shallow and broad and provides excellent gas detraining.

I think your other question was this: "Does the gas affect the liquid metal and the performance of other parts of the system?" It is particularly serious in pumps, and especially electromagnetic pumps, and provision must always be made to allow the pump to pump itself free. Although this is not very different from most liquid systems, if any cavitation occurs, the inlets and outlets are usually arranged so that accumulated vapors are blown free from the pump and do not reside at the inlet of the pump.

Mr. C. E. WEBER (USA): I should like to ask Mr. Bauer out of what material the superheater that failed from corrosion was made, and also if they have any idea as to what kind of corrosion failure took place.

Mr. BAUER (UK): The superheater tubes were made of stainless steel which was titanium stabilised, and it was thought that corrosion was due to minute traces of chloride in the water, but this has not been established very definitely.

Mr. S. SIEGEL (USA): My question concerns the practicability of using ammonia for cleaning large systems; that is, the actual reactor system, rather than the experimental equipment. Do you find it a little less obnoxious than cleaning with water and steam?

Mr. BAUER (UK): I answer this question with great diffidence, since our experience has not extended to anything like the large systems that Mr. Siegel has in mind. The largest system that I know of having been cleaned with ammonia is at a steam superheater plant, which is, of course, very small in comparison with what you are talking about. The method is fairly expensive, but the expense can be kept under control by recirculating the ammonia rather than throwing it away. This can be done by removing the sodium from the ammonia by water-titrating methods. This method should only be used for a really very high order of cleanliness. If you clean with water and steam, then in the case of any inaccessible places, such as small cracks and mechanical joints, the sodium will be covered by sodium oxide, and there is no means of shifting that with any amount of water washing. This can lead to difficulties, either corrosion or other troubles, in taking things apart; and in such a case the ammonia method has great advantages. But I think one has to look very carefully in each case and make up one's mind whether the price one pays is worthwhile. What one has to keep in mind is that the pressure of liquid ammonia is, I believe, about 125 or 150 pounds per square inch, so that the whole plant has to be designed to withstand such static pressures, because it is not always possible to chill a large plant down. Therefore, it is a fairly onerous operational demand, particularly in channels connected with electromagnetic pumps where such pressures can be quite troublesome.

Mr. TROCKI (USA): Mr. Bauer, you described an incident in your sodium system in which it became contaminated with oxygen. Would you care to comment on the specific measures taken to remove sodium hydroxide from the plant, and was any sodium residue encountered in the clean-up? Also, was water used?

Mr. BAUER (UK): I am afraid that in this particular incident it was difficult to know what to do. There was very little indication of what had happened. As a result, as so often happens on such occasions, everything was tried. First of all, an ammonia clean-up was done, but it was not entirely successful, since some parts of the system were completely blocked and inaccessible from either end. Sodium and water washes and acid washes were tried, and some of the tubes had to be pushed through mechanically in order to try to clean the thing up. It was a very lengthy and troublesome operation. I do not think anybody can claim that as a result of this experience they would know exactly how they should do it next time.

Mr. H. KRONBERGER (UK): Mr. Bauer has given a very comprehensive account of liquid metal-handling tanks. I should like to supplement this by commenting on the experience gained in the Research Development Branch of the Industrial Group of the United Kingdom Atomic Energy Authority over the last two or three years. The size of our equipment, and the costs, make ammonia-cleaning impractical, as Mr. Bauer himself has already pointed out.

We have had consistently good results with low-pressure steam cleaning, either in evacuated systems, admitting the steam at low pressure, or where the systems were not evacuated, by buffering the steam with nitrogen. We have been successful, even, in test rigs where cleanliness was highly important, such as test rigs for bearings running in sodium. The cleaning operation is monitored by charcoal being cooled with liquid nitrogen. The same method, by the way, is used for initial leak testing, and this has been described in a recent issue of the Journal of Scientific Instruments. Over the last two or three years we have not had any explosions, and we are quite confident that steam cleaning is the best technique to be used on large test rigs. Our experience in all branches of liquid metal technology confirms us in the belief that the handling of liquid metals will be only one of the minor problems in the design and operation of liquid metal reactors.

Mr. TROCKI (USA): May I ask a question in return? Did you include in your steam cleaning any high temperatures? We also did steam cleaning of rather large systems, and found it necessary to recycle or recirculate the nitrogen in a system, and admit just enough steam for the reaction rather than to use steam alone, because we found that where there was a considerable amount of sodium, the steam was not able to remove the heat sufficiently and we got, as a result, conditions which were dangerous to the equipment.

Mr. KRONBERGER (UK): I can confirm this because I have seen this happen once. After this we decided to monitor the reaction by measuring the amount of hydrogen continuously, the steam being fixed at a certain speed. I am afraid I have not the figure with me. Since then we have not had any hot spots. The hot spot was inside the convolution of the bellows. We quite obviously had admitted the steam too quickly. If one adopts the practice of measuring the hydrogen no difficulty will arise, and if you buffer with nitrogen you have additional control.

Session 19B.2

LIQUID METAL HEAT TRANSFER

LIST OF PAPERS

			Page
P/639	Heat transfer of molten metals	M. A. Mikheyev *et al.*	285
P/120	Liquid metal heat transfer predictions	R. N. Lyon	290
P/417	Liquid metal heat transfer	W. B. Hall	295
P/1103	A simple method for the comparison of reactor coolant efficiency	M. Hoyaux	302

Heat Transfer of Molten Metals

By M. A. Mikheyev, V. A. Baum, K. D. Voskresensky and O. S. Fedynsky, USSR

The prospect of the extensive use of nuclear units has advanced the problem of heat delivery from molten metals. The latter are convenient for transferring heat from the reactor to the working unit, especially because they may have a high temperature at low pressures with the consequent possibility of obtaining steam with high parameters in the energy cycle.

Water, gases, oils and other media which have the Prandtl number higher than 0.7 are widely used as cooling agents in heat exchangers. The laws of heat exchange for these liquids are well known.

The physical properties of molten metals differ radically from the properties of the liquids mentioned. The Prandtl number of molten metals is of the order 10^{-2}, and in many cases they do not moisten the heated surface. Therefore, the generally recognized heat exchange laws and the prevailing concepts about the heat transfer of "usual" liquids with low heat conductivity are inapplicable to molten metals. These specific features of molten metals were first discovered in the Soviet Union, in 1939, during experimental investigations on the heat transfer of mercury, conducted in connection with the study of the operation of mercury boilers.[1]

Investigations into the heat delivery of molten metals and of their alloys were continued at the institutes of the Academy of Sciences; heavy and alkaline metals have been used for this purpose. The choice of different metals for investigation was determined by the practical tasks and by the desire to study the largest possible interval of variation of the physical parameters of the heat-carrying agents. Hydraulics of the flow of molten metals were studied together with thermal research. As a result of extensive experiments it was established that the intensity of heat transfer depends upon conventional factors, both in the cases of the free and forced flow of molten metals. This interdependence is expressed in the form of relations between similarity criterions.

Investigations of thermal problems in the turbulent flow of molten metals in tubes were concentrated on the study of the underlying mechanism of the process and its dependence upon different factors varying in large intervals. These investigations were conducted with specialised units differing in means of heating and in methods of measuring the transferred heat flow, the metal flow and temperatures.

Original language: Russian.

The principal scheme of one of the experimental units with a heat exchanger in which a constant specific heat flow was maintained by means of an electrical heater is shown in Fig. 1. The circulation of the molten metal in the experimental loop was sustained by means of gear pumps, or centrifugal pumps.

The metal flow was measured by the calorimetrical method or by means of a magnetoelectric or volume flowmeter.

The experimental heat exchanger was made in the shape of a thin tube of stainless steel. To secure an even distribution of heat flow, the exterior surface of the experimental tube was covered with a thick layer of copper, by the electrolytic method. The temperature of the wall was measured by thermocouples. In all cases the distance between the thermocouple joint and the interior surface of the tube did not exceed 0.3–0.5 mm. In some units the temperature of the wall was measured by resistance thermometers. Thermocouples were used for measuring the temperature of the metal at the entrance to and exit from the experimental tube. The electromotive force of all the thermocouples was measured by the compensation method.

In order to compensate for the heat losses into the external space, an extra heater was placed above the principal one, and a thermometer was set between them. When the reading on the scale of the thermometer showed zero it meant that there were no external heat losses.

The cooler was built as a concentric tube system or as a steel rib welded to the tube of the loop. (See Fig. 1).

The rib together with the corresponding section of the tube was encased in a jacket which received cooling water from a small tank with a constant water level. The water level in the jacket and, consequently, the degree of immersion of the cooling rib were set in proportion to the utilized electrical power.

Heaters were mounted on the pump, on the tubing and on the container for the purpose of heating the unit.

Experiments with units of this kind were conducted as follows. To begin with, the air was pumped out, whereupon the unit was blown through by purified argon and pumped again. Then the unit was filled with metal under vacuum. After that, the remaining space was filled with purified argon under small extra pressure. Before the experiments, the

unit was heated with auxiliary heaters whereupon the main and compensational heaters were put into operation.

The required work conditions of the unit with necessary compensation for external heat losses in the working section were established by regulating the metal flow and power of the heaters, and by changing the speed of the flow or the water level in the cooler. When a steady state was attained, the electric power of the main heater, the metal flow and temperatures were duly recorded.

In order to obtain experimental data by another method, condensing steam was used in certain units as a heating agent and consequently the temperature of the wall along all the length of the experimental tube was practically constant.* Only mercury and a sodium-potassium alloy were used as cooling agents.

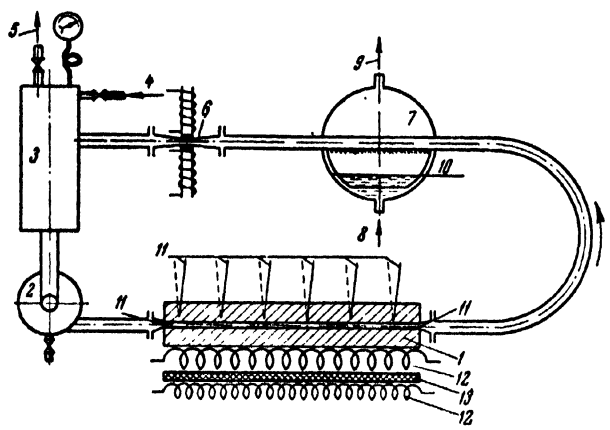

Figure 1. The principal scheme of the experimental unit: (1) experimental heat exchanger; (2) pump; (3) container; (4) argon; (5) to the vacuum pump; (6) flowmeter; (7) cooler; (8) water; (9) steam to condensator; (10) level of cooling water; (11) thermocouples; (12) electrical heaters (main and compensating); and (13) thermometer

The heat transfer of liquid metals was also studied under conditions when neither the heat flow nor the temperature of the wall were constant along the tube. In order to secure such conditions and to obtain an intensive heat flow the experimental tube was placed in an oil bath equipped with powerful electrical heaters, mixers and a thermostatic device.

Experiments with water were conducted for the preliminary control of all the experimental units. The results coincided well with the generally accepted heat exchange formulae for turbulent flow of "usual" ("Pr" > 0.7) liquids in tubes, thus confirming the method of investigation and the correctness of chosen experimental schemes.

Tubes with circular and fashioned cross sections were used in the experiments. Various metals and their alloys were used as cooling agents. Their choice, as it was already mentioned, was determined by the desire to study the largest possible interval for variations of physical parameters. Accordingly the investigations covered the heat exchange of mercury, tin, lead, bismuth, sodium and of bismuth-lead and sodium-potassium alloys.

* Special measures were taken to secure drip condensation.

The speed of the flow of molten metals varied, from 0.1 to 20 m/sec, the Reynolds number, from 1×10^4 to 6.5×10^5, the Prandtl number, from 4×10^{-3} to 3.2×10^{-2}, and the specific heat loading from 2×10^4 to 1×10^6 kcal/m^2-hr.

The objects sought were both the mean values of heat exchange coefficients taken along the length of the tube and the local heat exchange coefficients.

Data obtained were treated from the angle of similarity criterions.

This research led to the establishment of a general law based on more than 600 experimental points. It was also established that in the investigated interval of variation of the parameters the heat transfer rate of molten metals does not depend in practice upon the rate, direction and distribution of the heat flow over the heated surface of the tube.

By moistening the heating surface the cooling agent apparently exerts an indirect influence on the heat exchange. It may be presumed that oxides which offer additional thermal resistance to the heat flow drop out easily on the unmoistened heating surface.

The approximate rectification needed to account for the thermal resistance of the contact was determined by experiment. An interpolational formula was obtained for calculating the heat transfer in a turbulent flow of molten metals in tubes.

$$\mathrm{Nu} = 4.5 + 0.014\ (\mathrm{Re} \times \mathrm{Pr})^{0.8} \qquad (1)$$

Equation 1 is applicable to calculations for comparatively clean heating surfaces. In cases when the accumulation of oxides on the heating surface seems possible one may use as a first approximation, instead of Equation 1, the following formula obtained as a result of studies of liquid metals flow in oxidized (burnished) steel tubes, without corresponding protection from oxidation with the help of inert gases:

$$\mathrm{Nu} = 3 + 0.014\ (\mathrm{Re} \times \mathrm{Pr})^{0.8} \qquad (2)$$

To determine similarity criterions for Nu, Re and Pr in Equations 1 and 2 the physical parameters should be chosen according to the basis of the mean (along the tube) temperature of the cooling agent, the internal diameter of the tube being taken as the characteristic length. Equations 1 and 2 are applicable to long tubes with the ratio $l/d \geqslant 30$.

For calculating the heat delivery of molten metals flowing in short tubes $5 < l/d < 30$ the correction $\xi = 1.72\ (d/l)^{0.16}$ should be introduced in Equations 1 and 2.

Reports on many experiments relating to the heat transfer of molten metals were published recently in periodicals. Many of these, among them data on the most detailed study of the heat exchange of the bismuth-lead alloy conducted by Johnson and other authors[2] coincide with our data, confirming the above-mentioned conclusions about heat exchange in the region of small Prandtl numbers.

The known analytical solutions of Lyon[3] and Seban[4] have not been confirmed by experiment.

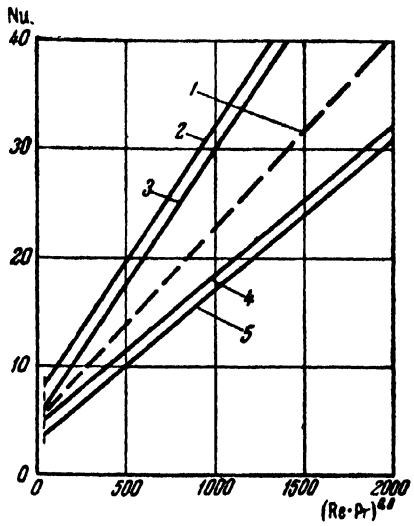

Figure 2. Experiment and theory compared: (1) Dwyer, 1954 (Lyon's theory with experimental correction); (2) Lyon's theory, 1951; (3) Seban's theory, 1951; (4) experiments of the A.Sc. of USSR, formula 1; and (5) experiments of the A. Sc. of USSR, formula 2

All the experimental data give lower values than the theoretical curves.† Lyon explains this discrepancy by the fact that the heating surface is not moistened by the metal. We believe that this discrepancy is due firstly to the incorrectness in the initial propositions of the said theories. The authors assume that each turbulent mole (finite mass of liquid) of the flowing cooler transfers heat across the stream in the same way as the quantity of motion. It is also assumed that throughout the mixing process the mole preserves its heat, i.e., that its temperature remains constant. It is known that one may use the analogy between heat transfer and quantity of motion transfer with satisfactory results only for "usual" liquids with low heat conductivity, for which $Pr \sim 1$. In the flow of molten metals, that have a high heat conductivity and $Pr \ll 1$, the heat content and the temperature of the turbulent mole on the path of transfer from one liquid layer to another changes and consequently the convective heat transfer of the mole in molten metals flow is relatively smaller than in the flow of "usual" liquids with low heat conductivity.

The theory based on these assumptions about the heat exchange process fits in well with the data produced by experiments.

In Fig. 2 the results of our experiments are compared with the theories of American authors.

It is noteworthy that Dwyer's latest conclusions[5] based on experimental studies have led him to diminish Lyon's result and to offer the following formula for calculating the heat delivery of heavy molten metals:

$$Nu = 4.9 + 0.018\,(Re \times Pr)^{0.8}$$

which in the range of $Re \times Pr$ varying from 1×10^3 to 2×10^4 gives a difference of 10% to 20% from values obtained by means of Equation 1.

In turbulent flow of liquids in tubes the heat transfer takes place through the turbulent mixing of the stream and through molecular conductivity of the cooler.

The relative part played by these means of heat transfer in the heat exchange process varies for coolers with different Prandtl numbers. In the turbulent flow of liquids with a small heat conductivity the heat exchange process (there being no boiling) is mainly determined by conditions of the flow of the cooler and is less influenced by the thermophysical properties of the cooler. One may therefore assume that the dependence of Nu on the Prandtl number is different for liquids with different thermophysical properties.

The choice of the system of similarity criterions and the corresponding treatment of different experimental data made it possible to determine the interdependence which defines unequivocally the general law governing the heat exchange process in a large interval of variation of criterions Re and Pr. This dependence is shown on Fig. 3 with experimental data for different metallic and non-metallic cooling agents, their Prandtl numbers differing more than on four orders.

These results are satisfactorily interpolated by the formula:

$$Nu = (3.2 + 0.021\,Re^{0.8} \times Pr^{n})K \qquad (3)$$

in which the exponent n is a continuous function of the Prandtl number.

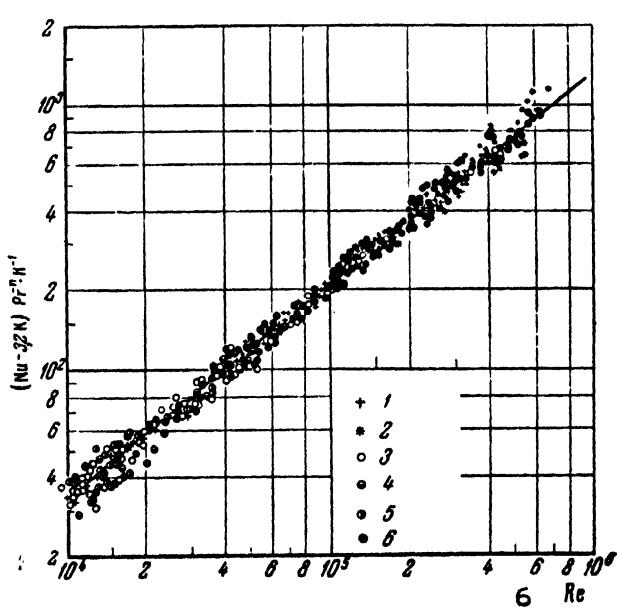

Figure 3. Relation among criterions Nu, Re and Pr in heat transfer of different turbulent flowing liquids: (1) gases (air); (2) water superheated steam; (3) water; (4) kerosene, acetone and others; (5) mineral oils; and (6) molten metals

† In a small interval of variation of the values ($Re \times Pr$) Lyon's theory is confirmed by Werner's experiments, conducted with the sodium-potassium alloy. Werner moistened (according to the author's instruction) the nickel surface of the tubes.

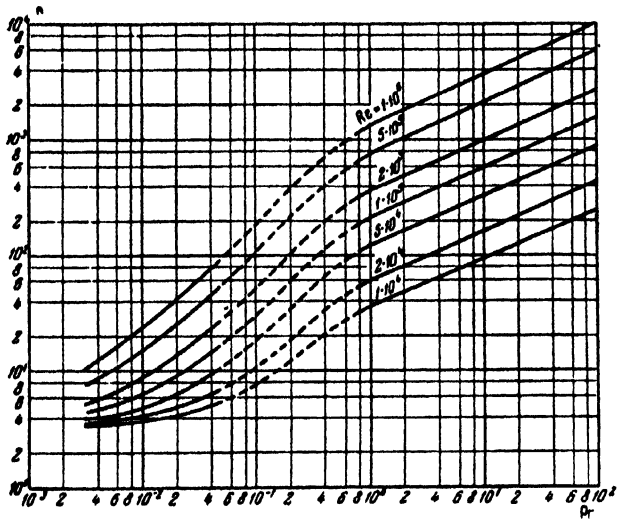

Figure 4. Generalized relation Nu/K = f(Pr) for Re = var

However, to simplify calculations it is sufficient in practice to take $n = 0.43$ for usual liquids with small conductivity (gases, gas mixtures, water, mineral oils and others) and $n = 0.90$ for molten metals.

Equation 3 is represented, in the form of a curve, in Fig. 4.

The coefficient $K = (\mathrm{Pr}_f/Pr_w)^{1/4}$ deduced from experiments[6] accounts for the influence of the physical parameters of the cooler on the heat exchange process.

In practice one may take $K = 1$ for molten metals.

Equation 3 is universal and applicable for calculating heat exchanges in the turbulent flow of any (molten metals included) cooling agents in "long" ($l/d \geqslant 30$) tubes.‡

Equation 3 takes into account the additional thermal resistance of oxides accumulated on the heating surface. That is why for clean surfaces and coolers having $\mathrm{Pr} \ll 1$ one must correct the values of Nu, calculated with the help of Equation 3, according to the correction

$$\mathrm{Nu}_{clean} = \mathrm{Nu} + 1.5$$

The comparison of Equation 3 with Equations 1 and 2, applicable only to molten metals, and with the formula of M. A. Mikheyev[7] that we count as the most reliable for calculating the heat delivery in the turbulent flow of usual liquids with a low heat conductivity, indicate that these formulas are in harmony with Equation 3.

In 1953 Hoffmann published a paper,[8] where a semi-empirical formula was offered for calculating the heat exchange for any values of Pr. Based on the Reynolds-Karman analogy that formula does not take full account of the influence of molecular heat conductivity in the heat transfer process by the turbulent flow of the cooler. For liquids with a low conductivity ($\mathrm{Pr} > 0.7$) the Hoffmann solution gives satisfactory results, but for molten metals the value of Nu calculated with the aid of this formula is twice the experimental value.

A detailed study was made of the heat transfer of heavy and alkaline molten metals and their alloys flowing in conditions of natural convection. Tubes and slabs were used in the experiments in question.

An analysis of the results of the study of the heat transfer of free-flowing usual liquids and molten metals furnished the bases for the general law governing the process in a large interval of variation of Gr and Pr numbers (Fig. 5).

The substitution of the curve shown on Fig. 5 by rectilinear sections depending on laws of 1/4 and 1/3 makes it possible to adopt for practical calculations of heat exchange with natural convection of any coolers including molten metals the equation

$$\mathrm{Nu} = C\mathrm{Gr}^m\mathrm{Pr}^n \qquad (4)$$

Values of the constants c and m in Equation 4 are chosen in dependence on the value of Gr:

Gr	C	m
$10^2 \div 10^9$	0.52	1/4
$10^9 \div 10^{13}$	0.105	1/3

The power of Prandtl number n is calculated through the equation $n = 0.3 + 0.02/\mathrm{Pr}^{1/3}$.

The physical parameters of coolers for calculating the similarity criterions are determined in this case by the mean temperature of the boundary layer.

Equation 4 on Fig. 6 is represented by a function $\mathrm{Nu} = f(\mathrm{Pr})$ with the number Gr as a parameter.

In order to calculate the hydraulics of the reactor-cooling system when metallic coolers are used it is necessary to have a correct idea about the character of the flow of molten metals in tubes and canals.

Since there was no certainty that the flow of molten metals was governed by the classical hydraulic laws, a study was made of the hydraulic

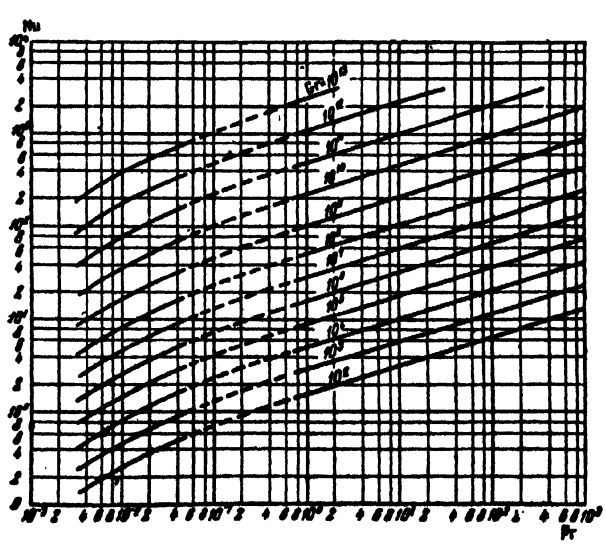

Figure 6. Generalized relation Nu = f(Pr) for Gr = var

‡ The choice of the determining temperature and of the characteristic length for calculations of similarity criterions, is indicated earlier.

resistance of polished steel and copper tubes to the isothermal and non-isothermal flow of heavy and alkaline molten metals. The pressure difference in the investigated tube was measured with the help of differential manometers filled with the studied liquid metal.

The flow of molten tin in oxidized (burnished) and tinned steel tubes was studied in order to ascertain the effect of the moistening of the heated surface.

The investigations have shown that the hydraulic tube friction resistance (in the experimental condition) does not depend on the moistening capacity of the liquid and that the hydraulic resistance coefficients in the tubes are equally dependent on the Reynolds number for metallic and non-metallic liquids. Special experiments revealed that this conclusion is also correct for local resistances.

From the above-said it follows that a quantitative analysis of the hydraulics of a reactor cooling system may be made with the help of ordinary hydraulic formulas.

SUMMARY

This paper contains a survey of the principal results of the investigations of the heat exchanges and hydraulics of molten metals flow conducted at the Academy of Sciences of the USSR.

These investigations shed new light on the heat exchange processes, covering as they do the unexplored field of liquid metallic coolers with a small Prandtl number.

The results obtained furnish the basis for a reliable quantitative analysis for the cooling of reactors by means of molten metals.

REFERENCES

1. Styrikovitz, M. A. and Semenovker, G. E., "Heat Exchange for Low Values of Prandtl's Number," Journal of Technical Physics, USSR, 10, N 16 (1940). Also The Soviet Kotloturbostroenie, N 9 (1940).
2. Johnson, H. A., Hartnett, J. P. and Clabaugh, W. J., "Heat Transfer to Molten Lead-Bismuth Eutectic in Turbulent Pipe Flow," Trans. ASME, 75, N 6 (1953).
3. Lyon, R. W., "Liquid Metal Heat-Transfer Coefficients," Chem. Eng. Progress, 47, N 2 (1951).
4. Seban and Shimazaki, "Heat Transfer to a Fluid Flowing Turbulently in Smooth Pipe with Walls at Constant Temperature," Trans. ASME, 73, N 6 (1951).
5. Dwyer, O. H., "Heat Exchange in LMFR Power Reactor," Nucleonics, *12*: N 7 (1954).
6. Aladiev, G. T., Mikheyev, M. A. and Phiedynsky, O. S., "Heat Exchange Dependence on the Direction of Heat Flow and on Natural Convection," Isvestia A.Sc. USSR, OTN N 11 (1951).
7. Mikheyev, M. A., "Heat Exchange in Turbulent Flow of Liquids in Tubes," Isvestia A.Sc. USSR, OTN, N 10 (1952).
8. Hofmann, E., Uber den allgemeinen Wärmeübergang der turbulenten Rohrstromung und Sinn der Kennzahlen. Forschung, 20, H.3 (1953).

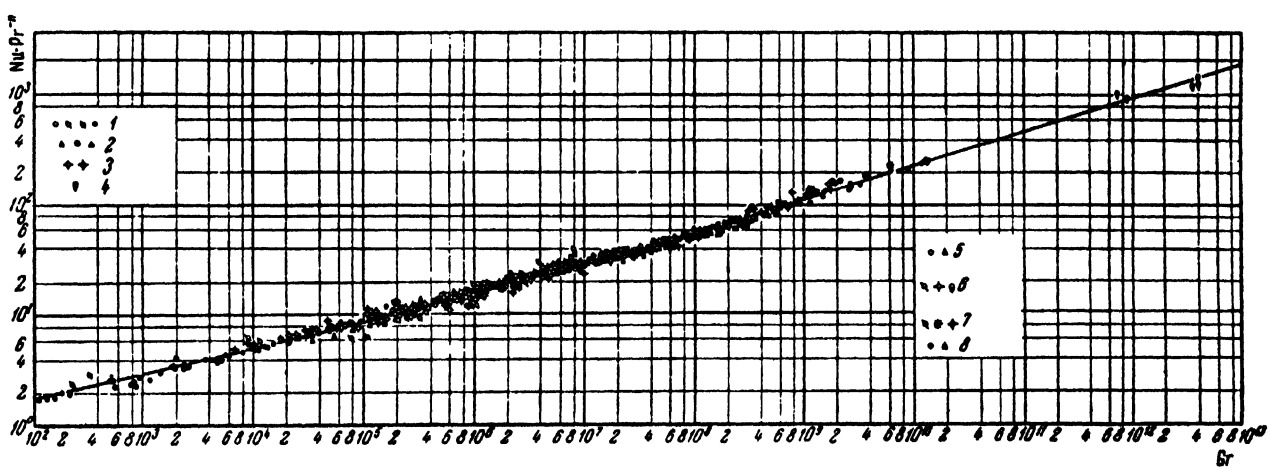

Figure 5. Relation among Nu, Re and Pr numbers in heat transfer of different liquids in conditions of natural convection: (1) tubes and wires; (2) slab; (3) balls; (4) balloons; (5) molten metals: mercury, tin, the bismuth-lead alloy, sodium; (6) gases: air, carbonic acid, hydrogen; (7) water; and (8) mineral oils

Liquid Metal Heat Transfer Predictions

By R. N. Lyon,* USA

The usefulness of liquid metals as reactor coolants is partly due to their high thermal conductivity which results in high heat transfer rates, with low temperature difference. But because liquid metals have higher thermal conductivity than non-metallic fluids, new equations must be developed to predict the heat transfer in cases where turbulent flow occurs. This fact was first discussed by Stirikovich and Semenovker[1], and first used theoretically by Martinelli.[2]

In a long, round tube for example, where heat enters uniformly along the tube wall, a general equation can be found for all fluids under any symmetrical flow régime:[3]

$$\frac{k}{hD} = 2\int_0^1 \frac{\left[\int_0^{S_2} S_1 V dS_1\right]^2}{S_2 K/k}\, dS_2 \qquad (1)$$

where k is the ordinary thermal conductivity of the fluid; K is the total local thermal conductivity of the fluid (ordinary conductivity k + eddy conductivity); h is the heat transfer coefficient (heat flow rate per unit area normal to the solid surface, divided by the difference between the temperature of the wall and the average temperature of the *flowing* stream); D is the tube diameter; S is the distance from the tube axis divided by the tube radius; and V is the local velocity of the stream divided by average velocity of the stream.

If it is assumed that the eddy diffusivities of heat and momentum are identical at each point, this equation can be solved graphically for turbulent flow using the local velocity data of Nikuradse,[4] and the results, as well as those of Martinelli, can be represented approximately by the equation for liquid metals in turbulent flow:

$$\frac{hD}{k} = 7 + 0.025\left(\frac{Du_m\rho c}{k}\right)^{0.8} \qquad (2)$$

where u_m is the average velocity of the fluid; c is the heat capacity of the fluid; and ρ is the density of the fluid.

As heat passes into the interior of the turbulent core, it is carried by two mechanisms in parallel. One is eddy conductivity, which carries essentially all of the heat into the turbulent core of ordinary fluids. The relative importance of this mechanism is given by the last term in Equation 2 which may be written, $0.025(\mathrm{Pe})^{0.8}$, where the term "Pe" stands for Peclet modulus.

The other mechanism for carrying heat into the turbulent core is ordinary thermal conduction, and its relative importance is 7 in Equation 2.

The comparative importance of turbulence and conduction in the turbulent core can be gathered from Table I.

From these figures it is seen that at $\mathrm{Pe} < 10^4$ the ordinary conductivity has an important influence on Nu, Nusselt modulus, because of conduction in the turbulent core.

A similar parallel heat flow takes place in the semi-turbulent buffer region near the tube wall. In this region, the relative importance of eddy transfer is related to the Prandtl modulus, $c\mu/k$, where μ is the viscosity of the fluid. For $\mathrm{Pr}<0.1$, which is true for most liquid metals, ordinary conduction controls in the buffer region, and the resistance of the region near the wall is relatively unimportant. For non-metallic fluids with Prandtl modulus usually greater than 0.5, eddy conductivities will be largely controlling in the turbulent core, and the resistance of the less turbulent region near the wall will be important because of the lower thermal conductivity.

In practical liquid metal-reactor applications, the range of Peclet modulus with turbulent flow will be between about 20 and 10,000.

It must be concluded, therefore, that the idea of a fictitious fluid film which incorporates all of the thermal resistance is of little use in predicting liquid metal heat transfer. In liquid metal heat transfer, important thermal resistance may extend far into the turbulent core.

It is apparent at once, as Stirikovich and Semenovker found experimentally,[1] that the equivalent

Table I. Relative Importance of Eddy Conduction in the Turbulent Core

Pe	$0.025\,Pe^{0.8}$	$\frac{0.025\,Pe^{0.8}}{7}$	$Nu = \frac{hD}{k}$
0	0	0.00	7
10	0.133	0.019	7.133
10^2	1.0	0.143	8.00
10^3	6.25	0.89	13.25
1.15×10^3	7.0	1.0	14.0
10^4	40	5.71	47
10^5	250	35.7	257
10^6	1330	190.	
10^7	10,000	1430.	

* Oak Ridge National Laboratory.

or hydraulic diameter cannot be used directly in relating heat transfer in differently shaped channels.

ROUND TUBES WITH CONSTANT WALL TEMPERATURE

It is found theoretically by Seban and Shimazaki[5] that the ordinary conduction contribution with constant wall temperature is about 5, compared with 7 when constant heat flows through the wall. Thus for constant wall temperature in a long tube, the heat transfer should be given by

$$\mathrm{Nu} = 5 + 0.025\ (\mathrm{Pe})^{0.8} \qquad (3)$$

OTHER THEORETICAL EQUATIONS

Other approximate theoretical equations of interest are:

$$\frac{2hd}{k} = 5.8 + 0.02\left(\frac{u_m \rho c d}{k}\right)^{0.8} \qquad (4)$$

for a channel between two plates with heating passing through only one side[6] where d is the distance between the plates, and

$$\frac{h(D_o - D_i)}{k} = 0.75\left(\frac{D_o}{D_i}\right)^{1/5} \times \left[7 + 0.025\left(\frac{(D_o - D_i)\, u_m \rho c}{k}\right)^{0.8}\right] \qquad (5)$$

for some annuli,[7] where D_o is the outer diameter, and D_i is the inner diameter.

A more complete presentation of theoretical expressions is given in the Liquid Metals Handbook.[7]

SHELL-SIDE HEAT TRANSFER

The baffled shell-side heat transfer coefficient of a tube-and-shell heat exchanger cannot be predicted by a simple theoretical approach because of the complicated fluid flow across the tubes. Tidball found that the empirical equation of Donohue[8] could be used to correlate data from a few early tests with sodium-potassium alloy.

More complete data by Tidball,[9] as well as data obtained by Brooks with sodium[10] and Hoe and Dwyer with mercury show that Donohue's Equation[11] may lead to predictions which are as much as ten times the experimentally determined value.

All of the data appear to be represented approximately by the expression:

$$\frac{hD_t}{k} = B\left(\frac{W}{D_t \mu}\right)^{0.6} \qquad (6)$$

where D_t is the diameter of the tubes; W is the mass flow rate of liquid metal across the tubes; and B is a function of the geometry of the tube and shell arrangement and of the Prandtl modulus. The term, B, is not well defined and is not necessarily the same for similar models of different scale.

COMPARISON OF THEORETICAL AND EXPERIMENTAL PREDICTIONS

Unfortunately, the theoretical expressions do not always predict exact values found in experiments.

A very complete summary of experimental liquid metal heat-transfer information in long and short circular tubes and in annuli, has recently been published by Lubarsky and Kaufman.[12] Figure 1 is taken from their report and shows the long tube data of many investigators after re-evaluation to a consistent basis. Equation 2 is shown as a solid line, and a new empirical equation proposed by Lubarsky and Kaufman is shown as a broken line through the bulk of the data.

$$\mathrm{Nu} = 0.625\ \mathrm{Pe}^{0.4} \qquad (7)$$

This equation predicts values of about one half those predicted by Equation 2 at Pe = 100 and Pe = 10^4, and values about thirty per cent below Equation 2 at Pe= 10^3.

Several reasons have been put forth by liquid metal investigators to explain the discrepancy between the theoretical prediction and the experimental results. Not all of the explanations have been carried to completion, but no single explanation has sufficed.

First let us examine the experiments briefly. It will be noticed that essentially all of the data of Isakoff and Drew[19] lie near the theoretical curve, as do some of the data of Johnson, *et al.* The data of Werner, *et al.*[22] with sodium-potassium alloy are not shown, but they also lie near the curve.

Experimental causes of low heat transfer which have been proposed are non-wetting of the wall, scale formation at the wall, gas entrained in the liquid (this is known personally to have been true in some of Stromquist's experiments and is also reported by Quittenton) and, as suggested by Trefethen,[23] a longitudinal conduction error in measuring the mean temperature of the heated or cooled stream.

Let us now examine the hypotheses for Equation 1. The most important postulates are: (1) well-established symmetrical velocity and temperature profiles and (2) constant heat flow rate through the tube wall regardless of location. In most of the experiments these requirements appear to have been met, except perhaps at low values of Pe where because of lower velocity some natural convection may have become important, or as suggested by Quittenton dissolved or entrained gas may be liberated and accumulate at poorly wet regions of the wall. Such a condition might explain the drastic drop in experimental Nu below Pe = 100.

It should be noted that Equation 1 predicts a minimum value of Nu = 4$\frac{4}{11}$ for classical viscous flow.

The most obvious weakness in the solution of Equation 1 to obtain the values approximated by Equation 2 is the postulate that the eddy diffusivity of momentum is numerically identical with the eddy diffusivity of heat.

Cope,[24] Trefethen,[13] and Kennison[25] have investigated the possibility that vorticity transfer rather than momentum transfer should be compared with heat transfer in the turbulent core.

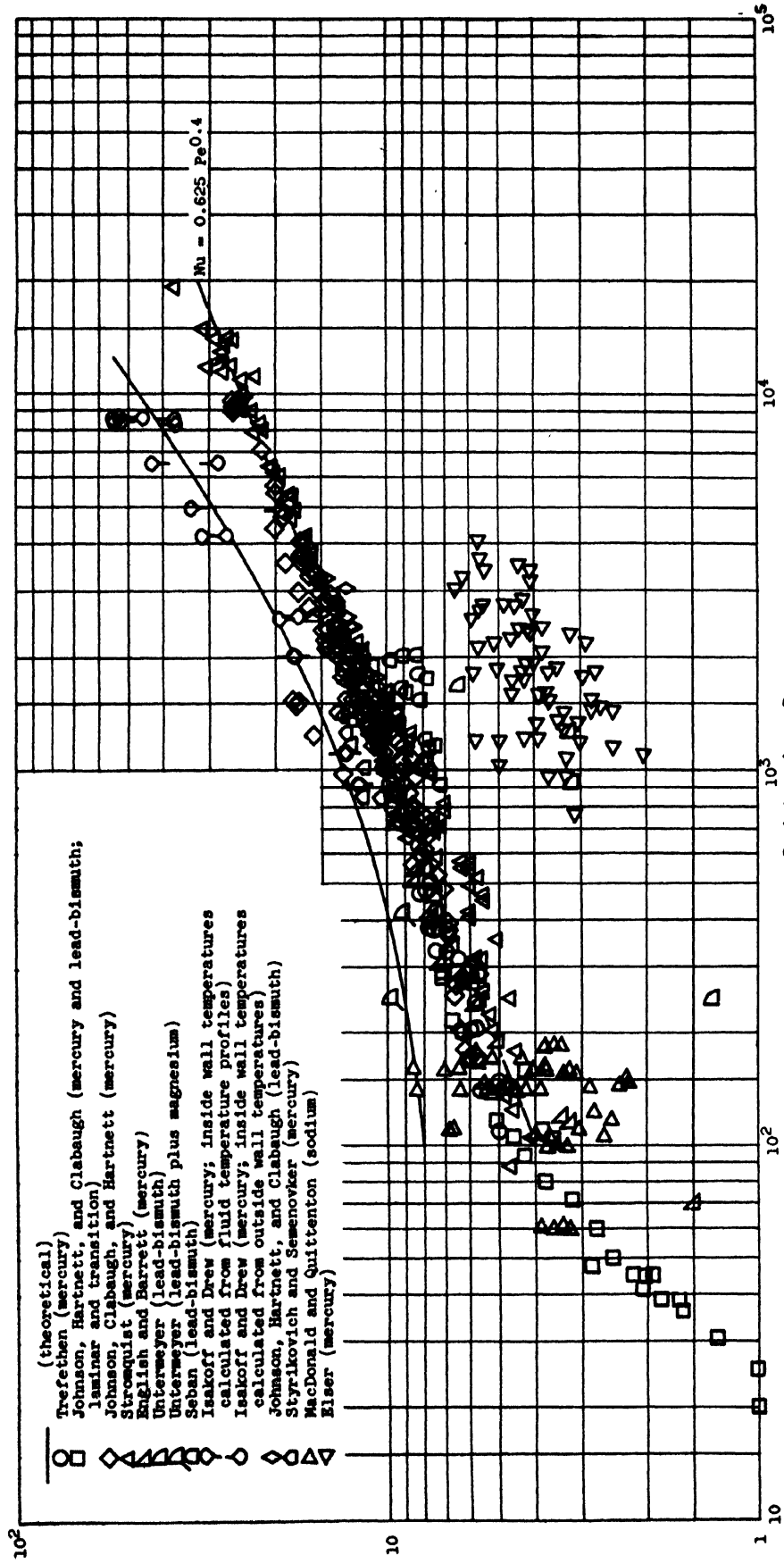

Figure 1. Experimental data for long tubes as re-evaluated by Lubarsky and Kaufman (ref. 12). The theoretical curve represents Equation 2. The original data were obtained from the following references, listed in descending order in the key at the upper left hand corner: 13, 14, 14, 15, 16, 17, 17, 18, 19, 19, 14, 1, 20, 21

Deissler[26] and Jenkins[27] have made modifications to the mixing length theory to allow for heat loss during radial transit of a particle or an eddy.

While difficult to visualize, it might be postulated that the ordinary thermal conductivity of the liquid may be affected by the high velocity gradients encountered in the turbulent core. On the other hand no such effect has been observed in the ordinary transfer of momentum at high velocity gradients.

Although each of these approaches offers a possible explanation, real understanding will probably come as a result of better basic experimental data. In this regard the work of Isakoff and Drew[19] is unique in the liquid metal field. Isakoff and Drew are the only experimenters who have actually measured the temperature and velocity profiles of a liquid metal stream inside a heat exchanger. Thus they were not only able to determine the overall conductance into the stream, but the total local conductivities as well. Their overall data agree with Equation 2 reasonably well, but the temperature profiles are not predicted by the theory as developed by Martinelli. (Fig. 2).

SHORT HEATED LENGTHS

Theoretical predictions for long tubes with short heated lengths have been made by Sanders,[28] by Poppendiek and Palmer[29] and by Deissler.[26] A finite difference solution of the short tube case has been made by Seban and Shimazaki.[30] In these cases the experimental data agree only approximately with the theoretical predictions although the data lie both above and below the prediction. In addition to the possible explanations listed for the case of long tubes, the lack of agreement here may also be due to inaccurate knowledge of the velocity profile of the stream as it enters the heated section. Another possible explanation is the difficulty of maintaining a sharp discontinuity in heat flux at the beginning of the heated section.

A comprehensive comparison between existing data and current theories for short heated lengths is presented by Lubarsky and Kaufman.[12]

CONCLUSION

In conclusion we find that the theoretical development is not quite satisfactory in predicting liquid metal heat transfer. The theory will at the present time provide a good guess within perhaps a factor of two. Good design must rely at present largely on overdesign using current empirical or theoretical equations, and on full scale mock-up tests.

Progress in theoretical development requires much more experimental work of the type performed by Isakoff and Drew. It is believed that theoretical development, based on this type of experiment and the accumulation of more operating data can result in much more accurate generalizations for the design of better liquid metal reactor systems. Such studies will also result in a better understanding of the basic laws of turbulent hydrodynamics, and turbulent heat transfer which are so important in all power reactor development.

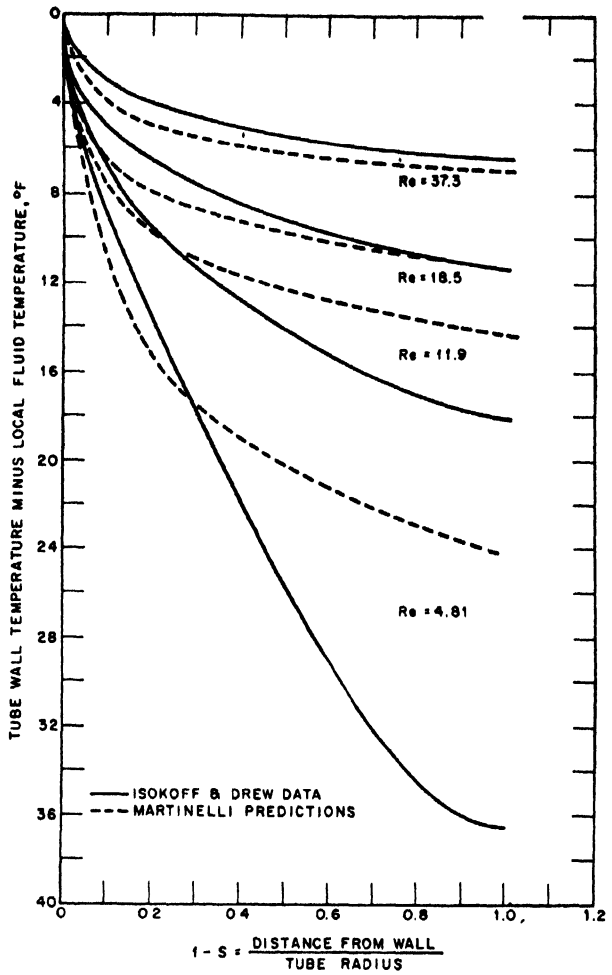

Figure 2. Comparison of temperature distribution data using mercury, Pr = 0.0239 with Martinelli's theoretical predictions (From Isakoff and Drew[19])

REFERENCES

1. Stirikovich, M. A. and Semenovker, I. E., *Heat Exchange at Very Low Pr Numbers,* J. Tech. Phys. (USSR) *10,* 1324–1330 (1940).
2. Martinelli, R. C., *Heat Transfer to Molten Metals,* Trans. Am. Soc. Mech. Engrs. *69*: 947–959, (1947). Minor numerical corrections are listed by Dr. Martinelli in a discussion of another paper, Trans. Am. Soc. Mech. Engrs. *71*: 802–803 (1949).
3. Lyon, R. N., *Liquid-Metal Heat Transfer Coefficients,* Chem. Eng. Prog., *47*: 75–79 (1951).
4. Nikuradse, J., *Gesetzmassigkeiten der turbulenten Stromung in glatten Rohren,* VDI Forschungsheft 356 (1932).
5. Seban, R. A. and Shimazaki, T., *Heat Transfer to a Fluid Flowing Turbulently in a Smooth Pipe with Walls at a Constant Temperature,* Am. Soc. Mech. Engrs., Paper No. 50–A–128 (1950).
6. Seban, R. A., *Heat Transfer to a Fluid Flowing Turbulently Between Parallel Walls with Asymmetric Wall Temperatures,* Trans. Am. Soc. Engrs., *72*: 789–795 (1950).
7. *Liquid Metals Handbook, Second Edition,* US Atomic Energy Commission (1952). Superintendent of Documents, Washington 25, D. C.

8. Donohue, D. A., Ind. Eng. Chem. *41*: 2499–2511 (1949).
9. Tidball, R. A., Mine Safety Appliances Company, Pittsburgh, Personal Communication (17 January 1955).
10. Brooks, R. D., Mech. Eng. *75*: 363 (1953).
11. Hoe, R. J. and Dwyer, O. E., *Heat Transfer to Cross-Flowing Mercury in Staggered Tube Banks,* Brookhaven National Laboratory (1954).
12. Lubarsky, B. and Kaufman, S. J., *Review of Experimental Investigations of Liquid Metal Heat Transfer,* Technical Note 3336, National Advisory Committee for Aeronautics (1955).
13. Trefethen, L. M., *Heat Transfer Properties of Liquid Metals,* Atomic Energy Establishment, Harwell, Berks (1 July 1950); NP-1788, US Atomic Energy Commission (31 March 1951).
14. Johnson, H. A., Hartnett, J. P. and Clabaugh, W. J., *Heat Transfer to Molten Lead-Bismuth Eutectic in Turbulent Pipe Flow,* Trans. Am. Soc. Mech. Engrs. *75*: 1191–1198 (1953); *Heat Transfer to Molten Lead-Bismuth Eutectic in Turbulent Pipe Flow,* Final Report, Inst. Engr. Res., University of California, Berkeley (15 November 1951); *Heat Transfer to Mercury in Turbulent Pipe Flow,* Inst. Engr. Res., University of California, Berkeley (July 1953); *Heat Transfer to Lead-Bismuth and Mercury in Laminar and Transition Pipe Flow,* Inst. Engr. Res., University of California, Berkeley (August 1953).
15. Stromquist, W. K., *Effect of Wetting on Heat Transfer Characteristics of Liquid Metals,* ORO-93, US Atomic Energy Commission (March 1953).
16. English, D. and Barrett, T., *Heat Transfer Properties of Mercury,* Atomic Energy Research Establishment, Ministry of Supply, Harwell, Berks (June 1950).
17. Untermeyer, S., Argonne National Laboratory, Personal Communication, (15 June 1949).
18. Seban, R. A., *Heat Transfer Measurements on Lead-Bismuth Eutectic in Turbulent Pipe Flow,* Inst. Engr. Res., University of California, Berkeley (15 June 1950).
19. Isakoff, S. E. and Drew, T. B., *Heat Transfer in Turbulent Flow in Mercury,* General Discussion on Heat Transfer, Inst. Mech. Engrs. and Am. Soc. Mech. Engrs.: 405–409 (1951).
20. McDonald, W. C. and Quittenton, R. C., *A Critical Analysis of Metal "Wetting" and Gas Entrainment in Heat Transfer to Molten Metals.* Preprint No. 8, Am. Inst. Chem. Engrs. (1953); Quittenton, R. C., *Direct Measurement of Film Coefficient of Heat Transfer to Molten Sodium Metal in Forced Convection,* Ph.D. Thesis, University of Toronto (1953).
21. Elser, D., *Warmeubergansmessungen an Quecksilber,* Schweitzer Archiv, pp 330–336 (November 1948). (English translation by Ronald Kay, Engineering Research Projects, University of California, Berkeley (1949).
22. Werner, R. C., King, E. C. and Tidball, R. A., *Heat Transfer with Sodium-Potassium Liquid Alloys,* presented at Annual Meeting, Am. Inst. Chem. Engrs., Pittsburgh (5 December 1949).
23. Trefethen, L., *Some Current Liquid Metal Heat Transfer Problems,* an outline of a paper presented at Massachusetts Institute of Technology, Summer Session on Modern Developments in Heat Transfer (July 1954).
24. Cope, W. F., *Heat Transfer to Mercury,* General Discussion on Heat Transfer, Inst. of Mech. Eng. and Am. Soc. Mech. Eng.: 453–458 (1951).
25. Kennison, R. G., *Vorticity Heat Transfer in Molten Metals,* Knolls Atomic Power Laboratory, General Electric Company, Schenectady, N. Y. (11 April 1952).
26. Deissler, R. G., *Analysis of Fully Developed Turbulent Heat Transfer at Low Peclet Numbers in Smooth Tubes with Application to Liquid Metals,* National Advisory Committee for Aeronautics, NACA RM E52FO5 (1952).
27. Jenkins, R., *Variation of Eddy Conductivity with Prandtl Modulus and Its Use in Prediction of Turbulent Heat Transfer Coefficients,* 1951 Heat Transfer and Fluid Mechanics Institute—Preprints of Papers, Stanford University,: 147–158 (20, 21, 22 June 1951).
28. Sanders, V. D., *A Mathematical Analysis of Turbulent Heat Transfer in a Pipe with a Surface Discontinuity at the Entrance,* M.S. Thesis, University of California (November 1946).
29. Poppendiek, H. F., *Forced Convection Heat Transfer in Thermal Entrance Regions, Part I,* Oak Ridge National Laboratory, ORNL-913 (1951); Poppendiek, H. F. and Palmer, L. D., *Forced Convection Heat Transfer in Thermal Entrance Regions, Part II,* Oak Ridge National Laboratory, ORNL-914 (1952).
30. Seban, R. A. and Shimazaki, T., *Calculations Relative to Thermal Entry Length for Fluids of Low Prandtl Number,* Institute of Engr. Res., University of California, Berkeley (10 January 1950).

Liquid Metal Heat Transfer

By W. B. Hall,* UK

ABSTRACT

The possible industrial applications for liquid metals as heat-transfer media and the theoretical approach to the problem of heat transfer with low Prandtl number fluids are discussed.

A description is given of experiments in which the heat-transfer coefficients between two annuli, each carrying a flow of liquid metal, were measured. Whilst a direct comparison with results obtained with a circular tube is not possible, the results are in quite good agreement with the theoretical values given by Lyon. A number of aspects of the work which are of interest in the design and operation of liquid metal circuits are discussed.

In the course of the work it was found that there were significant variations in temperature around the annuli carrying the liquid metal in the heat exchanger. It is thought that these variations were due to slight eccentricity of the exchanger tubes. An approximate theoretical treatment indicates that such variations are likely to be greater (when expressed as a fraction of the over-all temperature difference) in the case of liquid metals than in the case of fluids with a higher Prandtl number. In these experiments, where the heat flux was about 50 watts per cm^2, the temperature variations were quite small, but if full advantage is taken of the liquid metal to obtain high heat fluxes, they might be so large as to produce serious thermal stresses and distortion of the heat exchanger.

INTRODUCTION

In recent years considerable interest has been shown in the use of liquid metals as heat-transfer media. Their useful working range of temperature is as much responsible for this as their good heat-transfer properties. In the field of power generation by atomic energy, they are suitable coolants for nuclear reactors, and can be operated at sufficiently high temperatures to enable a high power-generation efficiency to be achieved. Other possible uses might be as a heat-transfer medium acting between the turbine and the boiler furnace in a steam reheat system in a power station; or between the two sides of a gas turbine heat exchanger. In both these cases the use of a liquid metal circuit might give a more economical arrangement of the plant.

Purely from a heat-transfer point of view, liquid metals are interesting in that they usually have a very low value of Prandtl number (ratio of kinematic viscosity or momentum diffusivity to thermal diffusivity) compared with all other fluids. Whereas with most fluids the convective heat-transfer process is governed very largely by the effect of turbulence on the diffusion of heat, with liquid metals the conductivity may be so high as to swamp the turbulent, or "eddy" conductivity. Empirical formulae based on heat-transfer data for gases and high Prandtl number fluids are not in agreement with liquid metal data; semi-empirical techniques involving the analogy between the transfer of heat and momentum in a pipe require modification to allow for ordinary conduction in the turbulent core.

Under the condition of very high heat flux which can be attained when using a liquid metal coolant any film of low conductivity material adhering to the heat transfer surface will cause an excessive temperature drop. It was this fact, coupled with the realisation that it might be somewhat difficult to prevent a certain amount of oxidation of sodium under plant conditions, which led to the decision to make the heat transfer measurements described below. The detailed experimental results and their analysis are given elsewhere (Hall and Jenkins 1955).[1]

THEORETICAL CONSIDERATIONS

The process of heat transfer from a solid surface to a fluid flowing past it takes place by two separate mechanisms. Firstly, heat will flow into the body of the fluid by the normal process of conduction: given the distribution of the velocity (parallel to the surface) with distance from the surface, it is possible to calculate the temperature distribution and evaluate the heat-transfer coefficient, if this is the only mechanism of heat transfer. Usually there is a second effect superimposed upon the first, due to turbulence in the fluid. In the earlier theories of turbulence, small masses of fluid were supposed to travel across the direction of the main flow and in doing so to transfer momentum between regions of different velocity and heat between regions of different temperature. The process is much the same as that of thermal conduction in gases, except that it takes place on the macroscopic rather than the molecular scale; its effect is to increase the apparent conductivity of the fluid. The present knowledge of turbulence is not sufficient to permit the *a priori* calculation of its effect on heat transfer, and the

* UK Atomic Energy Authority, Risley.

problem is usually approached from an empirical standpoint.

Empirical Approach

It may be shown that the experimental results for heat transfer by forced convection in a pipe can be expressed by a relationship such as

$$\frac{hd}{k} = f\left\{\frac{vd\rho}{\mu}, \frac{c\mu}{k}\right\}$$

or $$\mathrm{Nu} = f(\mathrm{Re}, \mathrm{Pr})$$

The advantage of using non-dimensional groups is merely one of simplification. The various physical quantities entering into the problem must be arranged in such a way that the equation is dimensionally consistent, and the above relationship is one way of expressing this condition. The functional relationship between the above quantities must be determined from the experimental data and cannot be assumed to be generally applicable outside the range of these data. The range of Prandtl number greater than unity has been covered fairly adequately by an equation of the form

$$\mathrm{Nu} = A \cdot \mathrm{Re}^m \cdot \mathrm{Pr}^n$$

where A, m, and n are experimentally determined constants. This expression is not in agreement with data for liquid metals which have a Prandtl number of the order of 0.01, and consequently a different empirical expression must be found for this part of the range. Lyon (1951) expresses the form[2,3]

$$\mathrm{Nu} = A + B(\mathrm{Re} \cdot \mathrm{Pr})^m$$

where A, B, and m are constants.

Analogies between Heat and Momentum Transfer

An alternative method of approach is to make use of the analogy between the transfer of momentum and the transfer of heat. Reynolds (1890) was the first to use this method,[5] followed by Prandtl and von Karman, and it has been applied quite successfully to the case of Prandtl number greater than unity. In the later developments of the analogy the fluid stream is divided into three regions: one close to the wall, where the flow is assumed to be laminar and heat is assumed to be transferred by the normal conduction process alone; secondly, a turbulent core, where it is assumed that the "eddy" or turbulent contribution to the conductivity is large compared with the molecular conductivity; and thirdly, a buffer region between the other two, where both mechanisms operate. The eddy diffusivity for momentum is determined from measurements of pressure drop along the pipe and velocity distribution across the pipe, and this value is assumed to be identical with the eddy diffusivity of heat in the heat-transfer calculation. Liquid metals differ from most other fluids in that they have a high thermal conductivity which cannot be ignored in relation to the eddy conductivity even in the turbulent core of the stream. Martinelli (1947)[4] has modified the analogy to take account of this fact. The main interest in the analogy between heat and momentum transfer is that it may be used as a test for theories of turbulence. For example, the assumption that the eddy diffusivities for heat and momentum are equal gives quite good results for high Prandtl number fluids; however, with these fluids the bulk of the temperature drop occurs in the laminar layer, so that they are not a good test of the validity of this assumption in the turbulent core. Liquid metals, for which the resistance of the laminar layer is relatively small, provide a better test for such theories.

Simplified Theoretical Analysis

With liquids of very high thermal conductivity it may be permissible to neglect the effect of eddy conductivity, at any rate for a Reynolds number below a given limit (about 10^5 in the case of sodium). In this case the heat-transfer problem reduces to the solution of the conduction equation with a convection term, for boundary conditions that the heat flux through the walls of the channel is uniform. This may be written

$$k\nabla^2 t - \rho v c \frac{\partial t}{\partial z} = 0$$

where $\partial t/\partial z$ is the temperature gradient in the direction of flow.

When fully developed conditions have been established, the distribution of v across the channel is known, and $\partial t/\partial z$ is constant across the channel, unless the temperature variation across the channel is large, k, ρ, and c may be assumed constant, and numerical integration of the equation can be made, giving the temperature distribution and the heat-transfer coefficient. This method is identical with that used in the case of laminar flow, as in both cases it is assumed that the transfer of heat is by conduction alone. The velocity distribution in a pipe is fairly flat under turbulent flow conditions, and quite a good estimate of the heat-transfer coefficient can be made by making v constant in the above equation. In a circular pipe this "slug" or "rod" flow solution leads to the result that the Nusselt number is constant and equal to 8, and for flow between infinite flat plates, one of which is insulated, the Nusselt number is 6. Trefethen (1951), in his work[6] on heat transfer between mercury in a tube and in an annulus, uses this concept of "slug Nusselt number" to separate the tube and annulus, heat-transfer coefficients. He assumes that the ratio of the actual Nusselt numbers for the tube and for the annulus at a given Peclet number is the same as the ratio of their slug Nusselt numbers. His experimental data support this assumption, and his method has therefore been used in this report.

DESCRIPTION OF APPARATUS

Experiments Using Sodium

A "figure of eight" circuit was adopted for the system, this method having the advantage that the

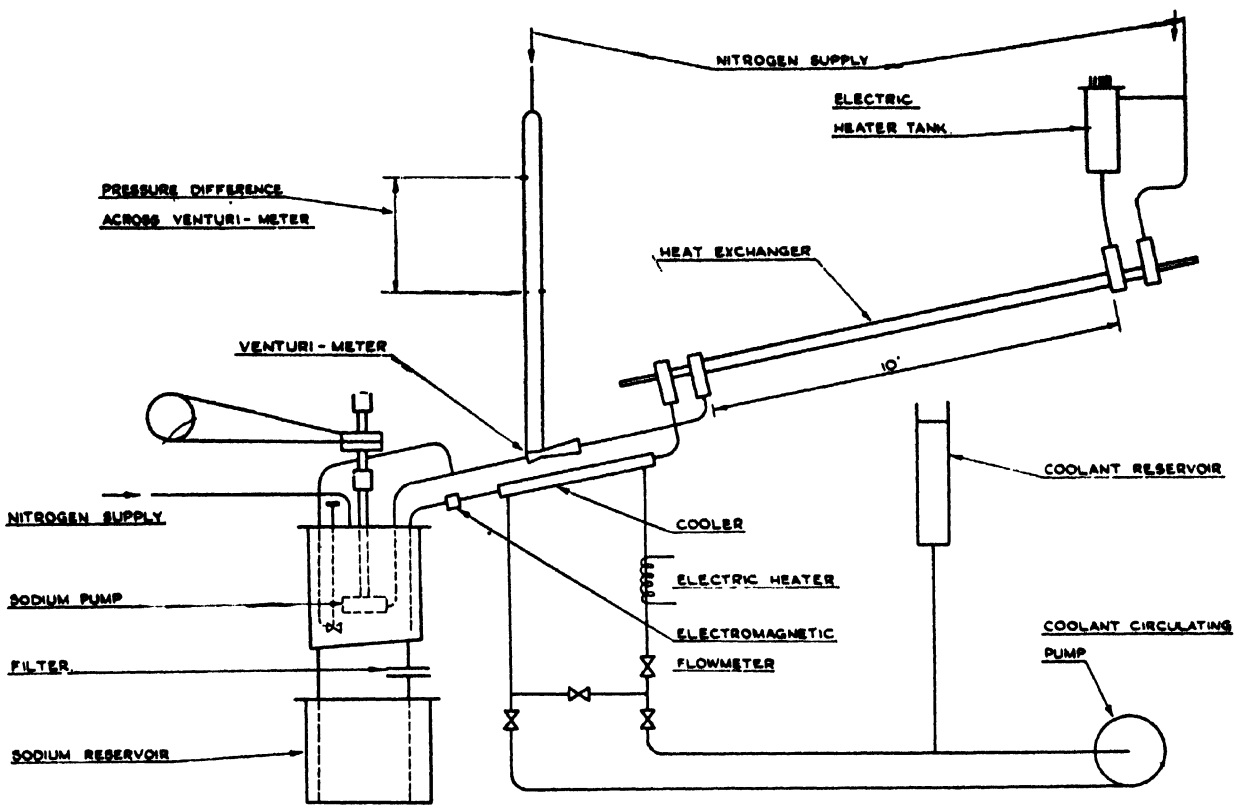

Figure 1. Sketch of apparatus

net heat input is considerably smaller than the heat transferred in the exchanger. The circuit is shown diagrammatically in Fig. 1, and was constructed entirely of mild steel. The exchanger consists of three concentric tubes, sodium flowing up the annulus between the outer and middle tubes through a heater, and back down the annulus between the middle and inner tubes. The heater maintains a temperature difference between the two streams of sodium, and as the mass flow is the same in each annulus, the temperature difference remains constant along the length of the exchanger (apart from a slight variation due to the change of specific heat with temperature). From the exchanger the sodium passes through a cooler where the heat put in by the heater is extracted, and thence through an electromagnetic flow-meter to the pump tank. The system is charged from a reservoir tank through a sintered stainless-steel filter.

The choice of a double annulus exchanger, rather than the more usual tube and annulus, enabled the temperature distribution along the length of each side of the exchanger to be measured. A thermocouple probe was constructed which could be inserted into the inner tube. As there is no heat flux through this tube, a thermocouple spring loaded on its inner surface could be relied upon to give the temperature of the sodium in contact with its outer surface. The corresponding sodium temperature in the outer annulus was measured by thermocouples brazed to the outer tube at intervals of one foot along the length of the exchanger. The construction of the exchanger is shown in Fig. 2. The annuli run into mixing pots at each end, and these pots are

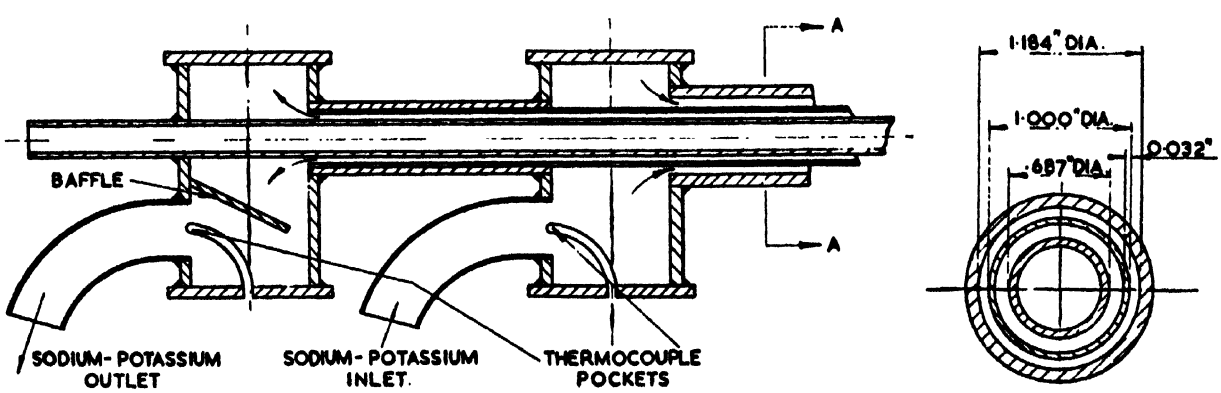

Figure 2. Sketch of end of heat exchanger

fitted with thermocouple wells. Four locating pins ⅛ inch in diameter are welded on the outside of the inner tube and on the inside of the outer tube at intervals of one foot along the exchanger so as to position the middle tube accurately.

The heat input was achieved by means of seven mild-steel-sheathed immersion-heater elements each rated at three kilowatts. Provision was made for switching in any number of elements, and one was operated from a variable transformer to give fine control. The cooler consisted of a jacket round the sodium pipe through which "Dowtherm A" (the eutectic mixture of diphenyl and diphenyl ether) was circulated. Heat was removed from the Dowtherm circuit by means of a water cooler.

The flow of sodium through the circuit was measured by means of a venturi meter. The tappings on the venturi were connected to vertical tubing, thus forming a sodium manometer. Potential tappings were brazed to these tubes at intervals of 10 cm along their length, and by making measurements of the potential difference between adjacent pairs of tappings when a current of about 10 amp was passed through the tubes it was possible to determine the level of the sodium. A nitrogen supply to the top of the manometer maintained the levels of the sodium at a convenient position for measurement. The difference in level between sodium in the two tubes could be measured to an accuracy of about 0.5 cm, or about 1 per cent. An electromagnetic flowmeter was also fitted in the circuit and calibrated against the venturi meter. This consisted of a permanent horseshoe magnet mounted on a section of the one-inch diameter pipe which had been flattened to a width of ½ inch; tappings were brazed to opposite sides of the pipe so as to measure the potential difference in a direction at right angles to the magnetic flux. The output from the flowmeter, which was of the order of 2 millivolts for maximum flow, was measured on a potentiometer.

A centrifugal pump was used to circulate the sodium, this being submerged below the sodium level in the pump tank. The pump shaft was carried on bearings outside the tank, and passed through a gland in the tank cover; as the sodium in the tank was blanketed with nitrogen, this gland was merely a gas-seal. A by-pass pipe on the pump delivery, terminating in a valve submerged in the sodium in the pump tank, enabled the flow through the exchanger circuit to be varied. The sodium level in the tank was determined by insulated electrodes passing through the cover; when the sodium made contact with these, indicator lamps were lit on the control panel.

Experiments Using Sodium Potassium (22 per cent Na)

As a result of the experiments with sodium it was decided that a shorter heat exchanger could safely be used without causing any difficulties from end effects; consequently the work was carried out on an exchanger 2.5 ft long. At the same time, a change from mild steel was made, and the centrifugal pump was replaced by a single-phase electromagnetic pump. The decision to use stainless steel was dictated by cleaning considerations rather than any fundamental objection to mild steel as a constructional material for sodium circuits.

Apart from these changes the apparatus remained substantially the same as for the work on sodium.

EXPERIMENTAL RESULTS

Over-all heat-transfer coefficients were determined from the temperature difference (as measured in the mixing pots) and the heat exchange calculated from the mass flow and the temperature rise from end to end of the exchanger. The temperature drop through the dividing wall could be calculated, but an assumption had to be made concerning the relative magnitudes of the coefficients in the inner and outer annuli. The basis of this assumption is mentioned above.

The results are presented below in Fig. 3.

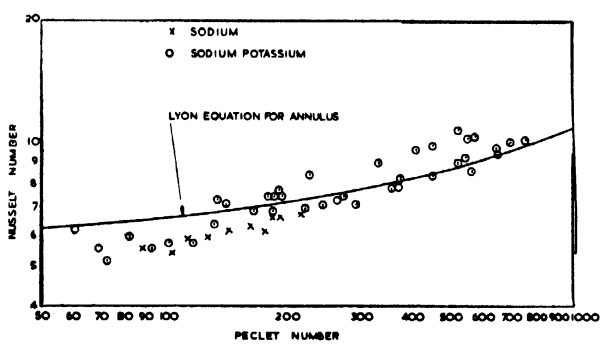

Figure 3. Results from double-annulus exchanger

In the tests using sodium, the temperature of the inner tube was found to be far from uniform round its circumference. Figure 4 shows a representative set of temperature distribution curves taken at intervals of two feet along the exchanger. In order to check the method of measurement, readings were taken with the sodium at approximately the same mean temperature in the exchanger, but with no input to the heater tank, and therefore no heat ex-

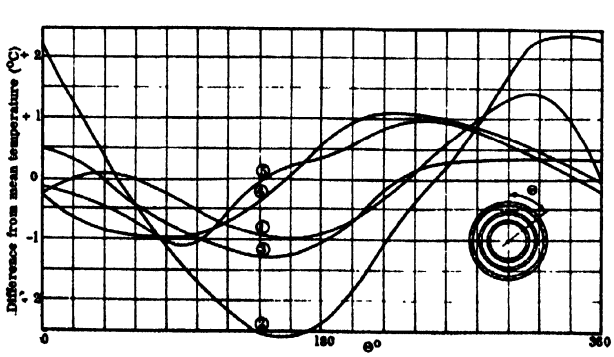

Figure 4. Temperature variation around inner tube. Numbers on curves refer to measuring stations situated at 2 ft—0 in. intervals along length of exchange

change; under these circumstances the temperature was uniform around the tube. Whilst the over-all variation in temperature in Fig. 4 is only three or four degrees, it is a significant fraction of the temperature difference between the two annuli, which was about 15°C in this case. It was impossible to account for this in terms of natural convection superimposed on the forced convection, and the variation appeared to be too systematic to be caused by fouling of the surface of the tube. However, the measurements were repeated after the apparatus had been cleaned, and the variation was still present. It is now thought that the effect is due to a slight eccentricity. Measurements taken from an X-ray of the exchanger show that the variations in width of the annulus are less than 0.010-inch, or 10 per cent of the width.

The exchanger used for the work on sodium potassium was concentric to the limit of accuracy of the measurements, and no significant circumferential temperature was found. However, some experiments were carried out on a heat exchanger in which the width of the annulus varied by about a factor of 2 around the circumference. Results were obtained using both water and sodium potassium as the heat-transfer medium. Figure 6 shows the temperature distribution around the circumference of the outer tube expressed as a fraction of the over-all temperature difference between the two streams of fluid.

DISCUSSION OF RESULTS

The generalized heat-transfer results shown in Fig. 3 have been calculated, using the normal definition of effective diameter (i.e., four times the cross-sectional area divided by the total perimeter, or, in the case of an annulus, twice the annular gap). It must be emphasized that the heat-transfer coefficients measured were the over-all coefficients from liquid metal, through the tube wall, to the other stream of liquid metal. The separation of the two liquid-metal heat-transfer coefficients is carried out merely so that the results can be compared with existing data; clearly there is no point in reproducing both coefficients for this purpose, and therefore only those for the inner annulus are shown in Fig. 3.

The results cannot be compared directly with the results of other workers, which are almost all for circular tubes, but they may be compared with an expression given by Lyon (1951)[3] for an annulus:

$$\mathrm{Nu}_{annulus} = 0.75\ \mathrm{Nu}_{tube} \cdot \left(\frac{r_o}{r_i}\right)^{0.3}$$

where r_o = outer radius of annulus, and r_i = inner radius of annulus.

The curve representing the above equation applied to the inner annulus is shown in Fig. 3. Lyon's theoretical values for circular tubes are compared with the experimental results of other workers in Lyon (1951).

Whilst the experimental results show a slightly greater rate of increase of Nusselt number with Peclet number than the Lyon equation, the agreement over the range tested is quite good. A few results have been obtained in the laminar-flow region of Reynolds number, and instead of giving a constant value of Nusselt number, as theory predicts, they continue to decrease as the Reynolds number decreases. However, the effects of heat losses and of conduction in the direction of flow of the liquid metal become important in this region and may possibly affect the results, which have therefore been rejected. A separate investigation using a modified apparatus is planned to resolve this point.

The main sources of inaccuracies in the experiments are probably the measurement of flow (± 5 per cent), and the measurement of temperature difference (± 3 per cent). It is felt that the over-all accuracy should be within ± 10 per cent. The experimental method is open to criticism on the following points. Firstly, the coefficients obtained include any end effects which may be present; this effect is probably quite small in view of the magnitude of the length to effective diameter ratio, which was approximately 350. It was hoped to separate this effect by making temperature measurements along the outer and inner tubes, but this was

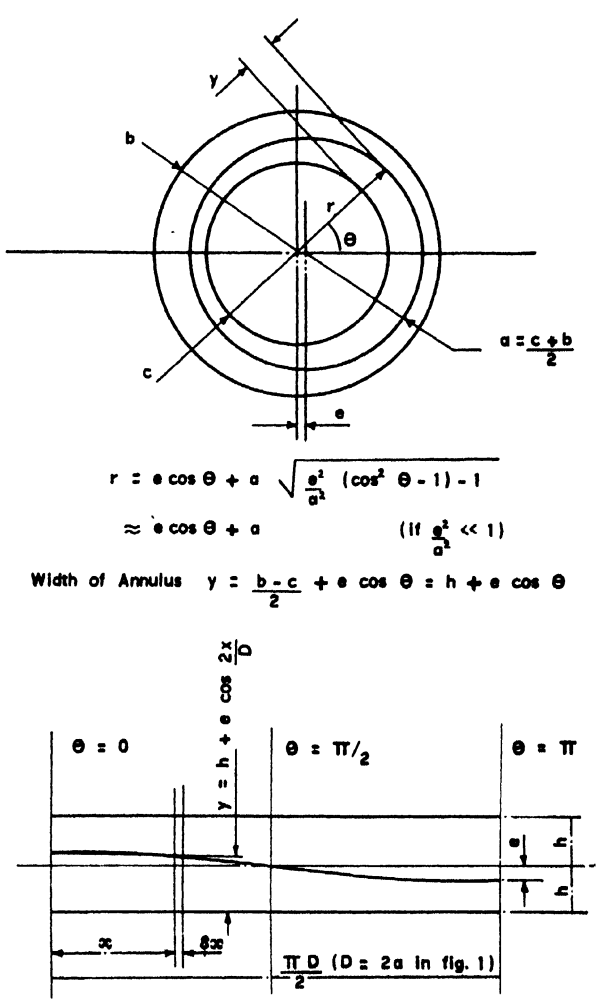

Figure 5

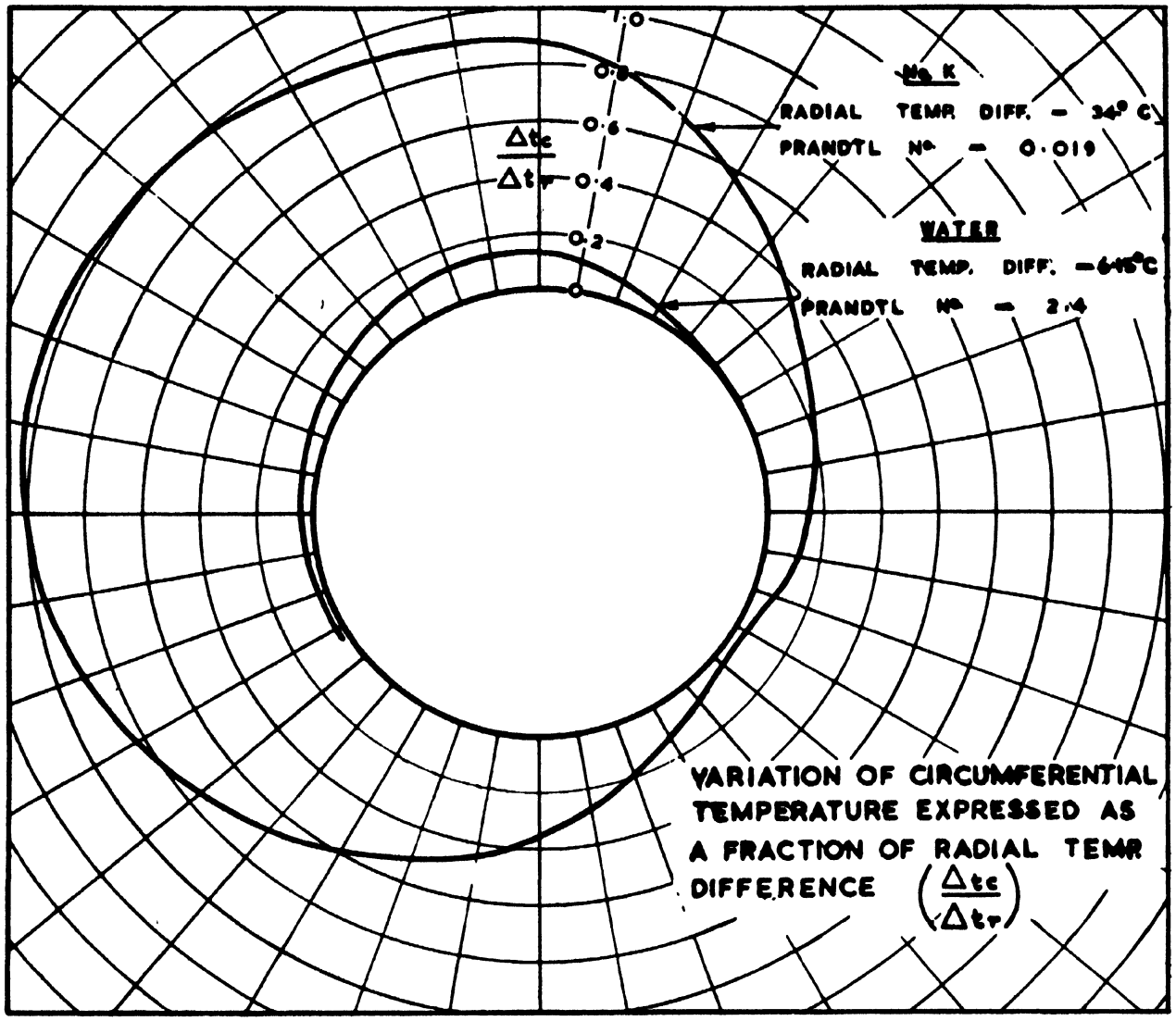

Figure 6

impossible owing to the temperature variation around the circumference of the tubes. Secondly, the circumferential temperature variation may influence the average heat-transfer coefficient. There is a tendency to assume that such variations are not likely to be as great with liquid metals as with higher Prandtl number fluids, but it is shown below that in fact the reverse may be true. Thirdly, it was necessary to make assumptions concerning the relative value of the coefficients for the inner and outer annuli. When this assumption is made, the results for the two annuli do appear to lie on the same curve, and, in any event, the slug Nusselt numbers for the two annuli are almost identical.

It is possible to make an estimate of the circumferential temperature variation which would result from a slight eccentricity of the middle tube of the heat exchanger (Hall, 1955). Such an exchanger is shown in Fig. 5 and it is assumed that the two fluid streams are in counterflow and that fully developed temperature distributions exist—that is, the temperature gradients in the direction of flow are uniform over the whole section. If the annuli are narrow compared with the diameter of the tubes they may be developed as shown in the lower sketch. Considering a section of width δx across both channels, it is clear that there is an excess of heat being brought by the fluid into the lower part of the section over that being removed from the upper part—in view of the greater cross-sectional area and, incidentally, the greater velocity. This excess of heat must be conducted away through the fluid in the x direction. This simplified problem may be solved and gives the result that the ratio of the maximum circumferential temperature difference, Δt_c, to the temperature difference between the two annuli in a radial direction, Δt_r, is given by

$$\frac{\Delta t_c}{\Delta t_r} = \left(\frac{D}{h}\right)^2 \times \frac{e}{h}$$

If $D/h = 5$ and $e/h = 0.01$ we see that the circumferential temperature variation is 25 per cent of the radial temperature difference. This is certainly

an overestimate due to the assumption that the temperature distribution is fully developed, but it does indicate that small variations in the width of the annulus could cause large variations in temperature in a circumferential direction.

It is interesting to compare the above analysis, which is appropriate to a fluid of low Prandtl modulus, with the results obtained with a fluid of high Prandtl modulus, such as a gas or a non-metallic liquid. In the latter case the resistance to heat transfer in a radial direction is largely confined to a thin boundary layer close to the dividing wall. Away from this wall the effective conductivity of the fluid is enormously enhanced by the turbulence in the stream. We can get an approximate idea of this case by taking the above analysis and imagining the dividing wall to have a large resistance to heat flow (this representing the relatively high resistance to heat flow in the boundary layers). This means that the temperature difference Δt_r will be increased considerably relative to Δt_o. Also in the case of a low-conductivity fluid (usually with a high Prandtl modulus) the conductivity of the metal wall is relatively high, and would tend to reduce any non-uniformity in temperature distribution. In the case of a liquid metal such as sodium, this effect would be negligible due to the high conductivity of the sodium relative to the conductivity of the wall.

One is therefore led to the conclusion that the temperature variations (expressed as a fraction of the over-all temperature difference) incurred as a consequence of slight inaccuracies in the manufacture of this type of heat exchanger are greater in the case of a low Prandtl modulus fluid (e.g., liquid metal) than in the case of a high Prandtl modulus fluid (e.g., gas or non-metallic liquid). This effect is not, of course, confined to heat exchangers of the above shape; thus in any heat-transfer apparatus involving the use of liquid metals the effect of inaccuracies in the shape of the exchanger, and the resulting thermal stresses, should not be overlooked. The results for water and sodium potassium mentioned "Experimental Results" and shown in Fig. 6 confirm these conclusions as far as the Prandtl Number effect goes.

CONCLUSIONS

Agreement between the two sets of results for sodium and for sodium-potassium alloy is good. The experimental curve of Nusselt number against Peclet number has a slightly greater slope than the Lyon equation for a similar annulus, otherwise agreement is good. No deterioration in heat-transfer coefficient due to oxide formation on the heat-transfer surfaces was noticed; this, however, would hardly have been expected, since the mass transfer of oxide in the liquid metal would lead to accumulation of oxide at the coldest point of the circuit, which was the cooler, and not the experimental heat exchanger.

NOMENCLATURE

ρ = density of liquid metal (gm-cm^{-3})
μ = viscosity of liquid metal (gm-cm^{-1}-sec^{-1})
k = conductivity of liquid metal (cal-cm^{-1}-sec^{-1}-°C^{-1})
c = specific heat of liquid metal (cal-gm^{-1}-°C^{-1})
v = velocity of liquid metal (cm-sec^{-1})
d = effective diameter of coolant passage (cm)
h = heat transfer coefficient (cal-cm^{-2}-sec^{-1} °C^{-1}) (h_i refers to inner annulus) (h_o refers to outer annulus)
Nu = Nusselt number, hd/k (dimensionless)
Re = Reynolds number, $vd\rho/\mu$ (dimensionless)
Pr = Prandtl number $c\mu/k$ (dimensionless)
Pe = Peclet number = Re · Pr (dimensionless)

REFERENCES

1. Hall, W. B. and Jenkins, A. E., *Heat Transfer Experiments with Sodium and Sodium Potassium.* J. Nuclear Energy *1*: 246–265 (1955).
2. Lyon, R. N. (editor), *Liquid Metals Handbook,* U.S.A.E.C. (1952).
3. Lyon, R. N., *Liquid Metal Heat Transfer Coefficients,* Trans. Amer. Inst. Chem. Engrs., 47, 75–79 (1951).
4. Martinelli, R. C., *Heat Transfer to Molten Metal,* Trans. Amer. Soc. Mech. Engrs., 69, 947–959 (1947).
5. Reynolds, O., *Papers on Mechanical and Physical Subjects,* Vol. 1, pp. 81–85, Cambridge (1890).
6. Trefethen, L. M., *Heat Transfer Properties of Liquid Metals,* U.S.A.E.C., NP 1788 (1951).

A Simple Method for the Comparison of Reactor Coolant Efficiency

By Max Hoyaux,* Belgium

A good reactor coolant must satisfy very severe requirements as regards heat transfer, pumping power, neutron absorption, etc. We wish to present here a simple method taking into account as many parameters as possible within very well-known formulae, but leading to a single coefficient involving them all, which would be a reasonable measure of the relative efficiency.

We assume, in the most general sense, a neutron diffusing medium, producing heat, and with a number of pipes to remove it; the number of pipes is n, their diameter, D, and their length L.

The basic equations can be stated as follows:

(a) The number N of neutrons absorbed per unit time is:

$$N = \frac{V\rho \mathrm{N}\sigma_a\phi}{M} \tag{1}$$

where V is total volume of the coolant $= n\pi D^2L/4$, ρ is density of the coolant, N is Avogadro's number, σ_a is neutron absorption cross-section for the coolant atoms, ϕ is neutron flux, and M is atomic mass of the coolant.

(b) The quantity of heat removed per unit time by the coolant is

$$Q = d\rho C(T_{rs} - T_{re}) \tag{2}$$

where d is volumetric rate of flow of the coolant $= n\pi D^2u/4$, u being the linear speed inside the pipes, C is specific heat per unit mass of the coolant, and $T_{rs} - T_{re}$ is temperature difference between output and input.

(c) The same quantity of heat must be transferred by convexion from the walls of the pipes into the coolant

$$Q = Sh(T_p - T_r) \tag{3}$$

where S is total external surface of the pipes, h is convexion transfer coefficient, and $T_p - T_r$ is temperature difference between wall and coolant.

We assume h to be given by the well-known McAdams formula for turbulent flow

$$h = 0.023 \frac{k^{0.6}u^{0.8}\rho^{0.8}C^{0.4}}{D^{0.2}\mu^{0.4}} \tag{4}$$

where k is thermal conductivity of the coolant, and μ is viscosity of the coolant.

There is some question about the validity of the McAdams formula for liquid metals. It is well known that if they do not wet the wall, this formula may be in error by a factor 5 to 10. But the addition of wetting agents may reduce the error to a factor 2. As will be seen later, a factor 2 is insufficient to render our conclusions incorrect.

(d) The pumping power W to force the coolant through the pipes is given, in thermal units and in the case of turbulent flow, by the formula

$$W = \frac{d}{J}\frac{2fLu^2\rho}{gD} \tag{5}$$

where J is the conversion factor of mechanical into thermal units, g is gravitation field at earth's surface, and f is friction factor, given by

$$f = 0.046\left(\frac{\mu}{D\rho u}\right)^{0.2} \tag{6}$$

The purpose of the calculation is to obtain, for different coolants, the number of calories removed per neutron absorbed in the coolant, that is, from Equation 1

$$q = \frac{Q}{N} = \frac{QM}{V\rho \mathrm{N}\sigma_a\phi} \tag{7}$$

all conditions being equal, that is: (a) the thermal power Q of the reactor, (b) the pumping power W, (c) the neutron flux ϕ, (d) the total length nL of the pipes,† and (e) the temperature differences $(T_p - T_r)$ and $(T_{rs} - T_{re})$.

We assume the diameter D and the speed u to be such that those conditions are satisfied for the chosen coolant.

We must calculate V in order to insert it in Equation 7. We have:

$$V = \frac{\pi}{4}(nL)\,D^2 \tag{8}$$

From Equation 2

$$nD^2u = K_1/\rho C \tag{9}$$

* Physics Research Laboratory of A.C.E.C., Belgian S.E.E.N.

† It does not seem possible to keep n and L constant separately according to the number of equations to be satisfied.

Table I. Liquids

Coolant	Isotop. abund.	k	ρ	$\mu(10^{-2})$	C	M	σ_a	$\frac{k^{2.5}\rho CM}{\mu^2\sigma_a}\left(\frac{C\mu}{k}\right)^{0.4}$	T_{melt}	T_{boil}
Hg	..	0.019	13.7	1.0	0.032	200.6	380	0.022	−39	357
Hg^{202}	29.6%	0.019	13.8	1.0	0.032	202	2.4	3.6	−39	357
Hg^{204}	6.7%	0.019	13.9	1.0	0.032	204	0.34	26	−39	357
H_2O	..	0.00154	1.00	0.18	1.05	6	0.22	0.91	0	(100)
D_2O	0.015%	0.00154	1.11	0.18	0.95	6.7	0.00037	570	3	(102)
56Na/44K	..	0.066	0.89	0.4	0.26	30.1	0.96	100	19	825
P	..	0.0005	1.7	1.2	0.2	31	0.19	0.004	44	280
K	..	0.09	0.82	0.35	0.19	39	1.97	87	62	760
Na	..	0.17	0.93	0.5	0.30	23	0.49	950	98	880
S	..	0.0003	1.6	>7	0.35	32	0.49	$<7\times10^{-5}$	115	445
44Pb/56Bi	..	0.025	10.2	1.5	0.035	208	0.094	74	125	1700
$44Pb^{208}$ +56Bi	50%	0.025	10.2	1.5	0.035	208.5	0.018	390	125	1700
38Pb/62Sn	..	0.05	8.5	1.0	0.05	152	0.53	108	183	..
$38Pb^{208}$ +$62Sn^{118}$	50% 24%	0.05	8.5	1.0	0.05	152	0.012	4800	183	..
Li	..	0.1	0.51	0.8	1.374	6.94	67	1.5	186	1317
Li^7	92.6%	0.1	0.52	0.8	1.37	7	0.033	3100	186	1317
Sn	..	0.08	6.7	1.5	0.065	118.7	0.65	110	232	2260
Sn^{118}	24%	0.08	6.7	1.5	0.065	118	0.02	3600	232	2260
98Pb/2Mg	..	0.04	10	2	0.04	207	0.17	82	250	..
Pb^{208} +2Mg	50%	0.04	10	2	0.04	208	0.002	6900	250	..
Bi	..	0.037	10	1.5	0.038	209	0.032	550	271	1477
Pb	..	0.037	10.4	2	0.037	207.2	0.17	65	327	1717
Pb^{208}	50%	0.037	10.4	2	0.037	208	0.00045	2400	327	1717
Mg	..	0.32	1.5	1	0.32	24.3	0.059	18,000	651	1103
Al	..	0.22	2.37	1	0.26	27	0.22	2900	660	2057

Table II. Gases

Coolant	Isotop. abund.	$k(10^{-4})$	$\rho(10^{-4})$ 1 atm	$\mu(10^{-4})$	C	M	σ_a	$\frac{k^{2.5}\rho CM}{\mu^2\sigma_a}\left(\frac{C\mu}{k}\right)^{0.4}$ 1 atm	30 atm
H_2	..	5.00	0.40	1.40	3.41	1	0.33	120×10^{-6}	3.5×10^{-5}
D_2	0.015%	4.00	0.85	2.00	1.7	2	0.00046	47,000 ..	1400 ..
He	..	3.98	0.80	3.20	1.7	4	0.008	2400 ..	71 ..
CH_4	..	0.72	3.30	2.10	0.59	3.2	0.26	3 ..	9×10^{-5}
H_2O	..	0.63	3.80	1.85	0.51	6	0.22	5.8 ..	17×10^{-5}
D_2O	0.015%	0.63	4.15	2.00	0.46	6.7	0.00037	3100 ..	94×10^{-5}
N_2	..	0.73	5.80	2.90	0.24	14	1.78	0.6 ..	1.7×10^{-5}
$(N^{15})_2$	0.38%	0.73	6.20	2.90	0.24	15	~0.00002	58,000 ..	1750×10^{-5}
Air	..	0.73	6.00	3.00	0.24	14.4	1.42	0.7 ..	2×10^{-5}
CO	..	0.54	5.80	3.00	0.24	14	0.0022	240 ..	7×10^{-5}
O_2	..	0.743	6.67	3.50	0.22	16	0.0002	4400 ..	130 ..
CO_2	..	0.50	8.15	2.70	0.22	14.7	0.0015	460 ..	13 ..
A	..	0.51	8.35	4.00	0.12	40	0.62	0.7 ..	2×10^{-5}

with

$$K_1 = \frac{4\,Q}{\pi\,(T_{rs}-T_{re})} \tag{10}$$

From Equations 3 and 4

$$D^2\,u^2 = K_2^{2.5}\,\frac{\mu}{k^{1.5}\,\rho^2\,C} \tag{11}$$

with

$$K_2 = \frac{Q}{0.023\pi(T_s - T_r)}\,\frac{1}{nL} \tag{12}$$

From Equations 5 and 6

$$u^7D^2 = K_3^{2.5}\,\rho^{-2}\,\mu^{-0.5} \tag{13}$$

with

$$K_3 = \frac{WJg}{0.023\pi}\,\frac{1}{nL} \tag{14}$$

From Equations 11 and 13

$$u = \left(\frac{K_3}{K_2}\right)^{0.5}\left(\frac{k}{\mu}\right)^{0.3}C^{0.2} \tag{15}$$

From Equations 11 and 15‡

$$D^2 = \frac{K_2^{3.5}}{K_3}\,\frac{\mu^2}{k^{2.5}\,\rho^2 C}\left(\frac{k}{C\mu}\right)^{0.4} \tag{16}$$

‡ We have not used Equation 9, which permits the calculation of n.

Inserting Equation 16 in Equation 8

$$V = \frac{\pi}{4}\,(nL)\,\frac{K_2^{3.5}}{K_3}\,\frac{\mu^2}{k^{2.5}\rho^2 C}\left(\frac{k}{C\mu}\right)^{0.4} \qquad (17)$$

and, finally, in Equation 7, taking into account Equations 12 and 13:

$$q = \frac{4(0.023\pi)^{2.5} Jg}{\pi N}\,\frac{(nL)^{1.5}(T_p - T_r)^{3.5} W}{Q^{2.5}\phi} \times \frac{k^{2.5}\rho C M}{\mu^2 \sigma_a}\left(\frac{C\mu}{k}\right)^{0.4} \qquad (18)$$

We can separate the right-hand side of this equation into three parts: the first one involves only universal constants; the second one involves pile characteristics—they are assumed to be kept constant in order to compare the coolants; the third one is a combination of coolant parameters: thermal conductivity, density, specific heat, atomic mass, viscosity and neutron capture cross section.

The values of

$$\frac{k^{2.5}\rho C M}{\mu^2 \sigma_a}\left(\frac{C\mu}{k}\right)^{0.4}$$

are listed in the following tables for several liquid and gas coolants considered as being not, or at least, not too much, subject to radiation damage. The thermodynamic constants are given around 300°C or at the melting point if higher; the cross sections are those for thermal neutrons.

Those tables allow a comparison of the different coolants on the basis of the accepted viewpoint, and some interesting conclusions may be drawn. Of course, they are generally well-known of the specialists, but the method in itself is interesting.

Among liquid coolants, comparison must include melting points that are listed too. Water, heavy water, NaK eutectic, sodium and bismuth seem the most promising apart from separated metal isotopes. The separation of isotopes is not interesting in the case of mercury, but seems promising for lithium, lead-tin alloy and lead-magnesium alloy. Magnesium should be extraordinary if the difficulties involved by the high melting point could be overcome.

Among gas coolants, the performance of N^{15} is probably purely academic. Apart from the isotopically pure materials and the too corrosive oxygen, we get confirmation that the best coolants are helium and carbon dioxide.

Very high quality coefficients are only significant if the structural material of the wall has a very high thermal conductivity and a very low neutron absorption cross section; otherwise, absorption and temperature drop in the wall will be many times in excess with respect to those in the coolant itself.

Another remark is that other hypothesis could be accepted at first sight as equally valuable; for instance, maintain n and L both constant and accept the value of $T_p - T_r$ as variable. In some respects, this conforms more to reality, but the difficulty is that, for a given fuel temperature, the output heat has no longer the same entropy, i.e., has different energetic values. Moreover, the quality coefficient obtained in this manner is independent of both k and ρ, so that it is not very satisfactory.

ACKNOWLEDGEMENT

The author wishes to acknowledge the interest shown by Mr. Van der Spek, Director of the Belgian S. E. E. N., and of Dr. Desirant, Director of the Physics Research Laboratory of A. C. E. C., as well as contributions of Mr. Erkes and Dr. Tavernier, of the S. E. E. N., and Dr. Michiels and Mr. Gans, of A. C. E. C.

REFERENCES

1. Goodman, Clark, The Science and Engineering of Nuclear Power.
2. Proceedings of the 1953 Conference on Nuclear Engineering, University of California.
3. Chemical Engineering (May 1954).
4. Smithsonian Physical Tables.
5. Handbook of Chemistry and Physics.
6. Handbook of Chemical Engineering.
7. C. E. A. N. Report No. 5000862.

Record of Proceedings of Session 19B.2

THURSDAY MORNING, 18 AUGUST 1955

Chairman: **Mr. L. Rotherham (UK)**

Vice-Chairman: **Mr. K. F. Alder (Australia)**

Scientific Secretaries: **Messrs. B. Prakash and C. A. Sastre**

PROGRAMME

P/639 Heat transfer of molten metals .....M. A. Mikheyev *et al.*

DISCUSSION

Mr. K. D. VOSKRESENSKY (USSR) presented paper P/639 as follows: I wish to report on the results of experimental and theoretical research on heat transfer by molten metals carried out at the Academy of Sciences of the USSR.

The authors of the paper are Mikheyev, Baum, Fedynsky and Voskresensky.

The problem of heat transfer in molten metals has arisen in connexion with the prospect that nuclear apparatus will be used on a large scale. It is convenient to use liquid metals for cooling the reactor and transferring heat to the power unit mainly because they can attain high temperatures at low pressures, which means that high steam parameters can be secured.

Water, gases, oils and other liquids with a Prandtl number higher than 0.5 have been widely used in heat exchangers as heat-transfer fluids. The conditions in which these liquids give up their heat have been studied in considerable detail. The physical properties of molten metals, however, differ very sharply from those of the "ordinary" liquids I have mentioned. Molten metals have Prandtl numbers of the order of 10^{-2}, and in many cases they do not moisten the heating surface. Hence, the conventional equations for calculating heat transfer and the conventional notions of the heat-transfer mechanism in turbulent flow of "ordinary" liquids are unsuitable for liquid metals. So far as we know, these features of heat transfer at low Prandtl numbers were first discovered in the Soviet Union fifteen years ago.

I will now go on to the substance of the paper. The main object of research was to determine the heat-transfer and hydraulic-resistance coefficients in the turbulent pipe-flow of liquid metals.

The experiments were conducted on rigs which differed from each other in the methods of setting the boundary conditions at the heating surface and of measuring the quantity of heat transferred, the temperature of the liquid metal and its flow rate.

Tubes of various sizes were used as heating surfaces, and mercury, tin, lead, bismuth, sodium and bismuth-lead and sodium-potassium alloys were used as heat-transfer agents. The physical characteristics of these metals were in many cases determined by experiment.

In the course of the experiments, the Reynolds number varied from 10^4 to 6.5×10^5, the Prandtl number from 4×10^{-3} to 32×10^{-3} and the heat-transfer rate at the heating surface did not exceed 10^6 kcal/m²/hr.

Data established by these experiments are:

The magnitude of the heat-transfer rate has practically no effect on the heat-transfer coefficient.

"Wetting" of the heating surface by the heat-transfer agent apparently has an indirect effect on heat transfer. It may be assumed that the oxides which offer additional thermal resistance drop out more readily on a heating surface which has not been moistened by the liquid metal.

The length of the heated area used was not more than 30 tube diameters.

An interpolation formula was obtained for heat transfer in long tubes ($l/d \geqslant 30$) with a clean heating surface in conditions under which the liquid metal was preserved from oxidation.

Equation 1 following was obtained for clean tubes with very good protection against oxidation.

$$\mathrm{Nu} = 4.5 + 0.014\ (\mathrm{Re} \times \mathrm{Pr})^{0.8} \qquad (1)$$

The following interpolation formula was obtained for heat transfer in long tubes with an oxidized surface and with insufficient protection of the liquid metal against oxidation, and is appropriate for use in approximate calculations:

$$\mathrm{Nu} \cong 3 + 0.014\ (\mathrm{Re} \times \mathrm{Pr})^{0.8} \qquad (2)$$

Heat transfer in short tubes ($5 \leqslant l/d \leqslant 30$) should be calculated by the equations which are true for long tubes and the results should then be multiplied by the corrective coefficient:

$$\xi = 1.72\ (d/l)^{0.16} \qquad (3)$$

The hydraulic resistance of the tubes under the conditions in which the experiments were conducted is not dependent on the wetting power of the liquid metal. Hence, the calculation of the hydrodynamics of a liquid metal cooling system for a reactor should be done by the conventional hydrodynamic formulae.

The results obtained agree satisfactorily with the published experimental findings of a number of other authors, e.g., Johnson.

It is useful to have a single formula for calculating heat transfer which will apply to both molten metals and ordinary liquids.

$$\mathrm{Nu} = (3.2 + 0.021 \times \mathrm{Re}^{0.8} \times \mathrm{Pr}^{n})K, \quad (4)$$

where $n = n(\mathrm{Pr})$. Approximated for molten metals, $\mathrm{Pr} \ll 1$, $n \cong 0.9$ and $K = 1$; for ordinary liquids, $\mathrm{Pr} \geqslant 0.7$, $n = 0.43$ and $K = (\mathrm{Pr}/\mathrm{Pr}_o)^{0.25}$.

Equation 4 satisfactorily interpolates the results of heat-transfer measurements for both molten metals and ordinary liquids.

In 1953, Hoffman also proposed a method of calculating heat transfer over a wide range of Prandtl numbers, but when $\mathrm{Pr} < 1$, his method gives results which differ appreciably from experimental findings.

Apart from the work recapitulated above, studies were made of heat transfer in relation to natural convection in large volumes of molten metals, which is also of importance and practice.

The results of these studies, together with the known data for ordinary liquids, are set out in the form of an interpolation formula covering a wide range of variations of the Gr and Pr numbers.

The theory of liquid metal heat transfer proposed by Lyon and other authors yields higher values than our own measurements (see Fig. 2 of P/639).

Let us examine the possible causes of this discrepancy.

With a constant heat loading at the heating surface, Lyon obtained the following expression for heat transfer in tubes:

$$\mathrm{Nu} = \frac{1}{2\int_0^1 \frac{[\int_0^R URdR]^2 dR}{R\left(1 + \frac{a_T}{a}\right)}} \quad (5)$$

This result was obtained without making any significant assumptions about the mechanism of turbulent heat transfer, and we regard it as an important scientific achievement, for which we are indebted to Mr. Lyon.

Mr. Lyon's further calculations must be approached with some reservation.

In calculating Equation 5, Mr. Lyon makes use of the analogy between turbulent heat transfer and momentum transfer and writes:

$$a_T = \nu_T$$

Furthermore, he uses the smoothed results of measurements by Nikuradse to calculate the field of velocities U.

Interpolating the results of these calculations, Lyon finds that:

$$\mathrm{Nu} = 7 + 0.025 \times (\mathrm{Re} \cdot \mathrm{Pr})^{0.8}$$

while our measurements give

$$\mathrm{Nu} = 4.5 + 0.014 \times \mathrm{Re} \cdot \mathrm{Pr})^{0.8}$$

The discrepancy between these results is due, in our view, to two causes. One is that the analogy between heat transfer and momentum transfer does not hold true in the turbulent flow of a molten metal, since the temperature of the particles in the turbulent liquid changes during their movement in the mixing process due to the high molecular conductivity of the metal.

The second reason for the discrepancy is that Nikuradse's measurements of the field of velocities give incorrect results near the tube walls. This conclusion is confirmed by the measurements made by Reichardt and Deissler about 1951.

On the basis of these hypotheses and on the assumption that the thermal resistance inside the turbulent field is small in comparison with its outside thermal resistance and that the proportion of the heat transferred by the field is not dependent on the molecular viscosity of the liquid, we get the following results from our calculation:

$$a_T = \beta \nu_T$$

$$\beta = A\left[1 - \exp\left(-\frac{1}{A}\right)\right]$$

$$A = K \cdot \frac{\nu_T}{\nu} \cdot \mathrm{Pr}$$

K can be regarded as constant to a first approximation. Its value must be determined by experiment.

If K is taken as 0.083 and the distribution of velocities U is calculated according to Reichardt (or Deissler), then interpolating the results of our calculations we obtain the formula

$$\mathrm{Nu} \cong 5 + 0.014\ (\mathrm{Re} \cdot \mathrm{Pr})^{0.8}$$

which agrees satisfactorily with the results of our measurements.

The concepts I have described are a development of Prandtl's ideas about the processes of turbulent mixture and are semi-empirical in character.

Further progress in this domain will probably be achieved by means of careful systematic measurements of the average temperature fields of liquid metals over a period in turbulent flow. For this reason the well-known experiments of Isakoff and Drew on this problem should be regarded as a very valuable beginning.

I must say in conclusion that the results of the liquid metal heat-transfer studies described in this paper are broadening our knowledge of heat-transfer processes, since they cover the little-studied field of coolants with low Prandtl numbers.

DISCUSSION OF P/639

Mr. W. B. Hall (UK): My first question concerns the correction given for short tubes. Presumably this was based on the measurement of local heat-transfer coefficients along the experimental heat exchanger. In this case was an allowance made for conduction in the direction of flow of the liquid metal in the layer of copper surrounding the tube?

My second question concerns the results shown in the correlation of a wide range of experimental results. I would like to know whether they were all obtained with a heat exchanger of the same size and shape in all cases? In fact were they all made on the same apparatus?

Mr. VOSKRESENSKY (USSR): In studying heat transfer in short tubes, we used thin-walled stainless steel tubes in which the effect of heat conduction along the tube walls could be neglected. As I understood him, Mr. Hall asked whether the interpolation of our results by means of Equation 3 is true only for tubes of a single size or for various tubes and whether it is true only for a particular design of apparatus or for apparatus of different designs.

The paper indicates that experimental apparatus of various designs were used in obtaining our results, but I only introduced one design into the paper as an example.

Mr. HALL (UK): Thank you. There is one short comment I would like to make on the work. In our work with sodium or sodium-potassium we have never found any reduction in the heat-transfer coefficient which could be attributed to oxide, or in fact any cause whatever. We feel that if oxide is present it will always certainly collect at a fairly localised point in the circuit, probably not in the heat exchanger but probably at a colder point. I am therefore rather surprised that it is suggested that a constant correction should be applied to the case where oxide is present in the circuit.

Finally, I would like to congratulate the author on the very wide range he has covered in his work, and I would very much like to see the actual measurements so that we can be sure we are all using the same physical properties to correlate results. Thank you.

Mr. VOSKRESENSKY (USSR): I thank Mr. Hall for his very interesting observation and would like to say that the measurements can be made available to him.

Mr. R. N. LYON (USA): I, too, would like to compliment the author on the very wide range of conditions and the wide range of experimental work, and also to compliment him on the additions to the theoretical development.

One point which left me a little unclear—as it apparently did the previous questioner—is this. In the correction for the impure materials, it seems a little surprising to me, if the oxide accumulates at the wall, that this should occur as a constant in the first term of that equation. One would expect it to become more controlled as the velocity increases. If I interpret your equation correctly, the resistance at the wall would appear to become less important as the velocity increases. I would think it is very fortunate that the people in the USSR should continue their work on liquid metals because, as was pointed out in the paper, the first published work in the field of liquid metals was by Stirikovich and Semenovker in Russia in 1940, and it is very gratifying to see that they are continuing their fine work.

Mr. VOSKRESENSKY (USSR): In reply to Mr. Lyon's observation about the constant correction to allow for the presence of oxides, I explained in the paper that the formula obtained in the presence of impurities is approximate and that this matter requires further research.

Mr. LYON (USA): There is one more comment which I forgot to make before. I, too, would like to emphasize the importance of the work of Issakov and Drewe in determining the temperature distribution in the stream. I feel that only by such studies can we get a really true fundamental understanding of the behavior of heat transfer in turbulent flow, and I would like to encourage anyone interested to carry on that type of work.

Mr. VOSKRESENSKY (USSR): I should like to thank Mr. Lyon for his extremely flattering remarks and to repeat that the problem of the thermal resistances set up by oxides has not been clarified sufficiently and requires further study.

Session 19B.3

CORROSION IN LIQUID METAL SYSTEMS

LIST OF PAPERS

		Page
P/119	Corrosion by liquid metals ..... L. F. Epstein	311
P/787	Observations on the corrosion of uranium in liquid sodium..... H. Mogard	318
P/829	Basic technology of the sodium graphite reactor..... S. Siegel *et al.*	321
P/122	Mass transfer in molten metal and molten salt systems ..... C. F. Bonilla	331
P/118	Corrosion problems with bismuth uranium fuels..... J. R. Weeks *et al.*	341
P/124	The solubility of structural materials in sodium..... R. A. Baus *et al.*	356
P/638	Behavior of the stainless steel 1X18H9T in contact with liquid lead and bismuth and their eutectic alloy at a temperature of 500° to 600°C..... L. I. Tsuprun and M. I. Tarytina	364

Corrosion by Liquid Metals

By Leo F. Epstein,* USA

APPLICATIONS OF LIQUID METALS

Most textbooks on corrosion phenomena concern themselves largely with the effects of solutions, aqueous and non-aqueous, of organic solvents, and of gases on solid materials. The effect of other types of inorganic liquids, fused salts or liquid metals, for example, have been largely ignored until fairly recently. But I should like to point out at once that there has been application of liquid metals, and a technology of liquid metal corrosion for some years now. Since the end of the Stone Age, man has had to melt metals in some stage of the process of fabricating them, and has been continuously interested in better materials for melting pots, crucibles, ladles, etc. In my presentation today, I shall try to direct your attention to the increasingly important role which liquid metals are playing in modern technology, and in particular the application to high temperature nuclear power systems. I hope you are all familiar with the *Liquid Metals Handbook,* published under joint AEC and Navy sponsorship,[1] which has already gone into its second edition and from which a great deal of my talk today will be derived.

Since 1922, the General Electric Co. has been operating turbines for the generation of electrical power using mercury vapor in place of the more conventional steam. The theoretical gain in thermodynamic efficiency made possible by the higher temperatures which are readily attainable with mercury have been achieved in practice. Thus, for example, the most efficient steam plant for which I could find data[1] requires 9200 BTU (2300 kcal) to produce 1 kwh of electrical energy; a mercury plant comparable in size (about 125,000 kw) requires only 8400 BTU/kwh (2100 kcal/kwh). The savings in fuel realizable by the use of the mercury cycle are sometimes sufficient to justify the much greater initial cost of mercury, as compared with steam, when integrated over the potential life of the power plant.

Some years ago, an American petroleum manufacturer advertised its "Mercury-made Oil" rather extensively. In the preparation of high-grade lubricating oil, the cracking process must be carried out with extremely accurate temperature control. Since 1926, this has been accomplished by using mercury as the thermostatting fluid in catalytic cracking systems.[1]

*General Electric Company, Knolls Atomic Power Laboratory, Schenectady, New York.

You may not be aware of the fact that in the United States the valves on all airplanes, most trucks, and a significant proportion of all passenger automobiles are cooled by liquid sodium.[1] This technique has been in use since 1928, and takes advantage of the extremely high heat transfer rates possible with this fluid. The problem with valves is to keep the seat cool. As you will note from Fig. 1, in a solid valve the seat temperature may get as high as 1280°F (693°C); but in a hollow sodium-filled valve, all other factors being equal, this temperature falls to 980°F (527°C). The temperature reduction of 300°F (166°C) is sufficient to give a very significant improvement in the service of these valves.

The use of Na and the liquid Na-K alloys as heat transfer fluids has been exploited on a large scale too. In 1943, the Dow Chemical Co. operated a system containing metallic sodium, and removed as much as a million and a half BTU/hr (440 kw).

These few examples are intended to emphasize the fact that for some years now, there have been significant numbers of applications of liquid metals in industry, and consequently a need for information on corrosion by these materials. Activity in this field has been considerably accelerated in the years since the war by the interest of the US AEC in liquid metals as heat transfer fluids. It is perhaps not necessary to go into the details of why this should be; but briefly, let me recall to you that fissioning uranium may be thought of as primarily an almost unlimited heat source. From the Smyth report, the critical mass of uranium-235 lies somewhere between one and 100 kg. The density of uranium metal is

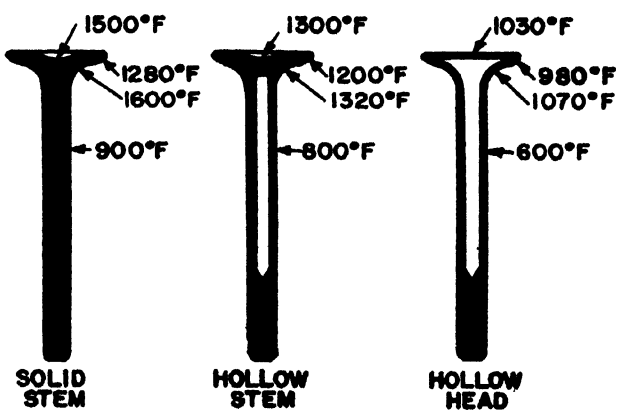

Figure 1. Effect of sodium cooling on valves

such that these masses would correspond to spheres about 5 to 20 centimeters in diameter; and in order to obtain useful energy from the fission process, it is desirable to remove from 10,000 to 100,000 kw from these sources. I do not wish to imply that nuclear reactors are no bigger than this; in actuality, of course, the uranium is diluted with other materials so that its volume is considerably larger than it would be if only pure uranium were used. Nevertheless, we are concerned with extremely concentrated power sources, and we require the most efficient possible heat transfer fluids to cool these reactors. An examination of a large number of liquids,[2] will show the outstanding value of liquid metals as heat transfer fluids from the point of view of the pumping horsepower required to maintain circulation (Table I). This is mostly due to the very high thermal conductivities of liquid metals, compared with other fluids. In addition to the low-pumping horsepower factor, liquid metals have the additional advantage of being monoatomic, thus avoiding the very serious problem of dissociation of polyatomic materials in the presence of the high radiation levels encountered in nuclear systems, a question related to the radiation damage effects which will no doubt be extensively discussed elsewhere at this Conference. For these reasons, the AEC has sponsored a program of research on liquid metals since about 1945, at many different sites, a few of which are listed in your abstracts. Similar studies have been in progress in Great Britain,[3] and no doubt in other countries as well. Many fluids—Hg, Na, Na-K, Pb, Bi, Pb-Bi eutectic, and others—have been studied, and the principal attention has been on high temperature applications. As you may have read, the Experimental Breeder Reactor now operating at the National Reactor Testing Station, Idaho, in the United States, uses sodium-potassium alloy (Na-K) as the heat transfer fluid; and the Submarine Propulsion Reactor (SIR) which our laboratory is now building uses liquid sodium.

LIQUID METAL CORROSION TESTS

The technique of testing corrosion in liquid metals is somewhat different from conventional corrosion research. In the discussion which follows, I shall be thinking mostly of the work which has been done in Schenectady on liquid Na and Hg, although the modifications in technique for other fluids will be obvious. In our work, we carry out tests which naturally fall into two large groups, the static isothermal tests, and dynamic tests with flowing liquids, most often with a ΔT as well (Table II). In static tests, a weighed sample of the solid metal whose corrosion properties are sought, is placed in a pot of the liquid metal, and held at temperature for the required length of time. On removal, it is examined (*a*) for weight changes (when it is possible to remove the excess liquid metal, as can be done with Na and Hg) or (b) metallographically to determine whether appreciable solution, pitting, etc., have occurred. Another kind of static test focuses attention on the liquid rather than the solid phase present: the apparent solubility and rate of solution of the solid in the fluid are measured as functions of time. These two kinds of isothermal tests logically supplement each other and a nice correlation between the two has been obtained in some cases. Figure 2 shows the kind of system normally used at KAPL for static pot tests with Na. The O-ring seal used to make the system tight is visible. The samples, usually in the form of weighed bars, with carefully prepared surfaces, are placed in the long tubular cups shown near the center of the photograph. These are in every case made of the same material as the metal being tested: we consider it quite important to have no material other than the metal being tested in contact with the sodium. You will note that 6 different samples can be examined simultaneously in this apparatus. After the system has been assembled, the sodium, purified as needed, is loaded into the pot through the filling ports shown. An inert atmosphere is maintained over the system, and it is heated externally for the required temperature and time. Figure 3 shows one of the static pot lines at KAPL, with 8 pots and their control systems. Similar set-ups can be found at most of the laboratories engaged in liquid metal corrosion work.

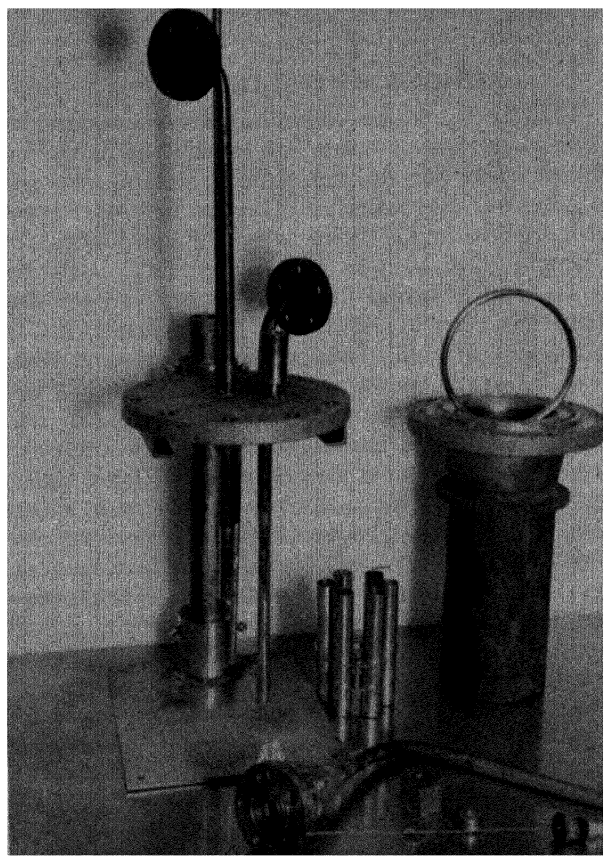

Figure 2. Static corrosion test pot

Table I. Comparison of Possible Liquid Coolants

Liquid	Heat transfer characteristics $H_2O = 1$		Comments
	Stream-line flow	Tur-bulent flow	
H_2O	1.0	1.0	Low Bp, 100°C
Na	0.2	2.0	Mp 97.6°C, reactivity
Sn	0.4	3.5	Mp 232°C
Hg	1.0	7.6	Low Bp, 357°C
Bi	1.5	12.0	Mp 271°C Yields Po
Cd	1.5	13.2	Mp 321°C
$NaNO_2$, $NaNO_3$, KNO_3	28.0	14.2	Mp about 200°C, radiation instability
Pb	2.4	17.8	Mp 327°C
Acetic acid	37.1	19.0	
Glycol	114.0	20.8	
Freon-12	30.7	21.6	Organic relatively unstable to heat and radiation
Aniline	105.0	35.5	
Diphenyl	113.0	45.7	
Naphthalene	163.0	64.6	
Glycerin	871.0	90.0	

In a "Merry-go-Round," an attempt to get at the effect of fluid flow velocity is made by rotating the solid test specimen under the liquid metal at high peripheral velocities, under isothermal conditions. Other constant temperature devices of this type have also been designed at other laboratories. But since the principal interest in liquid metal corrosion arises from heat transfer system applications where there will necessarily be a temperature gradient and fluid flow, results of dynamic tests under such conditions are considered of far greater value than any of the devices mentioned above. The simplest test unit in which these tests are made is the thermal convection loop, or "harp", shown in Fig. 4. Here advantage is taken of the fact that liquids expand on heating to produce flow. Figure 5 shows an ideal-

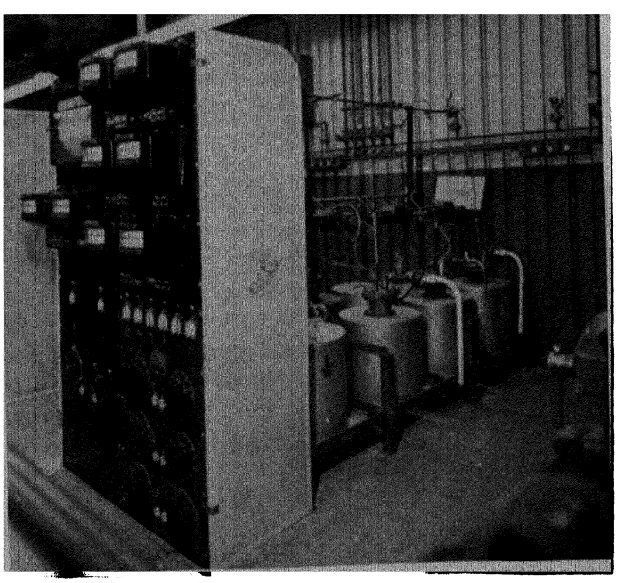

Figure 3. Kapl static corrosion pot line

ized thermal convection loop, and serves also to define the notation used in the figures which follow. The net flow and other characteristics of such a system depend to a marked extent on the hydraulic head, the vertical distance h between the hot and cold zones. The flow rates which can be achieved in such a harp, and the minimum amount of heat required (assuming no losses) to maintain it are shown in Figs. 6 and 7. The principal disadvantage of thermal convection loops is apparent from Fig. 6; even with quite large hydraulic heads, h, the flow rates which can be obtained are very small, not more than a few feet per second. It is for this reason that a great deal of effort has been devoted to pumped loops, in which either electromagnetic or mechanical pumps[1] are used. Systems of this type have been made in a wide variety of sizes, ranging

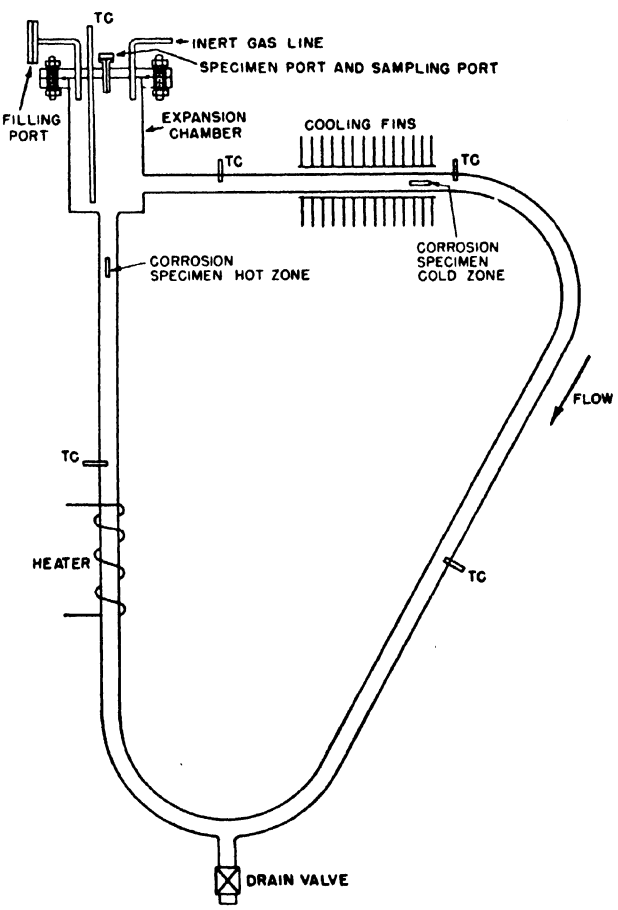

Figure 4. Typical thermal convection loop

from small laboratory experimental units to pilot plant size installations employing hundreds of gallons of fluid. With them corrosion tests can readily be made with flow velocities as high as 10 or 20 feet/sec (300 to 600 cm/sec).

I should like next to talk about some of the results of these corrosion tests in a few of the liquids of greatest interest. For service in mercury, nickel-free steels appear to be best since Ni is much more soluble than Fe in mercury (see Table III), and the nickel seems to be selectively dissolved out of alloys

Table II. Types of Liquid Metal Corrosion Tests

1. *Static tests* (isothermal, non-flowing liquid)
   - A. Static pot tests
   - B. Solubility studies
2. *Dynamic tests* (flowing fluids)
   - A. "Merry-Go-Rounds" and other isothermal devices
   - B. Systems with a temperature gradient
     - (1) Thermal convection loops ("harps")
     - (2) Pumped loops

which contain it, the 18-8 austenitic stainless steels for example. Plain carbon steels are excellent so far as resistance to liquid mercury is concerned, but because steels for mercury boiler tubes are required, in addition, to have a certain degree of high temperature strength and oxidation resistance, the material most commonly used is Sicromo 5S (Croloy 5Si) which contains 5% Cr, 0.5% Mo, 1.5% Si. In mercury boilers, magnesium is added to the Hg charge as a wetting agent; Mg is an excellent reducing agent, and some 20 to 100 parts per million by weight are enough to clean up the oxide films on steels and produce good wetting characteristics. In addition, there is a patented process for the inhibi- of corrosion of ferrous alloys (nickel free) by mercury: this consists in the addition of metallic titanium, one to ten ppm, to the Hg. The reasons why this works are somewhat obscure—perhaps a protecting film of an iron-titanium compound, Fe_2Ti or Fe_8Ti, is formed. In any case, its usefulness has been established by many years of operating experience with large scale plants. Other metals besides Ti can be used, Zr for example, with, however, a less economic inhibiting effect. In the paper to be presented here by the Brookhaven National Laboratory people,[4] the successful use of this inhibition technique with liquid Bi will be discussed, and there is some evidence of its value with other heavy metal fluids. All metals, in liquid mercury, appear to lose weight in the corrosion process.

This is in contrast to the behavior of metals in sodium or sodium-potassium alloy where metals may either gain or lose weight. In these liquid metal corrosion processes, a weight loss is almost always attributable to solution, either of the metal itself or of some minor constituent of the alloy. When weight gains are observed, these can usually be traced back to some chemical reaction in the system. In the case of Na and Na-K alloy, these reactions are most often due to the presence of small amounts of alkali metal oxides in the liquid. Quantities of oxygen in the range 0.001 to 0.01% are extremely important in this respect. Stainless steel, for example, gains weight in sodium due to formation of surface films of chromium oxides. A low-carbon steel loses weight

Table III. Solubilities in Liquid Mercury (parts per million)

T(°C)	Iron	Nickel
25	0.015	1.4
300	0.054	14.

continuously in Na: initially, this is almost entirely due to removal of carbon from the steel, a very rapid and effective process; after the steel has been thoroughly decarburized in this manner, further exposure to Na results in solution of the Fe itself with an accompanying weight loss, at a rate rather less than that for decarburization. Sometimes these weight loss and weight gain processes are combined, and it is difficult to separate them. Beryllium metal, for example, tends to reduce Na_2O, and gain weight in Na. The resulting BeO films are not, however, very adherent to the mother metal from which they are formed and tend to spall off, particularly at high liquid flow rates. Thus with this material, both positive and negative weight changes may be observed, depending on the precise way in which the corrosion tests are carried out. With the 18-8 stainless steels, and other ferrous alloys of interest for high temperature structural applications, penetration rates of 0.1 mil/year (0.0025 mm/year) or less are readily achieved if the oxygen content of the sodium, on which the corrosion rate is strongly dependent, is kept low enough.

Metallic lithium is of some interest. It seems to be very much like Na or Na-K, in its behavior, except that Li forms a highly corrosive nitride by reaction with air (in contrast to the other alkali metals which show no such reactions). Thus traces of nitrogen as well as oxygen in lithium appear to be quite important in accelerating the corrosion process.

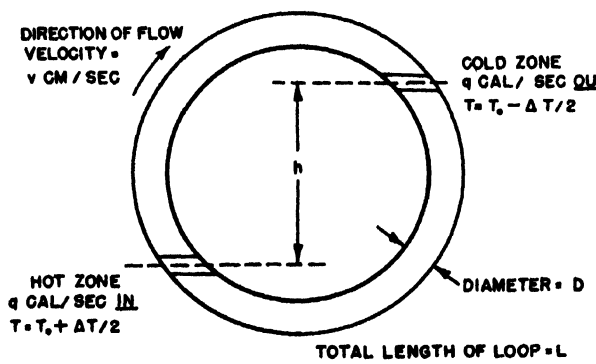

Figure 5. Idealized harp

Among the heavy metals, a great deal of attention has been devoted to lead and bismuth because of their very attractive nuclear properties. Some very fine work, at the University of California, at Stanford, at Brookhaven, and a number of other laboratories has shown that these metals cause rather strong intergranular attack, perhaps due to solution of grain boundary impurities. It is suspected that oxygen may be important in this process, but the exact role which lead and bismuth oxides play is still obscure. The addition of tin to various alloys in order to achieve lower-melting mixtures has often been considered, and has usually led to frustration and disappointment. Sn, by itself or in alloys, seems to be a very bad actor with respect to accelerating inter-

granular attack. As was noted above, there is some evidence that with these heavy metals, as in the case of mercury, the Ti or Zr inhibition process may be effective in reducing corrosion.

Just a word about gallium may be in order. The fact that this metal melts at about room temperature has made it the object of some study, in spite of its scarcity and high cost. Unfortunately, Ga seems to be almost a universal solvent for metals, and no satisfactorily resistant metallic container material for it at high temperatures has yet been found. Of course, Ga can be held in quartz, to temperatures where the solid begins to soften; you will recall that Ga in quartz thermometers have been made for use up to nearly 1000°.

In Table IV, the behavior of iron is compared, in liquid mercury and in liquid sodium. Note that while the equilibrium solubility of Fe is much higher in Na than it is in Hg, the corrosion rate is considerably less in the alkali metal. This immediately focuses attention on the fact that the equilibrium solubility is by no means the whole story, and that it is necessary to assume some difference in the mechanism of the corrosion process by the two solvents.

THEORY OF LIQUID METAL CORROSION

It is clear from the beginning that since liquid metals are excellent conductors, the electrolytic phenomena which are of predominant importance in aqueous corrosion can play no part in corrosion by metallic fluids. While some electrical phenomena have been observed in liquid metals (Na-K, for example, separates into its constituents somewhat under the influence of a strong electrostatic field) there is no evidence that electrical phenomena are of more than superficial interest and importance in these systems.

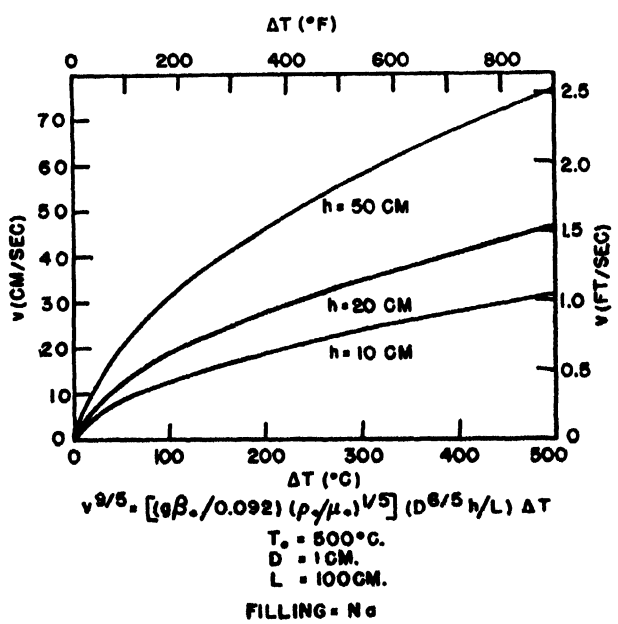

Figure 6. Flow velocity in a thermal convection loop

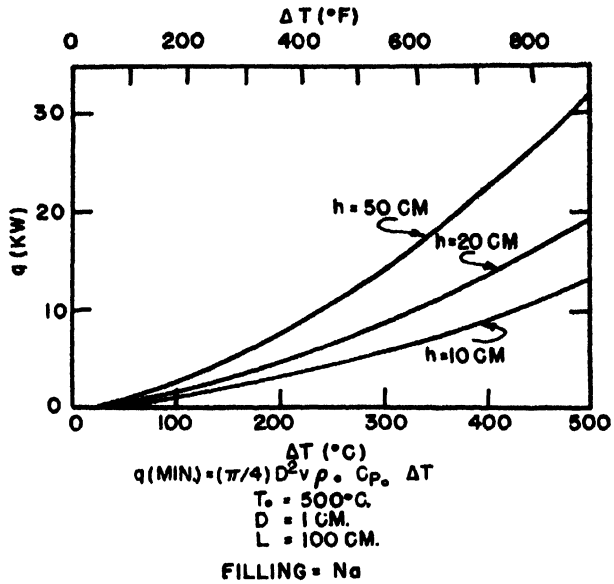

Figure 7. Minimum heat required in a thermal convection loop

There appear to be two principal modes of attack of liquid metals on solids: (1) by the process of solution, either of the major constituent of the alloy, or by leaching out a minor alloying element (as in the case of Ni from an 18-8 steel in Hg), or by solution of grain boundary constituents; (2) by chemical reaction, either of the liquid metal itself or of some impurity which it contains (oxide in the case of Na) with the solid.

In the case of solution attack, there appear to be two possible mechanisms. The heterogeneous diffusion of the solute atoms across the solid-liquid interface may be the slowest step; or alternately the rate-determining step may be the homogeneous diffusion of the solute through the solvent fluid. These two processes are illustrated, for Fe in Hg and Na, in Fig. 8. The second case, diffusion-limited attack is described by the following equation:

$$R_T = 0.023(\underline{D}/D)(vD/\nu)^{0.8}(\nu/\underline{D})^{0.4} \times (dS^\circ/dT)\Delta T \qquad (1)$$

where: R_T = corrosion rate (gm/cm²-sec), $\underline{D}$ = diffusion coefficient $\cong 2 \times 10^{-5}$ cm²/sec, D = diameter, v = flow velocity, ν = kinematic viscosity, μ/ρ, S° = equilibrium solubility, ΔT = temperature difference in a "harp" between hot and cold zones.

Table IV. The Corrosion of Iron by Liquid Sodium and Liquid Mercury—A Comparison

Property	*Mercury*	*Sodium*
Solubility		
100°C	0.015 parts per million	2 parts per million
700°C	1	18.3
Corrosion rate		
500°C	0.011 cm/year	0.0021 cm/year
700°C	0.30	0.0091
Rate of solution	Very fast (seconds)	Very slow (hours)

The chemical engineers in the audience will, I am sure, recognize the factor 0.023, and the exponents 0.8 and 0.4. This equation is very similar to one commonly used in heat transfer calculations, and was, in fact, derived by applying the analogy between heat and mass transfer. An equation of this type seems to represent the process of dynamic corrosion of Fe by Hg quite well. In the other case, where the rate at which the solid goes into solution is the rate determining step, the equation for the dynamic corrosion rate assumes a very different form, given in the following equation:

$$R_T = -(\alpha/2)(dS°/dT)\ \Delta T \times [1 + (2\alpha L/\pi Dv)^2]^{-1/2} \qquad (2)$$

In this equation, α is the specific solution rate constant for the process. If a solid of area A is immersed at time zero in a liquid of volume V, and the amount of solid constituent which is found in solution as a function of time is plotted, at constant temperature, the quantity $\alpha A/V$ is the initial slope of this curve, as illustrated in Fig. 9. The dynamic corrosion rate for solution-limited attack is directly proportional to this α, to the temperature coefficient of the equilibrium solubility $dS°/dT$, and to the ΔT in the system. Note that in contrast to the diffusion-limited attack, the flow velocity and the geometry of the system appear to have little bearing on the corrosion rate. There seems to be adequate evidence that the corrosion of iron by liquid Na is properly described by this latter process.

When corrosion results from chemical reaction, the rate at which the process proceeds will, in general, be describable in terms of ordinary chemical kinetics relationships, taking into account the specific reactions under consideration. There are few cases where such a treatment has been applied. In the case of the weight-gains observed in 18-8 and 25-20 steels in Na, the analysis has been made and seems to give satisfactory agreement with experiment.

In many cases of solution attack by liquid metals, the material dissolved out in the hot zone of the loop is in part precipitated in the cold zone, resulting in an over-all mass transfer. This leads to serious problems in some cases: in mercury boilers, for example, if the previously mentioned Ti-Mg treatment is not used, hundreds of pounds of ferrous metal may ultimately collect in the cooler portions of the system. The effects of these mass transfer phenomena are markedly aggravated when the dissolved material is radioactive. In reactor systems, the material dissolved out of the core, which is the hottest point, deposits in the external heat transfer system, resulting in undesirable long-lived radioactivity beyond the core shielding. Further, if the wall on which this precipitate is deposited is at a high enough temperature, the radioactive material diffuses into the solid to a significant extent, and is removable only with difficulty. Transfer of radioactivity by means of this solution-deposition mechanism may occur even in an isothermal system, due to random interchange of material between the solid and dissolved states; and because of this entropy effect, the over-all phenomenon is relatively insensitive to the magnitude of T in non-isothermal systems. A great deal of study has been devoted to this problem in the US, and while substantial progress has been made, much still remains to be done.

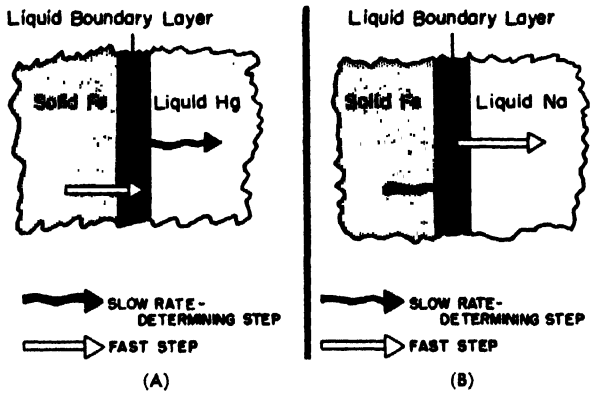

Figure 8. Mechanism of corrosion of iron by mercury and by sodium. (A) Because of the fast rate of solution, the boundary layer of Hg is always saturated with Fe. The rate at which metal is carried from the solid into the liquid stream is determined by the rate of diffusion of dissolved Fe through the Hg. (B) In liquid Na, the boundary layer is not saturated because of the slow rate of solution. The rate at which metal is carried from the solid into the liquid stream is determined by the rate of solution of solid Fe in the Na

SPECIAL TOPICS IN LIQUID METAL CORROSION

I should like to end this talk by mentioning briefly some phenomena which might perhaps each be the subject of a very lengthy discussion:

Heterometallic Effects

In many cases, if two dissimilar metals are immersed simultaneously in a liquid metal, the corrosion rates may be accelerated compared with the rates observed when only a single metal is in contact with the solvent. Examples are the Al-Fe pair, and the Cu-Ni couple in Na. In spite of the superficial resemblance to the acceleration of corrosion by electrochemical action, this phenomenon appears to occur only when there is strong compound formation or solid solution of the two constituents, and is largely a diffusion—solution rate—free energy effect.

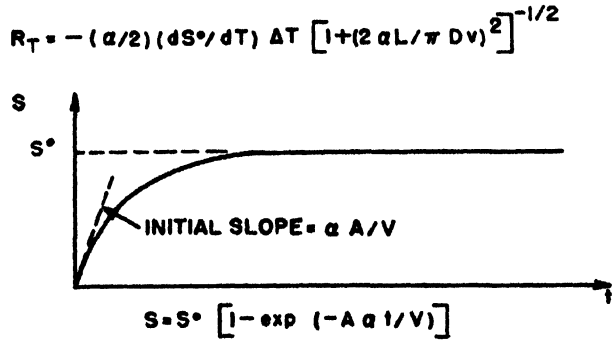

Figure 9. Solution rate limited corrosion

Welding and Diffusion Bonding

This is a most important phenomenon in alkali metals. If two pieces of solid metal in contact are immersed in liquid sodium at an elevated temperature (about 500°C for example), after some time the metals will be tightly welded together. The liquid seems to serve as a solvent bridge, and facilitates the transfer of atoms from one solid to the other. The strong reducing action of the alkali metals on the oxides of many heavy metals also seems to be of some importance in this process.

Carburization and Nitridification

The decarburizing action of Na on carbon steels has been mentioned above. Nitrogen can also be removed from a few steels in the same way. But sometimes, if a source of carbon or nitrogen is present in a Na system, along with a metal, such as a stainless steel, which can be nitrided or carburized, the solid may develop surface films due to these processes. This phenomenon seems to be closely related to the heterometallic mass transfer noted above, with the substitution of the non-metallic elements for the second metal.

Corrosion of Compounds and Non-Metallic Elements

Little has been mentioned in this discussion about the corrosion of solids other than metals by fluid metals. There is a rather extensive body of data on the corrosion of ceramics by liquid metals. In many cases, the corrosion of compounds depends largely on chemical effects; thus ceramics containing oxides that are thermodynamically reducible by Na would hardly be expected to be very resistant to this fluid. Often, with ceramics, the density, firing temperature, and the nature of the binder is extremely important in determining corrosion resistance. Thus, while single crystal Al_2O_3 (synthetic sapphire) is quite resistant to sodium, there are few Al_2O_3 ceramics which approach it in inertness.

Physical effects also have an important effect in the corrosion of many non-metallic solids. Graphite is drastically attacked by Na, possibly due to the penetration of the metallic atoms between the hexagon sheets which make up the graphite structure. Also, with porous solids, surface tension, and wetting phenomena are of considerable importance.

REFERENCES

1. Lyon, R. N., Ed., *Liquid Metals Handbook,* NAVEXOS P-733 (Rev.) 2nd Ed. Superintendent of Documents, US Government Printing Office, Washington (June 1952).
2. Goodman, C., Ed., *The Science and Engineering of Nuclear Power,* Vol. 1, Addison-Wesley Press, Cambridge, Massachusetts (1947).
3. Compare, for example, *A Report on the Proceedings of the Liquid Metal Utilization Conference,* A.E.R.E. X/R 1381, Her Majesty's Stationery Office, London (1954).
4. Weeks *et al.,* P/118, Session 19B, this Volume.

Observations on the Corrosion of Uranium in Liquid Sodium

By H. Mogard,* Sweden

In the binary system uranium-sodium there are no intermetallic phases formed and the mutual solubility of the elements is probably very small.[1,2] Nevertheless, an appreciable amount of uranium will appear in the sodium phase, when the two metals are heated together at temperatures below 600°C. Thus a uranium content of 0.1% to 0.5% was found in the preliminary tests. Evidently some corrosive action occurs. The purpose of the present investigation was to study the mechanism of this corrosion of uranium in liquid sodium and in this connection to find the effect of an intended inhibitor.

Oxygen, nitrogen, hydrogen, etc., are common impurities in liquid metals and these elements sometimes cause a corrosion of solid metals due to compound formation. From a thermodynamic point of view uranium will reduce any oxyde and nitride of sodium present, while the hydride is less likely affected. Sodium very easily combines with oxygen and consequently a formation of uranium oxyde may be expected when uranium is heated in presence of liquid sodium.

EXPERIMENTAL

Microscopic, X-ray and microhardness techniques were used for the study of the surface of the uranium specimens after isothermal heating in liquid sodium for periods of 1 month at 475°C and 600°C. Parts were loosened from the uranium surface by scraping with a diamond and analyzed for sodium and iron by means of chemical and spectrographic methods. The sodium was analyzed for uranium only.

The uranium was of a high purity and had been degassed by vacuum extraction at 600°C. The sodium was of a commercially p.a. quality (Merck) and contained about 0.04% oxygen.

Mild steel tubes of 12 mm id proved satisfactory as container material for the sodium-uranium test system. To minimize oxygen pick-up, the sodium was introduced into the container by a special technique. The steel tube, which had been closed tight at one end by flattening and welding, was electropolished and dried on the inside before charging with 3–5 gm pieces of electropolished and dried uranium. Two constrictions were applied above the final container space by pressing on the outside of the tube. About 8 gm of freshly cut sodium pieces were now placed on the upper constriction; the tube being rapidly connected to a vacuum pump and evacuated. Upon heating the sodium melted, passed through the narrow constrictions and entered into the lower container space. Argon was let in, the lower tube part cut off and the container brazed tight in a gas flame. Parallel experiments with glass tubes demonstrated that these constrictions on the tube acted as mechanical filters for the sodium oxyde.

Finally the steel container was enclosed in a Pyrex capsule which was filled with argon. In some corrosion tests calcium metal was tried as a deoxydizing agent for sodium and added to the tube in the form of powder together with the uranium pieces.

After heat treatment and crushing of the capsule the container was cut straight through by a saw, the sodium part being analyzed for uranium, the other part being treated in alcohol for freeing of the uranium specimen.

The metallographic preparation followed the ordinary sequence of operations: the specimen being mounted in Bakelite, ground on wet emery papers and finally polished on laps using diamond dust.

RESULTS

On heating uranium at 475°C in a sodium liquid, which had not been mechanically filtered from sodium oxyde, a scale of UO_2 is formed on the uranium surface (Fig. 1). The 110 plane of the UO_2 lattice was found oriented parallel to the surface of the specimen. The scale, which measured a thickness of about 100 μ, was dense and adhered quite well to the metal surface. However, it was brittle and, in consequence, UO_2 particles could be identified in the sodium phase, where about 0.5% U was detected chemically.

On filtering the sodium a thinner scale, or film (30–40 μ) appears on the uranium surface at 475°C (Fig. 2) and 600°C (Fig. 3). Microscopically two layers are easily observed as building up this corrosion film; the inside layer being dark, dense, adhesive and hard (600 VHN); the outside layer, however, being bright, porous and relatively soft (450 VHN). By X-ray analysis only a single phase, UO_2, could be detected in the film. In this case no pronounced orientation was detected.

At 600°C the corrosion front exhibits some isolated outbreaks into the uranium (Fig. 4) measuring a depth of about 100 μ, thus indicating a pitting attack.

* Dept. of Chemistry, Aktiebolaget Atomenergi, Stockholm.

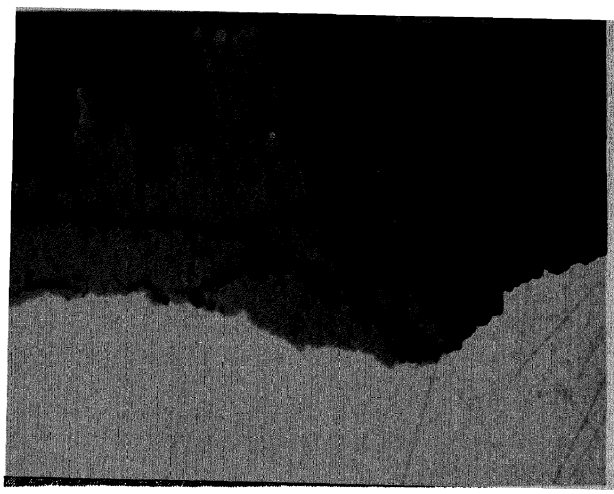

Figure 1. × 500, 475°C, 1 month. Dense UO_2-scale, formed in O-rich Na; the 110-plane of UO_2/U-surface; thickness 100 μ

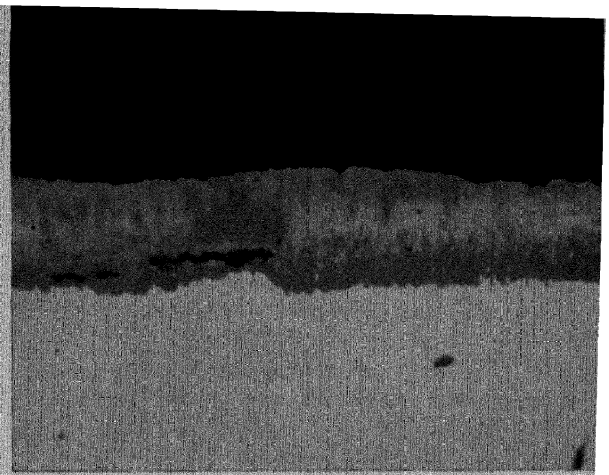

Figure 2. × 500, 475°C, 1 month. Two-layer film of UO_2 formed in Na containing initially about 0.04% O; thickness 30 μ

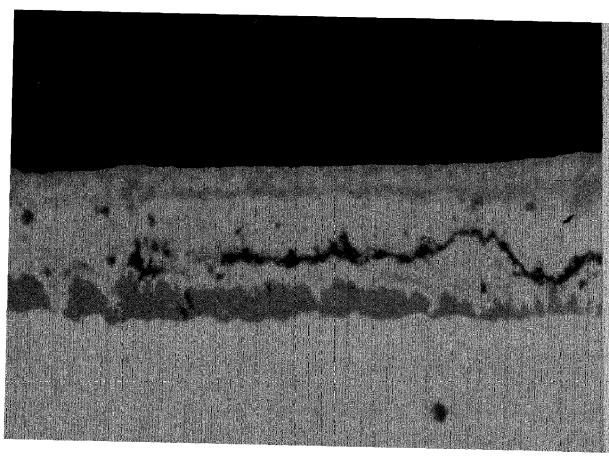

Figure 3. × 500, 600°C. Otherwise similar to Fig. 2; thickness 30 μ

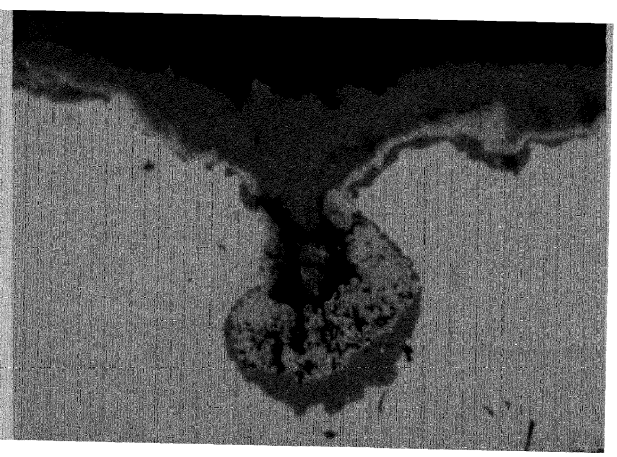

Figure 4. × 500, 600°C. Otherwise similar to Fig. 2; pitting 100 μ

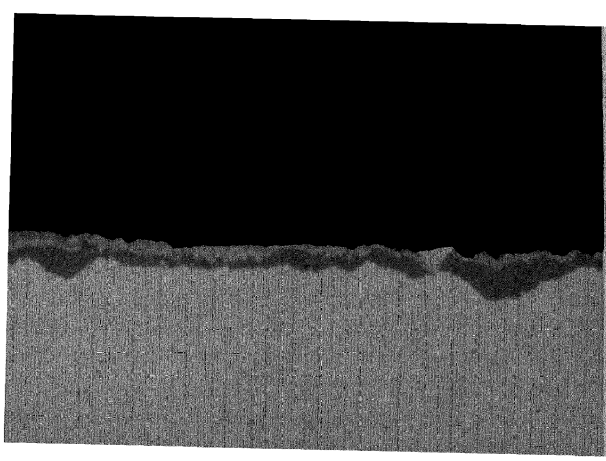

Figure 5. × 500, 475°C, 1 month. Two-layer film of UO_2 formed in Na initially containing about 0.04% O; 0.1% Ca added to Na; thickness 10 μ

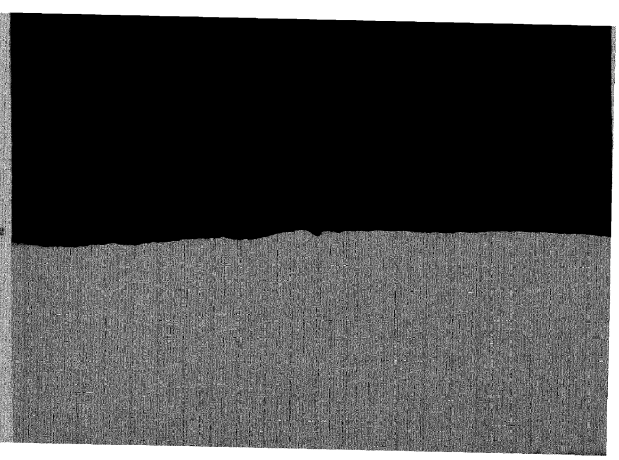

Figure 6. × 500, 8% Ca added to Na; otherwise similar to Fig. 5; U-surface almost bare

Figures 5 and 6 illustrate the effect of calcium as a deoxydizing agent for sodium, when tested at 475°C. The oxyde formation is obviously completely inhibited.

In these corrosion tests no significant amount of sodium or iron could be found on the corroded uranium surface. In the sodium phase the uranium content turned out to be less than 0.01%.

CONCLUSIONS

High purity uranium is attacked by the oxygen impurity in liquid sodium at temperatures up to 600°C. On the uranium surface a film of UO_2 forms, the rate of growth being dependent on the amount of oxygen in the sodium phase. However, the rate of corrosion measured over a test period of one month is fairly slow (30–100 μ/month).

When the corrosion proceeds at a rate of about 50 μ per month or less there is a two-layer UO_2 film formed which is composed of a dense and hard inside layer in close contact with the metal and a porous and less hard, non-orientated outside layer. The difference in nature of the two layers may be due to different nucleation and growth processes.

Calcium added to the sodium acts as a corrosion-inhibiting agent. In absence of a covering UO_2 film on the uranium surface no corrosion effects at all are observed at 475°C.

At 600°C the smooth UO_2 film is interrupted by corrosion pits penetrating into the metal.

The corrosion of uranium in sodium thus does not seem to be of a serious nature at temperatures around 500°C, provided that the sodium used is free from oxygen.

REFERENCES

1. Katz and Rabinowich, *The Chemistry of Uranium*, NNES, VIII–5 McGraw-Hill Book Co., Inc., New York, p 177.
2. Douglas, Thomas B., US AECD–3254 (Abstract).

Basic Technology of the Sodium Graphite Reactor

By Sidney Siegel, R. L. Carter, F. E. Bowman and B. R. Hayward,* USA

The Sodium Graphite Reactor is primarily intended for use as a central-station nuclear power source. It is a "thermal" reactor, with liquid sodium used for the heat transfer medium, graphite for the moderator, zirconium and stainless steel as the structural materials. The fuel elements are metallic uranium or thorium-uranium alloy, containing a few per cent of U^{235}. In order to achieve low-cost power, it is desirable to operate the reactor with the coolant near 1000°F. and the fuel element at temperatures substantially higher. The basic technology of the reactor thus concerns the properties of these materials and their reaction with each other, at the indicated temperatures, and in a thermal neutron flux of the order 5×10^{13} n/cm²-sec.

The phenomena which are of particular importance include the reactions between sodium and graphite, zirconium, and stainless steel; the behavior of graphite under the operating conditions; the behavior of metallic fuels under operating conditions. These subjects are discussed in the following sections.

REACTIONS BETWEEN SODIUM AND GRAPHITE

Chemical Effects

The central problem peculiar to the SGR is the reaction of sodium with graphite, or with any third material in contact with both. In all of the experiments on the corrosion of graphite by sodium, over the temperature range 450°C to 900°C, no positive evidence for the formation of sodium carbide has ever been observed. However, graphite exposed to sodium over this temperature range, in metallic capsules, has been observed to corrode. The conditions at which the corrosion becomes significant depend on the temperature and the capsule material.

The graphite tested was a molded type manufactured by the National Carbon Co., having a small grain size and an apparent density of 1.7 gm/cm³. Two series of samples were exposed, one in type 347 stainless steel capsules, the other in zirconium capsules. The loss in weight of the graphite samples and observations on the capsules are shown in Table I.

It thus appears that the rate of attack by sodium on graphite is primarily governed by the rate at which the container material can take up carbon, which probably is present in the sodium either as a dilute solution or as a suspension of small particles. Analyses of the sodium after the 750°C runs revealed a carbon content of the order 0.1 per cent. It is evident from the table above that in stainless steel containers sodium appreciably attacks graphite at about 600°C, while in zirconium the attack is slight even at 750°C.

Similar tests carried out on graphite which had been irradiated in a graphite moderated reactor for an integrated thermal neutron flux of the order of 10^{21} n/cm² exhibited substantially the same behavior.

Physical Effects

While the chemical attack on graphite in non-carburizing containers is negligible below 600°C, there are significant physical effects. The graphite tested has a fractional void volume of the order 25 per cent, of which about 90 per cent is interconnected to the surface. When graphite is immersed in liquid sodium, the graphite is wet by the liquid, at temperatures as low as 450°C. The available pore volume becomes completely filled by sodium under these circumstances.

Even if the graphite is only partially immersed in sodium, it will become filled with the liquid by capillary action at temperatures near 500°C. While no corrosion is observed, the permeation of the graphite is accompanied by a dimensional charge of the order +0.8 per cent.

The principal deleterious effect of sodium on graphite is thus not a chemical one, but the physical invasion of the pore volume of the graphite, and the resulting increase in neutron absorption cross sec-

Table I. Weight Loss of Graphite Samples

Temperature, °C	*Capsule material*	*%wt chg/ month*	*Effect on capsule*
450	347 SS	+0.06	No effect
525	347 SS	−0.2	No effect
600	347 SS	−0.4	Moderate carburization of SS
600	Zirconium	Negligible	No effect
675	347 SS	−7.5	Heavy carburization of SS
750	347 SS	−50.0	Heavy carburization of SS
750	Zirconium	−2.8	Slight carburization of zirconium
900	347 SS	−50.0	Massive carburization of SS

* North American Aviation, Inc., Nuclear Engineering & Manufacturing, Los Angeles, California.

tion. While the macroscopic cross-section Σ of the graphite alone is of the order 4×10^{-4} cm^{-1}, when it is permeated by sodium, $\Sigma = 3 \times 10^{-3}$. In order to avoid such a large cross section in the graphite it is necessary to physically separate the sodium from the graphite in the SGR. In addition, the dimensional change observed would impose a significant design problem.

REACTION OF SODIUM WITH METALS

Zirconium

The requirement for preventing contact between the coolant sodium and moderator graphite necessitates the selection of a can material which is compatible with both materials at the core temperatures and which provides the minimum of neutron absorption. The latter requirement immediately suggests zirconium and the consideration of other properties indicates that with proper precautions successful operation can be anticipated.

The use of zirconium as a sheathing material for the graphite does not involve substantial stresses; consequently, the low elevated temperature strength of the material offers no serious disadvantage. Since these moderator units are hexagonal sections eleven inches across the flats and ten feet long, the physical size presents certain assembly problems. The length of the weld seams involved in the fabrication of the can makes inconvenient the use of the conventional inert atmosphere glove-box techniques. Consequently, a process has been developed through an adaptation of the automatic inert gas shielded arc method which results in superior quality long seams.

Zirconium is a readily weldable metal, but good welding requires adequate shielding from the atmosphere, because of the high solubility of oxygen, nitrogen and hydrogen in zirconium. By employing a jig which provides the proper chilling, an inert gas backup beneath the weld deposit, and a torch with a trailing shield to permit complete protection of the weld metal as it cools, an essentially gas-free ductile weld can be consistently produced. For zirconium sheets of 0.035-inch thickness, that are used for the cans, no added metal is required and a tungsten electrode is employed. Filler metal in the form of zirconium wire can be used where heavier deposits are required.

In short, the problems in the manufacture and operation of a canned moderator of the type described involves only those created by the presence of sodium and graphite at the operating temperatures. Both the sodium and the graphite may be the source of impurities which can adversely affect the properties of zirconium. These problems arise primarily from the gas adsorption property of zirconium for which it has been conventionally described as a gas "getter". No evidence has been found to indicate a significant solubility of zirconium in sodium, or the converse, at temperatures even well above those considered in the sodium graphite reactor. The compatibility problem is one strictly dependent upon the contaminants in the sodium.

The ability of zirconium to remove oxygen from sodium is perhaps best demostrated by the free energies involved in the reaction:

$$Zr + 2Na_2O \rightarrow ZrO_2 + 4Na$$

	Free energy, kcal,	
Temperature, °K	Na_2O	1/2 ZrO_2
500	−83.0	−119.2
800	−72.4	−112.5
1000	−65.5	−108.0

Experimental evidence has substantiated predictions made on the basis of the free energy data. When zirconium is tested in hot oxygen-bearing sodium (it is very difficult to obtain and hold completely oxygen-free material) a weight gain accompanied by a black tightly adherent surface layer has been observed, which has been identified as the monoclinic form of ZrO_2. The rate of weight gain in zirconium is nearly independent of the oxygen content of the sodium, in the range above 0.005 weight per cent of oxygen. The rate of weight gain at 500°C in sodium, with oxygen contents from 0.005 to 5 per cent by weight, is about 0.04 mg/cm^2 per month.[1] At lower oxygen levels, of the order of 0.003 per cent, this rate of weight gain appears, based on a limited number of tests, to drop by a factor of about four. Very little is actually known about rates of oxygen pickup from sodium, since a major portion of the testing has been of one month duration with a single determination made at the end of the run. However, it seems reasonable to assume that once the oxide layer is established the rate is essentially equivalent to that found for gaseous oxygen. In this latter case it is known that after the initial formation of the oxide, diffusion of oxygen through this oxide layer is the rate determining factor. The oxidation rate curves appear to be parabolic at all temperatures up to 900°C.

Zirconium presents a complication not encountered in the oxidation of most materials, since it is capable of dissolving the oxide to form a solid solution. The current zirconium-oxygen phase diagram indicates a solubility of about 7 per cent by weight. It is this extensive solid solubility which presents the most serious problems with regard to the operation of zirconium in a sodium system. The diffusion rates of oxygen in zirconium at the temperatures of interest, namely 500°C to 650°C, have not as yet been established. A rough qualitative estimate can be made from data reported from the Knolls Atomic Power Laboratory.[2] These data indicate that oxygen, as measured by its effect on the hardness of zirconium, penetrates at the rate of about 0.0015 inch per month at 500°C and 0.002 inch per month at 650°C.

This hardness change points up the possibility of serious operational difficulty if zirconium is subjected to high oxygen content sodium over long periods of time. Treco[3] has reported the hardness versus oxygen content relationship for zirconium.

His data indicate a change of from R_A 21 at 0 per cent to R_A 60 at 2.5 atomic per cent. This hardness change is accompanied by a corresponding loss in ductility at 20°C. Treco points out, in fact, that as little as 2.0 atom per cent oxygen renders cold working and machining of zirconium impossible. This embrittlement of the surface affords an opportunity for impairment of the fatigue properties. Zirconium is a notch sensitive material and any surface cracking would result in rapid fatigue failure.

Fortunately, the reactor operation does not require the moderator cans to operate at low temperature. The embrittlement mentioned earlier is intrinsically a room temperature condition and the effects of oxygen have been shown to essentially disappear at temperatures of the order of 375°C. Bend tests on zirconium specimens run in sodium with sufficiently high oxygen contents to provide an oxygen-rich surface layer have indicated a serious ductility loss at room temperature; at 550°C however, these specimens exhibited properties similar to those found with unoxidized material. No surface cracking was noted at the higher temperatures.

Attention has been given to the effects of oxygen primarily because oxygen appears to be potentially the most serious problem. As pointed out earlier, zirconium is capable of dissolving both hydrogen and nitrogen in addition to oxygen. The solubilities of these gases are more or less interdependent and their effects upon physical properties are very similar. The diffusion rate of hydrogen in zirconium is very rapid, whereas that for nitrogen is relatively slow. In fact, it is reported that no diffusion of nitrogen has been detected below 800°C. This, of course, is for times relatively short as compared with the desired life of the moderator cans. In addition to this apparently low diffusion rate, the nitrogen problem is further minimized by the fact that nitrogen does not dissolve in nor react chemically with sodium, so that the opportunity for its transport to and contact with zirconium appears to be slight. Hydrogen on the other hand is readily soluble in sodium, and if present will easily find its way into the zirconium. The opportunity, however, for the introduction of hydrogen into the reactor system is appreciably less than that of oxygen and this fact plus the greater tolerable level in the zirconium tends to minimize the problem.

The problems of gaseous contamination if zirconium are eased because the deterioration of physical properties is small at the high operating temperatures. However, in view of the necessity for long moderator-can life, many years if possible, means for minimizing gaseous contamination are being developed. The most obvious precaution is, of course, to load the reactor, after thorough cleaning of the system, with the purest possible sodium. This is best and most conveniently accomplished by filtering the sodium at a temperature slightly above the melting point. The solubility of sodium oxide in sodium is temperature sensitive and by filtering at 250°C the oxygen content can be reduced to about 0.002 weight per cent. After loading and bringing the reactor to operating conditions, it is reasonable to expect that the reactor system may not be absolutely gas tight. It is therefore essential that provision be made to remove the contaminating gases introduced through unavoidable leakage. Here again advantage is taken of the temperature dependence of sodium oxide and hydride solubility. The sodium system is provided with "cold traps" which, by proper operation, are capable of removing these two impurities at significant rates. By maintaining a volume of sodium at a temperature slightly in excess of the melting point, in contact with the hot sodium in the system, advantage is taken of the low gas solubility at the low temperature to provide, essentially, a "sink" for these contaminants. Theoretical considerations which have been borne out by experimental evidence indicate that the oxygen and hydrogen level of the entire system can be brought down to and maintained at the solubility limit at the cold-trap temperature. Thus, an oxygen content of 0.002 weight per cent is theoretically possible in a suitably cold-trapped system. The rates at which these traps function may be exemplified by the theoretical capacity of the traps to be employed on the Sodium Reactor Experiment. Here in a system containing 50,000 pounds of sodium, one cold trap is capable of removing approximately 0.04 pound of oxygen per hour at an over-all oxygen level of 0.005 weight per cent in the system. The rate and extent of hydrogen trapping have not been investigated as thoroughly. However, it has been shown that the hydride can be cold trapped in a manner similar to the oxide.

It is possible that with a "gettering" material such as zirconium in the system the ability of the cold traps to retain the trapped oxygen may not be sufficient to prevent gradual contamination. While this problem is being investigated, alternate techniques are being developed. One of these which appears technically feasible is the use of a material thermodynamically capable of reducing ZrO_2, such as metallic calcium. Its solubility in sodium, and its nuclear characteristics as well as its apparent inertness with respect to zirconium, appear to make it completely suitable for use in minimizing the oxygen content of the sodium in the reactor system. However, any oxygen removed by the calcium results in particulate CaO in the system. This must be removed, possibly by filtering, to prevent possible erosion of surfaces, as well as plugging of narrow coolant passages. Another possible approach is the use of an insoluble material with superior "gettering" properties to zirconium. This "gettering" alloy presumably would have to be operated at a temperature at least as hot as the maximum encountered by the zirconium and possibly at an even higher temperature to be effective. Preliminary work indicates that a 50 atom per cent zirconium-titanium alloy will be effective for such use.[4] In contrast to the cold trap, a 50 atom per cent zirconium-titanium

alloy is capable of removing nitrogen as well as oxygen and hydrogen and consequently offers this advantage in addition to eliminating the problem of introducing particulate solids into the coolant stream. Operation of the SRE will establish the necessity for and the effectiveness of these various systems for contamination removal.

In order to monitor the contamination level of the sodium in the system and maintain a check on the effectiveness of the decontamination system, it is of course necessary to be able to quantitatively analyze the sodium at will during operation. Such analyses can be carried out using the so-called "plugging indicator". The operation of this device is based in principle on the variation of solubility of Na_2O in sodium with temperature, as shown in Fig. 1. The main sodium system (the oxide content of which is to be analyzed) is provided with a small side loop containing a plug having holes of the order of 0.050 to 0.060 inch in diameter. This plug section is provided with cooling so that its temperature can be carefully controlled. To make an oxide analysis, the temperature of the plug is lowered until a point is reached at which flow in the side tube ceases. This is an indication that precipitated oxide has filled the holes. The temperature at which this occurs corresponds to a definite solubility limit and this determines the oxygen level in the over-all coolant stream. By reheating the plug the precipitated oxide is redissolved and the indicator is returned to a condition suitable for another determination. This analytical procedure has shown excellent sensitivity, precision, and convenience.

Stainless Steel

In addition to the zirconium, the sodium-graphite reactor system necessarily involves the use of stainless steel in the core tank and piping system as well as, initially at least, the fuel element jackets. There is sufficient experience with sodium systems to indicate that with the austenitic type of stainless steel no serious corrosion problems, as such, exist. The surface oxidation produced by the contaminating oxygen in the sodium is inconsequential at reasonable oxygen levels. However, another phenomenon of similar nature but with radically different consequences has been observed. Mass transfer is involved, although the quantities with respect to weight are insignificant. The problem becomes significant because some of the material transported originates in the reactor core and consequently contains appreciable quantities of induced radioactivity. This, when deposited in locations external to the core, gives rise to accessibility difficulties in maintenance operations. These undesirable isotopes which are transported are for the most part impurities in the stainless steel, cobalt which is introduced with the nickel, and tantalum which accompanies the niobium in stabilized type 347 material. Also, it has been found that Mn^{54} resulting from an n–p reaction with Fe^{54} can under certain conditions become a very considerable contributor to the activity transfer problem.

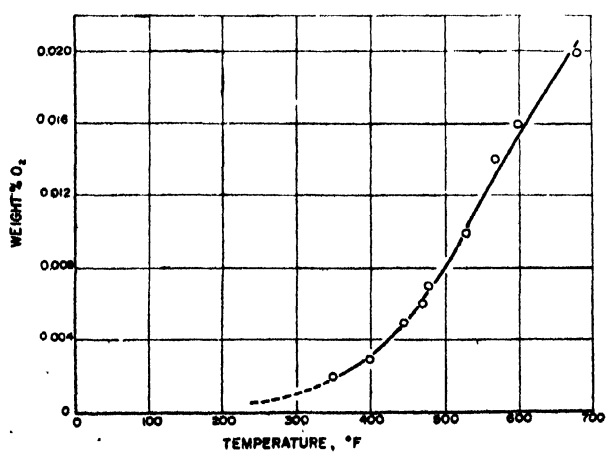

Figure 1. Solubility of Na_2O in sodium as a function of temperature

The actual mechanics of this transfer are not thoroughly understood. It is apparently not a matter of solubility alone, for experiments have shown that the precipitation and deposition is not restricted to, or even concentrated in, the coldest portions of the system. In fact, the deposition is apparently independent of temperature. The usual concept of mass transfer in liquid metal systems involves a thermal coefficient of solubility together with a thermal gradient which results in the over-all movement of material from the hot to the cold portions of the system. It has been demonstrated that the process is sensitive to the oxygen content of the sodium, the transfer rate varying directly with the oxygen content. Additional evidence of this oxygen dependence is offered by the fact that the additions to the sodium which most effectively inhibit the activity transfer are those which tie up the oxygen as insoluble oxides. To date barium has been found to be most effective in this regard. The process does not appear to be one of oxide formation, breakoff and settling out since the active isotopes diffuse into the surfaces upon which they are deposited, suggesting that they are deposited as atoms rather than as oxides or other compounds.

In any event, by controlling the oxygen content by the various available means, it appears possible to minimize the activity transfer to an extent such that no serious problem in the operation of a stationary power plant results.

BEHAVIOR OF GRAPHITE

Gas Evolution

The necessity to sheath the graphite, to separate it from the sodium coolant, makes it mandatory to investigate the problem of gas evolution from graphite under operating conditions. Commercial artificial graphite exhibits substantial sorption properties for all but chemically inert gases. Oxygen, nitrogen, hydrogen and carbon oxides are among the gases most strongly absorbed. All these gases are also

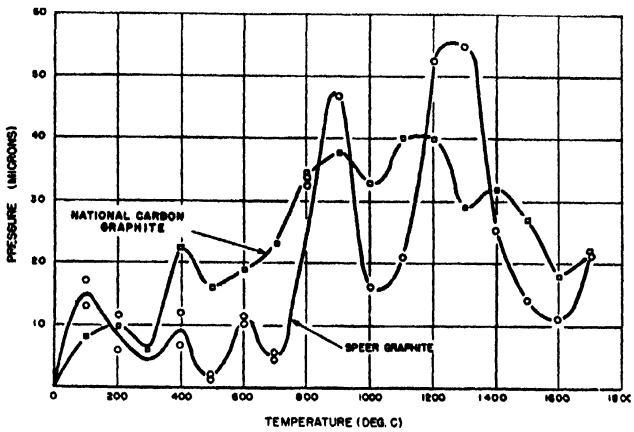

Figure 2. Differential curve of gas evolved at a succession of temperatures during the vacuum heating of graphite to 2000°C

readily absorbed at reactor operating temperatures by the zirconium employed to protect the graphite moderator from the sodium coolant, and may deteriorate the physical properties of the zirconium. High temperature vacuum degassing of graphite leads to evolution of volumes of gas ranging from 250 mm^3/gm for thoroughly graphitized materials to volumes tenfold greater for incompletely graphitized carbons.[5] These gases are apparently chemisorbed upon the surfaces of the intricate interconnected pore system of the graphite, preferentially at surfaces of high curvature.

The removal of gas from sorption sites can be stimulated thermally. Gas evolution rates are influenced by the thermal dissociation of chemical bonds between gas atoms and the solid, but are also dependent upon the diffusion rate through the pores of the gross graphite volume, as shown by the outgassing of helium gas observed at high temperatures from graphites previously outgassed and cooled in helium. A differential curve of the amount of gas evolved at a succession of temperatures during the vacuum heating two Speer Carbon Co. graphite specimens show reproducible characteristic structure, as is evident in Fig. 2. However, substantial differences appear between nominally similar grades of graphite obtained from different manufacturers, typified by the adjacent curve for a National Carbon Co. specimen.

Mass spectrographic analyses of the constituents in samples of the evolved gases are shown in Fig. 3 below.

No clear evidence for association between evolution rate maxima and identity of evolved species is evident. It is believed, therefore, that the structure of the gas evolution spectrum is associated with grain and pore size distribution.

A comparison of the integral gas desorption curve, Fig. 4, for purified spectrographic grade graphite with that for a similar unpurified commercial graphite suggests that most of the sorption sites from which gas is thermally desorbed below 1000°C are associated with impurity centers. Furthermore, the rate of sorption by purified graphite in which the graphite pores have been filled with helium gas is quite slow; open exposure to atmospheric gases for a period of several weeks is required to reach equilibrium. It is presumed that active sites initially protected by helium gas are reached by diffusion of gases from air into the graphite through micropores. The composition of the gas evolved at 1800°C, for graphites of various previous histories, and stored in air for several weeks, is tabulated below.

Graphite type	*H_2 released moles/gm*	*CO moles/gm*	*CO_2 moles/gm*	*Other moles/gm*
Normal	2.2×10^{-4}	7.2×10^{-4}	2.0×10^{-4}	1.7×10^{-4}
Purified, let down to He at 1300°C	4.1	1.4	0	0.4
Purified, let down to He at 200°C	4.5	0.9	0	0.3

Measurement of nitrogen adsorption isotherms in degassed graphite having received varying radiation dosages shows that the pore structure is modified by irradiation.[6] An increase in the large radius pore-surface area at the expense of pores of small size is inferred. For graphite enclosed in a gas-tight envelope during irradiation the evolved gas pressure was found first to rise, then to fall back to an intermediate value, Fig. 5. While confirmatory data are lacking, it is suggested that the dissociation of surface bonds, releasing adsorbed gas atoms at temperatures below those required for thermal decomposition, takes place at a rate dependent upon flux

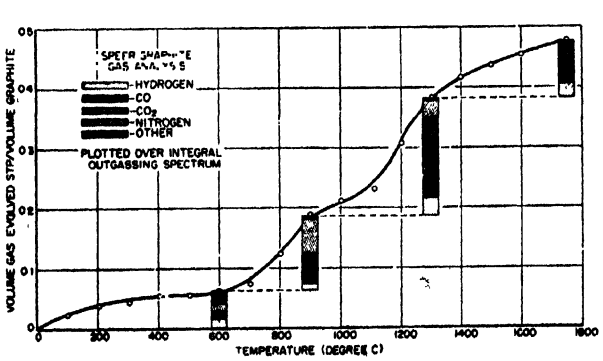

Figure 3. Mass spectrograph analysis of the constituents of the gases evolved from graphite

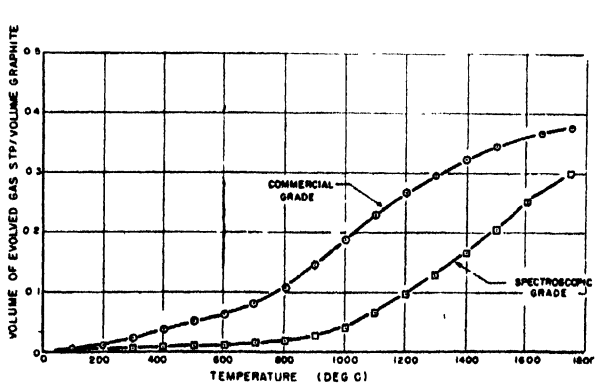

Figure 4. Integral curve of gas evolved up to temperature of measurement

intensity. Readsorption onto sites less vulnerable to radiation-stimulated decomposition takes place at a rate dependent upon the concentration of the gaseous species in the pore volume. The extent to which this readsorption prevents net release of gas under circumstances of practical interest remains to be determined.

The net volume of gas released from a given type of graphite on thermal annealing at 1800°C has been arbitrarily taken to represent the upper limit of the amount of gas which may become available as a result of operation at temperatures near 600°C in the sodium-graphite reactor. At this temperature the sheet zirconium metal surrounding the moderator elements reacts with N_2, CO, and CO_2 to rapidly form surface layers of nitride, carbide or oxide, while hydrogen readily diffuses into the metal. Calculations have been made for the 11-inch hexagonal graphite moderator elements, enclosed in cans of 0.035-inch thick zirconium sheet which are used in the Sodium Reactor Experiment. If the gas released from purified graphite of low initial gas content is entirely trapped by the zirconium, a surface concentration of 300 $\mu g/cm^2$ of oxygen would result. At the reactor coolant temperature of 500°C the diffusion rates of oxygen and hydrogen into zirconium are sufficient to lead to appreciable migration of surface oxygen and hydrogen throughout the solid zirconium. However, significant nitrogen and carbon penetration would be expected only at temperatures above 800°C.

No data are available on the combined effects of these contaminants upon the physical properties of zirconium metal. However, for 0.035-inch thick sheet the concentrations of oxygen resulting after homogenization of an oxide surface layer of the calculated density will be 0.06 weight per cent; the resulting hardness change in the metal for this concentration of oxygen is negligible. On the other hand, a homogenized hydrogen concentration of 370 parts per million results from the surface layer described. This is enough to lead to appreciable embrittlement of zirconium at temperatures below 300°C where hydride precipitation occurs. However, at reactor operating temperatures, the hydride will go into solution and little embrittlement is expected. The effect of relatively stable surface layers of nitride or carbide in retarding the initial penetration of the hydrogen into the zirconium is in the process of investigation.

Radiation Damage

While a very considerable volume of information on the effects of radiation upon numerous properties of graphite have been described recently by Eatherly[7] and Kinchin,[8] in this paper we consider only those changes which are of immediate practical importance to the reactor design and operating conditions. These include changes in the thermal conductivity, stored energy, lattice parameters and physical dimensions. While changes in electrical properties such as resistivity, magneto-resistivity and Hall effect are observable at fast neutron exposures of the order of 10^{15} n/cm^2, the onset of appreciable changes in such lattice properties occurs at about 10^{18} n/cm^2. The changes observed in these properties, for graphite exposed to reactor radiation near 30°C, are plotted in Fig. 6; it is evident that no saturation occurs. In a direction lying parallel to the most probable orientation of the expanding crystalline *c*-axis, very substantial physical distortion occurs. Of even greater potential significance in reactor design is the deterioration of the thermal conductivity by a factor of the order of fifty. The stored energy in the graphite lattice approaches that which would be associated with the conversion of amorphous carbon into graphite.

The effect of annealing such samples, previously exposed to radiation near 30°C, at a series of successively higher temperatures is shown in Fig. 7. It is evident that thermal annealing to 2000°C is accompanied by the return of all properties to substantially their initial values. Extensive studies of the kinetics of this return have yielded no simple description, but strongly suggest clustering of defects and the formation and migration of complex associations of interstitial atoms and lattice vacancies. Detailed discussion of these considerations form the subject matter of another paper.

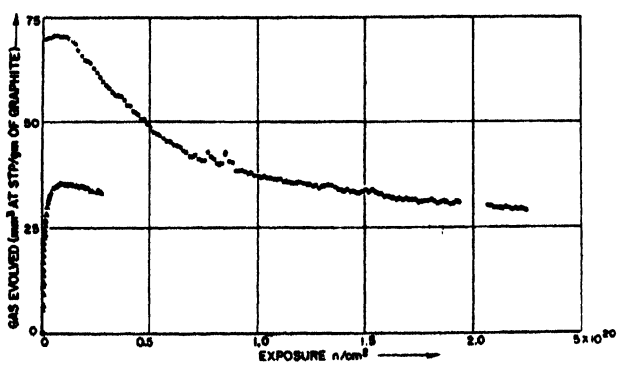

Figure 5. Gas evolved during exposure in reactor at approximately 150°C

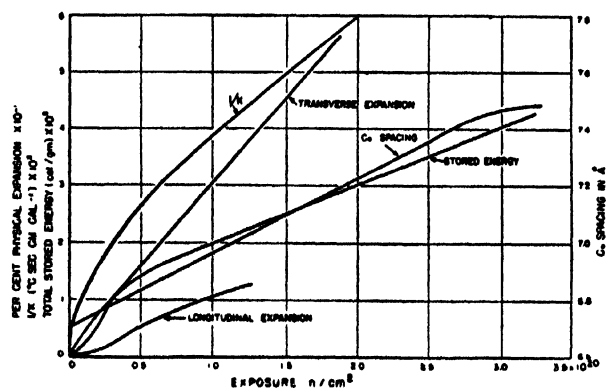

Figure 6. Change of properties during reactor exposure of graphite at 30°C

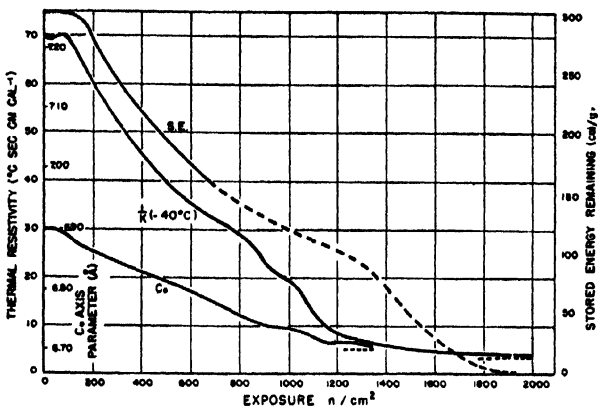

Figure 7. Change of properties during thermal annealing of graphite previously irradiated to 10^{20} n/cm² at 30°C

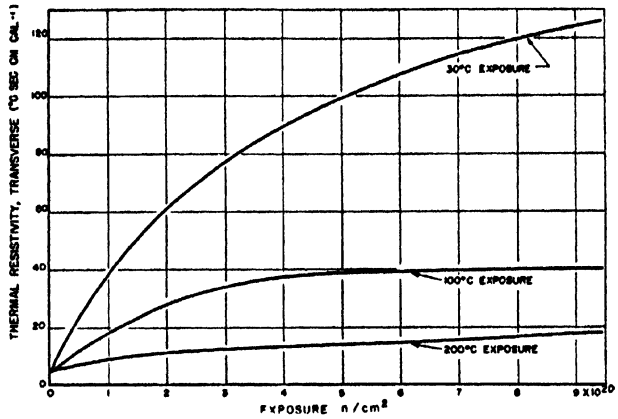

Figure 8. Change in thermal resistivity of graphite for irradiation at various temperatures

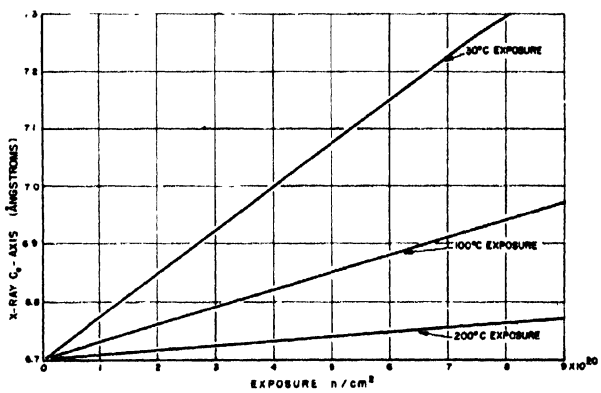

Figure 9. Change in lattice parameter of graphite for irradiation at various temperatures

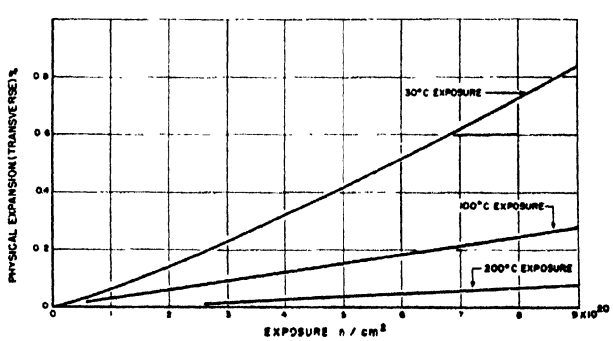

Figure 10. Change in physical dimension of graphite for irradiation at various temperatures

The relative roles of post-irradiation annealing and spontaneous annealing during irradiation have been examined by controlled temperature irradiations. The changes in thermal conductivity, lattice parameter, and physical dimensions transverse to the axis of extrusion of the graphite, which are observed after irradiation at higher operating temperatures, are shown in Figs. 8, 9, and 10. It is evident from these data that the changes produced during irradiation at the higher temperatures are much less severe than those observed at 30°C. Extrapolation of these data suggests that exposure at 600°C, the operating conditions in the SGR, will not produce significant deterioration of the graphite properties. The changes that are expected can be taken care of by appropriate design tolerances.

BEHAVIOR OF FUEL MATERIALS

Fuel Element Stability

The fuel rods in the SGR consists of cylindrical metal slugs contained within a thin-wall stainless steel jacket tube, and bonded to it by a thin annulus of liquid sodium-potassium alloy. The fuel element is a cluster of seven such rods. The fuel elements are supported vertically in the reactor, and the jacket tube thus provides the support required for the column of fuel slugs. In addition, the jacket serves to contain all fission and recoil products and prevents their accumulation in the coolant or in other parts of the coolant system.

A series of short slugs is used in preference to a single continuous rod to minimize warping tendencies arising from asymmetrical heating in the rods of the cluster. The liquid metal bond provides a good heat transfer medium and a free volume for thermal expansion and fuel slug distortion. By avoiding a strong metallurgical bond between the fuel slugs and the thin-walled jacket, the possibility of jacket rupture is reduced.

In a power-producing reactor, it is desirable to operate at the highest exit coolant temperature which material limitations permit, in order to maximize the thermal efficiency of the power plant. The fuel element surface in the SGR is therefore required to operate at 950°F or above. In order to produce economic power, it is desirable to generate as much heat as possible within each fuel element. The center of the fuel element experiences the highest temperature, and in the SGR this temperature has been initially limited to 1200°F, below the $\alpha \rightarrow \beta$ phase transition in uranium metal.

The radial temperature distributions in several fuel slugs at various heights in the center fuel channel of the SRE appear in Fig. 11, with coolant outlet temperatures of 885°F and 1135°F. It is evident, in the latter case, that the center portions of the fuel element are in the β phase, while the

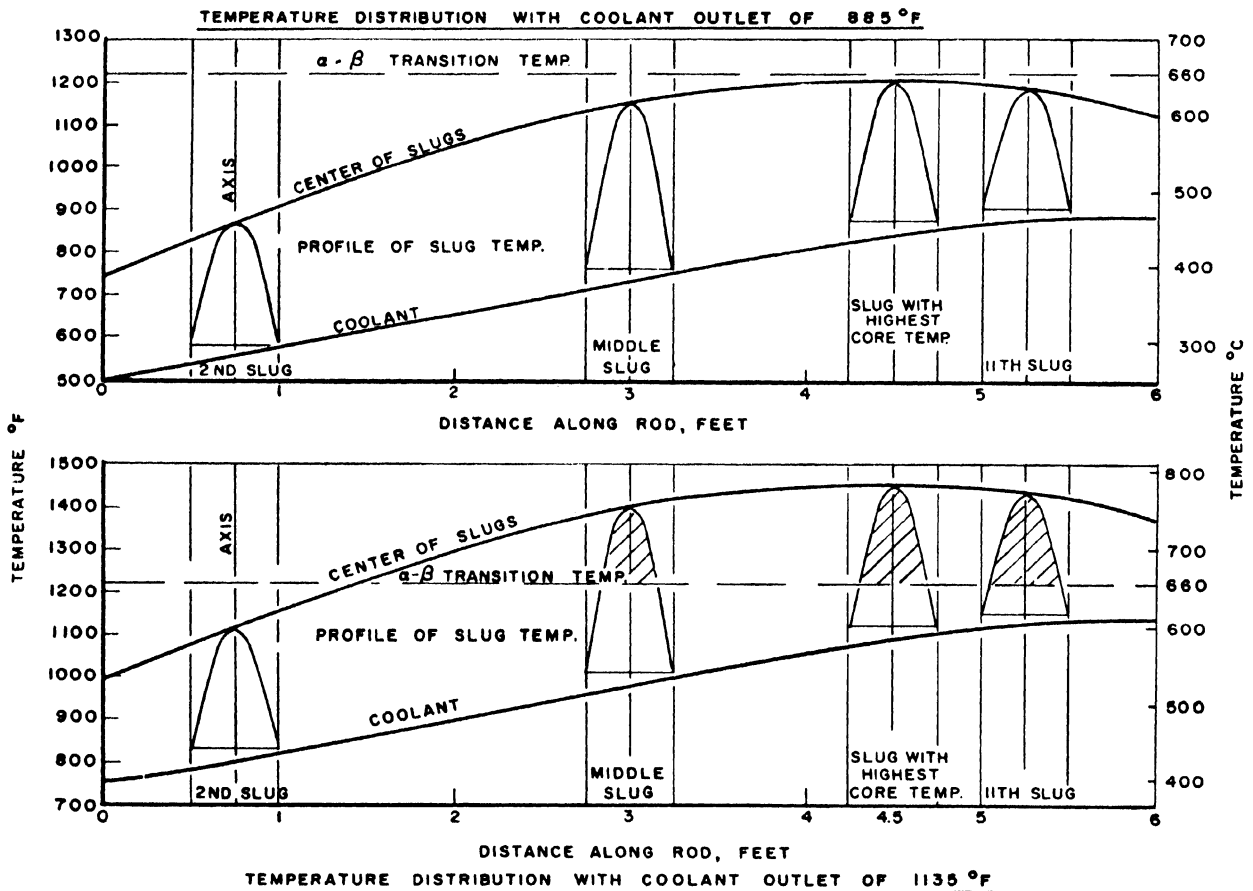

Figure 11. Plot of the radial temperature distribution in fuel slugs in the central fuel channel of the SRE, for two outlet coolant temperatures

outer portions are in the α phase. The behavior of fuel materials at these temperatures, and in operation with a phase gradient, are major problems of the SGR.

The anisotropic nature of α uranium leads to dimensional instability during irradiation or thermal cycling in the α phase, and the volume increase of 1.5 per cent at the α-β transition further aggravates these tendencies if a phase gradient exists in the fuel element. Experiments on a variety of metallic uranium fuel elements have indicated that thermal cycling may be used in place of radiation tests in screening materials for stability against radiation damage, or against the cycling effects *per se* present during reactor operation. The effect of thermal cycling on unalloyed uranium is shown in Fig. 12; cycling entirely within a single phase is far less damaging than the case where the cycles carry the sample through the β transition temperature, 660°C. Similar thermal-cycling tests from 200°C to 700°C on various alloys of uranium, produce the effects shown in Fig. 13. It is evident that some of the alloys are much more stable than the unalloyed metal.

It is believed that the improved stability of the alloys results from a combination of several factors. the α-β transformation is more sluggish, or may be absent, in the alloys. The alloying constituent improves the high temperature strength of the α phase, so that it can better constrain the expanding β phase, particularly in bi-phase operations. Alloying produces a fine grain-size and a more random grain orientation. In most of the alloys, specific methods

580° – 630°C	630° – 680°C	680° – 730°C
$\Delta l = +0.7\%$	$\Delta l = -31\%$	$\Delta l = -2.6\%$
$\Delta d = -0.4\%$	$\Delta d = +19\%$	$\Delta d = +2.4\%$

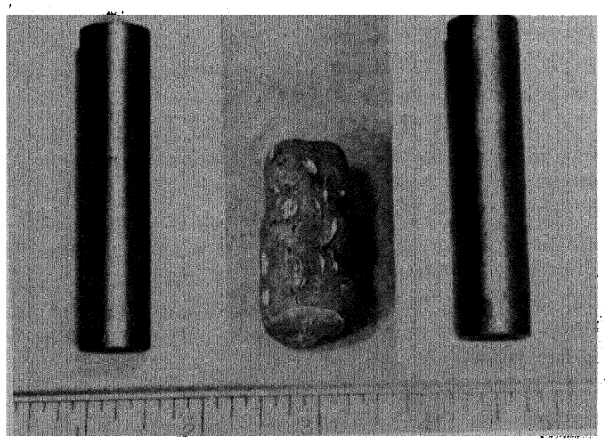

Figure 12. The effect of 200 thermal cycles on α-rolled uranium, over the temperature range indicated. Each cycle had a period of 15 minutes

of preparation, or heat treatments, are required to achieve the improved properties. Powder metallurgy or chill casting appear particularly promising.

It should be emphasized that the thermal cycle tests do not show complete correspondence with radiation tests. Materials which are stable with respect to the cycles, are not necessarily radiation stable, but those which are found unstable against thermal cycles are uniformly unstable against radiation. The thermal cycle tests thus serve as a convenient and rapid screening before the more difficult radiation tests. Radiation tests have been carried out in a variety of materials, generally at temperatures in the α-phase region. The results on three typical materials are given below, for an exposure in which 1 atom in 1000 have fissioned.

Material	*Fractional change in length*	*Fractional change in volume*
α-rolled uranium, no heat treatment	as much as +65%	+0.25%
α-rolled uranium heat treated from β phase	+1.2%	+0.25%
U–Zr alloy	+0.4%	+0.25%
Th–U alloys	Negligible	Negligible

The last entry in the table refers to a thorium base alloy containing a few per cent of uranium, and the results are preliminary.

Reactions Between Fuel and Jacket Materials

A further fuel surface temperature limitation is imposed by the interaction of the stainless steel jacket material and the uranium fuel slug. An iron-uranium eutectic exists which melts at 1320°F. At points where the uranium and jacket material are in contact, a layer of intermetallic compounds will form by interdiffusion, at a rate which depends on the fuel element surface temperature. The thickness of such a layer, formed by holding for 1 year at various temperatures, is shown in Fig. 14. This intermetallic layer gives rise to two major problems. First, it is quite brittle, and thus weakens the supporting stainless steel jacket during prolonged operation at normal operating temperatures. Second, the layer contains material of the eutectic composition which melts at 1320°F, so that in any power surge, failure of the fuel element cladding containing any of the eutectic is more likely.

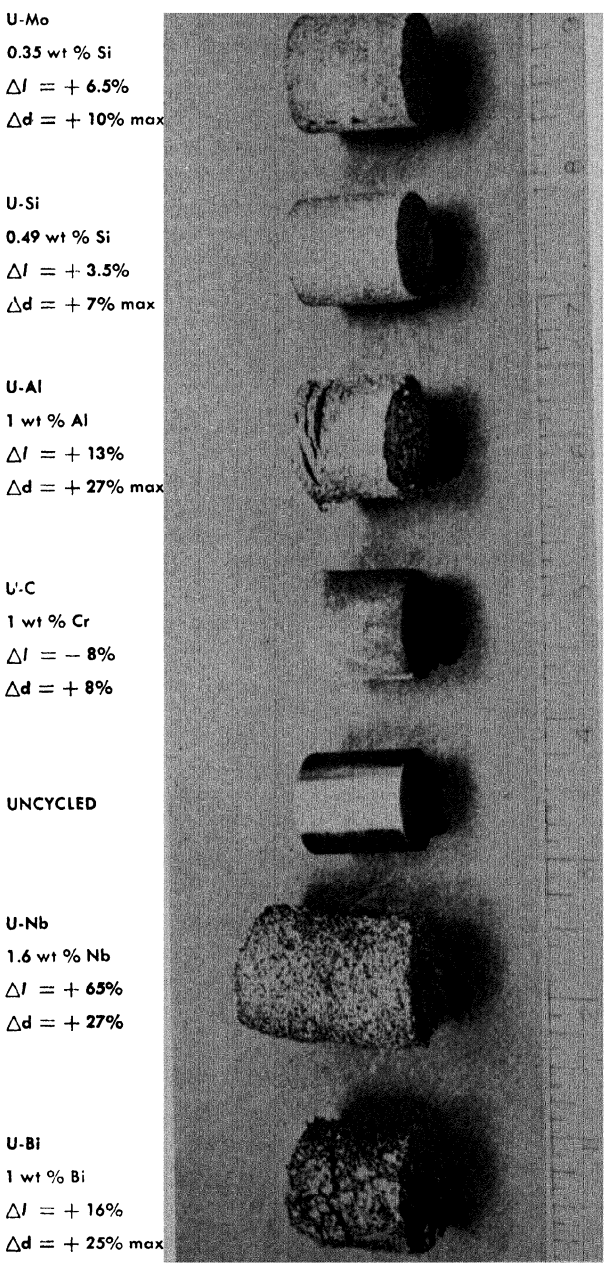

Figure 13. The effect of 500 thermal cycles, from 200° to 700°C, on various alloys of uranium. The original size of all specimens was approximately that of the uncycled sample

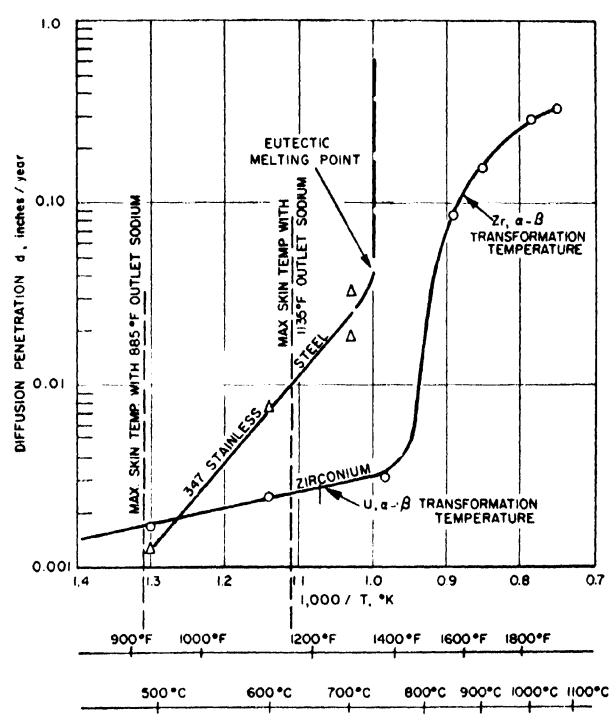

Figure 14. Thickness of interdiffused layer in uranium-zirconium system and in uranium-stainless steel system, which is produced in 1 year, at various temperatures

The oxide film normally present in uranium, the loose contact between the fuel slugs and the stainless steel, and the NaK layer interposed between them, all serve to alleviate this problem. However, as slug distortion occurs the degree of contact will become more intimate and the problem more severe. As is evident from the data for Zr in Fig. 14, the use of this material for cladding offers considerable improvement so far as the rate of interdiffusion is concerned. The strength of Zr at high temperatures is not adequate for a fuel element of the SRE type, but alloying additions may improve this property.

Data on the interdiffusion of thorium with possible jacket materials are not available; however, its melting point is much higher than that of uranium, and this suggests that diffusion rates at a given temperature are correspondingly lower.

SUMMARY

The materials problems which required exploration and satisfactory solution for the construction of the SRE relate to the behavior of graphite, zirconium, stainless steel and their interactions with sodium at temperatures near 1000°F. Of importance also is the stability of the fuel element material at these temperatures, under irradiation and thermal cycling conditions.

Graphite is not corroded by sodium at the temperatures present in the Sodium Graphite Reactor, but physical effects require that it be protected from liquid sodium by a low neutron-absorbing sheath, for which zirconium was chosen. The outgassing behavior of graphite at elevated temperatures, in the presence of radiation, presents problems in the design of the moderator container, and may influence the physical properties of zirconium. Methods of reducing the gas content of graphite are being investigated. The effects of radiation on graphite at and above 1000°F apparently will be negligible.

Zirconium and stainless steel are not corroded by sodium if the impurities in the liquid can be maintained at adequately low levels. This can be accomplished by cold-trapping or "gettering." The strength of zirconium and stainless steel at the normal operating conditions is adequate, but high temperature operation will require better materials.

Fuel stability under thermal cycling and irradiation conditions can be markedly improved by alloying and appropriate heat treatment. The maximum coolant temperature may be limited by interactions between the uranium and the jacket materials.

REFERENCES

1. Unpublished results by Brush, E. G., Knolls Atomic Power Laboratory, Schenectady, New York, USA.
2. Unpublished results by Koenig, R. F., Knolls Atomic Power Laboratory, Schenectady, New York, USA.
3. Treco, R. M., *Zirconium and Zirconium Alloys. A Symposium* . . . Presented to Members of the ASM During the Eighth Western Metal Congress and Exhibition, Los Angeles, March 23 to 27, 1953, Cleveland, USA (1953).
4. Personal Communications from Hayes, E. J., United States Bureau of Mines, Albany, Oregon, USA.
5. Norton, F. J. and Marshall, A. L., Trans. Am. Inst. Met. Eng. *156*: 351 (1944).
6. Unpublished work by Spalaris, C., General Electric Company, Richland, Washington, USA.
7. Eatherly, Walter, *Effect of Radiation Damage on Electrical and Thermal Properties of Graphite,* Bull. Am. Phys. Soc. *30,* No. 2: 8 (1955).
8. Kinchin, G. H., J. Nucl. Energy, *1,* 124 (1954).

Mass Transfer in Molten Metal and Molten Salt Systems

By C. F. Bonilla,* USA

Several nuclear reactor designs have been proposed in which the fuel is employed in solution in a molten metal or a molten salt. A principal feature of these liquid fuel reactors is that it should be possible to remove the fission products continuously by vaporization and/or by scrubbing with suitable liquid or solid adsorbents or reagents. Thus the inventory of fission product radioactivity could be kept at any desired low level, and the danger from that source in the event of an accident minimized. Also, neutron losses would be decreased.

To design equipment for the removal of fission products requires a knowledge of the mass transfer coefficients for the particular arrangements of the fuel and scrubbing phases contemplated. The heat transfer coefficients are also needed when appreciable heat is involved, as in vaporization and condensation. These mass transfer coefficients would also apply to other diffusion-controlled transfer processes, such as the dissolving or freezing of fuel into or out of the fuel solution, the freezing out of Na_2O from Na, the corrosion of metal pipes and containers by thermal differential solubility, etc.

Single film mass transfer coefficients have been reliably determined and dimensionlessly correlated for several two-phase arrangements employing water, organic solvents, and inorganic and organic solutes. Many more single-film heat transfer coefficients and correlations have been published for non-metallic fluids. It would be expected that all of these correlations can be applied to mass transfer in liquid metal and in liquid salt systems if it can be shown that several of them hold for these systems, and if the necessary physical properties of the liquids are available. This paper describes a small-scale but a broad research program under the author's direction that bears on these general goals. In all of the mass transfer tests only systems giving low solute concentrations and one or substantially one film resistance were employed.

INTERFACIAL CONTACT BETWEEN ONE SOLID AND ONE LIQUID PHASE

The highest liquid-metal heat transfer coefficients that have been observed agree with or slightly exceed available theoretical predictions. However, their average is ⅓ lower than theory at the same Peclet number and many results are only ⅕ of the maximum.[1] These results can not be explained satisfactorily by the degree of wetting of the solid by the liquid.[2] If the decrease is due to entrapped gas in the heat transfer tests or to restriction of electron transfer, no effect on mass transfer would be expected. However, if for the unwetted interfaces it is due to local surface cavitation caused by turbulence, or to the liquid bridging over microscopic concavities in the solid due to its high surface tension, mass transfer might be lower than at wetted interfaces. Two types of test were carried out to investigate this possibility.

In the first study[3] mercury at low absolute pressures was passed at a rapid uniform rate through an unwetted tube and observations made to indicate whether detachment occurred. The apparatus is shown in Fig. 1. *A* was a steel 5-liter mercury tank and *B* a quick-acting cock for starting and stopping the flow through needle valve *C*, constant level tank *D*, and excess mercury receiver *E*. The test section *F* was a 48-in. length of glass or polystyrene tubing selected for uniformity. The inner diameters of the tubes averaged 0.129 in. over their middle 2 ft, by weight of contained mercury and by sectioning and plug-gauging after the tests. The tube was connected by rubber pressure tubing at *S*, *G* and *H*. A toggle valve at *G* quickly turned the flow on and off, and a screw clamp at *H* regulated it. Receiver *J* was mounted on scales *K*, which with a stop-watch yielded flow rate. All tests tubes had flush 0.03-in. manometer connections at *L-L* over their middle 2 ft. The plastic tubes also had flush flat-ended steel No. 0 screw electrodes at *N-N*. To avoid burrs, close-fitting steel rods were inserted into the tubes before drilling and tapping, and turned before tightening the electrodes, then removed. Plastic cement sealed the electrodes. The test tube was held firm and straight on a board *R* pivoted behind *S* and held at *Q* at any desired inclination, as measured to 10 min of arc by a protractor with leveling bubble. For each run the inclination of *F* was pre-set, and the exact difference in level between *R-R* was maintained on *M* by adjusting *H*. The absolute pressure along *N-R-R-N*, read on *M* above the levels of *R-R*, was thus maintained constant. Runs were made at room temperature, at inclinations up to

---

* Including work by C. F. Bonilla, A. Gandek, M. Gutstein, B. Misra, C. R. Mitra, R. N. Roychoudhury, N. S. Shaikhmahmud, B. L. Tarmy, Columbia University; J. S. Bush, Westinghouse Electric Co.; H. T. Chu, M. W. Kellogg Co.; W. E. Dunn, C. Ferstenberg, DuPont de Nemours & Co.; B. Gross, North American Aviation, Inc.; F. H. Kant, Esso Research & Engineering Co.; A. Stalder, Ciba Pharmaceuticals, Basel, Switzerland; S. J. Wang, Air Products, Inc.

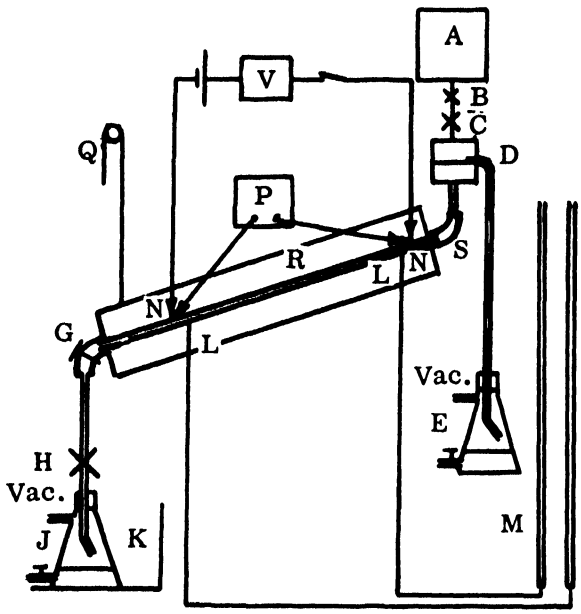

Figure 1. Apparatus for studying cavitation at tube walls

vertical, and, by varying the vacuum in E and J, at absolute pressures from 1000 to 100 mm of mercury. Figure 2 shows the friction pressure drop results as a Stanton diagram. No significant systematic error was evident. The position of the points above the smooth tube line is not unexpected in view of the small diameter. If significant slippage had occurred, the points would have fallen below the smooth pipe curve, presumably. The average velocity reached 60 ft/sec. The ratio (average velocity pressure/absolute static pressure), which with Reynolds number should control this phenomenon, reached 0.60 in the runs plotted. Observation of the voltmeter V and potentiometer P, and of reflections of spot-lights trained on the mercury, showed no fluctuations in any of the runs. It is concluded that under any conditions likely to be encountered in handling liquid fuels and coolants, no detachment from solid walls should be anticipated unless the usual cavitation criterion is reached, namely that the absolute pressure falls locally to the vapor plus gas pressure of the system.

In the other study[4,5,6] the interfacial thermal and electrical resistance was measured between absolutely horizontal iron, nickel, and stainless steel plates as the solid, and mercury as the static liquid, with and without sodium and magnesium wetting agents. Though it has not been established that poor wetting causes low heat transfer coefficients at clean surfaces, this is certainly a possible key factor. Also, electromagnetic sodium pumps and flowmeters generally are initially inoperative due to high liquid metal/solid metal interfacial electrical resistance, and until the wetting temperature is reached. An evident attack on the problem of liquid/solid contact is to measure simultaneously the thermal and the electrical resistance at the interface. Cells like that in Fig. 3 were employed. The top half is shown unassembled. A is the liquid metal chamber, formed of a thick-walled phenolic plastic cylinder B and solid metal plates CC'. Several surface finishes were employed, most frequently polishing with the finest emery paper. Wires DD' and the additional wires EE' are of the same composition (same thermoelectric potential) as plates CC'. Silicone rubber gaskets F isolate the plates and wires, and when bolts G are tightened through end-pieces H into the tapped holes in B a gas-tight cell results. A steel hypodermic needle tube J provides access. The outer surface of the cell is covered with Glyptal varnish, for further vacuum tightness. To fill the cell, it was evacuated for many hours with tube J rising vertically and the leveling bottle K low. K was then raised above the cell, filling it. In operation a steady fast flow of steam was passed through the top chamber and cooling water through the bottom. When steady temperatures were reached potentiometer P was connected to D' and E' and the potential read due to the differential thermocouple: wire/liquid metal/wire. Assuming D' was at steam temperature or somewhat lower, the temperature at the end of E' could be computed from the thermoelectric potential of this liquid metal/solid metal couple. For mercury and the dilute amalgams here employed, to iron and low carbon steel, e_0 in millivolts for one junction at 0°C and the other at t°C was found[7] to be:

$$e_0 = 0.01939t - 8.834 \times 10^{-6}t^2 - 9.675 \times 10^{-9}t^3 \quad (1)$$

within 1% from 0°C to 400°C. Next, switch S was closed, passing direct current I through the cell and

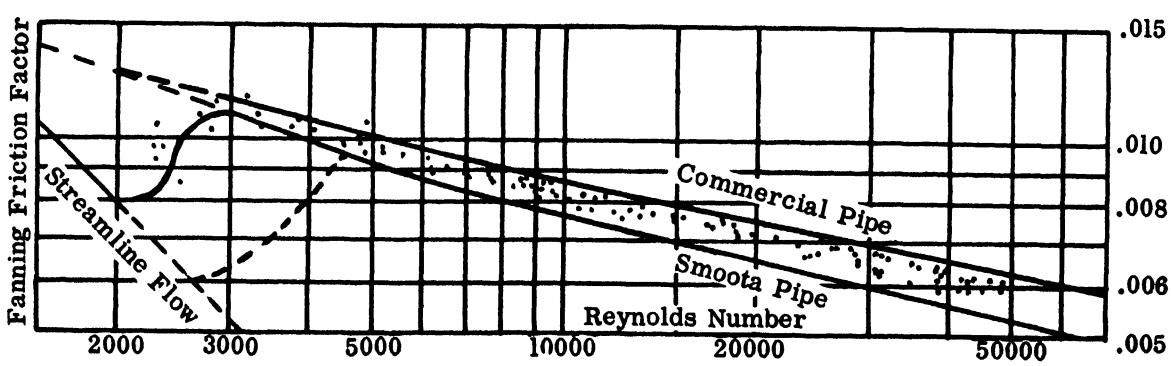

Figure 2. Stanton diagram for mercury in small unwetted tube

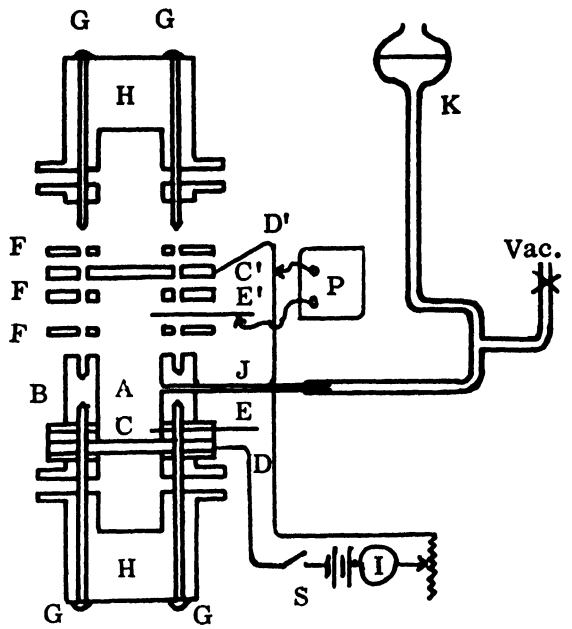

Figure 3. Interfacial resistance cell

potential $D'E'$ was read again. The algebraic difference between the two potentials is the electrical voltage drop $e_{C'E'}$ from C' to the top level of E'. The two potential measurements, with and without current, were repeated for EE' and again for ED. The interfacial thermal resistivity $1/h_c$ in °F × ft² × hr/BTU was obtained by correcting $\Delta t_{D'E'}$ for Δt across the mercury by linear extrapolation, assuming the thermal conductivity k_{Hg} constant. The formula is $h_c = k_{Hg}/(\Delta t_{D'E'} \times \overline{E'E}/\Delta t_{E'E} - \overline{D'E})$, where the bar means distance. The electrical interfacial resistivity r_c in ohms × ft² was similarly obtained by $r_c = (A'/I)(e_{D'E'} - e_{E'E}\ \overline{D_1E_1}/\overline{E_1E})$ where A' is the area. A typical run (lower or cold plate) is shown in Fig. 4. Similar results were obtained with carbon-steel and with stainless steel. The following conclusions apply to the separate resistances: $1/h_c$ fluctuated but did not drift greatly with time, was usually higher at the top plate (as might be caused by gas traces) but not always, and was affected only slightly by adding 0.05% or 0.1% sodium, or 0.002% or 0.004% magnesium, or by different mechanical surface treatments. Exposure to air increased $1/h_c$ somewhat. r_c fluctuated less in any run, but drifted slowly more with time and varied widely between different runs, surfaces, etc. It decreased more with Na and Mg additions. It was entirely unaffected by direction or magnitude of the current, which eliminates electron work function as a cause of thermal contact resistance. Both $1/h_c$ and r_c generally increased somewhat on cooling and decreased on heating, and both were entirely independent of pressure (from 2 to 40 cm of mercury above atmospheric), which eliminates large bubbles or flat gas spots as sources of thermal resistance. The Lorenz number for electrical/thermal resistivity for metals is theoretically 2.6×10^{-8} (BTU × ohm)/(hr × °R²), and most solid and liquid metals fall near it. The Lorenz number was computed as $(r_c h_c/T)$ for the interfacial resistances here found, ranging roughly from 100 to 10 times the theory without wetting additives, and down to 2 times theory with them. These and further results are still being analyzed, but indicate that electrons at liquid/solid metal interfaces flow only through "active centers," which increase in number with wetting agent additions, but cover only a tiny fraction of the surface otherwise. However, heat is also transferred by lattice vibrations across the full interface. Thus the full interface would be available for mass transfer if it was free of dirt, oxides, etc.

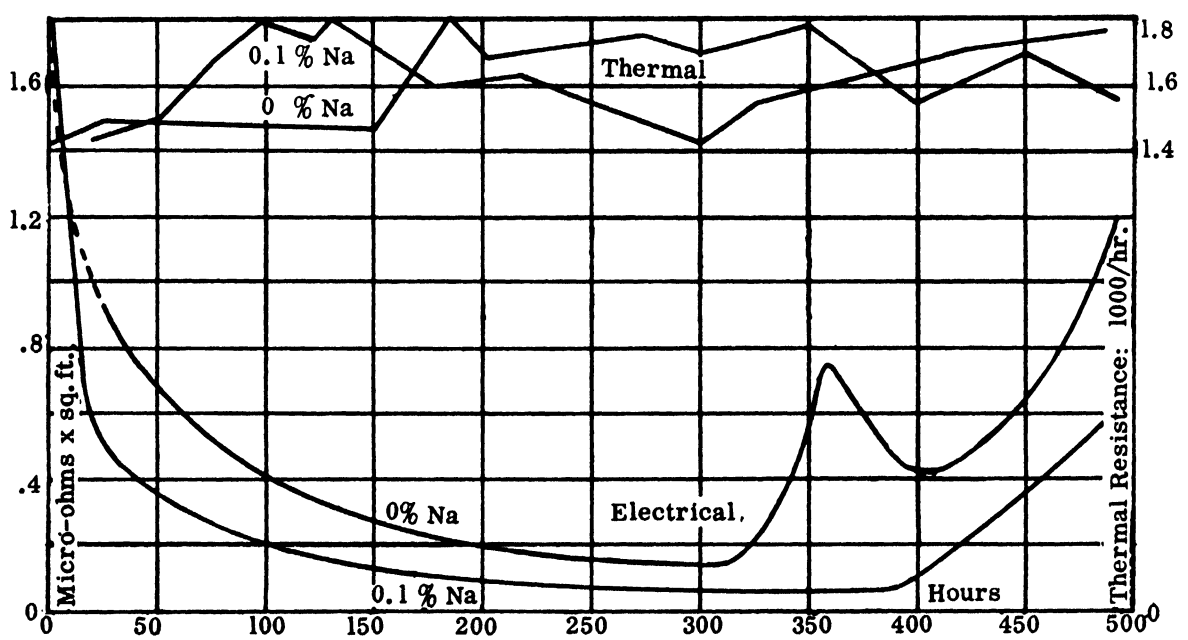

Figure 4. Thermal and electrical resistance of nickel/mercury interface vs. time at room temperature

METAL MASS TRANSFER BETWEEN ONE SOLID AND ONE LIQUID PHASE

The rate of dissolving of a solid metal into a liquid metal was investigated for the forced convection cases of flow inside of a pipe and through a randomly packed bed of spheres, and for natural convection outside of a horizontal cylinder.

For the first case the inner surface of a zinc tube was dissolved by a stream of pure room-temperature mercury flowing through it.[8] Zinc rods were cast by sucking molten 99.995% zinc up into ½-in. Pyrex tubes and allowing it to freeze. The rods were cut to a length of 2.1 in., drilled through axially on a lathe with a 0.140 in. extra long drill, and the end turned concentrically for a ½-in. length to an outer diameter of 0.350 in. and faced. These tubes were force-fitted at each end into a heavy-wall steel tubing with a 0.140-in. bore and a concentric 0.351-in. cup, so that the steel-zinc-steel bores formed a continuous tube. The apparatus (Fig. 5) consisted of a 3.5 liter steel tank A, submerged air inlet tube BC to produce constant mercury head, level gauge D, on-off cock E, drain pinch-clamp F, flow-regulating screw-clamp G, 50-diameter steel upstream-calming tube H, 15 diameter zinc test length I, downstream steel fitting J, glass receiver K, thermometer L, air vent M, rubber tube N, and 6 to 10 preweighed sample flasks O, each containing 30 ml of 1 M HCl. For a run, I was lightly amalgamated, G was preset, E suddenly opened, and a stop-watch started when mercury appeared at N. N was then pinched momentarily by hand at the end of each desired time interval (10 to 30 sec) until a new flask O could be moved under N. Immediately after the run E was closed and F drained, and each flask O weighed to obtain the mercury weight and thus flow rate over the interval. The zinc was dissolved in the HCl and determined by a recording polarograph. For every run the solubility of zinc C_i (about 2.15% by weight), and the "film" Schmidt number $Sc_f = (\mu/\rho d)_f$ computed from the average viscosity μ_f, density ρ_f, and diffusivity d_f at $C = (C_i/2 + C_2/4) = C_f$ were tabulated. For each interval the following average quantities were calculated, correcting as required for the change in diameter due to the dissolution of zinc: diameter D, velocity u, mass velocity G, outlet concentration C_2 (C_2 ranged from 0.01% to 0.03% by weight), rate of dissolving per unit wall area w, mass transfer coefficient $k_D = w/(C_i - C_2/2)$, mass transfer factor $j_D = (k_D/u)(Sc)_f^{2/3}$, and Reynolds number $Re = DG/\mu$ at $C = (C_2/2)$. j_D and Re for the intervals in each run fell close together, showing no significant deterioration of the surface. The points are compared in Fig. 6 with the Chilton-Colburn relation:[9]

$$j_D = (k_D/u)(Sc)_f^{2/3} = 0.023\ (Re)^{-0.2} \qquad (2)$$

Evidently, this relation is a conservative good fit with the data, which average 10% higher. The other data available are by Linton and Sherwood[10] for organic solids dissolving in water at $L/D = 6$ and 21. They show no effect of L/D, and roughly agree with these results in magnitude. Thus Equation 2 should be applicable to liquid metals in turbulent flow at L/D exceeding about 6, and probably with reasonable accuracy to lower L/D as well. The Leveque equation $j_D = 1.61\ (Re)^{-2/3}\ (L/D)^{-1/3}$ presumably holds in streamline flow.

Mass transfer in a firmly packed bed was studied by forcing mercury upwards through 99.9% lead spheres.[11] The apparatus was the one shown in Fig. 5, except that items H, I, J were replaced by a glass column with 7 to 10 thicknesses of 24-mesh per inch iron wire cloth at top and bottom, to distribute the flow and hold the bed compact. With 0.085-in. spheres, bed diameters and heights of ¾ × 1.9 in. and of 1 × 2.7 and 6 in. were used, and with 0.17-in. spheres a diameter and height of 1.43 × 6 in., respectively. Bed size sufficed to avoid wall error. Shortly prior to a run the spheres were weighed, then to obtain consistent results amalgamated by dipping into mercury through dilute nitric acid. The 6 runs each lasted 30 to 60 seconds, 3 to 5 sample flasks containing 50% acetic acid being used in each run. Mercury flow was obtained as before and lead was determined gravimetrically as the chromate to ±½%. The runs at the three higher Reynolds numbers showed relatively fast dissolving over the first interval. The other samples and other runs yielded con-

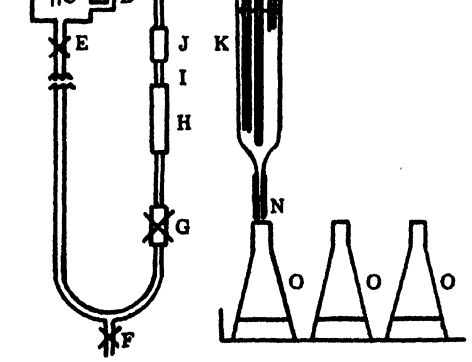

Figure 5. Apparatus for mass transfer from a zinc tube to mercury

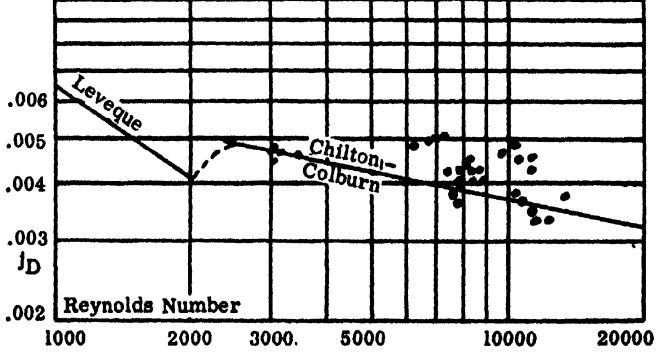

Figure 6. Correlation of mass transfer in a tube

sistent rates in any run. The flow rate and the outlet concentration C_2 extrapolated linearly back to the beginning of each run and the initial particle and bed dimensions were employed, since in some runs several % of the lead dissolved. The observed bed porosity X ranged from 0.45 to 0.56. C_2 ranged from 0.27% to 1.53%, and the logarithmic mean of C_i and $(C_i - C_2)$ was employed, or actually the number of transfer units NTU $= \ln[C_i/(C_i - C_2)]$. Results are compared in Fig. 7 with those of Gaffney and Drew,[12] as the principal previous study using liquids. For this purpose $j_D' = \text{NTU}/(aH)(\text{Sc})_f^{-0.58}$ was calculated, where a is the packing surface area per unit bed volume corrected to an infinite column and H is the bed height. Rather good agreement is obtained, the Gaffney and Drew curve averaging a slightly lower j_D'. The Reynolds number $\text{Re}_{p,s}$ employs particle diameter D_p and superficial velocity u_s. The equation of the straight dashed line is

$$j_D' = \frac{k_D}{u_s}(\text{Sc})_f^{0.58} = \text{Sc}_f^{0.58}$$

$$(a\,HTU)^{-1} = 0.90\,(\text{Re}_{p,s}/X)^{0.40} \qquad (3)$$

This line is more convenient for mathematical manipulations and should be adequately reliable for liquid metals, at least over the range $20 < (\text{Re}_{p,s}/X) < 2000$.

Mass transfer by natural convection was studied by dissolving horizontal cylinders of chemically pure zinc, tin, lead, and cadmium into stationary mercury at room temperature.[13] The apparatus, shown in Fig. 8, consisted of a specific gravity balance sensitive to 0.01 gm, a steel wire frame B holding the test cylinder C, and a counterweight D heavy enough to keep C submerged in the mercury bath E. A stationary platform with sponge rubber F supported the bath. The arm A was constrained by set screws so C could only move 1/64 in. Cylinders C were drilled through, and the ends shielded by rubber gaskets G, steel endpieces H, and a through-bolt. The zinc and cadmium cylinders were cast by sucking up into a glass tube and freezing, then turned smooth on a lathe. Lead and tin cylinders were extruded and only the ends machined. All were acid-

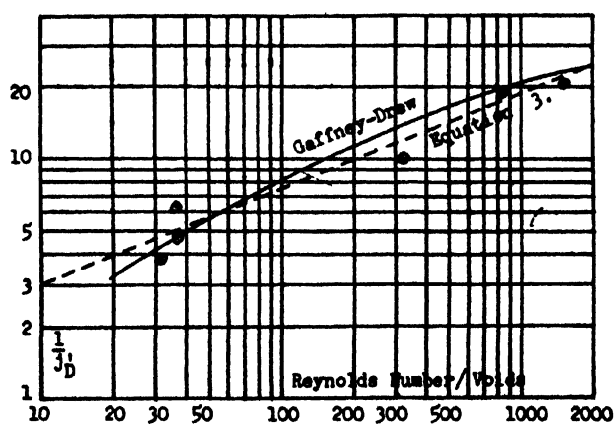

Figure 7. Correlation of mass transfer from a lead shot bed to mercury

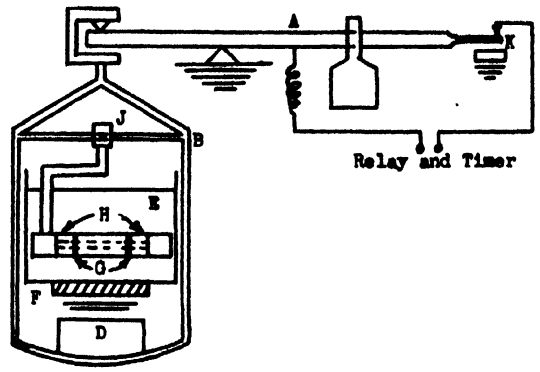

Figure 8. Apparatus for mass transfer from a horizontal cylinder by natural convection

dipped and amalgamated; tests showed that no difference in solution rate occurred whether the amalgamation was a long or short time beforehand.

To start a run the test cylinder was attached, then quickly lowered into the bath by rotating about J, a set screw at J tightened, and the buoyancy balanced. Thereafter the rate of dissolving was obtained over almost consecutive intervals. The riders were set so the test cylinder was up and the contact at K open. When enough metal dissolved for K to close, a vacuum tube relay and a holding relay started an electric clock. The riders were readjusted to a lesser buoyancy, and when K closed again the clock stopped and was read. Rates of solution fell off linearly and slowly with time. Results herein reported are all extrapolated back to initial conditions. The cylinders were placed near the center of the bath. Tests showed that rate of solution fell off when less than 1 kg of mercury was employed; 29 kg was normally used so the results apply to infinite ambient. End effect was measured for cadmium, the fastest dissolver, by testing ½-in. to 2½-in. lengths. Initial dissolving rate increased linearly as D/L decreased. Roughly, an infinite cylinder dissolved 5% faster than a cylinder with $L = 3D$. This correction to infinite cylinder, decreased by multiplying by the ratio (solution rate/cadmium solution rate), was applied to all runs. In correlating these results all the physical properties were taken at "film" concentration, namely ½ C_i. Physical properties were obtained from the literature, the major modification being a correction of diffusivity for concentration above zero. The correction, $\Delta d/d_0 = \partial \ln \gamma/\partial \ln N$ ranged from −50% with tin to +4% with cadmium, and was based on Richards' data[16] on amalgam concentration cells. All of the results are given in Fig. 9 as Sherwood number Sh_f vs Grashoff number for mass transfer × Schmidt number $(\text{Gr}_M \times \text{Sc})_f$. It is seen that they agree rather well among themselves, and with the corresponding heat transfer correlation[14] $\text{Nu}_f = 0.53\,(\text{Gr}_H \times \text{Pr})_f^{1/4}$. Thus, mass transfer by natural convection at long horizontal cylinders follows the relation

$$\text{Sh}_f = \frac{k_D D}{d_f} = 0.53\left(\frac{D^3\rho^2 g\beta_0(C_i - C)}{\mu^2}\frac{\mu}{\rho d}\right)_f^{1/4} \qquad (4)$$

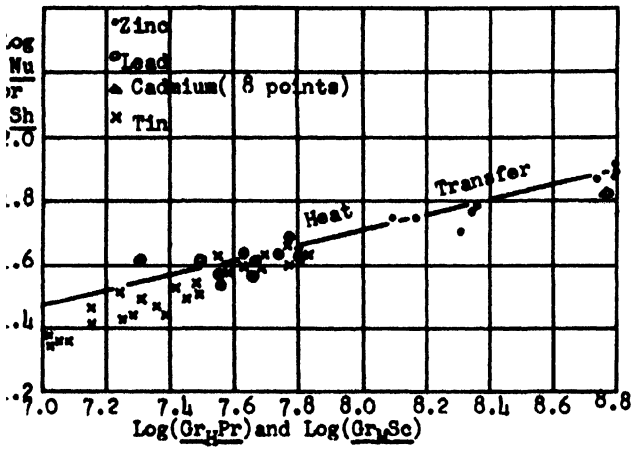

Figure 9. Natural convection mass transfer at horizontal cylinders

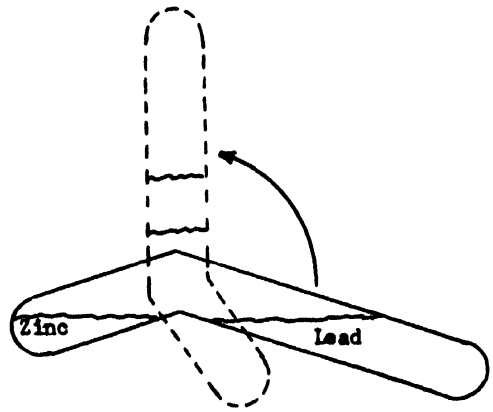

Figure 10. Liquid metal counter-flow apparatus

at least from $Gr_M \times Sc = 10^7$ to 10^9, and probably down to 10^8. Presumably all other well-established natural convection correlations for heat transfer to non-metals apply to mass transfer, including to liquid metals and salts. Thus, at $Gr_M \times Sc < 10^3$ the curve for horizontal cylinders probably starts to bend horizontal,[14] and when $(Gr_M \times Sc)/D^3$ reaches about 10^{11} ft^{-3} turbulence sets in[15] and Sh then increases rapidly.

MASS TRANSFER BETWEEN TWO LIQUID PHASES

The parallel or counter-flow of two liquid phases is attractive for fission product, and possibly heat removal from fuel solutions. The most compact arrangement would be droplets of one liquid passing by gravity or buoyancy through a continuous body of the other in an empty vessel, or "spray column." A packed column might also be employed. Unfortunately for the designer, the interface is mobile and variable, so that no good agreement is obtained by different workers, and no good general correlations are available. Single drops of known volume are the best-defined geometry. Unfortunately for the experimenter, he is restricted by the high reactivity with air, high surface tension, high temperatures and scarcity of suitable and convenient systems. However, two studies were carried out in this direction to obtain a feeling as to whether general mass transfer considerations held.

For liquid metal/liquid metal mass transfer lead and zinc were selected,[17] as this seems to be the only molten metal system below 600°C having only slight mutual solubility, thus yielding separate film coefficients. It also is used in the commercial Parks process for extracting silver from lead. Several apparatus were constructed for producing single drops of one of the metals, bringing them gently to the other liquid, letting them fall or rise through it, then removing them without further mass transfer. This turned out to be substantially impossible in small equipment without pumps. The only feasible simple device developed is that shown in Fig. 10. Into the shorter end of the bent Pyrex tube 8 gm of pure zinc were inserted and into the longer end enough lead to give full column heights of 3 to 10.5 in. Four runs employed 9 mm internal diameter tubing, and one other 6 and 13.6 mm. The tube was then evacuated and sealed, and placed in an oven at 450°C. When melted and isothermal, the tube was quickly but smoothly tilted 105 degrees so the lead poured on to the zinc and the zinc rose through the lead. It was then immediately removed and cooled in the vertical position. The tube was then broken open and the interfacial region discarded. Lead in the zinc pellet was determined gravimetrically as the sulfate. It increased linearly with the height of lead column and inversely with column diameter, and usually exceeded the solubility. Entrainment is suspected, and zinc phase film-coefficients can not be evaluated. Zinc in the lead was determined polarographically. In the bottom-most lead, where agitation would be violent, the zinc content was high. Thereafter and to the top in all runs it was uniform to $\pm 10\%$ at about 0.5%, compared to the solubility of 2.3%. Thus a lead phase film-coefficient of mass transfer could be computed based on the lead, zinc, or total volume, or on some model for the interphase area, and on an estimated contact time. Visual experiments with water and CCl_4 in similar tubes showed the water rising as one cylindrical globule through the CCl_4. This shape is also suitable for Higbie's analysis.[18] According to Higbie, k_D for the continuous phase film $= 2\ (d/\pi t_e)^{1/2}$, where t_e is the time of contact with the drop of an interfacial point in the continuous phase. The equations for the volume of a cylinder, the equality of the upward volumetric flow of zinc and the downward flow of lead, and the height of the globule $x(\Delta\rho/\rho_{Pb})$, equaling the velocity head of the lead and the friction between the lead and the zinc can be written in terms of the unknown height and diameter of the globule and velocities of the globule and of the lead. By elimination, these unknowns can be computed for each run, then finally t_e. The height came out to be 3 to 6 cm and t_e 0.11 to 0.18 sec. The "observed" k_D calculated as above is about 30 times Higbie's value. Evidently a single droplet was not obtained, but rather interfacial tension or the initial turbulence

broke up the zinc to many droplets. It seems likely from previous agreement of liquid metal mass transfer with non-metals that Higbie's equation would permit approximate prediction of mass transfer outside of drops where their size is known.

Mass transfer resistance within drops was studied by causing separate drops of c.p. LiCl-KCl eutectic to rise through various depths of liquid cadmium.[19] The runs were all near 808°F. By contacting the two phases in a sealed bulb at this temperature the solubility of cadmium in the salt was found to be 0.0623 weight % and of the salt in cadmium zero. The mass transfer apparatus was of Pyrex, and is shown in Fig. 11. To perform a run 100 gm of the salt were placed in chamber A and enough cadmium in chamber B to yield the desired depth (1.8 to 15 cm) over nozzle C. C was drawn down from 1.4 mm internal diameter tubing and ground to a 90 degree cone. The dry nitrogen system D was then attached and the apparatus placed in a constant temperature oven O at 808°F with an observation window. As the contents melted the nitrogen pressure was adjusted to keep the liquid interface in tube E. When the temperature was constant by thermocouple F, the nitrogen pressure was increased to 1.5 to 3 psig so as to obtain approximately one drop per second of salt flow into B. When most of the salt had been transferred the flow was stopped and the contents frozen quickly. Chamber B was then broken and the salt rod quickly sawed into 3 or 4 disks. excluding the bottom, and weighed. The disks were dissolved in water, and most of the salt solution decanted. The residue was dissolved in HCl and cadmium determined polarographically. In any run the disk compositions showed no trend with height, and were averaged. Two sizes of tips at C were employed, made by shrinking the capillary tube onto wires of diameter $D' = 1.00$ and 0.643 mm. They produced equilibrium drops with the volume of spheres of $D = 3.3$ and 2.8 mm.[20] There was negligible correction for speed of formation.[21] The steady rise velocities u were predicted[22] to be 23.5 and 22.6 cm per sec, respectively, based on 450 dynes/cm for the interfacial tension. For each tip, log $(C_i - C_2)/C_i$ vs height, and the least-squares straight lines, are plotted in Fig. 12. Since the differences are small, the average conditions and results were employed. Integrating[19] the drop concentration from C_i at breakaway position $H = 0$ to C_2 after a rise of H yields

$$\ln \frac{C_i - C_2}{C_i} = \ln \frac{C_i - C_1}{C_i} - \frac{6k_D}{\mu\rho D} H \qquad (5)$$

Thus, C_1 can be obtained from the intercept of Fig. 12 and k_D (= 0.042 cm per sec) from the slope. Setting $t_e = D/u$ and diffusivity d for cadmium = 2.2 times the Stokes-Einstein value,[23] the Higbie equation yields $k_D = 0.043$, in excellent agreement. Assuming constant salt-flow rate and a uniform mass transfer coefficient k_D' during the formation of the bubble, the expression

$$\frac{2C_i - C_1}{C_1} = \frac{4\rho N'}{3k_D'\left(\frac{11}{D'} - \frac{12}{D} + \frac{(D')^2}{D^3}\right)} \qquad (6)$$

can be derived,[19] where N' is drop rate per second. This yields $k_D' = 0.0044$ cm/sec from Fig. 12. Taking $N' = \text{sec}^{-1}$ and $t_e = 1$ second, Higbie's equation gives $k_D' = 0.0051$ cm/sec, in fair agreement. Presumably Higbie's equation would apply equally to mass transfer resistance in the continuous phase. Evidently mass transfer in the formation and rise or fall of droplets in liquid metal and liquid-salt spray columns can be at least roughly predicted for design purposes when droplet size is known.

PHYSICAL PROPERTIES FOR MASS TRANSFER CORRELATIONS

While mass transfer physical property data are not available for many liquid metals, salts, and conditions, they can usually be estimated with moderate precision from correlations, extrapolations, or similar substances. Diffusivity in liquid metals and interfacial tension between liquid metals and liquid salts are among the least available properties, and accordingly were somewhat investigated.

The literature was combed for liquid metal diffusivity values. These were then compared[23] with

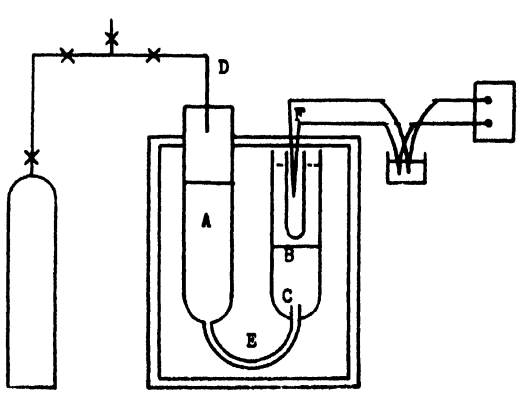

Figure 11. Apparatus for diffusional resistance within drops

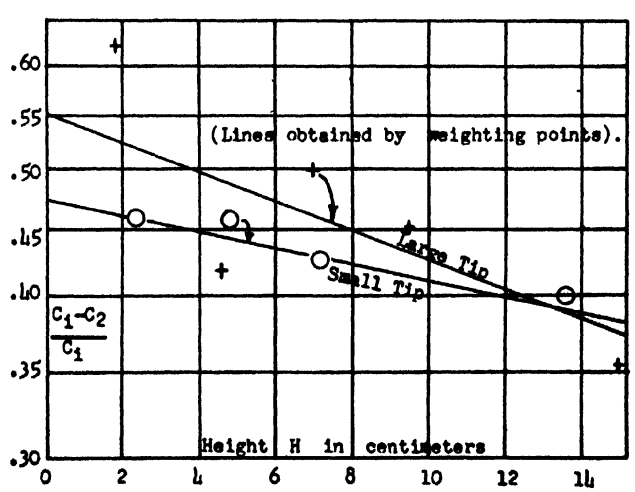

Figure 12. Fractional unsaturation of liquid salt drops versus rise.

the Stokes-Einstein equation

$$d = \frac{RT}{3\pi\mu N D_a} \qquad (7)$$

where μ is the viscosity of the medium and N is Avogadro's number. The atomic diameter of the solute atom, D_a, may be computed from the molar volume in the liquid form, considering the atom a sphere. Practically all the values found for d in the literature ranged from 1 to 2 times Equation 7. The only possibility of a general rule that was apparent was that solute alkali metals and metals of the same periodic table group as the solvent approached Equation 7, other combinations generally approaching twice Equation 7. For conservative design it seems advisable to use Equation 7 when a desirable mass transfer operation is taking place (i.e., fuel solution or fission product removal) and twice Equation 7 when an undesirable operation (i.e., corrosion).

The diffusivity of uranium in bismuth was measured approximately. A disk of natural U was inserted in a ½-in. fused quartz tube, the desired amount of cracked Bi added, and the tube evacuated, sealed, and inserted in a copper block in a vertical furnace kept at 500°C ± 1°C. A positive temperature gradient helped prevent natural convection. After 1 to 2 days the tube was removed and quenched from the bottom. The Bi rod was sectioned and polished and the U determined in a flowing gas counter. Employing standard unsteady-heat-conduction tables for a slab[14] and the observed fractional unaccomplished concentration change at the upper end of the rod yielded an average diffusivity of 2.24 ± 0.1 cm²/day, agreeing closely with Equation 7. Tests with Zn diffusing in Pb also agreed with Equation 7. A more detailed study of Cd and Zn, which are miscible, showed considerable variation of diffusivity with concentration at high concentrations. Thus the values given by Equation 7 should be considered approximations valid for low concentrations.

Antonoff's rule[24] states that the interfacial tension between two mutually saturated liquids A and B equals the difference between their surface tensions in the other vapor. Subsequent workers employed both surface tensions in the vapor of the liquid of the lower surface tension A. Harkins later showed[20] that it only holds if the spreading coefficient of A over B is positive. To test this rule with liquid metals and salts, and to obtain data for the specific system, the surface tension of KCl-LiCl eutectic and the interfacial tension between this salt and bismuth were determined.[25] The dropweight apparatus of Fig. 13 employed a ½-in. stainless steel cylinder A with a ⅛-in. stainless goose-neck B ending in a 90 degree conical tip C. A loosely fitting stainless plunger D slightly above C could be slowly screwed into the cylinder by turning the long threaded piston rod E in stationary nut F outside of oven O. The capillary was calibrated with runs on mercury in water, yielding 393 ± 12 dynes/cm, within 5% of

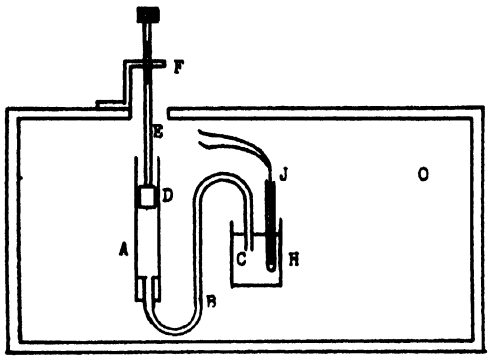

Figure 13. Drop weight interfacial tension apparatus

the best literature value of 375. A hot run was performed by inserting pure broken bismuth covered with graphite powder in A and inserting the apparatus into a thermally insulated air-recirculation oven O set to control at 820° ± 2°F. Beaker H with molten anhydrous eutectic salt and thermocouple J was then placed in position. When temperature was constant, rod E was turned slowly and uniformly so that it took 1 to 3 minutes to form about ¾ of the final drop, as seen through the viewing window. The oven fan was then turned off to minimize vibration, and the drop continued to grow by gravity flow until a minute or so later it fell to the bottom of the molten salt. The oven was then turned on again and the process repeated, either causing the next drop to fall with the previous one, or in a different region of the bottom of the beaker, or in a different beaker. Nineteen separate drops and 30 additional drops in groups of 3 to 7 each were recovered at an average break-off temperature of 810°F. By Harkins' correlation[20] the interfacial tension was obtained for each drop or group of drops and plotted on probability paper in Fig. 14. From the linearity of the plot it was concluded that any errors were random, rather than the higher values being better due to less vibration. The average was 240.0 ± 5.8 dynes/cm at the 99% confidence level. Three separate drops at 700°F and three at 900°F averaged 243.7 and 241.7 dynes/cm, respectively, so no significant effect of temperature exists. Three groups of 3 drops each of salt alone yielded a sur-

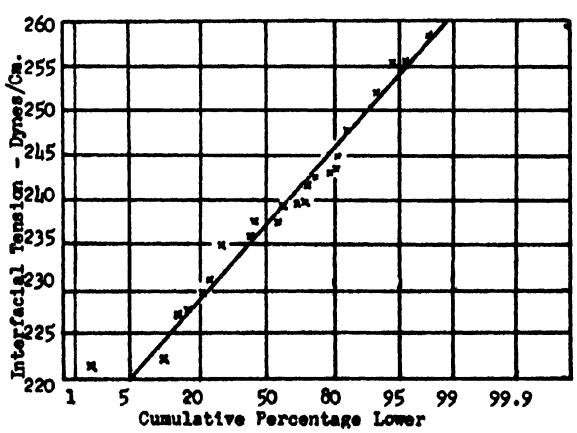

Figure 14. Probability plot of interfacial tensions

face tension of 118.2 dynes/cm (in air) with 0.7% average deviation. Qualitative tests did not show clearly whether the salt spreads on bismuth, but this will be assumed in view of the general spreading tendency of molten salts on metals. Based on a surface tension (in hydrogen) of 368 dynes/cm for bismuth[26] the Antonoff rule interfacial tension for bismuth/salt is 368 — 118.2 = 249.8 dynes/cm. This is only 4% above the observed average of 240.3, and would probably be closer if the surface tensions had been in pure salt vapor. It thus seems probable that Antonoff's rule holds in general for molten metal/molten salt interfaces.

FISSION PRODUCT REMOVAL BY VOLATILIZATION

The most economical method of inert gaseous or volatile fission product removal, where feasible, should be direct boiling out, or scrubbing out with an inert carrier gas such as helium. Some information was obtained for the design of such purification units.

For inert gases, of which Xe^{135} is the most important, the principal need in carrying out a stripper design is the solubility. However, it is so low that it can't be readily measured as gas volume. Accordingly attempts have been made to calculate it from theory, and to measure it by radioactivity.[27] Pure radioactive isotopes Xe^{133} (5.3 day), and I^{131} which produces Xe^{131} (12-day) are available from Oak Ridge. However, natural Xe activated for 5 days in the Brookhaven reactor at an average thermal neutron flux of 4×10^{12} neutrons/sec-cm^2 proved more convenient, even though the effective half-life is variable and under 2.3 days for the 3 to 4 days that the source is yet sufficiently strong for a solubility determination.

The principal single activities that were identified were the Xe^{125} (18 hr) and Xe^{133} (2.3 and 5.3 day) peaks. The Xe was counted with a Tl-activated NaI scintillation counter, cathode follower, linear amplifier, pulse-height analyzer, and scaler. For integral counting the best range was all energies over 0.35 Mev. The strongest peaks could also be used separately. Figure 15 shows the main apparatus. The activated Xe in shielded high-pressure shipping container A was admitted as required near atmospheric pressure to glass transfer container B with mercury

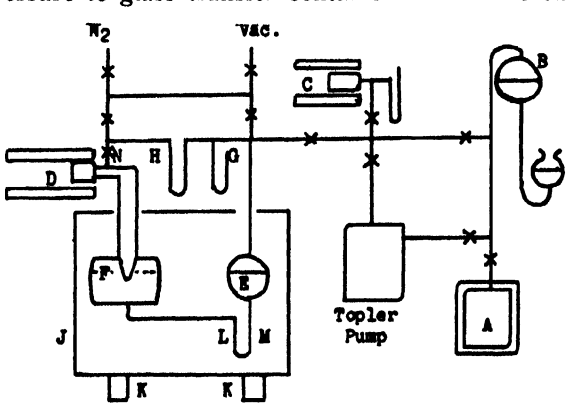

Figure 15. Apparatus for solubility determination of xenon in liquid metals

leveling-bulb. A sample of the Xe was trapped in counting chamber C, with its counter shield and manometer, to follow its decay. 130 ml saturator bulb E and desorber bulb F and connected tubing were of fused Vycor. Before a run about 95 ml of cracked bismuth were put into E and melted. Xe from B was then passed in to E to a pressure read on G. The lower level of the molten bismuth was kept at L by admitting nitrogen through N to counting chamber D (identical to C) to the proper differential pressure as indicated on H. Furnace J on rockers K was then tilted back and forth until the Bi was saturated with Xe. By quickly evacuating F to the predetermined pressure and shutting cock N, the Bi flowed into F until the final level was at M, as indicated on H. Furnace J was again rocked, to agitate the bismuth and to pump the desorbed gas through D (F is drawn rotated 90 degrees about its vertical axis, to show the partition). The radioactivity in D was followed until it passed its maximum, which occurred rapidly, within 1 to 2 minutes. C was also read regularly to provide the time-correction. The ratio R_{CD} of the counting rate at C to that at D at the same Xe pressure and temperature had previously been determined. The solubility N_V in volume fraction of Xe at saturating conditions P_E and T_E is

$$N_V = R_{CD} \frac{n_D}{n_C} \frac{P_C}{P_E} \frac{T_E}{T_C} \left(\frac{V_F'}{V_L} + \frac{V_D T_E}{V_L T_D} \right) \quad (8)$$

where P_C and T_C are the conditions in counting chamber C, n_C is the counting rate at C at the same time as n_D in D, V_F' is gas volume in F after the liquid of volume V_L is admitted, and V_D and T_D apply to chamber D. A simpler alternate procedure was also used on Bi and Na. Here the liquid metal was saturated with Xe then quickly frozen in the same vessel, excess Xe was evacuated thoroughly, the background activity in an attached counting chamber was determined, the metal was thawed or dissolved, and then the desorbed Xe counted.

Preliminary results indicate that the solubility in Bi of Xe at atmospheric pressure[27,28] is approximately 10^{-6} atom fraction. In sodium at 150°C the solubility is of the order of 6×10^{-6} and in mercury an order of magnitude smaller.[27] It may be assumed that solubility increases appreciably with temperature. Absolute solubility values computed by theory disagree widely with the experimental results. Empirical correlation of solubility of Xe and other rare gases vs internal pressure (or "solubility parameter") of the solvent, when extrapolated to the liquid metal yielded 100 times the observed solubility. Theoretical methods which explain deviations from ideality completely, or partially (Hildebrand's "regular" solutions) by van der Waals' equation yield solubilities many orders of magnitude too low. Evidently theoretical methods are not sufficiently developed to estimate the solubility of gases in liquid metals.

Heat requirements for continuous fission-product

volatilization processes will usually be taken from the sensible heat of the fuel stream, being made up in the reactor without boiling. If boiling at a heated solid surface is employed, as might be the case in processing a small side-stream, it is desirable for the liquid metal to wet the surface well. With liquid metals on a non-wetted surface, film-boiling and high surface temperatures may occur at very low heat velocities q/A,[29] or not be obtained even at high q/A.[7] With poor nucleation boiling may not occur at all, the liquid alternately superheating and flashing with violent bumping.[30] Multicomponent liquids would yield lower heat transfer coefficients, and experiments would be needed for reliable designing.

The condensation of single metal vapors on either wetted or non-wetted surfaces (see Fig. 16) has yielded heat transfer coefficients h that fall as low as 5% of the Nusselt theory.[31] The actual values of h so far obtained, however, range from 1500 BTU/hr × ft² × °F upwards, and are high enough not to be a design problem in this application. The tiny concentrations of fission products that could be obtained in a liquid metal fuel vapor with one vaporization should not affect these high coefficients significantly. For condensers handling multicomponent vapors or a non-condensible scrubbing gas the effective coefficient of heat transfer will be much lower. The usual analysis of simultaneous heat and mass transfer at the condenser surface should be applicable.

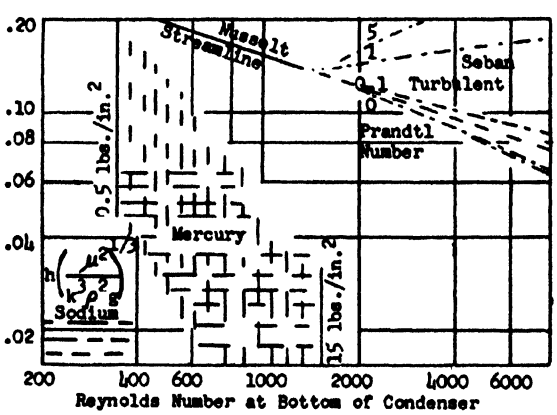

Figure 16. Condensation of single metal vapor on cylinders

REFERENCES

1. Lubarsky, B. and Kaufman, S. J., *Review of Experimental Investigations of Liquid-Metal Heat Transfer,* TN 3336, Nat. Adv. Comm. of Aero. (1955).
2. MacDonald, W. C. and Quittenton, R. C., *A Critical Analysis of Metal "Wetting" and Gas Entrainment in Heat Transfer to Molten Metals,* Preprint No. 8, Heat Transfer Symposium, St. Louis, Amer. Inst. of Chem. Engrs. (1953).
3. Gandek, A., *Flow Friction of Mercury in Tubes,* M.S. Thesis, Dept. of Chem. Eng., Columbia University (1950).
4. Bonilla, C. F. and Wang, S. J., *Interfacial Thermal and Electrical Resistance Between Stationary Mercury and Steel,* Report (NYO-3091, U.S. A.E.C. (1952).
5. Shaikhmahmud, N. S., Personal Progress Report (1954).
6. Gutstein, M., *Interfacial Thermal and Electrical Resistance Between Stainless Steel and Liquid Metals,* B.S. Thesis, Dept. of Chem. Eng., Columbia University (1955).
7. Busch, J. S., Chu, H. T. *et al., Boiling and Condensing of Liquid Metals,* NYO-3148, U.S. A.E.C. (1952).
8. Ferstenberg, C., *Mass Transfer to Mercury by Forced Convection,* M.S. Thesis, Dept. of Chem. Eng., Columbia University (1951).
9. Chilton, T. H. and Colburn, A. P., *Mass Transfer (Absorption) Coefficients,* Ind. & Eng. Chem. *26,* 1183 (1934).
10. Linton, W. H. and Sherwood, T. K., *Mass Transfer from Solid Shapes to Water in Streamline and Turbulent Flow,* Chem. Eng. Prog. *46,* 258 (1950).
11. Gross, B., *Mass Transfer in a Packed Column Using* [illegible] Thesis, Dept. of Chem. Eng., Columbia University (1953).
12. Gaffney, B. J. and Drew, T. B., *Mass Transfer from Packing to Organic Solvents in Single Phase Flow through a Column,* Ind. & Eng. Chem. *42,* 1120 (1950).
13. Dunn, W. E. Jr., *Mass Transfer from a Horizontal Cylinder in Natural Convection.* Ph.D. Dissertation, Dept. of Chem. Eng., Johns Hopkins University (1950).
14. McAdams, W. H., *Heat Transmission,* McGraw-Hill, New York (1954).
15. Hyman, S. C. *et al., Natural Convection Processes: I. ural Convection Processes: I. Heat Transfer to Liquid Metals and Non-Metals at Horizontal Cylinders,* Chem. Eng. Prog., Symposium Series *5,* 21 (1953).
16. Richards, T. W., *Electrochemical Investigation of Liquid Amalgams,* Carnegie Institution Publication No. 118 (1909).
17. Kant, F. H., *Mass Transfer in Liquid Metals,* M.S. Thesis, Dept. of Chem. Eng., Columbia University (1953).
18. Higbie, R., *The Rate of Absorption of a Pure Gas into a Still Liquid During Short Periods of Exposure,* Trans. Am. Inst. of Chem. Engrs. *31,* 365 (1935).
19. Tarmy, B. L., *Mass Transfer Between Fused Salts and Liquid Metal Phases,* M.S. Thesis, Dept. of Chem. Eng., Columbia University (1953).
20. Harkins, W. D., *The Physical Chemistry of Surface Films,* Reinhold Pub. Co. (1952).
21. Hayworth, C. B. and Treybal, R. E., *Drop Formation in Two-Liquid-Phase Systems,* Ind. & Eng. Chem. *42,* 1174 (1950).
22. Hughes, R. R. and Gilliland, E. R., *The Mechanics of Drops,* Chem. Eng. Prog. *48,* 497 (1952).
23. Bonilla, C. F., Roy-Choudhury, R. N. *et al, Mass Transfer in Liquid Metal and Fused Salt Systems,* NYO-3088, 3090, U.S. A.F.C. (1952).
24. Antonoff, G., *Sur la Tension Superficielle à la Limite de Deux Couches,* J. Chim. Phys. *5,* 372 (1907).
25. Shaikhmahmud, N. S., *Measurement of the Interfacial Tension of Bismuth Against KCl-LiCl Eutectic Mixture,* M.S. Thesis, Dept. of Chem. Eng., Columbia University (1953); NYO-3093, US AEC (1953).
26. Lyon, R. N., *Liquid Metals Handbook,* 2d Edition (1952).
27. Mitra, C. R., *Solubility of Xenon in Liquid Bismuth,* Preliminary Ph.D. Dissertation Report, Dept. of Chem. Eng., Columbia University (1954).
28. Weisman, J., Finston, H. L. and Samos, G., Brookhaven National Laboratory (1954).
29. Stalder, A., Personal Progress Report (1954).
30. Lyon, R. E. *et al, Boiling Heat Transfer with Liquid Metals,* Chem. Eng. Prog., Symposium Series (1955).
31. Misra, B. and Bonilla, C. F., *Heat Transfer in the Condensation of Metal Vapors,* Chem. Eng. Prog., Symposium Series (1955).

Corrosion Problems with Bismuth Uranium Fuels

By J. R. Weeks, C. J. Klamut, M. Silberberg, W. E. Miller and D. H. Gurinsky,* † USA

In one of the designs for a Liquid Metal Fuel Reactor under investigation at the Brookhaven National Laboratory, the fuel selected is a solution of uranium dissolved in Bi. The blanket or fertile material is a dispersion of an intermetallic compound of Th and Bi (probable composition Th_3Bi_5) in Bi. Graphite is being considered as the moderator for the core and blanket.

The choice of these materials has given rise to a number of corrosion and chemical problems. The problems that have been studied to date are the rate and extent of reaction of uranium with graphite, the reaction of U with materials of construction, and the mass transport of materials of construction (steels) by the U-Bi solution. The present status of this work is presented in the following.

THE REACTION OF URANIUM WITH GRAPHITE

Uranium is known[1] to form three stable carbides: UC, UC_2, and U_2C_3. Thus, it has been necessary to determine the rate and extent of the reaction of the U in the fuel with the C of the moderator. One way of preventing this reaction is to form a carbide on the surface of the carbon which is more stable than the uranium carbides. From experimental observations there was reason to believe that Zr as an additive might form such a carbide. Further, a private communication from L. Brewer[2] indicated that ZrC was more stable than the uranium carbides at 550°C.

Since experiments performed at 550°C in which U in Bi was contacted with graphite for 60 hours showed no reaction, a series of small graph-i-tite‡ crucibles were equilibrated with Bi and Pb-Bi solutions containing U and U + Zr under an He atmosphere at 1000–1200°C for approximately 100 hours. After cooling in the furnace, each crucible was removed and sectioned into slices. One cross-sectional slice was polished, and examined microscopically for carbide layer formation at the interface of the graph-i-tite and the metal. The containing graphite wall of one of the slices was machined to leave a thickness of about 0.010 inches. X-ray reflection patterns were taken through the remaining graph-i-tite to identify any surface deposits that might have formed at the carbon-bismuth interface.

The results obtained are summarized in Table I. It can be seen that when U was added to Bi in concentrations of 1% or less, no UC was detected at temperatures up to 1200°C (samples C_2, C_6, C_8). However, when the U addition was increased to 4.7% (sample H_2), surface deposits of carbide were noted at 1100°C. The addition of Zr to the liquid Bi in all samples at temperatures of 1000°C or higher produced surface deposits of a solid solution of ZrC + ZrN identifiable by X-ray diffraction, but invisible at 250X except at 1200°C (samples C_5, C_7, C_9). Only sample H_1, where the ratio of U to Zr added was nearly 50 to 1, appears to be an exception to this observation; there was some doubt whether the small amount of Zr added actually was present in the liquid metal in this sample. (Formation of the ZrC–ZrN layer was accompanied by a marked increase in the apparent "wetting" observed between the liquid metal and the crucible wall.)

The use of Pb-Bi eutectic rather than Bi as a solvent produced a marked increase in the amount of the UC but not of the ZrC formed. Microscopically visible deposits of UC were produced from 1% U alloys at 1000°C (sample C_{10}) and from 2% alloys at 900°C (sample T_2). However, the addition of 0.3% Zr to this same alloy prevented formation of UC, and produced a thin deposit of ZrC–ZrN solid solution not visible under magnification up to 500× (sample C_{11}). The addition of 0.36% Zr to a 4.2% U alloy in Pb-Bi prevented formation of UC in 100 hours at 1100°C (sample H_6). This corresponds to an added U to Zr weight ratio of 11.7 to 1, or atomic ratio of 4.5 to 1.

An attempt has been made to measure the thickness of the UC deposit produced in 100 hours as a function of temperature, in order to extrapolate the results to 550°C. The thickness of the layers was measured on samples H_2, T_1, and T_2. As these 3 results did not come from identical experiments with respect to concentration of U or nature of the solvent (both of which factors are suspected to influence the reaction), and, as the deposits of UC on graphite were not adherent or uniform, there was some hesitation in attempting to extrapolate these results. However, they did yield a nearly straight line when plotted as the logarithm of the thickness vs $1/T$. From the slope, an activation energy of 55,000 calories was calculated. Extrapolated to 550°C, the

* Brookhaven National Laboratory
† Prepared by J. R. Weeks, C. J. Klamut, and D. H. Gurinsky. Including work by J. E. Atherton, O. F. Kammerer, T. Sadofsky, B. Turovlin, R. J. Teitel, J. S. Bryner, D. W. Bareis, J. Weisman, R. W. Stoenner, and M. Slavin.

‡ Trade name for grade of graphite impervious to liquid metals produced by Graphite Specialties Corp., Niagara Falls, New York, USA.

Table I. Reaction Between Graph-i-tite Crucibles and U-Bi Solutions at Elevated Temperatures

Sample	Liquid metal	Additives (wt %)	Temp. °C	Time hr	Surface Deposits: Identified by X-ray diffraction	Surface Deposits: Visible at 250×
C_2	Bi	U –0.05	850	28	UN	None
C_3	Bi	U –0.32 Mg –0.19 Zr –0.11	850	42	MgO	None
C_5	Bi	U –0.42 Mg –0.18 Zr –0.18	1000	96	MgO ZrC + ZrN	None
C_6	Bi	U –1.0	1000	100	None	None
C_7	Bi	U –1.0 Zr –0.3	1000	100	ZrC + ZrN	None
C_8	Bi	U –1.0	1200	120	None	None
C_9	Bi	U –1.0 Zr –0.3	1200	120	ZrC + ZrN	Yes
H_2	Bi	U –4.7	1100	96	UC	Yes—est. 120 μ
H_1	Bi	U –4.2 Zr –0.09	1100	96	UC	Not examined
C_{10}	Pb–Bi eut.	U –1.0	1000	96	UC	Yes
C_{11}	Pb–Bi eut.	U –1.0 Zr –0.3	1000	96	ZrC + ZrN	None
T_1	Pb–Bi eut.	U –2.0	1000	100	UC	Yes—20 μ
T_2	Pb–Bi	U –2.0	900	100	UC	Yes—4 μ
H_6	Pb–Bi	U –4.2 Zr –0.36	1100	96	ZrC + ZrN	None
C_{14}	Pb–Bi	U –1.0	1000	96	Not examined	Yes
M_3	Pb–Bi	Zr –0.54	1000	100	ZrC	None
M_6	Pb–Bi	Zr –0.51	1100	96	ZrC	Yes—1.5 μ
M_{16}	Pb–Bi	Zr –0.52	1200	100	ZrC	Yes—3.5 μ
M_{17}	Pb–Bi	Zr –1.0	1200	100	ZrC	Yes—3.5 μ

thickness of film was of the order of 1 Ångstrom. This extrapolation is substantiated by the observations made at 550°C, i.e., no layer detectable microscopically or by X-rays.

The thickness of the ZrC–ZrN deposits as a function of temperature and concentration has also been investigated in Pb-Bi solutions (samples M_3, M_6, M_{16}, M_{17}). Samples M_{16} and M_{17} indicated little effect on the film thickness if the wt % of Zr was varied from 0.5 to 1.0. Sufficient data are not now available to permit a log thickness vs $1/T$ plot.

The effect of different types of graphite surfaces on the formation of UC from Pb-Bi eutectic was also investigated. Rods of graph-i-tite grade G,§ graphitar,¶ and AGHT** graphite were inserted in the graph-i-tite crucible of run C_{14}. The thickness of the deposits was essentially the same on all 4 types of samples.

The loose, non-adherent nature of the UC deposits (C_{14}) in contrast with the tightly adherent nature of the ZrC–ZrN (M_{17}) deposits is evident in Figs. 1 and 2. Perhaps the most striking demonstration of the ability of Zr additions of approximately equal atom % to prevent deposition of UC at the liquid metal-graphite interface is obtained when autoradiographs of cross sections of crucibles C_{14} and C_{11} are compared, as in Fig. 3. Here the concentration of U at the surfaces of the crucible and the graphite inserts is seen as the radiation halos outlining these surfaces. The addition of 0.3% Zr completely eliminated these halos. Since a much longer exposure was used in making the Zr-containing autoradio-

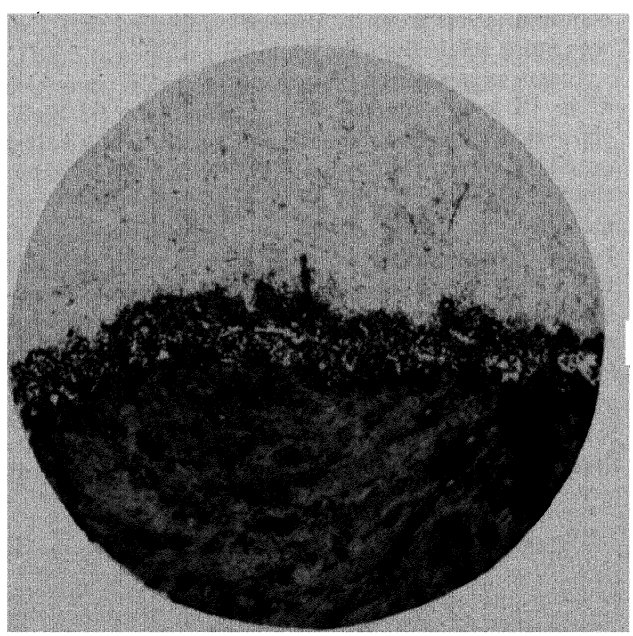

Figure 1. UC deposit on graphite from U-Pb-Bi at 1000°C in 100 hours. (Sample C-14; 250×)

§ An especially pure graph-i-tite containing little free carbon.

¶ A pressed natural graphite bonded with carbon.

** A pure, porous graphite.

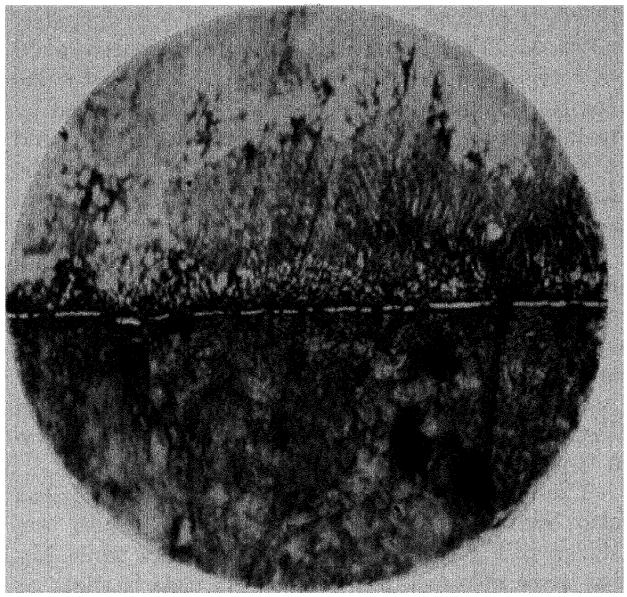

Figure 2. ZrC deposit on graphite from Zr-Pb-Bi at 1200°C in 100 hours. (Sample M-17; 250×)

graph, the distribution of U throughout the Pb-Bi matrix is visible.

The U–C reactions were also studied in an engineering type test. Steel (2¼ chrome†† and graphite were contacted with Bi containing Zr + Mg. The concentration of these elements in the Bi was followed. When no further drop in concentration was observed, a fixed quantity of U was added to the liquid alloy. The concentration of the U was then followed as a function of time. Two experiments which have been run over 2000 hours showed that after an initial loss of the order of 15%, the concentration of U remained constant for the entire period of the test. In another test which attempted to determine the relative stability of UC and ZrC, samples of a solid solution of ZrC–ZrN,‡‡ which analyzed 78.5% ZrC and 21.5% ZrN were activated in the BNL pile to a Zr^{95} activity of approximately 10^5 counts per minute per milligram. One-half gram of this sample was held at the bottom of a graphite crucible, 350 grams of molten Bi were vacuum filtered into the crucible, and the temperature raised to 550°C. A filtered liquid metal sample was taken after 24 hours equilibration time; no activity was observed in this sample. The subsequent operations performed on this experiment are outlined in Table II. The slight activity in samples 3–10 is definitely attributable to the U. When 0.0006 gram of the $Zr^{95}C$ was placed in the center of the 10 gram slug of Bi (so as to have maximum self-absorption) the counts per minute were found to be 1000 under this geometry. This corresponds to 60 ppm Zr in the Bi. Thus it can be concluded that ZrC does not react with Pb-Bi containing 1500 ppm U and 500 ppm Zr in 48 hours at 825°C.

†† Nominal compositions of the steels used in this work are given in Table V.

‡‡ Obtained from the American Electrometal Company, Yonkers, New York, USA.

LIQUID METAL Pb-Bi 1000°

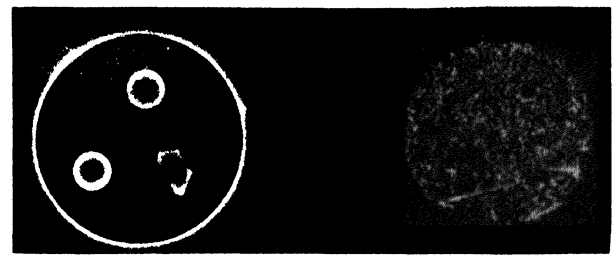

Figure 3. Autoradiographs of cross-sections of crucibles C-14 and C-11, showing elimination of deposition of UC on graphite surfaces by addition of Zr to the liquid metal

In general, from the experiments on U, Zr and C, it can be concluded that Zr prevents the formation of UC from U-Bi and U-Bi-Pb alloys under conditions that normally would result in the formation of UC. The Zr reacts to form a thin, adherent layer of ZrC–ZrN on the graphite surface. The amount of Zr required is less than ¼ the U atom concentrations in the liquid metal. The initial U loss noted in the composite tests (steel-graphite-U-Zr-Mg-Bi) may be due to a reaction of the U with the surface impurities of the steel.

STABILITY OF LIQUID METAL FUEL WITH RESPECT TO CONTAINER MATERIALS OTHER THAN GRAPHITE

The primary requisite of a material for a liquid metal fuel reactor must be its inertness to the fuel solution. In order to determine the stability of the U-Bi fuel with respect to steel, a number of experiments have been performed. These comprised (1) the effect of additives and steel corrosion products on the solubility of U in Bi, (2) a study of losses incurred on adding U to Bi in steel and (3) the effect of several deoxidants added to Bi on the losses noted in 2.

The Effect of Fe, Cr, Ni, Mg, and Zr on the Solubility of U in Bi

The solubility of U in pure Bi was determined both by a filtering and a settling method. The re-

Table II. Log of Experiment to Measure Reaction Between Radioactive ZrC and Liquid Bismuth Solutions

Step	*Added*	*Equilibration time (hr)*	*Temp. °C*	*Activity in 10 gram sample*
1	350 gm Bi–½ gm radioactive ZrC	24	550	None
2	500 ppm Mg to above	24	550	None
3	500 pm U to above	72	550	26 c/m
4	.....	96	550	19 c/m
5	1000 ppm more U added to above	48	550	90 c/m
6	61 gm Pb added to above	24	550	66 c/m
7	500 ppm Zr to above	72	550	70 c/m
8	Raised temp. to 725°C	24	725	50 c/m
9	Raised temp. to 825°C	24	825	40 c/m
10	.....	48	825	40 c/m

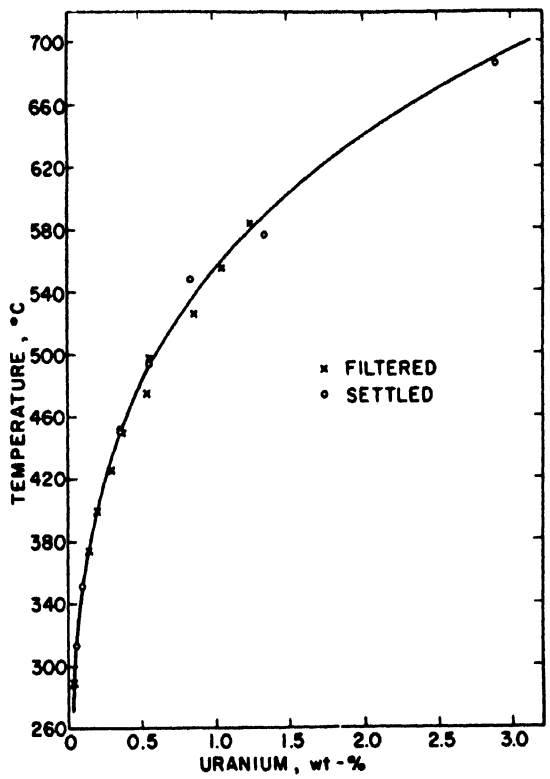

Figure 4. Solubility of U in Bi

sults obtained are shown in Fig. 4. This solubility curve can be approximated by the equation:

$$\log_{10} (\text{wt \% U}) = 3.13 - \frac{2550}{T\,(^\circ\text{K})} \qquad (1)$$

The accuracy of this curve to within normal analytical error (± 10%) has been substantiated by subsequent work at this laboratory.

The effect of Fe and Cr on the solubility of U in Bi has been investigated at 450°C using a filtration technique. The chemical analysis of the filtrates from the Fe crucibles in which the experiments were performed indicate that the solubility of U in Bi is not affected by the dissolved Fe. Two additional experiments were conducted to determine the stability of U-Fe intermetallic compounds in liquid Bi. Microexamination of the residue obtained from equilibration of UFe_2 with Bi at 800°C followed by filtration at 450°C showed that the UFe_2 had decomposed completely, forming U_3Bi_5 and small particles of Fe in the Bi. A specimen of UFe and U_6Fe eutectic decomposed partially, forming U_3Bi_5, and leaving lumps of what was presumed to be UFe_2 + eutectic. The filtrate from both experiments showed the normal U solubility. Although the results on Cr are not as conclusive, due to inadequate temperature control, they also suggest that Cr, like Fe, has little or no effect upon the solubility of U in Bi.

The effect of Ni on the solubility of U in Bi was determined at 450°C, using a graphite crucible lined with approximately 3 grams of Ni sheet. In duplicate tests, the Ni sheet dissolved completely; the filtrate contained 0.012 wt % U and approximately 1.8% Ni. This corresponds to approximately a 30 to 1 reduction in the U solubility. Two intermetallic compounds found in the residue were identified by metallographic and chemical analysis to be UNi_2 and UNi_5. No U_3Bi_5 was observed in the residue. The compound $NiBi_3$ precipitated in both filtrates upon cooling from 450°C.

A second series of experiments were performed to determine the effect of varying the Ni concentration on the solubility of U in Bi. Small, predetermined amounts of Ni foil were added to the U-Bi alloy, and the alloy equilibrated before filtering. The results obtained at 500°C and at 350°C are shown in Fig. 5. It can be seen that the presence of Ni causes a large decrease in the solubility of U in Bi.

The effect of Mg on the solubility of U in Bi has also been investigated at 500°C. The results are shown in Fig. 5 also. It can be seen that while Mg has some effect on the U solubility, this is slight at 500°C at low Mg concentrations.

The Solubility of U in Bi + Mg + Zr in Contact with a Chrome Steel

Since it has been suggested that additions of Mg and Zr to UBi solutions stabilized them in contact with graphite, and since corrosion studies (to be described) indicated that low alloy Cr steels stand up well in the presence of U-Bi solutions containing these same additives, the solubility of U in Bi containing Mg was determined in a 5 chrome steel crucible. Filtered liquid metal samples were taken over the temperature range 300–635°C. Next, Zr was added to the melt to make approximately 500 ppm and another series of liquid metal samples were taken. The samples were analyzed chemically for U, Fe, and Cr, and spectrographically for Mg and Zr. The results obtained are shown in Fig. 6. The data for the solubility of U in pure Bi are also shown for comparison. The Mg concentration averaged 1275 ppm and remained essentially constant throughout the experiment. When Zr was present, it averaged 400 ppm, except at temperatures below 400°C where 400 ppm is greater than saturation. Iron was present in all samples at approximately its normal satura-

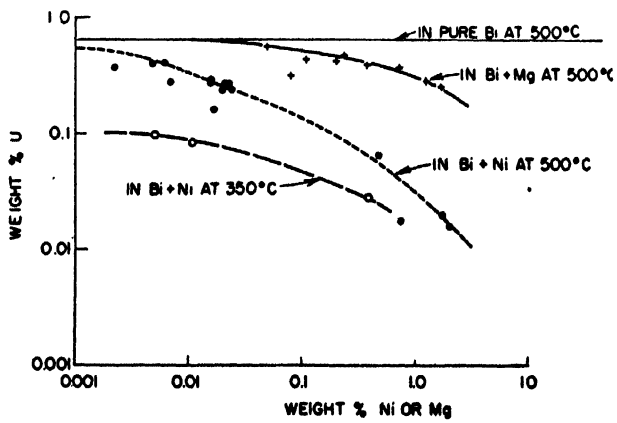

Figure 5. The effect of Ni and Mg on the solubility of U in Bi

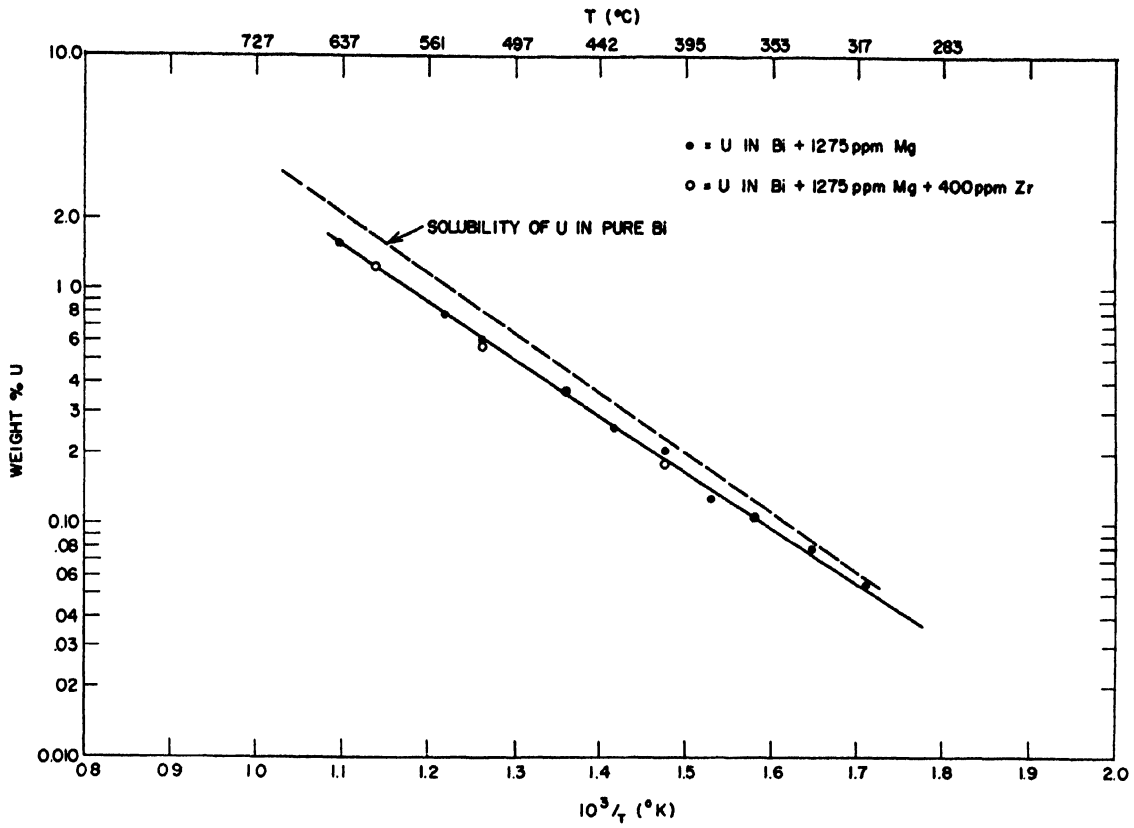

Figure 6. The solubility of U in Bi + 1275 ppm Mg + 400 ppm Zr in 5 chrome crucible

tion and Cr was less than 10 ppm in all samples. The results indicate that the effect of Mg on the U solubility becomes greater as the temperature is increased, and that 400 ppm Zr has no additional effect.

The Recovery of U upon Addition to Bi in Steel Systems

Considerable difficulty has been encountered in making quantitative U additions to liquid Bi in steel containers. Attempts to add the U, Mg and Zr simultaneously to the system nearly always resulted in large (50% or greater) initial losses of U. However, after this initial loss, the concentration of U in one loop (steel container) has remained constant at 450 ppm for over 17,000 hours.

Pre-conditioning the loops with Bi containing Mg and Zr for periods from 43 to 660 hours before adding the U improved the recovery of U in the liquid metal to 80–87% in 5 tests. The concentrations of U in these pre-conditioned steel containers has remained constant for 2500 hours of operation.

A series of 2¼ chrome steel "test-tube" experiments was performed to compare the relative abilities of various additions to Bi to pre-condition the steel surface in order to obtain a higher recovery of U in the Bi solution. One inch IPS 2¼ chrome steel pipes were pre-treated with Bi containing Mg + Zr, Th + Zr, and Ca + Zr additions until the concentration of these additives remained constant with time. Sufficient U was then added to each tube to make 1000 ppm and its concentration in the liquid metal was measured as a function of time. Pre-conditioning with 350 ppm Mg and 250 ppm Zr yielded a U recovery of 98% after 72 hours; the apparatus was shut down at this time for repair and the Bi solidified. Upon remelting the Bi, slight losses of Zr and Mg were noted, and the U concentration dropped to 75% of its initial value. It then remained constant for 2500 hours. Increasing the Mg concentration to 1000 ppm had no effect on the amount of U in solution.

Pre-treatment with 1000 ppm Mg and 250 ppm Zr in the liquid Bi gave a U recovery of 97% during the first 160 hours; this subsequently dropped to 84% and then remained constant for 800 hours.

Pre-conditioning with 200 ppm Th and 250 ppm Zr in the liquid metal gave a 100% recovery of U for over 800 hours. However, it was difficult to maintain Th concentrations in the alloy; additional amounts had to be added twice during the experiment, and the concentration of Th never stabilized. Pre-conditioning with 500 ppm Ca and 250 ppm Zr resulted in a 100% U recovery for over 1200 hours (duration of test).

These data indicate that the best recoveries of U are obtained when strong deoxidants such as Ca and Th are used.

CORROSION AND MASS TRANSFER OF Fe AND CHROMIUM BY LIQUID BISMUTH

Perhaps the major difficulty thus far encountered in the selection of a material for the liquid metal fuel container is corrosion and mass transfer. If a liquid

metal is convectively circulated through a closed loop by providing a temperature gradient on opposite sides of that loop, the temperature differential of the solubility of the container metal in the liquid metal will require the container material to dissolve continuously in the hotter portion of the loop (or hot leg) and to precipitate from the supersaturated solution in the colder portion of the loop (or cold leg). Such a system, assuming Fe as the container metal, is shown schematically in Fig. 7. In this comparatively simple 2-component system, six processes are continuously occurring as the Fe-Bi interface seeks to attain thermodynamic equilibrium throughout the loop. The six processes which will in time reach a steady state are: (1) dissolution of Fe from the wall of the hot leg into the quiet boundary layer of Bi, (2) diffusion of the dissolved Fe from the quiet boundary layer into the moving stream, (3) transport of the dissolved Fe by the moving stream of Bi from the hot to the colder regions of the loop, (4) nucleation of Fe crystals within the supersaturated liquid in the bulk stream or in the boundary layer, (5) transport of the Fe nuclei or crystallites into the quiet boundary film, or out of the cold leg into the hot zone, and (6) growth of the crystallites in the quiet boundary layer, accompanied by sintering of the particles one to another and to the wall to form a compact mass that ultimately plugs the loop and stops flow.

Any one of these six processes, or all of them in the steady state, may control the over-all mass transfer rate. In evaluating experimental data on corrosion, it becomes necessary to consider the possible effects of impurities in the liquid metal, alloying agents in the steel, and surface films at the steel-bismuth interface upon each of the six steps in the corrosion mass-transfer process.

It should be noted that a thermal gradient is not an essential driving force for mass transfer of a material by a liquid metal. Even in an isothermal system, far greater amounts of corrosion have been observed than equilibrium solubility would predict. When a polycrystalline metal is placed in contact with molten Bi, there is a difference in surface free energy between the different grains, grain boundaries, and the liquid metal due to crystal orientation, to grain-boundary disorder, and to segregation of impurities. Thus, extensive, selective attack or localized mass transfer may be observed in an isothermal system due to mechanisms that describe thermal mass transfer phenomena.

Historical Background

Published work on solution mass transfer by circulating liquid Bi (or any of the heavy liquid metals) is not extensive. Perhaps the earliest of interest to the present investigation was the development of the mercury boiler by the General Electric Company.[3,4] They performed an extensive series of mass transfer tests in steel systems utilizing a large number of metallic additives. All additives increased corrosion except Al, Cr, Ni, Ti and Zr. Of these, Ti and Zr inhibited corrosion and mass transfer most effectively.

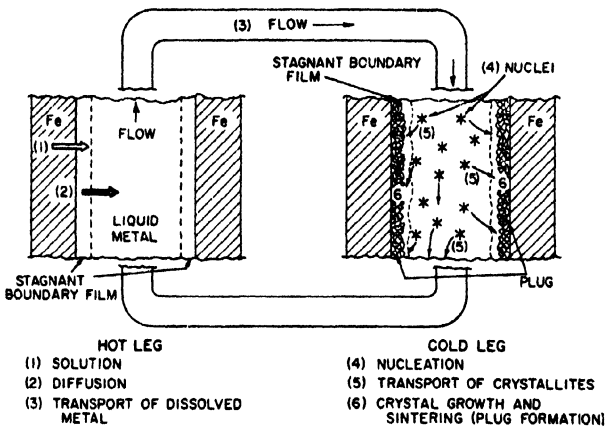

Figure 7

The early work on the corrosion resistance of materials to liquid Bi is reviewed in the Liquid Metals Handbook.[5] It was found that ferritic iron, low carbon steel, and the low alloy steels have good resistance to Bi at temperatures below their transformation temperatures, whereas the austenitic (Ni-bearing) stainless steels suffer pronounced attack in the temperature range 480–1200°C.

More recently Elgert and Egan[6] have investigated the resistance of steels to dynamic corrosion and mass transfer by liquid Bi. They attempted to control the process by using small amounts of Ti + Mg as inhibitors and by covering the metal with a protective coating such as an oxide or ceramic layer. They found a greater than 100-fold reduction in the corrosion rate of 5 chrome steel by adding more than 50 ppm Ti and 350 ppm Mg to a thermal convection loop with a temperature differential 700–615°C. Deoxidation of the system by adding Ca or Mg to the liquid metal had little effect on the corrosion rate. Pre-coating the steel with a heavy oxide film reduced the corrosion rate. Little correlation was observed between the corrosion rate and the Cr content of the steels; all runs testing only chrome alloyed steels, without additives to the liquid metal, gave excessive corrosion rates.

Recent work by Cygan *et al.*[7,8] at the North American Aviation Company, on mass transfer of low carbon and chromium steels by lead-bismuth eutectic, demonstrated that when a steel surface is not completely deoxidized, considerable difficulty may be encountered due to formation of a Bi_2O_3 plug in the cold leg. This difficulty was largely overcome by placing an alnico magnet in a quartz capsule inside an enlarged chamber at the exit of the cold leg, the life of one loop being increased more than thirty-fold by this unique device.

Recently, Terry and Skeats[9] have published an extensive bibliography on the available information on corrosion and handling of liquid Bi.

Selection of the System to be Studied

Based largely upon the experience gained in the development of the Hg boiler, the application of which to liquid Bi system was later substantiated by Elgert and Egan, it was decided to investigate the low chromium steels as container materials for U-Bi solutions, using metallic additives as inhibitors if necessary. Pre-oxidation of the steel surface to reduce mass transfer could not be considered due to almost certain loss of U from the fuel by reaction. Ni-bearing stainless steels also were not considered both because of their relatively poor resistance to attack by molten Bi and because of the large reduction in the solubility of U in Bi in the presence of dissolved Ni.

Of the two inhibitors discovered in the development of the Hg boiler, Zr has two advantages over Ti for use in a reactor fuel: it has a low capture cross section to thermal neutrons, and it is a fission product, and thus will be continuously generated within the liquid metal stream. Further, the demonstration that Zr will protect the U in the liquid Bi from reaction with the graphite moderator strengthened the hope that Zr could also be used successfully as an inhibitor to mass transfer of the container material by the liquid metal fuel. The following is a description of both the engineering and fundamental work that has been done and a discussion of the results obtained to date.

Static Tests

Static testing was the first method used to study corrosion of materials by liquid Bi. All static testing was done at a 550°C temperature. The apparatus used is shown in Fig. 8. Graphite was used to contain the test material because when U and Zr are added to the Bi, Pyrex or quartz is attacked by these materials, thus depleting them from the solution and because graphite is very slightly soluble in Bi and should not affect the test materials.[10] Separate tests to verify this showed that no carburization of the steel specimen was observed when Zr was present in the Bi even if the test was run at 750°C.

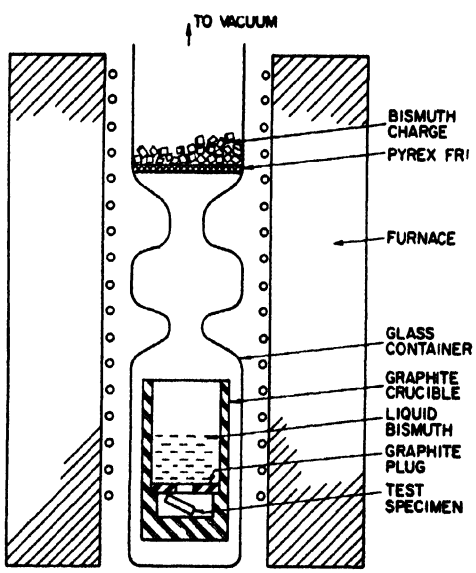

Figure 8. Static corrosion test apparatus

Two methods were used to purify the Bi metal prior to feeding it into the graphite crucible. One was to bubble purified H_2 through the molten Bi and then filter it into the crucible. The other was just to filter into the crucible. The oxygen content of the Bi thus treated was 2 and 4 ppm respectively. At the end of the test, i.e., 1000 hours at 550°C, the sample was removed from the furnace and the assembly immediately inverted. This operation decanted the Bi from the graphite crucible into the Pyrex reservoir. After cooling, the sample and graphite container were visually inspected for wetting. A transverse section was then cut from the specimen and chrome plated. It was then mounted in bakelite and prepared for metallographic examination in the usual manner. Table III shows some of the results obtained from these tests. The effect of Zr and other metals added to the Bi is evident. Typical methods of attack on pure iron and 2¼ chrome are shown in the microstructures, Fig. 9 and 10.

Loop Tests

A thermal convection loop is probably the simplest method to study the corrosion and mass transfer by a circulating fluid. Two types of loops are being used at BNL, the large bore loops shown in Fig. 11 and the small loops shown in Fig. 12. Since data can be obtained more rapidly in the small bore loops, they are being used for most of the experiments.

Flow through the loop is obtained by applying heat to the well-insulated hot leg and removing it from the cold leg. For high gradient runs, fans are used to help remove heat from the cold leg. The calculated flow through the small bore loops (0.622 inch id) is 0.1 ft/sec. All loops are run with a 550°C maximum temperature. Minimum temperatures are either 520°C, 470°C or 415°C, depending on the particular experiment. Temperatures are measured

Table III. Sample Results of Static Corrosion Tests on Various Materials in Liquid Bismuth—1000 Hours at 550°C

	Bismuth media chemical composition				*1×10⁻³ inches maximum penetration*
	Bi	*U*	*Mg*	*Zr*	
Armco	100	–	–	–	0.71
Armco	99.9	0.1	–	–	0.55
Armco	99.9	–	0.1	–	0.78
Armco	99.9	–	–	0.1	0
Armco	99.8	–	0.1	0.1	0
2¼ Chrome	100	–	–	–	0.59
2¼ Chrome	99.6	0.4	–	–	0.78
2¼ Chrome	99.8	0.1	0.05	0.05	0
5 Chrome	100	–	–	–	1.36
5 Chrome	99.4	0.4	0.1	0.1	0.34
304 SS	99.6	0.4	–	–	2.1
Moly	100	–	–	–	0

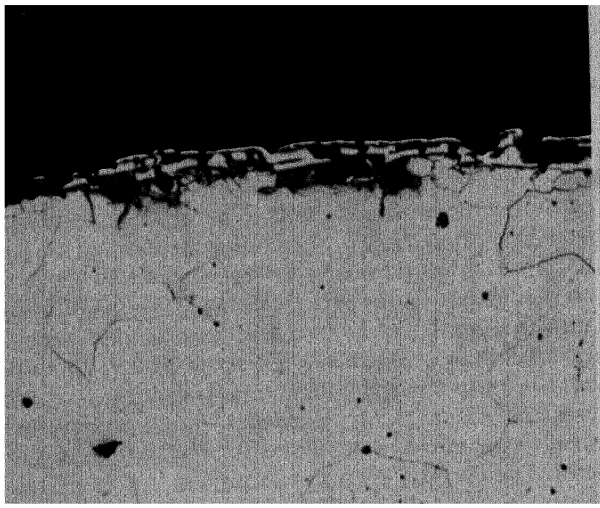

Figure 9. Armco iron: transgranular and intergranular attack by U-Bi solution; exposed 1000 hours at 550°C; 250×

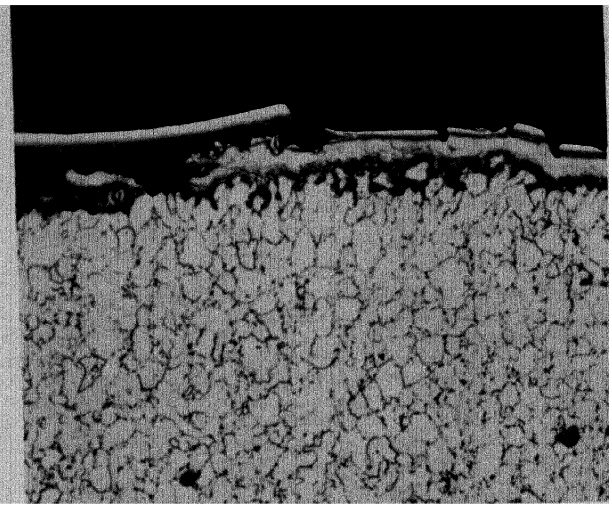

Figure 10. 2-¼ chrome steel; intergranular attack by U-Bi solution; exposed 1150 hours at 550°C; 250×

by thermocouples welded to the loop walls at various points. The actual bulk Bi temperature is measured with a long, thin, flexible thermocouple ⅛ of an inch in diameter. The thermocouple is inserted into the operating loop through a Wilson seal and pushed through the loop until the hottest and coldest bulk temperatures have been recorded. The loop gas outlets are connected to a suitable manifold so that the various operations such as H_2 treating of the Bi and pipe walls, filtering the Bi, and taking liquid metal samples can be accomplished without exposing the loop interior or the liquid Bi to air once the run has started. The air lock (see Figs. 11 and 12) facilitates inserting additives, temperature probes, and liquid metal extractors into the loop while it is in operation. All loops have a machined and polished corrosion sample which is fitted into the hot leg. This sample is examined metallographically for maximum penetration and mode of attack.

The general procedure for running a loop is as follows: (1) the entire system is leak tested, (2) the Bi and loop interior is dry H_2 treated at 500°C for 4 hours, (3) the Bi is filtered into the loop through a 35 micron type 410 steel filter, (4) the additives are inserted into liquid Bi and allowed to dissolve while loop is isothermal and (5) the gradient is applied and the test is run for the duration selected, or until flow stops. To detect build-up of plug material, gammagraphs are taken periodically.

The results of running some 25 loops indicate that the time required to plug completely a ½ inch IPS—2¼ chrome loop is approximately 300 hours when the circulating liquid is U-Bi and the temperature gradient is 40°C. A loop 1.7 inches-id made of 5 chrome silicon steel running under the above conditions (except 60 ppm Mg was added to the U-Bi) took 2441 hours to plug. A typical plug is shown in Fig. 13.

Several loops operating under the above conditions to which 250 ppm Zr has been added show no signs of plugging A ½ inch IPS 2¼ chrome and a 1.68-id 5 chrome silicon loop have now been circulating for 13,000 and also for 19,000 hours respectively.

A third loop containing 1000 ppm Zr and 1000 ppm Mg added to the U-Bi was shut down after 3000 hours of operation for metallographic examination. No transferred material was found in the cold leg and no corrosion of the standard sample in the hot leg was observed.

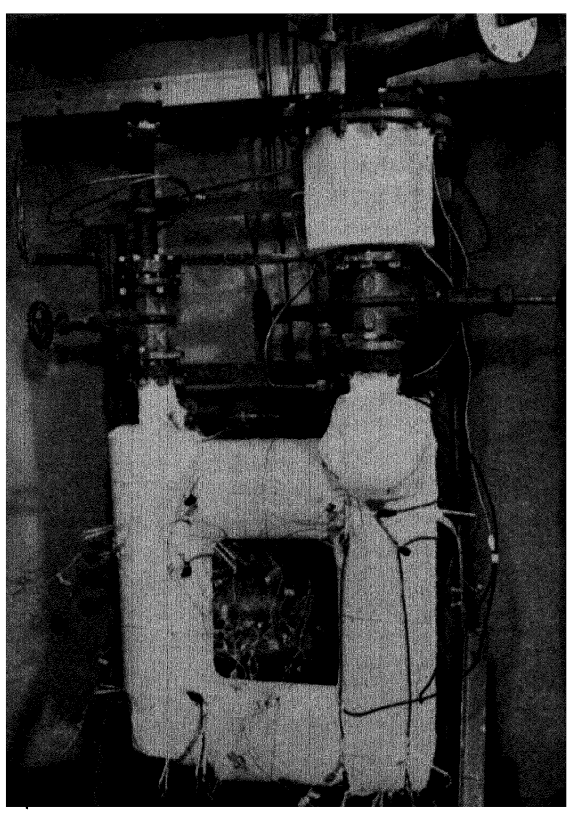

Figure 11. Large bore thermal convection loop

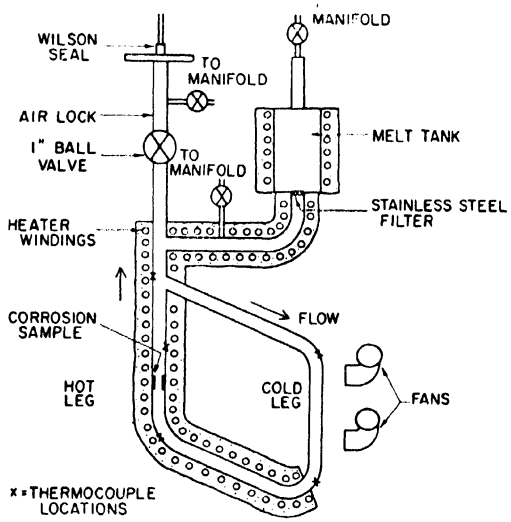

Figure 12. Small bore thermal convection loop

Recently, the temperature gradient has been increased to 150°C in loops containing 250 ppm Zr, 300 ppm Mg, + 1000 ppm U in the Bi. Radiographs of three of these loops showed transferred material in the cold leg soon after the gradient was applied. Two of these loops, (2¼ chrome, one is 0.622 id and the other 0.5 id) have now been in operation for over 1800 hours. The third loop, 5 chrome-silicon, was voluntarily shut down after 1060 hours at this high gradient. Metallographic examination showed the corrosion rate on the hot leg sample to be 2 mils/year. The transferred material in the cold leg weighed 500 mg.

One loop made of 5 chrome-silicon containing U-Bi to which 250 ppm Zr and 300 ppm Mg had been added, was run with a reduced size cold leg 0.312-inches id. The hot leg was 0.622 inches id. After 44 hours of operation, the temperature gradient rose from 150°C to 185°C indicating that a plug was forming. At 1100 hours, the gradient increased to 235°C. To determine whether the deposited material was well-bonded to the wall, the loop was tapped with a hammer. The ΔT dropped to 185°C, indicating that the plug was probably jarred loose from the cold leg. Again, at 2250 hours, the ΔT rose to 235°C at which time it was again tapped, and again the ΔT fell back to 185°C. The loop was then allowed to circulate undisturbed. Complete plugging occurred at 2400 hours.

To determine the effect of velocity on corrosion and mass-transfer, the pumped loop shown schematically in Fig. 14 has been constructed and is now in operation. The loop is constructed of 2¼ chrome steel. The maximum bulk Bi temperature is 520°C and the temperature gradient is 108°C. Flow is 1.2 gpm. Most of the loop is made of ¾ IPS pipe. A high velocity section ¼ inches id × 6 inches long located at the coldest point in the loop has a velocity of 8 ft/sec. A General Electric G3 electromagnetic pump circulates the Bi. Flow measurement is made with a submerged orifice located in the sampling

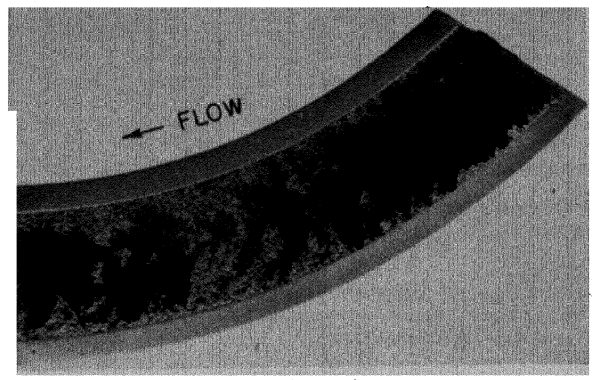

Figure 13. Typical plug formation

tank. Three standard corrosion samples are located at various portions of the loop and will be examined metallographically at the end of the 1000-hour run.

INVESTIGATION OF CORROSION FUNDAMENTALS

Recently, Shepard *et al.*[11] have made a detailed investigation of the effect of Ti, added as Ti metal or as TiH_2, upon the solution process of type 410 steel in liquid Bi and Pb-Bi eutectic contained in a Vycor capsule. They observed a slight inhibition in the solution of Fe, and a marked inhibition in the solution of Cr in the presence of Ti additions. The inhibiting effect increased with repeated re-use of the capsules. Subjecting a capsule previously contacted with Ti-Bi solution to fresh Bi without Ti showed a rapid recovery in the Fe solution rate, but much more persistence in Cr inhibition. They suggested tentatively that at least part of the inhibition involves a selective affinity of Ti for oxygen, and pointed out that Ti was a powerful promoter for wetting of the steel by the Bi. They also suggested that a barrier forms.

The Solubility of Fe, Cr, Zr and Mo in Liquid Bismuth

In order to investigate any possible effects of the Zr inhibitor upon the thermodynamics of the mass-transfer process, the solubility of Fe in liquid Bi was investigated as a function of temperature and the presence of additives in the liquid metal. The solubilities of Cr and Mo in liquid Bi have also been measured using the apparatus of Fig. 15. By means of this apparatus, it is possible to take a

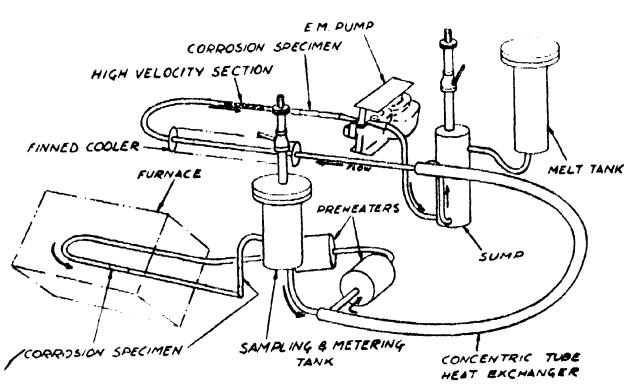

Figure 14. High velocity loop; piping and components

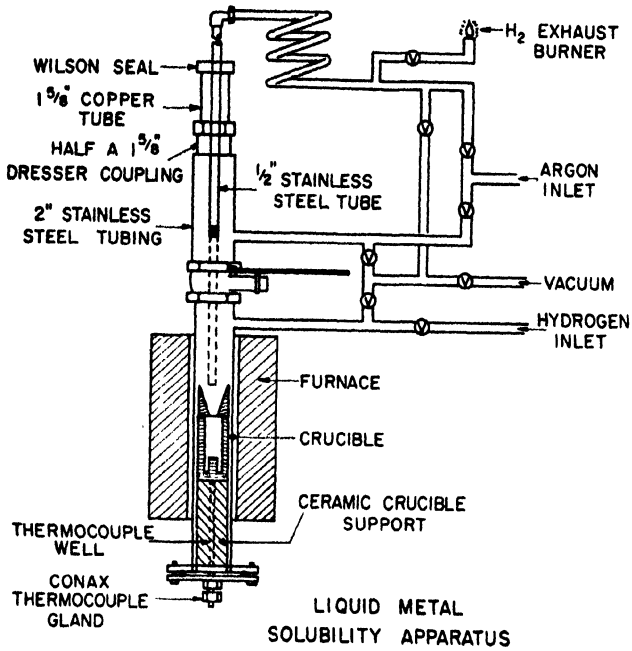

Figure 15. Apparatus for measuring liquid metal solubilities

series of filtered samples from the same batch of liquid metal without introduction of oxygen or nitrogen.

The solubility of Fe in Bi, in Bi + 0.1% Mg, in Bi + 0.1% Mg + 0.2% U, and in Bi + 0.1% Mg + saturation Zr was measured using a pure Fe crucible to which these additions were made. Similarly, the solubility of Zr in Bi + 0.1% Mg was measured using a pure Zr crucible. The results are shown in Figs. 16 and 17. U + Mg, in the quantities added, are seen to have no effect on the Fe solubility. This solubility can be represented approximately by the equation:

$$\log_{10} (\text{ppm Fe}) = 6.41 - \frac{4110}{T} \qquad (2)$$

to within ± 15% of the experimental data over the temperature range 450–650°C.

Zr is seen to increase slightly the Fe solubility; this increase was reproducible, and was measured during both cooling and heating cycles. The experimental data on the solubility of Zr in Bi can be approximated by the equation:

$$\log_{10} (\text{ppm Zr}) = 6.66 - \frac{2760}{T} \qquad (3)$$

to within ± 15% over the temperature range 300–625°C. Fe has no effect upon this solubility.

The solubility of Cr in liquid Bi was measured in a Cr-plated mild steel crucible in which was wedged an irregularly shaped lump of Cr metal. Some data on the Cr solubility were also obtained using an Mo crucible into which was wedged a lump of metallic Cr. The results using either method were identical within experimental error. The solubility of Cr in Bi is shown in Fig. 18. This curve can be approximated to within ± 15% of the experimental data between 400–635°C by the equation:

$$\log_{10} (\text{ppm Cr}) = 6.26 - \frac{3580}{T} \qquad (4)$$

Two attempts have been made to measure the solubility of Mo in Bi, using an Mo crucible; in one experiment Cr + Mg were present, in the other the

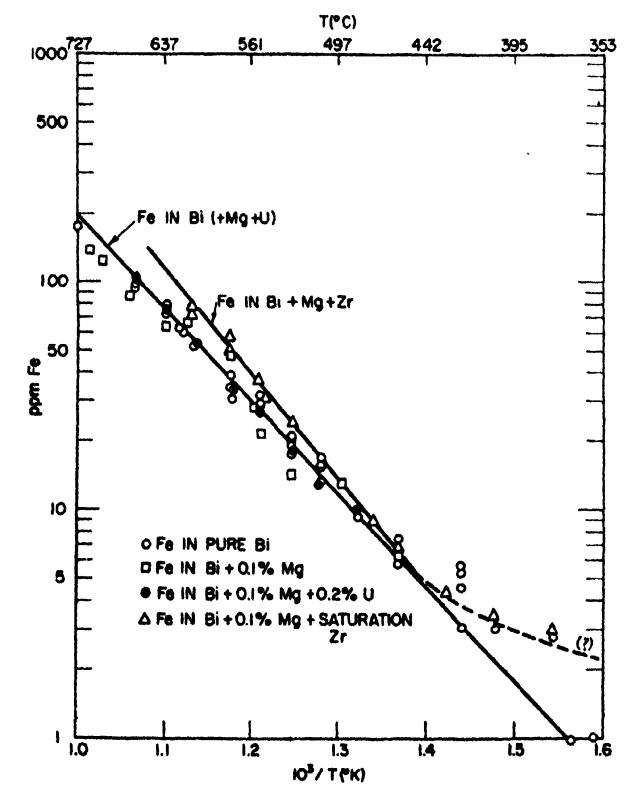

Figure 16. The solubility of Fe in Bi

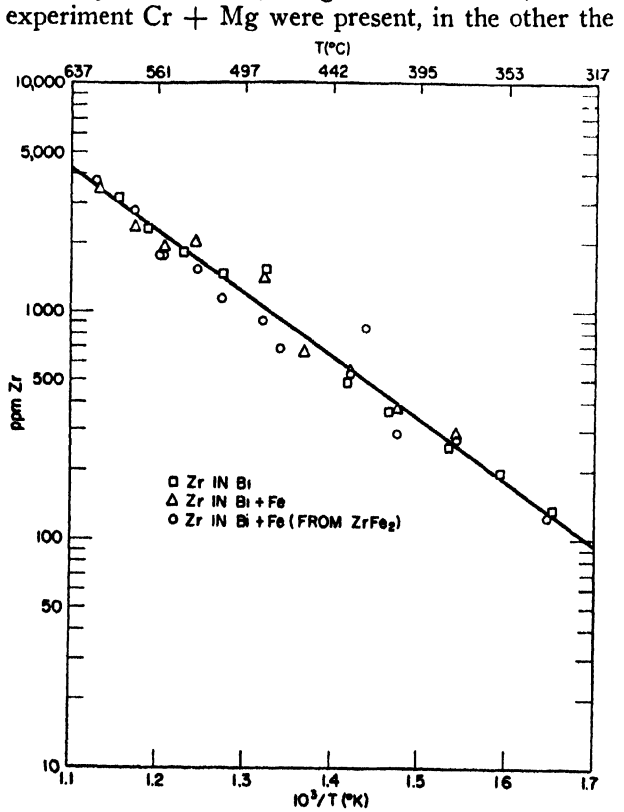

Figure 17. The solubility of Zr in Bi

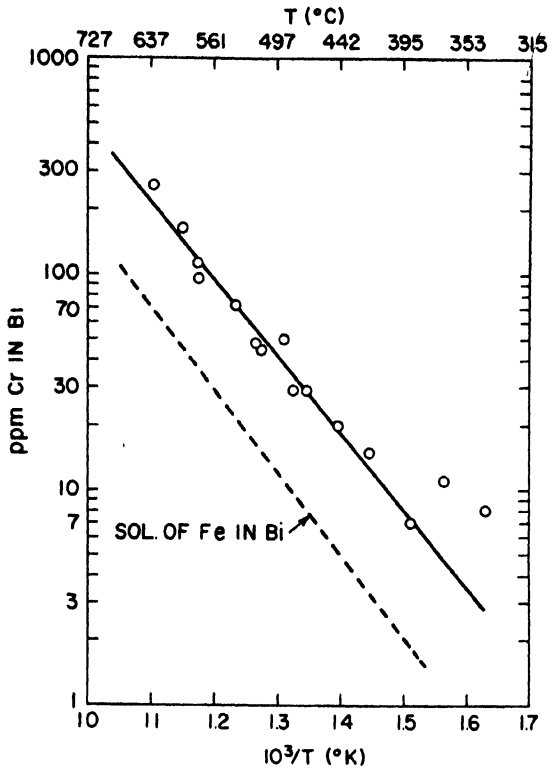

Figure 18. Solubility of chromium in bismuth + 500 ppm Mg

Mo crucible contained pure Bi. In neither case was Mo detected spectrographically (detection limit: 1 ppm) in any of the samples taken, at temperature between 350–750°C.

Since it has been speculated[4,6] that intermetallic compounds between iron and the Ti or Zr might play an important role in the inhibition mechanism, an attempt was made to investigate the behavior of Fe_2Zr intermetallic compound in contact with Bi. A 10-gram button of this alloy was wedged in the groove in the bottom of the pure Fe crucible, and the solubility measured as a function of temperature in the usual manner. It was found that the Zr and Fe dissolved each to its normal solubility limit in the presence of the other. A mass of particulate Fe was found in the residue upon cooling; some Fe_2Zr was also identified in the residue, although the original lump had completely disintegrated.

The Reaction Between Zr Dissolved in Bi and an Fe Crucible

Experimental evidence has been obtained for deposition of Zr on the surface of an Fe crucible, using a radioactive Zr tracer technique. The results of equilibrating a solution of Bi containing radioactive Zr in a pure iron crucible for one hour at 450°C are shown in Fig. 19. The measured activity on the crucible surface is plotted against ppm Zr in the Bi. This curve resembles a Langmuir adsorption isotherm; "saturation" of the surface appears to be nearly complete at about 10 ppm Zr in the Bi. The amount of deposited activity at "saturation" corresponds to approximately 1 Zr atom to every 8 Fe

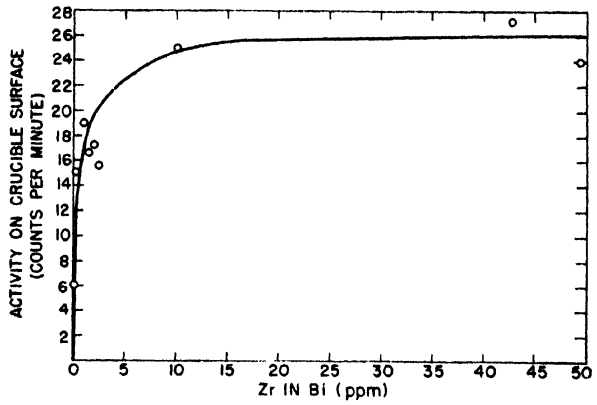

Figure 19. Deposition of Zr on Fe from liquid Bi at 450°C

atoms on the crucible surface, if the surface roughness factor of the crucible is taken to be 5. An adsorption energy of 17,000 calories per gram-atom Zr can be calculated from this curve, if it is assumed that this represents 450°C equilibrium.

Increasing the reaction temperature to 520°C and the equilibration time to 3 and 24 hours produced marked changes in the results obtained, as shown in Fig. 20. (The data obtained in 1 hour at 450°C are also shown here for comparison.) That the process occurring at 520°C is primarily film growth rather than adsorption is clearly demonstrated by the effect of time upon the amount of deposition. It should be noted also that this time effect is less important at higher concentrations of Zr in Bi; the 3 and 24 hour curves seem to approach one another as the Zr concentration increases above 75ppm.

The Effect of Zr and Bi on the Solution and Precipitation Rates of Fe from Bi

Since Zr has been observed to deposit upon the surface of an Fe crucible from Zr-Bi solutions, an attempt was made to measure the effect of this deposit upon the solution and precipitation rates of Fe from Bi in order to investigate the effect of the Zr upon the mass-transfer process.

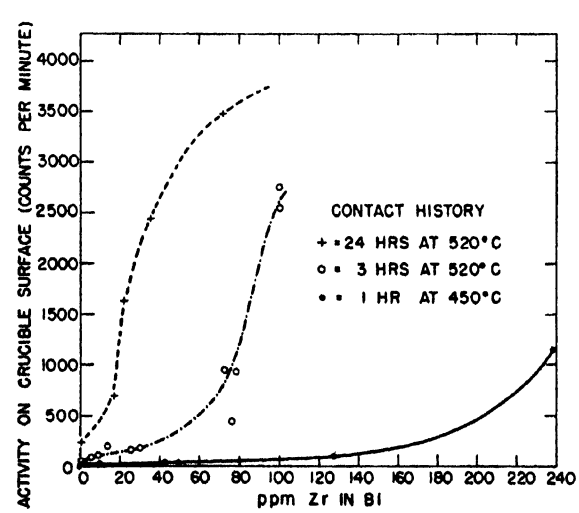

Figure 20. Deposition of Zr on Fe from liquid Bi

The equipment and sampling method used were the same as for the measurement of the solubility of Fe in Bi. Experimentally, after filtering the Bi into the crucible at 350°C, the crucible, liquid metal, and additives (if present) were equilibrated 24 hours (72 hours with Zr + Mg present) at some predetermined temperature, usually 400–450°C. The liquid metal was then sampled and the temperature raised to another predetermined value, usually 550°C or 615°C. The liquid metal was sampled at ½ to 1 hour intervals during equilibration. Metal additives were either present in the crucible under investigation at the time the Bi was filtered in, or were added during the original equilibration period.

In this manner, the amount of Fe dissolved as a function of time was measured at 615°C in a high purity Fe and in a 5-chrome crucible. The effects of Zr + Mg and of U + Mg on the solution process were also measured. The results obtained are shown in Fig. 21. The temperature cycle of the apparatus in terms of the solubility of Fe in Bi is also shown for reference. It can be seen that in pure Bi, Fe dissolved from both crucibles nearly as rapidly as the

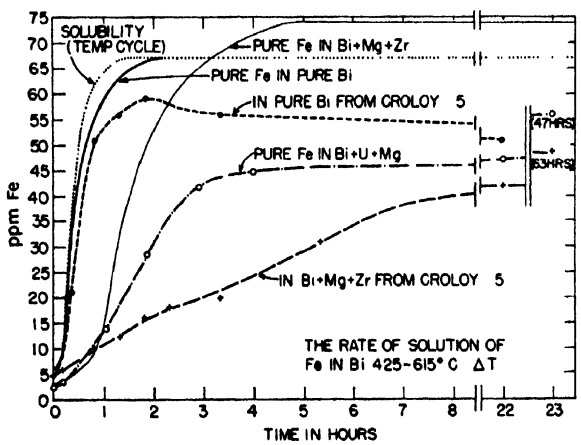

Figure 21

temperature was raised. The addition of Zr + Mg to the liquid Bi retarded the rate of solution of pure Fe considerably; the previously noted increase in the Fe solubility in the presence of Zr can also be observed in this curve. The addition of U + Mg to the liquid metal had an even greater effect than Zr + Mg upon the solution rate of pure Fe when measured in this manner. The retarding effect of Zr + Mg was much greater in the 5 chrome steel crucible than in the Fe crucible. The apparent maximum in the amount of Fe dissolved in pure Bi at approximately 2 hours is possibly due to subsequent dissolution of Cr displacing the Fe from solution, as was reported by Grassi, *et al.*[12] during dissolution of type 430 (16% Cr) steel in Pb-Bi eutectic alloy. These samples unfortunately were not analyzed for Cr.

The results of solution rate measurements at 540–550°C are shown in Fig. 22. The effect of the additives upon the precipitation process was measured in a similar manner. After the crucible and liquid

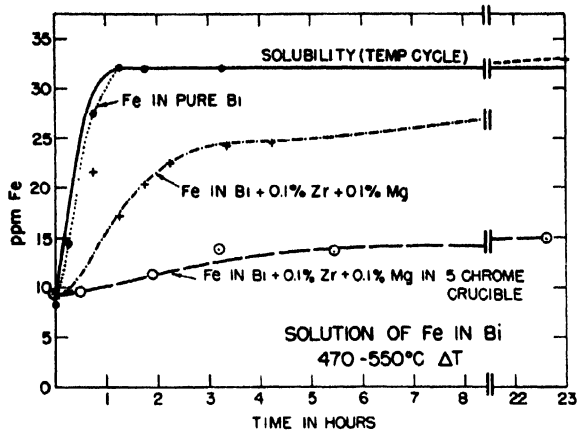

Figure 22

metal had equilibrated at the top temperature of the rate of solution run, the system was cooled to the original equilibration temperature (400°C or 450°C) and the liquid metal again sampled at intervals during equilibration. The results obtained in a pure Fe crucible at 425°C upon cooling from 615°C are shown in Fig. 23. The temperature cycle in terms of the solubility of Fe in Bi is shown for reference. Iron precipitated from pure Bi nearly as rapidly as the temperature was lowered. Zirconium + Mg caused a slight initial delay, followed by rapid precipitation of most of the excess dissolved Fe; however, precipitation of the last few ppm above saturation was very slow in the presence of Zr + Mg. In the presence of U + Mg, Fe precipitated more slowly than from pure Bi, but more rapidly than in the presence of Zr + Mg.

These effects become more apparent when the same data are replotted as the degree of supersaturation in the liquid metal (ppm in solution/equilibrium solubility as a function of time—Fig. 24). It can be seen that Zr + Mg stabilize the solution at a supersaturation of 2/1 for a period of time greater than 7 hours at this temperature. Uranium + Mg retard precipitation, but do not appear to stabilize the supersaturated solutions.

Precipitation data obtained in the 5-chrome crucible are shown in Fig. 25. In duplicate runs it

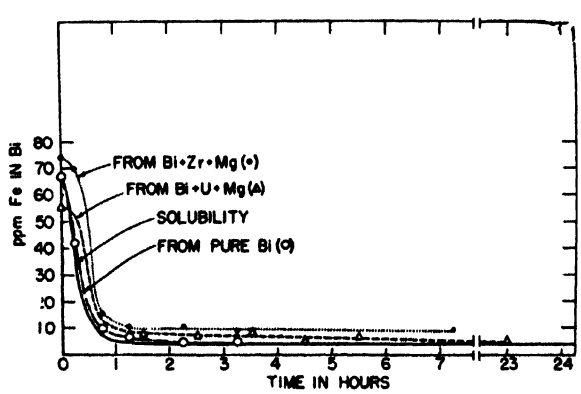

Figure 23. Precipitation of Fe from Bi in pure iron crucible, temperature cycle 615–425°C

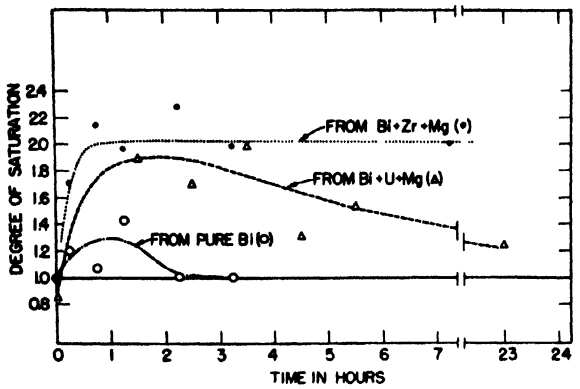

Figure 24. Precipitation of Fe from Bi in pure iron crucible, temperature cycle 615–425°C

was observed that the Zr + Mg stabilized the supersaturation of the solution at nearly 3.0/1 for periods greater than 24 hours. This degree of supersaturation suggests that mass transfer might be prevented in a circulating system in which the maximum supersaturation resulting from the temperature gradient does not exceed 3/1. In all of the test loops that have circulated for a long period without deposition, the gradient was low, so that this supersaturation was not exceeded.

Thus, it has been demonstrated that Zr + Mg as additives to the liquid metal affect both dissolution and precipitation of Fe from liquid Bi. These effects were observed to be greater in low Cr steel than pure Fe containers. Increasing the Cr content of the steel from 5% to 12% was found to have little effect upon the rate of solution at 600°C in the presence of Zr + Mg.

Radioactive Mass Transfer Measurements

In order to obtain mass-transfer data on a qualitative basis in a much shorter time than by running thermal convection loops, a "liquid metal convection pot" was constructed. With this apparatus it is possible to (1) measure mass transfer in a short time by the use of radioactive tracer, (2) circulate the liquid by thermal convection, (3) observe the test

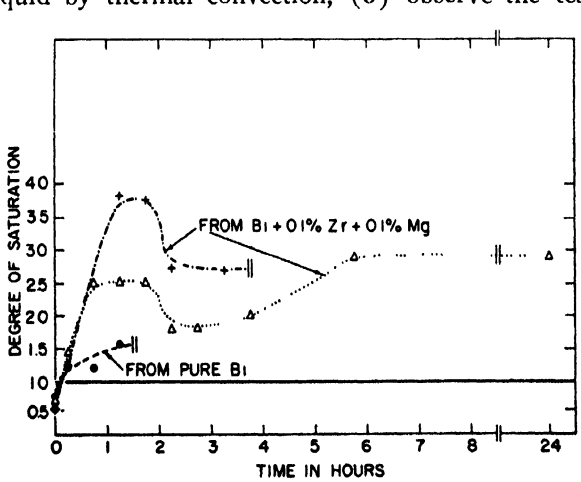

Figure 25. Precipitation of Fe from Bi in croloy 5 crucible, temperature cycle 615–425°C

materials during the run, (4) take liquid metal samples any time, and (5) purify the liquid metal. A small radioactive sample is placed in the hottest portion of the pot, and a similar non-radioactive sample in the coldest section. The normal temperature differential between the hot and cold samples, obtained during thermal convection in this apparatus is 25–35°C, with a hot sample temperature of 470–485°C.

Using pure Fe samples, mass-transfer rates have been measured in Bi, Bi + Mg, Bi + U + Mg, Bi + U + Mg + Zr, and Bi + Mg + Zr. The effect of varying the Zr concentration in this last system has also been investigated. The results are tabulated in Table IV. It can be seen that the change from an argon atmosphere of questionable purity (runs 3 and 4) to a purified helium atmosphere (run 18) produced a considerable drop in the amount of activity transferred. The addition of Mg (run 17) and Mg + U (runs 8 and 12) further reduced the mass-transfer rate. The addition of Zr + Mg, or Zr + U + Mg all but eliminated transfer under these conditions. For example, in run No. 14, the background averaged 0.8 and the cold sample 1.5 counts per minute over a 1-hour counting period. This should perhaps be regarded as no transfer within the accuracy of the experiment. With or without U, additions of Zr in all concentrations from 5 to 250 ppm appeared to be equally effective in reducing mass transfer, within the accuracy of the counting technique. The observation that as little as 5 ppm Zr prevents mass transfer at this temperature correlates with the nearly complete "saturation" of the Fe surface with Zr at 450°C from Bi containing 5 ppm Zr. Thus, the observations made from the results of the convection pot experiments tend to strengthen our conclusion based upon the surface reaction and static solution-precipitation rate experiments as to the mechanism of the inhibition of mass transfer of Fe by Zr.

Table IV. Relative Rates of Mass Transfer of Pure Fe in Bi in Graphite Thermal Convection Pot

	Additives (ppm)					
Run No.	*Mg*	*U*	*Zr*	*T max.*	*T*	*Transfer rate, mg/hr×10⁻⁶*
3*	–	–	–	467	32	430
4*	–	–	–	475	31	645
18	–	–	–	438	23	13
17	100	–	–	466	25	2
8*	130	800	–	484	48	1.2
12	400	2000	–	485	20	4.6
5*	100	700	200	472	28	0.8
6*	100	400	140	468	22	0.06
7*	100	600	200	457	31	0.2
9*	–	500	175	476	32	0.15
13	100	–	150	495	35	0.1
14	125	–	75	501	32	0.07
15	100	–	35	477	22	0.2
16	100	–	5	465	30	0.2

* Tank A atmosphere. Other runs in purified He atmosphere.

Table V. Approximate Analyses of the Irons and Steels Used in this Work

Material	C	Mn	Si	Cr	Mo	Ni	Fe	Cu	O_2	N_2
Pure Fe	0.003	Trace	Faint trace	0	Faint trace	0	–	Trace	0.012	0.00018
Armco	–	–	–	–	–	–	99+	–	–	–
2¼ chrome (Croloy 5)	0.15	0.30–0.60	0.50	2.00–2.50	0.90–1.10	–	bal.	–	–	–
5 chrome	0.15	0.30–0.60	0.50	4.00–6.00	0.45–0.65	–	bal.	–	–	–
5 chrome silicon	0.15	0.30–0.60	1.00–2.00	4.00–6.00	0.45–0.65	–	bal.	–	–	–
Type 410 steel	0.15	1.00	1.00	11.50–13.00	–	0.50	bal.	–	–	–
304 SS	0.08	2.00	0.75	18.00–20.00	–	8.00–11.00	bal.	–	–	–

DISCUSSION

The experimental data obtained suggest that the action of Zr as an inhibitor lies in its ability to form a deposit upon the Fe or steel surface. This deposit affects both the solution and precipitation processes: by acting as a diffusion barrier, it decreases the rate of solution of the container metal; by changing the nature of the Fe surface, it decreases the effectiveness of that surface as a nucleation site and decreases the tendency of the crystallites, once nucleated, to sinter together and to the container wall to form a compact mass or plug. Thus, the Zr affects directly steps 1, 4 and 6 of the mass transfer process, as outlined in Fig. 7.

The exact manner in which Zr produces these effects is not yet conclusively demonstrated. However, a possible mechanism can be proposed that is in agreement with the experimental data obtained to date.

It is felt that the Zr tends to react with the pure iron to form an adherant surface deposit of Zr-Fe intermetallic compound. Two intermetallic compounds, $ZrFe^2$ and $ZrFe^3$, exist in this system,[13] both are stable, congruently melting at 1610°C and 1520°C, respectively. A stable monolayer of either of these compounds at the Fe surface is a distinct possibility since the ratio:

$$n_{Zr} \times A_{Zr}/n_{Fe} \times A_{Fe}\S\S \qquad (5)$$

for both of these compounds is less than 1 (being 0.78 and 0.52 respectively). This is a unique property of the Zr-Fe alloy system; only Nb, Ta, and possibly Ti form a similar alloy system with Fe.

The "adsorption energy" calculated from the data of Fig. 19 is not out of line for formation of a deposit of a stable intermetallic compound of this type, although the higher temperature data suggest that this curve possibly is not a true adsorption isotherm.

It should also be noted, however, that Ti and Zr form two of the most stable carbides and nitrides known. It may, therefore, be that a Zr deposit on a steel surface might subsequently react with the C or N always present in commercial steels to form a surface layer of ZrC or ZrN, and that this layer might be the inhibitor. Attempts to identify the surface deposits by electron diffraction are presently planned. ZrN deposits have been identified by X-ray diffraction on a steel surface at 750°C in the presence of graphite, itself an abundant source of nitrogen. The solution rate of Fe in Bi + Mg + Zr is also being investigated in a carburized and nitrided steel crucible, where the tendency to form ZrC or ZrN might be high.

Since multilayer surface deposits of Zr were observed at 520°C, the presence of a possible diffusion barrier to solution in the hot region of the mass-transfer loops seems demonstrated. Since, however, only a "monolayer" was observed at 450°C, the effect of the Zr upon the cold-leg precipitation processes probably lies in the ability of the Zr monolayer to satisfy the free bonds at the Fe or steel surface. This action might greatly retard growth of the wall crystals or any of the crystallites nucleated in the solution phase, as Zr might be expected to react with their surface also.

Similarly, formation of such a surface deposit might effectively poison the ability of that surface to act as a nucleation site (step 4). A higher degree of supersaturation or super-cooling has been demonstrated to be necessary for precipitation to occur in the absence of a nucleation promotor or catalyst.[14,15] Furthermore, if inhibition of crystal-growth phenomena plays a part in this mechanism, the tendency of the precipitated crystals to sinter to one another and to the container wall to form a compact plug might also be greatly decreased. Thus, a loosely compacted deposit would be expected which would be jarred loose by tapping as described in the loop test.

§§ Where n_{Zr} is the number of atoms of Zr in a formula of the intermetallic compound, and A_{Zr} is the ⅔ power of the atomic volume of Zr, etc.

The apparent ability of the Mg + Zr additives to prevent the nucleated Fe crystals from sintering to each other and to the container wall suggests that a sufficiently high flow velocity through the cold region might sweep these particles through to the heated zone where, because of their relatively large surface area and short contact time with the dissolved Zr, they might dissolve at a much faster rate than the container walls. Thus, both the rate of corrosion of the container in the hot leg and the rate of plugging in the cold leg of an inhibited system might be substantially decreased, and the life of a liquid Bi heat exchanger considerably increased, particularly for a system where the flow velocity is high in the cold leg and low in the hot leg, giving the particles time to redissolve.

In conclusion, although it has not yet been established that the low chrome steels and graphite can be used as containing and moderating materials, the experimental and engineering evidence suggest that these materials show promise as construction materials for a reactor in which U-Bi is the fuel.

REFERENCES

1. Quill, L. L. (Ed.), *The Chemistry and Metallurgy of Miscellaneous Materials: Thermodynamics,* McGraw-Hill Co., Inc., New York (1950).
2. Brewer, L., Private communication to J.R.W. (December 1954).
3. Reid, R. C., *Mercury Boiler Treatment with Titanium and Magnesium Metals,* American Society of Mechanical Engineers: Tech. Paper No. 51-S-13 (1951).
4. Nerad, A. J., Private communication to R.J.T. (December 1951).
5. *Liquid Metals Handbook,* 2nd Edition, U.S.A.E.C. (1952).
6. Elgert, O. J. and Egan, C. J., *Dynamic Corrosion of Steel by Liquid Bismuth,* Report to U.S.A.E.C. No. MTA-12 (January 1953).
7. Cygan, R., *Circulation of Lead-Bismuth Eutectic at Intermediate Temperatures,* Report to U.S.A.E.C. No. NAA-SR-253 (October 1953).
8. Cygan, R., *Lead-Bismuth Thermal Convection Loop,* Report to U.S.A.E.C. No. NAA-SR-1060 (October 1954).
9. Terry, J. E. and Skeats, N. B., *Liquid Metal Coolants: A Bibliography,* Report No. AERE Inf/Bib 94 (July 1954).
10. Griffith, C. B. and Mallett, M. W., *The Solubility of Carbon and Oxygen in Liquid Bismuth,* J. Am. Chem. Soc. *75*: 1832 (1953).
11. Shepard, O. C., Morgan, J. R., Parkman, R. and Seibel, R. D., *Investigation of Materials for Use in a Heat-Transfer System Containing Liquid Lead or Bismuth,* Reports to U.S.A.E.C. No. AECU-2794 (December 1953) and AECU-2915 (June 1954).
12. Grassi, R. C., Bainbridge, D. W. and Harman, J. W., *Final Report on Metallurgical Investigation of Materials Subjected to Liquid Lead-Bismuth Alloy Environment,* Report to U.S.A.E.C. No. AECU-2201 (July 1952).
13. Wallbaum, H. J., *The Systems of the Iron Metals with Titanium, Zirconium, Columbium and Tantalum,* Archiv für das Eisenhüttenwesen *14*: 521-26 (1941).
14. Holloman, J. H. and Turnbull, D., *The Solidification of Metals and Alloys,* p. 1-19, AIME, New York (1951).
15. Turnbull, D. and Vonnegut, B., *Nucleation Catalysis,* Ind. Eng. Chem. *44*: 1292 (1952).

The Solubility of Structural Materials in Sodium

By R. A. Baus, A. D. Bogard, J. A. Grand, L. B. Lockhart, Jr., R. R. Miller, and D. D. Williams, USA

Radioactive structural materials dissolved by liquid sodium could cause engineering problems relative to shielding and maintenance access. Furthermore, if solubilities and transfer rates are high, the removal of metal from the hot to the cold part of a heat exchange system would present operational problems. The purpose of these investigations was to determine if an accessibility and shielding problem or a mass transfer problem existed in sodium-cooled systems.

SOLUBILITY OF IRON IN SODIUM

The solubility of iron in sodium was determined using radioactive iron-59. Sodium was distilled in vacuum onto the radioactive iron and was allowed to remain in contact with the iron for 2 hours. At the end of this time the sodium was removed without changing its temperature. The experiment was then repeated at a different temperature.

Table I. Solubility of Iron in Sodium Metal

Temp., °C	Grams Fe per gram Na	Grams of Na	Fe cpm*	Grams Fe per count
230	2.44×10^{-9}	16.7358	10.8	3.78×10^{-9}
232	0.90×10^{-9}	10.7006	1.4	6.81×10^{-9}
304	3.72×10^{-9}	17.1499	16.9	3.78×10^{-9}
329	2.68×10^{-9}	14.5333	6.7	5.84×10^{-9}
404	5.00×10^{-9}	9.8784	7.3	6.81×10^{-9}
483	5.75×10^{-9}	13.4423	1.3	5.91×10^{-8}
521	9.07×10^{-9}	9.9644	8.6	1.05×10^{-8}
544	10.6×10^{-9}	4.7999	7.5	6.8×10^{-9}

* Counts per minute, corrected for yield.

Table II. Solubility of Iron in Sodium Saturated with Na_2O

Temp. °C	Grams Fe per gram Na	Grams of Na	Fe cpm*	Grams Fe per count
205	0.78×10^{-8}	10.7973	1.8	4.59×10^{-8}
277	1.58×10^{-8}	6.3418	4.0	2.51×10^{-8}
331	1.52×10^{-8}	14.1926	37.0	5.84×10^{-9}
349	1.00×10^{-8}	10.7808	13.4	8.08×10^{-9}
380	1.47×10^{-8}	16.0779	5.1	4.59×10^{-8}
381	1.95×10^{-8}	7.5967	6.0	2.51×10^{-8}
391	1.72×10^{-8}	17.1676	78.0	3.78×10^{-9}
402	1.85×10^{-8}	14.7704	7.1	3.86×10^{-8}
431	2.03×10^{-8}	17.9393	17.8	2.05×10^{-9}
445	2.47×10^{-8}	10.7653	5.8	4.59×10^{-8}
469	2.76×10^{-8}	14.8311	109.0	3.78×10^{-9}
477	2.80×10^{-8}	14.1420	10.2	3.86×10^{-8}
524	3.90×10^{-8}	20.0720	20.3	3.86×10^{-8}
527	4.14×10^{-8}	12.9121	91.0	5.84×10^{-9}
559	3.85×10^{-8}	12.0190	22.6	2.05×10^{-8}

* Corrected for yield.

The apparatus used is shown in Fig. 1. Molten sodium was previously filtered into the charging vessel (A) and allowed to solidify in the glass tubes. As a sample was required it was melted into the type 304 stainless steel still, vessel (C), and distilled from there into the vessel (D) containing the radioactive iron. This vessel was also type 304 stainless steel. At the end of the two-hour soaking period the sample of sodium was forced into a previously weighed crucible in the sample receiver, (F). As the sodium was pumped out of the soaking vessel it passed through a nickel filter to remove particulate matter. Pumping was accomplished with purified nitrogen or argon by manipulating the stopcocks and mercury-leveling system.[1]

When the sample receiver was full, it was removed to an inert atmosphere. The sodium samples were then removed and weighed.

After reacting the sodium metal with alcohol and water, the iron was recovered with carrier as ferric oxide, purified, and the radioactivity in the pure ferric oxide measured.

The solubility of iron was determined in three different solvents, namely, pure sodium, sodium saturated with sodium oxide, and sodium containing sodium hydroxide.

Figure 2 shows the solubility curve for iron in pure sodium from the data in Table I.

The expression best fitting this data is:

$$\text{grams Fe/gram Na} = 2.28 \times 10^{-9} - 1.63 \times 10^{-11}T + 5.63 \times 10^{-14}T^2 \quad (1)$$

where T is expressed in degrees Centigrade.

The solubility of iron in sodium metal saturated with Na_2O follows the curve shown in Fig. 3. This is taken from data in Table II.

The curve follows the expression:

$$\text{grams Fe/gram Na} = 3.17 \times 10^{-8} - 1.71 \times 10^{-10}\,T + 3.51 \times 10^{-13}T^2 \quad (2)$$

where T is expressed in degrees Centigrade.

When sodium hydroxide is present the solubility of iron in sodium is shown by the graph in Fig. 4. This is taken from data in Table III.

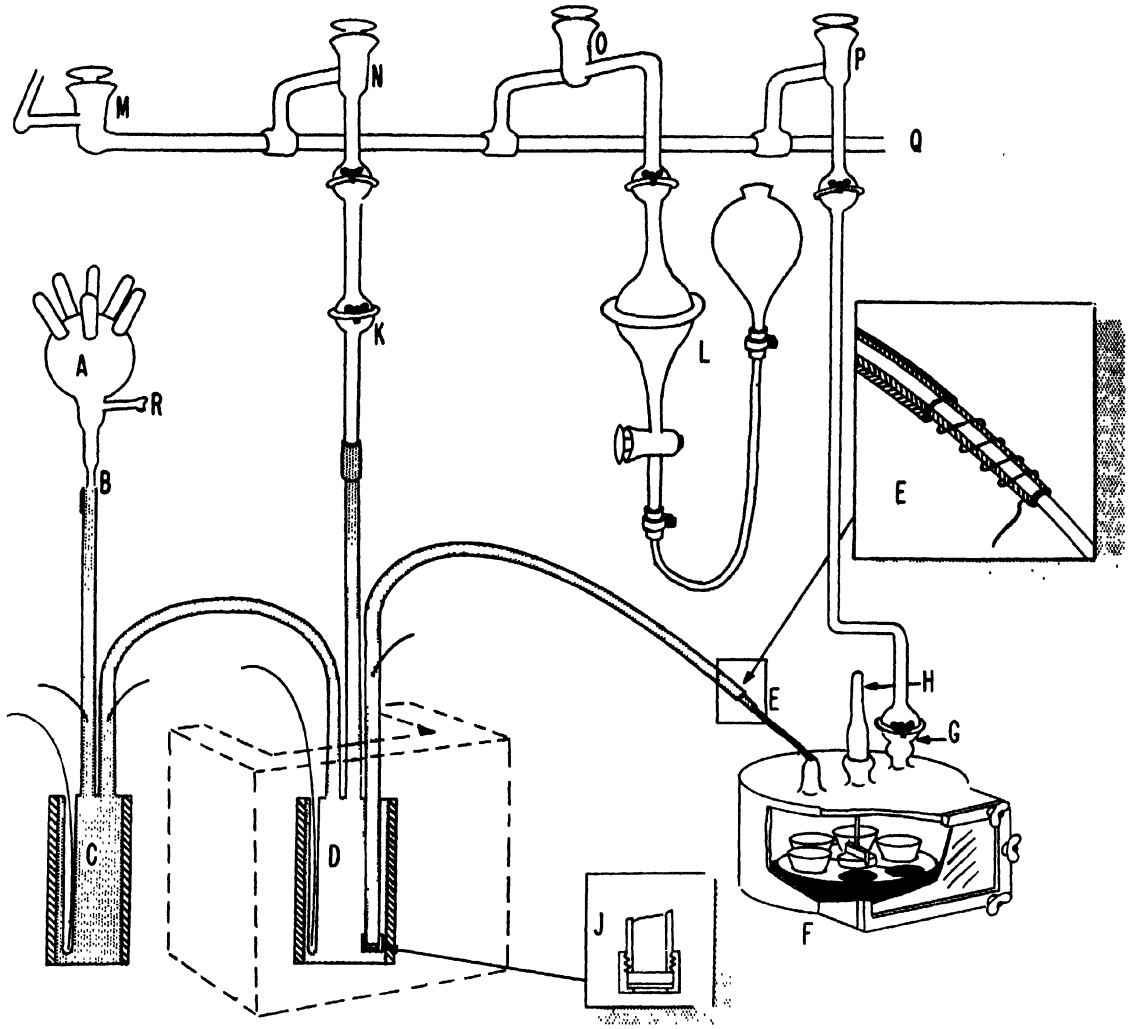

Figure 1. Iron solubility apparatus

Iron solubility in sodium containing sodium hydroxide follows the expression:

$$\text{grams Fe/gram Na} = 8.23 \times 10^{-10}\, T - 1.30 \times 10^{-7} \qquad (3)$$

where T is expressed in degrees Centigrade.

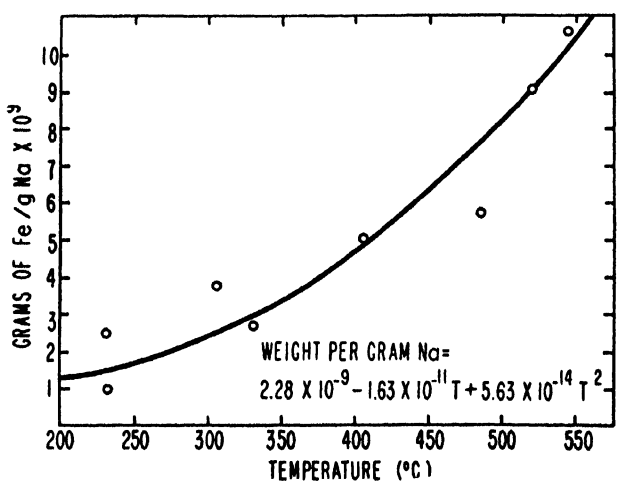

Figure 2. Solubility of iron in sodium metal

Each sample of sodium was in contact with radioactive iron for 2 hours. On the basis of data in Table IV this time is sufficient for equilibrium to be established.

It is apparent from this data that solubility is complete in a relatively short time. In one instance a sample was withdrawn after 15 minutes soaking and the value obtained for iron content was in agreement with similar samples soaked for two hours.

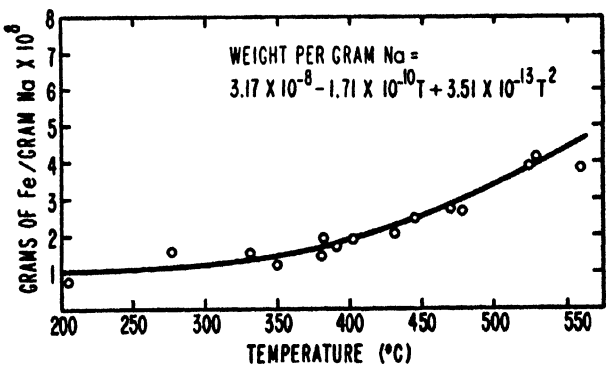

Figure 3. Solubility of iron in sodium metal with Na_2O present

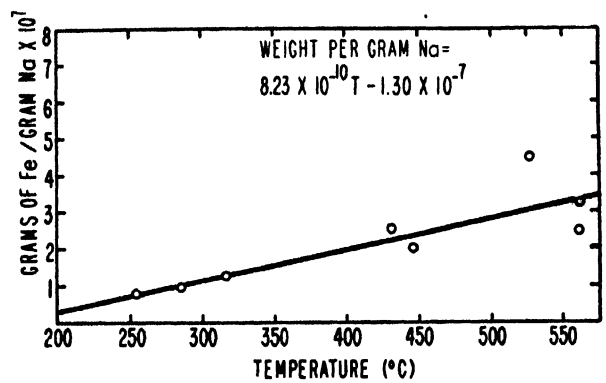

Figure 4. Solubility of iron in sodium metal with Na_2O and NaOH present

Table III. Solubility of Iron in Sodium with Sodium Hydroxide Present

Temp. °C	*Grams Fe per gram Na*	*Grams of Na*	*Fe cpm**	*Grams Fe per count*
253	0.81×10^{-7}	7.9932	42.7	1.51×10^{-8}
285	0.97×10^{-7}	11.7404	94	1.21×10^{-8}
316	1.25×10^{-7}	3.9254	32.5	1.51×10^{-8}
430	2.59×10^{-7}	16.8822	289	1.51×10^{-8}
445	2.03×10^{-7}	11.1600	187	1.21×10^{-8}
527	4.58×10^{-7}	7.8512	616	5.84×10^{-9}
561	2.47×10^{-7}	15.7481	258	1.51×10^{-8}
562	3.22×10^{-7}	11.1191	237	1.51×10^{-8}

* Corrected for yield.

The area of type 304 stainless steel exposed to sodium was approximately 36 square centimeters. Some solubility data were taken with a radioactive iron source of 50.4 cm^2 and some with a source of 0.11 cm^2 exposed to the sodium. The ratios of radioactive to non-radioactive areas were 1.40 to 1 and 3.06×10^{-3} to 1 respectively.

Solubility data taken with each source at comparable temperatures is given in Table V.

From this data it is apparent that an area ratio of 457 between the two sources has no significant effect upon the solubility values obtained in the type 304 stainless steel system.

The solubility of iron in sodium has been determined by other workers in the field. Epstein[1] determined the solubility of iron in sodium using an Armco iron system. Drugas and Kelman[2] have determined the solubility of iron in NaK alloy in an engineering system. These workers report solubilities of the order of 1×10^{-6} to 1.5×10^{-5} grams per gram of sodium. Mausteller and Batutis[3] have done engineering type experiments in which most values for iron concentration are of the order of 10^{-5} grams of iron per gram of Na.

These workers have determined iron almost exclusively by colorimetric methods, while our method has been almost exclusively radiochemical. Colorimetric procedures applied to our sodium samples indicate the iron content to be below the sensitivity of the method, 1×10^{-6} grams of iron per gram of sodium.

SOLUBILITY OF STAINLESS STEEL COMPONENTS IN SODIUM

The solubilities of type 347 stainless steel components were determined as the by-product of another experiment.

Figure 5 shows the apparatus used to study exchange and diffusion using sodium as the medium of exchange and transfer. Sodium at 425°C in the stainless steel tube (G) was electromagnetically stirred. A radioactive stainless steel source was mounted in the bottom of the sample holder (P). Type 347 stainless steel test specimens (O) and a sodium sample container were placed in the sodium.

Stainless steel test specimens were withdrawn for radioactive metal transfer measurements and sodium samples were withdrawn for oxygen analysis. At the end of the experiment the sodium was withdrawn at 425°C and analyzed for cobalt, tantalum, iron, antimony and other activities occurring in the source. Since all metal exposed to sodium was type 347 stainless steel, the calculations are based on the area ratio between radioactive stainless steel and non-radioactive stainless steel.

The radioactive source used in the first experiment was discharged from the reactor on 1 December 1951. The effective date of use was 1 April 1953, thus no short half life activities were present. A radiochemical analysis of the activities of interest is shown in Table VI.

It was assumed that the non-radioactive and radioactive stainless steel exposed to sodium contributed to the total stainless steel content of the sodium in a direct area ratio relationship. The ratio of total

Table IV. Effect of Contact Time on Iron Solubility

Soaking time in hours at 350°C	*Grams Fe per gram Na*
1	2.26×10^{-9}
2	2.70×10^{-9}
4	2.08×10^{-9}

Table V. Source Area Effect on Solubility of Iron

Temp. °C	*Grams Fe/gram Na*	
	0.11 cm^2	*50.4 cm^2*
342	1.33×10^{-8}	
350		1.21×10^{-8}
431		2.03×10^{-8}
445	2.47×10^{-8}	
524	3.90×10^{-8}	
527		4.14×10^{-8}

Table VI. Radioactive Components in Stainless Steel Source

Isotope	*Half-life*	*dpm/gm 4/1/53*	*% element in SS*
Co^{60}	5.3 yr	2.3×10^{10}	0.139
Ta^{182}	111 d	4.8×10^{8}	0.025
Fe^{59}	45.1 d	1.6×10^{7}	67
Fe^{55}	2.9 yr	1.1×10^{9}	
Sb^{124}	60 d	1.7×10^{8}	0.015

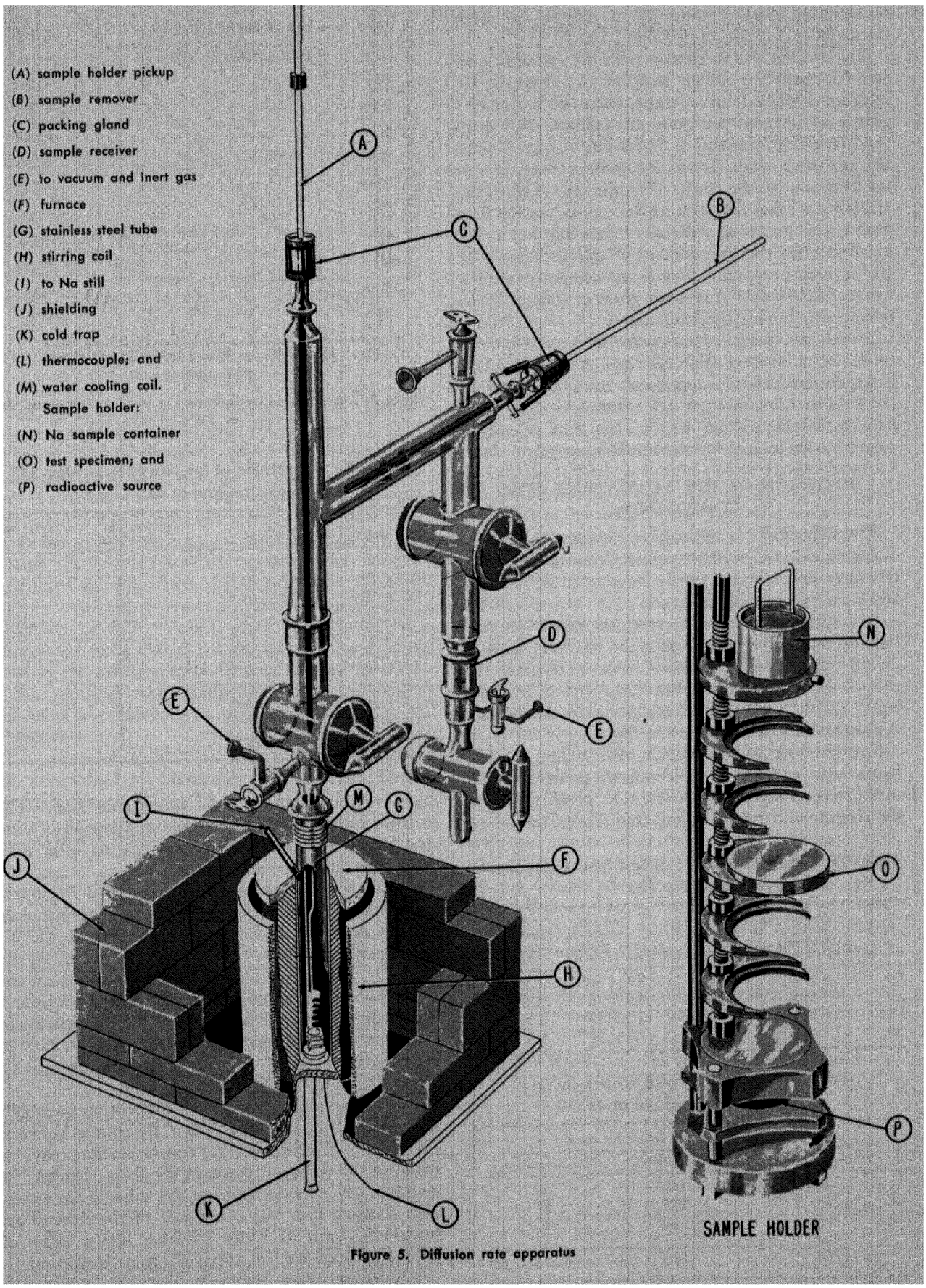

Figure 5. Diffusion rate apparatus

area to radioactive area was 48.5. Based on this assumption the solubility or equilibrium concentration of stainless steel components in sodium has been calculated and is shown in Table VII.

The sodium was in contact with the stainless steel for 762 hours. Sodium analyzed at intervals for oxygen contained an average value of 3×10^{-4} grams of oxygen per gram of sodium. The term "concentration" instead of "solubility" is used since the material available to the sodium may be restricted, as in the case of antimony, where the solubility at this temperature is approximately 0.23 grams per gram of sodium.[4] It should be noted, however, that the iron content of this sodium, 1×10^{-8} grams per gram of sodium, compares with a value of 2.2×10^{-8} grams per gram of sodium based upon iron solubility determinations.

A second experiment was performed using a fresh source of radioactive stainless steel. A cold trap was incorporated into the apparatus to remove sodium oxide. The level of radioactive stainless steel components in the sodium was so low that calculated concentration values were without meaning.

DEPOSITION OF TYPE 347 STAINLESS STEEL COMPONENTS

The deposition of radioactive components of type 347 stainless steel was determined from radioactivity measurements on specimens suspended in sodium and from the walls of the vessel.

In a system containing oxygen, the rate of deposition of radioactive components in stainless steel is directly proportional to time. Table VIII gives the rate of deposition versus time for a system containing 3×10^{-5} grams of oxygen per gram of sodium. A graph of this data is shown in Fig. 6.

The test specimen in contact with sodium for 762 hours was examined for depth of penetration of radioactive components. Table IX gives the data showing depth of penetration. One face of the specimen was removed in small increments (Δs). The activity remaining was measured in a low absorption and high absorption proportional counter after each increment was removed.

Table VII. Concentration of Stainless Steel Components in Sodium at 425°C

Element	Source activity dpm/gm of element	Activity dpm/100 gm Na	Element present from source, gm/100 gm Na	Total concentration, grams/gram sodium
Co	1.6×10^{12}	430	2.7×10^{-11}	1×10^{-11}
Ta	1.9×10^{12}	1170	6.4×10^{-10}	3×10^{-10}
Fe	1.6×10^{9}	44	2.7×10^{-8}	1×10^{-8}
Sb	1.1×10^{10}	2020	1.8×10^{-7}	9×10^{-8}

Table VIII. Deposition of Radioactivity on Type 347 Stainless Steel at 425°C

Exposure time (hours)	Counts per minute	
	Low absorption	High absorption
42	147	13
138	249	26
264	334	46
402	740	76
762	1176	138

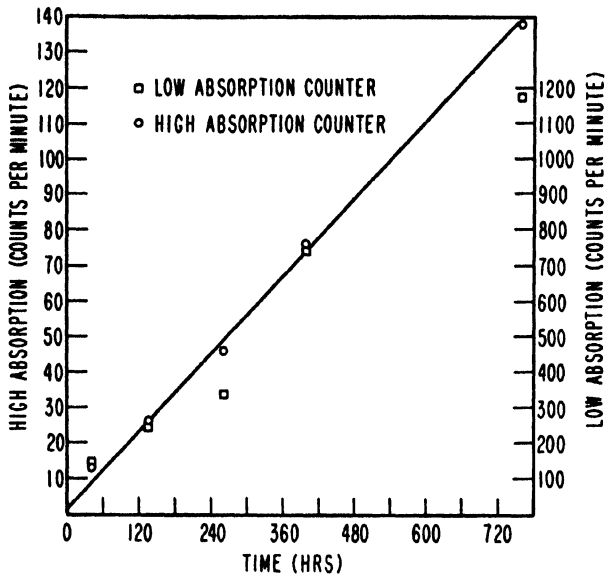

Figure 6. Deposition of radioactivity on type 347 stainless steel at 425°C

Table IX. Penetration of Radioactivity in Type 347 Stainless Steel at 425°C

Δs (cm)	$\Sigma \Delta s$ (cm)	cpm, low absorption	cpm, high absorption
0	0	1176	138
10.7×10^{-5}	10.7×10^{-5}	171	19
9.2×10^{-5}	19.9×10^{-5}	42	13
11.2×10^{-5}	31.1×10^{-5}	22	10
14.2×10^{-5}	45.3×10^{-5}	18	10
13.5×10^{-5}	58.8×10^{-5}	15	10
13.7×10^{-5}	72.5×10^{-5}	14	7
13.5×10^{-5}	86.0×10^{-5}	13	8
11.7×10^{-5}	97.7×10^{-5}	12	8
14.0×10^{-5}	111.7×10^{-5}	11	6
47.1×10^{-5}	158.8×10^{-5}	11	7

Figure 7 is a graph showing the total depth removed versus count rate. Under the circumstances of the experiment, 762-hours exposure at 425°C, approximately 99% of the activity is found in the first 25×10^{-5} cm. This conclusion is based on the assumption that the tail-off is due to the background counts from the edge and back of the test specimen. Furthermore, electropolishing to a depth of 25.4×10^{-4} cm removed all activity. The data for activity versus depth fits a diffusion mechanism.

On the assumption that low absorption and high absorption beta counting will differentiate between nickel-63 and cobalt-60, an approximation may be made of the diffusion constant for these elements in stainless steel. By determining the value of the diffusion constant that will allow a fit of the data to an integrated form of Ficks diffusion law a value of 2×10^{-15} cm^2-sec^{-1} is obtained for each element.

Absorption data indicated that the radioactive

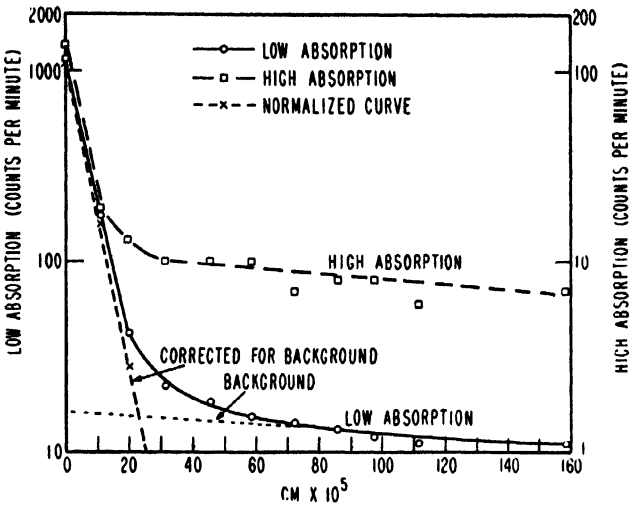

Figure 7. Penetration of radioactive components of type 347 stainless steel at 425°C

species were the same on all test specimens, regardless of the time of removal from the sodium.

The second experiment in which the oxygen was maintained at a low level and a fresh source was used is similar to the initial experiment in that transferred activity increased directly with time and the nature of the radioactive species deposited on the test specimens remained constant. The second experiment differed from the first in that the rate of attack was much lower for iron and cobalt. A comparison of these values is given in Table X.

Since the amounts of cobalt, tantalum and iron found in the sodium represent only a small fraction of that removed from stainless steel, these attack rates may be considered as transport rates for type 347 stainless steel.

The effect of oxygen on the transport rate has been determined by Mausteller and Batutis.[8] Their values are given in Table XI.

Table X. Attack Rates of Stainless Steel in Sodium at 425°C

	Stainless steel attack rate, micrograms/cm²/month	
Element	*No. 1*	*No. 2*
Co	0.3	0.05
Ta	0.8	1.40
Fe	1.6	0.17
Sb	180	48
Oxygen in Na	3×10^{-4} gm/gm Na	3×10^{-5} gm/gm Na

Table XI. Attack Rates of Stainless Steel in Sodium at 496°C

	Stainless steel attack rate, micrograms/cm²/month	
Element	*No. 1*	*No. 2*
Fe	2.5	40
Co	0.2	1
Ta	1	4
Mn	7.2	26
Oxygen in Na	3×10^{-5} gm/gm Na	1×10^{-4} gm/gm Na

The importance of oxygen content of sodium at low concentrations cannot be over-emphasized.

SATURATION RATE OF SODIUM WITH TYPE 347 STAINLESS STEEL COMPONENTS

The rate of saturation of sodium with components of type 347 stainless steel was determined by exposing a relatively large area of radioactive type 347 stainless steel to sodium in a type 347 stainless steel vessel. Duplicate determinations were made for 4 hours, 20 hours, and 240 hours. The concentration in sodium of the various components of stainless steel was calculated from the radioactivity in the sodium, the radioactivity of the source, and the area ratios between the source and inactive container.

The saturation vessel consisted of a type 347 stainless steel tube 1¼ inches outside diameter, 1 inch inside diameter and 8 inches long, fitted at the top with two type 347 stainless steel tubes, one for charging and the other for removing the source and the sodium. One of the tubes had a glass-to-Kovar seal to attach the apparatus to an inert gas system for sample removal. The radioactive source was a type 347 stainless steel accordion pleat made from a 15.2×10^{-3} cm thick sheet, 7.85 cm by 3.82 cm, and suspended in the sodium by a type 347 stainless steel wire. All saturation vessels were machined from the same bar stock and were fabricated so that sodium did not contact a weld. The steel for the activity sources was cut from a common sheet. The sources were irradiated together. Radiochemical and conventional chemical analyses were made on the source material. The analysis is shown in Table XII.

Solubility rate determinations were made by distilling sodium, at less than 0.1-micron pressure, into the saturation vessel containing the radioactivity, and then sealing the distilling tube with 500-mm pressure of nitrogen in the vessel. The apparatus was then placed in a controlled furnace at 425°C. At the end of the prescribed time, the saturation vessel was connected through a glass side-arm and break-off seal to auxiliary apparatus. The break-off seal was opened and the pressure checked to determine if leakage had occurred. With purified argon flowing through the system the radioactive source was removed and a sample of sodium withdrawn

Table XII. Analysis of Stainless Steel Source

Element	*dpm/gm of* SS 10/7/53*	*dpm/gm of† SS 1/1/54*	*Radiochemical analysis (%)*	*Chemical analysis (%)*
Fe	1.69×10^{10}	4.7×10^{9}	64.3	66.44
Co	7.27×10^{9}	7.1×10^{9}	0.071	0.10
Ta	2.74×10^{10}	1.6×10^{10}	0.088	0.07
Sb	1.71×10^{8}	6.4×10^{7}	0.004	Not found
Sn	1.95×10^{6}	1.7×10^{6}	..	0.005
Ag	1.44×10^{7}	1.2×10^{7}	0.0013	..
W	1.30×10^{7}	..	0.00090	..
Cr	5.2×10^{8} cpm	5.4×10^{7} cpm	..	18.85
Zn	1.34×10^{7}	1.3×10^{7}	0.0027	..

* Date of removal from reactor.
† Approximate date of experiments.

Table XIII. Radiochemical Analyses of Sodium from Saturation Rate Experiments at 425°C*

Element	4 hours dpm/100 gm Na	20 hours dpm/100 gm Na	240 hours dpm/100 gm Na
Fe^{59}	515	1660	1015
Cr^{51}	58 cpm	21 cpm	..
Co^{60}	1000	2150	1990
Ta^{182}	4900	21150	61000
Sb^{124}	2.2×10^6	1.6×10^6	3.4×10^6
Sn^{121}	6450	8450	9300
Ag^{110}	9.2×10^5	2.5×10^6	7.9×10^5
Zn^{65}	3.5×10^6	3.3×10^6	1.5×10^6

* Activities corrected to 1/1/54.

in a type 347 stainless steel ampule for oxygen analysis. The bulk of the sodium was then withdrawn at temperature. The oxygen analyzed 1×10^{-5} gm/gm Na or less in each case. The physical parameters of the experiments were the same in each instance with 43 grams of sodium, 86 cm^2 of non-radioactive area and 60.5 cm^2 of radioactive area. It should be noted that the inactive-to-radioactive-area ratio was 1.42 in these experiments while in previous work with radioactive stainless steel sources the ratios were 48.5 and 58.5 respectively.

The results of the radiochemical analyses of the sodium and the stainless steel containers are given in Tables XIII, XIV and XV.

This data indicates that, except for tantalum, the sodium is essentially at equilibrium with components of stainless steel after 4 hours at 425°C. Figure 8 shows the similarity of solution and deposition rates for iron, cobalt, and tantalum in 347 stainless steel. The data for each element is normalized to a common value. The rate of solution follows an exponential law. The deposition rate of stainless steel activity follows closely the solution rate of stainless steel activity. The ratios of deposited activity to that in solution for the elements tantalum, cobalt and iron are relatively constant at ratios of 4 to 40 for each experiment. The more soluble elements, antimony, tin, and silver have values of 0.05 to 0.002. This suggests, as indicated in earlier work, little exchange or transport of soluble elements as compared with relatively insoluble elements.

Antimony, silver, and zinc represented 98% of the activity in solution. The presence of the soluble elements in sodium is not of direct importance in accessibility to space outside the reactor, but their presence in sodium may be indicative of indirect influence by hole formation in the stainless steel or by effect on solubility of more important constituents.

The values obtained for equilibrium content of the sodium and rate of attack of stainless steel are in good agreement with the exchange experiments, where, as noted previously, the ratios of radioactive to non-radioactive areas are quite different. A summary of the rates of attack by sodium at low oxygen concentration of stainless steel for the exchange experiment and the saturation rate experiments is given in Table XVI.

Table XIV. Calculated Concentration of Type 347 Stainless Steel Components Dissolved in Sodium at 425°C

Element	4 hours gm/gram Na	20 hours gm/gram Na	240 hours gm/gram Na
Fe	1.8×10^{-9}	5.6×10^{-9}	3.8×10^{-9}
Cr	4.3×10^{-9}	1.7×10^{-9}	..
Co	2.0×10^{-13}	4.4×10^{-12}	4.2×10^{-12}
Ta	3.4×10^{-12}	1.5×10^{-13}	4.3×10^{-13}
Sb	3.3×10^{-8}	2.4×10^{-6}	5.0×10^{-8}
Sn	4.6×10^{-9}	6.0×10^{-9}	6.6×10^{-9}
Ag	2.4×10^{-8}	4.4×10^{-8}	3.1×10^{-8}
Zn	1.8×10^{-7}	1.7×10^{-7}	0.8×10^{-7}

Table XV. Radiochemical Analysis of Activity Deposited on Walls of Saturation Vessels

Element	Deposited activity in dpm at 425°C* 4 hours	20 hours	240 hours
Fe^{59}	3800	7000	8550
Co^{60}	4850	3800	5250
Ta^{182}	6.4×10^4	3.3×10^5	3.4×10^5
Sb^{124}	1700	1675	4700
Sn^{121}	25	200	125
Ag^{110}	1100	1400	5200

* Corrected to 1/1/54.

TANTALUM ISOTHERMAL EXCHANGE EXPERIMENT

Tantalum has been shown by previous experiments to be an important contributor to the activity levels deposited in type 347 stainless steel systems. Since transfer rates determined with stainless activities could have been affected by lack of availability of important minor constituents such as cobalt and tantalum it was considered worthwhile to study the transfer of tantalum to stainless steel. The exchange apparatus already described was set up with a tantalum source of large surface area to follow the rate of exchange of this single activity with type 347 stainless steel.

Stainless steel and tantalum tabs were exposed to the tantalum source in stirred sodium at 425°C. Stainless steel tabs were removed at intervals of 72, 312, 1224, 2136, 2712, and 3672 hours. Tantalum tabs were removed at 72 and 3672 hours. After the

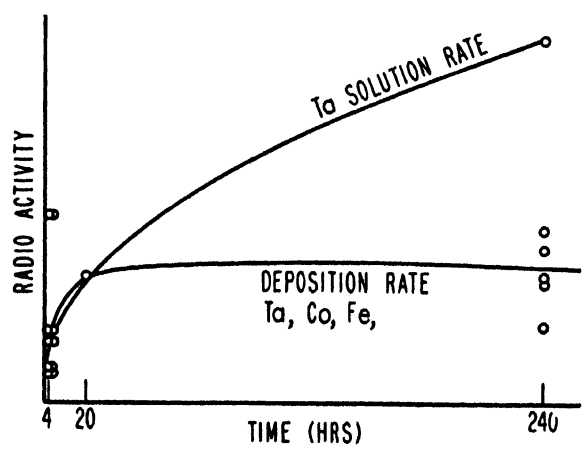

Figure 8. Solution and deposition rates for radioactive stainless steel components at 425°C

Table XVI. Comparison of Rates of Attack of Stainless Steel at 425°C

Element	Attack rate, micrograms/cm²/month: Exchange expt. No. 2 (2712 hr)	Attack rate, micrograms/cm²/month: Saturation rate expt. (240 hr)
Co	0.05	0.05
Ta	1.40	1.20
Fe	0.17	0.10
Sb	48	1000
Oxygen in Na	3×10^{-5} gm/gm of Na	1×10^{-5} gm/gm of Na

Table XVII. Tantalum Activity* Deposited on Stainless Steel and Tantalum Tabs

Time	S.S. tab	Ta tab
72 hours	111 cpm	111 cpm
3672 hours	839 cpm	14600 cpm

*cpm on scintillation counter corrected to 10/28/54. 1 mg source equivalent to 0.27×10^6 cpm.

removal of the last tabs at the 3672 hour point, three stainless steel tabs were added to the system and then removed at 1, 4, and 17 hours. The experiment was concluded with withdrawal, at temperature, of the container sodium and withdrawal of the cold trap sodium. Radiochemical analysis of the sodium samples and the solutions from electropolishing of the container and the cold trap was made.

Activity measurements of the stainless steel tabs indicated that tantalum transfer to stainless steel was proportional to the square root of time over the 3672 hour period. This means that transfer rates calculated as $\mu g/cm^2$/month will decrease with time. Transfer rates for tantalum to stainless steel were calculated as 0.6 $\mu g/cm^2$/month for 72 hours and 0.1 $\mu g/cm^2$/month for 3672 hours. These values are slightly lower than stainless steel transfer to stainless steel based on tantalum activity in previous work.

Comparison of radioactivity found on stainless steel and tantalum tabs shows the deposition rate to be the same initially but increasing for tantalum at a much greater rate than stainless steel as shown in Table XVII.

It might be conjectured from this data that atom exchange rates are comparable and that the tantalum diffusion rate is much greater in tantalum than in stainless steel and accounts for the greater activity deposited.

Three stainless steel tabs were added to the system at the conclusion of the experiment to determine if any immediate exchange of considerable magnitude would occur in an essentially saturated system. The results are given in Table XVIII.

The activity plotted versus the square root of time is a straight line passing through the origin. This indicates that an immediate exchange above that expected from diffusion did not occur. An extrapolation of the data to 72 hours gives a value of 230 cpm, near that of the initial 3-day tab value of 111 cpm.

The equilibrium concentration of tantalum found in the sodium at the end of the experiment was

Table XVIII. Tantalum Deposit on Stainless Steel in a "Saturated" System

Time	Activity/tab*
1 hour	29 cpm
4 hours	58 cpm
17 hours	92 cpm

*cpm on scintillation counter—corrected to 10/28/54.

1.6×10^{-8} grams Ta per gram of Na. This compares with an equilibrium value of 1×10^{-11} grams of Ta per gram of Na found with radioactive stainless steel sources.

The area ratio between tantalum exposed in the two cases is approximately 1300. It will be noted the concentration ratio is approximately 1600.

CONCLUSIONS

The values for concentration in sodium of type 347 stainless steel components are supported by radiochemical analyses from other engineering and laboratory systems, both isothermal and ΔT. The iron concentrations found by radiochemical techniques are a factor of 10^3 lower than those obtained at other laboratories by conventional chemical analysis. This discrepancy is at present under investigation. The transport rates for stainless steel are in agreement within an order of magnitude. It is recommended that for engineering calculations the transfer rates given in Table XVI be increased by a factor of 10 for a ΔT system operating at a maximum temperature of 425°C and 3×10^{-5} gram of oxygen per gram of sodium. As of now, the deposition rate should be treated as being directly proportionate to time.

If the sodium is drained from a reactor system, or if radioactive sodium is allowed to decay, it may be expected that transfer rates would not hamper accessibility to spaces outside the reactor compartment. However, Pepkowitz[5] has demonstrated an exponential rise in activity deposit with temperature. Furthermore, Mausteller[3] has shown that an oxygen content increase from 3×10^{-5} gram per gram of sodium to 1×10^{-4} gram per gram of sodium will result in an order of magnitude increase in transport rate. These facts emphasize the obvious precautions that should be observed.

It should also be noted that two of the principal activities deposited in the transport process, tantalum and cobalt, are present as impurities in type 347 stainless steel. Alternate materials free of these troublesome contaminants would be desirable.

REFERENCES

1. Epstein, L. F., "Preliminary Studies on the Solubility of Iron in Liquid Sodium," Science *112*, 426 (1950).
2. Drugas, P. G. and Kelman, L. R., "Equipment and Procedures for Studying the Equilibrium Solubility of Iron in NaK", ANL 5359 (4 September 1953).
3. Mausteller, J. W. and Batutis, E. F., "Mine Safety Appliance Co." Tech. Report 36 (16 March 1955).
4. Smithells, C. J., "Metals Reference Book," Interscience Publishers, Inc., New York, p. 335 (1949).
5. Pepkowitz, L. P. Private communication.

Behaviour of the Stainless Steel 1X18H9T in Contact with Liquid Lead and Bismuth and Their Eutectic Alloy at Temperatures of 500°C to 600°C

By L. I. Tsuprun and M. I. Tarytina, USSR

Liquid metals, and among them relatively low temperature melting lead, bismuth and their alloys, are promising as coolants for use in power reactors. That is why the interaction between liquid metals and structural materials with which they are in a direct contact is of great practical interest. The interaction of liquid metals with steel presents in this respect particular interest, for neither aluminium alloys (due to low melting point) nor zirconium and its alloys (because of their intense interaction with lead and bismuth) can be used for the fabrication of tubes, pumps and other structural parts operating in power reactors at elevated temperatures in contact with a eutectic lead-bismuth alloy.

An examination of the behavior of steels of various compositions at elevated temperatures in contact with a liquid eutectic lead-bismuth alloy was carried out under static and dynamic conditions to determine the possibility of using steel as a structural material for power reactors. The data of the research indicate that ordinary commercial stainless and heat-resistant steels do not sufficiently resist the attack of the eutectic lead-bismuth alloy at the temperature of the order of 600°C. Though iron and low carbon steels interact relatively less they cannot be used for the purpose because of their insufficient heat resistance.

In the present work the nature of the interaction between steel and the liquid metals—lead, bismuth and their alloys—under static conditions is revealed by the example of the widely used 18/8 steel; the report also presents data on inhibitors employed for the preservation of steel from the attack by the liquid eutectic lead-bismuth alloy. At the same time the work describes the method of a quantitative determination of the extent of steel damage by the attack of liquid metals.

The behavior of 1X18H9T stainless steel was examined at the temperatures of 500°C and 600°C in contact with pure liquid lead, bismuth and their alloys as well as with a eutectic lead-bismuth alloy containing small additions of nickel, calcium and barium as inhibitors. The effect of prolonged heating at the same temperature on the structure and the mechanical properties of 1X18H9T steel in an argon atmosphere was investigated for the sake of comparison.

Thin-walled tubes in a quenched condition were used for the examination; they were 9-mm od and had a wall thickness of 0.4 mm. The chemical composition of the steel is shown in Table I. The tests were conducted in the following manner. The specimen-tubes filled with a liquid metal and sealed by electric welding as well as empty tubes were heated in a resistance furnace in an argon atmosphere for 1000–1500 hours.

After the test the ends of the specimen-tubes were examined metallographically. The liquid metal was smelted out of the specimen-tube, the steel of the tube being tested by extension to determine the ultimate strength and the relative elongation.

The evaluation of the behavior of steel in contact with liquid metals was made on the basis of alterarations of the mechanical properties of steel, in particular, the reduced ductility properties in a tensile test as well as the depth of interaction in the surface layer, which was detected metallographically.

To study the nature of the interaction, composition changes in a liquid metal were determined together with the changes in the structure of the steel surface layer and in microhardness of structural constituents.

The data of the examination are summarized in Table II and in Figs. 1 and 2.

The examination established that prolonged heating of 1X18H9T steel at the temperature of 500°C in an argon atmosphere does not cause essential changes in either the mechanical properties or structure of a steel. After prolonged exposure at 600°C the relative elongation of the steel is reduced by 15%, ultimate strength somewhat increases; the formation of a carbide phase takes place at austenite grain-boundaries, grain size and hardness undergoing no changes.

The interaction between 1X18H9T steel and liquid bismuth, lead and their alloys occurs at temperatures of 500–600°C. It results in the alteration of the steel mechanical properties; relative elongation and ultimate strength are reduced. The changes in the steel mechanical properties are represented in Table II and in Fig. 1.

Original language: Russian.

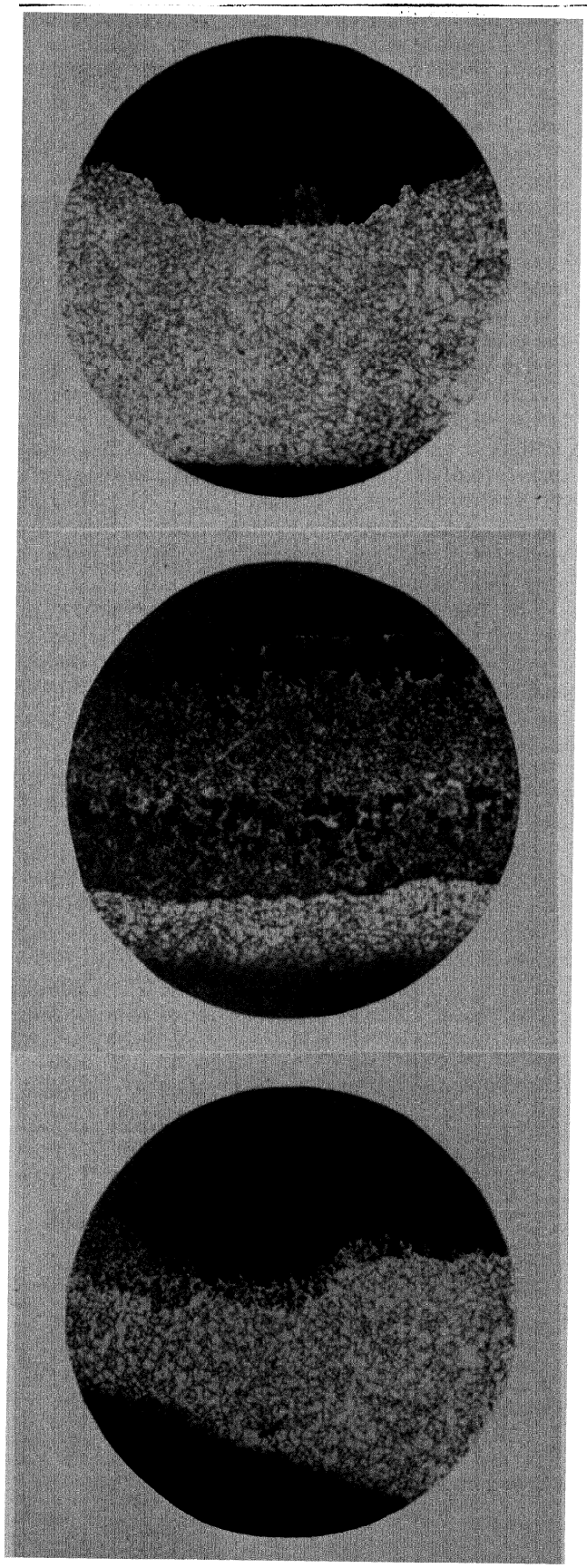

Figure 2. Photomicrographs of areas of interaction between 1X18H-91 steel and liquid metals: (top) lead, (center) bismuth, (bottom) bismuth alloy. × 130

The interaction is detected by the microscopic examination of the cross section of a specimen-tube in the form of dark areas in the steel surface layer (Fig. 1 *a, b, c*). Microhardness of such areas is less than that of steel and is several times more than that of low melting metals. Microhardness of metals of low melting point near the steel surface is increased several times. Steel microstructure and hardness are not affected by the interaction change in the same fashion as those of tubes without a liquid metal heated under the same conditions.

The maximum depth of the interaction zone is shown in Table II.

The corrosion rate of steel in liquid metals is calculated on the basis of the values of the interaction depth. It should be noted that such a calculation of corrosion rate is but approximate due to its un-uniformity. The values of the corrosion rate are represented in Table II.

It was observed in the process of the study that 1X18H9T steel, whose structure initially was that of austenite, assumes magnetic properties after testing in an eutectic lead-bismuth alloy.

X-ray diffraction patterns obtained from the specimens indicated that after the interaction α-phase appears in the steel surface layer. The chemical analysis detected the presence of nickel (to 1%) and of small amounts of chromium and iron in the eutectic lead-bismuth alloy smelted out of the specimen-tube.

It may be thus supposed that the interaction of 1X18H9T steel with a eutectic alloy results in "leaching" one alloy constituent, namely nickel, from the surface layer because of selective solution.

As a result of the reduced nickel content in the steel the face-centered cubic (austenitic) phase be-

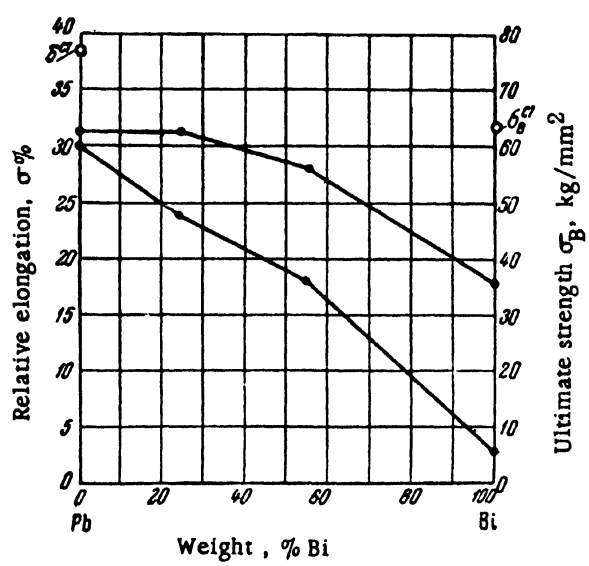

Figure 1. Alteration of mechanical properties of 1X18H9T steel tubes 9 × 0. 4 mm od after testing for 1000 hours at 600° in contact with liquid metals: lead bismuth and their alloys. $\delta, ^{ct}$, β^{ct} —relative elongation and ultimate strength of 1X18H9T tubes in their original condition

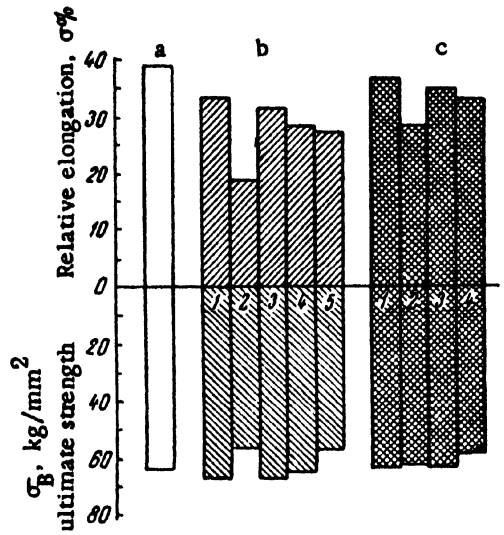

Figure 3. Diagram, illustrating change in mechanical properties of 1X18H9T steel tubes 9 × 0.4 mm od after testing at 500 and 600°: (a) original condition, (b) testing at 600° for 1000 hours, (c) testing at 500° for 1500 hours. (1) Tubes without liquid metal; (2) tubes with lead bismuth eutectic; (3) tubes with lead-bismuth eutectic with addition of Ni(0.6%); (4) tubes with lead-bismuth eutectic with addition of Ca(0.1—0.15%); (5) tubes with lead-bismuth eutectic with addition of Ba(0.1—0.3%)

comes unstable and the transformation to a body-centered cubic (ferritic) phase occurs.

From the examination of the binary equilibrium diagrams of the basic components of the steel and those of the eutectic alloy it follows that nickel solubility in lead at 327°C is 0.2%, nickel solubility in bismuth at 600°C amounting to 6%. Iron is almost insoluble in lead or bismuth. Chromium solubility in bismuth at 600°C is insignificant and in lead amounts to 1%.

The data of the research confirm the supposition that nickel "leaching" as well as partial solution of chromium take place when 1X18H9T steel interacts with a eutectic alloy.

A method of a preservation of the steel from the attack of a liquid eutectic lead-bismuth alloy was tried on the basis of this conclusion. It consists in the preliminary addition of nickel to the alloy at the temperature of 500°C.

The examination of 1X18H9T steel tubes tested at the temperatures of 500°C and 600°C in contact with the eutectic lead-bismuth alloy containing nickel (0.6%) indicated that the ultimate strength of the steel has practically not changed, the relative elongation has reduced very little (5–6%); the corrosion rate has been decreased two or three times (see Table III).

The presence of small additions of calcium or barium, which easily oxidize and form a thin isolating oxide film on the steel surface, in the eutectic lead-bismuth alloy reduces approximately two times the extent of the interaction between the steel and the liquid alloy (see Table III).

The films of calcium and barium oxides developed on the surface are barriers to solution or diffusion in the case of liquid metals affecting steel.

The nature of the interaction of the steel and the eutectic lead-bismuth alloy containing inhibitors (Ca, Ba, Ni) is the same as that between steel and a eutectic lead-bismuth alloy without inhibitors, the extent of the interaction being less.

Figure 3 illustrates the alteration of mechanical properties of 1X18H9T steel tubes after testing in

Table I. Chemical Composition of 1X18H9T Steel Tubes, 9 mm od and 0.4-mm Wall Thickness

Content of elements (weight per cent)						
C	*Ti*	*Cr*	*Ni*	*Si*	*Mn*	*S*
0.08	0.51	17.67	10.45	0.54	1.27	0.023

Table. II. Data of Examination of 1X18H9T Steel Tubes (9 mm od and 0.4 mm Wall Thickness) after Testing in Contact with Liquid Metals

	Ultimate strength σ_B *kg/mm²*	*Relative elongation* δ %	*% property changes of tubes, relative to* *Properties of tubes in original condition* σ_B	δ	*Properties of tubes heated without liquid metal* σ_B	δ	*Max. depth of interaction in microns* μ*	*Corrosion rate, mm/year*†	*Number of specimens tested*
1. Original condition	63	39	—	—	—	—	—	—	12
After testing at 600°C for 1000 hours									
2. Steel after heating (without liquid metal)	67	33	+ 6	−15	—	—	—	—	15
3. Steel tube with metal: lead	62	30	− 2	−23	− 7	− 9	60	0.5	6
bismuth	37	3	−41	−92	−45	−90	300	2.6	3
eutectic (Pb 44.5% Bi 55.5%)	56	18	−11	−54	−16	−45	160	1.4	9
alloy (Pb 75% Bi 25%)	62	24	− 2	−38	− 7	−27	40	0.4	3
After testing at 500°C for 1500 hours									
4. Steel after heating (without liquid metal)	64	36	+ 2	− 8	—	—	—	—	3
5. Steel tube with liquid metal: eutectic (Pb 44.5% Bi 55.5%)	63	28	0	−28	− 2	−22	80	0.5	3
6. Alloy (Pb 75% Bi 25%)	65	29	+ 3	−26	+ 2	−19	40	0.2	3

* Determined metallographically on cross section of specimen. † Calculated from the maximum depth of interaction.

Table III. Data of Examination of 1X18H9T Steel Tubes (9 mm od and 0.4 mm Wall Thickness) after Testing in Eutectic Lead-Bismuth Alloy with Additions of Inhibitors

	Ultimate strength σ_B kg/mm²	Relative elongation δ %	% property changes of tubes, relative to: Properties of tubes in original condition σ_B	δ	Properties of tubes heated without liquid metal σ_B	δ	Max. depth of interaction in microns μ*	Corrosion rate, mm/year†	Number of specimens tested
1. Original condition	63	39	—	—	—	—	—	—	12
After testing at 600°C for 1000 hours									
2. Steel after heating (without liquid metal)	67	33	+ 6	−15	—	—	—	—	15
3. Steel tube with liquid metal: eutectic with addition of Ca(0.1–0.15%)	65	28	+ 3	−28	− 3	−15	70	0.6	8
4. Eutectic with addition of Ba (0.1–0.3%)	57	27	−10	−31	−15	−18	70	0.6	9
5. Eutectic with addition of Ni (0.6%)	67	31	+ 6	−21	0	− 6	35	0.3	6
After testing at 500°C for 1500 hours									
6. Steel after heating (without liquid metal)	64	36	+ 2	− 8	—	—	—	—	3
7. Steel tube with liquid metal eutectic with addition of Ca(0.1–0.15%)	60	33	− 5	−15	− 6	− 8	40	0.25	3
8. Eutectic with addition of Ni (0.6%)	64	34	+ 2	−13	0	− 5	35	0.2	3

* Determined metallographically on cross section of specimen. † Calculated from the maximum depth of interaction.

contact with a eutectic lead-bismuth alloy with or without inhibition.

CONCLUSION

The investigation showed that the damage of 1X18H9T stainless steel in a eutectic lead-bismuth alloy at 500–600°C proceeds largely by the way of nickel "leaching" from steel.

The special additions of inhibitors—nickel, calcium, barium—reduce the interaction between the eutectic alloy and the steel. The presence of nickel, about 0.6%, in the eutectic lead-bismuth alloy preserves steel from the attack of the liquid alloy somewhat better than the presence of calcium and barium in the same alloy.

Technological operations necessary for the preparation of the eutectic lead-bismuth alloy with the nickel addition are considerably simpler than those in the case of calcium or barium additions to the same alloy.

The experiments similar to those described above were performed at temperatures of 300–450°C. In this case it is found that 1X18H9T stainless steel at the given temperature practically does not interact with the eutectic lead-bismuth alloy even without inhibitors.

Thus, stainless steel of type 18/8, 1X18H9T, should be considered to be capable of being used without essential interaction in contact with liquid eutectic lead-bismuth alloy without inhibitors for a long time at temperatures to 500°C.

In the case of the nickel or calcium additions as inhibitors to the liquid eutectic lead-bismuth alloy, an essential interaction at temperatures of the order of 600°C may be avoided.

For steel operating under dynamic conditions, it is necessary to take into consideration an erosion attack of a liquid metal on steel, which depends upon the flow of a liquid metal and the influence of temperature gradient on the mass transfer.

Record of Proceedings of Session 19B.3

THURSDAY MORNING, 18 AUGUST 1955

Chairman: Mr. L. Rotherham (UK)
Vice-Chairman: Mr. K. F. Alder (Australia)
Scientific Secretaries: Messrs. B. Prakash and C. A. Sastre

PROGRAMME

P/119 Corrosion by liquid metals ..... L. F. Epstein

P/787 Observations on the corrosion of uranium in liquid sodium ..... H. Mogard

P/829 Basic technology of the sodium graphite reactor ..... S. Siegel *et al.*

Discussion

Mr. L. F. Epstein (USA) presented paper P/119.

Mr. A. Kiessling (Sweden) presented paper P/787.

Mr. S. Siegel (USA) presented paper P/829.

DISCUSSION OF P/119, P/787 and P/829

Mr. W. B. Hall (UK): I should like to ask Mr. Siegel whether there has been any attempt to measure the temperature variations in a circumferential direction around the individual fuel elements. We have found that such temperature variations can be larger than would be expected with a liquid metal.

Secondly, I should like to ask him whether he feels that there is any possibility of restraining the growth as a result of thermal cycling by the can itself, or does it require too large and strong a can?

Thirdly, has he any views on the possibility of protecting graphite either by plating or by evaporating a thin layer on to the surface, rather than using sheet material?

Mr. Siegel (USA): In reply to the first question, concerning the circumferential variations in temperature, we have done experiments, which were described in a paper by Mr. Parkins* which was presented a few days ago, on the hydraulics of the fluid system. We find that the mixing which we obtain by the spiral wire wraps shown in his paper is very adequate. However, I must point out that, because of the geometrical configuration of the fuel elements, the power generation in an individual peripheral rod is not uniform, and so one can expect differences in temperature circumferentially for that reason.

With regard to the second question, the containment of the deformation of uranium by a sheath, we have shrunk stainless steel sheaths of various thicknesses on to uranium samples which we have cycled, but the thickness required to constrain substantially the growth makes it not practical.

In reply to the third question, on the use of something other than zirconium to protect the graphite from the sodium, we certainly have this in mind as an attractive avenue to explore, but our present attitude is a relatively conservative and perhaps expensive one; we are using a sheath about the integrity of which we have little doubt.

Mr. R. P. Hammond (USA): Has the removal of nickel from stainless steel by hot mercury a destructive effect on the structure of the metal, and has this some relation to the oxygen content of the mercury?

Mr. Epstein (USA): As you know, the essentially excellent mechanical properties of 18/8 steels depend on the stabilization of the thermodynamically metastable austenitic form, and this in turn depends on a delicate balance between iron, chromium and nickel. The removal of masses of nickel must have a tendency to cause transformation to the ferritic form, and this does lead to some deleterious effects, such as would be expected with this transformation. So far as I know, oxygen does not seem to have much to do with it, but our information is not very extensive, because these experiments have been done mostly in mercury treated with magnesium to keep down the oxygen.

Mr. J. M. Hutcheon (UK): Mr. Epstein says in his paper that graphite is drastically attacked by sodium. Mr. Trocki earlier said that alkali metals are compatible with graphite, and Mr. Siegel has indicated a basis for reconciling these views. I should like to ask Mr. Epstein whether he accepts Mr. Siegel's reconciliation or whether he would like to clarify his remarks in any other way.

Mr. Epstein (USA): I think that Mr. Siegel's work has been much more extensive than ours. It is true that by proper treatment of the graphite a greater stability than we ever saw has been obtained, but we still think that unjacketed graphite is a perilous material to handle in direct contact with sodium. I think that Mr. Siegel will essentially agree with that, since he must still jacket his graphite. I hope that he will correct me if I am wrong.

* P/499, Session 14A, Volume 3, these Proceedings.

Mr. SIEGEL (USA): The use of zirconium, as I indicated in reply to an earlier question, is necessary at the present time, we believe, because of the behavior of graphite in sodium. I would emphasize again, however, my opinion that it is not so much chemical corrosion at the temperatures concerned, but a physical invasion of the graphite by the sodium.

Mr. HUTCHEON (UK): Thank you very much. I should like to ask Mr. Siegel whether he has observed any difference in the behavior of different graphites with sodium according to their hardness, which might differentiate between solution of the graphite and actual removal of discrete particles.

Mr. SIEGEL (USA): I cannot answer the question. We did not thoroughly explore the differences between different types of graphite.

Mr. H. H. GOTT (UK): The migration of activated material from the structure of the reactive core round the cooling circuit has been mentioned. Is this deposited more or less indifferently in the coolers, or is there any evidence to suggest that it is co-precipitated in the cold traps, so that there may be an unusual build-up of activity there?

Mr. TROCKI (USA): Numbers of experiments have been conducted, including the release of radioactive material in systems with a temperature difference, some isothermal and some with a considerable amount of surface, like stainless steel fiber placed near the radioactive steel sample. It looked as if there were no particular preferential deposition of the stainless steel or the radioactive material anywhere in the circuit itself. There seems a difference of enrichment or some concentration of these materials in the cold trap, but, so far as their distribution within the heat transfer system itself is concerned, I do not think that we noted any particular concentration, except that possibly more material was concentrated near the radioactive source.

Mr. D. H. GURINSKY (USA): I should like to make some additional remarks with respect to the corrosion by bismuth in steel systems. Since the papers were prepared, some months ago, the evidence has been building up that the inhibition noted due to the addition of zirconium to bismuth is due to the formation of a very thin layer of zirconium nitride on the steel surface. This zirconium nitride is the result of the deposition of zirconium on the steel surface and migration, we think, of the nitrogen in the steel to meet that zirconium at the surface. We should also like to suggest that the inhibition noted in mercury systems is due to a similar mechanism due to titanium nitride being formed.

Mr. J. P. BAXTER (Australia): I should like to ask Mr. Siegel whether, in relation to the results which he gave us on the reactions between sodium and graphite and transport of graphite by sodium to other materials, he has any information on the possible acceleration of these processes or a change in their course under conditions of radiation.

Mr. SIEGEL (USA): Answering your question directly, we do not have evidence during exposure, but we have, as I pointed out in my talk, made similar experiments to those which I reported using graphite which had been irradiated to a fairly high degree, and we found no difference. That is all I can tell you at present.

Mr. M. J. LAVIGNE (Canada): I should like to ask Mr. Siegel what is the composition of this thorium-uranium alloy that he indicated.

Mr. SIEGEL (USA): The particular alloy that was mentioned, I think, had about 3½–4 per cent uranium.

Mr. LAVIGNE (Canada): Mainly thorium?

Mr. SIEGEL (USA): Yes, it is a thorium-based alloy such as would be used in a fuel element in the thorium breeder embodiment of a sodium-graphite reactor.

Mr. LAVIGNE (Canada): What is the surface condition of this uranium which was brought above the alpha-beta transition? When you operate in the range of about 1300°F and cool repeatedly, what is the surface condition or the condition of the uranium slugs?

Mr. SIEGEL (USA): One of the slides I did not show deals with that.* It is not possible to show it now. Perhaps I might try to describe our experimental results. We cycled the uranium in the alpha phase alone or in the beta phase alone, and we certainly observed a substantial amount of distortion of the surface, the growth depending on the nature of the material; for example, the slide I think was for an alpha-roll material. There is a significant amount of distortion on thermal cycling in a single phase. If the thermal cycling occurs through the phase boundary, however, the distortion is tremendously greater. These are thermal cycling experiments; they are not experiments so far carried out under entire reactor conditions.

* Paper P/829; Fig. 12.

Session 20B

CHEMICAL ASPECTS OF NUCLEAR REACTORS

LIST OF PAPERS

		Page
P/900	Chemical problems of power reactors ..... R. Hurst and J. Wright	373
P/821	Survey of homogeneous reactor chemical problems ..... C. H. Secoy	377
P/348	Behaviour of heavy water in piles of the C.E.A. ..... J. Chenouard *et al.*	384
P/535	Aqueous corrosion of aluminum alloys at elevated temperatures ..... J. E. Draley and W. E. Ruther	391
P/880	Corrosion of aluminium and aluminium alloys in aqueous solutions at high temperatures ..... K. Carlsen	397
P/411	Fundamental aspects of the corrosion of aluminium and their application to nuclear reactors ..... R. A. U. Huddle	403
P/537	Aqueous corrosion of zirconium and its alloys at elevated temperatures ..... D. E. Thomas	407
P/811	Aqueous uranium and thorium slurries ..... A. S. Kitzes and R. N. Lyon	414
P/536	Pressurized water reactor (PWR) water chemistry ..... T. Rockwell III and P. Cohen	423
P/412	Applications of square-wave polarography to analytical problems from experimental reactor loops ..... D. J. Ferrett and G. W. C. Milner	436

Chemical Problems of Power Reactors

By R. Hurst and J. Wright,* UK

The attainment of economic nuclear power will require the solution of difficult problems in physics, engineering, metallurgy and chemistry. Very frequently the interactions between these different disciplines will be complex, and the final solution may have to be a compromise, no one aspect being decisive.

On the chemical side there is the obvious need to seek streamlined and cheaper processes for winning uranium and thorium from their ores, and for making up these into suitable fuel elements. Equally there is a need to examine new methods for reprocessing exposed fuel to recover that part which is unburnt. Although these matters are most important in considering the choice of a reactor for power production, they are dealt with elsewhere, and the present paper is concerned with those chemical problems involved in establishing the correct design of the power reactor itself.

These problems become increasingly complex as we pass from consideration of low temperature air or water cooled research reactors to those working at much higher temperatures, cooled by gas, water at high pressure, or liquid metals. The development of liquid fueled homogeneous reactors, where the fissile material is in aqueous solution, in solution in a molten metal, or in a molten fused salt, has raised even more difficult problems, such as decomposition under radiation, corrosion of containing vessels, and continuous chemical treatment to remove fission product neutron absorbers.

The intense radiation present in a reactor core induces chemical reaction between components which are quite compatible in more conventional plant. Since radiation chemical reactions usually have lower temperature coefficients than the corresponding thermal processes, they are dominant in the lower temperature ranges and give place to normal chemical reactions as the temperature is increased. However, even at the higher temperatures, the character of the thermal process may be modified by the presence of reactive species produced by radiation.

In a reactor core, substances absorb energy from gamma radiation, from fast neutron scattering and the recoil atoms resulting from this process, and from nuclear reactions induced in the substance itself. The relative importance of these contributions varies considerably with the elemental composition of the substance and with the type of reactor and the position of the substance in it. In many systems the chemical effects of heavy particle radiation (e.g., recoil atoms) differ quantitatively, and even qualitatively, from those of lightly-ionizing radiation (e.g., gamma rays). It is necessary in such cases to know not only the total energy deposition but also how much is derived from each of the various types of radiation. A calorimeter designed to make these measurements[1] is in use at Harwell, and provides much valuable information. In most positions of a thermal neutron reactor, the energy deposition from fast neutron scattering is very small for elements above sulphur in mass number. In the case of hydrogen, however, this mode of energy deposition is dominant (about 90%). The contribution from gamma radiation increases with atomic number in accordance with the increase in absorption coefficient, but the energy derived from nuclear reactions is quite specific for each element. For example, in systems containing nitrogen, the nuclear contribution is high because a large fraction of the proton energy from the reaction $N^{14}(n,p)C^{14}$ is absorbed even in systems of quite small volume. In water-cooled or moderated reactors to which air has access this energy deposition has important chemical consequences. A special case of a nuclear reaction arises in systems containing fissile atoms, since a large fraction (80%) of the total fission energy is carried by the recoil fission fragments and all of this will be deposited within the system. This energy is the cause of the high rate of water decomposition in aqueous homogeneous reactors.

The energy quanta transferred to molecules from high-energy radiation are usually large compared with the kinetic energies of molecules at ordinary temperatures, and therefore most radiation-induced processes have quite low temperature coefficients. If the corresponding thermal reaction has a high activation energy, there will be quite a narrow temperature range above which the system will be thermally unstable and below which radiation instability will be most important. Some of our studies of gas-solid reactions illustrate this principle.

For reasons associated primarily with the availability of materials and established technology, the early stages of reactor development in the United Kingdom have been associated with gas-cooled and graphite-moderated systems. To enable natural uranium to be used and avoid the neutron absorption

* A.E.R.E., Harwell, Berks, England.

in material required to separate moderator and coolant, it is desirable that the two should be compatible under reactor conditions. Air and carbon dioxide both have suitable nuclear and chemical properties, and their reactions with graphite have been studied both in the absence and in the presence of reactor radiation.

The system graphite-oxygen is thermodynamically unstable under all conditions of practical interest, but the activation energy of about 40 kcal per mole for the thermal process is such that reaction rates are low at temperatures below 300 to 350°C in the absence of radiation. An air-cooled, graphite-moderated reactor would clearly be designed to operate at temperatures below this range if the two were to be in contact. It has been found that at these lower temperatures the radiation-induced oxidation of graphite is many times faster than the corresponding thermal process. The product of this reaction, carbon dioxide, is well known to be very stable under radiation as well as thermally, so that the process

$$C + O_2 \rightarrow CO_2$$

is virtually irreversible, and results in a loss of graphite with attendant decrease in moderating power and reduced mechanical strength of the graphite structure.

At high temperatures, carbon dioxide is reduced by carbon

$$C + CO_2 \rightleftharpoons 2\,CO$$

and the process is reversible. The equilibrium concentration of carbon monoxide increases rapidly with increased temperature and decreased pressure, but is very small at pressures above atmospheric and temperatures below about 400°C. The activation energy of the forward reaction is again high (about 60 kcal per mole) and the reaction rate is low for temperatures below 400 to 450°C in the absence of radiation. The radiation-induced reaction is many times faster than the thermal reaction at these lower temperatures. In a coolant circulating system the conditions will be complex and different equilibrium concentrations will apply for each point, depending not only on the temperature but also on the radiation intensity at that point. In general, coolant velocities will be such that true equilibrium will not be attained at each point, and the circulating gas composition will be depleted in carbon monoxide relative to the true equilibrium value at one position, and rich in carbon monoxide relative to the value for another position in the channel. Continuous circulation will result in carbon transport from the first type of position to the second. The temperature and radiation intensity distributions along reactor channels and the coolant velocity in the channels form a complex set of variables which have made it essential to carry out experiments in model channels under reactor radiation in order to derive data which can be applied directly to reactor conditions.

While the above examples indicate that radiation-induced processes may assume a dominant role when conditions have been chosen so that thermal reactions are small, the interplay of thermal and radiation-induced processes can be quite important in many cases. This is illustrated by the case of aqueous systems at high temperatures and pressures (up to 300°C and 2000 psi) where corrosion of the fuel element sheaths and structural materials (steels, zirconium alloys, aluminium etc.) is of major importance. Under radiation, water is decomposed to give very reactive hydrogen atoms and hydroxyl radicals and, at lower temperatures, hydrogen and hydrogen peroxide molecules.

$$H_2O \rightarrow H + OH$$

$$2H_2O \rightarrow H_2 + H_2O_2$$

At the higher temperatures, hydrogen peroxide will have only a transitory existence at most. The oxidizing species formed by radiation decomposition might be expected to have a marked effect on corrosion processes, but the presence of hydrogen, arising from the corrosion, will help to keep these species in check by ensuring the maintenance of the reaction chain:

$$H_2 + OH \rightarrow H_2O + H$$

$$H + H_2O_2 \rightarrow H_2O + OH$$

which leads to the re-formation of water.

Soluble corrosion products, especially those having ions of variable charge, may enhance the net water decomposition by removing free radicals which are essential for the back reaction. Such corrosion products must be continuously removed by passing a fraction of the water flow through an ion-exchange system to maintain the purity of the water. In water systems to which air has access, nitric acid is produced by the action of radiation. It is shown in another paper by one of us that this is a gas phase reaction which can be controlled by reducing the gas space under radiation; but the unavoidable remaining acid production must also be removed by the ion-exchange system in order to maintain the critical control of pH which is often needed to ensure minimum corrosion. In all these ways it will be seen that there is interaction between the main process, corrosion, and the different radiation-induced processes. They are so linked that it is difficult, and for most practical purposes irrelevant, to decide whether radiation has any direct effect on corrosion.

The types of radiation chemical problem considered above are such as may affect seriously the feasibility of a particular reactor system. At the stage of detailed design of a reactor it has been found that much more numerous questions are raised about the suitability of individual items of equipment for service under radiation conditions. Much has been published about the behavior of many of these

classes of materials under radiation (electrical insulators, elastomers, plastics, etc.) but the range of materials is so wide and the properties of interest so diverse that few general principles can be enunciated and empirical tests are usually necessary for each case.

These radiation decomposition and corrosion problems become very severe in the homogeneous fueled reactor, such as the HRE operated at Oak Ridge, Tennessee.[2]

In this reactor experiment, a solution of enriched uranyl sulphate in water was circulated through an 18-inch diameter steel sphere, in which the neutron chain reaction was sustained; the heat released was removed in a heat exchanger generating steam. In the core, the energy of fission decomposed water into a stoichiometric mixture of hydrogen and oxygen. This large volume of gas effectively sparged out the very small volume of rare gas (krypton and xenon) fission products. The gases were separated from the liquid fuel, and the hydrogen and oxygen catalytically recombined to water for return to the fuel solution storage tanks, while the rare gases were retained on charcoal absorbent beds. The experimental reactor was operated for several periods at a heat rating of one megawatt, and showed extremely good control and safety characteristics, since it had a very large negative temperature coefficient of reactivity due to changes in density of the fuel, and could not be made to "run away" either by normal transients or the most severe mal-operation.

Although interest in this type of reactor has been shown at Harwell for several years, actual work aimed at solving the design problems of such a reactor was not begun until 1954. Since then studies have been made on the basic physical chemistry of uranyl sulphate solutions at high temperature and pressure. Special autoclaves have been designed and built for measurement of vapour pressure and density, for determining solubilities of corrosion products and fission products, and for electrochemical studies of corrosion of steels and other materials. Special autoclaves for working in the large pile (BEPO) have also been used for determining the factors affecting the rate of break-down of water under irradiation, and for studies of corrosion in the fissioning fuel solution.

Some interesting results have been obtained by measuring the corrosion current-potential curves for stainless steels in sulphate media. Thus in 20% aqueous sulphuric acid both at room temperature and at 100°C, F.D.P. Steel (AISI 321) gives the normal sigmoid shaped curve, with large positive current (and corrosion) above + 1.0 volt, no corrosion below + 1 volt down to — 0.2 volt, and then a large negative current at lower potentials. In steels of types FMB (AISI 316) and FCB (AISI 347) although the region above + 0.1 volt was the same, on taking the metal to a slight negative potential a large *positive* current was found with considerable corrosion, rising to a peak about —0.1 to —0.2 volts and then changing to a large negative current on further reduction of potential.

At the same time engineering studies are being made of pumps, valves, heat exchangers, gas-liquid separators, and consideration given to the problems of the core design. By this means it is becoming clearer what are the problems which would arise in the design of a large reactor developing several hundred megawatts of heat. In this the core would be surrounded by a blanket of fertile material to absorb neutron leakage; with a core of uranyl sulphate of the isotope U^{233} the blanket would be an aqueous slurry of thoria. The indications are that if heavy water were used this reactor would be a thermal breeder. Consequently we are investigating in some detail the surface properties of thoria, measuring electrokinetic potentials and the changes upon irradiation, rheological behaviour, and retention of fission products. Thoria, sintered at 1700°C, was found to be positively charged on contact with water, and reversible anion exchange processes with hydroxyl groups on the surface have been followed until masked by ion absorption. Thoria which has been irradiated has a smaller zeta potential, and it is thought that this is due to the *F* centre defects neutralizing some of the exchange capacity. Chemical processes for the extraction of the uranium have been developed which promise to be quick and cheap. In case corrosion by the sulphate system should prove too severe, extensive work has also been done on the UO_3 hydrate systems, since such an oxide slurry could be used as an alternative core. By X-ray diffraction using a specially built Guinier camera, and by single crystal techniques it was possible to distinguish five crystallographically distinct hydrate phases; these were then characterised by analysis and thermogravimetry as UO_3, $2H_2O$ (probably monoclinic), UO_3, 1.0 H_2O (orthorhombic II, tablets) UO_3 0.8 H_2O (orthorhombic I, rods) UO_3, 0.5 H_2O (monoclinic, twinned rods), and a monoclinic phase only obtained in glass at 230°C.[3]

There is no doubt that an homogeneous reactor of this type would have many advantages and could play a large part in the development of economic nuclear power if the formidable problems of corrosion and of containment of the intensely radioactive solution could be solved successfully. It might be objected that the upper temperature of the core is limited to 300°C, so that steam for the turbines cannot exceed 500°F and 400 psi, but it must be said that if this steam should be really cheap a very satisfactory total system could be achieved.

Nevertheless for many applications, higher temperatures are called for, particular emphasis being placed on the possibility of using a gas turbine cycle, where cooling water is not available for a steam plant. There has therefore been an incentive to search for homogeneous fuels which might reach 500°C or more. Thus it might be possible to use a dispersion of uranium oxide in molten caustic soda as a homogeneous system, and some work has been

carried out on the physical chemistry in the molten salt. It has been a challenge to develop methods for studying rates of reaction between UO_3 and the caustic soda, and for measuring particle sizes and growth rates in the resulting slurry. Much attention has been given to the corrosion and mass transfer of container materials, and these difficulties appear to limit the upper operating temperature to about 550°C.

The most promising system for high temperature operation is the liquid metallic fuel, uranium dissolved in bismuth, on which much work has been done at the Brookhaven National Laboratory. Enough has been done already to show that a liquid metal fueled reactor is a feasible proposition and a satisfactory start has been made on the technological development, although there are obviously many difficulties to be overcome. The chief chemical problems are connected with the exploitation of one of the principal advantages of liquid fuels—the continuous removal of fission product neutron poisons. This may be effected by contacting with a fused salt—several low melting chloride eutectics have been tried and found promising. This whole subject of chemical activity in fused salts now appears to be very important to reactor chemistry in respect not only of fuels, but also in new methods of processing. It is important that work to determine the electrochemical series, the activities of ions, the extent of complex formation, and similar physico-chemical themes should be undertaken if full exploitation of high temperature systems is to be achieved.

REFERENCES

1. Anderson, A. R., *A Calorimeter for Measuring Energy Deposition from Pile Radiation,* A.E.R.E. Report C/R 1651, to be published.
2. Beall, S. E. and Winters, C. E., *The Homogeneous Reactor Experiment,* Chemical Engineering Progress, May, 1954.
3. Dawson, J. K. and Wait, E., *Some Aspects of the System UO_3-H_2O,* to be published.

Survey of Homogeneous Reactor Chemical Problems

By C. H. Secoy,* USA

During the course of the development of the Homogeneous Reactor project at Oak Ridge National Laboratory an extensive and vigorous research program dealing with the chemical problems of a water moderated homogeneous reactor was pursued. This paper presents a survey of some of the significant results of these researches. In many instances the research was exploratory only but was adequate to indicate general comparative feasibility. In other instances carefully performed, quantitative data were required in order for the results to be of any significance.

The initial problem was the selection of a fuel system with which one could be reasonably certain of satisfactory performance and which would minimize the probability of encountering operational difficulty. Therefore, it was necessary to understand and delineate the chemical phenomena which could occur in a homogeneous aqueous fuel system in order either to anticipate and avoid operational trouble or to correct it if it occurred.

The obvious general requirement is that the fuel system retain its homogeneity, especially with respect to the uranium fuel atoms, under all operating conditions. Picture, if you will, an n-dimensional space of homogeneity with dimensions for the concentration of each component of the system, for temperature, for pressure, and for each radiation type, intensity, and energy. The boundaries of this space are n-1 dimensional "surfaces" of non-homogeneity. One must find a system capable of existence within this space as determined by reasonable values of the parameters. These are fixed by the selected specifications of the reactor and the purpose for which it is intended. Furthermore, the point of normal operation within the space must be sufficiently distant from any of the boundary surfaces to allow considerable variation in conditions because of the practical limitations on the control of the reactor system.

Aside from this generality, the components of the system must be selected with neutron economy in mind. For the barest minimum the system must be capable of achieving criticality and, for economical operation, the maximum utilization of the available neutrons is a prime objective. Therefore components containing only atoms of reasonably low neutron capture cross sections may be used.

Finally, the system must be sufficiently noncorrosive to some otherwise acceptable container material to insure a reasonably long and safe lifetime for the reactor.

Early experiments involving the exposure of uranium salt solutions to the radiation of the Oak Ridge graphite reactor established the fact that hexavalent uranium was the stable oxidation state. Therefore, the program concerned itself with only uranyl compounds. The specific salts which will be discussed include uranyl nitrate, uranyl phosphate, uranyl chromate, uranyl fluoride, and uranyl sulfate. In the case of each of these, aqueous solutions of the stoichiometrically neutral salts are acidic because of hydrolysis. An increase of temperature promotes the hydrolysis reaction without exception, and thus one may obtain at elevated temperatures an acid-rich liquid phase and a basic or basic-salt solid phase from solutions which would otherwise be far from saturated. For this reason it is necessary to consider each as a three-component system, the components of which may be taken as UO_3, the respective acid anhydride, and water.

The data resulting from a study of the solubility of uranyl nitrate in water as a function of temperature are shown graphically in Fig. 1.[1] The significance of the data is simply that the solubility far exceeds that required for a reactor at all temperatures up to the congruent melting point of the dihydrate at 184°C. However, as shown in Fig. 2, at higher temperatures stoichiometric solutions of all concentrations undergo thermal decomposition of the nitrate ion and hydrolytic precipitation of a basic salt. If operation of a reactor at such temperatures was to be considered, the hydrolytic precipitation could be avoided by enriching the solution with nitric acid. The loss of oxides of nitrogen in the vapor phase would have to be compensated for by appropriate additions of acid. Under reactor radiation and in the presence of fission-recoil particles, uranyl nitrate solutions show an additional instability. Nitrogen gas as well as nitric oxide is produced even at lower temperatures.

The compound uranyl orthophosphate is insufficiently soluble in water to be of interest. At elevated temperatures such systems disproportionate into an

* Oak Ridge National Laboratory. Including work by J. W. Boyle, J. S. Gill, E. V. Jones, F. J. Loprest, H. F. McDuffie, H. A. Mahlman, W. L. Marshall, C. H. Secoy, M. D. Silverman, H. W. Wright, Oak Ridge National Laboratory; G. M. Watson, A. and M. College of Texas.

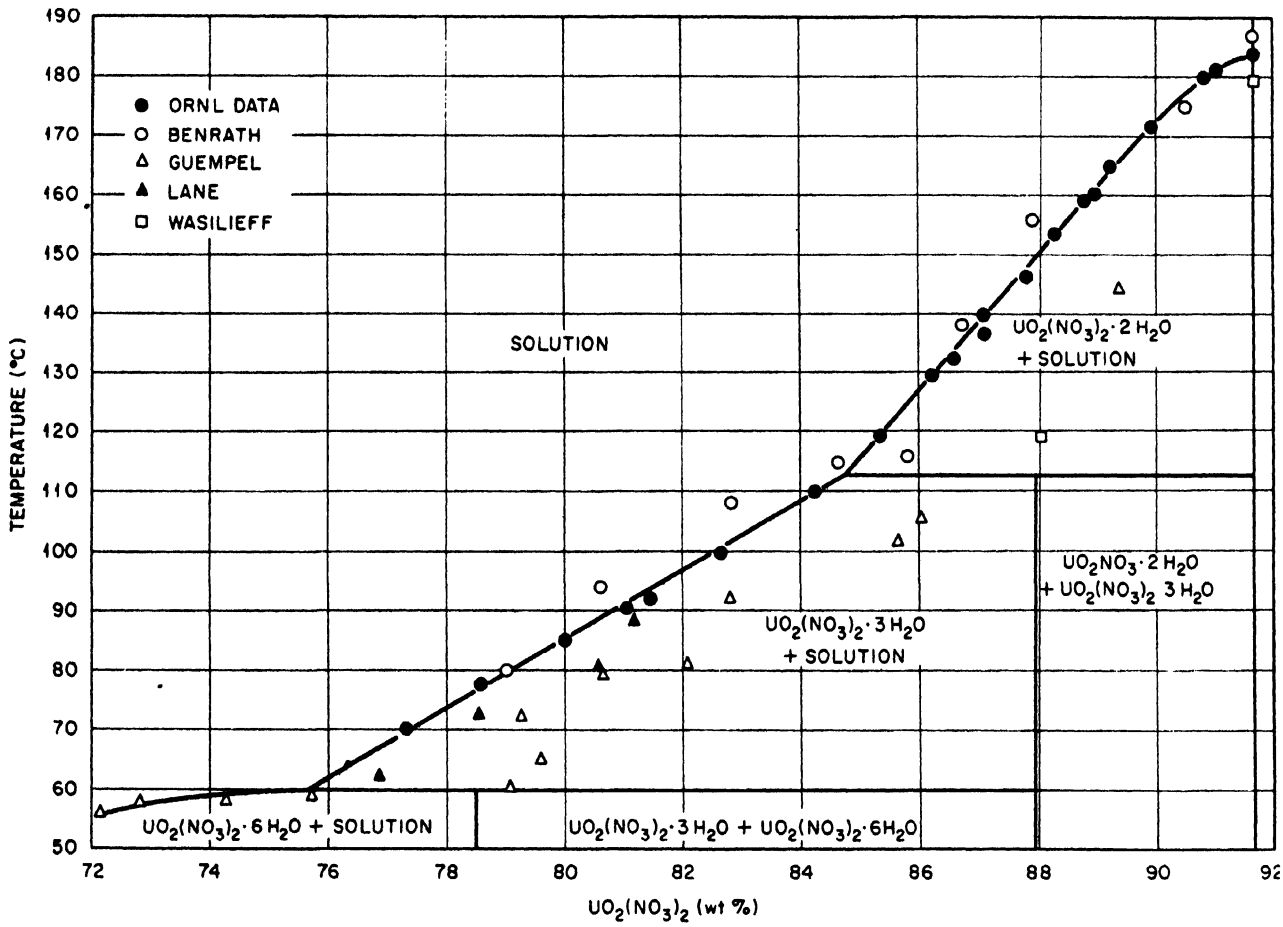

Figure 1. The solubility of $UO_2(NO_3)_2$ in H_2O

acid-rich solution in equilibrium with a basic salt. Thus by increasing the ratio of phosphate ion to uranyl ion, solutions stable to as high as 500°C and with adequate uranium content can be obtained. Such high phosphorus-to-uranium ratios detract from neutron economy and, probably more serious, the solutions are extremely corrosive to most of the desirable container metals and alloys. The phosphate ion has been shown to be adequately stable to reactor radiation.

The solubility of uranyl chromate as a function of temperature is shown graphically in Fig. 3.[2] The solubility increases rapidly from 25 to 66.3°C but is nearly invariant at higher temperatures. Here again, even though the solubility is adequate to be of interest, hydrolytic precipitation of a basic salt occurs as shown by the non-binary solid-liquid line in the diagram. Further experimentation has shown that this phenomenon may be easily avoided by the addition of excess chromic acid anhydride. In fact properly selected compositions undergo critical transformation without the appearance of a solid phase, the solute including the uranium being soluble in the supercritical fluid. However, reactor radiation has been shown to reduce hexavalent chromium to trivalent in solutions of a pH of 3 or less and the trivalent chromium is precipitated hydrolytically. Thus, for high temperature reactors, insufficient stability space appears available for safe, trouble-free operation. Further research may disclose a way around this difficulty. In so far as corrosion is concerned a few exploratory experiments have indicated that a chromatic system contained in some of the ordinary steels might be superior among those discussed here.

Uranyl fluoride is a highly soluble compound and its aqueous solutions are very attractive in so far as radiolytic stability and neutron economy are concerned. However, at elevated temperatures a different and interesting phenomenon occurs. This is the appearance of a two-liquid phase region or miscibility gap. The solubility data are shown in Fig. 4.[3] Region *K* in the figure represents unsaturated solution for the system. Line *ABCDE* is the uranyl fluoride solubility curve, transitions occurring in the solid phase at *C* and at *D*. The invariant point temperature along *GE* (333°) was fixed by liquefaction upon lowering the temperature of the solid ($\gamma UO_2F_2 \cdot 2H_2O$) which is stable above line *GE*. The region immediately above *FE* represents a two-liquid phase region. The minimum of the curve is not consolute in that the two phases involved at that point are not identical. The consolute temperature for the diagram occurs between 48.7 and 52.75%

UO_2F_2. On the left of this point in the figure the UO_3 rich phase appears as a second liquid upon raising the temperature while on the right the new phase is the water rich liquid. This fact constitutes evidence that the system is ternary and must be so depicted for complete understanding.

Solutions more dilute than approximately 25% UO_2F_2 yield a solid phase at temperatures indicated by line *JF*, well below the two-liquid phase region. This solid has been shown to be a solid solution of $UO_2(OH)_2$ and either $UO_2(OH)F{\cdot}\frac{1}{2}H_2O$ or $UO_2F_2{\cdot}H_2O$. Here, as in the previous cases, the hydrolytic instability can be prevented by enriching the system with the acidic component, HF. The only serious objection to the utilization of the fluoride system for high temperature reactor purposes is the expectation that corrosion rates would be prohibitively high. This expectation has been partially confirmed by experiment.

Uranyl sulfate is also a very soluble compound and one which has been shown to be completely stable under reactor radiation when in aqueous solution. The phase equilibria in the binary system, uranyl sulfate-water, are shown in Fig. 5.[4,5] The solubility of the stoichiometric salt remains far greater than required for a reactor fuel at all temperatures up to at least 400°C. A two-liquid phase region of somewhat greater scope than in the case of uranyl fluoride appears with solutions unsaturated with respect to the stoichiometric salt. The upper temperature limit of the two-liquid phase region is

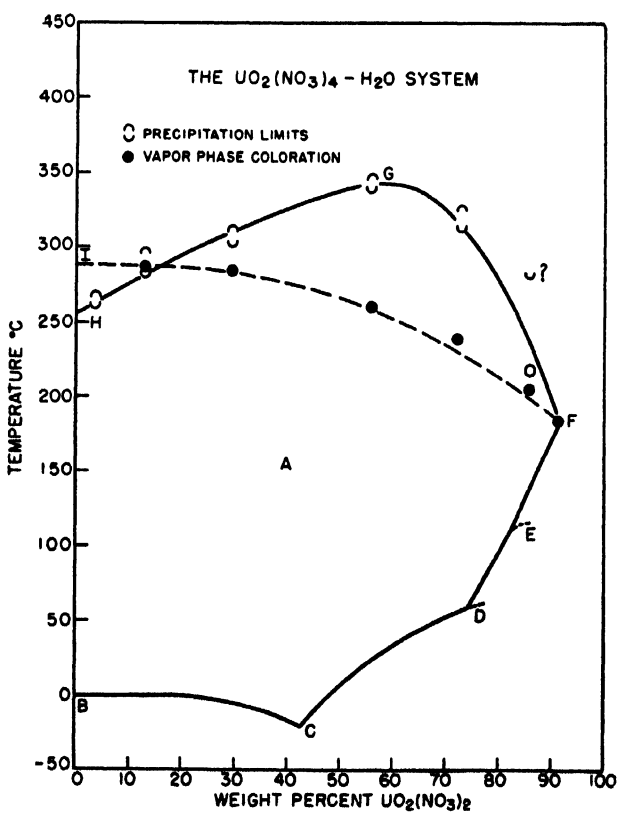

Figure 2. Thermal stability of uranyl nitrate solutions

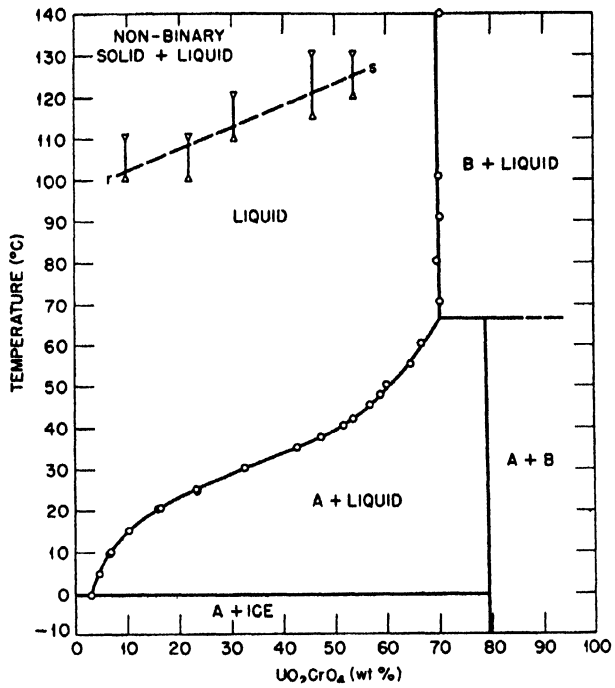

Figure 3. The system of UO_2CrO_4-H_2O

the critical temperature of the water rich phase, 374° ± 1.0°C. As in the case of uranyl fluoride the minimum temperature for the region is not consolute since the two phases are not identical. This established the fact that the region is ternary.

Studies of portions of the ternary system, UO_3-SO_3-H_2O have been made at 25, 100, 175, and 250°. Diagrams for these isotherms are shown in Fig. 6 to 9, respectively. The data on the SO_3 rich portion of Fig. 6 were calculated from the work of Colani.[6] It is evident from Fig. 6 that solutions with uranium concentrations in the range of general reactor interest are most endangered by the nearness of the UO_3 rich solubility curve. In fact as temperature is increased this curve moves to the left and, at 250° stoichiometric solutions of low concentration disproportionate into an acid rich solution and a precipitate of $UO_3{\cdot}H_2O$. If such solutions are to be used in a reactor at high temperatures the addition of sulfuric acid is necessary to maintain homogeneity. The introduction of corrosion products and fission products which contribute to the basicity of the system must also be compensated by the presence of excess acid.

Studies of the ternary system at higher temperatures at which the two-liquid phase separation may occur have not progressed sufficiently for a quantitative and complete picture to be presented. However a probably correct schematic understanding is possible. Fig. 10 presents data illustrating the effect of excess sulfuric acid on the temperature of appearance of the second liquid phase. From these curves one sees that as the sulfate to uranium mole ratio is increased the scope of the miscibility gap shrinks and the region moves to higher temperatures. Thus

it is possible to avoid the region completely by making the solution sufficiently rich in sulfuric acid. Points may be selected from the curves of Fig. 10 for the construction of isotherms in the ternary system. However, for a complete elucidation of this region, consideration of the composition of the vapor phase and of the effect of pressure is required.

Finally, we have remaining a consideration of the effects of reactor radiation on the solvent, water. The decomposition of water by fission recoil particles has been studied by several people[7] and the principal observations of concern are as follows. The primary products of the fission fragment impact are the free radicals, H and OH. These may react with each other in the fission track to produce H_2O, H_2, or H_2O_2. Therefore, the products of the forward reaction may be regarded as hydrogen molecules and hydrogen peroxide. On the other hand, the free radicals, H and OH, may escape from the fission track without interaction to react later with water molecules or other species present. These latter processes detract from the efficiency of the hydrogen and hydrogen peroxide production and, furthermore, give rise to high potentiality for the occurrence of either oxidation or reduction reactions involving the solute. For this reason ionic species capable of existence in more than one valence state are in a delicate and precarious balance in irradiated aqueous systems. This point has been illustrated by previous comments on the stability of hexavalent chromium and the observation that irradiated nitrate solutions yield nitrogen gas.

Returning to a consideration of the effects of the ultimate products of the radiolytic decomposition of water, the yields of hydrogen gas and hydrogen peroxide have been determined in several uranyl salt solutions.[8] Suffice it to say here that the yields expressed in molecules per hundred electron volts of

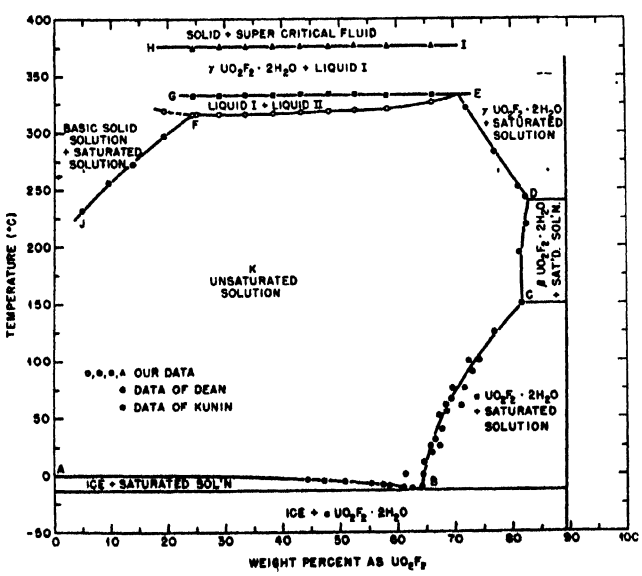

Figure 4. Phase equilibria of UO_2 and HF in stoichiometric concentrations

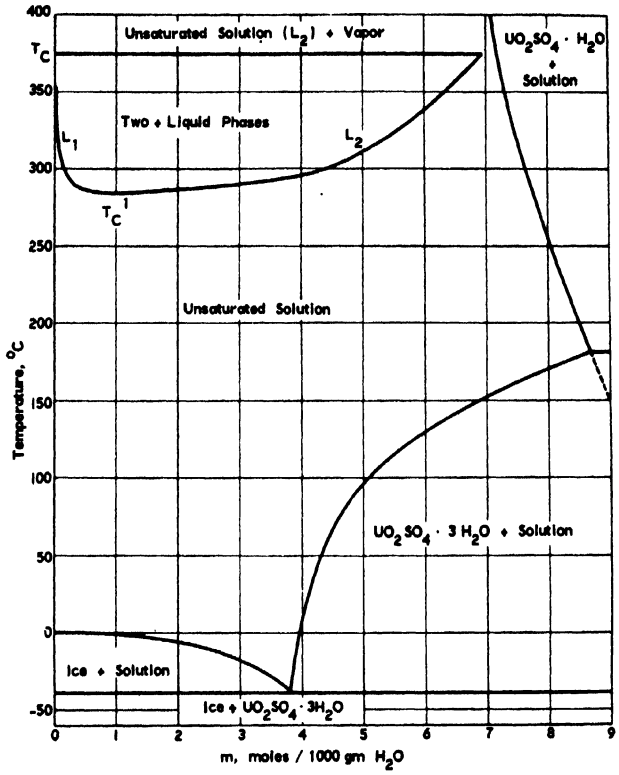

Figure 5. Phase diagram for the system uranyl sulfate-water

absorbed energy are essentially constant with temperature and vary only slightly for different uranyl salt solutions and for different uranium concentrations in moderately dilute solutions. For our purpose the yield of either hydrogen or hydrogen peroxide may be considered constant and equal to about 1.5 molecules per 100 electron volts.

Hydrogen peroxide may thermally decompose to form water and oxygen gas, or it may react with uranyl ion according to the equation,

$$UO_2^{++} + H_2O_2 = UO_4(aq) + 2H^+ \qquad (1)$$

The UO_4, being rather insoluble, may precipitate as $UO_4{\cdot}2H_2O$ if its solubility is exceeded or it may also thermally decompose according to Equations 2 and 3.

$$UO_4 = UO_3 + \tfrac{1}{2}\,O_2 \qquad (2)$$

$$UO_3 + 2H^+ = UO_2^{++} + H_2O \qquad (3)$$

Studies of the kinetics of the decomposition of peroxide in uranyl sulfate solutions have shown the rate to be first order with respect to the peroxide concentration, independent of the uranium concentration and, within limits, independent of the acidity of the solution. These studies were carried out by adding an amount of hydrogen peroxide, insufficient to precipitate uranium peroxide, to uranyl sulfate solutions and following the peroxide concentration with time. The reaction rates were determined at 53, 78, and 100°C for a variety of solutions. Figure 11 illustrates the data. The straight lines on the plot of logarithm of the peroxide concentration against time

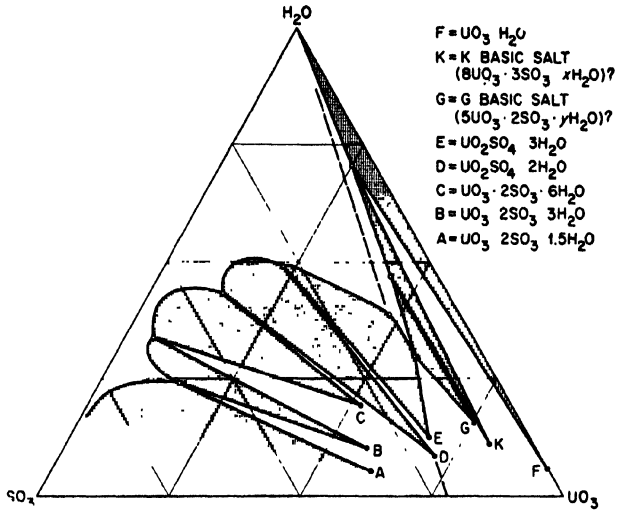

Figure 6. The system of UO_3-SO_3-H_2O at 25°C

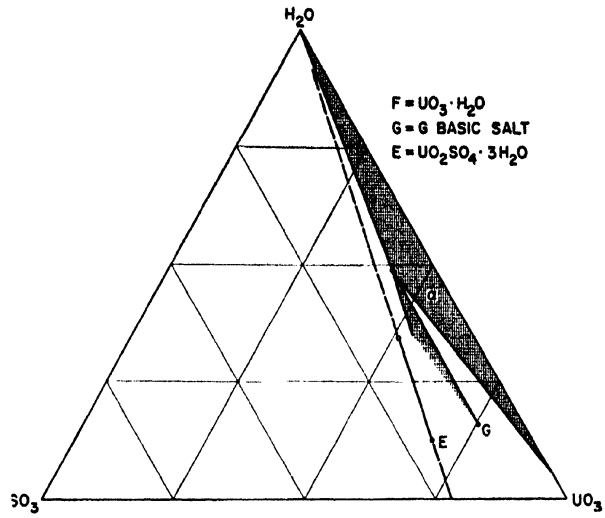

Figure 7. The system of UO_3-SO_3-H_2O at 100°C

establishes the first order dependence. Figure 12 shows the temperature dependence of the specific reaction rates for three different uranyl sulfate solutions. The slope of the lines indicates an activation energy of about 25.5 kilocalories. The fact that the three solutions gave different rate constants is attributed to differences in purity of the solutions. The pronounced catalytic effect of traces of certain ions on the decomposition of peroxide has long been known.[9] In order to test this hypothesis the effect of added ferrous ion was determined, the results being shown in Fig. 13. The presence of only a few parts per million of ferrous ion increases the rate many times.

For a specific solution at a specific temperature the decomposition rate can be expressed by the equation,

$$\frac{dC}{dt} = -kC \qquad (4)$$

in which C is the total proxide concentration in moles per liter at time, t, and k is the molar rate constant in the reciprocal of convenient time units, e.g., minutes. In the case of continuous production of peroxide, as in an operating reactor, the equation becomes,

$$\frac{dC}{dt} = K - kC \qquad (5)$$

where K is production rate and kC is decomposition rate.

In the steady state, dC/dt becomes zero and

$$K = kC_{ss} \qquad (6)$$

The production rate, K, in moles per liter per minute can be expressed in terms of the yield, G, in molecules per 100 electron volts and the average power density of the reactor, $P.D.$, in kilowatts per liter, by the equation,

$$K = 0.0052G \times P.D. \qquad (7)$$

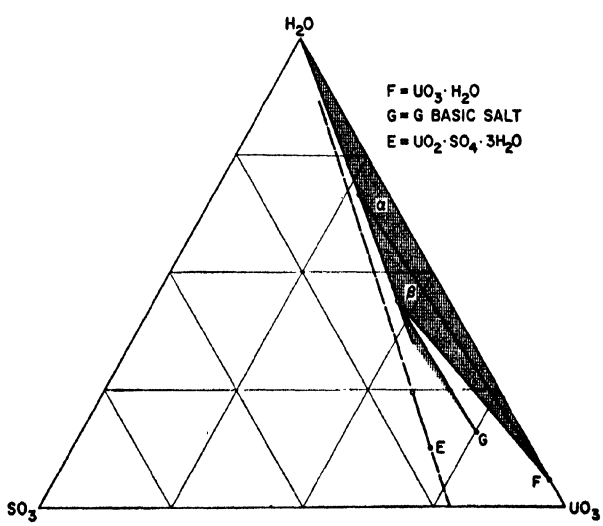

Figure 8. The system of UO_3-SO_3-H_2O at 175°C

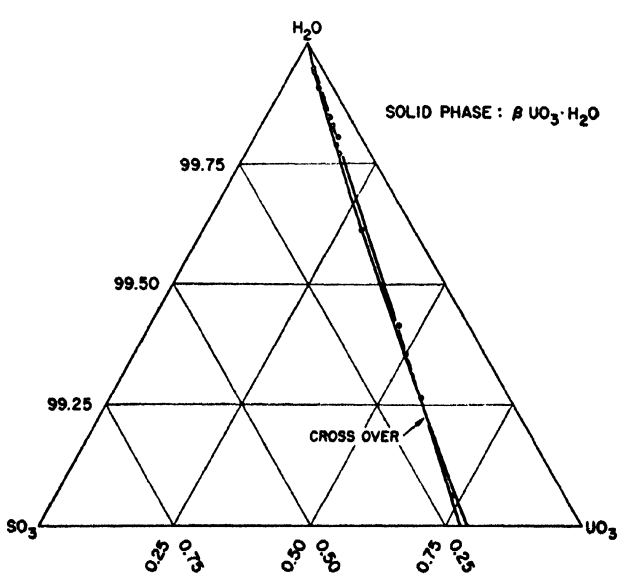

Figure 9. The system of UO_3-SO_3-H_2O at 250°C

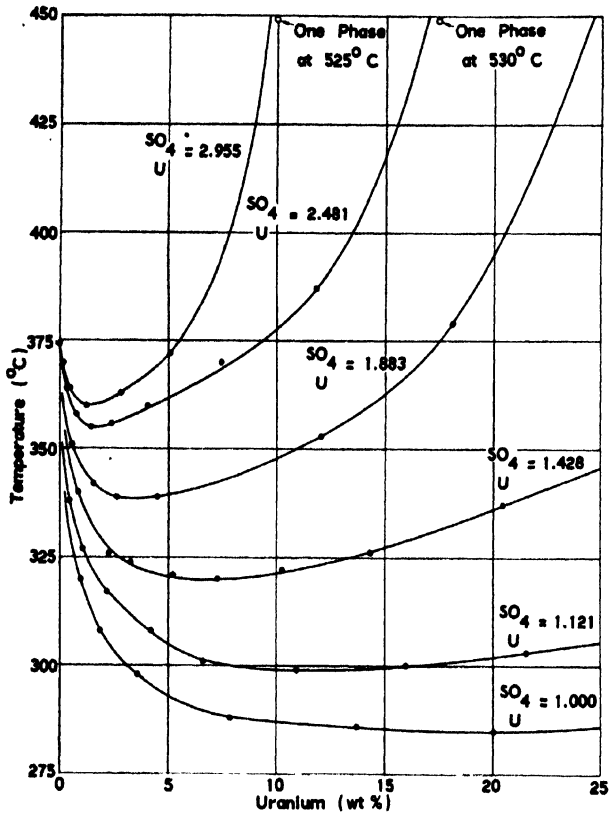

Figure 10. Coexistence curves for two liquid phases in the system UO_2SO_4-H_2SO_4-H_2O

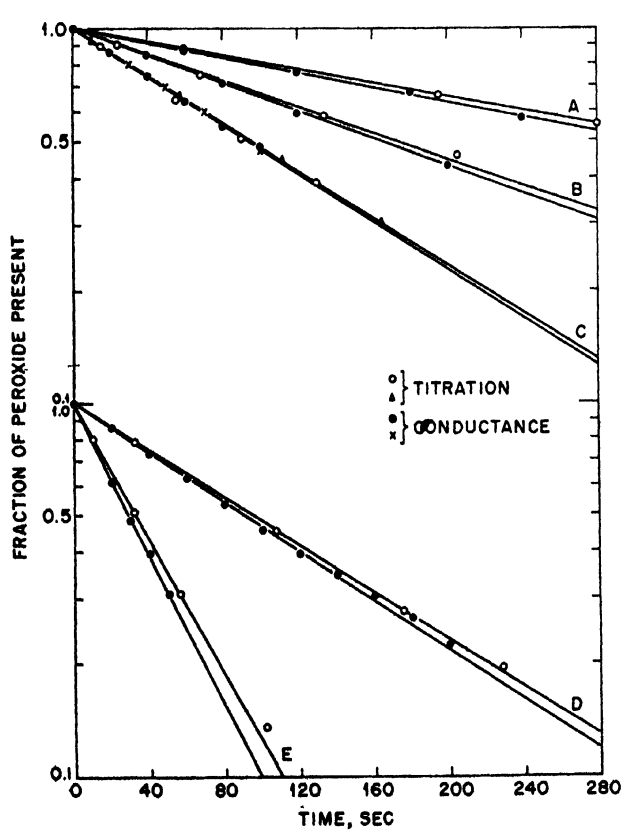

Figure 11. Correlation of chemical and conductance methods

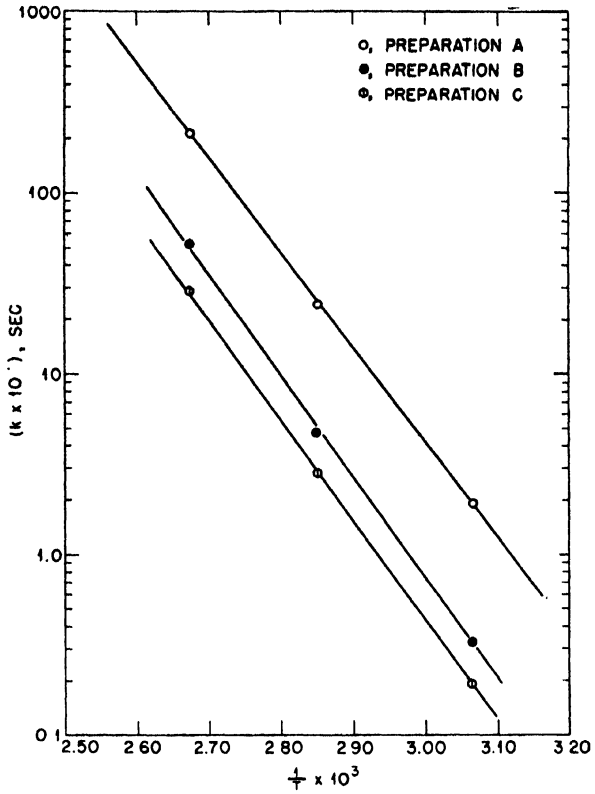

Figure 12. Peroxide decomposition as a function of temperature

Substituting in Equation 6, one obtains,

$$P.D. = \frac{kC_{ss}}{0.0052G} \qquad (8)$$

In order to avoid precipitation of uranyl peroxide in a reactor, C_{ss} must not be allowed to exceed the solubility of uranyl peroxide. Thus if one knows the decomposition rate constant, the solubility of uranyl peroxide, and the G value at a specific temperature, the maximum safe power level for the reactor at that temperature may be readily calculated. Because of the very great effect of traces of impurities on the value of k, this quantity should be experimentally determined on a sample of the actual reactor solution.

The effect of released gas, hydrogen plus a stoichiometric amount of oxygen from the peroxide decomposition, on the safety of homogeneous reactor operation has long been a matter of concern. The hazards were though to be two-fold. First, a sudden collapse of the gas bubbles and the accompanying sudden density increase might introduce an uncontrollable amount of excess reactivity. The operation of the Homogeneous Reactor Experiment at Oak Ridge has proven this a groundless fear in so far as operation at a power density comparable to the HRE is concerned. The large negative temperature coefficient of the density smoothed out steady power operation so that only very minor ripples in reactivity could be observed.

The second possible hazard was the chance that explosions of accumulated hydrogen-oxygen mixtures might occur with possible damage to the re-

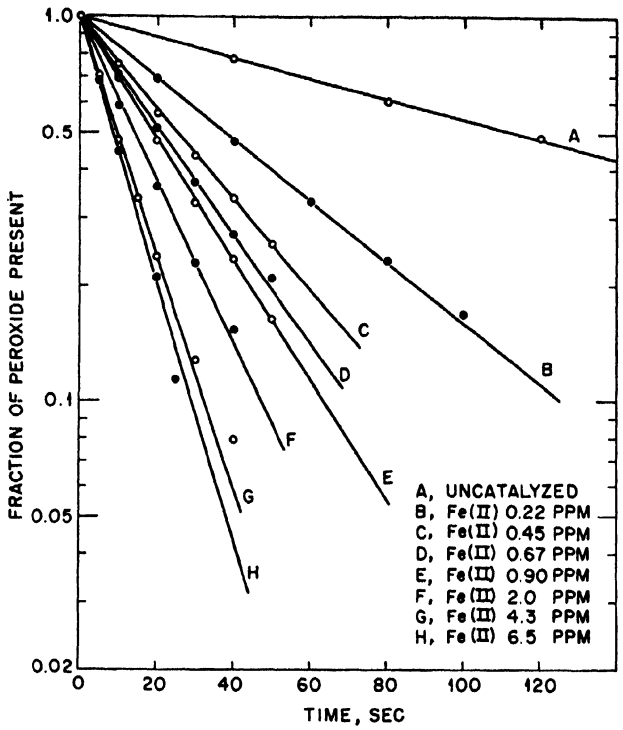

Figure 13. Catalytic effect of iron on peroxide decomposition

actor system. In the HRE this possibility was avoided by diluting the gas mixture with steam. The gas mixture was then bled to low pressure and, after condensing out the diluent steam, the hydrogen and oxygen were recombined in a hydrogen burner followed by a catalyst bed. Future engineering development will undoubtedly provide a means of controlled recombination of the gases at the pressure of the reactor.

The criteria which form the basis for a comparison of the relative merits of several aqueous homogeneous fuel systems have been presented. All of the systems discussed appear feasible for a comparatively low power reactor operated at 100°C or below. All have certain objectionable features for high power, high temperature operation. These have been pointed out. Only uranyl nitrate, in the Los Alamos Water Boiler, and uranyl sulfate, in the Oak Ridge Homogeneous Reactor Experiment, have been demonstrated by actual use in a reactor.

REFERENCES

1. Marshall, W. L., Gill, J. S. and Secoy, C. H., *The Uranyl Nitrate-Water System Above 60°*, J. Am. Chem. Soc., *73*, 1867 (1951).
2. Loprest, F. J., Marshall, W. L. and Secoy, C. H., *The System UO_2CrO_4-H_2O*, J. Am. Chem. Soc. (In press).
3. Marshall, W. L., Gill, J. S. and Secoy, C H., *Phase Equilibria of Uranium Trioxide and Aqueous Hydrofluoric Acid in Stoichiometric Concentrations*, J. Am. Chem. Soc., *76*, 4279 (1954).
4. Secoy, C. H., *The System Uranyl Sulfate-Water. I. Temperature-Concentration Relationships Below 300°*, J. Am. Chem. Soc., *70*, 3450 (1948).
5. Secoy, C. H., *The System Uranyl Sulfate-Water. II. Temperature-Concentration Relationships Above 250°*, J. Am. Chem. Soc., *72*, 3343 (1950).
6. Colani, A., *Etude du sulfate d'uranyl*, Bull. soc. chim., (4), *43*, 754 (1928).
7. Allen, A. O., Hochanadel, C. J., Ghormley, J. A. and Davis, T. W., *Decomposition of Water and Aqueous Solutions Under Mixed Fast Neutron and Gamma Radiation*, J. Phys. Chem., *56*, 575 (1952).
8. Boyle, J. W., Ghormley, J. A., Hochanadel, C. J., Kieffer, W. F. and Sworski, T. J., P/741, *The Decomposition of Water by Fission Recoil Particles*, Vol 7, Session 12B, these Proceedings.
9. Baxendale, J. H., *Decomposition of Hydrogen Peroxide by Catalysts in Homogeneous Aqueous Solutions*, Advances in Catalysis, Vol. IV, pp. 31-86, Academic Press, Inc., New York (1952).

Behavior of Heavy Water in Piles of the C.E.A.

By J. Chenouard,* G. Dirian* and E. Roth,† France

The Commissariat à l'Energie Atomique has built two heavy water piles, one at Châtillon and one at Saclay. These are known respectively as Zoé and P2. The Châtillon pile contains 1880 kg of natural uranium and 4.5 tons of heavy water. The Saclay pile contains 3 tons of natural uranium and 7.2 tons of heavy water. The maximum powers and fluxes obtained are, respectively, 150 kw and 2000 kw; 10^{12} and 8×10^{12} neutrons-cm^{-2}-sec^{-1}.

In these two piles we have carried out: (*a*) investigations on the isotopic composition of heavy water; (*b*) investigations of the gases evolved by the decomposition of the irradiated heavy water, and of their recombination; (*c*) periodical analyses for impurities.

ISOTOPIC COMPOSITION OF HEAVY WATER

The heavy water used, of Norwegian origin, has a molar composition in both piles of 99.74% D_2O ± .01%, and contains 0.22 mole % of O^{18}, instead of 0.20% as in ordinary water. The deuterium content, as monitored on samplings taken every three months at least, has not varied since the piles started up. Sampling is either by siphoning by means of a tube which goes direct into the vessel, or by aspirating at some point in the cooling circuit of the moderator.

MONITORING METHODS

Mass spectrometry is used as the reference technique and is coupled, in this concentration realm, with a technique of equilibrating the water and hydrogen. The material and methods used are similar to those described by Kirshenbaum.[1]

The drawback to this method is the dead time which elapses during the equilibration — a time set, in our laboratory, at a minimum of six hours. Thus, in spite of the sensitivity of the method and of the reproducibility of the results, the precision of which is estimated at ±0.005% in D_2O, we designed a method of analysis by absorption in the infra-red.[2]

At the moment we use two wavelength ranges:

1. That of the fundamental OH vibration at 2.98 μ, where, the molecular extinction coefficient is large. Isotopic analysis is obtained with an accuracy of ±0.01% when the thickness of the absorption cell does not exceed a few tenths of a millimeter. The detector used is a lead telluride cell, with a prism of lithium fluoride, and cell windows of quartz.

2. The region of overtone or combination frequencies, which makes it possible to measure the intensity of the combination band of HOD located at 1.66 μ. The measurement then can be carried out with simple equipment such as a glass prism spectrograph with glass absorption cells. The detector is a lead sulfide. However, the low molecular extinction coefficient in this range, requires utilization of a fairly thick cell, 1 cm approx., and limits the accuracy of the analysis to 0.1%. Utilization of an absorption thickness of 1 cm may facilitate the establishment of continuous purity control operations.

The impurities present in the heavy water may make these measurements more difficult and, in the case of the water in the Saclay pile, centrifuging or preliminary distillation is necessary, due to the presence of a suspension of aluminum hydroxide. The time for analysis of chemically clean water, including the sampling, is a few minutes.

QUANTITY OF GAS RELEASED

Case of the Châtillon Pile

The Châtillon Pile was equipped at first with uranium oxide rods and operated at a very low power, namely 3 kw, for the lack of a coolant. Under those conditions evolution of deuterium was, on the average, 1.5 liters N.T.P. per day. The elimination of the deuterium produced to avoid the formation of an explosive mixture was by purging the atmosphere of the pile with pure "R" nitrogen, as soon as the deuterium content reached 1.5% (which was very far under the explosive limit: approximately 8%). Following the replacement of the uranium oxide rods by the uranium metal rods, and the installation of a circulation system for the moderator, the production of deuterium at first increased proportionally to the pile power, which was brought up to 100 kw, then to 150 kw, and then continued to rise. It currently stands at 120 ± 15 cm^3 N.T.P. of deuterium per kwh produced by the pile instead of 20 ± 3 cm^3 per kwh under the initial conditions. Oxygen is not produced in a strictly stoichiometric proportion; at low power an oxygen deficiency of up to one-half of the theoretical amount could at times be noted. Some introduction of air, arising from the handling of the rods made it impossible to measure accurately the volume of oxygen released, but the deficiency from the stoichiometric composition requires the periodical

Original language: French.

* Stable Isotopes Section, Physical Chemistry Department of the C.E.A.

† Chief of the Stable Isotopes Section of the C.E.A.

Table I. Analyses of the Samples taken in 1954 and 1955 in the Heavy Water of the Piles

Dates	pH	Resistivity ohms/cm at 25°C	Impurities in ppm										D_2O_2 mole/l × 10^4	T μc/gm
			Al	Fe	Mg	Ni	Mn	Si	Cl^-	SO_4^{--}	N/NO_4^+	N/NO_3^-		
Pile Zoé														
18/1/54	5.5	36,700						2						
3/3/54			4		0.5	1	0.7	1						
25/5/54	4.6	24,100	2	0.5				1						
7/9/54	5.1[5]	17,000	0.5	0.5				1			<5	3		
4/11/54			1.5	1				1	12	20	2	4	3.2	3.6
18/2/54	4.5	19,400	10	0.5	0.5	0.5	0.3	1	12	25	5	6	4.6	5.2
5/5/54	3.9[5]	17,400	12	0.5	<0.3	<0.3	0.3	1	20	10		6	7	6.4
Pile P2														
29/3/54	3.3	13,800	10–15	3	0.7	1		1			<10	0.4		
22/4/54	3.4	10,800	7–8	1	0.5	1	0.3	1			4	0.2		
16/6/54	3.4	13,300	7	0.6	0.5			1						
22/6/54	3.3	13,400	7	0.6	0.5	0.5		1	22	9	7			
28/7/54	3.7	14,000	30	1	0.5	1		1						
8/9/54	3.7	13,400	20	0.5	0.5			1			5–10			
15/10/54	3.4	9600	140	1	1	1	0.5	1	15	13	5	4	1.2	15.3
8/2/55	3.4	8200	180	0.5	1	0.3	1	1	14	22	5	14	7.1	26
6/5/55	3.6	7400	280	1	5	0.5	≤0.3	1	30	12	5–10	9	8.6	39.5

Remarks: Concentration differences were noted in the heavy water located at various points along the pipes. Thus, variations which seem to be haphazard may take place in the contents observed as time goes by, which are due to the movements of water in the meantime. The moderator of Zoé circulates in temperature exchangers, that of P2 does not. In the water of P2, the presence of the hydrated alumina suspension causes the analyses made on the samples not to be very representative.

injection of small quantities of the gas in order to burn off excess deuterium.

The deuterium evolved has an isotopic composition different from that of the water in the pile. Hydrogen is preferentially released and the separation factor α, as measured, is 1.7.‡ It compares well, in order of magnitude, with the figure of 1.9 determined for the gas released by the action of X or γ rays on dilute solutions of heavy water in ordinary water.[3] The difference between the two figures may be due to errors introduced into our measurements by the uncertainty of the quantity of heavy water vapor entrained with the decomposition gases. The concentration of the deuterium released has been measured on the Châtillon pile following recombination with oxygen; the water produced, analyzing at 99.56%, is enriched by a small amount of the entrained vapor and has a composition which is essentially 99.74% D_2O. The correction needed in order to make allowance for this entrainment is not known exactly for the conditions under which we operate. Experiments carried out on the Saclay pile on the removal of entrained water vapor also gave a value of 99.56%. It might also be that deuterium and hydrogen are first produced in quantities proportional to their concentration in the liquid phase, and that the effect observed is due, in the first place, to the establishment of the equilibrium $D_2 + HDO \rightleftarrows HD + D_2O$, the constant of which is 3.11 at 25°C, and 2.78 at 50°C. The difference between the factor 1.7, as observed by us, and that of Weiss and his group, would then be due to a difference in the progress of this reaction. Other phenomena may come into play in this complicated isotopic effect: difference in the binding energies O–D and O–H, difference between the neutron capture cross section of H and D, etc.

‡ $\alpha = \left(\frac{H}{D}\right)_{gas} / \left(\frac{H}{D}\right)_{water}$

Case of the Saclay Pile

In this reactor, it took the gas release a certain time to become well established. Several months of low power operation then elapsed, corresponding to the production of 17,800 kwh before the first traces of deuterium appeared. Subsequently, after 300,000 kwh, the rate of evolution increased until it reached 8 cm^3 per kwh at a power of 1050 kw. At this point, following an incident, a certain quantity of oil contaminated the water in P2, and the gas release stopped completely. After purification of the water, as the reactor power increased, the amount of deuterium released increased progressively until it reached 120 cm^3 per kwh per day, where it remained stable. The energy produced during this period was 600,000 kwh.

Attention should be drawn to the fact that the amount of impurities in the liquid phase increased with deuterium production, without showing any evidence for quantitative parallelism (see Tables I and II). Observation relating to the amounts of oxygen evolved and to the isotopic composition of the deuterium are the same as for the Châtillon pile. The oxygen which has disappeared is probably used, in both cases, to oxidize the walls of the heavy water vessel, the rod cladding, and impurities in water.

It was observed in both piles, that the amount of gas released decreased with decreasing power and ceased with it. If, following a shut-down, the heavy water level is altered, for instance by the transfer of a fraction of the moderator present in the pile to

Table II. Production of Deuterium in the C.E.A. Piles

Date	Production of D_2 in cm^3 N.T.P per hour, per kw	Power in kw	Power delivered by the reactor since startup, in megowatt/hour
	Zoë		
May 1953	20	3	96
	Transformation of the reactor: uranium oxide rods replaced by metallic uranium rods; circulation of the heavy water started		
February 1954	21	0 to 150	194
April	45	100	240
May	52	1	273
June 1st	65	1	290
June 15	76	1	300
July 15	90	1	315
September	120±15	1	355
From January 1955 to June 1955	120	1	470 and beyond

		P2		
Date	D_2 production	Power in kw	Total power in Mwh	Observations
17/12/52 to 27/9/53	0	200 to 1000	18	
28/9/53 to 30/9/53	0.5	850	60	
30/9/53 to 1/10/53	0.7	850	80	
1/10/53 to 2/10/53	1.3	850	100	
2/10/53	4.5	850	110	
3/10/53	6	850	120	
23/10/53	6.25	800	199	
20/11/53	7	750	282	
18/1/54	9	1050	294	
				Pollution (oil)
19/1/54 to 20/1/54	3.7	1050	350	
22/1/54	1	1050	400	
23/1/54	0.7	1050	590	
14/3/54 to 22/3/54	0.05	1050	650	
	0	750	706	
				Heavy water purification
5/7/54 to 10/7/54	0	1100	881	
14/9/54	5	1000	886	
17/9/54	16	1400	926	
19/9/54	30	1400	1026	
19/9/54	42	1400	1040	
27/9/54	70	1400	1240	
4/10/54	70	1400	1430	
11/10/54	80	1400	1660	
25/10/54	120+10	1600	1903	
8/11/54	120+10	1500	2024	
From 8/11/55 to 1/6/55	120+10	≤2100	5300 and beyond	

the storage tank, this displacement of heavy water causes a release of dissolved gases. The maximum amount of the oxygen-deuterium mixture which can then be collected is about 2% of the moderator volume measured at N.T.P. If the pile is started up again following a sufficiently lengthy shut-down (several days) or again if the shut-down is accompanied by heavy water transfer, the gas release only attains its normal value once the moderator again becomes saturated with deuterium and with oxygen.

RECOMBINATION INSTALLATIONS

They were set up on the Saclay pile as soon as it was built, but on the Châtillon reactor, only when its power was increased. At Saclay, for safety reasons, recombination may be carried out, as desired by one or the other of two units mounted in parallel. The maximum processing capacity is 300 liters per hour of a stoichiometric mixture of deuterium and oxygen, diluted with nitrogen.

Recombination takes place by catalysis on palladium deposited on anhydrous alumina. The palladium content is 0.5% by weight. Platinum, which has often been used as a catalyst for the recombination of the explosive gas, appeared to us as being less active than palladium would be for the purposes of this recombination.

The catalyst acts at 30°C in a water vapor saturated atmosphere, and therefore requires pre-

heating in order to start the reaction which thereafter automatically maintains the temperature when the deuterium content of the gas is sufficiently high. In order to avoid deterioration of the catalyst, one should not allow the deuterium content to go beyond 4%, which would bring up the catalyst temperature to about 350°C. Under normal operating conditions it never exceeds 1%. Each one of the catalyst containers holds 12 liters of the catalyst and the spatial speed of the gases is approximately 3500. Prior to initiating the reaction, the catalyst is carefully treated with deuterium by exchange with heavy water vapor carried by a current of an inert gas. The only incident observed during operation was the deactivation of a charge of the catalyst, the palladium of which had been partially stripped from its carrier, probably by the heavy water carried along with the gases, which is slightly acid.

The deuterium content is estimated before and after passing the gas over the catalyst by means of thermal conductivity measurements using tungsten filaments, which are made very insensitive to variations in the water vapor content of the gas by an electrical device. The absolute precision of the measurements is $\pm$ 0.015%.§

The oxygen is measured with a magnetic susceptibility apparatus made under an O.N.E.R.A. license, which can detect 0.01% oxygen.

The readings obtained by the measuring devices are continuously recorded. Measurement of deuterium or oxygen dosage by the heating up of a catalyst has been given up: the catalysts used do not give sufficiently accurate results in the presence of large amounts of water vapor.

IMPURITIES

For each sample, the impurities are estimated semiquantitatively spectroscopically. The values obtained for some elements (aluminum, carbon, etc.) are confirmed by chemical methods; the conductivity and pH are measured, as well as the D_2O_2 content.

Tables I and II sum up for each pile the changes in the impurity contents and characteristic amounts. The amount of hydrated alumina is sufficiently large for an abundant milky suspension to be observed in the water of the Saclay reactor. Silicon, which was verified to be of normal isotopic composition, may arise from the silica gel dust brought into the lattice during drying. Iron, nickel and chromium are constituents of some parts of the stainless steel circuits. The ammonium and nitrate ions are probably produced by synthesis under the action of radiation, from either the nitrogen dissolved in the water, or that present in the atmosphere above the water and subsequently go into solution. This last hypothesis seems much more likely.[4] The Cl^- and SO_4^{--} ions are most likely due to accidental pollutions. The heavy concentration of anions accounts for the low pH and the low resistivities measured. In addition to the impurities measured spectrographically and by chemical methods, determinations of the half-lives and the energies of the activities observed in the heavy water of the Saclay pile show: magnesium with a 10-minute half-life; chromium with a half-life of 26.5 days, phosphorus 14.3 days, and sulfur 87.1 days.

To these activities, due to chemical impurities, let us add those pertaining to isotopes of oxygen and hydrogen. They are low average life activities, except for carbon-14 produced by the (n,α) reaction on oxygen-17, and for tritium produced by the (n,γ) reaction on deuterium. Carbon-14 was not looked for in our samples. In fact, it could also have been produced by the (n,p) reaction on dissolved nitrogen-14.[5] Tritium assays were computed with reference to standards supplied by Harwell. The contents mentioned in Table I are in good agreement with the evaluations made at first.

PRECAUTIONS AND REMEDIES AGAINST THE IMPURITIES

At first, the impurity most feared in heavy water was light water, and the dehydrating precautions taken are exceptionally stringent before heavy water is introduced into lattices which have been subjected to tightness tests with light water. Drying is achieved by circulation of "R" nitrogen¶ passed over silica gel charges which are regenerated several times during the operation, and controlled by special humidity monitoring devices of the thermal conductivity type.** Dehydration was stopped once the humidity content in the nitrogen fell below 0.02%. The total slight residual humidity, remaining in the reactor was estimated at 30 grams of water.

Experience shows that neither at the first startup nor thereafter is there any perceptible isotopic contamination. In order to avoid using non-metallic materials which contain substantial amounts of exchangeable hydrogen in contact with the heavy water, determination of light water brought in by contact with the raw materials of the gaskets, diaphragms, etc. of the heavy water circuits, was carried out under standard conditions. Table III gives a few results which place fluorocarbons, such as Teflon, at the head of the list of usable plastics. Unfortunately their mechanical properties, and, in the zones of intense activity, their resistance to radiation, are not as good as their water tightness. The polyethylenes, while they can be submerged in heavy water without any serious drawback, could not be used as pipes intended for circulation, for they are permeable and would permit certain exchanges with atmospheric moisture to take place. The natural and artificial rubbers (Perbunan) are convenient and relatively safe to use, although far from perfect. They have to be treated with deuterium before use.

§ See Appendix I.

¶ This gas, prepared by the Air Liquide Co., contains, according to our analyses, 99.99% of nitrogen, and only traces of oxygen and/or argon.

** See Appendix II.

Table III. Quantities of Light Water Which Appear in the Heavy Water in Contact with Non-metallic Materials

	Grams of H_2O per 100 gm of material	*Milligrams of H_2O per cm² of contact surface*	*Observations*
Polythene	0.2	0.0_6	Cleaning and drying of the materials under study are conducted under standard conditions, so that the results be comparable. Temperature, during exchange, is maintained at 25°C. Duration of contact, in every case, is greater than 10 days
Teflon	0.2	0.3	
Perbunan	0.5	0.5_4	
Chloroprene	0.4	0.7	
Natural rubber*	1.2	1.7	
Nylon	3	1.7	
Nylon treated with silicone oil	1.6_5	0.6	
Asbestos treated with Bakelite (Ferrodo)*	8–12	21	
Aradilte F*	3.6	2.1	
Aradilte-treated graphite*	3 6		

* Investigation stopped while the rate of water release still was appreciable.

The conventional remedies, in the presence of the other impurities, are distillation and ionic exchange.[6] We used certrifugation with good results for the purpose of rapidly separating small quantities of oil and water from P2. The alumina content was also reduced by this operation.

Preparations are being made to start ion exchangers. More particularly, a study was made of the treatment of the resins with deuterium. This is relatively easy, since, after drying in a heater, all the resins contained less than 1% of hydrogen by weight, either in an exchangeable form or in that of adsorbed residual water.

Thus, a single heavy water rinse is enough for complete deuterium treatment.

CONCLUSION

The behavior of the heavy water in the piles of the C.E.A. show that, while maintenance of the isotopic purity is not necessarily attended with all the difficulties which were first feared, maintaining the constancy of the gas release and of the impurity content is comparatively more difficult. We hope that continuous purification of the water present in the moderators with ions exchange resins, and maintenance of the piles in an atmosphere of helium will cause the values of the pH and of the electrical conductivity to go back to those of ordinary distilled water.

We also hope this will reduce the break-down rate of heavy water under irradiation, as well as the speed of formation of hydrated alumina by reaction with the walls of the vessel and the active rods.

APPENDIX I. CONTINUOUS DETERMINATION OF DEUTERIUM IN THE ATMOSPHERE OF THE C.E.A. PILES

It is necessary to work in the gaseous phase in order not to establish a continuous leak between the atmosphere of the reactor and the outside air.

Measurement by thermal conductivity was so adapted as to enable operations to be made in a saturated atmosphere, without the need for a thermostat.

The measuring device consists of two cells, *A* and *B*, made of two cylindrical housings bored from the same block of gold plated brass or stainless steel, operating at room temperature. The compensation cell contains dry nitrogen, the measuring cell is mounted in parallel in the path of the gases to be measured, which reach it only by diffusion. This conventional circuit makes the measuring device almost insensitive to variations in the gas output.

The filaments (tungsten: 32 mm long, diameter 0.011 mm) are placed in series in a Wheatstone bridge (see Fig. 1) to which a voltage of 2.5 v (current approximately 95 ma) is applied. The other two legs of the bridge consist of resistors *R* and *S*, 25 ohms, made of manganin.

Described overleaf there are a zero setting potentiometer (*Z*), and two electrical compensation devices.

G is a recording millivoltmeter of the Leeds and Northrup Micromax type. In the absence of the compensating device, this instrument gives approximately the following readings at 20°C (6.5 mv for

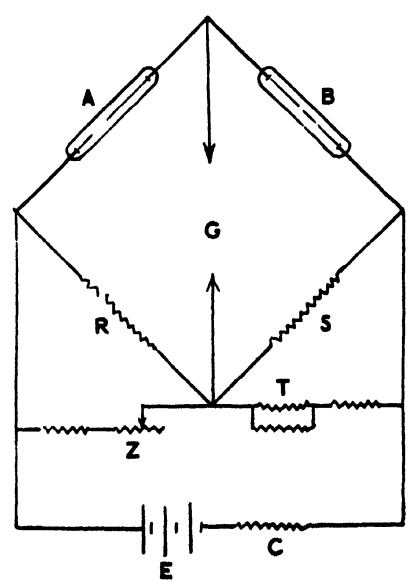

Figure 1. Deuterium measuring device; circuit diagram. A, B: Thermal conductivity cells; R, S: Secondary resistances; Z: Balancing resistance; T: Humidity compensating resistance; C: Room temperature compensating resistance; E: Constant voltage source; G: Indicator

a full scale deflection): + 2.4 mv for 1% of deuterium in the nitrogen; + 0.04 mv for 1% of oxygen in the nitrogen; + 0.5 mv for 1% of D_2O vapor in the nitrogen.

Calibration is affected by two parameters: the heavy water vapor content of the gas, which displaces the zero; the ambient temperature, variation of which alters the sensitivity of the device.

Compensation for the Effects of the Variations in the Heavy Water Content

The zero shift is not a linear function of the heavy water content. On the other hand, the same function is nearly linear at the dew point of the gas. In the vicinity of 20°C, a variation of 1°C in this temperature gives a deviation of ±0.04 mv.

On the other hand, heavy water vapor is the only component which, by variation in content, could affect the quaternary mixture to be measured. In fact, the concentration of oxygen varies parallel to that of the deuterium, except if there is an accidental entry of air or a substantial lack of oxygen due to the non-stoichiometric character of the dissociation gas. Furthermore, the thermal conductivities of oxygen and nitrogen are very similar. However, the concentration of heavy water vapor is solely a function of the temperature at the coldest point in the gas circuit. The effect of temperature variation is compensated for in the readings, which are linear, by connecting in parallel with resistor S, a thermosensitive resistor which functions over the cold spot. In our case, this point is at room temperature. The thermosensitive resistor consists of a nickel wire winding (temperature coefficient of resistivity: 0.006). The $(S + T)$ group is adjusted in order to get a temperature coefficient of 6.4×10^{-5}. The instrument used for measurements will then be practically insensitive to the variations in the heavy water vapor content.

Compensation for the Effect of the Variations in the Room Temperature

If the measuring bridge is energized at a fixed voltage of 2.5 v, the sensitivity of the device used for measurement decreases by 1.2% as the temperature of the medium goes up 1°C.

This variation in sensitivity is essentially due to a change in the power dissipated in the filaments, the resistance of which varies with the temperature (Joule effect).

Now, calculations show that one may stabilize the power dissipated from a filament fed by a fixed voltage, with respect to small variations in its resistance by connecting, in series with it, a fixed resistance of the same rating.

In actual practice, we use a 6 v voltage supply from a storage battery to feed a manganin resistance C (37 ohms) and the bridge across whose terminals there is a residual voltage of 2.5 v. The variation in the sensitivity of the measuring device is then reduced to 0.1% °C of variation in the ambient temperature.

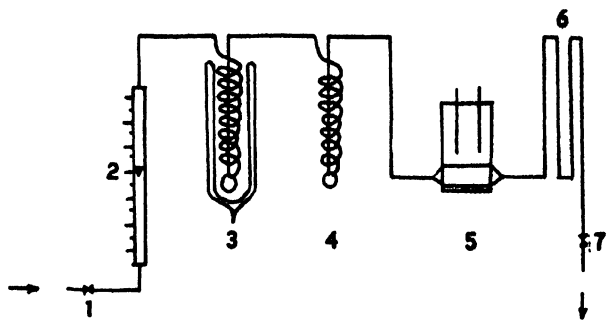

Figure 2. Moisture measuring arrangement: (1) feed control needle valve; (2) flowmeter; (3) drying coil; (4) reheating coil; (5) measuring cell; (6) outlet tube; (7) efflux needle vale

With these two compensating devices, it is possible to observe a volume concentration of 2×10^{-4} deuterium, and to measure those of the order of 10^{-2} with an accuracy of ± 2%, independently from variations in the output or humidity of the gases.

APPENDIX II: MEASUREMENT OF THE HUMIDITY

This depends on measurements of thermal conductivity (see Fig. 2). The cell block, similar to that used for the measurement of deuterium, is connected to a Wheatstone bridge directly energized by 6 v. Unbalance of the bridge is detected with a galvanometer having a sensitivity of 10^{-8} amp/mm, and an internal resistance of 96 ohms.

By observing these precautions, it is possible to observe, with a measure of certainty, the presence of water vapor of 2×10^{-5} by volume namely 1.5×10^{-2} gm per cubic meter, corresponding to a dew point of — 55°C. Concentrations of some 5×10^{-4} may be determined to ± 4%. The calibration curve is practically linear for gas content, in water vapor, from between the minimum and 1/1000.

In order to obtain the high sensitivity sought, a few units of 10^{-5} of vapor in the gas, the following precautions are necessary:

(*a*) The gas output, between 7 ml and 20 ml/sec, must be stable within ± 5%.

(*b*) A drift of the instrument zero, no matter how slight, rules out direct measurements with any sort of accuracy, since some 20 minutes elapse between consecutive measurements and the zero may drift by a quantity equivalent to the reading of a volumetric content of 2×10^{-5} water vapor. In order to solve the problem, the measurements are made differential by periodically drying the gas current in coil 3 (see Fig. 2) by means of a bath at 80°C. The gas is brought to room temperature within 1° (coil 4) before being passed through the measuring cell. Stability of the readings is achieved only 10 minutes after a change in the operational conditions.

(*c*) Where the gases escape to the free air after crossing the cell, a small cross section tube (6) makes it possible, thanks to the great linear speed of the gas current, to avoid back scattering of the atmospheric vapor which would interfere with the measurement of very dry gases.

(*d*) Apart from the measuring periods, the device must be kept shielded from atmospheric water: if not, it will work well only after flushing for several hours with dry gas.

REFERENCES

1. Kirshenbaum, I., *Physical Properties and Analysis of Heavy Water,* McGraw-Hill Book Co., Inc., New York (1951).
2. Lecomte, J., Ceccaldi, M. and Roth, E., *Dosage Isotopique de l'Eau par Mesure d'Absorption dans l'Infra-rouge,* Journal de Physique le Radium, *15,* 543–544 (1954).
Gaunt, J., *The Determination of Deuterium Oxide by Infrared Spectrometry.* The Analyst, *79,* pp. 529–592 (1954).
3. Kelly, P., Rigg, T. and Weiss, J., *Isotopic Composition of the Hydrogen Produced by the Action of Ionizing Radiations on Aqueous Solutions Enriched with Heavy Water,* Chemistry and Industry, *42,* 1291 (1954).
4. Primak, W. and Fuchs, L. M., *Nitrogen Fixation in a Nuclear Reactor,* Nucleonics, *13,* 38 (1955).
5. Barendregt, T. J. and Brakstad, K. H., *Corrosion and Impurities in the Heavy Water System of the Dutch-Norwegian reactor.* Chemical Engineering Progress, Symposium Series, *50,* 183 (1954).
6. Sivetz, M. and Scheibelhut, C. H., *Application of Mixed Bed Ion Exchange to Water Purification in Nuclear Reactors, 47,* 1020 (1955); McCorkle, W. H., *Heavy Water in Nuclear Reactors.* Nucleonics, *11,* 21 (1953).

Aqueous Corrosion of Aluminum Alloys at Elevated Temperatures

By J. E. Draley and W. E. Ruther,* USA

Aluminum is potentially a valuable material for use in nuclear reactors. It has a reasonably low capture cross section for neutrons, is readily available in sufficient quantity, its expense is moderate, and methods of fabrication and handling are well developed. For water-cooled reactors its use as cladding for fuel is feasible so long as its corrosion resistance is adequate; if it is to be used also for other structural members, then its strength and rigidity must also be considered.

At temperatures below 100°C the corrosion characteristics of aluminum and its alloys are generally well known. Although there appears to be a number of factors concerning the mechanism of corrosion which have not been well explained, there is a volume of information concerning its behavior in many aqueous environments. Exposure in distilled water is almost an exception. Although the general behavior of aluminum alloys in distilled water is known, the rate of the corrosion reaction appears not to have been well measured. Consequently a small amount of information concerning corrosion rates in distilled water at ordinary temperatures is given in this report as useful background for the higher temperature corrosion data.

Several investigators have observed the rapid initial corrosion of aluminum alloys in relatively pure water, usually followed by a much slower rate of reaction. Typically, however, such investigators have described the reaction as "ceasing" subsequent to the period of rapid reaction. Thus Bryan[1] observed that high purity aluminum continued to corrode at a rapid rate in boiling distilled water, but that the addition of a small amount of silicon in the metal was sufficient to give the type of corrosion characteristic of the commercial alloys.

At temperatures above the boiling point of water there is very little information concerning the corrosion of aluminum. There have been a number of installations in which steam has been carried in aluminum pipes, and aluminum pistons have been used in steam engines at temperatures as high as 400°C. Some investigators have observed rapid disintegration of the metal above certain critical temperatures. High purity aluminum has generally been agreed to be the poorest form of the metal for withstanding the corrosive effects of water at elevated temperatures.

It appears safe to say that most of the information concerning the corrosion of aluminum at elevated temperatures has been obtained within the Atomic Energy Program. Much of the work done at Argonne National Laboratory is summarized in topical reports.[2,3,4] Work at other installations has similarly been published in project reports. Reference will be made to the most interesting of these during the course of this paper.

CORROSION BELOW 200°C

In this region of temperature aluminum alloys corrode in distilled water and most dilute solutions in a fashion which might be called normal. Penetration of the metal is essentially uniform, small "etch pits" being formed in its surface. The attack shows the initial period of rapid reaction followed by a quite low rate of reaction, apparently linear (Fig. 1).

Amounts of metal corroded were obtained by careful chemical removal of corrosion product subsequent to test exposure without significant attack of the base metal, allowing direct weighing of the metal lost. The units used for the slopes of the linear curves (the corrosion rates) are milligrams per square decimeter per day (mdd), where 1 mdd is equivalent to an average penetration rate of 1.35×10^{-3} cm/year. The "corrosion rate" in distilled water at 50°C is observed to correspond to an average penetration rate of the metal of the order of 3×10^{-5} cm/year, after the first few days of exposure.

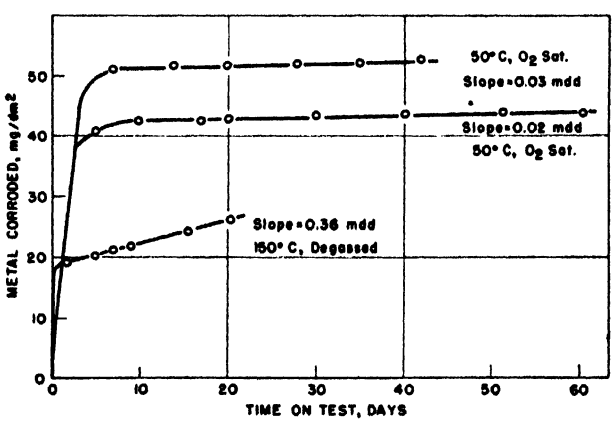

Figure 1. Corrosion of 2S aluminum in distilled water

* Argonne National Laboratory.

Table I. Nominal Compositions of Some Aluminum Alloys

Alloy designation	(Weight per cent) Copper	Silicon	Manganese	Magnesium	Nickel	Chromium	Zinc
2S (1100)*	(Minimum aluminum 99%)						
18S (2018)	4.0			0.6	2.0		
318S (2218)	4.0			1.5	2.0		
24S (2024)	4.5		0.6	1.5			
52S (5052)				2.5		0.25	
61S (6061)	0.25	0.6		1.0		0.25	
63S (6063)		0.4		0.7			
72S (7072)							1.0
75S (7075)	1.6			2.5		0.3	5.6
122	10.0			0.2			
A132	0.8	12.0		1.2	2.5		
142	4.0			1.5	2.0		
B195	4.5	2.5					
355	1.3	5.0		0.5			
356		7.0		0.3			

* Aluminum Alloy Assoc. new designation system given in parentheses.

The pH of the solution considerably influences the rate of corrosion of 2S aluminum. The pH of minimum corrosion appears to be that at which the solubility of the corrosion product is minimum.[2,5] At ordinary temperatures this is in the vicinity of 6.5. As the temperature is increased above 100°C, the pH of minimum corrosion appears to go down in much the same fashion as the concentration of the hydroxide ion goes up due to increased ionization of the water. The rate of corrosion of the metal is sensitive to the flow rate of solution past the metal surface at pH above that of minimum corrosion rate. Near the pH of minimum corrosion rate there is little effect of solution flow rate on the corrosion behavior. These factors are described in more detail in references 2 and 3, as well as the effects of several other variables of interest.

The dependence of corrosion rate of 2S aluminum† on temperature is shown in Fig. 2. In some instances it is likely that corrosion rates were not accurately determined. At the lowest temperatures, the rates were quite small and errors in weighing and removing corrosion product are significant. At temperatures above 100°C, samples were generally not stripped of corrosion product until the termination of the tests. Estimates of behavior during the tests are subject to error.

The discontinuous nature of the curve for distilled water is probably caused by a change in the structure of the corrosion product occurring in the vicinity of 100°C. Below that temperature it is Bayerite (β $Al_2O_3 \cdot 3H_2O$). At temperatures above 100°C it has been observed to be Boehmite (α $Al_2O_3 \cdot H_2O$). Corrosion rates in dilute sulfuric acid are seen to be consistently lower than those for distilled water except at the lowest temperature; they are generally higher in slightly alkaline solution. From work at lower temperatures it is quite probable that the latter difference would be accentuated by rapid flow of solution past metal surface. All data shown are from stagnant systems with no significant flow of solution past samples.

These corrosion rates have been corroborated by other experimenters. Link[6] observed corrosion in high purity water at temperatures up to 150°C to be essentially the same as that leading to the data of Fig. 2. He was unable to derive satisfactory corrosion rate curves due to difficulty in removing the corrosion product film without simultaneously dissolving significant quantities of the base metal. Since his tests were run at flow velocities up to 25 ft/second (7.6 meters/sec), it is indicated that at temperatures up to about 150°C very little effect of this variable is demonstrated in pure water. Strom and Boyer[7] and Strom, Boyer and Litz[8] obtained approximately the same corrosion rates as are shown in Fig. 2 for alloys 24S, 61S, 52S, and some Al-clad pieces (pure aluminum on 24S, and 72S on 75S). Atwood[9] has obtained corrosion rates for 2S aluminum in distilled water in the vicinity of 180°C which appear to be

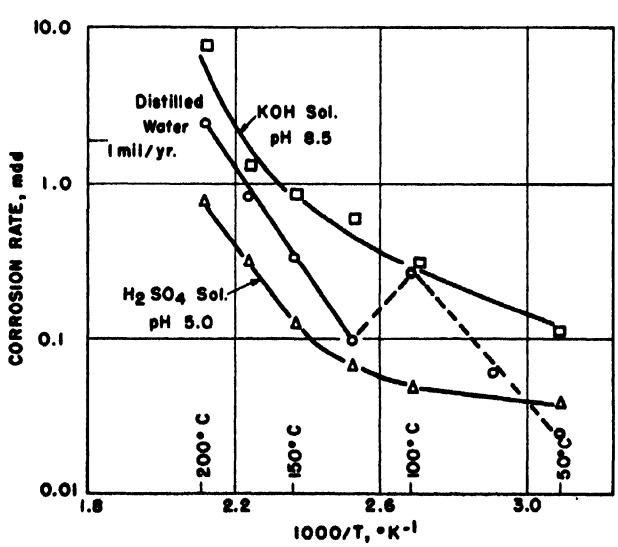

Figure 2. Aqueous corrosion of 2S aluminum

† Nominal compositions of American aluminum alloys to which reference is made are given in Table I.

higher than those of the curve in Fig. 2 by a factor of the order of 5. Flow rates in these tests were approximately 25 ft/sec (7.6 meters/sec). It does not seem possible to presume that these results are typical since there is some question whether occasional contamination of the distilled water occurred during the tests.

Crevice Effects

In some instances there has been observed an increased amount of corrosion in the crevices formed by close juxtaposition of aluminum samples. This effect has occurred even in water of high purity. The effect has been significantly worse where aluminum has been coupled to cathodic materials such as stainless steel or graphite. Experiments run at room temperature, at 100°C and 200°C showed considerable localized attack in the crevice on 2S aluminum coupled to graphite, both at room temperature and at 100°C. Exposures were 108 and 116 days. At 200°C no such harmful "crevice effect" was observed. 2S aluminum was also coupled with zirconium and with 63S–T aluminum in distilled water at 115 and 200°C. No effects of the coupling could be discerned. The effect did not occur at 50°C when the water contained 5×10^{-5} *M* hydrogen peroxide, both in Al/graphite and Al/stainless steel (18 Cr–8 Ni) couples. Analogy with observed corrosion of systems in which the metal surface area to solution volume ratio was quite large suggests the explanation that the water within the crevice did not remain of high quality during test (where the surface to volume ratio was large, the solution became alkaline, reaching a pH of about 8.5 in five days). This alkalinity would then reduce the resistance of the aluminum to anodic attack in those areas. In all galvanic couples the aluminum surface, where in free contact with distilled water, showed no unusual or heavy corrosive attack. The same galvanic crevice-accelerated corrosion of 2S coupled to stainless steel was noted by Nielson[10] in distilled water at 100°C.

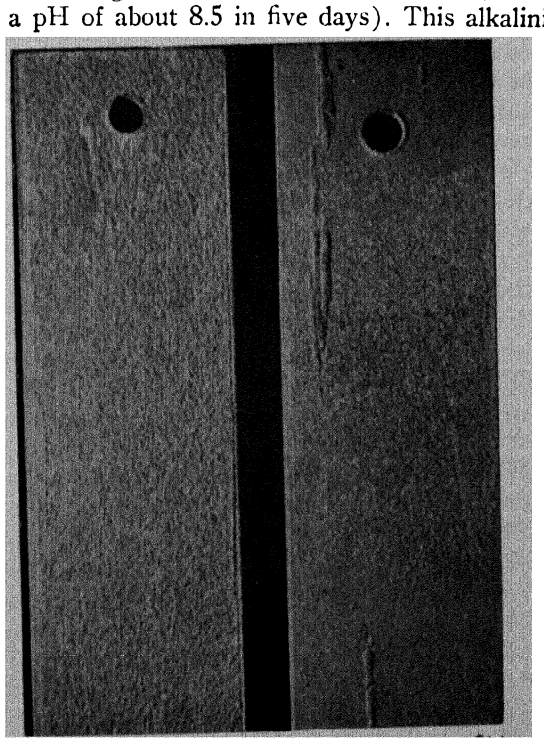

15,717 2×

Figure 3. Typical appearance of 2S aluminum after about two weeks in distilled water at 275°C

The magnitude of the problem of crevice corrosion at elevated temperatures is unknown. It appears to be considerably less a problem than below 100°. Nevertheless it is a subject worthy of investigation if it is desired to use aluminum in such environments.

CORROSION ABOVE 200°C

After a period of apparently "normal" corrosion, samples begin to show blisters forming on the surface as shown in Fig. 3, the attack apparently beginning at stringers and at grain boundaries. As testing time is increased these blisters grow larger, the surface roughens, and a type of attack proceeds in which the metal is penetrated much more rapidly, producing as product, mixtures of metal and oxide. At high temperatures, this type of attack occurs quite rapidly; samples of rolled 2S aluminum have completely disintegrated to oxide corrosion product in 4 hours exposure to distilled water at 315°C.

The time required to show this kind of penetrating attack has been observed to vary with the aluminum alloy used, with the mechanical treatment of the samples, and with the pH of the water. In general, these effects are qualitative only; that is, for most aluminum alloys the blistering attack always takes place at temperatures significantly above 200°C. The rate of the attack subsequent to blistering can be somewhat altered, and the time prior to its inception can be varied.

A large number of commercial aluminum alloys have been investigated.[11] Certain alloys show considerably greater resistance to the effect than 2S aluminum, including B195, 356, 142, Al-Si eutectic, 355, 122, A132, 24S, 18S.

It was observed that the harmful blistering attack and the subsequent rapid disintegration of the metal could be strikingly retarded or prevented by passage of an electric current to the sample such as to make it more anodic. Coupling to stainless steel or to zirconium reduced very considerably the nature of the attack. Direct passage of electric current from an external source similarly caused improvement. Even the most susceptible material, high purity aluminum, showed striking improvement at 250°C. The photograph in Fig. 4 shows the samples. In the steam phase anodic protection was not possible. In the liquid phase blister corrosion of the anode was almost prevented; the cathode corroded somewhat more than areas in the steam.

It is now believed that the explanation for the damaging attack of aluminum at elevated temperatures is that some of the hydrogen atoms produced in the corrosion reaction diffuse into the metal structure, mostly at structural defects, and, upon

combination to form molecular hydrogen, produce pressure pockets in small voids in the metal. As the weak metal yields, these pressure pockets cause the formation of blisters which subsequently rupture and let the water in. This produces new hydrogen, and the process is self accelerating. If the explanation is correct, two means of preventing the attack should be effective: (1) provision of cathode sites for the liberation of hydrogen so that hydrogen atoms will not be available to the aluminum metal surface, and (2) by making the aluminum impermeable to hydrogen diffusion. The latter method is perhaps impractical for 2S aluminum, although carefully vacuum cast metal does not appear to be susceptible to the blistering attack, as shown in Fig. 5. This is a sample of 2S aluminum which was carefully vacuum melted in an alundum crucible and then slowly cooled while still evacuated. It was exposed to distilled water for a total of 30 days at 300°C. Grain boundary areas appear to be delineated. The small pits noticed show rust color stains and are presumed to have resulted from the preferential corrosion of the iron-rich phase precipitated at grain boundaries. Unfortunately metal of this sort does not retain its apparent freedom from blistering attack when it is worked. Metal which was compressed in a tensile testing machine and metal which was cold rolled

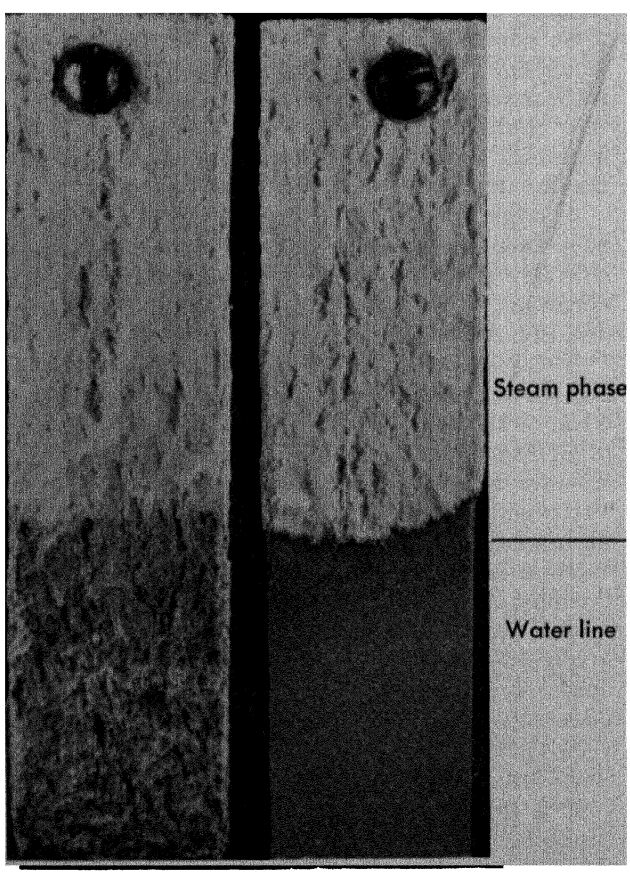

15,530 Cathode Anode 1.6×

Figure 4. High purity aluminum electrodes after 2 hours at 250°C in distilled water (current density 1.2ma/cm²)

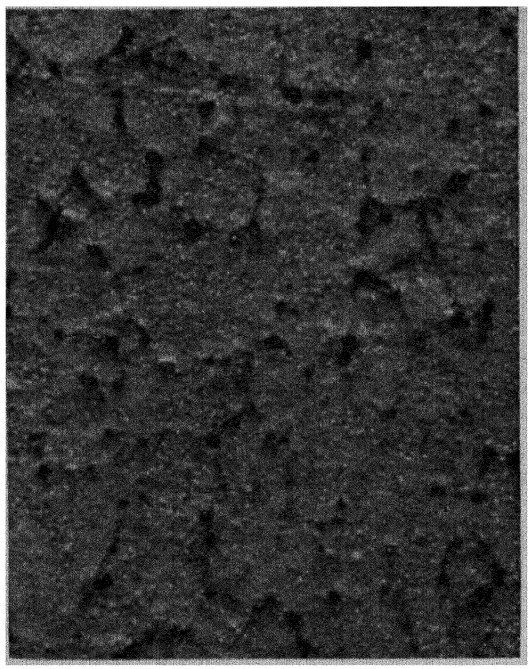

15,439 20×

Figure 5. Surface of vacuum melted 2S aluminum after 132 hours in distilled water at 300°C

completely lost resistance to this type of attack. Annealing in air or in vacuum at temperatures up to 550°C did not cause the return of the high degree of resistance to blister formation.

To provide cathode sites on the metal surface, solutions of certain reducible metal ions can be used instead of distilled water. Among reducible cations, those which produce metals of low hydrogen overvoltage are most useful. Solutions producing minimum corrosion in short tests were sulfates of cobalt, cadmium, nickel and copper. Nickel sulfate was chosen as the solute for further studies. From such solutions, nickel metal deposits at preferred cathode sites on the aluminum, as shown in Fig. 6. Presumably the hydrogen produced in the cathodic part of the corrosion reaction is liberated as a gas at these nickel dendrites. The concentration of the nickel salts required is not high: 5 parts Ni^{++} per million parts of water (by weight) appears to be sufficient to provide complete protection against blistering attack at 275°C. It is necessary to add acid to such solutions to prevent the formation of basic salts and their deposition on heated surfaces. Such acidified solutions produce excellent corrosion resistance of 2S aluminum, with respect both to the corrosion rate and the absence of blistering. In this environment however, stainless steel typically corrodes at an accelerated rate, so that it probably cannot be used. The longest test run to date was terminated after 124 days (20 parts per million Ni^{++}, as added, in a continuously refreshed autoclave) at 275°C without pH adjustment. In this instance heavy deposits of a basic nickel sulfate formed, but corrosion of the 2S aluminum samples was uniform

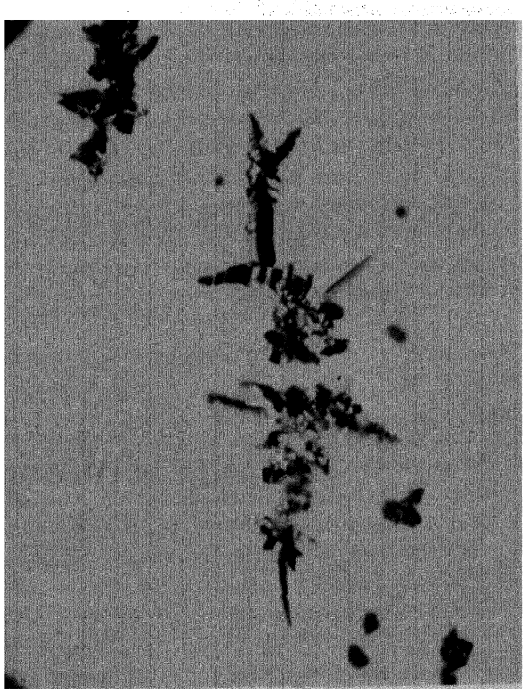

15,446 250×

Figure 6. Dendritic nickel deposited on 2S aluminum in nickel sulfate solution (50 ppm Ni^{++}) at 300°C

and moderately slow (apparently below about 20 mdd).

Instead of adding the nickel in solution, it can be applied to the surface of 2S aluminum samples. To date, samples coated with several tenths of a mil (0.0007 cm) of electroless nickel plate have withstood a loop corrosion test of over 80 days, having rapid flow of distilled water past the samples at a temperature of 315°C. One out of five samples failed. The other four have shown excellent resistance to corrosive attack, forming smooth blackened surfaces. Electroplated samples also hold up well. A six-weeks test (22 days at temperature) in a loop in which water at 260°C is recirculated past samples in the Materials Testing Reactor, however, has shown that a considerable fraction of the nickel plating was lost from the samples. It is probable that the lifetime of such plates is shorter in a neutron flux than in an ordinary corrosion test.

Aluminum-nickel alloys have been prepared in which the nickel-rich constituent appears as a second phase largely segregated at grain boundaries. Samples of these alloys show excellent resistance to blistering attack, presumably by the mechanism previously discussed. Only about 0.5% (by weight) is required for protection at 315°C and 350°C. Behavior is so good that in order to test rolled castings for quality a water temperature of 350°C has consistently been used. Many small melts of such alloys have been made at Argonne and on a sample basis by commercial suppliers such as Kaiser Aluminum Corporation and the Aluminum Company of America. Figure 7 illustrates the effect of varying nickel content while the other variables are held as constant as possible. This series of alloys was prepared by the Kaiser Aluminum Corporation. Sample appearance was good after test, with moderate smooth deposits of corrosion product forming on them. Note that the corrosion rate appears to be approximately the same for all the alloys, indicating no discernible advantage in adding more than about ½% nickel in alloys intended for use at this temperature. It is possible that long time testing might show differences not noticed in these tests. Although the weight gain curves are not reliable measurements of the actual corrosion rate, the data in Fig. 8 corroborate the estimate that very little of the corrosion product is lost from samples after the first few days on test. Data in this figure are from many castings (all tested after cold rolling) containing from about 0.5% to 2% nickel. These data must be regarded as preliminary in that small differences from casting to casting caused both by composition and mechanical preparation make quite inaccurate our estimated corrosion rates. However, these rates are probably roughly correct. Average penetration rates are:

0.0014 inch per year (0.0038 cm/yr) at 290°C;
0.0032 inch per year (0.0085 cm/yr) at 315°C;
0.009 inch per year (0.024 cm/yr) at 350°C.

Data from recirculating loops are as yet insufficient to allow estimation of corrosion rates. However, data at hand seem to indicate that in high purity water, 16 ft/sec flow rate, 315°C, corrosion of a 0.5% nickel alloy is faster than that observed in static tests. This alloy was also in the Materials Testing Reactor Loop Test at 260°C and 25 ft/sec (7.6 m/sec) water flow rate. Visual examination of the irradiated specimens did not reveal any striking difference from samples corrosion tested in autoclaves except for the rather large amount of magnetite which had deposited on samples and holders from the corrosion of the stainless steel loop components. Samples tested in the same loop outside of the irradiated zone showed corrosion which appeared to be greater than that occurring in the loops at Argonne. The factors responsible for this behavior are not known, but it is suspected that the quality of the water in the MTR

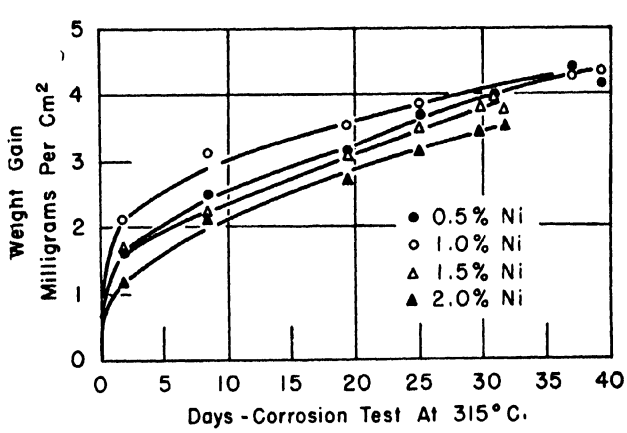

Figure 7. Effect of nickel concentration on the corrosion of nickel-2S aluminum alloys in distilled water at 315°C. (Alloys cast and rolled by Kaiser Aluminum Co.)

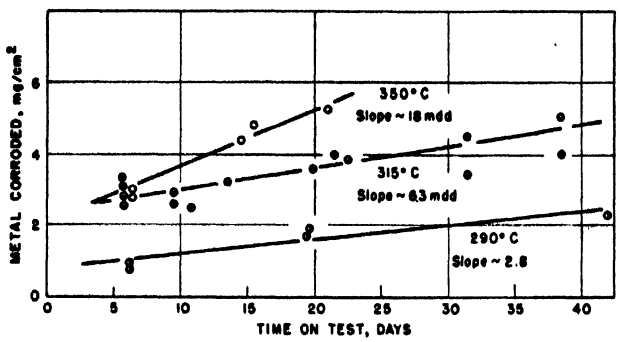

Figure 8. Corrosion of aluminum-nickel alloys in distilled water

loop was not in all respects satisfactory. This can be inferred from the unusually heavy deposit of magnetite. The impurity which might be expected to cause increased aluminum alloy corrosion rate would be hydroxide ion. There are at present no data which show clearly the effect of solution pH on the corrosion rate of such alloys.

The effects shown by added silicon and iron as ternary alloying elements in a 1% nickel alloy (high purity aluminum base) indicate that amounts of silicon greater than 0.1% cause rapid corrosion failure of the alloys at 350°C, while the iron additions from 0.2 to 1% appear to have made highly resistant alloys. Such alloys when properly made (must be homogeneous and sound) are completely impervious to the accelerated or blister attack which has been noticed on all other alloys. Further work to check the effects of the impurities which are common in commercially pure aluminum will be done. Present work will provide reliable values of corrosion rates at several values of temperature and pH, with and without rapid flow of water past metal surface.

PRACTICAL SIGNIFICANCE

With the elimination of the accelerating blister attack of aluminum in water at elevated temperatures, the only limitation on the material from the point of view of corrosion is the rate of chemical reaction of the material with the environment. Numerical values of corrosion rates at conditions which are of direct interest to reactor designers are probably not available. In particular, the effects of solution pH and flow rate on corrosion rate are not well known. However, there are now aluminum alloys known which can meet corrosion requirements for use in water at elevated temperatures, and it appears probable that water-cooled reactors will be built, using such alloys.

REFERENCES

1. Bryan, J. M., J. Soc. Chem. Ind. *69*:169 (1950).
2. Draley, J. E., Arendt, J. W., English, G. C., Story, E. F., Wainscott, M. M. and Berger, R. W., *The Corrosion of Aluminum in Dilute Solutions: Laboratory Studies,* CT-3027 (June 19, 1945).
3. Draley, J. E. and Ruther, W. E., *Aqueous Corrosion of 2S Aluminum at Elevated Temperatures,* ANL-5001, (February 1, 1953).
4. Draley, J. E. and Ruther, W. E., *Corrosion Resistant Aluminum Above 200°,* ANL-5430. In preparation Spring, 1955.
5. Groot, C. and Peekema, R. M., *The Potential pH Diagram for Aluminum,* HW-28556, (August 17, 1953); also Groot, C., *The Galvanic Corrosion of Aluminum,* HW-33881 (January 6, 1955).
6. Link, L., (Argonne National Laboratory) Private communication.
7. Strom, P. O. and Boyer, M. H., *Static Corrosion of Aluminum Alloys at 350F° and 480°F in Distilled Water,* LRL-64 (October, 1953).
8. Strom, P. O., Boyer, M. H. and Litz, L. M., *Aqueous Static Corrosion of Aluminum Alloys Coupled to Stainless Steel and Zirconium at 350°F,* LRL-74 (January, 1954).
9. Atwood, J., (Hanford Atomic Products Operation) Private communication.
10. Nielsen, N., (du Pont) Private communication.
11. Ayres, J. A. and Dillon, R., Private communication, General Electric Co., Hanford Atomic Products Operation.

Corrosion of Aluminium and Aluminium Alloys in Aqueous Solutions at High Temperatures

By K. Carlsen,* Norway

Because of its importance as a potential constructional material in power reactors, some investigations[1-5] have been carried out on the corrosion of aluminium in high temperature water. Unfortunately, most of these investigations are described in AEC publications which were not available to us when the present programme was planned. However, from what we could find out in the available literature, it appeared that although a number of commercial alloys had been tested, there had been no attempt to elucidate further the role of alloying in determining the corrosion behaviour of aluminium, and, in particular, the role of alloying elements that would be satisfactory from a neutron point of view. Neither had the effect of surface treatment, like for instance, anodizing, been examined.

That alloying might hold out some promise is indicated by the fact that very pure material has been reported[6] to disintegrate in steam at 300–350°C, while more impure material was found to have a better corrosion resistance. Obviously this is opposite to what presumably is the case at room temperature, and so it becomes imperative to examine in more detail the difference between high and low temperature corrosion characteristics.

No specific data were available on corrosion of aluminium alloys in the range of temperature of interest to us, namely around 230°C. We decided, therefore, to carry out tests at 230°C on a number of commercial alloys which would be suitable from a reactor point of view. Furthermore, we wished to obtain information regarding the importance of surface treatment and inhibitors. Finally, the work of Draley and Ruther[1] on the influence of pH made it desirable to include this variable in the experiments.

The investigation reported below, then, is the result of short time screening tests designed to select the most suitable materials and conditions for dynamic long-time tests in pressurized water.

Care should be exercised when judging the relative merits of the alloys; the tests being of very short duration, it may well be that samples which have shown promising behaviour in short-time tests, will turn out to be less so in long-time experiments.

*Joint Establishment for Nuclear Energy Research, Kjeller near Lillestrom.

EXPERIMENTAL METHODS

Samples, approximately 2.5 × 4 cm, were cut from rolled sheet, or, in the case of silumin, from cast bars. After electropolishing in a perchloric acid-alcohol bath, samples were washed carefully and dried. Silumin alloy samples could not be electropolished and were, therefore, ground on successive grades of emery paper.

In those cases where the influence of alloy composition and surface treatment was studied, specimens were supported on racks of quartz rods and placed in 2S aluminium containers filled with distilled water, which in turn were placed in a stainless steel autoclave. These tests lasted for 12 days and samples were removed every second day from the autoclave for weighing and microscopical examination.

Two such 12 days' tests were devoted to the study of the effect of gas atmosphere on corrosion. In one series, the autoclave was thoroughly flushed with nitrogen gas and finally filled with 5 atm of this gas; in another series, the same procedure was carried out with oxygen.

When the effect of additions to distilled water was being studied, the test sample and the test solution were placed in a small 2S aluminium container which was then sealed by means of argon arc welding. The atmosphere in these containers was normal air and the tests lasted for two days.

Throughout all these experiments the temperature was kept at 230°C ± 4°C by means of a thermostat.

After final exposure, the samples were in general treated with a hot solution of 4% CrO_3 and 10% H_3PO_4 (by weight) to remove the corrosion products, after which treatment they were again weighed.

In a few cases, a barrier layer thickness apparatus as described by Hunter and Fowle[7] was employed in order to study the anodic behaviour of corroded and un-corroded samples.

RESULTS

Effect of Alloying

Table I lists the commercial alloys studied, together with the composition and the rate of weight change observed in N_2 and O_2 atmospheres respectively.

The general appearance of the samples confirmed the results of Table I. The Reflektal alloy corroded

Table I. Rate of Weight Change in Milligrams/dm²/Day (mdd) of Commercial Aluminium Alloys in Distilled Water at 230°C

Denomination and composition of alloy	*After 12 days in N_2–atm*	*After 12 days in O_2–atm*	*$O_2 + N_2$ atm*
2S, commercial purity aluminium	2.9–3.9	3.2–3.5	—
4S, Al-1.2% Mn-1% Mg	4.8–5.2	4.7–5.2	—
F50S, Al-0.35% Mg-0.22% Si	4.3–4.4	3.9–5.0	—
Polital, Al-0.7-1% Si-0.55-0.75% Mn-0.65-0.85% Mg	3.6–3.8	3.8–4.5	—
Pantal, Al-0.6-1.4% Mg-0.6-1.2% Si-0.3-1.5% Mn	3.8	—	—
Reinaluminium, 99.5% Al	5.0	—	—
Silumin, Al-12% Si	4.4	—	—
54S, Al-4.2% Mg-0.8% Mn	—		123.0 (after 11 days)
BS-Seewasser, Al-2.4-4.0% Mg	—		380.0 (after 11 days)
Reflektal, super purity aluminium-0.5% Mg	—		Disintegrated
Super purity aluminium	—	—	Disintegrated

extremely rapidly and, after some time, the less pure alloys with high magnesium content (BS-Seewasser and 54S) also acquired a very bad appearance.

Among the rest of the alloys, the differences were not pronounced as regards the appearance and the table also shows that the differences in weight change are not very pronounced. However, with some certainty one can say that alloy 2S appears most promising, closely followed by Polital and Pantal.

The use of electropolished samples facilitated microscopical examination. The corrosive attack, which on visual examination seemed to be quite uniform, was found to be less so in the microscope. In the above mentioned series of alloys, intergranular attack was observed with certainty in Reflektal and also in the alloys high in magnesium. In the other alloys, intergranular corrosion was not encountered, neither was distinct pitting.

In this connection, the use of polarized light is of some interest. Under crossed Nichols, the uncorroded electropolished surfaces were completely black, except for a few light spots due to impurities. Corroded samples, on the other hand, were light grey under crossed Nichols, the corrosion products being shown clearly against the dark background. This, then, shows that corrosion at 230°C does not consist in the uniform thickening of a film. It was found that examination under crossed Nichols provided a sensitive means for detecting small amounts of corrosion, even when weight changes were negligible.

The very great difference in behaviour between the alloy based on super purity aluminum (Reflektal) and the rest of the alloys, and also the fact that super purity aluminium itself is known to disintegrate rapidly in water at high temperatures, suggested that one or more of the impurities present in commercial aluminium alloys are very effective in retarding corrosion at high temperatures.

In order to clear up this point, alloys based on super purity aluminium with additions of impurity elements were prepared. The additions were silicon, iron, and iron-silicon. Chromium was also added to one alloy since chromium improves the corrosion resistance in some cases.

The composition of these alloys and the results obtained are listed in Table II. It is evident that silicon is effective in reducing the amount of corrosion. The particular aluminium-silicon sample listed in the table had received a homogenizing heat treatment at 550°C and it was found that when such heat treatment was not carried out, i.e., when the structure consisted of pure aluminium and regions of aluminium-silicon eutectic, the samples exhibited nearly as low corrosion resistance as did super purity aluminium. Annealing at or below 450°C is not sufficient to improve matters, indicating that silicon must be finely dispersed throughout the matrix in order to be efficient.

Judging from the rate of weight change, 1% silicon is extremely effective in increasing the corrosion resistance of aluminium. The zero weight change is not, however, a true measure of the attack suffered, since both visual and microscopical examination clearly showed that corrosion had taken place. In fact, removal of corrosion products revealed that the alloy with silicon and iron addition, and the one with iron addition only, showed within experimental error approximately the same amount of corrosion as did the aluminium-silicon alloys. The aluminium-iron alloy had places where practically no corrosion had taken place, and both aluminium-silicon-iron and aluminium-iron had better appearance than aluminium-silicon after exposure.

The fact that aluminium-iron has such a good appearance indicates that iron is also effective in reducing corrosion at high temperatures. Unfortunately, this point cannot at present be decided upon conclusively since control analysis of the aluminium-iron alloy showed it to contain small amounts (0.008%) of silicon. At present, therefore, we can only say that

Table II. Effect of Additions of Alloying Elements on Corrosion of Super Purity Aluminium in Distilled Water at 230°C*

Alloy	*Rate of weight change (mdd)*	*Appearance*
Super-purity Al only	Sample disintegrated	Very bad
1% silicon added †	0.0	Good
0.23% silicon and 0.46% iron added†	18.2	Good
0.22% chromium added †	967.5	Very bad
0.4% iron added †	4.8	Good

* Tests lasting two days.

† O_2-atmosphere.

the iron seems to be a beneficial element but that it is not certain whether this beneficial action would be displayed if silicon were not present. If silicon must be present, the effect of iron might be to modify the distribution of silicon in a desirable way.

Both from the weight change and appearance it is quite evident that chromium is not capable of improving the corrosion resistance of super pure aluminium to any extent.

Effect of pH on Corrosion of 2S Aluminium

Draley and Ruther[1] emphasize the importance of pH in combating the corrosion of 2S aluminium. For this reason it was desired to include in the present investigation a study of the effect of pH, but preliminary experiments carried out showed that difficulties were encountered.

When small amounts of acid were added to distilled water at 230°C, it was found that the pH changed rapidly with time toward neutral values, thus rendering the interpretation of results difficult. The use of buffer solutions was contemplated but in order to vary the pH one would have to vary the components of the buffer, and in this way introduce new variables. It was concluded that the effect of pH could best be studied where a continuous replenishment of liquid could be effected. Since equipment for this type of experiment was not available, little effort was spent in pursuing the matter.

However, some results obtained in H_3PO_4 solutions and H_2SO_4 solutions are sufficiently interesting to merit mentioning. In H_2SO_4 solution with initial pH = 3.3 the rate of weight change appeared to be smaller than in distilled water. In H_3PO_4 solution with pH = 3.5 the initial rate of weight change was very much the same as in H_2SO_4 but after some days the rate was lower in H_3PO_4 than H_2SO_4. On the other hand, the sample from H_3PO_4 had a much more corroded look than the one from H_2SO_4. When the corrosion products were dissolved away, it was found that the ratio—weight of corrosion products/weight gain—indicated that no loss of corrosion products had taken place during the experiment itself. It was concluded, therefore, that the actual corrosion rates were proportional to the rate of weight change.

This was not so, however, in the case of H_2SO_4 with pH = 2.12. Here also the weight gains during corrosion were small, but removal of the corrosion products showed that great losses of corrosion products had taken place during corrosion. This finding is in agreement with the microscopical observations which showed that the film of corrosion products was undermined and peeled off, and was built up again successively. Following this undermining, extensive pitting was also observed.

The other alloys also showed less corrosion when pH was lowered from 6 to 3.5.

It is safe to say, therefore, that keeping the pH in the range 3.5–5.0 may retard corrosion, but it should be borne in mind that, if the pH is lowered below 3.0, serious acid attack may result.

Table III. Effect of Surface Treatment on Corrosion of 2S Aluminium in Distilled Water at 230°C

(Rate of weight change in mdd)

	N_2 atmosphere		O_2 atmosphere	
Treatment given	*After 4 days*	*After 12 days*	*After 4 days*	*After 12 days*
Electropolished only	8.6–9.1	2.9–3.9	11.8–16.7	3.2–3.5
Abraded with emery paper	10.0–15.5	4.5–4.3	13.9–18.0	3.7–3.9
Treated at 230°C with chromate-silicate inhibitor	6.0–8.9	2.5–3.8	—	—
Anodized and sealed in H_2O	7.4–8.3	−0.4–0.0	5.9–7.0	1.1–1.2
Anodized and sealed in Na-silicate soln.	4.6–6.4	0.2–0.7	4.7–5.7	1.5–2.4
Anodized only, no sealing	15.5–15.8	0.3–0.5	12.6–13.0	1.1–1.3

Effect of Surface Treatment and Surface Coatings

Table III gives the results of experiments on the influence of surface treatment. When one compares the electropolished samples with the abraded ones and with those which have received a treatment in inhibitor at 230°C before exposure, it is seen that the difference is more pronounced in the opening stages than later, but the difference is, in any case, not very marked. This is true also for the samples which have been anodically oxidized and sealed in hot water at 100°C.

The rest of the anodized samples seem to behave in a wholly different manner. Both the samples sealed in chromate, the ones sealed in silicate and the ones which had not received sealing treatment at all had high initial rates of weight change, the magnitude of which depended upon the sealing treatment, but after two days the rates dropped to low values. In one case a negative rate was found, indicating loss of material to the solution. If this were the case, the low rates of weight change may not be expressions of a low corrosion rate, since weight gains and weight losses could cancel each other. (In some experiments with anodized specimens where the test solution was in contact with the stainless steel autoclave, it was indeed found that anodized films could peel off.)

On the other hand, the experimental error is so large that the negative rate observed may not be significant and no weight losses may occur. In support of this view is also the fact that all the specimens in question showed nearly the same low rate of weight change. Furthermore, it was found in experiments with the barrier layer apparatus that samples sealed in chromate and those sealed in silicate had a barrier layer thickness corresponding to approximately 40 volts (i.e., an anodic potential of 40 volts had to be applied in order to obtain the same current density which would be obtained with a potential of 3 volts on an electropolished sample). This would indicate that a real protective layer is maintained during cor-

Table IV. Effect of Additions to Distilled Water on Corrosion of Aluminium at 230°C

Composition of aqueous solution	*Initial pH*	*Sample appearance*	*Rate of weight change in mdd after 2 days*
1% $K_2Cr_2O_7$	4.1	Very good but pitting	5.6
1% $K_2Cr_2O_7$ made neutral with NaOH	6.15	Fairly good	45.6
0.1% K_2CrO_4	8.05	Fairly good	38.5
1% $Al(SO_4)_3$	3.65	Very bad	—
1% Na-silicate	10.6	Very bad	—
1% $NaMoO_4$	6.7	Black, lot of pitting	—
Saturated As_2O_3-solution	2.7	Fairly good, but-extensive pitting	—
1% pyrogallol	5.7	Very good, but somewhat darkened	0.3
1% hydroquinone	3.95	Fairly good	3.1
1% pyridine	8.4	Bad	—
Dichromate-Na-silicate in proportion 1:1	6.75	Very good	0.9
Same in proportion 1:5	10.2	Very good	3.4
Same, proportion 1:10	10.8	Very good	4.1

rosion. In any case, it is obvious that long-time experiments are needed in order to clarify the importance of anodically oxidizing the samples.

Experiments were also carried out in order to see if surface coatings might have any use. Some samples were enamelled by a special enamel, designed to protect aluminium at elevated temperatures, but the results showed that the coating gave no improvements in corrosion resistance. The same was true for experiments in which chromium-plated samples and silicon-vapoured coated samples were employed.

Effect of Additions to Distilled Water

Some substances which are known[8] to inhibit corrosion of aluminium at low temperatures were tested at 230°C and the results are listed in Table IV.

For the solutions where the appearance of samples indicated severe corrosion, no figures of rate of weight change are given. These samples lost great amounts of corrosion products to the solution and information on weight changes might, therefore, lead to entirely misleading conclusions.

Also in those cases where actual figures are given, care should be taken in judging the relative merits of the solutions. In tests lasting only two days, the weight changes are small and the experimental error is consequently great. More emphasis should be put on the sample appearance and on the results of microscopical examination.

Of inorganic additions, As_2O_3 was used to gain some knowledge of the corrosion mechanisms. Since As_2O_3 is a cathodic inhibitor, it might give information as to the role of the cathodic reaction in the scheme. The results showed that As_2O_3 may inhibit corrosion but extensive pitting occurs.

Na_2MoO_4 was employed to see if the inhibiting effect of chromates is connected with the MeO_4^{--} group as such. As will be seen from the table, this was not found to be the case.

Sodium silicate gave very bad sample appearance but dichromate solutions produced beneficial effects. Sample appearance was very good and in the microscope no corrosion products could be seen under crossed Nichols. However, pitting was observed. When mixtures of dichromate and silicate were employed, the sample appearance again was very good and in addition there were no signs of pitting (after six days), thus indicating complete protection. From the table it appears that the best results were obtained with a mixture of 1:1. However, no difference between samples from the three solutions could be detected in the microscope. The gains in weight observed must be due to the building up of a film which is different from the corrosion products met with in other cases. This must be so because of the failure to observe any corrosion products on dichromate-silicate samples under crossed Nichols in the microscope.

When enough sodium silicate is added to dichromate, the latter is converted to monochromate and it was thought that this was the cause of the beneficial effect of the silicate. Accordingly, monochromate solution and dichromate solution made neutral with NaOH additions were employed in some experiments. The fairly great corrosion encountered in these solutions suggested that the silicate acts in a different way than to convert the dichromate to monochromate.

Of the inorganic inhibitors, pyrogallol seemed to be very good, leaving no corrosion products which could be detected under crossed Nichols. The darkening of the surface shows that decomposition of the compound occurs, a fact which will certainly prevent the use of pyrogallol in nuclear reactors.

The experiments mentioned in this section all refer to 2S aluminium. Silumin and SAP (sintered aluminium powder) samples were also employed in the dichromate-silicate tests, and the results obtained were similar to those obtained for 2S aluminium.

Effect of Atmosphere

From Table I it is seen that the results show no appreciable difference in behaviour due to O_2 or N_2 respectively.

For the anodized samples, there is no difference in behaviour during the first days, but after 12 days, O_2 samples have greater weight gains than N_2 samples. The difference is, however, small and is thought to be mostly due to experimental inaccuracies.

DISCUSSION

Mechanism of Corrosion

Draley and Ruther in their paper[1] have made some interesting suggestions as to the mechanism of corrosion at high temperatures. They emphasize strongly

that the initial amount of corrosion is greater than that needed to produce the protective layer and put forward two possible explanations. The first is that the iron in the metal causes alkalinity in the solution immediately adjacent to the metal, the second that "surface working and preferential etching on a microscopic or sub-microscopic scale might leave the surface metal atoms sufficiently distributed so that their configuration is not suitable for oriented growth of the protective film." It is of interest to look at these ideas in view of the results obtained in the present investigation.

When our results are plotted in the form of time-weight change curves, the slopes of the curves are very much the same as those obtained by Draley and Ruther, and the heights of intercept are not very different from those reported by these workers, so that we may conclude that also in the present investigation more metal is corroded away than needed to build up a protective layer. Now, if a minimum of silicon is needed to inhibit corrosion, then one would expect, according to the first assumption, that addition of iron to a pure aluminium-silicon alloy would tend to increase the amount of initial corrosion and, from the weight gains listed in Table III, this would indeed appear to be so. In fact, however, the corrosion of pure aluminium-silicon is as pronounced as that of aluminium-silicon-iron. Besides, the appearance is better, thus suggesting that iron has a beneficial rather than detrimental effect.

If alkalinity produced by iron was indeed the important effect, we might perhaps expect that presence of O_2, which would oxidize ferrous hydroxide to the ferric form, would give lower intercepts than when O_2 is absent. The present results on the influence of O_2 and N_2 do not show any such effect.

Draley and Ruther partly base their assumption of the role of iron on the brown discoloration of their samples. In the present investigation, no such discoloration was observed and it is concluded that in their case discoloration was caused by iron from the autoclave.

As to the second suggestion, the disturbance of the surface atoms, the fact that abraded specimens have a higher initial corrosion rate than electropolished ones might be taken to prove that the effect is a real one. On the other hand, the fact that electropolished samples also suffer high initial corrosion shows that this explanation alone is insufficient. Furthermore, it is possible to explain the difference between the two categories in another way, namely that the precipitated corrosion products, although not impermeable, set up a diffusion barrier which finally slows down the transport of ions through the layer to such an extent that the reaction after some time stifles itself. The effect of abrasion would be to increase the effective surface of the sample, thus increasing the amount of corrosion products needed to build up a layer of sufficient thickness. If this picture is accepted, it follows that the type of ions in the solution will influence the thickness and permeability of the outer layer, since the ions must in general be expected to affect the nucleation conditions in the layer.

It is possible that the action of dichromates could be explained on this basis. The chromate additions would act in such a way that a film is built up rapidly but since the film because of the high temperatures must be expected to have at least some permeability, it is possible that chromate will have to be supplied steadily to prevent the break-down of the film. If this is so, it would explain the observation made in this study that exposure to dichromate-silicon solutions at 230°C did not prevent corrosion when samples were exposed afterwards to distilled water.

Possible Alloy Development

It is interesting to consider whether new and more corrosion resistant alloys might be developed for high temperature use. Particularly in view of the difference between high and low temperature behaviour this would not appear impossible.

If it is true that silicon is the element which makes 2S aluminium so much more resistant than super pure aluminum, then one might believe that still better alloys might be produced by addition of more silicon. This may well be so, but the results on Silumin show that 12% silicon does not increase the resistance. However, it is possible that the best results will be obtained when the alloy contains the maximum of silicon atomically dispersed. If precipitation is not allowed to occur, this means a content corresponding to the solid solubility limit at the eutectic temperature.

It is stated that at room temperature silicon is a harmful impurity in aluminium[9] when present in amounts greater than the solid solubility, and magnesium a beneficial element with regard to corrosion resistance. Our experiments show that magnesium, particularly in greater amounts, cause increased corrosion at high temperatures. This again underlines the difference between high- and low-temperature behaviour.

It may indeed also be that iron, definitely an unwanted element at low temperatures, has a beneficial effect on the corrosion at high temperatures but, as has been pointed out previously, it is not yet known if this effect is always tied up with the presence and distribution of silicon.

By investigating further, then, the roles of silicon and iron in high temperature corrosion, it is possible that information might be gained which would lead to the development of more resistant alloys than 2S. In this connection, it should be mentioned that aluminium-silicon and aluminium-iron-silicon alloy must be expected to have good mechanical properties at high temperatures.

Finally, the effect of zirconium and beryllium additions to aluminium on corrosion behaviour should be studied.

Other Ways of Preventing Corrosion

Because of its stable oxide film and electro-positive nature of aluminium, it is doubtful whether coatings

of other metals or compounds could ever be successfully applied for the protection of aluminium in high temperature water. Anodic coatings seem to hold out greater promise and the matter should be investigated further. Inhibitors based on dichromate-silicate mixtures could be of great use, the same is true of pH-control, although the latter procedure cannot be expected to be as effective as suitably chosen inhibitors.

REFERENCES

1. Draley, J. E. and Ruther, W. E., *Aqueous Corrosion of 2S Aluminium at Elevated Temperatures,* ANL-5001.
2. Goldowski, N., *Corrosion of Aluminium at High Temperatures,* CT-3080.
3. Strom, P. O. and Boyer, M. H., *Static Corrosion of Aluminium at 350°F and 480°F in Distilled Water,* LRL-64.
4. Strom, P. O., Boyer, M. H. and Litz, L. H., *Aqueous Static Corrosion of Aluminium Alloys Coupled to Stainless Steel and Zirconium at 350°F,* LRL-74.
5. Grube, K. and Eastwood, L. W., BMI-T-38.
6. Guillet, L. and Ballay, M., Compt. rend. *189*: 551 (1929).
7. Hunter, M. S. and Fowle, P., J. Electrochem. Soc. *101*: 481 (1954).
8. Schenk, Max, *Werkstoff Aluminium und Seine Anodische Oxydation,* Bern 1948, p. 288.
9. BNFMRA Report No. RRA916, "The Effect of Impurities on the Corrosion of Aluminium and Its Alloys".

Fundamental Aspects of the Corrosion of Aluminium And Their Application to Nuclear Reactors

By R. A. U. Huddle,* UK

One of the major problems in the design of any water-cooled reactor is the prevention of corrosion. The low neutron absorption of aluminium suggests the use of this metal, providing its mechanical and corrosion characteristics are satisfactory for the particular application envisaged.

Aluminium has in fact been used extensively both in production piles and experimental reactors, not only for canning but also as a constructional material. However, as its corrosion resistance can be seriously impaired by the presence of very small quantities of certain ions in solution, as well as by contact with other metals, the factors responsible for this attack are worthy of consideration.

In this paper, the general principles of the corrosion mechanism as developed by the author[1] are introduced, and applied to the corrosion of aluminium in water at temperatures up to 100°C.

FUNDAMENTAL PRINCIPLES

Metallic corrosion is appropriately defined as the passage of metallic ions from the metal lattice into the ionic state. It is important to appreciate that the above definition includes the development of protective films as a corrosion process. In the case of aluminium this process is accompanied by a considerable decrease in the free energy of the system; however, the corrosion rate of aluminium is in no way related to this value as the rate is controlled entirely by the formation and breakdown of protective films. In water, the overall process of corrosion is best considered as a combination of the separate anodic and cathodic reactions. At the anode aluminium either dissolves as a soluble salt, or forms an insoluble hydroxide, hydrated oxide, or true oxide film.

In all anodic processes metal is destroyed—it passes into the ionic state—and excess electrons are left behind in the metal. It is the neutralisation of these excess electrons that constitutes the cathodic reaction. Unless either or both of these reactions are completely polarised (i.e., prevented) corrosion will proceed, the overall rate being determined by whichever reaction is the slower.

The Anodic Reaction

As defined above corrosion entails the passage of metallic ions into the ionic state; this is an anodic process which can take place either by metal dissolution or by the direct formation of a film. With aluminium it is doubtful whether metal dissolution as such (Equation 1) plays an important role except perhaps in the propagation of pits subsequent to film breakdown

$$Al \rightarrow Al^{+++} + 3e^- \qquad (1)$$

If the concentration of aluminium ions exceeds the solubility product of the hydroxide, precipitation will occur; this precipitation will take place away from the actual corroding surface, the degree of protection (if any) depending on the precise nature of precipitation.

The direct formation of bayerite, boehmite and the true oxide (Equations 2, 3 and 4) on the other hand all lead to the build up of passivity.

Hydroxide formation

$$Al + 3\,OH^- \rightarrow Al(OH)_3 + 3\,e^- \qquad (2)$$

Hydrated oxide formation

$$Al + 3\,OH^- \rightarrow AlO(OH) + H{\cdot}OH + 3e^- \qquad (3)$$

True oxide formation

$$Al + 3\,OH^- \rightarrow \tfrac{1}{2}Al_2O_3 + \tfrac{3}{2}\,H{\cdot}OH + 3e^- \qquad (4)$$

In this case the film is formed on the metal, growth occurring by a diffusion mechanism in which one or other (or possibly both) of the reacting species migrates through the film. In the case of a cationic diffuser it reacts at the outer surface, whereas with an anionic diffuser the reaction occurs at the metal interface.

Hydrated oxide formation which leads to passivity must not be confused with the solubility product precipitation mentioned above.

The Cathodic Reaction

Whatever the actual anodic process, the electrons left behind in the metal must be neutralised by a corresponding cathodic reaction. If this cathodic process can be restrained or prevented then the anodic process is likewise affected. This is an extremely important point as cathodic polarisation so often determines the overall corrosion process. Neutralisation of the electrons left as a result of the anodic reaction can proceed in one or more of the following ways:

(*a*) Metal deposition

$$M^{++} + 2e^- \rightarrow M \qquad (5)$$

* Atomic Energy Research Establishment, Harwell.

(*b*) Hydrogen evolution

$$2H^+ + 2e^- \rightarrow H_2 \quad (6)$$

(*c*) Cationic reduction

$$2M^{+++} + 2e^- \rightarrow 2M^{++} \quad (7)$$

(*d*) Anionic reduction

$$2X^{--} + e^- \rightarrow 2X^{---} \quad (8)$$

(*e*) Molecular reduction, e.g., oxygen absorption:

$$O_2 + 2H_2O + 2e^- \rightarrow 2OH^- + H_2O_2 \quad (9)$$

$$H_2O_2 + 2e^- \rightarrow 2OH^- \quad (10)$$

Metal deposition will take place if ions of a more noble metal are in solution, providing other characteristics of this solution do not inhibit such a reaction. Hydrogen evolution is dependent on the pH of the solution, the potential of the particular surface exposed, and the over-potential *especially at low over-potential cathodic phases*. Aluminium has a very high over-potential as evidenced by the absence of hydrogen evolution, when a specimen is cathodically polarised (in neutral solution) to —1.2 volts; i.e., a "hydrogen evolution" over-potential of at least 0.8 volts. Cationic, anionic and molecular reduction are dependent on the oxidation reduction potentials of the actual concentration of reacting species present at the cathode surface.

The reduction of oxygen is usually written as shown by Equation 11

$$O_2 + 2H_2O + 4e^- \rightarrow 4OH^- \quad (11)$$

However, it has been shown[2] that it actually proceeds in the two stages as given by Equations 9 and 10 above. Although kinetic studies have shown that the overall reaction is highly polarised, the major rate controlling factor (when the anodic reaction is uninhibited) is often the rate at which oxygen reaches the cathode surface, i.e., the concentration polarisation. This reaction leads to the direct formation of OH^- ions, a fact that may well account for the general attack on an aluminium specimen cathodically polarised in an oxygen containing solution. As oxygen is often necessary for the corrosion process to proceed, and as the corrosion product is usually an oxide (or hydroxide) it is often assumed that this oxygen reacts directly. However, our present knowledge suggests that such a simple mechanism is improbable, although such a reaction may take place through the catalysing action of certain complex ions containing oxygen as discussed below. It seems more likely that protective films are formed by direct reaction with hydroxyl ions from the solution, and that dissolved oxygen confines its activities almost entirely to the depolarisation of cathodic areas as given by Equations 9 and 10.

FILM GROWTH

As the passivity of aluminium is entirely dependent on the formation and maintenance of protective films, let us consider in some detail the factors determining the degree of protection afforded by these films.

A considerable amount of work has been carried out on anodised films on aluminium and the factors determining their rate of growth are fairly well understood.[3] The thickness to which these films (which have been shown to be the true oxide) grow is primarily dependent on the applied potential, the effect of temperature being subsidiary. Recent work[4,5] on the growth of boehmite and bayerite films has shown that they obey approximately the parabolic relationship. The rate of growth of bayerite is very much faster than with the true oxide, boehmite being intermediate.

These facts suggest that true passivity is largely dependent on whether or not the oxide, as opposed to the hydrated oxide or hydroxide, is formed. The conditions determining which particular corrosion product is formed appears to be dependent on the temperature and the composition of the solution. In water the film produced below about 70°C is bayerite, whereas above this temperature and up to at least 300°C boehmite is formed. The true oxide is only formed in certain "anodising" solutions. It is suggested that the presence of these "anodising" complex anions containing oxygen leads to the formation of true oxides as opposed to hydrated oxides and hydroxides, which would otherwise form in their absence, and that this factor is responsible for the increased corrosion resistance observed when such anions as chromates, silicates, etc., are present in solution. The extreme corrosiveness of distilled water and of some soft waters may well be due to the absence of any such oxygen-containing complex anions, as most natural waters contain silicate, carbonate etc. An excellent example of this occurred in the heavy water in DIMPLE.† To begin with, this heavy water was as pure as could be obtained and quite serious general corrosion of the search tubes occurred, producing a mass of gelatinous aluminium hydroxide. The addition of about five parts per million of silica was completely effective in preventing this attack.

The exact mechanism by which these complex ions impart a true oxide rather than a hydroxide has not been finally established. However, they will compete with the OH^- ions and other anions present in the water to participate in the reaction at the anode surface. If their adsorption is such as to exclude the OH^- ion from the reaction, it is suggested that the complex anion donates its own oxygen ion to the film regaining this ion from the solution. Certain of these complex ions are only effective in oxygen-containing solutions, indicating that the true function of the complex ion may well be to act as a catalyst in the anodic transfer of dissolved oxygen from the solution to the film. This situation can arise if the reduced form of the complex ion is not re-oxidised by water. If, however, the oxidation reduction potential of the anion is such that its reduced form can be re-oxidised by water the inhibitor should be effective in solutions free from oxygen.

† A heavy water zero energy assembly.

A consideration of the structure of these inhibiting complex anions suggests that their effectiveness is associated with the size (and charge) of the "nucleus" of the complex, the smaller the size (and greater the charge) the more effective the inhibitor. For example, chromates and borates are better inhibitors than sulphates and silicates, the chromium 6^+ and boron 6^+ ions being smaller than the sulphur 6^+ and silicon 4^+ ions.

The idea of a competitive reaction is most important, as illustrated by the anodic oxidation behaviour of aluminium. Sulphate is effective as an inhibitor (i.e., in donating oxygen ions rather than hydroxyl ions to the film) only when the OH^- ion concentration is low, i.e., in acid solution; in neutral solutions sulphate is ineffective. Furthermore, if ions such as chloride and fluoride are present which are corrosion accelerators as opposed to inhibitors, they may well cause failure by their actual incorporation in the lattice, resulting in a non-protective film, although their effect is generally attributed to their ability to peptise the oxide.

FILM BREAKDOWN

At temperatures below 100°C failure of the protective film can occur by two mechanisms:

1. If the composition of the water is such that the film is soluble, corrosion will proceed at a rate determined primarily by the solution kinetics of the film.

2. The application of an anodic or cathodic potential may affect breakdown either by modifying the film or by influencing the solution adjacent to the electrode surface.

If the pH is in the range 4–8, the rate of dissolution of the film is negligible unless perhaps such ions as chloride and fluoride are present. However, in both acids and alkali, dissolution of the film becomes appreciable, as evidenced by the corrosion of aluminium in these media.

Of all the common metals, aluminium is probably the most sensitive to anodic polarisation; it has been shown that in most waters the application of a small anodic potential leads to film growth.[6] However, above a certain critical value characteristic of the state of the film and the composition of the solution the film breaks down at isolated points,[7] any further increase of applied potential merely causing breakdown at other places with no increase in polarisation. Typical polarisation curves[8] for 99.8% aluminium in an untreated surface water are shown in Fig. 1. Immediately following film breakdown aluminium ions stream across the metal/liquid interface carrying the current into the solution. This incidentally relieves the potential adjacent to the point of breakdown and, therefore, reduces the probability of breakdown in the adjacent area, resulting in pitting corrosion. The concentration of aluminium ions in the solution adjacent to the point of failure soon exceeds the solubility product of aluminium hydroxide and a precipitate is formed. In the first instance, this precipitate is gelatinous; it hinders the migration of aluminium ions from the surface and a crystalline deposit soon forms around the point of attack. The reaction of aluminium ions with hydroxyl ions from the water produces acidity just at the point where no film exists; this acidity hinders, if not prevents film repair within the pit, and a state is reached where there is little or no resistance to the corrosion of the metal under the "barnacle" due to the film formation, *the rate of corrosion then being governed by the cathodic reaction.* This explains why oxygen is often necessary for pitting attack to develop, for if the cathodic reaction is polarised the anodic process will be affected in a similar manner. Once a "barnacle" has formed, therefore, the factors responsible for pit formation will no longer be essential for its continued growth.

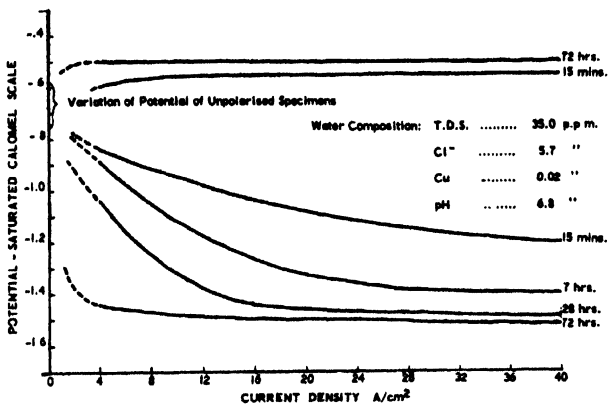

Figure 1. Polarization curves of 99.8% aluminum in an untreated surface water at 35°C

The critical potential of film breakdown is reduced by the presence of chloride and fluoride and increased by such ions as silicate, chromate, etc.,[6] probably by the mechanism discussed above. If chromates are present, the film formed in acid solution is the true oxide and as no pitting is ever observed when the true oxide is formed, it would appear that its breakdown potential is greater than the potential at which oxygen is evolved from solution.

Pitting will, therefore, occur in solutions containing sufficient chloride or fluoride to reduce the critical potential of film breakdown to a value at or below the natural corroding potential of the metal, or by the application of an anodic potential. This anodic potential can be derived from the following sources: (*a*) an applied emf from a battery or generator; (*b*) junction with a noble conductor, such as copper, silver, brass, mercury, graphite or sometimes even magnetite and steel; (*c*) cathodic metals re-deposited electrochemically from the corroding solution (copper, silver, mercury, etc.)[9] and (*d*) an oxidation-reduction reaction associated with molecular or ionic species in the water, e.g., oxygen reduction.

Whilst cathodic polarisation will reduce the probability of pitting corrosion it can in waters containing oxygen (and cations other than hydrogen) lead to film failure due to the alkalinity produced as a result of the oxygen reduction cathodic reaction. This pro-

duces general corrosion and is similar in nature to the attack observed when aluminium is corroded in alkaline solutions.

The most important aspect of the corrosion of aluminium in experimental nuclear reactors is the prevention of pitting. Whilst little difficulty is experienced in avoiding contact with noble conductors such as copper and graphite and also from stray currents, it is sometimes most difficult to avoid the presence of trace quantities of copper ions in solution. Experiments have shown that as little as one-tenth of a part per million copper ion in solution is effective in promoting pitting. Although the presence of anodic inhibitors is beneficial they are not always effective, and freedom from attack can only be achieved by elimination of these noble metal ions from solution. This imposes a severe limitation on the use of other metals containing copper in the primary circuit of the reactor.

ACKNOWLEDGEMENTS

The author wishes to acknowledge the help of Mr. J. Laing and Mr. N. J. M. Wilkins in the experimental work associated with this project.

REFERENCES

1. Huddle, R. A. U., *The Principles of Corrosion in Water and Aqueous Solutions and Their Application to Nuclear Reactors,* A.E.R.E. M/R 1313 (1955).
2. Heyrovsky, J., *The Processes at the Mercury Dropping Cathode,* Trans. Faraday Soc. *19*: 785 (1924).
3. Charlesby, A., *Ionic Currents and Film Growth of Thin Oxide Layers on Aluminium,* Proc. Phys. Soc., B. *66*: 317 (1953).
4. Hart, R. K., *The Oxidation of Aluminium in Wet and Dry Environments,* Thesis, University of Cambridge (1955).
5. Huddle, R. A. U. and Wilkins, N. J. M., *The Corrosion of Commercially Available "Pure" Aluminium in Demineralised Water between 125° and 300°C,* A.E.R.E. M/R 1669 (1955).
6. Huddle, R. A. U. and Wilkins, N. J. M., *The Critical Potential of Film Breakdown on Aluminium,* To be published shortly.
7. Huddle, R. A. U. and Laing, J., *Storage of Irradiated Cartridges,* A.E.R.E. M/R 293 (1948).
8. Huddle, R. A. U. and Laing, J., Unpublished work at A.E.R.E. (1948).
9. Huddle, R. A. U. and Wilkins, N. J. M., *Pitting Corrosion of Aluminium in Demineralised Water,* Comptes Rendu du XXVIIème Congres de Chimie Industrielle, Bruxelles, 1954.

Aqueous Corrosion of Zirconium and Its Alloys at Elevated Temperatures

By D. E. Thomas,* USA

High temperature water-cooled and moderated thermal reactors require a core structural material which is corrosion resistant and which has a low thermal neutron capture cross section. Conventional structural materials are unsuitable because they have either a high neutron capture cross section or inadequate corrosion resistance. Zirconium, however, is resistant to corrosion by high temperature water and has a low thermal neutron cross section. It was soon found, however, that maximum corrosion resistance is dependent upon the control of certain impurities in zirconium, and later that alloying effected improved corrosion resistance.

Cooperative work on the corrosion of zirconium and its alloys has been done at the following laboratories: Argonne National Laboratory, Battelle Memorial Institute, Nuclear Metals, Inc. (formerly Division of Industrial Cooperation, Massachusetts Institute of Technology), US Bureau of Mines, Albany, Oregon, and Westinghouse Atomic Power Division. Since much of the data is to be found in classified progress reports and committee reports which are not likely to become generally available, most of the references are made to individuals at the end of the paper.

Details of the testing procedures have been reported in the literature.[1] Briefly, corrosion test specimens of suitable size are bright etched in a solution consisting of 50 per cent distilled water, 45 per cent concentrated nitric acid, and 5 per cent hydrofluoric acid (48%), and rinsed prior to exposure. Specimens are suspended in stainless steel pressure vessels containing degassed high purity water at temperatures below the critical point (705°F, 374°C) at equilibrium pressure. Care is taken to exclude air from the system. The specimens are examined after exposure intervals of two weeks to two months and the change in weight is taken as a measure of the extent of corrosion.

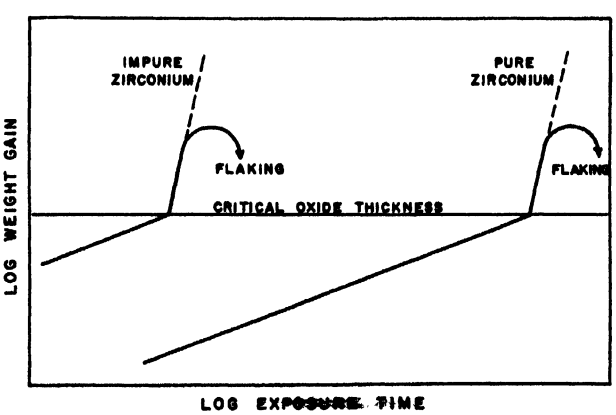

Figure 1. Schematic representation of the corrosion of unalloyed zirconium in high temperature water

CORROSION OF UNALLOYED ZIRCONIUM IN HIGH TEMPERATURE WATER

Kinetics

The general features of the corrosion behavior of unalloyed iodide process zirconium are to be discussed in the following paragraphs. A more detailed discussion than the following has been published.[1] The data generally refer to material which has been arc-melted and hot worked.

The course of corrosion of relatively pure zirconium is indicated schematically in Fig. 1 which is a logarithmic plot of weight gain versus exposure time. It will be noted that there is an initial period in which the rate of corrosion decreases with time followed by a period in which the corrosion rate is constant. The change in kinetics has been referred to as "breakaway." During the initial period the corrosion product is tightly adherent and in appearance ranges from interference colors to black, while in the second stage the corrosion product is white in appearance and flakes off, resulting in weight losses. The corrosion product formed in both stages is monoclinic zirconium dioxide, although there is some evidence that a small amount of the tetragonal modification is present during the very early stages.[2] The kinetics of the corrosion reaction may be described by the empirical equation:

$$\Delta m = kt^n \qquad (1)$$

where Δm is the weight gain per unit area, t is the time, and k and n are constants. The logarithmic form of Equation 1 is convenient in that the corrosion data are usually presented in logarithmic plots:

$$\log \Delta m = \log k + n \log t \qquad (2)$$

* Westinghouse Electric Corp., Atomic Power Division. Including work by C. R. Breden, Argonne National Laboratory; H. A. Pray, R. S. Peoples, Battelle Memorial Institute; T. T. Magel, K. S. Kneppel, Nuclear Metals, Inc.; E. T. Hayes, US Bureau of Mines, Albany, Oregon; and D. E. Thomas, K. M. Goldman, S. Kass, Westinghouse Atomic Power Division.

Thus, a plot of log Δm against log t yields a straight line having slope n and intercept k. As may be seen in Table I below the value of the exponent n of Equation 1 is about $\frac{1}{3}$, that is to say, corrosion of zirconium obeys approximately a cubic rate law during the first stage. The data in Table I represent a large number of samples of arc-melted iodide process zirconium which had been screened by means of a two-week corrosion test at 600°F (316°C) prior to arc-melting, and which had the composition indicated in Table II. The very pure material represented did not reach the second stage of corrosion or "breakaway" in the 200 days exposure at 550 or 600°F to which it was subjected. However, at 680°F (360°C) "breakaway" occurred in some samples as early as 7 days exposure and only 32% of the specimens had failed after 254 days. Because of the fact that "breakaway" is accompanied by spalling of the corrosion product, no reliable estimate has been made of the actual corrosion rate. However, the onset of "breakaway" in unalloyed zirconium signifies the end of useful life.

Table I. Rate Constants for the Corrosion of Zirconium in High Temperature Water

Temperature °F	Temperature °C	Pressure psi	k mg/dm²	n (dimensionless)
550	287	1084	2.4	0.270
600	316	1553	3.5	0.301
680	360	2705	5.9	0.330

The effect of temperatures may be seen in Table I. The logarithm of the constant k is approximately linear with the reciprocal of the absolute temperature. From such a plot an activation energy of 9400 cal/mol is obtained. However, not all of the temperature dependence is found in the constant k, since n also increases slightly with increasing temperature.

Effect of Impurities

By no means does all iodide zirconium behave as indicated above. In some cases "breakaway," or failure, is observed after only a few days exposure at 600°F (316°C), and in extreme cases complete disintegration occurs. Such behavior is due to the presence of impurities. In general, the initial mode of corrosion is interrupted when an oxide thickness corresponds to a weight gain of approximately 40 mg/cm². This critical oxide thickness for the onset of "breakaway" is indicated schematically in Fig. 1. The behavior of impure zirconium is also shown schematically in Fig. 1. The critical oxide thickness is reached in a time much sooner in the case of impure zirconium than in the case of the pure material.

The effects of the important impurities on corrosion resistance are summarized in Table II. Perhaps the most striking effect is that of nitrogen. Material containing more than 0.004 wt % suffers "breakaway" within a short time at 600°F (316°C), the time required for "breakaway" decreasing with increasing nitrogen content. Consequently nitrogen must be controlled to a maximum of about 0.005 wt % in all stages of metal production and fabrication. Similarly the corrosion rate increases with increasing carbon content, which must be kept to a minimum if maximum corrosion resistance is desired, a fact which precludes induction melting in graphite crucibles.

Other Effects

The corrosion behavior of zirconium is extremely sensitive to the condition of the surface prior to exposure. Surfaces machined with ordinary care exhibit in a short time white corrosion product indicative of "breakaway," and this effect has been associated with the presence of a layer of disturbed metal extending to a depth of 0.0015 to 0.002 inches below the surface.[8] It is therefore necessary to remove this disturbed metal by bright etching prior to corrosion testing.

The effect of deformation at temperatures ranging from room temperature to 1450°F (790°C) upon the corrosion rate is very slight.[3]

Table II. Effect of Impurity Content on the Corrosion Resistance of Zirconium in High Temperature Water

Impurity	Effect	Concentration at which effect is noted, wt %	Nominal composition, wt % arc-melted iodide Zr
N_2	Harmful	0.004	0.002–0.0025
C	Harmful	0.04	0.01
O_2	Very Slight	0.05	0.04
H_2	None	0.1	0.002
Ti	Harmful	0.1 to 20	0.002–0.003
Al	Harmful	0.1	0.0027 to 0.0037
Ca	Harmful	Uncertain	0.0025
Mg	Harmful	Uncertain	0.0010
Cl	Harmful	Uncertain	0.0015
Si	Harmful	Uncertain	0.002–0.007
Pb	Harmful	~0.01	0.0025
Hf	None	0–100	0.01–0.015
Cu	None	~0.1	—
W	None	~0.1	<0.01
Fe*	None	<0.1	0.037–0.049
Cr*	None	<0.1	0.001–0.0018
Ni*	None	<0.1	0.0025–0.0010

* Beneficial effects are found at about 0.1% of these elements.

The corrosion resistance of pure zirconium does not appear to be affected by heat treatment. However, arc-melted sponge zirconium exhibits impaired corrosion resistance when quenched from temperatures above the α-β transformation.

The presence of small amounts of various dissolved salts in the test water does not affect the corrosion behavior of zirconium, nor does the presence of up to a few hundred cubic centimeters of hydrogen, oxygen, or nitrogen per kilogram of water. However, the addition of 200 ppm of NaF leads to extremely rapid corrosion at areas of physical contact between specimens.

Effects due to the velocity of the test water, electrical coupling, and the presence of crevices are absent in the case of zirconium and its alloys.

Corrosion in Steam

The corrosion of zirconium in steam at 750°F (400°C) and 1500 psi was studied for the purpose of developing an accelerated test which would reflect the corrosion behavior of the material in hot water.[4] A completely satisfactory correlation was not found for unalloyed zirconium, although in many cases 750°F (400°C) steam test results paralleled those in 600°F (316°C) water. Pure zirconium exhibits quite erratic behavior in such a steam test and white corrosion product appears within 18 hours in many cases.

The reaction rate of zirconium in steam is sensitive to pressure. In tests at 750°F (400°C) steam, increasing the pressure from 15 to 1500 psi increased the weight gain by a factor of 20 to 40.

The steam test has been found useful particularly in alloy work. In view of certain known cases where corrosion in steam does not correlate with that in water it is necessary to confirm the steam test results by performing parallel water tests for new alloys.

CORROSION OF ZIRCONIUM-BASE ALLOYS

It is seen in the foregoing that unalloyed zirconium exhibits the undesirable phenomenon of "breakaway" which may occur at widely ranging exposure times. Furthermore, the corrosion rate after "breakaway" is too high for practical use. Thus, a major purpose in alloying is to provide more reproducible corrosion behavior, to eliminate or delay "breakaway," and to reduce the post "breakaway" corrosion rate. A further aim in alloying is to make it possible to employ the less expensive Kroll process sponge zirconium rather than iodide process material. Work of the latter type led to a certain amount of confusion concerning the effects of individual alloying elements because of the presence of beneficial as well as harmful impurities in the highly variable sponge zirconium. It should be recognized here that the gradual improvement in purity and uniformity of zirconium sponge effected by the US Bureau of Mines at Albany, Oregon, played a significant part in the success of the alloy development program. The data presented in the following refer exclusively to arc-melted material which has been hot worked to suitable size.

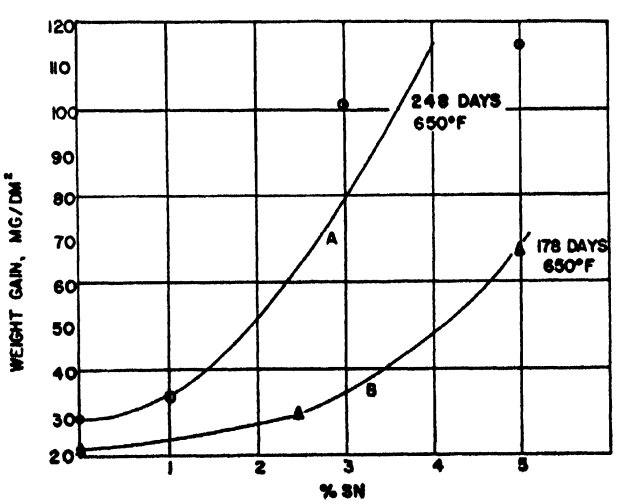

Figure 2. The effect of tin content upon corrosion resistance. Curve A represents a series of arc-melted crystal bar tin alloys melted by Battelle Memorial Institute. Curve B represents a similar series of alloys made by Westinghouse

Binary Alloys

Zirconium-Tin Alloys

Binary zirconium-tin alloys have been of considerable interest. These alloys corrode in much the same way as does unalloyed zirconium with the important exception that the oxide film remains adherent for a considerable period of time after "breakaway" occurs.[4] As may be seen in Fig. 2 the corrosion rate increases with increasing tin content in the range up to 5 wt % tin. This trend continues for higher tin contents. Test results on a number of ingots of iodide zirconium-2.5 wt % tin alloys containing less than 850 ppm of iron show that the onset of "breakaway" as indicated by the attainment of weight gain of 30–50 mg/dm² occurs at exposure times of 50 to 60 days at 600°F (316°C) as compared to something more than a year's exposure for crystal-bar zirconium. This effect becomes more pronounced at higher temperatures.

Table III. Concentration of Tin Required to Compensate for Various Concentrations of Nitrogen

Tin content, wt %	*Nitrogen content, ppm*
0.5	200
1.0	300
2.0	600
2.5	700
3.0	800

In addition to promoting the adherence of the corrosion product, tin tends to counteract the harmful effect of nitrogen. This effect was discovered independently by Battelle Memorial Institute[4] and Iowa State College, and is typified by the results shown in Fig. 3. It is seen that the addition of tin to an impure zirconium sponge base results in a considerable improvement in corrosion properties. It will be noted that there is an optimum tin content, in this case at about 0.5 wt % tin. As the tin content approaches this optimum value the harmful effect of nitrogen is counteracted, and as the tin content increases beyond this optimum value the normal increase in corrosion rate with increasing tin content becomes evident. With higher nitrogen contents, the amount of tin required increases and the optimum is shifted toward higher tin content. Based on a series of drip-melted zirconium-tin-nitrogen alloys, Magel and Kneppel[5] found the amount of tin necessary to cancel the effect due to various amounts of nitrogen. These data, shown in Table III, are based upon short term tests in 600°F water. Considerably lower permissible nitrogen contents are found when the corrosion test time or temperature is increased.

In this connection it should be pointed out that the corrosion resistance of zirconium-tin-nitrogen alloys does not equal that of pure zirconium.

Tin also tends to overcome the deleterious effects of aluminum and carbon. However, because these impurities are readily controlled, not much attention has been directed toward such effects.

The corrosion behavior of zirconium-tin alloys is not markedly affected by heat treatment. Alloys quenched from the beta phase field have somewhat higher corrosion rates than those slow cooled from the same temperature or those annealed in the alpha or alpha + compound fields.

Binary Alloys with Iron, Nickel, or Chromium

The effects of iron, nickel, or chromium as binary additions upon the corrosion resistance of zirconium are quite similar. In general, small additions of the order of 0.1 wt % improve corrosion resistance. From this point to about 0.5 wt % the corrosion resistance is fairly insensitive to composition, while additions above about 0.5 wt % result in decreased corrosion resistance in high temperature water. In the intermediate range best corrosion resistance is obtained when the alloys are heat treated in the α + compound phase field. When present above about 0.5 wt % these elements confer corrosion resistance in steam at 750° to 1500°F (400° to 816°C) superior to that of unalloyed zirconium, but have an adverse effect upon corrosion resistance in hot water. The effect of these elements appears to be additive when more than one is present.

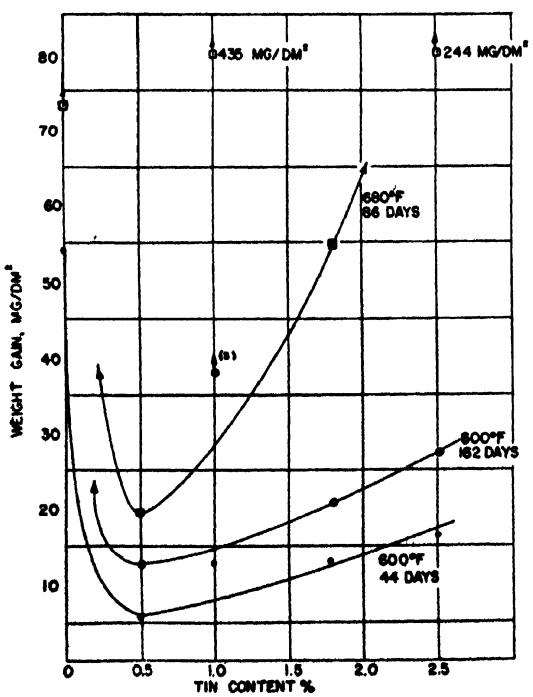

Figure 3. The effect of tin content on the corrosion resistance of arc-melted sponge base zirconium alloys. The poor corrosion resistance of the unalloyed material is due to 60 ppm of nitrogen. All alloys were made from the same batch of blended sponge zirconium

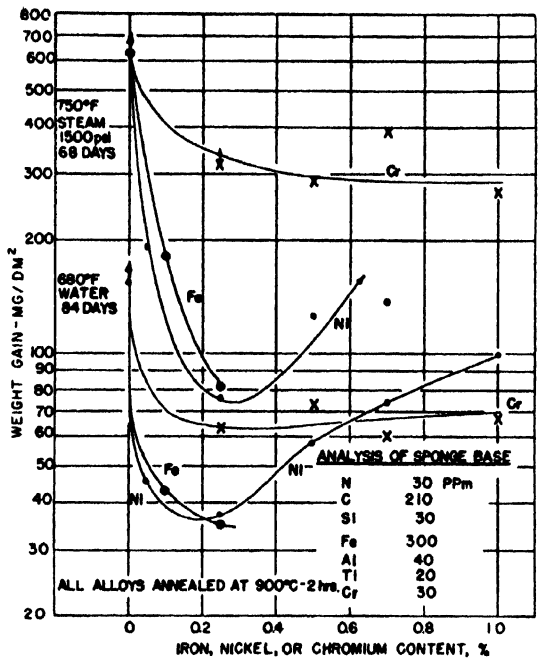

Figure 4. Corrosion of Zr-1.8 wt % n-base ternary alloys with iron, nickel, and chromium

Other Binary Alloys

Space does not permit a detailed presentation of the data on all of the alloying elements which have been investigated. There is, therefore, presented in Table IV a brief summary of the binary alloy systems which have been investigated together with a brief comment on the effect upon corrosion resistance.

Ternary and Higher Order Alloys

Zirconium-Tin Base Ternary Alloys with Iron, Nickel, or Chromium

The addition of small amounts of iron, nickel, or chromium has a very beneficial effect upon the corrosion properties of zirconium-tin alloys.[6] Figure 4 shows the weight gain after a given time as a function of ternary alloy concentration in a 1.8 wt % tin sponge-base alloy. The 1.8% tin alloy without ternary additions failed after 14 days in 680°F (360°C) water and 4½ days in 750°F (400°C) steam. However, the further addition of iron, nickel, or chromium produced a marked improvement. It will be noted that approximately 0.25 wt % of the ternary addition is required to achieve maximum corrosion resistance, and that nickel and iron appear to be more effective than chromium. Similar results were obtained at lower tin content and at 2.5 wt % tin. It is interesting to note in Fig. 4 that the steam test data reflect the same behavior as do the water test data.

Zirconium-Tin Base Ternary Alloys with Other Elements

The fact that tin is the most effective alloying element known for the purpose of counteracting impurity effects has led to the investigation of a number of ternary systems based on the zirconium-tin system.[6] None of these ternary additions has proved

Table IV. Summary of Corrosion Data on Binary Alloys[6]

Alloying element	*Range of composition, wt %*	*Effect*
Mo	0–10	Harmful
Nb	0–10	Tendency to counteract nitrogen. Much less effective than tin
Sb	10–30	Harmful
	0–3	Tends to counteract nitrogen. Much less effective than tin
U	0–100	Corrosion resistance decreases with increasing U content
Si	0–1	Harmful
Ti	0.1–100	Corrosion resistance extremely poor up to at least 20 wt %
Ta	0.05–10.0	Corrosion resistance decreased
Hf	0–2	No effect
Co	0–1.2	Corrosion resistance decreased slightly
W	0.7	Corrosion resistance decreased
Cu	0–1.5	Corrosion resistance decreased
Mn	0–5	Corrosion resistance decreased
Al,Cd,Ce,Ca,Mg Nd,Pb,Zn,La,Ga,V,Be	—	Harmful

to be as effective in improving corrosion resistance as has iron, nickel, and chromium. Among these investigated are manganese, tungsten, molybdenum, tantalum, titanium, copper, niobium, and oxygen.

Higher Order Alloys: "Zircaloy-2" and Related Alloys

The introduction of Zircaloy-2 has been instrumental in making it possible to use Kroll process zirconium sponge for commercial production of corrosion resistant material. This sponge-base alloy, developed by Westinghouse, contains 1.5 wt % tin, 0.12 wt % iron, 0.10 wt % chromium, and 0.05 wt % nickel. Nitrogen is controlled to 60 ppm maximum. The corrosion behavior of Zircaloy-2 in high temperature water and steam at a series of temperatures is illustrated in Fig. 5.[3,7] It is seen, for example at 680°F (360°C), that "breakaway" occurs at a weight gain of 34 mg/dm² after 112 days exposure. In contrast to the unalloyed material the "breakaway" time is quite reproducible and predictable. Furthermore, the term "breakaway" is now misleading since the corrosion rate after this time is linear and relatively low, and the corrosion product is adherent. Perhaps the term transition is more descriptive. Similar behavior is noted in 750°F (400°C) steam at which condition the transition occurs after 41 days after which the corrosion rate is 1.27 mg/dm²/day, while under similar conditions a 2.5% tin binary alloy reaches the transition after 7 days and has a post transition corrosion rate of 58 mg/dm²/day.

It will be noted in Fig. 5 that the exposure times required for transition at 600°F (316°C) have not been reached. However, it is estimated that a post transition corrosion rate of 0.065 mg/dm²/day begins after 1250 days exposure at a weight gain of 34 mg/dm². This corrosion rate was determined by first exposing samples in 750°F (400°C) steam for a time in excess of the transition time and then exposing the same samples at 600°F (316°C) and observing the corrosion rate.[8] A similarly determined post transition corrosion rate of 680°F (360°C) was in satisfactory agreement with that determined by continuous exposure to 680°F water.

Table V. Empirical Equations Describing the Corrosion Behavior[7,10] of Zircaloy-2*

Temperature °F	*°C*	*Pressure psi*	*Equation m in mg/dm², t in days*	
550	288	750	$\log\Delta m = 0.50 + 0.30 \log t$	
600	316	1553	$\log\Delta m = 0.74 + 0.26 \log t$	
680	360	2705	$\log\Delta m = 0.76 + 0.38 \log t$	Up to 112 days
			$(\Delta m\text{-}34) = 0.37\ (t\text{-}112)$	After 112 days
750	400	1500	$\log\Delta m = 1.10 + 0.32 \log t$	Up to 41 days
			$(\Delta m\text{-}41) = 1.27\ (t\text{-}41)$	After 41 days

* The values of the constants given in reference 10 are revised slightly here after eliminating material having miscellaneous heat treatments.

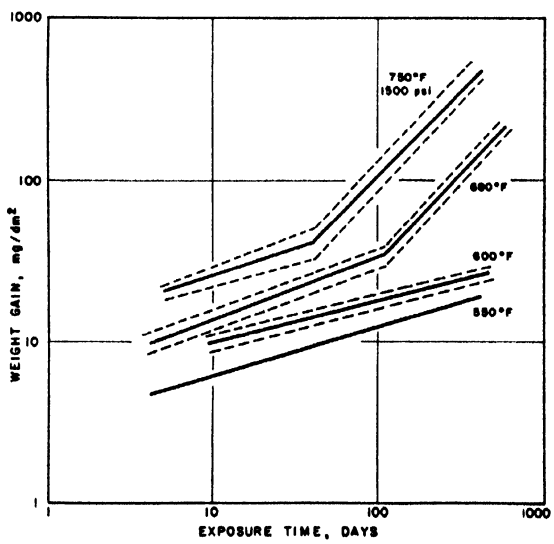

Figure 5. Weight gain—time curves of Zircaloy-2. Exposed to high temperature water and steam. The specimens exposed at 550, 680, and 750°F were previously annealed below 800°C. The specimens exposed at 600°F were in the hot rolled condition. Dotted lines indicate ± two standard deviations

Equations 1 and 2 may also be used to define the corrosion behavior of Zircaloy-2. The constants are given in Table V above, together with the equations defining corrosion behavior after the transition time.

The corrosion properties of Zircaloy-2 are relatively insensitive to heat treatment as may be seen in Fig. 6.[3,8,6] It will be seen that the weight gain after a given exposure time of 680°F (360°C) water or 750°F (400°C) steam is slightly higher for material annealed in the β-phase field than that for material annealed at lower temperatures. The corrosion rate

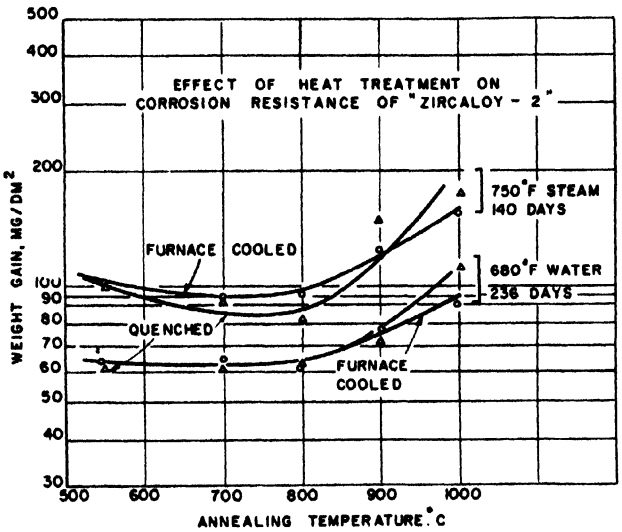

Figure 6.

is essentially unaffected by cooling rate from the annealing temperature. The effect of annealing temperature upon corrosion properties is believed to be associated with the presence of iron, nickel, and chromium since similar results are obtained when the tin content is varied from 0.7 to 1.5%.

The corrosion properties of Zircaloy-2 are insensitive to the concentration of alloying elements. The total iron, nickel, and chromium content may vary from 0.1 to 0.5 wt % without appreciable change in the corrosion rate in 680°F (360°C) water, while at 750°F (400°C) in steam the data suggest a minimum at about 0.3 wt %. The tin content may vary considerably without serious consequence. Data on alloys similar to Zircaloy-2 ((Zr-Sn-Fe, Zr-Sn-Ni) indicate that corrosion behavior improves with decreasing tin content, particularly when subjected to accelerated testing in 750°F (400°C) steam.[6]

Since nitrogen is the principal undesirable impurity encountered in practice, its effect upon the corrosion behavior of Zircaloy-2 is of great interest. Shown in Fig. 7 are corrosion data for Zircaloy-2 in which the nitrogen content varies from 40 to 190 ppm.[3,8] As indicated by the curve for 140 days exposure in 750°F (400°C) steam, a nitrogen content of about 100 ppm is without effect. However, it is important to note that the amount of nitrogen which is required to affect the weight gain depends upon the length of exposure. Thus the amount of nitrogen which can be tolerated will depend upon the severity of the application.

The effect of oxygen upon the corrosion properties of Zircaloy-2 within the range 400 to 2000 ppm is absent or very small. The effect of other impurities such as aluminum, lead, silicon, copper, and manganese is deleterious when present in quantities somewhat greater than those indicated in Fig. 5.[9] The amount by which those shown may be exceeded is not known with any degree of certainty.

Alloys containing up to 5% tin with iron, nickel, or chromium, singly or in combination may be considered to be similar to Zircaloy-2. Attempts to improve upon Zircaloy-2 have consisted first of lowering the tin content to achieve lower corrosion rates and longer transition times, and second of the addition of other elements.[6] Elements which have been added to Zircaloy-2 or to "Zircaloy-2 type" alloys without beneficial effect are niobium, molybdenum, titanium, and beryllium. Most promise appears to be in alloys containing 0.25 to 0.50 wt % tin with 0.25 to 0.40 wt % iron or iron plus nickel.

MECHANISM OF CORROSION

Since the mechanism of zirconium corrosion has been discussed in detail,[10] it is appropriate to mention here only the general nature of the argument. In the absence of impurities or alloying elements the corrosion rate of zirconium is limited by the diffusion of oxygen ions via oxygen ion vacancies from the oxide/water interface to the metal/oxide interface. This process is interrupted at the "breakaway" point which occurs when a critical film thickness has been attained. Thus the rate of diffusion of oxygen ions through the oxide governs the time necessary to reach "breakaway." If nitrogen is present in the metal and it is incorporated into oxygen ion sites in the growing oxide film as N^{+3}, additional vacancies are created with increase the rate of diffusion of oxygen ions and thus hasten "breakaway." Similarly, if tin is present and is incorporated into the oxide lattice on zirconium ion sites as Sn^{+3}, additional oxygen vacancies are created with a similar effect upon the diffusion of oxygen ions. If both tin and nitrogen are present an Sn^{+3} ion in the oxide lattice should tend to associate with an N^{+3} ion and an oxygen ion vacancy, thus tending to nullify the contribution of that vacancy to the diffusion current.

It is known that a portion of the hydrogen produced by the corrosion reaction diffuses through the oxide to the metal.[3] This fact is believed to be associated with the "breakaway" phenomenon. When sufficient

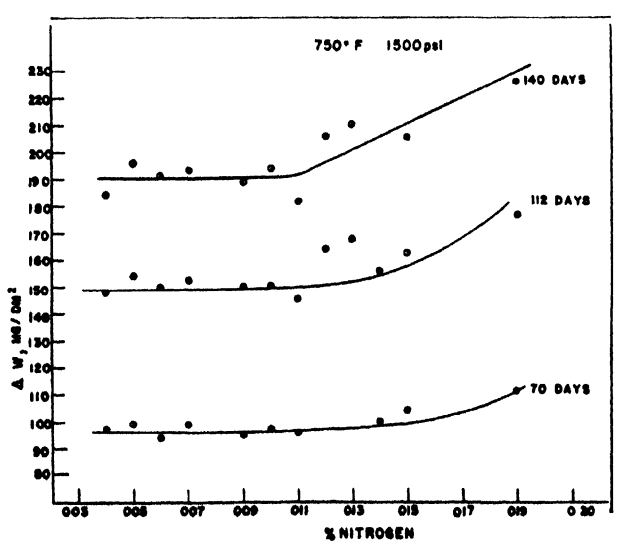

Figure 7. The effect of nitrogen content on the corrosion resistance of Zircaloy-2

hydrogen has diffused inward zirconium hydride may form at the metal/oxide interface with a resultant loss of coherency between metal and oxide. The alloying elements iron, nickel, and chromium may exert their beneficial effect by promoting the recombination of the nascent corrosion-product hydrogen to hydrogen molecules, thereby favoring the escape of hydrogen to the surrounding water.

The linear character of the corrosion kinetics after "breakaway" or after transition suggests that the corrosion rate is determined by diffusion through a protective layer of oxide next to the metal. This protective layer is presumably of constant thickness while the remainder of the oxide does not impede the transport of the reactants.

APPLICATION OF CORROSION DATA

Reference to Fig. 5 and Table V shows that Zircaloy-2 corrodes at a rate of 0.37 to 1.10 mg/dm^2/day after transition at 680° and 750°F respectively. Since this amounts to only 2 to 7 $\times$ 10^{-4} inches of metal corroded per year, it is obvious that the material has far greater corrosion resistance than is necessary from the structural standpoint in a nuclear reactor operating with water in the liquid state.

The limitation imposed by corrosion properties comes about under heat-throughput conditions.[11] In the case of a zirconium or Zircaloy-2 clad fuel element three temperatures are of interest. These are the surface temperature, the temperature at the interface between the corrosion product and the metal, and the maximum temperature of the fuel material in the interior of the fuel element. If one assumes a constant heat flux through the fuel element surfaces and a constant surface temperature, it is seen that the metal/oxide interface temperature will increase as the oxide thickness increases due to corrosion. This is of particular concern in the case of zirconium and its alloys because of the low thermal conductivity of zirconium dioxide. Furthermore, after "breakaway" or transition the corrosion rate is determined approximately by the temperature of the metal/oxide interface, since the corrosion rate in this stage is constant and presumably limited by diffusion through a relatively thin oxide layer of constant thickness lying immediately adjacent to the metal, the balance of the oxide film being nonprotective.

In the foregoing way it is seen that as corrosion proceeds under constant heat-throughput conditions the corrosion rate increases. The increase in corrosion rate and the increase in the maximum fuel temperature is calculable. The extent of corrosion may be considered excessive when either the cladding is penetrated or when the maximum fuel temperature becomes too high. Which of these occurs first depends upon the particular geometry of the fuel element, the nature of the fuel material, the surface temperature, and the heat flux.

It should now be evident that the corrosion resistance of the best zirconium alloys is necessary and desirable, and further that this corrosion resistance can be achieved only by careful control of impurities at all stages of processing, beginning with the Kroll process, and continuing through arc-melting, hot working, welding, and fabrication. While much can be done to detect off-composition and impure material by chemical and spectrographic analysis in the early stages of processing, corrosion testing of material samples or fabricated pieces is particularly valuable in detecting local contamination or segregation.

REFERENCES

1. Thomas, D. E., *Corrosion of Zirconium in High Temperature Water,* Nuclear Engineering, Part II, 16, AIChE (1954).
2. Schwartz, C. M., Vaughan, D. A. and Cocks, G. G., Battelle Memorial Institute.†
3. Goldman, K. M., Westinghouse Atomic Power Division.†
4. Pray, H. A. and Peoples, R. S., Battelle Memorial Institute.†
5. Kneppel, D. S. and Magel, T. T., DIC Massachusetts Institute of Technology (now Nuclear Metals, Inc.).†
6. Zirconium Alloy Corrosion Committee Reports (Committee members are listed at the beginning of the paper).
7. Kass, S., Westinghouse Atomic Power Division.†
8. Thomas, D. E. and Kass, S., Westinghouse Atomic Power Division.†
9. Hayes, E. T., U.S. Bureau of Mines, Albany, Oregon.†
10. *Metallurgy of Zirconium,* Ed. Lustman, B. and Kerze, F,. Vol. 4, Div. VII, NNES, McGraw-Hill Book Co. (1955)
11. Cohen, P. and Waldman, L., Westinghouse Atomic Power Division.†

† Private communication.

Aqueous Uranium and Thorium Slurries

By A. S. Kitzes and R. N. Lyon,* USA

Uranium slurries as homogeneous reactor fuels have the significant advantage over solutions of being less corrosive. In addition, slurries provide as high or higher neutron economy and share with other fluid fuels the advantages of greater simplicity within the reactor core, ease of loading and unloading, less expensive chemical processing, and the elimination of fuel element fabrication. These advantages were recognized early in the nuclear energy program over ten years ago when preliminary chemical and engineering studies were conducted by Vernon, Hiskey, Huffman and others at Columbia University and at the University of Chicago. Pumping tests at that time indicated that the UO_3 formed a hard cake in all stagnant regions, but more recently at Oak Ridge National Laboratory this has been found to be caused by impurities in the oxide.

Successful pumping of uranium oxide slurries at high temperatures for thousands of hours has led to new interest in this type of fuel. Of particular interest is the possibility of a plutonium power producer with a plutonium-bearing uranium slurry in a single region reactor or in the blanket of a two-region reactor. In this application the low corrosion rate of slurries offers a particular advantage over solutions because of the high attack rate of the solutions on stainless steels at high concentrations and high temperatures.

Of the thorium compounds which might be used in a thorium power breeder, thorium oxide slurries appear to be most promising. Uniform neutron absorption throughout the fertile material and ease of loading and unloading, absence of extraneous cladding, ease of chemical processing and the elimination of fertile element fabrication are advantages of a homogeneous fertile system. But thorium compounds for this application appear to be limited to thorium oxide, thorium carbonate, thorium fluoride or thorium oxyfluoride slurries or to thorium nitrate solutions.

Although corrosion-abrasion problems with thorium oxide slurries are known to exist, they have been found to be less difficult than expected. Based upon present knowledge there is little to be gained by using the more difficultly prepared fluoride or oxyfluoride slurries which hydrolyze into gelatinous mixtures at elevated temperatures. Thorium carbonate decomposes in water at elevated temperatures. Thorium nitrate with the use of N^{15}, may be the only thorium compound that merits attention in a fertile solution. However, the thermal and radiation instability of nitrates in general and the expense of N^{15}, reduce its value as a fertile compound.

Since the slurry behavior of uranium oxide differs from that of thorium oxide, this paper will consider the two oxides separately.

URANIUM OXIDE AND ITS SLURRIES

Chemical Stability of Oxide Slurries at Elevated Temperatures

On the basis of experiments at 250°C, it is concluded that of the common oxides of uranium (UO_3, U_3O_8, and UO_2), the trioxide is the most stable form in the hydrogen-oxygen environment expected in a reactor. Heating UO_2 and U_3O_8 slurries in a stainless steel bomb under equal pressures of hydrogen and oxygen at 150°C and above resulted in oxidation of a large fraction to the hexavalent state. In the case of uranium trioxide, however, only slight reduction occurred when the slurry was heated in the presence of a large excess of hydrogen. The data reported in Tables I, II and III were obtained by Morse and by Gillies.[1]

Uranium trioxide is stable in water at temperatures between 100°C and 300°C as the monohydrate. At room temperature, the conversion to the dihydrate is very slow. For these reasons $UO_3 \cdot H_2O$ appears to be a stable form of the oxide for use in a slurry reactor.

Preparation of $UO_3 \cdot H_2O$ Slurries

It has been found that this monohydrate can exist in three allomorphic modifications depending on its mode of preparation and treatment (Fig. 1).

A rodlet form of $UO_3 \cdot H_2O$ is produced if the anhydrous trioxide, formed by heating uranium peroxide at 300°C, is heated in water at 185°C to 300°C (Fig. 2). The rodlets can also be prepared by autoclaving at 250°C for at least 16 hours a slurry of uranium peroxide containing less than 50 parts per million uranyl nitrate as an impurity.

A platelet form of $UO_3 \cdot H_2O$ appears if the trioxide, made by decomposition of uranyl nitrate at 300°C to 400°C, is hydrated at 185°C to 300°C. Pulverized uranium trioxide rodlets digested at 200°C to 250°C convert to the platelet form, whereas pulverized uranium trioxide platelets digested at 150°C to 200°C transform into rodlets.

* Including work by members of the staff of the Homogeneous Reactor Project, Oak Ridge National Laboratory.

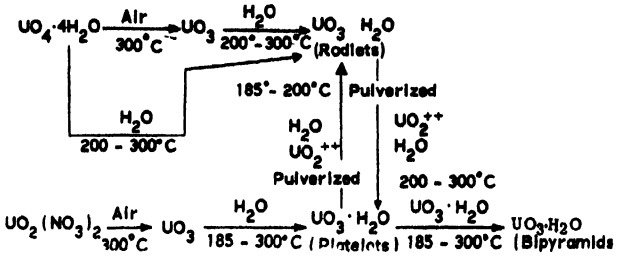

Figure 1. Preparation of $UO_3 \cdot H_2O$

Crystals which resemble truncated bipyramids are formed when either rodlets or platelets are heated with water containing several hundred parts per million of uranyl ions.

The rodlets are bright yellow in color, normally 1 to 5 microns in diameter and 10 to 30 microns long; the platelets are pale yellow in color, 6 to 50 microns on edge and about 1 micron thick; while the bipyramids are also pale yellow in color and several hundred microns along each edge. X-ray diffraction studies show that the rodlets, platelets and bipyramids all have an orthorhombic structure, but the crystal lattice parameters of each differs slightly from the others.

$UO_3 \cdot H_2O$ Slurry Characteristics

Easily suspended slurries have been prepared of both the rodlets and platelets. On the other hand, the bipyramids, because of their size, require violent agitation to keep them in suspension. With rodlets or platelets, slurries can be prepared which are dispersed and kept in suspension, by mild agitation, at both room temperature and at higher temperatures, even though settling occurs in stagnant water.

Slurries of the rodlets can be pumped satisfactorily at temperatures below 200°C, whereas, the slurries of the platelets, although easily pumped, have a tendency to form soft cakes on the pipe walls at temperatures above 200°C.

The solubility for pure $UO_3 \cdot H_2O$ in pure water is less than 10 parts per million at room temperature and is also low at high temperatures. As a result, pure $UO_3 \cdot H_2O$ slurries are essentially neutral. The presence of soluble uranyl salts of strong acids lowers the pH of the slurry, however, and increases the solubility of the oxide. In the preparation of UO_3 by the pyrolysis of $UO_2(NO_3)_2$ for example, residual nitrate can be trapped in the crystal and cannot be removed by washing. Such impure slurries release nitrate when the crystals are broken down in a pumping system and a corresponding reduction in pH occurs. Under extreme conditions the increased uranyl ion concentration in the supernate will cause serious crystal growth and the formation of hard cakes in stagnant regions. These cakes should not be confused with the soft cakes formed by pure platelets when pumped at elevated temperatures.

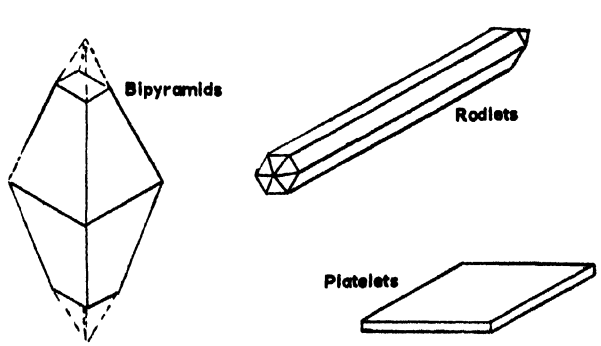

Figure 2. $UO_3 \cdot H_2O$ crystal habits

Table I. Oxidation of UO_2 Slurries upon Heating under Varying Partial Pressure of Hydrogen and Oxygen

Heating conditions		Gas pressure		Uranium oxidized,
Temp., °C	Time, hr	H_2, psi	O_2, psi	per cent
200	48	63.5	31.8	64.9
250	16		202	74.5
	16		378	82.2
	24	70	61.5	78.4
	24	70	175	91.4

Table II. Reduction of UO_3 Slurries at 250°C under Varying Partial Pressures of Hydrogen and Oxygen

	Gas pressure		Uranium reduced
Heating time, hr.	H_2, psi	O_2, psi	per cent
20	263	26.3	0.5
2	378	–	1.39
24	70	35	0
68	527	26.3	0.4

Table III. Oxidation of U_3O_8 Slurries on Heating for 24 Hours under Varying Partial Pressures of Hydrogen and Oxygen

	Gas pressure		Uranium oxidized,
Temp., °C	H_2, psi	O_2, psi	per cent
150	51.8	25.9	63.2
170	59.5	29.8	71.7
200	63.5	31.8	90.1
225	67	33.5	92.6
250	–	35	88.0
250	175	35	85.1
250	70	17.5	75.2
250	70	175	96.8

Properties of typical slurries prepared from the two crystal modifications of uranium oxide are shown in Table IV. Sedimentation of slurries prepared from both oxides are compared in Table V. It can be seen from these data that the platelets settle at a faster rate than the rodlets. It also appears that the platelets settle to a slightly higher bulk density.

A comparison of the results of particle size growth studies, as shown in Table VI, indicates that the particles of both oxides grow rapidly in the first two hours of heating at 250°C; then the rate of growth decreases markedly when the heating is extended to 24 hours. In these studies, at the end of 24 hours of heating, the equivalent spherical diameter was 3.9 mi-

Table IV. Summary of Properties of $UO_3 \cdot H_2O$ Slurries at Room Temperature

	Rodlets	Platelets
Color	Orange-yellow	Pale yellow
Size	1–5 microns in diameter	6–50 microns along each edge and 1 micron thick
Density (gm/cm³)	6.0	5.7
PH of slurry containing 25 gm U/l	6.3	6.1
Solubility in water (mg U/l)	1.4 at 25°C 1.0 at 90°C	2.6 at 24°C 4.5 at 95°C
Hydration number (moles H_2O per mole UO_3)	0.83–0.90	1.06
Behavior of slurry (250 gm U/l) on heating at 250°C for 24 hr	No agglomeration No caking	No agglomeration Slight caking

crons for the rodlets and 7.8 microns for the platelets using slurries containing 250 grams of uranium per liter of water in quartz capsules. Particle size analyses were made at room temperature by gravitational and centrifugal sedimentation.

Viscosity

For proper engineering design of systems requiring the pumping of slurries, the viscosity, density and other related physical properties of the slurries must be known as a function not only of the concentration of uranium but also of particle size.

The viscosity of $UO_3 \cdot H_2O$ slurries as a function of temperature is shown in Fig. 3. The data indicate no difference between the slurries of rodlets and platelets containing 250 gm U/l. Viscosity determinations were made by measuring the time required for a known volume of slurry to flow through a vertical tube of the proper dimensions. The pressure was fixed by the head of the suspension within the viscometer so that only the temperature and concentration could be varied for a given tube.

Plots of the fluidity (reciprocal of viscosity) versus concentration for fixed temperatures are shown in Fig. 4. The resulting isotherms when extrapolated to zero fluidity converge at a concentration of 890 gm U/l. This result is of interest since it is similar to the observed concentration of a settled slurry that has been heated at 250°C for 24 hours. The extrapolation in this fashion is not easily justified, and the result may be merely coincidental.

Table V. Representative Sedimentation Rates for $UO_3 \cdot H_2O$ Slurries at Room Temperature

Concentration (gm U/l)	Settling velocity (mm/sec)	
	Rodlets	Platelets
25	1.8	–
50	0.72	–
75	0.44	–
100	0.32	–
125	0.25	–
150	0.20	–
175	0.17	–
200	0.14	0.24
225	0.12	–
250	0.10	0.19
347	–	0.17
400	–	0.13
500	–	0.09

Heat Transfer by Forced Convection

Convective heat transfer data, obtained with a slurry of 250 gm U/l showed only about a 10 per cent reduction in heat transfer coefficient compared with that obtained under the same conditions with pure water. The data were obtained using the rod form of $UO_3 \cdot H_2O$ in a stainless steel system at a velocity of 10.5 ft/sec in a ¾ inch diameter tube, at about 150°C. Results of periodic heat transfer measurements at 150°C indicate that over-all heat transfer coefficient varies slightly with the concentration of oxide in the slurry. Using distilled water in the system, an average heat transfer coefficient of 656 BTU/hr-ft²-°F was obtained. Increasing the concentration of uranium from 50 gm/l to 250 gm/l decreased the overall heat transfer coefficient from 650 BTU/hr-ft²-°F to 600 BTU/hr-ft²-°F. The heat transfer coefficient for slurries did not vary with time, indicating that a film did not form on the heat transfer surfaces.

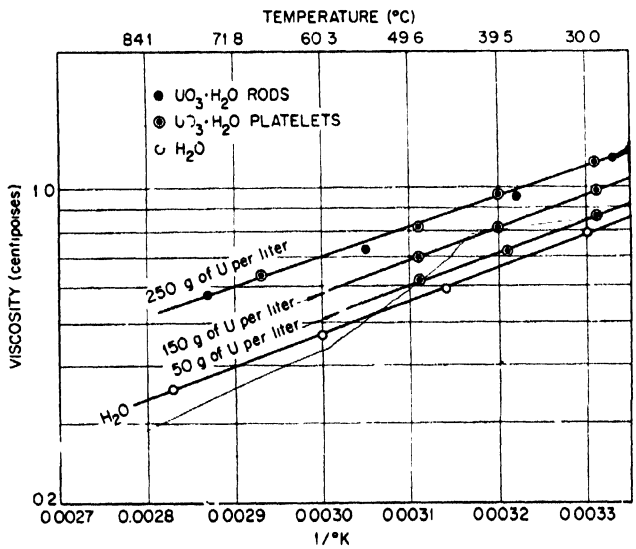

Figure 3. Viscosity of $UO_3 \cdot H_2O$ slurries as a function of temperature

Abrasion-Corrosion of Stainless Steel by $UO_3 \cdot H_2O$ Slurries

The attack of stainless steel system components by circulating uranium trioxide slurries at 250°C is essentially nil, even on pump impellers with a tip velocity of 120 feet per second.

These results were obtained in the system shown in Fig. 5 in which uranium trioxide slurries were circulated under a variety of conditions for thousands of hours.

The attack on the stainless steel components was measured in two ways: (1) by chemical analysis of slurry samples drawn from the system during operation, (2) by visual inspection of the pump impeller flow restrictor, and pipes after each test. Maximum velocity in the loop, excepting the pump, was 83 ft/sec which occurred at the throat of an orifice. Velocity of slurry in the straight runs of pipe and around the elbows was approximately 20 ft/sec.

Caking

The principal difficulty encountered in these circulation tests was the tendency to form soft cakes on the pipe walls during circulation at elevated temperatures. Rodlets, originally 2–3 microns in diameter by 15–30 microns long are apparently first abraded into spheres or ovals, 2–3 microns in diameter during circulation at 250°C, and then transformed into platelets which cake out on the pipe walls. The rodlets which appear to be the stable form at temperatures up to 200°C do not produce these cakes. No satisfactory explanation for this phenomenon has been found. However, the tendency of the $UO_3 \cdot H_2O$ to form such cakes at elevated temperatures can be greatly reduced by the use of appropriate additives.

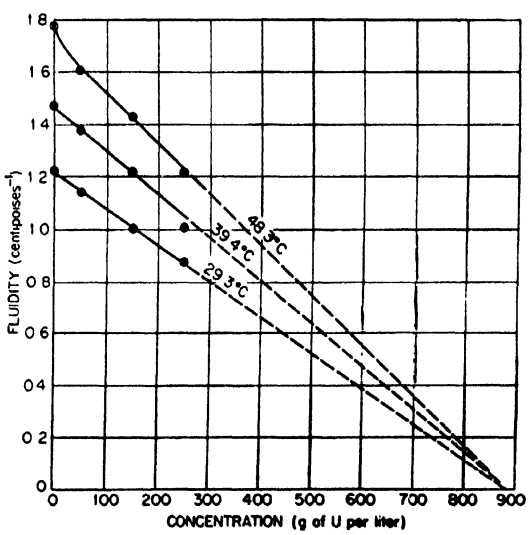

Figure 4. Fluidity of $UO_3 \cdot H_2O$ (platelet) slurries as a function of concentration

Alternative Uranium Slurries

Because of the caking tendency which caused difficulty in maintaining the concentrations of $UO_3 \cdot H_2O$ slurries during circulation at elevated temperatures, other uranium compounds such as uranyl carbonate and magnesium diuranate, were tested. These compounds were considered because they proved to be non-abrasive, non or only mildly corrosive, and because they have acceptable neutron economy. Unfortunately uranyl carbonate slurries were unsuitable because of their thermal instability at elevated temperatures. To prevent decomposition of the carbonate at higher temperatures excess CO_2 gas must be present at all times.

Table VI. Growth of Particles of $UO_3 \cdot H_2O$ on Heating at 250°C

Time, hr	*Equivalent spherical diameter of rodlets, microns*	*Equivalent spherical diameter of platelets microns*
0	0.5	1.8
1	3.0	4.8
2	3.1	6.2
4	3.2	6.0
24	3.9	7.8

Magnesium diuranate slurries were also found unsatisfactory during circulation at 250°C. Like the $UO_3 \cdot H_2O$ platelets, magnesium diuranate was found to produce soft cakes on the pipe walls. The pH of the slurry was above 10, which would enhance the attack on stainless steel if oxygen were present.

Zero Power Reactor Tests

The microscopic inhomogeneity of enriched rodlet slurry fuel was found to offer no serious difficulty in the operation of a zero-power homogeneous slurry reactor. In this reactor, suspension was established by a propeller type of mixer located near the bottom of the vessel. The reactor was extremely stable at any given stirrer speed. Changing the stirrer speed produced a change in nuclear reactivity which is attributed to a redistribution of the oxide when the stirrer was moving slowly, and to a change in the shape of a vortex type of concavity in the liquid surface when the stirrer was moving rapidly.

THORIUM OXIDE AND ITS SLURRIES

The behavior of thorium oxide slurries at elevated temperatures was found to be different than that of uranium oxide slurries. There are no phase transformations of the thorium oxide slurries at elevated temperatures, the erosive-corrosive attack on stainless steel at high velocity is many times greater than with uranium oxide and under some conditions thorium oxide slurries behave as non-Newtonian fluids so that the accepted correlations for pressure drop and heat transfer measurements are not valid without some modification.

Thorium oxide slurries show no crystal growth, and like uranium oxide slurries, they pump easily, are readily dispersible, and have a tendency to cake in the presence of some impurities. The average ultimate crystal size of thorium oxide prepared from the oxalate is about 200 Å, but these extremely small crystals are found as agglomerates ranging from 1 to 10 microns in diameter.[2]

Preparation of Thorium Oxide

Satisfactory thorium oxide for use in a high temperature circulating system can be prepared by controlled calcination of either thorium oxalate or thorium formate. In the oxalate procedure, the oxalate is precipitated at 40°C from a thorium nitrate solu-

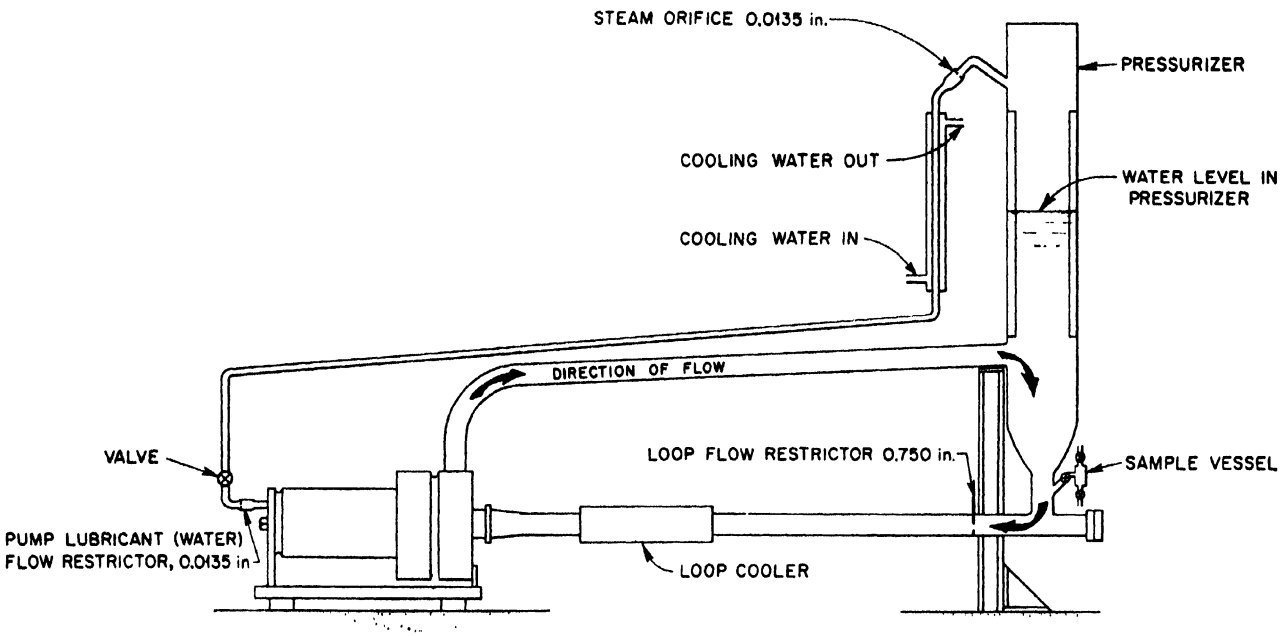

Figure 5. Schematic flow sheet for S loop

tion with solid oxalic acid, washed to remove the excess acid, and then calcined in three stages at 375°C, 525°C, and finally at 650°C or 800°C. In the formate procedure, thorium nitrate in solution is decomposed with formic acid at 95°C, washed to remove the excess acid, and then calcined at from 650°C to 800°C.

Sedimentation Rates

Sedimentation rates of thorium oxide slurries are not high, even at elevated temperatures, and no difficulty is encountered in redispersing the pure oxide after settling. The settling rates were determined by examination of motion pictures which were taken during sedimentation after a known quantity of slurry was sealed in a quartz capsule, 25 to 30 cm in length and 8 mm in diameter, heated to the desired temperature in a vertical tube furnace and agitated violently for 30 minutes to obtain a uniform suspension. The results are shown in Table VII. In these tests there was no difficulty in redispersing the solids and there was no severe packing even after standing for days.

Caking and Viscosity of ThO_2 Slurries

Caking of the solids on the pipe walls occurred during circulation at 250°C only when impurities were present. When circulated slurry was cooled below about 200°C a plastic mixture was obtained with many of the concentrated slurries. This phenomenon of thickening also occurs with many thorium oxide slurries, after violent agitation at room temperature. The rate at which the slurries become plastic depends upon the temperature at which the oxide is calcined —the lower the calcination temperature, the more readily the slurry becomes plastic with violent agitation—and on the amount and type of impurities present. Velocity gradient-shear stress diagrams, determined with a pipe line viscometer at room temperature for slurries prepared from oxide calcined at 650°C and 800°C, are shown in Figs. 6 and 7. In both cases the slurries were agitated in a baffled tank for 100 hours prior to loading into the viscometer. After mixing, distilled water was added to the concentrated slurry to make the diluted mixtures. The strain rates at the wall were computed from flow rate data by the method of Mooney.[8] Referring to Figs. 6 and 7, it will be seen that the slurries prepared from the two oxides behave as Bingham plastics—a finite yield stress was required to initiate flow. Once

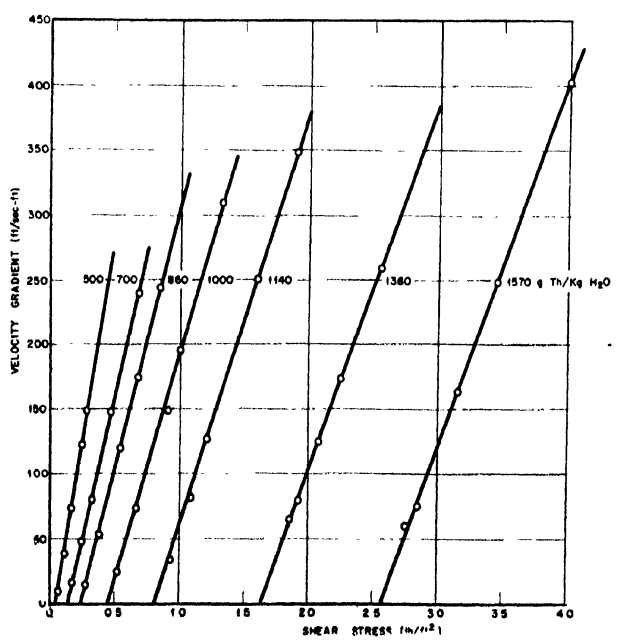

Figure 6. Shear diagram for slurry prepared from oxide calcined at 650°C

Table VII. Sedimentation Rates of ThO_2 Slurries at Elevated Temperatures

Slurry concentration (gm ThO_2 per kilogram of water)	*Rates of sedimentation (cm/sec)*				
	100°C	*150°C*	*200°C*	*250°C*	*300°C*
250	*	0.05	0.17	0.23	0.29
500	*	*	0.12	0.18	0.25
1000	*	*	*	*	*

* Solids are already in compaction.

the yield stress was exceeded for a given concentration of slurry, the apparent viscosity, defined as the shear stress divided by the velocity gradient, decreased as the velocity gradient increased. For approximately the same concentrations, the yield stresses for the slurries prepared from the oxide calcined at 800°C are less by a factor of three to four than those for the 650°C oxide.

Similar behavior was found for a slurry which has been prepared from oxide calcined at 650°C and pumped at 300°C for 300 hours as shown in Fig. 8. Data corresponding to all three figures are listed in Table VIII.

Minute additions of oxalic acid or other additives reduce drastically the viscosity of many plastic slurries at room temperature. In Fig. 9, the shear diagram for oxalate treated slurry is shown. Ten millimoles of oxalic acid per mole of thoria reduced the yield stress of the 600 gm/kg slurry from 0.37 lb/ft^2 to zero and reduced the coefficient of rigidity from 4.1 centipoises to 2.1 centipoises.

Pumping Characteristics of ThO_2 Slurries at Elevated Temperatures

Most of the pumping information reported in this paper was obtained in systems similar to that shown in Fig. 5. The slurries were easily pumped and readily dispersed after long shutdowns and there was no

Table VIII. Plasticity Parameters for ThO_2 Slurries at 25°C

Concentration gm Th/kg H_2O	*Coefficient of rigidity (centipoise)*	*Yield stress, lb/ft^2*
Slurry prepared from oxide calcined at 650°C		
500	2.35	0.05
700	3.32	0.14
860	3.58	0.26
1000	4.17	0.45
1140	4.62	0.82
1360	5.28	1.64
1570	5.25	2.58
Slurry prepared from oxide calcined at 800°C		
840	3.10	0.08
1120	4.05	0.19
1540	5.08	0.66
Slurry prepared from oxide calcined at 650°C and pumped at 300°C for 300 hours		
455	3.28	0.1
680	4.70	0.4
820	5.97	0.7
900	5.54	1.0

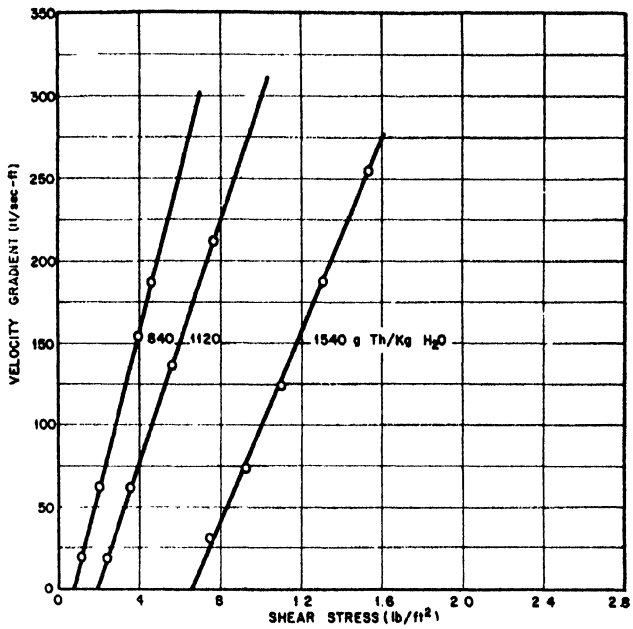

Figure 7. Shear diagram for slurry prepared from oxide calcined at 800°C

evidence of caking except with impure oxide. Although abrasion-corrosion problems were encountered the attack occurred exclusively in regions of high fluid velocity or high fluid acceleration where high shear or high impact forces would be expected. In straight pipes and standard elbows, with a velocity of 20–25 feet per second, the attack on stainless steel was essentially absent.

Several methods, other than designing for lower velocity, have been found to control attack in high

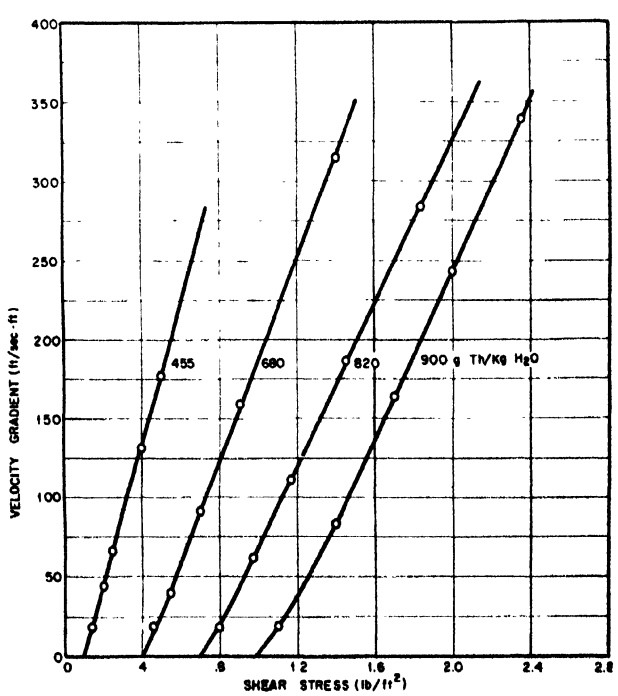

Figure 8. Shear diagram for slurry prepared from oxide calcined at 650°C and pumped at 300°C for 300 hours

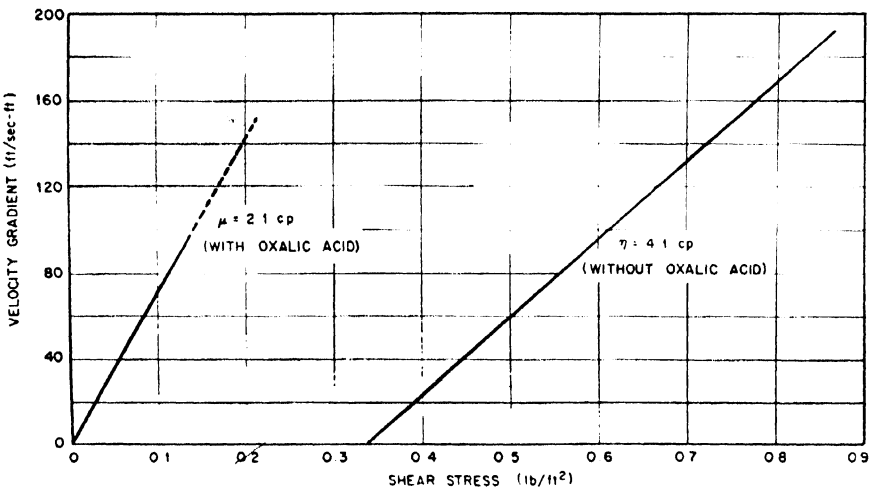

Figure 9. Effect of oxalic acid addition on the viscosity of ThO_2 slurries at 25°C

velocity regions. One method consists in substituting other materials for the stainless steel; another method is the control of slurry preparation; and a third method is by use of appropriate additives.

Resistance of Materials to Attack by Slurries

Tests with abrasion resistant and corrosion resistant metals indicate that corrosion plays an important role in the attack of high velocity thorium oxide slurries on metals. The results of experiments with corrosion resistant materials and with wear resistant materials are shown in Table IX and in Figs. 10 to 13. In the tests, four similarly shaped pieces of different materials were joined to form orifices through which the slurry was pumped at about 90 feet per second for about 140 hours at 250°C.

Table IX. Resistance of Construction Materials to Attack by ThO_2 Slurries Circulated at 250°C

Circulation time (hr)	*Thorium concentration grams/liter*	*Metal*	*Superficial Rockwell hardness*	*Weight change milligrams*
142	150	Inconel X	C-38	−17
142	150	17-4 pH stainless steel	C-37	−66
142	150	Titanium	B-80	+3
142	150	347 stainless steel	B-80	−69
141	300	Zirconium	B-88	−12
141	300	Zircaloy-2	B-95	−34
141	300	416 stainless steel	B-83	−1700
141	300	430 stainless steel	B-67.5	−269
137	300	Gold	*	−54
137	300	Platinum	B-77	−17
162	300	Stellite 98M2	C-58	−247
162	300	Zirconium	B-71	−17
162	300	Titanium	B-83	−18
162	300	347 stainless steel	B-80	−144
162	300	Carbaloy	C-92	†

* Too soft to measure hardness.
† Severely attacked, but shattered on removal from orifice holder so that the weight loss could not be determined quantitatively.

Referring to Table IX, it can be seen that those materials which formed a strongly adherent protective oxide film were resistant to the attack by the slurry. Apparently, the oxide film on the titanium, zirconium, and Zircaloy-2 was hard, unreactive and strongly adherent enough to withstand the abrasive action of the slurry; so the base metal was well protected from reaction with water. Gold and platinum, on the other hand, because they are chemically inert did not react appreciably when the base metal was exposed under these conditions. The attack on the two wear resistant materials, stellite 98M2 and carbaloy, may be due to attack on the cobalt which is a major constituent of stellite and is used as a binder in the sintered carbaloy.

Control of Attack on Stainless Steel by Thorium Oxide Slurry

The degree to which a high velocity slurry of a given concentration attacks stainless steel appears to be a function of the method of slurry manufacture and of the reagents added to the slurry. In general,

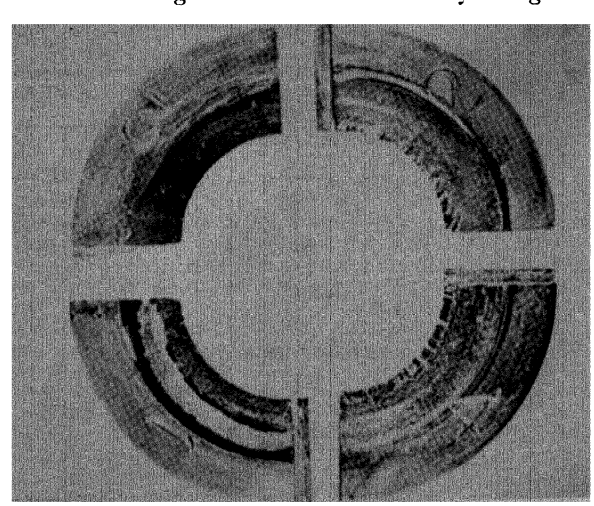

Figure 10. Upstream face of flow restrictor indicating the method of assembly; pits in inconel X (1) and type 347 stainless steel (4) indicate corrosion attack; dark area around opening on titanium (3) is black oxide film; sample 2 is Armco 17-4PH steel. 2X. Reduced 24%

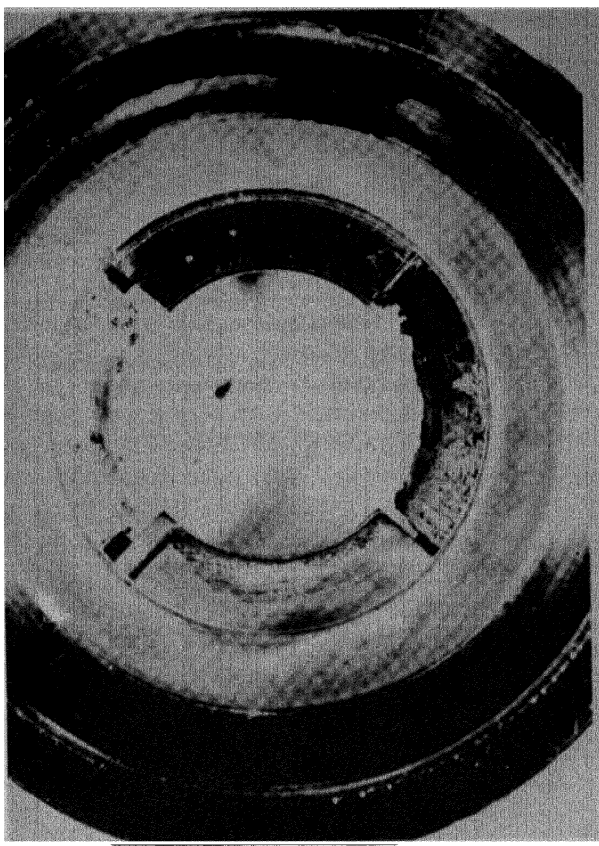

Figure 11. Downstream face of combination orifice; samples in clockwise order, zirconium, type 430 stainless steel, Zircaloy-2, and type 416 stainless steel showing corrosion attack on the stainless steels

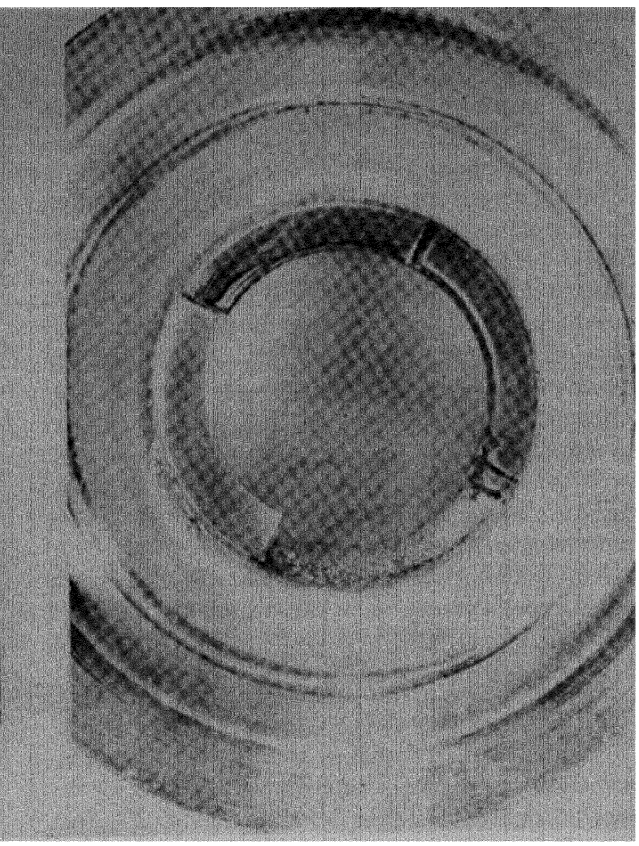

Figure 12. Upstream face of combination orifice used in run T-31; samples in clockwise order, zirconium, gold, type 430 stainless steel, and platinum

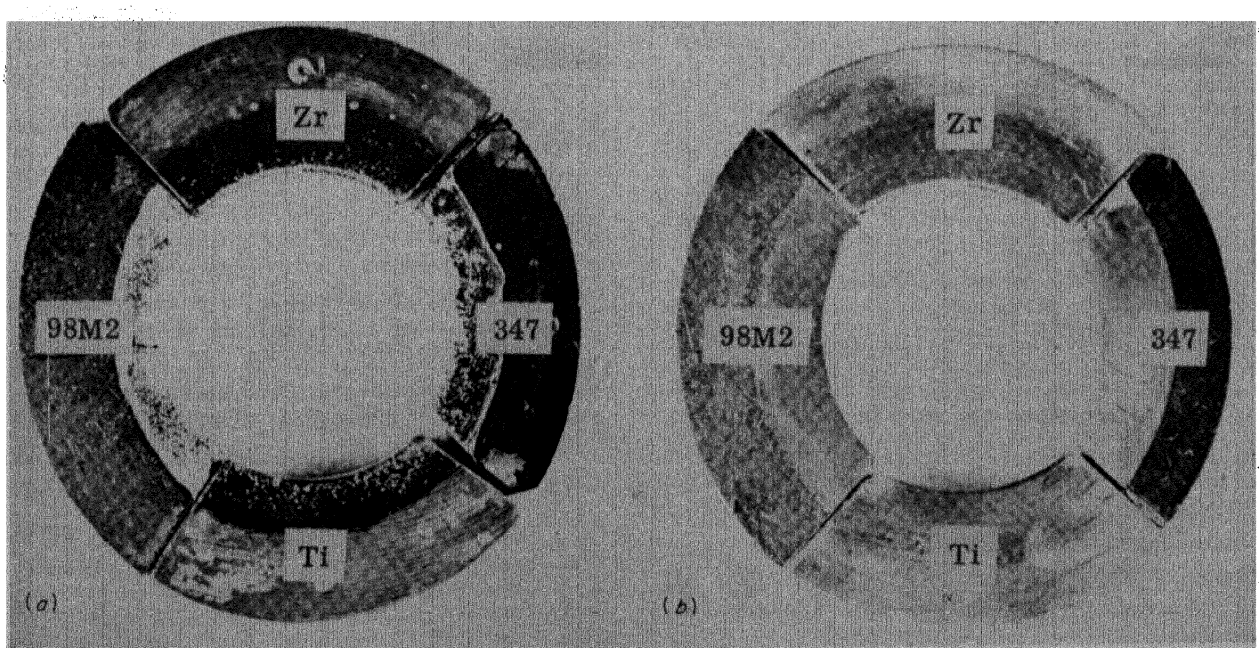

Figure 13. Composite flow restrictor showing attack on different metals by ThO_2 slurries at 250°C for 160 hr (run T-33), (a) Upstream face. (b) Downstream face. 2.5 ×. Reduced 19%

those materials produced by calcining the parent compound at high temperatures attacked stainless steel more rapidly than those calcined at low temperature. This is attributed in part to the higher crystallinity and stronger binding between crystallites. In Fig. 14, the relative attack at 250°C on stainless steel by slurries prepared from oxides calcined at 650°C, 850°C, and 950°C are shown as a function of circulation time.

Two other factors are the pH and the oxidation reduction potential of the slurry, since these factors would be expected to control the type and even existence of the protective oxide film. If impure oxide is used, the pH of a slurry may change during circulation, as the particles are broken down and the impurities are released into the water. In this connection, it is found with thorium oxide slurries, as with many other slurries, that the pH of the supernate is different from that of the slurry, when measured with a glass electrode and calomel reference electrode.

This is believed to be due to interaction of one or both of the electrodes with ions which are adsorbed on the particle surfaces.[4]

Pumps

The Westinghouse 100A pump, a canned rotor, 3450 rpm, centrifugal pump, was used in all circulation tests at elevated temperatures. The pump, designed to deliver 100 gpm with a head of 272 feet, has been operated successfully with slurries at 300°C and 1700 psi, Graphitar and stellite 98M2 are used for the bearing-journal assemblies. Very little difficulty has been experienced with this bearing-journal combination provided it is continuously flushed with water which contains no solids. A flow of as little as 1 liter per hour into the motor end of the pump has been found to be sufficient for bearing life of several thousand hours. It is believed that improvements can be made in the design which will permit much longer operation.

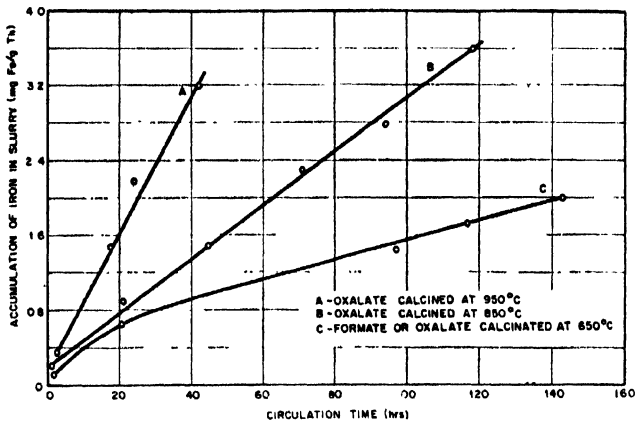

Figure 14. Attack on SS at 250°C by ThO_2 slurries prepared from oxide calcined at various temperatures

CONCLUSIONS

It is concluded that both slurry fuel and slurry fertile systems can be developed for nuclear reactors. In both cases sedimentation is less of a problem than the formation of plastic cakes either in the bulk of the material or at specific locations in the system. Abrasion and corrosion of stainless steel are essentially non-existent in $UO_3 \cdot H_2O$ slurry systems and in low velocity regions of ThO_2 systems.

The successful development of methods for handling uranium and thorium slurries at elevated temperatures provides additional means for utilizing the advantages of homogeneous power reactors.

REFERENCES

1. Gillies, D. M., "Some Studies of the Reactions of Uranium Oxides with Hydrogen, Oxygen and Water" (Columbia University), Report Number MDDC-647, United States Atomic Energy Commission, June, 1946.
2. Winfield, M. E., *et al., Australian Journal of Scientific Research,* Vol. 4, p. 648 (1951).
3. Mooney, Melvin, *Explicit Formulas for Slip and Fluidity, Journal of Rheology,* Vol. 2, No. 2, pp. 210-222, April, 1931.
4. Kruyt, H. R., *Colloid Science,* Vol. 1, Elsevier Publishing Company, New York.

Pressurized Water Reactor (PWR) Water Chemistry

By T. Rockwell III* and P. Cohen,† USA

When consideration was first given to constructing large pressurized water reactors, it was felt that the technology of handling water at 400–600°F in austenitic stainless steel systems was a relatively well known art. Application of this art to reactor systems, however, has turned up a number of problems. The purpose of this paper is to indicate what problems were considered, what steps were taken to investigate and to overcome these problems, and what the current state of knowledge is in regard to this technology. It is emphasized that these are engineering data, and the degree of really fundamental understanding of the mechanisms of these effects is small.

This discussion will be in three sections. First, we will discuss the basic potential problems: normal corrosion, effect of radiation on corrosion, etc., and summarize our current knowledge on each. Does radiation accelerate corrosion seriously? Under what conditions does fouling of heat transfer surfaces occur? What buildup of radionuclides takes place in reactor coolant? Second, we will discuss how these questions were attacked in the laboratory and what limitations must be attached to the answers: How are large numbers of autoclaves maintained at various conditions of temperature, gas content, and pH? Why does it generally require about a dozen men working for nearly two years to test a few grams of material surrounded by flowing water at 500°F in a significant neutron flux? How are specimens electrically heated without producing electrochemical effects which mask the deposition effects they are supposed to reveal? Third, we will consider the effects of this information on the design and operation of a large reactor plant. What precautions must be taken during construction to maintain adequate system cleanliness? How do dissolved gases affect warm-up and cool-down procedures? How is water sampling and analysis accomplished?

A final warning: These are interim data and conclusions. Experiments and analysis are continuing, and the data are only now being subjected to statistical scrutiny. Let us then proceed to:

* US Atomic Energy Commission.

† Westinghouse Atomic Power Division. Prepared by T. Rockwell, III and P. Cohen, including work by D. M. Wroughton, I. H. Welinsky, H. Glick, D. E. Thomas, Westinghouse Atomic Power Division; W. M. Haussler, US Atomic Energy Commission; C. R. Breden, C. H. Wohlberg, Argonne National Laboratory; and R. U. Blaser, Babcock and Wilcox Co.

THE BASIC PROBLEMS

Normal Corrosion

The development of zirconium cladding for fuel elements is a subject beyond the scope of this paper; we will note here only that from a water chemistry standpoint this development resulted in a fuel element cladding which presents essentially no corrosion problem (Fig. 1).

The gross corrosion of structural parts is also no problem. Not only is the average corrosion rate low, but no localized corrosion (pitting, intergranular or cracking) occurs. Table I summarizes the corrosion data for types 347 and 304 stainless steel, indicating the effects of dissolved hydrogen or oxygen, of temperature, of surface condition, and of velocity. None of the conditions tested led to structurally significant corrosion rates.

Many parts in the system, such as valve stems and seats, bearings, and parts of the reactor control mechanisms, required that metal parts rub against each other lubricated only by the hot water of the primary coolant system. For such use types 304 or 347 stainless steel are generally unsatisfactory. Therefore different materials had to be used which were required to meet not only the high corrosion standards, but also problems of wear and surface friction. Table II indicates the types and quantities of materials required. The use of these materials introduces potential problems of pitting corrosion, bi-metallic or "couple" corrosion, crevice corrosion, and other problems of this sort requiring a considerable expansion of the test program in order to ensure satisfactory operation.

It is concluded that normal corrosion in the absence of radiation can be satisfactorily handled with commercially available materials; the introduction of radiation, however, changes the picture considerably.

Effect of Radiation on Corrosion

Some general scattered literature exists in this field, most of which indicates that, although radiation tends to increase the rate of corrosion of metals in water, this can be without practical significance if the materials concerned produce a tight adhesive corrosion film. This conclusion is confirmed by tests on corroding material bombarded with deuterons from a cyclotron and from some in-pile corrosion specimens (see Table III).

Table I. Typical Corrosion of Stainless Steel Samples

a. Type 304 SS; Electrolytic Descaling; 500°F; water velocity 30 feet per second

Chemical addition	Time hours	Weight change rate, mg/dm²/month*	Corrosion rate by descaling, mg/dm²-month
O_2, 0–1 cm³/l	500	0	−8
		+3	−9
		+2	−7
	1000	0	−6
		+2	−3
		+3	−1
		+3	−3
	1500	+1	−3
O_2, 1–5 cm³/l	500	+3	−4
		+3	−2
		+2	−3
	1500	+1	−3
H_2, 100 cm³/l	500	+2	−1
		+3	−2
H_2, 50 cm³/l	500	+1	0
	1000	0	−1
H_2, 25 cm³/l	500	−2	−4

b. Effect of temperature on corrosion of stainless steel (347) 100 cm³ H_2 per kg, 20 feet per second as machined

Temperature, °F	Weight change, rate mg/dm²-month (1000 hr test)
500	−4.7 (avg, 12 samples)
600	−24 (avg, 5 samples)

* 165 mg/dm²-month = 0.001 inch per year.

c. Effect of surface treatment on corrosion of stainless steel; 304 and 347 SS, 600°F, 100 cm³ H_2 per kg, 1000 hr, 20 ft/sec

Material	Treatment	Appearance	Weight change rate, mg/dm²-month
347	As machined (63 rms)	Glossy, black	−24
			−24
			−24
			−23
			−23
347	Air oxidized, 48 hrs. at 800°C	Dull grey, (initially black, speckled)	−29
			−29
			−26
347	Electropolished† (–2 mils)	Glossy, light brown	− 2
			− 1
			− 1
347	20% HNO_3, 30 Minutes, 160°F	Glossy, black	−22
			−22
			−21
347	Pickled, 20% HNO_3, 5% HF, 10 minutes, 160°F	Glossy, black	−22
			−20
347	Pickled, 10% H_2SO_4 5 minutes, 160°F	Semi-glossy black with grey spots (initially brown speckled)	−19
			−17
304	As machined (63 rms)	Glossy, black	−24
			−22
			−20
			−16
			−15

† Only electropolishing seems to have any effect.

Table I—Cont'd

d. Effect of velocity on corrosion of stainless steel (304). In the absence of strong chemical effects, the influence of velocity is negligible. Velocity effects are noticeable in 0.1 M boric acid at 500°F.

Velocity, ft/sec	Weight loss rate mg/dm²-month
~ 0	1
2	8
36	11

e. Comparison of 304 and 347 SS; 600°F; 100 cm³ H_2 per kg, 1000 hr

	mg/dm²-month
347	−23 (avg, 5 samples)
304	−20 (avg, 5 samples)

f-1. Size consist of transported corrosion products of stainless steel (crud)‡

Particle size range, microns		Per cent first series
Greater than	Equal to or less than	
	0.5	44.0
0.5	1.0	30.7
1.0	1.5	18.1
1.5	2.0	5.4
2.0	2.5	1.5
2.5	3.0	0.4

‡ Technique: Demagnetized; light-field microprojector at 10,000; oil immersion.

f-2. Analysis of transported corrosion products of stainless steel

Element	Percentage
Cr	1.01
Ni	5.59
Fe	91.45
C	0.93
Si	0.30
Mn	0.78§

§ Spectrographic determination.

It is concluded that the acceleration of corrosion rate by radiation apparently produces no significant problems under the conditions tested to date. It is quite possible that other conditions (e.g., use of stainless steel clad fuel elements) might lead to trouble from this effect.

Table II. Materials Applications in Idaho Test Facility Primary System

Material	Percentage of total surface area
18-8 Stainless steel	79
Armco 17-4 Ph	9.3
Copper-nickel (70-30)	7.4
Monel	1.9
Inconel	1.4
AISI 410	0.5
Chrome plate	0.3
Stellited surfaces	0.1
Inconel X	0.1

Effect of Radiation on Water Chemistry

It is not possible to simulate completely the chemistry of water cooled reactor systems in the absence of radiation. Radiation acting upon water and its impurities creates compounds and ions not otherwise present and apparently precipitates colloids and produces other physical-chemical effects not fully understood. The water itself is decomposed into hydrogen, oxygen, hydrogen peroxide, and the various controversial complexes discussed in the literature. Conversely, an excess of hydrogen will, in the presence of sufficient ionizing radiation, tend to suppress the existence of free oxygen. Dissolved nitrogen, oxygen, and hydrogen combine under different circumstances to form ammonia, nitric acid, or various associated ions. Carbon from bearings or decomposed ion exchange resins yields carbon dioxide. These materials, of course, change the pH and electrical conductivity drastically, which in turn affects other chemical reactions. In addition, the problem of embrittlement of zirconium or steel by the dissolved nitrogen or hydrogen must also be considered.

The possibility was considered of hydrogen pressure developing between dissimilar metals (such as the reactor vessel and its cladding) due to a possible difference in diffusion rate of hydrogen through these materials. Diffusion measurements indicated that this would apparently not occur, and operation has not developed contrary evidence.

The effect of these chemical changes under irradiation is summarized in Table IV. The reader will note that some of the conditions can have serious practical consequences on the system and the plant design and operation must be devised to avoid these conditions.

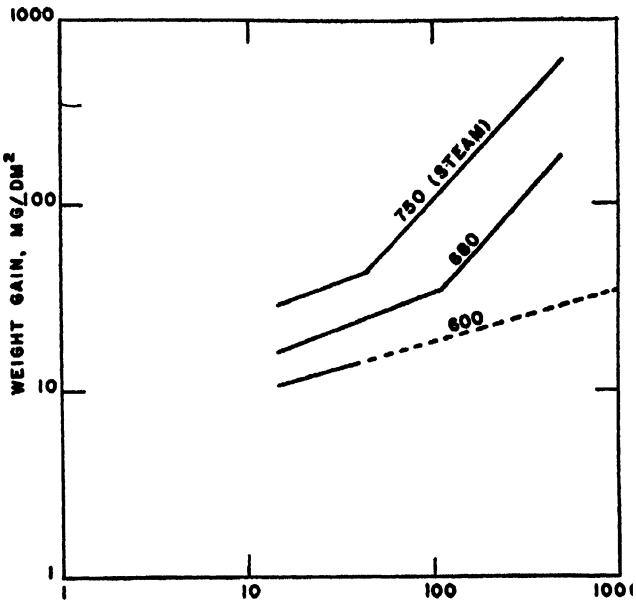

Figure 1. Typical corrosion of Zircaloy-2 autoclave tests

Table III. Effect of Irradiation on Corrosion

a. Deuteron bombardment on zirconium

1. Pre-irradiation does not affect corrosion rate.
2. Degassed water, 315°C.

Microampere-hours, cm²	*Film thickness, cm*
100	3×10^{-4}
200	5.8×10^{-4}
0 – for same time periods	One tenth of rates with simultaneous irradiation

b. Results of in-pile tests

1. Water temperature: 540°F.
2. Water velocity: 5–10 feet/sec.
3. Thermal neutron flux: approximately 10^{13} neutrons/cm² sec.

Material	*Total irradiation neutrons/cm²*	*Weight increase* of sample mg/dm²*
347 Stainless steel	0†	7
347 Stainless steel	10^{19}	10
Zr-Sn alloy	0†	4
Zr-Sn alloy	10^{19}	200
Fuel material clad with Zr-Sn alloy	0†	2
Fuel material clad with Zr-Sn alloy	10^{19}	140

* These specimens were never descaled. It is not known how much of this weight increase is due to corrosion film and how much to deposition of corrosion products from elsewhere in the loop. Significant deposition was evident on the irradiated specimens.

† All specimens were in the same loop for the same length of time, but the unirradiated specimens were outside the radiation field.

Table IV. Effect of Radiation on the Chemistry of the Coolant Water (Idaho Test Facility)

Plant condition	H_2	O_2	N_2	NH_3*	NO_3^-	*pH*	*Remarks*
1. No radiation	100 ppm	0.0	10.0	0.0	0.0	7.0	Reference condition
2. With radiation	100 ppm	0.0	10.0	0.4	0.0	9.1	NH_3 formed
3. With radiation	20 ppm	0.0	10.0	0.4	0.0	9.1	Reducing H_2 from 100 to 20 ppm has little effect
4. With radiation	5 ppm	0.03	10.0	0.4	0.0	9.1	At 5 ppm H_2, O_2 begins to appear
5. No radiation	0.0 ppm	15	80	0.0	0.0	7.0	Reference condition
6. With radiation	0.0 ppm	15	80	0.0	2.2	5.0	With O_2 present, NO_3^- appears, Cr attacked

* Corrosion tests with 10 ppm and 100 ppm of NH_3 in the water show no acceleration of corrosion of plant materials.

Effect of Radiation on Additives

Radiation decomposes many conventional boiler water additives such as hydrazine and morpholine (see Table V). Furthermore, many additives tend to accelerate water decomposition under some conditions, resulting in an intolerable amount of gas formation. Tests at the Chalk River reactor (NRX) at 200°F indicated that even a few parts per million of most additives would be unacceptable from this viewpoint, but later tests at 500°F and 2000 pounds per square inch did not produce such effects with the few materials tested. The reasons for these results are not understood. Additives also, in general, would present a problem of induced radioactivity and could possibly precipitate out in a radiation field. It has therefore been the practice to use only the purest water readily obtainable, and not to rely on any additives for inhibition of corrosion. The means for maintaining this water purity are described later in this paper.

Radioactivation of Water and Its Impurities

Even negligible corrosion rates (from a structural viewpoint) can produce significant amounts of corrosion products from the standpoint of radioactivity. For example, a rate of 10 mg/dm²/month, which is approximately that now occurring at the Idaho Test Facility, represents only 0.001 inch corrosion in 15 years, but this is still 30 grams/day total in the system. On a fresh metal surface, or one made of less resistant materials, this number could be as much as ten-fold higher.

Table VI lists the various radioactive nuclides identified in the water of the Idaho Test Facility. These are listed as equilibrium activities at full power. Also given in Table VI are the measured radiation levels which these radioactivities lead to within the shielded compartment housing the primary coolant system. There are also some data on air and surface contaminations which have resulted from various leakage and spillage of this water. It can be seen that these activities are quite satisfactorily low; maintenance of equipment in this system is done with relatively minor inconvenience without exposure to dangerous levels of radioactivity. The PWR is expected to have similar conditions, assuming that fission products can be kept from building up in the water.

Table V. Effect of Water Chemistry on Decomposition Reactions

a. Water dissociation

	H_2	O_2
Idaho Test Facility		
Corrosion products 0.5 ppm	7	0.02
LiOH, 2.5 ppm	7	0.02–0.03
Chalk River Test Loop		
Corrosion products, 0.25 ppm	10	0.25
1.0 ppm	10	0.25

b. Decomposition of additives

Morpholine: 85 per cent decomposition, 24 hours, at 525°F, 2.6×10^{13} nv (10 ppm initial conc.).

Hydrazine: complete decomposition in one-half hour under residual reactor gamma irradiation.

Fouling of Heat Transfer Surfaces

Even the small amount of corrosion product formed in these systems, if deposited on heat transfer surfaces, could decrease the overall heat transfer coefficient intolerably both by the temperature drop in the film, and because of the decrease in coolant flow due to the increased pressure drop. This has proved to be a significant radiation phenomenon.

In November, 1952, prior to starting up the Idaho Test Facility, it was reported that "with certain (not too pessimistic) assumptions, the conditions in the core after 3 weeks running without added hydrogen at 1% power or greater might be: (1) core friction factor doubled; (2) flow reduced by 10%; (3) thermal resistance of surfaces doubled which would raise the fuel surface temperature significantly. Under these conditions cleaning would be necessary after 2 to 6 weeks' operation in the power range."

The deposition is apparently caused by ionizing radiation, and also requires that certain chemical and physical conditions exist. Figure 2 and Table VII summarize the data obtained in accelerator-irradiated

Table VI

a. Radiochemistry of coolant–Idaho Test Facility

Nuclide	*Half-life*	*Specific activity**	*Source*
N^{16}	7.3 sec	100 μc/ml	O^{16} in H_2O
N^{17}	4.1 sec	800 neutrons/cm²/sec	O^{17} in H_2O
K^{88}	7.7 min	5×10^{-2} μc/ml	?
A^{41}	1.8 hr	4×10^{-2} μc/ml	Air in H_2O
F^{18}	1.9 hr	4×10^{-2} μc/ml	?
Mn^{56}	2.6 hr	0.5×10^{-2} μc/ml	Steel
Na^{24}	15 hr	$\sim 10^{-3}$ μc/ml†	Na in H_2O
Co^{60}	5.3 hr	2.5×10^{-5} μc/ml	Steel
Fe^{59}	45 days	1.1×10^{-5} μc/ml	Steel
Ta^{182}	111 days	0.6×10^{-5} μc/ml	Steel
Total crud	10–100μc/mg		

b. Effect on accessibility to system

1. The N^{16} activity creates a field of 100 to 1000 r/hr around the primary system during operation.
2. The N^{17} activity similarly causes an average neutron flux of 330 neutrons/cm²/sec during operation.
3. Fifteen minutes after shutdown, the loop activity is 0.05 to 0.1 μc/cm², giving a field of 2 to 200 mr/hr. At 100 hours it is down to 5 to 50 mr/hr.
4. Maximum surface contamination from spillage of primary loop water has been 50,000 cpm from a smear taken over 12 in². Normal surface activity is negligible.
5. Maximum air contamination during serious leakage of primary coolant into the shielded compartment has been 10^{-7} μc/cm². Normal air activity under the shield is less than 10^{-10} μc/cm².

* Saturation activity of primary coolant water at full power, full flow.

† Varies with rate of charging water.

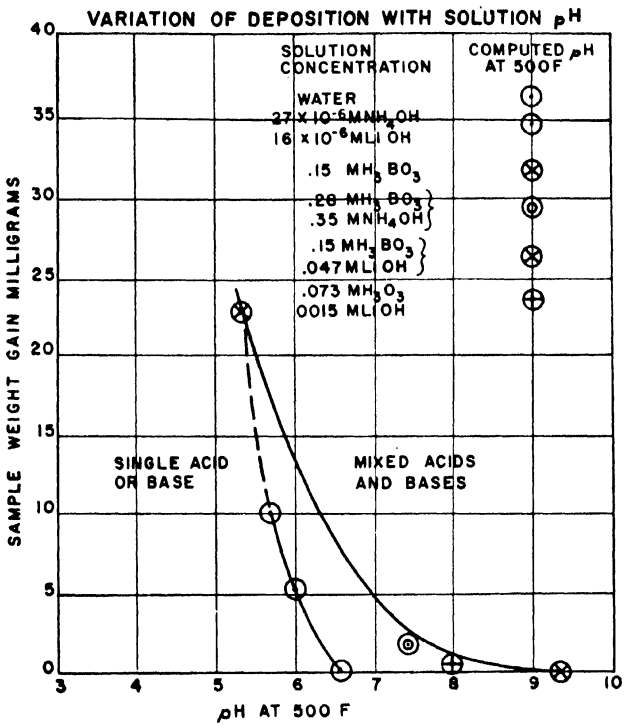

Figure 2a. Van de Graaf irradiation: effect of solution pH on deposition

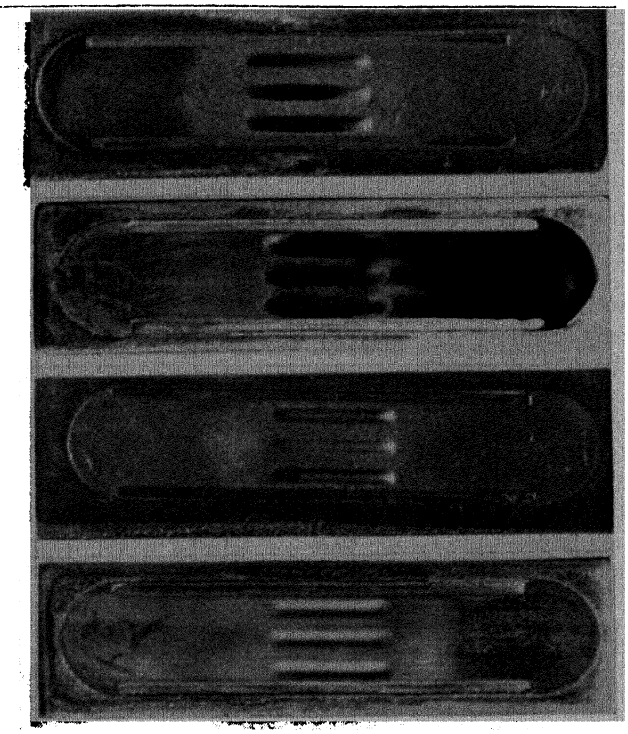

Figure 2b. Effect of pH on deposition of crud on irradiated zirconium surfaces in a circulating water system. (Loop: 500°F, 1500 psi, 8.7 ft/sec, 45 hr. No ion exchanger. Zirconium 9 mils thick. Crud added to system. Van de Graaf: 2 Mev, 100μa). Reading down: pH 6, first and second; pH 11 (LiOH), third and fourth

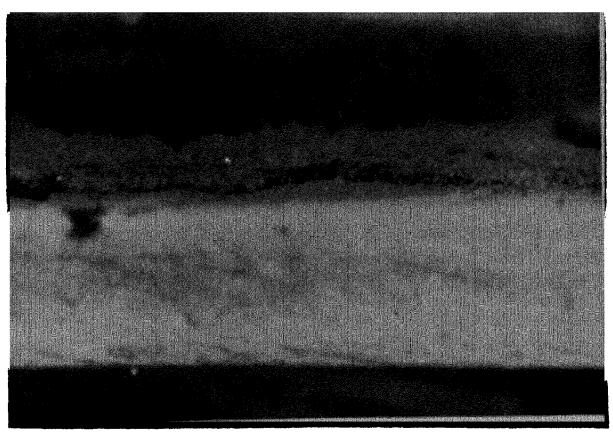

Figure 2c. Deposit on irradiated specimen 500°F, 20 cm^3 H_2 per kilo; heat transfer rate = 300,000 BTU per hour and $ft.^2$

loops and in-pile. We have been able to completely avoid the problem in reactor operation to date, but the effect is not well understood and the possibility of its occurrence in an operating plant with new conditions of flow, temperature and water chemistry cannot be overlooked.

Accumulation of Insolubles in Moving Parts

It was feared initially that this might be a serious problem. Experience with conventional steam plants indicates that some throttling valves and similar mechanisms through which large changes of water velocity occur can become traps for precipitated corrosion products. This has not been a serious problem in our reactor experience to date, although there are some circumstances under which it might be. Figure 3 shows a regulating valve stem from the Idaho Test Facility on which crud has built up. No other valves or mechanisms have given this trouble.

Effect of Water Chemistry on Friction of Rubbing Surfaces

Several experiments have been run in which the coefficient of friction between two surfaces rubbing in hot water is indirectly measured. These indicate a marked and little understood dependence upon water chemistry conditions. Table VIII summarizes the results of the few experiments done to date. An effort is being made to interpret and understand these effects, and experimental work is continuing. This phenomena is basic to the water reactor problem; more work is clearly called for and is being done.

Leaching of Fission Products from Fuel Elements

The above data and conclusions, and all of our reactor experience to date, is based upon no fission products in the water. Concentrations greater than 0.3 μc/ml will result in radiation levels around the system (within the shielded compartment) of greater than 200 mr/hr after reactor shutdown, which is the arbitrary limit which we set for easy maintenance. With fission product concentrations over 10 curies per gram in the fuel material, corrosion of one gram of fuel into the coolant or onto the walls will establish this condition. Experiments described later in this paper lead to these tentative conclusions:

1. Properly prepared uranium oxide is inert to high temperature water in the absence of oxygen. Under irradiation, the only significant fission products escaping to the water are the chains having volatile existence in excess of thirty minutes.

2. In contrast, uranium alloys fail completely after variable periods of exposure to water. The UO_2 particles retain a large fraction of their accumulated refractory fission products.

3. The gaseous and volatile fission products from oxide decay rapidly and their successors are largely soluble, short lived or very long lived, with only a few potentially troublesome species, such as Y^{93}, La^{140} and Ce^{143}.

4. The corrosion products of uranium and alloys studied are poorly transportable, accumulating on system surfaces, and at cracks and bends. Retention in the system is high.

5. Utilizing parameters based on the preliminary tests, an analytical comparison has been made of the contamination resulting from assumed rates of fuel element failures of oxide and metal fuel elements. The results indicate a substantial superiority of oxide fuel elements from the point of view of system contamination.

TECHNIQUES EMPLOYED IN WATER TECHNOLOGY DEVELOPMENT

Autoclaves

From the points of view of cost and simplicity, autoclaves are very attractive for corrosion testing in water at high temperature and pressure. Accordingly, much of the early work was done in this type of equipment. From subsequent work with more representative test conditions it was learned that autoclave tests are suitable primarily for: (1) materials not affected by velocity or coolant conditions, such as zirconium; (2) tests where low velocities or stagnant conditions are to be simulated; (3) tests where the major effect being studied is that of a stable chemical at relatively high concentrations (not velocity sensitive); (4) tests where a container is required for physical testing in water, such as wear or fretting; (5) tests where the distribution of corrosion products is not important.

Since the suitability of autoclaves must be established by testing in more complex equipment, they are most useful for conditions 2, 3, and 4. The difficulty of maintaining desired chemical conditions can be overcome by slowly pumping through the completely filled autoclaves test solutions of the desired composition, and this technique is sometimes employed.

Dynamic Loops

The next stage in the development of corrosion equipment was the pumped, isothermal loop. For this purpose totally enclosed centrifugal pumps were developed, which have operated for years at 2000 psi, 600°F without failure. Loop design has varied with designers and purpose but all have the same essential features as shown in Fig. 4; primary system including pump, test sections with sample holders, heaters, pressurizer, temperature and pressure regulators, feed pump, make-up water supply, sampling points. As interest developed, bypass purification systems were added, including coolers, filters, ion-exchangers, conductivity cells. Sample bombs for gas analyses, and gas addition systems were provided for corrosion testing.

Such loops have been built for corrosion testing with flow rates from 5 to 200 gpm (gallons per min-

Table VII. Effect of Water Chemistry on Deposition and Fouling. Heat transfer rate: 500,000 BTU per hr and ft²; zirconium tube; hot water heat source

Conditions*			Over-all heat transfer coefficient, BTU per hr and ft², °F
Ion Exchanger	O_2 conc. cm³/kl	pH	
Off	400–1100	5.6–5.9	2000
On	50–70	6.6–7.2	3300
On	100–200	7.4–7.8	3350
Off	30–50	6.0–6.7	1950
Off	<0.01	5.0–6.7	3000

Idaho Test Facility

The heat transfer characteristics of five fuel assemblies removed from the Idaho Test Facility after various periods of exposure varying from 3 months to 1 year have been studied by the cyclic heat transfer method. Observed coefficients have been the same as unirradiated assemblies within the ± 20 per cent limit of error of the method.

* These conditions were achieved in sequence on the same loop, by opening and closing the valve to the ion exchanger, and by adding and removing oxygen. Note that, not only do some conditions decrease the heat transfer coefficient, but that it is also possible to recover the higher value by restoring favorable chemical conditions.

Table VIII. Effect of Coolant Composition on Performance of Mechanisms

Composition, cm³ per kg*			
O_2	H_2	pH	Torque†, ft-lb
0.3	7.5	Neutral	4–5.5
0.01	7.5	Neutral	1.5–2.5
0.4	0.0	Neutral	5
0.6	7.0	Neutral	6
0.00	7.0	(Hydrazine added)	1.5–3.0
3.00	~0	Neutral	8.0
0.01	~0	(Hydrazine added)	1.5
0.03	5.0	10.0 (LiOH)	2.0
1.0	1.2	10.0 (LiOH)	6.0
0.03	1.2	10.0 (Hydrazine added)	2.5

* These conditions were obtained in sequence on the same loop. This demonstrates the reversibility and reproducibility of the phenomenon.

† This is an indirect measurement of the friction between rubbing parts.

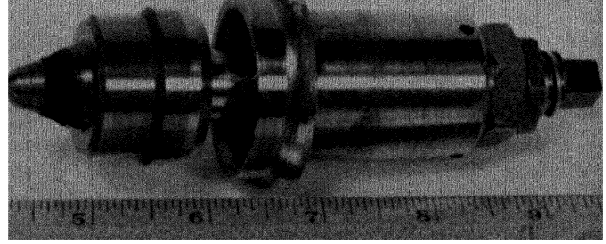

Figure 3. Crud on valve stem—Idaho test facility

ute), with test sections from ½-inch to 6-inch pipe size. Larger loops, for testing pumps, 4000 gpm, 10-inch pipe size have also been used for corrosion testing of the loop itself.

Non-Isothermal Dynamic Loops

Reactor systems operate non-isothermally. Accordingly, in the development work it became necessary to simulate this aspect in the test systems for these reasons: (1) to study corrosion under heat transfer conditions; (2) for fouling studies on heat transfer surfaces, and for heat transfer investigations; (3) to determine the effect of non-isothermal conditions on water chemistry.

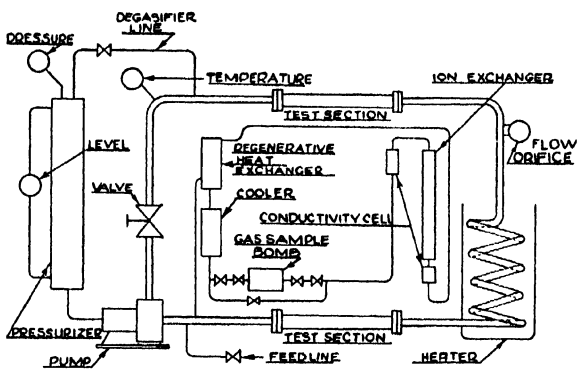

Figure 4. Diagrammatic typical dynamic corrosion loop

In the laboratory these objectives have been achieved in a variety of ways. Direct electrical heating of test specimens has been employed utilizing 400-cycle current to minimize electrolytic effects. Double circuits at different temperatures have been used, with the specimen the internal element of a double tube exchanger. Tubular samples have been heated by radiation sources.

The creation of non-isothermal conditions adds considerably to the complexity and cost of dynamic loops, but is essential for a full coverage in the laboratory of the problems of pressurized water reactor technology.

Studies with Radioactivity

Many of the problems of pressurized water reactor technology involve induced radioactivity and fission products. Problems derived from long-lived activities have been studied in the laboratory by the use of irradiated sources or separated fission products. Among these are the study of transfer of activity around a system by corrosion of irradiated metal, the corrosion of fuel and the distribution of fission products (long-lived), and the study of leakage problems.

Facilities have been developed in which sources up to ten curies have been used in the study of contamination and decontamination problems. The samples are loaded in a hot lab into a special transfer cask, and loaded therefrom into a shielded sample holder. The loops are unshielded, and after the desired activity level is reached, the sample holder is isolated. With only moderate precautions a close approximation to actual problem conditions has been achieved.

Studies with Radiation

Studies involving actual radiation processes are of the highest significance for the technology of pressurized water reactors. These include the investigation of the effect of radiation on fuels and structural materials, the effect of radiation on corrosion reactions and radiation chemical reactions in the coolant proper.

In the laboratory, for processes for which their radiations are appropriate, accelerators and gamma sources are of wide application. Deuteron bombardment has been used to study radiation effects on the corrosion of metals, and electron beams have been used for the study of radiation effects on chemical reactions. By the use of suitable thin windows these studies have been made in water at high temperature and pressure. Portable dynamic systems (the size of a small table) have been used in conjunction with a Van de Graaff generator for the study of "crud" deposition noted earlier.

Reactors provide the source of radiation of most general interest. For radiation chemistry studies small autoclaves have been used. By careful attention to design, these have been made usable at the highest available fluxes. For irradiation of appreciable quantities of fuel, particularly for the testing of prototype elements, large scale dynamic loops have been built, with suitable test sections inserted into reactors (in-pile loops). Tests in these loops provide a wide variety of information, since simultaneous studies can be made involving radiation stability, heat transfer and fouling, radiation chemistry, and radioactivity. Figure 5 shows an in-pile loop erected in the laboratory for tests prior to shipment to the reactor site.

In-pile loops, because of their coupling with reactors, must have a high degree of reliability and must include many of the features of reactor control systems. Because of the usual scarcity of space about reactors and shielding requirements, they usually must be built quite compactly. One hardly need add that they are also very expensive. The operating and size requirements for close simulation to the design problems of interest pose many problems. In-pile loops for pressures of 2400 pounds per square inch, temperatures of 600°F, test sections of three and four-inch pipe size are now in operation. Some in-pile loops have been designed for the study of problems resulting from failures of fuel elements and are capable of operating at activity levels of 10^7 to 10^8 disintegrations per milliliter per second. In others, the heat generation has exceeded 500 kilowatts.

The scarcity of suitable reactor facilities for engineering tests with in-pile loops, is one of the greatest problems in reactor development and additional facilities are being constructed.

Purification Experiments

A considerable effort was expended in the evaluation and development of a purification system for pressurized water reactors. Because of the importance of trace quantities of solubles (manganese particularly) high performance ion-exchangers were required. The finely divided state of the solid corrosion products of stainless steel dictated that filtration would have to be performed with fine pore size filters.

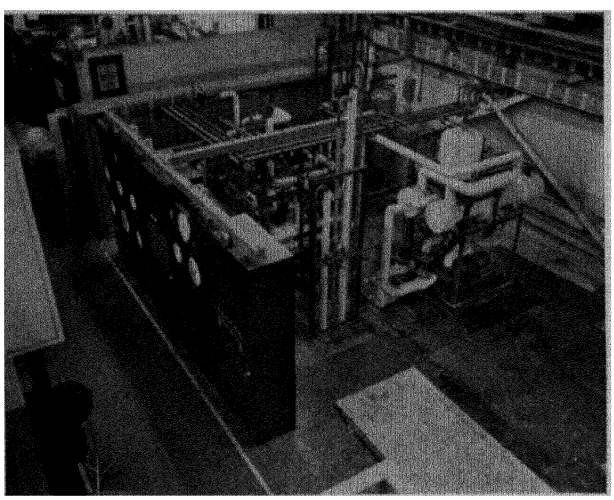

Figure 5. In-pile test loop-control panel-loop Dowtherm system

To meet these requirements studies were made of the following:

1. The performance of mixed-bed hydrogen, hydroxyl ion-exchangers at low and high pressure, and at influent concentrations of 100, 10 and 1 ppm sodium chloride.
2. The performance of similar ion-exchangers in a variety of loops including in-pile test loops.
3. Hydraulic filling and discharge techniques of full scale mock-ups.
4. Performance of 60, 20 and 10 micron mean pore-size sintered stainless steel filter plates.
5. Performance of model filter elements on large loops.
6. Autoclave and dynamic corrosion tests of filter materials.

From these experiments, materials and sizes for reactor components were selected. Additional work has since been done on improvements in application, such as:

1. Use of lithium, potassium or ammonium, and hydroxyl mixed bed resins.
2. Use of cation resins alone, particularly those stable at higher temperatures.
3. Use of magnetic and electrophoretic agglomerators for crud, coupled with filtration.
4. Use of bed filters, employing magnetite and zirconia.

For test purposes, ion-exchange materials are held in cans, which are in turn inserted into pressure vessels. Filter test elements, and filter bodies are also enclosed in pressure vessels. Continuous records of ion-exchanger performance are obtained with high pressure conductivity cells which are kept on stream continuously.

Wear and Bearing Tests

The evaluation and selection of materials for mechanical components presented the problem of wear testing in water at high temperature. Autoclaves were used as containers for the test elements and drive mechanisms were designed for two types of tests, shaft and journal (rotating) and piston cylinder (reciprocating). The rate of wear was determined as a function of material combinations, surface preparation, speed, temperature, load and chemistry of water. A very large effort was expended on this program, justified by the excellent performance in service of the wear materials selected. The outstanding chemical effects noted were the improved performance of 410 stainless steel at high pH (10.5) compared to neutral water, and the generally better performance of most materials in the presence of dissolved hydrogen (absence of oxygen).

Component Tests

Prototypes of all important components were thoroughly tested, evaluated and modified as required. Special facilities were constructed to test full size pumps, stop valves and control mechanisms. All units for the Idaho Test Facility were given production tests in the facilities previously used for development testing.

The High pH Program

The chemistry of pressurized water in stainless steel at high temperatures is markedly affected by the pH of the water. At pH values, cold, of 10–11, with strong bases, the distribution of corrosion products is substantially altered. The corrosion film is quite thick, compared to neutral water. The yield of transportable corrosion products is much lower than with neutral water. As noted earlier, the deposition of "crud" in irradiation fields is also inhibited by high pH.

In the period when the operating characteristics of pressurized water reactors with neutral water were not firmly established, a parallel effort was devoted to the study of the use of high pH. It was found by tests in both small and large systems that the pH could be maintained automatically by the use of basic mixed-bed resins in side stream purification systems. (LiOH, KOH). Carbonates are removed from the water, and soluble materials are as low or lower than in neutral water.

Operation of the Idaho Test Facility for short periods of time at high pH (10 with LiOH) indicated that the existing solid corrosion products were more filterable and that system activity increased slightly. Water dissociation did not increase. Tests on mechanisms indicated that their performance was not affected by high pH.

A hazard of high pH operation is the acceleration of corrosion by oxygen. At high pH attack on chrome-plate and stainless with the formation of

chromate is accelerated. In view of this consideration, and the so-far satisfactory performance in neutral water of the Idaho Test Facility, no further large scale testing at high pH is contemplated. For specific chemical problems, of course, the effect of pH is systematically investigated.

The Carbon Steel Program

The original selection of austenitic stainless steel for pressurized water reactor systems was dictated by the desire to minimize the various problems previously discussed. As soon as it became evident that these problems were not as serious as had been supposed work was started on the evaluation of carbon steel for reactor systems, in the interests of economy and the conservation of scarce materials.

Many of the problems investigated for stainless steel systems are being reinvestigated for carbon steel. Small and large loops of carbon steel have been built and large carbon steel components, including a boiler, are being studied in available stainless steel systems. The basic problems with carbon steel appear to be as follows. (1) high operating corrosion rates, 5 to 10 times that of stainless steel: (2) corrosion under "lay-up conditions" (system open for repairs).

Work is under way to develop conditioning treatments for carbon steel to reduce the high initial corrosion rates. Operating corrosion rates are being evaluated in terms of their effect on radioactivity and fouling of heat transfer surfaces. Means are being sought to protect carbon steel surfaces during lay-up. The techniques being utilized are essentially identical with those employed in the stainless steel studies.

The Fission Product Program

The obvious benefits from the use of high uranium content fuels in pressurized water reactors are accompanied by an increased release of fission products to the coolant upon fuel element cladding failure. Since clad integrity cannot be guaranteed, a systematic study has been begun of the mechanism, extent and effects of fission product release from high uranium fuels, both metallic and oxide.

Facilities have been installed for the study of fission product release from fuel elements irradiated at high temperature and pressure under conditions corresponding to power reactor operation. The fuel samples, both metals and oxide, have small holes to simulate cladding defects and the release therefrom of fission products and fuel corrosion products is determined during operation. The sample size of course cannot be reduced to the same scale as the test loop size corresponds to the power reactor size. Consequently, the tests as run give results comparable to the existence of some 500 similar failures in the projected reactor system. So far only a few such experiments have been run. In addition to the in-pile facilities, similar systems have been used for tests with pre-irradiated samples in which the consequences of fuel element failure have been investigated. Special systems have been designed for the investigation of the hydraulics of uranium corrosion products and for studies of contamination of surfaces by the released fission products, and their decontamination.

The current program is devoted to a detailed study of the release of fission products from UO_2, their distribution and removal from pressurized water system to permit a definitive evaluation of the problem.

Since other considerations may dictate the use of metal fuel materials, means are being sought to cope with the fission product problem from this source. Under study or being considered, are solid additives to promote transport, and solution agents to free fission products trapped in the particles of UO_2 resulting from corrosion.

PLANT DESIGN AND OPERATION

The previous pages have dealt with a laboratory viewpoint of water chemistry. In applying this to an operating reactor plant, a considerable change in emphasis inevitably took place. We will discuss this experience briefly.

System Cleanliness and Preconditioning

Early loop experience showed that, in spite of considerable care, an alarming quantity of grit, weld spatter, chips, and other foreign material became sealed with the system. It was thought in those days that much of the corrosion product found in the loop originated from this material. Extreme precautions were therefore taken to minimize this; "surgical cleanliness" was the term used.

Special cleaning and inspection specifications were issued to suppliers of components and to the plant construction contractor. Inspection of valves, pipe sections, etc. revealed that dirt was still present, so many components were disassembled and recleaned. Assembly was done in a dust-free area. Persons working around major openings in the primary system wore lintless, pocketless coveralls, shoe covers and gloves. Pipe sections were cleaned in organic solvent, nitric acid, then distilled water. Openings in cleaned sections were capped with special polyethylene caps until installation. Inventory was kept of tools, badges, buttons, and other items which could drop into the system. After final assembly and leak testing, water was circulated through the system, with a large filter screen installed in place of the reactor core. Figure 6 shows the material which was removed when the filter was withdrawn.

It is not known to what extent these precautions can be reduced, nor is it known how much initial dirt can be tolerated in a system. Although these precautions sound exacting, they can be followed rather inexpensively, and changes in these specifications will probably be made slowly.

After the system is intact, hot leakage and hydrostatic tests must be made. About two hundred hours of hot operation are thus obtained prior to initial criticality. The initial corrosion thus produced is thought to be a very important factor in determining later corrosion behavior, and it has therefore been

a practice to keep the oxygen concentration low for any operation above 200°F. Since no radiation is present during this period, hydrazine is used as an oxygen scavenger. About twice the stoichiometric amount is used; the excess is left in to decompose to harmless materials. This procedure appears to be quite satisfactory.

Some investigation is underway on the desirability of other preconditioning treatments to ensure that a stable corrosion film is established. Not enough has been done yet to evaluate the merits of such treatment.

Feedwater Treatment

Initially, feedwater was distilled, demineralized (by means of a mixed bed ion exchanger), and deaerated. Distillation is not essential to plant chemistry, and is a question of convenience. Deaeration can be eliminated if three potential troublemakers in air can be tolerated: argon, nitrogen, and oxygen.

Argon becomes A^{41} upon capturing a neutron, and can be a radiation hazard if the flux and dissolved air concentration are sufficiently high. If an abnormally high dissolved argon concentration were obtained, it would tend to concentrate in the gas bubble in the pressurizer and could present a gamma source which would inconvenience maintenance until it died down (A^{41} has a 1.8 hour half-life). If this occurred simultaneously with abnormally high leakage from the primary system into the air (e.g., via a large boiler leak, and thence to the air ejector) a problem could exist which would require some ventilation of the shielded compartment prior to entering for maintenance. Experience at the Idaho Test Facility has shown that no A^{41} radiation problem is obtained under the extremes of operation reached to date. No A^{41} problem is expected in PWR.

Nitrogen presents possible corrosion problems, but as noted in the previous section, investigation showed that these were tolerable. There is also a number of mechanical questions concerning any dissolved gases. These include cavitation at the pump intakes, pocketing in undesirable locations (such as pump windings which require water for cooling), bubbling in the reactor which could lead to reactivity fluctuations, and limitations on cool-down and warm-up procedures to ensure that gases do not come out of solution. These problems were first explored in connection with the use of dissolved hydrogen as a corrosion inhibitor (see below). It was concluded (and operation subsequently confirmed) that these problems would not present serious operating difficulties, although some modification to operating procedures would be required. For example, the system is not depressurized below 250 psi unless it is to be opened.

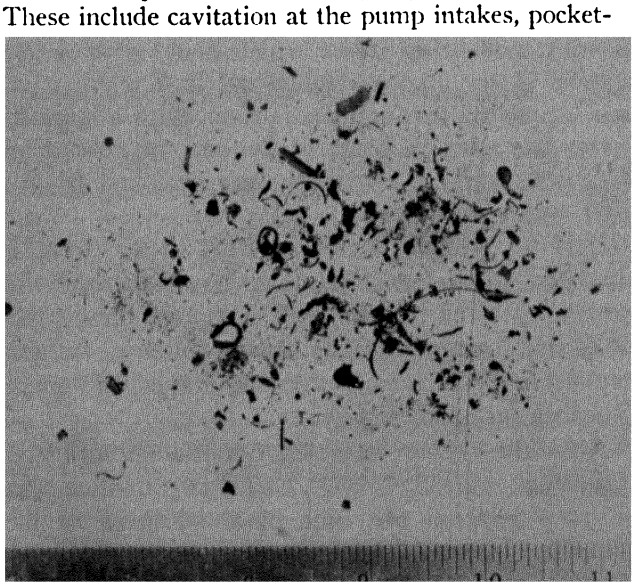

Figure 6. Debris collected during initial operations—Idaho Test Facility

Oxygen alone remains as an incentive to deaerate feedwater. Some work has been done with deoxygenating resins, but this has not been highly successful and was not followed further because experiments with feeding air-saturated water directly into the system began to show promise. Since August, 1954, the Idaho Test Facility has been operating on air saturated feedwater. This appears to be satisfactory when an excess of hydrogen is maintained in the system. Experiments are now under way in the plant to determine whether it is satisfactory to have no addition or control of hydrogen and merely allow the hydrogen produced by system corrosion to set its own concentration. We may have to choose between deoxygenation of feedwater and hydrogen addition to the system.

Corrosion Inhibitors

The use of hydrazine for precritical operation has been mentioned. For normal operation, hydrogen at a concentration of 100 cc, standard temperature and pressure, per kilogram of water was specified. This requirement was not accepted lightly by the plant designers and operators. In addition to the chemical and mechanical problems associated with dissolved gases which were noted above, there were questions associated with injection of the gas, measuring its concentration, distribution of the gas between the pressurizer bubble and the rest of the system, explosion hazards connected with venting and maintenance on the loop, and possible diffusion and leakage difficulties. A very thorough survey was made of these problems and it was concluded that operation with dissolved hydrogen was feasible and safe.

It should be noted that if all of the dissolved hydrogen in the system were released to the shielded volume, the average hydrogen concentration in that volume of air would not reach the lower limit of the explosive range. It is possible, of course, that local concentrations could be higher. For this reason, and to reduce the hydrogen inventory and consumption, it is desirable to lower the specified hydrogen concentration in the loop. Recent operational experience at the Idaho Test Facility indicates that 25–30 cm^3/kilogram is probably adequate, and the PWR specifications call for this concentration.

If the need to add, measure, and control hydrogen could be eliminated altogether, the injection system

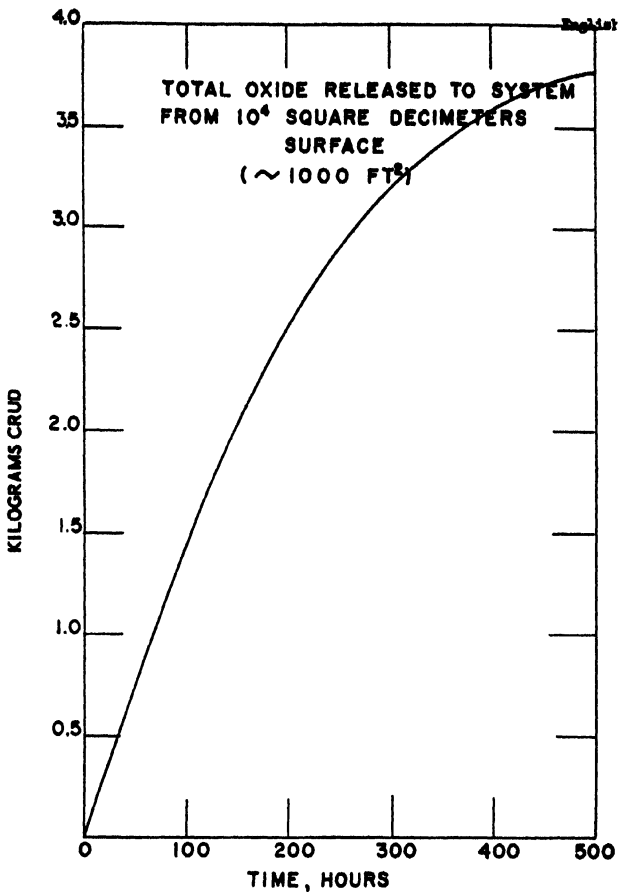

Figure 7. Corrosion products released to water—carbon steel system

and the sampling equipment devoted to gas analysis would not be necessary. This would be operationally desirable, but it has not yet been shown that such operation is feasible; considerable experimental effort is still underway. An unperturbed system tends to build up an equilibrium level of hydrogen from corrosion, ranging from 5 or 10 up to 30 cm^3/kilogram of water, depending upon the loop geometry and conditions. This concentration might be tolerable. but in an actual plant there is always the problem of significant quantities of air getting in during maintenance, filling, or by maloperation. There can then be a considerable quantity of oxygen, and little or no hydrogen, in the water, and this condition can lead to serious corrosion and sticking of mechanisms, as noted above. We are now investigating whether this condition would be tolerable with different materials than presently used; for example, chrome plate appears to be particularly sensitive to this condition.

Side-Stream Purification

Since corrosion products are continuously fed into the water, it is necessary to provide a place for them to go. There is some evidence that the soluble materials would reach a saturation level in the water which might be tolerable even without purification, but there is also some indication that insolubles are continuously produced from the soluble materials. Figure 7 shows the quantity of material which must be removed from the system in some way, if ordinary carbon steel is used for the system.

There is always appreciable leakage (several hundred gallons per day) of water past relief valves and discharge valves into discharge tanks—though leakage of coolant into the air is normally undetectably low. This provides a continuous purification, although only at a rate of a few per cent of the system volume per day. Figure 8 shows what equilibrium levels of "crud" (insolubles) would be expected if purification was accomplished only by leakage from the system.

The Idaho Test Facility is currently operating with only this leakage as purification, and plant conditions are superficially satisfactory. It is not yet known whether second order effects will build up to make such operation infeasible. With carbon steel systems, the higher corrosion rate is expected to make the feasibility of operating without any side-stream purification significantly less.

The Idaho Test Facility has a side stream of approximately 0.1% of the reactor coolant flow diverted through a mixed bed ion exchanger and through a sintered stainless steel filter. Figure 9 shows the crud levels expected at various purification rates, based on several corrosion rates. There are several possibilities for simplifying the purification system from a plant standpoint; these will be discussed separately below:

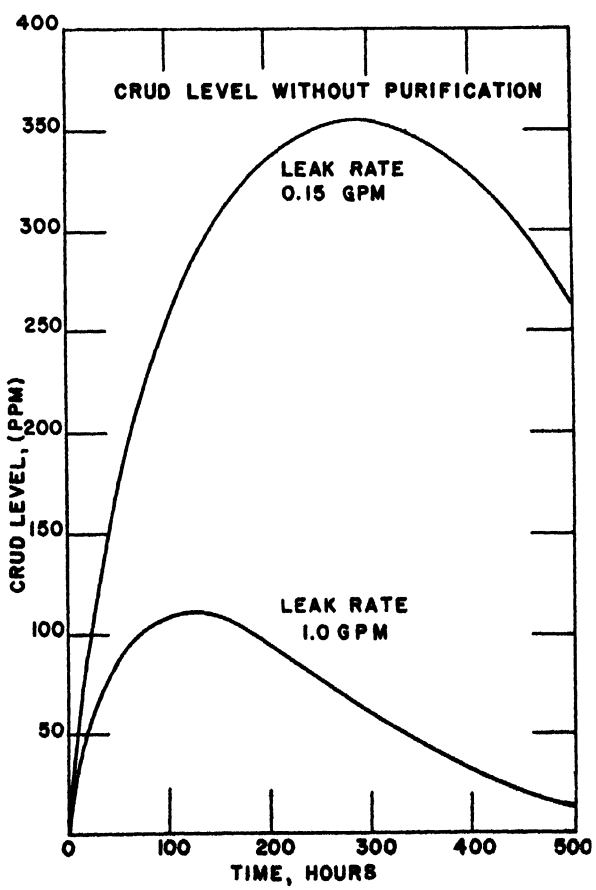

Figure 8. Crud levels without purification—carbon steel system

Filters

The sintered stainless steel filters were designed to hold many months' production of crud on their ten square feet of filter area. But, contrary to the laboratory experience, the filters at the Idaho Test Facility clogged with as little as one gram or less of crud. An arrangement was made to allow "backflushing", that is, water was run backwards through the filter, forcing the solids out into a tank external to the system. On occasions only five or ten minutes of flow through the filter built up the pressure drop from five or ten pounds per square inch to fifty. On other occasions trouble-free operation continued for two weeks or more.

This problem received a great deal of attention. The condition appeared to be a function of water chemistry, but could not be duplicated out of pile. It did not appear to result from drastic changes in the production rate of crud, although there did seem to be large variations in crud concentration during startup, apparently due to pockets being stirred up when the pumps were started up. The predominant effect appeared to be a change in the physical properties—the "filterability"—of the material. This is a well-known property of many metal hydroxides.

To minimize the amount of radioactive material discharged from the system, experiments were run to determine how little water was required to achieve an acceptable backflush. As little as five gallons could be used, if handled correctly. Later, the piping was changed to allow the material to be flushed back into the plant upstream of the ion exchanger, to be caught on the resin bed acting as a bed filter. This was moderately successful, but called for complex piping and several remotely operated valves under the shield, and it was later decided to remove the filter altogether and let the solids be continually filtered out by the resin bed. This now appears to be satisfactory and PWR is designed with such an arrangement: a resin bed and no separate filter.

Work is also underway to develop filters which will not be subject to the troubles encountered with the sintered metal units. It is obviously desirable to have a filter which does not require cooling the water. Zirconia or other particles in a bed may be the solution, and such filters are being tested.

Ion Exchanger

A standard commercial mixed bed (i.e., cation and anion removing) resin is used, designed to last six months to a year. About 40 cubic feet of resin are specified for PWR, to serve about 3000 cubic feet (20,000 gallons) of primary water. The resin has been shown experimentally to have more than adequate radiation stability, since only 10 to 30 curies of radioactivity will accumulate in the bed. But the resin must be kept below 130°F and therefore a heat exchanger must be provided to cool the water before it enters the bed. A temperature-operated protective valve is also provided. To recover some of the heat lost in cooling the water, a regenerative heat exchanger is also provided. The fine resin particles must be supported on a filter screen and further protection provided downstream in the form of an additional filter. It is obvious therefore that elimination of the ion exchange system would be an appreciable plant simplification.

Tests now in progress indicate that, just as it appears to be feasible to run with ion exchange and no filtration, it may also be feasible to run with filtration and no ion exchange. This would be a greater simplification in terms of equipment removed, but would not be satisfactory unless an operable high temperature filter were developed.

Coolant Sampling and Analysis

The PWR will have sample taps at the inlet and the outlet of the demineralizers and routine measurements will be made of gross radioactivity and for Sr^{89}, Sr^{90}, as an indication of fission products. Analyses may also be made for oxygen or hydrogen when desirable. A great deal of work has been done on coolant sampling and a lengthy treatise could be written on it. We will summarize the types of analyses made at the Idaho Test Facility and explain why it is now considered that they need not be made routinely to ensure satisfactory plant operation.

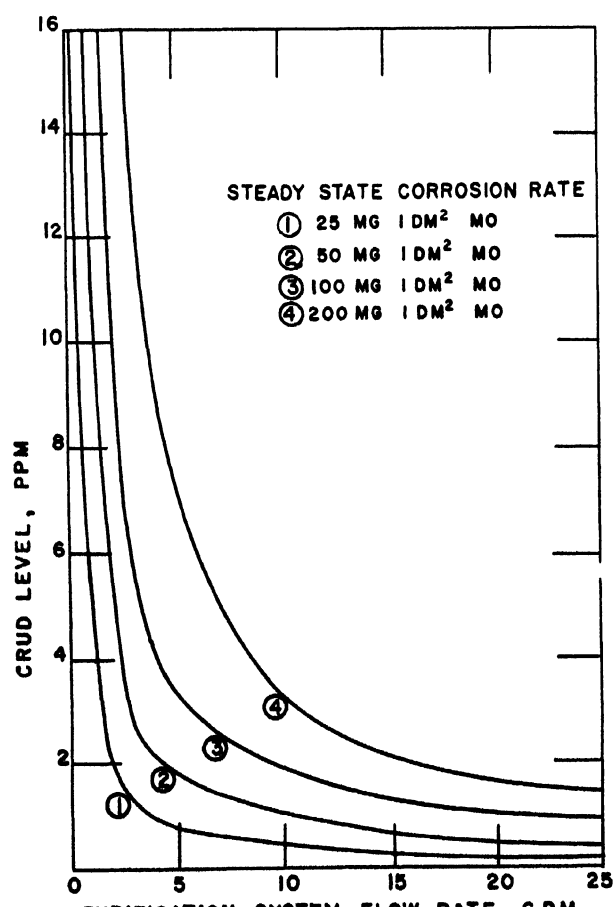

Figure 9. Crud levels with purification—carbon steel system

Electrical Conductivity

In-stream conductivity measurements are simple to make and may foreshadow problems sooner than any other variable. But conductivity can change with no significant problem occurring (e.g., when NH_3 production increases). It is concluded that radioactivity indicates directly the variable which should be watched and that knowledge of conductivity adds little to the operator's ability to control the plant chemistry.

pH

A similar argument holds for pH, although both of these variables are watched during chemistry experiments at Idaho.

Crud Level

It was initially assumed that the quantity of suspended matter in the system was the prime indication of the possibility of deposition. Several special pitot tubes were devised to bring streams of primary water into the sample shack without changing velocity (to prevent crud settling out). These had to be cooled and delayed approximately a minute to allow the seven-second N^{16} to decay. The water is then filtered and the solids weighed. This information is still gathered at Idaho but the technique is tedious, the sampling questionable, and the information so erratic as to be useless for plant control.

Gas Analysis

Analysis for dissolved gases is tedious and requires complex plumbing and analytical equipment. For following chemical experiments in the plant such information is essential. Removing a sample for analysis is the biggest operational and design complication. If it is desired to follow only hydrogen concentration, it is possible to measure the differential pressure across a palladium disc through which hydrogen diffuses. This device has been used experimentally but has not yet been completely proved out. A modified vacuum Winkler procedure and the Blacet-Leighton technique have both been used for oxygen analysis. Standard Orsat techniques have been used for hydrogen, carbon dioxide, and others.

Chemical Analyses

During certain tests, analyses have been made for CrO_4^-, NO_3^- or other specific ions expected to indicate incipient trouble. For example, an excess of oxygen will first attack chrome plate and analyses for CrO_4^- are made during tests which might lead to this condition.

Mechanical Indications

There are several sensitive mechanical indices to chemical trouble and these are routinely watched. One is friction of rubbing parts, as shown by the electric current drawn by control motors or valve operators. Another is indication that the "scram latches" on the control rods are sticking. Another indicator is pressure drop across the reactor. This has never shown any increase attributable to crud at the Idaho Test Facility, but it is calculated that a measurable increase in pressure drop would occur before the fuel element temperature would rise intolerably. Another criterion is flow through a throttling valve; the only crud accumulation noted to date has been in the control valve to the ion exchanger, and the flow through this valve is of course markedly decreased by even a small quantity of crud. All valve operation is watched, but so far no crud trouble has been detected there.

Waste Disposal

With the low radioactivity of water cooled plants, waste disposal poses little problem. *Filter backflush* has been eliminated. *Ion exchange resin* is backflushed once or twice a year into a shielded catch tank and later buried—the 1 to 10 curies representing little problem. The *coolant itself* is within lifetime drinking water tolerance for all nuclides within hours after removal from the system, even under extreme operating conditions. There are no gas disposal problems.

If *fission products* are present in significant quantities, then standard high-level radioactive waste handling procedures must be followed. PWR is providing for such a contingency.

Core Cleaning and Decontamination

Before initial plant operation, it was feared that deposition of crud in the core and of radioactive material on the piping might be so severe as to require a shutdown for cleanup and decontamination. Considerable effort was made to develop a satisfactory technique, but without significant success. Fortunately this did not turn out to be a problem. The core has required no cleaning, and components removed from the loop have needed only surface cleaning with commercial detergents and cleaners. Large components, exposed to the primary coolant for several thousand hours at temperature, measure only 10–50 mr/hr at contact.

Applications of Square-Wave Polarography to Analytical Problems from Experimental Reactor Loops

By D. J. Ferrett and G. W. C. Milner,* UK

ABSTRACT

The sensitivity of the Barker Square-Wave Polarograph makes analysis of very low concentrations of metal ions possible. Thus 0.1 ppm of reversibly reduced metal ions may be determined in 2 ml sample solutions. Moreover, the differential nature of the instrument allows the simultaneous determination of a number of metal ions. Fe, Cr, Mn and Ni can all be determined polarographically, and the technique is, therefore, well suited to the study of corrosion products from stainless steel experimental reactor loops. Fe may be determined in salicylic and citric acid solution, while Fe and Cr may be simultaneously determined in $5M$ sodium hydroxide, 3% mannitol solutions.

The polarographic steps for manganese and nickel in alkaline cyanide solutions have been studied, and the best conditions for the separation of the steps has been found in $1M$ KOH, $0.03M$ KCN containing sodium sulphite solution. Both these elements may be determined together.

With the use of the square-wave polarograph, it would appear to be possible to determine rapidly and accurately the principle corrosion products found in reactor loop-lines, down to 0.2 ppm on 2 ml or less of sample.

INTRODUCTION

One of the purposes of the experimental reactor loops being constructed at A.E.R.E., Harwell, is to obtain data on the corrosion problems associated with stainless steel/water systems. At the temperatures and pressures used, and under the high incidence of radiation that is possible, corrosion of the steel loop may take place, and it is obviously essential to have analytical techniques that can determine the extent of this corrosion. Besides studies of gas evolution, conductivity and pH, a knowledge of the ionic species present in solution is required. The small total volume of circulating liquid, often used in these experimental loops, limits the amount of water sample that can be withdrawn. Large replenishments of the volume will alter the reaction conditions considerably. Essentially an analytical method is required that will determine the various ions present at the ppm level in 1–2 ml of sample. In this paper the application of the Barker Square-Wave Polarograph to this problem is suggested.

DISCUSSION

The metal ions likely to be present as a result of corrosion are those of iron, chromium, manganese and nickel.

To determine these four elements with conventional polarographic equipment would involve a search for a base-solution in which the half-wave potentials of these elements were sufficiently far apart for their reduction steps to be clearly defined. Normal polarographic techniques are, however, insufficiently sensitive to determine ions at the ppm levels required and in general, the analysis of mixtures of reducible metal ions by classical polarographic techniques is often difficult. This is especially so, when it is necessary to determine the concentration of a metal ion in the presence of larger concentrations of other metal ions that are reduced at more positive potentials, or when it is necessary to determine the concentration of two metal ions whose half-wave potentials are so close together that their waves coalesce. Such difficulties are largely overcome in derivative polarography. In this technique various methods, e.g., the use of two electrodes,[1] or suitable circuit design,[2] enable the slopes of the classical current-voltage curves to be obtained automatically, and the normal polarographic step is recorded as a peak, whose maximum height is at the half-wave potential.

Derivative-type polarograms are also obtained when a small alternating potential is superimposed upon the normal slowly changing dc potential applied to the cell and the alternating component of the cell current is recorded. Breyer, Gutman and Hacobian[3] demonstrated the possibilities of this technique by obtaining separate peaks for the components of a mixture of Bi^{+++}, Sb^{+++}, Pb^{++}, Tl^{+}, In^{+++}, Cd^{++} and Sn^{++} in chloride-base electrolyte. These elements were present at concentrations of 10^{-3}–$10^{-4}M$.

In addition to the alternating component of current due to the reduction of metal ions at the dropping electrode, the double-layer capacity of the mercury/solution interface also gives rise to an alternating component. It is this factor that initially limited the extension of ac polarography to concentrations of reducible metal ions less than $10^{-4}M$.

Such difficulties are overcome in the square-wave polarograph designed by Barker.[4] Analytical applica-

*Atomic Energy Research Establishment, Harwell, Berks.

tions in this laboratory[5,6] have shown that mixtures of metals whose half-wave potentials are too close together for satisfactory polarographic determinations, may be determined with this instrument. Moreover, the levels at which these determinations may be carried out is at least a hundredfold less than with conventional polarographic equipment.

The highly increased sensitivity and resolution is obviously of great value in this type of study, but a limitation exists with the square-wave polarograph, for both these factors decrease rapidly when the reaction is irreversible. Manganese and nickel, for example, cannot be determined in acid solutions, but only when complexes are formed with high concentrations of strongly electro-negative ions, e.g., in 20*M* chloride[7] or in alkaline cyanide solutions.[6]

A simultaneous determination of Fe, Cr, Mn and Ni would, therefore, have to be carried out in some such medium, but under these conditions the iron and chromium steps are not separated. The procedure suggested here divides the sample; in one half iron and chromium are determined together, in the other manganese and nickel are determined together.

APPARATUS AND EXPERIMENTAL TECHNIQUE

The square-wave polarograph used was built to the design of G. C. Barker, by Electronics Division, A.E.R.E. and is the subject of British (709826) and foreign patent applications by the National Research Development Corporation.

The current-voltage curves were automatically recorded on a Honeywell-Brown potentiometer-type recorder. The polarographic cell of capacity 10 ml was constructed of Pyrex glass to the design of Figure 1. The cup A was designed to catch the mercury drops and prevent them from falling into a mercury pool anode. (Coalescence of the drop with the pool is not immediate and irregularities may produce disturbances in the strobing circuit.) The anode area was approximately 1 cm^2. An inlet tube was provided for nitrogen and a second tube for the withdrawal of excess mercury from the cup after prolonged electrolysis. The cell was fitted with a B19 socket, the capillary passing through the corresponding cone. The joint was left ungreased, as organic contaminants may enter the solution to be adsorbed at the double layer on the mercury drop and may reduce the peak height. The cell was thermostatted at 25 ± 0.1°C in a water bath.

The high sensitivity possible with the square-wave polarograph means that the reagents used have to be of the highest purity. Redistilled water of AR grade was further purified by passage through a mixed-bed ion-exchange column and was then sufficiently pure for general use. For determinations at concentrations of metal ion of 1 ppm or less, even greater precautions in the purification of the reagents are necessary.[5] The reagents used were of "Polaritan" standard when available. It is necessary for efficient operation of the strobing and amplifier circuits that the total series resistance of capillary and cell solution should not exceed 50 ohms. This was ensured by working with solutions with a total molality greater than 1.

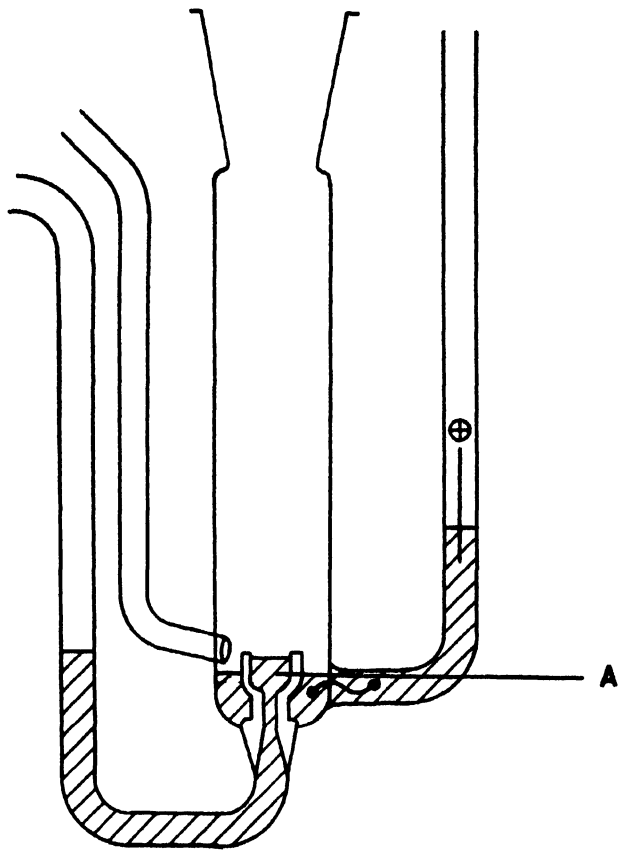

Figure 1. Polarograph cell

THE IRON/CHROMIUM SYSTEM

Any chromium present in the sample solution may be in a mixture of the chromic and chromate states. In this method, therefore, a preliminary oxidation step is incorporated to ensure that all the chromium is in the chromate state. The reduction step from chromate in sodium hydroxide has been shown to be reversible and to have a half-wave potential of —0.85 v vs S.C.E. (Standard Calomel Electrode).[8] Under these conditions however, any iron present will not be in solution unless complexed, and it is unfortunate that the half-wave potentials of most of the iron-complexes in sodium hydroxide lie very near to —0.85 volt. Thus although tartaric, salicylic, citric, mandelic, malonic, and glycollic acids, triethanolamine and diethylamine, potassium benzohydroxamate, tiron and sucrose were all found to form iron complexes which were reversibly reduced, none proved to be satisfactory for the iron/chromium system.

The only conditions found under which the iron and chromium steps were satisfactorily separated were the 3*M* NaOH 3% mannitol system used by Reynolds and Shalgosky.[9] Here the half-wave potential for iron is —0.81 v vs S.C.E. and that for chromium is —0.60 v. Neither step is however, very reversible. As Figure 2 shows, however, the reversibility increases with increase in hydroxide concentra-

tion from 1*M* to 5*M* NaOH. The increase in reversibility is only slight above 5*M*, and a 5*M* NaOH system was adopted as it is important to keep the concentration of base solution as low as possible to reduce impurity problems to a minimum.

The minimum concentration of mannitol necessary to ensure that all the iron was fully complexed was 3% at the iron levels studied; increasing concentrations of mannitol, up to 10% (the saturation concentration in 5*M* NaOH) had no effect on the size and shape of the steps. The base-solution used, therefore, for iron and chromium was 5*M* NaOH, 3% mannitol.

Standard solutions of iron were prepared from the spec-pure metal by dissolving it in a few millilitres of hydrochloric acid and heating with 60% perchloric acid until fumes of the perchloric acid appeared. The chromium solution was prepared from Analar chromic oxide. Final strengths of these solutions were about 10 μg/ml. A solution 10*M* NaOH, 6% mannitol was added to the required volumes of these standard solutions and these then diluted appropriately. Calibration graphs for these elements separately and together were prepared for the ranges 100 μg/ml to 0.8 μg/ml Fe and Cr. These are shown in Figure 3. The linearity enables both elements to be determined together down to these low levels.

The chromium step at 0.8 μg/ml was still well separated from the iron step and could easily be measured, even when the iron was in hundredfold excess. For iron and chromium solutions of 0.2 μg/ml clearly defined steps of 40 divisions (equivalent to 11 cm of recorder chart) were obtained. The baseline fluctuation at this sensitivity is ± 5 divisions, so that concentrations of these elements as low as 0.03 μg/ml may be detected with this technique.

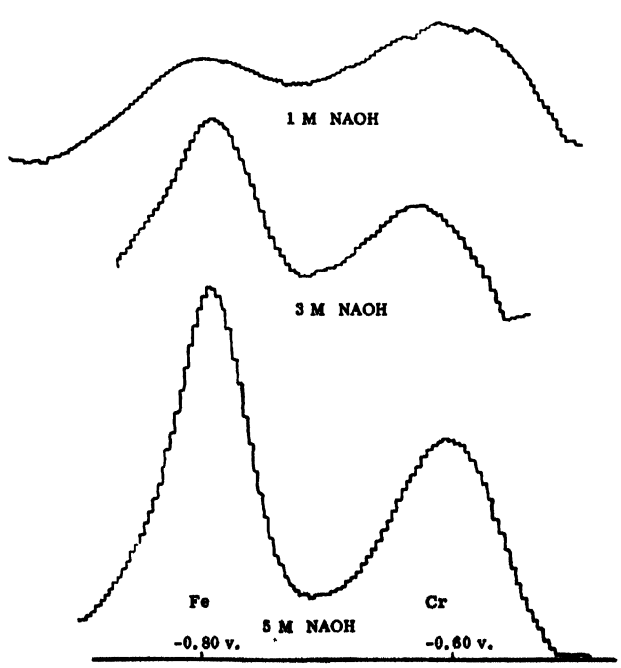

Figure 2. Variations in reversibility with NaOH concentration (all solutions 3% in mannitol). Concentrations: Fe ~ 10μg/ml, Cr ~ 6μg/ml

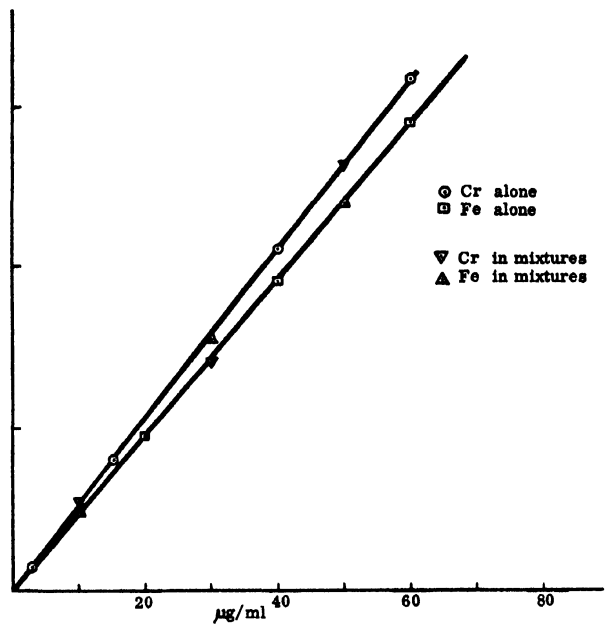

Figure 3. Peak-height for iron and chromium in 5M NaOH 3% mannitol

The sodium hydroxide contains sufficient iron to give a blank equivalent to 1 μg/ml of iron. This iron may be removed by controlled potential electrolysis[10], apparatus being available for this in the laboratory. There is no apparent chromium blank. Nickel does not give a step under these solution conditions; manganese gives a small drawn-out wave, $F\frac{1}{2} = -0.48$ v but does not interfere.

At these low chromium concentrations it is important to ensure that all the metal is fully converted to the chromate state and remains fully oxidized throughout. It is well known, for instance, that small traces of reducing agents likely to be present, e.g. nitrite ions, will readily reduce chromium at these low concentrations.

An ammonium persulphate oxidation procedure is the most satisfactory method of ensuring complete oxidation from the chromic to the chromate state at this level. It is, however, essential to ensure that no excess of persulphate remains after the oxidation, as this would interfere with a polarographic determination. Chromic ions are most rapidly oxidized in weakly acidic solutions; persulphate most readily destroyed in more strongly acid solution.

The procedure for the oxidation was, therefore:

Take 1 ml of the sample solution, in a 10 ml tall-form micro-beaker, add 0.1 ml of 10*N* sulphuric acid, 1 ml of 0.5% solution of ammonium persulphate and dilute to 3 ml with water. Cover the beaker, bring slowly to boiling point and then keep at near boiling for 15 min, maintaining solution level by replenishment with boiling water. Cool slightly. Add a further 0.4 ml of 10*N* sulphuric acid and simmer for 10 min allowing volume to decrease to about 2 ml. Cool. Add 2.5 ml 10M NaOH, 6% mannitol and dilute to 5 ml with water.

(When fuming with perchloric acid was tried, some chromium was always found finally in the reduced state. It had been reduced presumably by peroxide, or by chlorinated reducing agents produced by breakdown of the perchloric acid. It has been claimed[11] that this reaction can be prevented by rapid cooling after fuming, dilution with water, and boiling after the addition of a few drops of dilute potassium permanganate solution. The chromium was then determined by amperometric titration. We never found that this technique gave consistently reliable polarograms and at times high blanks were obtained. These were probably due to the polarographic reduction of break-down products of the perchloric acid.)

The persulphate oxidation procedure was tested by taking 1.0, 0.8, 0.6, 0.4, 0.2, and 0.0 ml of a chromic solution (approximately 20 μg/ml) prepared from chromic sulphate. These were then treated as described and the final chromium step plotted against concentration for this range of chromium concentrations (0.4–2 μg/ml Cr). Figure 4 shows this to be linear. Complete oxidation of the chronic ions was verified by taking an aliquot of a chromate solution through this procedure. The ratio of step heights of the two chromium-containing solutions was 1.98:1.

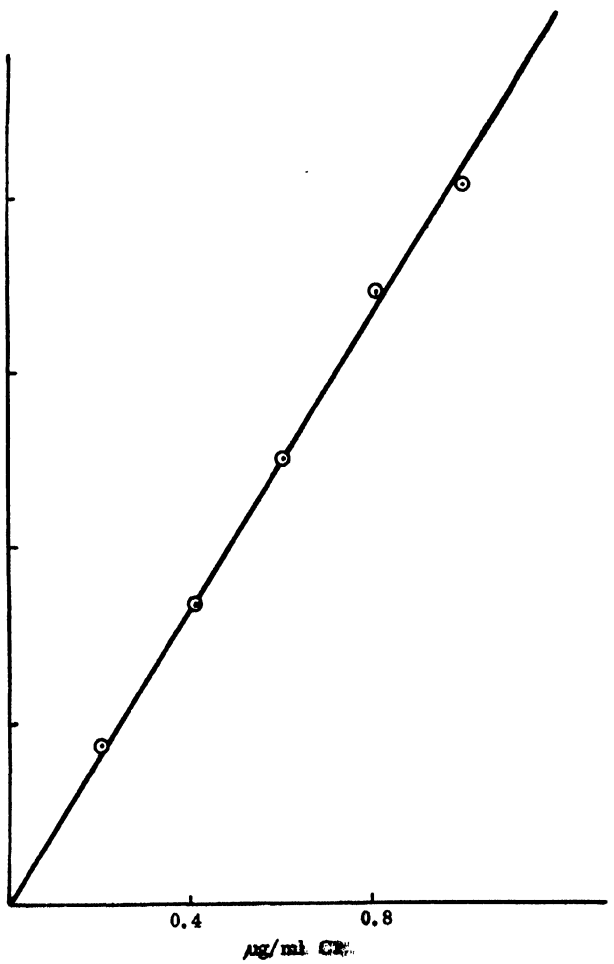

Figure 4. Peak-height for oxidised chromium (5M NaOH 3% mannitol)

An absorptiometric determination with diphenylcarbazide gave a result of 2.08:1. Solutions of iron were also taken through this oxidation procedure and the iron step-heights were found to be unchanged.

THE MANGANESE/NICKEL SYSTEM

Previous experiments[7] have shown that although nickel and manganese were not reversibly reduced in acid or neutral solutions, the reversibility of the electro-reductions increased considerably in alkaline cyanide solutions. Standard solutions of these two metals were prepared from the "spec-pure" metals, by dissolving them in hydrochloric acid and fuming with perchloric acid. Their strengths were about 100 μg/ml. A study of the various alkali cyanide ratios was made. For nickel it was found that:

1. In alkaline cyanide, the peak height for a solution of nickel (12 μg/ml) is comparable with that obtained for the same concentration of lead in chloride-base solution, showing that the reduction of the nickel-cyanide complex is fully reversible.

2. The half-wave potential of the nickel-cyanide complex becomes increasingly positive with increasing cyanide concentration, as indicated by the following:

Cyanide concentration, *M*	0.01	0.1	1.0
$E_{1/2}$, volts against the mercury-pool anode	−1.47	−1.42	−1.36

3. At cyanide concentrations of 0.03 *M*, 0.75 *M* and 5*M*, in the presence of 1*M*, 0.75 *M* and 5*M* hydroxide concentrations, respectively, there is a linear relationship between the peak height obtained and the nickel concentrations for the range 100–0.01 μg/ml nickel.

With manganese it was found that:

1. In alkaline cyanide, the height of the peak obtained showed that the manganese-cyanide complex was not reversibly reduced at low cyanide concentrations.

2. The peak height increased with increasing concentration of cyanide, showing increasing reversibility of the manganese-cyanide complex. The half-wave potential was, however, constant at about −1.35 volts against the mercury-pool anode, and

3. The manganese-cyanide complex formed was unstable in the presence of oxygen and was oxidised to manganese dioxide. This oxidation was rapid in solutions of low cyanide concentration, and slower but still troublesome at higher cyanide concentrations.

4. At cyanide concentrations of 0.03*M* and 5*M* in the presence of 1.0*M* hydroxide, there is a linear relationship between the peak-height obtained and the manganese concentration for the range 100–0.08 μg/ml manganese.

It can be seen from the above results that the most suitable cyanide concentration for the determination of nickel and manganese is about 0.03*M*. It is essential, however, to prevent oxidation and precipitation of the manganese under these conditions.

Complete de-aeration of the solution by prolonged bubbling with oxygen-free nitrogen (purified by pas-

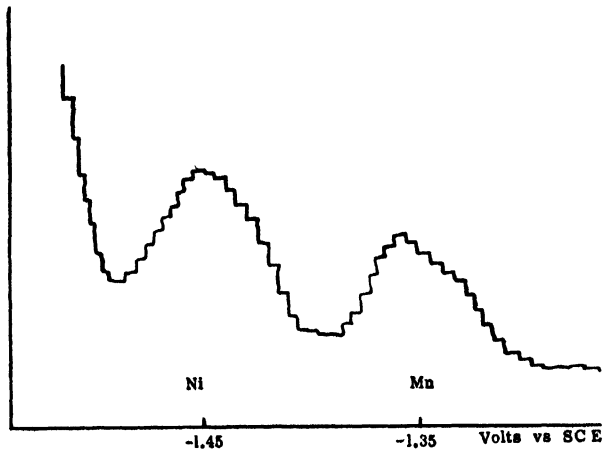

Figure 5. Square-wave polarograms for Ni and Mn 0.03M CN–, 1M OH–, Ni Mn ~ 1 μg/ml

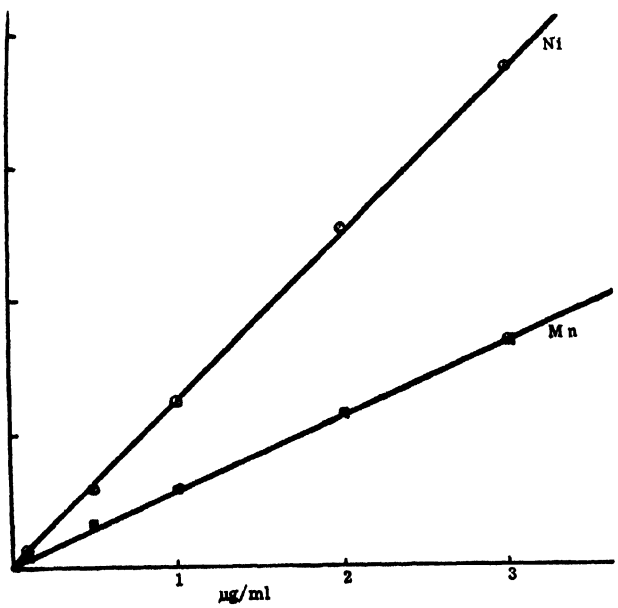

Figure 6. Peak-heights for mixtures of Ni and Mn. 0.03 M cyanide. 1M NaOH

sage through alkaline pyrogallol) and subsequent sealing of the cell delayed the time of precipitation, but there was still sufficient leakage of oxygen through the ungreased ground-glass joint of the cell to cause some precipitation during the determination. The addition of saturated sodium sulphite solution to that in the cell was found to prevent this precipitation.

The recommended conditions therefore for the determination of nickel and manganese are that the solution should be 0.03*M* in cyanide, *M* in hydroxide and that 0.1 ml of saturated sodium sulphite should be added to every 5 ml of the cell solution.

As can be seen from Figures 5 and 6, the two steps are clearly defined and the calibration graphs are still followed when the two metals are present together.

CONCLUSIONS

It has been shown that the Barker Square-Wave Polarograph should be applicable to the determination of corrosion products in solutions from experimental reactor loops. This is possible because the instrument has greater sensitivity and much higher resolution than a conventional polarograph. If 1 ml of sample is made 5*M* in NaOH, 3% in mannitol, iron and chromium may be simultaneously determined down to concentrations of 1 ppm and detected at levels of 0.2 ppm. If 1 ml of sample is made 1*M* in NaOH, 0.03*M* in cyanide, nickel and manganese may be simultaneously determined; the nickel at concentrations down to 0.4 ppm, the manganese down to 2 ppm; while these two metals may be detected at levels of 0.06 and 0.4 ppm respectively.

ACKNOWLEDGEMENTS

We are grateful to Mr. A. Bacon for carrying out the absorptiometric determinations of chromium.

REFERENCES

1. Airey, L. and Smales, A. A., Analyst, *75*: 287 (1950).
2. Leveque, M. P. and Roth, F., J. Chim. Phys. *46*: 480 (1949).
3. Breyer, B., Gutman, F. and Hacobian, S., Australian Sci. Res. *3*: 567 (1950).
4. Barker, G. C. and Jenkins, I. L., Analyst, *77*: 685 (1952).
5. Ferrett, D. J., Milner, G. W. C. and Smales, A. A., Ibid. *79*: 731 (1954).
6. Ferrett, D. J. and Milner, G. W. C., Ibid. *80*: 132 (1955).
7. Ferrett, D. J. and Milner, G. W. C., unpublished work.
8. Lingane, J. J. and Kolthoff, I. M., J.A.C.S. *62*: 852 (1940).
9. Reynolds, G. F. and Shalgosky, H. I., Anal. Chim. Acta. *10*: 273 (1954).
10. Meites, L., Anal. Chem. *27*: 416 (1955).
11. Parks, T. D. and Agazzi, E. J., Anal. Chem. *22*: 1179 (1950).

Record of Proceedings of Session 20B

THURSDAY AFTERNOON, 18 AUGUST 1955

Chairman: Mr. P. Savić (Yugoslavia)
Vice-Chairman: Mr. J. Shankar (India)
Scientific Secretaries: Messrs. J. Gaunt and D. J. Dewar

PROGRAMME

P/900	Chemical problems of power reactors	R. Hurst and J. Wright
P/821	Survey of homogeneous reactor chemical problems	C. H. Secoy
P/348	Behavior of heavy water in piles of the C. E. A.	J. Chenouard *et al.*
	Discussion	
P/535	Aqueous corrosion of aluminum alloys at elevated temperatures	J. E. Draley and W. E. Ruther
P/880	Corrosion of aluminium and aluminium alloys in aqueous solutions at high temperatures	K. Carlsen
P/537	Aqueous corrosion of zirconium and its alloys at elevated temperatures	D. E. Thomas
	Discussion	
P/811	Aqueous uranium and thorium slurries	A. S. Kitzes and R. N. Lyon
	Discussion	

Mr. R. Hurst (UK) presented paper P/900.

Mr. C. H. Secoy (USA) presented paper P/821.

Mr. E. Roth (France) presented paper P/348.

DISCUSSION OF P/900, P/821, P/348

Mr. J. Wright (UK): I would like to ask Mr. Secoy if he can say whether nitrogen evolution on irradiation of uranyl nitrate solution is a reversible process. One would expect that at some nitrogen pressure the re-formation of nitrate ion by the action of radiation on the gas phase would lead to equilibrium conditions.

Mr. Secoy (USA): I presume you mean the evolution of nitrogen gas from uranyl nitrate radiation. In the experiments which have been carried out so far no equilibrium has been reached. The actual rate —the yield—of nitrogen is not high; it is low, the *G* value being of the order of a few tenths, at the most.

Mr. J. A. Swartout (USA): Mr. Hurst mentioned that they had built autoclaves for determining factors affecting the rate of breakdown of uranyl sulfate and also water. I would like to ask whether they have obtained any results yet, and if so, without going into too much detail could he say what they are?

Mr. Hurst (UK): Our first experiments were done in thick-wall glass tubes and in these we have measured the solubility of one or two rare-earth solvents, chiefly in water. This work is just beginning. The solubilities are of the order of a fraction of a gramme per cm^3 as far as I recall. The autoclaves are still under construction and test, and we have not in fact conducted the experiments in the largest steel autoclaves as yet.

Mr. Swartout (USA): This is more of a comment than a question. In the French report it was pointed out that they used a catalyst of platinum suspended in aluminum. We have found that such platinum can be highly contaminated with chloride. We ran into this trouble at least once, and we found it necessary to wash the catalyst thoroughly or have special preparations made for such use.

Mr. Roth (France): We use palladium and not platinum, but, of course, we wash the catalyst very thoroughly before putting it into operation and we check by passing heavy-water vapour over this catalyst that no impurities are entrained. Only then do we put the catalyst into the recombination unit.

Mr. E. Rometsch (Switzerland): Is it possible to remove the alumina by ion exchanger or by centrifugation, or is there any soluble aluminium oxide remaining in the solution as a colloid?

Mr. Roth (France): It is not possible to extract the aluminium by centrifugation, but we believe that the soluble part can be separated by ion exchange. Centrifugation, of course, only permits separation of the insoluble parts.

Mr. J. E. Draley (USA) presented paper P/535 as follows: Aluminum alloys are valuable materials for use in nuclear reactors because of their availability, fabricability, and reasonable cost, coupled with adequately low neutron cross section. For water-

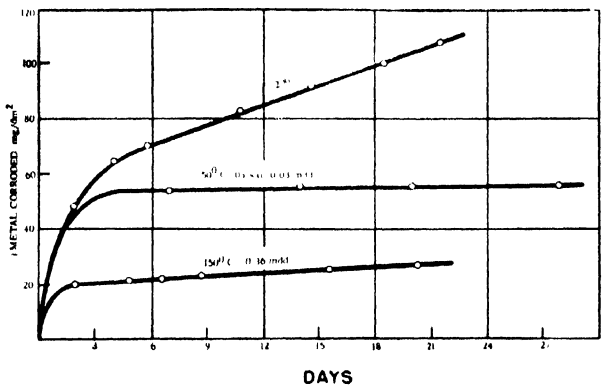

Slide 1. Corrosion of commercially pure Al in H_2O

cooled reactors their use as cladding for fuel elements is feasible so long as corrosion resistance is adequate; if they are to be used also for structural members, then strength and rigidity must be considered.

In distilled water the corrosion of most commercial alloys is very similar to that of the commercially pure metal. Corrosion behavior for 2S aluminum, the American commercially pure aluminum, in distilled water is illustrated in Slide 1.

You will note that the characteristic initial period of rapid reaction is followed by an apparently continuous period of constant corrosion rate. In the test at 50°C the water was saturated with oxygen at 1 atmosphere, and at 150°C and 200°C the water was essentially gas free. The two tests were run in stainless steel autoclaves with the aluminum samples insulated from the steel equipment. For all three tests fresh distilled water was continuously added at a low rate.

The "corrosion rates" after the initial period of rapid reaction are shown on the slide in terms of milligrams of metal corroded per square decimeter of sample surface per day of exposure. For those unfamiliar with the terms I may explain that 1 microgram per square decimeter per day (1mdd) is equivalent to an average penetration rate for this metal of 13.5 microns per year, so that the corrosion at 50°C is seen to be quite a small number.

The pH of the solution considerably influences the rate of corrosion of commercially pure aluminum. The pH of minimum corrosion appears to be that at which the solubility of the corrosion product is a minimum. At ordinary temperatures this is in the vicinity of 6 to 6.5. As the temperature is increased above 100°C, the pH of minimum corrosion appears to go down in much the same fashion as the concentration of the hydroxide ion goes up due to increased ionization of the water. Below 100°C, where there are more data to prove the point, the rate of corrosion of the metal is sensitive to the flow rate of solution past the metal surface at pH considerably displaced from the minimum in the corrosion rate versus pH curve. Near the pH of minimum corrosion rate there is little effect of solution flow rate on the corrosion behavior.

The dependence of corrosion rate of commercially pure aluminum on temperature is shown in Slide 2 (Fig. 2 of P/535).

Three environments were used—a dilute KOH solution, distilled water, and dilute sulfuric acid solution. Rather good fits to straight lines were obtained for the logarithm of rate versus reciprocal of absolute temperature for distilled water and the acid at temperatures above 100°C; a discontinuous curve for distilled water is readily apparent.

It is believed that the explanation for the unusual nature of the curve in distilled water is associated with the change in the structure of the corrosion product in the general vicinity of the boiling point. Below this temperature it is Bayerite, the trihydrate of aluminum oxide, and above is Boehmite, the monohydrate of aluminum oxide. These tests were static; that is, there was no significant flow of solution past sample surfaces. It is believed that considerably higher corrosion rates would be observed at pH 8.5 if a significant solution flow rate were used.

At temperatures much above 200°C, samples show a period of apparently "normal" corrosion followed by the formation on the surface of blisters. This "blistering" attack apparently begins at stringers and grain boundaries and other minute imperfections in the surface metal structure. As testing time is increased, these blisters grow larger, the surface roughens, and rapid penetration of the metal occurs, producing mixtures of metal and oxide. At high temperatures this type of attack occurs quite rapidly; Slide 3



Slide 3

shows a sample of rolled, commercially pure aluminum after four hours exposure to distilled water at 315°C.

The rapidity with which this sample failed in corrosion test is not typical of normal metal; it can be made to occur by providing metal in the most sensitive condition.

It is believed that the explanation for the damaging attack at elevated temperatures is that some of the hydrogen atoms produced in the corrosion reaction diffuse into the metal structure and form molecular

hydrogen, producing pressure pockets in small voids in the metal. As the weak metal yields, these pressure pockets cause the formation of blisters, which subsequently rupture and let in water. This produces new hydrogen, and the process is self-accelerating. If the explanation is correct, two means of preventing the attack should be effective: (1) provision of cathode sites for the liberation of hydrogen gas so that hydrogen atoms will not be available to the aluminum metal surface, and (2) by making the aluminum impermeable to hydrogen diffusion. Only the former method will be discussed here. This type of protection may be called anodic protection.

The most susceptible material to this kind of damaging attack is high purity aluminum. An illustration of the improvement caused by making such material the anode is shown in Slide 4 (Fig. 4 of P/535).

These two samples were partially immersed in distilled water at 250°C for two hours with a current density of 1.2 milliampere per square centimeter of sample in the water. The water levels during the test can be seen very readily, somewhat less than halfway up the sample. Heavy corrosion occurred in the steam phase where little or no current was passing. The amount of corrosion observed on the cathode was greater than that in the steam phase. The damaging attack was almost prevented for the anode.

Perhaps a practical way of applying anodic protection is to add to the solution cations of reducible metals. From these solutions, tiny dendritic metal deposits occur on the aluminum surface. These then can act as cathode sites for the liberation of hydrogen. Among the reducible cations, those which produce metals of low hydrogen overvoltage will be most valuable. The corrosion of commercially pure aluminum in a nickel sulfate solution containing 5 milligrams of nickel ion per liter plus sulfuric acid to control the pH at 3.5 is illustrated in Slide 5.

The temperature for this test was 275°C. Incidentally, it is necessary to add the acid to avoid the formation of basic salts in such a system; otherwise a basic nickel sulfate will precipitate at high temperatures. In the absence of the nickel sulfate solution, rapid disintegration of the metal would have begun after 10 to 14 days of testing.

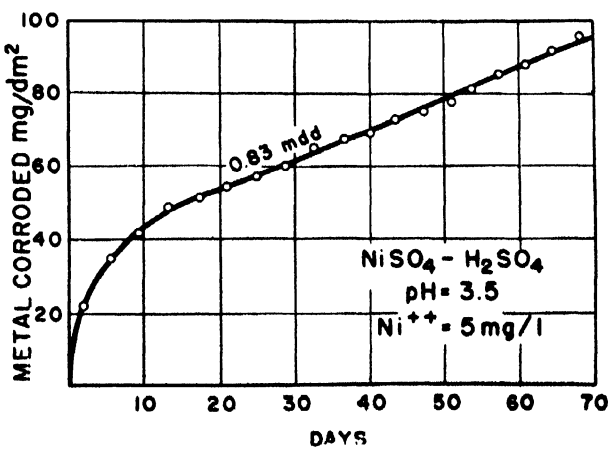

Slide 5. Corrosion of commercially pure Al

The low corrosion rate observed is perhaps characteristic of the corrosion of aluminum alloys in water at this pH. The primary function of the nickel ion added is to prevent the rapid attack due to the penetration of hydrogen. Although the hydrogen penetration can also be prevented by maintaining nickel ion concentration in the solution at higher pH values, such conditions are probably impractical due to the formation and deposition of basic nickel salts. Acidifying the solution is necessary for the prevention of this deposition.

Aluminum-nickel alloys have been prepared in which the nickel-rich constituent appears as the second phase, largely segregated at grain boundaries. Samples of these alloys show excellent resistance to "blistering" attack, presumably by the same mechanism. About ½ per cent (by weight) is required for protection of commercially pure aluminum at temperatures as high as 350°C. The corrosion curves are similar to those for aluminum alloys at low temperatures, as was illustrated in Slide 1.

Table I. Corrosion Rate for Aluminum-Nickel Alloys in H_2O

Alloy	*°C*	*mdd*
Al + 0.5% Ni	250	2.4
	290	3.4
Al + 0.5 − 2% Ni	315	6.3
Al + 1% Ni	350	18

Corrosion rates subsequent to the first few days of exposure for some nickel alloys are given in Table I on this page. At 250°C and 290°C the alloy was made by the addition of 0.5% nickel to commercially pure aluminum. The greatest impurities present in this material are iron (0.2–0.5%); copper (of the order of 0.2%), and silicon (up to about 0.2%). There is some indication that a small amount of iron should be present in order to achieve protection against "blistering" attack. At 315°C the corrosion curve was made up from data obtained using samples made of many nickel concentrations ranging from 0.5 to 2%. Aluminum melting stock was high purity aluminum in two instances, and commercially pure aluminum in all others. We are not certain that we can get such consistently good results with high purity material. It is now believed that fortuitous contamination of the high purity base melt by iron was responsible for the satisfactory behavior of such alloys. Although the beneficial effect of added iron has been demonstrated, it is not yet clear that its presence is essential.

It is to be remembered that distilled water is considerably more alkaline than the pH of minimum attack at elevated temperatures. As a consequence, one should anticipate that corrosion rates would be increased by causing the water to flow past metal surfaces.

This point is illustrated in Slide 6, where the difference between corrosion in static distilled water and that where the water was circulated past sample surfaces at a rate of approximately 20 ft/sec (6.1 m/sec) is shown. By analogy with behavior at low temperatures, this accelerated corrosion caused by high flow rate should not occur near the pH of minimum corrosion rate. Whether this is true has not yet been determined, although the effect of flow rate has been shown to be less at pH 5 than in pH 7. These pH values were measured at room temperature.

There are other alloying constituents which can provide protection against the damaging attack due to hydrogen penetration of high purity aluminum. Copper, cobalt, iron and platinum show strong protective tendencies, but do not provide complete protection when present to the extent of 2 per cent. It is possible that alloys containing larger amounts or mixtures of these constituents would be satisfactory. Such higher alloys might also be developed to provide high temperature strength. In particular copper and iron alloys would be expected to show real benefit in this regard.

With the elimination of the accelerating "blister" attack of aluminum in water at elevated temperatures, the only limitation on the material from the point of view of corrosion is the rate of chemical reaction of the material with the environment. Corrosion rates at conditions which are of direct interest to reactor designers are probably not available. However, there are now aluminum alloys known which can meet corrosion requirements for use in water at elevated temperatures, and it appears probable that water-cooled reactors can be built using such alloys.

Mr. K. CARLSEN (Norway) presented paper P/880.

Mr. D. E. THOMAS (USA) presented paper P/537.

DISCUSSION OF P/535, P/880, P/537

Mr. T. ARNET (Switzerland): I would like to make a few remarks about corrosion tests on aluminum which were made in Switzerland. In a frame of 99.5 per cent aluminum several test rods with a diameter of 10 mm and a length of 32 mm were simultaneously tested in an autoclave at 200°C. Distilled light water was used as the corrosion medium. The duration of the tests depended on the speed at which hydrogen was produced, as a protection plate burst at a pressure of about 100 atmospheres. The apparatus used is shown in Slide 7.

The first tests showed that destruction was far quicker with 99.99 per cent aluminum called "Raffinal," than with 99.5 per cent pure aluminum. This was not altogether expected, as the resistance of aluminum against corrosion usually increases with increased purity. Tests were therefore made to find out what impurities caused these varied properties and to examine whether the resistance could be increased by means of certain additions. Practically all

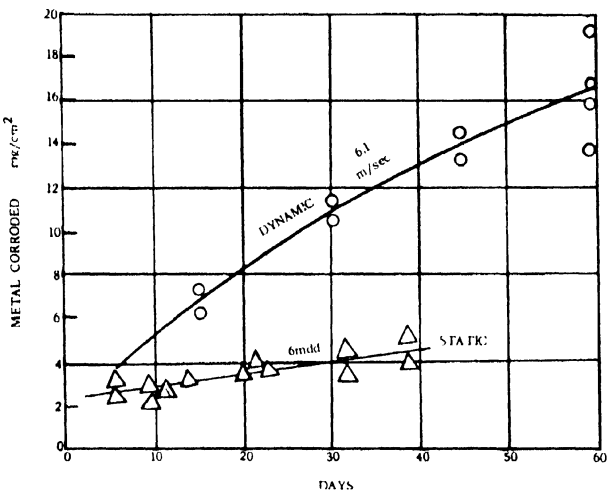

Slide 6. Corrosion of Al-Ni alloys in water at 315°C

elements which, on account of their metallurgical and physical behavior seemed likely to produce the desired results, were added to Raffinal and 99.5 per cent aluminum. It was not possible to remove the layer of corrosion by normal means, so that the weight increase is shown as a function of the time in the following slides.

Slide 8 shows the properties of Raffinal with various additions. The additions were used for the different curves, magnesium, silicon, etc., in various proportions from 0.5 to 5.0 per cent: copper, magnesium, titanium, iron 0.5 and 1 per cent, and iron and silicon together.

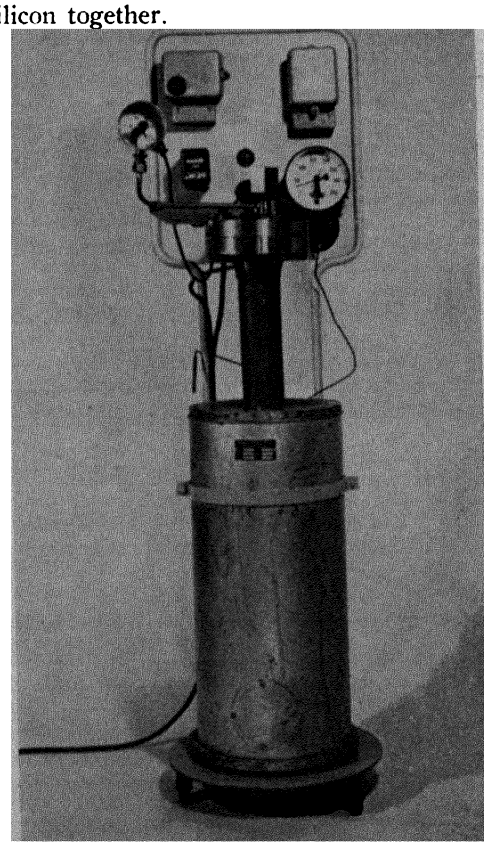

Slide 7

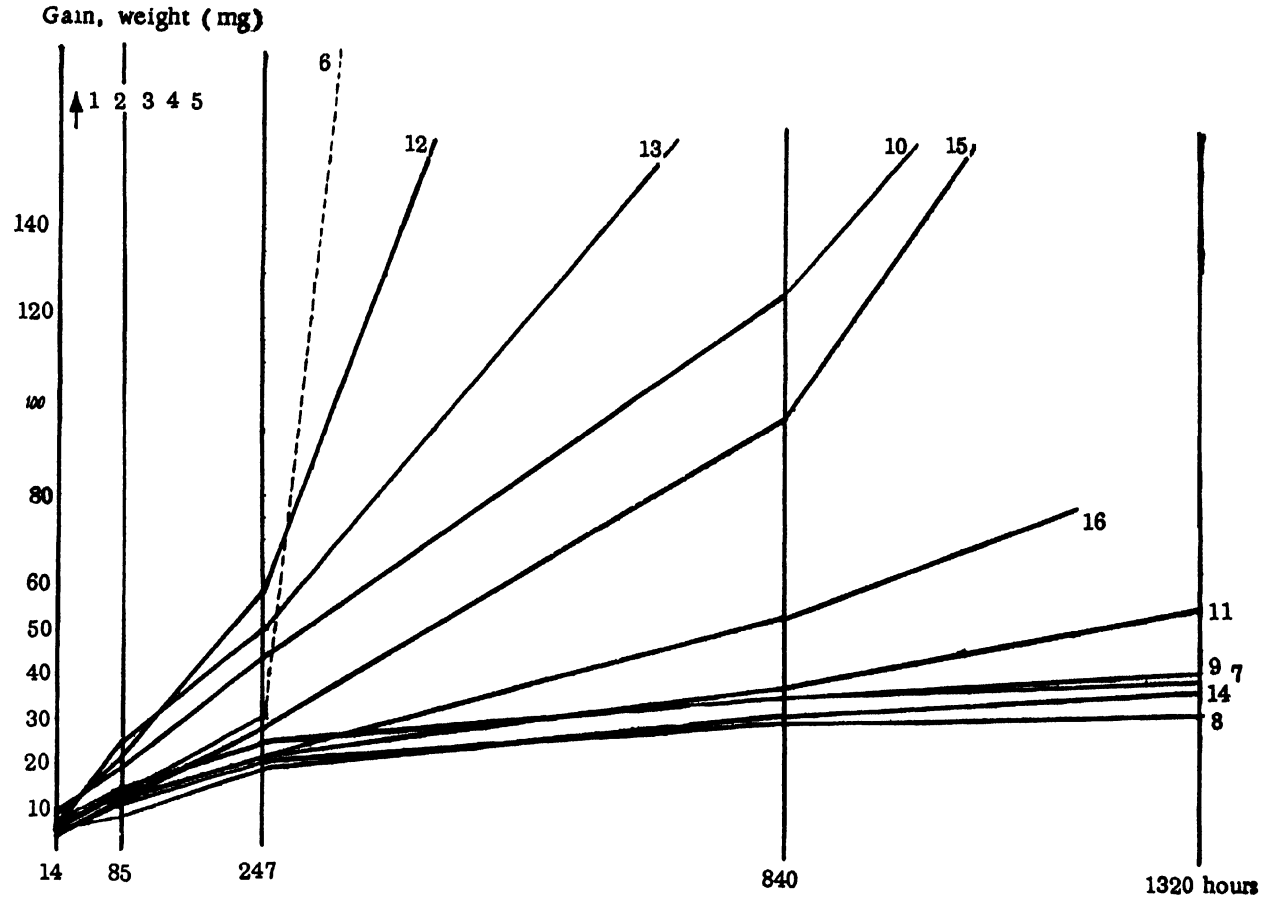

Slide 8. Corrosion in flowing water at 200°C; curve 1: raffinal; curve 2: raffinal plus 1.0% Mg_2Si; curve 3: raffinal plus 0.2% V; curve 4: raffinal plus 0.5% Zn; curve 5: raffinal plus 0.5% Si; curve 6: raffinal plus 1.0% Si; curve 7: raffinal plus 2.0% Si; curve 8: raffinal plus 5.0% Si; curve 9: raffinal plus 0.5% Cu; curve 10: raffinal plus 0.3% Cr; curve 11: raffinal plus 0.2% Ti; curve 12: raffinal plus 0.5% Fe; curve 13: raffinal plus 1.0% Fe; curve 14: raffinal plus 0.5% Fe plus 0.5% Si; curve 15: Al 99.5 raffinal plus 0.3% Fe; curve 16: Anticorodal raffinal.

Slide 9 shows the same alloys after having been cold-worked by 50 per cent before the test.

Slide 10 shows the properties of 99.5 per cent aluminum with additions, and the properties of some of the more common aluminum alloys.

Slide 11 shows 99.5 per cent aluminum samples having been cold-drawn before the test.

Slide 12 shows the weight increase of Raffinal samples in mg/dm²/day (mdd).

Slide 13 shows the results of similar tests on 99.5 per cent aluminum and aluminum alloys.

In short, the following conclusions can be made: All additions to Raffinal increases its resistance to water at 200°C although the results vary considerably. Additions of 0.5 per cent copper, 2–5 per cent of silicon and the joint addition of iron and silicon were particularly favorable. The addition of 0.5 and 1 per cent silicon inhibited the reaction only.

Additions to 99.5 per cent aluminum can be favorable as well as the contrary. Considerable improvements were again made with the addition of 0.5 per cent copper. Sintered aluminum powder, called "SAP", however, showed the best properties. Earlier experiments with this material gave bad results. It must therefore be determined whether slight structural or analytical irregularities caused the deviations. The slide of the weight increase in mdd shows clearly that various materials, for instance Anticorodal (51S), have good properties at the beginning which deteriorate rapidly later on.

Further tensile tests on 99.5 per cent aluminum, 51S and 52S, under various conditions showed a considerable reduction in the tensile strength after exposure for 666 hours. The elongation, however, also increased considerably, so that it is clearly an effect of the heat treatment. Tests with solutions containing chromate and chromic acid as inhibitors showed bad results, as pitting clearly took place.

Mr. Draley (USA): My first question is to Mr. Carlsen: have you made any attempt to determine whether the barrier layer film formed on aluminum in the silicate chromate inhibiting solution is different from that formed in the absence of the inhibitors? My second question is, do you expect that this inhibition will be permanent?

Mr. Carlsen (Norway): As to the first question, we have not done any measurements of the barrier layer thickness. I am sure it would be very interesting to do so, and I should like to make that kind of experiment in future.

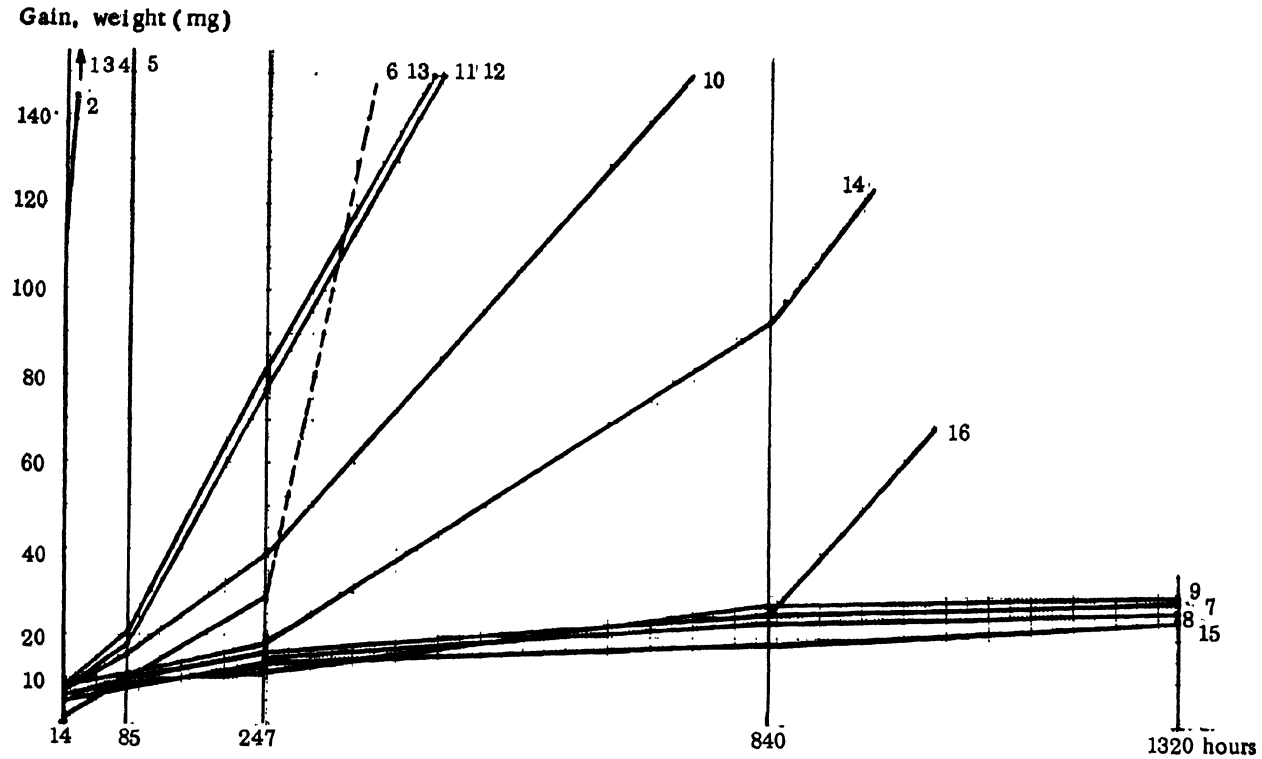

Slide 9. Corrosion in flowing water at 200°C. (50% cold-washed); curve 1: raffinal; curve 2: raffinal plus 1.0% Mg_2Si; curve 3: raffinal plus 0.2% V; curve 4: raffinal plus 0.5% Zn; curve 5: raffinal plus 0.5% Si; curve 6: raffinal plus 1.0% Si; curve 7: raffinal plus 2.0% Si; curve 8: raffinal plus 5.0% Si; curve 9: raffinal plus 0.5% Cu; curve 10: raffinal plus 0.3% Cr; curve 11: raffinal plus 0.2% Ti; curve 12: raffinal plus 0.5% Fe; curve 13: raffinal plus 1.0% Fe; curve 14: raffinal plus 0.5% Fe plus 0.5% Si; curve 15: Al 99.5 raffinal plus 0.3% Fe; curve 16: anticorodal raffinal.

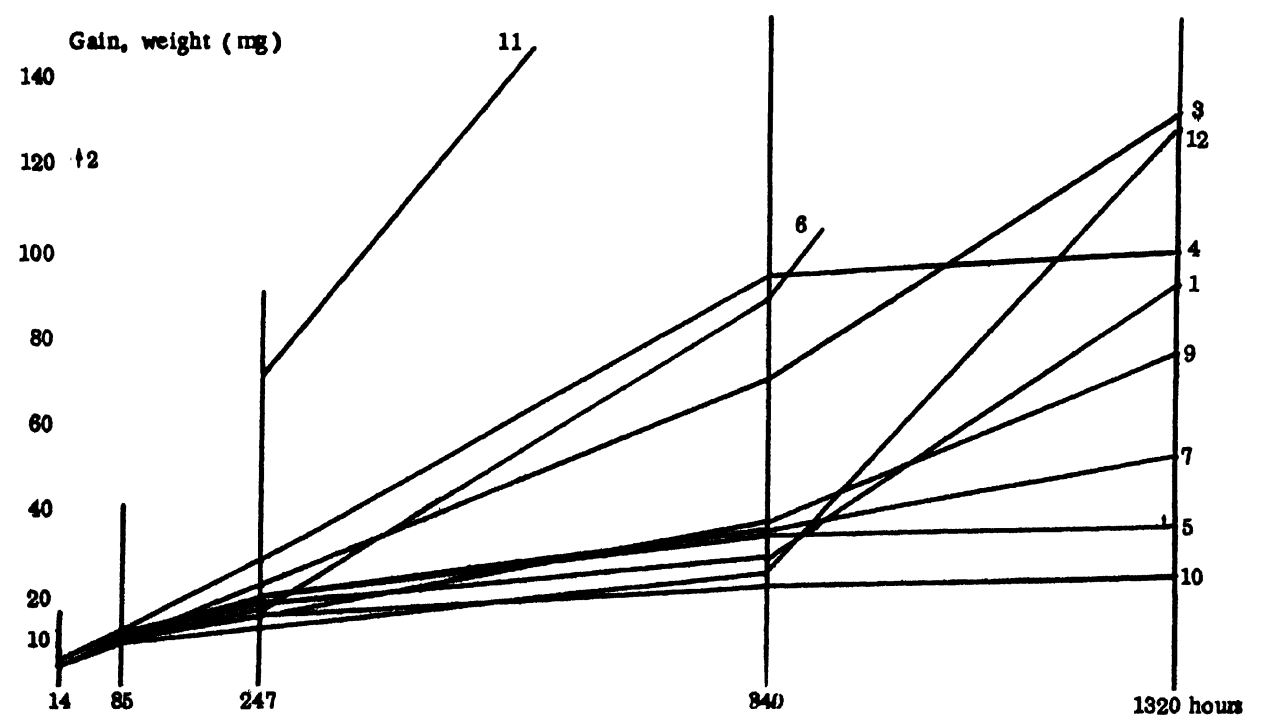

Slide 10. Corrosion in flowing water at 200°C; curve 1: Al 99.5%; curve 2: Al 99.5% plus 1.0% Mg_2Si; curve 3: Al 99.5% plus 0.2% V; curve 4: Al 99.5% plus 0.5% Zn; curve 5: Al 99.5% plus 0.5% Cu; curve 6: Al 99.5% plus 0.3% Cr; curve 7: Al 99.5% plus 0.2% Ti; curve 9: Al 99.2%; curve 10: SAP; curve 11: peraluman 30; curve 12: anticorodal B.

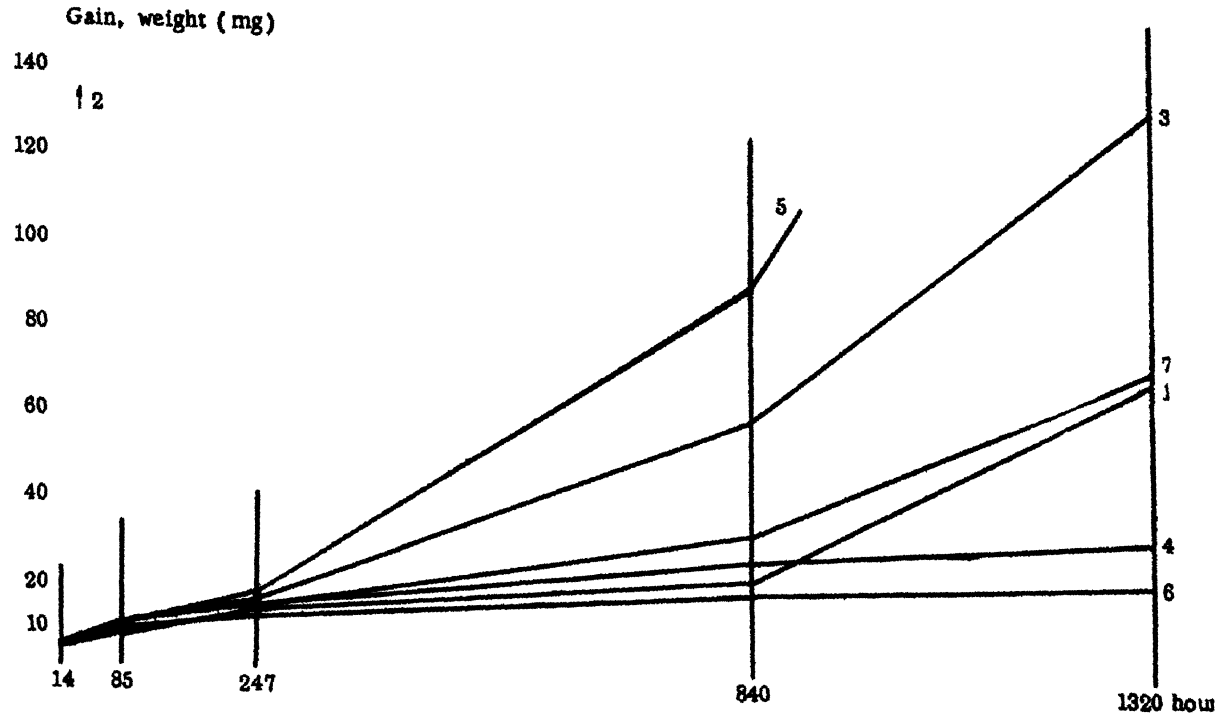

Slide 11. Corrosion in flowing water at 200°C. (50% cold-washed); curve 1: Al 99.5%; curve 2: Al 99.5% plus 1.0% Mg₂Si; curve 3: Al 99.5% plus 0.5% Zn; curve 4: Al 99.5% plus 0.5% Cu; curve 5: Al 99.5% plus 0.3% Cr; curve 6: Al 99.5% plus 0.2% Ti; curve 7: Al 99.5% plus 0.2% V.

As to the second point, I mentioned that these experiments were screening tests, and accordingly they were run for only a short time. None of the chromate inhibitors was run for more than six days. The small increases in weight that we obtained seemed to decrease as a function of time. However, I would not like to say what would happen after those six days, and in order to ascertain this we should have to conduct some more experiments.

Mr. M. J. LAVIGNE (Canada): I notice that for the most part these papers have been given by chemists. Personally I have nothing against chemists except that none of them has indicated the metallurgical condition of the material, and I think it is most important to find out what we are dealing with before we make any corrosion tests. Mr. Draley and I have had some long discussions together. Mr. Carlsen has not mentioned at all the metallurgical condition of his material. Mr. Thomas approached it a little. I would like to find out from the three of them if they have found any difference in the behaviour of their materials when they have different metallurgical conditions, because somebody mentioned in the discussion that he was trying to use pure material such as 99.5%—which is not a very pure material. We have tried 99.9984% aluminium, and we were quite surprised and quite shocked to find that it corroded intergranularly at 100°C in pure water, with pH near 7. By increasing the purity we have not found any difference, but I understand that French workers have found a slight difference in the corrosion. We have found that the metallurgical condition bears quite a bit on the behaviour of the material, and seems to be associated with the grain size and the orientation between contiguous crystals, and that is the main thing; the solubility of nickel in aluminium is very low, so with the addition of nickel it may move to the grain boundary and may act as cathode sites for the discharge of hydrogen; but I think it does first decrease the degree of misfit between the contiguous crystals.

Mr. DRALEY (USA): I did mention some things concerning the metallurgy of aluminum alloys and particularly alloys containing nickel. I said the nickel was in the form of second phase and almost completely in grain boundaries. You would be interested to know of the work which concerns the relative roles of iron and nickel. I mentioned that we were interested in it, that there was considerable improvement by using both as contrasted to one, although nickel was the better of the two when used solely. Photomicrographs have shown us that we can see precipitation of the second phase caused by the addition of nickel at grain boundaries, and clean structure within the grains; this is using high purity aluminum. When we add iron to high purity aluminum we find most of the precipitate shows up throughout the grains, so that the two seem to act with each other to meet the objective of getting very fine and very well dispersed cathodic precipitate throughout the metal. This is a theory we are working on. The point at which you can find the precipitate corresponds rather well with the point at which protection against hydrogen penetration occurs. Also, a rule of thumb which applies to this and at least three other alloy systems that I know, is that when you do rely on precipitate to do you some good in corrosion resistance, the finest grain material

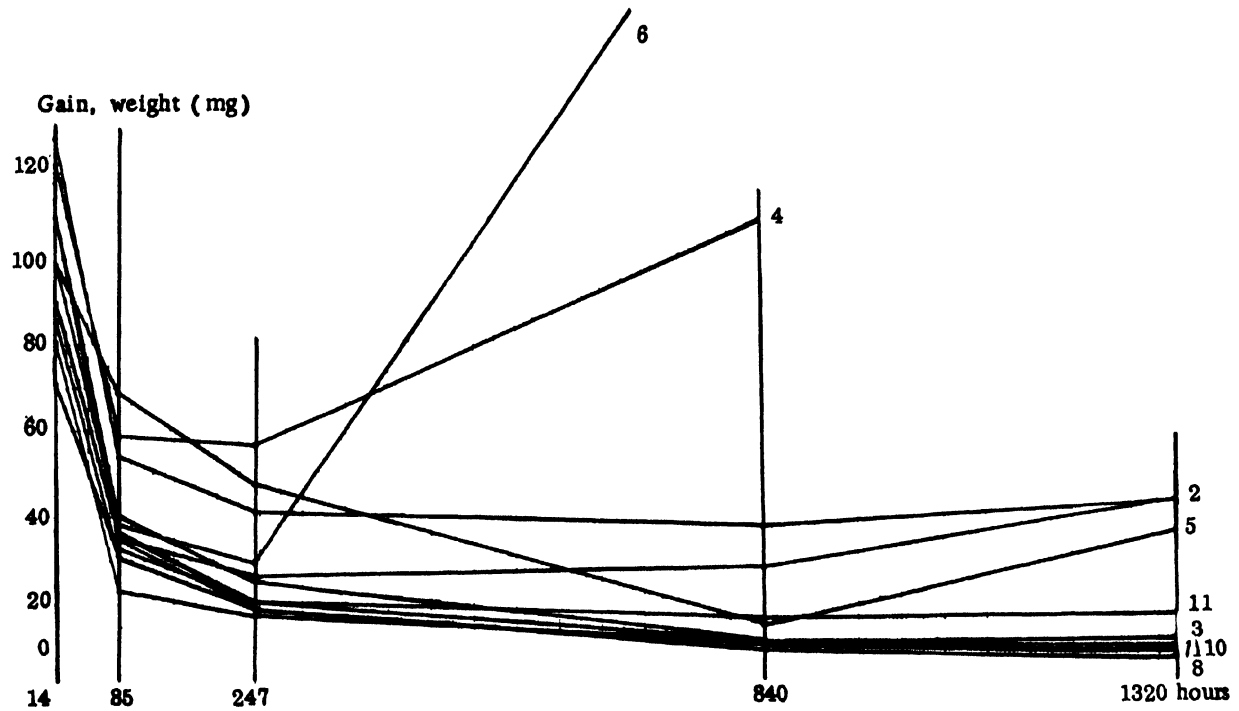

Slide 12. Corrosion in flowing water at 200°C; curve 1: raffinal plus 0.5% Cu; curve 2: raffinal plus 0.3% Cr; curve 3: raffinal plus 0.2% Ti; curve 4: raffinal plus 0.5% Fe; curve 5: raffinal plus 1.0% Fe; curve 6: raffinal plus 1.0% Si; curve 7: raffinal plus 2.0% Si; curve 8: raffinal plus 5.0% Si; curve 9: raffinal plus 0.5% Fe plus 0.5% Si; curve 10: Al 99.5% raffinal plus 0.3% Fe; curve 11: anticorodal raffinal.

is generally the best as is the finest precipitate and the most randomly dispersed precipitate are the best.

Mr. THOMAS (USA): I thank Mr. Lavigne for his reference to chemists, but I do not happen to be one. However, I am sorry if my paper conveyed the idea that we have not considered the effect of structure upon corrosion, because we certainly have done so. I did not, however, mention it as I spoke. In general, it seems that in pure zirconium the effect of heat treatment is very small. In alloys of the Zircoloy-2 type, it appears that the maximum corrosion resistance occurs when the alloying elements are permitted to precipitate in fairly fine dispersion.

Mr. CARLSEN (Norway): In a paper of that length one had to restrict oneself. The alloys we tested were cold-rolled samples except 2S which was cold-rolled in the first instance. We decided to investigate 2S more thoroughly to compare the behaviour with metal of super purity. In that connexion we carried out experiments on cold-rolled samples with different heat treatments. We quenched them from 550°C, some were furnace-cooled, and some were used in the cold-rolled condition. We did not find any difference whatsoever in the general corrosion rates although there were some minor differences in the microscopic behaviour of the samples. I cannot remember exactly the microscopic features, but I do not think they were very important for the corrosion resistance of the samples.

Mr. LAVIGNE (Canada): I think the behaviour of the super pure aluminium, the high purity aluminium, and 2S under cold working is completely different. High purity aluminium may re-crystallize during rolling, which would give a completely different structure. Therefore you cannot compare the two under the same conditions. You have to be quite careful, if you want to reproduce the metallurgical conditions, to vary your reduction of area during rolling, and make some X-ray analyses of the material to find out if it has re-crystallized or whether it is in the cold-worked condition; because we found out that high purity aluminium, that is the 99.9984 cold-rolled, with very careful passes of 1 to 3000 of an inch per pass, from 5 per cent to 50 per cent, did corrode intergranularly at 100°C, but the 60 per cent cold-worked up to 92 per cent cold-worked did not corrode intergranularly at 100°C. If you first did annealing to the material standing up to 100°C and annealed at 400°C, to make sure it did not re-crystallize, everything corroded. If you add only 0.08 per cent silicon to high purity aluminium and followed the same procedure in that cold-rolling, using the same amount of reduction per pass, you did not get any corrosion whatsoever in the rolled condition. Even 5 per cent cold-working stopped intergranular corrosion. If you annealed it to complete crystallization it corroded intergranularly.

Mr. CARLSEN (Norway): We did not work with super-purity aluminium heat-treated in different ways, and in connexion with the 2S I can only say that we re-crystallized it but did not take any X-ray pictures. I used electropolished samples so that I could confirm in a microscope whether the samples had re-crystallized or not. In those samples which were cold-rolled the grains were elongated as you find in the cold-rolled material and in the other cases it was coarse grains obtained by the re-crystallization.

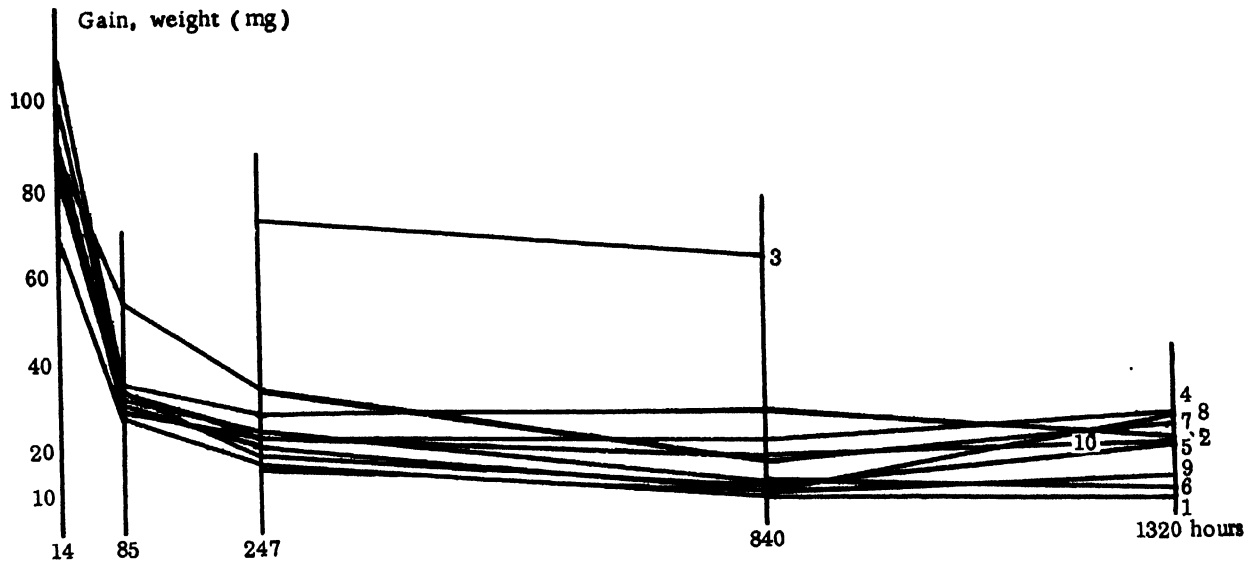

Slide 13. Corrosion in flowing water at 200°C; curve 1: SAP; curve 2: Al 99.2%; curve 3: peraluman 30%; curve 4: anticorodal; curve 5: Al 99.5%; curve 6: Al 99.5% plus 0.5% Cu; curve 7: Al 99.5% plus 0.3% Cr; curve 8: Al 99.5% plus 0.2% V; curve 9: Al 99.5% plus 0.2% Ti; curve 10: Al 99.5% plus 0.5% Zn.

The VICE-CHAIRMAN: The subject seems to be an extremely interesting one, but I suggest that further discussion should be carried on outside this hall. It is obvious, however, that in this field of corrosion, team work between the metallurgists and the chemists is most desirable.

Mr. R. N. LYON (USA) presented paper P/811.

DISCUSSION OF P/811

Mr. K. DAWSON (UK): I should like to comment that the results which we have obtained on the UO_3-water system, and which are in the process of publication elsewhere, indicate that the rod form ($UO_3 \cdot 0.8\ H_2O$) is unstable with respect to the platelet form ($UO_3 \cdot 1.0\ H_2O$) in water above 200°C, and that the conversion is not reversed on heating in water below 200°C. In this respect, our results do not appear to agree with the present paper. The upper limit for the stability of these two forms in water is given by Kitzes and Lyon as 300°C. Our results indicate that the transformation to $UO_3 \cdot 0.5\ H_2O$ takes place at as low a temperature as 280°C. Since this temperature is in the region of operation of a possibly slurry reactor, could Mr. Lyon give any information on what would be the ultimate form of the hydrate obtained by rapid cycling of the slurry above and below this transition temperature? Would it be $UO_3 \cdot 1.0\ H_2O$ or the hemihydrate, or a mixture? The form obtained would presumably affect the pumping characteristics of the slurry.

I have a second question relating to fission product poisons. One of the advantages of the homogeneous solution reactor fuel is that removal of fission product poisons and radiation damage products may be performed continuously. Has Mr. Lyon any comments on how this may be achieved in a slurry fuel?

Mr. LYON (USA): With respect to the first comment, we also found that the platelet form did not convert to the rod form unless the platelets were very finely pulverized first, and then, apparently because of the reduced size, solubility was sufficient to permit it to convert over to the rod form. If it was not pulverized, but simply heated in a bomb without pulverizing it, conversion did not take place. We concur completely about that.

With regard to upper temperatures, most of our tests were conducted at 250°C, though a few bomb tests were run at temperatures approaching 300°C, and the upper figure I am sure is more accurate as you put it than as we listed it, and we would be willing, at least tentatively, to accept your figure.

With regard to what happens in cycling, I assume you mean above and below monohydrate conversion. We have so little experience from that aspect of the matter that I am afraid I cannot give you any information. Most of our tests were run at 250°C with uranium.

The next question was in regard to fission products. The range of the fission products is, of course, a measurable amount, and it is possible, although I cannot say this definitely, that if the particle size is quite small the fission fragments may move from within the particle into the surrounding medium and remain outside without being held in the particle; but I have no information on whether this is the case.

Mr. H. de BRUYN (Netherlands): I should like to make a few remarks with respect to the choice of the most suitable uranium oxide as a fuel for a homogeneous reactor. As you know, we advocate the use of uranium dioxide. I want to point out that in our opinion a hydrogen atmosphere is to be preferred to an oxygen atmosphere, because the decomposition rate of the water decreases with the hydrogen pres-

sure. Therefore, the decomposition gas is diluted beyond the explosion limit with hydrogen, about 5–10 times, and this dilution corresponds to a hydrogen-oxygen ratio of about 20. In this case, however, $UO_3 \cdot H_2O$ is not stable according to your Table II, whereas UO_2 remains stable, according to Ipatiev and other Russian authors. Secondly, we think that a well-defined particle size is very useful in order to ensure that the fission products mainly enter the water phase. Therefore, we prefer an oxide which does not show recrystallization or crystal growth under the circumstances to be expected in the reactor. Thirdly, we prefer to avoid platelet-shaped particles as they will produce cakes in the pipeline. Even when the platelets are colloid-chemically stable, cakes will occur, which is a well-known phenomenon in practice, for instance in the case of shale suspensions. The cakes are soft when the suspension is stable, and hard when the suspension is not stable, or in cases where recrystallization is possible. Fourthly, with respect to abrasion-corrosion, I must admit that platelet-shaped particles are preferable. However, the results of your experiments with ThO_2 suspensions give us good hope that by a proper choice of the construction material, especially in bends or in general at those points of the circuit where high velocities or velocity gradients are to be expected, erosion and corrosion will be minimized.

Beside these remarks on the choice of UO_2 or UO_3 as the most suitable fuel material, I would like to make a few other comments on your paper. I should be very interested to know whether you noticed the so-called "sigma" phenomenon when you measured the viscosity of your suspensions, or, in other words, did you obtain the same viscosity with viscosimeter tubes of different diameter? Moreover, one would expect an influence of the rate of shear in this case of rod-shaped or platelet-shaped particles, even when the suspensions are colloid-chemically stable. The difference in rheological behaviour between $UO_3 \cdot H_2O$ and ThO_2 suspensions may be attributed to the fact that your $UO_3 \cdot H_2O$ suspensions are colloid-chemically stable, whereas your ThO_2 suspensions are not. I should be glad to know whether you noticed an influence of the pH on the rheological properties of the ThO_2 suspensions which, as we know, are positively charged in pure water.

With respect to your remarks on the measurement of the pH of a suspension, I would add that in my opinion the only proper pH definition of a suspension is the pH value of the equilibrium liquid, which is approximately equivalent to the supernatant liquid after centrifuging.

Mr. Lyon (USA): With regard to the proper oxide to use in a reactor, I would agree, of course, that in a hydrogen atmosphere, UO_2 would be the stable form, and the question merely resolves into one of whether you wish to have an oxidizing solution or a reducing solution in the reactor. I am sure that with the system that you have in mind you have a stable form with UO_2, and we believe that in the system we have in mind we will have UO_3 as a stable form. I would hesitate to comment on which is the better situation to have.

With regard to crystal size, the first uranium trioxide which we used had very large platelets. The platelets seemed to grow and to cake. We found that this was due principally to the presence of a small amount of uranyl nitrate which was not decomposed in the formation of the oxide, and that when the oxide was purified the crystal size was greatly reduced and did not grow above the order of 5–10 microns along the side of the platelets. The size seemed to be stable at about that point. The presence of a very small amount of nitrate, however, caused crystals to grow, and a large amount of uranyl nitrate converted the platelets to bipyramids. The soft cakes which we found had formed with the small platelets could be ameliorated to some extent by the addition of some additives. One additive which was found to be useful was monosodium phosphate. I should point out that we tried some of the other methods, but they increased the pH to the point where the attack was more severe.

With regard to viscosity, as I recall, the viscosities were measured with a rotating type of viscosimeter, so that I am afraid that I cannot answer your question on the effect of viscosimeter diameter. One reason for the difference between the viscosity behavior of thorium oxide and that of uranium oxide was of course, that we were using a much higher concentration in the case of thorium oxide. I think the uranium oxide would not have displayed Newtonian behavior if we had measured slurries with higher concentrations. We have noticed the effect of pH on the viscosity of thorium oxide, and this seemed to be associated to some extent with deflocculation of the thorium oxide. There have been some other materials which we have found reduced the viscosity of thorium oxide slurries but again it appears to be a question of deflocculating the thorium oxide.

Mr. C. H. Secoy (USA): If I understood correctly, Mr. de Bruyn used, as one of his arguments in favor of the reducing atmosphere and therefore in favor of UO_2, the statement that the radiolytic decomposition of water was reduced by the presence of hydrogen gas. I think, if you will look into it carefully, this is not so in the presence of fission-recoil particles. The statement he makes is correct in the radiolysis of pure water without any fission fragments present, but in the presence of fission-fragment particles I think you will find that any reasonable hydrogen pressures have no measurable effect on the rate of production.

Mr. R. F. S. Robertson (Canada): Mr. Boyd, at Chalk River, has done some work on the viscosity of UO_3 slurries, and he has worked from 350 grams per liter up to 2000 grams per liter, and he did definitely find non-Newtonian behavior for the UO_3 slurries.

Session 21B

CHEMICAL PROCESSING OF IRRADIATED FUEL ELEMENTS

LIST OF PAPERS

			Page
P/414	Criteria for the selection of separation processes	C. M. Nicholls	453
P/413	Chemical principles in the separation of fission products from uranium and plutonium by solvent extraction	J. M. Fletcher	459
P/822	Reprocessing of reactor fuel and blanket materials by solvent extraction	F. L. Culler	464
P/541	The processing of uranium-aluminum reactor fuel elements	F. L. Culler, Jr. and F. R. Bruce	484
P/349	Solvent extraction of plutonium from uranium irradiated in atomic piles	B. Goldschmidt *et al.*	492
P/785	The extraction of uranium and plutonium with tetrabutylammonium nitrate, cupferron and neocupferron as complexing agents	E. Haeffner *et al.*	498
P/540	Solvent extraction separation of U^{233} and thorium from fission products by means of tributyl phosphate	A. T. Gresky	505
P/824	Practical limitations of solvent extraction processes	R. E. Tomlinson	511
P/551	The chemical processing of aqueous homogeneous reactor fuel	D. E. Ferguson	514
P/765	The characteristics of liquid-liquid extraction equipment as applied to radioactive processing	H. R. C. Pratt	520
P/539	Solvent extraction separation of uranium and plutonium from fission products by means of tributyl phosphate	J. R. Flanary	528
P/543	Experience with a direct maintenance radiochemical processing plant	R. B. Lemon and D. G. Reid	532
P/547	Nuclear reactor fuel dissolution	D. L. Foster *et al.*	546
P/548	Removal of fission products from stainless steel	D. O. Campbell	551
P/549	High-level sampling devices for radiochemical plants	J. W. Landry	555

Criteria for the Selection of Separation Processes

By C. M. Nicholls,* UK

The following criteria are considered:

1. Process selection; general processes: (*a*) selectivity, (*b*) radiation and chemical stability, (*c*) low corrosion characteristics, (*d*) short reaction times and process continuity, (*e*) safe operation; solvent extraction processes: (*a*) low mutual solubility, (*b*) low inflammability hazard, (*c*) physical characteristics desirable for efficient contactor operation, (*d*) minimum volume fission product effluents.

2. Equipment selection: factors affecting the selection of equipment are discussed; the effect of the presence of high levels of radiation on such selection is emphasized.

3. Plant lay-out: the detailed laying-out of plant can have a large influence on both capital and operating cost.

4. Plant location: in the case of present separation plants serving reactors whose sole function is to produce fissile material, the plant has been located as near as possible to the reactor. In the case of experimental reactors and nuclear power stations this is not necessarily the most economic location. The arguments in favour of large, centralised processing facilities are presented. Factors affecting the choice of a radiochemical separation plant are compared and contrasted with those affecting other types of chemical plants.

In the early stages of any atomic energy programme so many demands are made on the available research effort that it has never been possible to achieve the full benefits that can come from detailed costing of several possible alternative processes. It has always been necessary to rely on judgment rather than the easier but longer course of relative costing and the success of projects has depended on the soundness of judgment of the design teams based on the scientific and technical information and experience available at the time. Since the first processes for separating uranium and plutonium from fission products were devised, considerable experience has been gained and continuing research has widened our knowledge of possible separation methods so that it is now possible to draw up guiding criteria that may be helpful in the selection of processes and equipment, in laying-out plant and selecting suitable sites for the plant.

The objective of the separation process is assumed to be to provide a service to power or experimental reactors. The processing may be necessary for several reasons. It may be required to recover fissile material, the loss of reactivity due to poisoning may have become excessive or the fuel or its container may have failed by chemical, metallurgical or physical action.

Three general specifications are possible for such separation processes depending on the proposed use of the recovered fissile material and the fabrication methods used for re-making fuel elements for the reactor.

1. Complete separation of the fertile material, the fissile material and the fission products.

2. Separation of the fission products away from the fissile and fertile materials which are then metallurgically reformed and refabricated into fuel elements under α-active conditions.

3. Separation of the neutron-absorbing poisons with little or no decontamination from γ-emitters. This necessitates the metallurgical reforming treatments and fuel refabrication processes being carried out under γ-active conditions.

These three specifications can call for quite different types of process and equipment. Since processing by the first specification has become the conventional route this type will be considered in detail.

PROCESS SELECTION

General Processes

A plant working such a complete separation process must enable the following to be performed with safety:

1. Isolate substantially pure uranium and pure plutonium from a wide variety of elements, generally called fission products, with mass numbers ranging from 72 to 158.

2. Since the fissile material is very valuable, the losses of this precious material must be extremely small. Recoveries of 99.9 per cent or better in sections of plant are not uncommon.

3. The fission products have a great nuisance value and, in this type of plant, must be eliminated to an extremely high degree. The fission product decontamination factor for the uranium may be 10^6–10^8. The decontamination factor is defined as the ratio of the fission product activity per unit weight of uranium entering the plant to that leaving the plant.

In order to meet these requirements, the process selected must be extremely specific for a few elements and should preferably lend itself to a fractionating

* Atomic Energy Research Establishment, Harwell, England.

technique if cumbersome, expensive operations are to be avoided. The presence of intense radiation must not impair the selectivity and the chemicals should be mutually stable under the selected conditions of operation. The presence of very high levels of radiation brings other demands on process selection. Since servicing, inspection and replacement of plant may be impossible or very costly, chemicals with objectionable corrosion properties must be avoided and the selected processes must be operable by remote control. Because of these servicing and accessibility implications it is highly desirable to eliminate the fission products as soon as possible and as completely as possible in order that a minimum of plant shall suffer from these limitations and that non-productive, fission product waste-treatment plants shall be kept to a minimum.

Apart from possible advantages such as cheapness of operation, uniformity of product and minimum losses that can often result from using continuous rather than batch processes, in processes handling radioactive materials there are two unique factors that may weigh heavily when balancing a choice between batch and continuous operation. The volume of material held-up in vessels very largely affects the amount of shielding required from γ-emitters and has a considerable bearing on possible criticality hazards when handling fissile materials. Provided short reaction times are involved, continuous processes lead to smaller hold-up volumes for the same throughput than do batch processes.

Owing to the toxic, radiation and criticality hazards associated with some of the materials to be processed, safety consideration will need even more careful study than is usual in process selection. The introduction of hazards additional to those inherent in the materials handled should be avoided. The influence of criticality on separation processes is the subject of separate papers to this Conference.[1,2,3] With attention focussed on the radioactive materials, there is a danger of less than due attention being paid to "inactive" chemicals which may bring inflammability, carcinogenic and other dangers to plant operators. The possibility of long-term, accumulative toxic effects from new or even common chemicals must be watched for when developing new processes. The following sources of hazard are of particular importance in a chemical plant[4] and should be taken into consideration when comparing possible separation processes: (1) corrosion, (2) heat sensitivity, (3) fire or explosion, and (4) toxicity.

Solvent Extraction Processes

It has now become well-known that continuous counter-current solvent extraction processes have been applied to these separations with considerable success.[5,6,7] Guiding criteria can be suggested for these processes with the generalisations above. Low mutual solubility is desirable if expensive solvent losses are to be avoided and the most favourable extraction characteristics obtained. The extraction of single components is expressed by the distribution or partition coefficient. For normal batch extraction these coefficients must be higher than for continuous (or batch) counter-current fractionating extraction where a high value may not necessarily be advantageous owing to the limit in the phase flow ratios that can be efficiently used in some types of extracting equipment, e.g., in packed columns. The separating power of a solvent for two solutes is frequently expressed by the ratio of the partition coefficients and this ratio may frequently vary from about 500 to 5000 for some of the solvents used for separating uranium from fission products. The value for the separating power for a given pair of solutes in a given solvent will be affected by the concentration of the solutes, the temperature, the relative volumes of the phases and by adventitious impurities in the solvent. The following process variables affect the performance of a continuous extraction unit: (1) temperature, (2) composition of aqueous and solvent phases, (3) relative flow ratios of phases, (4) number of stages, and (5) location of feed point.

These are not independent variables (see Alders[8]) but are factors to be taken into account when equipment is being considered for a solvent extraction process. High concentrations of solutes, particularly when due to "accumulation" at different stages, can cause trouble with solid deposition and even complete blockage of equipment. Or a viscous third liquid phase can be formed, interfering with the flow of liquids and causing premature flooding. These "accumulation" phenomena frequently limit the ratios of solvent and aqueous phase flow rates that can be used and limit the value of high partition coefficients. It is desirable that components extracted into the solvent can be completely removed, for example by washing with water, for completeness of recovery of valuable material and because small quantities of the solute in the recycled solvent can have a great influence on the losses of that component in the raffinate. The effect of this "re-entry value" of the solvent has been discussed by Alders.[8]

The selection of equipment for liquid-liquid contacting and the effect of the physical characteristics of process systems on the performance of this equipment is discussed in another Conference paper.[9]

In addition to the desirability of eliminating the fission products as soon and as completely as possible, it is a very valuable feature of some of these solvent extraction processes that they can be operated free from dissolved salts other than those resulting from dissolving the reactor fuel element in nitric acid. Often this results in an effluent from the first extractor containing virtually all of the fission products free from other salts with the result that the volume of the effluent can be considerably reduced by evaporation. Sometimes the volume can thus be reduced more

than fifty-fold with considerable reduction in the cost of storage of these wastes. The economic advantages of this volume reduction are shown in Fig. 1. Before a decision can be reached to reduce the volume by evaporation, the possibility of violent reactions between the dissolved or entrained solvent and hot nitric acid must be considered. In general, it is imperative that entrainment be reduced to a minimum and the dissolved solvent removed or destroyed under controlled conditions. The removal can be accomplished either continuously or batch-wise by contacting of the aqueous stream with air or steam, operations known as air or steam stripping.

Equipment Selection

The presence of radioactive materials imposes restrictions on the selection of equipment above those that would apply for a more conventional plant and these restrictions must be taken into account when selecting a process. The extent to which servicing can be carried out governs the design specification and the type of equipment that can be employed. This is demonstrated by the classification of plant in Table I. The figures given for the total activity present in a cell are only relative and would be affected by the size of plant and of containing cell. Also, the remarks on the possibility of entering the cell are only a rough guide and are subject to variation for different types of plant.

The plant servicing philosophies that may be employed also affect the equipment selection. The following can be considered: (1) contact servicing; (2) contact servicing after decontamination; (3) remote servicing—repair; (4) remote servicing—replacement; and (5) no servicing—built-in spares.

Harty (Hanford[11]) has discussed the design philosophy of remote maintenance, for which he lists the following advantages and disadvantages.

Advantages	*Disadvantages*
1. Operations and maintenance can be conducted safely.	1. Design is more difficult.
2. On-stream efficiency is high.	2. Fabrication and construction take more time.
3. Capital investment per unit of throughput is low.	3. Initial investment, neglecting throughput, is higher.
4. Flexibility for process changes and increased capacity is available.	

The choice of the servicing philosophies to be adopted must depend on the plant in question and the resources of the design and construction organization concerned. In some cases all five of the servicing types may be applied at different parts of a plant, the compromise and selection aiming at producing the cheapest, reasonably flexible plant.

While the servicing philosophy can affect the selection of plant, there are some generalisations that hold for any radioactive plant. Extreme reliability is most desirable and this usually comes with simplicity. Subject to this reliability requirement, the equipment selected is much the same as for a standard chemical plant, standard equipment being used wherever possible. Very special pre-installation inspection and performance specifications are necessary in order to

Table I. An Activity Classification of Plant:[10] Design and Servicing Implications

Grade	*Total activity present in cell*	*Possibility of entering cell*	*Design notes*
1. Extremely high activity	>1000 curies	No entry at all	No relaxing of design specification possible. All servicing must be done from outside shielding by remote control.
2. Very high γ-activity	100–1000 curies	Short entry (2–30 minutes) after extensive decontamination, assuming ease of decontamination is made a feature of the design of vessels and plant.	Slight relaxing of design specification is possible if plant is required for short time service only. For plant required to work for a long life Grade 1 design specification is necessary.
3. High γ-activity	1–100 curies*	Entry possible after draining plant and a limited amount of decontamination, particularly if some local shielding is used.	Careful use of some conventional plant items may be permissible.
4. Low γ-activity	<1 curie*	Entry may be possible during operation, particularly if local shielding is used.	Conventional plant items can be used.
5. α-activity only	—	Entry possible at any level of activity for unlimited periods. (Wearing protective clothing and mask).	Owing to intense toxicity plant should be inside "fume cupboard" or "dry box" type of cell and should be leak proof.

* These figures are very much dependent on the size of plant and containing cell.

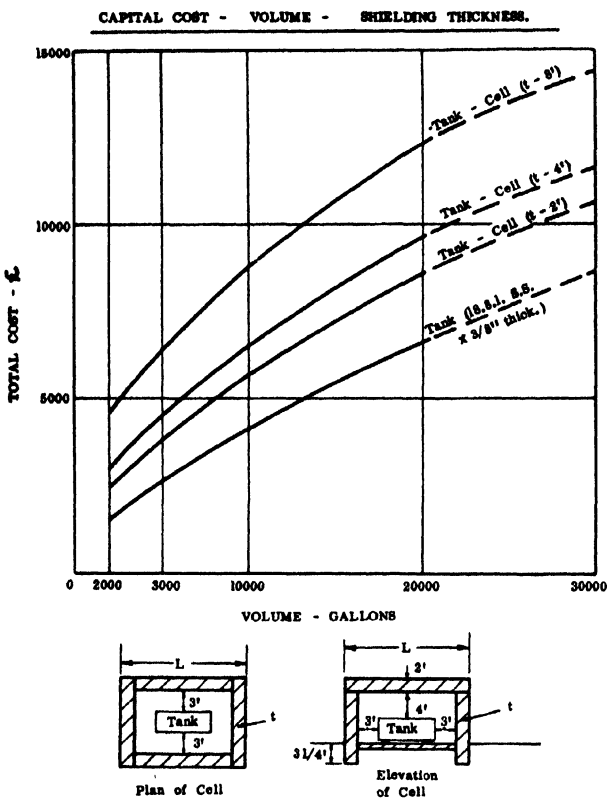

Figure 1. The relative cost of storing fission product wastes

achieve this reliability and some items must be specially developed. Equipment must be leak-proof. This leads to avoiding the use of valves wherever possible on lines carrying radioactive solutions. If valves have to be used, they must incorporate extraordinary features to prevent gland leakage, and leak detectors may be desirable. Normally, welded joints are preferred to flanges and very high standards of welding technique and inspection are essential. The plant is usually designed so that it can be drained and decontaminated. Methods of elevating solutions can be placed in the following order of reliability: vacuum transfer, air-lifting, direct pumping; the second calling for special equipment to remove contamination from the air and the last requiring special precautions against leakage, totally enclosed, canned rotor pumps being an example of the lengths to which it is sometimes necessary to go. The advantages of selecting processes that lead to low hold-up of process liquors has been mentioned. Frequently equipment can be selected to give features perhaps more necessary with radioactive than inactive applications. An example is given in Table II where the performance of two designs of small continuous evaporator a compared.

The very much smaller hold-up has been achieved in the much simpler, cheaper climbing film evaporator at the expense of greater activity entrainment in the condensate and higher pressure drop. This much lower hold-up would have a considerable effect on the amount of shielding required from γ-radiation and might have been a valuable feature in removing a criticality hazard if fissile material had been involved. This example lists most of the features to be looked for in evaporators handling radioactive liquids, low hold-up, low corrosion rate and high decontamination factor being most important. Considerable information has been published on evaporation of radioactive liquids, usually waste streams,[13,14,15] on entrainment[16] and on methods of treatment of aerosols[17] so that suitable equipment can usually be designed for these formidable evaporator specifications.

PLANT LAYOUT

As with the equipment to be used, a rough idea of the plant as a whole must be in mind early in the process development stages. In any chemical plant, details of the laying-out of the plant can have a large influence on both capital and operating costs. This is even more the case in highly radioactive plant where design of the shielding can play a large part in determining the layout of the plant that the shielding must house. Remote operation by itself is not new to chemical technology. Centralised instrument control panels are standard practice in conventional chemical plant since these forms of control usually result in considerable savings in operating costs by a reduction in man-power and by greater uniformity of products. Many modern chemical plants could not be operated without the fine degree of control possible with these instruments. In radioactive plants, where remote operation is a safety necessity, these techniques can be applied to even greater advantage.

The features of a highly radioactive plant that largely govern the detailed lay-out are the following: (1) the design of the shielding; (2) the compartmentation and segregation of parts of the plant of varying degrees of activity; (3) ventilation requirements; (4) the servicing philosophy adopted. If remote replacement of key plant items is planned this will call for special plant lay-out. For contact servicing rapid access to plant may be vital; (5) the nature of the effluents and methods of treatment; (6) the numbers and location of sampling points; (7) the degree to which the process lends itself to complete automatic remote control; (8) the type of equipment that is available can play a predominant role. For example, in plants handling liquids, the following govern the lay-out: methods of liquid handling, whether by gravity flow or pumping; the types of contacting equipment available, whether vertical or horizontal; the numbers and sizes of inter-unit buffer storage or process tanks that have to be used; and (9) contamination control both as it affects equipment location, e.g., preventing active solutions backing up inactive pipe-lines, and personnel, clothing, washing, eating, smoking and sanitary regulations.

These notes on plant lay-out must be sketchy and generalised. It is hoped that they may serve as a guiding background to the type of thinking that must be applied when converting a test-tube process to a plant conception. The earlier this thinking can be applied the more profitable will be the process development efforts and the more elegant will be the plant

Table II. Comparison between Experimental Pot-type and Climbing Film Continuous Evaporators[12]

Property	*Pot-type*	*Climbing film*
1. Duty	To evaporate 100 litres of feed a day, giving a three fold volume reduction. Feed: Radioactive 0.6*M* in HNO_3	Same
2. Size	Cylinder 1 ft diameter by 2 ft high, with dished ends. Surmounted by packed column 3 in diameter by 6 ft high. Surface area in contact with liquid = 5.5 ft^2	Tube 0.3 in diameter by 5 ft long. Surmounted by a packed column 2 in. diameter by 2 ft long. Surface area in contact with liquid = 0.472 ft^2
3. Hold-up	14–15 litres	0.11 litres
4. Over-all heat transfer coefficient	200 BTU/hr-ft^2-°F	440 BTU/hr-ft^2-°F
5. Decontamination factor	3×10^7	2×10^5 (could be better if longer packed column was used)
6. Corrosion-penetration rate	0.001 in./yr	0.0028 in./yr
Production* contamination	9.3μg/ml of concentrate	2.2μg/ml of concentrate
7. Ability to cope with foaming such as is liable to occur with this type of feed.	Foaming would cause flooding in the packed column which would have serious results	Only probable noticeable effect would be increase in pressure drop in evaporator. No serious results.
8. Pressure drop	10 in. water	4 ft water

* The evaporators were made of similar grades of stainless steel.

PLANT LOCATION

The location of a separation plant in relation to the reactor requiring this service must sometimes be considered almost as soon as the requirement for processing is conceived. There is a trend in reactor development to regard the chemical processing and the reactor as a single unit. The possible simplified processes associated with homogeneous reactors may be cited as an example of this trend. In this case the processing may consist of merely filtering insoluble fission products from the circulating solution of fissile material. On the other hand, with solid fuels there are strong economic arguments in favour of transporting the discharged fuel to a centralized processing plant. This is because both the capital and operating costs of most plants fall markedly with throughput. Furthermore, the staff operating power plants will probably very much prefer to pay for a processing service than to have to do the processing on the power-station site.

Apart om these special features, the location of a plant to process nuclear fuels is subject to the same considerations as any other chemical plant, each type of plant merely accenting different factors. Vilbrandt[18] cites the following as major factors in locating a chemical industry: (1) raw materials, (2) market, (3) transportation, (4) labour, (5) plant requirements, and (6) power. He cites a further seventeen minor factors which include waste disposal, oil structure and climatic conditions.

A nuclear separations plant would place waste disposal very high on the list; soil structure might be very important if massive concrete shields were involved and climatic conditions could not be ignored. An electrochemical plant may require that power supplies are considered the most important and a plant extracting a small quantity of precious metal from large amounts of ore would probably best be situated at the source of the raw material. Thus the analytical procedure for locating any chemical plant is the same. The accent is placed on different factors depending on the nature of the industry concerned.

REFERENCES

1. Callihan, A. D. *et al.*, P/834, *"Small Thermal Homogeneous Critical Assemblies"*, Volume 5, Session 20A.3, these Proceedings.
2. Horton, C. C. and McCullen, J. D., P/428, *"Plutonium—Water Critical Assemblies"*, Volume 5, Session 20A.3, these Proceedings.
3. McKay, H. A. C. and Nicholls, C. M., P/454, *"The Criticality Safety of Chemical Plant Producing Fissile Materials"*, Volume 13, Session 18C.1, these Proceedings.
4. Perry, J. H., Editor, *Chemical Engineer's Handbook*, Second Edition, p. 2913, McGraw-Hill Book Company (1941).
5. Ohlgren, H. A., Lewis, J. G. and Welch, M., Nucleonics, Vol. *13*, No. 3, p. 18 (March 1955).
6. Culler, F. L., P/822, *"Reprocessing of Reactor Fuel and Blanket Materials by Solvent Extraction"*, Volume 9, Session 21B, these Proceedings.
7. Lawroski, S., P/823, *"Survey of Separation Processes"*, Volume 9, Session 22B.1, these Proceedings.
8. Alders, L., *Liquid-Liquid Extraction*, Elsevier Publishing Company (1955).

9. Pratt, H. R. C., P/765, *"The Characteristics of Liquid-Liquid Extraction Equipment as Applied to Radioactive Processing"*, Volume 9, Session 21B, these Proceedings.
10. Nicholls, C. M. and White, A. S., Chemistry and Industry No. *3*, p. 51 (17 January 1953).
11. Harty, W. M., "Chemical Engineering Progress Symposium Series No. 13", Nuclear Engineering—Part III, Vol. *50*, p. 115 (1954).
12. Pepper, D., A.E.R.E., Harwell, Report in preparation.
13. Browden, F. N., Ind. Eng. Chem., *43*, p. 1502 (1951).
14. Horrigan, R. V. and Fried, N. M., Brookhaven National Laboratory Report, B.N.L., 121 (1951).
15. McCullough, G. E., Ind. Eng. Chem., *43*, p. 1505 (1951).
16. Montross, C. F., Chem. Eng., *60*, No 10, p. 213 (1953).
17. Smith, I. J., *"A Survey of the Published Literature Concerning the Removal of Aerosols"*, to be published—Trans. Inst. Chem. Engs. (London).
18. Vilbrandt, F. C., *Chemical Engineering Plant Design*, McGraw-Hill Book Company (1942).
19. Hayes, T. and Clegg, G. D., A.E.R.E. Harwell, Private Communication.

Chemical Principles in the Separation of Fission Products from Uranium and Plutonium by Solvent Extraction

By J. M. Fletcher,* UK

Solid reactor fuels require processing periodically for one or more reasons. There may be structural damage, due to radiation or the formation of fission products; and there may be depletion of the fissile material with an undesirable accumulation of fission product poisons. Recovery of the fuel and its reconstitution into new fuel elements is necessary. One well-established but elaborate method for this operation is to separate the fissile and source material from the radioactive fission products, so that the manufacture of further fuel may be carried out in a manner comparable to that for natural uranium, i.e., without the hazards introduced by β and γ radiation from fission products. This separation problem can conveniently be undertaken, after dissolving the fuel in an acid such at nitric acid, by various chemical methods: one of these is by solvent extraction using suitable organic solvents flowing counter-current to the nitrates in aqueous solution.

The flowsheet for a plant to carry out such a solvent extraction process will be based:

1. On factors which make the plant convenient to operate: thus the choice of solvent is influenced by its boiling point, inflammability, solubility in aqueous solutions, etc., while corrosion and the tendency to form precipitates or sludges need to be avoided.
2. On the chemical characteristics, e.g., equilibrium and kinetic data, relating to the various nitrates present in the system, and the effect on them of valency changes, temperature, concentrations, etc.

This paper deals with point 2.

REQUIREMENTS

As a general case, the processing of 1000 kg of a reactor fuel, initially natural uranium, will be considered. It is supposed that there has been fission of 1 kg (mainly U^{235}, but some Pu), corresponding to approximately 1000 mwd/t; and that after removal from the reactor the fuel has been cooled for 100 days, and dissolved in nitric acid to give a solution 1*M* in uranyl nitrate. The important constituents present in the resulting solution are given in Table I.

The object of the process may be envisaged as the recovery of uranium and plutonium (either separately or together) for further use, and the segregation of the fission products in some form where they present no hazard. A solvent extraction process accomplishes this by taking advantage of the varying extent to which the elements present form nitrato complexes which are extractable by the organic solvent chosen.

CLASSIFICATION OF NITRATO COMPLEXES

Nitrato complexing of metals in aqueous solutions is usually small in comparison with complexing by other ligands such as fluoride, phosphate, oxalate ions: but for the uranyl, plutonyl, and nitrosylruthenium (RuNO) radicals, and for certain of the metals of Table I in their tetravalent form, it is considerably greater than for other valency states of these metals and for other fission products. Three main groups of nitrato complexes may be postulated:

Metal or radical	*Species in organic solvents*
Group A: relatively strong	
UO_2(II), PuO_2(II)	Di and trinitrato complexes
Pu(IV), U(IV), Zr(IV), Ce(IV)	Tetra- and hexanitrato complexes
(RuNO) (III)	Trinitrato complexes
Group B: relatively weak	
Pu(III), Y, Ce(III), La, Pr and other rare earths, Nb	Trinitrato and higher complexes
Group C: very weak or existence doubtful	
Cs	
Sr, Ba	
Mo, Tc	
Ru(IV), Rh	

URANYL NITRATE

It has been known for a long time that uranyl nitrate can be extracted from an aqueous phase by a wide range of solvents; many of them, e.g., ethers, ketones, possess a donor oxygen atom which plays an important part in the extraction process. In an aqueous solution of uranyl nitrate there are present, not only hydrated uranyl ions UO_2^{2+}, but also a series of hydrated nitrato complexes, $[UO_2NO_3]^+$, $[UO_2(NO_3)_2]$, $[UO_2(NO_3)_3]^-$; at room temperature, there is rapid equilibrium between the nitrato species. The formation of the higher nitrato complexes is promoted by the presence of nitrate ions, which in the feed solution (for this solvent extraction process) may be present as nitric acid or as other nitrates

* Atomic Energy Research Establishment, Harwell, near Didcot, Berks.

Table I. Important Constituents in a Solution Obtained by Dissolving 1000 kg of Uranium Irradiated to 1000 Mwd/t and Cooled 100 Days

Fissile and source material	*Valency*	*Approx. weight*	*β-activity, curies*	*γ-activity* curies*
Uranium	6	998 kg	0.6†	0.03†
Plutonium	4.6	0.8 kg	–	–
Fission products				
Caesium	1	110 gm	3000	2300
Strontium	2	40 gm	45,000	Nil
Barium	2	40 gm	Nil	Nil
Yttrium	3	20 gm	60,000	Nil
Lanthanum	3	40 gm	Nil	Nil
Cerium	3.4	100 gm	170,000	12,000
Praseodymium and other rare earths	3	155 gm	12,000 (from Pm)	Nil
Zirconium	4	115 gm	70,000	65,000
Niobium	Various	5 gm	110,000	105,000
Molybdenum	Various	85 gm	Nil	Nil
Technetium	Various	25 gm	Nil	Nil
Ruthenium	Various	55 gm	55,000	20,000
Rhodium	Various	12 gm	Nil	Nil
Other elements	–	40 gm	1000	–
Total for fission products in solution		842 gm	526,000	204,300
Add fission product rare gases and halogens removed during dissolving		140 gm	500	–
Total for fission products		982 gm		

* Includes activity from short-lived daughters of UX_1, Cs, Sr, Ce, and Ru.
† For UX_1 in equilibrium with U^{238}.

added intentionally for this purpose; thus $[UO_2NO_3]^+$ may predominate in $[NO_3^-] \sim 4M$,[1] and $[UO_2(NO_3)_2]$ in concentrated nitric acid.[2] The uncharged dinitrato complex and the anionic trinitrato complex[2] are soluble in many organic solvents, so that by agitating the aqueous solution with a suitable organic solvent for a few seconds, a substantial fraction of the total uranium is transferred to the organic phase. Examples of the distribution of uranyl nitrate between aqueous and organic phases are given in Table II. Values of the observed distribution of uranium for various solvents and conditions depend (*a*) on the formation constants for the nitrato species in both the aqueous and organic phases, and (*b*) on the solubility of each particular nitrato complex in the two phases. The solubilities of the dinitrato, and more particularly of the trinitrato complex, are considerably greater in many organic solvents (where the dielectric constant is low) than in aqueous solutions; therefore, though only a small fraction of the uranyl radicals may exist in a particular aqueous solution as higher nitrato complexes, relatively large amounts pass into the organic phase, since the equilibria are shifted, e.g.

$$\underset{\text{aqueous}}{[UO_2 6H_2O]^{2+}} \rightarrow \underset{\text{aqueous}}{[UO_2(NO_3)_2]} \rightarrow \underset{\text{solvent}}{[UO_2(NO_3)_2]}$$

After such agitation, the organic phase contains not merely organic molecules but water and nitric acid (if aqueous nitric acid is present); the molar concentrations of these are considerable (Table III) and their relative amounts affect the proportion of the various nitrato complexes in the organic phase in a similar manner to what occurs in an aqueous phase.[2] The transfer of uranyl nitrate to the organic phase is accompanied by additional water,[3] indicating that uranyl nitrate can exist in organic solvents as aquo-nitrato complexes; in particular organic solvents (*S*) there is also evidence that non-aquo complexes, e.g. $[UO_2(NO_3)_2S_2]$, are formed. In principle, there appear to be two stages; firstly, the extraction of complexes in which aquo groups are present in the co-ordination complex; secondly, the replacement, probably as a slower process, of some or all of these aquo groups by the solvent.

THE SOLVENT EXTRACTION OF NITRATES

There is little difficulty in devising a counter-current system by which uranium, as uranyl nitrate, and plutonium, as Pu(IV) or plutonyl nitrate, are effi-

Table II. Distribution of Uranyl Nitrate between Water and Various Organic Solvents at 25°C. Aqueous Phase at Equilibrium

Organic solvent	*Distribution coefficient (organic/aqueous in terms of molalities for 0.2 molal uranyl nitrate*	*1 molal uranyl nitrate*	*Ref.*
Diethyl ether*	0.003	0.14	4
Dibutyl cellosolve	< 0.001	0.026	5
Dibutyl carbitol	0.01	0.32	5
Penta-ether	0.12	1.0	5
Methyl isobutyl ketone	< 0.004	0.16	5
Cyclohexanone	0.17	0.9	5
Isoamyl alcohol	0.004	0.15	5
Tributyl phosphate	5.5	1.8	6

* At 18°C.

Table III. Concentrations of Water and Nitric Acid in Organic Solvents in Equilibrium with Aqueous Nitric Acid

Organic solvent and its aprox. molarity in organic phase	*Aqueous phase* $[HNO_3]$ *M*	*Organic phase* $[HNO_3]$ *M*	$[H_2O]$ *M*	*Ref. and temp.*
Diethylether	0.5	0.022	0.5	7
(10*M*)	1	0.09	–	22 ± 2°C
	2	0.5	–	
	4	2.6	4.9	
Dibutyl carbitol	0.5	0.028	0.6	8
(4*M*)	1	0.13	0.8	25°C
	2	0.62	1.5	
	4	2.1	3.6	
Penta-ether	0.5	0.15	2.8	8
(3*M*)	1	0.55	5.9	25°C
	2	1.4	9.9	
	4	2.7	11	
19% tributyl	0.5	0.045	0.185	9
phosphate	1	0.14	0.22	20°C
(0.7*M*)	2	0.29	0.22	
	4	0.51	0.11	

Table IV. Distribution Coefficients between Organic and Aqueous Phases for U, Pu and F.P. Nitrates at 20–25°C*

Metal or radical	Molarity	Distribution coefficient (O/A) For I	II	III	Refs.
UO_2(II)	10^{-2} to 10^{-3}	5	30	very high	10
PuO_2(II)	10^{-2} to 10^{-3}	0.7	3	very high	10
Pu(IV)	10^{-2} to 10^{-3}	1.3	20	very high	10
Zr(IV)	Tracer	0.01	1	1‡	10
Ce(IV)	Tracer	0.01	0.2	–	11
(RuNO) as trinitrate	10^{-2} to 10^{-3}	10	0.01	very high	10
Pu(III)	10^{-2} to 10^{-3}	0.015	0.01	–	10
Ce(III)†	Tracer	0.04	0.02	10	11
Y(III)	Tracer	0.01	0.02	–	11
Nb	Tracer	0.01	0.01	–	10

* Stirring times from ½ to 5 minutes. *Organic phase:* 20% tributyl phosphate (with hydrocarbon diluent and in equilibrium with respect to water and nitric acid with the aqueous phase). *Aqueous phase at equilibrium:* I, 1*M* HNO_3; II, 6*M* HNO_3; III, 0.1*M* HNO_3, 6*M* $NaNO_3$.

† For Ce(III), data are for 50% TBP.

‡ Value applies to aqueous phase with 1*M* HNO_3, 5*M* $NaNo_3$.

ciently extracted from a nitric acid (or nitric acid + nitrate) solution of the fuel. The distribution coefficients for the elements listed in groups *B* and *C* above are usually very much lower (Table IV) than the values for U and Pu, and their separation efficiency will depend primarily on physical features (e.g., disentrainment) of the extraction system. However, the fission products which are in group *A* with U and Pu, include γ-emitters Zr and Ru (cerium is normally present as Ce(III)). Even if only 5% of the total Zr and Ru accompanies the uranium and plutonium into the organic phase, there is carried forward, per 1000 kg of fuel, about 4000 γ-curies to be removed at later stages. Assuming that it is the intention to extract plutonium as Pu(IV) and PuO_2(II) with uranium as UO_2(II), there is therefore particular interest in the individual differences between the nitrato complexes of U and Pu on the one hand, and those of Zr and Ru on the other hand since, with this knowledge, the separation factor for fission products may be improved.

Uranyl and Plutonyl

Conditions for the formation in aqueous solution of uranyl and plutonyl nitrato complexes are similar. Spectrophotometric and other measurements provide a semi-quantitative measure of the extent of complexing at various concentrations of nitric acid or other nitrates. For plutonyl nitrate, changes in the height of the 502 mμ peak have been correlated with changes in the distribution coefficient.[12] Hydrolysis (with the formation of polynuclear species) which is only slowly reversible, is unimportant up to pH 4. A wide variety of conditions therefore enables these forms of U and Pu to be extracted from aqueous solution by organic solvents; also, in the so-called stripping section of counter-current extraction systems, if the solvent phase is washed with dilute nitric acid, uranyl and plutonyl nitrates can still be made to emerge quantitatively in the organic phase. In the presence of inextractable inorganic nitrates (MNO_3) in the aqueous phase and with [HNO_3] low, the distribution coefficients (*D*) increase with [MNO_3] for a large number of solvents; the major reason is the promotion of nitrato complexing by the common ion effect.

With nitric acid as the source of nitrate ions, although there is at first an increase of *D* with [HNO_3], a maximum value of *D* is usually reached at 6 *M* HNO_3 in the aqueous phase.[10,12] Although the common ion effect initially increases *D*, the combined effects (*a*) of the reduced degree of ionisation of aqueous nitric acid and, (*b*) its increasing concentration in the organic phase, become increasingly important as [HNO_3] increases and may even lead to a decrease in *D*.[13]

Pu(IV) and Zr(IV)

The characteristics of Pu(IV) and Zr(IV) nitrates are conveniently considered together. Hydrolysis with the formation of slowly reversible polynuclear products becomes of major importance at low acidities: with the relatively low concentrations of these elements in the system under consideration, the onset of such hydrolysis can be taken approximately as pH = 1 for Pu(IV), and pH = 0 for Zr(IV). Complexing of Pu(IV) to [$Pu(NO_3)_4$] is followed in concentrated nitrate solutions by the formation of the anions [$Pu(NO_3)_5$]$^-$ and [$Pu(NO_3)_6$]$^{2-}$: the formation constants for the similar nitrato complexes of Zr(IV) appear to be lower, the situation being complicated by the existence of zirconyl, ZrO or $Zr(OH)_2$(II) species.[14] Advantage can be taken of this behaviour of Zr(IV), by employing relatively low nitrate concentrations to give a good separation factor of Pu and U from Zr.

Ruthenium

Separation from fission product ruthenium is simple, if it exists in the fuel solution as Ru(IV), since nitrato complexing of this form is very weak.[15] Treatment of irradiated fuel with nitric acid, leads

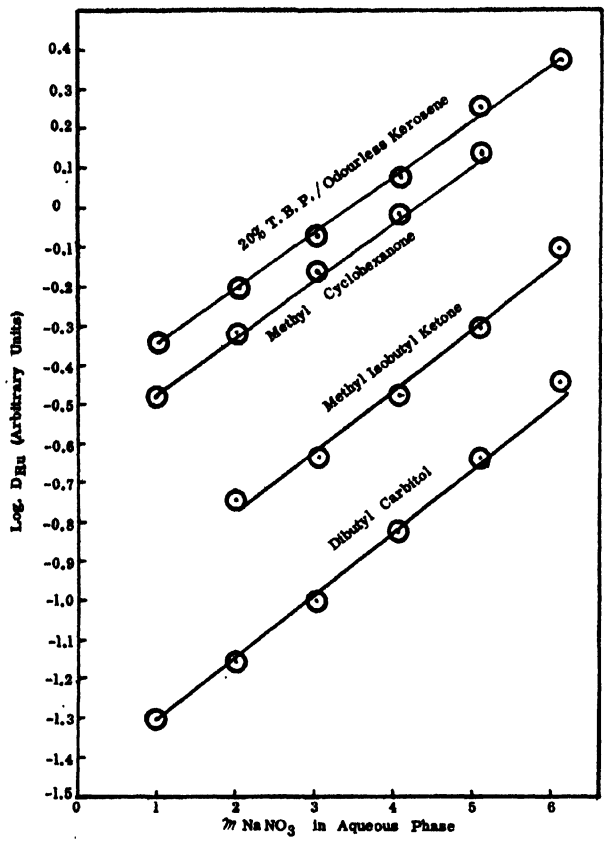

Figure 1. Salting-out of $RuNO(NO_3)_3$ by sodium nitrate

however to nitrosylruthenium compounds which display the characteristics of octahedral six coordination compounds of the transition metals in forms such as Co(III) and Pt(IV).[16]

The formation of nitro as well as of nitrato (RuNO) complexes is to be expected. The outstanding way in which the nitrato complexes of (RuNO) differ from those of (UO_2), (PuO_2), Pu(IV) and Zr(IV), is in their slow rates of formation and of reaction. Kinetic effects, which for practical purposes can be ignored for all the latter radicals, can play an important part in purification from ruthenium. As for other metals or radicals, the presence of nitrate ions in aqueous solution leads, at equilibrium, to increasing proportions of the higher nitrato complexes of nitrosylruthenium. Thus the proportion present as the trinitrate, $[RuNO(NO_3)_3(H_2O)_2]$, has been found to increase from about 4% in 1*M* HNO_3 to 35% in 6*M* HNO_3.[17] This complex is readily soluble in many organic solvents, whereas the solubility of the lower, di- and mono-nitrato complexes is very considerably less. Unlike the other nitrato complexes considered in this paper, it is sufficiently unreactive at temperatures between 0°C and 20°C for measurements of its distribution coefficient to be made, for short times of stirring, without serious interference from the presence of other nitrosylruthenium species, which are formed slowly by hydrolysis or by further nitration. Thus with increasing concentrations of inextractable metallic nitrates in the aqueous phase, log *D* increases linearly with $[MNO_3]$[18] as a result of Setchenow salting-out from the *aqueous* phase (Fig. 1). But with increasing concentrations of nitric acid (part of which passes into the solvent phase), log *D* decreases nearly linearly with $[HNO_3]$ as a result of Setchenow salting-out from the *solvent* phase.[10] On the other hand, for periods of stirring, which are long in comparison with the times of the nitration and denitration reactions (these occur both in the aqueous and in the organic phases), the shape of the log *D*: $[HNO_3]$ curve[19] becomes similar to that for uranyl nitrate, etc.

In the separation of uranium and plutonium from fission products by solvent extraction, decontamination from ruthenium is therefore a complex function (*a*) of the solvent, (*b*) of the nitrate and nitric acid concentrations of the aqueous feed and stripping solutions, (*c*) of these concentrations in the organic phase at different stages of the extraction system, and (*d*) of the number of stages and the hold-up per stage in the extraction system employed.

TEMPERATURE AND VALENCY CHANGES

There is a variation in the distribution coefficients for metallic nitrates with temperature due to transfer to the organic phase being accompanied by the evolution of heat. In the absence of salting-out agents, *D* has been found[20] to be about twice as great at 0°C than at 25°C. Of the metallic nitrates considered, all except plutonium are relatively free from valency changes in a number of solvent extraction systems based on nitric acid or nitrates. Any tendency for plutonium to be reduced to Pu(III) (in which form nitrato complexing is weak, as for the trivalent rare earths) may lead to incomplete extraction of plutonium. Irradiation of the solutions by the fission products contained in them, and the presence or absence of nitrous acid and of organic decomposition products, can all affect the proportions of plutonium in the three valency states Pu(III), Pu(IV) and PuO_2(II).

Attention to the chemical principles described, combined with sound chemical engineering of the extraction system, can lead to a counter-current solvent extraction process in which the fission product contamination of uranium and plutonium is reduced in one extractor by about 10,000.

REFERENCES

1. McKay, H. A. C., *The Physical Chemistry of Uranyl Nitrate Solutions,* Chem. & Ind.: 1549 (1954).
2. Kaplan, L., Hildebrandt, R. A. and Ader, M., *The Trinitratouranyl Complex in Ketonic Solvents and The Absorption Spectra of Uranyl Nitrate in Organic Solvents,* ANL-4520 and 4521 (1950).
3. Katzin, L. I. and Sullivan, J. C., *The System Uranyl Nitrate-Water-Organic Solvent,* AECD-2537 (1948). Also Gardner, A. W., McKay, H. A. C., Mathieson, A. R. and Warren, D. T., *The Partition of Uranyl Nitrate between Water and Organic Solvents,* Parts I and III, Trans. Faraday Soc. *47*: 428 (1951), and *48*: 997 (1952).
4. Lofthouse, E. and Smith, A. J., Results, quoted in Ref. 5, (Table 1), from report (dated 1948).

5. Glueckauf, E., McKay, H. A. C. and Mathieson, A. R., *The Partition of Uranyl Nitrate between Water and Organic Solvents,* Part II, Trans. Faraday Soc. *47*: 437 (1951).
6. Waind, G. M. and Healy, T. V., *The Effect of Diluents on the Solvent Extraction of Nitrates,* A.E.R.E. C/R 773 (1952).
7. Sutton, J., *Distribution of Nitric Acid between Water and Ether,* A.E.R.E. C/R 438 (1949).
8. Glueckauf, E. and McKay, H. A. C., unpublished results, Chemistry Division, A.E.R.E.
9. Healy, T. V. and Ford, D. L., unpublished results, Chemistry Division, A.E.R.E. Also Alcock, K., Grimley, S. S., Kennedy, J. and McKay, H. A. C., *The Extraction of Nitrates by Tributyl Phosphate,* Part I, submitted to Trans. Faraday Soc. (1955).
10. Fletcher, J. M., *et al.* Results obtained in the Chemical Processing Group, A.E.R.E.
11. McKay, H. A. C., Alcock, K. and Scargill, D., *The Extraction of Some Rare Earths by Tributyl Phosphate,* A.E.R.E. C/R 1514 (1954).
12. Healy, T. V. and Gardner, A. W., *Solvent Extraction of Pu(VI) from Nitrate Solutions,* A.E.R.E. C/R 800 (1952).
13. McKay, H. A. C., P/441, *Tributyl Phosphate as an Extracting Agent for the Nitrates of the Actinide Elements,* Volume 7, Session 10B.2, these Proceedings.
14. Lister, B. A. J. and McDonald, L. A., *Some Aspects of the Solution Chemistry of Zirconium,* J.C.S., 4315 (1952).
15. Anderson, J. S. and McConnell, J. D. M., *Ruthenium(IV) Nitrates,* J. Inorganic and Nuclear Chem. (in course of publication).
16. Fletcher, J. M. and Martin, F. S., P/437, *The Chemistry of Ruthenium,* Vol. 7, Session 9B.2, these Proceedings.
17. Fletcher, J. M., Jenkins, I. L., Lever, F. M., Martin, F. S., Powell, A. R. and Todd, R., *Nitrato and Nitro Complexes of Nitrosylruthenium,* J. Inorganic and Nuclear Chem. (in course of publication).
18. Martin, F. S., unpublished results, Chemistry Division, A.E.R.E.
19. Sangster, D. F., Results obtained in Chemical Engineering Division, A.E.R.E.
20. Jenkins, I. L., *et al.,* unpublished results, Chemistry Division, A.E.R.E.

Reprocessing of Reactor Fuel and Blanket Materials by Solvent Extraction

By F. L. Culler,* USA

A survey of the reprocessing technology of irradiated reactor fuel elements by solvent extraction must cover the work of hundreds of people and data contained in thousands of detailed reports. In preparing such general summary, much detailed data must be omitted, data on such important subjects as chemical variables, engineering and plant construction information, and specific costs. Probably the most useful information that can be presented is the chemical flowsheets for solvent extraction processes and a cursory discussion of the most important chemical and engineering process variables. This survey is supplemented by detailed papers in the proceedings of this meeting, to which reference is made wherever such a reference is appropriate. Unfortunately, it is not possible to give proper credit to individuals, companies, and national laboratories that have contributed to the reprocessing technology. Suffice it to say that the work of many people and of all groups engaged in the atomic energy program in the United States, Great Britain, and Canada has contributed to the information presented in this summary.

This paper is divided into four major sections:

"Fuels and Reprocessing Requirements" is a general discussion of the nature of fuels for which chemical processing flowsheets have been developed, the time required for decay of radioactive contaminants before processing is started, fission product decontamination, and the separation required for fissionable and fertile materials and their neutron-produced daughters.

"Chemical Processing Flowsheets" is a presentation of chemical flowsheets for reprocessing fissionable and fertile materials by solvent extraction.

"Auxiliary Processes" discusses supporting processes, such as solvent recovery, iodine removal, and isolation procedures for fissionable products.

"Equipment and Engineering Concepts" reviews the types of contactors that have been used for solvent extraction. A general discussion of design of radiochemical processing facilities covers maintenance philosophies and waste disposal. Relative costs of functional areas of a typical radiochemical processing plant are given.

* Oak Ridge National Laboratory. Including work by E. D. Arnold, J. R. Flanary, W. B. Lanham, A. T. Gresky, D. C. Overholt, A. C. Jealous, H. E. Goeller, W. G. Stockdale, R. W. Stoughton, S. W. Peterson, Oak Ridge National Laboratory; W. A. Rodger, Argonne National Laboratory; and personnel at Argonne National Laboratory, Knolls Atomic Power Laboratory, Hanford Engineering Works, California Research and Development Corporation, University of California Radiation Laboratory and other development sites.

FUELS AND REPROCESSING REQUIREMENTS

The possibility of extracting useful power from fission caused by thermal or fast neutrons in nuclear fuels consumed in reactors is commanding world-wide attention. The fuels that have been proposed for fission release of recoverable energy are U^{235}, U^{233}, and Pu^{239}. U^{235} occurs in nature at a concentration of 0.71% in natural uranium, but the other two must be produced by neutron capture in the fertile materials Th^{232} and U^{238}. In the light of our present knowledge, these are the only elements that can be made available in quantities large enough to support fission-produced power on an economic scale.

It is fortunate that each fission event in U^{235} produces, per fission, an average of 2.5 ± 0.1 neutrons in addition to approximately 193 Mev of energy available as heat. Fission neutrons can be absorbed in fertile atoms, U^{238} or Th^{232}, to produce theoretically more fissionable material than has been consumed. The thermal-neutron capture cross sections for these fertile materials are well-established as $\sigma_a = 7 \pm 0.4$ barns for thorium and $\sigma_a = 2.8$ barns for natural uranium. The U^{233} and Pu^{239} produced are desirable nuclear reactor fuels, possibly more desirable than U^{235} under some circumstances. Thus we have the first and possibly most pertinent reason for chemical reprocessing of nuclear reactor fuel: the recovery of fissionable elements produced by neutron capture.

The fission-product mass yield curves for thermal neutron fission of U^{235} and Pu^{239} are well known.[1] Although the thermal and fast yield curves of U^{235} differ slightly from those for plutonium-239, they are close enough that they need not be considered separately from the standpoint of chemical reprocessing. Of importance to the chemists and the engineers concerned with fuel reprocessing are the atomic number and decay characteristics of the fission products. These properties determine the difficulty of separation and the degree of separation required. It is necessary to consider another property of the fission products of interest, namely, the neutron capture cross section. Fission product poisons must be removed periodically from reactor fuels to prevent neutron capture sufficient to seriously affect the neutron economy of the

reactor. Thus there are two groups of fission products that are of interest in chemical processing, the active isotopes of relatively long half-life and significant yield which must be removed from a desirable product to eliminate radiation hazard, and the active or inactive products which have high thermal-neutron capture cross section.

From a capture-cross-section standpoint, the fission products can be divided into three groups: (1) those which can be removed as a rare gas of which Xe^{135} ($\sigma_{ab} = 3.5 \times 10^6$ barns); (2) those with capture cross sections below 100 barns, which are the bulk of the fission products; and (3) those of capture cross section higher than 100 barns, most of which fall in the rare-earth fraction of the periodic table and are easily removed by the solvent extraction processing techniques.

Decay Period

The decay period for fuel is desirably long enough to allow decay of the active fission gases Xe^{133} and I^{131}; however, it is usually determined by the time required for one of the following heavy-element chains to decay:

In thorium:

$$Th^{232}(n,\gamma) \longrightarrow Th^{233} \xrightarrow[23.5\ \text{min}]{\beta^-} Pa^{233} \xrightarrow[27.4\ \text{d}]{\beta^-} U^{233} \qquad (1)$$

$$Th^{232}(n,\gamma) \longrightarrow Th^{233}(n,\gamma) \rightarrow Th^{234} \xrightarrow[24.1\ \text{d}]{\beta^-} Pa^{234} \xrightarrow[6.7\ \text{hr}]{\beta^-} U^{234} \qquad (2)$$

In uranium:

$$U^{238}(n,\gamma) \longrightarrow U^{239} \xrightarrow[23.5\ \text{min}]{\beta^-} Np^{239} \xrightarrow[2.33\ \text{d}]{\beta^-} Pu^{239} \qquad (3)$$

$$U^{235}(n,\gamma) \longrightarrow U^{236}(n,\gamma) \rightarrow U^{237} \xrightarrow[6.7\ \text{d}]{\beta^-} Np^{237} \qquad (4)$$

The required decay period for natural uranium or for thorium can be obtained from curves shown in Fig. 1.[2] For uranium, the decay period is determined by Np^{239} or possibly by U^{237} decay. For fuels which are initially enriched in U^{235}, the U^{237} usually controls the length of the decay period. In establishing the curves shown in Fig. 1, it was assumed that the uranium or thorium product from a solvent-extraction plant should not emit more radiation than could be tolerated in direct handling of the product. Shorter decay periods than those indicated can be used with the following results: (1) radiochemical processing may be complicated by relatively large quantities of I^{131} and Xe^{133}; (2) uranium and thorium may be produced which contain enough β-emitting isotope to make remote handling of products and refabrication of metal fuel assemblies necessary; and (3) losses of neutron-capture-produced fissionable material may be high if the neptunium or protactinium have only partially decayed.

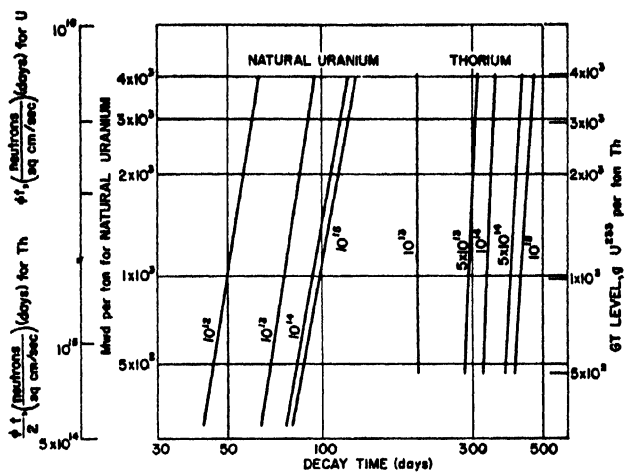

U^{235} enrichment (%)	Additional decay time required (days)	U^{235} enrichment (%)	Additional decay time required (days)
2	10	30	37
5	19	40	40
10	26	50	42
15	30	100	49
20	33		

Figure 1. Time required for U^{237} from uranium and Th^{234} from thorium to decay

The decay period is an important economic consideration in chemical reprocessing and in nuclear power economics. Interest must be paid on the value of fissionable and fertile material in decaying fuel elements. For some power reactor proposals, these inventory charges are of such importance that short decay periods, in some cases 10–20 days, are required. The solvent extraction processes are not necessarily applicable to short-decayed fuels of high burn-up because of radiation damage to solvent.[3]

Required Decontamination Factors from Fission Products

Reactors that are capable of producing useful economic power must operate at relatively high neutron flux levels and must consume a reasonable fraction of the fissionable material in the fuel. Solvent extraction processes have been developed to provide the necessary decontamination of fission products from fissionable and fertile material for high burn-up and appropriate cooling periods. The curves in Fig. 2[4] show the required β-decontamination factors for varying flux-time product versus a constant times the decontamination factor divided by the megawatt-days per ton of fuel. The curves are drawn for 10-days' decay; by applying reduction factors indicated for additional decay periods, it is possible to estimate within 30% the required β-decontamination factors for chemical processing. In preparing these curves it was assumed that fissionable and fertile products require decontamination to their background activity levels to permit subsequent direct handling.

Table I. Fission Products Important in Chemical Reprocessing

Fission product	Fission yield (%)	Half-life	Radio-activity	Energy (Mev)	Absolute curies per gm U^{235} burned,* after 10 days' decay
Ru^{103}	3.0	45 d	β	0.35	27.9
			β	0.66	27.9
			γ	0.31	27.9
Ru^{106}-Rh^{106}†	0.5	290 d	β	2.30‡	0.9
			β	3.55‡	7.26
			γ	0.52‡	0.9
			γ	0.73‡	0.9
			γ	1.25‡	0.09
Zr^{95}-Nb^{95}†	6.2	65 d	β	0.39	99.7
			β	1.12	2.17
			γ	0.21	95.5
			γ	0.73	91.0
			γ	0.94	6.94
Nb^{95}	6.2	38.7 d	β	0.15	97.2
			γ	0.76	97.2
Ce^{141}	6.1	28 d	β	0.44	75.0
			γ	0.13	75.0
Ce^{144}-Pr^{144}†	5.2	275 d	β	0.35	56.7
			β	1.80‡	5.7
			β	3.05‡	49.9
			γ	0.20‡	52.7
			γ	1.25‡	5.7
Kr^{85}	0.33	9.7 yr	β	0.7	0.43
Sr^{89}	4.7	54 d	β	1.46	78.6
Sr^{90}-Y^{90}†	5.2	25 yr	β	0.53	2.7
			β	2.18‡	2.7
Y^{91}	5.6	57 d	β	1.54	107.5
Te^{130}-Te^{130}†	0.4	32 d	β	1.8‡	6.7
			γ	0.11	6.7
			γ	0.3‡	6.7
			γ	0.8‡	6.7
Cs^{137}-Ba^{137}	6.1	33 yr	β	0.52	2.17
			β	1.19	0.11
			γ	0.67‡	2.17
Ba^{140}	6.2	12.8 d	β	0.47	18.4
			β	1.00	58.6
			γ	0.53	18.4
La^{140}†	6.2	40 hr	β	0.91	12.96
			β	1.40	58.3
			β	2.18	9.73
			γ	0.49	7.33
			γ	0.87	9.73
			γ	1.65	65.5
			γ	2.14	5.64
Pr^{148}	5.6	13.8 d	β	0.84	64.5
Nd^{147}	3.0	11.8 d	β	0.37	13.03
			β	0.95	19.56
			γ	0.58	13.03
Pm^{147}	3.0	3.7 yr	β	0.22	9.9
All other radioactive fission products			β		46.3
			γ		27.8
Total			β		960
			γ		628

* These numbers are based on the assumption that no radioactivity has been removed from the feed by volatilization of ruthenium or by scavenging of zirconium and niobium (i.e., by the "head-end" treatments).

† Quantity of emitted radioactivity is governed by decay of long-lived parent.

‡ Activity due to daughter element.

Fission Products of Importance in Chemical Reprocessing

After a decay period of 10 days the fission products that are of primary interest in chemical processing are those listed in Table I.

The number of absolute curies per gram of U^{235} burned can be corrected for any decay period by applying the decay correction factors shown in Fig. 2. For use in determining the curies of specific fission products present, individual decay factors can be determined from the half-lives given in Table I.

For each level of total power production from nuclear fission, there is an equilibrium quantity of fission products of long half-life. The equilibrium concentration of individual fission products can be calculated from the following equation, starting with $n = 0$, $t = 0$:

$$n = \frac{R}{\lambda}(1 - e^{-\lambda t}) \qquad (5)$$

where n = weight of isotope, R = weight of isotope produced per unit time, λ = decay constant in appropriate units, and t = decay time in appropriate units. At varying times, depending on the half-life of the fission product, each fission product will approach a limiting concentration, which is

$$n = R/\lambda \qquad (6)$$

at infinite time. From this simple relation it is possible to estimate fission product quantities involved in long-term waste disposal problems in a nuclear power economy.

Required Decontamination from Heavy Elements

The degree of separation of the heavy isotopes produced by neutron capture in Equations 1–4 is determined by the allowable radioactivity in a product, by the allowable concentration of one element in another, which depends on the neutron cross section, or by the loss represented by the presence of one product in another. In addition to the capture-produced isotopes (Pa^{233}, Th^{234}, Np^{239}, U^{237}, and Np^{237}) shown in these equations, others are produced by double neutron capture, which may assume some significance if fissionable and fertile materials are recycled through many exposures in a reactor.

CHEMICAL PROCESSING FLOWSHEETS

Solvent extraction processes have been developed for the following purposes: (1) separation of plutonium from natural uranium; (2) separation of enriched uranium from aluminum and other diluents and cladding materials; and (3) separation of U^{233}, protactinium, and thorium.

Solvent extraction technology has progressed to the point that any of the above fissionable and fertile materials can be separated from each other, from fission products, and from inactive diluents and contaminants. Nitric acid is a reasonable dissolution agent. For materials such as stainless steel and zir-

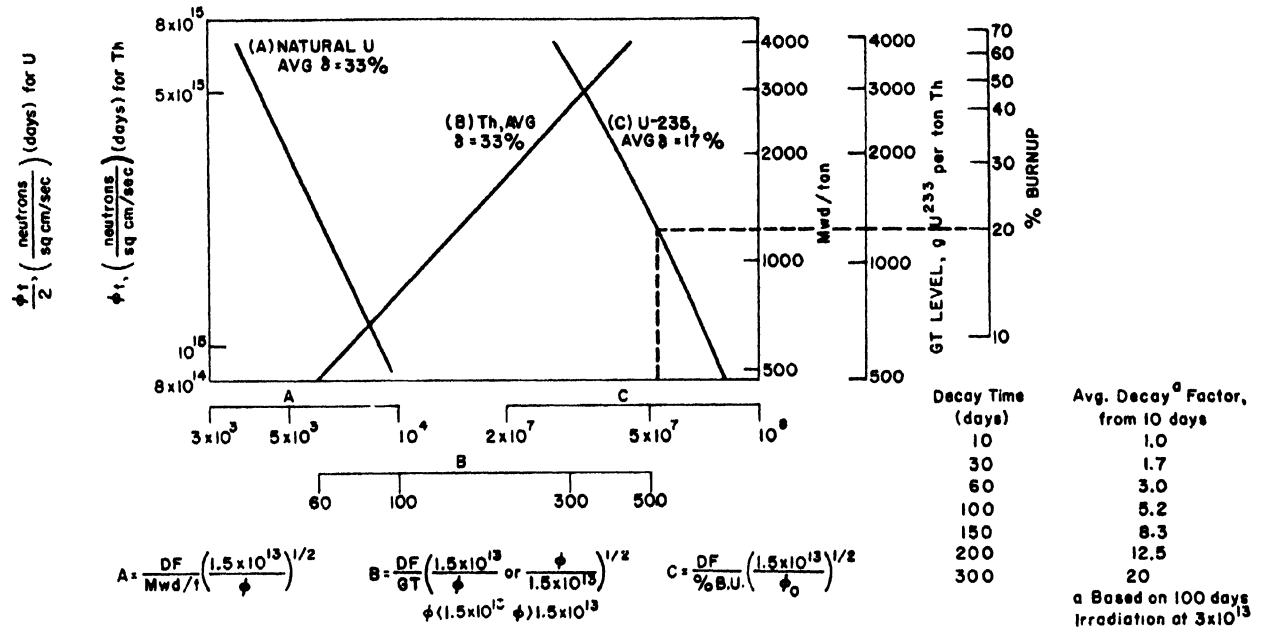

Figure 2. Required decontamination factors for irradiated natural uranium, enriched uranium, and thorium. Base on background activity of 10^9 disintegrations/min/kg; decay time, 10 days. Consider the following example: Assume that U^{235} was irradiated to 20% burnup at flux of 10^{14}; the decontamination factor $= 20 \times 5.3 \times 10^7 \times (6.67)^{1/2} = 10^9$ after 10 days decay and 3.3×10^8 after 100 days. (ϕ_0 = initial flux; flux increases with burnup in order to maintain constant power)

conium which are nitric acid insoluble, other mineral acids may be used for the primary dissolution; before solvent extraction is performed, however, the nitrate ion can be added either as nitric acid or as a salt such as aluminum nitrate to make the extraction take place from a nitrate system.

The choice of the organic solvent depends upon the selectivity of the solvent for the desired products, the ease with which products can be stripped from the organic material after the primary extraction, chemical and radiation stability of the solvent, immiscibility of the organic-aqueous mixture, specific gravity of the organic as compared with the aqueous streams, interfacial tension, recoverability, viscosity, toxicity, flammability, and cost. Many organic solvents are suitable in the solvent extraction of fissionable and fertile materials. Some of the solvent systems that have been investigated are listed in Table II. Around them and aqueous nitrate systems have been developed the processes listed in Table III.

The Redox Process

Both uranium and plutonium are extracted by hexone from concentrated aqueous nitrate solutions, while fission products are only very slightly extracted. At the low acidities required for solvent stability and best decontamination, Pu(IV) may hydrolyze to the non-extractable polymeric form, and in addition is not extracted as well as Pu(VI); extraction of plutonium is therefore preceded by oxidation of plutonium to the VI state with sodium dichromate at elevated temperatures.

The Redox process is a three-column cycle in which plutonium and uranium are separated from each other and from the bulk of the fission products. The feed solution is an acid deficient uranyl nitrate containing sodium dichromate to oxidize the plutonium. Both uranium and plutonium are extracted with acidified hexone, and the organic extract is scrubbed in the same column with acid-deficient aluminum nitrate. In a second column the plutonium is stripped from the organic by reducing plutonium to the inextractable III state without affecting the uranium. To prevent uranium stripping, the reducing solution contains aluminum nitrate and it is scrubbed with additional solvent before leaving the column. The uranium is then stripped from the organic phase in a third column by dilute nitric acid.

The uranium product from the first cycle is evaporated and put through second and third uranium cycles. The scrub solutions may contain a reducing agent to provide additional separation from plutonium.

The plutonium product from the first cycle, already salted with aluminum nitrate, is oxidized with dichromate and then decontaminated by additional solvent extraction cycles. The plutonium is extracted with acidified hexone and scrubbed with oxidized acid-deficient aluminum nitrate in one column and stripped with dilute nitric acid in a second column. A reducing agent is not required in the scrub stream, as in the

Table II. Extractants for Solvent Extraction Processes

Solvent	*Alternate name*	*Diluent*	*Used to separate*	*Salting agent*
Ethyl ether	Diethyl ether	None	U from ores	$Ca(NO_3)_2$, $Mg(NO_3)_2$
Hexone	Methylisobutyl ketone	None	U, Pu from fission products	$Al(NO_3)_3$
TBP	Tri-*n*-butyl phosphate	Kerosene fraction	U, Pu and Th from fission products and U and Th from ores	HNO_3
Carbitol	Dibutyl ether of ethyleneglycol	None	U, Pu from fission products	HNO_3
Pentaether	Dibutyl ether or tetraethyleneglycol	None or butyl ether	U, Pu from fission products	HNO_3
Trigly	Triglycol dichloride	None	U, Pu from fission products	$Al(NO_3)_3$
TTA	Thenoyl trifluoroacetone	Benzene	Pu from fission products	None
DIPC	Diisopropyl carbinol	None	U from fission products	None
OPPA	Dioctyl pyrophosphoric acid	Kerosene fraction	U recovery from ores	None
Cellosolve	Ethyleneglycol monobutyl ether	None	U from fission products	$Al(NO_3)_3$
DIPE	Diisopropyl ether	None	U from fission products	$Al(NO_3)_3$

Table III. Processes for Chemical Separation of Fissionable and Fertile Materials

Process	*Organic solvent*	*Aqueous solvent*	*Irradiated metal feed*	*Salting agent*
For separation and decontamination of U and Pu				
Redox	Hexone	HNO_3	Natural U, Al can	$Al(NO_3)_3$
Metal recovery	12.5% TBP in hydrocarbon	HNO_3	Caustic precipitated U, fission products	HNO_3
Purex	30% TBP in hydrocarbon	HNO_3	Natural U, Al can	HNO_3
TTA chelation	0.25*M* TTA in hexone	HNO_3	Natural U, Al can	$Al(NO_3)_3$
For separation and decontamination of enriched U and Al				
25	Hexone	HNO_3, $Hg(NO_3)_2$ catalyst	U-Al alloy	$Al(NO_3)_3$
25, TBP	5% TBP in hydrocarbon	HNO_3, $Hg(NO_3)_2$ catalyst	U-Al alloy	HNO_3-$Al(NO_3)_3$
For separation of U^{233}, Pa, and Th				
Interim-23, hexone	Hexone	HNO_3, F^- catalyst	Th, Al can	$Al(NO_3)_3$, HNO_3
Interim-23, TBP	1.5% TBP in hydrocarbon	HNO_3, F^-+Hg^{++} catalyst	Th, Al can	$Al(NO_3)_3$, HNO_3
Thorex	42.5% TBP in hydrocarbon	HNO_3, F^-+Hg^{++} catalyst	Th, Al can	$Al(NO_3)_3$, HNO_3

first-cycle partitioning column, where separation from uranium is accomplished. The plutonium solution from the strip column of the second cycle is then salted with $Al(No_3)_3$ and put through a third cycle similar to the second.

Waste volumes can be decreased by using the aqueous waste solutions from the second and third cycles in making up scrub solution for the earlier cycles.

A simplified Redox flowsheet is given in Fig. 3.[7] Decontamination factors that have been demonstrated for two cycles of the Redox process are given in Table IV.

Table IV. Redox Decontamination Factors

	log D.F.					
	1st cycle		*2nd cycle*		*Over-all 2 cycles*	
Constituent	*U*	*Pu*	*U*	*Pu*	*U*	*Pu*
Gross γ	3.7	3.9	1.8	2.9	6.5	7.7
Gross β	3.9	4.3	1.8	2.9	6.0	7.5

The TBP Metal Recovery Process

Precipitation processes for the recovery of plutonium from irradiated natural uranium have been developed which do not recover decontaminated ura-

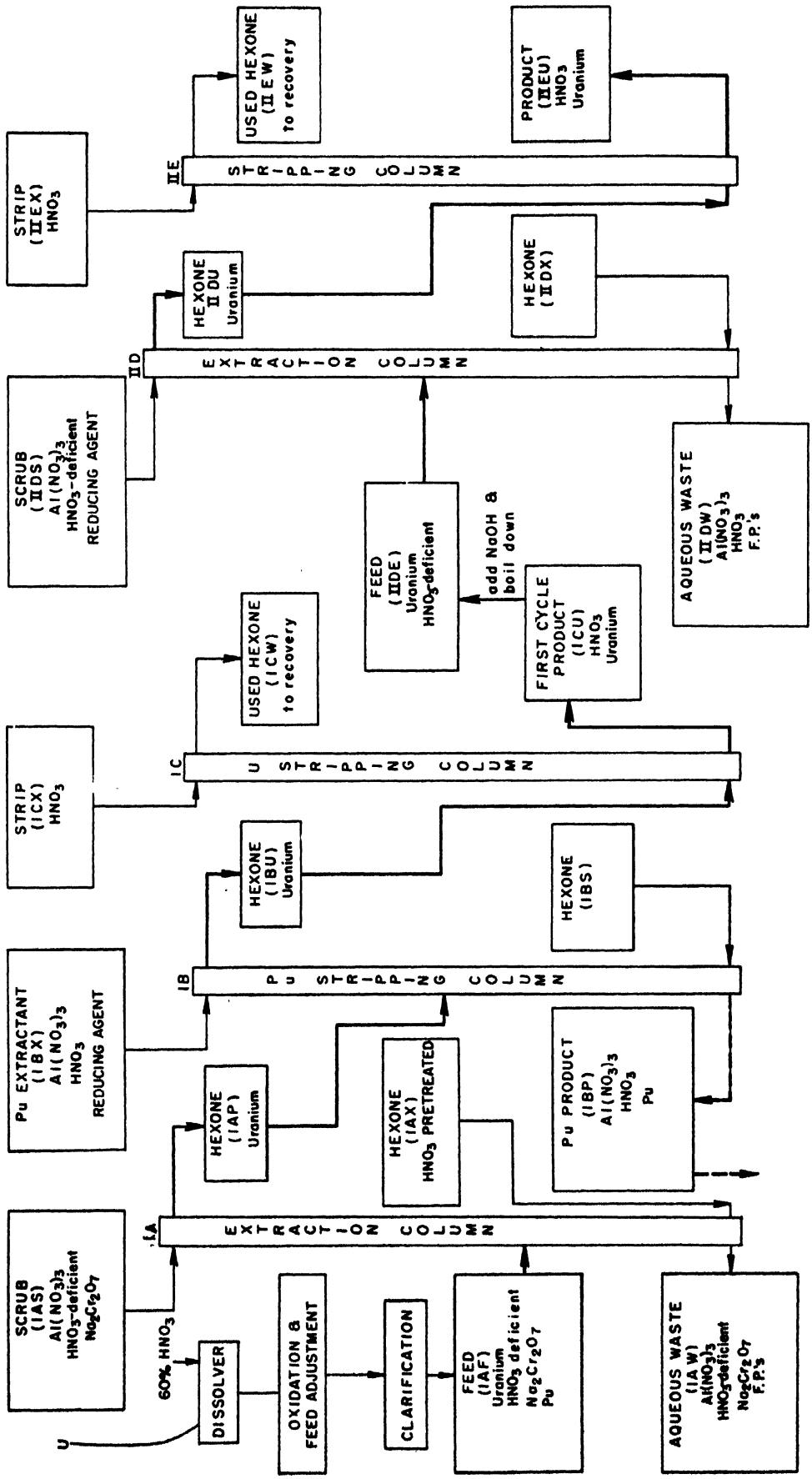

Figure 3. Schematic flowsheet for first Redox cycle and second uranium cycle

nium from fission product wastes. The uranium and fission product raffinates from such a process must be stored; this is best done after the wastes are neutralized with sodium carbonate and sodium hydroxide. Uranium can be decontaminated from fission products by solvent extraction with TBP, in a process similar to the Purex process with the omission of the partitioning column. Any traces of plutonium which remain in the feed go into the first cycle aqueous waste; the extraction column is operated under reducing conditions, maintained by a reducing agent in the scrub, so that plutonium is not extracted.

The waste solution containing solids can be removed from the waste storage tanks as a slurry, concentrated by evaporation, and dissolved in nitric acid. The resulting solution is further concentrated and centrifuged to remove the remaining insolubles which are returned to waste storage. The solution that is solvent-extracted contains nitric acid, sodium nitrate, and some sulfate and phosphate ions, along with uranium. Although sulfate and phosphate interfere with uranium extraction under some conditions, the nitrate concentration in the feed can be made sufficiently high to prevent serious interference with uranium extraction. The solution is extracted with tributyl phosphate in hydrocarbon diluent, and is scrubbed with a solution of nitric acid and a suitable reducing agent. The extract is then contacted with dilute nitric acid to strip the uranium into the aqueous phase. Uranyl nitrate product is finally concentrated by evaporation and possibly denitrated if uranium oxide is a desired product.

For the recovery of uranium from wastes which have decayed for two years or longer, one cycle of decontamination is sufficient. After shorter decay, additional cycles may be required.

A flowsheet for the TBP metal-recovery process is not included, since it is very similar to that of the Purex process. Decontamination factors attainable are given in Table V.

Table V. TBP Metal Recovery Decontamination Factors

Constituent	*log D.F., one cycle*	*Constituent*	*log D.F., one cycle*
Gross γ	4.7	Total rare earths	5.3
Gross β	4.4	Pu	2.5

Product uranium has 30–90% of the activity of natural uranium in secular equilibrium with its decay products. These data are valid for uranium solution that has decayed longer than two years, and from which plutonium has been removed by a process which recovers plutonium only.

The Purex Process

Jacketed uranium metal is charged into a dissolver where the customary aluminum sheath is preferentially dissolved by a sodium hydroxide-sodium nitrate solution. The uranium is then dissolved in nitric acid. The concentrated uranyl nitrate-nitric acid solution is withdrawn, filtered to remove silica and aluminum particles, and adjusted to the feed concentration. Finally, the plutonium is quantitatively stabilized to the tetravalent state, the form most readily extracted by TBP, and the feed is ready for solvent extraction. Batch or continuous dissolution of uranium metal can be used.[8]

The metal feed is extracted with TBP diluted with a kerosene-type carrier. Here conditions of flow and salting strength are regulated in such a manner that the uranium and the Pu(IV) are coextracted almost quantitatively, leaving most of the fission products and other impurities in the aqueous phase. Under these conditions some fission products are also extracted, but these are partially backwashed into a nitric acid stream flowing counter-currently to the solvent stream. The bulk of the radioactive and nonradioactive impurities leave as an aqueous waste stream, and the organic product stream is passed into a second contactor for U-Pu partitioning.

In the second contactor uranium and plutonium are separated by reducing the latter to the highly aqueous-soluble trivalent state. Salting strength and flow conditions are controlled in such a manner that separation of the two products is virtually complete, the aqueous plutonium stream leaving the lower end of the column while the uranium remains in the organic phase.

The uranium-bearing organic solvent is passed into the bottom of a third column, where the uranium is stripped from the organic with water. The stripped organic is reconditioned for subsequent reuse in the process.

The dilute plutonium stream flows directly to the second cycle for continuous feed make-up, in which the salting strength is raised by addition of nitric acid and the Pu(III) is oxidized to Pu(IV). The plutonium is extracted by the solvent to complete its separation from residual activity. The organic product stream flows into a second contactor where the plutonium is again reduced to the trivalent form and is stripped into an aqueous hydroxylamine sulfate solution. At this point, the product stream is concentrated by sorption on and elution from a cation-exchange resin bed. Additional purification is realized from this step such that the over-all separation of plutonium from fission products can exceed 10^7.

The aqueous uranium stream from the first cycle flows to a continuous evaporator and is concentrated and then adjusted with nitric acid. Following this the uranium is extracted and is scrubbed in a manner similar to that of the first-cycle extraction. The extracted uranium is stripped into water in a second column and is concentrated in a second evaporator. The concentrate is passed through a bed of silica gel which absorbs trace fission products to complete the removal of fission-product activity. The uranyl nitrate concentrate then is calcined to uranium trioxide.

Since the solvent is re-used, it is sent to a solvent-recovery area after each passes through the system, where it is washed with a sodium carbonate solution

and then with dilute acid, to remove the traces of strongly complexed radioelements and the TBP degradation products. Over-all solvent losses can be maintained as low as 0.01%.

The aqueous wastes from the solvent-extraction cycles are concentrated, and nitric acid is simultaneously distilled and recovered. Other nitric acid is recoverable from the slug dissolution and denitration operation so that nearly all the acid employed in the process is available for re-use. The main incentive, however, for acid recovery is the reduction in volume of active wastes, which must be stored indefinitely.

For feeds containing large concentrations of fission products (i.e., those which result from high reactor burn-up and/or short decay periods), an additional cycle of extraction on both the uranium and the plutonium streams may be required. In addition, a feed oxidation and filtration step may be added prior to the preparation of first-cycle feed. This treatment is carried out by adding potassium permanganate to the feed solution, warming and centrifuging off the resulting manganese dioxide. The permanganate is reduced to manganese dioxide by the combined effect of heat and radiation. Plutonium is oxidized by both permanganate and manganese dioxide to Pu(VI), which is not adsorbed on manganese dioxide. The small amount of uranium and plutonium occluded by the precipitate is washed out with dilute nitric acid and recycled to the next batch of dissolver solution. The manganese dioxide centrifuge cake is subject to further reduction to manganous ion under the action of intense radiation. Feed preparation is completed by adding nitrite, which reduces Pu(VI) back to Pu (IV), and adjusting the uranium and acid concentrations to the specified values. The precipitation of manganese dioxide scavenges traces of solids from the solution.[6]

A schematic chemical flowsheet for the Purex process is shown in Figs. 4, 5, and 6. Flanary has reviewed the complete Purex process.[9]

Attainable decontamination factors after solvent extraction of U and Pu through two cycles of solvent extraction are given in Table VI; additional decontamination for uranium after silica-gel adsorption and for plutonum after ion exchange also are shown.

Table VI. Purex Decontamination Factors

	log D.F.			
	After 2 cycles of solvent extraction		*After sorption*	
Product	β	γ	β	γ
U	6.82	6.43	6.99	6.81*
Pu	6.89	6.30	7.51	7.20

* Residual fission product β and γ activities in the uranium product were 3% and 100%, respectively, of those of natural uranium in secular equilibrium with its decay products, for fuel that had decayed about 100 days.

A Chelation Process for Separation of Uranium, Plutonium, and Fission Products

It is possible to separate plutonium, uranium, and fission products by a chelation process that uses thenoyl trifluoroacetone (TTA). In this process plutonium in the tetravalent state is first extracted away from uranium and all fission products except zirconium with a TTA solution in benzene (Fig. 7). Traces of fission products are scrubbed from the plutonium-zirconium-bearing solvent with nitric acid. The plutonium is then selectively stripped from the solvent with dilute nitric acid containing a reducing agent, which reduces the plutonium to the insoluble trivalent state. After the zirconium has been removed by a nitric acid-oxalic acid solution scrub, the solvent is ready for re-use.

The uranium, which is contained in the aqueous raffinate from the plutonium extraction cycle, can be extracted with a TTA solution in hexone. The solvent containing the decontaminated uranium is stripped with nitric acid. Part of the decontaminated uranyl nitrate solution is returned to the uranium extraction contactor and used to scrub residual fission products from the uranium-bearing solvent.[10]

The comparative advantages of this process are that only one cycle each is required for plutonium and uranium decontamination, and that the radioactive waste streams contain only dilute nitric acid and oxalic acid, which simplifies the waste disposal problem. The process has the marked disadvantage, however, that the rate of chelation is slow.

The 25 Process, Hexone Solvent

The separation and decontamination of enriched uranium from fuel elements such as those used in the Materials Testing Reactor, the Swimming Pool Reactor, or the Aquarium Reactor can be accomplished by solvent extraction with hexone from nitric acid solutions. The process is similar to the Redox process except that the separation and decontamination of plutonium is not required since only small quantities of plutonium are produced in enriched uranium fuels. The plutonium in the feed stream to the 25 process follows the fission products into the aqueous waste from the first- and second-cycle extraction columns. Aluminum present as a uranium diluent and cladding material in the fuel element serves as the salting agent in the solvent extraction process.

The process developed for recovery of uranium from nitric acid solution containing aluminum consists in the following steps: dissolution of uranium or uranium-aluminum alloy in nitric acid with mercuric nitrates for aluminum dissolution; feed clarification by filtration without filter aid through a sintered stainless-steel filter; feed adjustment to acid deficiency; and separation of the uranium from fission products and plutonium in three cycles of solvent extraction, using methylisobutyl ketone as the solvent. Plutonium is separated from the uranium in the second cycle after being reduced to the trivalent inextractable state with a reducing agent added with the scrub stream. Small quantities of plutonium are discarded with the fission products if the fuel is highly

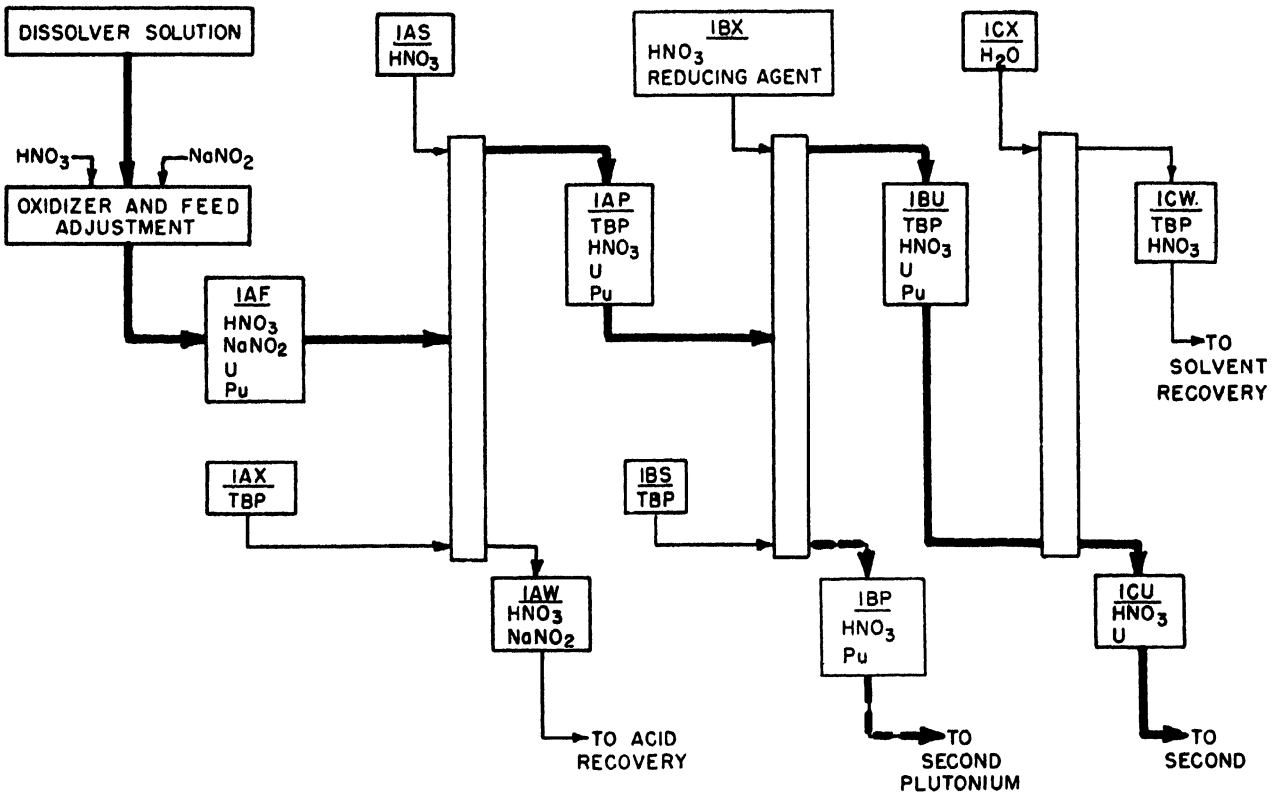

Figure 4. Purex process: first cycle chemical flowsheet

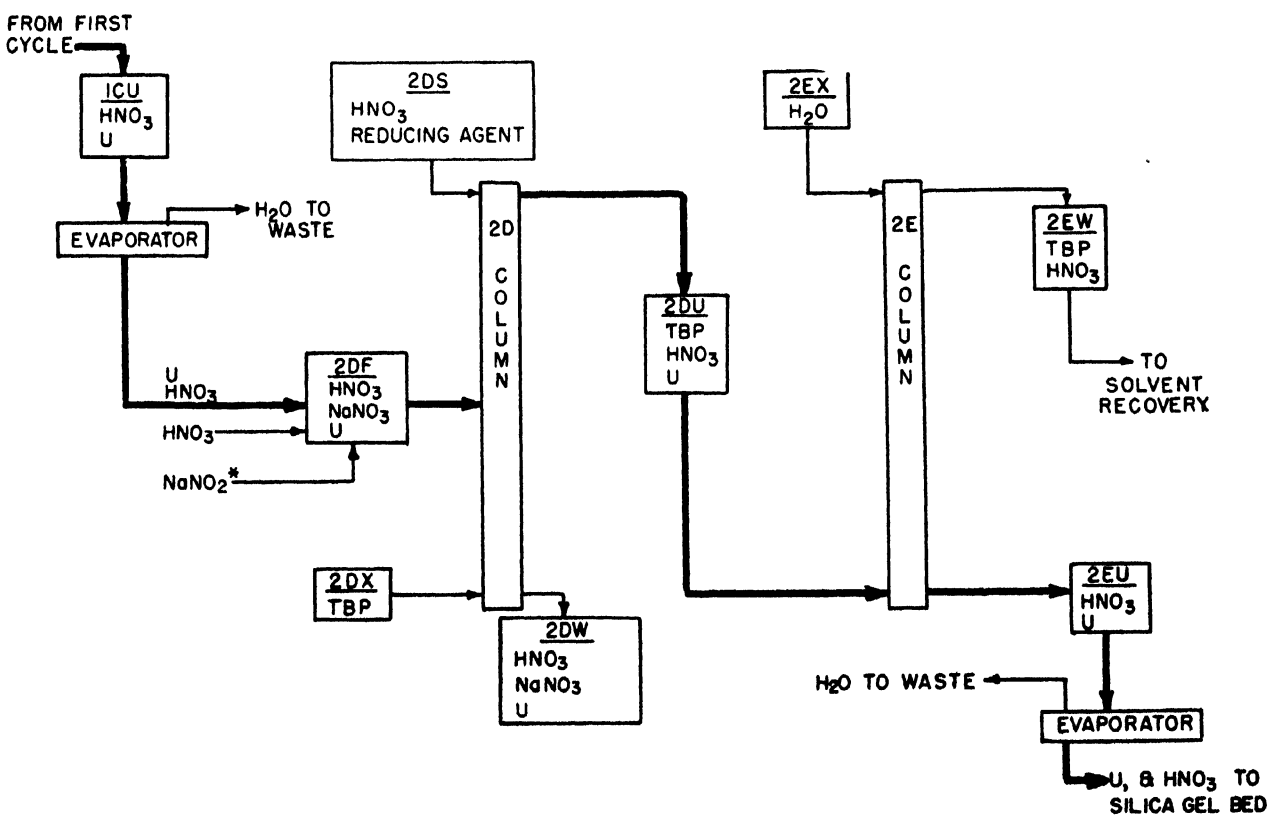

Figure 5. Purex process: second uranium cycle chemical flowsheet

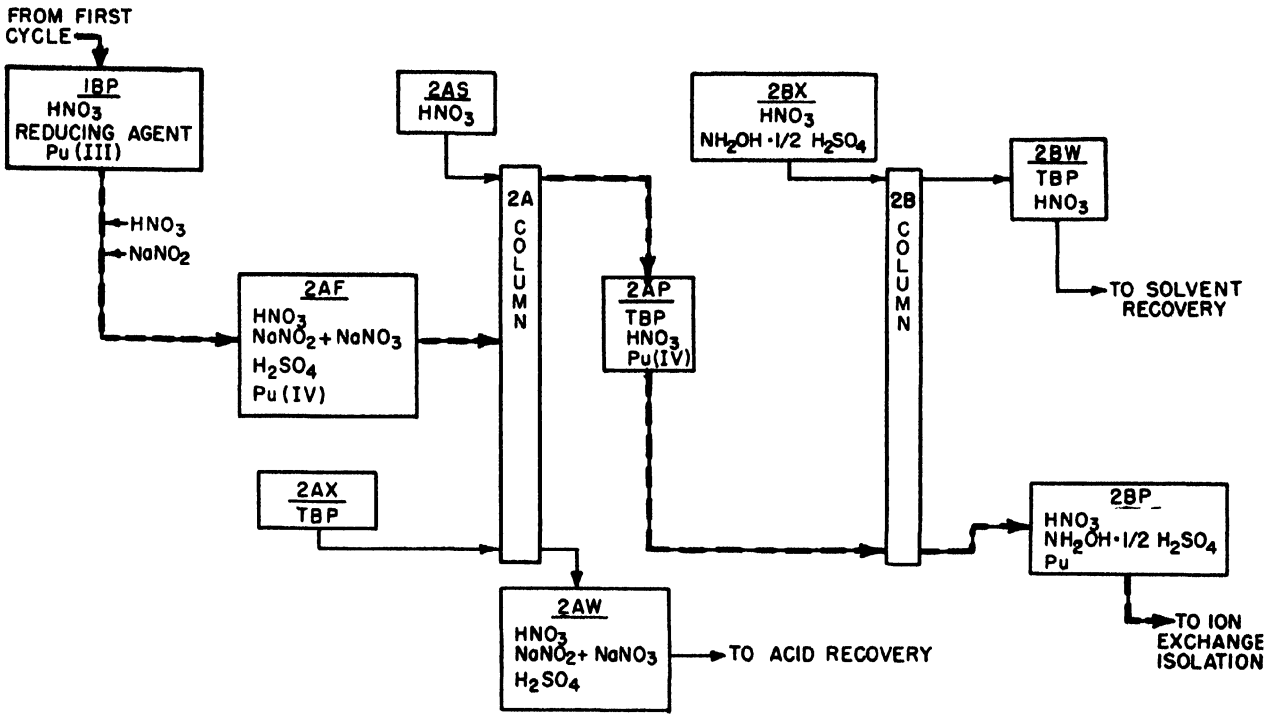

Figure 6. Purex process: second plutonium cycle chemical flowsheet

enriched. If partially enriched fuels are used, a modification of the Redox process can be used to recover plutonium.

An over-all chemical flowsheet showing two cycles of solvent extraction is given in Fig. 8. Decontamination factors for two cycles of hexone extraction are given in Table VII.

A more detailed description of the Hexone-25 process can be found in a paper by Culler and Bruce.[11]

The 25 Process, Tributyl Phosphate Solvent

Tributyl phosphate in hydrocarbon diluent may offer some advantages over hexone for the extraction of uranium from solutions containing aluminum. For the TBP 25 process the fuel dissolution and feed preparation steps are similar to those described for the hexone process except that acid rather than acid-deficient conditions are used. The TBP process for uranium-aluminum alloy processing is a modification

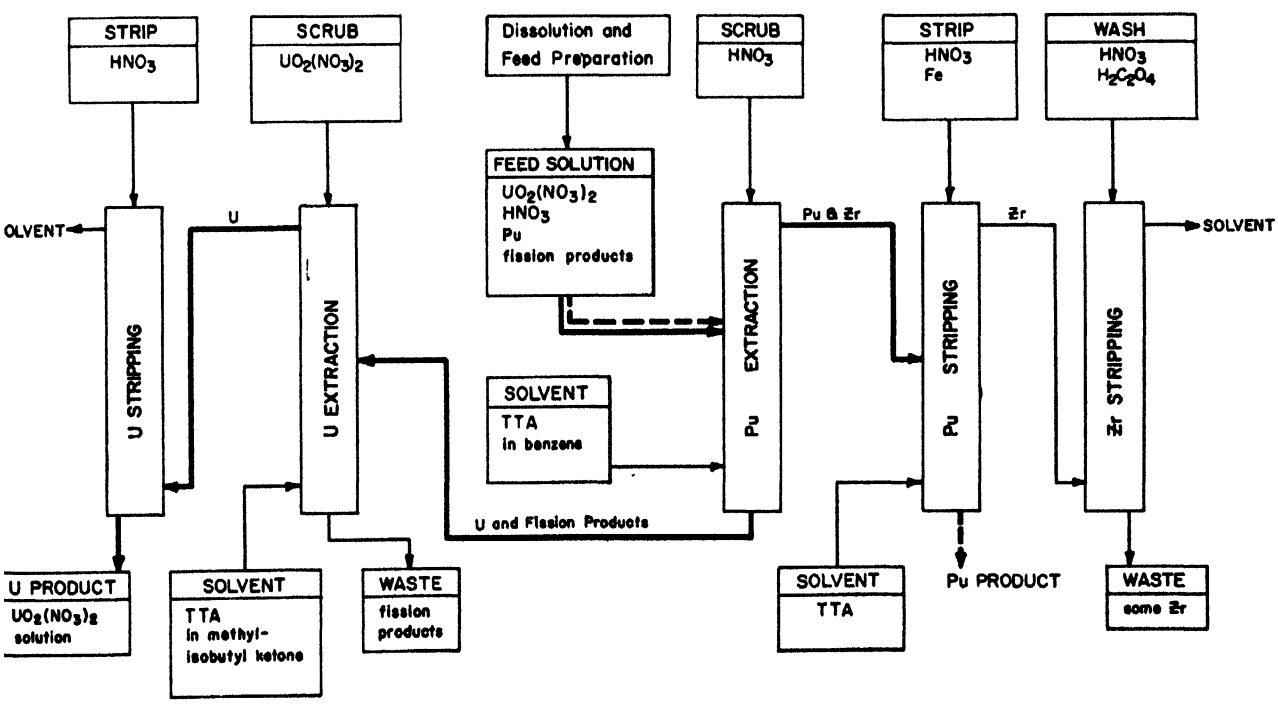

Figure 7. Schematic flowsheet for U, Pu, and fission product separation by TTA chelation

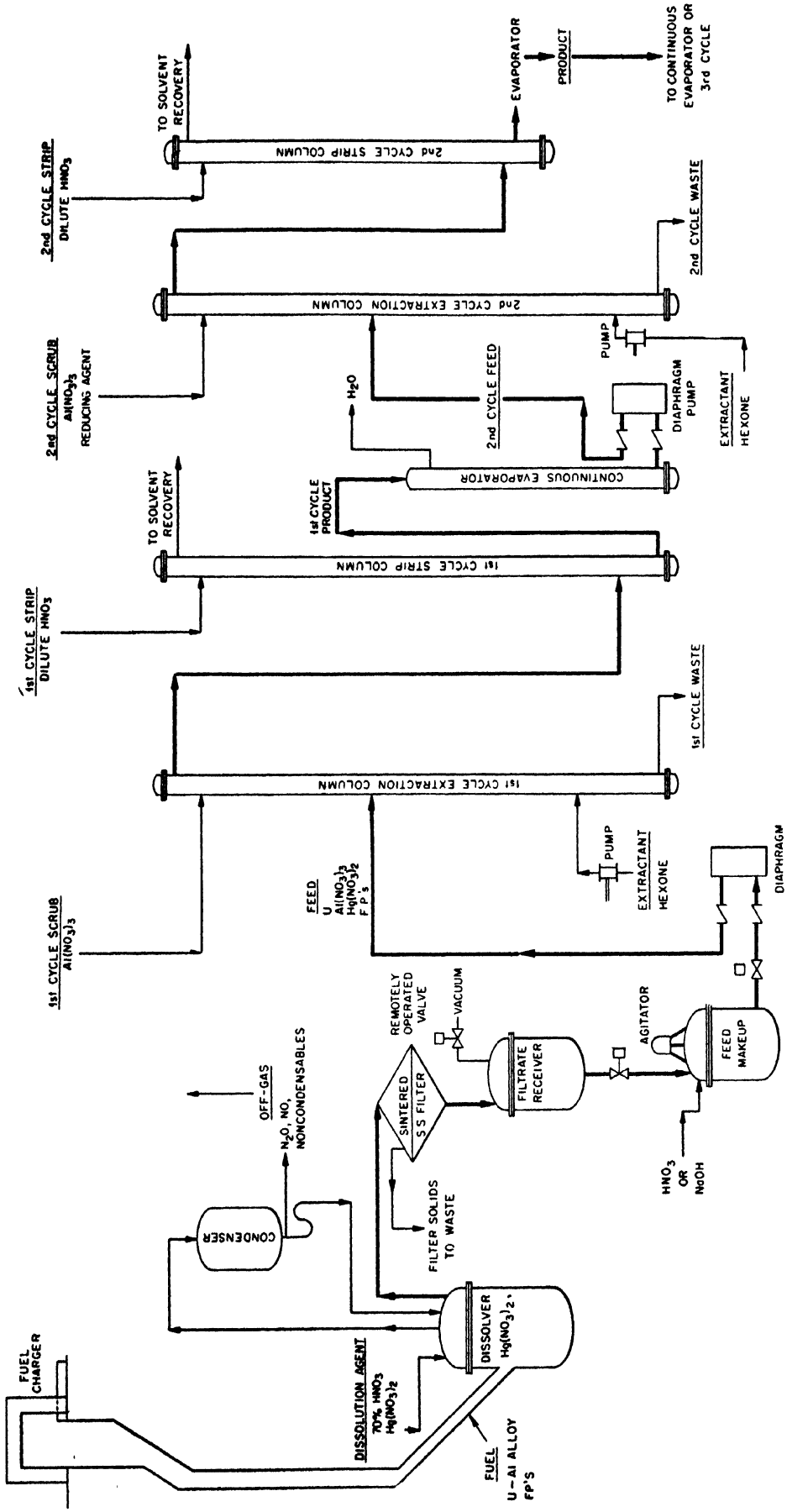

Figure 8. Schematic flowsheet: two cycles of hexone solvent extraction for uranium-aluminum alloy

Table VII. Hexone-25 Decontamination Factors

Constituent	log D.F. 1st cycle	2nd cycle	Over-all
Gross β	4.04	2.41	6.45
Gross γ	3.84	2.36	6.20
Pu α	1.30	1.95	3.25

of the TBP extraction process for plutonium and uranium (Purex process).[9] Laboratory test results with high levels of activity for a TBP uranium-aluminum alloy process have been established. A schematic flowsheet is shown in Fig. 9.

The feed solution, containing aluminum nitrate and uranium, is solvent-extracted with TBP in hydrocarbon diluent under acid, rather than acid-deficient conditions. The organic stream in the compound extraction-scrub column is scrubbed with a solution of aluminum nitrate and nitric acid. Uranium is stripped from the organic phase in a second column with dilute nitric acid. This aqueous product is evaporated and used as feed to a second extraction cycle where TBP in hydrocarbon diluent is used as the extractant. A reducing agent is added to the nitric acid scrub to reduce any plutonium to the nonextractable Pu (III) state. Product from the second-cycle stripping operation is passed through a silica-gel bed to ensure removal of the last traces of fission products. After the silica bed adsorption, uranium may be concentrated by evaporation or by sorption and elution from an ion-exchange resin.

Decontamination factors and losses are given in Table VIII. A more complete description of this process is given in a paper by Culler and Bruce.[11]

Table VIII. TBP-25 Process Decontamination Factors

Constituent	log D.F. 1st cycle	2nd cycle
Gross β	5.48	>2.48
Gross γ	3.17	3.40
Pu	>4.00	>2.00

The Hexone-23 and Interim-23 Processes

These processes are designed for the specific recovery of U^{233} from irradiated thorium metal. The former may be utilized only on long-decayed material (material that has decayed until U^{233} losses as protactinium are very low), since it does not provide effective separation from the highly radioactive Pa^{233}, whereas the latter can be used after very short decay periods. The aqueous wastes from these processes contain the thorium, fission products, and/or Pa^{233} and must be permanently stored in stainless steel tanks. Neither process is designed to recover and decontaminate thorium.

The Hexone process (Fig. 10), similar in many respects to the 25 process, utilizes acid-deficient aluminum nitrate as the aqueous salting agent to permit effective U^{233} extraction and decontamination. Thorium is sufficiently inextractable in the hexone to permit separation factors of greater than 10^4. Decon-

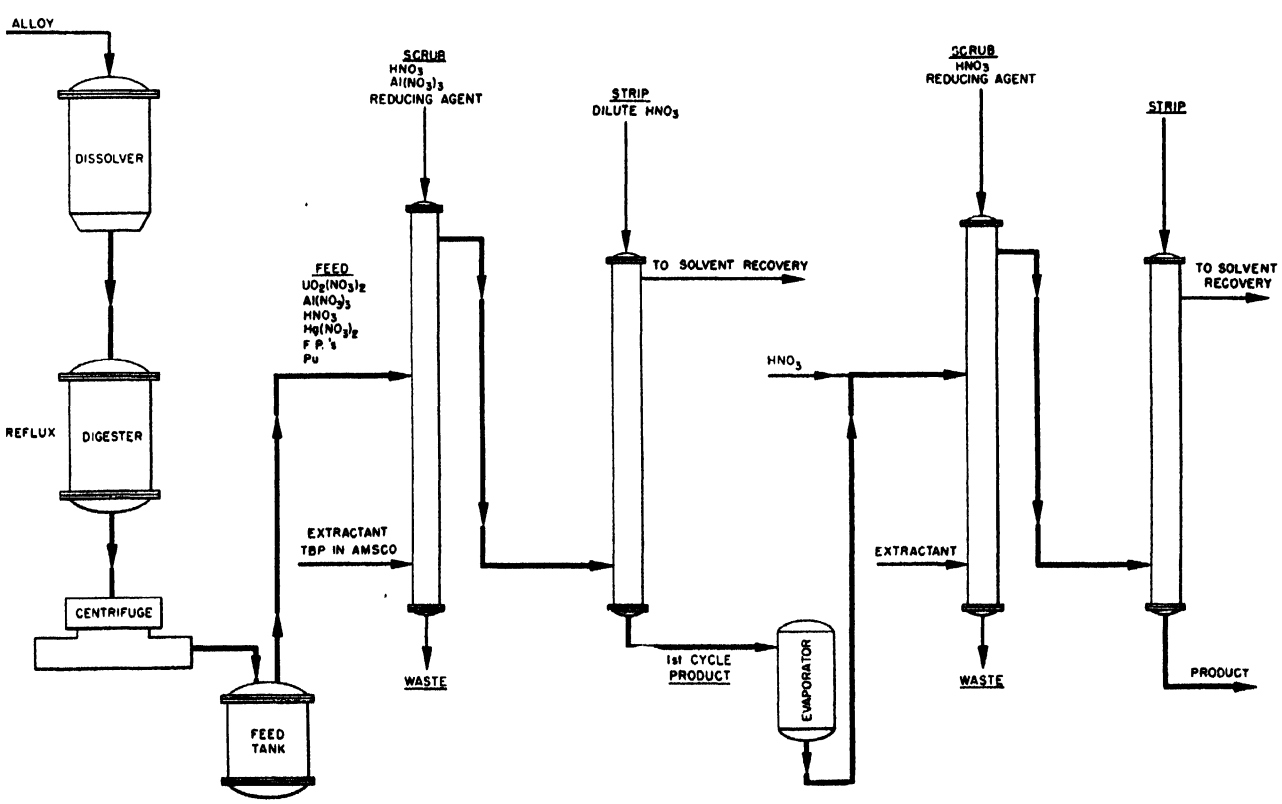

Figure 9. Schematic flowsheet, TBP-amsco extraction of uranium-aluminum alloy

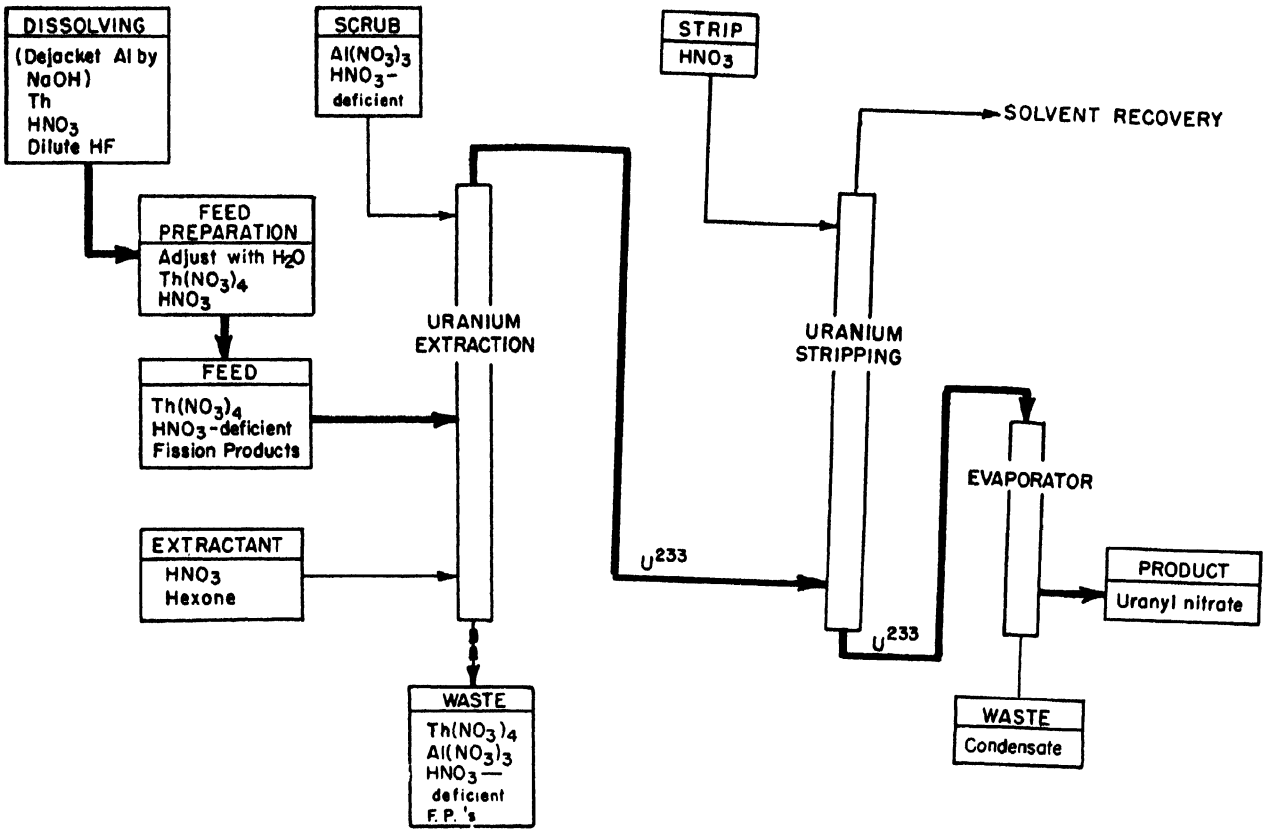

Figure 10. Chemical flowsheet for the hexone interim-23 process

tamination factors for most fission products are greater than 10^5. The decontaminated product is stripped from the hexone into nitric acid, subsequently evaporated and given a final clean-up in laboratory equipment.

The Interim-23 process (Fig. 11) utilizes TBP in an aromatic-free paraffinic diluent as the preferential U^{233} extractant. Such a system offers excellent separation of the product from highly radioactive materials, as well as from the thorium. The product is stripped into dilute nitric acid; passed through a silica-gel column for adsorption of traces of fission products; through a small resin column for removal of ionic impurities, such as corrosion products and thorium; and finally through a larger resin column for sorption of the U^{233}. This series of continuously operated steps is effective for the final concentration and decontamination of the product from both radioactive and ionic impurities. After its subsequent elution from the column as uranyl acetate, the product can be precipitated as the peroxide, and finally redissolved in nitric acid. Total fission product activity in the final uranyl nitrate can be as low as 50 counts per minute per milligram of U^{233}.

The Thorex Process

The Thorex process has been developed for separating and decontaminating thorium, U^{233}, and Pa^{233} from neutron-irradiated thorium. It is a solvent-extraction process which employs tri-*n*-butyl phosphate as the extractant, nitric acid catalyzed with fluoride ion as the thorium-dissolution agent, and either aluminum nitrate or nitric acid as the salting agent. The U^{233} product is isolated by ion exchange.

A fertile element such as irradiated thorium metal jacketed with aluminum is dissolved in concentrated nitric acid. The catalysts fluoride ion and mercuric ion are used to catalyze the reaction of thorium and aluminum, respectively. Excess nitric acid is required to dissolve refractory thorium oxide, which may be present in thorium metal. Feed dissolution is followed by a digestion step for the removal of excess nitric acid.

The aqueous feed is introduced near the middle of the compound extraction-scrub column. An aqueous scrub solution of acid deficient aluminum nitrate, ferrous sulfate, and dilute phosphoric acid enters at the top of the column. Tributyl phosphate diluted with Amsco 125-82 (an inert paraffinic diluent) extracts the thorium and U^{233}. The primary TBP-nitrate complexes of these elements are $Th(NO_3)_4 \cdot 4TBP$ and $UO_2(NO_3)_2 \cdot 2TBP$. The corresponding complex of nitric acid is $HNO_3 \cdot TBP$.

In TBP extraction of thorium it is essential that the diluent be free of aromatic organic compounds to prevent the formation of two phases in the organic streams. A second organic phase results from the extraction of a polymerized TBP complex of thorium (corresponding to the complex ratio equivalent of $Th(NO_3)_4 \cdot 2.5TBP$ by small traces of aromatics in the paraffinic diluent.

Decontamination from rare-earth fission products and from protactinium is sensitive to the degree of saturation of the organic solvent. The organic effluent is not fully saturated with thorium; however, near the feed plate saturation is almost attained, owing to reflux in the scrubbing section. This saturation with thorium suppresses the extraction of the rare-earth fission products, which would be extracted in the presence of a large excess of TBP and which normally undergo extensive reflux in the lower section of the extraction column. Owing to the nitric acid-deficient conditions of the aqueous phase, the Pa^{233} and most of the troublesome fission products are not extractable; however, the aqueous scrub solution provides for additional removal of these from the product extract. Phosphate ion is included in the scrub solution to assist in decontamination from protactinium, and ferrous ion is included to prevent extraction of an oxidized chromium compound that is produced during the head-end treatment of the feed.

The aqueous phase from the extraction column, contains aluminum nitrate, is acid deficient, and contains any Pa^{233} that has not decayed to U^{233} fission products and other impurities. It is reduced in volume by evaporation to permit minimum storage volumes.

The organic extract from the extraction column, containing Th^{232}, Th^{234}, U^{233}, and traces of fission products and any Pa that may be present is introduced into the middle of the partitioning column. The thorium is stripped into an aqueous phase of nitric acid, which flows down the column; this aqueous solution is scrubbed by the organic stream of TBP introduced in the bottom of the column. The aqueous strip stream represents the combined flow of a nitric acid solution introduced some distance below the top of the column and a water stream introduced at the top of the column. Aqueous conditions are thus maintained slightly acidic, which will permit thorium stripping into the aqueous stream and retention of the U^{233} in the organic stream. The water stream entering the top of the column permits some U^{233} reflux, but it is necessary to remove nitric acid from the organic phase so that the subsequent uranium stripping cycle will operate at maximum efficiency.

The organic effluent from the partitioning column, containing all the U^{233} and traces of nitric acid is passed to the bottom of the uranium stripping column. An aqueous phase of dilute nitric acid is introduced at the top of the column and serves to strip the U^{233} from the rising organic stream. The aqueous effluent is then passed through a silica-gel column for removal of trace quantities of fission products; a small column containing cation exchange resin for the retention of traces of thorium and corrosion products; and a larger cation exchange for concentrating and further decontaminating the U^{233} product. The effluent from this column is discarded to chemical waste. Product is eluted by a solution of ammonium acetate and acetic acid.

A schematic flowsheet for a one-cycle Thorex process is given in Fig. 12. Details of the Thorex process are given in a paper by Gresky.[12]

Decontamination factors for one cycle of extraction are given in Table IX. One cycle of extraction may not provide adequate decontamination of ruthenium in the thorium stream for highly irradiated feeds.

AUXILIARY PROCESSES

Solvent Chemistry and Recovery

Hexone used in the extraction of uranium and plutonium from fission products can be treated and recycled for re-use with very low over-all solvent loss. Hexone as purchased from the vendor may contain

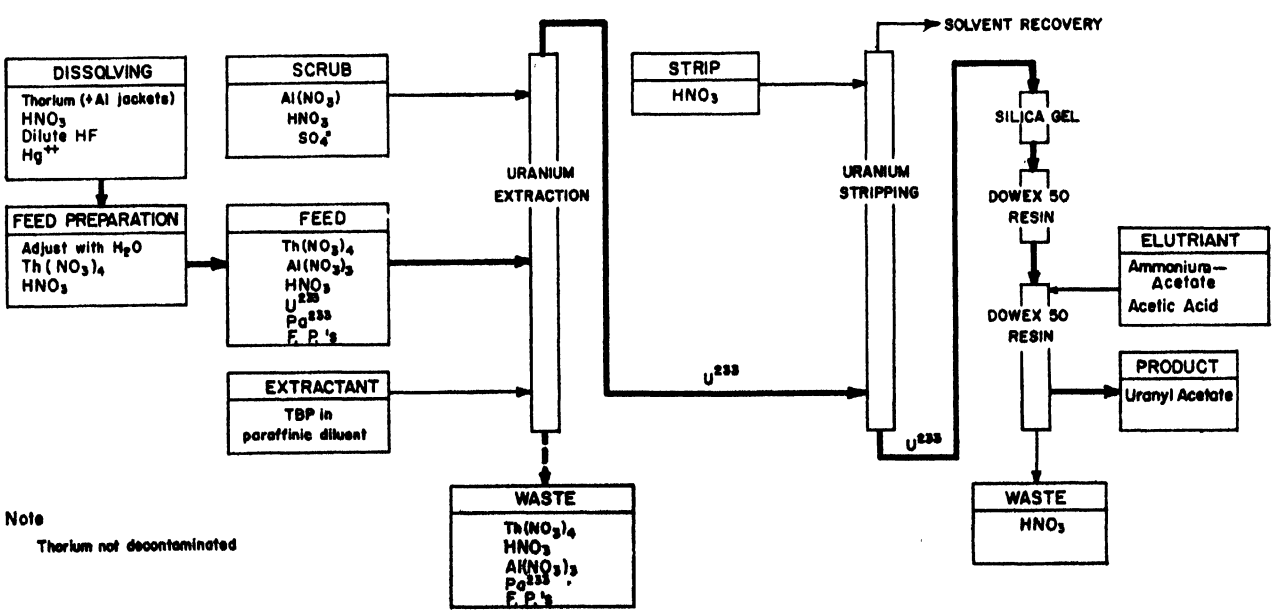

Figure 11. Chemical flowsheet for TBP Interim-23 process

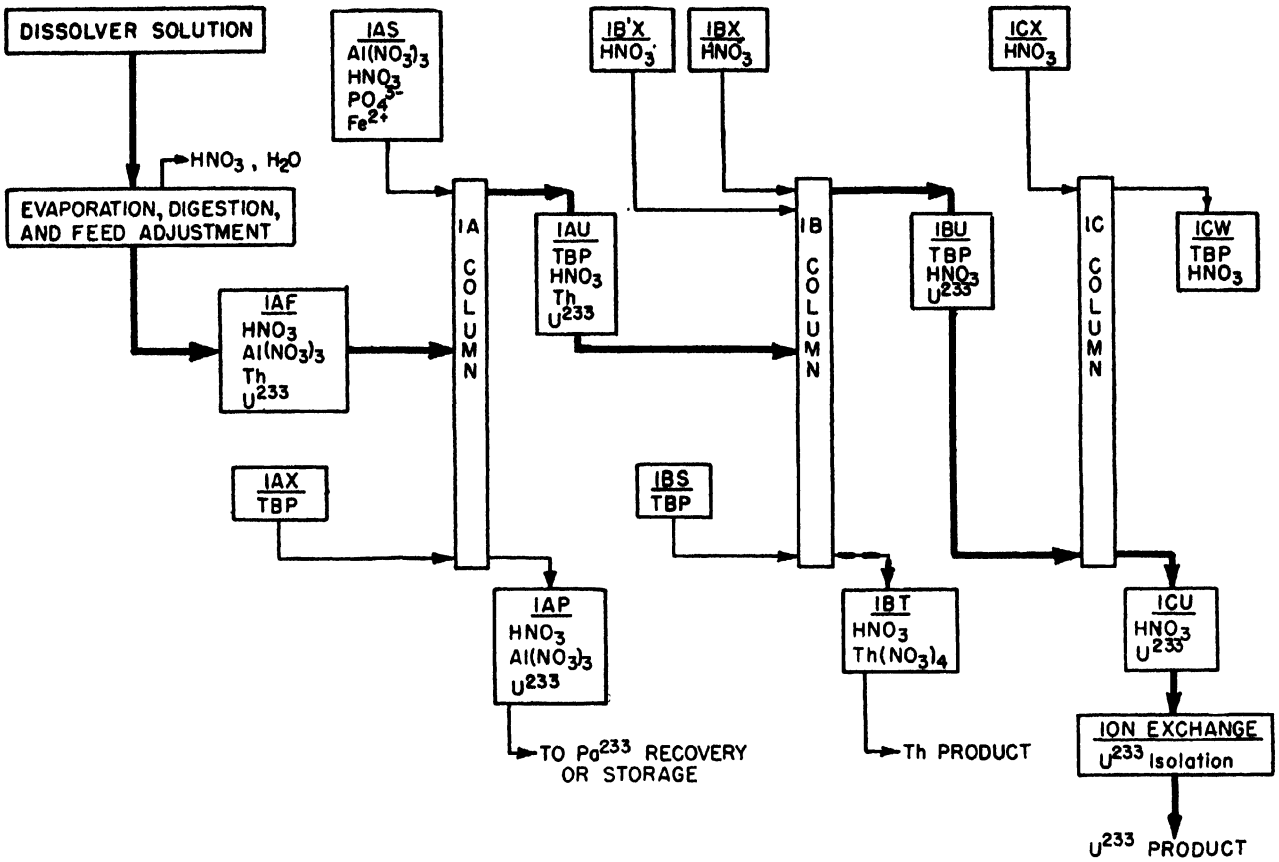

Figure 12. Thorex process chemical flowsheet

such impurities as mesityl oxide, methylisobutyl carbinol, and an aromatic substance, possibly mesitylene. These impurities, which decrease the uranium and fission-product separation, are all oxidizable and may be destroyed and removed by agitation of the solvent with a sodium dichromate-nitric acid solution, followed by washing with sodium hydroxide solution and stream distillation from a sodium hydroxide heel. This procedure is also adequate for removing fission-product contamination from used solvent. Investigation of the stability of hexone to radiation is reported in a paper by Cathers.[3]

Experience with commercial grade tributyl phosphate (TBP) indicated that certain impurities [traces of butanol and of mono- and dibutyl acid phosphate (MBP and DBP)] present were harmful in radiochemical separation processes. Separation of uranium and plutonium from fission products was not so effective with commercial TBP as with butanol-free TBP, the difference being due to an increased (fivefold) β-activity distribution coefficient in the scrub section.

Although TBP is satisfactory initially, continued use of the solvent results in gradual degradation. The alkyl acid phosphates have a marked effect on plutonium behavior in the Purex process, the DBP by its strong complexing of Pu(IV) and the MBP by its tendency to form a precipitate with Pu(IV). These contaminants are known to react similarly with U(VI) and would pose a problem in TBP systems demanding extremely high uranium recovery. Owing to the complexing action of DBP, Pu(IV)

Table IX. β, γ Decontamination, Th-U Separation in the Thorex Process

Factor	*log of factor*				
	Over-all	*Through A-column*	*Through B-column*	*Through C-column*	*Through isolation**
	Thorium Product				
Pa^{233} γ decontamination	4.30	4.23	4.30	....	....
Total rare earths (TRE) β decontamination	5.30	5.28	5.30	....	....
Th-U^{233} decontamination	3.00	....	3.00	....	....
Pa^{233} γ decontamination	6.84	4.23	4.30	4.61	6.84
TRE β decontamination	8.30	5.28	6.30	7.30	8.30
U^{233}-Th separation	7.30	....	4.30	5.00	7.30

* Includes silica-gel column plus cation sorption and acetate elution. Further decontamination from radioactive and ionic constituents is obtained in the subsequent peroxide precipitation step.

loss during stripping becomes excessive unless the DBP concentration is kept very low. However, complexing of Pu(III) by the organic-soluble DBP is relatively weak. At DBP concentrations up to 0.01%, plutonium may be readily reduced and stripped. The behavior of the aqueous-soluble MBP has not been thoroughly studied, but no major process difficulties associated with this contaminant have been encountered.

Owing to the acidic natures of MBP and DBP, they are readily removed from the used solvent by washing with a dilute sodium carbonate or caustic solution and then with dilute nitric acid. This procedure also removes traces of uranium and residual fission products. The solvent is reconditioned after each pass through the process, and all fresh solvent is treated the same way before use.

Laboratory studies indicated that Amsco 123-15 naphtha is generally acceptable for use as the solvent diluent in the Purex process. Although tests indicated that this material is not appreciably affected by the chemical environment and radiation exposure, the cumulative effects of such exposures in extended reuse could not be predicted. Another diluent, Amsco 125-82, is used for the Thorex process.

Off-Gas Iodine Removal

Irradiated fuels after decay periods of as much as 100 to 130 days contain enough residual I^{131} to require iodine removal before dissolver gases can be discharged to the atmosphere. Iodine can be removed from gas streams by reaction with heated silver or with silver nitrate in a packed tower. A column, packed with silver nitrate coated Berl saddles, removes 99.9% of the iodine from a dissolver off-gas. Most of the iodine is removed in the first few inches of packing.[13]

EQUIPMENT AND ENGINEERING CONCEPTS

Types of Contactors Used for Solvent Extraction

The principal types of continuous contactors used in the liquid-liquid extraction of fissionable and fertile material are gravity columns, including packed and perforated-plate columns, and powered contactors, including pulsed columns and mixer-settlers.

The packed tower (Fig. 13) contains some form of a packing, such as stainless steel Raschig rings, to provide a tortuous route for the droplets of dispersed phase to follow through the continuous phase, enhancing the contact of the two phases. The type of packing used for a given application depends largely on the chemical nature of the system and the processing requirements, while the packing depth (packed height) depends on the degree of separation required.

Mixer-settler equipment, which can be operated at high stage efficiency can be used. Horizontal type mixer-settlers usually require less height but greater canyon length than vertical solvent extraction columns of the same processing capacity. Pump-type mixer-settlers have been developed (Fig. 14).[15] In

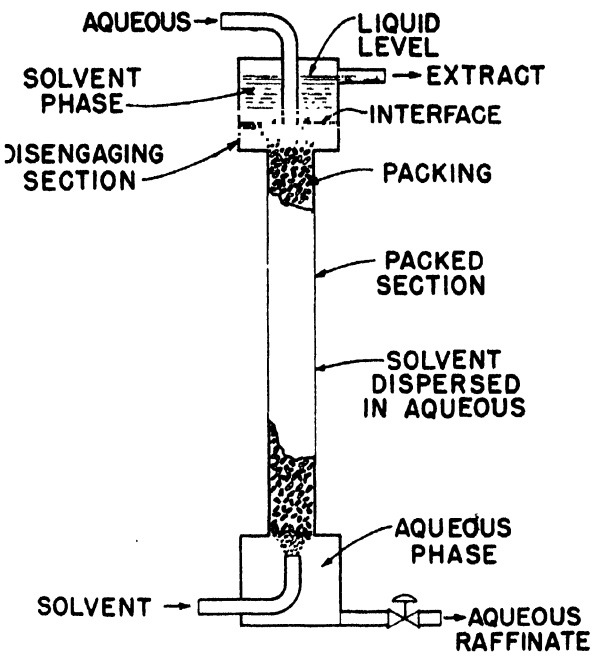

Figure 13. Solvent extraction packed column

this compact mixer-settler, the mixing chambers are separated from the pumping chambers by partitions. A centrifugal pump agitator in each mixing chamber picks up both incoming phases in a hollow vertical shaft and discharges them radially, intimately mixed, into the adjacent settling zone, thus producing the necessary hydraulic head for stage-to-stage flow and maintenance of the liquid-liquid interface in the desired position in each stage. The two-phase flow in each settling zone is concurrent while flow between stages is countercurrent. There are no submerged seals or bearings; the motor-impeller assembly may be removed or replaced by remote control.

The pulsed perforated-plate column (Fig. 15) was originally described by Van Dijck,[16] and other data on pulsed column development have been published.[17,20] It provides a significant, often more than twofold, reduction in column height from the heights needed with a conventional packed column. In the pulsed column an up-and-down pulsing motion is superimposed on the net counter-current flow of the liquid phases through a series of stationary, spaced, horizontal perforated plates. As an alternative to the

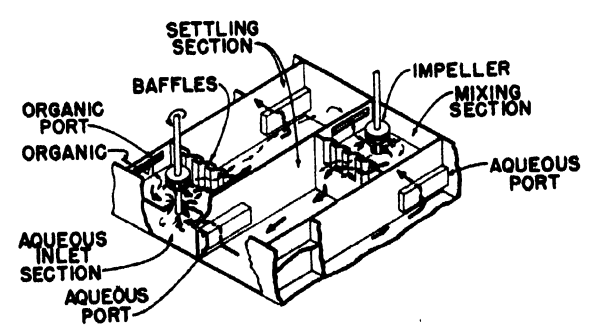

Figure 14. Schematic cutaway of solvent extraction pump-type mixer-settler

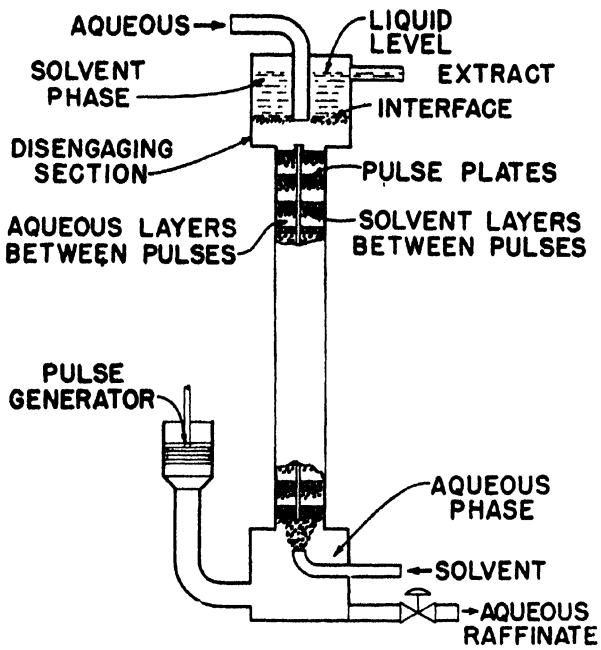

Figure 15. Solvent extraction pulse column

perforated plates, a pulsed column may employ Raschig rings or other packing.

In the case of perforated-plate columns the pulsing also performs another important function in that it provides the means of counter-current flow of the aqueous and organic phases. The specific gravity difference between the two phases is usually not sufficient to cause a significant counter-current flow through the small holes in the perforated plates. Consequently, the net flow of the light phase up and the heavy phase down the column is caused almost entirely by the actions of the pulse generator and the stream pumps.

The most important advantage of pulsed columns over packed columns is the fact that, for the same extraction duty, they can be made much shorter. Additional advantages are a less pronounced dependence of extraction effectiveness (H.T.U. values) on the throughput rate and, in the case of sieve-plate columns, the greater ease of a temporary shut-down and start-up with the characteristic of very little flow through the plates in the absence of pulsing. The need of a pulse generator, with its initial cost and maintenance requirements, is a disadvantage.

Design Concepts

Any detailed discussion of the engineering and equipment design which must be done for a radiochemical plant cannot be summarized in a paper such as this. However, a survey of solvent extraction technology would be incomplete without some general discussion of possible approaches for equipment and plant design.

A typical radiochemical processing plant has certain basic functional components. These components, which may be considered as unit processes, can be grouped as follows: (1) storage of irradiated reactor fuel or fertile reactor elements to permit decay of short-lived fission products; (2) dissolution of fuel elements in the appropriate chemical reagent and subsequent clarification and chemical adjustment to provide feed for the separation process; (3) storage of feed solutions until introduced into the separation process; (4) separation of fissionable or fertile materials from fission products and transuranic elements; (5) collection and analysis of fission-product-bearing waste streams; (6) collection of product, analysis, and preparation for shipment; and (7) preparation, distribution, and recycling of chemical process reagents.

To support these main line chemical processes and to handle highly radioactive wastes, the following supporting facilities are required: (1) analytical laboratory; (2) waste processing, storage, and disposal of both liquid and gaseous wastes; (3) maintenance shops and personnel; (4) service facility for production and distribution of all common process services; (5) mechanical handling equipment for manipulating shielded fuel carriers, etc; (6) health physics facility and personnel for biological protection of operating personnel; (7) security and protection facilities and personnel; (8) site development such as roads, main power distribution, primary water supply, sewage disposal, etc; and (9) facilities for all standard administrative functions.

The design and conception of a radiochemical plant involves consideration of many factors that are foreign to standard chemical plant design. A limited number of these has been selected for discussion.

A choice between batch and continuous processing must be made. Batch processing is advantageous for good fissionable material accountability since the location of all fuel material in the processing plant can be determined by following discrete batches through a processing plant with remote instrumentation and analytical control. The advantages of continuous processing are reduction of the number of process pieces, and hence the cost, and in the greater compatibility of continuous techniques with criticality control of solutions containing U^{235} or Pu^{239}.

Criticality of solutions in the chemical plant must be considered. Critical conditions of systems containing fissionable material result from the accumulation of a sufficient mass of fissionable material in a geometric configuration which minimizes loss of neutrons produced by the fission of the fissile element adequately to allow a chain reaction to progress. Solutions containing U^{235} or Pu^{239} can be made to go critical, or can do so by accident, during chemical processing. Obviously, the chemical plant designer must provide a system in which it is impossible to produce critical conditions.

A thick radiation shield is required to provide protection for operating and maintenance personnel. All process lines, contaminated air, liquid wastes, and radioactive auxiliary equipment must be shielded. Shields in a radiochemical plant are erected for the biological protection of operating personnel from penetrating γ rays emitting by decaying fission prod-

1 watt = 9.35 × 10⁷ r/sec (S = TOTAL EMISSION)
$\mu_\gamma = 3.5 \times 10^{-5}$/cm, 0.05 Mev < E < 4 Mev
$\mu_\beta = 2.7 \times 10^{-3}$/cm
1 watt = 9.41 × 10⁷ r/8 hr AT 1 cm ($\mu_\gamma S$ – γ ENERGY ABSORBED/cm²·cm OF PATH)
= 1.18 × 10⁷ r/1 hr AT 1 cm
= 1.96 × 10⁵ r/1 min AT 1 cm
1 watt = 7.27 × 10⁹ r/8 hr AT 1 cm ($\mu_\beta S$ – β ENERGY ABSORBED/cm²·cm OF PATH)
= 9.10 × 10⁸ r/1 hr AT 1 cm
= 1.51 × 10⁷ r/1 min AT 1 cm
1 watt = 169/E curies (E = ENERGY OF PARTICLES OR PHOTONS, IN Mev)
= 6.24 × 10¹² Mev/sec = 6.24 × 10¹⁸ ev/sec

S — EMISSION FROM POINT SOURCE
S_L — EMISSION FROM UNIT LENGTH OF LINE SOURCE
S_A — EMISSION FROM UNIT AREA OF PLANE SOURCE
S_V — EMISSION FROM UNIT VOLUME OF VOLUME SOURCE
ϕ — ANGLES (AS SHOWN) IN RADIANS
σ — ABSORPTION COEFFICIENT OF SHIELD MATERIAL
ν — ABSORPTION COEFFICIENT OF SOURCE MATERIAL
t — THICKNESS OF SHIELD MATERIAL
r, R — RADII OF CIRCULAR SOURCES
η — THICKNESS OF VOLUME SOURCES
Σ — EFFECTIVE THICKNESS OF VOLUME SOURCES
a, b, c, d — DISTANCE OF SOURCE FROM OBSERVER

$F_0 = -E1(-b) = \int_b^\infty \frac{e^{-x}}{x}dx$

$F_1 = E(b) = b\int_b^\infty \frac{e^{-x}}{x^2}dx$

$\mathcal{F}(\phi\theta) = \int_0^\phi e^{-\Sigma\sec\phi}d\phi$

TYPE SOURCE	UNSHIELDED	SPEC. CONDITIONS	SHIELDED
POINT SOURCE 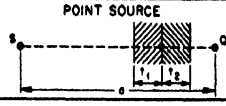	$E_A = \frac{\mu S}{4\pi a^2}$		$E_A = \frac{\mu S}{4\pi a^2} e^{-\Sigma\sigma t}$
LINE SOURCES STRAIGHT LINE 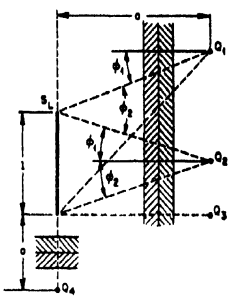	AT Q_1 $E_A = \frac{\mu S_L}{4\pi a}(\phi_2 - \phi_1)$		$E_A = \frac{\mu S_L}{4\pi a}\left[\mathcal{F}(\phi_2\theta) - \mathcal{F}(\phi_1\theta)\right]$
	AT Q_2 $E_A = \frac{\mu S_L}{4\pi a}(\phi_2 + \phi_1)$		$E_A = \frac{\mu S_L}{4\pi a}\left[\mathcal{F}(\phi_2\theta) + \mathcal{F}(\phi_1\theta)\right]$
	$E_A = \frac{\mu S_L}{2\pi a}\phi$	$\phi_1 = \phi_2$	$E_A = \frac{\mu S_L}{4\pi a}\mathcal{F}(\phi\theta)$
	$E_A = \frac{\mu S_L}{4a}$	$l = \infty$, $\phi_1 = \phi_2 = \frac{\pi}{2}$	$E_A = \frac{\mu S_L}{4\pi a}\mathcal{F}\left(\frac{\pi}{2}\theta\right)$
	AT Q_3 $E_A = \frac{\mu S_L}{4\pi a}\phi$	$\phi_2 = 0$	$E_A = \frac{\mu S_L}{4\pi a}\mathcal{F}(\phi\theta)$
	$E_A = \frac{\mu S_L}{8a}$	$\phi_2 = 0$, $l = \infty$	$E_A = \frac{\mu S_L}{4\pi a}\mathcal{F}\left(\frac{\pi}{2}\theta\right)$
	AT Q_4 $E_A = \frac{\mu S_L}{4\pi}\left[\frac{1}{a} - \frac{1}{a+l}\right]$	$\phi_1 = \phi_2 = 0$	$E_A = \frac{\mu S_L}{4\pi}\left[\frac{1}{a} - \frac{1}{a+l}\right]e^{-\Sigma\sigma t}$
	$E_A = \frac{\mu S_L}{4\pi a}$	$\phi_1 = \phi_2 = 0$, $l = \infty$	$E_A = \frac{\mu S_L}{4\pi a}e^{-\Sigma\sigma t}$
RING SOURCE 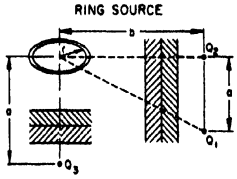	AT Q_1 $E_A = \frac{\mu S_L r}{2}\left[(a^2+b^2+r^2)^2 - 4b^2r^2\right]^{-1/2}$		$E_A = \frac{\mu S_L r}{2}\left\{\left[(a^2+b^2+r^2)^2 - 4b^2r^2\right]^{-1/2} - \frac{\Sigma\sigma t}{a}\left[(a^2+b^2+r^2)^{-1/2} + \frac{3rb}{8}(a^2+b^2+r^2)^{-5/2} + \cdots\right] + \frac{1}{2}\left(\frac{\Sigma\sigma t}{a}\right)^2\right\}$
	AT Q_2 $E_A = \frac{\mu S_L r}{2}\left(\frac{1}{b^2 - r^2}\right)$	$a = 0$	
	AT Q_3 $E_A = \frac{\mu S_L r}{2(a^2+r^2)}$	$b = 0$	$E_A = \frac{\mu S_L r}{2(a^2+r^2)}e^{-\frac{\Sigma\sigma t\sqrt{a^2+r^2}}{a}}$
PLANE SOURCES DISK SOURCE 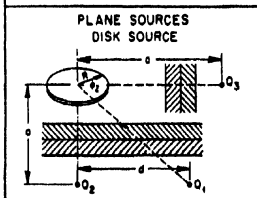	AT Q_1 $E_A = \frac{\mu S_A}{4}\ln_e\frac{R^2+a^2+d^2+\sqrt{(R^2+a^2-d^2)^2+4a^2d^2}}{2a^2}$		$E_A = \frac{\mu S_A}{4}\left\{\ln_e\frac{R^2+d^2+a^2+\sqrt{(R^2+a^2-d^2)^2+4a^2d^2}}{2a^2} - \frac{2\Sigma\sigma t}{a}\left[\sqrt{a^2+d^2+r^2} - \sqrt{a^2+d^2}\right] + \frac{1}{2}\left[\frac{R}{a}(\Sigma\sigma t)\right]^2\right\}$
	AT Q_2 $E_A = \frac{\mu S_A}{4}\ln_e\frac{R^2+a^2}{a^2}$	$d = 0$	$E_A = \frac{\mu S_A}{2}\left[F_0(\Sigma\sigma t) - F_0\left(\frac{\Sigma\sigma t}{a}\sqrt{a^2+R^2}\right)\right]$
	AT Q_3 $E_A = \frac{\mu S_A}{4}\ln_e\frac{d^2}{d^2-R^2}$	$a = 0$	$E_A = \frac{\mu S}{4\pi(a+z)^2}e^{-(\nu z + \Sigma\sigma t)}$
INFINITE PLANE 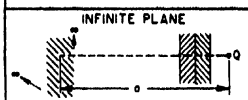			$E_A = \frac{\mu S_A}{2}F_0(\Sigma\sigma t)$
SOLID SOURCES INFINITE SLAB 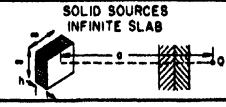	$E_A = \frac{\mu S_V}{2\nu}\left[1 - F_1(\nu h)\right]$		$E_A = \frac{\mu S_V}{2\nu}\left[F_1(\Sigma\sigma t) - F_1(\Sigma\sigma t + \nu h)\right]$
CYLINDRICAL SOURCE 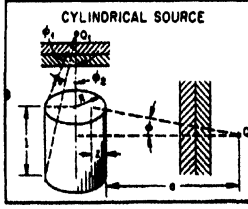	AT Q_1 $E_A = \frac{\mu S_V}{2\nu}\left\{\left[1 - F_1(\nu h)\right] - \left[\frac{1 - F_1(\nu h\sec\phi_1)}{\sec\phi_1}\right]\right\}$	UPPER LIMIT	$E_A = \frac{\mu S_V}{2\nu}\left\{F_1(\Sigma\sigma t) - F_1(\Sigma\sigma t + \nu h) + \frac{F_1\left[(\Sigma\sigma t + \nu h)\sec\phi_1\right]}{\sec\phi_1} - \frac{F_1(\Sigma\sigma t\sec\phi_1)}{\sec\phi_1}\right\}$
	$E_A = \frac{\mu S_V}{2\nu}\left\{\left[1 - F_1(\nu h)\right] - \left[\frac{1 - F_1(\nu h\sec\phi_2)}{\sec\phi_2}\right]\right\}$	LOWER LIMIT	$E_A = \frac{\mu S_V}{2\nu}\left\{F_1(\Sigma\sigma t) - F_1(\Sigma\sigma t + \nu h) + \frac{F_1\left[(\Sigma\sigma t + \nu h)\sec\phi_2\right]}{\sec\phi_2} - \frac{F_1(\Sigma\sigma t\sec\phi_2)}{\sec\phi_2}\right\}$
	$E_A \cong \frac{\mu S_V}{2\nu}(1 - \cos\phi)$ | $E_0 = \frac{\mu S_V R^2}{2\nu a}$	$\nu h > 3$–5 | $R \cong 0$	
	AT Q_2 $E_A = \frac{\mu S_V R^2}{2(a+z)}\mathcal{F}(\phi\theta^0)$ $\theta^0 = \nu z$	Q AT $\frac{1}{4}$	$E_A = \frac{\mu S_V R^2}{2(a+z)}\mathcal{F}(\phi\theta^0)$ $\theta^0 = \nu z + \Sigma\sigma t$

Figure 16. Shielding equations for homogeneous β and γ sources

ucts; the shielding of α particles presents no problem because of the short range of these particles in any material; beta particles are stopped by shields much thinner than those required for the penetrating photons of γ rays. A summary of useful shielding formulas for various cases is given in Fig. 16.[21]

Radioactive decay cooling can be accomplished in water-filled basins or "canals," which provide thermal cooling for fuel elements from reactors as well as providing a γ-ray shield. A water shield for storage and cooling of radioactive materials is reasonably inexpensive. Bulk shielding is usually concrete and ranges in thickness from 1 ft to 6 ft.

Special shields for plant appurtenances such as samplers (Fig. 17)[22] pump blisters, carriers, and dissolver chargers (Fig. 18) usually are made of lead because of its higher density and consequent lower volume requirement. Lead shielding specialties are even more expensive than concrete mass shielding, since normally they are integrated with some mechanical handling device for radioactive materials.

All process equipment must be operated remotely from outside a processing cell. For each process vessel a liquid level indicator and a specific gravity indicator-recorder are required. If temperature is important, a remote-reading temperature recorder is necessary. All valves inside processing cells must be bellows- or motor-operated; they must also be packless and contain no plastic seats or poppets (Fig. 19). The measurement of flow of radioactive solutions is greatly complicated because of lack of accessibility for maintenance and possibly low volumetric flow rates.

All equipment used in handing radioactive solutions must be as maintenance-free as possible. Complicated processing equipment with moving parts requiring lubrication cannot be used. Pumps that have packings are not used since all packings require replacement. Extensive and expensive precautions must be taken to assure good workmanship in all equipment; all piping must be absolutely leak-tight. Equipment that may require frequent maintenance is removed from processing cells and installed in shielded, accessible compartments. Materials of construction must be resistant to process and decontaminating solutions.

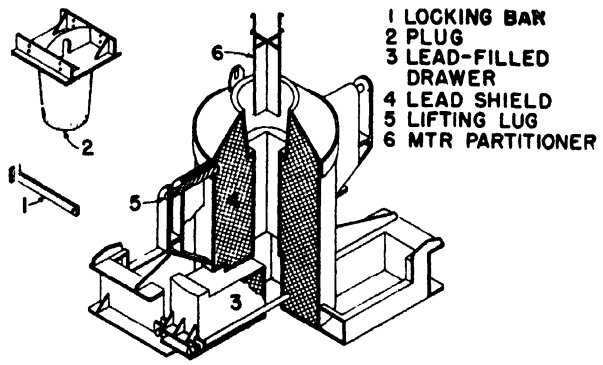

Figure 18. Fuel assembly charger

Most decontaminating reagents are liquids and are usually corrosive; mineral acids and combinations of same are used extensively. Process equipment and piping must therefore be resistant to the corrosive attack of decontaminating reagents.[23] To prevent the exterior of process vessels and piping in a process cell from becoming permanently contaminated, the same corrosion resistance must be provided. Therefore the use of stainless steel for all equipment and piping inside processing cells is advisable. Equipment supports are commonly stainless steel or carbon steel coated with corrosion-resistant organic coatings. The concrete surfaces in a processing cell must also be protected. Stainless steel floors are frequently used. Walls are carefully finished to a smooth surface, etched with acid, and coated with protective organic coatings.

In spite of all precautions to prevent equipment or piping failure, it must be recognized that some maintenance will be required. Three basic philosophies for maintenance systems can be used:

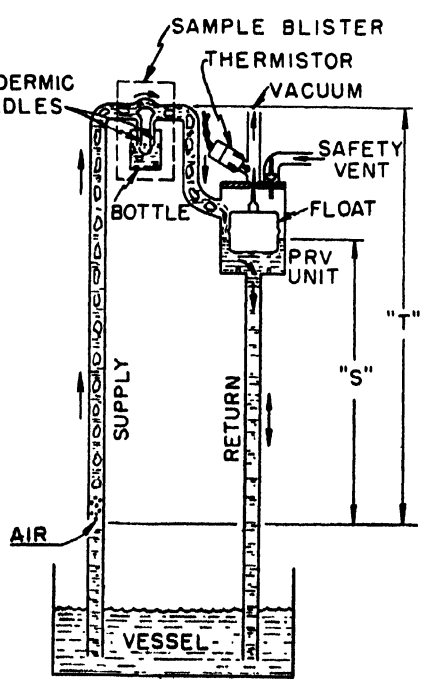

Figure 17. Sampler loop

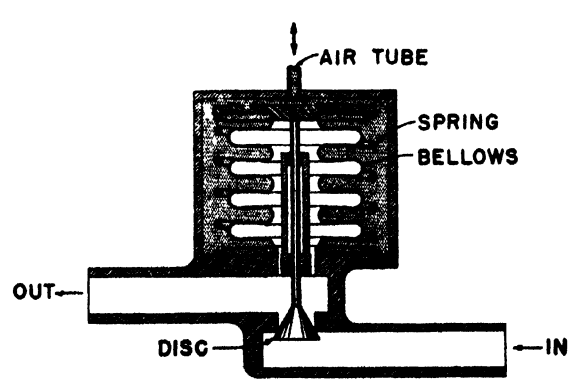

Figure 19. Bellows valve assembly

1. Remote maintenance: equipment and piping designed so that it can be removed by remotely operated mechanical devices, discarded, and replaced.

2. Direct maintenance: equipment and processing cells designed so that decontamination from fission product activity can be done preceding direct repair.

3. Underwater maintenance: equipment installed as for direct maintenance but located so that mechanical operations can be accomplished through a water cover if necessary; process cell built so that equipment can be covered with sufficient water for shielding during maintenance.

REFERENCES

1. Coryell, C. D. and Sugarman, N. (eds.), *Radiochemical Studies: The Fission Products,* National Nuclear Energy Series, Div. IV, Vol. 9, Appendixes A and B, McGraw-Hill, New York (1951).
2. Curves prepared by Arnold, E. D., Oak Ridge National Laboratory.
3. Cathers, G. I., P/743, *Radiation Damage to Radiochemical Processing Reagents,* Volume 7, Session 11B, these Proceedings.
4. Curves prepared by Arnold, E. D., Oak Ridge National Laboratory.
5. Rodger, W. A., "Radioactive Wastes: Treatment, Use, Disposal," Chem. Eng. Progress, *50*: pp. 263-5 (1954).
6. Data developed at Knolls Atomic Power Laboratory by Albaugh, F. W., Callis, C., Hill, O., Zebroski, E. L. and Haas, W. O., *et al.*
7. Process development work at Argonne National Laboratory; later at Oak Ridge National Laboratory.
8. Foster, D. L., Savolainen, J. E. and Wymer, R. G., *Nuclear Reactor Fuel Dissolution,* Session 21B.
9. Flanary, J. R., P/539, *Solvent Extraction of Uranium and Plutonium from Fission Products with TBP,* Volume, 9, Session 21B, these Proceedings.
10. Based on work done by Thomas, J. R. and Crandall H. W., California Research and Development Corporation, and Hicks, J. E. and Rubin B., Radiation Laboratory, University of California.
11. Culler, F. L. and Bruce, F. R., P/541, *The Processing of Uranium-Aluminum Reactor Fuel Elements,* Volume 9, Session 21B, these Proceedings.
12. Gresky, A. T., P/540, *Solvent Extraction Separation of U-233 and Thorium from Fission Products by Means of Tributyl Phosphate,* Volume 9, Session 21B, these Proceedings.
13. Data developed at Hanford Engineering Works and Knolls Atomic Power Laboratory.
14. Data developed at Hanford Engineering Works and Knolls Atomic Power Laboratory.
15. Coplan, B. V., Davidson, J. K. and Zebroski, E. L., "The Pump-Mix Mixer Settler, A New Liquid-Liquid Extractor," *Chem. Eng. Progress, 50*: 403-8 (1954).
16. VanDijck, W. J. D., U.S. Patent 2,011,186 (13 August 1935).
17. Sege, G. and Woodfield, F. W., "Pulse Column Variables," *Chem. Eng. Progress, 50*: 396-402 (1954).
18. Ibid., "A Louver-Plate Redistributor for Large-Diameter Pulse Columns," *Chem. Eng. Progress Symposium Series, 50*: No. 13 (1954).
19. Thornton, J. D., *"Recent Developments in Pulse Column Techniques,"* ibid.
20. Jealous, A. C. and Johnson, H. F., *"Power Requirements for Pulse Generation in Pulse Columns," Ind. Eng. Chem.* (in press, June 1954).
21. Prepared by Goeller, H. E., Oak Ridge National Laboratory.
22. Landry, J. W., P/549, *High Level Sampling Devices for Radiochemical Plants,* Volume 9, Session 21B, these Proceedings.
23. Campbell, D. O., P/548, *The Removal of Fission Products from Stainless Steel,* Volume 9, Session 21B, these Proceedings.

The Processing of Uranium-Aluminum Reactor Fuel Elements

By F. L. Culler, Jr. and F. R. Bruce,* USA

The recovery and decontamination of enriched uranium fuel elements of the type used in the Materials Testing Reactor, in the Swimming Pool Reactor, or from any reactor which uses fuel elements of aluminum-clad uranium-aluminum alloy can be accomplished by organic solvent extraction from nitric acid solution. Fuel elements in an enriched fuel reactor require reprocessing after only part of the U^{235} has been consumed for any one or a combination of the following reasons: (1) depletion of U^{235} content of the reactor core and build-up of fission product poisons to the point where the reactor is subcritical; (2) corrosion of the fuel element by coolants; (3) dimensional changes in the fuel element due to heat or radiation; and (4) corrosive or mechanical failure of the fuel element.

The unconsumed enriched U^{235} must be chemically separated from fission products, inert fuel diluents and impurities, and heavy elements resulting from neutron capture by fertile materials present in the fuel mixture and by parasitic capture of neutrons by the fuel itself. This chemical purification has been accomplished by the use of selective organic solvents such as methylisobutyl ketone (hexone) and tributyl phosphate (TBP) dissolved in an inert organic diluent such as aromatic-free kerosene. A chemical description of these two processes follows. Each process will decontaminate enriched uranium from fission products to background activity level and will separate plutonium by factors of 10^4 to 10^6.

FUEL MATERIAL

Materials Testing Reactor fuel assemblies consist of thin concave uranium-aluminum alloy sheets, each clad in aluminum, held together at the sides by an aluminum plate into which each fuel sheet is brazed. At the time of discharge, after approximately 15% of the U^{235} has been fissioned at a specific power of 10 kw per gram of U^{235}, the fuel assembly contains about 2×10^8 curies of fission product activity and small quantities of plutonium and other transuranic elements.

COOLING PERIOD BEFORE CHEMICAL PROCESSING

Enriched uranium fuel elements are stored under water before chemical processing to allow for the decay of fission product activity. The period of decay allowed for uranium fuels usually is determined by the quantity of U^{237} produced by the following reaction during irradiation.

$$U^{235}(n,\gamma)\ U^{236}(n,\gamma)\ U^{237} \xrightarrow{6.9\ d} Np^{237} \quad (1)$$

U^{237} will be present in product uranium that has been decontaminated from fission products; it must be allowed to decay before uranium of low activity background can be produced. If the U^{237} is allowed to decay before chemical processing, the decay period also allows time for fission product activity level reduction of approximately 10^4. At decay periods over 100 days, the action fission gases I^{131} and Xe^{133} have decayed, and other fission products such as Ba^{140} (12.8 d)—La^{140} (40.0 hr) have been reduced. La^{140} decay is desirable before processing since this isotope emits a 2.1-Mev γ photon which controls chemical plant shield thickness for periods of less than 90 days.

REQUIREMENTS FOR CHEMICAL PROCESSING

If it is assumed that uranium must be sufficiently decontaminated from fission products to allow direct handling during refabrication to fuel elements, gross decontamination factors of 10^8 must be obtained after irradiated fuel has been cooled for a period of 100–140 days. To eliminate the hazard from parasitically produced plutonium, decontamination factors of approximately 10^4 must be achieved for this element. Because of the value of enriched fuel, over-all process losses for uranium should not exceed 0.1%, with losses of about 0.05% in solvent extraction cycles. Since only small quantities of plutonium are produced when enriched U^{235} fuel is used, processes developed for highly enriched uranium allow plutonium to follow the fission product waste streams. Contamination of the uranium product by such non-active impurities as aluminum, iron, and sodium must not exceed several thousand parts per million.

From an engineering standpoint, the chemical process should be capable of remote operation, since all equipment must be placed in cells shielded with 4 ft or more of concrete. Operations must be mechanically simple, since maintenance is difficult and expensive. A processing plant is designed with sufficient shielding to protect operating personnel from receiving more radiation than 30 mr per 40-hr week, which is 0.1 tolerance.

* Oak Ridge National Laboratory. Including work by W. B. Lanham, J. R. Flanary, F. R. Bruce, H. K. Jackson, W. K. Eister, W. H. Baldwin, E. O. Nurmi, D. L. Foster, J. H. Goode, D. E. Ferguson, R. E. Blanco, A. T. Gresky, Oak Ridge National Laboratory; D. G. Reid, Phillips Petroleum Company, Idaho Falls, Idaho; T. C. Runion, National Lead Company, Fernald, Ohio, *et al.*

An important consideration in vessel design and equipment location for plants which process enriched U^{235} is the prevention of criticality. Criticality control can be maintained by limiting the weight of U^{235} in each process vessel, by dilution, or by using equipment of a shape which allows sufficient neutron loss from the uranium-bearing solution to prevent criticality under any loading conditions.

STEPS IN THE HEXONE EXTRACTION PROCESS

A process for recovery of uranium from nitric acid solution containing aluminum may consist of the following steps: dissolution of uranium or uranium-aluminum alloy in 60% nitric acid with mercuric nitrate as catalyst for aluminum dissolution; feed clarification by filtration; feed adjustment to the desired aluminum nitrate, and nitric acid concentrations; and separation of the uranium from fission products and plutonium in three cycles of solvent extraction, using methylisobutyl keteone as the solvent. Plutonium is separated from the uranium in the second cycle by reducing it to the trivalent inextractable state. Small quantities of plutonium are discarded with the fission product waste if the fuel is highly enriched. An over-all chemical flowsheet showing two cycles of solvent extraction is given in Fig. 1. If partially enriched fuels are used, a modification of the Redox process[1] can be used to recover plutonium.

Dissolution

The first chemical operation following cooling is the dissolution of fuel assemblies in nitric acid. Nitric acid dissolves finely divided aluminum quite readily, but, because of the formation of passive surfaces of aluminum oxide, thick pieces of the metal are incompletely dissolved. Mercury catalyzes the reaction of nitric acid with aluminum and allows complete dissolution, as a result of aluminum amalgamation and galvanic effects. Dissolving procedures for all fuel elements that contain aluminum include the use of mercuric nitrate (1 to 2% of the weight of the aluminum in the assembly) as a catalyst. Dissolution of uranium metal in dilute nitric acid involves the primary reaction

$$U + 4NO_3 \rightarrow UO_2(NO_3)_2 + 2\,NO + 2\,H_2O \qquad (2)$$

However, when acid concentrations greater than 8 *M* are used, reactions involving 8 and 5 moles of nitric acid per mole of uranium also occur, with the liberation of nitrogen dioxide. Based on experimental results, the over-all reaction can be approximated by the equation

$$U + 4.8\,HNO_3 \rightarrow UO_2(NO_3)_2 + 2.4\,H_2O + 1.2\,NO_2 \qquad (3)$$

Similarly, the dissolution of aluminum in nitric acid involves a number of reactions which may be approximately summarized in the over-all reaction

$$Al + 3.75\,HNO_3 \xrightarrow{Hg^{++}} Al(NO_3)_3 + 0.225\,NO + 0.15\,N_2O + 0.1125\,N_2 + 1.875\,H_2O \qquad (4)$$

All the above reactions occur in the course of a normal dissolving, and it is difficult to predict accurately on the basis of stoichiometry the quantity of nitric acid required. Dissolution in the presence of excess metal makes possible acid-deficient solutions which are desirable in the solvent extraction operation. An acid-deficient solution may be defined as one containing more hydroxyl ions than are formed by the hydrolysis of aluminum nitrate and uranyl nitrate.

Batch and continuous dissolving procedures are reviewed in more detail by Foster, Wymer, and Savolainen.[2]

Feed Preparation

Feed volumes in the chemical reprocessing of uranium-aluminum are determined by the quantity of aluminum in the fuel element rather than the uranium content. From braze metal used in the fabrication of fuel elements of the Materials Testing Reactor type and from impurities in aluminum itself, silica is introduced into the feed stream so that a filtration or centrifugation step is required. Siliceous precipitates in feed cause emulsions to form during solvent extraction; these collect at the interface in the solvent contactor and eventually cause flooding. Sufficient silica can be removed by filtration through a bare 10-micron pore size sintered stainless steel filter.

Solvent Extraction

Uranyl nitrate behaves as a strong electrolyte in aqueous solution, being almost completely dissociated into uranyl (UO_2^{++}) and nitrate (NO_3^-) ions. However, as an undissociated molecule, $UO_2(NO_3)_2 \cdot 3H_2O$, it is soluble in many organic solvents, including methylisobutyl ketone. The introduction of a common ion, in this case NO_3^-, into the aqueous solution shifts the equilibrium toward the molecular form and enhances the extraction of uranyl nitrate by the solvent. Aluminum nitrate is an obvious choice as salting agent in the processing of uranium-aluminum alloy since it is present in high concentration in the dissolver solutions, and is inexpensive enough to be added in scrub solutions and second- and third-cycle feeds.

The general scheme of uranium purification by solvent extraction involves a series of extraction-stripping cycles. Uranium is preferentially extracted with methylisobutyl ketone from an aluminum nitrate solution. Most fission products, which are much less extractable than uranium, remain in the aqueous phase. In a second operation uranium-bearing solvent is brought into contact with dilute nitric acid and the uranium and the small fraction of fission products extracted from the radioactive feed are back-extracted (stripped) into the aqueous phase. A new feed is prepared from this solution, and the extraction-stripping cycle is repeated for additional separation from fission products. For reactor fuels such as those from the Materials Testing Reactor, three cycles are required before the uranium is sufficiently free of fission products to permit handling without shielding.

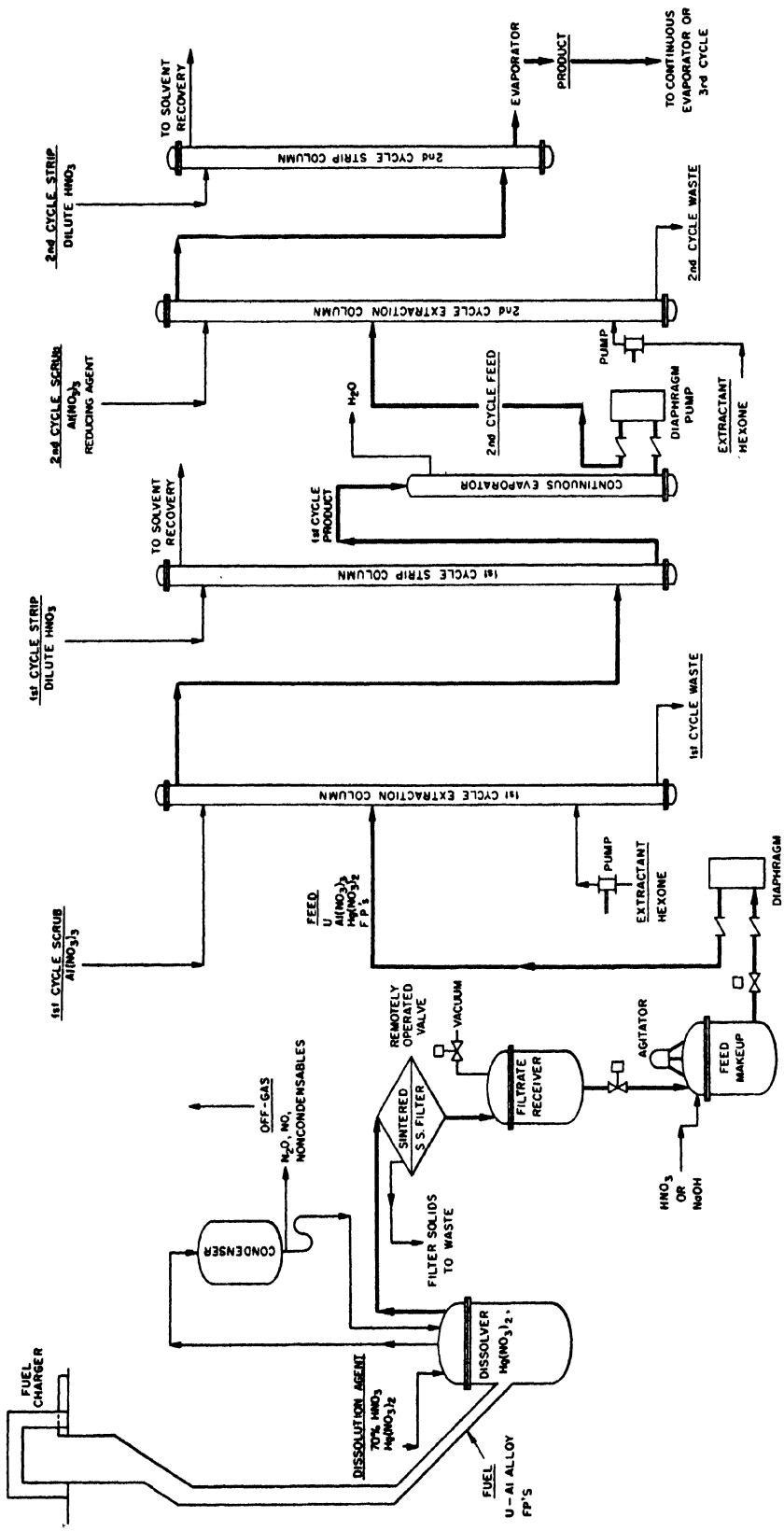

Figure 1. Schematic flowsheet: two cycles of hexone solvent extraction for uranium-aluminum alloy

1. First Cycle Extraction Step

The initial separation of uranium from fission products is carried out in a compound solvent-extraction contactor in which the aqueous feed solution is introduced about halfway between the top and bottom of the column. Hexone is introduced as the discontinuous phase near the bottom of the column and flows upward counter-currently to the downward-flowing aqueous phase. Essentially all the uranium is extracted by the organic phase. After passing the aqueous feed inlet, the solvent rises through the upper part of the column, where it comes in contact with a fresh aluminum-nitrate scrub solution which has been introduced near the top of the column. The upper portion of this column is known as the "scrub" section, and the portion below the feed inlet, as the "extraction" section.

The loss of uranium in the extraction section is a function of the uranium extraction factor and of the number of extraction stages (length of column). The extraction factor is the product of the distribution coefficient and the ratio of the solvent and the aqueous flow volumes.

The extraction of fission products is far less complete than that of uranium, and their separation from uranium is essentially independent of the number of extraction stages. The separation is primarily affected by chemical variables which alter the distribution coefficients of uranium and fission products; the maximum separation occurs when the distribution coefficients of the uranium and the fission products differ by a large amount. The process variables that have the greatest effect on the uranium and fission-product distribution coefficients are the concentrations of aluminum nitrate and nitric acid. The results of distribution-coefficient determinations made under varying conditions (see Fig. 2) show that, qualitatively, uranium and fission products are affected in the same

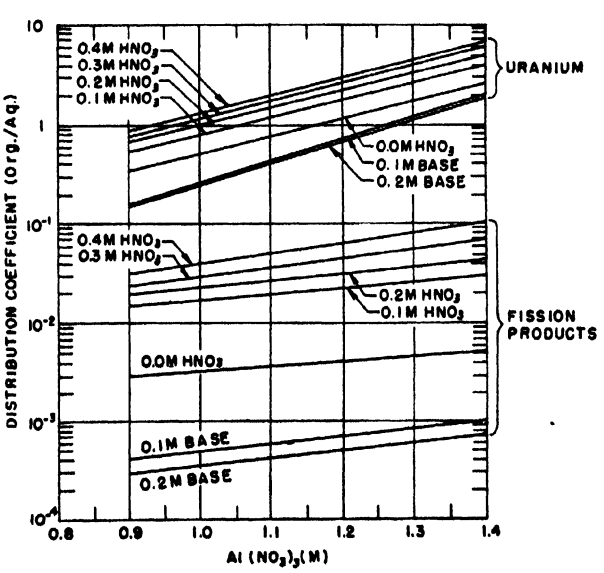

Figure 2. The effect of $Al(NO_3)_3$ concentration on the distribution coefficients of uranium and fission products in methylisobutyl ketone extractions at various HNO_3 concentrations

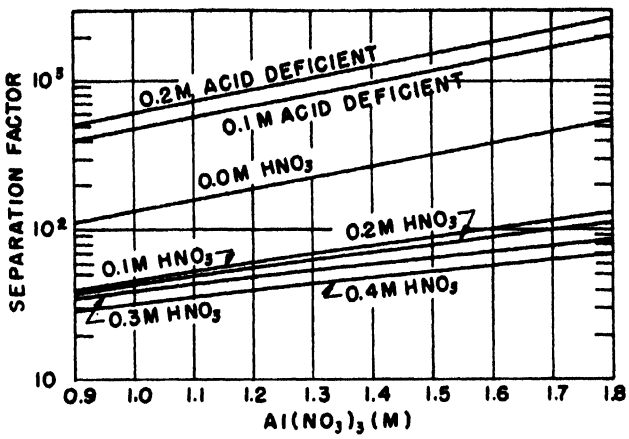

Figure 3. Effect of $Al(NO_3)_3$ concentration on the separation factor at various HNO_3 concentrations

manner by changes in aluminum nitrate and acid concentrations, but that they differ quantitatively. This difference is more apparent when the ratio of the uranium to the fission-product distribution coefficient (separation factor) is plotted as a function of aluminum nitrate and acid concentrations (see Fig. 3). The separation of the uranium and the fission products is increased to a greater extent by changes in acid concentration than by changes in aluminum nitrate concentration. The performance of fission products in hexone solvent extraction is discussed in detail in a paper by Bruce.[3]

Distribution coefficients of both uranium and gross gamma fission product activity are influenced to approximately the same extent by temperature changes (see Fig. 4). Consequently, the degree of separation of uranium from fission products that is achieved in hexone extraction is not appreciably affected by temperature. However, it is desirable to maintain a constant uranium distribution coefficient in a solvent extraction process at all times, so the temperature should remain constant. A 5% variation in the uranium distribution coefficient results from a temperature change of 6%.

Since a uranium concentration gradient exists in a continuous solvent extraction column, the effect of uranium concentration on the uranium distribution coefficient was investigated. It was found that the uranium distribution coefficient in hexone extraction was independent of the uranium concentration in the aqueous phase in the range between 2 and 5 gm per liter. At aqueous phase uranium concentrations below 2 gm per liter, there was evidence that the distribution ratio increased significantly (Fig. 5). Uranium concentrations of from 1–10 gm per liter in hexone have little effect on the uranium distribution coefficient. Thus for feeds containing several grams of uranium per liter, such as those resulting from the solution of uranium-aluminum alloy, uranium distribution coefficients are relatively independent of uranium concentration in either phase.

In continuous liquid-liquid extraction column operation, the aqueous phase with a relatively high oxi-

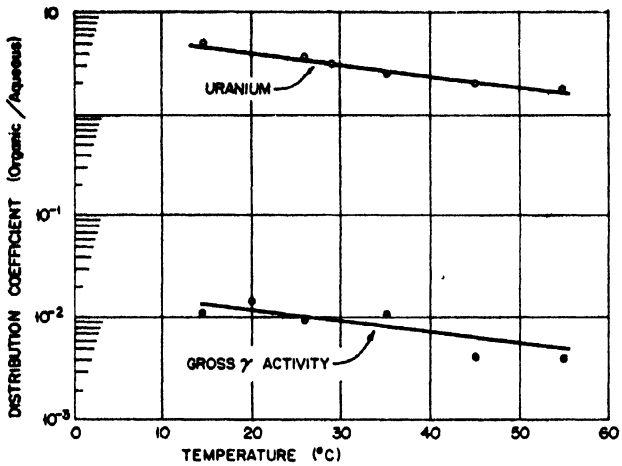

Figure 4. The effect of temperature on the distribution coefficients of uranium and fission products

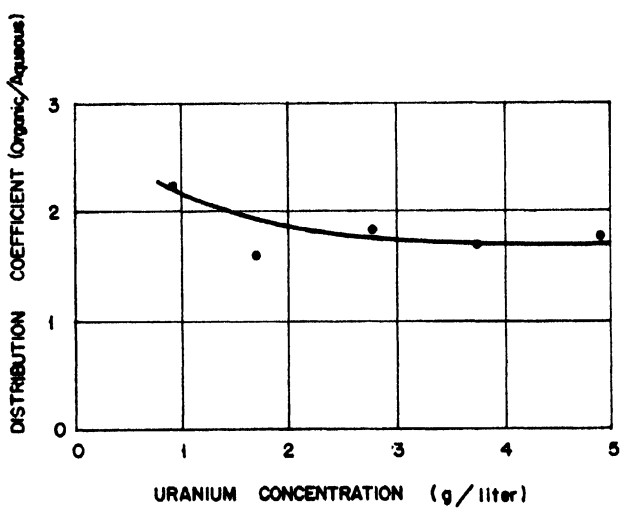

Figure 5. Effect of uranium concentration on the distribution coefficient in equal-volume hexone extraction at 30°C

dation potential, saturated with hexone and containing fission products, is in contact for a relatively long time with the extracting solvent. Solvent decomposition, which might impair decontamination, could occur from radiation damage or from oxidation. In order to investigate this possibility, an aqueous phase containing aluminum nitrate, nitric acid, sodium dichromate, 5 gm of uranium per liter, and fission products was contacted with an equal volume of hexone, and samples were removed after agitation times varying from 5 min to 17 hr. This study showed that the extraction of fission products is independent of phase contact time. The effect of extraction conditions and radiation on hexone degradation is further discussed by Cathers.[4]

2. First Cycle Scrubbing Step

The greatest separation of uranium from fission products takes place in the extraction section; however, it is possible to effect some additional decontamination in the scrub section. In this section of the extraction column, the transfer of uranium and fission

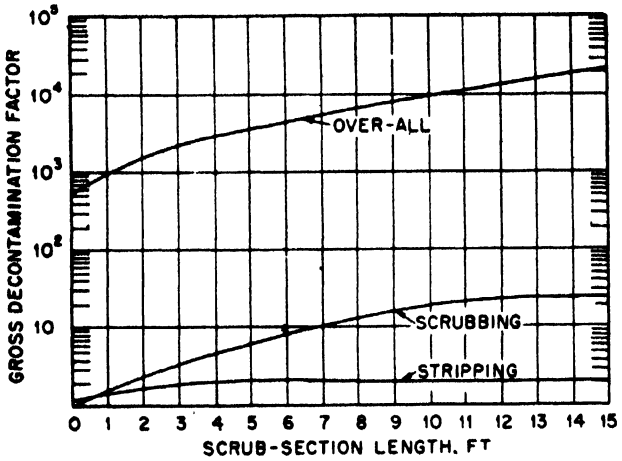

Figure 6. Gross beta decontamination as a function of scrub-section length

products is the opposite of that in the extraction section: from the solvent into the aqueous scrub solution. The amount of uranium refluxed in the scrub section is almost independent of the number of stages, whereas the fission-product reflux is quite dependent upon the number of stages. Accurate prediction of fission-product behavior in the scrub section from the distribution coefficients in the extraction section is not possible since some of the fission products apparently exist in several forms with different extraction characteristics. As the less extractable forms are removed in the extraction section and the scrub section, the distribution coefficient approaches that of uranium and further separation from uranium becomes very difficult. The number of scrub stages (length of column) which can be used efficiently, must be determined empirically. This was done for one of the process flowsheets considered, with the results shown in Fig. 6. In this case, the use of more than about 12 ft of scrub section did not improve decontamination in the scrub section.

As in the extraction section, reduction of the aluminum nitrate and acid concentrations enhances the back-extraction of fission products into the aqueous phase. It is apparent, therefore, that a low aluminum nitrate concentration is desirable in the scrub section. Under these conditions, the transfer of uranium to the aqueous phase is also increased, and the refluxed uranium is returned to the extraction section and is re-extracted into the solvent.

3. First Cycle Stripping Step

The uranium-bearing solvent from the extraction-scrubbing column is introduced at the bottom of a second column and flows upward countercurrently to the dilute nitric acid introduced at the top of the column. Owing to the low nitrate concentration, uranium is stripped (back-extracted) into the aqueous phase. Very little separation of uranium from fission products occurs (about a factor of 2) during this operation, since the conditions favor concentration of fission products in the aqueous phase.

The purpose of this step is to return the uranium to aqueous solution so that a new feed solution may be prepared for a subsequent extraction-scrubbing-stripping cycle in which further separation of uranium from fission products can be obtained.

Second Cycle

The first solvent-extraction cycle yields a product which contains a small quantity of fission products and some of the plutonium in the original fuel assembly. The function of the second cycle is to purify further the uranium with respect to fission products and to reduce the plutonium concentration to less than 1 part per 10^8 parts of uranium.

The second cycle employs conditions similar to those used in the first cycle. In addition, a reducing agent is added to the scrubbing solution to reduce plutonium to its trivalent state, which, under flowsheet conditions, has a distribution coefficient (organic/aqueous) of about 6×10^{-4}. Plutonium is not extracted into the hexone phase under reducing conditions, while uranium, which is not reduced, is extracted into the organic phase.

Alternate chemical flowsheets are available for the second cycle, one for batch and one for continuous operation. The procedure for batch operation consists in evaporating the first-cycle product and adding aluminum nitrate and ammonia to produce a feed of the same composition as the first-cycle feed. Thus the second-cycle feed composition is approximately the same as that of the first cycle, but the feed preparation is a batch operation, requiring additional tanks for feed adjustment and storage. In the second method of operation the first-cycle product is continuously evaporated to concentrate the uranium. This provides a feed that is somewhat acid, but the acidity is neutralized in the extraction column by acid-deficient scrub solution. The chemical conditions for the extraction section of the second cycle are made the same as for the first cycle by increasing the aluminum nitrate concentration of the scrubbing solution and by changing the flow ratio of the feed and scrub solutions. If, as shown in the flowsheet, continuous evaporation of the first cycle strip column product is used with adjustment of feed composition, the operation of the two cycles becomes truly continuous.

Third Cycle

At the end of two cycles of operation the uranium has been decontaminated and concentrated to the point that it may be finally purified by further solvent extraction on a laboratory scale behind light shielding.

However, the same results can be obtained by inclusion of a third cycle in the process. The third-cycle conditions are essentially a repetition of those of the second cycle. For the third cycle, a second-cycle stripping product is continuously concentrated, extracted into the solvent, scrubbed, and then stripped from the solvent. The principal difference in the two cycles is the omission of a reducing agent in the third cycle in order to reduce final product contamination.

SOLVENT CHARACTERISTICS AND PURIFICATION

The physical properties of the solvent, methylisobutyl ketone, are given in Table I. As purchased, it may contain such impurities as mesityl oxide, methylisobutyl carbinol, and an aromatic substance, possibly mesitylene. These impurities, which decrease the uranium and fission-product separation, are all oxidizable, and may be destroyed and removed by agitation of the solvent with sodium dichromate-nitric acid solution, followed by washing with sodium hydroxide, and steam distillation from a sodium hydroxide heel. This procedure is adequate for the removal of possible fission-product contamination from the recycled solvent.

Hexone is soluble to approximately 2% by weight in the aqueous phase. Water is soluble to approximately 2% by weight in hexone. This small mutual solubility does not influence uranium recovery or decontamination. It does make it necessary to strip solvent from all aqueous phases to prevent high solvent losses and high explosion hazard in aqueous raffinates. This solvent removal from aqueous streams is accomplished by boiling off approximately 5% of the aqueous phase; this fraction contains 100% of the dissolved hexone, which forms an azeotrope with water boiling at 87.9°C containing 75.7% hexone at 760 mm Hg.

RESULTS OF LABORATORY TESTS

Demonstration Runs

In two cycles of solvent extraction, the β, γ, and plutonium activities were reduced by factors of 2.9×10^6, 1.6×10^6, and 1.8×10^3, respectively (Table II). The activity of the final product was below the background activity of unirradiated enriched U^{235} after two cycles of extraction; for more radioactive feeds than those used in the pilot plant tests, three cycles of solvent extraction are required to decontaminate to background.

TRIBUTYL PHOSPHATE EXTRACTION OF URANIUM ALUMINUM ALLOY

Tributyl phosphate (TBP) in a suitable diluent will selectively extract uranium from fission products and

Table I. Physical Properties of Methylisobutyl Ketone

Specific gravity at 20°C	0.8024
Boiling point at 760 mm Hg pressure (°C)	116
Vapor pressure at 20°C (mm Hg)	15.7
Flash point (°F), tag open cup	81
Solubility in water at 20°C (%)	2
Solubility of water in methylisobutyl ketone at 20°C (%)	2.2
Viscosity, centipoise at 20°C	0.585
Latent heat of vaporization, cal/gm	86.5
Limits of flammability in air, vol %	
Upper	8.00 at 100°C
Lower	1.34 at 50°C
Latent heat of azeotrope with water (75.7% hexone, 87.9°C)	9500 cal/gm of azeotrope

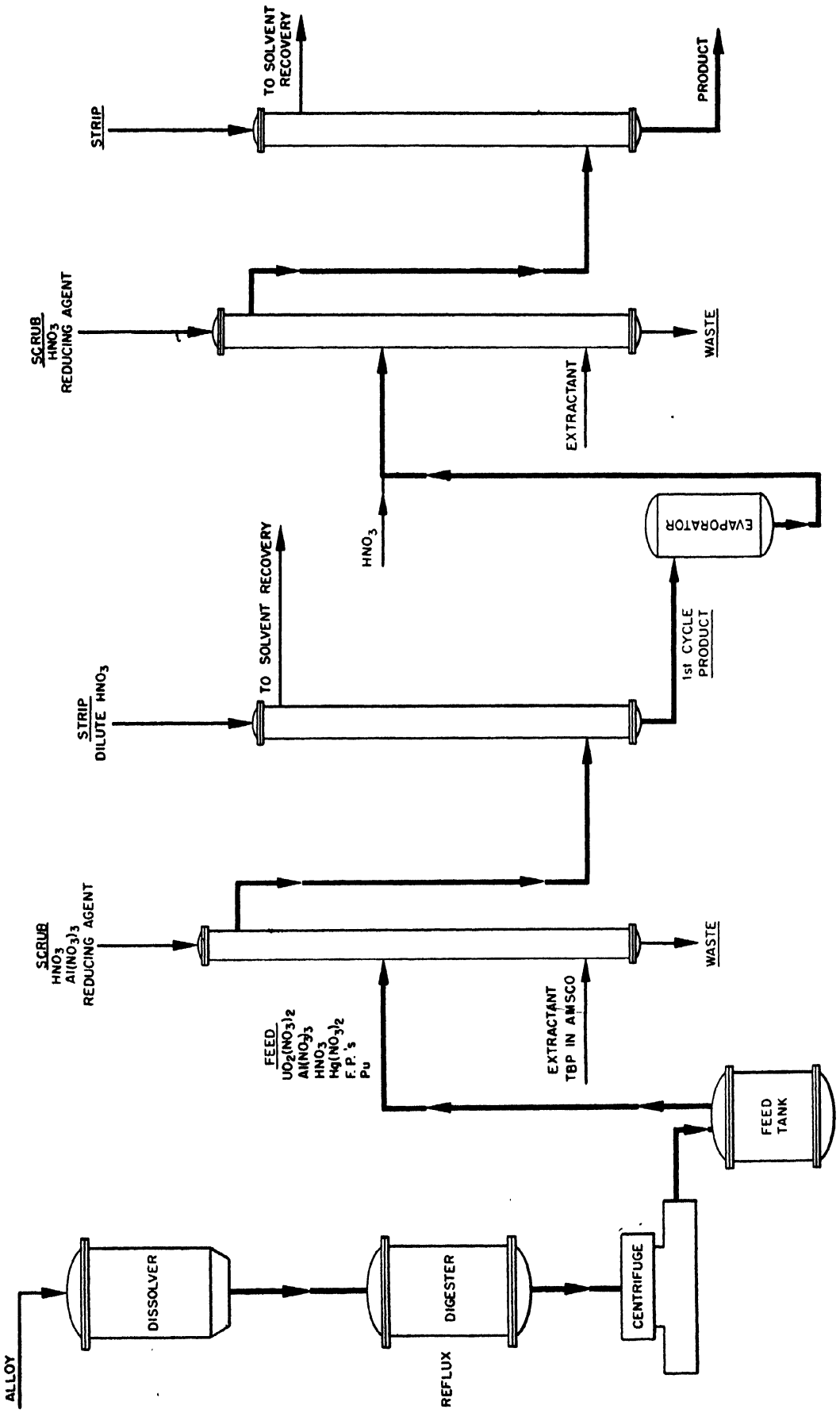

Figure 7. Schematic flowsheet, TBP-amsco extraction of uranium-aluminum alloy

Table II. Decontamination of Enriched Uranium

	Decontamination factors*		
Constituent	*First cycle*	*Second cycle*	*Over-all*
Gross β	1.1×10^4	2.6×10^3	2.9×10^6
Gross γ	7.0×10^3	2.3×10^3	1.6×10^6
Pu α	20	90	1.8×10^3

* The decontamination factor is defined as the fission-product activity/unit of uranium in the feed divided by the fission-product activity/unit of uranium in the product.

aluminum. This solvent offers the following advantages over hexone: (1) higher β and γ decontamination factors; (2) higher flash point in solvent; (3) less reactivity with concentrated nitric acid; (4) lower mutual solubility between aqueous and organic phases. Fuel dissolution and feed preparation for a TBP flowsheet are similar to the steps described for the hexone process, except that acid rather than acid-deficient conditions are used. Acid conditions are necessary to prevent emulsion formation in the solvent-extraction column. The TBP process for uranium-aluminum alloy processing is a modification of the TBP extraction process for plutonium and uranium reviewed by Flanary.[5] The chemical nature of the solvent extraction is discussed in the above reference along with data on diluents, solvent stability, solvent treatment, and performance of uranium and fission products. The process conditions and laboratory test results with high levels of activity for a TBP uranium-aluminum alloy process have been established. A schematic flowsheet is shown in Fig. 7.

Uranium losses are consistently low in the solvent extraction and solvent recovery wastes. Plutonium decontamination factors exceed 10^4 and possibly 10^5. Solvent can be recycled after simple washing with 0.1 *M* sodium carbonate, followed by a water wash in an extraction column similar to the primary solvent extraction unit. Two cycles of solvent extraction are adequate to decontaminate uranium to background activity level.

The TBP extraction process can be used, with minor modifications, to recover and decontaminate uranium from solutions containing fuel diluents other than aluminum.

This process yields the following over-all decontamination factors in laboratory-scale apparatus:

	1st cycle	*2nd cycle*
Gross β	3×10^5	$>3 \times 10^3$
Gross γ	1.5×10^3	2.5×10^6
Pu	$>1 \times 10^4$	$> 10^2$

ENGINEERING DESIGN AND EQUIPMENT DISCUSSION

A discussion of the type of equipment used and operating experience in a direct maintenance plant which separates uranium from irradiated uranium-aluminum-alloy fuel elements is given by Reid and Lemon.[6] A more general discussion of the types of equipment used, the maintenance provisions, general engineering concepts, and relative cost data are given in a survey paper by Culler.[7] Harty[8] has published a paper describing generally the engineering approach to the design of remotely maintained solvent extraction plants. Sege and Woodfield have published articles dealing with a pulse column for use in uranium solvent extraction.[9,10] Thornton[11] has recently published information on pulse column variables. The general literature contains many excellent papers on solvent extraction theory and on the performance of different types of solvent extraction contactors. Jealous and Johnson[12] have published a paper on power requirements in pulsed extraction columns. Coplan, Davidson, and Zebroski have described a pump-mix mixer-settler which can be used as a solvent extractor in radiochemical processing.[13]

REFERENCES

1. Lawroski, S., *et al,* work on the Redox Process at Argonne National Laboratory.
2. Foster, D. L., Wymer, R. G. and Savolainen, J. E., P/547, *Nuclear Reactor Fuel Dissolution,* Volume 9, Session 21B, these Proceedings.
3. Bruce, F. R., P/719, *The Solvent Extraction Chemistry of Fission Products,* Volume 7, Session 9B.1, these Proceedings.
4. Cathers, G. I., P/743, *Radiation Damage to Radiochemical Processing Reagents,* Volume 7, Session 11B, these Proceedings.
5. Flanary, J. R., P/539, *Solvent Extraction Separation of Uranium and Plutonium from Fission Products,* Volume 9, Session 21B, these Proceedings.
6. Reid, D. G. and Lemon, R., P/543, *Experience with a Directly Maintained Solvent Extraction Plant,* Volume 9, 21B, these Proceedings.
7. Culler, F. L., P/822, *Survey of Solvent Extraction Processes,* Volume 9, Session 21B, these Proceedings.
8. Harty, W. M., *The Design Philosophy of Remote Operation and Maintenance of Separation Facilities,* Chemical Engineering Progress Symposium Series, *50,* No. 13 (1954).
9. Sege, G. and Woodfield, F. W., *Pulse Column Variables,* Chemical Engineering Progress, *50*: (August 1954).
10. Sege, G. and Woodfield, F. W., *A Louver-Plate Redistributor for Large-Diameter Pulse Columns,* Chemical Engineering Progress Symposium Series, *50,* No. 13 (1954).
11. Thornton, J. D., *Recent Developments in Pulse Column Techniques,* Chemical Engineering Progress Symposium Series, *50,* No. 13 (1954).
12. Jealous, A. C. and Johnson, F. H., *Power Requirements for Pulse Generation in Pulse Columns,* Industrial and Engineering Chemistry (June 1955).
13. Coplan, B. V., Davidson, J. K. and Zebroski, E. L., *The Pump-Mix Mixer-Settler, A New Liquid-Liquid Extractor,* Chemical Engineering Progress, *50* (August 1954).

Solvent Extraction of Plutonium from Uranium Irradiated in Atomic Piles

By B. Goldschmidt,* P. Regnaut,† I. Prevot,‡ France

SUMMARY

Description of the conditions for separating plutonium, fission products and uranium by selective extraction of the nitrates by tributyl phosphate diluted by a paraffin hydrocarbon, comprising a simultaneous extraction of plutonium and uranium, followed by re-extraction of plutonium after reduction by hydrazine and by ferrous sulfamate, and re-extraction of uranium.

Since the decontamination ratios are insufficient in this first stage, decontamination processes are also described which make is possible to obtain separately the desired ratios for uranium and plutonium by means of another extraction cycle with the same solvent, followed by precipitation of uranium oxalate and plutonium oxalate. Finally, a description is also given of the beginning of the operation, which consists of dissolution of the active uranium in nitric acid with the addition of oxygen (which makes possible nitric acid economy, avoids the release of nitrous fumes and makes possible the recovery of the gaseous fission products). A description is also given of the final concentration of the fission products in the form of a concentrated solution, after destruction of nitric acid by the addition of formaldehyde.

INTRODUCTION

The purpose is the separation (as complete as possible) of plutonium, uranium more or less depleted in U^{235}, and fission products. In particular, the decontamination of uranium and plutonium by removing the γ-radioactive fission products must reach a ratio of 10^6 to 10^7, so that their subsequent treatment without any protection against γ rays might later be countenanced.

The volume of the solution of the fission products will be reduced as much as possible in order to facilitate storage.

The method is based on the solubility of uranium and plutonium nitrates in the oxygenated organic solvents.

As early as 1942, Seaborg and his team on the Chicago Metallurgical Project had decided that the solvent extraction method was one of the general methods most readily applicable to this difficult problem.

One of us (B. Goldschmidt) who had had the good fortune of working at that time with Seaborg, went back in 1944 to the solvent extraction process in the course of work carried out by the Chemistry Division of the Anglo-Canadian Atomic Energy Group. This work led to a plutonium extraction process which later was used industrially. In all these studies, one of the difficulties encountered was the need for using a mineral nitrate as a salting-out agent in the aqueous phase in order completely to extract the uranium into the solvent.

Our attention was drawn in 1951 to publications relating to the extraction of metals by tributyl phosphate (see bibliography of important articles at the end of this paper) and, in particular, to the fact that this solvent could extract uranyl nitrate without a salting-out agent. We then decided to study the possibility of using this solvent for the extraction of plutonium. In view of the favorable results obtained in preliminary tests, we devoted the main efforts of our team from 1951 to 1953 to perfecting the process described in this paper, which has been working perfectly on an industrial scale since 1954 on uranium rods corresponding to a reactor power of 500 kw per tonne of uranium. This industrial adaptation of the method was carried out by the St. Gobain Company which built the plutonium extraction plant of our Marcoule Center.

GENERAL

Properties of Tributyl Phosphate (TBP)

(*a*) It does not require any salting-out agents, which facilitates subsequent concentration of the fission products to a small volume.

(*b*) It extracts uranyl and plutonium(IV) nitrates remarkably well, and only a small fraction of those of the fission products.

(*c*) It is not sensitive to concentrated nitric acid or to radiation.

(*d*) Without any drawback for extraction, it can be mixed with other organic liquids which normally do not dissolve uranium. This makes it possible, by reducing its viscosity and density, to improve separations.

(*e*) It is neither volatile nor inflammable at ordinary temperatures.

Original language: French.

* Directeur du Département de Chimie au C.E.A.

† Chef du Service Plutonium au C.E.A.

‡ Service Plutonium au C.E.A.

These special properties are due to the fact that this is not a simple solvent, but rather a complexing agent. With the nitrates, complexes such as: $UO_2(NO_3)_2 \cdot 2TBP$ and $Pu(NO_3)_4 \cdot 2TBP$ are obtained.

We studied the extraction of uranium, plutonium and fission products in the laboratory. We used various diluents such as debutylether and xylene, and finally adopted a saturated hydrocarbon fraction with a high boiling point (170/240°C), having a specific gravity of 0.750, which has the advantage of giving, with tributyl phosphate, a practically non-inflammable mixture of low specific gravity.

Extraction of Uranium and Plutonium

We give in Table I a few particularly characteristic results (in all the following, the values indicated for nitric acidity and uranium or plutonium contents refer to the aqueous phase in equilibrium with the solvent).

Table I. Uranium Extraction

(a) As a function of uranium concentration: Solvent used; TBP 40% in a paraffin compound diluent; nitric acidity, 2N

U concentration (gm/liter)	*Distribution coefficient for U* $(C_{org.}/C_{aq.})$
10	5.7
50	2.6
100	1.45
250	0.62
400	0.39

(b) As a function of acidity

U content (gm/liter)	*Nitric-acidity (Normality)*	*Distribution coefficient for U* $(C_{org.}/C_{aq.})$
10	0.6	3.3
	1.5	4.3
	2.0	5.7
	3.0	7.2
50	0.6	2.1
	1.5	2.4
	2.0	2.6
	3.0	2.7
400	0.6	0.38
	1.5	0.39
	2.0	0.39

The results for plutonium extraction (Table II) were obtained with a solvent containing 33% tributyl phosphate.

The solutions used are nitric solutions of plutonium in the oxidized condition (valency IV, and exceptionally VI).

We noted no influence of the plutonium concentration up to a concentration of 500 mg/liter. Under the influence of reducing agents (hydrazine, hydroxylamine, ferrous sulfamate), plutonium is trivalent. In the absence of a carrier, Pu(III) has but a small distribution coefficient. It remains practically in the aqueous phase.

Table II. Plutonium Extraction

(a) Plutonium alone: influence of acidity

Acidity (normality)	*Distribution coefficient*
0.5	1.05
1.4	2.3
2.8	10.0

(b) Plutonium in the presence of uranium: influence of U concentration (acidity 2N)

U content	*Distribution coefficient*
0	5.5
50	0.21
350	0.18
420	0.10

(c) Influence of sodium nitrite

	Acidity	*Distribution coefficient*	
		without nitrite	*with nitrite*
Pu alone	1.8 *N*	0.39	0.68
Pu in presence of U (50 gm/l)	3 *N*	4.8	8.0

Total Extraction of Fission Products

After four to six months of decay, the fission products consist essentially of long-lived products (cesium, strontium, rare earths, zirconium, niobium, ruthenium).

It is known that, in this group of elements, tributyl phosphate can extract only the rare earths, the zirconium, the niobium, and possibly ruthenium.

At low acidities (less than 2 *N*), and in the presence of strong uranium concentrations, the distribution coefficients dropped very rapidly.

As an indication, Tables III and IV are a few values obtained on uranium solutions irradiated for one year, after six months of decay. The values of the two tables refer to β-activity. In fact, analyses have shown that the entrained activity was due ex-

Table III. Influence of Uranium Concentration (Acidity: 2N) on Fission-Product Extraction

U concentration (gm/liter)	*Over-all decontamination coefficient*
0	8.5×10^{-3}
10	3.1×10^{-2}
50	2.1×10^{-2}
100	1.7×10^{-2}
250	1.6×10^{-2}
400	1.6×10^{-2}

Table IV. Influence of Acidity on Fission-Product Extraction (100 gm/l U)

Acidity (normality)	*Over-all decontamination coefficient*
0.6	1.4×10^{-2}
2.0	1.7×10^{-2}
3.0	2.6×10^{-2}

clusively to zirconium-niobium (γ-emitters, 0.75 Mev, soft β). Thereafter, if decontamination is calculated with respect to γ-activity, values of the order of 1 to 2 $\times 10^{-2}$ are obtained, the acidity and uranium concentration acting in the same way as for β particles.

Conclusion

Taken as a whole, the above results show that:

(*a*) The distribution coefficients decrease in the direction: uranium, plutonium, fission products, with a very low value for the latter.

(*b*) The presence of uranium considerably reduces plutonium and fission product extraction.

(*c*) The increase in the acidity brings about an increase in extraction for all elements, an influence which is less and less perceptible as the uranium concentration increases.

(*d*) The presence of an oxidizing agent such as NO_2^- enhances plutonium extraction.

(*e*) Trivalent plutonium is practically not extracted at all, except for the very strong acidities or in the presence of a salting-out agent.

Bearing these findings in mind, we have designed our process, which consists of two principal stages:

(*a*) Tributyl phosphate counter-current extraction of an aqueous solution obtained by nitric dissolution of irradiated uranium. The ratios of the outputs are so calculated as to get an outlet solvent which has the highest possible uranium concentration. Under these conditions, fission products decontamination is a maximum. Plutonium is quantitatively extracted, but accumulates in large quantities in the extractant, due to the poor distribution coefficients of the element in the presence of a great deal of uranium.

(*b*) The uranium- and plutonium-containing solvent is treated by a reducing aqueous solution. Use is made of hydrazine at the low plutonium concentrations, and of a hydrazine-sulfamate mixture at high concentrations.

Plutonium, reduced to the trivalent state, returns to the aqueous solution, and is thus separated from uranium.

DESCRIPTION OF THE PROCESS

The process consists of the following phases: (1) separation of the rod from the cladding, (2) nitric dissolution of the rod, (3) solvent extraction of the uranium and plutonium, (4) reducing re-extraction of plutonium, (5) concentration of the aqueous solution of the fission products, (6) aqueous re-extraction of uranium, and recovery of the solvent, (7) concentration of the plutonium, and (8) final purification and decontamination of the plutonium.

Cladding Separation

One may use: (*a*) either a mechanical technique, which has the advantage of being independent of the metal used for the cladding, or (*b*) a chemical process: for aluminum cladding, sodium hydroxide; for magnesium cladding, 0.5*N* nitric acid.

Nitric Dissolution

The rods are dissolved by 12*N* nitric acid at boiling temperature (approximately 110°C). The reaction begins only at the boiling point, and considerable heating is needed at the start. Thereafter, since the reaction is exothermal, the external heat needed is small.

Adding oxygen during the reaction makes it possible to reoxidize the nitrous vapors produced. This reoxidizing phenomenon is not instantaneous, and takes place only at a low temperature. It is made quantitative by operating as follows:

The equipment used for dissolution is surmounted by a condenser column. The oxygen supply is adjusted so as to suppress the release of gases. The amount of oxygen needed gives information as to the status of the dissolution process.

The method§ has three main advantages: (*a*) nitric acid consumption is a minimum, namely 2 moles of acid per atomic weight of uranium; (*b*) a warning is given at the end of the reaction; and (*c*) any production of nitrous vapors is avoided, and it is possible to recover gaseous fission products such as krypton and xenon.

Following cooling off, the solution is adjusted to the optimal concentrations for extraction, namely uranium, 1.65*M* and nitric acid 1.7*N*. The temperature of crystallization is below 10°C.

Extraction

The solvent used is made up of tributyl phosphate diluted to 40% in a saturated hydrocarbon which has a high boiling point.

Tributyl phosphate must be very pure and, particularly, free of mono- and dibutyl acids, which favor the extraction of zirconium and niobium.

The operation is carried out by counter-current process, in a battery of six mixer-separators. The solvent recovered at the outlet is washed again in two additional mixer-separators by 3 or 4*N* nitric acid which re-extracts approximately 70% of the fission products entrained. The acid used for this washing is re-introduced one stage after the aqueous phase entrance.

The ratio of solvent/aqueous phase is kept at about 2.8 so as to obtain an output solvent containing a uranium concentration.

This output solvent contains the whole of the uranium and at least 99.8% of the plutonium. It carries approximately 5% of the β-activity, and 1% of the γ-activity.

Plutonium Re-extraction

Plutonium reduction is carried out in a battery of four mixer-separators. The aqueous output phase, which contains Pu(III), is treated in two mixer-separators by fresh solvent in order to remove the uranium(VI) which has followed the plutonium in the aqueous phase.

§ This method was developed in our laboratory by P. Faugeras.

The reducing solution used depends on the plutonium concentration.

For low plutonium concentrations, use is made of a hydrazine solution having the following characteristics: acidity, 0.2*N*; hydrazine, 0.3*N*.

However, we noted that this re-extraction, which is rapid and nearly complete up to 1 γ/cm^3, decreases very rapidly when the plutonium concentration increases (95% for 1 γ/cm^3–50% for 10 γ/cm^3–30% for 50 γ/cm^3).

Thus, it is necessary to use a reducing agent which acts faster than hydrazine. We chose ferrous sulfamate, and used for concentrations of 2γ and above, the following solution: acidity, 0.2*N*; hydrazine, 0.3 *N;* ferrous sulfamate, 0.0025*M*.

We purposely reduced the sulfamate concentration as low as possible in order not to load unduly the final plutonium solution with iron.

The presence of hydrazine seems to prevent any unduly rapid reoxidation of the ferrous salt.

The acidity must be low, in order to favor re-extraction of the plutonium, but it must not fall below 0.1*N*, in order to avoid plutonium hydrolysis.

The re-extraction affords a first concentration of plutonium. The following ratios are taken for the outputs of the various phases: charged solvent/washing solvent = 2.5; total solvent/aqueous phase = 7.0.

The contact times in the mixers were about 3 minutes, and the separation times about 20 minutes.

Fission Product Concentration

The solution of fission products coming from the extraction is concentrated by distillation, and its volume reduced by a factor of approximately 100. This can be done either with two evaporators in series or else by successive evaporations of various charges in a single evaporator.

The first method is to be preferred, since it makes it possible to work on a smaller total activity.

During evaporation, the nitric acid is concentrated and reaches 13*N*, which causes difficult corrosion problems for the equipment. In order to rule out this difficulty, we designed a technique which makes it possible continuously to destroy the nitric acid:

Use is made of formaldehyde which reduces nitric acid on warming, according to the following reaction:

$$3\,HCHO + 4\,HNO_3 = 3\,CO_2 + 5\,H_2O + 4\,NO$$

In fact, formic acid is used as an intermediate product. Indeed, formic acid is found again in the solution when the final acidity is below 0.8*N*.

The reaction can start of itself, when large quantities of concentrated acid and formaldehyde are mixed. However, a certain time may elapse before it starts. Then it can run away.

In order to avoid any runaway reaction, it is necessary that the quantity of one of the two reagents remain very small.

In order to avoid any delay at the start, it is desirable to operate at a temperature higher than 85°C, and, if necessary, to start the reaction with nitrous vapor.

In practice, the process is carried out as follows:

The liquid to be concentrated is brought to the boiling point, after which a 30% formalin solution is injected continuously, starting the reaction with a trace of sodium nitrite. The formalin output is so adjusted as to follow the evaporation step by step; the nitric acid concentration must always remain close to normal.

Finally, a concentrated solution of the fission products, which can be stored as is, is obtained, or else it can be reduced to the solid state by total evaporation or adsorption on clay.

The activity of the distillates is 10^{-4} to 10^{-5} times that of the solution of the fission products at the start. This seems to be due to mechanical entraining phenomena.

Re-extraction of Uranium, and Solvent Recovery

Uranium is re-extracted by water, using 2 volumes of water for each volume of solvent. This operation is carried out, counter-currently, in a battery of six mixer-separators. The process is completed by a sodium carbonate wash, which retains the last traces of uranium and absorbs the small quantities of mono- or dibutyl acid which might have been formed by hydrolysis of the solvent. The outgoing solvent is recycled.

The uranium is treated in order to reduce residual contamination. Solvent extraction can be repeated.

To this end, the aqueous phase due to the extraction of the solvent (which has a concentration of approximately 0.25*M* uranium) is concentrated by evaporation to the initial characteristics (U = 1.65 *M*, free HNO_3 : 1.7*N*).

It is treated counter-currently in a new battery of mixer-separators, as was explained in connection with the initial solution. Note that the absence of plutonium makes it possible to make the battery lighter, and to take out one plate at least.

The solvent thus obtained then is re-extracted into twice its volume of water.

From this last solution, uranium finally is recovered by oxalic acid precipitation.

Since the zirconium and niobium oxalates are soluble in an acid medium, a new decontamination factor of approximately 20 is obtained thereby. However, we observed that the most quantitative precipitation of uranium was obtained with some excess of oxalic acid (1.2 to 1.5 moles per atomic weight of uranium). Following precipitation, the supernatant solution will still contain approximately 4 gm of uranium (element) per liter.

The initial acidity of the solution has but very little influence on precipitation.

The centrifuged and washed uranium oxalate then is dried at a temperature of 125°C. This gives an oxalate monohydrate. More complete calcination (temperature above 310°C) in a reducing atmosphere causes the transformation into the oxide UO_2, from which it is easy again to get to the fluoride UF_4, then to the metal by reduction with calcium.

Plutonium Concentration

The aqueous solution from the re-extraction contains all the plutonium (approximately 0.5 gm/l). Sodium hydroxide is added. A uranate precipitate is formed and carries down the plutonium hydroxide. Precipitation must be carried out at a pH of 8 or 9. Any substantial excess of alkali causes the precipitate to be peptized and makes separation difficult.

The mother liquors are separated by centrifuging. The precipitate is then re-dissolved by nitric or hydrochloric acid, according to the techniques adopted for subsequent purification. These techniques, which can be used alone or in combination, are: (*a*) solvent extraction (tributyl phosphate); (*b*) oxalic acid precipitation; (*c*) ion exchange resins; and (*d*) solvent extraction of various complexes.

The precipitation conditions for (*a*) and (*b*) are much more severe for plutonium than they are for uranium. They are substantially the following: acidity, 0.7*N* nitric acid or hydrochloric acid; oxalic acid, 2.2*M* per atomic weight of plutonium. Small variations around these values bring about a noticeable loss of plutonium due to solubility.

The zirconium and niobium oxalates remain in solution, as well as a large part of possible inactive impurities such as iron.

The interest of the method lies in the solubility of plutonium oxalate in an acid medium, which makes it possible to make several successive precipitations. Each one of these reduces the residual γ-contamination by a factor approximately 20.

On the other hand, plutonium is finally obtained in a form which is practical for its subsequent utilization.

For (*c*), anion exchange resins are the most used. In particular, tetravalent plutonium forms, in a nitric solution, an anionic complex $Pu(NO_3)_6^{2-}$ which is fixed very well on the resins of the quaternary ammonium type.

Along the lines of (*d*), solvent extraction of various complexes, use may be made of the plutonium complexes with the β diketones and fluorinated diketones (TTA). Plutonium gives complexes with these products which can be extracted by aromatic hydrocarbon or chlorinated solvents. Purification is obtained by working in a well-defined pH range.

The quaternary ammonium salts form complexes of the $Pu(NO_3)_6(NR_4)_2$ type with plutonium(IV) in nitric solution, and these can also be extracted in chlorinated or aromatic solvents.

The quaternary ammonium salts which we used are of the

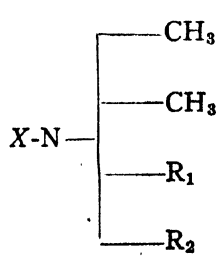

type, in which R_1 and R_2 are paraffin radicals containing 8, 10 or 12 carbon atoms. These salts are soluble in a number of solvents, such as chloroform or benzene.

On mixing such an organic solution with a nitric acid solution of plutonium, the latter is extracted while uranium is extracted only in very small quantities.

Some results obtained with didecyldimethylammonium are given in Tables V and VI. Analysis shows that the entrained activity consists almost entirely of ruthenium.

Table V. Influence of Reagent Concentration in the Organic Phase*

Reagent concentration	*Pu distribution coefficient*	*U distribution coefficient*
1%	0.4	0.012
2%	0.5	0.022
3%	2.2	0.034
4%	5.0	0.044
5%	8.0	0.053

* Aqueous phase used: Pu(IV) nitrate (U = 300 gm/liter, free acidity : 0.8 *N*). Reagent: benzene solution of quaternary ammonium.

Table VI. Influence of Uranium Concentration*

U concentration gm/liter	*Pu distribution coefficient*	*β-activity distribution coefficient*
125	50	5.5×10^{-3}
250	45	3×10^{-3}
375	6.1	10^{-3}
500	1.4	

* Aqueous phase used: solution of uranium which has been irradiated for a year and then allowed to decay for 6 months. Free acidity: 0.8 *N*. Reagent: benzene solution containing 10% quaternary ammonium.

The distribution coefficients for uranium, plutonium and the fission products increase with acidity. This increase is particularly important for plutonium, particularly in the vicinity of the neutral point.

Even at neutrality, plutonium and uranium remain completely in the aqueous phase.

These results account for the operating technique used: an aqueous nitric acid plutonium phase 0.8*N* in free acidity, which can contain up to 300 gm/liter of uranium, is extracted by a 5% benzene solution of didecyldimethylammonium nitrate. Counter-current operation is employed.

The solvent phase which contains the plutonium then is rewashed twice: (1) volume for volume, by a 0.8 *N* nitric acid solution, which reextracts approximately 70% of the entrained uranium and 10% of the plutonium; (2) by half its volume of neutral water, which re-extracts all of the remaining plutonium (90%).

CONCLUSION

The above-mentioned treatment makes possible the extraction of plutonium with an efficiency of more than 97%.

Uranium is recovered with a minimum yield of 99%.

The decontamination ratios for β- and γ-emitters reach values of the order of 10^6 and 10^7 for the two products.

REFERENCES

1. Warf, J. C., *Extraction of cerium (IV) nitrate by butyl-phosphate,* AECD 2524 (1947), declassified on March 11, 1949.
2. Anderson, Marion R., *Distribution of thorium nitrate between water and a mixture of butyl phosphate and butyl ether,* ISC 116, USA 8, 8 2147 (1950).
3. Moore, L. R., *The mechanism of extraction of uranium by T. B. P.,* AECD 3196 (1951).
4. Hahn, H. T., *The mechanism of uranium extraction by T. B. P.,* NSA 9, 2, 585 (1954).
5. Peppard, D. F., Gray, *Séparation du Cm et du Pu par T. B. P.,* US Pat. 2, 683-655 (July 1954).
6. Hall, G. R., *Séparation de l'Am du Pu par T. B. P.,* J. Chem. Soc., p. 2214 (1954).
7. Segré, G. and Woodfield, F. W., *Pulse column variables —solvent extraction of uranyl nitrate with T. B. P. in a 3 inches diameter pulse column,* Chem: Eng. Prog.— symposium série n° 13, 50, 179 (1954).
8. Ohlgren, Lewis and Weech, *Reprocessing reactor fuels,* Nucleonics p. 18 (March 1955).

The Extraction of Uranium and Plutonium with Tetrabutylammonium Nitrate, Cupferron and Neocupferron as Complexing Agents

By E. Haeffner, G. Nilsson and A. Hultgren,* Sweden

In recovering fissionable material from uranium fuel elements, it is often of interest to have methods for the separation of relatively small amounts of plutonium from uranium, not only for industrial use but also in the laboratory for analytical or preparative purposes. Solvent extraction has proved to be a useful tool for the separation of actinide elements in all these respects. With a multi-stage countercurrent extraction process a fractionation of even closely related elements may be obtained. The selectivity of the extraction can in many cases be increased by the use of an organic complexing agent. There are many organic substances known to form chelate compounds with uranium and plutonium which can be used for extraction purpose. In studying these matters, a series of extraction experiments has been done with TBAN (tetrabutylammonium nitrate) cupferron, (nitrosophenyl hydroxylamine ammonium) and neocupferron (nitrosonaphthyl hydroxylamine ammonium) as complexing agents. Part I of this paper describes the TBAN experiments, and part II deals with factors influencing the chloroform extraction of the cupferron and neocupferron complexes.

TETRABUTYLAMMONIUM NITRATE AS COMPLEXING AGENT

Synthesis

As tetrabutylammonium nitrate could not be obtained commercially it was synthetized in the following way. First tetrabutylammonium iodide (TBAI) was made from tributylamine and butyl iodide according to the reaction:

$$(C_4H_9)_3N + C_4H_9I = (C_4H_9)_4NI$$

The solution was heated to 80–90°C for a few minutes. Tetrabutylammonium iodide crystallized after cooling the solution to room temperature. The yield after 24 hr at room temperature is 50–60%, but it can be considerably increased as tetrabutylammonium iodide is continuously crystallizing. The raw product was purified by recrystallizing twice from a water solution. The resulting product has a melting point of 146–147°C. The solubility is about 30 gm/l at 30°C and about 90 gm/l at 85°C.

From TBAI the TBAN was produced by a reaction with silver nitrate,

$$(C_4H_9)_4NI + AgNO_3 = (C_4H_9)_4N \cdot NO_3 + AgI$$

The silver nitrate solution was added to the heated TBAI-solution under agitation. AgI was removed by filtration and the TBAN extracted by chloroform. The chloroform was evaporated and the product dried at 80–90°C. The end product had the melting point 118–119°C. The yield of the last reaction was about 80%.

EXPERIMENTAL

The distribution of uranium between chloroform and a water solution containing uranyl nitrate, tetrabutylammonium nitrate (TBAN), nitric acid and, in some experiments, ammonium nitrate, has been studied while varying the concentration of each of the mentioned constituents.

The water solutions were prepared by adding calculated amounts of the following six standard solutions:

1. A solution of $UO_2(NO_3)_2 \cdot 6H_2O$ containing 300 mg U/ml. The solution was analysed by a gravimetric and a colorimetric method.
2. 5.05 *M* HNO_3. Standardized by titration with 0.02 *M* NaOH and phenol red as indicator.
3. 14.53 *M* HNO_3. Standardized by titration with 0.02 *M* NaOH and phenol red as indicator.
4. TBAN-solution containing 500 mg/ml, standardized by weighing.
5. 10.0 *M* NH_4NO_3 solution, standardized by weighing.
6. Pu(VI)-solution containing 4 μg Pu/ml.

A volume of 5 ml of the aqueous solutions, containing the intended amount of solutes, was vigorously shaken for 3 min with the same volume of chloroform in a graded centrifuge tube. The phases were then separated by centrifuging for 3–4 min. The volume of the organic phase increased and the water phase decreased according to the amount of U-TBAN complex extracted. At TBAN-concentrations of 100 mg/ml and 150 mg/ml the change in volume of the aqueous phase was respectively 12% and 18%. At the addition of TBAN to the uranyl nitrate solution the U-TBAN complex precipitated but dissolved again in the chloroform phase.

* Aktiebolaget Atomenergi, Department of Physics, Stockholm, Sweden.

ANALYSIS

At small concentrations of uranium, 4 ml were taken for analysis from each phase, but usually 2 ml were sufficient. To these 2 ml, concentrated H_2SO_4 was added in a Kjeldahl-flask, which was heated until the evolution of SO_3 fumes. In about 15 min 3 ml portions of concentrated HNO_3 were carefully added and heated until all nitrous fumes had disappeared. The content was then again oxidized with a few portions of 3 ml 30% H_2O_2 and the clear yellow solution analysed according to the colorimetric method described by Davenport and Thomason.[1] The following procedure was used:

An aliquot of the solution containing 1.0–1.5 mg U was transferred to a 25 ml volumetric flask. Ammonia was then added to alkaline reaction and 2 ml of a 10% solution of ammonium thioglycolate was added. After the addition of 2 ml $NH_3(1+1)$, the volumetric flask was filled to the mark with water. The extinction of 1 cm solution was measured in a colorimeter (Fisher Electrophotometer, Fisher Scientific Co., Pittsburgh, Pa, USA) with a blue filter at 425 mμ and within 30 minutes after the addition of thioglycolate. After a correction proportional to the H_2SO_4 content, the method gave good results.

Each value was measured five times with zero correction of the instrument between readings. Good linearity was found up to a concentration of 1.6 mg U in 25 ml.

In all distribution experiments both phases were analysed and the result was controlled by noting the phase volumes and comparing the amount of uranium found in both phases with the amount of uranium initially added. In most cases all uranium was found within 1–3%, which is the accuracy of the volume readings.

Activity Measurements

From each phase in the plutonium distribution experiments 100 or 250 λ were taken and evaporated on aluminum disks. Ammonium nitrate and organic matter were then decomposed and destroyed in a furnace at 600°C. The activity was measured in an α-scintillation counter. The plutonium initially added

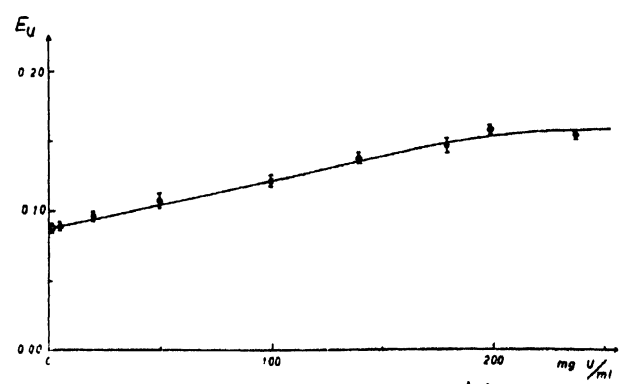

C_{HNO_3} = 163 M C_{TBAN} = 50 mg/ml

Figure 1. Diagram showing E_U as a function C_U^{aq}

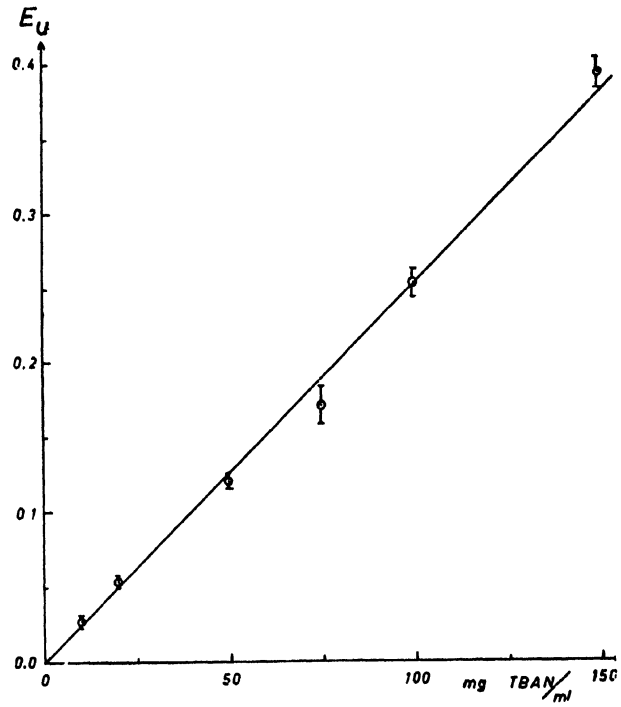

C_{HNO_3} = 163 M C_U = 240 mg/ml

Figure 2. Diagram showing E_U as a function of C^{aq}_{TBAN}

to the water phase was usually recovered within 2% in the two phases after the distribution experiment. In some experiments activity measurements were used also for the analysis of uranium.

Results

The following type of abbreviations is used:

C_U^{org} = concentration of uranium in the organic phase

C_{TBAN}^{aq} = concentration of TBAN in the aqueous phase before extraction, unless otherwise stated.

In the first series of experiments the distribution of uranium between chloroform and a water solution initially containing 50 mg TBAN/ml and 1.63 *M* HNO_3 was studied. The result is given in Fig. 1, which shows the distribution factor for different concentrations of uranium in the water phase. When the uranium concentration increases, the distribution factor (E_U) slowly increases to reach a limiting value of 0.15.

In Fig. 2 the value of the distribution factor for different concentrations of TBAN is shown. The concentration of nitric acid and uranium in the water phase before extraction was kept constant. It is found that the distribution factor is proportional to the concentration of TBAN.

In Fig. 3 the results of another two series of measurements are given. The distribution factor has been determined for different concentrations of free nitric acid. In this case the distribution factor approaches a limiting value of 0.34 when the initial concentration of C_{TBAN} is 50 mg/ml (0.164 *M*), and 0.9 when the

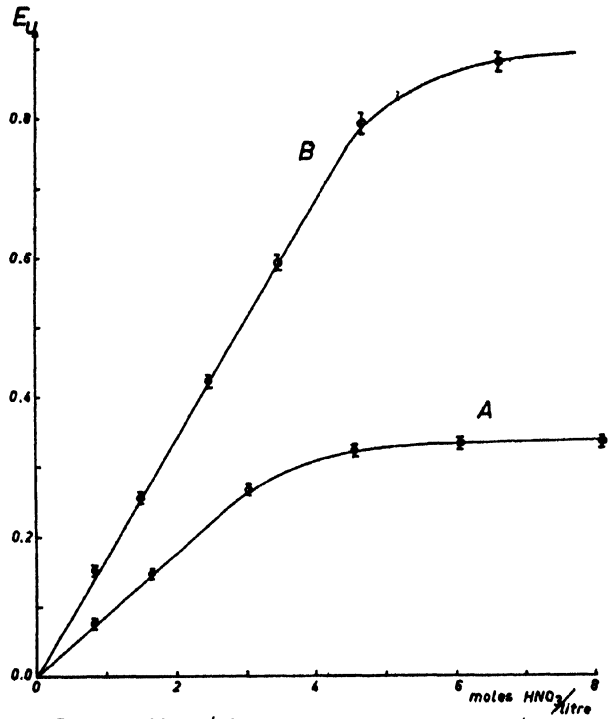

Figure 3. Diagram showing E_U as a function of $C^{aq}_{HNO_3}$

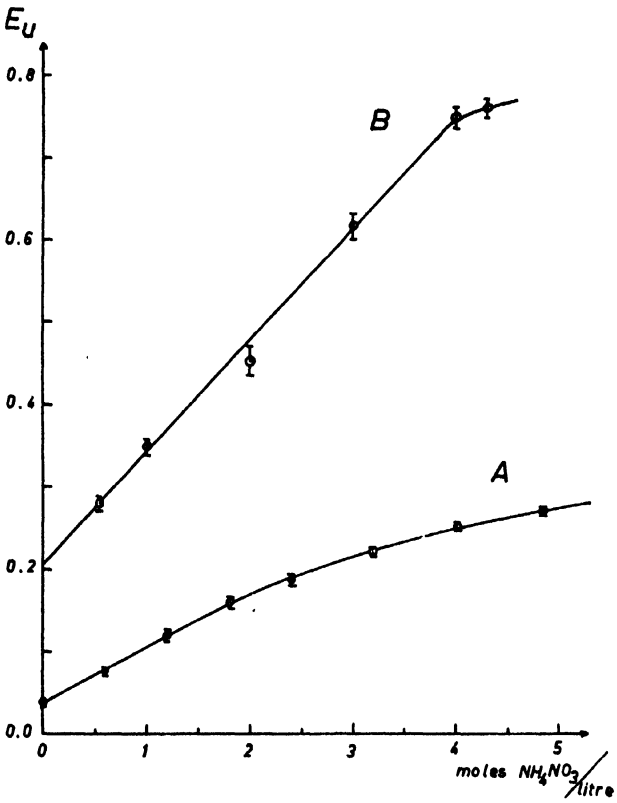

Figure 4. Diagram showing E_U as a function of $C_{HN_4NO_3}$

TBAN concentration is 100 mg/ml. The concentration of uranium was 120 mg/ml before extraction in both cases.

In the next two series of experiments, ammonium nitrate was added to the aqueous phase in different amounts, while the concentrations of uranium, TBAN, and, when present, nitric acid were kept constant. The distribution factor is given in Fig. 4.

The concentration of nitric acid and ammonium nitrate were co-ordinated in the following experiment in such a way that $C_{HNO_3} + C_{NH_4NO_3} = 7$ M and the partition of uranium and plutonium was measured at different pH. The TBAN concentration was 50 mg/ml in the uranium experiment and 25 mg/ml in the plutonium experiment.

Because of the high extraction efficiency, the percentage of plutonium found in the organic phase was chosen as ordinate in Fig. 5 instead of the distribution factor. The uranium values are given in the same way for comparison. As the TBAN concentration was only 25 mg/ml in the plutonium experiment, uranium values for this TBAN concentration have been calculated and are shown in the dotted curve in Fig. 5. The calculation is based on the result given in Fig. 2, and equal phase volumes are assumed. As the phase volumes are only approximately equal, the dotted curve is not exactly true, but gives an indication of the possibilities of separating uranium and plutonium under the conditions mentioned.

Finally, some extraction experiments were performed with different TBAN concentrations; first with plutonium alone, then with both plutonium and uranium in the same solution. The analysis was done by measuring the activity from uranium and plutonium separately in a 24-channel pulse analyser.[2] The results are shown in Table I where the extracted fractions of uranium (calculated from the results previously given in Figs. 1, 2 and 5) are also shown for comparison with the values actually found.

The ratio, R, between the fractions of plutonium and uranium extracted has evidently a maximum at a TBAN concentration of about 2 mg/ml. The R-values are, however, strictly valid only for the uranium concentration used, 6 mg/ml and will decrease somewhat with increasing uranium concentration. The decrease is due to the simultaneously increasing distribution factor for uranium.

Discussion

It is possible to define a thermodynamic partition coefficient p_A^T as the ratio between the activities of a solute A, distributed between two immiscible solvents a and b

$$p_A^T = \frac{[A]_a\,(f_A)_a}{[A]_b\,(f_A)_b} = p_A\,\frac{(f_A)_a}{(f_A)_b} \qquad (1)$$

At low concentration the ratio $(f_A)_a/(f_A)_b$ is close to unity and within a small concentration range it is nearly constant. The observed partition coefficient is thus practically independent of the solute concentration under these conditions.

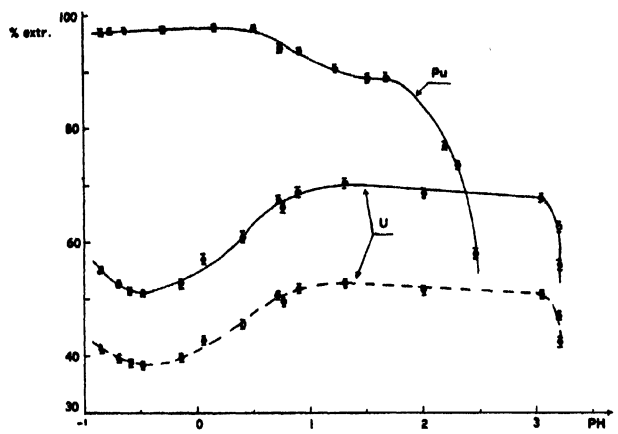

C_{TBAN} = 25 mg/ml C_U = 24 mg/ml
C_{Pu} = 4400 cpm/ml $C_{HNO_3} + C_{NH_4NO_3}$ = 7.0 M

Figure 5. Diagram showing the fraction of U and Pu extracted versus acidity

Equation 1 is valid only for molecular species or ions common to both phases. If dissociation or association occurs in one or both phases, the ratio $[A]_a/[A]_b$ is not independent of the total solute concentration in either phase.

For the practical use of solvent extraction the prime interest is, however, to know the fraction of a certain solute present in one phase. This fraction can be characterized as the distribution factor E_A and thus represents the ratio between the analytically determined total concentrations $(C_A)_a$ and $(C_A)_b$ of element A in the two phases a and b. In the experiments described, the distribution factor for uranium, E_U, and for plutonium, E_{Pu}, has been determined by the extraction of water solutions of different compositions.

Summarizing the results it is found that E_U is linearly dependent on the initial HNO_3, TBAN, and, when NH_4NO_3 is present, also NH_4NO_3 concentrations. It is also found that E_{Pu} is much larger than E_U at certain conditions (Fig. 5 and Table I).

Uranyl nitrate is very soluble in many alcohols, esters, ethers, and ketones but insoluble in chloroform or other halogenated compounds. Although uranyl nitrate is a strong electrolyte in dilute water solution, changes in the absorption spectrum of the UO_2^{++} ion on the addition of nitrate ions[3] support as Irving[4] points out the hypothesis of covalent bonding between UO_2^{++} and NO_3^- rather than that of ion pair association. Measurements of the osmotic coefficient in saturated solutions of uranyl nitrate indicate that up to 20% of undissociated $UO_2(NO_3)_2 \cdot aq$ may be present.[5] The formation of covalent bonds between uranyl and nitrate ions is consistent with the existence of the ion $UO_2(NO_3)_3^-$ and the formation of the double nitrates $UO_2M(NO_3)_3$ and $UO_2M_2(NO_3)_4$, where M can be NH_4, $N(CH_3)_4$ or $N(C_2H_5)_4$ among others.

On the basis of these facts and the experimental results it seems highly probable that the complex entering the chloroform phase can be written $UO_2N(C_4H_9)_4(NO_3)_3$ or $UO_2[N(C_4H_9)_4]_2(NO_3)_4$ with the addition of water or solvent molecules to fill the coordination number.

CUPFERRON AND NEOCUPFERRON AS COMPLEXING AGENTS IN NITRIC ACID SOLUTION

Cupferron is rapidly destroyed in nitric acid solutions, and this acid has therefore been avoided in cupferron extraction processes. As cupferron, however, has shown good separation properties in other acid media and the processing of uranium fuel elements often takes place in the presence of nitric acid, it is of interest to study the rate of decomposition and the possibilities of using cupferron as a complexing agent in spite of its destruction by nitric acid.

Neocupferron has not been so extensively studied as a chelating agent but it can be expected to behave as cupferron in most respects. It seems, however, to possess properties which make it more suitable than cupferron in nitric acid solutions.

Trivalent and tetravalent plutonium can be extracted as cupferrates from an aqueous acid solution to a chloroform phase, whereas hexavalent plutonium does not extract equally well.[6] As far as is known,

Table I

	Pu alone Activity cpm/100*			*Pu + U†*													
				Org. phase					*Aq. phase*								
C_{TBAN} *mg/ml*	*Org. phase*	*Aq. phase*	*% Pu extr.*	*λ in sample*	*Tot cpm*	*% Pu*	*cpm Pu*	*cpm U*	*λ in sample*	*Tot cpm*	*% Pu*	*cpm Pu*	*cpm U*	*% Pu extr.*	*% extr. found*	*% extr. calc.*	*R*
0.2	0.5	138.1	0.3	–	–	–	–	–	–	–	–	–	–	–	–	0.23	~1
1.0	13.7	132.3	9.40	250	40.4	68.7	27.8	12.6	50	218.9	25.9	56.7	162.2	9.82	1.55	1.78	6.3
2.0	61.6	89.0	40.9	100	62.9	83.4	52.4	10.5	50	203.0	22.6	45.9	157.1	36.4	3.34	3.51	10.9
5.0	123.8	26.3	82.5	100	138.5	78.1	108.2	30.3	50	150.8	10.8	16.3	134.5	76.9	10.1	8.3	7.5
10.0	137.3	10.3	93.0	100	193.1	71.8	138.7	54.4	50	139.8	4.38	6.1	133.7	91.8	16.9	15.4	5.4
25	From Fig. 5		97.7	50	169.4	71.6	121.6	47.8	50	107.3	2.5	2.5	104.8	98.0	31.2	31.2	3.1

**Pu alone*
C_{Pu} ≃ 1450 cpm/ml
C_{HNO_3} = 3 M
$C_{NH_4NO_3}$ = 4 M

†*Pu + U*
C_{Pu} ≃ 1450 cpm/ml
C_U = 6 mg/ml
C_{HNO_3} = 3 M
$C_{NH_4NO_3}$ = 4 M

$$R = \frac{\%\ \text{Pu extr.}}{\%\ \text{U extr.}}$$

no extraction experiments on plutonium using neocupferron as chelating agent have been reported.

The separation obtained with a chelating agent of this type is, among other things, a function of the concentration of chelating agent and the acidity. As, however, the cupferrates are destroyed by nitric acid, the amount extracted is also a function of time, i.e. the time between the addition of complexing agent and the extraction of the metal complex to the chloroform phase. When dissolved in the chloroform phase the complex is not so rapidly destroyed by nitric acid.

Experimental

Owing to the small amount of plutonium available, the volume of the aqueous phase was limited to one or two millilitres. To this water phase, which contained trace amounts of plutonium, nitric acid and, in some cases, iron, a water solution of the complexing agent was added. The solution contained in a test tube was shaken in a mechanical shaker for five seconds and was then allowed to stand a predetermined time. After that time the aqueous phase was vigorously shaken for one minute with an equal volume of chloroform, and then the phases were separated by centrifuging the test tube for five minutes. Increasing the shaking time had very little effect on the amount of plutonium extracted.

The content of plutonium in the chloroform phase was determined by evaporating 0.1 ml chloroform on an aluminum disk, destroying organic matter at 600°C, and measuring the activity in an alpha scintillation counter. From a measurement in the same geometry of the specific activity of the Pu stock solution, the extracted fraction of plutonium could be calculated.

To purify the commercially available qualities of cupferron and neocupferron, they were recrystallized several times from methanol before use. New aqueous solutions of the reagent were prepared for every experiment and the chloroform used was of analytical grade.

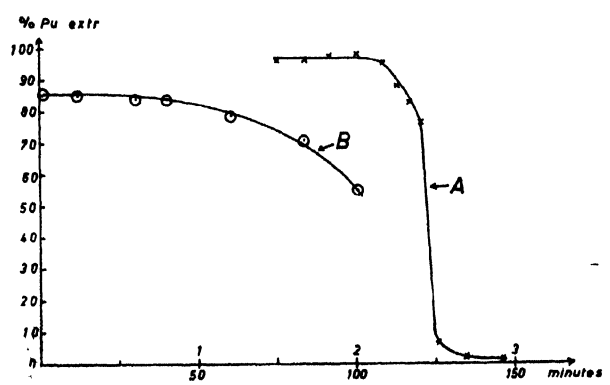

A = Cupferron (upper time scale)
B = Neocupferron (lower time scale)

Figure 6. The extraction of Pu as a function of the time interval between the addition of complexing agent and the start of extraction

Results

In the first three series of extractions, (Figs. 6, 7 and 8), the fraction of plutonium extracted was determined as a function of the time interval between the addition of complexing agent and the start of extraction.

In Fig. 6 cupferron and neocupferron are compared under identical conditions. The complexing agents had in these experiments a concentration of 0.014 *M* in a 1.9 *M* nitric acid solution.

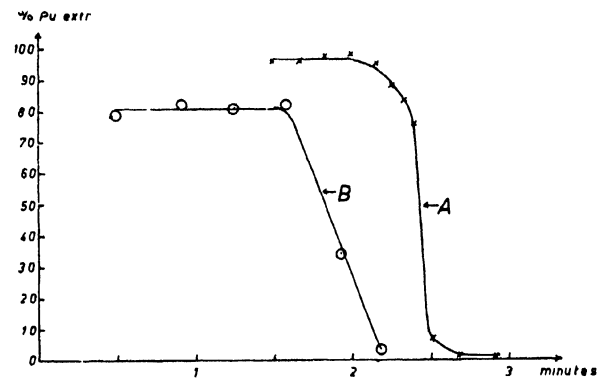

A: 0.014 M Cupferron; 1.9 M HNO_3
B: 0.014 M Cupferron; 1.9 M HNO_3 and 0.0025 M Fe

Figure 7. The fraction of Pu extracted from a water solution

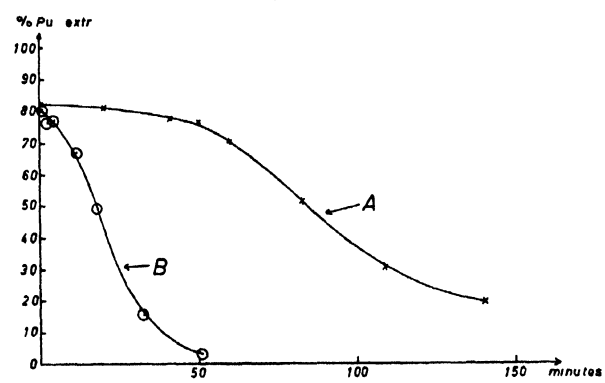

A: 0.0023 M Fe; 0.014 M Neocupferron; 1.9 M HNO_3
B: 0.0023 M Fe; 0.014 M Neocupferron: 3.7 M HNO_3

Figure 8. The fraction of Pu extracted from a water solution

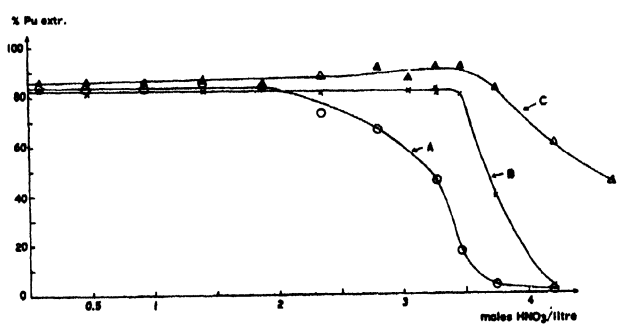

A: 0.01 M Neocupferron
B: 0.06 M Neocupferron
C: 0.0167 M Fe(Neocupferron)$_3$ + 0.01 M Neocupf. in excess = 0.06 M Neocupferron

Figure 9. The fraction of Pu extracted after a time interval

The addition of iron (0.0025 M) in an aqueous phase of the same composition as above has the effect of decreasing the fraction of plutonium extracted by cupferron as shown in Fig. 7.

Figure 8 gives the result of extractions intended to show the effect of increasing the nitric acid concentration at constant iron and neocupferron concentrations.

Another series of experiments was performed in exactly the same way except that the time interval was fixed at one minute and the nitric acid concentration was varied. The results are shown in Fig. 9.

Discussion

From the extractions plotted in Fig. 6 it is seen that cupferron extracts plutonium slightly better than neocupferron but is much more sensitive to nitric acid. The time interval for good extraction is about twenty times greater in the neocupferron case.

The extracted amount of plutonium decreases when iron is added to the aqueous solution (Fig. 7). That this must be the case is shown as follows:

Making the simplifying assumptions that the water phase contains only the species NO_3^-, A^-, M_1A_n, M_2A_m, M_1^{n+}, and M_2^{m+}, and the organic phase only M_1A_n, M_2A_m, and HA, it is shown in the appendix that:

$$q = \frac{K_1^n\, K_3\, K_5\, V_o}{\left(\frac{[H_3O^+]^n}{[HA]_{aq}^n} + K_1^n\, K_5\right) V_{aq}} \qquad (2)$$

where

$$[HA]_{aq} = \frac{[HA]^0\, V_{aq} - m[M_2A_m]_o\, V_o}{K_2\, V_o} \qquad (3)$$

This is valid if M_1 is present in trace amounts only and $[HA]^0$, K_2 and K_4, are large. The symbols used in the equations have the following meaning: q = total amount of M_1 in org. phase/total amount of M_1 in aq. phase; M_1: Pu; M_2: Fe; HA: complexing agent; $[HA]^0$: initial concentration of HA in aqueous phase; V_{aq}: volume of aqueous phase; V_o: volume of organic phase; K_1: dissociation constant of HA; K_2: distribution factor of complexing agent; K_3: distribution factor of M_1A_n; K_4: distribution factor of M_2A_m; K_5: complexing constant of M_1A_n. Obviously $[M_2A_m]_o$ in Equation 3 decreases the value of q in Equation 2.

The extracted amount of metal ion, which is initially available in trace amounts in the aqueous phase, evidently decreases if macro amounts of another extractable ion are added. The effect is also seen if curve B in Fig. 6 is compared with curve A in Fig. 8.

Table II

HNO_3 M	Fe mg/ml	U mg/ml	Neocupf. conc.	% Pu ex.	% U ex.
0.467	0.935	10.7	[illegible]	94.4	0.28
3.05	0.935	10.7	0.06	90.9	Undetectable

Increasing the neocupferron concentration ($[HA]_o$) makes it possible to extract the plutonium in more acidic solutions. This follows from Equation 2 and is seen experimentally in Fig. 9. If neocupferron is added partly as $Fe(Neocupf.)_3$, a slightly better extraction is obtained (Fig. 9).

Less than 1% uranium(VI) is extracted to a chloroform phase by neocupferron in the nitric acid concentration range 1–4 M. The results of two experiments with uranium(VI) and Pu present are given in Table II.

Owing to the instability and complexity of the system it is hard to make any quantitative conclusions from the experiments. It is, however, obvious that neocupferron is more suitable than cupferron in nitric acid solutions and that a good separation from uranium(VI) is obtained.

APPENDIX

For the meaning of the symbols see preceding section. The following primary assumptions are made:

1. The only existing metal complexes are M_1A_n and M_2A_m.

2. The water phase contains only NO_3^-, H_3O^+, OH^-, A^-, HA, M_1A_n, M_2A_m, M_1^{n+} and M_2^{m+}.

3. The organic phase contains only M_1A_n, M_2A_m and HA.

4. Activity coefficients are unity.

Then the following relations are valid:

$$K_1 = \frac{[H_3O^+][A^-]}{[HA]} \qquad (1)$$

$$K_2 = \frac{[HA]_o}{[HA]_{aq}} \qquad (2)$$

$$K_3 = \frac{[M_1A_n]_o}{[M_1A_n]_{aq}} \qquad (3)$$

$$K_4 = \frac{[M_2A_m]_o}{[M_2A_m]_{aq}} \qquad (4)$$

$$K_5 = \frac{[M_1A_n]_{aq}}{[M_1^{n+}][A^-]^n} \qquad (5)$$

From the assumptions made, it follows that

$$q = \frac{[M_1A_n]_o\, V_o}{([M_1^{n+}] + [M_1A_n]_{aq})\, V_{aq}} \qquad (6)$$

Combining with Equations 3, 5, and 1 gives

$$q = \frac{K_1^n\, K_3\, K_5\, V_o}{\left(\frac{[H_3O^+]^n}{[HA]_{aq}^n} + K_1^n\, K_5\right) V_{aq}} \qquad (7)$$

Further,

$$[HA]^0\, V_{aq} = [HA]_o\, V_o + [HA]_{aq}\, V_{aq} + n[M_1A_n]_{aq}\, V_{aq} + n[M_1A_n]_o\, V_o + m[M_2A_m]_{aq}\, V_{aq} + m[M_2A_m]_o\, V_o + [A^-]\, V_{aq}$$

If M_1 is in trace amounts and $[HA]$ is large, this reduces to

$$[HA]^0 = [HA]_{aq} + [HA]_o\frac{V_o}{V_{aq}} + [A^-] + m[M_2A_m]_{aq} + m[M_2A_m]_o\frac{V_o}{V_{aq}}$$

Combining with Equations 2, 1, and 4 gives

$$[HA]^0 = [HA]_{aq}\left(1 + K_2\frac{V_o}{V_{aq}} + \frac{K_1}{[H_3O^+]}\right) + m[M_2A_m]_o\left(\frac{V_o}{V_{aq}} + \frac{1}{K_4}\right)$$

As K_4 is large, $K_2 \sim 10^2$, $K_1 \sim 10^{-5}$ and $[H_3O^+] > 10^{-2}$ this reduces to

$$[HA]_{aq} = \frac{[HA]^0 V_{aq} - m[M_2A_m]_o V_o}{K_2 V_o} \quad (8)$$

REFERENCES

1. Davenport, W. H., Jr. and Thomason, P. F., *Determination of Uranium (VI) in Presence of Anions,* Anal. Chem. *21*: 1093 (1949).
2. Dardel, G. V., *A Portable 24-channel Kicksorter,* AB Atomenergi, Dept. of Physics, Stockholm, Sweden (1954).
3. Betts, R. H. and Michels, Rita K., *Ionic Association in Aqueous Solutions or Uranyl Sulfate and Uranyl Nitrate,* J. Chem. Soc.: S286-294 (1949).
4. Irving, H. M., *Solvent Extraction and its Applications to Inorganic Analysis,* Quarterly Reviews *5*: 200-226 (1951).
5. Glueckauf, E. and McKay, H. A. C., *Possible F-shell Covalency in the Actinide Elements,* Nature *165*: 594 (1950).
6. Fryxell, R. and Kleinschmidt, R., *Some Factors Affecting the Cupferron Extraction Procedure for Estimation of Trace Amounts of Plutonium,* MDDC 461.

Solvent Extraction Separation of U^{233} and Thorium From Fission Products by Means of Tributyl Phosphate

By A. T. Gresky,* USA

A possible solvent-extraction process for separating and decontaminating thorium, U^{233}, and Pa^{233} from neutron-irradiated thorium uses nitric acid as the thorium dissolution agent, tri-*n*-butyl phosphate (TBP) as the extractant, and aluminum nitrate and nitric acid as the aqueous salting agents. The U^{233} is finally isolated by ion exchange.

The economics of nuclear power producers that utilize thorium–U^{233} breeding require that such a process recover more than 99% of the fissionable U^{233} and the source Th^{232}; recontaminate the U^{233} and thorium from highly radioactive or high cross-section fission products before it is used in the reactors, both for personnel safety and maintenance of good neutron economy; and be able to process the thorium after short cooling periods because of inventory charges on the valuable reactor fuel U^{233}. The last provision is significant and demands that the process efficiently separate and recover the highly radioactive Pa^{233} parent of U^{233}. This isotope, a β-γ emitter with a half-life of 27.4 days, will normally account for more than 95% of the β-γ radioactivity in the irradiated thorium at the time of reactor discharge. The complex thorium irradiation scheme, a U^{233} fission-product yield curve, and flux-time-production curves are shown in Figs. 1–5.

Since a basic requirement for this process is remote and continuous operability with short cooled feed material and/or decontamination and recovery of the short-lived Pa^{233}, a primary factor governing process design is the order of product separation. There are four products to be considered: U^{233}, thorium, Pa^{233}, and fission products, the last being treated as waste. In order to expose the process solvent to a minimum of radiation and to permit a minimum of heavy shielding for the equipment, the order chosen is: (1) separation of the highly radioactive protactinium and fission products from the uranium and thorium products; (2) separation of the thorium from the U^{233}, (3) isolation of the U^{233}.

The length of the cooling period prior to processing is important. Owing to the complicated chemistry of protactinium and the problems of physically handling large quantities of the radioactive Pa^{233}, long cooling periods before chemical processing would be favored, i.e., periods sufficiently long to ensure insignificant waste losses of potential U^{233} and a minimum radiation level in the process solutions. About 200 days would normally permit U^{233} losses of less than 0.5% and would also permit decay of the 24.1-day Th^{234} (UX_1 and UX_2) radioactivities, which would otherwise contribute to the background radioactivity in the thorium product. However, up to two years would be required to absolutely eliminate Pa^{233} radioactivity as a problem in β-γ decontamination of products. Such a period would pose significant inventory problems and would probably not be economically allowable. For this reason, the process was made sufficiently flexible to permit processing of either long or short cooled irradiated thorium.

PROCESS FLOWSHEET

The general characteristics of the process are given in the flowsheet, Fig. 6. The irradiated thorium metal, or oxide, is dissolved in a nitric acid solution containing fluoride ion as a catalyst. The thorium nitrate solution is adjusted to feed specifications and is introduced into the first column, where the thorium and U^{233} are extracted by the TBP; Pa^{233} and fission products remain in the aqueous phase. An aqueous scrub solution of acid-deficient† aluminum nitrate containing phosphate ion is introduced at the top of this column to remove small amounts of Pa^{233} and fission products from the organic product stream. The aqueous stream leaving the bottom of the column is concentrated by evaporation and is then introduced into a smaller recovery system where the Pa^{233} is removed on a carrier; fission products remain in solution and are routed to radioactive waste storage. The organic stream, containing the decontaminated thorium and U^{233}, flows continuously to the middle of a second column, where the thorium is preferentially stripped into dilute nitric acid solution introduced at the top of the column. An organic scrub stream is introduced into the bottom of this column to re-extract small amounts of U^{233} from the aqueous stream, and the latter proceeds to an evaporator for

* Oak Ridge National Laboratory. Including work by E. D. Arnold, M. R. Bennett, A. T. Gresky, W. T. McDuffee, J. E. Savolainen, R. P. Wischow, Oak Ridge National Laboratory; S S. Brandt, DuPont, Savannah River Plant, Ga.; D. C. Overholt, F. L. Steahly, Carbide & Carbon, South Charleston, W. Va.

† Refers to a deficiency of free nitric acid, in solutions of hydrolyzed nitrate salts, e.g., of aluminum or thorium. Such solutions may be considered to contain quantities of "basic" salts such as $Al(OH)(NO_3)_2$ or $Th_2(OH)(NO_3)_7$; however, they have acidic reactions, i.e., from pH 2.0 to pH 4.0.

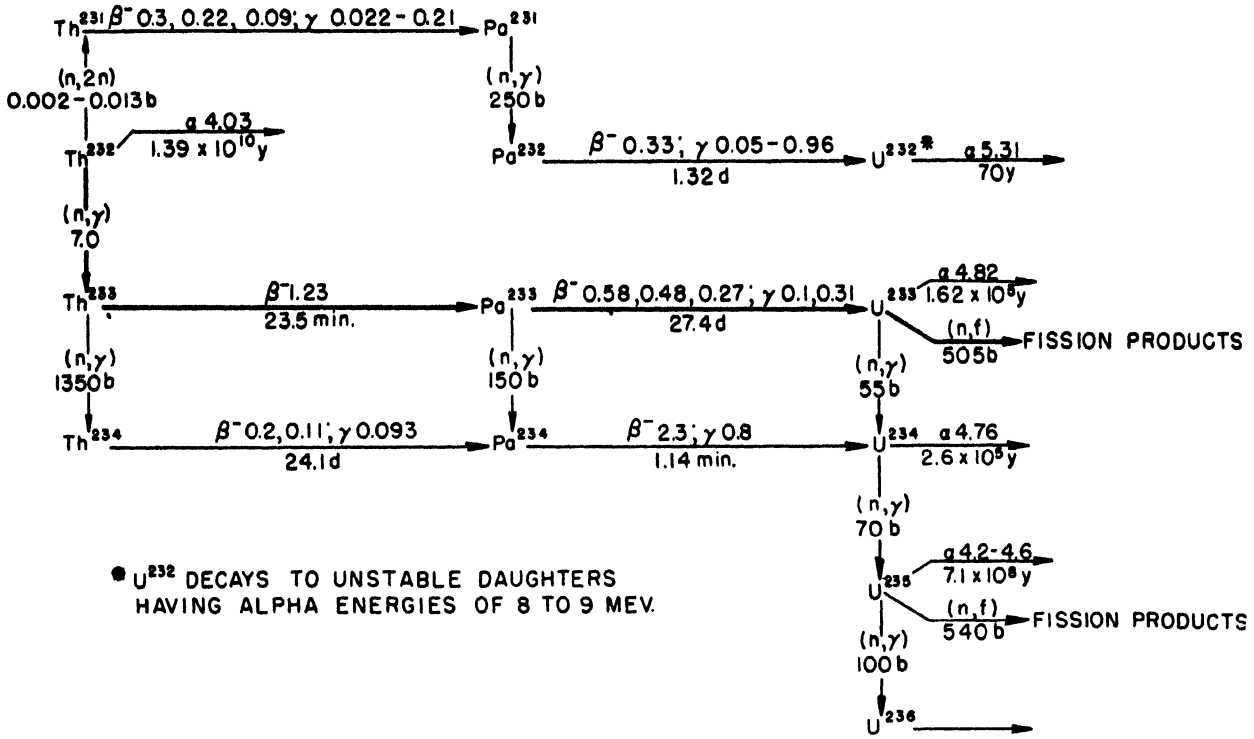

Figure 1. Nuclear reactions occurring in neutron irradiation of thorium

concentration of the thorium product. The organic stream, containing the U^{233}, flows continuously to the bottom of a third column, where the uranium product is stripped into a slightly acidic water solution and is then passed through an ion-exchange resin column for concentration and final purification. The organic stream finally flows continuously to a solvent-recovery column where acidic decomposition products of TBP are removed by washing with dilute sodium carbonate solution. The recovered solvent is centrifuged, and recycled in the process.

Results from laboratory countercurrent tests indicate that the thorium-U^{233} separation factor, i.e., the ratio of the relative concentrations of these elements in the feed and product streams, was about 10^4. The product decontamination factors obtainable through the solvent extraction cycles are shown in Table I. These values are based on laboratory data from countercurrent studies made at reduced activity levels.

Additional beta-gamma decontamination of the uranium product by a factor of about 10 is obtainable in the final ion-exchange isolation system. The concentrated thorium nitrate product will generally be stored for periods of time sufficient to permit decay of the Th^{234} and Pa^{233} contaminants.

Most of the Pa^{233} product is expected to be recoverable to carriers from the radioactive aqueous stream from the first extraction column. It is anticipated that the concentrated product will be stored in an appropriate system to permit its decay to U^{233}. The daughter U^{233} can then be readily extracted from the concentrates.

Thorium Dissolution

Aluminum-jacketed thorium slugs can be dissolved in a nitric acid solution containing fluoride and mercury. Essentially stoichiometric quantities of nitric acid are required to simultaneously dissolve the thorium and aluminum. The fluoride and mercuric ions are required to catalyze the thorium-nitric acid and the aluminum-nitric acid reactions, respectively. An excess of nitric acid appears to dissolve a highly stable thorium oxide impurity which is present in irradiated metal slugs. This material is deep-blue in color and resistant to attack by nitric acid, hydrofluoric acid, and aqua regia. It apparently develops as a result of electron displacement during neutron irradiation, which may explain the color phenomenon. No "blue thoria" has been encountered in dissolver solutions of unirradiated thorium; however, it is recognized that ThO_2 is a metallurgical impurity. Dissolution of this material was important since it represented potential process losses of both the thorium and the associated U^{233}. It also could plug filters or small equipment lines owing to its high density and fine particle size. In addition to dissolving the "blue thoria," the excess nitric acid permitted more rapid dissolution rates and provided optimum final solution conditions for the subsequent head-end treatment, or feed-preparation cycle.

Feed Adjustment and Digestion

The metal feed normally contains significant amounts of metallurgical impurities, such as elements and compounds of beryllium, silicon, calcium, mag-

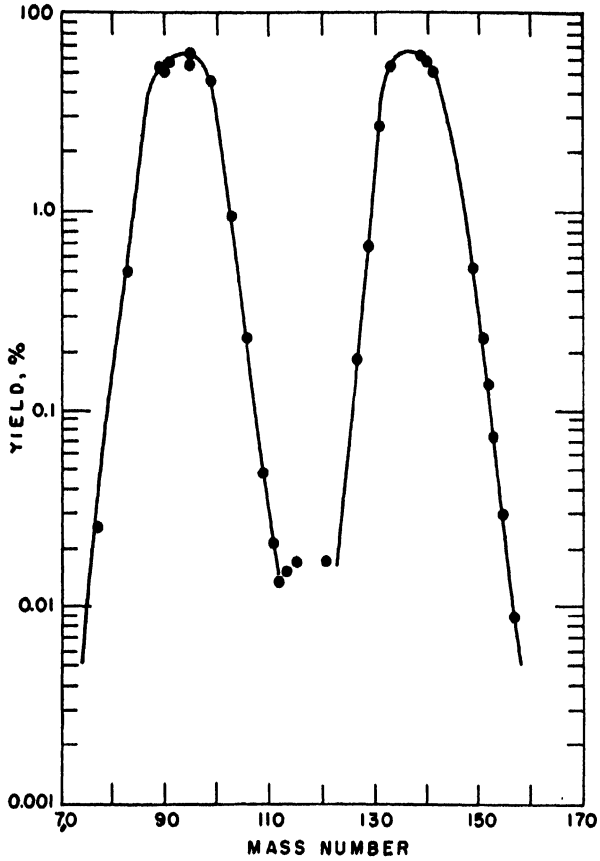

Figure 2. U^{233} fission product yield curve

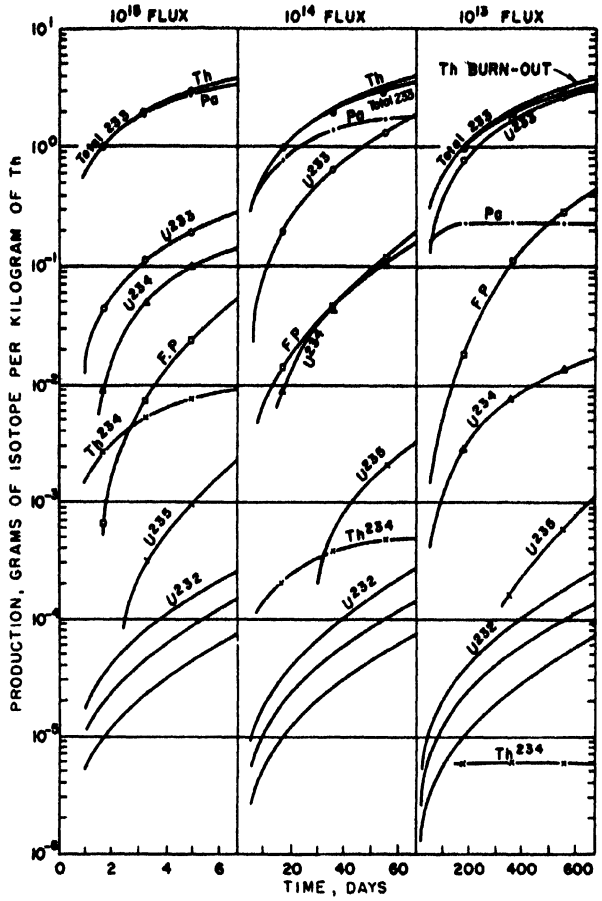

Figure 3. Summary of Th^{232} irradiation data

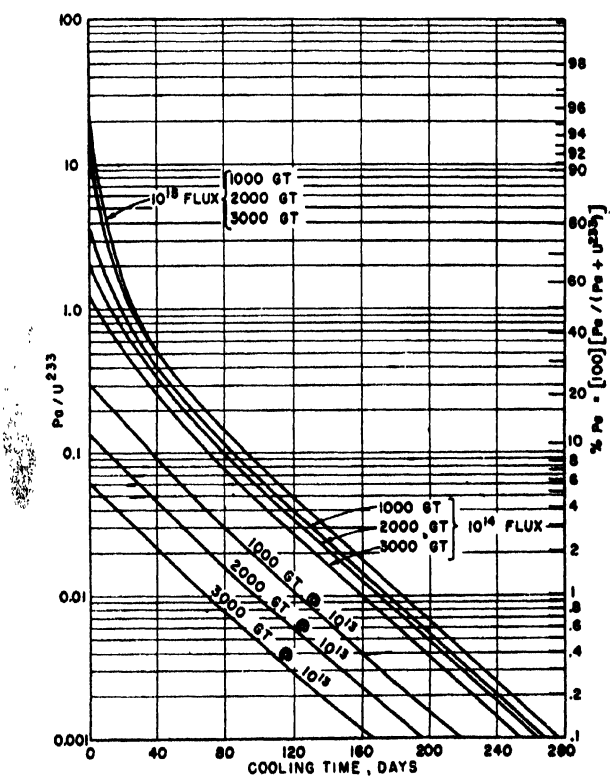

Figure 4. Effect of the extent of irradiation and cooling time on the Pa/U^{233} ratio. The "GT" level represents the grams of fissionable material produced per ton of source material

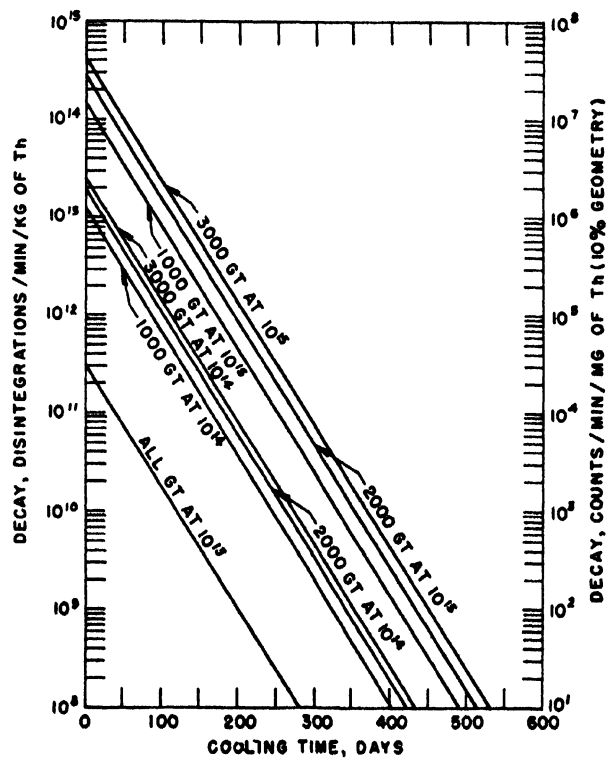

Figure 5. Decay of Th^{234}. (See Fig. 4 for explanation of "GT")

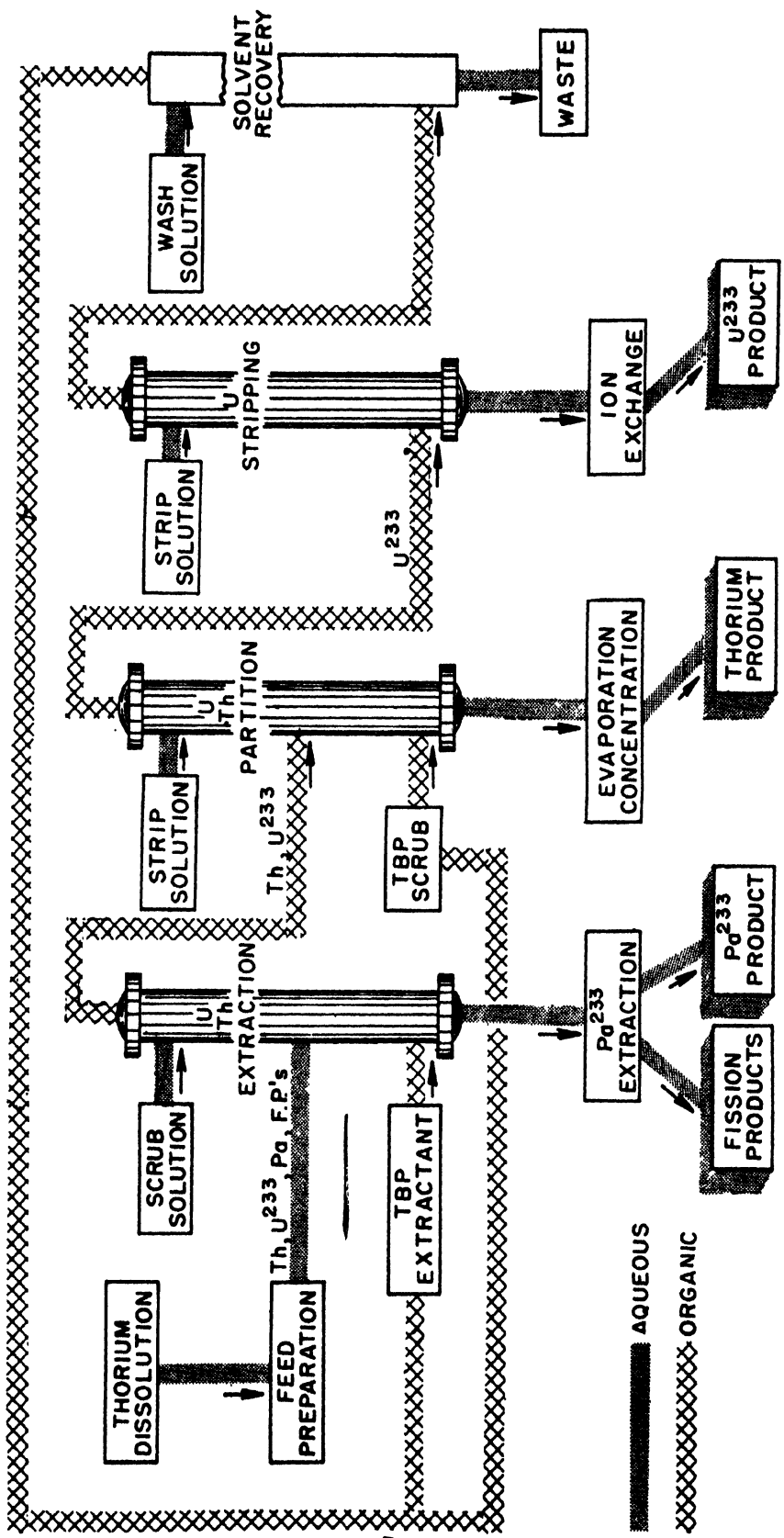

Figure 6. Process flow diagram for the separation of uranium from irradiated thorium

nesium, niobium, iron, chromium, and nickel, which are potential sources of trouble in the subsequent processing. Insoluble silicon compounds of these metals promote emulsions in the solvent extraction contractors, and some of these impurities are highly refractory claylike materials, which become distributed through the equipment and tend to become surface-active carriers of radioactivity. A feed treatment, consisting of dehydration of silicic acids and/or the dissolution of the clays, was developed to minimize these effects.

The excess nitric acid and a portion of the free acid, formed by the hydrolysis of the thorium and aluminum nitrates, are evaporated from the dissolver solution. Under these solution and temperature conditions, stable silicas are formed that are not harmful in the subsequent extraction cycle. The residual nitric acid-deficient thorium and aluminum nitrate solution of high concentration is then digested at an elevated temperature. Finally the solution is diluted with water to provide the conditions specified for the aqueous feed to the extraction column. The nitric acid condensate is recovered for use in the next dissolving operation.

Thorium and U^{233} Extraction and Pa^{233} Recovery

The aqueous feed is introduced near the middle of the extraction column; an aqueous scrub solution of aluminum nitrate, containing ferrous sulfate and phosphoric acid, enters at the top of the column. The extractant, TBP in an inert paraffinic diluent, flows upward through the column and extracts the thorium and U^{233}. The primary TBP-nitrate complexes of these elements are $Th(NO_3)_4 \cdot 4TBP$ and $UO_2(NO_3)_2 \cdot 2TBP$. The corresponding complex of nitric acid is $HNO_3 \cdot TBP$.

Table I. Solvent Extraction Decontamination Factors

	Decontamination factor	
Element	*Th product*	*U^{233} product*
Th^{234}		1×10^4
Pa^{233}	4×10^5	4×10^6
Total rare earths	1×10^5	2×10^6

The organic phase in the column becomes nearly saturated with thorium. This condition gives decontamination from the rare-earth fission products, which would be extracted in the presence of a large excess of TBP and which normally are extensively refluxed in the lower section of the extraction column. Owing to hydrolysis effects of the nitric acid-deficient conditions of the aqueous phase, the Pa^{233} and most of the troublesome fission products are not extractable; however, the aqueous scrub solution provides for additional removal of these from the product extract. Phosphate ion is included in the scrub solution to assist in decontamination from protactinium, and ferrous ion is included to prevent extraction of an oxidized chromium compound, a corrosion product, that is produced during the head-end treatment of the feed.

The aqueous phase from the extraction column contains aluminum nitrate, Pa^{233}, fission products, and other impurities. It is evaporated to permit minimum storage volume and/or the high aluminum nitrate concentrations that may be required for salting in subsequent Pa^{233} recovery cycles or for solvent extraction of the U^{233} daughter.

The optimum Pa^{233} extraction cycle has not been firmly established. Several alternate techniques have been considered, but the most practical evolved to date consists of adding sodium chromate, concentrating the stream by evaporation, and then filtering or centrifuging the resultant precipitate of basic aluminum chromate. A minimum volume of noncorrosive radioactive aqueous wastes results from this procedure, and the Pa^{233} is concentrated owing to the small volume of the carrier precipitate. The precipitate can be readily redissolved by acidification as may be required for subsequent processing steps. Decay of the Pa^{233} to U^{233} in the carrier or the extraction-column effluent before further processing is preferred; relatively simple solvent-extraction techniques are available for uranium recovery.

Thorium and U^{233} Partition and Thorium Recovery

The organic extract from the extraction column, containing Th^{232}, Th^{234}, U^{233}, and some contaminating Pa^{233} and ruthenium, flows continuously to the middle of the partitioning column. The thorium is stripped into an aqueous phase of dilute nitric acid, which flows down the column and is scrubbed by an organic stream of TBP in a hydrocarbon diluent introduced into the bottom of the column. Small amounts of U^{233} that are stripped into the aqueous phase are re-extracted by the organic scrub entering the bottom of the column; therefore, the aqueous effluent contains principally the thorium, including Th^{234}, along with smaller quantities of Pa^{233} and ruthenium. This stream is fed to a continuous evaporator which is designed to permit maximum distillation of the TBP that contaminates the product stream.

U^{233} Stripping and Recovery

The organic effluent from the partitioning column, containing all the U^{233} and, having a low nitric acid concentration, flows continuously to the bottom of the uranium stripping column. An aqueous phase of dilute HNO_3 is introduced at the top of the column and serves to strip the U^{233} from the rising organic stream. The aqueous effluent is then passed through (1) a silica gel column for removal of trace quantities of Pa^{233}, niobium, and zirconium, (2) a small column‡ containing a cation-exchange resin for retention of traces of thorium and corrosion products,

‡ This column initially becomes saturated with U^{233}, but this is gradually displaced by the more strongly sorbed thorium and corrosion products.

and (3) a larger column of cation-exchange resin for sorbing and further decontaminating the U^{233} produced.

The effluent from this column is discarded to chemical waste. When a sufficient quantity of U^{233} has been sorbed on the resin column, the product is eluted by a solution of ammonium acetate and acetic acid. The uranyl acetate is readily converted to other compounds as required by the user.

Solvent Recovery

The organic effluent from the stripping column is cascaded to a solvent-recovery column, where it is washed with sodium carbonate to remove nitric acid and acidic TBP decomposition products, i.e., mono- and dibutyl phosphates. As the solvent leaves this column, it is centrifuged to ensure removal of any entrained decomposition products and then is pumped to storage for recycle in the process system.

Practical Limitations of Solvent Extraction Processes

By R. E. Tomlinson,* USA

The practical application of basic process data to the construction and successful operation of a solvent extraction facility for the recovery of fissionable materials requires a thorough understanding of the process data and an appreciation for the types of processing problems likely to be encountered. The purpose of this paper is to discuss the types of problems encountered, with typical examples, and to discuss briefly the need for adequate piloting of a process before constructing a production facility.

DISCUSSION

The processing problems typically encountered in the operation of solvent extraction facilities may be grouped in the following categories: (1) the coexistence of two or more chemical compounds of a given element with widely different solvent extraction characteristics, (2) the process abnormalities engendered by the presence of hydrolysis products of process chemicals, (3) the presence of solid impurities which adsorb certain fission products and contaminate product solutions by entrainment, and (4) the presence of emulsifying agents which may severely reduce the operating rates and decontamination factors obtainable. These types of problems are discussed individually below.

CHEMICAL SPECIE

The process characteristics of a given fission product are frequently complicated by its coexistence in two or more chemical combinations with widely different extractabilities in a given solvent. This characteristic is sometimes further complicated by a relatively slow rate of transition from one chemical form to another, giving rise to a seemingly anomalous behavior pattern. Perhaps the best example of this phenomenon is that of ruthenium in the Redox process. Suppose a piece of irradiated uranium is dissolved in nitric acid and the solution mixed with aluminum nitrate solution to approximate the composition of the aqueous phase in the extraction section of a Redox IA contactor. If this solution is agitated with methylisobutyl ketone, commonly called hexone, a fraction of each chemical component present in the system is extracted into the hexone. At equilibrium, the ratio of the concentration of a given component in the hexone phase to the concentration of that component in the aqueous phase is called the distribution coefficient, designated as E_d^0. Under the conditions noted above, the distribution ratio for ruthenium would be observed to be about 0.005 to 0.01, some variation of this ratio resulting from differences in techniques used in preparing the initial solutions. If the hexone solution obtained above were rapidly and repetitively agitated with, and separated from, successive portions of an aqueous solution of aluminum nitrate simulating the scrubbing action of the IA Contactor, and the distribution ratio of ruthenium determined for the last contact, a value of approximately 10 would be obtained. If the two solutions from the last contact were held and recontacted the next day, a distribution ratio of about unity would be observed. This seemingly anomalous behavior is the result of at least three chemical forms of ruthenium being fractionated by the solvent extraction process and re-establishing equilibrium concentrations of the chemical species in each phase with time. A proposed explanation of these phenomena, with appropriate equilibria and rates of approaching equilibrium, is presented in Fig. 1.

It is thus evident that, while the "*A*" form of ruthenium constitutes less than one per cent of the total ruthenium present, it is the controlling specie with respect to the decontamination factor obtainable. The process must be engineered either to reduce the distribution ratio of this form of ruthenium to a value permitting its removal in the aqueous phase or to accelate its rate of change into another chemical form having a lower distribution ratio.

HYDROLYSIS

Hydrolysis phenomena may limit the efficacy of a given process in one of two ways. In one case, an element of process importance may undergo partial and reversible hydrolysis to produce a chemical form much less extractable than the unhydrolyzed form, the extent of the hydrolysis reaction being controlled by the hydrogen ion concentration. In the other case, a component in the system may be slowly and irreversibly hydrolyzed, with small concentrations of the hydrolysis products exerting pronounced effects on the distribution ratios of the elements being extracted.

As an example of the first case, the distribution ratios of uranium and plutonium in Redox-type systems are noted below, showing the dependence of these ratios on the pH of the aqueous phase.

* Hanford Atomic Products Operation. Including development work performed at Argonne National Laboratory, Hanford Atomic Products Operation, Knolls Atomic Power Laboratory, and Oak Ridge National Laboratory.

Table I. Distribution Ratio of Designated Elements in Redox-Type Systems. Aqueous phase: 1.0M $Al(NO_3)_3$, plus HNO_3 or NaOH. Organic phase: Methylisobutyl Ketone (Hexone)

pH of aqueous phase	*Distribution Ratio, E_a^0*		
	U(VI)	*Pu(VI)*	*Pu(IV)*
0.0	2.1	3.2	3.0
0.5	1.6	2.9	0.85
1.0	1.3	2.7	0.27
1.5	1.0	2.5	0.09
2.0	0.78	2.2	0.03
2.5	0.6	2.0	0.01

An inspection of Table I reveals that, while hexavalent uranium or plutonium may be extracted into hexone at relatively high pH, the tetravalent plutonium may be extracted only when the pH is held to a much lower value. The distribution ratios of some of the fission products, particularly ruthenium, exhibit a pH dependence similar to that of tetravalent plutonium, making it desirable to operate the Redox process at a high pH. The adequate recovery of plutonium at high pH thus requires that the plutonium be held in the hexavalent state by the use of an adequate oxidizing agent, taking care that the oxidizing potential is kept low enough to obviate the decomposition of the solvent.

In those processes employing tributyl phosphate as the solvent, the irreversible hydrolysis of tributyl phosphate assumes process importance. The rate of this hydrolysis is determined primarily by the concentrations of tributyl phosphate and hydrogen ion, and by the temperature of the system. The hydrolysis product dibutyl phosphate forms tight complexes with extractable ions such as uranium, plutonium, and zirconium; thereby increasing the carrying power of the solvent for these elements. This phenomenon tends to increase the losses of the products uranium and plutonium via the stripped solvent, and to increase the contamination of the recovered product by fission products such as zirconium. Any monobutyl phosphate formed may increase product losses by forming a precipitate with uranium or plutonium and carrying the product with the aqueous raffinate.

SOLID IMPURITIES

The successful operation of any solvent extraction process requires scrupulous cleanliness to minimize the presence of solids of small size. The presence of relatively large particles having a density greater than that of the aqueous phase may be tolerated if the contactor is designed to operate in their presence. Particles less than a few microns in diameter, however, tend to associate themselves with the interfaces of the dispersed and continuous phases, thereby tending to be carried by the dispersed phase. If these materials adsorb some of the radioactive ions, such as zirconium or niobium are adsorbed on siliceous materials, then these contaminants may be carried with the product stream and thus limit the decontamination factor obtainable.

EMULSIFYING AGENTS

The successful operation of a solvent extraction process requires successive, intimate contacts followed by a clean separation of the two phases. Many compounds, such as gelatinous materials, precipitates involving monobutyl phosphate, colloidal silica or alumina, etc., promote emulsification and hinder the separation of the two phases. The entrainment of contaminated aqueous phase in the solvent phase containing the desired products can seriously reduce the decontamination factor obtainable in that contactor. In severe cases, the degree of emulsification can prevent the countercurrent flow of the two phases

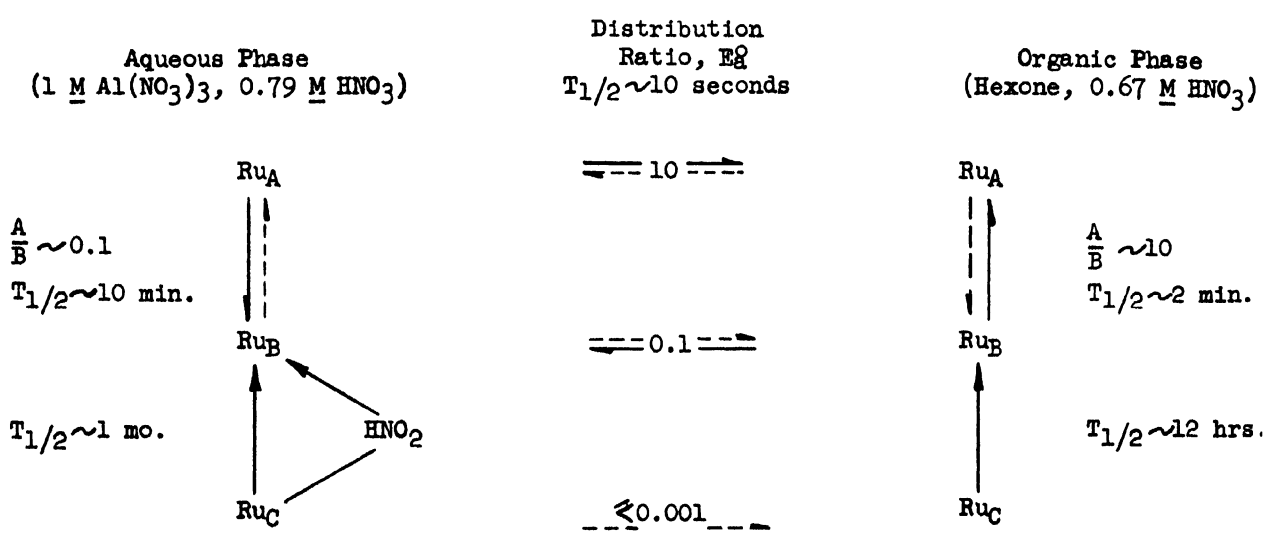

E_a^0: Ration of concentration in solvent to concentration in aqueous at equilibrium

$\frac{A}{B}$: Ratio of equilibrium concentrations of Species A to Species B in phase indicated

$T_{\frac{1}{2}}$: Half time to reach equilibrium

Figure 1. Proposed explanation of the behavior of ruthenium

through the contactor. Here, again, the solution of the problem lies in prevention by excluding the impurity which promotes emulsification.

PILOTING THE PROCESS

Many of the problems discussed above are of a type not necessarily observed in laboratory-bench-scale investigations, but prove to be serious impediments to the successful operation of a production facility. In many cases, the problem becomes apparent only after a process is in operation for many hours or days. When encountered, the definition and resolution of the problem may require extensive and continued experimentation. Should it be imperative that the process be utilized to produce an urgently needed product, the delays engendered by such problems may be very costly and embarrassing to the operating and development personnel. The best insurance that a given process will produce satisfactorily is obtained by constructing and operating a pilot plant prior to the start-up of the production facility and, preferably, prior to its design and construction. The cost of such a pilot plant program is usually recovered via decreased plant modification costs and increased productivity from the start of production plant operations.

The Chemical Processing of Aqueous Homogeneous Reactor Fuel

By D. E. Ferguson,* USA

The successful operation of the experimental homogeneous reactor at Oak Ridge National Laboratory has demonstrated the basic feasibility of aqueous homogeneous reactors. The use of a two-region thorium breeder reactor of the aqueous homogeneous type is of considerable interest for the production of economic power because of its inherent simplicity.[1] Such reactors have a central core containing the fuel surrounded by a blanket of thorium. The fuel is a heavy water solution of $U^{233}O_2SO_4$, which also serves as neutron moderator and heat transfer medium. Excess neutrons produced in the core are absorbed in the thorium blanket, which may be composed of thorium dioxide suspended in heavy water.

With a reactor core 5 ft in diameter, 360,000 kw of heat can be produced from a fuel solution of 0.011 *M* $U^{233}O_2SO_4$ (see Table I). The total volume of the core system, including heat exchanger, pump, and piping is 10,000 liters, of which only 1850 liters is contained in the core tank itself. The amounts of U^{233} in the core system is about 20 kg. In a blanket with a thorium concentration of 1380 gm/kg D_2O, allowing the U^{233} concentration to build up to 4.1 gm/kg D_2O will give a heat production of 80,000 kw in the blanket. The heat produced in both core and blanket will make 100,000 kw of useful electricity. The chemical processing of the fuel solution and blanket slurry of this reactor is discussed in this paper.

CORE PROCESSING

Chemical processing of the reactor fuel solution, or core processing, has the objective of maintaining the level of neutron-absorbing fission products and corrosion products at an acceptable level. If the fuel solution is kept free of neutron poisons, this reactor will produce in the blanket 21% net more U^{233} than is consumed in the core.[1] As neutron-absorbing materials are allowed to build up in the core, this net U^{233} production or breeding gain drops off. It is not economically feasible to process at a rate that will maintain the fuel free of neutron poisons. However, fission and corrosion product removal on a continuous basis at a rate sufficient to maintain the core poison fraction at about 0.06 appears reasonable. (The poison fraction is defined as the macroscopic neutron capture cross section of impurities divided by the total macroscopic neutron-absorption cross section of U^{233} in the fuel solution.)

The neutron poisons are primarily fission product rare gases, rare earths, iodine, cesium, and corrosion products of stainless steel (see Table II). The concentration of rare gases may be reduced by a factor of about 10 in this reactor by mechanically degassing the fuel solution. This is accomplished by centrifuging out the gases as they form, recombining the radiolytic D_2 and O_2, and venting the noncondensable gases from the reactor. In small-scale tests the stable state of iodine under these conditions is the elemental form. In this form iodine tends to pass into the vapor phase.

Table I. Characteristics of a Two-Region Thorium Breeder Reactor. Electrical Output: 100,000 kw

	Core	*Blanket*
Core diameter (ft)	5	...
Blanket thickness (ft)	...	2.5
Average temperature (°C)	275	280
Heat output (kw)	360,000	80,000
Total volume (liters)	10,000	14,000
U^{233} concentration (gm/kg D_2O)	2.5	4.1
Thorium concentration (gm/kg D_2O)	...	1380
Pa^{233} concentration (gm/kg D_2O)	...	1.6

Table II. Poison Fraction of the Major Neutron Poisons of Breeder Core. Reactor Operated with No Removal of Poisons

	*Poison fraction**		
Poison	*After 10 days' operation*	*After 30 days' operation*	*After 120 days' operation*
Rare gases	0.064	0.065	0.068
Rare earths	0.012	0.019	0.042
Iodine	0.003	0.004	0.004
Cesium	0.001	0.002	0.008
Corrosion products†	0.005	0.008	0.031
Others	0.000	0.001	0.003
Total	0.085	0.099	0.156

* Macroscopic neutron capture cross section of poison divided by total neutron absorption cross section of U^{233} in the fuel solution.

† Based on an assumed stainless steel corrosion rate of 0.0005 in./year.

* Oak Ridge National Laboratory. Including work by D. E. Ferguson, P. N. Haubenreich, I. R. Higgins, K. A. Kraus, R. A. McNees, G. E. Moore, and M. E. Whatley, Oak Ridge National Laboratory.

Therefore, degassing also may effectively remove this fission product.

Requirements for a satisfactory process for removing the nongaseous fission and corrosion products from the fuel solution include: fuel cleanup without grossly altering the fuel composition; maintaining low inventories of fissionable material and D_2O in the plant; low losses and low costs. The process need not completely decontaminate the fuel—removal of only the bulk of the neutron-absorbing impurities is required. This may be accomplished by a simple procedure such as ion exchange or by taking advantage of the low solubility of the rare earths, iron, and chromium at the temperature of the reactor.

A schematic flowsheet for removing fission products from the fuel solution by ion exchange is shown in Fig. 1. In this process 300 liters of fuel solution are removed from the core each day. After 5 days' storage for decay of short-lived fission products, the solution is passed through a 2-liter bed of cation exchange resin of the sulfonated phenolic type that has been previously loaded with U^{233} recovered from the reactor blanket. Most of the fission products in the fuel are more strongly sorbed on the resin than the uranyl ion and displace the uranium from the resin. By this means the fission products are concentrated on the resin bed along with approximately 100 gm of U^{233}. Laboratory results indicate a removal of 95% of the rare earths, about 80% of the strontium, and 30% of the cesium by this method. No data are available on nickel removal; however, nickel should be removed by the same order of magnitude as strontium. This method does not significantly alter the fuel solution, and the treated fuel can be returned directly to the reactor. The fission products collected on the resin bed can be eluted along with nickel and residual U^{233}, about 100 gm, with a nitric acid solution. The U^{233} then can be recovered from this solution in the thorium-blanket processing plant. The principal advantage of the ion exchange method is its simplicity. The major limitations of the process result from radiation damage to the resin and the insolubility of several fission and corrosion products.

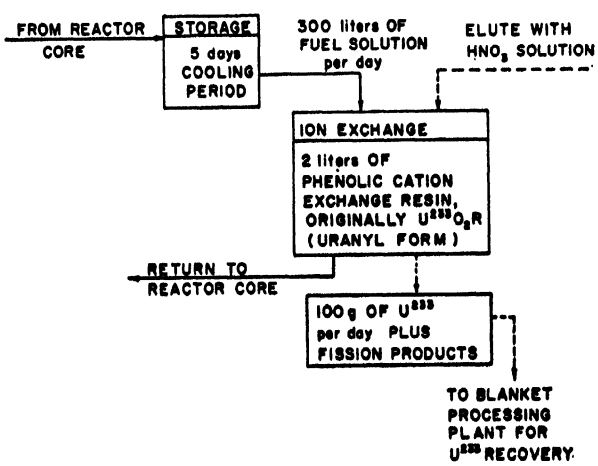

Figure 1. Schematic flowsheet for thorium breeder reactor fuel processing by ion exchange

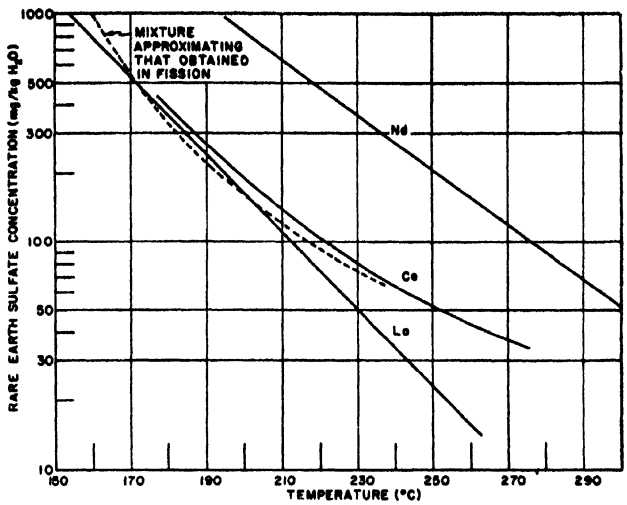

Figure 2. Solubility of rare-earth sulfates of 0.02M uranyl sulfate solution

The phenolic resins, such as Dowex 30 or Amberlite IR-105, are the most stable of the organic exchange resins.[2] They lose about 1% of their capacity when exposed to 1 watt-hr of ionizing radiation per gram of dry resin. Under the conditions outlined in Fig. 1, and, assuming an optimistic cycle time of 3 hr for resin loading and elution, the resin would be exposed to a minimum of 10 watt-hr/gm and would lose at least 10% of its capacity. For this reason it must be discarded after being used only once. The use of a resin less stable to radiation, such as a sulfonated polystyrene type which loses about 15% capacity per watt-hr/gm, would require a cooling period of 100 days to limit the resin capacity loss to 10%. Another problem introduced by the intense radioactivity is contamination of the deuterium in the fuel solution with hydrogen from the resin by radiation-induced exchange. The seriousness of this problem has not been determined. Using an inorganic exchange medium that contains no hydrogen would eliminate the limitation of radiation damage, since inorganic compounds are comparatively stable to radiation. This would permit processing with essentially no decay time. However, a suitable inorganic exchange medium has not been found for this application.

If an ion exchange process is used for removing impurities that are in solution in the fuel at room temperature, provisions also must be made for removing precipitated impurities such as iron, chromium, barium, and zirconium. These substances which precipitate at elevated temperature are only slightly redissolved when the fuel solution is cooled, and must be removed as solids.

The build-up of nongaseous fission product poisons in the reactor fuel may also be controlled by taking advantage of the low solubility of the rare earth sulfates at elevated temperature. All the rare earth fission products exhibit decreasing solubility in dilute

uranyl sulfate solution with increasing temperature (see Fig. 2). In general, at elevated temperature the solubility of the light rare earths is extremely low and the solubility increases as the molecular weight increases. In all cases the concentration of rare earth fission products in the reactor can be controlled to maintain a total poison fraction of 0.06 by removing the insoluble rare earth sulfates as they form at the reactor operating temperature. Based on the solubilities at 275°C given in Fig. 2, the poison fraction for neodymium is estimated to be 0.01 and about the same, for all other soluble rare earth fission products, for a total of only 0.02. Many of the other fission and corrosion products are only slightly soluble under reactor conditions. For instance, barium, strontium, zirconium, iron, and chromium can be expected to reach their solubility limit after only a few days of reactor operation. Of the major neutron poisons listed in Table II, only cesium and nickel have solubilities great enough to contribute significant poison to the reactor if the solids are removed as they are formed. The concentration of the soluble impurities can be controlled by removing a small fraction of the core solution for comprehensive clean-up in the blanket process.

Possible methods of removing the insoluble impurities at elevated temperature are settling, filtration, and centrifugation. Settling has the disadvantage that a large volume of fuel solution must be held in a semi-stagnant state at high temperature and pressure. There is also some doubt that these solids would settle as non-radioactive materials do in laboratory experiments because of the presence of bubbles of steam and radiolytic gas formed as a result of the intense radioactivity of the fission products. The disadvantage of filtration is the problem of cooling the solid cake on the filter because of the very high energy released from the radioactive solids. A continuous centrifugal device, which discharges the solids as a slurry, appears most attractive. Such a device, which has been tested in the laboratory, is a liquid-solid cyclone separator, or hydroclone.

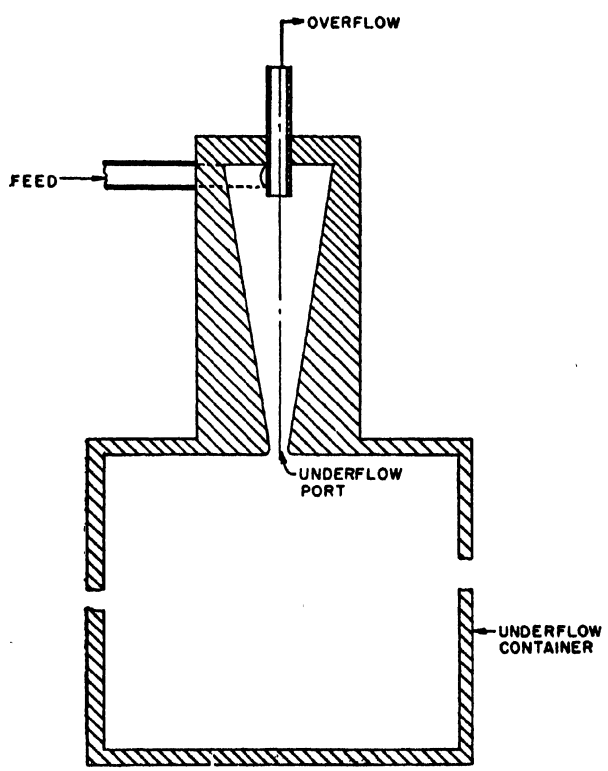

Figure 3. Schematic cross section of hydroclone separator

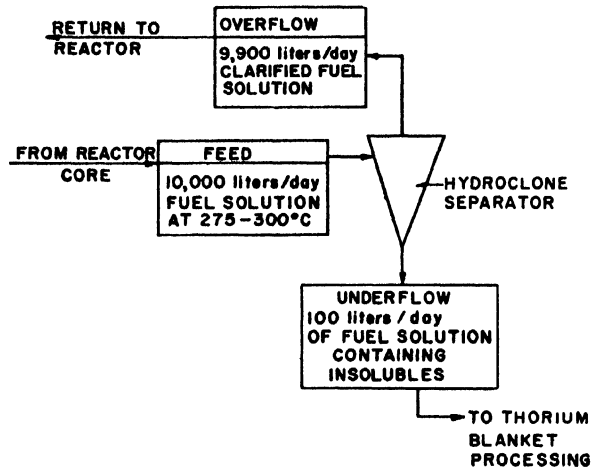

Figure 4. Schematic flowsheet for core solution processing by solids removal

A hydroclone consists of a cone into which a dilute slurry is introduced tangentially at the top (see Fig. 3). The solid particles are concentrated near the wall of the cone and flow down into an underflow container. The clarified liquid is withdrawn at the top through a tube or vortex finder, inserted down through the top of the hydroclone. In laboratory tests of a hydroclone model at room temperature, 70% or more of thorium dioxide particles suspended in water was removed, to give a concentration ratio of about 1000. This ratio compares the solids concentration in the underflow container to the solids concentration in the feed. The particles used in these tests were predominantly 1–5 microns in size. A hydroclone can be expected to perform even better at elevated temperatures than at room temperature, since both the viscosity and density of dilute aqueous solutions decrease with increased temperature.

A schematic flowsheet for core processing by a hydroclone liquid-solid separator is shown in Fig. 4. This process consists in continuously passing the fuel solution containing insoluble fission and corrosion products through the hydroclone separator at a rate of 10,000 liters/day. The solids are concentrated into about 100 liters/day of solution in the hydroclone underflow container, and the 9900 liters/day of clarified overflow are returned to the reactor core. The U^{233} contained in the 100 liters/day fuel collected in the underflow container can be recovered along with the U^{233} from the blanket by the thorium blanket processing scheme to be discussed later. The 100 liters/day removal rate of fuel from the core adequately controls the concentration of soluble impurities.

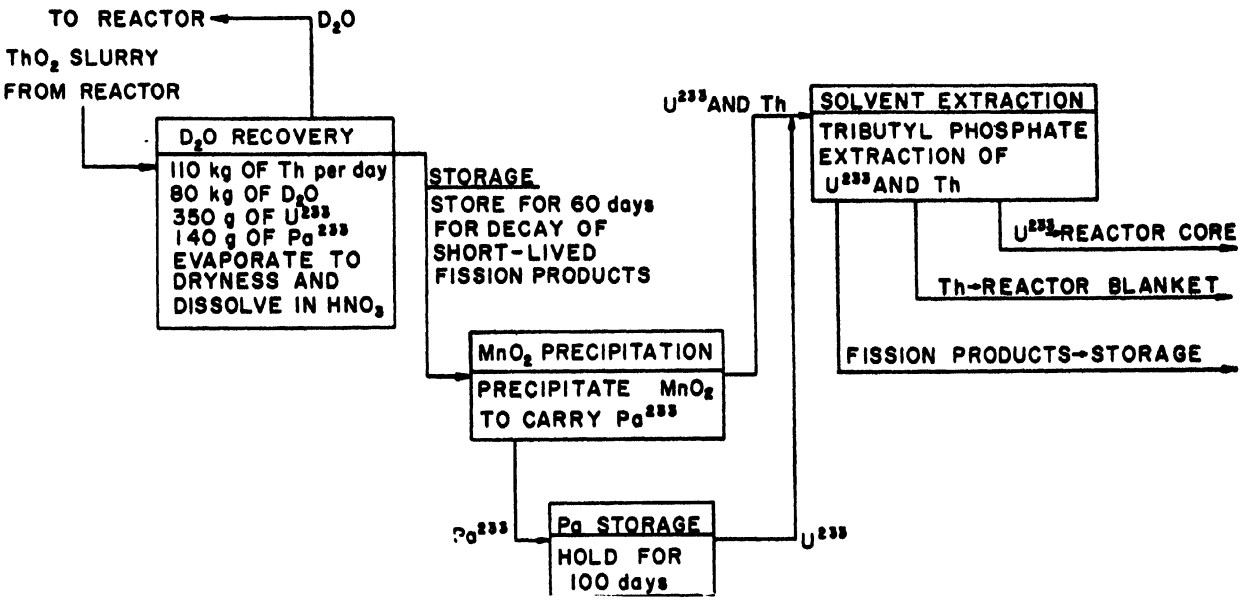

Figure 5. Schematic flowsheet for thorium blanket processing by precipitation and solvent extraction

The chief disadvantage of core-processing by liquid-solid separation is that the fuel solution is left saturated with the low-solubility materials. There is a tendency for these materials, especially the rare earth sulfates, to precipitate out and cling to hot metal surfaces with which a saturated solution comes in contact. Since metals inside the reactor, especially the core tank, are heated by intense γ-radiation, they may be hotter than the fuel solution, and rare earth sulfates and other low-solubility materials may deposit on these surfaces. The ion exchange method previously described does not have this disadvantage, since it is possible by ion exchange to keep the concentration of rare-earth sulfates below their solubility limit.

THORIUM BLANKET PROCESSING

Processing of the thorium blanket is required for recovering the bred U^{233} to replenish that which is burned in the core and to remove the neutron poisons, primarily fission products, which are produced in the blanket. The blanket process must be capable of recovering both the U^{233} and thorium in a form suitable for return to the reactor, and the process must provide for the safe disposal of the fission products. When the thorium oxide is removed from the blanket it contains roughly one-third as much Pa^{233} as U^{233}, in addition to fission products. Either steps must be taken in the process to recover and store the protactinium for subsequent decay to U^{233}, or the thorium may be stored until essentially all the protactinium has decayed to U^{233} before processing. The first step in the blanket-processing after recovery of heavy water by evaporation is dissolution of the thorium oxide. Attempts to leach U^{233}, protactinium, and fission products from irradiated thorium dioxide with mineral acids and complexing agents have been unsuccessful. Only by the complete dissolution or metathesis of the thorium dioxide has adequate removal of uranium and protactinium been accomplished. After the thorium dioxide has been dissolved, thorium, uranium, and protactinium may be separated from each other by a number of techniques, including ion exchange, crystallization of the nitrates, solvent extraction, precipitation, or a combination of these methods.

One attractive combination of methods is isolation of protactinium by carrier precipitation on manganese dioxide, followed by a tributyl phosphate solvent extraction recovery and isolation of uranium and thorium from fission products. This process is illustrated schematically in Fig. 5. When manganese dioxide is precipitated from a $1M$ nitric acid solution of thorium nitrate, 95% or more of the protactinium in solution is carried on the manganese dioxide. The chief disadvantage of this method of recovering protactinium is that little separation is gained from several fission products, including zirconium, niobium, and ruthenium. After the protactinium has decayed to U^{233}, it is still necessary to separate the U^{233} from these fission products. This can be done by feeding a nitric acid solution of the manganese dioxide cake, after 100 days' decay, to the solvent extraction process for U^{233} recovery.

An attractive solvent extraction process for separating thorium, uranium, and fission products is discussed in detail in another paper.[3] The process consists in a simultaneous extraction of uranium and thorium from a nitrate solution with a hydrocarbon solution of tributyl phosphate, selective removal of thorium from the solvent with dilute nitric acid, and removal of the uranium with water. This process will recover greater than 99.9% of the thorium and uranium, sufficiently separated from fission products to be handled without massive shielding. The disadvantages of solvent extraction are the complexity of the

process and the cooling time required, about 60 days, for decay before processing to prevent excessive radiation damage to the solvent.

The extent of radiation damage to the tributyl phosphate solvent in the process is determined by the radiation intensity of the feed solution and the time the solvent is in contact with this radioactive solution. To limit the exposure of the solvent to 0.5 watt-hr/liter,[2] with a reasonable contact time of 10 min, the β-radiation level of the aqueous phase must not exceed 3 watts/liter. If only the blanket material were processed, a decay period of 30 days would be sufficient to reach this level; however, when the fission products from the core solution are added to the blanket material, either as the hydroclone underflow or as the eluant from an ion exchange process, a decay period of at least 60 days is required to attain a solvent exposure level of 0.5 watt-hr per liter.

Uranium, protactinium, and thorium can be effectively separated by anion exchange on a quaternary amine styrene polymer (see Fig. 5). Both protactinium and uranium are strongly sorbed by the strong-base anion exchange resins from 8*M* hydrochloric acid solutions. Thorium is not appreciably sorbed by the resin. The uranium and protactinium can be selectively eluted with about 4*M* hydrochloric acid. With this concentration of hydrochloric acid the protactinium appears first in the eluant followed by the U^{233}. The limitation on this method of processing is radiation damage to the organic exchange resin. With an optimistic assumption for cycle time of 10 hr, a decay period of about 100 days is required to limit the capacity loss of the anion-exchange resin to 10% per cycle.

It is also possible to separate thorium from uranium and fission products by selective crystallization from concentrated nitric acid solutions. About 80% of the thorium contained in boiling 16*M* nitric acid can be crystallized with separation from rare earth fission products by a factor of 10. Separation from uranium and almost all other fission products is by a factor of 100 or more. Repetition of the crystallization step after further evaporation and proper recycling of the thorium nitrate crystals can yield any desired recovery of thorium with sufficient separation from fission products for return to the reactor. While this process is not subject to limitations of radiation damage, the many evaporations and recycles make it much more complicated and unwieldy than the solvent extraction process.

After recovery and separation from the fission products, uranium and thorium must be converted back to a heavy water uranyl sulfate solution and heavy water slurry of thorium dioxide, respectively. The uranium as uranyl nitrate or uranyl chloride product solution from the separation process can be very simply converted to uranyl sulfate by ion exchange. The uranyl sulfate can be dried by evaporation and redissolved in heavy water. Thorium can be precipitated from a chloride or nitrate solution as either the hydroxide or oxalate and then converted to dry thorium dioxide by calcination.

COMPARISON OF METHODS

The final choice of a method of chemical-processing for a power-producing reactor must be based on economy as well as feasibility. From the standpoint of feasibility, both ion exchange and solids removal are attractive methods of core-processing. Both appear capable of maintaining the neutron poisons in the core at an acceptable level. About the same capital expenditure and operating cost would be expected for the two methods, since both are simple, compact processes which require a minimum of attention. However, the ion exchange method has the disadvantage that appreciable inventories of U^{233} and D_2O are necessitated by the 5-day fission products decay period before processing. The materials in storage for this decay period represent a 20% increase in U^{233} and D_2O inventory for the core system. Therefore, unless a suitable radiation-resistant ion exchange medium is developed, the solids removal method appears the more attractive from the standpoint of economy.

For the blanket process, the comparative economics of the many possible methods is much more complex. The choice of the most economical method must depend on a detailed analysis of capital, operating, and inventory costs of the various feasible chemical separation methods. Such an analysis is beyond the scope of this paper. However, the following general conclusions can be drawn, based primarily on chemical feasibility of the separation methods previously discussed. Ion exchange and solvent extraction are not attractive methods of isolating Pa^{233} owing to radiation damage of the organic reagents used. Therefore, a precipitation process, such as carrying Pa^{233} on manganese dioxide from a nitrate solution, appears the most attractive. For the separation of thorium, U^{233}, and fission products, tributyl phosphate solvent extraction appears to be the most effective and straightforward method; however, the inventory of material necessitated by the 60-day decay period required to prevent excessive damage to the solvent is certainly an economic disadvantage. Compared to solvent extraction, the ion exchange method

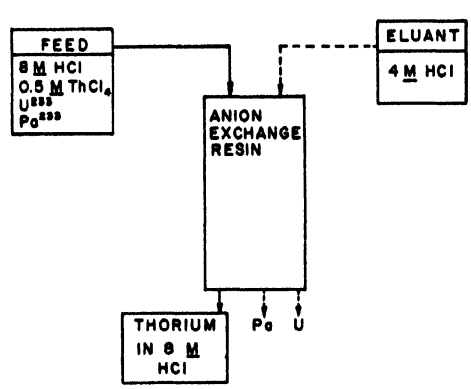

Figure 6. Anion exchange separation of thorium, U^{233}, and Pa^{233}

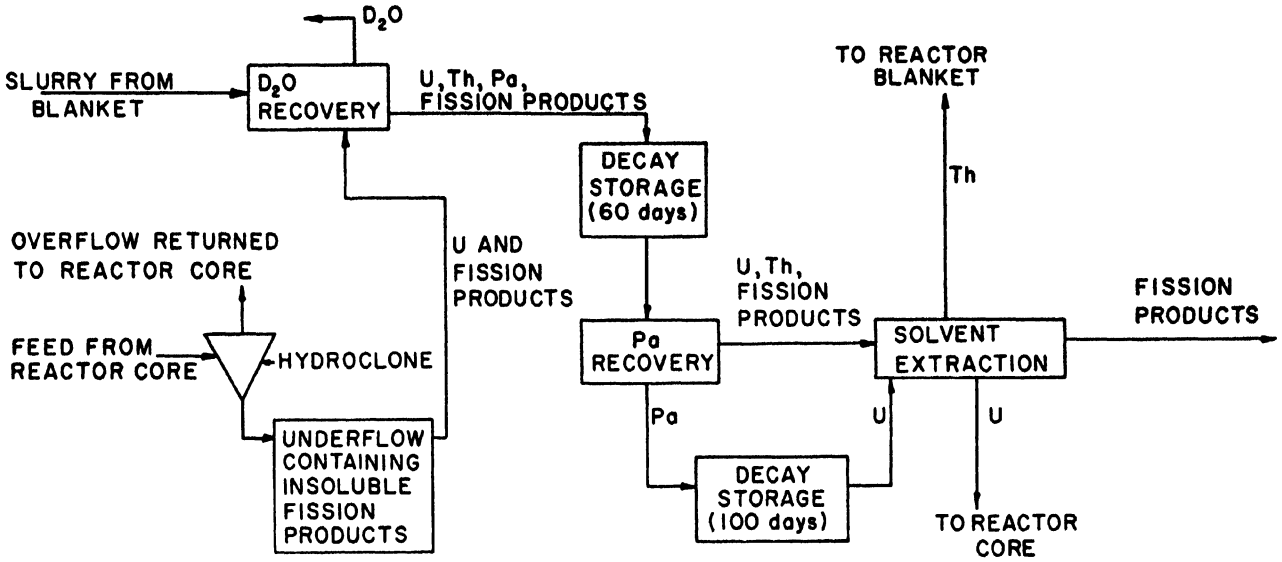

Figure 7. Schematic flowsheet for thorium breeder reactor core and blanket processing

has the marked disadvantage that the chloride solutions are corrosive to common materials of construction. The many evaporations and recycles necessary in the recrystallization method make it much more complicated than solvent extraction.

Figure 7 illustrates how solids removal from the core can be tied in with the thorium blanket process to give an integrated reactor process. The small underflow from the hydroclone separator containing the insoluble fission products can be added directly to the blanket slurry withdrawn for processing. After heavy-water recovery by evaporation from the combined streams, the thorium, uranium, protactinium, and fission products are dissolved in nitric acid and stored for 60 days. After the decay period, protactinium can be recovered by precipitation and the uranium, thorium, and fission products separated by solvent extraction. The U^{233}, after conversion to a UO_2SO_4-D_2O solution, can be returned to the reactor core, and the thorium, after conversion to an oxide slurry, returned to the blanket, completing the cycle.

REFERENCES

1. Briggs, R. B. and Swartout, J. A., P/496, *Aqueous Homogeneous Power Reactors,* Volume 3, Session 12A, these Proceedings.
2. Cathers, G. I., P/743, *Radiation Damage to Radiochemical Processing Reagents,* Volume 7, Session 11B, these Proceedings.
3. Gresky, A. T., P/540, *The Solvent Extraction Separation of U^{233} and Thorium from Fission Products,* Volume 9, Session 21B, these Proceedings.

The Characteristics of Liquid-Liquid Extraction Equipment as Applied to Radioactive Processing

By H. R. C. Pratt,* UK

Chemical-processing operations associated with nuclear reactors resemble one another to the extent that they all involve the separation of a fissile element from highly active fission products and from inactive or source material. Within this broad similarity, however, many differences occur, according to the type of reactor with which the process is associated. Thus, fuel elements based on plutonium or enriched U^{235} require somewhat different treatment from those comprising natural uranium. Again, different treatment is required for breeder reactor "blanket" containing U^{238} or thorium as fertile materials, while the possible introduction in the future of reactors containing liquid metal or metal slurry type fuels is likely to require entirely different methods of processing.

Of the four methods suggested in the Smyth report[28] for the processing of natural uranium fuel elements, viz., precipitation, solvent extraction, distillation, and ion exchange, extraction appears for the present to have general acceptance. This process consists in principle in the dissolution of the irradiated rods in nitric acid, followed by "conditioning," i.e., adjusting the concentrations of uranium, acid and salting-out agent to the appropriate values. The resulting solution is then extracted with a suitable solvent, generally a higher ketone or substituted ether, or a solution of tributyl phosphate in a non-polar solvent such as kerosene.[2,15,23] The extract contains substantially the whole of the uranium and plutonium, while the greater part of the fission products pass out with the waste aqueous stream. The plutonium is then separated by reduction to a lower valency state, followed by extraction with a solution of salting-out agent. The uranium is recovered from the residual solution of backwashing with water. The plutonium and uranium solutions can be further purified by repeated cycles involving extraction into solvent followed by backwashing.

The design of suitable equipment for the present purpose introduced many new problems, not the least of which was the requirement that the plant should operate for prolonged periods behind concrete shielding with little or no maintenance. It is, therefore, appropriate to review the progress which has been made in the development of such contactors and the problems still facing the designer in the prediction of their leading dimensions.

* Atomic Energy Research Establishment, Harwell.

BATCH AND CONTINUOUS OPERATION

Radioactive separations are carried out by the process known as double-solvent extraction, in which the solutes, i.e., uranium, plutonium and fission products, are distributed between two solvents, one of which is water or an aqueous solution. This process is normally carried out continuously, as shown in Fig. 1 for the case of the primary separation of uranium and plutonium from fission products. Thus, referring to the diagram, the feed, consisting of a solution of the fuel elements in nitric acid and suitably conditioned, enters the contacting section of the column at F and descends countercurrent to an ascending stream of solvent which enters at the base. In the extraction section of the column, below the feed when using solvents lighter than water, the uranium and plutonium together with a proportion of the fission products are extracted by the entering solvent. The fission products are largely removed from the extract in the washing section of the column, i.e., the section above the feed inlet, by means of the entering stream of stripping agent, which comprises an aqueous solution of a suitable salting-out agent. The solvent extract leaving the top of the column thus consists mainly of uranium and plutonium nitrates and passes on to the later stages of the process.

As an alternative to the continuous method of operation it is possible to employ batch fractional extraction, analogous to batch fractional distillation.[24] A typical method of double-solvent batch operation is shown in Fig. 1*b*; in this process the initial charge, consisting of an aqueous solution of fuel rods suitably "conditioned", is treated with the extraction solvent in mixer (A). The extract then passes up the extraction column countercurrent to a descending stream of aqueous stripping agent which removes the fission products. The extract leaving the column enters the solvent-removal unit, whence the solvent is recycled to the main extraction column. If desired, a part of the concentrated extract phase may be refluxed to the column as shown in order to provide an additional degree of freedom for control of the product composition (i.e., radioactivity in the present case). The remainder of this stream is withdrawn as product and further processed in a similar manner to

separate the uranium and plutonium. The aqueous phase leaving the column passes to the water-removal unit, whence the water is recycled if desired. As the extraction proceeds the composition of the extract starts to deteriorate, and it is then diverted to the intermediate fraction tanks, as in batch distillation. When the whole of the uranium and plutonium is extracted the process is stopped, and the residue in the charge tank, comprising an aqueous solution of fission products, is disposed of in the appropriate manner. The intermediate fraction is recycled with the next charge and hence does not accumulate.

The solvent-removal units (noting that water is one of the solvents in this particular case) can take a number of forms, depending upon the relative volatilities of solvents and solutes. In the present case the solutes are non-volatile, and the solvent-removal units can take the form of simple extraction (stripping) columns, evaporators or a combination of the two. It is convenient to use evaporators wherever possible, either with or without extractors, since, with evaporators of the climbing-film type, it is possible to dispense with pumps for the circulation of the various streams. At the same time the rates of circulation of the solvents can be controlled by controlling the heat input to the evaporators, thus eliminating the need for flowmeters.

Although the continuous process would obviously be used in any plant where sufficient material is coming forward to warrant substantially continuous operation of the plant, it is less suitable when processing small amounts of special material, i.e., enriched fuel from experimental high-flux reactors. In this case it is probable that a truly continuous plant would require columns of too small a diameter to be practical, in which case it would need to be operated intermittently. Under such conditions quantities of off-grade material would be obtained during start-up and would need to be re-introduced into the process, always a difficult problem. Under such circumstances, therefore, it may well be found preferable to install larger diameter columns and operate on the batch principle, since there is then no problem in the disposal of the intermediate fractions. A batch plant has the additional advantage that it is much more flexible, as is the case with batch distillation, so that the same unit can be used for a variety of duties.

Batch operation can also prove useful as an experimental tool in the development of new processes, since it is possible to scale up directly from the batch to the continuous process, as with distillation. For this purpose the flexibility of batch operation is again of great value.

SELECTION OF CONTACTOR

As stated earlier, the requirements of radioactive-processing are much more stringent than those encountered generally in the chemical industry. The

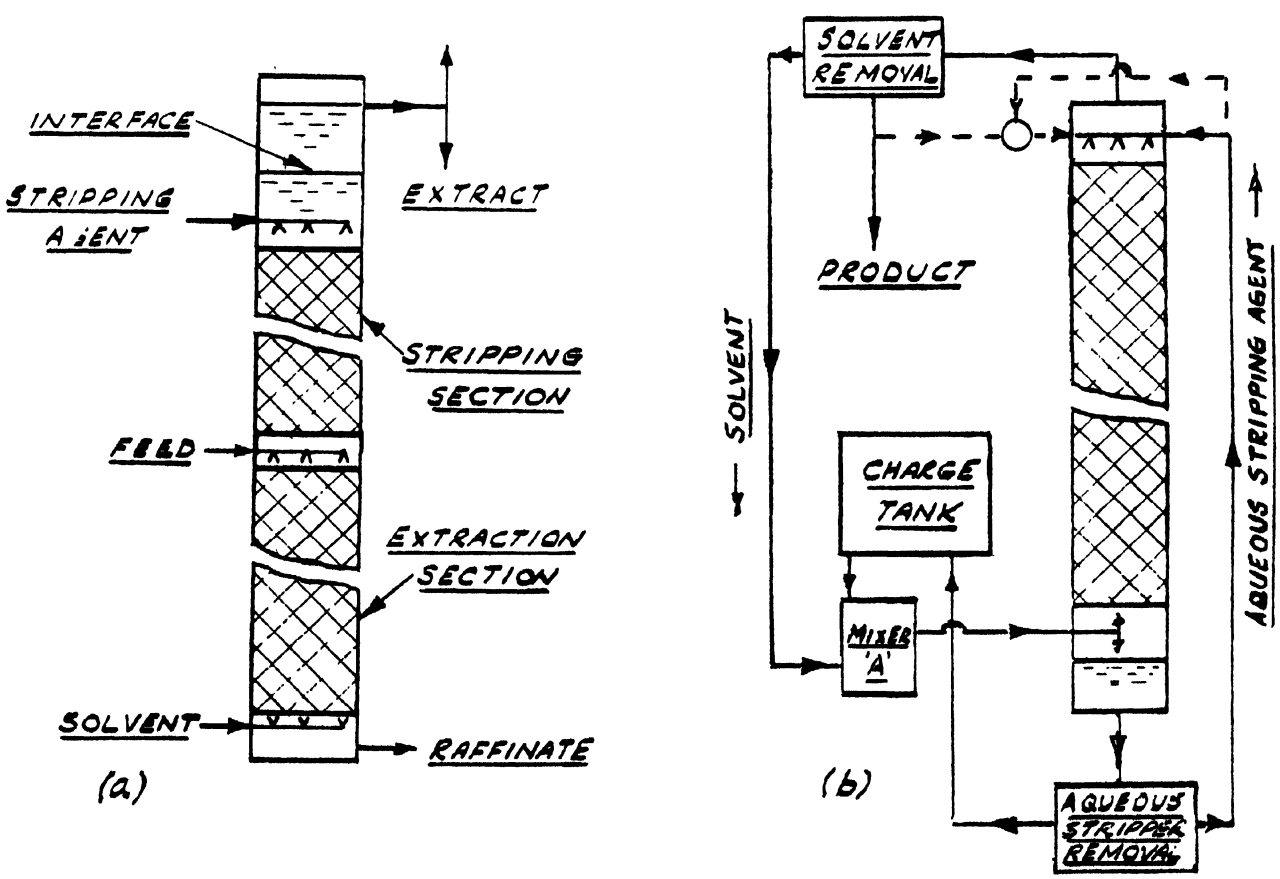

Figure 1. Continuous and batch methods of processing

features which must be taken into account in the selection and design of contacting equipment are summarised below:

1. The plant must be capable of operation for long periods without maintenance behind heavy shielding.
2. Moving parts in contact with the process liquors should be eliminated or reduced to a minimum. In particular, submerged bearings on rotary shafts and conventional stuffing-boxes and mechanical seals are completely inadmissible.
3. The geometry of the equipment should be such that criticality, in the nuclear sense, cannot occur when it is filled with process liquors.
4. Gaseous effluents should be avoided as far as possible in view of the risk of carry-over of radioactive spray.
5. It must be possible to drain and wash out the plant by remote control.
6. Weirs, orifices, etc., should be eliminated altogether or made as large as possible in order to reduce the danger of blockage by solid matter.
7. The contactor should be as compact as possible, the height in particular being reduced to a minimum, to reduce shielding costs. Other things being equal, a horizontal type contactor is preferable to a vertical type.
8. Automatic controls on active streams should be kept to a minimum, owing to the difficulty of obtaining satisfactory control valves.

The brief description given below of the types which most nearly fulfill the above requirements is based on a recent review classifying all types of extractor.[25]

Non-Mechanical Contactors

The most suitable types of non-mechanical contactor are the packed and the perforated plate columns (cf Fig. 2.) Both have the disadvantage that the H.E.T.S. is comparatively large, necessitating high columns with consequent heavy shielding costs, although on the other hand the complete avoidance of moving parts is a great advantage from the maintenance point of view. An additional disadvantage of the perforated plate column is the risk of blockage of the orifices by solid matter, i.e., interfacial "crud." On the other hand, the comparatively low performance of packed columns often necessitates the introduction of perforated plates at intervals of 3 to 6 feet for the purpose of re-mixing the phases and reducing longitudinal circulation. These should be designed with a small number of comparatively large holes since the solvent phase which coalesces beneath the plates is effectively re-dispersed and broken down into small droplets when it re-enters the packing.

Mechanical Columns

Conventional mechanical columns, e.g., of the rotary annular, rotary disc and multistage-mixer types are generally not suitable for radioactive-processing in view of the need for a comparatively large number of stages, requiring long columns with consequent internal shaft bearings. They may possibly be used, however, in cases where the level of γ-radiation is low and maintenance is not unduly difficult.

Many workers in the nuclear energy field have shown interest in recent years in the pulsed plate

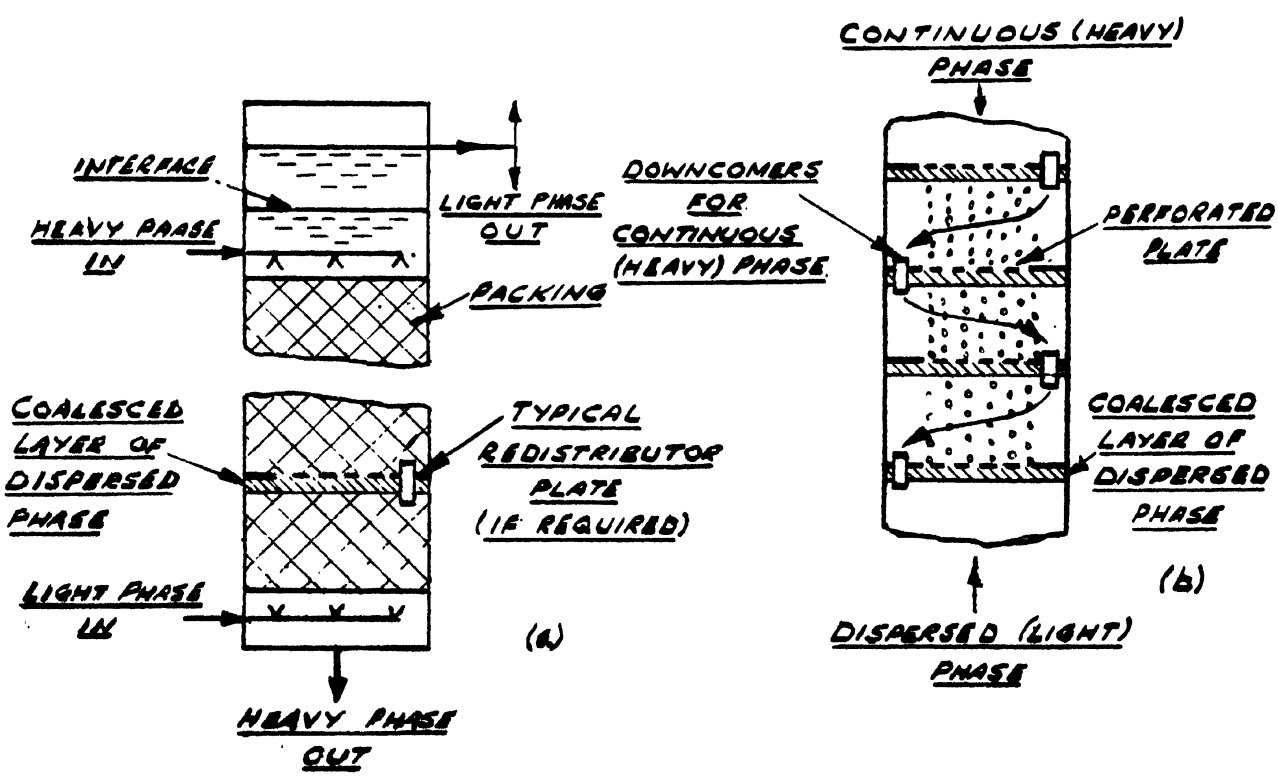

Figure 2. Typical arrangements of packed (a) and perforated (b) plate columns

column,[1,3,12,29,30,31] which was proposed by van Dijck in 1934 as an alternative to his oscillating plate column.[34] This contactor comprises a vertical column with closely spaced perforated plates, without downcomers or risers for the continuous phase, in which a suitable mechanism is used to impart a reciprocating motion to the liquid. By this means the droplets are broken down to such an extent that the height is reduced by a factor of two to three as compared with packed columns. At the same time the contacting section is self-cleaning by virtue of the breaking-up of agglomerates of solid matter by the pulsing action.

The main disadvantage of pulsed columns arises from the fact that the types of pulsing mechanism normally used, i.e., valveless pumps, oscillating diaphragms or bellows, are in contact with highly active liquid, making maintenance difficult if not impossible. This disadvantage may be overcome, although not very satisfactorily, by pulsing the entering inactive light phase. A more satisfactory solution is the method of air pulsing recently described by Thornton,[31] although this requires a greater power input than mechanical pulsing methods. In this method, shown diagrammatically in Fig. 3, an air cylinder is used to produce the pulse by alternately compressing and decompressing the air above the surface of the liquid in the connecting line between the pulse cylinder and the base of the column. The resulting movement of the liquid in this line transmits the pulse to the column itself. This method has been used successfully to pulse a column of 6-in. diameter with a height of contacting section of 20 feet, pulse rates of 2-3 cycles/sec with amplitudes of ½ in.–¾ in. easily being obtained. As the column height is increased, however, the pulse amplitude and/or frequency diminishes due to the greater inertia of the column of liquid; this limitation manifests itself in the case of normal mechanically-pulsed columns in the onset of cavitation.

Although experience to date with the air-pulsed column is comparatively limited, it shows promise of being one of the most satisfactory contacting devices for the earlier stages of a radioactive processing plant. For the later stages, where the level of γ-activity is lower and limited maintenance is possible, normal mechanically-pulsed columns are acceptable.

Mixer-Settlers

In the mixer-settler contactor the phases are mixed together repeatedly in a series of stirred vessels, followed by settling chambers in which phase separation takes place (cf. Fig. 4). Many variants of this type of extractor have been described in the literature, and their classification has been attempted by Davis, Hicks and Vermeulen[7] (cf. also Pratt[25]).

Vertical mixer-settlers can be eliminated from consideration for the present purpose for the same reason as the mechanical columns, i.e., on account of the necessity for internal bearings. Horizontal mixer-settlers, on the other hand, are more suitable since the mixers in each stage can generally be carried in external bearings, thus making limited maintenance possible. It should be noted, however, that the geometry of mixer-settler equipment is less favourable from the criticality point of view when processing enriched fuels.

Two types of mixer-settler contactor have recently been described[5,7] which merit consideration for radioactive processing; both are multicompartment forms of the well-known Holley-Mott[14] contactor shown in Fig. 4*a*. The unit described by Coplan and Zebrowski (Fig. 4*b*) is particularly interesting in that the pumping action of the mixing impellers is used to control the interface level in all the settling chambers except the last.

DESIGN OF CONTACTING EQUIPMENT

The design of extraction equipment involves initially the determination of two basic parameters; namely, the capacity, which fixes the diameter of column or size for settling chamber for a given output, and the duty, which is determined by the degree of separation required and governs the height of column or the number of stages required. The capacity is dependent upon the flood-point of the equipment for the particular liquid-liquid system in use, and is determined by hydrodynamical considerations alone. The duty, on the other hand, is primarily a matter of mass transfer and is a much more complex matter.

Up to the present it has been normal in the case of radioactive processing to determine the size of equipment required by purely empirical methods, using inactive process solutions. Thus, runs are carried out with solutions of non-irradiated fuel elements, to which are added, if desired, tracer amounts of fission product activity and also, in the later stages of the work, plutonium. The flow rate at which flooding takes place is first determined, and then, operating at somewhat lower flows, extraction runs are carried out and the results interpreted in terms of the H.E.T.S. or H.T.U. Such experiments must be carried out, at least in the later stages of the work, with equipment as close as possible in cross section to that of the final plant units. The height or number of stages should, however, be less than that ultimately required in order to study the effect of mean concentration in the H.E.T.S., H.T.U. or stage efficiency.

Experimental work of the type described above is inevitably expensive and time-consuming, and much effort has been devoted to the problem of predicting column capacity and performance. The present state of knowledge in these two fields will therefore be reviewed briefly below.

Determination of Column Diameter

The limiting capacity of a column extractor is governed by the flood-point, i.e., the flow rate at which, for a given flow ratio, the dispersed phase is rejected from the column at the continuous phase outlet. For most types of column the flood-point can be calculated from the equation relating the hold-up of dispersed phase to the flow rates of the phases,[11] thus:

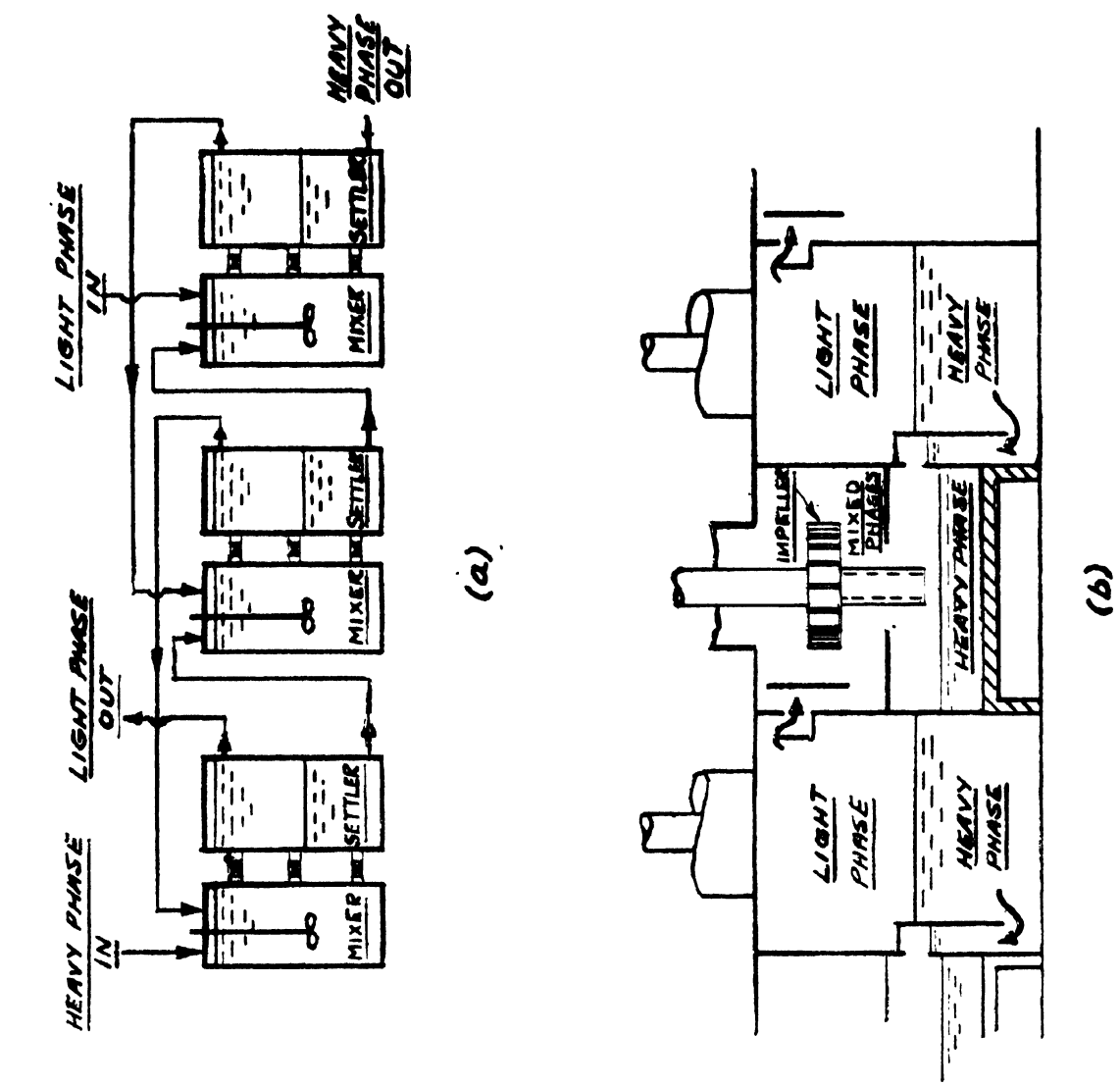

Figure 4. Typical mixer-settler contactors showing: (a) Holley-Mott type; and (b) pump-mix box contactor

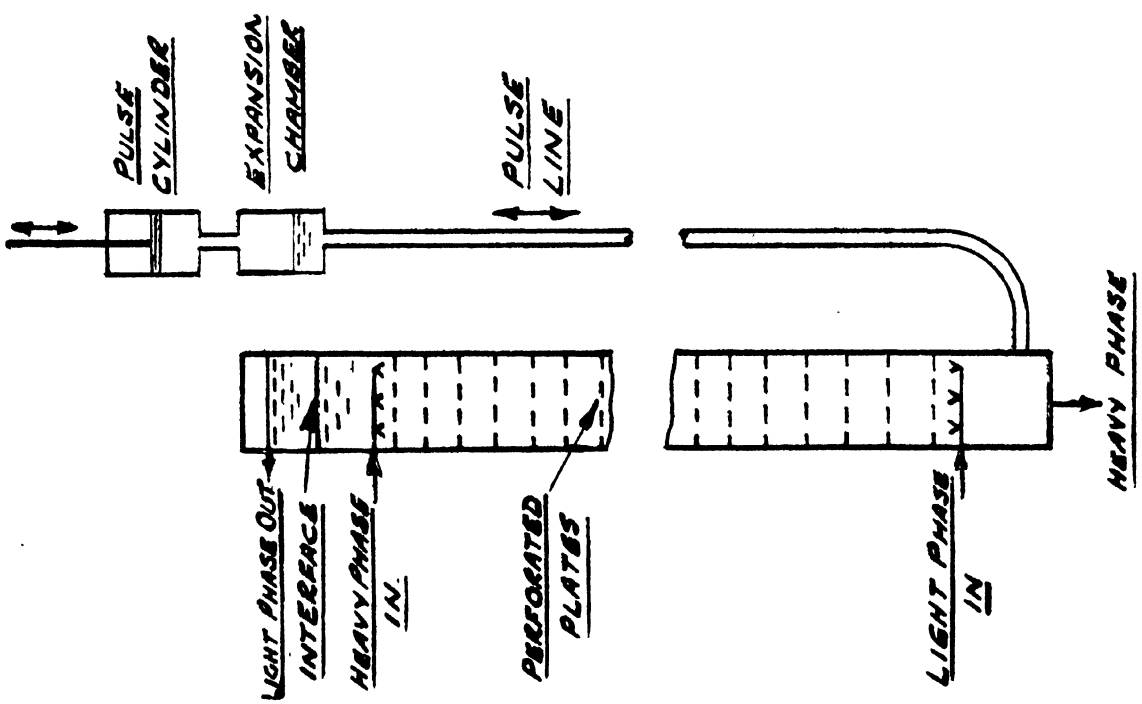

Figure 3. Arrangement of air pulsed column

$$V_d + \frac{x}{1-x} V_c = \bar{v}_0 \epsilon x(1-x) \qquad (1)$$

In Equation 1 $\bar{v}_0$ is termed the "characteristic droplet velocity," and is effectively the mean droplet velocity when $V_c = 0$ and $V_d \to 0$. Introducing the condition that the flow-rates are a maximum 32:

When

$$dV_d/dx = 0: V_c = \epsilon\bar{v}_0 \ (1-2x_f) \ (1-x_f)^2 \qquad (2)$$

and when

$$dV_c/dx = 0; V_d = 2\bar{v}_0\epsilon x_f^2 \ (1-x_f) \qquad (3)$$

The hold-up at flooding, x_f, is obtained in terms of the flow ratio $L_R(=V_d/V_c)$ by eliminating $\bar{v}_0$ between Equations 2 and 3, thus:

$$x_f = \frac{(L_R^2 + 8L_R^{\frac{1}{2}} - 3L_R}{4\ (1-L_R)} \qquad (4)$$

Either Equations 2 or 3 together with Equation 4 can be used to predict the flood-point, provided the characteristic velocity is known. The problem of predicting the flood-point therefore reduces to that of predicting $\bar{v}_0$ in terms of physical properties, column geometry, rotor speed, etc. Correlations of this parameter have been obtained for a number of types of column, and have been reviewed by the present writer.[27] In the case of packed columns Equations 2–4 predict the upper transition rather than the flood point, above which the shape factor of the droplets changes and the flow rates increase at constant hold-up. Correlations of the true flood-point for these columns have been given by several workers.[6,8,13,16]

For design purposes the column cross section should be selected so that it operates at 50–60% of the calculated flooding rate. The same method can be applied to packed columns, although in this case it is more convenient to calculate the cross section from Equation 1 assuming a hold-up of 15–20%. In some cases the solute effects discussed below result in a reduction in hold-up and an increase in the flood-point, but an allowance for this can only be made on an experimental basis. They do not normally occur with uranium systems unless an undistributed component such as nitric acid is present in the entering solvent.

In the case of perforated plate columns the throughput is best determined by means of the orifice equation, assuming suitable values of the height of the layer of coalesced layer of dispersed phase below (or above) the plates. Orifice coefficients for this purpose have been satisfactorily correlated by Major and Hertzog.[21]

Column Height

The number of theoretical stages or over-all transfer units required for a given separation can be calculated by well-established methods,[33] using values of the partition coefficient obtained experimentally for a range of concentrations of solute and salting-out agent. Before the actual column height can be specified, however, it is necessary to know the H.E.T.S. or over-all H.T.U., and the prediction of this would require the assessment of four basic parameters, viz. (*a*) the interfacial area of contact to the phases, (*b*) the individual "film" mass transfer coefficients for transport of the solute to and from the interface, (*c*) the longitudinal mixing factor, which results in a reduction in effective driving force for the transfer, and (*d*) interfacial effects, i.e., interfacial resistance due to slow heterogeneous chemical reaction, interfacial oscillation and spontaneous emulsification. Some success has been obtained in the determination and correlation of the first three of these factors in the single case of packed columns[27] but the effect of the fourth can only be found by experiment, as will be seen below.

Several attempts have been made to assess the magnitude of the interfacial effects.[26] In particular, Murdoch and Pratt[22] measured the interfacial resistance in the transfer of uranyl nitrate in a wetted wall column, while Lewis studied interfacial effects in the transfer of both organic solutes[17] and uranyl nitrate[18] in a specially designed transfer cell. In both cases definite slow steps were found in the transfer of uranyl nitrate, but Lewis found with the organic solutes that the interfacial resistance was sometimes positive and sometimes negative. The latter result was ascribed to additional turbulence resulting from interfacial oscillation or "pulsation," which had previously been observed in separate experiments with single droplets.[19] An additional interfacial effect, spontaneous emulsification, has been observed by McBain and coworkers,[20] who considered that it was due to molecules of solvent being carried across the interface with the solute into the other phase and isolated there. Finally, Gayler and Pratt[10] observed with packed columns that the transfer of organic solutes, e.g., acetone, across the interface from solvent to water phase resulted in a coalescence of the droplets with reduction in interfacial area and an increase in H.T.U. Separate single droplet experiments confirmed that pulsation occurred under these conditions. However, when the direction of transfer was reversed pulsation was generally not observed and coalescence did not occur in the packed column, although the over-all mass transfer coefficients (calculated on an area basis) appeared to be enhanced by as much as 100–200% as compared with values predicted from individual coefficient data obtained by the Colburn and Welsh method.[4]

It may be concluded from these results that the over-all interfacial effect is too complex to predict, except by experiment. Hence for packed columns it is necessary to carry out model experiments with a small column using the actual system under consideration, and to compare the experimental and predicted values of the over-all H.T.U. This gives a factor which includes all the interfacial effects and can be used to correct the predicted values for the full-scale unit.[27] It should be noted in this connection that while the transfer of uranyl nitrate by itself ap-

pears to take place under substantially quiescent conditions, without interfacial oscillation or droplet coalescence, the presence of an undistributed solute such as nitric acid may alter conditions markedly.

For other types of column contactor it is not yet possible to apply this method since, owing to lack of droplet size data, the interfacial area cannot be calculated. However, the following expression can be used as an alternative basis for the interpretation of the model experiments for mechanical columns:

$$(\text{H.T.U.})_{oc} = (\text{H.T.U.})_c + \frac{V_c}{HV_d}(\text{H.T.U.})_d \quad (5)$$

Equation 5 shows that, provided the "film" values of the (H.T.U.) are constant, a plot of $(\text{H.T.U.})_{oc}$ against V_c/HV_d should give a straight line of slope $(\text{H.T.U.})_d$ and intercept $(\text{H.T.U.})_c$. In general, the assumption that the film H.T.U.'s are constant is not valid, but for mechanical columns it is found that the power input required to break down the droplets is such that a very high degree of turbulence is induced in the continuous phase.[32] Hence the continuous phase resistance is normally relatively small, i.e., $(\text{H.T.U.})_c$ is small and can be assumed constant; in addition, it is found that $(\text{H.T.U.})_d$ for a given system can generally be correlated in a relatively simple manner in terms of column size and geometry, rotor speed, etc. Consequently, the data obtained in the model tests are plotted in the manner described above, and the resulting value of $(\text{H.T.U.})_d$ is substituted in the appropriate correlating equation to obtain the value for the full-scale column. This is then substituted in Equation 5 together with the value of $(\text{H.T.U.})_c$ from the model test to give $(\text{H.T.U.})_{oc}$. For uranium systems it is necessary to carry out the experiments over a range of compositions so that values of $(\text{H.T.U.})_{oc}$ can be calculated as a function of composition.

To conclude with a note of warning, it should be remembered that the methods of interpreting model tests discussed above are still in the development stage. Consequently, while the evidence to date suggests that they are perfectly reliable, some caution should be exercised for the present when applying them to complex systems such as those encountered in radioactive processing.

Mixer-Settlers

The design of mixer-settlers is not yet on a sound fundamental basis, and there is a wide variety of types to choose from, as mentioned already. The choice must therefore depend to some extent on the designer's judgement and perhaps on his personal preferences.

The mixer-settler has the inherent advantage that the stage efficiency can readily be adjusted to be of the order of 90% or more, and the number of stages required for a given duty can therefore be calculated from equilibrium data. Mixing must of course be adequate and there are limitations on the agitator speed if the dispersed phase is not to be broken up so fine as to reduce its settling rate and thereby reduce capacity. The stage efficiency may be reduced if the dispersed to continuous phase ratio is very low or if a slow homogeneous chemical step takes place during the transfer. This difficulty can generally be overcome by arranging to recirculate part of the separated dispersed phase back from the settling to the mixing chamber, so that the ratio of the two phases in the mixing chamber is independent of the flow ratio. This ability to adjust residence time is a factor which favours the mixer-settler in cases where a slow chemical step affects the transfer.

It is less easy to determine the dimensions of a mixer-settler for a given capacity, or alternatively to predict the capacity of a given unit. It may be anticipated that the capacity would be governed by the settling rate of the emulsion formed in the mixing chamber, provided that coalescence at the interface itself is not unduly slow. Although it is possible in principle to predict the settling rate by means of the usual drag coefficient correlation for spheres, this first requires a knowledge of the variation of droplet size in the mixing chamber with rotor speed, scale of the equipment, and physical properties. An ingenious method of determination of droplet size in mixer settlers using a photoelectric probe has been described recently by Vermeulen and co-workers,[9,35] and it is to be hoped that further work on these lines will lead eventually to the development of a sound method for the prediction of mixer-settler performance.

For the present it is necessary to design mixer-settler equipment by experimental work with the actual system to be used. This involves separate investigations of the effect of agitator speed on stage efficiency and on capacity. While model tests may be of some assistance in this respect, it is generally necessary, unless large factors of safety are introduced, to test one or two stages at full size.

NOMENCLATURE

Symbols

c = Concentration of solute, lb-mols/ft^3 or gm-mols/cm^3

c^* = Concentration of solute at equilibrium with other phase, lb-mols/ft^3 or gm-mols/cm^3

H = Partition coefficient, $= c_d/c_c$ (See refs. 22 and 26 for the definition of H when the equilibrium line is curved)

H.T.U. = Height of a transfer unit, ft or cm

L_R = Flow ratio, V_d/V_c

V = Superficial flowrate of phase in empty column, ft/hr or cm/sec

$V_0, \bar{v}_0$ = Characteristic droplet velocity, i.e., velocity of droplets when $V_c = 0$ and $V_d \rightarrow 0$

x = Fractional hold-up of dispersed phase in column voids

ϵ = Fractional voidage of packing

Subscripts

c = Continuous phase
d = Dispersed phase
f = Value at flood-point
oo = Over-all value based on continuous phase

REFERENCES

1. Belaga, M. W. and Bigelow, J. E., U.S. A.E.C. rpt. KI-133 (1952).
2. Benedict, M., Ind. Eng. Chem. *45*: 2372 (1953).
3. Cohen, R. H. and Beyer, G. H., Chem Eng. Prog. *49*: 279 (1953).
4. Colburn, A. P. and Welsh, D. G., Trans. Amer. Inst. Chem. Eng. *38*: 179 (1942).
5. Coplan, B. V., Zebrowski, E. L. and Davidson, J. K., Chem. Eng. Prog. *50*: 403 (1954).
6. Crawford, J. W. and Wilke, C. R., Chem. Eng. Prog. *47*: 423 (1951).
7. Davis, M. W., Hicks, T. E. and Vermeulen, T., Chem. Eng. Prog. *50*: 188 (1954).
8. Dell, F. and Pratt, H. R. C., Trans. Inst. Chem. Eng. *29*: 89; 270 (1951).
9. Fick, J. L., Rea, H. E. and Vermeulen, T., U.S. A.E.C. rpt. UCRL-2545 (April 1954).
10. Gayler, R. and Pratt, H. R. C., Trans. Inst. Chem. Eng. *31*: 69 (1953); also unpublished work.
11. Gayler, R., Roberts, N. W. and Pratt, H. R. C., Trans. Inst. Chem. Eng. *31*: 57 (1953).
12. Griffith, W. L., Jasny, G. R. and Tupper, H. J., A.E.C.D.-3440 (1952).
13. Hoffing, E. H. and Lockhart, F. J., Chem. Eng. Prog. *50*: 94 (1954).
14. Holley, A. E. and Mott, O. E., B.P. 321, 200 (7 March 1928).
15. Jay, K. E. B., "Britain's Atomic Factories", H. M. Stationery Office (1953).
16. Kafarov, V. V. and Planoskaya, Zhur. Prik. Khim, *24*: 624 (1951).
17. Lewis, J. B., Chem. Eng. Sci. *3*: 248; 260 (1954).
18. Lewis, J. B., (Private communication).
19. Lewis, J. B. and Pratt, H. R. C., Nature, *171*: 1, 155 (1953).
20. McBain, J. W. and Woo, T. M., Proc. Roy. Soc. *163A*: 182 (1937); Kaminski, A. and McBain, J. W., Proc. Roy. Soc. *198A*: 447 (1949); McBain, "Colloid Science'," D. C. Heath & Co. (1950).
21. Major, C. J. and Hertzog, R. R., Chem. Eng. Prog. *51*: 17-J (1955).
22. Murdoch, R. and Pratt, H. R. C., Trans. Inst. Chem. Eng. *31*: 307 (1953).
23. Ohlgren, H. A., Lewis, J. G. and Weech, M., Nucleonics, *13*: 18 (March 1955).
24. Pratt, H. R. C., Chem. Eng. Sci. *3*: 189 (1954); cf. also Ind. Chem. *30*: 437 (1954).
25. Pratt, H. R. C., Ind. Chem. *30*: 475, 597 (1954).
26. Pratt, H. R. C., Ind. Chem. *31*: 63 (1955).
27. Pratt, H. R. C., Ind. Chem. (to be published) (1955).
28. Smyth, H. D., "A General Account of the Development of Methods of Using Atomic Energy for Military Purposes Under the Auspices of the U.S. Government", H.M.S.O. (1945).
29. Stephenson, R., Chem. Eng. Prog. *49*: 340 (1953).
30. Sege, G. and Woodfield, F. W., Chem. Eng. Prog. *50*: 396 (1954).
31. Thornton, J. D., Chem. Eng. Prog., Symposium Series No. 13, *39*: (1954).
32. Thornton, J. D. and Pratt, H. R. C., Trans. Inst. Chem. Eng. *31*: 289 (1953).
33. Treybal, R. E., "Liquid Extraction", McGraw-Hill Book Co. (1951).
34. Van Dijck, W. J. D., U.S.P. 2011, 186 (16/2/34).
35. Vermeulen, T., Williams, G. M. and Langlois, G. E., Chem. Eng. Prog. *51*: 85-F (1955).

Solvent Extraction Separation of Uranium and Plutonium From Fission Products by Means of Tributyl Phosphate

By J. R. Flanary,* USA

A continuous solvent-extraction process has been developed which uses tributyl-*n*-phosphate (TBP) as the solvent and nitric acid as the salting agent for the isolation of uranium, plutonium, and fission products from irradiated metallic uranium reactor fuel. Tributyl phosphate is less volatile and has a higher flash point than methylisobutyl ketone used in earlier processes. Nitric acid can be distilled off and reused in the process; this yields a lower waste volume than when aluminum nitrate is used as the salting agent.

The fuel rods, after irradiation, contain nearly equivalent weights of plutonium and mixed fission products which are small fractions of the uranium present. Processing this irradiated uranium, after 90 to 120 days' standing to permit decay of short-lived radioelements, by the flowsheet (Fig. 1) has given the following beta and gamma activity decontamination factors for uranium and plutonium:

After 2 cycles of solvent extraction:

	β	γ
U	6.6×10^6	2.7×10^6
Pu	7.7×10^6	2.0×10^6

After 2 cycles of solvent extraction plus adsorption:

	β	γ
U	9.9×10^6	6.5×10^6
Pu	3.2×10^7	1.6×10^7

PROCESS STEPS

All steps in the process except feed preparation are continuous, and recent developments indicate that continuous feed preparation may be feasible. Pulse columns are used for contacting the organic and aqueous phases and have proved to be very efficient and reliable. The process consists of the following steps: (1) fuel dissolution and feed adjustment; (2) first cycle extraction, partitioning, and stripping of uranium and plutonium; and (3) separate second cycles of extraction and adsorption for purification of plutonium and uranium. The solvent is reconditioned and reused.

Fuel Dissolution and Feed Adjustment

The irradiated uranium slugs are charged into a vessel where the silicon-bonded aluminum sheath is preferentially dissolved in sodium hydroxide. The uranium is then dissolved in nitric acid at 105°C. About 4.5 moles of nitric acid are consumed per mole of uranium dissolved.[1] The uranyl nitrate–nitric acid solution is filtered to remove solids (e.g., silica, undissolved aluminum), after which final feed adjustment is made by addition of nitric acid.

Some disproportionation of Pu(IV) to Pu(III) and Pu(VI) occurs during the holdup in the batch dissolution procedure where the acidity is low prior to adjustment. Therefore, after acid adjustment, nitrous acid is added to convert the plutonium to the Pu(IV) form, which is the most stable and also the most highly complexed by TBP

$$Pu(III) + HNO_2 + H^+ \rightarrow Pu(IV) + NO + H_2O \quad (1)$$

$$Pu(VI) + HNO_2 + H_2O \rightarrow Pu(IV) + NO_3^- + 3H^+ \quad (2)$$

First Cycle Extraction and Partitioning of Uranium and Plutonium

The uranium and plutonium are extracted from the metal solution by TBP, diluted with an inert hydrocarbon of low viscosity and specific gravity. The two metals are subsequently separated and each is eventually extracted back into an aqueous medium. In the first extraction the aqueous acidic metal solution enters the column near the midpoint and flows downward; the organic phase enters the bottom of the column and flows upward. Flow conditions and salting strength are so regulated that uranium and Pu(IV) are extracted almost quantitatively, leaving most of the fission products and other impurities in the aqueous phase.

After extracting the metal, the organic phase, which is nearly saturated with uranium, is scrubbed in the upper part of the column with nitric acid to backwash any extracted fission products before it passes out the top and on to the midpoint of the second (partitioning) column. A high degree of saturation is maintained to maximize throughput and restrict fission product extraction. The aqueous solution, containing the bulk of the fission products, is drawn off the bottom of the first column.

In the partitioning column the plutonium is reduced to Pu(III) in the presence of dilute nitric acid, which is introduced at the top of the column. Plutoni-

* Oak Ridge National Laboratory. Including work by S. V. Castner, L. E. Line, Jr., J. Reilly, DuPont, Savannah River Plant, Ga.; J. R. Flanary, A. T. Gresky, R. G. Mansfield, Oak Ridge National Laboratory; W. B. Lanham, D. C. Overholt, Carbide and Carbon Chemicals Co., South Charleston, W. Va.

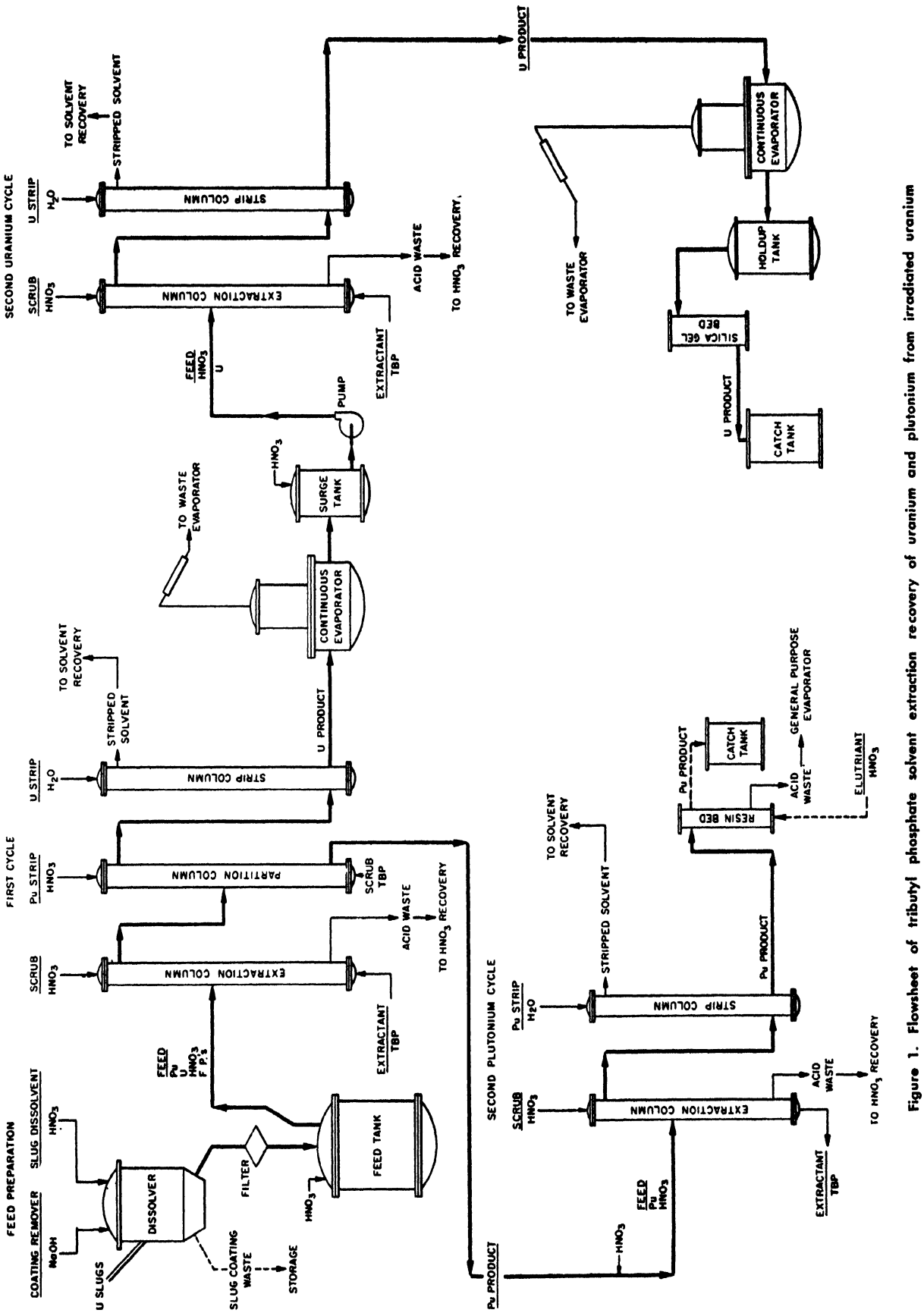

Figure 1. Flowsheet of tributyl phosphate solvent extraction recovery of uranium and plutonium from irradiated uranium

um(III), which has a very low distribution coefficient, 0.02 under these conditions, and part of the uranium are stripped from the organic solvent into this acid stream. The aqueous stream is scrubbed with TBP, introduced at the bottom of the column, to re-extract the uranium. The aqueous plutonium solution flows continuously to the second plutonium cycle; the organic uranium solution is fed to the bottom of a third column where the uranium is stripped with water, and is then fed to the second uranium cycle. At this point the products are decontaminated from gross fission products by a factor of 10^3-10^4.

Extraction column conditions are chosen for maximum uranium and plutonium and minimum fission product extraction as determined by the relative complexing action of TBP. The reaction of uranyl nitrate with TBP is

$$UO_2^{++}{}_{aq} + 2NO_3^-{}_{aq} + 2TBP_{org} \rightarrow UO_2(NO_3)_2TBP_{2\ org} \quad (3)$$

If activity coefficients are neglected, the equilibrium constant, K_m, for this equation is approximately 22 for TBP diluted with an inert hydrocarbon; it is nearly independent of hydrogen ion concentration. Similar complexes are formed by TBP with nitric acid, $K_m = 0.177$, and with Pu(IV) and Pu(VI). In nitric acid concentrations greater than $1M$, an equation involving second-power TBP dependence and fourth-power nitrate dependence fits most of the data with a K_m value of 3.0 for Pu(IV).

Equation 3 may be rewritten as

$$\text{U(VI) D.C.} = K_m(NO_3^-)^2{}_{aq}\,(TBP)^2{}_{org} \quad (4)$$

where the uranium organic/aqueous distribution coefficient, D.C. (O/A), is defined as the ratio of the uranium concentration in the solvent to that in the aqueous phase.

The relative complexing power of TBP is illustrated by the results of batch equilibration of TBP with a nitric acid solution of uranium, plutonium, and mixed fission products, with conditions adjusted to yield about 60% uranium saturation of the solvent. The D.C. (O/A) for U(VI), Pu(IV), and Pu(VI) is 8.1, 1.5, and 0.6, respectively; that for the bulk of the fission products is 0.002. Hence, a high degree of separation is possible.

From Equation 4 it may be seen that the complexing action of TBP is affected by the nitrate ion concentration of the aqueous phase and the concentration of TBP.

Extraction of uranium and Pu(IV) into the organic phase gradually increases with increasing nitrate ion concentration. With the rare earths and other fission products the distribution is the opposite (see Table I).

The uranium distribution coefficient (O/A) decreases as 100% uranium saturation of the solvent is approached. Also, with a high uranium saturation less plutonium and fission products are extracted (see Table II). The proper saturation point for maximum decontamination consistent with efficient product extraction is determined from the extraction factor, i.e., the ratio of the amount of product in the solvent phase to that in the aqueous phase multiplied by the ratio of organic to aqueous flow rates: Extraction factor = D.C. × vol of organic phase/vol of aqueous phase.

Plutonium Purification

For additional separation from fission products, the plutonium is processed through a second solvent extraction cycle in a manner similar to that previously described. The aqueous Pu(III) solution is treated continuously with a threefold excess of sodium nitrite at room temperature. The following reaction occurs:

$$Pu(III) + H^+ + HNO_2 \rightarrow Pu(IV) + NO + H_2O \quad (5)$$

After adjustment to the appropriate salting strength with nitric acid, the Pu(IV) is then again extracted with TBP. As the nitric acid concentration increases the salting strength for Pu(IV) increases rapidly, and rare-earth extraction remains low (see Table III).

The organic phase, after scrubbing with nitric acid to backwash extracted fission products, passes to a

Table I. Distribution of Uranium, Plutonium, and Fission Products as a Function of Nitric Acid Concentration in the Primary Extraction*

HNO_3 in aqueous phase (M)	Distribution coefficient, O/A			
	U	Pu(IV)	Gross β	Total rare earths
0.5	1.18	0.10	0.0008	0.0004
2	2.84	0.46	0.0008	0.0005
3	3.28	0.59	0.0010	0.0004
4	4.28	1.11	0.0023	0.0004
5	4.16	1.55	0.0034	0.0002
6	3.61	2.62	0.0041	0.0001

* Aqueous: nitric acid solution of U, Pu, and mixed fission products. Solvent: TBP in Amsco 123-15. Equilibration time: 5 min; temperature: 25°C.

Table II. Distribution of Uranium, Plutonium, and Fission Products as a Function of Percentage Uranium Saturation of Solvent*

Uranium saturation of solvent (%)	Distribution coefficient (O/A)			
	U	Pu(IV)	Gross β	Total rare earths
28.0	16.7	4.0	0.013	0.0096
37.0	13.7	3.7	0.011	0.0073
45.6	12.1	2.3	0.0065	0.0048
54.9	10.2	1.3	0.005	0.0032
61.7	7.9	1.6	0.0035	0.0021
70.2	6.4	1.3	0.0025	0.0014
72.0	5.4	1.1	0.0018	0.0011
77.2	4.5	1.0	0.0015	0.0007
82.4	3.6	0.79	0.0011	0.004
86.8	2.3	0.57	0.007	0.002

*Aqueous: nitric acid solution of U, Pu, and mixed fission products. Solvent: TBP in Amsco 123-15. Equilibration time: 5 min; temperature: 25°C.

second column where the plutonium is stripped into water. Final product concentration is achieved by ion exchange.

Uranium Purification

The aqueous stream from the first cycle is continuously evaporated and adjusted to proper feed concentration by addition of nitric acid.

The uranium is extracted with TBP under conditions similar to those of the first cycle. The uranium is stripped from the organic phase with water, and the aqueous effluent is evaporated. At this point the product meets β-activity specifications, but it contains two to three times the permissible amount of γ-activity.

The uranium is finally purified by passing the concentrate through a column packed with silica gel. It also acts as a filter; any insoluble matter present in the concentrate collects near the top of the bed, and is subsequently backwashed when adsorbed activity is eluted with dilute oxalic acid. Integral decontamination factors of about 20 are obtained by silica gel adsorption.

SOLVENT CHEMISTRY

Pure tributyl phosphate is a water-white, somewhat viscous liquid (see Table IV) used industrially as a plasticizer and antifoaming agent. Early experience with this solvent indicated that the fission product β-activity in the first cycle product was five times as great with commercial-grade TBP as with butanol-free TBP. Monobutyl acid phosphate, which is aqueous-soluble, is also present in commercial-grade TBP. No major process difficulties associated with this contaminant have been encountered, although it forms precipitates with Pu(IV). The acidic phosphate impurities and traces of uranium and fission products are easily removed from the used solvent by washing with dilute sodium carbonate or hydroxide solution followed by dilute nitric acid washing. All new and used solvent is treated in this manner before use or re-use.

The TBP concentration is limited by its relatively high viscosity and density. Desirable physical properties are attained by blending the solvent with an inert hydrocarbon of low specific gravity and viscosity to permit greater dispersal and more rapid phase disengagement. The diluent used, Amsco 123-15, has a specific gravity of 0.788, a flash point of 143°F, and a Saybolt viscosity at 100°F of 31 sec. The diluent is composed of 83% paraffins, 11% aromatics, and 6% naphthenes. Although the diluent becomes yellow upon contact with aqueous streams containing nitrous acid, the extent of nitration under process conditions is very slight and not significant.

The selection of Amsco 123-15 in preference to other hydrocarbons with similar physical properties and chemical compositions was based on the following criteria: (1) high flash point, (2) nontoxicity, (3) noncorrosiveness to stainless steel, (4) purity, (5) radiation stability, and (6) low affinity for fission products.

Table III. Distribution of Pu(IV) and Fission Products as a Function of Nitric Acid Concentration in the Plutonium Purification Cycle*

	Distribution coefficient (O/A)			
HNO_3 (M)	*Pu(IV)*	*Gross β*	*Gross γ*	*Total rare earths*
0.7	1.5	0.018	0.013	0.013
2.0	8	0.020	0.023	0.020
4.0	25	0.023	0.060	0.017
6.0	35	0.026	0.15	0.010

* Aqueous: nitric acid solution of Pu and mixed fission products. Solvent: TBP in Amsco 123-15. Equilibration time: 15 min; temperature: 25°C.

Table IV. Properties of Tributyl Phosphate

Chemical formula	$(C_4H_9)_3PO_4$
Molecular weight	266
Color	Water white
Odor	Mildly sweet
Refractive index at 20°C	1.4245
Viscosity at 25°C	3.41 centipoises
at 85°C	38.6 Saybolt sec
Boiling point at	
760 mm Hg	289°C
15 mm Hg	173°C
1 mm Hg	121°C
Specific gravity at 25°C	0.973
Freezing point	−80°C
Flash point, Cleveland open cup	294°F
Dielectric constant at 30°C	7.97
Solubility in water at 25°C	0.6 vol %
Solubility of water in TBP at 25°C	7 vol %

REFERENCE

1. Foster, D. L., Savolainen, J. E. and Wymer, R. G., P/547, *Nuclear Reactor Fuel Element Dissolution*, Volume 9, Session 21B, these Proceedings.

Experience With a Direct Maintenance Radiochemical Processing Plant

By R. B. Lemon and D. G. Reid,* USA

It is not possible to burn up completely the fissionable material from the fuel elements in a nuclear reactor because the depletion of the fissionable material, the build-up of fission product poisons and radiation damage to the elements eventually requires their replacement. Economical operation of a reactor requires that the unconsumed fissionable material be recovered from the spent fuel elements. This paper describes a successfully operating plant for the recovery and decontamination of fissionable material from fuel elements. Its purpose is to summarize the features of this plant and the experience gained during its operation. As reprocessing operations must always be considered as an integral part of any nuclear reactor program, it is hoped that this information will be of value to those planning reactor programs in the future.

The Idaho Chemical Processing Plant is located at the National Reactor Testing Station near Idaho Falls, Idaho. The plant was specifically designed for processing uranium-aluminum alloy fuels such as those used in the Materials Testing Reactor, although spare cells were provided for the addition of processing facilities for other fuel types and for other radiochemical processes. The development of the solvent-extraction process used in the plant was carried out by the Oak Ridge National Laboratory. The plant was designed by Oak Ridge and the Foster-Wheeler Corporation and constructed by the Bechtel Corporation. Initial startup and operation was carried out by the American Cyanamid Company of New York early in 1953. The present operating contractor is the Phillips Petroleum Co. of Bartlesville, Oklahoma.

The Idaho plant is the first Atomic Energy Commission fuel element processing facility that has been designed for direct, rather than remote, maintenance. No provisions have been made for remotely-controlled removal or repair of the process equipment. Thus in the event of equipment failure or the necessity of modification, chemical solutions must be used to decontaminate the equipment before personnel can be allowed access to the process areas to carry out the required work. As the radioactive solutions processed contain as much as 150 curies of radioactivity per liter, effective procedures for decontamination are an absolute necessity for the successful operation of this type of plant.

* Phillips Petroleum Company, Atomic Energy Division, Idaho Falls, Idaho.

PROCESS DESCRIPTION AND RESULTS

The process in use at the Idaho plant for recovering uranium from spent uranium-aluminum alloy fuels was developed at the Oak Ridge National Laboratory. The process consists of three basic steps: dissolution of the uranium, aluminum elements in nitric acid; adjustment of the dissolver solution to a composition suitable for extraction; and separation of the uranium from the fission products and plutonium in three cycles of liquid-liquid extraction, employing methylisobutyl ketone (hexone) as the solvent. The solvent extraction cycles are operated continuously while the other portions of the process are carried out as batch operations. A simplified flowsheet of the process is shown as Fig. 1.

Fuel Cooling

The reactor fuel elements are stored ("cooled") under water before processing to allow U^{237} formed during irradiation to decay to a level such that it does not appreciably affect the radioactivity of the uranium product so it can be handled without shielding. During this cooling period the fission product activity is also reduced by radioactive decay.

Dissolution

The aluminum alloy fuel elements are dissolved at boiling temperature in nitric acid containing mercuric nitrate catalyst. Different dissolution procedures must be developed for each type of fuel element processed, as the dissolution rate varies markedly with the alloy composition, exposed surface area, thickness of the fuel elements and concentrations of nitric acid and mercuric nitrate.

Feed Preparation

Solid material in the feed solution, if present, is removed by filtration by means of vacuum through a sintered stainless-steel filter. The filter is cleaned, when necessary, by backwashing with sodium hydroxide solution. Uranium losses with the filter cake amount to about 0.05 per cent of the total feed.

The feed solution is adjusted to a composition suitable for extraction by concentration and the addition of ammonium hydroxide.

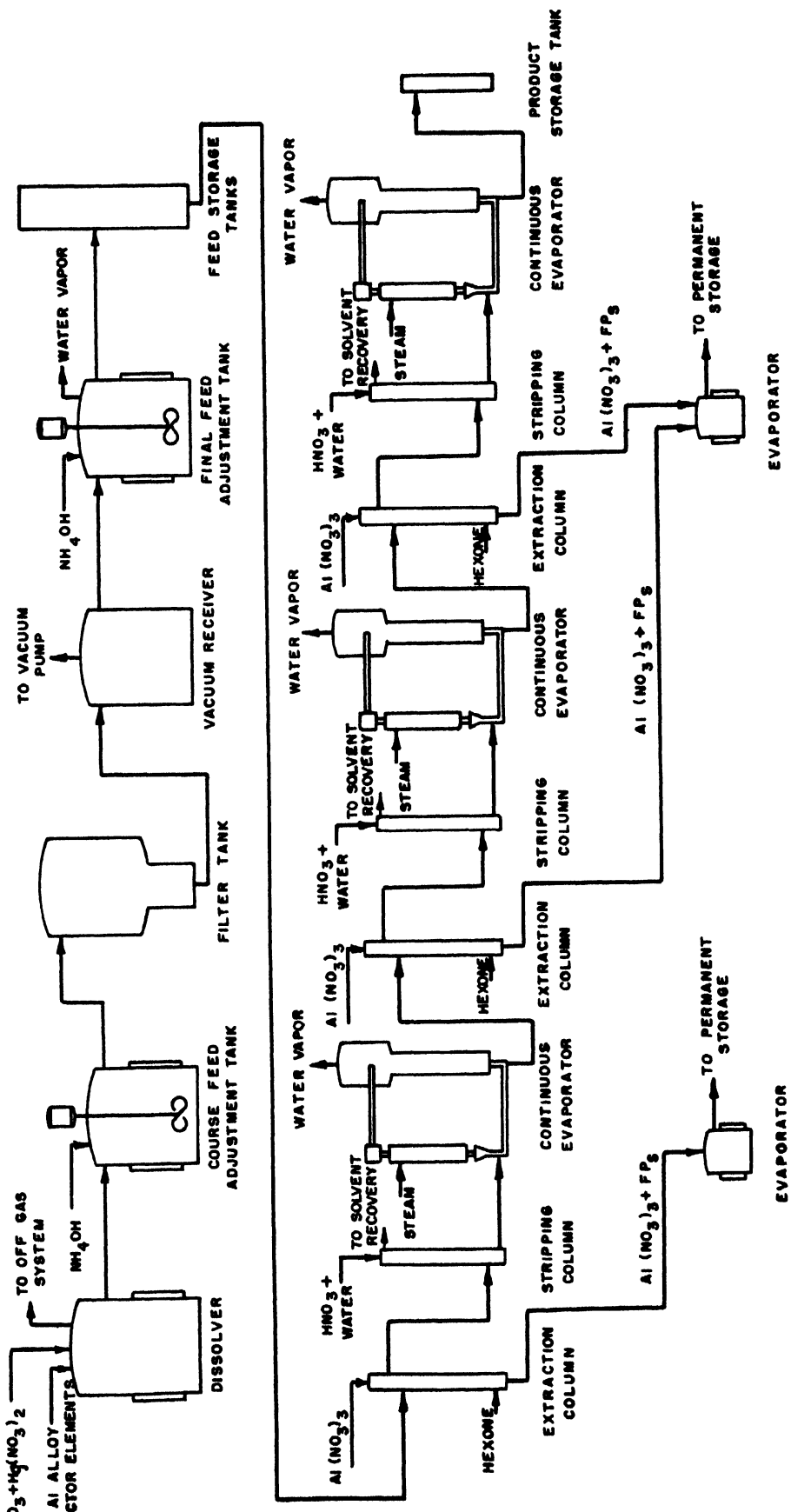

Figure 1. Simplified flow sheet for aluminum alloys

Solvent Extraction

The solvent extraction process involves a series of extraction-stripping cycles as shown on the simplified flowsheet (Fig. 1). Uranium is extracted with hexone from aluminum nitrate solution in the lower section (extraction section) of the extraction columns. Most of the fission products remain in the aqueous phase, as the fission products are considerably less extractable than uranium. The uranium-hexone extract rises into the upper section (scrub section) of the extraction column where additional fission product decontamination is accomplished by scrubbing with a counter-flowing stream of aluminum nitrate solution. The solvent, containing the uranium and some fission products, is contacted with dilute nitric acid in a second column and the uranium and fission products are stripped into the aqueous phase. A new feed is prepared from this solution by concentration in an evaporator and the extraction-stripping cycle is repeated for additional fission product decontamination. The aluminum nitrate salting agent for this extraction is provided in the extraction column scrub stream. Three extraction-stripping cycles are required before the uranium is sufficiently free of fission products to permit handling without shielding. Plutonium follows the same path as the fission products in the extraction cycles. A reducing agent, ferrous sulfamate, is added to the second cycle scrub stream to enhance over-all plutonium decontamination.

Uranium waste losses from the columns during a typical processing run totalled 0.15 per cent of the uranium fed. About 0.04 per cent of this loss was contained in the first extraction column waste. The balance of the loss was due mostly to column upsets, as each of the other column waste streams normally contain less than 0.01 per cent loss.

Gross fission product beta- and gamma-radioactivity decontamination factors for the over-all process are over 10^6. Typical fission product decontamination factors for each solvent extraction cycle are given in Table I. Ruthenium is the fission product limiting decontamination and is the only fission product that has been found in significant quantities in the final product stream.

Table I. Fission Product Decontamination Factors

Extraction cycle	*Decontamination factors* *	
	Beta	*Gamma*
First	9.5×10^8	3.8×10^8
Second	50	49
Third	5.6	7.0
Over-all	2.6×10^6	1.3×10^6

* The decontamination factor is defined as the ratio of the radioactivity initially associated with the feed uranium to the radioactivity associated with the product uranium.

Waste Handling

Equipment is provided for recycling process wastes high in uranium back to the process when necessary. Normally, liquid wastes from the processing operations are concentrated to the minimum volume possible without crystallizing and stored in underground, stainless-steel storage tanks.

The first-cycle extraction waste storage tank is equipped with internal cooling coils for the removal of heat generated by fission product decay. It is necessary to cool this tank to minimize corrosion.

Second- and third-cycle extraction wastes and all other concentrated wastes are stored together in a second underground tank system. It is not necessary to cool this system because of the relatively low radioactivity level.

Medium activity level wastes such as the condensates from the evaporation of the extraction column wastes and the filter backwash solutions are collected in the process equipment waste system and evaporated. The condensate is sufficiently decontaminated for discharge to the ground, and the concentrate is stored with second- and third-cycle wastes. A continuous-feed, thermosyphon-type evaporator equipped with a bubble cap de-entrainment tower is used to concentrate these wastes. The evaporator bottoms are dumped to the second- and third-cycle waste storage system periodically. Decontamination factors of about 10^4 are realized with this evaporator, where the decontamination factor is defined as the ratio of the activity in the feed to that in the condensate.

A second radioactive waste system collects wastes from laboratory and process area drains with activity levels low enough that they can normally be discharged directly to the ground. These wastes can be routed to the process equipment waste evaporator if necessary.

During a normal processing run, about 7×10^{-7} curie of radioactivity is discharged to the ground for each curie of activity in the fuel elements processed. About 1×10^{-7} curie of this activity is contained in the process equipment waste evaporator condensate with the balance coming from the low-level waste system discharges and the overflow water from the fuel element storage basin. Wastes discharged to ground are mixed with various cooling-water, steam condensate and other non-radioactive waste water streams before discharge to the ground. The combined waste stream flows through a continuous recording monitoring station before discharge. The combined stream meets drinking-water tolerances for radioactive contamination as given in the National Bureau of Standards Handbook 52.

Solvent Recovery

The spent solvent from the stripping columns is recovered for re-use in the process. It is first contacted with sodium hydroxide and the solvent-sodium hydroxide mixture is then fed continuously into a four-plate bubble-cap fractionating tower where the hexone is distilled to remove completely solvent decomposition products and fission product contamination. Essentially all of the solvent is recovered in this

manner and solvent losses average only about one per cent during normal operation.

PLANT FACILITIES

Design Philosophy

Direct Maintenance

The Idaho Chemical Plant was designed for direct maintenance. The process equipment is designed with sufficient capacity to allow periodic shutdowns for maintenance operations. The equipment is of simple mechanical design for easy decontamination and repair and contains a minimum of moving parts. Solution addition funnels and outlets to the waste system are provided to facilitate decontamination with chemical solutions. Critical items such as transfer jets, valves and pumps are installed in pairs or alternate transfer routes are provided so that failure of one equipment piece will not require a process shutdown for repair. The use of valves and pumps is held to a minimum. Much of the equipment with a high maintenance potential, such as Lapp Pulsafeeder pumps and samplers, has been placed in shielded cubicles located outside the hot cells. To minimize maintenance requirements during the processing of radioactive solutions, all equipment is leak-tested and operated on simulated process solutions before actual radioactive processing operations begin. Stainless-steel liners and spray nozzles are provided in the process cells to facilitate external decontamination of the equipment and the cells. The direct maintenance philosophy allows a maximum amount of process equipment to be placed in each cell as no provision is made for removal by remote methods. Permanently installed ladders and platforms are provided in many cells to allow maintenance personnel easy access to otherwise hard-to-reach equipment.

Shielding

The radioactive process and auxiliary equipment is shielded either by the cell walls or by unit shielding when outside the cells. In general, the shielding is designed to reduce the radiation intensity to less than 1 mr/hr in the zones to which personnel normally have access.

Critical Mass Control

As fissionable materials are processed, there is always a chance of accumulating a critical mass. The process and process equipment must, of course, be designed to prevent critical conditions. Each process vessel is made safe by one of the following methods:

1. Limited concentration, in which the concentration of the solution is held within the range where a chain reaction is not possible.
2. Mass limitation, where the quantity of fissionable material allowed in the vessel is kept below the amount that can go critical under any possible condition.
3. Safe geometry, where the vessel diameter is such that critical conditions can never be achieved because of high neutron loss. Vessel spacing is such that interaction between vessels is minimized.

All vessels in the continuous feed storage, extraction, waste and product areas are of safe geometry. Vessels one step removed from the continuous equip-

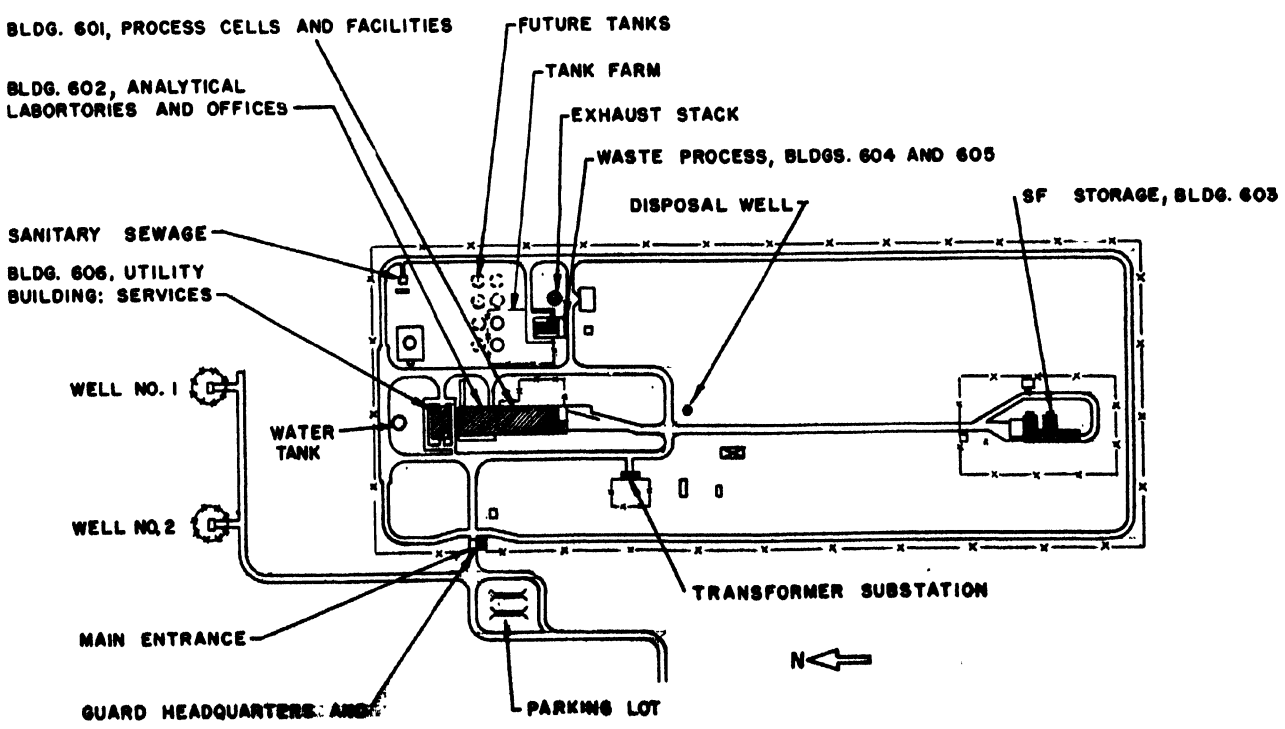

Figure 2. Plan for the chemical-processing area

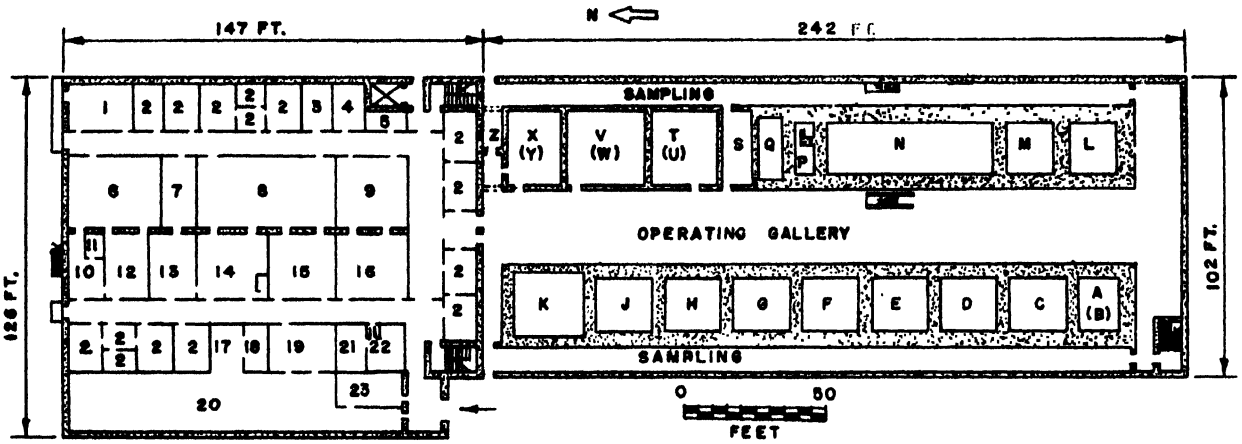

Figure 3. Plan at operating-corridor level, process and laboratory buildings. Building 602, laboratory and administration; (1) stock, (2) office, (3) dish wash, (4) health physics, (5) emergency wash, (6) instrument laboratory, (7) counting room, (8) warm laboratory, (9) sample dilution, (10) optical laboratory, (11) dark room, (12) chem. spec. preparation, (13) mass-spec. preparation, (14) mass-spectrometer, (15) cold laboratory, (16) warm miscellaneous, (17) drying room, (18) men's shower, (19) men's wash room, (20) locker room, (21) women's wash room, (22) locker room, (23) clothing. Building 601, process cells; (C) feed preparation, (D) feed preparation, (J) hot salvage, (K) solv. recovery, (N) feed storage, (P) 1st cycle extrac., (Q) 2nd cycle extrac., (R) upper part of "S", (S) 3rd cycle extrac., (T) solvent pumb room, (U) 1st cycle aq. raff. treat., (V) decontamination, (W) 1st cycle solv. raff. treat., (X) sample dilution, (Y) 2nd and 3rd cycle raff. treat., (T through Y on 2 levels), (Z) 3rd cycle prod. storage

ment are mass or concentration limited and critical conditions are prevented by rigid process control measures.

Process cell floors are so pitched that, in the event of a major spill, solution depth cannot exceed an "always-safe" depth. A geometrically-safe sump with an alarm and steam jet is placed at the low point in each cell.

There are no gravity-flow connections between process tanks containing uranium and waste collection drains. All floor drains are normally closed by an air-operated valve to prevent entry of uranium to the waste system.

Arrangement

The plant is located in a fenced area approximately ⅗ mile long by ⅕ mile wide. Within this area all fuel element storage, processing, waste disposal, and service facilities are located as shown in Fig. 2. All processing facilities, the fuel storage basin, and waste storage tanks are underground, extending, in the case of the process building, to a point 55 ft below grade.

A plan view of the process and laboratory and administration buildings is shown as Fig. 3.

The process building, which houses the bulk of the processing equipment, is approximately 240 ft long, 100 ft wide, and 60 ft deep at maximum depth. These dimensions exclude the steel and Transite building which covers the roof deck and houses the chemical make-up area. Cells average 20 ft square by 40 ft deep and are shielded with 2 to 5 ft of normal concrete, depending upon the activity level of the material being processed in the cell.

Figure 4 shows a section through the process building taken through the feed preparation and feed storage cells.

The process instruments and controls are located on panels in the center of the operating corridor. Solution addition, service and instrument lines enter the cells through offset pipe sleeves through the cell walls adjacent to the operating corridor. Personnel access to the cells is through labyrinth corridors and doors from the access corridor.

A "hot" analytical facility (Cell X) is located in the process building. This area is used primarily for storage of high-radioactivity-level samples and for housing dilution and decontamination equipment for preparation of the samples for removal to the laboratory building.

The laboratory and administration building adjoins the process building on the north. This building houses the administrative offices, cafeteria, telephone exchange, first aid facilities, low-radiation-level analytical laboratories, process development laboratories, and maintenance shop. The analytical laboratory floor is located on the same level as the process operating gallery and is shown on Fig. 3.

The service building which houses the steam plant, electrical equipment, the heating and ventilating equipment and other service equipment adjoins the laboratory and administration building on the north side.

The basin for the storage of incoming fuel elements is located approximately ⅛ mile south of the process building as shown on Fig. 2. The fuel elements are stored under water in stainless-steel buckets suspended from a system of overhead tracks in two storage basins in this building. The building also contains two transfer basins for the loading and unloading of fuel element carriers under water and a transfer canal for movement of the buckets between the storage and transfer basins. The basin water is continually recirculated through a filter so that it will be kept clear.

The waste disposal building and waste storage tank farm are located to the east of the process building.

The waste disposal building houses tanks for the temporary storage of radioactive wastes, the process equipment waste evaporator, the exhaust fans for process cell ventilation and the Fiberglas filters and exhaust equipment for the vessel ventilation systems. The 250 ft stack for discharge of waste gases and ventilation air is located next to the waste building. The waste tank farm contains the stainless-steel tanks and auxiliary equipment for storage of the radioactive process wastes.

Ventilation System

All process areas are kept under a negative pressure of about 0.2 inch of water with respect to the personnel areas to prevent the spread of radioactive contamination. The ventilation system is designed to provide twenty air changes per hour to the process cells to sweep out any solvent vapors that might accumulate and cause an explosion hazard.

Fresh air under a positive pressure is supplied to the process building after being washed and heated in the service building. This air is distributed to the nonradioactive areas of the building and drawn into the cells and sample corridors. The main air flow to the cells is through louvred doors in the access corridor. The air is exhausted from the cells and sample corridors via the vent tunnels and delivered to the stack via a connecting duct and two fans in the waste disposal building. The main exhaust air is not cleaned before discharge through the stack since all process equipment operates under a slight vacuum, making the possibility, therefore, of contaminating the cell air very remote.

All process vessels, except for the dissolving vessels, are ventilated through a closed system designed to keep the vessels under a negative pressure of one inch of water with respect to the cells. A condenser is provided on the main header to remove steam vapors which enter this system during steaming of the process vessels for decontamination. The ventilation gases from this system are filtered through a packed-bed Fiberglas filter in the waste disposal building before passing through the exhaust blowers to the stack.

The dissolver vessels and sampling stations are ventilated by similar systems. The dissolver system is designed to provide a pressure differential of up to 10 inches of water during fuel element dissolutions. Vacuum is drawn on the system by a steam jet ejector in the waste disposal building. The sampler off-gas system provides a minimum air velocity of 100 linear ft/min through any opening in the sampler stations by means of two exhaust blowers located in the process building.

PROCESS EQUIPMENT

Most of the process equipment items are standard commercially-available items which have been thoroughly evaluated to make sure they are suitable for use in this type of plant. A few of the items were specially designed to meet the process requirements and were built by commercial fabricators.

Process Vessels

The process vessels are fabricated of Type 347, 304ELC or 309SCb stainless steel as this material is highly resistant to corrosion by the nitrate ion contained in the process solutions and does not require annealing after welding. In general, Type 309SCb is used only for dissolver vessels which contain high concentrations of nitric acid and are subject to operation at boiling temperatures. These construction materials have proven highly satisfactory and there have been no corrosion failures in the plant.

All vessels are of standard all-welded construction and were built by commercial fabricators.

Vessels that are emptied by jet suction usually are fabricated with a reverse-dish head on the bottom so that they may be almost completely emptied by a suction line located at the low point of the head. Some vessels emptied by bottom outlets do not have reversed heads. All vessels requiring agitation are equipped with air spargers and a few also have mechanical agitators. Vessels requiring heating and cooling have external steam and water jackets; no internal coils are provided.

Vessels originally installed in the plant did not have internal spray nozzles. It has been found desirable to provide spray nozzles in all new vessels to allow spraying of decontaminating solutions against the upper areas of the vessels.

Condensers are of conventional shell and tube construction. Cooling water is admitted to the shell side.

The solvent extraction columns are fabricated from standard-sized pipe and are packed with stainless steel Raschig rings. Aqueous outflow from the column is controlled by air pressure applied to the column discharge loop. The diameters of the columns are small enough that they are geometrically safe with respect to nuclear chain reactions.

Thermosyphon-type, critically-safe, continuous evaporators are used for concentrating the intercycle feed and final product streams. The steam jacket on the evaporator tube bundle is separated from the tube sheets at the ends of the bundle so that leakage from these tube sheets will fall to the floor rather than entering the steam chest.

Piping and Valves

Process lines are Type 347 stainless-steel tubing or schedule 40 pipe. Ventilation lines are of Type 347 while instrument tubing is either Type 347 or 304 stainless steel. In some cases 309SCb stainless steel is used for dip tubes normally in contact with nitric acid solutions at boiling temperatures. Remotely controlled valves in the process areas are of Type 347 stainless.

Lines and valves are sloped to drain by gravity, when possible. Most valves are installed at a 45-degree angle with the horizontal plane to insure good drainage.

All lines of less than 1-in. diameter in the original installation were of tubing and connected by non-

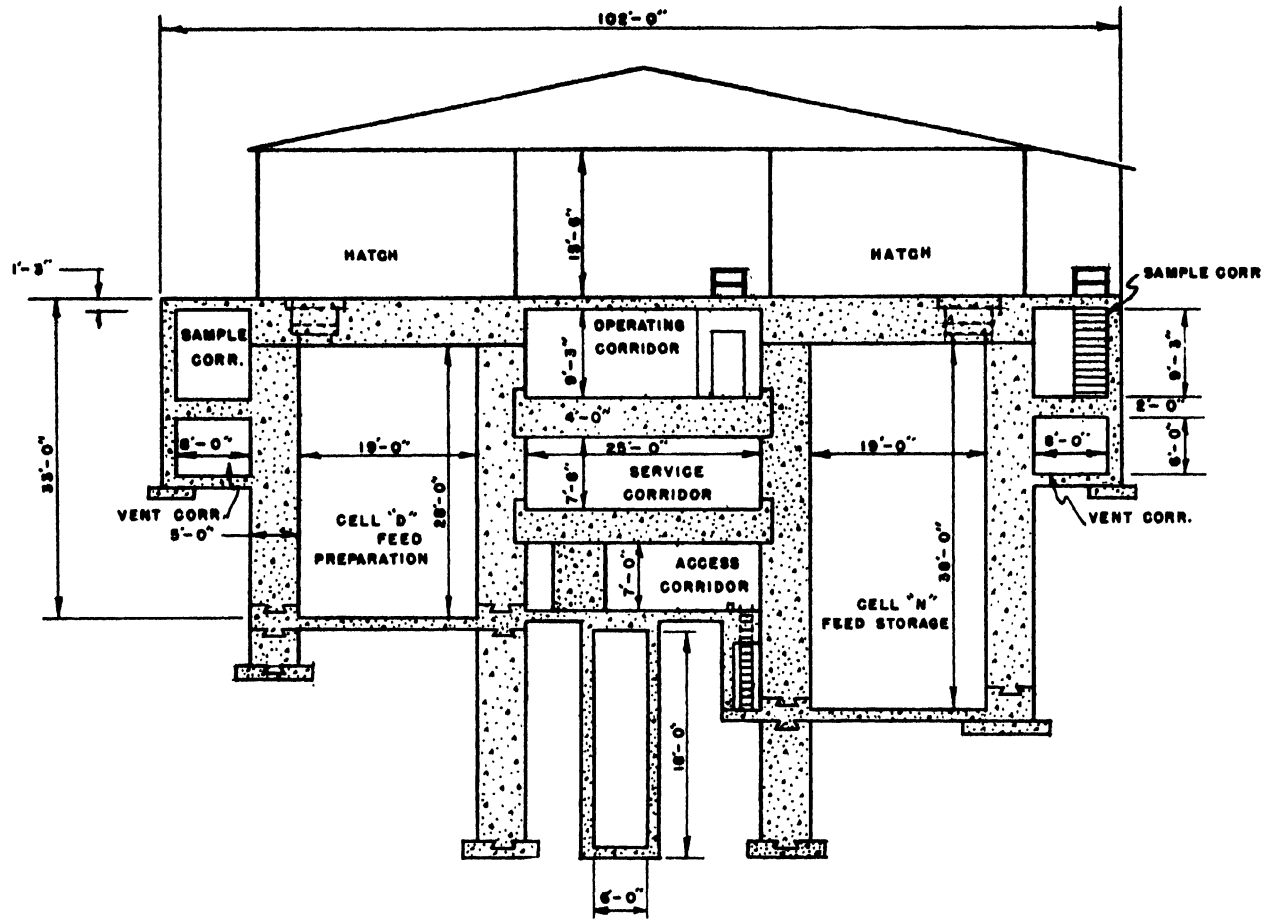

Figure 4. Cross section of process building at cells D and N

gasketed tubing connectors. Lines of 1-in. diameter or larger were of Schedule 40 pipe connected by welding. The welded lines have served satisfactorily whereas the tubing connectors have shown a tendency to leak as evidenced by a high degree of external contamination in the cells. Much of the original tubing has been replaced with all-welded pipe and all new piping is of all-welded construction.

A minimum number of valves is installed in the process areas. Mason-Neilan bellows-sealed valves operated by air pressure are used almost exclusively. The bellows is enclosed by an all-welded housing which prevents solution leakage in the event of bellows failure. The air pressure controls are located on the operating corridor panel boards. These valves are of the on-off type which do not control flow rates. In critical locations, two Mason-Neilan valves are usually installed in parallel so that failure of one will not cause a process shutdown. Where prevention of valve leakage is critical, two valves are installed in series. Some of these extra valves were not provided in the original installation but were added at later dates. Only two flow control valves are used on radioactive lines in the plant. These are air-operated diaphragm valves used to control the outflow rate of the third-cycle product evaporator and the feed rate to the process equipment waste evaporator. These valves are located in relatively low-radiation-level zones.

The remote valves have given satisfactory service in most cases, although a few of the Mason-Neilan valves have either leaked excessively through the seat or failed in the shut position. The bellows seals have failed in several cases but the bellows housing prevented any loss of solution. Valve failures have never caused a process shutdown because of the installed-spare and alternate-route philosophies.

Mechanical Equipment

Pumps

Lapp Insulator Co. Pulsafeeders with two diaphragm heads connected by a liquid piston line filled with kerosene are used for feeding radioactive streams to the extraction columns and solvent recovery still. The drive mechanism and one diaphragm head of these pumps are located outside of the process cells. The remote heads, which are the only parts of the pumps handling radioactive solution, are located within the cells or in shielded areas just outside the cells. Two pumps are installed in the same service so that failure of one pump does not require a process shutdown while the pump is repaired. A remote head pump installation is shown schematically in Fig. 5.

The only difficulties that have been experienced with these pumps are air-locking in the kerosene line and plugging of the check valves. Kerosene line air-locking can be minimized by installing lines of at least ½-in. diameter and installing the lines in such a way that sharp bends and level spots are not present. Check valve plugging occurs infrequently and is easily remedied by steaming out the head through permanent auxiliary lines, installed for this purpose, from the service areas.

Agitators

Mechanical agitators are installed on some of the feed preparation vessels, on the hexone-sodium hydroxide mixing pots which feed the solvent still and on some of the process equipment waste and cell floor drain waste collection tanks. Most of the agitators were originally installed with water-cooled mechanical seals. Some of these failed and were replaced by graphite-impregnated lead packing rings. These rings operate satisfactorily but do allow some leakage of radioactive vapor. It has since been found that the agitators on the feed preparation vessels are not necessary as air sparging through the existing spargers provides adequate agitation. It has also been found that the hexone-sodium hydroxide mixing pots, which have no spargers, do not require agitation. Thus the mechanical agitators on these vessels are no longer used. The mechanical agitators are still used on the waste collection tanks because they provide somewhat better agitation than spargers because of the horizontal shape of these tanks.

Steam Jets

Almost all solution transfers in the plant are made with steam jets. This method of transfer is easily adapted to remote control and is essentially trouble-free.

The steam lines supplying the jets are all vented into a common header through ¼-in. gate valves with a $\frac{1}{16}$-in. hole drilled through the gate. The operator closes the vent valve before turning on steam to the jet and opens it again immediately after turning off the steam. If he fails to open it there is sufficient air leakage through the $\frac{1}{16}$-in. hole to prevent vacuum formation when the steam condenses which would cause solution to back up the steam line.

Special Equipment

Samplers

Samples of the radioactive process solutions are necessary for process control purposes and for accurate accounting of the fissionable material.

A sampler system was specially designed to meet the particular needs of the plant. As can be seen in the building sectional view in Fig. 4, special sampling corridors were constructed at operating corridor level for each cell bank. Samplers for several cells were grouped so that a continuous 4.5-in. lead shield having one entry for a sample carrier and a single set of sample handling tongs could be used. Figure 6 shows a single air operated sampling jet, tongs and shield. The sampling tip is filled with two hypodermic needles which punch through the neoprene cap on the sample bottle. The sample bottles are removed from the sample carrier, conveyed to the sample jet and raised to sampling position. The sample is drawn by drawing a vacuum on the bottle, with the air jet, through the short needle which in turn draws process solution from the vessel to be sampled through the sampling line and long needle into the bottle. Solution is drawn through the bottle and returned to the process vessel for a few minutes before the jet is turned off and the bottle removed. Air bleed orifices are provided in sampler intake lines having

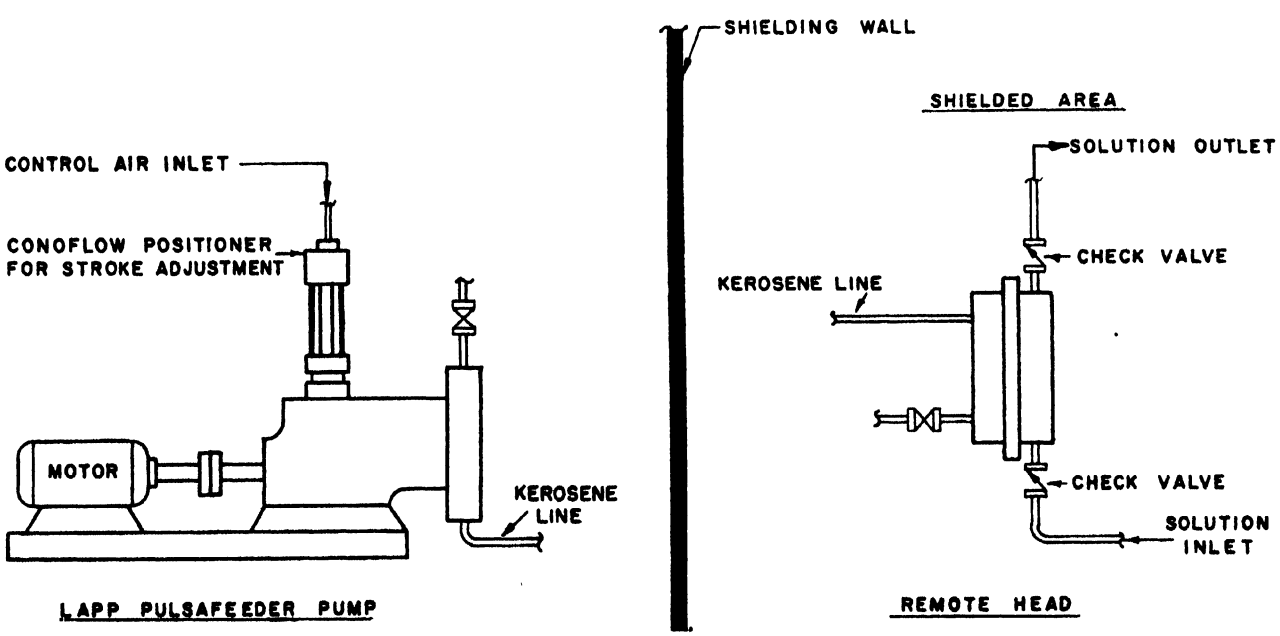

Figure 5. Remote head pump

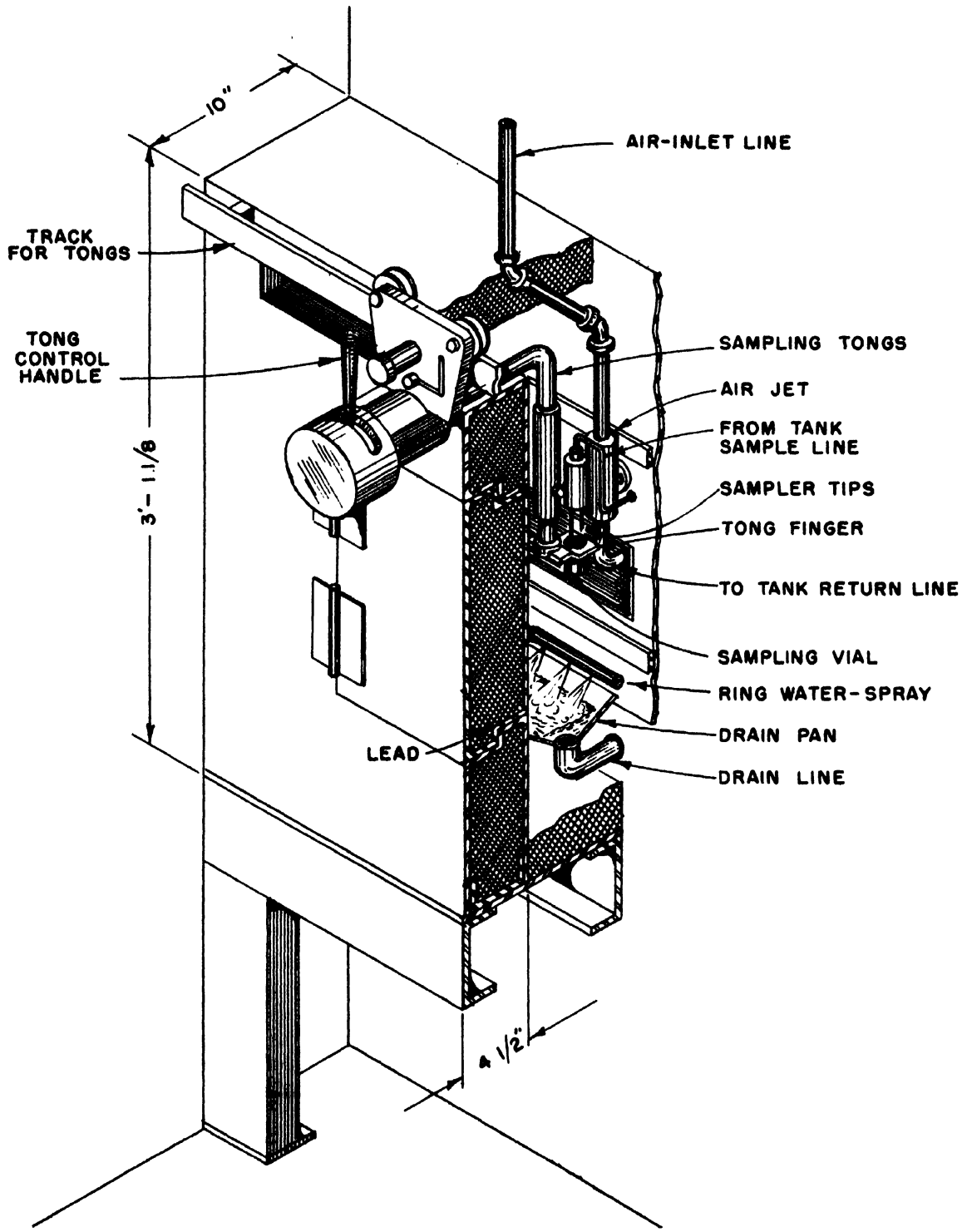

Figure 6. Sampling station

a fluid lift greater than 17 ft to provide an air lift effect and thus reduce the jet vacuum requirements. The sampling operation is viewed through a lead-glass window located directly in front of the sampler tip. The filled sample bottle is returned to the sample carrier and removed from the sampling station for delivery to the analytical facilities.

The samplers require a fair amount of maintenance but, in general, the sampling system as described above is quite satisfactory.

Product Handling Equipment

The product solution from the third-cycle evaporator is collected in two transfer vessels. It is then transferred batch-wise into the product cell collection vessels by applying air pressure to the transfer vessels. The product is drawn from these vessels by vacuum into either of two product bottle filling burettes. The product is drained from the burettes to the product shipping containers by gravity. The product container is sampled and then weighed on a balance accurate to the nearest one gram of weight. The container is then placed in a second container ("bird-cage") with outside dimensions such that the possibility of assembling a critical mass with a number of product containers is minimized.

Filter Handling Equipment

A star-shaped filter element made of sintered type 304 stainless-steel is used for clarification of the feed solution. The element is enclosed in a casing designed to prevent damage by twisting during installation or removal. A threaded connector at the bottom of the element screws into the bottom of the filter tank when the element is installed. The filter is installed or removed by a long handled wrench which fits into the slots in the casing. The wrench and element are raised or lowered by a winch. Used elements are pulled out of the feed preparation cell into a shielded carrier that travels along a track at the top of the cell. This method of filter handling has proven very satisfactory except for the stainless-steel threads which are subject to galling.

INSTRUMENTATION

Standard industrial instruments are used throughout the plant for remote control of the process operations. In general, simple recording instruments are used for the batch-operated portions of the process where the process operations are controlled manually. In the continuous extraction cycles, automatic control instruments are used extensively although some stream flows are controlled manually.

Many types of radiation and contamination monitoring equipment are also used in the plant for the protection of personnel and to monitor the decontamination performance of the process. These instruments are also commercially available types.

Most of the process control instruments are the air-purge type. The instrument panels are located in the operating corridor. The instrument lines are run across the ceiling of the operating corridor, so that there is always a point higher than the process vessel being served, through the cell wall, and to the vessel.

There are no flow measurement instruments in the radioactive portions of the plant. Flow rate control, when necessary, is accomplished with manually- or automatically-controlled metering pumps. The flow rates are checked by observing the decrease in level in vessels or burettes provided for this purpose.

Solution heads and specific gravities from which volumes are determined are measured by pneumatic instruments using an air-purge system. Purge air is admitted to the instrument lines through rotameters and bubbles out through the instrument dip legs in the process vessels. The differential pressure across two dip legs is measured by a transmitter or aneroid manometer which actuates the pen on the recording unit. Knowing the location and spacing of the dip legs allows the calculation of the density and solution head and thus the solution volume from the differential pressure readings.

The aqueous-solvent interface position in the solvent-extraction columns is recorded and controlled by a similar system. The instrument dip legs in the column measure the differential pressure across the interface which is an exact indication of the interface position because the densities of both phases are known. The controller output air pressure is fed through a reducing relay to the column jackleg pressure pot to control the aqueous outflow rate and thus the interface position.

The intercycle evaporators are also controlled by pneumatic recording instruments. The steam rates to the evaporators are controlled by the head measurement while the product outflow rate is controlled by the evaporator density. The output air pressure from the density controller actuates metering pumps in the case of the first- and second-cycle evaporators and an air-operated diaphragm valve for the third-cycle evaporator and thus regulate the product output rate.

Extremely accurate measurements of the solution volume in the feed preparation tanks is necessary for plant input measurements. Manometers are installed in parallel with the recording instruments for these tanks to provide a constant check of the head measurement.

Most of the pneumatic instruments are hooked into alarms which sound when the liquid level or density goes out of the normal operating range.

Liquid level displacement meters are used for measuring solution weights in the product transfer pots and product loading burrettes. As the level in the vessel rises, a float displaces more liquid. The displacement force thus generated causes a slight rise of the float which in turn rotates a torque tube through a small angle. A transmitter translates the rotation of the torque tube into output air pressure proportional to the solution head which is transmitted to a recorder. This type of instrument is not suitable for use in

high-radiation-level locations because the transmitter must be located next to the vessel where it would not be accessible for servicing.

Electrodes are used for actuating sump alarms and indicating high liquid levels in tanks such as filtrate receivers which are operated under vacuum. These have not proven entirely satisfactory as salt deposited on the insulation from the process solutions eventually couses a short circuit. Air-purge systems are being developed to replace the electrodes in some locations. On some sumps the electrode alarm automatically actuates a steam jet which empties the sump.

Thermocouples are used for temperature indication in remote locations. The thermocouples are installed in stainless-steel wells in the process vessels so that they do not come in contact with the process solutions. The thermocouples are connected into conventional indicating or recording units on the panel boards.

DECONTAMINATION OF EQUIPMENT FOR MAINTENANCE

As radiation levels in the process cells are estimated to run as high as 10^6 r/hr during operation, the process equipment must be decontaminated before personnel can enter the cells to perform maintenance work. During plant operation very little maintenance has been required as evidenced by the fact that the plant has averaged greater than 98 per cent on-stream operating time for all processing runs. During 14 months of actual processing operations it has only once been necessary to enter a high-radiation-level cell. However, the plant has been decontaminated twice during scheduled shutdown periods; once to allow for general maintenance work on the equipment and once to allow construction personnel to enter the plant to install additional processing equipment. During this second shutdown some general maintenance was also performed.

It is difficult, as yet, to predict the frequency of shutdowns for decontamination and general maintenance actually needed for a direct maintenance plant for this type. Based on experience to date it appears that about 30 days per year should be allowed for this purpose while another 30 days should be allowed for emergency maintenance and the correction of process difficulties.

Decontamination Methods

The thorough flushing of process solutions from the process vessels is the first step in decontamination operations. This is accomplished by water and dilute acid flushing and steaming of the vessels with steam admitted through the spargers or solution addition funnels. Appreciable quantities of uranium are usually recovered in the first flushes and they must either be sent on through the process or to the salvage equipment for eventual recovery. In some cases steam and acid flushes will decontaminate the equipment sufficiently to allow small maintenance jobs to be carried out without additional decontamination.

After flushing, the equipment is decontaminated further with chemical solutions. Chemical decontamination procedures are based mainly on past experience gained at both this plant and the Oak Ridge National Laboratory pilot plant where the Materials Testing Reactor recovery process was developed. The mildest decontaminating agents are used first followed by the more corrosive solutions. The standard decontamination agents usually used are: (1) 10% nitric acid, (2) 10% citric acid, (3) 10% sodium hydroxide-2.5% tartaric acid, (4) 10% oxalic acid, (5) 0.003*M* periodic acid and (6) 3% sodium fluoride-20% nitric acid. These solutions are normally used in the order listed except that the 10% nitric acid flush is usually repeated after use of each of the other solutions. The use of each solution is usually continued until it no longer proves effective.

The vessels are filled to slightly over normal working volume with the decontaminating solutions, heated by steam sparging or jacket steam, and agitated during the contact period. The solutions are usually held in the vessels for 8 hours at boiling or near-boiling temperature. Exceptions to this are oxalic acid solution which is heated to a maximum of 75°C and sodium fluoride-nitric acid solution which is left in contact with the vessels for a maximum time of about one hour at room temperature. The solutions are transferred between vessels during the operations to decontaminate the transfer lines. Spent decontamination solutions are disposed of to the process equipment waste system.

Although some of the decontaminating solutions used do attack stainless steel to a slight extent, the short contact times used keep the vessel corrosion to a minimum. Examination of the interior surfaces of some of the vessels after two thorough decontaminations showed that corrosion during the decontamination operations was negligible.

Off-gas lines, vent lines, knockdown towers and other equipment not normally contacted with process solutions are decontaminated by steaming. Chemical solutions can also be backed into these lines by overfilling the process vessels but this is seldom necessary.

During the internal decontamination operations, the external surfaces of the equipment and cells are decontaminated by spraying water and/or admitting steam to the cells. When the cell radiation levels are low enough the residual external contamination is removed by direct scrubbing with detergent and chemical solutions.

Sampler stations are decontaminated by recirculating decontaminating solutions from the process vessels through the samplers, steaming down the sampler lines and internal portion of the stations and cleaning up residual contamination with detergent and chemical solutions.

Contamination spread to the personnel areas is cleaned up by scrubbing or, in the case of bad spills, by removing sections of the asphalt tile.

During all decontamination operations Health Physics personnel are present to monitor radiation

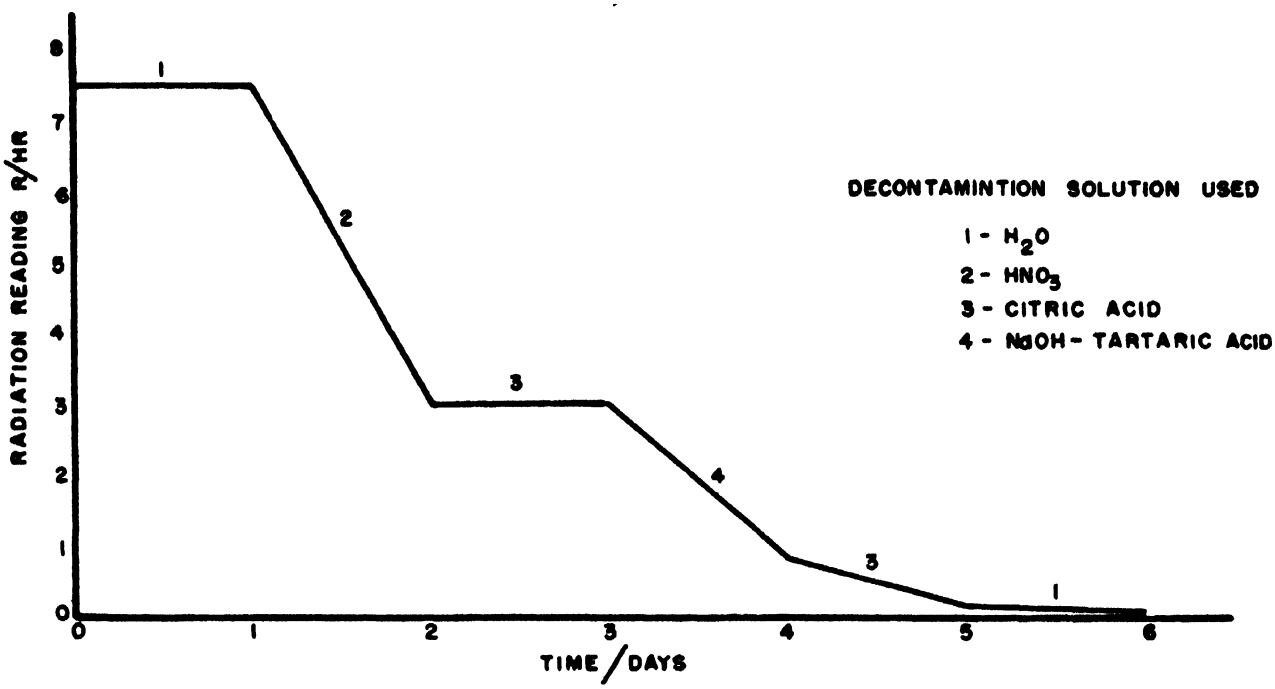

Figure 7. First decontamination of dissolver C-101

levels and safeguard the operating maintenance personnel from overexposure.

EFFICIENCY

The only time that entrance to a high-radiation-level cell was necessary during plant operation occurred during the first plant run. Fuel elements cooled for two years and longer were processed during this run and thus the decontamination before entering the cell was somewhat easier than would be possible during a short-cooled fuel-processing run. The feed stream radioactivity level was about 10 curies† per liter during this run.

During this run the first-cycle extraction column feed pot became plugged and it was necessary to shut down the extraction process. The contents of the column were jetted to the salvage equipment and the column was steamed for thirty minutes. The column was then flushed with water and jetted to salvage again. The radiation level at the column was found to be 1500 mr/hr at this time and maintenance personnel were allowed to enter the cell with limited working time. The line to the feed pot was removed and the nozzle capped and the feed pot and line to the column were flushed with steam and water to bring the feed pot radiation level down to 500 mr/hr. Two new sections of pipe were installed and the columns were started up and operated satisfactorily. The total plant down time was twenty-five hours. The weekly radiation exposure limit (300 mr/hr) was reached by four maintenance and two operations personnel during these operations.

† Radioactivity concentrations given in this report are based on beta radioactivity counting of actual process solution samples on the second shelf of a beta proportional counter. Counting efficiency is assumed to be 10 per cent.

Following the first relatively low radiation level run (feed activity of 10 curies per liter), the equipment in the feed preparation, first extraction cycle and first-cycle aqueous waste cells was decontaminated to make it possible to enter the cells and check the equipment and make minor repairs. The radiation levels in the remaining cells requiring entrance were low enough after flushing during the process shutdown to allow maintenance work to be carried out without decontamination. The extent of the decontamination required in each cell was determined by the time required to complete the work based on a maximum average daily radiation dose of 60 mr.

Decontamination progress curves for two typical process vessels, a dissolver vessel and the first-cycle extraction column are shown in Figs. 7 and 8. Radiation levels at contact beginning after the initial flushing at the time of shutdown are plotted against time on these figures and the decontamination methods used are indicated.

The dissolver required six days of decontamination with water, nitric acid, citric acid and sodium hydroxide-tartaric acid solutions to reduce the contact reading from 7.5 to 0.05 r/hr. The decontamination results for this vessel are typical of the results obtained for all the feed preparation vessels.

Steaming of the extraction column and removal of the packing reduced the radiation level from 20 r/hr down to 0.5 r/hr. No other decontaminant was used. The comparative ease with which this column was decontaminated in comparison with the batch-operated feed preparation vessels indicates that the continuous operation of equipment without intermittent idle time and operation at room rather than boiling temperatures makes the vessels easier to decontaminate.

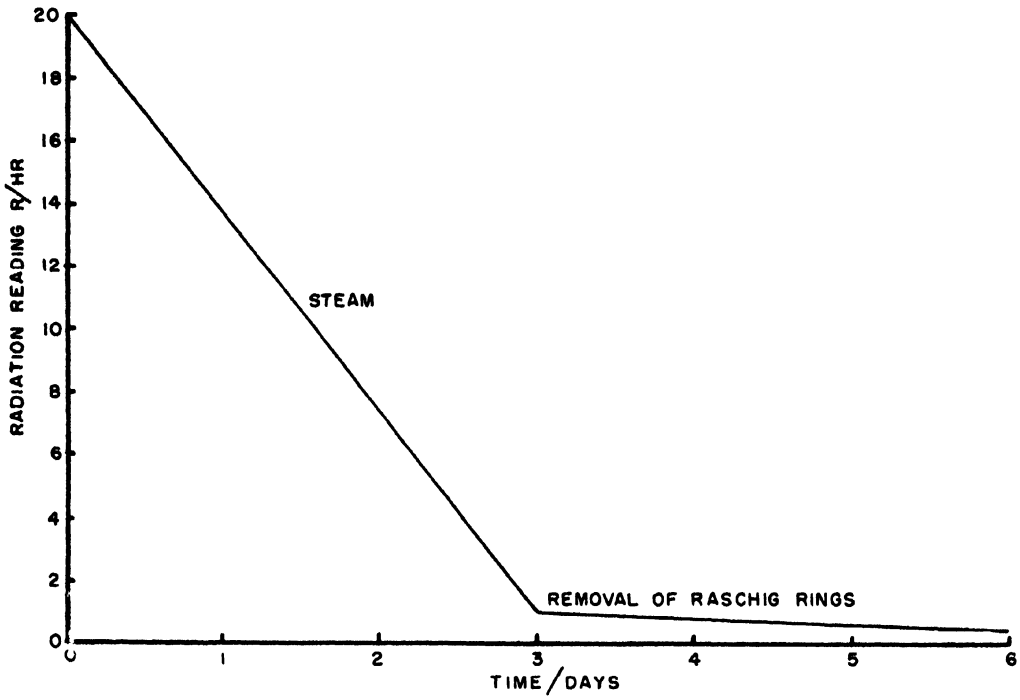

Figure 8. First decontamination of extraction column P-102

The second plant decontamination was much more difficult to carry out than the first. Just prior to this decontamination short-cooled feed solutions of 150 curies per liter had been processed. Also, the decontamination had to be continued to much lower radiation levels (< 7.5 mr/hr general background) so that construction personnel, who were unfamiliar with the effects and techniques for the control of radiation, could be allowed safe access to the process areas for nearly unlimited working times. Several months but only a limited number of personnel were available for this decontamination so that decontamination was not carried out at anywhere near the speed with which it could be accomplished on an emergency basis. From ten to thirty days were taken to decontaminate each process vessel. It is believed that a single cell could be completely decontaminated in about one week with efficient scheduling of operations and sufficient manpower. It is also believed that a complete plant decontamination could easily be carried out in less than 30 days using only the personnel normally employed to operate the plant.

Because of the high radiation level of the vessels at the end of the run, it was not possible to enter the cells and determine radiation levels at the individual vessels. For example, just after decontamination operations had started the level just inside the dissolver cell door was over 100 r/hr. In many cases two or more decontamination steps were finished before it was possible to monitor the process vessels to determine the effectiveness of the decontamination procedures.

Cell C (dissolving and feed preparation) proved to be the most difficult area to decontaminate. The radiation level at the entrance to this cell was 30 r/hr after seven days of internal decontamination. After external decontamination of the vessels and additional internal decontamination with the standard solutions up to and including sodium hydroxide-tartaric acid the average radiation level at contact with the vessels was 1.5 r/hr. Oxalic acid solution was used next with little effect. Treatment with periodic acid followed by nitric acid proved to be very effective at this point and the radiation levels at contact were reduced from about 1.2 r/hr to about 250 mr/hr after several treatments. A few lines and vessels required additional treatment with sodium fluoride-nitric acid solution. The decontamination of the C Cell vessels required an average time of twenty-three days to reduce the average radiation levels at contact to 60 mr/hr. It is interesting to note that about 75 per cent of the time used was required to reduce the level from 5 r/hr to 60 mr/hr.

Decontamination progress for a dissolver vessel during the second decontamination is shown in Fig. 9. The curve shows an increase in radiation level after some decontamination steps; this is believed due to cross-contamination from other vessels during the transfers of decontaminating solution. The results shown for this vessel are similar to those obtained for all dissolver cell vessels.

Similar procedures were followed for the other process cells and the results were similar except that decontamination was easier and was usually accomplished in less time.

The first extraction column required 15 days to reduce the radiation level to 280 mr/hr at contact as compared to the six days required for nearly complete decontamination after the first run. Steam, nitric acid, citric acid and sodium hydroxide-tartaric acid

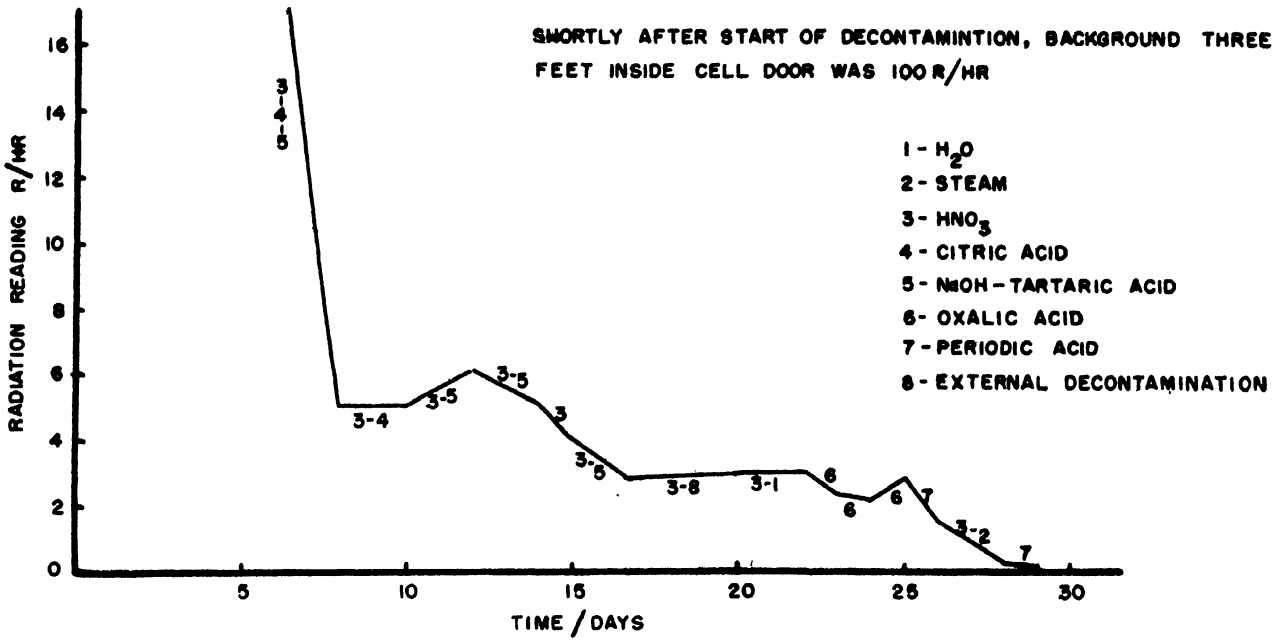

Figure 9. Second decontamination of dissolver C-101

solutions were required to complete the decontamination. These results again illustrate the ease of decontamination of continuous equipment operated at room temperature as compared with batch equipment operated at boiling.

Advantages over Remote Maintenance

The choice between design of radiochemical processing plants for direct instead of remote maintenance should be made primarily on the basis of plant scale. In plants designed for the recovery of plutonium from large quantities of irradiated natural uranium, or in other large-scale plants, it may be desirable to provide for remote maintenance or removal of some of the equipment as the large-scale equipment in these plants would be hard to decontaminate and maintain directly primarily due to its large size. On the other hand, it is believed that design for remote maintenance would be very costly for an enriched uranium processing plant because the many small-diameter critically-safe vessels required would be very difficult to adapt to the special connectors, piping jumpers and other specialized apparatus required for remote maintenance plants.

Direct maintenance plants can be built using commercially available equipment and equipment fabricated using standard industrial techniques. The cell space can also be used more efficiently as the equipment pieces can be stacked two or three high. These factors add up to an appreciable saving in initial plant cost which, it is believed, more than offsets the costs and time consumed for equipment decontamination prior to maintenance operations.

The operating experience at the Idaho Chemical Plant has definitely proven the feasibility of designing and operating a production-scale radiochemical plant using direct maintenance techniques. This experience has shown that a properly designed direct maintenance plant requires essentially no maintenance within the "hot" cells. Maintenance operations should be required in the cells for only five reasons: (1) equipment failure because of corrosion, (2) mechanical equipment failures, (3) remote valve failures, (4) plugging of the lines or equipment and (5) solution leaks because of faulty construction or use of unreliable connection methods. Experience has shown that proper choice of construction materials, installation of spare equipment, location of all equipment with a high maintenance potential in cubicles outside the cells, reduction of the number of valves to the absolute minimum, provisions for flushing the equipment from cold areas, welding all piping connections and thoroughly leak-testing all equipment with freon and simulated process solutions before startup can all but eliminate these potential maintenance problems.

Nuclear Reactor Fuel Dissolution

By D. L. Foster, J. E. Savolainen and R. G. Wymer,* USA

The dissolution of heterogeneous nuclear reactor fuel elements is necessary for chemical processing to recover fissionable and fertile materials. A change of state is thus brought about from solid fuel to liquid feed solution. In this paper, chemical and engineering data are presented for dissolution systems for representative nuclear reactor fuel elements. The materials considered are uranium metal, uranium-aluminum alloy, aluminum jackets, thorium metal, and zirconium-clad uranium-zirconium alloy. Batch-pot dissolution techniques may be most satisfactory for many applications. However, continuous dissolution methods with intermittent charging of metal, continuous addition of dissolvent, and continuous removal of product are of interest.

The dissolution chemistry of nuclear fuel elements is concerned with reaction rates for various fuel materials in various dissolvent systems. Nitric acid dissolution has been used for uranium, uranium-aluminum alloy, and thorium. Sodium hydroxide could be considered for dissolution of aluminum jackets and uranium-aluminum alloy. Fuel elements containing zirconium can be dissolved in hydrofluoric acid.

The equipment used in dissolution includes three major units: (1) the fuel charger, (2) the vessel, and (3) the off-gas system. The chargers could be shielded casks capable of controlled discharge of fuel elements, or a remote crane-type unit to charge the fuel elements from buckets. Conveyor-type chargers may be used with both batch and continuous dissolvers.

Dissolver vessels are of three general types—pot, column, and slab. The choice depends on the critical mass of the fuel being processed and the shape of the fuel element. Pot-type dissolvers are operated either batchwise or continuously; column and slab dissolvers are continuous-type units.

The off-gas system is concerned primarily with disposal of the gaseous radioactive fission products and removal or recovery of the chemical reaction products.

CHEMICAL REACTIONS AND RATES

Typical fuel dissolution methods use a nitric acid dissolvent, with an appropriate catalyst when necessary with fuel elements made of uranium, thorium, and uranium-aluminum alloys. These elements are encased in an aluminum jacket which is removed by chemical dissolution. In the case of uranium metal, for example, the aluminum jacket is removed chemically by dissolution in sodium hydroxide–sodium nitrate solutions, leaving the uranium unaffected. Similarly, dissolution temperatures studied have usually been the boiling temperatures of the dissolvent solution, the dissolution rates being higher at elevated temperatures.

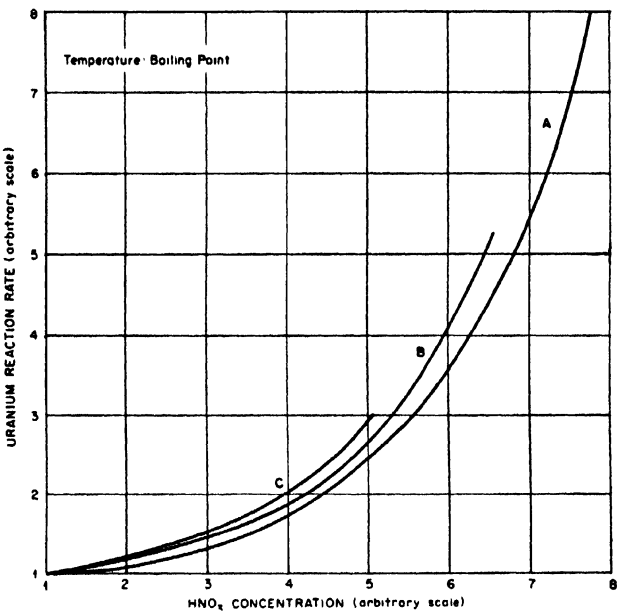

Figure 1. Dissolution rate of uranium metal as a function of nitric acid and uranyl nitrate concentrations. Uranyl nitrate concentrations: A, B, C

Uranium Metal

Uranium metal dissolves readily in boiling nitric acid to yield uranyl nitrate. The stoichiometric acid requirements are variable, depending on dissolution conditions. With 55% nitric acid (11.7 *M*) the reaction for batch dissolution is, approximately,

$$U + 4.5\ HNO_3 \rightarrow UO_2(NO_3)_2 + 1.57\ NO + 0.84\ NO_2 + 0.0005\ N_2O + 0.043\ N_2 + 2.25\ H_2O$$

Increased acid economics can be obtained by oxygen or air oxidation of the nitrogen oxide fumes, which are a product of the dissolution reaction, followed by their absorption in water to form reusable nitric acid.

* Oak Ridge National Laboratory. Including work done at Argonne National Laboratory, Lemont, Ill.; California Research and Development Co., Livermore, Calif.; Hanford Atomic Products Operation, Richland, Wash.; Idaho Chemical Processing Plant, Idaho Falls, Idaho; Knolls Atomic Power Laboratory, Schenectady, N.Y.; Oak Ridge National Laboratory, Oak Ridge, Tenn.; Savannah River Laboratory, Augusta, Ga.; University of California Radiation Laboratory, Berkeley, Calif.

The dissolution rate of uranium increases with increasing acid concentration. The presence of the uranyl nitrate product does not inhibit but, instead, increases dissolution rates at fixed acidities (see Fig. 1). Since similar increases in uranium dissolution rates are observed when nitrate salts, for example, calcium and aluminum nitrates, are added to the nitric acid dissolvent, the effect is attributable to the increased nitrate ion concentration rather than to the uranyl ion.

Some chemical additives that are known to form complex ions with the uranyl ion markedly increase the initial dissolution rate in batch dissolutions. Among these are hydrofluoric acid, calcium fluoride, sodium sulfate, ammonium silicofluoride, and phosphoric acid. These additives, with the possible exception of phosphoric acid, do not produce significant time savings in an over-all batch dissolution cycle. It seems likely, therefore, that their catalytic effect is inhibited by the increasing uranyl ion concentration.

Uranium-Aluminum Alloy and Aluminum Jackets

Uranium-aluminum alloys and aluminum jackets dissolve in both nitric acid containing mercuric ion as a catalyst and in NaOH (caustic) solutions.

Nitric Acid—Mercuric Nitrate System

The stoichiometry of the reaction between nitric acid and aluminum or its alloys depends strongly on the acid concentration. At acid concentrations of about 4 *M*, the reaction is, approximately,

$$\mathrm{Al} + 3.75\ \mathrm{HNO_3} \xrightarrow{\text{catalyst}} \mathrm{Al(NO_3)_3} + 0.225\ \mathrm{NO} + 0.15\ \mathrm{N_2O} + 0.1125\ \mathrm{N_2} + 1.875\ \mathrm{H_2O}$$

$$(\Delta H = -190\ \text{kcal})$$

The presence of uranium does not significantly change the reaction from that for pure aluminum.

Aluminum and its alloys are protected from nitric acid attack by a coherent film of aluminum oxide. The catalytic action of mercuric ion in this system involves reduction of mercury at the surface of the aluminum metal to produce an amalgam which prevents further formation of the protective oxide film. The amalgamated area then reacts with the nitric acid, producing aluminum nitrate and metallic mercury. This process continues until a balance is reached between the reduction of mercury by the aluminum and the dissolution of mercury by the nitric acid solutions. Above a certain mercuric nitrate concentration, variations in this concentration have little effect on the uranium dissolution rate (see Fig. 2).

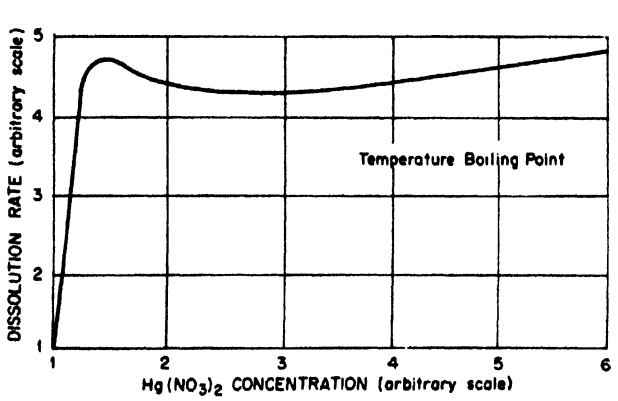

Figure 2. Initial dissolution rate of uranium-alloy in nitric acid as a function of mercuric nitrate concentration

The dissolution rates in the mercury-catalyzed system vary in a complex way with acid concentration, passing through a maximum. Unlike the effect of an increase in the uranyl nitrate concentration, as the aluminum concentration builds up in the dissolver, the dissolution rate decreases rapidly. Dissolution rate data are difficult to reproduce accurately, and are of little practical value unless obtained with samples of the metal of interest.

Caustic and Caustic-Nitrate System

The caustic dissolution of aluminum and uranium-aluminum alloys follows heterogeneous first order kinetics laws. The rate equation is:

$$\ln (c_0/c_t = kst/v$$

where c_0 and c_t are the caustic molar concentrations initially and at time t, respectively; s is the available surface area of aluminum or alloy, in square centimeters; t is the time in minutes; v is the dissolvent volume in liters. If either s or v is not constant (s is not constant when a dissolution is carried to completion), this variable must be introduced into the differential rate expression as the appropriate function of caustic concentration. In general, the caustic-nitrate system gives specific dissolution rates about 1.5 times larger than the pure caustic system for equal caustic concentrations in the dissolvent. However, no rate law has been determined for the caustic-nitrate system.

The reaction of aluminum with sodium hydroxide is

$$\mathrm{Al} + \mathrm{NaOH} + \mathrm{H_2O} \rightarrow \mathrm{NaAlO_2} + \tfrac{3}{2}\ \mathrm{H_2}$$

When sodium nitrate is present hydrogen gas evolution is suppressed:

$$\mathrm{Al} + \mathrm{NaOH} + \mathrm{H_2O} \rightarrow \mathrm{NaAlO_2} + \tfrac{3}{2}\ \mathrm{H_2}$$
$$\mathrm{NaAlO_2} + 0.9\ \mathrm{NaNO_2} + 0.15\ \mathrm{NH_3} + 0.2\ \mathrm{H_2}$$

The mole ratio of sodium nitrite to ammonia gas in the product is variable, and depends on the total and relative amounts of sodium hydroxide and sodium nitrate in the dissolvent. The resulting solutions are fairly stable toward crystallization but are not thermodynamically stable. A convenient concentration range for sodium hydroxide in the dissolvent is 3–8*M*. Solutions containing 3*M* sodium hydroxide and 3*M* sodium aluminate are stable indefinitely at room temperatures as supersaturated solutions. At low caustic concentrations the $\mathrm{NaOH/NaAlO_2}$ mole ratio must be increased to reach the same degree of stability.

In the caustic dissolution of irradiated uranium-aluminum alloy the bulk of the fission products is

precipitated with the uranium solids. Cesium, iodine, zirconium, and niobium are the major contaminants of the liquid phase, of which zirconium and niobium are not present to more than several tenths of a per cent of their total amounts.

Thorium Metal

Thorium metal, like aluminum metal, can be readily dissolved in boiling nitric acid if a catalyst is employed. Fluoride ion, at concentrations low enough that corrosion of processing equipment is not prohibitive, is an effective catalyst for thorium metal dissolution. The thorium dissolution rate increases with increasing nitric acid and fluoride ion concentrations.

These phenomena may be qualitatively interpreted by assuming that a tenacious thorium oxide film covers the metal and prevents its attack by the nitric acid. Thorium oxide itself is only slowly soluble in nitric acid. Fluoride ion provides a mechanism whereby thorium oxide can be rapidly dissolved. Since thorium forms stable fluoride complexes and a relatively insoluble salt, if high concentrations of thorium nitrate are present, fluoride ion is removed by complex ion formation and precipitation, thereby effectively lessening its catalytic effect.

Uranium-Zirconium Alloy

Zirconium metal and alloys dissolve very rapidly in aqueous hydrofluoric acid. The dissolution rate is controlled by the rate of addition of hydrofluoric acid. After the zirconium is in solution, nitric acid is added to dissolve the uranium.

DISSOLUTION EQUIPMENT

The fuel element shape and the possibility of accumulating a critical mass of fissionable material are governing factors in determining the size and shape of the dissolving vessel (see Fig. 3). When fuels with high fissionable material content are processed, either the mass or the geometry must be controlled. With mass control the amount of fuel charged is below the minimum required for a critical mass regardless of geometry. With geometry control the dimensions of the vessel are fixed so that criticality cannot occur regardless of size of charge. As the fissionable material concentration of the fuel increases, the dissolver must become smaller in one or more dimensions.

Dissolving vessels are either pot, column, or slab type (see Fig. 3). Each type finds its best application with a particular type of fuel.

Pot Dissolvers

A pot dissolver is a vessel having a height/diameter ratio approximately 1/1. Although this type of dissolver may be used for enriched fuels, its best application is in the processing of fuels containing low concentrations of fissionable material. If the fuel mass is restricted by criticality, the capacity of the vessel for highly enriched fuels becomes small.

The pot dissolver is usually operated batchwise. The normal procedure followed in this type of operation is to charge the fuel to the dissolver together with sufficient dissolvent to dissolve a portion of the fuel. The entire fuel charge is not usually dissolved since, as the surface area approaches zero, an extremely long dissolving time is required. The dissolvent reacts with the fuel at boiling conditions under slightly subatmospheric pressure until the proper concentration is reached. This final concentration is usually determined by the specific gravity of the dissolver contents. The subatmospheric pressure operation, approximately 10 inches of water vacuum, is employed to prevent leakage of radioactive contamination into the operating area.

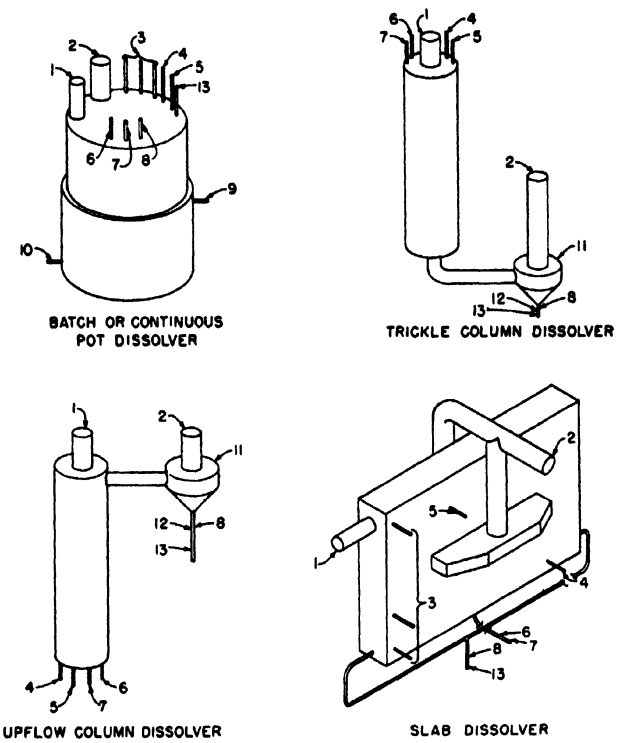

Figure 3. Various types of dissolvers for nuclear reactor fuels. (1) Fuel loading port; (2) line to off-gas equipment, condenser, etc.; (3) liquid-level specific gravity probes; (4) thermocouple well; (5) pressure tap; (6) feed inlet; (7) condensate return line; (8) sampler; (9) pipe for jacket steam and water; (10) condensate drain; (11) product gas-disengaging cyclone; (12) product specific gravity determiner; (13) product transfer line

Continuous pot dissolution has been demonstrated. In this type of operation both fuel and acid are continuously charged and product is continuously removed. At steady state the metal surface area is maintained large and the metal is kept submerged in liquid of product concentration. There is a constant rate of off-gas and heat evolution. Therefore, the auxiliary equipment, such as condensers, piping, and gas processing equipment, can be designed to handle the mean processing load rather than a peak load. In addition, continuous pot dissolution will produce a more consistent product than other methods of continuous dissolution.

In a batch pot dissolver the vessel must be large enough to contain the total charge of dissolvent plus

fuel and must have sufficient freeboard to allow for liquid-vapor disengaging. This volume is usually a factor of 2–3 greater than the metal plus liquid. The cross-sectional area of the dissolver must be sufficiently large to limit the boil-up rate resulting from the heat of reaction to less than 40 lb of steam per hour per square foot. Another fact to be considered is that there must be sufficient fuel surface area to produce the desired product at the desired rate.

The design factors for a continuous pot dissolver are the same as for a batch dissolver, but the vessel size can be much smaller for a given capacity since the liquid volume in the continuous pot is determined by that necessary to cover the metal, rather than by the amount of metal to be dissolved, and by product concentration.

Column Dissolvers

The column dissolver vessel has two dimensions restricted for criticality reasons. Its operation is much the same as that of a packed column containing three phases: solid (nuclear reactor fuel), liquid (dissolvent), and gas (reaction product). There are two practical methods of operation of this unit, depending upon the direction of flow of each phase. In one method, the "trickle" type, all phases flow down the column with a continuous gas phase. In the second method, the "up-flow" type, the liquid and gas phases flow up the column, and the solids move down. The liquid phase is continuous at the bottom. In column-type dissolver operation, the volumetric flow ratios are of the order of $1/10^2/10^5$ for the solid, liquid, and gas phases, respectively. The gas phase is therefore more likely to be continuous at the top of the upflow column.

Both types of operation of a column dissolver have been shown to produce similar results. Because of the nature of the operation, the product concentration fluctuates over a fairly wide range around a mean value. Channelling of the dissolvent is probably the main cause of this fluctuation. Channelling occurs in any packed column operation, and in this case it is aggravated by the constantly changing physical dimensions of the fuel packing. This is, however, probably the best type of equipment for dissolving most enriched fuels. A typical dissolution rate curve for the trickle dissolver is shown in Fig. 4.

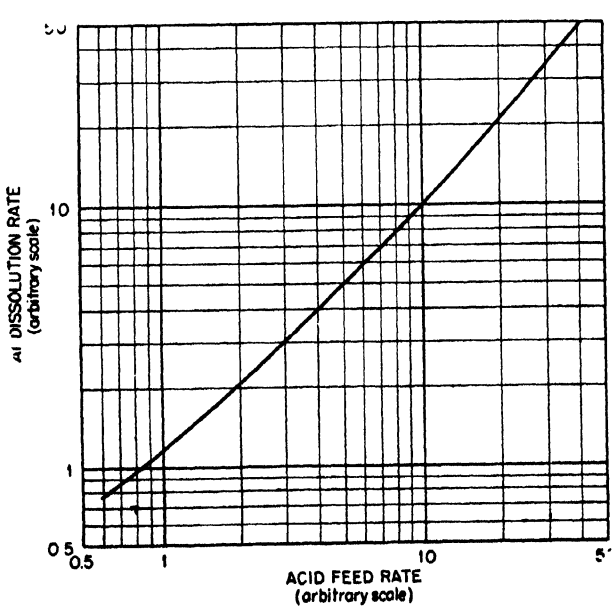

Figure 4. Dissolution rate of aluminum slugs in a trickle dissolver as a function of acid feed rate

Slab Dissolvers

A slab dissolver has one of its dimensions restricted for criticality reasons, and is used for processing enriched fuels whose shapes are too unwieldy for column dissolver packing. Examples of such shapes are long cylindrical or tubular fuel elements; these can be laid horizontally, one atop another in a long, narrow chest, or "slab." The awkwardness of loading these elements usually restricts the dissolving operation to a semicontinuous one, with batchwise loading of fuels and continuous addition of dissolvent and removal of product.

Off-Gas Equipment

Dissolver off-gases are processed to remove radioactive components that constitute a health hazard. At the same time gaseous reaction products are removed. The off-gas processing equipment for nitric acid dissolutions is described since it is typical. Where caustic or caustic-nitrate is used as dissolvent, the radioactive off-gas treatment is essentially the same as for nitric acid, except that hydrogen or ammonia gas disposal equipment must be substituted for nitrogen oxide recovery equipment.

In nitric acid dissolution, the heat generated is usually so great that 90–95% of the gas that leaves the dissolver is steam. The gases remaining after the steam has been condensed are principally oxides of nitrogen, with radioactive (and other) gases present as minor constituents. The radioactive gases are iodine, xenon and krypton. The iodine, if released to the atmosphere, would constitute a health hazard and so must be removed. The equipment used for processing gases from a typical batch uranium dissolution includes a condenser for steam removal and acid recovery, a silver nitrate tower for radioactive iodine absorption, and a sorption column for final nitrogen oxide recovery.

The first piece of equipment in the dissolver off-gas system is the condenser. If the condenser is connected so that the gases enter the top and leave the bottom, much better absorption of NO_2 by the condensed water vapor will be accomplished. This is because the condensate drains down the condenser tubes, rendering the entire tube area available for NO_2 sorption. The resulting acid can be returned to the dissolver, reducing the acid required for the metal dissolution.

To remove iodine from the off-gas stream, the gas is passed through a packed tower where the packing is coated with silver nitrate. The iodine in the gas

reacts with the silver nitrate to form silver iodide. Before the gas is admitted to the tower, it must be preheated to about 200°C. At temperatures of 100°C, nitric acid condenses on the packing and stops absorption. In experimental studies, iodine retention was not complete after approximately 40% of the silver nitrate had been converted to the iodide. The bed may be renewed by flushing with a silver nitrate solution, which removes the silver iodide, and at the same time recoats the packing. The entering hot gas dries the bed, leaving a coating of silver nitrate. After iodine removal, the gases may be vented to the stack.

Removal of Fission Products From Stainless Steel

By D. O. Campbell,* USA

The decontamination of equipment used for handling solutions containing fission products has long presented a problem. Decontamination of large apparatus, such as that used in chemical plants for processing irradiated materials and reactor fuels, is necessary for modification of the equipment or for direct maintenance. An alternative, remote maintenance is more expensive and less flexible than direct. Chemical plants for processing radioactive materials are generally constructed of stainless steel, and the material to be processed is usually in a nitric acid or nitrate solution. The results of an investigation of the fission product contamination of type 347 stainless steel from nitric acid solutions and of the effectiveness of several reagents for subsequent removal of the fission products from the surface, i.e., decontamination, are discussed in this paper.

Radioactive contamination on stainless steel is either adsorbed on the surface or has not penetrated very deeply, and a large part of it may be easily removed. Decontamination methods usually involve one or more of the following: detergent cleaning, forming a soluble complex of the contaminant, solution of the contaminant in strong acid, and removal of the surface by physical or chemical means. Since some of these methods corrode the surface, a corrosion study is a necessary corollary to a decontamination study.

Complexing agents and strong acids easily remove 90% or more of the contamination; removal of the remainder becomes increasingly difficult. Eventually rather violent means must be applied, and very often they meet with relatively little success. Initial decontamination must therefore be interpreted separately from the very difficult subsequent decontamination, after most of the fission products have been removed.

The contaminating solutions used in this work were about $2M$ in nitric acid and contained various fission products (see Table I). Some contained large amounts of uranium and a little plutonium, but others did not. The β-active fission products were largely rare earths, and the γ-activity was due mostly to niobium and zirconium. The actual amounts of the fission products varied somewhat, depending on the cooling time of the solution. Most experiments were done with solutions that had cooled from 2 to 6 months.

The test coupons, about 4 cm^2 in total area, were cut from bars of type 347 stainless steel. Some were used as cut, some were ground with carborundum, and some were polished to a mirror finish. After exposure to the fission product solution, the coupons were rinsed with water to remove all water-soluble fission products and any residual solution.

Contamination levels on coupons exposed to the solutions for several days were normally about 500 mr/hr β and 100 mr/ γ-activity. However, the contamination on the first coupon exposed to a solution reached a level several times this. The level decreased for subsequent coupons contaminated in the same solution, and levelled off at these values after three to five coupons had been contaminated. All coupons showed essentially the same relative amounts of fission products (see Table II). The primary contaminant was always niobium, there was some zirconium, and the other fission products contributed less than 1% of the gross contamination. The γ-contamination is the most important insofar as equipment decontamination is concerned. The presence of uranium in the contaminating solutions had no apparent effect.

Since a single isotope is responsible for most of the contamination, a simple relation between the contamination level and the concentration of contaminants might be expected. In Fig. 1 is shown a log-log plot derived from the classical, or Freundlich, adsorption isotherm. The slope is very close to 1. This increase in contamination level with concentration

Table I. Fission Products in Contaminating Solution*

	Percentage of gross activity due to components					
	Zr	*Nb*	*Ru*	*Total rare earths*	*Cs*	*Sr*
β	9	1	5	70	2	12
γ	37	47	8	3	3	0

* Gross γ-activity, $\sim 2 \times 10^6$ cpm/ml; scintillation counter. Gross β-activity, $\sim 1.5 \times 10^6$ cpm/ml; end window counter, 10% geometry.

Table II. Fission Product Contaminants on Type 347 Stainless Steel

Experiment No.	*Percentage of gross activity due to components**							
	Niobium		*Zirconium*		*Ruthenium*		*Rare earths*	
	β	γ	β	γ	β	γ	β	γ
1	68	93	15	1.6	..	1.0	..	1.0
2	74	87	5.6	0.8	0.6	0.2	0.1	..
3	..	95	..	4.7	0.3	..	..	0.05

* Others less than 1%. The percentages do not add to 100 because of lack of precision in some of the analytical methods.

* Oak Ridge National Laboratory.

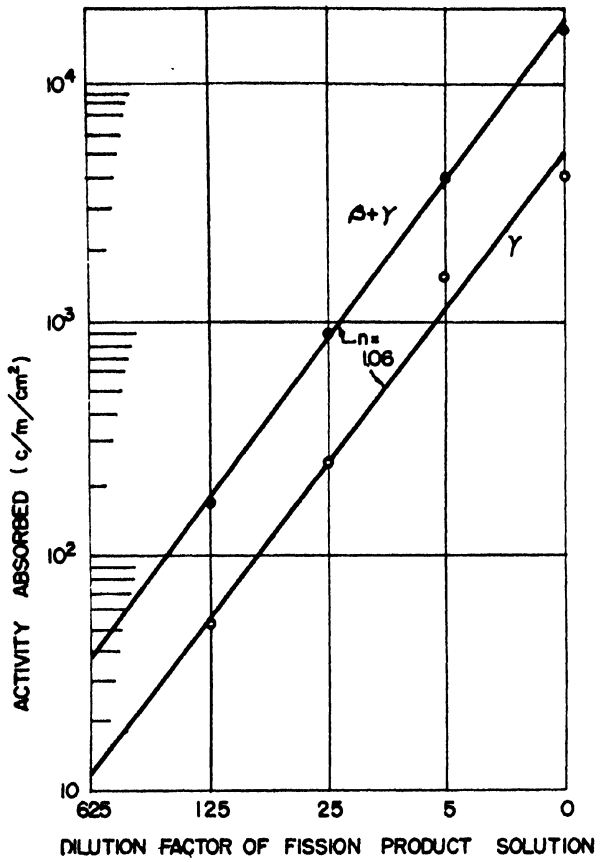

Figure 1. Contamination of type 347 stainless steel with various concentrations of fission product solution (HNO_3 = 2.2 M) according to Freundlich isotherm

explains why a spill of fission products that concentrates or evaporates to dryness contaminates the surface to such a high level.

Since niobium and, to a lesser extent, zirconium are the most important contaminants, the problem of decontamination is one of removing these from the surface. Every reagent which significantly decontaminated stainless steel was found, by radiochemical analysis, to have removed from the surface more of these two elements than anything else. During decontamination zirconium and niobium remained the most important contaminants, and it appears that they are the most difficult fission products to remove. This is especially true of niobium, which, after considerable decontamination, has been found to be the only significant fission product still present on the surface.

The most effective decontamination reagents are fluoride solutions. Three per cent hydrofluoric acid in 20% nitric acid has been used most often; it has been reported to give as good a decontamination as any fluoride solution, and with minimum corrosion. The use of fluorides depends on whether or not the corrosion can be tolerated. Since these decontamination reagents contain large amounts of fission products after use, they must be stored, and the long-time storage of fluoride solutions also presents a very serious problem.

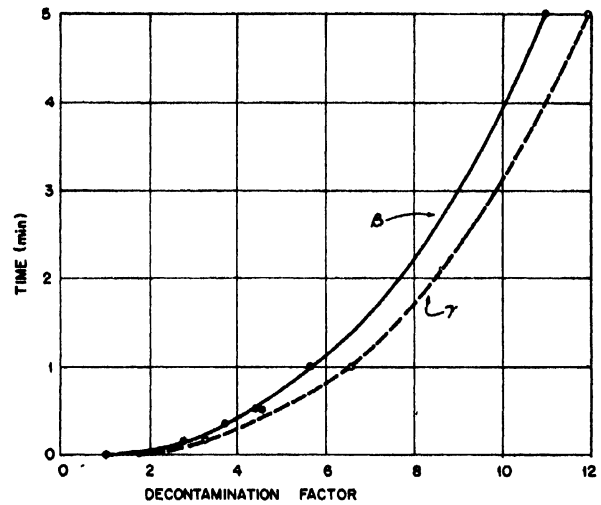

Figure 2. Rate of decontamination with 3% HF-20% nitric acid

Figure 2 shows the rate of decontamination of type 347 stainless steel with a 3% hydrofluoric acid-20% nitric acid reagent at room temperature for the first 5 min. The decontamination factor, i.e., the ratio of radioactivity on the steel before treatment to that after treatment, is plotted against time. The β-decontamination factor is smaller than the γ. A decontamination factor of more than 10 was observed in 5 min. Decontamination factors up to a thousand have been observed in an hour. No corrosion of the stainless steel surface was evident after 5 min, at 500× magnification, but it was evident after longer exposure. The corrosion appeared as a rather general attack, which is much less serious than pitting or intergranular corrosion. The corrosion rate at 25°C has been reported to be less than 0.1 mil/hr. If this corrosion can be tolerated and the problem of storing the used reagent is not prohibitive, the 3% hydrofluoric acid-20% nitric acid solution can be recommended. However it probably should be used only if less corrosive reagents do not give sufficient decontamination.

The next most effective reagent, which is relatively noncorrosive, was an alkaline tartrate-peroxide solution. Sodium hydroxide and alkaline tartrate solutions have been used before, but the addition of hydrogen peroxide definitely improves their effectiveness. In Fig. 3 the decontamination factor is shown as a function of time for sodium hydroxide and a solution of 10% sodium hydroxide-2.5% sodium tartrate-2.5% hydrogen peroxide. The concentrations of the three constituents are not critical since corrosion is negligible, but the decontamination effectiveness appears to fall off if the concentrations are reduced to less than half these values.

It is apparent that the alkaline tartrate-peroxide is much more effective than sodium hydroxide alone. Another interesting fact is that during the first minute the β-decontamination factor is larger than the γ; this was observed with all reagents except the fluorides. After this, β- and γ-decontamination factors are the same, but, because of the initial difference,

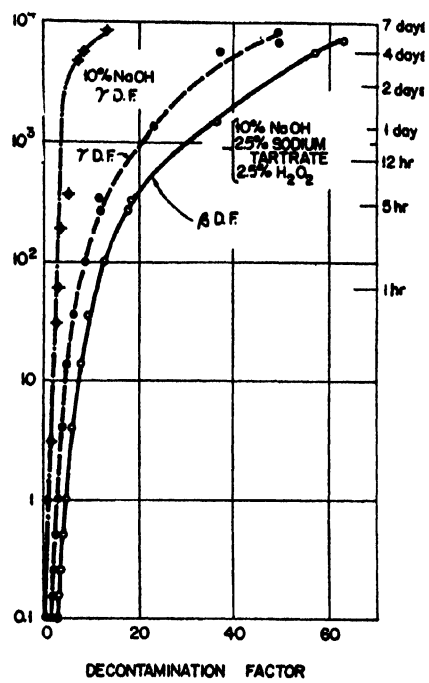

Figure 3. Decontamination of type 347 stainless steel by sodium hydroxide and alkaline tartrate-peroxide

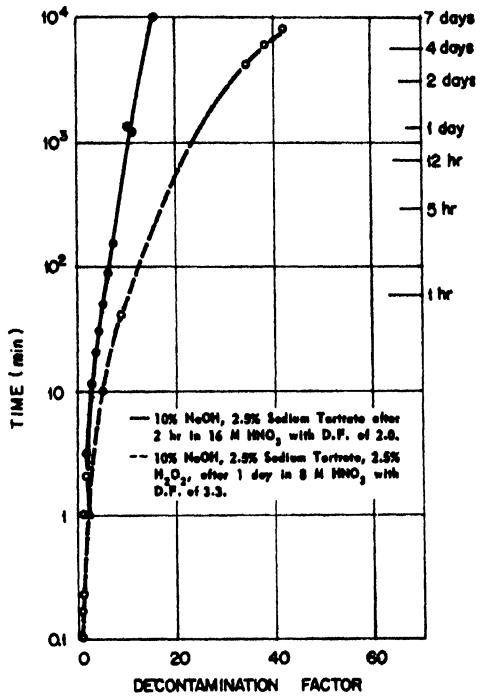

Figure 4. Decontamination of type 347 stainless steel by alkaline tartrate and alkaline tartrate-peroxide following initial decontamination by nitric acid

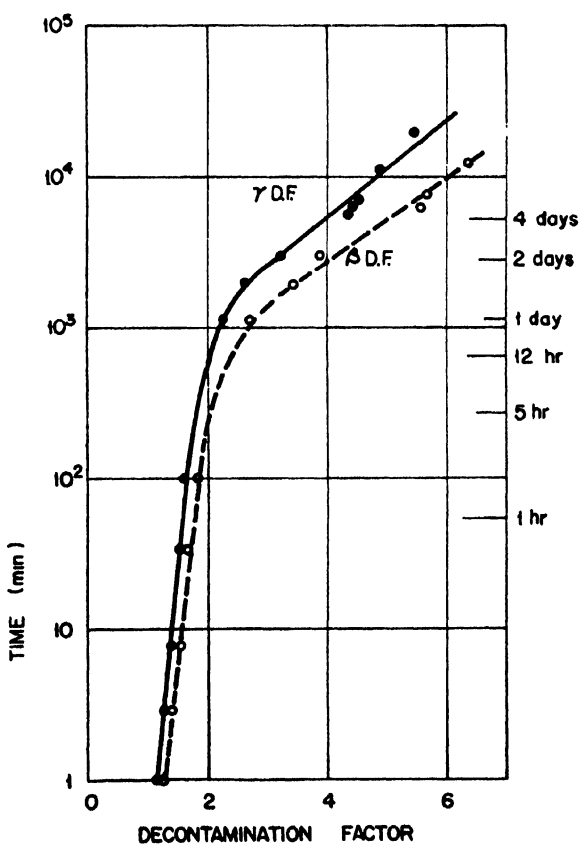

Figure 5. Decontamination of type 347 stainless steel by 16M nitric acid

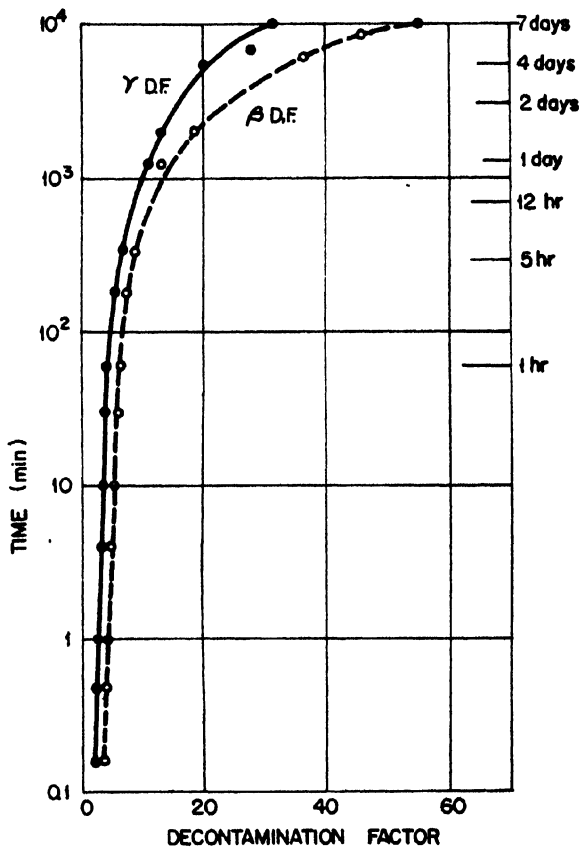

Figure 6. Decontamination of type 347 stainless steel by 5% oxalic acid

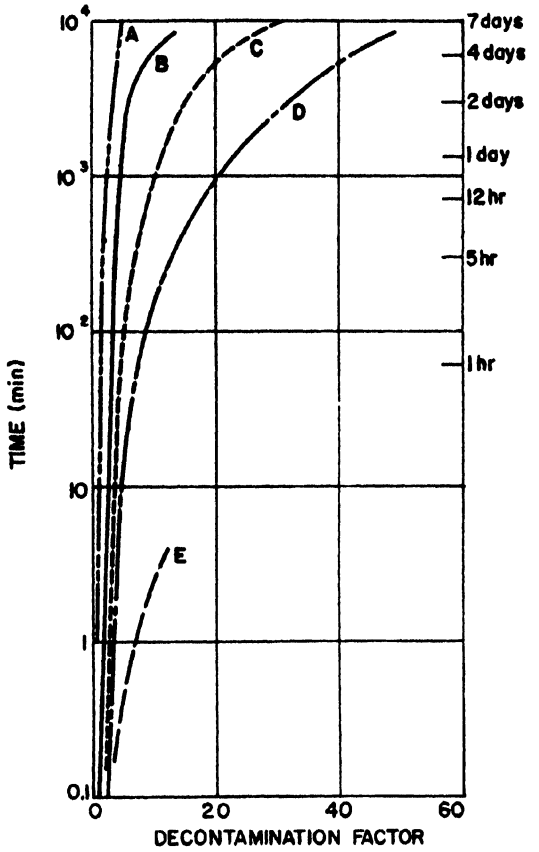

Figure 7. Summary of γ-decontamination of type 347 stainless steel by various reagents. (A) 16M HNO_3; (B) 10% NaOH; (C) 5% oxalic acid; (D) 10% NaOH, 2.5% sodium tartrate, 2.5% H_2O_2; (E) 3% HF, 20% HNO_3

the over-all β-factors are greater. It is believed that this is due to the quick removal of those fission products that are strong β-emitters, relative to the rate of removal of niobium, which is a strong γ- but weak β-emitter.

Figure 4 is a similar graph, comparing alkaline tartrate-peroxide to the alkaline tartrate without peroxide. The peroxide clearly improves the decontamination. In both cases the coupons were previously decontaminated by a factor of 2 to 3 with nitric acid.

The rate of decontamination decreases with time, and after a few days it becomes practically constant at 6% removal of activity per day. Decay of niobium could account for only 2% per day. Treatment with nitric acid, 8 to 16*M*, for an hour, following alkaline tartrate-peroxide, gave a small decontamination factor, normally less than 2, but subsequent treatment with alkaline tartrate-peroxide was then more effective. Decontamination factors of the order of 10^4 were obtained by several successive treatments with nitric acid for an hour followed by alkaline tartrate-peroxide overnight.

Nitric acid was the least effective decontamination reagent tested (see Fig. 5). Decontamination factors of only 2 to 3 were obtained in a day with this reagent. Actually, in a plant operation, the first treatment with nitric acid may be much more effective because it dissolves most solids and precipitates in the system, and these carry large amounts of fission products. Again, the rate of decontamination levels off at about 6% removal of activity per day after several days.

It should be mentioned, however, that nitric acid was an extremely effective decontaminant for stainless steel exposed to a different contaminating solution—one which was an acid deficient, concentrated salt solution. The solution contained protactinium as well as fission products, and the important contaminants in this case were protactinium and niobium. A decontamination factor of 200 was observed in 30 min with nitric acid.

Decontamination with 5% oxalic acid is much superior to nitric acid (see Fig. 6). Although oxalic acid has been reported to be corrosive, scouting tests have shown corrosion of type 347 stainless steel to be less than 1 mil/year in 5% oxalic acid.

The effectiveness of the several reagents are indicated by the γ-decontamination factors plotted in Fig. 7. Nitric acid was the poorest reagent tested. The 10% sodium hydroxide was slightly better, and the 5% oxalic acid was still better. The 3% hydrofluoric acid-20% nitric acid solution gave the best contamination. However, decontamination with alkaline tartrate-peroxide solution was quite good and its use resulted in less corrosion.

In summary it may be said that decontamination is improved by repeated treatment with several reagents. For rapid and satisfactory decontamination, it is recommended that alternate contacts be made with 8 to 16*M* nitric acid for at least an hour and alkaline tartrate-peroxide for several hours or overnight. This cycle should be repeated until the desired decontamination has been obtained. The occasional use of oxalic acid solution may aid decontamination considerably.

High-Level Sampling Devices for Radiochemical Plants

By J. W. Landry,* USA

Sampling of liquids in a radiochemical plant is necessary for process control and for accountability. It is chiefly by analysis of samples that process variables are followed, such as density, acidity, radioactivity, contamination, amount of corrosion products, viscosity, and presence of phases and suspensoids. Account of valuable materials like uranium is kept as a result of analysis of samples.

The first requirements of the sampling device are that it take a sample representative of the process liquid and that the amount taken be sufficient for analysis. Radiochemical process liquids can present serious radiation and chemical hazards to personnel, and the sampler must operate with complete safety to personnel. Radiochemical materials are valuable as well as dangerous, and the sampler must remove no material from the process except the sample. Because radiochemical equipment is subject to dangerous contamination, great reliability is necessary in the sampling equipment; sampler maintenance operations must be infrequent and easily performed. A method of dispatching the sample to the analytical laboratory must be provided. A means for direct viewing of the process liquid is an advantage.

Six sampling devices in use at the Hanford, Savannah River, Idaho, and Oak Ridge radiochemical processing plants are described. All six use a recirculating loop to remove solution from the process vessels. Other parts include the air lift, jet, tips, package or container, conveyor, and shield.

Operating personnel draw the samples from special rooms or galleries, separated from the process areas by 4–6 ft of shielding. The galleries are situated higher than the process areas to prevent drainage of process liquids through the sampler lines into the sampling galleries and to provide good drainage back into the process vessels between samplings. Because the process areas are remote from the sampling station, samples are drawn through lines that are very long relative to the volume of sample taken and the sample supply line must be rinsed with many volumes of liquid in order that the sample will be representative. In the arrangement known as the "recirculating loop," the sample supply line is continuously rinsed with the liquid being sampled and the rinse is sent through a return line to the originating vessel.

* Oak Ridge National Laboratory. Including work done at Hanford Atomic Products Operation, Richland, Wash.; Idaho Chemical Processing Plant, Idaho Falls, Idaho; Oak Ridge National Laboratory, Oak Ridge, Tenn., and Savannah River Laboratory, Augusta, Ga.

Recirculation is produced by an air lift and/or a jet; these devices were selected because of their reliability. A combination of air lift and jet (Fig. 1) produces greater recirculation potential than would either by itself. Opposing potentials of 30 ft between process vessels and samples are common, and the combination of both air lift and jet is in predominant use in the samplers described. The air-lift operation consists of bubbling air, or nitrogen, into the sample supply line. The resulting density reduction causes the liquid to rise in the line. Optimum air-lift performance results from starting the air lift at the interior vessel terminus of the sample supply line. In some cases, in order to gain ease of installation and freedom from certain crystallization effects, performance is comprised by starting the air lift in the sample supply line at the vessel exterior. The bubble rate is controlled by an orifice accessibly located. The jet is similar to an aspirator except that it is adapted to the transfer of liquid. The sample supply line, which contains the air lift, is 4–16 mm inside diameter in the six samplers being described. Five of the six samplers contain the jet in the sample return line, and a return line of 16 mm inside diameter is used to accommodate the jet discharge.

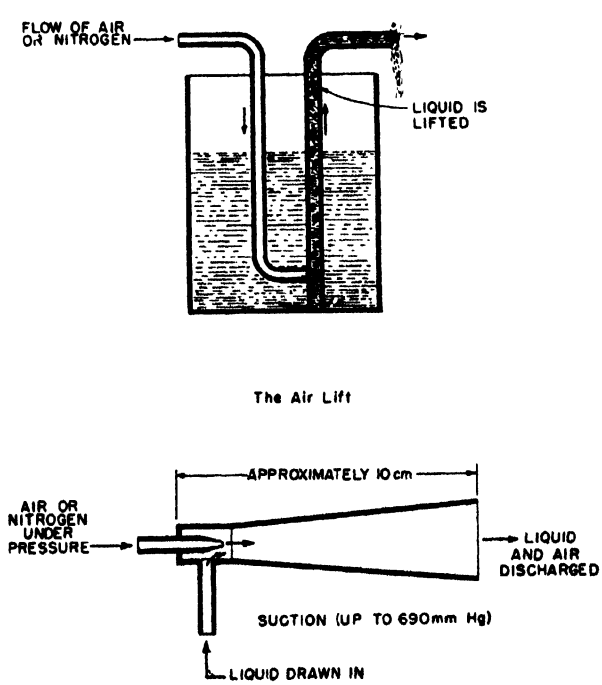

Figure 1. Air lift and jet

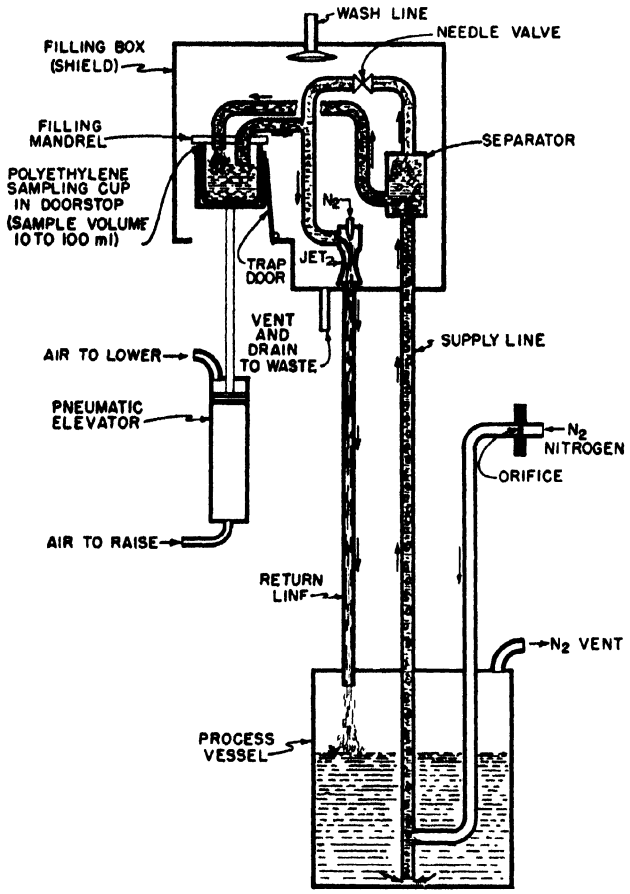

Figure 2. One type of sampler in use at the Hanford plant

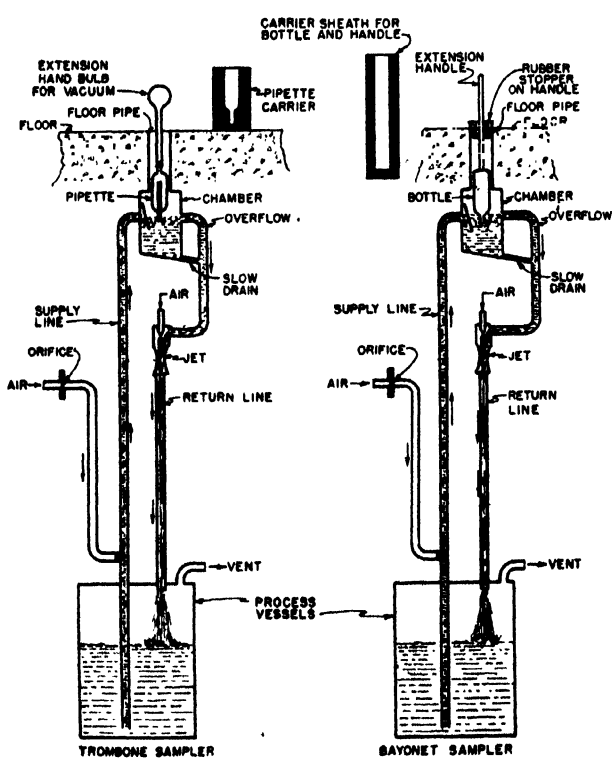

Figure 3. Trombone and bayonet samplers

The tips are simply the connections between the sampler lines and the sample packages. Formerly the sampler lines terminated in a rubber stopper onto which the package could be attached. The current trend is to the use of hypodermic needles and penetrable-top packages.

The package is either a bottle or cup. Pyrex bottles of about 15 ml capacity are generally used, although in some cases these are being replaced with nonwetting plastic bottles to prevent plating effects from certain materials in the samples. Access is via screw type caps with Buna-N inserts for needle entry. Two of the samplers that will be described use bottles with conical bottoms. One type of sampler uses a plastic cup of 100 ml capacity as the package.

The sampling package is usually held in a light portable shield, generally known as the "doorstop." After receiving the sample, the package and doorstop are transferred to a larger mobile shield for removal to the analytical laboratory. In one sampler the doorstop is built into an automatic chain conveyor.

The shield is composed of several inches of steel, lead, concrete, or glass and encloses those sampler parts which might otherwise irradiate operating personnel. Much of the sampler operation, including "handling" of the bottle, is performed through the shield.

Three types of samplers in use at the Hanford plants are described. The first type draws samples of 10 to 100 ml volume and the other two types, known as the "bayonet" and the "trombone" samplers, are used for sample volumes of 0.5 to 5 ml. These three samplers recirculate process solution by means of a jet located in the sample line; they differ in packaging methods.

In the first type (Fig. 2), the plastic sampling cup with the carrier is placed on the elevator and is raised through the trapdoor into the shielded filling box until the cup seals with the mandrel. A stream of liquid from the process vessel is drawn through the inlet line, separator, and sample cup by the action of the jet, which discharges the stream back to the process vessel. The jet in many instances must lift the liquid 30 ft from the vessel. The jet is aided by an air lift in the supply line. Nitrogen is used to operate the jet and air lift. The nitrogen bubbles from the air lift are removed at the separator. The needle valve atop the separator is adjusted so that all the nitrogen bubbles and only a little of the liquid bypasses the sampling cup. The nitrogen from the lift and the nitrogen to operate the jet are removed through the vent on the process vessel. The volume of sample is set by the level at which the jet suction line terminates in the cup. After a representative sample has been obtained in the cup, the cup is lowered from the filling box, and by use of hand tongs is capped and taken in a shielded carrier to the analytical laboratory. As soon as the cup is lowered from the mandrel the vacuum is released and the sampler lines drain back to the process vessel. The exterior of the filling box including the shield is 5 ft 3 in. high by 2 ft 9 in. wide by 1 ft 6 in.

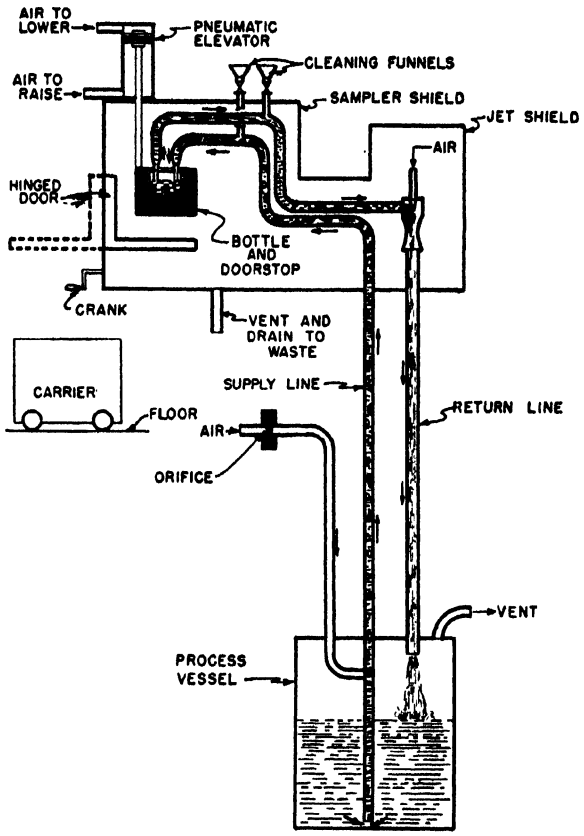

Figure 4. The SRP sampler

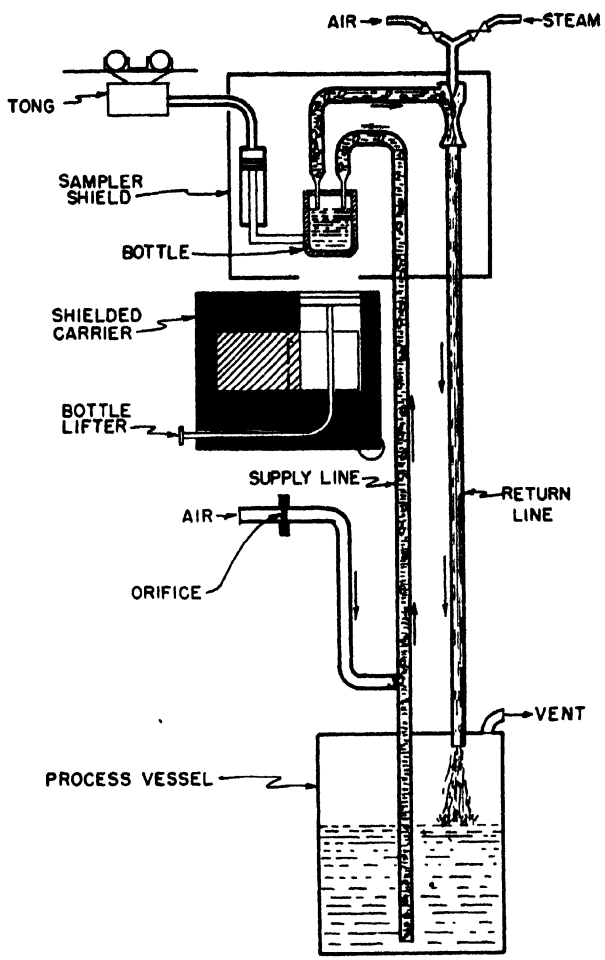

Figure 5. One type of sampler used at the Idaho plant

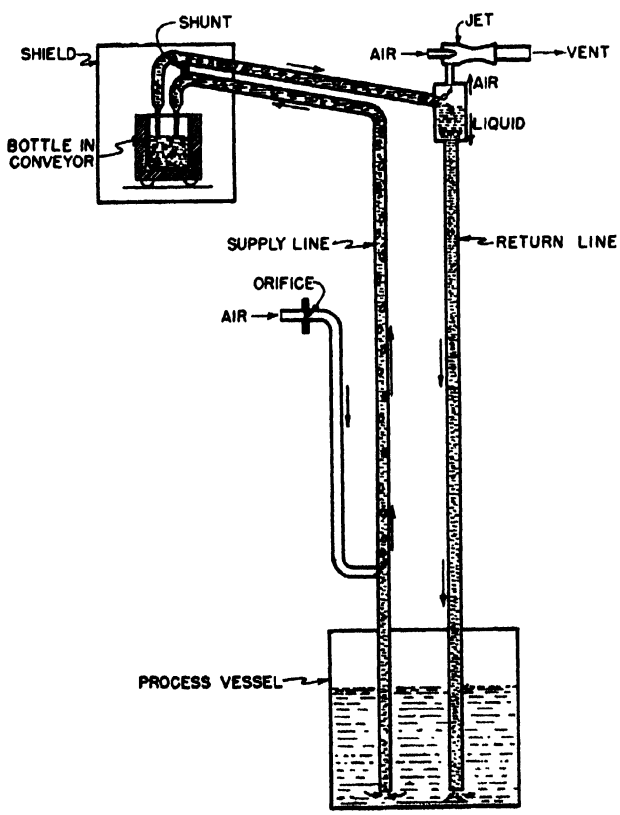

Figure 6. The Oak Ridge plant sampler

deep. The filling box is provided inside with a sprinkler and drain for washing.

The trombone and bayonet samplers (Fig. 3) are used for 0.5-to 5-ml samples of the less radioactive process liquids. Process liquid is recirculated through a chamber shielded beneath the floor. In the trombone sampler a pipette with a plastic well at the tip is lowered on an extension just within the chamber liquid. A hand-operated vacuum bulb draws liquid into the pipette. The extension is used to transfer the filled pipette to a shielded carrier, where the well is unscrewed from the pipette and is left in the carrier for transport to the analytical laboratory.

The bayonet sampler is similar to the trombone sampler except that a Saran bottle on an extension handle is used in place of the pipette arrangement. The bottle is necked down to a tip which is lowered into the chamber. After the bottle is in place, the jet reduces the pressure in the chamber and bottle alike during the recirculation period. When the jet is turned off, the chamber is vented by the return line and this forces liquid from the chamber into the bottle. The bottle and handle are transferred to a carrier sheath and carried to the analytical laboratory.

With one type of high-level liquid sampler, in use at the Savannah River plant (Fig. 4), the hinged door

in the shield is opened for the doorstop with bottle to be hoisted onto the door bracket, and the door is closed. A reversible crank mechanism lifts the cover from the doorstop, withdraws a drip drain from beneath the needles, and moves the doorstop and bottle beneath the two needles. The pneumatic elevator raises the doorstop and forces the penetrable-top bottle onto the needles in sampling position. An air lift-jet combination recirculates the process liquid and supplies the sample. The sample volume depends on the level of the return needle in the sample bottle. After the sampling, the bottle and doorstop are lowered into the mobile carrier for transportation to the analytical laboratory. The shielded sampler is about 5 ft long by 4 ft high by 2 ft wide. Cleaning funnels are provided for servicing the sampler lines, and the enclosure has facilities for washing the interior.

The Idaho plant uses a type of sampler in which the bottle is brought to the sampling station in a mobile shielded carrier and is raised from this into a port in the sampler enclosure (Fig. 5). A track-mounted tong services several samplers and operates through a slot in the shield to raise the bottle from the port up onto the tips to receive the sample. The recirculating air lift and jet are used in conjunction with hypodermic needles and a penetrable-top bottle. The sample is drawn, returned to the carrier, and moved to the analytical laboratory without personnel exposure. A rotating drawer within the carrier removes the sample from the entrance to a central point for maximum shielding. The jet can be cleaned by steam.

A recently developed sampler in use at Oak Ridge (Fig. 6) uses an air lift for recirculation. The jet passes no liquid but serves only as a vacuum supply to provide submergence for air-lift operation. Penetrable-top bottles are brought into shielded enclosures, 10 to each enclosure, by a chain conveyor which automatically positions 30 bottles beneath 30 sets of hypodermic needles, corresponding to 30 sampling points in the process. The tubes carrying the needles flex 2 in. in a 5-ft span, within the 5-ft gallery wall. The depth of the needle penetration into the bottle determines the sample volume. A shunt at the needles provides recirculation rates through the bottle nine times greater than those provided by the needles, and representative samples are rapidly obtained. The external measurements of the enclosures are 2 ft 4 in. long by 1 ft 8 in. wide by 11 in. deep. From 1 to 30 samples are drawn simultaneously and automatically transported to an unloading station at the analytical laboratory without personnel exposure.

Record of Proceedings of Session 21B

FRIDAY MORNING, 19 AUGUST 1955

Chairman: Mr. R. Spence (UK)

Vice-Chairman: Mr. H. R. Sethna (India)

Scientific Secretaries: Messrs. D. J. Dewar and J. Gaunt

PROGRAMME

P/414	Criteria for the selection of separation processes	C. M. Nicholls
	Discussion	
P/822	Reprocessing of reactor fuel and blanket materials by solvent extraction	F. L. Culler
P/540	The solvent extraction separation of U^{233} and thorium from fission products by means of tributyl phosphate	A. T. Gresky
P/349	Solvent extraction of plutonium from uranium irradiated in atomic piles	B. Goldschmidt *et al.*
P/785	Extraction of uranium and plutonium with tetrabutylammonium nitrate, cupferron and neocupferron as complexing agents	E. Haeffner *et al.*
P/824	Practical limitations of solvent extraction processes	R. E. Tomlinson
	Discussion	
P/551	The chemical processing of aqueous homogeneous reactor fuel	D. E. Ferguson
	Discussion	

The Chairman: Ladies and gentlemen, the various methods for the generation of nuclear power which have been discussed at this Conference all depend on the process of nuclear fission. The fissile nucleus breaks up into two lighter nuclei which fly apart with very great kinetic energy, so producing heat which can be converted into power. These fission products were first identified by Hahn and Strassmann in 1939, and in doing so they established for the first time that the absorption of neutrons by U^{235} leads to fission. It has given great pleasure and satisfaction to all of us that Mr. Hahn has been able to attend this Conference and to take the Chair at some of our meetings. This morning we shall discuss chemical processes for the separation of irradiated fissile material, several of which have already been applied in great industrial plants. These plants descend in direct line from those experiments carried out only a few short years ago, with feeble radioactivities, in the laboratories of Mrs. Joliot-Curie in Paris and of Hahn in Berlin.

Not only do we obtain the lighter fission product elements as a result of the nuclear chain reaction but many heavy element isotopes are formed by neutron capture processes as well, the fissile isotopes Pu^{239} (formed from U^{238}) and U^{233} (formed from Th^{232}) being the most important. It has been necessary, therefore, to devise processes for the recovery of pure uranium and plutonium or uranium and thorium from irradiated fuels and blanket materials and to collect the fission products together in a form suitable for storage or subsequent use.

As we have heard in previous papers at this Conference, the efficiency of any nuclear power programme depends not only on the efficiency of the nuclear reactor itself but equally on the efficiency of processes in all the other stages of the fuel cycle.

In the case of solid fueled reactors, the fuel must be removed after a certain period on account of the development of structural damage, due either to radiation or to some other operating factor, or on account of the growth of neutron absorbing fission products. The problem, so far as power reactors are concerned, is to remove the bulk of the fission product poisons, to separate, if necessary, the fissile material which has been produced in the reactor and to refabricate the fuel element. It is important that there be no significant loss either of fissile or of fertile material. The amount of loss which can be permitted depends on the type of reactor and fuel cycle under consideration. For example, in a reactor such as the fast reactor using highly enriched fuel, which must be recycled many times, the processing loss must be very low indeed as otherwise it might easily happen that more fissile material is lost in the processing plant than is burned up in the reactor. On the other hand, if very long irradiation periods could be achieved in natural uranium reactors, greater losses could be tolerated

in the chemical plant provided the process was very cheap and simple.

You will see from the papers which are to be presented this morning that solvent extraction processes are available which will separate uranium and plutonium almost quantitatively and which will give a far higher decontamination from fission products than is required in a power reactor programme. Ideally, one should remove only that fraction of the fission products which has an appreciable adverse effect on the operation of the reactor. This would mean the handling and refabrication of highly radioactive materials. Unfortunately, few if any metallurgical plants are equipped to do this at the present day and it seems likely that processes such as solvent extraction, which readily yield products which can be treated in existing plants and which therefore confer greater flexibility, will hold the field in the immediate future. This morning we are being presented with a great wealth of data on solvent extraction which should be of profound interest and value.

I have spoken so far only of the problem of solid fuelled reactors. Reactors with liquid or fluidized fuels offer special opportunities for continuous chemical processing in a plant which would virtually be an integral part of the reactor. The most elegant of these systems which has so far been described is the aqueous homogeneous reactor and we are fortunate in having an important contribution from the Oak Ridge National Laboratory describing the techniques which they have developed for continuous separation of fission products.

I would like to conclude my remarks by emphasizing firstly that efficient chemical processing is a vital factor in any nuclear power programme, and secondly that the chemical plant cannot be considered in isolation from the reactor. Each reactor and fuel cycle has its own special requirements and each offers different opportunities to the chemist and chemical engineer.

Mr. C. M. NICHOLLS (UK) presented paper P/414.

DISCUSSION OF PAPER P/414

Mr. TOMLINSON (USA): The question of remote versus contact maintenance for separation facilities has received considerable study in the United States of America, since contact maintenance requires a smaller capital investment than does the utilization of remote maintenance techniques. The feasibility of contact maintenance has been established with dealing with up to 100,000 curies at a time, provided that up to several weeks of interrupted production may be tolerated in case of equipment failure in a very radioactive zone. The cost of non-productive time is a function of the throughput of the plant, and the choice of contact or remote maintenance is largely determined by the production demands made on the facility. A compromise maintenance method is currently under study whereby contact methods will be utilized if practicable, but provision is made to flood the cell with water and manipulate the equipment with long-handled appliances under direct observation.

Mr. NICHOLLS (UK): These comments are extremely useful and are in line with our experience, although our experience probably does not go up to the activity mentioned. There is one very obvious point which I might make; when a plant is to be flooded it is assumed that the criticality implications will have been taken into account.

Mr. TOMLINSON (USA): It is obvious that when we flush the cell we have already cleaned out the equipment.

Mr. F. L. CULLER (USA) presented the following summary of papers P/822 and P/540: During the preceding two weeks we have heard frequent mention of the importance of radiochemical reprocessing in the economics of nuclear power production by many physicists and reactor engineers. Almost without exception their prognostications for economic power have parenthetic statements such as: "assuming that adequate, inexpensive chemical reprocessing is available."

The frequency with which the solvent extraction method for reprocessing has been mentioned is a clue to the amount of basic and applied development which has been devoted to this technique and to the importance of this step in the production of economical nuclear power. It is my privilege to report on the work of many hundreds of individuals and of well-directed technological teams in the United States who have developed the solvent extraction reprocessing of fissionable and fertile materials. The published Proceedings of the Conference contain many papers which expand upon and supplement the information which I shall present.

In deciding what to cover in this oral presentation, I have elected to discuss the mechanisms involved in the processes involving the two most versatile solvents, tributyl phosphate and methylisobutyl ketone, for the separation of plutonium and uranium and for the separation of uranium and thorium; and then to present schematic flowsheets for three possible processes.

The solvent extraction technique belongs to the general class of processes in which the fissionable and fertile materials are separated completely from fission products.

Chemical processing of reactor elements normally is preceded by a period of decay cooling between the time of discharge of fuel or fertile material from the reactor and the start of chemical processing.

The time that a reactor fuel or blanket material is allowed to decay between discharge from a reactor and the start of chemical reprocessing is a variable dependent upon the nature of the irradiated material, the specific power of the reactor, the time of irradiation, and the nature of the chemical process to be applied. For solvent extraction processes, this period is desirably long enough to allow decay of the active

fission gases Xe^{133} and I^{131}; however, it is usually determined by the time required for the decay of one of the following heavy-element chains.

For uranium:

$$U^{238}(n,\gamma) \longrightarrow U^{239} \xrightarrow[23.5\ min]{\beta^-} Np^{239} \xrightarrow[2.33\ d]{\beta^-} Pu^{239}$$

$$U^{235}(n,\gamma) \longrightarrow U^{236}(n,\gamma) \rightarrow U^{237} \xrightarrow[6.7\ d]{\beta^-} Np^{237}$$

For thorium:

$$Th^{232}(n,\gamma) \longrightarrow Th^{233} \xrightarrow[23.5\ min]{\beta^-} Pa^{233} \xrightarrow[27.4\ d]{\beta^-} U^{233}$$

$$Th^{233} \xrightarrow{(n\,\gamma)} Th^{234} \xrightarrow[2.41\ d]{\beta^-} Pa^{234} \xrightarrow[6.7\ hr]{\beta^-} U^{234}$$

For uranium the decay period is determined by Np^{239} or possibly by U^{237} decay. Shorter decay periods than those required by these decay chains can be used with the following probable results: (1) radiochemical processing may be complicated by relatively large quantities of I^{131} and Xe^{133} and by the higher activity level of process solutions; (2) uranium and thorium may be produced which contain enough β-γ-emitting isotopes to make remote handling of products and refabrication of metal fuel assemblies necessary; and (3) losses of neutron-capture-produced fissionable material may be high if the neptunium or protactinium have only partially decayed.

The solvent extraction processes are somewhat limited in their applicability to short-decayed fuels of high burn-up because of radiation damage to solvent, which should not exceed from 0.2 to 2 beta watt-hours per liter of solvent. This can be controlled by regulating the time of contact between the active solution and the solvent itself, so that it is not so serious a limitation as it may sound.

A process that is satisfactory for the recovery of fissionable and fertile material must separate fissionable and fertile material from each other, while simultaneously separating both from fission products and inactive chemical contaminants. The high selectivity of certain organic solvents for this purpose makes solvent extraction rather ideal for radiochemical separations.

Solvent extraction of uranium, plutonium and thorium from an aqueous phase containing high concentrations of nitrate ions is possible because of the solubility of the nitrates of these elements in certain organic solvents. Nitric acid therefore is the logical dissolution agent for fuel elements. For materials such as stainless steel and zirconium which are nitric acid insoluble, other mineral acids such as hydrofluoric acid and sulfuric acid can be used for the primary dissolution; but before solvent extraction, nitrate ion is added either as nitric acid or as a nitrate salt.

The choice of the organic solvent depends upon the selectivity of the solvent for the desired products, the ease with which products can be removed from the organic material after the primary extraction, chemical and radiation stability, interfacial tension, recoverability, viscosity, toxicity, flammability, and cost. Certain solvents, namely, methylisobutyl ketone and tri-*n*-butyl phosphate, have all the desirable properties for the recovery and decontamination of fissionable and fertile materials. With them, the processes shown in Table I are possible.

Table I. Selected Solvent Extraction Processes

Process	*Solvent*	*Salting agent*
Redox	Hexone	$Al(NO_3)_3$
Metal Recovery	Tributyl phosphate	HNO_3
Purex	Tributyl phosphate	HNO_3
TTA Chelation	Thenoyl trifluoroacetone in benzene	$Al(NO_3)_3$
25	Hexone	$Al(NO_3)_3$
25, TBP	Tributyl phosphate	HNO_3–$Al(NO_3)_3$
Interim-23, Hexone	Hexone	$Al(NO_3)_3$, HNO_3
Interim-23, TBP	Tributyl phosphate	$Al(NO_3)_3$, HNO_3
Thorex	Tributyl phosphate	$Al(NO_3)_3$, HNO_3

You will note that methylisobutyl ketone (hexone) can be used for the separation and decontamination of uranium and plutonium, separation and recovery of U^{233} from thorium, and the recovery of enriched uranium from a non-fertile diluent such as aluminum. In each process the extraction occurs from an aluminum nitrate salted system.

Tributyl-*n*-phosphate (TBP) can be used to separate and decontaminate uranium and plutonium; to recover uranium from fission-product-bearing waste from which plutonium has been removed; to separate enriched uranium from non-fertile diluents such as aluminum; and to separate and decontaminate U^{233}, thorium, and protactinium. With TBP the extractions occur from nitric acid salted systems. TBP is diluted usually with an inert hydrocarbon diluent similar to kerosene or saturated kerosene fraction. Now let us consider the mechanism of extraction of fissionable and fertile materials.

Uranium and plutonium, and some of the fission products always exist in aqueous systems as ionized ions of formulae corresponding to UO_2^{+2}, PuO_2^{+2}, etc. Th^{+4} and Pu^{+4} exist probably unhydrolyzed but they are surrounded by waters of hydration. In systems containing anions such as NO_3^-, Cl^-, and other anions, U, Pu, and Th form anionic complexes. Undissociated nitrate complexes form solvents with the organic extractants with the equations shown below.

For hexone:

$$UO_2^{++} + 2\,NO_3^- + 4\,H_2O \rightleftarrows UO_2(NO_3)_2 \cdot 4\,H_2O \quad (1)$$

$$UO_2(NO_3)_2 \cdot 4H_2O + n\ \text{MIBK} \rightleftarrows [UO_2(NO_3)_2 \cdot 4H_2O \cdot n\ \text{MIBK}]_{org} \quad (2)$$

(similarly for Pu^{+4} and some fission products)

For TBP:

$$UO_2^{++} + 2\,NO_3^- + 2\,TBP_{org.} \rightleftarrows [UO_2(NO_3)_2(TBP)_2]_{org.} \quad (1)$$

$$Pu^{+4} + 4\,NO_3^- + 2\,TBP_{org.} \rightleftarrows [Pu(NO_3)_4(TBP)_2]_{org.} \quad (2)$$

$$Th^{+4} + 4\,NO_3^- + 4\,TBP_{org.} \rightleftarrows [Th(NO_3)_4(TBP)_4]_{org.} \quad (3)$$

(similarly for some fission products)

In the case of hexone the undissociated nitrates, along with waters of hydration, are soluble in the organic phase, where the solvate is formed. With TBP a complex involving the TBP molecule is formed to provide the organic soluble compound. Thus, there is a difference in mechanism between hexone and TBP extraction that results in constant distribution coefficients for hexone, but varying distribution coefficients for TBP dependent upon a power function of uncomplexed TBP concentration and nitrate concentration.

Now let us consider the effect of salting strength in the aqueous phase. From the equation expressing the equilibrium between the dissociated strong electrolyte and the hexone solvated complex, it is obvious that extraction into hexone is favored also by high aqueous phase nitrate concentrations. For both hexone and TBP systems the additions of nitrate forces the extraction of metal nitrates into the organic phase.

For TBP, adding the nitrate as HNO_3 is satisfactory since the extraction of fission product nitrates by TBP can be suppressed by operating the systems so that the organic phase is nearly saturated with the more tightly formed uranyl nitrate-TBP complex.

For hexone, salting agents such as $Al(NO_3)_3$ or NH_4NO_3 must be used to obtain the necessary nitrate salting strength without making the aqueous phase highly acidic, a condition which favors the extraction of fission products. $Al(NO_3)_3$ or ammonium nitrate, by forming such hydrolysis compounds as $Al(OH)_2^+$ or NH_4OH and by hydrated ions effectively increase the nitrate concentration by binding water molecules in the aqueous phase. Systems containing amphoteric aluminum can be made deficient in free acid by the formation of such basic complexes as $Al(OH)_2^+$. In hexone systems and in the extraction of Th^{+4} by TBP, acid deficiency in the aqueous phase allows certain of the fission products whose nitrates are organic soluble under acidic conditions to hydrolyze to organic insoluble complexes, or possibly to be reduced to a valence state in which their nitrates are inextractable.

We come now to the mechanism for the separation of uranium and plutonium in both hexone and TBP systems.

If it were not for the existence of the several oxidation states of uranium and plutonium, and particularly for the differences of these various states in aqueous nitrate systems, the separation one from the other would be rather difficult since, in general, their chemistry is relatively the same. Fortunately, their chemistry, while quite similar in the same valence state, is markedly different in different valence states. The most stable valence state of uranium is the U(VI), the condition of uranium in nitric acid solution.

The nitrate of U(VI), and for that matter the nitrate of U(IV), is soluble in hexone or TBP. The most stable valence state of Pu is Pu(IV), the nitrate salt of which is soluble in TBP. The nitrate salt of Pu(VI), which can be produced by the addition of an oxidant such as $Na_2Cr_2O_7$ to nitric acid, is soluble in hexone.

However, the nitrate salt of Pu(III), the second most stable valence state of Pu, is only very slightly soluble in either TBP or hexone. Extractable Pu (IV) can be reduced to the inextractable Pu(III) state without reducing U(VI). This is the basis for separating uranium and plutonium. This is illustrated by the typical distribution coefficients shown in Table II.

Table II. Distribution Coefficients with TBP and Hexone

	TBP D.C. (O/A) with HNO_3 Salting agent	*Hexone D.C. (O/A) with $Al(NO_3)_3$ Acid deficient*
U(VI)	8.0	~1.5
Pu(IV)	1.5	1.6×10^{-2}
Pu(VI)	0.6	7.6
Pu(III)	0.02	4.5×10^{-4}
Fission products	0.002	$\sim 6 \times 10^{-4}$

In the TBP process the distribution coefficients vary with the quantity of extracted material in the organic phase. The distribution coefficients in this slide would be lower than shown if the organic phase were near saturation.

Thus a countercurrent system in which saturation is maintained near the feed point for high fission product decontamination and fresh TBP at the bottom of the contractor for high uranium recovery provides an idealized process. If the organic phase rising above the feed point is scrubbed with an aqueous phase containing no uranium, additional fission product decontamination can be removed.

Let us now consider the mechanism for the separation of U^{233} and thorium.

Hexone can be used to separate U^{233} and thorium, since thorium nitrate is not appreciably soluble in hexone. However, thorium follows the fission products in this process and requires subsequent separation with other organic solvents or by other chemical methods.

TBP can be used to separate thorium, U^{233} and Pa^{233} which follows the fission products. Thorium and uranium are extracted under high salting conditions and fission products and Pa, and then separated from each other under low salting conditions where the difference in distribution coefficient between U and Th provides the basis for separation.

Decontamination from fission products has been mentioned. As might be expected, some fission products (or more exactly, some fission product nitrates) are more soluble in organics than others. Table III lists the fission products of importance in solvent extraction.

Table III. Fission Products of Importance in Solvent Extraction

Periodic group	*Isotope*
0	Kr^{85}, Xe^{133}, Xe^{135}
I	Cs^{137}, Cs^{135}
II	Sr^{89}, Sr^{90}, Ba^{140}
III	Y^{91}, Y^{90}, Ce^{141}, Ce^{144}
IV	Zr^{95}
V	Nb^{95} (daughter of Zr^{95})
VI	Se, Te
VII	I^{131}
VIII	Ru^{103}, Ru^{106}–Rh^{106}

The products in Groups I and II of the periodic table show very low solubility in organics. Group III elements including the rare earths, and excluding cerium, are similarly easily separable. Of the elements in Groups IV and V only zirconium and its decay daughter, niobium, are difficult to separate. Group VI fission products have very long or very short half-lives and are, therefore, not important if the cooling period before processing is longer than 20 days to allow for the decay of the 67-hour half-life Mo^{99}. Iodine in Group VII is important because it reacts with many organic solvents and is extracted. In Group VIII, ruthenium is difficult to separate because of its many valence states and its very complex chemistry.

The decontamination of uranium and plutonium using TBP has been mentioned previously, the mechanism being one of saturation of the organic phase with the more tightly bound U-TBP complex for those fission products whose nitrates are appreciably soluble in the TBP phase.

For hexone processes the decontamination from fission products is dependent upon the free nitric acid concentration in the aqueous phase. An aqueous solution highly salted in aluminum nitrate can be made "basic" in the sense that no free acid exists; however, the pH of an "acid deficient" system is less than 7. The distribution coefficient of those fission products with hexone soluble nitrates is much more sensitive to the acidity of the solution, particularly in the "acid deficient" range. This is possibly due to the greater hydrolysis of fission products than either UO_2^{++} or PuO_2^{++}.

This is illustrated in Slide 1 in which the separation factor between uranium and fission products is plotted against acid concentration at constant $Al(NO_3)_3$ concentration. You will notice that the marked change on each side of the neutral point is several tenths in terms of pH. The separation of fission products from thorium and uranium by TBP

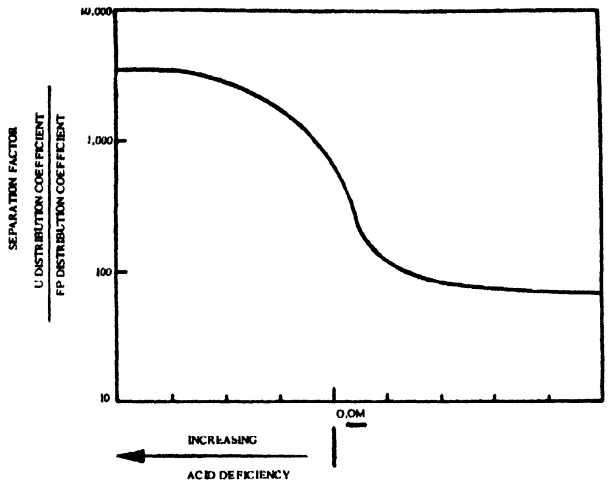

Slide 1. Separation factor vs free acid in hexone extraction

employs both the saturation of the organic phase with the more extractable $Th(NO_3)_4$ to suppress the extraction of those fission products whose nitrates are soluble and the acid deficient aluminum nitrate salted aqueous phase.

The Purex Process

Now let us consider the TBP process for separating uranium and plutonium, using tributyl phosphate —the so-called Purex process. A schematic flowsheet for the separation and decontamination of uranium and plutonium using TBP is shown in Slides 2 and 3.

Uranium metal is charged into a dissolver where the customary aluminum sheath is preferentially dissolved by a sodium hydroxide-sodium nitrate solution. The uranium is then dissolved in nitric acid. The concentrated uranyl nitrate-nitric acid solution is withdrawn, filtered to remove silica and possibly aluminum particles, and adjusted to the feed concentration. Finally, the plutonium is quantitatively stabilized to the tetravalent state, the form most readily extracted by TBP, and the feed is ready for solvent extraction.

The metal feed is extracted with TBP diluted with a kerosene type carrier. Here conditions of flow and salting strength are regulated in such a manner that the uranium and the Pu(IV) are coextracted almost quantitatively, leaving most of the fission products and other impurities in the aqueous phase.

In the second contactor uranium and plutonium are separated by reducing the latter to the highly aqueous-soluble trivalent state. Salting strength and flow conditions are controlled in such a manner that separation of the two products is virtually complete, the aqueous plutonium stream leaving the lower end of the column while the uranium remains in the organic phase.

The uranium-bearing organic solvent is passed into the bottom of a third column, where the uranium is stripped from the organic with water. The stripped organic is reconditioned for subsequent re-use in the process.

The dilute plutonium stream flows directly to the second cycle for continuous feed make-up in which

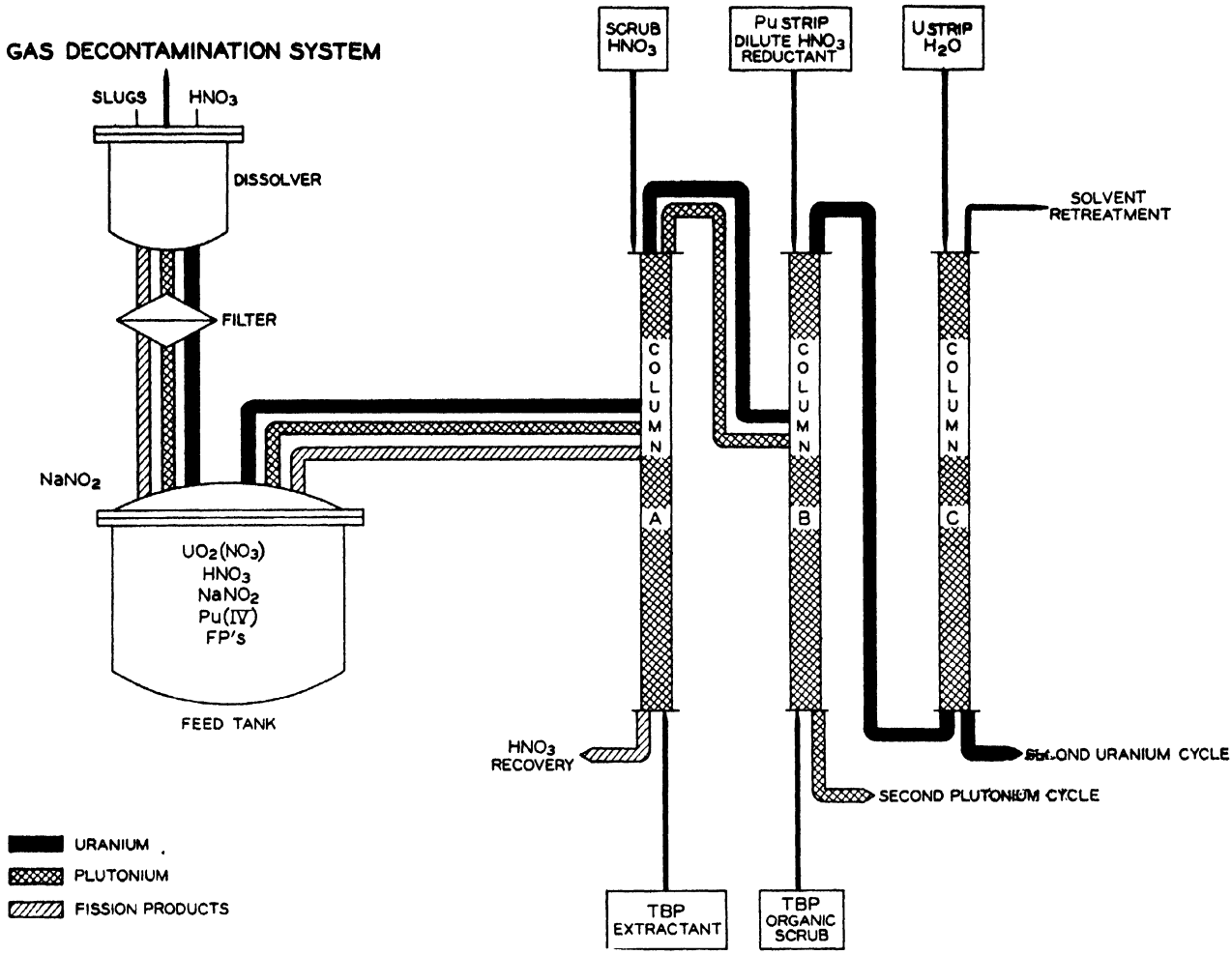

Slide 2. Purex process—first cycle flowsheet

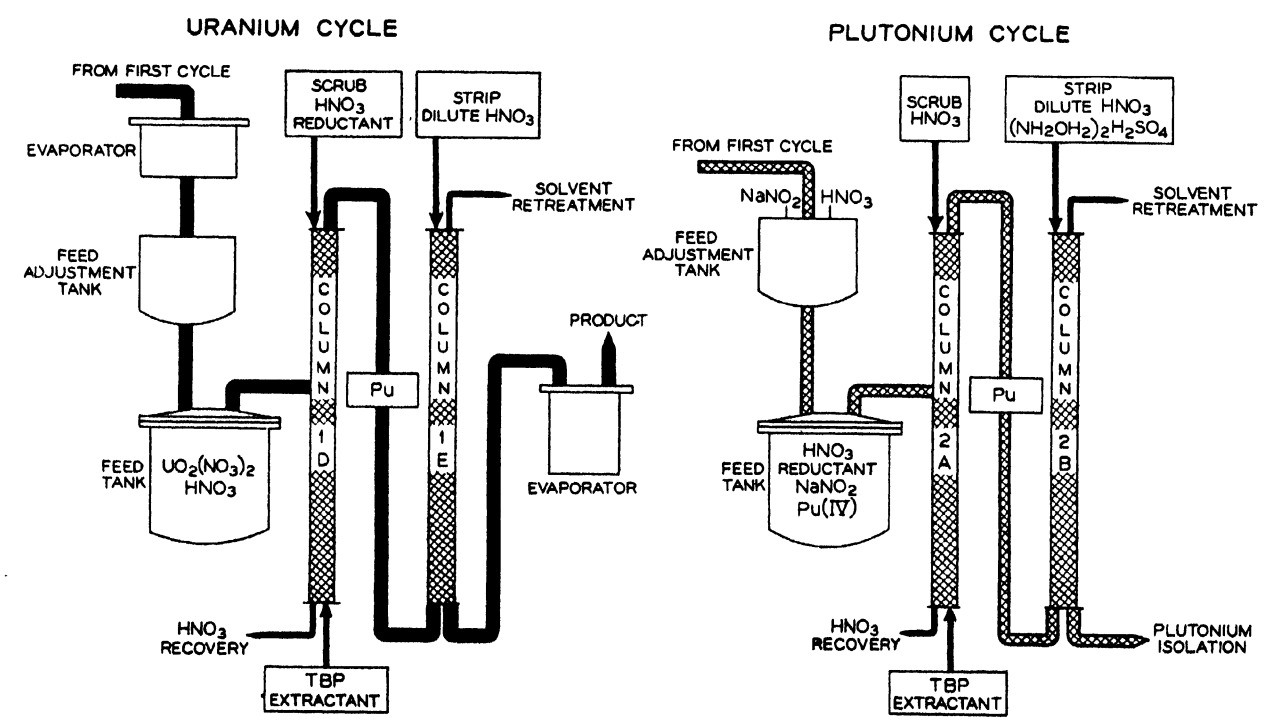

Slide 3. Purex process—second cycle flowsheet

the salting strength is raised by the addition of nitric acid and the Pu(III) is oxidized to Pu(IV), (Slide 3). The plutonium is extracted by the solvent to complete its separation from residual activity. The organic product stream flows into a second contactor where the plutonium is again reduced to the trivalent form and is stripped into an aqueous hydroxylamine sulphate solution. At this point, the product stream is concentrated by sorption on and elution from a cation-exchange resin bed. Additional purification is realized from this step such that the over-all separation of plutonium from fission products can exceed a factor of 10.

The aqueous uranium stream from the first cycle flows to a continuous evaporator and is concentrated and then adjusted with nitric acid. Following this, the uranium is extracted and is scrubbed in a manner similar to that of the first-cycle extraction. The extracted uranium is stripped into water in a second column and is concentrated in a second evaporator. The concentrate is passed through a bed of silica gel (which adsorbs trace fission products) to complete the removal of fission product activity. The uranyl nitrate concentrate then can be calcined to uranium trioxide or converted to other uranium salts, and upon leaving the solvent extraction system the uranium is usually below its normal background.

Since the solvent is re-used, it is sent to a solvent recovery area after each pass through the system. Here it is washed with a sodium carbonate solution and then with dilute acid to remove the traces of strongly complexed radioelements and the TBP degradation products. Over-all solvent losses can be maintained as low as 0.01 per cent.

A modified Purex flowsheet can be used to recover enriched uranium from inactive diluents and fission products.

Redox Process

The Redox process is a three-column solvent extraction system in which plutonium and uranium are separated from each other and from the bulk of the fission products. The feed solution is aluminum nitrate salted, acid deficient uranyl nitrate containing sodium dichromate to oxidize the plutonium to Pu(VI). Both uranium and plutonium are extracted with acidified hexone, and the organic extract is scrubbed in the same column with acid-deficient aluminum nitrate. In a second column the plutonium is stripped from the organic by reducing plutonium to the inextractable III state without affecting the uranium (Slide 4).

The uranium product from the first cycle is evaporated and put through a second cycle (Slide 5) and possible third uranium cycle depending upon how radioactive the feed material is at the beginning. The

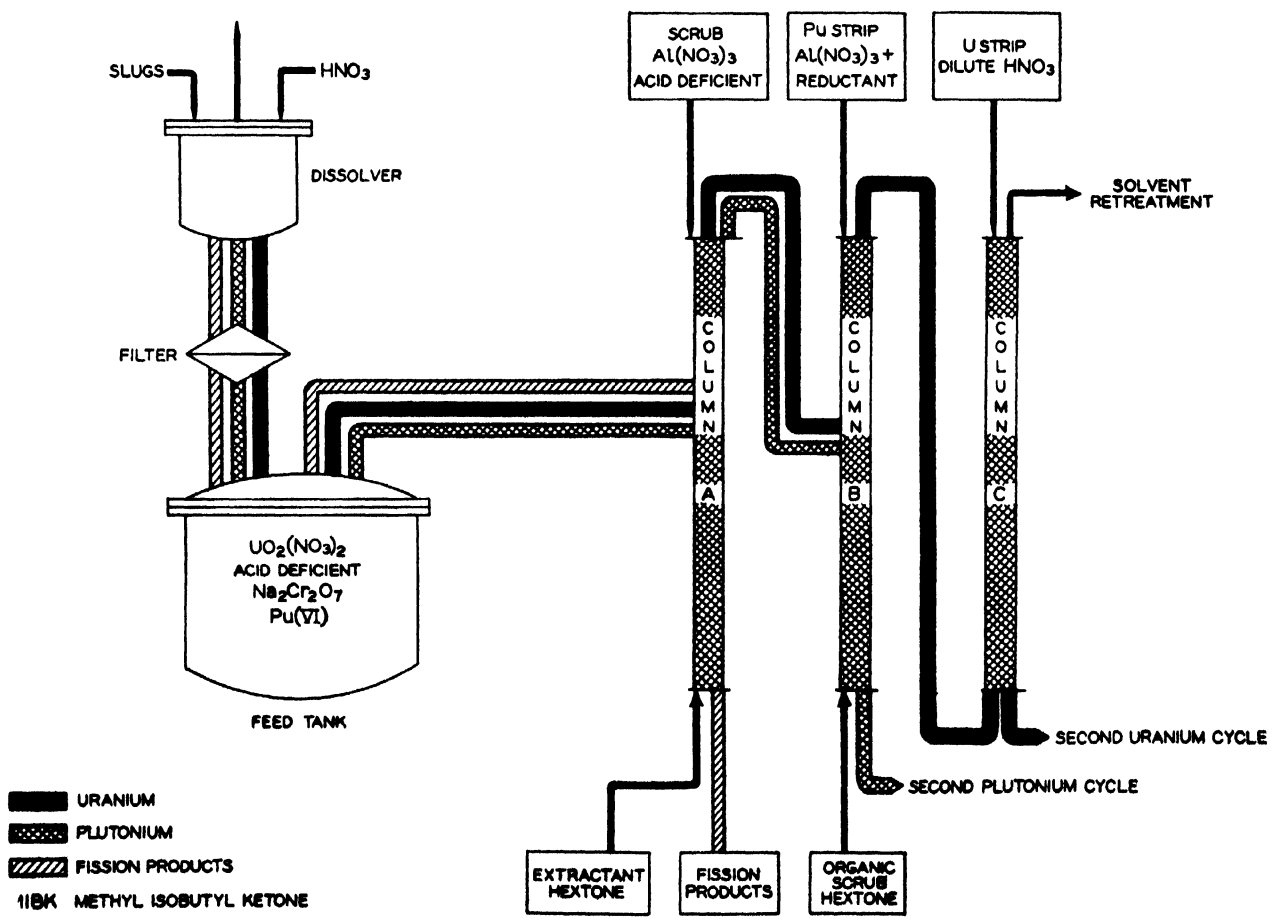

Slide 4. Redox process—first cycle flowsheet

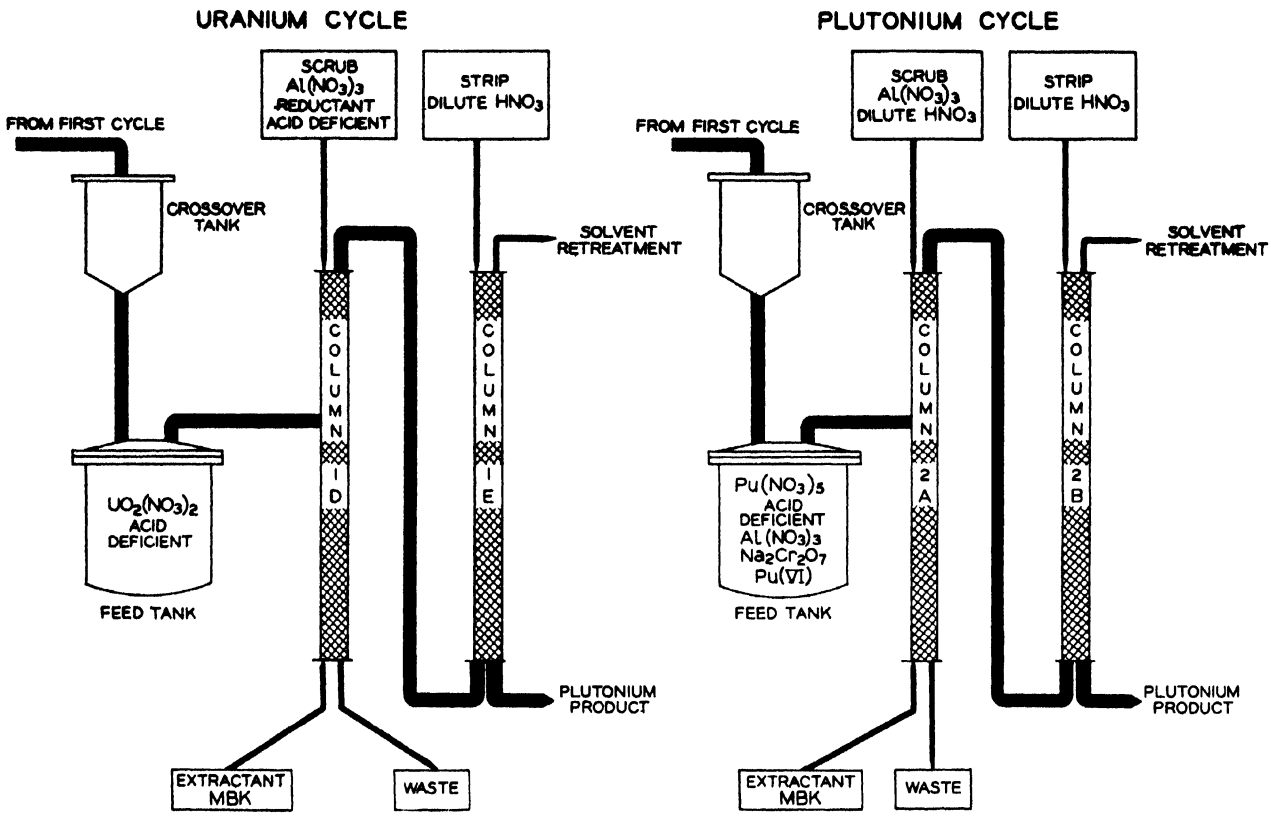

Slide 5. Redox process—second cycle flowsheet

scrub solutions may contain a reducing agent to provide additional separation from plutonium.

The plutonium product from the first cycle, already salted with aluminum nitrate, is oxidized with dichromate and then decontaminated by additional solvent extraction cycles. The plutonium is extracted with acidified hexone and scrubbed with oxidized acid-deficient aluminum nitrate in one column and stripped with dilute nitric acid in a second column. A reducing agent is not required in the scrub stream, as in the first-cycle partitioning column, where separation from uranium is accomplished. The plutonium solution from the strip column of the second cycle can be salted with $Al(NO_3)_3$ and put through a third cycle similar to the second, if necessary for product decontamination.

A modified hexone flowsheet can be used to recover enriched uranium from inactive diluents and fission products. This is the so-called 25 process.

Over-all Fission Product Decontamination Factors

The TBP and hexone processes described provide decontamination from fission products by repetitive re-extraction to reduce the activity in uranium and plutonium product streams to the natural background activity level. Table IV gives the fission product decontamination factors for these processes.

The Thorex Process

The process for the separation of thorium, U^{233}, protactinium and fission products uses tri-*n*-butyl phosphate as the active extractant. Extraction occurs from an aqueous nitrate solution prepared by dissolving thorium in nitric acid (Slide 6).

Nitric acid dissolution of thorium metal canned in an aluminum can can be accomplished by adding concentrated HNO_3, containing fluoride and mercuric ions to a dissolver holding an excess of the metal at all times. The fluoride and mercury serve as catalysts in the reaction of HNO_3 with thorium and aluminum, respectively.

Excess nitric acid is evaporated from the dissolver solution and is recovered by fractionation for reuse. The thorium and aluminum nitrate residue is concentrated to an essentially molten state of the salts. This residue is subsequently diluted with water to prepare the proper salt concentrations for feeding to the solvent extraction contractors. This step may seem a little bit unusual; it is used to dehydrate compounds of silica which go along with both the aluminum, the canning material possibly, and with the thorium metal.

Table IV. Fission Product Decontamination Factors for Purex and Redox

	Log D. F. after 2 cycles of extraction		*Log D. F. after extraction plus sorption*	
Constituent	*U*	*Pu*	*U*	*Pu*
TBP gross β	6.82	6.89	6.99	7.51
gross γ	6.43	6.30	6.81	7.20
Hexone gross β	6.50	7.7	–	–
gross γ	6.0	7.5	–	–

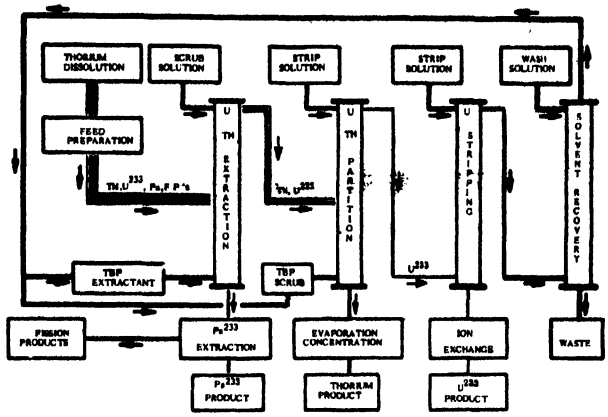

Slide 6. Process for separation of thorium, U^{235}, Pa^{233}, and fission products

This aqueous feed enters the first contractor at approximately the mid-point where it mixes with a down-flowing scrub solution made up of aluminum nitrate containing small amounts of ferrous and phosphate ions. In the bottom section of this contractor, this combined aqueous stream is equilibrated with an up-flowing organic stream containing tributyl phosphate in an inert, paraffinic diluent and the thorium and U^{233} are extracted, leaving the Pa^{233} and fission products in the aqueous "waste" stream. In the top section of this contactor where the extract flows continuously against the aqueous scrub solution, traces of Pa^{233} and certain fission products are further removed from the thorium and U^{233} products in the organic phase.

The organic extract then enters at approximately the middle of the second contactor where a down-flowing stream of dilute nitric acid serves to preferentially strip the thorium nitrate, leaving the U^{233} in the extract. A small stream of fresh organic extractant which enters the bottom of the contactor flows upward and re-extracts traces of U^{233} which has been stripped along with the thorium. The organic extract, containing now only U^{233} leaves the top of the second contactor and proceeds to the bottom of a third contactor where the U^{233} is stripped into a down-flowing stream of water. The dilute uranyl nitrate solution is then passed through a silica gel column for removal of trace fission product and possibly Pa^{233} colloids and finally to a cation-exchange resin system where traces of thorium and corrosion products are further removed and where the U^{233} is finally sorbed and concentrated. This product is subsequently eluted from the resin as a concentrated uranyl acetate solution (other eluting acids can be used), which is subsequently treated in reduction steps as required for preparing the U^{233} for re-use in the reactors.

The depleted organic extractant passes from the top of the third contactor to a solvent recovery contactor where it is washed by an aqueous sodium carbonate solution to remove the undesirable acidic decomposition products of TBP, (that is, mono- and dibutyl phosphoric acids). The solvent is subsequently centrifuged to assist in the trace removal of entrained decomposition and fission products, and is then recycled as extractant to the first and second contactors.

The aqueous "waste" stream from the first contactor, containing the fission products and quantities of Pa^{233}, the concentration of which varies, depending on irradiation and cooling conditions, would be sent to interim storage facilities until the Pa^{233} decays to U^{233}, isotopically purified by virtue of prior removal of uranium and thorium isotopes, is subsequently extracted away from the fission products, again by use of a TBP solution, and is isolated by ion exchange for return to reactor cycles. The residual fission product wastes are then routed to permanent storage facilities. Note that this does not contain an isolation step for Pa.

(An alternate Pa^{233} and/or U^{233} recovery cycle has also been developed, to eliminate the need for interim Pa^{233} decay, and involves the "carrying" of Pa^{233} on a solid "carrier" of basic aluminum chromate. This represents a means for isolating and concentrating, by a factor of about 50, the Pa^{233} product so that small interim storage systems would be sufficient to allow for decay of U^{233}. The U^{233} after decay would be subsequently recovered from the carrier concentrates by solvent extraction. The fission product wastes from the "carrying" step could be routed immediately and directly to permanent storage.)

A summary of fission product decontamination factors for the thorium and U^{233} products is shown in Table V. Additional cycles of extraction, similar in most respects to that presented, can be used to increase decontamination from fission products.

Table V. Solvent Extraction Decontamination Factors

Element	*Decontamination factor* *Th product*	*U^{233} product*
Th^{234}	....	1×10^4
Pa^{233}	5×10^4	4×10^6
Total rare earths	1×10^6	2×10^6
Thorium-uranium separation factor $\cong 1 \times 10^4$		

A thorium-U^{233} separation factor of 10^4 is also indicated. This factor is further increased for the U^{233} product during the ion exchange step.

Let us now look more carefully at the mechanisms of separation for this process. Unlike the processes for uranium and plutonium, in which the separation of Pu from U is accomplished by changing the oxidation state of plutonium, the separation of U^{233}, thorium, and protactinium depends upon differences in solubility of the undissociated nitrates of these elements in the TBP phase. Distribution coefficients for U, Th, Pa, and HNO_3 into dilute TBP from a non-salted aqueous phase are shown in Slide 7.

Obviously, there is sufficient difference in distribution coefficients to provide adequate separation of the products desired. The distribution coefficient for tho-

rium can be improved by the addition of an inextractable salting agent or by increasing HNO_3 concentration in the aqueous phase, as shown in Slide 8. This shows the effects of various salting agents on the extraction of thorium, the distribution coefficient of thorium and the distribution coefficient of nitric acid into TBP. Nitric acid extracts readily into the organic phase so that aluminum nitrate is favored. However, increasing the nitrate salting strength also increases the extraction of fission products and protactinium, particularly if the free acid concentration in the aqueous phase is high.

In the Thorex process, separation from fission products and from protactinium is obtained by saturating the organic phase with uranium and thorium which form much stronger TBP complexes, thus preventing mass transfer of fission products.

Slide 9 shows the effect of TBP saturation on the distribution coefficient of cerium, typical of the rare-earth fraction. This backsalting effect is insufficient for high separation factors from fission products such as zirconium, niobium and ruthenium and protactinium so that it is necessary to operate the extraction and scrubbing contactor under acid deficient conditions, the effects of which were discussed earlier in this paper. The presence of $Al(NO_3)_3$ in the aqueous phase makes it possible to operate with a deficiency of free acid and yet not precipitate any of the aqueous phase components. To illustrate the marked effect of acid deficiency on fission products, let us look again at Slide 1. Protactinium probably hydrolyzes to a colloid form of the hydroxide, which is

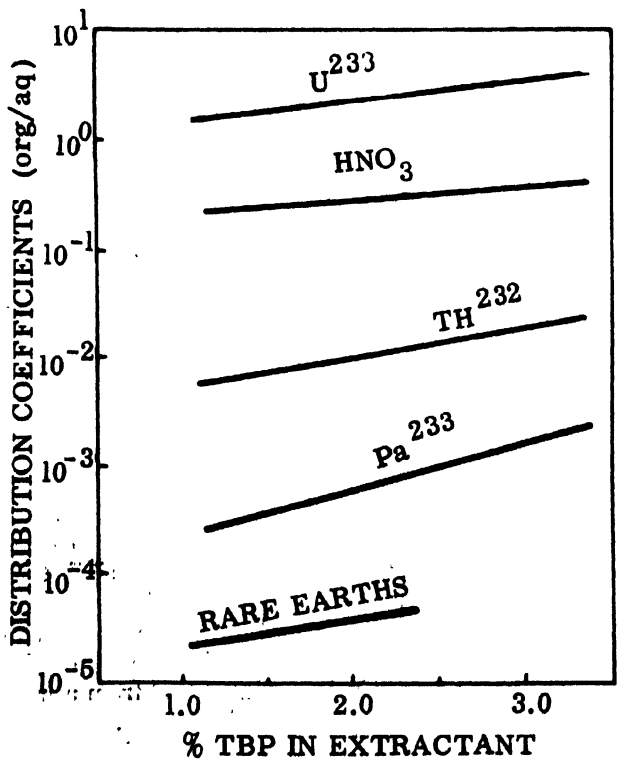

Slide 7. Distribution of thorium and its irradiation products in very dilute TBP solvents

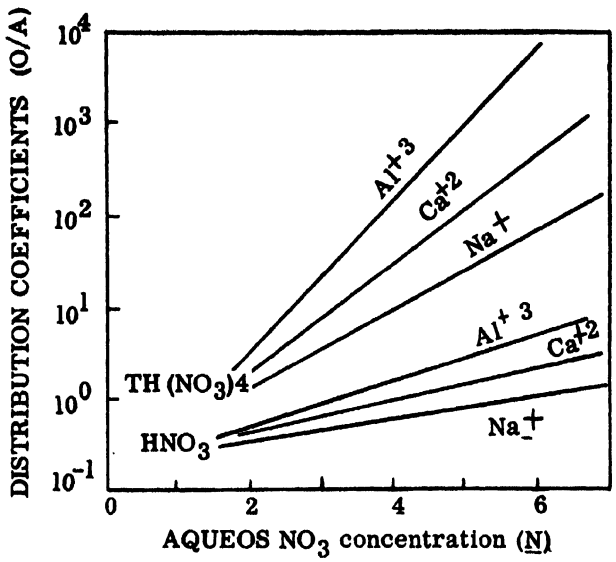

Slide 8. Distribution of Th and HNO_3 in 30% (1M) TBP as a function of the aqueous salting agent

inextractable and passes out with the fission products. There are possibly other mechanisms.

The solvent extraction principle provides a basis for the reprocessing of spent reactor fuel elements. Research and development has shown that the technique is applicable to a variety of fuel materials. High decontamination from fission products, high separation of fissionable and fertile materials and low overall product losses are proven characteristics of solvent extraction systems.

Mr. B. Goldschmidt (France) presented paper P/349.

Mr. E. Haeffner (Sweden) presented paper P/785.

Mr. R. E. Tomlinson (USA) presented paper P/824. In addition to the four processing problems mentioned in the second paragraph of paper P/824, he mentioned a fifth problem—process and equipment limitations arising from the choice of materials of construction. He later commented on this problem as follows:

The choice of materials with which the process equipment is constructed can affect both process performance and longevity of the process equipment. For example, Tygon (a plasticized copolymer of polyvinyl halides) exhibits good resistance to attack by nitric acid systems; its use in solvent extraction work is undesirable, however, since the plasticizer tricresyl phosphate is slowly extracted into the process streams and contributes to the formation of emulsifying materials. Similarly, polymerized tetrafluorethylene (Teflon) is an excellent material for gaskets for solvent extraction equipment. After it has been exposed to about 1000 roentgens of beta-gamma radiation, however, it begins to become brittle and undergo chemical decomposition with the liberation of fluorine. This halide greatly accelerates the corrosion of stainless steels in contact with nitric acid systems. The corro-

sion of stainless steels by nitric acid is also accelerated by the presence of hexavalent chromium ion. It is thus evident that the choice of materials of construction must be made carefully, considering both the effect of the material on the process and the effect of the process chemicals on the materials.

DISCUSSION OF P/822, P/540, P/349, P/785, P/824

Mr. H. A. C. McKay (UK) : There are two comments I would like to make on Mr. Culler's paper. The first is to cast a certain amount of doubt on the formula for the thorium nitrate-TBP complex. In both P/822 and P/540 this is given as thorium nitrate with four TBP's. However, if one makes a saturated solution of thorium nitrate in TBP one gets more thorium nitrate dissolving than would be permitted by this formula. By analogy with the other tetravalent metal nitrates I think we would have expected to have two TBP's rather than four.

The second comment is a rather more general one and concerns what I think is a somewhat important difference between TBP and ethereal or ketonic solvents. To illustrate this, we will consider the extraction of uranyl nitrate, say, in the presence of nitric acid. Both these compounds form complexes with TBP, and when you extract with TBP you get a competitive effect, so that each of them hinders the extraction of the other. On the other hand, if you consider the extraction with ethers or ketones, you get a co-operative effect. This is because in these latter solvents trinitratouranyl species are involved. This means, for example, that you get better extraction of uranyl nitrate in the presence of nitric acid than you would in the presence of lithium nitrate which does not extract into the solvent and form such compounds. You get a similar co-operative effect with, for example, plutonium in these solvents, and equally a competitive effect in tributyl phosphate.

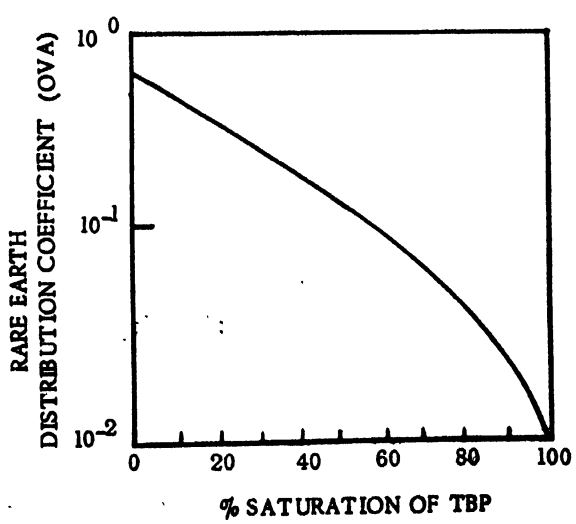

Slide 9. Rare-earth (Ce group) distribution coefficients as functions of TBP saturation with thorium, where 100% ≡ $Th(NO_3)_4 \cdot 4$ TBP. Fission product decontamination by saturation

Mr. Culler (USA) : Mr. McKay's comments are appreciated. He is not alone in doubting the complete validity of the thorium TBP four complexes. However, we have used it as a working hypothesis for process development, and it has been satisfactory. There has been some reason for doubting whether this is accurate; studies on this are continuing.

We appreciate, too, his comments pointing out a fine difference in the mechanisms between TBP and hexone.

Mr. J. M. Fletcher (UK) : I would like to ask Mr. Culler two questions. The first is in relation to his opening remarks in which he described and mentioned the economics of these chemical separation processes. I would like to ask him whether he can say what value or cost is attributed to solvent extraction processes in the estimates of nuclear power along the lines we have heard in some of the earlier papers in the A Sessions, where the cost of power was given and obviously had to include some element for reprocessing after, say, 3000 megawatt days per ton. It would be interesting to know what value Mr. Culler gives for solvent extraction and purification by the solvent extraction process.

Secondly, as this is a point which is not covered in his paper, how does he think that the solvent extraction process can be modified to deal with some of the newer types of fuel elements about which we have heard, in which there is bonding between the uranium fuel and the containing or cladding material? We also heard a few days ago in these B Sessions about the use of the uranium oxide fuel in the pressurized water type of reactor. Does he feel that the solvent extraction process can be readily applied to this sort of fuel?

Mr. Culler (USA) : The first question is rather difficult to answer, concerning what allowances are made for chemical reprocessing in the estimates which have been prepared concerning the economics of various reactor fuel recycle recombinations. I think, generally speaking, one could say something like this: Assuming that the power will sell at 7–8 mills per kwh, the chemical cost possibly should not exceed 20 per cent of the total cost of power; some estimates have been prepared on this basis. In certain of the process techniques with which we are most familiar, for example, the economics of the aqueous homogeneous systems on which Mr. Ferguson will report, this cost can be two to three mills total, including inventory, storage, fuel cost and so on.

For the uranium-plutonium systems, or for reactors like the MTR, it is a little more difficult to define, but the total processing cost, I should say, could never exceed 2½ dollars to 3 dollars per pound for uranium, with the plutonium cost included. However, I think you might wish to get comments from Mr. Lawroski and others, concerning this question. It is difficult to answer exactly.

The second question, concerning how the solvent extraction processes might be modified to take care of the more refractory type of fuel elements, is pri-

marily a consideration of how one would get these materials into aqueous solution. It is possible to dissolve stainless-steel elements in sulfuric acid. These solutions are then converted into the nitrate form by the addition of salting agents such as aluminum nitrate, or nitric acid. For other fuel materials there are possible dissolving techniques. There is a separate paper (P/547) in the published Proceedings of this session on dissolving metals of interest in a power economy. There are methods for dissolving zirconium and zirconium-clad fuels, using concentrated hydrofluoric acid, which is again converted back to the nitric acid form, putting through TBP extraction. I think that any fuel element that is used can eventually be dissolved and processed. Whether or not this would be economic is quite another question, and I would not say that we can safely assume that this is the case.

Mr. M. BENEDICT (USA): I just wanted to ask Mr. Culler for a few details of the processes which he described. In the Purex process, how is the plutonium stabilized in the tetravalent state prior to extraction in the first column; and in the Redox process what reducing agent is used to bring plutonium into the trivalent state during extraction in the second column? I failed to note the particular agent that was used.

Mr. CULLER (USA): Answering the second question first, I did not say what particular agent was used. A number of reducing agents can be used—hydrazine, hydroquinone, etc., from which you can take your choice and chances.

Answering the first question, plutonium is stabilized to the plus 4 state. If it is in nitric acid solution, there is a disproportionating between plutonium 3, 4 and 6. By the addition of nitrous acid it is possible to convert the plus 3 plutonium to plus 4 with the evolution of NO, at the same time converting the plus 6 state to the plus 4, which reaction produces a nitrate ion and free hydrogen ions. This step is quite effective and it is done with relatively dilute nitrous acid or sodium nitrate simmered for a period of time to allow the reaction to proceed to completion.

Mr. P. REGNAUT (France): I should like to ask Mr. Culler two questions about the separation of thorium from U^{233}. The first concerns the apparatus for dissolving thorium metal. I would like to know what kind of material is used to withstand the corrosive action of the mixture of nitric and hydrofluoric acid, and some typical corrosion rates.

My second question concerns the extraction of the thorium in tributyl phosphate diluted with a paraffin solvent. We noticed that as the concentration of thorium increases, the organic phase separates into two phases. The phenomenon seems not to occur when an aromatic diluent is used. I should like to know whether you have discovered a diluent which, while enabling extractions of concentrated thorium to be made, retains all the other necessary qualities, such as stability towards nitric acid and radiation low density and non-inflammability.

Mr. CULLER (USA): In answer to the first question, about materials of construction for dissolving thorium metal using a trace quantity of fluoride ion and concentrated nitric acid, we have normally used type 309 columbium-stabilized stainless steel. In order to give us maximum corrosion resistance in very carefully welded vessels using 25-12 welding rod we have heat-treated at 1950° to 2050° to circumvent intergranular attack on the weld. The corrosion rates during certain parts of the dissolving cycle are quite low, because the trace of fluoride is completely complexed by the thorium or aluminum that is present. However, during the digesting step which I mentioned, where the excess nitric acid is evaporated after dilution and in which the salts are concentrated essentially to molten salt form, there is a short period of time when the corrosion rate is relatively high—it may be somewhere around 15 to 20 mils a year. However, the time during which the solution remains at this concentration is relatively short, so that we have not experienced serious corrosion difficulties.

The second question concerns the diluent used for TBP in the Thorex process. We are using a kerosene type of diluent very highly refined to remove aromatics and unsaturates. The brand we have found most satisfactory is Amsco 125/82. This means nothing to you, but I am sure you can buy it.

The problem of three-phase or essentially two-phase formation is, as you suggest, from our experience a function of the impurities in the diluent. The diluent which we buy is carefully pre-treated, and we have no third-phase difficulties with relatively concentrated TBP organic streams. We have taken great care to remove all unsaturates, and we have not experienced two-phase formation. We have had no difficulty with this in continuous process.

The CHAIRMAN: The next questions are directed to paper P/349. We have received a question from Mr. G. T. Seaborg (USA): "Do you recover, or intend to recover, neptunium-237, and how?"

Mr. GOLDSCHMIDT (France): I would call that a boomerang type of question because (*a*) we have not had time to study the problem, (*b*) we intend to study it, and (*c*) it would be much easier to study it if Mr. Seaborg would tell us what neptunium does in the process.

Mr. SEABORG (USA): I do not know.

Mr. GOLDSCHMIDT (France): Thank you.

Mr. BRUCE (USA): There are two questions I would like to ask of Mr. Goldschmidt on his very interesting paper. The first is this. He notes that anion exchange is employed for the concentration and purification of the plutonium product. I wonder if he would say a little more about the considerations which have led to the selection of anion exchange for this work rather than cation exchange.

The second question I would like to ask is, why is

a mixture of N_2H_4 and $Fe(NH_2SO_3)_2$ employed as reducing agent for concentrated plutonium solutions rather than N_2H_4 or $Fe(NH_2SO_3)_2$ alone?

Mr. GOLDSCHMIDT (France): The answer to the first question is, I think, that plutonium giving anion complexes, anion exchange, is much more selective than cation exchange.

In answer to the second question, we started with N_2H_4, which worked quite nicely on low concentrations. At high concentrations we added $FE(NH_2SO_3)_2$. If we had used $Fe(NH_2SO_3)_2$ from the beginning it would have worked all the way. That is why we used the two reducing agents in our process.

Mr. HAEFFNER (Sweden): In your paper you have given several methods for final purification of plutonium. Which of these methods are you actually using in your plant, and what is its efficiency as regards plutonium recovery and fission product decontamination?

Mr. GOLDSCHMIDT (France): The one we are using is the oxalate, and I think I gave the purification coefficient, which is about 20. As to the recovery, we can only recover whatever plutonium stays in solution and put it a step backwards.

Mr. HAEFFNER (Sweden): In your paper it is stated that by using sodium nitrite as an oxidizing agent in a solution containing plutonium in valent states 4 and 6, the partition coefficient, where 33 per cent TBP solvent is used, is increased from 4.8 to 8.0. Have you some experimental or other evidence for your opinion that plutonium 4 is oxidized by sodium nitrite?

Mr. GOLDSCHMIDT (France): I think perhaps we have badly explained in our paper what we wanted to say. I think the answers to that question were given very clearly by Mr. Culler a few moments ago. Nitrite stabilizes plutonium to valency 4.

Mr. TOMLINSON (USA): We are interested in the mechanical de-jacketing of irradiated fuel elements. Could you give us an idea of the equipment being used?

Mr. GOLDSCHMIDT (France): That is a tough question for a chemist. We are using mechanized de-jacketing for the rods of our first graphite pile, but they are rather special because they are 12-inch-long canning rods rather smaller than those you have in your Brookhaven pile, so it means you get 40 kg in one single de-jacketing operation. I am unable to give you the exact details because I do not know them.

Mr. V. G. TIMOSHEV (USSR): I have a question to put to Mr. Tomlinson. I should be very grateful if he would give his opinion on the limitations of the use of tributyl phosphate from the standpoint of the greatest possible acidity and from that of the greatest possible gamma activity of the solution.

Mr. TOMLINSON (USA): TBP is quite stable in the presence of nitric acid, and concentrations up to 15 or 16 molar nitric acid may be used in the presence of pure TBP. However, the kerosene diluent we normally use begins to suffer degradation in the range of 6 to 8 molar nitric acid.

As far as the radiation limits are concerned, we note that TBP diluted with kerosene type of diluent is usable at room temperature up to the range of, say, several hundred curies per liter.

Mr. D. E. FERGUSON (USA) presented paper P/551.

DISCUSSION OF P/551

Mr. E. GLUECKAUF (UK): I should like to ask Mr. Ferguson what percentage, by weight, of the fission products has been found, in actual tests, in the gas fraction of a homogeneous reactor or loop.

Mr. FERGUSON (USA): I do not think that we have made any measurements that would give an answer to your question. In the Homogeneous Reactor Experiment, of course, the gaseous phase of the reactor, after the recombination of the hydrogen and oxygen, was worked out on a charcoal bed. However, I do not think that we have made any attempt to determine what fission products showed up in the off-gas from the reactor.

Mr. BROWN (USA): I should like to know how the radiation effect on the ion exchange resin manifests itself.

Mr. FERGUSON (USA): We observed a drop in the capacity of the resin in this case for absorbing uranium.

Session 22B.1

CHEMICAL PROCESSING OF IRRADIATED FUEL ELEMENTS *(concluded)*

LIST OF PAPERS

			Page
P/823	Survey of separations processes	S. Lawroski	575
P/350	Method for separation of uranium-233 from thorium irradiated in atomic piles	A. Chesne and P. Regnaut	583
P/544	Pyrometallurgical processing of nuclear materials	H. M. Feder	586
P/545	The purification of uranium reactor fuel by liquid-metal extraction	A. F. Voigt	591
P/542	High temperature fuel processing methods	E. E. Motta	596
P/550	High temperature processing systems for liquid-metal fuels and breeder blankets	O. E. Dwyer *et al.*	604
P/546	Decontamination of irradiated reactor fuels by fractional distillation processes using uranium hexafluoride	H. H. Hyman *et al.*	613

Survey of Separations Processes

By S. Lawroski,* USA

When fossil fuels are burned to produce heat, essentially complete consumption of fuel is obtained at once. Therefore, there is no fuel recovery problem. Nuclear reactors do not give this completeness of fuel burn-up because of premature adverse reactivity change or physical damage of fuel. Consequently, several cycles of burn-up and intervening recovery operations are necessary to get the equivalent of a complete utilization of fuel. A separations process for the fuel recovery must, therefore, be capable of high yields and low cost per cycle. Moreover, ideally the process should accomplish this with a minimum of hold-up time to avoid a large inventory of fissionable material.

The degree of decontamination required of reprocessing steps may vary widely. For example, with homogeneous reactors it is generally conceded that partial decontamination will suffice. This is expected to be done continuously on at least a portion of the fuel circulated through the reactor. While only partial decontamination is needed, it must be derived without deleterious effects on reactor operation. This means that the purification process must be reliably continuous and must not introduce into the fuel substances which are harmful to reactor operation. In the cases of heterogeneous reactors, substantially complete decontamination has been demanded as of the present. This permits direct-contact fabrication of fuel assemblies from the recovered fuel. Such a restriction limits the selection of separations processes to those capable of thorough decontamination. The problem is further complicated in many instances by the use of fuels, fuel claddings, and bonding materials which are extremely difficult to dissolve and to handle conveniently during reprocessing. The successful development of methods for remotely fabricating fuel elements for heterogeneous reactors would alleviate the demands on separations process decontamination for such reactors. The result would be a wider choice of processing schemes. It is believed that some of these have good prospects of minimizing the total costs in a reactor complex to produce power.

Many different separations methods are being investigated for reactor fuel recovery and purification. They are listed in Table I. These are in various stages of study or development in order to permit the optimum selection of reprocessing methods for various reactors. The review here will be concerned with the other principal separations methods. They are (1) precipitation, (2) ion exchange, (3) fractional distillation, and (4) pyrometallurgical or high temperature processes.

PRECIPITATION PROCESSES

Precipitation methods have played a major role in laboratory investigations of the fission process. Numerous examples of these methods and their uses for laboratory separations have been described.[1,2] Therefore, this discussion will be confined to large-scale applications of this type of separations method.

The most important example is the Bismuth Phosphate Process, which uses $BiPO_4$ and LaF_3 as carrier precipitation agents. It has been the most thoroughly investigated and developed of all the precipitation methods and has culminated in a successful production-scale use of the process to recover and decontaminate plutonium from irradiated natural uranium.

Table I. Separations Methods for Fuel Recovery and Purification

Precipitation
Ion exchange
Fractional distillation
Pyrometallurgy (high temperature)
Solvent extraction

The Bismuth Phosphate Process recovers plutonium but not uranium. The uranium is, however, recoverable from the process wastes by other methods. The Bismuth Phosphate Process accomplishes the quantitative separation of plutonium from uranium and fission products according to the schematic flowsheet given in Fig. 1. Separation of plutonium from uranium and from some of the fission products is obtained in an early process step, designated in Fig. 1 as "Extraction Step." At this stage, the uranyl nitrate feed solution is first treated with $NaNO_2$ to adjust the valence of plutonium to +4. A complexing agent for uranium, SO_4^{--}, is also added. Then a co-precipitation of $BiPO_4$ and plutonium phosphate is arranged. Meanwhile, the complexing action of sulfate prevents the precipitation of uranium at this point. Following the extraction step, the precipitate is dissolved in nitric acid and two cycles of decontamination of the plutonium are performed by means of $BiPO_4$ precipitations. Each of these cycles has a

* Argonne National Laboratory.

product precipitation and a by-product precipitation step. A product precipitation refers to one in which plutonium has been brought down with the precipitate. A by-product precipitation is one in which the plutonium remains in solution. These two modes of precipitation are effected with +4 and +6 states of plutonium in the product and by-product precipitations, respectively. Following the two decontamination cycles with $BiPO_4$, there is a series of operations termed collectively as "Concentration Step." This comprises a $BiPO_4$ by-product precipitation, a LaF_3 cycle of by-product and product precipitations and, finally, a metathesis of the LaF_3 product precipitate with KOH to give a mixture soluble in nitric acid for ultimate plutonium isolation. The final isolation of plutonium is performed by a peroxide precipitation with H_2O_2.

The concentration of plutonium in the early stages of the process is very small so that carrier precipitation with $BiPO_4$ is necessary. Both trivalent and tetravalent plutonium can be co-precipitated with this reagent, but the tetravalent form is more effectively co-precipitated. Valence adjustment of plutonium to +4 is obtained with $NaNO_2$ in the extraction step and with Fe^{++} elsewhere. When by-product precipitations are desired in the process, various oxidants, such as BiO_3^-, MnO_4^-, or $Cr_2O_7^{--}$ have been used to obtain the plutonium in the +6 state.

Various provisions are undertaken to improve decontamination in individual process steps. Additions of scavenging agents, such as inactive cerium or zirconium ions, are employed for purposes of maximizing radioactive zirconium and niobium carry-down in

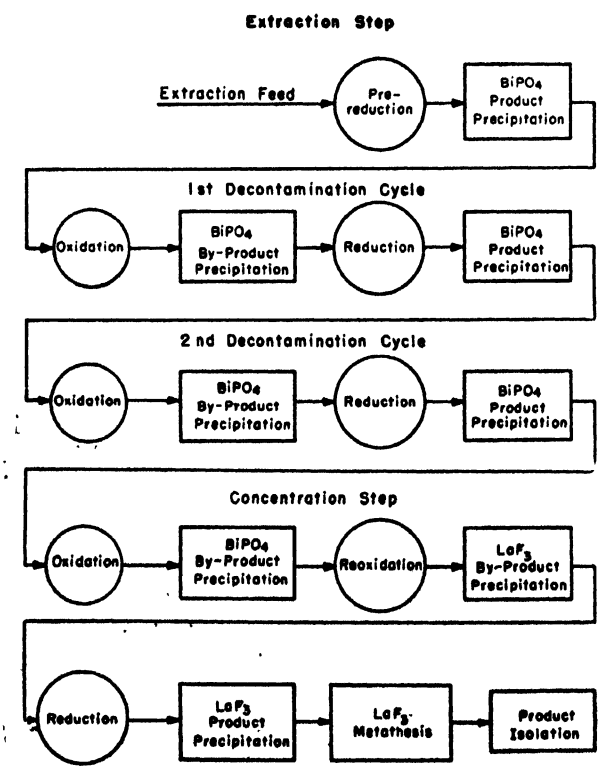

Figure 1. Schematic flowsheet for Bismuth Phosphate process

Table II. Typical Decontamination Factors Obtained with Bismuth Phosphate Process

Operations step	Decontamination factor	
	Individual	Over-all
Extraction	7.5	7.5
First decontamination cycle	150	1.1×10^3
Second decontamination cycle	90	1×10^5
Concentration	100	1×10^7

by-product precipitations. On the other hand, solubilizing or complexing reagents, such as fluosilicates, are added in product precipitations to minimize radioactive zirconium carry-down.

It is interesting to note here that the details of this process were worked out before there were more than trace amounts of plutonium available. Nevertheless, the production-scale performance of the process was remarkably good from the start-up of the plant. The over-all recovery of plutonium has been above 95 per cent for the Bismuth Phosphate Process. The loss of 5 per cent or less is rather evenly distributed to the various waste streams. Typical decontamination factors obtained in the course of the different process steps are given in Table II. From these data it is evident that thorough decontamination of plutonium from fission products is achieved.

The separation of uranium from plutonium in the extraction step is also excellent as indicated by low uranium content in the plutonium product from the process.

Another precipitation method intended for large-scale purposes is one that has been developed for recovery of uranium from the Bismuth Phosphate Process. The method has been successfully tested on a pilot-plant scale. Decontamination of the uranium is accomplished by repeated crystallizations of uranyl ammonium phosphate. The continuous and adequate purification of fuel solutions from certain of the aqueous homogeneous reactors appears promising with a precipitation-type method according to currently available results. The method is believed to be simpler and more economical than other types thus far studied.

Before concluding this brief review of precipitation processes, it should be pointed out that experience has shown them to be flexible and also comparatively easy to scale-up from laboratory results. This is because the large-scale equipment is generally very simple in design. Probably the most complicated piece of equipment is that required for the solid-liquid separations. Centrifugation has been the preferred method for this operation, at least in the case of the Bismuth Phosphate Process. Remote operation and maintenance have proved feasible for large-scale installations.[8] There are, however, two significant disadvantages which should be mentioned relative to precipitation-type separations processes. The precipitation methods are (1) not as adaptable to continuous operation as, for example, solvent extraction or fractional distillation methods, and (2) not

as capable of achieving high yields of recovery as some of the other methods.

ION EXCHANGE PROCESSES

A large number of anion and cation exchangers are available commercially. A partial list of these, according to name, manufacturer, type, and capacity, is given in Tables III and IV.[4]

Recent syntheses of certain organic polymers have resulted in a number of ion exchange resins with improved properties in such respects as capacity, concentrating factor, chemical and radiation stability, and regenerative behavior. Techniques of continuous ion exchange operation with either bead or membrane form have also been developed recently.[5,6,7,8] All of these factors can be expected to extend the application of ion exchange processes in connection with fuel recovery and purification.

In the atomic energy program, ion exchange methods have been very extensively used in the laboratory to make very difficult separations. The most outstanding examples have been the isolation and concentration of individual heavy elements and, similarly, of individual fission products of the rare earth group. The use of complete ion exchange processes for fuel recovery and purification has been studied in the laboratory and in small-scale pilot plant installations. It has not yet gone beyond this stage.

One of the most important larger-scale applications of ion exchange methods has been in auxiliary steps with other basic types of separations processes. Ion exchange has proved to be a very effective method

Table III. Commercially Available Anion Exchangers

Name	*Manufacturer*	*Type*	*Total capacity*	
			Milli-equivalents per gram	*Milli-equivalents per ml*
Amberlite IR4B	Rohm and Haas	Weak base	10.0	2.5
Amberlite IR-45	Rohm and Haas	Weak base	6.0	2.0
Amberlite IRA-410	Rohm and Haas	Strong base	2.5	1.0
Amberlite IRA-400	Rohm and Haas	Strong base	2.3	1.0
De Acidite	Permutit	Weak base	9.3	1.5
Duolite A-2	Chemical Process	Weak base	7.0	1.2
Duolite A-3	Chemical Process	Weak base	6.8	1.1
Ionac A-300	American Cyanamid	Intermediate base	7.4	1.5
Wofatit M	I. G. Farben	Weak base	–	1.2
Alumina	–	Amphoteric base	0.01	–
Dowex 2 (Nalcite SAR)	Dow Chemical	Strong base	2.3	0.9
Dowex 1	Dow Chemical	Strong base	2.4	1.0

Table IV. Commercially Available Cation Exchangers

Name	*Manufacturer*	*Type*	*Total capacity*	
			Milli-equivalents per gram	*Milli-equivalents per ml*
Amberlite IR-100	Rohm and Haas	Phenolic methylene sulfonic	1.75	0.65
Amberlite IR-105	Rohm and Haas		2.70	1.00
Dowex 30 (Nalcite MX)	Dow Chemical		4.00	1.35
Duolite C-3	Chemical Process		3.25	1.00
Ionac C-200	American Cyanamid		2.70	0.81
Wofatit P	I. G. Farben		1.35	0.53
Wofatit K	I. G. Farben		2.50	1.00
Wofatit KS	I. G. Farben		2.45	0.90
Zeo Rex	Permutit		2.70	0.89
Zeo Karb	Permutit	Sulfonated coal	1.62	0.60
Amberlite IR-120	Rohm and Haas	Nuclear sulfonic	4.20	2.15
Dowex 50 (Nalcite HCR)	Dow Chemical		4.25	2.20
Alkalex	Research Products	Carboxylic	4.95	1.80
Amberlite IRC-50	Rohm and Haas		10.0	4.20
Duolite CS-100	Chemical Process		3.85	1.11
Permutit 216	Permutit		5.30	1.70
Wofatit C	I. G. Farben		7.00	2.50
Montmorillonite	–	Aluminum silicate	0.8 –1.2	–
Koalinite	–		0.06–0.10	–
Glauconite	–		0.18–0.2	–
Permutit	Permutit		1.0 –3.0	–
Decalso	Permutit		–	–
Zeo Dur	Permutit		–	–
Silica gel	–	Silicic acid	0.01–0.04	–

for concentrating solutions of plutonium, enriched U^{235}, or U^{238}. Comparative studies which have been conducted on various ways to concentrate intermediate or final product streams (such as from solvent extraction separations processes) have resulted in the conclusion that ion exchange is superior to evaporation or precipitation schemes. Firstly, it is a more convenient method than evaporation for accomplishing large-volume reduction factors. Secondly, it is less likely to introduce impurities such as corrosion products in the case of evaporation methods, and added chemical reagents in the case of precipitation methods. Thirdly, it frequently achieves significant additional purification in the course of concentrating a particular product stream from main line separations processes. In some instances, the amount of purification is enough to enable elimination of a complete cycle of solvent extraction.

Concentration factors in excess of 100-fold have been demonstrated with simple ion exchange operations on plutonium and other heavy element-containing solutions. At the same time, 2 to 10-fold or more decontamination from zirconium and niobium is often obtained. Some ruthenium removal is also effected. Organic exchangers have been most often used for this purpose. Silica gel, however, has been very successfully used to clean up concentrated uranium solutions from solvent extraction processes. The losses of valuable material have been negligible in applying ion exchange to concentration or added purification steps.

Other significant large-scale utilizations of ion exchange have been in conjunction with the preparation of pure process waters and with the decontamination of large volumes of low-level radioactive wastes from reprocessing or major laboratory installations.[8]

As mentioned previously, laboratory and small-scale pilot plant tests of ion exchange processes have been made for fuel recovery and purification. Intensive work on this approach was temporarily interrupted in favor of methods which offered prospects of earlier development and less trouble from radiation problems. The early work was done with about 10 wt % uranyl nitrate solutions from irradiated natural uranium. The recovery of plutonium exceeded 97 per cent, which compared favorably with the yields of other methods being studied at that time. However, the gross beta and gamma decontamination factors were only about 30 to 300. In addition, the resins available in early work on ion exchange were quite sensitive to chemical and radiation effects. Recently available resins appear to be considerably more stable against chemical and radiation effects. Therefore, it is reasonable to expect that there will be a renewed interest in ion exchange methods for reprocessing operations. Some of this interest is already evident in connection with continuous processing of solutions from aqueous homogeneous reactors. Work with both inorganic and organic forms of ion exchangers is in progress for this reprocessing problem.

Table V. Properties of Non-volatile Fission Product Fluorides

Compound	Melting point, °C	Boiling point, °C
CsF	684	1251
SrF_2	1300–1400	2460
BaF_2	1280	2260
YF_3	>1000	
LaF_3	>1000	
CeF_3	1324	
PrF_3	1370	
ZrF_4	*	
CeF_4	1460	

* Sublimes at 500°C.

FRACTIONAL DISTILLATION PROCESSES

The potentiality of fractional distillation for fuel recovery has always appealed to chemists and chemical engineers working on separations problems in the atomic energy program. An important reason for this attitude has been the fact that the basic principles and technology of fractional distillation have been so well developed. Another [illegible] influence has been the economically attractive possibility of recovering uranium directly as UF_6 by this separative method. Obviously, this form of uranium product from a process would be advantageous when the recovered uranium is to be sent to a diffusion plant for enrichment. If the recovered uranium is to be converted to metal it is significant that UF_6 can be readily reduced to UF_4 which in turn, is readily convertible to metal. One other important factor in favor of a fluoride system is the background of experience in the diffusion plants with this system.

The choice of a fluoride system for a fractional distillation process is logical for, at least, the reasons just mentioned. As other possible feed systems are examined, further advantages of a fluoride system become apparent. The volatility of UF_6 is substantial at reasonable temperatures. This is not the case with other known stable compounds of uranium. From a separations standpoint, it is very encouraging to find that the volatilities of the fission product fluorides are appreciably different from that of UF_6. This is illustrated in Tables V and VI, which summarize the boiling points for a number of fission product fluorides and of UF_6. It is evident that practicable separation of UF_6 from the fission product fluorides should be achievable by efficient fractional distillation. With few exceptions, the fission product fluorides are less volatile than UF_6. For this reason, substantial decontamination is likely even with a crude distillation. Complete decontamination requires more efficient distillation. These predictions have been verified with distillations of feed solutions prepared by various techniques of fluorination.

Much of the effort on the research and development of fractional distillation processes has been concerned with the preparation of fluoride feed solutions from irradiated uranium fuel. Various approaches have been necessary because the starting fuel

Table VI. Volatile Fission Product Fluorides in order of Decreasing Volatility

Compound	Melting point, °C	Boiling point or sublimation point, °C
AsF_5	−79.8	−53.2
TeF_6	−37.8	−38.3
RuF_6*	?	?
IF_7†	5–6	4.5
MoF_6‡	17.5	35.0
UF_6	64.02§	56.4
AsF_3	−6.0	58.0
Te_2F_{10}†, ¶	−14.0	60.0
IF_5	8.5	97.0
NbF_5	78.9	233.3
RuF_5	106.0	313.0
TeF_4	129.6	371.3**

* Recently reported as very volatile and highly reactive. No conclusive evidence of its formation in fluoride process feed.

† No evidence of its presence in fluoride process feed.

‡ Mo is a short-lived fission product.

§ Triple point.

¶ Reported as relatively unstable.

** Decomposes at approximately 194°C.

may be pure uranium metal, mixtures of uranium and diluent metals, or various uranium compounds such as oxides and salts.

The fluorination of uranium metal with elemental fluorine was attempted at an early stage. Control of this gas-solid reaction has proved to be extremely difficult and even hazardous, because the effective rate of heat transfer is too slow to dissipate the enormous heats of chemical reaction. A practical solution to this problem has been found in the use of liquid-phase fluorinating agents, such as ClF_3 (chlorine trifluoride), BrF_3 (bromine trifluoride), and BrF_5 (bromine pentafluoride). These interhalogen compounds, particularly BrF_3, have convenient liquid ranges, as shown in Table VII.

The dissolution and complete fluorination of uranium metal can be satisfactorily effected with BrF_3 or with ClF_3-HF mixtures at temperatures and pressures such that the liquid phase of the fluorinating agent can be maintained. The liquid phase of the fluorinating agent provides adequate heat transfer from metal to solution. The vaporization and condensation of vapors from dissolver solution provides for the necessary removal of the heat of chemical reaction. It is important that metal always be covered with solution; otherwise, the character of reaction may revert to that of a gas-solid reaction and result in the same problems and hazards as obtained with elemental fluorine.

Subsequently, fractional distillation of the resulting dissolver solution can decontaminate the uranium from the fission products. Small-scale demonstration tests have been conducted on fractional distillation of fluoride feeds from ClF_3-HF or BrF_3 dissolutions of irradiated uranium. The effectiveness of decontamination in such tests is indicated by data in Table VIII, which are for ClF_3-HF dissolver solutions. Very encouraging results on decontamination have also been observed in laboratory fractional distillations of fluoride feed solutions prepared from BrF_3 dissolutions of irradiated uranium. Reliable figures for UF_6 recovery are not available because the demonstration tests have been conducted on a relatively small scale. The results are, however, encouraging, and no difficulty is expected in regard to recovery of purified UF_6.

It should be noted here that plutonium remains in the non-volatile residue. The reason for this is that, unlike uranium, plutonium is not fluorinated to the volatile form, PuF_6, under the usual dissolution conditions. Recovery of plutonium from the residue can be obtained by aqueous processes such as solvent extraction. The residues are dissolved in dilute $Al(NO_3)_3$ solution for solvent extraction purposes. The fact that plutonium is fluorinated only to the non-volatile lower fluorides is advantageous for reprocessing irradiated, highly-enriched uranium by fractional distillation methods. In this instance, plutonium recovery is not important and the small amount usually present is desirably directed to the fission product wastes. On the other hand, the failure of these dissolving methods to yield volatile PuF_6 is a distinct disadvantage for application of this separations method to irradiated natural uranium. In this instance, recovery of plutonium as well as of uranium is desired.

Cost estimates have been made for the recovery of uranium by fractional distillation and the recovery of plutonium from the residue by solvent extraction. They show only a slight advantage for the combination of these processes as against the use of a solvent extraction process alone for recovery of both of the products.

There are known methods for the preparation of

Table VII. Properties of UF_6, Br_2, F_2, HF and Some Interhalogen Compounds

	UF_6	F_2	BrF_3	ClF_3	BrF_5	Br_2	HF
Molecular weight	352.07	38.00	136.92	92.46	174.92	159.83	20.01
Boiling point, °C	56.4*	−187.92	125.75	11.75	42	58.78	19.54
Melting point, °C	64†	−217.96	8.77	−76.32	−61.3	−7.3	−83.07

* Sublimation point.

† Triple point.

Table VIII. Decontamination by Fractional Distillation Method (Irradiated Uranium Dissolved in ClF_3-HF)

	Decontamination factors	
	Beta	*Gamma*
Evaporation from dissolver solution	about 10^4 to 10^5	–
Fractional distillation of above overhead	about 10^2 to 10^3	10^3
Over-all for both operations	about 10^7	10^7

PuF_6, but they are not convenient for large-scale operations which begin with irradiated uranium metal. Work is in progress with the objective of finding more satisfactory conditions under which both plutonium and uranium may be obtained as volatile hexafluorides. Success in this respect, together with practical methods of handling PuF_6, would make the fractional distillation method a superior separations process for irradiated natural uranium. Until then, its outstanding promise is for the reprocessing of highly enriched uranium where the plutonium problem is absent. Of course, there are other situations where the plutonium problem is also absent and where this method may be used to complete purification of uranium. Some obvious examples are ore concentrates and uranium product streams from intermediate stages of solvent extraction processes.

Enriched fuels are frequently manufactured with major amounts of alloying agents. Some of these alloy mixtures are not amenable to nitric acid dissolution nor even to interhalogen dissolution at convenient temperatures. Successful dissolutions of such alloys have been accomplished at 500–700°C with fused salt mixtures through which HF is first dispersed, followed by either F_2 or BrF_5. As much of the fluorination and dissolution as possible is effected with HF, which is relatively inexpensive. The resulting UF_4 is fluorinated completely to UF_6 by F_2, or preferably by BrF_5 which can be more easily recycled than F_2. Other refractory reactor fuels, such as oxides and salts of uranium, may be similarly dissolved and completely fluorinated.

The dissolver solutions prepared in the manner described above are stripped of UF_6 content with considerable decontamination of UF_6 obtained at the same time. The overhead vapors are then fractionally distilled to complete the purification of UF_6. The fission products are principally in the fused salt mixture, which may be a better storage medium than aqueous solutions for long-term storage of these by-products.

The potency of the aforementioned dissolution procedure poses problems of containment, especially at the F_2 or BrF_5 addition step. Nickel and Monel are only moderately satisfactory materials of construction. However, both of these materials have been found very satisfactory for laboratory and pilot plant work on BrF_3, BrF_5, and ClF_3-HF metal dissolutions at moderate temperatures and subsequent fractional distillations.

The various fluorinating procedures which have been developed enable dissolution of an imposing number of contemplated reactor fuels. It is anticipated that this will ultimately result in extensive applications of fractional distillation methods for fuel reprocessing.

The direct distillation of molten, irradiated uranium to recover and concentrate plutonium will be reviewed under Pyrometallurgical Processes

PYROMETALLURGICAL OR HIGH TEMPERATURE PROCESSES

The development of high power-density reactors and high burn-up fuels may aggravate the problems of spent fuel reprocessing. Conventional methods may require extended cooling periods of the fuel prior to reprocessing in order to avoid deleterious irradiation effects. Therefore, research and development work on pyrometallurgical, or so-called high temperature, processes has been undertaken in an effort to find a suitable way of processing short-cooled, highly irradiated fuels.[9,10] These methods would enable heterogeneous reactor fuels to be processed with some of the advantages that accrue with continuous processing of aqueous homogeneous reactor fuels. They may also have possibilities for use in preceding more conventional processing for purposes of initial bulk reduction of radioactivity levels or crude concentration of fissionable substances.

If the irradiated, fertile and fissionable materials can be processed as molten metals, not only would the above aims be realized but some other benefits may be obtained. Since the pyrometallurgical schemes avoid bulk chemical conversion during purification, the usual need for converting uranium or plutonium salts back to metal would be avoided. The purified material as obtained is ready for fabrication into new fuel elements. Variations in fuel alloy compositions which sometimes cause difficulties in aqueous processing systems may be of much less concern in pyrometallurgical processes. Finally, the fission products are isolated in a very compact form and, therefore, are more likely to be suitable for utilization or disposal. The principal objectives of these processes are otherwise similar to those of other types of processes.

The development of pyrometallurgical processes has been along two lines. One of these is concerned with reactor blanket processing and the other with reactor core processing. It is not anticipated that these would give more than partial decontamination. Thus, after many recycles with pyrometallurgical processing, special treatments may be necessary to remove at least some fraction of the elements which have not been removed. The pyrometallurgical operations, however, must be able to concentrate fissionable substances from blanket material and satisfactorily remove from core material those fission products which have high cross sections or interfere with the fabrication qualities of the fuel.

The three types of pyrometallurgical operations which have received the most attention for blanket

Table IX. Vacuum Volatilization of Plutonium from Molten Uranium

Temperature, °C	Area, cm²/gm	Time, min	Per cent volatilized
1680	0.7	40	91
1680	0.4	140	99

processing to concentrate plutonium are: distillation, salt extraction, and molten metal extraction. Thermodynamic evaluations[11,12] and experimental demonstrations have been conducted with encouraging results; however, the engineering feasibility and the economic advantages have yet to be determined.

Plutonium can be concentrated by vacuum distillation from molten uranium at 1500–1800°C. Over 99 per cent removal has been effected and the experimental results agree with theoretical calculations. Table IX contains the results of two typical runs. The two major problems are the materials of construction and the design of the plutonium collectors.

The salt extraction of plutonium from molten uranium has been successfully accomplished with halides such as UF_4 or $MgCl_2$. The distribution of plutonium in the system molten UF_4-molten uranium metal is such that, at equal weight ratios of salt to metal, 90% of the plutonium goes into the salt phase. By repeating the extraction, it should be possible to obtain all the plutonium from the uranium. Although in this procedure the uranium remains in its metallic state, the plutonium is recovered as the fluoride or chloride and later must be reduced to metal.

Extraction with fused salts is also being developed for purification of the fuel from liquid metal homogeneous reactors.[10] If the spent molten fuel, such as uranium in liquid bismuth, is contacted with a molten salt mixture it has been found that most of the rare earth fission products are transferred into the salt phase. A large fraction of the fission products, which are important from the cross-section standpoint in a thermal reactor, are removed in this way.

The third method under examination is the use of molten metals as extractants. Both silver and magnesium are immiscible with molten uranium and have favorable capacities for plutonium extraction. The plutonium distribution ratios (by weight) are about 2.0 for either the magnesium or silver system. The results in Table X indicate that the fraction of plutonium extracted by magnesium is independent of plutonium concentration, at least over a 300-fold range. When magnesium is used, the extraction step operation must take into account the high vapor pressure of magnesium at the melting temperature of uranium. When silver is used, the subsequent separation of plutonium from silver is a difficult one. At present, distillation of the silver is the preferred method for its removal.

These molten metal solvent extractions recover plutonium but are not highly selective in so far as separation of uranium or plutonium from fission products is concerned. This is illustrated by the data in Table XI.

A smaller amount of effort has been expended on a continuous recrystallization or zone melting process for purification, but the results are not encouraging. In order to realize the theoretical separations factors, it has been necessary to process at extremely slow rates (less than $\frac{1}{250}$ linear inch per hour).

In the recycle of fuel from heterogeneous reactor cores, the primary objective is the removal of fission products. There is no real need to separate the uranium from the plutonium when reprocessing the core. To accomplish purification of core material, two different approaches are being studied. One is by oxidative slagging and the other by electro-refining. If spent fuel is melted in the presence of a very limited amount of oxygen the most stable oxides are formed preferentially. They are the oxides of cerium and rare earths. Upon liquation, these oxides float to the surface and may be skimmed off. As in all other pyrometallurgical operations, the rare gases and the halogens bubble off and are vented during the melting of the fuel. The fission products of intermediate volatility (cesium, strontium, lanthanum, and barium) diffuse into the crucible and through the slag layer. The oxygen needed for the slagging operation is supplied by the use of oxide crucibles, by control of the furnace atmosphere, or by the addition of oxides directly to the melt. Representative data from a typical run are shown in Table XII. Other substances, such

Table X. Plutonium Extraction in the Molten System Uranium-Magnesium

Pu concentration in irradiated U, parts per million	Weight ratio U/Mg	% Pu in Mg phase
0.3	1.0	60
23	0.9	60
55	0.7	71
97	1.0	67

Table XI. Extraction of Irradiated Uranium with Silver

Element	% extracted by silver*
Cs	96
Sr	94
La	89
Ce	86
Zr	73
Pu	65

* Equal weight ratios of silver and uranium employed.

Table XII. Oxidative Slagging

Element	% of original amount remaining in purified metal ingot*
Uranium	94
Plutonium	94
Cesium	0.1
Rare Earths	1.0
Zirconium	34
Ruthenium	95
Strontium	0.02

* 4 hr at 1200°C in an oxide crucible.

as graphite, may be added to improve removal of zirconium and some of the other fission products. From Table XII it will be noted that only ruthenium is not affected. Other noble metal fission products and niobium and molybdenum probably behave like ruthenium.

The second approach to fission product removal for core processing is electro-refining. If the heavy metals are transported through a molten bath of alkali or alkaline earth halides (mixtures of chlorides or fluorides), the noble metal-fission products collect as an anode sludge. The rare gases are vented off at the anode. The active metal-fission products tend to build up in the salt bath. As a result of this build-up, the bath must be replaced or separately processed to keep the decontamination factors high. In most of this work to date, it has been convenient to use as a cathode some metal that forms a low-melting alloy with uranium so that the product can be continuously removed from the cell as a liquid. On small-scale runs, the material recovered at the cathode represents 98% of the metal leaving the anode and decontamination factors of 100 to 300 have been obtained for cesium, strontium, zirconium, and ruthenium. Of all the pyrometallurgical processes, electro-refining is the only one that separates the bulk of the noble metals from the uranium.

Another solution to the core processing problem may be the use of a scheme similar to the deBoer process. Uranium is iodized and then reclaimed as metal by hot wire (or tube) decomposition of the volatile UI_4. The only fission products that appear to transfer appreciably with the uranium are zirconium and niobium. However, cold trap arrangements can be used to effect better separations of zirconium and niobium iodides from the uranium iodide. The fate of plutonium has not yet been determined. Another application of the deBoer method which appears promising is the separation of U^{233} from irradiated thorium.

The experimental results obtained to date are very encouraging for the development of one or more high temperature processes suitable for short-cooled, highly irradiated fuels. However, the problem of equipment development is quite formidable and has yet to be completely resolved. Some alleviation of the crucible problem is expected through the use of a lower temperature system than that of pure molten uranium; that is, small additions of certain metals will be employed to lower the melt temperatures. In addition, although the decontamination factors obtained are quite adequate from a reactor standpoint, they are not sufficient to enable direct fabrication of the fuel elements. Therefore, the problems of remote-control fabrication must be simultaneously solved to realize the advantages offered by pyrometallurgical processes. The recycle of many types of fuel eventually produces an accumulation of enough uranium or thorium isotopes and other transuranic elements so as to require at least some remote fuel fabrication. Therefore, one must be careful in cost estimates not to over-penalize the pyrometallurgical processes for their modest decontamination factors.

ACKNOWLEDGEMENTS

The information presented in this review is based on work by many people from the following organizations: Ames Laboratory, Argonne National Laboratory, Brookhaven National Laboratory, Hanford Atomic Products Operation, K-25 Laboratory, Knolls Atomic Power Laboratory, North American Aviation, Inc., and the Oak Ridge National Laboratory. The author acknowledges very gratefully the contributions of all these people to the subject discussed in this survey.

REFERENCES

1. Seaborg, G. T. and Katz, J. J., *The Actinide Elements,* National Nuclear Energy Series, Division IV, Vol. 14A, McGraw-Hill Book Co., New York (1954).
2. Coryell, C. D. and Sugarman, N., *Radiochemical Studies: The Fission Process,* National Nuclear Energy Series, Division IV, Vol. 9, McGraw-Hill Book Co., Inc., New York (1951).
3. Harty, W. M., *The Design Philosophy of Remote Operation and Maintenance of Separations Facilities,* Chemical Engineering Progress Symposium, Series No. 13, Part III: 115-121, Vol. 50 (1954).
4. Kunin, R. and Myers, R. J., *Ion Exchange Resins,* John Wiley and Sons, Inc., New York (1950).
5. Hiester, N. K., Fields, E. F., Phillips, R. C. and Radding, S. B., *Continuous Countercurrent Ion Exchange with Trace Components,* Chemical Engineering Progress *50*: 139-150 (1954).
6. Higgins, I. R. and Roberts, J. T., *A Countercurrent Solid-Liquid Contactor for Continuous Ion Exchange,* AECU-2546 (1952).
7. Kunin, R. and McGarvey, F., *Ion Exchange,* Industrial and Engineering Chemistry *47*: 565-575 (1955).
8. *Ion Exchange Symposium,* Industrial and Engineering Chemistry *47*: 46-101 (1955).
9. Brewer, L., *High Temperature Decontamination and Separation Process,* UCRL-314 (May 6, 1949).
10. Raseman, C. and Weisman, J., *Liquid-Metal-Fuel Reactor Processing Loops,* Chemical Engineering Progress Symposium Series No. 12, Part II: 153-172, Vol. 50 (1954).
11. Glassner, A., *A Survey of the Free Energies of Formation of the Fluorides, Chlorides and Oxides of the Elements to 2500° K,* ANL-5107 (August, 1953).
12. Quill, L. L., *The Chemistry and Metallurgy of Miscellaneous Materials: Thermodynamics,* National Nuclear Engery Series, Division IV, Vol. 19B, McGraw-Hill Book Co., Inc., New York (1950).

Method for Separation of Uranium-233 from Thorium Irradiated in Atomic Piles

By A. Chesne,* and P. Regnaut,† France

Uranium-233 is one of the nuclear fuels of the future. It is the purpose of this paper to describe an extraction technique for U^{233} from reactor irradiated thorium.

It will be remembered that the formation of U^{233} is brought about by the action of slow neutrons on thorium-232 atoms. The intermediate elements which appear in the process are thorium-233 and protactinium-233.

The half-life of the first element, 23.5 minutes,[1] is such that a few hours are enough to ensure its complete decay.

The second element has a half-life of 27.4 days.[2]

By allowing the activity of the irradiated sample to decay for three to four months, the protactinium and fission product activities are considerably reduced. The latter are due to the fission of Th^{232} by fast neutrons. In the treated samples, their activity was negligible as compared to that of protactinium after a decay period of three months.

Thus, the problem of separating U^{233} from irradiated thorium is closely allied to that of isolating protactinium-233, which is the main β, and γ emitter.

This element shows a tendency to hydrolyse, even in a fairly acid medium, and we have endeavored to prevent the formation of the colloidal form during processing, either by working in a highly acidic medium, or else in the presence of a complexing agent.

On the other hand, the quantities of U^{233} and protactinium-233 are small as compared with those of Th^{232}. In the case of uranium, the uranium/thorium ratio is close to 10^{-4}, and protactinium, under the conditions mentioned above, it is from 10^{-5} to 10^{-6}.

PRINCIPLES

The separation method for the three elements is based on the differences in their respective behaviors in a hydrochloric acid medium. Uranium and protactinium [3,4] give negatively charged complexes which can be fixed on anion exchange resins. Thorium, under the same condition, is not fixed.[5]

The study was carried out by stirring for two hours, a certain quantity of a strongly alkaline resin (A'300 D—Philips & Pain), with solutions of the three elements at various acidities. The analysis of the phases in equilibrium gives a measure of the degree of fixation.

The results are as follows:

(*a*) For uranium, the distribution coefficient *Kd*, which is low up to an acidity of 0.5*N* increases progressively. From 6*N*, one gets values higher than 400 and over 1000 with 8*N* HCl.

(*b*) For protactinium from 0.5 to 4*N*, *Kd* is practically constant and close to 4. From 4*N*, it increases very rapidly and reaches 450 in 8*N* HCl.

(*c*) There is practically no thorium fixation, regardless of the acidity.

These results show that it is possible to separate quantitatively uranium and protactinium from thorium by passing an 8*N* HCl solution of the three elements through an anion exchange resin column.

Elution of the protactinium is feasible in a 4*N* HCl medium,[5] but we felt it was preferable to use an 8*N* HCl solution, 0.1*M* in $(NH_4)_2SiF_6$.

Under these conditions, the distribution coefficient of uranium is practically not affected, in contradistinction to that of protactinium. The last named probably gives complexes of another form, as shown by Kraus and Moore,[6] which are fixed to a much smaller degree.

Uranium elution then is carried out in an 0.5*N* HCl medium.

Summing up, processing consists of the following operations: (*a*) dissolving the irradiated metal, and (*b*) fixing the protactinium and uranium, (*c*) carrying out selective elution of the elements, and (*d*) recovering HCl and thorium.

PROCESS

Dissolving

Attack of the metal by hydrochloric acid is rapid and considerable heat is evolved but, as already pointed out,[7] it is not complete. Traces of silicofluoride make it possible to dissolve thorium and to obtain a clear solution.

We used 11*N* acid brought to *M*/100 in ammonium silicofluoride. The acid must be added cautiously in order to avoid a possible runaway reaction.

Following filtration, in order to eliminate the traces of insoluble material, the solution is adjusted with concentrated hydrochloric acid to a free acidity of 8*N*. Under those conditions, the concentration is

Original language: French

* Plutonium Division, C.E.A.
† Chief, Plutonium Division, C.E.A.

somewhere between 0.5 and 0.6*M*, and the $(NH_4)_2SiF_6$/Th ratio is approximately 0.003.

Fixation of Protractinium and Uranium

The solution thus obtained is passed over a column filled with a 300 D resin (Philips & Pain). It is an anion exchanger of the divinylbenzene type, which has amine and oxy-amino groups.

The resin is used in the R-Cl form, and the speed at which the solutions are passed over the resin column is set at 2 $cm^3/cm^2/min$.

At the outlet of the column, the liquid passes an ionization chamber connected with a recorder, which makes it possible to check that the absorption process is developing normally, and later to verify the elution of the protactinium.

The presence of traces of ammonium silicofluoride does not affect the fixation of protactinium, in view of the considerable excess of thorium, which complexes the SiF_6^{--} ions.

Some other elements (iron, in particular) are separated from the thorium along with uranium and protactinium,[8] giving anionic complexes under the conditions mentioned above.

Following the passing of the solution, and in order to eliminate the last traces of thorium, the column is washed with an 8*N* hydrochloric acid solution.

The required volume is approximately 10 times that of the resin. The thorium so recovered contains less than 2×10^{-3} of the protactinium initially present.

Fractionated Elutions

During the elutions, we kept the same rate of passage as during fixation and washing.

Protactinium begins to appear following the use of a fairly reduced volume of eluant. The passage of a volume equivalent to six times the resin volume makes it possible to extract the protactinium nearly quantitatively. However, the last traces are difficult to remove by elution.

Thereafter, one can carry out the elution on uranium with dilute hydrochloric acid. We used 0.5*N* acid for this operation, and an eluant volume eight times that of the resin.

Under these conditions, less than 1% of the uranium and protactinium remain on the resin.

The solution used for the elution of the uranium-233 still contains an activity which corresponds to $\frac{1}{500}$ of that initially present.

Let us draw attention to the fact that additional decontamination of the uranium may be achieved by bringing this solution to the following conditions: HCl acidity, 0.1*N*; F^-, 0.01*M* to 0.02*M*.

This new solution is passed through a Permutite cation exchange resin C.50 (Philips & Pain)—similar to Dowex 50—this resin being in the RH form.

In contradistinction to uranium, protactinium is fixed but little.

Elution then is carried out with a 0.1*N* solution and 0.01*M* HCl solution in NaF in order to remove the last traces of protactinium.

Elution of the uranium with 4*N* hydrochloric acid occurs. The decontamination factor is at least 100.

Recovery of Hydrochloric Acid and Thorium

The various fractions obtained are:

(*a*) An 8*N* solution of HCl arising from the dissolving solution passed down the column, and from washing this column. This fraction is richest in hydrochloric acid and contains all the thorium.

(*b*) The protactinium solution, eluted by 8*N* HCl and 0.1*M* in $(NH_4)_2SiF_6$.

(*c*) A uranium solution, eluted by 0.5*N* HCl.

Fraction (*a*) is processed in two stages (Fig. 1).

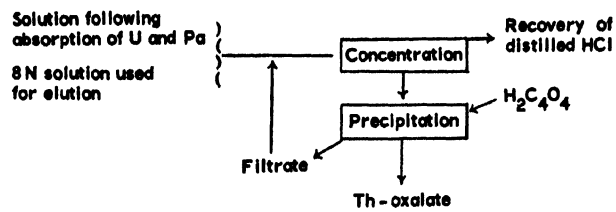

Figure 1. Scheme of the treatment of fraction (a)

1. The thorium is concentrated up to 2*M*, and the hydrochloric acid distilled off is recovered.

2. The concentrated solution is precipitated by an amount of oxalic acid of less than 5% the quantity theoretically necessary to precipitate the thorium quantitatively.

Following filtration of this oxalate, the acid solution, which still contains a little thorium, is placed with the next (*a*) batch which will undergo the same treatment.

Thorium is thus recovered in the form of an oxalate, which can thereafter be calcinated to oxide, and transformed into fluoride for retransformation to metallic thorium.

The major part of the hydrochloric acid contained in fraction (*b*) is recovered, by being concentrated by a factor 10. The distilled acid is recovered.

Hydrochloric acid from fraction (*c*) is not recovered, since it makes up only a very small percentage of the acid used.

The hydrochloric acid balance sheet can be summed up as follows:

Origin	*Used in % of total HCl*	*Recovered in % of total HCl*
Dissolving and adjusting to 8*N*	69.0	85.0
Washing the column following fixation	16.5	
Elution of the protactinium	13.8	13.0
Elution of the uranium	0.7	–
	100.0	98.0

Here, as an indication, are the quantities of uranium consumed: 40% hydrochloric acid, approximately 15% by weight of thorium; ammonium silicofluoride, approximately 3% by weight of thorium; and oxalic acid, a weight comparable to that of the thorium.

CONCLUSION

The method just described affords a means of achieving good separation of the three elements, each

of them being extracted in a yield of better than 98%.

At the outlet of the resin column, the residual protactinium contamination of the thorium and U^{233} is approximately 2×10^{-8}.

By additional treatment on a cationic resin, one may reach 2×10^{-5} for U^{233}.

The main difficulty encountered is due to the choice of the materials which most resist hydrochloric acid attack, particularly for distillation operations.

REFERENCES

1. Nuclear Data, p. 262.
2. Nuclear Data, p. 264.
3. Kraus, Kurt A. and Moore, Georgie E., *Adsorbtion of Pa from HCL solutions by anion exchange resins*, J. Am. Chem. Soc., *72*: 4293 (1950).
4. Kraus, Kurt A. and Moore, Georgie E., *Anion exchange studies: Pa in some HCL-HF mixtures. Separation of Nb, Ta and Pa*, Rep. ORNL 673 (13 November 1950).
5. Kraus, Kurt A. and Moore, Georgie E., *Anion exchange studies: separation of Pa and Fe by anion exchange in HCL-HF solution*, J. Am. Chem. Soc. *77*: 1384-84 (1955).
6. Kraus, Kurt A. and Moore, Georgie E., *Anion exchange studies: Pa in some HCL-HF mixtures; separation of Nb, Ta and Pa*, Rep. ORNL 673 (13 November 1950).
7. Newton, Hyde and Meinke, *Solution of thorium metal and thorium dioxyde*, Rep. AECD 2750, Procedure 90-4, p. 8, declassified on 12-2-1949.
8. Moore, Georgie E. and Kraus, Kurt A., *Adsorption of iron by anion exchange resins from hydrochloric acid solution*, J. Am. Chem. Soc. *72*: 5792 (1950).

Pyrometallurgical Processing of Nuclear Materials

By H. M. Feder,* USA

The purpose of this paper is to present a detailed examination of one process, namely, oxidative slagging. This process is designed to remove from irradiated uranium or uranium-plutonium alloy a significant fraction of the fission product elements in order to permit the re-use of the metal as pile fuel. The success of the purification will be judged by the mechanical strength, thermal stability, radiation damage stability and nuclear properties of the purified material.

THEORY

Brewer[1] examined the thermodynamic and volatility data available in 1945 and arrived at the following conclusions:

1. Maintenance of molten uranium at a sufficiently high temperature would effect the removal of volatile fission elements: Xe, Kr, Rb, Cs, Sr, Ba, I, Sn, Cd, and Sb.
2. Addition of oxygen to molten uranium would affect the removal of all the rare-earth elements, including yttrium, in an oxide layer which would separate as a floating scum or onto the walls of the container.
3. The addition of carbon to molten uranium would affect the removal of zirconium and niobium as a light carbide scum.

Tables I-III present some thermodynamic data of interest at an arbitrarily chosen temperature, 1500°K, in the liquid uranium range. Some minor modifications have been made in the thermodynamic data from available compilations[2-6] as a result of more recent information on heats of combustion, high temperature heat capacities, etc. The application of these data to the problem at hand should, of course, be made with reasonable caution because of departures from ideality of real solutions. For example, the partial pressure of, say, tellurium above its solution in molten uranium may differ greatly from its ideal value because uranium tellurides may be stable at the temperature in question. Likewise, although the equilibrium constant corresponding to the following reaction

$$\mathrm{Sr}(l) \times \tfrac{1}{2}\,\mathrm{UO_2}(s) = \mathrm{SrO}(s) + \tfrac{1}{2}\,\mathrm{U}(l)$$
$$\Delta F^\circ_{1500} = -3.2 \text{ kcal} \qquad (1)$$

is calculated to be 2.9, the actual equilibrium constant for this distribution reaction may be very significantly different when radiostrontium and its oxide are present at low concentrations in solution in uranium and uranium dioxide, respectively.

EXPERIMENTAL

Clean uranium discs weighing 100–200 grams were used. These had been previously irradiated in a reactor to a total exposure of about 2 kilowatt-hours per gram and the radioactivity allowed to decay to a convenient level for handling.

The shielded furnace used for the high temperature studies is shown schematically in Fig. 1. Prior to each experiment the furnace tube and crucibles were given a preliminary outgassing treatment at 800°C and less than 0.1-micron pressure. Melting and slagging were conducted in a slow stream of highly purified helium. The auxiliary gas handling train is shown in Fig. 2. The entire assembly is pictured in Fig. 3; the lead brick shielding walls have been removed from around the furnace box for greater visibility.

After the metal was held at temperature for the time desired, the slag was separated by either chemical or physical means. In the former case the ingot was furnace-cooled and the slag, which had formed a definite layer at the crucibles walls and top surface (Fig. 4), was chemically removed by differential etching with nitric acid. Physical separation of slag and metal was accomplished by bottom-pouring. Very clean separation of slag and metal could be achieved by careful technique. The results of the two methods of slag separation were indistinguishable.

Analyses for the elements were performed by conventional radiochemical and wet chemical methods.

Table I. Vapor Pressure of Some Elements and Compounds at 1500°K

Substance	*P, mm Hg*
Se, Kr, Xe	$>>10^5$
Rb	3.3×10^4
As	3.2×10^4
Cd	3.0×10^4
Cs	1.6×10^4
Zn	1.1×10^4
Te	1.9×10^3
UI_3	3.3×10^2
Sr	2.7×10^2
Sb	1.1×10^2
Ba	4.2×10^1
UBr_3	3.0×10^1
Elements occurring in fission not listed	<10

* Argonne National Laboratory. Including work by H. M. Feder, N. Chellew, M. Ader and C. Cushing, Argonne National Laboratory.

Because the short-lived radiomolybdenum isotopes had decayed out, a sensitive colorimetric method[7] for the estimation of inactive, fission product molybdenum in uranium was developed. The precision of most of the radiochemical analyses was about ±10% (relative). However, at very low levels of residual activity (<1%) the analyses are probably reliable only to within a factor of two because of difficulties of sampling and cross-contamination.

RESULTS

Approximately forty experiments were performed. Some of the variables which were examined were: time, temperature, size and configuration of charge, crucible material, and the effect of carbon addition. In the tables which follow, experiments are compared which are most nearly alike with respect to unlisted variables.

The significant variations of residual activities with time at temperature are shown in Table IV. Apparently the processes responsible for the loss of the elements listed are not complete in a half-hour. More extended periods at temperature (to eleven hours) showed that after four hours further action was negligible. One notes also that after a half-hour the residual contents of cesium, strontium, and rare earths are the same within experimental error. This observation may be interpreted as indicating the approximate equality of the diffusion coefficients of these elements in uranium solution. Undoubtedly, the time required to achieve a nearly steady state with respect to these elements varies with the size and configuration of the charge and other factors. For most of the experiments to be discussed a four-hour run duration was arbitrarily selected.

Table II. (Gibbs) Free Energy of Formation of Oxides at 1500°K

Oxide	$-\Delta F°$ (kcal/gm-atom oxygen)
1/3 La_2O_3	109.7
1/3 Ce_2O_3	107.0
1/3 Nd_2O_3	105.7
SrO	102.0
1/3 Pu_2O_3	99.0
1/2 UO_2	98.9
1/2 ZrO_2	97.0
BaO	95.0
NbO	66
1/2 MoO_2	38
1/2 TeO_2	4.7
Cs_2O	3.6
1/2 RuO_2	−2.7

Table III. (Gibbs) Free Energy of Formation of Carbides at 1500°K

Carbide	$-\Delta F°$ (kcal/mole)
ZrC	43.1
UC_2	33.8
UC	−35
PuC	<33
Mo_2C	−3
Carbides of Ru Rh, Pd	< 0

Table IV. Residual Activity of Fission Elements as a Function of Time at 1200°C

Experiment number	Crucible material	Time (hr)	Per cent of original concentration		
			Cs	Sr	Rare-earths
7	UO_2	0.5	13	11	11
2	UO_2	4.0	3.0	1.7	0.9
9	MgO	0.5	20	18	21
6	MgO	4.0	2.9	1.7	1.8

Table V shows the effect of temperature on the residual content of some fission elements. An increase in temperature markedly lowers the retention of cesium and strontium without noticeably affecting the retention of the other elements. The elements cesium and strontium are those for which evaporation was expected to be a significant method of removal.

The effect of charge configuration is shown in Table VI. Although some of the entries in this table are not in line, a tendency towards greater retention of activity in thicker ingots is clearly evident. The ingot used in Experiment 9 (Table IV) was three times as thick as that used in Experiment 7. The influence of diffusional distance on the retention of activities during the period when the retention is diffusion controlled may be seen.

Some results of experimentation with various crucible materials are shown in Table VII. The refractory oxides were the purest materials available, except for zirconia, which contained a few per cent of lime for stabilization. The oxides are listed in the order of decreasing thermodynamic stability at 1200°C. The residual content of rare-earth activity exhibits a variation which suggests that the removal of the rare-earth elements may be limited by an oxidation-reduction equilibrium with the refractory oxide used. The

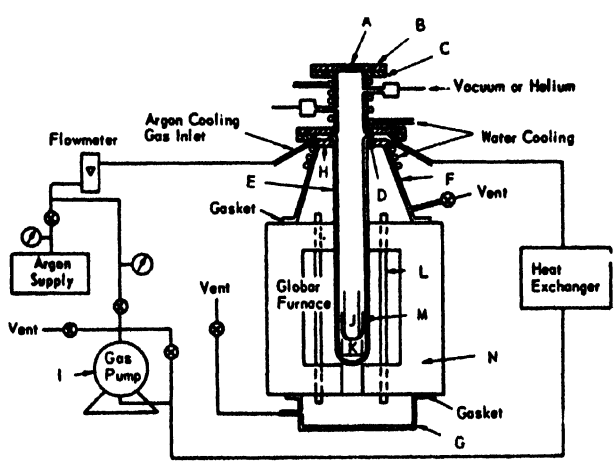

Figure 1. High temperature melting furnace with Argon cooling and blanketing system; (A) sight glass; (B) top flange; (C) head; (D) gasket (argon cooled); (E) porcelain tube; F) shroud; (G) sealing pan; (H) supporting baffle; (I) Roots-Connersville gas pump; (J) crucible; (K) crucible support; (L) globar heating element; (M) tantalum pail; (N) refractory brick; (↗) pressure gauge; (X) valve

Table V. Residual Activity of Fission Elements as a Function of Temperature after Four Hours

Experiment number	Crucible material	Temp. (°C)	Per cent of original concentration							
			Cs	Sr	Rare-earths	Te	Zr	Nb	Ru	Mo
27	Al_2O_3	1200	0.15	0.17	0.52	55	47	102	108	97
24	Al_2O_3	1310	0.027	0.0085	0.71	79	55	92	104	96

Table VI. Residual Activity of Fission Elements as a Function of Diffusional Distance after Four Hours at 1200°C

Experiment number	Thickness of ingot, cm (average)	Per cent of original concentration			
		Cs	Sr	Rare-earths	Ce
8	0.51	1.4	0.3	1.9	–
2	0.63	3.0	1.7	0.9	0.4
5	1.22	3.6	0.1	1.2	1.4
6	1.47	2.9	1.7	1.8	1.9
11	2.44	5.7	6.5	12	–

same marked variation is not characteristic of strontium; other evidence, however, indicates that this arises from the fact that both oxidation and vaporization are significant processes for this element. No influence of crucible material is discernible in the behavior of cesium, which is removed entirely by vaporization and/or diffusional processes.

The residual activity of zirconium was indifferent to the crucible material employed; moreover, no exchange of radiozirconium with the zirconia crucible took place. These facts implied that zirconium was being removed by a process other than oxidation. Liquation of zirconium carbide, formed as a result of the presence of 100–500 ppm of carbon impurity in the metal, seemed to be a very likely method of removal. This mechanism was strikingly confirmed by experiment number 25 (Table VIII) in which a graphite rod was dipped into the molten uranium for one-half hour during the course of a four-hour run. The results are shown in Table VIII.

Concentration of zirconium on the surface of the graphite rod and depletion of zirconium in the melt as a result of carbon addition are apparent. A similar effect for niobium, although much less marked, was also observed. Previous experiments without added carbon had failed to show any significant separation of niobium from uranium. As expected, ruthenium showed no tendency to separate from uranium by preferential carbiding.

In addition to the experiments already discussed, many further experiments were conducted. These led to the following findings which are presented without detail:

1. Radiocesium was obtained in good yield by condensing the evaporated activity on a cold finger above the molten uranium.

2. The incorporation of the non-volatilized fraction of the cesium into the oxidic portion of the slag was shown to be consistent with the notion that lattice imperfections in the uranium dioxide (to the extent of about 10^{-3}%) act as traps for cesium atoms.

3. Tellurium was found to be non-volatile under conditions reported. The loss of tellurium into the slag appeared to be affected by the rare earths, even

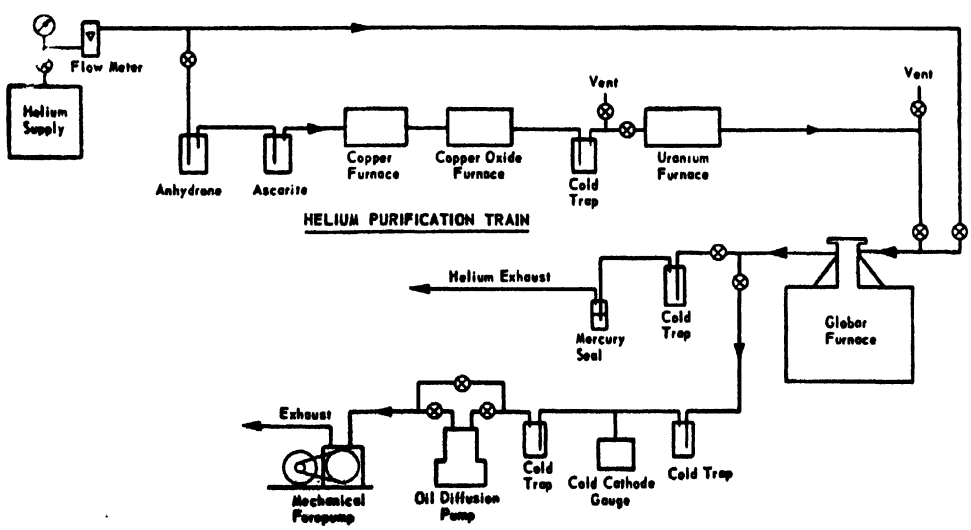

Figure 2. Experimental furnace auxiliary system

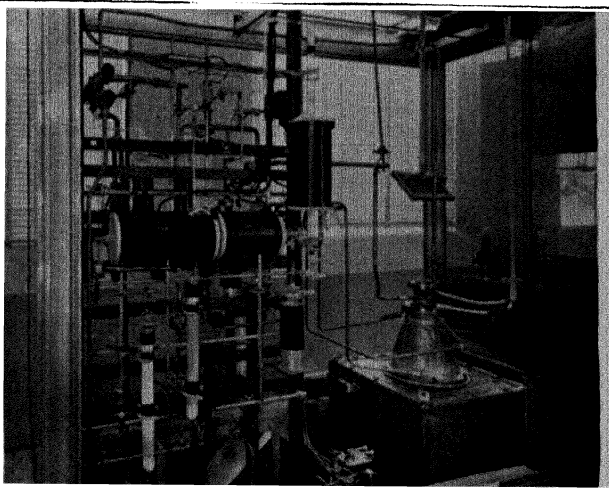

Figure 3. View of uranium melting furnace

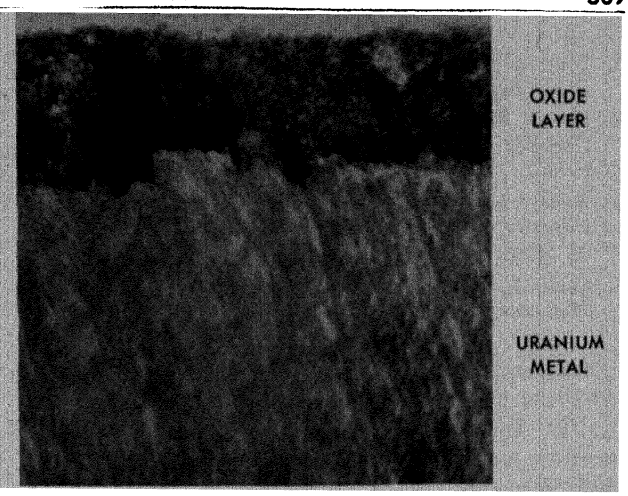

Figure 4. Photomicrograph of uranium ingot: vertical section at crucible (MgO) wall. Test conditions: 2 hr at 1200°C; flowing helium atmosphere. Photographic scale: 1 cm = 10 microns

at tracer levels of the elements. Upon addition of inactive cerium at 0.1–0.2% concentration to the melt, tellurium removal into the slag became nearly quantitative. The incorporation of stable rare-earth tellurides in the slag has been postulated.

4. The addition of small amounts of boron, nitrogen or silicon had no pronounced effect on the behavior of the fission elements investigated in the oxidative slagging process.

5. The distribution of plutonium, ruthenium, niobium and molybdenum, which are not removed in the oxidative slagging process, was not affected by significant increases in their concentrations.

6. The slag produced in this process consists of 10-40% weight of uranium dioxide, small amounts of uranium carbide, and entrapped uranium metal. The fraction of the original metal which may be lost to slag is a complex function of many variables. By proper attention to experimental details slag losses as low as two per cent may be realized.

Table VII. Residual Activity of Fission Elements as a Function of Crucible Material after Four Hours at 1200°C

Experiment number	*Crucible material*	*Per cent of original concentration*			
		Cs	*Sr*	*Rare-earths*	*Zr*
23	BeO	0.1	2.9	4.2	31
19	MgO	0.1	0.1	1.5	44
15	ZrO_2	0.5	0.1	0.9	36
16	Al_2O_3	0.1	0.1	0.4	48

Table VIII. Effect of Scavenging with Graphite on Fission Product Removal at 1200°C

Experiment number	*Location*	*Per cent of starting material*			
		U	*Zr*	*Nb*	*Ru*
27	Slag	2.3	53	1.7	1.6
	Ingot	97.6	46	100	106
25	Slag	2.2	31	1.5	0.9
	Graphite rod	3.4	65	8.2	3.4
	Ingot	94.1	2.9	90	91

7. Plutonium was preferentially incorporated in the slag by a small factor which varied from 1.0 to 1.4. No significant loss of plutonium by volatilization occurred under the experimental conditions chosen.

8. By pouring the purified metal way from the slag, good physical separation has been demonstrated on a kilogram scale.

DISCUSSION

The success of the oxidative slagging process cannot be judged until the criteria listed in the opening paragraph are applied to significant quantities of purified metal. Currently available information indicates that the removal of fission products by this process will yield reactor fuel with the required low parasitic capture cross section, particularly if the fuel is to be used in a fast neutron pile. Because the fission product elements that are removed by this process are those which have low solubility in solid uranium or which form brittle intermetallic compounds with uranium, the mechanical strength of the purified metal is not expected to be adversely affected. Some of the metals, for instance niobium and molybdenum, which will accumulate as a result of reprocessing by oxidative slagging, are known to have rather beneficial effects on the stability of uranium to thermal cycling.

One may conclude that on the basis of performance, speed, simplicity, compactness and economy, oxidative slagging appears to be a quite promising reprocessing method for certain types of heterogeneous, fast neutron power reactors, provided that problems of remote fuel element fabrication and testing can be successfully solved.

ACKNOWLEDGEMENTS

The author wishes to acknowledge with gratitude the following persons who assisted in this work by experimentation, design and consultation: B. Blumenthal, J. H. Schraidt, H. Smith, D. C. Hampson, D. P. Krause, R. P. Larsen, C. E. Crouthamel, H. H. Chiswick, J. Faris, L. Burris.

REFERENCES

1. Brewer, L., *High Temperature Decontamination and Separation Process,* UCRL-314 (1945).
2. Kelley, K. K., *The Thermodynamic Properties of Metal Carbides and Nitrides,* Bureau of Mines Bulletin 407 (1937).
3. Kelley, K. K., *High Temperature Heat-Content, Heat-Capacity, and Entropy of Inorganic Compounds,* Bureau of Mines Bulletin 476 (1949).
4. Quill, L. L. (Ed.), *The Chemistry and Metallurgy of Miscellaneous Materials: Thermodynamics,* National Nuclear Energy Series, Division IV, Vol. 19B, McGraw-Hill Book Co., New York (1950).
5. Brewer, L., *et al., The Thermodynamic Properties and Equilibria at High Temperatures of the Compounds of Plutonium,* Paper 6.40 in *The Transuranium Elements,* McGraw-Hill Book Co., New York (1949).
6. Glassner, A., *A Survey of the Free Energies of Formation of the Fluorides, Chlorides, and Oxides of the Elements to 2500°K,* ANL-5107 (1953).
7. Crouthamel, C. E. and Johnson, C. E., *Thiocyanate Spectrophotometric Determination of Molybdenum and Tungsten,* Anal. Chem. *26*: 1284 (1954).

The Purification of Uranium Reactor Fuel By Liquid-Metal Extraction

By A. F. Voigt,* USA

In a reactor which is operated at a high enough level to provide useful power, it will be necessary to reprocess the fuel at regular intervals to accomplish at least one of three different objectives. If the fuel is a solid metal, radiation damage may cause distortion of the metal leading to failure of the fuel elements. Under some conditions fission products of high neutron capture cross section may accumulate to the point where their removal is essential to efficient operation. It may be necessary to add new fissionable material to replace that which has been burned out.

If a reactor is operated primarily for the production of power, it appears to be possible to make use of relatively simple types of processing to accomplish these ends. These processing methods apply to a solid or liquid metal fuel reactor and do not destroy the metallic state of the fuel. They thus involve fewer chemical steps than aqueous processing methods and could, consequently, be more economical. However, at least at the present state of the art, they are not quantitative to the degree that is required if the purified material is to be handled without shielding. The degree of removal of fission products which will permit the direct handling of partially spent fuel material is very high and the methods to be described do not meet this criterion. Thus the refabrication of the fuel element must be a part of a remotely controlled operation, and of necessity the fuel element design must be kept simple. If this type of processing can be adopted, the entire reactor is affected. One set of problems which accompany aqueous processing is replaced by another set unique to this type of processing.

Early work in this laboratory, begun in 1942, showed that in metallurgical operations such as melting in oxide or graphite crucibles, high percentages of the fission products were removed, some by volatilization, others by selective oxide or carbide formation. Other experiments showed that the fission products could be extracted into a second metal phase by processes analogous to aqueous-organic liquid extraction. A number of metals, notably the rare earths, copper, silver and magnesium are at least partially immiscible with uranium in the molten state. When melted with uranium these form two-phase systems which separate on standing into uranium-rich and extractant-rich layers.

The early experiments were concerned primarily with the behavior of plutonium which was found to extract readily into silver and weakly into the other extractants which were investigated. These experiments were performed on a limited scale with tracer quantities of plutonium but the data indicated roughly a 90-95 per cent removal of plutonium in one contacting operation with an equal volume of silver.

Although liquid metal extraction was shown to produce some separation, the process was not considered feasible for systems which required that the fuel or any product be decontaminated to the extent which would permit unshielded handling. Research on this type of processing was therefore set aside until in recent years power reactor concepts evolved in which such processing could be an important part.

The renewed program in the Ames Laboratory has been concerned with liquid metal extraction using silver, cerium, lanthanum and magnesium as extractants. All of these display the proper liquid immiscibility with very little liquid solubility.

EXPERIMENTAL

Materials

As the working fuel for these experiments three different materials were employed in order to vary over a wide range the amounts of fission products and plutonium present in the uranium.

Irradiated Natural Uranium

Fuel samples exposed for various lengths of time in the reactor at the Oak Ridge National Laboratory provided sources containing plutonium in concentrations varying from about 2 to 250 parts per million. This material contained detectable amounts of radioactive isotopes of nearly all the major fission products except molybdenum and zirconium. Thus the behavior of most of the fission products and plutonium could be followed in the extraction process.

Uranium-Chromium Eutectic

Because the melting point of the U-Cr eutectic at 20 atomic per cent chromium, is much lower at 859°C

*This paper represents work done in the Ames Laboratory of the US Atomic Energy Commission, Iowa State College, Ames, Iowa, by the following: F. H. Spedding, I. B. Johns, T. A. Butler, F. J. Woller, A. H. Daane, E. H. Dewell, R. G. Clark, J. E. Gonser, J. F. Haefling, K. L. Malaby, A. F. Voigt and others with assistance by the Analytical Groups of the Laboratory under C. V. Banks and V. A. Fassel and Metallurgical Groups under P. Chiotti, O. N. Carlson and D. J. Peterson.

than that of uranium at 1132°C, it may lend itself more readily to remote fabrication. Interest in this alloy has been high and a number of extraction experiments have been performed on it. The material used in these experiments was prepared in the Ames Laboratory and sent to Oak Ridge for irradiation. Of the series one sample was irradiated for several months and cooled for a similar period. The remainder were irradiated 7 days and cooled for another 7 days.

The latter group contained tracers for all the major fission elements but very little plutonium (about 0.5 ppm).

The long-irradiated sample had plutonium at a level of about 11 ppm with the fission products at a corresponding level. However, no analysis could be made for those fission products such as molybdenum, which have only short-lived isotopes.

Artificial Mixtures

In a power reactor it would be economical to use a fuel rod as long as possible before reprocessing it. At what point reprocessing becomes absolutely essential depends on the reactor design, but it is certainly at a point where the fission product content would be quite high, too high to permit handling in the existing Ames Laboratory facilities. Since the behavior of the fission products might depend on concentration, it was desired to conduct experiments on a fuel containing fission products at the expected level. In order to do this, artificial mixtures of fission product elements and uranium which have been called "fissium" were prepared. In these experiments the fissium contained the less volatile elements of high yield: zirconium, molybdenum, ruthenium and one or more typical rare earth. The concentration was that which would be found in a uranium fuel in which two per cent of the atoms had been fissioned. The thermal fission yield curve[1] was used to calculate the weights of the fission products expected by summing the yields of all stable and long-lived fission product isotopes for each element. The material was made up to contain 1.18 gm of zirconium, 0.69 gm of ruthenium, 0.76 gm of molybdenum, and 3.40 gm of rare earths per kilogram of uranium. In a number of the experiments these metals were irradiated at the Argonne National Laboratory reactor to produce radioactive tracers. The behavior of the element in the processing could then be followed by radiochemical analysis.

Extractant Metals

The silver used in the extractions was 99.9+% pure electrolytic crystals. The cerium and lanthanum metals were prepared in the Ames Laboratory. The lanthanum analyzed ~ 99.5% pure. The grades of cerium varied between 91% Ce and 99.5% Ce. Impurities in all these samples were predominantly other rare earths.

Equipment and Procedure

Most of the extractions were run using an induction furnace to provide heating and stirring. About 150 gm of uranium and an equal volume of the extractant were used in each experiment. The metals were placed in graphite or tantalum crucibles, surrounded by thermal radiation shields to reduce the rate of cooling and placed in a quartz envelope which was sealed and evacuated. A high vacuum was maintained during the heating process. Temperatures were read with an optical pyrometer using a mirror and window system. After the heating period the samples were allowed to cool by radiation. Cooling was slow enough so that the two phases, though violently mixed by the induction stirring, were completely separated by gravity during the cooling period before they solidified.

Graphite crucibles were removed from the outside of the specimens by a remote mechanical operation before sectioning the melt for samples; tantalum crucibles were left on. Sectioning was done with a slow speed slitting saw which was found to give far less contamination of the surroundings than high-speed abrasive wheels. Sections were taken across the crucible, with care to avoid the interface in either metal sample. Thus, any concentration of material at the interface went undetected. The samples of both phases were dissolved and analyzed by radiochemical methods which are largely standard,[2] though the presence of large amounts of an extracting metal made it necessary to adapt old and develop some new methods.

At the beginning of the present program, analyses were made for a large number of the fission products, as many as could be detected by their radioactivity. As the program progressed, it became apparent that many of these were of very low abundance in spent fuel and of no particular consequence as reactor poisons and analysis of them was discontinued.

The pattern followed in the analytical procedure was to add carriers for all of the important fission products to the acid solutions of the metals and separate each fission product from a different aliquot of this solution. Chemical recovery of the original carrier was determined and the counting rate of the sample was corrected to what it would have been with 100% chemical recovery. At least four replicates of each analysis were made until agreement indicated that fewer replicates would suffice, but duplicates were run in all cases.

RESULTS

Analyses for each fission product were made in samples taken from the original metal, the final uranium phase and the extractant metal phase. By the use of the first two of these, the results are reported in terms of a decontamination factor, the ratio of the counting rate from each particular fission product per gram of the original metal to its counting rate per gram of the final metal. These counting rates are, of course, proportional to the amount of fission product expressed in any other consistent units. The analyses of the two final phases are used to determine a distribution coefficient which, in our results, is expressed as the counting rate per gram of extractant

divided by the counting rate per gram of final metal. This can be converted to a distribution coefficient defined on the basis of moles of each phase by multiplying it by the ratio of the molecular weight of the extractant to that of uranium.

The decontamination factor is thus a measure of the removal of fission products and plutonium by all methods, including extraction, volatilization, crucible reactions, and surface accumulation whereas the distribution coefficient measures only the extraction. The percentage of the original fission products which were recovered can also be estimated giving a measure of the amount removed by volatilization and side reactions.

Irradiated Natural Uranium

Experiments on pure uranium as the extracted phase were run on material which had received irradiation to produce three different levels of plutonium and fission products. Analytical results showed the plutonium levels to be about 2, 18 and 230 parts per million in these samples. The first of these was used for preliminary experiments which are not reported in the table; the second and third are referred to as medium and high level.

Silver extractions were made in graphite at temperatures of 1200°C and heating times of about 20 minutes. The results of Table I are based on three experiments at the medium level and two at the high level.

Extractions of the irradiated uranium with rare earth metals were successfully carried out in tantalum. Graphite was unsatisfactory because it reacts with the rare earth metals to form carbides. Heating was as before at 1200°C for about 20 minutes.

Extraction data in Table II are from single experiments except for the medium level lanthanum column which is the average of two runs.

Uranium-Chromium Alloy

Extractions of the U-Cr eutectic were made at 1050–1150°C for periods of 20 to 40 minutes using the induction heating method and tantalum crucibles as the extraction vessels. Results in Table III are in most cases the average of two separate experiments.

Artificial Mixtures

The "fissium" mixture of fission elements and uranium was treated in a manner similar to that used in the previous experiments. To study the effect of technique on the results, several experiments were run in sealed bombs heated by resistance furnaces and inverted frequently during the heating period. No significant differences were observed in the extractions obtained by this method. Extractions were made using the regular induction heating procedure for 20 to 40 minutes with no consistent differences. Consequently all runs with a given metal are averaged in Table IV. The number of replicates was varied from two to five in the determination of distribution coefficients. The decontamination factors are the averages of two runs.

The attempt was made to find out whether molybdenum could be removed from uranium with magnesium and with the magnesium alloys of tin, zinc and aluminum. In all cases the distribution coefficient was less than 0.2.

Table I. Extraction of Uranium with Silver

Fission product	Decontamination factor fission product content		Distribution coefficient fission product content	
	Medium	High	Medium	High
Cs	29	1000		~10
Sr	14	420		400
La	9		6.3	
Ce	11	55	18	270
Zr	3.0		1.4	
Te	2.6		2.1	
Ru	~1	1.04	0.02	0.03
Pu	3.7	5.1	4.6	7.0

Table II. Extraction of Uranium with Rare Earth Metals

Fission product	Decontamination factor fission product level		Distribution coefficient fission product level	
	Medium	High	Medium	High
		Cerium		
Cs	85	2420	0.16	0.43
Sr	28	260	0.39	0.85
Ce	6.9	9.8	11	23
Ru		1.17	0.18	0.71
Pu	1.50	1.58	0.95	1.02
		Lanthanum		
Cs	56	280	0.26	0.20
Sr	37	17	4.4	0.09
Ce	15.7	16.4	44	41
Ru	1.15	1.19	0.42	0.28
Pu	1.28	1.22	0.65	0.56

Mutual Solubilities

It is important to know the amount of uranium which passes into the extractant phase and, conversely, the amount of extractant which goes into the uranium phase. These mutual solubilities have been determined for most of these systems and a considerable temperature dependence has been found. Results given here are those observed at temperatures within 100 degrees of the melting point.

The solubility of silver in uranium at 1135°C is 0.03% and in the uranium-chromium eutectic at 960°C, 0.02%. Uranium is soluble in silver at 1135°C to the extent of about 4%. When the eutectic was equilibrated with silver at 960°C, the silver was found to contain 2.8% uranium and 0.03% chromium.

In the cerium-uranium system at 1150°C the solubility of cerium in uranium was found to be 1.2% while that of uranium in cerium was 3.6%. The uranium-chromium eutectic at 970°C dissolved 1.5% cerium and the cerium contained about 2.5% uranium and 0.4% chromium. As far as is known lanthanum resembles cerium in its behavior towards uranium.

DISCUSSION

A number of generalizations can be drawn from the observations of these experiments. The fission

Table III. Extraction of U-Cr Alloy

Fission product	Decontamination factor using extractant				Distribution coefficient of extractant			
	Ag	Ag*	Ce	La	Ag	Ag*	Ce	La
Cs	3.8	14.6	15	3.0	2.3	1.08	1	1.7
Sr	9.4	10.1	15	5.2	8.8	9.5	5	1.1
Ba	9.7		50	5.2	7.9		6	1.0
Y	7.1	8.1	34	3.5	8.1	9.2	63	4.6
La	8.6		210	4.9	9.7		475	6.5
Ce	12	8.4	43	3.0	18	12	94	4.5
Zr	7.8	10.6	37	1.7	1.5	2.2	6.7	0.26
Nb			1.2	1.2			0.2	0.01
Mo	1.25		2.5		0.06		0.03	
Ru	1.2		1.6	1.4	0.04		1.2	0.23
Te	1.5		75	5.3	3.2		98	2.0
Pu	13.5	6.8	1.4	1.13	21	8.3	0.64	0.52

* Higher content of fission products and plutonium, see text.

products can be divided into a number of groups with similar behavior within the group. The more volatile ones such as cesium, strontium and barium are removed effectively by volatilization and the extent of this removal increases markedly as the amount of the fission product present is increased. The decontamination factors observed for these elements give a good indication of the removal which might be expected in such a process, i.e., up to 99.9+% removal in a single heating operation. The distribution coefficients observed for these elements are not very meaningful and represent only a transitory state observed as the system approaches equilibrium, since at equilibrium these elements will have a very low concentration in either phase. The increase of removal with concentration indicates that at a concentration corresponding to 2% burn-up these elements would be quantitatively removed and, conversely, that fissium containing these metals would be extremely difficult to prepare. Leaving them out of the fissium mixture seemed justifiable for this reason.

The rare-earth metals, including yttrium, form another group. They are not volatile but are quite readily extracted into silver, with distribution coefficients of the order of 10 and decontamination factors in the same range. As gauged by the per cent recovery figure, crucible and interface reactions may remove an average of 15 to 20 per cent of the rare earths, the higher values being obtained in graphite crucibles. Extraction of rare earth fission products into rare earth extractants was high, as would be expected and the distribution was close to that which would be indicated from the solubility of rare earth metals in molten uranium. Particular values which were low were probably the result of a slow approach to equilibrium.

Table IV. Extraction of Fissium

	Decontamination factors		Distribution coefficients	
	Ag	Ce	Ag	Ce
Zr	2.7	2.5	0.6 ± 0.3	0.8 ± 0.2
Mo	1	1	0.02 ± 0.015	0.04 ± 0.01
Ru	1	1.9	0.02 ± 0.015	1.0 ± 0.2
Nd	9	20	3.7 ± 2	30 ± 20

Zirconium and tellurium apparently behave similarly in the extractions, although due to its low fission yield less attention was paid to tellurium. A single extraction with silver or cerium gives removal of better than 60 per cent of the zirconium. The recovery was sometimes low which may have been the result of reactions with the crucible. Indications were found for the diffusion of zirconium activity into tantalum crucibles.

The elements most difficult to remove from uranium by liquid-metal extraction are ruthenium and molybdenum, two of the most abundant in yield. No extraction conditions were found which would remove more than 10 per cent of the molybdenum and in general its extraction coefficients were in the range of 0.01 to 0.1. Ruthenium can be extracted with cerium with a distribution coefficient of near unity, with lanthanum the value is about 0.3 and with silver 0.02.

The fission yield of niobium is not high enough to be of much concern, but the few experiments which were run indicated that it might also be difficult to remove.

Of most vital concern to a reactor scheme is the behavior of plutonium in the processing cycle. It is apparent from the results that silver could be used in an extraction step designed to remove plutonium. The distribution coefficient is about 6 making the transfer of plutonium to silver a logical step in the regeneration of a uranium fuel. Experiments at higher plutonium level will be necessary before this process can be stepped up to the pilot plant stage since the extraction coefficient seems to depend on the concentration of the plutonium.

The removal of plutonium by rare earth extractants is marginal, not enough to be considered effective and too much to call it insignificant. Further research in this direction may uncover another extractant of more definite properties.

The lack of reproducibility which is apparent in some of the results is possibly explainable by the reason of the very low concentration of the materials being studied in these systems. In the fissium samples these concentrations were in the range of 0.05 to 0.3 per cent which is about a hundred times their value in

the irradiated uranium. Minute traces of impurities such as oxide, carbide or fluoride in the original uranium metal might under these conditions markedly change the behavior of particular elements. The erratic nature of some of the results at the lower fission product concentrations was one reason for going to the higher levels and fissium. Conversely, it is felt that the behavior of the elements in the fissium extractions may be more representative of the actual extraction characteristics of these elements.

CONCLUSIONS

It has been shown on the laboratory scale that uranium metal in which fission has been occurring for some time in a nuclear reactor can be reprocessed for continued use by simple metallurgical methods. Melting the solid fuel will remove the deformations which result from radiation damage and restore to the metal its original metallic properties. If this melting is done in vacuum, volatile fission products including xenon, the halogens, the alkali and alkaline earth metals will distill out. Using an inert atmosphere instead of vacuum would allow less removal by this method although some of these elements would be released even in this case.

Contacting the molten metal with silver will extract most of the plutonium, the rare earths, and zirconium fission products but will leave the ruthenium and molybdenum largely unaffected. A series of extractions with fresh silver as in a repeated batch or continuous extract or would increase the plutonium removal and should make it essentially quantitative.

Thus a vacuum melting process involving contacting with silver would remove the plutonium and all of the important fission products except ruthenium and molybdenum. The resulting uranium would contain only 200 to 300 parts per million of silver. In the molten state the proper quantity of fissionable material could be added to restore the nuclear characteristics of the original fuel. Refabrication of the fuel elements by some remote casting technique would then permit the reuse of the fuel immediately. Thus the fuel would need to be out of the reactor only a short time and the inventory of fissionable material would need to be little more than that which is actually in the reactor.

The extractant phase will, of course, require additional processing to recover the plutonium and the uranium which it dissolves, concentrate the fission products and, preferably, to purify the silver for reuse. While these steps could be accomplished by aqueous chemistry, the advantages of pyrometallurgical processing will not be fully exploited until non-aqueous methods are found for these steps. Research is pointed toward the development of non-aqueous steps which could be used to purify the silver and recover the plutonium and uranium. It is expected that such methods can be developed.

An additional advantage of this type of processing would be that the radioactive fission product wastes would be in a much smaller volume than is the case in aqueous processing, and thus easier to dispose of or to use for industrial radiation sources.

It is reasonable to expect that the pioneering work done now in this little known area of chemistry and chemical engineering will be the basis in a few years of a processing industry for power reactors. The production of radiation sources for radiography, food sterilization, plastic polymerization aids, medical radiology, and many as yet undeveloped uses would be an auxiliary part of this industry.

REFERENCES

1. *The Plutonium Project,* J. Am. Chem. Soc. 68: 7411 (1946).
2. Coryell, C. D. and Sugarman, N., eds, *Radiochemical Studies: The Fission Products,* Part VI, Nat. Nuc. En. Ser., Div. IV, Vol. 9, Book 3, McGraw-Hill Co., Inc., New York (1951).

High Temperature Fuel Processing Methods

By E. E. Motta,* USA

The need for lower cost fuel processing and refabrication processes to serve the new nuclear power industry has stimulated an interest in high-temperature processes. These methods keep reactor-irradiated uranium metal in the metallic form during fission product removal and re-enrichment. In this manner the expense of dissolving and diluting the bulk uranium metal and then later reducing it again to the metallic form is eliminated. A typical fuel cycle would follow four major steps: (1) decladding of fuel; (2) removal of fission elements and plutonium by high temperature processes and re-enrichment by addition of plutonium or U^{235} metal, if desired; (3) recasting into billet form; and (4) recladding the fuel for re-entry into the reactor.

Such a process should eventually be made remote, continuous and automatic. Since the basic nature of these operations is very similar to those now found in metal producing and metal working mills, there seems to be a strong chance that these processes will prove practical and lead to substantial economies.

BASIC CHEMISTRY OF HIGH-TEMPERATURE SEPARATIONS PROCESSES

The basic chemistry of the pyroprocessing methods under study at North American Aviation, Inc. was developed in small-scale experiments. To date, four methods of separating plutonium and fission products from uranium have shown enough promise to be considered for test in larger scale experiments. These methods are:

1. Direct distillation—Pu and volatile fission products are distilled from uranium at 1600° to 1700°C;
2. Fused salt extraction—Pu and some fission products are extracted from molten uranium by fused UF_4 or mixtures of fluorides;
3. Magnesium extraction—molten magnesium, immiscible with molten uranium extracts Pu and fission products by direct solvent action;
4. Solid scavenging—certain refractory oxides, when used as containers for molten uranium, remove some fission products.

The distribution of plutonium and fission products in these experiments has been investigated first with tracer-level activities and later with actual irradiated reactor fuels. The results obtained with the two activity levels were in good agreement, indicating that extrapolations to higher fuel burnup levels are warranted.

Direct Distillation of Plutonium and Fission Products from Molten Uranium

The vapor pressure of plutonium is several hundred times as great as that of uranium at a given temperature. In spite of the low concentration of plutonium in natural uranium fuels, a simple calculation showed that an effective separation from uranium could be obtained by distillation.[1]

The evaporation was tested with a few grams of uranium in a small CeS crucible in vacuum from 1500°C to 1680°C. The results obtained with tracer level plutonium (0.03 μg Pu/gm U) are shown in Fig. 1.[2] It may be seen that at 1600°C and 1680°C the measured fraction evaporated was essentially that expected from the calculations based on Raoult's law. At 1495°C the experimental data fell below the theoretical for some unknown reason.

A series of experiments was made at higher plutonium levels. For this work small pieces of reactor fuel containing about 0.01 per cent plutonium were used.[3] These results are reported in Table I. The per cent of plutonium evaporated was found to be in good agreement with the calculated values.

The evaporation of fission products observed was substantially that expected from their vapor pressures. Table II gives the vapor pressures of some of the elements of interest and Table III shows the results obtained. The volatile fission products were effectively removed from the uranium, while nonvolatile ruthenium was not. These results indicate that the elements with vapor pressures higher than plutonium will be removed by evaporation, while those with lower vapor pressures will not be removed.

Fused Salt Extraction

The free energy of formation of PuF_3 is somewhat more negative than that of UF_4 at the melting point of uranium. Therefore, plutonium is expected to concentrate in a fused UF_4 slag in contact with molten irradiated uranium. The degree of extraction of plutonium from pieces of uranium reactor fuel by UF_4 and mixtures of UF_4 with other salts was studied in a series of experiments.[4] One to two grams of salt were melted with 5 to 15 grams of uranium in graph-

* North American Aviation, Inc., Nuclear Engineering and Manufacturing, Los Angeles, California. Including work by D. Bareis, R. Barney, A. Buyers, D. Cubicciotti, C. Dowler, J. Foltz, W. Gardner, B. Johnson, F. Keneshea, R. Lineberry, F. Rosen, A. Saul, S. Yosim, C. Young, North American Aviation, Inc., Nuclear Engineering and Manufacturing, Los Angeles, California.

Table I. Plutonium Evaporation from Pieces of Reactor Fuel

Corrected temp., °C	Surface area of evap., cm²	Wt. of samples, gm	Time of evap., sec	at/w*	% Pu evaporated	
					Measured	Calculated
1680	1.4	3.60	8400	3800	98.6	99.2
1680	2.3	3.30	2460	1700	90.9	89
1600	1.7	3.79	14480	6500	96.6	97
1600	2.1	5.63	9900	3700	90	86
1600	1.1	2.74	1800	740	23	33

*at/w = (area)(time)/(weight).

Table II. Vapor Pressures of Some Elements at 1680°C

Element	Vapor pressure, atm
Cs	90
Te	60
Sr	4
Ba	1
Ce	3×10^{-3}
La	6×10^{-4}
Pr	3×10^{-4}
Pu	1×10^{-4}
Y	2×10^{-5}
U	8×10^{-7}
Zr	2×10^{-7}
Ru	10^{-10}
Nb	10^{-11}

Table III. Fission Product Evaporation from Pieces of Reactor Fuel

Temperature, °C	at/w	% Activity found in residue						
		Pu	Ce	R. E.*	Sr	Cs	Te	Ru
1680	3800	1.4	2	1	1	0.2	5	100
1680	1700	9.1	3	2	2	0.2	2	100
1600	6500	3.4	1	1	2	0.1	3	75
1600	3700	10	7	2	2	0.3	3	90
1600	740	77	7	4	4	0.2	7	95

* R. E. = rare earth elements.

Table IV. Pu Extraction by Fused Fluorides

Mole fraction UF_4	Mole fraction other salts	% Pu in salt	Equilibrium constant, K_e
1.0	–	92	4.4
1.0	–	95	5.2
1.0	–	96	5.3
1.0	–	96	4.4
1.0	–	85	4.0
0.46	0.14 CaF_2 0.40 LiF	95	5.5
0.17	0.22 CaF_2 0.61 LiF	99	6.3
0.02	0.98 LiF	94	6.5
0.17*	0.22 CaF_2	99	–

* Three cycle run (i.e., three fresh batches of salt contacted individually with metal).

ite crucibles at 1300°C. The mixture was cooled rapidly, the salt phase separated from the metal and both phases analyzed for plutonium fission products.

The plutonium data for these experiments are given in Table IV. The plutonium extraction was good; more than 90% was removed in most cases. Differences between the experiments result from the variation in the amounts of metal and salt. The agreement among the data is shown by the consistency of the equilibrium constants given in the last column. These equilibrium constants are calculated for the reaction:

$$\tfrac{1}{3}\ Pu + \tfrac{1}{4}\ UF_4 = \tfrac{1}{3}\ PuF_3 + \tfrac{1}{4}\ U$$

The extraction of fission products by the fused fluorides was essentially that expected from the free energies of formation of their fluorides. In Table V is a compilation of free energies of formation, and in Table VI are some representative data for fission product extraction by fused fluorides. It may be seen that the fission products reported were all extracted efficiently as expected from the free energies of formation of their fluorides. Ruthenium, which was not found to be extracted by the salt, has a small free energy of formation of fluorides. Thus, the results observed in the fused fluoride extractions were generally those expected from the free energy data.

Magnesium Extraction

Since magnesium is immiscible with molten uranium,[5] it seemed a possible reagent for the extraction of plutonium and fission products from uranium. No reliable method of predicting the mutual solubilities of metals exists; therefore, the effectiveness of extraction by magnesium was measured experimentally. The amount of extraction was determined by heating a few grams of magnesium with a few grams of

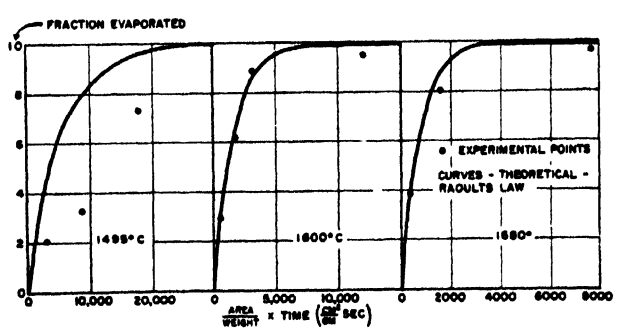

Figure 1. The evaporation of tracer plutonium from uranium

Table V. Standard Free Energies of Formation of Fluorides at 1500°K

Fluoride	$-\Delta F°$ 1500°K, kcal per equiv.
SrF_2	116
CaF_2	115
BaF_2	115
LaF_3	113
LiF	112
CeF_3	111
NbF_5	109
MgF_2	100
PuF_3	96
ZrF_4	90
CsF	87
UF_4	85
NbF_5	74
TeF_6	32

uranium fuel at 1150°C.[6] The mixture was contained in a tantalum crucible in a steel bomb because of the high vapor pressure of magnesium.

The degree of plutonium extraction depended on the ratios of amounts of magnesium and uranium as expected. The data are given in Table VII, the last column of which gives the distribution constant defined by:

$$K = \frac{\text{conc. of Pu in Mg per mole of Mg}}{\text{conc. of Pu in U per mole of U}}$$

It may be seen that magnesium does extract plutonium well, since as much as 94% was removed in one experiment. The distribution constant, K, was essentially constant at about 0.23 over a wide range of plutonium concentration and ratio of amounts of magnesium to uranium.

The extraction of fission products by magnesium is shown in Table VIII. Of the fission products

Table VI. Fission Product Extraction by Fused Fluorides

Salt mixture (mole fractions)	% Activity removed from uranium			
	Ce	R. E.	Sr	Cs
UF_4 = 0.17 CaF_2 = 0.22 LiF = 0.61	85	88	91	90
UF_4 = 0.46 CaF_2 = 0.14 LiF = 0.40	96	99	99	99
UF_4 = 0.02 CaF_2 = 0.98	99	99	99	99

Table VII. Plutonium Extraction by Magnesium

Pu conc, ppm	Wt ratio U/Mg	Equilibrium Pu distribution		K
		% in U	% in Mg	
0.03	0.50	18	–	0.23
0.3	0.96	36	60	0.21
8.1	5.97	71	23	0.25
23	0.88	29	60	0.22
50	0.92	25	57	0.28
55	0.92	25	71	0.19
74	0.83	28	67	0.22
97	1.0	37	67	0.19
97	0.11	3.4	94	0.30
97	3.42	64	19	0.20

studied, only ruthenium is not well extracted; however, when sufficient magnesium is used, even the ruthenium is extracted to some degree. In the case in which the uranium to magnesium ratio was 0.11, almost all of the rare earths and cesium and strontium were removed; most of the tellurium and some of the ruthenium, thus showing magnesium capable of purifying the uranium quite effectively.

Magnesium, because of its volatility, lends itself nicely to a recycling scheme of the Soxhlet type. By this method, plutonium and fission products can be

Table VIII. Distribution of Fission Products between U and Mg at 1150°C

Wt ratio, U/Mg		0.11	3.42	0.83	0.88	0.96	0.50
Conc Pu, ppm		97	97	74	23	0.3	0.03
Ce	% in U	1	11	5	6	3	2
	% in Mg	99	80	92	80	102	93
	K	1.1	2.8	1.6	1.4	3.2	2.5
R. E.	% in U	0.4	16	8	14	30	10
	% in Mg	92	71	95	83	72	76
	K	2.8	1.8	0.97	0.55	0.23	0.46
Cs	% in U	1	9	6	11	74	73
	% in Mg	90	54	90	65	25	19
	K	1.1	3.6	1.3	0.73	0.034	0.019
Sr	% in U	1	16	10	15	67	64
	% in Mg	92	70	91	73	30	36
	K	1.1	1.8	0.76	0.51	0.048	0.029
Te	% in U	19	10	4	8	3	4
	% in Mg	92	34	47	91	94	82
	K	0.05	3.1	2.0	1.0	3.2	1.2
Ru	% in U	49	99	95	94	94	83
	% in Mg	46	1	5	2	1	3
	K	0.011	0.004	0.005	0.006	0.006	0.0011

Table IX. Standard Free Energies of Formation of Some Oxides at 1500°K

Oxide	$-\Delta F°$ 1500°, kcal per gm atom of oxygen
ThO_2	115
CaO	114
BeO	112
La_2O_3	112
Ce_2O_3	107
Nd_2O_3	107
MgO	103
SrO	102
Al_2O_3	102
UO_2	99
ZrO_2	97
PuO_2	96
NbO	66
Cs_2O	4
RuO_2	−3

effectively extracted from molten uranium by distilling and condensing magnesium into a crucible containing the molten uranium and allowing the contaminated magnesium to overflow into a pot where it is redistilled. Small scale experiments of that type are in progress.

Oxide Scavenging of Molten Uranium

When irradiated uranium is melted in an oxide crucible, there is some reaction between the oxide and the fission products in the uranium. The fission products whose oxides are more stable than uranium oxide concentrate in the oxide phase. In Table IX are given the free energies of formation of oxides of interest. The rare earths in particular would be expected to be removed from uranium by an oxide treatment, while plutonium should remain in the metal almost entirely.

The data observed with a zirconia crucible[7] are shown in Table X. In general, the results were as expected. The fission products whose oxides are stable (cerium, rare earths, strontium) and the volatile fission products (cesium, tellurium) were effectively removed. The others were not. Some of the plutonium was found in the oxide phase in these zirconia experiments; however, where urania or thoria crucibles were used, very little plutonium was transferred to the oxide phase.

The data observed with a urania crucible at 1450°C are shown in Table XI. The results are essentially the same as those observed with a zirconia crucible except that 5% or less of the plutonium moved into the oxide phase.

HIGH TEMPERATURE SEPARATIONS PROCESSES—HOT CELL WORK ON THE KILOGRAM SCALE

When it appeared that high temperature partial decontamination methods were technically feasible on the 5 to 15 gram laboratory scale, it was decided to test these methods on the kilogram scale in a hot cell. The activity levels and plutonium content of the fuel required the design of special apparatus to be operated remotely within the NAA hot cells. The primary purpose of the tests was not to demonstrate a complete fuel cycle. The purpose was rather to confirm at the kilogram scale the results obtained with 5 to 15 gram samples of uranium fuel. Moreover it was thought that a closer insight into the engineering problems associated with these methods could be obtained by working with kilogram quantities of fuel.

Table XI. Distribution of Fission Elements and Pu between a Uranium Oxide Crucible and Molten Uranium at 1450°C

	% activity			
	Run 1		Run 2	
Element	In metal	In oxide	In metal	In oxide
Pu	96	5	95	5
Sr	<1	82	<1	84
Ce	<1	106	<1	93
R. E.	<1	96	<1	93
Te	13	14	5	4
Cs	<1	2	<1	3
Ru	100	trace	100	trace

Distillation of Plutonium and Fission Elements from Molten Uranium

Because of the previous laboratory scale results with the plutonium distillation separation method, it was one of the first methods chosen for scale-up in the hot cell experiments. Tests were made with unirradiated and tracer irradiated uranium to develop the high temperature vacuum furnace components. Then ex-

Table X. Distribution of Fission Products and Pu between a Zirconia Crucible and Pieces of Uranium Reactor Fuel at 1300°C

	% activity found							
	Run 1		Run 2		Run 3		Run 4	
Element	In metal	In oxide	In metal	In oxide	In metal	In oxide	In metal	In oxide
Pu	70	20	84	17	75	25	71	24
Sr	1	53	<1	48	1	42	1	44
Ce	1	72	<1	53	<1	83	<1	87
R. E.	1	67	<1	55	<1	45	1	45
Te	34	7	<1	6	26	6	16	2
Cs	<1	6	<1	4	<1	4	<1	8
Ru	100	0	100	0	100	0	100	0

periments with actual reactor fuels were conducted.

Uranium dioxide was found to be a fair container material for molten uranium at 2000°K. A useful technique consisted of painting less expensive magnesium oxide crucibles with a UO_2 slurry. A typical assembly of uranium ingot, crucible, tantalum susceptor, tantalum radiation shields and silica container is shown in Fig. 2. The lid assembly consisting of tantalum condenser-radiation shields and silica cover is shown in Fig. 3. The arrangement of the furnace components with the crucible assembly partly withdrawn is presented in Fig. 4.

The furnace components along with the necessary sampling devices had to be enclosed in a plastic container to confine the activities. Figure 5 shows the scale-up equipment within the hot cell, while Fig. 6 is a view of the working face of the hot cell. A report has been written describing in detail the scale-up equipment developed to perform the high temperature separations.[8]

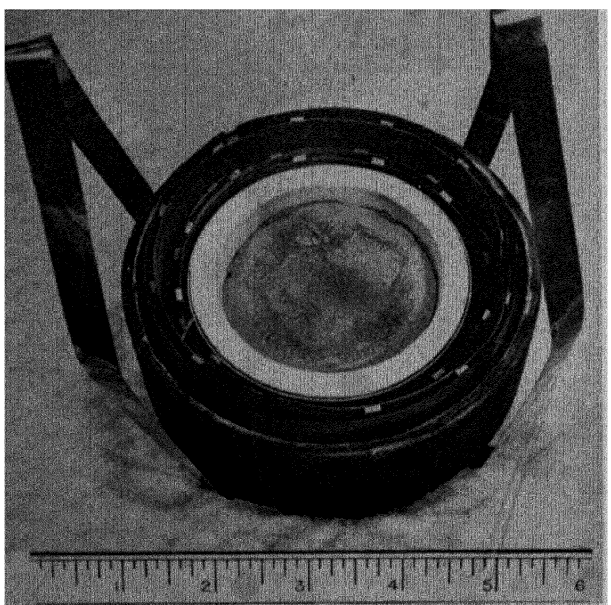

Figure 2. Crucible assembly for the 1-kilogram scale furnace

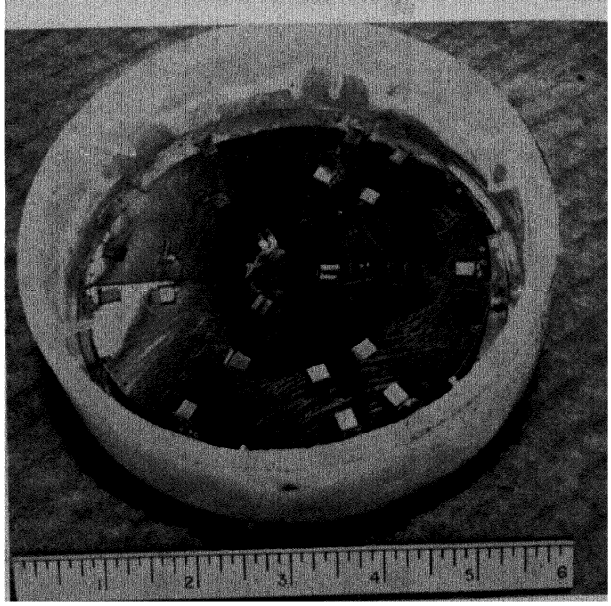

Figure 3. Crucible lid assembly

Results of two experiments on plutonium distillation from kilogram quantities of spent reactor fuel are presented in Table XII. Condensation and recovery of the vaporized plutonium was only 60 to 70 per cent efficient. Complete plutonium recovery could be obtained with an improved condenser design.

Uranium Oxide Scavenging of Molten Uranium—Kilogram Scale

For certain power reactor fuel cycles, removal of plutonium from used fuel is not desired. Decontamination by oxide scavenging lends itself well to such a fuel cycle, since plutonium is not appreciably removed by the oxide phase.

The oxide scavenging experiments were performed at the kilogram level in the same apparatus used for plutonium distillation. Results of decontamination studies on kilogram quantities of irradiated fuel by oxide slagging at 1300°C are presented in Table XIII. Removal of some fission products resulted from volatilization since all experiments were performed in vacuum. An average of 1 per cent of plutonium was unaccounted for in these experiments.

Fused Salt Extraction—Kilogram Scale

Two salt extractions of irradiated uranium were completed. They demonstrated the extraction of plutonium with molten fluoride salts. Preliminary melts were made with unirradiated natural uranium for the purpose of developing sampling and handling techniques.

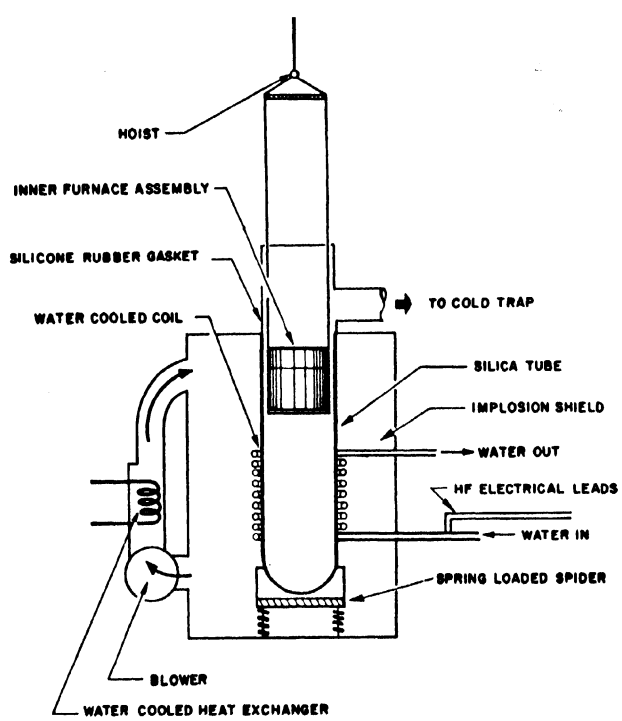

Figure 4. Diagram of furnace

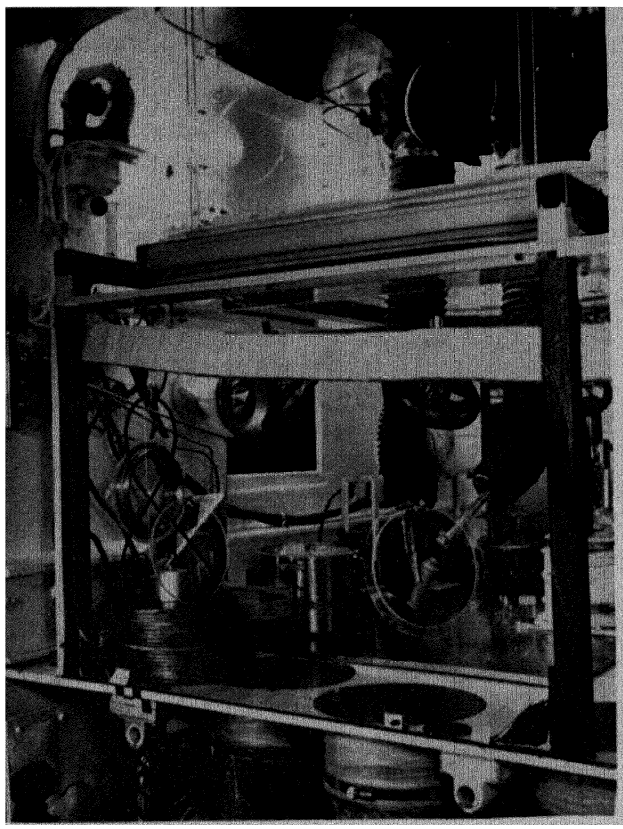

Figure 5. One-kilogram scale experiment in hot cell

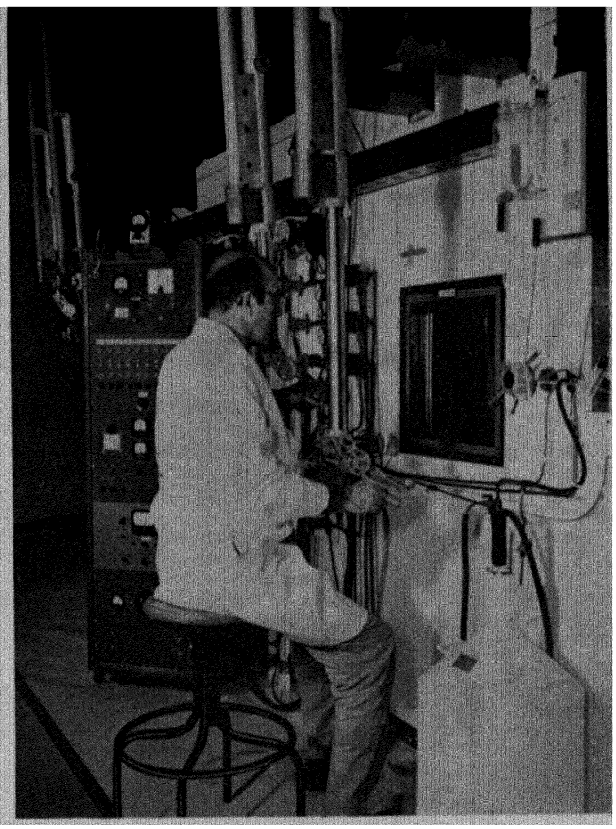

Figure 6. Working face of NAA hot cell

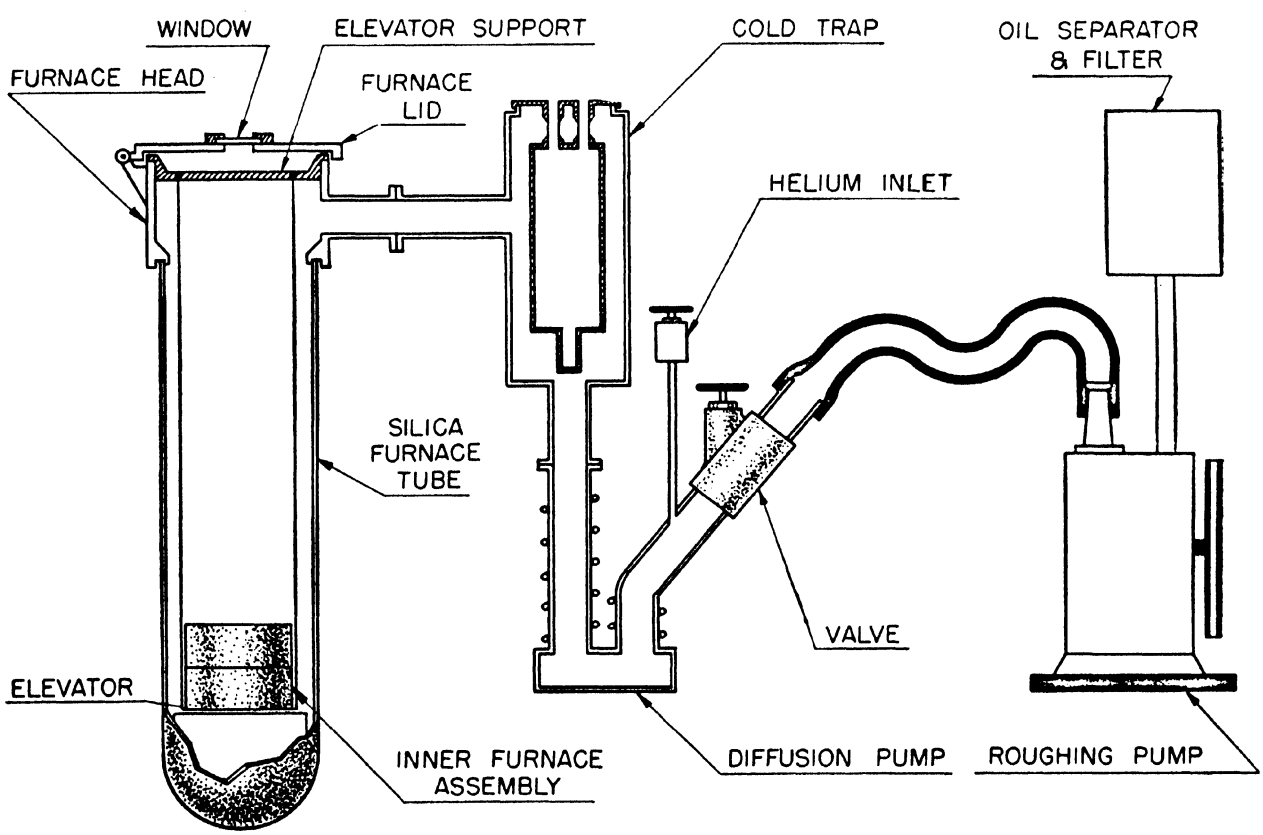

Figure 7. Vacuum system diagram

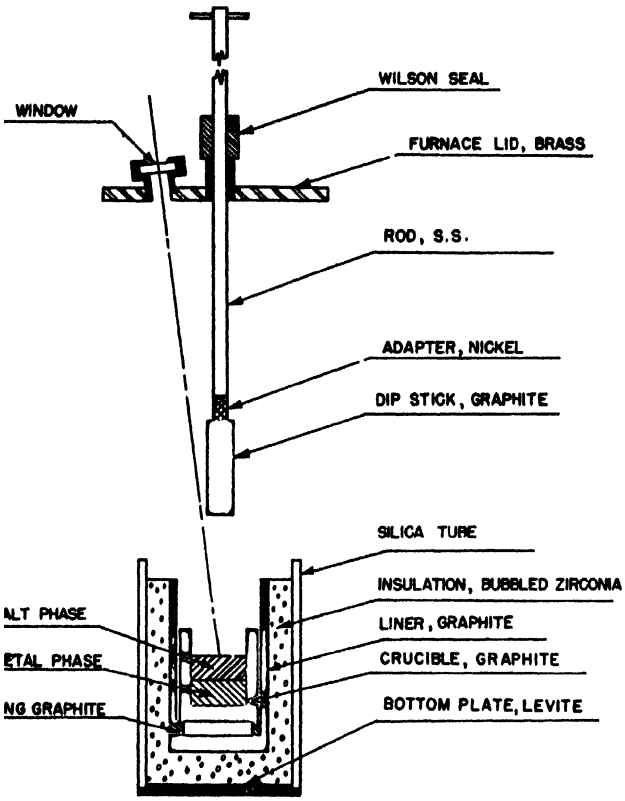

Figure 8. Inner furnace assembly and furnace lid detail for fused salt extraction experiment

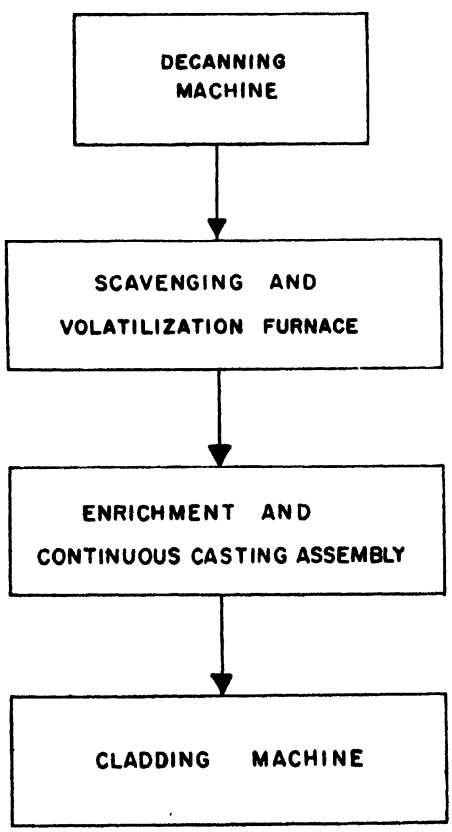

Figure 9. Automatic sequence for high-temperature pilot plant

Table XIV lists the conditions and data obtained from the hot cell tests with irradiated uranium. The vacuum furnace shown diagramatically in Fig. 7 was used with the lid and inner assembly shown in Fig. 8. It should be noted that increasing the contact time increased the degree of plutonium extraction into the salt phase.

ILLUSTRATIVE PROCESS FLOW SHEETS

It is reasonably clear that in order to achieve minimum costs for fuel processing and refabrication a series of automatic industrial-type machines and furnaces will need to be developed which declad, partially purify, re-enrich, and re-clad the uranium metal fuels. Although these assemblies seem intricate, various elements of such machines already exist and more complex processing machines have already been designed, built and operated. A grouping of such machines and automatic furnaces would resemble a production line and should be associated with fuel processing rates of at least 1 ton per day. Continuous casting and cutting of metals should be applicable. Figure 9 summarizes schematically the sequence of events which might be carried out in a pilot plant.

A number of illustrative flowsheets are summarized in Fig. 10. After oxide scavenging four methods are available, depending on the nature of the fuel cycle of the particular reactor. For two-region uranium breeder reactors, a process such as

Table XII. Removal of Plutonium from Irradiated Uranium by Direct Distillation

Wt U, gm	*Area/wt, cm²/gm U*	*Temp, °C*	*Observed % Pu removed*
831	0.06	1710–1730	74
890	0.06	1730–1775	76

Table XIII. Removal of Fission Products during Uranium Oxide Scavenging of Irradiated Uranium at 1300°C

Wt U, gm	*% Fission products removed*				
	Ce	*R. E.*	*Sr*	*Cs*	*Ru*
893	88	78	87	91	3
989	99.6	99	82	90	8
936	98	98	73	97	7
948	96	97	70	66	8

Table XIV. Fused Salt Extraction

General conditions:
U = 850 gm — Fluoride salt = 210 gm
Pu = 8.4 mg/gm of U (initial) — UF_4 = 25 mole % of salt
Pressure = ½ atmosphere of helium — Temperature = 1225°C (maximum); a rapid heating rate

Hot cell run no.	*Time at 1225° C (min)*	*% Pu in salt*	*% Pu in metal*
7	10	58	41
8	70	90	9

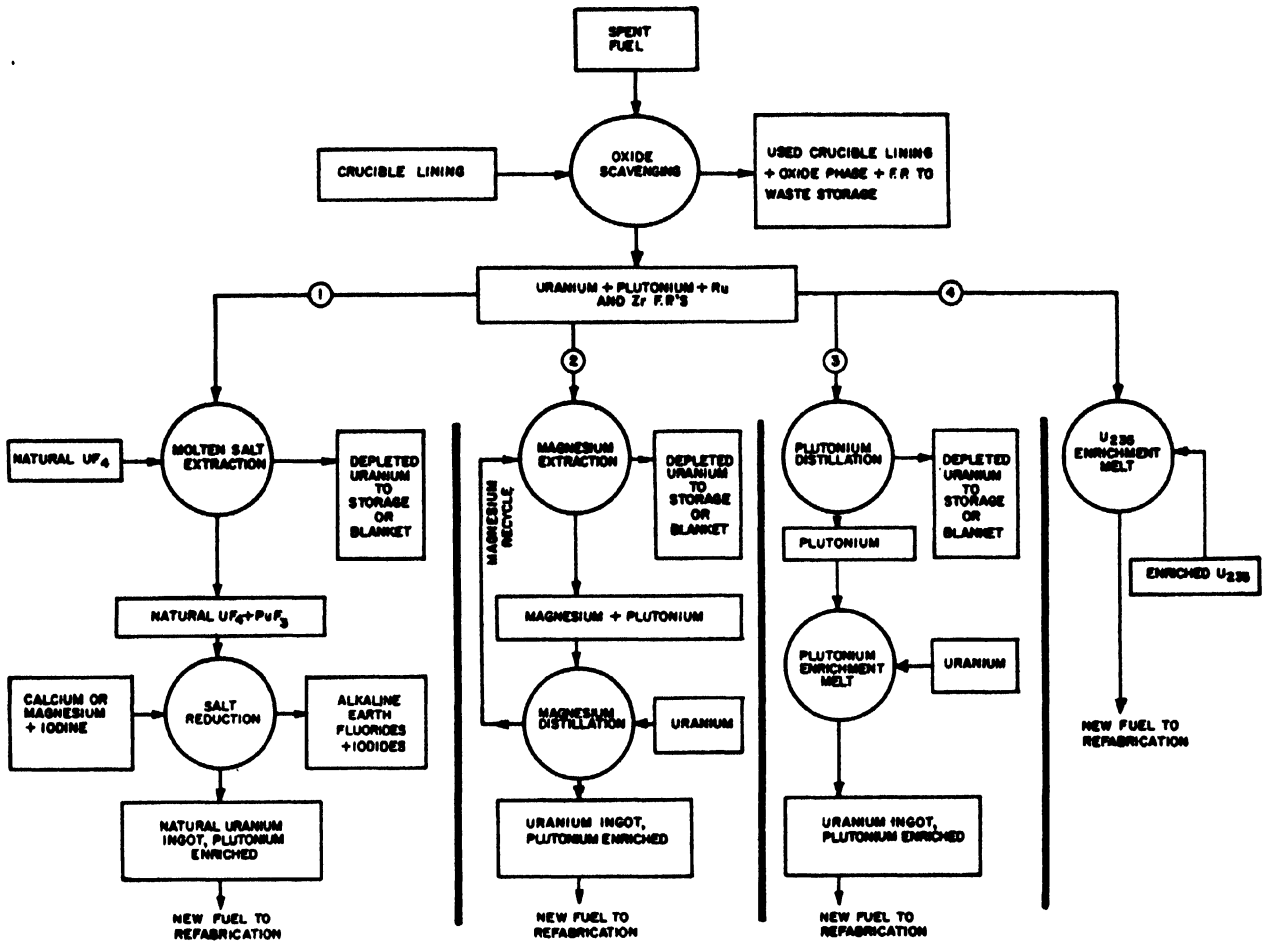

Figure 10. Pyroprocessing flow sheet

1, 2 and 3 would be used. For internal uranium breeders, method 4 would be most applicable.

REFERENCES

1. Rosser, W., "Theoretical Rate of Volatilization of Pu from a Dilute Solution of Pu in U," NAA-SR-218 (24 February 1953).
2. Cubicciotti, D., "The Volatilization of Tracer Pu from Molten U Metal," NAA-SR-242 (22 May 1953).
3. Cubicciotti, D., "The Evaporation of Pu from Small Pieces of U Reactor Fuel," NAA-SR-1057 (15 October 1954).
4. Buyer, A., "The Distribution of Pu and Long-Lived Fission Products Between Molten Irradiated U and Fused Fluorides," NAA-SR-1157 (15 March 1955).
5. Tracy, J., *et al*, "The Magnesium-Uranium Alloy System," ISC-377 (June 1953).
6. Barney, R. and Keneshea, F., "The Distribution of Pu and Fission Products Between Molten Uranium and Magnesium," NAA-SR-1324, to be published.
7. Saul, A. M., "The Removal of Certain Fission Products from Molten Irradiated Uranium by Solid Oxides," NAA-SR-1361, to be published.
8. Foltz, J. R., Gardner, W. J. and Rosen, F. D., "Apparatus and Procedures for High Temperature Processing in the NAA Hot Cells," NAA-SR-1227, to be published.

High-Temperature Processing Systems for Liquid-Metal Fuels and Breeder Blankets

By O. E. Dwyer, R. J. Teitel, R. H. Wiswall, Jr.,* USA

The liquid-metal fuel reactor (LMFR)† being developed for power purposes at the Brookhaven National Laboratory in the United States is a thermal-breeder or converter reactor and uses as a fuel a dilute solution of uranium, magnesium, and zirconium in liquid bismuth. The breeding is done in a blanket surrounding the core of the reactor and the most promising blanket material is a thorium-bismuthide slurry in bismuth. Since the η values at thermal energies for both U^{235} and U^{233} are relatively low—2.08 and 2.31 respectively—it is necessary to maintain low concentrations of fission products in the fuel for good neutron economy, and in order to breed with a "g" value significantly greater than unity. At the low concentrations required, the rate of fuel processing is necessarily high when one thinks in terms of the pounds of fuel which must be handled per day; but for a high-density liquid like U-Bi, where continuous operation can be used, the actual flow rates of fuel through the processing equipment are estimated to be less than one gal/min for reactors having heat rates as high as 1000 Mw. In other words, with a liquid fuel, the economics of the situation are probably such that the concentration of fission products in the fuel should be low. In the LMFR, the fission products can be divided arbitrarily into three groups: (a) those which are appreciably volatile at the operating temperatures of the reactor, (b) those which form chlorides that are more stable than UCl_3, and (c) those which form chlorides less stable than UCl_3. For convenience, the names of these three groups have been abbreviated to FPV, FPS, and FPN respectively. It is proposed to remove the first group by a volatilization process, either one of gas sparging or vacuum desorption; the second by a fused-salt extraction process; and the third by a combination of salt extraction, metal extraction, distillation, and wet chemistry. In a commercial LMFR, the individual concentrations of these three groups would of course be determined by economic considerations, but it is felt that their combined poisoning effect would probably be less than 5%, i.e., the total fission products in the fuel would absorb less than $\frac{1}{20}$ as many neutrons as the uranium. In this paper, for purposes of discussion, a nominal poisoning of 1% will usually be assumed for each of the three groups. As reactor poisons, the first two groups are by far the worst; the first because of Xe^{135} with its 2.6×10^6 barn cross section, and the second because of the rare earths, particularly Sm^{149} with its 47,000 barn cross section. Because of the relative innocuousness of the FPN's as a group, little attention has been given to the task of removing them from the LMFR fuel; and consequently little space will be devoted to them in this paper.

POISONING EFFECTS OF FISSION PRODUCTS

FPV's

Where the fissile material is U^{233}, it is estimated that the FPV's represent about 28% by weight of the total fission products produced. This is based on the assumption that as much iodine and bromine leave the fuel with the FPS's as leave with the FPV's. It is further estimated that, for a uranium concentration of 1000 ppm, a FPV concentration of about 18 ppb‡ in the fuel is equivalent to 1% poisoning. In the case of U^{235}, the FPV's are a slightly smaller fraction of the total fission products, but for 1% poisoning their concentration would be slightly greater. For a typical 500-Mw reactor with a hold-up in the fuel system of 300,000 lb, the average residence time of the FPV's is estimated to be about ½ hr. In arriving at the above values, the thermal cross section for Xe^{135} was taken as 2.6×10^6 barns and those for all other nuclides were assumed to be negligible. Many of the cross section values used in this paper were taken from a Brookhaven Laboratory report soon to be published.[1]

FPS's

To explain the method of determining the poisoning effect of this group of fission products, the following treatment is given.

The fission products extractible by the fused salt are Rb, Sr, Y, Cs, Ba, La, Ce, Pr, Nd, Pm, Sm, and Eu. Table I gives the yields of fission products for

* Brookhaven National Laboratory. Including work by J. S. Bryner and M. Brodsky.

† A general paper on the LMFR entitled "Liquid-Metal Fueled Power Reactor" by F. Miles and C. Williams will be found in P/494, Volume 3, Session 11A, these Proceedings.

‡ "1 ppb" is a weight fraction of 10^{-9}.

Table I. Fission Chains from U^{235} Relative to FPS's

Mass no.	% yield	Fraction in FPS's	Mass no.	% yield	Fraction in FPS's
81	0.18	0.50	142	5.68	1.00
83	0.62	0.15	143	5.35	1.00
85	1.55	0.15	144	4.75	1.00
87	2.80	0.20	145	4.00	1.00
88	3.64	0.20	146	3.15	1.00
89	4.40	1.00	147	2.45	1.00
90	5.13	1.00	148	1.85	1.00
91	5.60	0.95	149	1.28	1.00
92	5.73	0.05	150	0.82	1.00
127	0.21	0.50	151	0.49	1.00
131	3.0	0.35	152	0.26	1.00
133	6.74	0.10	153	0.11	1.00
137	6.15	0.90	154	0.05	1.00
138	6.36	0.90	155	0.03	1.00
139	6.34	1.00	156	0.02	1.00
140	6.23	1.00	157	0.01	1.00
141	6.00	1.00	158	0.002	1.00

the pertinent chains (for U^{235}) and the estimated atom fraction of each chain which is extracted from the FPS group.

From Table I, the average mass number of the FPS's is calculated to be 128.2, and their weight per cent of the total fission products turns out to be 43.0.

There are six nuclides which are particularly bad poisons and these are Nd^{143}, Nd^{145}, Sm^{149}, Sm^{151}, Eu^{155}, and Gd^{157}. For this reason, these six nuclides must be given special consideration. As a result, we now have three subgroups of FPS's—Group A, consisting of the chains listed in Table I minus chains 143, 145, 149, 151, 155 and 157; Group B consisting of chains 143, 145, 149, 151, and 157 minus the six high-poison nuclides listed above; and Group C consisting of the six nuclides. Group A is shown in Table II.

Table II. FPS's in Group A for U^{235}

Mass no.	(% yield) X (fraction in FPS's)	Assumed cross section, barns
81	0.09	2.6
83	0.09	10.
85	0.23	1.
87	0.56	0.14
88	0.73	0.005
89	4.40	110.
90	5.13	1.
91	5.32	1.52
92	0.29	0.2
127	0.10	6.7
131	1.05	600.
133	0.67	29.
137	5.53	2.
138	5.72	0.6
139	6.34	8.4
140	6.23	1.
141	6.00	10.
142	5.68	1.8
144	4.75	4.8
146	3.15	9.8
147	2.45	60.
148	1.85	3.3
150	0.82	2.9
152	0.26	150.
153	0.11	420.
154	0.05	5.5
156	0.02	750.
158	0.002	4.

From the information given in Table II, the average cross section for Group A is calculated to be 23.7 barns. The poisoning effect of this group is relatively small and assumed to be the same for all conditions of reactor operation. The poisoning effects of the other two groups vary appreciably with operating conditions, and the methods used in estimating them will now be explained. The following treatment is based on the continuous removal of the FPS's, the existence of steady-state conditions, and the assumption that all the FPS's transfer from the metal to the salt phase to the same degree. The concentration of a given nuclide in the fuel stream depends upon a number of processes which govern its rate of formation and its rate of removal or disappearance from the system. The following rates are involved:

1. Rate of formation from fission

$$\frac{dN}{dt} = N^{235} V_c \sigma_{5f} \phi f \qquad (1)$$

2. Rate of fomation from neutron capture

$$\frac{dN}{dt} = N_t V_c \sigma_t \phi \qquad (2)$$

3. Rate of formation resulting from decay of parent

$$\frac{dN}{dt} = \lambda N_p V_t \qquad (3)$$

4. Rate of disappearance by decay

$$\frac{dN}{dt} = \lambda N V_t \qquad (4)$$

5. Rate of disappearance by neutron capture

$$\frac{dN}{dt} = NV_c \sigma \phi \qquad (5)$$

6. Rate of disappearance by extraction in fused salt

$$\frac{dN}{dt} = V_s k N \qquad (6)$$

Of course, not all of the above processes apply in a particular case. In fact, for practical purposes, process No. 2 can be neglected entirely. It so happens that none of the really serious poisons have significant rates of formation as a result of neutron capture, owing to the low cross sections of the neutron-capturing species. From the above equations, the steady-state concentration of a chain-initiating nuclide or a nuclide whose precursors have negligibly short half-lives is given by the equation

$$N = \frac{N^{235} V_c \sigma_{5f} \phi f}{\lambda V_t + V_c \sigma \phi + V_s k} \qquad (7)$$

For a nuclide inside the chain ends, the equation is

$$N = \frac{\lambda_p N_p V_t}{\lambda V_t + V_c \sigma \phi + V_s k} \qquad (8)$$

and for a chain-terminating nuclide, the equation is

$$N = \frac{\lambda_p N_p V_t}{V_c \sigma \phi + V_s k} \qquad (8a)$$

Using the above equation, the concentrations of each of the nuclides in the six high-cross-section, rare-earth chains can be determined; although it is necessary to assume certain cross sections for the lower cross-section species. These, however, have relatively slight poisoning effects. As examples, Tables III and IV show the calculated results for groups B and C, respectively, for the following operating conditions: 1000 ppm U^{235} in fuel, 150 tons fuel in system, 500 Mw reactor, 75 ft^3 fuel in core, and 20-day residence time for FPS's in fuel.

Table III. FPS's in Group B for U^{235}

Nuclides	*Calculated fraction of total chain*	*Chain yield, %*	*Assumed cross section*
143 chain minus Nd	0.857	5.35	50
145 chain minus Nd	0.072	4.00	10
149 chain minus Sm	0.609	1.28	50
151 chain minus Sm	0.000	0.49	—
155 chain minus Eu	0.000	0.03	—
157 chain minus Gd	0.649	0.01	1000

Table IV. FPS's in Group C for U^{235}

Nuclide	*N atoms/cm³*	*Barns*
Nd^{143}	3.72×10^{15}	290
Nd^{145}	1.81×10^{16}	52
Sm^{149}	1.51×10^{15}	47,000
Sm^{151}	1.92×10^{15}	7200
Eu^{155}	1.67×10^{14}	13,000
Gd^{157}	4.10×10^{12}	160,000

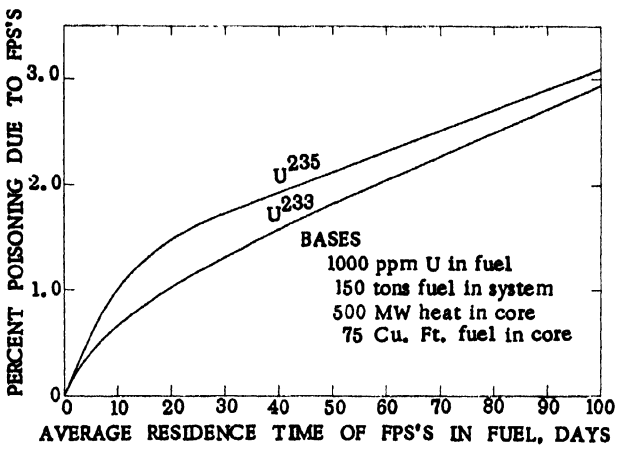

Figure 1. Poisoning effect of FPS's in LMFR

From the information given in Tables II and III, the average cross section of all the FPS's minus the six worst nuclides is found to be 25.6 barns. This value along with those given in Table IV permits the calculation of the poisoning effect. For the conditions listed above, this comes out to be 0.58% which is the percentage of neutrons captured by the FPS's relative to the total absorption in uranium. Calculated poisoning effects for certain typical operating conditions are shown in Figs. 1 and 2 for both U^{233} and U^{235}. It is seen that, other things being equal, the poisoning effect with U^{235} is appreciably greater than that with U^{233}. This is mainly due to the much higher fission yields of the rare earths in the case of U^{235}.

FPN's

As stated earlier, this group of fission products is inherently far less poisonous than the other two and therefore can be allowed to build up in the fuel stream to much higher concentrations. They may be removed continuously, maintaining a constant concentration in the fuel, or they may be essentially completely removed at certain intervals of time. In the latter case, these intervals could be as long as several months without their cumulative poisoning

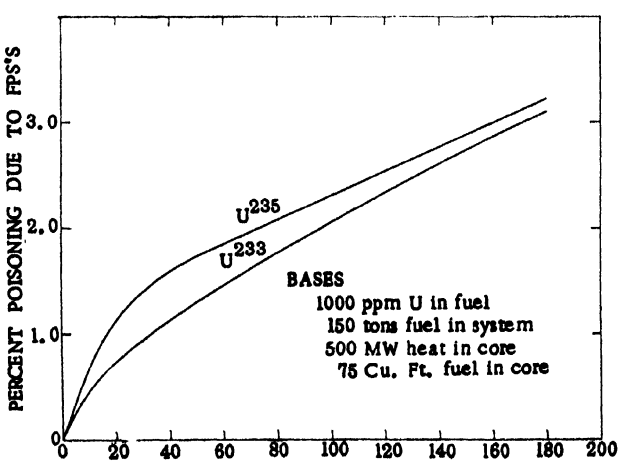

Figure 2. Poisoning effect of FPS's in LMFR

effect becoming excessive with respect to those of the other two groups. For lack of space, this group will not be considered further in the present paper.

CHEMISTRY OF FPS EXTRACTION FROM U-Bi

The chemistry of the removal of the FPS's from the LMFR fuel is based on their selective oxidation by fused chloride salts.[2] Table V gives the free energy of formation per atom of chlorine, at 500°K, for the chlorides of a number of elements of interest in the present case. This quantity gives a direct measure of chemical stability or relative ease of oxidation. The free energies of the rare earth chlorides on this basis all exceed 70 kcal.

Table V. Free Energies of Formation of Certain Chlorides

Compound	$-\Delta F$, kcal/gm-atom Cl	Compound	$-\Delta F$, kcal/gm-atom Cl
KCl	93.1	$MgCl_2$	66.8
$BaCl_2$	92.8	UCl_3	62.2
CsCl	91.7	UCl_4	53.9
LiCl	88.8	$CrCl_3$	34.7
NaCl	87.4	$FeCl_2$	33.2
$CaCl_2$	86.4	$NiCl_2$	29.0
$LaCl_3$	75.4	$BiCl_3$	22.2

One would predict, from inspection of Table V, that if a metal phase containing Bi, U, and Ce were contacted with a salt phase containing $MgCl_2$ the reaction

$$3MgCl_2 + 2\,Ce \rightarrow 3Mg + 2\,CeCl_3$$

should take place, and that the salt and metal products of the reaction should go into the corresponding bulk phases. The uranium, on the other hand, should not react significantly and remain in the metal phase.

The free energies given in the table for cesium, barium, and lanthanum are representative of those of all the other elements in the Periodic Table subgroups to which these elements belong. That is, all the fission products which are in columns IA, IIA, and IIIA of the Periodic Table, including the rare earths, form chlorides more stable than UCl_3.

The choice of oxidant is important. The three most likely oxidants now being considered are $MgCl_2$, UCl_3, and $BiCl_3$. The first of these has the advantage that the oxidation potential of the system $MgCl_2$-Mg can be adjusted by control of the concentrations of the two species, within a reasonable range, to a point at which the FPS's can be removed from the bismuth without extracting appreciable uranium. A separation factor is defined by

$$\frac{(\text{ppm FPS in salt}) \,/\, (\text{ppm U in salt})}{(\text{ppm FPS in metal}) \,/\, (\text{ppm U in metal})}$$

and, according to the simple theory presented above, values of this factor as high as 10,000 are possible; but practically, they are found to be in the order of 100 when the proper concentrations of Mg and $MgCl_2$ are used which nevertheless is still very good for engineering purposes. The concentrations of Mg and $MgCl_2$ will always be greatly in excess of those of the FPS, making the oxidation potential practically independent of the degree of completion of the desired reactions, which is a real advantage from an engineering standpoint. Systems of this type have come to be referred to as "buffer" systems, in the usual chemical meaning of the word.

With UCl_3 as the oxidant, uranium is added to the metal which means that in actual practice this method of FPS removal has the advantage of adding uranium make-up to the fuel. The stoichiometric relationships are such, however, that the FPS's will not transfer sufficient uranium to replace that which is consumed. The additional uranium can be transferred with magnesium.

$BiCl_3$ is a very strong oxidizing agent and one which does not add a solute to the fuel. It must, of course, be added to the carrier salt in just the right amount to extract the FPS's and not the uranium. It should give the same separation factors as those attainable with $MgCl_2$. The FPS's are, as it were, titrated out. This type of extraction system has been called "stoichiometric" to distinguish it from the buffer system described above.

The composition of the carrier salt for the $BiCl_3$ is not critical. Any low-melting mixture of chlorides which are at least as stable as $MgCl_2$ could be used, as for example the ternary NaCl-KCl-$MgCl_2$ mixture which melts at 396°C.

PROCESS DESIGNS FOR FPS REMOVAL

Use of Buffer System

A flowsheet, with typical numerical values, explaining the removal of FPS's from the LMFR fuel and based on the "buffer" chemical system described earlier in this paper, is shown in Fig. 3. The flow rates, concentrations, and equilibrium stages indicated on this diagram are based on a core heat rate of 570 Mw and a FPS concentration in the fuel of 15 ppm. For a U^{235} concentration of 600 ppm this would amount to about 1.5% reactor poisoning. The numerical values in the flowsheet are based on the following four assumptions: (*a*) no entrainment; (*b*) partition coefficients for FPS's and a U between salt and metal phases are constant over concentration ranges involved; (*c*) all FPS's have the same partition coefficients; (*d*) the separation factor

$$\frac{(\text{ppm FPS in salt}) \,/\, (\text{ppm U in salt})}{(\text{ppm FPS in metal}) \,/\, (\text{ppm U in metal})}$$

is the same for all extraction columns and equals 100. This value is one which is practically attainable with the system U-Bi-Mg/KCl-LiCl-$MgCl_2$, where the salt phase is mainly the KCl-LiCl eutectic. The individual values for the FPS and U partition coefficients between salt and metal phases depends on the buffering action, and therefore, the concentration, of the mag-

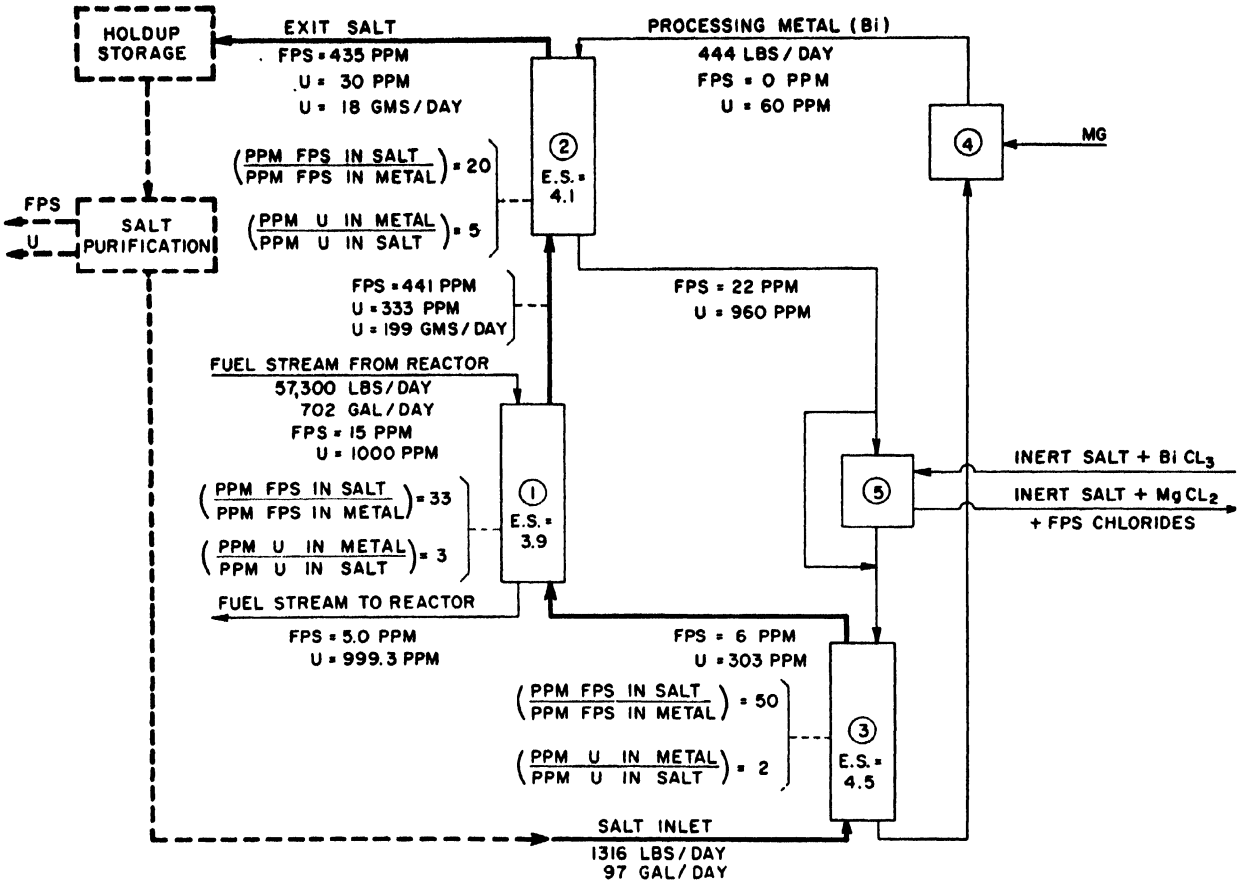

Figure 3. Proposed flowsheet for FPS removal from LMFR fuel using "buffer" method

nesium in the metal. The process outlined in Fig. 3 does not represent a careful optimization of the several operating variables but is nevertheless believed to be typical as far as indicated sizes, concentrations, and flow rates are concerned.

Columns 1, 2, and 3 are countercurrent extraction columns of 3.9, 4.1, and 4.5 equilibrium stages, respectively. They could all be spray columns in which the liquid metal fuel fell in the form of fine droplets through the slowly rising salt. The columns should preferably contain some baffling to prevent vertical mixing of the salt. Viscosity, interfacial tension, and density conditions are such as to make the metal-salt system an ideal one for this type of operation. Carryover, or entrainment, as judged on the basis of small-scale laboratory experiments should be negligible. The relative velocity of the falling metal with respect to the rising salt is about 2 ft/sec. This, together with the fact that the flowing streams are very small, means that the diameters of the columns are also very small. For example, Column 1, the largest, would need to be more than 3 or 4 inches in diameter. The heights of the columns will depend on their efficiencies and the separations required, but in any case, it is expected that they would not need to be taller than 2 or 3 feet. The height of column equivalent to a theoretical stage has not yet been quantitatively determined.

In Column 1, the fission products are extracted from the fuel; in Column 2, the uranium is recovered from the salt leaving Column 1; and in Column 3, the uranium is recovered from the processing metal stream by the incoming salt. The same salt stream passes through all three columns. The partition coefficients, indicated on the flowsheet, are varied between all three columns by changing the oxidation-reduction potential in each by varying the Mg concentration in the metal phase. Column 2 is more reductive than 1 to promote transfer of uranium to the metal phase, while Column 3 is more oxidative than 1 to promote transfer of uranium to the salt. Units 4 and 5 in the flowsheet are for adding Mg to, and removing Mg from, the processing metal stream to give the desired partition coefficients in Columns 2 and 3. The Mg could be added by means of an electrochemical cell in which Mg and Bi are the anode and cathode, respectively, and in which the salt bridge could consist of the ternary KCl-LiCl-$MgCl_2$. Or, the Mg could be added mechanically in the form of a bismuth solution. Item 5 is a salt-metal contactor in which sufficient $BiCl_3$, a very strong oxidant, is added to the carrier salt to oxidize the desired fraction of the magnesium without oxidizing a significant amount of uranium.

After leaving Column 1, the salt must be cooled to remove decay heat; but heat exchangers have not

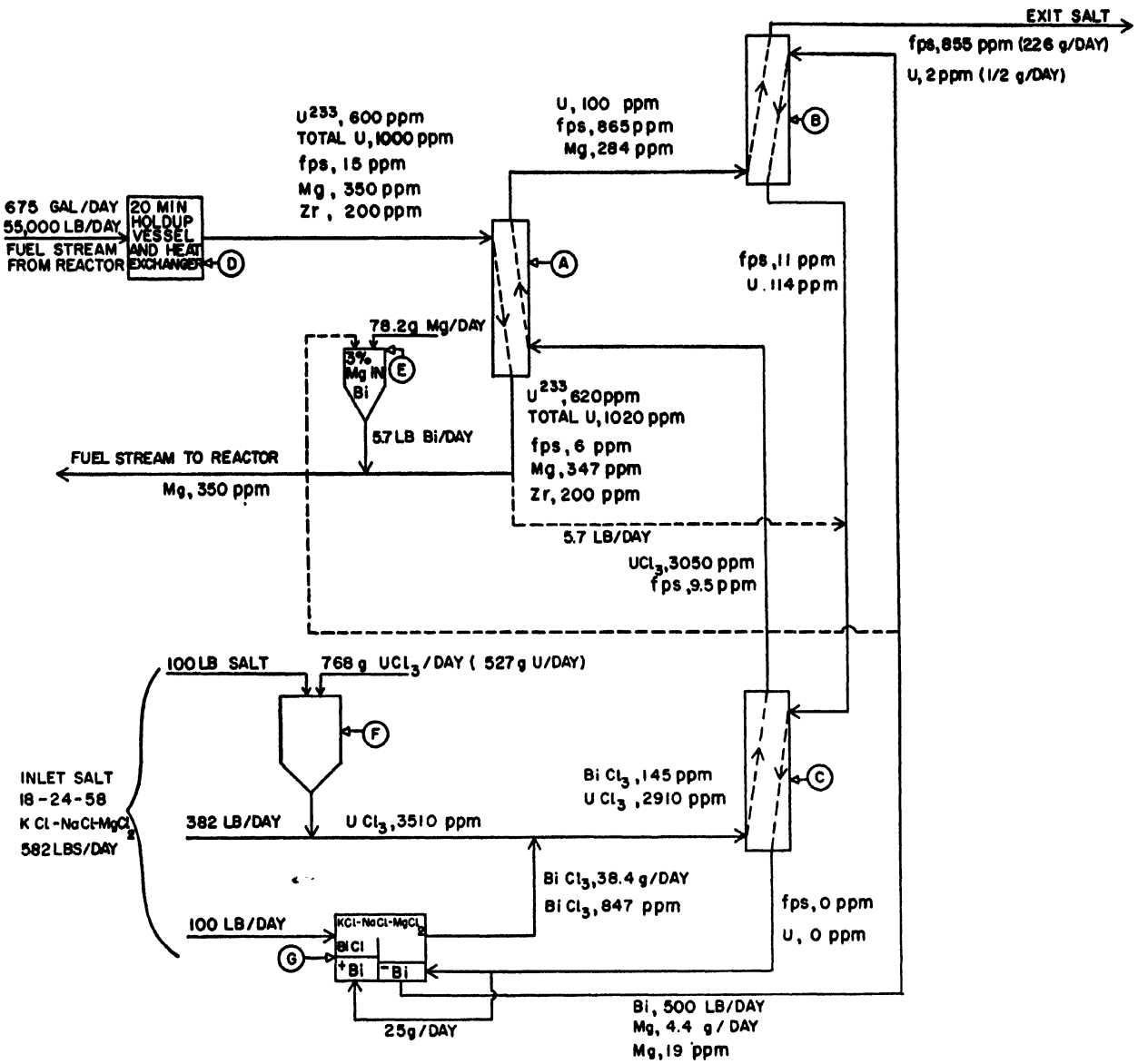

Figure 4. Proposed flowsheet for FPS removal from LMFR fuel using "stoichiometric" method

been included in the figure for sake of simplicity. The question of heat release from the FPS's will be discussed in a later section of this paper. The dashed portion of the flowsheet in Fig. 3 is simply a schematic representation of the salt decontamination step as it relates to the main processing plant.

Use of Stoichiometric System

A second flowsheet for a proposed LMFR fuel-processing plant, based on the "stoichiometric" chemical system, is shown in Fig. 4. From an engineering standpoint, the two flowsheets are very similar. The second flowsheet is based upon a 500 Mw heat rate in the reactor core, U^{233} as the fissile material, and 1.0% poisoning due to FPS's.

Referring to Fig. 4, the fuel from the reactor is first held up in a heat exchanger, D, allowing the fission products to "cool off," before it flows through extraction Column A. In this column, approximately two-thirds of the FPS's are removed from the fuel; but before it is returned to the reactor, its Mg concentration is brought up to its original value, by adding about once daily a 3% solution of Mg in bismuth. The UCl_3 carried in the salt from Column A is nearly all recovered in Column B by contacting the salt with a Mg-Bi solution. The uranium, accompanied by a small amount of FPS's, is recovered from the metal stream leaving Column B by contacting it with the incoming salt in Column C. The electrochemical cell, G, introduces $BiCl_3$ into the inlet salt stream and magnesium into the processing metal stream in the proper stoichiometric quantities to accomplish the two-step transfer of the uranium from the out-going salt to the ingoing salt. UCl_3 is added to the salt stream from mixing tank F at the required rate to supply the necessary U make-up to the fuel stream. In other words, UCl_3 as the oxidant in the salt simultaneously removes the fission products and adds

U to the fuel. The stoichiometric quantities are such that a small amount of Mg must be oxidized along with the FPS's in order to add the required amount of uranium. The UCl_3 addition of 768 grams/day does not include the U make-up required for neutron capture by the U. If it is not desired to add the uranium to the fuel by this method, then the oxidizing constituent would be $BiCl_3$.

In the stoichiometric system, a typical carrier salt would be the NaCl-KCl-$MgCl_2$ eutectic.

The salt stream, of course, becomes very radioactive and must be cooled. As in Fig. 3, the heat exchangers for this have been omitted. It is pointed out again that the numerical values shown in Fig. 4 are not the result of careful economic optimization but are nevertheless believed to be fairly representative of commercial operation.

It will be noticed that the flow rates shown in Figs. 3 and 4 are very small, which means that the equipment is correspondingly small. The largest conduit lines need to be no greater than ¼ inch in diameter and the largest contactor column, 3 inches in diameter. The small equipment, which is a consequence of the facts that the operation is continuous and that the chemistry is non-aqueous, means that the amount of shielding required, though thick, is not expansive. From the standpoint of investment costs, instrumentation and control equipment will be major items. It is expected that electrochemical cells can be used for adding small amounts of solutes to both salt and metal streams and that e.m.f. cells can be used for control of concentrations of critical materials. Stainless steels of both the austenitic and ferritic types have proven to be very satisfactory materials of construction for equipment handling fused chlorides, as long as the systems are quite oxygen free. At Brookhaven, the following steels have been in common use: 18 Cr, 10 Ni, Cb stabilized (U.S. type 347) and 13.5 Cr (U.S. type 410 S.S.).

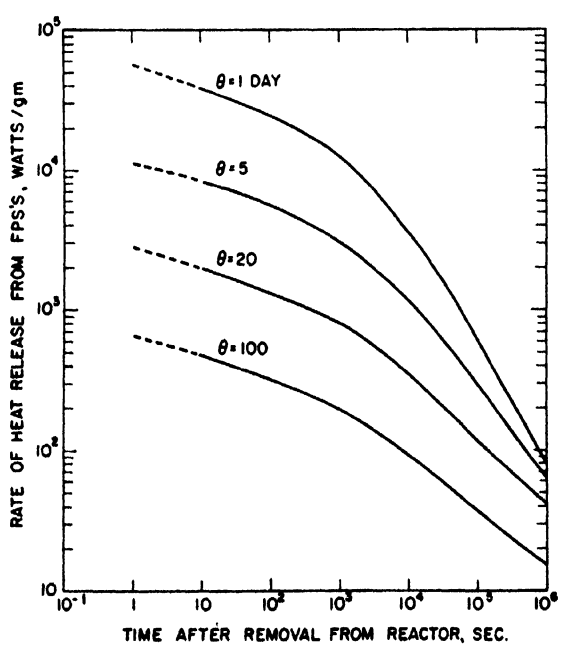

Figure 5. Rates of heat release from FPS's

Pre-treatment and conditioning of equipment before use includes such operations as electropolishing, degassing under high vacuum at temperatures in the neighborhood of 800°C, and contacting with Mg-Bi solutions. It is essential that the equipment and piping be absolutely gas tight. This calls for either canned-rotor or canned-motor pumps and bellows-sealed valves and pressure transmitters.

The LMFR, due to the rapid removal of the FPV's and FPS's from the fuel, is capable of providing very young fission products for irradiation purposes. Moreover, since they are present in fluid streams, they are easily adapted to on-the-spot gamma-radiation facilities. The fused salt mixture containing the FPS's is a particularly good source of high-intensity ionizing radiation, because heat removal from the salt is not a serious problem. The radiation associated with the salt-extracted FPS's in a large plant, say one of 500–1000 Mw heat rate, can be as great as several million curies. It is assumed that high-intensity gamma-radiation facilities would be associated with a commercial LMFR power plant.

After a suitable storage period, the salt can be purified for re-use. Complete decontamination is unnecessary. The FPS's can be removed from the salt by contacting it with liquid lead containing a strong reductant like Mg or Ca; and they could then be removed from the lead by direct oxidation by an air stream. Alternatively, they could be left in the lead for indefinite storage.

HEAT RELEASE FROM FISSION PRODUCTS

An important consideration in the design of processes and equipment for handling radioactive fission products is the problem of heat generation. This is particularly true in the present case, because of the relatively short age of the fission products at the time of their removal from the fuel. In the case of the FPS's, for example, the typically high rates of heat release are given in Fig. 5. This plot gives the specific heat rates for the FPS's as a function of average residence time in the reactor fuel and time after removal from the fuel. The curves were calculated on the basis of fission-product heat-release data obtained from the Argonne National Laboratory[3] which were extrapolated with the aid of the Way-Wigner[4] expression for fission-product decay heat.

BLANKET MATERIAL AND PROCESS

This discussion of the blanket material and processing method, necessarily brief, will be limited to the basic chemical metallurgy and conceptual process design. Details on experimental methods and techniques and physics and economic considerations will appear in future publications.

The blanket design proposed for the LMFR utilizes a dispersion of Th_3-Bi_5 in molten bismuth. The concentration of thorium in this dispersion is between 10% and 12% by weight. This concentration permits

good neutron economy with reasonably high fluidity. It is expected that the concentration of the radiation products—protoactinium and uranium—would be in the order of 100 ppm under steady-state operation.

Probably, the best method of producing the dispersion is that which involves the use of thorium powder and which has already been published.[5] A typical microstructure of a solidified dispersion produced by this method is shown in Fig. 6. Experience has indicated that the stable, steady-state particle size is in the order of 100 microns.

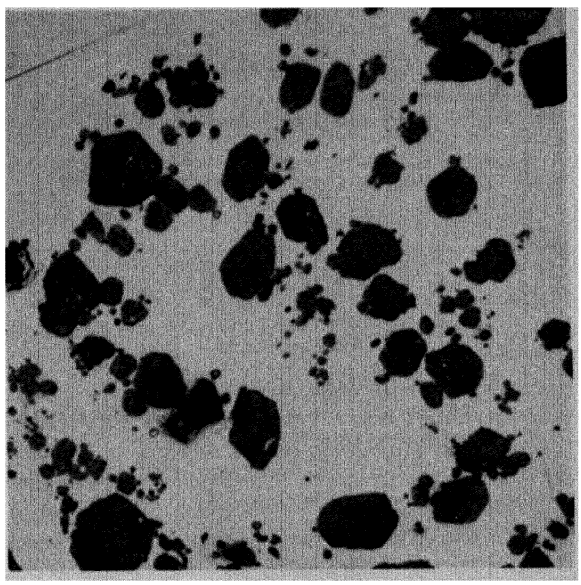

Figure 6. Microstructure of Th-Bi dispersion (powder method) air etched, 100×

The proposed process for recovering the bred uranium from the blanket dispersion is based on the transfer of the uranium from the solid particles to the liquid metal phase. In this transfer, the equilibrium distribution is such that a large portion of U (and possibly Pa) goes into the liquid phase. In a typical experiment; an alloy, consisting of 5% w/w thorium and 100 ppm uranium in bismuth was placed in a special impervious-graphite crucible above a graphite frit located half-way down the crucible. The entire assembly was then heated in a vacuum to 1000°C, well above the liquidus temperature. The Th_3Bi_5 compound was then allowed to precipitate by cooling the mixture to 350°C. After a short equilibration period, an inert gas was admitted forcing some of the liquid phase through the filter into the lower half of the crucible. Chemical analyses of the residue and filtrate indicated that the ratio of the concentration of uranium in the solid to that in the liquid phase was 6. The value of the same ratio for the thorium was 5000. Such results indicate that it should be possible to effect the separation of the bred uranium from the fertile material by allowing it to transfer to the liquid phase. Uranium and protactinium can then be recovered from the separated liquid phase by some oxidation process.

The solubilities of uranium and thorium in bismuth, which are of fundamental importance to the process, are given in Fig. 7. The corresponding data for protactinium are not yet available. In the transfer of the radiation products from the solid phase to the liquid, their concentrations in the bismuth should not exceed their solubility limits when the mixture is cooled for thorium separation.

Conceivably, the simplest method for transferring the radiation products from solid to liquid phases is to allow them to diffuse from one to the other. Such experiments are now in progress and quantitative results are not yet available. An alternative way of rapidly transferring the radiation products from solid to liquid phases is to dissolve the particles by increasing the temperature and then re-precipitating them. The big drawback to this scheme, however, is that the newly-formed particles are platelets, instead of equiaxed particles as before. These platelets, which are about 25 microns thick and up to 1 cm in diameter, greatly decrease the fluidity of the dispersion. This difficulty can be circumvented by partial, instead of complete, dissolution of the original dispersion. Apparently, the nuclei retained upon partial dissolution cause equiaxed particles to re-form upon subsequent cooling. In some experiments it was possible to dissolve as much as 80 per cent of the solids and still retain equiaxed particles upon cooling.

For a 500 Mw (heat rate) reactor, it is estimated that approximately 20 tons of blanket material would be processed per day. Figure 8 presents a proposed flowsheet, showing typical concentrations, based upon the partial-dissolution process described above. First,

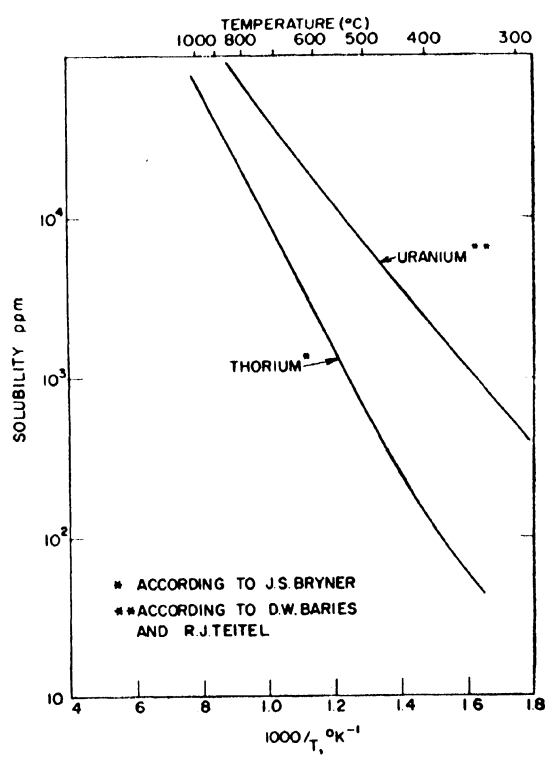

Figure 7. Solubility of uranium and thorium in bismuth

the concentration of thorium in the blanket effluent is reduced to 5% by dilution with bismuth, in order to reduce the dissolution temperature and later to facilitate phase separation. The dispersion then passes through a graphite-lined pipe, wherein its temperature is raised to 850°C and then lowered to 350°C. During this temperature cycle, 60% of the solids dissolves and re-precipitates. The dispersion then enters a centrifugal separator for removal of a portion of the liquid phase whence the residual dispersion is returned to the blanket, after its thorium concentration has been brought back up to 10%. The radiation products can be separated from the remaining thorium by one of three possible methods, depending upon the ultimate use of the bred fuel. These methods are: oxidation followed by wet-chemical processing, oxidation and extraction by fused salts followed by centrifugation, and distillation of bismuth followed by centrifugation to give a concentrated U-Bi alloy.

Rates of particle growth and settling are two pertinent factors relating to process design. On the basis of extensive experimental results, however, it appears that neither of these will present undue enginering difficulties.

EXPLANATION OF SYMBOLS AND ABBREVIATIONS

Symbols

f = fraction fission yield
k = ratio (atoms FPS/cm³ of salt)/(atoms FPS/cm³ of fuel)
N = concentration of a given nuclide in fuel, atoms/cm³
N_p = concentration of parent nuclide in radioactive decay, atoms/cm³
N_t = concentration of target nuclide in neutron capture, atoms/cm³
N^{235} = concentration of U^{235}, atoms/cm³
t = time, seconds
V_c = fuel volume in core, cm³
V_t = fuel volume in reactor system, cm³
V_s = salt flow rate, cm³/sec
θ = average residence time in fuel, days
λ = radioactive decay constant

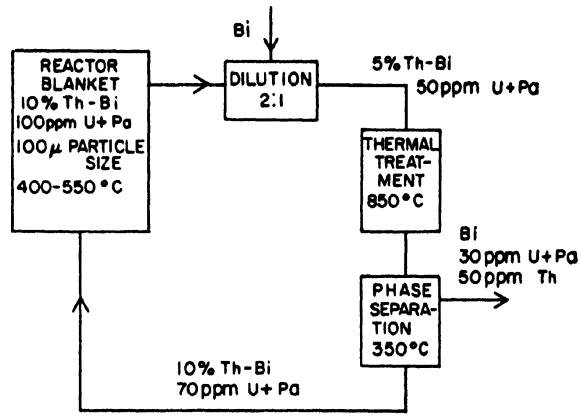

Figure 8. LMFR blanket process

σ = thermal-neutron cross section for N, barns
σ_t = thermal-neutron cross section for target nucleus, barns
σ_{sf} = thermal fission cross-section for U^{235}, barns
ϕ = thermal neutron flux, neutrons/cm²sec

Abbreviations

E.S. = equilibrium stage in mass transfer
FPN = non-volatile fission products which form chlorides less stable than UCl_3
FPS = non-volatile fission products which form chlorides more stable than UCl_3
FPV = volatile fission products

REFERENCES

1. Hughes, D. J. and Harvey, J. A., *Neutron Cross Sections*, Brookhaven National Laboratory Report, BNL-325 (May 1955).
2. Bareis, D. W., Wiswall, R. H. and Winsche, W. E., *Processing of Liquid Bismuth Alloys by Fused Salts*, Chemical Engineering Progress Symposium Series, Vol. 50, No. 12 (1954).
3. Steinberg, E. P., Argonne National Laboratory, Lemont, Illinois, U.S.A., Private Communication.
4. Wigner, E. P. and Way, K., Paper 43, *National Nuclear Energy Series*, Div. IV, Vol. 9, McGraw-Hill Co., Inc., New York (1951).
5. Teitel, R. J., Gurinsky, D. H. and Bryner, J. S., *Liquid Metal Fuels and Breeder Blankets*, Nucleonics, 12, No. 7: 14-15 (1954).

Decontamination of Irradiated Reactor Fuels by Fractional Distillation Processes Using Uranium Hexafluoride

By H. H. Hyman, R. C. Vogel and J. J. Katz,* USA

INTRODUCTION

Heterogeneous reactors generally employ fuel elements of limited useful life. When such elements are removed from a reactor, they are intensely radioactive. In spite of the difficulties this radioactivity introduces into reprocessing steps, the uranium or other heavy metal content of the fuel elements usually justifies decontamination and re-use.

Why Uranium Hexafluoride?

Of the many techniques suggested for uranium decontamination and recovery, those employing uranium hexafluoride are interesting for two principal reasons. Distillation of volatile materials is a well-established purification procedure. Both at the laboratory and engineering levels experimental techniques and process performance may be based on wide experience. A second and perhaps more important factor is related to the special role of uranium hexafluoride in the isotope separations program. The fissionable isotope content of spent uranium fuel elements is usually lower than that of fresh fuel elements. The most appropriate use of the recovered uranium may well be as feed to some stage in an isotope separations process to permit concentration of U^{235}. For these situations the production of uranium hexafluoride may be a required step. Therefore the direct production of this compound and its use in the purification appears to be a very direct processing technique.

Perhaps the most important handicap faced by decontamination processes using uranium hexafluoride lies in the required use of fluorine. The technological problems associated with the production and handling of fluorine are far from negligible, especially when coupled to those problems associated with handling large amounts of radioactivity.

Rationale of Liquid Phase Fluorination

Uranium metal may be directly converted to the hexafluoride by combustion in an atmosphere of fluorine. The conversion to uranium hexafluoride releases a very large amount of heat (2.2×10^3 kcal/kg). When large quantities of metal are involved, it has not proved practical to remove this amount of heat when generated in a solid-gas reaction. Even for fuel elements where the uranium is enriched and only small amounts need to be processed at a time the direct gaseous fluorination is not satisfactory. Therefore the practical methods of producing uranium hexafluoride discussed in this paper are liquid phase reactions in which the heat may be removed by well-established procedures so as to permit moderately rapid fluorination of the fuel element.

The liquid phases suitable for fluorination may be conveniently divided into two groups: a low temperature group, consisting primarily of halogen fluoride solutions, e.g., bromine trifluoride or chlorine trifluoride; and a high temperature group, consisting primarily of fused metallic fluorides. High temperature fluorinations pose additional engineering problems associated with accelerated corrosion but many of the alloys suggested for reactor fuel elements do not yield uranium hexafluoride in the available low temperature fluorinating media.

Scope of the Paper

This paper will discuss briefly the basic chemical information useful in the development of a uranium hexafluoride separations process. It will then describe in some detail a laboratory investigation of the conversion of uranium metal fuel elements to uranium hexafluoride employing bromine trifluoride dissolution and the auxiliary problems associated with such an approach to uranium decontamination.

Next will be discussed the alternative approaches which may be employed for more refractory fuel elements and finally those aspects of fluorine technology will be touched on where progress in recent years has increased the probability of successful application of the chemical principles emphasized in this paper.

CHEMISTRY OF SOME PERTINENT FLUORIDES[1,2]

Fluorides of Uranium[3]

Several fluorides of uranium have been prepared and characterized. Uranium in its compounds shows several valences (3, 4, 5, and 6) and, at least in solid systems, complex fluorides are found in which the effective uranium oxidation state varies from the lowest to the highest value.

* Argonne National Laboratory. Including work by O. DuTemple, J. Fischer, L. Gaumer, H. H. Hyman, J. J. Katz, M. Levenson, R. D. Long, W. J. Mecham, R. Liimatainen, J. G. Schnizlein, Jr., W. Seefeldt, P. Seufzer, I. Sheft, L. Stein, R. Steunenberg, R. C. Vogel, S. Vogler.

Uranium Hexafluoride[3,4,5]

Uranium hexafluoride may be formed quantitatively from almost all uranium compounds or alloys by one or another of the fluorinating reagents employed in this program. It is stable to thermal decomposition up to very high temperatures. While moderately reactive towards water and hydrogen-containing material in general, it may be stored and handled in a variety of construction materials (e.g., dry glass). Uranium hexafluoride is a volatile solid (triple point: 64.02°C at 1137 mm). This behavior is typical of molecular lattice compounds when valence number and coordination number coincide.

Uranium Tetrafluoride

Uranium tetrafluoride is a nonvolatile, insoluble, refractory compound. It may well play a role as intermediate in a process yielding uranium hexafluoride. Uranium tetrafluoride may be prepared from either the metal or other uranium compounds using hydrofluoric acid as a source of fluorine rather than the more expensive elemental form. Uranium tetrafluoride may subsequently be converted to the hexafluoride by bromine trifluoride or a similar reagent with minimum net fluorine consumption. The other uranium fluorides may appear as unstable intermediates in the fluorination process, but are otherwise of no interest to the program.

THE FLUORIDES OF PLUTONIUM[6,7]

The fluorides of plutonium have been less thoroughly investigated than the corresponding uranium compounds. The trifluoride, tetrafluoride, and hexafluoride have been prepared in pure form and are well characterized. As might be expected, the trifluoride is more stable to oxidation than the corresponding uranium compound; the hexafluoride less stable to reduction or decomposition. The low temperature fluorinations in which uranium is converted to the hexafluoride usually yield the nonvolatile plutonium fluorides.

The Fission Product Fluorides

Volatile Fission Product Fluorides

The volatile fission product fluorides vary considerably in their process importance. Niobium and ruthenium are serious contaminants in irradiated uranium. The fluorinating procedures used in this work usually produce the pentafluorides (RuF_5, b.pt., 313°C; NbF_5, b.pt., 233.3°C). Their separation by distillation from uranium hexafluoride is quite practical. Such separations, in fact, are usually much easier than might be anticipated. Pentafluorides in general show a strong tendency to form the hexafluoro-anions. This behavior reduces their volatility from ionizing solvents, e.g., bromine trifluoride.

Molybdenum hexafluoride (b.pt., 35.0°C) might well be one of the more troublesome fission products to separate from uranium. However, the longest lived radioactive molybdenum isotope is the 67-hr Mo^{99}, and a short cooling time removes the radioactive species.

Tellurium, and to a lesser extent iodine, are the only fission product activities whose separation from uranium poses a significant problem. Thorough decontamination of uranium from fission product activity might require a decontamination factor for tellurium of 10^2–10^4. While significant quantities of both the less volatile tellurium tetrafluoride (b.pt., 371.3°C) and the more volatile tellurium hexafluoride (b.pt., −38.3°C) have appeared in the experiments described below, it should not be difficult to design equipment to effect an adequate separation of hexafluoride from either species.

Yost and Clausen[8] have reported the existence of an intermediate fluoride which has been confirmed by English and Dale[9] as Te_2F_{10} (b.pt., +54°C). Distillation would not be easy for the separation of uranium hexafluoride from this compound. Fortunately, the conditions under which it is formed appear to be limited and high yields are not expected under process conditions. A more troublesome aspect of uranium-tellurium separation appears to be the possible reduction of the tellurium hexafluoride to non-volatile tellurium at one stage of the separations process and its reoxidation to the hexafluoride under conditions and in such a way that tellurium accompanies uranium in its final distillation. The chemistry of the tellurium fluorides in bromine trifluoride is not adequately established. Although empirically adequate decontamination may be achieved under specified conditions this area certainly merits further study.

The principal tellurium nuclide Te^{129m} decays via an isomeric transition to the short-lived, γ-emitting Te^{129}. In gaseous tellurium hexafluoride this transition is accompanied by a Szilard-Chalmers decomposition of the molecule which complicates analytical procedures for tellurium based on radioactivity.

Iodine is fluorinated to the pentafluoride under most of the procedures discussed below. In bromine trifluoride solutions this compound shows a lower volatility than its boiling point might suggest and is not usually a serious problem in uranium fractions. For the same reason, however, the separation from bromine trifluoride does not appear to be too practical and recycled bromine trifluoride would almost certainly contain a steady state concentration of this fission product.

Nonvolatile Fission Product Fluorides

In the case of the nonvolatile fluorides the solubility is of considerable process significance.[14] Cesium and strontium fluorides tend to be significantly soluble in ionizing solvents, specifically bromine trifluoride. The trivalent rare earth fluorides are much less so. The actual solubility product in process solutions may not be exceeded due to the low concentration by weight of these rare earth fission products. However, it might be anticipated that any insoluble fluoride, including the protective films on metal equipment, will act as absorbent or carrying

agent for these insoluble fluorides and remove them from solution.

The Halogen Fluorides[10,11]

The halogen fluorides have been studied in increasing detail in recent years; however, they are still unfamiliar to most laboratory workers. They are powerful oxidizing agents and ordinarily cannot be prepared without the use of elemental fluorine itself. They are easier to store and transport than fluorine. Chlorine trifluoride is prepared by a gas-phase reaction between chlorine and fluorine in a heated cell. In the case of bromine trifluoride, fluorine bubbled through a liquid phase containing bromine is sufficient.

The behavior of the halogen fluorides as solvents can be most readily correlated in terms of non-aqueous solvent acid-base theory.[10,11,12,13] In the more familiar acid-base treatments, compounds are considered according to their ability to gain or lose a proton. In the halogen fluoride systems the fluoride ion occupies an analogous though complementary relationship, i.e., gain of a fluoride ion is equivalent to loss of a proton.

Bromine Trifluoride

Of the halogen fluorides, bromine trifluoride has perhaps the most convenient liquid range and shows the widest range of chemical properties. Primarily for these reasons, most of the low temperature fluorinations investigated at Argonne employed bromine trifluoride as the primary solvent.

Bromine trifluoride is a straw-colored liquid, readily obtained in a pure state by distillation. It is a good electrical conductor and a good solvent for both fluorine ion donors and acceptors, as well as for saturated volatile compounds such as uranium hexafluoride.

Bromine trifluoride, like most other solvents, is not capable of dissolving salts which give polyvalent cations. Therefore, no solubility is found for the rare earth fluorides or those of zirconium, thorium, and plutonium which do not appear to be acidic enough in this solvent to form complex fluoride anions.[14]

Mixtures of bromine pentafluoride and bromine or lower bromine fluorides react to give the trifluoride rapidly at 150°C or higher. However, nonequilibrium may be maintained at low temperatures for some time. Conversely, disproportionation of bromine trifluoride may occur to a slight extent at high temperature. However, the free energies of formation of the varying species and the exact equilibrium conditions are not yet established.

In connection with this program, a number of phase diagrams have been prepared for bromine trifluoride systems. Some have been published previously. In the bromine-bromine trifluoride condensed system[15] a liquid immiscibility gap with a consolute point at 55.5 ± 0.5° at 60 ± 5 mol per cent bromine was found. The pure components were the only solid

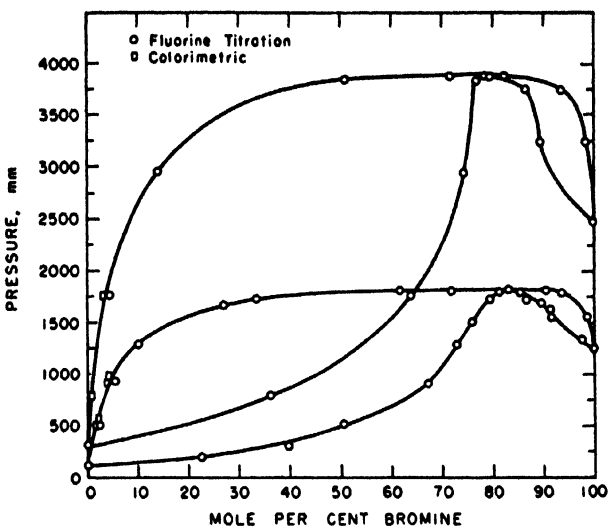

Figure 1. Liquid-vapor equilibria bromine-bromine trifluoride 75°C and 100°C

phases observed down to −10°C. The three condensed binary systems, uranium hexafluoride-bromine,[16] uranium hexafluoride-bromine trifluoride, and uranium hexafluoride-bromine pentafluoride[17] were all simple eutectic types, and the solid phases in equilibrium with the saturated solutions were the pure components. Ternary and higher systems have not yet been studied.

The liquid-vapor equilibria in the system bromine trifluoride-bromine pentafluoride are as yet unpublished and have been found to be close to ideal. Complete isotherms have been measured at 50, 75, 100, 125, and 150°C and the 1 atmosphere isobaric diagram was determined. These data have been treated by modern solution theory and will be reported elsewhere.

The liquid-vapor equilibrium in the system bromine-bromine trifluoride is also still unpublished and has proved to be quite interesting. The 75 and 100°C isotherms have been determined. At both temperatures, the system exhibits azeotropes at pressures

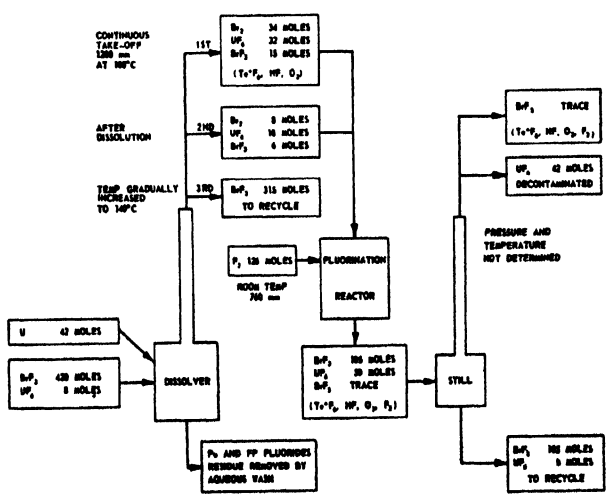

Figure 2. Continuous product removal flowsheet for processing natural uranium

greater than the sum of the pressures of pure bromine and bromine trifluoride. This is indicative of another molecular species, perhaps bromine monofluoride, coexistent in the vapor phase with bromine and bromine trifluoride. The data are illustrated in Fig. 1. Further work is now being done on this equilibrium between bromine and bromine trifluoride using a spectrophotometric technique, and other attacks on this system are planned.

Other Halogen Fluorides

Chlorine trifluoride and bromine pentafluoride have also been employed as fluorinating agents. Since neither is a good fluoride ion acceptor, they are poor electrical conductors and less reactive towards metals in the liquid phase. They dissolve acids (HF, SbF_5) to form more reactive solutions.

Fluoride Volatilities

Many of the literature values for the vapor pressure of volatile fluorides have been accumulated by Ruff and his students.[2] The interest in this problem in United States Atomic Energy Laboratories has resulted in improved values for a number of compounds. Table I summarizes the best current values for the vapor pressure of volatile substances encountered in this program.

PROCESS OF METALLIC URANIUM FUEL ELEMENTS

An important group of fuel elements consists primarily of uranium metal. While usually protected by an exterior can, the fuel element itself contains only a limited amount of foreign material. While such a fuel element may be made from enriched uranium, the most important systems of essentially pure uranium fuels are those in which the bulk of the uranium is U^{238} and plutonium is an important fissionable constituent. Under specific conditions the amounts of plutonium may vary from parts per mil-

Table I. Vapor Pressure Equations for Substances Encountered in the Fluoride Volatility Process

Compound	Boiling point (°C)	Melting point (°C)	$\Delta H_v(L)$ (kcal/mol)	$\Delta H_v(S)$ (kcal/mol)	Vapor pressure equation	Reference
F_2	−187.92	−217.96	1.51		liq.: $\log P = -442.72/T + 9.1975 - 0.013150T$	(18)
ClF	−100.8	−154	5.3		liq.: $\log P = 15.738 - \frac{3109}{T} + \frac{1.53 \times 10}{T^2}$	(19)
TeF_6	−38.9	−37.8	4.5	6.7	sol.: $\log P = 9.1605 - \frac{1471.4}{T}$	(8)
					liq.: $\log P = 7.091 - \frac{9.88}{T}$	(20)
Cl_2	−34.05	−100.98	4.9	6.5	liq.: $\log P = 7.773 - \frac{1160}{T}$	(21)
					sol.: $\log P = 9.950 - \frac{15301}{T}$	
ClF_3	11.754	−76.32	6.6	8.5	liq.: $\log P = 7.36711 - \frac{1096.917}{t + 232.75}$	(22)
HF	19.54	−83.07	1.9	3.0	liq.: (50-760 mm) : $\log P = 7.3739 - \frac{1316.79}{T}$	(1)
					liq.: (760-3581 mm) : $\log P = 7.51 - \frac{1357}{T}$	ANL
BrF_5	42.2	−61.3	7.2	9.2	liq.: $\log P = 6.4545 + 0.001101t - \frac{895}{t + 206}$	ANL
UF_6	54.6	64.02	6.9	11.5	sol.: $\log P_{mm} = 6.38363 + 0.0075377t - 942.76/(t + 183.416)$ liq.: $\log P_{mm} = 6.93718 - 1091.537/(t + 217.32)$	(4)
PuF_6	62.3	0.7	7.4	12.1	liq.: $\log P = 7.7039 - 1617.8/T$ sol.: $\log P = 10.87553 - 2645.3/T$	(7d)
Br_2	58.78	−7.3	7.3	10.0	liq.: $\log P = 63420 - \frac{1577.6}{T}$	ANL
IF_5	100.5	9.4	9.9	13.7	sol.: $\log P = 11.764 - \frac{3035}{T}$	(23)
					liq.: $\log P = 8.6591 - 2159.0/T$	
BrF_3	125.75	8.77	9.5	11.4	liq.: $\log P = 7.65752 - 1627.5/(t + 215)$	ANL
NbF_5	229	78.9	12.7		liq.: $\log P = 8.3716 - \frac{2779.3}{T}$	(25)
RuF_5	313	105	16.8	23.1	liq.: $\log P = 7.607 - \frac{2770}{T}$	(7b)
					sol.: $\log P = 13.62 - \frac{5052}{T}$	
TeF_4	193.8° Dec. 371.3° B.P.	129.6	8.2	14.5	liq.: $\log P = 5.6397 - 1786.4/T$	(26)
					sol.: $\log P = 9.0934 - 3174.3/T$	

lion to several per cent. The concentration of fission products and the required purification of the product uranium hexafluoride may also vary between fairly wide limits. While some care need be exercised in extrapolating from data reported here to fuel elements whose composition is significantly different, it is hoped that enough of the general principles will be emphasized to permit such reasonable extrapolations.

At this point we need not concern ourselves with the first step in the processing line, the removal of the can. Either mechanical or chemical methods are available and usually will be necessary since the materials of construction employed in protecting uranium from corrosion have been invariably those not readily attacked by the low temperature fluorination procedures.

A typical process flow sheet is shown in Fig. 2. The important process features include the uranium dissolution conditions, the fate of the plutonium, the uranium purification, the halogen fluoride recycling and waste disposal.

Uranium Dissolution

The dissolution of metallic uranium in bromine trifluoride solution may be made to proceed smoothly at virtually any desired rate. The bromine generated by the reaction may be refluorinated with elemental fluorine either directly in the dissolver itself or in some subsequent vessel. The heat generated by the dissolution may be readily removed, either with a cooling jacket or cooling coils or by permitting the solution to boil and removing the heat in a reflux condenser. The uranium hexafluoride produced by the reaction is dissolved in a mobile liquid which may be pumped or otherwise transferred to either a batch-still or a continuous distillation system. The plutonium and the major portion of the fission products are left as a compact, non-volatile residue. Treating the plutonium is a special problem which is discussed briefly below.

Kinetics of Uranium Dissolution in Bromine Trifluoride

The dissolution of uranium in bromine trifluoride has been studied in some detail. The goal is a uniform, reasonably fast, and controllable reaction rate. While the reaction is complex, a range of empirically satisfactory dissolving conditions have been established.

Like all heterogeneous reactions the exact rate of dissolution is a function of the geometry of the solid and system. Like most metals dissolving in acid, the rate is a function of the purity and local crystal orientation in the metallic structure as well as the surface area and degree of agitation. Therefore, a complete kinetic study is long and complex. While Tables II and III quote measured penetration rates for specific solutions on uranium at specific temperatures, these must be taken as indicative rather than values which may be used for the accurate prediction of the time required to dissolve a specific batch of uranium. In particular, those data on Table III based on specially purified and metallurgically treated uranium metal are substantially slower than those found for ordinary irradiated specimens.

Pure bromine trifluoride attacks metallic uranium only slowly. The addition of bromine pentafluoride probably reduces this rate; the addition of bromine increases it. For the purest uranium and best bromine trifluoride the activation energy of the reaction appears to be between 6 and 7 kcal, corresponding to a doubling in rate for every 20 or so degree rise in temperature. It is postulated that the primary metal acid reaction involves the transfer of electrons from a metal to a characteristic cation, and that the order of attack is

$$Br^+ > BrF_2^+ > BrF_4^+$$

If a fluorine ion acceptor, e.g., SbF_5, is added to the solution, the dissolution rate is accelerated in spectacular fashion.

Table II. Selected Experiments on the Dissolution of Uranium* in Bromine Trifluoride Solution

Dissolving medium†	*Temperature °C*	*Incubation time, ‡ hr*	*Final penetration rate, mm/hr*
$BrF_3 + Br_2$ (as generated)	45	12	0.4
$BrF_3 + Br_2$ (10 mole %)	45	0	0.4
$BrF_3 + Br_2$ (as generated)	65	3	1.0
$BrF_3 + Br_2$ (as generated)	90	0.6	1.2
$BrF_3 + Br_2$ (10 mole %)	65	0	1.3
$BrF_3 + SbF_5$ (5 mole %)	65	0	12
$BrF_3 + KF$ (5 mole %)§	65	0.8	0.7
$BrF_3 + F_2$ (added as consumed)	140	0	0.7
BrF_5	65	90	0.03
$BrF_3 + BrF_5$ (30 mole %)	65	4.5	0.8

* Early experiments made on available uranium of unspecified purity, not, however, an unsuitable reactor fuel.

† In each case uranium hexafluoride is present as generated. The final concentration of UF_6 was about 10 mole %.

‡ During the incubation period the reaction proceeds at a slowly increasing rate. Heat must be supplied to maintain the temperature. As the concentration of reaction products increases the rate of reaction and heat evolution increases, boiling starts and the sample dissolves rapidly at the rate shown in the next column.

§ A substantial amount of uranium was found as a non-volatile complex compound, yielding BrF_3 on ignition, yielding U(IV) on hydrolysis, and containing potassium, uranium, and fluorine.

Table III. Selected Experiments on the Dissolution* of Purified Uranium in Bromine Trifluoride Solution

Dissolving medium†	*Temperature, °C*	*Penetration rate,‡ mm/hr*
BrF_3	65	0.010 ± .001
	85	0.015 ± .001
	105	0.036 ± .001
$BrF_3 - Br_2$ (5 mole %)	85	0.05 ± .006
(10 mole %)	85	0.08 ± .006
$BrF_3 - UF_6$ (5 mole %)	85	1.6

* Dissolution rate is measured by weight loss in a highly purified uranium cylinder rotating at a peripheral speed of 3000 cm/min over a 15-minute interval.

† No appreciable change in concentration took place during the experiment.

‡ Each value except the last is the average of several runs.

Uranium hexafluoride itself would not be expected to be an acid in bromine trifluoride. However, it accelerates too markedly the rate of dissolution, at least in the moderate temperature range. The behavior of uranium hexafluoride may be correlated with the acid base concept by assuming the existence of significant quantities of an intermediate UF_6^- or $UF_6^=$ anion in a system in which uranium metal is dissolving.

Since these products which accelerate the rate of dissolution of uranium in bromine trifluoride are produced by the dissolution, the simple closed system dissolution of uranium in bromine trifluoride is autocatalytic. If such a system is heated to some moderate temperature, it is easy to divide the dissolution into two stages: an incubation period in which heat must be put in to maintain the temperature and only a small reaction is taking place; and a vigorous reaction period in which cooling is required to dissipate the heat of the reaction which may take place as rapidly as the experimenter is willing to permit.

On the other hand, if the products of the reaction are removed as rapidly as they are generated by distillation or an inert gas purge or even if the bromine is destroyed by continuous admission of fluorine as the reaction proceeds, a higher temperature is required in our equipment for speedy dissolution.

The effect of uranium hexafluoride generated during dissolutions conducted under a fluorine atmosphere is obscure. The actual dissolution rates observed under these conditions are not substantially higher than might be anticipated for pure bromine trifluoride at the temperature employed. A detailed discussion of this point must be postponed.

While some of the details of the uranium dissolution remain obscure, it might be mentioned that the dissolution of uranium metal in nitric acid is about as complex and on the whole no better understood. From the practical point of view, there appears to be no problem in the readily controllable liquid-phase dissolution of uranium metal in bromine trifluoride solutions at a convenient rate. Optimum conditions can only be established for a more completely specified fuel element and dissolver. Although laboratory operations have been confined to batch-type dissolutions, a flowsheet which involves continuous removal of the products of the dissolution is obviously adapted to the design of continuous dissolution equipment.

Other halogen fluoride solutions may be employed. A group at Oak Ridge[7b] has investigated the chlorine trifluoride-hydrogen fluoride system as a solvent with very comparable results.

Plutonium Behavior in a Fluoride Volatility Process

The fate of plutonium in a process aimed at the recovery of uranium is of obvious interest. Using a high temperature procedure such as the ignition of uranium in an atmosphere of gaseous fluorine, a substantial fraction of the plutonium is converted to a volatile form and carried with the uranium. Procedures have been developed for removing this plutonium from a uranium hexafluoride gas stream with rather high efficiency, for example, by absorption on alundum.[7a] Earlier investigations with bromine trifluoride dissolutions of irradiated uranium containing small amounts of plutonium (ca 10 parts per million) gave uranium hexafluoride fractions with detectable plutonium concentrations corresponding to a few tenths of a part per million of plutonium in uranium. It was feared that a similar fraction of the plutonium would be volatilized when uranium containing a higher concentration of plutonium was employed. The presence of parts per million of plutonium in uranium hexafluoride would be undesirable in the final product. Experiments on plutonium compounds as well as slightly irradiated uranium pointed to a substantially lowered volatile plutonium product if bromine were eliminated from the dissolution media either by continuous refluorination or continuous removal of the volatile components. In view of the improved control of the dissolution procedure observed when these procedures were employed, they were adopted for most of the laboratory dissolution and decontamination experiments and the amount of plutonium in uranium hexafluoride fractions reduced below the limits of analytical detection. Recent experiments in which more concentrated plutonium alloys have been treated in the presence of bromine have failed to confirm the fears of higher plutonium content in the volatile fraction.

It may be mentioned that an intensive effort was made to produce plutonium hexafluoride in high yield by some suitable modification of the low temperature halogen fluoride procedure. No approach has been successful. If plutonium hexafluoride is contacted with bromine trifluoride, it is reduced to the tetrafluoride, an extremely insoluble species. While in principle this procedure might be reversed by rapid removal of plutonium hexafluoride if a mobile equilibrium could be established, in practice the rate of dissolution of the tetrafluoride has never been speeded up sufficiently to permit a useful yield.

If all volatile material is removed from the dissolver, via the vapor phase, the residual nonvolatile plutonium and fission product fluorides may be periodically washed from the dissolver with an aqueous aluminum nitrate or similar solution capable of solubilizing these fluorides. Such a solution might be processed by solvent extraction methods discussed elsewhere in these Proceedings. This procedure is completely satisfactory from a chemical point of view. It does offer engineering difficulties in view of the incompatibility of bromine trifluoride solutions and aqueous solutions and the potential hazards involved in employing such solutions in the same equipment. The serious corrosion problems presented by alternate use of aqueous solutions and bromine trifluoride appear to have been solved.

To reduce these problems, the plutonium might be removed from the dissolver as a slurry in liquid

bromine trifluoride and concentrated in a small auxiliary vessel where subsequent operations might present a substantially reduced hazard. This procedure would probably involve including a finely divided insoluble fluoride, e.g., aluminum fluoride, in the bromine trifluoride menstruum. Alternatively, a high temperature fluorination of the residual plutonium might be employed for this step. Both of these procedures are chemically feasible and offer engineering problems of some difficulty.

The Purification of the Uranium Hexafluoride

The distillation and purification of uranium hexafluoride, both in discussion and in practice, may be conveniently considered in two steps, i.e., more volatile and less volatile impurities. In the more volatile category we have the macro impurities, bromine pentafluoride, hydrogen fluoride, and radioactive fission product tellurium as the hexafluoride. Bromine or bromine monofluoride might be a more volatile impurity; however, it appears best at the present time to refluorinate any bromine in the system before the distillation purification. The separation of bromine pentafluoride and uranium hexafluoride would be the most difficult single distillation separation encountered based on the vapor pressure of the pure materials (cf. Table I).

The design of a separation still to remove more volatile constituents is complicated by the high triple point pressure of uranium hexafluoride (1137 mm of mercury at 64.02°C). To maintain a liquid phase at all times, the still must be under pressure unless the uranium is present as a dilute solution. Batch equipment, such as has been operated on the laboratory scale at Argonne National Laboratory for the decontamination runs summarized in Table IV, has not on the whole been very satisfactory. Neither high yield nor specially pure uranium hexafluoride has been obtained.

A variety of dissolution and feed treatments was employed. In each case the distillations were performed in a nickel distillation column containing a two-foot section of randomly packed nickel helices. Decontamination factors for tellurium have varied widely, due at least in part to operational difficulties. The equipment was not designed to minimize recontamination with separated tellurium. Various reflux ratio and temperature control methods were tried. Repeated single stage separations on a vacuum line have yielded higher decontamination factors up to approximately 4000, and some larger scale tellurium-uranium separations in continuous equipment tested at Brookhaven National Laboratory[7c] gave more consistent decontamination factors close to 1000. In the Oak Ridge studies employing chlorine trifluoride no difficulty was found in achieving decontamination factors for tellurium of 10^6.[7b] These numbers tend to confirm the feasibility of tellurium-uranium separations, though it cannot be regarded as a completely solved problem.

Table IV. Selected Laboratory Experiments in the Decontamination of Uranium by Distillation*

Uranium collected in best cut (% of feed)	*Decontamination factors†*		
	Gross β	*Gross β-γ*	*Te‡*
20	10^5	3×10^8	50
60	10^5	6×10^8	5
15	10^5	10^4	100
45	2×10^5	5×10^4	1000

* In each case, the uranium was dissolved in bromine trifluoride and the bromine refluorinated either with fluorine or chlorine trifluoride. The resulting solution was distilled through a laboratory column and several fractions collected. While the best cut was usually better than 90% UF_6 no material free of interhalogens was collected.

† Decontamination factor is defined as (counts/min/gm U in feed)/(cpm/gm U in best cut).

‡ Depending on irradiation and cooling time, the fraction of radioactivity attributable to tellurium may vary considerably. In the data reported Te was the only important residual fission activity except in the last run. In this run, the best uranium fraction was collected just before distillation of the bromine trifluoride. In this fraction 50% of the γ-activity was due to iodine.

In practice the distillation of uranium hexafluoride and its separation from less volatile constituents has proved to be much more readily accomplished on the laboratory scale than the separation of more volatile constituents. A short and uncomplicated distillation tower yields uranium hexafluoride essentially free of either bromine trifluoride or any significant fission product impurity less volatile than the uranium hexafluoride.

Although no implications may be drawn at this point as to the need for multiple processing procedures for uranium decontamination, it is worth noting that the specific fission product troublesome in the volatility processing, i.e., tellurium, is not a significant impurity in uranium decontaminated by solvent extraction processes; likewise, the principal impurities found in uranium decontaminated by a solvent extraction process, i.e., Ru and Zr, are not found as significant contaminants in the distillation separation.

Halogen Fluoride Recovery and Waste Disposal

As the flowsheet in Fig. 2 shows, bromine trifluoride is recirculated to the dissolver. The bromine trifluoride appears to be readily separable by simple distillation from all the fission products except the iodine. Since this reagent would be re-used immediately in the dissolver, no real decontamination is required. The 8-day half-life of the iodine limits the ultimate activity to what appears to be a tolerable amount. A separate iodine recovery step should be technically feasible though not really justified. The bulk of the fission product waste will be concentrated with the plutonium and will ultimately appear as wastes from the plutonium processing.

PROCESSING OF IRRADIATED ENRICHED REACTOR FUELS USING URANIUM HEXAFLUORIDE

Many of the power reactors in the United States, either proposed or in use, use enriched uranium as the fuel. In most of these reactors the fuel is diluted

with some inert material. It is believed that the use of uranium hexafluoride suggests sufficiently simple recovery schemes for these enriched reactor fuels that costs for equipment, shielding, and for labor in plant operation are markedly decreased. It is hoped, as in the processing of plutonium-uranium alloys, that the simplifications will be great enough that they will more than compensate for the use of the rather expensive reagent fluorine.

Since most of the fuel elements of enriched reactors currently under consideration are not easily fluorinated at modest temperatures by reagents such as fluorine, bromine trifluoride or chlorine trifluoride, attention has been directed toward high temperature fluorination procedures. The following information is offered in the spirit of a progress report since laboratory and pilot plant studies, both at Argonne and Oak Ridge are still being carried out.

General Outline of Sodium Fluoride-Zirconium Fluoride Approach

Zirconium-containing fuel elements are immersed in molten sodium fluoride-zirconium fluoride at perhaps 600 to 700°C. A typical melt contains 45 mole % zirconium fluoride. The fuel element is dissolved in the melt by bubbling anhydrous hydrogen fluoride through it. Hydrogen is given off. An inert gas is passed through the melt to sweep out the hydrogen and the uranium fluoride dissolved in the melt is then fluorinated to the hexafluoride and distilled. This fluorination can be carried out with fluorine, bromine trifluoride, bromine pentafluoride, and probably chlorine trifluoride.

The ratio of zirconium metal dissolved to fused salt used in the dissolving operation is so selected that on dissolving a batch of fuel elements the zirconium concentration increases from 45 to perhaps 55 mole%. The bulk of the fission products should remain behind in the fused salt media. After a batch of fuel elements has been dissolved and the uranium volatilized from the melt a fraction of the melt is discharged to waste. The melt composition is then readjusted to 45 mole% by adding sodium fluoride.

The waste from this process might be poured into cans or long pipes and capped for storage. The volume of the fused salt waste is less than one-tenth that of a solvent extraction scheme worked out for the recovery and decontamination of uranium from a zirconium-containing fuel element. The corrosion problems to be overcome in the dissolving vessel are quite serious and represent a major hurdle for this type of process.

Hydrofluorination Studies

A systematic series of hydrofluorination runs was performed on zirconium metal, giving the results indicated in Table V. The data show that the rate is proportional to the 0.75 power of time but that there is only a small temperature coefficient for the dissolution rate (activation energy, 6 kcal per mole). It should be emphasized that the dissolution rates reported are very much functions of the geometry of the experimental equipment and are useful only in estimating the rates in other pieces of equipment.

Selection of Fused Salt System

The selection of the sodium fluoride-zirconium fluoride fused salt system as a dissolving medium probably requires some explanation. One reason is that zirconium is a likely major component of reactor fuels. A second reason for its selection is that there is a liquid phase region in the composition range from 45 to 55 mole% zirconium fluoride above 550°C. In the processing scheme outlined it is necessary to keep within these composition limits and above 550°C.

Fluorination of Uranium in the Melt to the Hexafluoride

The experimental work on the fluorination of the fused salt systems resulting from the hydrofluorination step has been done with fluorine, bromine pentafluoride, and bromine trifluoride. Since corrosion and efficiency data are lacking it is still too early in the developmental program to determine which fluorinating agent is best. The interhalogen fluorinating agents have the advantage of being easily condensible as contrasted to fluorine. This may be a point of some importance, since it is difficult to imagine that this type of gas-liquid reaction could be run with high fluorinating efficiency. It will therefore be nec-

Table V. Dissolution of Zirconium Metal by Hydrofluorination in Fused Sodium Fluoride-Zirconium Fluoride*

Run time, hours	Temperature, °C	Amount dissolved, %	Penetration rate, mm/hr	HF addition rate, gram/min	HF efficiency, %
1	700	30	0.34	0.62	16
2	700	41	0.23	0.56	12
3	700	69	0.26	0.53	14
4	700	86	0.24	0.58	12
2	700	34	0.19	0.11	48
2	700	54	0.30	0.62	14
2	700	60	0.34	1.43	7
3	600	56	0.20	0.63	11
3	800	100	0.38	0.59	18

* Melt volume: 50 ml. Initial melt composition: 1 mole NaF, 1 mole ZrF_4. Coupon: Zr Metal, 1 inch × 2 inches × 0.1 inch; approximate weight, 20 grams. Pressure: 1 atmosphere. Conditions: Hydrogen fluoride bubbled through fused salt.

essary to recirculate, in some manner, the excess fluorinating agent. In the case of fluorine this involves the use of a fluorine pump. Such a piece of equipment will probably become radioactive and will probably be difficult to maintain in good operating condition. If easily condensible fluorinating agents such as the interhalogens are used the excess fluorinating agent can be easily recycled.

The Use of Fluorine as the Fluorinating Agent

The following experiment was done to investigate the use of fluorine as a fluorinating agent. A zirconium-uranium alloy, high in zirconium, was dissolved in an equi-molar sodium fluoride-zirconium fluoride melt at 600°C by bubbling hydrogen fluoride through the system. After the dissolution was complete, fluorine was bubbled through the melt for 5 hours at 600°C with an efficiency of 21%. Analysis of the melt showed that 0.3% of the uranium remained in the salt residue. It can therefore be concluded from this typical experiment that uranium can be readily recovered from the melt.

The Use of Interhalogens as the Fluorinating Agent

Since no data are available on the use of bromine trifluoride or bromine pentafluoride at 600°C, blank experiments were done by bubbling the interhalogen through the sodium fluoride-zirconium fluoride fused salt system. Both bromine trifluoride and bromine pentafluoride reacted to the extent of 5 to 10%. The product of the experiment with bromine trifluoride contained bromine and with bromine pentafluoride contained bromine trifluoride, indicating reduction rather than disproportionation.

It was found that zirconium metal as well as uranium could be dissolved quite rapidly at about 630–650°C using either bromine trifluoride or bromine pentafluoride. However, if all the zirconium in a zirconium matrix fuel were fluorinated, there would have to be some strong compensating economic advantage for the use of bromine pentafluoride to fluorinate the bulk constituent. It was also found that in two hours at 630°C all the uranium was recovered within analytical accuracy when uranium tetrafluoride was fluorinated in equi-molar sodium fluoride-zirconium fluoride with bromine pentafluoride.

Fission Product and Plutonium Separation

It can be expected that uranium hexafluoride will be separated from the nonvolatile fission products directly. The recovered uranium hexafluoride can readily be purified by redistillation as described previously. Of course, it is an objective of the developmental work to retain as much of the fission products as possible in the fused salt since this simplifies the waste disposal problem. However, our laboratory group has not yet done experiments on the behavior of fission products and plutonium with bromine pentafluoride as a fluorinating agent.

Application to Other Enriched Reactor Fuels

A number of exploratory experiments have been made to determine if this method of processing reactor fuels could apply to other fuels besides the zirconium matrix type.

At 600°C in a fused salt melt stainless steel type 347 was penetrated by fluorine at the rate of 0.3 mm/hr, but only 0.05 mm/hr by hydrogen fluoride at 700°C. Uranium trioxide and U_3O_8 were readily converted to the hexafluoride at 700°C by fluorine.

RECENT CONTRIBUTIONS TO FLUORINE TECHNOLOGY

In conjunction with the development of methods of processing reactor fuels using fluorine chemistry, it has been necessary to solve a number of practical problems. Some of the practical lessons in the handling of interhalogens are discussed below. The ignition of uranium and of other materials in fluorine and interhalogens has been investigated. Corrosion studies of a number of different types have been carried out, although much more work in this field remains to be done. A pilot plant for testing the flowsheet of Fig. 2 has been built.

Handling the Halogen Fluorides

The halogen fluorides are among the more potent oxidizing agents available. The stability of hydrogen fluoride is so great that all other hydrogen-containing materials react vigorously to yield this compound. Once it is recognized that contact between the halogen fluorides and any readily oxidizable or hydrogen-bearing material usually results in a vigorous reaction, the materials can be handled safely.

Laboratory work with bromine trifluoride can be done in quartz apparatus. Only occasionally, especially when halogen fluoride-hydrogen fluoride mixtures are involved, is quartz appreciably attacked in short experiments. Quartz has been used for windows on optical cells of various types although the windows must be replaced from time to time. Fortunately for the large scale use of the halogen fluorides, common metals such as iron, nickel, aluminum, magnesium, and copper form coherent protective films which make their use as construction materials practical. Mild steel is ordinarily employed in equipment for the production of the crude halogen fluorides, and steel containers are used in shipping these reagents. However, especially in the presence of moisture and the resulting hydrogen fluoride, corrosion of steel containers is quite evident, and substantial quantities of ferric fluoride are found in these reagents. Nickel or Monel have been favored at Argonne for the construction of semi-permanent laboratory equipment. Nickel bomb-tubes have been used with bromine trifluoride at temperatures in excess of 350°C without visible attack. Nickel welds appear to be as impervious to attack as the base metal itself. Aluminum is a possible material of construction although our laboratory group

has had unfavorable experiences with aluminum equipment which was alternately exposed to atmospheric moisture and interhalogens. All metal equipment will deteriorate to a certain extent under these conditions, but aluminum seems worse than nickel or Monel. Copper is less satisfactory than nickel or Monel. However, since it is so easy to construct equipment from copper it has been used by our group.

Another type of material which can successfully be used is the highly fluorinated plastics. For example, Teflon (polymerized tetrafluoroethylene) and Fluorothene (polymerized monochlorotrifluoroethylene) are both safe in ordinary laboratory practice. The latter material, of course, has the virtue of being transparent. Our laboratory group has made extensive use of Fluorothene test tubes.

One of the most critical laboratory equipment components is the valve. Those of the packless variety are generally favored for this type of work. The most frequently used valve in our group has been the Hoke (411-417 series) ¼-inch Inconel diaphragm valve with a Monel body and seat and a Duranickel spindle. Teflon diaphragm valves such as the brass Imperial "Red Head" model are suitable for some applications, as are the brass or bronze bellows types represented by the Crane ¼-inch unit. A particularly useful model for small apparatus is the Hoke (No. 1103) model with a Monel body and bronze bellows. Monel bellows valves are also available from both Hoke (No. 1132) and Fulton-Sylphon.

CORROSION STUDIES

Corrosion of Possible Equipment Materials in Interhalogen Systems

Long term corrosion studies have been conducted on several materials of construction commonly used for interhalogen systems. The observed corrosion rates in mils per year are presented in Table VI. It will be noted from the data that nickel and Monel, both welded and unwelded, K-Monel and Inconel appear to be excellent materials of construction for interhalogen use. Duranickel, Incoloy and aluminum might be useful in non-critical applications. Magnesium appears to be a material of construction which might merit further consideration. Nicloy-9 corroded quite seriously.

Corrosion of Possible Construction Materials by Aqueous Systems

Since the present scheme of processing plutonium-uranium alloys by a fluoride volatility method suggests the removal of plutonium and fission product fluorides from the Monel or nickel vessel by washing it with an aluminum nitrate solution, it is appropriate to investigate the corrosion under these circumstances.

The corrosion of Monel by aqueous aluminum nitrate is acceptable only in a narrow range of conditions and might become serious because of maloperation of equipment or operational mistakes. It is believed that nitrous acid is an intermediate species in the corrosion mechanism since the corrosion is probably due to nitrate oxidation of the metal. This hypothesis offers the possibility of inhibiting corrosion by nitrous acid removal through additions of sulfamic acid, ferrous sulfate, urea, or other similar reagents. It was found that sulfamic acid was the most effective additive.

The conditions of the experiments and typical data are presented in Fig. 3 to illustrate the effects of time and sulfamic acid concentration. The upper curve shows the total corrosion at a particular time by an aluminum nitrate solution in the absence of sulfamic acid. The lowering of the corrosion rate with time is associated with the consumption of acid during the test.

Table VI. Corrosion in Interhalogen Systems at 125°C¶

Metal	Time of exposure (weeks)	Penetration in mils per year: Pure BrF_3* Vapor	Pure BrF_3* Interface	Pure BrF_3* Liquid	10% BrF_5 – 90% BrF_3 Vapor	10% BrF_5 – 90% BrF_3 Interface	10% BrF_5 – 90% BrF_3 Liquid	10% Br_2 – 90% BrF_3 Vapor	10% Br_2 – 90% BrF_3 Interface	10% Br_2 – 90% BrF_3 Liquid
Nickel	11	+†	+	+	+	0.006	0.012	+	0.002	0.004
Welded Nickel	11	+	0.0004	+	0	0.012	0.005	+	0.001	0.006
Monel	11	+	+	0.005	+	0.025	0.029	+	0.020	0.024
Welded Monel	11	+	+	0.005	0.004	0.029	0.018	+	0.015	0.033
K-Monel	11	0.0002	0.003	0.007	0.009	0.031	0.036	0.008	0.025	0.034
Inconel	11	0.0005	0.010	0.027	0.0008	0.045	0.046	+	0.029	0.041
Duranickel	4	0.12	0.28	0.30	0.23	0.30	0.26	0.30	0.37	0.37
Incoloy	4	1.3	3.2	3.6	1.4	1.5	1.7	0.74	1.0	0.9
Aluminum‡	4	0	0.71	0.70	0.19	0.10	+	0	0.17	+
Magnesium§	4	-	-	+	5.3	-	+	-	-	+
Stainless Steel	1	2.8	3.6	3.4	11	6	6.9	1.3	2.0	2.0
Mild Steel	1	4.9	7.7	7.8	-	16	19	2.7	4.9	4.1
Nicoloy-9	1	-	74	-	-	160	-	-	27	-

* The exposure time for pure bromine trifluoride to nickel through Inconel was 20 weeks instead of 11.

† + indicates a weight gain.

‡ Concentrated HNO_3 wash used to remove fluoride film from aluminum.

§ No method devised for film removal without attack of coupon. Weight changes are of the same order of magnitude as Duranickel, so penetrations should be of the same order of magnitude.

¶ 1⅜ in. × 1⅜ in. × 1/16 in. coupons initially polished with fine steel wool and scouring cleanser paste, washed, degreased and dried at 110°C. Supported in interhalogen between Teflon spacers. Fluoride films removed with 1 *M* $Al(NO_3)_3$, 0.05 *M* sulfamic acid, pH 0.5.

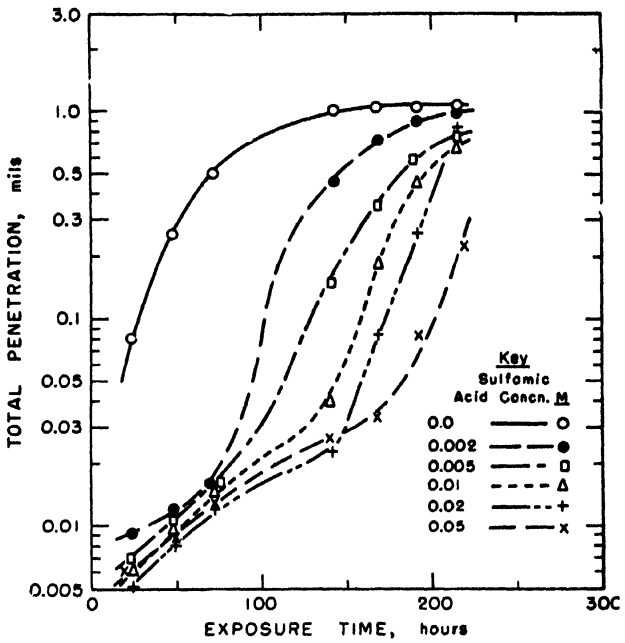

Figure 3. Inhibiting nitrate (125 ml 0.1M Al-nitrate, pH 0.5) corrosion of Monel with sulfamic acid at 70°C in N_2 atmosphere. Two 1× 1 × 1/32 in test coupons used, washed with Br F_3

The corrosion inhibition is shown to increase with increasing sulfamic acid concentration. The inhibiting effect is appreciable for 75 hours at a sulfamic acid concentration of 0.005*M*. This inhibiting effect decreases the corrosion by a factor of about 30. For 0.01*M* sulfamic acid the effect lasts for about 140 hours and for 0.05*M* about 175 hours. It is important to emphasize that in this type of operation the total penetration is a function of the ratio of metal area to solution volume, and that the variable of solution pH is controllable only at the beginning.

Monel Corrosion in Cyclic Exposure to Aqueous and Interhalogen Systems

Since it is proposed in the processing of plutonium-uranium alloys to expose alternately the dissolving vessel to interhalogen and to aqueous systems it is necessary to examine the corrosion resulting from this type of cyclic operation. A cyclic operation was set up to duplicate that which might be expected in a typical separations plant using the flowsheet shown in Fig. 2.

Coupons of nickel, welded nickel, Monel, welded Monel, K-Monel, and Inconel were weighed at the completion of the first, second, third, tenth, twelfth, and fourteenth cycles. The attack was uniform throughout the test and a weight loss corresponding to about 0.005 mil per cycle were found for all coupons. From these corrosion data it appears feasible to cycle between interhalogen and aqueous systems under conditions similar to those in the experiment.

Corrosion Studies in Fused Salt Melts

Some preliminary information is available from a corrosion program just started to determine a suitable material of construction and manner of design for the dissolver vessel needed in the fused salt method of processing enriched reactor fuels. Since steps in which the fluorinating agents are employed appear to be the most corrosive the experiments were started on these steps. The hydrofluorination step has been observed to give rather mild corrosion problems.

Some experiments have been done at 700°C with an equimolar mixture of sodium and zirconium fluorides. The melts were continuously sparged with helium or a helium-fluorine mixture. In 24 hours with helium sparging alone, Inconel showed a penetration of 3 mils per month while the Monel and nickel samples showed slight weight gains. In a second test with a helium sparge for 19 hours and fluorine plus helium for 5 hours the penetration rates for Inconel, Monel, and nickel were 160, 71, and 67 mils per month, respectively. In a third experiment in which the fused salt was sparged with helium for 3 hours and with helium plus fluorine for 3 hours the penetrations for Inconel, Monel, and nickel were 42, 15, and 12 mils per month. The latter corrosion rates were calculated on the basis of the exposure time to fluorine. All nickel samples showed evidence of grain growth.

Corrosion experiments have also been started using bromine pentafluoride as the fluorinating agent. The experiments show that corrosion is quite severe at the equipment locations where bromine pentafluoride gas directly impinges. The problem is apparently not as serious in other locations and may be solved by proper equipment design.

Although it is expected that corrosion will be serious in a processing scheme of this type there are several possible ways of approaching the problem. The dissolver vessel might be made of a less expensive material than nickel, with less corrosion resistance. The dissolver would then be frequently removed and used as a waste storage container. Another way of solving the problem might be to keep solid salt along the vessel wall and internally heat the melt by passing a current through it. The nickel electrodes would be periodically replaced. This procedure has been tried and it seems feasible.

In summary it can be said that although the corrosion problems of this type of process are serious, the fused salt processing scheme for enriched reactor fuels is simple enough that rather extreme solutions are justified.

THE BEHAVIOR OF VARIOUS MATERIALS IN FLUORINATING MEDIA AT ELEVATED TEMPERATURES

The experiments described below were undertaken to determine the behavior of uranium in bromine trifluoride at higher temperatures and to define an upper temperature limit for safe dissolving procedures. For comparison purposes, the reactions between uranium and chlorine trifluoride, bromine pentafluoride, and fluorine were studied, but to a lesser extent than the uranium-bromine trifluoride

reaction. Hazardous conditions were found to exist in the uranium-vapor reactions at elevated temperatures with each of these fluorinating reagents; conditions of "ignition" of the uranium were determined. It should be emphasized that in fluorinating uranium it is advisable to keep the uranium covered with interhalogens. The results of test exposures of some other pertinent materials are given below.

Description of Apparatus and Procedure

The apparatus and procedures used in these experiments will be described in detail in a forthcoming publication.

The bromine trifluoride and uranium were usually heated separately; then the liquid bromine trifluoride was flashed into the reaction cell to a level completely covering the uranium. The reaction cell was designed so that the uranium could be watched during the experiment. The uranium was in the form of a cube, slightly less than ¼ inch on each side, with a circular hole in one face into which an Inconel-Constantan needle thermocouple was inserted. The sample was supported in the field of view by the thermocouple and isolated from the walls of the cell; heat loss from the sample by conduction was thereby minimized. The reaction could be carried out in the liquid phase, or the liquid level could be lowered to expose completely the uranium to vapor by opening the drainage valve. In the latter case, some liquid remained in the bottom of the cell and maintained its vapor pressure in the system. The surface of the uranium cube probably remained wet for a short time after the liquid was drained off; the conditions were therefore not representative of a true solid-vapor reaction but of a situation which might occur in process work. Most of the experiments were done in this manner, but, for comparison, uranium was also exposed to bromine trifluoride vapor without first being wetted by liquid, and the behavior was affected by the change of conditions.

In experiments with chlorine trifluoride and bromine pentafluoride, the high vapor pressures restricted the temperatures to which the liquid phases could be heated. Uranium was heated to 170°C in liquid bromine pentafluoride, then the liquid was drained off, and the temperature was increased further with only vapor in the reaction cell. The vapor-phase fluorinations in chlorine trifluoride were carried out by condensing a small amount of liquid in the cell, then vaporizing it completely by raising the temperature. An approximate threshold temperature was determined for the ignition of uranium in each reagent.

Test specimens of aluminum, copper, iron, magnesium, zirconium, and Fluorothene were machined into ¼-inch cubes and tested in the manner described above for uranium. Since the apparatus was constructed of nickel, Monel, Inconel, brass, quartz, and Teflon, some knowledge of the reactivity of these materials was also obtained.

DISCUSSION OF RESULTS

Uranium Exposed to Liquid Reagents

In all exposures of uranium to liquid halogen fluorides, the uranium dissolved smoothly and the temperature remained constant or rose slowly due to the heat liberated by the reaction. Temperatures of 210, 170, and 70°C were reached with bromine trifluoride, bromine pentafluoride, and chlorine trifluoride, respectively.

Uranium Exposed to Gaseous Reagents

In all experiments in which uranium was first covered with liquid bromine trifluoride and then exposed to bromine trifluoride vapor at 150°C or higher, ignition of the test specimen occurred. The temperature rose slightly for about one or two minutes, then surged abruptly above the melting point of uranium. Usually the Inconel-Constantan thermocouple also melted, indicating that the temperature exceeded 1400°C at the peak. The pressure increased only slightly during ignition.

The data for ignition of uranium in bromine trifluoride vapor after immersion in liquid are given in Part A of Table VII. The "Initial Uranium Temperature" is the temperature at which the liquid level was lowered, exposing the uranium to vapor, and the "Contact Time" is the elapsed time in the vapor before ignition. It can be seen that at 150°C or higher, ignition usually occurred within several minutes. No ignitions were observed below 150°C. This lower temperature limit is not sharply defined, however, and is probably dependent upon such conditions as the surface-to-volume ratio of the uranium, the surface pretreatment, and especially the heat transfer to surroundings.

The addition of uranium hexafluoride or bromine to the bromine trifluoride raised the threshold temperature for ignition slightly. Both of these substainces, therefore, appear to be inert diluents in the vapor-phase reaction. Since uranium hexafluoride

Table VII. Ignition of Uranium Metal in Vapor-Phase Fluorination; Some Typical Runs*

Reagent (vapor)	*Initial U temperature, °C*	*Ignition temperature, °C*	*Vapor contact time, min*
Part A: Uranium exposed to vapor after immersion in liquid			
BrF_3	155	185	8
BrF_3	135	150	20
BrF_3	150	150	2
BrF_3	160	160	2
BrF_3+UF_6†	160	170	17
BrF_3+Br_2‡	135	160	14
Part B: Uranium exposed to vapor without prior liquid immersion			
BrF_3	25	190	68
BrF_3	25	190	70

* Approximately 3 grams of alpha-rolled uranium used in each experiment. Pressure = vapor pressure of liquid reagent at indicated temperature.
† Initial solution composition 10.3 mole % UF_6.
‡ Initial solution composition 17 mole % Br_2.

and bromine are both more volatile than bromine trifluoride, their concentrations in the vapor phase in these experiments were higher than the solution concentrations given in Table VII.

The results of two experiments in which uranium was heated in bromine trifluoride vapor without prior immersion in liquid are given in Part B of Table VII. Here the "Contact Time" is the entire period of heating from room temperature to the ignition temperature. The uranium ignited at 190°C in both experiments. This indicates that the ignitions at lower temperatures were largely due to liquid bromine trifluoride adhering to the surface of the uranium. The surface liquid would be expected to provide a high initial reaction rate and high output of heat.

Uranium was also found to ignite in vapor-phase reactions with bromine pentafluoride, chlorine, and fluorine. The minimum temperatures at which ignitions were produced in these reagents were 225°, 205°, and 260°, respectively. The lowest ignition temperature of uranium in chlorine trifluoride vapor (205°) differed but little from that in bromine trifluoride vapor (190°) in the experiments in which the uranium was not first wetted by liquid. During an ignition, the pressure usually rose slightly and then dropped to a final value only two or three per cent below the initial value.

Other Materials, Liquid and Gaseous Reagents

The behaviors of other materials were investigated in liquid bromine trifluoride (up to about 200°C), bromine pentafluoride (up to 120°C). Investigations in gaseous bromine trifluoride, bromine pentafluoride, chlorine trifluoride, and fluorine up to temperatures of about 400, 350, 340, and 360°C, respectively, were also carried out. All of the test specimens were ¼-inch cubes except the platinum, which consisted of 1-gram pieces of 10-mil foil wrapped around the tip of the needle thermocouple. In the vapor-phase experiments, the liquid beneath the specimen was usually vaporized completely before the final temperature was reached.

Aluminum, copper, iron, and magnesium were attacked very little by any of the reagents. The ¼-inch cubes usually lost or gained a few milligrams as the result of corrosion or surface fluorination.

Platinum readily dissolved in liquid bromine trifluoride at 150°C and was not tested further.

Zirconium was only slightly attacked by liquid bromine trifluoride and bromine pentafluoride but proved to be unstable in the vapor-phase reactions. The test specimens ignited in vapor-phase reactions with chlorine trifluoride and fluorine. In one experiment with bromine trifluoride vapor, no noticeable changes occurred, but in all subsequent vapor exposures the zirconium became heavily coated with a thick white scale, and rapid temperature surges were recorded.

Fluorothene ignited in vapor-phase reactions with chlorine trifluoride and fluorine. Although it did not ignite in the vapors of bromine trifluoride and bromine pentafluoride, the number of experiments was too small to establish this with certainty. It probably cannot be considered safe for use with the latter two reagents above 125°C.

The Teflon gaskets used to seal the windows of the reaction cell did not react noticeably below 200°, but at higher temperatures they occasionally caught fire in the fluorinating agents. The nickel, Monel, and Inconel parts of the apparatus were stable in all of the experiments. The brass parts were slightly corroded but remained serviceable. The quartz windows were etched by the halogen fluorides. However, they remained transparent while wetted with liquid and could be used for a number of experiments before replacement became necessary.

ACKNOWLEDGEMENTS

The authors have profited greatly by discussions with the personnel of Brookhaven National Laboratory, Los Alamos National Laboratory, North American Aviation, and the groups in the K-25 plant and in the Chemical Technology Division at Oak Ridge National Laboratory. We regret that space does not permit a more personal acknowledgement.

REFERENCES

1. Simons, J. H., Editor, *Fluorine Chemistry,* Academic Press, New York, N. Y. (1950).
2. Ruff, O., *Fluorine and Its Compounds,* Ber. 69A; 181 (1936). (And many earlier papers.)
3. Katz, J. J. and Rabinowitch, E., *The Chemistry of Uranium,* National Nuclear Energy Series, Division VIII, Vol. 5, McGraw-Hill Book Co., Inc., New York.
4. Oliver, G. D., Milton, H. J. and Grisard, J. W., *Vapor Pressure and Critical Constants of UF_6,* J. Am. Chem. Soc., *75*: 2827 (1953).
5. Stein, L. and Vogel, R. C., *Refractive Indices of Systems UF_6–BrF_3 and UF_6–BrF_5,* J. Am. Chem. Soc. *76*: 6028 (1954).
6. Seaborg, G. T. and Katz, J. J., *The Actinide Elements,* National Nuclear Energy Series, Division IV, Vol. 14A, McGraw-Hill Book Co., Inc., New York (1954).
7. Unpublished Research from: (*a*) Oak Ridge National Laboratory, Oak Ridge, Tennessee; (*b*) Research Laboratories, K–25 Plant, Carbon and Carbide Division, U. C. and C., Oak Ridge, Tennessee; (*c*) Brookhaven National Laboratory; and (*d*) Los Alamos National Laboratory.
8. Yost, D. M., and Clausen, W. H., *The Thermochemical Constants of the Hexafluorides of Sulfur, Selenium and Tellurium,* J. Am. Chem. Soc., *55*: 885 (1933).
9. English, W. D. and Dale, J. W., *Te_2F_{10},* J. Chem. Soc.: 2498 (1953).
10. Greenwood, N., *Physico-Chemical Properties of the Interhalogen Compounds,* Rev. Pure Appl. Chem. *1*: 84–120 (1951).
11. Sharpe, A. G., *Interhalogen Compounds and Polyhalides,* Quart. Rev. 4: 114 (1950).
12. Emeleus, H. J. and Woolf, A. A., *Bromine Trifluoride as an Ionizing Solvent,* J. Chem. Soc.: 2865 (1949).
13. Banks, A. A., Emeleus, H. J. and Woolf, A. A., *Electrical Conductivity of Chlorine Trifluoride, Bromine Trifluoride and Iodine Pentafluoride,* J. Chem. Soc.: 2861 (1949).
14. Sheft, I., Hyman, H. H. and Katz, J. J., *Solubility of Some Metal Fluorides in Bromine Trifluoride,* J. Am. Chem. Soc. *75*: 5221 (1953).

15. Fischer, J., Steunenberg, R. K. and Vogel, R. C., *Phase Equilibria in the Condensed System Bromine-Bromine Trifluoride*, J. Am. Chem. Soc. *76*: 1497 (1954).
16. Fischer, J. and Vogel, R. C., *Solid-Liquid Phase Equilibria in the Condensed System Bromine-Uranium Hexafluoride*, J. Am. Chem. Soc. *76*: 4862 (1954).
17. Fischer, J. and Vogel, R. C., *Phase Equilibria in the Condensed System Uranium Hexafluoride-Bromine Trifluoride and Uranium Hexafluoride-Bromine Pentafluoride*, J. Am. Chem. Soc. *76*: 4829 (1954).
18. Aoyama, S. and Kanda, E., *Studies of Fluorine at Low Temperatures*, Bull. Chem. Soc., Japan *12*: 409 (1937).
19. Ruff, O. and Laass, F., *Constants of Chlorine Fluorides*, Z. anorg. u. allgem. Chem. *183*: 214 (1929).
20. Henkel, P. and Klemm, W., *The Vapor Pressure of Selenium Hexafluoride and Tellurium Hexafluoride*, Z. anorg. u. allgem. Chem. *222*: 65 (1935).
21. International Critical Tables, McGraw-Hill Book Co., Inc., New York (1926).
22. Grisard, J. W., Bernhardt, H. A. and Oliver, G. D., *Thermal Data, Vapor Pressure and Entropy of ClF_3*, J. Am. Chem. Soc. *73*: 5725 (1951).
23. Rogers, Max J., Speirs, John T., Thompson, H. B. and Panish, M. B., *IF_5, Freezing and Boiling Point, Heat of Vaporization, Vapor Pressure-Temperature Relationship*, J. Am. Chem. Soc. *76*: 4843 (1954).
24. Oliver, G. D. and Grisard, J. W., *Thermal Data, Vapor Pressure and Entropy of BrF_3*, J. Am. Chem. Soc. *74*: 2705 (1952).
25. Junkins, J. H., Farrar, R. F., Jr., Varber, E. J. and Bernhardt, H. A. *Preparation and Physics Properties of NbF_5*, J. Am. Soc. *74*: 3464 (1952).
26. Junkins, J. H., Bernhardt, H. A. and Barber, E. J., *Preparation and Properties of TeF_4*, J. Am. Chem. Soc. *74*: 5749 (1952).

Record of Proceedings of Session 22B.1

FRIDAY, 19 AUGUST 1955

Chairman: **Mr. J. P. Baxter (Australia)**
Vice-Chairman: **Mr. F. H. Spedding (USA)**
Scientific Secretaries: **Messrs. B. Prakash and J. Gaunt**

PROGRAMME

P/823 Survey of separations processes ..... S. Lawroski

P/350 Method for separation of uranium-233 from thorium irradiated in atomic piles ..... A. Chesne and P. Regnaut

P/544 Pyrometallurgical processing of nuclear materials ..... H. M. Feder

P/545 The purification of uranium reactor fuel by liquid-metal extraction ..... A. F. Voigt

DISCUSSION

Mr. S. LAWROSKI (USA) presented paper P/823 as follows:

Simultaneously with the development of nuclear reactors for the economic production of power there is needed the development of improved methods for fuel recovery. In this presentation I should like to review some of these methods or separations processes as they are sometimes called.

In the normal course of reactor operation several cycles of burn-up and intervening recovery operations are necessary to obtain the equivalent of a complete utilization of reactor fuel. Therefore, a separations process must strive for high yields and low cost per cycle. It should accomplish this with a minimum of hold-up time to avoid a large inventory of fissionable material. Of course, if the process can recover economically other constituents such as expensive alloying ingredients so much the better.

The degree of purification required of a reprocessing step may vary widely. For example, with homogeneous reactors it is generally conceded that partial decontamination will suffice for reprocessing the fuel. In the case of heterogeneous reactors, substantially complete decontamination has been demanded thus far. This is so as to enable direct-contact manufacture of reactor fuel elements from recovered fuel. If remote fabrication of fuel elements can be conducted economically, then partial decontamination would also be adequate for heterogeneous reactors. The result would be a wider choice of recovery schemes for the reprocessing engineer and improved prospects for minimizing the total costs in a reactor complex to produce power.

Many different separations methods are being studied for fuel recovery purposes in the United States. They are listed in Slide 1 (Table I of P/823).

As Mr. Culler has previously reviewed the last item shown, solvent extraction with organic solvents from aqueous solutions, this review will only be concerned with the first four methods.

There are numerous references to precipitation methods for laboratory separations in the literature. My comments will be confined to a method which has been used for large-scale purposes. I refer, in this instance, to the Bismuth Phosphate Process. It has been used for some time to recover plutonium from irradiated natural uranium and was worked out very sucessfully when only traces of plutonium were available. This process accomplishes the purification of plutonium according to the flowsheet given schematically in Slide 2 (Fig. 1 of P/823).

The separation of plutonium from uranium and from some of the fission products is obtained in the "Extraction Step." In this step a co-precipitation of plutonium phosphate with bismuth phosphate is arranged. Then the precipitate is dissolved in nitric acid and two cycles of decontamination are performed on the plutonium. Each of these cycles consists of a product and a by-product precipitation step with bismuth phosphate. Next, there is a series of operations termed collectively as "Concentration Step."

Typical decontamination factors obtained in the course of the different steps of this process are shown in Slide 3 (Table II of P/823).

In addition to the thorough purification from fission products illustrated by these data, the process gives an excellent removal of uranium as evidenced by the low uranium content in the plutonium product. The recovery of plutonium has also been good. Uranium is not recovered but is recoverable by other methods.

Experience has proved this process to be flexible and easy to scale-up reliably from laboratory-size experimentation. This is because the large-scale equipment necessary is generally very simple in design. Remote operation and maintenance have proved feasible for the process. There are two sig-

nificant disadvantages to this type of process as compared with solvent extraction or fractional distillation type methods. One of these is the lesser adaptability to continuous operation and the other is the somewhat lower yields that can be readily obtainable.

I should next like to remark briefly on the application of ion exchange methods to fuel recovery.

In the atomic energy program, ion exchange methods have been very extensively used in the laboratory to effect very difficult separations. The use of complete ion exchange processes for fuel recovery and purification has been studied up through small-scale pilot plant installations. The work has not yet gone beyond this stage.

However, there has been an important larger-scale application of ion exchange methods for auxiliary steps with other basic types of separations processes. For example, ion exchange has proved to be a very effective method for purposes of concentrating intermediate or final product streams of plutonium, uranium-235 and uranium-233 from solvent-extraction type plants. Because it often purifies as well as concentrates such streams, it has sometimes enabled a solvent extraction cycle to be eliminated.

Other significant large-scale uses of ion exchange have been in conjunction with the preparation of pure process waters and with the decontamination of large volumes of low-level radioactive wastes.

Recent syntheses of certain organic polymers have resulted in a number of ion exchange resins with improved properties in such respects as capacity, concentrating factor, chemical and radiation stability, and regenerative behavior. Techniques for continuous ion exchange operation have also been developed recently. All of these factors may lead to a renewal of interest in the more extensive use of ion exchange for fuel recovery purposes.

The next basic method for full recovery I should like to discuss is that of fractional distillation. This method has always appealed to chemists and chemical engineers working on separations problems in the atomic energy program. One of the reasons for this attitude has been the fact that the basic principles and technology of fractional distillation have been so well developed. Another significant influence has been the economically attractive possibility of recovering uranium directly as the hexafluoride and, hence, a direct tie-in with diffusion plant operations.

From a separation standpoint, it is very encouraging to find that UF_6 has a substantial volatility which is also appreciably different from the volatilities of the fission product fluorides. This is illustrated in Slides 4 and 5 (Tables V and VI of P/823).

These give the boiling points of a number of fission product fluorides. With a few exceptions, the fission product fluorides are less volatile than UF_6. For this reason, substantial decontamination is achievable even with a crude distillation. More complete purification of UF_6 would naturally require more efficient distillation.

Much of the effort on the research and development of fractional distillation processes has understandably been concerned with the preparation of fluoride feed solutions from irradiated uranium fuels. The extreme variation in compositions of these fuels has necessitated a number of approaches to the dissolution problem.

The fluorination or uranium metal with elemental fluorine has proved to be extremely difficult and even hazardous. A practical solution to this problem has been found in the use of liquid-phase fluorinating agents, such as ClF_3–HF or BrF_3. These compounds have convenient liquid ranges as shown in Slide 6. (Table VII of P/823).

Demonstration tests have been conducted on fractional distillation of fluoride feeds from interhalogen dissolutions of irradiated uranium metal. The effectiveness of this procedure is indicated by the results summarized in Slide 7 (Table VIII of P/823).

I should like to point out that plutonium largely remains in the nonvolatile residue. The reason for this is that, unlike uranium, plutonium is not fluorinated to the volatile form, PuF_6, under the usual condition of dissolution with ClF_3–HF or BrF_3. This is a most acceptable situation when one is reprocessing highly enriched uranium and plutonium recovery is unimportant. On the other hand, the procedure is not so attractive for processing irradiated natural uranium for plutonium recovery. In this case, the uranium is recovered all right but the plutonium must be recovered by some other method such as solvent extraction. Work is in progress with the object of finding satisfactory conditions from an engineering standpoint, which yields the plutonium as well as the uranium as the volatile hexafluorides.

Enriched fuels are frequently manufactured with major amounts of alloying agents. Some of these alloy mixtures are not amenable to dissolution with nitric acid nor even with the liquid-phase fluorinating reagents I have just mentioned. Successful dissolution of many such alloys have been accomplished at 500–700°C by fluorinations with HF and F_2 dispersed in a fused salt mixture.

The various fluorinating procedures which I have mentioned enable the dissolution of an imposing number of contemplated reactor fuels. It is expected that at least some of these will contribute to the successful application of fractional distillation methods for fuel reprocessing.

I would now like to discuss briefly pyrometallurgical or high-temperature processes which we are investigating for fuel recovery purposes. In these schemes it is envisaged that the irradiated materials will be processed while held principally in the form of molten metals. That is, it is intended to avoid bulk chemical conversion during purifications operations. If successful, it would mean the achievement of more compact plants, immediately high concentration of fission products for use or disposal and possibly even the recovery of valuable fuel alloying ingredients. It is not anticipated that any of these

high-temperature processing methods would give more than the partial decontamination which is necessary to reconstitute the fuel for satisfactory reuse. Therefore, remote fabrication of fuel is an essential adjunct to these methods of reprocessing.

The development of pyrometallurgical processes has been along two general lines or objectives. In the case of blanket processing, the objective is principally to concentrate the bred fissionable material to a level which is adequate for replenishing the core. In the case of core processing, the objective is to achieve enough removal of those fission products which interfere with satisfactory reactivity or physical properties of the fuel.

For blanket reprocessing, three high-temperature procedures are being studied or considered as prospective means for concentrating plutonium. We have not yet conducted work on thorium blankets by these procedures.

Plutonium can be concentrated by vacuum distillation from molten uranium at 1500–1800°C. As much as 99 per cent plutonium removal has been obtained in laboratory tests of this method as illustrated in Slide 8 (Table IX of P/823.)

Another method of concentrating plutonium from molten uranium is by solvent extraction with fused salts such as UF_4 or $MgCl_2$. Although the uranium is largely recovered as metal, the plutonium is recovered as the fluoride or chloride and later must be reduced to metal.

The third method under examination is again by solvent extraction but, in this instance, with molten metals as extractants. Silver and magnesium have been examined for this purpose. Both are immiscible with uranium and have favorable capacity for extraction of plutonium from the uranium. Inasmuch as the use of silver as an extractant will be discussed later by Spedding, I will present at this time some information on magnesium only.

Slide 9 (Table X of P/823) shows the per cent of plutonium extracted from molten uranium when about equal weight ratios of uranium and magnesium are equilibrated.

With regard to core processing two methods have been studied with encouraging results. They are oxidative slagging and electro-refining.

If spent fuel is melted and held in the presence of a limited supply of oxygen, decontamination from many fission products is achieved in much the same way that highly chemically reactive impurities are removed in the manufacture of steel. The supply of oxygen may arise from the use of oxide crucibles or from the oxygen in the metal or atmosphere.

Representative data from an oxidative slagging experiment are given in Slide 10 (Table XII of P/823).

It will be noted that the combination of slagging plus contribution by volatilization has resulted in a good decontamination from cesium, rare earths, and strontium. Zirconium has only partially been removed and ruthenium not at all. Other noble metal fission products and niobium and molybdenum are expected to behave like ruthenium. This behavior of the latter two may not prove to be so objectionable inasmuch as they are often beneficial as alloying materials in fuel technology. Many variables in oxidative slagging have been investigated and undoubtedly some of these will be discussed later by Feder.

The second approach to fission product removal for reactor core processing, namely electro-refining, has also shown promising results from laboratory experiments on irradiated metal.

In closing I should like to add that just because the high-temperature methods were initially stated to require remote fabrication of fuel, the same thing may hold for whatever degree of decontamination is obtained in a reprocessing scheme. This stems from the fact that continued re-cycling of fuel may result in the accumulation of non-fission product constituents which might make remote fuel fabrication mandatory.

Mr. P. REGNAUT (France) presented paper P/350.

Mr. H. M. FEDER (USA)presented paper P/544.

Mr. F. H. SPEDDING (USA) presented paper P/545.

DISCUSSION OF P/823, P/350, P/544 AND P/545

Mr. E. GLUECKAUF (UK): First, I want to comment that Mr. Lawroski's Tables III and IV hardly do justice to the ion exchange resins available in Europe. To give an example, there are available the strongly acid resins Zeokarb-225 and 325 and the strongly basic resins De-acidite FF, made by the British Permutit Company, which have formed the basis of most of our research.

In addition, I would like to ask Mr. Lawroski a question. He mentioned in his paper a complete ion exchange process for fuel recovery. Apparently this has not been very economical, because it was not carried beyond the pilot plant stage, but it would be of interest to know, from a purely research point of view, if Mr. Lawroski or one of his colleagues could give any individual stages in this process, particularly the first step, which would have to involve the treatment of the large quantity of uranium in the solution.

Mr. LAWROSKI (USA): With regard to Mr. Glueckauf's first statement, I would like to assure him that I did not intend to slight the talents of the ion exchange makers in Europe. For that matter, I am sure that I failed to include a large number of United States made resins which have only recently become available for experimental purposes.

With regard to the use of ion exchange processes for a complete recovery method, the work which I referred to in my paper was done some ten years ago, and was done with irradiated uranium with concentrations of about 20 weight per cent uranyl nitrate. However, work at that time was on the basis

of exploring as many methods as possible to find one which offered immediate prospects of some high decontamination factors; and when the results initially obtained showed decontamination factors of the order of 300, this alone was a discouragement, particularly when the precipitation and solvent extraction methods on the basis of initial experiments offered very good hopes of fairly thorough decontamination. Moreover, the techniques, which have been worked out recently by, for example, Mr. Higgins at Oak Ridge on continuous ion exchange made the radiation problem—that is, damage to the ion exchange—a serious one. It is quite possible that with the continuous ion exchange methods which may be used now and with a little more chemical and radiation stability, and also with the inorganic type resins, it may be possible to work out a complete ion exchange process for continuous recovery in lieu of such processes as solvent extraction.

Mr. K. DAWSON (UK): One of Mr. Feder's tables gives the effect of varying fission products in the oxidative slagging process. I would like to know whether he can give us any information on the useful lives of these various crucible materials, as this must be an important factor when one is working under remote handling conditions.

Mr. FEDER (USA): I cannot answer your question as to the useful lives under large-scale conditions, as we have had too little experience with this. However, I will say that the penetration or corrosion of a well-fired crucible by the molten uranium is rather small, and the effect is now being investigated in a quantitative fashion.

Mr. G. L. MILES (Australia): First, I have a number of comments and one or two questions to put to Mr. Lawroski. In his paper, Mr. Lawroski refers to the difficulty of containing fluoride melts in the presence of fluorine or bromine trifluoride. This problem may be simplified if electrodeposition instead of volatilisation is used for the recovery of the uranium, so eliminating the need for fluorine or bromine trifluoride. Has this been studied in the United States?

The second point is, the chemical separation of the more noble fission products from uranium can only be achieved by processes involving the complete oxidation (or halogenation) of metallic fuel. Mr. Lawroski has mentioned fluoride volatilisation and electro-refining as two examples of this process. Another type of halogenation process which has been studied at Harwell makes use of the dissolution of uranium in fused lead chloride-potassium chloride melts. This gives a preferential chlorination of uranium, plutonium and the more electropositive fission products and leaves ruthenium, niobium, etc., associated with lead in the metallic phase. Subsequent recovery of uranium from the chloride melt can be achieved by preferential reduction with, for example, magnesium.

My third point refers to a statement in Mr. Lawroski's written paper. I am sure that Mr. Lawroski would agree that the statement "that there is no real need to separate the uranium from the plutonium when reprocessing the core" represents only an initial target for pyrometallurgical processing. While several recycles of fuel may be possible, eventually the depletion of U^{235} will necessitate the rejection of uranium from the fuel cycle, and at this stage recovery of the plutonium is obviously desirable.

Finally, in Table IX, what percentage of uranium was volatilised? You only give volatilisation figures for the plutonium.

Mr. LAWROSKI (USA): In regard to the first point, on the corrosion problem of the inter-halogens, we have not had very serious problems with just the use of such things as chlorine trifluoride and bromine trifluoride. When we have gone to these temperatures of 500°C or 600°C, using fluorine as well as the fused salt mixture, we have run into numerous problems. The HF step, which is the one which precedes the fluorine dispersion step to get as much fluorination as possible done with cheap fluorine, has not been a serious corrosion problem. We have followed with interest the selective reduction of oxygen in molten metals with such things as lead chloride. However, we have not done any work as yet, but we have certainly followed the United Kingdom work with considerable interest.

With regard to the amount of uranium volatilized in a vacuum distillation, the volatility of uranium is several hundred-fold less than that of plutonium at the temperature of, I think, 1680°C mentioned in the table so that while the plutonium obtained would not be free of uranium, redistillation, however, would give you high concentration of plutonium.

Mr. G. L. MILES (Australia): I have several points to raise in connection with Mr. Feder's paper. In the chemical processing group at Harwell we have been working for some time on a variety of high-temperature processing methods, and it may be of interest to compare some of our results with those described in Mr. Feder's paper.

Firstly I would like to emphasise that our results are in substantial agreement and that we support Mr. Feder's general conclusions concerning the potential advantages and disadvantages of pyrometallurgical processing. There is however a number of differences in detail, and one difference in the interpretation of the slagging process to which I would like to draw attention.

Considering first the time of processing: It is our experience at Harwell that a separation of fission products similar to that described in Mr. Feder's paper can be achieved in from 15 to 30 minutes. This is using either a resistance-heated furnace or induction heating, in the same temperature range, and on a scale of from 10 to 1000 grams of uranium.

Secondly, as regards scale of processing: we have no evidence of a falling-off in the efficiency of the process with increasing size of sample in the 10 to

1000 gram range, and in fact, from the point of view of uranium losses, the larger scale experiments were most encouraging.

Thirdly I have a point on plutonium behaviour. We found a slight tendency for plutonium to be preferentially oxidised. This may be overcome either by increasing the scale or by the addition of a little calcium during the melting process. This does not adversely affect the fission product decontamination.

As to zirconium behaviour, while we found that the behaviour of zirconium is extremely variable, we have not been able to correlate significant improvement with graphite addition.

As to crucible material, except in the case of zirconia crucibles, in which (speaking from memory) we have reduced the zirconium activity by isotopic exchange, we have not obtained any evidence for a dependence of fission product separation upon the material of the crucible.

I would like to bring these points quickly together, in terms of the mechanism of the process. The evidence of a large number of experiments which we have carried out at Harwell does not support the theory that the surface of the crucible plays a very significant role in determining fission product removal. In particular I would like to cite the results of scaling-up on time of processing, the independence of crucible material, and the small activity remaining associated with the crucible walls.

On the other hand I would like to emphasise that for burn-up of a few hundred megawatt days per ton, for natural uranium, the concentration of fission products in the uranium will be less than the stoichiometric equivalent amount of light element impurities such as oxygen, nitrogen, carbon, silicon, etc., initially present, in all but the purest uranium. It is suggested that the results which have been described could be due to reaction of electropositive fission products with impurities initially present within the uranium metal.

Mr. FEDER (USA): I think that Mr. Miles has, in his last statement, practically resolved the source of the differences between our results in saying that at very low concentration of fission product elements in the presence of significantly larger concentrations of oxygen, carbon, nitrogen and so forth, the reaction with the impurities already present will be controlling rather than the reaction with the crucible surface. I would deduce from the fact that Mr. Miles found his reactions were not diffusion controlled, were not influenced by the crucible material, that indeed this is the case, that is the uranium which he had been using contained, I would suggest, sufficiently large quantities of oxygen, nitrogen or carbon so that the diffusion to the surface of the crucible would not be important. I can only suggest that this is a likely explanation, and inasmuch as we know that the uranium we were using was rather low in oxygen content it fits the picture quite well.

There are two other comments that I would like to make in replying. One is that the process which we are attempting to perfect is one in which we will be dealing with very high burn-up materials, of the order of 2 per cent fission of total atoms, so that it is almost certain we cannot count on contained impurities in the metals to do the slagging.

Another point I wish to make is that I do not know whether it was quite clear to Mr. Miles that we did find some preferential incorporation of plutonium in the slag. This is stated in the paper.

Mr. MILES (Australia): I would like to make one very brief comment about the uranium used. The degree of burn-up in our experiment was very close indeed to those used in the Argonne experiments described in the paper, and a very quick calculation shows that it would be necessary to use exceedingly pure uranium indeed if the light element concentration was going to be low enough to be less than the equivalent of the fission products produced.

Mr. C. M. NICHOLS (UK): First of all, I would like to ask Mr. Feder whether he would care to comment on the precise implications of the different types of heating, high-frequency versus resistance-heating.

It would be rather interesting to have comments from both Mr. Feder and Mr. McKenzie from Canada on my second question. Mr. Spedding has referred to the use of the artificial alloy "fissium" for this high-temperature processing. All of us who are involved in this type of work have to find something to work on. I wonder if he would care to comment on the reproducibility of the results obtained with these artificial alloys when he comes to refer to radioactive alloys later on?

Mr. FEDER (USA): Taking up these two points in sequence, the majority of our laboratory experiments have been done with resistance heating, and a number have been done subsequently on a larger scale also with high-frequency heating. From the process standpoint I believe there is no significant difference, with perhaps the exception that if the high-frequency heating is done directly on the metal rather than on a susceptor, the resulting violent agitation of the metal may make the separation of phases more difficult, and is to be avoided.

With regard to the second question, it is recognized to be very difficult to incorporate in the so-called fissium alloys the more volatile constituents in order to simulate the high burn-up slip one wishes to simulate. We have recently attempted to overcome this difficulty of alloying essentially immiscible powdered material with uranium by going from the usual technology of alloying to a powder metallurgical technology, and we have had made for us some large quantities of uranium containing a large variety of fission elements—I think some seventeen fission elements—present in proper proportions, made by powder metallurgy at 800°C. Our experiments with this material—which have not been reported in the paper—indicate that the results with those higher

concentrations in a material which fairly well simulates the pure material, are very very comparable with those obtained in the laboratory as stated in the paper.

D. E. McKENZIE (Canada): I have two short comments. My first, with regard to what Mr. Feder had to say, is that I was inclined to agree with Mr. Nicholls that it is very difficult to duplicate neutron irradiated uranium. However, this powder technique may give that duplication.

My second comment is that we agree with Mr. Feder's results on the effect of time in the removal of fission products from uranium, that is oxidation of slag. This is because Canada obtains its uranium metal from the United States, and so I think this again shows it is the uranium metal that does this. But I also agree with Mr. Feder; I think it means the United States has pure uranium metal.

Mr. S. MALY (Czechoslovakia): In his paper, Mr. Spedding speaks of the removal of fission products from liquid uranium by extraction with liquid metals, such as, silver, zirconium, thorium and magnesium.

I would like to ask him whether the Ames laboratory, or any other American laboratory, has experimental data relating to the extraction of liquid salts, for example, the extraction by liquid magnesium chloride—$MgCl_2$. How are the fission products extracted by liquid magnesium or by the liquid chloride respectively, if indeed the two methods are comparable?

Mr. SPEDDING (USA): We have, of course, done considerable work in making metals and having the slags above the metals as we melt them, and we have observed what materials go into the slags and what stay with the metals. We have not done this for radioactive samples, and as far as my laboratory is concerned I cannot say much about it. I think that work has been done elsewhere in the United States with molten fluorides in contact with metals and the oxide, not in the molten state, in contact with them. I cannot give you the details, but I believe that they are available, and I suggest that the questioner should talk to Mr. Lawroski about this.

Mr. LAWROSKI (USA): Magnesium chloride and uranium trifluoride and tetrafluoride have been used for the extraction of plutonium from molten uranium, and, in the case of experiments using equal weight ratios, at least 90 per cent of plutonium was extracted in a single operation. There was no reason to believe that further contacts would not give more complete recovery of plutonium. I believe that a paper by Mr. Parker, of North American Aviation, which was submitted for these proceedings, has more information on the use of salts for plutonium extraction.

Mr. FEDER (USA): I have one observation on the question from Czechoslovakia, which perhaps is not completely elucidated, with regard to the results obtained when contacting or extracting molten uranium with liquid salts. These results have been generally in full agreement with those which can be deduced theoretically from the available thermodynamic data, assuming that the action is one of cation exchange between the various salts involved.

Mr. J. M. FLETCHER (UK): I should like to ask Mr. Lawroski one question. He says that cost estimates should be made for the recovery of uranium by fractional distillation of the fluorides and recovery of the plutonium from the residue, on the one hand, and the complete solvent processes on the other. In making this comparison, has he been able to take fully into account the disposal of waste products, and does he think, looking further ahead, as these two types of processes develop, that one is more likely to proceed on economic lines than the other?

Mr. LAWROSKI (USA): The economic comparison of solvent extraction for the recovery of both uranium and plutonium first with the use of fractional distillation to recover uranium and solvent extraction for the plutonium, was made in a very preliminary fashion. The storage costs of waste were assumed to be about the same for the two, inasmuch as solvent extraction was involved with the major portion of the fission product in any case; although the volumes of the fission product were considerably less with the fractional distillation process, the cost of having another plant tended to balance the savings.

Cost estimating is extremely difficult at the present time because there has been a lack of standardization of fuels. Not until we can say that there are many reactors using the same kind of fuel can we make precise cost estimates.

Session 22B.2

SEPARATION AND STORAGE OF FISSION PRODUCTS

LIST OF PAPERS

		Page
P/415	Chemical processing of fission product solutions ..... E. Glueckauf and T. V. Healy	635
P/552	The design and operation of high level waste storage facilities ..... C. R. Anderson and C. A. Rohrman	640
P/553	Processes for high level radioactive waste disposal ..... L. P. Hatch *et al.*	648

Chemical Processing of Fission Product Solutions

By E. Glueckauf and T. V. Healy,* UK

SOURCES OF FISSION PRODUCTS

The subsequent discussion is pertinent to fission products which are obtained from the highly active waste stream of solvent extraction plants in which practically all the plutonium and uranium of the highly irradiated uranium metal rods has been removed with HNO_3 as salting out agent. The waste stream would contain the fission products as nitrates, some unextracted uranyl nitrate, dissolved impurities from the uranium metal, corrosion products and traces of solvent plus its radiation breakdown products. The main electrolyte constituent of the solution would be the nitric acid itself and the total fission products would be a very small proportion, the actual amount depending on the burn-up of fuel in the reactor. The radioactivity and to a certain extent the constituents of the fission product solution will depend on the irradiation time of the uranium and the length of cooling time after removal of the fuel from the reactor.

CONCENTRATION BY EVAPORATION

As dilute nitric acid is the main constituent of these waste fission product solutions, they can be easily concentrated by evaporation down to less than 1% of their original volume. The evaporation should be preceded by a steam strip to remove solvent and most of the solvent decomposition products, which otherwise may give rise to violent reactions during the concentration process. The primary object of the evaporation is to reduce the fission product solution to small bulk and throw away the distillate. Entrainment of spray in the distillate must therefore be avoided and no volatile fission product activity must be produced. Radioactive ruthenium is normally found in the reduced form in nitric acid solutions and as such is not volatile. However, it can be oxidized to the volatile tetroxide by hot concentrated nitric acid and then can actually be quantitatively distilled from fission product solutions of $15N$ HNO_3 by evaporation at atmospheric pressure to near dryness.[1] The oxidation (and therefore distillation) rate of ruthenium is partially dependent on the nitric acid acidity, as is illustrated in Table I.

Time of contact at a constant reflux temperature also affects the oxidation rate. In addition there is a salt-concentration effect illustrated by Table II. This displays the results of a distillation at atmospheric pressure of previously reduced ruthenium, from concentrated fission products at an acidity of $15N$ HNO_3.

Distillation of fission product solutions at low pressures and low acidities reduces the amount of volatile ruthenium, less than 0.01% being distilled at acidities below $13N$ at atmospheric, and still less at lower pressure.[1,2] However, the effects of time of contact is shown by the fact that, after 70 hours reflux of $12.1N$ acid fission products, about 5% of the ruthenium was distillable. In practice, evaporation of nitric acid solutions of fission products at low pressure and temperature may be carried on to a saturated solution, over a reasonable time, without causing the distillation of more than 10^{-6} of the ruthenium.

RECOVERY OF CAESIUM-137 AND STRONTIUM-90

These are two of the longest-lived fission products. They are also the two fission products most likely to be utilised commercially, caesium as a gamma source and strontium as a pure β source. Several methods of separation are described below.

Separation by Drying, Roasting and Leaching

Fission product solutions are taken to dryness to remove all nitric acid and water; then the dry material is roasted for about an hour at 300°C, whereby all the nitrates except those of the alkali and alkaline earth metals are decomposed into oxides.[3] The solid is then leached with warm water which dissolves out the caesium and strontium nitrates, leaving behind all the water insoluble oxides. Usually about 95% of caesium and up to 85% of the strontium can be extracted. The original fission product solutions can be evaporated to very small bulk under a vacuum of about 100 mm pressure where, at about 70°C, a constant boiling mixture of $11N$ HNO_3, but no ruthenium will distil over. In order to avoid volatilisation of Ru during the roasting, excess formaldehyde may be cautiously added in small quantities to the fission product solution until all the nitric acid has decomposed, the remaining solution taken to dryness, and roasted at 300°C. The roasting temperature is critical to ±10°C, otherwise the leached material either contains too many impurities (at < 290°C), or retains too much caesium and strontium with the

Table I

HNO_3 acidity	$5N$	$11N$	$13N$	$14N$	$15N$
Per cent Ru in distillate	None	None	0.01%	0.2%	1.5%

* Atomic Energy Research Establishment, Harwell, Berkshire, England.

Table II

% solution distilled	12	37	56	67	75	85	89	94
% ruthenium distilled	0.3	1.0	2.5	3.2	4.7	13	25	49

oxides (at > 310°C). The individual fission product nitrates decompose at different temperature—the order of their decomposition being similar to the order of their basicity. The least basic are the most readily decomposed in the order: Zr (200°) Ce(III), Sc, Yb, Tm, Er, Ho, Tb, Sa, Gd, Nd, Pr and La (300°) Sr, Ba, (> 600). The major individual constituents of the fission product solutions, ferric nitrate and $UO_2(NO_3)_2$, also decompose below 300°C, but there is usually some small contamination of uranium and lanthanum in the leached out solutions. Table III gives the leaching results for the nitrates decomposed at different temperatures. The figures are the percentage of the metals leached out with one hot water wash after roasting the fission products for one hour.

Table III

Roasting temp (°C)	*180*	*250*	*300*	*350*	*450*	*600*
Metal nitrate	*(% leached out)*					
Caesium	100	100	95	85	50	2
Strontium	100	100	85	10–2	1	0
Uranium	100	50	5	2	0	0
Iron	18	10	0	0	0	0
Cerium	100	30	4	0	0	0
Fission products	65	20	8	2–5	1.5	0.3%

The large decrease in the amount of strontium leached out with water between roasting temperatures of 300°C and 350°C was found to be due to oxidation of the chromium impurity to chromate which forms an insoluble Sr-salt. Addition of barium nitrate, either initially to the fission product solution, or as a leaching wash helps to overcome this effect and separates up to 80% of the strontium after roasting at 350°C. Only traces of ruthenium are leached out from the solids roasted above 250°C. Other metals can be eluted by using complexing agents or dilute acids. The whole of the solids can subsequently be dissolved in boiling 5*N* HNO_3.

Precipitation of Fission Products as Hydroxides

This requires, in addition to the concentration of the fission products, the removal of nitric acid down to low acidity. Concentration has been discussed previously and the removal of nitric acid is described later. Three methods of precipitation studied at Harwell are all based on raising the pH of the solution so that only the caesium and strontium fission products remain in solution. These methods are (*a*) direct precipitation of fission products by addition of ammonia solution, (*b*) electrolytic removal of nitric acid using a semi-permeable anionic exchanger membrane accompanied by continuous precipitation of the hydroxides produced and (*c*) removal of nitric acid by passage through an anion exchange resin in the OH form, where the precipitable hydroxides are removed.

(a) Precipitation by Ammonia

Strong ammonia is added with continuous stirring to the low acid solution of concentrated fission products, until a fixed pH is reached, depending on the conditions required.[4] The fission products gradually precipitate as the pH rises, but a clean chemical separation does not occur. If the precipitation is stopped at pH 6, practically all the strontium and caesium, but no iron, remain in solution but so also does a large proportion of the fission products. At the higher pH of 8 some strontium is entrained with the precipitate which now contains most of the fission products. The following table shows the effect of pH on the precipitation. Table IV gives the percentage of individual fission products found in the filtrate.

These figures vary somewhat; the greater the proportion of iron present, the lower is the strontium content of the filtrate.[6] The precipitate is easily and quickly filtered, or alternatively decanted. This is important, as ageing effects occur with the precipitates which affect the composition of the two phases.

(b) Electrolytic Precipitation Using Anionic Exchanger Membranes

The type of electrolytic cell which can be used[5] consists of two compartments separated by an anion permeable membrane (Permaplex A 10) which has adequate radiation stability. The solutions are circulated by means of an air lift, the catholyte passing from the cell through a filter which continuously removes the precipitate and thence back into the cell. The maximum radiation dose for a three fold increase in the transverse resistance of wet "Permaplex A 10" membranes is of the order of 10^9 roentgens and from this one may estimate a useful life of about 40 days for membranes with one side in contact with a 6-mm layer of solution of specific activity of 1000 curies/litre.[8]

The pH increases with electrolysis and a series of hydroxide precipitates are formed as shown in Table V. We see that it is impossible to separate individual metals by this means, but group separa-

Table IV

	Cs	*Sr*	*Ce*	*Ru*	*Total F.P.'s*
pH of solution 6.2	100	98	77	–	68
pH of solution 8.0	97	77	0.3	4	4

Table V

pH 2–3.5	Fe^{+++}, Zr and some Ru
pH 3–5	Mainly uranium
pH 5–8	All rare earths, Fe^{++}, Ni, Co, Al

Table VI

% nitric acid	99	95	90	85	80	75	72	66
Milligrams Sr/litre	1.3	1.1	1.0	1.8	3.2	7.1	13.7	120

tion may be attained, and in fact, all the cationic species are removed from solution except members of Group 1A and 2A of the Periodic Table, since the pH values attained are insufficient to precipitate the alkaline earth hydroxides. 85% of caesium and strontium fission products remain in the solution, the remainder being adsorbed on the precipitate due to the very large excess of iron and uranium.

(c) Precipitation on Anionic Resins in Hydroxide Form

The above two methods required the filtration of the fission product hydroxides from the solutions containing caesium and strontium. In a highly radioactive system, particularly on a large scale, filtration is a complex operation and it was realised that considerable advantages would result if precipitation could be effected by passage of solutions through strongly basic anion exchange columns[7] instead of by addition of aqueous alkalis. This procedure would not involve the addition of any other electrolyte and since precipitation of the hydroxides would occur in the column, the anion exchange resin functions both as precipitant and as a filter aid which retains the precipitates. Experimental work showed that no free precipitates were visible but, instead, the deposited hydroxides formed a firm layer surrounding the resin beads. Obviously, the mechanism differs from that occurring in liquid solutions, as a very dense and adhering precipitate is formed which differs markedly from the gelatinous and almost colloidal precipitates which are often obtained during normal alkali precipitations. This method of precipitation was found to give a good separation of caesium from the rest of the fission products, but the strontium was largely retained, at least in the presence of the large amounts of iron contained in these fission product solutions. This process also lends itself to the separation of caesium and strontium by passage through an anion exchange resin in the carbonate form, where the strontium is retained quantitatively on the resin, while all the caesium goes through into the filtrate.

Direct Precipitation of Caesium and Strontium

Removal of Strontium by Precipitation from Nitric Acid

The nitrates of barium and strontium have low solubilities in concentrated nitric acid.[9] More detailed data about the solubility of strontium have now been ascertained using tracer strontium-87.[10] The results given in Table VI are the solubilities as milligrams strontium per litre of solution at 25°C, the nitric acid solutions being per cent by weight.

This extremely low solubility of strontium in concentrated nitric acid can be utilized to remove all the strontium from fission products as a large scale manufacturing process. The actual amount of strontium removed from fission products by precipitation with nitric acid is dependent upon the nitric acid concentration, the concentration of fission products and other electrolytes and the quantity of carrier added. The large amount of iron nitrate present in concentrated fission product solutions acts as a salting out agent and improves the strontium precipitation. Table VII shows the decrease in the strontium solubility caused by 16 grams of iron as nitrate per litre of nitric acid, at 25°C.

The salting out effect of iron nitrate is further demonstrated in Table VIII where the nitric acid concentration is fixed at 72%.

Still more effective is the addition of a carrier. The carrier efficiency decreases in the order Sr, Ba, Pb.

Strontium-90 is the most toxic isotope of the fission products and its complete removal would ease the disposal problem. 99–100% removal of strontium may be obtained by addition of the appropriate amount of fuming nitric acid to the concentrated fission products, with or without lead carrier. A second precipitation with lead carrier gives a decontamination factor of 10^4.

The process for separation of strontium-90 by nitric acid precipitation from concentrated fission product solutions is in use at R.C.C. (Radiochemical Centre) Amersham.[11] Strontium is first precipitated from 68% HNO_3 which avoids the co-precipitation of cerium and is later purified by two precipitations from 80% nitric acid. This furnishes a material of 98% radiochemical purity.

Removal of Caesium from Fission Products by Precipitation

Caesium salts of hetero-poly acids are insoluble in acid solution and Feldman and Glendenin[12] used this property to separate caesium from rubidium by precipitation of caesium silicotungstate. Caesium is precipitated quantitatively by sodium phosphotungstate from concentrated acid solutions of fission products, but a great excess of phosphotungstate is required at very high acid concentrations. R.C.C. Amersham are at present extracting caesium from concentrated fission products 8*N* in nitric acid by phosphotungstate precipitation.[18] More than 99.5% of the caesium is precipitated from the fission products in this way. The Cs-phosphotungstate is then dissolved in dilute caustic soda and reprecipi-

Table VII

Wt % nitric acid	90	80	72	67	63	58	52	48
Milligrams of Sr/litre of solution	1	1	4	10	17	65	76	92

Table VIII

Iron in grams per litre	0	4	8	16	32	40
Strontium in milligrams per litre	13.7	7	5	4	3	3

tated again. After a few minor purification steps the radiochemical purity of the Cs^{137} is 99.9% and the chemical purity (apart from the small amount of rubidium present) is 98%.

One possible drawback with this system is that excess phosphotungstic acid remains with the residual fission products. This heteropoly acid can easily be removed (1) by precipitation with ammonia from the residual fission products or (2) by solvent extraction of the phosphotungstic acid.[14] The latter is soluble in alcohols, esters, ethers and ketones and its partition coefficient in dilute nitric acid varies from 200 in favour of dibutyl carbitol, 100 in diethyl ether to 30 for dibutyl cellosolve.

Caesium Alum

This procedure is based on the low solubility of caesium alum in the presence of high concentrations of the lighter alkali alums. It involves neutralizing the fission product wastes with alkali, until a pH of about 2 to 4.5 is reached. An amount of potash alum equivalent to twice its solubility at 25°C is added to the warmed solution. On cooling, over half the potash alum is precipitated carrying between 95% and 100% of the caesium with it.[15] Repetition of this procedure several times with fresh potash alum produces a highly concentrated caesium alum. This caesium can be separated from the aluminium and alkali metal contaminants by ion exchange methods. This process gives unsatisfactory yields when carried out in dilute acid solutions.

Tetraphenyl Boron Caesium

This salt is very insoluble in water (4.4 milligrams/litre) and has solubility product for caesium of 10^{-9}.[16] More than 99.5% of the caesium is precipitated from fission product solutions by addition of an aqueous solution of tetraphenyl boron sodium at a pH of 2–4. This precipitate is extremely fine, settles only slowly and needs to be filtered through a fine sinter. On heating this caesium complex salt to 600°C, it loses boron and decomposes to caesium oxide. Similarly, heating the salt with sulphuric acid furnishes caesium sulphate direct.

Nickel Caesium Ferrocyanide

The fission product solutions can be treated with nickel ferrocyanide at a pH of 4. Under these conditions nickel caesium ferrocyanide is precipitated. The caesium is recovered from the complex by calcination followed by leaching with water.[17]

None of the last three methods of caesium precipitation is very suitable for use with acid fission product solutions as, at the low pH values of 2–4 it is difficult to avoid precipitation of at least a minor proportion of the fission products and of a substantial proportion of the impurities (iron).

REMOVAL OF NITRIC ACID

Three ways of removing nitric acid from concentrated fission products, without addition of electrolytes to the solutions, are discussed below.

Solvent Extraction of Nitric Acid

Nitric acid can easily be extracted from highly acid solutions by polar solvents of the ether, ester and ketone type; but extraction efficiency falls off rapidly at concentrations below 1*N*.[18] The solvent is easily stripped of nitric acid by washing with water and so regenerated for further use. Thus, with the aid of a counter current flow and a series of extraction stages, the bulk of the nitric acid can be efficiently extracted into a solvent.[19] To avoid extracting also some of the fission products into the organic phase, the counter current extraction has to contain a stripping section. The details vary, depending on the nitric acid and fission product concentrations in the original aqueous phase and also on the particular characteristics of the solvent chosen for extraction.

Anionic Membrane Electrolysis

Acids can easily be removed by electrolysis through an anion semi-permeable membrane (e.g., Permaplex A 10). The equipment resembles that mentioned previously.

Removal of Nitric Acid with Formaldehyde, Formic Acid or Nitric Oxide

Nitric acid reacts with formaldehyde in a similar manner to its reaction with most reducing agents. The two equations below indicate the typical course of reaction where R is the reducing agent.

Reaction in concentrated HNO_3

$$2H^+ + 2NO_3^- + R = RO + 2NO_2 + H_2O \qquad (1)$$

Reaction in dilute HNO_3

$$2H^+ + 2NO_3^- + 3R = 3RO + 2NO + H_2O \qquad (2)$$

At intermediate acidities both nitric oxide and nitrogen peroxide are found as reduction products. Under certain conditions there is quite an appreciable induction period before reaction commences and the reaction may be initiated by dissolving small amounts of nitrogen peroxide in the mixture. This fact has similarly been noted in copper/nitric acid mixtures and has led to the suggestion[20] that the mechanism of oxidation of metals involves nitrogen peroxide, and thereafter nitrous acid.

The nitric acid/formaldehyde reaction using this mechanism leads[21] to Equations 3, 4 and 5.

$$N_2O_4 + H_2O = H^+ + NO_3^- + HONO \qquad (3)$$

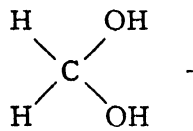

$$+ 2HONO = 2H_2O +$$

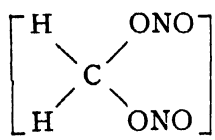

$$\rightarrow 2H^+ + CO_2 + 2NO \quad (4)$$

$$4H^+ + 4NO_3^- + 2NO \rightleftharpoons 3N_2O_4 + 2H_2O \quad (5)$$

with the two resultant Equations 6 and 7 for dilute and concentrated acid respectively, linked by the equilibrium of Equation 5.

$$4HNO_3 + 3H{\cdot}CHO = 4NO + 3CO_2 + 5H_2O \quad (6)$$

$$4HNO_3 + H{\cdot}CHO = 4NO_2 + CO_2 + 3H_2O \quad (7)$$

Equation 7 predominates over the acid range 16–8 *N* and Equation 6 over the range 8–1 *N*. The speed of reaction increases with acidity, the reaction at 100°C being almost instantaneous at acidities greater than 8*N*. A study of the reaction rate over the acid range from 8 to 1 *N* at 100°C and over the acidity range from 11 to 1 *N* at 60°C indicates an apparent third order reaction for the nitric acid at constant formaldehyde concentration, the values for *K*, the reaction rate constants at these temperatures, being 9.1×10^{-4} and 2.76×10^{-4} litres^2-moles^{-2}-sec^{-1} respectively. Reaction of formaldehyde with nitric acid at or below 1*N* acid strength furnishes largely formic acid and nitrogen peroxide:

$$HCHO + 2HNO_3 = HCOOH + 2NO_2 + H_2O \quad (8)$$

Formic acid itself reacts with nitric acid according to the Equations 9 and 10 below. The former is the prime reaction over the acidity range 16–8 *N* and the latter over the range 8 to 0.5 *N*.

$$4HNO_3 + 2HCOOH = 2CO_2 + 4NO_2 + 4H_2O \quad (9)$$

$$4HNO_3 + 6HCOOH = 6CO_2 + 4NO + 8H_2O \quad (10)$$

Here too, the rate at 100°C indicates a third order reaction for the nitric acid at constant formic acid concentration over the range 15 to 2 *N* with a reaction rate constant of 4.7×10^{-4} litres^2-moles^{-2}-sec^{-1}. This is about half the rate for the formaldehyde/nitric acid reaction at 100°C.

We have therefore two reagents for reducing nitric acid acidity, one about twice as vigorous as the other, and both producing only water and gaseous products except at acidities below 1*N* acid.

Nitric oxide alone will also reduce the nitric acid content very efficiently from 16*N* down to 8*N* by simply blowing the gas through the warm acid solution whereby nitrogen peroxide is produced in accordance with Equation 5.

Application of these methods to the removal of nitric acid from concentrated fission product solutions gives good results. As the concentrated fission product solutions contain large proportions of ferric and uranyl nitrates, the reaction rate of the acid with both formaldehyde and formic acid is increased appreciably because both these electrolytes catalyse the speed of the reactions. The formaldehyde treatment has proved successful both as a continuous and as a batch process[22] in removing nitric acid from fission product concentrates. By allowing a pretreatment of the 15*M* nitric acid feed with the exhaust gases containing nitric oxide, the consumption of formaldehyde is halved. The consumption rate so obtained is approximately three moles of nitric acid destroyed per mole of formaldehyde used.

REFERENCES

1. Healy, T. V. *et al.*, Experiments on Oxidation and Distillation of Ruthenium, A.E.R.E. C/M 210.
2. Waste Disposal, KAPL 604 and 649.
3. Healy, T. V. and Ford (Miss) B. L., unpublished work.
4. Healy, T. V., Brown, P. E. and Ford (Miss) B. L., Separation of Caesium and Strontium from F.P.'s by Ammonia Precipitation, A.E.R.E. C/M 208.
5. Littlejohn, A. C. Separation of Fission Products by Electrolytic Precipitations A.E.R.E. C/R 1537.
6. Payne, W. E. *et al.*, Primary Precipitation of Undesirable Cations from F. P. Feed Solution, PDB 77.
7. Glueckauf, E. and Roberts, P. J. P., Precipitation Separations without Filtration, A.E.R.E. C/R 1443.
8. Barker, G. C. and Gardner, A. W., Radiation Effects on Anion Exchange Membrances, A.E.R.E. C/M 207.
9. Willard, H. H. and Goodspeed, E. W., Separation of Sr, Ba and Pb from Ca and other metals by pptn. as nitrates, Ind. Eng. Chem. (Anal. Ed.) Vol. 8, 1936, 414.
10. Healy, T. V. and Brown, P. E., unpublished work on Sr extraction from F.P.'s.
11. Carter, P. E., of R.C.C. Amersham, private communication.
12. Feldman, M. H. and Glendenin, L. E., Identification and Yield of Rb^{86} in Fission, NNES Part IV, Vol. 9, p. 654.
13. Carter, P. E., Precipitation of Caesium as Phosphotungstate, A.E.R.E. C/R 1231.
14. Wu, H., The chemistry of phosphotungstic acids and allied substances, J. Biol. Chem. *43*, 190 (1920).
15. Gresky, A. T., Recovery of Cs^{137} from ORNL Radiochemical Waste, ORNL 742, AECD 2999.
16. Geilmann, W. and Gebauhr, W. Pptn. of the alkali metals as tetraphenyl boron compounds, Z. Anal. Chem. *139*, 161 (1953).
17. Glueckauf, E., private communication.
18. Sutton, J., Distribution of Nitric Acid between Water and Ether, A.E.R.E. C/R 438
19. Peacegood, J. A. *et al.*, Removal of Nitric Acid by Solvent Extraction, Risley Report No. 8027 and 8050.
20. Yost, D. M. and Russel, H., System of Inorganic Chemistry, Prentice Hall, New York, N. Y. (1944).
21. Healy, T. V. and Ford (Miss) B. L., The destruction of Nitric Acid by Formaldehyde, Part I, A.E.R.E. C/R 1339.
22. Morris, J. B., The Reaction of Nitric Acid with Formaldehyde, A.E.R.E. CE/R 1490.

The Design and Operation of High Level Waste Storage Facilities

By Cleve R. Anderson and Chas. A. Rohrman,* USA

DEFINITION AND NATURE OF THE WASTES

With the development of the plutonium producing reactor, along with the complex chemical separations processes for product recovery, the need for suitable methods for disposing of the wastes from these processes was met in the simplest manner commensurate with the nature of these wastes. They were stored underground in steel-lined concrete tanks.

In this paper the storage of high level waste is discussed from the design and operation standpoints as related to containers, energy release, radiological safety and economics. These problems are of concern in any location. Specific solutions which are utilized today in production plants will be emphasized. In addition, alternate solutions to the various problems will be considered.

The wastes from separations processes in use today are aqueous, salt solutions. In order to minimize the corrosion characteristics the wastes are normally made alkaline and may contain substantial amounts of insoluble matter. The wastes are intensely radioactive from the contained fission products and, therefore, require extensive shielding. This radioactivity is dissipated within the volume of stored waste and results in the continuous evolution of heat. For the high level wastes, facilities must be included to dispose of this heat.

With the development of power producing reactors the problems of storing the wastes are intensified. Minimum volume is desired. This results in greater concentration of fission products, salts and insoluble matter. The heat disposal problem is also increased because of the increased concentration of fission products. In addition similar economy moves will take place at the power producer itself. The fuel will be irradiated for a longer time and at greater intensity; higher neutron fluxes will be used. These factors generate correspondingly greater concentrations of fission products in the fuel which must subsequently be processed for purification and recovery. In order to simplify the separations processing, irradiated fuel, after discharge from the reactor, is stored for a period to eliminate certain fission products by radioactive decay.

The term "high level waste" used in this paper is considered to relate to waste originating from fuel which has had an exposure in excess of 2000 kilowatt hours per kilogram. Exposures greater than one hundred times this value are proposed for nuclear power production.

The high level wastes have initially an extremely high activity. The average half-life of such waste is at first quite short, being of the order of a few weeks. As the elements of short half-life disappear, the average half-life increases because of the greater fraction of the longer lived isotopes remaining in the wastes. In the typical wastes strontium-90 and cesium-137 are the radioisotopes of longest half-lives.

The objective of a separations process is to recover in greatest possible yield elements such as uranium, thorium and plutonium. However, even from the most efficient process, concentrations of plutonium in separations plant wastes are so high that this element alone, with its long half-life (24,000 years) and extreme biological toxicity, requires the utmost assurance against uncontrolled release of such material to the ground or into any area where it may be taken up by plant or animal life. This necessitates extreme protective measures to assure the provision of storage vessels of the greatest possible dependability. In areas adjacent to population centers or near an easily penetrated ground water table, auxiliaries are required for decontaminating the vapor or liquid streams prior to release.

PROBLEMS

Storage Methods

Storage of high level wastes requires long-term confinement with a high degree of assurance against release of the contained radioactivity to the environs.

Underground Tanks and Auxiliaries

The usual method for storing high level wastes involves containment in steel-lined concrete tanks buried sufficiently deep to provide earth shielding against the intense radioactivity. Although some installations may indicate justification for storage in the acid condition in stainless steel, large installations have used ordinary steel with the wastes maintained in the alkaline condition.

Auxiliary equipment required for an operable storage system includes delivery lines, vapor lines, condensers, vapor filters, stacks, cooling water supply, provision for instrumentation, alternate routings,

* Hanford Atomic Products Operation, General Electric Company.

and spares for critical services. The attached sketch (Fig. 1) shows a typical storage facility. For complete storage facilities, including tanks and auxiliaries, recent cost figures have been less than seven cents per liter. Additional storage capacity can be provided for appreciably less than seven cents per liter by planning the maximum utilization of facilities which are common to a complete storage area. These common facilities include condensers, de-entrainment devices, filters, emergency water supply and the exhaust system.

Alternate Methods

Alternate methods for high level waste storage must have cost or process advantages over storage in steel tanks in order to justify the program of development work to make these alternate methods available for production plants.

Alternate storage methods which are being considered include: (1) Fusion of dry radioactive wastes in glass; (2) Preparation of concrete from liquid radioactive wastes; (3) Fixation of wastes in montmorillonite clay with firing to about 1000°C; (4) Disposal of liquid wastes in abandoned, deep wells.

High level wastes decay initially at a rapid rate. After five years there remains only a few per cent of the original activity. For the first three methods mentioned it would appear reasonable to allow activity reduction by decay to continue for a five-year period before fixing the activity for permanent storage. The fourth method of disposal in abandoned, deep wells has three major disadvantages:

1. The activity disposed to ground is no longer under control. Undesirable ground-water contamination can result due to soil or rock leaching from the chemical, radiological and temperature effects of the wastes.

2. Reclamation of the fission products for industrial use would be improbable.

3. Long-term legal and public responsibilities are not compatible with this method of disposal.

Economics

The cost of high level waste storage by presently used underground tanks has been cited in the general literature as being extremely high. The experience in actual production plants has definitely established the converse to be true. In order of magnitude, waste storage costs can be expected to be appreciably less than 1% of the sales value of electricity from a nuclear reactor.

Storage costs can be markedly reduced after the majority of the short half-life fission products have decayed. A period of about five years interim storage would be required after which the remaining fission products (about 2%) would be concentrated by removal of inert material and then placed in permanent storage. A further possibility for volume reduction would be the recovery of specific isotopes for use as industrial radiation sources.

Energy Release

The energy accumulation in stored wastes results from the self absorption of the radiation from the decaying fission products. The rate of energy release is dependent on the duration and intensity of the irradiation to which the fuel has been exposed and also on the age of the waste since exposure was terminated. On a unit basis, the energy release from a high level waste may be regarded as small. However, the large volume of wastes which may be handled, the unique character of the internal energy release which is not subject to controlled change, and the heterogeneous nature of the wastes which encourage segregation or non-uniform distribution of the fission products in the waste body make the design problem complex for the disposal of the released energy.

High level wastes, as earlier defined, may exhibit an energy release of up to one watt per liter. By comparison with normal heat sources this is a very low rate. However, with millions of liters of such waste in storage, the magnitude of total heat released as water vapor is substantial even when appreciable heat loss to the ground occurs.

The low release rate per unit of volume or per unit of surface area also results in very low rates of convection within the liquid. This, in turn, encourages the development of superheat. In addition the formation and deposition of precipitates concentrate some of the fission products, which contribute to the heterogeneous nature of the energy release phenomenon. Heat is stored as superheat in the liquid and also in the precipitates. Eventually the unstable system is disturbed by liquid movement and the heat, in the form of steam, is released suddenly, initiating rapid boiling with steam releases on the order of ten to twenty times the nominal heat liberation rate. Because of the pressure which is developed by the steam surge, coupled with the pressure drop restrictions in the vapor headering system, the eruptions are cyclic and continue at intervals of about half a minute until the available stored energy has been exhausted. Prolonged boiling at much higher than nominal rates without spectacular pressure increases has also been observed.

The self-heating phenomenon has been used to concentrate the waste and thus achieve additional economies in the cost of waste storage. Although the actual cost of heat alone to achieve the same degree of concentration as that obtained by utilization of the heat resulting from radioactive decay is truly minor, the design, construction and operation of evaporation facilities are certain to be expensive. It is recognized that the eruption phenomena aggravate the storage problem. Present operations with adequate condenser capacity, together with the pressure relief and de-entrainment facilities are operating with complete confinement of activity. Sufficient information has been obtained to show that only moderate agitation is needed to eliminate the eruption problem. The most practical alternate is to store dilute wastes for a period, then utilize evaporation for ultimate con-

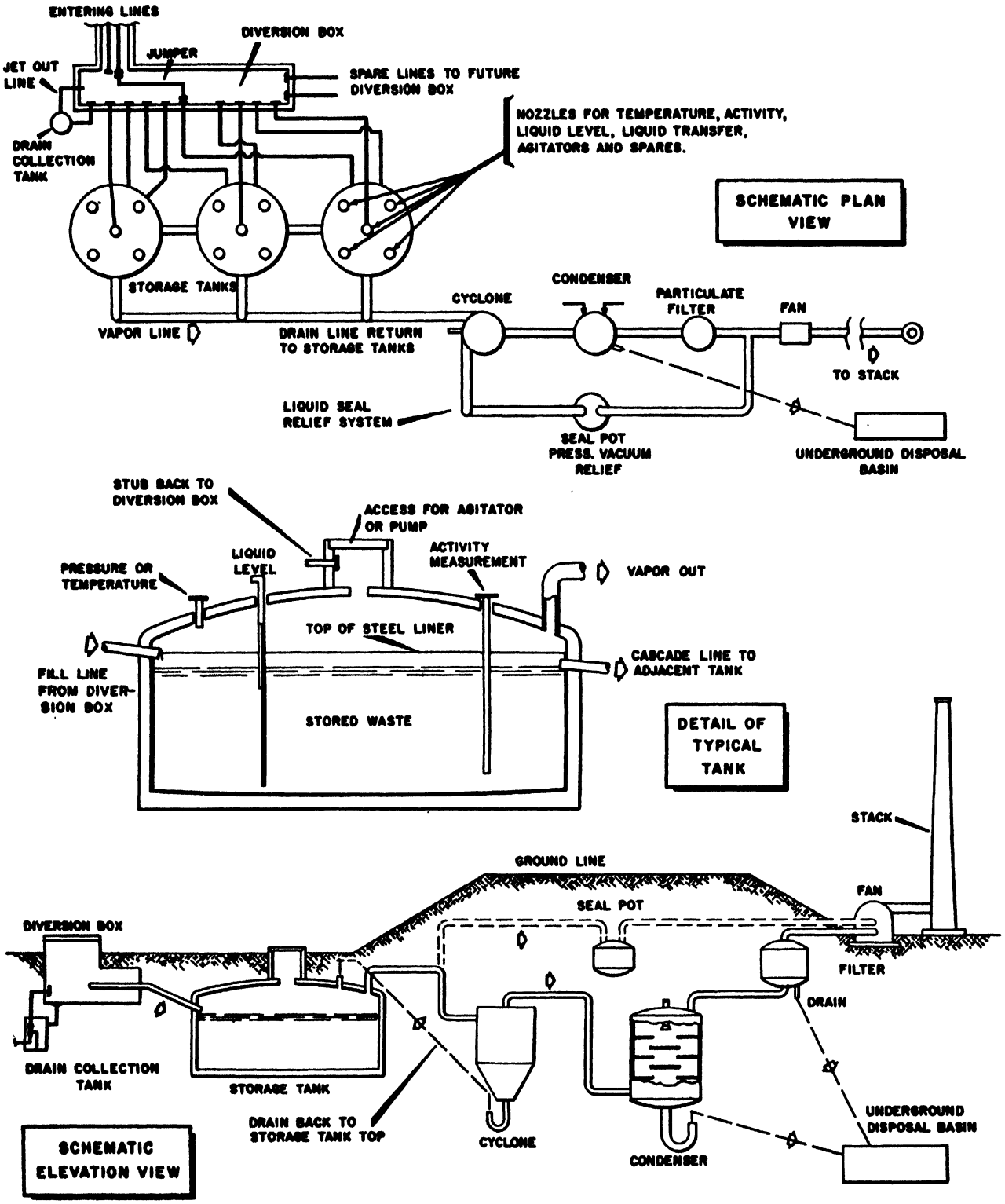

Figure 1. Typical high level waste storage facility

centration and final storage after a large fraction of the self heat has been dissipated from the dilute media.

At the present time, fairly representative information is available on energy release from separations process wastes. However, conservative designs are retained for the size of the storage facility as well as the size of the auxiliaries such as vapor headering, condensers, de-entrainment facilities, instrumentation and emergency supply for coolant.

Radiological Safety

General Considerations

The goal for radiological safety is to avoid all unnecessary exposure to ionizing radiation since it is not desirable to depart from the natural conditions under which man has developed. However, man has always lived in a field of ionizing radiation. There is a lower limit of continuous exposure to radiation that is (unavoidably) tolerated by man. There is, on the other hand, a much higher level of exposure that is definitely known to be harmful. Between these two extremes there is a level of exposure, in the neighborhood of 0.1 roentgen per day, that experience to date shows to be safe for the individual concerned.[1]

Efforts are made to prevent the accumulation of dangerous quantities of radioisotopes in the body. Radioisotopes may enter the body by way of food and water, in the air, through wounds and abrasions, and through pores of the skin. The physical state and the chemical properties of a specific radioisotope determine the type of radiation hazard and to some extent the degree of retention in the body and magnitude of hazard. Other important factors that determine the radiation hazard are the quantities of radioactive material involved, the facilities and equipment available for handling radioisotopes, the training and experience of those working with the radioactive material, and the respect they have for appropriate radiation protection standards and procedures.

Some radioisotopes can be expected to enter the body. Levels of maximum permissible exposure have been established to serve as guides to safe operation and levels of exposure.[2] Future information may show these values to be conservative. However, bearing in mind that in the future it may become necessary to lower some permissible limits, a factor of safety is used in the design and operation of permanent installations where large quantities of radioactive material are involved. This is particularly important in cases in which provisions of additional protection later would be very difficult and expensive.

Environmental Conditions

Air

Airborne radioactive particles and volatilization of certain fission products pose extremely difficult containment problems. Any method for high level waste disposal must be scrutinized for these contamination possibilities.

Methods which retain the high level wastes in a liquid state at relatively low temperatures result in little, if any, fission product volatilization or airborne radioactive particles. Proposed processing methods which require the handling of solids or conversion by fusion at elevated temperatures, however, can be expected to pose difficult control problems in both of these respects. It is visualized that a basic process may be developed for solids storage of high level wastes which has attractive economic advantages when only the storage problem itself is considered. However, when provisions for reasonable control of environmental conditions are included it is expected that costs for any solids storage system will exceed those of the present tank storage method.

The provisional levels of permissible concentration of radioactive contaminants for use in or beyond the control area in air are 10^{-9} microcuries per milliliter of beta or gamma emitter and 10^{-7} microcuries per milliliter of alpha emitter.

Since the spread of radioactive contamination in the ground follows the path of movement of the waste liquids, knowledge of the mechanics of flow in the ground is vital. Successful analysis of the patterns of contamination developed in the ground thus requires a detailed knowledge of the soils and the sediments underlying the disposal sites, including their relative efficiencies (permeabilities) in transmitting the waste liquids. Soils of high permeability generally do not decontaminate the waste liquids as well as those of lower permeability but higher exchange capacity (soils containing clays) or soils that may chemically react with the waste solutions. Once these factors are recognized and evaluated, predictions of the behavior at disposal sites become possible.[3]

Population

The discharges both to the air and to ground water are controlled such that concentrations at public access do not exceed limits specified as the maximum permissible concentrations of radioisotopes in either air or water. Although dilution factors as a function of distance provide an additional safety factor for dispersion of sporadic peak emissions of radioisotopes to the air, dilution by natural air flow is not completely dependable.

Climate

An arid climate is most favorable for waste disposal, especially for condensate disposal to ground. In one location, test data indicate that if all the normal rainfall percolated through the soil bed, up to four hundred years might be required to effect a measurable migration.

In a wet climate, by contrast, the water table can be expected to be relatively near the surface. Water displacement through the soil can be expected to be rapid due to the heavy rainfall. Ground-water travel can also be expected to be relatively fast. Under these conditions, condensate waste disposal to ground is limited to materials of less than permissible concentrations for water.

Personnel Protection on Site

General Considerations

Persons working in zones where radiation hazards are present are kept fully informed as to the nature of the hazards and the protective measures required. A manual of radiation protection standards contains the latest policies for control of radioactive materials and radiation hazards.

It is the established policy that maximum permissible exposure limits to radiation and radioactive contamination, as recommended by the National Committee on Radiation Protection, be used as the official standards. An essential part of the National Committee's recommendation is that they are based on presently available information and cannot be regarded as permanent. For this reason, and on general grounds, it is accepted practice that exposure to radiation be kept at the lowest practicable level in all cases.

Problems in Handling Liquid Wastes

No real change in industrial technique, other than shielding, is required in handling liquid wastes. The movement of material is in pipes which minimize the chance for escape of radioactive material. Diversion of flows is accomplished by remote routing arrangements.

Operating personnel are shielded from the radiation by thick concrete walls with daily exposure levels normally less than 10% of the accepted allowable levels. Maintenance such as pump or jet replacements, line reroutings or equipment repair, is done remotely without exposing personnel. In certain cases, where contact maintenance is necessary and is economically justified, a piece of equipment will be decontaminated to a low activity level. The fact that only radioactive liquids have been in contact with the equipment facilitates decontamination work. The decontamination work itself is usually done by using liquids such as acid solutions.

Escape of radioactive material from process lines or vessels does not pose a difficult problem with liquid wastes. The plant design encompasses cell floor drainage pits and means for washing down the equipment, cell walls and floors. The cell drain wastes are collected in the liquid form for ultimate disposal, either to underground storage or to ground, depending on the type and the activity level.

Problems Visualized in Handling Solid Wastes

Special equipment and handling techniques will have to be developed for any of the proposed solids-handling types of high level waste disposal, such as fusion in glass, setting of wastes in concrete or adsorption and firing of clay. The special problems which can be introduced by a solids-handling method as compared to liquid waste handling are:

1. Spread of contamination throughout the processing area by spalling, spilling or mechanical failures.
2. Control of aerosol contaminant spread to the environs in the event of dusting of the solids. Requirements here would appear to be an efficient filtering system for the ventilation air leaving the process cell as well as development of equipment-cleaning or washdown procedures for equipment replacement.
3. Control of contaminant spread beyond the processing area as a result of volatilization by heat of certain fission products. Elaborate scrubbing or chemical reactors may be required to contain volatilized fission products since only a few micrograms can represent one curie of activity. Decontamination factors in the order of 10^6 to 10^8 may be required in the process exit air in order to keep the environs contamination within currently accepted limits.
4. Resolution of the mechanical gadgets for solids handling to allow remote operation and maintenance of the process equipment.

These personnel protection problems for solids waste disposal appear to require several years of development work before solids-handling methods for waste disposal can be competitive on a large production scale with the present, liquid waste, handling methods.

The amounts of high level wastes are increasing yearly as is the knowledge of the exposure effects on man and his environs. In certain cases, as more knowledge is gained, permissible exposure limits have been reduced. It is firmly believed that the first criterion of any large-scale disposal method must be that the high level wastes are fully contained in a specific area and under control at all times.

STORAGE IN PRODUCTION PLANTS

Storage Tanks

High level wastes are stored in reinforced concrete tanks which are lined with steel. The inside diameter of such storage containers is approximately twenty-five meters. For shielding against the hazardous radiation the tanks are placed several feet in the ground. The concrete is formed around the steel liner which extends nearly to the concrete dome. In one design the tanks have an annulus between the steel and the concrete with the lower portion of the concrete vessel also lined with steel. This annulus provides a sure means for prompt detection of leaks in the steel tank. The dome of concrete which is joined to the vertical walls completes the storage vessel. Filling lines enter the tanks above the steel liner. The reinforced concrete provides the necessary support against the hydrostatic load. The concrete and steel construction for these facilities requires the highest quality of materials and workmanship. All welding on the steel liners is inspected by X-ray photographic methods. On the basis of such inspection, defects are corrected.

A number of nozzles enter the tank through the dome to provide means for temperature, pressure, liquid-level and radiation measurement; and for sampling and installation of auxiliary equipment for liquid transfer or agitation. A waste storage area consists of a number of tanks. Several wells are dis-

tributed in the storage area to permit ease in monitoring the earth sub-structure to determine evidence of leakage from any tank.

Filling of the tanks may be done individually or by cascading from one tank to another. Wastes are delivered to the farm in alkaline condition in fairly high concentration with respect to soluble salts. Wastes are transferred from the separations plants by means of pumps or steam jets. Detailed records are kept of all deliveries from the separations plants to the storage area. Discrepancies in deliveries, liquid-level measurements or increase in activity at monitoring wells are used to establish leakage. In over ten years of experience with the storage of high level wastes no evidence of tank failures has been established.

In order to provide volume for some years of operation, several tanks are built at one time. Tank volumes have ranged from two to five million liters.

The delivery of waste to individual tanks is carried out through a diversion box, also of thick concrete construction. It is sunk in the ground and has a thick concrete cover which can be removed. Routing of wastes to specific tanks is accomplished by means of jumpers which are placed in the diversion box and attached by remote-viewing methods (mirrors) to give the required diversion of the waste without exposure of personnel to a direct beam of radiation from lines within the box. These jumpers are rigid sections of pipe to which accurately positioned heads are attached which can be engaged and disengaged to the similarly positioned stubs which lead to the tanks being filled. Although valves would be of great utility here, no valve has been considered sufficiently leak proof and indefinitely reliable without maintenance to be accepted for this service. All long runs of pipe which carry high level waste are placed in concrete troughs with suitable provisions for expansion and movement of the pipes caused by temperature changes. The troughs drain to the diversion box which in turn may drain into a catch tank from which contaminated leakage can be readily delivered to the storage tanks or disposed of in other ways. In addition to the nozzles for the introduction of instruments for determination of temperature, pressure, liquid level and radioactivity, spare nozzles are provided to allow continuation of such monitoring, if a certain nozzle becomes inoperable because of mechanical failure or contamination. Also nozzles are provided for unspecified future uses such as sampling points, places for introduction of agitation devices or equipment needed to transfer the wastes to other tanks, if intolerable leakage in any tank develops.

Laboratory tests on the liquid and vapor phases of boiling wastes showed a maximum corrosion rate of 0.01 centimeter penetration per year for type SAE 1020 mild steel. Operation of the storage facility under boiling conditions continues for only a few years. Photographic examination of the walls of storage tanks which were emptied after about eight years of continuous waste storage service showed no evidence of gross corrosion.

The self-heating of high level wastes requires vapor and condensate handling facilities. Such facilities are designed on the basis of peak rather than routine conditions. Factors of ten to twenty times nominal boil-off rates are used for the design of the vapor and auxiliary condensing facilities.

Groups of tanks with the essential auxiliaries such as diversion boxes, vapor headering, and condensing system and emergency water supply system are designed so that additional tanks can be added later at minimum cost to obtain maximum utilization of common facilities. Adequate spare lines and tie-in points are always provided.

Operation

Filling of tanks is a routine operation once the desired diversion box connection is made. Although with the wastes at the lower end of the high level range there is advantage in energy concentration in filling a series of tanks by cascading from one to the other, the general practice for high level wastes is to fill tanks individually which requires more frequent changes in routings at the diversion box. Although this may be regarded as an unimpressive operation, the needs for personnel protection, precautions to be taken against the spread of contamination and minimum contamination of expensive equipment make such an apparently simple change a costly and time consuming effort.

Vapor System

Unless adequate cooling capacity is provided in the storage tank, high level wastes are likely to be maintained at the boiling temperature for a period of some years. The presence of precipitates which concentrate fission products can result in temperatures at the tank bottom, which are above the boiling temperature of the liquid waste. Temperatures as high as 176°C have been observed. In storage systems, temperatures in excess of this figure must be anticipated. Cooling coils have been provided in some waste tanks for heat removal. Potential coil failure with cooling water contamination may be regarded as a disadvantage of this method. However, in storage tanks which are not cooled, the vapors evolved from the boiling wastes must be condensed and disposed of externally or returned as liquid to the tank. Economic considerations favor external disposal of the condensed vapors to effect volume reductions. Although the heat from the vapors may be transferred to the atmosphere by means of air condensers, such condensers become large for high heat duties and, furthermore, do not have sufficient flexibility in the handling of vapor surges.

In order to capitalize on the potential volume reduction possible by removal of the self generated water vapor from the storage system, it is necessary to provide a vapor system which encompasses the following:

1. A means for removing the entrained droplets of liquid waste and their attendant activity.

2. A means of dissipating or recovering the heat content of the water vapor which exists essentially as atmospheric steam.

3. A means of handling energy releases which are approximately tenfold the magnitude of the normal, operating, energy release.

4. A safety release mechanism which will provide the most orderly vapor release in the event of complete failure of the normal system.

5. Standby facilities to take care of periods of emergency power stoppages or interruption to the flow of coolant.

Contamination control requires that the vapors leaving the storage system be essentially free of activity. The primary control point on entrainment is a standard mist separator with a secondary control being obtained in the contact type condensers which are used for heat removal. The factors of economy and collection efficiency, which in normal plant practice are primary considerations, are secondary to the considerations for minimum maintenance and long life expectancy.

Three types of commercially available separators which show the most promise are the cyclone, the wire-mesh entrainment remover, and the Calder-Fox orifice-type mist collector. For the plant installations, the cyclone has been used as it appears to offer the highest life expectancy combined with assured continuous operation. The orifice type has a high collection efficiency but is subject to fouling because of the small, 2-mm diameter holes in the collector plates. The wire-mesh entrainment remover has a major disadvantage for continuous radioactive service in that the mesh which would become highly contaminated must be periodically removed.

Although storage tanks are of massive construction they have limited resistance to pressures much above or below atmospheric. The vapor system must, therefore, be designed to provide adequate relief for both positive and negative pressures. Present tanks are satisfactory for excess pressures of about 250 mm Hg. Empty tanks should not be exposed to pressures greater than about 15 mm Hg below atmospheric.

Cooling System

In the vapor system the mist separator is followed by a condenser. There are no particular requirements for the quality of cooling water above that normally considered in industry, such as freedom from corrosive agents and excessive concentrations of insoluble matter. The selection of the condenser is determined by availability of water, economic, environmental, climatic and geologic factors. Where both the condensate and the used cooling water can be discarded, the contact condenser has the cost advantage over the surface condenser as well as requiring less cooling water due to closer temperature control between outlet water and inlet vapor. The disadvantage is the need to dispose of the total effluent whereas only condensate need be disposed to the soil structure from surface condensers.

Where economic conditions require it, recirculation of coolant may be applied by the usual industrial techniques. However, means for detecting leaks of activity into the coolant must be provided as well as alternate routings in case of such leakage. Where extreme conservatism in design must be exercised, closed system cooling may be provided.

The disposal of the water used to take up the heat from the waste storage facilities is determined by the environmental and geological conditions. Where there is adequate assurance against in-leakage of activity the used coolant may be returned to the source—stream, lake, ocean or it may be discarded to the earth. Where coolant and condensed vapor are combined as from the contact type condensers there may be objectionable levels of activity present. In such cases, disposal may be to the ground in acceptable areas, or some treatment method would be required such as ion exchange to assure adequate clean-up of this waste.

Ground Monitoring

Local conditions of soil, ground-water table, rate of ground-water flow, and proximity to populated areas determine the extent of contaminated water disposal to ground. In certain locations no water above the permissible limit established by the United States National Committee on Radiation Protection is allowed to be discharged to the soil. Other locations with more favorable ground-water table and ground-water flow have capitalized on the natural ionic characteristics of the soil for disposal to ground of condensates resulting from concentration of the stored wastes.

In disposal to the ground of the low radioactivity, aqueous distillates, soil tests are made for each specific area used. It has been demonstrated by both laboratory and field tests that of the radio elements of greatest concern, ruthenium moves farthest in soil, followed in order by cesium, strontium, and the rare earths. It has also been demonstrated that some non-radioactive salts provide ions that are markedly more mobile than are the radioisotopes. Field studies have established that when the nitrate ion is present in the wastes, it will lead all the radioisotopes and other non-radioactive ions in rate of migration. Sufficient nitrate ion is normally present in related waste streams so that nitrate ion monitoring of the underground water provides effective control of ground water contamination.

The removal of cations from the soil is possible and is dependent on the solution composition. Once in equilibrium with a given solution, the soil will remain in adsorption equilibrium until the solution composition changes. The degree of cationic saturation can be expected to vary with concentration. Large quantities of leaching solutions are required, however, to effect measurable changes in the soil adsorption. Locations with low rainfall and good ionic

characteristics in the soil may find little, if any, migration of activity once the condensate discharge to ground is stopped.

An extensive network of ground-water monitoring wells in and about the disposal area establishes the water table gradients. These, combined with measurements of the travel of certain ions in the underground water, establish the travel time for the shortest route to the perimeter of the isolation area.[3]

Radiological Disposal Limits

The hazards considered in the present disposal of radioactive wastes result from any movement of isotopes in the ground water to points of public usage either directly from wells or by dilution into streams or rivers. Appropriate limiting concentrations at the possible points of use are considered to be one tenth of those listed by the United States National Committee on Radiation Protection.[2]

Each stream proposed for ground discharge is studied carefully before disposal to ground. The examinations include the salt contents, concentrations of individual isotopes, tests on representative soils and investigation of the disposal site. In general, limits are placed on the total volumes discharged and monitoring wells are drilled as necessary to measure movement through the soils and concentrations in the ground water, if any. In addition, the stream is sampled, either by a proportional sampler or by spot samples, depending upon the method of discharge. An audit is maintained on the total amounts discharged and the isotopic composition.[3]

REFERENCES

1. National Bureau of Standards, United States Department of Commerce, Handbook 59, "Permissible Dose From External Sources of Ionizing Radiation" (1954).
2. National Bureau of Standards, United States Department of Commerce, Handbook 52, "Maximum Permissible Amounts of Radioisotopes in the Human Body and Maximum Permissible Concentrations in Air and Water" (1953).
3. Parker, H. M., "Ground Disposal of Radioactive Wastes at the Hanford Site," (4 June 1954).

Processes for High Level Radioactive Waste Disposal

By L. P. Hatch, W. H. Regan, B. Manowitz and F. Hittman,* USA

Waste disposal problems in the field of atomic energy will depend in considerable measure on the type of chemical treatment used in the processing of spent uranium fuels. For this reason alone it is necessary that a number of disposal methods be investigated. This paper presents a discussion of two approaches to the problem which are currently under study at Brookhaven National Laboratory.

ULTIMATE DISPOSAL OF WASTES UTILIZING MONTMORILLONITE CLAY

There are at least two major objectives which should be met in the disposal of the waste fission products from an atomic power industry.

1. The disposal must be permanent if it is to be considered adequate.
2. The total cost of disposal must be only a small proportion of the cost of producing atomic power.

Even though intense development work in the field of atomic power production has been progressing rapidly over the past decade, it is still too early to state realistic economic goals in the waste disposal problem. It simply is not enough to generalize on what should be achieved and give as a basis of comparison the cost of storing long-lived wastes in tanks. Experience in this country to date with storage in tanks is mostly reassuring in its own right, but the extent of that experience covers a range in time of less than one-half the half-life of the important isotopes strontium-90 and cesium-137. In short, the lack of any real assurance of permanence in disposal by storage in tanks makes it virtually impossible to assess the total cost over centuries of time. The replacement and repair of the containers themselves, as well as the safe transfer of contents to new containers and disposal of old ones are among the items which should be included in estimates of cost. The continuous monitoring to detect the first signs of any escape of radioactive contents from the system and the extensive investigations of geochemical characteristics of adjacent regions are also possible major contributors to disposal costs.

Although the element of cost in waste disposal, by itself, has a purely practical significance, it does serve to point up the much more important matter of safeguarding the environment. Indeed, it is not being realistic to draw conclusions with respect to cost without also considering environmental safety. To simplify matters, therefore, it may be well to consider waste disposal costs as an integral part of the cost of processing the reactor fuels, and thus relate it to the cost of power production. The factor of safety, then, should be weighed independently on its own merits.

No general discussion of waste disposal in an atomic power industry under present-day conditions can properly exclude consideration of the direct method of discharge to the oceans.[1] Undoubtedly there are many advocates of that method who are able to find strong supporting arguments. Since, however, by its very complexity, the subject of disposal to the ocean is a very broad one, and no comprehensive conclusions can be drawn until after a great deal of difficult testing by use of the oceans themselves, no further consideration of the subject is made in this paper. As one last thought, however, it may not be amiss to reassert, in view of the broad implications of this conference, that the oceans and the living things contained therein are of fundamental importance to us all—a matter which warrants our deepest concern in any wholesome plan for a world-wide atomic energy industry. Suffice it to say, then, that the authors are primarily interested in the development of methods of permanently confining the fission wastes in compact form on land areas.

One approach to the problem of ultimate disposal of radioactive wastes which has been in effect at Brookhaven National Laboratory over the past six years is based on the premise that the dependable life of large physical containers, tanks and the like, fabricated from reasonably available structural materials, would not be adequate for safely holding large quantities of the wastes over several centuries of time. Quite obviously, such a broad premise must be qualified in a number of ways, and there may well be exceptional circumstances in which certain special containers would be considered satisfactory. By and large, however, it is assumed that by chemically compounding the fission elements into solid substances already known to be highly stable in the environment, a much more secure method of containment would be obtained. Since the fission products, with the exception of ruthenium, are largely cationic in aqueous solution, and since it is well known that some of the natural clays have good capacity for chemical exchange of cations, the investigation at Brookhaven has centered on the

* Brookhaven National Laboratory.

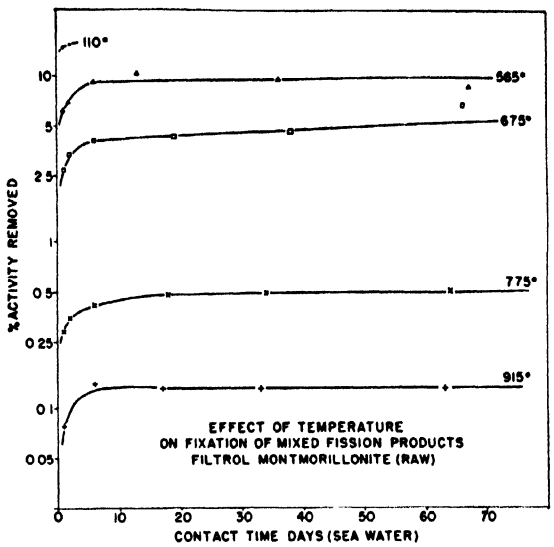

Figure 1. Fixation of fission products on montmorillonite clay

use of clays of the montmorillonite group. Three results of the investigation stand out thus far:[2]

1. The capacity for cation exchange is found to be 1.2 milliequivalents per gram of clay.

2. Ruthenium, possibly as an anion, is not effectively exchanged on the clay.

3. The exchange capacity is reduced essentially to zero by heating the clay to about 1000°C.

By this latter device the cations then on the clay are firmly fixed in place and it is in this sense that the quality of permanence in disposal is to be determined. That is to say, the fission products fixed on the clay would not be dispersed into natural waterways and, thus, would be highly restricted from ever finding their way into the body fluids of plants and animals. So long as the fired clay was confined, a major step would have been taken in securing safe disposal of the fission products without any significant reliance on the use of tanks or similar containers.

Here again, we must attempt to qualify what is being implied, for no disposal system will be perfect, and we must look to the results of experiments in which fired clay containing fission products has been contacted directly with representative solutions such as sea water. The percentage of the fission products removed from the clay as a function of time of contact is given in Fig. 1. The influence of heating to high temperature is clearly seen, and it is very important to note that after a few days, no progressive removal is perceptible during the 80-odd days of the experiment.† More investigation along these lines is necessary before far-reaching conclusions can be drawn.

Since the mechanism of incorporating the fission products into the clay is ion exchange, it is fundamental to the most efficient use of the clay that the concentrations of extraneous cations, which may be present in the solutions as a result of processing the parent reactor fuels, be at a practical minimum. No limiting value for such concentrations can be given for it depends heavily on the nature of the competing ion but, as an example, it is found that for sodium ions a concentration of $0.05N$ is very satisfactory, while for some multi-valent ions such as aluminum, the level should be much less than $0.05N$. Sodium is of particular interest because its hydroxide is commonly used in the neutralization of acid waste solutions. Aluminum and zirconium, for example, would be present in wastes from processing solid fuels in which these elements were alloyed with uranium. These examples are but a few among the many possible combinations that will be encountered in any ion exchange or similar process for treating waste solutions. Accordingly, in all the work on the clays we have set up two principal objectives; (1) a pre-treatment of the raw waste solutions designed to reduce or prevent the admission of extraneous ions, and (2) direct adsorption of radioactive ions on the clay. The extent to which the first step is accomplished becomes a very good measure of the possible success of the second step.

As an important example of the first objective, the removal of nitric acid by volatilization and by electrolysis using ion-selective membranes are highly desirable over the use of caustic. Likewise, the separation of aluminum or zirconium from the fission products by first converting to the oxides on heating and then leaching with water or dilute acid, shows much promise. Not all of the fission products are leached away in this manner. However, by this method it appears that the aluminum or zirconium, with whatever fission products remain after leaching, are converted into a stable form suitable for ultimate disposal; the leached fission products would then be fixed on the clay. Enough work has been done along these lines to demonstrate the feasibility of such separations process in conjunction with the use of the clay. Figure 2 shows a diagram of one type of membrane unit with which a reduction of nitric acid concentration to less than $0.08N$ with satisfactory consumption of electric current has been demonstrated. Exposure of the membranes to radiation from high-level activity wastes has not revealed serious limitations with respect to the use-life of the membranes. Possibly, the most difficult problems will be associated with the design of membrane units in order to provide for mechanical maintenance and and servicing. It now appears evident that, for our purposes, a combination of initial removal of nitric acid by volatilization and final reduction by use of membranes will prove most economical.

Results on the adsorption of mixed fission products on montmorillonite clay following acid reduction is shown by the curves in Fig. 3. Here the sodium hydroxide is added to neutralize acid in the concentration $0.02N$. The clay is formed into permeable beds by extruding small rods of a mixture of clay

† A continuation of this experiment revealed no change after one year.

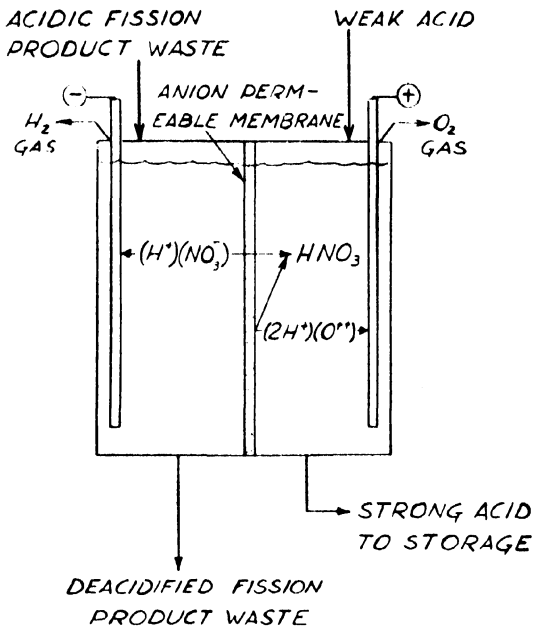

Figure 2. Deacidification process using ion selective membrane

and water (Fig. 4). A series of columns of clay, each about 1-foot long and containing about 15 grams of clay, was arranged so that three successive columns were used at a time. By adding a fresh column at the downstream end and removing a spent column at the upstream end, the system was operated in a counter-current fashion and the quality of the effluent was maintained. In this experiment a decontamination factor (measured by composite activity counting) of about 5000 was obtained. Much longer paths of contact with clay would be available in any commercial-scale plant, however, and greater decontamination factors would be possible, but we are not yet in a position to generalize in this respect.

It is not the purpose in writing this paper to present the results of laboratory experiments in any full detail, but it may be significant to report on a recent run in which the behavior of strontium in the presence of all other fission products was specifically observed. Strontium was chosen for the reason that it appears to be less reactive with the exchange sites on the clay than the other fission products (as before, ruthenium is excluded from this consideration). In the experiment, five columns of clay were used with three on stream at a time. The feed solution was made up as follows: Sr, 0.1 meq/liter; Ba, 0.06 meq/liter; Cs, 0.07 meq/liter; Y, 0.08 meq/liter; La, 0.1 meq/liter; Ce, 0.07 meq/liter; Pr, 0.1 meq/liter; Nd, 0.3 meq/liter; ZrO, 0.24 meq/liter; and Na, 50.0 meq/liter.

The Sr^{90} activity was 2.7×10^5 cpm/ml. After 70 hours of operation 10 liters of solution had moved through the system, and the concentration of strontium in the effluent had varied between values based on $C = 10$ and 20 counts per minute per ml. The decontamination factor for strontium, therefore, was more than 10^4 and, on the basis of 10 ml of fired clay in each column, the volume of decontaminated liquid was about 200 times the volume of the fired clay.

As already pointed out, the clay is not known to have any significant capacity for adsorption of ruthenium. In fact, it has been found that a high percentage, if not all, the ruthenium in certain waste solutions passes readily through the clay columns. There is reason to presume, therefore, that a good separation of ruthenium from the other fission products may be possible by use of the clay. The problem of disposal of ruthenium would remain but, as a separated fission product having a half-life of only about one year, the disposal problem would be much reduced. As one possible alternative we are investigating the extent to which ruthenium may be incorporated in glass or ceramic bodies. It has already been found that ruthenium-bearing residues from effluent solutions fused with particles of ground glass shows no perceptible loss of ruthenium on contact with 6*N* nitric acid. It is quite possible,

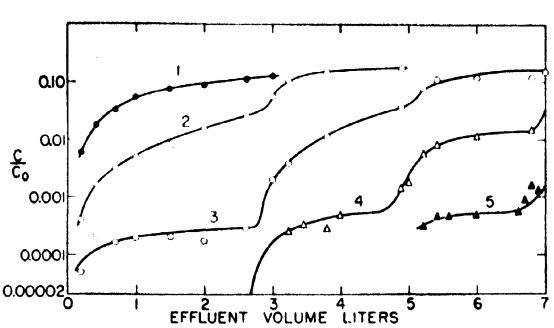

Figure 3. Cation exchange of fission products on clay

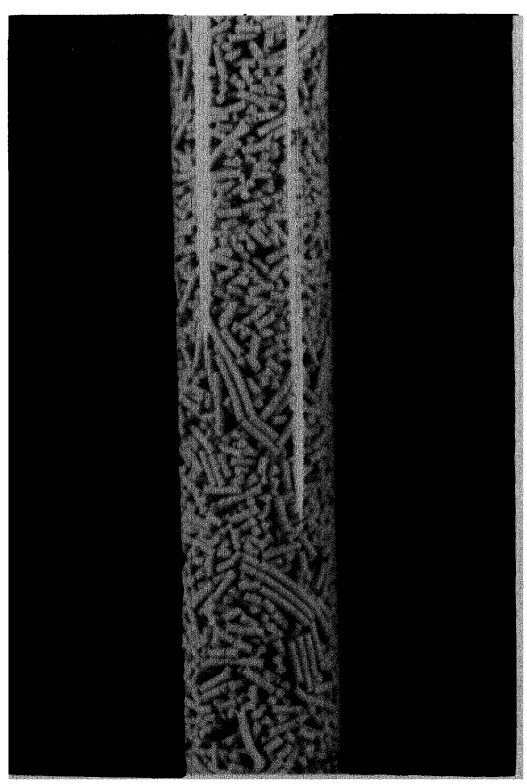

Figure 4. Extruded clay

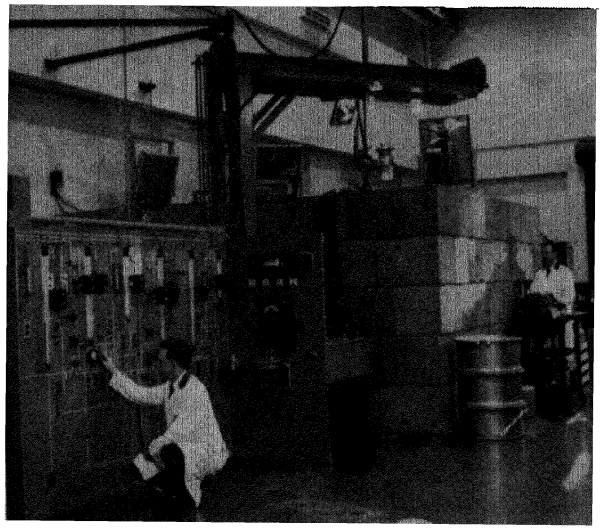

Figure 5. Pilot plant for clay process

moreover, that ruthenium-106 with its daughter rhodium-106 represents a valuable source material for use in irradiation in industrial processes. The short half-life, as compared with that of cesium for example, would be a disadvantage in one important respect, but it can be considered as a possible advantage with regard to such matters as obsolescence and ultimate disposal.

About two years ago our investigations of montmorillonite clay were considered sufficiently promising that a test of the process on a more realistic scale was warranted. Consequently, a pilot plant (shown in Fig. 5) was constructed, and put into operation the first of this year. Briefly, the plant comprises a series of four columns of clay mounted in a vertical line with suitable mechanical manipulators so that the columns can be moved individually in a direction counter-current to the flow of fluid. Containers made of refractory materials are enclosed in stainless steel jackets joined at the mid-section by means of demountable quick-opening bands, all of which is shown in Fig. 6. Spent columns of clay are fired in a high temperature kiln. All mechanical operations on the pilot plant have proved to be satisfactory and the entire plant is designed for treating high activity level wastes. To date two runs have been made, each utilizing a feed solution containing representative amounts of the fission products as stable elements, together with 0.2*N* sodium nitrate. In the first run tracer amounts of fission products from actual wastes were added. In the second run strontium-90 was added. Results of both runs were in good agreement with results of similar experiments using laboratory-scale equipment.

The advantages gained in contacting the solution and the clay in a counter-current fashion are very substantial as would be the case for any mass transfer system. Counter-current operation in the pilot plant by shifting the columns from one position to another presents the advantage of conserving equipment such as pipes, valves, etc. However, it does present problems regarding such matters as safety and economy in operation wherein refractory vessels containing large amounts of radioactive solids would be handled. For these reasons, among others, we now propose to base the design of a commercial-scale waste disposal plant on the principle of using stationary columns and providing for counter-current operation by periodically shifting the course of the feed streams. Of first importance in such a design is the need for a suitable large-size refractory container for the clay and with the necessary inlet and outlet conduits built into the container itself so that interconnection without the use of jackets is obtained. The development of such a container is being explored by the Refractory and Insulation Corporation, 120 Wall Street, New York City, and a picture of their latest product is shown in Fig. 7.

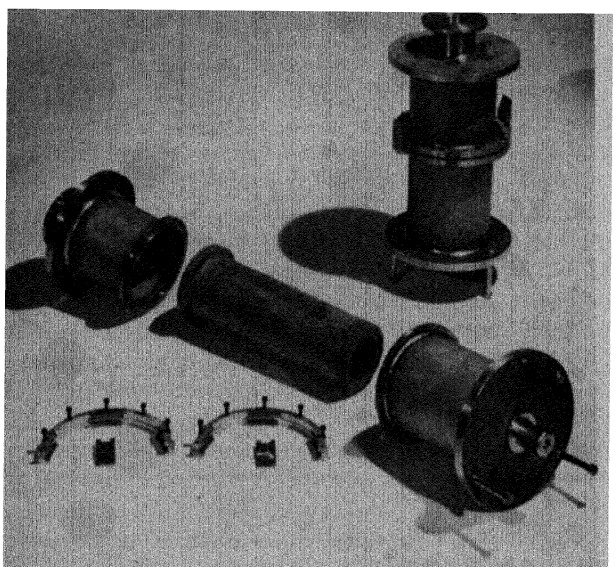

Figure 6. Pilot plant column assembly



Figure 7. Commercial scale container for clay beds

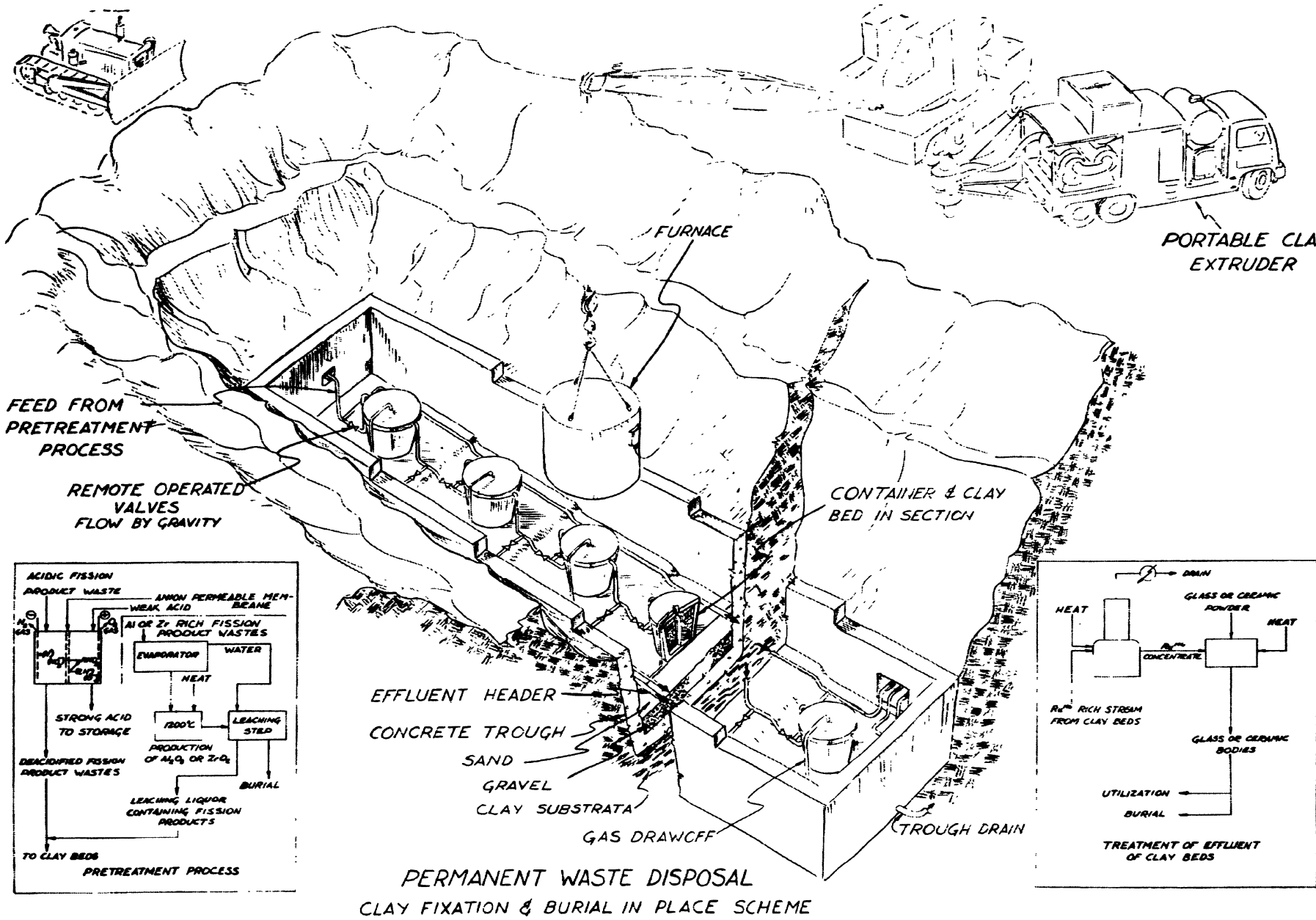

Figure 8. Conceptual design of commercial scale waste disposal plant utilizing clay

A perforated disk for supporting the clay is placed near the bottom of the container and the inlet solution is fed to the space below the disk through a pipe located along the center of the container. The course of the solution is downward through the pipe, upward through the disk and the bed of clay, outward through the overflow pipe near the top, and thence to the next column. The layout of a plant using these containers is shown in Fig. 8. Fluid flow by gravity is shown [illegible] the plant but an inexpensive air-driven piston pump is available which has the advantage of being easily removed from the system for replacement. Provision is made for firing the clay with the aid of a portable bell furnace, as shown, or by utilizing the heat associated with decay of the fission products, or a combination of the two methods. Self-heating is entirely feasible and would mainly introduce problems of controlled insulation.

From the standpoint of simplicity and economy such a design as is shown in Fig. 8 presents a number of advantages.* The beds of clay would be formed in place for final burial and it would be required only that they be adequately covered after the firing operation. No movement of radioactive solids would be involved, and no handling of large containers would be necessary. The problems of maintenance of equipment would tend to be minimized and the need for large buildings would be eliminated. On the basis of the tentative design shown in Fig. 8 it is possible to give a very rough estimate of the cost of permanent waste disposal in terms of the cost of power production. Considering the relatively small volume of wastes from one reactor of 500 megawatt capacity, the cost of disposal would be in the range, 2% to 3% of power costs at 0.007 dollars per kwh. However, if wastes from several reactors are processed in one central disposal plant large reductions in cost with respect to both capital investment and operations can be envisioned.

CONVERSION OF AQUEOUS WASTES TO ANHYDROUS MELTS

To reduce the hazards and costs involved in storing highly radioactive wastes, it is proposed to dewater and fuse the voluminous liquid wastes to a compact fused salt. After dehydration, the wastes would be in the form of a mixture of insolubles and dried salts which can be fused upon further heating. Any solids which do not dissolve in the fused salt can be occluded or fluxed by having an adequate amount of fusible salt present in the waste. Because of the neutralization step, the aqueous wastes which are presently being stored as 20 to 30 wt % salt solutions contain large quantities of $NaNO_3$. Having a relatively low melting point (308°C), fused sodium nitrate can serve as a fluxing agent for the other solids including the fission products which are present in the waste streams. In waste streams where this "built in" fluxing agent is not present, other low temperature melting salts can be added to serve as fluxing agents for the de-watered wastes. The fluxing constituent is necessary because it gives mobility to the concentrate product (i.e., it can be pumped) and because it serves as a medium through which the heat of radioactive decay can be removed from the waste product. The conversion of the aqueous wastes to a fused salt reduces the volume of waste which has to be stored, and because the fused salt can be stored as a solid in the final container, the potential hazard of storing a mobile liquid is decreased.

MELT STORAGE TANKS

The melt storage tanks would be of mild steel construction. Conservatively, the melt process is capable of achieving a volume reduction factor of 2 to 3. Thus, relatively few melt storage tanks would provide long-term storage.

From the potential hazard point of view, the melt storage system would greatly reduce the risks involved in solution storage, and, in fact, should be relatively stable and safe. As conceived, the final storage system is a large underground concrete enclosure containing a number of flat mild-steel pans. A dehumified ventilation system provides corrosion-free natural convection cooling for the melt-containing pans. The pan geometry is chosen to provide optimum surface areas for cooling and for possible gassing due to radiation damage. A feed distribution system would permit the gain of decay time by sequence filling. Even in the event of a major accident involving the exposure of large volumes of the melt to wind and weather, the activity would be leached or eroded from the melt with difficulty, so that a major accident involving exposure of the melt would result in a disagreeable cleanup job rather than a disaster.

Preliminary calculations have been made to determine the extent of the temperature build-up which can be expected in the fused salt product from the heat of radioactive decay. In these calculations decay times of 90 days and 1 year were used. The heat generations of 90-day-old and 1-year-old fused salt waste were assumed to be 24 BTU/hr/gal and 8 BTU/hr/gal of melt, respectively. The ambient air temperature was assumed to be 80°F, and the over-all heat transfer coefficient was taken as 2 BTU/hr/ft²/°F. Figure 9 shows the maximum temperature to be expected in the 90-day-old waste as a function of salt cake thickness, and Fig. 10 shows the same relationship for 1-year-old waste.

If a limit of 700°F (approximate melting point of melt product) is placed on the maximum allow-

* The authors wish to acknowledge the extensive contributions of Dr. H. C. Thomas of Yale University, Dr. W. S. Ginell of Brookhaven, and George P. Simon formerly of Brookhaven and presently with the Atomic Power Division of Westinghouse Electric and Manufacturing Company, in this investigation. T. V. Sheehan, D. W. Huszagh, and B. R. Gibbs of the Mechanical Engineering Department at Brookhaven carried out much of the work in the preparation of the engineering designs.

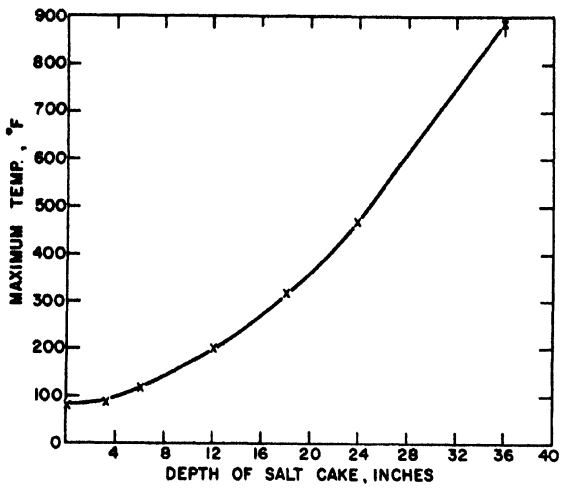

Figure 9. Temperature distribution in salt cake after 90 days cooling

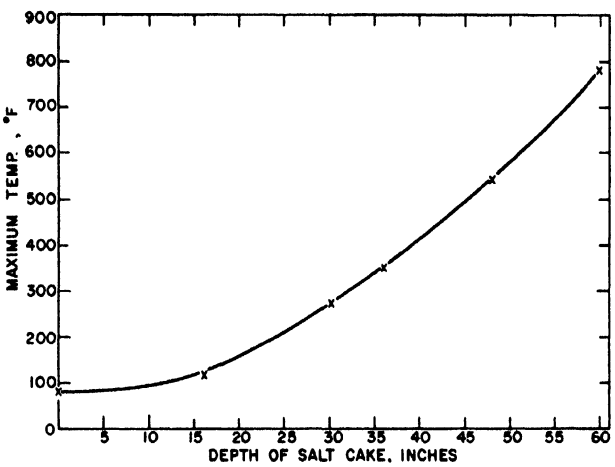

Figure 10. Temperature distribution in salt cake after 1 year cooling

able salt temperature (which would occur at the center of the salt cake), a cake depth of approximately 30 in. is permissible with the 90-day-old waste. This depth would result in a maximum surface temperature of only 190°F. If 1-year-old waste is processed, a 55-in. salt cake appears permissible without exceeding a maximum salt temperature of 700°F. The maximum surface temperature under these conditions would be approximately 150°F.

DEVELOPMENT OF EQUIPMENT

The following criteria were established for the concentration equipment:

1. It must be mechanically simple.
2. The entire concentration sequence (i.e., dewatering, drying, and fusing) should take place in one piece of equipment.
3. It must operate continuously.
4. Operation of the equipment should involve a minimum amount of manual process operations.

Figure 11 shows the process flow sheet for a pilot plant unit designed to meet the above criteria. The salt solution is fed continuously from the feed tank to the calciner by means of a centrifugal pump. The rate of flow is controlled by means of throttling valves and is measured by a flowrator. The feed enters the calciner body at the cold end (200°F) where the solution is dehydrated, and as the auger moves the dried salts toward the discharge end the temperature of the salt is raised until it fuses. The fused salt is then discharged continuously to a heated sump for transfer to a final container. The water vapor and oxides of nitrogen which are given off during the calcination pass through an entrain-

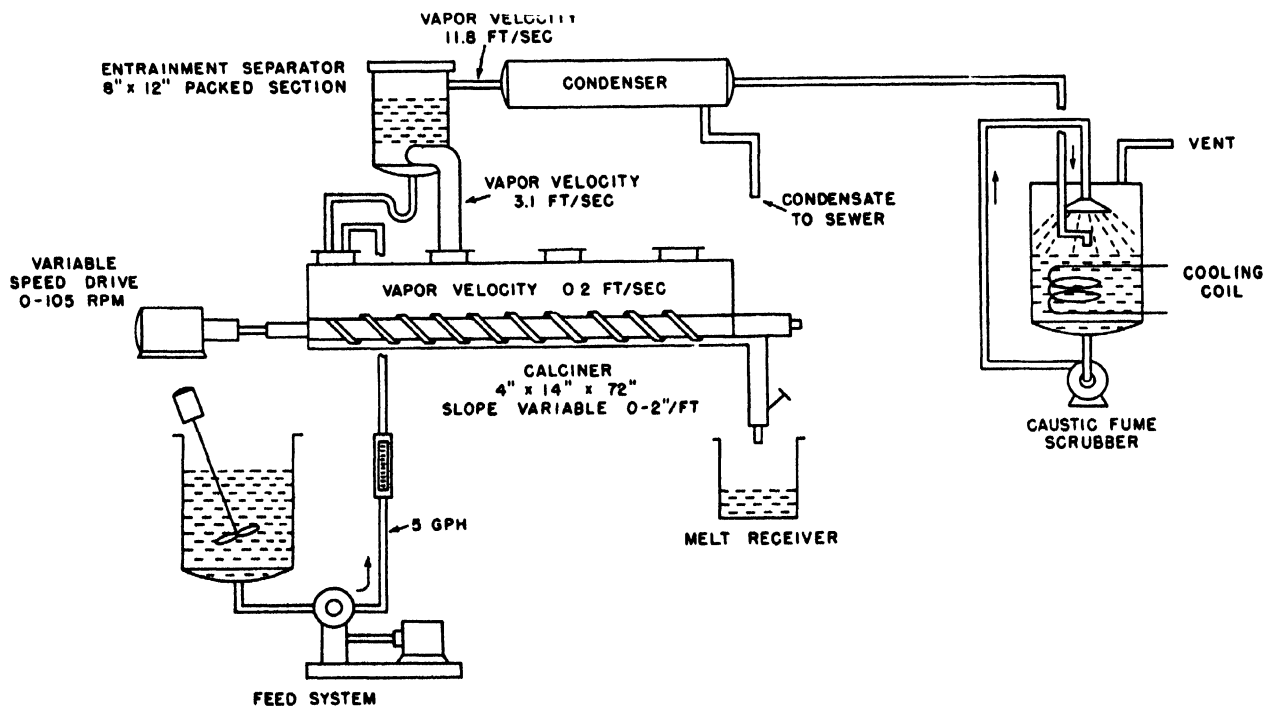

Figure 11. Calciner pilot plant process flow sheet

ment separator to a condenser where all the water vapor is condensed and received in a condensate receiver. Any oxides of nitrogen which do not dissolve in the condensate pass through a caustic scrubber where they are removed by reaction with 25% NaOH.

Figures 12 and 13 describe a pilot plant constructed to test this process. The entire calciner plant, except for the caustic scrubber, is constructed of stainless steel (Types 347 and 304). All heating is done by means of U-shaped strip heaters and No. 20 stainless steel braided-Nichrome resistance wire. The heating of the calciner is controlled by nine separate circuits. The heat output of each circuit can be varied by means of a voltage regulator. Temperature measurements are made at 32 points on the calciner assembly. These temperatures are recorded continuously on a Brown multipoint recorder. A thermal overload switch in the temperature recording circuit, prevents temperatures from exceeding 1000°F anywhere on the calciner body.

A half section of 4-in. Schedule 40 Type 347 stainless steel pipe, 6-ft. long, serves as the trough of the calciner. A rectangular-shaped dome is welded to the trough. Standard pipe flanges serve as inspection ports and connections for the feed and vent lines. The entrainment separator contains a wire basket, 8-in. by 12-in. high, packed with stainless steel mesh. It is designed for a vapor velocity of 0.75 to 1.0 ft/sec. The mesh has a wire diameter of 0.0045 in. and a packing density of 15 lb/ft.[3] A 4-in. stainless steel twist auger (Fig. 14) is supported at the driven end by an external ball bearing. Its entrance into the calciner body is sealed by means of a stuffing box. At the discharge side of the calciner the auger rides in a graphite sleeve. The auger can be installed and removed easily by removing the rear flange and inserting or removing the auger through the rear of the calciner. The entire plant is mounted on a single platform whose slope can be varied by means of a screw type jack. Figures 15 and 16 are construction photographs which show the pilot plant before insulation was completed. Figures 12 and 13 show the completed calciner plant. The U-shaped cross section of the calciner body makes it possible to observe the operation of the equipment through the observation ports and offers a large free volume above the process stream, but it also results in the anomalous heating of the calciner body and poor utilization of heat input.

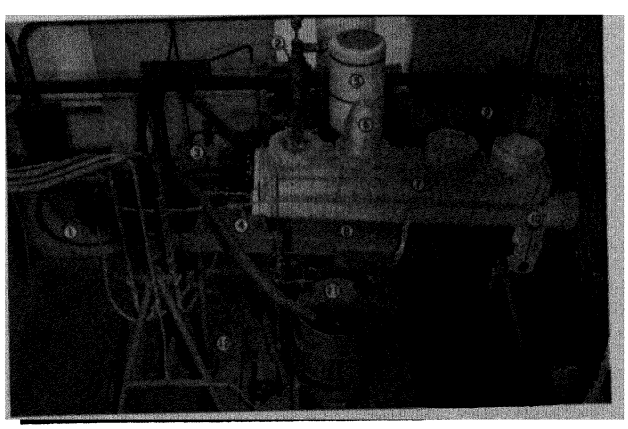

Figure 12. Photograph of completed calciner pilot plant: (1) variable speed drive; (2) condenser; (3) flexible coupling; (4) auger shaft; (5) de-entrainment separator; (6) vapor line; (7) calciner body; (8) variable slope mounting platform; (9) viewing ports; (10) product discharge line; (11) feed tank; (12) screw type jack

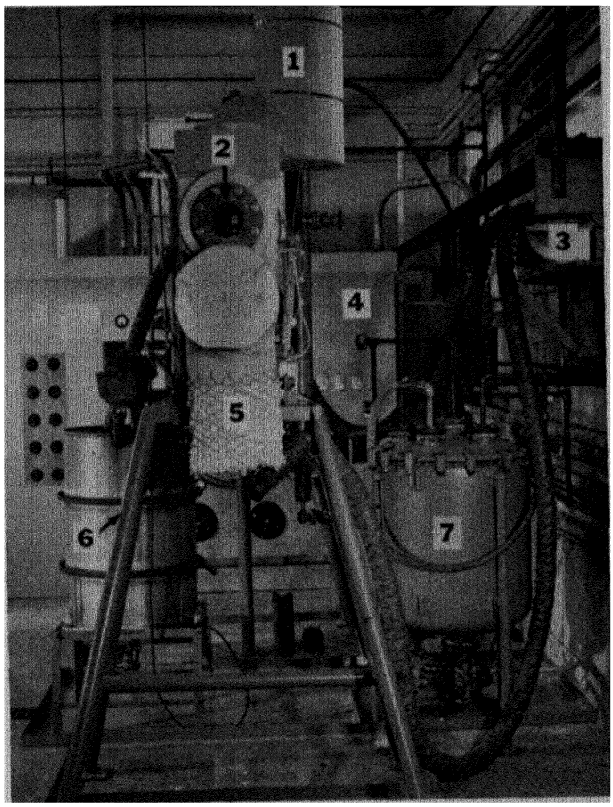

Figure 13. Photograph of completed calciner pilot plant: (1) de-entrainment separator; (2) viewing port; (3) exhaust fan; (4) operating panel board; (5) heated sump; (6) calciner support; (7) caustic scrubber

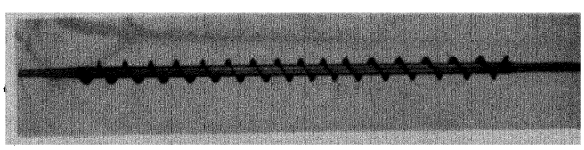

Figure 14. Auger drive for calciner

The greater part of the process heat for the calciner is provided by the U-shaped strip heaters located uniformly along the bottom half of the calciner body. The heated section of the strip heaters extends about 8 in. from the bottom of each side of the calciner body.

During operation the liquid height in the calciner is kept at about 1 or 2 in. Therefore, a portion of the heat does not have direct access to the process liquid. This results in the maximum calciner body temperatures occurring in the middle and upper section, and limits the production capacity and thermal efficiency of the unit.

The lower section runs between 200°F at inlet and 700°F at outlet, while the upper sections run at much higher temperatures (900°F). The thermal overload switches prevent these upper section temperatures from exceeding 1000°F. The upper sections also expand a greater amount longitudinally than the lower sections, which causes a slight tilting of the end plates on the calciner body.

The external bearing mount for the auger shaft is attached directly to the front end plate. Thus, the shaft is deflected down when the calciner body is at operating temperatures. The resulting misalignment with the variable speed drive shaft is taken up by the flexible coupling.

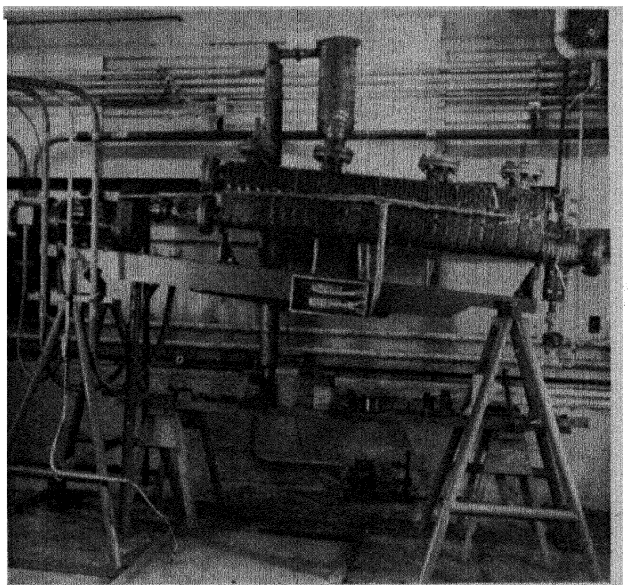

Figure 15. Construction photograph of calciner pilot plant

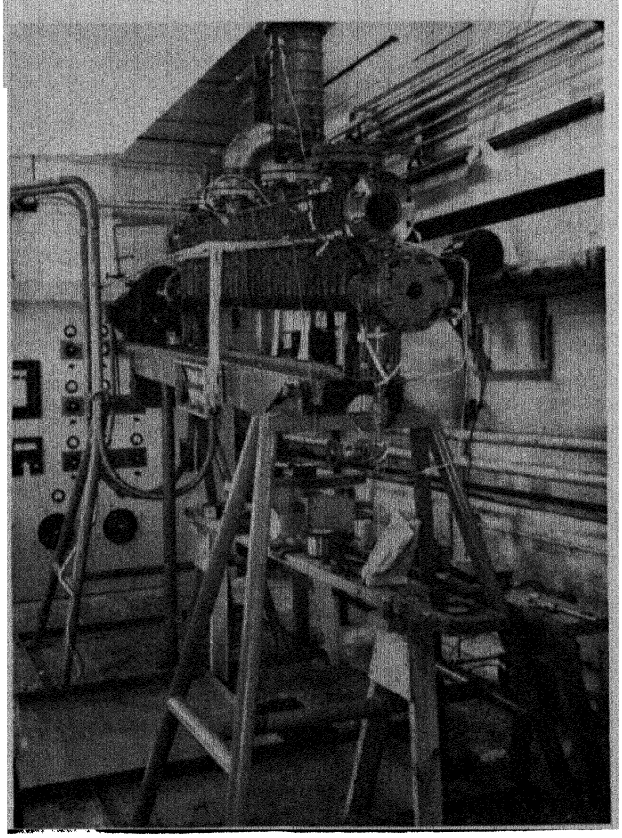

Figure 16. Construction photograph of calciner pilot plant

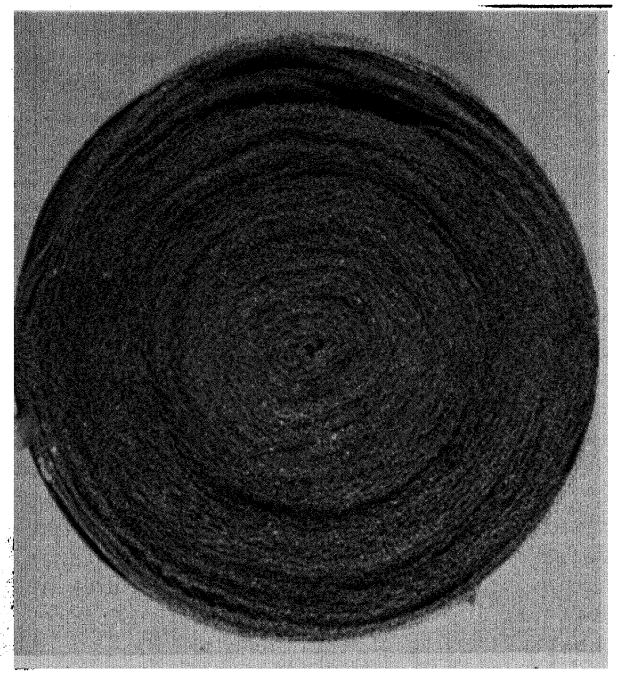

Figure 17. Stainless steel de-entrainment unit at start of run

The calciner plant was shaken down in a start-up run in which a 50% $NaNO_3$ solution was used as feed. In starting up, the entire unit was brought up to temperature slowly. It was impossible to maintain a temperature gradient of 500°F between the cold and hot ends during this period because of the conductivity of the steel calciner body. However, a temperature gradient of 300°F was achieved. After a heat-soaking period of 4 hr the feed was started at 3 gal/hr and the heat inputs were adjusted so that the cold end of the calciner operated at 200°F and the hot end at 700°F. After approximately 1 hour of operation, molten $NaNO_3$ was discharged from the calciner. Since the discharge line was not running full, cold air was sucked into the calciner which tended to cool off the discharge line. It was therefore decided to operate the unit by discharging the melt intermittently. Thereafter, the discharge valve was opened only when the heated sump (see Fig. 13) was filled. After equilibrium conditions were established, the plant operated satisfactorily for a period of 16 hr.

In order to check the capacity of the equipment, a second run was started in which 35 wt % of $NaNO_3$ solution was used as feed. After equilibrium conditions had been attained at a feed rate of 3 gal/hr, the feed rate was raised incrementally. Appropriate increases in heat input followed each feed rate increase. This process was continued until some factor in the operation of the equipment proved to be limiting. In order to operate at feed rates above 5 gal/hr, it was necessary to keep the temperature at the cold end of the calciner at approximately

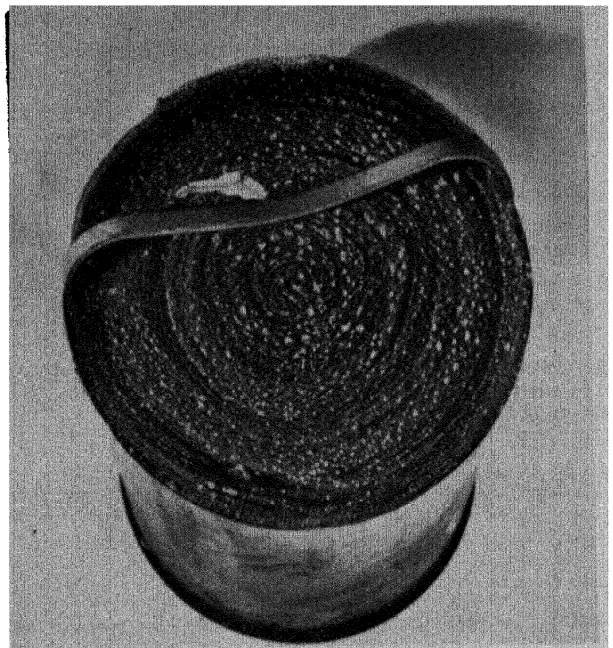

Figure 18. Stainless steel de-entrainment unit at end of run, top view

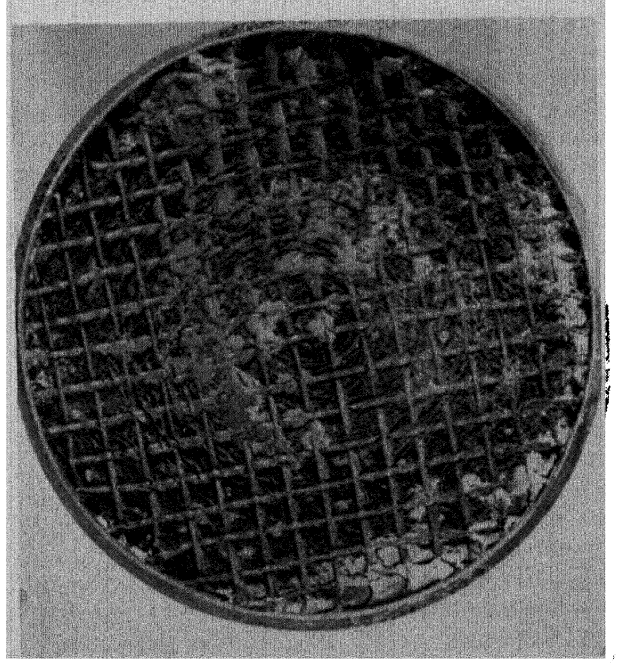

Figure 19. Stainless steel de-entrainment unit at end of run, bottom view

600°F. This proved to be a limiting factor, since the aqueous feed impinged upon a layer of fused salt (melting point, 587°F) near the feed entrance point and formed numerous aerosols which eventually plugged the bottom of the packed section in the entrainment separator and thereby pressurized the unit. In order to determine the nature and extent of this problem, the plant was shut down and the entrainment separator inspected. Figures 17, 18 and 19 on this and the previous page, show the results of this inspection.

Figure 17 is a photograph of the entrainment packing before the run was started. Figures 18 and 19 show the bottom and top of the entrainment separator basket after the run was completed. It can be seen that a large amount of salt had caked on the bottom of the packed section and that some salt was even carried through to the top of the packing.

The results of this run emphasized the necessity of maintaining the temperature of the calciner section nearest the feed entrance point below the melting point of the salts, and in all subsequent runs this temperature was never allowed to exceed 300°F.

After the packing in the entrainment separator was replaced with clean stainless steel mesh, a 29-hr run was completed in which a feed was used which consisted of 6 wt % $Fe(NO_3)_3 \cdot 9H_2O$ and 24.0 wt % $NaNO_3$. In this run the $Fe(NO_3)_3$ decomposed to Fe_2O_3 and the fine particles of Fe_2O_3 were in turn fluxed by the $NaNO_3$ to form a uniform dense salt cake product. Most of the NO_2 vapors resulting from the thermal decomposition of the $Fe(NO_3)_3$ dissolved in the condensate, and the small amount which did not, was removed by the caustic scrubber.

Condensate samples were taken during the run and evaporated to dryness to determine the amount of entrained salt present. In all cases this amounted to approximately 0.1 gm of salt per 100 ml of condensate. Since the feed stream contained of the order of 50 gm of salt per 100 ml of water, this represents a decontamination factor of approximately 500.

After completion of the third run, the graphite sleeve in which the auger rides at the hot end of the calciner was removed and inspected. Figure 20 shows the condition in which this bearing surface was found. Considerable embrittlement and erosion

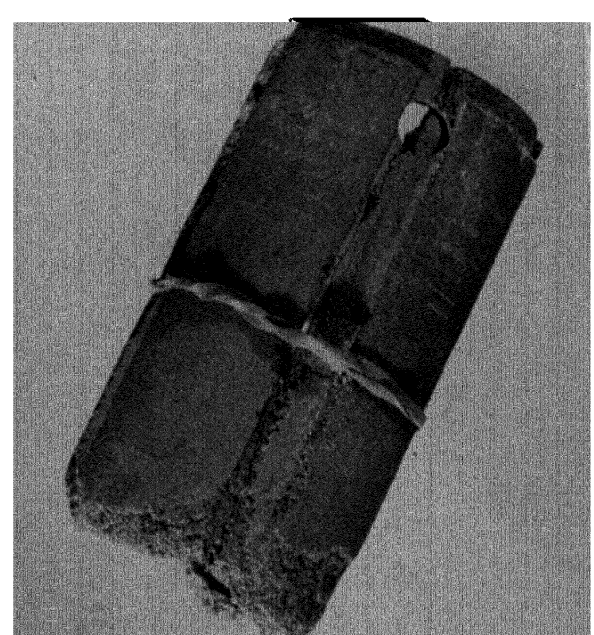

Figure 20. Graphite bearing after calciner run

had taken place, and the sleeve had cracked longitudinally. The graphite sleeve was replaced by a new one, and a program has been initiated to find a more suitable high temperature resistant material for calciner service.

SUMMARY OF RESULTS

The calciner plant has been operated successfully in processing simulated high activity waste streams containing 30 wt % salt. These waste streams were converted by the calciner on a continuous basis to anhydrous free-flowing melts. The pilot plant equipment has operated successfully for a total of 150 hr and has produced approximately 1500 lb of fused salt product.

ACKNOWLEDGEMENTS

The authors acknowledge the contributions to the research effort covered by this paper to Robert J. Isler, Samuel Zwickler, Harold Wanger, Fred Pallas, and Lincoln Stoughton.

REFERENCES

1. Hatch, L. P., "Ultimate Disposal of Radioactive Wastes," American Scientist, Vol. 41, No. 3 (July 1953).
2. Ginell, W. S., Martin, J. J. and Hatch, L. P., "Ultimate Disposal of Radioactive Wastes," Nucleonics, Vol. 12, No. 12 (December 1954).
3. Manowitz, Bernard and Hatch, L. P., "Process for High-Level Waste Disposal," Chemical Engineering Progress Symposium Series, Vol. 50, No. 12 (1954).

Record of Proceedings of Session 22B.2

SATURDAY MORNING, 20 AUGUST 1955

Chairman: Mr. A. J. Cipriani (Canada)
Vice-Chairman: Mr. A. R. Torky (Egypt)
Scientific Secretaries: Messrs R. Hara and D. J. Littler

PROGRAMME

P/415 Chemical processing of fission product solution . . E. Glueckauf and T. V. Healy

P/552 The design and operation of high level waste storage facilities . . . . . C. R. Anderson and C. A. Rohrman

P/553 Processes for high level radioactive waste disposal . . . . . L. P. Hatch *et al.*

DISCUSSION

Mr. E. GLUECKAUF (UK) presented paper P/415 as follows: Chemical processing of fission product solutions is done mainly for two reasons.

First, we may require bulk reduction, which would be economical for storage, transport or chemical operations; secondly, we may desire the recovery of individual fission products.

The fission product solutions in which we are most interested contain mostly nitric acid, and then corrosion products, fuel impurities and lastly the fission products, all in a very large volume.

The sequence of operations, therefore, is first of all concentration, secondly, if so desired, de-acidification, and thirdly, individual separation. In ordinary industrial chemistry such operations would hardly invite comment, but with fission products the operations are more complicated, because (*a*) the materials are highly active, and (*b*) there is a difficult waste disposal problem. Not only must the apparatus be so simple that it can be operated, serviced and removed by remote control, but any chemical substance added in bulk increases the disposal problem unless it can be extracted inactive. The only way in which it can be removed inactive is via the gas phase. We therefore consider it almost an axiom that no chemical should be used in bulk which cannot be removed as gas or vapour. Hence we use nitric acid as salting-out agent in solvent extraction processes.

Our first important process with fission product solutions is therefore concentration by distillation of nitric acid. In this case the distillate should be of such purity that it can be re-used or thrown away. This requires very high decontamination of the vapour. The dangers are due to spray entrainment and to volatile fission products such as iodine or ruthenium. Iodine can be dealt with generally by ageing, on account of its short life. Ruthenium has a half-life of about one year and is volatile as RuO_4. The volatility depends on the acidity of the solution. It increases sharply at higher acidity. It also depends on the electrolyte content of the solution.

Slide 1 (Table II of P/415) shows the results of distillation, the ruthenium being clearly more volatile from the more concentrated solutions which arise at the end. Time also is a very important factor. In $12N$ HNO_3 immediate distillation volatilizes only 10^{-3} per cent ruthenium, but boiling under reflux for 70 hours followed by distillation of the solution volatilizes as much as 5 per cent.

However, taking all these factors into account, it has been possible to achieve decontamination by a factor of more than 10^7 by evaporating the nitric acid at low acidity, low pressure and with low hold-up volume.

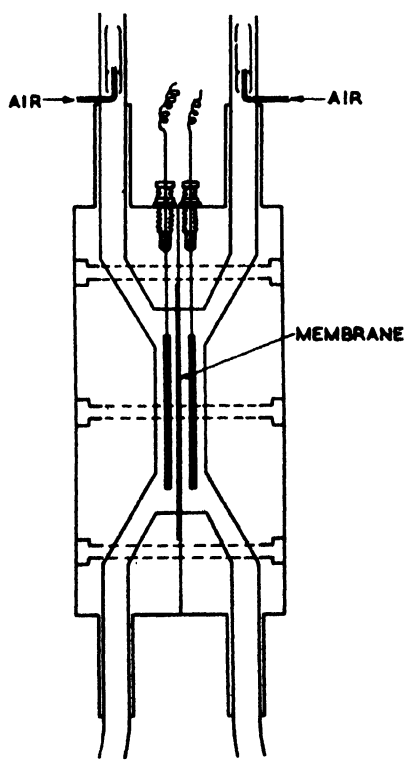

Slide 2

Having concentrated our original solution by a factor of 50 or more, the next operation is de-acidification.

We have investigated four treatments, namely evaporation to near dryness and subsequent dilution; solvent extraction of HNO_3; anionic membrane electrolysis; and destruction of HNO_3 with formaldehyde. Evaporation can be carried out in the same way as distillation. Low temperature, low acidity and good reducing conditions are desirable if ruthenium is to be retained in the solid. For solvent extraction of nitric acid, ethers, ketones and esters have been found useful, and reduction of acidity to 0.1 or 0.2*N* can be achieved in this way.

A fairly new method of de-acidification is electrolysis through an anion-semipermeable membrane.

Slide 2 shows the two-compartment cell with a separating membrane. As the nitrate ion moves through the membrane, and as the equivalent amount of hydrogen is evolved at the cathode, electrolysis results in the removal of nitric acid from the cathode compartment and its accumulation in the anode compartment. The nitric acid so removed is not entirely inactive, as the anionic fission products, SeO_4^{--}, TeO_4^{--}, and TeO_4^{-}, as well as a proportion of ruthenium, are eventually found in the anode compartment, together with the nitric acid.

A very effective method is the destruction of HNO_3 with formaldehyde. Three main reactions can occur, according to the concentration of the nitric acid.

Above 8*N*:

$$4HNO_3 + CH_2O \rightarrow 4NO_2 + CO_2 + 3H_2O$$

Between 1 and 8*N*:

$$4HNO_3 + 3CH_2O \rightarrow 4NO + 3CO_2 + 5H_2O$$

Below 1*N*:

$$2HNO_3 + CH_2O \rightarrow 2NO_2 + HCOOH + H_2O$$

The first two reactions show an observable induction period which is due to the NO_2 or N_2O_4 playing an important part in the reaction mechanism.

Also important is the reaction between NO and nitric acid, which can serve to destroy nitric acid at concentrations above 8*N*.

Having dealt with the problems of concentration and de-acidification, we can turn our attention to chemical separations. Our efforts to separate fission products have largely been centered on the isolation and removal of caesium and strontium from the bulk of the fission products, as the complete separation of these long-lived fission products facilitates the disposal of the bulk fission products. In principle, one can precipitate either the other fission products leaving caesium and strontium in solution or vice versa. Both types of procedure were investigated, and according to the starting solutions and according to the aim to be achieved, both have their uses.

We now come to the methods investigated.

These were, first, roasting and leaching; secondly, precipitation of hydroxides by ammonia, by electrolysis, and by anionic resins; thirdly, precipitation of strontium by concentrated HNO_3; and, fourthly, precipitation of caesium. Both the first and the second methods leave caesium and strontium in solution.

To go into detail; in the roasting and leaching process the fission product solutions are evaporated to complete dryness. In an oxidizing atmosphere ruthenium can be completely removed by evaporation as RuO_4 and can be isolated in this way. Alternatively, if $H \cdot CHO$ is added as a reducing agent, volatilization of ruthenium can be prevented. The dry solids are then roasted at 300°C and under these conditions the soluble nitrates of many metals are decomposed to insoluble oxides, the decomposition temperatures of the nitrates varying with their basicity.

The decomposition temperatures are as follows: 200°C for iron and zirconium; 250°C for rare earths and UO_2^{2+}; 600°C does not yet decompose strontium and caesium. This should permit a perfect separation for both caesium and strontium by leaching, but when dealing with our particular fission solution, the results were less favourable for strontium than was expected.

Slide 3 shows the leachability curves of the various fission products as functions of the roasting temperature, and while caesium can be almost quantitatively leached from the product, strontium partly remains behind. This was found to be due to the chromium content of our solutions which resulted in the formation of insoluble strontium chromate. The addition of Ba salt would reduce strontium retention, but would not avoid it completely.

Precipitation with ammonia can be carried out in a conventional manner, and I confine myself therefore to the results only, which are dependent on the final pH of the precipitation.

Slide 4 (Table IV) of P/415) gives the amount of fission products left in the filtrate, and it can be

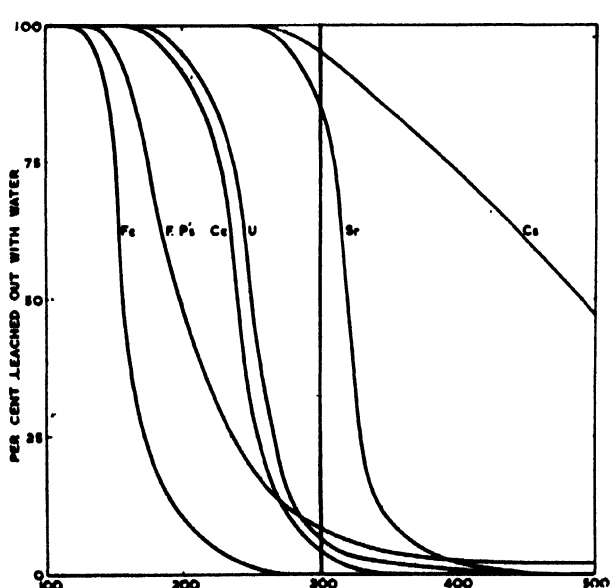

Slide 3

seen that at pH 6, most of the cerium is still in solution, but at pH 8 only caesium and strontium, apart from a small ruthenium contamination, are left. For an electrolytic precipitation we can use the type of cell using an anion-permeable membrane, shown in Slide 5.

The current is passed until the increased pH in the cathode compartment causes the precipitation of hydroxides. Both cathode and anode solutions are circulated rapidly by means of an airlift or Sprengel pump. The cathode solution is constantly filtered to avoid blocking, and the acidity of the anode compartment is kept at a low value by passing it through a bed of basic anion exchanger. The ions were found to precipitate at varying pH values as shown in Slide 6 (Table V of P/415).

Caesium, strontium, rubidium, and barium only remained in the solution, which was free from ruthenium. However, on account of the very large excess of iron, there was some occlusion of caesium and strontium in the hydroxides, and the yield of both was only 85%.

Coming now to precipitation by basic resins, our method was based on the use of anion exchange resins in the OH-form as precipitating agents. Passing a slightly acid solution through a column filled with OH-resin; precipitation takes place around the particles. The precipitate remains firmly attached; thus no filtration is needed.

Slide 7 shows clearly that after precipitation there is practically no flocculent precipitate present, but that the precipitate clings firmly to the resin spheres. There is no precipitation in the spheres, which can be shown by drying and crushing the spheres of resin, when the precipitate-shells flake off.

Slide 8 shows the broken-off shell of the hydroxide precipitation after drying. We found that if the fission product solution is passed through a column of resin in the OH form, only caesium, rubidium, strontium and barium remain in the effluent solution. The same method can be applied for the separation of caesium from strontium and barium by passing the resultant solution, after concentration, through a small column of anion exchanger in the carbonate form. This removes all the strontium and barium, and the filtrate from this column contains caesium and rubidium only.

We come now to individual precipitations: first, strontium. The best reaction for the removal of strontium is the classical precipitation with concentrated nitric acid. The solubility is low enough to precipitate the fission products strontium and barium without a carrier, though the addition of lead improves the yield further.

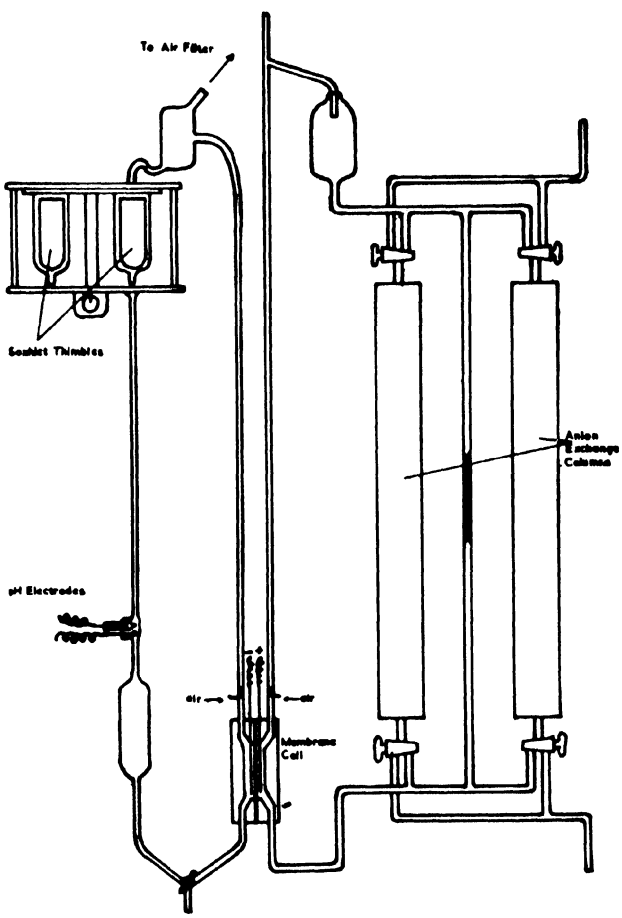

Slide 5

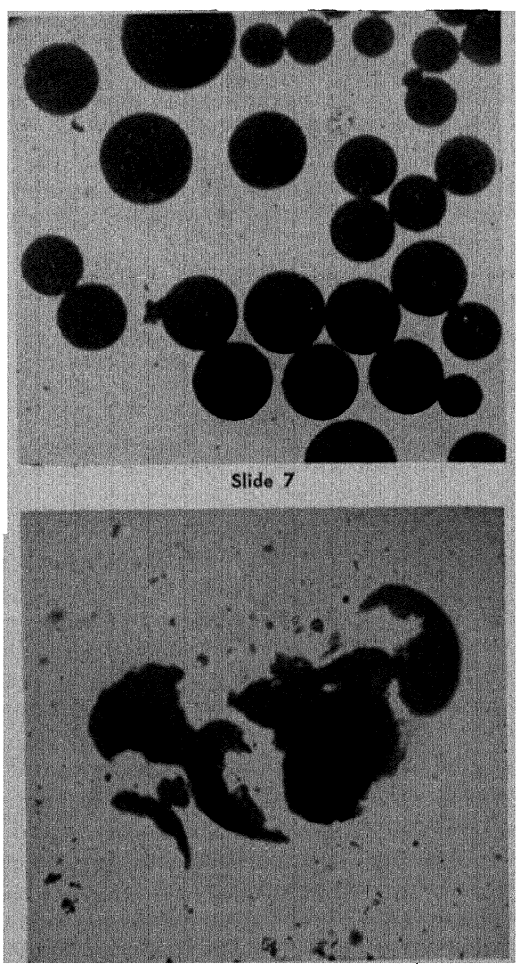

Slide 7

Slide 8

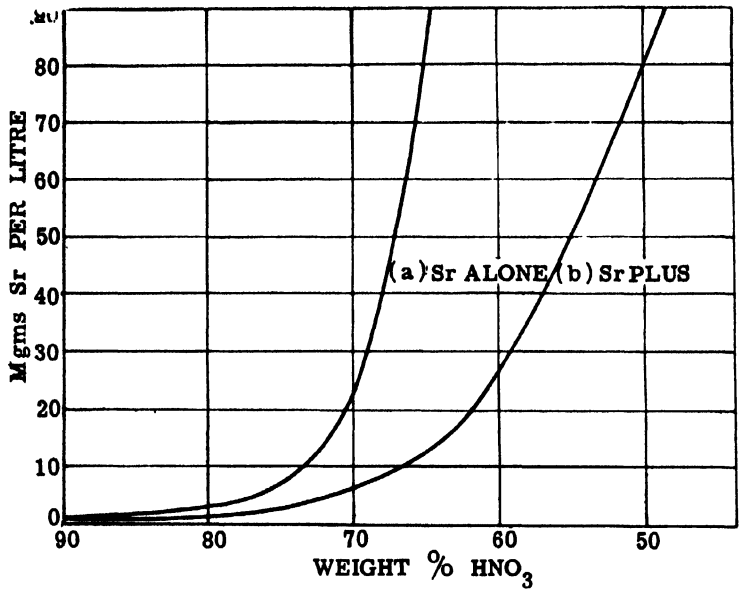

Slide 9

Slide 9 shows the solubility curves of strontium. It will be noted that the presence of ferric nitrate reduces still more the low solubility, thus improving the strontium yield.

Quite a large number of reactions have been found useful for the precipitation of caesium from fission product solution. It may be precipitated with hetero-poly acids as caesium-silico-tungstate or caesium-phospho-tungstate; as caesium-alum; as tetraphenyl-boron-caesium; and as nickel-caesium-ferrocyanide. The precipitation with hetero-poly acids can be carried out in fairly acid solutions, while the other reactions require a substantial de-acidification to a pH between 2 and 4. All of them precipitate caesium with a very good yield.

The reactions discussed in this paper do not claim to exhaust the field, but they offer a good starting point for further investigations, which may soon cover a very much wider range of fission products.

Mr. H. M. Parker (USA) presented paper P/552 as follows: The paper relates to the handling of radioactive wastes from chemical processing of nuclear fuel in what is best described as semi-permanent storage. Special emphasis is given to problems that arise with "high level wastes." This term can be applied to wastes originating from fuel exposed to 2000 kwh or more per kilogram (of natural uranium).

The initial activity of such wastes is high, but it decays according to the well-known power function for a general fission product mixture. After several years the significant activity is associated with the fission products Sr^{90} and Cs^{137}, and with such traces of plutonium or related heavy elements as originally escaped separation.

The design problems for waste storage are largely conditioned by three factors arising from the radioactivity. These are:

1. Protection against gamma radiation from the wastes during storage or transfer to storage.

2. Prevention of environmental hazards by escape of radioactive material to the ground, where it could enter a water table, or to the atmosphere as entrained mist or spray.

The second factor establishes the need for storage vessels of great dependability, with auxiliary equipment to control escaping vapors.

3. Evolution of heat, which is particularly significant for high level wastes.

In conventional terms, the energy release in separations plant waste is small, up to about 1 watt per liter, but its management is complicated by large volumes involved and non-uniform distribution promoted by the tendency to form precipitates in wastes normally made alkaline to minimize corrosion.

The low rate of heat release leads to poor convection in the liquid wastes and encourages development of superheating. Random disturbances then lead to sudden release of heat as steam. The additional pressure developed in the venting system temporarily suppresses the eruption. Cyclic eruptions at intervals of about half to one and a half minutes may result.

The short-term energy release can reach 10 to 20 times the nominal heat liberation rate. At other times, prolonged boiling at higher than nominal rates without spectacular pressure increase may occur. The eruption phenomena aggravate high level storage problems and require conservative design of vessels and auxiliary equipment to accommodate peak releases. Moderate induced circulation of the wastes has been found to control or even eliminate the eruption problems.

Storage Tanks

Wastes are stored in reinforced concrete tanks lined with steel. Tank diameter is about 25 meters and the volume 2 to 5 million liters. Radiation shielding is achieved at low cost by burying the vessels 2 or 3 meters underground.

Concrete is formed around the steel liner and the vessel completed by a concrete dome. Filling lines enter above the steel liner.

Structural strength is provided by the concrete and primary integrity against escape of liquids by the steel liner. Both components require high quality of material and workmanship.

Nozzles enter the tank through the dome to provide access for temperature, pressure, liquid level and radiation measurements, and for equipment for liquid transfer or agitation.

A waste storage area, or farm, conventionally includes a number of these tanks. Wells around the tanks provide one means of leak detection.

Tanks may be filled individually or in cascade. Wastes are delivered by pumps or steam jets in alkaline condition at fairly high concentration of soluble salts (say 10% or more by weight). Delivery records are kept, and these, with liquid level measurements and monitor well readings, indicate leakage. Actually in 10 years' local experience no leak has occurred.

Connection to specific tanks is controlled through jumpers or connectors in a shielded diversion box. Radiation protection is maintained by positioning and connectng the jumpers by remotely operated means. All transfer pipes from the separations plants are in concrete troughs which prevent promiscuous leakage of wastes to ground. Run-off for these troughs and the diversion box goes to a catch tank from which it can be delivered to the storage tanks.

Filling of the tanks is a routine operation, with a choice of either cascade or individual filling. For the less active wastes, cascading is advantageous because there is a concentration in the first tank of a train, and the liquid in later tanks can be transferred or additionally treated more easily.

Corrosion in the steel liners does not exceed 0.01-cm penetration per year under severe boiling conditions. As the severity of boiling will progressively decrease, it is expected that the life of the liner as computed from this maximum corrosion rate will be conservative. Tanks examined after 8 years of operation have shown no evidence of significant localized corrosion. During the period of severe boiling, the vapor handling system must be carefully operated.

Vapor System

Temperature in the tank, especially near the bottom, can rise as high as 175°C, which is above the boiling point of the waste. The operating choices are to provide cooling coils or a system to handle vapor release. The second is the method of choice. There are two hazards involved: (1) structural damage by excess vapor pressure; and (2) environmental contamination by radioactive spray carried by the vapors. Contamination is controlled by primary deentrainment of spray (as in a cyclone) and condensation of vapor in a contact or surface condenser. The choice here depends on whether contaminated condenser water can be run into the ground. If residual activity prohibits this, the less efficient surface condenser must be used and the active condensate returned to storage, if necessary.

In either case the residual non-condensable gas passes through a filter for final clean-up of contaminants and on to release through a stack. Protection against damage from excess vapor pressure is provided by an emergency by-pass. Provision is also made to prevent negative pressure. Although the tanks would withstand a positive pressure of about 250 mm Hg, they are sensitive to sub-atmospheric pressure in excess of 15 mm Hg.

Alternate Methods of Storage

Alternate methods for high level waste storage must have cost or process advantages over storage in steel tanks to justify the programme of development work to make other methods available for production plants.

The present method is described as semi-permanent. The urgency to provide permanent methods depends on the location of the tanks. In the present case at our site, the depth and characteristics of the underground soil are such that late failure of tanks would not be intolerable. With tanks a short distance above a mobile and accessible water table, the incentive to develop permanent methods would be great.

Some of the methods considered are: (1) Fusion of dry radioactive wastes in glass; (2) Stabilization of wastes in a concrete mixture, possibly with disposal in the ocean; (3) Fixation of wastes in montmorillonite clay with firing to about 1000°C; and (4) Disposal of liquid wastes in abandoned deep wells.

The high level wastes initially decay at a rapid rate. After five years there remains only a few per cent of the original activity. For the first three suggested permanent disposal methods, it would be reasonable to begin storage in the semi-permanent system and fix the activity after 5 or more years.

The fourth system does not seem to be attractive. The active material in deep wells is beyond the control of the operator. One would need assurance that no geological-hydrological process or man-induced process, such as pumping for other purposes, could transfer contamination to available water sources. Long term public responsibilities are difficult to reconcile with this method.

In addition, reclamation of specific fission products for industrial use would be difficult or impossible.

Economics

The cost of high level waste storage by presently used underground tanks has been cited in the general literature as being extremely high. Actual experience in production plants does not support this. The cost is currently about 7 cents per liter. However, with plausible assumptions on the operation of commercial power reactors, it appears that waste

storage costs would be appreciably less than one per cent of the sales value of electricity.

Storage costs can be markedly reduced in many cases after an interim storage of 5 years or so. Residual active fission products can be separated for permanent storage, and large volumes of liquid discarded. Another promising avenue of cost reduction is the recovery of specific isotopes for use as industrial radiation sources.

Mr. B. MANOWITZ (USA) presented paper P/553.

DISCUSSION OF P/415, P/552 AND P/553

Mr. GLUECKAUF (UK): We have found that the reproducibility depended considerably on the initial stages of the process; in other words, if one starts with a highly acid solution which then has to be electrolyzed for a long time before precipitation takes place, and there is considerable reduction in particular of the uranium to uranium(IV), the situation is rather different in this case than if one de-acidifies the solution beforehand and starts with a 0.1*N* solution where the uranium is practically all in the uranyl state and afterwards precipitates at a pH between 3 and 5. If there is a substantial reduction of uranium to uranium(IV), the precipitation of the uranium(IV) takes place together with the zirconium and iron and one has effectively a different situation.

One of the difficulties we have found in our experimental laboratory work—I should like to say this has not been carried to any pilot stage—was that with the electrodes we used, we tended to get formation of precipitate on the electrodes if we allowed the uranium to reduce to the (IV) stage.

If the acidification proceeded first to 0.1*N* solution, things went comparatively smoothly. We were specially interested in this matter not so much in obtaining the strontium and caesium but to see whether this leads to complete removal of these materials. As this part was not so successful and some 15 per cent of caesium and strontium remained with the rest of the fission products, we did not carry the experiments to any pilot plant stage.

Mr. C. M. NICHOLLS (UK): I have more of a comment than a question. Reference has been made to the formaldehyde reaction with nitric acid. There is a rather nice continuous application of this in the following manner. It is said that under low acid conditions the gaseous product was predominantly NO. By feeding in the nitric acid at the top of the column and the formaldehyde below, we have the advantage of continuous operation, which means that the hold-up of material is small and we have the most economical use of the formaldehyde reacting with nitric acid. This is one of the things that chemical engineers like to play with; it lends itself to all the classical methods of treatment.

The CHAIRMAN: I should like to address a comment to Mr. Manowitz on his paper. During the high-temperature treatment of the materials for fixing activity, is there any serious problem with volatile activity leaving the kilns and other high-temperature furnaces which he uses?

Mr. MANOWITZ (USA): So far I believe that only laboratory work has been done on this problem, but some volatile activities do escape. I can make no further comment than that.

Mr. GLUECKAUF (UK): Mr. Manowitz has described his very elegant methods of absorbing fission products on clays after these clays have been extruded. I should like to comment that some experiments have also been made by us using not clays but sand such as green sand. These sands have a much better percolating property and can be used in columns without any special treatment; in other words they need not be put into "spaghetti" form. We have heated them to above 1000°C and found, as was to be expected, that the property of retention of the fission product under those conditions is exactly the same as that of the ordinary clays. They have perhaps the disadvantage that the capacity is usually smaller, about one third that of the clays, because of the silica part of the sand. I might perhaps ask Mr. Nicholls or Mr. Hutcheon to say something about a variation of the clay treatment.

Mr. J. M. HUTCHEON (UK): We have carried out work with montmorillonite clays on similar lines to those which have been described. This work has been done at Harwell. Instead of extruding the clays with water to give more or less stable granules, we have bonded the clay particles with ethyl silicate previously hydrolyzed with alcohol. This gives us firm, hard granules without sacrificing too much in the way of diffusion characteristics, because we can keep an open porous structure. The process is certainly more expensive than that described by Mr. Manowitz, but there may be some advantages, since it makes it possible to prepare the adsorbent at some central spot and take this as pre-formed material to the desired site for adsorption.

We have taken these experiments to the stage where we have adsorbed trace activities on the clays, and we have fired them to temperatures of upwards of 1000°C. Our work differs from his, however, in another respect, in that we are not putting a complete range of fission products on our clays. I am thinking primarily of strontium and caesium solutions, from which the bulk of the fission products and other materials such as iron have been previously removed by some alternative process.

Mr. MANOWITZ (USA): We are very interested in the Harwell work on clays. I wonder whether the British workers would care to comment on the previous question, of the possible volatiles involved in firing clays to 1000°C?

Mr. GLUECKAUF (UK): We did not watch out for volatility. In the case of the green sand to which fission products have been adsorbed, we were able to heat it higher than 1000°C, to about 1200°C, and even with acid and salt solution treatment at high

temperature we were unable to get off any activity. Apparently the whole of the silica is fused to a glass.

Mr. C. A. MAWSON (Canada): In Canada we have been interested in the disposal of acid wastes of high activity containing about 2.5*N* nitric acid, and we have used a mineral known as nepheline syenite which is the raw material of opal glass. It comes by the mountain and costs about 10 cents a pound. It has the admirable property, for the purposes in which we are interested, of forming a very pleasant dry gel when mixed with acid solutions. We have a pilot plant in operation at Chalk River in which we mix the 2.5*N* acid solution with the nepheline syenite and fuse the mixture at a temperature which I have forgotten, but which I think is slightly below 1000°C. It then forms this opal glass material. Tests have shown that a very slight amount of activity can be leached from the surface of the glass by water, but after a very short time almost no activity comes off at all. We have not tested the results of prolonged irradiation on the glass, but, apart from the possibility that it might break down after long periods of irradiation, the product is satisfactory and the process, I think, will turn out to be reasonably cheap.

Session 23B.1

DISPOSAL IN THE GROUND

LIST OF PAPERS

			Page
P/565	Disposal of liquid wastes to the ground	R. E. Brown *et al.*	669
P/12	Waste disposal into the ground	C. A. Mawson	676
P/564	Problems of ground disposal of nuclear wastes	C. V. Theis	679
P/554	Disposal of high level radioactive liquid wastes in terrestrial pits	E. G. Struxness *et al.*	684

Disposal of Liquid Wastes to the Ground

By R. E. Brown, H. M. Parker and J. M. Smith,* USA

Large nuclear reactor and radiochemical separations plants produce radioactive wastes which cannot be released directly to the public domain because of their toxicity. As the conservative alternate of storage of all such wastes is economically prohibitive, disposal to ground of certain wastes was considered as a possibly feasible method.

This paper relates the generally favorable experience of ground disposal at the Hanford plant over the past decade. Experience here, while based on specific local conditions, is believed to be useful for guidance in economical radioactive waste-disposal methods in the development of peaceful uses of atomic energy at other locations.

FACTORS GOVERNING GROUND DISPOSAL

In considering the feasibility of disposal of radioactive wastes to ground, the factors requiring evaluation include:

1. The chemical and radiochemical content of the waste.
2. The effectiveness of retention of the radioisotopes in the available soil column above the ground-water table.
3. The degree of permanence of such retention, as influenced by subsequent diffusion, leaching by natural forces, and additional liquid disposal.
4. The natural rate and direction of movement of the ground water from the disposal site to public waterways, and possible changes in these characteristics from the over-all liquid disposal practices.
5. Feasibility of control of access to ground water in the affected region.
6. Additional retention, if any, on sands and gravels in the expected ground-water travel pattern.
7. Dilution of the ground water upon entering public waters.
8. Maximum permissible concentrations in public waters of the radioelements concerned.

NATURAL CONDITIONS AT HANFORD

The Hanford Works lies in south-central Washington in a structural and topographic basin of volcanic rocks traversed by the Columbia River. The region is characterized by a low (17 cm) annual rainfall and by a deep water table with a relatively low gradient, consequent in part upon that low annual rainfall. The region is underlain by basaltic lavas and associated pyroclastic rocks and other sedimentary interbeds of the Columbia River basalt series. These rocks, generally of high impermeability, are in turn overlain by a series of unconsolidated and semi-consolidated sediments consisting of lacustrine and fluviatile sands, gravels, silts and local clays of Pleistocene and later ages. The groundwater table lies at a depth of about 100 meters beneath the radiochemical separations plants and in the sediments overlying the basalt. The Columbia River, at a distance of 13 to 16 kilometers from the separations plants, constitutes the base level of the water table. The entire land area of interest for waste disposal is controlled by the Atomic Energy Commission.

LABORATORY STUDIES

The concentration of radioisotopes by adsorption on soil particles was early recognized as a possible method for the decontamination of process waste solutions. The soil materials with an average exchange capacity of about 0.05 milliequivalents per gram of soil and a depth to the water table of approximately 100 meters presented a potentially large reservoir for the adsorption and retention of radioisotopes. Thus if only 0.001 of the cation exchange capacity were used to adsorb Sr^{90}, a soil column one-meter square and 100-meters deep could retain about 60,000 curies of that nuclide.

Laboratory experiments were conducted to determine the behavior of the more important radioisotopes in soils representative of the materials, underlying the disposal sites. Studies were made with distilled water, salt solutions, or synthetic waste solutions all containing added radioactive tracers. Verifications of these studies were made with actual process waste solutions.

While the recovery of plutonium in the separations process is highly efficient, small amounts of it are unavoidably discharged to ground in the waste streams together with fission products and uranium. The radioisotope Pu^{239} was studied intensively because of its high radiochemical toxicity.

Laboratory equilibrium adsorption studies showed that plutonium is almost completely adsorbed over a wide pH range; the data are shown in Fig. 1a. The decreased adsorption at higher pH values is believed due to the formation of different ionic or molecular species presently undefined.

* Radiological Sciences Department, Hanford Atomic Products Operation, General Electric Company, Richland, Washington.

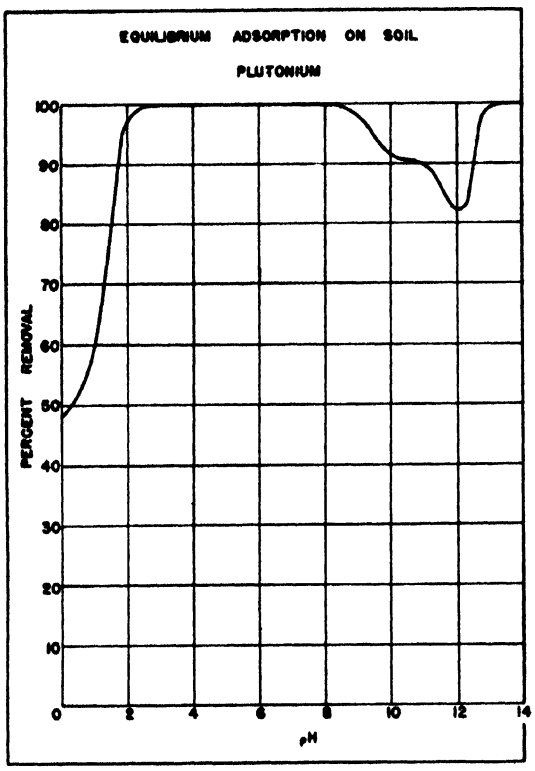

1(a)

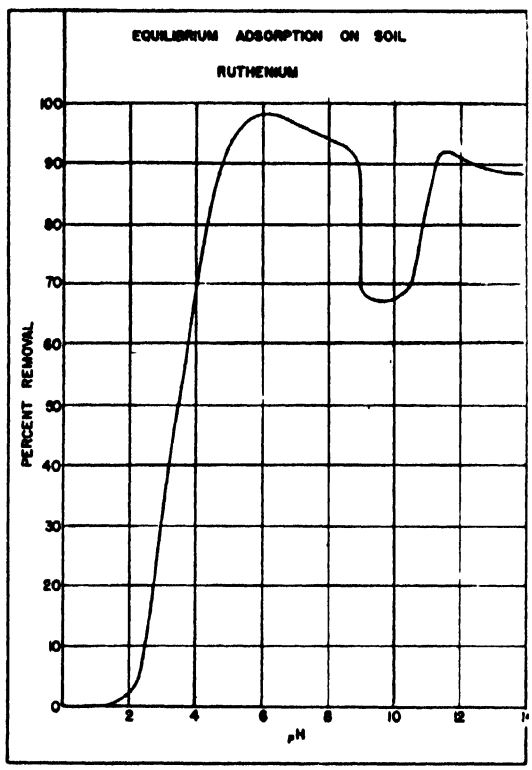

1(b)

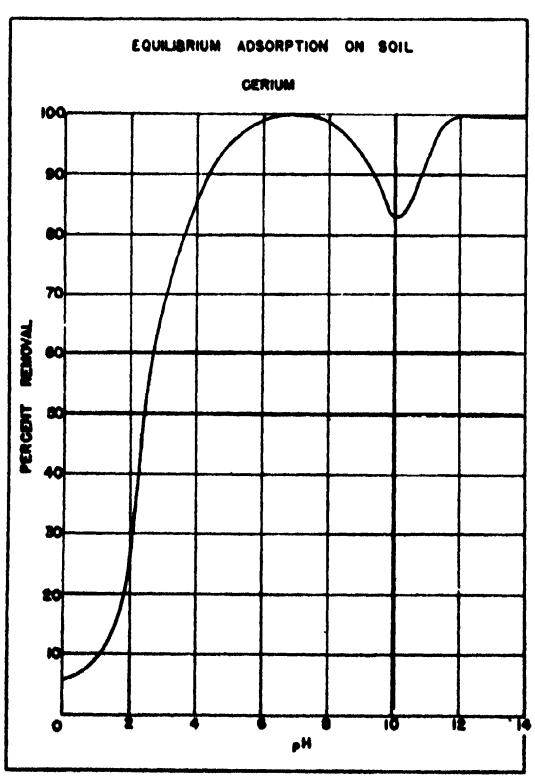

1(c)

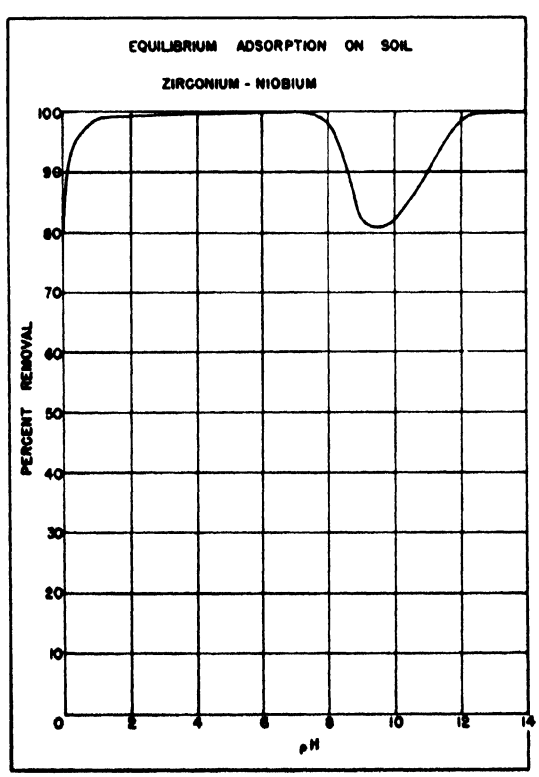

1(d)

Figure 1

The presence of monovalent ions (Na^+) or divalent ions (Sr^{++}) in the solution had no apparent effect on the adsorption of plutonium by soil while trivalent ions (such as Al^{+++}) reduced it markedly.

The difficulty encountered in the removal of adsorbed plutonium from soil by extraction with salt solutions suggested that adsorption processes more complicated that simple ion exchange may be involved.

Further laboratory work showed that plutonium may exist in solution as a complex ion under certain conditions, as in oxalic acid solution for example. In this case, the plutonium is readily adsorbed on soil columns and on anion resin exchange columns at pH 1. Similarly, ammonium acetate or calcium acetate solutions extracted plutonium from its adsorbed condition on a soil column.

Ruthenium appears abundantly in most process waste streams because of the large yield in uranium fission. The chemistry of this element suggests that it may exist as a cation, an anion, or as a neutral molecule depending on the conditions. This was borne out by its behavior in laboratory soil column work using pure solutions of Ru^{106}. Figure 1b illustrates the adsorption of cationic ruthenium at various pH values. When actual process waste stream samples were used, however, ruthenium was not readily adsorbed on soil columns and significant concentrations were found in the first effluent issuing from such a column.

A small amount of work with Ce^{144} indicated that adsorption is almost complete from neutral solutions; the curve illustrating the effect of pH is shown in Fig. 1c. That for the Zr^{95}-Nb^{95} system is in Fig. 1d.

Representative soils were equilibrated with chloride solutions of cesium, strontium, and yttrium containing Cs^{137}, Sr^{90}, and Y^{90}; concentrations of the cation were multiples of the soil saturation capacity and solution weights were ten times that of the soil. As generally found in soils-work of this kind, the absolute adsorption of each ion increased with increasing solution concentration but the percentage adsorption decreased therewith; the decrease was insignificant up to approximately one-tenth of the saturation capacity of the soil but then became rapid with further concentration increase.

For these radioisotopes, as in the cases previously discussed, the equilibrium adsorption of trace amounts was affected by changes in the pH of the solution. Results of experiments are shown in Figs. 2a, b, and c. The reduction in cation adsorption with lowered pH in all these cases was attributed to the competition of H^+ for available exchange sites.

In other experiments, soil samples were treated with successive increments of Cs^+, Sr^{++}, and Y^{+++} solutions. The limiting saturation capacity was greatest for Y^{+++} and least for Cs^+. Ten increments of a given concentration of a cation did not produce the degree of saturation given by one increment of a solution ten times as concentrated. The effect of high Na^+ concentrations on the adsorption of Cs^+ is shown in Fig. 2d.

The removal of cations from a soil on which they have been adsorbed is of importance in the disposal of radioactive wastes into the ground. The system, solution-adsorbed cation-soil, is not static but dynamic so that the degree of cationic saturation of a soil layer will vary as the solution composition varies.

The laboratory work showed that removal of adsorbed Cs^+, Sr^{++}, and Y^{+++} was brought about by leaching with acids, salts, or water. Removal by acids was most rapid and complete being dependent upon the hydrogen-ion concentration. Sodium ion, as $NaNO_3$, was likewise effective in the removal of Cs^+ from the soil as was CO_2-saturated water which simulated percolating ground water. The data from the latter experiments indicated that if all the normal rainfall in the region percolated through the bed, up to 400 years would be required to reduce the adsorbed Cs^+ content of the soil by 50% when initially only 0.01 of the soil capacity was cesium-saturated. Furthermore, the cesium so removed would enter into exchange with deeper layers of the soil thereby increasing the net time of retention.

FIELD DISPOSAL PRACTICES AND OBSERVATIONS

Ground disposal of radioactive wastes at Hanford is accomplished by release to sumps 3 to 6 meters below the ground surface, and therefore high above the ground water. The sub-surface sumps have been constructed in various forms to achieve economy and adequate percolation rate. Figure 3 indicates the general arrangements of open-bottomed "crib" boxes, tile fields similar to those in general use in sanitary service, and rock-filled "caverns", which have been employed. Experience has indicated the need for prior evaluation of percolation rates attainable at the disposal location to assure that instantaneous and average stream flows can be handled without upward movement to ground surface. In some cases where the duration of usage of a facility is short, say several days, open trenches have been used with the earth cover replaced as soon as the disposal is completed. Open ponds have been found usable only for streams of very low activity density. Otherwise, contamination on the dried peripheral sediments is subject to movement by the winds, and contamination of wildlife making use of the water source has been noted.

Test wells were drilled around crib facilities to determine the distribution of the radioisotopes in the soil. Sampling of the sediments provided information on both this pattern and the composition of the strata encountered. A typical example of such a pattern showing the differentiation which occurs between individual isotopes is given in Fig. 4. In general, it has been found that ruthenium is the most mobile radioactive ion, with cesium of interest because of its long half-life and intermediate mobility. Ions of great biological significance. such as plu-

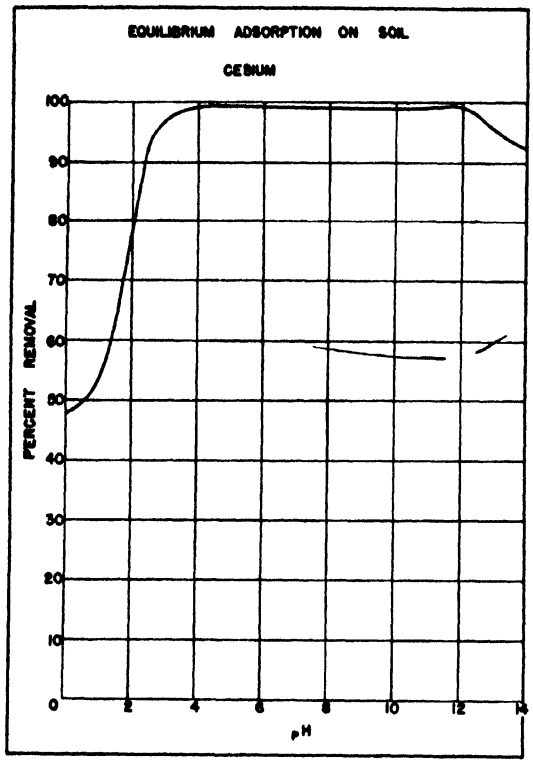

2(a)

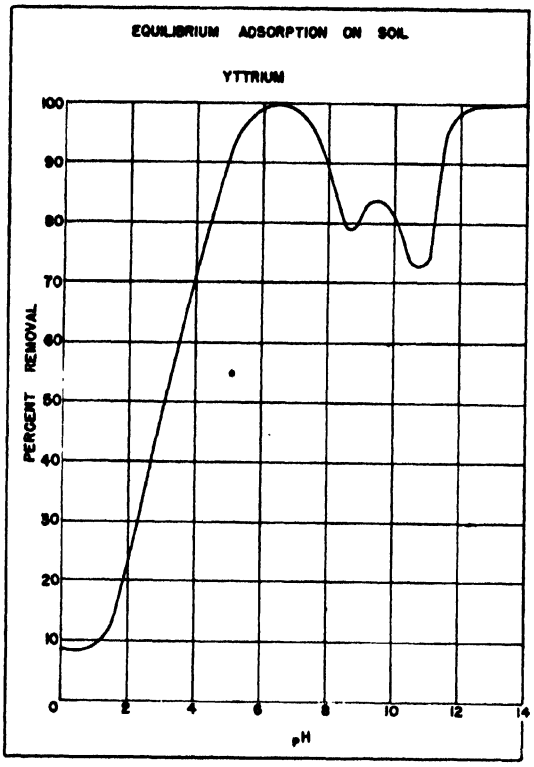

2(c)

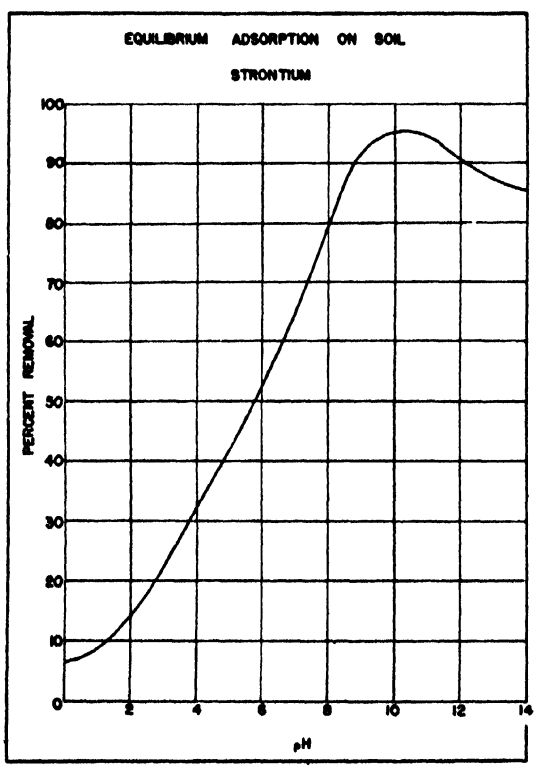

2(b)

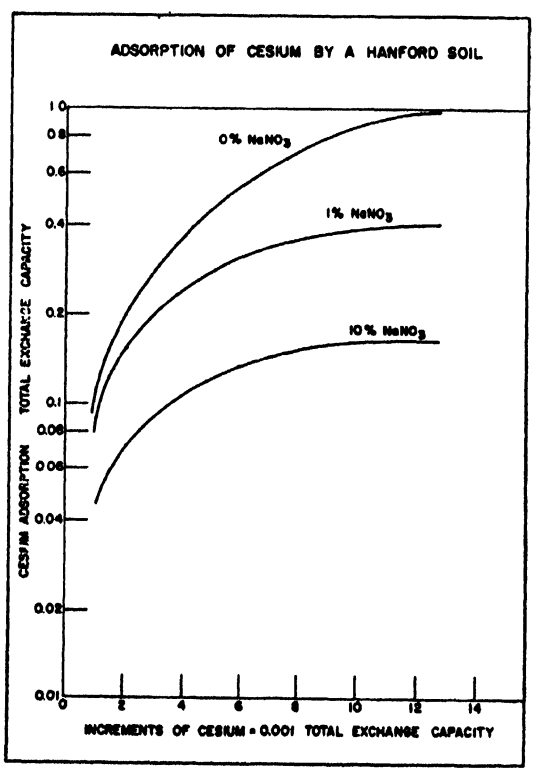

2(d)

Figure 2

tonium and strontium are generally retained quantitatively by the soils immediately surrounding the disposal point. The inclination of the general pattern in Fig. 4 is attributed to the inclined attitude of strata of varying permeability. The influence of total salt content of the waste was illustrated by findings at two disposal sites; one which received about 8000 curies of fission products in low salt waste resulting in no detectable ground-water contamination; and the second which received about 800 curies of fission products in the same volume of high-salt waste resulting in ground water contamination of 4×10^{-6} $\mu c/cm^3$.

Waste streams to the ground are generally limited by the ion exchange capacity of the intercepted soil column. In several cases it has been possible to remove specific hazardous radioisotopes such as Sr^{90} and Cs^{137} from the original liquid and thus produce a waste suitable for ground disposal from one which would otherwise require storage. Dilution of waste before disposal is contraindicated since the uptake per gram of soil will be higher from a more concentrated solution even though the percentage uptake is not as great. This permits maximum utilization of the ion-exchange capacity of the soil column, although care must be taken to avoid leaching by later additions of solutions of lower concentrations.

Ground-water contamination patterns detected around the experimental reverse wells provided a valuable index to the rate of movement of the ground water in the disposal region. The movement rate as estimated from adjacent monitoring wells for this pattern was of the order of 7 meters per month. This estimate was later confirmed by measurement of patterns indicated by nitrate and other ions not readily retained by soil. Ground-water movement in the disposal region was influenced by the changes in gradient induced by the formation of ground-water mounds from the very large volume disposal of nonradioactive cooling water in surface ponds. These mounds, which have reached elevations of 20 meters above the normal water table, are located around the periphery of the disposal area and have flattened the natural gradient in this region. These mounds have had a profound effect on the direction as well as the rate of local ground-water movement and provide a controlling factor in the location of new disposal sites.

Investigations of the regional ground-water movement and permeability of soil have indicated the presence of ancient river channels which provide possible avenues for accelerated movement to the river. Relative ground-water velocities at various points have been obtained by measuring the rate of dilution of electrolytes in individual wells, together with conventional draw-down tests. The ground-water movement time from the separations plants to the river is dependent on the disposal location with respect to the ground-water mounds. Present estimates of the minimum time of movement are of the order of fifty years.

PRESENT DISPOSAL PRACTICES

Advantage is taken of laboratory and field investigations to expand the use of ground disposal for significant economy in waste handling. The release of radioactive wastes to ground is regarded as ground storage rather than uncontrolled disposal, as disposal criteria are based on prevention of escape to public waters. Based on a travel time to the river of fifty years, significant ground-water contamination at the disposal site with radioelements of half-lives greater than three years is not permitted. When trace contamination is detected by routine sampling of ground-water and water-table sediments in the monitoring wells at each disposal site, use of the affected soil column is discontinued, and operation of a new soil column is initiated. To avoid interference of adjacent contaminated soil columns, the disposal facilities are laterally separated at least 30 to 50 meters.

Process waste streams placed in ground storage are those remaining after most of the fission products have been removed and routed to underground tank storage, and include low salt condensates from high activity waste volume reduction steps, condensates from fission product heat self-concentration of stored wastes, moderate activity density supernatants from the later stages of the separations processes, and dilute solutions resulting from process leakage and process equipment decontamination operations. Each such stream proposed for ground disposal is evaluated to determine the chemical and radiochemical composition, and the retention capacity of the proposed disposal site soils for the waste.

The permissible volume per unit cross section of soil column is prescribed from these data. For low salt wastes the capacity of the disposal soil column is high (up to 2×10^5 liters per square meter in some cases). Control is provided by monitoring the downward progress of the contaminated pattern by wells at the disposal site. For high salt wastes strict control of volume is required, and may be in the range of 500 to 3000 liters per square meter to avoid significant contaminant breakthrough to the ground water. For certain wastes which exhibit early breakthrough characteristics in laboratory tests, disposal to ground is limited to that volume which can be retained in the soil column without any liquid penetration to ground water. This volume is on the order of 40 to 60 liters per square meter. In this case additional safety is provided as it is conservatively assumed that no adsorption on the soil will occur.

Present disposal criteria provide safety factors, in that no advantage is currently taken of the increase in intercepted soil-column cross section caused by lateral spread as the solutions encounter lower strata of decreased permeability, of the probable adsorption which would occur in waste movement through the ground-water sands and gravels, and of the dilution of the ground water upon entering the river. It has been estimated from rainfall in the watershed that

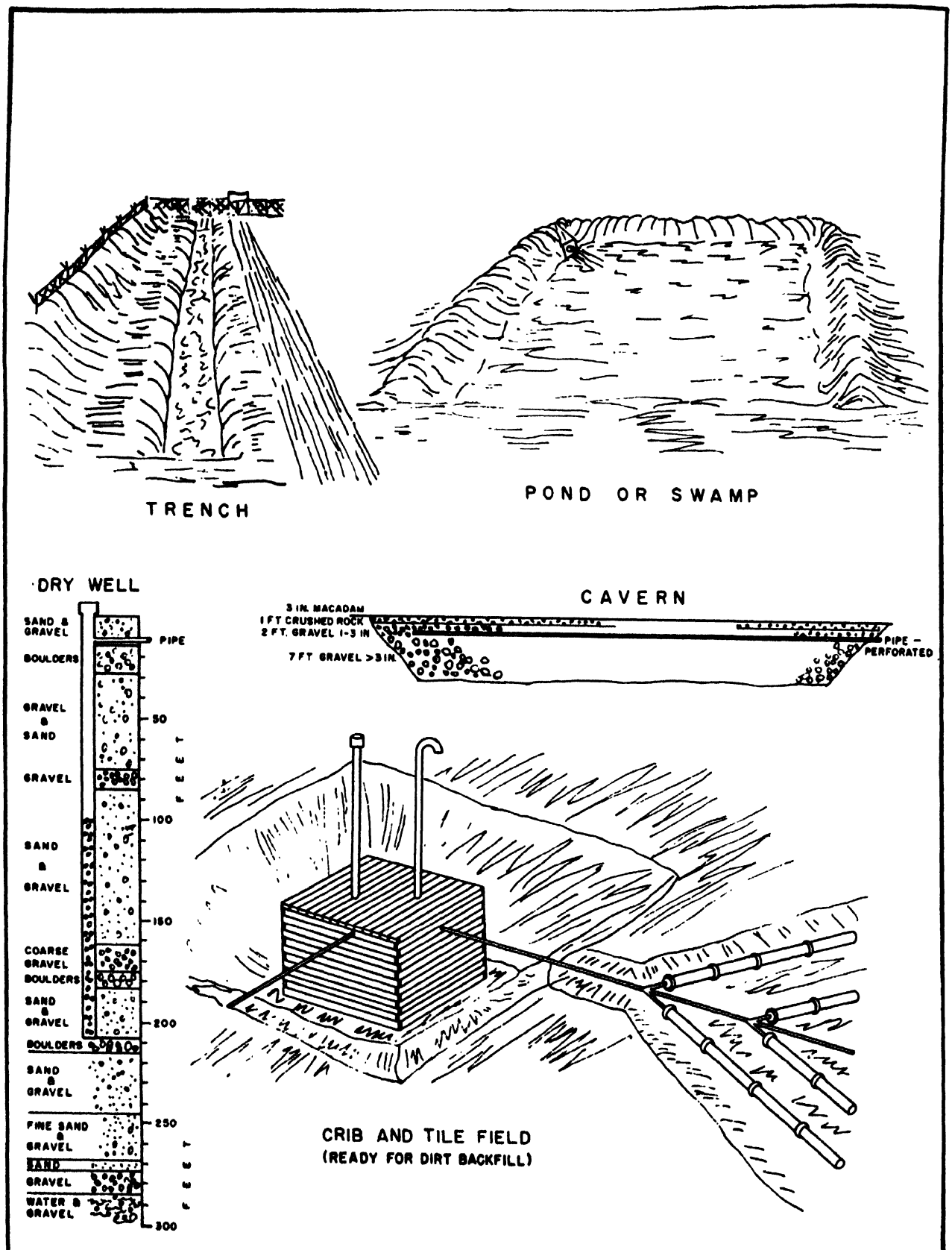

Figure 3. Typical ground disposal facilities

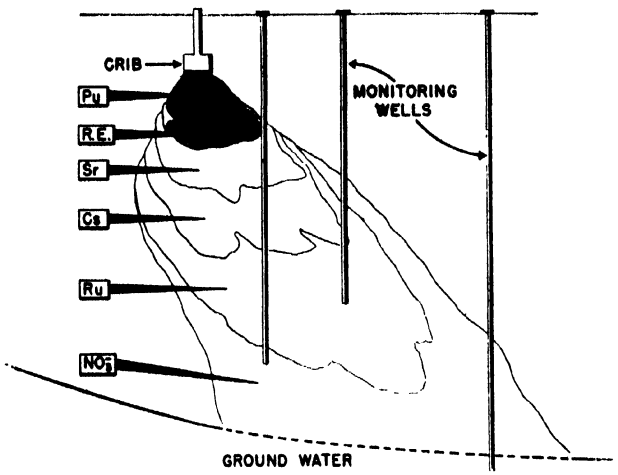

Figure 4. Ground storage of wastes

ground water in this region contributes only about 0.02% to the Columbia River flow.

Some 8×10^{10} liters of essentially non-radioactive process cooling water have been released forming the previously mentioned ground-water mounds. Advantage is taken to place the radioactive waste disposal sites in adjacent positions of resulting low ground water gradient to reduce possible movement rates. Approximately 10^9 liters of active wastes containing several hundred thousand curies of fission products have been stored in such sites in the first decade of operation.

The specific experiences at this location cannot be applied to other locations without field and laboratory evaluation of local problems. The economic incentives to apply to the ground storage method where feasible are high. This account serves to guide the establishment of ground disposal criteria at other atomic energy installations.

Waste Disposal Into the Ground

By C. A. Mawson,* Canada

The establishment of an atomic energy project is soon followed by the production of a variety of radioactive wastes which must be disposed of safely, quickly and cheaply. Experience has shown that much more thought has been devoted to the design of plant and laboratories than to the apparently dull problem of what to do with the wastes, but the nature of the wastes which will arise from nuclear power production calls for a change in this situation. We shall not be concerned here with power pile wastes, but disposal problems which have occurred in operation of experimental reactors have been serious enough to show that waste disposal should be considered during the early planning stages.

SITE SELECTION

Waste disposal should be a factor in the selection of a site for a reactor and chemical processing plant. Serious thought must be given to the fact that, in addition to the material foreseen by the chemical engineers as a continuing product of normal operation, accidents will happen. Faults will develop in the processing plant which will cause spills of radioactive solutions, equipment will become so highly contaminated that it is not economically recoverable, and our experience has shown that a reactor can break down in such a way that millions of litres of radioactive water create an urgent disposal problem. Accidents result in emergencies and, when emergencies arise, it is convenient to have an area close at hand where radioactive material can be dumped without fear of contamination of ground water supplies.

It is a mistake to assume that when a solution is run into the soil it will soon be diluted by the ground water. This water moves slowly and is not mixed by turbulence and temperature changes in the same way as surface water, so the solutions may move a long way without much mixing or dispersion. Pollution control depends more upon filtration, adsorption and chemical reaction with the soil than upon dilution in the general body of the water table, but observation of the movement of the ground water is necessary to estimate the speed and direction of travel of solutions put into the ground. The knowledge we need for choice of a ground disposal area includes, therefore, information on the chemical and physical nature of the soil, including its neutralizing capacity and its cation exchange capacity, and also data on the movement of ground and surface water.

Useful knowledge of the chemical and physical nature of the soil can be gained by laboratory experiments on core samples, but the application of such studies to forecasting the results of waste disposal in the field depends on factors which cannot be controlled from the laboratory. The stratification of the soil is of great importance in translocation of water because much of the movement may occur through narrow soil horizons which are difficult to recognize and isolate in core samples. In some types of overburden, such as wind-blown sand, the surface topography may bear little relation to the direction of movement of ground water and hidden formations of bedrock may give rise to relatively fixed reservoirs of water from which there is only slight surface run-off. On the other hand, what appears at the surface to be a soil-filled rock basin may have deep drainage through fissures or channelling.

Before deciding the site of a disposal area, a geological survey should be done. This would begin with a surface reconnaissance of the proposed plant area by a geologist. Selected locations would be mapped by aerial survey methods to give a $\frac{1}{2400}$-scale map with 2-metre contours. A surface geological survey would then place on the map all rock outcrops, soil types and surface drainage. The approximate profile of the subsurface bedrock would next be determined by seismic technique. Finally, the best area would be chosen and drilled in detail to test the character of the overburden, its grain size and its water content. The water table would be accurately located and the bedrock profile determined. The drilling programme would provide samples for laboratory work on soil permeability, porosity, adsorptive capacity and retention.[1]

This programme seems at first sight to be very elaborate and expensive but it is a brief summary of the work undertaken at Chalk River to investigate our disposal area. Such work should be done before dumping of wastes into the ground has begun.

DISPOSAL OF "HOT" WASTES

We have no experience of the disposal of "hot" wastes into the ground. Such wastes result from the concentration of processed rod solutions and contain mixed fission products giving about 10^9 disintegrations per second per millilitre and are about 7-molar in nitric acid. They are stored below ground

* Biology Research and Radiation Hazards Control Division, Atomic Energy of Canada Limited, Chalk River, Ontario, Canada.

in stainless steel tanks which have shown no sign of corrosion over a period of more than six years. Tank storage is not permanent disposal, and experimental work is in progress for fixing the hot waste in a form for safe disposal.

DISPOSAL OF "COOL" WASTES

Our "cool" wastes contain 2.5-molar nitric acid and, in some cases, 4-molar ammonium nitrate. Their radioactivity is about 10^6 disintegrations per second per millilitre. Experimental disposals of these wastes have been made into the ground. Laboratory experiments have shown that our sandy soil is surprisingly efficient in the neutralization of acid and this has been confirmed by drilling in the field. About 54,000 litres of a waste containing 2.5-molar nitric acid were dumped into a pit 4-metres deep during January, 1955. A drill hole was sunk on May 1, 1955, about 15 metres from the edge of the pit in the presumed direction of the ground-water flow. Although radioactivity was detected in the drill hole, no free acid was present.

In another experiment 6800 litres of a different "cool" waste, containing 2-molar nitric acid and 4-molar ammonium nitrate, was run into a lime-filled pit 4-metres wide and 4-metres deep. The soil at field capacity holds about one third of its volume of water so, when all the liquid had sunk into the ground, the lower level of the radioactive area should have been about 1½ metres below the bottom of the pit, or 5½ metres from ground level. The liquid disappeared very rapidly in spite of the fact that the bottom of the pit was at the level of the water table. A drill hole was made several months after completion of the disposal at about 6 metres from the edge of the pit in the presumed direction of ground water flow. A sharply defined zone of intense radioactivity was found at a depth of 5½ metres which continued to a rather ill-defined lower limit at about 7½ metres. This seems to show that, although the waste had travelled a lateral distance of 6 metres and had sunk for a distance of 1½ metres through the water table, it had dispersed very little in its vertical dimension.

Our drilling programme has not gone far enough (May 12, 1955) to define the leading edges of the radioactive regions produced by experimental disposals. However, in the case of cooling water which was pumped to the burial ground after the pile accident in December, 1952, the situation is clear. Radioactive material in solution and in suspension was run into trenches cut in the sand. The total volume dealt with in this way was about 5×10^6 litres, containing 10^4 curies of long-lived fission products. The trenches were 5-metres wide, 3½-metres deep and about 300 metres in total length. A drill hole sunk on May 6, 1955, 12 metres from the edge of one of these trenches, showed no sign of radioactivity. A hole sunk through the middle of the trench showed radioactivity starting at the bottom of the trench and extending to a depth of 3½ metres. The core has not yet been analysed, but a core-sample taken about a year previously in a similar position showed that most of the radioactivity had been held near the surface in spite of the very large volume of water which had washed through the soil.

These field observations confirm laboratory results from radioactive burial ground soil which was leached with various solutions. The most efficient leaching solution (Table 1) was ammonium chloride, followed by hydrochloric acid, citric acid, sodium hexametaphosphate, ammonia, sodium hydroxide, trisodium phosphate and water, in that order. Alkaline solutions percolated through the soil very slowly, owing to action on the organic constituents. These experiments illustrate the importance of keeping detailed records of ground disposals made to ensure that fixed material is not leached by disposals.

Table 1. Disposal Area Soil Containing Fission Products (mainly Sr^{89}, Sr^{90}, Cs^{137}, Cs^{134} and Ce^{144}) Leached with Solutions Likely To Be Put into the Ground

Leaching solution	*Amount leached (Relative only)*
NH_4Cl (1.0M)	100
HCl (0.01M)	87
Citric acid (0.1M)	82
Sodium hexametaphosphate (0.02M)	59
NH_4OH (1.0M)	31
NaOH (1.0M)	12
Trisodium phosphate (0.01M)	12
Water	6

Table 2. Sr, Cs and Ce Bound to Separate Fractions of Disposal Area Soil. Activity Extracted from Soil in Successive Treatments

	cpm/100 gm whole soil		
Treatment	*Sr*	*Cs*	*Ce*
1. $CaCl_2$ wash	9.8×10^5	2.4×10^5	0
2. H_2O_2 (destroys organic matter)	1.6×10^6	1.7×10^5	0
3. Dispersion in Na_2CO_3	0	3.2×10^5	0
4. Separation of soil fractions; fractions dissolved in HF			
Sand	0	2.9×10^5	5.7×10^2
Coarse silt	0	3.1×10^5	3.6×10^3
Medium silt	0	1.2×10^5	2.1×10^3
Fine silt	0	1.9×10^5	8.1×10^2
Coarse clay	0	4.3×10^5	3.1×10^3
Medium and fine clay	0	2.6×10^5	1.1×10^4

Particle size analysis of radioactive soil from the burial ground has given some information on the relative efficiency of the soil constituents in holding fission products (Table 2). Our soils consist mainly of sand, but the small proportion of clay and silt is responsible for much of the fixation. Strontium is easily exchanged and can be eluted with calcium chloride solution, but much of the caesium and all the cerium resist this treatment. Caesium is fixed in the inter-layer spaces of the mica-type minerals vermiculite and illite, while cerium is fixed in inverse proportion to particle size. This suggests that fixa-

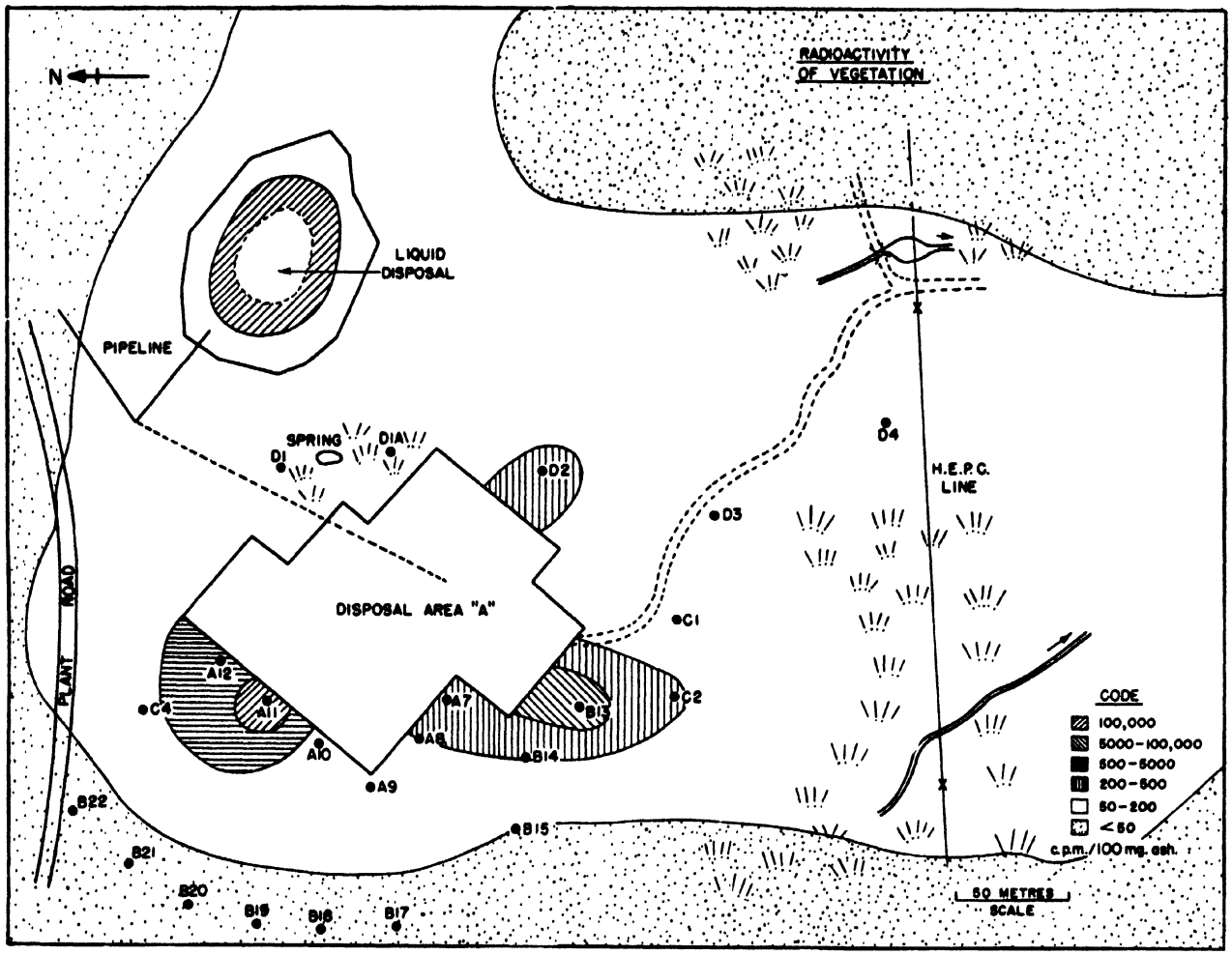

Figure 1

Table 3. Radioactivity Held by Separated Fractions of Sand in Disposal Area Soil

Mineral	*cpm/gm*
Feldspar	22,800
Hornblende	2535
Quartz	524

tion of cerium depends on the surface area of the grains and recalls the behaviour of ferric oxide, which is known to form a thin layer over soil particles. The larger sand particles bind a small amount of caesium very firmly, but, as our soil consists mainly of sand, a high proportion of the bound caesium is held in this way. The feldspar fraction of the sand is responsible for this binding (Table 3), and it is suggested that caesium may be fixed by a coating of layer silicate which is formed on the surface of the feldspar grains by weathering.

We have not carried investigations far enough to be able to give a detailed picture either of the physics and chemistry of our soil or the field behaviour of fission products in our burial ground. Extensive investigations of radioactivity in trees surrounding the burial ground and sampling of ground water from shallow bore-holes have shown that no appreciable contamination has progressed beyond about 60 metres from the burial ground fence. Figure 1 shows a map of a disposal area with the bore-holes marked as circles. The ground to the south-west of the area fence is thickly covered with trees, and the movement of ground water is from north-east to south-west. Contours of relative radioactivity have been drawn showing that some movement has been detected in a southwesterly direction, but only very slight traces of activity have been found in the water of the swamp marked in the south-west corner of the map. Some of the deciduous trees near to the fence have taken up a great deal of radioactive material—for example, one poplar tree contains about 40 mc of Sr^{90}, whereas neighbouring jack-pines are relatively inactive. Surveys of the outfall of the springs and streams along the bank of the Ottawa River have shown no evidence of contamination but, until the deep drilling programme is complete, we shall be unable to be sure that nowhere between surface and bedrock is there any evidence of radioactive contamination beyond the area defined by radioactivity found in the trees and bore-holes.

REFERENCE

1. Buffam, B. S. W., letter dated 6 January 1955 to W. J. Bennett.

Problems of Ground Disposal of Nuclear Wastes

By Charles V. Theis,* USA

The present methods of storage of high-level nuclear wastes are expensive, and in so far as they involve storage near the ground surface and above potable water-bearing formations they are potentially hazardous. No division of science regards with favor the disposition of radioactive wastes in the environment with which that division is most familiar. Nevertheless, the wastes are present and some method of disposal must be found. Disposal to the ground has many ostensible advantages. It is comparatively inexpensive and sufficiently permeable beds are present beneath most sites for nuclear plants.

Disposal of nuclear waste to the ground involves the placement of a complex chemical solution into a complex natural environment. It may be planned that the waste seep away or that it be retained. It may be planned that the waste be placed in a formation already saturated with a natural liquid or that it be placed in unsaturated ground high above the water table. Geologically, the environment may consist of (1) sandy, relatively permeable formations, (2) permeable cavernous formations, (3) jointed or otherwise fractured rocks, (4) relatively impermeable shales, or (5) deposits of salines — rock salt and gypsum. Although any decision as to the use of the ground in any particular locality obviously must be preceded by consideration of the particular waste and its relation to the particular environment, this paper will attempt to describe some of the factors to be considered for any of the combinations suggested above.

DISPOSAL THROUGH DEEP WELLS INTO FINELY POROUS FORMATIONS

Much of the land area of the earth is underlain by sediments, some of which at most localities are permeable enough to accept quantities of liquids of the order of magnitude of the waste expected from a nuclear plant. Such a means of disposal would be the most generally accessible and, at least ostensibly, the least expensive to the average plant. However, geographic, chemical, radiologic, and hydraulic factors which restrict this type of disposal must be considered. The most important of these factors are touched upon below.

Probably the first requisite for an injection well is that it be cemented and thoroughly sealed to a point below the potable water-bearing formations. This is generally a legal requisite for all injection wells and oil wells, at least in the United States—a requisite set by the need to protect potable waters. It is apparent that much greater precaution would necessarily be taken to protect potable waters from radioactive solutions.

A second requisite for an injection well is the elimination of any suspended solids in the waste. Any sandy formation will act as a perfect filter, and any injection well will become plugged in a short time if any solids are present. Injection wells are used widely for repressuring oil fields, for the disposal of waste from chemical processing, and for return of cooling water that has been drawn from the ground. Almost without exception, difficulty is encountered with suspended solids, and elaborate precautions are taken to avoid getting any solid materials into the system. Rather commonly the injection well is periodically pumped in order to recondition it. This recourse would be difficult if not impossible for wells into which radioactive liquids had been put. It is probable that, in order to be put in wells, most nuclear wastes would have to be pre-filtered, with consequent production of a radioactive cake on the filter which would cause in its turn another problem of disposal.

A third requisite is chemical compatibility of the injected waste and the solid and liquid substances into which it is injected. In the process of water flooding of oil fields it is generally necessary to pretreat the driving water in order to prevent loss of permeability in the formation into which it is injected. Whenever possible the water used is that which has been derived from the same formation. Difficulties arise from reactions between the introduced water and the natural water and between introduced water and the materials of the formation, from corrosive products of the well casing, and from swelling of the clay minerals of the formation due to changes in the liquid environment.

Sandy formations in general contain quartz, a varying proportion of clay minerals, and a cementing material which is frequently calcium carbonate. Feldspars may be present in comparatively large amount. Accessory minerals may be of many kinds[1] and may contain most of the chemical elements, of which iron, manganese, and magnesium are probably the most important in connection with waste disposal.

Acids, hydroxides, and some neutral salts break down the structure of clay minerals even in weak

* US Geological Survey.

solutions.[2] Pressure, such as would be encountered at depth, and higher temperatures, such as would be generated by undiluted or little diluted wastes, accelerate the process.[3] In nitrate solution any calcium carbonate present probably would become soluble and might cause compaction of the formation. Inasmuch as the formations are likely to be in equilibrium with neutral or somewhat alkaline waters, any iron or aluminum carried in an acid solution may begin to precipitate as the hydrogen ion is adsorbed by the clay minerals and the solution becomes less acid.

The problem of putting a complex waste containing, at best, considerable concentrations of zirconium, molybdenum, barium, strontium, and the rare earths, and, at worst, molar concentrations of aluminum and hydrogen ion into a complex earth medium will be difficult and may be insoluble. At best, a rigorous geological exploration of the formation to obtain cores for testing, a rigorous series of experiments on the reactions between the waste and the natural medium, and finally a rigorous control of the character of the waste, permitting no change from time to time, would be necessary.

It would seem that particular combinations of waste chemicals and available sandy formations may be found, making possible the use of particular sandy formations for disposal of particular nuclear wastes. However, it seems evident that chemical incompatibility of waste and formation will greatly restrict the use of such formations for nuclear waste disposal.

A fourth requisite for injection wells for nuclear waste is that no other wells pierce the injected formation within the area that will be contaminated. At least one waste disposal to the ground has been voluntarily stopped because the waste reached the ground surface through other wells after being placed in a sand at a depth of about 800 feet.[4] Many areas of active petroleum exploration are pierced with deep holes. Those areas in which exploration was conducted years ago before controls by public agencies were formed may contain unknown abandoned wells. The hazard in such cases is not so much appearance of waste at the surface, but dissemination of waste into potable water-bearing formations near the surface without any sign at the surface. Much effort has been spent in some areas of artesian wells to plug abandoned wells to prevent the loss of water from these aquifers to shallower aquifers under less head. The prevalence of such holes for oil exploration in a number of areas further restricts the localities where nuclear wastes could be stored.

A fifth requisite for injection wells is that the hydraulics of its movement be understood in as great detail as possible. The movement of a waste in a formation depends on the hydraulic properties of the formation and the contained liquid. The density of the natural aqueous liquids of the formations of the earth ranges from 1 to 1.2 or perhaps a little higher. A nuclear waste put into a formation may therefore be lighter or heavier than the liquid into which it is put. If it is of different density there will be differential movement between the two liquids. The general motion, however, will be that of the natural liquids. It will be assumed in the immediately following discussion that the waste has about the same density as the natural liquid.

Ground water moves through our productive aquifers typically at a rate of the order of magnitude of a decimeter or a fraction of a foot per day. In deep-lying consolidated formations the average rate of movement, because of the generally lesser permeability of the deeper formations, probably is typically of the order of a meter or a few feet per year.

A waste injected into a well moves from the place of injection under the increased head imposed by the injection and also under the hydraulic gradient under which the natural liquid is moving. In a homogeneous and isotropic formation, the mathematics of ground-water flow is analogous to that of the conduction of heat or electricity, with the concept of hydraulic head taking the place of that of temperature or voltage and permeability that of thermal or electrical conductivity. Hence the shape and size of a volume of waste in the ideal formation can be computed. If wastes of the same viscosity and density are injected at a fixed rate into such a formation, the waste volume will approach asymptotes parallel to the direction of flow of the natural liquid in the formation and distant from the well an amount a. It will approach a point up-gradient a distance b from the point of injection, where the imposed hydraulic gradient will equal the oppositely directed natural gradient. Its course down-gradient will be governed by the imposed and natural gradients and it will reach a distance c in the time t. The volume of waste will be included in a rectangle given by the asymptotes and perpendiculars drawn at the distances b and c. These distances are given by the following formulas:

$$a = Q/2PID$$

$$b = Q/2\pi PID$$

$$t = (\rho/PI)\,[c - b \ln (1 + c/b)]$$

in which
Q = the input into the well per unit time (l^3t^{-1}); P = permeability of the formation with respect to the particular liquid in volume per unit area per unit time. (lt^{-1}); D = thickness of permeable formation (l); ρ = porosity of the formation (dimensionless); and I = natural hydraulic gradient (dimensionless).

For a permeable aquifer such as those from which potable water supplies are drawn, if Q = 6000 liters (1325 gal) per day, P = 25 darcies (= about 500 US gal/day-ft^2 = 2.3 $\times$ 10^{-2} cm^3/sec-cm^2), $I = 10^{-3}$, D = 100 ft (30 meters), and ρ = 0.2, the dimensions would be: a = 13.25 ft = 3.975 meters, b = 4.2 ft = 1.3 meters, and c = 43.7 ft

(= 13.1 meters) after 100 days of injection and 353 ft in 1000 days. For a more or less typical deep-lying aquifer in which P = 0.5 darcies (= about 10 US gal/day-ft^2 = 4.6 × 10^{-4}cm^3/sec-cm^2) and with other quantities the same, a = 662.5 ft = 197.75 meters, b = 210 ft = 65 meters, and c = 17 ft (5.1 meters) in 100 days and about 58 ft (= 17.3 meters) in 1000 days. Inasmuch as the waste volume can move no farther in any direction than it does directly down-gradient, in the latter case the limits would not have been approached within the time given and the volume would be essentially a cylinder of radius 17 feet after 100 days and 58 feet after 1000 days of injection.

Probably no formation is uniformly porous at all horizons and hence such distances as given cannot be expected to closely limit the distance to which contamination would spread. The waste would be expected to move farther in the more permeable beds and less far in the beds less permeable than the average. As the permeability commonly varies widely through a vertical section, a considerable factor of safety would be necessary in any place. Differences in viscosity between waste and natural liquid also would modify the shape of the waste volume.

In a poorly permeable formation, in which the volume of waste injected would take more or less the shape of an expanding cylinder, the volume occupied would be only 5 to 10 times the volume of liquid injected. After injection ceased the volume of waste would drift with the movement of the natural liquid and, in a poorly permeable formation in which the natural movement was a few feet a year, would pass through a very large volume, because of its large cross section, before going far. If it were put in a quite permeable formation it would be entrained in the more rapidly moving liquid and be pulled out in a narrower cross section. In the latter case it would pass through a greater volume of material, in which it might exchange some of its ions, in a given time, but through less material in a given distance than in the former case.

Another characteristic of movement of ground water that might affect the emplacement of wastes is the leakiness of confining beds. Our prominent artesian aquifers seems to discharge commonly by seepage through the confining beds. A waste injected under pressure in most confined formations would tend to pass through the confining beds into upper formations. The mathematics of such injection would be basically the same as that for the discharge of an artesian well.[5] It probably would be advisable to have one or more discharging relief wells out of range of the injected waste, to relieve the pressure in the formation and for monitoring.

Differences in density between the waste and the natural liquid may cause differences in the pattern of movement of the waste. If considerable differences in density exist the probability of entrapment should be considered.[6]

A final characteristic of ground-water hydraulics has significance regarding waste injection. Fresh water in artesian aquifers along the seacoast in general discharges by upward percolation through so-called confining beds into overlaying aquifers. The fresh water is bounded beyond a more or less curved interface by static salt water. The zone beyond the interface seems to give a possibility for the placement of wastes if the hazards of plugging of wells can be overcome. Presumably, relief wells could be drilled in the vicinity to reduce the pressure resulting from injection and probably to furnish water for dilution.

Such placement necessarily would be made well beyond the interface in order to prevent future contamination of fresh water. Salt water is intruding in many aquifers upon the coast today and contaminating them because of heavy pumping of fresh water farther inland. Some of the brackish water is used for cooling and industrial purposes. It will be difficult to predict the possible extent of intrusion a century or more in the future before isotopes of intermediate half-life decay. The extent and mechanics of mixing of the two waters during intrusion of sea water needs investigation before future hazards of emplacement in salty ground water can be evaluated.

One of the greatest problems connected with disposal of radioactive wastes into the earth is that of heat generation. The temperatures that would be reached in a mass of waste that would be decreasing in heat-generating ability with time, that would be moving in two dimensions, largely radially in poorly permeable formations or largely in a band in more permeable formations, where ion exchange in the sediments may or may not change the pattern of heat production, while the heat is conducted away in three dimensions, probably cannot be computed directly. With knowledge of the hydraulic constants of the formations, the ion-exchange capacity of the formation materials for the radioactive components of the particular waste, and the heat-generating characteristics of the waste, the temperatures can be approximately computed by the assumption of heat sources of varying strength at proper spacing.

The following table of thermal conductivities of sedimentary rocks is selected from a much longer list which gives references to the individual determinations.[7]

It would appear from preliminary computations that 100-day-old wastes, generating over 1000 calories per day per liter at the time of injection, and placed near the surface at a rate of 6000 liters a day, would be likely to reach boiling temperatures. If an injection well carrying wastes of much higher level became plugged, the static column of waste could geyser, thus relieving the pressure within the aquifer, and under some conditions might cause the waste contained in the aquifer to burst into steam.

INJECTION INTO CAVERNOUS ROCKS

Injection of wastes into cavernous rocks, such as limestones, might eliminate at least some of the difficulties caused by precipitation of included chemicals and consequent plugging of finely porous formations. The most cavernous and most permeable limestones are a product of solution by moving ground water and the best known are in the zone of potable water. Petroleum is recovered from porous limestones beneath unconformities, from dolomitized limestones, from fractures in limestone, and even exceptionally from caverns. The small pores in some limestones, as in oolitic and dolomitized limestone, would not present an advantage to waste disposal because of size of pore. In the types of porosity caused by solution, movement of waste would in general be more erratic and less predictable than in sandy formations. In limestone having this type of porosity, the permeability may be high and the porosity low, with the result that wastes might spread more widely in them than in sandy formations. Of course, being more widely spread, they would not form as concentrated a source of heat.

Table I. Thermal Conductivity of Rocks

Rock	*Temperature* (°C)	*Conductivity cal/ sec-cm-°C*
Limestone, dolomitic, Queenston, Ontario	123	3.4×10^{-3}
	177	3.4
	254	3.3
	332	3.2
Marble (17 varieties)	30	$7.7\text{–}5.0\times10^{-3}$
Proctor, Vermont,		
Parallel to bed	0	7.36
	100	6.0
	200	5.2
Perpendicular	0	7.2
	100	5.7
	200	5.1
Quartzitic sandstone		
Parallel to bed	0	13.6
	100	10.6
	200	9.0
Perpendicular	0	13.1
	100	10.3
	200	8.7
"Recrystallized sandstone"	30	11
"Hard sandstones"		10.8–6.2
Sandstone, Boreland Bore	17	10
"Soft sandstones"		4
Slate, Wales		
Parallel to schistosity		6.7
Perpendicular to schistosity		3.9
Slate	30	4.7
Shale		4.1–2.4
"Very fine-grained"	17	1.4
"With sand"	17	2.8
Gerhardminnebron Bore (Witwatersrand)		
From 6457 feet	25	6.6
From 4190 feet	25	4.4
Silty clay	17	3.7
Silt, Hankham (borehole)	17	4.4
"Uncemented"	17	5.3
"Micaceous, argillaceous"	17	2.5
Fireclay, Boreland Bore	17	4.4
Red marl, Holford	17	5.25
Gray marl, Holford	17	2.2, 3.5
Rocksalt, Holford	17	17.2

DISPOSAL INTO UNSATURATED SEDIMENTS

In finely porous unconsolidated materials in arid regions where the water table is very deep, some possibility seems to exist for the disposition of wastes into the unsaturated materials above the water table. If the quantities of waste put into such materials were closely computed with relation to the character of the material, it should be possible to hold the material to a low degree of saturation so that the waste would not descend to the water table. After use of an area for disposal, the surface of the ground necessarily would be sealed to prevent the blowing of dust and the entry of more water from rain. The waste would be spread over a great volume of material and hence would have a large opportunity for ion exchange and other forms of adsorption. Some types of waste probably would evaporate owing to the heat produced. Vapor transfer from warm to cool levels probably would not be significant as the long-lived isotopes could not thus be moved. The possible movement of water in the liquid phase down the thermal gradient would need further investigation.

The obvious disadvantages of such a type of disposal would be that the radioactivity would be held close to the surface of the ground, that it would be above the water table and therefore potentially able to drain to potable water bodies, and that cover over the area would have to be maintained for a long future period. Experimentation along this line probably would be done best on a small mesa in arid country.

RETENTION IN PITS

Inasmuch as dispersal into porous formations imposes many problems, planned retention in artificial cavities offers some possible advantages.

In most areas of sedimentary rocks and in many areas of Pleistocene glaciation, formations of poorly permeable shale and clay are present. Pits or caverns could be constructed at moderate expense in these materials and, if at the surface, backfilled with coarse crushed rock capped by sand for an entrainment filter, as has been suggested at Oak Ridge. In such a structure almost any desired temperature could be attained between boiling and fusion, depending on the age and dilution of the wastes and on the horizontal area and depth of the cavity.

Asphalt and other liners have been proposed to seal surface pits, but it would seem to a hydrologist that, to minimize hazard, final reliance must be on the geological formation itself. Probably no naturally occurring shale or clay formation could be considered impermeable enough to retain—to the degree necessary—high-level radioactive liquids containing long-lived isotopes, because of the presence of joint cracks and more permeable layers.

However, all the properties of the wastes that would make injection into porous formations difficult would be helpful in sealing any small fractures and sandy layers if it were planned to retain the wastes. Particulates would help to seal the pit, and if it were possible to develop enough silica by acid reaction with the clay materials, or to cause precipitation of aluminum or iron hydroxides within the pores by reducing the acidity of the solutions by ion exchange, it would seem possible to seal the area sufficiently to permit deposition of even high-level wastes. If these processes are to take place, it probably would be advisable to condition the pit for a time before permitting substantial precipitation of waste salts on its bottom.

The hazards after abandonment of a filled pit would depend to a great extent on the position of the pit with reference to the water table, and on whether the process of sealing was successful. If the surrounding material had been rendered impermeable and no checks or cracks developed during cooling, no ground water would move through the pit to pick up soluble precipitates. If well above the water table, the material in the pit probably could be preserved from solution by rendering the land surface impermeable. It probably would be possible in many shale bodies to lower the water table artificially by pumping a little water periodically from wells upgradient from the abandoned pit. However, if such maintenance were necessary except as an emergency, it would make disposal expensive, unless only short-lived isotopes were involved.

Geologically, salt deposits seem to offer the least hazard for the disposal of high-level wastes. Cavities can be made in salt by either solution or mining. Generally, no ground-water movement occurs in salt; most, if not all, salt mines are dry even where they are far below the water table. Salt deposits occur in many places throughout the world. If areas and beds containing potassium or other valuable salts, and salt structures associated with oil production are avoided, probably no over-all economic loss would be suffered by dedicating some salt deposits to the storage of wastes. Salt is plastic under load and therefore probably more free than any other rocks from earthquake hazard. It has a melting point of only 800°C, and hence the temperature of any wastes put into it probably would have to be kept below this temperature. Solubility would be no problem with wastes already at the point of saturation. Typically, caverns in salt would be connected to the surface through wells or shafts, which probably would permit using a closed system, condensing the escaping steam and returning it to the cavern again with any entrained or volatile isotopes.

The chief apparent disadvantage of the use of bodies of salt for disposal of liquid waste is the necessity for transportation from the reactor or processing plant. In particular areas the possibility that gypsum or anhydrite beds carrying water may be present would need investigation. Such water doubtless would be impotable, but attention would have to be given to the possibility of escape of waste products along such beds. If shafts or wells were sunk through potable-water zones to salt at depth, the upper zones would have to be protected from possible contamination.

CONCLUSIONS

1. With present reactor technology, salt deposits seem to offer the best hope for disposal of high-level wastes.

2. Disposal of dense wastes to porous formations at depth will present many problems concerning the prevention of clogging.

3. If technology advances to the state that wastes can be prepared without the addition of preponderant quantities of inert salts, or if the problems of injection can be solved, wastes must be diluted or aged to the point that they cannot steam even in the case of a shutdown.

4. Artificial caverns or pits in non-fractured and non-cavernous rocks of very low permeability seem to offer the best possibilities for local disposal in most places, provided it can be assured that reactions will occur which will virtually seal the pit from ground-water movement during and after its use.

5. The two isotopes Cs^{137}, with a 33-year half-life, and particularly Sr^{90}, with a 20-year half-life and very low tolerance, tremendously increase the hazard of ground disposal. If these two isotopes could be removed, ground disposal of some type might be feasible in many places. The over-all cost of waste disposal might be less if more money were spent on treatment and less on storage or disposal.

6. No disposal to the ground should be made without the advice of thoroughly competent geologists and hydrologists, who should be informed about the nature of the waste problems involved.

REFERENCES

1. Twenhofel, W. H., *Principles of Sedimentation,* McGraw-Hill Co., Inc., 287-288, New York (1950).
2. Nutting, P. G., *The Action of Some Aqueous Solutions on Clays of the Montmorillonite Group,* U. S. Geol. Survey Prof. Paper *197*: 219–233 (1943).
3. Grim, R. E., *Clay Mineralogy,* McGraw-Hill Co., Inc., New York, p. 296 (1953).
4. Harlow, I. F., *Waste Problem of a Chemical Company,* Industrial Engineering Chemistry *31*: 1345–1349 (1929).
5. Jacob, C. E., *Radial Flow in a Leaky Artesian Aquifer,* Trans. Am. Geophys. Union *27*: 198–205 (1946).
6. Hubbert, M. K., *Entrapment of Petroleum under Hydrodynamic Conditions,* Bull. Am. Assn. Petroleum Geologists *37*: 1954–2026 (1953).
7. Birch, Francis, et al., *Handbook of Physical Constants* Geol. Soc. Am. Special Papers No. *36*: 251–258 (1942).

Disposal of High Level Radioactive Liquid Wastes in Terrestrial Pits

By E. G. Struxness, R. J. Morton,* and C. P. Straub,† USA

Storage of high level radioactive liquid wastes in suitable underground tanks has been practiced at all atomic energy installations since the start of the industry. At the Oak Ridge National Laboratory (ORNL) concrete gunite tanks with a total capacity of 1,104,000 gallons have been in use since 1944 for the storage of neutralized, metal recovery, process wastes and miscellaneous radioactive wastes.[1]

In June, 1949, a pot-type, internal steam-coil heated evaporator having a design capacity of 300 gallons of water per hour was installed to reduce the volume of currently produced waste by a factor of 10 to 15. Early in 1951, in spite of this volume reduction, it was soon evident that the limit of available tank capacity was being approached, and the high cost of additional tank space prompted consideration of the use of earth pits for waste storage and disposal. In July, 1951, Waste Pit 1 was located and constructed in a Conasauga shale formation within the ORNL controlled area. Since then two additional waste pits have been built. Originally wastes were transferred to the pit by tank truck; at present wastes are pumped through a 7000-foot, 2-inch diameter, welded steel pipeline.

These waste pits supplement tank facilities in that they are used for the storage of intermediate level radiochemical wastes containing $\frac{1}{300}$ to $\frac{1}{30}$ curies of activity per gallon. Metal wastes are still stored in the concrete waste tanks, dilute liquid wastes are discharged into the White Oak Creek drainage system, and solid wastes are buried in a similar Conasauga shale formation. Sanitary sewage is collected in a separate system and is discharged to White Oak Creek following primary treatment and chlorination. The layout of the waste storage and disposal facilities is shown in Fig. 1.

Storage in structural tanks has a number of limitations including finite capacity, uncertain durability, vulnerability to accidents, and high costs. Since the average half-life of a mixture of 100 days aged fission products is about 20 years, storage for at least 200 years must be considered. This long time storage focuses attention on the need for very large tank capacity, and upon the problems of structural disintegration due to corrosion, chemical action, and long continued exposure to radiation. Uncontrolled release of tank contents, as a result of disruption of the tank by an accident such as an earthquake or explosion, could be disastrous. Experience shows that tank storage is expensive as indicated by cost estimates of $0.75 to $2.00 per gallon of tank capacity.

* Oak Ridge National Laboratory.
† US Public Health Service.

THE CONCEPT OF GROUND DISPOSAL

Potentialities of the Soil

That soils have the property of exchanging ions from solutions in contact with them has been known for some time. This knowledge has been applied to removal of radioactive materials (primarily cations) from waste solutions. Among the first to point to the possible use of soil for retaining radiosotopes were Jacobson and Overstreet.[2] The capacity of a soil for the removal of specific radioactive materials is influenced by the concentration of the ions to be exchanged, the kind of ion and its valence state, the electrolyte or salt concentration of the waste liquid, the chemical composition of the waste solution, the texture and properties of the soil, and the pH of the waste solution and soil. Due to the large areas and volumes of soil available in most locations, the potential capacity for sorption of wastes is great. The effect of the other factors will be discussed in more detail later.

From the viewpoint of safety, soils tend to resist disruption and dispersal by accident and tend to retain the radioactive materials attached to them. In the case of a change in waste composition from an alkaline to an acid waste, there is the possibility of leaching the previously fixed material and moving it downstream with the ground water. It is believed that disposal in terrestrial pits will prove more economical than the current practice of tank storage.

Complete Retention

For complete retention, the pit should be located in an impervious soil formation. Unless the soil in which the pit is located is naturally impervious, it must be lined to prevent passage of radioactive materials into the ground water. An impervious seal may result from the interaction of the waste material and the soil, as in the case of an acid waste solution in contact with a limestone or dolomitic rock formation. Whether the liner is prepared, or is formed as a result of chemical interaction, it must

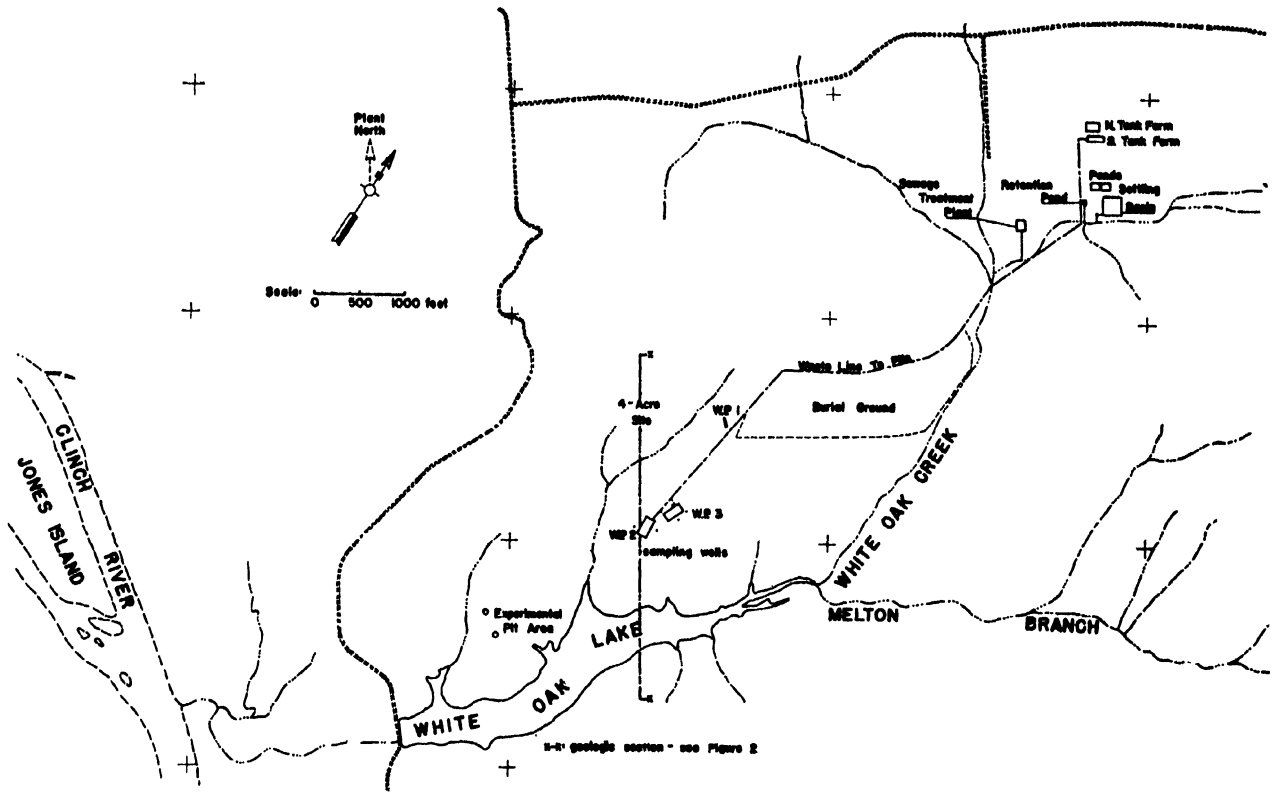

Figure 1. Disposal of high level radioactive liquid wastes in terrestrial pits

be temperature stable, resistant to chemical action of the waste solution, resistant to the effects of continuous radiation, and economical.

To increase the probability of complete retention and to decrease the accident hazard, measures to immobilize the mass of waste material within the pit are under consideration. Evaporation, either solar or due to the heat of radioactive decay, may be effective for immobilization. However, evaporation to dryness presents the possible hazard of air contamination by radioactive particulates. Another means of reducing movement is by admixture with solid materials such as slurries of clay or fluxing agents.

A major limitation in application of the concept of complete retention in soil pits is that impermeable soil formations are generally non-existent. In most locations the soils may be somewhat pervious and the sub-surface rock structure may contain fissures and faults. The rate and direction of flow and elevation of the ground water will have a bearing on the location and construction of the pit. In the location, design, and operation of a retention waste pit the potential health hazard due to radioactive aerosols, shielding, ground water contamination, and uptake by vegetation must also be considered.

Partial Retention and Seepage

In partial retention and seepage, use is made of the ion exchange properties of the soil surrounding the pit to separate out and hold some of the radioactive constituents of the waste. An ideal arrangement would be one in which all of the radioisotopes were removed from the waste solution and fixed to the soil as the solution passes through the first few inches or feet of pit wall or bottom. In practice removal does not occur in the first few inches or feet and some of the factors influencing the use of such pits will be pointed out.

Between these two extremes—complete retention and partial retention and seepage—many intermediate schemes may be considered. For example, a pervious liner may be installed which has a high exchange capacity for the more critical radioisotopes in the wastes. Permanence of fixation is a major consideration in this type of installation. The useful life of such a liner will be predicated on its total exchange capacity.

Another application of this concept would be for the disposal of pretreated wastes, the more critical nuclides having been removed prior to discharge to the soil. In general the critical nuclides include those of maximum abundance, high toxicity, and long half-life such as Sr^{90}-Y^{90}, Sr^{89}, Zr^{95}-Nb^{95}, Cs^{137}-Ba^{137}, Ba^{140}-La^{140}, Ce^{144}-Pr^{144}, and Pm^{147}.

The major limitation of this method of disposal is that control of the wastes is lost once they leave the confines of the pit and, unless fixation takes place close to or at the point of contact, there is danger of contaminating the ground water. Because of this limitation, the method may have to be used principally for the disposal of low activity wastes. Other disadvantages are that retention is reduced due to the presence of high concentrations of non-

Table I. Waste Pit Characteristics

Waste pit	*1*	*2*	*3*
Design capacity in gallons	180,000	1,000,000	1,000,000
Dimensions (length, width, depth), in feet	100 × 20 × 15	210 × 100 × 15	210 × 100 × 15
Period of use	8/1/51–10/5/51	6/20/52–1/18/55	1/24/55–4/22/55
Volume of waste added, in gallons	123,000	1,331,760	541,800
Beta activity of wastes added, in curies	389	15,975	10,491
Radioisotopes present, per cent of total			
Cs^{137}–Ba^{137}	60	60	77
Ru^{106}–Rh^{106}	40	40	12
Sr^{90}–Y^{90}			11
pH of waste solution	~12.5	~12.5	~10–11
Approximate construction cost, per million gallons capacity	$14,500	$14,500	$14,500
Approximate cost per gallon of waste capacity, in cents	1.45	1.45	1.45
Approximate cost per gallon of waste added, in cents	2.12	1.09	<2.68

radioactive ions, and generally only cations will be removed. In the case of a highly acid waste, only zirconium and niobium are removed, all other ions move through the soil and are taken out only after the pH of the waste solution is changed following contact with the soil.

ORNL EXPERIENCE AND STUDIES RELATIVE TO GROUND DISPOSAL

At the Oak Ridge National Laboratory site, located in the Appalachian Plateau, there are four primary rock formations identified as Rome sandstone and shale, Conasauga shale, Knox dolomite, and Chickamauga limestone, shown in the geologic section in Fig. 2. Of the formations, the Conasauga shale was considered most suitable for the location of terrestrial waste pits, because it was the most impermeable, was not subject to solution, and was at least 1500 feet thick. Ground water in the area occurs under water-table conditions and at depths ranging from ground water seeps at the surface to about 35 feet.

Experience with Low Level Wastes

As indicated earlier, three waste pits have been located in the weathered Conasauga shale overburden, and to date have received the quantities of wastes reported in Table I along with other pertinent details. The wastes added to Pits 1 and 2 were highly alkaline (pH, 12.5) evaporator concentrates, with an activity of about $\frac{1}{30}$ curie per gallon, mainly as cesium and ruthenium (60 per cent Cs^{137}-Ba^{137} and 40 per cent Ru^{106}-Rh^{106}). The wastes added to Pit 3 are less alkaline (pH about 10–11), are more dilute by a factor of 10 to 15, and contain measurable amounts of strontium in addition to the cesium and ruthenium (about 77 per cent Cs^{137}-Ba^{137}, 12 per cent Ru^{106}-Rh^{106}, and 11 per cent Sr^{90}-Y^{90}). The total solids concentration of the waste added to Pits 1 and 2 averaged about 34 to 35 per cent of which the principal stable constituents were Na^+, NH_4^+, and NO_3^-, and that added to Pit 3 was more dilute by a factor of 10 to 15.

Sampling and radio-logging wells have been provided for the purpose of monitoring and have shown that radioactive ruthenium and stable NO_3^- pass through the Conasauga shale formations. In the case of Pit 2, six weeks after the introduction of the wastes, ruthenium and nitrates were found in a sampling well 85 feet distant. No evidence of radioactive cesium or any other radioactive cations in any of the wells has been observed in the three years of operation. Breakthrough of radioactive ruthenium and stable nitrate to a surface stream 500 feet distant from the pit took place after two years of operation. The underground movement of the wastes corresponded with geologic and hydrologic findings of ground water flow in the disposal area.

Box turtles native to the area were found dead; symptoms indicated that ingestion of the high concentration of nitrates (approximately 15,000 mg/liter of NO_3^-) contained in the seepage liquid was the probable cause of death. Because of its public health implications, the movement of stable NO_3^- through the soil is of considerable interest. Public health agencies have assigned a limit of 10 mg/liter nitrate nitrogen to ground water supplies. The possible contamination of ground water aquifers with high nitrate waste solutions should definitely be avoided.

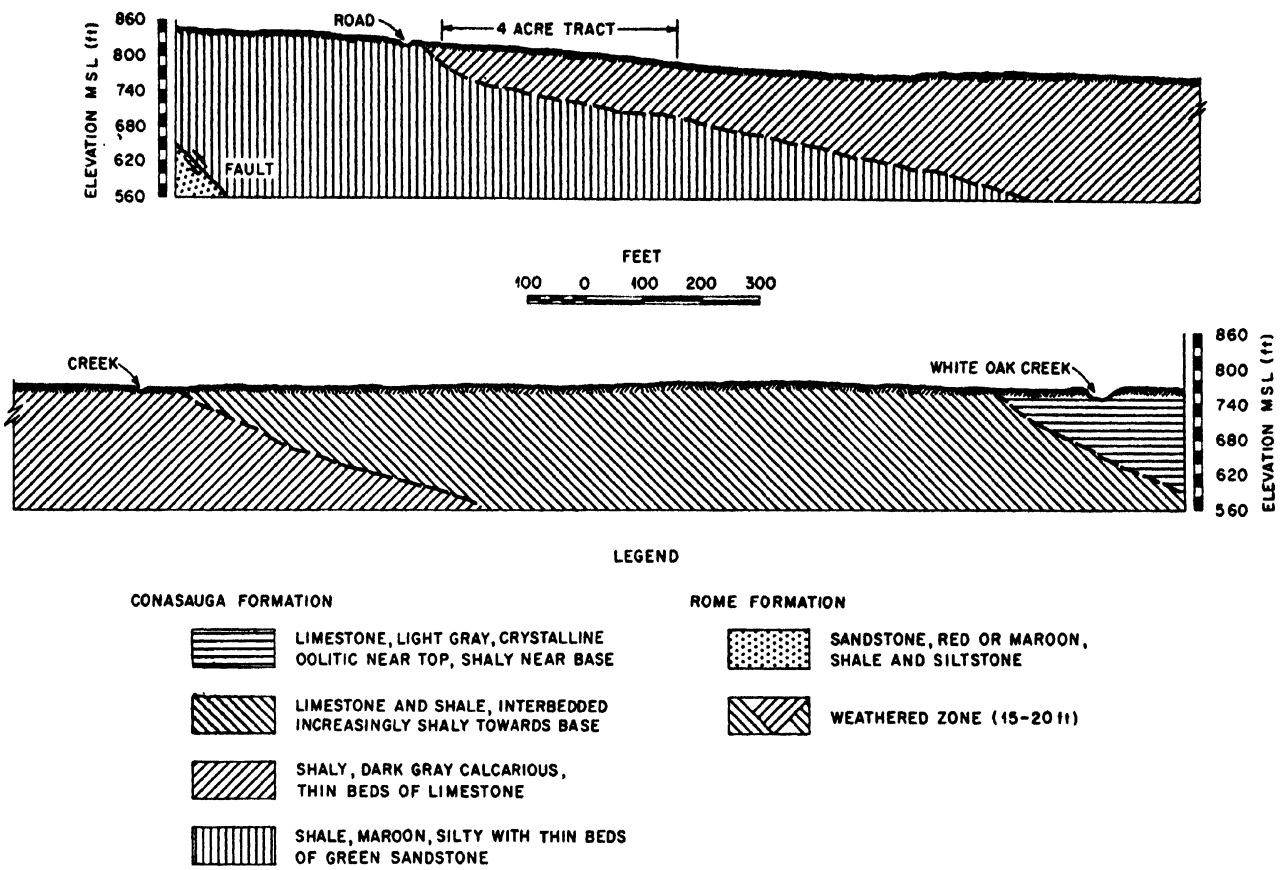

Figure 2. Generalized geologic section, waste disposal area, Oak Ridge National Laboratory

The construction cost of about 1½ cents per gallon of waste capacity shown in Table I for terrestrial pits may be compared with the estimated cost of 75 cents per gallon capacity for a gunite-lined, stainless steel tank. Use of these pits has resulted in a saving of at least $63,000 per year as compared with storage in underground tanks.

Laboratory Studies

Laboratory studies included a consideration of the properties of the soil and the effect of waste solutions on these properties; of the desirability of pre-treatment of the wastes in order to make them more suitable for disposal into the soil, to remove the more hazardous constituents, and to dissipate the decay heat; of the feasibility of liner materials of bituminous or mineral origin; of the possibility of fixing the activity to ceramic masses; and of the control of the aerosol problems.

Properties of Local Soil

The adsorptive behavior of local soils with respect to the major long-lived fission products (Sr^{90}-Y^{90}, Zr^{95}-Nb^{95}, Cs^{137}, and Ru^{106}) was studied. It was found that little adsorption of the isotopes named occurred on soils saturated with carrier solutions of these isotopes, with the exception of zirconium and niobium, from the $0.2M$ HNO_3 and $1.6M$ $Al(NO_3)_3$ solution; but in aqueous solutions (pH $\geqslant$ 3) removal (with the exception of cesium) followed that predicted from the Hofmeister lyotropic series—ions of higher valence being more strongly

Table II. Uptake of Cations by Textural Fractions of Conasauga Shale

Textural fraction mesh/inch (1)	*Cation exchange capacity - meq/100 gm*		*Estimated total bases* meq/100 gms* (4)	*H^+ meq/100 gm by difference* (5)=(3) - (4)
	Strontium (2)	*Ammonium acetate* (3)		
6–8	13.5	16.8	5.3	11.5
10–20	22.3	18.9	–	–
20–40	21.9	20.7	6.0	14.7
40–80	18.8†	20.6	–	–
<120	17.0	16.2	4.1	12.1

* Ammonium acetate extraction from cation exchange capacity determination analyzed for Ca, Mg, Na, and K.
† 40–120 mesh/inch.

adsorbed than those of lower valence. From the H^+ saturated soil, for example, the order of removal was $Nb^{95} = Zr^{95} \geqslant Cs^{137} > Ru^{106} > Y^{90} > Sr^{90}$. The adsorptive capacity of soils for cesium as a function of the cesium concentration was determined in an effort to explain its greater tenacity at low concentrations. It was found that the adsorption of cesium ions followed the Langmuir isotherm and that at lower concentrations the exchange capacity of a given soil was much less than its saturation capacity. Saturation capacity is also a function of the kind of soil and its textural fraction. For example, the cation exchange capacity of the soil two feet below the surface was found to be 5 milliequivalents per 100 grams (meq/100 gm), whereas the textural fractions of the semi-weathered rock material 15 feet below the surface yielded a capacity of 16 to 20 meq/100 gm. As indicated in Table II, the uptake of strontium by the various textural fractions is of the same order of magnitude as the cation exchange capacity determined by the ammonium acetate method.[3]

Undisturbed core samples of the same semi-weathered rock material had a strontium uptake capacity averaging 9 meq/100 gm, again demonstrating the inefficiency of the natural material as compared with saturation capacity values of 16 to 20 meq/100 gm. After completion of the tests, the cores were broken apart and showed that the greater part of the strontium uptake occurred along the crevices and, at the flow rates studied (k_{20} approximately 5×10^{-4} cm/sec),‡ advantage is not taken of the exchange capacity of the centers of the rock fragments.

A study of the neutralizing ability of the Conasauga shale showed that in passing through 1500 gm of shale the pH of 100 ml of the acid aluminum nitrate solution was changed from less than 1.0 to approximately 1.5.

Flow rates of tap water and acid aluminum nitrate solutions through the soil were determined and the results are indicated in Table III. As shown there appeared to be no consistent ratio between the k_w and k_a values.

Cores were also collected in such a manner that vertical permeability and permeability perpendicular and parallel to the stratification could be determined. Permeability values (k_{20}) of 3×10^{-3} cm/sec were found for vertical flow, and 1×10^{-3} and 4×10^{-3} cm/sec, respectively, for flow normal and parallel to the stratification.

‡ k_{20} = permeability in cm/sec corrected to a temperature of 20°C.

Pretreatment of the Wastes

Because of the movement of ions from acid waste solutions, and particularly the movement of cationic strontium in aqueous wastes, separation of the critical radionuclides was indicated. Two procedures using the acid aluminum nitrate waste solution have been studied: (1) neutralization by the addition of sodium hydroxide to complex the aluminum present followed by the addition of carbonate to precipitate the strontium, and (2) precipitation of the critical nuclides in the acid waste. In the latter procedure, copper ferrocyanide is used for the precipitation of ruthenium and cesium, barium sulfate for cerium and strontium, cerium oxalate for yttrium, and zirconyl phosphate for zirconium and niobium. A decontamination factor§ of 10 to 20 has been obtained using both procedures, but the second is preferred since preliminary estimates of the chemicals required indicate a cost of 5 to 6 cents per gallon of waste treated as compared with 10 to 20 cents for neutralization.

Removals of the more critical radioisotopes will alleviate the problem of boiling in pits and will reduce the hazard from aerosol contamination. The wastes discharged to the pit will be less hazardous and the lower temperatures of the waste solutions may permit use of asphalt and other bituminous liners which are unstable at high temperatures (see next section). Pretreatment will add to the cost since storage facilities will have to be provided for the small volume of highly active materials contained in the precipitates.

Liner Materials

The resistance of asphalt liners to radiation damage, chemical disintegration, and temperature stability has been examined.¶ Under a dose of 5×10^8 roentgens, tars did not undergo any appreciable change. Asphalts increased in volume up to 70 per cent, emitted H_2 gas, and became honeycombed, but did not lose their properties of ductility and cohesion. The asphalts and tar maintained their characteristics while in contact with water, acid aluminum nitrate, and neutralized aluminum nitrate solutions. At temperatures above 70°C, they became hard and brittle and were unsuited for liner materials. The k_{20} values were 10^{-10} and 10^{-11} cm/sec.

§ Decontamination factor (D.F.) = Influent activity/Effluent activity.

¶ These studies have been carried out cooperatively with C. D. Watson, Chemical Technology Division, ORNL.

Table III. Relative Permeability of Rock Cores to Tap Water and Acid Aluminum Nitrate Waste Solutions

	Permeability, cm/sec				
Sample number	*1*	*2*	*3*	*4*	*5*
Tap water (k_w)	1.2×10^{-3}	3.5×10^{-4}	1.0×10^{-3}	4.4×10^{-4}	1.8×10^{-6}
Acid waste (k_a)	5.7×10^{-4}	4.0×10^{-4}	0.8×10^{-3}	2.6×10^{-4}	2.2×10^{-6}
Ratio (k_w/k_a)	2.1	0.9	1.2	1.7	0.8

Another possible liner material is a local clay** which gave k_{20} values of 10^{-10} cm/sec when placed and packed at a moisture content just below the lower plastic limit. No measurable differences were observed when distilled water and alkaline solutions were placed in contact with the liner material. This material could not be used in contact with acid wastes. Dilutions of the clay with as much as 75 per cent sand to increase its physical stability did not increase the permeability value.

Gels produced by the interaction of limestone or dolomite with acid waste solutions to form liners were investigated and found promising for pits containing acid wastes.

To confirm laboratory data on the use of clay and asphalt type liner materials, experimental sections employing these liners were placed in Waste Pit 3 and are being observed under actual field conditions. There has been no detectable leakage through a ½ inch asphalt membrane in the side of Waste Pit 3. The clay lined unit leaked; the permeability was found to be 10^{-7} cm/sec. There appeared to be no difference in the radioactive components present, however, the pH of the solution changed from about 10 to 6 in passing through the clay membrane. Stability studies on a clay strip liner three feet in width indicated severe damage from erosion.

Fixation in Ceramic Mixtures

The possibility of incorporating radioactive isotopes, contained in an acid aluminum nitrate solution, into a ceramic body for the safe and economical disposal of high level radioactive wastes is under investigation. The method involves mixing 250 ml of aluminum nitrate solution (1.6*M* $Al(NO_3)_3$ and 0.2*M* HNO_3) with 30 grams Chickamauga limestone (80 mesh per inch), 30 grams of sodium carbonate, and 200 grams of Conasauga shale (80 mesh per inch) to form a gel or slurry. This is dried and sintered at 1935°F to 2000°F for 6 hours, to produce a mass in which the isotopes may be fixed and which is resistant to aqueous leaching. In one experiment Sr^{90} was added as a tracer and none was found in the distilled water leach solution after 10 days contact. Further investigation is directed toward obtaining more economical mixtures which will sinter at lower temperatures. The compositions studied include several local shales, limestone, sodium carbonate, phosphate tailings, and fly ash. Apparatus has also been constructed to determine if Sr^{90} is released during firing.

It is hoped that sufficient heat (from radioactive decay) is available for the fusing process; if not, external heat will have to be supplied. Studies are now in progress to determine the amount of heat available from decay and the actual amounts of heat required to fuse the various ceramic mixtures.

** Spinks Ball Clays, a product of the H. C. Spinks Clay Company, Paris, Tennessee.

De-entrainment of Evolved Aerosols

The amount of aerosol evolution from a boiling liquid may be expressed by a decontamination factor of about 10^{12} (required for very high level boiling liquid to the activity in the condensate. Experiments with a gently boiling sodium aluminate solution showed decontamination factors of 10^5 to 10^7 due to boiling alone. To attain a decontamination factor of about 10^{12} (required for very high level waste solutions) entrainment separators having a decontamination factor of about 10^7 will be needed. River sand is being considered for this purpose.

The results of a series of tests using river sand are plotted in Fig. 3 and show the existence of an aerosol size for maximum penetration through the bed. With small sizes, rapid diffusion of the particles results in low penetration values; with larger sizes, gravity settling and inertial impaction are effective. The combination of these effects results in the optimum penetration as shown. The establishment of the size for maximum penetration is very important, since beds tested with this aerosol size will give better removals of smaller or larger particles.

As shown in Fig. 3, the decontamination factor is better than 10^3 for the most penetrating particle at a linear velocity of 0.04 ft/min through the bed, which is equivalent to about 0.1 pounds of water vapor per square foot per hour. This gives an overall decontamination factor of at least 10^8 for a 5-inch bed of sand at this flow rate for combined distillation and filtration. It seems quite likely that a bed thickness of less than 3 feet will be needed to obtain the required 10^{12} decontamination factor, at a velocity equivalent to 0.1 pounds of water vapor per square foot per hour.

Hydrologic and Geologic Investigations of the "Four Acre Site"

Since experience at ORNL in the disposal of radioactive liquid wastes into the ground has been confined to the disposal of intermediate level wastes considerable additional information on the geologic and hydrologic features of the area is needed before high levels of wastes may be discharged into the same formation. Thus an extensive study of a site, known as the "four acre site" to determine its suitability for high level waste disposal via terrestrial pits is being made.

To determine the physical properties of the soil and rock which underlie the site selected, a program that includes geologic mapping, test drilling, pressure tests, and pumping tests is being conducted.

Examination of the cores obtained indicated that from land surface to a depth of 10 to 20 feet the area is underlain with a weak, silty, punky clay. This grades downward into less weathered shale. Pressure tests of the borings also indicated that below a depth of about 100 feet the rock in the vicinity of the borings is quite impermeable, accepting about 0.3 gallons per minute at pressure of

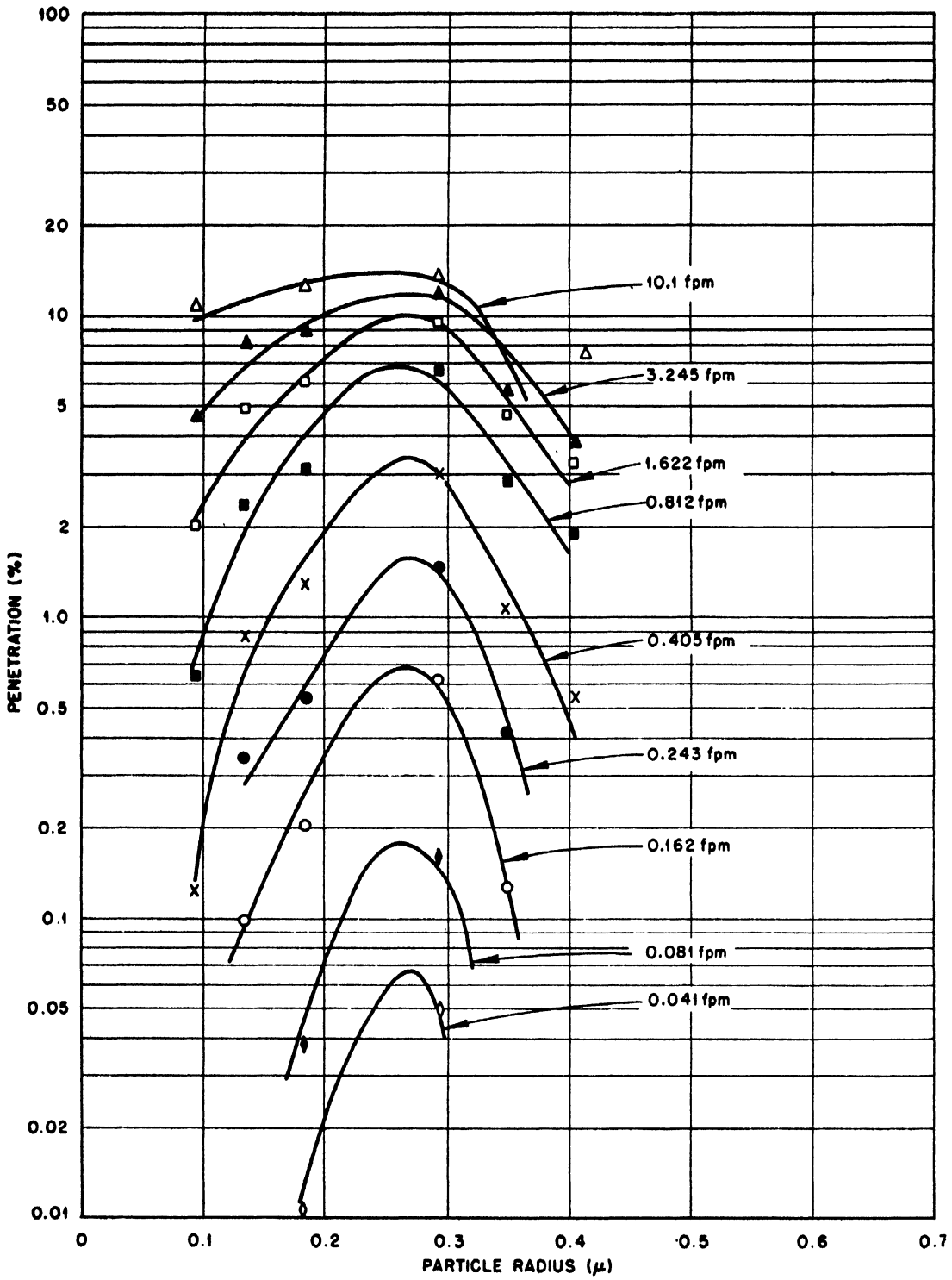

Figure 3. Aerosol penetration through a sand bed: penetration vs particle size

30 pounds per square inch (gage). Discharging well pumping tests will be conducted and analyzed to determine the coefficients of transmissibility and storage of the underlying rock, parameters that control in part the rate of ground water movement. All of the core borings have been equipped with recording gages which obtain continuous records of fluctuations of water level.

DISCUSSION AND CONCLUSION

The experience with the disposal of intermediate level liquid wastes in terrestrial pits at ORNL shows that pits have certain advantages over evaporation and storage in tanks. However, before this experience can be applied directly to the disposal of high level liquid wastes, more laboratory and field pilot plant data are needed. Some of the factors requiring

further evaluation include (1) the effects of interaction between soil and the waste materials, (2) the movement of critical nuclides through various soil formations, (3) the effects of high concentration of stable salts such as aluminum, nitrates, and various solvents and complexing agents upon the ability of the soil to retain radionuclides, and (4) the underground flow pattern of waste solutions as compared with ground water.

Although study of these factors is to continue at ORNL, there is need for similar studies at other sites where soil disposal is contemplated. Such studies will expand the information on the feasibility of this method for the safe and economical disposal of high level liquid wastes.

It is recognized that, in addition to terrestrial pits in surface strata, other containment formations exist, which under suitable conditions may be advantageous for high level liquid waste disposal. Some of the formations that have been suggested include salt deposits, deep excavated holes, regional aquifers, structural troughs, and closed valleys.

A thorough hydrologic and geologic study of proposed ground disposal sites is essential. The geology must be known to determine the suitability of available formations, particularly the stratigraphy, structure, texture, composition, and base exchange capacity. The important hydrologic factors include ground water elevation, the rate and direction of ground water flow, and the permeability and porosity of the formations.

In spite of the precautions taken in the location and design of terrestrial pits for the disposal of high level liquid wastes, unusual care must be exercised to prevent health and safety hazards resulting from the uncontrolled release of critical contaminants to the environment. The disposal of power reactor process wastes, for example, may involve megacurie quantities of fission products daily in a variety of situations. For this reason, extensive monitoring facilities, including observation and sampling wells and reliable instrumentation, will be required.

The construction cost of simple terrestrial pits for the disposal of ORNL wastes has been about 1½ cents per gallon of capacity as compared with 75 cents per gallon for steel-lined gunite concrete tanks. Assuming that such pits can be adapted for the successful disposal of high level wastes, it is reasonable to expect that the cost of construction will be intermediate between these figures.

ACKNOWLEDGEMENTS

The authors acknowledge the assistance of the following in the preparation of this paper: T. W. Bendixen, M. I. Goldman, Bernd Kahn, K. E. Cowser, J. W. Thomas, R. M. Richardson, J. M. Warde, E. J. Witkowski, and C. D. Watson.

REFERENCES

1. Browder, Frank N., *Liquid Waste Disposal at Oak Ridge National Laboratory,* Ind. Eng. Chem., *43*: 7, 1502 (July 1951).
2. Jacobson, Louis, and Roy Overstreet, *The Uptake by Plants of Plutonium and Some Products of Nuclear Fission Adsorbed on Soil Colloids,* Soil Sci., *65*: 129 (1948).
3. Wilcox, L. V., and Hatcher, J. T., *Methods of Analysis,* Rubidoux Laboratory, US Department of Agriculture. Washington, D. C. (1952).

Record of Proceedings of Session 23B.1

SATURDAY MORNING, 20 AUGUST 1955

Chairman: Mr. A. J. Cipriani (Canada)

Vice-Chairman: Mr. A. R. Torky (Egypt)

Scientific Secretaries: Messrs R. Hara and D. J. Littler

PROGRAMME

P/565	Disposal of liquid wastes to the ground	R. E. Brown *et al.*
P/12	Waste disposal into the ground	C. A. Mawson

DISCUSSION

The CHAIRMAN: We come now to a very important phase in the operation of atomic energy plants, that of waste disposal. The types of wastes of which we are talking today are not the concentrated wastes which one expects and stores and keeps for some future date when we will be able to deal with them, but wastes arising by the way, especially from chemical plants and from cleaning up contamination incidents. These wastes usually appear in very dilute form, and economy forbids that they be evaporated into nice little packages and stored away, with materials from which they arise. It is fairly common practice today to throw these wastes away, but when one does so one must be sure that they do not come into contact with human beings through either the food they eat or the water they drink.

This problem of waste disposal is not easy to solve. So far two methods in general have been adopted for dealing with these wastes, one being to put them into the ground, the other to put them into the sea. Wastes put into the ground are immediately lost to sight, but this is not sufficient reason for forgetting about them; we have to know what is [illegible] where they are going, and this entails a good deal of work on soils and the following of ground water, if it exists, in which these wastes may travel. It is quite possible that in the future siting of chemical plants the availability of suitable ground for waste disposal may be a big factor in locating these installations. The one other factor would be transportation facilities.

Mr. H. M. PARKER (USA) presented paper P/565 as follows:

This paper relates the generally favorable experience of ground disposal at the Hanford plant over the past decade. Experience here, while based on our specific local conditions, is believed to be useful for guidance in economical radioactive waste disposal methods in the development of peaceful uses of atomic energy at other locations.

In considering the feasibility of disposal of wastes to ground, the following factors must be evaluated: (1) the chemical and radiochemical content of the waste, (2) the effectiveness of retention of the radioisotopes in the available soil column above the ground water table, (3) the degree of permanence of such retention, as influenced by subsequent diffusion, leaching by natural forces, and additional liquid disposal, (4) the natural rate and direction of movement of the ground water from the disposal site to public waterways, and possible changes in these characteristics from the over-all liquid disposal practices, (5) feasibility of control of access to ground water in the affected region, (6) additional retention, if any, on sands and gravels in the expected ground water travel pattern, (7) dilution of the ground water upon entering public waters, and (8) maximum permissible concentrations in those public waters of the radioelements concerned.

First a few words on our particular local situation. The Hanford Works lies in south-central Washington in a basin of volcanic rocks traversed by the Columbia River as shown in Slide 1. The region is



Slide 1

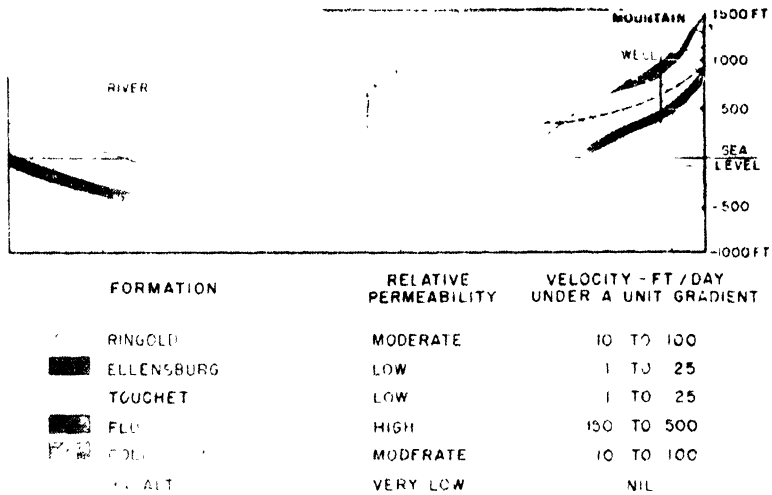

Slide 2. Typical geological strata at Hanford

characterized by quite low annual rainfall (less than 20 cm per annum) and by a water table with a relatively low gradient, resulting in part from the low rainfall.

Chemical-separations plants are located broadly in the centre of the slide, an area which is some 100 meters above the ground water table and at a distance of 13 to 16 km from the river, as the river follows this bend, which forms the base of the water table.

The location is rather uniquely favorable because the disposal points have an aspect bounded by the river over about 240 degrees, and by a ridge of quite impermeable hills over the remaining 120 degrees, so effectively we have a private basin in this area. The entire land area of interest for waste disposal is controlled by the Atomic Energy Commission.

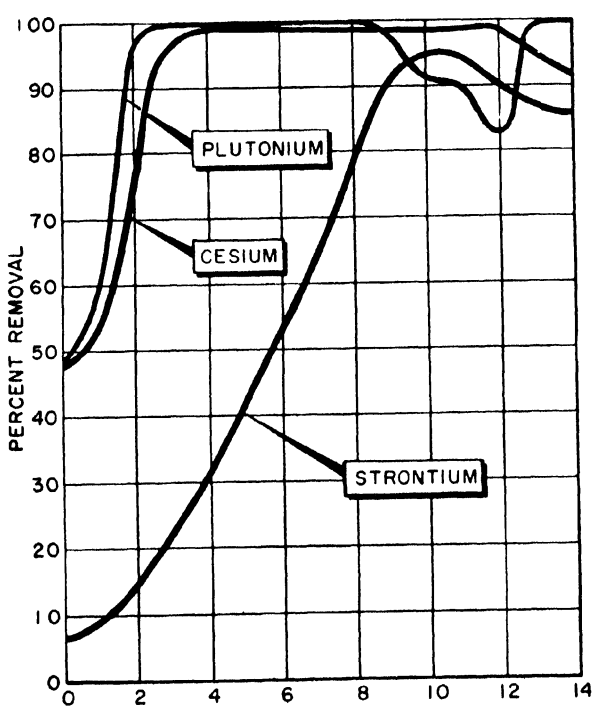

Slide 3. Equilibrium adsorption on soil

Slide 2 shows a cross-section of the typical geological strata at Hanford. The region is underlain by basaltic lavas of low permeability. These are overlain by a series of unconsolidated and semi-consolidated sediments consisting of lacustrine and fluviatile sands, gravels, silts and clays. The permeability of these structures ranges from low to high over the zone of interest.

The next few slides will indicate the work which we feel is needed in soil science.

Slide 3 represents the retention of three of the more critical materials (plutonium, cesium and strontium) in laboratory conditions on soil. A strong characteristic of our studies with the particular soil materials at Hanford is that plutonium, rather fortunately, is extremely well retained under almost all conditions. In looking at the plutonium curve, one finds a peculiar shape in the region of pH 10–12. This we feel is due to the existence of plutonium in various complex forms in this range. Also with respect to plutonium we feel that the difficulty encountered in the removal of adsorbed plutonium from soil by extraction with almost any plausible solution strongly suggests that in this case processes decidedly more complicated than the obvious simple ion exchange are involved.

Slide 4 gives similar data for various other elements. One of these, ruthenium, is to be regarded as of major interest. Again one finds the peculiar bumps in the region generally of pH 10 for all the materials mentioned here. Ruthenium has to be regarded with great suspicion. As we well know its chemistry is peculiar in our conditions. It can exist as a cation, an anion or as a neutral molecule, and the curve given here refers only to ruthenium existing in the cation form. One must study also the effects of cation concentration in these cases. Always the absolute adsorption increases with increasing solution concentration, but per cent absorption decreases and this must be measured in

order to choose the most favorable concentrations for disposal. One must do measurements for successive increments of these radioactive solutions to find what happens when more fluid is passed into a soil already contaminated by, say, last week's disposal.

In Slide 5 some work of that kind is included. The abscissa represents successive increments of cesium addition to soil up to 14 increments, each being 0.001 of the total exchange capacity; so if one thinks of the stage at ten increments if adsorption continued unhindered, we would reach the point which says 1 on the vertical scale. You see it falls slightly below that for a pure cesium solution. Then one must find out what happens with the addition of a wide variety of possible interfering materials. In this slide sodium nitrate is taken as such a material, and we find, going through the various curves a very marked reduction in the retention of cesium. All these factors—not only for sodium but for all reasonably interfering ions—have to be measured in all these cases. It is interesting to pass CO_2-saturated water through soil columns to find out what can be done in the way of removal of materials.

At least as important as retention measurement is a study of processes that could subsequently release materials adsorbed on soil. The cation exchange mechanism is, of course, dynamic at all times, and is reversible. We have examined such matters as removal of Cs, Sr and Y by leaching with acids, salts and water. Removal by acids can be rapid and complete. Sodium quite readily displaces cesium, and cesium is also removed by CO_2-saturated

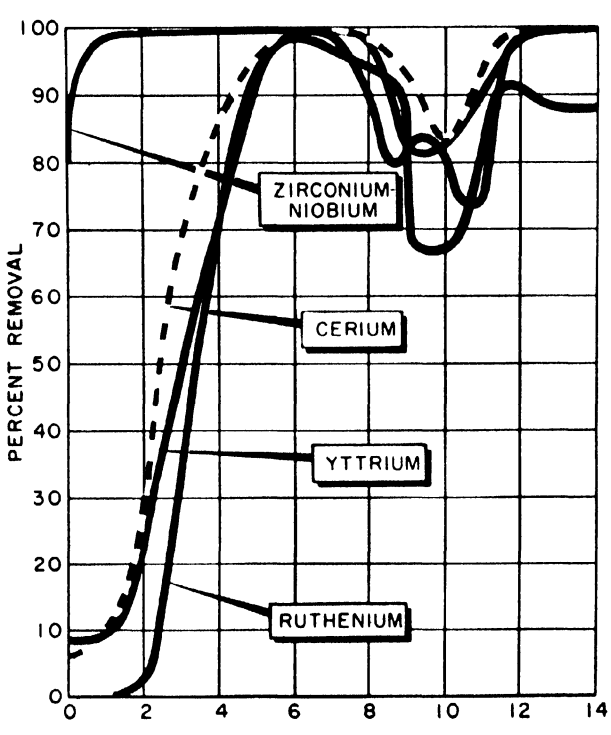

Slide 4. Equilibrium adsorption on soil

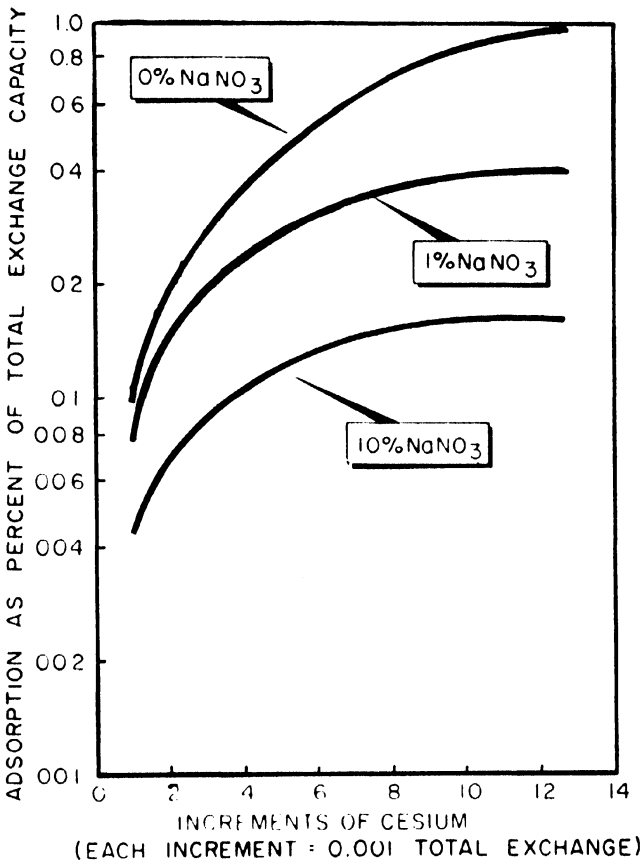

Slide 5. Adsorption of cesium by a Hanford soil

water, simulating percolating rain water. We find that 400 years of our local rain would remove 50 per cent of the cesium initially at 1 per cent saturation.

I have now a few notes about our field disposal practices. We use a variety of methods and devices, all of which are conventional.

For disposal of unusual waste of a non-recurrent nature we use a simple trench as shown in Slide 6. We dig the trench, pour in the liquid, cover the whole thing up with soil kept for that purpose, put a label on the top and forget about it.

Ponds are fine devices for large volumes of waste which are normally not contaminated at all, but which may from time to time have a small amount of accidental contamination. A pond with

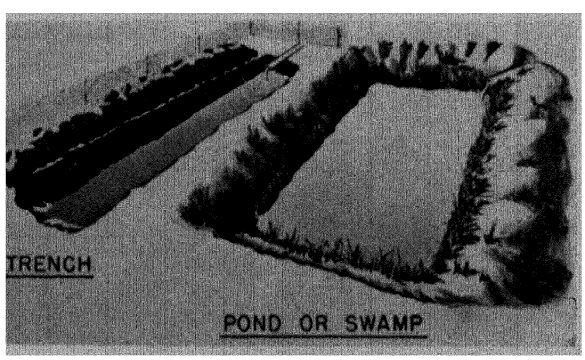

Slide 6. Typical ground disposal facilities

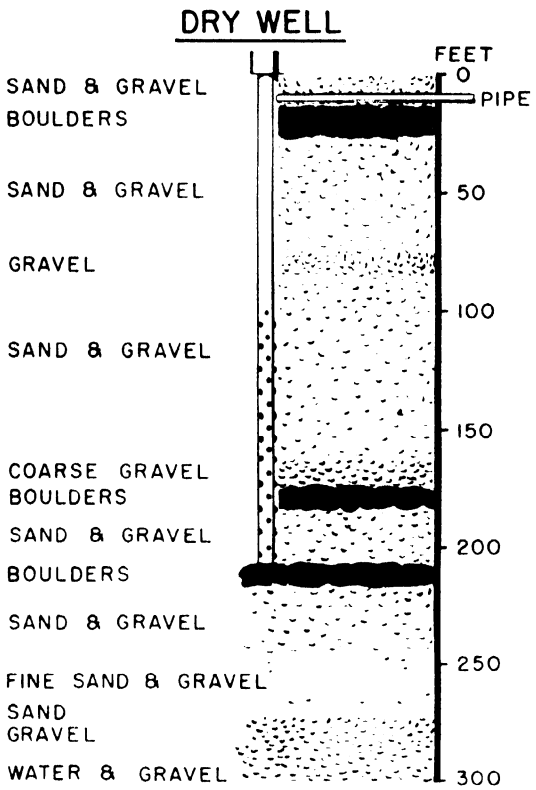

Slide 7. Typical ground disposal facility

a fluctuating level is dangerous, because then the dried sediment around the edge is picked up by the wind and we have to chase it through the whole meterological system.

We have experimented with dry wells or reverse wells (see Slide 7), but this is a bad method, because the natural protection of the long path to ground water is by-passed.

Slide 8 shows a widely used facility in our practice, the so-called crib, an open structure into which liquid is poured. It is necessary to determine the capacity of this system to take a given flow rate and to engineer it accordingly. On the right is shown the tile field, which comes into play only if we have miscalculated the percolation rate or if, as sometimes happens, the crib changes its properties and becomes blocked up.

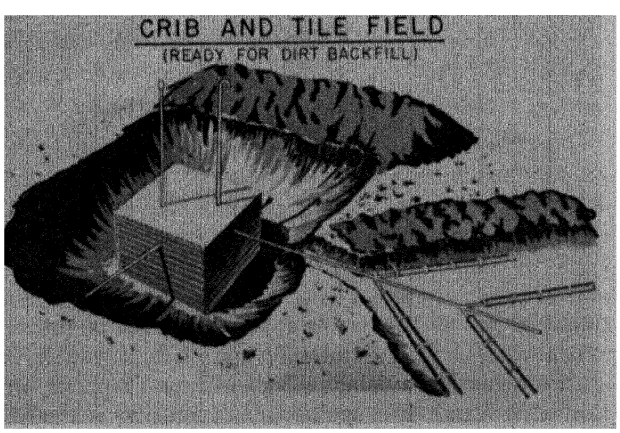

Slide 8. Typical ground disposal facility

Slide 9 shows a device which we have found to be most favorable for large-scale disposal. It is simply a bed of rock, the whole covered with an impervious layer so as to minimize leaching by rain later. Test wells are drilled around crib facilities to determine the distribution of the radioisotopes in the soil. Sampling of the sediments provides information on both this pattern and the detailed composition of the strata encountered.

A typical example of such a pattern showing the differentiation which occurs between individual isotopes is given in Slide 10. In general, it has been found that ruthenium is the most mobile radioactive ion, with cesium of interest because of its long half-life and intermediate mobility. We find that we can get the leading front in all cases by a purely chemical determination of nitrate concentration, which must be a great disappointment to the radiochemists.

Waste streams to the ground are generally limited by the ion exchange capacity of the intercepted soil column. In several cases it has been possible to remove specific hazardous radioisotopes such as Sr^{90} and Cs^{137} from the original liquid and thus produce a waste suitable for ground disposal from one which would otherwise require storage. Dilution of waste before disposal is contra-indicated. There is a tendency for engineers to specify a concentration limit for a waste, and if a waste which is offered to you has five times that concentration you are apt to dilute it to get the concentration which is laid down

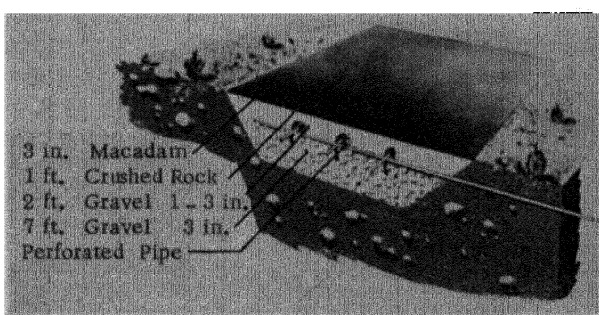

Slide 9. Typical ground disposal facility, cavern

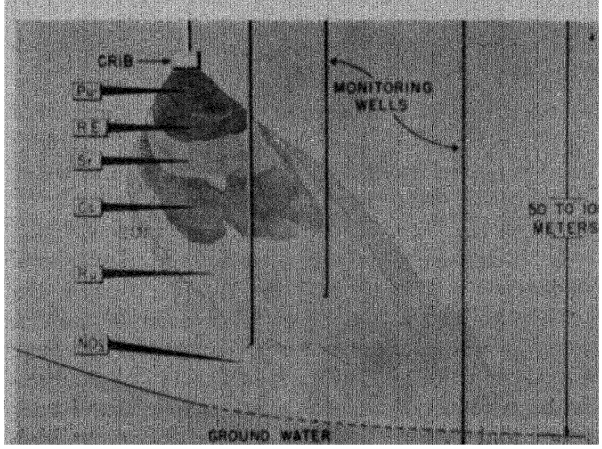

Slide 10. Ground storage of wastes

in the textbooks. This is the worst way to approach a disposal problem of this kind; it is always better to keep the volume as small as possible and use high concentration, because although the percentage at any one point in the soil may fall by the dilution method, the total retention will always increase.

Ground water contamination patterns detected around experimental reverse wells provided a valuable index to the rate of movement of the ground water in the disposal region. The movement rate as estimated from adjacent monitoring wells for this pattern was of the order of 7 meters per month. This estimate was later confirmed by measuring of patterns indicated by nitrate and other ions not readily retained by soil. Ground water movement in the disposal region was influenced by the changes in gradient induced by the formation of ground water mounds from the very large volume disposal of non-radioactive cooling water in surface ponds. These mounds, which have reached elevations of 20 meters above the normal water-table, are located around the periphery of the disposal area and have flattened the natural gradient in this region. These mounds have had a profound effect on the direction as well as the rate of local ground water movement and provide a controlling factor in the location of new disposal sites.

Investigations of the regional ground water movement and permeability of soil have indicated the presence of ancient river channels which provide possible avenues for accelerated movement to the river. Relative ground water velocities at various points have been obtained by measuring the rate of dilution of electrolytes in individual wells, together with conventional drawdown tests. The ground water movement time from the separation plants to the river depends on the disposal location with respect to the ground water mounds. Present estimates of the minimum time of movement are of the order of fifty years. We believe that we shall have no trouble for several hundred years, but our calculations are made on a 50-year basis.

The original practice of ground disposal was considered to be a temporary reasonable expedient. With the body of hydrological and soil science information developed, we now feel that an intelligent management of ground disposal is possible. Release is controlled ground storage rather than uncontrolled disposal. The basic policy is to avoid ground water contamination. If this should occur with short-lived isotopes, no harm is done. We load up a soil column until it is on the point of breaking through the water table and then seal the top.

Because Ru^{106} conveniently leads the more dangerous Cs^{137} and Sr^{90}, its arrival can be used to signal abandonment of a disposal facility. New ones can be safely built at a spacing of 50 or even 30 meters.

Process waste streams placed in ground storage are those remaining after most of the fission products have been removed and routed to underground tank storage, and include low salt condensates from high activity waste volume reduction steps, condensates from self-concentration of stored wastes, moderate activity density supernatants from the later stages of the separations processes, and dilute solutions resulting from process leakage and process equipment decontamination operations. Each such stream proposed for ground disposal is evaluated to determine the chemical and radiochemical composition, and the retention capacity of the proposed disposal site soils for the waste.

The permissible volume per unit cross section of soil column is prescribed from these data. We can say that about 10^{11} liters of essentially non-radioactive water has been released in this way, and 10^{9} liters of radioactive wastes containing several hundred thousand curies of fission products. That is our experience for the last ten years.

Mr. C. A. MAWSON (Canada) presented paper P/12 and read the text. At the end of the written paper he added the following:

I will now add a little information on later drillings since the paper was written. Drillings have been made further into the swamp in the bottom [illegible] corner (see Fig. 1 of P/12), and a radioactive layer has been found at a depth of 40 feet actually in the swamp. The contamination factor, however, is very very large indeed. This radioactive water was giving only about 50 counts per minute per millilitre, but nevertheless there was no trace of this either in the trees or in the shallow bore-holes. The 40 foot bore-holes, however, did give evidence of this, and as an example of the very great variation in conditions of the ground water and sub-surface soil, I might mention that a bore-hole was made only about 10 metres away from the one which struck radioactive material, and this one gave us an artesian flow. Now this is an illustration I think of the detail into which one must go in order to arrive at an accurate idea of what is going on underneath the ground. In planning disposal areas it is essential that they should be investigated in quite considerable detail, especially where one is dealing with rocks, such as limestone, which are permeable, or rocks which may contain fissures, or areas in which one can anticipate laminar distribution of gravel and this kind of thing. It is no good just taking a look at the surface of the ground and hoping to get very much idea of what is going on underneath.

DISCUSSION OF P/565 AND P/12

The CHAIRMAN: These two papers, although the subject has been the same—that of pouring radioactive materials into the ground—have described quite different situations. On the one hand, Mr. Parker's paper has involved the putting of radioactive materials into the ground where they cannot possibly get to the water table, and this is indeed a most conservative and safe approach if you have such a situation available. Mr. Mawson's paper, on the other hand, has spoken about putting materials directly into the water table. I do not think it is

the intention at Chalk River to continue this practice indefinitely until we know what is the result. It is in fact a large tracer experiment which was forced upon us at a time when the only alternative was to put it into the Ottawa River, and I think everyone will agree that it is far better to put it into the ground than directly into the water supply, which you would not like it to reach.

Mr. S. B. MORRIS (USA): Our area is one with a large amount of ground-water development, in which we have had half a century of detailed experience in spreading water on the surface or spreading water in wells to increase ground water replenishment, and in connection with that we have found the surface application of the water most effective; but it does require the cleaning of the surface area by scarifying to maintain the percolation rates. In putting water underground by wells we have found it necessary to filter the water and also to chlorinate to prevent growths taking place within the gravels which restrict the percolation rates. We have had a number of rather serious samples of contamination by toxic wastes since the area has become heavily industrialized, by such matters as chromium and that coming from chromium plating works, and also from phenols which have shown a rather extensive movement in the ground water basins. I mention this along with the fact that there is going to be an ever-increasing demand upon ground water represented by two fundamental elements: first, supplemental irrigation of crops, such as we see in Geneva during the summer period, mostly by individual development of ground water, and secondly by air-conditioning demands, so that it is very important that ground water should be adequately protected in anticipation of its subsequent use.

Mr. C. N. WATSON-MUNRO (Australia): I would like to ask the Canadian representative about the question of black flies and things which the black flies live on when they are not living on the scientists at Chalk River, and whether they have carried any substances from the burial ground elsewhere.

Mr. MAWSON (Canada): I will answer that question in a rather more general field than that of black flies. In general we have done extremely detailed ecological investigations of living creatures of all kinds around the disposal area and around the river, and we can say that there has been no appreciable contamination of livestock of any sort in the area—nothing which is significant. There has been activity detected in the river to about four miles down river, but these have been totally insignificant amounts. You must remember that in our liquid disposals into the ground we do not have the conditions which were described by Mr. Parker; we do not have standing water to any very geat extent, because this stuff disappears into the sand very quickly, and we do not have a condition in which there is a swamp with a lot of vegetation growing round it and wild fowl feeding on it. We do have ponds which have minute amounts of activity where frogs live, but the animals and fish which we have been able to investigate up to now have not been radioactive in the sense that they can be any danger at all to anybody or anything.

Mr. E. GLUECKAUF (UK): Both Hanford and the Canadian station at Chalk River are in the fortunate position of being very far away from inhabitated areas and, in order not to get a completely wrong conception of the picture in highly populated countries, I should like to say that, although we have given considerable consideration to the problem of soil disposal, we have at Harwell not come to the conclusion that we know sufficient about the movement and the reaction taking place in the ground for us to consider disposing of substantial quantities of radioactivity in the ground. I think the situation which we are planning is more in the nature of the treatment of solutions which will remove everything from radioactive materials by ordinary conventional water treatment, except things like strontium and perhaps ruthenium, and then placing these solutions into large prepared beds of clay or green sand materials which are not free dispersers but which are contained in large concreted containers, so that there is still the possibility of looking at the effluent which comes out from these materials. This is more or less a controlled ground disposal where the ground is brought especially to the station and eventually may be left, after contamination, in the particular position in which it has been deposited. It is now done largely in containers underground so that the ground can be covered over at a later date, and no futher influx of water will take place.

Mr. K. Z. MORGAN (USA): I would like to say that in our area for the past ten years we have been experimenting in the disposal of fairly high-level radioactive waste in open ponds, and we find that, if the area can be carefully monitored with wells, this seems to be one of the most promising methods of disposal. We have disposed of many thousands of curies of contamination, mixed fission products, and we found our type of soil (red clays and shales) very efficient in the retention of this contamination. We believe that if you have accurate monitoring systems to keep track of the movement of the contaminants in the soil, this is a much better and more promising method of disposal than retention in underground tanks, where you may be subject to failure at a later date. I would like to say also that at present in connection with our extrapolation into the future we are much interested in this as a possibility for the disposal of waste from reactors used for fuel. Under such circumstances you have a new problem injected, and that is that there would be enough energy in the fluid operating to bring it to the boil and to boil the fluid to dryness and, by our calculations, to melt the soil in the immediate neighborhood. We are looking into this particular matter and we believe that this, too, offers a great

deal of promise for the disposal of radioactive wastes associated with power plants. In such cases the material becomes fixed to the rock as the soil cools, and then the problem is one of air-contamination at these higher temperatures.

Mr. PARKER (USA): I want to make it clear that we do not dispose of significantly contaminated material in open ponds. We use such ponds for waters in which there is a very low probability of contamination, recognizing that from time to time very small amounts have been released by that method. But the main disposal facilities are built anywhere from three to six meters underground, this being necessary because if one miscalculates the percolation rate the water can be forced upwards and get into the root systems of plants, and three meters is the minimum and five meters probably the reasonable depth for disposal facilities.

Session 23B.2

DISPOSAL IN THE SEA

LIST OF PAPERS

		Page
P/418	The discharge of radioactive waste products into the Irish Sea. Part I: First experiments for the study of movement and dilution of released dye in the sea ..... H. Seligman	701
P/419	The discharge of radioactive waste products into the Irish Sea. Part 2: The preliminary estimate of the safe daily discharge of radioactive effluent ..... H. J. Dunster	712
P/420	The disposal of waste products in the sea. Part 3: The experimental discharge of radioactive effluents ..... D. R. R. Fair and A. S. McLean	716
P/569	Disposal of radioactive wastes at sea ..... C. E. Renn	718

The Discharge of Radioactive Waste Products into the Irish Sea

PART 1. FIRST EXPERIMENTS FOR THE STUDY OF MOVEMENT AND DILUTION OF RELEASED DYE IN THE SEA

By Henry Seligman,* UK

Before the erection of an atomic energy production plant on the coast of the Irish Sea, it was essential to make an estimate of how much radioactivity could be disposed continually into the sea without danger to the neighborhood or to animal and plant life. Therefore experiments were undertaken which should establish the order of magnitude of radioactivity which could be so disposed and give the length of the necessary pipeline for this discharge into the sea. At the same time the influence of the tide and weather conditions for discharge had to be investigated. The purpose of the experiments could be summarized as to study: (1) the movement of effluent released at a certain time into the sea under various conditions of tide and wind; (2) the dilution with time of the released material; and (3) the changes in 1 and 2 when the release takes place at different distances from the shore.

Not enough data were available to establish a reliable theory to determine the movement of effluent and rate of dilution after discharge. However, details about tidal streams on the Cumberland Coast were available from which it could be deduced that a floating object would move around a narrow ellipse of between 3 and 6 miles long during a tide. It was likely that the ellipse would be almost parallel to the shore. For a number of reasons superimposed motions were expected, but this information was too inaccurate and it was decided that large scale trials should be undertaken.

Radioactive material was not available in large enough quantities at that time to make such experiments and, quite apart from it, even if available, could not have been used, in order not to prejudge the issue under investigation. Therefore it was decided to use a dye as tracer. An estimate showed that one ton of dye would be needed for an experiment if the sensitivity of determination was of the order of 1 part in 10^9.

After preliminary experiments fluorescein was chosen as it had a high enough sensitivity for detection, could be easily matched and measured against standard solution and was readily and cheaply available. The main disadvantage was the fading of such a solution under the influence of sunlight, but it was thought that following up of an experiment for 12 hours would give sufficient data. The experiments could be done at night and the fading effect was therefore not a serious drawback.

The site was the West Cumberland Coast and the experiments extended over 14 miles along that coast. The distance between the high and low water marks was between 300 and 500 yards along that coast. the main disturbances of the water flow were caused by the rivers Ehen and Calder entering the Irish Sea in the experimental area.

The fluorescein dye solution was released by one of the ships during the evening hours and after certain time intervals the ships steamed slowly through the dye patch, sampling the water continuously. Near the coast where the water was too shallow for the ships to operate, dinghies were used for the sampling. All ships and dinghies were plotted by radar based on shore and a telecommunication system was installed in all ships. Aerial photographs were taken during a number of the trials.

The ships were motor fishing vessels of the Royal Navy (see Fig. 1). They had a displacement of 150 tons and were run by diesel engines with a maximum speed of 10 knots and a minimum speed of 3½ knots. The three motor fishing vessels were slightly modified for the experiments. Each had a sampling boom attached to the bow with the help of which it was possible to suck in sea water continuously from three



Figure 1. H.M.S. Toiler and M.F.V. 1555 in Queens Dock, Whitehaven

* Atomic Energy Research Establishment, Harwell, Berks, England.

different depths (1 ft, 6 ft and 12 ft). The sampling boom could be raised and lowered for entering the harbour. The water was pumped through polythene tubes by self-priming pumps which could deliver a thousand gallons per hour with a suction lift of 25 ft. The pumping rate was so high that the time from the entry of the sample into the boom to the entry into the sampling bottle was only five seconds which corresponded to less than 10 yards at the slowest speed of the ships. Fifteen samples could be taken every two minutes which corresponded to a set of samples from the three mentioned depths every 40 yards.

The ships were also fitted with a small laboratory where the samples were analysed. This was done by comparing the samples under ultraviolet light with standard solutions. All equipment was fixed as the motor vessels occasionally rolled considerably. One vessel did all the dye releases and was adapted so that two fuel tanks could be used to hold 10 tons of solution which in our case was a concentrated fluorescein solution having the same density as sea water.

The position of the ship was determined by radar to an accuracy of $\pm$ 10 yards at distances up to 10,000 yards, and so the samples taken at certain times could be correlated to definite positions. The course of all three ships was plotted in turn every 90 seconds.

The experimental procedure was as follows:

12-oz blocks of fluorescein were dissolved to give a 6.7 per cent fluorescein solution and 10 tons of this solution was transferred by a road tanker to the harbour and the tanks of one motor vessel filled with it. The vessels had to steam out of harbour at high tide, usually in the afternoon or early evening. Then radio contact was established with the shore, the clocks synchronised and special weather broadcasts were given which were prepared specially for these experiments for this area.

The dye discharge ship went then to the releasing point chosen and the solution was discharged into the sea with the help of a pump. The discharge time varied between 15 and 20 minutes and the course of the ship was plotted during that time by radar. After that one motor fishing vessel kept sight of the dye patch by using a search-light, and before each sample run started, flares were dropped around the perimeter of the patch and then the vessels were ordered into position for the sampling run.

Usually the patch was cigar-shaped and one vessel sampled along the main axis of the patch, whilst another one crossed several times the patch at right angles. The third ship usually took "deep sea" samples just outside the visible surface patch as special sampling apparatus had been constructed for this purpose.

Samples were usually analysed in the periods between two sample runs, and each ship had a crew of three for this purpose on board, two scientists and one deck hand. Up to 150 samples were obtained during one sample run. In most cases the samples had to be diluted with sea water before they could be checked against the standard solution. The sample runs were made at certain intervals throughout the night and even during the following day as long as measurable concentrations of fluorescein could be seen before the sunlight would fade the dye.

There are too many results to give them all in detail here. The general results and conclusions are considered in the following:

Altogether eleven experiments were carried out, of which nine were dye releases from the ship and two were dye releases through a temporary pipeline built into the sea. The ship releases took place at various distances between 2100 and 5300 yards from the high water mark, in different weather conditions and at different stages of the tide.

The highest concentration observed was 10^{-4} of the original concentration. The movement of the fluorescein patch parallel to the coast was bigger further from shore. The highest concentration found on the shore was 10^{-5} on the day of release and 10^{-7} 24 hours after the release.

To evaluate the results iso-concentration curves were plotted for the three investigated depths, namely 1 ft, 6 ft, and 12 ft. In each run the following information was obtained:

The position of the area with the greatest concentration in relation to the point of release, the area where the concentration was higher than 10^{-9} of the original concentration and the maximum concentration observed. It had been theoretically predicted that the area in which the concentration was greater than C would be logarithmetically related to the concentration C. From this equation one could get three other quantities: (1) The calculated maximum concentration at which the area would be zero; (2) The area (b) the material would cover if it were all at the maximum concentration; and (3) The total quantity of fluorescein per unit depth ($b \times C_{max}$), when integrated over the known depth of the sea could be compared with the total quantity of fluorescein originally released.

As an example more detailed results are given for Test Series No. 10 in graphs giving: (1) details of the course of the ships during each run; (2) the iso-concentration curves for each run at the three depths measured; and (3) the logarithmic dependancy of the concentration C, versus the area where the concentration is bigger than C.

The movement of the patch which was observed was analysed for the trials, and it could be divided into the movements due to tidal streams and the movement due to the influence of wind. The values for the movement due to tidal streams agreed very well with the data obtained from British Admiralty publications. They gave a mean value for the tidal drift of 0.74 $\pm$ 0.8 as compared with the Admiralty value of 0.75 knots. The total movement was about 4½ miles, without taking the winds into account. The only available theory predicts that westerly

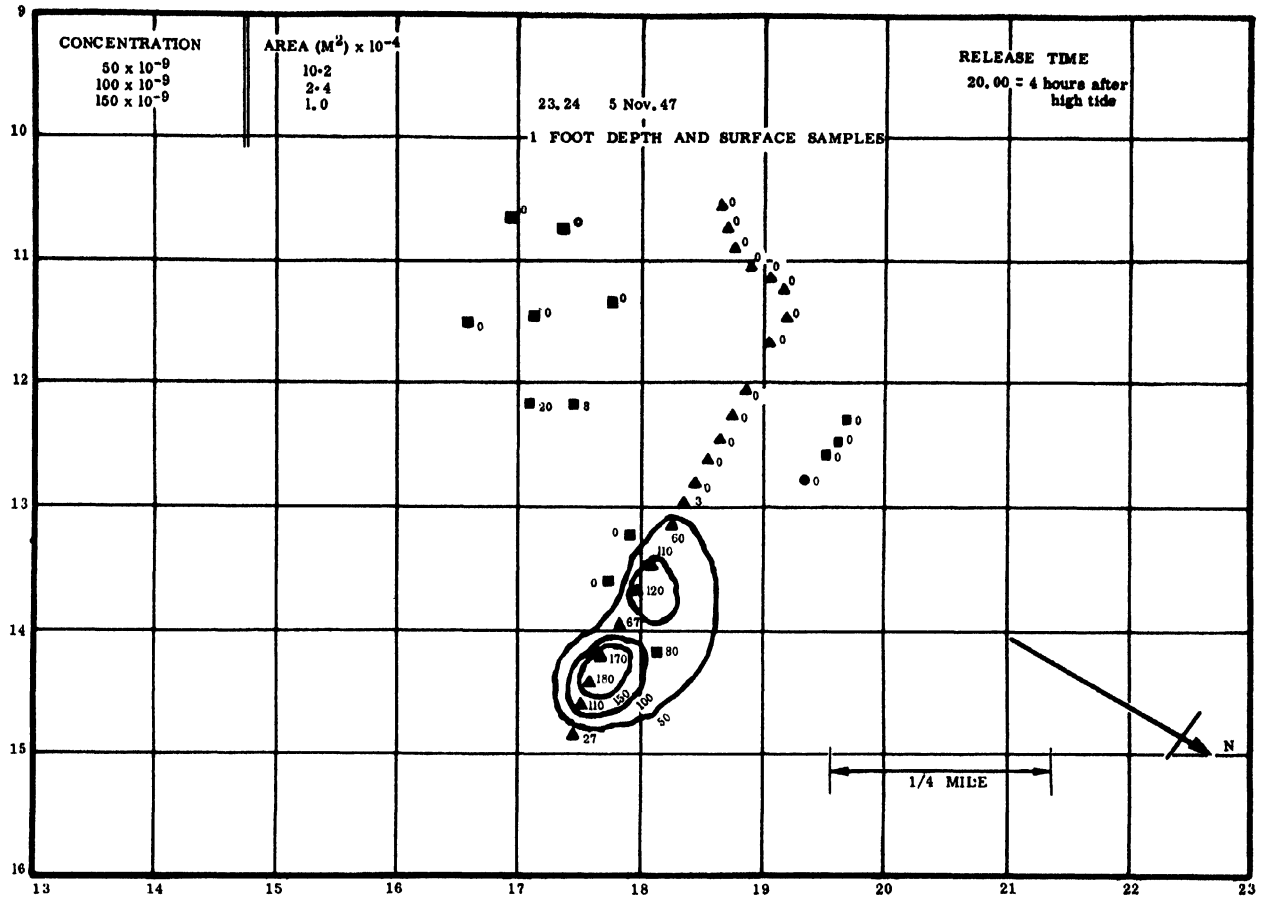

Figure 2. Test series 10, run 1

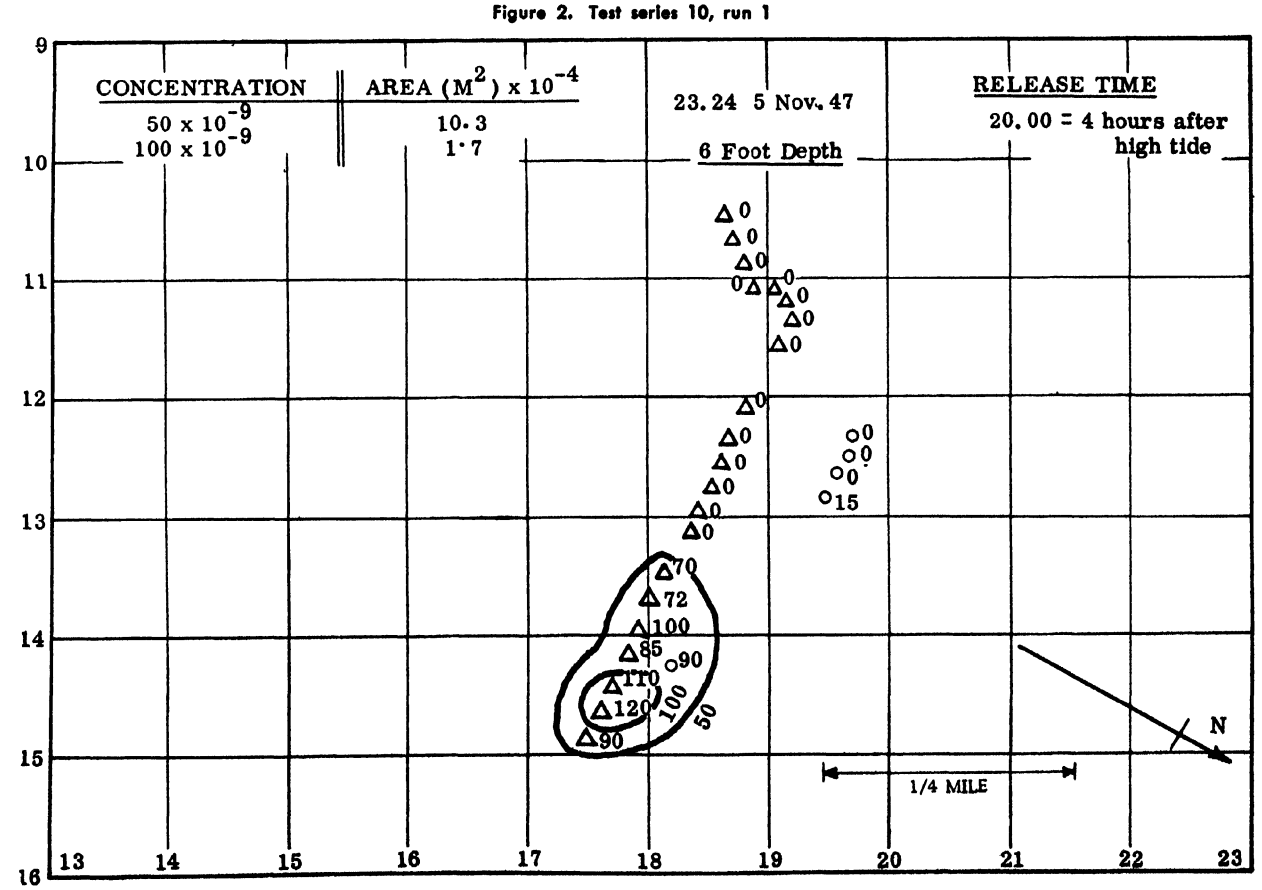

Figure 3. Test series 10, run 1

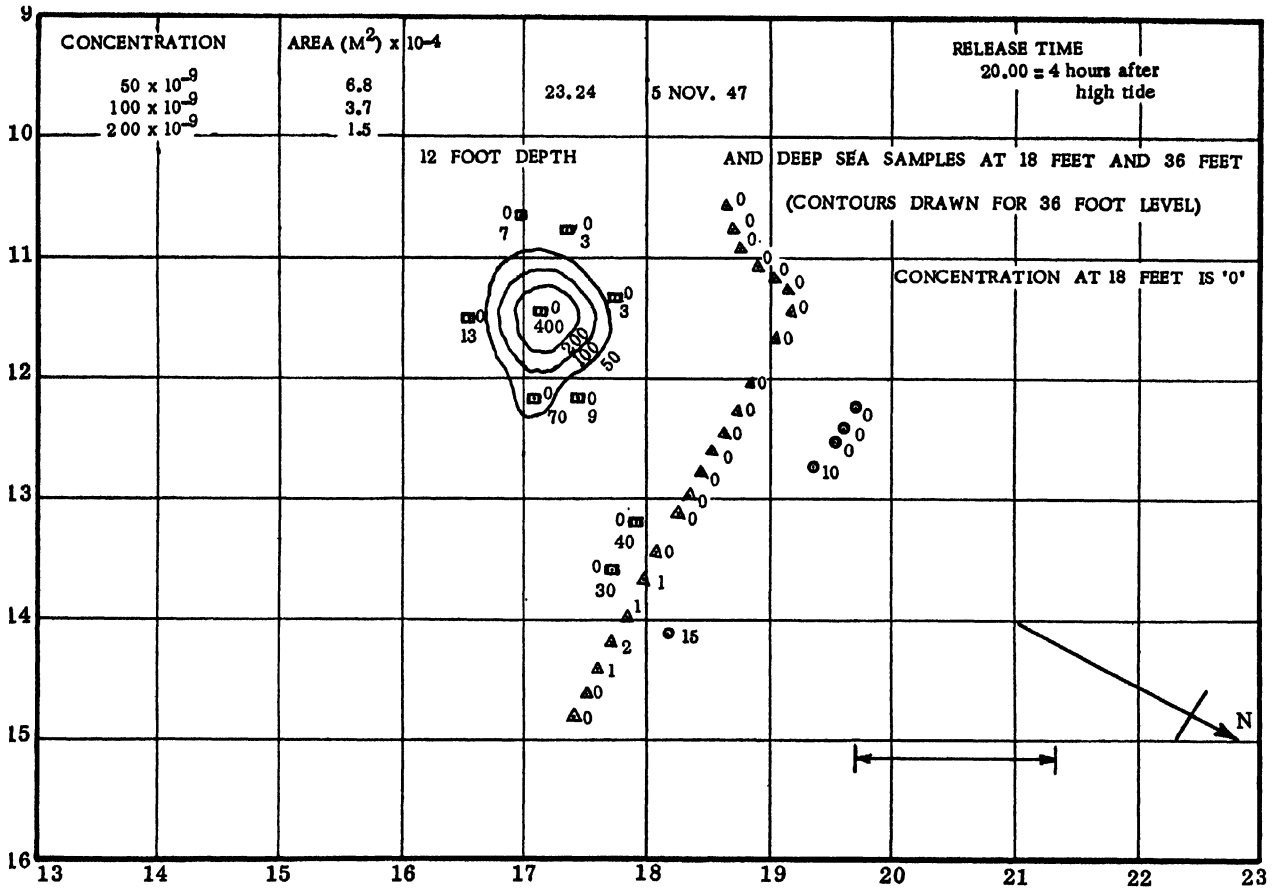

Figure 4. Test series 10, run 1

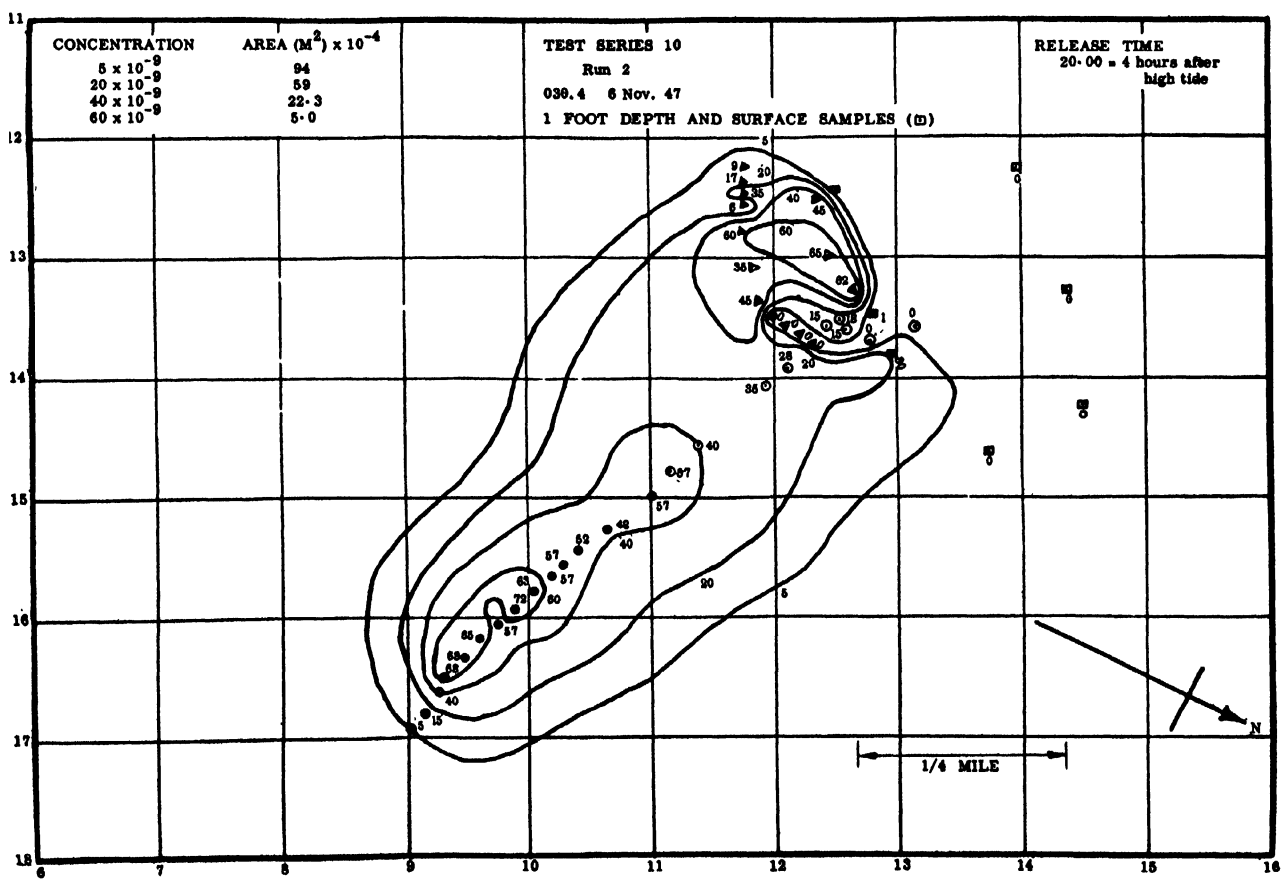

Figure 5. Test series 10, run 2

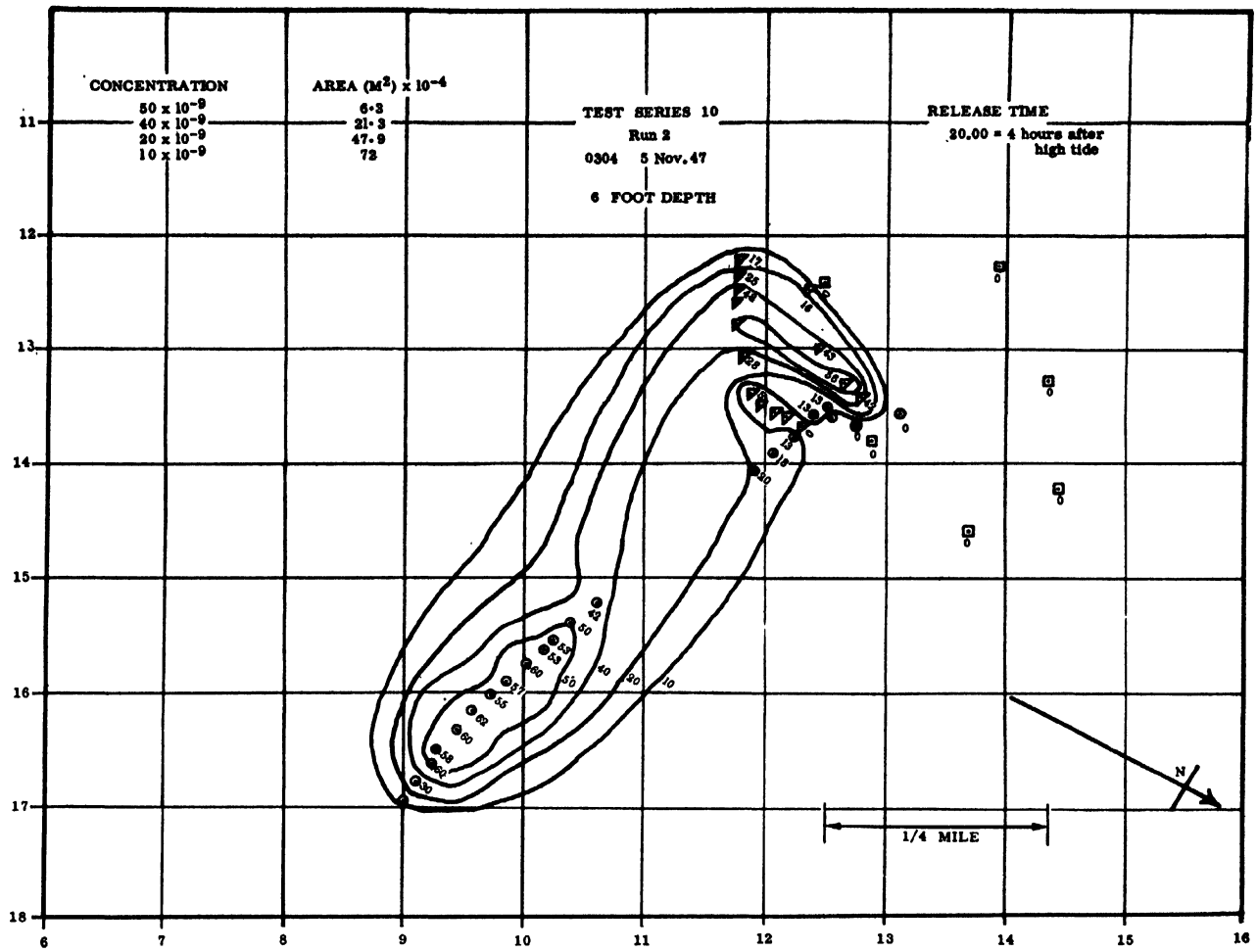

Figure 6. Test series 10, run 2

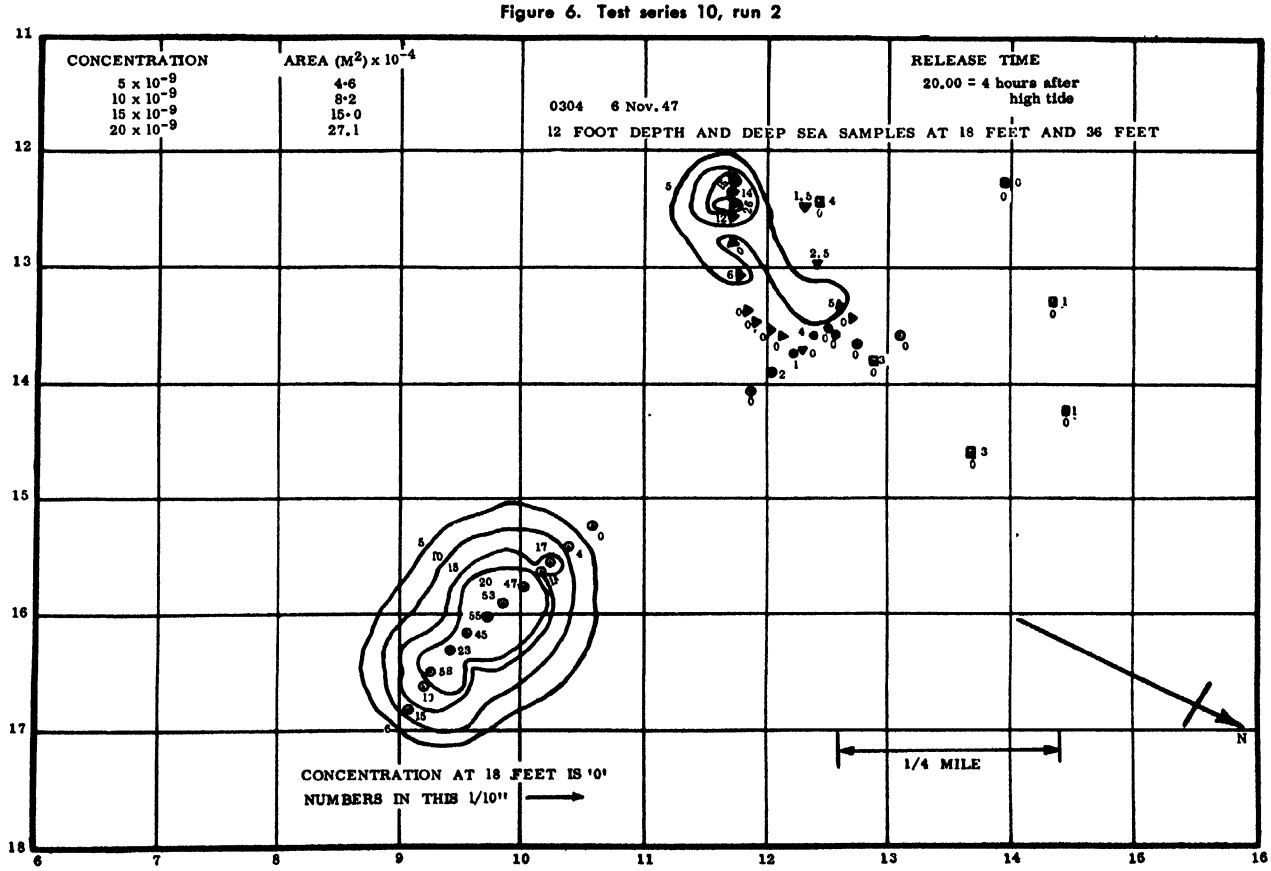

Figure 7. Test series 10, run 2

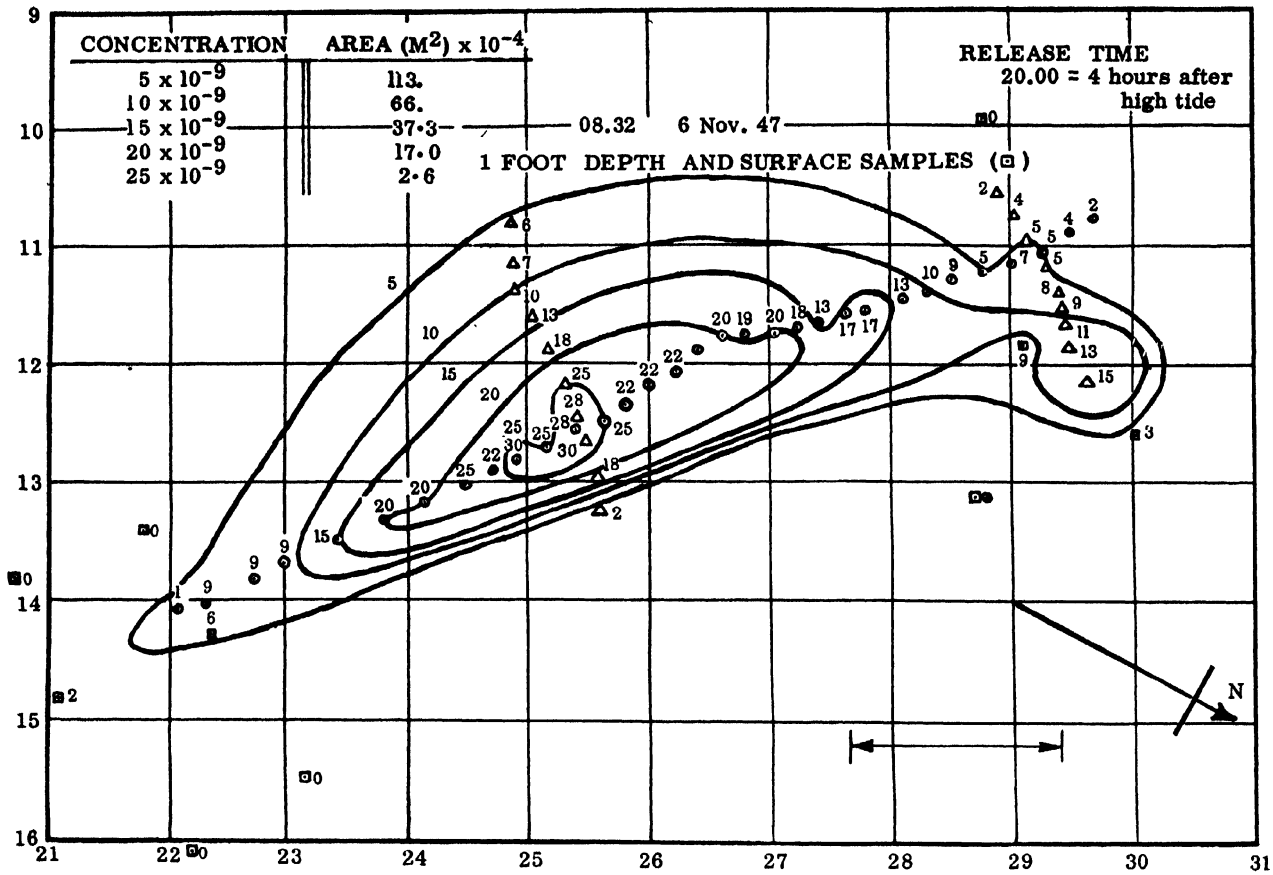

Figure 8. Test series 10, run 3

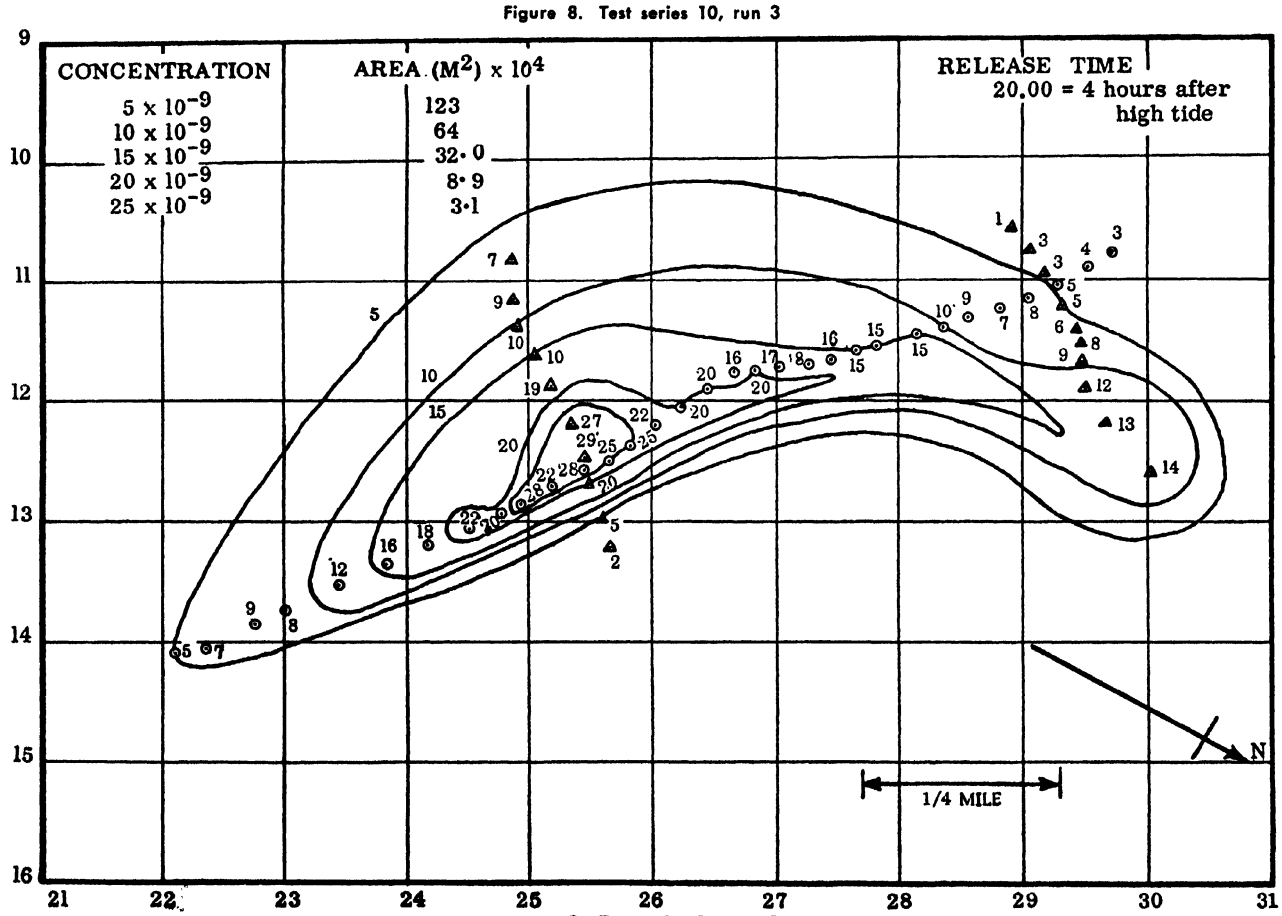

Figure 9. Test series 10, run 3

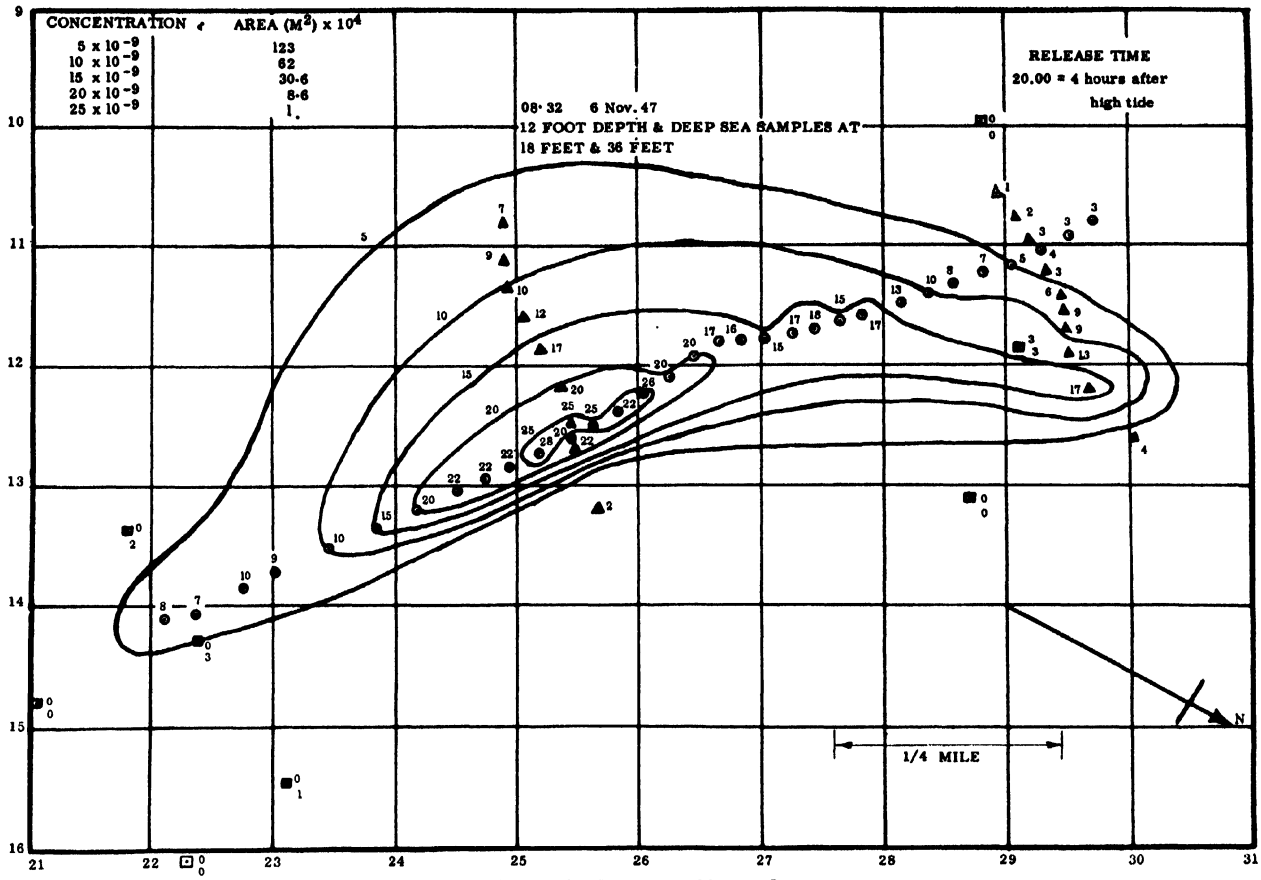

Figure 10. Test series 10, run 3

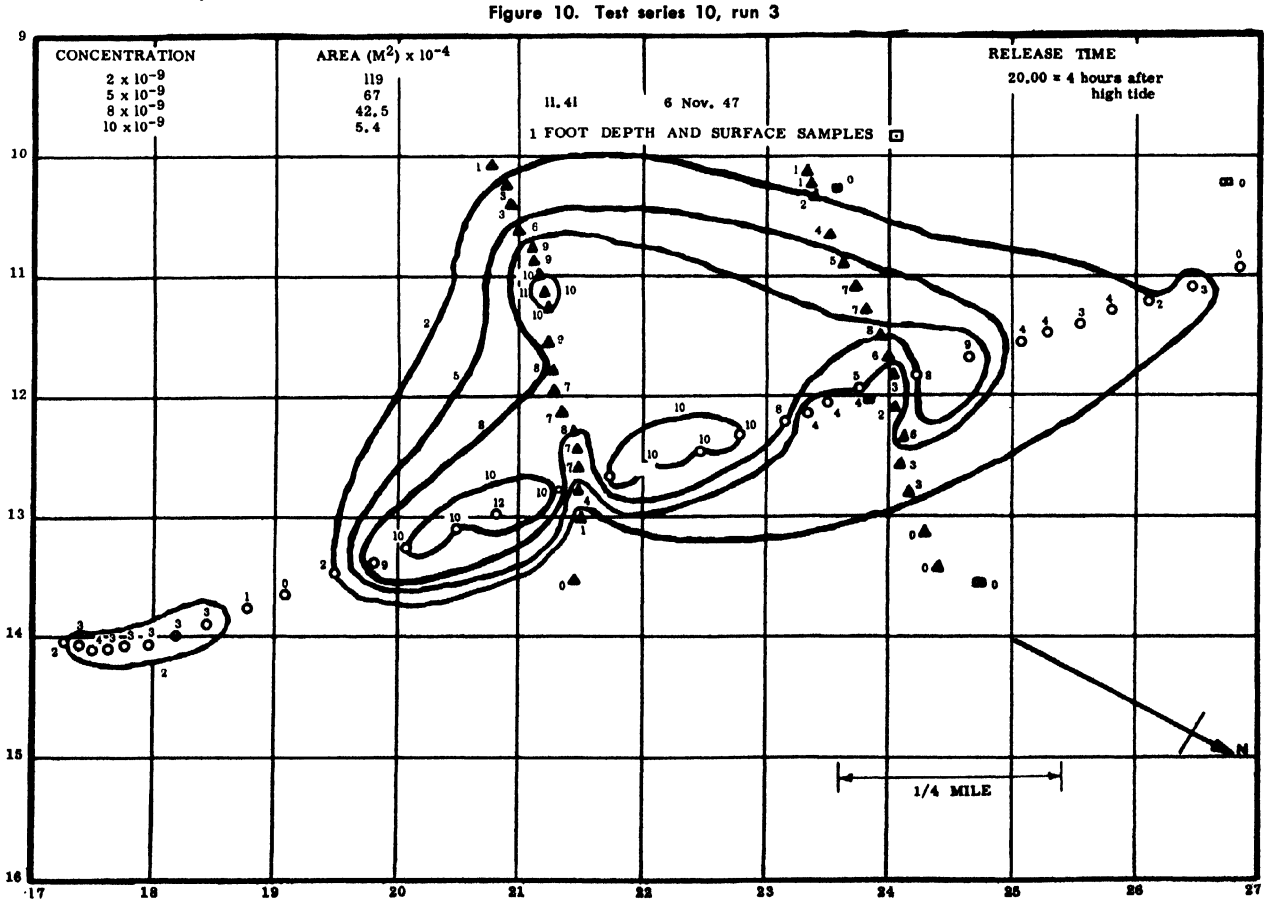

Figure 11. Test series 10, run 4

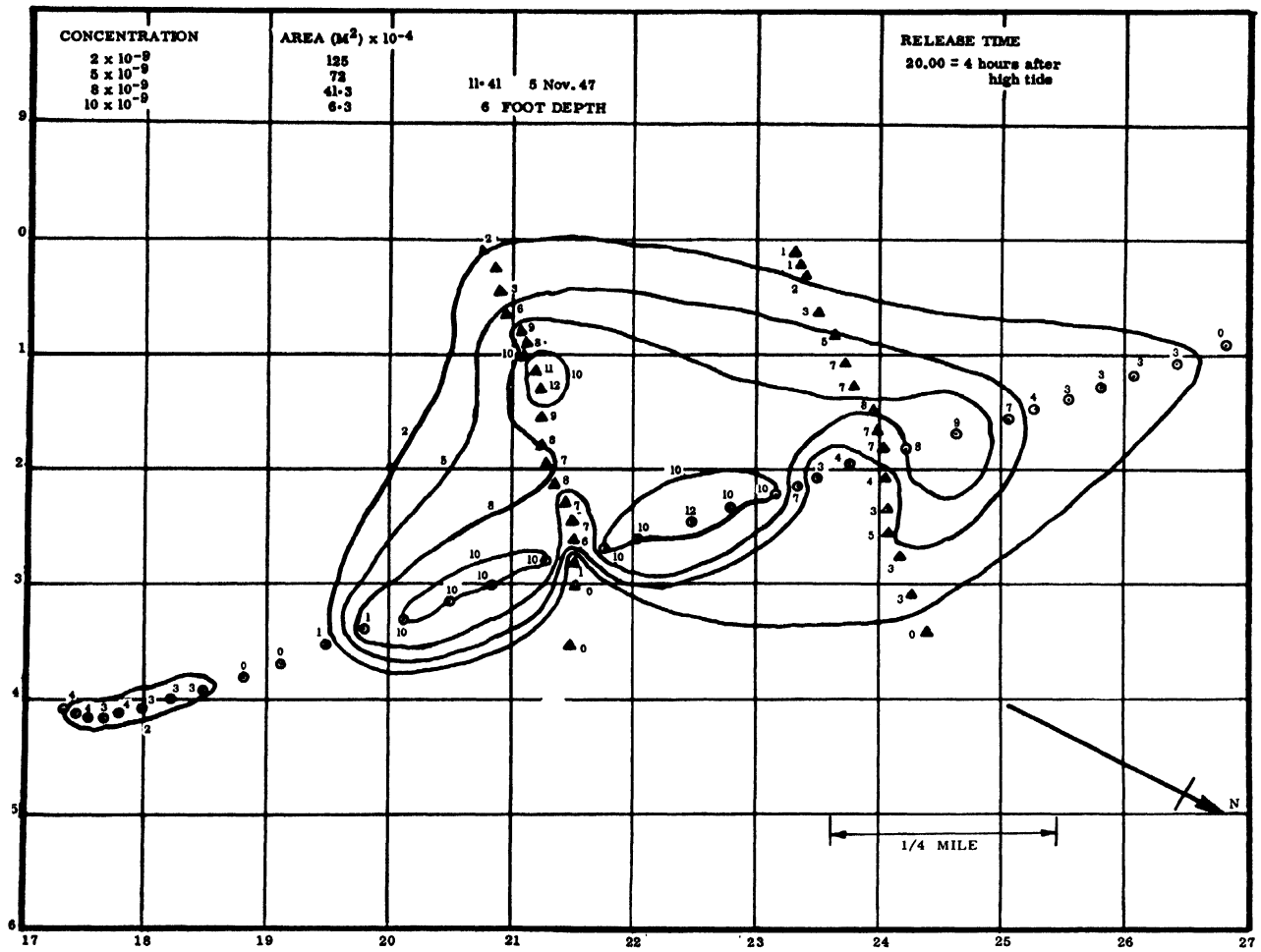

Figure 12. Test series 10, run 4

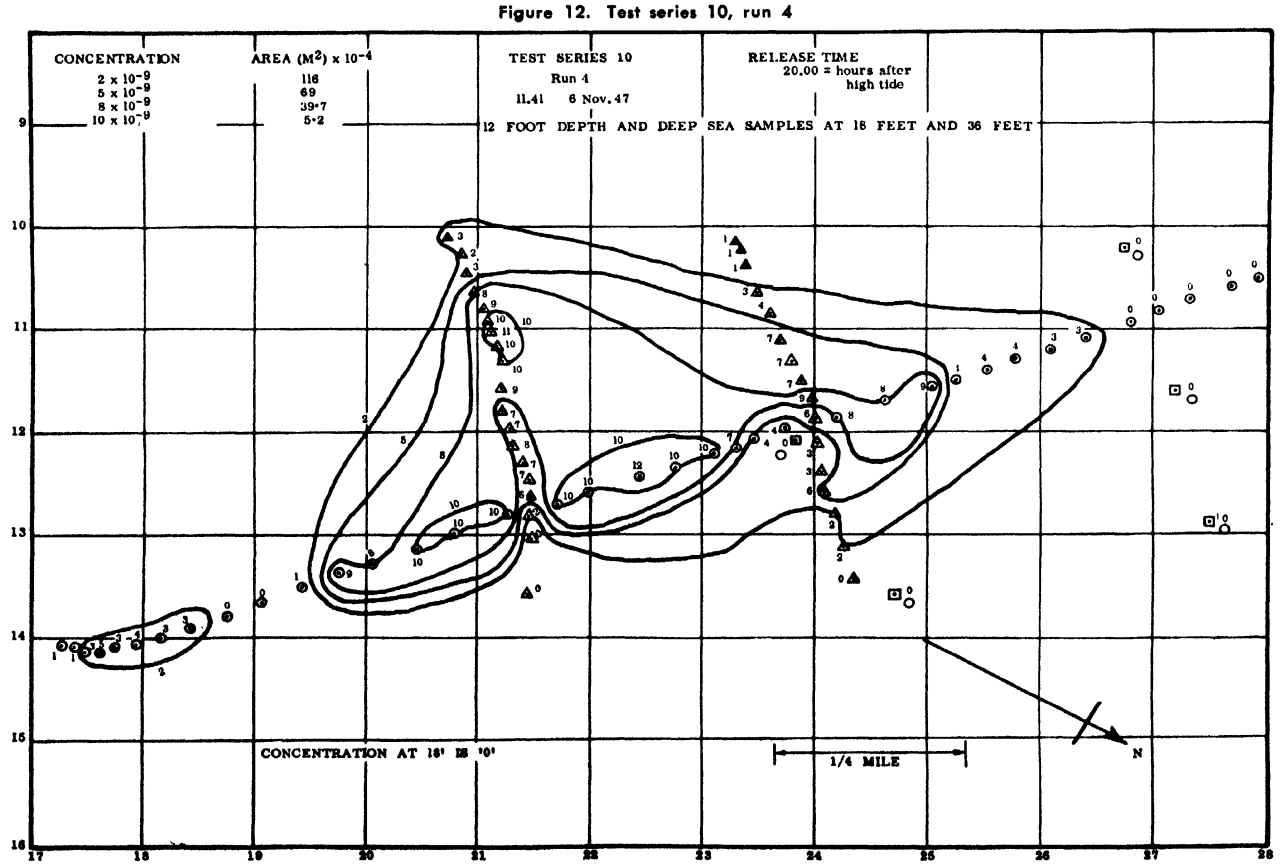

Figure 13. Test series 10, run 4

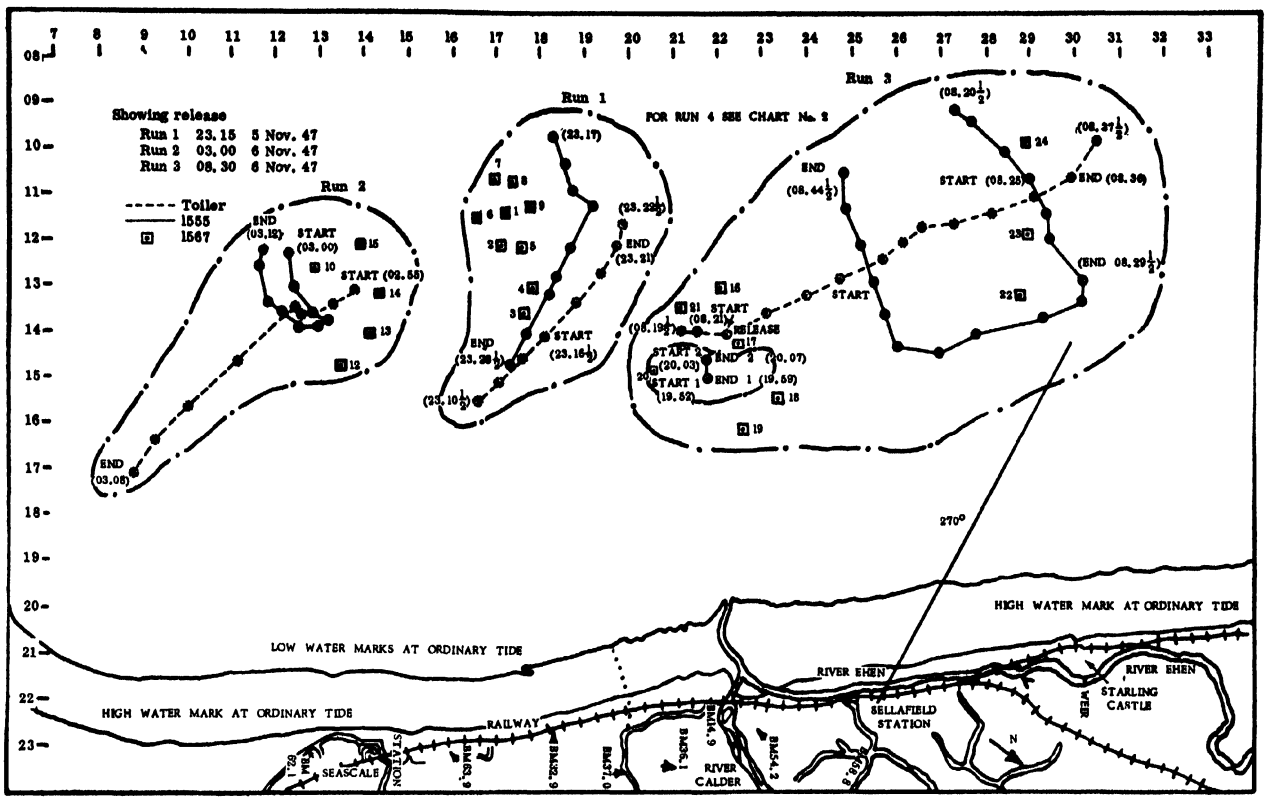

Figure 14. Test series 10, chart 1

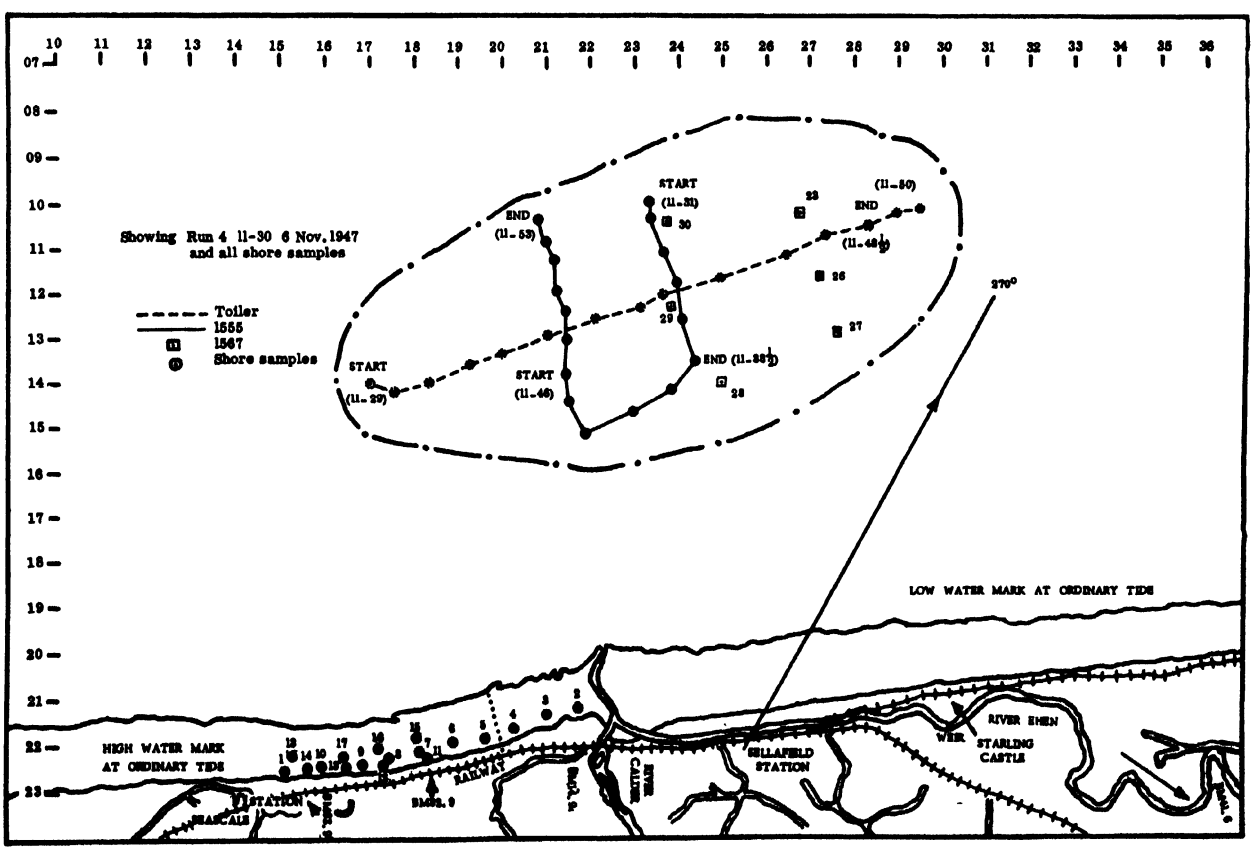

Figure 15. Test series 10, chart 2

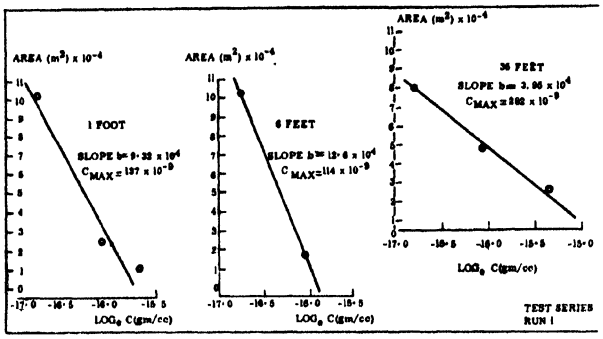

Figure 16. Test series 10, run 1

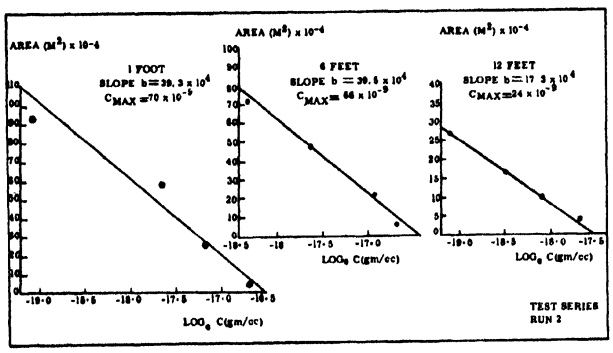

Figure 17. Test series 10, run 2

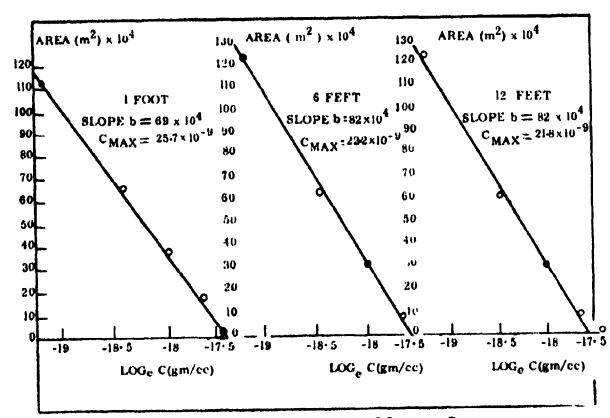

Figure 18. Test series 10, run 3

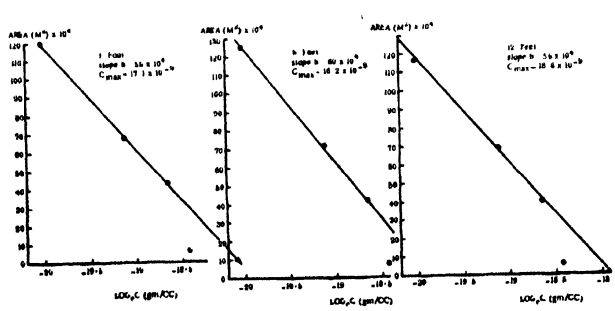

Figure 19. Test series 10, run 4

winds are expected to produce a southerly drift. However, in these trials we found just the reverse and an on-shore (westerly) wind gave northerly drifts and southerly drifts were only observed when we had east or southeast winds. The reason for this, according to Scott who analysed these results, is that the main assumption that we have an ocean of infinite extent is invalid as the trial area was most likely part of an eddy current. Therefore it was not possible from these trials to make any reasonable predictions of wind effects upon the movement of effluent, except to note the observations during the conditions encountered.

Scott's calculation, based on Taylor's theory of statistics of turbulence, predicted that the fluorescein after release should form an oval patch and he calculated that the area where the concentration is bigger than C should be related as follows:

$$A = 2\pi\sigma_x\sigma_y(\log C_{max} - \log C)$$

where σ_x and σ_y are the quantities giving the dispersion of the dye parallel and at right angles to the coast. No perfect oval patch was ever observed, and the distortion could always be attributed to the fact that, firstly, the dye was not released at one place, owing to the movement of the tide during the release, and secondly that some distorting eddy currents existed. But even in this distorted shape the area concentration relationship mentioned was valid.

$2\pi\sigma_x\sigma_y C_{max}$ is the quantity of fluorescein per unit depth and as no large change of concentration with depth was found up to the depth measured, it could be assumed that throughout an experiment the quantity of dye released divided by the depth of the sea would be constant. This was found to be approximately true in these trials. As C_{max} gets smaller with time $2\pi\sigma_x\sigma_y$ should increase. The decrease of C_{max} with time was as follows:

Directly after release: 10^{-4} times the original concentration

2–3 hr after release: 6×10^{-6} times the original concentration

9 hr after release: 10^{-6} times the original concentration

12 hr after release: 5×10^{-7} times the original concentration

15 hr after release: 4×10^{-7} times the original concentration.

However, the values of $2\pi\sigma_x\sigma_y C_{max}$ obtained from the graphs of area versus log C were consistently lower than the quantity of dye released, divided by the depth of sea in that area. In fact it was almost consistently a factor of 3. The reason for this could not be established.

By extending the theoretical treatment, Scott calculated the concentration that one might expect on shore from a continuous discharge of radioactive effluent of Q curies per second through a pipeline of various different distances. Due to the beforementioned discrepancy in the amount of fluorescein discharged into the sea and the integrated amount measured the data could be analysed in two different ways. One could either distrust some of the iso-concentration curves and put the emphasis on the value C_{max} or one could try to use the area b.

Table I shows the concentrations calculated on the assumptions that 100 curies per day are released and owing to bad weather conditions the activity may accumulate for 50 days.

Table I. Concentrations Based on Assumption of 100 curies per day, Accumulating for 50 days

Distance of point of discharge (yards)	*Estimated concentration (unit = 10^{-10} curie/litre)*	
	Calculation 1	*Calculation 2*
380	1020	310
660	430	150
1200	120	63
2080	19	22
3800	0.33	3.8
4660	0.03	1.6

In Calculation 1 C_{max} is the foundation for the calculation, and in the second the area b has been assumed accurate. Considering these two extremes one is up to 3800 yards from the discharge point still within a factor of 10 of an estimate which seemed to be good enough for these preliminary experiments. By establishing these figures and having had the most difficult weather conditions it was thought that no further trials were required, although these trials were originally only intended to be preliminary ones. The effluent pipe was designed on the basis of the results from these experiments.

ACKNOWLEDGEMENTS

The experiments were carried out in the second half of 1947 and were under the over-all direction of Dr. E. Bretscher. Co-operation was obtained from the Royal Navy, Air Force and Army. Air Vice-Marshall Davis coordinated the Services. I am indebted to many of my colleagues who helped with these experiments. J. M. C. Scott was responsible for the theoretical part and John Wright was responsible for most of the detailed planning and the issue of the original report.†

† AERE C/R 210.

The Discharge of Radioactive Waste Products into the Irish Sea

PART 2. THE PRELIMINARY ESTIMATE OF THE SAFE DAILY DISCHARGE OF RADIOACTIVE EFFLUENT

By H. J. Dunster,* UK

The first work undertaken in the study of the fate of radioactive effluent to be discharged from Windscale Works to the sea at Sellafield was the study of dispersal of fluorescein reported by Seligman in Part 1 of this paper. This was followed by a preliminary assessment, the aim of which was to estimate the effect of radioactive effluent on man and his environment and thus to set limitations on the quantity discharged so that the local inhabitants would be neither harmed nor inconvenienced.

THE BASIS OF THE PRELIMINARY ASSESSMENT

The effluent was expected to amount to several hundred cubic metres per day and to contain small quantities of chemical wastes and a low concentration of fission products, uranium and plutonium. As the effluent leaves the pipeline it is immediately diluted with a large volume of sea water and then further diluted by the process of eddy diffusion which has been discussed in Part 1 of this paper. The diluted effluent is then removed from the area between Cumberland and the Isle of Man by a mixture of eddy diffusion and non-tidal currents. In this way it is still further diluted to insignificant levels and eventually removed from the Irish Sea through North Channel. Figure 1 shows the location of Windscale Works in relation to the Irish Sea.

While these hydrodynamic processes are causing continual dilution of the effluent, others, mainly chemical and biological, are causing local concentration of the radioactive constituents in fish and seaweeds and on sand and mud. It is principally these local concentrations which may affect members of the general public. Both fish and seaweed from this area are sources of food and the sandy beaches all along this coast are greatly used by holiday makers and it was necessary to estimate the possible ingestion of radioactive materials as well as any exposure to external radiation. Once acceptable levels had been defined for ingestion and exposure, it was possible to fix the maximum permissible amounts of radioactive material in the discharges.

The main steps in the preliminary assessment were then as follows: (1) The estimation of activity levels in the sea resulting from a unit daily discharge; (2) The estimation of the relationship between activity levels in the sea and those in fish, seaweed, and shore sand; (3) The selection of suitable criteria of safety for the exposure of members of the public; and (4) The relating of these factors to set safe limits of discharge of radioactivity.

It must be emphasised that these estimates had to be made well before the completion of the chemical plant giving rise to the effluent. The first estimates were in fact made about three years beforehand and the more detailed assessment described here was completed about two years later.

THE LEVELS OF ACTIVITY IN THE SEA

The main data from which it was possible to estimate the expected levels of activity in the sea were the results of the fluorescein experiments described by Seligman in Part 1 of this paper. These were supplemented by measurements of tidal streams, by studies of the effect of wind on water movement and by studies of the variation of salinity with position. Some work was also done by discharging fresh water from the effluent pipeline and measuring local variations of salinity.

Measurements with current meters and drift poles showed no clear non-tidal current off the Cumberland Coast and a programme of drift-bottle releases was started. The strandings of these bottles were largely determined by the action of the winds on the surface waters: a problem which has been extensively discussed by Munk[1] and by Sverdrup *et al.*[2] Nevertheless a study of the time and place of the strandings from a series of regular releases, interpreted with the help of the data on wind-produced water movement, showed that while there was some systematic flow to the west in the channel north of the Isle of Man and to the north in North Channel, there was little or no current between Cumberland and the Isle of Man apart from tidal streams and wind-produced movement.

This conclusion was confirmed by a study of the salinity data for the Irish Sea, using a method developed by Bowden.[3] When this method was applied to the channel east of the Isle of Man it was found that the main method of removing fresh water from

* Atomic Energy Research Establishment, Harwell, England.

this channel was by eddy diffusion and not by a steady current.

It was then possible to apply the results of this work to predict the behaviour of the effluent.

For a unit discharge of 1 curie per day in a volume of several hundred cubic metres it was expected that the concentration in the sea within a mile or so of the pipeline would not exceed 4×10^{-8} microcuries per millilitre in average conditions. No build-up was expected because the eddy diffusion process was thought to be adequate to disperse the effluent except possibly in calm weather with wind speeds below about 7 miles per hour. Such conditions are rare on this coast and were not likely to present any serious problems.

THE LEVELS OF ACTIVITY ON THE SEA-BED AND SHORE

The process by which activity concentrates on the sea-bed and shore is one of chemical adsorption onto the surface of the particles. The concentration per unit mass is thus very dependent both on the chemical element involved and on the particle size of the sand or mud. As soon as laboratory work was started it became clear that the apparent concentration factor depended primarily on the extent to which very fine particles had settled and this made it very difficult to relate the laboratory experiments to the conditions in the sea.

For the purpose of this assessment it was eventually decided to use a concentration factor (activity per gramme of sand/activity per gramme of water) of 1000 for yttrium, cerium and the rare earths, of 100 for ruthenium and caesium and of 10 for strontium. It was expected that in very calm conditions, when the fine particles in the sea settle out as a temporary deposit of mud, some of these figures might be underestimates. From this work it was possible to estimate the expected activity level of the sea-bed.

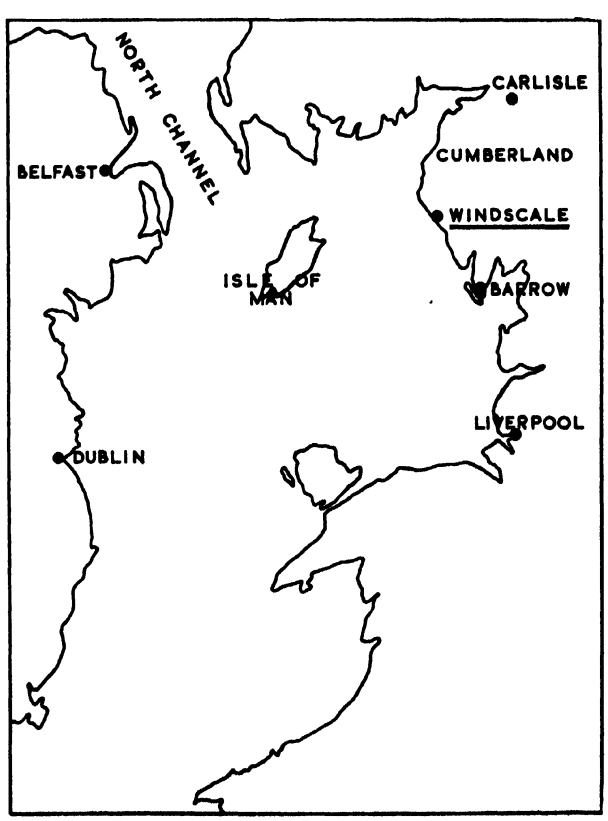

Figure 1. Windscale works, Cumberland, and its site on the Irish Sea

Prediction of the activity of the shore presented greater difficulties because of the uncertainty of the activity level of the water near the shore. From the diffusion measurements it seemed that the activity of water at the shore would be a factor of at least 50 below that near the outlet but, because there is an inshore movement of sand in this area, this factor was not used in the assessment and it was assumed that the shore and the sea-bed would be equally active.

THE LEVELS OF ACTIVITY IN FISH

The estimation of the activity level of fish around the effluent discharge point is a most complex problem involving the biological behaviour of the radioactive components of the effluent.

The biological aspects of this problem were extensively studied by the Fisheries Laboratory of the Ministry of Agriculture and Fisheries who carried out a large scale programme of marking of plaice, the fish of principal commercial interest in the area. From this work they were able to establish that plaice remained in the vicinity of the pipeline for some months, with some local seasonal movement, and that a large proportion of the maturer fish would be landed within a few months of leaving the pipeline area.

The second part of the problem was tackled both by the Fisheries Laboratory and by a biological team at Windscale and two methods were employed. The first of these involved keeping fish in tanks of sea water containing measurable amounts of the active element being studied. Some of the fish were then sacrificed at suitable intervals and the activity of their various parts determined. This method gives a measure of the final value of concentration factor and of its rate of rise. The second method, "the method of natural isotopes" gives only the saturation concentration factor and can be used only for elements normally present in sea-water and fish. If the ratio of the concentration of the inactive element in fish and sea-water can be measured analytically this inactive concentration ratio is a measure of the upper limit of the radioactive concentration factor. Analytical work was therefore carried out on a range of fish tissues and the results were compared with the published data on concentrations in sea-water.

From a combination of these methods it was possible to make estimates of the concentration factors to be expected in fish caught in or around the region of the outlet. The values adopted are shown in Table I. They apply to the edible parts of such fish

Table I. Expected Concentration Factors for Edible Fish Tissue (Wet Weight)

Element	*Concentration factor used in this assessment*	
Strontium		1
Yttrium		5
Caesium		7
Cerium		12
Ruthenium	Guessed	5
Plutonium	Guessed	50

as plaice, dabs, skates and rays. Later developments of these investigations confirmed most of these figures but showed that the true figure for plutonium was nearer unity.

THE LEVELS OF ACTIVITY IN SEAWEED

In most coastal areas of the United Kingdom the possible activity of seaweed would be only a minor problem. However an edible seawood, *Porphyra umbilicalis,* grows on the Cumberland coast and is commercially harvested on a small scale.

The concentration factor was again studied for the edible weed both by tracer studies in tanks and by analytical methods. Typical tracer work has also been reported by Spooner.[4] At the time of this assessment most of the data on *Porphyra umbilicalis* was based on analytical work very close to the limit of detection. Table 2 shows the figures used in this assessment.

The later work showed that the true figures for yttrium, cerium, ruthenium were all at least a factor of 10 higher than those used here. This error was partly offset by the fact that the weed only grows between high and low water lines and is thus not exposed to the full concentration of activity in the sea-water near the outlet. Seligman's work had suggested that this factor would be at least 50 but for this assessment it was assumed to be only 10 because of the paucity of the data on concentration factors.

CRITERIA OF SAFETY FOR THE EXPOSURE OF MEMBERS OF THE GENERAL PUBLIC

As a result of some 50 years of experience with the effects of X-rays and gamma rays on the human body and of about 30 years experience of the effects of radium fixed in the human body there is now widespread agreement on the levels of radiation to which it is safe to expose people as part of their conditions of work. This agreement is exemplified by the reports of the International Commission on Radiological Protection[5] which have recommended a basic maximum permissible level of 0.3 roentgen per week for occupational exposure to gamma radiation and corresponding maximum permissible concentrations of radioactive substances in air and water. Before these figures can be applied to the problems of liquid waste disposal, a further factor has to be considered—by how much should the recommended occupational levels be reduced before they can be applied to the general population? It was decided that the policy in Cumberland should be to ensure that no one would be exposed to radiation equivalent to more than one tenth of the occupational levels recommended by I.C.R.P. At the same time, the assumptions made about the time spent on the shore, and the amount of fish and seaweed eaten were such that very few people would approach this limiting exposure and the great majority of those who might possibly be exposed would receive very much lower levels of radiation.

The maximum permissible level applied to achieve these conditions on the shore was 5×10^{-3} microcuries per gramme of shore sand—a level which even if widespread would permit of regular exposure amounting to about 1 hour per day. For fish and seaweed the occupational levels for drinking water were applied directly to the edible parts. These limitations certainly satisfied the required safety conditions.

Finally, because of the unsatisfactory nature of much of the data, it was thought necessary to apply a safety factor of 10 over and above the intrinsic safety factors of some of the individual stages of the calculation.

THE RECOMMENDED PERMISSIBLE DISCHARGES

By relating the data given above and the criteria of safety, it was possible to arrive at the corresponding maximum permissible discharges expressed in curies per day. These are shown in Table 3. Only the most restrictive figure is given for each element; the cause of the restriction is also shown.

Small quantities of other radioactive materials were expected to occur in the effluent and, because time did not allow the necessary detailed investigations to be made, these were controlled by setting a limit of 50 curies per day on unspecified beta-emitters. Any additional alpha-emitters were classed with plutonium in the total of 0.1 curies per day. Finally the possible effects on man by routes not so far considered in detail were checked. These routes

Table II. Expected Concentration Factors for Edible Seaweed (Wet Weight)

Element	*Concentration factor used in this assessment*	
Strontium		0.5
Yttrium		30
Caesium		5
Cerium		25
Ruthenium	Guessed	10
Plutonium	Guessed	500

Table III. Estimated Maximum Permissible Discharges from Windscale Works to the Sea

Element	*Maximum permissible discharge (curies/day)*	*Cause of the restriction*
Strontium	2	Fish
Yttrium	10	Sea shore
Ruthenium	100	Sea shore
Caesium	100	Sea shore
Cerium	10	Sea shore
Plutonium	0.1	Seaweed

included bathing, handling of fishing gear, breathing salt spray or sand, and the use of seaweed as a fertiliser. The possibility of a reduction of the number or quality of the fish in the area was also considered. It was quite clear that none of these effects would be of any significance at the discharge levels recommended.

These limits on the proposed discharges were thus expected to give complete protection to members of the population at large. However, because of the various safety factors included in the assessment, it was expected that the final limits would be unnecessarily restrictive. To confirm this, and to enable a more accurate assessment to be made, a further programme of laboratory and field work was initiated. The most important part of this work was the period of experimental discharges reported in this paper.

REFERENCES

1. Munk, W. H., *The Critical Wind Speed for Air/Sea Boundary Processes,* Journal Marine Research *6*: No. 3 (1947).
2. Sverdrup, H. V., Johnson, M. W. and Fleming, R. H., *The Oceans,* published by Prentice-Hall (1949).
3. Bowden, K. F., *Processes affecting the salinity of the Irish Sea,* Monthly Notices of the Royal Astronomical Society, Geophysical Supplement *6*: No. 2 (1950).
4. Spooner, G. M., *Observations on the Adsorption of Radioactive Strontium and Yttrium by Marine Algae,* Journal Marine Biological Association U.K. *28*: 587 (1949).
5. International Commission on Radiological Protection, *Recommendations,* (1950 and 1953). British Journal Radiology *24*: 46, (1951). British Journal Radiology *27*: 245, (1954) British Journal Radiology, Supplement No. 6 (1955).

The Disposal of Waste Products in the Sea

PART 3: THE EXPERIMENTAL DISCHARGE OF RADIOACTIVE EFFLUENTS

By D. R. R. Fair and A. S. McLean,* UK

The indiscriminate discharge of radioactive liquid effluents into the sea might be expected to give rise to a variety of problems. How these problems were assessed before effluents were discharged from Windscale Works into the Irish Sea, and the limitations which were recommended in consequence, have already been described in this group of papers. It will be noted that these first recommendations contained substantial factors of safety which were expressly included to allow for limited knowledge about the ultimate fate of radioactive effluents discharged into the sea; consequently the planning and operation of the Works were heavily restricted. It was decided therefore to carry out a series of investigations which included laboratory work (this has already been described) and the discharge of radioactive effluent into the sea on an experimental basis, so that the maximum amount of information could be gained about the processes involved in the dissemination of radioactive effluents in the sea. It is the purpose of this paper to describe these experiments, and to summarise the results and the conclusions which were drawn from them.

The materials used in the experiments were effluents in that they arose from time to time as wastes in various stages and states of operation of the works chemical group. They were treated, however, so as to satisfy the fundamental criteria of the experiment:

1. That there should be a large margin of safety —for this reason, substantial factors of safety were deliberately introduced.
2. That the quantities of radioactive materials should be just large enough to provide positive results from the sampling programme.
3. That the radioactive composition of the effluent should approximate consistently to a predetermined pattern.
4. That the volume and chemical nature of the effluent should be similar to that expected to arise regularly as normal effluent.
5. That the experiment should continue for several months to facilitate the study of the effects of varying weather conditions and of saturation processes.

Detailed records were kept of the quantity and composition of the material put to sea throughout the experiment.

A pipeline had already been laid from the works extending out into the sea for nearly two miles and it was by this means that the effluent was released into the sea, discharges being made over a period of two or three hours immediately after high water.

A comprehensive sampling plan was devised so that the levels of activity resulting from the discharges could be recorded, particular attention being paid to fish, seaweed, the sea-bed and the shore as these had appeared to be of special importance in the preliminary survey. The quantity of radioactivity to be discharged was low and it was expected that it would be diluted in sea-water to a level below the limit of detection, except in the immediate neighborhood of the point of discharge; observations made in the course of the experiment showed that this was the case. For this reason the experiment was not designed primarily to test the assumptions made at each step in the deductions described in the previous paper; its aim was to test the validity of the conclusions about the relationship between given levels of discharge and the resultant levels of activity at the end points of the various chains through which the effluent might become a hazard to mankind.

As a result of observations made during the experiment and of information which was later available from other sources it became possible to review the criteria of safety which were to be applied in considering the possible hazard to the population at large. In each case, the appropriate maximum permissible level was taken to be one tenth of the corresponding figure for occupational exposure to radiation. The following figures were adopted:

Shore sand: 25×10^{-3} μc/gm. Any individual could safely spend about a hundred hours a year on shore contaminated consistently at this level.

Sea-bed mud: 10^{-1} μc/gm. It has been shown experimentally that fishermen can safely handle gear trawled over a sea-bed contaminated consistently at this level.

Fish (flesh): Ten times the maximum permissible level for any radioisotope in drinking water. It has been shown that if this is the *maximum* level of contamination, then the *average* level throughout the fishing ground in question is safe by a substantial margin.

Edible seaweed: Ten times the maximum permissible level for any radioisotope in drinking water.

* U.K.A.E.A., Risley.

It has been shown that if this is the *maximum* level of contamination, then the *average* level throughout the harvesting area in question is safe by a substantial margin.

It is now possible to make a comparison between the levels of activity found in samples and the above assumed criteria and so to gauge the degree of safety inherent in the discharge of the quantities of radioactive materials used in the experiments. The figures given for the mean daily-discharge rates in the following table have been averaged over a period of many months; likewise the levels of activity reported in samples are in all cases averages of large numbers of individual sample results.

Nuclide(s)	*Mean daily discharge (curies)*	*Nature of sample*	*Mean activity of sample (μc/gm)*	*Assumed criterion of safety (μc/gm)*
Plutonium–239	0.05	Fish	4×10^{-7}	3×10^{-5}
		Seaweed	3×10^{-8}	3×10^{-5}
Strontium–90	7	Fish	2×10^{-7}	8×10^{-6}
		Seaweed	2×10^{-7}	8×10^{-6}
Ruthenium–106	16	Fish	1×10^{-5}	1×10^{-3}
		Seaweed	3×10^{-5}	1×10^{-3}
		Sea-bed	5×10^{-4}	1×10^{-1}
		Shore sand	7×10^{-6}	25×10^{-3}
All beta-emitters (excluding ruthenium–106)	35	Fish	4×10^{-5}	1×10^{-3}
		Seaweed	7×10^{-6}	1×10^{-3}
		Sea-bed	2×10^{-3}	1×10^{-1}
		Shore sand	3×10^{-5}	25×10^{-3}

The first and most obvious conclusion that can be drawn from these figures is that the external radiation arising from beta-emitting nuclides is insignificant by comparison with the hazards arising from the ingestion of activity in fish flesh or in seaweed; were it not for the risk of ingestion, it would clearly be possible to discharge some thousands of curies of these materials each day without risk. It will be seen, in fact, that, with the exception of plutonium, which is restricted by the contamination of fish flesh, the discharge of activity is limited in all cases by the contamination of seaweed and this must be regarded as a rather unusual complication. It is concluded that the original estimates of the maximum permissible daily-discharge rates were conservative by factors varying from 5 in the case of Ru^{106} to 100 in the case of Sr^{90}.

These experiments have helped to define the limits of the value of the pipeline method of disposal of radioactive liquid effluents into the sea. It has been shown that, in the conditions encountered in the sea in the vicinity of Windscale Works, several hundreds of curies of beta-emitting isotopes and several hundreds of millicuries of alpha-emitters can be disposed of daily in this way with safety. Were it not for the unusual problem connected with the harvesting of edible seaweed in that region, larger figures could be envisaged, especially for the bulk of the beta-emitting nuclides.

It is unlikely that the discharge of small amounts of radioactivity could cause any significant disturbance of the marine ecology; nevertheless, the effects of external and internal irradiation of fish and other forms of marine life are not well understood and this aspect would require further study in the event of any proposal to release very large amounts of radioactive wastes in the oceans.

Disposal of Radioactive Wastes at Sea

By Charles E. Renn,* USA

At this present moment there is no practical working program for the continuing disposal of power reactor wastes at sea. Our experience with sea disposal has been limited to small amounts of low level wastes developed in a variety of laboratories and installations.

Detailed analyses of the conditions for safe and economical waste disposal are being made with the aid of leading American oceanographers and waste disposal specialists. The studies, to date, show that some misapprehensions exist and that an extensive series of basic investigations must be made before sea disposal can be recommended. In this paper we will briefly review the hopes and limitations for sea disposal of reactor wastes as we know them today.

DISPOSAL OF WASTES IN "DEEP HOLES" IN THE OCEAN

It has been pointed out frequently that there are limitless opportunities for disposal of wastes in sequestered areas of the ocean bed. There exist, the argument runs, a number of deep holes, or basins, in the ocean, which contain cold, salt water so dense that they mix very slowly, if at all, with overlying water. Obviously, if lightly encased wastes are dropped into these areas, or if heavy, saline-type wastes are piped down into these basins, the wastes will be contained long enough to permit fission decay to safe levels. We would know where the wastes are; they would be effectively locked up; and the whole operation would be quite economical.

When we examine this concept in detail, however, we discover a number of limitations. First, oceanographers do not agree that such deep areas of stable water exist. If water masses were static for many centuries, the deep water of the ocean floor would warm from heat of the earth's crust. There should be a slight rise in temperature immediately over the sea bottom. The existing temperature data, and there is a great deal of this, show only a few areas where temperature variations in the deep water exceed those due to pressure. Information on the rate of mixing and turn-over of deep water is limited. The more recent critical studies show vertical mixing of the ocean waters to be much more rapid than we had anticipated some years back.

Some oceanographers suggest that the time of mixing in the Atlantic may be as long as 1500 years. Others propose a much shorter time. The problem is of great intrinsic interest and is being pursued intensively by physical oceanographers.

In addition to this, there is some evidence to indicate that there may be periodic and uncontrolled types of overturn due to prolonged variations in the ocean surface temperatures. For example, the existence of oxygen in the deep Atlantic waters strongly suggests that this bottom water must have been at the top not much more than 100 years ago. At about this time a series of severe winters with continuing cool summers may have produced large masses of surface water of low temperature and high density which displaced the stagnant oxygen-free water of an earlier period. Although there is a great poverty of adequate early weather records, the incidents during Napoleon's march on Moscow and other accounts in the history and literature of the time, suggest that this may have been such a period of prolonged cooling. The possibility certainly exists that we may have relatively short-period convective overturns of the ocean waters due to unusual local cooling conditions at the water surface.

It goes without saying that oceanographers are greatly concerned with the dimensions of this stability limit. The dimensions of the so-called basins, the rate of flow across rims and low margins are also factors of great concern. While the sonic fathometer has greatly increased our knowledge of the topography of such areas, detailed knowledge of the densities, temperatures, oxygen concentration and other factors require laborious, time-consuming, and expensive deep sea sampling, analysis of carefully taken samples, and critical correlation of much data.

DISPOSAL OF ATOMIC ENERGY WASTES INTO CANYONS OF THE CONTINENTAL SHELF

It has been proposed even more frequently that packaged masses of fission wastes be dropped into one or more of the many deeply cut canyons that break the face of the North American continental shelf. These areas have the advantage of being relatively close to shore, of having well-defined configurations, and being readily located by sonic soundings, and loran navigation. We should know where the waste is, in this case, and we should be able to get to the dumping areas with a minimum of time and cost.

The submarine geologists point out, however, that the canyons themselves are produced by local insta-

* The Johns Hopkins University.

bilities. These gullies are scoured at relatively frequent intervals by what are submarine mud-slides. There seems to be no disagreement about this. The slides occur every two or three years, and in some localities oftener. Detailed observations of the phenomena are being made on the West Coast. A number of studies has also been made on the Atlantic Coast. Some especially provocative information has grown from an inspection of the records of cable breaks in the areas of such submarine earthquakes and land-slides. These suggest that the flowing mud and sand that erodes the canyon bottom reaches high velocities, in the order of 15 to 50 miles an hour. Movement over the bottoms is sufficiently rapid to keep them scoured hard and clean; and density currents project mixed sands and silt for miles beyond the mouths of the canyons, a phenomenon that is demonstrated by repeated strata of fines in cores that have been taken in the deeps beyond the shelf.

This description shows us that packaged wastes will undoubtedly receive rough treatment if they are deposited in the bottoms of the canyons. We would not, in fact, know where the waste was. We could not be sure that it was being contained. It would be extremely difficult to conceive of inexpensive packages designed to withstand the tumbling, grinding, and scouring of submarine mud-flows. We know nothing of the fate of any activity freed in the deep sea dust-storm that develops with these flows. It is possible that activity will be adsorbed on the fines. Our limited knowledge of the degree of uptake and of the behavior of wastes as they exist makes predictions impossible.

DISPOSAL OF FISSION WASTES INTO DEEP SEA MUDS

Another recommendation has received considerable publicity, that atomic wastes be packaged in suitable shaped containers, flown or carried to sea, and dropped or projected at high velocities to be buried in the deep oozes of the sea bottom or in the soft delta muds of our various rivers. This idea seems to be especially appealing.

A review of the possibilities from this method shows that aside from the rather specialized and expensive requirements for packaging and transport, there is very little likelihood that either shaped or unspecialized masses will sink into the bottom. First, there are few accessible places where the bottom is sufficiently light and permeable. This word "ooze" has had especial quality in misleading thought on ocean disposal. In most areas, with the exception of harbors and recent delta deposits, the fines of the bottom have achieved a degree of consolidation that more approximates putty and stiff clays. Only a very thin layer exists in unconsolidated form. Our experience with wrecks, sunken buoys, and more recently with mines and depth charges dropped from planes, shows us that any degree of useful penetration is extremely unlikely. With the practical densities that can be achieved, marine geologists all agree that the drums, cubes, and spheres, shaped-objects that rest on the sea bottom would continue to rest on the bottom long past the period of useful decay of the fission products themselves. We would be able to secure natural containment in only a few selected sites. Dumping of shaped charges itself, while dramatic, has little practical advantage in sea disposal. Experiments with cylinders and other shapes show that terminal velocities in the water is usually reached at about 60-feet drop through the water, after which the object tumbles down at a velocity of approximately 20–25 feet per second to crash against the bottom. Shaped, finned charges have a somewhat higher terminal velocity, determined by skin friction in water. There would be no gain from dropping these from high altitude for deep sea disposal.

There are, however, certain soft spots where natural containment of packaged wastes may be possible. Submarine geologists point out that one very desirable characteristic is that the bottom disposal areas themselves may be contained by some sort of natural rim. We have, for example, mud pockets in the Gulf of Maine. These exist in relatively shallow areas of 90 to 120 fathoms and might be considered accessible. Disposal operations in the Gulf of Maine, a heavily fished part of the world in which deep sea trawling operations are becoming more frequent, at least present problems in public relations. There are also contained areas in the deeper parts of the Gulf of Mexico, where the bottom is relatively unconsolidated and where heavy masses might be expected to sink for eventual cover.

Disposal in the so-called unconsolidated silts of the estuaries requires a careful and detailed analysis of estuarian geology. Some sections of the Mississippi Delta have histories indicating some permanence.

It is important to view these points critically since it is easy to be plausible in discussions of unknown phenomena, especially in discussions of behavior of the ocean waters and bottoms where our common, real information, practically speaking, is at the level of folk lore. Some time ago a proposal was made that wastes from one of our very large installations be cast in the form of large air-borne concrete torpedoes, carried to the coast and dropped off the mouth in soft mud of one of our larger rivers. Aside from the transportation difficulties, a quick glance at the coast and geodetic map would have shown that the area recommended was not a soft, muddy bottom, but a shallow, coral plateau with a hard bottom, and swept to depths of 300 to 400 feet by the north-flowing Gulf Stream. The site certainly represented the least desirable type of permanent burial place. I mention this case as an example of the somewhat superficial type of examination that has been given to the problem of ultimate disposal at sea generally.

DISPOSAL OF LOW LEVEL ACTIVITIES AND RADIOACTIVE TRASH AT SEA

We do actually dispose of small quantities of radioactive wastes at sea. Most of this material can be

classified as laboratory and experimental installation wastes, including small amounts of concentrates that cannot be disposed locally at several of our coastal AEC and contractor installations. They include broken glassware, experimental animals, reagents, contaminated equipment, cloths and paper, liquid waste concentrates. These are packaged in a variety of ways. One common method is to encase the material in concrete to form packages of sufficient size to furnish shielding for safe shipment, and to weight the mass for deep sea sinking. Blocks as large as 12 tons are routinely disposed, although most of the sea disposal material of low level concrete-embedded wastes is cased in 55 gallon, 30 gallon, or 5 gallon drums. Each installation has its own practice in the preparation of these drums.

The ocean carrier facilities that are attached to these disposal operations are furnished by reciprocal government services. Along the Atlantic Coast, the US Army disposes of wastes from several installations as part of their waste or outdated ammunition-disposal program. These are carried to sea on large ammunition barges and dumped in pre-selected ammunition burial areas beyond the edge of the continental shelf in 1200 fathoms of water. The US Coast Guard also disposes of packaged waste. On the West Coast, the US Navy disposes of packaged trash and waste from its own installations and from Atomic Energy Commission contractor installations. In addition, much smaller quantities of waste are disposed by private contractors as part of salvage and hazardous chemical disposal operations. An even smaller quantity has been handled as a courtesy by oceanographic and marine laboratories having adequate ship facilities. These represent courtesy services to their respective universities.

We may say of these small operations that there is nothing in them that can be applied to disposal of high level wastes represented by reactor wastes. The poundage cost is high, and the type of light, temporary shielding yielded by concrete-loaded drums is totally inadequate for individual shield requirements of high level wastes. The costs of these operations, including all phases, are completely out of line with anything that may be practicably attached to power development. Roughly, experience with low level waste gives us a costs figure of approximately $10 per cubic foot for final disposal.

In the case of these low level wastes we make no effort to monitor the disposal area, and we have no information whatever upon the durability and condition of the containers. It is reasonable to assume that the levels will never produce hazardous concentrations, even when assimilated by plankton organisms and other forms that may be in the area. A practical working test of the procedure, which on the surface would seem somewhat uncontrolled, and possibly much overdesigned, is that there have been no repercussions from the practice.

The disposal of wastes by private companies from high level operations may be anticipated from the power reactor development presents many problems that are quite different from those attached to government operations. The possibilities for exchange of service, for example, are distinctly limited. Cost of equivalent labor to private operations is frequently much higher. Even more significant is the fact that surplus labor, or emergency and auxiliary labor required for handling of high level wastes in preparation and transport are unavailable in private operation. For example, it is quite possible, in emergencies, for an AEC or contractor installation to draw on its secretarial staff, machine shop help, or ground crew to assist in a radioactive mop-up operation so that the necessary exposures may be shared among a large number of people. This reduces the amount of shielding and special precautions that are necessary in the packaging and handling operations. It is unlikely that our labor unions will favor such exchange of service and quite unlikely that a power operation will contain the reservoir of emergency assistance needed. This requires an entirely different type of design, and that is possible in experimental units.

OCEANOGRAPHIC REVIEW OF WASTE DISPOSAL CRITERIA

At intervals over the past year we have conferred with leading American oceanographers concerning the development of suitable criteria for safe disposal of radioactive wastes at sea. Prior to our review, the Committee on Radiological Hazards of the US Atomic Energy Commission had recommended that all waste disposed at sea be contained in suitable, permanent containers. It is not clear what the structure of such permanent containers for sea disposal might be, but this seems like a safe suggestion in view of almost total absence of information at that time on the magnitude of the waste anticipated from a working reactor program.

Oceanographers point out that we do not yet have the techniques for determining the boundaries of dispersal from any large discharged mass of free wastes. Some very important unknowns enter. First, we have little previous knowledge of the behavior of heavy, saline solutions injected into large water masses such as the ocean, in dimensions that represent disposal of free waste at sea. Second, we have no adequate monitoring technique for judging the dispersal or containment of any large mass of radioactive wastes. If we are to dispose of some millions of curies of wastes at sea in some hopeful deeps offcoast, we face the primary limitation of precision navigation of the dumping and monitoring vessels. Some fixed point must be established. It appears that deep sea buoys represent the simplest and most satisfactory method of marking the burial site and the area to be monitored. The type of activity-sensing equipment required represents another special problem. If such equipment is to be lowered and powered through cables, the reliable performance and useful life of a power-conducting cable becomes a

limit. The pressures developed by winding two miles or more of conductor-type cable on a winch drum are very great. These combined with the changing tensions upon such a system restrict reliable life of a unit fed and sensed through a cable to 20 or 30 lowerings. The time required for such a sampling program is great and the operations conducted by specialists are necessarily expensive. There are also unsolved problems of background level and error induced by absorption of activity upon the submerged equipment itself. These are limitations that cannot be taken lightly. Ideally, of course, a system of automatic monitoring by a grid of planted equipment capable of delivering a signal to a surface station is most desirable, but this is still in the dream stage. So far we have not even developed design plans for an experiment to determine the pattern of diffusion and movement of free waste in the sea.

Such an experiment is necessary. Although the volume of the sea is great, mixing in the whole ocean is unlikely. Wastes may be expected to move much more rapidly in horizontal mixing than in vertical mixing, although the vertical dimension adds a most important element. In design of dispersal experiments we must know where to look for the wastes and must have some idea of how much will be at sampling points. Precision sampling represents a great instrumental and technical problem.

ASSIMILATION OF RADIOACTIVITY BY PLANKTON AND ORGANISMS IN THE SEA

The biologists, marine ecologists and fisheries investigators are concerned with the potential hazards associated with assimilation and concentration of fission products by plants and animals in the sea. In the short-lived category of fission products, iodine would appear to be most significant. This, fortunately, has a short half-life. Strontium and caesium are much more significant in aged wastes. Some marine forms are known to substitute strontium for calcium in their structure and it is possible that this component will be concentrated. Little is known concerning the fate of caesium.

It is anticipated, from experiments with other natural waters, with silts and with adsorbing surfaces, that much of the strontium and caesium in the water will become associated through adsorption or reaction with particulate stuffs of the sea water system and that these will follow the sediments.

There is some apprehension of the effects of high levels of activity upon societies of marine plants and animals. Interdependent communities are more sensitive to changes in the environment than individual species. A small change in predator population, for example, permits a large shift in the food species, or a small decline in food resources may wipe out a species that is not directly sensitive to radiation. Ecological changes are, of course, possible, and so far we have made no attempts to assess them quantitatively in the sea.

DISPOSAL OF PACKAGED AND BULK WASTE AT SEA

A very large fraction of the costs of ultimate disposal of reactor wastes promises to come from the costs of shielding required for safe transport, and from shipping costs of massive shielding. Heavy shielding must be provided if the waste is to be moved by common carriers, and if it is to move through shipping centers. If expendable shielding is used, the costs of return shipping will be saved, but the costs of expendable shielding must be entered. Concrete appears to be the most economical combination container and shield that may be expended. Concrete, with relatively low density, on the other hand, has bulk and structural limits.

A transportation system that uses returnable permanent shielding permits the use of denser, stronger, and less bulky structures, but increases capital costs and return shipping costs will be almost identical with the outgoing costs. The waste discharges to the sea from permanent shield containers, or as an unshielded solid or liquid which will ultimately mix with sea water.

We have had some experience with the surface disposal of dense, inactive liquid industrial wastes. In the cases that were studied, it was interesting to discover that dilution proceeded so rapidly during the downward travel of the waste in the sea that dilutions of roughly a million times were achieved through one hundred feet vertical profile. This emphasizes the relative magnitude of horizontal mixing in the sea.

Very clearly then, any liquid bulk wastes must be discharged directly into the stratum where dilution is desired. It also indicates the degree of precision required in sounding and sampling during monitoring and experimental operations—it is impossible to know, at the moment, within 200 to 300 feet where the sampling equipment may be at the end of a 20,000-foot line. The behavior of a weighted cable suspended in the open sea is not comparable to the conductor of an oil well probe.

INTERESTS OF OCEANOGRAPHERS IN DISPOSAL OF RADIOACTIVE WASTES

Physical and chemical oceanographers and marine biologists have been interested for some time in the potentialities of disposing of radioactive wastes at sea. Only recently, with the development of the fission industry, have they become acquainted with the magnitude of the waste problem. It must be realized that we have few specialists in the sciences of the sea who can guide us, and that these men are occupied with a wide variety of problems. We will need their help, and we will need to help them to enlarge their studies rapidly to provide necessary information of the sea. If the fission power industry becomes a reality, we will need to know much more about the ocean than we do now.

Record of Proceedings of Session 23B.2

SATURDAY MORNING, 20 AUGUST 1955

Chairman: Mr. A. J. Cipriani (Canada)
Vice-Chairman: Mr. A. R. Torky (Egypt)
Scientific Secretaries: Messrs. R. Hara and D. J. Littler

PROGRAMME

P/418 The discharge of radioactive waste products in the Irish Sea. Part 1: First experiments for the study of movement and dilution of released dye in the sea ..... H. Seligman

P/419 The discharge of radioactive waste products into the Irish Sea. Part 2: The preliminary estimate of the safe daily discharge of radioactive effluent ..... H. J. Dunster

P/420 The disposal of waste products in the sea. Part 3: The experimental discharge of radioactive effluents ..... D. R. R. Fair and A. S. McLean

P/569 Disposal of radioactive wastes at sea ..... C. E. Renn

DISCUSSION

The CHAIRMAN: We shall now pass to the next aspect of waste disposal, that is, disposal into the sea. The sea is one of the most attractive places into which to throw things; it is the largest body of water we know, it is not potable and the only thing that really comes out of it that we are interested in is food such as fish, maybe seaweed, and a few other things. The indiscriminate disposal of wastes into the sea, however, has its uncertainties. The sea has been used in two ways for waste disposal, one in which the waste has been solidified in some form such as concrete and thrown into very deep portions of the ocean, the other in which the liquid material has been put to sea in pipe-lines. Again, when one does this it is necessary to forecast the fate of such material, whether it is going to be washed back on to the shore where it will come into contact with human beings, or whether it will get on to the fishing banks in some way and contaminate edible fish. This problem is a small one at the moment because the amount of wastes which we now possess could easily be put into the sea if we thought this was all that we would ever have, but with the advent of power piles and the spread of nuclear energy plants throughout the world this will in turn become a most significant problem, and a great deal of study is necessary before it can be said that the sea can be used indiscriminately.

Mr. H. SELIGMAN (UK) presented paper P/418.

Mr. H. J. DUNSTER (UK) presented paper P/419.

Mr. D. R. R. FAIR (UK) presented paper P/420 and prefaced his presentation with the following comment:

I should like to emphasize, as did the Chairman in his opening remarks, that it is important to recognize that this group of papers is concerned solely with the disposal of relatively low-level active liquids which arise in an atomic energy programme. It is not concerned with the very highly active fission product liquors produced during the chemical processing of irradiated uranium.

Mr. W. D. CLAUS (USA) presented paper P/569.

DISCUSSION OF P/418, P/419, P/420 AND P/569

The CHAIRMAN: It is evident from what has been said that the same principle is involved in getting rid of wastes into the ground and into the sea. This principle is that it is not considered good practice just to throw the waste into either place without regard to its fate; in other words, quite extensive studies must be undertaken to see what is happening and to ensure that these wastes will not come into contact with humans in one way or another.

Mr. F. G. KROTKOV (USSR): Studies made in the Soviet Union have shown that in disposing of liquid radioactive wastes in natural waters one cannot rely on the uniform dilution of the radioactive products by the large masses of water of the river or sea concerned. First, adsorption of radioactivity by muds and bottom deposits is of substantial importance; their content of radioactive products may be many times greater than that of the water itself. Secondly, the adsorption and accumulation of radioactive materials from the water by water organisms must be borne in mind. Experiments carried out in the USSR show that the accumulation of radioactive materials in the bodies of water organisms can become very great and can exceed their concentration in the water by as much as 1000 or even 10,000 times. Hence, even when the average concentration

of radioactive substances in the water is not high, contamination of fish and other aquatic species for food may occur.

Thus, the checking of health conditions in open waters into which sewage water containing radioactive substances is discharged requires not only radiometric inspections of the water and bottom deposits but also inspections of water organisms.

We feel that even if the natural waters are very extensive, as in the case, for example, of the Irish Sea, which, as we have seen from Mr. Dunster's paper, is used for radioactive waste disposal, they are not a reliable and safe burial ground for the radioactive wastes deposited in them.

All waters, especially the larger expanses, have more or less well-marked currents, and the process whereby the contaminated currents near the bank mix with the entire mass of river water takes place over a distance measured in tens of kilometers.

In that area, therefore, until mixing is complete, the concentration in the contaminated currents may be greater than the maximum permissible.

It seems to us that the problem of radioactive waste disposal cannot be solved at the level of any single country; it calls for sanitary control at the international level.

Mr. R. R. D. REVELLE (USA): As an oceanographer I was very much impressed with the careful work which has been done by the Windscale people in the Irish Sea. I was a little surprised to hear it repeated more than once that the seaweed represents a very unusual problem, particularly coming from a country so close to Scotland, where there is, in Scotland, a thing called the Scottish Seaweed Association, which firmly believes that at least 20 million tons of seaweed per year can be harvested in the whole world. This is about equivalent to our total catch of fish.

I would also like to comment on Mr. Claus' paper that the problem of the rate of exchange between the deep water and the surface water, where fish and marine plants of importance to man live, is certainly a difficult one. There are two or three areas in the world where we have an idea that this is quite a slow growth, namely the Black Sea and the Caribbean where hydrogen sulfide is in the water. The existence of the hydrogen sulfide is due to the reduction of the sulfate by anaerobic bacteria in the bottom muds and its presence there indicates that the rate of exchange of the surface waters is so slow that in fact no exchange takes place over a period of several thousands of years. These hydrogen sulfide basins, leaving out economic considerations, certainly would represent places which would be quite safe over long periods of time.

One more thing which has been implied but not stated is the buffer action of the sea water, particularly in the case of strontium. There are something like 10^7 megatons of strontium in ocean water, and even with a very large-scale disposal of radiostrontium into the sea the specific activity would be very low. Fortunately enough, the next most important of the fission products is cesium. There are 700 megatons of cesium in the ocean, and the specific activity of cesium deposited from a large-scale atomic program would also be quite small.

Another matter is this: the seas are international; they bathe all continents, and are the concern of all peoples, and I think that in this particular problem of waste disposal at sea international co-operation and international interest should certainly be very high.

Mr. MAWSON (Canada): I would like to support the comments of Mr. Revelle, Mr. Claus and Mr. Krotkov. It is obvious to us all that if once things get loose in the sea it is a matter of interest to everybody. Also, if things get loose in a long river which flows through several countries, the people who are at the mouth of the river, at the receiving end of a series of disposals, are liable to become very worried about the situation. I would like to support the feeling which appears to be expressed here that waste disposal is a thing which we cannot regard as our own private business, to go dumping stuff wherever we like, and it is an urgent matter, I think, that some kind of international agreement should be arrived at on the whole general policy of the disposal of radioactive wastes.

The CHAIRMAN: I have a question to Mr. Dunster from Mr. R. F. Foster (USA) which I will read: "I have been very much interested in the work done in the Irish Sea in the experiments with the concentration in fish; were seasonal cycles and food chains considered?"

Mr. DUNSTER (UK): They were considered, but when this work was done they were not in fact investigated in detail. Much, however, of the basic analysis worked on the assumption that the fish cannot concentrate by any route radioactive isotopes by a factor greater than they concentrate inactive isotopes. Calculations of this sort take complete account of food chains. Additional work has been done and is still going on on the uptake by fish through food chains, but is difficult to do on the basis of yearly cycles because it is difficult to reproduce under laboratory conditions the natural habitat of the fish.

Mr. W. G. MARLEY (UK): I agree with the sentiments expressed in regard to the international nature of this problem, but I would like to press for the carrying out of experiments to provide the scientific data on which some international agreement could be reached on this subject. It seems to me that we need experiments on the spread of radioactivity in deep parts of the ocean as well as in the shallow areas. Such experiments can be carried out at levels which in themselves would cause no harm, and this would provide the scientific data on which reasonable international understanding could be reached. In the work of the United Kingdom in the Irish Sea very great care was taken over the ex-

ploratory experiments, and the work is in the nature of establishing by direct experimental observation what the build-up is into human food through all the biological food chains. This is the kind of work which I think needs to be done, and I would press and invite countries which have an opportunity of carrying out experiments, particularly in the ocean depths near their coasts, to do this so that we can have the fundamental data. I think it would be a mistake to try to legislate on the subject before we know what the scientific facts are.

Mr. CLAUS (USA): I would like to comment on what Mr. Marley has just said. In the United States we have a great deal of interest in carrying out a practical experiment for determining what is the result of the disposal of a quantity of radioactive material somewhere in the deep sea. We are discussing this question at intervals with the oceanographers, but it is going to take a little time before we can decide exactly what kind of experiment needs to be performed. Once it is agreed what we are trying to learn and how we are planning to go about it, we will see if some suitable mechanism cannot be set up for carrying out the experiment. Certainly it would be an expensive one. In addition to that, we do feel that other nations will also have some interest in this, and I think that rather than carry out such an experiment on entirely unilateral lines we will attempt to get into touch with those who also have an interest in this type of thing, to consult with them and have at least their concurrence before we carry out the experiment.

Mr. BREITENBERGER (Singapore): I would like to put a question to the Windscale group. If I remember correctly, the tides between the Isle of Man and the Cumberland coast are somewhat peculiar and result in the formation of standing waves. That would mean that if you discharge your waste a few hours after high water it would be carried away both ways in a roughly northerly and southerly direction. I wonder if that has perhaps facilitated your disposal problem?

Secondly, the tidal flow in the Irish Sea is generally somewhat more turbulent than in other areas, and I wonder whether that fact has particularly facilitated disposal.

Mr. DUNSTER (UK): The first point, about the run of the tides, was to some extent taken into account by the timing of the discharges. They are regularly discharged from high water onwards for the next three hours. At this stage the local tidal stream is fairly rapidly in a general N.N.W. direction. By the time slack water occurs discharges have ceased, but unfortunately the patch of activity is carried back to the neighbourhood of the discharge point for the next high water, so that I do not think the flow of tidal streams is of particular advantage in this area; in fact, as I mentioned, the basic mechanism for removal of effluent, fresh water run-off, etc., from land is almost entirely turbulent diffusion, and here I would agree with the last speaker that we have been greatly helped by the fact that the turbulent diffusion in this area is quite considerable. Except in exceptional conditions there is complete vertical mixing in this part of the sea, with the result that we get a good deal of dilution in this way. In fact I would draw one distinction here between the method of disposal applied to this effluent and the methods referred to in ground disposal of effluents of a not very dissimilar character. In the case of the effluent discharged to sea we are aiming at dispersal down to concentration levels which we can demonstrate to be harmless. In the case of ground disposal the primary aim, as I see it, is to maintain the active constituents of the effluent as closely under control as possible so that one knows exactly where they are. In the case of the sea we are more concerned with the levels than with the location.

Session 23B.3

AIRBORNE PROBLEMS

LIST OF PAPERS

		Page
P/571	Air and gas cleaning for nuclear energy processes ..... L. Silverman	727
P/567	The variation of effluent concentrations from an elevated point source ..... M. E. Smith	736
P/1051	The system of routine observations of radioactivities in the air, rain-water and sea-water in Japan ..... Central Meteorological Observatory, Tokyo	745
P/1056	Method of measurement of radioactive dusts in the upper air by radiosonde ..... C. Ishii	747
P/353	Measurement of radioactivity in the atmosphere and pollution in the vicinity of an atomic center ..... J. Labeyrie and J. Weill	752
P/975	Determination of atmospheric radioactivity ..... F. Barreira and M. Laranjeira	756
P/995	The fast ionization chamber in the study of α radioactivity in air ..... U. Facchini and A. Malvicini	761
P/788	Properties of electrostatic precipitators for the measurement of radioactive aerosols ..... A. Bergstedt	764

Air and Gas Cleaning for Nuclear Energy Processes

By L. Silverman,* USA

Air and gas cleaning for nuclear energy processes differs from other industrial problems in two major respects. The first is the high order of toxicity of the contaminants (in most instances) and the other is associated with the condition that the decontaminating device may in operation become a radiation source or health problems may arise in disposal of collected materials. Contamination from radioactive gases and particulate matter in solid or liquid forms comprises the physical state of the materials producing aerosol cleaning problems. Because of their high toxicity the degree of cleaning necessary is much more severe than ordinary non-radioactive materials with one or two exceptions (such as beryllium) in order to satisfy health and safety requirements.

In nuclear energy applications of air- and gas-cleaning problems arise from the mining, refining, and production of metals such as urnaium and thorium. In nuclear reactor operation, because of the need for providing cooling air for reactors or shielding, contamination can result from induced radioactivity in particulates conveyed by the cooling air if it is not adequately prefiltered. The cooling air may also become contaminated with radioactive gases or particulates resulting from failure or erosion of fuel elements.

Processing of reactor elements or slugs results in gaseous and particulate emanations which create radioactive aerosols requiring nearly complete removal from the air stream before release to the atmosphere. Laboratory and pilot production of special isotopes and metals usually involve aerosol contamination. Recovery of certain materials for reuse and isotope separation processes must also be recognized as operations which create radioactive airborne contaminants.

The concentration or reduction of bulk volume of solid wastes by incineration and the evaporation of liquid wastes each involve airborne particulates which require special treatment. In most instances the air and gas cleaners by their recovery function provide solid or liquid contaminated materials which must be processed or handled. The exact nature of the contaminants is not primarily the concern of this presentation but by way of definition it should be pointed out that in gaseous form they range from rare gases, such as argon (A^{41}), which are difficult to recover, to highly corrosive acid gases from metal extraction processes such as hydrogen fluoride corrosive acid gases from metal extraction processes (HF). Solid and liquid particulates may be organic or inorganic and may range in size from less than 0.05 microns (μ) to 20 μ. The finest particulates arise from metallurgical fumes evolved by burning or vaporization and the coarest are acid mist droplets which are low in specific gravity and thus may remain suspended in larger sizes for longer periods.

* Harvard University.

TYPES OF EQUIPMENT EMPLOYED AND THEIR CHARACTERISTICS

Like all other new processes, nuclear energy applications in early developments were hampered by a lack of information on performance of equipment. In the beginning of the US program, because of limited knowledge, it was necessary to apply devices which had been designed or developed for other purposes. As a result there were several instances where industrial dust control equipment was applied and subsequently failed to give adequate performance. The severe cleaning requirements imposed by the low permissible concentrations specified for release to the atmosphere means that efficiencies exceeding 99% for aerosol particulates less than one micron (1 μ) are frequently necessary. With some higher specific activity materials of long half-life efficiencies a thousand times greater than this are often required. It is customary, because of these exacting demands, to talk of decontamination factors or penetration values (1 — efficiency) rather than efficiency. A factor of 10 means an efficiency of 90%, similarly a factor of 1000 indicates 99.9% removal. In some problems factors as great as 10^6 may be necessary for safe operation.

In industrial applications three factors are of prime importance in defining air- or gas-cleaner performance. These are efficiency, resistance to flow, and life. The two most important in nuclear applications are the first and the last. The necessary power consumption to overcome resistance to air or gas flow cannot be disregarded but can be provided within reasonable limits without difficulty.

In commercial practice[1] efficiency may be expressed on a weight basis, on a weight basis for certain particle size ranges, on a stain discoloration or surface area evaluation, and by actual numbers of particles. Since most radioactive contamination is on an activity for equivalent mass basis the weight efficiency for certain particle size ranges is a reliable

method although rapid testing of units with fine aerosols ($< 0.5\ \mu$) may be done with light obscuration procedures using controlled particle size aerosols such as dioctyl phthalate.

Life of the cleaning unit in service is of great importance and is related to efficiency and resistance since retention of particulates on filters influences flow resistance and life in relation to power consumption. Life becomes of special interest in minimizing exposure of individuals who may become exposed when changing or cleaning components or units. For this reason remote-controlled or constant resistance automatically cleaned methods are the optimum for nuclear applications.

Nuclear energy operations range from the handling of large volumes of materials of low activity, as in refining, to the handling of less than gram quantities of intense activity in research or recovery operations.

Because of limited knowledge as to performance of various kinds of equipment on radioactive gases and particulates and since our various atomic energy activities may involve expenditure of millions of dollars per year on such equipment, a thorough program of evaluation, development in the field of air- and gas-cleaning research was initiated at Harvard in 1950. Two years earlier a preliminary survey and research program was started to develop the extent of applications and survey the general problem.

The survey and a review of general activities within the US resulted in the publication of a handbook[2] for use by the various facilities. This handbook incorporates a number of test results obtained in laboratory and field studies under the Harvard program as well as elsewhere in the US atomic energy and related research facilities.

Air- and gas-cleaning equipments of most available types have been used and several have application for the operations involving nuclear development. These range from simple inertial collectors to high efficiency filters or electrostatic precipitators. Modifications and technical variations of these devices have also been made. A summary of the usual applications and characteristics of the many devices employed is listed in Table I. Some of the methods are used in combination or series and, in some instances, are similar to devices widely used for other industrial problems. Exceptions are the higher efficiency final filters and prefilters and deep beds of fibers. The high efficiency space filter[8] was developed for special applications as required by AEC, and will be discussed in detail below. Since its development however, commercial application has been made in pharmaceutical manufacture and fine instrument assembly plants. Specific and extended performance data on various collectors for inert and radioactive aerosols are given in our annual reports (see references in footnote of Table I).

A distinguishing feature of atomic energy applications in most operations (except refining) is the low loadings or concentrations of materials to be exhausted. This is apparent when the quantities of material involved are understood. In certain instances this simplifies the control and in others it often complicates matters. Beyond refining operations, loadings lie in the range of 1 to 10 times that of outdoor air. This means that life of equipment for certain applications is manifold as compared to usual process wastes and makes certain approaches applicable which would be impractical from a life standpoint on industrial process wastes of high effluent particulate concentrations.

In reactor air cooling it becomes paramount to remove particulates from the cooling air to prevent them from becoming radioactive. It also improves the heat transfer characteristics of the surfaces because their coefficients remain uninfluenced by deposition. In nuclear energy processes it is desirable to clean as close to the source of contamination as possible to avoid deposition and accumulation in ducts and piping which can in some instances also become radiating sources requiring shielding. Cleaning close to the source sometimes involves problems of high temperature in thermal reaction processes and may require unique approaches, some of which will be discussed below. Highly corrosive gases and the need for minimal maintenance have required the use of special materials.

SPECIAL PROBLEMS REQUIRING DEVELOPMENT AND RESEARCH

In the handling of many nuclear energy processes as indicated above, commercial equipment has become available through efforts by manufacturers and the assistance of the federal atomic energy agency and its contractors. In this discussion examples of particulate removal will be given followed by approaches used for gas problems.

Particulate Removal

The high efficiency asbestos-cellulose filter (Fig. 1) is one example where the efforts of the US Army Chemical Corps on gas mask development were applied by them to a space filter for protective shelters. From this point an improved form was developed of increased capacity and life for application to atomic energy problems. This filter, which shows a decontamination factor of nearly 5×10^3 on $0.3\ \mu$ particles improves in performance within a short time when placed in service because of the particulate deposition. It has had wide use in nuclear energy problems. For example, it has been used to clean air from air cooled reactors for chemical processing operations and for general laboratory hood and glove box discharge cleaning. As originally developed it was indicated that the filter should not be used for resistances above 2 inches of water because of excessive power consumption and possible structural failure or rupture of the cemented filter element. In practice, however, these filters have been used for resistances as high as 8 to 10 inches with a material increase in life (although not in linear proportion).

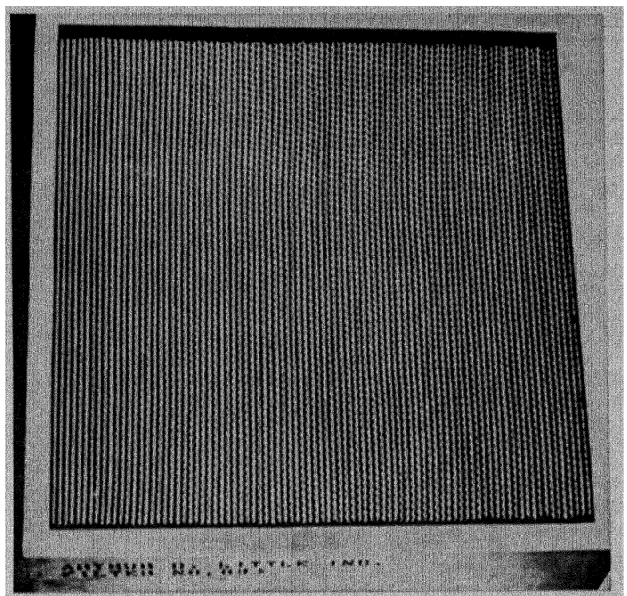

Figure 1. Cellulose-asbestos filter as used for high efficiency filtration of air. Unit shown is 24 in. × 12 in. and filters 1000 ft³ per min of air

It was also observed quite early in this development that it would be advantageous to protect the filter and increase its life by using a roughing or prefilter to remove the coarser particles and a fraction of finer particles. To date this has proved a very practical matter and most applications have involved having a spun glass filter as a pre-filter and a significant improvement in life has been obtained even though efficiency has not been increased. The practical life of these filters has proved to be much greater than originally anticipated and in many instances they have been left in service two to three years.

One of the major weaknesses of the cellulose-asbestos filter is its inability to withstand more than small amounts of corrosive gases or acid mists and also it is limited to temperatures below 100°C. Another limitation is the fact that the material used is not fireproof although it can be treated with a fire retardant. The inherent danger lies with ignition and dispersal of retained contaminants or in the collection of pyrophoric materials which can burn a hole through the media at the point of contact. Where the cellulose filter has been applied to reactor gas cleanup, spray cooling has been used to reduce gas temperatures. Roughing filters precede the final filters and well filtered water is necessary for preventing aerosol formation from the cooling spray.

Because of these limitations studies were initiated to develop an all-mineral filter. Two types of media have been formulated: one an all-glass formulation utilizing a combination of 1.5 micron and 0.5 micron fibers,[4] and the other a combination of the coarser size and Bolivian blue asbestos as used in the cellulose type. These have been fabricated into two kinds of units: one a metal frame[5] type utilizing an aluminum foil corrugated separator similar to the kraft type used in the cellulose model and the other[6] incorporating an all-glass frame and asbestos separators. Both of these media give performances comparable to the cellulose-asbestos formulation. In the case of the all-glass type, efficiencies far exceeding the earlier media have been reported for bacteria by Decker, *et al.*[7] Some filters fabricated with this media have already been placed in service. In applications for chemical exposure, wood frames and the vinyl adhesive have withstood most mineral acid attack. A recent development[8] has been a ceramic fiber 50% Al_2O_3 and 50% SiO_2, known as Fibrafrax which, although brittle and fragile, has been formulated into filter webs capable of withstanding 1000°C. The glass web or paper formulations employ a plastic binder which decomposes at temperatures above 250°C and tensile strength is lost. The only serious limitation to the glass or mineral media is attack by alkalis or hydrofluoric acid.

Another approach to the chemical resistance problem has been the development of papers from fine plastic fibers such as styrene or amid polymers. Papers comparable to the mineral fiber formulations have been developed and these resist all mineral acids and alkalis.

Another application of glass fibers has been the development of extended life graded layer filters for handling dissolver off-gas or vessel vent gases. This application has used chemically resistant glass in various diameters from 25 μ to < 1 μ placed in layers of varying density and thickness. Studies by Blasewitz and Judson[9] using a methylene blue and dissolver off-gases give performance and life characteristics for pilot studies. Full size installations have been in service for almost two years and show close to predicted resistance and life on radioactive aerosols. They are used for low loadings of radioactive particulates of acids and metal contaminants.

Sand or gravel in graded layers were used for cleaning general cell ventilation gases which were a problem before the glass fiber data were obtained. The greater porosity and smaller unit physical size with these fibers make them more suitable and capable of longer life in comparable sizes to present sand filters. A concrete lined pit can be filled with fibrous material in graded formulations on a porous supporting tile duct. An area large enough to handle the total gas volume at velocities of 20 feet per minute is the design criterion. Life of 15 to 25 years can be incorporated at extremely high efficiencies before the filter is abandoned.

Filters whose resistance increases in service and become highly radioactive because of their activity must be remote from personnel. For this purpose we have developed a variable compression filter[10] as shown in Fig. 2, which can be controlled remotely by means of a mechanical linkage or a motor. The unit incorporates compressed layers of spun fiber glass arranged so they can be relaxed or released in compression gradually as resistance increases. This permits the collected particulates to penetrate further into the media. Efficiencies well above 95% can be

Table I. Operational Characteristics of Air Cleaning Equipment*

Type of equipment	*Particle size range mass median microns*	*Per cent efficiency for size in col. 2*	*Velocity ft/min*	*Pressure loss: inches of water*	*Approximate cost/cfm $*	*Current application in US atomic energy program*
Simple settling chambers	>50	60 to 80	25 to 75	0.2 to .5	0.05	Rarely used.
Cyclones, large diameter	>5	40 to 85	2000 to 3500 (entry)	0.5 to 2.5	0.10 to 0.25	Precleaners in mining, ore handling, and machining operations.
Cyclones, small diameter	>5	40 to 95	2500 to 3500 (entry)	2 to 4.5	0.25 to 0.50	Same as above.
Mechanical centrifugal collectors	>5	20 to 85	2500 to 4000	–	0.20 to 0.35	Same as large cyclone application.
Baffle chambers	>5	10 to 40	1000 to 1500	0.5 to 1.0	0.05	Incorporated in chip traps for metal turning.
Spray washers	>5	20 to 40	200 to 500	0.1 to 0.2	0.10 to 0.20	Rarely used, occasionally as cooling for hot gases.
Wet filters	Gases and 0.1–25 μ mists	90 to 99	100	1 to 5	0.09 to 0.10	Used on laboratory hoods and chemical-separation operations.
Packed towers	Gases and soluble particles 5 μ	90	200 to 500	1 to 10	0.40 to 0.80	Gas absorption and precleaning for acid mists.
Cyclone scrubber	>5	40 to 85	2000 to 3500 (entry)	1 to 5	0.25 to 0.40	Pyrophoric materials in machining and casting operations, mining and ore handling. Roughing for incinerators.
Inertial scrubbers power-driven	8 to 10	90 to 95	–	3 to 5 HP per 1000 cfm	0.15 to 0.25	Pyrophoric materials in machining and casting operations, mining and ore handling.

* References for this table are:

First, M. W., *et al., Air Cleaning Studies,* Progress Report for Feb. 1, 1950 to Jan. 31, 1951. Harvard School of Public Health, NYO 1581, Waste Disposal.

First, M. W., *et al., Air Cleaning Studies,* Progress Report for Feb. 1, 1951 to June 30, 1952. Harvard School of Public Health, NYO 1586, Waste Disposal.

Friedlander, Sheldon, *et al., Handbook on Air Cleaning,* US Atomic Energy Commission (September, 1952).

Blasewitz, A. G., *et al., Filtration of Radioactive Aerosols by Glass Fibers,* Part One, General Electric Co., Hanford Works, Richland, Washington, HW20847, (1951).

Silverman, L., *Laboratory Design for Handling Radioactive Materials,* Panel Discussion. BRAB conference report No. 3, (Nov. 27 and 28, 1951). Available from Building Res. Ad-

obtained at reasonable resistances. The phenolic bonded flexible fiber glass gives resilience to the media to maintain shape as the compression is relaxed. Fiber glass media in this form has considerable acid and temperature resistance (to 170°C).

One important application for refining operations may be mentioned and that is the use of continuously or automatically cleaned pressed wool or synthetic felts. These are made in the form of bag units which are cleaned by high velocity jets. Rotary arm- and disk-type units are two new forms which appear useful for heavy loading applications. The major advantage of this type for refining and fabrication operations with radioactive metals is that constant resistance maintains uniform ventilation rates at the hood at the contamination source. The greater capacity cubic feet per minute per square foot of cloth area (cfm/ft^2 or filter velocity) reduces the number of bags or compartments and minimizes maintenance and replacement.

Mixed particulates such as acid mists and solids are common contamination forms and the fiber glass devices mentioned above are applicable. The use of continuously wetted fiber beds and dry filters is another approach to solving this problem. Wet collection procedures cannot be made as inherently efficient because entrained moisture or misting creates effluents not readily captured. Wet collectors in general, therefore should be followed by some dry collection procedure for most high efficiency requirements.

At our Air Cleaning Laboratory we have devoted considerable study to wet cell units followed by dry pads.[11] This type of device has been used for cleaning of laboratory hood effluents when connected to a central exhaust system. The test data presented in reference cited show this type of unit is primarily an excellent gas adsorption system because of the excellent extended surface provided by the fiber glass packs (8-inch thick cells of 250 micron glass in 8 pounds per cubic foot density). On a basis of these tests, a composite unit employing Dynel and Saran plastic fibers was studied for combined hydrogen fluoride gas and mist adsorption.[12] This gas adsorption unit indicates removal above 99% of hydrogen fluoride gas and for particulates in the 1 micron range 85 to 95%. If large amounts of

Table I. Operational Characteristics of Air Cleaning Equipment—continued

Type of equipment	*Particle size range mass median microns*	*Per cent efficiency for size in col. 2*	*Velocity ft/min*	*Pressure loss: inches of water*	*Approximate cost/cfm $*	*Current application in US atomic energy program*
Venturi scrubber	>1	99 for H_2SO_4 mist. SiO_2, oil smoke, etc. 60 to 70	12,000 to 24,000 at throat	6 to 30	0.50 to 3.00	Incorporated in air-cleaning train of incinerators.
Viscous air conditioning filters	10 to 25	70 to 85	300 to 500	0.03 to 0.15	0.004 to .006	General ventilation air.
Dry spun glass filters	5	85 to 90	30 to 35	0.1 to 0.3	0.02 to 0.04	General ventilation air. Precleaning from chemical and metallurgical hoods.
Packed beds of graded fibers. 1 to 20 μ. 40 inches deep	<1	99.90 to 99.99	20	10 to 30	1.0 to 5.0	Dissolver off gas cleaning.
High efficiency cellulose-asbestos filters	<1	99.95 to 99.98	5 through media 250 at face	1.0 to 2.0	0.04 to 0.06	Final cleaning for hoods, glove boxes, reactor air and incinerators.
All-glass web filters	<1	99.95 to 99.99	5 through media 250 at face	1.0 to 2.0	0.07 to 0.10	Final cleaning for hoods, glove boxes, reactor air and incinerators.
Conventional fabric filters	>1	90 to 99.9	3 to 5	5 to 7	0.30 to 1.00	Dust and fumes in feed materials production.
Reverse jet fabric filters	>1	90 to 99.9	15 to 50	2 to 5	0.50 to 1.00	Dust and fumes in feed materials production.
Single stage electrostatic precipitator	<1	90 to 99 90–95 on metallurgical fumes	200 to 400	0.25 to 0.75	0.50 to 2.00	Final cleanup for chemical and metallurgical hoods. Uranium machining.
Two stage electrostatic precipitator	<1 to 5	85 to 99	200 to 400	0.25 to 0.50	0.25 to 0.50	Not widely used for decontamination.

visory Board, National Research Council, Washington, D. C.
Dennis, R., *et al., Performance of Commercial Dust Collectors* (Report of field tests), Harvard School of Public Health, NYO 1588, Waste Disposal, (November, 1953).
First, M. W., *et al., Air Cleaning Studies,* Progress Report for July 1, 1952 to June 30, 1953. Harvard School of Public Health, NYO 1591, Waste Disposal.
Dennis, R., *et al., How Dust Collectors Perform,* Chemical Engineering, *59*:196, (Feb., 1952).
Dennis, R., *et al., Dust Collectors Tested in Field,* Chemical Engineering, 187–189 (May, 1954).
Johnson, G. A., *et al., Performance Characteristics of Centrifugal Scrubbers,* Chemical Engineering Progress, *51*:176, (April, 1955).

fine radioactive particulates ($< 1\ \mu$) are present such mists should include a filter type comparable to the cellulose-asbestos made with plastic fibers. Plastic filter web material, in quantity enough for this purpose, can readily be made if necessary as the technique has been well established. Another case of combined mixed particulates is associated with radiochemical laboratory use of perchloric acid. A small composite unit comprising a wetted cell-pack mist eliminator and all-mineral filter has been developed for this purpose as shown in Fig. 3. This device can be placed inside typical laboratory hoods as described.[3] It is thus possible to eliminate all organic materials in the cleaner with which perchloric acid might react. Sufficient cleaning is provided so that there is no danger of perchlorates forming in ducts or on succeeding dry hood filters. With this unit in place perchloric acid operations are safely performed in hoods provided with fiber glass prefilters and cellulose-asbestos final filters. Additional filtration was necessary because of the high specific activity of the isotopes involved in the perchloric digestions. The perchloric acid scrubber unit involves minimal duct surface before cleaning of effluent vapor. Similar problems have arisen in interhalogen chemical use in uranium metallurgy. Since these reactions were to be conducted in protected hoods, as mentioned above, some additional consideration was necessary to remove the interhalogen decomposition products. Chlorine trifluoride (ClF_3) and bromine trifluoride (BrF_3) react violently on contacting air to form intermediate gases such as hydrogen fluoride, chlorine, chlorine monoxide, chlorine dioxide, hydrogen bromide and hydrogen chloride. The use of aluminum wire filters or packed beds of limestone or shell natron was proposed to replace the fiber glass prefilters in hood operations. When using larger quantities of materials for recovery and treatment operations the scrubbing system developed by Liimatainen and Levenson[14] gives greater life and less maintenance. It consists of a series of ejector type nozzles followed by a metal demisting screen. High removal of halogen gases was readily obtained but particulate removal was less satisfactory.

Radioactive Gas Cleaning Problems

Radioactive gases created by reactor neutron flux on cooling air such as A^{41} and certain radioactive

gases (Kr^{89}, Kr^{91}, Xe^{140}, Xe^{141}) which decay to radioactive particulate matter are not easily removed by conventional approaches. Decay products may form after the latter gases pass through filters. One method of handling A^{41} and the decay products is based on meteorological dilution and dispersion from tall stacks. If large amounts of rare gases are involved adequate dispersion may depend upon meteorological conditions for proper operation.

The gases may be condensed and adsorbed on activated charcoal at extremely low temperatures using liquid nitrogen and similar refrigerents where it is economically feasible. The cost of such systems per cubic foot of air treated is so high that the method is only feasible for small volumes. Another approach for such volumes is compression and storage of the gases in chambers and permitting it to decay. For small volumes of gases this may be more economic than low temperature adsorption.

For gases such as iodine-131, because of its release in volume during dissolver operations, research has been devoted to methods for its removal from effluent gas streams. Scrubbing with spray or baffle plate scrubbers utilizing caustic adsorbents only yields efficiencies of 60 to 80% and removes some oxides of nitrogen simultaneously, neutralizing some caustic. Use of silver reactions was applied so that with a silver reductor unit composed of a tower packed with saddles coated with silver nitrate and maintained at an elevated temperature gives the highest removal of iodine compounds. These units are used in series with the fiber glass. Tests with this reactor have resulted in iodine removal with efficiencies greater than 99.99%. Most of the units installed have remained in operation for periods beyond two years. Difficulties have only resulted if excessive temperatures develop in the silver reactor thus stripping it of silver. Reaction gases with long half-life are fortunately quite limited in number. Some gases may be more difficult to remove than particulates. In these cases as a safeguard to all large scale operations producing large volumes of particulate areosols or gases, a stack should be provided to prevent difficulty from failures in cleaning equipment. The stack also provides an added dilution factor for minimizing health hazards. It should be emphasized however, that the first possible cleaning at the source within economic reason must be provided before considering dispersion to the atmosphere.

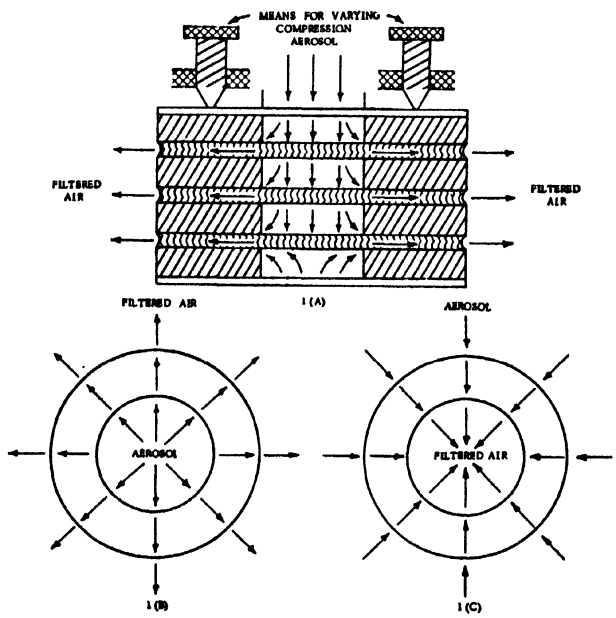

Figure 2. Variable compression filter as developed for remote control of resistance and utilizing a bonded fiber glass media

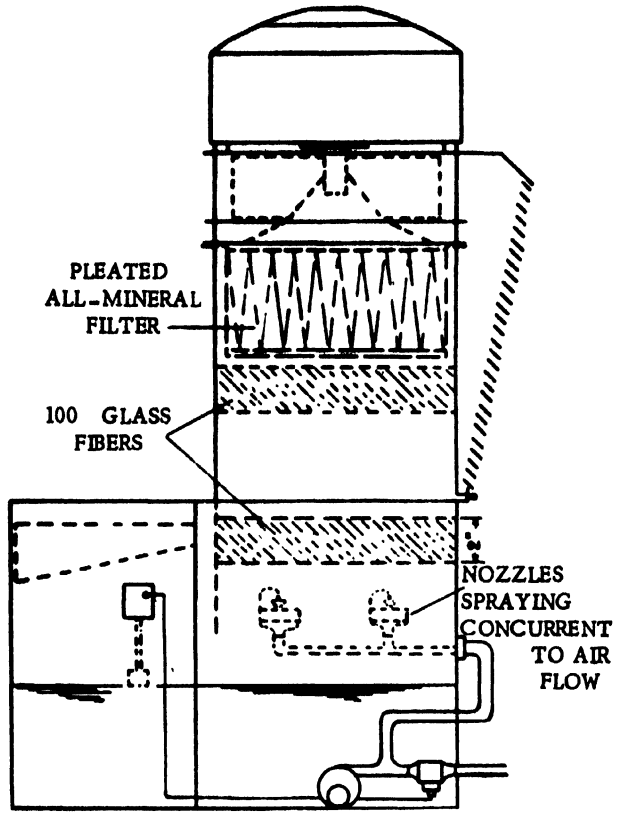

Figure 3. Schematic diagram of perchloric acid hood scrubber unit

Incineration and Evaporation

The problem of reducing solid and liquid wastes is of major concern in the nuclear energy field. To reduce the volume of low-activity waste tenfold by incineration or to reduce liquid waste 100 fold, or to its solid content, by evaporation has been investigated at many locations by the Atomic Energy Commission and its contractors. Incinerator development has been a major problem and should also incorporate an optimum gas cleaning system. High temperatures are developed, ranging from 500 to 1000°C, therefore it is necessary to provide cooling before particulate removal in most instances. Cleaning incinerator effluent gases consists primarily of removing particulates. There are situations where carbon isotopes may be involved and production of $C^{14}O$ or $C^{14}O_2$ can be of concern. Usually this problem is rare and after burners and alkali scrubbers can be employed to remove the carbon gases formed. Sulfur gases which can be formed may also

be absorbed by conventional methods of recovery, acid mist may be removed by filters. The approach at the present time is to reduce gas temperature so that final cleaning may be with a cellulose-asbestos filter ($< 100°C$) or an all-glass filter ($< 275°C$). Reducing gas volume by spray cooling or wet scrubbing minimizes the physical capacity of the final cleaning equipment. The type of gas-cleaning equipment applied to incinerators may be spray towers with elaborate scrubbers such as the Venturi scrubber in series and finally filtration through a spun glass prefilter with a final filter of cellulose-asbestos. Reheating may be necessary to prevent condensation on filters. A serious difficulty associated with incinerator operation is that improper combustion results in tar formation. Carbonaceous particulates which are gummy or sticky may rapidly plug high efficiency cleaners. Proper incineration will reduce some of the problems in the gas cleaning. Steam addition may increase particle size in some instances and if excess steam is available it can be utilized in steam scrubbers for capturing aerosols.

The problem of evaporation of liquids in regard to aerosol production depends on the method employed for reduction of liquid volumes. The highest efficiency in reducing volume is obtained by vapor compression evaporation. Filtration of entrained mist is done by means of fiber glass. Manowitz and his co-workers[15] have studied vapor compression equipment incorporating fiber glass filters for reducing radioactive particulates. They were able to obtain 100 fold reduction in liquid waste volume. Fiber glass filters gave decontamination factors ranging from 10^6 to 10^7. Fiber glass layer composition is similar to those employed for air or gas filtration purposes of coarser aerosols. A 3-foot layer of 14 to 20 micron fiber glass has a bulk density of 5 pounds per cubic foot at velocities of 60 feet per minute. This velocity is higher than used for direct aerosol filtration but it is apparently feasible where steam condensation takes place simultaneously. In evaporation of liquid wastes, rapid boiling or ebullition should be avoided as it produces droplets which may contain entrained solids. Upon evaporation these particles become an aerosol cleaning problem. At low temperatures these particulates can be cleaned by any of the methods described above for high efficiency removal. If the gas stream is saturated with moisture, condensation may result and all-glass filters would be needed.

In the perchloric acid scrubber described earlier the final all-mineral filter can be washed and cleaned several times. This removes the entrained acid but does not remove particulates imbedded in the fibers. It is apparent that fiber glass media can filter saturated gas streams without difficulty.

Methods of Evaluating Equipment Performance and Problems in Selection

Of major concern in evaluation of air cleaners has been the method of sampling and rating performance. To obtain an overall evaluation requires more than a single test aerosol. A single aerosol is useful for rapid rating of high efficiency filters where each must be tested to meet specific requirements. The dioctyl phthalate (DOP) condensation aerosol of 0.3 micron diameter which is nearly homogeneous is a simple technique for mass testing. Rapid measurement of aerosol concentration is done with a light scattering (forward) photometer. Since DOP is a liquid droplet however, results are not the same as obtained with solid particulates. For potential nuclear energy applications of devices or methods we use a number of aerosols made by dispersing of solid particulates or by spraying liquids containing dissolved salts (such as copper sulfate or uranium nitrate) which can be made into solid particulates of controlled size. Liquid smokes made from oil vapor condensation or burning tobacco are also employed. The size of the aerosol series used ranges from less than 0.1 micron (vaporized metals) to particles in the 1 to 5 micron range made from redispersed reduced solids such as talc, fly ash, calcium carbonate, and other mineral dusts. For high specific gravity simulation iron powder spheres prepared from iron carbonyl may be used. Performance should be based on efficiency by weight or weight efficiency for a specific particle size. We also employ stain or discoloration evaluation and for extremely toxic aerosols numbers of particles penetrating.

Cleaning Gases from Power Reactors

Particulates from power reactors come from two major sources. These are identified with conditions at the inlet and outlet of the reactor cooling air or its shield cooling air. The cleaning of air entering the reactors minimizes deposition and induced radioactivity. The degree of cleaning necessary for gases leaving the reactor depends upon the reactor design and the amount of precleaning. Regardless of the reactor design there will likely be gas generation somewhere in the system with possible entrainment of particulates. In present reactor designs some portion of the system may involve gas or air contamination. In the design stage, of course, this gas evolution or air contamination should be kept minimal. Certain package types may not involve gas in quantities until reprocessing of fuel elements. In cleaning reactor produced gases and particulates the methods which have been described above can be applied and the importance of reducing the gas volumes involved cannot be over emphasized.

The problems of cleaning associated with air-cooled reactors are more acute if rupture of fuel elements takes place in operation or if serious erosion of surfaces results. The important feature to bear in mind, however, is that contamination loadings will be low unless a large number of fuel element failures takes place. The reactor system should be safeguarded against any large numbers of slug or element ruptures by interlocking controls and warning devices. Should a catastrophic or multiple failure

reaction take place, the downstream filter should be capable of retaining most of the volatilized material. Devices as mentioned are available which will permit cleaning of gases at high temperature and where necessary should be constructed to allow high resistances to develop for extended life of the unit. Research is now directed towards developing devices which will operate continuously at temperatures above 500°C. This conditon also makes tall stacks much more effective for dispersion of radioactive gases and any discharged particulates.

New Methods of Gas Cleaning

Several new methods of gas cleaning have been developed by research sponsored by the Atomic Energy Commission. Many of these procedures have been described briefly in a recent paper by the writer.[8] Utilization of electrostatic forces at reduced costs and the development of devices which can operate continuously at high temperatures are two examples. A recent paper from this laboratory[17] describes a new method of electrostatic separation utilizing continuous friction charging of fabrics and appears promising for precleaning use. Figure 4 shows a schematic diagram of this unit. It cannot be used for saturated aerosols and acid-contaminated air streams. The use of inexpensive slag or mineral wool is being explored at our laboratory for high-temperature gas cleaning.[17] This method involves re-use of the wool by washing and drying. Similar methods of research at the University of Illinois[18] have indicated the possible use of electrified sprays or electrified filters for air- and gas-cleaning work. Electrification can be done at fairly low voltages in the case of the filter. Electrostatic precipitator voltages are probably necessary in the case of the spray collecting device. Since most of these devices are in the state of early development it is not possible at the present time to indicate more than their potential application to nuclear energy systems.

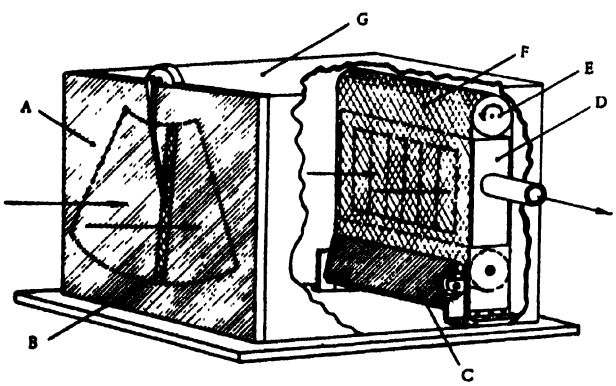

A - ORLON SCREEN
B - WOOL COVERED WIPER BLADE
C - ORLON COVERED PADDLE
D - PERFORATED LUCITE BOX
E - LUCITE ROLLER
F - WOOL BELT
G - MASONITE BOX

Figure 4. Continuously friction charged electrostatic air filter utilizing synthetic and wool fabrics

SUMMARY

Problems in air and gas cleaning which result from the handling, metallurgy, reactions and applications of nuclear energy processes are discussed in detail. Processes which create aerosols and their behavior are described briefly with emphasis on those aspects which differ from handling or combustion of ordinary materials. Cleaning requirements are considered for protection of personnel engaged near operations as well as the general public. Special emphasis is devoted to the aspects of cleaning gases from power reactors and their relations to the basic economics of the overall problem.

The paper includes performance data for various devices on radioactive and inert aerosols encountered in mining, feed materials production, metallurgical reactions, reactor operation, isotope production and handling and special problems such as incineration of contaminated waste materials.

Methods of evaluating equipment performance and problems in the selection and operation of equipment are of special concern and are discussed in detail.

New methods of gas cleaning developed by research at Harvard and elsewhere for needs of the US Atomic Energy Commission and its contractors such as high temperature and corrosion resistant filtration media are mentioned. Areas in which further research is needed and the importance of reducing air- and gas-cleaning costs in relation to operating economics are emphasized.

REFERENCES

1. Silverman, L., *Performance of Industrial Aerosol Filters,* Chemical Engineering Progress, *47*:462, 1951.
2. Friedlander, S., Silverman, L., Drinker, P., and First, M. W., *Handbook on Air Cleaning,* US Atomic Energy Commission, US Government Printing Office, September, 1952.
3. Stafford, E., and Smith, W. J., *Dry Fibrous Air Filter Media,* Industrial and Engineering Chemistry, *43*:1346, 1951.

4.a Anonymous, *Paper from Glass Fibers,* National Bureau of Standard Technical Report 1607, Washington, D. C., November, 1951.

b Anonymous, *Fiberglas Products for Paper Making,* Owens-Corning Fiberglas Corporation, Newark, Ohio. Bulletin GL2.A1, February, 1954.

c Smucker, C. A., and Marlow, W. C., Jr., *Application of Glass Fibers in Filtration Processes,* Industrial and Engineering Chemistry, *46*:176, 1954.

d O'Leary, M. J., Scribner, B. W., Missimer, J. K., and Erving, J. J., *Manufacture of Paper from Glass Fibers,* TAPPI *35*:289, 1952.

5. Smith, W. J., *Non-Combustible and Chemical Resistant Air Filters for High and Low Temperature Use,* Air Cleaning Seminar, Ames Laboratory, September 15–17, 1952. US Atomic Energy Commission, WASH 149, March, 1954.
6. High Temperature All-Glass Ultra Filter. Mine Safety Appliances Company, Pittsburgh 8, Pa., 1954.
7. Decker, H. M., Harstad, J. B., Piper, F. J., and Wilson, M. C., *Filtration of Micro-organisms from Air by Glass Fiber Media, Heating, Piping and Air Conditioning, 26*: 155, 1954.

8. Silverman, Leslie, *New Developments in Air Cleaning,* American Industrial Hygiene Association Quarterly, *15:3,* 1954.
9. Blasewitz, A. G., and Judson, B. F., *Filtration of Radioactive Aerosols by Glass Fibers,* Air Repair, *4*: 223, 1955.
10. Silverman, Leslie, and First, M. W., *Edge and Variable Compression Filters for Aerosols.* Industrial and Engineering Chemistry, *44*:2777, 1952.
11. First, M. W., Moschella, R., Silverman, L., and Berly, E. M., *Performance of Wet Cell Washers for Aerosols,* Ibid, *43*:1363, 1951.
12. Berly, E. M., First, M. W., and Silverman, L., *Recovery of Soluble Gas and Aerosols from Air Streams,* Ibid, *46*: 1769, 1954.
13. Silverman, Leslie, and First, M. W., *Hood Scrubber Unit for Perchloric Acid,* Harvard School of Public Health, NYO 1589, US Atomic Energy Commission, November 30, 1954.
14. Liimatainen, R. C., and Levenson, M., *Absorption of Some Halogen Gases from Air by a Limestone Bed and a Spray Tower,* Argonne National Laboratory, Lemont, Illinois, ANL–5015, April 1, 1953.
15. Manowitz, B., Richards, P., and Horrigan, H., *Vapor Compression Evaporation Handles Radioactive Waste Disposal,* Chemical Engineering *62*:194, 1955.
16. Silverman, L., Conners, E. W., and Anderson, D. M., *Mechanical Electrostatic Charging of Fabrics for Air Filters,* Industrial and Engineering Chemistry, *47*:952, 1955.
17. Silverman, L., *Technical Aspects of High Temperature Gas Cleaning for Steel Making Processes,* Air Repair, *4*:189, 1955.
18. Kraemer, H. F., *Properties of Electrically Charged Aerosols,* University of Illinois, Engineering Experiment Station, Technical Report No. 12, (COO–1013), March 31, 1954.

The Variation of Effluent Concentrations from an Elevated Point Source

By M. E. Smith,* USA

Measurement of the dispersion of an oil-fog test effluent from a 355-foot source has been one of the outstanding features of the meteorological program at Brookhaven National Laboratory since 1949. In this paper, the results of more than 100 individual field tests contribute to a study of the time and space variations of concentrations. However, even this analysis can hardly be called complete, since sufficient data are available only for the analysis of typical daytime dispersion cases. The measurements of nuclear radiation from the cooling air of the reactor could have been used to provide additional information, but it is felt that a study of the oil-fog concentrations alone is more valuable. Treatment of two completely different effluents in the same paper would be likely to result in confusion rather than clarification of the problem. Furthermore, radiation effects can be computed from concentration estimates in a relatively straightforward manner, but it is nearly impossible to define point concentration values from measurements of radiation from A^{41}.

INSTRUMENTATION

The meteorological installation, oil-fog test facility and local topography have been described previously by Beers,[1] Lowry,[2] Singer and Smith.[3] A 420-foot tower supports wind and temperature instruments as well as a test stack from which oil-fog is emitted. The oil-fog is produced by condensation rather than combustion, and the resulting aerosol consists of droplets ranging from 0.005 to 3.0 μ with a mean radius of 0.3 μ. The settling rate is negligible when compared to natural diffusion processes, and both evaporation and coagulation effects are believed minor. The effluent may therefore be treated as a true aerosol.

The oil-fog has been measured by two very different techniques. Photometric densitometers, operating on the basis of the 90-degree scattering of visible light, have been used for continuous measurements at ground-level. Since these instruments are expensive and a vehicle is required for the operation of each unit, not more than three have been used at one time. A second method, involving the collection of oil-fog on molecular filters, and measurement by a fluorometric device has been used during the past two years. This method permits measurements at a large number of points, but gives no indication of short-term variations. The calibration of both systems has been accomplished in a virtually airtight room having a volume of 200 m^3. Oil-fog is introduced in known amounts by a miniature of the large field generator.

Laboratory accuracy has not been achieved with either of the field sampling techniques. In fact, it is quite difficult to evaluate certain aspects of this problem of accuracy, since no method of testing the sampling techniques has been found that does not also have relatively large errors. It is necessary, therefore, to use comparisons for an over-all evaluation of accuracy. The light-scattering and fluorometric techniques are good checks against each other. The former is very sensitive to variations in particle size but cannot "lose" an appreciable quantity of the effluent in the process of sampling. Exactly the reverse would be expected of the filter-fluorometer method. The data are subject to an over-all check by comparison with the measurements of the radiation from the A^{41} contained in the nuclear reactor cooling air. These measurements, described by Lowry[4] and Singer[5], are of a different type altogether. The effluent is an inert gas not subject to any depletion other than an accountable radioactive decay. Also, the sampling devices are sensitive to both β and γ radiation and therefore reflect a complex integration of effects from a large portion of the cloud rather than a small volume. Despite these and other important differences, predictions of the radiation based on oil-fog measurements have been accurate to within a factor of 2. Furthermore, the comparisons have shown no tendency to change with distance, and this certainly should be apparent if the oil-fog suffered serious depletion after leaving the stack.

Thus, the oil-fog data summarized are believed to be accurate to $\pm$ 50%. The data obtained after 1951 are almost certainly more accurate than this, but it would be incorrect to assign greater reliability to the combined results.

The accuracy of the meteorological instruments is of course much easier to evaluate. Complete reports of this work have been published previously by Mazzarella,[6] and Mazzarella and Kohl.[7] It is important in this analysis to recognize that the wind direction measurements are reliable only to $\pm$ 3.0 degrees, and that map locations may have directional errors of the same order. Therefore, the

* Brookhaven National Laboratory.

Table I. Relation of Gustiness Classes and Meteorological Conditions*

Gustiness classification	Mean wind speed (m-sec^{-1})	Mean lapse rate T_{410}-T_{37} (°C)	Qualitative description of meteorological conditions	Behavior smoke plume	% frequency of occurrence
A	1.8	−1.25	Sunny skies, light variable winds.	Erratic movement of plume in loops and separate puffs.	1
B_2	3.8	−1.60	Similar to A, stronger winds.	Similar to A, but more consistent direction.	3
B_1	7.0	−1.20	The typical daytime condition. Sunny to partly cloudy skies, moderate winds.	Considerable vertical and horizontal motion with loops in plume, but rather steady direction of motion.	42
C	10.4	−0.64	Overcast skies and moderate to strong winds.	Cone-shaped plume with very consistent dimensions and no evidence of loops or breaks.	14
D	6.4	+2.00	Clear to partly cloudy nights with light surface winds. The typical nocturnal conditions.	Fanning plume with no appreciable vertical motion and weak horizontal dispersion.	40

* The winds, lapse rates and general weather conditions usually associated with the Brookhaven gustiness classes are shown. Their frequency of occurrence and rough description of smoke behavior are also included.

relation between the indicated mean winds and the locations of the samplers is reliable to only ± 6.0 degrees. The wind speed measurements are accurate to ± 0.2 m-sec^{-1} and the temperature differences to ± 0.1°C.

SAMPLING PROCEDURES

The oil-fog sampling instruments have been used in three different ways. The first and most common are continuous records of concentration at a fixed point over time periods ranging from a few minutes to several hours. It is from these densitometer records that all data on short-term variations are obtained. The densitometers have also been used to obtain series of traverses perpendicular to the wind direction. These give fair estimates of the mean crosswind profiles of the concentration and good estimates of plume width. In the third procedure, ten or more filter samplers have provided more accurate measurements of the crosswind profiles. Mention should also be made of the large number of visual and photographic observations which, although qualitative, have served to eliminate faulty data and improve the reliability of the sampling system.

METEOROLOGICAL CLASSIFICATION

In order to prevent an analysis of this type from becoming too involved, it is necessary either simply to list the concentration data together with the associated meteorological information, or to sort them on the basis of some simplified classification of weather conditions. Largely for convenience, these data are separated in accordance with the gustiness classification described by Singer and Smith.[8] The gustiness classes are based on the variability of the horizontal wind direction at stack height (355 feet). Sample sections of the horizontal direction records are shown in Fig. 1. The frequency of occurrence is shown in Table I together with other pertinent information. The following sections themselves reveal some of the deficiencies of the classification, but it has been found suitable for the separation of major differences in dispersion and for the prediction of ground-level concentrations at this site.

MATHEMATICAL CONSIDERATIONS

The formula developed by Sutton,[9] serves as a mathematical model for the dispersion. As has been noted recently by the author,[10] this selection is more a matter of convenience than theoretical preference, since no treatment now available can be described as a general solution of the problem. The form used in this analysis is given in Equation 1.

$$\overline{X} = \frac{2Q}{\pi C_y C_z \bar{u} x^{2-n}} \exp\left[-\frac{1}{x^{2-n}}\left(\frac{y^2}{C_y^2} + \frac{h^2}{C_z^2}\right)\right] \tag{1}$$

where $\overline{X}$ = mean concentration (gm/m^3), Q = rate of pollutant emission (gm-sec^{-1}), C_y = horizontal diffusion parameter (m$^{n/2}$), C_z = vertical diffusion parameter (m$^{n/2}$), u = mean wind speed (m-sec^{-1}), x, y = downwind and crosswind distances (m), h = stack height (m), and n = index of turbulence (dimensionless).

Since one of the main purposes is to summarize the Brookhaven results for comparison with others,

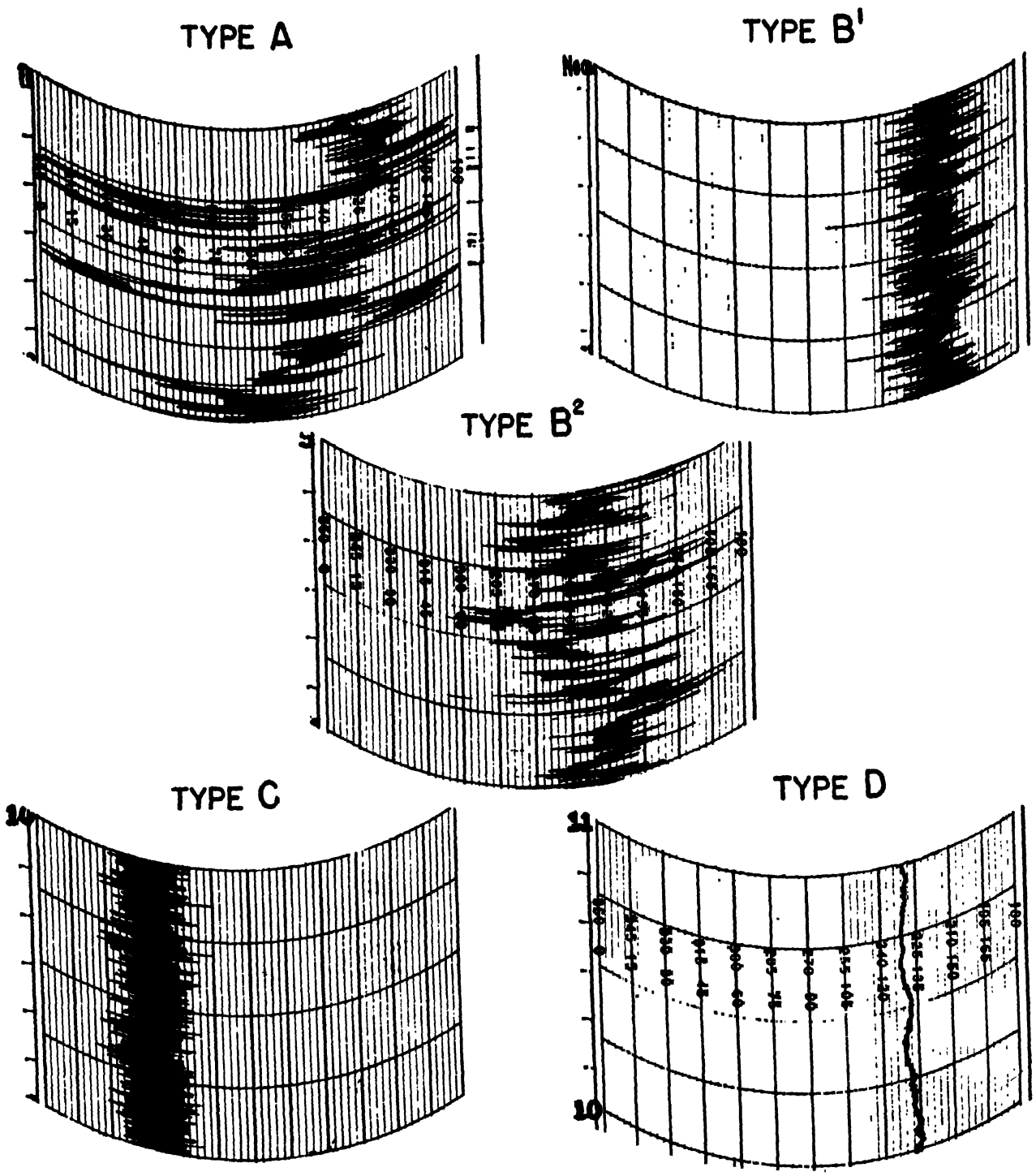

Figure 1. Gustiness classification. Sections of horizontal wind direction records are shown illustrating the five classes of wind gustiness

the concentration values are converted to the dimensionless quantity $X\ uh^2/Q$, although they will still be referred to concentrations. The reader is warned that the use of this form does not imply that direct comparison with data obtained from very different sources should give satisfactory results. C_y and C_z almost certainly vary significantly with height and probably with surface roughness also. The physical significance of the parameter n is somewhat uncertain, but it too may vary with height and terrain factors.

Some readers may wish to review the actual concentration measurements. The necessary values of u and Q are given in Table VIII, and a constant stack height of 108 meters is used, since the plume seldom rises significantly above the stack top.

In a study involving turbulence it is always necessary to select time intervals to be used as basic averaging periods. In so doing, one influences the study by excluding or including variations of certain periods from the definition of turbulence. In the Brookhaven case, a one-hour period was chosen in accordance with the large scale of the problem and the initial interest in a relatively long-term radiation dosage. Thus, the most intensive work has been directed toward the prediction of mean concentrations for one-hour periods. Data for shorter intervals have been treated as deviations.

TIME-MEAN CONCENTRATIONS

The most complete mean concentration data from tests are those obtained during the sunny skies and moderate winds of the B_1 gustiness class. In fact, the data are sufficient to allow consideration of variations with wind speed as well as distance. Accordingly, the time-mean concentration values are divided into low and high wind speed groups in Tables II*a* and II*b*. Data lying within ± 5.0 degrees of the plume centerline, as indicated by the mean wind direction, are included.

The first point of interest is the obvious deviation of certain tests from the relatively smooth concentration-distance relation suggested by the majority of the results. Tests 54–19, 50–9 and 54–21 in Table II*a* and 54–16 in Table II*b* are the most apparent misfits. No simple and complete explanation of these deviations has been found. However, the remaining data give fairly consistent patterns indicating a maximum concentration between 0.8 and 1.0 km in the 0–8.9 m-sec^{-1} group and at about 1.3 km in the $\geqslant$ 9.0 m-sec^{-1} set. The lack of data at distances other than those indicated does not mean that measurements were never made at such points, but rather that the attempts gave results below the sensitivity of the instrumentation.

One reason for the wide variability of the data given in Tables II*a* and II*b* is certainly that the relation between the indicated and true plume centerlines is difficult to specify. Two of the causes of this, wind direction and map errors, have been mentioned previously. In addition, the variation of wind direction with height is recognized as a contributing factor. The validity of this can be shown by an analysis of the crosswind traverse and filter data which automatically define the actual centerline at ground-level. A significant improvement in the definition of the concentration-distance relation is shown in Table III, in which only tests of the crosswind type are used.

Similar tabulations of data for the A, B_2 and C gustiness types are not included because the number of suitable runs in each of these groups is insufficient. This is not surprising in view of the infrequent occurrence of the types and the fact that precipitation often accompanies the C conditions. However, partial data and visual observations have permitted evaluation of diffusion parameters for the B_2 and C cases as well as the B_1. The estimates completed in 1953 are shown in Table IV. These values of n, C_y and C_z have been used to prepare the ground-level concentration patterns given in Figs. 2, 3 and 4. It should be noted that only half of the full horizontal plot is shown, and that the scale in the y-direction is exaggerated for clarity.

Comparison of the B_1 plot with the actual data (Tables II*a* and II*b*) shows that some revision is needed. The distance of the predicted maximum is nearly correct for the 0–8.9 m-sec^{-1} wind group, but the value of 0.226 seems high. However, it must be admitted that it is extremely difficult to locate a sampler at the exact position of the maximum, and the value is probably nearly correct. It is quite evident that the prediction underestimates

Table IIa. Time-Mean Concentrations within ± 5.0 degrees of the Indicated Centerline of the Plume.* B_1 gustiness; winds 08.–9 m-sec^{-1}

Distance from source (km)	Mean concentration $\left(\frac{Xuh^2}{Q}\right)$	Length of test (min)	Test No.
0.70	0.026	60	54–2
0.77	0.083	52	22
1.00	0.151	37	50–3
1.00	0.118	58	50–6
1.10	0.041	135	54–15
1.10	0.086	54	51–9
1.20	0.037	54	51–9
1.20	0.095	83	52–4
1.40	0.018	116	54–19
1.50	0.011	76	50–9
1.90	0.131	106	54–21
1.90	0.049	92	51–9
2.25	0.054	46	50–3
2.40	0.052	70	51–1
2.50	0.049	43	50–6
3.60	0.015	95	51–1
3.98	0.031	70	52–3
4.40	0.003	80	50–9
4.40	0.027	74	51–9

* The variation of mean concentrations with distance is shown for low and high wind-speed groups in the *a* and *b* sections of this table respectively. Concentration values are actually in dimensionless units of Xuh^2/Q, as is true for all data.

Table IIb. Time-Mean Concentrations within ± 5.0 degrees of the Centerline of the Plume. B_1 gustiness; winds $\geqslant$ 9.0 m-sec^{-1}

Distance from source (km)	Mean concentration $\left(\frac{Xuh^2}{Q}\right)$	Length of test (min)	Test No.
1.10	0.073	95	52–1
1.20	0.120	120	54–6
1.30	0.134	90	52–2
1.30	0.125	59	54–3
1.50	0.019	150	54–16
1.50	0.102	140	54–6
1.70	0.095	86	52–6
2.00	0.040	180	54-8
2.30	0.066	90	52–2
2.50	0.027	86	52–6
5.10	0.053	86	52–6

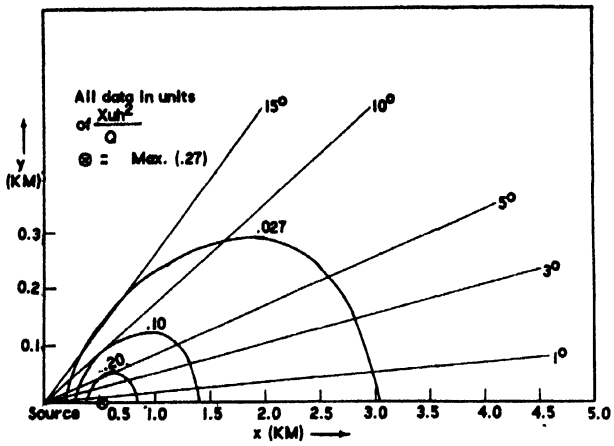

Figure 2. Isolines of ground-level concentration—B_2 gustiness. Horizontal plot of ground-level concentrations computed from the Sutton equation with n, C_y and C_z values for B_1 case derived at Brookhaven

the distance of the maximum with winds $\geqslant$ 9.0 m-sec^{-1} and here also the predicted maximum is somewhat above that shown by the actual data. The set of parameters gives a good indication of the limits of the plume as defined by 10% of the predicted centerline concentration. Table III shows the comparison between plume boundaries obtained from filters and traverses and the computed values. Taken together, the data indicate a need for a revision in the B_1 classification, as well as some alteration of the values of the parameters. The existing B_1 class clearly includes too wide a range of dispersion conditions.

Even though it is impossible to substantiate directly the reliability of the B_2 and C predictions, an examination of Figs. 2 and 4 show the qualitative differences from the B_1 case. The maximum concentration is found close to the source in the B_2 case and the value of 0.270 is the highest observed. The C case on the other hand, is accompanied by a lower maximum value of 0.148 at a distance of 2.0 km. In practice, the gradation from high-maximum mean concentrations with the B_2 condition to lower values with the C case is accentuated by the fact that the typical wind speeds increase in the same order.

Some mention should be made of the A gustiness at this point. It is impossible to define a suitable estimate of a mean concentration distribution since the case is characterized by extreme variability of the light wind flow. All that can be accomplished is a description of the peak concentrations observed.

SHORT-PERIOD MAXIMA

Although long-term mean data are adequate for many problems at this site, the interest of others is often directed to the short-term peak values. The tests in which the photometric densitometers have been used provide reliable records of fluctuations as short as 5 seconds duration. It would be possible to prepare sets of parameters for Equation 1 to predict the maximum values for any desired time period. However, ratios of the short-period maxima to the long-term means are simpler to compute and equally suitable for most purposes.

As in the earlier portion of this analysis, it is possible to give a reasonably complete summary of the B_1 gustiness class, but only a rough approximation for the B_2 and C groups. From the visual appearance of the three types of dispersion and recognition of the predominance of large, convective eddies in the B_2 cases, one would anticipate that the largest ratios would accompany this condition and that the C group would show the smallest. That the data shown in Table V do not fulfill this expectation is probably a reflection of the inadequate number of B_2 tests.

The decrease of the ratios with distance in the B_1 condition is an interesting feature. It may reflect the more complete mixing of the effluent with increasing distance; it may also be concerned with the inadequacy of the classification itself. No positive answer can be given at present.

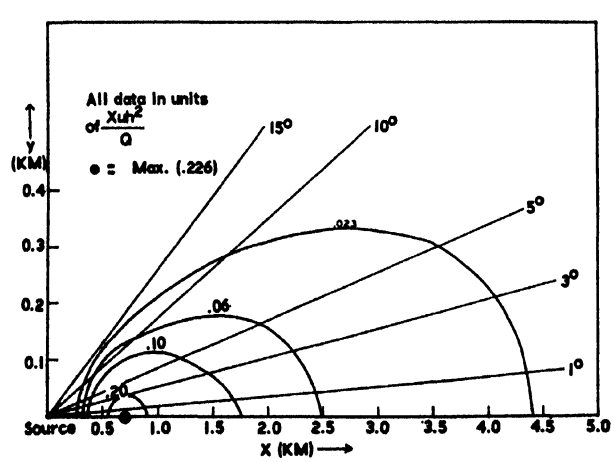

Figure 3. Isolines of ground-level concentrations—B_2 gustiness. Horizontal plot of ground-level concentrations computed from the Sutton equation with n, C_y and C_z values for B_2 case derived at Brookhaven

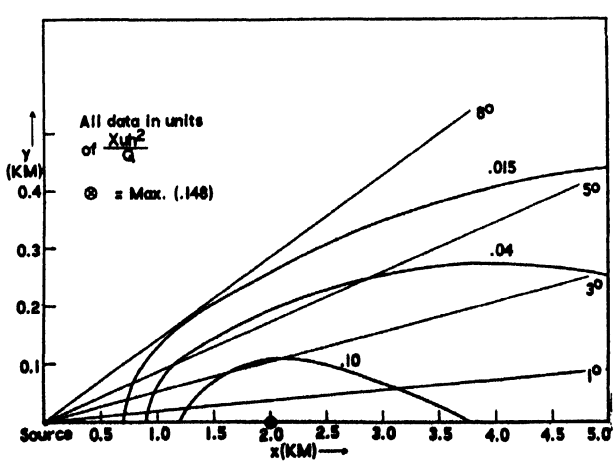

Figure 4. Isolines of ground-level concentrations—C gustiness. Horizontal plot of ground-level concentrations computed from the Sutton equation with n, C_y, C_z values for C case derived at Brookhaven

Table III. Relation of Plume Width to Distance from the Source.* B_1 gustiness

Distance downwind (km)	Observed centerline concentration $\left(\frac{Xuh^2}{Q}\right)$	Plume half width†		Test No.
		Observed (deg)	Computed (deg)	
1.1	0.132	10	13	52–1
1.2	0.125	9	13	54–3
1.2	0.116	13	13	51–9
1.2	0.132	12	13	52–4
1.3	0.176	14	12.5	52–2
1.4	0.120	14	12.5	54–6
1.7	0.124	10	12	52–6
1.9	0.157	12	12	54–21
2.3	0.090	10	12	52–2
2.5	0.100	9	12	52–6
3.6	0.015	9	12	51–1
4.0	0.041	11	12	52–3
4.4	0.038	10	12	51–9
5.1	0.067	8	12	52–6

* Measured and computed angular plume widths are shown for the B_1 gustiness class only. Since these tests include only those in which the true centerline was known, the concentration values are believed more reliable than those in II*a* and II*b*.

† (Angular distance at which 10% of centerline value occurs).

Table IV. Diffusion Parameters for Prediction of Hourly Mean Concentrations from the 355-ft. Test Stack*

Gustiness classification	n	C_y	C_z
B_2	0.17	0.31	0.36
B_1	0.28	0.40	0.39
C	0.48	0.54	0.34

* The n, C_y and C_z values used with the Sutton equation are shown. No values are included for the A and D gustiness classes because neither is properly described by the equation.

In addition to the ratios of short-period maxima to long-term means, an indication of the absolute maximum values that have been observed is of interest. Presentation of these data as a function of distance but without regard to other factors emphasizes the characteristics of dispersion associated with the gustiness classes. In Table VI it is easily seen that the peak concentrations are exclusively associated with B_2 gustiness close to the source and B_1 conditions in the intermediate distance range. At distances beyond 5.5 km, the C gustiness predominates. The D-B_1 class is a transitional type discussed in a later section. The order of progression with increasing distance certainly should be A, B_2, B_1 and C, and it is believed a matter of chance that an A case does not appear among the absolute maximum values.

A similar presentation of the time-mean concentrations is given in Table VII to complete the study of absolute maximum values. In this analysis also, the lack of a B_2 case close to the source probably reflects chance and inadequate data.

PERSISTENCE OF EFFLUENT AT SAMPLING POINTS

The data presented in preceding sections have indicated that the typical process of dispersion during the daytime cannot be completely described in terms of hourly mean concentrations, since the effluent moves past a fixed sampler in a series of puffs or eddies. An analysis of maximum concentration values has been used as an additional measure. Another study of interest is the percentage of time that effluent is found at given sampling points. This is presented in Table VIII, in which the B_1 and C data are listed in order of increasing distance, and the corresponding mean wind speeds are added for comparative purposes. The tabulation for the B_1 case shows no conclusive relation with either wind speed or distance, although one might have anticipated the latter effect on the assumption of more complete mixing of the effluent further from the source. The lack of such a relationship probably reflects the major importance of the large, long-period eddies in controlling the position of the entire plume with reference to all stations within 10 km.

The three cases representing the C gustiness are included because it is believed that they are typical, even though it is not possible to offer statistical proof. The long-period eddies appear to be less prominent under these conditions, and one would expect relatively continuous concentrations at points near the plume centerline. With similar reasoning, the B_2 condition should show low percentage, but the data are inadequate to warrant any firm conclusion.

DISPERSION UNDER STABLE CONDITIONS

Special mention must be made of the D gustiness class since concentration data are not presented. The

Table V. Average Ratios of Peak to Time-Mean Concentrations*

Gustiness type	Distance from source (km)	Ratios of peaks to mean concentration for complete test					No. measurements used
		5-sec	1-min	4-min	12-min	24-min	
B_1	0.5 to 2.0	12.8	7.9	5.0	3.1	1.8	14
B_1	2.1 to 5.5	6.6†	5.5	3.6	2.1	–	7
C	All	2.7	2.1	1.9	1.4	–	3
B_2	All	9.3	5.2	4.0	3.1	2.1	3

* In the Brookhaven work, short period concentrations are usually treated as deviations from the long-term values. The observed ratios are shown. No data are included for the A gustiness type because of the wind fluctuations and inability to select an appropriate location for extended observation.

† The observed individual ratios in the 5-second, B_1 cases ranged from 29.8 to 2.8.

reason for this is that effluent from the test stack remains aloft during temperature inversions, and a fully satisfactory method of obtaining measurements has not been perfected. The lack of data does not suggest that the case is unimportant. If the point of emission were below the general level of the terrain, the D condition would become a matter of vital interest since the concentrations within the plume remain greater than in any other case, and the frequency of occurrence is high (40% of all hours). Therefore, the photographic and visual observations are summarized.

The effluent plumes have been followed with vehicles and aircraft to distances as great as 25 miles, yet oil-fog has never been detected at ground-levels while an inversion was present. The oil-fog disperses in the shape of a narrow cone close to the stack, gradually widening horizontally but not vertically as it moves downwind until it assumes the appearance of a flat sheet at great distance. Two distinct forms of inversion plumes have been detected. In the one case, long-period, horizontal eddies give the trail the appearance of a meandering river. In the other, the meandering is absent and the trail takes a simple, wedge-shaped form. Many estimates of the width of the trail leave little doubt that the most common horizontal angle at which the lateral dimension of the trail expands is 3 degrees.

Table VI. Variation of Peak Concentrations with Distance

Distance from source (km)	Peak concentrations* $\left(\frac{Xuh^2}{Q}\right)$ 5-sec	1-min	Gustiness type	Test No.
0.26	2.100	–	B_2	23
0.36	1.300	–	B_2	23
0.70	2.500	1.000	B_2	51–11
0.75	2.610	1.621	B_1	50–6
0.77	1.200	–	B_1	22
1.00	1.099	0.814	B_1	50–3
1.10	1.463	0.501	B_1	54–19
1.20	1.340	0.690	B_1	50–3
1.50	1.320	1.069	B_1	54–6
1.90	0.407	0.387	B_1	54–21
2.20	0.524	0.374	B_1	50–3
3.00	0.525	0.400	B_1	51–2
5.00	0.254	0.246	B_1	51–2
5.70	0.318	0.303	C	51–4
6.00	0.156	–	D–B_1	11
6.20	0.152	0.145	C–D	51–5
13.00	0.049	–	D–B_1	11

* Data have been selected from the records to suggest the envelope of the probable over-all maxima. The relation of the gustiness classes to the peak values is noteworthy.

Table VII. Variation of Maximum Time-Mean Concentrations with Distance

Distance from source (km)	Time-mean* concentration $\left(\frac{Xuh^2}{Q}\right)$	Gustiness type	Test No.
0.70	0.038	B_1	54–2
0.75	0.120	B_1	50–6
0.77	0.083	B_1	22
0.80	0.137	B_1	53–2
1.00	0.151	B_1	50–3
1.10	0.132	B_1	52–1
1.30	0.238	B_1	54–3
1.50	0.102	B_1	54–6
1.90	0.157	B_1	54–21
2.30	0.090	B_1	52–2
2.50	0.100	B_1	52–6
4.00	0.041	B_1	52–3
5.00	0.107	B_1	51–2
5.10	0.067	B_1	52–6
5.70	0.117	C	51–4
6.20	0.095	C–D	51–5

* Only tests of at least 30-minute duration are used.

Table VIII. Per Cent of Time Effluent Present at Sampler* During Tests $\geq$ 30 Minutes

Distance (km)	Time oil-fog present (%)	Wind speed ($m\text{-}sec^{-1}$)	Test No.
	B_1 gustiness		
0.7	69	3.5	50–6
0.8	61	4.0	22
1.0	81	3.5	50–6
1.0	86	8.5	50–3
1.1	44	5.0	54–15
1.4	91	6.0	54–19
1.5	64	5.5	50–9
1.5	74	10.0	54–16
1.5	58	10.5	54–6
1.9	96	8.7	54–21
2.0	57	10.5	54–8
2.2	93	8.5	50–3
2.4	69	8.0	51–1
2.5	91	3.5	50–6
3.6	47	8.0	51–1
4.4	83	5.5	50–9
	Mean 73%		
	C gustiness		
4.0	100	8.8	15
5.7	73	8.5	51–4
6.2	100	7.5	51–5

* All units within ±5 degrees of indicated centerline. The effluent in lapse conditions is seldom present continuously at a sampling location.

TRANSITIONAL CONDITIONS

No description of pollution from the test stack would be complete without some reference to transitional periods. Changes from one gustiness class to another are normally uncomplicated in terms of concentration values. However, the transition from stable to unstable conditions or vice-versa is often noteworthy. The breakdown of a well-established D gustiness into an A, B_2 or B_1 classification is often productive of high ground-level concentrations. Close to the tower, these peak values are similar to those of the A or B_2 class, but at greater distances the values are usually higher than are ever found otherwise. This is because they result from a sudden overturning of the highly concentrated inversion plume. The peak values given for 6.00 and 13.00 km in Table VI were obtained during such cases, and the 13.00 km measurement is the most distant ever made in the entire test series. This

overturning or fumigation seldom occurs with wind speeds above 6 m-sec^{-1}, and normally does not last for more than 30 minutes. Figures 5 and 6 show the appearance of the plume before and after such a fumigation.

The change from lapse to inversion conditions may also give rise to unusual concentration measurements. In this transition, effluent from a lapse condition may be trapped in an inversion layer forming near the ground, with the result that the concentration remains nearly constant in a small area for one hour or more. The values of such concentrations are not necessarily high. Only the duration is unusual.

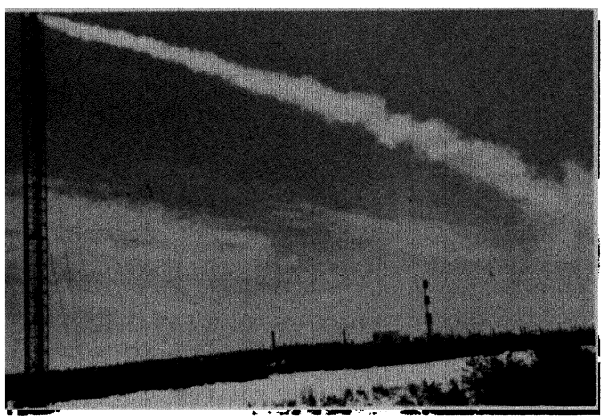

Figure 5. Inversion oil-fog plume—Brookhaven test stack. The photograph is taken just prior to the change from an inversion to lapse condition, but the trail is still typical of the D gustiness

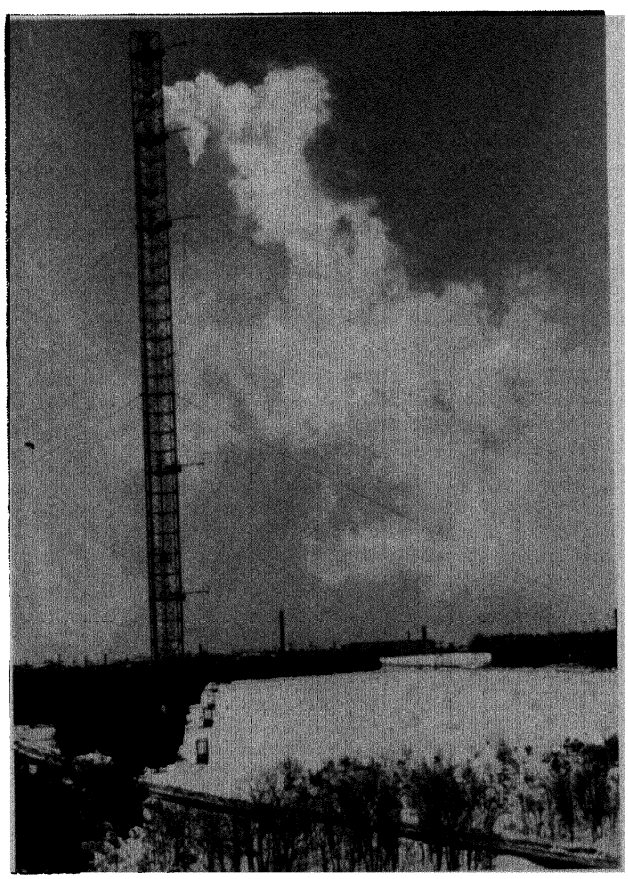

Figure 6. Lapse oil-fog plume—Brookhaven test stack. This photograph was taken about 30 minutes after Fig. 5. The inversion has been replaced by a lapse temperature structure, and the effluent plume is now typical of the A gustiness

CONCLUSIONS

The foregoing analysis has given a relatively complete survey of dispersion patterns from a specific, elevated point source. The quantitative data, though incomplete, suffice to show that an orderly gradation of dispersion conditions exists, and that a generally acceptable prediction of the ground-level concentrations can be achieved during lapse conditions. The qualitative measurements made under inversions indicate that concentrations can be predicted in this case also.

The gustiness classification developed in the earlier phases of the work at Brookhaven correctly separates the major types of dispersion but needs considerable improvement. In particular, the B_1 category includes too wide a variety of conditions. Additional classification criteria are needed, very probably including some reflection of the importance of eddies of different periods. More complete and more accurate field data are required for revision of the classification and for the establishment of new values for dispersion parameters.

The tests show that the most suitable type of field sampling includes a large number of accurate devices operated simultaneously. Methods that do not permit evaluation of pertinent data, such as plume centerline locations, from the field data may give rise to serious errors.

The importance of time in such analyses is emphasized by the relationships presented. It is apparent from the wide variations observed that the results of any field experiments will be a function of time, at least up to periods of one hour.

The current meteorological-research program at Brookhaven is based on these conclusions, and many of the deficiencies of the earlier work are being eliminated. However, this program can produce results for only one site, and similar work in other localities is needed for a more complete understanding of atmospheric dispersion.

ACKNOWLEDGEMENTS

It must be apparent that this paper summarizes the efforts of a number of persons rather than that of an individual. Of the present and past members of the Meteorology Group, the late Norman R. Beers deserves foremost credit for conceiving the original installation and program. Philip H. Lowry and Irving A. Singer have made major contributions in the development of the program and analysis of data. The original instrumental work and basic sampling techniques are largely credited to Daniel A. Mazzarella, and the development and perfection of them has been carried on by Robert M. Brown, and Frederick E. Bartlett. George Potts has assisted in many aspects of both the field sampling and the

Table IX. Pertinent Data Major Oil-Fog Test Runs

Test No.	Date	Starting time (EST)	Length of Run (min)	Mean wind Dir. (deg)	Mean wind Speed ($m\text{-}sec^{-1}$)	Rate of emission (gm/sec)	Equipment*	Lapse rate $T_{410}-T_{37}$	Gustiness type
7	1/14/49	–	–	290	7.0	43.5	D	0.0	C
11	3/3/49	0652	79	315	8.0	26.8	D	+2.0	D–B_1
15	3/14/49	1640	41	211	8.8	20.0	D	−0.5	C
22	5/13/49	1418	52	145	4.0	24.4	D	−1.2	B_1
30	8/9/49	0449	170	272	5.0	38.1	D	−1.0	D–B_1
50–1	8/8/50	1401	87	275	3.5	48.5	D	−1.3	B_1
50–3	9/15/50	1343	97	212	8.5	Var	D	−0.7	B_1
50–4	9/18/50	0920	82	Var	1.0	34.0	D	−1.3	A
50–5	9/20/50	1223	87	055	5.4	33.0	D	−1.3	B_1
50–6	10/2/50	1347	134	150	3.8	34.7	D	−1.2	B_1
50–7	10/5/50	1048	42	177	5.8	31.4	D	−2.0	B_1
50–9	10/31/50	1400	110	325	5.5	42.3	D	−1.6	B_1
51–1	1/26/51	1307	83	300	8.0	36.1	D	−1.7	B_1
51–3	3/6/51	0644	164	Var	0.5	37.0	D	+5.0	D–A
51–4	3/27/51	1806	72	195	8.5	32.5	D	−0.1	C
51–5	4/24/51	1825	66	174	7.5	47.0	D	−0.7	C
51–9	10/25/51	1518	54	064	6.0	42.0	D–T	−1.4	B_1
51–11	11/21/51	1440	42	285	3.5	43.6	D	−1.5	B_2
52–1	1/16/52	1425	95	320	9.0	35.0	D–T	−1.4	B_1
52–2	1/24/52	1400	90	290	12.8	44 8	D–T	−1.3	B_1
52–3	4/7/52	1105	70	348	4.5	43.(	D–T	−1.2	B_1
52–4	3/7/52	1432	83	339	6.0	45.0	D–T	−1.1	B_1
52–6	4/17/52	0900	86	148	11.1	48.1	D–T	−1.4	B_1
53–2	12/2/53	1037	71	330	10.5	41.0	F, D	−1.7	B_1
53–3	12/3/53	1059	71	309	1.5	46.0	F, D	−1.3	A
54–1	1/7/54	1037	68	300	10.0	42.0	F, D	−1.5	B_1
54–2	1/26/54	1352	60	207	8.8	43.0	F	−1.4	B_1
54–3	2/5/54	1345	59	288	11.0	41.0	F, D–T	−1.6	B_1
54–6	3/16/54	1330	140	315	10.5	42.0	F, D	−1.8	B_1
54–7	4/2/54	1000	90	210	11.0	42.0	F	−1.9	B_1
54–8	4/6/54	1315	180	200	10.5	40.0	D	−0.9	B_1
54–10	5/5/54	0850	117	345	7.8	44.0	D	−2.3	B_1
54–11	6/2/54	1200	75	110	7.5	39.0	F	−1.0	B_2
54–15	7/23/54	0915	138	345	5.0	41.0	D	−2.3	B_1
54–16	8/6/54	0850	150	341	10.0	44.0	D	−1.7	B_1
54–17	8/18/54	0918	86	375	1.7	43.5	D	−1.5	B_2
54–19	11/9/54	1410	125	329	6.0	36.0	D	−0.8	B_1
54–21	11/11/54	1300	180	226	8.7	31.0	F, D	−1.4	B_1

* *Equipment:* D, photometric densitometer; F, filter units; D–T, densitometer traverse.

analysis. In the preparation of this paper, Mr. Bartlett, June Crane, and Carolyn Smith have given invaluable assistance.

REFERENCES

1. Beers, N. R., *Stack Meteorology and Atmospheric Disposal of Radioactive Waste,* Nucleonics *4* : 28–38 (1949).
2. Lowry, P. H., *et al., Ground-Level Measurements of Oil-Fog Emitted from a Hundred-Meter Chimney,* Meteorological Monographs, *1* : 30–35 (1951).
3. Smith, M. E., and Singer, I. A., *Applicability and Key to Meteorological Punch Card Data,* April, 1950–March 1952, BNL 288 (T–48), (1954).
4. Lowry, P. H., *The Theoretical Ground-Level Dose Rate from the Radioargon Emitted by the Brookhaven Reactor Stack,* BNL 81 (T–19), (1950).
5. Singer, I. A., *A Comparison of Computed and Measured Dose Rates from Radioargon Emitted by the Brookhaven Reactor Stack,* BNL 292 (T–49), (1954).
6. Mazzarella, D. A., *Wind Tunnel Tests on Seven Aerovanes,* Review of Scientific Instruments *25* : 63 (1954).
7. Mazzarella, D. A., and Kohl, D. K., *Temperature Measurements on a 420–ft. Tower,* Instruments and Automation, V. 27, No. 8 (1954).
8. Singer, I. A. and Smith, M. E., *Relation of Gustiness to Other Meteorological Parameters,* Journal of Meteorology, V. 10, No. 2: 121–126 (1953).
9. Sutton, O. G., *The Theoretical Distribution of Airborne Pollution from Factory Chimneys,* Quarterly Journal of the Royal Meteorology Society, *73,* 426–36 (1947).
10. Smith, M. E., and Singer, I. A., *Sampling Periods in Air Pollution Evaluations,* Third National Air Pollution Symposium, Pasadena, California. (1955) (In press).

The System of Routine Observations of Radioactivities in the Air, Rain-Water and Sea-Water in Japan

By CMO,* Japan

Observations of radioactivity contained in the airborne dusts, rain, snow, and sea-water have been carried out by many research workers in Japan since last spring who volunteered in the work for the purpose of protecting public safety. On 1st April, 1955, government routine observations were started at 16 weather stations including one weather ship. The main purpose of these investigations is to find distribution and change of radioactive contaminations of the air on a synoptic meteorological and climatological basis.

THE PROCEDURES EMPLOYED IN MEASUREMENTS

Dust particles in the air are collected by two different methods. One is to receive falling dusts in a porcelain vessel of about 30 cm × 30 cm × 5 cm filled with a thin layer of water which is exposed to the outer air for a few days (water vessel method). The other is to collect airborne dusts near the ground on a filter paper attached to the cylindrical impactor of 3 cm diameter by aspirating a few cubic meters of air (filter paper method). The former is used to determine the total contamination received on a unit area of the surface of the earth and the latter to measure the radioactivity suspended in a unit volume of air. Other methods of dust collection, gummed-paper method and electric dust collector, are also under investigation at the present time.

Rain-water is collected every day in a funnel-shaped glass receiver of 25.2 cm diameter at 9 a.m. for determining the mean concentration of activity for the daily total rainfall. To find the change in activity for the duration of rainfall, a constant volume of rain-water, 100 cm^3, equivalent to 1 mm of rainfall, is collected from the beginning of precipitation in a specially designed glass bottle. When unusually high activities are expected in the rain-water, a large volume of water is collected for radiochemical analysis in a large funnel receiver of 100 cm × 150 cm width which is made of wooden body covered with a polyvinyl sheet.

Snow samples are received every day in a cylinder vessel made of plastics at 9 a.m. Samples from different depths of accumulated snow are occasionally collected for examination.

Sea-water in the Pacific is collected occasionally on board the weather ship, when abnormal gamma activity coming from the sea surface is detected by a scintillation counter installed aboard the vessel.

Samples of rain-water, usually 100 cm^3 at a time, are evaporated, and after drying the residues in planchets, the activities are measured by a G-M counter. Usually the time interval of 500 counts of the G-M counter is read. Before and after the measurement of a sample, the counts during 10 minutes are also read to determine the effect of the background.

The rate of decay of activity is measured in a planchet for the estimation of the nature of the active substances. It is believed that a large part of the natural activity is lost in 6 hours after the time of collection of the sample.

Efficiency of measurement is calibrated at definite time intervals with standard samples under the same geometrical conditions.

Snow samples are melted and activities are measured by the same method as above. Activities of dust particles which are collected by the water-vessel method are measured with the same procedure. Those which are collected by the filter-paper method are measured by inserting the paper in a planchet.

Activities in sea-water are coprecipitated with a small amount of barium sulphate and ferric hydroxide.

Table I. Network of the Routine Observations of the Radioactivities

Weather station	*Location* Long.	Lat.	*Height (m)*	*Classification**
Kagoshima	130°33′ E	31°34′ N	5.4	B
Fukuoka	130 23	33 35	3.6	A
Muroto	134 11	33 15	186.1	B
Yonago	133 21	35 26	7.9	B
Osaka	135 32	34 39	8.0	A
Hachijojima	139 47	33 06	81.3	B
Fujisan	138 44	35 21	3773.0	B
Wajima	136 54	37 23	6.9	B
Tokyo	139 46	35 41	5.8	A
Akita	140 06	39 43	9.9	B
Sendai	140 54	38 16	39.8	A
Kushiro	144 24	42 59	33.5	B
Sapporo	141 20	43 03	18.1	A
Wakkanai	141 41	45 25	3.2	B
Torishima	140 18	30 29	82.5	B
Weather Ship	135 00	29 00		C

* *A* denotes a station measuring rain-water, dusts by water-vessel method and filter-paper method, and collecting rain-water for radiochemical analysis; *B* denotes a station measuring rain-water and dusts by water-vessel method; *C* denotes a station measuring rain-water and sea-water.

* Observation Division, Central Meteorological Observatory, Tokyo.

The network of the routine observation of the radioactivities is shown in Table I. Table I shows the name, location, height above the mean sea level, and the classification of the observations.

INFORMATION SYSTEM AND FUNCTION OF CMO

Results obtained at each station are reported every ten days to the Central Meteorological Observatory (CMO) in Tokyo. However, in case any unusually high value of contamination is detected, it is reported immediately by telegram.

Distribution and change of activity are investigrated by experts at the center (CMO) on a synoptic meteorological and climatological basis. Compiled results are released in printed or other appropriate form for use by government agencies. The radiochemical analysis of water or dusts which are sent from local stations is also carried out at CMO.

Calibrations of the G-M counter of each station, supply of the equipments used in routine observations and the improvements of the methods and instruments are also carried on at the center (CMO).

Method of Measurement of Radioactive Dusts in the Upper Air by Radiosonde

By Chihiro Ishii,* Japan

Although several data are reported concerning the radioactivity of precipitated water and dust on the earth,[1,2,3] the distributions of these sources in the upper atmosphere are not observed directly. The measurement of the vertical distribution of these sources in the air will be important to solve the problems of radioactive contamination of air,[4,5] and of its climatological effects on the earth.

Moreover, if this type of measurement is made to a large extent and in detail, the results will be also available for the identification of the so-called "Air-Mass" in the synoptic analysis of meteorology.

For this purpose, two methods of observation are used; one is the survey of gamma-ray intensity by sending detectors into the upper atmosphere by balloons and by airplane; the other is the direct collection of air-borne dusts by means of an impinging apparatus attached to an airplane. The former measurements are carried out by the author and his collaborators and the latter are done by Dr. Y. Miyake.

THE APPARATUS FOR GAMMA-RAY DETECTION

The gamma-ray detector consists of a bundle of Geiger-Müller counters in which a single counter A is surrounded by six counters B as shown in Fig. 1. The charged particles which discharge the central counter A must discharge at least one of the outer counters B. On the other hand, most gamma rays penetrate the outer counters without giving rise to discharge. Therefore, by taking the anti-coincidence measurement $A - B$, a gamma ray is detected only in the event that the central counter A is discharged.

All these counters are the self-quenching type, filled with alcohol and argon in the usual content, and the walls are made with 1-mm thick aluminum tube of 3-cm diameter. The center wires are 0.1-mm tungsten. The effective length of each counter is about 28 cm. In later experiments, the length of the central counter is nearly one-half that of the outer counters.

The number of pulses of anti-coincidence $(A - B)$ is indicated by the motion of an arm driven by the clock-work escapement and gear system after being reduced through a scaling circuit (scale of two). This arm slides on the signal board connected with transmitter in radiosonde. One of the typical circuit diagrams used in the balloon flight experiment is shown in Fig. 1,† and its side view is shown in Fig. 2.

The number of counts per unit time interval, i.e., the intensity of gamma radiation, is transmitted to the receiver on the ground as a change of signal together with other signals concerned with the meteorological factors of the upper air.

The efficiency of the Geiger-Müller counter for gamma-ray detection is estimated at 0.8% by making use of radium as a standard gamma-ray source. This estimate does not seem to be unreasonable as compared with other references.[6] The detection efficiency of Geiger-Müller counter for gamma-radiation varies with the energy[6] but the weighted average energy of radium gamma radiation is regarded as not so different from that of artificial radioactive substances; according to one reference,[7] the average energy of the latter is around 0.7 Mev.

As there are several narrow gaps among the outer counters B, and in the axial direction of the counter bundle, some charged particles are able to discharge the central counter A without causing the discharge of one of the outer counters B. This gives a false count for $(A - B)$. Consequently a correction must be made for this leakage in anti-counters B. The correction factor for this is calculated by considering the geometrical conditions of the counter arrangement, and is found to be 2–4%. This means that 2–4% of the total flux of charged particles is observed as a gamma ray owing to gaps between the outer counters.

The resolving time of the mechanical system is nearly 0.05 second, and this is tested by comparison with high-resolving circuit systems using a strong gamma-ray source. Thus, the reliable limit of the counting rate is estimated at 600 counts per minute.

However, miscounts are found in actual records which seem to be attributable to some phenomenon like electric discharge in low-pressure air. From the latest experiments in the laboratory, we have found that this kind of discharge occurs below a pressure of 50 millibars and that it increases with decrease in pressure.

* Director of Geoelectric and Geomagnetic Laboratory, Meteorological Research Institute, Tokyo.

† The circuit designed for the balloon flights is not restricted to the one shown here, but others are almost the same in principle.

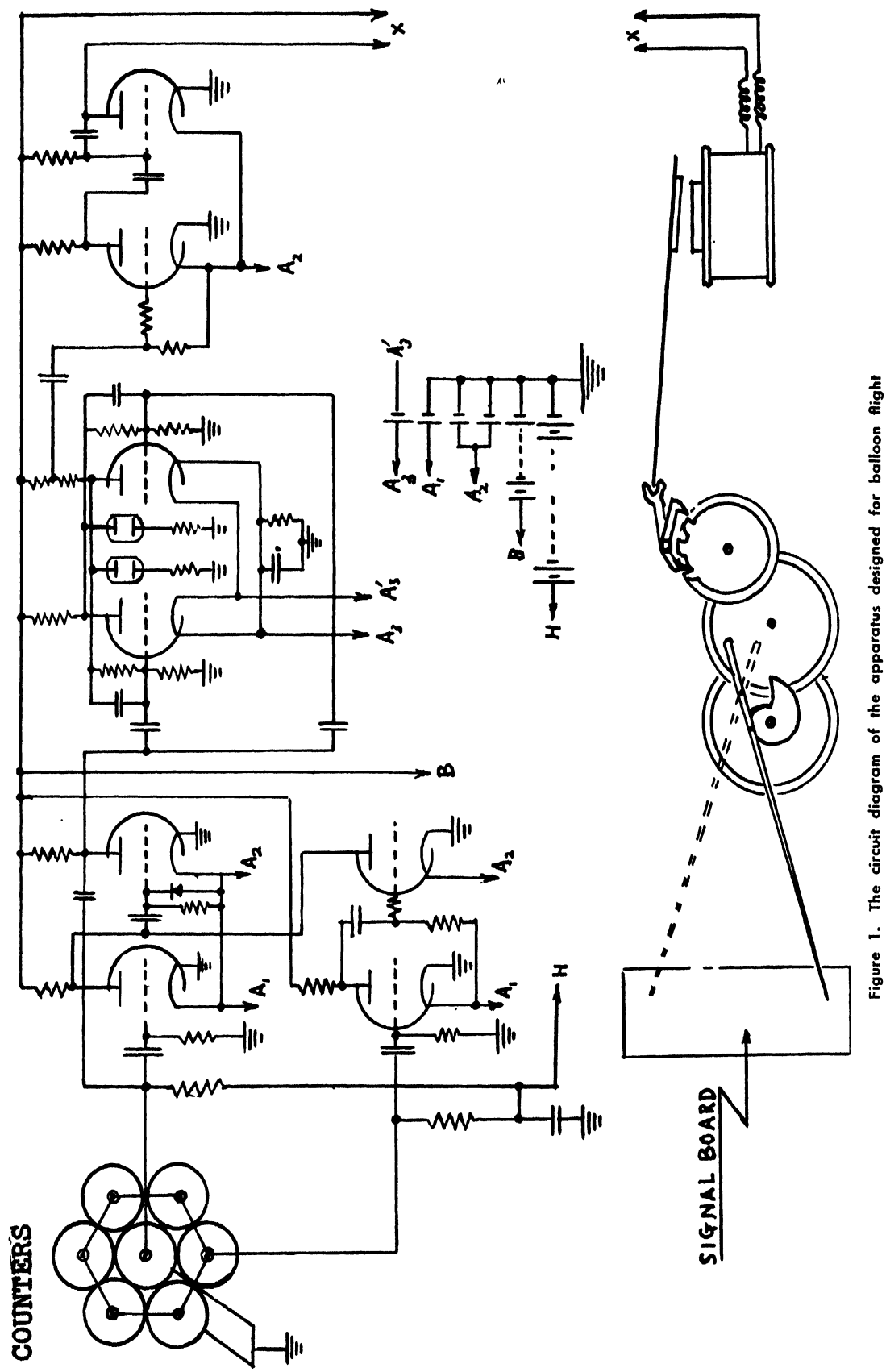

Figure 1. The circuit diagram of the apparatus designed for balloon flight

The high tension supply for the Geiger-Müller counters is taken from two batteries of 500 v connected in series, primary batteries of water-instilled-type are used for A and B sources of anti-coincidence and scaling-circuits, and a Model RSB 52 primary battery of 7.5 v is used for the power supply of the transmitter circuit (see Fig. 1).

The whole of this apparatus is constructed in a spherical gondola which is about 50 cm in diameter and is made with wisteria tendrils as shown in Fig. 2. The bottom part thereof is covered with aluminum foil and the surface of each set is colored with carbon black for the purpose of heating by insolation. Moreover, all parts of the apparatus except the antenna are enveloped in a thin polyethylene sheet. In this way, the temperature inside the gondola is kept above 5°C by insolation during flight and can prevent deterioration of the counter due to cooling in the upper atmosphere. Furthermore, two thermometers with electric contacts at 0°C and 40°C respectively are attached to the surface of the counters for checking the counter temperature so that when the counters are acting below 0°C or beyond 40°C, an alarm signal is transmitted.

The total weight of the apparatus is nearly 5 kg, and three or four rubber balloons for aerological routine work are used in one flight. To get the desired velocity in ascension, the lift of each balloon is determined from the table prepared from the data of previous experiments on balloon flights,[8] and the maximum height of the flight, corresponding to the burst of the balloons, is also estimated from the same table.

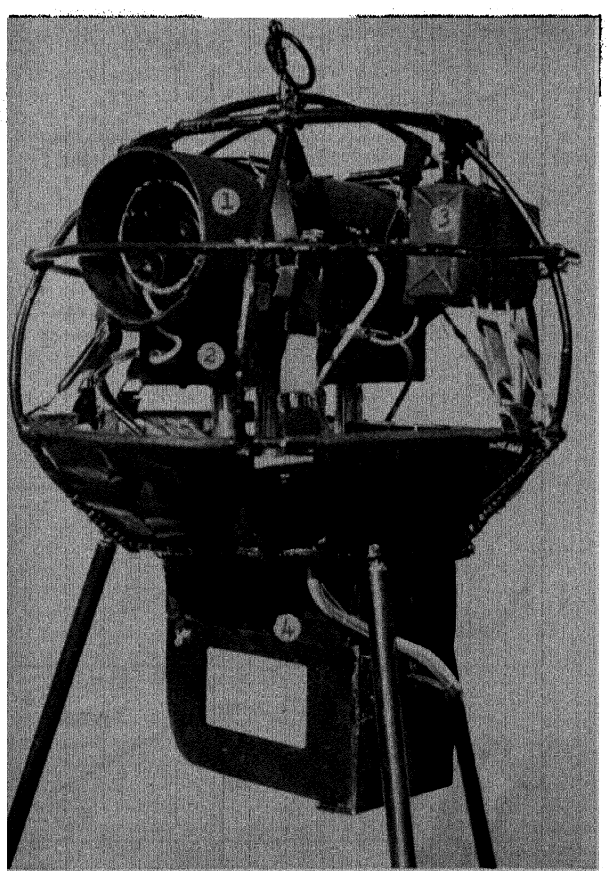

Figure 2. The side view of the whole set: (1) bundle of counters, (2) anti-coincidence circuit, (3) high-tension battery for counters, (4) mechanical system and transmitter

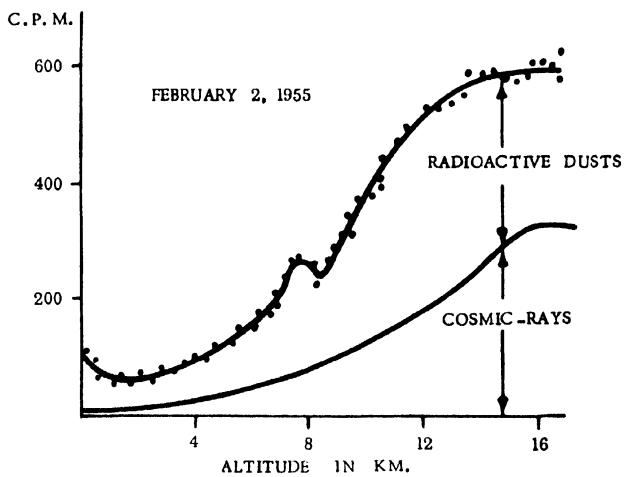

Figure 3. One of the observed data of gamma-ray intensity without corrections

EXPERIMENTS AND THE RESULTS OF GAMMA-RAY MEASUREMENT

Four gamma-ray observations have been made by balloon and two by airplane as a check on the measuring instruments, and one dust observation is performed by airplane. The dates of flights are shown in Table I, and one of the observed results is given in Fig. 3.

From Fig. 3, we can see that the radioactivity increases with altitude much more rapidly than the increase of the photon component of cosmic-rays and that the increase fluctuates somewhat. However, the large fluctuation corresponds to a temperature inversion in the atmosphere.

From the meteorological point of view, it is plausible that contamination increases just below the inversion layer owing to the accumulation of floating dusts in the air by convection. It is obvious that the decrease in counts just above the ground is due to the decrement of natural radioactive substances with altitude.

Table I

Date	*Flight*	*Location of flight*	*Subject*
1954			
Aug. 3	Airplane	Tokyo	Gamma-ray intensity and dust
Aug. 13	Balloons	Tateno*	Gamma-ray intensity
Dec. 23	Balloons	Tokyo	Gamma-ray intensity
1955			
Jan. 13	Airplane	Tokyo	Gamma-ray intensity
Feb. 2	Balloons	Tokyo	Gamma-ray intensity
Feb. 22	Balloons	Tateno	Gamma-ray intensity

* Tateno, the site of the Aerological Observatory is 50 km north of Tokyo.

DETECTION OF RADIOACTIVE DUSTS OF ARTIFICIAL ORIGIN BY AN IMPINGING METHOD

On the other hand, Y. Miyake and Y. Sugiura at this Institute tried to determine the radioactive substance in the air by airplane on August 3, 1954, above Tokyo area and its neighborhood.

Ordinary impinging type of dust collectors were used. A total of 6.3 m^3 of air was passed through four impinger bottles, each filled with about 70 cm^3 of distilled water. The altitude at which sampling of the air was done was between 1–3 km above the ground. After radon and thoron daughters had decayed, the radioactive substance dissolved in water was co-precipitated with a small amount of barium sulphate and ferric hydroxide and its activity was measured by a G-M counter.

The result showed a total activity of 3.2 ± 1.3 cpm/l which was equivalent to about 2×10^{-18} curie/cm^3 of air.

The rate of capture of air-borne dusts by the impingers is unknown, but, usually it may be considerably lower for particles smaller than 1 μ. Therefore the measured value might be considerably less than the total amount of radioactive dusts suspended in the air; however, it is of importance that the presence of the radioactivity of artificial origin was confirmed in the upper air.

ANALYSIS OF THE DATA

In order to get the actual distribution of radioactive dusts in the atmosphere from the observed data of gamma-ray intensity, the contributions from following points must be taken into account: (1) the photon component in cosmic rays; and (2) the charged particles in cosmic rays.

The contribution of (1) is estimated from the results obtained from similar observations,[9,10,11] considering the latitude effects of cosmic radiation.

For the estimation of the contribution of (2), the computation of the leakage factor was made by three different methods and the results were found to agree within the values of 2–4% corresponding to the difference in geometrical conditions of the counter-bundle as remarked in the previous section. Then the correction for (2) is easily obtained by using the altitude dependence of the total intensity of cosmic radiation in our latitude.

With regard to correction (1), the assumption is made that the intensity of the photon-component in cosmic-rays is proportional to that of the soft component of cosmic-rays, and the numerical values are deduced for our latitude from data obtained in the United States. The change of cosmic radiation intensity with altitude is taken from the literature.[12,13]

Finally, it is convenient to express the content of radioactive substances in the air by the unit of curie per cm^3. To do this, the following relation can be used, namely, the relation between the number of counts per minute by the counter, N, and the content of the radioactive source, m_0 in curies per cm^3.

$$N = \int_{r=0}^{\infty}\int_{\phi=0}^{2\pi} 2\int_{0=\theta}^{\frac{\pi}{2}} \frac{i_0}{4\pi}\cdot\frac{S(\theta)}{r^2}\,e^{-\frac{r}{\lambda}} \cdot r^2\sin\theta\cdot d\theta\cdot d\phi\cdot dr$$

$$= S_0\cdot m_0\cdot 3.7\times 10^{10}\cdot\lambda\cdot f\cdot 60$$

$$m_0 = \frac{N}{S_0\cdot\lambda\cdot f}\cdot 4.5\times 10^{-13}$$

where the identity, $i_0 = 3.7 \times 10^{10} m_0$, is used as this is the number of disintegration per second from a radioactive substance of concentration m_0 curies per cm^3.

$S(\theta)$ is the effective cross-sectional area of the central counter in cm^2 and is given by $S(\theta) = 2bl \sin\theta + \pi b^2 \cos\theta$ where b and l are the radius and the effective length of the central number in cm, respectively, and θ is the angle between the incident radiation and the axis of the counter. Thus S_0 becomes $\pi b(b+1)$.

f is the gamma-ray detecting efficiency of the counter and is taken as 0.8% from the laboratory experiment described above.

$1/\lambda$ is the gamma-ray absorption coefficient of air in cm. This is a function of gamma-ray energy that increases with a decrease in gamma-ray energy.

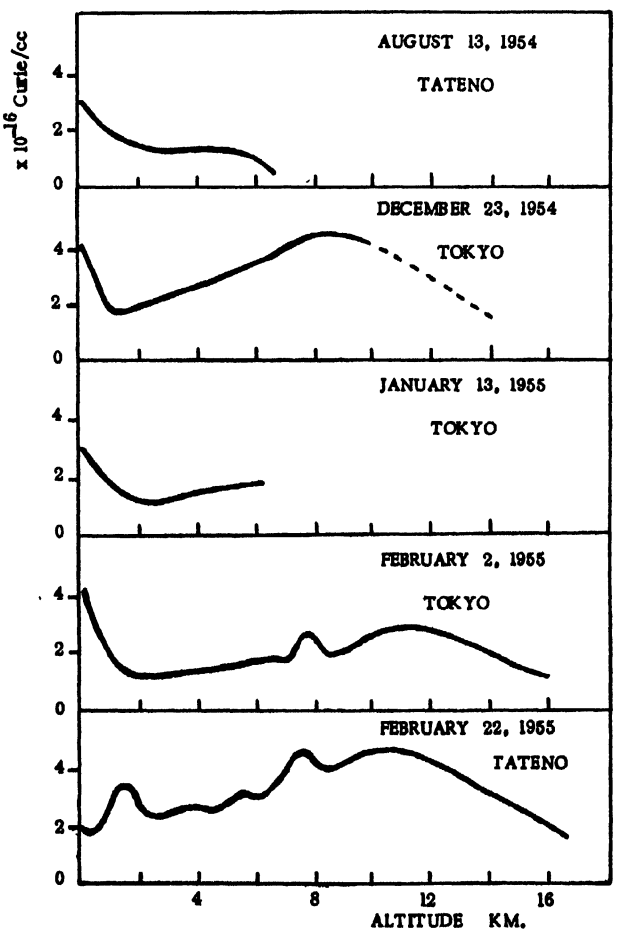

Figure 4. The observed vertical distributions of radioactive substances in the atmosphere

In the numerical computation, we took the value $\lambda = 1.07 \times 10^3$ cm, assuming the average energy of artificial radioactive substances as 0.7 Mev as mentioned above.[7]

It should be noted that the number of counts per unit time, N, is proportional not only to m_0 but also to λ, and the latter is inversely proportional to the density of air. This is the reason why the efficiency of the measurement of radioactive contamination by means of a gamma-ray detector increases in the upper air. The results obtained from the above computation are represented in Fig. 4.

According to the results from the dust-collecting measurement performed by airplane on August 3, 1954, the mean density of artificial radioactive dust around 1–3 km altitudes is the order of 10^{-18} curie per cm^3 and the same order of radioactive contamination is found from the surface of the rubber balloons used in the flight from Tateno on August 13 and retrieved near Tokyo on the next day.

It seems, therefore, that these are not inconsistent with the values obtained from our gamma-ray measurement which are the order of 10^{-16} curie per cm^3 as the content of the radioactive dusts in the troposphere, if the collecting efficiency of the impinger and the rubber-balloon surfaces is taken into account. Moreover, these data are consistent with the roughly estimated values from the measurement of the radioactivity of rain, etc. Our measurement, however, is restricted in the troposphere owing to disturbances that occur in the electric system at the extremely low pressure. In this respect the improvement of the instrument is now under consideration.

ACKNOWLEDGEMENTS

These experiments were performed through the co-operation of the Aerological Section in the Central Meteorological Observatory, Tokyo, the Aerological Observatory, Tateno, and the Tokyo Air Port Aviation Weather Service, Haneda. The observations by airplane were carried out through the kindness of the aviation section of the Asahi Press.

REFERENCES

1. Miyake, Y., *The Artificial Radioactivity in Rain Water Observed in Japan from May to August, 1954,* Papers in Met. Geophys. *5*: 178–181 (1954).
2. Morio, Masao, *The Radioactive Dust from the Nuclear Detonation,* Bull. of Inst. Chem. Res. Kyoto Univ. Supplementary issue: 1–133 (November 1954).
3. *Thirteenth Semiannual report of A.E.C.* (Monitoring System in USA).
4. Otsuka, R. and Shimada, K., *On the Upper Air Currents in Low Latitudes of the Northwestern Pacific Ocean at Beginning of March 1954,* Jour. Met. Soc. Japan *32*: 225–239 (1954).
5. Arizumi, N., *On the Distribution of Ash-fall,* Jour. Met. Soc. Japan *32*: 303–35 (1954).
6. Curan, S. C. and Cragg, J. D., *Counting Tubes.*
7. Hirschfelder, J. O., David, B., Parker, *et al., The Effect of Atomic Weapons* (1950).
8. Ishii, C., Maeda, K. and Minagawa, O., *Report on the Floating Balloon Experiments for Cosmic-Ray Measurements,* Kenkyu-jiho, *6*: 405–418 (1954). (This is described in Japanese).
9. Rest, R. G., Reiffel, L. and Stone, C. A., *Note on Soft Gamma-Component of Cosmic-Rays,* Phys. Per. *81*: 894–895 (1951).
10. Reiffel, L., Stone, C. A. and Rest, E. G., *Scintillation Spectrum from Cosmic Ray at 30,000 ft,* Phys. Rev., *82*: 121–122 (1951).
11. Reiffel, L. and Burgwold, G. M., *Low Energy Events in Cosmic Radiation,* Phys. Rev. *95*: 1294–1295 (1954).
12. Neher, H. V., *Recent data on Geomagnetic Effects,* Progress in Cosmic-Ray Physics. I (1952).
13. Hayakawa, S., *Structure of Cosmic-Ray,* Kagaku *22*: 278–285, (1952). (This is described in Japanese).

Measurement of Radioactivity in the Atmosphere and Pollution in the Vicinity of an Atomic Center

By Jacques Labeyrie,* and Jacky Weill,† France

The C.E.A. is particularly interested in the study of atmospheric radioactivity since it is necessary that it make sure that the atmosphere is not contaminated in the neighborhood of its installations, especially:

(*a*) In the neighborhood of uranium mines where large quantities of radon and of ore dust may be in suspension in the air;

(*b*) In the neighborhood of atomic reactors where the cooling gases are contaminated with argon-41 to a varying degree and where, in the event of an accident, fission products in the form of smoke may be projected into the atmosphere;

(*c*) In the vicinity of hot laboratories or of plants in which irradiated fissionable materials are being treated and where large quantities of radioactive gases (xenon, krypton, iodine or fission products in the form of smoke or fog) might be released.

This has led the C.E.A. to develop equipment designed for permanent operation with a minimum of supervision, mostly in incompletely equipped and protected sheds, but capable of detecting all radioactive gases and smokes or fogs of the types indicated above.

The sensitivity of this type of equipment must be sufficient to detect all dangerous elements, even if present only at a concentration very much below the accepted tolerance dose.

This equipment now has been perfected to the point where it is in use in a certain number of stations in the region of Paris. It is proposed to equip several other stations in the country with these same devices within the next six months.

These are essentially of two types: one, called "Babar" is designed for monitoring fumes (or smokes), fogs and dusts[1] (Fig. 2); the other type, meant for the measurement of gases, is called a differential ionization chamber (Fig. 3). Figure 1 shows a diagram of a station equipped with these two devices.

"BABAR"

This apparatus consists of the following: (*a*) a two-stage air aspirator (capacity: 50, 100 and 150 liters/minute, under a pressure of 100 cm H_2O); (*b*) A special cellulose filter tape, green Schneider type (stopping power: 75% for the aerosols of methylene blue of an average size of 0.3 μ); this tape unwinds continuously and slowly (at a speed of 0.20, 1, or 5 mm/minute) and catches the dusts contained in the aspirated air; the magazine holds about 40 meters of this filter tape;

Suction through the tape is by means of the circular hole of diameter 35 mm, located at a short distance (which can be varied from 0 to 15 mm) below the thin window (2 mg/cm²) of a semi-proportional bell-type counter (type CEA 8 AP 7) having the same area as the exhaust hole. After a period ranging from 3 to 50 hours, the filter tape then passes under a second radiation detector consisting of a photo-multiplier (DuMont 6291) customarily equipped with an α-ray scintillator (thin layer of ZnS covered with 0.6 mg/cm² of aluminum).

The first detector, which may work either as a semi-proportional counter (counting α rays only) or as a Geiger counter (counting $\alpha + \beta + \gamma$ rays) is used to investigate the activity of the dust, fume or fog residues left on the filter immediately after they have been caught. The signals are transmitted to a 25 cm channel recorder (Meci, micromax) through a pre-amplifier and an integrator; moreover, if re-

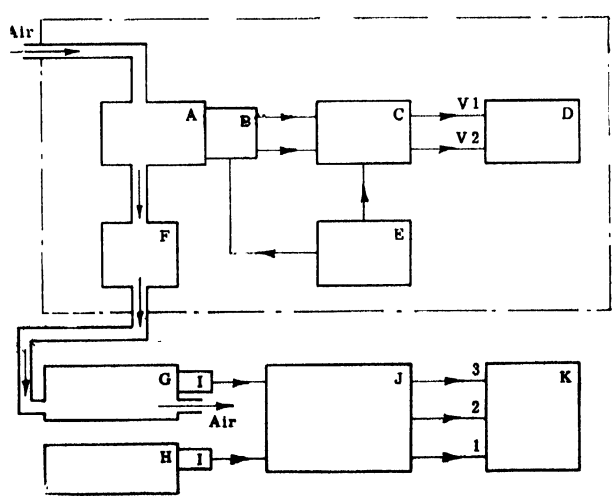

Figure 1. Diagram of station: (A) filter and aspirator; (B) GM counter (V1) photomultiplier fitted with scintillator (V2); (C) amplifiers and integrators; (D) two track recorder; (E) supply of high voltage and very high voltage current; (F) filter removing dust passing the aspirator collector; (G) open ionization chamber; (H) closed ionization chamber; (I) dc preamplifiers; (J) symmetrical dc amplifiers; (K) three-track recorder

Original language: French.

* Chef de la Section d'Electronique Physique au C.E.A.
† Ingénieur au C.E.A.

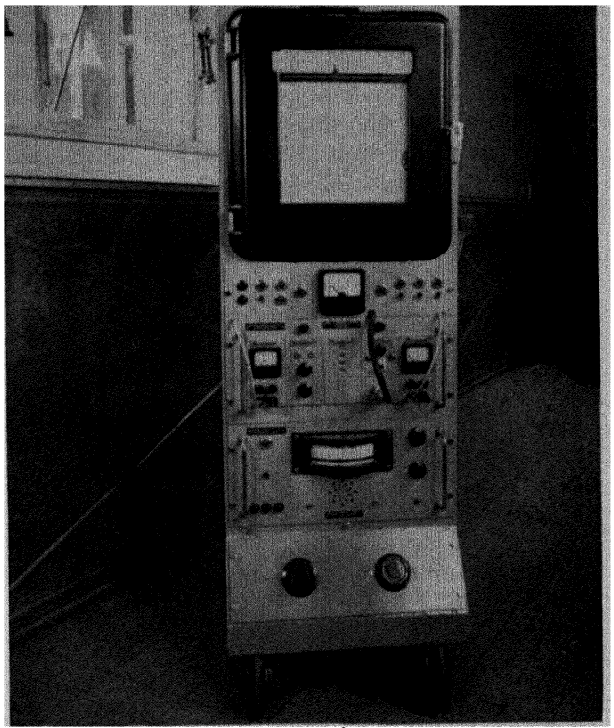

Figure 2

quired by high counting rates, two decade scalers may be added (standard type unit of the C.E.A.).

The second detector is used for the purpose of measuring the residual activity at the end of the time interval indicated above, when the slight activity of the element searched for makes it imperative to differentiate it from the greater activity of another short half-life element. This occurs, for instance, when the concentration of plutonium aerosols in air is to be measured, the tolerance dose (2×10^{-12} curies per m^3 of air) of which produces in this equipment about four counts per minute. This low activity is concealed by the natural radioactivity of the atmosphere due to the radon derivatives which are always present in it in appreciable concentration. The average value of this concentration in the region of Paris produces about 200 counts in the first detector per minute; since the half-life of the radon derivatives is about half an hour, this natural activity of the dust will have become negligible at the end of six hours as compared to that due to plutonium if the latter is present in the air at a concentration equal to the tolerance standard. In the same way, the concentrations of uranium, radium, polonium, thoron, or (by changing the scintillator) strontium, etc. can be measured. The signals given by the second detector are recorded by means of a special integrator on the same recorder as those of the first detector. A 5-cm thickness of lead protects the latter against stray γ-radiation.

The device runs continuously without any supervision, consumes about 400 watts (115 to 250 volt, 50 cycles/sec) and weighs about 60 kg.

Sampling of air in suspected places can be carried out at distances of up to 100 meters from the apparatus by means of a flexible metallic hose having a diameter of 40 mm.

Calibration is effected by the aspiration of standard aerosols tagged with radon descendants. These standard aerosols are formed by the fixation of radon descendents on iron oxide fumes, or local atmospheric dusts. Preliminary studies have permitted determination of the proportion of the active deposit which attaches itself to the aerosols as a function of various parameters: concentration and dimensions of the aerosols, dimensions of the chamber where the fixation process takes place.[2]

The sensitivity of the device for the various radioactive aerosols is indicated in Table I.

DIFFERENTIAL IONIZATION CHAMBERS

This equipment is used for measuring the concentration in the air of active gases such as $C^{14}O_2$, A^{41}, Rn^{222} etc. The filtered air (generally the air leaving the "Babar" is used for this purpose), is continuously fed into a big metallic ionization chamber in the form of a parallelepiped ($2.4 \times 1.1 \times 0.4$ m). The effective volume of this is about 850 liters. A second chamber, identical with the former one, but without any air circulation, is placed close to it. After amplification by means of a symmetrical amplifier, the currents obtained from each of the two chambers

Table I. Sensitivity of "Babar"*

Aerosols	*Tolerance dose (in curies/m³)*	*Reading of "Barbar" for a tolerance dose (in counts per minute)*	*Practical limit of sensitivity (in tolerance doses)*
U, natural	2×10^{-11}	35	1/20†
Pu soluble	3×10^{-13}	0.3	5†
Pu insoluble	2×10^{-12}	2	8/10†
Rn (descendants)	10^{-8}	10^{-4}	1/100
Ra	2×10^{-12}	2	8/10
$Sr^{90}Y^{90}$	10^{-10}	2×10^{2}	1 1/100†
Na^{24}	2×10^{-16}	2×10^{6}	1/10,000

* Unwinding speed of the filter paper strip 1 mm/minute capacity: 100 liters/minute.

† Deferred (by 10 hours).

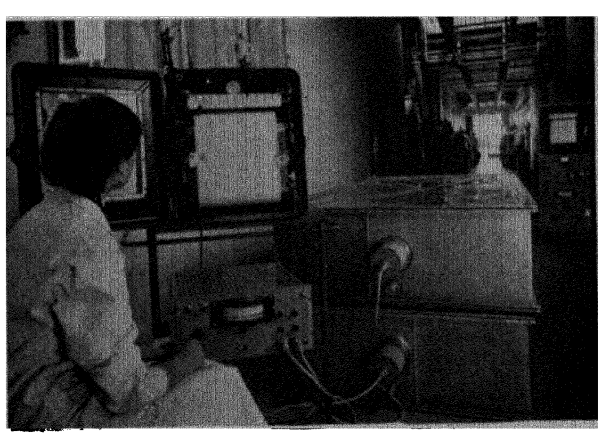

Figure 3

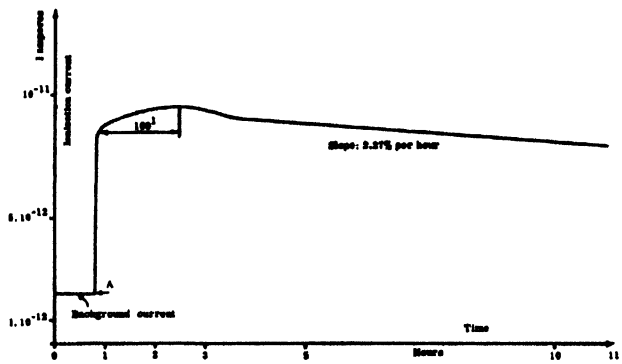

Figure 4. Calibration of differential chambers by radon: background current chamber volume 1 m³; introduction in A of about 16^{-9} curie of radon

are recorded, as well as the difference between them.

In a non-contaminated place and under a light roof, the background current of the closed chamber (due to cosmic rays and local γ rays) is of the order of 2×10^{-12} amperes; usually, that of the open chamber is the same; however, on certain days, it might be larger than the former by several ten per cent because of the presence of natural radon, the concentration of which in the air at times increases by an order of magnitude.

A radon concentration of 10^{-8} curies per m³ of air causes an increase of about 6×10^{-12} amperes, when the formation of an active deposit is taken into account (see Fig. 4).

An argon-41 concentration of 10^{-6} curies per m³ of air causes a current increase of 8×10^{-12} amperes. It may be deduced from this that about 35 cm of the path taken by the β rays of argon-41, on an average, is used in the chamber.

Figure 5 shows the activity measured simultaneously in three chambers through which successively the same gaseous current has passed, after introducing in one of them, at zero time one liter of air containing 10^{-6} curies of argon.

Figure 6 shows an example of the triple recording mentioned above, which has been obtained in a typical night during which there was an inversion of

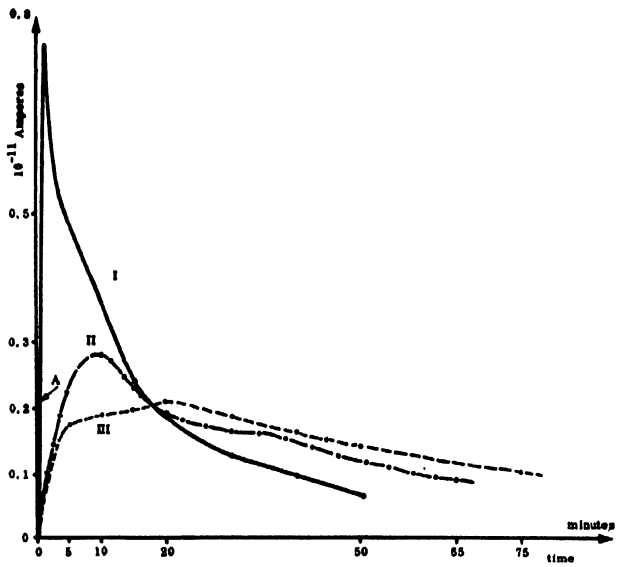

Figure 5. Calibration of differential chambers by means of argon. Introduction of argon-41 into three chambers connected in series; introduction in A of 8×10^{-7} curies of argon-41: (I) curve obtained in the first chamber, (II) curve obtained in the second chamber, (III) curve obtained in the third chamber

the temperature gradient in the region of Paris. This activity is due to the radon continually released from the soil.

Figure 7 shows another recording of increased activity (amounting to 8.5×10^{-10} curies of radon per cubic meter) likewise due to an inversion. The

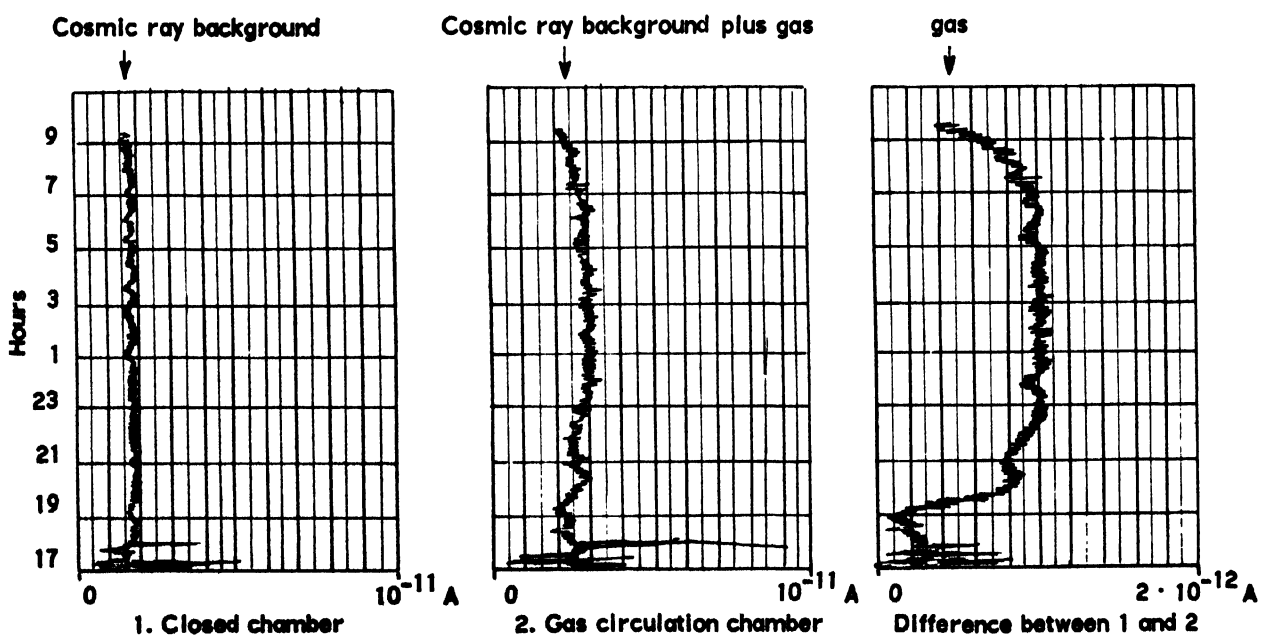

Figure 6. Two 1000-litre chambers in opposition

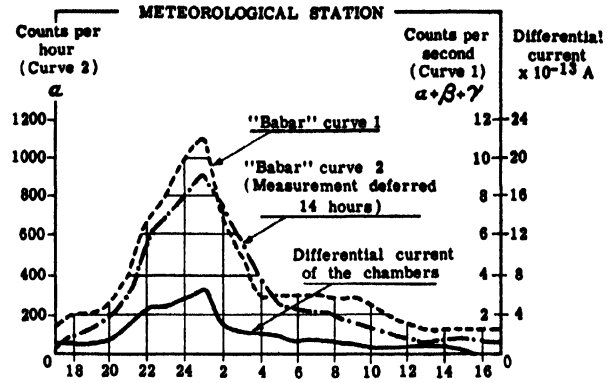

Figure 7. Meteorological station. Simultaneous recording of the differential current and of the instantaneous (1) and deferred (2) curves from "Babar"

indicated values are those of the difference between the currents in two chambers of the first "Babar" detector which measure, in this instance, the activity due to the radon descendents, and of the second "Babar" detector, which measures the activity due to the thoron derivatives. (The latter which are about one hundred times less abundant than those of the radon require deferred detection). Since the air output is about 60 liters per minute, the sensitivity indicated on Curve 1 on Fig. 7 is about ⅔ of that indicated in Table I.

Examination of the tracings made during 1954 by two of these stations, located 20 km (13 miles) from each other in the region of Paris, shows that the activity due to radon varies in the same way, at the same time, and with nearly the same amplitude at the two stations.

REFERENCES

1. Labeyrie, J., *Pellé M. Enregistreur pour aérosols radioactifs,* J. Phys. Rad. *14* : 477 (1953).
2. Labeyrie, J., Thesis, *Mesure des concentrations des aérosols radioactifs,* Paris (1953).

Determination of Atmospheric Radioactivity

By F. Barreira and M. Laranjeira,* Portugal

Among the various procedures that have been used for the determination of atmospheric radioactivity,[1-13] one of those offering the best possibilities consists of collecting dust on a filter paper. Two main variants of this procedure have been used.

In one of them, collection is made on filter paper, and the active deposit is measured after an appropriate time has elapsed;[8,10] in the other one, use is made of a paper tape unwinding in such a fashion that the collecting surface is continuously renewed.[11,13] The detectors used in each procedure have been of widely varying types (proportional counters, G. M. counters, scintillators).

In our work, we have used the first variant with a G. M. counter, for beta particles.

In so far as natural radioactivity is concerned, the active deposit fixed on the filter consists solely of the solid daughter products of radon and thoron. On the other hand, the atmospheric activity due to thoron and its descendants is only about 5% of that due to radon and its descendants.[5] Moreover, the half life of ThB (10.6 hours) makes the activity retained on the filter and originating from this family negligible, for sampling times of several hours. For these reasons we will assume, in the following, that the active deposit solely consists of daughter products of Rn.

Atmospheric turbulence may break the radioactive equilibrium between radon and its descendants, particularly starting with RaD (19.5 years), so that, as regards the radioactive deposit on the filter, only short-lived daughter products RaA, RaB, RaC, RaC' will be of interest to us. For these, experience shows that, for a normal atmosphere, the hypothesis of radioactive equilibrium with Rn is justified.

In the experimental setup used by us, we employed only the beta activity alone from the emitters RaB and RaC. In dealing with the identification of the products deposited on the filter paper, we shall show that these radioelements were the ones actually detected.

The choice of this modus operandi was based on the fact that the absorption due to the penetration of the dust particles in the filter paper is very much less intense than it is for the alpha particles, so that errors due to depth variations are thus reduced from one experiment to the next. It seems to us, moreover, that the computation of the Rn content of the air is more likely to give errors when alpha emissions from RaA and RaC' are used, because of the interposition of two other radioelements (RaB and RaC) between them.

Original language: French.

* Centros de Estudos da Energia Nuclear, Laboratorio de Fisica, Lisboa.

MATHEMATICAL STUDY OF THE INCREASE IN THE BETA ACTIVITY OF THE RaB AND RaC DAUGHTER PRODUCTS ON THE FILTER

For a mathematical study of the increase in the beta activity present on the filter we shall consider: (1) the formation of RaB by alpha decay of the RaA deposited on the filter, under a constant flux; (2) the collection of atoms of RaB, under a constant flux, and their decay; (3) the formation of RaC by the decay of the RaB present at each moment on the filter, and (4) the collection of RaC atoms under a constant flux and their decay.

Let $(N_0)_A$ be the number of atoms of RaA deposited per minute; N_A the number of atoms of RaA present on the filter at time t, and λ_A the radioactive constant of RaA. We then have:

$$\frac{dN_A}{dt} = (N_0)_A - \lambda_A N_A \qquad (1)$$

and by integration

$$N_A = \frac{(N_0)_A}{\lambda_A}\left(1 - e^{-\lambda_A t}\right) \qquad (2)$$

The number N'_B of RaB atoms present at time t and due to RaA decay will be given by:

$$N'_B = \frac{(N_0)_A}{\lambda_B}\left(1 + \frac{\lambda_B}{\lambda_A - \lambda_B} e^{-\lambda_A t} - \frac{\lambda_A}{\lambda_A - \lambda_B} e^{-\lambda_B t}\right) \qquad (3)$$

If $(N_0)_B$ is the number of RaB atoms deposited each minute under a constant flux, we get:

$$\frac{dN_B}{dt} = (N_0)_B - \lambda_B N_B \qquad (4)$$

Equation 3 and the integral of Equation 4 give for the total number of RaB atoms:

$$N_B = \frac{(N_0)_B}{\lambda_B}\left[1 + \frac{\lambda_B}{\lambda_A} + \frac{\lambda_B^2}{\lambda_A(\lambda_A - \lambda_B)} e^{-\lambda_A t} - \frac{\lambda_A}{\lambda_A - \lambda_B} e^{-\lambda_B t}\right] \qquad (5)$$

by assuming that a radioactive equilibrium exists between radon and its daughters, down to RaC, which balance may be considered as a secular one, the increase of RaC due to the RaB present will be given by:

$$N'_C = \frac{(N_0)_B}{\lambda_C}\left[1 + \frac{\lambda_B}{\lambda_A} - \frac{\lambda_B^2\lambda_C}{\lambda_A(\lambda_A-\lambda_B)(\lambda_A-\lambda_C)}e^{-\lambda_A t} + \frac{\lambda_A\lambda_C}{(\lambda_A-\lambda_B)(\lambda_B-\lambda_C)}e^{-\lambda_B t} - \frac{\lambda_B\lambda_A(\lambda_A-\lambda_C)-\lambda_B^2(\lambda_B-\lambda_C)}{(\lambda_A-\lambda_B)(\lambda_A-\lambda_C)(\lambda_B-\lambda_C)}e^{-\lambda_C t}\right] \quad (6)$$

The collection of RaC under a constant flux when the equilibrium is taken into consideration, gives:

$$N_C = \frac{(N_0)_B}{\lambda_C}\cdot\frac{\lambda_B}{\lambda_C}\left(1 - e^{-\lambda_C t}\right) \quad (7)$$

The sum of Equations 6 and 7 gives the number N_C of RaC atoms present at instant t.

A study of Equation 5, and of the sum of Equations 6 and 7 shows that the collection of beta emitters on the filter and their formation may be considered, according to the established hypotheses, as a secular equilibrium, whereby the filter activity tends to reach a limit with the passing of time.

When the values of the radioactive constants are substituted for these constants themselves, there will result, for the absolute activities of RaB and RaC respectively, at time t:

$$A_B = \lambda_B N_B = (N_0)_B\,(1.114 + 0.015\,e^{-\lambda_A t} - 1.129\,e^{-\lambda_B t}) \quad (8)$$

and

$$A_C = \lambda_C N_C = (N_0)_B\,(1.849 + 0.002\,e^{-\lambda_A t} - 4.991\,e^{-\lambda_B t} + 3.145\,e^{-\lambda_C t}) \quad (9)$$

and the total absolute activity will then be given by:

$$A_t = A_B + A_B = (N_0)_B\,(2.963 + 0.017\,e^{-\lambda_A t} - 6.125\,e^{-\lambda_B t} + 3.145\,e^{-\lambda_C t}) \quad (10)$$

The curves corresponding to Equations 8, 9, and 10 have been drawn on Fig. 1 in percentages, and the three equations have been normalized for $t = \infty$.

In order to express $(N_0)_B$ as a function of the atmospheric concentration of radon, and A_t, as a function of the activity a_t, measured at each instant during the sampling, we shall bring the following magnitudes into the computation:

C = concentration of Rn in the air, in curies/liter.

D = pump output in liters/min.

k = counting efficiency coefficient of the system for the beta radiation under consideration. In fact, for an appropriate distance, the detection coefficients of RaB and RaC may become nearly equal, as was shown experimentally for our system. Nevertheless, a slight modification in the following calculations, which can readily be made, allows for the introduction, if need be, of two coefficients, k_B and k_C, for the two emitters concerned.

r = filter efficiency in the collection of radioactive dusts.

q = coefficient of loss by beta absorption on the paper. For the mass thickness of the filter paper, it is not necessary to use two different coefficients, q_B and q_C respectively, for the two radioelements.

a_t = activity in counts per minute, at each instant of the sampling.

f_t = value of $A_t/(N_0)_B$ given by Equation 10. In the case where k_B and k_C are different, we must consider Equations 8 and 9 separately.

The number $(N_0)_B$, of RaB atoms deposited per minute will be given by:

$$(N_0)_B = 3.7 \times 10^{10} \times 60 \times \frac{CDr}{\lambda_B} \quad (11)$$

On the other hand:

$$a_t = qkA_t \quad (12)$$

and, generally:

$$a_t = q\,(k_B A_B + k_C A_C \quad (12')$$

From Equations 10, 11, 12, we can deduce the values of the Rn concentration in curies/liter:

$$C = 1.164 \times 10^{-14} \times \frac{a_t}{krqDf_t} \quad (13)$$

When Equation 12′ is used instead of Equation 12, we get:

$$C = 1.164 \times 10^{-14} \times \frac{a_t}{rqD(k_B f_{Bt} + k_C f_{Ct})} \quad (13')$$

where

f_{Bt} and f_{Ct} are the values of $A_B/(N_0)_B$ and $A_C/(N_0)_B$ respectively, derived from Equations 8 and 9.

For atmospheres with low pollution, the values of a_t are rather low, and the accuracy of the method is improved when, instead of the a_t activities, the number of counts m_t recorded during time 0-t, is used:

$$m_t = \int_0^t qkA_t\,dt = qk\,(N_0)_B \int_0^t f_t\,dt = qk\,(N_0)_B F_t \quad (14)$$

The value of C then will be given by:

$$C = 1.164 \times 10^{-14} \times \frac{m_t}{krqDF_t} \quad (15)$$

and, in case different values of k were considered. the following would be obtained as above:

$$C = 1.164 \times 10^{-14} \times \frac{m_t}{rqD(k_B F_{Bt} + k_C F_{Ct})} \quad (15')$$

Table I gives the values of f_t and of F_t. Because of the form of Equation 10, the values of $f_t/f\infty$

coincide with those of $A_t/A\infty$ shown on Fig. 1. On Fig. 1*A*, the curve representing function $F_t = \phi(t)$ is drawn.

EXPERIMENTAL SETUP

A diagram of the system used when making the measurements is shown on Fig. 2*a*, and the details of the filter holder and of the detector monitor are shown on Fig. 2*b*.

Whatman No. 41 filter paper was used, as employed by other authors.[9,14,15,16]

For this filter paper a value of 0.85 may be given for the coefficient of efficiency in the fixation of radioactive particles.[9,14,15]

The detector being utilized is a Philips Geiger-Müller 18.514 tube with a mica window of 4 mg/cm².

Under the indicated experimental conditions, a value of the *kq* product has been determined with artificial isotopes having an energy comparable to that of radioactive particles of RaB and RaC, and such values have been found that 0.15 may be taken as their average.

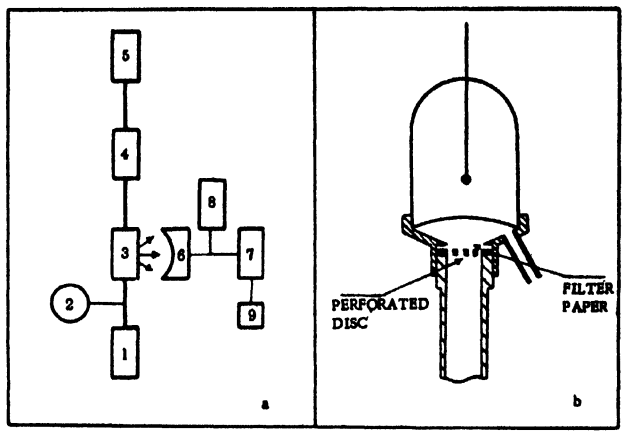

Figure 2. (a) Diagram of equipment: (1) flowmeter; (2) manometer; (3) filter holder; (4) desiccater; (5) exhauster; (6) counter; (7) integrator; (8) high voltage; (9) recorder; and (b) Filter holder counter unit

The air flux, in all determinations, was measured with a type 126 flowmeter produced by the "Rotameter Manufacturing Co., Ltd.", placed as shown on the diagram.

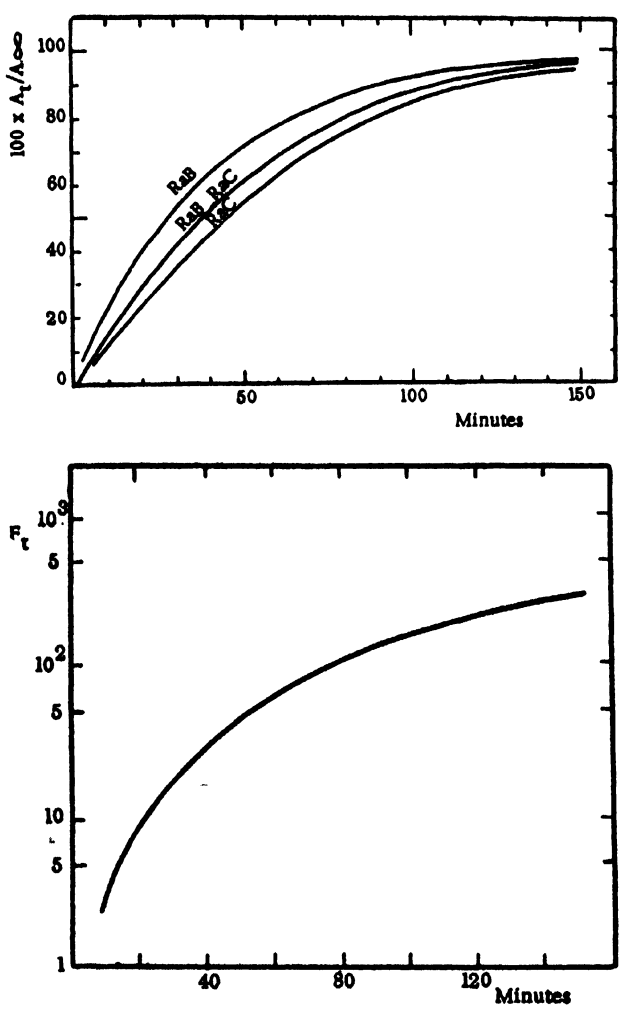

Figure 1. (above) Increase of β-activity on the filter paper Figure 1a. (below) Curve showing Function $Ft = \phi(t)$

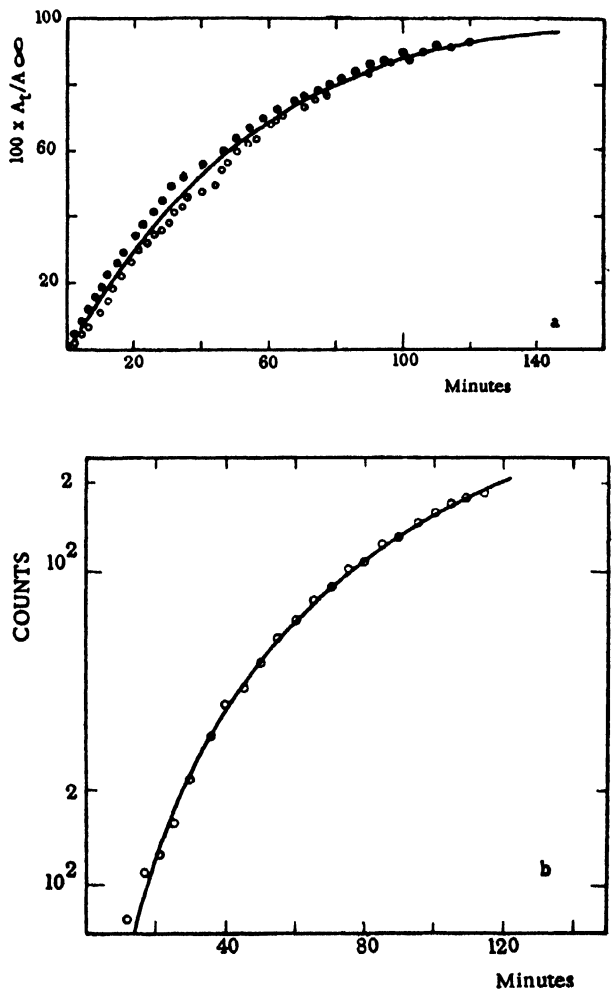

Figure 3. Theoretical and experimental curves showing activity increase on the filter paper: (a) (above) differential curve; (b) (below) integral curve

EXPERIMENTAL RESULTS

Various tests were carried out with an integrator connected to a recorder, in order to verify the agreement between the curves expressing Equations 10 and 14 and the values obtained by experiment.

From Figs. 3*a* and 3*b* it can be seen that the agreement between the theoretical curves and the experimental values is good, both as regards activities at each moment of sampling and the number of counts recorded within the interval 0–*t*. With the latter procedure, the agreement is still better, as could be foreseen, since the errors made are smaller.

Thus the experimental facts justify the assumptions made in arriving at Equations 13 and 14.

ELECTROSTATIC EFFECT ON THE DUST DEPOSIT

During the first stage of the work, we ascertained that radioactive saturation of the filter was obtained at the end of a sampling period of from 40 to 60 minutes. From that time on, activity remained perfectly constant.

The filter paper holder initially was glass and was electrically insulated. This has been eliminated by making a good contact between the filter paper and ground, and agreement between the theoretical and experimental curves has been reached.

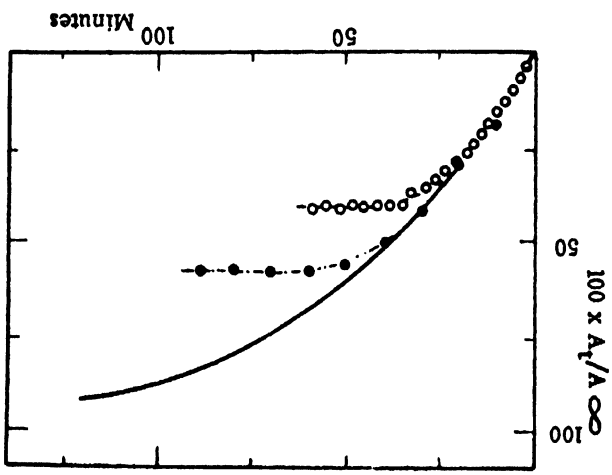

Figure 4. Electrostatic effect

We have interpreted this fact as follows: friction of the air passing through the filter produces electric charges, and these create a field which stands in the way of the depositing of radioactive particles when the system is insulated. From this moment on, the activity of the filter will remain constant, contrary to what is to be envisioned from the theoretical curve, because a state of equilibrium will be reached. Grounding will eliminate this difficulty and the deposit will be normal again. Figure 4 points out this electrostatic effect.

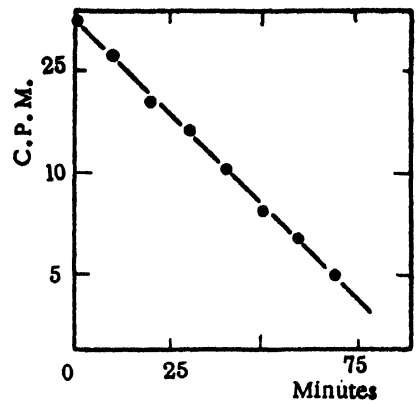

Figure 5. Decay curve for a source taken from a normal atmosphere

IDENTIFICATION OF BETA EMITTERS DEPOSITED

This identification is carried out summarily by the approximate determination of the half-life and maximum beta energy.

Figure 5 shows the decay curve of a sample taken in the open air. The half-life found is 27.5 minutes.

Figure 6 shows the decay curve and beta absorption curve in aluminum of a sample taken in a radon-contaminated atmosphere. The decay curve reveals the "transient equilibrium" which, in its final part, leads to a 27-minute half-life.

Analysis of the absorption curve in aluminum leads to maximum energies of 3.0 Mev, 0.73 Mev,

Table I. Values of f^t and F^t

t minutes	f_t	F_t
0	0.000	0.00
10	0.450	2.04
20	0.866	8.82
30	1.237	19.43
40	1.559	33.31
50	1.822	50.52
60	2.046	69.78
70	2.226	91.26
80	2.381	114.12
90	2.500	138.49
100	2.596	164.08
110	2.672	190.39
120	2.734	217.48
130	2.784	244.95
150	2.853	301.57
∞	2.963	-

Table II

Date	Hour	Rn content, curie/l
18/6/54		1.1×10^{-18}
19/6/54		0.5
5/7/54		2.4
21/10/54		1.5
13/11/54		0.5
16/11/54		1.5
3/2/55		2.3
4/2/55		1.3
11/2/55	10.30	4.2
	11.30	2.9
	12.30	2.0
	14.15	0.8
	15.15	0.9
	16.15	0.7
24/5/55		1.5
25/5/55		1.4
6/6/55		0.4

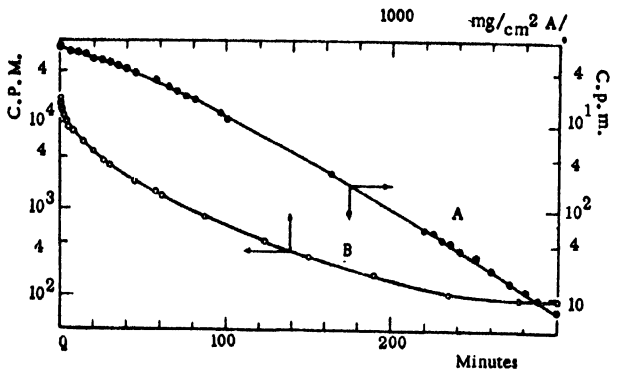

Figure 6. Decay (A) and absorption (B) curves of a source taken from an atmosphere polluted by Rn

and to a component of 1.05 Mev. Within the limits of error of the method, these values agree with the half lives and beta energies of RaB and RaC.

RADON CONCENTRATION IN THE AIR

With the values determined experimentally and by means of Equations 13 and 15, the values shown on Table II for Rn concentration in the air have been determined by various experiments lasting several months. As is well known, the average content of Rn in the atmosphere is 10^{-13} curie/l.

REFERENCES

1. Norman, Holter J. and Glasscock, R., "Tracing Nuclear Explosions," Nucleonics, *10,* 8, 10 (1952).
2. Aliverti, G., De Maio, A., Lovera, G. and Perilli-Fedeli, R., "Autoradiografie Dell'Aerosol Atmosferico," Nuovo Cimento, *XII,* 270 (1954).
3. Hudgens, J. E., Benzing, R. O., Coli, J. P., Meger, R. C. and Wilson, L. C., "Determination of Radium or Radon in Gases, Liquids and Solids," Nucleonics, *9,* 2, 14 (1951).
4. Delibrias, Mme. G., "Dosage du radon dans l'air," J. Phys. Rad., *15,* 78A (1954).
5. Wilkening, M. H., "A Monitor for Natural Atmospheric Radioactivity," Nucleonics, *10,* 6, 36 (1952).
6. Erdik, Enis, "Etude de la radioactivité alfa, de l'atmosphère d'un laboratoire par des émulsions nucléaires," J. Phys. Rad., *15,* 445 (1954).
7. Malvicini, "Camera a scintillazione per la misura dell'emanazione contenuta nell'aria," Nuovo Cimento, *XII,* 821 (1954).
8. Delibrias, Mme. Georgette and Labeyrie, Jacques, "Propriétés, doses de tolérance, et dosage des aérosols presentant une radioactivité alfa," J. Phys. Rad., *14,* 407 (1953).
9. Alercio, John S., Harley, John H., "Evaluation of Alfa-Particle Absorption by Filter Paper," Nucleonics, *10,* 11, 87 (1952).
10. Anderson, W., Mayneord, W. V. and Turner, R. C., "The Radon Content of the Atmosphere," Nature, *174,* 424 (1954).
11. Mansfield, T. H., "Continuous Air Monitor," Nucleonics, *10,* 9, 55 (1952).
12. Labeyrie, J. and Pellé, M., "Enregistreur pour aérosols radioactifs," J. Phys. Rad., *14,* 477 (1953).
13. Watts, Brauner, Burgwald and Reiffel, "Monitor Measures Air and Surface Contamination," Nucleonics, *13,* 1, 51 (1955).
14. Stokinger, H. E., and Laskin, S., "Air Pollution and the Particle-Size Toxity Problem," Nucleonics, *6,* 3, 15 (1950).
15. Harley, J. H., "Sampling and Measurement of Airborne Daughter Products of Radon," Nucleonics, *11,* 7, 12 (1953).
16. Tsivoglou, E. C., Ayer, H. E., Holaday, D. A., "Occurrence of Monequilibrium Atmospheric Mixtures of Radon and its Daughters," Nucleonics, *11,* 9, 40 (1953).

The Fast Ionization Chamber in the Study of α Radioactivity in Air

By U. Facchini, A. Malvicini,* Italy

In a recent paper[1] we studied the behaviour of argon-nitrogen mixtures as the filling gas of a fast ionization chamber and we showed that the electron collection in these mixtures is not practically influenced by small quantities of oxygen.

The curves of Fig. 1 give the pulse amplitude of uranium α particles, obtained with a usual gridded ionization chamber.

In case *A* we have a mixture of great purity (99.99%) consisting of A (98%) and N_2 (2%).

In case *B* we have the same mixture contaminated with about 0.25% of oxygen.

The pulse amplitude is not significantly affected by oxygen above a given voltage. This behaviour is understood when we take into account the fact that the average energy of electrons in the studied range of voltage is around 1 ev and that at this energy the absorption cross section of oxygen is particularly low.

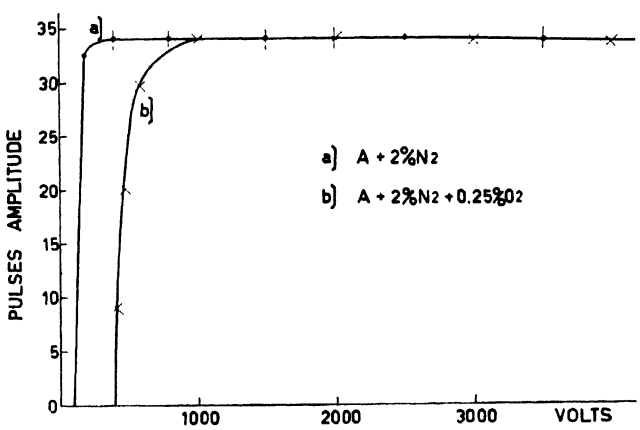

Figure 1. Pulses versus voltage

With such mixtures it is possible to operate a fast ionization chamber easily and quickly, thus avoiding the necessity of the good vacuum and the careful purification of gases required when using unmixed pure gases, such as argon or nitrogen. It should be added that the linearity of the chamber for α particle spectra measurements is as good as in the case of pure gases.

Two kinds of experimental apparatus have been prepared for the study of air activity.

The first, shown in Fig. 2, is made up of a conventional gridded chamber connected with a mechanical pump and with a container of the mixture A (98%)-N_2 (2%).

After the alpha-emitting samples are placed in the chamber, it is evacuated in 30 sec by the pump.

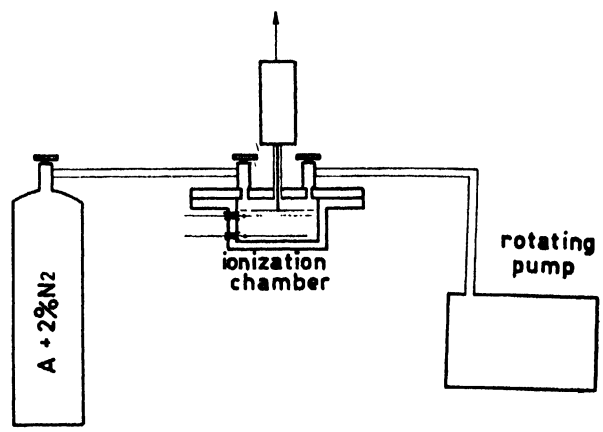

Figure 2. Experimental assembly

Then the chamber is filled to the desired pressure with gas mixture.

The chamber is then ready for functioning. The whole process of introducing the sample and preparing the chamber takes just a few minutes.

The second apparatus consists of a chamber similar to the first one but the sample can be introduced from the side so that only traces of air penetrate the chamber during the operation.

A slow flow of the filling mixture reduces the air contamination to a sufficient extent.

The air, which is under examination is sucked through an electrical discharge between a few score of sharp points and an aluminum plate.

In this way most of the radioactive contamination contained in the air is deposited on the plate in a thin layer.

The plate is quickly put in the ionization chamber and the energy spectrum of α particles is measured at different times.

The results obtained with ordinary air are shown in Fig. 3 (*A, B, C*) the quantity of air under examination being one cubic meter and the time of flow about 20 minutes. The air was taken in the basement of our laboratory.

* Laboratori CISE, Milano.

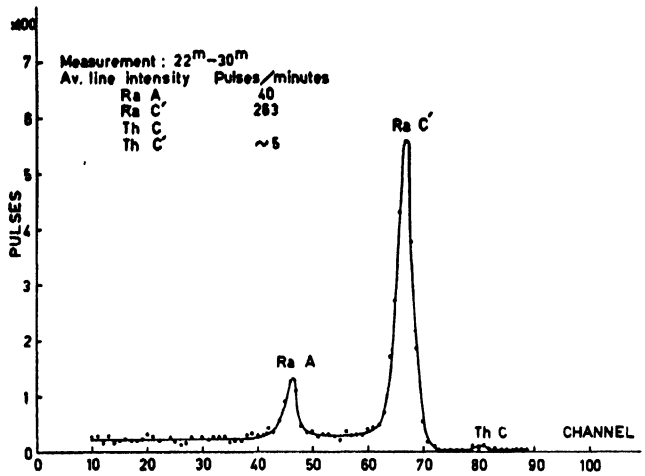

Figure 3A. α-spectrum from ordinary air: air volume, 1.06 m³; time of flow, 20 min

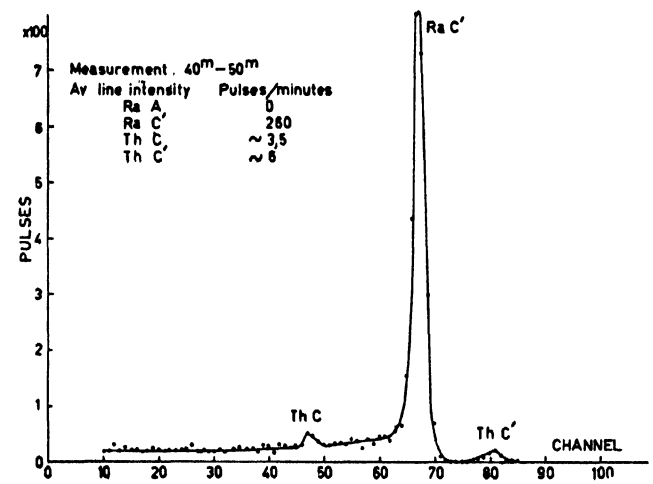

Figure 3B. α-spectrum from ordinary air: air volume, 1.06 m³; time of flow, 20 min

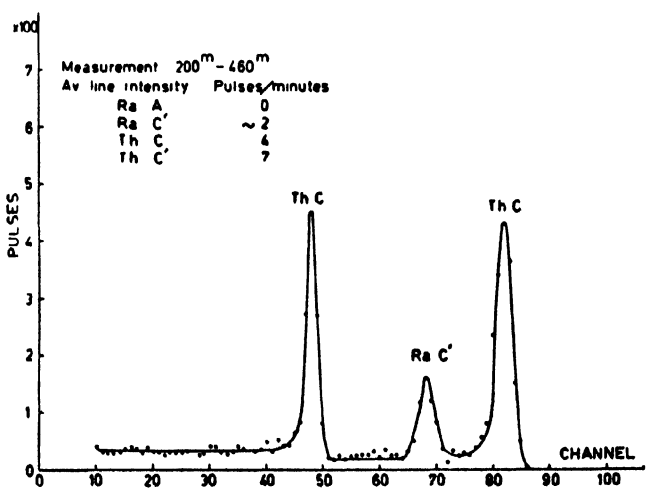

Figure 3C. α-spectrum from ordinary air: air volume, 1.06 m³; time of flow, 20 min

The spectrum taken between the 22nd and 30th minute after the beginning of the flow is shown in Fig. 3A where the line of RaA (5.99 Mev) and of RaC' (7.68 Mev) can be noted. The spectrum in Fig. 3B was taken between the 40th and 50th minute. It can be seen that the RaA line has disappeared and the small peak at 6.05 Mev is due to the ThC; the ThC' line at 8.77 Mev is clearly visible.

In Fig. 3C, corresponding to a time between the 200th and the 460th minute, it is noted that the RaC' line has decayed while the ThC and ThC' lines have maintained a steady intensity.

The figures are in agreement with the well-known decay schemes of these radionuclides. Taking into account the decay time of the different nuclides it is possible to obtain their relative concentration in air. When the method is calibrated, the absolute concentrations are obtained easily.

The method described is very sensitive: ordinary air can be analyzed without any difficulty. The yield of collection of radioactive deposits is greater than 50%. The background of the ionization chamber is often less than 1 pulse per minute and depends on the cleanness of the electrodes; this background is made up of pulses of different amplitude.

When an α-particle line is measured by means of a pulse analyzer the pulses are collected by a certain number of channels (5–6).

The background pulses in these channels form only a small percentage of the total background; i.e. 2 to 3 pulses/hour. It is therefore possible to reveal a line of α-particles when the total number of pulses on the corresponding channels is of the order of 20 pulses/hour.

When, for instance, the analyzed volume of air is 1 cubic meter, a radionuclide can be detected when its concentration in the air is of the order of 5×10^{-18} curie, a very low concentration.

The method described above can be used for studying air contaminated with α active elements such as Pu, U, Po etc. This will be of interest to uranium or plutonium plants and hot laboratories

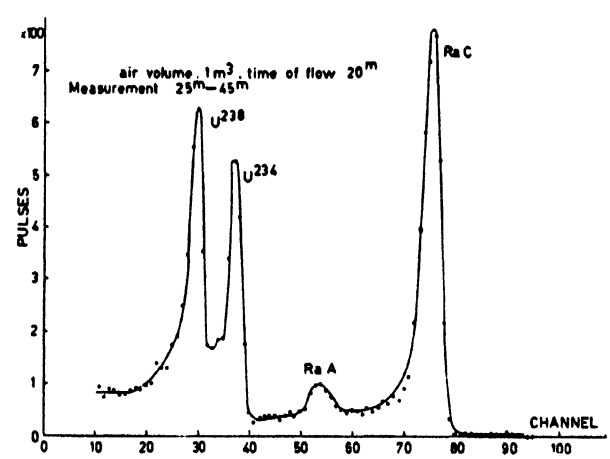

Figure 4. α-spectrum from air contaminated with uranium

where the air is contaminated. Figure 4 shows the α-spectrum obtained from 1 m^3 of air taken in a uranium workshop.

The uranium activity can be easily and quickly measured and distinguished from the usual α lines (RaA, RaC', etc.) of ordinary air, without having to wait for the decay of these lines. This is also true in the case of plutonium where the method described can be even more useful.

REFERENCE

1. Facchini, U. and Malvicini, A., Nucleonics, *13*, No. 4, 36–37 (1955).

Properties of Electrostatic Precipitators for the Measurement of Radioactive Aerosols

By Allan Bergstedt,* Sweden

One of the main problems in the application of the electrostatic precipitator to the sampling of radioactive aerosols is to maximize the amount of dust collected in unit time on a restricted collection surface, i.e., to get a high precipitation rate. The restriction on the area of collection is obvious as the limit of sensitivity in the measurement will be set by the surface density of the radioactive source. The precipitation rate is determined by the effective drift velocity of the dust particles towards the collection surface. In a careful analysis by W. Deutsch[1] of the charging and precipitation process in a Cottrell-type precipitator it was shown that the particle drift velocity was due to electrical forces on the particles and that the electric wind effect in the corona discharge only resulted in an increased turbulence in the gas. The effective particle velocity in the precipitator to be described is easily made more than a factor of ten higher than the limiting particle velocity given for a Cottrell-type precipitator.[2] The results from some of the measurements reported here indicate that the increased particle velocity is due to electric wind effects.

The importance of the particle drift velocity is evident from the expression for the efficiency p of the electrostatic precipitator,[2,3]

$$p = \frac{n_0 - n}{n_0} = 1 - e^{-\frac{Sv}{q}}$$

where n_0 and n are the number of particles per unit volume of air at the input and output, respectively. S is the collection surface area, v is the particle drift velocity towards this surface and q is the air flow rate through the precipitator. For constant efficiency p and air flow rate q an increase in v gives a corresponding reduction in S. The precipitation rate is directly proportional to the product of efficiency and air flow rate. When q is increased the function pq tends towards a saturation value equal to Sv. When used for the sampling of radioactive aerosols the following advantages will be gained by operating the precipitator in the saturation region.[4]

(a) The precipitation rate will be maximal for a given collection surface area.

(b) The precipitation rate will be nearly independent of the air flow rate.

(c) The dust collected will be almost uniformly distributed over the collection surface.

ELECTROSTATIC PRECIPITATOR

The electrostatic precipitator in shown in Fig. 1. In a cylindrical cavity a circular electrode with a number of discharge points is mounted on a tubular insulator. The discharge points are facing an aluminium tape on which the dust is collected. The air passes the discharge region between the points and the surface of the tape and out through the insulator. On the back side of the tape there is a suction plate, which prevents the tape from being sucked into the precipitator cavity as this has a lower pressure than the surroundings. This precipitator is used in a continuous moving tape air monitor. A portable dust sampler using the same type of precipitator was used in the measurements. In the portable dust sampler using the same type of precipitator was plate. These instruments are described in another paper.[4] The measurements reported here were made on alpha active radon products. A flow type proportional counter† having uniform sensitivity over the collection surface was used.

MEASUREMENT OF COLLECTION EFFICIENCY

The measurements were performed in a room containing a large amount of uranium ore, giving an increase in the natural aerosol activity by a factor of more than 10. Wilkening[5] has shown that the distribution of the natural aerosol activity is sharply peaked with 5% of the total activity on particles with a diameter of less than 0.005 microns and 10% on particles larger than 0.035 microns. The efficiency measurements have also been made on pure natural activity, giving the same results but with a lower accuracy.

The efficiency as a function of the air flow rate was measured at a corona current of 1.5 ma and a point to plane distance of 5.60 mm. Another sampler working in parallel at constant efficiency and flow rate was used to standardize the measurements. The result obtained is shown in Fig. 2.

The curves in the diagram are the theoretical values of p and pq as a function of q. The experimental values are marked as small circles. The agreement with theory is very good (within 1.5%)

* Aktiebolaget Atomenergi, Department of Physics, Stockholm, Sweden.

† An independent contribution by A. Franzon.

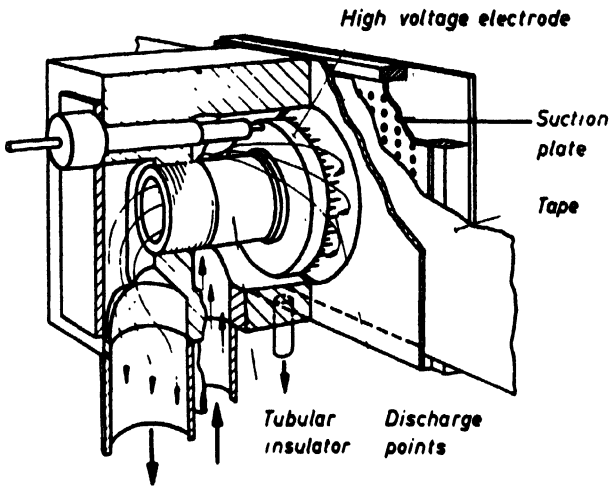

Figure 1

in the normal operating range, i.e., for $q > 0.3$ m³/min. For low flow rates, however, the efficiency measured is much lower than the theoretical value. Experiments with a glass plate covering the precipitator in place of the aluminium plate, and a very dense artificial aerosol permitting observation of the stream lines in front of the discharge head have been made. From these it is evident that the lowering of the efficiency is due to a change in the stream line picture at low flow rates. At high flow rates the turbulence is very high in this region, giving an isotropic mean flow of air. At very low flow rates there usually is a preferred direction of flow from the edge of the electrode to the exhaust at the centre. This tends to make the effective collection surface smaller, resulting in a lower efficiency. At low flow rates some of the stream lines apparently never go through the discharge region between the points and the plate but pass between the tips of the needles and the electrode surface. This gives a shunting of the precipitator. Further experiments are being made with the points projecting less than 1 mm from the surface of the electrode to reduce this latter effect.

EFFECTIVE PARTICLE VELOCITY

The effective velocity v of the particles has been measured as a function of the corona discharge current i for different point to plane distances. The measurements were made with two portable dust samplers, one serving as a standard. The same aerosol as in the previous measurements was used. The air flow rate was constant equal to 0.575 m³/min. The efficiency at this flow rate, at a corona current of 1.60 mA and for a gap distance of 5.60 mm was determined from the previous measurements to be 16.6%. The collection surface is 16.0 cm². This gives the value of the exponent Sv/q, as $p = 1 - e^{-Sv/q}$. With the aid of this value of the efficiency at the operating point stated, the relative pq values in the following parallel measurements were normalized. From these normalized values of p the effective velocity v was calculated as a function of the current i. The result is shown in Fig. 3.

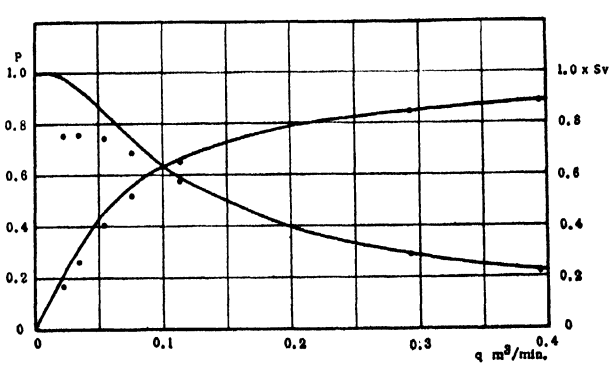

Figure 2

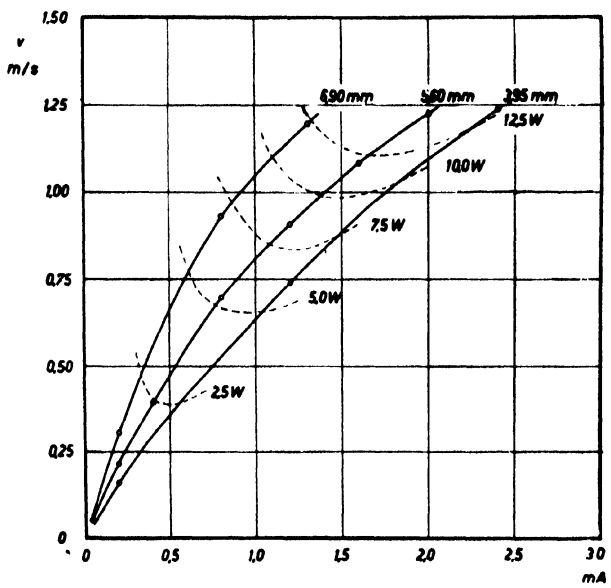

Figure 3

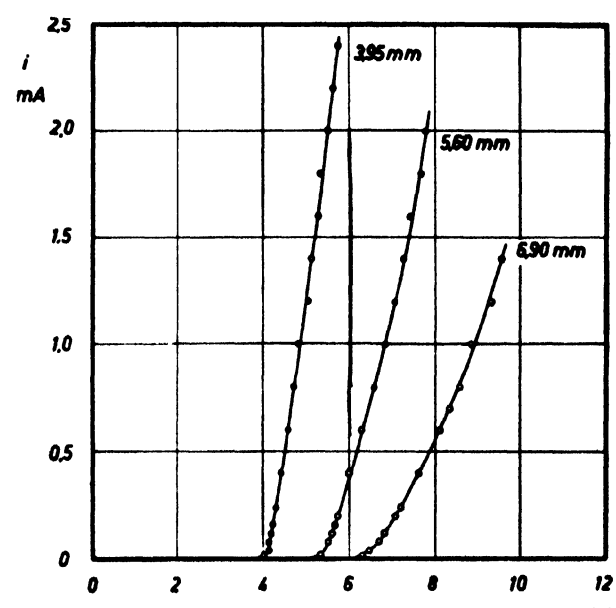

Figure 4

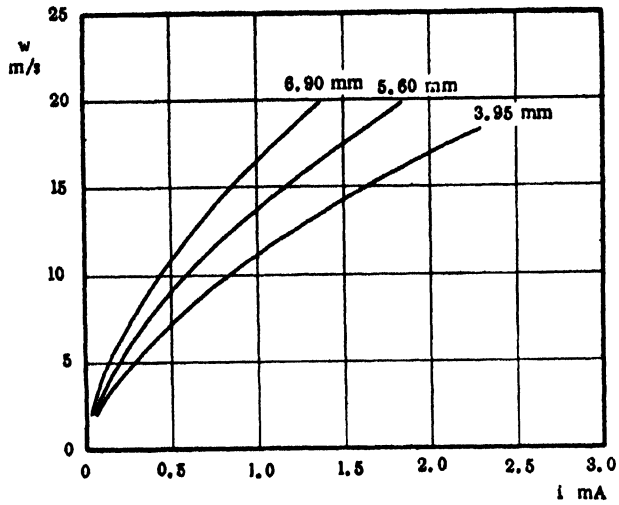

Figure 5

The particle velocity v is shown as a function of the current i for three different point to plane distances: 3.95, 5.60 and 6.90 mm. The current-voltage characteristics of the corona discharge were also measured at these distances, and are shown in Fig. 4.

From these the electrical power input to the precipitator as a function of current has been calculated and is also shown in Fig. 3. It is evident from these curves that for a given power input a higher particle velocity is obtained at large gap distances, if this is greater than approximately 5 mm. The current range shown in the diagrams is well within the existence range of the corona discharge. The number of discharge points is 120. In the continuous air monitor a current of 3 ma is used, the maximum power output of the supply being 28 watts.

PRECIPITATION MECHANISM

To explain the high particle velocity attained in these precipitators the following mechanism was proposed.[4] In the broom-shaped discharge the ions will transfer momentum to the air molecules, creating a wind towards the collection surface. The aerodynamic stream lines of the electric wind bend off and pass through a thin layer close to the surface, outwards from the center of the area hit by the ions. The space between the separate discharges must be large enough to admit the return flow. In the space charge region the electric field strength is low, but immediately in front of the surface there is a steep change of the potential giving a large gradient. The particles will take up some charge while passing the space charge region and are rapidly transported to this layer of high field strength. The precipitation rate in the layer will then be relatively high, though the linear air velocity is also high.

Of special interest is the form of the curves shown in Fig. 3, which can be approximated by the function $v = \alpha\, i^{2/3}$. α is constant within $\pm$ 5%, except at very low currents. This result may be interpreted in the following way. The current-voltage characteristic of the corona discharge is approximately given by the Townsend expression $i = kV\ (V-V_o)$, where k is a constant and V_o is the corona starting voltage. The total power input is $i \cdot V$ watts, and we may consider the part $i \cdot V_o$ as the power lost in the discharge. The maximum available power for imparting an ordered movement to the gas in the discharge is then $P_m = i(V-V_o)$. The sum of the cross sections of the point discharges at their greatest diameter is approximately equal to $S/2$, as measured on the collection plate. If P_m is set equal to the power necessary to accelerate the air to the velocity w, we get

$$P_m = \frac{1}{2}\rho\,\frac{1}{2}\,S\,w^3 = i(V-V_o), \text{ or}$$

$$w = \left(\frac{4}{k\,\rho\,S}\right)^{1/3} i^{2/3}$$

where ρ is the air density.

The electric wind velocity calculated from this equation is shown in Fig. 5. A mean value of k has been used, obtained from the current-voltage characteristics shown in Fig. 4. The relative positions of the curves in Fig. 3 and Fig. 5 are the same. As seen in the diagrams, the electric wind velocity calculated is about 20 times larger than the effective velocity of the particles. As the real collection surface is only one half the total, this means that the effective velocity of the particles is approximately one-tenth the electric wind velocity. A rough estimate of the electric wind velocity has been made by measuring the displacement of the discharges when the precipitator is operated at low current and high air flow rate. These estimates show that the wind velocity calculated is within a factor of 2 of that observed.

It is concluded that the electric wind contributes to the particle drift velocity in these precipitators. A complete verification of the precipitation mechanism proposed would entail measurements of the electric potential in the discharge, in particular at the collection surface.

REFERENCES

1. Deutsch, W., *Ist die Wirkung der elektrischen Gasreinigung dem elektrischen Wind zu verdanken?* Ann. der Physik *9*, 5 Folge: 249–64 (1931).
2. Engel, A. v and Steenbeck, M., *Elektrische Gasentladungen*, Band 2, Springer, Berlin (1934).
3. Deutsch, W., *Bewegung und Ladung der Elektrizitätsträger im Zylinderkondensator*, Ann. der Physik *68*: 344 (1922).
4. Bergstedt, A., To be published.
5. Wilkening, M. H., *Natural Radioactivity as a Tracer in the Sorting of Aerosole According to Mobility*, R.S.I. *23*: 13 (1952).

Record of Proceedings of Session 23B.3

SATURDAY MORNING, 20 AUGUST 1955

Chairman: Mr. A. J. Cipriani (Canada)
Vice-Chairman: Mr. A. R. Torky (Egypt)
Scientific Secretaries: Messrs. R. Hara and D. J. Littler

PROGRAMME

P/571 Air and gas cleaning for nuclear energy processes ..... L. Silverman

DISCUSSION

The CHAIRMAN: Airborne problems constitute one of the greatest hazards in atomic energy installations because it is largely through the air that individuals get radioactive materials into their bodies. The cleaning of air in atomic energy installations might be compared with the cleaning of air in bacteriological installations.

Mr. L. SILVERMAN (USA) presented paper P/571 as follows:

Air and gas cleaning for nuclear energy processes differs from general industrial problems in two major respects. One is the toxicity of the contaminants (higher in most instances) and the other the fact that the cleaner in operation may become a radiation health problem directly or in disposal of collected materials. Radioactive gases and particulate matter (solid or liquid) are the aerosol cleaning problems. Because of their high toxicity the degree of cleaning necessary in order to satisfy health and safety requirements is much more severe than with ordinary materials.

Air and gas cleaning problems arise from the mining, refining, and production of uranium and thorium. In providing cooling air for reactors or shielding, contamination can result from induced radioactivity in cooling air particulates if they are not adequately prefiltered. Cooling air may also become contaminated with radioactive gases or particulates resulting from failure or erosion of fuel elements.

Processing of reactor fuel elements creates radioactive aerosols requiring their nearly complete removal before release to the atmosphere. Laboratory and pilot production of special isotopes and metals; recovery of certain materials; and isotope separation processes are operations which also create problems of airborne radioactive contaminants.

Reducing bulk volume of solid wastes by incineration and evaporation of liquid wastes each produce airborne particulates which require special treatment. The air and gas cleaners by their recovery function provide solid or liquid contaminated materials which must be processed or handled. The contaminants range from rare gases difficult to recover, such as argon (A^{41}), to highly corrosive acid gases such as hydrogen fluoride (HF). Solid and liquid particulates may be organic or inorganic and range in size from less than 0.05 microns to 20 microns. The finest particulates arise from the burning or vaporization of metals and the coarsest are acid mist droplets.

In the early days of the US program, devices which had been designed or developed for other purposes were used. There were many instances where industrial dust control equipment did not give adequate performance. Requirements imposed by low permissible concentrations mean that efficiencies exceeding 99 per cent for particulates less than one micron are frequently necessary. For higher specific activity materials of long half-life efficiencies a thousand times greater are required.

Factors of prime importance are efficiency, resistance to flow, and operating life. The most important in nuclear applications are the first and the last. Power to overcome resistance can be provided within reasonable limits without difficulty.

Since most radioactive contamination is on an activity for equivalent mass basis, the weight efficiency for certain particle size ranges is reliable. Rapid testing of units with fine aerosols is often done with light obscuration procedures.

Unit life in service is of great importance and is related to efficiency and resistance since retention of particulates on filters influences flow resistance and their life in relation to power consumption. Filter life becomes of special interest in minimizing exposure of individuals required to change or clean components. Remote controlled or constant resistance automatically cleaned methods are therefore the optimum for nuclear applications.

Operations may range from the handling of large volumes of materials of low activity, as in refining, to the handling of less than gram quantities of intense activity in research or recovery work.

Air and gas cleaning equipment of most available types have been used. These range from simple inertial collectors to high efficiency filters or electrostatic precipitators. Modifications and technical variations of these devices have also been made. A summary of the usual applications and characteristics of the many devices employed is listed in paper P/571. Because of limitations of time I cannot present the table here.

A distinguishing feature of atomic energy applications in most operations (except refining) is the low loadings or concentrations of materials to be exhausted. This is apparent when the quantities of materials involved are understood. Except for refining operations, loadings lie in the range of one to ten times that of outdoor air. Equipment life for certain applications therefore is manifold as compared to usual process wastes and makes certain approaches applicable which would be impracticable from a life standpoint on industrial process loadings.

In reactors it is essential that we remove particulates from the cooling air to prevent induced activity. Doing this however maintains the initial heat transfer characteristics of the surfaces. It is desirable to clean as close to the source of contamination as possible to minimize deposition and accumulation in ducts and piping. In some instances these become radiating sources requiring shielding. Cleaning close to the source sometimes involves problems of high temperature in thermal reaction processes and as in the case of corrosive gases requires special materials.

I will now show some of the cleaning equipment applied and its applications.

Those who have seen the exhibits both here and at the Palais des Expositions may have seen this filter shown in Slide 1 (Fig. 1) of P/571.

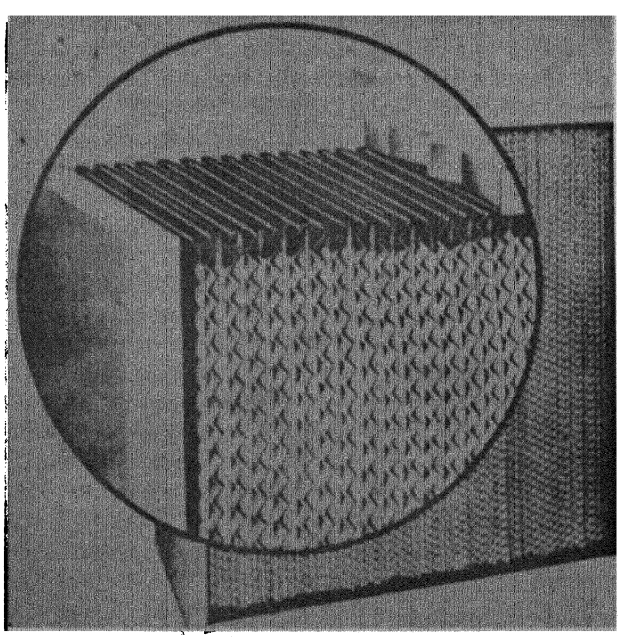

Slide 2

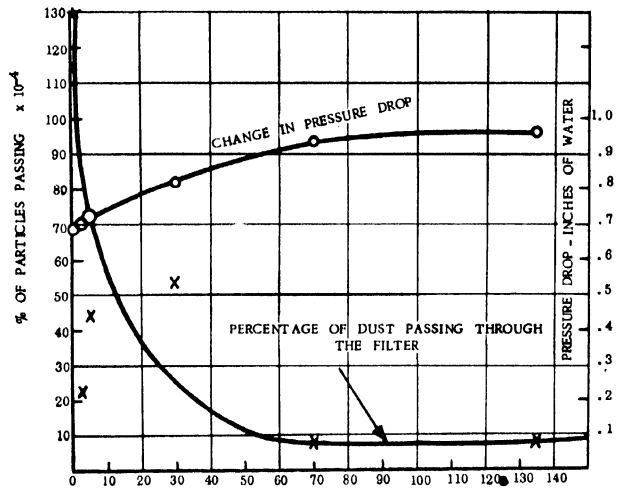

Slide 3. Effect of running time on efficiency of AEC filter paper at a flow rate of five linear feet per minute

Slide 2 shows the structure of this filter in detail. The paper is folded into many pleats separated by corrugated paper separators. The life of this filter is very good in terms of the type of loading to which it is exposed, and its efficiency exceeds 99.98 per cent, or a decontamination factor of at least 10^4. It improves in service.

Slide 3 shows the change in resistance with time over hours of operation, and shows that the efficiency increases as dust is deposited within the filter. The efficiencies actually are given in terms of what you might call the decontamination factor, and the factors are at least 10^4 in removal.

Slide 4 shows the exposure of the filter over several months and indicates the progressive increase in resistance as compared to other types of filter media and indicates the loadings. These are atmospheric dust loadings which are comparable to reactor cooling air operations, and shows the filter has an excellent life. In practice, however, these filters have been used for resistance as high as 8 to 10 inches with increased life. It is advantageous to protect the filter and increase its life with a prefilter. With a spun-glass prefilter a significant improvement in life has been obtained.

The cellulose-asbestos filter is unable to withstand more than small amounts of corrosive gases and is limited to temperatures below 100°C. The media is not fire-proof although it can be made fire retardant. Danger is inherent with ignition and dispersal of retained contaminants. Pyrophoric materials cause damage at their point of contact. In reactor gas clean-up, spray cooling is used to reduce gas temperatures. Prefilters precede the final one and very clean water is necessary for preventing spray aerosol formation.

Because of these obvious limitations an all-mineral filter was developed. Two types of media have been formulated. One, an all-glass formulation utilizing a combination of 1.5-micron and 0.5-micron fibers and the other a combination of the coarser size glass and

asbestos. These have been fabricated into units, one a metal frame type utilizing an aluminum foil corrugated separator similar to the kraft type used in the cellulose model, and the other incorporating an all-glass frame and asbestos separators. Both give performance comparable to the earlier type. In the all-glass media, efficiencies far exceeding the earlier one have been reported for bacteria by Decker, *et al.*

Filters fabricated with this media have already been placed in service. In chemical exposures, wood frames and the plastic adhesive resist most mineral acids. A recent development has been a ceramic fiber 50 per cent Al_2O_3 and 50 per cent SiO_2, known as Fibrafrax which, although brittle and fragile, has been formulated into filter webs capable of withstanding 1000°C. The glass formulations employ plastic binders which decomposes at temperatures above 250°C, and much tensile strength is lost. The only serious limitation to the glass of mineral media is attack by alkalis or hydrofluoric acid.

Another approach to the chemical resistance problem has been the development of papers from fine plastic fibers such as styrene or amid polymers. Papers comparable in performance to the mineral fiber formulations and which resist mineral acids and alkalis are available.

Glass fibers are also used in extended-life graded layer filters for handling dissolver-off gas or vessel vent gases. This application incorporates chemically resistant glass in various diameters from 25 μ to 1 μ placed in layers of varying density and thickness. Full-size installations have been in service for over two years and give low resistance and long life on low loadings of radioactive aerosols.

Sand or gravel in graded layers was used for cleaning general cell ventilation gases before the glass fiber data were obtained. The greater porosity and smaller size with glass fibers make them more feasible than present sand filters. A concrete lined pit may be filled with fibrous material in graded formulations on a porous supporting tile duct. An area large enough to handle the total gas volume at velocities of 20 feet per minute is the design criterion. Fifteen to twenty-five years of use at extremely high

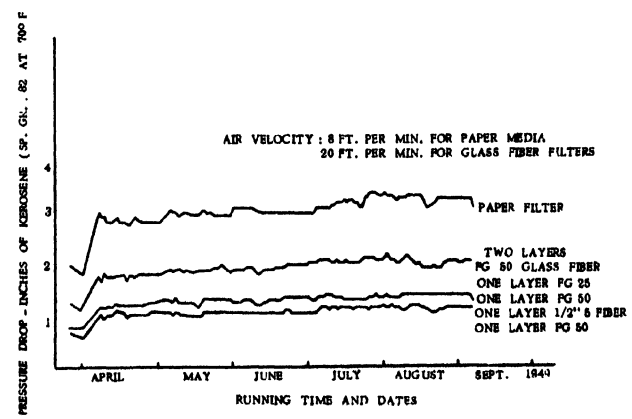

Slide 4. Pressure drop across filter media samples during test run, spring and summer 1949, Brookhaven

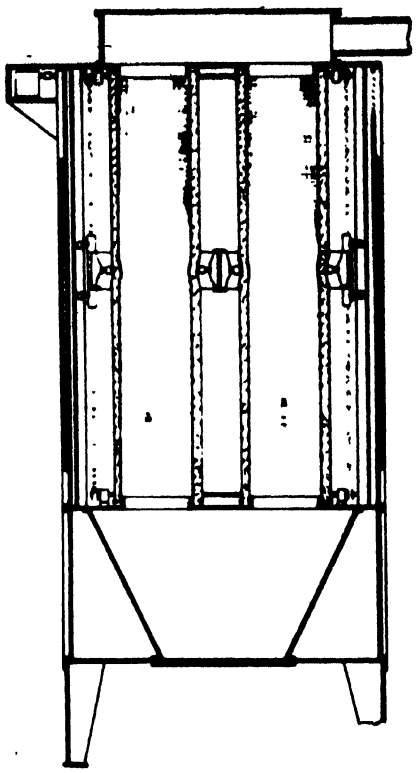

Slide 6. Section through reverse jet filter

efficiencies will be obtained before the filter is replaced.

For filters the resistance of which increases rapidly in service and becomes highly radioactive must be remote from personnel.

We have developed a variable compression filter as shown in Slide 5 (Fig. 2 of P/571) which can be controlled remotely by means of a mechanical linkage or a motor. The unit incorporates compressed layers of spun fiber glass arranged so they can be gradually released in compression as resistance increases. Collected particulates thus penetrate further into the media. Efficiencies well above 95 per cent can be obtained at reasonable resistances. The phenolic bonded flexible fiber glass gives resilience to the media to maintain shape.

One important application for refining operations may be mentioned and that is the use of continuously or automatically cleaned pressed wool or synthetic felts. These are made in the form of bag units which are cleaned by high velocity jets. Rotary arm and disc type units are two new forms which appear useful for heavy loading applications (Slide 6).

The major advantage of this type for refining and fabrication operations where heavy loadings occur with radioactive metals is that constant resistance maintains uniform ventilation rates. The greater capacity, cubic feet per minute per square foot of cloth area (cfm/ft^2 or filter velocity) reduces the number of bags or compartments and minimizes maintenance and replacement.

Mixed particulates such as acid mists and solids are common and the fiber glass devices mentioned

above are applicable. The use of continuously wetted fiber beds and dry filters is another approach to solving this problem. Wet collection procedures cannot be made as inherently efficient because entrained moisture or misting creates effluents not readily captured. Wet collectors in general therefore should be followed by some dry collection procedure.

At our Air Cleaning Laboratory we have devoted considerable study to wet cell units followed by dry pads. This type of device has been used for cleaning of laboratory hood effluents when connected to a central exhaust system. Studies show that this type of unit is an excellent gas absorption system because of the extended wetted surface provided by the fiber glass packs. A composite unit employing Dynel and Saran plastic fibers was developed for combined hydrogen fluoride gas and mist absorption. This unit removes 99 per cent of hydrogen fluoride gas and 85 to 95 per cent particulates in the 1 micron range. If fine radioactive particulates ($< 1\ \mu$) are present, units should include a plastic fiber filter type comparable to cellulose-asbestos. Mixed particulates are also associated with radiochemical laboratory use of perchloric acid. A small composite unit comprising a wetted cell, mist eliminator, and an all-mineral filter has been developed for this purpose as shown in Slide 7 (Fig. 3 of P/571).

This device fits into typical laboratory hoods. It is thus possible to eliminate all organic materials in the cleaner with which perchloric acid might react. Removal eliminates the danger of perchlorates forming in ducts or on succeeding dry hood filters. With this unit perchloric acid may be used in hoods provided with usual filters. Similar problems have arisen in interhalogen chemical use in uranium metallurgy. Since these reactions take place in protected hoods, additional treatment was necessary to remove the interhalogen decomposition products such as hydrogen fluoride, chlorine, chlorine monoxide, chlorine dioxide, hydrogen bromide and hydrogen chloride. Aluminum wire filters or crushed limestone packs can be used in hoods, but for larger quantities of materials a scrubbing system is required. It consists of a series of ejector type nozzles followed by a metal demisting screen. High removal of halogen gases was readily obtained but particulate removal was less satisfactory.

Radioactive gases created by reactor neutron flux on cooling air such as A^{41} and certain radioactive gases (Kr^{89}, Kr^{91}, Xe^{140}, Xe^{141}) which decay to radioactive particulate matter are not easily removed by conventional approaches. Decay products may form after the latter gases pass through filters. At present the method of handling A^{41} and the decay products is based on meteorological dilution and dispersion from tall stacks. If large amounts of rare gases are involved adequate dispersion may depend upon meteorological conditions for proper operation.

The gases may be condensed and absorbed on activated charcoal at extremely low temperatures using liquid nitrogen and similar refrigerants where it is economically feasible. The cost of such systems per cubic foot of air treated is so high that the method is only applicable to small volumes. Another approach for such volumes is compression and storage of the gases in decay chambers.

For reactive gases such as iodine-131, released in volume during dissolver operations, use of silver reactions was applied. A silver reductor unit composed of a tower packed with saddles coated with silver nitrate maintained at an elevated temperature gives the highest removal of iodine compounds. These units are used in series with fiber glass filter. Iodine removal efficiencies are greater than 99.99 per cent. Most of the units have been in operation for periods beyond two years. Reaction gases with long half-life are fortunately quite limited in number. Some gases may be more difficult to remove than particulates. In these cases as a safeguard to all large scale operations producing large volumes of particulate aerosols or gases, a stack should be provided to prevent difficulty from failures in cleaning equipment. The stack also provides an added dilution factor for minimizing health hazards. It should be emphasized however, that cleaning at the source within economic reason must be provided before considering dispersion to the atmosphere.

The problem of evaporation of liquids in regard to aerosol production depends on the method employed for reduction of liquid volumes. The highest efficiency in reducing volume is obtained by vapor compression evaporation. Filtration of entrained mist is done by means of fiber glass.

Particulates from power reactors come from two major sources. These are identified with conditions at the inlet and outlet of the reactor cooling air or its shield cooling air. The cleaning of air entering the reactors minimizes deposition and induced radioactivity. The degree of cleaning necessary for gases leaving the reactor depends upon the reactor design and the amount of precleaning.

A number of new methods of gas cleaning has been developed by research sponsored by the Atomic Energy Commission. We recently described a new method of electrostatic separation utilizing continuous friction charging of fabrics. This appears promising for precleaning use. Slide 8 (Fig. 4 of P/571) shows a schematic diagram of this unit. It cannot be used for saturated aerosols and acid-contaminated air streams.

DISCUSSION OF P/571

The CHAIRMAN: This air and gas cleaning is a very special art. It is necessary but expensive. For those who have not yet started to build such plants, there are a few words of wisdom which we have learnt from experience and which I might pass on to you.

The first is, do not filter any more air than you have to. The second is, do not let in any circumstances maintenance people and others put airducts

throughout the plant, because if you do you will find yourself with a tremendous number of ducts about which you know nothing, and which may or may not need filtering. This leads to a very embarrassing situation.

Mr. R. SPENCE (UK): In defence of maintenance engineers, in view of the Chairman's remarks, I would say that we have this problem of a great deal of ducting in our laboratories at Harwell, but the answer is that the maintenance staff are equally responsible with the scientists. If you have a high order of maintenance, you can rely on your maintenance staff to do the work. I think the answer is that the maintenance engineers must be, as I feel that ours are, sufficiently scientifically-minded to appreciate the difficulties and the problems.

The CHAIRMAN: Are there any other questions about air filtration or air cleaning?

Mr. SILVERMAN (USA): Because of limitations of time, I could not go into the meteorological aspects of the problem that we have in air contamination, which is similar to that which one might consider in the case of large bodies of water. We must consider, in handling any rare gases that might be created by processing of reactor operation, that a certain amount of atmospheric dispersal is permitted, but this must be done under very carefully controlled conditions and with the help of meteorologists.

PEACEFUL USES OF ATOMIC ENERGY:

Proceedings of the International Conference in Geneva, August 1955.

The following is a complete listing of the sixteen volumes which comprise this publication, together with the main subjects covered by each volume.

VOLUME 1

The World's Requirements for Energy: The Role of Nuclear Power

World Energy Needs
Capital Investment Required for Nuclear Energy
The Role of Thorium
The Role of Nuclear Power in the Next 50 Years
Education and Training of Personnel in Nuclear Energy
Economics of Nuclear Power

VOLUME 2

Physics, Research Reactors

Special Topics in Nuclear Physics
Fission Physics
Research Reactors
Research Reactors and Descriptions

VOLUME 3

Power Reactors

Experience with Nuclear Power Plants
Fuel Cycles
Design of Reactors for Power Production
Power Reactors, Prototypes

VOLUME 4

Cross Sections Important to Reactor Design

Equipment and Techniques Used in Measuring Cross Sections Important to Reactor Design
Cross Sections of Non-Fissionable Materials: Delayed Neutrons
Cross Sections of Fissionable Materials
Properties of Fissionable Materials

VOLUME 5

Physics of Reactor Design

Integral Measurements
Resonance Integrals
Fission Product Poisoning
Criticality in Solutions
Zero Energy and Exponential Experiments
Zero Energy Experiments on Fast Reactors and Reactor Kinetics
Reactor Theory

VOLUME 6

Geology of Uranium and Thorium

Occurrence of Uranium and Thorium
Prospecting for Uranium and Thorium

VOLUME 7

Nuclear Chemistry and the Effects of Irradiation

The Fission Process
Facilities for Handling Highly Radioactive Materials
Chemistry of Fission Products
Heavy Element Chemistry
Effects of Radiation on Reactor Materials
Effects of Radiation on Liquids
Effects of Radiation on Solids

VOLUME 8

Production Technology of the Materials Used for Nuclear Energy

Treatment of Uranium and Thorium Ores and Ore Concentrates
Production of Metallic Uranium and Thorium
Analytical Methods in Raw Material Production
Production Technology of Special Materials

VOLUME 9

Reactor Technology and Chemical Processing

Waste Disposal Problems
Metallurgy of Thorium, Uranium and their Alloys
Fabrication of Fuel Elements
Liquid Metal Technology
Chemical Aspects of Nuclear Reactors
Chemical Processing of Irradiated Fuel Elements
Waste Treatment and Disposal
Separation and Storage of Fission Products

VOLUME 10

Radioactive Isotopes and Nuclear Radiations in Medicine

Isotopes in Medicine and Biology
Therapy
Diagnosis and Studies of Disease

VOLUME 11

Biological Effects of Radiation

Modes of Radiation Injury and Radiation Hazards
Mechanisms of Radiation Injury
Protection and Recovery
Genetic Effects
Human Implications

VOLUME 12

Radioactive Isotopes and Ionizing Radiations in Agriculture, Physiology, and Biochemistry

Isotopes in Agriculture
Radiation-induced Genetic Changes and Crop Improvement
Tracer Studies in Agriculture
Animal Physiology
Plant Biochemistry
General Biochemistry

VOLUME 13

Legal, Administrative, Health and Safety Aspects of Large-Scale Use of Nuclear Energy

Legal and Administrative Problems
Reactor Safety and Location of Power Reactors
Safety Standards and Health Aspects of Large-Scale Use of Atomic Energy

VOLUME 14

General Aspects of the Use of Radioactive Isotopes: Dosimetry

Isotopes in Technology and Industry
General Uses, Production and Handling of Radioactive Isotopes
Dosimetry

VOLUME 15

Applications of Radioactive Isotopes and Fission Products in Research and Industry

Radioactive Isotopes in Research
Radioactive Isotopes in Control and Technology
Fission Products and their Applications

VOLUME 16

Record of the Conference

Opening of the Conference and the Presidential Address
International Co-operation in the Peaceful Uses of Atomic Energy
Closing Presidential Address
Evening Lectures
Author Index and Paper Index

SALES AGENTS FOR UNITED NATIONS PUBLICATIONS

ARGENTINA
Editorial Sudamericana S.A., Alsina 500, Buenos Aires.

AUSTRALIA
H. A. Goddard, 255a George St., Sydney; 90 Queen St., Melbourne.
Melbourne University Press, Carlton N.3, Victoria.

AUSTRIA
B. Wüllerstorff, Markus Sittikusstrasse 10, Salzburg.
Gerold & Co., Graben 31, Wien.

BELGIUM
Agence et Messageries de la Presse S.A., 14-22 rue du Persil, Bruxelles.
W. H. Smith & Son, 71-75, boulevard Adolphe-Max, Bruxelles.

BOLIVIA
Librería Selecciones, Casilla 972, La Paz.

BRAZIL
Livraria Agir, Rio de Janeiro, Sao Paulo and Belo Horizonte.

CAMBODIA
Papeterie-Librairie Nouvelle, Albert Portail, 14 Avenue Boulloche, Pnom-Penh.

CANADA
Ryerson Press, 299 Queen St. West, Toronto.
Periodica, Inc., 5112 Ave. Papineau, Montreal.

CEYLON
Lake House Bookshop, The Associated Newspapers of Ceylon, Ltd., P. O. Box 244, Colombo.

CHILE
Librería Ivens, Casilla 205, Santiago.
Editorial del Pacífico, Ahumada 57, Santiago.

CHINA
The World Book Co., Ltd., 99 Chungking Road, 1st Section, Taipeh, Taiwan.
Commercial Press, 211 Honan Rd., Shanghai.

COLOMBIA
Librería América, Medellín.
Librería Nacional Ltda., Barranquilla.
Librería Buchholz Galería, Bogotá.

COSTA RICA
Trejos Hermanos, Apartado 1313, San José.

CUBA
La Casa Belga, O'Reilly 455, La Habana.

CZECHOSLOVAKIA
Ceskoslovensky Spisovatel, Národní Trída 9, Praha 1.

DENMARK
Einar Munksgaard, Ltd., Norregade 6, Kobenhavn, K.

DOMINICAN REPUBLIC
Librería Dominicana, Mercedes 49, Ciudad Trujillo.

ECUADOR
Librería Científica, Guayaquil and Quito.

EGYPT
Librarie "La Renaissance d'Egypte," 9 Sh. Adly Pasha, Cairo.

EL SALVADOR
Manuel Navas y Cía., 1a. Avenida sur 37, San Salvador.

FINLAND
Akateeminen Kirjakauppa, 2 Keskuskatu, Helsinki.

FRANCE
Editions A. Pedone, 13, rue Soufflot, Paris V.

GERMANY
Elwert & Meurer, Hauptstrasse 101, Berlin-Schoneberg.
W. E. Saarbach, Gereonstrasse 25-29, Köln (22c).
Alexander Horn, Spiegelgasse 9, Wiesbaden.

GREECE
Kauffmann Bookshop, 28 Stadion Street, Athens.

HAITI
Librairie "A la Caravelle," Boîte postale 111-B, Port-au-Prince.

HONDURAS
Librería Panamericana, Tegucigalpa.

HONG KONG
The Swindon Book Co., 25 Nathan Road, Kowloon.

ICELAND
Bokaverzlun Sigfusar Eymundssonar H. F., Austurstraeti 18, Reykjavik.

INDIA
Orient Longmans, Calcutta, Bombay, and Madras.
Oxford Book & Stationery Co., New Delhi and Calcutta.
P. Varadachary & Co., Madras.

INDONESIA
Pembangunan, Ltd., Gunung Sahari 84, Djakarta.

IRAN
"Guity", 482 Avenue Ferdowsi, Teheran.

IRAQ
Mackenzie's Bookshop, Baghdad.

ISRAEL
Blumstein's Bookstores Ltd., 35 Allenby Road, Tel-Aviv.

ITALY
Librería Commissionaria Sansoni, Via Gina Capponi 26, Firenze.

JAPAN
Maruzen Company, Ltd., 6 Tori-Nichome, Nihonbashi, Tokyo.

LEBANON
Librairie Universelle, Beyrouth.

LIBERIA
J. Momolu Kamara, Monrovia.

LUXEMBOURG
Librairie J. Schummer, Luxembourg.

MEXICO
Editorial Hermes S.A., Ignacio Mariscal 41, México, D.F.

NETHERLANDS
N.V. Martinus Nijhoff, Lange Voorhout 9, 's-Gravenhage.

NEW ZEALAND
United Nations Association of New Zealand, C.P.O. 1011, Wellington.

NORWAY
Johan Grundt Tanum Forlag, Kr. Augustsgt. 7A, Oslo.

PAKISTAN
Thomas & Thomas, Karachi.
Publishers United Ltd., Lahore.
The Pakistan Cooperative Book Society, Dacca and Chittagong (East Pak.).

PANAMA
José Menéndez, Plaza de Arango, Panamá.

PARAGUAY
Agencia de Librerías de Salvador Nizza, Calle Pte. Franco No. 39-43, Asunción.

PERU
Librería Internacional del Peru, S. A., Lima and Arequipa.

PHILIPPINES
Alemar's Book Store, 749 Rizal Avenue, Manila.

PORTUGAL
Livraria Rodrigues, 186 Rua Aurea, Lisboa.

SINGAPORE
The City Book Store, Ltd., Winchester House, Collyer Quay.

SPAIN
Librería Bosch, 11 Ronda Universidad, Barcelona.
Librería Mundi-Prensa, Lagasca 38, Madrid.

SWEDEN
C. E. Fritze's Kungl. Hovbokhandel A-B, Fredsgatan 2, Stockholm.

SWITZERLAND
Librairie Payot S.A., Lausanne, Genève.
Hans Raunhardt, Kirchgasse 17, Zurich 1.

SYRIA
Librairie Universelle, Damas.

THAILAND
Pramuan Mit Ltd., 55 Chakrawat Road, Wat Tuk, Bangkok.

TURKEY
Librairie Hachette, 469 Istiklal Caddesi, Beyoglu, Istanbul.

UNION OF SOUTH AFRICA
Van Schaik's Bookstore (Pty.), Ltd., Box 724, Pretoria.

UNITED KINGDOM
H.M. Stationery Office, P. O. Box 569, London, S.E. 1 (and at H.M.S.O. Shops).

UNITED STATES OF AMERICA
International Documents Service, Columbia University Press, 2960 Broadway, New York 27, N. Y.

URUGUAY
Representación de Editoriales, Prof. H. D'Elía, Av. 18 de Julio 1333, Montevideo.

VENEZUELA
Librería del Este, Av. Miranda No. 52, Edf. Galipan, Caracas.

VIET-NAM
Papeterie-Librairie Nouvelle, Albert Portail, Boîte Postale 283, Saigon.

YUGOSLAVIA
Drzavno Preduzece, Jugoslovenska Knjiga, Terazije 27/11, Beograd.
Cankarjeva Zalozba, Ljubljana, Slovenia.

Orders and inquiries from countries where sales agents have not yet been appointed may be sent to: Sales and Circulation Section, United Nations, New York, U.S.A.; or Sales Section, United Nations, Palais des Nations, Geneva, Switzerland.